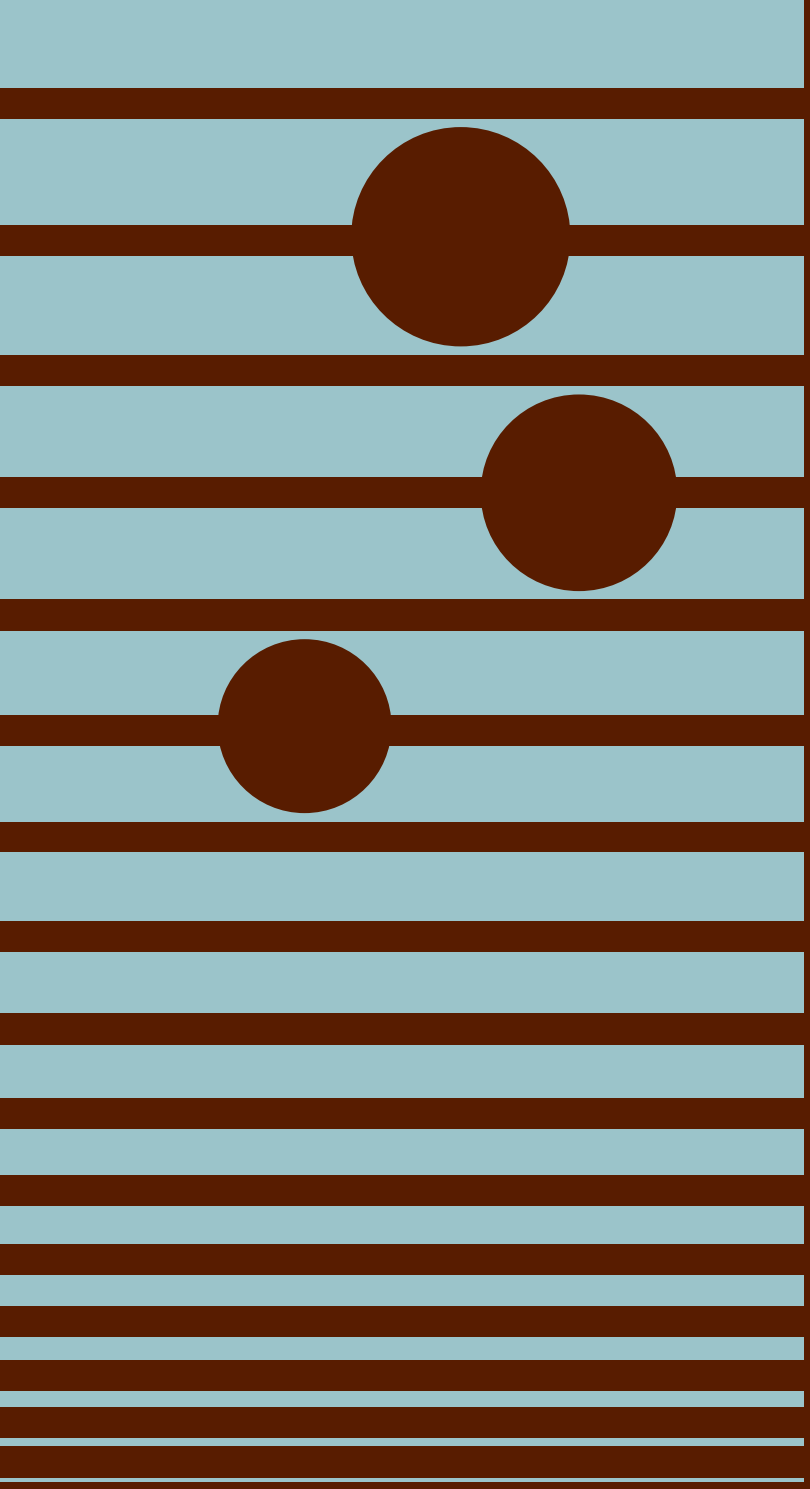


Editors:
Xueqiu He
Hani Mitri
Baisheng Nie
Yunhai Wang
Ting X. Ren
Wenxue Chen
Xiangchun Li

Progress in Mine Safety Science and Engineering II

CRC Press
Taylor & Francis Group
A BALKEMA BOOK

This page intentionally left blank

PROCEEDINGS OF THE 2ND INTERNATIONAL SYMPOSIUM OF MINE SAFETY SCIENCE AND ENGINEERING, BEIJING, CHINA, 21–23 SEPTEMBER 2013

Progress in Mine Safety Science and Engineering II

Editors

Xueqiu He, Hani Mitri, Baisheng Nie, Yunhai Wang, Ting X Ren, Wenxue Chen & Xiangchun Li

North China Institute of Science and Technology, Beijing, People's Republic of China

CRC Press
Taylor & Francis Group
Boca Raton London New York Leiden

CRC Press is an imprint of the
Taylor & Francis Group, an **informa** business

A BALKEMA BOOK

Sponsored by China Academy of Safety Science and Technology, North China Institute of Science and Technology

Co-sponsored by China University of Mining and Technology (Beijing), McGill University, National Safety Council, University of Wollongong and Mining Products Safety Approval and Certification Center

CRC Press/Balkema is an imprint of the Taylor & Francis Group, an informa business

© 2014 Taylor & Francis Group, London, UK

Typeset by V Publishing Solutions Pvt Ltd., Chennai, India
Printed and bound in Great Britain by CPI Group (UK) Ltd, Croydon, CR0 4YY

All rights reserved. No part of this publication or the information contained herein may be reproduced, stored in a retrieval system, or transmitted in any form or by any means, electronic, mechanical, by photocopying, recording or otherwise, without written prior permission from the publisher.

Although all care is taken to ensure integrity and the quality of this publication and the information herein, no responsibility is assumed by the publishers nor the author for any damage to the property or persons as a result of operation or use of this publication and/or the information contained herein.

Published by: CRC Press/Balkema
P.O. Box 11320, 2301 EH Leiden, The Netherlands
e-mail: Pub.NL@taylorandfrancis.com
www.crcpress.com – www.taylorandfrancis.com

ISBN: 978-1-138-00122-0 (Hbk + CD-ROM)
ISBN: 978-1-315-77012-3 (eBook PDF)

Progress in Mine Safety Science and Engineering II – He et al. (Eds)
© 2014 Taylor & Francis Group, London, ISBN 978-1-138-00122-0

Table of contents

Preface xix

Academic technology committee xxi

1 *Coal mine safety*

Study on integrated fire-fighting technology of fully-mechanized caving mining of the deeply inclined combustible thick seam 3
H. Wu, C. Xu, S. Yuan, H. Yao & Z. Zheng

The research on disturbed effects of polyurethane material's expansion pressure upon mine disaster prevention 9
G. Zou, F. Zhang & Y. Song

Research on the application of monitoring techniques of micro-seismic to water inrush forecast in Wutongzhuang Coal Mines 15
Y. Bai & J. Wang

Study on the safety advancing speed of aquifer-protective mining working face in the shallow thick coal seam 19
Y. Liu

The design of rapid prediction system on coal seam gas content 27
Y.T. Liu, J. Liu, S.Q. Ma & W. Di

Research and application of technique of injecting liquid CO_2 in goaf of Shigang coal mine to preventing fire 31
X.L. Tong, Z.A. Huang, Y.H. Zhang, Y.F. Zhang & X.T. Wang

Research on wind tunnel reducing ventilation resistance 37
J.G. Zhang

Research on the application of controllable circulatory ventilation in the mine 41
J.G. Zhang

Research on terminal mining support technology of the hard stratified roof in the fully mechanized coal face 47
L. Chen, G.Q. Hao, P. Liu & Sh.Ch. Peng

Comparative experimental study on dynamic mechanical properties of anthracite and limestone 51
Y.C. Miao & Y.K. Fu

Research on the burst triggering mechanism under the coupling action of higher stress and gas pressure 57
L. Qi, X. Chen, G. Cheng & Y. Cheng

Characteristics of electromagnetic signals obtained during blasting rupture of coal in excavating workface 63
C. Wang, C. Li, J. Wang, P. Hu, Y. Cui & X. Xu

Detection method and abnormal characteristics analysis of TEM in coal mine 71
Q.H. Liang

Calculation of the natural wind pressure of mine based on working-condition adjusted of mine main fan 77
L. Chen

Study on new hydraulic support and technology of top-coal caving at the ends of fully-mechanized working face 81
Y. Liu

Study of reliability of on-line monitoring system for mine hoist braking system 87
H.B. Qiao, K. Liu, Y.L. Wang & H. Yu

Study on the prediction model of gas emission for coal beds based on the EMD and BP-ANN 93
L.N. Zhang, D.C. Lin & J. An

Electromagnetic method in detecting water hazards in coal mining face 99
X. Shi & Y. Hou

Evaluation and applicability study on prediction methods of water inflow in mines 105
H.Q. Lian, X.X. Xia, B. Xu & H. Xu

The application research of mine gas and the fire-reversed stove gas mixing 111
G. Meng & H. Guo

Technology of controlling upper corner gas by pneumatic fan with vortex zone replacement 115
X.X. Chen, W.G. Jin, L. Gong & H.T. Li

The prospecting technology for water enrichment of water-inrush geological structure in mine 121
W. Yang

Determination of mine ventilation resistance and analysis on ventilation systems in the No. 4 mine of Pingdingshan Coal Field 127
Y. Hu, Y.F. Weng & L. Zhang

Design of mine monitoring system based on ZigBee and CAN 131
D. Liu, J. Wu & H. Liang

Development and application of gel foam materials for fire prevention and extinguishing 135
Z. Xie, T. Luan & Y. Zhang

The research on water inrush from overburden and early warning technology according to electrical characteristics in Qidong mine 143
Y. Zhang & H. Huang

Study of key technology for gob-side entry retaining in high gas coal face 149
J. Xing, P. Dang, Z. Li & W. Li

Fractured zone roof grouting reinforcement technique 153
Z.W. Zhu & C. Wang

Method of choosing optimal features used to Intrusion Detection System in coal mine disaster warning internet of things based on Immunity Algorithm 157
J.W. Zhao, Y. Hu, L.M. Sun, S.C. Yu, J.L. Huang, X.J. Wang & H. Guo

Non-Darcy seepage and stopped floor water inrush prevention 163
J. Wu & S. Yin

The study on the principle of the compound perforating technology to improve rate of gas extraction 167
J.D. Xu & X. Yang

Method of detecting in coal mine disaster warning internet of things based on SVM intruders optimized by Genetic Algorithm 171
C.L. Wang, L.M. Sun, S.C. Yu, J.L. Huang, X.J. Wang & H. Guo

Experimental study on the impact of complex surfactant in coal-water contact angle 175
L. Jin, N. Jiang & S. Chen

Research on method of automatic recognition of coal mine water inrush sources based on Immune Algorithm and Back Propagation Neural Network 179
S.C. Yu, L.M. Sun, J.L. Huang, X.J. Wang & H. Guo

Gas drainage technology of inner interlocked low tail laneway in extraordinarily high gas working face 185
Q. Ye, Z.Z. Jia, H.Z. Wang & Y. Pi

Research on airflow catastrophic of side branches induced by gas pressure in upward ventilation 191
A. Zhou, K. Wang, Z. Wu & Y. Jiang

Experimental study of horizontal strata deep rock roadway crack propagation and strength criteria 199
M.C. He, Y.Y. Peng, F. Zhao, Y.B. Wang, Y. Zhang, Y.Q. Sun & W.L. Gong

Research on the performance of foam agent used for mine fire prevention 205
Z.J. Tian, X.L. Zhang, R.Y. Zhou & Q. Ye

Research on efficient dust suppression measure in full-mechanized mining face 211
G.J. Yi, M.X. Jia, J.H. Wang & S.M. Wang

Risk analysis of 18 kinds of coal spontaneous combustion at Huanghua port 217
J.S. Zhang, S.M. Wang, X.L. Zhang & H.Q. Xiong

An LCA-based health damage evaluation method for coal mine dust 223
R. Tong, Y. Zhai & X. Li

The controlling techniques on floor heave of large cross section mining roadway with complicated surrounding rock 231
Q.F. Zhao, Y.H. Wang, Y.D. Liu, H.T. Li, J.J. Shi & L.Y. Shi

Study on the inhibitor rate evaluation by thermal analysis method 237
C. Xu, Z. Zheng, S. Yuan, H. Yao & H. Wu

Determination of goaf "three zones" scope in Pang Zhuang mine and fire prevention technology 245
Z. Xie & K. Wang

Active pressure determination under the condition of rapid determination of gas pressure 249
S. Yang, G. Cheng & L. Qi

Study on effect of gas adsorptive constant under electro magnetic fields exerted 253
L. Zhang, X. He, J. Yue & E. Wang

Hazard prediction and prevention of rock burst in island working face 257
S.S. Guo

Research on technology of paste-like filling mining under villages 263
Y. Dong, Y.C. Huang, L.C. Shao, K. Wang & Z.J. Duan

Study of rockbolts nondestructive detecting based on improved immune Danger Theory 269
X. Sun, Y. Zhao, J. Cheng & X. Sun

Experimental study on fireproofing performance of active explosion suppression system 275
Y.Y. Wang, J.F. Wang, Y.L. Zhang, J.M. Wu & S. Liu

Influence of concentration distribution on gas explosion shockwave in tunnels 279
J. Chen, L. Pang & Q. Ma

The application of the relaxative operator theory to predict the emission volume of gas in coal mine 283
L. Tan, Y. Xue & H. Ju

Outburst prevention technology and effects of hydraulic flushing with effects of pressure relief and increasing permeability 287
W. Meng & B. Li

Experimental research on major properties of the sealant to control toxic and harmful gases leakage in coal mine 293
J. Li, F. Song & H. Kang

A new borehole arrangement for draining the methane in mining induced fractured zone and the utilization of the drained methane in Yangquan Nanzhuang Coal Mine 299
D. Zhang, J. Zang, Y. Jiang & K. Wang

The empirical analysis of ARIMA multiplicative seasonal model to forecast the total number of coal mine accidents 305
L. Liu, H. Yao & L. Tan

Monitor and control node in coal production safety based on LonWorks Fieldbus 309
T. Zhang

Study on subsidence reducing technique by continuously filling grouts into stope overburden bed-separation along the dip 313
X. Fan, X. Fan, P. Wang, L. Zhou, Z. Wang & J. Zhao

Optimization of roadway layout and its effect analysis for lower protective seam in fully mechanized caving mining 319
Z. Chang, Q. Hui, Y. Li, Z. Wang & J. Zhao

Safety evaluation model and application for purification device of sour natural gas based on risk 327
J. Yi, M. Zong & W.H. Wang

Coal mine comprehensive safety information management system based on the cloud computing 331
S.Y. Liu & T.Y. Xiong

Treatment methods of coal mining subsidence area at South Lake in Tangshan city, Hebei province 335
C. Xu, Y. Chen & Z. Li

TBM tunneling in squeezing ground: Problems and solutions 339
H.S. Ma, J. Wang & L.J. Yin

On the best escape route with multiple optimization objectives during mine fire time 347
W.M. Gai, W.M. Gai, Y.F. Deng, J. Li, Y. Du & B. Cao

Mine sewage control system using PLC technology 353
J. Jiang & X. Zhang

A brief analysis of electromagnetic interference caused by the electrical and electronic equipments in the underground coal mine safety monitoring system 359
X. Hu, J. Wang, X. Li & F. Ding

The desorption laws and diffusion model of coal gas in different particle size 363
C. Wang, S. Li, J. Liu, Y. Qin & Z. Shen

Research on heat damage control and combined technology of waste heat utilization 369
J. Ma

Research on mine refrigeration of large mines with large mining depth 373
Y. Niu & J. Wang

Application feasibility study of single based station CORS in deformation monitoring of mine slope 379
Q.B. Wei, W. Li, L.B. Gao, C. Wang & Q.L. Li

Study on building permanent underground refuge chamber in Dayangquan Coal Mine 383
T. Zhang, L. Jin, N. Gao & X. Huang

Study on distribution law of lead abutment pressure in fully mechanized caving face with large mining height 389
F.L. He, Z.Y. Liu, T.D. Li, S.R. Xie, H.K. Wu & Z. Wei

The explosion-proof design of Abandoned Mine Detection Robot 395
L. Lei, B. Zhu & R. Jia

Study on the regulation of water hazards and prevention work in Yima Coalfield 401
S.Y. Li, Z.Q. Ma, M.L. Ren & X.L. Zhang

The safety technology of head rope replacement in large friction hoisting mine 407
A.T. Balkema, G. Westers, M.J. Dong & F.Y. Jia

Kinetics study on anthracite coal oxidation at low temperature by thermal analysis 411
X.X. Zhong, G.L. Dou, Y. Chen & D.M. Wang

Research on thermal stability of new-style foamed gel 417
S. Yu, H. Zhao, X. Chen & G. Meng

The application research of K shortest path algorithm in avoiding mine disaster 423
F. Wang, H.G. Guo & G.J. Lu

Study on goaf spontaneous combustion prediction simulation of gas-drainage in spontaneously flammable and thick coal seam 427
Z. Zheng, Q. Zhang, C. Xu, C. Ma, H. Yao & H. Wu

A study of GM (1, 1) residual correction model in gas concentration prediction of heading face 433
B. Wu, Z. Liu, Y. Zhou & P. Lou

Study on barrier door of gas explosion with foam ceramics as the main body 439
J.H. Sun, Z. Qu, H.Y. Fan & C.R. Wei

Prediction of coal and gas outbursts with random forests 445
Y. Lin, X. Lu & J. Fan

Goaf frictional ignition and its control measures in underground coal mines 451
G. Wang, T.X. Ren & C. Cook

The water hazards caused by burst of overburden strata separation and the control strategies 461
J.M. Wang & H. Huang

Research on multivariate hierarchical analysis and evaluation on rock burst hazard 467
Z. Yu, F. Jiang, Q. Zhu & J. Li

Study on stability of thick-hard key stratum based on numerical simulation in longwall mining 477
Z. Yu, F. Jiang, Q. Zhu & S. Zhu

Research on the free radical affecting methane outburst within coal under the electromagnetic radiation 483
M. Shang-Quan & F. Jing

Study on safety monitoring system of mine machine 487
W. Zhao, S.M. Wang & S. Qiao

2 *Metal and nonmetal mine safety*

Numerical investigation of three-point bending fracture test on granite 493
H.J. Wang, D.A. Liu, J.R. Niu, Z.D. Cui & F. Zhao

Potash exploration overview and safety considerations in Canada 499
J. Han, L. Piché & P. Geo

Experimental study on high temperature shear strength parameter of salt rock 505
K. Fang, Y.P. Li, W.W. Bi & J.P. Wu

3 *Mine product testing technology and safety symbol management*

Fast verification method of mining mechanical anemometers based on wind speed equivalent weight 511
W.Y. Ni & W.M. Gai

Development of a new kind of safety helmet of underground miner for emergent hedge 515
X.M. Liu, Y.K. Gao, Z.A. Huang, Y.H. Zhang, Y.F. Zhang & Q. Zhao

The research of dynamometer for anchor cable in mine tunnel based on the industrial Ethernet 521
X. Li, X. Li, H. Feng & J. Liu

Research on safety lead-acid battery charger in coal mine 527
Q.Z. Zhang & M.Y. Xu

Studies on the large capacity mine lithium ion battery intelligent charger 531
Z. Quan-Zhu, S. Xiao-Lei, D. Yong-Hong & M. Hong-Mei

The structural optimization and numerical simulation of wet centrifugal precipitator in fully mechanized heading face 537
H.F. Yao & P.J. Hu

Literature-based study of warning sign and of its effectiveness 543
C. Ma, S. Jia & Y. Zhang

Study on special protective clothing of coal mine 551
J. Yao & D. Tian

4 *Mine rescue tools and techniques*

How to improve the psychological quality of mine rescue commanders and fighters 559
Q.Z. Li

Assessment of Emergency Preparedness Effects of work safety in Xinjiang autonomous region of China based on weighted Rank Sum Ratio 563
W. Zhang, F. Kong & T. Jiang

Application of reverse circulation DTH hammer in mine rescue drilling 567
F. Kong & X. Lai

Study on chemical oxygen source in underground emergency refuge system 571
S. Wang, L. Jin, S. Liu & Z. Zhang

A probe into the working procedures of crisis public relations in mine disasters 577
X. Shao, H. Xu & J. Tang

Mine rescue training programs and research 583
H. Xie & T. Yan

An completeness evaluation method of community emergency response plan 587
G. Ren

Analytical and improvement research on emergent evacuation system of terminals based on behavioral mode characteristics 593
H.X. Hao

5 *Mine safety management and standardization*

Forecasting of coal mine CBM productivity based on wavelet transform 601
H.Q. Zhou & B. Cheng

Discuss on safety training of coal enterprises 605
Q. Du & B. Kou

Study on problems of safety culture construction in coal mine and the countermeasures 611
Y. Zhao & Y. Wang

Game model and analysis of market-based refined safety management in a coal mine enterprise 615
Y. Weng

Analysis on the factors' characteristics of coal miners' safety behavior based on trajectory crossing 619
R. Ni

Human behavior classification and application in the field of work safety 625
Y. Zhang & L. Pan

Study on coal mine hazard information management system based on PDCA 631
X. Zou, H. Guan, Z. Yu, Z. Guo & Z. Zhao

Application of optimized decision-making system in coal mine hidden dangers information management 637
S.Y. Liu, M. Zhu & L. Peng

Systems thinking theory in the safety production management system construction 641
H. Liu & X.L. Wang

Research on the safety prevention measures of mine water disaster in Shaqu coal mine of Liulin region 647
X.H. Wang, Y.B. Wang, J.H. Cheng, J.J. Fan, H.J. Xu, X. Zhang & Z.W. Liu

Application of the combination forecasting method in coal mine accidents forecasting 653
J. Li & Y. Ning

A statistical analysis of coal gas explosion accidents in China 659
Y. Cui, B. Xie, J. Cao & C. Wang

Construction way on the team safety culture in coal mine 665
D. Tian, J. Yao & H. Xu

Research of distributed monitoring and management system of mine ventilation 669
X.L. Liu, B. Shen, L.H. Li, S.W. Ren, L. Zhang, K.Q. Cheng & X.Z. Xu

Selection of coal mine accident cases for training 673
W. Yang, K. Zhu, S. He, Y. Zhang & S. Gao

Research on relationship between coal mine safety input and safety performance based on system dynamics 679
B. Wu & Z.F. Liu

Study on information disclosure of especially serious accident 685
B. Wu & Z. Chen

Analysis of regularity and occurrence causes of coal-gas dynamic disasters accidents 689
W. Sheng, Z. Sheng, M. Gao & L. Yang

Comparative study on the investigation mechanisms for coal mine work safety accidents in China and USA 693
G. Mei & L. Liu

Implementation of Kaizen in enterprise HSE management 699
X. Niu, P. Yang & M. Qu

Analysis on the reasons and response measures for accidents of dangerous chemicals transport 705
Q. Bu, J. He & X. Tong

Coal mine accident human error model construction and team safety management mode analysis 711
J. Chen, Q. Cao & Y. Yang

Analysis on ERP implement in coal enterprises based on management mechanism innovation 717
Y. Wang, J. Wang & S. Shao

Application of fuzzy comprehensive evaluation for mining idlers' performance 721
Y. Xing

Function principle and empirical research of "zero accident" concept 725
Z.M. Liu, G. Fu & H.B. Pei

Analysis and statistics of workers' unsafe acts in coal mine gas explosion 731
W. Yin, G. Fu, P. Gao & C. Yang

Study on STOP applied to safety management of coal mine 737
Y. Yao

The implications of behavior-based accident causation "2-4 model" in the prevention of coal mine roof accident 741
P. Gao, G. Fu & W.T. Yin

Research on safety management capability of coal enterprises of strategic orientation 745
H.L. Qi & Y.C. Ning

Influence of underground noise to people's unsafe behavior in coal mines 749
G.Y. Cheng, S.J. Chen, J.L. Qi & Y. Cheng

A brief analysis on Chinese classical philosophical thoughts and the idea of safety 753
G. Xu & G. Xu

Social structural analysis of mine accident 759
F. Lu & Y. Yan

Discussion on the management system innovation about safe development of China coal mining industry 763
J. Zhang

Grey system theory-based overseas investment risk assessment for mining enterprises 769
J. Han

Cause analysis of behavior of the secondary accidents in coal mines and the prevention 775
S. Zhang, G. Fu & S.H. Shi

Analysis on relationship of construction accident probability and safety training 783
Z.M. Liu, G. Fu & H.B. Pei

6 *Mine safety science and theory*

Analysis of mine pressure factor of dynamic disasters to coal seam with large dip angle 791
G.Q. Hao & C. Li

Mechanical mechanism analysis of forming grouting seepage channel in clay sand medium 795
H. Shi & D. Tian

Mechanism study on gas diffusion through coal particles base on mass transmission fundamental 799
Z.L. Wang

Cooling parameters fitting analysis in long distance excavation roadway 803
Z. Chu, X. Zhang, J. Ji, Y. Zhang & W. Baoqi

Study on acoustic emission and damage during the failure of coal rock 807
Y. Wu, H. Liu & S.M. Zeng

Study on numerical simulation for the fracture law of gob-side entry retaining roof 811
J.J. Shi, H.Y. Shi & J.Zh. Guo

Numerical simulating research on changing law of humidity in refuge chamber 815
Y.H. Zhang, Q. Zhao, Z.A. Huang, Y.F. Zhang, Y. Tian & Y.K. Gao

Medium characteristics and water transmissibility of carbonate strata on Ordovician top in Pingshuo, China 821
Y.M. Qi, H.B. Bai, X.E. Zhao & B. Luo

The abutment pressure distribution of extremely thick seam top coal caving longwall panel: A case study 827
H. Nan

Research on the fractal characteristics of pore structure of coal particles based on low temperature nitrogen adsorption method 831
L.C. Dai, B.S. Nie & L. Li

Research on experiment test system of mechanism of fame propagation for gas and coal dust explosion 837
L. Zhang, L. Liu & J. Xu

Numerical simulation of W-type ventilation in goaf of spontaneous combustion and gas migration 843
J.J. Liu, D. Wang & J.L. Gao

Numerical simulation study on permeability and humectant properties of coal seam water injection under high water pressure in long drilling hole 851
Y.B. Yu, W.M. Cheng, G. Zhou, L.J. Chen, L. Zhang & G.M. Liu

Dimensionless analysis in mathematical model of gas emission in coal particles 857
Y.P. Qin, Y.J. Hao, P. Liu & J. Wang

Analytical study of the time varying diffusion law of the gas in the pea coal 863
B. Cheng & H.Q. Zhou

Safe and high-efficient mining model in old mining area and resource integration mines 869
H.T. Li, L. Zhang, Y.F. Weng, H.T. Li & J.G. Yang

A numerical simulated study on the permeability and the rule of stress distribution on working face 875
X. Song & Z. Xie

Study on the optimization of ventilation system in Zhongxing coal mine 879
X. Song & Z. Xie

Multifractal characteristics of coalfield faults and gas-geological significance 883
P. Chen, E.Y. Wang, Z.T. Liu & Z.Y. Sun

The reasonable narrow coal pillar width along gob research of the deep dynamic pressure conditions 891
Z.W. Zhu & Z.J. Wen

The mechanism of coal fatigue failure and its numerical analysis under pulsating water pressure 897
H. Zhu, M. Zhang, J. Shen, B. Lei & G. Jia

The law of gas releasing in heating and oxidation process of coal 903
H. Wang, B. Yu, X. Cui, M. Chen & L. Geng

A new mathematical model of the relationship between gas desorption index of drill cuttings and gas content 907
K. Shen & H.Q. Zhou

Based on simulate test to research the law of CO newly generated when external oxygen involved during the coal breaking process 911
X. Wu, Q. Qi, X. Zhou, Z. Dong, S. Huang & Z. Liu

Feasibility of mining under water based on detecting height of water flowing fractured zone 915
B. Gao, Y. Liu & T. Yuan

Study on the deformation mechanism of deep soft rock tunnel and its control 923
H. Luan, D. Kong, Z. Wang & W. Sun

Theoretic seepage model of "water-rock-structural plane" considering the hydro-mechanical coupling mechanism 927
K. Man, J. Wang, R. Su, X. Liu, Y. Zhao & B. Zhao

Laboratory study and prediction on coal permeability of Qinshui Basin 935
G.Q. Zheng, B.C. Ling, X.Z. Zhu, J. Pan, Z.J. Pan, L.D. Connell & S.H. Tang

Impact of air-return lane and gas drainage lane spacing on surrounding rock stress 943
Y.C. Lyu, M. Wang & Y.W. Wang

Research on distribution and evolution patterns of abutment pressure in front of the fully-mechanized working face of "three-soft" coal seam isolated island 949
W.Q. Xu, E.Y. Wang, Z.T. Liu, E.K. Hou, S.J. Wang & Z.S. Deng

Study on safety theory of rheology-mutation based on system life cycle 957
X.Q. He & D.Y. Zhao

The law of gas accumulation in top-carving area of roadway and its treatment method 963
C. Chen, B. Wu, H. Wang, Y. Ding, X. Cui & Y. Zhu

Unsafe act analysis on major and particular major flood accident in coal mine 969
Y. Chun, J. Dong, B. Lu, S. Shi, S. Yuan, P. Gao, Z. Chang, Z. Chen & G. Fu

Numerical study of fluid flow and convention heat transfer in sandstone as a porous media 977
W.L. Gong, D. Liu, P.Y. Guo, H. Zhang, Y.B. Wang, Y. Zhang, B.J. Liu & Y.Q. Sun

Research on the adaptability large mining height fully-mechanized mining equipment to panel mining of unstable coal seam 983
H.X. Wen, Y.D. Liu & X.T. Meng

The study on dynamic early-warning of coal face gas emission based on extension theory 987
B. Lei, B. Wu, Y. Peng & C. Wang

Study on mining pressure appearance feature in shallow-buried fully-mechanized longwall face 993
Y.F. Ren

Numerical simulation of blasting effects on soft coal under different confining pressure 997
H.Q. Zhu, S.H. Zhu, G.W. Jia & Z.Y. Song

The research of high-altitude mine ventilation optimization decision theory based on Analytical Hierarchy Process (AHP) 1003
H. Wang & K. Zhang

Study on the stability of roof based on Mathews method in deep mining 1009
B. Zhang, C. Wang & L. Wang

Burning characteristics of No. 6 coal seam at mine field's two wings in Cuijiazhai mine 1013
Y.H. Wang, H.T. Li, Q.F. Zhao, J.J. Ren, S.S. Yang & Z.J. Shu

Study on influence of propane for the generating kinetics of multi-component gas hydrate 1017
Q. Wu, Q. Wu, B. Zhang & X. Gao

Microcirculation of air leakage of gob-side coal pillar in fully-mechanized face 1023
H.Q. Zhu, S.H. Zhu, S.L. Feng & G.W. Jia

Effect of hydrate crystal type on mechanical properties of gas hydrate-bearing coal 1029
Q. Wu, F. Zhu, X. Gao & B. Zhang

Numerical study of heat convection caused by two-phase flow confined in underground heat-exchange tunnel 1033
W.L. Gong, D. Liu, Y.Q. Wu, Y.Y. Peng, Y. Zhang & B. Liu

The research of realizing the mine safety of ascending vessel undertake force by using 2 force stem mechanical characteristics 1041
A.T. Balkema, G. Westers, F.Y. Jia & M.J. Dong

Research quantitative model of gas pressure gradient and in-situ stress in complex tectonic outburst coal seam 1045
D.X. Qin, M.B. Zhang, B.L. Lei, X.Y. Kang & A.Y. Zhu

Experimental research on movement law of coal-bed methane including temperature and confining pressure effects 1051
Y. Kang, X. Gao & C. Pan

Experimental simulation for "sorting" effect after gas and coal outburst in blind draft 1055
B.S. Nie, W.X. Hu, L.L. Yang & J.W. Chen

Study on the law of mining-induced fractures field evolution based on similar simulation experiment 1061
Y. Wu, B. Wu, M. Hua & Z. Guo

Study on abrasivity characteristics of surrounding rock in long inclined-shaft of coal mine by TBM techniques 1067
H. Jiang, Y. Jiang & J. Zhang

Protected range extension of mining underlying protective seam with long distance 1073
T. Yu, J. Sun, P. Lu & H. Guo

Study on Weijiadi coal mine geological structure characteristics and gas occurrence regularity 1079
S. Shao & J. Zhang

Numerical simulation on goaf gas extraction by the ground drilling 1083
Z. Ma, J. Zhang, Y. Xie, Q. Feng & J. Dang

Study on the similar experimental model and flow field distribution law of stope 1087
Y. Qin, S.Q. Yang, C.L. Jiang, J.Y. Lun, G.X. Zhang & J. Niu

Uncertainty analysis and evaluation of gas flow measurement 1095
P. Lu

Coupling model and its application to dynamic failure for hard coal containing gas 1099
C. Wei, H. Li & B. Li

Experimental investigations on gas emission rules during fully-mechanized developing entries in deep and high-gas coal seams 1105
F.B. Liu & Y.S. Wang

Application of optical fiber oxygen sensor in coal mines 1109
Y. Zhao, Y. Wei, Y. Li, T. Zhang, W. Zhao, L. Lv, T. Liu & C. Wang

Variation characteristics of coal and gas outburst accident and its quantitative analysis based on FAHP 1113
X.J. Lv, M.H. Geng & X.G. Zhang

The causes of sinking columns in North China coal fields and their permeability identification 1121
L. Xu & J. Wang

Characteristics of in-situ stress field in northern Tianshan Mountain mining areas 1127
S.K. Zhao

Distribution and genesis of H_2S abnormity area in gas of Shigejie Coal Mine 1133
L. Lu, X.H. Fu, Y. He & C.L. Jiao

Rock slope surface monitoring technologies with focus on ground-based synthetic aperture radar 1137
H. Mitri & I. Vennes

Stability analysis on pillar for point-pillar mining of karst water mine 1145
S.G. Fu & K.L. Xu

Characters and control measures of unsafe operation behaviors in colliery accidents 1151
M. Shang-Quan, M. Zheng, X. Li & F. Jing

High gas drainage lane design parameter simulation research 1159
Z. Wang & H. Li

7 *Occupational health and safety in mines*

SWOT analysis of aging mines' low carbon development 1169
H. Ma, H. Lian & H. Zhu

Study on the information management mode of occupational hazard supervision 1175
H. Bai & Y. Weng

Study on factors of asphyxiation & poisoning and its preventive measures in underground mining 1179
G. Mei

8 *Petroleum and natural gas exploitation*

Preventive maintenance planning strategy of natural gas pipelines based on risk inspection 1187
H.X. Li, W.H. Wang, B.J. Sun & R.Z. Dong

Collision behavior mechanism between drill pipe and coal hole wall during gas extraction drilling 1193
X. Han, Z. Tie, D. Li, L. Zhang & C. Shi

Research on leak accident risk of typical heavy-caliber long-distance natural gas transportation pipeline 1199
S. Zhang

Safety evaluation model of oil depot based on BP neural network 1205
Y. Yang, G. Luo, Y. Gu & C. Zhu

9 *Other related topics*

Protection for the occupational safety right of workers and China's legislative practice 1213
F. Lu

Analysis on the styles of young miners subculture 1217
Y. Fang & X. Tian

The industry transformation in resource-exhausted city based on safety science 1221
H. Yao

Application of the analytic hierarchy process on the tender invitation and evaluation of mine safety equipments 1229
Y. Song & L.P. Liu

Fault characteristics and the tectonic evolution in Changdi area of the Bohai Bay Basin 1235
X. Li, W. Wang, B. Zhang & L. Zhou

Regression model analysis on relativity between coal mine output and safety 1241
L. Song, L. Yang & C.J. Zhang

Construction of mine safety explicit knowledge map 1245
W. Wang, W. Dai & Q. Sun

The distribution and influencing factors analysis of coal consumption of China based on quantile regression 1249
P. Cheng & Y. Kong

Coal fines production in different drainage stages and its influence on productivity 1253
S. Hou, X. Wang, M. Wu, X. Wang, Z. Jing & A. Zheng

Research on the relationship among safety labor division, safety specialization and safety marketization 1259
Y. Weng

Study on effectiveness of coal mine reorganization systems based on game model 1263
Y. Bi & X. Zhang

A study on accounting and measurement of resources and environment value in Beijing region 1267
P. Bai & Q. Duan

Early-warning models of regional work safety risk in Chongqing city and Ningbo city, China-based on partial least squares regression 1273
T.H. Jiang & D.Y. Zhao

Study on the hydrogeochemistry and isotope characteristics of Ordovician groundwater in Yanzhou coalfield, North China 1279
Y. Han, G. Zheng, J. Pan, G. Wang & Z. Li

Discussion on application of strength reduction FEM based on bishop method of soil slope 1287
W. Yu & J. Cai

Experimental study on macro-micro mechanism of the marble during unloading damage process 1291
Y. Cong, Z. Wang & L. Zhang

Graded classification of mine environment geological problems 1297
Q. Chen, W. Sun, Q. Wu & S. Xi

Preliminary study on safety audit 1305
S.M. Wang, J. Xu & X.F. Liu

Author index 1313

This page intentionally left blank

Progress in Mine Safety Science and Engineering II – He et al. (Eds)
© 2014 Taylor & Francis Group, London, ISBN 978-1-138-00122-0

Preface

As societies continue to grow and develop, the demand for energy has been on the rise worldwide. In China, coal is still one of the principal energy resources and more coal mining projects are needed in the future. As mining operations continue to increase their production rates and discover more ore reserves, the problems of mine safety science and engineering have become more present. There is a greater need more than ever before to better understand these problems. Based on the success of first international symposium on mine safety science and engineering, the second conference also brings together researchers from around the world to present and discuss their research findings on mine safety techniques and technologies, methods and approaches, as well as problems and issues, all with the goal that we improve the safety of our mines worldwide.

In this symposium, the peer reviewed papers were published in this proceeding, which is very important to share mine safety technology with worldwide researchers. And we hope to see you in next conference in the future.

This page intentionally left blank

Progress in Mine Safety Science and Engineering II – He et al. (Eds)
© 2014 Taylor & Francis Group, London, ISBN 978-1-138-00122-0

Academic technology committee

DIRECTOR OF ACADEMIC TECHNOLOGY COMMITTEE

Zhou Shining, *Academician of the Chinese Academy of Engineering, Beijing, China*

V-DIRECTOR OF ACADEMIC TECHNOLOGY COMMITTEE

He Xueqiu, *North China Institute of Science and Technology, Beijing, China*
Hani Mitri, *McGill University, Montreal, Canada*

MEMBER OF ACADEMIC TECHNOLOGY COMMITTEE

Shi Lin
Luo Haizhu
Jiang Yaodong
Wang Jiren
Li Shugang
Tang Chunan
Zhao Yangsheng
Erik Westman
Guo hua
Naj Aziz
Mani Ram Saharan
Raghu Arunachalam
David D. Wagner
Hu Qianting
Zhang Jianguo
Yu Bin
Li Side
Yang Daming
Yin Guangzhi
Jin Longzhe
Wang Jiachen
Wu Chao
Dou Linming

This page intentionally left blank

1 *Coal mine safety*

This page intentionally left blank

Progress in Mine Safety Science and Engineering II – He et al. (Eds)
© 2014 Taylor & Francis Group, London, ISBN 978-1-138-00122-0

Study on integrated fire-fighting technology of fully-mechanized caving mining of the deeply inclined combustible thick seam

Haijun Wu
Mine Safety Technology Branch, China Coal Research Institute, Beijing, China

Changfu Xu
Mine Safety Technology Branch, China Coal Research Institute, Beijing, China
Faculty of Resources and Safety Engineering, China University of Mining and Technology, Beijing, China

Shasha Yuan
Faculty of Resources and Safety Engineering, China University of Mining and Technology, Beijing, China

Haifei Yao & Zhongya Zheng
Mine Safety Technology Branch, China Coal Research Institute, Beijing, China

ABSTRACT: To solve the technical problem of spontaneous combustion prevention and control in fully mechanized caving mining gob of deeply inclined thick coal seams, the characteristics of spontaneous combustion of deeply inclined was analyzed systematically. Based on the selection of index gases and determination of spontaneous combustion danger zone, the technology of low air quantity ventilation, nitrogen injection in goaf, buried grouting, injection FR-1 inhibition and inserting and masonry retaining walls can be used for ensuring the safety and efficiency of the 065-2 fully mechanized caving face. The research results have an important demonstration guidance significance and application for fire prevention in the gob and safety production of other similar mines.

1 INTRODUCTION

The deeply inclined seams are defined by the coal seams which pitch are between 35~55° (Wu et al. 2000). Their reserves account for 14% of total coal reserves in China. More than 50% of the mining coal seams in west are the deeply inclined seams mainly distributed in the Sichuan, Xinjiang, Gansu, Fujian, Guangdong, Inner Mongolia and northeast provinces (regions). The deeply inclined seams are difficult mining for low mining production efficiency, bad safety benefits and harsh operating environment (Zhang et al. 2010). So the major coal producing countries exploit hardly these kind seams. Only a few countries are small-scale mining for experimental study. The technology of fully mechanized coal mining of the deeply inclined seams has been obtained success in different degree in China. But there are still some questions about spontaneous combustion prevention and control, which need deeply research and practical explore (Li 2006, Zhang 2009).

The 065-2 working face in gushan mine of Inner Mongolia Pingzhuang Co., Ltd. is the main production face, of which the average length is 926 m and the average inclination length is 78 m. The industrial reserves are 91.6 million tons and mining period is 1 year. Whether can safe and highly efficient extraction or not directly affects the economic and social benefits of gushan mine. It is the current pressing issues. The average mineable thickness of the coal seam is 7.5 m. The seam inclination is 34 degrees. And mining method is the technology of fully mechanized coal mining of the steeply dipping thick seam. Spontaneous combustion of the 065-2 working face is serious and its spontaneous combustion stage is one to three months. There are the fire areas of shallows mall coal mine and gushan No. 1 mine around the work-face. The upper of the 065-2 working face is goaf of the 065-1 working face, where exist coal spontaneous combustion hidden trouble and menace seriously the safety of the coal production. Although some measures of spontaneous combustion prevention and control have been taken to the fire area of shallows mall coal mine and gushan No. 1 mine, there is still of big hidden danger. Meanwhile, it is a new technical problem of spontaneous combustion prevention and control of the fully mechanized coal mining of the steeply dipping thick seam.

2 THE CHARACTERISTICS OF SPONTANEOUS COMBUSTION IN GUSHAN MINE

1. Strong coal spontaneous combustion tendency. The spontaneous combustion stage of seam containing fusains is general one to three months and the shortest one is only 15 d.
2. Slow drawing speed of working face. The geological conditions of coal seam are complicated because the major tectonic is faults and intrusions in the area. Meanwhile, there are unclearly small coalfield fire areas.
3. The falling height and volume increases and the uncertainty and concealment of fire location strengthen for large inclination (Chang et al. 2009).
4. Mine fire generally occurs in deep area where has a certain distance from coal exposed surface.
5. It is difficult to achieve the requirements of fire prevention and control of the traditional anti-fire fighting methods such as thick loess grouting, spraying separating agent and so on for large inclination.

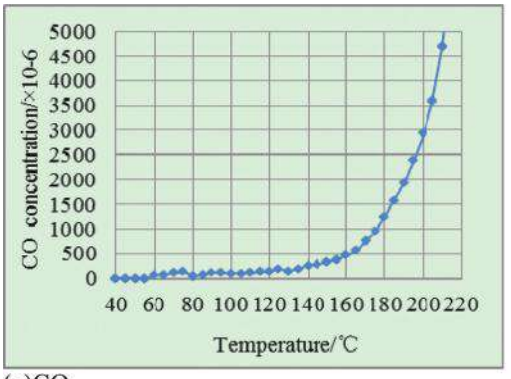
3 PREDICTION TECHNOLOGY OF COAL SPONTANEOUS COMBUSTION

3.1 *Index gases*

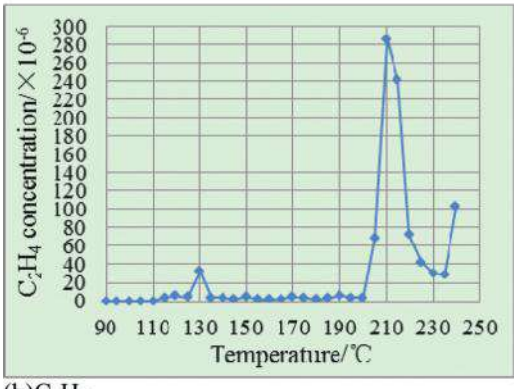
As shown in Fig. 1, the appearance temperature of CO is about 55°C. When the temperature is lower than 130°C, CO concentration presented linear increase and when the temperature is higher than 130°C, its concentration presented exponential increase. In the case of the air volume is not mutated, when CO concentration is high and rapid increase, it shows that coal there is some trends of coal spontaneous combustion, which can judge the degree of development of the coal spontaneous combustion.

The appearance temperature of C_2H_4 is about 109°C. C_2H_4 concentration presents a tendency of slow increase at first and afterwards it decreases between 110°C~130°C. It is a lower value between 140°C~200°C. When the temperature is higher than 200°C, the gas concentration increases rapidly, then it becomes smaller.

The ignition temperature of the coal samples is about 340°C according to spontaneous combustion characteristics experiments of coal samples of the 065-2 working face in gushan mine. The spontaneous combustion index gas system with CO for main index gas and C_2H_4 for auxiliary was established when the effective forecasting temperature was below 220°C.



(a)CO



(b)C_2H_4

Figure 1. Relationship between the gas generation concentration and temperature.

3.2 *Distribution regularity of spontaneous combustion "three zone" in goaf*

The distribution of oxygen concentration in goaf is one of the important criterions of spontaneous combustion danger zone (Sudhish C.B. 1985). Grasping the distribution law is the important basis and dependence of effective technical measures to prevent coal spontaneous combustion. The variation of oxygen concentration in goaf with the advance of the working face was detected by the embedded bundle tube sampler (see Table 1).

The spontaneous combustion "three-zone" is divided in goaf using O_2 index. The oxidation zone is defined by the area of the oxygen concentration which is from 18% to 8% (Wang 2008). It would be possible to obtain the range of spontaneous combustion "three zone" that non-ignition zone is 0~15 m, the spontaneous combustion zone is 15~45 m and the suffocative zone is over 45 m.

Table 1. Monitoring results of goaf oxygen concentration in the 065-2 working face.

Embedding goaf distance/m	Oxygen concentration (O_2%) of the measuring points				
	1#	2#	3#	4#	5#
0	20.2	20.20	19.82	19.78	19.56
3	19.97	19.67	19.21	19.13	17.46
7	19.91	19.45	18.78	18.50	15.35
10	19.81	19.23	18.08	16.68	14.9
15	19.40	19.11	16.9	14.76	11.50
22	17.51	18.16	15.5	12.12	11.10
24	14.32	18.01	15.3	11.34	9.26
27	9.12	17.87	14.06	10.51	8.24
36	7.43	16.54	12.63	8.13	7.84
39	7.02	14.07	12.14	7.87	7.54
42	6.78	10.27	10.87	6.93	7.10
45	6.43	7.91	8.76	6.64	7.08
48	6.12	7.08	7.84	6.27	6.83
57	5.68	6.02	7.35	5.02	5.64
60	5.21	5.57	6.13	4.65	5.48
63	4.88	5.02	5.49	4.34	5.21

4 INTEGRATED FIRE-FIGHTING TECHNOLOGY OF 065-2 WORKING FACE

4.1 *Low-volume air ventilation*

Theory research and production practice shows that using the low-volume air ventilation in the working face to reduce breathing of gob effectively is the fundamental technology for spontaneous combustion prevention in goaf (Zhou et al. 2010). In order to get the effect rule of air volume changes on the spontaneous combustion "three zones" in gob, the change rules of oxidation heating zone in goaf under different air volumes have been simulated, and air volumes of simulation are respectively 642 m^3/min, 800 m^3/min, 900 m^3/min, 1000 m^3/min. The change rules of spontaneous combustion "three zones" of goaf in simulation results are shown in Table 2.

As seen in Table 2, with the increasing air volume of working surface, the position of oxidation heating zone moves to the deep gob, and rendering the trend that the width of oxidation heating zone increasing obviously. From the angle of preventing spontaneous combustion in gob, it should be minimized the width of oxidation heating zone as much as possible and the air volume of working face as low as possible. So the lowest supplying air volume of 065-2 mechanized caving face should be 525 m^3/min which is calculated according to «Coal Mine Safety Regulations» and «Operating procedures of 065-2 mechanized caving Face». Considering the instability of ventilation status in working surface, air volume can be increased moderately and the reasonable air volume range of 065-2 mechanized caving face is 578 to 656 m^3/min according to the air volume surplus coefficient of 1.1 to 1.25.

Table 2. Change rules of spontaneous combustion "three zone" with different air volume.

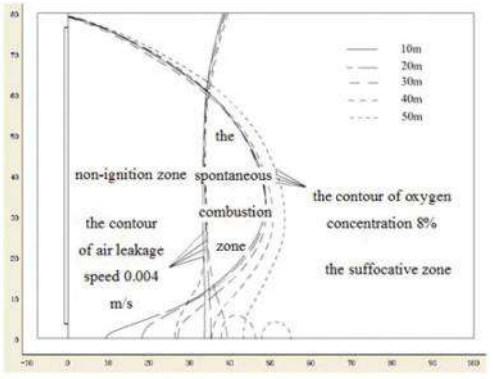
Air volume (m^3/min)	Starting position/m	End position/m	Spontaneous combustion width/m
642	7	49	42
800	12	55	43
900	15	58	43
1000	17	60	43

4.2 *Nitrogen injection against fire in goaf*

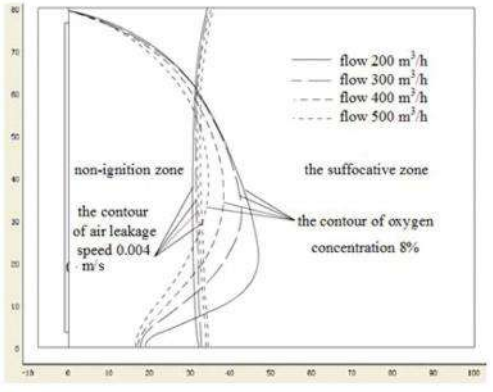
The reasonable nitrogen injection capacity and place are the key technical parameters of nitrogen injection against fire in gob, and they play the important role in effect test of spontaneous combustion prevention and safety production (Li 2003). The influence of nitrogen injection quantity on the law of spontaneous combustion "three zone" in goaf distribution was studied by using the numerical simulation method. Combined with the spontaneous combustion period of work seam and the advancing degree of working face, the reasonable nitrogen injection position and quantity in 065-2 fully mechanized caving face have been confirmed. As shown in Fig. 2, the reasonable nitrogen injection position is 15~35 m in mined-out area and the reasonable nitrogen injection quantity is 250~350 m^3/h.

4.3 *Embedded pipe grouting in upper corner of coal face*

Embedded pipe grouting is a traditional technology for preventing spontaneous combustion in GOAF, which can fill float coal gap and inhibit the oxidation process and the heating rate of the float coal. 2.5-inch 24 meters grout iron pipes were buried along ventilation roadway in the course of actual mining of 065-2 working face. From the open-off cut, pipe should be cut off once every 48 meters along with the working face advanced. The standard of grouting quantity is seeing pulp (or water) at the position after the hydraulic supports in down-corner angle. To insure the slurry concentration, water soil ratio is not more than 4:1. Inject sludge into the gob timely along with mining work.



(a)Nitrogen injection quantity



(b)Nitrogen injection position

Figure 2. Influence of nitrogen injection quantity and position on the law of spontaneous combustion "three zone" distribution.

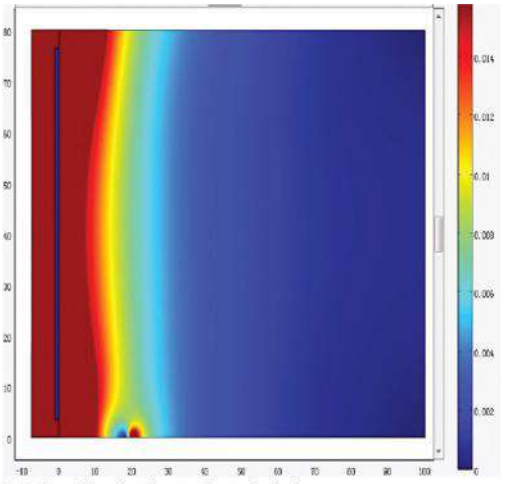
4.4 *The diaphragm walls*

Fig. 3 shows that the comparison of the air leakage between building diaphragm walls and without diaphragm walls.

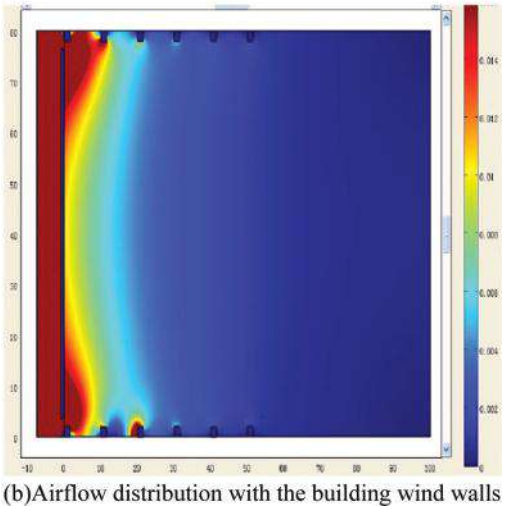
As shown in Fig. 3, the diaphragm wall in the upper and lower crossheading is effective technical measures to control gob air leaking and prevent float coal spontaneous combustion (Tang et al. 2012). Along the direction of the working face, a diaphragm wall with size of 2 × 1.5 × 2.6 m was separately built every 10 meters at the roof caving line of the upper corner and down corner using bags filled with loess and crushed coal.

4.5 *Injecting FR-1 inhibitor*

In order to produce safely and go over the fire zone successfully, mixed the FR-1 polymer liquid foam inhibitor and water according to the proportion of 1:2 (Xu 2010). Use special foam device to create the inhibitor foam. And then put out fire



(a)The distribution of goaf airflow



(b)Airflow distribution with the building wind walls

Figure 3. The comparison of the air leakage between building diaphragm walls and without diaphragm walls.

by means of pour this material into the hidden danger areas of spontaneous combustion through compressed air pipe or inert gas injection pipe. PU's foam equipment consists of special pump, solvent tank, foam maker and air line and so on. The equipment and technology of system bubble is shown in Fig. 4.

In across fire area stage, 135 detection holes were drilled and FR-1 inhibitor was injected into the 37 high-temperature ones. FR-1 inhibitor was introduced into the detection holes in amount of 25~100 kg daily and fill volume of 11.75~45.5 m^3. The total amount of injecting FR-1 inhibitor was 2.5 t and fill volume was 1125 m^3. Injecting FR-1 inhibitor played a significant role in

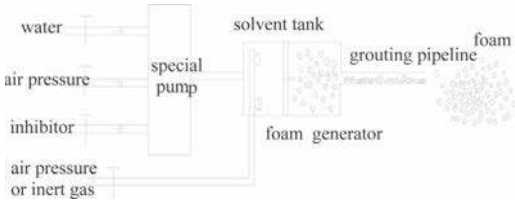
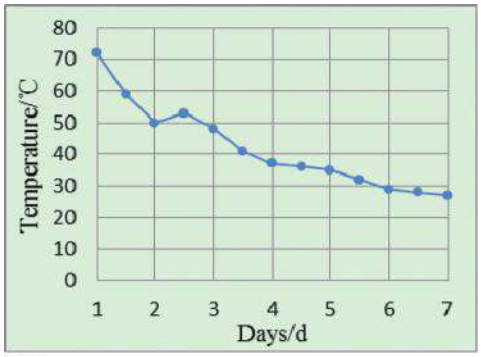
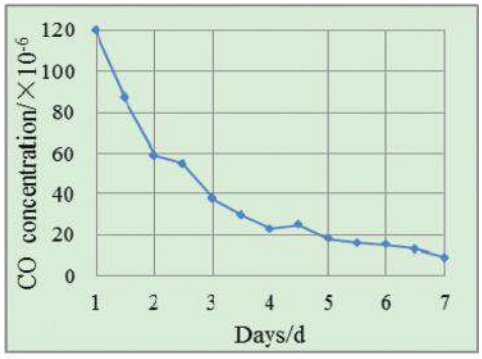


Figure 4. Equipment and technology of system bubble.



(a)Temperature



(b) CO

Figure 5. Variation of the extinguished parameters after pouring FR-1 inhibitor.

eliminating the high temperature point and preventing coal mine fire. Take B4-2 drilling of fire zone in guxin small coal mine as an illustration. CO concentration was 0.012%, O_2 concentration was 4.3%, and the gas temperature was 72°C. Inject the foam inhibitor 100 Kg to the beyond-standards danger zone by B4-2 drilling. The volume of the foam filling was 45.5 m^3 according to foam multiple of 500. Then, validate the effect through adjacent boreholes. The results of test are shown in Fig. 5. The results show that CO concentration and gas temperature decrease with injection time increased. The two indications reduced to the fire zone extinction standard of coal mine safety regulation within 4 to 5 days.

5 CONCLUSIONS

1. Based on the characteristic experiment of coal sample in spontaneous combustion, the relation of concentration and temperature of index gas generated in low temperature oxidation combustion was studied. The index gas system of spontaneous combustion was set up with CO, C_2H_4 subsidiary. The distribution of "three zones" of spontaneous combustion is determined with the oxygen concentration method. And the result shows that non-ignition zone is 0~15 m, the spontaneous combustion zone is 15~45 m and the suffocative zone is over 45 m.
2. The influence of air volume to "three zones" of mined-out area is studied with numerical simulation method, and the reasonable air volume for 065-2 fully mechanized caving face is 578~656 m^3/min. The influence of injection capacity of nitrogen to the "three zones" distribution of 065-2 fully mechanized caving face is analyzed with the method of the combination of mined-out area monitoring and numerical simulation, and the reasonable injection capacity of nitrogen is 250~350 m^3/h. The reasonable injection place of nitrogen is 15~35 m in mined-out area.
3. For the 065-2 fully mechanized caving face is crossing fire area and the point is spontaneous combustion prevention, on the basis of advanced detection and prevention of fire area, the comprehensive fire prevention technology of plugging leakage channel of the gob, nitrogen injection with buried pipe in upper and lower corner of mining face and low concentration gel injection with buried pipe in upper corner have been used. It has prevented the spontaneous combustion of 065-2 fully mechanized caving face efficiently, and has created the history of safely and efficiently crossing the continuous 260 m fire area in fully mechanized caving coal face of deep dip angle thick seam, which is 920 m long and with serious spontaneous combustion.

ACKNOWLEDGEMENTS

The authors gratefully acknowledge foundation by Technology Innovation Fund of China Coal Science and Engineering Group (2012MS001), Technology Innovation Fund of China Coal Research Institute (2010CX09).

REFERENCES

Chang S.Q., Wang G.P. & Li Z.Q. 2009. Research and application on comprehensive fire preventing and extinguishing technique large DIP angle of fully mechanized coal face. *Energy Technology and Management*, (6):83–85.

Li X.Z. 2006. Research of Coal Spontaneous Combustion Prediction of the Gob of a High Inclination-angle Coal Seam Named 1409 Working Face in HuaFeng Mine. Xi'An: Xi'An University of Science and Technology.

Li Z.X. 2003. Numerical simulation and parameter determination of nitrogen injection process in fire prevention and extinguishing in fully mechanized longwall top-coal goaf. *China Safety Science Journal*, 13(5):54–57.

Sudhish C.B. 1985. Spontaneous combustion of coal and mine fires. Dhanbad: Central Mining Research Station.

Tang M.Y., Dai G.L., & Qin R.X., et al. 2012. Numerical analysis of air-leakage law in goaf of fully mechanized face. *Journal of Central South University (Science and Technology)*, 43(4):1494–1498.

Wang D.M. 2008. Mine fires. Xuzhou: China University of Mining and Technology Press.

Wu Y.P., Yuan D.F., & Zhang M.F. 2000. Study on the elementary problems of full-mechanized coal mining in greater pitching seam. *Journal of China Coal Society*, 25(5):465–468.

Xu C.F. 2010. Experiment Research on the characteristics of 065–2 coal seam spontaneous combustion in the gushan nine. Fuxin: Liaoning Technical University.

Zhang Y.L., Li K.F., & Ren S.G. 2010. Overlying strata movement property of fully mechanized caving mining in steep inclined steam. *Journal of Xi'An University of Science and Technology*, 30(2):150–153.

Zhang Y. 2009. Comprehensive fire fighting technology in high inclined underhand stopping full-mechanized caving face and application. *Safety in Coal Mines*, 40(12):37–39.

Zhou X.H., Bi B., & Qi Q.J., et al. 2010. Numerical simulation of preventing and extinguishing measures of fully mechanized caving face in gushan coal mine. 2010 (ShenYang) International Colloquium on Safety Science and Technology.

Progress in Mine Safety Science and Engineering II – He et al. (Eds)
© 2014 Taylor & Francis Group, London, ISBN 978-1-138-00122-0

The research on disturbed effects of polyurethane material's expansion pressure upon mine disaster prevention

Guanghua Zou & Fengyan Zhang
North China Institute of Science and Technology, Beijing, China

Yanbo Song
Xingtai Tongcheng Coal Mining and Technology Co., Ltd., Hebei, China

ABSTRACT: With the practical effects on the rock mass space of improving the broken structure, transferring the failure mechanism, reinforcing fracture network, the polyurethane material is widely applied to the prevention of mine disasters by sealing and plugging method. Furthermore, due to the nature of expansibility, the polyurethane material produces the disturbed effects on the surrounding rocks, which causes the polyurethane material to fill in and compact the broken rock mass in further and strengthens the elastic modulus of rocks themselves, the expectation of improving the intensity of the broken rock mass achieves correspondingly.

1 PREFACE

Coalmine production, being performed underground, is imperiled by such disasters as water, fire, gas, coal dust and roof; especially the gas and coal dust explosion along with underground fire will bring an enormous damage to coal mines. To remove the poisonous gas in laneways and recover the ventilation system in dealing with explosion accidents, it is necessary to restore the destroyed ventilating devices quickly. In case of fire, it is obliged to do the hermetic seal promptly to have fire under control. The waterproof plugging material made of polyurethane elastomer, therefore, is applied to the hermetic sealing in the mine work underground.

The waterproof plugging material made of polyurethane elastomer is the resin of dual component organic polymer with such features as durability, non-shrinking, expansibility, glutinosity, impermeability, fire retardation. This kind of material should be operated with grouting pumps in coal mines underground, injecting the polyurethane agent group A and B into the sealing place in terms of the corresponding volume ratio and producing polymerization reaction to form the strengthening solid fillings. As the low viscosity of agent group A and B allows the material to permeate into the hairline cracks of the rock mass and foam to cement it firmly. Meanwhile, polyurethane material is capable of sealing gas drainage holes and the cracks around the holes to improve the effect of the mines gas drainage, of reinforcing the coal pillars of gob-side gateway and broken coal pillars and of decreasing air leakage to prevent the spontaneous combustion in the goaf. Besides, with the contribution to the reinforcement of fragile coal roof (or rock roof) and the precaution of roof fall by reinforcing the excavation and the roof of mining face, the polyurethane material is supportive of ensuring the workers' security and accelerating the production through blocking the passing water and wind to reduce and eradicate the leakage. According to the theories and practice researches, in terms of a appropriate proportion, the application of polyurethane material effectively reduces the exposed structural plane of surrounding rocks due to that the internal friction angle of the coalition is improved by an average of 10% and the cohesion by 15%.

Through constraining and consolidating the regional fractures, it increases the intensity through organic material directly filling and grouting strengthening coagulation broken free surface, to develop the anti-deforming capability of weak planes by penetrating and strengthening the rough fracture surface sliding friction, to improve the overall resistance to deformation of surrounding rock stiffness, which converts surrounding rocks stability from the weak planes control to the grouting coalition control.

Through the organic grouting and reinforcing, it changes the fractures of surrounding rocks and the rock mass from the state of biaxial stress to three dimension which strengthens the weak surface on both sides of the constraints and the continuity, transforming the failure mechanism of rock mass from the original fissure extension into the shear

failure under the action of maximum shear stress, or the tensile failure in the perpendicular direction to the minimum principal stress.

Through the organic grouting and reinforcing, it changes the proportion among the items in rock mass, developing a large system, the network skeleton structure, in broken rock mass and increasing the integrity and the resistance to external force damage.

2 EXPANSIVENESS

The expansiveness of the polyurethane slurry, as one of the important technical parameters of grouting of the organic material, can be measured with expanding multiple and expansion pressure.

2.1 *Expansion multiple*

The slurry expansion multiple along with the response time is the critical parameter for slurry grouting behavior. Greatly influenced by foaming agent added in the slurry, the expansion multiple is also related to the gas generation and its rate in the reactive process of components A and B. Expansion multiple is calculated by densimetry, which can be demonstrated by the ratio of pure slurry weight to gel weight in the same volume after the slurry reaction expansion, the expansion multiple of polyurethane material is commonly between 1~15. As far as the common polyurethane material concerned, the relation curves of the effect from the expansion multiple of slurry on the materials performance can be admeasured in a closed mould, and the relations of, elastic modulus and expansion multiple can be shown in figure 1and 2.

The figures above indicate obviously, the expansion coefficient of material which leads to degrading the resultants' mechanical performance is in the range of 1.5~2.0, and improving the expansion coefficient in further causes no reduction in the resultants' mechanical performance, after all, in most cases of deformation the expansion coefficient hardly impacts on the gel mechanical performance.

2.2 *Expansion pressure*

In the grouting process, the reaction gas generation and expansion pressure of material produce the disturbance effect of slurry and further penetration, of which the analysis on the generated gas in polyurethane material reaction and the properties of generating expansion pressure is the start point for further study on organic grouting reinforcement materials behavior. Related to the expansion multiple of material reaction, the expansion pressure of slurry reaction reaches the maximum

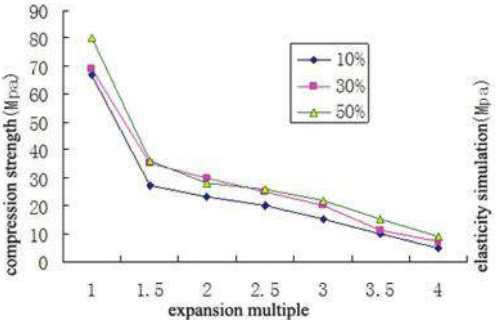


Figure 1. The relation curve of compression strength and expansion multiple.

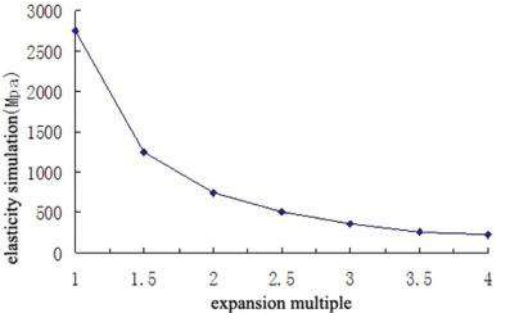


Figure 2. The relation curve of elasticity simulation and expansion multiple.

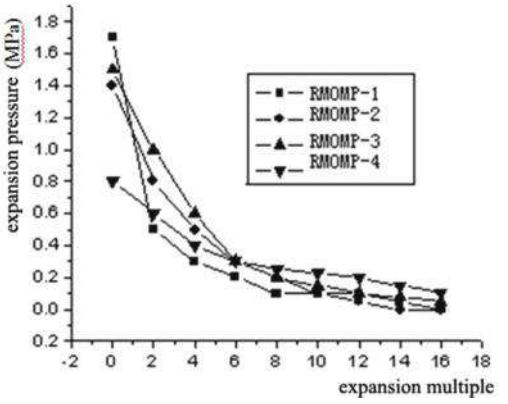


Figure 3. The relation curve of expansion pressure and expansion multiple.

under the condition of rigid constraints, however, with the increase of the material expansion multiple and the decrease of constraints, the will significantly decay, as shown in figure 3.

The slurry in grouting produces large amounts of CO_2 gas and the foaming agent into the slurry

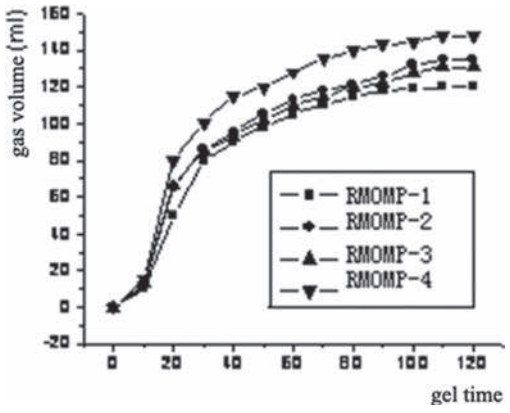


Figure 4. The curve of gas volume vs. gel time.

subsequently gasifies with the increasing of reaction temperature, being released with CO_2 from the reaction system. The gas amount and producing speed of slurry in the reaction is also one of the most important indicators for grouting. It is shown clearly in figure 4 that in the reaction the total producing amount of the gas is related to the amount of foaming agent added in the material because it produces less gas in 1 type due to the amount of foaming agent added in the slurry is only 10%, while in 4 type 25% foaming agent in the slurry leads to more gas production.

3 EXPANSION PRESSURE DISTURBANCE EFFECTS

To assume the strengthened rock stratum as the ideal elastic plastic material, in which the slurry spreads the way on its own power, producing the stress on the surrounding rock stratum and filling the cracks within the rocks, therefore, under the grouting pressure, the slurry is squeezed into the fractures and making its way to diffusion and penetration. If injected into the surrounding rocks with high pressure, the two components of polyurethane material will bring the chemical reaction in the rock mass, producing the expansion pressure and making the slurry diffusing and penetrating towards the deeper fissures till the end of the reaction.

Furthermore, under the pressure of pump and expansion all together, the spreading slurry can not only fill the fractures within the rock mass connected to others but also compact the small enclosed fissures and consolidate the broken rock mass further to increase the elastic modulus and accordingly improve the strength of broken rock mass accordingly.

The research demonstrates that the form of the slurry infused into the rock mass is irregular, which can be reduced to the approximate cylindrical in order to calculate the disturbance effect of expansion pressure. The form will be changed from the state of elastic deformation to plastic one with grouting pressure increasing around the injection holes, then it can be analyzed by the elastic-plastic theory.

Provided that under the co-action of the grouting pressure and the expansion pressure (pr), three regions will be formed surrounding the grouting pipe zone. They are the grout filling region (I), the plastic deformation region (II) and the elastic deformation region (III) of the grouting coalition. To presume that the hydrostatic stress of the injection holes is $p_{0,}$ the penetration radius of slurry is r and the radius of grouting pipe is r_0, then the stress boundary condition is

$$\begin{cases} \sigma_r = -p_c & (r = r_0) \\ \sigma_r = -p_0 & (r \to \infty) \end{cases} \tag{1}$$

$$\begin{cases} \sigma_r = -p_r & (r = r_0) \\ \sigma_r = -p_c & (r \to \infty) \end{cases} \tag{2}$$

By the differential equation of ax symmetric plane problem, physical equation and geometric equation, we get the radial stress σ_r as $r = R_0$, tangential stress σ_θ and displacement Ur:

$$\sigma_r = -p_c, \sigma_\theta = -2p_0 + p_c,$$
$$U_r = \frac{1+\gamma}{E}\left[p_c - 2(1-\gamma)p_0\right]r_0 \tag{3}$$

In the formula above, E and γ present the elastic modulus of the coalition and Poisson ratio respectively

To presume that the principle press of the coalition is $\sigma_1 = \sigma_r$, $\sigma_3 = \sigma_\theta$, when the strength condition, Mohr-Coulomb, is met, it will be changed into the plastic state. The strength condition is expressed by:

$$\sigma_\theta - \sigma_r = -2(C\cot\varphi + \sigma_r)\frac{\sin\varphi}{1+\sin\varphi} \tag{4}$$

In this formula, C and φ present the adhesion stress of the coalition and internal friction angle, with the above expression (4) substituted into this formula, we can conclude:

$$\sigma_r = \left(p_r + C\cot\varphi\right)\left(\frac{r_0}{r}\right)^{\frac{\sin\varphi}{1+\sin\varphi}} - C\cot\varphi$$
$$\sigma_r = -p_c, p_c = p_0\left(1+\sin\varphi\right) - C\cos\varphi \tag{5}$$

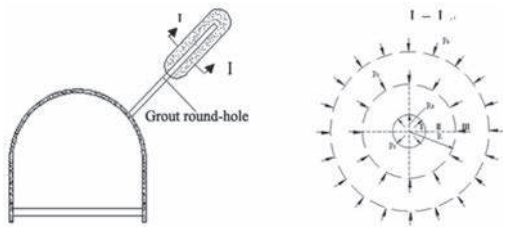


Figure 5. Grout round-hole & different stress regions resulting from grouting.

Then, there comes the formula:

$$C\cos\varphi + C\cot\varphi - p_0(1+\sin\varphi) = (p_r + C\cot\varphi)\left(\frac{r_0}{r}\right)^{\frac{\sin\varphi}{1+\sin\varphi}} \quad (6)$$

To expand this formula, we get the relation of penetration radius r and the expansion pressure p_r:

$$r = \left[\frac{C\cos\varphi + C\cot\varphi - p_0(1+\sin\varphi)}{p_r + C\cot\varphi}\right]^{-\frac{1+\sin\varphi}{\sin\varphi}} r_0 \quad (7)$$

To assume that hydrostatic stress p_0 = 3.5 MPa with the internal friction angel ranging from 37.8° to 38.5° and the internal friction force ranging from 6.8 to 7.1 MPa, the relation between the expansion pressure changes and penetration radius can be calculated in terms of the formula (7). The curve is shown by figure 6. According to the empirical data on spot, the graph of the relation between the expansion pressure changes and the grout quantity can be shown as figure 7.

From figure 6 and 7, it can be concluded that the disturbance effect of the slurry expansion pressure grout increases the diffusion radius of the slurry in the rock mass; meanwhile, the grouting quantity is also improved with the expansion pressure increasing, with conducive to the grouting.

The disturbance effect produced by expansion pressure above can be analyzed further by the circular tube model of porous media.

Taking the expansion pressure of polyurethane material into consideration, that is,

$$\Delta p' = p_0 - p_1 + p_2,$$

to expand

$$Q = \frac{4\pi k_g}{\mu_g}\sqrt{3\Delta p\gamma_g r_0^3}$$

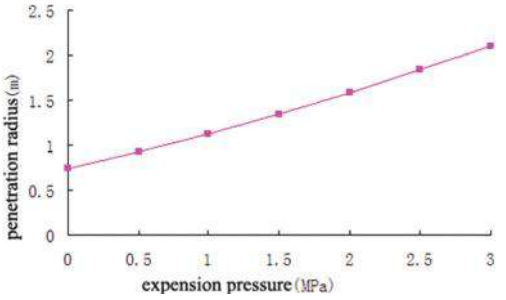


Figure 6. The curve of expansion pressure vs. penetration radius.

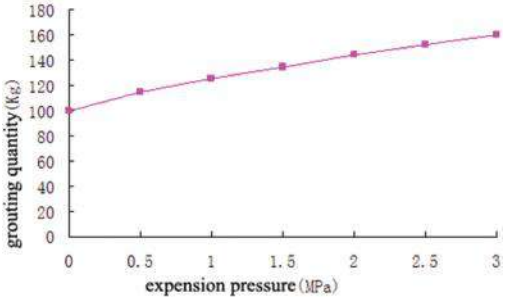


Figure 7. The curve of expansion pressure vs. grouting quantity.

and

$$r = \frac{\mu_g Q^{\frac{2}{3}}}{3}\sqrt[3]{\frac{\mu_g}{2\pi^2 k^2\gamma_g^2 p}}$$

along with the formula

$$Q = V\omega t = \omega t\kappa_g J^{1/2},$$

we get

$$dp = -\frac{1}{\gamma_g}\left(\frac{Q\beta}{4\pi r^2 tk}\right)^2 dr \quad (8)$$

To do integral on both sides of the above formula, there comes;

$$\int dp = -\frac{1}{\gamma_g}\left(\frac{Q\beta}{4\pi tk}\right)^2 \int r^{-2} dr,$$

the solution for it is

$$p = \frac{1}{3\gamma_g}\left(\frac{Q\beta}{4\pi tk}\right)^2 r^{-3} \quad (9)$$

With the boundary conditions, when $r = r_0$, $p = p_1 + p_2$, when $r = R$, $p = p_0$, thus, we get the following expressions:

$$p_1 + p_2 = \frac{1}{3\gamma_g}\left(\frac{Q\beta}{4\pi tk}\right)^2 r_0^{-3} \tag{10}$$

$$p_0 = \frac{1}{3\gamma_g}\left(\frac{Q\beta}{4\pi tk}\right)^2 r^{-3} \tag{11}$$

Then, we draw a conclusion of

$$\begin{aligned} Q &= \frac{4\pi kt}{\beta}\sqrt[3]{3\Delta p'\gamma_g r^3} \\ &= \frac{4\pi kt}{\beta}\sqrt[3]{3(p_0 - p_1 + p_2)\gamma_g r^3} \end{aligned} \tag{12}$$

Because the slurry diffuses spherically, so

$$Q = \frac{4}{3}\pi r^3 n; \Delta p' = p_1 - p_0 + p_2,$$

set into the formula above, there comes:

$$\begin{aligned} \Delta p' &= \frac{1}{3\gamma_g}\left(\frac{Q\beta}{4\pi k}\right)^2 (r_0^{-3} - r^{-3}) \\ &= \frac{1}{3\gamma_g}\left(\frac{\beta}{3tk}\right)^2 r^6 (r_0^{-3} - r^{-3}) \end{aligned}$$

For r_0 is rather smaller than r_1 then comes the formula

$$\Delta p' = \frac{1}{3\gamma_g}\left(\frac{\beta}{3tk}\right)^2 r^6 r_0^{-3}$$

The deformation is

$$r = \sqrt[3]{\frac{3kt}{\beta}} \bullet \sqrt[6]{3\Delta p'\gamma_g} \tag{13}$$

Ultimately, we obtain the strengthened grouting material with expansion pressure, of which the calculation formula of grouting quantity and penetration radius is:

$$Q = \frac{4\pi kt}{\beta}\sqrt[3]{3(p_1 - p_0 + p_2)\gamma_g r^3} \tag{14}$$

$$r = \sqrt[3]{\frac{3kt}{\beta}} \bullet \sqrt[6]{3\Delta p'\gamma_g} \tag{15}$$

In the formula,

κ–The penetrating coefficient of rock stratum, m/s;

κ_g–The penetrating coefficient of the slurry in rock stratum, $\kappa_g = \kappa/\beta$, m/s.

β–The viscosity ratio of slurry vs. water

n–The porosity factor of rock stratum with slurry

P_2–The expansion pressure value of grouting slurry

The formula (14) shows that grouting quantity is in direct proportion to the penetrating coefficient of the slurry in rock stratum, the sum of grouting and expansion pressure, the grouting time, and the drilling diameter but in inverse proportion to the slurry viscosity.

In $Q = (4\pi kt/\beta)\sqrt[3]{3(p_1 - p_0 + p_2)\gamma_g r^3}$, the main factors influencing on grouting quantity are such penetrating coefficient of rock stratum with slurry, grouting time, drilling diameter, grouting and expansion pressure and slurry viscosity. On condition that other factors are in certain cases, the analysis on the impact of grouting and expansion pressure upon grouting quantity is that the grouting pressure is the leading factor in the process, during which with the occurrence of polyurethane material's expansion pressure and without altering the grouting pressure, the total pressure difference grows to increase the grouting quantity.

It is clear that in the transfusion process of polyurethane material, the more the gas moles are produced, under the certain effect of grouting pressure; the easier it is to overcome the resistance of static grout and the viscous resistance created by slurry solidification, which is advantageous to grouting.

The gas produced outside of the gel will generate new additional grouting pressure while the one inside will form the forming structure together with gel to strengthen the force of slurry-proof or the anti-permeability. Along with the continuous grouting, more and more slurry becomes concreting to fill in the cracks.

4 CONCLUSION

1. The slurry expansiveness of polyurethane material is one of the important technical parameters of organic material grouting, which can be measured by expansion multiple and pressure.
2. As the grouting material made of polyurethane with expansion and penetrating pressure, the formula for calculating the grouting quantity and penetration radius is

$$Q = \frac{4\pi kt}{\beta}\sqrt[3]{3(p_1 - p_0 + p_2)\gamma_g r^3}$$

$$r = \sqrt[3]{\frac{3kt}{\beta}} \bullet \sqrt[6]{3\Delta p' \gamma_g}$$

Under the condition of the same grouting parameters, the disturbance effect of expansion pressure produced by the strengthening slurry of polyurethane grouting will promote the penetration radius and grouting quantity of grouting coalition, providing the grouting with the positive effects.

REFERENCES

[1] Yang Ping, Peng Zhenbin, Li Fenqiang. Study on the reinforcement mechanism and calculation model of tunnel grouting. Mining and metallurgical engineering, 2005, 25(1):3~5.

[2] Zhou Weiyuan Yang Reqiong. The mechanism of grouting with the high pressure. Xiong Houjin editor: new international anchoring and grouting progress. Beijing: China building industry press, 1996.

[3] Song Yanbo. Organic high water material grouting of water plugging mechanism and engineering application research, Beijing: China University of Mining & Technology (Beijing) doctoral thesis, 2004.

[4] Zou Guanghua. Using organic materials broken surrounding rock reinforcement mechanism research and engineering application, Beijing: China University of Mining & Technology (Beijing) doctoral thesis, 2008.

[5] Miao Runtao, Liu Wutuan, Guo Shengmao. Application and practice of block up water grouting process in Industrial Minerals and Processing, 2005, 10:33–35 (in Chinese).

[6] E. Nonveiller. Grouting Theory and Practice. Elsevier Science Publisher B.V., The Netherlands, 1989.

[7] Arrind. V. Shroff. Grouting Thchnology in Tunneling and Dam Construction, 1993:21~23.

[8] Yesilnacar, M I. Gouting applications in the Sanlinurfa tunnels of GAP, Turkey[J]. Tunneling and Underground Space Technology,2003,18(4):321~323.

[9] David Ho, Williams Gill, Charles Huang. High performance Light-weight PU Shoe Sole Material Based on New Polyether Polyols. Proceeding of PU-tech Asia, 1997, (5):221~223.

[10] Masri SF, Chassiakos AG, Gianghey TK, Identification of nonlinear dynamic system using neural networks, J. App. Mech, 1993, 60(3):38~42.

[11] Baldwin, J.L., Bateman, R.M., Weatley, C.L., Application of a neural network to the problem of mineral identification from well logs, 3rd Mgls. Borehole Geophys. For Mineral, Geotech. & Groundwater Appl. Int. Symp, 1989. 10, The Log Analyu, 30(5)1990:8~11.

Progress in Mine Safety Science and Engineering II – He et al. (Eds)
© 2014 Taylor & Francis Group, London, ISBN 978-1-138-00122-0

Research on the application of monitoring techniques of micro-seismic to water inrush forecast in Wutongzhuang Coal Mines

Yue Bai & Jingming Wang
North China Institute of Science and Technology, Sanhe City, Hebei Province, China

ABSTRACT: Water inrush from coal floor is that limestone water with high pressure under the coal seam erupts out from the aquifuge strata and the strata are broken during mining activities. Therefore, the micro-seismic will take place when coal floor strata crack. Consequently, to monitor the micro-seisms and position focal areas become the effective methods to figure out the possible inrush places. The technique on week seismic monitoring to forecasting water inrush from coal floor in Wutongzhuang Coal Mine, Fengfeng Coal Field was applied to and it is found that micro-seisms happened in the deep coal floor confining strata, in the ahead area of mining face while the seisms takes place in shallow area in the goof; the seisms appears far more frequently and its active time is much longer in the pin off area of faults than in any other intact coal floor areas and places of the faults; the place where the seismic frequently happens is easy to cause a water eruption. These phenomena are complied with the inrush mechanism of "pressured water progressively intruding up into the floor aquifuge". The monitoring result indicates that the fracturing or micro-seismic focuses and water inrush can be forecasted by means of calculating mechanics semesters inversely and mining simulation. The technique is significant to safety and efficiency production in mining and no doubt has bright future in its practical application because the water inrush is one of the main water hazards in north China coal field where is the main coal productivity area.

1 INTRODUCTION

The water inrush out from coal floor and sinking columns are one of the worst hazards in the north China coal field. According to the statistics, there have been 1282 cases for hazards resulting from water inrush from coal floor and sinking columns in the north China coal field, around 220 cases of mine flooded among them, since 1955. Consequently with the economical loss of 30 million R.M.B. Yuan. Fengfeng Coal Mining Area is one of typical areas with heavy mine flow, with hundreds of water hazards because of water inrush from the coal floor, six mines or work face flooded, among which, Wutongzhang Coal Mine share 6 water hazards caused by water inrush out from coal floor, with 17 mortality, once mine blood and work face blood respectively. Hence, investigation on the mine water hazards control is very important to safe and efficient production. Wutongzhuang Coal Mine has such a typical characteristics in the north China coal field by its hydrogeological features that the technology of water hazards control in this mine is applicable to other north China-typed coal mines.

Many hydrogeologists have been involved in the predicting or forecasting study of water hazards caused by water inrush from coal floor and sinking columns. The researches have figured out that the water hazards caused by water inrush from coal floor and sinking columns is the result from the impermeable stratum failure. Consequently, some scientists had utilized the techniques on monitoring the stress, strain, water temperature and pressure (Wang Jingming 1998), and the others using the supersonic methods (Wang Zuoyu & Liu Hongquan 1992, Chen Feng et al. 2000), and gradually in China begins the technology of micro-seism to tentatively forecast the water hazards in the coal mines (Yang Tianhong et al. 2007) in Sanhejian Coal Mine, Xuzhong (Yang Fuxing 2007) and Huafeng Coal Mine, Xinwen (Wang Jingming et al. 1996), without engineering tests. The authors utilized the technique to monitoring the water disaster from coal floor and sinking column in Wutongzhuang coal mine, and obtained validated achievements that combination of monitoring the position and regulation of a micro seismic with the hydrogeology analysis is feasible to forecast the hydrogeological conditions in the coal floor strata and sinking columns.

2 THE HYDROGEOLOGICAL CONDITIONS OF WUTONGZHUANG COAL MINE

Located at the bottom of Shanxi Group, Permian system, the major coal seam No. 2 in

Wutongzhuang Coal Mine is about 35 m to 50 m over Ye Qing limestone aquifer, and 140 m over Ordovician limestone reservoir. Without any water disaster happened in excavating coal No. 2 at other coal mines in Fengfeng Coal Mining Area, hence the hydrological condition at Wutong Coal Mine was also thought to be simple. However, there were several water disasters happened in mine construction period and operation period. The first disaster happened during excavation of the transfixion between working shaft and auxiliary shaft at station level, and caused 17 deaths. The second hazard happened in 3 first work faces due to water inrush from coal floor, and brought production stop. The third happened when the north main ventilation tunnel was excavated close to the strongly permeable sinking column and caused an water inrush with flowage of 130 m^3/h. The 24 sinking columns had been detected in the recruit geological exploration, among which three were validated, and 2 of them were strongly permeable. Therefore water inrush from coal floor and sinking column seriously threaten the coal mine both in safety and efficiency. And these have become the one of main factors to constrain the production progress. In order to predict, forecast the water disasters and to ensure the safety production, the Micro-seismic Monitoring technique was applied to industrial tests for the water inrush both from coal floor and sinking column at the work face 182106, in Wutongzhuang Coal Mine.

The work face 182106 is 505 m–707 m deep. The upper gateway and lower gateway are –506 m and –327 m in elevations respectively, and slope distance between the two gateways is from 65 to 165 m. The mining height is 3.4 m. Work faces 182105 and 182301 remain un-mined in the east and west. When the lower gateway was heading, the sinking column X3 with its diameter of about 30 m had exposed; Two faults of less than 2 m in throws had been found in the work face and faults F2 of 20.0 m maximum fall expanding from upper side work face to and tip off at the working face, as shown in Figure 1. The main work of the research was to monitor the sinking column activities and fault F2 extension.

3 SYSTEM CALIBRATION AND MONITORING METHOD

After installed and modulated, the MSM was calibrated. The parameters, such as elastic wave traveling velocity in coal floor strata, the average traveling speed in the surrounding rocks, energy attenuation rule etc. were obtained by site tests to ensure the of monitoring net to be reasonable. Both the compensation errors of every sensor and the consistency for reaching time of the waves were gained and calibrated by blasting after the MSM system had been set up.

The blasting wholes were drilled in the coal roof of monitoring areas in work face 182106. The explosive parameters can be seen at Table 1. Because the arriving time of wave P (longitudinal wave) was used in plotting wave emission source, the speed and structure of wave P are interested.

5 sensor holes and 2 calibrating blast holes were laid out in the coal floor of work face. The sensor hole are named as B1 to B5, and the calibrating blasting holes are named as C1–C2.5 three dimension sensors named as S1 to S5 were distributed in the 5 boreholes, which S4 and S5 was close to the fault in order to monitor the fault activity. Because the area between lower gateway within borehole B4 to B5 and upper gateway within borehole B1 to B3 abnormal in hydrogeology according electricity sound respecting, the 8 one dimension sensors named as D1~D8 were added there. Two one dimension sensors named as D9 and D10 were set up at the edge of sinking column due to the sinking column was dangerous in hydrogeology. The sensors layout can be seen in Figure 1 and parameters of borehole is shown in Table 2.

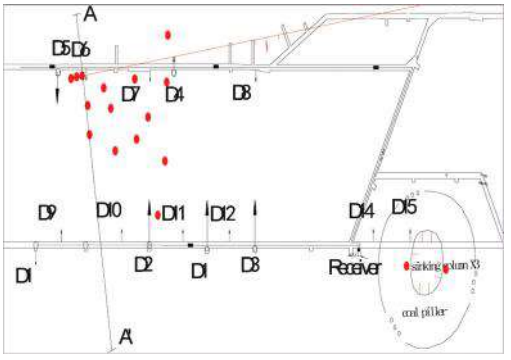


Figure 1. Chart of the sensors layout and micro-seismic plane distribution in coal floor strata.

Table 1. Parameters of Calibrating Blast.

Explosion style	Explosive (kg)	Kind of explosive	Roll length (m)
once	16.6	gel	6
Distance from blast point to sensor (m)		Distance from blast to coal roof	Blast Borehole dip (^{0})
32		27.7	60

4 THE RESULTS AND VALIDATION

4.1 *The results*

The micro-seismic can be classified into 3 phases according to their frequency and intensity, e.g. the energy accumulation phase, frequent micro-seismic phase and aftershock phase.

The energy accumulation phase: this phase covered the 115 m from the cut off to the working face. Small energy events had happened in this period at areas close to the lower gateway and the edge of sinking column, without failure in the coal floor with bigger energy.

Frequent micro-seismic phase: When the work face advanced to 115~180 m from January 25 to 28, there were 6 among 8 micro-seismic of bigger energy events took place in the phase, as shown in Table 2. Especially, 3 stronger micro-seismic occurred concentrically at the point of 45 m ahead of working face. Seismic source's depth was 25–28 m under the floor. Geology map indicated that the micro-seismic source was located at fault pin off area. According to the displacement of micro-seismic source, the fault was considered to have extended by 8 m and 12 m both in height and length during mining.

After shock phase: After January 8, only 3 microseisms with stronger energy happened in lower area of work face in the range of 181 m~291 m from the cut off during the phase, while 2 micro-seismic events with small power were detected at nearby sinking column X3 apart from work face by 425 m and 315 m respectively. Apparently, the two small power events had nothing to do with mining.

The micro-seismic events on coal floor distributed at plane and section is shown in Figure 1 and Figure 3.

4.2 *The analysis of the results*

According to Figure 1 and Figure 2, the micro-seismic appearing on the floor of work face 182106 mostly happened in lower part between the detecting holes D4 and D5. The reasons were considered as follows: (1) Based on the theory of mining pressure, The closer to lower part of inclined work face, the greater mining pressure is, and the more intensive damage of the coal floor strata. (2) the integrality of coal floor strata is ruin at lower part. Although there was no macro-factures at the fault pin off, some micro crack had been found to a limited extension because the fault F106-1 went into the interior of work face through the lower gateway of work face. According to the fracture mechanics and damnification mechanics, the stress is easy to accumulate at the end of the fault to make the fault expand.

Table 2. The parameters of borehole and sensors (only some listed).

Hole name	Sensors mane	Sensor type	Distance to cut off (m)
B1	S1	3 dimension	162.56
B2	S2	3 dimension	285.67
B3	S3	3 dimension	400.08

Dip angle (°)	Depth of holes (m)	Remark
–45	15	Hole in floor
–30	25	Hole in floor
–30	25	Hole in floor

Table 3. The main factors of micro-seismic at work face 182106 (some data omitted from volume limitation).

Time	X	Y
2006-12-25 12:43:26	22990	18760
2006-12-25 12:48:57	22930	18765
2006-12-26 5:18:49	22980	18646
2006-12-26 13:35:33	22955	18712
2006-12-28 6:25:57	23000	18650
2006-12-28 10:12:18	22987	18695

Z	Energy (no dimention)	Remark
–470	134991150.4	
–468	/	Small energy event
–380	58092376.89	
–370	/	
–400	13277253.87	Small energy event
–424	/	
–371	26711970.64	Small energy event

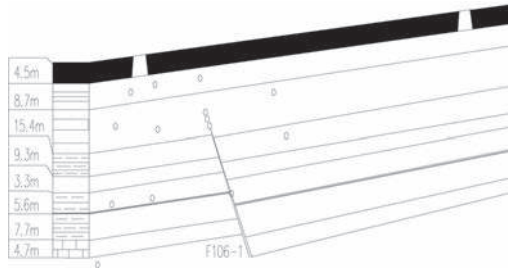


Figure 2. Projection of section A-A' for micro-seismic on floor of work face 182106.

During monitoring, 3 micseismic events with bigger energy were recorded. This means 3 propagations of the fault. There were only an interval of 5 minutes between the first and second events (as shown in first two records in Table 2). These could

be considered as the results of same mining pressure activity. The third micro-seismic event had an interval of 70 hours from the first, when the work face was advanced by about 10.5 m. Based on the former measurement to the mining pressure in Wutongzhuang Coal Mine, the roof pressure period was between 8–12 m, so the last micro-seismic event should belong to resulting from another mine pressure.

The micro-seismic event happened during mining made unfavorable effects in hydrogeology. When the sensor was receiving the micro-seismic signals, the floor of coal floor crack with big noise, and then water gushed out at the flowage of 60 m^3/h from Carbinous limestone aquifer, which was almost the same as the water inrush from coal floor as the result of floor breaking with a coinstantaneous blare happened in a work face in Coal Mine No. 2, Fengfeng Coal Area in 80's last century. It is proof that micro-seismic detecting method is an effective technique to predict water inrush from coal floor.

We can consider the pin off of the fault F106 as a hidden part of the fault under the coal floor, i.e. the fault extending down into Ordovician limestone with bigger fault throw in lower and smaller in above, as shown in Figure 2. The upward propagation of the fault testified by 2 micro seismic is confirmed with the water inrush mechanism of water progressive upward intrusion.

During detecting, there was no micro-seismic events caused by mining happened in sinking column. The reason could be as follows: (1) Because the fillings in the sinking column was mixed and lack of integrality, the fillings' brittle fracture was replaced by its plastic deformation during a mining. (2) The sinking column was grouted and the protective coal pillar was arranged. This also means that the size of the coal pillar is enough to stand the mine pressure.

4.3 *Engineering validating*

In order to detect the fault F106-1's water conductivity before mining, two boreholes through the fault were dilled and there was no water flow from the holes, indicating that the fault was impermeable under undisturbed conditions. After the water inrush happened in fault during mining, one of the holes was redrilled, and water flowed out at the rate of 30 m^3/h. This indicated that the fault became "active", and the fault zone became permeable.

5 CONCLUSION

With the whole monitoring procedure on the micro-seismic happened on floor of work face 182106 in Wutongzhuang Coal Mine which has a complicated hydrogeological condition, We have achieved the following ultimatums:

There were 25 micro-seismic events happened on coal floor of work face during the mining activity, among which 8 times of the events had the bigger energy, mostly appearing on the weakness of the floor in lower part of the work face.

Three biggish micro-seismic events occurred in the fault pin off area during mining, with the interval of micro-seismic consistency with the period mine pressure on the roof. The fault had extended for 12 m, according to recording of micro-seismic monitor. The activities of fault resulted in the water inrush from floor confirm with the mechanism of water inrush during groundwater progressive intrusion process.

The micro-seismic event has a distinct advanced sign that can be important basis for water inrush forecasting in coal mine.

There was no micro-seismic event happened in sinking column and the permeability had no obvious change with mining activities.

REFERENCES

Chen Feng, et al. 2000. Research on Characteristic of Ultrasonic Spectrum in the Course of Rock Rupture by Pressing and Shearing. *Engineering Geology Academy Paper*, 164–168, 8(2).

Cui Sanyuan. 2005. Predicting Method Study on Water Disaster of Coal Mine by Mach Information Resources. *Journal of Physical and Chemical Exploring*, 557–560, 29(6).

Wang Jingming, et al. 1996. Mechanism On Progressive Intrusion of Pressure Water up into Protective Aquclude and its Application to Predition of Water Inrush In coal Mine. *Journal of Coal Science & Engineering.* 12, 9–16.

Wang Jingming. 1998. Monitoring Technique on Water Inrush From Coal Floor and Its Application. *Mine Design*. P. 32–34.

Wang Jingming. 2004. Mechanism of Water Inrush Out Of Coal Floor By Progressive Intrusion And Its Application To Water Hazards Prediction, *Doctor Thesis*, P. 2–4.

Wang Zuoyu & Liu Hongquan. 1992. Mining technology under high water pressure of aquifer. *Coal Publishing house*.

Yang Fuxing. 2007. The Micro-seismic Inspecting Technique on Bursting of Impacted Underground Pressure and Coal and Water Gushing, *Journal of Science and Technique of Coal*. P. 26–28, 35(1).

Yang Tianhong, et al. 2007. State of The Art of Inrush Models in Rock Mass Failure and Developing Trend for Prediction and Forecast of Groundwater Inrush. *Chinese Journal of Rock Mechanics and Engineering*. P. 268–277, Feb.

Progress in Mine Safety Science and Engineering II – He et al. (Eds)
© 2014 Taylor & Francis Group, London, ISBN 978-1-138-00122-0

Study on the safety advancing speed of aquifer-protective mining working face in the shallow thick coal seam

Yude Liu
Key Laborary of Mine Disaster Prevention and Control, Yanjiao, Beijing, China
College of Safety Engineering, North China Institute of Science and Technology, Yanjiao, Beijing, China

ABSTRACT: Based on the domestic and foreign research conclusions and based on the 2_{-2} coal seam as the research object, thought of "working face advances speed depending on the overlying strata water seepage velocity" is proposed by analyzing the mechanism and key of aquifer-protective mining in shallow coal seam (working face advances speed can make broken key strata body closing before upper water seepage to mined-out area). According to the seepage theory and empirical formulas and the measured data etc., seepage time formulas and calculation of ground water in upper strata of working face is made for every classification of aquifer-protective mining. According to the key strata theory and geological data of Shendong Mine Area, initial or periodic breaking space of overlying strata is calculated for each class. Thus, the working face advance speed of each class is calculated and identified. Meanwhile, the length range of safety aquifer-protective mining face is determined by the lower limit of working face's promoting speed and cutting speed of combine. The aquifer-protective mining technology system is perfected furthermore, and theoretical guidance is provided for security applications of shallow seam aquifer-protective mining technology.

1 INTRODUCTION

Aquifer-protective mining is aimed at avoiding damage to the water-bearing structure of aquiferous layers in the process of mining by applying appropriate methods. Even there is some damage which may cause loss of some water, but the damage can be recovered within a certain period of time and it does not affect the minimal water-bearing level for the growth of ground flora.

Domestic scholars carried out in large scale field measurements. Their thorough research involved the basic mechanical properties of the major groups between coal seams and aquifer rocks. This consisted of the evolution of fractures, load transfer mechanisms, features of water-resisting and water-conduction and the relationship between major related factors of mining. Various methods and means were used, revealing the deformation and failure format of different rocks, the roof breakage mechanism and the apparent ground pressure and determined the aquifer-protective action of water-resisting layers and the controllability of water-conducting fissures.

Using Coal Seam 2_{-2} in the Shendong Mine as our research object, we analyzed the mechanism and key of aquifer-protective mining of shallow coal seams and classified its applicable conditions by using the Integrative Index Method of multi-factors. The key point in aquifer-protective mining is to ensure that the fracture zone does not break over the aquifer or the fracture which can conduct water will be closed and keep equilibrious by controlling the controllable factors under different natural conditions. The classification system has been established, as shown in Table 1.

In order to further improve aquifer-protective mining technical system, we have analyzed particularly the mining speed of each class based on the relevant theory and geology, technical conditions which may provide some theoretical directions for the application of aquifer-protective mining technology of thick coal seam.

2 GEOLOGIC ASPECTS OF SHENDONG MINE AREA

The structure of Shendong Mine Area is simple, and contains mainly Jurassic strata which with 185 m of average thickness. It has the characteristics of shallow buried depth, and thin bedrock, and thick loose sand and rich phreatic water.

2_{-2} coal seam in Shendong Coal Field belongs to Yanan group of Jurassic mid-formation, while, ranges in thickness from 3.93 to 6.71 m, and is as much as 6.18 m in average thickness. The configuration of 2_{-2} coal seam is so simple that contains about 1 to 3 strata of black shale which ranges in thickness from 0.12 to 0.37 m. The essence of black

Table 1. Classification system of aquifer-protective mining in shallow coal seams.

Class	Classes name	Main features
I	Safety aquifer-protective mining class	The bedrock thickness is usually bigger than 80 to 85 m, which meets the demand for the thickness of waterproof protection rock pillars prescribed in The Regulations of Coal Pillars Leaving and Mining in Main Lanes under Buildings, Water Body, and Railways.
II	Long-wall easy aquifer-protective mining class	The bedrock thickness is usually bigger than 70 to 75 m, the buried depth is over the shallow limit, and it has the features of compound key strata. In this case, aquifer-protective mining is relatively easy.
III	Long-wall moderate aquifer-protective mining class	The bedrock thickness is generally bigger than 60 to 65 m, having the features of single key strata or compound key strata, lying between easy aquifer-protective mining area and difficult one.
IV	Long-wall difficult aquifer-protective mining class	The bedrock thickness is usually bigger than 50 to 55 m, the buried depth is less than the shallow limit, and it has the features of single key strata. With mining at the working face, steps in the overlying rock can easily go down as a whole, and the coming pressure becomes intense.
V	Short-wall continuous water preservation continuous mining class	The bedrock thickness is usually bigger than 35 to 40 m, having the features of single key strata, and long-wall mining is not suitable.
VI	Short-wall interval water preservation continuous mining class	The bedrock thickness is usually less than 35 to 40 m, but bigger than 15 to 20 m, having the features of single key strata, and continuous mining is not suitable.
VII	Short-wall single chamber water preservation continuous mining class	The bedrock thickness is usually less than 15 to 20 m, and single chamber or room arrangement is suitable.

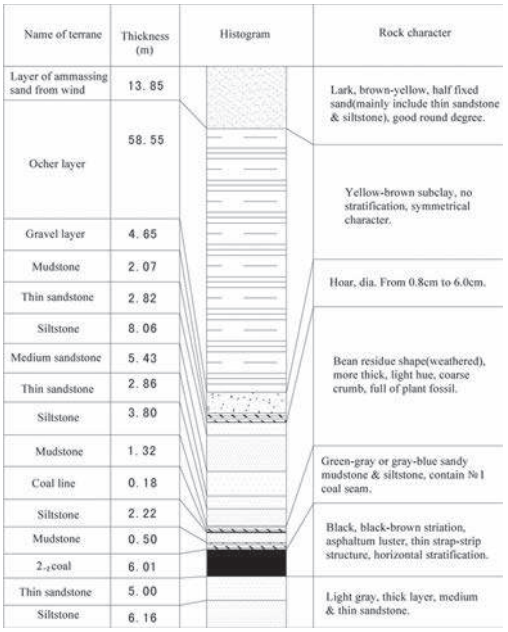


Figure 1. Pole diagram of 2–2 coal seam.

shale, commonly, is mudstone except be charcoal mudstone in some areas. Consequently, 2_{-2} coal seam could belong to stabile thick coal seam. See Fig. 1.

Underground water is mainly supplied by atmospheric precipitation, and classified three classes which are respectively the pore phreatic water of Cainozoic unconsolidated strata, the cranny phreatic water and pressure water of Mesozoic, the hole fissure phreatic water of burnt rock.

Based on the geological conditions, the long-wall fully mechanized mining technology of higher min-ing height and short-wall continuous mining technology have been used in Shendong Mine Area. The ratio of mining and caving is 1:1.3, and the caving step distance is 0.8 m. The working face's roads are supported by the combined support mode of bolt and anchorcable. The hydraulic supports among working face are ZFS-6000/17/33 type, are amount of 131 supports in the longest section of working face. Three supports are laid at each end of working face which is 6500/20/32 type.

3 TO DETERMINE THE MINING SPEED OF AQUIFER-PROTECTIVE MINING

Based on the mechanism of aquifer-protective mining, the working face's advancing speed of safety aquifer-protective mining of each class must satisfy the following conditions: the advancing speed can make the broken rock body of overlying strata to be closed before the aquifer water seep to the goaf after mining.

The speed can be shown and calculated by follow formula:

$$v_m > L_z / t_s \quad (1)$$

where, v_m is the working face's advancing speed, m/d; L_z is the initial or periodic broken distance of key layer, m; t_s is the seepage time of upper aquifer water.

3.1 *Seepage velocity*

a) The Laws of turbulent motion and laminar flow motion
Usually, the water's laminar flow motion of smaller seepage in the joints rocks obeys the Darcy Law, namely:

$$V = k \cdot I \quad (2)$$

where, V is the seepage speed of water; k is the seepage coefficient which depends on the physical characteristics of rocks; I is the water head gradient which means the water head loss of each unit length of the distance.

If in the larger gap strata or the water head gradient higher, the water move subjects to the turbulent motion laws which is as the follow:

$$V = k \cdot I^{1/2} \quad (3)$$

b) Cubic Law
According to the Cubic Law, fracture is formed by the smooth, flat, infinite long parallel plates without filling medium, and the water flow between the plates is viscous incompressible flow which is permanent laminar flow. Thus, according to the basic principle of fluid mechanics, the discharge per unit width through the crack surface i.e. q can be calculated by the follow formula:

$$q = \frac{\gamma \cdot a^3}{12 \cdot \mu} \cdot J_f \quad (4)$$

where, a is the breadth fracture; γ is the liquid unit weight; μ is the flow dynamics viscous coefficient of water; J_f is the hydraulic slope along the direction of fracture surface. According to Darcy Law, the above formula is formed as follows:

$$u = k \cdot J_f; \quad k = \frac{g \cdot a^2}{(12 \cdot \mu)} \quad (5)$$

where, g is the gravity acceleration.

c) Experience formula
Nolte show after test that if the mechanical gap width a_m replaces the crack width a, then the Cubic Law will not stand, and established the following empirical formula through the flow capacity test of fractures under the different normal stress action:

$$q = q_0 + C(a_m)^p; \quad a_m = a_{\max} - a_0 \quad (6)$$

Where, $a_{\max}$ is the closed maximum degree of fracture; a_0 is the compression value of fracture under the stress action; q_0 is the basic flow value of fracture when produced the greatest compression; C is constant.

Nolte concluded that the p value is about equal to 8 by test using quartz-feldspar fracture. Consequently, the empirical formula of seepage coefficient as follows according to Nolte experimental formula:

$$k = \frac{g \cdot a_m^{(p-1)}}{12 \cdot \mu} \quad (7)$$

d) Seepage coefficients influenced by mining
Louis established the following empirical formula of the relationship between the normal stress α and the permeability coefficient k of rock according to some pressure water test's result of drillings:

$$k = k_0 \cdot k_m \cdot e^{-\alpha \cdot \sigma} \quad (8)$$

where, k_0 is the initial permeability coefficient; k_m is the influence coefficient by mining (To take 5 to 10 in the long-wall working face, and take 10 to 15 in the short-wall face); α is the correction coefficient of mining in the shallow coal seam, takes 0.001 to 0.01; σ is the normal stress ($\sigma = \gamma h$), MPa; γ is the rock density, kN/m^3; h is the depth, m. According to the relation between the seepage and stress, permeability coefficient of overlying strata can be calculated after mining in the long-wall working face, see Table 2.

Table 2. The permeability coefficient expectation of overlying strata above long-wall face.

cover depth (m)	Initial permeability coefficient, i.e. k_0 (m/d)				
	0.005	0.015	0.025	0.045	0.065
60	0.0291	0.0874	0.1457	0.2622	0.3788
65	0.0279	0.0836	0.1393	0.2507	0.3621
70	0.0266	0.0799	0.1331	0.2397	0.3462
75	0.0255	0.0764	0.1273	0.2291	0.3310
80	0.0243	0.0730	0.1217	0.2190	0.3164
85	0.0233	0.0698	0.1163	0.2094	0.3025
90	0.0222	0.0667	0.1112	0.2002	0.2892
95	0.0213	0.0638	0.1063	0.1914	0.2764

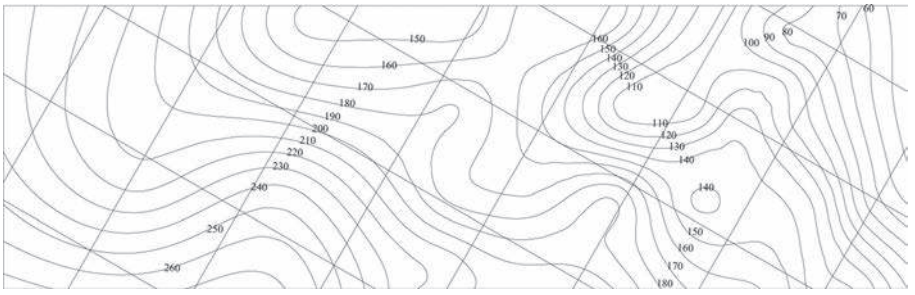


Figure 2. The local hydraulic equivalent line of Shendong Mine Area.

Table 3. The calculation results of seepage speed of overlying strata in strong water area.

Strata	k_0 (m/d)	I	Thickness of unconsolidated formation (m) 60	70	80	90
Weathered zone	0.045	15	6.786	6.755	6.725	6.695
Zhiruo group	0.055	15	9.330	9.288	9.247	9.205
Yanan group	0.025	15	6.126	6.098	6.071	6.044

Table 4. The calculation results of seepage speed of overlying strata in weak water area

Strata	k_0 (m/d)	I	Thickness of unconsolidated formation (m) 60	70	80	90
Weathered zone	0.045	15	4.128	4.091	4.054	4.018
Zhiruo group	0.055	15	9.082	9.000	8.920	8.840
Yanan group	0.025	15	4.587	4.546	4.505	4.465

e) Measurement data
According to the field geological data of the detailed survey, it is known that the aquifer thickness of surface loosed strata in Shendong Mine Area is commonly between 0 m to 20.0 m. The buried depth of phreatic water is about 6.73 m to 10.17 m; the water hydraulic gradients changes greatly between 0.12 m to 13.92 m, and its average is about 10.0 m. The local hydraulic equivalent line is as shown in Figure 2.

The permeability coefficient of Jurassic Zhiruo group is 0.0535 m/d; and the permeability coefficient of No. 5 sect of Yanan group is 0.0253 m/d.

f) To estimate the seepage speed
Based on the above theoretical analysis and measured data and Turbulence Flow Law, we estimate the seepage speed of bedrock and weathered strata as follows by considering safety coefficient k_s (to take 1 to 5), see Table 3 and Table 4.

g) To estimate the seepage time after mining
Passing progress of phreatic water from fracture zone to the goaf after passed the water-resisting layer of weathered zone is very short and quickly. So, the seepage time can be approximately equal to the time through weathered zone strata and origin strata without fracture. According to the measured data, the height of fracture zones above long-wall face of shallow coal seam is commonly 45 m or so, when the mining height is taken 5 m to 6 m in Shendong Mine Area now.

Consequently, we may calculate the phreatic water's seepage time of aquifer-protective mining condition's each class according to the seepage speed of Table 4 by taking 45 MPa as the comprehensive strength of overlying strata, and see Table 5 and Table 6.

3.2 *To calculate the broken distance of key strata*

a) The initial broken distance
Based on the key strata theory, the calculation formula for initial broken distance L_c of roof key layer according to mechanics model of fixed supported girder is as follows:

$$L_c = h\sqrt{\frac{2R_t(1-\psi)}{q}};\quad q = \frac{E_1 h_1^3 \sum_{i=1}^{n}\gamma_i h_i}{\sum_{i=1}^{n} E_i h_i^3} \tag{9}$$

where, q is the weight of key strata and above strata; ψ is the mining damage factor of key strata (its value ranges from 0.1 to 0.5, here is 0.4 according to numerical simulation result); R_t is the available extension strength of key strata (σ_c); E_i is the elastic modulus of No. i layer strata, MPa; h_i is the thickness of No. i layer strata, m; γ is the bulk forces of No.i layer strata, kN/m^3; n is the number of restrained overlying strata by key layer (synchronization deformation to key layer). The calculation parameters are seen in Table 7.

b) The periodic broken distance

The major damage in the form of key layer strata is tension destroy. The fracture position in advance of key layer strata just is the position of immediate roofs periodic broken. So the periodic broken distance of key layer strata can be defined. The periodic broken distance L_z of key layer is calculated by the following formula according to the theory of half infinite long girder on the elastic foundation:

$$L_z = l_z + \frac{1}{\omega}\arctan\left(\frac{2}{3\cdot\omega\cdot l_z + 2}\right) \tag{10}$$

where, L_Z is the suspended stretch length of key layer, can be calculated by the following equation:

$$3\cdot q_1\cdot l_z\cdot e^{-\frac{\omega}{\sqrt{2}}x_1}\left(\frac{2\sqrt{2}+\omega\cdot l_1}{\omega}\sin\frac{\omega}{\sqrt{2}}x_1 + l_1\cos\frac{\omega}{\sqrt{2}}x_1\right) - h_1^2\cdot\sigma_c = 0$$

$$x_1 = \frac{\sqrt{2}}{\omega}\arctan\frac{\sqrt{2}}{\sqrt{2}+\omega\cdot l} \tag{11}$$

c) To calculate the broken distance of key layer above shallow coal seam

From the above formula, we select four models (Table 8) to calculate.

According to the related parameters of each stratum, the first and periodic broken distance of key layer strata of different strength and thickness are calculated, such as Table 9 shows.

From the Table 9, the periodic broken distance of key layer strata is general 21 m to 28 m, and the initial broken distance is about 50 m to

Table 5. The expectation of seepage time in weak water area.

Sort	Thickness of bedrock (m)	Mining height (m)	Height of cranny zone (m)	Height of origin rock without cranny (m)	Weathered zone (m)	See page time (d)
I	>80	<6.0	40–52	27.72	6	>4.5
II	70–80	<6.0	40–52	17.72	6	3.5
III	60–70	<5.5	40–50	8.83	6	2.5
IV	50–60	<4.0	35–45	0.1	6	1.5
V	35–50	3.0–6.0	30–45	0	5.3	1.2
VI	15–35	3.0–4.0	16–22	0	0	0
VII	<15		10–15	0	0	0

Table 6. The expectation of seepage time in strong water area.

Sort	Thickness of bedrock (m)	Mining height (m)	Height of cranny zone (m)	Height of origin rock without cranny (m)	Weathered zone (m)	See page time (d)
I	>85	<6.0	40–52	32.72	6	>4.5
II	75–85	<6.0	40–52	22.72	6	3.5
III	65–75	<5.5	40–50	13.83	6	2.5
IV	55–65	<4.0	35–45	5.1	6	1.5
V	40–55	3.0–6.0	30–45	0	5	1.2
VI	20–40	3.0–4.0	16–22	0	0	0
VII	<20		10–15	0	0	0

Table 7. The calculation parameters of pressure step distance of key layer.

Strata	Bulk forces (t/m^3)	Elastic modulus (MPa)	Remark
Loosed layer	1.8	5.6	To unite and combine the adjacent strata with similar characteristic
Weathered zone	2.2	8	
Overlying bed rock	2.3	25	
Key strata	2.5	30	
Immediate roof	2.4	12	
Coal seam	1.3	3	

Table 8. Calculation type model of key layer's broken distance.

Strata	The thickness of strata (m) I	II	III	IV
Loosed strata	65	72	72	80
Weathered zone	6	6	6	6
Overlying bedrock	20	20	25	30
Key layer	5	10	15	20
Immediate roof	10	10	10	10

Table 9. The calculation result of broken distance of key layer.

Thickness (m)	Broken distance (m)	Intention strength of key layer (MPa) 20	30	40	60	80
20	*Lc*	33.7	41.5	48.2	59.4	68.9
	Lz	15.8	19.3	22.4	27.5	32.0
15	*Lc*	34.9	43.1	50.0	61.7	71.7
	Lz	16.3	20.0	23.2	28.7	33.6
10	*Lc*	43.7	53.9	62.6	77.1	89.1
	Lz	21.8	25.3	29.7	37.5	44.2
5	*Lc*	58.2	71.3	82.1	100	115
	Lz	29.5	37.7	45.0	57.6	68.5

Table 10. The corresponding mining speed of each class.

Sort	Cycle broken distance (m)	Seepage time (d)	Advancing mining speed (m/d)
I	30~35	>4.5	<10
II	30~35	3.5~4.5	>10
III	30~35	2.5~3.5	>15
IV	30~35	1.5~2.5	>25
V	30~35	1.0~1.5	>35
VI	30~35	0.5~1.0	>45
VII	Mining room is disposed in a single decorated form, and the aim of mining at no falling down of roof		

60 m, under the condition that the strength of overlying strata is 35 MPa, and the thickness of key layer strata is 10 m to 15 m.

3.3 *To determine the mining speed of each class*

The mining speed of long-wall face is major relevant to the length of working face and cutting speed. And the mining speed of short-wall face is major relevant to such factors as the length of working face, the cutting mode and the granularity of mining rooms.

According to the above calculation of the seepage time and key layer strata's periodic broken distance, the relevant mining speed of each class is calculated, and the results is listed in Table 10.

3.4 *To determine the range of working face length by the mining speed*

In order to aquifer-protective mining, the working face's length of each class is calculated by the following formula:

$$L_{face} \le \left(t_{work} \cdot v_{cut} \cdot d_{cut}\right) / v_{face} \tag{12}$$

where, L_{face} is the length of working face, m; t_{work} is the working time of working face each day; v_{cut} is the cutting speed of combine, m/h; d_{cut} is the cutting distance of combine, m; v_{face} is the advancing speed of working face, m/d.

The cutting speed of combine of long-wall working face in Shendong Mine Area is chosen 480 m/h, and the cutting distance is chosen 0.86 m. For short-wall face, it is equivalent to 15 m/h to 20 m/h of cut-ting speed, 10 m of cutting distance that the cutting speed of continued mining machine is 7.6 m/min, and 3 to 4 mining rooms is mining in one hour considering the preparing time. Consequently, the working face length of each class may be calculated as Table 11.

Table 11. The corresponding working face's length and speed of each class.

Sort	Advancing speed (m/d)	Upper limit of working face's length (m)
I	<10	
II	>10	750
III	>15	500
IV	>25	300
V	>35	80~100
VI	>45	60~80
VII	Mining room is disposed in a single decorated form, and the aim of mining at no falling down of roof	

4 CONCLUSIONS

Based on the mechanism and key of aquifer-protective mining, we put forward the idea that the working face's advancing speed is decided by the seepage velocity of water through the overlying strata, i.e. the time of working face's pass through the initial and periodic broken distance is less than the time of the above water seepage to working face. This time of long-wall general is 10 m/d to 15 m/d, and must be more than 25 m/d at the difficulty of aquifer-protective mining.

The length range of the safety aquifer-protective mining face has been determined by the lower limit of working face's advancing speed and the cutting speed of combine. Long-wall working face may be more than 300 m, and short wall working face generally is not more than 100 m.

ACKNOWLEDGEMENTS

Financial support for this work, provided by the research fund of North China Institute of Science and Technology (No. A09002, Title: Preliminary Study on Mechanism and Technology of Aquifer-protective Mining in Shallow Coal Seam, 2009) and the basic scientific research grants funded of central universities and colleges (No. E1204, Title: The research and analysis of coal mine water treatment technology, 2012), and the Teaching Research Project of North China Institute of Science and Technology (Title: The Optimization Research of Teaching System Based on Enterprise and Student Feedback Information, 2011), is gratefully acknowledged.

REFERENCES

Chen P & Zhang YT. coupling analysis of seepage/stress for jointed rock [j]. Chinese Journal for Rock Mechanics and Engineering, 1999, 13(4):299–308.

Huang QX. Simulating on damage law of disturbed thick sandy soil layer and transference of load in shallow seam [J]. Journal of Chang' an University (Natural Science Edition) 2003, 23(4):82–83.

Liu YD, et al. Study on the pattern and the application of short-wall continuous mechanical mining in shallow coal seam with thin bedrock [J]. Journal of Safety Science and Technology. 2010.

Louis C. Rock hydraulics. Rock Mechanics. 1974.

Ma LQ. Study on Distribution Characteristics and Control Technology of Water Conduction Channels Cranny in Shallow Sand-Bedrock-Coal Seam [D]. Xuzhou: Doctor Dissertation of China University of Mining and Technology, 2007.

Nolte DD, et a1. The fractal geometry of flow paths in natural fractures in rock and the approach to percolation. Fractals in Geophysics. 1989.

Qian MG, et al. Key Strata Theory in Underground Control. Xuzhou: China University of Mining & Technology Press, 2000 (In Chinese).

Shi BQ & Hou ZJ. Research on coal mining method with water conservation in Yushen Mining Area [J]. Coal Engineering, 2006, (1):63–65.

Wang A. Modern Manufacturing Techniques in Shendong Hundred million tons Mine Area. Peking: Coal Industry Press, 2005 (In Chinese).

Yi MS. Study and Application of Key Strata Theory in Shallow Seam of Shendong Mining Area [D]. Xuzhou: Doctor Dissertation of China University of Mining and Technology, 2008.

Zhang D, et al. Preventing and controlling techniques of ecological environments in Shan-Xi and Inner Mongolian mine are [C]. Journal of Coal Science & Engineering. Vol. 13 No. 4 Dec. 2007, 471–475.

This page intentionally left blank

Progress in Mine Safety Science and Engineering II – He et al. (Eds)
© 2014 Taylor & Francis Group, London, ISBN 978-1-138-00122-0

The design of rapid prediction system on coal seam gas content

Yong-Tao Liu, Jia Liu, Shang-Quan Ma & Wei Di
North China Institute of Science and Technology, Lang Fang, Hebei Province, China

ABSTRACT: In this paper, coal seam gas content forecast needs to test and analyse the gas content of the coal sample. Gas desorption rate of coal sample gradually reduced with time extension, so we need to use a very low pressure loss of the gas flow sensor for testing. In order to adapt to the demand, the instrument design uses micro electro mechanical system (MEMS) flow sensor FS4001, to realize the collection of gas flow through the mixed signal processor 12 bit A/D conversion. According to coal sample gas desorption power function relationship between the rate changing over time, automatic matching is deduced under the natural state sample total coal desorption of gas. This instrument has realized the data acquisition, storage of more groups, curve display, time setting, desorption rate total logic deduction, the loss in fitting and so on in the field of micro gas measurement with its good application prospect.

Keywords: MEMS, flow sensor, curve fitting, least square method

1 INTRODUCTION

How to quickly and accurately determine the coal seam primitive gas content, is a topic on research field of coal mine gas prevention and control. Coal seam gas content is the basis to determine the gas emission data, is one of the important parameters of designing mine gas drainage and mine ventilation. The existing measuring equipment's function is not complete and it's intelligent degree is not high, so there is an important theoretical significance and practical value to design and develop a high performance of coal seam gas content tester (QI Li-ming 2007).

This article mainly introduce based on micro electro mechanical system (MEMS) flow sensor FS4001-200—CV—CH4 desorption of gas in coal bed recorder in the research and design method. For trace, low pressure loss and the volume of a gas flow velocity measurement.

The PC software design, using VC++ to program development, completed the linear fitting based on nonlinear least squares curve fitting and design, thus made further precise calculation and post-processing on lower machine data.

2 EXPERIMENTAL PRINCIPLES AND METHODS

2.1 *Basic principles of gas flow sensor FS4001-200—CV—CH4*

FS4001 is an application of micro electro mechanical system (MEMS) sensor chip technology, silicon chips use mechanical and electrical characteristics of micro-scale thermal film type sensor. It is not simply to miniature mechanical and electrical function on a chip, but adopt the modern materials technology and large scale integrated circuit technology combined with access to new features. MEMS chips can be obtained by some micro mechanical and electrical devices that cannot achieve the effect.

Hot membrane type gas flow sensor is made by using the principle of heat conduction and heat dissipation. Sensor adopts thermal quality gas flow sensor chip, belongs to the mass flow sensor of flowmeter. It measures the gas flow by gas flow field changes through the produced heat. The variation and the fluid velocity, heating current, surface temperature of the hot film, from these relations can be derived thermal membrane retention of heat Q and the relationship between the fluid velocity v (Sang Xiaowei 2009). Due to different quality of the gas changes have different impacts on the thermal field, as a result, the sensor measured by the flow of mass flow rate, and therefore there is no need to compensate temperature and pressure. At the same time, the adoption of multiple sensors, and micro heat source technology, make it have the excellent zero point stability, short response time and low loss characteristics (Li Caichun 2009; Fujita H 1995).

Unlike other MEMS sensor technology, FS4001 chip integrate a multiple of sensors on a single sensor. Chip surface adopted passivation of ceramic material with high thermal conductivity, in guarantee the sensor has a minimum of traffic at the

same time to avoid direct contact with the sensor and gas medium to improve its reliability. When there is no gas medium through the MEMS sensor chips, sensors keep a stable temperature field (distribution of temperature) around. When gas medium flows through the sensor, because of the fluid medium taking away heat, the temperature field leads a local temperature distribution (Wu Y 1992; Toda K 1996). Measuring principle is shown in Figure 1.

The local temperature field depends on the quality and velocity of fluid medium, integrates on a chip of the sensor to measure temperature distribution through calibration. The specially designed signal processing circuit will be converted to mass velocity and mass flow rate of medium into a linear relationship between output voltage value (Durst F 2003).

2.2 *Research of prediction system's function*

The gas content data recorder was designed with a scientific desorption method, desorption steps method is to use the common coal core tube coal core drill, when the coal core is putting forward after the orifice, then use the tank to seal the acquisition of coal sample containing gas, sample desorption instrument has been applied to the determination of coal gas desorption quantity law changing over time, and according to the exposure time of coal sample calculated the sampling gas quantity loss in the process. Then sent sample coal seal whose desorption law has been measured to the lab, determinate the residual gas content in coal core. After adjustment for temperature and pressure, with desorption gas quantity (including desorption quantity and loss quantity) and the sum of residual gas volume. Divided by the weight of coal core, the gas content of coal are obtained. The method for determining coal bed gas content adapt to take in geological exploration drilling coal core determination of coal seam gas content and gas composition.

Concrete steps as follows: first of all from coal seam drilling and sampling by coal core pipe, coal sample gas content including gas analytic data before crushing (measurement process for the first time, this process needs to measure before crushing coal sample methane desorption gas quantity Q_2, Q_1 and the loss) and crush after desorption data (second determination process, determination of the process after crushing the gas desorption quantity Q_3). The desorption rate of Q_2 meets regular pattern as shown in Figure 2, system makes use of these data using the following formula to fitting.

$$V_t = V_0 (1+t)^{-k} \tag{1}$$

In The Formula,

V_t – desorption rate of desorption gas at time t, ml/min;

k – constant;

V_0 – coal gas desorption rate at start ($t = 0$) desorption time, ml/min.

Then the processor according to the test data Q_2, where V_0 and fitting out the coefficient k, then generation back expression formula for V_t, according to the coefficient of the known formula exposure period of gas loss quantity Q_1. Last measured pieces begin to the end of the desorption time the total cumulative desorption volume in Q_3, When the desorption amount is less than 1 ml/min, instrument automatically end the Q_3 measurement, process and save the data.

The total gas content is calculated:

$Q_{content}$ – coal seam gas-bearing capacity, ml/g;

Q_1 – loss of gas quantity, ml;

Q_2 – desorption gas quantity before coal sample pieces, ml;

Q_3 – desorption gas after coal sample pieces, ml;

M – the total quality of the coal sample, g;

M_0 – pieces with the quality of the coal sample, g.

According to this formula, only the instrument keyboard input samples of coal sample total mass M and crushing coal quality M_0, can the total gas content Q always is deduced.

At the end of data processing, Q_1, Q_2, Q_3 and Q the total value can query and display at any time. Cumulative desorption rate desorption rate curve changes over time can query and display (Zhang Yanwen 1998).

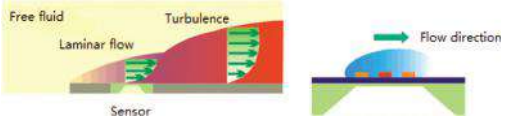


Figure 1. Sensor working principle diagram.

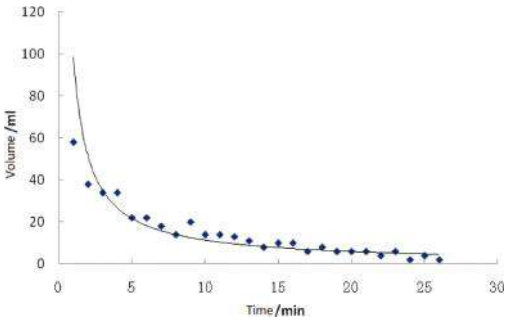


Figure 2. Desorption rate curve diagram.

2.3 *Under machine design*

The system uses MSP430F149 do give priority to the controller, cooperate with FS4001 gas mass flow sensor complete the gas content test. The whole function circuit includes MCU module, ferroelectric storage module, clock module, keyboard module, LCD display module, USB communication circuit module unit (Ji Liming 2010).

System uses the unit circuit design and has a high integration. This is to ensure the stability of the instrument, but also increases the difficulty of the system software design. The core and difficulty of the instrument design is that each point data of Q_2 fitting the curve of the value of Q_1 and Q_2 desorption rate being derived.

Due to the processor's operation limited ability, Q_1 data fitting process cannot use all Q_2 value to accurately fitting the Q_1 numbers. So system adopted nearby principle, according to the initial point of three numbers to the power function $V_t = V_0(1+t)^{-k}$ make a list of equations. Calculate starting rate V_0 and time constant k, again make t equal to 1, 2, 3 respectively where V_0 into the formula. Finally obtaining data values V_1, V_2, V_3, which is deduced from Q_1 result.

System programming difficulty and core focus on the LCD display curve fitting, data fitting and menu interface design.

2.4 *Experiment data comparison*

The group data, by one machine to the USB port to PC intelligent gas content prediction system. Run the PC software, set the COM port and baud rate, input to upload data from the instrument category, run the upload menu. PC interface is shown in Figure 3.

Software adopted two methods of data fitting processing, traditional curve fitting and nonlinear least square fitting. Through the test of the two methods, multiple linear regression coefficient was 0.991308 and 0.988942, respectively, the resulting fitting error controlled within 2%. After the treatment in choosing a good similarity, input the value of the specific test points number and M, M_0 data make a process for our needed results and saved to the database. Measurement data for Q_2 and fitting data Q_1 can be derived through the first interface, curve distribution can be copied or printed directly.

In view the data interface, data query process can be set according to place, time, total Q threshold alone or integrated query. We need to research and analysis of data directly to the graphics print or export to excel spreadsheet. As exporting data shown in Figure 4, including 1 fitting for piecewise curve fitting of data, 2 fitting for the least squares fitting of curve data.

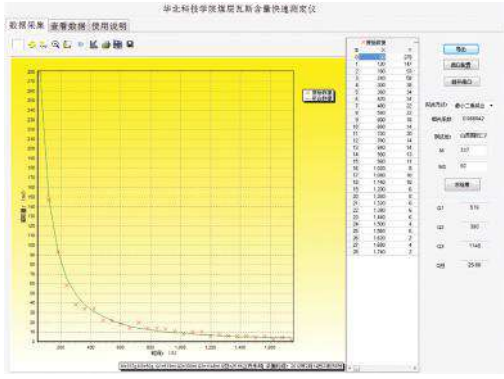


Figure 3. PC data fitting processing interface.

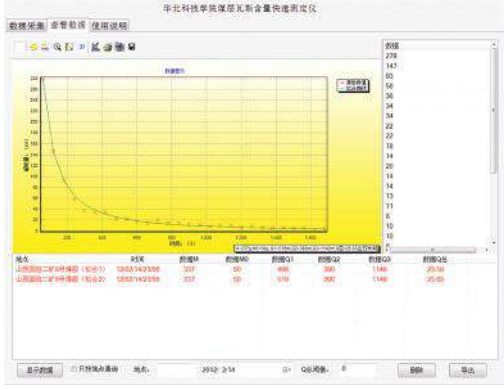


Figure 4. Data query interface.

3 CONCLUSION

Design of the instrument has features of small volume, light weight and good timeliness. When the gas desorption quantity is less than 1 ml/min the design can automatically complete the data processing, there's no need for staff to intervene to realize the intelligent operation of the equipment. The system reduces power consumption through a variety of software and hardware optimization, so it can meet for a long time, more group testing. Instrument connected to the computer through USB ports and the data transfer is accurate, stable and easy to operate. Design to the existing instrument can't display curve, can't direct the logic of the fitting, and derive the total gas desorption quantity shortcomings and so on has carried on the research and improvement. The successful design of the instrument to the underground coal seam gas content provides a good scientific method for fast measurement and support.

ACKNOWLEDGEMENTS

The authors gratefully acknowledge supported by the Fundamental Research Funds for the Central Universities (3142013095).

REFERENCES

Durst F, et al. 2003. The development of a pulsed-wire probe for measuring flow velocity with a wide bandwidth. *International Journal of Heat and Fluid Flow*, 24(1):11–13.

Fujita H, et al. 1995. A thermistor anemometer for low—flow-rate measurement. *IEEE Transactions on Instrumentation and Measurement*, 44(3):779–782.

Ji Liming, et al. 2010. New coal seam gas content accurate determination method, *Journal of Mining and Safety Engineering*, 1:111–115 (in Chinese).

Li Caichun, et al. 2009. Based on the method of constant temperature thermal membrane type gas flow sensor design. *Sensor and. Micro System*, 6:104–109 (in Chinese).

Qi Li-ming, Wang, et al. 2007. Study on the coal gas pressure dynamic distribution law in the front of tunneling place. *Journal of the Sout—Hern Aferican Institute of Mining and Metallurgy*, 107(7):431–433 (in Chinese).

Sang Xiaowei, et al. 2009. Comparison of several kinds of coal bed methane content measurement method, *China Coal Bed Methane*, 3:27–28 (in Chinese).

Toda K, et al. 1996. Simple temperature compensation of thermal air flow senso. *Sensors and Actuators A*, 57(3):197–201.

Wu Y, et al. 1992. The design and analysis of an imp roved high air flow meter with analog/digital filters. *IEEE Transactions on Instrumentation and Measurement*, 41(6):791–796.

Zhang Yanwen, et al. 1998. Micro gas flow sensor, *Sensor Technology*, 2:43–45 (in Chinese).

Progress in Mine Safety Science and Engineering II – He et al. (Eds)
© 2014 Taylor & Francis Group, London, ISBN 978-1-138-00122-0

Research and application of technique of injecting liquid CO_2 in goaf of Shigang coal mine to preventing fire

Xin-Long Tong, Zhi-An Huang, Ying-Hua Zhang, Yan-Feng Zhang & Xin-Tong Wang
State Key Laboratory of High-Efficient Mining and Safety of Metal Mines, University of Science and Technology Beijing, Ministry of Education, Beijing, China

ABSTRACT: The extinguishing effect of liquid CO_2 is significant, but fire preventing technology with liquid CO_2 is not mature in coal mines. Against characteristics and laws of spontaneous combustion of residual coal in goaf, mechanism of preventing and extinguishing fire with liquid CO_2 was analyzed. Through carrying out temperature programmed experiments on coal samples, concentration and producing rate of CO, oxygen concentration and consuming rate of oxygen and other relating parameters under conditions of pure air and different concentrations of CO_2 were compared and analyzed. According to fire preventing theory and technology with liquid CO_2, combining with the actual situation of 15109 fully mechanized caving face of Shigang mine, a reasonable fire preventing system of injecting liquid CO_2 into goaf was built up, and then changes of gases and temperature in goaf were continuously monitored. Results show that liquid CO_2 has remarkable effect on fire prevention, and the system of injecting liquid CO_2 runs well, which prove that the proposed fire preventing technology has certain reference value to similar mines.

1 INTRODUCTION

According to statistics, as one kind of major energy in China, coal accounts for more than 85% of amount of domestic production and consumption of primary energy, so it occupies an important place in national energy structure. However, spontaneous combustion of coal has been so serious that it threatens safety production of mines heavily, and it has been such a major scientific challenge that it has not been completely resolved by any country until now.

As a kind of inert material, CO_2 has been widely used for prevention of various fire disasters, and it can control even extinguish various fire disasters in a very short period of time. It has so many advantages such as strong fire-fighting capability, short fire-fighting time, wide fire-fighting range, low pollution to environment and so forth, so it has been the first choice for dealing with various ground fire disasters. As technology constantly develops, CO_2 has been also applied for preventing fire in coal seam, and good effects have been achieved, but due to existing problems in fields of storage, transportation, cost and crafts, it still cannot be applied widely like nitrogen (Li 1998). In recent years, as storing technology of liquid CO_2 becomes mature, liquid CO_2 has been applied for dealing with various ground fire disasters more and more widely. Some mines at home and abroad have tried to apply liquid CO_2 to control Fire District, and fire extinguishing effects of liquid CO_2 have been remarkable, but research on adopting liquid CO_2 for preventing and extinguishing fire is still very limited, leading to immature of this technology.

The environment of spontaneous combustion of coal in goaf of mechanized caving face was analyzed, and technique of injecting liquid CO_2 into goaf to prevent and extinguish fire was studied, aiming to effectively prevent occurrence of spontaneous combustion of coal in goaf.

2 ANALYSIS OF ENVIRONMENT OF SPONTANEOUS COMBUSTION OF COAL IN GOAF AND MECHANISM OF PREVENTING AND EXTINGUISHING FIRE WITH LIQUID CO_2

Spontaneous combustion of coal starts at physical adsorption of oxygen which provides energy for coal-oxygen chemisorptions by releasing heat. Coal is a kind of natural adsorbent, being able to absorb inorganic substances such as CH_4, CO_2, N_2 and organic substances such as methanol and benzene (H 2002). Adsorbing capacities and speeds of coal against different substances are different. According to soluble mechanism, gas with higher boiling point and critical temperature can more easily spread into all pores of coal, and can be more easily absorbed by coal. Boiling points and critical temperatures of four gases which are CO_2, CH_4, CO and N_2 are shown in Table 1.

Capacity and speed of coal adsorbing CO_2 are all better than coal adsorbing other gases. Quantum

Table 1. Boiling points and critical temperatures of four gases.

Gas	CO_2	CH_4	CO	N_2
Critical temperature/K	304.2	191.1	132.8	126.2
Boiling point/K	194.7	109.2	81.5	77.4

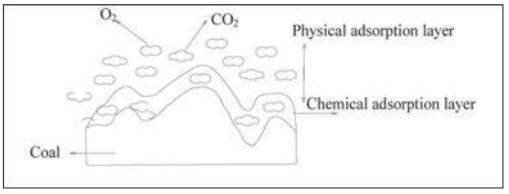


Figure 1. Schematic diagram of CO_2 inhibiting coal-oxygen physical adsorption.

chemical study on interaction between coal surface and CO_2 has shown that coal adsorbing CO_2 is physical adsorption which can be multilayer adsorption and relatively stable (Cui 2005, Jiang 2006). When coal surface needs to adsorb gas molecules, CO_2 molecules can be stably adsorbed on surface of coal sooner than oxygen molecules. Therefore, when there are a variety of gases at the same time underground, CO_2 can be quickly adsorbed by coal, wrapping coal body and preventing oxygen from contacting coal, so spontaneous combustion of coal can be inhibited (Liu 2006).

Schematic diagram of CO_2 inhibiting coal-oxygen physical adsorption is shown in Fig. 1.

As a kind of inert material, once injected into fire preventing area, CO_2 can evaporate and then spread to fill space rapidly, driving O_2 in hazardous areas to make the Fire District suffocate as result of lacking oxygen or inhibit spontaneous combustion of coal. Steaming of liquid CO_2 needs to absorb large quantities of heat, which make temperature in dangerous area decrease. Except the general role of preventing fire of inert gas, liquid CO_2 has its unique fire preventing characteristic such as wide cooling range, obvious effect, high inerting speed and great perfusion flow (Han 2009).

Liquid carbon dioxide achieves fire-fighting purposes by following three ways (Zhao 2010):

1. Effect of separating oxygen and covering. Spontaneous combustion of coal is result of coal-oxygen compounding reaction, as oxygen is a necessary condition of oxidation reaction. If there is no oxygen or only little oxygen, spontaneous oxidation of the coal would be interrupted or inhibited.
2. Effect of cooling and lowering the temperature. Liquid CO_2 can quickly cool off high temperature coal body and suppress temperature of coal rising, so spontaneous combustion of coal can be prevented.
3. Effect of inerting and suppressing explosion. Vaporizing CO_2 can dilute content of combustible gas and oxygen and make degree of inerting of gases in space of Fire District become larger and larger, which can hinder formation of activation center and make explosive gas reflect inerting explosive characteristic.

3 EXPERIMENTAL RESEARCH OF LIQUID CO_2 AFFECTING SPONTANEOUS COMBUSTION OF COAL

When heat released by coal-oxygen chemical reaction is more than distributing heat, temperature of coal rises and causes fire, so spontaneous combustion of coal can happen (Deng 2003). This process was simulated under experimental condition, and through injecting liquid CO_2, changing laws of coal's temperature, oxygen consuming amount, CO producing amount as well as relating parameters of other gases during this process were all studied. Experimental conditions were as follows:

1. Quality of samples are 1.0 kg, which was got by crushing and sieving raw coal and taking 20 g of coal particles with granularity of following ranges: 0~0.9 mm, 0.9~3 mm, 3~5 mm, 5~7 mm, 7~10 mm;
2. Heating rate: 0.5 °C/min (room temperature to 110 °C); 1 °C/min (110~210 °C); 2 °C/min (210~330 °C);
3. Liquid CO_2 injecting frequency was every time temperature rising 20 °C;
4. Liquid CO_2 injecting volume was 100 ml/min, as concentrations of CO_2 were respectively 9%, 17%, 25%, and 38%. Different concentrations of liquid CO_2 were injected into different coal samples, and then temperature-programmed experiments were carried out. Four groups of coal samples from least to most of concentration of liquid CO_2 injected were respectively numbered 1#, 2#, 3# and 4#, and the group of coal samples not injected liquid CO_2 was numbered 5#.

Schematic diagram of experimental apparatus is shown in Fig. 2, and curves of concentration of O_2, CO and CH_4 changing with temperature are respectively shown in Fig. 3–Fig. 5.

According to Fig. 3, through comparing and analyzing curves of concentration of O_2 changing with temperature, what can be known are as follows: CO_2 has great influence on concentration of O_2, and concentration of O_2 of coal samples under condition of pure air is larger than that of coal samples injected CO_2. As temperature rises, concentration of

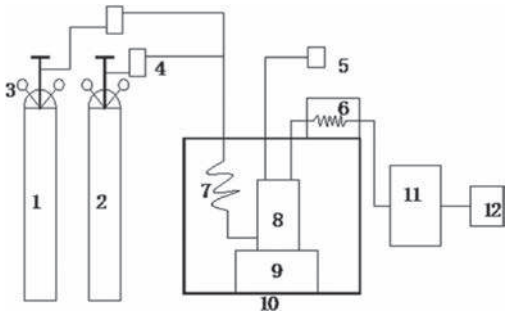


Figure 2. Schematic diagram of experimental apparatus.

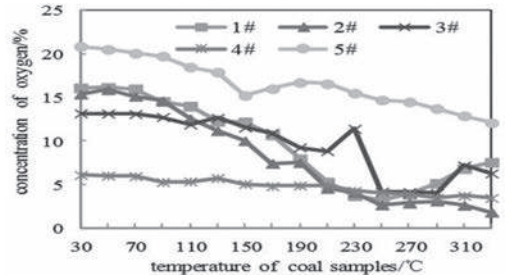


Figure 3. Schematic diagram of experimental apparatus.

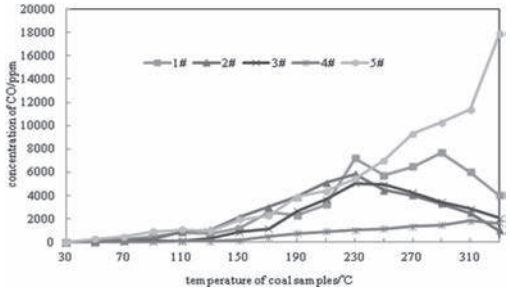


Figure 4. Curves of concentration of CO changing with temperature.

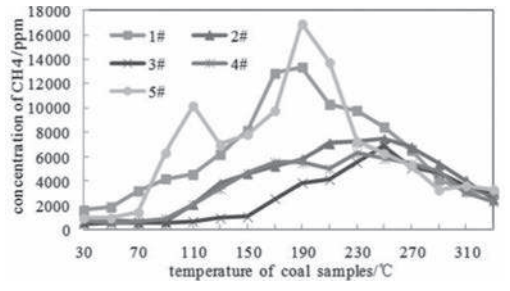


Figure 5. Curves of concentration of CH_4 changing with temperature.

O_2 decreases. Coal-oxygen oxidation reaction weakens and eventually stops due to lacking oxygen.

According to Fig. 4, through comparing and analyzing curves of concentration of CO changing with temperature, what can be known are as follows: as temperature rises, concentration of CO of each group of coal samples increases. Curves of concentration of CO of coal samples injected liquid CO_2 are all lower than that of raw coal samples, and with concentration of liquid CO_2 injected increasing, these differences become more obvious, which proves that Coal-oxygen oxidation reaction increases as temperature rises concentration of CO produced by oxidation of 1# ~ 4# coal samples are less than that of raw coal samples under influence of CO_2.

According to Fig. 5, through comparing and analyzing curves of concentration of CH_4 changing with temperature, what can be known are as follows: in temperature range of 130 °C~330 °C, CH_4 is produced by pyrolysis of coal which only has something to do with temperature, CH_4 produced by 5# coal samples is far more than that produced by other groups of samples, which proves that in high temperature range, CO_2 can significantly reduce methane producing amount and can inhibit coal producing CH_4 by oxidation pyrolysis.

4 EXPERIMENTAL RESEARCH ON THE TECHNIQUE OF INJECTING LIQUID CO_2 INTO GOAF OF SHIGANG MINE FOR PREVENTING FIRE DISASTER

4.1 *Overview of mine and mining face*

Shanxi Shigang Coal Mine has field area of about 7.479 square kilometers, and its recoverable reserves is 31 million tons.

The experiment mining face is NO.15109 mining face which lies at NO.1 mining area. Its trending length is 560 m, incline length is 157 m, and area is about 87250 m^2. Its coal seam has stable occurrence and complex structure, with maximum, minimum and average total thickness being respectively 7.73 m, 6.85 m and 7.23 m. There are generally two layers of rock in the coal seam, as one layer with thickness 0.28 m lies at position where is 2.36 m below roof and the other layer with thickness 0.35 m lies at position where is 0.47 m above backplane. There are joints developing in the coal seam.

4.2 *Injecting process of liquid CO_2*

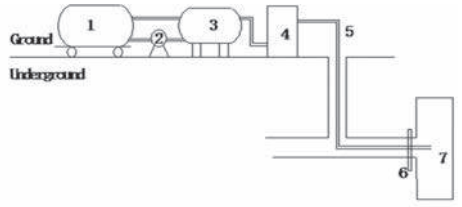
According to actual situation and environmental conditions of NO.15109 mining face of Shigang coal mine, considering cost and other relating factors, method of vaporization perfusion from ground was adopted, that is to say, liquid CO_2 is transported from chemical plant to mine by

specialized transport tank lorry and imported to low temperature storage tank, and then vaporized on the ground by external vaporizer, and finally transported to via pipeline to goaf or Fire District for fire prevention. Liquid CO_2 equipments are installed on ground near wellhead and connected to underground fire-fighting pipes so that a stationary fire-fighting system can be built up. The process map of injecting CO_2 is shown in Fig. 6.

4.3 *Arrangement of data acquisition system of injecting liquid CO_2*

Data acquisition includes gas sampling and temperature acquisition. Manual sampling method was adopted on purpose of saving cost. Temperature were measured by using TES-1310 digital thermometer, compensation wire with indexing number KC and K(CA)NiCr/NiAI thermocouple and data then was recorded. Gas samples were carried back to ground and analyzed with chromatograph.

Data acquisition system was arranged at return airway of 15109 mining face, and spacing of measuring points was 70 m. The first measuring point is 5 m away from the front of initial releasing mouth. Method of burying pipes for observation was adopted, as three beam tubes and three survey lines were buried at bottom of right side ditch of 15109 mining face, and two-inch steel pipe was used as their protective casing. A temperature probe and a beam tube dust filter were set up at each measuring point. The schematic diagram of arrangement of measuring points is shown in Fig. 7.



1 - liquid CO_2 tank lorry, 2 - booster pump, 3 - low temperature storage tank, 4 - carburetor, 5 - injecting pipeline,6 - closed wall, 7 - goaf

Figure 6. Process map of injecting CO_2.

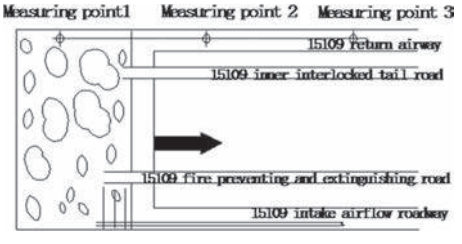


Figure 7. A schematic diagram of arrangement of measuring points.

4.4 *Monitoring and analysis of experimental effect of injecting liquid CO_2*

4.4.1 *Changes of gas concentration and temperature in goaf of 15109 mining face*

When 1 # measuring point is 35 m away from the mining face, namely injecting mouth is 30 m away from the mining face, liquid CO_2 was begun to be injected continually. In order to better monitor and analyze fire preventing effect of injecting liquid CO_2 into goaf and grasp change of gas concentration in goaf and distributing law of the three zones, temperature was measured and gas samples were analyzed continually for three months at the three measuring points at air returning side of goaf.

Changes of concentration of CO, CO_2 and O_2 at air returning side of goaf in situation of continuous injection are respectively shown in Fig. 8–Fig. 10.

As Fig. 8 shows, before injecting liquid CO_2, with the mining face advances, concentration of CO in goaf gradually increases, especially when distance between 1# measuring point and mining face is more than 30 m, concentration of CO rapidly increases, as maximum concentration reaches

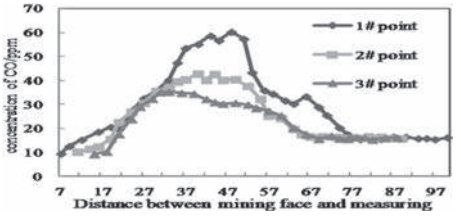


Figure 8. Change of concentration of CO.

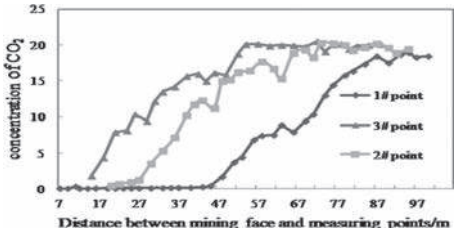


Figure 9. Change of concentration of CO_2.

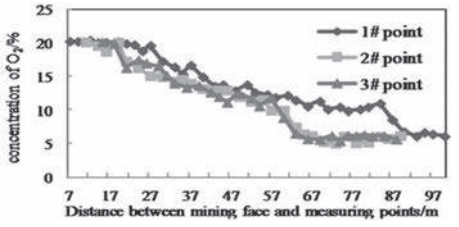


Figure 10. Change of concentration of O_2.

60 ppm. As liquid CO_2 is continuously injected, concentration of CO quickly decreases, and ultimately maintains at a low level, which shows that 1# measuring point quickly passes through oxidized spontaneous combustion zone and gets into choking zone. What can be seen from results of 2# and 3# measuring points is that under condition of continuously injecting liquid CO_2, concentration of CO at each measuring point all firstly increases a little but then decreases rapidly, finally maintains at low level of about 15%. Therefore, the inhibiting effect against spontaneous combustion of residual coal of continuously injecting liquid CO_2 in goaf is very good.

As Fig. 9 shows, after injecting liquid CO_2 in goaf, concentration of CO_2 in goaf significantly increases, as maximum concentration reaches more than 20%. When measuring points are relatively close to the mining face, concentration of CO_2 is relatively low, mainly because falling rock gap near the mining face is large and air leakage in goaf is serious as leakage flow can transfer and dilute CO_2. The nearer to the mining face, the larger the effect is. However, at position far away from the mining face, air leakage is little and concentration of CO_2 is relatively large. As depth of goaf increases, falling rocks are gradually compacted and transferring effect of CO_2 stream is inhibited, so concentration of CO_2 increases and finally reaches balanced state (Wang 2011).

As Fig. 10 shows, width of area where concentration of O_2 maintains in range of 10%~18% gradually shortens, and this kind of area advances a lot. That is to say, under condition of continuously injecting liquid CO_2, oxidized spontaneous combustion zone gradually shortens.

4.4.2 *Analysis of test results of gas concentration at the upper corner of 15109 mining face*

In order to ensure concentration of O_2 in 15109 mechanized caving face above safe value and prevent a large number of toxic and harmful gases from gushing out, gas concentration at the upper corner of 15109 mining face was continuously monitored for a month. Changes of concentration of O_2, CH_4, CO and CO_2 at the upper corner are respectively shown in Fig. 11–Fig. 14.

As can be seen from Fig. 11 to Fig. 14, continuous injection of liquid CO_2 has little influence on concentration of O_2 which basically maintain at about 20%, but it has greater influence on CO as concentration of CO decreases and finally maintains at about 5ppm, moreover, it has little influence on CH_4 as concentration of CH_4 only changes a little. After the injection, concentration of CO_2 increases and ultimately maintains at about 0.18%. Therefore, continuously injecting CO_2 into goaf is feasible and safe.

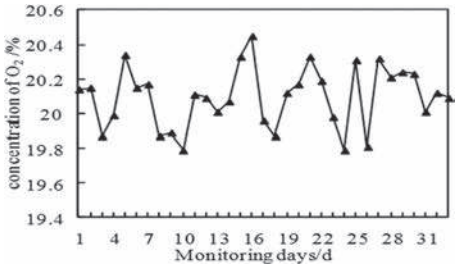


Figure 11. Change of concentration of O_2 at the upper corner.

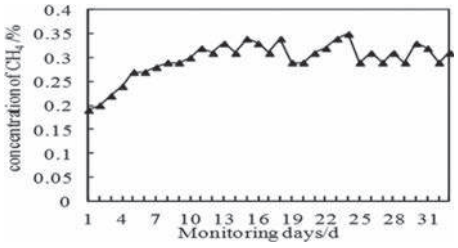


Figure 12. Change of concentration of CH_4 at the upper corner.

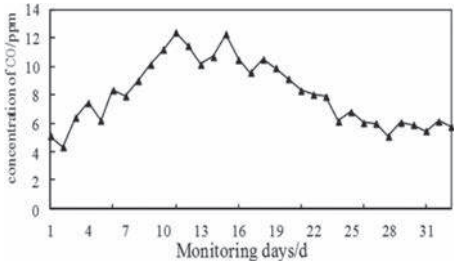


Figure 13. Change of concentration of CO at the upper corner.

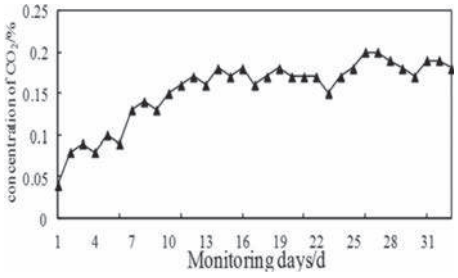


Figure 14. Change of concentration of CO_2 at the upper corner.

4.4.3 *Changes of three zones of spontaneous combustion in goaf*

Through analyzing change of concentration of O_2 in goaf, what can be known is that under condition of continuously injecting liquid CO_2, at

Table 2. Change of three zones of spontaneous combustion after injecting CO_2 into goaf of 15109 mining face.

Three zones	Heat dissipation zone	Oxidized spontaneous combustion zone	Choking zone
Concentration of O_2 /%	>18	10~18	10
Width of zone before injecting CO_2/m	30	30~87	>87
Width of zone after injecting CO_2/m	19	19~60	>60

position about 19 m away from the mining face, concentration of O_2 decreases to below 18% and oxidized spontaneous combustion zone is reached, and at position about 60 m away from the mining face, concentration of O_2 decreases to below 10% and choking zone is reached. Changes of three zones of spontaneous combustion after injecting CO_2 into goaf can be seen from Table 2. As Table 2 shows, after the injection, oxidized spontaneous combustion zone advances 11 m and shortens 16 m, and choking zone advances 27 m, which together prove that continuously injecting CO_2 into goaf has great inhibiting effect on spontaneous combustion of residual coal and good fire preventing effect.

4.4.4 *Analysis of effect of injecting liquid CO_2 into goaf*

In goaf of 15109 mining face of Shigang mine, through nearly three months of continuous monitoring, what can be known is that with amount of injection increasing, concentration of O_2 at each measuring point all decreases and ultimately maintains at about 6%, concentration of CO_2 maintains at about 20%, and temperature at deep position of goaf maintains at about 20 °C, moreover, concentration of CO maintains at relatively low level, which all together prove that the technique of injecting liquid CO_2 into goaf for fire prevention can effectively inhibit formation of hot spots in goaf and prevents coal spontaneous combustion of residual coal (Li 2008).

5 CONCLUSIONS

1. In addition to the general role of preventing fire of inert gas, liquid CO_2 has its unique fire preventing characteristic such as wide cooling range, obvious effect, high inerting speed and great perfusion flow. Its fire-fighting mechanism mainly reflects in the following three respects: effect of separating oxygen and covering, effect of cooling and lowering the temperature and effect of inerting and suppressing explosion.
2. Results of the temperature-programmed experiments show that CO_2 has good inerting effect on spontaneous combustion of coal, but it is easily influenced by concentration and ambient temperature. When concentration is over 20%, CO_2 has obviously inerting effect and the higher the temperature is, the stronger inerting effect is; moreover, CO_2 with low concentration has inerting effect in low-temperature stage, but its inerting effect in high-temperature stage is not obvious.
3. As CO_2 is injected continuously, concentration of O_2 at each measuring point all decreases and ultimately maintains at about 6%, concentration of CO_2 maintains at about 20%, and temperature at deep position of goaf maintains at about 20 °C, moreover, concentration of CO maintains at relatively low level, which all together prove that the technique of injecting liquid CO_2 into goaf for fire prevention can effectively inhibit formation of hot spots in goaf and prevents coal spontaneous combustion of residual coal.

REFERENCES

Cui, Y.J., Zhang, Q., Zhang, Y. et al. 2005. Adsorption of different rank coals to single component gases. Natural Gas Industry 25 (1): 14–16.

Deng, J., Xu, J.C. 2003. Perspectives on spontaneous combustion mechanism and prediction theory of coal. Journal of Liaoning Technical University 22 (4): 455.

H, W., B, Z., M, K. 2002. Kinetic modeling of low temperature. Combustion and Flame 131(7): 452–469.

Han, G., Liu, S.Y. 2009. Application of liquid carbon dioxide fire extinguishing in practice. Coal Technology 28 (4):107–109.

Jiang, W.P., Cui, Y.J., Zhang, Q. 2006. The quantum chemical study on the coal surface interacting with CH4 and CO_2. Coal Society 31 (2): 35–39.

Li, C.X. 1998. Entire of China's coal mine safety. Beijing: Coal Industry Press.

Li, S.R. 2008. Experimental study on performance that carbon dioxide inhibits coal oxidation and spontaneous combustion. Xi'an: Xi'an University of Science and Technology.

Liu, C. 2006. Research of coal spontaneous combustion laws and preventing technology in easy self-ignition coal seam exploiting without coal pillar. Xi'an: Xi'an University of Science and Technology.

Wang, Z., Gao, M. 2011. CO_2 Fire Extinguishing Technique in steep seam. Mining Science and Technology 39 (3): 49–50.

Zhao, X.X. 2010. Application of liquid carbon dioxide fire extinguishing. Heilongjiang Science and Technology Information (30): 65.

Progress in Mine Safety Science and Engineering II – He et al. (Eds)
© 2014 Taylor & Francis Group, London, ISBN 978-1-138-00122-0

Research on wind tunnel reducing ventilation resistance

Jing-Gang Zhang
Institute of Resource and Safety Engineering, China University of Mining and Technology (Beijing), Beijing, China
Key Laboratory of Mine Disaster Prevention and Control Technology in Hebei Province, China
College of Safety Engineering, North China Institute of Science and Technology, Beijing, China

ABSTRACT: Wind tunnel is defined to connect the main fan and shaft tunnel. Wind tunnel ventilation resistance has always been a big problem of mine ventilation resistance. This article analyses measured the ventilation resistance of many wind tunnels. Based on the theoretical analysis about reasons, it is concluded that there are many reasons contributing to a larger ventilation resistance, at the same time it puts forward the improvement to decrease the ventilation resistance, save energies and achieve good economic benefits.

1 INTRODUCTIONS

The wind tunnel is the connection of the main fan and shaft tunnel. Because of big ventilation quantity and pressure difference between inside and outside, it should try to reduce the ventilation resistance and reduce the air leakage. Though its short length, resistance loss often has accounted for more than 10%, some 50%, or even far more than mine design hypothesis of 200 Pa in the sinking and driving system (not including wind tunnel). As far as possible measures are required taking to reduce the ventilation resistance in the design, construction and use of wind tunnel. According to the requirements of the wind tunnel, ventilation resistance should be less than 0.0196 N.s^2/m^8, generally not more than 0.0490 N · s^2/m^8~0.0980 N · s^2/m^8.

2 THE CONDITION OF WIND TUNNEL VENTILATION RESISTANCE

In order to know wind tunnel well, we research and refer to the materials of 13 wind tunnels. Was found wind ventilation resistance of the mine situation what was found about ventilation resistance follow as in the table 1.

As known from Table 1:

1. As a result of different forms, construction qualities and management levels, the ventilation resistance R, resistance loss h, ventilation resistance of adit of sinking and driving system resistance percentage K value vary considerably. R varies from 0.016 N · s^2/m^8 to 1.232 N · s^2/m^8; K varies from 6.58 to 75.16%. (Cai Wei 2004)
2. Ventilation resistance of wind tunnel is greater than 0.0196 N · s^2/m^8, while 53.8% of the wind tunnels R are larger than 0.098 N · s^2/m^8 and R of three wind tunnels are larger than 0.294 N · s^2/m^8, the largest 1.232 N · s^2/m^8.
3. The ht of 50% of the wind tunnels researched in the survey is more than 200 Pa, the largest 1097.6 Pa.
4. The K of 76.9% of the wind tunnel researched in the survey is more than 10%, among which K of three wind tunnels is more than 50%, the largest one is 75.6%.

The data above show that quite a great part of output energy from some mine main fan is consumed in the wind tunnel, sometimes 50%. Ventilation resistance of many wind tunnels is larger than 0.0490 N · s^2/m^8~0.0980 N · s^2/m^8. Attention should be paid.

3 THE THEORETICAL ANALYSIS ON THE RESISTANCE OF WIND TUNNEL

3.1 *Analysis of friction resistance*

Friction resistance is produced due to mutual friction between air, shaft wall and air micelle when air flows along the tunnel. Its formula is:

$h_f = \frac{\alpha L U Q^2}{S^3}$ h the

In the formula: is refered as friction resistance, Pa; Q is referred as air volume through tunnel, m^3, L is referred as length of the air flowing through shaft, m; α coefficient of the friction resistance, N · s^2 / m^4; U section perimeter, m; h_t

We can adopt the following methods to reduce friction resistance of wind tunnel from above formula:

1. Reduce the coefficient of friction resistance α.
2. Guarantee enough sinking and driving section. As other parameters are constant, the area of sinking and driving section expands 33%, h_f can be reduced by 50%.

Table 1. Summary about ventilation resistance of the wind tunnel.

Mine fan system	The wind adit section S_t (m^2)	Wind speed V (m/s)	Air volume Q (m^3/s)	Mine resistance h_m (P_a)	Adit wind resistance h_t (P_a)	K = ht/h_m × 100 (%)	Wind tunnel resistance Rt (N . s^2/m^8)
1	7.66	9.5	72.8	940.8	138.1	14.68	0.026
2	2.2	10.2	22.6	217.5	19.6	9.09	0.038
3	3.39	4.38	14.9	363.5	272.7	75.6	1.232
4	5.95	10.1	60.1	815.3	242.0	29.66	0.067
5	5.6	11.3	63.3	216.5	284.2	13.12	0.070
6	2.8	18.5	52.0	379.2	196.0	51.68	0.072
7	4.75	9.5	45.3	1372	196.0	14.3	0.095
8	6.7	12.9	96.7	3067.4	1097.	35.78	0.117
9	4.0	16.4	65.6	1117.2	539.0	48.2	0.125
10	2.66	26.6	70.9	1342.6	807.5	60.14	0.160
11	3.0	9.99	29.9	446.8	147.0	32.8	0.163
12	5.1	3.34	17.0	1430.8	94.0	6.58	0.325
13	2.39	7.6	18.2	519.4	117.6	22.6	0.352

3. Choose a sinking and driving which has a smaller perimeter. Under the condition that sinking and driving section is of the same area, the perimeter of the circular section is the minimum, while arch section fades to it, and the circumference of rectangular or trapezoidal section is the larger.
4. As far as possible to shorten the length of the wind tunnel.
5. Avoid wind too centralized in the tunnel.

3.2 *Analysis of local resistance*

Due to The cross section of mine, change of direction and bifurcation or convergence and so on, local resistance makes uniform flow in the local area affected and damaged, resulting changes in wind velocity field distribution and eddy current and so on, and causes the wind energy loss. Generally experience formula of local resistance is: $h_l = RLQ^2 = \frac{u_1^2 \xi_1 \rho}{2}$ or $RLQ^2 = \frac{u_2^2 \xi_2 \rho}{2}$ In the formula: ξ_1 is the average wind speed before air flow into local resistant objects; μ_1 is the coefficient of corresponding local resistance, dimensionless; ξ_2 is the average wind speed after air flow into local resistant objects; u_1 is the coefficient of corresponding local resistance, dimensionless; h_1 is for local resistance Pa.

4 THE ANALYSIS OF THE CAUSES OF THE LARGER VENTILATION RESISTANCE

Combining the wind tunnel involved in the survey and basic situations of wind tunnel, we analyse what increases ventilation resistance in the production, and then get the actual factors influencing ventilation resistance.

4.1 *Unreasonable construction form of wind tunnel*

The three basic forms of wind tunnel:

1. The oblique type (Figure 1): Between the return air shaft and fan there is 45°or so inclined lane connection. This form of wind tunnel adopts comparative gentle dip and reduces the resistance caused by turning. With a simple structure and the wind tunnel is very short, the ventilation resistance is relatively small. (Cheng Shaoren & Cheng Jianjun 2006).
2. The line type (Figure 2): due to the special geologies or design factors, we cannot use a plain tunnel to connect directly to the return air shaft, but have to use inclined tunnels with some sharp turnings and plain tunnels to compose wind tunnels. The ventilation resistance is greater by increasing the length of tunnel, setting nasty angle of inclined lane.
3. The vertical shaft type (Figure 3): due to the design or other causes, wind tunnel cannot adopt the up type, but connects a few plain tunnels (or inclined lanes) with return air shafts. The ventilation resistance of this type is large. The reason is there are many sharp turnings surely increasing the length between two points of tunnel and the defects in the tunnel design, water spray is bigger, and these reasons comprehensively lead to the large resistance of wind tunnel.

Above the analysis, we can conclude that the oblique type is the best construction form of wind

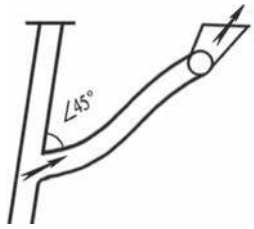


Figure 1. The oblique type.

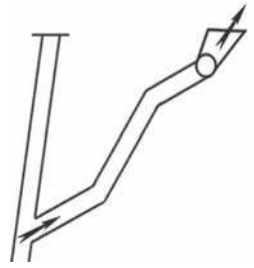


Figure 2. The line type.

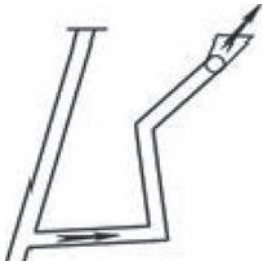


Figure 3. The shaft type.

tunnel, which has the minimum ventilation resistance, while shaft type is the worst and line type is medium.

4.2 *Unreasonable length and excessive turnings in designing wind tunnel*

In the practical production, unreasonable length of wind tunnel has a direct effect on the ventilation resistance. The unreasonable turns in the wind tunnel are caused by the unreasonable length.

Too many turnings directly lead to increase length of the wind tunnel; an elbow bend not only increases length of tunnel, but also increases ventilation resistance in the turning. The length of wind tunnel ranges generally from 35 m to 50 m, but some wind tunnels turn 2 or 3 elbow bends, causing a lot of local losses. Some of losses are from thoughtless designs, while some are caused by reconstructing old wind tunnels, others are because of contrary air flow directions between axial fan and wind shaft, artificially increase the ventilation resistance. Or not according to the design requirements to construct and artificially increase the number of turning, poor quality of construction cause large local ventilation resistance with rough and not gentle corners.

4.3 *Unreasonable design for wind tunnel section*

The wind tunnel section is so small that it results large wind velocity. The design of the wind tunnel is matched with power of a fan; it does not result in too large wind speed, which effects ventilation resistance.

4.4 *Unreasonable organization management for wind tunnel*

1. Laying multiple pipes and piling a lot of float coals cause to increase resistance of wind tunnel.
2. The air volume is not only that from the mine underground, but also all the air leakage. A large number of shaft head air leakage increase air volume of the wind tunnel and resistance. In addition, a large number of air leakages forming intersection of cold and warm air cause perennial water spray by in the wind tunnel and increase the ventilation resistance of the mine. (Cheng Genyin et al., 2009).

4.5 *For other reasons*

Due to the sudden changes in the connection of wind tunnel and wind shaft, larger local ventilation resistance is formed. Some wind tunnels inside may suddenly become larger or smaller. Unreasonable use of gate put in the wind tunnel regulating air cause the wind tunnel additional resistance.

5 MEASURES TO REDUCE VENTILATION RESISTANCE

5.1 *Design wind tunnels*

Other comprehensive factors should be considered when designing wind tunnel, the following terms about designing should be paid attention to:

1. Using Single oblique type to fit the layout of wind tunnel.
2. Wind tunnel is directly linked with the shaft together and tries to reduce the number of turning, which angle is less than sixty. All the connection corners should be smooth, especially the inside corner, which should be put into a double curves, we should use a sleek obtuse angle bend instead of an elbow bend.

3. Large enough section, which makes its wind speed less than 10 m/s and not more than 15 m/s, it is appropriate to use a round or close to a round section. (Wang Junliang et al., 2006).
4. The joint of wind tunnel and wind shaft should avoid a sudden narrow or expansion, within the range of wind tunnel, the areas with the different sections should have a gradual transition.
5. Trying to shorten the length of the wind tunnel as far as possible. (Xin Guanglong et al. 2004).
6. In the installation of main fan the centerline of wind tunnel is consistent with the axis of axial flow fan, and centrifugal fan must be vertical to axis.
7. Building it by lying bricks or stones and cement finishing wall, keep the surface neat and reduce the air leakage on the wind tunnel wall.
8. Getting rid of obstacles to keep air ways clear and make the total resistance of wind tunnel less than 200 Pa and l0% of total resistance of all mine ventilation system.

5.2 *Usage and management*

No special necessities, wind tunnel is not compatible for other purposes (such as laying pipes and cable, etc.). Often clear the tubes, stone, coal dust and debris inside the wind tunnel. Take effective measures to minimize the ground air leakage.

5.3 *Transform seriously unreasonable wind tunnel*

Some wind tunnels can adopt one or several measures to reduce the ventilation resistance. Wind tunnels affected negatively by a long length and too many quarter turns with large R_t, h_t, K must be transformed. (Zhu Kai et al., 2004).

Take the wind tunnel for example, before transforming it has a steel reinforced concrete structure and a rectangular cross-section, its specifications: width 2.0 m, height 2.1 m, section area is 4.2 m^2. To meet the requirements the area of wind tunnel section is expanded to at least 1.6 m^2. An air corridor (steel air duct) is added between reverse wind crossing of the centrifugal fan and the derrick of main shaft in the reconstruction design. To expand the wind tunnel section, we can parallel a new air way with the original wind tunnel. New air way has a square section (1.5 m *1.5 m) and steel plate (thickness is 10 mm). One end of it connects to the derrick of main shaft while the other end connects with the reverse wind crossing. The outlet is sealed with a 10 mm thick steel plate, then exit is cut in the junction, thus fresh air ways and two joint points are welded firmly. It is shown in the Figure 4. After transforming ventilation resistance of wind tunnel drops to 0.057 $N \cdot s^2/m^8$, resistance reduces 205.01 Pa, underground air volume increases by 9.33 m^3/s, thus further improving the condition of mine ventilation.

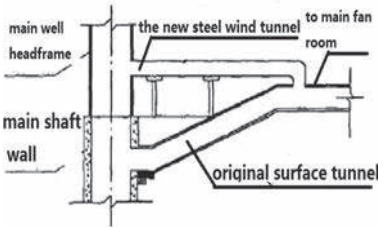


Figure 4. Wind tunnel reconstruction plans.

6 SUMMARIES

In conclusion, the output energy of the mine main ventilator is quite consumed in the wind tunnel; some may reach 50% or even more. There are many reasons contributing to it. Although ventilation resistance is usually very large, the benefit is very considerable as long as we take measures in the design, construction and reconstruction links to reduce the ventilation resistance. So it is not dispensable to reduce the ventilation resistance when it comes to developing ventilation potential, saving energy, and achieving good economic benefits. In some cases, it is expanding measures such as underground roadway with large range of influence, quantities less effective, fast, saving a lot of advantages of electrical energy. So to achieve the purpose of developing the scientific concept, it requires us flexible in the application and comprehensively developing.

ACKNOWLEDGEMENT

The work is partly Supported by "the Fundamental Research Funds for the Central Universities" No. 3142013103 and No. AQ1204B.

REFERENCES

Cai Wei 2004. Mine ventilation system safety evaluation and its application. *Journal of coal,* (23): 195–198.

Cheng Genyin et al. 2009. Measurement and analysis of ventilation system resistance in the Baishan coal mine. *Chinese journal of safety science*, 12 (2): 101–105.

Cheng Shaoren & Cheng Jianjun 2006. Measurement of mine ventilation resistance and analysis of several problems. *Journal of coal mining*, (121): 73–74.

Wang Junliang et al. 2006 Transformation and application of wind tunnel on coal surface of Spring. *Shandong coal science and technology* 90 (2): 101–105.

Xin Guanglong et al. 2004. Questions and answers of coal mine safety rules one ventilation and three preventions. Beijing: coal industry press.

Zhu Kai et al. 2004. The practical research on performance test of main fan in the Qianjiaying coal mine. *Journal of safety science*, 78 (3): 65–63.

Progress in Mine Safety Science and Engineering II – He et al. (Eds)
© 2014 Taylor & Francis Group, London, ISBN 978-1-138-00122-0

Research on the application of controllable circulatory ventilation in the mine

Jing-Gang Zhang
Key Laboratory of Mine Disaster Prevention and Control Technology in Hebei Province, China
Institute of Resource and Safety Engineering, China University of Mining and Technology (Beijing), Beijing, China
College of Safety Engineering, North China Institute of Science and Technology, Beijing, China

ABSTRACT: This paper focuses on the analysis of the controllable circulatory ventilation technology which is a new economical and practical ventilation technology. It can effectively solve the problem of partial air supply shortage in the large mine caused by the over-large production layout. According to Lizhuang Coal Mine's condition, I have analyzed its ventilation's problems. I think we can apply the controllable circulatory ventilation to this mine. In this paper I also propose three implemental projects, choose the most suitable one after the analysis and compare and put forward the security technology measures that should be noticed in the use of the controllable circulatory ventilation.

1 CONTROLLABLE CIRCULATORY VENTILATION

1.1 *Definition of controllable circulatory ventilation*

Controllable circulatory ventilation system is a new technology developed with the need of tunneling and recovery safety of ventilation. When conventional methods cannot solve the problem or are economically unreasonable, the controllable circulatory ventilation technology is a good choice. It can increase air flow, improve the climate conditions and save ventilation cost. As it is showed in Figure1.1, controllable circulatory ventilation system refers that we can control part of air flow artificially letting them flow through the same place many times and be used repeatedly. The word "controllable" has two meanings: There should be impetus to provide energy. Let artificially some backed air flow into the intake airway and be mixed with fresh air; Control the amount of the circulated air and make sure the mine gas density in the mixed intake air and return current is less than that in the Rules of Coal Mine' Safety. Its method is setting a ventilation fan between the intake air and the return current or in the inside of the airs. Thus the return current can cycle and the ventilation fan is called gas circulator.

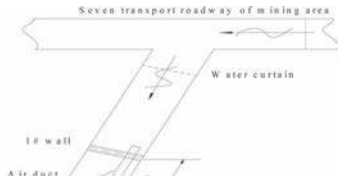


Figure 1. Controllable circulatory ventilation system.

1.2 *Circulatory ventilation system and its features*

Take the lane linking intake airway and return current way as the circulation duct and install a gas circulator. In the figure1.1 the area of 5-2 is the circulated area. Circulation rate F refers to the ratio between the circulate wind and the actual air volume in the work face. That is $F = Q_{5-2}/Q_{3-4}$. The figure F reflects the circulated levels of the airflow. Assuming the mine gas Q_1 (m^3/s) in the area comes from the work face, the volume of the fresh air Q_1 in the work face does not change with the airflow's circulation. There is not mine gas in the fresh air and compared with the airflow's volume Q_1, the mine gas' discharged volume q1 is very small. According to the relevant formula, every branched air flow and gas concentration in steady state are:

Air-intake shaft in work face:

$$Q_{2\text{-}3} = Q_1/(1-F) \quad \rho_{2\text{-}3} = F \times (q_1/Q_1)$$

Airs return way in work face:

$$Q_{4\text{-}5} = Q_1/(1\text{-}F) \quad \rho_{4\text{-}5} = q_1/Q1$$

Circulation duct:

$$Q_{5\text{-}2} = Q_1 \times F/(1-F) \quad \rho_{5\text{-}2} = q_1/Q_1$$

Airs return way in the system:

$$Q_{5\text{-}6} = Q_1 \quad \rho_{5\text{-}6} = q_1/Q_1$$

From the above formulas we can know that except for mine gas density in the intake airway in the work face, mine gas density in the other branches has no relation to the airflow's circulation. It depends on the discharged gas volume in the work face and the supplied amount of the fresh air. The highest point of the mine gas' density in the system is still within that in the return current. (Du tailiang 1997).

1.3 *Advantages of the controllable circulatory ventilation*

1. The application of the controllable circulatory ventilation, especially using it with dust removal fan will play a very significant effect on decreasing dust and improving climate in the work face.
2. In the circulatory area, the controllable circulatory ventilation can increases the effective air flow in the work and regulate the temperature and humidity in the mine. Circulatory ventilation in the contact lane can reduce the fresh volume that main fan supplies to the circulatory area and expand the scope where main fan supply air. (Ian Lowndes & Cem Sensogut 1990).
3. Controllable circulatory ventilation can save ventilated power consumption. When we use controllable circulatory ventilation, the main ventilator's power remains unchanged, but it extra increases gas circulator's power consumption. While the conventional ventilation system gets the effective air volume it needs through the main ventilator's self-regulation. So the main ventilator's power is improved accordingly.

2 PROBLEMS IN THE VENTILATION SYSTEM

2.1 *Survey of mine*

At present LiZhuang Mine Company's actual production capacity is 400,000 tons. Its main coal seam is coal 3. The mine is a mine with low density gas. Its mine seam has the tendency to combust spontaneously. It has not had the internal-caused fire. Coal dust has the explosion hazards. It takes comprehensive dust prevention measures and has explosion-proof facilities. The mine has not had gas and coal dust explosions. Its ventilation mode is central tied for spare. Air gets into the mine from the auxiliary shaft and returns from the main shaft. Main ventilator is 4-72-11 No20B centrifugal fan with motor power for 160 KW. Ventilation negative pressure is 2000 Pa and air volume is 2500 m^3/min. Fresh airflow gets into the mine through the auxiliary shaft and is divided into two parts at the bottom of the mine: one part gets into the v dark tilt for second level heading through the east motor lane; the other part goes downhill and gets into five or seven mining district alongside the east rail. Return current gets into the main return airway alongside each mining's return airway and drainages from the main shaft to the surface.

2.2 *Problems of mine ventilation system*

1. Lack of mine airflow
   When 3512B in the fifth mining area is finished, the mine production is concentrated in seventh district, in which air volume the mine requires is 2818 m^3/min.
   Q mining required = $(Q_{3704} + Q_{3702A} + Q_{3702B\ driving} * 2 + Q_{3701driving} * 2 + Q_{D\ mining} + QD_{\ pump} + Q_{two\text{-}level} * 2 + QII_{\ excavation\ horizontal\ pump} + Q + Q_{other\ storerooms}) * 1.15 = (360 + 280 + 320 + 200 * 2 + 200 * 2 + 50 + 50 + 200 * 2 + 60 + 80 + 50) * 1.15 = 2818\ m^3$/min
   Main ventilator's actual air volume is 2600 m^3/min.
2. The length of the airflow line in the seventh mining district and the two horizontal airflow line has a large disparity. The seventh mining district has insufficient air volume. It affects the mine production. The mine's work face is concentrated in the seventh mining district. The second level is the mining level. The length of the airflow path in the seventh mining district is 6610 m while that in the second level is 1060 m. The second level does not form a production system. The seventh mining area is the main production area with two production work faces 3,704 on ramen and 3702A, and 4 excavation work faces. The air volume that the seventh mining district requires is 1860 m^3/min. According to the ventilator's capacity, the intake air volume that the seventh mining district uses is 1400 m^3/min. According to the layout of the Lizhuang mine, 3702A should be finished in June, 2010 when horizontal has formed system and the seventh mining district need reduce the air volume it requires, thus ease the tension of air volume. At present, if the seventh district cannot reduce air volume it requires, it will directly affect the mine's production.

2.3 *Necessity of the controllable circulatory ventilation*

Controllable circulatory ventilation should be best used in the boundary mining area. When the airflow line is too long, mining area is lack of air volume or it is not technically feasible and economically reasonable to replace ventilation or have large scale of shaft engineering, on the premise to ensure safety produce, using controllable circulatory ventilation is an efficient way (Niu baohu 2002). Lizhuang Mine is a mine with low density gas and the density of the mine is very low. Its mine seam has not the tendency to combust spontaneously. It is possible to use the controllable circulatory ventilation. According to the seventh mining district's actual condition, using controllable circulatory ventilation is a reasonable technological project to solve air volume's shortage in the seventh mining district. To increase effective air volume by application of controllable circulatory ventilation must increase the return current's density. Gas emission in Lizhung Mine is very small. Return current's gas density in the seventh mining area is 0.1%, and that of carbon dioxide is 0.25%. Using controllable circulatory ventilation has little effects on the increase of the gas density.

3 FIX OF THE CONTROLLED CIRCULATORY VENTILATION TECHNOLOGY IN THE SEVENTH MINING AREA, LIZHUANG MINE

3.1 *Fix of the controllable circulatory ventilation area*

Lizhuang coal mine's main production area is in the seventh district, at the same time opens up the second level. During the transitional period, according to the mining area's geology, production conditions and taking the seventh mining area being a remote place into consideration, it is fixed as the circulatory ventilation area.

The problem that the circulatory air needs to solve is the seventh mining area's ventilation during the producing period. Circulatory duct in different locations, circulatory air's zone and circulatory efficiency are also different.

According to the lane's layout in the seventh mining area, Lizhuang coal mine and through the technical and economic comparison, we decide to use the original contact lane between the seventh haulage way in the back of substation and the rail lane in the seventh mining area (the seventh mining area's intake airway). (See Figure 2). Specific circulatory parameters are seen as in table 1.

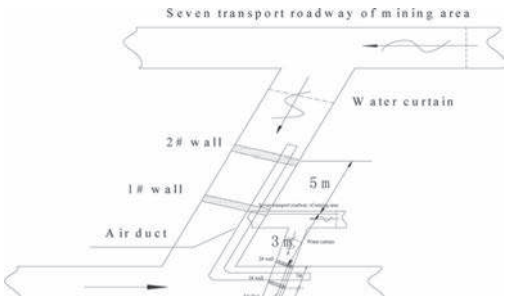


Figure 2. Program a.

3.2 *Design of controllable circulatory ventilation*

1. Selection of the project

According to safety, reliability, easiness to perform and full use of the existing lane and equipment, I design the following programs in accordance with the different layout of the circulatory duct:

Program A: Single wall type, see as figure 2. Set a confined wall in contact lane, 3~5 m away from the intake air side. Install a gas circulator in the wall and link the ventilator's exit to a silencer on which link a rubber wind tube. The wind tube should be laid along the seventh mining area's inner track road. Electromechanical device should be put outside the confined wall near the track road (where fresh air flows). Spray sprinkler should be set in the contact lane of the confined wall before the ventilator's entrance. The program is characterized by small engineering and simplicity. But the confined wall has the problem of serious air leakage. When throttle is open, it will affect the airflow's stability, thus having a less security.

Program B: Double wall type, see as Figure 3. Set the first confined wall in contact lane, 3~5 m away from the intake air side and the second 5 m away from the first confined wall. The gas circulator is installed in the second wall and the silencers are put in both the exit and the entrance of the ventilator. The silencer at the exit of the ventilator is set in the second confined wall. This silencer is linked with a rubber wind tube and connects with the iron wind tube set in the first confined wall. The layout of the iron wind tube's exit is in compliance with the wall of the seventh mining area's track lane along which the rubber wind tube's elbow makes transition. Thus it makes two water curtains for transport lane (large lane of the return current) and contact lane. The program is characterized by the fact that the confined wall has small amount of air leakage and small security. But the amount of engineering is larger than the program A.

Program C: Partition type, see as Figure 4. Set a confined wall 3 m away from the intake air side and fix the ventilator in the wall. Set another confined

Table 1. Table of circulatory parameters.

Circulatory range	Ventilator's working way	Security	Fresh air's volume (m^3/min)	Maximum of circulatory air volume (m^3/min)	Total air volume (m^3/min)	Circulation rate (%)
Mining area-7	Press	Safe	1480	500	1980	26.3

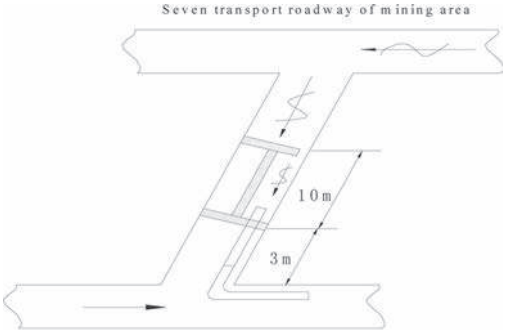


Figure 3. Program b.

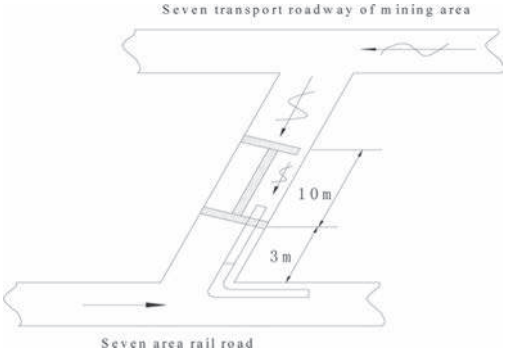


Figure 4. Program c.

wall 10 m away from the first confined wall. Separate this 10 m lane by wind wall and form a purified room by loading a ventilator and setting firefighting water curtain. The other side place electromechanical device and monitoring instrument and it also works as the personnel guards' room. Set throttle on each wind wall. The program is characterized by safety, small leakage and good cleaning effect. It also has a guards' room, but it is a large engineering and the lane need a large cross section.

By comparing the three kinds of programs, we can know program A is less secure, program C requires a large section of roadway which is a large engineering. So choose program B.

2 Engineering design of controllable circulatory ventilation

Use the contact lane between track road and the large transport lane in the seventh mining area as the cycle duct. See as Figure 3.1 Set two confined walls in the cycle duct. The first wind wall is 3 m away from the track road and a wind tube is place in the wall with a throttle. The second confined wall is 5 m away from the first confined wall in which set a silencer and throttle. The two wind walls are all set cable holes and pressure measured holes and the walls are built by stones. As it is showed in Figure 3.2, water curtain is set between the large transport lane and the contact lane in the seventh mining area. There are also CO and CH_4 probes before the entrance of the ventilator to measure the ventilating status of the circulatory current.

3 Selection and installation of the circulatory ventilator

1 Selection of the circulatory ventilator

Basis of the circulatory ventilator's selection: based on the required air volume, wind resistance and the established circulation rate in the circulatory area, and taking the match of the circulatory ventilator into consideration, we can know the wind pressure that the circulatory ventilator produce.

Parameters of the circulatory ventilator:

Air volume $Q_f = 500$ m^3/min

Wind pressure $H_f = (R_{2+} R_c + R_3) + R_4 = 1.156 \times 31.72 + 0.092 \times 8.32 = 1161.7 + 6.3 = 1168$ Pa

We can choose 3 BKJ66-11 NO4.5, two sets of which operate simultaneously, the other for standby. Its properties are:

Q_f = 170~300 m^3/min, H_f = 1000~1900 Pa, N = 8 KW, n = 2950 rpm its performance.

2 Installation of the circulatory ventilator

Circulatory ventilator is fixed on the circulatory duct's shelf. Place one circulatory ventilator on the lower deck and two on the upper deck. The interval distance is 0.2 m among the ventilators and ventilator on the lower deck is 0.3 m away from the lane's floor. There is a silencer on both the exit and entrance of the ventilators. Air regulator is set at the entrance of the ventilator. A sealed cover is placed at the entrance of the alternate ventilator

Table 2. List of each program's devices.

Program	Airtight wall	Air door	Remarks
A	One (one door)	Φ600 mm iron fan drum 3 m (the length of joint is 1 m), a number of rubber fan drum	Connect three fans (two working, one standby)
B	Two (two doors)	Φ600 mm iron fan drum/3 m (the length of joint is 1 m), a number of rubber fan drum	Connect three fans (two working, one standby)
C	Three (three doors)	Φ600 mm iron fan drum 3 m (the length of joint is 1 m), a number of rubber fan drum	Connect three fans (two working, one standby)

to prevent airflow's short circuit. To ensure that airflow is short circuit when the ventilator stops running, the following measures should be taken: wind tube in the exit falls down by its own gravity when the ventilator stops working and the current flows out from the auto-confined circulatory ventilator; fix a wooden cover on the entrance of the ventilator and seal it manually when the ventilator stops working.

4 Electrical equipment

Electrical equipment should be installed reliably to ensure circulatory ventilator works continuously and normally. Explosion-proof switch and other electrical equipment's should be installed in the fresh current outside the confined wall near the big track lane in the circular duct. It requires using "three spot, methane and carbon monoxide atresia".

5 Eliminating of the noise, dust and fire

To reduce the noise, install a FJZX-1-silencer on the two ends of the ventilator, letting the ambient noise is less than the regulation's requirement. Let the circulatory current gets through the water curtain which is placed in the seventh mining area's big transport lane and contact lane to be purified before flows into the ventilator. Thus it can eliminate the dust and fire, and reduce its heat.

6 Others

Install CO and CH_4 probes before the circulatory air duct, 5 m away from the entrance of the ventilator to achieve unrestricted power failure alert and make sure the circulatory ventilator's wind, electricity, CO and methane closed. At the same time special attention should be paid to eliminate the fires caused by external reasons in the circulatory area by using reliable measures.

3.3 *Safety and technical measures of the controllable circulatory ventilation*

To ensure the security of the controllable circulatory ventilator, the following safety measures must be strictly observed:

1. Ensure circulatory ventilator works continuously and normally and power should be safely supplied 24 hours. On special circumstances, it can have power cut when it is approved by the mine's chief engineer and measures has taken. (S.Tate 1994).
2. When the circulatory ventilator stops supplying air, original ventilation system must return to work to prevent current in the circulatory duct from short circuit. When the ventilator stops, personnel on the duty in the mine must report this to the mine's dispatcher and organize personnel to deal with immediately. When restart the circulatory ventilator, power must be restored manually.
3. Sealed devices should be installed at the wind tube's entrance of the circulatory ventilator. Once the ventilator stops working, block the circulatory wind's duct immediately.
4. In the circulatory area, thorough measures must be taken in case of fire, so flame retardant duct must be used.
5. Install CH_4, CO probes at the entrance and the exit of the circulatory duct. When the gas density rises to the limited level, it should ensure the power failure and alarm, and restores the original ventilation system.
6. Purify the airflow by the water curtain before the circulatory air enters into the ventilator, letting the dust in the mixed air is not more than the regulation's standard.
7. A silencer is set at both the entrance and the exit of the circulatory ventilator, letting the noise around the circulatory ventilator is less than the regulation's requirement.
8. Establish specialized responsibility and make clear divisions for each people's responsibility. Implement concerning administration. Ask expert people to manage circulatory ventilation system and send specialized people to the underground on duty in each class.
9. Strengthen safety supervision for the ventilation in the circulatory area, establish parameter recording account for CH_4, CO, air volume, dust and circulatory air system, and write circulatory fan's running. (Weimin Hu et al. 1998)

10. Install U water meters on the two sealed walls in the circulatory air duct to check changes of pressure. If the system's pressure is abnormal, the entire circulatory system must be checked immediately.
11. When there are serious disasters (CH_4, fire, flood, dust, and so on) in the circulatory area, circulatory ventilator must be stopped immediately and normal ventilation system should be restored. The disasters should be handled according to the disaster prevention and treatment plans.

4 CONCLUSION

According to the theoretical analysis of the controllable circulatory ventilation system as well as the system's practical application in Lizhuang coal mine, we get the following conclusions:

1. The use of controllable circulatory ventilation can improve the mining face's effective air volume in the mining area, and improve work face's climate condition to achieve ventilation and energy saving.
2. The use of controllable circulatory ventilation can meet the seventh mining area's required air volume 1860 m^3/min. The visible natural wind volume is 1400 m^3/min. When the controllable circulatory ventilation is used, the air volume it supplies to mining area is 500 m^3/min. Compared with the improved air volume that the main ventilator supplies and the auxiliary ventilator, mine's total in and out air is small and we have less energy consumption. Rate of the mine's effective air volume is improved.
3. To ensure the safety of controllable circulatory ventilation, safety technical measures must be strictly observed.

ACKNOWLEDGEMENT

The work is partly Supported by "the Fundamental Research Funds for the Central Universities" No. 3142013103 and No. AQ1204B.

REFERENCES

Du tailiang 1997. Mine controllable circulation air-circulation rate in the system analysis and optimization.*Coal engineer,* (2): 35~38.

Ian Lowndes & Cem Sensogut 1990. Computer simulation of radon contamination levels around controlled district recirculation circuits. *Mining Science Technology*, (10): 177~188.

Niu baohu 2002. Development and research status of controllable circulation ventilation. *Coal mine security*, (12): 18–20.

S. Tate 1994. United Kingdom local and regional circulation of air in coal mines. *Shaanxi coal technology*. (1): 57–63.

Weimin Hu et al. 1998. Non-steady-state study on gas distribution of controllable circulation ventilation system.*Coal*, 23 (3): 283~288.

Progress in Mine Safety Science and Engineering II – He et al. (Eds)
© 2014 Taylor & Francis Group, London, ISBN 978-1-138-00122-0

Research on terminal mining support technology of the hard stratified roof in the fully mechanized coal face

Li Chen, Guo Qiang Hao, Ping Liu & Shi Chao Peng
Hebei University of Engineering, Handan, Hebei, China

ABSTRACT: Combined the condition of the roof with the terminal mining process under fully mechanized coal mining face, caving and the stress of the roof is analyzed. And based on the analysis a strong stratified roof support scheme was put forward in Rongtai mine, which worked successfully in the field. This technical experience not only creates a good convenience for the Fast Moving, shortens the time slope expansion to dismantling equipments at the terminal mining process, but also achieves a reduction in cost and increases efficiency at the same time. In addition, it has a strong promotional value.

1 INTRODUCTION

The retracement of fully mechanized working face is an important process of mining, which affects the speed of Face Moving, Mine Safety and Efficiency directly (Li & Liu 2010, Zhao 2005, Zhao 2009, Wang & Zhang 2009, Zhang & Zhang 2009). So, the key of high production and high efficiency in coal mines is Fast Moving, and how to choose a reasonable support method to maintain the stability of back channel becomes the key technology of Fast Moving (Yang & Lian 2006, Liu 2004, Li 2006).

When Full-mechanized working face is stopped, the surrounding rocks get closer to the working face, thus, the rib spalling gets more and more serious, however, recycling supports requires a large secure space, in order to recycle supports safely, the support method which commonly used at the terminal mining of fully mechanized coal face is combined support that the combination of network, rope and anchor net, and it creates a secure condition for recycling supports.

In order to improve the existing support form at the terminal mining of fully mechanized working face, We put forward a reformational and experimental scheme that no networks and ropes are used when supporting the roof of 10104 working face according to the data of roof dynamic observation and the manage experience of working face in two full-mechanized working faces called 10102 and 10104 of Rongtai coal mine.. And this scheme can meet the requirement which evacuate supports safely and efficiently and the roof management requirement, shorten the time which prepare the mining expansion and the cycle time of moving, then more time can be used for goaf protection, so its technical and economic benefit is obvious.

2 GETTING STARTED

The 10104 face is the first nearly flat and fully mechanized mining face in Rong tai coal mine, and it has been finished mining. Its face length is 180 m, face advance length is 863 m, and coal-seam thickness is steady, the average thickness is 2.79 m, the angle is about 1~8°.The geologic structure in this face is simple, the attitude of coal is gently, no fault, no magmatic, no collapse column exists in this face, but there are rolling folds in the floor; the roof consists of the thickness of the roof for 9 m, pale, dense and uniform limestone with horizontal bedding; the floor consists of thickness of 3.5 m, light gray, tidal flat depositional environment of mixed flat and marsh sedimentary mudstone. The columnar section is shown in figure.1.

3 THE PARAMETERS OF SUPPORTING

According to the analysis of "three parts on the transverse" and "three parts on the vertical" and the 9 meters' roof which consists of layered limestone. We use the support method in the mining face, it ensures the secure withdraw of the equipments in the fully mechanized mining face, combined with the conditions of the roof and floor.

3.1 *Operation without online and onrope*

At the terminal mining process, the first row of bolts are started constructing away from stopping line 9 meters, the bolts are made of steel with thread, the model is φ22 mm × 2000 mm, the distance between two bolts is 1500 on the vertical,1800 on the transverse. All the bolts are equipped with

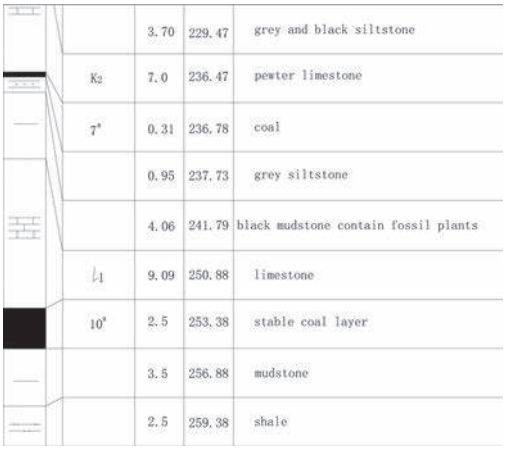


Figure 1. The columnar section of rock in 10104 mining face.

anchor agent to ensure the supports can be not buried by the gangues which come from the carving zone when the hydraulic supports are retreated. The supporting scheme is shown in figure 2.

3.2 *Support design of back channel*

When listing facts use either the style tag List signs or the style tag List numbers.

3.2.1 *Construction technology*

The back channels are started broadening as the mining face is 3 meters' distance to the stopping line, stop moving the supports, meanwhile, separate all of the advancing jacks of the supports and the scraper conveyor, use hydraulic props to accomplish the operation that moving the scraper conveyor, erect a hydraulic prop between the scraper conveyor and the supports every 3~5 supports, adopt the way that the emulsion is offered in a distance to move the scraper conveyor, clear the float coal in front of the supports and beside the supports before moving the supports, people are forbidden stranded at the mining face channel when scraper conveyor is moved by hydraulic props.

3.2.2 *Support parameters design*

Back channels' height is 3 meters; its width is also 3 meters. Adopting the bolts which made of steel with thread and the model is φ22 mm × 2000 mm to support the roof. The distance between two bolts is 1500 on the vertical, 1100 on the transverse, and they are equipped with mesh reinforcements and ladder beams; there is a row of strand anchor cable in the roof, the model of the strand anchor cable is φ17.5 mm × 6000 mm, the distance between two

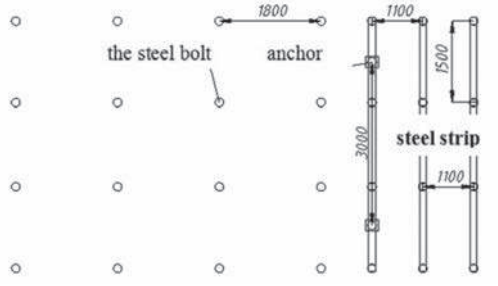


Figure 2. The supporting scheme.

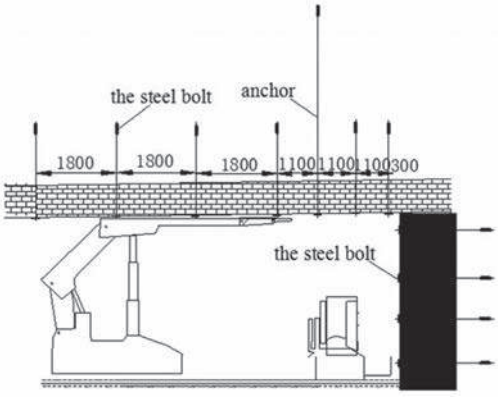


Figure 3. The construction design.

adjacent strand anchor cable is 3 meters, and every strand anchor cable is equipped with the metal pallet which the model is 300 mm × 300 mm × 16 mm and 3 cartriges (one is high-speed, anther two are medium-speed). Laying plastic mesh which the model is 3000 mm × 1200 mm on the coal wall and making it connect to the anchor net; the model of the bolt is φ18 mm × 1600 mm, the distance between two adjacent rows is 800 mm × 1000 mm, and every bolt is equipped with an anchor agent. The construction design is shown in figure 3.

4 TECHNICAL AND ECONOMIC BENEFIT ANALYSIS

4.1 *Technical efficiency analysis*

We can ensure the stability of the roof and the safety and the portability of the back channel with the combined support of bolts, anchor cables and supports.

Adopting double shield to control the trigonal area effectively. Hydraulic props were used to expand the trigonal area once upon a time, but,

they could affect the adjusted direction of supports when the supports were cycled, and, hydraulic props should be erected, then cycled frequently, it make workers be of high labor intensity and high risk. By using the double shield can shorten the workers' labor intensity, provide the work efficiency and raise the safety.

There are no support nets between roof and top beam of the supports, so, it can not cause the auxiliary work which are caused by broken the top wire in the withdrawal period, and the roof behind the shield supports can collapse fully as the shield supports are moved forward, and it would not appear the flap top phenomenon in a large area.

Adopting the channel which transport the supports, by this way the workers can avoid the auxiliary work caused by the wipe angle, the bracket line, the corners and the derailment of loaded car for transportation.

According to the analysis of the data about roof bedding separation in the condition without online and onrope, it shows the roof is stable, and roof bedding separation is not obvious.

4.2 *Economic benefit analysis*

By the reform of supporting way of last roof of hard roof, the duration Shorten seven days in the tunnel expansion and labor cost has been saved by ¥127,000, the cost of materials is reduced by more than ¥106,000.The reform achieves cost efficiency, minimize labor intensity of workers, and improve the speed of face removing in overall and save time. This way effectively avoid the Problem of coal wall spalling or ground up and other secondary issues, which are caused by a long time of the working surface ending mining or dead time of the face mining equipment. This process is the accumulation of advanced experience quick moving of fully mechanized coal face and has more important practical significance.

5 CONCLUSIONS

Through the analysis of the supporting effect and the concrete construction technique, the adoption of the supporting method can effectively control the shelves space roof surrounding rock. Meanwhile, it can make the surrounding rock steady, and fully meet the requirements of the use of the roadway, so that it can achieve the expected effect of support. The construction is simple and convenient, and it is easy to operate, and we can get good economic benefit. It is feasible in technology and theory, and provides new experience and methods for the strong stratified roof at the end of the fully mechanized coal face mining support.

REFERENCES

Li, Y.S. & Liu Y.C. 2010. Application of anchor mesh supporting in the fully-mechanized face retreat channel. *Coal science and technology* 38(4):35–36.

Li, Y.F. 2006.The practical experience on preparations before the moving of fully mechanized mining face. *Waterpower mining and pipeline transportation* (1): 48–49.

Liu, C.Z. 2004.The bolt support at the terminal mining process in fully mechanized mining face. *Coal mine technology* 24(5):76–77.

Wang, H.B. & Zhang, L.X. 2009. Research on the support form at the terminal mining in fully mechanized mining face. *Mining machinery* 37(7):16–19.

Yang, X. & Lian, J.J. 2006. The roof control of the retreatment of supports at the terminal mining process in fully mechanized mining face. *Waterpower mining and pipeline transportation* 6(2):38–39.

Zhang, W. et al. 2009. Simulation analysis on the effect of combined support at the back channel with large section in large mining height mining face. *Coal mine engineering* 37(7):16–19.

Zhao, J. 2005. The technology and application of large cross-section retreat channel bolt support. *Coal science and technology* (11):5–7.

Zhao, Z.Y. & Qi, G.H. 2009.The construction technology which under the condition with dynamic pressure in fully mechanized working face of channel which retreat equipments. *Coal mine safety* 42(12): 50–53.

This page intentionally left blank

Progress in Mine Safety Science and Engineering II – He et al. (Eds)
© 2014 Taylor & Francis Group, London, ISBN 978-1-138-00122-0

Comparative experimental study on dynamic mechanical properties of anthracite and limestone

Yong-Chun Miao
School of Resources and Safety Engineering, China University of Mining and Technology (Beijing), Beijing, China

Yu-Kai Fu
Coal Mining and Designing Department, Tiandi Science and Technology Co., Ltd., Chaoyang District, Beijing, China

ABSTRACT: In order to understand the failure mechanism of rock under dynamic loading, such as explosion, impact and earthquake, the different impact speed experiments of anthracite and limestone sample were conducted by using Φ50 mm Split Hopkinson Pressure Bar (SHPB) experiment system. The experimental results showed that the dynamic mechanical properties of Anthracite and limestone are obviously different. The dynamic stress-strain of anthracite is generally has leaping features. Obvious nonlinearity is presented in the initial rising stage and the degree of nonlinearity is inversely proportional to the impact velocity. However, dynamic stress-strain curve of limestone is a straight line in the initial stage, the deviation of linear slope is small. The stage has linear-elastic properties; Anthracite and limestone both have the tendency of increasing impact rate while the plastic deformation and the ultimate strength increased. Whereas the plastic deformation of limestone is smaller than the plastic deformation of anthracite. According to the dynamic stress-strain curve, the dissipated energy of anthracite and limestone and the dissipated energy of anthracite and limestone both has the weak power function increasing trend with the increasing of the impact rate based on calculation.

1 INTRODUCTION

With the rapid development of the national economy and the increased mining depth coal and rock dynamic disaster is increasing ay by day. In order to ensure life safety, safe, reasonable and efficient mining method are very necessary. Then the research on dynamic mechanical properties of underground rock is also very important[1]. Almost all of the dynamic disaster, such as broken rock, rock burst, coal and gas outburst and other dynamic disasters had certain correlation with the rock failure under impact load and stress wave's propagation in the rock[2]. Because research on the dynamic mechanical properties of rock is minimal in our country, many law needs to refer to foreign data[3,4], which leads to the lack of theoretical basis in China. Rock burst and other dynamic disaster tend to occur in coal seam with limestone roof. Therefore, in order to effectively control the mine dynamic disasters, we must reveal its dynamic mechanical properties, thus it is very important to do the comparative study on dynamic mechanical properties of coal and limestone.

The research on the dynamic mechanical properties of rock is earlier in Europe and United States[5]. Hydraulic pressurizing or drop hammer test method was used in early stage. The hydraulic pressure method by B. Bresler[6] could achieve the strain rate of 1 s^{-1}. And the drop hammer test method used by B. P. Hughes[7,8] could reach to 10 s^{-1}. Because of the inertia of the drop hammer, it was hard to ensure that experimental results measured by drop hammer test method were the real dynamic properties of material. SHPB method was used to test the dynamic mechanical properties of concrete by L.E. Malvern[9]. This method reduced the influence of inertia effect and the loading strain rate could reach 103s^{-1}. Through this method we have a new understanding with strain rate sensitivity of concrete material. In 1984, the mechanical characteristics of coal under quasi static load and impact load were studied by Klepaczko from Canadian Manny Ba University[10], whose research results showed that coal modulus was not sensitive to the strain rates in a certain range of strain rates, but when strain rates exceeded the critical value, the elastic modulus and the crack propagation would have an obvious different law and increased in linearity with the increase of strain rate.

Wu and Gao[11] had studied on the mechanical properties of Yangquan coal under the

10^{-1}~104 MPa/s loading rate with the fast loading machine, the results of the research showed that coal tensile, compressive strength and elastic modulus have increased as the loading rate increased. Shan[12] of domestic scholar studied anthracite in Yunjialing coal mine with SHPB experiments, and believed that dynamic stress-strain curve showed the nonlinearity in the initial stage and the degree of nonlinearity is inversely proportional to the impact velocity. Many scholars had only studied qualitatively the dynamic mechanical properties on coal and rock, but had not studied the difference of dynamic properties of two kinds of rocks. This paper aims to study the difference of dynamic properties of coal and limestone and to carry out quantitative analysis on the dissipated energy through impact experiment of coal and limestone under different speeds.

Dynamic mechanical experiments were completed with SHPB test device from China University of Mining and Technology (Beijing), The Split Hopkinson Pressure Bar (SHPB) is currently widely used to study dynamic strain rate. Using φ50 mm SHPB test device, dynamic mechanical properties of coal and limestone under different strain rates were analyzed and mechanical properties of coal and limestone were explained from the structure.

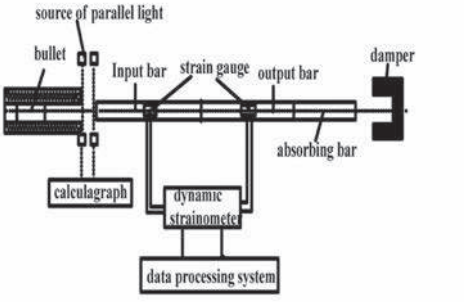


Figure 1. SHPB experimental system.

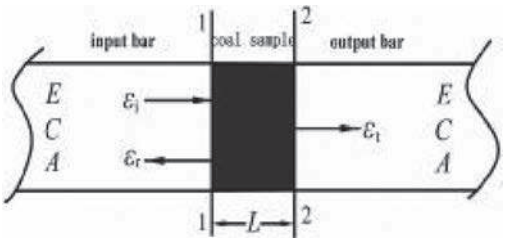


Figure 2. Principles of SHPB experiment.



Figure 3. Physical map of the SHPB test system.

2 SHPB EXPERIMENTAL SYSTEM

2.1 *Sample preparation*

Coal and limestone samples are both cylinder-shaped, and have size of Φ50 mm × 50 mm. Parallel degree was controlled within the range of 0.02 mm error in the sample processing to guarantee the surface cleanliness. In order to reduce the friction effect between the pressure bar and the specimen, ensure good contact and meet the SHPB uniformity assumption, graphite lubricant is evenly smeared on the two ends of specimens.

2.2 *SHPB experimental system and device*

Dynamic mechanical experiments was completed with SHPB test device from China University of Mining and Technology (Beijing), The SHPB device consists of an impact rod (bullet), input and output bar, the test samples are sandwiched between the input and output bar. The typical SHPB experiment system, principle and object diagram are respectively shown in Fig. 1, 2, 3.

The bullet has the diameter of 50 mm and the length of 400 mm. The input and output bar are both 50 mm in diameter, 2000 mm in length, made of steel and 200 GPa in elastic modulus. Semiconductor strain gauge was symmetrically attached to the central location of input and output bar.

The basic principle of SHPB experiment is the stress wave propagation theory in elastic slender bar, which is based on two basic assumptions that one is one-dimensional assumption (also known as plane assumption) and other is uniform stress assumption. The one-dimensional assumption considered that each cross section in elastic bars always keeps the plane state in the propagation process of the stress wave in the slender bar. Uniform stress assumption assumed that the stress

wave propagation repeated 3~4 back and forth in the specimen and the stress was equal everywhere. The simplified calculation formula is as follows:

$$\dot{\varepsilon}(t) = -\frac{2C_0}{L}\varepsilon_r(t) \tag{1}$$

$$\varepsilon(t) = -\frac{2C_0}{L}\int_0^t \varepsilon_r(t)dt \tag{2}$$

$$\sigma(t) = \frac{A_0 E_0}{A}\varepsilon_t(t) \tag{3}$$

In the formulas, $\dot{\varepsilon}(t)$, ε(t), $\sigma(t)$ is respectively strain rate, strain and stress. C_0 is the elastic wave velocity in pressure bar, 5060 m/s. E_0 is the elastic modulus of bar material, 200 Gpa. A_0, L is respectively cross-sectional area and length of specimen, The impact velocity of experiment was controlled within 2~6 m/s. Because the impact velocity of bullet is provided by high pressure gas, the impact speed of coal and limestone samples will vary slightly.

3 DYNAMIC MECHANICAL ANALYSIS

3.1 *Waveform curve analysis of anthracite coal and limestone*

The striking bars (bullets) acquired a certain speed from gas power, then did central collision with the input bar, a pressure pulse εi was generated by input bar and propagated along the axial of bar, the pressure pulse spread to the specimen, since the wave impedance of input bar and specimen was different, stress wave will generate multiple reflection on both ends of the specimen surface and lead to uniform deformation of specimen. Part of the input stress wave propagated output bar through the specimen (the transmitted wave εt), the transmitted wave was captured by the absorbing bar, finally was absorbed by the damper, another part became the reflected wave εr, and returned the input bar, the signal was collected by the strain gauge arranged in input and output bar.

In the Φ50 mm SHPB system, the incident bar impacts anthracite coal and limestone specimens under the different impact velocity, strain curve obtained in the input and output bar is shown in Fig.4 and Fig.5.

The figure 5 shows that incident wave and reflected wave of anthracite has a good agreement. Meanwhile, the corresponding transmission wave descend immediately at maximum stress and wave shape performs linear attenuation. The speed of attenuation (the slope of line) is related to the loading intensity and the degree of fragmentation of samples. This phenomenon indicates that the

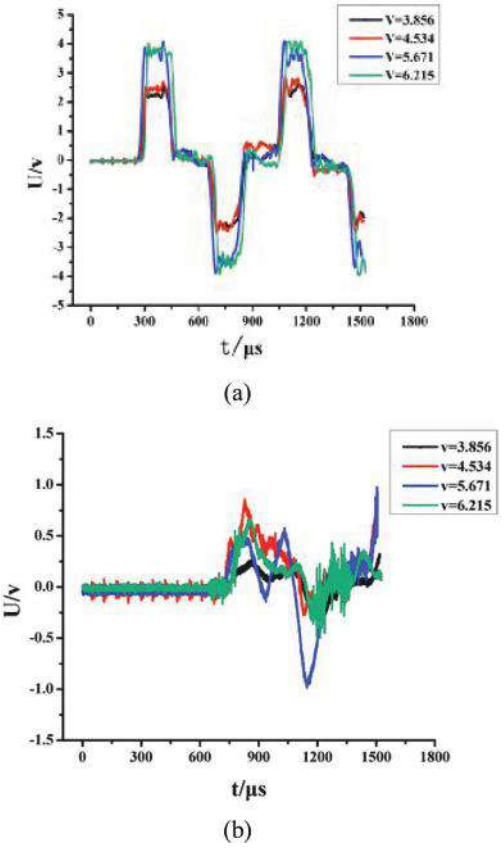


Figure 4. (a) incident wave and reflected wave of anthracite; (b) transmission wave of anthracite.

anthracite specimen has badly damaged and generate cracks, the wave will be reflected at the crack free surface.

The reflection wave form of limestone is "W" shape and the second wave trough is shallow. this indicates that the limestone specimens has not badly damaged, Moreover, the transmitted wave does not descend immediately at maximum stress, but lasts a period of time, which shows that limestone specimens did not serious damage like the anthracite. From the waveform curve anthracite coal and limestone, there are significant differences between the two materials in terms of dynamic mechanical properties.

3.2 *Dynamic stress-strain curve of anthracite coal and limestone*

Elastic modulus (E) of steel pressure bar in experiment is equal to 206000 MPa. Wave velocity C_0 is equal to 5060 m/s, cross-sectional area A is equal to 625 πmm^2, the specimen thickness L = 50 mm.

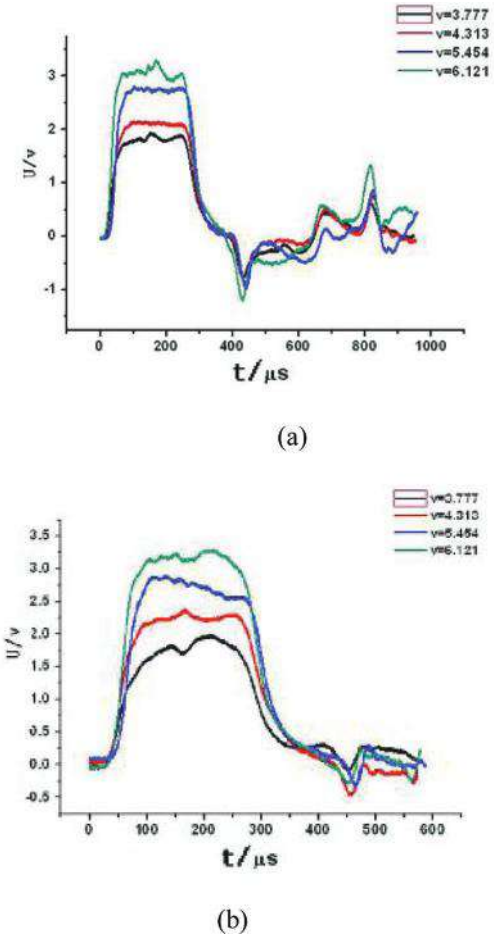


Figure 5. (a) incident wave and reflected wave of limestone; (b) transmission wave of limestone.

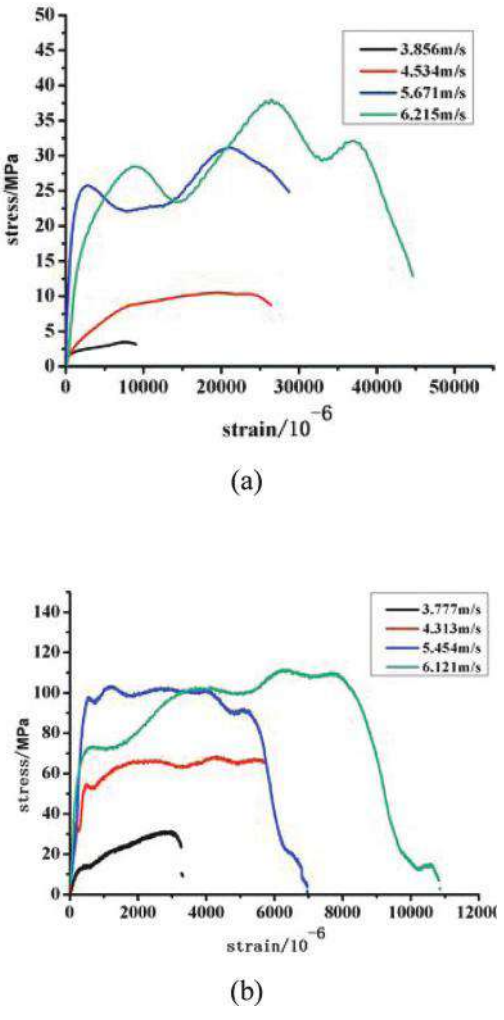


Figure 6. (a) Dynamic stress strain curve of anthracite; (b) Dynamic stress strain curve of limestone.

The dynamic stress-strain curve of specimen was obtained through (1), (2), (3) formula. The stress-strain curve of specimen is shown in Fig.6.

As shown in Fig.6, dynamic stress strain curve of anthracite was markedly different from limestone. The stress and strain of anthracite in general are characteristic of leap before the maximum value. After rising to the first maximum, stress decreases firstly and then increases to a maximum value with increasing strain. In the initial stage, dynamic stress strain curve of anthracite shows obvious nonlinearity, which is more obviously with the decrease of the rate. The slope of curve is also increasing with the increase of impact velocity in the initial stage, but different is relatively large. The faster impact rate increases, The greater the plastic deformation of anthracite coal is. However, the dynamic stress strain curve of limestone is basically a straight line at the initial stage. Deviation is smaller with different rate, the segment can be very good overlap. It is believed that rock in this stage is linear elastic. From the Fig.6, we can also see that strain of limestone is significantly less than anthracite. The curve have the same properties that the faster impact rate increases, The greater the plastic deformation of limestone is.

Compared with limestone, the anthracite has bigger porosity, more endogenous fracture and stronger plastic deformation. Whereas, limestone has more strength, brittleness and homogeneity. Therefore, part of crack propagates and part of crack closes due to endogenous fracture in the impact process of anthracite coal, and the properties of strain hardening will appear. Moreover, this

properties is more sensitive to high strain rate, but not sensitive to low strain rate. while in the impact process of anthracite coal, the strain hardening properties is not obvious and more insensitive to high strain rate due to Limestone's uniformity, good compactness, and little cracks.

3.3 *Coal and rock dynamic comparative analysis of the impact of failure modes*

As can be seen from experimental results, anthracite sample at 75–125s-1 strain rate, cylindrical sample were destroyed by the impact occurred. When the strain rate is low (75–82s-1), there is a higher degree of fragmentation close to the incident lever, and near the side of the transmission lever broken a lesser extent, it shows that the stress wave in the process through the specimen, in the incident lever side of the crack growth due Anthracite coal sample, absorbing part of the stress wave energy, causing the stress wave attenuation occurs, so that the end of the specimen can not be broken for the specimen to provide enough energy; As the strain rate increases, the pieces of specimen damage scale was significantly decreased, while the number of fragments increased significantly, showing that a strong correlation between strain rate, and anthracite coal sample crushed particles are relatively uniform, but particle dispersion is not.

Sandstone specimen strain rate of 75s-1 there was a certain crack, but not destroyed. In the 82–125s-1 strain rate range, the effect of cylindrical specimens under attack and damage, and equally close to the incident lever side of the lever features a high degree of fragmentation. The fragmentation character of sandstone samples and anthracite coal is markedly different, sandstone sample crushing particle morphology varies widely, the discrete particles is large, especially in the effect of 125s-1 strain rate, the local sample crushed into powder, partial sample also retains good integrity, this is mainly due to the large number of irregular sandstones cracks, bubbles and other defects result in the strike, the local stress concentration of the first failure occurs, resulting in crushed particles discrete greater.

3.4 *Breaking dissipation energy analysis of anthracite coal and limestone*

When rock was subjected to dynamic loads, the nonlinear deformation was also significantly increased with the impact velocity (strain rate) increased. The breaking dissipation energy also could be used to measure the difficult degree of rock breaking in addition to breaking strength and elastic modulus[13].

The dissipation energy of sample E_s is:

$$E_s = E_I - E_T - E_R \tag{4}$$

The incident energy E_I, reflex energy E_R, transmission energy E_T is respectively:

$$E_I = \frac{A_0}{\rho C_0}\int_0^T \sigma_I^2(t)dt \tag{5}$$

$$E_T = \frac{A_0}{\rho C_0}\int_0^T \sigma_T^2(t)dt \tag{6}$$

$$E_R = \frac{A_0}{\rho C_0}\int_0^T \sigma_R^2(t)dt \tag{7}$$

In the formulas, $\sigma_I(t)$, $\sigma_T(t)$, $\sigma_R(t)$ is respectively the incidence, reflection and transmission stress at some point. Compressive stress is positive for the incident and transmitted stress. However, tensile

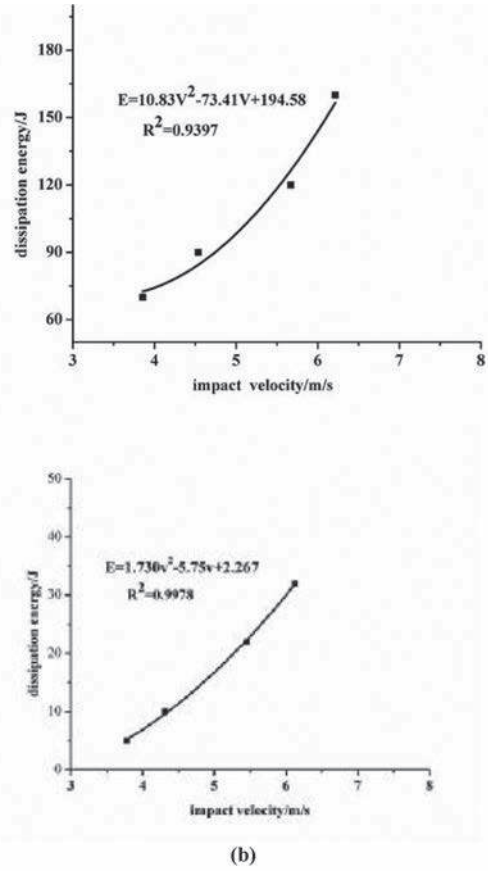


Figure 7. (a) Energy dissipation curve of anthracite coal; (b) Energy dissipation curve of limestone.

stress is positive for reflecting stress. ρ, C_0 respectively represents press bar density and stress wave velocity of elastic bar. T represents the continued time of stress wave. A_0 represents the cross sectional area of elastic bar.

According to the dissipated energy formula that was used in the SHPB dynamic impact rock specimen, incident energy, reflex energy and transmission energy could be calculated under different impact rate. Finally the change tendency of dissipation energy with the impact velocity was shown in Fig. 7.

As seen from the Fig.8, the dissipative energy of anthracite coal and limestone has a increasing tendency that shows a weak power function relationship or linear relation, and the growth rate of energy dissipation is faster with the increase of impact speed. In other words, the dissipation energy and the degree of fragmentation of anthracite is larger, higher than that of limestone in the same impact rate.

4 CONCLUSIONS

The impact experiments of anthracite and limestone samples were conducted by using Φ50 mm split Hopkinson pressure bar (SHPB) experiment system, the dynamic mechanical properties of samples are analyzed under impact loading. Finally, the relationship between the dissipation energy and impact velocity is studied. The main conclusions are as follows.

Dynamic stress strain curve of anthracite was markedly different from limestone, in general are characteristic of leap. In the initial stage, dynamic stress strain curve of anthracite shows obvious nonlinearity, which is more obviously with the decrease of the rate. However, the dynamic stress strain curve of limestone is basically a straight line at the initial stage, deviation is smaller with different rate and the segment can be very good overlap. It is believed that rock in this stage is linear elastic. Anthracite and limestone have both the tendency of the plastic deformation and the ultimate strength increases with the increase of the impact rate, but the plastic deformation of limestone is smaller than the plastic deformation of anthracite.

With the increasing of impact speed, the dissipative energy of anthracite coal and limestone has a weak power function increasing tendency and the growth rate of energy dissipation is faster for anthracite. That is to say anthracite could absorb more energy and show more broken than limestone in the same impact rate.

ACKNOWLEDGMENT

The authors would like to thank The National Natural Science Funds (51074167) and the Fundamental Research Funds for the Central Universities (2010YZ04) for supporting this research.

REFERENCES

[1] Liu XH, Zhang R, Liu JF. Dynamic test study of coal rock under different strain rates. Journal of Coal Science & Engineering 2012; 37: 1528–1534.

[2] Li XB, Gu DS. Rock impact dynamics. Chang SHA: Central south university of technology press; 1994.

[3] Voss K H. New stowing material and raw coal bunkers in the coal mining industry. Glueckauf and Translation 1987; 123: 289–295.

[4] Coles E F. Development of a vertical bucker level indicating system. Colliery Guardian 1982; 230: 596–597.

[5] Moomivand H. Effect of size on the compressive strength of coal. In mining science and Technology 1999; 399–404.

[6] Bresler B, Bertero VV. Influence of high strain rate and cyclic loading of unconfined and confined concrete in compression. Heidebrecht A C, Emery J J, Speirs J W, et al, ed. Proceedings of Second Canadian Conference on Earthquake Engineering. Ontario, Hamilton: McMaster University; 1975, p. 1–13

[7] Hughes B P, Gregory R. Concrete subjected to high rates of loading in compression. Magazine of Concrete Research 1972; 24: 25–36.

[8] Hughes BP, Watson AJ. Compressive strength and ultimate strain of concrete under impact loading. Magazine of Concrete Research 1978; 30: 189–199.

[9] Malvern L E, J enkins D A, Tang T, et al. Dynamic compressive testing of concrete. Ross C A, Thompson PY, ed. Proceedings of Second Symposium on the Interaction of Non-Nuclear Munitions with Structures, Florida: Department of Defense; 1985, p. 194–199.

[10] Klepaczko J R, Hsu T R, Bassim M N. Elastic and pseudoviscous properties of coal under quasi-static and impact loadings. Canadian Geotechniacl Journal 1984; 21: 203–212.

[11] Wu MB, Gao JG. Experimental study of the dynamic characteristics of the Yangquan Coal. Journal of Coal Science & Engineering 1987; 12: 31–38.

[12] Shan RL, Cheng RQ, Gao WJ. Study on dynamic constitutive model of anthracite of yunjialing coal mine. Chinese Journal of Rock Mechanics and Engineering 2006; 25: 2258–2263.

[13] Li LY, Xu ZQ, Xie Hp, et al. Failure experimental study on energy laws of rock under differential dynamic impact velocities. Journal of Coal Science & Engineering 2011; 36: 2007–2011.

Progress in Mine Safety Science and Engineering II – He et al. (Eds)
© 2014 Taylor & Francis Group, London, ISBN 978-1-138-00122-0

Research on the burst triggering mechanism under the coupling action of higher stress and gas pressure

Liming Qi & Xuexi Chen
Key Laboratory of Mine Disaster Prevention and Control, Hebei, China
Safety Engineering College of North China Institute of Science and Technology, Beijing, China

Genyin Cheng & You Cheng
Science and Technology Division of North China Institute of Science and Technology, Beijing, China

ABSTRACT: Along with deep mining of coal mine, in the condition of higher stress and gas pressure, the burst triggering mechanism will change. Firstly, according to the distribution of the stress and gas pressure in the front of working face, and there are some broken coals in the top of burst coal seam, and combining with characteristic, the physical mechanical model of burst coal was constructed in the condition of higher stress and gas pressure; then, the mechanical mechanism of burst coal was analyzed, and the theoretical formula of burst energy was deduced. The results show the relative motion is rolling friction between burst coal and roof in the condition of higher stress and gas pressure, and the relative motion is sliding friction between burst coal and floor in the other conditions, the burst energy increase with the depth of burst spot by exponential law. Therefore, in the condition of higher stress and gas pressure, the elastic deformation energy of coal (rock) and the expansion energy of gas release instantly, On the one hand, the burst energy increases, On the other hand, the resistance falls. Therefore, the action mechanism which prevents and controls the burst by enhancing the distressed zone width is improving the energy consumption of burst happening.

1 PREFACE

With the increment of mining depth, there are a series of new phenomena on deep rock mechanical behavior, and the most prominent is the "three high and one disturbance" complex mechanical environment (i.e. "three high" refer to high ground stress, high temperature and high gas pressure are, and "one disturbance" refers to the excavation disturbance strongly) (HU Qian-ting, et al. 2007, Liu Weidong, & Zhang Rongyu. 2006, Pan Liyou, et al. 2006). In the depth environment, coal (rock) and gas dynamical disasters (such as rock burst) which are related closely to stress and mining disturbance is also increasing in coal mining engineering, and showing a new and more complicated disaster characteristics. In order to effectively prevent the occurrence of burst, scholars at home and abroad have carry out a series of fruitful work, bring forward the burst generating mechanism (such as strength theory, energy theory, stiffness theory, impact orientation theory and instability theory), and the rock burst prediction index (such as elastic deformation energy index, impact energy index and dynamic failure time). The above-mentioned achievements have been widely used in coal mine (F. Otuonye, & J. Sheng. 1994, Germanovich L N, et al. 1993, K. Sato, & Y. Fujii. 1989, Lama R D, & Bodziony J. 1998, Li S, & Zhang H W. 2002, QI Li-ming, et al. 2007, Qi Qingxin, & Dou Linming. 2008). Although the great achievements of burst stress have been made at home and abroad, the research which the coupling action of higher stress and gas pressure lead to the disasters in deep mining is still less. Theoretical researches have been carried out on the burst stress trigger mechanism in this condition, and it may provide theoretical guidance to the prevention and cure of coal (rock) dynamical disaster in deep mining.

2 THE COAL MECHANICAL MODEL UNDER THE COUPLING ACTION OF HIGHER STRESS AND GAS PRESSURE

In the front of working face, firstly, the stress increases, secondly, decreases, finally, tends to be stable. Gas pressure increases gradually, and eventually tends to be stable. For the coal seam prone to burst, there is a thin layer of smash coals (about 0.1 m to 0.2 m) between the coal seam and roof (Huang RQ, & Wang XN. 1999, Jin Liping, &

Xian Xuefu. 1993, QI Li-ming, et al. 2007, Xie Heping, & Pariseau W C. 1993, Zhang Wanbin, et al. 1992, ZOU yin-hui, et al. 2007). The coal would be fractured in the front of working face in the condition of stress-concentrated, turn from elastic state to plastic state, and at the same time, a large number of high-pressure gases were desorbed. The air flows into the top of the coal seam along the seam cracks, and the soft broken coal between coal seam and roof was ejected out under the action of high-pressure gas flow, leaving a little of rigid coal particles between coal seam and roof, and it is shown as figure 1.

In the front of working face, when the coal turns from elastic state to plastic state, the elastic deformation energy would release. The amount of energy directly depends on burst energy index, the release speed depends on the dynamic failure time, and the amount of releasing energy depends on the relative size of these two indicators in unit time (Li Zhonghua, & Pan Yishan. 2002, Lin Baiquan, & Cui Hengxin.1998, Litwiniszyn J.1990, Paterson L. 1986, S. Murakami. 1983). The greater of releasing energy is in unit time, the higher of additional stress. Coal does not belong to the rigid body; therefore, the energy will be spread to the mining face by the form of stress wave.

In the process of stress wave spreading to the working face, coal body along the way will absorb some of the energy and distort under the disturbance of stress wave. Because of deformation and instability of coal in the front of mining face, the consumed energy is different in the different condition of stress and gas pressure. A unit coal close to mining face wall maybe occur bending deformation and even instability collapse under the affect of stress wave, and the burst takes place in the macro.

Under the effect of stress wave, the mechanical model of each unit coal can be simplified as follows: stressed at both left and right sides, the bottom is fixed, and has some shear strength, and the upper end contacts with roof through a spherical

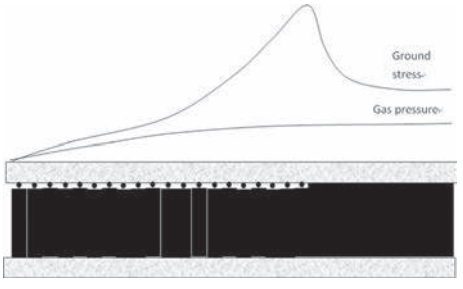


Figure 1. The structure diagram of coal and rock before burst happening.

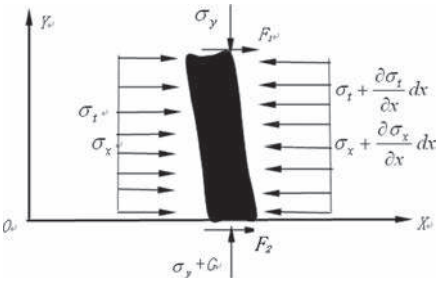


Figure 2. The stress diagram of burst coal body.

coal, and the relative motion between it and spherical coal belongs to rolling friction.

When the elastic deformation energy and the gas expansion energy released by coal burst is higher and the additional stress reaches a certain level enough to overcome the rolling frictional resistance at the top and the sliding frictional resistance at the bottom of coal seam, on the one hand, the coal was stressed and compressed further, on the other hand, the displacement towards to the low stress area (roadway coal wall) takes place, and it is shown as figure 2.

The coal in condition of forced state can be simply regarded as the cantilever beam, and both left side and right side are forced, and at the same time, the free end is also forced by the focusing load, and the whole coal (including the bottom of coal) will make a displacement.

3 THE STRESS ANALYSIS OF COAL BODY UNDER THE COUPLING ACTION OF HIGHER STRESS AND GAS PRESSURE

σ_y is the force which can act on coal seam and be perpendicular to direction of burst and MPA. according to the basic knowledge of rock mechanics, in the region of high-point stress, the stress increases exponentially basically. Therefore, it can be expressed by formula 1

$$\sigma_y = \sigma_{b_1} e^{b_1 x} \tag{1}$$

In formula 1, σ_{b_1} is the compress stress at roadway coal wall, MPA; b_1 is the coefficient describing the rate of stress change, m^{-1}; x is the depth from coal wall, m.

To the coal under the action of high stress and gas pressure, rolling friction at top and sliding friction at bottom, rolling friction and sliding friction per unit area can be expressed by formula 2–3.

$$\mu_g \sigma_y = \mu_g \sigma_{b_1} e^{b_1 x} \tag{2}$$

$$\mu_h \sigma_y = \mu_h \sigma_{b_1} e^{b_1 x} \tag{3}$$

In formula 2–3, μ_g is the rolling friction coefficient; μ_h is the sliding friction coefficient.

The additional stress generated by the release of elastic deformation energy and gas expansion energy can be expressed by formula 4.

$$\sigma_t = \sigma_{b_2} e^{b_2 x} \tag{4}$$

In formula 4, σ_t is the additional stress generated by the release of elastic deformation energy and gas expansion energy, MPA; σ_{b2} is the residual stress when elastic wave transmitted to the roadway coal wall, MPA; b_2 is the coefficient describing the rate of stress change, m^{-1}.

The coal is compressed by the action of additional stress, and the stress both left side and right side will change and achieve stress equilibrium within a short time. Then, at left side, the stress can be expressed by formula 5.

$$\sigma_x = K \sigma_{b_1} e^{b_1 x} \tag{5}$$

In formula 5, σ_x is the stress at left side, MPA; K is the coefficient of side stress.

The balance equation was built by making use of force analysis, as shown in formula 6.

$$\begin{aligned}&(\sigma_x + \sigma_t) Lm + \mu_g \sigma_y L dx + \mu_h \sigma_y L dx + \rho m L a dx \\ &= \left(\sigma_x + \frac{\partial \sigma_x}{\partial x} dx + \sigma_t + \frac{\partial \sigma_t}{\partial x} dx \right) Lm\end{aligned} \tag{6}$$

Where L = the depth of coal where burst takes place, m; m = the thickness of coal seam, m; ρ = the density of coal, kg/m^3; a = the acceleration of coal element which is analyzed, m/s^2.

The formula 6 can be simplified, as shown in formula 7.

$$\left(\frac{\partial \sigma_x}{\partial x} + \frac{\partial \sigma_t}{\partial x} \right) m - \mu_g \sigma_y - \mu_h \sigma_y = \rho m a \tag{7}$$

Putting formula 1, 4 and 5 into formula 7, the formula 8 may be obtained.

$$\begin{aligned}&(K b_1 \sigma_{b_1} e^{b_1 x} + b_2 \sigma_{b_2} e^{b_2 x}) m - \mu_g \sigma_{b_1} e^{b_1 x} \\ &- \mu_h \sigma_{b_1} e^{b_1 x} = \rho m a\end{aligned} \tag{8}$$

The formula 8 can be simplified, as shown in formula 9.

$$a = \frac{(K b_1 m - \mu_g - \mu_h) \sigma_{b_1} e^{b_1 x} + b_2 m \sigma_{b_2} e^{b_2 x}}{\rho m} \tag{9}$$

According to the Newton's laws of motion, the formula 10 may be obtained.

$$V = at \tag{10}$$

Where V = the overall motion velocity of the coal element which is analyzed, m/s; t = the time of acceleration, s.

In the whole accelerated motion process, the displacement of coal accelerated motion is the distance from the initial position to coal wall, and the formula 11 may be obtained.

$$x = \frac{1}{2} a t^2 \tag{11}$$

The coal element can obtain kinetic energy, and it may be expressed by formula 12.

$$dW_1 = \frac{1}{2} \rho m L dx V^2 \tag{12}$$

Where W_1 = the needed energy of entire coal body motion, MJ.

Putting formula 10 and 11 into formula 12, and the formula 13 may be obtained.

$$dW_1 = \rho m L a x dx \tag{13}$$

Putting formula 9 into formula 13 and the formula 14 may be obtained.

$$dW_1 = ((K b_1 m - \mu_g - \mu_h) \sigma_{b_1} e^{b_1 x} + b_2 m \sigma_{b_2} e^{b_2 x}) x L dx \tag{14}$$

The formula 15 is the integral of formula 14.

$$\begin{aligned}W_1 = {} & (K b_1 m - \mu_g - \mu_h) \sigma_{b_1} L \left(\frac{x}{b_1} - \frac{1}{b_1^2} \right) e^{b_1 x} \\ & + m \sigma_{b_2} L \left(x - \frac{1}{b_2} \right) e^{b_2 x} \\ & + \frac{(K b_1 m - \mu_g - \mu_h) \sigma_{b_1} L}{b_1^2} + \frac{m \sigma_{b_2} L}{b_2}\end{aligned} \tag{15}$$

4 THE BURST TRIGGERING MECHANISM UNDER THE COUPLING ACTION OF HIGHER STRESS AND GAS PRESSURE

According to formula 15, the thickness (m) and the width (L) are both constant to some working face, and the energy to move coal is proportional to the initial stress of coal and the additional stress generated by the release of elastic deformation energy

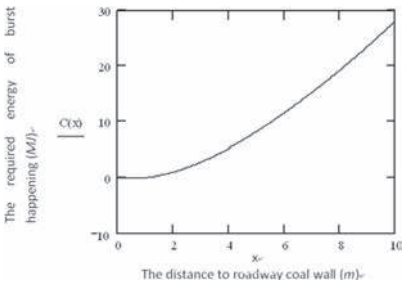


Figure 3. The relationship diagram between burst energy and burst depth.

and gas expansion energy, and it is inversely proportional to the friction stress at the top and bottom of coal seam; the relationship between it and burst depth is complicated, and it is very difficult to determine directly, and the burst energy change curve with the depth of burst can be drawn out by mathematical software, as shown in figure 3.

To coal in the condition of high ground-stress and gas pressure, because a large number of coal and rock elastic deformation energy and gas expansion energy can be released instantaneously, original stress and additional stress of burst coal is higher, and the existence of high gas pressure and crushed coal changed the frictional resistance form of burst coal, reducing friction force. According to formula 15, the energy that may be used to move coal increases greatly, and the risk of burst happening rises sharply.

The longer distance from the position of burst happening to coal wall, the higher energy required to move coal by burst, the smaller risk of burst occurrence in the same conditions. The mechanism of actual prevention measures of burst (including relieve-shot, seam water injection and hydraulic cutting seam) is increasing the width of distressed zone in the front of working face and tunnel, and the distance from the position of burst happening to coal wall is enhanced, and the energy that is consumed because of coal motion increases sharply, and the risk of burst happening falls in effect.

5 CONCLUSION

1. The mechanical model of burst coal was constructed under the coupling action of higher stress and gas pressure. In the process of bursting and moving, the relative movement between roof and coal seam belongs to rolling friction, and moreover the relative movement between floor and coal seam belongs to sliding friction.
2. In the condition of high ground stress and gas pressure, the elastic deformation energy of coal (rock) and the expansion energy of gas release instantly, not only providing enormous energy and impetus for the occurrence of burst, but also changing the mechanical action between burst coal and roof. The resistance of burst reduces, and the risk of burst occurrence rises significantly.
3. The mechanical mechanism of burst coal was analyzed in the condition of high ground stress and gas pressure, the theoretical formula of burst energy was deduced, and it increases exponentially with the burst depth; therefore, by making use of various pressure relief measures, increasing the distressed zone width, the level of energy consumption of burst happening will rise greatly, and its risk will be reduced.

ACKNOWLEDGEMENTS

Thanks to the supporters. The Project Supported by National Natural Science Foundation of China (No. 51204070), Hebei Province Key Basic Research Project (No. 11965629D), Fundamental Research Funds for the Central Universities (No. 2012E1202 and No. 2011SYSJJ01) and Program for New Century Excellent Talents in University (No. NCET-11-0837).

REFERENCES

Germanovich L N, et al. 1993. A model of the deformation and fracture of brittle materials with cracks under un-axial compression. *Mechanics of solids* 28(1):116–128.

Hu Qian-ting, et al. 2007. New technology of outburst danger prediction by gas content. *Journal of China Coal Society* 32(3):276–280.

Huang R Q, & Wang X N. 1999. Analysis of dynamic disturbance on rock burst. *Bulletin of Engineering Geology and the Environment* (57):281–284.

Jin Liping, & Xian Xuefu. 1993. The Study of Outburst-Proneness of Coal Seam Via Experiments and fuzzy Comprehensive Judgement. *Journal of Chongqing University* (6): 114–119.

Lama R D, & Bodziony J.1998. Management of outburst in underground coal mines. *Int. J. Coal Geology* 35(1): 83–115.

Li S, & Zhang H W. 2002. Coal and gas outburst model recognition and regional prediction. *Proceedings of Mining Science and Safety Technology*: 331–334.

Li Zhonghua & Pan Yishan. 2002. Analytical Solution of Rock burst on Working Surface. *Journal of Liaoning Technical University* (1): 40–42.

Lin Baiquan & Cui Hengxin.1998. *Theory and Technology of Gas Prevention in Mine*. Xuzhou: China University of Mining and Technology Press:80–95.

Litwiniszyn J. 1990. Rarefaction shock waves,outbursts and consequential coal damage. *Int.J. Rock Mech. Min. Sci. & Geomech. Abstr* 20(27):535–540.

Liu Weidong & Zhang Rongyu. 2006. A review on mechanism of rock burst. *Mining Engineering* 4(2): 12–14.
Murakami S. 1983. Notion of continuum damage mechanics and its application to anisotropic creep damage theory. *Engng. Mater. Technol* (105):99–105.
Otuonye F, & Sheng J. 1994. A numerical simulation of gas flow during coal/gas outbursts. *Geotechnical and Geological Engineering* (12): 15–34.
Pan Liyou, et al. 2006. *Practical Technology of Rock burst Forecast and Prevention*. Xuzhou: China University of Mining and Technology Press: 45–60.
Paterson L. 1986. A model for outburst in coal. *Int. J. Rock Mech. Min. Sci. Geomech. Abstr* (23):327–332.
Qi Li-ming, et al. 2007. Analysis on the Gas Pressure Measurement Result Revision on the Basis of Gas Loss Quantity Before Bore Being Sealed. *Journal of China Coal Society* 32(1):60–63.
Qi Li-ming, et al. 2007. Study on the Coal Gas Pressure Dynamic Distribution Law in the Front of Tunneling Place. *Journal of the Southern Aferican Institute of Mining and Metallurgy* 107(7):431–433.
Qi Qingxin & Dou Linming. 2008. *Theory and Technology of Rock burst*. Xuzhou: China University of Mining and Technology Press: 10–30.
Sato K, & Fujii Y. 1989. Source Mechanism of a Large Scale Gas outburst at Sunagawa Coal Mine in Japan. *Pageoph* 129(3):325–343.
Xie Heping, & Pariseau W C. 1993. Fractal Character and Mechanism of Rock Burst. *Int.J, Rock Mech. M in, Sci. & Geomech. Abstr* 30(4):343–350.
Zhang Wanbin, et al. 1992. Status and development of rock burst research and prevention in China. *Journal of China Coal Society* (3): 27–25.
Zou Yin-Hui, et al. 2007. Trial research about forecasting outburst by making use of gas content. *Mining Safety and Environment Protection* 34(4):4–6.

This page intentionally left blank

Progress in Mine Safety Science and Engineering II – He et al. (Eds)
© 2014 Taylor & Francis Group, London, ISBN 978-1-138-00122-0

Characteristics of electromagnetic signals obtained during blasting rupture of coal in excavating workface

Chuan Wang, Chengwu Li, Jingui Wang, Po Hu, Yongguo Cui & Xiaomeng Xu
Faculty of Resource and Safety Engineering, China University of Mining and Technology, Beijing, China
State Key Laboratory of Coal Resources and Safe Mining, China University of Mining and Technology, Beijing, China

ABSTRACT: In order to study the electromagnetic radiation characteristics of coal-rock-mass under strong impact loadings, the ZDKT-1type transient magnetic vibration detection system is set up in the 21180 excavating workface of TIAN AN TEN MINE in Pingdingshan Coal Group to collect the transient electromagnetic signals during the blasting process. The transient electromagnetic signals are obtained, and a pulse component is extracted from it, and then a low frequency component is gained by the Ensemble Empirical Mode Decomposition method. Based on this, the characteristics of each component and the reconstructed signal are studied. The results show that: (1) an obvious electromagnetic emission phenomenon is observed with a distance of 200 meters away from the working face during the blasting process; (2) the reconstructed EMR signal is gained by mixing the two components, the waveform presents a high amplitude pulse rising in the initial phase and then presents as a lower amplitude damp feature; (3) the pulse number of the pulse component has a good relationship with the blasting holes and blasting charge quantity, and the low frequency component has a longer wavelength, can transmit much further. Thus, both the two components have great significance for monitoring or predicting coal and rock dynamic disasters.

1 INTRODUCTION

Coal rock dynamic disasters such as rock burst and coal and gas outburst have always been major problems in coal mining. A lot of researches prove that coal and rock dynamic disaster is a result of coal and rock rupture quickly, being subject to the comprehensive action of stress and the physical chemistry inside and outside the body. Coal/rock undergoing deformation and failure emits many forms of energy, among which is electromagnetic radiation (EMR) (Wang & Zhao 2013).

The term EMR was first proposed in the 1920 (Cohen 1914), and between the 1960s and 1980s, nonlinear theoretical issues were studied, such as effects of stress on the magnetic field, electric field, magnetic induction intensity and heat induction in elastic solids and unveiled a research direction on EMR emitted by elastic media under stress (Jordan & Eringen 1964). EMR phenomenon during rock failure was found and investigated (Hanson 1982). Thereafter, several researchers studied the characteristics of EMR emitted by marble, granite and other hard rocks, and applied the EMR in earthquake forecasting (Yoshino 1989, Parrot 1989, Khatiashvili 1989). Studies on EMR produced by the deformation and failure of coal and other low strength rocks in coal-bearing strata started from 1990s (He & Liu 1995). Over the past several decades, this issue of EMR in the process of coal and rock rupture instability has aroused much concern. Many scholars have studied this issue with fruitful results. EMR characteristics, mechanism and propagation law of coal and rock material have been studied in depth (Wang & He 2009).

The experiment researches of EMR wave in the deformation and fracture process of coal under stress by slow or static load lasts ten minutes or more. Experiment results indicate that the EMR wave has a wide frequency scale. Its frequency spectrum appears as the shape of 'M' (Wang & He 2009). To study the EMR characteristics of coal under fast and dynamic loading, coal or rock crash experiment was conducted with high velocity impact at the speed over tens meters per second (Wan 2008a, b, Li & Wan 2009, Liu 2011, Li et al. 2012a). Even more, the EMR characteristics of rock mass under blasting stress wave impact was tested (Guo et al. 1999, Jin et al. 1997). The results revealed that the magnetic field varied obviously in a short distance of coal sample area during the process of coal dynamic impact, and its duration is shorter than 2 seconds and the frequency is less than 40 Hz (Li et al. 2012a).

But in the actual mining environment, the wavelength of high frequency EMR signal is so short that its propagation distance in coal and rock mass is within about 20 m (Jia 2010), and would be vulnerable to mechanical and electrical equipment of high-frequency interference effects. Low frequency electromagnetic wave has a lower attenuation in coal mass medium, could transmit much further, be well capable of anti-interference (Jia 2010).

Therefore the study on the characteristics of low frequency EMR of large scale coal-rock-mass under the impact load has great significance for the predication of coal and rock dynamic disasters. For blasting in coal mining process make coal and rock mass under intense dynamic loading, the ZDKT-1 type transient magnetic resonance detection system developed by China University of Mining & Technology (Beijing) was set up in blasting excavating work face for field test research of the EMR during coal body blasting destruction.

2 THE FIELD TEST DETAILS

2.1 *The field test system*

The ZDKT-1 type transient magnetic vibration detection system was developed for the varied magnetic field detection in the experiments related to coal and rock dynamic rupture.

It consists of magnetic field detector, signal transmit cable, and monitoring substation (underground), network switch and the host computer (on the ground). The EME signal generated during coal-rock deformation and fracture in the excavating workface is received by an electromagnetic antenna. Considering the signal is too weak and apt to be affected by the surrounding noise, an amplifier is set to amplify the forwarding gain. And then the data signal via a data collector is obtained (sample rate is 3000 s^{-1}). Then the data is transferred to an embedded computer for processing as electric current. Finally, the detector is connected to the host computer on the ground through electric cable and the network. Fig. 1 shows a schematic diagram of the system.

The detector contains 4 parts: electromagnetic signal acquire antenna, signal amplifier, data collector and embedded computer. The detector is installed on the left wall with 1.5 m over floor, and the antenna is kept towards the workface horizontally.

2.2 *Introduction of the test field*

The test was carried out in the 21180# excavating workface of TIAN AN TEN MINE in Pingdingshan Coal Group. There has been happened serious

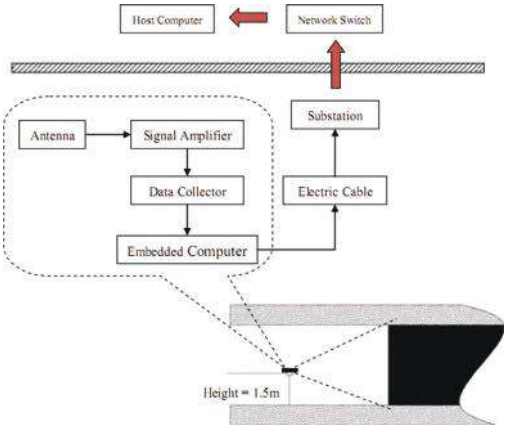


Figure 1. The transient magnetic resonance detection system schematic diagram.

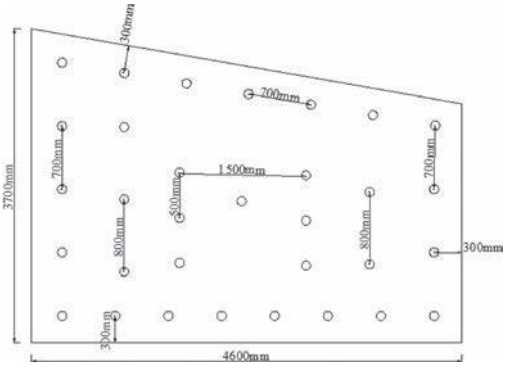


Figure 2. Layout plan of blasting holes.

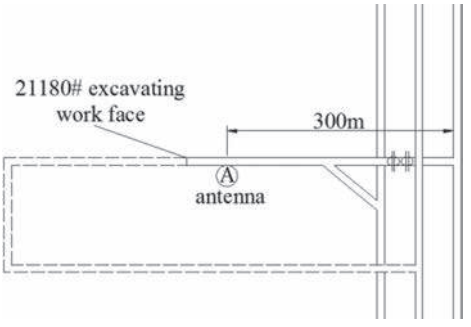


Figure 3. The detector installation project plan.

coal and rock dynamic disasters this coal mine. The thickness of the excavated coal seam is 2.0~2.6 m, with dip angle of 6°~12°. The 21180# tunnel net sectional area is designed about 13.8 m2, and the design length is 1095 m, using blast excavating. Fig. 2 shows the layout plan of blasting holes.

Table 1. The blast excavating parameters record.

Number of the Blasting holes	Blasting charge quantity (stick)	Excavating length (m)	Distance to the detector (m)
42	1	0.8	188.2
46	0.5	0.8	189
49	1	0.8	189.8
54	1	0.8	190.6
54	1	0.8	192.2
45	1	0.8	194.6
50	0.5	0.8	195.4
44	1	0.8	196.2
45	0.5	0.8	197
50	0.5	0.8	197.8
45	0.5	0.8	198.6
48	0.5	0.8	199.4
44	0.5	0.8	201
45	1	0.8	201.8
41	1	0.8	202.6
41	1	0.8	203.4
37	1	0.8	204.2
36	1	0.8	205
40	0.5	0.8	205.8
35	1	0.8	206.6
35	0.5	0.8	207.4
49	0.5	0.8	208.2

The transient magnetic resonance detector is set at a permanent position staying 300 meters away from the tunnel opening. Fig. 3 shows the detector installation project plan.

The blast excavating work takes three shifts a day. Table 1. shows the record of blasting holes and other blast parameters in some excavating periods.

2.3 *The detected electromagnetic signal*

The obvious electromagnetic signal was detected by the ZDKT-1 magnetic vibration detector during the blasting process. Fig. 4 shows a detected electromagnetic signal during the blasting process.

It can be seen from fig. 4 that the magnetic field varied obviously in the area 200 m away from the working face during blasting process.

3 THE ANALYSIS METHOD OF THE DETECTED SIGNALS

Fig. 4 indicates that the detected signal contains a lot of noise so that the time domain feature is inconspicuous. In order to get the authentic EMR signal from the detected signal, the process of decomposition and reconstruction of the signal is needed.

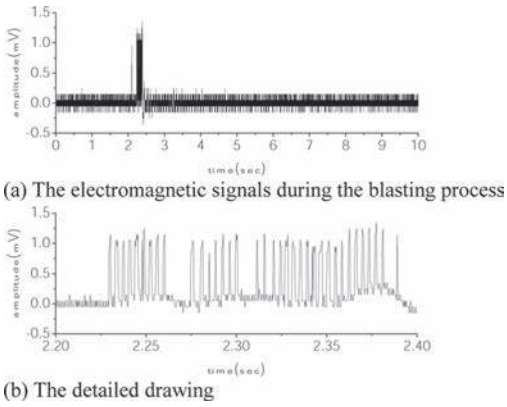


Figure 4. The electromagnetic signal during the blasting process.

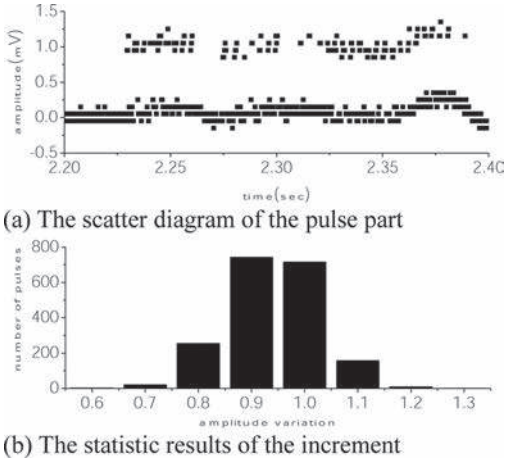


Figure 5. The increment of the pulse part.

3.1 *Extracting the pulse component from the detected signal*

The scatter diagram of the pulse part shows in fig. 5(a). The pulse part seems to have a stabile increment. To verify the hypothesis, the statistic of the increment of the pulse part in all the 27 signals has been done. Results are shown in fig. 5(b).

The results show that the value of pulse increment is still at 0.8~1.1 mV. Considering the amplitude of the noise, the real increment is 0.94 mV. For the amplitude of the pulse part presents so stable, to further observe the composition and structure of the detected signal, the pulse part should be extracted first. Fig. 6 shows the extracted results.

It is revealed from Fig. 6(a) that the pulse part focused in a short time with a stable amplitude. Contrasting fig. 6(c) and fig. 6(d), it is known that

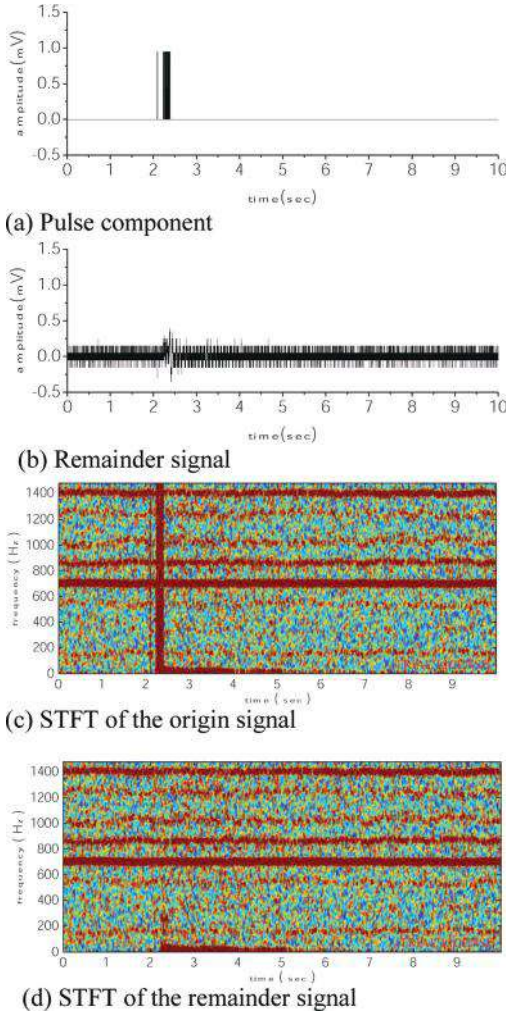


Figure 6. The pulse component extracted result.

the pulse component extract process has reduced the false frequency composition, making the remainder signal's frequency spectrum much more authentic.

3.2 *The decomposition of the remainder signal*

Fig. 6(d) emphasizes that the remainder signal greatly varies in low frequency range, but still contains a lot of noise, leading the time domain feature inconspicuous (see fig. 6(b)). Thus, the signal is paroxysmal, and its frequency and time domain statistical characteristics change over time, belonging to the non-stationary random signal. As an adaptive time-frequency signal analysis method, Empirical Mode Decomposition (EMD) has been successfully used by scholars in all fields to handle multiple nonlinear and non-stationary signals (Wu & Huang 2009, Semion et al. 2004).

Wu and Huang proposed a new concept of 'Ensemble Empirical Mode Decomposition method' (EEMD). Literature [18] has reported the detailed proceeding of EEMD method. Non-stationary random signal can be effectively decomposed into some Intrinsic Mode Functions (IMFs) by EEMD method. The valid signal waveforms of the random signal can be determined from these IMFs. These IMFs can be combined into different filters to remove the noise components or do special analyses. The low pass filter can be expressed as the following formula:

$$x_{lk}(t) = \sum_{i=k}^{n} h_i(t) + r_n(t) \tag{1}$$

where $h_i(t)$ is the IMF_i, and $r_n(t)$ is the remaining component of the decomposition.

These spatial filters preserve the nonlinear and non-stationary of the signal. And filtering and denoising or signal spectrum analyzing techniques on the basis of EEMD method have confirmed the potential superiority in many aspects, such as micro-seismic monitoring and blasting vibration signals application and the like (Liu et al. 2011, Li & Zhang 2006, Ling & Li 2004, Li et al. 2012b).

Thus, in order to obtain the authentic waveform from the remaining signal, the EEMD method was used. As shown in fig. 7, the remaining signal was decomposed into 14 IMFs from high frequency to low via EEMD, and each IMF has an independent physical significance.

As shown from the result by EEMD, IMF_h1-IMF_h4 are high energy noise components, IMF_h5 with a short abnormal part, and the abnormal part in IMF_h6~IMF_h14 are longer. There should be an index to determine which IMF could be selected as valid components. The amplitude enlargement ratio K can be defined as the judgment standard. The index K can be expressed as below:

$$K = A_1 / A_2 \tag{2}$$

where A_1 is the maximum amplitude of the abnormal part, A_2 is the normal part of the amplitude.

The K value of each IMF is shown in fig. 8.

The K value of IMF_h1 equals 1, meaning that this component hasn't changed during the blasting rupture of coal. Similarly, IMF_h2~IMF_h4 can also be seen as noise. The amplitude of IMF_h5~IMF_h14 has been enlarged more than 2 times, therefore they can be seen as the valid components of the remaining signal. The filter as formula (1) expresses can be used to mix the valid components

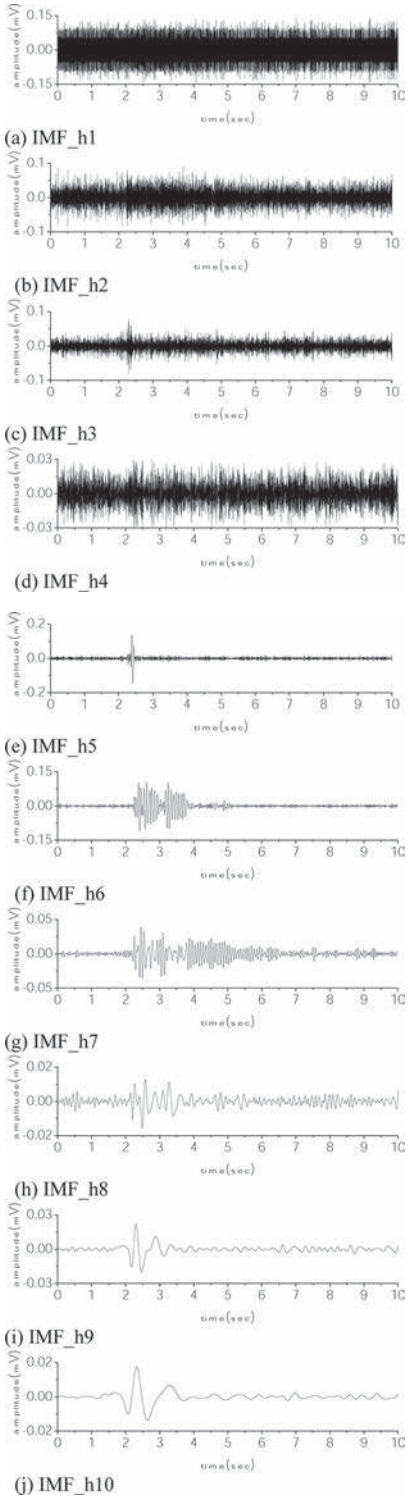


Figure 7. (*continued*).

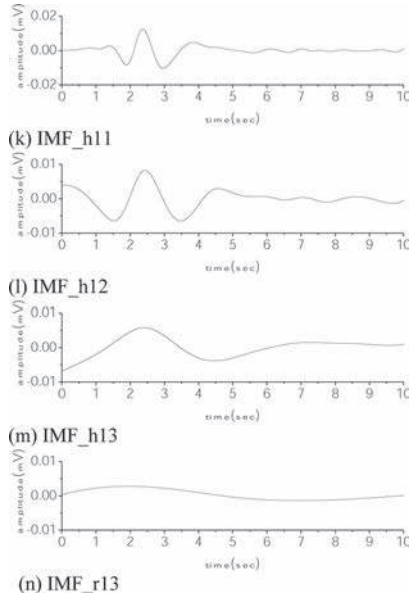


Figure 7. EEMD result of the Remainder signal.

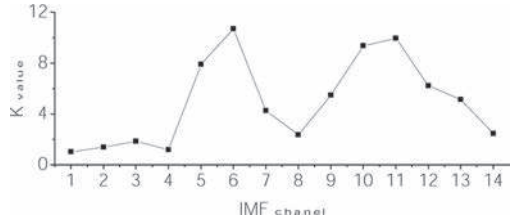


Figure 8. The K value of each IMF.

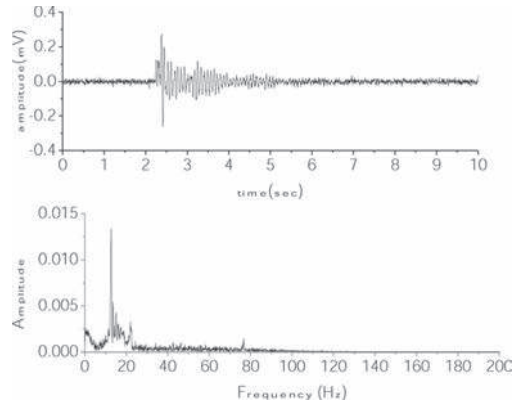


Figure 9. The waveform and FFT spectrum of the valid component in the Remaining signal.

together with another component of the EMR signal (shown in fig. 9).

Fig. 9 reveals that via EEMD method, the signal's time domain feature can be obviously distinguished, and the undesired signal can be perfectly wiped off, illustrating that the transient non-stationary nature of EMR signal detected during the coal mass blasting rupture has been fully preserved by EEMD method.

The frequency of the valid signal component focused under 25 Hz, thus this component is a low frequency EMR signal, lasting for about 3~4 seconds with a damp trend.

3.3 *Reconstruction of the EMR signal*

From the above analyses, it reveals that coal mass blasting rupture generates two kinds of EMR, pulse EMR and low frequency EMR. The two kind signals are mixed together to get the whole authentic EMR signal.

As shown in fig. 10, the reconstruction of the EMR signal waveform presents a high amplitude pulse rising in the initial phase and then presents as a lower amplitude damp feature. The method is used to other signals detected, and similar results are obtained.

4 RESULTS AND ANALYSIS

The EMR signals during coal blasting rupture process are composed by a pulse component and a low frequency component. The pulse number of each pulse component and the maximum amplitude and signal energy of each low frequency component are calculated. Table 2. presents the result calculated.

The pulse number and pulse duration have a good linear relationship (fig. 11), the slope is 0.00094, meaning the duration of per pulse is nearly 0.001s. The FFT spectrum of pulse

Table 2. The calculated result of each components.

	Pulse component	Low frequency component	
Signal Number	Pulse number	Max amplitude (mV)	Energy (mV^2)
1	39	0.19	316.50
2	7	0.07	289.84
3	40	0.27	450.11
4	67	0.25	419.33
5	64	0.24	443.60
6	11	0.18	426.87
7	22	0.20	317.65
8	30	0.27	498.60
9	16	0.13	258.73
10	14	0.19	336.35
11	3	0.12	295.23
12	7	0.12	291.23
13	25	0.14	321.66
14	62	0.31	413.49
15	44	0.21	406.06
16	35	0.15	416.47
17	27	0.26	426.52
18	19	0.34	639.86
19	4	0.14	366.00
20	25	0.19	363.15
21	2	0.12	290.82
22	3	0.12	400.28

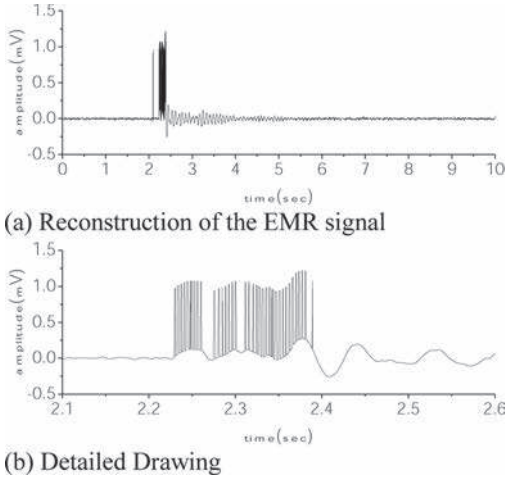


Figure 10. Reconstruction of the EMR signal.

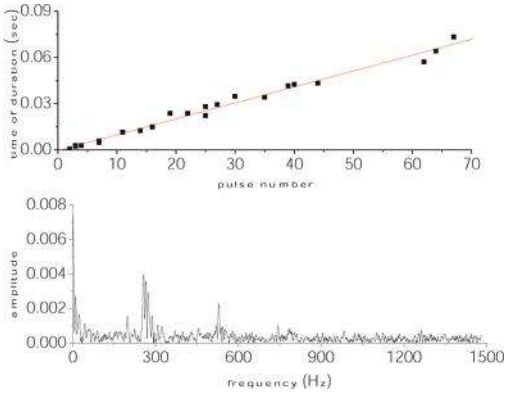


Figure 11. Relationship between pulse number and duration of pulse components and its FFT spectrum.

component indicates a wide range, but the main frequency range is focused about 250~280 Hz.

The low frequency component energy depends on its amplitude. And the maximum amplitude is related to the pulse number of the pulse component. Fig. 12 and fig. 13 present the relationship between them.

As indicated in fig. 12 and fig. 13, the maximum amplitude of the low frequency component increases with the pulse number, and has a positive relationship with its energy.

The intensity of the electromagnetic signal emerged during coal blasting process must be associated with blasting holes and charge quantity. Fig. 14 presents the relationship between them.

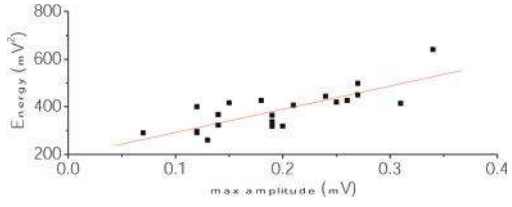


Figure 12. Relationship between maximum amplitude and energy of low frequency components.

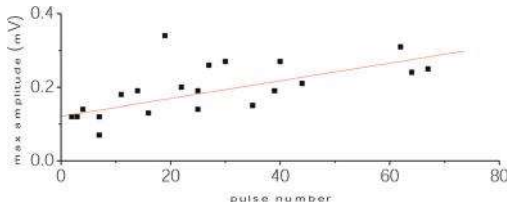


Figure 13. Relationship between maximum amplitude of low frequency components and pulse number of pulse components.

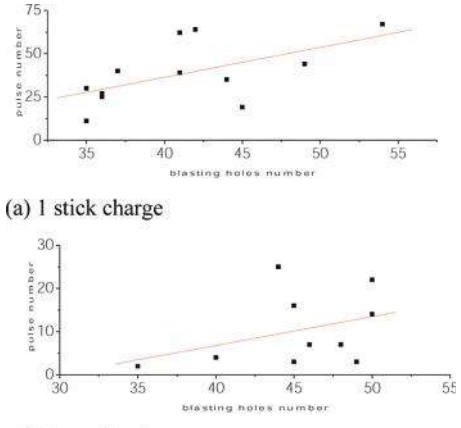


Figure 14. Relationship between pulse number and blasting holes at different charge quantity.

Fig. 14 indicates that the pulse number has an increasing trend as the number of blasting holes increases. Contrasting fig. 13 (a) with fig. 13 (b), it can be confirmed that the blasting charge quantity affects the pulse number sharply, but there exists large discreteness which need further study.

From the above analysis, it can be deemed that two kinds of EMR emerged in the process of blasting shock wave propagation in coal matrix. One is pulse radiation produced by the impact of coal or rock burst. The other is low frequency radiation caused by the rubbing effect on the coal fracture surface with the shock wave.

5 CONCLUSIONS

The field test result of EMR signal emerged during the blasting process in the excavating workface and analyses suggest that:

1. The obvious transient electromagnetic signal is observed during the blasting process with a distance of 200 meters away from the working face, and the electromagnetic signal detected can be decomposed into a pulse component and a low frequency component. When the two components mixed up to a reconstruct signal, the waveforms presents a high amplitude pulse rise in the initial phase and then presents as a lower amplitude damp feature.
2. The main frequency of the pulse component ranges from 250 Hz to 280 Hz, the duration time of a single pulse is nearly 0.001s. And the pulse number has a good relationship with the number of the blasting holes. Hence, the pulse component has much information of the impact frequency, benefits for the coal and rock dynamic disaster monitoring or forecasting.
3. The low frequency component lasts for about 3~4 seconds, with its maximum amplitude and energy related to the blasting holes and blasting charge quantity. Especially its frequency ranges about 0~25 Hz, with a longer wavelength, and can be transmitted much further. It proves that the low frequency EMR has great significance for non-contact and long-distance early warning of coal and rock dynamic disasters.

REFERENCES

Cohen L. 1914. Electromagnetic radition. Frank Inst177: 409.

Guo Ziqiang, Luo Xianglin, Qian Shuqing. 1999. Electromagnetic emissions during quarry blasting. Chinese Journal of Geophysics, 42(6): 834–840.

Hanson D R. 1982. Electromagnetic radition from rock failure. Int J Rock Mech Min Sci 4:77.
He Xueqiu, Liu Mingju. 1995. Electromagnetic dynamics of coal containing gas destruction. Xuzhou: China University of Mining and Technology Press.
Jia Huilin. 2010. Study on Regularity and Mechanism of Low-frequency Electromagnetic Signals in Deformation and Fracture of Coal and Rock under Load. Xuzhou: China University of Mining and Technology.
Jin Anzhong, Zhao Qiang, Liu Xiqiang. 1997. Result of electromagnetic radiation of rock in small scal abserved from field experiment. Acta Seismologica Sinica, 19(1): 45–50.
Jordan N F, Eringen A C. 1964. On the static nonlinear theory of electromagnetic thermoelastic solids-I. Int Eng Sci 2:59–95.
Khatiashvili N G, Perel'man M E. On the mechanism of seismo-electromagnetic phenomena and their possible role in the electromagnetic radition during periods of earthquakes, foreshocks and aftershocks. Phys Earth Planet Inter. 1: 169.
Li Chengwu, Xie Beijing, Yang Wei. 2012a. Characteristics of transient magnetic nearby field in process of coal impact damage. Chinese Journal of Rock Mechanics and Engineering, 31(5): 973–981.
Li Chengwu, Xie Beijing, Yang Wei. 2012b. Coal impact damage SHPB testing signal de-noising based on HHT method. Journal of China Coal Society, 37(11): 1796–1820.
Li Xibing, Wan Guoxiang, Zhou Zilong. 2009. The relation between the frequency of electromagnetic radiation (EMR) induced by rock fracture and attribute parameters of rock masses. Chinese Journal of Geophysics: 253–259.
Li Xibing, Zhang Yiping, Zuo Yujun. 2006. Filtering and denoising of rock blasting vibration signal with EMD. Journal of Central South University (Science and Technology), 37(1): 150–154.
Ling Tonghua, Li Xibing. 2004. Laws of energy distribution in different frequency bands for blast vibration signals. Journal of Central South University (Science and Technology), 35(2): 310–315.
Liu Jikun, Li Chengwu, Wang Cuixia, Zhang Ruming. 2011. Spectral characteristics of micro-seismic signals obtained during the rupture of coal. Mining Science and Technology (China) 21(5):641–645.
Liu Wenzhen. 2011. Experimental Study on Dynamic Mechanical Properties of the Coal under Impact Load. Hefei: AnHui University of Science and Technology.
Parrot M, Mogilevsky M M. VLF emissions associated with earthquakes and observed in the ionosphere and the magnetosphere. Phys Earth Planet Inter 1:86–99.
Semion, K. etc. 2004. On the Hilbert-Huang Transform Data Processing System Development. IEEE Aerospace Conference Proceedings.
Wan Guoxiang, Li Xibing. 2008a. Relationship between the electromagnetic radition and rock masses parameter during rock failure. Mechanics and Practice, 30(2): 70–73+77.
Wan Guoxiang. 2008b. Study on the characteristics of the electromagnetic emission and acounstic emission in rock under stress wave. Changsha: Central South University: 15–67.
Wang Enyuan, He Xueqiu, Li Zhonghui. 2009. Coal and Rock EMR Technology and its Application. Beijing: Science Press.
Wang Enyuan, Zhao Enlai. 2013. Numerical simulation of electromagnetic radition caused by coal/rock deformation and failure. Int J Rock Mech Min Sci 57: 57–63.
Wu Z H, Huang N E. 2009. Ensemble empirical mode decomposition: a noise-assisted data analysis method. World Scientific.
Yoshino T, Tomizawa I. 1989. Observation of low-frequency electromagnetic emissions as precursors to the colcanic eruption at Mt. Mihara during November, 1986. Phys Earth Planet Inter 1:2.
Zhao Mingsheng, Liang Kaishui, Luo Yuanfang. 2011. Application of EEMD in Blasting Vibration Signal De-noising. Blasting, 28(2): 17–20+59.

Progress in Mine Safety Science and Engineering II – He et al. (Eds)
© 2014 Taylor & Francis Group, London, ISBN 978-1-138-00122-0

Detection method and abnormal characteristics analysis of TEM in coal mine

Qing-Hua Liang
Chongqing Research Institute of China Coal Technology and Engineering Group Corporation, Chongqing, China

ABSTRACT: Based on mine transient electromagnetic theory, combined with the mine transient electromagnetic method (TEM) detection test, this article studied detection method, abnormal characteristic and accuracy rate of mine TEM, in order to provide the reference to underground coal mine. The results showed that: mine TEM had obvious reaction to each water abnormal body, and it presented different abnormal characteristics. Based on the test statistics, the integral detection success rate of TEM was 86.2% by the analytical methods and techniques. Also, the false anomaly detection may occur, while the body containing water can be detected with this method. From the current practice experience, mine TEM may make more prediction, and rarely misses predictions. Mine TEM is a more practical geophysical method to detect water damage in the underground mine.

1 GENERAL INSTRUCTIONS

At present, to the geophysical equipment of detecting water damage in China, the geophysical equipments that can be used to underground mine mainly include Direct Current method (DC), Transient Electromagnetic Method (TEM), Ground Penetrating Radar (GPR), radio wave penetration, etc (Dong Shuning 2008). DC in space, has some unsatisfactory application effects; GPR instrument, influenced by mine explosion-proof requirements and full-ection distance is short for water damage, generally 30–50 m; radio wave penetration mainly be used to detect coal mining face. One of the advantages of TEM is that is able to penetrate the shield layer of high resistivity, plus it has better resolving power to the high resistivity layer overlying stratum or structure. It is particularly sensitive to water-containing body of low resistivity, and the range of detection is extensive (Zhang Yunxia 2004). Therefore, in recent years, it was spreaded in the application of advanced detection in China, Most coal mines are equipped with TEM devices, but the detection analysis and recognition of anomaly is not enough, Sometimes there are some analysis errors. Based on this situation, and years of experience the author, summarized TEM detecting method, studied the characteristics of each water conductivity anomaly body and application in coal mine, and examined detection accuracy rate, to provide reference for the coal mine detection.

2 TEM DETECTION PRINCIPLE

TEM is a method of detecting medium resistivity, which launches a pulsed magnetic field to the underground by the no earth return or grounding line. It observe the two induction eddy current field which are caused by underground medium using the coil or grounding electrode during a pulse magnetic field intermittently (Yue Jianhua 2003).

The basic theory of mine (full-space) TEM is basically in line with that of ground TEM. But the difference between them is that mine TEM can only be detected by multi-tum small loops, because it is used in the limited space of underground tunnel. There are certain multiples between full-space and half-space for late apparent resistivity of TEM. Therefore the late apparent resistivity of mine TEM can be calculated through the half-space TEM apparent resistivity multiplied by a coefficient K_m, mine TEM apparent resistivity ρ_τ formula is (Liu Zhixin 2008, Yu Jingcun 2007).

$$\rho_\tau = K_m \times 6.32 \times 10^{-12} \times (S \times N)^{2/3} \times (s \times n)^{2/3} \times (V / I)^{-2/3} \times t^{-5/3} \quad (1)$$

In the formula, K_m is the calculation coefficient of mine TEM apparent resistivity, and the general value is 500~2000; S is the transmitting loop area; N is transmitting loop turns; V is induction voltage; I is power supply current intensity; s is receiving loop area; n is receiving loop turns; t is the time when the second field declines. The apparent

resistivity calculated with half-space TEM is small, but it won't affect the judgment of abnormal.

3 MINE TEM DETECTION METHOD

The operating mode of Mine TEM is changeable. According to the antenna arrangement, the author classified and summarized the detection methods of mine TEM. At present, Mine TEM generally use overlapping loop device which can illustrate the work mode of underground mine antenna.

3.1 *Fixed translation method*

Fixed translation method is the detecting method which places the transmitting antenna and the receiving antenna in parallel, then moves them gradually. This method is mainly used in detection for underground coal mining working face or bottom hidden containing water.

This method is usually constructed with antenna artificially, moving once in every 5 m or 10 m till the completion of detecting the tunnel. At present, we mostly select a tunnel of coal face to detect. If the working face width is greater than 150 m, we recommend adopting two tunnels to detect, and the detection method is shown in Figure 1.

3.2 *Angle—conversion method*

Conversion angle method is the detecting method which turns the transmitting antenna and the receiving antenna at a certain angle to detect the front fan-shaped region. This method is mainly used to detect the hidden water-containing body when working on the single-entry tunnel progress.

Using this method to detect, the antenna is changed to a certain angle, generally 10°. A driving face can be changed at an angle from left to right or from top to bottom with the completion of two lines, to observe the water—containing bodies' condition in the front of driving face. In order to ensure the accuracy, the driving machine should be back more than 20 m in acquisition. Detection method is shown in Figure 2.

3.3 *Integrated method*

The so-called integrated method is a combination of fixed translation method and conversion angle-conversion method; this method mainly used when there is major water damage in front of blind tunnel.

As shown in Figure 3, we start from the left side of the driving face. Firstly, we make the transmitting antenna and the receiving antenna face the left side of the tunnel to measure up, and then rotate the overlapping loop antenna, rotating the normal direction of the antenna into a 60°, a 45°, and a 30° compared with the left side of the tunnel. According to the width of excavated section, the measuring points of which the working area is just opposite these 3 antennas are fixed. Then to the right side, measuring points are symmetrically

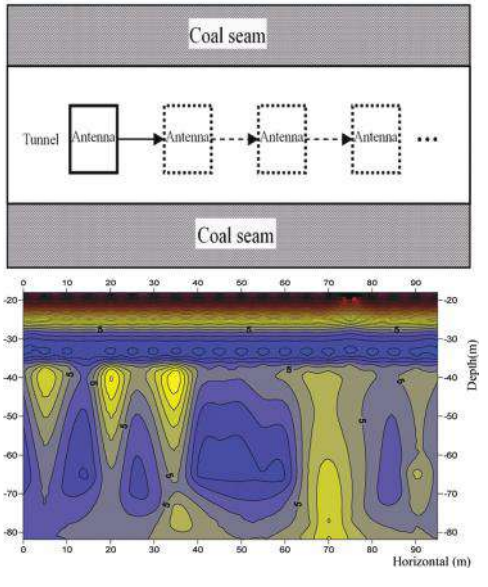


Figure 1. Schematic diagram and result map of fixed translation method.

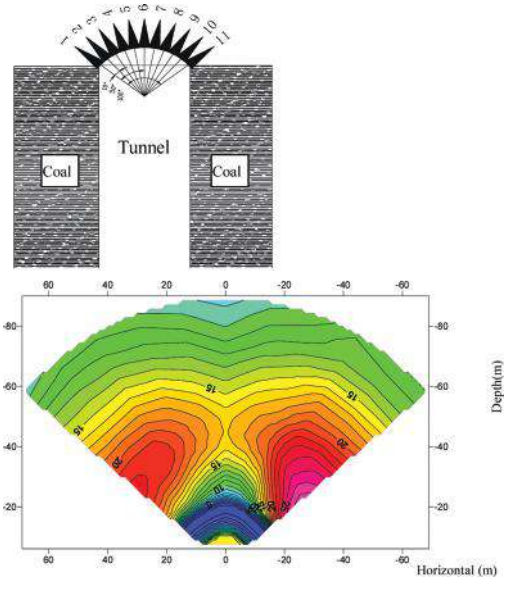


Figure 2. Schematic diagram and result map of conversion angle method.

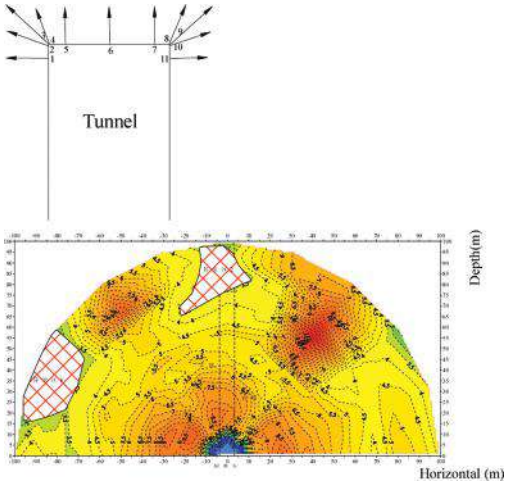


Figure 3. Schematic diagram and result map of integrated method.

arranged (Wang Dongwei 2011), so the data can be collected from multiple angles, rotation, combined with translation.

4 ABNORMAL CHARACTERISTICS ANALYSIS OF MINE TEM

In most working coal seam, the main water filling, the sandstone fracture water and limestone kart' s fissure water, the deep Ordovician limestone water and goaf water. Water channel is tectonic fracture zone and water flowing fracture in the roof caused by coal mining exploitation. The abnormal characteristics studies of fault, collapse column and goaf have a strong guiding significance for qualitative analysis of TEM abnormal condition.

4.1 *Abnormal characteristics analysis of fault fissure water detection*

In the coal mine, the fault structure in Local areas developed and the roof was broken. If the overburden is aquifer, then water in fissure will develop. Then here shows that the amplitude contour fluctuation will be increased in the apparent resistivity contour map, the change of regional variation of apparent resistivity will be larger, and there will be discontinuous small scope in low resistivity zone.

Figure 4 is the case of detecting fault fissure water in front of the driving face in Shanxi mine. From the chart, we can see that there is a small and low resistivity anomaly area located near the front of driving face 90 m. After drilling to prove, the location of the 90 m ahead is water point with low

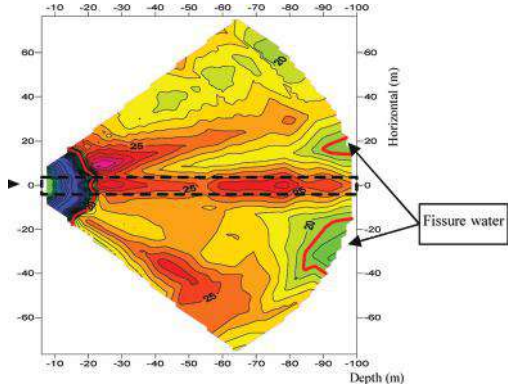


Figure 4. Apparent resistivity contour map caused by fault.

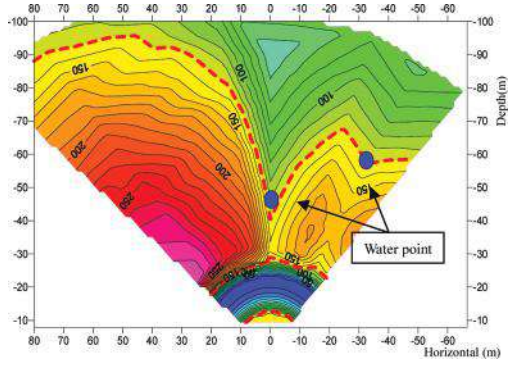


Figure 5. The apparent resistivity isopleths map when the goaf water.

resistivity abnormity which is caused by the fault fissure water.

4.2 *Abnormal characteristics analysis of goaf water detection*

In the goal water filling condition, the apparent resistivity contour shows low-resistivity in a wide range; the apparent resistivity value is associated with the containing water condition, and the continuity of low-resistivity abnormity is better. If more water was heaped up, then electromagnetic waves can't pass through, and the deep area in the contour map shows low-resistivity abnormity.

Figure 5 is a detection result map of Shanxi mine, and detecting location is return air driving face. Within 90 m in front of the detected location, there is a low-resistivity abnormity area. Located in front of driving face right ahead of 48 m, abnormal area range is relatively large and the apparent resistivity value is small. We conclude that this

area is rich of water. After verification by drilling, the water point exists in 50 m in front of the area, another water point exists in 65 m ahead on the 30 degrees right side

4.3 *Abnormal characteristics analysis of not filling water collapse column detection*

In case of not filling water, collapse column or fault crush is seriously broken with low conductivity compared with its surrounding rocks. Also it shows high-resistivity abnormity, which is reflected in the high-resistivity area of resistivity contours.

Figure 6 is an example of collapse column with no filling water in Shanxi mine, whose detecting location is track driving face. There is a high-resistivity abnormity area in front of detection area. Through verification, there is a subsided column of a diameter of 25 m and not filling water.

4.4 *Abnormal characteristics analysis of filling water collapse column detection*

In case of filling water, presents high conductivity compared with its surrounding rocks and low-resistivity abnormity which is reflected in the low resistivity area of the resistivity contours.

Figure 7 is an example of water filled subside column in Shanxi mine, whose detecting location is the air return driving face. In front of 90 m, there is an abnormal area, located right ahead of 40 to 90 m of tunneling head, in the direction of left 45 m to right 60 m.This abnormal area range is relatively large with low resistivity value, thus we concluded that it is rich in water resources. After verification by drilling, the area in front of the 46 m is water point, in addition, another water point is in the right 20 degrees ahead of 51 m of this area, which is a diameter of hydraulic 20 m subsided column.

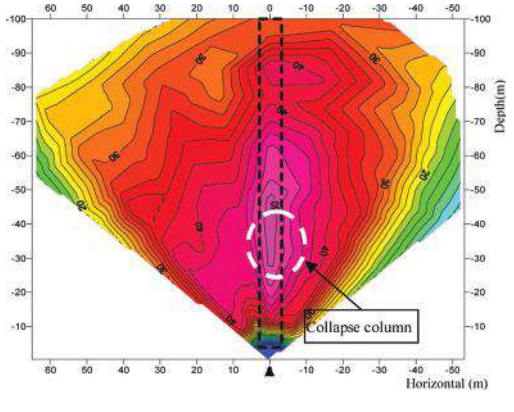


Figure 6. The apparent resistivity isopleths map of not water filled subsided column.

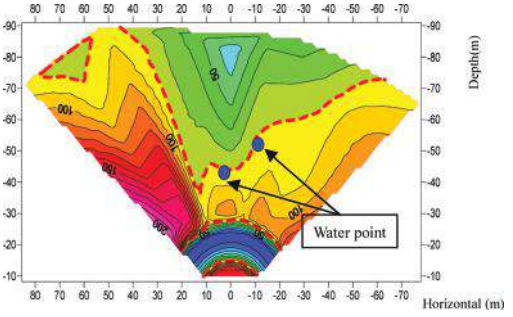


Figure 7. The contour map of water filled subsided column detecting TEM apparent resistivity.

4.5 *Abnormal characteristics analysis of water flowing fractured zone detection*

At present, the methods of determining the maximum height of coal seam water flowing fractured zone have the empirical formula method, field test method and numerical simulation method etc. The actual measurement data is the main method to determine water flowing fractured zone (Wang Shuangmei 2006). Field measurements have the mine TEM, water injection test method, ultrasonic imaging method and high density resistivity method etc.

We can study the coal mining water flowing fractured zone by mine TEM. At a certain angle detected the roof of the coal face. With the fixed translation method, we can get an overburden containing water abnormal situation of a coal mining working face. The following figure is a detecting effect chart of water flowing fractured zone in Shanxi mining coal, with 60 degrees of detection angle. From the map view, the basic abnormal area is the blue region; abnormal position exists in 52 m. Through the calculation of the triangular relationship, we can draw that the height of water flowing fractured zone is about 45 m. After the mine.

5 THE ACCURACY OF THE EXPERIMENTAL STUDIES ON MINE TEM DETECTION

Combined with the specific situation in Changping Mine Field, through the tracing detection test for mine containing water structure, this part studied the accuracy of TEM in Changping Mine.

Changping Mine is substitute of Wangtaipu coal mine in Shanxi Coal Group, the coal seams are composed of the Taiyuan group and Shanxi group. This mine now is exploited No. 3 coal seam; the problem of mine water inflow is roof water leakage and goaf seepage but no large water

damage in mine. The main hazards are goaf ponding of two village-run coal mines: Wangbao and Gaoliang coal mine which are near the southeastern boundary. We should detect and investigate on the distribution of two village-run coal mine, in order to prevent causing water inrush through the goaf seeper area.

Considering that it exist 20 m blind areas in mine TEM, We need to avoid blind areas in mine detection. After a lot of practice, we adopt the mine TEM tracking detection used as shown in Figure 9. The detection distance is 100 m, and the driving distance is 80 m; the next cycle reaches 80 m to detect. In accordance with such 80 m cycle detection, we can avoid blind area.

TEM experiment in Changping Mine started from September 6, 2011 to December 9, 2011, and a total number of TEM detection was 29 times with 2715 m prediction distance. The overall situation of abnormal test is shown in Table 1.

Through a lot of practice in mine, we got a wealth of mine TEM data. Typical anomaly of detection is showed in Figure 10.

From the analysis of table 1, abnormal frequencies of detection were 16 times; the number of

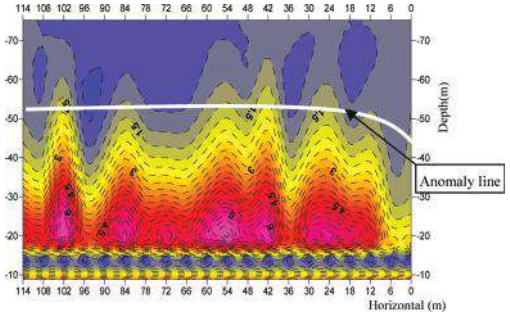


Figure 8. The sounding chart of water flowing fractured zone of TEM verification, the detection result is accurate.

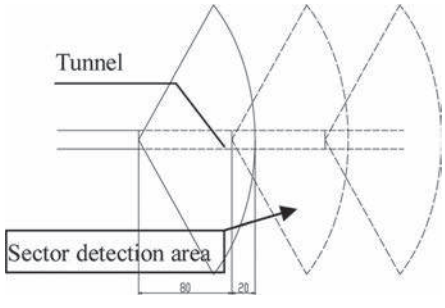


Figure 9. The track layout of sector detection the driving face.

Table 1. Abnormality detection table.

Total times of detection	Times of detected anomalies	Times of successful prediction	Times of turnover
29	16	16	0
Abnormal times	Extra times of prediction	Times of successes	Success rate of detection
12	4	29–4 = 25	25/29 = 86.2%

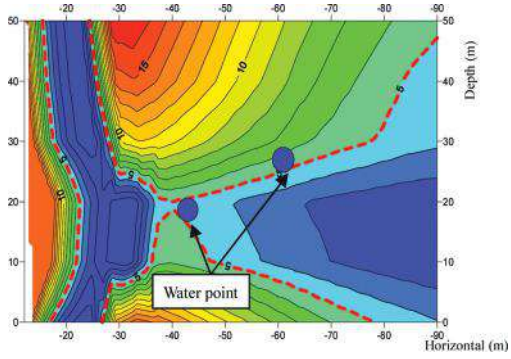


Figure10. The contour map of apparent resistivity for 13131 tunnel detection.

successful prediction was 16 times. From the total number of detection, extra times of prediction were 4 times, the total number of detection was 29 times, so the overall detection rate of success was 86.2%. From the detection accuracy of statistical data, we can see that mine TEM could present false anomaly in detecting, but this would detect basically to the existence water containing body ahead. From the current practice, TEM may forecast too much, but it rarely missing, which shows that TEM has good accuracy in coal mine application.

6 CONCLUSIONS

1. By analyzing TEM response characteristics of typical water flowing abnormal body, this article concludes that apparent resistivity contour is low resistance in a large scope when goaf or large collapse column is in the water filling conditions, and the continuity of low resistivity anomaly is better; when the small fault is in the case of water flowing, and the amplitude contour fluctuation is increased, the change of region apparent resistivity gets greater, and discontinuous low-resistivity abnormal zone exists on a small scale; abnormal body of no water flowing subsided column shows the

characteristics of high-resistivity; application of TEM can detect accurately for the exploitation of water flowing fractured zone, anomaly characteristics are manifested as anomaly low resistivity of large-area.

2. According to the arrangement of antenna, this paper summarized that the detection methods of TEM include fixed translation method, angle-conversion method and integrated method. Fixed translation method is fit for detecting in coal mining face or tunnel roof and floor, angle-conversion method and integrated method are fit for detection of driving face.
3. Through the actual verification detection to the mine TEM by the analytical methods and techniques mentioned above, the author concluded that through statistical analysis, the integral detection success rate of mine TEM was 86.2%. The detection could be false abnormity, but this method would be able to detect when it existed containing water bodies ahead. From the current practice, TEM may forecast too much, but it rarely misses a little, so it is the practical method to detecting containing water bodies in coal mine.

REFERENCES

Dong Shuning, et al. 2008. Practical technology and equipment for mine water prevention and control. *Coal Science and Technology* 36(3): 8–11.

Liu Zhixin 2008. Study on the distribution and application of mine transient electromagnetic field. *China University of Mining and Technology, Xuzhou*.

Wang Dongwei, et al. 2011. Application of mine transient electromagnetic method to advanced detecting of roadway head. *Chinese Journal of Engineering Geophysics* 8(4): 403~407.

Wang Shuangmei 2006. Summary of research methods on height of transmissive fracture belt. *Jiangsu Geology* 30(1): 64~66.

Yu Jingcun 2007. Mine transient electromagnetic exploration. *China University of Mining Press, Xuzhou*: 50~75.

Yue Jianhua & GAN Huichun 2003. Mine transient electromagnetic method and its application. *Chinese Geophysical Society Annual Conference*.

Zhang Yunxia et al. 2004. The application of transient electromagnetic method in the work of mine flood damage control. *Chinese Journal of Engineering Geophysics*1(5): 418–423.

Progress in Mine Safety Science and Engineering II – He et al. (Eds)
© 2014 Taylor & Francis Group, London, ISBN 978-1-138-00122-0

Calculation of the natural wind pressure of mine based on working-condition adjusted of mine main fan

Li Chen
Hebei University of Engineering, Handan, Hebei, China

ABSTRACT: This paper states the theoretical basis and application method of using the working-condition adjusting of mine main fan to calculation of natural wind pressure, and tested and verified through the practice. Compared with the traditional calculation methods, this one overcomes the error and inconvenience of the traditional ones which derives from many factors. And verifying the method by using it in the engineering case, results show that it is a theoretically feasible, computing fast, accurate calculation method to calculate natural wind pressure.

1 INTRODUCTION

Natural wind pressure is the necessary data of the mine ventilation design and technical management of mine ventilation (Liu 2003). In the use of mechanical ventilation of mine, natural wind pressure can be both main fan ventilation with power, increase air volume of mine; and may be hampering the main fan ventilation resistance, reduce the air volume of mine, reverse, and even lead to safety accident (Liu 2005). The existence of the natural wind pressure will result in changes of the parameters of the mine ventilation network (Hu & Xu 2008), and has important influence on the stability of mining area romantic (Tan *et al*. 2005). So, accurately measure the size of the natural wind pressure mine, grasp its change law, it is of important significance for the mine ventilation design and ventilation safety management.

2 CHARACTERISTICS ANALYSIS ON NATURAL WIND PRESSURE TRADITIONAL MEASUREMENT

2.1 *Partition calculation method*

It is showed in figure 1. This method is also called the direct calculation method (Hu *et al.* 2009). After the fan is stoped, set up a seal in the total wind or use the gate is closed adit wind to partition wind flow, take advantage of the differential manometer to determine the sealed adit wall or wind pressure difference on both sides of the gate, the reading of the differential manometer is the natural wind pressure in mine. This method is simple, but you need to stop the fan, it is a great influence for production and safety in mine. And

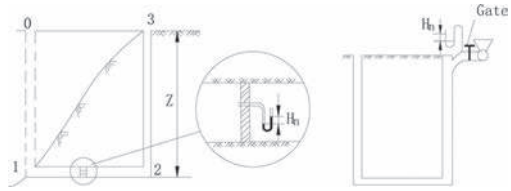


Figure 1. Calculation of the cutting airflow.

the fan is not allowed to stop, this method is inconvenient to use.

2.2 *Average density calculation method*

It is showed in figure 2. This method is also called the indirect calculation method (Hu *et al.* 2009). Through measuring the average density of roadway air flow to calculate the natural wind pressure of Mine. formula is:

$$H_n = gZ(\rho_{m1} - \rho_{m2}) \tag{1}$$

where H_n = natural wind pressure; g = acceleration of gravity; Z = height difference; ρ_{m1} = the average density of the inlet air; ρ_{m1} = the average density of the return air.

When this method is used, the fan can run normally, it does not affect the production and safety. But for the large depth, and a lot of roadway and complex ventilation system, you need to set up multiple measuring points, a heavy workload for measuring and computing is needed, and you will take a long time to measure the average density of the air. This method can not be directly concluded the natural wind pressure value of the ventilator in the multiple levels of multi loop ventilation system.

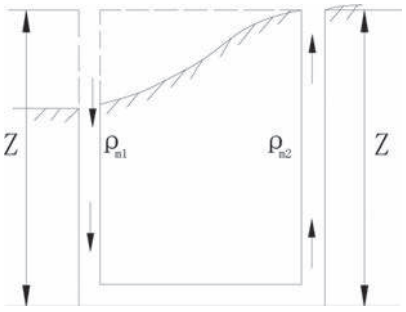


Figure 2. Calculation of the average density.

2.3 *reverse ventilation calculation method*

Using the data of the reverse ventilation in mine, according to the formula (2) to calculate the natural wind pressure of mine (Liu 2005, Liao 2013):

$$H_c = \frac{H_{yq} \cdot Q_c^2 - H_{cq} \cdot Q_y^2}{Q_c^2 + Q_y^2} \tag{2}$$

Where Q_c = mine air quantity of exhaust ventilation; Q_y = mine air quantity of reverse ventilation; H_{yq} = the relative total pressure in mine of reverse ventilation; H_{cq} = the relative total pressure in mine of exhaust ventilation.

This method needs the data of the exhaust ventilation maneuver, but the cycle of the exhaust ventilation maneuver in mine is too long, so the application of the method is restricted.

In addition, there is "Komarov" experience formula method (Bao 2000), but the error of this method is too big.

In view of the above shortcomings of the methods of natural wind pressure calculation, in order to adapt to the condition of large coal mine of natural wind pressure calculation, such as multi levels, well depth, tunnel complex, it can adjust the fan operation condition to calculate mine natural wind pressure, This method can make up the shortcomings of traditional method, realize the accurate and rapid computation.

3 THE THEORETICAL BASIS ON WHICH CALCULATING NATURAL WIND PRESSURE BY ADJUSTING OPERATION CONDITION OF THE FAN

It is necessary to adjust the operation points of the fan usually because of the changes of fan performance and the changes of natural conditions, such as the increase or decrease of the extracting coal face length, the metastasis of the extracting coal faces, the changes of gas emission. It is one of the convenient conditions to calculate natural wind pressure by working-condition adjusted of the fan.

In the mines ventilated by mechanical power, ventilation resistance of the mine is over comed by combination of the static pressure of fan and the natural wind pressure, with the joint effort of which the ventilation process is accomplished.

According to the resistance law:

$$H_n + H_f = R_m Q^2 \tag{3}$$

Where H_f = Fan's static pressure; R_n = Mine's total wind resistance; Q = Mine total air volume.

In the formula (3), H_f and Q can be measured directly, H_n and R_n are unknown. Adjusting operation point of fan, H_{1f} and Q_1 which correspond to H_f and Q can be obtained, substituting H_{1f} and Q_1 into formula (3).

$$H_n + H_{1f} = R_m Q_1^2 \tag{4}$$

Combining equations (3) and (4), and solving the natural wind pressure, that is

$$H_n = \frac{H_f - H_{1f}}{Q^2 - Q_1^2} Q^2 - H_f \tag{5}$$

The formula (5) is the theoretical basis on which calculating natural wind pressure by adjusting operation points of the fan.

In order to reduce error, the operation points of fan can be adjusted two times, three times or n times, therefore, different H_{2f}, H_{3f}, ……, H_{nf} and Q_2, Q_3, ……, Q_n can be obtained. Similarly, different equations can be obtained.

$$H_{2n} = \frac{H_{1f} - H_{2f}}{Q_1^2 - Q_2^2} Q_1^2 - H_{1f}$$

$$H_{3n} = \frac{H_{2f} - H_{3f}}{Q_2^2 - Q_3^2} Q_2^2 - H_{2f}$$

$$H_{nn} = \frac{H_f^{n-1} - H_f^n}{(Q^{n-1})^2 - (Q^n)^2} (Q^{n-1})^2 - H_f^{n-1}, (n = 1,2,3,\cdots,n) \tag{6}$$

To ensure accurate results, calculating the average for its many times, that is

$$\bar{H}_n = \frac{H_n + H_{2n} + \cdots + H_{nn}}{n}, (n = 1,2,3 \ldots, n) \tag{7}$$

4 APPLICATION PROJECTS

Now, taking the data which is tested by working-condition adjusted of fan three times in a mine

for example to describe application steps and processes which calculating natural wind pressure by working-condition adjusted of fan.

In the data obtained by working-condition adjusted of fan, extracting 3 sets of data of wind pressure and air volume, numbering and grouping them successively, dividing the data for each test into A, B, C three groups.

Combining arbitrary two sets of data like AB, AC, BC of wind pressure and air volume, substituting them into equation (5) and calculating, a set of data on natural wind pressure can be obtained. To reduce calculation error and ensure accurate results, the data can be combined many times to be calculated, and be substituted into equation (7), finally, the average value can be obtained. Calculation results are shown in table 2.

Compared with the calculation results in table 2 and the results calculated by traditional density calculation method, the comparative analysis on the error is shown in table 3.

Table 1. The performance test data of the axial flow fan in one mine.

The number of tests	The adjustment of operation condition	Sets of data	Static pressure of fan (Pa)	Air volume of fan/ (m^3/s)
1	1	A	1646.73	60.73
	2	B	1775.08	62.99
	3	C	1919.26	65.43
2	1	A	1982.53	42.62
	2	B	2129.57	44.21
	3	C	2378.57	46.78
3	1	A	1769.95	44.35
	2	B	1968.73	46.69
	3	C	2098.67	48.16

Table 2. Calculation and error analysis of natural wind pressure of mine.

The number of tests	The combination of data	Natural wind pressure (Pa)	Average value (Pa)
1	AB group	46.259	48.419
	AC group	48.393	
	BC group	50.605	
2	AB group	–47.911	–48.154
	AC group	–48.180	
	BC group	–48.371	
3	AB group	65.370	64.234
	AC group	64.474	
	BC group	62.859	

Table 3. The comparative analysis on the error.

The number of data	Natural wind pressure/Pa		Relative error/%
	Traditional algorithms	Working-condition adjusted method	
1	48.957	48.419	–1.11
2	–49.032	–48.154	–1.82
3	62.978	64.234	1.96

5 CONCLUSIONS

Using the method of working-condition adjusted of mine main fan to calculate natural wind pressure of mine can make calculation convenient, time-saving and accuracy, besides, the approach has a solid theoretical foundation, it is a new mean and method to calculate natural wind pressure. It can not only test the performance of main fan in mines but also calculate the natural wind pressure of mine, to be more important, it can provide accurate basis for management of ventilation equipments.

The data must be integral and rational when using the working-condition adjusted of main fan to adjust data. To ensure the accuracy of the results of natural wind pressure, a few more sets of data can be chosen to calculate respectively, finally, the average value can be obtained.

REFERENCES

Bao, G.C. 2000. The indirect calculation of natural wind pressure and curve drawing. *Coal mine safety,* 30(3):3–5.

Hu, M.S. & Xu, W.Z. 2008. A study of the effect of natural wind pressure on the ventilation network's stability. *Coal engineering*, (11):72–74.

Hu, W.M. et al. 2009. *Mine ventilation and safety*. Xuzhou: China university of mining press.

Li, L. 2013. Research and application on the method which to calculate natural wind pressure of mine. *Energy technology and management,* 38(1):79–81.

Liu, C.S. 2003. The calculation of natural wind pressure. *Coa*, l(1):12–15.

Liu, D.W. 2005. A method which to calculate natural wind pressure of mine through reversing ventilation. *Coal mine safety,* 36(7):10–13.

Tan, Y.Z. et al. 2005. The effects of natural wind pressure on the stability of the mining face's ventilation system and the prevention methods. *The journal of Shandong university of science and technology (natural science edition)*, 24(4):7–16.

This page intentionally left blank

Progress in Mine Safety Science and Engineering II – He et al. (Eds)
© 2014 Taylor & Francis Group, London, ISBN 978-1-138-00122-0

Study on new hydraulic support and technology of top-coal caving at the ends of fully-mechanized working face

Yude Liu
Key Laboratory of Mine Disaster Prevention and Control, Yanjiao, Beijing, China
College of Safety Engineering, North China Institute of Science and Technology, Yanjiao, Beijing, China

ABSTRACT: Based on the top-coal caving fully-mechanized working face No. 43B2 at Wangzhuang Coal Mine, we have analyzed the moving law of overlaying strata above the ends of working face, and determined the relationship between the end-support and surrounding rock, and designed the new top-coal caving hydraulic end-support i.e. the host-vice transitional inner-end-support and the symmetric end-support, and then mathematical simulated and analyzed the caving character of top-coal at the ends of working face. We have solved two key problems in the design process of end-support; one is that the end-support has enough space to place the rear conveyor of working face, other one is that the loose drop-coal on the floor can be carried into the high troughs of conveyor head and tail. The core content of new end-support includes the low coal-raking system which has the tilt scraper and the symmetric pair wheels and the high coal-caving system which has the unsymmetrical pair-open troughs. It should improve the coal recovery significantly, produce good economic and social benefits, and have very important significance and broad application prospect that to solve the difficult problem of top-coal caving at the ends of fully-mechanized working face.

1 INTRODUCTION

Since 2000, the fully-mechanized top-coal caving mining technology has become main method of thick coal seam in China which has basically instead of the fully mechanized layered mining and its application range is growing.

At present, the recovery rate of top-coal caving mining is not high, is relative less than of layer mining. The loss rate which makes the recovery rate of fully mechanized top-coal caving working face to be averaged 81~83% contains process loss about 7~12%, initial and ending cutting loss about 1%, two ends loss about 4~5%.

The layout of head, tail and transmission device of front and rear conveyors needs a large support space and high support strength, and makes the process more complex. On the other hand, the ends of working face are more difficult to maintain at the condition of top-coal caving. So the ends of fully mechanized top-coal caving working face used to be support by no-caving or less-caving traditional support mode such as individual hydraulic prop, bolt supports, common hydraulic supports or transitional supports and so on.

In order to achieve the purpose of high production and efficiency, it is inevitable trend that using hydraulic end-support at ends of working face which can be put down top-coal and favorable support. Therefore end-support can produce remarkable economic and social benefits, has very important significance and broad application prospect.

2 RESEARCH FOUNDATION

The fully mechanized working face No. 43B2 which is buried depth of 237~256 m exploits 3# coal seam. This coal seam deposits in Shanxi Group of Permian system, is thickness of 7.4 m and an average angle of 3.5°. The rock character of roof and floor can be seen in Figure 1.

Serial number	Roof and floor	Average layer thickness /m	Histogram	Strat name	Petrographic description
1	Basic strata	3.70		Fine sandstone	Gray, fine grain, composition of quartz, feldspar. Contain mica piece.
2	Immediate roof	3.30		Mudstone	Black, compact, and including a large number of plant fossils
3	Coal seam	7.40		3' coal seam	Coal seam structure /m 0.55 (0.05) 0.29 (0.22) 4.08 (0.06) 0.53 (0.12) 0.8 (0.03) 0.67
4	Immediate floor	0.90		Mudstone	Black, compact, and including plant fossils
5	Basic floor strat	1.60		Fine sandstone	Gray, fine grain, composition of feldspar, quartz. Contain mica piece.

Figure 1. Strata histogram of working face No. 43B2.

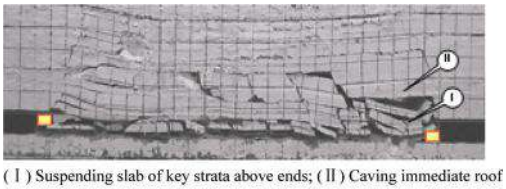
The ratio of mining and caving is 1: 1.3, and the caving step distance is 0.8 m. The working face's roads are supported by the combined support mode of bolt and anchor-cable. The hydraulic supports among working face are ZFS-6000/17/33 type, are amount of 131 supports in the longest section of working face. Three supports are laid at each end of working face which is 6500/20/32 type.

3 STRUCTURE CHARACTERISTIC ABOVE THE ENDS OF FULLY-MECHANIZED TOP-COAL CAVING WORKING FACE

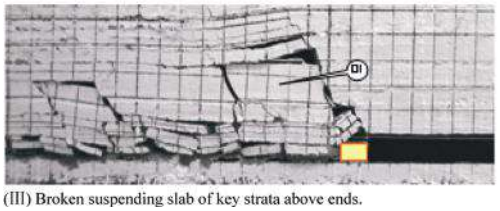
After top-coal caving, above the ends there is a certain area of hanging slab which is periodically broken and hinged joint to rock-mass of goaf along with the advancing of working face.

This is shown in Figure 2.

Above the ends of working face, the roof strata can form a structure of arc triangle suspension slab which is as shown in Figure 3, and be supported mainly by the ends' supporting, coal wall front of working face, waste rock rear of working face, and protective pillar of roadway.



(I) Suspending slab of key strata above ends; (II) Caving immediate roof



(III) Broken suspending slab of key strata above ends.

Figure 2. Caving characters of overlying strata above the ends of fully-mechanized top-coal caving working face.

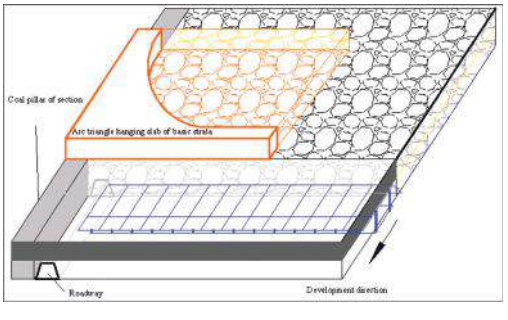


Figure 3. The structure of arc triangle hanging slab above ends of working face.

Therefore at the conditions of top-coal caving, there may be two relations as follows between supports and surrounding rock:

a. "Supports and cracking rock" structure: the triangle suspension slab has hinged structure with the fracture rock inside goaf. Under the cover of slab, the collapsed loose body of immediate roof and coal may pile up on the supports naturally.
b. "Supports and cracking rock and rock beam" structure: The fractured arc triangle slab, which its' two ends hinge to the fracture rock of goaf and the no-broken rock strata above the pillar of roadway, forms a monoclinic hinged structure.

4 NEW HYDRAULIC END-SUPPORT OF TOP-COAL CAVING AT ENDS OF WORKING FACE

According to the falling features of overlying strata and top-coal above the ends of working face, we have developed the new hydraulic supports which can make the top-coal to cave at the ends of working face. The collocation mode of those supports is as shown in Figure 4.

4.1 *Key problems*

To achieve the purpose of top-coal caving at the ends must solve two key problems:

a. End-support has enough space to place the rear conveyor.
b. The loose cracking coal on floor can be carried into the troughs of conveyor head and tail.

4.2 *Host-vice type transitional inner-end-support*

The stereo effect of transitional inner-end-support is as shown in Figure 5.

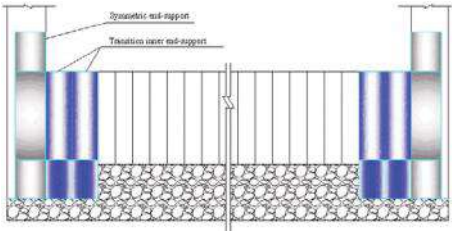


Figure 4. The layout of new end-supports at ends of working face.

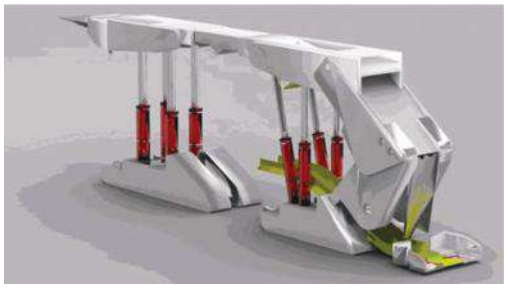


Figure 5. Virtual effects of host-vice type transitional inner-end-support.

4.2.1 *Host-vice type*

It makes the rear scraper conveyor to locate in a larger space that adding a vice support behind the normal (host) support. See Figure 6.

4.2.2 *Low coal-raking system*

The coal-raking system with tilt scraper and symmetric wheels is put under the low coal-caving window, rakes the cracking drop-coal on the floor into the high troughs of scraper conveyor's head and tail.

The system consists of high segment, middle segment and low segment. The low segment is joined to the base of supports. The high segment hinges to the trough ledge of scraper conveyor in the way of sliding round, and hinges to the middle segment in the turn way. The dip angle of the middle segment isn't more than 25°. See Figure 7.

4.2.3 *High coal-caving system*

The coal-caving system with unsymmetrical pair open troughs (one longer and one shorter) is designed in the middle of support's top beam. The open troughs joins to support's top beam in the way of sliding round, in order to adapt to the continuous caving of top-coal at different location of scraper conveyor.

The single open directional moving baffle plate is installed at the side of shorter trough, in order to improve the efficiency of coal loading, while at the same time the fixed baffle plate is installed at one trough ledge of scraper conveyor. See figure 8 shown.

4.3 *Symmetrical-type end-support*

Base on the host-vice transitional support, it is consisted of similar symmetrical end-support that to add an inverted part of support at roadway area. The virtual effect of symmetric-type end-support is as shown in figure 9. Its principle and size data of the low coal-raking system and the high coal-caving system are basically same as the transitional inner-end-support.

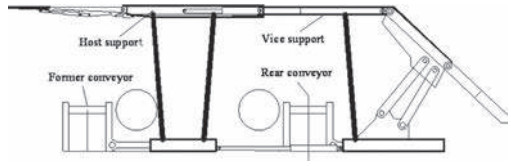


Figure 6. The space relation between supports and conveyors at ends of working face.

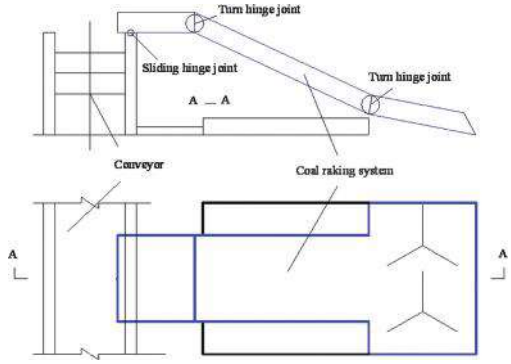


Figure 7. The coal-raking system with tilt scraper and symmetric wheels.

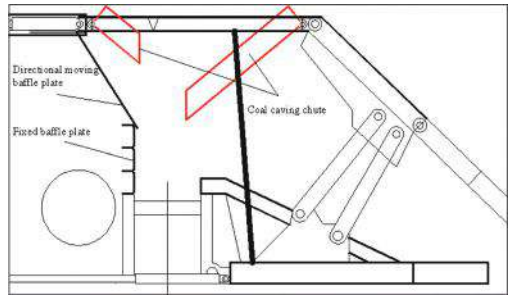


Figure 8. The coal-caving system with unsymmetrical pair open troughs.



Figure 9. The virtual effect of symmetric type supports at ends of working face.

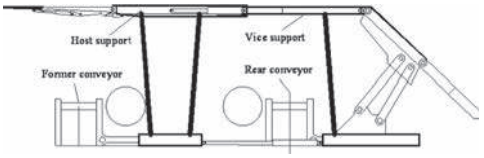


Figure 10. The structure of symmetrical end-support.

The inverted part of support plays an advance supporting role to improve processing efficiency, safety and reliability of the working end; on the other hand, improves the stability of overall support, see Figure 10.

4.4 *Basic parameters*

4.4.1 *Working resistance*

The reasonable working resistance of support can be calculated by Load Estimation Method and Theoretical Analysis Method.

The need working resistance of support is as follows by Load Estimation Method:

$$P_1 = 642.32 \times 9.0 \times 1.5 = 8671.32 \text{ kN} \quad (1)$$

While, the need working resistance is as follows by Theoretical Analysis Method:

$$P_2 = 5939.4 \text{ kN} \quad (2)$$

Therefore, the support resistance of new hydraulic end-support of fully-mechanized top-coal caving working face should be more than 8672 kN/frame.

4.4.2 *Initial support force*

Initial support force should not be too big, generally is not less than 60% of working resistance.

According to the geological conditions of Wangzhuang Mine, the initial support force takes 80% of working resistance of new end-support i.e. 6937 kN/frame.

4.4.3 *Structure height*

The height of end-support may be determined by the structural thickness of coal seam. According to the domestic experience and the size of basic supports in 43B2 working face, the minimum support height of new end-support is 1.90 m, and the maximum is 3.90 m.

4.4.4 *Structure width*

According to the theory and mining practice of top-coal caving, the short axis Lb of ellipsoid in top-coal caving space can be calculated by the following formula:

$$L_b = (0.15 \sim 0.21)\, h \quad (3)$$

In the formula: L_b is ellipsoid's short axis, m; h is the top-coal caving height, m.

To take the condition of 3# coal seam into the formula gets the conclusion:

$$L_b = 0.585 \sim 0.819 \text{ (m)} \quad (4)$$

The reasonable support width and caving step distance should be integer times of L_b in order to achieve the maximum limit of top-coal caving. So, the width of new end-support is chosen to 1.75 m.

5 ANALYSIS OF TOP-COAL CAVING CHARACTER AT WORKING FACE ENDS

It is calculated and analyzed by UDEC3.0 software that the six main influence factors of top-coal caving character i.e. the mining-caving ratio,

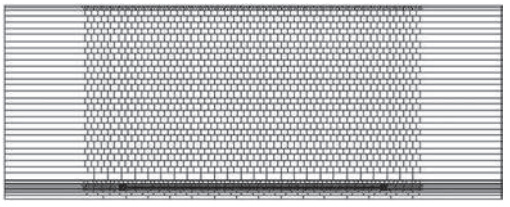


Figure 11. The model of numerical simulation.

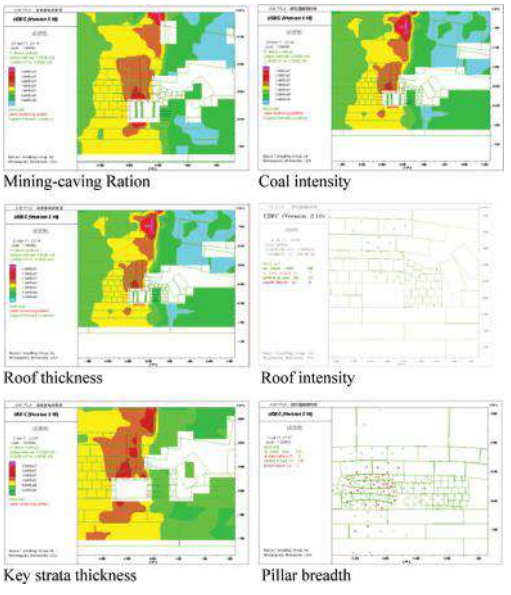


Figure 12. Some demonstration of mathematical simulation results of top coal caving characteristic at ends of fully-mechanized working face.

Table 1. The influence law of top-coal caving at ends of fully-mechanized working face.

Effect factor	Simulation scheme	Influence law
Mining-caving ratio	1:1, 1:2, 1:3 (Coal thickness is 7.4 m).	The ratio of mining and caving height is the bigger, and the caving of top coal at ends is the better.
Coal intensity	f = 1.5, 2, 3, 4 and 5 (Mining-caving ratio is 1:2).	The Coal intensity is the bigger, and the caving of top coal at ends is the more poor.
Roof thickness	38 m, 28 m and 4 m (mining height is 7 m).	When the immediate roof thickness is not enough to be full of the goaf, the immediate roof thickness is the bigger, and the caving of top coal at ends is the weaker. Otherwise the thickness of immediate roof has less action on the top-coal caving.
Roof intensity	20 MPa and 30 MPa (coal intensity is 20 MPa).	It goes against the top-coal caving that when the immediate roof strength is less than coal seam strength, otherwise is in favor of the top-coal caving. And it makes the immediate roof and top-coal to deform and destroy integrally that when the immediate roof strength equals to coal seam strength.
Key strata thickness	3 m, 4 m and 8 m (roof thickness is 4 m).	The key strata thickness is the bigger, and the carrying capacity of key strata's arc triangle slab at ends is the stronger, and the caving of top-coal is the weaker.
Pillar breadth	No mining; leave lane along goaf; pillar breadth is 5 m, and 30 m respectively.	The breadth of coal pillar is the smaller, and the breakage of top-coal is the more serious, and the caving of top coal is the easier, and the support of ends is the more difficult.

immediate roof thickness and strength, key strata thickness, coal seam intensity, coal pillar width etc. The numerical calculation model is shown in Figure 11. Its floor boundary is vertical fixated, and both side boundaries are horizontal fixated. Material constitutive model is Moore-coulomb model.

The simulation process is as follows: from the equilibrium calculation of original rock stress to the calculation of bolt support along with roadway excavation, then to the cutting advance of top-coal caving working face, and to the output of result. Part of the calculation results is shown in Figure 12.

The top-coal caving law at the ends of fully mechanized face can be obtained by summary of simulation results, and seen Table 1.

6 CONCLUSIONS

New top-coal caving end-support has the coal-caving system and the coal-raking system. This end-support is an innovation of top-coal caving hydraulic support, and can improve the recovery of coal, and make the distinct economic and social benefits.

At the condition of top-coal caving, the overlying strata can form the arc triangle slab which may break periodically at the ends of working face.

By the application and observation of top-coal caving at the ends of 43B2 working face, it is known that the periodical pressure step is average of 14.3 m, and the biggest incidence is average of 2.05 m, and the excessive amount of recovery coal is 54966.6 t, and the recovery rate is improved about 5.8%.

ACKNOWLEDGEMENTS

Financial support for this work, provided by NCIST Research Fund Project (Title: Preliminary Study on Mechanism and Technology of Aquifer-protective Mining in Shallow Coal Seam, 2009) and NCIST Teaching Research Project (Title: The Optimization Research of Teaching System Based on Enterprise and Student Feedback Information, 2011; the fundamental research funds for the

central universities, No 3142013035) is gratefully acknowledged.

REFERENCES

Chen J B, et al. 2008. The implementation and study of end support at top coal caving fully-mechanized workface. *Coal Science & Technology Magazine*, 14 (2): 33–37.

Dai J, et al. 2004. Elastic analysis of suspended triangle roof plate with curve side on the end of sublevel caving mining face. *Chinese Journal of Rock Mechanics and Engineering*, 23 (2): 16–21.

Du J P, et al. 2009. Mining Science. Xuzhou: China University of Mining & Technology Press.

Li C J & Li S W 2008. Roof control technology for large unsupported roof at face end of coal mining face. *Coal Science and Technology.* 36 (8): 26–30.

Liu Y D, et al. A new type of hydraulic end-bearing supports for fully-mechanized top caving working face. *Patent: 201010586162.X. 2010*.

Ma Q Y, et al. 2001. Break of main roof ahead of workface and ground pressure. *Journal of China Coal Society*, 26 (5): 473–477.

Qian M G, et al. 2000. Key Strata Theory in Underground Control. Xuzhou: *China University of Mining & Technology Press*.

Qin L Y & Zhang L Y 2000. Study on the roof structure and stability of fully-mechanized coal face End, *Coal Science & Technology Magazine* 6 (3): 14–16.

Wei J P, et al. 1999. The experimental studies of rock pressure during fully mechanized mining with sublevel caving. *Journal of Taiyuan University of Technology*, 30 (3): 331–335.

Zhu H C, et al. 2004. Numerical modeling methods and application for jointed rock mass, part 2: application in engineering practice. *Chinese Journal of Rock Mechanics and Engineering*, 23 (20): 3444–3449.

Progress in Mine Safety Science and Engineering II – He et al. (Eds)
© 2014 Taylor & Francis Group, London, ISBN 978-1-138-00122-0

Study of reliability of on-line monitoring system for mine hoist braking system

Hong-Bing Qiao, Kai Liu, Yi-Lun Wang & Hua Yu
China University of Mining and Technology (Beijing), Beijing, China

ABSTRACT: The reliability of the mine hoist braking system, directly determines the coal production safety and worker safety in the hoisting transportation process. This paper proposes an on-line monitoring system of mining hoister braking system based on fault tree analysis, which sets up the fault tree of the mine hoist braking system and determines the monitoring points. We design the on-line monitoring system of mining hoister braking system based on Siemens's PLC. The monitoring system capable of providing on-line monitoring and providing HCI (Human-Computer Interaction) can be used as the assisting tool of running and maintenance of the hoister.

1 INTRODUCTION

The reliability of the mine hoist braking system, directly determines the safety of workers in the process of transportation. Relevant data show that coal mine safety accidents caused by the braking system failure account for over 60% of the total mine accidents, having caused great economic losses and casualties.

More and more enterprises want to be able to schedule maintenance in time, to realize the predictive maintenance, to manage the equipment more effectively, to curb accidents, and improve the comprehensive benefit of enterprises according to the braking system the real-time state of work. Therefore, mine hoisting mechanism system real-time monitoring equipment based on modern monitoring technology must be developed. The traditional mechanism of hoist braking system can judge one single limitation. When the abnormal occur, simple alarm instructions come into use. This pattern cannot systematically, scientifically reflect the reliability of the mechanism of the whole hoist braking system so that great potential safety hazard exists in the production process. The comprehensive evaluation of the reliability of the hoist braking system should be employed, thus establishing fault tree of the mechanism of hoisting braking mine system security to determine various monitoring points.

Using Siemens PLC as the core, designs the real-time monitoring system of the hoist braking system, which can be used as a staff member to management and maintenance of auxiliary hoist analysis tools. The main features include real-time online monitoring, human-computer interaction interface.

2 FAULT TREE OF HOIST BRAKING SYSTEM

2.1 *Modeling of the fault tree analysis of braking safety system*

Insufficient braking torque is the major failure of mine mechanism dynamic system through summarizing dynamic failure caused by the mine accident reasons of the hoist braking mechanism. All the fault parameters of each parameter is not isolated, but interrelated and interacted in the braking process. Fault tree analysis is intuitive, flexible, convenient and universal, especially suitable for the failure analysis and research of braking system. Therefore, by using the fault tree analysis method in this paper, deduce the braking safety failure events graphically, analyze and reason the system fault and failure of the system components relates in together organically, find out all the reasons causing brake failure, evaluate the reliability of braking system. (Zhang 2007).

2.2 *The determination of monitoring points*

To determine the reasonable monitoring point is the key to the successful monitoring system, all other work is for its services. Reasonable monitoring stations can be determined through shoe safety fault tree analysis and the point of geometric and physical relationship. Indirect monitoring points are derived from the direct transformation of monitoring data.

Experience reference points are determined by the experience of the field specialist.

Indirect monitoring: shoe clearance (4 groups), brake shoe wear and tear (4 groups), state of

spring (group 4), temperature rise rate of brake rubber blocks (4 groups), change rate of the working oil pressure, oil pump reaction time (2 groups), export/working oil pressure differential, the deflection of brake disc, symmetrical gap (4 groups).

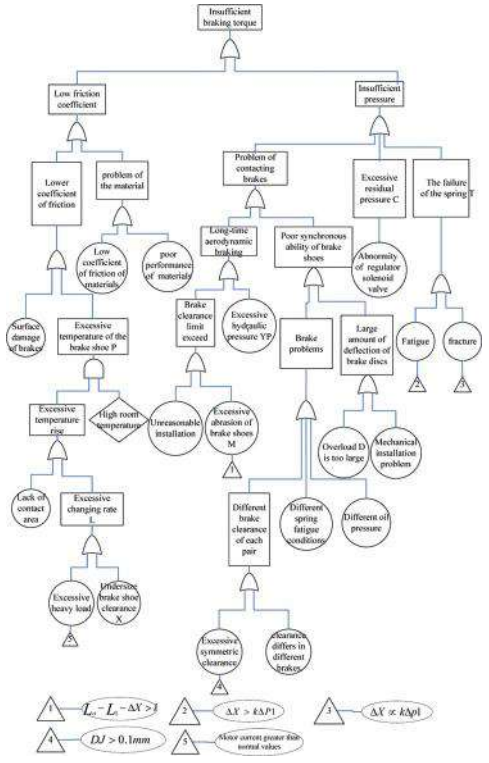


Figure 1. The Security fault tree of hoist braking system.

Experience reference points: shoe quality, spring time, installation of brake shoe, brake disc.

The nature of the brake-shoe is easy to loss, which directly indicates that the block has the characteristics of real-time relative variations. Clearance of the brake shoe is a very active parameter. The deflections of brake disc, the oil pressure of the hydraulic pressure station and degree of the fatigue and damage of the disc springs also have effects on it. The direct reaction in the braking system is reflected by the performance of the brake shoe clearance. So the clearance of the brake shoe is the key parameters of safety of real-time monitoring of brake shoe.

Mathematics and physics relationship between Indirect monitoring points and direct monitoring points monitoring are as follows:

Brake clearance: L; Brake shoe clearance: X = L.

Symmetrical clearance: DJ = Xa – Xb

Xa/Xb are same set of brake shoe clearance respectively.

$$\begin{cases} \Delta X = k\Delta P1 \\ \Delta X = \chi_n - \chi_1 \end{cases}$$

Spring deformation caused by difference of oil: ΔX

ΔP1 = P1n–P11, P1n, P11 are the working oil pressure when the brake loose brake at 1/n times respectively; x1, xn are brake clearance when loose the brake after braking at 1/n times respectively.

Disc spring deformation:

$$T = \begin{cases} \Delta X > k\Delta P1 & (\text{Spring fatigue}) \\ \Delta X \propto K\Delta P1 & (\text{Spring fracture}) \end{cases}$$

Differential pressure: JP = CP – YP YP is the hydraulic station when brake is in loose condition.

Table 1. Direct monitoring points.

Monitoring points	Monitoring sensor type	Sensor installation
Brake clearance L (4 groups)	High-frequency eddy current sensor	Sensor installed on the brake block, surface parallel to the brake shoe back
Skin temperature of brakes (4 groups)	Infrared temperature sensor	
The oil pressure of the hydraulic pressure station YP	Hydraulic sensor	The installation of main loop of the hydraulic station
Safe brake hydraulic pressure on Level 1 ZP	Hydraulic sensor	Pipeline of spring energy accumulator in tube B
Hydraulic pressure of hydraulic station export CP	Hydraulic sensor	Installation of the hydraulic pump inlet
Load current D	AC current sensor	Ammeter circuits
Oil temperature of the Tank YW	Thermocouple	Installation of the tank
Room temperature	Thermocouple	

The residual pressure: oil pressure in the hydraulic station when braking.

The deflection of brake disc: PB = MAX(ΔX), ΔX is for the clearance of symmetric brake shoes.

Temperature rise of Brake shoe: S = J – W.

Temperature rise rate of brake shoe: L = S/t1, t1 is sampling time.

Rate of oil pressure change in hydraulic station: YPL = ΔYP/t2, t2 is the sampling time.

3 DESIGN OF MONITORING SYSTEM

3.1 *Design of system function*

This system can be used as management and maintenance of auxiliary analysis tools of hoist machine for the staff, so as to curb major accidents and prolong the service life of equipment, and ensure the normal production. The purpose of its main features includes real-time online monitoring and human-computer interaction. (Qiao et al. 2010).

3.1.1 *The function of the real-time online monitoring*

Monitoring system requires for real-time monitoring on the mechanism of dynamic system, and processors are applied to collect data for analysis, judgment. When the clearance of brake-shoe exceeds the specified value or the symmetrical clearance of brake-shoe exceeds threshold value or hydraulic pump station works abnormal, various kinds of fault conditions can trigger alarm or forecasting warning. This has the following functions to the coal mine production work:

1. Remind staff in a timely manner to adjust and repair the equipment, ensures reliable braking brakes, and ensure safety in production enterprises.
2. Ensure brake-shoe clearance and Symmetrical clearance of each pair, to guarantee the braking stability, so as to prolong the life of the hoist mechanical system, reduce the major security incidents caused by the damage of roller and reducer. At the same time, for real-time and high precision monitoring of brake shoe wear and tear, it can replace mechanical switch for wear of brake shoe.
3. Ensure the reliable operation of the hydraulic pump station, make the staff in a timely manner to maintain and improve its reliability and service life.

3.1.2 *The human-computer interaction interface function*

In order to highlight the principle of "people-oriented", humanization interface is set up to facilitate staff to maintain and manage the mine hoist. It provides staff with comprehensive, intuitive information, to ensure that the hoist system for efficient maintenance and management.

3.1.3 *The selection of the main controller*

Main controller is the core of the monitoring system, which determines the design of the hardware system and software system the whole monitoring system of. So the type of main controller should be firstly determined, and then to determine the implementation scheme of the whole system based on the selection of main controller. Currently, microcontroller, DSP and programmable controller (PLC) is widely used. Having compared the performance of the three, PLC facilitate to the subsequent development of system, is more suitable in the mine production environment. So PLC is elected as main controller system.

3.2 *Design of the hardware system*

The designs of hardware system and type selection directly influence the overall performance of the system. This section details design principles of the hardware circuit, aiming at the need of function of the modular design. Touch screen with PLC is used as the main scheme, and it introduces the selection of the main function module, performance and advantages.

3.2.1 *The CPU module*

S7–200 series PLC is developed and produced by Germany's Siemens Company, which is a small modular PLC with stacked structure. PLC S7-200 PLC not only has the basic control functions, but also characterized by compact structure, low cost, strong communication and network. It can be applied for simple control situation, suitable for the complex automatic monitoring and control system; can also make network control system, which has the very high performance price ratio. The model number of this article chooses—CPU226 is the most advanced CPU of S7-200PLC series. (Chen 2009).

3.2.2 *The main function module*

System configuration is the first step in using PLC. It is the key step of allocation of appropriate systems to give full play to the function and effect of PLC to achieve better economic benefits. The CPU module, power module, memory and extension module should put into comprehensive consideration when carrying on the system configuration. It neither lost any item in system configuration, but also is higher than the user's actual requirements.

3.2.3 *Selection and installation of sensors*

According to the specific purpose, objects and environment, selecting the appropriate sensor is the primary problem when measuring a certain value. Effect of the measurement depends largely on whether the selection of sensors is suitable.

1. Considering the working environment and the actual condition of mine production, where the characteristic is full of dust, high variation in relative temperature and humidity, this article selects the high precision non-contact eddy sensors to ensure the accuracy of measurement. This type of sensor is divided into high frequency reflection type and low frequency transmission type two kinds. Considering the object to be tested—the physical structure of disc brake, high frequency reflection type is optimal. (Wang 2004).
2. The system selects the IRTP series sensor to monitor the temperature of the brake shoe. IRTP sensor series are economical temperature sensors. Monitoring accuracy is not affected by pollution, moisture and the influence of electromagnetic interference environment.
3. HYDAC ETS4000 series temperature sensor is chosen for the oil temperature.
4. Hydraulic sensor selects CYAT type pressure sensor, which has high measuring accuracy, stable and reliable performance, good sealing performance.
5. Use thermocouple to measure the hydraulic oil temperature and room temperature.
6. We choose HB1701S series DC power supply produced by Shanghai FUJIDQ electric company as system sensor power source. The output voltage can be freely chosen from 0~30V, and output current can be continuously adjusted within 0~30 A.

3.3 *Design of the software system*

PLC of S7-200 series apply software STEP7-Micro/WIN32 software to complete programming, alignment, and online monitoring.

3.3.1 *Design of the sampling programs*

Monitoring points of monitoring safety system of the mine hoist use signal sampling process shown in figure 2, to reduce the errors affecting the decisions of the system.

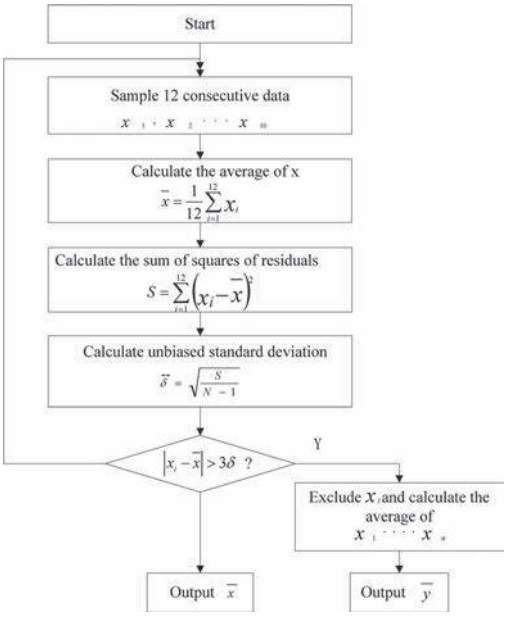


Figure 2. Signal sampling process.

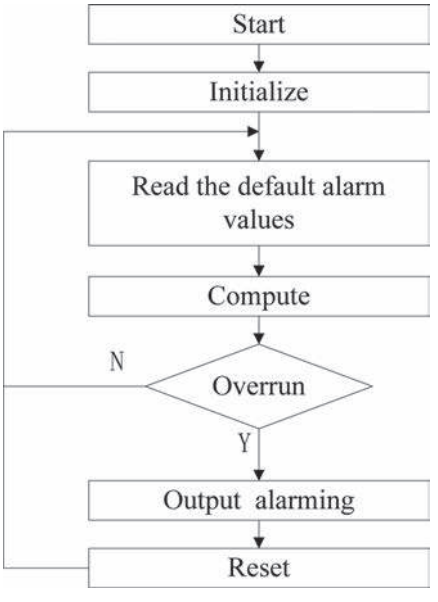


Figure 3. The main flow of alarming.

3.3.2 *Design of the alarm system*

Alarm program for braking safety monitoring system is very important. PLC system is required for logic operation and it sends the signal into human-machine interface. According to the relationship of direct monitoring points and indirect monitoring points, the state of alarms can be determined. It includes the following aspects: the brake clearance alarm, residual pressure alarm, oil pressure alarm, disc spring state alarm, excessive brake shoe wear alarm, oil filter state alarm, brake shoe temperature alarm, the oil temperature alarm, over-

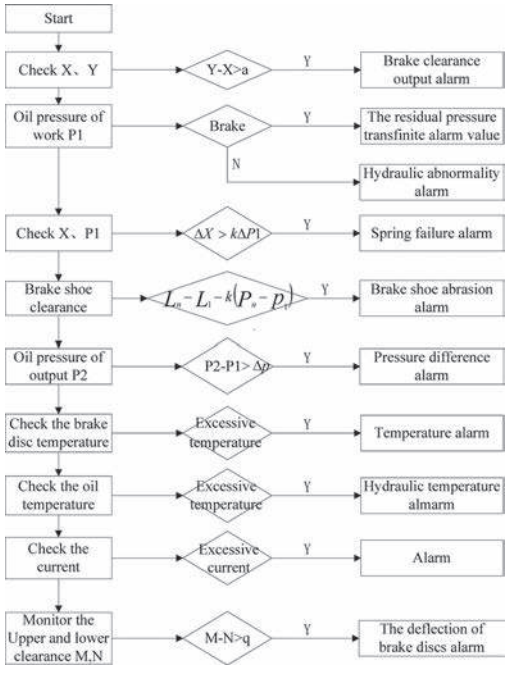


Figure 4. The flow of alarming.

load alarm and deflection of brake disc overload alarm.

3.3.3 *Design of man-machine interface*

Man-machine interface development environment of the brake safety monitoring system:

SIMATIC WinCC Flexible is a kind of innovative HMI software under Windows, which is used in control and automated monitoring process in the factory. All this engineering software allows for configuration in operator panel based on SIMATIC HMI (Windows) - from the control panel of minimal solutions to the PC. (Shijian Luo & Shouqian Sun 2002).

Brake safety monitoring system of human-machine interface mainly includes display, query functions, operating permissions. Show features include display parameters of monitoring system in real time, display and indicated the situation of braking system failures, historical curve of monitoring parameters. Query function is able to refer the braking system failure records at any time. Operation permissions is set up in order to ensure relevant staff only to view or modify the information of the monitor system, such as settings of the alarm values.

REFERENCES

Dongya Chen, 2009 Application of PLC in mine hoist control system. *Electronic Technology; 2009: 47–48.*

Hongbing Qiao et al. 2010. The Safety Monitoring System for Mine Hoisting Machine Brake Shoes. *ICEEE2010, Volume 7.*

Liqun Wang 2004. Monitoring method of the disc brake clearance based on eddy current sensors. *Coal Mine Machinery: 122–123.*

Meng Zhang 2007. Causes of hoist braking failures and preventive measures. *Sci-Tech Information Development & Economy: 270–271.*

Shijian Luo & Shouqian Sun 2002. *The man-machine interface design*. Beijing: Mechanical Industry Press.

Shuguang Wang et al. 2007. *S7–200 PLC application basis and examples*. Beijing: People's Posts and Telecommunications Press.

Yanjie li et al. 2008. *S7-200 PLC principles and practical guide for development*. Beijing: Mechanical Industry Press, 2008.

This page intentionally left blank

Progress in Mine Safety Science and Engineering II – He et al. (Eds)
© 2014 Taylor & Francis Group, London, ISBN 978-1-138-00122-0

Study on the prediction model of gas emission for coal beds based on the EMD and BP-ANN

Li-Ning Zhang & Da-Chao Lin
North China Institute of Science and Technology, Architecture Engineering College, Yanjiao, Beijing, China

Jing An
North China Institute of Science and Technology, Telecommunications College, Yanjiao, Beijing, China

ABSTRACT: Based on the research of existing gas emission methods and technique, this paper firstly points out the problems of present prediction ways for gas emission. Takes the coalface gas emission of a coal seam as example, collects its gas emission measured data. On this basis, the prediction model of gas emission for coal beds based on the EMD and BP-ANN set up, the intrinsic mode functions, that is, IMF components, are obtained by the EMD analysis of the historical recording dada of gas emission, and after the prediction of each intrinsic mode is carried out by the extrapolation of its regression function determined by the BP-ANN, then the prediction result of gas emission is derived through the reconstruction summing all prediction results corresponding to different intrinsic modes. From an application example related to the monitoring data it can be seen that the introduction of EMD method into the theoretical modeling to predict the gas emission from the coalface obviously improves the accuracy in comparison with the conventional BP-ANN method, to have the prediction results agreement with the monitoring data. The study is to provide important scientific basis and decision support for more reliably and accurately gas disaster warning.

1 INSTRUCTIONS

At present, mine gas is the major risks affecting coal mine production safety in China, the safety problems caused by the gas accounted for over 80% of coal mine production safety accidents, and its casualties account for 90% of all serious accidents' casualties (Li & Jing 2007), Especially the gas explosion accidents, which have caused worst human and economic losses. From 2004 to 2009, various national coal mine accidents caused more than 10 people died approximately 225 cases, 5280 people deaths, of which including 147 gas accidents, 3,667 people deaths, accounting for 65.3% and 69.5% respectively. After restoration efforts, the industry in recent years, coal mine production safety situation in China is a little better. But the coal mine production safety situation is still grim, the total accidents is still too large, serious accidents have occurred from time to time. Based on the statistical data of the state production safety supervision and Management Bureau in 2010 and other statistical data, in 2010 China's coal mine gas accident occurred 135 cases, killed 593 people (Chen & Zhao 2012). Therefore, the coal mine gas disaster is one of the key factors to the coal industry production safety in china. Research shows that, in order to solve the gas disaster problem fundamentally, accurate prediction of mine gas emission is the key[1].

In recent years, the gas emission forecasting technology has been gained more and more attention in the world's coal-producing countries, they put a lot of human and financial resources to conduct technical researching, have obtained many reference experience and research results.

Such as British established the Airey method considering the time and mining conditions for the influencing factors, Germany is presented the Winter method to dynamic forecast the mining working face gas with time series, and the Pittsburgh mining research institute of United States etc.

The gas emission prediction study in China's coal mine started relatively late, for example, Qu Fang proposed the fully mechanized workface gas emission prediction method based on the initial velocity of gas emission (Qu et al. 2004); Yuan Dong-sheng applied three-dimensional grey trend surface analysis method to the prediction of gas emission (Yuan & Hao 2004); Xia Hong-chun proposed the prediction method of deep mine area gas

[1] Sponsors: The basic research costs of national universities: JCB2013B08

emission based on least square method (Xia et al. 2002), which established a linear regression equation between the working surface mining depth and the relative gas emission by using the method, and using the equation to predict gas emission from the deep region; Chen Fu-yong applied numerical analysis to gas emission prediction for mine untapped area (Chen 2004), which made fitting analysis on the existing discrete data of gas emission and depth by using the numerical analysis method, to find the approximate function between the gas emission amount and the mining depth, thus realizing the untapped area gas Emission prediction; Wu Ai-you introduced the grey theory into the gas emission prediction and established the prediction mode (Wu et al. 2005); Zhao Chao-yi applied the genetic programming to coalface gas Emission prediction (Zhao & Yuan 1999), to establish the prediction model of coal face gas emission. However, the above method is essentially pay more attention to the fitting effect of gas emission data that has occurred, applies only to the critical gas explosion forecasting, also cannot meet the early warning requirements (Hu 2001).

In addition to statistical mathematics, theory of gray system modeling method, the application of nonlinear theory and artificial intelligence method are also greatly enriched the theory means of gas emission prediction and gas time forecast based on observation data. For example, Liu Xin-xi put forward a method to predict the mine gas emission amount based on BP artificial neural network (Liu & Wang 2002); Xue Peng-qian considered the problems of slow convergence speed, easily falls into local optimization when use the traditional neural network method to solve nonlinear problems, proposed a new wavelet neural network method for gas emission prediction, which not only made full use of the time-frequency localization properties of wavelet transform, but also combined with neural networks self-learning ability, and established the prediction model (Xue et al. 2006); Wu Cai-fang combined neural network and genetic algorithm organically, with the neural network theory as the foundation, using genetic algorithm to optimize the hidden layer neurons and the number of connection weights in the network, established the gas content prediction model (Wu & Zeng 2003). But the above approaches has at least a fatal defects in the following two aspects, one is the excessive dependence on the monitoring data that can't be taken into account the real mechanism link between them and their real physical process, two is no observational existing data for a new mine, so there is no guidance to its design on the whole.

Obviously, the limited observational data alone does not fully reproduce all the characteristics of the problem. More importantly, for a time series, we can use only the time variable, it shows the features contained linking the clue is not clear. However, the literature studies provide some inspiration (Wang 1999), which can seek the changing characteristic of gas emission under different time scales by signal decomposition, considering different gas emission control mechanism should have different time scale effects, the link between the gas emission variations and its intrinsic physical mechanism is expected to explore through the difference of the time scales. However, the wavelet transform of digital signal analysis techniques are based on a pre-selected basis functions on the characteristics, does not meet the physical mechanism varies with time.

On the other hand, for its good adaptive decomposition effect, the empirical mode decomposition (EMD) method proposed by Huang et al in 1998 provides a possible approach to solve this problem (Huang et al. 1998). Based on the EMD method, it can make directly decomposed to the observed gas emission data, the approximately orthogonal intrinsic mode function (IMF) can be obtained, whole emission observations is the sum of these IMF components.

At the same time, considering the advantages and shortages of neural network in recent years in the treatment of prediction problems (Liu & Wang 2002, Zhu et al. 2007), this paper presents a new prediction method for coalface gas emission based on the EMD and BP-ANN. By using the gas emission historical data, obtains its intrinsic mode functions (namely IMF component) through the EMD decomposition, then corresponding respectively to each intrinsic mode make forecast by using the function fitting method of ANN, on this basis, different intrinsic mode prediction results were synthesized, reconstructed and synthesized, thus obtaining the theoretical prediction results for gas emission. Examples analysis of monitoring results show, compared with the conventional neural network method and other forecasting methods, the EMD method is greatly improving the prediction accuracy, whose prediction results are very consistent with the actual monitoring data.

2 THE DYNAMIC PREDICTION MODEL ESTABLISHMENT OF EMD-ANN

2.1 *The basic principle of EMD*

The intrinsic mode extraction of gas emission monitoring value can be achieve through the EMD method, although the EMD method has not been strictly theoretical proved, however, it has

got good results in many applications, also found some physical contact between it and some physical mechanisms.

According to Huang et al, intrinsic mode components should meet the following two conditions (Huang et al. 1998):

1. In the whole component signals, the number of zeros and poles are equal or different at most one;
2. For any point in the signal, the envelope determined by the local maximum point and the envelope determined by the local minimum point, whose average value is zero.

The time series signal of monitoring data is decomposed into several IMF and EMD steps as follows. Firstly, to identify all extreme points for the monitoring data signals x (t), then, the upper envelope $e_{sup}(t)$ and the lower envelope $e_{inf}(t)$ of $x(t)$ are respectively fitted by using all the maxima points and minima points, and they meet the following relationship:

$$e_{inf}(t) \le x(t) \le e_{sup}(t) \tag{1}$$

Set the average value of $e_{sup}(t)$ and $e_{inf}(t)$ with $m(t)$, there is:

$$m(t) = [e_{sup}(t) + e_{inf}(t)]/2 \tag{2}$$

Let the $x(t)$ minus the $m(t)$,

$$c(t) = x(t) - m(t) \tag{3}$$

The $c(t)$ to see as a new $x(t)$, repeat the above process, until the resulting $c(t)$ and the last calculated $c(t)$ satisfy the given consistency determination conditions, it can filter out the first order IMF component $c_1(t)$ from the original time series signal. At the same time, there is:

$$m_1(t) = x(t) - c_1(t) \tag{4}$$

Set $m_1(t)$ as a new $x(t)$, using the same method that can filter out the other IMF component sequentially.

At last, $x(t)$ can be expressed as

$$x(t) = \sum_{k=1}^{n} c_k(t) + m_n(t) \tag{5}$$

n is the number of decomposition, it is the number of IMF components determined by the monitoring signal features, namely the total number of intrinsic mode, $m_n(t)$ is the residual after decomposition.

Because of the time curves of gas emission is not very complex (He et al. 2008), so in strike the upper and lower envelope, the study used cubic spline interpolation. In addition, the data mirror extension method is applied to eliminate end effect (Lee et al. 2009).

2.2 *Forecasting model of BP neural network*

Artificial neural network (ANN) is a new subject produced in the late 1980s with rapid development, is an information processing system based on the imitation of human brain structure and function. At present, the ANN has been widely applied to all areas of our lives.

The typical BP neural network has three layers, namely: input layer, hidden layer and output layer, to achieve full connectivity between each layer, seen in figure 1. The detailed prediction process can refer to the literature[9].

By using the gas emission historical data, obtains its intrinsic mode functions (namely IMF component) through the EMD decomposition, then corresponding respectively to each intrinsic mode make forecast by using the function fitting method of ANN, on this basis, different intrinsic mode prediction results can be synthesized and reconstructed, thus obtaining the theoretical prediction results for gas emission.

The prediction accuracy using average relative error (MRE) is:

$$MRE = \frac{1}{n}\sum_{i=1}^{n} \left| (y_i - \hat{y}_i) / y_i \right| \times 100\% \tag{6}$$

In the formula, y_i is the monitoring values, $\hat{y}_i$ is the predictive value.

3 EXAMPLE

Taking the coalface of Dongpang coal mine in Xingtai as an example, the mine is the most abundant coal resources in Xingtai mining area, whose annual production capacity about 1.8 million tons.

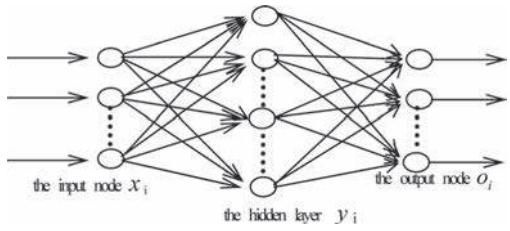


Figure 1. The typical BP-ANN model.

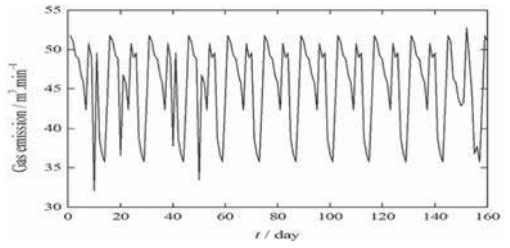


Figure 2. the monitoring results of coalface gas emission.

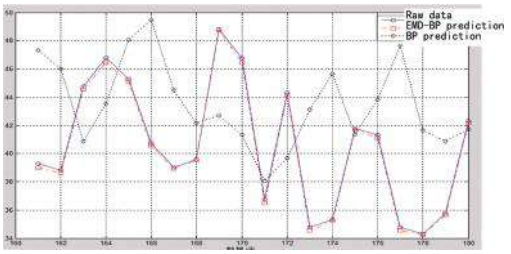


Figure 3. Comparison between measured and two predicted results.

The 6_{-2} coal seam is the main mining seam, integrated mining face in high gas zone. Select the top 160 gas observation data as the theoretical modeling sample data, as shown in Figure 2, the remaining 20 gas observation data as the test sample data, to make empirical study.

Six IMF components of the sample data are obtained through EMD analysis, therefore, the relevant mine gas emission in coal face changes over time contains total of six natural modes. Make predict to these six intrinsic modes separately through BP neural network, the prediction results from 161 day to 180 day are obtained after accumulative synthesis of each intrinsic mode prediction results as shown in Figure 3. It is not difficult to see, the prediction results based on EMD and BP-ANN are in good agreement with the actual test results, the prediction result of BP-ANN is clearly much worse. The average relative error is only 2.08%, while the latter is as high as 19.47%.

As can be seen, in the gas emission prediction modeling of coalface, when let the monitoring results as the modeling data, the gas emission laws in different time scales is difficult to fully revealed, to establish a theoretical model to predict the effect is not ideal, the introduction of the intrinsic mode in some extent overcome this deficiency. Although the application of the above examples may not reflect the whole features of gas emission problem, but the prediction results in Figure 3 at least one side confirmed the good predictive ability of EMD and BP-ANN prediction modeling for coalface gas emission. In addition, the theoretical modeling and calculation process of this method is relatively simple, and without excessive pursuit of how to optimize and select calculation parameters and other details, showing good engineering application value.

4 ANALYSIS AND CONCLUSION

This study reviews the existing gas emission prediction technology, designs and proposes a new prediction model for gas emission based on EMD-BP ANN, and apply it to the forecasting process of mine gas emission. The results show that, the model is feasible and effective, and can be used to predict the gas emission dangerous for large-scale coal seam. By predicting that if the gas emission abnormal, we can take the following measures to control:

1. Strengthen geological exploration work, seriously and comprehensively analyze the geological conditions before the mining face production, use vibration shot release the gas in advance if necessary.
2. Strengthen the management of the ventilation system, to ensure that the system is reasonable and effective, the air is sufficient.
3. Strengthen safety monitoring system repair and management, ensuring normal operation of the system. All mining face must be required to install gas automatic alarm and cut-off device, wherein the abnormal gas zone in high gas area, to achieve "three special two locking."
4. Strengthen gas prediction. Check the gas concentration each shift on coal hole of all underground mining working face, to predict the gas changing trends of the coalface forward direction through gas concentration changes analysis, and to take effective preventive measures in advance.
5. Strengthen the maintenance and management of electromechanical equipment, and resolutely put an end to electrical equipment explosion and illegal operation phenomenon.

In actual mine engineering, because there are many factors influencing the gas emission, the characteristics of coal seams and geological characteristics vary, so how to scientific and comprehensively extract the various factors influencing gas emission, is a further research topic.

REFERENCES

Chen Fuyong. Application of numerical analysis in gas emission prediction for untapped area of mine [J].

Mining Safety & Environmental Protection, 2004 (4):43–56.
Chen Juan, Zhao Yaojiang. Statistical analysis and enlightenment of Chinese coal mine accidents in the past ten years [J]. Beijing: State Production Safety Supervision Administration, 2012, (3):137–139.
He Liwen, Shi Shiliang, Song Yi, et al. Complexity and measurement of complex degree of gas emission in heading faces of coal mine [J]. Journal of China Coal Society, 2008, 33 (5): 547~550.
Huang N E, Shen Z, Long S R, et al. The empirical mode decomposition and the Hilbert spectrum for nonlinear and non-stationary time series analysis [J]. Proceedings of the Royal Society of London Series A, 1998, 454(1971):903~995.
Lee Y S, Tsakirtzis S, Vakakis A F, et al. Physics-based foundation for Empirical Mode Decomposition [J]. AIAA Journal, 2009, 47(12): 2938~2963.
Li Bingang, Jing Xingpeng. Prediction of Gas Emission status and progress [J]. Shangxi coal, 2007(5):20–22.
Liu Xinxi, Wang Peng-fei, etc. Mine gas emission prediction based on BP-ANN [J]. Safety and Environmental Engineering, 2002, 9.
Qu Fang, Liu Gong, Zhao Hongliang, etc. The gas emission prediction of fully-mechanized working face based on the initial velocity of coal wall gas emission [J]. Coal Mine Safety, 2004(3):50–53.
Wang Hongyu. The analysis and processing of non-stationary random signal [M]. Beijing: National Defense Industry Press, 1999.
Wu AiYou, Tian Yunli, Song Yi. Grey System Theory in Gas Emission Prediction [J]. Journal of China Coal Society, 2005, 30 (5):589–592.
Wu Caifang, Zeng Yong. Study of gas content prediction based on Genetic Neural Network [J]. Earth Science Frontiers, 2003, 3.
Xia Hong Chun, Cheng YuanPing, Li Shunfeng. The gas emission prediction of deep mine area mine based on the least squares method [J]. Mining Safety & Environmental Protection, 2002, 29(4):13~16.
Xue Pengqian, WU Lifeng, Li Haijun. Prediction of gas emission based on the wavelet neural network [J]. China Safety Science Journal, 2006, 2.
Yuan Dong-sheng, Hao Tian-xuan. Three-dimensional gray trend surface analysis in Gas Emission Prediction [J]. Chinese coal, 2004, 127 (1):44~45.
Zhao Zhaoyi, Yuan Xiu-gan, SUN Jinbiao. Application of genetic programming in coalface gas emission prediction [J]. Journal of Basic Science and Engineering, 1999 (7):32–36.
Zhu Hongqing, Cang Wenjie, Zhang Bin. Different source gas emission prediction model of working face based on BP artificial neural network and its application [J]. Journal of China Coal Society, 2007, 32(5):504~508.

This page intentionally left blank

Progress in Mine Safety Science and Engineering II – He et al. (Eds)
© 2014 Taylor & Francis Group, London, ISBN 978-1-138-00122-0

Electromagnetic method in detecting water hazards in coal mining face

Xianxin Shi & Yanwei Hou
Xi'an Research Institute of China Coal Technology and Engineering Group Corporation, Xi'an, Shaanxi, China

ABSTRACT: Water hazards in mining face are prone to cause inrush accidents and result in production interruption, even lead to underground water flooding, injuries or deaths. Pre-proved water hazards with known distributions in the mining face followed with effective water prevention measures taken are crucial for preventing or reducing flooding accidents and ensuring safe and high-efficient coal production. Due to the sensitivity of Coal Mine Electromagnetic Method towards water-bearing body with low resistivity, this sensitivity plays a unique role in detecting water hazards in coal mining face. This Paper introduces the working principles and construction methods of Mine High-density Electrical Method, Voice Frequency Electric Perspective Technique and Mine Transient Electromagnetic Method applied for detecting water hazards in mining face; describes the application effects for the detections of water hazards on the floor in coal mine roadway, in Working Face and in Single Entry Mine Tunnel respectively. Focuses are rested on the methods, principles and effects of Voice Frequency Electric Perspective Technique and Mine Transient Electromagnetic Method for coal mine detection. Finite Element Method (FEM) is used for simulating the underground potential of point electric source and the response of abnormal body with low resistivity both in homogeneous half-space in purpose to explain the basic theory of Electric Perspective. The application cases show that Coal Mine Electromagnetic Method is sensitive to the water-bearing body with low resistivity, possesses higher resolution capability for water-bearing geologic body when closely to target detection layer or the geological body, is one of efficient method to detecting water hazards in working face.

1 INTRODUCTION

Hydro-geological conditions for coal mines in China are complicate with severe water hazards. Coal mine water hazard, the second disaster, second only to gas explosion accident, ranks the first when counting the economic losses comparing with other disasters.

Water inrush accidents for coal mines mainly occur in mining face, especially in heading face. According to the statistics made by the Accident Investigation Department of State Administration of Coal Mine Safety, there are altogether 24 water hazard accidents occurred for coal mines nationwide with the death toll up to 122; within which, 8 are of less severity: 6 accidents happened in heading face, 1 in mining face; for 5 severe accidents, 3 in heading face and 2 in mining face. As a result, making studies on detecting water hazards in mining face, taking precise positioning theories and methods, checking out water-bearing position, water-bearing geological body and potential water flowing channel in mining face and evaluating the influence taken by water-bearing body towards mining are of great importance, and all of these are the crucial measures for preventing and solving water accidents for coal mines.

Electromagnetic methods adopted to detect hydrogeological condition of coal mines can be classified into two main types, ground electromagnetic method and mine electromagnetic method. Taking forecasting of water hazard in coal mines for example, our country has formed an integrated geophysical prospecting technology system in the long-term production and practice, giving priority to the mine electrical exploration and taking technologies like mine high-resolution earthquake exploration, radio-wave penetration, down-hole microgravimetry, radioassay and infrared temperature measurement as auxiliaries, all of which provide effective technical measures for safe production of coal mines and play an unique role in water prevention and control of coal mines (Chu Shaoliang 1996, Yue Jianhua & Liu Shucai 2000). At present, the commonly-used mine electrical exploration methods include mine DC electrical method, electric transmission tomography, mine transient electromagnetic method and etc., which are mainly applied to hydrogeological detection on supply source of mine water-gushing, insidious water-conducting passage, fissure zone, thickness of aquifuge, water-bearing formations in front of heading face of the roadway and etc., as well as detection on small water-bearing formations

and karst collapse columns in the coal face (Liu Qingwen 2001, Wang Guohua et al 2003, Guo Chun et al 2006).

2 MINE HIGH-DENSITY RESISTIVITY METHOD

2.1 *Detection principle, method and technology*

Mine high-density resistivity method is a combined method with multi-device and multi-electrode-distance, integrating electrical section method and electrical depth-measuring method into one. For the application of the mine high-density resistivity method, it is only needed to once set dozens or hundreds of electrodes at measuring points with a certain distance from each other, whose density, usually 1–10 m, is much higher than that of normal mine DC electrical method. Figure 1 is distribution schematic diagram of measuring points of the high-density resistivity method. If the array distance of electrodes is "a", the measuring electrode distance is $x = n \cdot a$, in which $n = 1, 2, \ldots$ in sequence. Each electrode distance moves point by point from left to right according to the form of fixed device to finish the data acquisition of this electrode distance. For one electrode distance, the result is equivalent to that of the resistivity section method, while observation on different electrode distances at the same record point is equivalent to an electrical depth-measuring point. For the convenience of actual work and facilitating the realization of automatic measurement of apparent resistivity, Wenner array, Schlumberger array, dipole-dipole array and monopole–dipole array are always adopted by the high-density resistivity method system. Detecting depth of the resistivity method increases along with the increase of distance between power-supply electrodes C1C2 and when the isolation coefficient "n" increases in sequence, the electrode distance between C1C2 increases gradually, as well as its capability of response to deep underground medium. Measurement result of the high-density resistivity method is usually recorded at the midpoint of observing electrodes P1P2 and the point location of a depth of na.

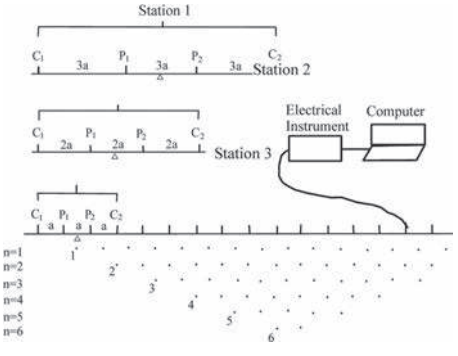


Figure 1. Schematic diagram of electrode array pattern and measuring point distribution of the mine high-density resistivity method.

Compared with normal mine electrical depth-measuring method and mine electrical section method, the mine high-density resistivity method has features like high efficiency in construction and abundant information acquired. It can use measurement results of different device forms to calculate different ratio parameters and show the abnormal information, and also be capable to suppress inference and decompose compound anomaly to a certain degree. Due to its outstanding effect, it becomes one of the ideal methods for mine geophysical prospecting

2.2 *Application effect*

The following is the introduction of detection condition of hidden trouble of water gushing from the floor in the excavation roadway of Coal Face 1116 of Shaanxi Xinghuo Coal Industry Co., Ltd., adopting the mine high-density resistivity method. The Coal Face 1116, located in the south wing of Xinghuo Mine Field. The mining coal seam is 11# and its thickness is about 4.69 m and the average angle of inclination is 3.5°. Roof of the excavation roadway of the coal face is sandy mudstone, mudstone and siltite; and the floor is mudstone with Ordovician limestone below. Task of this detection is to detect the water-conducting formation of fracture zone, fissure development zone and etc. and the scope of water-rich area 80 m below the floor of the excavation roadway of Coal Face 1116, in order to provide basis for design of water prevention, control scheme, arrangement and implementation of the water prevention and control engineering to ensure the safe mining on the coal face.

Figure 2 and Figure 3 are the floor detection results respectively of headentry and tailentry of Coal Face 1116 by adopting the mine high-density resistivity method.

As is shown in Figure 2, the resistivity on this section changes greatly both longitudinally and transversely, indicating the relatively complicated geoelectric structure. In the diagram, change from

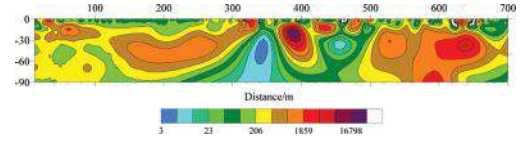


Figure 2. Headentry resistivity at coal face 1116 that detected by high-density resistivity method-depth section.

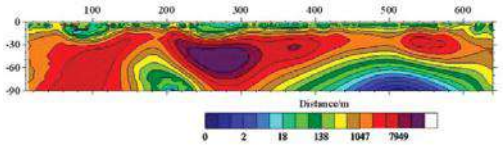


Figure 3. Tailentry resistivity at coal face 1116 that detected by high-density resistivity method-depth section.

blue to red represents the change of apparent resistivity from low to high. There are mainly two places where the apparent resistivity is lower than the wall rock in Figure 2, and they are shown as blue low-resistivity abnormal zones.

Based on the analysis of apparent resistivity value, we take the abnormal segment with its apparent resistivity lower than 30Ω.m as low resistivity segment, and regard it as possible hidden trouble of water gushing. Therefore, two low resistivity anomalies are outlined according to the above principle. One of which with 332–355 m as its horizontal extent and 50 m approximately as its central buried depth on section; the other one with 440–470 m as its horizontal extent and 40 m as its central buried depth. The explanation on low resistivity in Figure 3 can be made in the same way: 490–520 m as horizontal extent and 85 m as its central buried depth. Thereby, drilling hole layout and verification can be adopted by mining party when abscissa of haulage way is at 510 m and abscissa of air-return way is at 345 m respectively. As the maximum water discharge is 67 m^3/h and 45.7 m^3/h respectively when drilling enters into the abnormal zone, grouting shall be taken to bottom plate immediately to reinforce.

The detection achievements of mine high-density resistivity method provides scientific basis for design of water prevention, control scheme, arrangement and implementation of the water prevention and control engineering at Coal Face 1116. Relying on these results, the coal floor of abnormal zones of this mine have been processed by drilled grouting; after the transformation of grouting, coal mined safely from this coal face has reached 210 thousand tons.

3 ELECTRIC TRANSMISSION TOMOGRAPHY

The principle of the electric transmission tomography is similar to that of mine radio-wave penetration method and the difference is that the electric transmission tomography adopts stable and constant current field. Actual construction layout is one-supply and multi-collection, forming a densely-covered bidirectional sector observation system

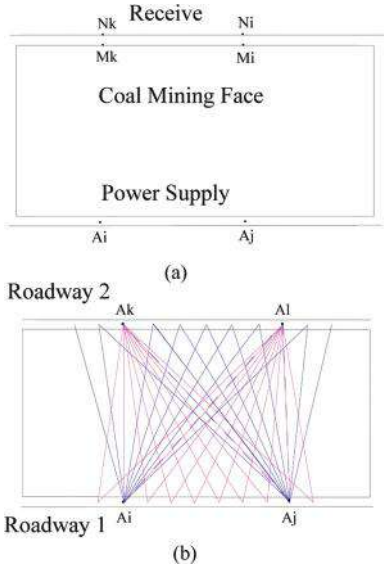


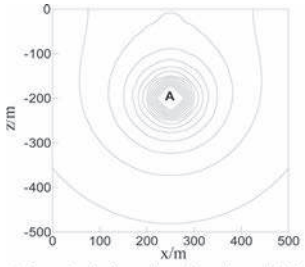
Figure 4. Layout diagram of down-hole electric transmission measurement.

(Figure 4), to research the distribution rules of electric fields in coal faces between two roadways as well as in the wall rock.

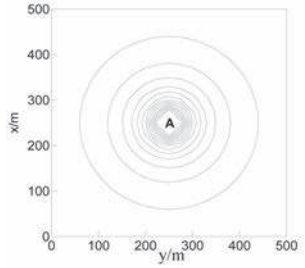
3.1 *Basic principle of detection*

Its basic principle of detection can be interpreted by 3-D finite element simulation (Zhou Xixiang & Zhong Benshan 1986). Suppose the earth resistivity is 100Ω.m, the point power supply is placed 200 m deep underground, and equipotential diagrams of longitudinal section (Figure 5-a) and transverse section (Figure 5-b) of the stable and constant current fields generated by the underground point current source A can be provided, then we can find that on the transverse section of point power supply, the equipotential lines are a group of concentric circles. When a low-resistivity abnormal body of 10Ω.m resistivity is placed at the position with horizontal coordinates of X = –200 m and Y = 0 m and 60 m below the point power supply A, the anomaly response calculated is shown in Figure 6. Influence of the abnormal body on spherical-shell equipotential lines is that changes of equipotential lines around the abnormal body are greatest and the farther the equipotential lines are from the abnormal body, the less the changes are. Generally speaking, when the spherical-shell equipotential lines are near to the abnormal body, they will show the low-resistivity characteristic (attracting current) of the latter.

It is indicated by three main diagrams of the 3-D finite element simulation shown above that

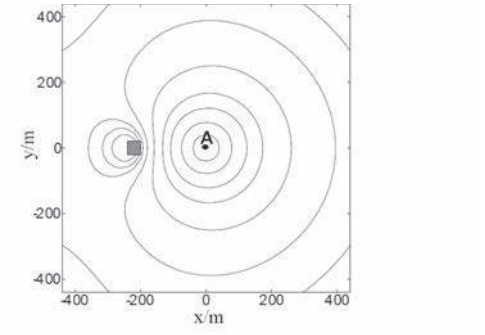


(a) Longitudinal section of equipotential lines of point source 200m deep underground (earth resistivity: 100Ω.m)



(b) Transverse section of equipotential lines of point source 200m deep underground(earth resistivity: 100Ω.m z=-200m)

Figure 5. Longitudinal and transverse sections of underground point source



Earth resistivity: 100Ωm; Abnormal body: 40m×40m×40m, 200m below the power supply A; Resistivity: 10 Ω.m

Figure 6. Abnormal body response on the plane 200 m deep underground.

the potential lines of relatively deep down-hole power supply are basically free from influence of the semi-space; the abnormal body below the source influences distribution of plane potential lines of the source; according to the principle of electrical method, electrical difference between the abnormal body and wall rock, scale of the abnormal body and distance between the abnormal body and source will all influence the amplitude of anomaly, which is the basic principle of using monopole-dipole device to carry out down-hole electric transmission.

3.2 *Application example*

In the following part, results of water gushing detection by electric transmission tomography at Coal Face 1031 in Taoyuan Coal Mine of Anhui Huaibei Mining Group are introduced.

3.2.1 *Geological profile*

Coal Face 1031 in Taoyuan Coal Mine mines coal seam No. 10, with burial depth is 327–445 m. Strata in roof and floor of coal seam No. 10 usually are siltstone, fine sandstone or interbedding of siltstone and packsand, which water-bearing feature is weak; about 58 m below the floor of coal seam No.10, there is a stratum of Taiyuan formation limestone (limestone No. 1) of a thickness of 2–3 m, which is one of the major aquifers of mine.

The Taoyuan formation limestone and sandstone in roof and floor of the coal seam are all pressure-bearing aquifers, containing extremely inhomogeneous water; their water-bearing feature is mainly subject to karst, hole and fissure development degree. If partial fissure formation or water-bearing formation of the stratum is within high degree scope of water-conducting fissure development, they will extremely possible to threaten the safe mining at coal faces, and even lead to water trouble accidents. Therefore, it is required to find out hydrogeological conditions in the coal face in advance, in order to provide basis for water prevention and control before mining and implementation of appropriate technical measures during mining.

3.2.2 *Detection effect*

Figure 7 is the achievement diagram of electric transmission detection on water-bearing feature of strata near to segment below the floor of Coal Face 1031 by a certain depth. As is shown in the diagram, values of apparent electric conductivities of strata in the segment are changing within 0.16–8.2 S/m, with an average of 1.5 S/m. According to the general rule, that is, if the electric conductivity is high, the water-bearing feature will be good, we can come to the conclusion that the water-bearing abnormal zones in the coal face are mainly in the inner segment (southern segment), which shall be treated with water prevention & control measures during mining at the coal face.

4 MINE TRANSIENT ELECTROMAGNETIC METHOD

4.1 *Method introduction*

The mine transient electromagnetic method is very sensitive to water-bearing low-resistivity bodies

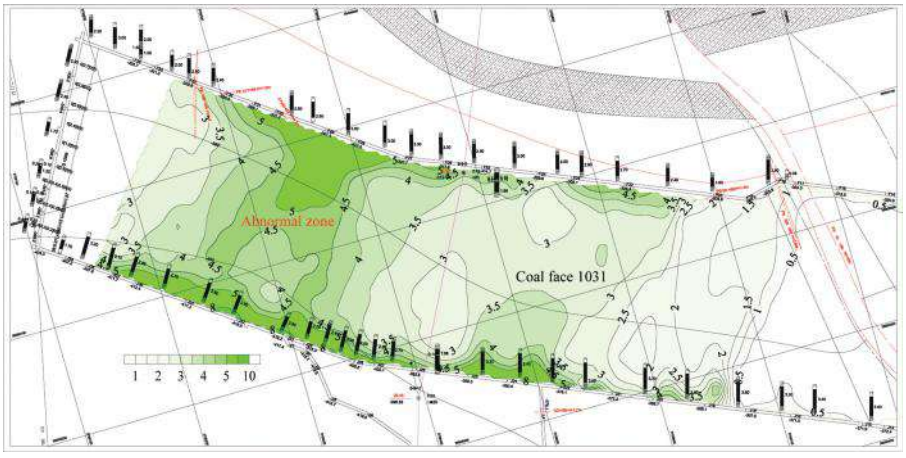


Figure 7. Plane figure of apparent electric conductivity by electric transmission tomography in the coal seam floor of coal face 1031.

and of fine directional property (orientational property); as a result, it can be applied to downhole omnibearing detection (not only available in front of heading end, but also for detection of lateral wall of roadway and roof, floor of coal seam and etc.); In addition, its advantages like long detecting distance and quick construction create a bright prospect for its application in detecting hidden trouble of water gushing at coal face.

4.2 *Calculation of apparent resistivity by the mine transient electromagnetic method*

The apparent resistivity of the mine transient electromagnetic method is a comprehensive reflection of electric conductivity of the whole-space stratum, and its formula is (Jiang Bangyuan. 1998):

$$\rho_\tau = C\frac{\mu_0}{4\pi t}\left[\frac{2\mu_0 SN}{5t(V/I)}\right]^{\frac{2}{3}} \tag{1}$$

In the formula, C is whole-space response coefficient; S is area of receiving coil; N is the number of coil windings of; t is attenuation time of the secondary field; and V/I is normalized induced voltage value.

4.3 *Conversion between time and depth by the mine transient electromagnetic method*

According to the fact that the underground induced current is distributed like rings and the "smoke ring effect" theory of electromagnetic field transmission, the vertical spreading speed vs and depth D of the electromagnetic field under random distribution condition of conductive medium are:

$$v_s = \alpha\frac{\sqrt{\gamma}}{\sigma_i\mu a}\times\left\{C_1+(C_1^2+2)^{\frac{1}{2}}+\left[1+C_1\Big/(C_1^2+2)^{\frac{1}{2}}\right]\gamma C_2\right\} \tag{2}$$

$$D = v_s t_i \tag{3}$$

While C_1 and C_2 are determined by the following formula:

$$C_1(\gamma) = \frac{3\sqrt{\pi}}{4}\left[1-\frac{\gamma}{4}-\sum_{k=2}^{\infty}\frac{(2k-3)!!}{k!(k+1)!}\left(\frac{\gamma}{2}\right)^k\right] \tag{4}$$

$$C_2(\gamma) = \frac{3\sqrt{\pi}}{4}\sum_{k=0}^{\infty}\frac{(2k-1)!!}{k!(k+1)!}\left(\frac{\gamma}{2}\right)^k \tag{5}$$

In the formula, $\gamma = \sigma_i\mu\alpha^2/4t_i$; σ_i is apparent resistivity corresponding to time t_i; α is whole-space response coefficient; a is area of transmitting loop; τ is time constant; and $\mu \approx \mu_0 = 4\pi \times 10^{-7}$ H/m.

According to the apparent resistivity-time curve actually measured, the apparent resistivity-depth curve can be acquired through the conversion by (2) and (3), thereby the corresponding relation between electrical distribution and depth of the conductive medium can be determined.

4.4 *Application example*

4.4.1 *Geological profile*

Coal-bearing series in this area is typical North-China type Permo-Carboniferous system, coal

series stratum overlaid by Jurassic system, tertiary system and quaternary system. Basic formation of the mine field is a uniclinal structure; the direction of strata is 300–330°; inclined direction is 210–240° and the angle of inclination is 12–30°.

4.4.2 *Field working method, technology and working parameters*

In view of the field working conditions, device of coincident loops is used to measure; additionally, method test has been implemented according to actual field conditions in order to increase signal-to-noise ratio to the largest extent. The final working parameters selected are as follows: transmitting wire frame: 1.3 m × 1.3 m (10 windings in total); receiving wire frame: 1.1 m × 1.1 m (20 windings in total); emission current: 20 A; delay time of sampling: 20 ms; superposition times: 256 times.

4.4.3 *Detection result*

3-D all-wave processing and analysis on data acquired through the measurement shall be carried out, including wave filtering, smoothing, forward calculation and inversion; especially aiming at influences of metal brackets, rails and etc. in the roadway on the distribution of transient electromagnetic field, simulation should be done by finite-difference time-domain method to eliminate them; anomaly of low-resistivity geological body to be detected should be given prominence to, and resistivity section diagrams with the processing results should be drawn; then conclusions and interpretations should be given according to the spatial changing conditions of resisitivities reflected by the section diagrams.

Figure 8 is the vertical section figure of pilot detection in blind roadway by the down-hole transient electromagnetic method. As is shown in the diagram, there is an obvious low-resistivity abnormal zone about 275–320 m in front of the excavation face, and the center is at 310 m. After analyzing based on the geological condition, we deduce that the anomaly is reflection of the fissure zone of water-bearing formation. In the process of subsequent roadway excavation, water-bearing fissure zone is found at 282–317 m, whose amount of water gushing is 60 m^3/h. Due to the water detection & drainage adopted by the mine, safety of the excavation construction is ensured. Thereby the detection result of mine transient electromagnetic method is verified.

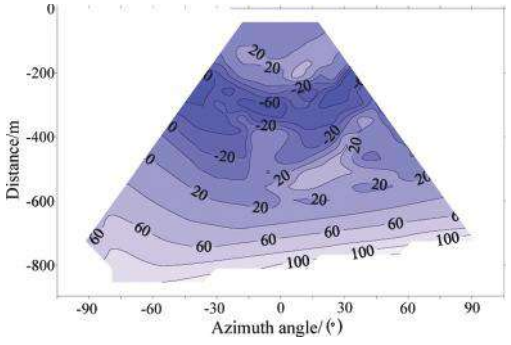


Figure 8. Resistivity section diagram of pilot detection in blind roadway of coal mine by the mine transient electromagnetic method.

5 CONCLUSION

Based on electrical differences between rocks, the electromagnetic method exploration is the main method for mine geophysical prospecting. Because of its sensitivity to water-bearing low-resistivity bodies, it shows a strong superiority in aspects of solving mine structures related to water and evaluating the water-bearing property. It has been proven by practice that the mine electromagnetic method is simple in construction, fast and economic, is an effective method for detecting hidden trouble of water gushing from the coal face and can provide reliable and correct basis for design of water prevention and control scheme for the coal face, as well as layout and implementation of water prevention and control project; thereby it plays an unique role in water prevention and control work of the coal mine and is very significant for ensuring the safe mining at the coal face.

REFERENCES

Chu Shaoliang. 1996. *Application of Mine Geophysical Prospecting*. Beijing: China Coal Industry Publishing House.

Guo Chun, et al. 2006. Prediction of Water Disasters Ahead of Tunneling in Coal Mine Using Continuous Detection by UWTEM. *Seismology and Geology* 28(10):456–462.

Jiang Bangyuan. 1998. *Applied Near-Zone Magnetic Source Transient Electromagnetic Exploration*. Beijing: Geological Publishing House.

Liu Qingwen. 2001. Pilot Detection for Down-Hole Electrical Method and its Application. *Coal Geology & Exploration* 29(5):60–62.

Wang Guohua, et al. 2003. Application of Down-Hole DC Electrical Method in Pilot Detection at Tunneling Face. *Coal Science & Technology*31 (Album):42–45.

Yue Jianhua & Liu Shucai. 2000. *Mine DC Electrical Exploration*. Xuzhou: Press of China University of Mining & Technology.

Zhou Xixiang & Zhong Benshan. 1986. *Value Simulation Technology for Electrical Exploration*. Chengdu: Sichuan Publishing House of Science & Technology.

Progress in Mine Safety Science and Engineering II – He et al. (Eds)
© 2014 Taylor & Francis Group, London, ISBN 978-1-138-00122-0

Evaluation and applicability study on prediction methods of water inflow in mines

H.Q. Lian
North China Institute of Science and Technology, Yanjiao, Hebei, China
China University of Mining and Technology, Beijing, China

X.X. Xia, B. Xu & H. Xu
North China Institute of Science and Technology, Yanjiao, Hebei, China

ABSTRACT: After studying domestic and foreign related literatures, the prediction methods of existing water inflow in mines were summarized and analyzed in this study from two aspects, which are distributed-parameter method and lumped parameter approximation. Simultaneously, taking the Xinwen mining area as an example, numerical method, analysis method and analogue method were used to evaluate the water inflow in mines. Moreover, the characteristics and applicability of prediction methods were evaluated compared with the measured data. The evaluation results showed that: when the hydrogeology information file is enough in studied area, the numerical method can be used to predict water inflow in mines. When the research materials is not enough, the numerical method can be used to predict, meanwhile the analytical method need to be used as a comparison at the same time. For the newly-built mine, when the hydrogeology parameter is insufficient, the hydrogeology analogue method can be used to predict the water inflow. This study has certain guidance on choosing prediction methods at the analogous conditions in mine flow.

1 INTRODUCTION

How to accurately predict the water inflow in mines is an important issue during coal mining process, and that's also what the experts try to solve at home and abroad. Although many scholars have done a lot of work from different aspects and use different methods (Chen & Liu 2009) over the past few years. However, there still exist large errors between the predicted data and the measured data, and the biggest one can be more than ten times. The reasons causing the errors of prediction water inflow in mines can be mainly summarized in the following three aspects: failure to identify hydrogeological conditions, the selected hydrogeology parameter lacking represent activeness, improperly choosing the mathematical model (Dong 1995). Therefore, appropriately choosing the method of prediction water inflow in mines is an important way to reduce the errors. In this study, Xinwen mining area is chosen as study object. Meanwhile, the results of different prediction methods are analysed for water inflow in mines. Taking the recent actual measured data as a comparison, the applicability of the prediction water inflow is evaluated in mines under the areas condition.

2 OVERVIEW ON PREDICTION METHODS

Domestic and foreign scholars have done a lot of researches on prediction water inflow in mines, and summed up various prediction methods by practice. One is distributed parameter method, and the other is lumped parameter method (Du & Deng 2009). The most typical ones are: numerical method (Ma & Li 2011), analytical method (Song & Yang 2009), neural network method (Wen 2009) water balance method (Wu 2009), and hydrogeological analogy method (Zhang & Xu 2012) Distributed parameter method is represented by partial differential equations. Lumped parameter method is represented by ordinary differential equations. Figure 1 shows the classification on methods of prediction water inflow in mines.

2.1 *Numerical method*

1. Principle and application conditions
   Numerical method is an approximate calculation method, which is developed with the appearance of electronic computer, and is widely used recently. Theoretically, it is a method of approximate solutions for solving partial differential equations. The practical application of

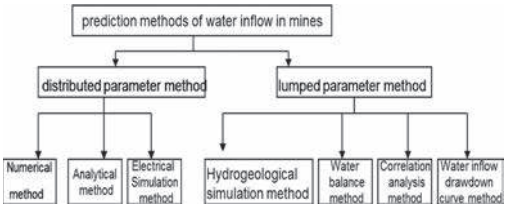


Figure 1. The classification on prediction methods of water inflow in mines.

this method can fully meet the precision need, and it also can solve many complex problems of water inflow in mines. What's more, numerical method can be very effective to the situation of simple hydrogeological conditions and simple aquifer system in the study areas.

2. Calculation method

Now the finite element method and the finite difference method are two commonly used numerical methods.

The finite element method: the finite element method is dividing the areas to be solved into finite units, and constructs the basis function in the unit. Then it constructs the shape function, and takes shape function as the approximate solution, finally uses Galerkin method or the principle of minimum potential energy to get the approximate value of the node.

The finite difference method: The finite difference method is replaced differential coefficient by difference quotient. So do the boundary conditions and initial conditions, turning the problem for determining solution to a algebraic equation set. Its essence is replacing the partial differential equation of groundwater movement by the corresponding differential equation approximately, and then solving the differential equation.

2.2 *Analytical method*

1. Principle and application conditions

The analytical method is one of the methods widely used in prediction of water inflow in mines and it is applicative to any roadway systems. The analytical method is based on the modeling requirement of analytical solution. Used the groundwater dynamics principle, and could be used to predict water inflow in mines after establishing an analytic formula of the ideal model.

2. Calculation method

The basic theorem of movement of the groundwater flow is Darcy's theorem. All the analytical formulas are based on or derived from it. The analytical method that is most commonly used is the well flow equation. It is basic formula can be divided into two categories: steady flow formulae (Dupuit Formula) and non-steady flow formula (Theis formula).

When using the analytical method, steady flow theory can solve two issues: predicting the totally water inflow in mines if maximum water drawdown of the mining level is known. The use of non-steady flow theory can solve the three problems: Predict water inflow in mines if the drawdown data and unwatering time is known. Predict the drainage time if the drawdown and drainage capacity is known. Predict the drawdown data of water level if the drainage capacity and unwatering time is known.

2.3 *BT neural network method*

1. Principle and application conditions

Artificial Neural Network (ANN) integrated the organization and function of applying engineering technology and computer. it is means to simulate the biological neural network. Artificial neural network is an artificial intelligent system which connects into a network through a large number of artificial neural cells that are similar with natural nervous system cells. The system realizes parallel distributed processing of knowledge.

2. Calculation method

BP network is divided into the input layer, hidden layer and output layer three layers and the full link of layers structure. Output layer can have multiple points (neurons). Hidden layer can be separated into multiple layers. If the number of hidden layer units is free to design, then uses three S-shaped, which can approach to any continuous function in arbitrary precision. Choose 3 layer networks (hidden layer is the first layer) will not affect the accuracy of the network, but also can improve the speed of the network.

2.4 *Water balance method*

1. Principle and application conditions

The water balance method is based on the principle of water balance, to find out the relationship between income and expenditure parts on water balance when mining the mine. It is applicative to the water-filled deposit of the non-seepage groundwater movement and simple water-equilibrium conditions. Therefore, find out the groundwater recharge and discharge conditions in the mining areas, research mine changes in the unwavering process, rationally confirm the balanced project as well as the data then can be combined the water balance calculation.

2. Calculation method

Through the study of the groundwater dynamics laws, establish the changing relationship between income and expenditure parts of groundwater in the mining area and in a certain period (equalization period), to establish a balanced equation to predict the water inflow of the mining area. Basic balance equation:

$$Q = Q_c + Q_y + Q_h + Q_{yh} + Q_r - (Q_c/ + Q_y/ + Q_h/ + Q_{zh}/ + Q_r/) - Q_{ch}$$

In the equation:

Q – The possible water inflow of the mining, m^3/d;

Q_c, Q_c/ – The underground runoff lateral inflows and the lateral leakage amount, m^3/d;

Q_y, Q_y/ – Leaky recharge and leaky excretion, m^3/d;

Q_h, Q_h/ – River recharge and drainage amount to the river, m^3/d;

Q_{yh}, Q_{zh}/ – Meteoric recharge and evaporation consumption, m^3/d;

Q_r, Q_r/ – Artificial recharge and manually pumping (row) amount outside the mine, m^3/d;

Q_{ch} – The amount of growth or consumption of aquifer storage capacity in unit time, m^3/d.

Storage capacity to a confined aquifer is the elasticity, diving watering layer is static reserves, for the steady state, this is 0.

2.5 *Hydrogeological simulation method*

1. Principle and application conditions

The hydrogeological simulation method is based on stable flow, uses the geological and hydrogeological conditions similarity, the drainage or gush material of the mine with the similar mining method to predict water inflow of the new mine. The application premise of this method is that the new mine has the similar conditions as the old one does, and the old mine should have a long-term observational data, to make sure the reliability of the mathematical expression between the water inflow and influencing factors, so it is just an approximate calculation method.

2. Calculation method

Hydrogeological simulation method mainly includes the rich water factor comparable method and the analogy method per water inflow.

① The rich water factor comparable method

It is based on the known mine rich water factor to prediction the neighboring new mine with the similar hydrogeological conditions and similar mining methods, namely:

$$Q = K_P P = \frac{Q_0}{P_0} P$$

In the equation:

Q – Water inflow of new designed mine (m3/a);

Q_0 – Water inflow of known old mine (m3/a);

P_0 – Production of known old mines (t/a);

P – Production of designed new mine (t/a)

② The analogy method of per water inflow

The physical meaning of per water inflow mine is the average actual water inflow in per unit drawdown and per mining area of the mine. If mine inflow water quantity (Q_0) is changing with the mining area (A_0) and water drawdown (S_0), the unit inflow water quantity (q_0) is

$$q_0 = \frac{Q_0}{F_0 S_0}$$

In the equation:

q_0 – Per water inflow of per area of production mine (m^3/H);

Q_0 – Total water inflow in mines (m^3/d);

F_0 – Roadway mining area of production mine (m^3);

S_0 – Water decreasing level of production mine (m);

According to the Per water inflow of per area of production mine, you can calculate total water inflow of deigned mine similar with other hydrogeological conditions:

$$Q_m = q \cdot F_m \cdot S_m$$

In the equation:

F_m – Designed mining area of designed mine (m^2)

S_m – Designed average water decreasing level of designed min (m)

3 PREDICTIONS AND ANALYSIS ON WATER INFLOW IN MINE

3.1 *Study areas*

Taking Longgu, Jiyang and Zhaoguan three mines of Xinwen Mining, as key study areas. And Longgu mine is located in Shandong Province, Heze county, main mining 3 # coal seam, with the complex structure. Jiyang mine is located in the north of the Yellow River, mining depth from-280 m to-750 m. Zhaoguan mine is located in Zhaoguan town, Dezhou Qihe County, and the earthquake

intensity is 6 degrees. And there are four principal coal seams in this court.

The main stratum of the study areas is Ordovician system, the black coal system and permian system, the Jurassic system Cretaceous system the Tertiary system and the Quaternary system. the coal system stratum is respectively the black coal system Benxi Group, the Taiyuan Group, and permian system Shanxi Group. The major aquifers in mines are: Quaternary conglomerate aquifer, Tertiary conglomerate aquifer, Permian Shanxi Group sandstone aquifer, Carboniferous Taiyuan Group limestone aquifer, Carboniferous limestone aquifer and Benxi Ordovician limestone aquifer.

Through studying the collections the materials of three mines in the area, its purpose is obtaining the hydrogeology parameter. The hydrogeology parameter directly affects the reliability and accuracy of the prediction data. Information of three mines is shown as Table 1.

3.2 *Different prediction methods of water inflow in mines*

Under the different situation, chooses LongGu, ZhaoGuan, and Jiyang mines as example. Using numerical method, analytical method and hydrogeology analogue method to predict the water inflow in mines. Analyzes errors of various prediction methods, to select the most suitable method to predict water inflow under similar conditions.

1. Numerical methods
   Since the mines have a wealth of information, and have a reasonably high hydrogeological parameters. The study takes the Longgu mining as an example, using numerical simulation method to research water inflow in mines. The results of water inflow in mines of major aquifer are shown in Table 2.

   Table 2 shows that the data of prediction of water inflow in mines by numerical method changes a little the error is smaller, compared with the actual data, So, the model satisfy the accuracy of prediction, can be used to predict water inflow.

   There are two reasons: ① Calculation method is not fully fit the actual groundwater flow movement. This is one of the main causes to the error. ② Lacks the understanding of hydrogeological conditions. Although the study area has accumulated a certain amount of research, still lacks observation materials and hydrogeological parameters of the groundwater.
2. Analytical method
   Using the analytical method to predict the water inflow of Longgu, Zhaoguan and Jiyang, three mines. The results are shown in Table 3.

   Table 3 show that there exist some errors between the prediction data and the actual data, especially for Longgu, Zhaoguan mines, which have a bigger errors by analytical method.

   There are three reasons: ① the complexity of boundary conditions and the aquifer medium, which will take water inflow errors. ② selecting the applicable formulas: the Dupuit equation is the steady flow of groundwater, but using the analytical method to predict water inflow in mines, the drawdown range from tens of meters to several hundred meters, is not a slowly varying flow. ③ errors from selecte impact radius, impact radius in mines is impossible symmetrical.
3. Hydrogeological simulation method
   Using hydrogeological simulation method to prediction water inflow of zhaozhuang and Jiyang mine, The prediction results are shown in Table 4.

Table 1. Collection information.

Mine	Information	Hydrogeological parameters accuracy
Longgu	Rich	Higher
Zhaoguan	General	General
Jiyang	Less	Lower

Table 2. The prediction results on water inflow in mines by numerical method.

Mine	Aquifer	Numerical simulation water inflow (m^3/h)	Actual water inflow (m^3/h)
Longgu	Shanxi3 sand	236	250
	Shanxi3 gray	845	720

Table 3. The prediction results of water inflow by analytical method.

Mine	Prediction aquifers	Water inflow (m^3/h)	Actual water inflow (m^3/h)
Longgu	Shanxi group 3 sand	343.4	250
	Shanxi group3 gray	834	720
Jiyang	10# aquifer roof	414.8	543
Zhaoguan	11# and 13#	2564.4	1669.2
	–415 m horizontal	343	245

Table 4. The prediction results of water inflow in mines by hydrogeological analogy method.

Mine	Water inflow Prediction (m^3/h)	Actual water inflow (m^3/h)	Formula expression
Zhaoguan	934		$Q_{set} = Q_{set} \times \sqrt{\frac{F_{real\text{-}time}}{F_{the}}} \times \sqrt{\frac{S_{real\text{-}time}}{S_{set}}}$ $F_{real\text{-}time}$ actual mining area $S_{real\text{-}time}$ levels of actual deep
Jiiyang	853	350	F_{the} anticipated mining area S_{set}, it is expected that water level down deep

Table 4 show that the hydrogeology analogue method has limited, can just be used for the approximate calculation.

There are two reasons: ① the hydrogeological conditions difference between existing materials of the water inflow in mines and the budgetary exploration areas. ② determining the analogy coefficient.

4 EVALUATION ON ERROR ANALYSIS AND APPLICATION

4.1 *Error analysis*

According to the all aspects of prediction the mine water inflow, the reason that may cause the prediction distortion of the mine water inflow can be summarized as follows:

1. Lacking the knowledge of hydrogeological conditions in mines, and non-identifying mine hydrogeological conditions
2. Improperly selecting the hydrogeological conceptual model. If the hydrogeological parameters data incorrectly or partition errors, boundary conditions or flow forms generalized improperly, will affect the accuracy of the results.
3. Mathematical model distortion. Usually, it is difficult to accurately describe the complex hydrogeological conditions and mining system with mathematic expressions. So to establish the mathematical model is hard, and slightly carelessness can make mathematical model distortion.
4. The well building engineering and the mining process in mine area are different from groundwater numerical simulation. Besides, the actual mining coal project unceasingly excavates according to the working area at time, while the numerical simulation treatment process does not simulate the groundwater by stages according to the actual coal mining project, instead it takes the mining time as the beginning stage of numerical simulation, and takes the finishing point of mining process as the end stage. Thus there exists some certain difference between prediction steps and actual mining engineering.
5. Influence on mining coal craft, well building practice and mining rate affected to predict water inflow in mines

4.2 *Evaluation on prediction methods and applicability of water inflow in mines*

1. Evaluation on applicability of numerical method
   Advantages: ① it can consider many factors, it has strong ability of adapting to boundary condition, is good at describing the non-isotropic and characteristics of aqueous medium, is easy to deal with the source and converge terms in control equation, it completely considers the non-linear problem about pressure-bearing turning to non-pressure in the process of pelting the deep sparse falling; ② It well solves various ground-water flow conditions under complex condition, and has the high precision; ③ The eological models by numerical method can clearly reflect the distribution information of each stratum.
   Disadvantages: ① modeling and operating work are heavy and time-consuming; the load of memory and computation is huge. ② It needs to revise water inflow in mines repeatedly, to make computation water levels of numerous controlled points drop to the designed requirements. ③ It needs the high systematic characteristics and accuracy of materials.
2. Evaluation on applicability of analytical methods
   Advantages: ① Analytical method in predicting water inflow in mines is simple and convenient; ② It is applicable to any type of roadway, as well as the water inflow in mines calculation of specialized unwatering drainage device.
   Disadvantages: By theoretical analysis and practice know that the method is not suitable for water inflow of large drawdown irregular mine calculations prediction.
3. Applicability evaluation of hydrogeological analogy methods
   Advantages: ① when hydrogeological conditions are quite simple, water inflow is not big and the mine of hydrogeology work degree is

low, it is available to use analogue method. ② When being used for the long-history production, we can forecast the water inflow of new expanded working area according to the actual draining water material of previous horizontal, or according to the draining water material of production working area, and the effect is good.

Disadvantages: ① When dynamic changes of influencing factors in mines water filling cannot be considered thoroughly, then we cannot use this method to forecast water inflow; ② When lacking of similarity under the geological and mining engineering conditions, it cannot be used too.

In summary, the analytical method operates simply, fast and economically, but the simplification of boundary and selection of parameter affect prediction accuracy. It is suitable for predicting water inflow under simple hydrogeological conditions, as well as simple boundary conditions; the numerical method is suitable for solving complex problems because of its quick computation, high prediction accuracy, simple computational method and economical, but it is an approximate estimation method and is suitable for the old mine with similar hydrogeological conditions and long-term water volume observation materials.

Therefore, in order to satisfy the accuracy and having the hydrogeology detailed material may use the numerical method to predict water inflow in mines. When lacking enough research area materials, may use the numerical method to predict water inflow by simulation, and simultaneously use the analytical method as comparison. The newly-built mine, when the hydrogeology parameter is insufficient, may use the hydrogeology analogue method to predict.

5 CONCLUSIONS

From the contents discussed above, the following conclusions can be draw: The prediction of water inflow in mines must follow three principles: finding out different conditions, using representative calculated parameters, and selecting the proper mathematical model. No matter which method is used to predict water inflow in mines, the amount of increment of mine groundwater must be calculated., Moreover, the rationality of calculating water inflow from the water balance must be considered in mines In order to obtain accurate water inflow data successfully, it is necessary to analyze hydrogeological conditions carefully to select the appropriate water inflow calculation methods. Different method has its special using conditions, and in the practical application, different methods. Then select quite accurate one by comparing and comprehensive analyzing water inflow in mines, only by this way can we accurately conform to the practical prediction of water inflow. We recommend that when predicting water inflow in mines, it is better use numerical simulation method, and then take other analogy extrapolating methods as supplement.

ACKNOWLEDGEMENTS

Thanks to the supporter. This work was supported by the National Natural Science Foundation of China (41072188), Program for New Century Excellent Talents in University (NCET-11–0838), "Twelve Five" plan to support the implementation of national science and technology programs (2012BAK04B04), 973 program (2013CB227903), Central Universities Fundamental Research (AQ2013B01), Hebei Natural Science Foundation (E2013508123).

REFERENCES

Chen Mingzhi, Liu Shucai & Yang Guoyong. The Development of Mining Water Inflow Predict Method [J]. *Engineering Geophysics*, 2009, v.601:68–72.

Dong Xingwen. Mine water inflow calculation and maximum parameter determination—On the southern karst mine water balance prediction method [J]. Acta Geologica Sichuan, 1995, 01:75–80.

Du Minming, Deng Ying Er & Xumo. Review of Methodology for Prediction of Water inflow in mines [J]. *Sichuan Geology*, 2009, v.29; No.9701:70–73.

Ma Xiuyuan& Li Yifan,. Numerical methods in the mine water inflow prediction [J]. *Shandong University (Engineering Science)*, 2011, v.41; No.18905: 86–91.

Song Chunhui, Yang Yunlong & Guo Jifeng. Analysis in mines Water Inflow Prediction of several common methods [J]. *Information Development & Economy*, 2009, v.19; No.22310:177–178.

Wen Wenfu & Cao Liwen. Analogy method and the analytical method in a mine discharge prediction analysis and comparison [J]. *Chinese coal*, 2011, v.37; No.42007:38–40.

Wu Cuijuan. A study on the nervous network based mine water inflow predictions [J]. *Chinese coal,* 2009, v.35; No.39910:105–108 + 113.

Zhang Shuai Wei, Zhang Qingfeng, Xu Zhijun & Zhang Fei. Analytical Prediction Cambrian limestone aquifer water inflow [J]. *Science Communication,* 2012, No.6912:157–158.

Progress in Mine Safety Science and Engineering II – He et al. (Eds)
© 2014 Taylor & Francis Group, London, ISBN 978-1-138-00122-0

The application research of mine gas and the fire-reversed stove gas mixing

Guangxue Meng & Hong Guo
North China Institute of Science and Technology, Beijing, China

ABSTRACT: Currently on combustible gas safety studies mostly for single gas, and the study of multivariate mixed gases is less, only a handful of concentration explosive limits data reports[1,2]. This article proposes a application security research program about mixing two different sources, mine gas and fire-reversed stove gas which makes a detail about the theoretical analysis of the program' feasibility, the determination method of mixed gas explosion limit, and the process of using test unit to test determination. Finally, it introduces the safety measures, which should be taken in practical application.

1 INTRODUCTION

Mine gas is one of the main safety problems in coal production, which does great harm to coal mine safety production and people's life and property. Since 1980s, people pay more and more attentions to the comprehensive utilization of mine gas. At present, the widely used technique is pumping coal seam gas by gas drainage pumps, and compress it by gas compressor, and then used in industrial and civil fuel, or power generation, etc. According to this way, not only improve the safety of coal mine production, but also relieve the strain on energy, protect the environment, which achieves "to use for extraction, from extraction to promote safe" virtuous circle development of coal mines.

But the gas concentration and volume are greatly influenced by the resources of the mine and the geological conditions. If the gas pumping capacity reduction for some reason, it will affect the normal supply of gas users. The usually method is shutting down part of users, and shuts down all users gradually, causing a serious waste of original network and equipment.

In order to solve the problem, ensure the gas users of normal air supply, it puts forward under the condition of the mine gas reducing using a network of mine gas and the fire-reversed stove gas mixed with implementation plan. Not only has simple system, convenient management, less investment, more effect, but has the good social benefits and economic benefits as well. In order to use mixed gas safely, this article introduces the program's the feasibility analysis and safety testing.

2 FEASIBILITY RESEARCH

2.1 *Explosion limit of flammable gas*

Mine gas and fire-reversed stove gas are of high quality energy, they have their own explosion properties. After mixing them, their explosion characteristics will change.

Whether the combustible gas in the air will explode or not when it meets fire, which is associated with combustible gas concentration. This range is called explosion limit. We call the lowest concentration of combustible gas in the air explosion when it meets fire (in volume percent) the lower explosive limit; highest combustible gas concentration said the explosion limit. To avoid mixed gas exploding, we should find the gas explosive limits of each component.

2.2 *The algorithm of a single flammable gas explosion limit*

According to the requirement of number of oxygen atoms and combustion reaction, considering the oxygen content in air, we can determine the explosion limit of flammable gas:

$$X_{下} = \frac{100}{4.76(N-1)+1}\% \tag{1}$$

$$X_{下} = \frac{100}{4.76N+4}\% \tag{2}$$

where $X_{下}$ = The lowest limit of a single gas explosion; $X_{上}$ = The highest limit of a single gas

Table 1. The limit of a single flammable gas explosion.

Name	Molecular formula	Highest explosion	Lowest explosion
Hydrogen	H_2	75%	4%
Carbon monoxide	CO	74.2%	12.5%
Acetylene	C_2H_2	81%	2.2%
Ethylene	C_2H_4	32%	3.1%
Methane	CH_4	15%	5%
Ethane	C_2H_6	13%	2.9%
Propane	C_3H_8	9.5%	2.1%
Butane	C_4H_{10}	8.4%	1.9%
Pentane	C_5H_{12}	7.8%	1.4%

explosion; and N = The number of oxygen atoms when the combustible gas fully burning.

The above formulas calculate several single combustible gas explosion limit parameters are shown in Table 1.

2.3 *The calculation method of multiple gas explosion limit*

Firstly, we should make sure the proportion and form of the mixed gas. Secondly, we should benchmark the gas components. In other words, we convert it to pure gas composition, no air base composition and the gas composition. Thirdly, we should find out the explosion limit of the unit gas. Fourthly, we should calculate the explosion limit of the pure combustible gas, no air flammable gas. Fifthly, we should calculate the overall gas (including gas, inert gases (CO_2,N_2) and air) explosion limit in the air.

We can use the Lee Chatelle Formula to calculate the explosion limit of Compound and mixed steam.

2.3.1 *The calculation method of L*

No oxygen and inert (CO_2,N_2) of combustible gas explosion limit for L is:

$$L = \frac{100}{\sum_{i=1}^{n}(X_i / L_i)}\% \tag{3}$$

where X_i = An unit gas percentage (%); and L_i = An unit gas explosion limit.

2.3.2 *The calculation method of L_n*

L_n – The explosion limit of no oxygen containing inert gas (CO_2,N_2) is:

$$L_n = L \times \frac{(1 + X_N / (1 - X_N)) \times 100}{(100 + L \times X_N / (1 - X_N))}\% \tag{4}$$

where X_N = A inert gas percentage.

Table 2. The compositions of fire-reversed stove gas (%).

H_2	CO	CH_4	C_2H_6	CO_2	N_2	O_2
34.0	6.9	7.0	0.9	8.5	41.9	0.8

Table 3. The calculation results.

Mine gas accounted for the proportion of mixed gas (%)	0	20	40	60	80	100
The proportion of combustible gas (%)	95.4	82.3	69.2	56.2	43.1	30
The highest limit of flammable gas explosion (%)	62.01	50.35	40.21	30.56	22.58	15
The lowest limit of flammable gas explosion (%)	8.52	8.03	7.59	6.84	6.11	5
The difference of the flammable gas concentration exceeds the upper limit (%)	33.39	31.95	28.99	25.64	20.52	15.0

2.3.3 *The calculation method of L_N*

L_N – The explosion limit of oxygen containing inert gas (CO_2,N_2) is:

$$L_N = L_n(1 - X_{Air})\% \tag{5}$$

Where X_{Air} = The air percentage.

2.4 *The test data*

The volume fraction of methane in the mine gas is 30% and the air is 70%. The fire-reversed stove gas of compositions are shown in Table 2:

According to three different proportions, the original gas composition, no gas composition of air, no air and inert gas, we make hundreds of testing and calculating. We choose the calculation results of mine gas accounts for each of the gas sample components were 100%, 80%, 60%, 40%, 20%, 0.0%. The result is shown in Table 3. The analysis diagram as shown in Figure 1.

According to calculation results and analysis diagram, we can see when the explosion limit of combustible gas is between 15% and 20%, it is safe to use.

3 THE EXPLOSION LIMIT TEST

In addition to the theoretical analysis, we carry on the experiment of the explosion limit and the

actual measurement of the fire-reversed stove gas and mine gas in different proportion mixing.

3.1 *The explosion test method and test apparatus*

We usually use the propagation method to test explosion limit. The device is shown in Figure 2.

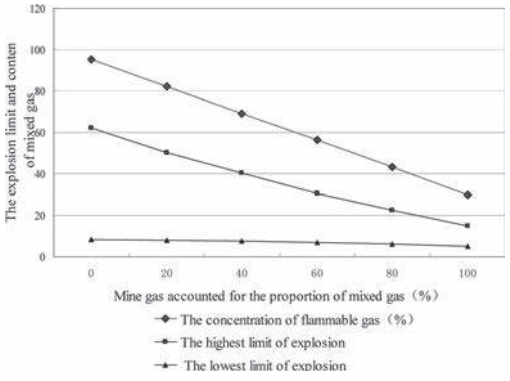
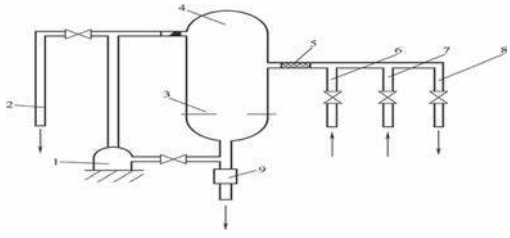


Figure 1. Result analysis.



Where 1-Circulating pump; 2-Pick up mercury manometer 3-Electrode; 4-Explosion tube; 5- Resistance fire net; 6-Pick up air; 7-Pick up samples; 8-Pick up vacuum pump; 9-Discharge air.

Figure 2. Explosion test apparatus.

The main components used 150 cm long, diameter of 7 cm hard glass tube explosion, tungsten rod ignition electrode diameter is 1.5 mm, pressure gauge, flow meter, circulating pump, etc.

Test principle: First of all, we should pump the air of the blast pipe, and then we should make it with a fixed pressure and temperature of a certain concentration of combustible gas and air. After mixing them averagely, we use the ignition electrode to light it, studying the communication situation of the fire. Flame propagation of low concentration or high concentration (gas volume percentage) is the lowest explosion limit and the highest explosion limit in a certain pressure and temperature.

3.2 *The test results*

The test condition: The initial temperature is $T_0 = 20 – 34$ °C; the initial pressure is $P_0 = 13.320 – 34.550$ Kpa. The reactor seals Mixture test results are shown in Table 4.

The results are shown that no matter what proportion to mix the mine gas and the stove gas, it will not explode, which is conformed to the analysis and calculation.

4 THE RESEARCH CONCLUSION AND SAFETY MEASURES IN PRACTICAL APPLICATION

4.1 *The research conclusion*

Through many calculations and tests, we can put forward it: with the stove's gas qualified (<0.8%) and mine gas (>30%) of different mixing proportion are outside the range of explosion, which is safe to use. After the trial is successful, we test three different gases, the coal gas, mine gas furnace and coking coal gas, which is also successful.

Table 4. The experimental results.

Constituent	O_2	CO_2	CO	H_2	CH_4	N_2	C_nH_m	Calorific value (KJ/M3)	The experimental results
Mine gas	15.5	0.85	/	/	28.6	55.1	/	10416.4	
Fire-reversed stove gas	0.40	7.30	34.05	48.82	3.03	6.15	0.25	11038.04	
Mine gas: Stove gas (1:2)	5.45	5.05	22.75	32.50	11.0	22.47	0.23	10886.77	Security
Mine gas: Stove gas (1:1)	8.00	4.07	17.06	24.40	15.85	30.41	0.22	10823.38	Security
Mine gas: Stove gas (2:1)	10.47	3.00	11.36	16.30	20.10	38.57	0.20	10739.23	Security
Mine gas: Stove gas (n:m)		…	…	…	….	…	…	…	Security
Air: Stove gas (1:2)	10.64	3.66	17.02	24.41	1.52	42.62	0.13	5524.61	Explosion

According to the result of three mixed gas test, mine gas concentration is above 30%, with qualified the fire-reversed stove gas and qualified coking coal gas by different mixing ratio, which is the same safe to use.

4.2 *The safety measures*

When using the gas and the fire-reversed stove gas mixing application we should take security measures.

1. We must guarantee the quality of produced gas, oxygen content is below 0.8%.
2. Mine gas concentration requires to more than 30%.
3. To send the fire-reversed stove gas and mine gas at the same time to arrival piping, together with sending the pressure to the gas holder.
4. Stove gas and mine gas should be analysis on a regular basis to ensure that the two gas conform reach the requirements of the specifications and standards, or stop gas holder.

5 CONCLUSION

According to the algorithm analysis and experiment, mixing the mine gas with two gas or even more, if we use it under a certain condition, we can use it safely. The technology has practical application in some coal enterprises.

REFERENCES

Deng Jun, et al. 2007. Experimental Study on Explosive Oxygen Concentration of Coal Mine Combustive Gases. *Safety in Coal Mines*, 6.

Hu Yao-yuan, et al. 2002. Study on The Explosive Limit and Its Container Factor of Polybasic Explosive Mixture Gas Conlaining H2, CH4 and CO. *Sci. China. Ser B*, 32(1).

Huang sheng-chu, et al., 2009. Coalbed methane development and utilization-China:Status and future development, *China Coal*, 35(1).

Liu Bin, 2007. The Recommended Calculation Method of Organic Combustible Gas Explosion Limit. *Journal of Kunming University of Science and Technology (Science Edition)*, 32(1).

Liu wen-ge, et al. 2009. China's coal mine ventilation gas utilization potential and economic analysis. *China Coalbed Methane*, 6(6):3–8

Lu Xiao-qing. 2004. Researches on The Conditions and Possibilities for Mixed Gases Explosion. *Industrial Safety and Dust Control*, 3.

Progress in Mine Safety Science and Engineering II – He et al. (Eds)
© 2014 Taylor & Francis Group, London, ISBN 978-1-138-00122-0

Technology of controlling upper corner gas by pneumatic fan with vortex zone replacement

X.X. Chen, W.G. Jin, L. Gong & H.T. Li
Key Laboratory of Coal Mine Disaster Prevention and Control, Hebei, China
North China Institute of Science and Technology, Beijing, China

ABSTRACT: Because of high inclination angle and thick coal seam in fully mechanized coal face S204 in QiJiapomine, using U-type ventilation can easily result in gas overrun in upper corner. After the analysis of main source and accumulation causes of upper corner gas in fully mechanized coal face. The technology of managing upper corner gas by Pneumatic fan with vortex zone replacement is researched. The best installation location and technical parameters of pneumatic fan have been determined through numerical simulation methods, and the process parameters and the engineering implementation method of replacing upper corner are determined according to the pneumatic fan parameters. Application results show that after the technology has been carried out, gas concentration in upper corner decreased up to 61.78%, and the gas overrun has been effectively controlled, gas control effect is remarkable.

1 INTRODUCTION

Qi jiapo Mine of Baoji Qinyuan Coal Industry is a low gas mine, average relative gas emission is 4.6 m^3/t. Because of high inclination angle, upper corner in working face as leak points of goaf air flow can easily form gas accumulation zone if use U-type ventilation mode is used[1]. And upper corner gas would easily lead to gas overrun and bring great hidden danger to safety production if it is not properly controlled. How to effectively control the upper corner gas in working face is an urgent problem.

The main technologies of controlling upper corner gas in working face in the world scope are as follows: change the ventilation system, airflow dilution method, tail lane method, isostatic pressing method, fan pumping method, gas drainage method, etc[2,3,4]. These methods all play a certain effect in controlling upper corner gas. For instance, changing ventilation system could effect a radical cure for the gas accumulation in upper corner, but roadway maintenance and project cost is large. Airflow dilution is an economic method and simple to install, but the introduction of air volume is limited, ventilation resistance will increase, and operating environment would be narrowed. Tail lane method has a well effect for gas emission, but it is not suitable for the working face of easily spontaneous combustion because it will increase amount of engineering quantity, ventilation resistance and air leakage in goaf. Facilities of isostatic pressing method is installed in return airway and needed to be opened and closed frequently, a large number of gas would gush out once the ventilation system changed or the isostatic pressing facilities are destroyed. Fan pumping method can effectively solve gas overrun in the upper corner, but the fan is hard to install and operate, when the fan stops working, it will cause the problem of gas overrun. Gas drainage method is flexible and effective to control upper corner gas, but the drainage system must be installed, and the project quantities of installation is large. Qi Jiapo mine is a low gas mine and gas drainage system is not installed. After fully comparing the advantages and disadvantages of upper corner gas control technologies, the method of controlling upper corner gas by Pneumatic fan with vortex zone replacement in fully mechanized coal face S204 is researched, concentration of upper corner gas has been effectively controlled and safety production in working face has been guaranteed.

2 MAIN SOURCES AND ACCUMULATION ORIGIN OF UPPER CORNER GAS IN MECHANIZED COAL FACE S204

The fully mechanized coal face S204 is located in the south limb of Qi Jiapo mine, the average inclination angle of the coal seam is 15°, and the average thickness is 8.0 meters, the length of the lower roadway is 1560 meters and the upper roadway is 1500 meters, inclination length of working face is about 180 meters, U-type ventilation mode is used

in the working face. According to the field test data, it can found that along the inclination direction of the working face, the gas concentration changes little from the air inlet side to the middle of working face, but increases rapidly from the middle of working face to the upper corner, especially near the return air side in the range of 30 to 40 meters. This is because airflow takes goaf gas into the middle of working face where gas begins to accumulate. The monitoring point that perpendicular to the coal wall in the working face shows that the gas concentration in goaf side is much higher than that is found in coal wall side, which indicates that the goaf gas is the main headstream in working face.

Using U-type ventilation and under the air pressure between intake and return air way in working face, upper corner as the air leakage point in working face is the only way by which the emitted gas in goaf and airflow pass. Wind speed is very low in upper corner near coal wall and goaf side, and the wind current is located in vortex state. A large number of high concentration gas which emitted from goaf is difficult to enter into the main airflow due to vortex motion, and this motion leads to circulatory movement of high concentration gas and local gas accumulation near upper corner.

3 TECHNOLOGY OF CONTROLLING UPPER CORNER GAS BY PNEUMATICFAN

3.1 *Introduction of pneumatic fan function*

FQ series mine pneumatic fan is developed by China University of Mining and Technology, the working medium and the power of the motor are compressed air. Output shaft are installed at the both ends of fan, fan blade is installed in the front end and linen wind wheel driven by the fan airflow is installed in the back, and there has an incomplete circular air outlet in the linen wind wheel. Thus, blade and line wind wheel would be rotated by the fan when the fan is working, and a certain frequent and disturbed jet which can reach the range of 8 meters to 15 meters would be generated in a conical area, so it is suitable for blowing dead space of ventilation, especially for harmful gas accumulation in upper corner.

3.2 *Numerical simulation technical parameters of pneumatic fan for managing upper corner gas*

According to the mining conditions in working face S204, some parameters such as the average inclination of coal seam is 15°and the main airflow speed is 1.6 m/s, are input into FLUENT software. After the numerical simulation analysis for the effect of different location and technical parameter of pneumatic fan in upper corner field, the obtained data is shown in Figure1 to figure 4, it shows streamline distribution of flow field on the condition that the

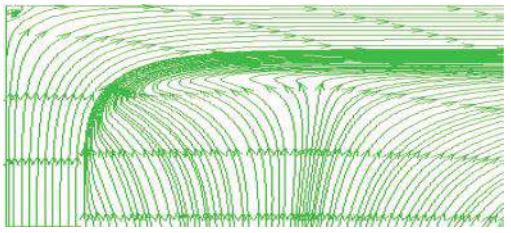


Figure 1. 4 meters away from the outer side wall in upper.

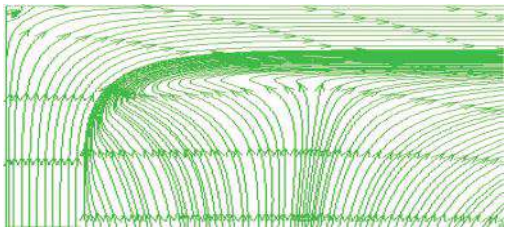


Figure 2. 5 meters away from the outer side wall in upper.

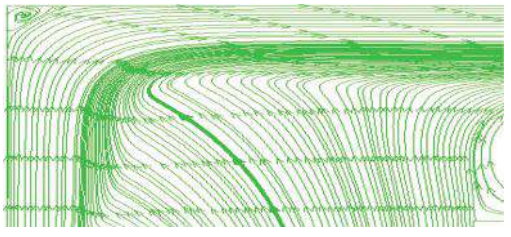


Figure 3. 7 meters away from the outer side wall in upper.

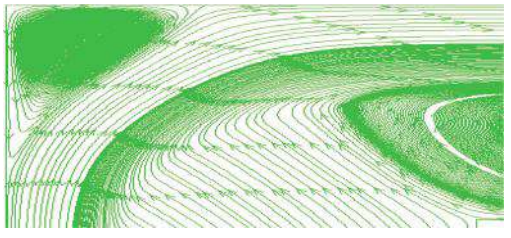


Figure 4. 9 meters away from the outer side wall in upper.

angle between airflow direction of pneumatic fan and main airflow direction is 0°, the vertical distance from the outer side wall in upper roadway to the pneumatic fan is 4 meters, 5 meters, 7 meters, 9 meters respectively. When the vertical distance mentioned above was 4 meters or 7 meters, there still existed a small vortex zone in upper corner; when the vertical distance was 5 meters, the vortex zone in upper corner was completely disappeared and maximum range appeared when the distance was 9 meters.

Figure 5 to 8 is the velocity vector diagram of upper corner field on the condition that the angle between airflow direction of pneumatic fan and main airflow direction is 0°, the vertical distance mentioned above is 5 meters, the exit velocity is 15 m/s, 20 m/s, 25 m/s, 30 m/s respectively. As is shown in the diagram, the exit velocity of pneumatic fan is different, the effects on the velocity vector in upper corner field is different. When the exit velocity of pneumatic fan is 15 m/s, 20 m/s, 30 m/s respectively, a small range of low velocity area is still existed in upper corner and the area would have disappeared when the exit velocity is 25 m/s.

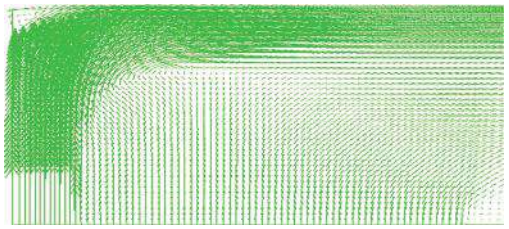


Figure 5. Exit velocity is 15 m/s.

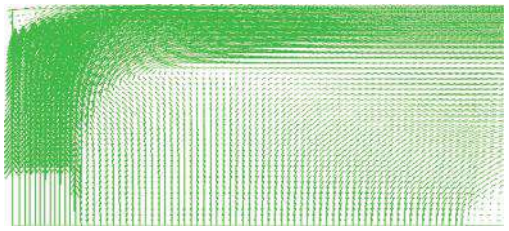


Figure 6. Exit velocity is 15 m/s.

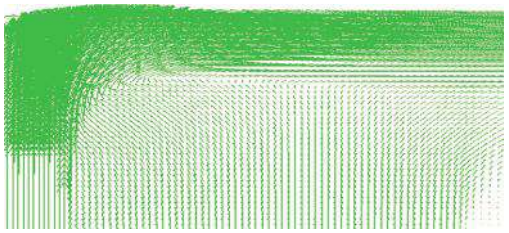


Figure 7. Exit velocity is 25 m/s.

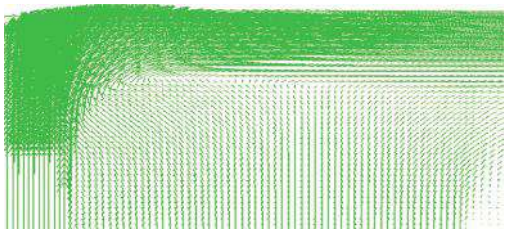


Figure 8. Exit velocity is 30 m/s.

Figure 9 to 11 is the streamline diagram of pneumatic fan under different exit airflow direction.

Though the analysis of numerical simulation mentioned above, the best installation parameters of pneumatic fan for eliminating the vortex zone in upper corner can be obtained. Namely, the vertical distance from the outer side in upper roadway to the pneumatic fan is 5 meters, the exit velocity of

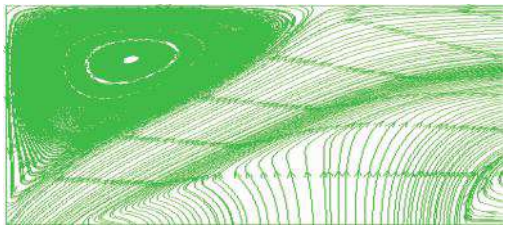


Figure 9. The angle between airflow direction of pneumatic fan and main airflow direction is 30°.

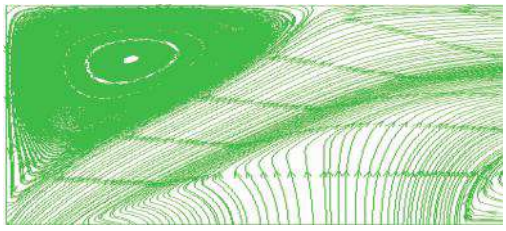


Figure 10. The angle between airflow direction of pneumatic fan and main airflow direction is 45°.

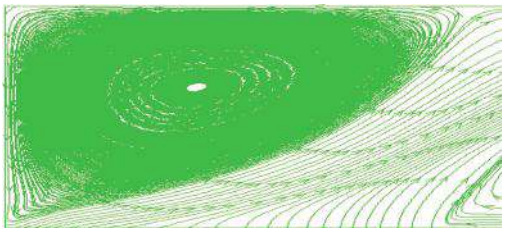


Figure 11. The angle between airflow direction of pneumatic fan and main airflow direction is 60°.

pneumatic fan is 25 m/s, the angle between airflow direction of pneumatic fan and main airflow direction is 0°.

4 CONTROLLING UPPER CORNER GAS BY VORTEX ZONE REPLACEMENT

Vortex zone replacement is used with pneumatic fan. This method uses some chemical material which is good at sealing and inflaming retarding(just like Hassfu) to replace the vortex zone generated in upper corner field, which can eliminate the space of upper corner gas. Meanwhile, in order to make upper corner gas flow with the main return air smoothly, the outer boundary of replacement in replacement area is made into an arc shape for reducing the wind resistance and facilitating the gas flow according to the morphological characteristics of out boundary in vortex zone.

The project of vortex zone replacement is shown in Figure 12. The technological parameters of replacement management is determined by the parameters of pneumatic fan, the details are as follows:1) The center angle corresponding to the arc AC is 60°, 2) The vertical distance of AB is 3.0 meters, 3) The horizontal distance of BC is 2.0 meters, 4) The height of airtight wall and replacements equals the roof of upper roadway, 5) The normal distance from pneumatic fan to BC is 5.0 meters, 6) Pneumatic fan is fixed on the posterior column of end support, and 5 meters away from the upper beam, 7) The type of pneumatic fan is FQ-80/5.0, set the exit velocity to 25 m/s. 8) The angle between airflow direction of pneumatic fan and main airflow direction is 0°.

Implementation methods of replacement management project are as follows:

1. Using plastic bags with crushed coal to build vertical airtight walls from scraper conveyers to outer side walls in upper and lower roadway respectively, as is shown in Figure 4. The outside part of airtight wall in lower roadway was sprayed by Hassfu in order to improve the effect of preventing air leakage in lower roadway.
2. Measuring the length of Arc AC in Figure 4 to prepare for spraying Hassfu.
3. Spraying Hassfu on the air tight wall downward from the upper roadway, filling vortex zone that is need to be replaced.
4. Because the first-formed outer boundary of replacements Arc AC is relatively coarse. After the initial spraying, in order to improve the efficiency of ventilation, some modifications should be carried out to make the Arc AC more smoothly.
5. Fixing the pneumatic fan to the posterior column of end support, and making the outlet direction of fan to the outer boundary of replacement area, meeting the angle requirement between the airflow direction of pneumatic fan and the main airflow direction.
6. Connecting the pneumatic fan to the air duct in upper roadway so that the fan can be obtained power.

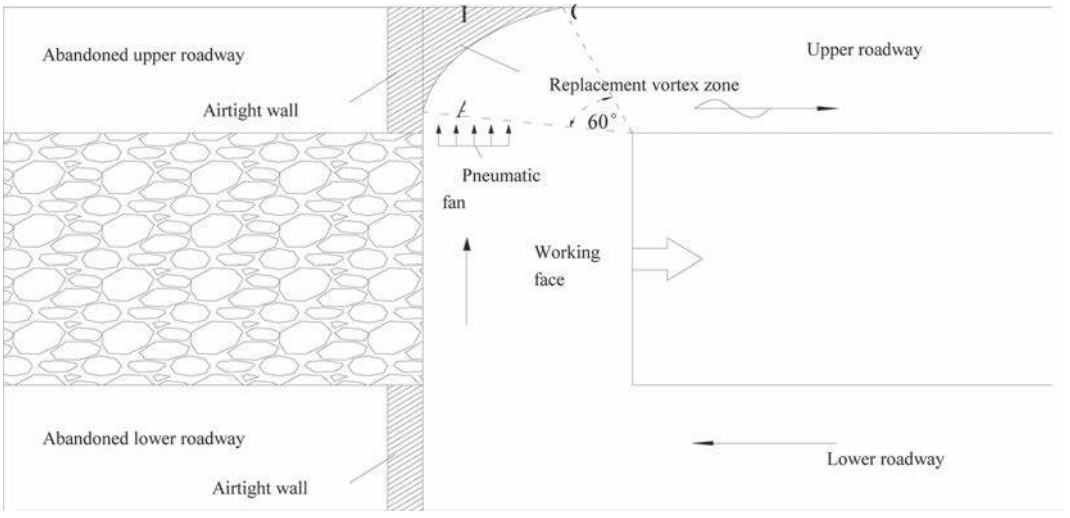


Figure 12. The streamline diagram under different location of pneumatic fan in upper corner field.

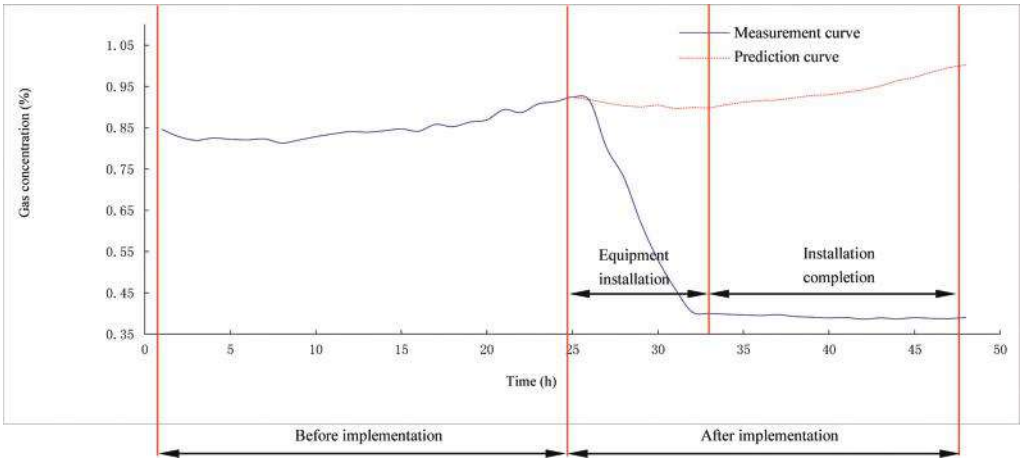


Figure 13. The streamline diagram under different location of pneumatic fan in upper corner field.

5 APPLICATION EFFECT EVALUATION

In order to evaluate the effect of adopting gas control techniques, according to the previous gas concentration before the technology implementation, the later gas concentration can be predicted by grey theory method when the techniquesare not adopted. The gas concentration before adopting gas control techniques in working face S204 at different time is 0.846, 0.822, 0.820, 0.839, 0.858, 0.894, 0.924 respectively, the data is measured in every 4 hours. Figure 5 shows the change curve and the prediction curve of gas concentration in upper corner before and after implementing the technologies.

From the figure we can see that the gas concentration in upper corner shows a rising trend before the technology implementation, but after the technology implementation, the gas concentration decreased sharply at first, and then decreased slowly. There is a big gap between predicted values and measured values, and this gap has a trend of widening. It shows that the technology can effectively control the gas concentration in upper corner. Taking the last data in the day as an example, after the technology implementation, the gas concentration is 0.390%. However, according to the prediction results, the gas concentration will rise to 1.002% without the measures. Therefore, it can be seen that the upper corner gas concentration totally decreased by 61.78% after the measures, thus, the gas controlling effect of this techniques are extremely remarkable.

6 CONCLUSION

1. Upper corner in fully mechanized coal face which uses U-type ventilation is likely to locate in vortex state. A large number of gas emitted from the goaf is hard to enter into the main airflow, which can cause the circular movement and accumulation of gas in upper corner.
2. The installation parameters of pneumatic fan has a significant impact on the effect of eliminating the vortex zone, the optimum parameters of pneumatic fan are as follows: the vertical distance from pneumatic fan to the outer side wall in upper roadway is 5 meters, exit velocity is 25 m/s, the angle between airflow direction of pneumatic fan and main airflow direction is 0°.
3. When vortex zone replacement is adopted to control the upper corner gas, relative technology parameters should be determined based on the parameters of pneumatic fan, and the outer boundary of replacement in replacement area should be made into an arc shape for reducing the wind resistance and facilitating the gas flowing.
4. The comparison between the measured and predicted results shows that the gas concentration in upper corner decreased sharply after implementing the technologies, and the highest decreasing value could reach 61.38%. Desirable results achieved in fully mechanized coal face S204 where gas emission is relatively low.

ACKNOWLEDGEMENTS

Thanks to the supporter. This work was supported by the New Century Excellent Talents in University (NCET-11–0837); Fundamental Research Funds for the Central Universities (2011SYSJJ01).

REFERENCES

Bi, D.C. & Zhang, C.J. 2007. *Effect of upper corner gas drainage in upper corner and goaf [J]. Coal Society*, 2007. (11):13–15.

Lin, B.Q. & Zhou, S.N. 1997. *Methane controlling technique at the upper corner of the goaf in U-type ventilation face [J]. Journal of China Coal Society*, 1997.22(5):509–513.

Mi, X.K. 2009. Gas control at upper entry corner of coal face [J]. *Coal Technology*, 2009.(28):32–34.

Qiao, Z.K. 2012. *The research on numerical simulation of the gas migration in the comprehensive mechanized upper-coal caving goaf [M]*. Taiyuan University of Technology.

Wang, H.L. 1994. The experience of upper corner gas drainage by pneumatic fan [J]. *Coal Engineer*, 1994. (3):45–47.

Progress in Mine Safety Science and Engineering II – He et al. (Eds)
© 2014 Taylor & Francis Group, London, ISBN 978-1-138-00122-0

The prospecting technology for water enrichment of water-inrush geological structure in mine

Wuyang Yang
School of Safety and Engineering, North China Institute of Science and Technology, Sanhe, Hebei, China

ABSTRACT: Karst collapse column, fracture, gob area are the main geologic structures that causing the mining water inrush. Through the comparing research on the application of every kinds of geophysical prospecting, the 3D seismic exploration is adopted to find out the type, size, and distribution of water inrush geological structure, and the transient electromagnetic method and SYT electromagnetic sounding method is used to prospect the watery feature of water inrush structure. The research suggests that the formation water abundance is relative to the size of the apparent resistivity, the watery layer has low apparent resistivity while the low and non-watery layer have high apparent resistivity. The water enrichment of geological structure was analyzed according to horizontal and longitudinal apparent resistivity contour map. This study will provide geological basis for danger evaluation of water inrush. The prospecting results in Huainan mining area suggest that there are two collapse columns in the detection region, the northwest collapse column is free from water and the east one is high with water. The actual laneway shows the data is coincide with the prospecting results, which provides a efficient integrated geophysical method for prospecting the water enrichment of geological structure.

1 OVERVIEW

During the coal mine production, when the excavation roadway runs into karst collapse columns, fault fracture zones, or gob area, the geological hazards, such as coal and gas outburst, roof falling and water-inrush, would be likely to happen. Recent years, several domestic major coal mine accidents are primarily caused by these structures, especially when touching the upper or lower aquifer, the geological structure bearing water would possess the necessary conditions of bursting mine water-inrush (Hu Weiyue & Tian Gan 2010). It is very important to prospect the geological structure type timely and accurately and carry out research on its water enrichment and water storage capacity for predicting mine geological hazards.

2 WATER ENRICHMENT FEATURES OF GEOLOGICAL STRUCTURE AND ITS PROSPECTING METHOD SELECTION

The geological structure, especially the fracture structure, destroys the integrity of aquifuge, meanwhile weakens the water isolating properties and offers a leaking passage to ground water. For different development stages, geological structures are distinct in water enrichment features: the Karst collapse column often forms in areas with soluble rocks. Its water enrichment varies with different development stages. At the rapid development stage of collapse columns, its fillers have not been compacted, featuring high porosity, cavities, water filling and strong water conductivity. Once exposed or touching the affected zone, it will lead to water-inrush accident (Liu Guolin et al. 2009, Yin Shangxian et al. 2008). Upon formation, the fracture will possess the possibility of water enrichment and conductivity, but different types of fracture has different impacts on water enrichment. Featuring weak water enrichment capacity, the compress-shear fracture plane usually contains no water and performs water isolating functions. However, featuring strong water enrichment capacity, the tensor-shear plane usually contains water, especially when communicating with the aquifer. The water enrichment of old mining areas is very complicated and the major reason for water enrichment differences lies in whether the mining areas have been refilled and the saturation of refilling.

Due to the concealment and complexity of water enrichment of geological structures, it is very hard to achieve desired objectives by determining its distribution and properties through conventional geological surveys, especially for the geological structure buried deeply in the ground. For example, it has problems with accuracy for the survey of old mines to be conducted by examining the mining drawing and conducting the survey

of surface cracks (Cheng Jianyuan et al. 2008). Practice shows that the combination of integrated geophysical prospecting and a few underground boreholes can help find out the properties of water-inrush geological structures. At present, the main geophysical prospecting methods to detect geological structure consist of seismic prospecting, transient electromagnetic method, direct current electric method and controlled-source audiomagnetotellurics as well as SYT electromagnetic sounding method (Wang Junru et al. 2002, Ma Zhaofeng 2010, Yu Youshun et al. 2007, Xiang Shoulong 2006, Wang Yanwei et al. 2009). When prospecting on the surface, the seismic prospecting is sensitive to the geological structure type and its occurrence but dull to water enrichment feature. Resistivity method, transient electromagnetic method, controlled-source audiomagnetotellurics and electromagnetic wave method are sensitive to low resistivity good conductor and water enrichment. Due to different working environment of detecting area, different physical properties of rocks and ores, every detecting method has its own application conditions. Single geophysical prospecting may lead to the multiplicity of the outcome, so it is very important to find out efficient prospecting method.

Because of different geological structure depth and surface environment, the combination of geophysical prospecting will have a great impact on the final outcome of its water enrichment prospecting. In several mines of Huainan Coal Mine, the three dimensional seismic method was used to detect the geological structure and finally determined its type, size and distribution range. In Pansan Coal Mine, the corresponding ground location of water-inrush geological structure prospected by seismic prospecting is waterlogged area. It is very hard for many conventional geophysical prospecting methods to prospect on the water, so the combination of transient electromagnetic method and SYT electromagnetic sounding method was selected in this study, to expect a good application effect.

3 GEOPHYSICAL PROSPECTING THEORIES OF WATER ENRICHMENT

3.1 *Transient electromagnetic method*

Transient electromagnetic method solved geological problems by using ungrounded loop or electrode to generate the primary electromagnetic field in pulses and using the loop or grounded electrode to observe the spatial and temporal distribution of the secondary electromagnetic field generated by underground eddy current that was sensed by the first electromagnetic field. this method is sensitive to the underground good conductor medium (low resistivity object), suitable for the evaluation of the water enrichment of faults and fractures, water enrichment prospecting of collapse columns and old mining areas and classifying of roof, floor of coal seam including the aquifer and aquifuge, characterized by alarm to abnormal terrestrial electricity, restriction without electrode contact, strong penetrating and covering ability, subtle volume effect, quick construction and high efficiency. In case of water enrichment, the apparent resistivity will reduce, so this method is an efficient way to explore the hydrogeololgy.

The PROTEM plus 67 transient electromagnetic prospecting system made in Canada was adopted to carry out the detection in the research area on ground.

3.2 *The SYT electromagnetic sounding technique*

The SYT electromagnetic sounding technique is a type of passive electromagnetic system. When the electromagnetic wave which comes from magnetosphere, ionosphere and atmosphere, enters the earth and transmits through underground media, it meets with interfaces with different electric characteristics underground, reflection and penetrating transmission accordingly occurs. A portion of electromagnetic wave is reflected upwards back to the earth surface, the attenuation of its frequency quantum can be calculated through the low frequency window ending frequency formula of the geomagnetism field (Geoff A. Burrell & Leon Peters, JR. 1979, Wang Wenxiang & Yang Wuyang 2002).

$$f = \frac{k\rho}{(H+A)^2} \tag{1}$$

In which, f as the ending frequency (Hz), ρ as the average resistance (Ω·m) of the geological mass at a certain depth, H as the depth (m) of a certain geological mass, k as a constant (9.4×10^5), A as a specific constant, obtained from experiment.

Through derivation, the energy of a certain frequency electromagnetic waves reflects back to the earth surface can be expressed as:

$$V_{fi} = n\frac{\gamma\sigma^2\rho^2}{(H+A)^4} \tag{2}$$

where $n = \dfrac{2\alpha BC_i k^2(10^2-10^3)^2(1-2v)^2}{E^2}$

In formula (2), γ as the reflection factor of interface, σ is the body stress value (MPa), υ is the Poisson

ratio, E is the elasticity amount (GPa), B represents the sensitivity of the transducer (dB), C_i is a variation value which greater than 0 but smaller than 1, α as frequency selection bandwidth of equipment (Hz).

From the formula, it can be known that the reflecting amount of electromagnetic energy is related to the resistivity of underground medium and reflection coefficient of an interface. By calculating the measured data, we can get the apparent resistivity of various depths under each measure point. Research shows that in general, in case of development or water enrichment, the rock crack will be enhanced in absorption of electromagnetic wave, so the energy of electromagnetic wave reflected back weakens a lot and the calculated value of apparent resistivity was low. Accordingly, It can be inferred whether it contains water and its water enrichment degree.

Employ SYT geophysical devices to prospect within the research area.

4 WATER ENRICHMENT PROSPECTING PRACTICE OF WATER-INRUSH GEOLOGICAL STRUCTURE

At present, when prospecting and researching the hydrological conditions in an area, we usually adopted integrated geophysical prospecting. Namely, carry out exploration and investigation of the geological structure and then use electric methods to prospect the water enrichment of the geological structure on ground.

Huainan Coal Mine of research areas is located in the southern margin of the North China plate. Its structural form is a tectonic basin running nearly east-west. The north and south side of the basin collided and formed an imbricate nappe structure and its inside is wide and shows a syncline structure running north-west, forming a synclinorium in Huainan. Pansan Coal Mine is located in the middle of the Huainan synclinorium and the limb of the south-east of Chenqiao anticline and the limb of nappe structure.

From old to new, the layers within the research area are Ordovician system, Carboniferous system, Permian system, Triassic system, Tertiary system and Quaternary system. The coal-bearing stratum is Permo-Carboniferous system. The thin seam of carboniferous Taiyuan group system is nonproductive. The Permian system contains main productive coal seams including 33 coal seams, the primary mineable coal bed are 13–1, 11–2, 8, 4 and 1.

4.1 *Achievements of three-dimensional seismic exploration*

The early three-dimensional seismic exploration found out two geological abnormal objects, located in the northwest and southeast of the prospecting area. In the seismic time section, the standard reflection waves are leaped and disappeared. The layer and seismic attributes of identified geological abnormal objects by seismic exploration shows obvious features of collapse columns. Figure 1 shows the time section of the geological abnormal objects developing at coal seam 8. The number in this figure means the position of the coal seam. Figure 1a is the time section crossing long axis of the collapse column (geological abnormal objects) and its section direction is NE24°. It developed in the west of the prospecting area, featuring small distribution area, elliptic distribution and its long axis was 70 meters and minor axis 40 meters. Figure 1b is the time section along the minor axis of the collapse column (geological abnormal objects) and its section direction is 114°. It developed in the east of the prospecting area, featuring big distribution area and its long axis was about 120 meters and minor axis 100 meters.

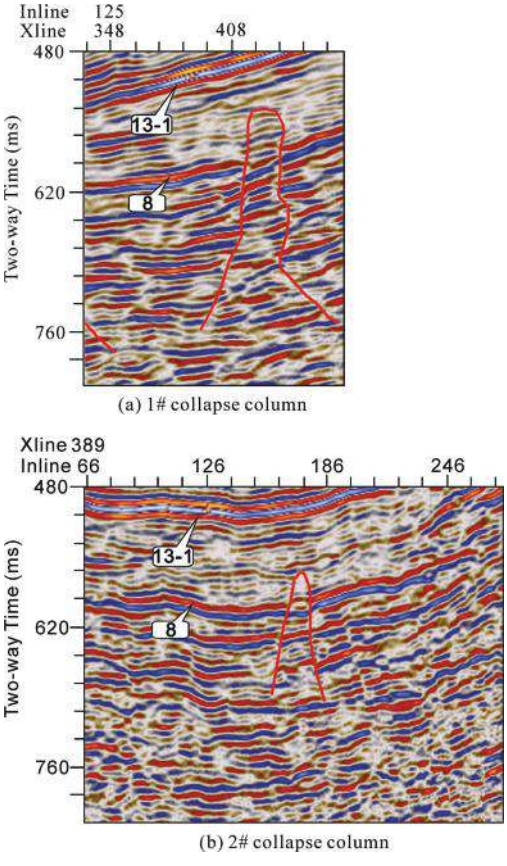


Figure 1. Show up of collapse column on time section of No. 8 coal seam.

The plane configuration of the collapse column was shown in the Figure 2.

4.2 *Prospecting areas and layer positioning*

Take the geological abnormal objects identified by three-dimensional prospecting as the main prospecting area and assign grid measure point in prospecting area with a internal of 25 m, 13 survey lines, 33 measure point on each survey line and a area of 300 m 800 m, as shown in the Figure 2. The dot and line space of the transient electromagnetic method and electromagnetic sounding method are the same.

The transient electromagnetic method equip with high resolution central loop device, emit with a 800 m × 800 m single-turn loop, occupy an area of 200 m^2 and supply with 18 A current and worked within the measure point area covered by the 1/5 of the center loop emitting area. With a sounding depth of 400 m~1500 m, the electromagnetic sounding method prospect point by point.

By prospecting, we should first check up the water enrichment and its distribution area of the geological abnormal objects in the coal strata and then analyze the water enrichment and conductivity of the geological abnormal objects in deep layers as limestone of Taiyuan formation and Ordovician limestone.

4.3 *Data processing method and material interpretation principles*

As for transient electromagnetic method, ρ_s (apparent resistivity) and h_s (apparent depth) can be obtained by conversion. On basis of this, we can conduct topographical correction and elevation correction according to materials concerning measure, geology and misering. The SYT electromagnetic sounding method can form two kinds of drawing by adopting the microcomputer processing software to calculate the apparent resistivity of various depths at each landmark: (1) Contour map of apparent resistivity of horizontal section at different depths used to analyze the coal seam position and the water enrichment and distribution area of layers. (2) Contour map of vertical survey line resistivity used to analyze vertical water enrichment situations.

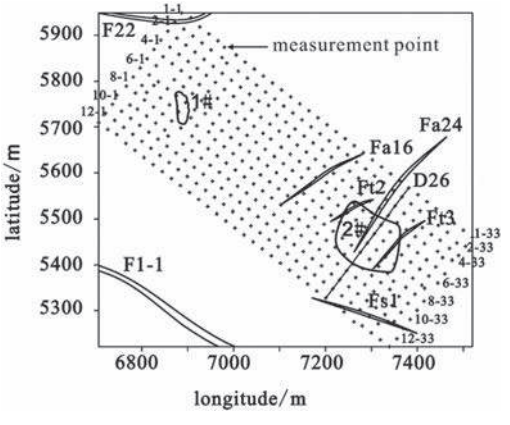


Figure 2. The distribution map of measurement point.

Explain the water enrichment of rock strata. The profile map was based on the horizontal changing features of the apparent resistivity. The explanation principle is: water enrichment area abnormity is the reflection of low resistivity. The stronger the water enrichment is, the low the resistivity is, which was show on the profile map in form of a through featuring "two high and one low". (It is also called "v" style relatively low resistivity). The explanation of the water enrichment area on the profile map is based on the changing of the apparent resistivity. Water enrichment areas are mainly the closed circle of low resistivity on the profile map and the closed circle of minimum is strong water enrichment areas. Moreover, the lower level of the closed circle of minimum is weak water enrichment areas.

Within the prospecting depth, analyze the water enrichment of the target layer through the contour map of horizontal section resistivity at different depths and form a vertical terrestrial electricity section of geological abnormal objects.

4.4 *Geological structure water enrichment analysis*

4.4.1 *Water enrichment of horizontal section*

Take the –650 level coal seam 8 and -800 level limestone of Taiyuan formation as an example for the horizontal section and analyze the structure water enrichment. Figure 3 is –650 level horizontal contour map of apparent resistivity of two method.

Figure 3a is the outcome of SYT electromagnetic sounding method. There is large low value area but the level of 1# collapse column lie in the high value area of apparent resistivity with low water enrichment. The northwest of 2# collapse column is low value area of resistivity with strong water enrichment capacity and meanwhile there is also low value water abundance area in parts of the fault. Figure 3b is the outcome of transient electromagnetic method. The area of 1# collapse column is middle and high resistivity with low water enrichment but the west of 2# collapse column is low value area of apparent resistivity with abundant water. Around the area of the two collapse columns, the outcomes of the two methods are basically the same.

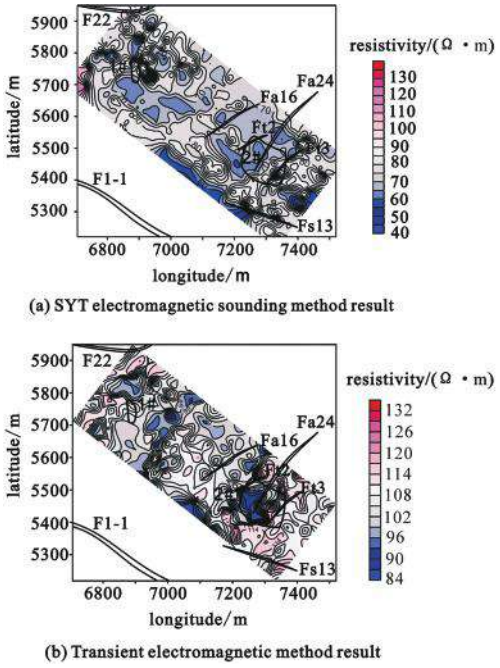


Figure 3. –650 level (8# coal) contour map of horizontal section of apparent resistivity.

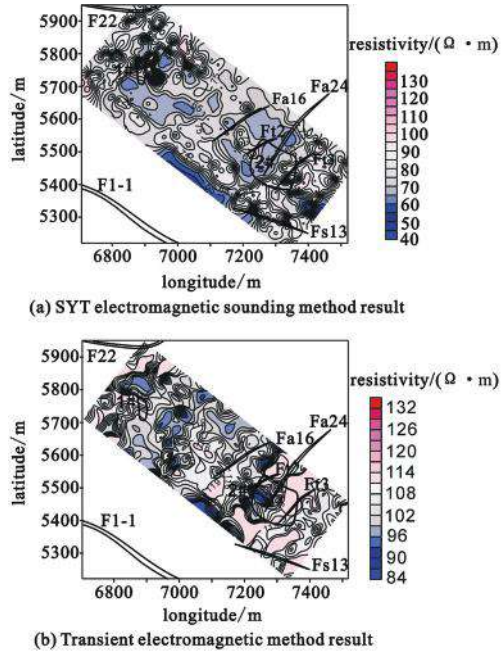


Figure 4. The apparent resistivity contour of –800 level.

The lower of the coal strata lays limestone of Taiyuan formation and Ordovician limestone. In these layers, the water enrichment area water enrichment degree is similar to coal strata.

Figure 4 is the -800 level horizontal contour map of apparent resistivity at the layer of limestone of Taiyuan formation.

In Figure 4a, the area of 1# collapse column is a middle and high value with low water enrichment and the west of 2# collapse column is low value with abundant water, but compared with the coal seam 8, this area is relatively low in water enrichment. In Figure 4b, the abnormal 1# collapse column is high value with scarce water and 2# collapse column lies in low value area. Compared with the coal seam 8, the low value area becomes smaller and part of the west is abundant in water. the prospecting outcome of the two method shows that, at the –800 level, the area of 2# collapse column reduced in the water enrichment.

4.4.2 *Water enrichment of vertical section*

From the analysis of all horizontal sections, we can know that the eastern 2# collapse column has strong water enrichment capacity, so we use the transient electromagnetic method. Figure 5 shows an apparent resistivity sectional map of the D26 line in the middle of the collapse column, it's location is showing in Figure 3. It is a abnormal low resistivity area of –850 to –600 level with a width of 76 m, demonstrating features of the collapse column, which was consistent with the outcome of the horizontal section. Known from the each vertical section, the west of the 2# collapse column has a strong connectivity with the upper and lower aquifer but the southeast relatively weak.

4.5 *Roadway disclosure validation*

Soon after the geophysical prospecting, the roadway of coal seam 8 ran through the geological abnormal part determined by the three-dimensional seismic method. The roadway materials showed that the 1# geological abnormal objective is a collapse column and contains no waters, which is consistent with the explanation of prospecting outcome.

Figure 6 is a sketch of a collapse column section disclosed by coalface. From the disclosure, characterized by mix of big and small rocks, the side of the geological body has the general features of collapse columns. From the analysis of rock fillers, the rock is loose and vulnerable and the rock moves up and has many scoring, which was the result of secondary agent. There was a rock with normal bedding in the middle of the geological abnormal objects, which was caused by the roof falling of the coal seam 8. It has a normal falling

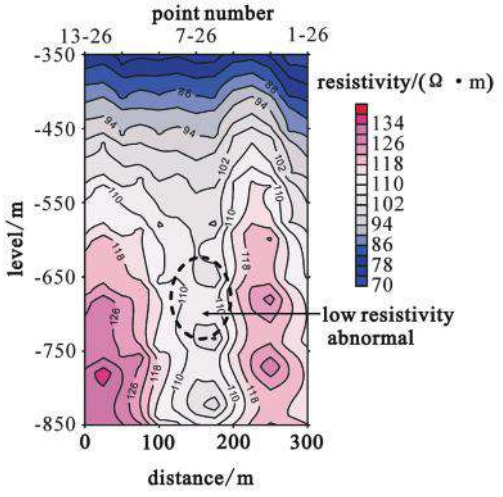


Figure 5. The D26 line apparent resistivity section of Transient Electromagnetic Method.

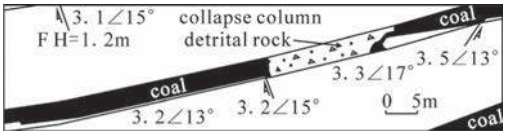


Figure 6. Coalface disclosure Sketch of the 1# collapse column section.

distance with the normal rock strata. The high crack in the geological abnormal object developed and from the distribution, its long axis is 70 m and its minor axis is 30 m.

The water enrichment and distribution range of the 1# collapse column are basically consistent with the prospecting outcome.

The Prospecting outcome of 2# collapse column needs further validation by roadway disclosure.

5 CONCLUSION

Two geological abnormity bodies, named with 1# and 2#, were recognized by three dimensional seismic prospecting method in the prospecting areas. These two abnormity bodies were judged as collapse column from their development features.

The outcome of the transient electromagnetic method and SYT electromagnetic sounding method shows that the 1# collapse column (geological abnormity bodies) in northwest was not water enrich. This outcome was proved by the roadway disclosure. The east of 2# collapse column was partly water abundant and there is hydraulic connection between the upper and lower aquifer in the west of the collapse column and the vertical section through the middle of the collapse column. This needs to be paid more attention in the future roadway excavation.

Materials revealed by some roadway are highly consistent with the outcome of integrated geophysical prospecting. Therefore, combination of transient electromagnetic method and SYT electromagnetic sounding method can be used to find out the water enrichment of the geological structure efficiently, this will provide relatively reliable geological basis for the safety production of coal mines.

REFERENCES

Cheng Jianyuan et al. 2008. The detection technology of excavated region in coal mine and case study. *Journal of China Coal Society*, 33(3): 179–182.

Geoff A. Burrell & Leon Peters, JR. 1979. Pulse propagation in lossy media using the low-frequency window for video pulse radar application. *Proceedings of the IEEE*, 67(7): 981–990.

Hu Weiyue & Tian Gan 2010. Mine water disaster type and prevention and control countermeasures in China. *Coal Science and Technology*, 38(1): 92–96.

Liu Guolin et al. 2009. The study on water conductivity of paleo-sinkholes in North-China-Type coalfields. *Journal of Safety Science and Technology*, 5(2): 154–158.

Ma Zhaofeng 2010. Application on transient electromagnetic method of coal mine in exploring water yield property of karst collapse column. *Coal*, 19(2): 21–23.

Wang Junru et al. 2002. The application of shallow seismic exploration to the detection of rock stratum collapse in mined-out areas. *Geophysical and Geochemical Exploration*, 20(1): 75–78.

Wang Wenxiang & Yang Wuyang 2002. The Shun theory and natural electromagnetic method exploration. *Shanxi People's Publishing House*, Xi'an : 73.

Wang Yanwei et al. 2009. The application of syt natural electromagnetic wave method in the detection of the mined-out areas. *Sci-tech information development and economy*, 19(4): 164–166.

Xiang Shoulong 2006. Water-rich subsided column investigation through the use of Controlled-Source Audiomagnetotellurics. *Coal Geology of China*, 18(supplement): 64–72.

Yin Shangxian et al. 2008. The study on collapse columns and it's water inrushing of north China coal field. *China Coal Industry Publishing House*, Beijing.

Yu Youshun et al. 2007. Application of direct current sounding on detection of collapsing karst column in coal mine. *Resources Environment & Engineering*, 21(6): 736–738.

Progress in Mine Safety Science and Engineering II – He et al. (Eds)
© 2014 Taylor & Francis Group, London, ISBN 978-1-138-00122-0

Determination of mine ventilation resistance and analysis on ventilation systems in the No. 4 mine of Pingdingshan Coal Field

Yang Hu, Yi Fei Weng & Lin Zhang
Key Laboratory of Mine Disaster Prevention and Control, North China Institute of Science and Technology, Beijing, China

ABSTRACT: Determination of resistance of mine ventilation system is an important part of safety production of coal mine and ventilation safety management, the size of the resistance directly influence the effect of the mine ventilation. In order to understand the No. 4 Mine of Pingdingshan Coal Field mine ventilation resistance and its distribution, the optimization of mine ventilation system, selected major determinations, based on the basis of the barometer method for determination of resistance to the mine, and according to the results of mine ventilation system are analyzed.

1 METHOD FOR DETERMINATION

Currently, the determination of mine ventilation resistance in common use precision digital barometer.

Determination method is mainly divided into two point method and synchronization method. Using the method of base point to determine the mine ventilation resistance, it has the characteristics of time saving, labor saving, fast speed, the more commonly used method is the method of base point. Point method is that a barometer is placed in well or at a point well, at a certain time measured pressure reading and record the time of determination and the changes of surface and atmospheric pressure, which is to correct of pressure data of downhole measurement; Another barometer meter air pressure numerical along pre-selected route by point and records the time measurement.

According to the basic point method, the ventilation resistance between two points by using the following formula calculation (Chen Shaoren & Cheng Jianjun 2006, Chen Zhou, et al 2006):

$$h_i, h_{i+1} = (P_i - P_{i+1}) + (H_i - H_{i+1}) \times (\rho_i + \rho_{i+1}) \times \frac{9.81}{2} + \left(\frac{\rho_i v_i^2}{2} - \frac{\rho_{i+2} v_{i+1}^2}{2} \right) + P_{di} - P_{di+1} \quad (1)$$

where h_i, h_{i+1} i and $i + 1$ are ventilation resistance, *Pa*; P_i, P_{i+1} i and $i + 1$ are absolute pressure value, Pa; H_i, H_{i+1} i and $i + 1$ are elevation, *m*; ρ_i, ρ_{i+1} i and $i + 1$ are air density, Kg/m^3; v_i, v_{i+1} i and $i + 1$ are wind speed, *m/s*; P_{di}, P_{di+1} i and $i + 1$ are ground atmospheric pressure variation value when reading, *Pa*.

2 DETERMINATION OF ROUTE CHOICE AND THE ARRANGEMENT OF MEASURING POINT

Determination of route is from the inlet shaft through air location to return all flow route without wellhead installation drag facilities a flow line, it can control the whole network of a ventilation system, and can facilitate the understanding of all kinds of roadway resistance distribution.

Measuring point layout should meet the following requirements:

1. Section is regular, consistent with the wind conditions.
2. Local resistance measuring point road material requirement is: before 3–4 times and 8–12 times after lane width.
3. Measuring point should be located where elevation locations can be found.
4. The measuring distance between two adjacent points is generally 200 *meters*, instrument readings should be greater than 19.62 *Pa*.
5. Measuring point should be located in a safe place.

3 DATA PROCESSING

3.1 *Parameter calculation*

When the working of underground actual measurement end, we must carefully collate and calculate

the actual measurement data (Cheng genyin, et al 2005).

1. Air volume calculation

$$Q = S \times V \tag{2}$$

Where S is Roadway break area of test point, m^2; V is mean wind speed of test point, m/s.

2. Ventilation resistance

$$h_i, h_{i+1} = \left(P_i - P_{i+1}\right) + \left(H_i - H_{i+1}\right) \times \left(\rho_i + \rho_{i+1}\right) \times \frac{9.81}{2} + \left(\frac{\rho_i v_i^2}{2} - \frac{\rho_{i+2} v_{i+1}^2}{2}\right) + P_{di} - P_{di+1}$$

3. Roadway windage

$$R_{1-2} = \frac{h_{i,i+1}}{Q^2} \qquad NS^2/m^8 \tag{3}$$

Roadway standard windage

$$R_{0,1-2} = \frac{\rho_0 R_{1-2}}{\rho_{1-2}} \qquad NS^2/m^8 \tag{4}$$

Where ρ_0 is reference value of underground air density, $\rho_0 = 1.2\ mg/m^3$; $\rho_{1\text{-}2}$ is average of the air density between two section, mg/m^3.

4. Roadway meters wind resistance

$$R_{r100} = \frac{100 R_r}{L_{1-2}} \qquad NS^2/m^8 \tag{5}$$

Where R_r is friction windage of measured straight roadway, NS^2/m^8; $L_{1\text{-}2}$ is distance between the two measuring points, m.

5. Coefficient of frictional resistance

$$\alpha = \frac{R_r S^3}{LU} \qquad NS^2/m^4 \tag{6}$$

Where L is length of measuring roadway, m; U is circumference of the measuring roadway point section, m; Standard value of airway friction resistance factor

$$\alpha_0 = \frac{\alpha \rho_0}{\rho_{1-2}} \qquad NS^2/m^4 \tag{7}$$

3.2 *Data processing principle*

1. The air volume between the measurement section, roadway basal area and perimeter take the calculated average between two points.
2. The air volume is too small or the roadway with throttles, if slightly speed wind table cannot be started, the air flow according to the node flow closed principle, composed of adjacent tunnel air volume calculation.
3. Due to the resistance measurement time is long, everyday air volume has changed, even the same day, a measuring section due to the approaching tunnel door open or vehicles, air volume changes, may cause joint air flow imbalance, the volume takes two point average.
4. If the actual measurement data of manifest error, we use the same lane other measured results by analogy. Small wind amount measuring section, differential pressure is too small, the reading error is larger, this segment has no analogy.
5. The existence of local resistance measured not by analogy.

4 ANALYSIS OF THE RESULTS

4.1 *Resistance measurement result analysis*

In May 25, 2012, the No. 4 Mine of Pingdingshan Coal Mine finished the ventilation resistance, resistance measurement result analysis and opinion as follows:

1. WuJiu mining area of the first level determination results for 4023 *Pa*, compared to draught fan working pressure 3980 *Pa*, WuJiu mining area in measuring resistance of main draught fan working pressure is larger than 43 *Pa*, the error of 1.08%, in the allowable error less than ±5%.
2. The JiSan mining area of the second level determination results for 4067 *Pa*, and draught fan working pressure 4010 *Pa* (Dongtai), measuring the resistance of main draught fan working pressure greater than 57 *Pa*, error is 1.42%, the allowable error of less than ±5%. Determination of GengYi mining area are: 3723 *Pa*, and draught fan working pressure 3760 *Pa* (West), measuring the resistance of main draught fan working pressure is smaller than 37 *Pa*, error is 0.99%, the allowable error of less than ±5%.
3. In third level of determination results for 1770 *Pa*, and compared to draught fan working pressure the 1780 *Pa*, measuring resistance than the main draught fan working pressure too small for 10 *Pa*, error is 0.56%, the allowable error of less than ±5%. Ding Jiu area determination results for: 1781 *Pa*, 1780 *Pa* compared with draught fan working pressure, measurement of resistance than the main draught fan working pressure too small for 1 *Pa*, error is 0.05%, the allowable error of less than ±5%.

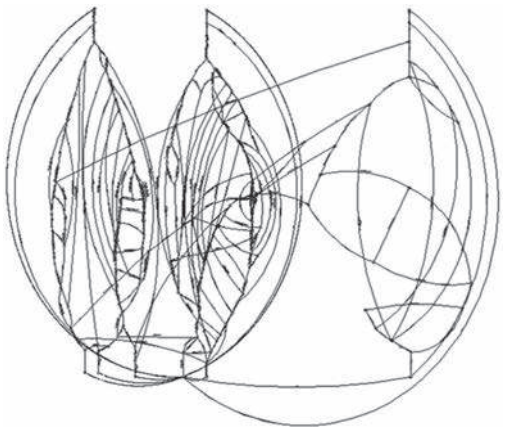


Figure 1. Mine ventilation chart.

Through the calculation, the three shaft system errors are within the allowable error less than ± 5%, basically conforms to the mine ventilation reality, the results can be used for the ventilation system transformation.

4.2 *Mine each air shaft system resistance distribution analysis*

Through the calculation of mine ventilation network and analysis of mine, the WuJiu mining area into, use, air return section resistance percentage of 14.21%:41.9%:43.89%, the JISan mining area into, use, air return section resistance percentage 22.67%:51.45%:25.88%, the GengYi mining area into, use, air return section resistance, percentage of 25.81%: 37.14%:37.05%; the third level into the mining area, use, return period of resistance percentage of 68.92%:18.18%:12.9%; the DingJiu mining area into, use, air return section resistance percentage 54.54%:36.83%:8.63%; The individual location of total return is affected by mining roadway in serious deformation, the roadway contraction section smaller, and the bend more, causing the return air resistance is too large, should focus on the main return airway ventilation resistance area for the expansion and maintenance of transformation, in order to reduce the resistance of ventilation. Mine ventilation network solution shown below.

5 CONCLUSION

1. For a air volume 24750 m^3/min old mine, ventilation resistance, 4010 *Pa*, it indicate the ventilation system line is longer, resistance is bigger. For high resistance of roadway must accelerate roadway repair strength, timing fixed object specific arrangements, to reduce the resistance of ventilation system, better play the main draught fan performance.
2. To further strengthen the management of mine ventilation technology, improve the basic technical work, improve the whole level of management of "one ventilation and three prevention".

GRATITUDE

Research findings of this paper Originate "Greenhouse gas recover from coal mines and unmineablecoalbeds and conversion to energy", Grant agreement no: 268194.

REFERENCES

Chen Shaoren & Cheng Jianjun. Mensuration of mine ventilation resistance and analysis of several problems. *Coal Mining Technology*, 2006, 11(1):72–74.

Chen Zhou. et al. Data adjustment method of resistance measurement for mine ventilation and its application. *China Mining Magazine*, 2006, 15(10):105–108.

Cheng genyin. et al. Measurement and Analysis of resistance in ventilation system of Jinpushan. *China Safety Science Journal*, 2005, 15(9):67–72.

Wang Guochen. Ventilation resistance mine measurements and computer processing systems research. *China Mining Magazine*, 2007, 16(5):107–109.

This page intentionally left blank

Progress in Mine Safety Science and Engineering II – He et al. (Eds)
© 2014 Taylor & Francis Group, London, ISBN 978-1-138-00122-0

Design of mine monitoring system based on ZigBee and CAN

Deguo Liu & Jinshun Wu
North China Institute of Science and Technology, East Yanjiao, Beijing, China

Hao Liang
Department of Scientific Research Collaboration of Jiuquan Satellite Launch Center, East Yanjiao, Beijing, China

ABSTRACT: The current coal monitoring system is analyzed in the paper. We design the new structure of coal wireless monitoring system based on the ZigBee and CAN Technology. The coordinator node is designed using 89C51 and CC2420. Further more, the router node and the end node are designed using CC2530 and the sensors such as temperature, humidity and gas sensors.

1 INTRODUCTION

The environmental parameters in coal mining should be monitored in real time. The current monitoring system in coal mining collects the environmental information from the sensors by the cables. The sensors and the monitoring centers are connected by the cables directly. The information of temperature, humidity and gas is sent to the monitoring centers on the ground. Now, with the developments of the ZigBee and CAN technology, the new wireless monitoring system combining the ZigBee and CAN is studied. The environmental information is collected by the wireless sensor networks underground. Then the information is sent to the ground monitoring centers in real time by the CAN bus. The new wireless monitoring system is low power consumption and flexibility. The system use wireless network and CAN technology. It is easy to lay and expand. The environment information can be transmitted over long distance. The system is suitable for the monitoring of mine environment.

2 SYSTEM VIEW

The current cable monitoring system which is connected by the cables underground demonstrated in Figure 1. The monitoring system includes the sensors, the monitoring stations, the Bus, the Modem and the host monitoring computers. The information is collected by the sensors underground and then the information is sent to the stations by the cables. The information is sent to the modem by the Bus and the information is sent to the host computers on the ground by the cables or optical cables.

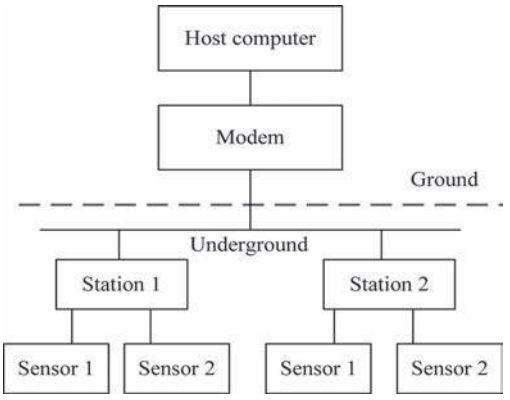


Figure 1. Current monitoring system.

The stations and the sensors are connected directly with the cables. Due to the limitations of the mine, maybe it is difficult to lay the cables between the stations and the sensors somewhere. On the other hand, the cable will perish or be eroded, that is hidden danger to monitoring system. Therefore, there are some defaults for the system with the cables.

The monitoring system based on ZigBee and CAN technology is shown in Figure 2. The monitoring system includes the host computer, the CAN bus, the coordinator, the router node and the end node.

The environmental information is collected by the end nodes directly. The end node is composed of the sensors and the microprocessor which possesses the Zigbee protocol stack. The end nodes which are carried by the workers or the mechanical equipments in the mine collect the environmental

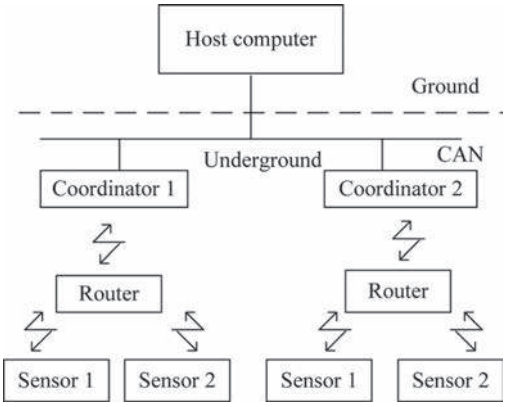


Figure 2. Monitoring system based on ZigBee and CAN technology.

information. The information is transmitted to the router node or the coordinator over the wireless. The end nodes are the reduced function devices (RFD) which can only collect and transmit the information.

The environmental information which is collected from the router nodes directly or collected from the end nodes can be routed to the coordinator. In comparison with the end nodes, the router nodes have the lager transmission power and they are fixed on the wall of the tunnels. The router nodes are the full function devices due to the routing function.

The coordinator node receives the information from the router nodes over the wireless, meanwhile, it converges and deal with the data. Then, the data is transmitted to the host computer over the ground. The coordinator is the important node in the system. The coordinator which is the full functional device (FFD) builds the networks and receives the data from the router nodes or end nodes. The coordinator node can also control the router nodes or end nodes.

The host computer with the monitoring software deals with the data from the mine. The data can be analyzed and stored. Then it can also be shown by the LCD screen or be printed in real time. The data is transmitted between the host computer and the coordinators by the CAN bus. The CAN bus adapts the non-destructive arbitration technique, which can avoid the bus collision. It ensures the capacity and the rate of the data. From Figure 2, we see that the data is transmitted between the coordinator node and the router node or the end node over the wireless. It is flexible to install the node underground over the wireless. Further more, it avoids the dangers of the cables such as the aging, the breakage and the corrosion of the cables. Therefore the wireless monitoring system is suitable to the mine.

3 THE COORDINATOR NODE

From the analysis above, we can conclude that the coordinator is an important node which collect and transmit the data. The structure of the coordinator is shown in Figure 3.

The coordinator node use 89C51 which is from the Intel Company as the microprocessor. The CAN bus controller use SJA1000 from the Philips company. Since the 51 series microprocessor can connect directly with the CAN bus controller, it is easier to design the hardware. In order to use 51 series microprocessor, the "MODE" foot of SJA1000 should be set to high level. Due to the special environment underground, the jamming of the wireless network is serious. The CAN bus between the host computer and the coordinator node can decrease the jamming underground. The Highly integrated CAN controllers SJA1000 can realize the bus access priority and hardware filter. The PCA82C250 which is the transceiver for CAN bus can support more than 110 nodes. The communication distance, the precision and reliability are improved by the PCA82C250 transceiver.

In order to enhance the anti-interference capability of the system, the optical isolators 6 N137 module is adapted between the transceiver and controller of the CAN bus.. The CC2420 module is the RF transceiver between the coordinator and the router node or the end node. First the RF transceiver CC2420 receives the information and transmit to the 80C51 microprocessor, then the information is transmitted to the host computer by the CAN bus. The keyboard module, the LCD display module and the alarm module are designed on

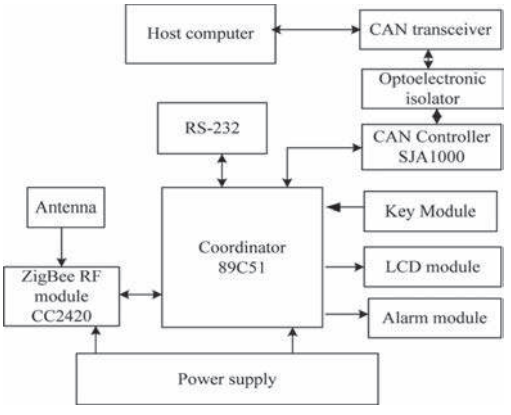


Figure 3. The Coordinator node.

the coordinator node. The environmental parameters upper and lower limits are set by the keyboard module. The LCD displays the function menu and the environmental parameters. When the end node is separated from the network or the environmental parameters overrun the limits, the alarm module will send alarm information. The RS232 is used to debug the program.

4 THE ROUTER NODE

The router node collects the environmental parameters and relays the information. The structure of the router node is shown in Figure 4.

The router node includes the CC2530 chip, the sensors, keyboard and the led. The CC2530 is a true system-on-chip solution for ZigBee applications. The CC2530 combines the excellent performance of a leading RF transceiver with an industry-stand enhanced 8051 MCU and in-system programmable flash memory.

The sensor monitors the gas, the temperature and the humidity underground. In order to detect the methane, the TGS813 which is a tin dioxide (SnO_2) semiconductor is a general purpose sensor with sensitivity to a wide range of combustible gases. The conductivity of SnO_2 is low in clean air. But the conductivity of SnO_2 increases depending on the detectable gas concentration in the air. TGS813 has the long life and low cost. The sensor module can convert the change in conductivity to an output signal according to the gas concentration.

The digital temperature-humidity sensor SHT11 is used to detect the temperature and the humidity underground. The temperature and the humidity can be detected by the SHT11 sensor at the same time. The operating range of the temperature is –40~+123.8°C, the temperature accuracy is ±0.4°C. The operating range of the humidity is 0~100%RH, the humidity accuracy is 3%RH. The information of the humidity and the temperature is transmitted to CC2530 micro processor by the SCK and the DATA line. Then the environmental information is sent to the coordinator node bye the antenna. It will explode when the concentration of the methane is 5%–15%. Therefore, the router node will alarm when the concentration of the methane is more than 3%.

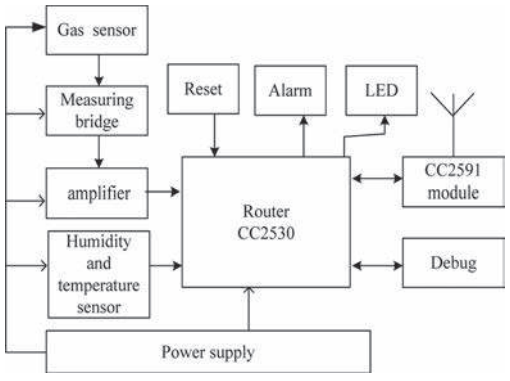


Figure 4. The Router node.

In order to improve the sensitivity and the transmission power, the CC2591 as the broadband RF front end is used. The TPS73033 power supply is used in the design. The TPS73033 module can change the input volt 3.3~6V to the steady output volt 3.3V.

5 THE END NODE

The end node is only responsible for the collection of the environmental parameters. The structure of the end node is similar to the router node. In order to reduce the cost, the end node has no the module of broadband RF front end CC2591. The transmission range of end node is shorter than that of the router node. The end nodes collect only the information. The router node can not only collect the information but also relay the information.

6 CONCLUSION

The current monitoring system underground is analyzed. Then the new monitoring system underground based the ZigBee and the CAN technology is discussed. The coordinator node, the router node and the end node are designed. The new monitoring system base on the Zigbee and CAN technology underground can monitor the environmental parameter underground and display the information. The new system is suitable to the complex environment underground and it will play a great role in the coal mine safety monitoring system.

ACKNOWLEDGEMENT

This paper is supported by the Fundamental Research Funds for the Central Universities (3142013056, 3142013095).

REFERENCES

Akhondi, M.R. et al. 2010. Applications of Wireless Sensor Networks in the Oil, Gas and Resources Industries, 24th IEEE International Conference on

Advanced Information Networking and Applications. Perth, WA. pp: 941–948.
CC2420 2.4GHz IEEE 802.15.4/ZigBee-ready RF Transceiver. http://www.chipcon.com.
Qandour, A. et al. 2012. Applied application of sensor networks in underground mines, Networking, Sensing and Control (ICNSC), 2012 9th IEEE International Conference. pp: 256–260.
Sun, B.S. et al. 2010. Design of the mine gas sensor based on zigBee. Proceedings of the Third International Symposium on Computer science and computational Technology (ISCSCT'10). Jiaozuo, P.R China, 14–15. pp:077–081.
Wang Q.Z. et al. 2008. Application Study of Mine Alarm System based on ZigBee Technology, Proceeding of the IEEE International conference on Automation and Logistics, (ICAL2008), Qingdao, China. pp:2637–2540.
Zigbee Alliance Website http://wwwzigbee.org.

Progress in Mine Safety Science and Engineering II – He et al. (Eds)
© 2014 Taylor & Francis Group, London, ISBN 978-1-138-00122-0

Development and application of gel foam materials for fire prevention and extinguishing

Zhenhua Xie, Tingting Luan & Yu Zhang
Civil and Environment Engineering School, University of Science and Technology Beijing, Beijing, China

ABSTRACT: Because the geological conditions of coal in goaf with high dip and hard roof are complex, and the law of air leakage is complicated and changeful, so the risk of coal spontaneous combustion in goaf is higher, and need to take effective measures for fire prevention and extinguishing. Through theoretical analysis and experimental research, this paper determines the appropriate foaming agent, foam-stabilizing agent, gelling agent, cross-linking agent in gel foam materials. The optimum formula for gel foam materials by experimental study is: foaming agent compound with sodium laureate and SDS at the ratio of 2:3, concentration for 0.6%; foam-stabilizing agent CMC concentration for 0.1%; gelling agent AM concentration for 0.3%; cross-linking agent MBA concentration for 0.3%. This gel foam materials have excellent inhibitor performance and sealing performance for the spontaneous combustion prevention. The gel foam materials were grouted to goaf of 7162 working face in LongDong coal mine for fire prevention and extinguishing. The results in monitoring sites show that the gel foam materials had effectively restrained spontaneous combustion in goaf, and guaranteed the safety mining.

1 INTRODUCTION

Coal spontaneous combustion is one of the major disasters in coal mines, wasting a lot of coal resources, and affecting the coal mine safety production. At present, the process of fully mechanized top coal caving, which has advantages of high mining intensity, high efficiency, good economic returns and etc., are widely used in coal mining, but the caving height of fully mechanized face goaf is big, float coal is more and uneven distribution, which result in the increase of spontaneous combustion risk in goaf (Yan Wei 2010). Especially the goaf with high dip angle and hard roof caving has a greater risk of coal spontaneous combustion. The main reasons are that: fully mechanized mining technology is difficult, which is easy to cause advance speed of the working face slowly or stopping mining and make the oxidation time of floating coal too long in goaf; in addition, coal seam roof is hard, and coal pillar is easy to compression crushing, and the caving filling in goaf is not dense, which increases air leakage. Therefore, we must take the targeted measures for fire prevention and extinguishing to control coal spontaneous combustion in goaf.

At present, conventional methods to control coal spontaneous combustion in goaf include grouting, nitrogen injection, inhibitors injection and etc. fire-fighting technology (Qin Botao 2007, Chan Yafei 2008). In recent years, by the study of coal spontaneous combustion mechanism and new materials, new fire prevention and extinguishing technology can be implemented and applied, such as gel (Deng Jun 2011), atomization inhibitor (Deng Jun 2012), three-phase foam (Xie Zhenhua 2011), etc. but as a result of the restriction of technical and economic aspects, while these materials is used in single, there are still shortcomings such as high cost, incomprehensive effect, and they also cannot satisfy requirements for fire prevention and extinguishing of large dip angle, hard roof caving mining face and etc. special conditions.

Through theoretical analysis and experimental research, the paper developed a fire prevention and extinguishing material with the advantages of synthetic gel and three-phase foam, namely, a fire prevention and extinguishing material of gel and foam, which has excellent inhibitor performance to coal spontaneous combustion and sealing performance to air leakage in goaf. Using gel foam materials can effectively prevent the coal spontaneous combustion in goaf with large dip angle and hard roof caving of 7162 working face in Long Dong coal mine.

2 THE FORMULA OF GEL FOAM MATERIALS FOR FIRE PREVENTION AND EXTINGUISHING

2.1 *Composition and fundamental characters of gel foam*

Gel foam is a kind of decentralized system of which gas dispersed evenly in the gel, which is produced

by the reaction of gelling agent, foaming agent, foam-stabilizing agent, cross-linking agent, etc (A.M.Tafreshi 1999). After gel foam fluid formed foam under the action of foaming agent, the gelling agent and cross-linking agent distributing evenly in the foam wall react cross-linking, forming the gel of cubic reticular structure containing gas. The liquid phase of the gel foam is water, and generally gas phase is nitrogen.

Gel foam combines the advantages of gel and three-phase foam, and overcomes their shortcomings, its character mainly contains:

1. The liquidity of pure gel is bad, and the flow rate and diffusion range is small. Gel foam can be transported smoothly higher and farther range after adding gel into gas phase medium.
2. Large flow gel foam can cover the loose coal in goaf, and have a good effect on cooling and insulating air. So it can effectively restrain spontaneous combustion, and guarantee the highly efficient and safe backstopping.
3. Gel foam has good sealing performance. When the foam is broken, the gel in the foam continues to play a role of sealing and covering, and ensure the constancy and validity of sealing.
4. Gel foam expansion ratio is high, making the gel foam cost of unit volume greatly decreased.

2.2 *The research of gel foam formula*

After gelling agent and foaming agent dissolving and being stirred evenly, we add cross-linking agent and foam-stabling agent and agents form foam rapidly through mechanically foaming. The gelling agent and cross-linking agent in the foam wall set off cross-linking reaction, forming three-dimensional network spatial structure, making up the skeleton of foam, which makes gel foam have incomparable stability and strength than common water-based foam (Asghari, K. 2005, Gupta, D.V.S. 2005).

2.2.1 *The selection of foaming agent and concentration determination*

According to the influencing factors of gel foam performance and selecting principle of foaming agent (Chen Qibin 2007, Gu Xuerong 2005, Romero-Zeron, L.2006), and on the basic of fully analysis and comparison, we select 7 kinds of foaming agents—sodium dodecyl benzene sulfonate (ABS), lauryl sodium sulfate (SDS), sodium laurate, Dodecyl Trimethyl Ammonium Chloride (DTAC), fatty alcohol polyoxyethylene lauryl ether sulfate sodium (AES), A alkenyl sulfonic acid sodium (AOS), Cetyl Trimethyl Ammonium Bromide (CTAB)—to measure their foaming capacity. Take a certain quality of foaming agent by analytical balance, putting it into a 250 mL beaker, then add 50 mL water from LongDong coal mine, dissolving in the constant temperature water bath to ensure that the temperature of foaming-agent water solution can stay at 25°C. After foaming one minute in the Waring Blender, pouring it into graduated cylinder and measuring foaming volume. The experimental results are shown as Fig. 1.

From Fig. 1 we can see that with the increase of concentration of foaming agent, foam volume also increases rapidly; and when the concentration of foaming agent reach a certain value. This is because when the concentration of foaming agent reaches its critical micelle concentration, the gas-liquid interface has been full of foaming agent, and the surface tension of solution will no longer continue to decline.

Under the same concentration of foaming agent, the foaming capacity of sodium laurate, SDS and DTAC is significantly stronger. They can respectively reach 460 mL, 500 mL and 480 mL when the concentration is 0.6%. This is mainly because the surface tension of the solution is lower than the solution containing ABS, AES, AOS and CTAB after adding sodium laurate, SDS and DTAC, which reduces the surface energy of the liquid and is conductive to foam.

Then select sodium laurate, SDS and DTAC to compound with each other. We can know from the experimental results that foaming agent after compounding has better effect on foam expansion and foam stability than single foaming agent. Foaming performance is the best compound at the ratio of 2:3~3:2, and its foaming capacity firstly increases then decreases. We can see by comparing 3 kinds of compounding results that compound with sodium laureate and SDS at the ratio of 2:3 has the best performance, and foam volume reaches up to 630 mL, significantly higher than the other two 460 mL and 500 mL. So we select sodium laurate and SDS to be foaming agent compound at the ratio of 2:3.

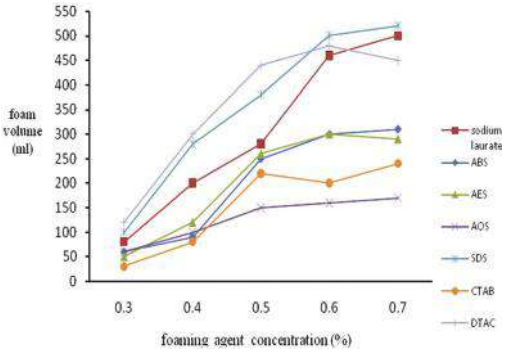


Figure 1. Foaming capacity curve of foaming agent.

Finally, research the influence of concentration of foaming agent on foaming performance by change the concentration of foaming agent. The results are shown as Fig. 2.

We can know from Fig. 2 that with the increasing of the concentration of foaming agent, foaming performance also enhances. When the concentration is greater than 0.6%, foam volume increases slowly. This is because when the concentration exceeds 0.6%, the surface tension of the seriflux falls difficultly, and foaming agent has formed micelles in solution. So we finally determine the concentration of the foaming agent being 0.6%.

2.2.2 *The selection of foam-stabilizing agent and concentration determination*

According to the foam-stabilizing mechanism and demand of foam-stabilizing agent, and through analysis and comparison (Wang Qiwei 2008, Dong, Y.S. 2005), we select 6 kinds of foam-stabilizing agents—starch, glycerol, poval (PVA), Polyacrylamide (PAM), Hydroxyl Ethyl Cellulose (HEC), Carboxy Methyl Cellulose (CMC)—to measure their foam-stabilizing capacity. Measure the foam-stabilizing effect under the same condition of foaming agent compound sodium laurate and SDS at a ratio of 3:2 (concentration for 0.6%) and concentration of foam-stabilizing agent for 0.1%. The results are shown as Table 1.

We can see from Table 1 that the foam produced by system containing HEC and CMC have the longest stability time (more than 4h), but adding different foam-stabilizing agent has influence of different level on system foaming. The foam-stabilizing mechanism of starch, PVA, PAM and HEC is to increase the viscosity of foam and decrease the liquidity of foam. The increasing of foam liquid viscosity are contradictory to the decreasing of surface tension, bringing some bad effects on foaming. Although glycerol has some function of foam-boosting, its foam-stabilizing performance is low, and can't meet the requirement of the field use. The adding of CMC can increase the viscosity of foam liquid, reduce the liquidity; at the same time, it can enhance the structural stability of foam liquidity membrane, making foaming agent molecules distributing orderly on the foam liquidity membrane, and giving foam good elasticity and self-healing ability. So we select CMC to be foam-stabilizing agent. The best concentration of CMC is 0.1% by concentration experiment.

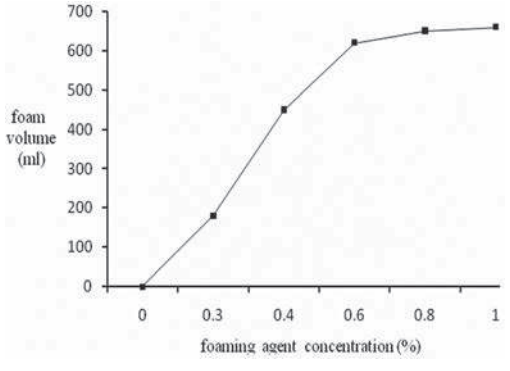


Figure 2. Foaming capacity curve of foaming agent.

Table 1. Different foaming-stabilizing agents' influence on foam volume and stability time.

Foam-stabilizing agent	Starch	Glycerol	PVA	PAM	HEC	CMC
foaming volume (mL)	480	650	520	560	510	620
foamstabilizing time (min)	180	190	210	225	315	295

Table 2. Components concentration relational tables of gelling time and gel foam.

Gelling agent	Concentration (‰)	Cross-linking agent	Concentration (‰)	Gelling time (min)
AM	3	MBA	1	–
	3		2	72
	3		3	14
	4		1	52
	4		2	25
	4		3	8

2.2.3 *Concentration determination of gelling agent and cross-linking agent*

Through theoretical analysis and literature analysis (He Li 2006), select Acrylamide (AM) to be gelling agent and N, N'-methylene-bis-acrylamide to be cross-linking agent, and measure gel time and gelatinous modality of different concentrations. Measure gel time of the respectively reaction of gelling agent AM at 2 concentrations of 0.3% and 0.4% and cross-linking agent at 3 concentrations of 0.1%,0.2% and 0.3%. The results are shown as Table 2.

It will be best that the gel time of gelling agent and cross-linking agent is shorter than the half-time of surfactant forming foam, but it can't be too fast. There is an induction period in the cross-linking

reaction between adding cross-linking agent into gelling agent and viscosity rising. After that, the viscosity increases along with the change of time, and go through a steady-state cross-linking stage.

We can know from Table 2 that under the condition of the same concentration, gel time decreases with the increasing of the concentration of cross-linking agent. When the concentration of gelling agent is 0.3% and the concentration of cross-linking agent is 0.1%, it can't gel; when the concentration of MBA increases to 0.2%, it can gel after 72 min, but its gelling is weak and can not conform to the requirements of the use; when the concentration of MBA increases to 0.3%, gelling time is 14 min, and gel time is appropriate, and gel strength can also meet the requirements. When the concentration of gelling agent is 0.4% and the concentration of cross-linking agent is 0.1%, it takes 52 min to gel, and it is too long; when the concentration of MBA increases to 0.2%, under the condition of less gelling agent and cross-linking agent, gelling time is just 8 min, so it is bad for long distance pipeline transportation. So, both of the two kinds of formula of gelling agent concentration for 0.3%+cross-linking agent concentration for 0.3% and gelling agent concentration for 0.4%+cross-linking agent concentration for 0.2% can meet the requirements of gel foam.

2.2.4 *Determination of gel foam formula*

Determine the best formula of gel foam by comparing experimental results of foam volume, and check the influence of each component on the gel foam. The experimental results are shown as Table 3.

The foaming capacity of the gel foam increases with the increasing of the concentration of the foaming agent, and up to a certain concentration, the concentration of the foaming agent increases but its foaming capacity basically remain unchanged, and 6‰ is the best concentration; but the foam volume decreases with the increasing of the concentration of gelling agent, because the adding of gelling agent makes system viscosity increase, and make it more difficult to overcome surface tension forming foam; concentration of cross-linking agent have less influence on the foaming capacity. It needs some time for cross-linking agent and gelling agent react, to make gelling agent react cross-linking to form gel.

The optimum formula for gel foam materials by experimental study: foaming agent compound with sodium laureate and SDS at the ratio of 2:3, concentration for 0.6%; foam-stabilizing agent CMC concentration for 0.1%; gelling agent AM concentration for 0.3%; cross-linking agent MBA concentration for 0.3%.

3 PERFORMANCE TEST OF GEL FOAM MATERIALS FOR FIRE PREVENTION AND EXTINGUISHING

3.1 *Inhibitor performance test of gel foam*

At present, there are two common methods of testing the inhibitor performance of materials for fire prevention and extinguishing: one is testing the percentage ET of the amount difference of CO released before and after the coal sample processed by inhibiting and the amount of CO released coal sample unprocessed by inhibiting to be the inhibitor rate (Tian Zhaojun 2010); and the other one is testing the percentage Eco of the temperature difference of coal sample before and after processed by inhibiting and the temperature of the coal sample unprocessed to be the inhibitor rate (Lu Wei 2005, Glenn, Gregory M. 2008,).

Experimental facility is shown as Fig. 3. It includes gas supplying system, programmed temperature system and sample analysis. Gas supply system includes air compressor pump, reducing valve, flow control valve and display instrument, and connect them with copper tube in turn. Programmed temperature system includes thermostat and programmed heating controlling facility. Install spiral preheating tube and sample can in the thermostat, and the temperature controlling precision is 0.1°C.

The experimental coal sample is from 7162 working face in LongDong coal mine. Break up the

Table 3. Experiment results of gel foam formula.

Experiment	Composite foaming agent concentration (%)	Foam-Stabilizing concent ration (%)	Gelling agent concentration (%)	Cross-linking agent concentration (%)	Faom Volume (mL)
Formula 1	0.6	0.1	0.3	0.3	620
Formula 2	0.6	0.1	0.4	0.2	570

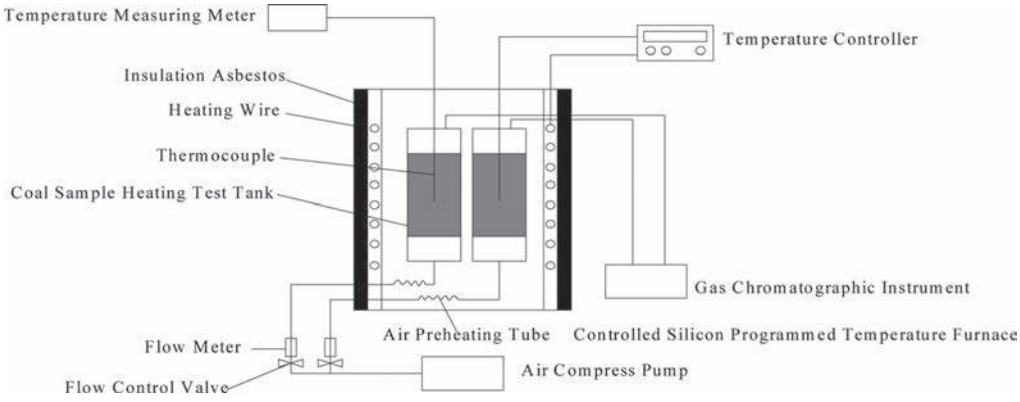


Figure 3. Testing device diagram of the inhibitor performance.

coal sample, take and compound the same weight of coal sample of different granularities which are <0.9 mm, 0.9~3 mm, 3~5 mm, 5~7 mm and 7~10 mm as the experimental coal sample. Add $CaCl_2$ into the mine sample to compare, because $CaCl_2$ is traditional inhibitor for the spontaneous combustion agent. Weigh up three portions 1.0 kg coal sample, and compound respectively: the raw coal sample, coal sample with 10% $CaCl_2$, coal sample with 1% gel foam. After compounding coal sample and inhibitor evenly, ventilate and dry it in room temperature for 24h to constant weight. Put the sample after processing into the coal sample can, under the condition of not passing oxygen into it, and set temperature control furnace running at 30°C constantly. When the temperature of coal sample rises up to 30°C, pass dry air at s flow rate of 100 mL/min, and start programmed temperature and the heating rate is 1°C/min.

Record the coal sample temperature per 15 min, and analysis the content of indicator gas CO by using gas chromatograph instrument. And we get three portions of the coal sample temperature changing rule with the increasing temperature of furnace and the indicator gas CO released in the process of oxidizing and heating up. It is shown as Fig. 4.

We can know from Fig. 4 that under the same temperature conditions, the CO released coal samples processed by the gel foam is much lower than the raw coal samples. The inhibitor rate Eco is 45% at 100°C. We can know from the data of temperature changing (data omitted) temperature of the coal sample processed by the gel foam and $CaCl_2$ is lower than the raw coal sample in the same heating time, and the inhibitor performance of gel foam excels significantly than $CaCl_2$. When the temperature of furnace is 180°C, the inhibitor performance of gel foam is the best (ET = 25%).

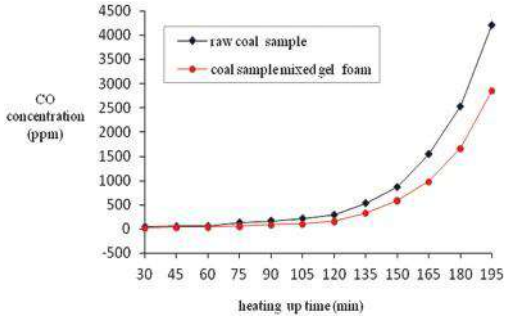


Figure 4. Relations between CO concentration and coal-sample heating-up time.

3.2 *Sealing performance test of gel foam*

Put the coal sample processed by the gel foam into the homemade test-tube of sealing pressure, and make sure the dry air at the entrance of the tube decompressed and pressure controlled by the reducing valve, and test the pressure at the entrance of the tube by pressure gauge. Test the pressure at the exit of the tube after sealed by the coal sample processed by gel foam by pressure gauge. Figure out the pressure difference between entrance and exit, and assess the sealing performance of gel foam.

Break up the new coal sample, take and compound the same weight of coal sample of different granularities which are <0.9 mm, 0.9~3 mm, 3~5 mm, 5~7 mm and 7~10 mm as the experimental coal sample. Weigh up three portions 1.0 kg coal sample, and compound respectively: the raw coal sample, coal sample with 1% water-based foam, coal sample with 1% gel foam. Put the coal samples into the test tube, and seal the whole system. Improve the pressure at

the entrance of the tube gradually, and get the pressure difference between entrance and exit. Test the minimum pressure when the gas breakthrough the block.

After putting the raw coal sample into the test tube, the pressure difference between the two ends of the test tube has no obvious rise, and once gas appears at the outlet, the pressure difference will decreases soon, and gas rips through. After putting the coal sample processed by the water-based foam into the test tube, the inlet pressure can reach up to about twice as high as the outlet, but it can't last long, so the sealing performance is not obvious. After putting the coal sample processed by the gel foam into the test tube, the inlet pressure can reach up to about 6 times as high as the outlet, and the sealing performance is obvious. We can see from the sealing tests of three different samples that sealing strength of the material of gel foam is highest.

4 GENERAL SITUATION OF WORKING FACE

The 7162 working face of LongDong coal mine has recoverable coal reserves of 576200 t, Working face length of 800 m, slope length is 150 m, coal seam thickness is 5.2 to 6.9 m, the average coal thickness is 5.4 m, coal seam dip angle is 22° to 31°, and the average inclination is 25°. Adopt longwall light fully mechanized sub-level caving mining, a mining caving, low recovery rate, remaining coal of goaf is more. The 7162 roof litho logy is mainly for the fine-grained sandstone and sandstone, belonging to the hard roof, roof first cross step distance is 50 m, showed the cycle pressure, cross step down distance is about 30 m, so as goaf compaction time extended, there is a lot of space porosity and air leakage seriously.

The 7162 coal seam spontaneous combustion in coal seams, with explosion risk, has a low gas level. The geological structure of the face is more complex, roadway excavation revealed 13 faults. F114, F108, as the working face advancing and after the demolition process, the protection pillar will withstand the huge rock pressure, the 5 faults will have a greater impact on protection pillar integrity. Fault at the top of the coal is difficult to put a net retention caused by a large number of coals in goaf. As affected by the F108 fault, the face lower half in the F108 fault at the jumping surface, there is a gap of 2 m. Leave here 45 m pillar, surrounded by the pressure of coal pillar crisp formed float coal accumulation; create conditions of coal spontaneous combustion. The 7162 working face goaf has a high risk of coal spontaneous combustion.

5 APPLICATION EFFECT ANALYSES OF GEL FOAM MATERIALS

According to the field monitoring results of coal temperature and gas concentration, combining with the results of numerical simulation, perfusion gel foam for easy spontaneous combustion area of the 7162 working face in LongDong coal mine. Coal temperature in goaf has been monitored in real-time after perfusion, five measure points has been put along the working face in goaf, as shown in Fig. 5.

Part temperature monitoring results of 7162 fully mechanized face in goaf are shown in Table 4.

Seen from Table 4, the temperature of remaining coal with less than 26 m from the working face rises very slowly, This shows that roof caving rock of this area is in loose accumulation state, the pore is more and larger, air leakage intensity is big, and coal spontaneous combustion will not occur; temperature of remaining coal rises significantly within the scope of 34 m ~ 110 m from the working face, which shows that remaining coal in

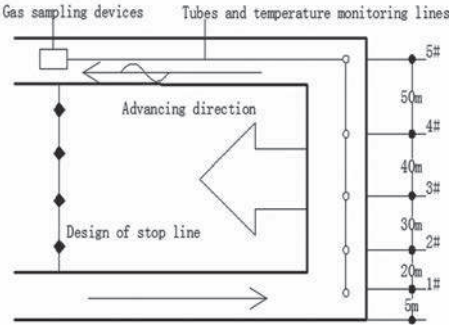


Figure 5. The layout of observation points in goaf.

Table 4. Temperature monitoring data in goaf.

Distance from the working face/m	Temperature/°C				
	1#	2#	3#	4#	5#
0	28.5	28.7	28.6	28.8	29.6
5	29.2	29.5	29.3	29.6	30.3
17	31.6	31.4	31.2	31.7	31.6
26	35.2	33.4	34.5	33.8	35.2
34	37.8	37.5	37.7	36.9	38.6
44	41.2	41.5	41.8	41.3	42.3
59	46.7	47.5	47.2	47.2	47
70	49.7	50.8	51.9	51.2	51.5
87	55.4	55.3	56.4	56.5	53
104	54.2	59.7	61.8	59.6	50.1
117	52.7	57.3	61.4	57.3	48.1
139	48.3	52	53.5	51.5	46.2
153	45.6	46.8	48.2	48.4	44.2
174	41.9	42	43.3	44.4	40.4

this region is oxidation heating as the growth of the time, leading to coal spontaneous combustion. Taken injected gel foam material can effectively prevent the occurrence of spontaneous combustion. The temperature of remaining coal with more than 100 m from the working face begins to reduce slowly, because rock heat dissipation makes oxidation heating gradually disappear, the temperature of remaining coal returns to normal.

6 CONCLUSIONS

1. The gel foam combination of the advantages of gel and three-phase foam has good fire prevention and extinguishing performance.
2. By theoretical analysis and experimental research, selecting sodium laurate and SDS as foaming agent, CMC as form-stabilizing agent, AM as gelling agent, an MBA as the cross-linking agent.
3. The optimum formula for gel foam materials by experimental study is: foaming agent compound with sodium laureate and SDS at the ratio of 2:3, concentration for 0.6%; foam-stabilizing agent CMC concentration for 0.1%; gelling agent AM concentration for 0.3%; cross-linking agent MBA concentration for 0.3%. The gel foam materials have excellent inhibitor performance and sealing performance for the spontaneous combustion prevention.
4. The gel foam materials were grouted to goaf of 7162 working face in LongDong coal mine for fire prevention and extinguishing. The results in monitoring sites show that the gel foam materials had effectively restrained spontaneous combustion in goaf, and guaranteed the safety mining.

ACKNOWLEDGEMENTS

The authors gratefully acknowledge foundation by the national "Twelve—Five" Science and technology support program project of China (project No. 2012BAK09B05).

REFERENCES

Asghari, K., Taabbodi, L., Dong, M.A new gel-foam system for water shutoff purposes in wormhole reservoirs Source: SPE/PS-CIM/CHOA International Thermal Operations and Heavy Oil Symposium Proceedings, v 2005, p A423-A428, 2005.

Chan Yafei, Wang Jiren, Deng Cunbao, etc. Study on influences of different inhibitors on coal spontaneous combustion [J]. Journal of Liaoning Technical University (Natural Science), 2008, 27(1):1–4.

Chen Qibin, MA Baoqi, Ni Binghua. Effects of Several Factors on the Properties of a Foamed Gel [J]. Journal of East China University of Science and Technology (Natural Science Edition), 2007, 33(1):71–74.

Deng Jun, Wang Nan, Wen Hu, etc. Study on characters of high-water fire prevention gel [J]. Journal of Xi'an University of Science and Technology, 2011, 31(2): 127–131.

Deng Jun, Wu Huiping, Ma Li, etc. Experimental Research on Atomizing Performance of Coal Spontaneous Combustion Inhibitors [J]. Safety in Coal Mines, 2012, 4 (5):15–18.

Dong, Y.S.; Liu, B.; Lin, P.H.; Zhang, Q.G.; Pu, Y.P. Macroporous hydroxyapatite scaffold fabricated by foam impregnation Source: Key Engineering Materials, v 288–289, p 565–568, 2005.

Glenn, Gregory M.; Klamczynski, Artur; Chiou, Bor-Sen; Orts, William J.; Im, am, Syed H.; Wood, Delilah F. Temperature related structural changes in wheat and corn starch granules and their effects on gels and dry foam Source: Starch/Staerke, v 60, n 9, p 476–484, September 2008.

Gu Xuerong, Zhu Yuping. Gel chemical[M].Beijing: Chemical industry press, 2005.

Gupta, D.V.S., Leshchyshyn, T.T., Hlidek, B.T. Surfactant gel foam/emulsions: History and field application in the western canadian sedimentary basin, Source: Proceedings—SPE Annual Technical Conference and Exhibition, p 4543–4549, 2005, Proceedings—SPE Annual Technical Conference and Exhibition, ATCE 2005.

He Li, Jiang Zhong- an, Zhong Mao- hua. Study and application on optimum gel inhibitor for coal spontaneous combustion by orthogonal test method[J]. Journal of Safety Science and Technology, 2006, 2(4):40–44.

Lu Wei, Wang Deming, Chen Ge, etc. Research on Programmed Temperature-rise Oxidation Method Used for Evaluating Performance of Inhibitors of Coal Spontaneous Combustion [J]. Mining Safety & Environmental Protection, 2005, 32(6):12–14.

Qin Botao, Wang Deming. Present Situation and Development of Mine Fire Control Technology [J]. China Safety Science Journal, 2007, 17(12): 80–85.

Romero-Zeron, L., Kantzas, A. Evolution of foamed gel confined in pore network models Source: Journal of Canadian Petroleum Technology, v 45, n 11, p 51–62, November 2006.

Tafreshi, A.M., Marzo, M.di.. Foams and Gels as Fire Protection Agents[J]. Fire Safety, 1999, 33(4): 295–305.

Tian Zhaojun, Wang Deming, Xu Yongliang, etc. Research of Foam Gel Using for Fire Prevention and Gas Plug [J]. Journal of China University of Mining & Technology, 2010, 39(2): 169–172.

Wang Qiwei, Zheng Jingtang, Cao Xulong, etc. Foam capacity in tertiary oil recovery and applicati on in pilot [J]. Journal of China University of Petroleum, 2008, 32(3):93–98.

Xie Zhenhua, Li Xiaochao. Application of Three-phase Foam Technology for Spontaneous Combustion Prevention in Longdong Coal Mine. Procedia Engineering, 2011, 26: 63–69.

Yan Wei, Zhao Changhong. The Analysis and Safety Technology of full-mechanized mining technology in steeply inclined coal seam [J]. Shandong Coal Science and Technology, 2010, 20(1): 112–113.

This page intentionally left blank

Progress in Mine Safety Science and Engineering II – He et al. (Eds)
© 2014 Taylor & Francis Group, London, ISBN 978-1-138-00122-0

The research on water inrush from overburden and early warning technology according to electrical characteristics in Qidong mine

Yunhai Zhang
Wanbei Coal Power Group Company, Suzhou, China

Hao Huang
North China University of Science and Technology, Beijing, China

ABSTRACT: The water hazards from overburden seriously threatened the mining safety in Qidong coal mine and the early warning technology to prevent the disaster become an urgent problem to solved. Electrical prospecting theory illustrates that before the water inrushes from the overburden aquifers into coal mine, the geoelectric characteristics of overburden strata will change. In combination with hydrological observation online system, monitoring and analyzing the electric field through the network parallel electrical method successfully predicted water inrush from roof aquifers in the working face 7130 and the losses were avoided. The tests found that the apparent resistivity and the potential changes simultaneously with the water levels in boreholes and 20 ~ 30 m ahead of water inflow. This provides a reliable practical significance for the early warning of roof water inrush.

1 INTRODUCTION

Due to complicated hydrogeological conditions, the Qidong coal mine has occurred many water hazardsfron the overburden aquifers. Such as, the water in rush from the No. 4 pore aquifer in the working face 3222 in 2001. On September 16, 2002, a heaver water hazard with max flow of 227 m^3/h happened again in the working face 3221. As the two strong aquifers --pore aquifer and sandstone aquifer in the overburden exists, mining activities is always in the dangerous conditions.

Water disaster from alluvium aquifers is a common form in both Lianghuai coal field and west Shangdong coal field. This cases over six billion tons of coal reserves unminable. Therefore monitoring roof water disaster harbingers and making early warning are significant to release the coal reserves, ensure the production safety in Lianghuai and Western Shangdong coal mines areas.

Experts and scholars have done a lot of research work in our country and put forward a series of theoretical methods. In terms of mechanism of roof water inrush, Liu Tianquan proposed overburden failuredoctrine, according to the overburden deformation characteristics and water conductivity overburden can be divided into "three zones". Professor Gao Yanfa proposed "four band" model for rock movement. Ming-Gao Qian has proposed "Masonry beam" mechanical model and "key strata theory", SONG Zhen Qi supposed mining pressure in the overburden as "passing rock beams" (Miao 2004, Zhang 2008, Wang 2007), Wang Jingming (Wang & Yu 2010) proposed a new type hazards due to "strata separation water " and its treatment method.

In terms of roof water disasters forecasting warning, Wu Qiang forward "three figures—double indexes "to predict roof water inrush disasters quantitatively; Many scholars introduce the numerical simulation technology for safety evaluation and zoning. Since roof water inrush involves multiple factors, the traditional warning technology is constricted due to a single factor analyses (Wu & Wang 2007, Chen & Liu 2010).

The parallel electrical tests in Qidong Coal Mine achieved good results, and early warning of schedule comply with the design requirements. This technology for under the threat of "the fourth aquifer" in Lianghuai mining areas have promotion value.

2 ROOF WATER INRUSH EARLY-WARNING MECHANISM BASED ON ELECTRIC FIELD

Sandstone water inrushes into the mine along the roof collapse caused fissures electrical changes ahead is the foundation of electrical method early warning.

In process of coal mining, the overburden lose support, the original stress state changes, roof strata movement, deformation even aving. If the cracks spread achiveaquifer, which above roof and it is likely to become into underground aquifer water channel. Actually, in the process of overburden caving with collapse Angle existing, the farther at the top of the rock burst or bending deformation, the more advanced (fig. 2–1). At the same time, damage or deformation of rock permeability coefficient has changed (Wang & Dong 2005), as shown in figure 2–2.

The figure shows that the stope shear stress contours and permeability coefficient are extended forward at the top, which will cause an increase in overburden and overburden fracture water level changes, which will become sign of water hazard warning.

Besides changes in mechanical properties of rock, the electrical significant changes of destroyed rock will occur. When rock under high natural stress state, due to the pressure, the solid particle land area will increase, the resistivity value decreased; When stress more than rock mass itself strength, rock mass rupture, the resistivity value will rise. According to field exploration theory, rock resistivity values determine apparent resistivity values

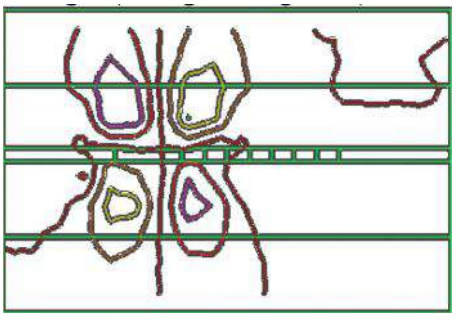


Figure 1. Stope surrounding shear stress contours map.

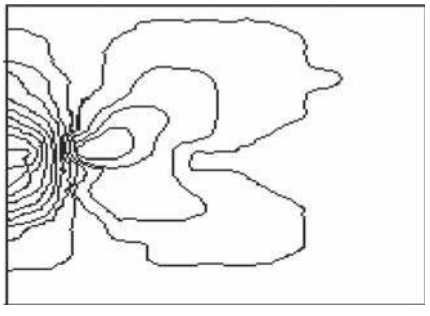


Figure 2. Incremental permeability coefficient contour map.

change, though the apparent resistivity prospecting methods to discovery stress state and deformation and failur of rock mass. If the damage zone does not contain water, the resistivity values will rise, the amplitude more greater, the destruction more completer; if damage zone filled with water, within resistivity values of the damage zone will be significantly reduced.

Groundwater during exercise interact with media various in rock, in the solid, liquid medium generate the electric field exception, the use of natural electric field anomaly in geotechnical engineering seepage studies have actually been applied. The indoor transient response experimental study, which combine earth's natural electric field with the person workshops shaw that (Liu, et al. 2009): Water seepage resulting resistivity significantly lower and supply current significantly increased; The potential of natural electric field and primary field is far higher than that of water-filled the potential of the medium, the position; as time goes by, the electrode potential and the power supply current is increased. Through monitoring of ground electric field can be visually the change of rich water condition of medium, the seepage velocity, seepage saturation state, etc. Therefore, water seepage caused the ground electric field anomalies, through to the electric field anomalies inversion groundwater seepage process inevitably, so as to achieve early warning of roof water disasters.

3 PRINCIPLES OF PARALLEL ELECTRICAL WARNING

Parallel electrical technology is a real-time field observation technology, which is characterized at the same time of the power supply, continuous measurement of all measured electrode potential duration curve, obtained through the excitation current and the potential of space-time curve can decompile a natural field for arbitrary electrode, primary field, the response of the secondary field potentials (Figure 3-1), At the same time, according to the electrode combination of three-dimensional coordinates, Complete three-dimensional calculation of apparent resistivity conventional.

Three-dimensional arrangement of electrical observations in Figure3–2 shows, designing 1 to 47 electrodes are arranged in order, through the electrode loop and synchronous parallel measurement of power form the whole space included roadway current line distribution. 1,6, the 12th electrode is formed when the space current power line distribution. Parallel electrical work is divided into AM and ABM method: AM method powered electrode when working from the 1st cycle to 47 electrodes,

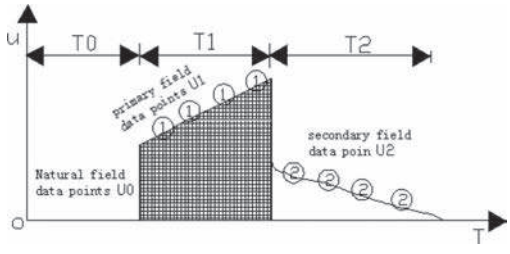


Figure 3. Response potential.

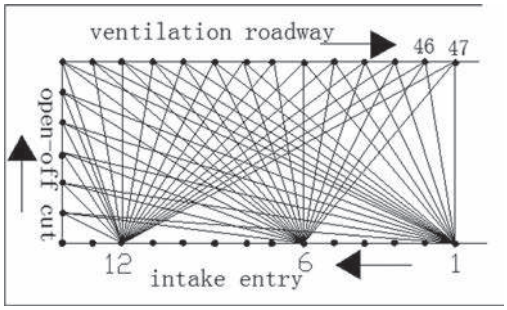


Figure 4. The three-dimensional electrical method electrode layout and the current line.

parallel acquisition and other measuring electrode common reference electrode potential difference; ABM method of operation, the electrodes 1 to 47 sequentially assume A, B power supply, the other measuring electrode parallel acquisition difference potential of the reference electrode and the common, measurement electrode is not idle.

4 PRACTICAL APPLICATION

4.1 *Working face overview*

Qidong Coal Mine coal working face 7_1 30 is located in 3th mining area in the east wing of mine field, under great threat of fourth aquifer (the fourth aquifer) of unconsolidated aquifers. The working face orientation is 355 °~35 °, dip is 11°~14 °. The main roof is light gray, sandstone, average 14.4 m; Immediate roof is a dark gray mud rock, the average thickness 1.7 m. In accordance with on-site geological analysis, the II blocks has a large risk to the production of working face. Combined with the actual monitoring work mainly analyzed the block, (Fig 5).

The fourth aquifer total thickness of the working face $7_1$30 Roof about 3.7~38. 21 m, lithology particle coarsening of the sand and clayey sand, there are also gravel and gravel. High crack detection drill field results show that after working face advancing 30 m seam mining "two band" basically

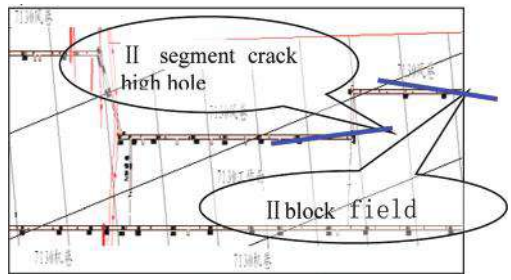


Figure 5. Working face 7130 layout and engineering overview map.

formed in the region. In the top plate 14.75 m of 7_1 coal formed capcaving zone ceiling, Fractured height is 40 mat the top, mining thickness calculated in accordance with 3 m, caving ratio of 4.55, split-production ratio of 13.4. This indicates that Working face $7_1$30 Mining overburden rock fissures height likely to achieve "the fourth aquifer" bottom border, may become water channel guide of the "the fourth aquifer", threatening the safety of mining working face.

4.2 *Early warning project arrangement*

The arrangement form used in the electrode cables buried inside seam roof, electrical meter installed in the tunnel behind, linked ground monitoring station through the underground cable.

II blocks arranged toward the plane of the roof drilling. Field observation wells are arranged along the direction of Wind Tunnel Working face, At the front 14 m lane S18 measurement points are arranged drill field. Drill1 where in the holes arranged 48 electrodes, the electrode spacing of 2 m, 32 electrodesare arranged in the hole2, an electrode spacing of 3 m.

4.3 *Analysis*

1 Natural potential changes

Working face 7130 segment roof crack high detection hole data suggest that two drilling natural potential fluctuation has positive correlation with block period of water yield of working face 7130. the natural potential in drilling increases, the water amount of working face increases (Figure 7), which is mainly due to the high crack deflection drilling work within all things, drilling electrode direct contact with roof water, the natural potential changes in direct response to the changes of the water.

2. Related changes of excitation current

Figure 8 shows the excitation current in the event of an increasing trend after the working face amount

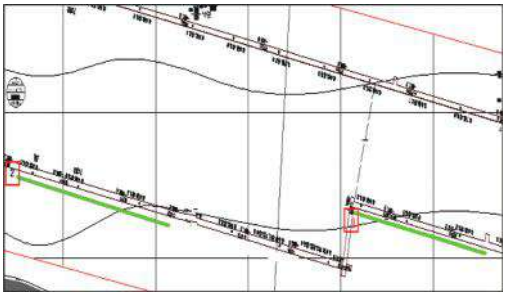


Figure 6. Working fac 7130 roadway monitoring system electrical schematic plan view layout.

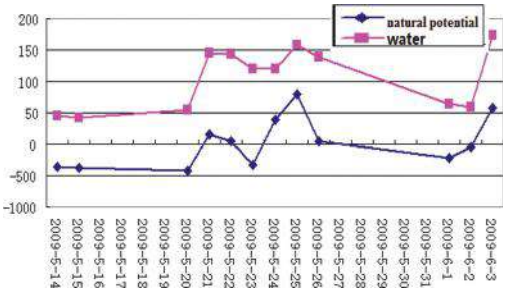


Figure 7. Working face 7130 block water borehole drilling natural potential and dynamic curve.

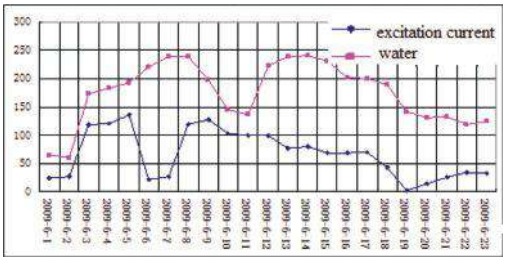


Figure 8. Working face 7130 II Stage #17 electrode excitation current related water figure (current: mA).

of water in the next 2 to 3 days or less appeared an increasing trend, when the excitation current is reduced, working face out of water also decreased slightly. Because drilling electrode arrangement on the roof, when roof water after drilling electrode, electrode exciting current to increase drilling, but this roof seepage water is not the working face, so you can predict the future of working face water 2~4 days there will be a larger increase.

Compareing excitation current curve and the curve of water, it shows that the excitation current rise rate change point corresponds to the future of water rise. Observational data found that S_I that

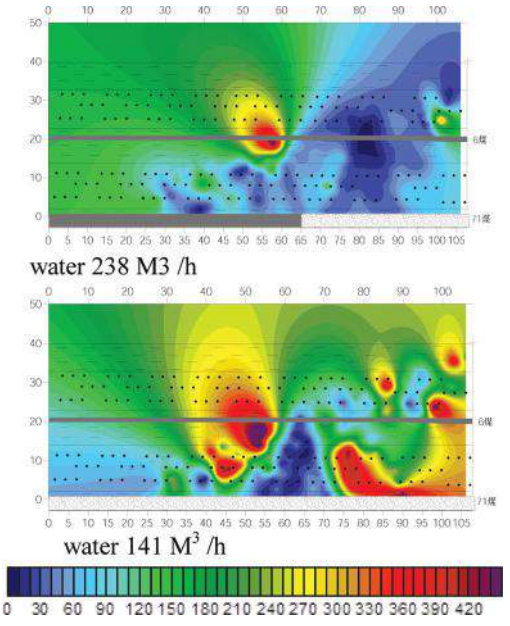


Figure 9. Working face 7130 stage apparent resistivity change map.

the excitation current rate of rise is 3.5 mA / h was water inrush predictors, the higher the rate of rise, indicating that the larger water.

3. Changes of resistivity

Because the roof water seepage areas generally are a relatively low resistance area, by the monitoring results show that the low resistance detection area of the roof area has a certain change in the process of mining face. When the low resistance region developed up and down, the amount of water in working face increases (Figure 8 Left figure), when the low resistance region narrow, and the probe resistivity overall tended to increase, the working face water has decreased (Figure 8 Right figure). Through this period the roof monitoring activities indicate that inthe detection area less than 25Ω · m below of the low resistance region are roof water seepage area, By analyzing low resistance region changes in the spatial morphology and characteristics, which possess the roof water seepage regional space distribution characteristics.

5 CONCLUSIONS

According to mining theory, when roof collapse caused by mining communication with fractured porous and fractured aquifers caused when water

seepage along the damage zone, thus forming the roof water damage. In the percolation process, the natural potential, the excitation current and the apparent resistivity and other parameters of the geoelectric field will produce spatial transient response. Therefore, by inversion of geoelectric field anomaly floor water damage can be predicted. By the study of Qidong Coal Working face 7130, it can be found that:

1. The location of groundwater seepage through natural potential rise, with advanced sensing capabilities. Natural potential increase in the time direction airspace consistent with the seepage flow. Natural potential isochron indicating extreme points seepage locations.
2. Excitation current degree of water saturation of the aquifer is sensitive, after the excitation current in the event of an increasing trend the working face amount of water in the next 2 to 3 days or less appeared an increasing trend, when the excitation current is reduced, working face out of water is also slightly reduced.
3. Resistivity exploration analysis result is helpful to water seepage from roof area of space positioning, the morphological changes of the low resistivity zone corresponds to roof water seepage regional variation. By analyzing the low resistance region's development, the evolution of morphology, we can determine the seepage area development and change, at the same time forecasts the location of the future effluent preliminary.

REFERENCES

Chen Peipei & LiuXiue. 2010. Mine roof water inrush warning system research and application. *Coal Science Academic,* 38 (12):93–95.

Liu Shengdong, & Wu Rong 2009. new three-dimensional parallel electronic prospecting and mine water disaster exploration. *coal society*, 34 (7):928–932.

Liu Shengdong, et al. 2009. Based on groundwater flow in response to the electric field of the mine water hazard warning experimental study. *Rock Mechanics and Engineering*, 28 (2):272–268.

Miao Xiexing, et al. 2004. *Mining seepage theory. Science Press* Beijing.

Wang Jingming & Dong Shuning, 2005. Mine water inrush disaster early warning principle and its application. *Coal Geology & Exploration*:33 (8), 1–4.

Wang Jingming & Yu Daohui. 2010. Secondary seam roof abscission layer causes water damage simulation study *geotechnical engineering report*, 32 (2):230–236.

Wang Xin. 2007. Coal mine roof water inrush mechanism discussion. *Journal of coal mining*, 12 (5):75–77.

Wuai-Xiang & Wang Yi Ming. 2007. Geoelectric field leaching solution for fractured rock seepage characteristics of the study. *Rock Mechanics and Engineering*, 26 (5): 972–976.

Young Choi & Liu Shengdong 2012. Based on the response to the electric field of the mine roof water inrush simulation. *Geophysical and Geochemical Exploration*, 36 (2):221–223.

Zhang Yan. 2008. Prevent seam roof water into the mine collapse warning system. *Coal Research Institute*, Xi'an.

This page intentionally left blank

Progress in Mine Safety Science and Engineering II – He et al. (Eds)
© 2014 Taylor & Francis Group, London, ISBN 978-1-138-00122-0

Study of key technology for gob-side entry retaining in high gas coal face

Jiliang Xing
School of Resource and Safety Engineering, China University of Mining and Technology (Beijing), Beijing, China
Shanxi Coking Coal Group Wulin Coke Development Co., Ltd., Fenyang, Shanxi Province, China

Peng Dang, Zheng Li & Wenchao Li
School of Resource and Safety Engineering, China University of Mining and Technology (Beijing), Beijing, China

ABSTRACT: In order to solve the problem of gas control in high gas coal face, gob-side entry retaining technology was implemented to achieve Y-shaped ventilation. Based on the working-face 18205 in Tunlan Mine, aiming at the force condition of different width of roadway-side filling body under the second mining influence, numerical simulation analysis was done, combining with field practice, and the conclusion was that the reasonable width of filling body was 2.5 m. Force analysis inside it showed that shear failure occurred. The both inside and outside reinforcement measure was adopted, installing bolting with net outside the filling body and steel fabric inside the filling body, and the gaps in the filling body were sealed by guniting. Gas comprehensive control technologies were put forward including gas drainage by buried pipes in filling body and inclined bed plate tunnel. Field observations showed that the pressure of gob-side entry retaining was steady and the treating effect of gas was remarkable, achieving great economic and security benefits.

Xishan Coal Electricity Group Company is a coking coal production base in China, the mining of coal seam exploitation takes medium-thick seam and thin seam as the principal thing. The company-owned Tunlan Mine is a high gas mine. Such as the relative gas emission rate of No.8 coal seam is 8.63~15.49 m^3/t, gas pressure is 1.9 MPa, working faces exploit at the same time, drivage-mining link is tense. The entry protection coal-pillar is generally 20 m between sections, and the coal face reserves tail roadway of gas, leading to the low recovery rate of coal resources and the difficulty of gas control. According to the specific conditions of Tunlan Mine, the technology for gob-side entry retaining adapted to the Tunlan Mine was discussed, realizing the Y type ventilation. The application value of it is very important for solving the gas governance problems, improving resource recovery rate, relieving the tension of drivage-mining link, achieving safety, high efficiency and sustainable development of mine.

1 GENERAL SITUATION OF WORKING-FACE

Working-face 18205 of Tunlan Mine is a gob-side entry retaining face, mainly exploiting No.8 coal seam. The average coal thickness is 3.29 m, the dip angle of coal seam is 4 °~6 °, main roof of coal seam is siltstone which is 4.21 m, immediate roof of coal seam is limestone which is 2.42 m, immediate floor is mudstone whose thickness is between 0 m and 1.2 m, the main baseboard is medium-sandstone which is 2.08 m. The trend length of coal face is 1592 m, and the inclined length is 211 m. Two lane roadways and a borrowed one, paralleling to each other, realized the Y type ventilation. The orbital gateway is a gob-side entry retaining roadway, which is rectangular cross-section, 3.5 m high and 5.5 m wide, and the plane of fracture is 19.25 m^2, supported by anchor with network. The layout of roadway pattern is shown in figure 1.

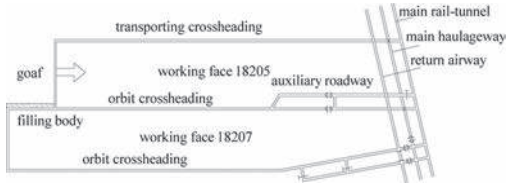


Figure 1. Roadway layout in gob-side entry retaining working-face.

2 STRESS ANALYSIS AND REINFORCEMENT OF ROADWAY-SIDE FILLING BODY

2.1 *The determination of the width of roadway-side filling body*

Roadway-side filling body is arranged between worked out section and orbital crossheading. In order to determine the reasonable width of the filling body, the numerical simulation software FLAC^{3D} conducted stress analysis of filling body whose width is 2.0 m, 2.5 m and 3.0 m, under the second mining influence (Shi & Shi 2012, Chen et al. 2012), according to geological conditions of mining.

From the size of bearing pressure and the damage area of the 2.0 m, 2.5 m and 3.0 m wide filling body in front of the coal face by 30 m, 60 m and 90 m, we could know that, three kinds of filling body under the front abutment pressure were mainly not damaged, and all can meet the requirements of gob-side entry retaining. The front support pressure of the 2.0 m wide filling body is relatively large, and the requirement of the filling material strength will be relatively high. When the width of filling body is 3.0 m, each filling step's filling slurry requirement increases, which will increase the cost, and according to the current conditions of Tunlan Mine, the filling time will take more half an hour than before. When the width of the filling body is 2.5 m, the demand for filling body strength and the actual filling workload are more reasonable. Therefore, the width of the filling body is 2.5 m. Further theoretical analysis of stress distribution for this wide filling body was conducted.

2.2 *Internal force analysis of roadway-side filling body*

The roadway-side filling body was poured integrally by pasty concrete material, each filling's length is 2.4 m and width is 2.5 m. The width of filling body in mined-out area and the orbital crossheading is 1.6 m and 0.9 m respectively. Concrete is a kind of solid which has a lot of micro fractures, and its damage process is the development process of cracks. Concrete is a kind of heterogeneous material, and stress concentration often occurs on the combined surface of the aggregate and mortar, which is the main reason of concrete cracking. The experimental study of concrete strength failure criteria shows that, concrete materials mainly have two damage forms, tensile and shear, and Chinese scholars have derived the expression for calculating the shear strength which is suitable for the concrete (Li & Liu 1993), as follows:

$$\frac{\tau}{f_c}=\frac{1}{K+1}\sqrt{1+(K-1)\frac{\sigma_x}{f_c}-K\left(\frac{\sigma_x}{f_c}\right)^2} \tag{1}$$

$$K=\left(\sqrt{1+\tan^2\varphi}+\tan\varphi\right)^2=\frac{1}{2}\frac{f_c}{f_t} \tag{2}$$

$$\tan\varphi=\frac{\sqrt{2}}{4}\cdot\frac{(f_c-2f_t)}{\sqrt{f_c f_t}} \tag{3}$$

where, f_c = uniaxial compressive strength of concrete; f_t = uniaxial tensile strength of concrete; f = internal friction angle of material.

Substituting the related parameters of the filling material and the stress distribution of filling body under the second mining into the expression of shear strength calculation of concrete, the shear stress of filling body is 5.2 MPa, but the maximum shear stress of concrete is 3.7 MPa through the experimental analysis, and shear failure would occur inside the filling body. Therefore, the filling body should be reinforced to increase its strength and play the support efficiency.

2.3 *The reinforcement of filling body*

2.3.1 *The inside reinforcement of filling body*

In order to increase the strength of the filling body, 5 pieces of steel mesh were placed in, realizing the reinforcement of the filling body (Yang et al. 1999). Steel mesh specifications are length (2250 mm) and height (3000 mm), using the steel bar of 8 mm diameter, and the steel mesh grid size is 150 mm and 150 mm. ①There were three pieces of steel mesh perpendicular to the orbital crossheading's two sides and floor, and they were linked with a deformed bar, whose diameter was 16 mm and length was 2100 mm. ②Two pieces of steel mesh were placed parallel to both sides of the orbital crossheading, and connected by the wire as a whole with the previous three pieces of steel mesh.

2.3.2 *The outside reinforcement of filling body*

On the surface of filling wall, three rows of Φ14 type bracket, length 2.6 m, with four holes were arranged along the roadway. Every two brackets interconnected mutually, and the steel mesh of No.8 and left-handed special thread steel anchors ranked IV which was super strength pre-tension formed the combination support. Diamond metal net was adopted on the uneven filling wall. The anchors' specification was Φ20-M22-1600 mm. Each anchor was extended and anchored by the medium speed resin cartridge of Z2355; the interrow spacing is 900 mm × 800 mm (Li et al. 2011). On the basis of anchor joint reinforcement of steel strip and bar-mat reinforcement, in order to prevent the surrounding rock from weathering, 50 mm thickness concrete was jetted to seal the surface of filling body.

Due to the roof and floor of the roadway were not flat and the float coal of bottom board was not clear in time, or the influence of the filling process, the filling body contacted leaky and stressed unevenly, creating gaps. In order to prevent the leakage of gas, the gaps should be sealed by guniting.

3 THE TECHNICAL MEASURES OF GAS COMPREHENSIVE CONTROL

The working face uses gob-side entry retaining technology, realizing Y type ventilation of two downcast airways and one return air course, which means that the transporting crossheading is the main downcast airway and the orbit crossheading is the auxiliary downcast airway, retaining the entry to return air. The single coal seam gas drainage methods could not meet the production requirements according to the practice of coal seam gas drainage technology of Tunlan Mine in recent years. The extraction system in working-face 18205 used ground extraction pump downhole movable extraction pump and burying pipes in filling body to jointly drainage gas in coal seam and adjacent layer. The reasonable drainage drilling parameters was determined according to the theory of ground stress, gas geology and rock movement (Chen et al. 2012). The gas emission of the working-face 18205 has greatly improved than the working-face 18203, since using Y type ventilation. But it made bottom gas relatively high, leading to bubbling phenomena, sometimes causing gas transfinite accident, and bringing difficulty to the gas control. Only by increasing air flow rate, the bottom gas has not been fundamentally improved, and the main fan negative pressure would increase and the effect was poor. In order to solve this problem, inclined bed plate tunnel drainage gas technology was adopted in the working-face 18205.

4 FIELD MEASUREMENT OF LANE SIDE FILLING BODY STRESS AND ANALYSIS OF GAS CONTROL EFFECT

4.1 *Filling body stress observation project*

The stress observation of gob-side entry retaining filling body provides the science evaluation basis for the inspection filling effect. According to the mechanical principle and the actual situation of the underground pressure in Tunlan Mine, at the distance of 10 m to open-off cut, 5 points, each interval to 10 m, and another 5 points, each interval to 50 m, were decorated. Two hydraulic pillows were arranged in each observation point of filling body. The height from hydraulic pillow to the floor was 1.75 m and to the both sides of the filling body edge was 1 m. The total observation distance was 300 m.

4.2 *Actual measurement analysis of filling body*

In accordance with stress observation project of the filling body, the stress of it under the second mining influence was observed. The filling body's force was 2~4 MPa and the load anchor's force was 5~25 MPa, which explained that the filling body stress was poor under the second mining influence. Combining with the two sides' displacement of gob-side entry retaining, roof abscission layer observations, the whole pressure of gob-side entry appeared stable, and the width of 2.5 m could satisfy the production requirement.

4.3 *Analysis of gas control effect*

Fully mechanized mining working-face 18205 used Y type ventilation system and gas comprehensive control technology of burying pipes in filling body and inclined bed plate tunnel. Gas extraction effect was obvious. The gas emission from working-face 18205 during mining significantly reduced compared with already picked working-face 18203. The average gas emission of working-face 18203 was 54 m^3/min, and the maximum was 83 m^3/min, while the average gas emission of working-face 18205 was 24 m^3/min, and the maximum was 34 m^3/min. The working-face 18205 gas emission during mining gradually reduced after stoping 850 m, with the bed plate tunnel drainage system forming. The average gas emission was 20 m^3/min and reduced 4 m^3/min than before. This technical measure reduced the concentration of gas and achieved a very good extraction effect.

5 CONCLUSIONS

According to the stress numerical simulation analysis and field production practice of 2.0 m, 2.5 m, 3.0 m wide gob-side entry retaining filling bodies under the influence of second mining, the reasonable width was 2.5 m. The reinforcement measures, as field observations shown, that the anchor belt net was arranged inside the filling body and steel mesh was arranged outside the filling body, could prevent generating shear failure in the filling body, enhance its strength, exert its support performance, and make the gob-side entry retaining mine pressure appear stable.

Gob-side entry retaining working face realized Y type ventilation system. Gas comprehensive control technology, burying pipes in filling body and inclined bed plate tunnel, improved the gas

extraction rate greatly and reduced the working face gas emission, and solved gas overrun problem of the gas coal face effectively, achieving good economic and security benefits.

REFERENCES

Baogui Yang, Henghu Sun, Huasheng Liu, Jinan Wang. 1999. Reinforcement's effects to the backfill body of high water material. *Journal of University of Science and Technology Beijing* 21(5):421–424.

Hong Li, Xila Liu. 1993. Shear strength calculation based on concrete failure criterion. *Engineering Mechanics* 10(1):52–60.

Jianjun Shi, Haoyu Shi. 2012. Simulation research on the law of strata behavior in gob-side entry retained. *China Coal* 38(10):42–4.

Nong Li, Duanming Hou, Jingqiang Bian. 2011. Research and practice of gob-side entry driving support technology for combined roof. *China Coal* 37(2):56–8.

Yanke Chen, Dingding Yang, Xiulei Jiang. 2012. Stereo methane drainage technology of protective coal-seam mining face in Guqiao Colliery. *Coal Mining Technology* 17(5):84–7.

Yong Chen, Jianbiao Bai, Ying Xu, Taolei Zhu, Jun Long, Wentao Kang. 2012. Rational determination on width of support mass along side of gateway retained goaf. *Mining Engineering* (5):4–7.

Progress in Mine Safety Science and Engineering II – He et al. (Eds)
© 2014 Taylor & Francis Group, London, ISBN 978-1-138-00122-0

Fractured zone roof grouting reinforcement technique

Zhu-Wu Zhu
College of Natural Resources and Environmental Engineering, Shandong University of Science and Technology, Qingdao, Shandong, China

Can Wang
Shandong Tengzhou Chenlong Energy Sources Group Co. Ltd., Tengzhou, Shandong, China

ABSTRACT: When the working face advancing to the fractured zone, it often encounters the fractured roof in coal mining, which poses a serious safety hazard to underground construction. However, fractured roofs caused by geological structures such as faults, folds and gob area support pressure effects are often encountered in underground mining. Employing the method of strengthening the roof support to control the surrounding rock can hardly achieve the desired security, especially for the fractured roofs happened in gateway, which is likely to cause material waste and limited supporting effect. Therefore, the paper combines fractured roadway surrounding rocks support pressure distribution, starting the change of the nature of the surrounding rock, by injecting Malisan to change the fractured state of the surrounding rock, so as to achieve effective control of the surrounding rock fractured effect.

Keywords: fractured zone, surrounding rock control, grouting reinforcement, roof

1 INTRODUCTION

Coal roof fracturing is one of the hazards of the coal mine production safety. Every year, roof-fall accident caused great casualties, so exploring ways to strengthen the control of gateway roof to help to reduce such safety accidents is worth to study. The roof control of face can be achieved by changing the mining process to strengthen the roof control of hydraulic support, while the supporting effect of strengthening roof support to control fractured roof is limited in both roadways of gateway. A coal mine located in Jinin city, Shandong province employs the method of injection Malisan to change the fractured state of the surrounding rock, to change the block surrounding rock into surrounding rocks of continuity, solidity and integrity, so as to effectively control the surrounding rock fractured state and ensure the coal mine production safety.

2 FRACTURED ROADWAY SURROUNDING ROCKS SUPPORT PRESSURE DISTRIBUTION

On one hand the roadway surrounding rock fracturing is caused by the geological structure, on the other hand, it is caused by support pressure due to mining. Support pressure is generated in the island face, of which the support pressure distribution is similar to the shape of a saddle. By the superposition of mining support pressure and distribution support pressure, it forms a strong concentration of support pressure in the roof coal in the both sides of face. With advancing of the face, this area continues to move forward, and the surrounding of main roof has varying degrees of fractures when the face advancing. The time of main roof collapse in both sides of face is not merely affected by dynamic load, but also by the impact of other factors such as suspending area of main roof in both sides of the mined area and crushed extent of remaining coal pillars, because the badly fracture with burstiness is easier to induce roof accident.

The support of gateway fracture section often employs single hydraulic prop, or building sheds, bolt-mesh-anchors, and cribs. However, those supporting method only controls from external causes, of which supporting effect is limited, wastes a lot of support material, and cannot guarantee the ideal control effect. Therefore, a good supporting effect can be achieved by changing the nature of the surrounding rock to control the roadway deformation and roof fracture.

Affected by support pressure, roadway roof is fractured, it is feasible to employ the method of grouting reinforcement to change the fractured state of surrounding rock (Ge 1996, Yang et al. 1997). Employ Malisan N of Yanzhou Haokeweibo

Mining Engineering Co., Ltd. as the chemical material to reinforce surrounding rock, and respectively apply injection reinforcement to roadway both sides, roof and PVIs, depending on different parameters at different circumstances. In the initial stage of face rib spalling and roof falling, using Malisan material to reinforce or Rockxiu to fill.

3 MALISAN N PERFORMANCES

Malisan N has a high degree of adhesion and good mechanical properties, which can highly adhered with the strata, and its good flexibility and toughness can ensure it withstand the subsequent ground movement, which can maintain the same life span with the face. When the production is injected into the strata, low viscosity mixture is maintained for a few seconds, then penetrates into small cracks and expands, thus effectively strengthening and sealing the processed region. Details are shown in Table 1. Its resin and catalyst for two-component material are in a leading position in the world and have a history of 40 years.

The application scope of Malisan N: cracks and unstable strata reinforcement, water inlet and strata seal, rock reinforcement, and rock rivet seal.

4 MALISAN N REINFORCEMENT PROGRAM

Affected by fault F2 geological structure, rocks within the scope of 50 m near 1311 mining face belt roadway fault F2 outburst, and the coal fractured has lost its integrity and continuity. When the face advancing to the position of fault, roof accident is easily induced, thus resulting in stop production and affecting face advancing. By the mine feasibility studies, chemical material reinforcement roadway processing is implemented in the 1311 face belt roadway structure developed zone and partial fracture zone. Employ Malisan N reinforcement material, and the specific methods are as follows (Chu 2007, Gao 2005):

Table 1. Malisan N technical data.

Project		Resins	Catalysts
Basic ingredients	Density at 25℃(g/cm3)	1.04	1.23
	Viscosity at 25℃(MPa•s)	200	210
	Mixing ratio(Volume ratio)	1	1
	Storage period at 25℃(months)	6	6
	Storage Temperature (℃)	5-30	5-30
	Package	25kg Plastic bucket	30kg Plastic bucket
Polymerization products	Application temperature (℃)	15	25
	The initial viscosity (MPa • s)	450	250
	Start of the reaction (minutes)	1:15	0:45
	The foam time (minutes)	2:10	1:25
	Expansion ratio	2	2
	Pressure(MPa)	>10	>10
	Adhesive strength (MPa)	>1	>1

(1) According to the site examination, drill pores in roadway vault fracture section using pneumatic drill or Roof bolter, pore size is Φ42 mm-Φ45 mm, pore depth is 3 m, row distance is 3 m, grout after pore finished. And then drill pores in roadway vault angle, pore size is Φ42 mm-Φ45 mm, pore depth is 4 m, spacing is 2 m, row distance is 3 m, grout after pore finished.

According to the roadway fracture condition, for example of 5 m coal pillar, drilling with coal electric drill is suggested. Pore size is Φ42 mm-Φ45 mm, pore depth is 2.5 m, spacing is 2 m, and row distance is 3 m, triangular configuration. Put the sealing in the position of 1.5 m and start grouting.

(2) According to site condition, if the first pore grouting volume is controlled in approximately 4 barrels of material, which reflects that this roof is quite fractured and cracks are developed.. If the Malisan material cannot be injected into the cracks, which reflects that the cracks are not developed. The grouting volume is determined by site conditions. Grouting can be guaranteed according to the site condition, the first cycle grout four pores, then view the grouting and effects. The reinforcement length is approximately set as 117 m.

5 MALISAN GROUTING PROCESS

Specific process is shown as Figure 1.

6 MALISAN GROUTING PROCESS

Malisan N dosage can be expected based on the coal volume in designed grouting reinforced region. Specific calculation is shown as formula (1):

$$Q = VrC \tag{1}$$

In the formula:
- Q – designed Malisan N dosage, t;
- V – volume of grouting reinforced region (see formula (2) below), m^3;
- R – density of the coal, $r = 1.4$ t/m^3;
- C – amount of Malisan N grouting in per ton of coal, 0.5%;

$$V = (\pi(R^2 - r^2)/2 + AB - ab) \times L / \sin\delta \tag{2}$$

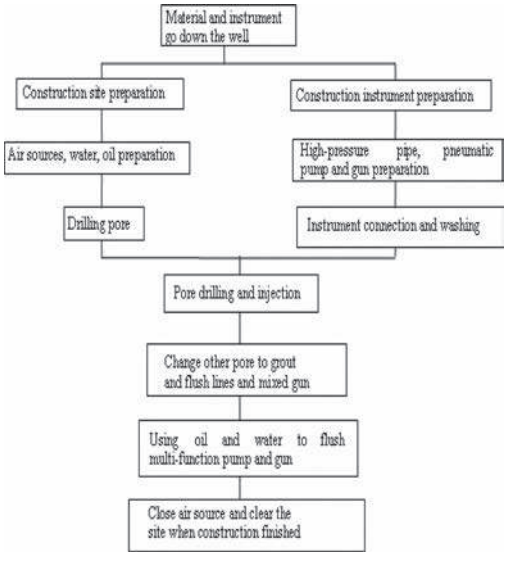


Figure 1. Malisan Grouting Process.

Among them:

R,r – the inner and outer radius of grouting reinforced region, $R = 4.45$ m, $r = 2.06$ m;

A,a – width of grouting reinforced region and non- reinforced region in roadway sides, $A = 7.6$ m, $a = 3.6$ m

B,b – height of roadway, $B = 1$ m, $b = 1$ m

L – coal seam thickness, $L = 3.03$ m;

δ – angle of coal seam, $\delta = 10°$.

Put each parameter into the formula, and calculate $Q = 3.5$ t., the dosage of Malisan N is 3.5 t. Malisan N resin and catalyst mixture ratio is shown as: volume ratio is 1:1, mass ratio is 1:1.17.

7 MINING CONTRAST UNDER SIMILAR CONDITIONS

1305 face and 1311 face are in the same mining area, with similar geological conditions, and both encountered faults in roadways. Because no corresponding roof reinforcement measures were implemented when 1305 face advances cross the fault, head face roof collapse is induced when 1305 face advances cross the fault, which causes great difficulty in safety production, and wastes large amount of materials in roof and buttock control. The material inputs are shown as Table 2.

The total cost of materials is 35983.75 yuan, and raw coal output influence by crossing fault is 5990 t.

Similarly, when 1311 face haulage roadway advances across the fault, Malisan injection is implemented to reinforce the roof, put Malisan 3.5 tons, the unit price is 10,000 yuan per ton, the total investment is 35,000 yuan. No coal wall spalling happens when crossing fault, and no face roof-fall accident is caused, which not only ensures safety production, but achieves economic benefit.

Table 2. Materials cost schedule due to face roof and buttock fracture support.

Material name and specifications	Quantity	Unit price	Total Price yuan
Semicircle wood 1.8×1.5m	498block 12.7m^3	796.46yuan/m^3	10115.04
Semicircle wood 1.8×2.5m	168block 7.2m^3	796.46yuan/m^3	5734.51
Anchoring agent	600strip	2.05yuan/trip	1230
I-steel 2.5m	30strip	79.5yuan/m	2385
Railway 7m	2strip	399.6yuan/strip	799.2
Shearer pick	60bunch	106yuan/bunch	6360
Face anchor (with bedding and cap)	480 strip	17yuan/ suit	8160
Wooden anchor plate	300piece	4yuan/ piece	1200

8 CONCLUSIONS

Employing Malisan N as reinforcement material can ensure no spalling or roof-fall happens in 1311 mining gateway development zone and partial section, which enhances coal carriage capacity. Through the reinforcement of roadway surrounding rock can strengthen the integrity of roadway surrounding rock and improve the overall carriage capacity of the surrounding rock, thereby eliminating the security risks of roadway roof fracture.

Through injecting Malisan N to change the nature of the surrounding rock can achieve the purpose of control of surrounding rock, which not only reduces the waste materials of roadway reinforcement support, but achieves good control, high security and low cost.

ACKNOWLEDGMENTS

This work is supported by National Basic Research Program of China under Grant No.2012CB72310402, National Natural Science Foundation of China under Grant No.51244010, Science Research Innovative Group of College of Resources and Environmental Engineering of SDUST No.2012ZHTD06. New Teachers' Fund for Doctor Stations of Ministry of Education under Grant No.20123718120009.

REFERENCES

Chu F. 2007. New Mali Powder Used in Liuqiao No. 1 Coal Mine. Coal Technology 26(1):99–100 (in Chinese).

Gao Z.G. 2005. Application of Malisan grouting reinforcement in roof management of fully-mechanized working face. Coal Mining Technology 10(5):53–54 (in Chinese).

Ge J.L. 1996. Study of Grouting Reinforcement Mechanism of Soft Rock Roadway and Grouting Technology Problem. Xuzhou: China University of Mining and Technology (in Chinese).

Yang M.J. et al. 1997. Exploration of Cement Grouting Penetration Mechanism. Mechanics in Engineering 19(5):45–47 (in Chinese).

Progress in Mine Safety Science and Engineering II – He et al. (Eds)
© 2014 Taylor & Francis Group, London, ISBN 978-1-138-00122-0

Method of choosing optimal features used to Intrusion Detection System in coal mine disaster warning internet of things based on Immunity Algorithm

Jun-Wei Zhao, Ying Hu, Li-Min Sun, Sheng-Chen Yu, Jiang-Lan Huang, Xiao-Ju Wang & Hui Guo
Key laboratory of Mine Disaster Prevention and Control Technology in Hebei Province, Beijing-East, Yanjiao, China
North China University of Science and Technology, Beijing-East, Yanjiao, China

ABSTRACT: In order to improve the detection rate of new intruders in coal mine disaster warning internet of things, a new method of Intrusion Detection System (IDS) based on immune algorithm and Back Propagation Neural Network (BPNN) is developed in the paper, on the base of analysis on the network data. In this method, Immune Algorithm (IA) is used to preprocess the network data, extract key features and reduce dimensions of network data set by feature analysis, then BPNN is adopted to classify the data (program) and recognize intruders. Experimental results show that the method is feasible and efficient, and the detection right rate of intruders in internet of things was above 97%.

Keywords: Intrusion Detection System (IDS); Feature selection, Immunity Algorithm (IA), Back Propagation Neural Network (BPNN)

1 INTRODUCTION

The Internet of things is an important part of the new generation of information technology. The Internet of things is an internet of the connection of objects. The dynamic safety early warning system of the coal mine disaster base on the internet of things is a new method and new means to protect the mine safety and is a complicated system project integrated with the coal mine safety theory internet of thing technology and the early warning technology. The system structure of the dynamic early warning system could be divided into three structures, as a sensing layer, a transmission layer and a application layer and could realize the management of the mine safety information system, the dynamic warning of the Coal Mine disaster, the joint sharing of the safety information, the experts system of the disaster prevention and control and other functions. The dynamic early warning system could integrate the available resources and realize the coordinative management and control of the personnel, machine, equipment and basic infrastructures within the production network under the complicated environment.

The manipulations may take the form of attacks by skilled malicious hackers, or script kiddies using automated tools. Intrusion Detection System (IDS) is used to detect all types of malicious network traffic and computer usage that can't be detected by a conventional firewall. This includes network attacks against vulnerable services, data driven attacks on applications, host based attacks such as privilege escalation, unauthorized logins and access to sensitive files, and malaria (viruses, Trojan horses, and worms).

An IDS is composed of several components: Sensors which generate security events, a Console to monitor events and alerts and control the sensors, and a central Engine that records events clogged by the sensors in a database and uses a system of rules to generate alerts from security events received. An IDS also is a large and complicated project. Now, there are yet many weaknesses in IDS, it should be improved.

IDS includes choosing a set of features, building up a set of attack models or normal models, matching or comparing the models with activation of now executed program, obtaining the difference of the built models and activation of now executed program, and alarming.

An IDS is a large and complicated project. Now, there are yet many weaknesses in IDS, it should be improved (YU, 2009). IDS includes choosing a set of features, building up a set of attack models or normal models, matching or comparing the models with activation of now executed program, obtaining the difference of the built models and activation of now executed program, and alarming.

Currently, how to extract the appropriate features for IDS is less studied. This article will do some research on this issue.

In IDS, to choose a set of features is very important (YU, 2008). If the set of features used in IDS are chosen wrongly, no matter how perfect next later works are, the final results of IDS are wrong. In addition, action classification in IDS is completed through mathematics method, which requires that number of features is small. How to determine a good group of features and how to classify and recognize intruders are important in IDS (Rao & Yang, 2003). The solutions to the problems are provided in the paper. In this paper, Immune Algorithm (IA) is used to preprocess the network data, to determine a good group of features, and the Back Propagation Neural Network (BPNN) is adopted to classify and recognize the intruders. Experimental results show that the method is feasible and efficient. The approach is introduced in follow sections.

2 BACK PROPAGATION NEURAL NETWORK (BPNNN)

In paper, the Back Propagation Neural Network (BPNN) is used to class and recognize intruders and normal programmes. The BPNN abstracts and simulates some basic characters of human brain by mathematical approaches. BPNN is a nonlinear information processing system that simulates the structure and its function of human brain.

The essence of the material that follows is the use of a multitude of elemental nonlinear computing elements (called neurons) organized as networks reminiscent of the way in which neurons are believed to be interconnected in the brain.

The resulting models are referred to by various names, including neural networks, neurocomputers, Parallel Distributed Processing (PDP) models, neuromorphic systems, layered self-adaptive networks, and connectionist models. Here, we use the name neural networks, or neural nets for short. We use these networks as vehicles for adaptively developing the coefficients of decision function via successive presentations of training sets of patterns.

Pitts [1943] proposed neuron models in the form of binary threshold devices and stochastic algorithms involving sudden 0–1 and 1–0 changes of states in neurons as the bases for modeling neural system. Subsequent work by Hebb [1949] was based on mathematical models that attempted to capture the concept of learning by reinforcement or association.

More recent results by Rumelhart, Hinton, and Williams [1986] dealing with the development of new training algorithms for multilayer perceptions have changed matters considerably. Their basic method, often called the generalized delta rule for learning by back propagation provides an effective training method for multilayer machines. Although this training algorithm cannot be shown to converge to a solution in the sense of the analogous proof for the single-layer perception, the generalized delta rule has been used successfully in numerous problems of practical interest. This success has established multilayer perception-like machines as one of the principal models of neural networks currently in use.

2.1 *Perception for two pattern classes*

In its most basic form, the perception learns a linear decision function that dichotomizes two linearly separable training sets. Figure 1 shows schematically the perception model for two pattern classes. The response of this basic device is based on a weighted sum of its inputs; that is,

$$d(x) = \sum_{i=1}^{n} w_i x_i + w_{n+1} \tag{1}$$

which is a linear decision function with respect to the components of the pattern vectors. The coefficients $w_i, i = 1,2,\ldots,n,n+1$, called weights, modify the inputs before they are summed and fed into the threshold element. In this sense, weights are analogous to synapses in the human neural system. The function that maps the output of the summing junction into the final output of the device sometimes is called the activation function.

When $d(x) > 0$ the threshold element causes the output of the perception to be +1, indicating that the pattern x was recognized as belonging to class w_1. The reverse is true when $d(x) < 0$. This mode of

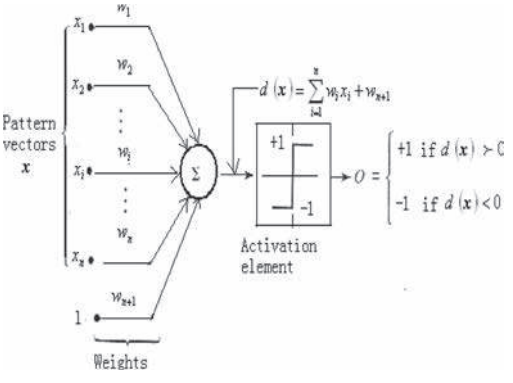


Figure 1. Two equivalent representations of the perception model for two pattern classes..

operation agrees with the comments made earlier in connection with $(d_i(x) - d_j(x) = 0)$ regarding the use of a single decision function for two pattern classes. When $d(x) = 0$, x lies on the decision surface separating the two pattern classes, giving an indeterminate condition. The decision boundary implemented by the perception is obtained by setting Eq. (1) equal to zero:

$$d(x) = \sum_{i=1}^{n} w_i x_i + w_{n+1} = 0 \tag{2}$$

$$w_1 x_1 + w_2 x_2 + \cdots + w_n x_n + w_n = 0 \tag{3}$$

which is the equation of a hyper plane in n-dimensional pattern space. Geo-metrically, the first n coefficients establish the orientation of the hyper plane, whereas the last coefficient w_{n+1} is proportional to the perpendicular distance from the origin to the hyper plane. Thus if $w_{n+1} = 0$, the hyper plane goes through the origin of the pattern space. Similarly, if $w_j = 0$, the hyper plane is parallel to the x_j-axis.

The output of the threshold element in Fig. 1 depends on the sign of $d(x)$. Instead of testing the entire function to determine whether it is positive or negative, we could test the summation part of Eq. (1) against the term w_{n+1}, in which case the output of the system would be

$$O = \begin{cases} +1 & if \sum_{i=1}^{n} w_i x_i \succ -w_{n+1} \\ -1 & if \sum_{i=1}^{n} w_i x_i \prec -w_{n+1} \end{cases} \tag{4}$$

This implementation is equivalent to Fig. 1 and is shown in Fig. 1, the only differences being that the threshold function is displaced by an amount $-w_{n+1}$ and that the constant unit input is no longer present. We return to the equivalence of these two formulations later in this section when we discuss implementation of multilayer neural networks.

Another formulation used frequently is to augment the pattern vectors by appending an additional $(n + 1)$st element, which is always equal to 1, regardless of class membership. That is, an augmented pattern vector y is created from a pattern vector x by letting $y_i = x_i$, i=1,2,…,n, and appending the additional element $y_{n+1} = 1$. Equation (1) then becomes

$$d(y) = \sum_{i=1}^{n+1} w_i y_i = w^T y \tag{5}$$

where $y = (y_1, y_2, \ldots y_n, 1)^T$ is now an augmented pattern vector, and $\boldsymbol{w} = (w_1, w_2, \ldots w_n, w_{n+1})$ is called the weight vector. This expression is usually more convenient in terms of notation. Regardless of the formulation used, however, the key problem is to find $\boldsymbol{w}$ by using a given training set of pattern vectors from each of two classes.

2.2 *Training or learning*

The BPNN is based on the use of sample patterns to estimate statistical parameters of each pattern class. The patterns (of known class membership) used to estimate these parameters usually are called training patterns, and a set of such patterns from each class is called a training set. The process by which a training set is used to obtain decision functions is called learning or training.

The patterns (of known class membership) used to estimate these parameters usually are called training patterns, and a set of such patterns from each class is called a training set. The process by which a training set is used to obtain decision functions is called learning or training.

The training patterns of each class are used to compute the parameters of the decision function of BPNN corresponding to that class. After the parameters in question have been estimated, the structure of the BPNN is fixed, and its eventual performance will depend on how well the actual pattern populations satisfy the underlying statistical assumptions made in the derivation of the classification method being used.

The statistical properties of the pattern classes in a problem often are unknown or cannot be estimated. In practice, such decision-theoretic problems are best handled by methods that yield the required decision functions directly via training. Then, making assumption regarding the underlying probability density functions or other probabilistic information about the pattern classes under consideration is unnecessary.

3 IMMUNITY ALGORITHM

Immunity algorithm work in the same way the biological immunity principle does. According to biological immunity principle, the biology immune system produces automatically the corresponding immune body (antibody) against the antigen through the cell fission and the disintegration, to resist the antigen that invades the life body. This process is called the immunity reply. In the immunity reply process, part of antibodies is preserved as memory cell. When the similar antigen invades the life body once more, the memory cell is activated and produces rapidly the massive immune bodies. This causes that 2nd reply is more intense than the primary reply, which manifests memory function of

the immune system. A kind of immune body and another kind of immune body are also promoted and suppressed mutually, to maintain the multiplicity of the immune body and the balance of immunity. This kind of balance is carries on according to the density mechanism, namely the density of the immune body is higher, the immune body is suppressed more; The density of antibody is lower, the antibody is promoted more. This manifests self-adjustment function of the immune system.

The immunity algorithm is a new method developed recently in the artificial intelligence, which is a new algorithm that is designed under enlightenment of the biology immune system.

In the immunity algorithm, the antigen is corresponding the objective function and variant kind of constraint conditions; and the immune body (antibody) corresponds with the optimal solution. The kissing degree between the antibody and antigen corresponds with the match degree of solution and the objective function.

3.1 *Encoding methods*

In the immunity algorithm, encoding method of the immune body and antigen mainly has three kinds, that is, the binary code, the real number code and the character code, and in minor case, the grey code (gradation) is used, and so on. Binary code has merits of strong search ability, simple crossover and variation operation. Therefore, the binary code method is selected in this article. As to P attributes of the network data, each attribute is expressed by the binary string which is E in the length. The decimal base value in correspondence with this binary value represents the weight value of the attribute. Therefore, each immune body contains $P \times E$ binary code.

3.2 *Methods for computing immune body density*

Immune body density is mainly used to maintain multiplicity of the immune body, and raise the partial search ability. The methods for computing immune body density are mainly ones based on Euclidean space distance and information entropy. The latter is used in this article, to compute immune body density. Information entropy is used in indicating multiplicity of the immune body in the community. The immune body density is computed and obtained by average information entropy of a group of the immune bodies.

3.3 *Method for computing the affinity between immune body and antigen*

The affinity between immune body and antigen is used in indicating the degree in which the immune body recognizes the antigen. In this article, BPNN, which is a classification method, is applied to obtain the rate of alarm missing and the rate of false alarm, then compute the affinity between immune body and antigen.

3.4 *Steps of immunity algorithm*

The immunity algorithm step proposed in this article is as follows:

1. Analysis question: Analysis and understand the characteristic of solution, and design the appropriate coded form of the solution.
2. Initialization: Initialize immune body group as well as memory storehouse (base). Set the initial values of immune body group size n and memory storehouse size m.
3. Evaluate each immune body in the immune body group: Expectation reproduction rate of the immune body is taken as the standard evaluate index of immune body in this algorithm. The index is determined together, according to immune body density and affinity between the immune body and the antigen.
4. Save the superior immune body to memory storehouse (base): The immune bodies are ordered by descent, according to expectation reproduction rate. Save the former m immune bodies with higher expected reproduction rate into memory storehouse (base).
5. Judge whether the stop condition satisfies: Yes, then algorithm stops; otherwise, continues the operation of the next step.
6. Production new community: Based on the fourth step computed result, the selection, crossover and variation operations of each immune body in each immune body group are carried on, to obtain new community, according to its expectation reproduction rate. The new generation of community is constituted of the new community obtained just about and m individuals in the memory storehouse together.
7. Change to the step 3, and continues to carry out.

4 THE INTRUSION DETECTION SYSTEM MODEL BASED ON THE AI-BPNN

The essential idea of BPNN classification is to use a gradient method to modify weights and thresholds of BPNN to make the square sum of error of network output minimum, so that the two classes of data become linearly separable, as far as possible. The pretreatment of the data and features used in IDS is carried on with the immunity algorithm, to withdraw main attribute features related with intrusion detection. The classification of the data

processed is carried on with BPNN. The outline of the concrete IDS model based on the AI-BPNN is: (1) network data set, (2) immunity pretreatment, (3) BPNN training, (4) BPNN sorter, (5) policy-making response (react).

5 EXPERIMENTS AND RESULT ANALYSIS

The data used in the experiment is KDD CUP 99 data sets. This data set provides 9 week's network connection data that gathered from on a simulation local area network. Each record in the data set has contains 41 features and 1 marking of kind. The record in the data set has been divided into 5 kinds, namely normal connection (Normal) denial of service (DoS), the unauthorized remote service to login (R2 L), the unauthorized access to the local super user's privilege, scanning and probing (Probing).

Because primitive data sets of KDD CUP 99 are too huge, in order to carry on the confirmation to the algorithm, the representative data sets had chosen in this article, to product stochastically training set and test set, which have contained 5072 and 5280 records separately. In the practical test, the mean value of 10 test results is taken as the test finishing result. The practical immunity algorithm parameters are as follows:

The community size is 120, alternate number is 50 generations, the memory storehouse size is 7, crossover rate is 0.5, and the variation rate is 0.02.

The BPNN is made of three layers, the first layer is made of 22 nodes, the second layer consists of 25 nodes, and the last layer consists of a node, whose value is 0 for normal users, 1 for the intruder. After the BPNN is trained successfully, that is, its weight and threshold values are selected, the procedures running in the network can be monitored and evaluated with the neural network. Experimental result is as shown in Table 1.

The experimental results show that correct recognition rate is enhanced greatly by method developed in the paper, while the rate of false alarm rises lightly.

Table 1. Comparisons of correct identification rates for intruders in some different IDSs.

Method for IDSs	The rate of alarm missing	Correct recognition rate
BPNN	4.5%	80.2%
Immunity algorithm (IA) + BPNN	4.7%	97.3%

6 CONCLUSION

In data used in Intrusion Detection System (IDS), there are non-correlated or the redundancy features which causes performance of IDS to drop. Other, in data used in IDS, the dimension of features is higher. Thus, the extraction of characteristic was carried on in the paper. Considering the global restraining of immunity algorithm as well as the immune body multiple features, it was proposed to carries on pretreatment of the data and extraction of essential attributes with the immunity algorithm, then classify and recognize intruders with BPNN. IDS model based on the AI-BPNN was established. The experiments indicated that this algorithm was feasible and effective, and the detection right rate of intruders in internet of things was above 97%.

ACKNOWLEDGEMENTS

This work was financially supported by "the Fundamental Research Funds for the Central Universities of China" (JSJ2013B09, 3142013103, JSJ2013B02, JSJ1207B, 2011B029, 2011B028).

REFERENCES

X. Rao, & S.Q. Yang 2003. An Intrusion detection system based on Support Vector Machine, *Journal Sofeware*, 14(4):798–803.

Yu Sheng chen 2008. Solution to Character Compression of Intrusion Detection System In Controllable and Trustednet Works, *International Conference on Information Technology an Environmental System Sciences (ITESS'2008),* 704–710.

Yu Sheng-chen 2009. Method for Getting Inter-Independent Features Used to Intrusion Detection System In Controllable and Trusted Networks, *GCIS 2009,* 461–465.

This page intentionally left blank

Progress in Mine Safety Science and Engineering II – He et al. (Eds)
© 2014 Taylor & Francis Group, London, ISBN 978-1-138-00122-0

Non-Darcy seepage and stopped floor water inrush prevention

Jinsui Wu
Department of Faculty of Earth Resource, China University of Geosciences, Wuhan, China
Department of Basic, North China University of Science and Technology, Beijing, China

Shangxian Yin
Department of Safety Engineering College, North China University of Science and Technology, Beijing, China

ABSTRACT: Using Forchheimer and non-Darcy seepage theory, revealed the mechanism of water inrush from the structure of nonlinear dynamics system instability perspective. Research shows that: Mine water inrush is related to the porosity of rock, particle diameter, mechanical properties of penetrating liquid, and the velocity of flow etc. The smaller of porosity and particle diameter, the larger of Reynolds number for causing loss of stability of seepage, i.e. the steady state is not easy to lose; otherwise, the larger porosity and particle diameter, the smaller of Reynolds number for causing loss of stability of seepage, the steady state is easy to lose.

1 INTRODUCTION

Broken rock of mining is caused by coal mining, the permeability coefficient of fractured rock mass is higher several orders of magnitude than porous rock, Along with the influence of confined water or near the high pressure gas, and the seepage is non Darcy flow, prone to the seepage mutation. The origin of coal mine gas and water inrush accidents is mining fracture seepage in rock and mutation. Therefore, Study of non Darcy flow has important significance for the prevention and control of mine disaster, new technology can be developed based on the governance of coal mine of seepage disasters.

2 THE THEORY OF NON-DARCY SEEPAGE

Darcy's law was established by Darcy in 1856 (Darcy 1856), which is a standard approach in investigation of single phase fluid flow in microscopically both disordered and homogeneous porous media. The Darcy's law is often written as

$$-\nabla P = \frac{\mu}{K}\vec{V} \tag{1}$$

In Eq. (1), the permeability K is an intrinsic property of porous media. If the velocity becomes large enough, the Darcy's law is no longer sufficient. To describe the nonlinear flow in porous media, a quadratic term was introduced by Dupuit (Dupuit 1863) and Forchheimer (Forchheimer 1901) to generalize the flow equation, i.e.

$$-\nabla P = \frac{\mu}{K}\overline{V} + \beta\rho\overline{V}^2 \tag{2}$$

In Eq. (2), the factor β is generally called Forchheimer coefficient, is also called non-Darcy factor.

A most commonly used special form of Eq. (2) is Ergun equation (Sabrl Ergun 1952), which is a macro-scale model and is based on the hydraulic radius model

$$\frac{\Delta P}{L} = \frac{150\mu(1-\varepsilon)^2 v_s}{D_P^2\varepsilon^3} + 1.75\frac{1-\varepsilon}{\varepsilon^3}\frac{\rho v_s^2}{D_p} \tag{3}$$

Where P is the pressure, L is the length along the macroscopic pressure gradient in porous media, v_s is superficial velocity, μ is dynamic viscosity of fluid, ε is porosity of porous media, and D_p is average diameter of particles, ρ is density of fluid. The constants 150 and 1.75 in Eq. (3) were obtained from fitting 640 experimental data on spheres of different diameters. Compared Eq. (3) with Eq. (2), we get

$$K = \frac{D_P^2\varepsilon^3}{150(1-\varepsilon)^2} \tag{4}$$

$$\beta = 1.75\frac{1-\varepsilon}{D_p\varepsilon^3} \tag{5}$$

3 THE NONLINEAR DYNAMICS MODEL OF LAYERED ROCK MASS SEEPAGE

3.1 *The nonlinear dynamics model*

Set stope floor is composed of N layers of rock, i is rock number, see Figure 1, for the one-dimensional passive flow, while ignoring the volume and compressibility of water, the control equation for the rock dynamic system (Shu J S et al 2004, Schiavi C & Guglielmone F. 2012, Miao X Y et al 2007, Sun M G et al 2005)

$$\frac{\partial p}{\partial t} = -\frac{1}{\rho_0 \phi_0^{\,i} c_t^{\,i}} \frac{\partial w}{\partial x} \tag{6}$$

$$\frac{\partial w}{\partial t} = \frac{1}{c_\alpha^{\,i}} \left[-\frac{\partial p}{\partial x} - \frac{1}{\rho_0} \left[\frac{\mu}{k_i} w + b_i w^2 \right] \right] \tag{7}$$

When the system is in equilibrium, $\frac{\partial p}{\partial t} = 0$, $\frac{\partial w}{\partial t} = 0$, integral above second balance, and the sum of *i*, get

$$G_p = Aw + Bw^2 \tag{8}$$

In which

$$A = \sum_{i=1}^{n} \frac{h_i \mu}{\rho_0 h k_i} \tag{9}$$

$$B = \sum_{i=1}^{n} \frac{h_i b_i}{\rho_0 h_i} \tag{10}$$

$$G_P = \frac{p_0 - p_n}{\sum_{i=1}^{n} h_i} \tag{11}$$

The existence criteria of seepage system equilibrium state for the above layered rock mass is

$$D = A^2 - 4BG_p \tag{12}$$

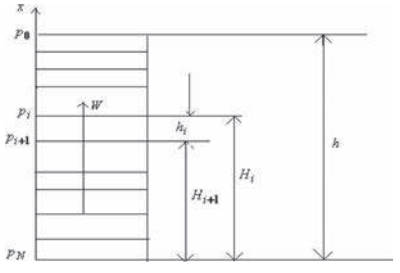


Figure 1. Dynamic model of rock seepage.

When D < 0, There is no equilibrium state, the system is not stable, we get specific instability conditions

$$g = \frac{4 \sum_{i=1}^{n} \frac{h_i b_i}{\rho_0 h_i} \frac{p_0 - p_n}{\sum_{i=1}^{n} h_i}}{\left(\sum_{i=1}^{n} \frac{h_i \mu}{\rho_0 h k_i} \right)^2} \tag{13}$$

From equation (4), (5), (13), we know, when $g < 1$, the occurrence of water inrush accidents is not caused by seepage instability.

Now we calculate the bottom floor is a single rock, the conditions of water not inrush, i.e. i = 1

$$g = 4 \frac{\Delta p b}{L \mu^2} \rho_0 k^2 = 4(bk\,\mathrm{Re} + (bk\,\mathrm{Re})^2) < 1 \tag{14}$$

Substituted the equations 4 and 5 into equation 14, we get

$$bk\,\mathrm{Re} = \frac{1.75 D_p\,\mathrm{Re}}{150(1-\phi)} \tag{15}$$

From equation 14, we get $-1.207 < bk\,\mathrm{Re} < 0.207$, From Eq. 15, we know that $bk\,\mathrm{Re} > 0$, Therefore, when $bk\,\mathrm{Re} <$ **0.207** satisfied, water inrush is not caused by seepage instability. i. e.

$$\frac{1.75 D_p\,\mathrm{Re}}{150(1-\phi)} < 0.207 \tag{16}$$

Change equation 16 to equality

$$D_p\,\mathrm{Re} = \frac{150 * 0.207(1-\phi)}{1.75} \tag{17}$$

The particle average diameter are respectively equal to 20 mm, 15 mm, 10 mm, 5 mm, get the relation of Reynolds number and porosity, see Figure 2.

From Figure 2 we can see that, when the Reynolds number in the corresponding figure below, floor water inrush will not caused by seepage instability, When the Reynolds number in the corresponding figure above, Floor water inrush will be caused by seepage instability. Figure 2 also shows that, the smaller of porosity and particle diameter, the larger of Reynolds number for causing loss of stability of seepage, i.e. the steady state is not easy to lose; otherwise, the larger porosity and particle diameter, the smaller of Reynolds number for causing loss of stability of seepage, the steady state is easy to lose.

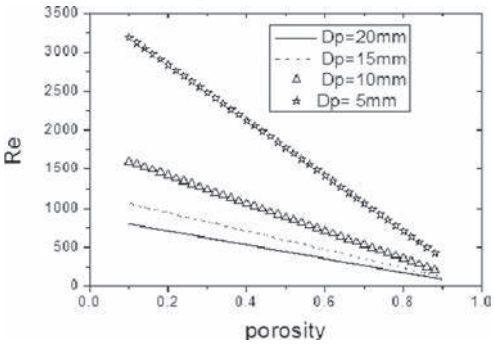


Figure 2. Relationship between Reynolds number and porosity.

4 CONCLUSION

Mining rock mechanics is a new subject for mechanics and mining engineering cross growth point, study on percolation theory is an important research direction. The seepage of mining rock mass which is fragmentation as the basic medium characteristic, has high nonlinear dynamic and random. Test method for new development, and on the basis of research, using random method and nonlinear dynamic systems is feasible. This paper mentioned some developments of this theory, further research is need to Continue.

ACKNOWLEDGEMENTS

The authors gratefully acknowledge foundation by the China National Nature Science Foundation of China (No. 51204069, 51074075, 41072188), the twelfth five year national science and technology support program (2012BAK04B04), The Central College Fund (NO. JCB2013B02).

REFERENCES

Darcy H. 1856. *Les Fontaines Publiques de la Ville de Dijon*. Paris:Dalmont.

Dupuit J. 1863. *Estudes Theoriques et Pratiques sur le Mouvement des Eaux*. Paris: Dunod.

Forchheimer P. 1901 Wasserbewegung durch Boden. *Z. Ver. Deutsch. Ing.,* 45:1782–1788.

Miao Xie xing, et al. 2007. Rock mass seepage and mine disaster prevention and control, *Journal of Xi'an Petroleum University*, 22:74–77 (in Chinese).

Sabrl Ergun. 1952. Fluid Flow through Packed Columns, *Chemical Engineering Progress*, 48:89–94.

Schiavi C & Guglielmone F. 2012 Pennella and U. Morbiducci, Acoustic method for permeability measurement of tissue-engineering scaffold. Measurement Science and Technology, 23:105702.

Shu J S, et al. 2004. Imploring on assumetion for water pressure distributing on failure surface in rock slope [J]. *Journal of China University of Mining and Technology,* 33(5):5092512.

Sun M G, et al. 2005. The mechanism of water inrush of based on the layered rock mass seepage instability conditions, Journal of China University of Mining and Technology, 34(3):284–288.

This page intentionally left blank

Progress in Mine Safety Science and Engineering II – He et al. (Eds)
© 2014 Taylor & Francis Group, London, ISBN 978-1-138-00122-0

The study on the principle of the compound perforating technology to improve rate of gas extraction

Jing-De Xu & Xin Yang
North China Institute of Science and Technology, Beijng, China

ABSTRACT: For the issues that low permeability coal seam gas extraction does not have obvious effect and low gas extraction rate, we propose the perforating technology which has been applied maturely in oil and gas exploration to increase coal seam porosity and improve gas extraction effect. Through analysing the feasibility of perforating technology applied in gas extraction and improving gas extraction rate, we can provide the evidence for the next step to carry out field testing and theoretical analysis roundly.

1 THE PRACTICAL BACKGROUND OF PERFORATING TECHNOLOGY

Due to coal and geological conditions, most of the high gas and outburst mines are difficult to extract in China, the fundamental reason is that coal seam permeability is poor. For low permeability and high gas coal seam, adopting conventional method to extract coal seam gas has the problems of long gas extraction cycle and low gas drainage efficiency. The main factor which determines whether coal seam permeability is good or bad is porosity of coal seam; therefore, the key measure to increase the coal seam porosity is to improve the gas extraction effect. (Lin 2006, Lin 1996, Hu 2002, Wan 2003 & Fushun 1984)

Over the years, the studies on gas extraction technology in China and abroad focuses on the goal of improving the coal seam permeability. The basic principle is using specific technology to change the original structure of coal, increase the porosity of coal seam with the help of outside force. The adopted technologies include Hydraulic Cutting Seam, Hydraulic Fracturing, Loose Blasting, Densely Borehole, Cross Borehole, Deep Hole Presplitting blasting and ect. (Zhou Zhou 1990 & Cheng 2009). Among these technologies, Hydraulic Fracturing and Deep Hole Presplitting blasting technology are more widely used.

Hydraulic Fracturing technology can use slotting to relieve coal seam pressure, cause deformation and damage of coal seam through underground stress, and increase the number of fractures in coal seam, so as to increase coal seam permeability (Sun 2010). However, the technology requires specialized fracturing equipment, relatively large quality and volume of conventional hydraulic fracturing equipment, it is inconvenience to transport, needs to prepare space for equipment and operating personnel to active. In the process of water injection, it needs to control the water injection pressure and fracturing time, the preparatory process is complex and the fracturing time is longer.

The Deep Hole Presplitting blasting technology is to use blasting stress wave as energy of destroying coal, the stress wave produces stress wave and superimpose each other in the process of stress wave propagating to the depths; it further accelerates the destruction of the coal, thus increasing the permeability. However, the technology needs to calculate and control parameters such as the blast hole depth, charge length in the hole, hole sealing, easy to produce misfire and thus leaves hidden danger.

In order to improve extraction rate and ensure safety, the new technology and new process must be developed. This paper mainly discusses the feasibility of compound perforating technology applied to the coal mine gas extraction.

2 THE PRINCIPLE OF COMPOUND PERFORATING TECHNOLOGY TO IMPROVE COAL SEAM PERMEABILITY

2.1 *The introduction of principle of perforating technology*

The perforating technology has became the main technical means to explorate the oil and gas field in China and abroad, at present the perforation completion has been widely used to mine oil and gas in the world (Joseph R.H. et al.). In China the perforation completion operation has been used in the oil and gas since 1950s and after development of 50 years, we have achieved remarkable achievements not only on the perforating technology but also on

the performance and supporting of perforating equipment. The main principle of the perforating technology is to use cavity effect to make the energy of explosive explode work on the shaped charge liner; then producing metal jet of high temperature, high pressure and high speed, penetrating the casing pipe and object and forming channel of certain depth (Wang 2002, Yuan 2002 & Wang 2006). The cavity effect refers to the product of explosive explode flying outward along the normal direction of explosive surface under high temperature, high pressure and high speed. Therefore, after exploding the explosive on the groove, there will appear a puff of agminated, high speed and high pressure explosive product stream; this makes the released chemical energy from explosive explode get together in a certain range. This is shown in Figure 1.

The compound perforating (Simon L. et al. 2004 & Jim G. et al. 1999) technology is a collection technology of perforation and high-energy gas fracturing, at the same time of perforating, the gas fracturing is conducting to the stratum, forming multiple cracks, increasing coal seam permeability and improving the ability of flow conductivity of coal gas.

2.2 *The mechanism of compound perforating technology crack coal*

During operation, the detonating cord ignites the propellant while detonating the perforating charge. First of all, the perforating charge penetrates the gun body and coal and forms a gallery between drilling and coal. Then the solid propellant explodes the second time, and instantly follows the high temperature airflow. Under the effect of dilate and extrude of high pressure gas, it washes out and fractures the perforating channel, forms crack of radial direction and axial direction and expand to multi-directions. Moreover, it forms multi-direction net crack in the coal channel and expand the perforating depth, increases coal seam porosity, improves coal seam permeability; and thus improves the effect of gas extraction.

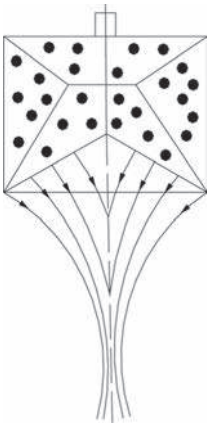


Figure 1. The principle of the perforating technology.

The feasibility of the compound perforating technology applied to improve the permeability of low permeable coal seam is mainly manifested in the following several aspects:

1. The oil and gas generally occurred in around the non-permeability rock, it reserves in adsorption state in the coal rock crack, this point is similar with the gas occurrence condition.
2. The explosive used in the perforating technology belongs to civilian explosive materials, it is conventional initiating explosive device and widely used in coal mine, and the management of explosive belongs to the normal management.
3. It is more safety than the deep hole presplitting blasting. After perforating, the residual metallic object in the object (coal seam) cannot produce or carry any oxidant (or oxygen in the air); therefore, the possibility of coal seam gas explosion is very small.
4. The perforating technology is maturely used in the oil and gas industry, it has easy popularization and application, simple technique, low cost and is easily to be operated and promoted.

3 THE EQUIPMENT AND PROCESS OF PERFORATING TECHNOLOGY

3.1 *The perforating equipment*

The perforating equipment includes perforating charge, perforator, gun body and the core part is perforating charge.

1. Perforating charge
   The perforating charge is made based on the principle of cavity effect; different shape explosive has different energy transfer ways. This is shown in Figure 2.
2. Perforator
   The perforator is cascaded of dozens of perforating charge to hundreds of perforating charge; this is the tool that uses the detonator and detonating cord to detonate the perforation. It can be divided into perforator with gun body and perforator without gun body. The perforator with gun body refers to the perforating charge equipped in the sealed steel tube; the perforator without gun body refers to single sealed perforating charge connected by seal wire, metal rod or thin metal belt, it perforates directly in the well.

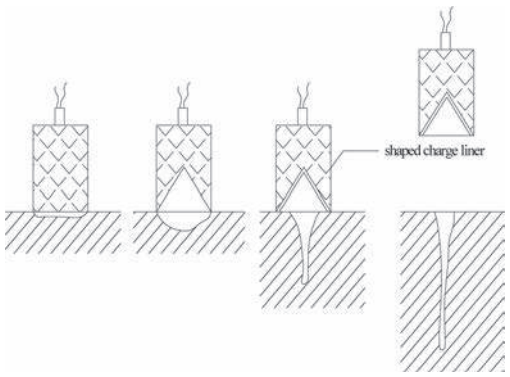


Figure 2. Different shape explosive has different destructive effect.

3. Gun body
   The gun body is an important part of a perforator, the main function as a carrier is to confine and absorb the energy produced by the perforating charge (the perforator without gun body do not have gun body).

3.2 *The perforating process*

According to process, the perforating can be divided into overbalanced perforating, underbalanced perforating, super-overbalanced perforating.

According to conveyed way, the perforating can be divided into cable conveyed perforation and tubing conveyed perforation (Wee H.L. 2002).

The cable conveyed perforation uses the cable (divided into perforator with gun body and perforator without gun body) to convey the perforator to underground by casing pipe or oil tube. It uses the perforating depth control technology to locate to align the target zone. Then the instrument on the ground supplies power to the perforation priming device and detonate the perforator; this can perforate the casing pipe, cement sheath, target zone and establish gallery between shaft and target zone.

The tubing conveyed perforation refers to concatenating all the perforators, which are used for perforating the oil and gas layer, into the end of the tube. This will form a hard-wired sting to run down to the well. By measuring the magnetic positioning curve or radioactivity curve, modifying the alignment of the depth allows perforator to correctly align with the perforation layers. Through using percussive type and pressurized type, these two types of detonating perforator perform a perforation to the destinated layers. During the perforating operations of highly deviated wells, horizontal wells, heavy oil wells, high pressure gas wells, sand wells and low permeability formations, each of them has their own unique advantages.

4 APPLICATION OF COMPOUND PERFORATING TECHNOLOGY TO IMPROVE THE RATE OF GAS EXTRACTION TECHNOLOGY ROADMAP

During the process of implementing the perforating technology into the oil and gas wells, the operations personnel are constructing on the ground. The issues related to construction process safety hazard is small, as a result, the probability of injury is very small as well. Meanwhile, coal mine production environment determines that workers and perforation preparation works have to be under the same operating environment during perforating process. Since there is a security risk, ensuring the safety of mine workers is the primary issue. The general technical routes are:

1. Measure the elastic modulus of coal and rock, the permeability and other basic parameters; the use of specialized software; the simulation for perforating fracture distribution formed by perforating in the operating environment. This information will all serve as reference for the trial.
2. According to the numerical simulation results, people select the appropriate perforating equipments, determine the drilling parameters (drilling diameter, length, spacing, angle, etc.) and sealing lengths.
3. After complete drilling, confirm the length of ignition wire according to the depth of drilling, then connect the ignition wire to the detonator wring in the perforating gun.
4. Using a dedicated thruster (such as stemmer) to drill the determined perforating charge into the hole bottom. Based on the actual needs, the perforating charge can be concentrated to perform a perforating operation.
5. When using hole sealing device for sealing, the sealing material has to be polyurethane, and the sealing length must not be less than 10 m, the ignition wire should be protected well when sealing, short circuit or open circuit is forbid to appear.
6. Performing a perforating operation after connecting the ignition wire to the initiation instrument well and electrifying in the safety area, the working process of perforating gun is shown in Figure 3.
7. After the operation is done and the job-site safety is confirmed, one must measure and record the data for the gas flow and density inside the hole. Such data will be compared with

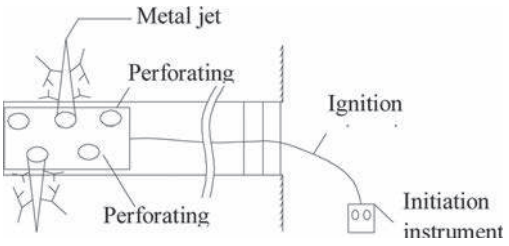


Figure 3. The process of perforating gun installation and perforating.

the gas parameters before implementing the perforating operation, and conclusions should be drawn.

REFERENCES

Cheng Y.P., Fu J.H. & Yu Q.X. 2009. Development of gas extraction in coal mine technologies in China. *Journal of Mining & Safety Engineering* [J], (2):127–139.

Fushun Institute of China Coal Research Institute, 1984. *Translations of gas extraction in coal mine technology* [M]. Beijing: China Coal Industry Press.

Hu Q.T. 2002. Research of efficient coal and ourtburst prevention technologies[J]. J*ournal of Huainan Industry College* 22(4): 11–14.

Jim Gilliat, Phillip M.S. & Robert H. 1999. A review of field performance of new propellant/perfortating technologies, *Paper SPE 56469, presented at the 1999 SPE Annual Technical Conference and Exhibition held in Houston*, *Texas*, (11), 3–6.

Joseph R Hearst, Philip H Nelson, and Frederick L. Well Logging for Physical Properties. *A Handbook for Geophysicists, Grologists, and Engineers*, New York: 427.

Lin B.Q. & Zhang J.G. 1996. *Theory and technology of gas extraction in mine* [M]. Xuzhou: China University of Mining Press.

Lin B.Q. & Zhai C. 2006. Mechanism of gas explosion in coal exploitation and its preventive measures[J]. *Journal of Mining & Safety Engineering* 23(1):19–23.

Moreo CE. 1883–1888. On Certain Phenomena Produced by Detonation of Gun Cotton. *NewPort Natural History Soeiety*. Proeeedings. Report No.6.

Neumann M. Einiges uber brisante Sperengstoffe. 1911. Zeitehrift fur Angewandte Chemie. *Wtrrenburg. Germany*: 2233–2240.

Newmann E. 1914. New hollow bodies of High Exposive Substanees. *Zeitsehrift fur das Gesamte Sehiess-und Sprengstof fweeen*. Darmstradt, Germany: 183–187.

Simon Labrunie, José A. Carrillo & Pierre Bertrand, 2004. Numerical study on hydrodynamic and quasi-neutral approximations for collisionless two-species plasmas, *Journal of Computational Physics*, 200(1):267–298.

Sun B.X., Wang Z.F. & Wu H.R. 2010. The application of Hydraulic Fracturing in gas extraction[J]. *Coal Science and Technology*, 119(11):78–80.

Wan Z.F. 2003. Discussions of problems and countermeasures for gas extraction in coal mine in our country [J]. J*iaozuo Institute of Technology* (4):241–246.

Wang H.D. & Sun X.B. 2006. Summary of development of perforating technology both in China and abroad. *Explosive Materials* 35(3):33–36.

Wang Y.P. & Huang Y.S. 2002. Status and trends of compound perforating technology[J]. *Explosive Materials* 31(3):30–34.

Wee H.L. 2002. Oil well perforator design using 2D Eulerian code, *International Journal of Impact Engineering*, 27:535–559.

Yuan J.C. 2002. Status and development of perforating technology in China [J]. *Technology of Well Logging* 26(5):421–425.

Zhou S.N. 1990. Mechanism of gas flow in coal seam [J]. *Journal of Coal* (1).

Zhou S.N. & Sun J.Z. *Theory and applications of gas flow in coalseam* [A].

Zou L.Z. & Shi H.G. 2012. Review and comments of main perforating technology development in China and abroad. *Oil Equipment* 26(4): 34–37.

Progress in Mine Safety Science and Engineering II – He et al. (Eds)
© 2014 Taylor & Francis Group, London, ISBN 978-1-138-00122-0

Method of detecting in coal mine disaster warning internet of things based on SVM intruders optimized by Genetic Algorithm

Chang-Li Wang, Li-Min Sun, Sheng-Chen Yu, Jiang-Lan Huang, Xiao-Ju Wang & Hui Guo
Key Laboratory of Mine Disaster Prevention and Control Technology in Hebei Province, Yanjiao, Beijing-East, China
North China University of Science and Technology, Yanjiao, Beijing-East, China

ABSTRACT: In order to improve the detection correct rate of intruders in coal mine disaster warning internet of things, Support Vector Machine (SVM) classifier and Genetic Algorithm (GA) are applied synthetically to detect intruders in coal mine disaster warning internet of things in this paper. SVMs, as a new pattern classification technique, have been well recognized as a powerful computational tool for nonlinear problems. However, the standard SVMs are inefficient to achieve expected performance due to limitations in single kernel function. To enhance the SVMs' learning process and achieve expected performance, a hybrid kernel function has been proposed, which is composed of RBF kernel and polynomial kernel. GA is used to optimize the parameters of hybrid kernel to control misclassification. Experiments based on real-world data indicate that hybrid kernel SVM optimized by GA is higher in recognition accuracy than the general SVM and the detection right rate of intruders was above 91% for the KDD CUP 1999 data.

Keywords: Intruders, Support Vector Machine (SVM), Genetic Algorithm (GA)

1 INTRODUCTION

Software trespass can take the form of a virus, worm, Trojan horse, One of the two most publicized threats to security is the intruder (the other is viruses), generally referred to as a hacker or cracker. An intrusion is a formal term describing the act of compromising a system. And detecting either failed or successful attempts to compromise the system is called intrusion detection. In a nutshell, intrusion detection systems or IDS do exactly as the name suggests: they detect possible intrusions. The goal of IDS tools is to detect computer attacks or illegal access, and to alert the concerned people about the detection or security breach. An IDS installed on a network can be viewed as a burglar alarm system installed in a house. Though their methods are different, when an intruder/attacker/burglar is present, both can detect them, and both subsequently can issue some type of warning signal or alert (Rao, 2003).

Intrusion detection techniques can be partitioned into two main approaches: misuse detection and anomaly detection. Misuse detection methods attempt to model attacks on a system as specific patterns, and then systematically scan the system for occurrences of these patterns. Anomaly detection methods attempt to establish each user's normal activity profile, and to flag deviations from the established profile as possible intrusion attempts.

The intrusion detection problem is pattern classification problem in essence. Over the past decade, a lot of techniques, which involve the Bayesian parameter estimation (YU, 2008), data mining, artificial neural network techniques and support vector machine, etc have been applied to the field of intrusion detection.

As a good classifier, Support Vector Machines (SVM) certainly can perform better than some other methods, because it has higher generalization capabilities and is able to maximize the generalization performance of a trained classifier. In SVM, each kernel function has its own characteristic. Smits has pointed out that polynomial kernel function is a global kernel with weak learning ability and strong generalization ability, while RBF kernel is a local kernel function with just opposite characteristics. The 'good' characteristics of two or more kernel functions should be combined in order to enhance the whole performance of the SVM.

Thus, we make a combination of polynomial kernel and RBF kernel as the kernel of SVM. Genetic Algorithm (GA) is used to optimize the parameters of the hybrid kernel. In the application results, standard SVMs have been compared with SVMs with single kernel optimized by GA in the paper.

The rest of the paper is as follows. The necessary background knowledge is described in section 2. The dataset and the model of algorithm used in this paper are described in section 3. Experiment results are reported in section 4. Section 5 is conclusions.

2 PRINCIPLES OF HYBIRD-KERNEL SVM

A Support Vector Machine (SVM) is a class of supervised machine learning techniques. It is based on the principle of structural risk minimization. The ideal of SVM is to search for an optimal hyperplane to separate the data with maximal margin. Let *d*-dimensional input x belong to two classwhich was labeled

$$y_i\left(x_i, y_i\right), i=1,\ldots,n, x \in R^4, y \in \{+1,-1\}$$

his can be achieved by:

$$y_i[(w \cdot x_i)+b]-1+\xi_i \geq 0, \quad i=1,2,\ldots,n \tag{1}$$

If the data are not linearly separable, one can introduce slack variables ξ_i and instead minimize a modification of the above.

$$\min \phi(w)=\frac{1}{2}(w \cdot w)+C\sum_{i=1}^{n}\xi_i \tag{2}$$

Where C is a constant chosen a-priori.

In order to solve this problem, one can introduce Lagrange multipliers and consider the dual problem, under the constraints,

$$\sum_{i,j=1}^{n} a_i y_i=0, \ a_i \geq 0, \ i=1,2,\ldots,n \tag{3}$$

The optimal problem now is,

$$Q(a)=\sum_{i,j=1}^{n} a_i-\frac{1}{2}\sum_{i,j=1}^{n} a_i a_j y_i y_l (x_i \cdot x_j) \tag{4}$$

This is a two optimal problem, the only answer exists. According to Kuhn-Tucker condition, this optimal problem must satisfy,

$$a_i(y_i(w \cdot x_i+b)-1)=0 \tag{5}$$

Hence only the points x_i which satisfy, change equation will have non-zero Lagrange multipliers. These points are termed Support Vectors (SV). All the SVs will lie on the margin and hence the number of SVs can be very small. Consequently the hyperplane is determined by a small subset of the training set. Hence the solution to the optimal classified problem is given by,

$$f(x)=\operatorname{sgn}\left(\sum_{i=1}^{n} a_i^* y_i (x_i x)+b^*\right) \tag{6}$$

As the training of SVM is equivalent to solving a linearly constrained convex quadratic programming problem, the solution of SVM is always global optimal and absent from local minima. Actually, the solution is determined by only support vectors, which are a subset of training data points, so it can be represented sparsely.

Hybird kernel can be expressed in: $K=\sum \lambda_i K_i$, where K_i form a family of various kernel functions. The hybird coefficients λ_i are either simply required to be nonnegative or determined in the such way that the hybird kernel is positive semi-definite. So the hybird kernel function can be described as following ormula:

$$K=\lambda_1 K_{poly}+\lambda_2 K_{RBF}$$
$$S.T.\begin{cases}\lambda_1+\lambda_2=1\\ \lambda_1,\lambda_2 \geq 0\end{cases} \tag{7}$$

3 GENETIC ALGORITHM (GA)

GA is an artificial intelligence procedure based on the theory of natural selection and evolution (Chen, 2007). It is inspired by and named after biological processes of inheritance, mutation, natural selection, and the genetic crossover that occurs when parents mate to produce offspring. GA differs from conventional non-linear optimization techniques in that it searches by maintaining a population of solution from which better solutions are created rather than making incremental changes to a single solution to the problem.

Two important issues in GA are the genetic coding used to define the problem and the evaluation function, called the fitness function. Each individual solution in GA is represented with a string called the chromosome. The initial solution population could be generated randomly, which evolves into the next generation by genetic operators, such as selection, crossover and mutation. The solutions coded by strings are evaluated by the fitness function.

4 INTRUSION DETECTION MODELS BASED ON HYBIRD KERNEL SVM OPTIMIZED BY GA

4.1 *Hybrid kernel function*

Common kernel functions are divided two categories, global kernel functions and local kernel function. Global kernel function can display a perfect level of generalization performance, but its learning ability is poor. When global kernel function is used, the data points which are far between them can also affect the value of kernel function. On the other hand, local kernel functions have good learning ability, but their generalization performance

is poor and the dataset affect the value of kernel function only in small domain.

4.2 *GA-optimized procedure*

In intrusion detection, there are two types of misclassification errors. The type I of error occurs when non-intrusion are classified into intrusion group. The type II of error occurs when intrusion are classified into normal group. So the fitness function can be set as follows:

$$f = M(1 - TDR - FDR) \tag{8}$$

GA has been used to optimize RBF kernel width parameter σ^2 and punitive coefficients C_1, C_2 when $p = 1$ and $p = 2$ (p is the power of polynomial kernel) respectively. Here C_1, C_2 are the loss costs of and type II of errors. Chromosome length is 3; genetic algorism adopts real-valued encodings. The initial population is set to be 30. The True Detection Rate (TDR) measures the percentage of data correctly classified in the test set. The False Detection Rate (FDR) measures the percentage of data falsely classified in the test set that are detected falsely. M is an amplifying coefficient which ensures the change of fitness function is observable. We use proportional algorithm operator and arithmetic crossover algorithm, non-uniform mutation, mutation rate is set to be 0.07, $\lambda \in [0, 1]$, step length is 0.05 and the evolving generation is 2000. Some experimental results are reported in the following sections.

The GA-optimized procedure is as follows:

1. Initial Population
2. GA operation
3. Fitness Function Calculation
4. Maximum generation, If satisfies, then go to the step (5); If does not satisfy, go to the step (2).
5. Get optimized hybrid kernel SVM parameter

We have given a new intrusion detection model as follows:

1. Network Dataset;
2. GA parameter optimized by GA;
3. Classification by Hybrid kernel SVMs with optimized parameter;
4. Recognize possible intruders.

5 EXPERIMENTS AND RESULTS ANALYSIS

5.1 *Data set used in the experiments*

The dataset used is the KDD CUP 1999 data, which consists of approximately 4,900,000 data instances. Each instance is a 42-dimensional vector (label included). Each of the dimensions corresponds to an extracted feature value from a connection record obtained from the raw network data. The extracted features included the basic features of an individual TCP/IP connection, such as its duration, protocol type, number of bytes transferred, etc. Some of the attributes are nominal-valued. some of them are continuous-valued, and some are discrete-valued. Attacks fall into four main categories:

DoS: denial-of-service, e.g. SYN flood;
R2 L: unauthorized access from a remote machine, e.g. guessing password;
U2R: unauthorized access to local superuser (root) privileges, e.g. various "buffer overflow" attacks; Probing: surveillance and other probing, e.g. port scanning.

Each instance is a 42-dimensional vector (label included). There are eight discrete attributes, thirty-three continuous attributes and one label attribute.

5.2 *Experiments results*

To evaluate our method, we randomly chose 8,000 unique samples from the 10% sample of KDD Cup 1999 for our experiment, 5,000 samples are used to train the model and 3,000 to test. Since the KDD Cup 1999 is concerned with multi-classification. So we construct separately four classifiers to train dataset.

We compare the result based on our method with the result based on standard SVMs and SVMs with single kernel optimized by GA. The experiment results of four classifiers are shown in Table 1.

Based on those results, we can see the intrusion detection system based on ours method do not increase the training time of support vector

Table 1. Performance comparison of three methods.

Datasets	Algorithm	Accuracy (%)	False rate (%)
Probe	SVM	80.4	5.39
	SVM+GA	84.3	1.43
	Ours method	91.6	0. 61
DoS	SVM	81.3	5.58
	SVM+GA	85.7	1.52
	Ours method	90.5	0.37
U2R	SVM	81.8	5.07
	SVM+GA	84.6	0.89
	Ours method	90.7	0.50
R2L	SVM	82.7	4.73
	SVM+GA	87.3	0.79
	Ours method	92.3	0.52

machines classifier and can give higher recognition accuracy than the general SVM.

6 CONCLUSIONS

When Hybrid kernel SVM improved by GA is used as IDS, the overall performance of IDS can improved. Experiment results shown that this method was useful and the detection right rate of intruders was above 95% for the KDD CUP 1999 data. The study is motivated by the need to effectively control misclassification error and enhance the learning and generation performance of SVMs. We turn to hybird-kernel SVM composed of Polynomial kernel and RBF kernel which have been proved to be of compensatory characteristics. In order to control misclassification error, we use GA to optimize the parameters of hybird kernel function. All of above represent the feasibility and advantage of our method. But there are many respects which need the further study inevitably.

Future work is to improve the algorithm itself, we will reduce the degree of sensitivity of algorithm to noise, so as to improve the detection rate and lower rate of false positives further

ACKNOWLEDGEMENTS

This work was financially supported by "the Fundamental Research Funds for the Central Universities of China" (JSJ2013B09, JSJ2013B02, JSJ1207B, 2011B029, 2011B028)

REFERENCES

Chen Guoliang 2007. *The genetic algorithm and applies.* Beijing: People's posts and telecommunications publishing press, 37–38.

X. Rao 2003. An Intrusion detection system based on Support Vector Machine, *Journal Sofeware*, 14(4):798–803.

YU Sheng-chen 2008. Solution to Character Compression of Intrusion Detection System In Controllable and Trustednet Works. *International Conference on Information Technology Environmental System Sciences (ITESS'2008)*, 704–710.

Progress in Mine Safety Science and Engineering II – He et al. (Eds)
© 2014 Taylor & Francis Group, London, ISBN 978-1-138-00122-0

Experimental study on the impact of complex surfactant in coal-water contact angle

Longzhe Jin & Nannan Jiang
School of Civil and Environment Engineering, Beijing University of Science and Technology, Beijing, China

Shaojie Chen
School of Safety Engineering, North China Institute of Science and Technology, Beijing, China

ABSTRACT: The seam water injection is one of the coal dust prevention measures. However, due to the hydrophobic coal, the wetting effect of clean water is not ideal. By adding manner of the single surfactant and the two surfactants mixed in the water, the surface tension of the solution and the contact angle of 3 groups of coal samples were measured in this article. The experimental results show that two formulations, P_1: Fatty alcohol amide with Alkyl quaternary ammonium salt ratio of 2:1; P_2: JFC with Triton X-100 at a ratio of 1:1.

1 INTRODUCTION

Pre-wet coal is the most fundamental and the most effective means to reduce the dust which is caused by mining, loading and shipment of the coal. However, due to the poor wettability of the coal, only the water injection speed is low, and water capacity can not reach the dustproof requirements. When the surface active agent is added into the water, it can reduce the surface tension and wetting angle of the aqueous solution, thereby enhancing the ability of the solution wetting coal along the coal body fractured surface. Usually, according to its structure, surface active agent can be divided into cationic, anionic, non-ionic and mixed, which can reduce the surface tension of water, and change the characteristics of its contact angle. But for the cationic surface active agent, the cation is strongly adsorbed on the surface of the coal, which makes the coal surface leaving dehydrated state so that the absorbent capacity of the coal reduces, not achieve wetting coal acts. So, cationic surfactants are not suitable for coal seam water injection.

2 EXPERIMENTAL METHOD

2.1 *Coal sample preparation*

Particle size of 200 mesh accounted for more than 80% of the pulverized coal used in the experiment, and compressed into a diameter of 13 mm, a thickness of 2–3 mm coal cake. The coal cake was soaked in a saturated saline 24th, for the contact angle measurements.

2.2 *Measurement of surface tension and contact angle*

Bulleted lists may be included and should look like this:

- This experiment uses the FTA200 table interface analyzer to measure the contact angle and surface tension between the liquid and solid. Surface analyzer survey liquid and solid, shows the interfacial tension. The standard deviation of the contact angle measurement is smaller than 1°. The standard deviation of surface tension measurement is smaller than 0.5 m $N \cdot m^{-1}$.

3 SURFACTANT FORMULATION RESEARCH

Surfactant formulation starts from monomeric surfactants, then carry out the compound after choose preferably, control the type and proportion of the surfactant complex to alter the nature of the mixed solution. At last, elect a final surfactant formulation preferably which is based on surface tension and contact angle data.

3.1 *Study of the single surfactant*

According to the measurement of the wetting time of the prepared solution, the test surfactant is finally selected to the JFC, fatty alcohol amides, alkyl quaternary ammonium salt and Triton X-100 solution, which is in the ratio of the content of active agent and $CaCl_2$ is 1:9. Prepare of the salt solution of a concentration of 0.8% of the active

agent firstly, gradually dilute to 0.1%, 0.05% and 0.025% concentrations of the active agent solution. The experimental results are shown in Table 1.

As can be seen from Table 1, the JFC solution of high concentration (0.1%) of smaller surface tension, and the contact angle is small. But in the JFC solution of the medium (0.05%) and low (0.025%) concentration, the surface tension and contact angle are not big; fatty alcoholsamide, and Triton X-100 is low changes in solution surface tension of the medium and high concentrations, each concentration of fatty alcohol amides corresponding to the contact angle is small; In the Alkyl quaternary ammonium salt solution with low, medium and high concentration, the surface tension is larger, only high contact Angle is small, other concentration contact Angle is bigger. So, for single surfactant, the test is needed to find the compound formula to reduce contact Angle.

3.2 *Study of the complex surfactant*

When two kinds of surfactant are Compounded, choosing surfactant concentration was 0.05%, and the proportion of the two kinds of surfactant was 1:1. Preliminarily select two suitable compound formula, then do the concentration distribution in detail. The experimental results are shown in Table 2 and Table 3.

According to Table 1, the surface tension and contact angle of Fatty alcohol amide and Alkyl quaternary ammonium salts complex solution and JFC and Triton X-100 complex solution are less, it is necessary further study these detailed formula.

Derived from Table 2.2: the surface tension of 1:1 fatty acid amide and alkyl quaternary ammonium compound solution is minimum, corresponding to three sets of coal samples' contact angles which are small too. The surface tension and contact angle of JFC with Triton X-100 1:1 mixed solution are small. Both aboved solution can be studied in detail. Other complex formulations' surface tension and contact angle are big, which are not suitable for complex tests.

According to Table 3, 1) amide of fatty alcohols and alkyl quaternary ammonium salt ratio of 2:1, surface tension when compared with 1:1 is slightly higher, but the effect of the contact Angle of three kinds of coal sample decreased, better effect than 4:1 and for the most appropriate ratio formula is amide of fatty alcohols and alkyl quaternary ammonium salt ratio of 2:1. 2) For JFC and Triton X-100 in addition to the 1:1 ratio, the surface tension of the solution are rising with other proportion. The contact Angle of different coal sample has the tendency of increase, with the rest of the proportion is not suitable for carrying out the test. 3) The compound formula was finally determined:

Table 1. The surface tension and contact angle of salt solution.

Solution	Concentration (%)	Surface tension (dy/cm)	Contact angle (°)		
			1#	2#	3#
JFC	0.1	23.4	8.0	12.1	12.9
	0.05	26.3	20.8	34.4	31.7
	0.025	32.5	30.9	44.0	31.9
Fatty alcohol amide	0.1	23.7	9.3	13.5	12.1
	0.05	23.1	7.2	17.0	21.2
	0.025	25.8	15.2	20.5	26.4
Alkyl quaternary ammonium salts	0.1	28.5	7.6	11.4	14.5
	0.05	32.2	21.3	32.3	29.5
	0.025	38.8	36.0	43.0	46.3
Triton X-100	0.1	26.2	15.5	7.9	12.5
	0.05	26.5	21.7	40.8	37.4
	0.025	26.9	27.8	45.1	39.0

Table 2. 1:1 ration of surfactant solution of surface tension and contact angle.

Solution	Concentration (%)	Surface tension (dy/cm)	Contact angle (°)		
			1#	2#	3#
Fatty Alkyl	0.05 0.05	22.3	15.7	10.7	13.7
Fatty TritonX-100	0.05 0.05	24.9	9.2	8.2	24.6
JFC Alkyl	0.05 0.05	28.2	18.6	21.9	32.6
Alkyl TritonX-100	0.05 0.05	23.0	3.9	7.9	26.2
JFC TritonX-100	0.05 0.05	23.5	9.2	29.5	12.6
JFC Fatty	0.05 0.05	23.5	8.4	23.4	20.4

Table 3. The detailed formula surfactant solution of surface tension and contact angle.

Solution	Concentration (%)	Ratio	Surface tension (dy/cm)	Contact angle (°)		
				1#	2#	3#
Fatty alcohol amide Alkyl	0.05 0.05	1:1	22.3	15.7	10.8	13.7
		2:1	22.7	11.1	9.4	14.0
		4:1	22.8	22.3	13.5	8.3
JFC Triton X-100	0.05 0.05	1:1	23.5	9.2	29.5	12.6
		2:1	25.6	31.5	7.7	30.6
		4:1	24.6	29.4	9.5	13.0
		1:2	24.5	22.9	32.5	16.4
		1:4	26.7	15.8	26.1	30.0

based on the detailed proportion of surfactant with surface tension and contact Angle data contrast, getting the optimal formula.

4 CONCLUSIONS

Selected four kinds of surfactants on single surfactant measurement, it can be seen that the contact Angle is smaller in the relatively high concentrations of surfactant; In the low concentration of the contact Angle is bigger. Thus, it is necessary to do the two surfactant test. Comparison by the surface tension and contact angle, the optimal formula are P_1, P_2. P_1: The surface tension is 22.70 dy/cm, when the ratio of amide of fatty alcohols and alkyl quaternary ammonium salt is 2:1; P_2: The surface tension is 23.51 dy/cm, when the ratio of JFC and Triton X-100 are 1:1. For P_1, P_2, according to the choice of different coal condition such as the critical surface tension of the specific analysis.

ACKNOWLEDGEMENTS

This paper is supported by National Natural Science Foundation of China (Grant no. 51074015) and the Special Funds of Central Colleges Basic Scientific Research Operating Expenses (Grant no. 2011B01).

Consistency of style is very important. Note the spacing, punctuation and caps in all the examples below.

REFERENCES

Chen SJ, et al. 2012. Measurement and analysis on critical surface tension of caol. *Safety in Coal Mines* 43(11):161–162. (in chinese).

Cheng Y, et al. 2006. Study of adding surfactant to seam water injection. *Safety in Coal Mine* (3):9–12. (in chinese).

Fu G, et al. 2002. *Coal mine dust control:20–25*. Beijing: China University of Mining and Technology Press. (in chinese).

Huo LJ, et al. 2011. Application practice on surfactant in coal seam water infusion. *Coal Tecnology* 30(5):106–108. (in chinese).

Wu C & Gu DS. 2001. The improvement of addition of sodium sulfate on wettability of coal dust by anionic surfactants. *Journal of Safety and Environment* 1(2):45–49. (in chinese).

Yan ZJ, et al. 2011. The influence of coal sample preparation method on the determination of coal-water contact angle analysis. *Journal of North China Institute of Science and Technology* 8(2):66–69. (in chinese).

This page intentionally left blank

Progress in Mine Safety Science and Engineering II – He et al. (Eds)
© 2014 Taylor & Francis Group, London, ISBN 978-1-138-00122-0

Research on method of automatic recognition of coal mine water inrush sources based on Immune Algorithm and Back Propagation Neural Network

Sheng-Chen Yu, Li-Min Sun, Jiang-Lan Huang, Xiao-Ju Wang & Hui Guo
Key Laboratory of Mine Disaster Prevention and Control Technology in Hebei Province, Beijing-East, Yanjiao, China
North China University of Science and Technology, Beijing-East, Yanjiao, China

ABSTRACT: In order to improve the discrimination accuracy of underground water source, a method on recognition of flood water based on immune algorithm and Back Propagation Neural Network (BPNN) is developed in the paper by studying and analyzing the water chemical data. In this method, Immune Algorithm (IA) is used to preprocess the flood water data, extract key characteristics and reduce dimensions of experiment data set by characteristic analysis method, then BPNN is adopted to classify and recognize the flood water data. Experimental results show that the method is feasible and efficient, and the detection right rate of flood waters was above 93%.

Keywords: Water inrush source recognition, Mine water-bursting, Immune algorithm, Back Propagation Neural Network

1 INTRODUCTION

Over the years, the prevention and treatment of mine water disaster is always an important question for study or discussion of scientist, engineer and producer relevant to the research in the science field. In hydrogeochemical (referred to as the "water chemical") detection technology, the source of water (headwaters, waterhead) is analyzed and determined according to the ground water quality test results (CAO, 2010). More than eight indexes of water are tested generally on the ground. The method technology is an important means of mine water prevention and control work. In some complex area effect in recognition of mine water inrush, it is significant. It is a rapid, economic and practical method. At present, several following methods are commonly used. (1). mine water source is recognized by characteristic ion or ion ratio method; (2) Source of mine water in inrush (Chung, drench, collapse) is recognized synthetically by the water quality analysis and the isotopic analysis method; (3) Water source is determined by artificial tracer method; (4) Source of mine water in inrush is recognized by the establishment of mathematical distinguishing model. For example, through research, the people of a unit think that the content of NO_3^{-1} in Ordovician limestone water is 9~10.5 mg/L, the content of NO_3^{-1} in the water in other water-bearing stratum (aquifer) is very low. According to this result, with the help of the content of NO_3^{-1}, they determine whether Ordovician limestone water is projecting. However, the actual conditions are quite different with the results which are got in this manual and single index method, in some complex area. In addition, the computational efficiency of fuzzy clustering algorithm is very high, but its main shortcoming is that the model selected often does not reflect the probability structure of ground water quality index data, so the results obtained with these methods cannot reflect the real situation of data structure. In fact, mine water hazard source identification system is a complex project, not a simple classification problem. The many problems need to be studied further, for example, how to reduce the redundancy of the data to be analyzed, how to select the best characteristics, etc.

In this paper, a plurality of data of analysis of ground water quality test were pre-processed with Immune Algorithm (IA). The key characteristics of coal mine water inrush source data are extracted by characteristic analysis method. The complexity of the data is reduced by reducing the dimensionality of the data set. With the help of the data after dimension reduction, the Back Propagation Neural Network (BPNN) is trained. The coal mine water inrush source is recognized by the trained BPNN. Experiments show that if the source of mine disaster water is identified by the method developed in the paper, its accuracy can reach 93%. The more detailed introduction on the method is given below.

2 THEORY ON IDENTIFICATION OF MINE DISASTER WATER SOURCE

That mine water chemistry data are treated and the water sources are identified by mathematical model, is the inevitable result of the combination of modern geochemistry, mathematics and computer science. The process steps of recognizing water sources are as follows (Zheng, 2004):

1. According to the actual situation, first of all, the water chemistry model (or library of the water sample) of a mine, or an area (for example, Lu'an Group's mine), or water source in China's mine is established. The water sources in China's are mainly sandstone water, water in Ordovician limestone, the water in Tai limestone, the water in old lane and the cavity mined.

   In the mine that is mined below shallow sea, the mine water sources is mainly seawater; In the mine that is mined below reservoir or lake, the mine water source is mainly reservoir or lake water.
2. To obtain a plurality of indicators of water quality analysis in laboratory: for example, K^+, Ca^{2+}, Mg^{2+}, SO_4^{2-} (sulfate), PH, Fe (iron), NO_2^- (nitrite), I (iodine) and T (temperature).
3. To establish a mathematical modeling method for judging water inrush, such as application of artificial intelligence method to determine the source of water.
4. When the water is determined to be the Ordovician limestone, or water-accumulating old kiln and gob area water, which may bring about water disasters in coal mine, the preventive measures can be taken. When the water is determined to be the other water or water with small harm, the coal mine can be mined normally.

3 IMMUNE ALGORITHM (IA)

Immune algorithm is a new algorithm which is designed in recent years according to enlightenment of the biological immune system (Mo & Jin, 2002).

Antigen, namely, an alien cell, everything which is not physical things will be probably antigen, for example, pathogen, pollen, a transplanted organ. Antibody is able to swallow the antigen. The molecule of antibody is a kind of protein, for example, white blood cell.

According to the biological immune principle, with the help of the division and differentiation of cell, the biological immune system produces automatically corresponding antibody against the antigen which invades life body. This process is called immune response. In the immunity reply process, part of antibodies is preserved as memory cell. When the similar antigen invades the life body once more, the memory cell is activated and produces rapidly the massive immune bodies. This causes that 2nd reply is more intense than the primary reply, which manifests memory function of the immune system. A kind of immune body and another kind of immune body are also promoted and suppressed mutually, to maintain the multiplicity of the immune body and the balance of immunity. This kind of balance is carries on according to the density mechanism, namely the density of the immune body is higher, and the immune body is suppressed more. The density of antibody is lower, the antibody is promoted more. This manifests self-adjustment function of the immune system.

Immune Algorithm (IA) is essentially a new algorithm for searching for multimodal function and global optimization. It has the ability of massively parallel processing information, the ability of strong learning, the ability of memory, the ability of recognition, adaptability and robustness, the ability of self-organization and the ability of maintaining the diversity.

In the immunity algorithm, the antigen is corresponding to the objective function and variant kind of constraint conditions; and the immune body (antibody) corresponds with the optimal solution. The kissing degree between the antibody and antigen corresponds with the match degree of solution and the objective function.

That a set of characteristics for identification of mine water hazard source are selected by immune algorithm is proposed in this paper. This group of characteristics is few, and the classification ability is strong. With this group of characteristics, the accuracy rate of the recognition of mine water is high. In this paper, the quantitative weight represents the importance of characteristics.

In the immune algorithm, the problem is solved as antigen, the antigen corresponding to the objective function and constraints, antibody corresponds to the solution of the problem, namely the antibody corresponding to the optimal solution, between antibody and antigen affinity corresponds to matching and objective function.

1. Coding mode

   In the immune algorithm, the antibody and antigen encoding are binary code, code and character code. There are a few gray coding. Binary search capability, but also has the advantages of simple operation of the cross, variation. Therefore, this paper uses binary coding.

   For the P attribute of mine water hazard source data, namely P characteristics, each attribute is represented by the length of the E binary string. The decimal number correspond-

ing binary represent the weight value of the attribute. Each antibody contains P × E binary.

2. Initial antibody population
   Randomly generated in the solution space of the N candidate solution as the initial antibody, which is randomly selected characteristics group N, N is the number of antibody group.
3. Calculation methods of antibody concentration
   Antibody concentration is mainly used to maintain the diversity of antibodies, improve the local search ability. Antibody concentration calculation method is based on the Euclidean distance between antibodies and information entropy method based on two. This paper adopts the method based on information entropy. Information entropy (Information Entropy) used to indicate that the population diversity of antibodies, antibody concentration obtained by the method of antibody population average information entropy.

   A number of N antibody, gene number of antibodies for M, allele number is S. First define the symbol (~) probability in loci, i.e.:

$$p_{ij} = \frac{\text{The total number of i symbols appear in locus j}}{N}$$

   As the information entropy of the gene, defined as:

$$H_j(N) = -\sum_{i=1}^{N} p_{ij} \log_2 p_{ij} \tag{1}$$

   The average information entropy for the whole group:

$$H(N) = \frac{1}{M} \sum_{j=1}^{M} H_j(N).$$

   At this time, the antibody, affinity, i.e. similarity of antibodies and for: $ay_{vw} = \frac{1}{1+H(2)}$, Among them: $H(2)$ is the average information entropy antibody and antibody group, if $H(2) = 0$, and the same, then the antibody. The concentration of antibody: $C_v = \frac{1}{N} \sum_{W=1}^{N} aC_{VW}$, Among them: $aC_{vw} = \begin{cases} 1 & ay_{vw} \succ Tac1 \\ 0 & other \end{cases}$, for a given threshold.
4. Calculation method of affinity between antibody and antigen
   Antibody and antigen affinity for the antibody to the antigen that the degree of recognition, using the Back Propagation Neural Network (BPNN) to get false negative rate and false positive rate as a method to identify mine water, then calculate affinity.

   Against the group of antibodies by decoding operation, into various attributes of mine water source identification data (characteristics) of the weight value, the weight value of 6 characteristics larger as the input of BPNN, and then use BPNN to record data for training and recognition.

   Coal mine water inrush source data reference standard set, get the recognition of the false positive rate and false negative rate. The affinity between antibody and antigen is defined with the false positive rate and false negative rate. The formula for the definition:

$$ax_v = \frac{1}{a_1 \times e_v + a_2 \times m_v} \tag{2}$$

   Where a_1 and a_2 determined with the experience value.
5. The reproduction rate of computing antibody expectations
   On the basis of antibodies expected breed rate selection operation, concentration of the natural immune system regulation mechanism, namely the antibody concentration low promotion, suppression of antibody concentration is high, thus maintaining the diversity of antibodies, prevent the algorithm into premature convergence; antibody and antigen affinity of antibody development to better control of the individual direction.

   Antibody expectation reproduction rate:

$$e_v = \frac{ax_v}{c_v}$$

6. New antibody group
   Arrangement of the descending antibody group according to expectation reproduction rate, and taking the first antibody composition of parent population, antibody at the same time, before the specified number of deposited into the memory. Select, crossover, mutation operation of parent groups are new groups, and then remove the memory antibody from memory, together constitute a new generation of antibody population.
7. Termination Rules
   The running of immune algorithm is stopped with the number of iterations. After all the iterative operation is finished, the individual in memory is the optimal solution of immune algorithm.

4 BACK-PROPAGATION NEURAL NETWORK

The study results of modern neurophysiology and anatomy show that, the human brain is extremely complex, which is consisting of 101000 million neurons, which are intertwined, and constitute a reticular structure. The human brain can finish such as intelligence, thinking, emotion and other senior neural activity. It is considered to be an information processing system which is the most perfect, the most effective. Back Propagation Neural Network (BPNN) is an abstraction and simulation of some basic characteristic of the human brain by mathematical method. It is a nonlinear information processing system of imitating human brain structure and function. The essence of BPNN reflects a functional relationship between the input and output of the network. By selecting different model structures and the activation function, the different neural network can be formed, to obtain different relationship of input and output, and achieve different design purpose, complete different tasks. Neuron is the basic processing unit of neural network. Neuron is generally nonlinear element with multiple input and single output. The output of neuron is not only influenced by the input signal, but also affected by other factors within neurons, so in the modeling of artificial neurons, an additional input signal, known as the deviation (bias), sometimes called threshold, is often also added.

For example, for a neuron with n input component, the input components of the $x_j(j - 1,2,...n)$, the corresponding weight coefficients w_{j1}, w_{j2}, w_{j3},...,w_{jn}, namely the

connection weights, indicate synaptic connection strength between synaptic 1, 2, 3....., N and the j neuronal.

For the convenience of analysis, we divide the process into three mathematical calculation steps:

1. The weighted – each input signals are weighted in different degree weights coefficient;
2. Sum – sum of the combination effect of all of input signals are calculated;
3. Mapping – the output results are calculated by transfer function.

The biological neuron response process is described in the mathematical equations in follow.

Column vector represents the input vector:

$$X = [x_1 \cdots x_2 \cdots x_n]^T \tag{3}$$

Row vector $\boldsymbol{w}_j$ represents connection weights vector of the neural:

$$W_j = [w_{j1} \cdots w_{j2} \cdots w_{jn}] \tag{4}$$

Pure input s_j of the neurons j is:

$$S_j = \sum_{i=1}^{n} w_{j1} + \theta_j = W_j X + \theta_j \tag{5}$$

Where θ_j in the formula —— threshold.

After pure input of the neuron is alternated with transfer function, the input y_i of the neurons is:

$$y_i = f(S_j) = f\left(\sum_{i=1}^{n} w_{ji} x_i + \theta_j \right) \tag{6}$$

If the θ_j is processed in $x_0 = 1$ method, then the formula (4) expressed as:

$$y_i = f(S_j) = f\left(\sum_{i=1}^{n} w_{ji} x_i \right) = f\left(W_{ji} x_i \right) \tag{7}$$

Thus, with formula, we describe the process of obtaining the information of response to the signal received by a neuron.

For the various topologies of BPNN, its operation process can be divided into two stages: The first stage is learning (or training) of BPNN; the second stage is association of BPNN (namely, to recognize the source of water of water- inrush).

In the learning process of BPNN network, through inputting some sample patterns to the BPNN network, the weights of each layer of BPNN are adjusted constantly by following the learning rules, the algorithm, so that the input and output of BPNN approximate the given sample model to a certain precision.

The essence of BPNN learning is that BPNN recognizes the inherent law in the information through the input and output information. Learning methods can be divided into two kinds: one kind is supervised learning or learning with teacher; another is the unsupervised learning or teacherless learning. On the basis of weight adjustment way, learning can be divided into off-line learning and on-line learning.

Table1. Comparison of results of identification hazard water source by methods and method developed in the paper.

Different recognition methods	Identification of hazard water source correct rate
Method developed in the paper	93%
Manual single index method	43%
Cluster analysis method	71%
Method of fuzzy cluster analysis	75%
Discriminative analysis	70%

Table 2. The part of the data and results of identification hazard water source by method developed in the paper.

Recognition results	Actual water types	Temperature (T)	Chlorine (Cl^-)	Kalium (K^+)	Calcium (Ca^{2+})	(Mg^{2+})	(SO_4^{2-})	PH	Fe	NO_3^{-1}	I
Sandstone Water	Sandstone Water	35	106.0	16.51	571.44	164.320	495.0	7.328	0.310	237.45	1.220
Ordovician limestone water	Ordovician limestone water	45	184.0	57.83	783.05	367.190	1125.787	7.591	2.640	46.0	1.540

A learning process of BPNN consists of two sub-processes: the forward propagation of the input data and the reverse propagation of error. The weights and threshold of BPNN are adjusted by the gradient method, so that sum of square error of BPNN output is minimum. In the algorithm, firstly, the network weights and threshold are given small initial value, and then, with selecting a training sample set, the error relative to this sample set is computed. If the gradient of each layer can be known, according to the learning rule, the connection weights and thresholds are updated, until the algorithm convergence.

5 MODEL OF IDENTIFICATION OF MINE WATER HAZARD SOURCE BASED ON AI-BPNN

The mine water hazard source identification data are pretreated by Immune Algorithm (IA), to extract the main characteristics associated with the water source identification. The processed data are classified and recognized with the BPNN. The specific steps of recognition of the water source are as follows:

(1) to obtain a plurality of data set obtained by analysis and test of ground water quality; (2) The data set is pretreated by Immune Algorithm (IA); (3) BPNN is trained by the data set pretreated; (4) The mine water source is recognized by the trained BPNN; (5) The decision response to result of recognition.

6 RESULTS AND DISCUSSION

In this paper, with the water samples in mine and borehole in a gold mine of Hebei area and the coal mines of Lu'an Group, the water sources were recognized with a plurality of index data obtained by analysis and test of the ground water quality. The water sources of flooding to mine of the two mining area are mainly divided into 4 categories: water in Ordovician limestone water, sandstone, Tai limestone water, the old kiln water, ground water and fault oxidation zone water. The results of water resource recognized by the method developed in the paper in the two mine area are given in Table 1.

From Table 1 and Table 2, we can see that the right rate of water-bursting source identification obtained by several different methods is different. The right rate of water-bursting source identification obtained by the method developed in the paper is the highest, which proves that the method developed in the paper is effective and feasible.

ACKNOWLEDGEMENTS

This work was financially supported by "the Fundamental Research Funds for the Central Universities of China" (JSJ2013B09, JSJ2013B02, JSJ1207B, 2011B029, 2011B028).

REFERENCES

Cao Xue-Chun 2010. Hydrochemical classification and identification for groundwater system by using integral multivariate statistical models, *Journal of China Coal SocietyJournal.* 14(8):18–20.

Mo Hongwei & Jin Hong-zhang 2002. Immune algorithm principle and application. *Aeronautical computing technology,* 32(4):24–25.

Zheng Gang 2004. Research of Water Inrush Resource Based on Hydrochemical Character in Similar. *Coal minee safety*, 35(1):24–25.

This page intentionally left blank

Progress in Mine Safety Science and Engineering II – He et al. (Eds)
© 2014 Taylor & Francis Group, London, ISBN 978-1-138-00122-0

Gas drainage technology of inner interlocked low tail laneway in extraordinarily high gas working face

Q. Ye, Z.Z. Jia, H.Z. Wang & Y. Pi
School of Energy and Safety Engineering, Hunan University of Science and Technology, Xiangtan, Hunan, China
Hunan Province Key Laboratory of Safety Mining and Technology of Coal Mine, Xiangtan, Hunan, China

ABSTRACT: The gas emission of 33207 working face is extraordinarily high, according to the characteristics of coal seam occurrence and gas emission in 33207 working face, the gas emission rate and the gas emission sources were measured and analyzed by the element method, and then the law of gas emission and gas migration were obtained. According to previous experience and gas control technologies, the gas drainage technology of the upper corner by the inner interlocked low tail laneway was adopted, based on the U type ventilation and the gas drainage from extracting seam. Finally, its drainage technique, application conditions and problems were acquired. By using these measures, the gas emission and gas over-limitation of 33207 working face was solved effectively, and the risk of coal and gas outburst was eliminated, thus ensuring safety production. The gas drainage technology of the upper corner by the inner interlocked low tail laneway can offer the instruction for similar working faces with extraordinarily high gas emission.

1 GENERAL SITUATION AND EXISTING PROBLEMS OF 33207 WORKING FACE

The III_2 coal seam is the upper adjacent seam of III_3 coal seam, which is an unworkable coal seam and has unstable occurrence, its average thickness is 0.6 m, and the average distance from III_3 coal seam is 25 m. The IV_1 coal seam is the lower adjacent seam of III_3 coal seam, which is also an unworkable coal seam and has unstable occurrence, its average thickness is 1 m, and the distance from III_3 coal seam is 12–15 m. The III_3 coal seam has three working faces: 33206 working face, 33207 working face and 33208 working face. The 33207 working face is the main working face, its length and crossheading length are 156 m and 1596 m, respectively; the left of 33207 working face is the 33206 working face which will be mined out soon, and the right of 33207 working face is the 33208 working face which is being prepared. The thickness of III_3 coal seam is 2.6–4.5 m, the average is 3.9 m; and the inclination angle of III_3 coal seam is 0°–15°, the average is 5°. The structure of III_3 coal seam is simple: the false roof consists mainly of carbon mudstone and carbon shale, with a thickness of 0.1–0.3 m; the immediate roof is mainly composed of siltstone and fine sandstone, with a thickness of 9.8 m; and the floor consists mainly of fine sandstone, with a thickness of 8.17 m. At the beginning of production, the coal mine has potential safety hazards; because the absolute gas emission rate is 115.8 m^3/min, the relative gas emission rate is 42.72 m^3/t, and moreover, the gas emission has an obvious increase tendency.

According to the gas emission from the mined working faces and 33207 working face, the main problems in 33207 working face were found as follows: (1) both the upper and lower adjacent seams of III_3 coal seam (i.e. the III_2 coal seam and the IV_1 coal seam) are unworkable, and they are fairly close to III_3 coal seam; thus the gas emission rate from the adjacent seams is so great that the gas concentration in 33207 working face is frequently in the critical state and the gas concentration in the upper corner of 33207 working face often exceed limitation; (2) the U+L ventilation mode was adopted in 33206 working face, the coal spontaneous duration is short, the coal spontaneous combustion is easily caused by the air leakage from the gob, which has negative influence on production; (3) the existing ventilation system and gas drainage measures cannot solve the gas overrun efficiently.

2 ANALYSIS ON GAS EMISSION LAW OF 33207 WORKING FACE

The gas emission in mined working faces, field measure results and theoretical analysis showed that the gas in 33207 working face is mainly from mining coal seams, adjacent seams (including wall rocks), and gobs, the gas from adjacent seam

enter the mining coal seam and the gob through wall rock fractures. The gas emission sources in 33207 working face were measured by the element method; the results showed that the air leakage rate from the gob is –27 m^3/min, the gas emission rate from the gob is 2.81 m^3/min, the gas emission rate from the coal wall and the fallen coal is 0.887 m^3/min. According to the measure data, the results can be obtained as follows: (1) the gas emission rate from the gob accounts for 76% of the total gas emission rate, the gas emission from the coal wall and the fallen coal accounts for 24%, more than 91% of the gob gas passes through the upper corner and enters the 33207 working face; (2) the air leakage quantity into the gob from the element where the upper and lower corners are and the air leakage quantity from the gob are obviously larger than that in other elements, which shows that the measures on stopping air leakage from the upper and lower corners can efficiently prevent and control gas emission from the gob; (3) the gas concentration is fairly large within the range of 30–50 m from the upper corner, and the gas concentration in the upper corner is obviously larger than other elements, which indicates that the gas emission zone is mainly around the upper corner; thus the key of gas prevention and control in 33207 working face focuses mainly on the gas control in the upper corner. To solve gas emission and gas over-limitation in 33207 working face, based on previous experience and gas control technologies (Lin & Cui 1998, Lin & Hu 2006, Lin & Zhang 1996, Ye et al. 2006, Yu 1992, Zhang et al. 2006, Zhou 1999), the U type ventilation and the gas drainage from extracting seam were used, and then the gas drainage technology of the upper corner by the inner interlocked low tail laneway was analyzed and practiced.

3 GAS DRAINAGE TECHNOLOGY OF UPPER CORNER BY INNER INTERLOCKED LOW TAIL LANEWAY

3.1 *Principle of inner interlocked low tail laneway*

The inner interlocked low tail laneway is located in the windward side of the upper corner in the fully mechanized caving face and in the top layer of the coal seam, meanwhile, drainage pumps are used for gas drainage, which ensures that the inner pressure of the inner interlocked low tail laneway is lower than the ventilation pressure of the return airway, making the air inlet constantly in a low pressure area. This has two functions (Hao 2006): on one hand, a greater air suction flow field exists in the air inlet of the inner interlocked low tail laneway, and a very obvious "air curtain wall" is formed, which drains high concentration gas in the upper corner and makes the gob gas move towards the inner interlocked low tail laneway; on the other hand, the inner interlocked low tail laneway communicates with the gob, and a ventilation channel is formed, which closures the gob gas between the inner interlocked low tail laneway and the intake airway, greatly reducing gas emission from the gob, so as to prevent and control gas in the upper corner of the gob.

3.2 *Characteristics of inner interlocked low tail laneway*

The characteristics of the inner interlocked low tail laneway can be described as follows:

1. Gas split-flow: the inner interlocked low tail laneway is an important channel of gob gas spit-flow, which changes the gas emission path, reduces the gas pressure in the upper corner, and thus guarantees production safety in the mining face; the larger the proportion of gas quantity drained by the inner interlocked low tail laneway is, the less the gas entering the return airway will be and the lower the gas concentration in the return airway will be.
2. Generating negative pressure point: the tail of the inner interlocked low tail laneway straightly enters the gob and generates the negative pressure point, which makes the gob gas move towards the inner interlocked low tail laneway and prevents the gob gas from moving towards the working face and the return airway (namely, closures the gob gas between the inner interlocked low tail laneway and the intake airway), thus reducing gas quantity into the upper corner and solving the problem on gas accumulation in the upper corner effectively. The motion of negative pressure point depends on the roof caving, generally speaking, the better the effect of roof caving is and the shorter the distance between the negative pressure point and supports is, the better the effect of gas drainage will be.

3.3 *Layout of inner interlocked low tail laneway*

The measure on gas concentration in the gob indicates that the gas concentration is increasing within a 30 m range from working face to the gob, which is the accumulation region of high concentration gas in the gob. Besides that the roof caving lags behind the coal cutting; thus, along the trend of working face, the air inlet of the inner interlocked low tail laneway must stretch into the coal wall of the gob above 8 m (namely, the air inlet of the inner interlocked low tail laneway must be behind the air return inlet of the mining field at working face more than 8 m), so as to collect the

gas emitted from the gob along the airflow direction. Along the vertical direction of working face, the air inlet of the inner interlocked low tail laneway is near 5 m vertically above the floor of the mining field at working face, so as to collect gas emitted from the coal (rock) of the gob roof after releasing pressure.

3.4 *Design of inner interlocked low tail laneway*

A great deal of gas emitted from the 33207 gob enters working face via the upper cutting-off line, thus generating gas over-limitation between the upper supports, at the top of the upper supports, at the tail beam, and in the upper corner. In order to solve this problem, according to the gas flow theory on pore medium of mining field, a gas drainage laneway at the roof is laid along the coal seam roof and parallel to the return airway, which is referred to as 33207 inner interlocked low tail laneway. The 33207 inner interlocked low tail laneway is laid at 5 m location below the return airway and parallel to the roof, its cross section area is 3.8 m × 2.4 m; and it will cave spontaneously with advancing working face (see Figs. 1–3). The mining of 33206 working face which is immediately adjacent to 33207 working face has influence on the coal within 33207 inner interlocked low tail laneway; for example, the pressure on coal seam is fairly large, the coal is instable, and part of coal seam is separated. During the mining at working face, the key of designing the inner interlocked low tail laneway is that the inner interlocked low tail laneway cannot cave before the top coal caving by fully-mechanized supports and can ensure the air return channel unobstructed. If the inner interlocked low tail laneway above the supports falls down, the gas at the end of supports is difficult to drain after the top coal caving; if the reserved inner interlocked low tail laneway before the working face falls down and communicates with the working face, the ventilation system of the working face is

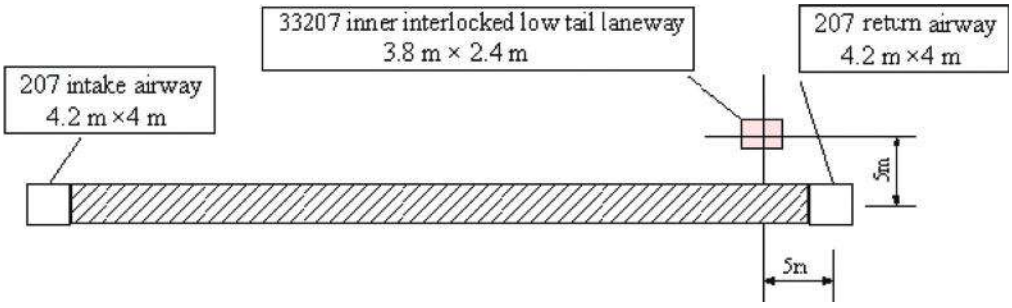


Figure 1. The structure diagram of 33207 inner interlocked low tail laneway.

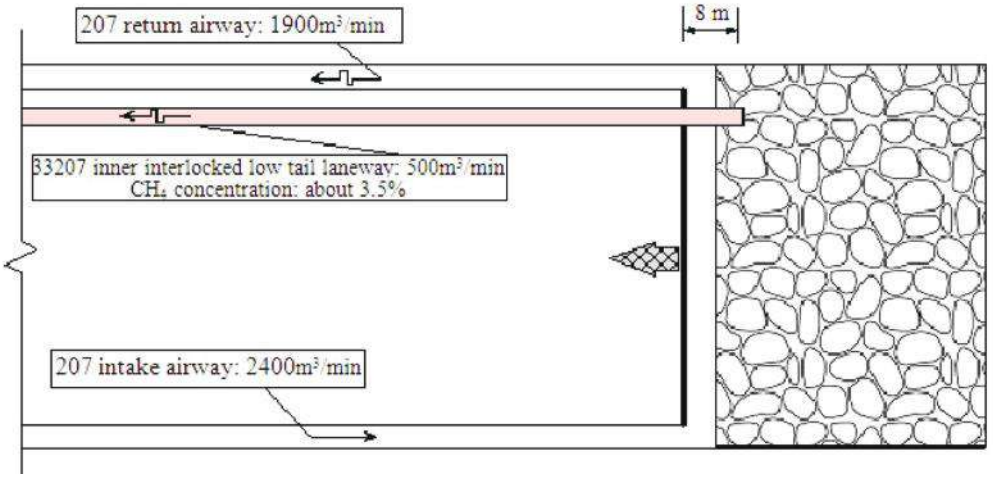


Figure 2. The plan of 33207 inner interlocked low tail laneway.

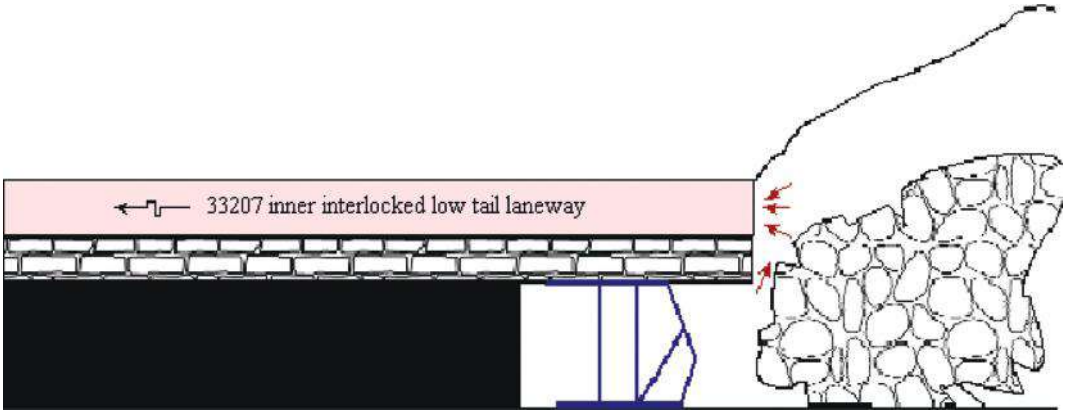


Figure 3. The side elevation of 33207 inner interlocked low tail laneway.

disordered and the coal cannot come out normally from the working face; therefore, the most important is that the coal pillars from the position above the supports to the inner interlocked low tail laneway and the coal pillars from the position before the working face to the inner interlocked low tail laneway cannot cave. In order to achieve the effect of the inner interlocked low tail laneway in mining process, the support on the roof and the wall of the inner interlocked low tail laneway should be strengthened, a rock layer with a thickness of at least 1.2 m should remain at the floor and the support top (as shown in Fig. 1 and Fig. 3). In the mining process at 33207 working face, in order to acquire the changes of roof and coal, the working face roof below the inner interlocked low tail laneway and a range of 10 m at the end of supports should be monitored in real time, thus providing a basis for further improvement in the layout of the inner interlocked low tail laneway.

4 PROBLEMS ON GAS DRAINAGE TECHNOLOGY OF UPPER CORNER BY INNER INTERLOCKED LOW TAIL LANEWAY IN PRACTICE

The theoretical analysis and field practice show that gas emission rate from the gob is large, the gas drainage in the gob is a vital part of gas control, and the inner interlocked low tail laneway can drain the gas in the upper corner effectively. Meanwhile, in practice, the following problems should be paid attention to:

1. The thickness of coal between the inner interlocked low tail laneway and the working face should be controlled strictly (Xue & Zhang 2007).

   In tunneling, according to the height design of the inner interlocked low tail laneway, the height design of the working face, and the coal seam thickness, the construction should be implemented in strict accordance with the design. The method for drilling holes into coal seam floor from the inner interlocked low tail laneway is used, and the thickness between the inner interlocked low tail laneway and the roof of the working face can meet the design; so that the caving of the inner interlocked low tail laneway caused by the insufficient thickness in the front or upper of supports is avoided, thus making the ventilation system work normally.
2. The negative pressure of the inner interlocked low tail laneway must be satisfied firstly (Wang 2004).

   The practice in the mining process at 33207 working face found that the relative pressure difference between 33207 inner interlocked low tail laneway and the return airway of 33207 working face must be satisfied firstly, which is the precondition to ensure that 33207 inner interlocked low tail laneway works effectively. The relative pressure difference between the mouth of 33207 inner interlocked low tail laneway and the return airway of 33207 working face is 450–550 Pa by adjusting the adjusting wall. Meanwhile, sufficient air quantity should be guaranteed in 33207 inner interlocked low tail laneway and cannot make gas emission from the gob increase.
3. The effect of coal caving at the supports of tail segment must be ensured (Wang 2004).

   According to the principle of the inner interlocked low tail laneway, the gas split-flow in the gob can achieves good results, only when the outlet of the inner interlocked low tail laneway in the gob is unobstructed. Based on the field observation, the gas emitted from the coal within the range of 10 m near the upper corner

can be drained mainly by the air quantity in the upper corner; therefore, in the process of mining, the coal caving is carried out reasonably according to the specific situation of the roof, which can be controlled effectively in the field, and also changes the negative pressure point of the inner interlocked low tail laneway in the gob. The practice has proved that on the premise that the gas problem in the upper corner is solved effectively, it is better that the negative pressure point moves forward; because when the negative pressure point moves backward, the influence on the gob is relatively large, directly showing that the windblown mine gas concentration is large, thereby increasing the gas emission quantity in the area, which is bad for gas control.

4. The air leakage at the roof of the inner interlocked low tail laneway and the roof of transportation roadway should be prevented (Wang 2004).

   If human factors or objective factors make the inner interlocked low tail laneway and the transportation roadway air leakage, then the system will become an U type ventilation system and the inner interlocked low tail laneway will not work. When the air leakage appears; corresponding measures should be adopted, for example, the air duct cloth is covered at the air leakage spot of supports' canopy or the adjusting wall is constructed at the mouth of the inner interlocked low tail laneway to adjust the air quantity of the inner interlocked low tail laneway, meanwhile, the air brattice is hung at the drive end unit to solve the gas accumulation in the upper corner.
5. The support management of the inner interlocked low tail laneway and the roof management below the inner interlocked low tail laneway should be strengthened (Xue & Zhang 2007).

In general, the inner interlocked low tail laneway is laid immediately adjacent to the return airway; in the process of the support design, the roof pressure between roadways and the dynamic pressure should be taken into account; especially in the mining process, the effect of the inner interlocked low tail laneway should be considered fully, that is to say, the support strength should be considered fully, otherwise, once the mining causes the collapse of the inner interlocked tail roadway, all the previous efforts will be wasted.

During the period of mining, the roof management below the inner interlocked tail roadway is also very important, pulling supports must be in time or in advance, supports must be tightened, and the face sprag must be reinforced. Besides that the mining height must be controlled strictly at coal-cutting, in order to prevent the working face and the inner interlocked low tail laneway cutting through; meanwhile, the support maintenance in this segment should be strengthened so as to avoid the negative influence of support faults on advancing.

5 EFFECT AND ASSESSMENT OF GAS CONTROL

Based on the U type ventilation and the gas drainage from extracting seam, which were adopted at working face, the gas drainage technology of the upper corner by the inner interlocked low tail laneway was analyzed and practiced. The gas in the gob and the upper corner of 33207 working face with extraordinarily high gas emission was controlled effectively by adopting this gas drainage technology, which improves the production capacity of the working face.

1. Based on the measure and analysis on gas emission, the migration law and gas emission sources at 33207 working face were obtained: the gas concentrations increased gradually from the inlet side to the return air side, the gas concentration from the air inlet to the middle of working face is not high, the gas concentration from the middle of working face to the upper corner is relatively high, especially, the gas concentration within a range of 30–50 m near the return air side is higher. The region near the upper corner is the high gas concentration area, and is also the main channel where the gob gas enters the working face; thus the emphasis of gas control at the working face is to avoid the gas over-limitation in the upper corner, which can be solved by the inner interlocked low tail laneway.
2. When the inner interlocked low tail laneway is adopted to drain gas in the upper corner; a greater air suction flow field exists in the air inlet of the inner interlocked low tail laneway, and a very obvious "air curtain wall" is formed, which drains high concentration gas in the upper corner and prevents the gas in the gob moving towards the working face and the return airway, thus achieving the purpose of gas control in the upper corner.
3. In practice, the following aspects should be paid attention to in the layout and management of the inner interlocked low tail laneway: firstly, the thickness of coal between the inner interlocked low tail laneway and the working face should be controlled strictly; secondly, the relative pressure difference between the inner

interlocked low tail laneway and the return airway should be ensured within a appropriate range, the sufficient air quantity should be guaranteed in the inner interlocked low tail laneway and cannot make gob gas emission increase; thirdly, the coal caving should be controlled, which can increase the permeability of the inner interlocked low tail laneway, and cannot make the inner interlocked low tail laneway lose the effect of gas drainage due to the short circuit of air flow; fourthly, the inner interlocked low tail laneway should be laid in the roof fracture zone, and the distance between the inner interlocked low tail laneway and the floor of the working face should be chosen according to the characteristics of coal occurrence, so as to avoid the phenomenon that the coal winning machine cuts through the inner interlocked low tail laneway; fifthly, the support management of the inner interlocked low tail laneway and the roof management below the inner interlocked low tail laneway should be strengthened.

ACKNOWLEDGEMENT

This work is supported by the National Natural Science Foundation of China (51004048). The support is acknowledged with thanks.

REFERENCES

Hao, Y.J. 2006. Research on the gas control technique in comprehensive machined coal-mining face in the inner alternated tail tunnel, *Sci-Tech Information Development & Economy* 16(16):273–274.

Lin, B.Q. & Cui, H.X. 1998. *Gas control theory and technology in coal mines*. Xuzhou: China University of Mining & Technology Press.

Lin, B.Q. & Hu, D.M. 2006. *Gas occurrence law and gas control technology of coal seam.* Xuzhou: China University of Mining & Technology Press.

Lin, B.Q. & Zhang, J.G. 1996. *Gas drainage theory and technology in coal mines*. Xuzhou: China University of Mining & Technology Press.

Wang, Z.Y. 2004. The application of inner interlocked tail road in 2308 comprehensively mining sub-level work face at Si He coal mine. *Journal of North China Institute of Science & Technology* 1(4):70–78.

Xue, J.Z. & Zhang, Q. 2007. The application and practice of tail-roadway laid within inner face in high gas mine. *Shanxi Coal* 27(2):49–51.

Ye, Q. Lin, B.Q. & Jiang, W.Z. 2006. The study of methane outflow law in coal mining face, *China Mining Magazine* 15(5):38–41.

Yu, Q.X. *Gas prevention and control in coal mines*. Xuzhou: China University of Mining & Technology Press.

Zhang, J.G. Lin, B.Q. & Ye, Q. 2006. Research on technology of draining methane off shallow boreholes in a stress-relaxation area of working face. *Journal of Mining & Safety Engineering* 23(4):432–436.

Zhou, S.N. 1999. *Gas occurrence and flow theory of coal seam*. Beijing: China Coal Industry Publishing House.

Progress in Mine Safety Science and Engineering II – He et al. (Eds)
© 2014 Taylor & Francis Group, London, ISBN 978-1-138-00122-0

Research on airflow catastrophic of side branches induced by gas pressure in upward ventilation

Aitao Zhou, Kai Wang, Zeqi Wu & Yifeng Jiang
School of Resource and Safety Engineering, State Key Laboratory of Coal Resources and Mine Safety, Beijing, China University of Mining Research on Airflow Catastrophic of Side Branches Induced by Gas Pressure in Upward Ventilation and Technology, Beijing, China

ABSTRACT: In order to analyze the law of airflow catastrophic of side branches induced by gas pressure in upward ventilation after dynamic of outburst disappearing, one dimensional unsteady-state flow momentum equation of gas flow is established. Combined with circuit airflow pressure balance equation, this equation is used in static and dynamic analysis on airflow catastrophic of side branches induced by gas pressure in upward ventilation. The research results show that gas pressure is produced in upward ventilated roadway when gas flowed by; when the gas pressure is great enough, the air flow in side branches reverses. Whether the air flow in side branches reverse is affected by their own length and initial velocity. In order to prevent the air flow reversal in the side branches, it is necessary keep the fan normal operating, and avoids adding resistance in external system. The research results may be of important theoretical and practical significance for outburst accident rescue as well as effective prevention of the occurrence of secondary accidents.

1 INTRODUCTION

Once coal and gas outburst occurs, shock wave and gas flow is produced transiently (Wang and Zhou et al, 2012; Wang and Zhou et al, 2011; Wang and Zhou et al, 2012; Wang and Zhou et al, 2012; Wang and Zhou et al, 2011; Zhang and Wang et al, 2010; B. Basil Beamish and Pete J. Crosdale, 1998), which induces mine airflow catastrophic in two ways: (1) The overpressureof outburstshock wave (C.Y. Chen, 2010; Wang and Zhou et al, 2012), when the resistance is lower than the outburst overpressure in one roadway, the airflow will reverse in the roadway. (2) The gas pressure (Y. Zhou and X.S. Wang, 2000; Fluegge G, 1969). After the dynamic of outburst disappears, gas pressure induces airflow catastrophic further. Upward ventilation system is widely used in working face. But few studies have been done on the law of airflow catastrophic of side branches induced by gas pressure in upward ventilation (W. Dziurzynski and J. Krawczyk, 2008; F. Otuonye and J. Sheng, 1994; W. Y. Cheng and G.X. CHEN, 2000; Zhang and Sun et al, 2007; A. Britan and G. Ben-Dor et al, 2006; Cheng and Liu et al, 2004). This paper established one dimensional unsteady-state flow momentum equation of gas flow after dynamic of outburst disappears, which, combined with circuit pressure balance pressure equation, is used in static and dynamic analysis on airflow catastrophic of side branches induced by gas pressure in upward ventilation. The research results are of important theoretical and practical significance for outburst accident rescue as well as effective prevention of the occurrence of secondary accidents.

2 MECHANISM OF AIRFLOW CATASTROPHIC INDUCED BY GAS PRESSURE

Gas pressure is practically the increment of natural pressure when outburst occurs. Because density of the gas containing high-concentration methane is lower than that of the air, after outburst occurs, the differential of density leads to pressure difference. This gas pressure can be defined as, where C is gas concentration (%), ρ_a is air density (kg/m^3), ρ_m is density of gas with methane (kg/m^3), Z is height differential of roadway (m). Characteristic of gas pressure are as follows:

1. Gas pressure is proportional to height differences of the roadway. The greater the height differences are, the greater gas pressure is. In entries, height difference is small, as well as the gas pressure; gas pressure is not obvious in entries. But when flow of high-concentration methane flows though inclined drifts or vertical shafts, gas pressure is quite obvious.

2. The higher the methane concentration of air flow is, the greater the gas pressure is. When methane concentration in roadways falls to zero, gas pressure is not existence.
3. When gas pressure produced in upward ventilated roadways, its direction is the same as fan pressure, which is positive for the fan; when gas pressure produced in downward ventilation roadways, its direction is opposite to fan pressure, which is negative for the fan.

3 ESTABLISHMENT OF ONE DIMENSIONAL UNSTEADY-STATE FLOW MOMENTUM EQUATION

This equation considers gas flow in roadways as one dimensional fluid flow, properties of gas flow are uniform in the same section of roadways. Considering flow of micro-unit along roadway branch *i* as object of study, the one dimensional unsteady-state flow mometum equation is as follows:

$$\rho \frac{du}{dt} = -\frac{\partial P}{\partial s} + \rho F - j - j_D \delta(s - s_D) + h_f \delta(s - s_f) \quad (1)$$

Where:

$\frac{du}{dt}$ is acceleration of airflow micro-unit (m/s^2), $\frac{\partial P}{\partial s}$ is press acts in *s* direction per unit volume (N/m^3), ρF is body force on per unit volume, $F = -g\frac{dz}{ds}$ is average density of airflow micro-unit (kg/m^3), g is acceleration of gravity (m/s^2), z is elevation ofroadway i (m), j is resistance of per unit longth (Pa/m), j_D is pressure drop by regulator at s_D(Pa), h_f is pressure of fan at *si*(Pa), $\delta(s–s_D)$, $\delta(s–s_f)$ is dirac δ function, when $s \neq s_D$, $\delta(s–s_D) = 0$; when $s \neq s_f$, $\delta(s–s_f) = 0$; when $\varepsilon > 0$, $\int_{s_D-\varepsilon}^{s_D+\varepsilon} \delta(s - s_D)ds = 1$, $\int_{s_f-\varepsilon}^{s_f+\varepsilon} \delta(s - s_f)ds = 1$; The last two terms show that pressure drop by regulator and pressure of fan are variables related to position, and that they located at corresponding positions s_D and s_f. In this equation, s is space coordinate along axial direction of roadways (m), s_D is coordinate of points where there is a loss (m). s_f is coordinate of fan's position (m).

Integrating along roadway *i* from $s = 0$ to $s = Li$. Because on-way resistance is: $\int_0^{L_i} jds = R_i|Q_i|Q_i$, and $R_i$is windage of roadway *i*, $R_i = \frac{\lambda\rho_i}{8}\frac{L_i U_i}{A_i^3}$, Ns^2/m^8; A_i is section area of roadway, m^2; $Q_i = u_i A_i$, is volume flow rate, m^3/s. pressure drop of road *i* $H_i = -\int_0^{L_i} dP_i$, equation (1) can be translated into:

$$\rho_i L_i \frac{du_i}{dt} = H_i - g\int_0^{L_i} \rho dz - R_i|q_i|q_i - j_{D,i} + h_{f,i} \quad (2)$$

Let $K_i = \frac{\rho_i L_i}{A_i}$, $u_i = u$ is air flow velocity of roadway *i*, m/s, $\rho_i = \frac{1}{L_i}\int_0^{L_i} \rho ds$ is average density of the air flow in roadway *i,* one dimensional unsteady-state flow momentum equation is established:

$$H_i = K_i \frac{dQ_i}{dt} + g\int_0^{L_i} \rho_i dz + R_i|Q_i|Q_i + j_{Di} - h_{fi} \quad (3)$$

4 THEORETCAL ANALYSIS AIRFLOW REVERSAL OF SIDE BRANCHES INDUCED BY GAS PRESSURE IN UPWARD VENTILATION

When outburst occurs in mine, airflow catastrophic will occur in intake airways connected with the source of outburst because of the great impact force produced by gas flow transiently released and of the gas pressure after the dynamic of outburst disappears, of which the most typical is airflow reversal of side branches. Therefore, this paper will use one dimensional unsteady-state flow momentum equation established above to analyze law of airflow reversalof side branches induced by gas pressure when upward ventilation airflow catastrophic occuring.

4.1 *Static analysis of airflow reversal of side branches induced by gas pressure in upward ventilation*

Fig 1 is schematic diagram of Gas flow in upper ventilation (Y Zhou, 2006).

Side branch b is considered as object of investigation, and by branch b, the ventilation network can be divided into two parts: the left part and the right part; Branch a is the roadway with a large amount of gas influx because of outburst, C branch can be divided into BF and FA, where FA is atmospheric branch; h_i represents gas pressure in branch a; and h_v fan pressure in the left; R_i synthesized windage of branch a; R_0 synthesized windage of left part; Q_0 represents air quantity of the left part, Q_i the right; R_b and Q_b represents windage and air quantity of side branch b respectively.

On condition that the original wind direction from A to B remains the same, establishing airflow pressure balance pressure equation along circuit

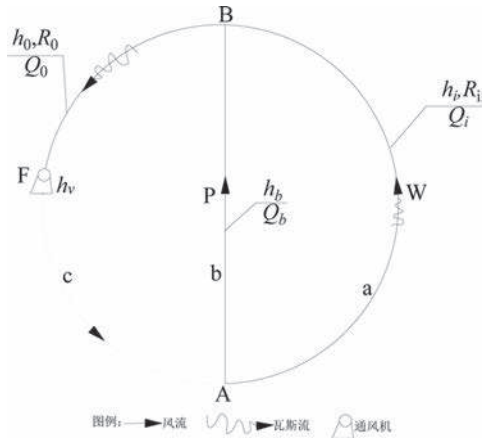


Figure 1. Gas flow in upper ventilation.

FAPB:

$$h_v = R_0 Q_0^2 + R_b Q_b^2 \tag{4}$$

Also, establishing airflow pressure equation along circuit FAWB:

$$h_v + h_i = R_0 Q_0^2 + R_i Q_i^2 \tag{5}$$

The two formulas subtracting and devition:

$$\frac{h_i}{h_v} = \frac{R_i Q_i^2 - R_b Q_b^2}{R_0 Q_0^2 + R_b Q_b^2} < \frac{R_i Q_i^2}{R_o Q_o^2} \tag{6}$$

When airflow direction in branch b remain the same and $Q_b > 0$, $Q_b > Q_i$.

So it can be deduced that:

$$\frac{h_i}{h_v} < \frac{R_i}{R_0} \tag{7}$$

According to inequality (7), the following conclusion can be drawn:

1. After outburst occurs, if cannot be controlled timely, great gas pressure will be produced in upward ventilated airways methane flowing by. When hi is great enough, airflow in side branch b will reverse.
2. In order to prevent airflow reversing in side branches, a h_v big enough is need to guarantee. Therefore, it is necessery to keep the fan normal operating, avoid adding resistance in external system, and keep R_0 as low as possible.
3. Taking measures in outburst branch a to increase resistance to increase internal windage R_i, which can reduce air supply to outburst branch, then reduce gas pressure, and have the effect of stability of the side branch airflow.
4. Airflow direction in side branches has nothing to de with its own windage.

4.2 *Dynamic analysis of airflow reversal of side branches induced by gas pressure in upward ventilation*

Practically, in the process of outburst, the quantity of gas released is changing. Correspongdingly, flow in the network is consequentially a dynamic process. It can be said that dynamics is the basic feature of the state of flow after outburst. Therefore, it is very necessary to consider the dynamic feature of airflow when analyzing airflow catastrophic induced by gas pressure.

Circuits airflow pressure balance equation is still tenable to dynamic network flow. Press differences between the first note and the last note can be obtained one dimensional unsteady-state flow momentum equation. For easy analysis, assuming that branch a, branch b and branch c has the same section area.

First of all, considering the condition that airflow remain the same direction in any branch, and define that: velocity of airflow is positive when airflow direction remain the same as it is before outburst, when the opposite is negative. Solve the press differences between two ends of branch a, b and c in Fig. 1 respectively, based on the one dimensional unsteady-state flow momentum equation.

1. Branch b

$$H_{APB} = -\int_{APB} \frac{\partial p}{\partial x} dx \tag{8}$$

Where:

H_{APB} is press difference between note A and B in branch b(Pa).

By substitution of the formula (3) and the equivalent diameter $d = \frac{4A}{U}$ into formula (8), and regardless of other additional power and resistance loss, the conclusion is drawn as followed:

$$H_{APB} = -\int_{APB} \left(\rho \left(\frac{\partial u}{\partial t} + \rho g \sin a + \frac{\lambda \rho u^2}{2d} \right) \right) dx \tag{9}$$

Where: a is inclination of branch b.

Because there is no gas flow in branch b, density of airflow in this branch can be consider as constant, viz:

$$\rho_b = \rho_0 = const \tag{10}$$

Where:

ρ_b is density of airflow in branch b (kg/m^3), ρ_0 is density of airflow in the network before outburst (kg/m^3).

Institute formula (10) into formula (9), the result is:

$$\begin{aligned} H_{APB} &= \rho_0 \left(\frac{\partial u}{\partial t} + \frac{\lambda u^2}{2d} \right)_b L_b + \rho_0 g \sin a L_b \\ &= \rho_0 \left(\frac{\partial u}{\partial t} + \frac{\lambda u^2}{2d} \right)_b L_b + \rho_0 g (z_B - z_A) \end{aligned} \tag{11}$$

Where:

L_b is length of branch b(m), Z_A is height of note A(m), is height of note B(m).

2. Branch c

FA is atmospheric branch, so wind pressure in this branch is 0, and:

$$H_{BFA} = H_{BF} - h_v = -\int_{BF} \frac{\partial p}{\partial x} dx - h_v \tag{12}$$

Where: H_{BFA} is pressure differences between the first note B and the last note A in branch c(Pa), H_{BF} is pressure differences between two ends of BF in branch c(Pa), h_v is pressure of fan (Pa).

By institution of formula (3) and the equivalent diameter $d = \frac{4A}{U}$ into formula (12), it is obtained that:

$$\begin{aligned} H_{BFA} = &\int_{BF} \left[\rho \frac{\partial u}{\partial t} + (\rho - \rho_0) g \sin a \right] dx \\ &+ \int_{BF} \frac{\lambda \rho u^2}{2d} dx + \rho_0 g (z_A - z_B) - h_v \end{aligned} \tag{13}$$

Let, $h_{BFA} = -\left\{ \int_{BF} \left[\rho \frac{\partial u}{\partial t} + (\rho - \rho_0) g \sin a \right] dx \right\}$, formula (5.15) becames:

$$H_{BFA} = \underbrace{-h_{BFA}}_{(1)} + \underbrace{\int_{BF} \frac{\lambda \rho u^2}{2d} dx}_{(2)} + \underbrace{\rho_0 g (z_A - z_B)}_{(3)} - \underbrace{h_v}_{(4)}$$

Where, the 2nd term is the whole frictional resistance of branch c, and the 3rd term is position pressure differences between two ends of branch c when airflow is steady state; the 4th term h_v is the power of fan, and the first h_{BFA} is gas pressure in static analysis. Obviously, h_{BFA} contains more than gas pressure in static analysis. h_{BFA} not only contains the partial gas pressure caused by density differential, but also contains extra power produced by flow with variable velocity of airflow (resistance).

3. Branch a

$$H_{AWB} = -\int_{AWB} \frac{\partial p}{\partial x} dx \tag{14}$$

Where:

H_{AWB} is pressure differences between the first note A and the last note B of branch a(Pa).

By institution of formula (3) and the equivalent diameter $d = \frac{4A}{U}$ into formula (14), it is obtained that:

$$\begin{aligned} H_{AWB} = &\int_{AWB} \left[\theta \rho \frac{\partial u}{\partial t} + (\rho - \rho_0) g \sin a \right] dx \\ &+ \int_{AWB} \frac{\lambda \rho u^2}{2d} dx + \rho_0 g (z_B - z_A) \end{aligned} \tag{15}$$

Let, $h_{AWB} = -\int_{AWB} \left[\rho \frac{\partial u}{\partial t} + (\rho - \rho_0) g \sin a \right] dx$ and formula (15) becomes:

$$H_{AWB} = \underbrace{-h_{AWB}}_{(1)} + \underbrace{\int_{AWB} \frac{\lambda \rho u^2}{2d} dx}_{(2)} + \underbrace{\rho_0 g (z_A - z_B)}_{(3)}$$

Any term has the similar meaning with branch c.

Based on circuit wind pressure balance equation, it is obtained in the circuit constructed with branch a and b that:

$$H_{AWB} - H_{APB} = 0 \tag{16}$$

By institution of formula (15) and (11) into formula (16), it is obtained after simplification that:

$$h_{AWB} + \rho_0 \left(\frac{\partial u}{\partial t} \right)_b L_b = \int_{AWB} \frac{\lambda \rho u^2}{2d} dx - \rho_0 \left(\frac{\lambda u^2}{2d} \right)_b L_b \tag{17}$$

Again based on circuit wind pressure balance equation, it is obtained in the circuit constructed by branch b and c that:

$$H_{BFA} + H_{APB} = 0 \tag{18}$$

By institution of formula (13) and (11) into formula (18), it is obtained after simplification that:

$$h_{BFA} + h_v - \rho_0 \left(\frac{\partial u}{\partial t} \right)_b L_b = \int_{BF} \frac{\lambda \rho u^2}{2d} dx + \rho_0 \left(\frac{\lambda u^2}{2d} \right)_b L_b \tag{19}$$

Let formula (17)/(19):

$$\frac{h_{AWB}+\rho_0\left(\frac{\partial u}{\partial t}\right)_b L_b}{h_{BFA}+h_v-\rho_0\left(\frac{\partial u}{\partial t}\right)_b L_b}=\frac{\int_{AWB}\frac{\lambda\rho u^2}{2d}dx-\rho_0\left(\frac{\lambda u^2}{2d}\right)_b L_b}{\int_{BF}\frac{\lambda\rho u^2}{2d}dx+\rho_0\left(\frac{\lambda u^2}{2d}\right)_b L_b}<\frac{\int_{AWB}\frac{\lambda\rho u^2}{2d}dx}{\int_{BF}\frac{\lambda\rho u^2}{2d}dx}$$

viz:

$$\frac{h_{AWB}+\rho_0(\frac{\partial u}{\partial t})_b L_b}{h_{BFA}+h_v-\rho_0(\frac{\partial u}{\partial t})_b L_b}<\frac{\int_{AWB}\frac{\lambda\rho u^2}{2d}dx}{\int_{BF}\frac{\lambda\rho u^2}{2d}dx} \quad (20)$$

Inequality (20) is deduced out under the condition that the airflow direction in branch b remains the same. It can be proved that inequality (20) will not be tenable when airflow in branch b stagnating or beginning to reverse. So inequality (20) is the conditional inequality guaranteeing airflow in branch b remains the same.

Practically, the process of airflow reversal in side branch b is a process that its wind quality becomes smaller and smaller, and tends to 0, which becomes negative at last. In the process that airflow tends to reverse but before it reverses, the velocity of airflow in branch b is always becoming smaller, that is inequality $\frac{\partial u}{\partial t}|_b<0$ is always tenable. So inequality (20) can be modified into:

$$\frac{h_{AWB}-\rho_0\left|\frac{\partial u}{\partial t}\right|_b L_b}{h_{BFA}+h_v+\rho_0\left|\frac{\partial u}{\partial t}\right|_b L_b}<\frac{\int_{AWB}\frac{\lambda\rho u^2}{2d}dx}{\int_{BF}\frac{\lambda\rho u^2}{2d}dx} \quad (21)$$

Let: $x_1=\left|\frac{\partial u}{\partial t}\right|_b L_b$, $x_2=h_{AWB}$, $x_3=h_v+h_{BFA}$, the left side of inequality (21) can be expressed as:

$$\frac{h_{AWB}-\rho_0\left|\frac{\partial u}{\partial t}\right|_b L_b}{h_{BFA}+h_v+\rho_0\left|\frac{\partial u}{\partial t}\right|_b L_b}=\frac{x_2-\rho_0 x_1}{x_3+\rho_0 x_1} \quad (22)$$

Let $H(x_1,x_2,x_3)=\frac{x_2-\rho_0 x_1}{x_3+\rho_0 x_1}$, it is obtained that:

$$\frac{\partial H}{\partial x_1}=-\frac{\rho_0(x_2+x_3)}{(x_3+\rho_0 x_1)^2} \quad (23)$$

Based on the circuit wind pressure balance equation in the circuit constructed with branch a and c, it is obtained that:

$$h_{AWB}+h_v+h_{BFA}=\int_{AWB}\frac{\lambda\rho u^2}{2d}dx+\int_{BF}\frac{\lambda\rho u^2}{2d}dx \quad (24)$$

The right side of Equation (24) is always more than 0, and the left is equivalent with x_2+x_3, so $x_2+x_3>0$; and therefore, $\frac{\partial H}{\partial x_1}=-\frac{\rho_0(x_2+x_3)}{(x_3+\rho_0 x_1)^2}<0$.

Formula (23) shows that, $H(x_1,x_2,x_3)$ is decreasing function of the left of inequality (21) about $\left|\frac{\partial u}{\partial t}\right|_b L_b$. That is the bigger $\left|\frac{\partial u}{\partial t}\right|_b L_b$ is, the easier formula (23) will tenable, and the less possible airflow reversal occurs in branch b. Therefore, the greater the air flow velocity in branch b is before it contains methane, inevitably, the greater the rate velocity changing with time $\left|\frac{\partial u}{\partial t}\right|_b$ if it deduces to 0 in the same time. Therefore, it can be concluded qualitatively that: when upward ventilated branches filled with methane, it is difficult for airflow reversing in side branches that has great length and original velocity. That is, when outburst occurs, airflow reversal of side branches in upward ventilation is related with the length and original velocity of the branch.

4.3 *Comparison of static and dynamic analysis*

After outburst, when methane exits in upward ventilated branches, by the static method, whether airflow reversal will occur in side branches has no relation to its own windage. While in dynamic analysis, airflow reversal of side branches in upward ventilation is related with the length and original velocity of its own. According to the calculation formula, the length of roadways is a important factor that affects their windage. Consequently, there are some contradictions between the conclusions of static and dynamic analysis. The reason is that the contradictions are caused by the ignorance of dynamic changes in static analysis of the flow in network after outburst. Steady flow is assumed in static analysis, which is to say $\frac{\partial u}{\partial t}=0$. But in practical process, the flow is unsteady, even dramatic changing, in the network. Therefore, the steady assumption of static analysis is deviated from the fact obviously in a outburst in networks. And because of $\frac{\partial u}{\partial t}=0$, there will naturally not appear $\left|\frac{\partial u}{\partial t}\right|_b L_b$ in the conclusion of static analysis. For side

branch b, $\rho_0 \left|\frac{\partial u}{\partial t}\right|_b L_b$ in inequality (21) is actually hysteresis effect of flow inertia on airflow changing. The fundamental limitation of static analysis is not considering dynamics of flow, thus ignoring the inertia effect of airflow. According to the analysis of the dynamic method, although it cannot be said that airflow reversal of side branches must be related to its own windage (because length is just one of the factors that influence windage, windage can be the same with different length), at least it can be believed that the conclusion of static analysis that airflow reversal of side branches has nothing to do with windage is somewhat limited. Except this, other conclusions of static analysis have no contradiction with that of dynamic analysis, which can, therefore, still be considered reasonable.

5 CONCLUSIONS

1. After outburst occurs, great gas pressure will be produced in upward ventilated airways methane flowing by. When gas pressure is great enough, airflow in side branches will reverse.
2. In order to prevent the air flow reversal in the side branches, it is necessary to keep the fan normal operating, and avoid adding resistance in external system.
3. When outburst occurs, airflow reversal of side branches in upward ventilation is related with the length and original velocity of the branch.
4. The conclusion of static analysis that airflow reversal of side branches has nothing to do with windage is somewhat limited.

ACKNOWLEDGEMENTS

The authors are grateful to National Natural Science Foundation of China (No. 51304213, 51174212), the Open Funds of State Key Laboratory Cultivation Base for Gas Geology and Gas Control—Henan Polytechnic University (WS2012A01, WS2013A03) and the Fundamental Research Funds for Central Universities (2010QZ05, 2013QZ01).

REFERENCES

Basil B. Beamish, Pete J. Crosdale, 1998.Instantaneous outbursts in underground coal mines: An overview and association with coal type [J].International Journal of Coal Geology, 35:27–55.

Britan, A., Ben-Dor, G., Shapiro, H., 2006. Shock wave attenuation by grids and orifice plates [J]. Shock Waves, 16:1–15.

Chen, C.Y., 2010. Numerical simulation on airflow effects in local ventilate network of gas explosion [D]: Huainan: Anhui university of science and technology. (In Chinese)

Cheng, W.Y., CHEN G.X., 2000. Shock wave formation and model establishment induced by coal and gas outburst [J]. Safety in Coal Mines, 2000(9):23–25. (In Chinese)

Cheng, W.Y., Liu X. Y., Wang K.J. et al, 2004. Study on regulation about shock-wave-front propagating for coal and gas outburst [J]. Journal of China Coal Society, 29(1):57–60.(In Chinese).

Dziurzynski, W., Krawczyk, J., 2008. Computer simulation of air and methane flow following an outburst in transport gallery D-6, bed 409/4 [J]. The Journal of The Southern African Institute of Mining and Metallurgy, 108:139–145.

Fluegge, G. 1969. Druckgefaelle zur beurteilung der stabilitaet von wetterstroemen [J]. Glueckauf—Forschungshefte, 30(3):135–145.

Krah, W., Kruszynski, M., Trutwin, W., 1969. Gas concentration in mine heading, diffusion phenomena beingtaken into account. Bulletin del, a cademie polonaise des sciences, Series des science techniques volume XVII, No. 7~1969.

Otuonye, F., Sheng, J., 1994. A numerical simulation of gas flow during coal/gas outbursts [J]. Geotechnical and Geological Engineering, 1994(1):15–34.

Wang, K., Zhou A.T., Zhang J.F. et al, 2011. Study of the Propagation Characteristics of Shock Wave and Gas Flow during Coal and Gas Outburst at the Roadway with a Right-angled Bend [J]. Journal of China University of Mining & Technology, 40(6):865–869. (In Chinese).

Wang, K., Zhou A.T., Wei G.J., 2012.Study of the formation and propagation characteristics of shock wave and gas flow of outburst at straight roadway[J]. Journal of Mining & Safety Engineering, 29(4):559–563. (In Chinese).

Wang, K., Zhou A.T., Wei G.J., 2012. Influences of roadway cross-section variation on outburst shock wave propagation [J]. Journal of China Coal Society, 37(6): 983–987. (In Chinese)

Wang, K., Zhou A.T., Zhang J.F. et al, 2012. Real-time numerical simulations and experimental research for the propagation characteristics of shock waves and gas flow during coal and gas outburst [J]. Safety Science, 50(2012):835–841.

Wang, K., Zhou A.T., Zhang P. et al, 2011. Study on the propagation law of shock wave resulting from coal and gas outburst. Journal of Coal Science & Engineering, 17(2):142–146.

Wang, K., Zhou A.Z., Zhang J.F. et al., 2012.Real-time numerical simulations and experimental research for the propagation characteristics of shock waves and gas flow during coal and gas outburst [J]. Safety science, 50(4):835–841.

Zhang, J., Sun Y.R. et al, 2007. Study on propagation law of shock wave induced by coal and gas outburst [J]. Mining Safety & Environmental Protection, 34(5):21–23 (In Chinese).

Zhang, J.F., Wang K., Wei C.P., 2010. Formation and propagation of shock waves during coal and gas outbursts [J]. Journal of Mining & Safety Engineering, 27(1):67–71. (In Chinese).

Zhou, Y., 2006. Research on thermo dynamic phenomena of fire in tunnel and network [M]. Xuzhou: China University of Mining and Technology Press. (In Chinese).

Zhou, Y., Wang X.S., 2000. On the air flow reversal in airway parallel to ascensionally ventilated airway o n fir e [A]. Progress in Safet y Science and Technology (Vo l. II) – Proceedings of the 2nd International Symposium on Safety Science and Techno logy [C]. Beijing: Chemical Industry Press. 720–724.

This page intentionally left blank

Progress in Mine Safety Science and Engineering II – He et al. (Eds)
© 2014 Taylor & Francis Group, London, ISBN 978-1-138-00122-0

Experimental study of horizontal strata deep rock roadway crack propagation and strength criteria

M.C. He, Y.Y. Peng, F. Zhao, Y.B. Wang, Y. Zhang, Y.Q. Sun & W.L. Gong
State Key Laboratory for Geomechanics and Deep Underground Engineering, Beijing, China
School of Mechanics and Civil Engineering, China University of Mining and Technology, Beijing, China

ABSTRACT: In order to obtain deep mine of layered rock mass surrounding rock stability, we carried out physical modeling to study the deformation and failure processes of roadways subjecting to a plane loading scheme. The variation of inner strain of the model in the whole process were recorded by strain gauges and camera separately. Then the crack initiation and propagation during failure process of the tunnel were analyzed by combining the stress filed in the physical model and the experimental photos. As a conclusion, under geostress caused by gravity and tectonic factors, crack initiation occurs at the bottom of the tunnel at first. Then the cracks appear on the side and top of the tunnel. Ultimately, general failure of the tunnel is credited to crack propagation, coalescence with the increasing loads.

1 INTRODUCTION

With the increment of 100–250 m every ten years for the excavation depth in mine in eastern China, it can be noted that many coalmine will enter into 1000–1500 m depth (He 2004). Due to the complex environment where the deep rock mass stay (high stress, high temperature, high karsts water pressure and intense exploitation disturbance), deep rock behave great difference in mechanical properties comparing to that in shallow mining (He & Qian 2010). And most of the coal-bearing strata with layered structures are located in the tunnel of the hard roof and floor where the dynamic disasters such as rockburst and coal and gas outburst often met. Thus, investigation of deep mining stability of coal stratum is of important significance.

Many researchers have done a great amount of research on the stability of roadway surrounding rock. For example, the effect of stress field direction on roadway surrounding rock stability has been studied (Huang et al. 2012). Numerical simulation is applied to study the case of Jin Chuan deep tunnel (Yi 2012). And the numerical analysis methods of rock mass and principle of geo-mechanical model test have been clearly pointed out (Zhang et al. 2005). To date, it is difficult to get satisfactory answers by the field study and numerical simulation (Jing 2003, Huang et al. 2013) since the complex factors involved in the mining stability. Therefore, the laboratory studies of stability in the coal strata mining need to be addressed (Kittitep & Decho 2010). Using the geo-mechanics model tests, the rock deformation regularities during the large underground caverns excavation have been investigated (Xie et al. 1995, He 2011, He et al. 2010, Gong et al. 2013). These results are mainly focus on the simulation the stratified rock excavation. However, the paper (Zhou et al. 2006) has discussed the stress distribution characteristics and its variation with the different bedding dip without consideration of the micro-and inhomogeneous structure of rock influence on the entire field stress. The paper (E.T. Ooi & Z.J. Yang 2009) presents an extension of the recently-developed finite element–scaled boundary finite element (FEM–SBFEM) coupled method to model multiple crack propagation in concrete. This paper (Dongwoo 2011) is proposed for simulation of crack propagation in heterogeneous media including randomly distributed voids or inclusions. According to the variation law of stress intensity factors of crack tip I and II in different directions, the new criterion of fracture mode and failure for mixed crack of rock under the compressive loading condition was proposed (Guo et al. 2002). To study the surface crack development and distribution in layered salt rock subjected to the uniaxial compression, the fluorescence and mesomechanical techniques were employed (Li et al. 2011). The paper (Bao et al. 2013) has obtained the surface crack formation mode of layered rock under uniaxial tension by numerical simulation. But the above research cannot reproduce the structure effect of field engineering rock because of the laboratory size in the mode. The large-scale physical model experimental study has been carried out by the State Key Laboratory for Geomechanics

and Deep Underground Engineering (Beijing). And the existing researches are mainly focused on the roadway stability in horizontal layered rock decrypting the infrared characteristics during the rock failure process (He et al. 2010, He et al. 2009, Gong et al. 2013). But the crack propagation and coalescence variation law are rarely seen.

Great number of engineering practice show that large scale physical model experimental is the effective means to reproduce and analyze the stability of coal stratum. Thus, this paper presents the large scale physical model experimental study of the crack propagation during failure process of roadway in horizontal soft rock stratum. The crack formation, propagation until coalescence are all analyzed and the failure mechanism of soft rock roadway are deeply discussed from the crack aspect. All these results are expected to be helpful for the deep recognizing and understanding the law of roadway destruction.

2 MODEL AND EXPERIMENT DESIGN

2.1 *Geological background*

Based on the geological structure of Qishan coalmine in Xuzhou, this paper had simulated the horizontal contacted roadway in north wing track which lied in the depth of −1000 m. This roadway which is the main development roadway has the length of 650 m. To the north, it contacts with −850~−1000 downhill of the north wing track. To the south, it links the −850 downhill of the contacted track. According to the geological profile, the −1000 contacted roadway of horizontal north wing track which is actually the crossing layer roadway passed through 1# and 3# coal stratums three times respectively and 4# coal seam twice. It can be noted that the lithology is mainly sandy mudstone, mudstone and sandstone. The original rock mechanical parameters of the three types of rock mass for the roadway simulation of geological structure are listed in Table 1.

2.2 *Model design*

The 'YDM–C Geological Disaster Simulation Testing Machine', was used to accommodate the physical analogue model and apply boundary loads. The testing machine consists of main stand, hydraulic loading-control system, and data collection system. The test machine was use for two purposes, i.e. roadway tunnel excavations under plane loading conditions and deformation and failure of the underground openings under plane loading conditions.

Based on the original rock mechanical parameters, the author suggested that the similar material could be simplified into the sandstone, shale and coal three physical finite element plate (PFESA) to simulate the geological structure of the practical engineering. This geomechanical model test adopted different plates of five kinds of dimensions and their geometric dimensions and mechanical parameters are shown in Table 2.

2.2.1 *Similarity parameters of model*

The dimensions of the PFESA model were 1600 × 1600 × 400 mm, and the roadway excavation zone was designed as a cubic space with a

Table 1. Main physical and mechanical parameters of engineering rock mass.

Rock mass	Volu-metric weight (kN/m^3)	Compressive strength (MPa)	Elastic modulus (GPa)	Poisson ratio	Friction angle (°)
Sandstone	26.55	63.98	25.77	0.151	33.71
Mudstone	25.78	43.78	21.01	0.127	36.35
Coalseam	13.50	26.15	4.51	0.358	40.07

Table 2. Parameters for basic elementary sheet.

Size (cm)	Simulated rock mass	Ratio of water to gypsum	Volu-metric weight (kN/m^3)	Compressive strength (MPa)	Elastic modulus (GPa)
40 × 40 × 3	Sandstone	0.8:1	14.68	6.75	1.28
40 × 40 × 2	Mudstone	1:1	11.25	4.66	0.94
40 × 40 × 1	Coalseam	1.2:1	8.4	3.38	0.81
40 × 20 × 3	Sandstone	0.8:1	14.68	6.75	1.28
40 × 20 × 2	Mudstone	1:1	11.25	4.66	0.94

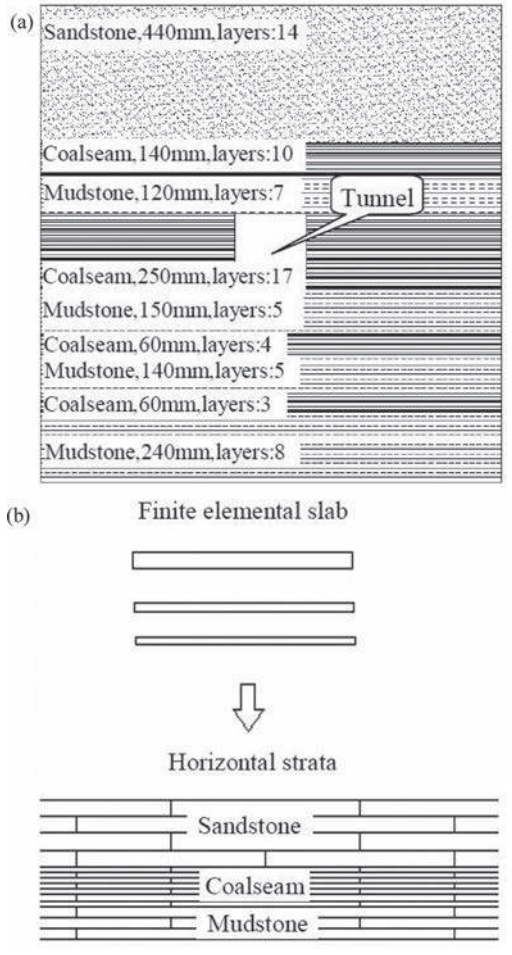


Figure 1. Similarity model; (a) Simulated rock types; (b) Model-making process.

face area of 250 × 200 mm^2 and tunneling length of 400 mm. The geometric scale factor α_t, defined as the ratio of the dimension of the real rock mass to the physical analogue model, was determined as $\alpha_t = 10$. Thus the model can simulate a rectangular-shaped underground cavern with the width of 2.5 m and height of 2 m (see Fig. 1a) and a dimension of the surrounding rock mass of 16 × 16 m, which was the typical configuration and dimension of the underground roadway found in China. According to the uniaxial compressive strength of the real rocks and the maximum loading capacity (5 MPa) of the testing machine, the force scale factor α_σ was evaluated as $\alpha_\sigma = 8$. In addition, for the sake of calculating the body force (i.e. the unit weight, see Table 1), we need to define a body force scale factor α_γ, which can be derived by $\alpha_\gamma = \alpha_\sigma/\alpha_t = 8/10 = 0.8$.

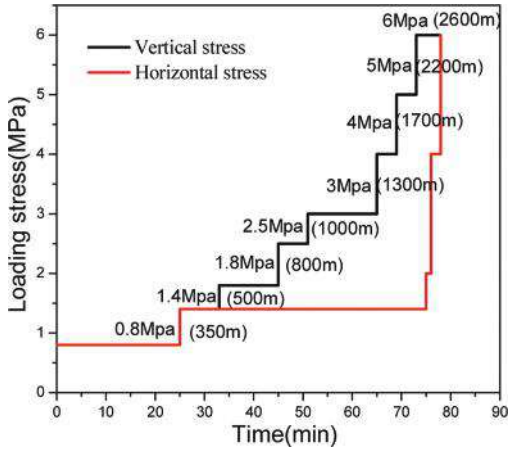


Figure 2. Loading scheme.

These force scale factors were used in the tests for fabrication the artificial materials of the PFESA model (see Table 2). The model is divided into nine layers with the help of the geological column map of Qishan. The lithology and thickness for each layer, number of layers for plate are described in Fig. 1a,b. And the roadway located in the central model.

2.2.2 *Loading design of model*

This experimental design aims at simulating the overload failure mode of roadway under the gravity stress and tectonic stress. First, simultaneously increase the vertical and horizontal loads to the stress state corresponding to the depth of −350 m (both vertical and horizontal stresses are 0.8 MPa). Secondly, load the vertical and horizontal stresses to the state of −500 m depth and keep constant. Then, load the vertical stress progressively for the research on the crack propagation. Last, retain the vertical stress, and then increase the horizontal stress progressively until the total destruction of model to study the effect of horizontal tectonic stress on the failure process of roadway model. Fig. 2. shows the loading curves of roadway.

3 STRESS FIELD DISTRIBUTION

3.1 *Analysis of stress*

Strain gauges were placed at the key point in the surround rocks shown in Fig. 3. Two strain gauges were used at each of the measuring point for capturing straining in the x and y directions respectively. Dense distribution of the gauges was utilized in the near-face region and sparse-arrangement for the far-field region.

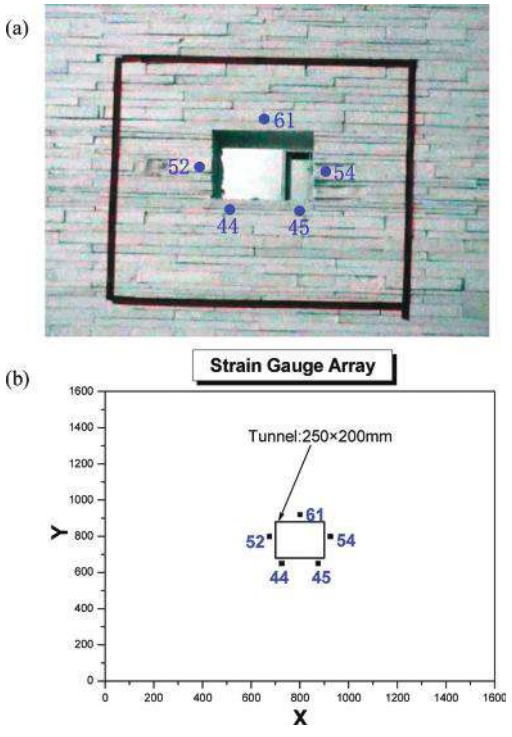


Figure 3. Key point strain gauge array; (a) Physical model; (b) Strain gauge array.

During our test, external stresses were applied in the vertical and horizontal directions which correspond to a quasi-plain stress states. In-plane strains were measured during the tests. The rock stratum is inclined horizontally, thus the vertical and horizontal stresses acted in the beddings can be recognized as the major and intermediate principal stresses. Consequently, the measured strains at each of the point are the major and moderate principal strains under the condition the deformation is pure elastic. Utilizing formula (1), the principal stresses, sigma 1 and 2, can be given:

$$\left.\begin{aligned}\sigma_1 &= \frac{E}{1-v^2}(\varepsilon_1 + v\varepsilon_2)\\ \sigma_2 &= \frac{E}{1-v^2}(\varepsilon_2 + v\varepsilon_1)\\ \tau_{\max} &= \frac{E}{2(1+v)}(\varepsilon_1 - \varepsilon_2) = \frac{\sigma_1 - \sigma_2}{2}\end{aligned}\right\} \quad (1)$$

where σ_1,σ_2 are the maximum principal stress and minimum principal stress in the plane; $\varepsilon_1,\varepsilon_2$ are the strains on the principal stress direction and $\tau_{\max}$ is the maximum shear stress in the plane.

3.2 *Brittle fracture G criterion*

Assume that there is an infinite glass plate thickness of B. After being stretched, Glass plate are fixed on both ends. If the plate subjected to uniform tensile stress, the strain energy stored in per unit volume is: $\sigma_e/2 = \sigma^2/2E$. If cut a crack length of 2a in the center of the plate, due to the crack surface stress disappear, releasing part of the elastic strain energy. At this point, the state of plane stress is: $U = \pi\sigma^2a^2B/E$. On the other hand, surface crack propagation into a new need to absorb energy as follows: $S = 4aB\gamma$, where γ is the surface energy required by forming new surface per unit area and 4aB is the area of the crack surface on both sides combined.

If the strain energy release rate dU/dA (dA = 2Bda) is equaled to the energy absorption rate required by forming new surface dS/dA, crack has reached a critical state, at this time, a slight interference will make crack expands itself, enter into unstable state. If the energy absorption rate is greater than strain energy release rate, crack is stable, otherwise, the crack is unstable. So as to conclusions:

$$\left.\begin{aligned}&\frac{d}{dA}(U-S) > 0, \text{ Unstable}\\ &\frac{d}{dA}(U-S) = 0, \text{ Critical state}\\ &\frac{d}{dA}(U-S) < 0, \text{ Stable}\end{aligned}\right\} \quad (2)$$

where $G_I = dU/dA$ is the strain energy release rate and $G_{IC} = dS/dA$ is the energy absorption rate. Subscript I representative type I crack, the critical condition of the crack is: $G_I = G_{IC}$ (2). Formula (2) is called the brittle fracture G criterion.

4 CRACK GROWTH ANALYSIS

As the vertical stress is loaded to the third stage, the floor heave occurs firstly in the roadway. Then the tensile crack and shear crack appear at the left side of the roadway, continually propagate, converge and coalesce. And shear crack generate at the right side of the roadway afterwards and appear at the top region latest. The critical stress state for the last total destruction of the roadway is 6 MPa of the horizontal stress and 6 MPa of the vertical stress. In the next section, the crack initiation, propagation and coalescence in the floor and left side of the roadway are analyzed respectively. Because of the later occurrence of the crack in right side and roof of the roadway and the little variation, these will not be analyzed in this paper.

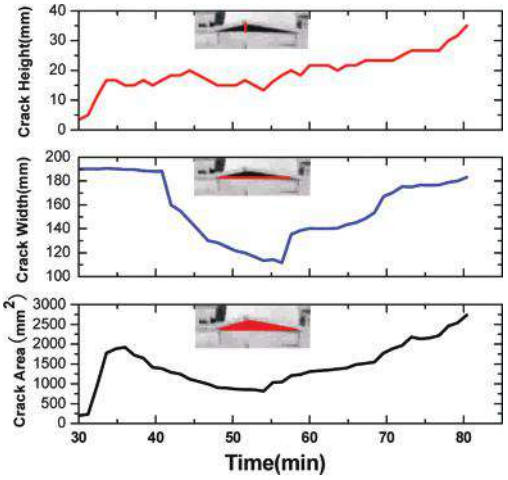


Figure 4. Relation between geometric parameters of crack and time.

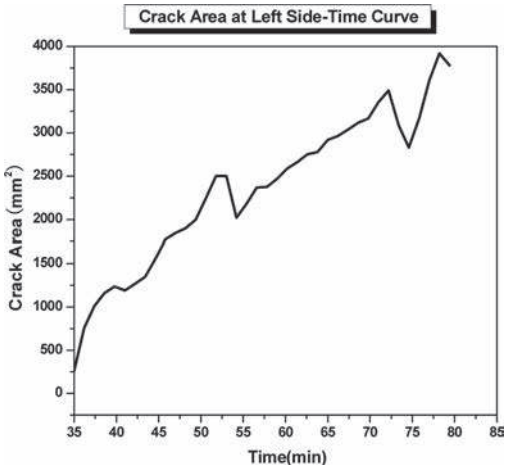


Figure 5. Crack area at left side-time.

4.1 *Analysis of the cracks at bottom of the roadway*

In order to analyze the change process of the cracks which are under sustained loading condition at the bottom of the roadway, in this paper, the length, width and area of the cracks at the bottom of the roadway are measured. Relationship of geometric parameters of crack and time is plotted in Fig. 4.

From Fig. 4, we can conclude that the trend of cracks in the bottom of the roadway as follows: 1) The length of crack is bigger and bigger indicating that the crack has extended along the height direction; 2) The crack width has little change and experience a descent stage. It can be seen that roadway width deformation is obviously in this period. After that, the width increase due to the new crack appearance. 3) The crack area is rising sharply at the beginning, representing the produce process of crack, then the area retain stable. And the descent stage is the result of fracture of gypsum plate. Last, the area is steadily rising indicating the overall crack area is being larger.

4.2 *Analysis of the cracks at left side of the roadway*

In order to analysis the change process of the cracks which are under sustained loading condition at left side of the roadway, the area of the cracks in the left side of the roadway are measured. The crack area-time curve is shown in Fig. 5.

From Fig. 5, we can obtain the trend of crack at left side of the roadway as follows: Crack area has an ascendant trend as the whole except slight fluctuations. With the increase of load, three tension cracks sequentially appear at the left of the roadway. With the experiment performing, cracks continually propagate, converge and coalesce until the left side wall of the roadway collapsed. Large stress accumulation in the model is generated due to the friction between the rock layers movement at the left side of the roadway.

5 CONCLUSION

1. With increase of the roadway depth, the left side and the right side of the roadway are subjected to tensile, shear, or combined stress state. Thus, tension crack, shear crack or mixed mode crack are existed in these locations.
2. During the failure process, floor heave appears first in the roadway tunnel. Propagation of fractures leads to the further development of the floor heave. It indicates that the floor is weaker than the sides of the roadway in horizontal strata.
3. Under the increase of loads, there are three independent tension cracks firstly arise on the left side wall. As further increase of the loading, cracks continually propagate, converge and coalesce leading to the penetrating cracks on both sidewalls and the floor until complete failure of the roadway.

ACKNOWLEDGEMENT

Financial support from the Special Funds for the National Natural Science Foundation (Key Project) under Grant No. 51134005 is gratefully acknowledged.

REFERENCES

Bao Chunyan, Tang Chunan, Tang Shibin, Cai Ming, Yu Qun. 2013. The formation mode and mechanism research of surface crack of bedded rock under uniaxial tension [J]. *Chinese Journal of Rock Mechanics and Engineering*, (3):474–482.

Gong W.L., Gong Y.X., Long A.F. 2013. Multi-filter analysis of infrared images from the excavation experiment in horizontally stratified rocks. *Infrared Physics & Technology*, (56):57–68.

Gong W.L, Wang J, Gong YX. 2013. Thermography analysis of a roadway excavation experiment in 60° inclined stratified rocks. *International Journal of Rock Mechanics and Mining Sciences*, (60):134–147.

Guo Shaohua, Sun Zongyi, Xie Xiaoqing. 2002. The research on mode and criterion of rock fracture under compressive stress [J]. *Chinese Journal of Geotechnical Engineering,* (3):304–307.

He Manchao. 2004. The symposium of the eighth national rock mechanics and engineering academic conference [C]. *Chinese Society for Rock Mechanics & Engineering,* (5).

He Manchao, Qian Qihu. 2010. The Basis of Deep Rock Mechanics [M]. Beijing: *Science Press*, 8(6).

Huang Longxian, Yang Tianhong, Li Xianguang, Zheng Chao. 2012. The influence of stress field direction on the stability of surrounding rock in the roadway [J]. *China Mining,* (4):105–107.

Huang Feng, Zhu Hehua, Xu Qianwei, Cai Yongchang, Zhuang Xiaoying. 2013. The effect of weak interlayer on the failure pattern of rock mass around tunnel – Scaled model tests and numerical analysis. *Tunneling and Underground Space Technology,* (35):207–218.

He Manchao. 2011. Physical modeling of an underground roadway excavation in geologically 45°inclined rock using infrared thermography. *Engineering Geology,* 121(3):165–176.

He M.C., Gong W.L., Zhai H.M., Zhang H.P. 2010. Physical modeling of deep ground excavation in geologically horizontal strata based on infrared thermography. *Tunneling and Underground Space Technology*, 25(4):366–376.

He Manchao, Gong Weili, Li Dejian, Zhai Huiming. 2009. Physical modeling of failure process of the excavation in horizontal strata based on IR thermography. *Mining Science and Technology (China)*, 19(6):689–698.

He Manchao, Jia Xuena, Gong Weili, Faramarzi Lohrasb. 2010. Physical modeling of an underground roadway excavation in vertically stratified rock using infrared thermography. *International Journal of Rock Mechanics and Mining Sciences*, 47(7):1212–1221.

Jing L. 2003. A review of techniques, advances and outstanding issues in numerical modeling for rock mechanics and rock engineering. *International Journal of Rock Mechanics and Mining Sciences*, 40(3):283–353.

Kittitep Fuenkajorn, Decho Phueakphum. 2010. Physical model simulation of shallow openings in jointed rock mass under static and cyclic loadings. *Engineering Geology,* 113(1–4):81–89.

Li Lin, Chen Jie, Jiang Deyi, Yang Chunhe, Liu Chun. 2011. The analysis of surface crack propagation on bedded rock salt under uniaxial compressive stress[J]. *Rock and Soil Mechanics*, (5):1394–1398.

Ooi, E.T., Yang, Z.J., 2009. Modeling multiple cohesive crack propagation using a finite element–scaled boundary finite element coupled method. *Engineering Analysis with Boundary Elements*, 33(7):915–929.

Sohn Dongwoo, Jae Hyuk Lim, Young-Sam Cho, Jeong Ho Kim, Seyoung Im. 2011. Finite element analysis of quasistatic crack propagation in brittle media with voids or inclusions. *Journal of Computational Physics*, 230(17):6866–6899.

Xie Mowen, Yang Shuqing, Liao Yelan. 1995. Study and practice of stability for tunnel group in alternative stratified rocks [J]. *Chinese Journal of Rock Mechanics and Engineering*, 14(2):131–137.

Yi Yongliang. 2012. Numerical simulation study of stability of surrounding rock in deep roadway in Jin shan[J]. *Technology and Enterprise Development,* (15):83–86.

Zhang Qiangyong, Li Shucai, Jiao Yuyong. 2005. Numerical analysis of rock mass and experimental principle and engineering application of geomechanics model [M]. *China Water Power Press.*

Zhou Xiaojun, Gao Yang, Li Zelong, Yang Changyu. 2006. Experimental study on the uneven rock pressure and its distribution applied on a tunnel embedded in geologically bedding strata [J]. *Modern Tunneling Technology*, (1):12–21.

Progress in Mine Safety Science and Engineering II – He et al. (Eds)
© 2014 Taylor & Francis Group, London, ISBN 978-1-138-00122-0

Research on the performance of foam agent used for mine fire prevention

Zhao-Jun Tian, Xiao-Lu Zhang, Rong-Yi Zhou & Qing Ye
School of Energy and Safety Engineering, Hunan Province Key Laboratory of Safe Mining Technology of Coal Mine, Hunan University of Science and Technology, Xiangtan, Hunan, China

ABSTRACT: Foam agents have been widely applied to mine fire prevention, and its performances determine its using effects and economic benefits. This paper explored the mechanism of foam formation and rupture as well as parameters of foaming properties. Many factors that could exert influences on the foaming performance and the foam stability were discussed, such as foaming agent itself (the concentration, the kind and its molecular structure), mixed surfactant, salt, temperature, pH, surface-active nanomaterial and polymers, and some methods were put forward to improving the performance of foam agent.

1 INTRODUCTION

Foam fire prevention technology has been applied to mine fire prevention for more than fifty years. Its mechanism is that the heat taken away through the evaporation of foam could reduce the heating rate of coal and the generated water vapor would isolate the oxygen existing in the environment. The coal spontaneous combustion is the main factors of mine fire, accounting for the total of 85%–90%. To address this problem, domestic and foreign scholars have conducted a lot of researches. Three-phase foam, containing solid, liquid, gas material, developed by China University of Mining has been applied to many mines. The results of application indicated that the process was simple, the effect of fire prevention was obvious, and foam could stack up to a sufficiently height to prevent the continuation of temperature at high fire point. The gel foam setting gel and foam with excellent properties of fire prevention in one has high foam stability and foam ductility.

However, foam performance is still not well meet the actual production. The stabilization time had only 8–24 hours, and its life cycle could hardly satisfy the demand. Thus, raw material had to be pumped into frequently. The gel foam also has its own shortcomings. For example, it requires foaming agent possess excellent performance to reduce production costs and expand its scope of application. The improvement of the foaming performance of foaming materials not only can drop the cost, but also increase the volume of foam per unit time. All of these could be conductive to applying the accumulation and scalability of foam material more effectively. Thus, it is of great significance to improve performance to promote the application of fire prevention and improve its performance in mine further.

2 MECHANISM OF FOAM GENERATION AND RUPTURE

When pumped gas into or stirred, the aqueous solution containing surfactants can generate bubbles wrapped with film. The surfactants are distributed on the internal and external surface of film. Surfactant molecule is a kind of amphoteric molecule, which contains both hydrophilic groups and hydrophobic groups at the same time. Its hydrophobic hydrocarbon chains spread into the gas phase and hydrophilic polar groups insert into water. In virtue of high gas volume fraction, bubbles could float above water spontaneously, contact with air, and then stack up on the surface of liquid to form foam. To maintain its mechanical stability, the foam generally is rendered as polyhedral shape. It is a dispersion of gas dispersed in liquid, belonging to unstable system thermodynamically. And it has more free energy than the sum of air and liquid. As a result, the foam will break down and the total free energy of the system reduces. The rupture of foam is mainly caused by the drainage when the gas defuse through membrane, the gravity and the difference of pressure at each point in the film.

3 PARAMETERS OF FOAM PERFORMANCE

Parameters of foam performance mainly include the foaming performance and the foam stability. Foaming agent is a kind of surfactants with excellent foaming performance. It can reduce the surface tension of aqueous significantly and make it easier to produce foam. Generally, the ability of reducing the surface tension is used to represent the foaming performance of agent. The stronger the ability is, the better foaming performance present. But it is not on the contrary. The formation of foam is a dynamic process, accompanying with the rupture. Therefore, good foam stability can not only increase the amount of formation, but also improve the quality. It is an important prerequisite to improve foaming performance. At present, many scholars are keen to improve the performance indirectly by improving the foam stability. The surface viscosity and the surface flexibility are main factors affecting agent foam-stabilizing properties. The former, which can be used to measure the ruggedness of adsorption film, is produced by monolayer composed of active molecules on the surface. Because the ruggedness determines the film strength, the viscosity will affect foam stability. The latter could restore the film thickness to promote its stability when foam suffer from mild local impact and prevent film from.

4 FACTORS AFFECTING FOAM PROPERTIES AND WAYS OF IMPROVING FOAM PERFORMANCE

4.1 *Foaming agent own factors*

Foaming agent own factors is the fundamental factor affecting foam properties, mainly in the type and the concentration of the foaming agent and the molecular structure.

4.1.1 *Types and concentration of foaming agent*

The performance of different foaming agent varies. It is mainly related to the nature of its own, such as some special groups and its adaptability to the external environment. Foaming agent concentration also exert influence to foaming properties. When the concentration is less than the critical micelle concentration(cmc), the increase of solution concentration will increase the adsorption capacity, reduce the surface tension and enhance the foam strength. But the stability of formed foam is poor. When the concentration is above the cmc, the surface tension can't be reduced by increasing the concentration, but increase slightly. However, the solution surface will form increasingly dense film because of the enrichment of foaming agent. Thus, the stability of formed foam increases. When the concentration is continued to a certain extent, the foam liquid content will be reduced and the fragility of film increases. As a result, foam become more unstable.

3.1.2 *Molecular structure of foaming agent*

The increase of carbon chain of foaming hydrophobic groups within a certain range could enhance the cohesive force among the molecular chains, which makes the interface of film have greater flexibility and stronger mechanical strength. However, when the carbon chain continues to increase, the foaming power will be reduced. For the long carbon chain hardens the film and reduces its flexibility. The hydration of agent hydrophilic groups could form a very thick water film around itself, which turns free-flowing water into bound water with poor mobility. As a result, it increases the viscosity of the liquid film, slows the rate of thinning liquid film owing to gravity drainage and stabilizes the foam stability. Therefore, foam stability can be improved by the addition or deletion of the length of carbon chain. Generally, strong hydrophilic groups matched with suitable hydrophobic groups can be used to produce a better foaming agent.

In addition, part of the hydrocarbon chain can be also replaced by some special reactive groups to obtain some outstanding properties original structure do not have. Aydogan put forward a novel asymmetric Bola surfactant-FHUB through replacing part of hydrocarbon chains by fluorocarbon chains with strong rigidity. This substance has strong hydrophobic and oleo phobic. The aggregation ability, the mobility and the dispersion coefficient is also good. Such surfactants are not very sensitive to changes of ion concentration existed in solution. Besides, the grows of fluorocarbon chain could lead to the reduction of limit surface tension and the increase of Krafft and cmc. Therefore, it can greatly improve the foaming performance and the foam stability.

4.2 *Mixed surfactant*

It is a common means of improving foaming properties by compounding surfactants. On the one hand, owing to the intermolecular interactions, the electrostatic repulsion between polar groups decreases and surfactant molecules will be arranged more closely. On the other hand, hydrocarbon chains would attract each other because of the hydrophobic effect. Therefore, it is easier for surfactant molecules to aggregates to form micellar in the interior of solution, and surfactant molecules are arranged more closely and have a greater adsorption capacity in the surface adsorption layer. Those surfactants synergies can not only increase foaming

performance and foam stability significantly, but also reduce the cost of the surfactants and the damage to the environment. Therefore, there is profound significance and broad prospects in improving economic efficiency and popularization.

There are some common complex systems, such as anionic/anionic, anionic/cationic, anionic/amphoteric, anionic/nonionic, male/non-ionic mixed surfactant and so on. Compared with other combinations, anion/cation, anionic/amphoteric show a better synergistic effect.

4.2.1 *Anionic/Cationic mixed surfactant system*

Recent studies negated the prospective that the negative effect produced by anionic/cationic mixed surfactant system would result in loss of surface activity. Instead, they found that these systems had good foaming capacity and low surface tension. The electrical interaction between the two surfactants reduces the effectiveness and the efficiency of the surface tension as well as the critical micelle concentration of the system, increase the adsorption of active agent at liquid surface and the strength of film, Improves the stability of foam, and increase the foaming height, which showing a significant synergistic effect. During tests of SDS/OB-2 composite system, Chen Weizhang found that the foaming height increased rapidly with the addition of OB-2 and reached the maximum height at 245mm when (SDS): m (OB-2) was 1:3. Similarly, SDBS/OB-2 composites exhibited a good composite effect also. Minimum value of the surface tension was 2312mN·m-1 and maximum foaming height was 214mm when m(SDBS):m(OB-2) was 2:1.

4.2.2 *Anionic/amphoteric mixed surfactant system*

Amphoteric surfactants have some advantages, such as low irritation, good resistance to hard water, excellent biodegradability, etc. Regrettably, its price is too expensive. In the anionic/amphoteric mixed surfactants system, cheaper anionic surfactants not only can be used to replace amphoteric surfactants, but also compensate for shortcomings of anionic surfactants. As positive charges exist in amphoteric surfactant molecules, there is a strong electrical interaction between anionic surfactants and amphoteric surfactants and display an excellent synergy and great practical value.

4.3 *Polymer*

Numerous studies results showed that there were significant interaction between polymer and surfactant. The surface tension of ordinary polymer/surfactant mixture solution is often higher than singles. The reason is that part of surfactants are adsorbed by polymer and the concentration of free surfactant in solution drops. After polymer are added into the agent, the mechanical strength of foam film enhanced through increasing the viscosity of liquid phase on the one hand. On the other hand, the polymer can slow down the liquid expulsion rate and the film thinning speed, increase the apparent viscosity of the liquid film, and make the foam film more flexible. Besides, the coadsorption of foaming agent and polymer molecules on gas/liquid interface make the solution more tenser and increase the the draining period and the stability. Therefore, the polymer plays the role of foam stabilizer. By observing changes of the bulk viscosity and the surface tension of mixed solution, the interaction between polymer and surfactants can be studied. Du Jianfen conducted comparative experiments to analyze DP-4 foam performance under high temperature and pressure. Single and composite foam system and the system with the addition of 2% crude on the basis of original were researched in this study. He came to the conclusion that composite foam system with polymer had better foaming capacity and foam stability than single system without polymer. In addition, the polymer concentration was another important factor affecting foaming performance. When the concentration was too high, the film thickness could not be restored; while the concentration was too low, the self-repairable ability and foam stability of film became poor because of low elasticity.

4.4 *Inorganic salts*

In the practical application, various salts inevitably exist in the aqueous solution of foaming agent. Generally, the performance of Ionic surfactants is susceptible to electrolyte while it is not for non-ionic surfactants. As for ionic surfactants, the adsorption of agents can be increased significantly when a certain amount of inorganic electrolyte was added into solution. The reason is that increasing the concentration of inorganic ions appropriately makes more counter-ions permeate adsorption layer. And these ions would combine with ionic surfactant molecules, weakening the electrical repulsion between surface-active ions. Then, adsorbed molecules are arranged more closely. However, when the salt concentration is too high, it will compress the diffuse double layer. These changes weaken the electrostatic repulsion between surfaces and make the film more easier to thinning and rapture, which exert negative impact on foaming performance. A study certificated that the half-life of foam had nearly doubled when the NaCl concentration was 0.0125% than those without salt. Nevertheless inorganic salts began to play a serious negative role on foam stability after the NaCl concentration reached at 0.1%.

4.5 *Temperature*

Wang Xianguang tested the foam properties of SDBS (Sodium dodecyl benzene sulfonate) and three kinds of ABEPS (Alkyl benzyl group of homogeneous polyoxyethylene ether sulfonate) at different temperatures in experiment. The data showed that the foaming performance of surfactant solution would be improved with the rising of ambient temperature, while the foam stability was declining. Within the appropriate range, the foam temperature is conducive to reduction of the surface tension, which increased total area of film formation in unit time and enhanced the foaming capacity. As the temperature continued to rise, the evaporation and the discharge of water film quickened, which thinned the film and reduced solution viscosity. On the other hand, the increased molecular motion and the thermal expansion of gas volume also thinned the film. In addition, elevated temperature reduced the hydration of hydrophilic surfactant molecule. Meanwhile, the reduced cohesion between hydrophobic carbon chain and repulsion between film weakened film strength. Taking all factors, the foam stability decreased.

4.6 *pH*

Liu Zhaowen studied the effect of pH on foam performance with certain complex systems, and found that the pH had a great impact on the forming properties. Under acid conditions, the foaming capacity of complex systems was weak. As the pH increasing, the foaming capacity enhanced and reached maximum at pH 7. However, it presented in the opposite under alkaline conditions. Zhang Qun studied the forming capacity and form stability of different varieties of oleic acid solution at different pH. They found that the capacity was very weak when pH<7, then gradually increased with the increase of pH when pH>7, and achieve the finest effect at pH 10. Other experiments showed that the change of PH values have few effect on foam properties of non-ionic surfactant solution. However, it affected the foam stability of ionic surfactant aqueous solution greatly. The effect of pH on foam varied with the composition of the solution. The main cause is that the change of pH affects the force between active substances or between active substance and water. In practical application, the value of pH should be adjusted to a reasonable range based on the degree of sensitivity to pH about that system.

4.7 *Surface-active nanoparticles*

Some surface-active nanoparticles with suitable hydrophilic-lipophilic properties can be adsorbed at the air/liquid interface, forming monolayer or multilayer particles which is similar to surfactant adsorbed monomolecular layer. This structure can stabilize the gas/liquid phase and play the role of foaming and stabilizing foam. Binks obtained a stable foam system with silanized SiO_2 particles, and improved the foaming performance and foam stability greatly by adjusting the hydrophobicity of particles with the use of NaCl. Cui Yanzhen conducted a comparative experiment targeted at nano calcium carbonate—surfactant mixed system. When different concentrations of SDS were added into 1% dispersion of nano-$CaCO_3$, she found that instant foam volume increased with the increase of the SDS concentration and the effect was more pronounced than single SDS system. When the SDS concentration range is lower than the cmc, the foam volume of mixed system is also lager than single system. Apparently, nano-$CaCO_3$ with SDS produced a significant synergistic effect in foaming and foam stability.

5 SUMMARY AND OUTLOOK

In summary, the performance of the foam material was affected by many factors, such as foaming agent characteristics (the concentration, the kind and its molecular structure), mixed surfactant, salt, temperature, pH, nanomaterials with surface activity and polymers. We should consider to seek ways to improve foam performance according to the mechanism of these effects of factors, and make full use of all the advantages of foam in the field of fire prevention, such as simple preparation, low cost, few resources consumed and so on. It is proved to be an effective way to improve the effect of coal spontaneous combustion. In addition, we can mix it with other fire prevention material, included nitrogen, sediment and gel to make a mixture. Not only can it save resources, but also it is of significant economic value for its better fire prevention performance than single material.

ACKNOWLEDGEMENTS

This work was financially supported by Educational Department of Hunan Province (11C0540), the Research Fund of The State Key Laboratory of Coal Resources and Mine safety, CUMT (09KF01), Key Laboratory of Gas and Fire Control for Coal Mines (China University of Mining & Technology), Ministry of Education (GFCKF201107), Open Research Fund Program of Hunan Province Key Laboratory of Safe Mining Techniques Of Coal Mines (Hunan University of Science and Technology) (201004) and College

Students Research Learning and Innovative Experiment Project of Hunan University of Science and Technology (KDCX1101).

REFERENCES

Aydogan N & Abbott NL. Effect of Electrolyte Concentration on Interfacial and Bulk Solution Properties of Ferrocenyl Surfactants with Anionic Headgroups[J]. *Langmuir*, 2002, 18:7826–7830.

Chen WeiZhang, et al. Study on Super Foamability of Solution System of Composite Surfactants[J]. *Fine and Specialty Chemicals*, 2007, 15 (3/4):21–27.

Chen Zuzhang & Zhao Qingming. Application of Three-phase Foam in Mine Fire Prevention[J]. *Coal Mine Modernization*, 2010, 3:26–28.

Cui Yanzhen. Study on Formability and Foam Stability of Calcium Carbonate Nanoparticles-surfactant Mixtures[D]. Wuxi City:University of the South, 2009:17–25.

Du Jianfen, et al. Experimental Study of DP-4 Foam Performance at High Temperature/High Pressure[J], *Engineering of Oil & Gas*, 2008, 37(3):223–225.

E. Dickinson, et al. Factors controning the Formation-and Stability of Air Bubbles Stabilized by Partially Hydrophobic Silica Nanoparticles[J]. *Langmuir*, 2004, 20:8517–8525.

Jiang Qingzhe, et al. Surfactants Science and Applications [M]. China Petrochemical Press, 2009:296.

Lin Yihua. Application of Three-phase Foam Fire Extinguishing Technology in Dazhuang mine[J]. *Zhongzhou Coal*, 2009, 1:92–93.

Liu Chaowen, et al. Experimental Study of High-performance Foam—a Separate Chemical Agent Carrier for Coal Spontaneous Combustion[J]. *Mining Safety & Environmental Protection*, 2009, 36(5):3–5.

Tian Shuicheng & Fan Yukai. Application of Three-phase Foam Fire Extinguishing Technology in Qinyuan Mine [J]. *Shanxi Coal*, 2010, 3:76–78.

Tian Zhaojun. et al. Research of Foam Gel Using for Fire Prevention and Gas Plug[J]. *Journal of China University of Mining & Technology*, 2010, 39(2):169–172.

Wang Deming. Mine Ventilation and Safety [M]. Xuzhou: China University of Mining and Technology Press, 2007:317–318.

Wang Xianguang, et al. Foam Properties of ABEPS Series Anionic-Nonionic Surfactants[J]. *Oilfield Chemistry*, 2009, 26(4):357–361.

Yao Dagang. Application of Three-phase Foam Fire Extinguishing Technology [J]. *Coal Mining Technology*, 2009, 14 (1):96–97.

Ye Zhongbin, et al. Interaction of Hydrophobically Associating Polymer and Surfactant[J]. *Journal of Southwest Petroleum Institute*, 2003, 25 (1):55–58.

Zhang Guoshu, et al. Ventilation Safety Science [M]. Xuzhou: China University of Mining and Technology Press, 2008:246–248.

Zhang Peng. Study on Foam Fluid Stability and the Behaviors and the Performance of Foam in Porous Media[D]. Jinan City:ShanDong University, 2005:37.

Zhang Qun, et al. Effect of pH Value on the Foaming Properties of Oleic Acid[J]. *Journal of Jinan University(Science and Technology)*, 2006, 20(1):31–34.

Zhou Yawen, et al. Study on Mixed System of Zwitterrionic and Anionic Surfactants[J]. *Journal of Beijing Technology and Business University(Natural Science Edition)*, 2008, 26 (5):5–9.

This page intentionally left blank

Progress in Mine Safety Science and Engineering II – He et al. (Eds)
© 2014 Taylor & Francis Group, London, ISBN 978-1-138-00122-0

Research on efficient dust suppression measure in full-mechanized mining face

G.J. Yi, M.X. Jia, J.H. Wang & S.M. Wang
China University of Mining and Technology (Beijing), Beijing, China

ABSTRACT: Aiming at the actual situation of #131419 fully mechanized face, testing in the field and analyzing the problems in the fully mechanized face, including water quality, nozzles, coal shearer's spray and dust reduction system, closing between the hydraulic support, finding the reasons for large dust concentration. From system point of view, the author improves the original dust suppression, uses the new engineering and technical measures, including magnetized water, changing material of nozzles, optimizing the spraying system for coal shearer, closing dust source between the hydraulic support and so on, finally uses the new efficient dust suppression measure in #131419 working face of Laowuji Coal Mine with on-site detection, make the conclusion finally: by taking the new efficient dust suppression measure, the dust suppression efficiency of working face is more than 80%, especially the respirable dust is greatly reduced and the workers exposed dust is reduced.

1 INTRODUCTION AND BASIC SITUATION OF THE WORKING FACE

At present, the attention degree of most mines for underground dust prevention is not enough, the dust control engineering techniques is relatively single, resulting in that the dust concentration seriously exceeded the national standard. On the system level, through the analysis of the existing problems in the system, this paper puts forward some improvability measures for the existing dust removal system in Laowuji mine #131419 working face, including engineering technical measures, such as the use of magnetized water, selecting new nozzle, improving coal winning machine internal and external spray system, optimizing frame dust source closed systems and so on. On a whole, the underground coal dust is under control, the dust concentration of fully-mechanized face is greatly reduced, and the working environment of work face is improved.

The maximum trend length in #131419 of Laowuji Coal Mine is 1053 meters, the minimum trend length is 1030 meters, and the average trend length is 1042 meters. The thickness of mineable coal averaged at 2.8 meters and the dip of the coal averaged at 10°. The capability is 1.5t/m^3.

The coal mining method in #131419 is the strike longwall retreating method and the coal mining technology is Coal Mining Technology, which uses the ZY3300/15/28 Hydraulic Support at the same time the MXG-250/600QWD Double Cylinder Shearer.

The Mining Face uses SGZ730/400-type scraper conveyor, the roadways and transportation lanes use SGW-40T-730/110 Crossheading Conveyor as well as STJ-800 Belt Conveyor.

The #131419 working face adopts dynamical pressure water infusion in exploitation process to prevent dust, uses ZYG—150 which total weight is below 2 tonnes, hole diameter is 75 mm, the drilling length is greater than 50m, drilling machine drilling in the upper and lower roadways meanwhile seaming water infusion bi-directional.

2 LAYOUT OF TEXT PROBLEMS IN ORIGINAL DUST REMOVAL SYSTEM

The respirable dust concentration of the #131419 work surface in the working environment is more than 10 mg/m^3, at the same time, the maximum concentration of respirable dust appears at 5 meters after advancing support, reaching at 129 mg/m^3. In addition, near the shearer and the upper and lower end, the concentration of respirable dust averaged at more than 20 mg/m^3 which is great harm for workers. The reason producing such a large amount of dust, after analysis and experimentation, is that the original dust removal system exist the following problems.

2.1 *The problems of water*

All tables should be numbered with Arabic numerals. Headings should be placed above tables, left justified. Leave one line space between the heading and the table. Only horizontal lines should be used

within a table, to distinguish the column headings from the body of the table, and immediately above and below the table. Tables must be embedded into the text and not supplied separately. Below is an example which authors may find useful.

2.2 *The problems of nozzle*

Due to using traditional materials-brass nozzle in #131419 working face, this type of spray nozzle are likely to cause destruction of the surface material owing to high velocity flow erosion and corrosion in the process of using, which make nozzle increase the amount of water but decrease the degree of spray.

2.3 *The problems of spray and the dust reduction system for coal*

Coal mining machine uses MG700 series of spray and dust reduction system for coal, the Interior Spray System comes with appliances, which is fixed inside the coal machine fuselage, whose nozzles are relatively settled, and the water pressure is lower (1~3MPa), in a word, the efficacy of actual removing of dust is just so so. The nozzles in External Spray System put direct jet to use, the water is not completely atomizing, which waste much of water and in contrary, the effect of dust removal is reduced.

2.4 *No closing between the hydraulic support*

Supporting of hydraulic support in Full-mechanized Mining Face is a major source of dust and moving hydraulic support often can cause a grate deal of dust for supporting process. The #131419 working face does not do enough protective measures for dust falling in this respect, which results in the dust concentration rising rapidly. After measured, the highest concentration of respirable dust appears at 5 meters behind moving hydraulic support and can reach for 129 mg/m^3.

3 OPTIMIZATION IN DUST-FALLING SYSTEM

Aiming at the original dust-falling system problems, the author has improved the original system by doing experiments and determining in the locale, at last, the author put forward specific measures as follows.

3.1 *Using magnetized water to reduce dust*

In order to solve the problem of water quality, the author does experiment of magnetized water to reduce dust in the laboratory, noticing the water of coal-water surface tension and contact angle changes which are shown in the following Figure 1 and 2.

By the figures we can know, the surface tension of water continue lower when the magnetic field intensity is between 0.5–0.7T, at the same time, the water is more easy moist coal and spray dust; the water-coal contact corner is linear decrease when the magnetic field intensity is between 0.6–1.2T and the law is obvious; the water-coal contact corner is reach for the minimum number 29.2° when the magnetic field intensity is 1.2T, that is reduced by half and has obviously effects.

By the magnetic experiments, we decided to use permanent magnet to magnetize the water considering both cost-effectiveness and security performance in #131419 working face. The permanent magnet was made up of two magnets whose diameter is 100mm and thickness is 15mm; we can figure out that the magnetized pipeline's length is 2 m based on the water's velocity and the time of magnetization.

In addition, it is important that the water should be filtered in underground first before magnetized. The reason is that if the water is filtered in the ground and then transported to working face by pipeline, in this process, there may produce other impurities which could reduce the fog effect.

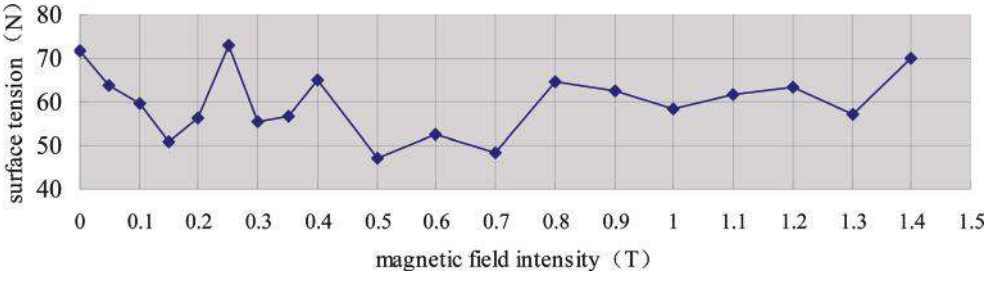


Figure 1. The relationship between surface tension of water and magnetic field strength.

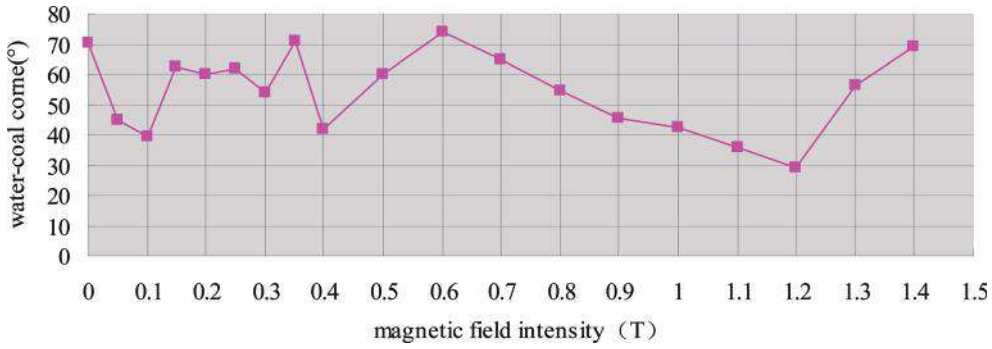


Figure 2. The relationship of coal water contact angle and the magnetization strength.

3.2 *The improvement and arrangement of nozzles*

Having done with the things above, then what we should do is improving the original nozzles in the system. The working face was using copper material nozzles which have several defects. In contrast, ceramic material nozzles have other advantages such as strong corrosion resistance capability, abrasion resisting, high strength, hardness and other advantages, so it can perfectly overcome the defects of copper material nozzles. After detecting in site, the author decides to use ceramic material nozzle whose aperture is 1.5 mm.

After determined the material of nozzles, and then we should optimize the arrangement of nozzles which influences a lot on the effect of spraying dust. Only when the nozzle's spray wraps up totally the shearer drum, can the spray dust spray dust results. Therefore, the principle for the arrangement of nozzles is that the nozzle's spray wraps up totally the shearer drum. In #131419 working face, after repeatedly experiments, we install 3 high pressure nozzles on each spray device which are mutually staggered. The water can be formed fog flow screen when it arrives at the coal shearer's drum and totally cover dust source. In order to control maximized of shearer cutting coal dust, the nozzles should point to the shearer's gear and keep an appropriate distance. According to the actual condition of the underground, the spray device is welded on the shearer traction motor parts to ensure the water-fog can be blowed to the dust source from time to time.

3.3 *The improvement of the spraying for coal shearer*

The author introduces the optimizations for spray and nozzles; here we introduce the improvement of the spraying for coal shearer. According to the actual circumstances, there exists lots of problems on the outer and inner mist spray at the coal shearer in the working face, such as low spray pressure and others. The authors do the following optimization for the spray device of coal shearer.

1) The improvement of internal spraying device
Because the water's pressure of water pressure is low, firstly we should increase the pressure of the water. The larger water pressure is essential to ensure the effect of spray. Secondly, we should increase the number of filtering of the water and setup several different precision filters along the liquid pipeline to ensure the quality of water and to prevent the spray nozzle clogging at the same time.

2) The improvement of external sprayer device
The improvement of external sprayer device in coal mining process is the main force to spray dust system in the working surface, so we do more improvements for it. The improved high-pressure shearer spray of dust reduction system contains water filtration system, booster pump, pressure reducing valve, coal shearer with high pressure spray device, as shown in the following Figure 3:

1. The water filters with high performance multilayer coagulation has better effects. The impurity filtering accuracy is below 1.8 μm and the filtering speed is between 0~100 L per minute and the working pressure is 0.3~2.5 MPa. The water filters installed in the water supply pipeline, which can filter water as well as protect booster pump.
2. The supply of high pressure water and spray system is the key technology to high pressure spray dust in coal mining machine. This system uses TQB80/12–5 booster pump whose quantity of flow is 80L per minute and pressure 0~12.5 MPa. The booster pump is installed on the shearer, the low-pressure water is changed

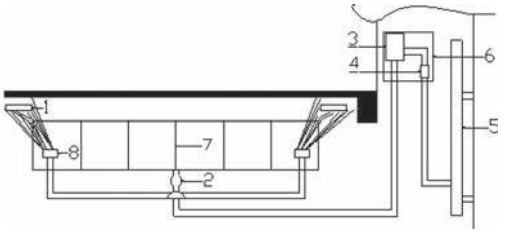


Figure 3. Shearer' high pressure outside the spray dust suppression system.

into high-pressure water through the filter and then delivers to the coal shearer sprayer device to produce high-pressure spray.

3. The system uses Y42X pressure reducing valve whose nominal diameter is 25 mm and adjustable pressure ranges 1.6~10 MPa. The working principle is that the pressure changes through throttle valve. The inlet pressure can be reduced at the outlet, when the quantity of flow and pressure change, the water can keep stable due to its media power. In order not to influence the water pressure of coal shearer, the pressure reducing valve is installed before water pipeline.
4. The high pressure spray device adopts single hole nozzle which has a far range, big flow and high degree of atomization. High pressure water spray can surround the head of the coal shearer with the help of cohesion, intercept and diffusion effect of water spray to reduce dust. In addition, a high concentration of fog particle has the effect of filtering working surface to air flow, which, to some extent, purifies the working surface wind.

In order to meet the field conditions, we do the tests repeatedly and find that the spray effect reaches for maximum effect when the high pressure of the system is 4.0 MPa and quantity of flow is 12.24 L per minute. The effective range of the system is 2.85 meters and the maximum range can reach for 3.8 meters.

3.4 *The arrangement of spray point in the working face*

Above are improvements respectively of spray water, spray nozzle and outer and inner mist spray at the coal cutter, next the spray system only has the last step of work, namely reasonable layout of the spray point when the shearer is on work. The coal cutting speed of shearer in the #131419 face is 6m per minute, the center spacing of stents is 1.5m, so the time that the shearer required to pass through each bracket is 15s, therefore, fully mechanized mining face live stent spray can layout in the following manner:

1. When the shearer cuts coal upstream, NO. 4, NO. 9 and NO. 14 spray device on leeward side of the coal miner driver spray tracking the shearer, the spray time is 30s. When the shearer walk through a stent distance, NO. 4, NO. 9 and NO.14 on the downwind side of the original coal miner driver has been spray for 15s. At this time, NO. 3, NO. 8 and NO. 13 on the downwind side of the original coal miner driver began to spray; spray time is the same as 30s. Along with the shearer, the stent spray opens one by one.
2. When the shearer cuts coal downstream, NO. 5, NO. 10 and NO. 15 spray device on the leeward side of the coal miner driver tracking the shearer, the spray time is 30s. The circulating mode is the same as above.

3.5 *The improvement of closed system among hydraulic support*

There is not too many protection measures in this aspect in #131419 working face which result in the dust concentration increases rapidly when moving the hydraulic support. According to measure, the concentration of respirable dust is highest after 5 meters of moving hydraulic support and is up to 129 mg/m^3. In order to reduce the amount of dust when moving hydraulic support, the author has done experiments of closed system among hydraulic support to dust source in #131419 working face.

(1) The material of closing dust source between hydraulic supports. According to the performance of hydraulic support, the field conditions and industrial reality also satisfied the closed material characteristics to dust source. The original materials have been chosen as follows: a tank chain sheet structure made of zero copper; knitted rubber rope net structure; high elastic fibers (spandex); high elastic bandage; a rubber band, rubber (board).

Through the market survey and feasibility analysis, we decide to use rubber, rubber wire with the elastic bandage and spandex fabric as elastic material to the closed device. It is seen from surface, there is a great difference between various materials, rubber has several features such as good elasticity, good sealing, no net export, but easy to tear, and the performance would reduce when adding flame retardant. At the same time, elastic bandage resists tearing, easy installation, easy to add conductive wire, but the flame is not good and the dust effect is not good. It is very difficult to find the appropriate size of the loom in the testing phase.

By collecting the related information widely on the elastic material exploring in-depth on domestic rubber industry and textile industry, we preliminarily determine using rubber, rubber thread, and

spandex. Based on understanding of domestic rubber and textile industry technology, through laboratory experiments, including the determination of stress-strain properties, tensile fatigue properties, electrical properties, abrasion resistance and flame retardant properties, and finally we choose the elastic rubber silk bandage material as the appropriate closed material.

(2) The design plan for closed system among hydraulic supports. The material for dust separation is made of high elastic bandage and iron clamp assembly. The performance of closed dust source device demands high standard on chemical and physics performance such as strength, elasticity, flame retardant, antistatic, and corrosion. According to the factors of low temperature underground, humid conditions and the motion characteristics hydraulic support, the high elastic bandage was preferred to as dust prevention materials. The high elastic bandages are made into trapezoid whose length is between 1.6–2 meters. At the same time, in order to avoid the punch local shear connection of the bandage and angle iron too much, ensuring the closed dust source device durable, these were connected by the iron clamp. The iron clamp can wrap the bandage edge that can avoid stress concentrating in a vulnerable area, and can transform it into the edge with the bandage iron clamp of the shear stress, to enhance the service life of apparatus.

4 EFFECTS OF OBSERVATION

The improved measures were applied in the fully-mechanized face, the dust removal effect of the working face was observed, as shown in Table 1:

Through observation, after the #131419 working face adopted the optimized dust removal system, the efficiency of reducing dust reached 80%, while using the traditional dust removal methods, such as ventilation and dust control, could only reach about 40%, so the optimized dust removal system can better improve the working environment, and it could be more beneficial to the health of workers, and provide guarantees for the safety production of coal mine.

Table1. Comparison of before and after optimization.

Position of the observation	The original concentration/mg·m^{-3}	The optimized the concentration /mg·m^{-3}	Efficiency of dust-fall/%
The unde end of face	16.44	3.32	79.8
10 m away from working face	16.84	3.54	78.9
Face site of shearer driver	58	11.58	80.0
The upper end of face	22.04	4.39	80.0

ACKNOWLEDGEMENTS

This work is supported by the National Natural Science Foundation of China (No. 51174209) and the Fundamental Research Funds for the Central Universities (CUMTB, No. 2009QZ06).

REFERENCES

Jiang, G.X. 2010. The comprehensive dust technology of fully mechanized top coal caving mining face. *Hebei Coal* (6):26–28.

Kou, L.W. et al. 2011. Fully Mechanized Caving Face Spray Dust Removal Technology and Its Application. *Industrial Automation* (1):75–77.

Mao, J. & Bi, C.F. 2006. Research on improvement of shearer spray device. *Mining Machinery* (9):24–25.

Ren, H.H. et al. 2011. Dust control technology of fully mechanized top-coal caving working face in chengzhuang mine. *The Mine Safety and Environmental Protection* 38(3):57–59.

Shen, J.W. 2010. A research on a highly efficient dust suppression technology used in a longwall face in Zhaozhuang Coal Mine.*China Coal* 36(4):96–98.

Wang, X.Q. et al. 2008. Analysis on Spraying Nozzle and Design. *Coal Mine Machinery* (3):15–16.

Zhao, Z.B. 2008. Physicochemical properties of magnetized water and coal seam injection mechanism. *Journal of Liaoning Technical University (Natural Science)* 27(2):92–94.

Zhao, H.Z. & Chang, H.H. 2003. Improvement in MG200 Coal conversion spray system. *Shanxi Coal* 23(1):49–50.

Zhou, G. et al. 2009. Optimal Design of Dust-settling Device by Water Spraying for Power Support in Full Mechanized Caving Face Annually Producing 6 Million Tons of Coal. *Journal of Shandong University of Science and Technology* 28(4):82–86.

This page intentionally left blank

Progress in Mine Safety Science and Engineering II – He et al. (Eds)
© 2014 Taylor & Francis Group, London, ISBN 978-1-138-00122-0

Risk analysis of 18 kinds of coal spontaneous combustion at Huanghua port

J.S. Zhang, S.M. Wang, X.L. Zhang & H.Q. Xiong
China University of Mining and Technology (Beijing), Beijing, China

ABSTRACT: In order to select 6 kinds of coal which are large spontaneous combustion tendency used in experimental study and analysis of the storage in the 3nd silo at Huanghua port, storage coal evaluation modal is established to compare the spontaneous combustion tendency of all 18 kinds of coal. The results show that properties indicators suitable for the quantitative analysis are selected from many factors that influence the coal spontaneous combustion, establishing evaluation system to analyze the storage coal tendency of spontaneous combustion at port; the 4 selected coal internal indicators can be used to establish fuzzy evaluation factors and then evaluation degree of coal spontaneous combustion; the 6 selected kinds of coal are suitable for storage in the 3nd silo and provide support for the experimental study and security storage period calculated in later.

1 INTRODUCTION

Huanghua port has completed 3nd silo construction of the coal storage system. Compared to the yard storage, silo closure and low heat dissipation are more likely to appear high temperature. This requires to explore the coal's which are stored in silo oxidation process and safety storage measures. Beause Huanghua 3nd siol are the largest group of coal storage system now, and can draw lessons from foreign related case is less, given the above situation, we need to select the appropriate coal used in experimental study and analysis.

Now some researchers studied on the tendency of coal spontaneous combustion which occur in goaf (Cao 2009, Shi et al. 2001, Lu & Geng 2009, Yu et al. 2004), mine(Ding & Di 2005) and coal mining working face(Deng et al.2011). Methods including Grey Relational Analysis (Wu et al. 2011), Grey Slope Relational Analysis (Jin et al. 2012), Fuzzy Evaluation (Ding & Di 2005, Deng et al. 2011, Zhou & Qi 2011) and so on, but little research for storing coal's comparison of spontaneous combusion tendency, and there do not have a unified, comprehensive evaluation indicator system. Taking into account tendency of coal spontaneous combustion cotains some vague, ambiguous terms, this paper which combines academic study and practical experience in the production establish an evaluation indicator system of Huanghua port's coal, and then vague comprehensive evaluation model on the tendency of those coal spontaneous combustion to select 6 kinds of suitable coal. The method combines with the characteristics of coal to determine the indicator weight and to ensure scientific and accuracy of evaluation conclusion through the fuzzy calculation.

2 ANALYSIS ON SPONTANEOUS COMBUSTION

2.1 *Coal introduction of Huanghua port*

A total of 18 kinds of coal at Huanghua port, mainly contains Low ash coal, Shenyou series coal, Waigou series coal, Meager lean coal and Shenhun series coal, in those coal, Waigou series come from collaborative coal mines, while others from coal mine which belongs to Shenhua group.

2.2 *The influencing factors of storage coal spontaneous combustion*

This paper studies the size of storing coal spontaneous combusion tendency at Huanghua port, so external factors are not taken into account. Based on the mechanism of coal spontaneous combustion (Wang 2007), The internal factors of coal spontaneous combustion are the metamorphic degree of coal, the composition of coal rock, the sulfur content in coal, the particle of coal, the pore characterisitic, the degree of crushing, the gas content in coal and the moisture content (Wu et al. 2011, Wang 2007). Now analyze the effect degree of different factors on coal spontaneous combustion.

1. The sulfur content in coal. Sulfide majority of pyrite in coal, the chemical equation in burning of sulfide and element sulfur is:

$S+O_2 = SO_2$

$4FeS_2+15O_2+2H_2O = 2Fe_2(SO_4)_3+2H_2SO_4$

Both of those chemical reaction equations are exothermic reaction, and when the products meet water, they will combine with strong oxidizing acid and release large amounts of heat. A huge amount of thermal accelerate the speed of coal oxidation, thus promote the spontaneous combustion. The study found that under the condition of the same coal property, the higher sulfur content, the easier oxidized(Wen et al. 2011).

2. The grade of coal. Coal grade indicates the metamorphic degree of coal, commonly said by volatile content. The lower the coal quality, the higher the content of volatile, while at the room temperature oxidation of coal are mainly depends on the content of volatile. According to the observations and statistics, even under the same conditions of open storage, taking incidence of spontaneous combusion into account, high volatile content coal is twice bigger than low volatile content coal (Wang 2004).
3. The moisture content in coal. How much moisture content in coal on the influence degree of the coal spontaneous combustion are different. Lab studies have shown that when the moisture in coal is lower than 12%, the moisture will produce wet heat to promote spontaneous combustion, but when the moisture in coal more than 12%, due to large amounts of water evaporation remove heat and spontaneous combustion tendency decline (Wang 2004, Zhou & Wen 2009). The Huanghua port coal moisture is greater than 12%, so the moisture for this port of coal spontaneous combustion is suppressed.
4. The ash in coal. The coal ash is a residue when coal sample complete combustion under prescribed condition. It is an important indicator in the study on the characteristics and utilization of coal quality. Coal ash can reduce coal oxidation heat per unit of mass, while the higher the coal ash, the lower the effective yield of carbon, then the more difficult to spontaneous combustion of coal.
5. The particle size of coal. As can be seen from the port date in Table 1, the particle size of 18 species coal is roughly same in Huanghua port. So the effect of particle size are the same on all coal spontaneous combustion at Huanghua port, hence this factor can disregard.

Moreover, the gas content in coal belongs to the nature of coal rock, but research object for the port storage of coal in this paper, so don't consider the influence of the coal gas content in coal spontaneous combustion.

3 THE ESTABLISHMENT OF EVALUATION SYSTEM

Fuzzy comprehensive evaluation method which based on fuzzy mathematics is a method of quantitative evaluation. According to the features of Huanghua port and characteristics of storage coal, through the selection of evaluation subset, setting of remark set, and the decision of membership degree, establish evaluation system for this port coal.

3.1 *Determination of factors in evaluation*

Because there is no national standands on impact indicators for storage coal spontaneous combustion, the impact indicators is more variety and the influence is bad master of coal spontaneous combustion, so it is particularly important to develop an evaluation system for storage coal spontaneous combustion. According to the analysis of influencing factors on coal spontaneous combustion of the port, establish factor set X = {moisture, ash, volatile, sulfur}. Research found that the coal composition content record in the form of interval, in order to ensure accuracy and convenience of quantitative research results, by using averaging method to determine the content of composition and then to number different kinds of coal. Eeach component content of 18 kinds of coal as shown in Table 1.

3.2 *To determine the weight of line matrix A*

In comprehensive evaluation, taking into account the influence degree of each indicator for coal spontaneous combustion is different. Therefore it is necessary to determine the weight of each influence factor, according to literature (Jin et al. 2012, Wang 2007) and analysis of the evaluation factors can determine the weight of line matrix A = [0.2, 0.1, 0.4, 0.3].

3.3 *To calculate membership function and establish a matrix of fuzzy relation*

For spontaneous combustion tendency of storage coal at Huanghua port, X represents the evaluation set while Y represents remark set.

X = {moisture x_1, ash x_2, volatile x_3, sulfur x_4};

Y = {easy spontaneous combustion y_1, spontaneous combustion y_2, possible spontaneous combustion y_3, not spontaneous combustion y_4};

Based on the fuzziness of coal spontaneous combustion standard, it is reasonable to use the membership which is determined by membership function division classification boundary. Combined with moisture, ash, volatile, sulfur, a total of 4 internal indicators on effect of coal spontaneous

Table 1. Quantification of the content of 18 kinds of coal.

Number	Coal type	Moisture	Ash	Volatile	Sulfur	Particle size
1	Low ash coal	16	7	34.0	0.4	25
2	Shenyou 1–5800	13	12	28.0	0.4	25
3	Shenyou 2–5800	17	12	34.0	1.0	25
4	Shenyou 3–5800	15	13	34.0	1.0	25
5	Waigou 1–5500	17	12	27.5	0.65	25
6	Waigou 2–5200	20	16	25.5	0.75	25
7	Waigou 3–4800	20	30	26.5	1.0	25
8	Waigou 4–4500	15	35	26.5	1.0	25
9	Waigou 5–4200	12	40	26.5	1.25	25
10	Meager lean coal 1–5200	15	28	15.0	1.0	25
11	Meager lean coal 2–4800	15	35	15.0	1.0	25
12	Meager lean coal 3–4500	10	40	15.0	0.8	25
13	Meager lean coal 4–4200	10	45	28.0	0.8	25
14	Shenhun 1–5500	17	12	25.5	0.55	25
15	Shenhun 2–5200	20	16	25.5	0.65	25
16	Shenhun 3–4800	20	20	25.5	0.65	25
17	Shenhun 4–4500	25	20	24.5	0.75	25
18	Shenhun 5–4200	28	15	25.0	1.0	25

Table 2. Membership degree of different coal's evaluation factors.

Number	Coal type	Moisture x_1	Ash x_2	Volatile x_3	Sulfur x_4
1	Low ash coal	0.63	0.99	0.93	0.29
2	Shenyou 1–5800	0.77	0.86	0.66	0.29
3	Shenyou 2–5800	0.59	0.86	0.93	0.36
4	Shenyou 3–5800	0.68	0.84	0.93	0.36
5	Waigou 1–5500	0.59	0.86	0.66	0.47
6	Waigou 2–5200	0.45	0.77	0.57	0.54
7	Waigou 3–4800	0.45	0.46	0.62	0.72
8	Waigou 4–4500	0.68	0.34	0.62	0.72
9	Waigou 5–4200	0.81	0.23	0.62	0.90
10	Meager lean coal 1–5200	0.68	0.50	0.10	0.72
11	Meager lean coal 2–4800	0.68	0.34	0.10	0.72
12	Meager lean coal 3–4500	0.90	0.23	0.10	0.54
13	Meager lean coal 4–4200	0.90	0.14	0.66	0.54
14	Shenhun 1–5500	0.59	0.86	0.57	0.40
15	Shenhun 2–5200	0.45	0.77	0.57	0.47
16	Shenhun 3–4800	0.45	0.68	0.57	0.47
17	Shenhun 4–4500	0.23	0.68	0.53	0.54
18	Shenhun 5–4200	0.09	0.80	0.53	0.72

combustion tendency, according to the averaging method defines the respective membership functions on the remark set Y. Because the effect of moisture and ash to coal spontaneous combustion at this port is in reverse, its membership functions need to take the opposite values. The indicators of membership function are as follows.

$$X_1(x)=\begin{cases}0.1 & x=10\\ 1-\left[0.1+(x-10)\times\dfrac{0.9}{30-10}\right] & 10<x<30\\ 1 & x=30\end{cases}$$

$$X_2(x)=\begin{cases}0 & x=6\\ 1-(x-6)\times\dfrac{1}{50-6} & 6<x<50\\ 1 & x=50\end{cases}$$

$$X_3(x)=\begin{cases}0.1 & x=15\\ 0.1+(x-15)\times\dfrac{0.9}{35-15} & 15<x<35\\ 1 & x=35\end{cases}$$

$$X_4(x)=\begin{cases}0 & x=0\\ x\times 0.9\div 1.25 & 0<x<1.25\\ 0.9 & x=1.25\end{cases}$$

For the evaluation of 18 kinds of coal sanple consider moisture, ash, volatile and sulfur for single factor evaluation, so can use the fuzzy matrix respresents the relationship between X and Y. Then evaluation matrix R can be get.

R =

$$\begin{bmatrix}
0.63 & 0.77 & 0.59 & 0.68 & 0.59 & 0.45 & 0.45 & 0.68 & 0.81 & 0.68 & 0.68 & 0.90 & 0.90 & 0.59 & 0.45 & 0.45 & 0.23 & 0.09\\
0.99 & 0.86 & 0.86 & 0.84 & 0.86 & 0.77 & 0.46 & 0.34 & 0.23 & 0.50 & 0.34 & 0.23 & 0.14 & 0.86 & 0.77 & 0.68 & 0.68 & 0.80\\
0.93 & 0.66 & 0.93 & 0.93 & 0.66 & 0.57 & 0.62 & 0.62 & 0.62 & 0.10 & 0.10 & 0.10 & 0.66 & 0.57 & 0.57 & 0.57 & 0.53 & 0.53\\
0.29 & 0.29 & 0.36 & 0.36 & 0.47 & 0.54 & 0.72 & 0.72 & 0.90 & 0.72 & 0.72 & 0.54 & 0.54 & 0.40 & 0.47 & 0.47 & 0.54 & 0.72
\end{bmatrix}$$

According to the weight vector A, weight of moisture, ash, volatile and sulfur can be get which are 0.2, 0.1, 0.4, 0.3 respectively. thus

$n\neq 1$, A = [0.2, 0.1, 0.4, 0.3]

A is a fuzzy set of evaluation factor set X, by using fuzzy transform.

B = AR

= [0.68, 0.59, 0.68, 0.70, 0.61, 0.56, 0.60, 0.63, 0.71, 0.44, 0.43, 0.41, 0.62, 0.55, 0.54, 0.53, 0.49, 0.53]

Here, B for fuzzy sets on the comment set Y, is the comprehensive evaluation results. The order of spontaneous combustion of 18 species coal sample by B is:9# coal, 4# coal, 3# coal, 1# coal, 8# coal, 13# coal, 5# coal, 7# coal, 2# coal, 6# coal, 14# coal, 15# coal, 16# coal, 18# coal, 17# coal, 10# coal, 11# coal, 12# coal.

4 THE EVALUATION RESULTS AND DISCUSSION

According to the fuzzy relation matrix analyse the degree of coal spontaneous combustion danger of Huanghua port.

1. 1# coal which is called low ash coal spontaneous combustion tendency is quite high, but the port date shows that the storage and export capacity of such coal is less and is not stored in silo. So the size of the spontaneous combustion of such coal can not consider.
2. From the date of port, the waigou series coal are stored in the yard, so should exclude the influence of 9# coal, 8# coal, 7# coal and 6# coal.
3. For the meager lean coal, because of its low volatile content and high ash content, the spontaneous combustion tendency of this coal is lower than those of other types. By fuzzy comprehensive evaluation can also be seen that the ranking of spontaneous combustion tendency is low of this coal, so can eliminate the meager lean coal, that is, excluding 13# coal, 10# coal, 11# coal, 12# coal.

Based on the above three circumstances, the spontaneous combustion tendency of port coal is: 4# coal, 3# coal, 5# coal, 2# coal, 14# coal, 15# coal, 16# coal, 18# coal, 17# coal. this need 6 kinds of coal, so we should select larger coal spontaneous combustion tendency as experimental coal. Both 3# coal and 4# coal are shenyou series coal and they are similar to the possibility of fire, so select one of the two as the experimental coal, in this experiment 3# coal is selected. According to the above analysis, larger of spontaneous combustion tendency and selected as experimental coal are: 3# coal, 5# coal, 2# coal, 14# coal, 15# coal, 16# coal. They are shenyou 2, waigou 1, shenyou 1, shenhun 1, shenhun 2, shenhun 3.

Through the work mentioned above, storage coal spontaneous combustion evaluation system, evaluation factors and quantitative evaluation method are initially obtained. Through exploration solve the evaluation problem of coal spontaneous combustion tendency of port. In this paper, the results selected six kinds of coal can use for the later experimental study on its performance, and simulation study on its storage in silos. Provide support for the security operation of 3nd silo in Huanghua port.

5 CONCLUSION

1. This paper analyzes and builds the spontaneous combustion tendency fuzzy comprehensive evaluation system of port storage coal, completed quantitative evaluation analysis of 18 kinds of coal in Huanghua port. Results show that this evaluation system can be used to assess the capacity of coal spontaneous combustion of storage coal.
2. To select moisture, ash, volatile and sulfur 4 internal indicators which influent port storage of spontaneous combustion, can be used to evaluate the spontaneous combustion tendency of port coal storage. Geological conditions and external factors have little use to coal spontaneous combustion tendency of port, so it does not take into account in the selection factors.
3. Analysis on the assessment results found that the order of larger capacity of port storage coal and higher tendency of coal spontaneous combustion is: Shenyou 2, Waigou 1, Shenyou 1, Shenhun 1, Shenhun 2, Shenhun 3.

ACKNOWLEDGEMENTS

This work is supported by the National Natural Science Foundation of China (No. 51174209) and the Fundamental Research Funds for the Central Universities (CUMTB, No. 2009QZ06).

REFERENCES

Cao, M. 2009. Study on Evaluation of Coal Spontaneous Combustion Risk. Anhui: Anhui University Of Science & Technology.

Deng, J. et al. 2011. Fuzzy Clustering and Pattern Recognition of Characteristic Information in Coal Spontaneous Combustion. *Journal of Xi'an University of Science and Technology* 31(5):505–509.

Ding, D.T. & Di, X.Q. 2005. Study on Multilevel Fuzzy Comprehensive Evaluation Method for Danger of Mine Spontaneous Fire Disaster. *Coal Science and Technology* 33(3):58–60.

Jin, M.Y. et al. 2012. Grey Correlation Degree Analysis for the Weight of Coal Spontaneous Combustion Influencing Factors. *Safety in Coal Mines* 43(12):173–176.

Lu, G.B. & G, M. 2009. Spontaneous Combustion of Coal Mined-out Area and Its Mechanism of Control Research. *Journal of Liaoning Technical University (Natural Science)* 28(9):28–30.

Shi, B.M. et al. 2001. Comprehensive Evaluation and Application of Coal Spontaneous Combustion. *Mining Safety & Environmental Protection* 28(6):1–3.

Wang, D.M. 2007. Mine Ventilation and Safety. Xuzhou: China Mining University Press.

Wang, J.H. 2004. Discussion on the Cause Analysis and Control Measures of Coal Spontaneous Combustion in Thermal Power Plant. *China Occupational Safety and Health Management System Certification* 1:60–61.

Wen, H. et al. 2011. Experiment Research on Effect of Sulfur on Characteristic Parameters of Coal Spontaneous Combustion. *Safety in Coal Mines* 42(10):5–7.

Wu, Z.Y. et al. 2011. Grey Slope Correlation Degree Analysis of Coal Spontaneous Combustion Affecting Factors. *Safety in Coal Mines* 42(3):109–112.

Yu, M.G. et al. 2004. Evaluation and Analysis Influential Factors of Coal Spontaneous Combustion in Wuda Mine Goaf. *China Safety Science Journal* 16(4):97–100.

Zhou, J. & Kang, W.C. 2009. Study on Causes of Coal Spontaneous Combustion and the Countermeasures. *Railway Freight Transport* 12:24–26.

Zhou, X.H. & Qi, Q.J. 2011. Fuzzy Comprehensive Evaluation of the Spontaneous Combustion Tendency of Coal. *Coal Geology & Exploration* 39(6):16–19.

This page intentionally left blank

Progress in Mine Safety Science and Engineering II – He et al. (Eds)
© 2014 Taylor & Francis Group, London, ISBN 978-1-138-00122-0

An LCA-based health damage evaluation method for coal mine dust

Ruipeng Tong & Yabing Zhai
Faculty of Resources and Safety Engineering, China University of Mining and Technology (Beijing), Beijing, China

Xiaodong Li
Department of Construction Management, School of Civil Engineering, Tsinghua University, Beijing, China

ABSTRACT: The health problems caused by coal mine dust are growing worse, causing mine workers serious health damages as well as economic losses. This study is based on the Life Cycle Assessment (LCA) and the coal mine unit process decomposition method, which are combined with the related environmental health and pathology. This study establishes the type indicators of coal dust health damage through collecting coal dust inventory data and it builds an assessment model that uses the health injury factors and the damage quantitative indicators. A monetization analysis is then used as the basis of a quantitative evaluation method that contains a collection of the inventory data, the type indicators of health damage, and the comprehensive quantitative values of health damage. After the application of this method within the coal mine, this study then goes on to examine society's willingness to pay for health damage caused by dust is obtained in both construction and production industries. This study shows that this method is able to quantitatively assess the extent of health damage caused by dust in the mine life cycle. Consequently, it can be used as the basis for decision making and can be provided for the use of the management of mining occupational health

1 INTRODUCTION

The effects of economic globalization mean that the health and safety damage in many workplaces is getting worse. Many developing countries in the global economy are undergoing occupational accidents and occupational diseases that arise because of rapid industrialization. Mining plays a significant role in rapid economic development. Indeed, it is one of the most important industries promoting global economic development. However, poor working conditions and serious hazardous substances in the mines can lead to a high incidence of occupational diseases, which are a serious threat to the workers' safety. China is currently the world's major coal production center. It is also one of the most affected countries by industrial disease and it suffers the world's highest incidence of occupational diseases that have been caused by the coal industry (Zou, C.Q. & Shao Q., 1999; Chen, W.H., 2006). In 2010, China's coal mines had the largest number of occupational disease cases when compared with the country's other industries. There were a total of 13968 cases of emerging diseases, accounting for 51.28% of the total number of cases (Li, F.X., 2011). Harmful toxic factors in the coal mines include mainly physical factors (such as dust, noise, heat, and hand-transmitted vibration) and toxic substances (such as CO, CO_2, SO_2, NO_2 and H_2S). However, coal dust is the most important factor among all of these harmful factors (Ai, H, 2012). For example, pneumoconiosis is an industrial disease that is caused by coal dust; it is also the major occupational disease in the coal industry accounting for about 50% of China's total cases of pneumoconiosis. The increasingly serious health damage caused by coal dust has attracted the attention of both domestic and foreign scholars and a large body of research has been conducted on this problem.

Some developed countries (such as the U.S., UK, and Australia) have had perfect researches on the health damage caused by coal dust. For example, in addition to related legislation, these studies have shown that the establishment of an occupational health management system can effectively control the incidence and mortality rate of coal mining occupational diseases. For example, Australia had set up a statutory body called *The Joint Coal Board* to control the incidence of pneumoconiosis and achieves good results. The Australian pneumoconiosis detection rate has gone from 16.0% in 1948 down to 0.5% in 2000 (Kizil, G.V. & Donoghue, A.M., 2002). Donoghue uses the *risk = probability × consequence* formula to conduct a risk assessment of the elements of coal mining that can cause damage (Donoghue, A.M., 2000). He also uses this formula to achieve a semi-quantitative method

for each risk factor, which are sorted according to the different degrees of harm. His results show that coal dust causes the most serious damage to the health of coal miners. Research has also been carried out on the relationship between the mechanism of occupational diseases and mortality, which is based on health pathology. For example, in the UK, Miller (Miller, B.G.1985) and Mcvitte (Mcvitte, J.C.1990) studied the public health and epidemiological effects of pneumoconiosis from a medical point of view and they proposed that there was a relationship between pneumoconiosis pathology and mortality. Many developed countries started to research the health damage caused by coal dust quite early in the history of the coal industry. Consequently, they established occupational health management systems and evaluation methods to a relatively sound level.

There are many domestic studies of the damage that coal dust does to health. The main themes of the current studies are listed below, including a brief description of their contents and deficiencies:

- Most analysis conforms to the status quo of the damage that coal dust causes to health, including the morbidity, and mortality of pneumoconiosis.
- Some studies find that there are problems that arise during the current domestic prevention of coal dust underground and in the control of pneumoconiosis. These studies have proposed a number of appropriate measures to improve this situation, including government and corporate management improvements, and the establishment of an occupational health management system.
- However, most of these studies conduct a qualitative discussion of the damage that coal dust does to the health of miners. Consequently, they lack a systematic theoretical and empirical analysis, and quantitative evaluation of the risk factors.
- Most of these studies have only focused on the health damage coal workers may suffer during the coal production and they lack an overall view of the full life cycle assessment. Consequently, their view of the prevention and the range of occupational injury are too narrow.

The LCA theory contains four phases, which are: definition of the purpose and scope of the study, inventory analysis, impact assessment and interpretation of the results (Ge, J. & Gong, M., 2008). Many studies in China have used the LCA theory in construction, agriculture, air conditioning manufacturing, automobile manufacturing, waste disposal and other fields. However, these studies have tended to focus on the size of the environmental impact analysis and they have rarely taken health damage into account. In view of this, this study will use LCA theory to assess the health damage caused by coal dust. Consequently, by expanding the assessment scope and the content of the study we can achieve new ideas for the quantitative evaluation of coal dust exposure.

2 THE ESTABLISHMENT OF DUST HEALTH DAMAGE EVALUATION SYSTEM IN COAL MINES

2.1 *Unit resolution and scope determination*

The decomposition research of the unit stage is very important to integrally collect the dust emissions in each stage of coal's life cycle. Combined with the actual situation of coal mines in China, the life cycle of a coal mine can be divided into: an exploration and construction stage, a production stage, an expansion stage, and a scrap processing stage (Fig 1). Although coal dust is emitted throughout the whole life of a coal mine, the quantity of pollution is unequal in each of the stages. Consequently, this study decomposes the unit of mine life cycle. To provide a basis for controlling measures, reverse tracking of the evaluation results is used to get the main components of health effects during application in a specific evaluation.

2.2 *Inventory analysis*

This study uses inventory analysis to identify and collect the inputs and outputs of the coal mine life cycle (e.g. the input of energy and material, output of dust, CO_2, and SO_2). According to the dates collected, the inventory date can be transferred into the total resource consumption and emissions of harmful substances. Without immediately connecting with the input of energy and materials in the construction and production period, coal dust is mainly caused by coal and rock crushing. Therefore, the dates of total dust emission, dust concentration in each stage, population density in each working location, space model area and the duration of the occupational disease will be collected, and the output of energy and materials will not be considered.

It should be noted that these coal mines lack relevant date records in the total emission of coal dust. The main dust production sites underground are: heading face, coal working face, shotcreting operating point, and transfer point. The dust is imported into the return air shaft through wind currents and indirect total dust emissions can be achieved as long as we get the dates of dust concentration in the air shaft and in the total return air volume.

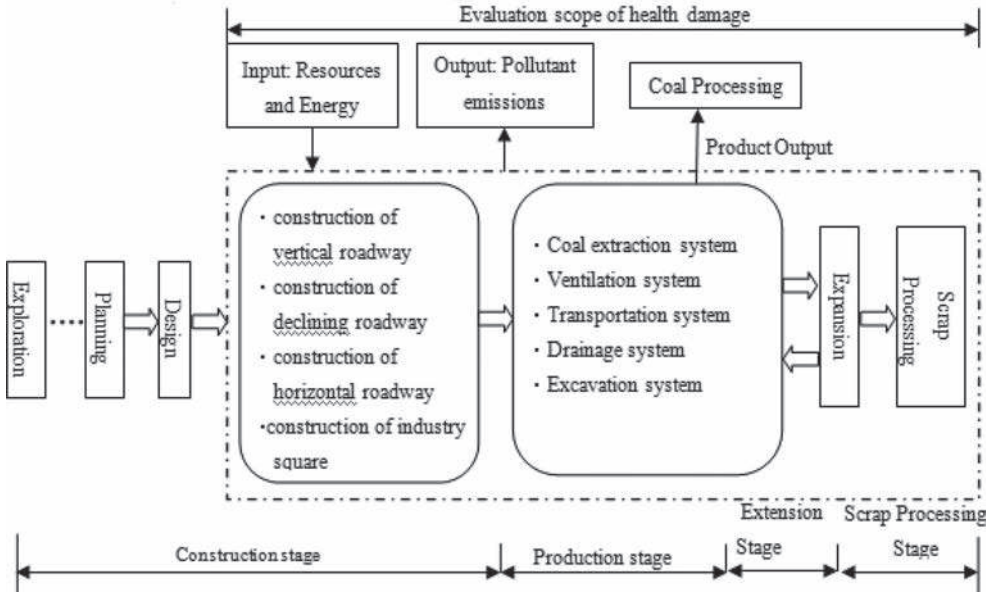


Figure 1. Evaluation of a coal mine life cycle.

2.3 *Impact assessment*

Impact evaluation has been considered to have the highest technical content, to be the most difficult, and also to be the most imperfect link of the four stages in LCA, whose main aim is classification, characteristic and quantitative. Currently, there is no clearly unified evaluation criterion between inventory dates and health damages(Gao, F., 2008). Therefore, it is important to establish a set of comprehensive and quantitative methods to transfer inventory dates into health damages.

2.3.1 *Classification*

Coal dust can lead to many health damages, such as pneumoconiosis, chronic obstructive pulmonary disease (COPD), cardiovascular disease, cerebrovascular diseases and acute respiratory infections (ARI), which all belong to diseases of the respiratory system. Therefore, the health damages caused by dust are classified into respiratory system related damage indicators.

2.3.2 *Characterization*

Characterization is able to help us choose a way to measure the impact of coal dust on the human body at various stages by quantifying the impact of dust into the same shape or by size of the same unit (Deng, N.S. & Wang, X.B., 2003) so that the severity of health damage caused by dust can be seen intuitionally. This method uses the disability adjusted life years (DALY) (WHO, 1987) to characterize dust damage to the human body because the DALY has a high degree of universality and monetization potential for various diseases (Murray, C J., 1994). Then, to convert the incidence of health damage terminal into the same quantitative indicator, impact pathway analysis (IPA) is used to determine the equivalent factor between different pollutants and quantitative indicator.

IPA can quantify the impact of substances on human health by tracing the active path of various pollutants in its life cycle. The IPA has three steps: fate analysis, effect analysis and injury analysis. Fate analysis places the health damage factors that are collected in the inventory analysis into a concentration of added value within the scope of the research space because (according to the research results of pathology) most of the quantitative analysis of relationship between the concentration of harmful substances and health damage terminals are studied in pathology. Effect analysis translates the concentration's diversification of health damage factors into the morbidity's diversification of health damage terminal and it is based on the results of epidemiological studies. Injury analysis translates the morbidity's diversification of health damage terminals into the added value of quantitative indicators (i.e. DALY). Consequently, IPA can ultimately convert coal dust emissions into the value of quantitative indicators of health damage by establishing an equivalent relationship between dust emissions and quantitative indicators.

• *Fate analysis*

The destination factor is an important parameter in fate analysis. It is a ratio between the added value of pollutant concentration in a specific environment and the annual emissions of pollutants in the same environment. The fate factor F_i is calculated as follows:

$$F_i = C_i / M_i = 1/f_0 \quad (1)$$

Where C_i is the added value of dust concentration in the air, μg·m^{-3}; M_i is the dust emissions form mine phased in a year, μg; f_o is the amount of air exchange between the inside and outside of the coal mine in a year, m^{-3}/a. Since the mine has a separate ventilation system, the annual ventilation rate of a coal mine can be regarded as the amount of air exchange.

We can then put the annual emissions of pollutants into the added value of pollutant concentration in the range of research space by using the destination factor. The conversion formula is as follows:

$$C_i = F_i \times M_i \quad (2)$$

• *Effect analysis*

Epidemiological studies often use unit risk factor (URF) to characterize the quantitative relationship between the pollutants and the health damage effects. The URF is a person's added value of number of cases of health damage terminals, which are caused by increasing the unit concentration of pollutants in their living environment. The URF can obtain the added value of number of cases of health damage terminals that is caused by increasing the unit concentration of dust in life cycle of the coal mine, which is considered as effectors. URF is calculated as follows (Hofstetter, P, 1998):

$$E_{ij} = P_d \times S \times UR_{ij} / L_t \quad (3)$$

Where E_{ij} is the effectors, case (μg·m^{-3}·a); P_d is the population density within the model space, person/m^2; S is the area of space model, m^2; UR_{ij} is the URF of health damage terminal j, caused by dust, case (μg·m^{-3}); and L_t is the average life of the population who are influenced by harmful substances, y (70 years).

The URFs of those health damage terminals have been measured and calculated as shown in Table 1(WHO, 2000):

We can obtain the added value of number of cases of health damage terminals by using the effectors and combining with the results of the fate analysis, which is caused by the emissions of harmful substances in a year. This is calculated as follows (Hofstetter, P, 1998):

$$T_{ij} = E_{ij} \times C_i \quad (4)$$

Table 1. The Unit Risk Factors of those health damage terminals.

Pollutant	Health damage terminals	UR_{ij}
Dust	Pneumoconiosis	7.7E-3
	COPD	6.0E-4
	Cardiovascular	5.3E-4
	Cerebrovascular disease	5.3E-4
	ARI	6.3E-3

Where T_{ij} is the added value of number of cases of health damage terminals, which is caused by the emissions of harmful substances in a year, case/a.

• *Injury analysis*

The DALY concept includes the years of life lost (YLL) and the years of life with disability (YLD), which is calculated as follows:

$$DALY_j = YLL_j + YLD_j \quad (5)$$

Where YLL_j is the YLL that are caused by the health damage terminal j of unit case, y/case; YLD_j is the YLD that are caused by the health damage terminal j of unit case, y/case.

Meanwhile, YLDj is calculated as follows:

$$YLD_j = L_j \times D_j \quad (6)$$

Where L_j is the duration of health damage terminal j, y/case; D_j is the disability weight of health damage terminal j.

The duration of health damage terminal can be determined according to the study of hygiene. The duration of curable diseases is formed from the onset and persists to the cure. The duration of the incurable disease is defined as the lifetime spent sick. The average of the onset of pneumoconiosis is 42 years old, so the average duration of pneumoconiosis is 20 years (Qu, S.Y. & Huang, W.L., 2012). The lifespan of cardiovascular and the cerebrovascular disease is an average of five years less than normal. The durations of related diseases are shown in Table 2:

When calculating YLD, the disability weight is used to assess the extent of damage to health of different disability statuses. A figure of 0 is considered to be completely healthy, a figure of 1 represents death; therefore, the severity of damage to human health caused by other health damage terminals is assigned form 0 to 1. The World Health Organization has identified 22 symptoms that are indicative of disability and their disability weight is used in the Global Burden of Disease Study. This present study determines the disability weight of related diseases based on the Global Burden of Disease Study (see Table 3).

Table 2. The average duration of the health damage terminals.

Health damage terminals	Duration
Pneumoconiosis	20a
COPD	10a
Cardiovascular	25a
Cerebrovascular disease	25a
ARI	14d

Table 3. The disability weight of the health damage terminals.

Health damage terminals	Disability weight (Dj)
Pneumoconiosis COPD	0.25
	0.15
Cardiovascular	0.24
Cerebrovascular disease	0.24
ARI	0.08

Finally the added value of the years of life lost (U) caused by the health damage terminal j, which is aroused by the dust emissions in the space model during a year, can be obtained via equation (4) and equation (5).

2.3.3 *An analysis of weights*

To determine which health damage type indicator gains from character analysis in terms of economic significance, the mine life cycle evaluation system uses the monetization method to determine the weights of each evaluation type. The monetization method has been internationally recognized and it has been applied in a number of systems; for example, the environmental priority strategies (EPS) system and TELLUS (Steen, B, 1996; Tellus Institute, 1992). The monetization method includes the contingent valuation method (CVM), hedonic pricing method (HPM) and willingness to pay (WTP). According to the related research at home and abroad, this study will use WTP. The WTP is the currency value that is willing to be paid to reduce the risk of death and disability. It is also used to measure and quantify the economic burden of diseases that are invisible.

After the fate analysis, effects analysis and injury analysis, an evaluation system will transform inventory analysis results into the size of health damage terminal which indicated by quantitative indicators (i.e. DALY). Weight analysis is to determine the WTP value in the unit's DALY value of life year (VLY), using the method of monetizing to determine the size of health damage terminal. To get VLY, the value of human life should be first determined and then converted into the value of a year of healthy life. The formula for calculating the life value of coal miners is as follows:

$$V_k = K \times D_k \times M_{v+m}/(S \times D) \tag{7}$$

$$K = K_1 \times K_2 \times K_3 \times K_4 \tag{8}$$

Where V_k is the economic value of the lives of miners, D_k is the average working day in their lifetime, M_v+_m is the last year's net output value of the enterprise, S is the last year's average number of employees of enterprise, D is the last year's working of the enterprise, K is the coefficient of the value of life, k_i is a person's coefficient of age, coefficient of level of education, coefficient of post and coefficient of skill levels(i is form 1–4).

Combined with the actual production of the coal mine, we can value K_1 as follows: age between 20–25, then K_1 takes the value of 0.85, age between 26–30, then K_1 takes the value of 0.95, age between 31–40, then K_1 takes the value of 1.0, age between 41–45, then K_1 takes the value of 0.95, age between 46–50, then K_1 takes the value of 0.9; $K_2 = m/22$, m is the somebody's actual education years, if he or she is an illiterate, K_2 takes the value of 0.2;we can value K_3 as following: Mining cadres takes the value of 1.1, district cadres take the value of 1.05, General Workers takes the value of 1.0; we can value K_4 as following: senior professional title takes the value of 1.15, medium grade professional title takes the value of 1.1, the primary title take the value of 1.05, General Worker takes the value of 1.0(Wang, Y.H. & Li, X.Y., 2004).

To determine the WTP value in the unit's DALY, the life value of one year must be calculated again after getting the value of the lives of miners, the equation is as follows:

$$VSLY = \frac{VSL}{\left[1-(1+r)^{-n}\right]/r} \tag{9}$$

Where $VLSY$ is the miner's life value of a year, VSL is the life value of miners, n is the life years that workers expect to remain, r is discount rate which is 4% in this paper (Friedrich, R, 2004).

The VSLY calculated above is the WTP value in the unit's DALY. Finally, the product of the health damage life of miner (U) and the WTP value in the unit's DALY is the monetary loss value of health damage caused by dust (V).

3 APPLICATION TO A COAL MINE

A coal mine in Shanxi Province that is 6.5 km long from north to south, 4.3 km wide from east to west

and covers an area of 19.59 km^2 was selected as the case. Its geological reserve is 259.62 Mt, the design reserve is 200.798Mt, and the developed reserve is 141.623Mt. The annual design production capacity of the mine is 4.0 Mt/a and the length of its service is 35 years. The engineering quantity is 32839.17 m during the mine construction, including the main and auxiliary shaft, return air shaft, shaft station and rock roadway. The central parallel exhaust system was adopted in mine production stage, selecting two BD-Ⅷ-10-No29 contra-rotating axial-flow fans with frequency control; the motor power is 2 × 280kw. In the production phase, the total air flow is 8100 m^3/min, the maximum exhaust air volume of the ventilator is 11000 m^3/min. Since the required air ventilation is less in construction than the production period, the total air volume is also less (about 4000 m^3/min). The coal dust emissions were 112 kg/a and 220 kg/a during the construction phase and in the early period of production. This increased to 140 kg/a using the optimization of coal dust reducing measures in the production period. The mine's net output is RMB680 million in 2012. During the mine's construction period there were on average 100 workers underground. During production the annual staff is about 8120, including about 400 workers on the morning shift, and about 200 workers on the afternoon and evening shift; therefore, the average working number is 300 workers.

The calculation parameters for the health loss of health damage terminal that is caused by coal dust in the construction phase are shown in Table 4.

Table 4 shows that the years of life lost caused by dust emissions in the construction phase is 2.7014 years according to the table above. The society's WTP value is RMB208, 000.

After optimizing the dust measures, the calculation parameters for the health loss of health damage terminal that is caused by the dust in the initial stage of production is shown in the Table 5 and the calculation parameters for the health loss of health damage terminal that is caused by the dust after optimizing the dust measures is shown in the table 6.

Table 5 shows that the years of life lost caused by dust emissions in the initial stage of production is 5.9003 years. The society's WTP value is RMB454, 300.

Table 6. The calculation parameters for the health loss of health damage terminal caused by the dust after optimizing the dust measures.

Table 6 shows that the YLL caused by dust emissions after optimizing the dust measures in the production phase is 3.8035 years and society's WTP value is RMB292, 900.

Table 4. The calculation parameters for the health loss of health damage terminal in the construction phase.

Health damage terminal Unit	F m^{-3}	M μg	E case/(μg·m^{-3}·a)	DALY y/case	U y/a	V ten thousand
Pneumoconiosis	4.8E-10	1.1E+11	1.1E-3	20.0	1.2	9.24
COPD	4.8E-10	1.1E+11	8.5E-4	16.5	0.7	5.39
Cardiovascular	4.8E-10	1.1E+11	7.6E-4	11.0	0.45	3.46
Cerebrovascular disease	4.8E-10	1.1E+11	7.6E-4	11.0	0.45	3.46
ARI	4.8E-10	1.1E+11	9.0E-3	3.0E-3	1.4E-3	1.0E-2
Total					2.7014	20.8

Table 5. The calculation parameters for the health loss of health damage terminal caused by the dust in the initial stage of production.

Health damage terminal Unit	F m^{-3}	M μg	E case/(μg·m^{-3}·a)	DALY y/case	U y/a	V ten thousand
Pneumoconiosis	2.3E-10	2.2E+11	2.5E-3	20.0	2.5	19.25
COPD	2.3E-10	2.2E+11	1.9E-3	16.5	1.6	12.32
Cardiovascular	2.3E-10	2.2E+11	1.7E-3	11.0	0.9	6.93
Cerebrovascular disease	2.3E-10	2.2E+11	1.7E-3	11.0	0.9	6.93
ARI	2.3E-10	2.2E+11	2.0E-2	3.0E-3	3.0E-3	2.3E-2
Total					5.9003	45.43

Table 6. The calculation parameters for the health loss of health damage terminal caused by the dust after optimizing the dust measures.

Health damage terminal Unit	F m^{-3}	M μg	E case/(μg·m^{-3}·a)	DALY y/case	U y/a	V ten thousand
Pneumoconiosis	2.3E-10	1.4E+11	2.5E-3	20.0	1.6	12.32
COPD	2.3E-10	1.4E+11	1.9E-3	16.5	1.0	7.70
Cardiovascular	2.3E-10	1.4E+11	1.7E-3	11.0	0.6	4.62
Cerebrovascular disease	2.3E-10	1.4E+11	1.7E-3	11.0	0.6	4.62
ARI	2.3E-10	1.4E+11	2.0E-2	3.0E-3	1.9E-3	1.4E-2
Total					3.8035	29.29

In the case study above, it can be seen that the years of life lived with disability caused by dust emissions in the construction phase is 2.7014 years and society's WTP value is RMB208, 000. Consequently, the economic significance is that the health damage caused by dust emissions in the production phase is equal to the loss of 2.7014 healthy years and RMB208, 000 is required to be paid to counteract this loss. Consequently, the evaluation result shows that pneumoconiosis is the most serious occupational disease during the total cycle of a coal mine, which is followed by COPD and cardiovascular disease. In addition, the dust health damage of production phase is more serious than that of the construction phase. The health damage after optimizing the dust measures is obviously lower before the improvement. The years of life lost caused by dust in the earthwork construction is 2.61, which is obtained from similar researches in architecture (Zhang, Z.H., 2008), and the value caused by toxic vapors during interior decoration is 0.29 years (Li, X.D. & Gao, Y.X., 2013). Comparing these three values, it can be seen that the coal mine dust inflicts more serious damage.

Since coal mines are generally sealed at the end of their working lives when they move into the scrap processing stage, this stage is less damaging to human health. Consequently, this study has not made a detailed evaluation of this stage.

4 CONCLUSION

This study is able to draw a number of conclusions. In contrast to the methods used in previous studies, this method has been able to apply LCA theory to study the damage that coal dust does to health. It has also been able to identify effects of coal dust throughout the range of a coal mine's full life cycle, including four stages of construction, production, expansion, and scrap processing. The evaluation methods between dust and the degree of health damage terminal are established on the basis of inventory collection.

After determining the health damage caused by dust and willingness to pay values, we find that coal miners experience more years of life lost than construction workers. According to their economic significance and model evaluation, the results indicate that coal dust poses a serious health risk and can cause considerable damage to the human body.

The dust's severity of damage in different stages of coal mine can be seen directly in the evaluation results. In addition, since the unit risk factors of health damage terminal caused by coal dust are different, the years of life lost from these health damage terminals are also different; therefore, we have been able to reach the degree of damage of health damage terminal in each stage.

The degree of health damage caused by coal dust has been significantly cut down since coal mines have taken mitigating measures to cut down on coal dust in the air. This model can be used to evaluate the merits after these measures have been taken.

Our method has used the relationship between the added value of concentration of the damage factors and the disease rate of health damage that is terminal in the epidemiological; however, there are other damage factors (such as the vibration, noise and temperature factors) that are harmful to people because they transmit energy. Consequently, our concentration value cannot be used to represent the amount of freed energy. Therefore, more research needs to be done before this method can be used to measure the health effects of other occupations.

ACKNOWLEDGEMENTS

The work was financially supported by the National Science Foundation of China (No. 51204188) and the Fundamental Research Funds for the Central Universities (No. 2011QZ04).

REFERENCES

Ai, H. (2012). Application of evaluation unit principle of classification in the coal mine occupational hazard evaluation. *China Science and Technology Information* 18:109–110.

Chen, W.H. (2006). Research advances and perspectives of prevention and control of pneumoconiosis in China. *China Personal Protective Equipment* 24 (9):513.

Deng, N.S. & Wang, X.H.(2003). Life cycle assessment. Beijing, *Chemical Industry Press*.

Donoghue, A.M.(2000). The degign of hazard risk assessment matrices for ranking occupational health risks and their application in mining and minerals processing. *Society of Occupation Medicine*: 118–123.

Friedrich, R (2004). New elements for the assessment of external costs from energy technologies. Final Report to the European Commission. Stuttgart: DG Research, *Technological Development and Demonstration (RTD)*.

Ge, J & Gong, M (2008). Life cycle assessment in building load quantitative evaluation. *Nationwide Building Physics academic papers*: 700–704.

Gao, F (2008). Life cycle assessment and its application in China Industry. Beijing, *Beijing University of Technology*.

Hofstetter, P (1998). Perspectives in Life Cycle Impact Assessment: A Structured Approach to Combine Models of the Technosphere, Ecosphere and Valuesphere. Dordrecht, the Netherlands: *Kluwers Academic Publishers*.

Kizil, G.V. & A.M. Donoghue (2002). Coal dust exposures in the longwall mines of New South Wales, Australia: a respiratory risk assessment. *Society of Occupation Medicine* 52 (3):138–149.

Li, F.X. (2011). Mine occupational hazards and countermeasures. *Occupational Health Engineering*:499–501.

Li, X.D. & Gao, Y.X (2013). Health damage assessment of interior decorations based on LCA methodology. *Journal of Tsinghua University* 53 (1):66–71.

Miller, B.G. (1985). Dust exposure, pneumoconiosis, and mortality of coal miners. *British Journal of International Medicine*: 723–733.

Mcvitte, J.C.(1990). Pneumoconiosis in coal miners. *Postgraduate Medical Journal*:618–631.

Murray, C.J. (1994). Quantifying the burden of disease: The technical basis for disability adjusted life years. *Bulletin of the World Health Organization* 72(3):429–445.

Qu, S.Y. & Huang, W.L.(2012). Research for the actuality and analysis for countermeasures of the occupational disease in coal mine. *China Coal Industry Medicine* 15 (4):568–570.

Steen B (1996). EPS-default valuation of environmental impacts from emission and use of resources, version 1996, AFR Report 111. Stockholm: *AFN, Swedish EPA*.

Tellus Institute (1992). The Tellus packaging study. Boston: *Tellus Institute*.

Wang, Y.H. & Li, X.Y.(2004). Study on Economic Evaluation of Life Value Lost in Coal Mine Accident. *China Safety Science Journal* 14 (8):28–30.

World Health Organization, Regional Office for Europe (1987). Air quality guidelines for Europe. Copen hagen: *WHO Regional Publications*.

World Health Organization (2000). Air Quality Guidelines for Europe. Geneva, Switherland: *World Health Organization*.

Zhang, Z.H. (2008). Health impairment due to building construction dust pollution. *Journal of Tsinghua University* 48 (6):922–925.

Zou, C.Q. & Shao, Q. (1999). Contribute to the global elimination of pneumoconiosis. *Journal of Industrial Hygiene and Occupational Diseases* 17 (1): 2–4.

Progress in Mine Safety Science and Engineering II – He et al. (Eds)
© 2014 Taylor & Francis Group, London, ISBN 978-1-138-00122-0

The controlling techniques on floor heave of large cross section mining roadway with complicated surrounding rock

Q.F. Zhao, Y.H. Wang, Y.D. Liu, H.T. Li & J.J. Shi
Key Labaratory of Mine Disaster Prevention and Control of Hebei Province, Sanhe, Hebei, China
Safety Engineering College, North China Institute of Science and Technology, Sanhe, Hebei, China

L.Y. Shi
China Coal Ping-shuo Group Co., Ltd, Shuozhou, Shanxi, China

ABSTRACT: In order to control the severe floor heave of large cross section mining roadway in No. 1 Coal Mine of China Coal Ping-shuo Group Co., ltd, the various controlling measures are simulated by numerical simulation software FLAC, such as floor bolting, pressure-relief groove and floor drilling, and the stress distribution and displacement characteristics of the roadway floor are analyzed in the condition of different measures. Additionally the combinatorial controlling measure of reinforcement method (floor bolting) and pressure relief method (pressure-relief groove) is put forward. The engineering test results show that the maximum displacement and the maximum rate of floor heave are within the controllable range. Thus the combinatorial controlling technique can effectively control the floor heave and keep the surrounding rock stable.

1 INTRODUCTION

The large cross section roadway of the fully mechanized top-coal caving is a special type of roadway affected by mining. This type of roadway is more serious than common mining roadway in the damage of surrounding rock, mainly in the concentration of floor rock horizontal stress and the change of shear stress, especially roadway passes fault, or the distance between two working faces is too small, or the interaction of multiple coal seams is obvious, and so on. (He, M.C. et a1. 2009, Yang, B.S. & Geng, X.L. 2012, Jiang, Y.D. et a1. 2004). In recent years, many scholars at home and abroad carried out the beneficial exploration on the mechanical mechanism of floor heave and the controlling measures in order to control floor heave effectively, such as reinforcement method, pressure relief method and comprehensive treatment method. But the control effect of each method varies widely due to the different engineering geological conditions. (Luo, Y.Q. et a1. 2005, Wang, W.J. & Hou, C.J. 2003, Guo, B.H. & Lu, T.K. 2008).

On the basis of former researches, this thesis tends to continue studying the stress field in floor strata of large cross section mining roadway with complicated surrounding rock, and analyzes the advantages and disadvantages of various technologies for controlling floor heave by using the numerical simulation software FLAC. Additionally the combinatorial controlling technique has been used in the auxiliary haulage roadway of No.4108 fully mechanized top-coal caving working face. The operation results show that this control technique has achieved favorable effects.

2 GEOLOGICAL CONDITION OF MINING ROADWAY

The No. 4108 fully mechanized top-coal caving working face is located in the Tai-xi mining area of No. 1 Coal Mine of China Coal Ping-shuo Group Co., ltd, it is adjacent to No. 4107 working face, its southern part is undeveloped areas, its eastern part is the chain pillar for protecting the haulage entry, its western part is Shi-xi Coal Mine. The length of No. 4108 working face is 2596 m along the strike direction, the width is 300 m along the tilt direction and the surface is hilly land. The ground elevation is from 1284 m to 1409 m, and the working face elevation is from 1050 m to 1170 m. The thickness of No.4 coal seam is from 6.05 m to 11.33 m, its dip angle is from 9° to 11°. The inclined-longwall fully mechanized top-coal caving method is adopted in the working face. The cross-section of auxiliary haulage roadway is gradient trapezoid, sectional width is 5.0 m, and sectional height is 3.4 m. During the period from May to October, 2011, the floor heave which happened in the auxiliary haulage roadway was significant.



Figure 1. Floor heave of auxiliary haulage roadway in No. 4108 working face.

The maximum of floor heave was from 900 mm to 1400 mm, as shown in Figure 1.

3 SIMULATION ANALYSIS OF FLOOR HEAVE UNDER THE ORIGINAL SUPPORTING CONDITIONS

3.1 *The geological background and numerical calculation model*

Numerical calculation model is established by using three-dimensional finite-difference software FLAC to simulate floor heave of large cross section mining roadway in No. 4108 working face. The model length is 250 m along the strike direction, its width is 200 m along the tilt direction and its vertical height is 115 m. Vertical load is applied on the upper boundary of the model according to the static weight of overlying strata. Horizontal constraints are imposed on both sides of the model. Horizontal and vertical constraints are imposed on bottom boundary of the model. Due to the study on mechanical behavior of floor failure, Mohr-Coulomb yield criterion is used to judge rock damage. (Li, Z.G. 2012, Li, X.H. et a1. 2003). The numerical modeling diagram is shown in Figure 2.

3.2 *Simulation analysis of floor heave under the original supporting conditions*

3.2.1 *The original supporting parameters*

The sectional supporting system is bolt-mesh-anchor on the roof of auxiliary haulage roadway. Each row is installed 6 bolts which are made of non-longitudinal reinforcement deformed steel bar, inter-row interval is 900 mm × 900 mm, each row is hung a steel belt, ϕ12 mm × 4600 mm. Anchor cable processed by using steel strand wires, ϕ17.8 mm × 7300 mm, is centered double row arranged, inter-row interval

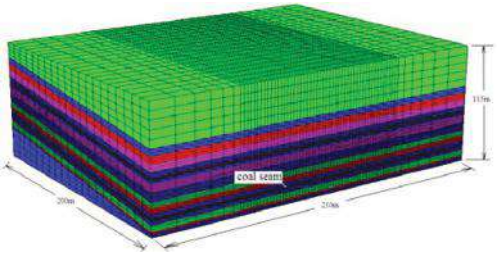


Figure 2. Numerical calculation model.

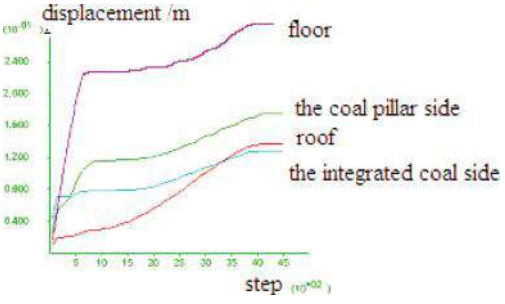


Figure 3. Displacements of surrounding rock.

is 2000 mm × 2700 mm. Each row is installed 3 bolts which are made of ordinary carbon structure round steel in both sides of the roadway, inter-row interval is 1200 mm × 900 mm.

3.2.2 *Simulation results of floor heave*

Before the simulation operation, displacement measuring points are arranged in floor, roof and both sides at different depths (located at 0 m, 1 m, 2 m, 3 m, 4 m) in order to monitor surrounding rock displacement.

First, the floor heave is larger than the amount of both side's convergence and roof sagging, as shown in Figure 3. The floor heave is generally of slope shape with the bigger heave on the coal pillar side and the smaller on the integrated coal side. Due to the large horizontal stress and the constraint role of the integrated coal beside the roadway, laminar floor strata move to free space of mining roadway, resulting in slope shape floor heave in large cross section roadway in the fully mechanized top-coal caving working face. (Gao, M.Z. & Jing, H.Q. 2012). This result is in conformity with the field measurement.

Second, the amount of floor heave at different depths is different. The deformation of floor surrounding rock located in 2 m is bigger. The displacements show a sharp growth trend to the surface of the floor. The floor strata deformation located in 5 m is smaller.

4 NUMERICAL SIMULATION ON THE VARIOUS MEASURES OF CONTROLLING FLOOR HEAVE

According to the actual geological conditions of large cross-sectional mining roadway in No.1 Coal Mine of China Coal Ping-shuo Group Co., ltd, this paper has designed three control schemes for floor heave on the basis of the original supporting parameters. The three schemes are floor bolting, pressure-relief groove and floor drilling. The research results can provide decision-making reference for field implementation.

4.1 *Floor bolting*

Numerical simulation shows that the plastic zones firstly appear in the corners of the floor. The floor heave is mainly caused by the floor strata crowding into roadway and both sides sagging. Therefore, the controlling of the floor corners is very important in large cross section mining roadway.

4.1.1 *Layout scheme*

The type of floor bolts is extension-length anchored, which are made of non-longitudinal reinforcement deformed steel bar, and the angle is 45° between the floor bolt and the horizontal plane.

4.1.2 *The effect on controlling floor heave*

The simulation results indicate that the plastic zones of surrounding rock begin to develop from the floor corners where the scope of plastic zone is biggest. The floor bolts which have been installed immediately after the exposure of surrounding rock improve the floor strata strength, change the regional stress distribution, and reduce the bottom horizontal stress. Therefore the floor bolts play a positive role in resisting floor heave.

4.2 *Pressure-relief groove*

4.2.1 *Layout scheme*

Pressure-relief groove is excavated on the floor near the side of coal pillar. (Sun, J. & Wang, L.G. 2011). Considering the convenience for transportation and pedestrian safety, the groove width is 300 mm. The Figure 4 shows stress distribution and displacement characteristics of floor strata at different depths of the grooves, such as 0.2 m, 0.3 m, 0.5 m, 0.7 m, 1.0 m, 1.3 m, 1.5 m.

4.2.2 *The effect on controlling floor heave*

First, the growing trend of floor heave has been effectively controlled by cutting pressure-relief groove. The floor strata move to the groove free space so as to reduce the amount of floor heave.

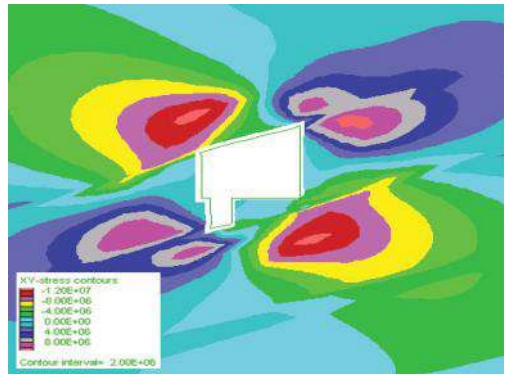


Figure 4. Shear stress distribution of the pressure-relief groove.

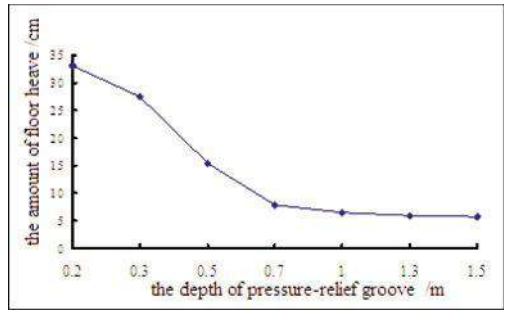


Figure 5. Displacement curve of floor strata after cutting pressure-relief groove at different depths.

If the groove is longer and wider, this kind of phenomenon could be more obvious.

Second, the scope of plastic zone in floor corners is influenced by cutting pressure-relief groove at different depths. The pressure-relief groove can transfer high stress to the deeper strata. The deformation energy can be released. Additionally the groove cutting and roadway excavation should be constructed simultaneously in order to make the cutting of pressure-relief groove become a part of roadway excavation.

Third, the displacement curve of floor strata after cutting pressure-relief groove at different depths is shown in Figure 5. When the groove depth is less than 0.5 m, the amount of floor heave is still large and the controlling effect is not obvious. When the groove depth is 0.7 m ~1.0 m, the amount of floor heave has reduced effectively, the inflexion point is found at the curve. Based on site conditions and the actual operation, the depth of pressure-relief groove is determined as 0.7 m ~1.0 m.

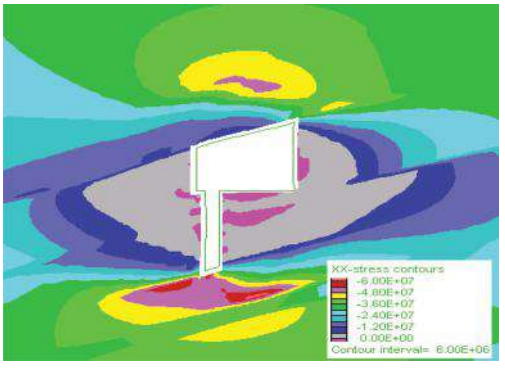


Figure 6. Horizontal stress distribution of the floor drilling.

4.3 *Floor drilling*

4.3.1 *Layout scheme*

Based on site conditions and the convenience of traffic, boreholes are drilled in the floor strata near the side of coal pillar. The borehole's diameter is 42 mm. (Wang, W.J. & Feng, T. 2005). Figure 6 shows the stress field and displacement distribution of floor boreholes at different depths, such as 1.0 m, 1.5 m, 2.0 m, 2.5 m, 3.0 m, 3.5 m.

4.3.2 *The effect on controlling floor heave*

First, the numerical simulation results show that the floor boreholes can transfer high stress to the deeper strata, the shallow strata stress can be reduced significantly. This result has ensured the stability of the large cross section mining roadway. But the convergence of roadway sides affected by floor drilling is not obvious.

Second, the stress redistribution around the boreholes is an important factor which results in the generation of the loose zone and plastic zone. Under the action of high stress, deep strata have the trend to move towards to the free surface. Therefore, the amount of floor heave in the deep strata is decreased.

Third, compared with other controlling measures, the initial moving point of the floor strata is deeper by adopting the floor boreholes, the boreholes are drilled much deeper than pressure-relief grooves. So the construction period is longer and the actual operation is more complicated.

4.4 *Comparative analysis on the different measures of controlling floor heave*

Through the comparative analysis on the above control schemes of floor heave, the key parts of controlling floor heave are the floor corners and floor rock affected by mining. The first program is reinforcement method, floor bolting, changing the stress distribution, reducing the horizontal stress and strengthening the overall strength of surrounding rock. The second program is pressure relief method, pressure-relief groove, providing the free space for high horizontal stress transfer. The third program is pressure relief method, floor drilling, although floor strata stress can also be significantly reduced, but the construction is too complicated. Based on the practical conditions of large cross-sectional mining roadway, the combinatorial controlling technique of reinforcement method (floor bolting) and pressure relief method (pressure-relief groove) is put forward. This combinatorial technique could be able to give full play to their respective advantages.

5 ENGINEERING PRACTICE

5.1 *Floor bolting reinforcement supporting at floor corners*

According to the results of numerical simulation and in-situ operation conditions of No.1 Coal Mine of China Coal Ping-shuo Group Co., ltd, the whole train of thought is identified as: on the basis of the original supporting parameters in large cross section mining roadway, the control technology of floor bolting reinforcement supporting at floor corners is adopted. The floor bolts are extensible anchoring, made of non-longitudinal reinforcement deformed steel bar, the bolt diameter is 22 mm, its length is 2400 mm, and the angle between the floor bolt and the horizontal plane is 45°. The supporting parameters are shown in Figure 7. Field application shows that floor bolting can limit the expansion of plastic zone, prevent floor heave, and improve the overall supporting effect of large cross section roadway.

5.2 *Pressure-relief groove cut in floor*

According to the results of numerical simulation, the parameters of pressure-relief groove are identified, its width is 300 mm, and its depth is 800 mm. Considering the convenience for transportation and pedestrian safety, pressure-relief groove excavated in floor corners (the junction between coal pillar and floor) should be filled up with flexible materials such as sawdust, fine sand and so on. The strength of the filling material should not be greater than floor rock. This technical innovation not only realizes horizontal stress transferring to the groove, but also prevents the floor strata from expanding up under the influence of water. The layout parameters of pressure-relief groove and the actual operation are shown in Figure 8.

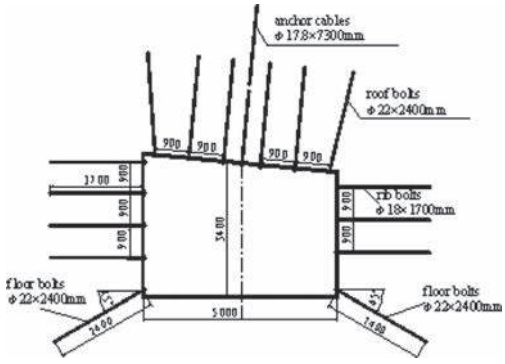


Figure 7. Schematic diagram of floor bolting reinforcement supporting.

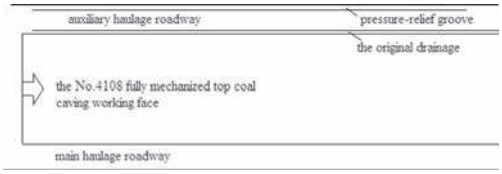


Figure 8. Pressure-relief groove layout parameters.

5.3 *Controlling effects on floor heave*

Trough the above technical measures, the industrial application have been carried out in the auxiliary haulage roadway of No.4108 working face. The technicians have monitored the amount of floor heave at the same time. The monitoring results show that the maximum displacement of floor heave is 232 mm and the maximum rate is 19.3 mm/d. The maximum displacement and rate are within the controllable range, as shown in Figure 9. Compared with the former supporting measures, the gradually decreased tendency of floor heave at the auxiliary haulage roadway has presented through the combinatorial controlling technique. Thus, the combinatorial controlling technique can effectively control the floor heave and keep the surrounding rock stable. The actual operation is shown in Figure 10. In practice, the technique has ensured that the pedestrian and material transportation are unimpeded and has achieved good technical and economic benefits.

6 CONCLUSIONS

Firstly, engineering practice shows that the combinatorial controlling technique of reinforcement method (floor bolting) and pressure relief method (pressure-relief groove) has achieved remarkable

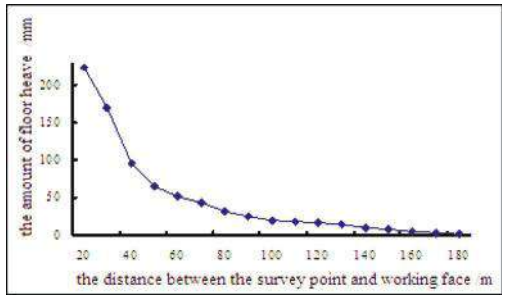


Figure 9. Displacement curve of floor heave by adopting the combinatorial controlling technique.



Figure 10. The actual operation by using the combinatorial controlling technique.

effects. This technique can effectively control floor heave within the allowed range and keep the surrounding rock stable.

Secondly, this technical innovation of pressure-relief groove not only realizes horizontal stress transferring to the groove, but also prevents the floor strata from expanding up under the influence of water. The pressure-relief groove cutting and roadway excavation should be constructed simultaneously. The cutting of pressure-relief groove becomes a part of roadway excavation. Considering the convenience for transportation and pedestrian safety in the large cross section mining roadway, pressure-relief groove is excavated at the floor corner (the junction between coal pillar and floor), which should be filled up with flexible materials such as sawdust, fine sand and so on.

Thirdly, the numerical simulation method can reveal the stress and deformation characteristics of floor surrounding rock with various kinds of controlling measures, this is conducive to optimizing the design scheme, reducing the testing time and improving economic and social benefits.

ACKNOWLEDGEMENTS

This work was financially supported by the Fundamental Research Funds for the Central Universities (3142013035); the Fundamental Research Funds for the Central Universities (3142013100).

REFERENCES

Gao, M.Z. & Jing, H.Q. 2012. Mechanical analysis of asymmetric floor heave of roadway. *Journal of Anhui University of Science and Technology (Natural Science)* 32(4):38–43.

Guo, B.H. & Lu, T.K. 2008. Analyses of floor heave mechanism and cutting control technique in deep mines. *Journal of Mining and Safety Engineering* 25(1):91–94.

He, M.C. et a1. 2009. Research on mechanism and application to floor heave control of deep gateway. *Chinese Journal of Rock Mechanics and Engineering* 28(Supp):2593–2598.

Jiang, Y.D. et a1. 2004. Research on floor heave of roadway in deep mining. *Chinese Journal of Rock Mechanics and Engineering* 23(14):2396–2401.

Li, X.H. et a1. 2003. Controlling floor heave with strengthening roof in gateway by numerical analysis. *Journal of China University of Mining & Technology* 32(4):436–439.

Li, Z.G. 2012. Prevention of floor heave in roadway influenced by dynamic pressure induced by mining. *Coal mining technology* 17(5):52–55.

Luo, Y.Q. et a1. 2005. The reason caused floor heave of drift and its preventive measures at 1178 m sublevel of No.2 mine area in Jin-chuan. *China mining magazine* 14(6):73–76.

Sun, J. & Wang, L.G. 2011. Numerical simulation of grooving method for floor heave control in soft rock roadway. *Mining Science and Technology (China)* 21(1):49–56.

Wang, W.J. & Hou, C.J. 2003. New development of mechanism and control technique study of extraction opening floor heave. *Journal of Xiangtan Mining Institute* 18(1):1–6.

Wang, W.J. & Feng, T. 2005. Study on mechanism of reinforcing sides to control floor heave of extraction opening. *Chinese journal of rock mechanics and engineering*24(5):808–811.

Yang, B.S. & Geng, X.L. 2012. Research on floor heave mechanism of thick seam roadway in wu-yang coal mine and its control. *Journal of mining and safety engineering* 29(1):8–13.

Progress in Mine Safety Science and Engineering II – He et al. (Eds)
© 2014 Taylor & Francis Group, London, ISBN 978-1-138-00122-0

Study on the inhibitor rate evaluation by thermal analysis method

Changfu Xu
Faculty of Resources and Safety Engineering, China University of Mining and Technology, Beijing, China
Mine Safety Technology Branch, China Coal research institute, Beijing, China

Zhongya Zheng
Mine Safety Technology Branch, China Coal research institute, Beijing, China

Shasha Yuan
Faculty of Resources and Safety Engineering, China University of Mining and Technology, Beijing, China

Haifei Yao & Haijun Wu
Mine Safety Technology Branch, China Coal research institute, Beijing, China

ABSTRACT: Based on thermal analysis kinetics and combined the thermo-gravimetric experiments of two coal samples: 065–2 working face of Gu-Shan Mine and silk carbon layer with STA449C TGA Test System, calculated the kinetic parameters of two coal samples and coal added inhibitor kind, and quantitatively analyzed the activation energy in the reaction stage. The results show that the inhibitor rate is defined as a percentage of the activation energy difference between the original coal samples and adding inhibitor ones compared with the original coal samples activation energy in oxygen increasing stage and the best inhibitor ratio parameters of FR-1 is 1:2 in Gu-Shan Mine. Validated inhibition effect of FR-1 through field application, which effectively prevented spontaneous combustion of 065–2 working face and guaranteed to produce safely and go over the fire zone successfully. The results have theoretical and practical significance to select inhibitors of spontaneous ignition of coal and find the optimum ratio parameters.

1 INTRODUCTION

The coal spontaneous combustion in coal mine shaft is one of current coal production significant natural disasters (Li 1998). Mining the spontaneous combustion tendentious coal bed mine occupies the similar mine 47% in our allocation and key coal mine, which has more than spontaneous combustion 300 times every year. In addition another spontaneous combustion tendentious coal bed, the number will reach 600 times every year, causing the giant person casualties and the economic loss and threatening the coal mine safety seriously, affecting the coal mine economic efficiency (Luo et al. 2003, Wang 2005).

The inhibitor is a kind of effective measures to prevent coal spontaneous combustion (Jiao et al., 2012). At present, inorganic salt solution and silicone gel used inhibitors are used in China (Wang et al. 1990, Zhang 1999), inhibiting major mechanisms of which are liquid membrane preventing oxygen and reducing temperature theory. Its main drawback is the high cost of fire prevention, unguaranteed inhibition effect, few sources of drugs and difficult purchase. In recent years, lots of new type inhibitor have been developed, such as DDS series composite inhibitor, polymer emulsion inhibitor, water soluble inhibitor and powder thermal protection agent and so on (Zhang et al. 1995, Dong 1997, Yang et al. 1999). So, it is extremely important to quantitatively determinate the inhibition effects and rates of coal inhibitors. However, it has not been a good way to identify resistant effect. In China, inhibition rate has being been adopted that a percentage of the CO difference between the original coal sample and adding inhibitor one compared with CO of the original coal sample at 100°C. However, the short comings of this method (Lu et al. 2005) are that the measuring apparatus is relatively complicated and test time is too long. This article discusses a new method of thermal analysis, which is convenient for practical application for simple measuring device and reliable test result.

2 EXPERIMENTAL APPARATUS AND CONDITIONS

Thermo-gravimetric analysis of this experiment is carried out on STA449C TGA Test System (Fig. 1). Experiment conditions: ①Sample size: 200 item;



Figure 1. STA449C TGA Test System.

②Heating rate: 5°C/min; ③Initial temperature: 25°C, end temperature: 800°C, ④Experimental atmosphere gas: Nitrogen and Oxygen (4:1); ⑤The initial sample quality: 15 mg~20 mg.

3 COAL OXIDATION REACTION KINETICS MODEL

3.1 *Activation energy*

Activation energy is the minimum energy required to start a chemical reaction (Liu et al. 1999, Deng 2006), which can be thought of as an energy "hill" or barrier that must be crossed before reactants can proceed to form products.

3.2 *Kinetic model of coal combustion*

Reaction kinetics of coal combustion in oxygen-enriched environment is investigated by non-isothermal method in this work. The reaction kinetic equation of coal combustion can be expressed as (Liu et al. 2005, Li 2007, Shan et al. 2005, QI et al. 2010):

$$\frac{d\alpha}{dt} = Ae^{-\frac{E}{RT}} f(\alpha) \tag{1}$$

$$\alpha = \frac{m_0 - m_1}{m_0 - m_\infty} \times 100\% \tag{2}$$

$$f(\alpha) = (1 - \alpha)^n \tag{3}$$

Where A is pre-exponential factor, min^{-1}; E, activation energy, kJ/mol; R, general gas constant, 8.314×10^{-3} kJ·mol^{-1}·K^{-1}; α mass conversion fraction; n, reaction order. $f(a)$ is the reaction mechanism function; m_0, mass of the sample at the beginning of reaction; $m_\perp$, mass of the sample at the end of reaction; m_t, mass of the sample at time t.

The parameters E and A of the coal samples were obtained from the kinetic analysis of TG data. The Coats-Redfern method has a great advantage of simplicity among the kinetic approaches and is extensively acknowledged. The reaction kinetic equation can be deduced as:

$$\ln[\frac{g(a)}{T^2}] = \ln\{\frac{AR}{\beta E}[1 - \frac{2RT}{E}]\} - \frac{E}{RT} \tag{4}$$

Since the E value is large, 2RT/E can be approximately equal to zero. According to the chemical reaction order, formula left on reciprocal temperature.

$1/T$ for the photo shows a straight line. As a result, E can be calculated from the slope, and A can be calculated from the intercept.

4 EXPERIMENTAL RESULTS AND ANALYSIS

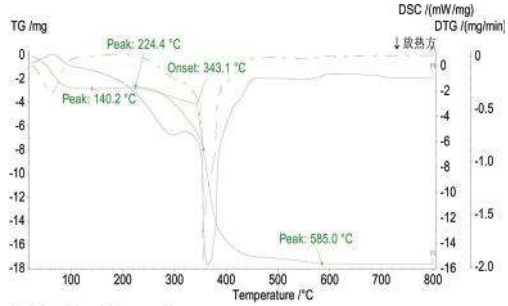
In order to find the optimal ratio of FR-1, coal samples (coal sample of 065–2 mine face and silk carbon layer) were immersed respectively in the different proportions inhibitor(the volume ratio of Foam Retardant-1 and water is 1:1, 1:1.5, 1:2, 1:2.5, 1:3) for one day. Then the coal samples were dried two days in desiccators. The experiments were carried out using Simultaneous Thermal Analysis STA449C produced by Nietzsche of German.

4.1 *Thermo-gravimetric characteristics analysis*

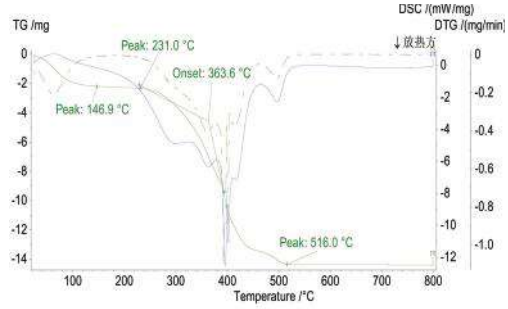
TG is based on continuous recording of mass changes of a sample of material, as a function of a combination of temperature with time, and additionally of pressure and gas composition. The TG curves reflect weight changes of coal sample in the process of coal oxidation caused by coal oxygen complex and various gases desorption and escape.

Several combustion parameters such as temperature of water the best evaporation (T_1), the beginning pyrolysis temperature (T_2), ignition temperature (T_3) and burnout temperature (T_4) were achieved by analyzing the TG and DTG curves.

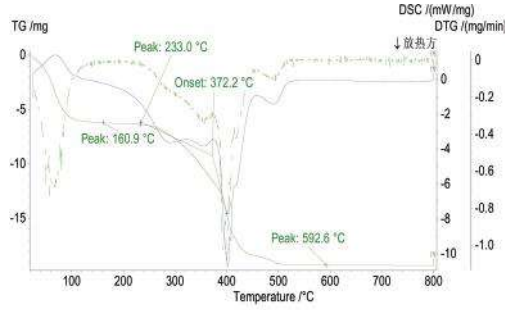
As shown in Fig. 2, whether additional inhibitor or not, the general trend of coal samples TG curves are divided into five stages: Water evaporation to weight lessness (T_0~T_1), oxygen increase to heavy (T_1~T_2), coal thermal decomposition (T_2~T_3), the combustion (T_3~T4) and the burnout ($T > T_4$); The weight of the coal sample have been basically reduced because he physical oxygen role are suppressed after adding the inhibitor to coal samples. And the quality of the coal samples reduced slowly



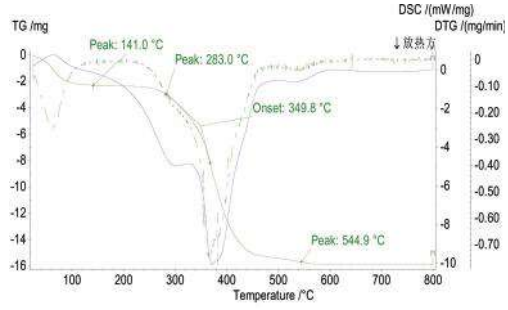
a) No. 3 coal sample



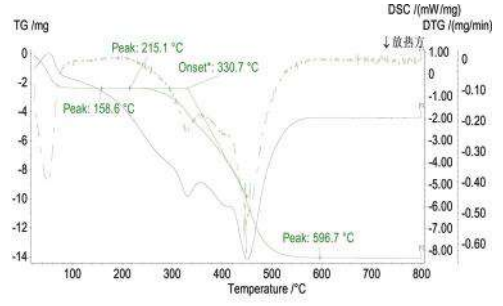
b) No. 3 coal sample at 1:1.5



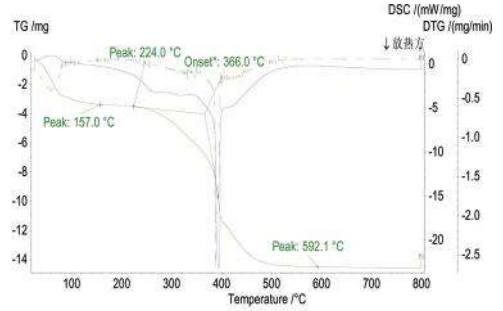
c) No. 3 coal sample at 1:2



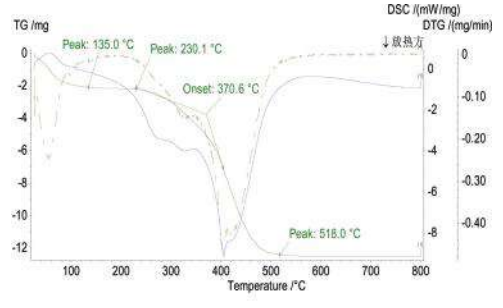
d) No. 3 coal sample at 1:2.5



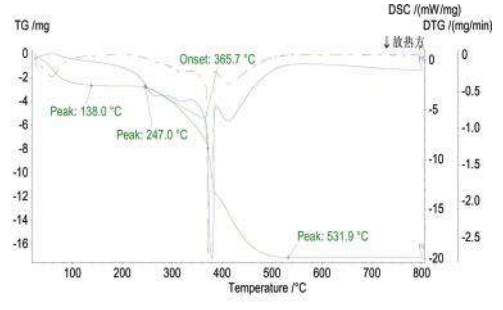
e) No. 8 coal sample



f) No. 8 coal sample at 1:1.5



g) No. 8 coal sample at 1:2



h) No. 8 coal sample at 1:2.5

Figure 2. TG & DTG curves of 3 and 8 samples at different inhibitors ratios.

Table 1. Characteristic temperature of different samples at different inhibitor ratio.

Sample Number	Inhibitor ratios	Characteristic temperature			
		T_1	T_2	T_3	T_4
No. 3	0	140.2	224.4	343.3	585.0
	1:1.5	146.9	231.0	363.6	516.0
	1:2	144.0	233.0	372.2	592.6
	1:2.5	141.0	283.0	349.8	544.9
No. 8	0	158.8	215.1	330.7	596.7
	1:1.5	157.0	224.0	366.0	592.1
	1:2	160.0	230.1	370.6	518.0
	1:2.5	138.0	247.0	365.7	531.9

for the weak oxygen-absorbing effect in the oxidation weight gain stage (T_1~T_3).

As observed from Table 1, the ignition temperature T_3 of coal samples increased after adding inhibitor; when the inhibitor ratio was 1:2, it reached the maximum value on the same coal sample.

4.2 *Kinetic Parameters*

According to Esq. 4, if a correct model is select for the reaction, the plot of $\ln[g(a)/T^2]$ versus $1/T$ will be linear with high-correlation.

By comparing correlation coefficient r in Table 2, it found that the correlation coefficients r of the coal samples in different reaction stages are bigger using first-order reactions than others, which

Table 2. Correlation coefficient of the different reaction models of different samples at different inhibitor ratios.

No.	Ratios	Stages	Correlation coefficient *r*								
			Reaction order			Phase interfacial		Diffusion model			
			0	1	2	R_2	R_3	1	2	3(J)	3(G-B)
3	0	T_0—T_1	0.91947	0.96890	0.92236	0.89965	0.93590	0.86030	0.88992	0.93590	0.90587
		T_1—T_2	0.92122	0.97404	0.81136	0.95066	0.96222	0.92742	0.94371	0.96222	0.95046
		T_2—T_3	0.93542	0.96054	0.73758	0.94849	0.95551	0.93945	0.94717	0.95551	0.95008
		T_1—T_3	0.96293	0.95506	0.28602	0.96303	0.92198	0.92117	0.91971	0.92198	0.92220
	1:1.5	T_0—T_1	0.86270	0.98208	0.92049	0.93339	0.96448	0.89748	0.93223	0.96448	0.93968
		T_1—T_2	0.95409	0.97907	0.87640	0.97186	0.97266	0.96171	0.96791	0.97266	0.97538
		T_2—T_3	0.96676	0.98566	0.78270	0.97957	0.98408	0.97012	0.97665	0.98408	0.98017
		T_1—T_3	0.98936	0.98131	0.34830	0.98645	0.98564	0.99053	0.98902	0.98654	0.98828
	1:2	T_0—T_1	0.84884	0.97897	0.93392	0.92131	0.95599	0.88556	0.92211	0.95599	0.92846
		T_1—T_2	0.92596	0.96334	0.87687	0.95376	0.96105	0.93794	0.94660	0.96105	0.95830
		T_2—T_3	0.95233	0.98019	0.75911	0.97054	0.97779	0.95744	0.96697	0.97779	0.97144
		T_1—T_3	0.99457	0.99185	0.47027	0.99461	0.99379	0.99527	0.98876	0.99379	0.98847
	1:2.5	T_0—T_1	0.86307	0.97380	0.92094	0.92644	0.95641	0.89353	0.92125	0.95641	0.93290
		T_1—T_2	0.95466	0.95374	0.37481	0.95176	0.95545	0.96138	0.96016	0.96455	0.97121
		T_2—T_3	0.92450	0.96536	0.84188	0.94946	0.95874	0.92929	0.94288	0.95874	0.96363
		T_1—T_3	0.97868	0.96919	0.33514	0.97524	0.97649	0.98105	0.97938	0.97649	0.97852
8	0	T_0—T_1	0.58141	0.88955	0.97226	0.74178	0.83445	0.68985	0.75874	0.83445	0.77952
		T_1—T_2	0.91771	0.97725	0.80798	0.95269	0.96616	0.92258	0.94454	0.96616	0.95017
		T_2—T_3	0.93858	0.95872	0.66135	0.95130	0.94800	0.93172	0.93804	0.94800	0.94237
		T_1—T_3	0.95174	0.9729	0.33596	0.96600	0.90942	0.90851	0.90621	0.90942	0.90978
	1:1.5	T_0—T_1	0.71600	0.90636	0.94004	0.82180	0.88016	0.77590	0.82406	0.88016	0.84001
		T_1—T_2	0.87897	0.92477	0.84979	0.91300	0.92500	0.89758	0.90714	0.92500	0.92213
		T_2—T_3	0.94375	0.97445	0.76313	0.96240	0.97086	0.94985	0.95972	0.97086	0.96417
		T_1—T_3	0.99077	0.98712	0.51801	0.99059	0.99038	0.99202	0.99191	0.99038	0.99138
	1:2	T_0—T_1	0.61184	0.86901	0.90497	0.74172	0.81744	0.67447	0.73427	0.81744	0.76358
		T_1—T_2	0.73388	0.86375	0.72388	0.81588	0.86375	0.78390	0.82467	0.87092	0.83948
		T_2—T_3	0.89711	0.95426	0.58433	0.92908	0.94432	0.90748	0.92567	0.94432	0.93245
		T_1—T_3	0.99481	0.99377	0.50000	0.93778	0.94226	0.99552	0.95003	0.94226	0.94772
	1:2.5	T_0—T_1	0.68922	0.93365	0.88412	0.82109	0.88758	0.75417	0.81078	0.88758	0.83863
		T_1—T_2	0.69663	0.72578	0.23908	0.71862	0.77014	0.75615	0.76580	0.77014	0.76789
		T_2—T_3	0.87720	0.94366	0.65362	0.91459	0.93220	0.88920	0.91055	0.93220	0.91844
		T_1—T_3	0.92564	0.91210	0.13953	0.92113	0.92785	0.93485	0.93227	0.92785	0.93098

indicates the stages meet first-order reactions in the reaction model; adding the inhibitor into coal samples, $T_0 - T_1$ and $T_2 - T_3$ stage basically meet first-order reactions in the reaction model; $T_1 - T_2$ stage belongs to three-dimensional reaction in diffusion mechanism model and $T_1 - T_3$ stage belongs to the one-dimensional model of diffusion mechanism reaction.

Kinetic parameters of various coal samples in different inhibitor ratios with the different reaction models of combustion reaction are calculated respectively from experimental data: apparent activation energy (E) and apparent frequency factor (A) of the reactions.

Calculating results are listed in Table 3.

4.3 *Optimal ratio of FR-1*

As shown in Fig. 3 and Fig. 4, the activation energy of 8 coal sample is lower than the one of 3 coal sample, indicating that the coal spontaneous combustion tendency of the carbon layer with wire is larger than the ordinary one, more likely to catch fire.

But the coal ignition activation energy of coal samples added inhibitor become smaller than coal samples without the inhibitor.

On the one hand, T_1-T_3 stage of coal samples with the inhibitor belong to one-dimensional reaction of the reaction diffusion mechanism model rather than first-order reactions in the reaction model. On the other hand, because the water content of FR-1 Foam inhibitor reaches as high as 90%, Liquid films are formed, what cut off oxygen and reduce the temperature before 100°C. The coal water evaporation is decreasing; to a certain point, resistance change into promoting the coal spontaneous combustion with the temperature increasing.

The activation energy of ignition and ignition temperatures at different inhibitors ratios are shown in Fig. 5. As inhibitors ratio decreases, the ignition activation energy first increase, then reduce. When the ratio of FR-1 is 1:2, all ignition activation energy reaches maximum value, which mean best resistance ratio.

Table 3. Kinetic parameters of different samples at different inhibitor ratios.

Number	Ratios	Stages	*E* (kJ/mol)	*A*	*r*
No. 3 (working face)	1:1.5	$T_0 - T_1$	33.37	12487.32	0.98208
		$T_1 - T_2$	104.69	4.62×10^9	0.97538
		$T_2 - T_3$	109.45	4.2×10^8	0.98566
		$T_3 - T_4$	90.62	5.72×10^5	0.91125
		$T_1 - T_3$	113.10	2.31×10^8	0.99053
	1:2	$T_0 - T_1$	36.04	37845.96	0.97897
		$T_1 - T_2$	56.28	189018.90	0.96334
		$T_2 - T_3$	104.08	1.26×10^8	0.98019
		$T_3 - T_4$	52.55	722.47	0.95645
		$T_1 - T_3$	126.14	3.68×10^9	0.99627
	1:2.5	$T_0 - T_1$	36.66	48268.97	0.97830
		$T_1 - T_2$	98.59	2.25×10^7	0.97121
		$T_2 - T_3$	177.78	7.10×10^{14}	0.96536
		$T_3 - T_4$	68.81	13158.41	0.84959
		$T_1 - T_3$	115.32	5.33×10^8	0.98105
No. 8 (the carbon layer)	1:1.5	$T_0 - T_1$	31.78	6517.061	0.90636
		$T_1 - T_2$	114.76	1.05×10^{11}	0.92500
		$T_2 - T_3$	97.88	51221216	0.97445
		$T_3 - T_4$	91.07	583994.8	0.88925
		$T_1 - T_3$	112.95	3.77×10^8	0.99202
	1:2	$T_0 - T_1$	38.01	80222.42	0.86901
		$T_1 - T_2$	80.28	15076600	0.87092
		$T_2 - T_3$	103.58	1.38×10^8	0.95426
		$T_3 - T_4$	133.67	8.13×10^8	0.92102
		$T_1 - T_3$	130.42	1.17×10^{10}	0.99552
	1:2.5	$T_0 - T_1$	34.69	24152.88	0.93365
		$T_1 - T_2$	66.15	56800.61	0.77014
		$T_2 - T_3$	107.20	2.92×10^8	0.94366
		$T_3 - T_4$	82.75	161183.4	0.88977
		$T_1 - T_3$	114.51	4.10×10^8	0.93485

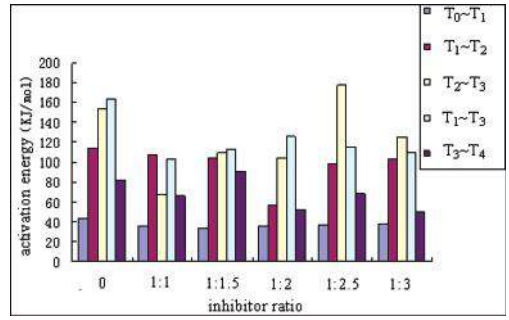


Figure 3. Activation energy of each stage of No.3 sample at different inhibitor ratios.

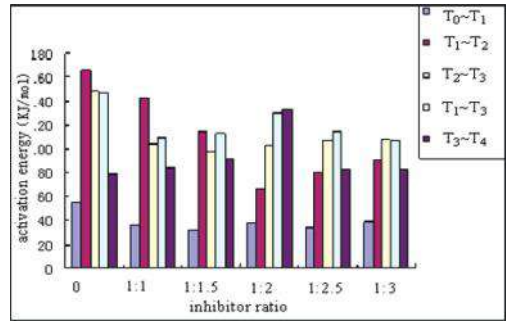


Figure 4. Activation energy of each stage of No.8 sample at different inhibitor ratios.

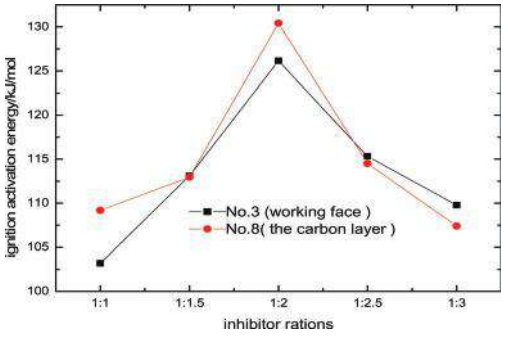


Figure 5. The activation energy of ignition at different inhibitors Ratios.

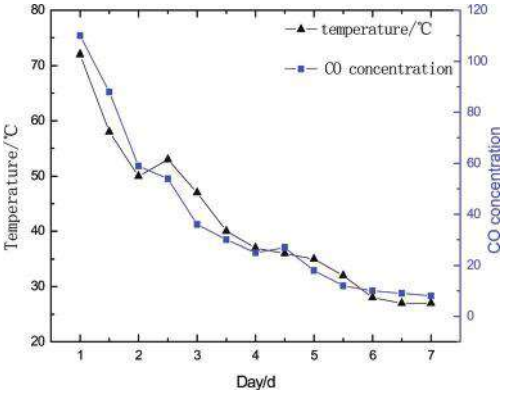


Figure 6. Variation of temperature and CO concentration after pouring FR-1 retardant.

4.4 *The inhibitor rate*

The percentage of activation energy differences of oxygen stage ($T_1 - T_3$) between the original coal samples and adding inhibitor ones compared with the activation energy of the original coal samples is called inhibitor rate. The inhibitor rate value can be taken from Eq.5:

$$E = \frac{B - A}{A} \times 100\% \tag{5}$$

Where E is resistance rate, A is activation energy in oxygen stage ($T_1 - T_3$) of the original coal samples and B is activation energy in oxygen stage ($T_1 - T_3$) of adding inhibitor coal samples in the same test condition.

Thus, resistance rate of No.3 and No.8 samples in the inhibitor ratio 1:1, 1:1.5, 1:2 1:2.5, 1:3 are as follows: 5.86%, 8.18%, 50.63%, 13.52%, 9.57%; 13.64%, 30.54%, 59.96%, 51.41%, 45.6%.

5 APPLICATION OF FR-1

In order to produce safely and go over the fire zone successfully, mixed the FR-1 polymer liquid foam inhibitor and water according to the proportion of 1:2. Use special foam device to create the inhibitor foam. And then put out fire by means of pour this material into the hidden danger areas of spontaneous combustion through compressed air pipe or inert gas injection pipe. PU's foam equipment consists of special pump, solvent tank, foam maker and air line and so on.

Take B4–2 drilling of fire zone in Gu-Xin small coal mine as an illustration. CO concentration was 0.012%, O_2 concentration was 4.3%, and the gas temperature was 72°C. Inject the foam inhibitor 100 Kg to the beyond-standards danger zone by B4–2 drilling. The volume of the foam filling was 45.5 m^3 according to foam multiple of 500. Then, validate the effect through adjacent boreholes. The results of test are shown in Fig. 6.

The results show that CO concentration and gas temperature decrease with injection time increased. The two indications reduced to the fire zone extinction standard of coal mine safety regulation within 4 to 5 days. That is to say air temperature of detection zone decreased to below 30°C, the oxygen concentration is reduced to below 5%, the concentration of carbon monoxide reduced to below 0.001%. Injecting FR-1 polymer liquid foam inhibitor played a significant role in eliminating the high temperature point and preventing coal mine fire.

6 CONCLUSION

Based on the TG/DTG profiles, the kinetics parameters such as activation energy (E) and frequency factor (A) were obtained by Coats-Redfern method. The following conclusions can be drawn:

1. The best inhibitor ratio of FR-1 in Gu-Shan Mine is 1:2.
2. The inhibitor rate is defined as the percentage of activation energy in oxygen increasing stage ($T_1 - T_3$) between the original coal samples and adding inhibitor ones compared with the original coal samples activation energy. It had theoretical and practical significance to select inhibitors of spontaneous ignition of coal and find the optimum ratio parameters.

ACKNOWLEDGEMENTS

The authors gratefully acknowledge foundation by Technology Innovation Fund of China Coal Science and Engineering Group (2012MS001), Science and Technology Development Fund of China Coal Research Institute (2012 JC11).

REFERENCES

Dong, X.L. 1997. Experimental investigation into the DDS inhibitors to suppress the spontaneous ignition of coal. *Fire Safe Science*, 6(1):20–26.

Deng, C.B. 2006. Study on coal spontaneous combustion mechanisms and the spontaneous combustion danger index. Docter's Thesis, Liao Ning Technical University.

Jiao, X.M. Wang, D.M. & Zhong, X.X. 2012. Experiment study on different retarder affected to critical temperature of Coal Spontaneous Combustion. *Coal Engineering*, 2:88–91.

Li, X.C. 1998. *China coal mine safety compilation*. Beijing: Coal Industry Press.

Liu, J. Wang, J.R. & Sun, B.Z. 1999. A study on the theory of activation energy of coal. *Journal of China Coal Society*, 24(3):316–320.

Luo, H.Z. & Liang, Y.T. 2003. Current status and perspective of forecast and prediction techniques for spontaneous combustion of coal. *China Safety Science Journal*, 13(3):76–78.

Lu, W. Wang, D.M. & Chen, k. 2005. Research on programmed temperature-rise oxidation method used for evaluating performance of inhibitors of coal spontaneous combustion. *Mining Safety &Environmental Protection*, 2005, 32(6):12–14.

Liu, J. Chen, W.S. & QI, Q.J. 2005. Study on the spontaneous combustion tendency of coal based on activation energy index. *Journal of China Coal Society*, 30(1):67–70.

Li, Z.J. 2007.Investigation on the mechanism of spontaneous combustion of sulphide ores and the key technologies for preventing fire. Docter's, Thesis, Central South University.

Qi, Q.J. Xu, C.F. & Zhou, X.H. 2010.Experimental research on resistance effect and technical parameters of FR-1 foam inhibitor.//Proceedings of 2010(Shenyang) International Colloquium on Safety Science and Technology, 273–277.

Shan, Y.F. Wang, J.R. & Deng, C.B. 2008. Study on influences of different inhibitors on coal spontaneous combustion. Journal of Liaoning *Technical University (Natural Science)*, 27(1):1–3.

Wang, X.S. & Zhang, G.S. 1990. *Mine fire prevention*. Xuzhou: China University of Mining and Technology Press, 27–30.

Wang, D.M. 2005.*Mine ventilation and safety*. Xuzhou: China University of Mining and Technology Press.

Yang, Y.L. Yu, S.J. & Zhang, R.Y. 1999. Study on new stopping agent of preventing coal spontaneous combustion. *Journal of China Coal Society*, 24(2):163–166.

Zhang, R.W. & Li, Z.H. 1995. Study on new type of gel inhibitor and its application. *Journal of China University of Ming &Technology*, 24(4):46–51.

Zhang, R.Y. 1999. Fire-fighting materials and separate chemical agents against coal spontaneous fire. *Mining Safety &Environmental Protection*, (1): 6–7.

This page intentionally left blank

Progress in Mine Safety Science and Engineering II – He et al. (Eds)
© 2014 Taylor & Francis Group, London, ISBN 978-1-138-00122-0

Determination of goaf "three zones" scope in Pang Zhuang mine and fire prevention technology

Zhongpeng Xie
Faculty of Resources and Safety Engineering, China University of Mining and Technology, Beijing, China
Safety and Environmental Engineering Institute, Capital University of Economics and Business, Beijing, China

Kai Wang
Faculty of Resources and Safety Engineering, China University of Mining and Technology, Beijing, China

ABSTRACT: According to Pang Zhuang mine 7431 fully mechanized caving face situation, along the goaf orientation layout of 4 measuring points and determination of goaf gas composition, using three order spline interpolation methods, according to O_2, CO concentration determined "three zones" scope and the residual coal in the oxidation zone time. Finally, According to the "three zones" determine the implementation technology of fire prevention and control techniques, effectively prevent the spontaneous combustion of residual coal in goaf and ensure the safety of coal mining face.

1 INTRODUCTION

Goaf is one of major hazard source in coal major disasters; many accidents and mine are almost in goaf with some factors. With the development of mining technology, spontaneous combustion risk of the residual coal in the goaf will become more and more serious. In recent years, with the continuous development of high yield and high efficiency new technology, increasing mining intensity range, mining empty area expands unceasingly, especially in fully mechanized top coal caving goaf spontaneous combustion of coal seam, left a large number of coal, the coal spontaneous combustion fire prevention in goaf of fully mechanized top coal caving mining becomes the key factor of success.

Analysis of spontaneous combustion of Residual coal in goaf, Determination of the actual condition of "three zones" distribution of goaf, spontaneous combustion danger area and morphology For determine the ventilation mode, the optimization of ventilation parameters and Determining safe speed of coal mining face, Ensure that the goaf float coal spontaneous combustion danger does not appear have very important realistic meaning (Yang et al. 2000, Shi & Qin 2012).

2 GENERAL SITUATION OF WORKING FACE

Pang Zhuang mine 7431 working face of coal seam belongs to coal 7# and the coal seam thickness change range is 2 ~ 5 m, the average thickness of 3.5 m. The gateroad of working face strike length is 1200.7 m and Slope length is about 120 m. Working face ventilation by using "U" type ventilation. According to the mine gas classification, Pang Zhuang mine belongs to the high gas mine, coal dust has explosion hazards, Coal seams have spontaneous combustion tendency, and the spontaneous combustion grade is I or II that is easy to spontaneous combustion or spontaneous. Coal spontaneous combustion period is generally 5 to 12 months, the shortest was 1 ~ 3 months.

3 "THREE ZONES" DIVISION OF GOAF

With the working face advance, because of the mine pressure, when the coal caving zone from loose (cooling zone) gradually into the roof separation zone, Falling rocks began to pressure, and gradually the compaction, the porosity decreases, air resistance increases, the air leakage intensity is prone to state of spontaneous combustion of residual coal, At this time Significant increase in temperature, decrease of oxygen concentration, carbon monoxide concentration increased (Oxidation zone) (Li et al. 2011).

With the working face further advance, when the falling rock gradually Enter the compaction zone, because the air leakage is reduced, the oxygen concentration is difficult to sustain the spontaneous combustion of residual coal, originally residual coal in spontaneous combustion state but

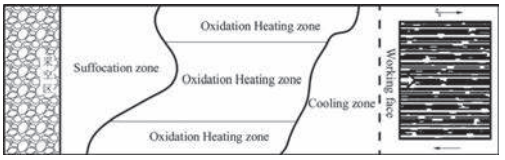


Figure 1. The goaf spontaneous combustion danger zone static distribution diagram.

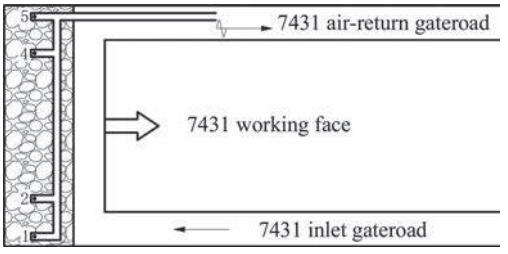


Figure 2. The temperature measuring and sampling test point arrangement schematic diagram of 7431 working face.

also because of hypoxia and asphyxia. Now the temperature began to decline slowly, carbon monoxide concentration gradually slowing down (Suffocation zone) (Yang & Cheng 2011).

In addition, because of the goaf Fresh air lane within the fresh air leakage, so the oxygen concentration decreased slowly while the Return air lane within the Air leak congruence, Airflow by oxidation and resulting gas influx, oxygen concentration decreased rapidly and Carbon monoxide concentration is relatively high. "three zones" distribution diagram is shown in Figure 1.

4 GOAF "THREE ZONES" OF MEASUREMENT AND ANALYSIS

4.1 *The establishment of beam tubes sampling analysis system*

Pang Zhuang mine 7431 working face Slope length is about 120 m, In the Supply and return air side respectively, the arrangement of 2 measuring points, Each measuring point embedding a beam tube (with the working face advancing step by step, 4 points respectively into the cooling zone, spontaneous combustion zone and suffocation zone), in the pumping station with explosion-proof pump pumping gas, sampling gas composition analysis by China University of Mining and Technology spontaneous combustion simulation dedicated chromatography laboratory. Sampling test point arrangement diagram is shown in Figure 2.

4.2 *Determine the goaf width of "three zones"*

Based on the comprehensive analysis of O_2 and CO concentrations of 4 Measuring point along the goaf strike length, concentration changes of O_2 and CO of The air intake side of 1 and 2 point and The return air side of 4 and 5 points is shown in Figure 3 and Figure 4.

First point from Figure 3, Figure 4 shows oxygen concentration of the inlet side was significantly higher than the return air side, and CO concentration of the air inlet side of was significantly lower than the return air side, This is mainly because the air inlet side leakage is large, there have been fresh

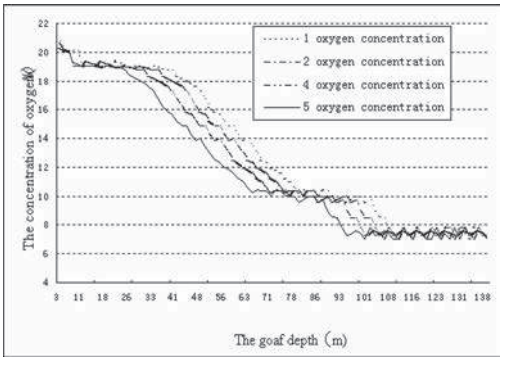


Figure 3. The O_2 concentration along the goaf depth diagram.

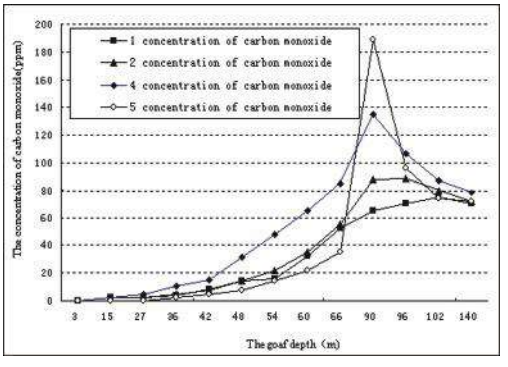


Figure 4. The CO concentration along the goaf depth diagram.

air supplement to dilute the concentration of CO, and take some of the heat, And higher CO concentration of the return air side is due to the return air side oxidation more intense consume large amounts of oxygen, this is caused by oxidation of goaf coal Produces CO With the continuous accumulation of air leakage to the return air lane.

Table 1. Division of distribution table of goaf "three zones" According to the O_2/CO concentration.

Measuring point	Cooling zone (m)	Spontaneous combustion zone (m)	Suffocation zone (m)
1(O_2/CO)	30/28	106/102	106/102
2(O_2/CO)	28/27	101/98	105/98
4(O_2/CO)	19/15	96/94	96/94
5(O_2/CO)	13/14	90/88	90/88

Table 2. Working face goaf "three zones" Range table.

Measuring point Position	Cooling zone (m)	Spontaneous combustion zone (m)	Suffocation zone (m)
Air intake side	0~27	27~106	106
Return air side	0~13	13~96	96

Second point with the working face advancing O_2 concentration of goaf decreased, and the concentration of CO increased gradually. Comprehensive analysis of goaf oxygen, carbon monoxide, the parameters of coal oxidation and spontaneous combustion "three zone" is classified by oxygen concentration: (O_2) > 19% is cooling zone, 15%< (O_2) < 19% is spontaneous combustion zone, (O_2) <15% is Suffocation zone. On the basis of changes in concentration of oxygen and CO, By using MIN-MAX optimization theory (Chen & Wang 2009), According to the concentration of oxygen and reference CO concentration classified: The minimum value of the two in cooling zone, The maximum value of the two in spontaneous combustion zone and the range of "three zones" in goaf, as shown in Table 1, shown in Table 2.

5 GOAF FIRE PREVENTION MEASURES

5.1 *Fire prevention mechanism of three-phase foam*

China University of Mining and Technology developed a fire new technology of three-phase foam for preventing spontaneous combustion of coal (Zhang et al. 2006). Three-phase foam fire extinguishing technology Take materials, gas liquid solid three phase fire extinguishing performance As a whole, Make full use of coverage of fly ash or yellow mud and Asphyxiant of nitrogen and water cooling for fire prevention and control(Smith & Lazzara 1998). Field application shows: treatment and prevention of three-phase foam fire extinguishing technology of spontaneous combustion, large fire of coal in goaf and ignition location unknown area, Fully mechanized caving face high and tunnel High fire, inclined downward goaf of fully mechanized caving face spontaneous combustion of coal, the result is quite remarkable (Li 2006). The fire extinguishing mechanism:

First point seal the coal, isolation of oxygen, plugging leakage channel and fracture of coal body.

Second point heat absorption and cooling, reduces coal body and the surrounding environment temperature.

Third point reduces the goaf oxygen concentration, inhibiting oxidation of coal, coal spontaneous combustion of asphyxia.

Fourth point Wetting coal, increase the moisture of coal.

And so on inhibiting production of coal free radicals, blocking the chain reaction of free radicals in the existing (Kang & Chen 2010).

5.2 *Process perfusion of three-phase foam*

First point three-phase foam preparation

For the appropriate concentration of slurry, the first station ahead of supply 10 min water in the grouting, grouting pipe flushing; then began to injection the mud; when the slurry injection foaming agent to the location, Start the screw pump, the foaming agent according to the quantitative ratio into the grouting pipe; When the mixed liquid slurry and foaming agent reaches foaming device, then open the gas valve to supply, three-phase foam formed at this time into the need to fire prevention area, three-phase foam filling process is shown in Figure 5.

Second point perfusion of three-phase foam

In the working face of the air inlet side along the goaf embedded 5–10 m length of the thick wall steel pipe as the foam injection pipeline, the movement mainly uses the face hydraulic support for traction, foam injection tube moving with the working face advancing. Foam injection port position should be inserted into the working face goaf spontaneous combustion zone, i.e. away from the work face scraper-trough conveyer 5–10 m range.

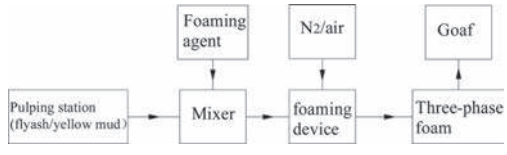


Figure 5. Three-phase foam perfusion flow chart.

6 CONCLUSIONS

First point with the working face advancing, the oxygen concentration of goaf each measuring point decreases gradually, spontaneous combustion "three zones" of goaf has been moving forward.

Second point in 7431 working face goaf oxygen concentration and CO concentration actual measurement, using the MIN-MAX optimization theory to determine the "three zones" width of working face goaf, from the working face mining deep space 0 ~ 27 m for the scattered tropical, 27 ~ 106 m is oxidized zone, More than 106 m is suffocative zone.

Third point according to the actual situation of the "three zones" of working face goaf put forward the corresponding Fire prevention measures of three-phase foam. Three-phase foam Fire prevention, not only make the goaf oxygen concentration greatly reduced, but also quickly reduce the residual coal temperature, can effectively prevent the spontaneous combustion of coal.

And so on During the whole goaf of temperature measuring and sampling observation (A range of about 140 m), the data analysis results measured by each: Spontaneous oxidation of Residual coal in goaf is always in the latent period, self-heating period (Generally self-heating Early period) two stages, no occurrence of spontaneous combustion of coal in goaf. But in the Fresh air lane side away from the work face about 90 ~ 100 m and return air lane side about 85 ~ 96 m "spontaneous combustion zone" range. CO appeared wave crest. These shows in these areas (especially in the Fresh air lane side) are high temperature heat source and the local coal spontaneous combustion is more intense.

REFERENCES

Chen, C.-H., Wang, Z. (2009) Study on Resembling Simulation Experiment of Spontaneous Combustion in Goaf, *Journal of Liaoning Technical University (Natural Science) (China)*, 28, 1–3.

Deng, J., Xu, T.-M. & Xu, J.-C. (2002) Analysis of the Danger Zone Liable to Spontaneous Ignition Around Coal Roadway at Fully Mechanized Long Wall Top-Coal Caving Face, *Journal of Coal Science & Engineering (China)*, 8, 55–59.

Kang, X., Chen, C.-H. (2010) Percolation Theory of Irregular Medium Stope and Prevention of Spontaneous Combustion in Goaf, *Journal of Liaoning Technical University (Natural Science) (China)*, 29, 8–10.

Li, D.-Y., Jiang, D.-J. & Jia, H.-L. (2011) Bu Liangou Coal Mine Extra-thick Coal Seam Fully Mechanized Caving Mining Face of Spontaneous Combustion " Three Zones " Distribution. *Coal engineering (China)*, 5, 42–46.

Li Z.-X. (2006) Numerical Simulation Application of Goaf Spontaneous Combustion in Blasting Coal of Roof, *Science and Technology for Safety Production of China (China)*, 27, 35–39.

Smith A C, Lazzara C P. (1998) Inhibition of Spontaneous Combustion of Coal, Report of Investigation United States. *Bureau of Mines, Pittsburgh, PA (USA)*, 41.1–41.4.

Shi, L., Qin, R.-X. (2012) Determination of Goaf "Three Zones" Width in Fully Mechanized Caving Minim and Fire Prevention Technology. *Coal technology (China)*, 11, 95–98.

Yang, S.-Q., Cheng, T. (2011) Theoretical Analysis and Numerical Simulation of Influence of Thechange of Negative Pressure and Air Volume of Inner Interlocked Tail Road on Coal Spontaneous Combustion, *Journal of China Coal Society (China)*, 36, 308–312.

Yang, S.-Q., Zhang, R.-W. & Di, Z.-Q. (2000) Distribution Regularity of Spontaneous Combustion Threezone in Goof of Full-mechanized Coal Faces. *Journal of China University of Mining & Technology (China)*, 9, 104–107.

Zhang, X.-H., Liu, C. & Zhou, J.-S. (2006) Modeling of Flow Field and Partition of Spontaneous Combustion Danger Zone in Gob of Fully Mechanized Caving Face, *Journal of Xi`an University of Science and Technology (China)*, 26, 6–9.

Progress in Mine Safety Science and Engineering II – He et al. (Eds)
© 2014 Taylor & Francis Group, London, ISBN 978-1-138-00122-0

Active pressure determination under the condition of rapid determination of gas pressure

Shu Yang, Genyin Cheng & Liming Qi
North China Institute of Science and Technology, Yanjiao, Beijing, China

ABSTRACT: The gas pressure in coal seam is one of the important basic parameters. Accurate and quick determination of the gas pressure in the coal seam has not only great significance for the determination of gas content in coal seam, for the control of mine gas emission, for gas drainage, and for the prevention of coal and gas outburst, but also has economic and social benefits for the safe production of coal mine. There are direct method and indirect method on the determination of gas pressure in the coal seam. Direct determination method includes active manometry and passive manometriy. This paper, on the premise of active manometriy, explores a method to rapidly determine gas pressure.

Keywords: gas pressure, manometric method, grouting hole

The prevention of gas accidents is the key of the key in the coal mine security work. To effectively prevent and control gas accidents, we must first accurately measure the gas pressure. In general, two broad headings of methods are proposed, —direct determination method and indirect determination method. The pattern of direct determination method includes active manometric method and passive manometric method. Active manometry is to measure the pressure by aerating compensation gas into coal seam through the drill hole so as to balance the gas pressure, and therefore to determine the gas pressure. The compensation gas can be high-pressured Nitrogen N_2 high-pressured carbon dioxide CO_2 or other inert gas. The barometric pressure of compensation gas should be slightly higher than the expected gas pressure in coal seam. The passive manometry is to measure the gas pressure through the natural infiltration of the gas into coal seam after the drill hole sealed, to achieve the balance of gas pressure.

According to an incomplete statistics, the successful rate of drilling manometry is no higher than 70%, and the scrap rate of some manometry hole is as high as 50%. Besides, it often takes the passive manometry at least about a month or several months to complete one measure cycle—(Xun Bingxing, et. al, 2010) This manometry, with relatively long measure cycle, low success rate and high error risks, wastes a lot of financial resources, delays the production cycle, leads to wrong technical judgment, and has high potentiality of accidents. Therefore, this paper expects to explore a determination method or approach, under the premise of active manometry, to promote the rapidity and accuracy of gas pressure determination.

1 GAS FLOWING LAW AROUND THE MANOMETRIC DRILL HOLE AND ITS MATHEMATICAL MODEL

1.1 *Gas pressure in coal seam*

The gas pressure in coal seam refers to the pressure of the gas contained in the coal seam. The determination method is to drill holes in the coal seam, bury piezometric tube, grout and seal holes, install pressure gage. The determination of the gas pressure under steady situation is the coal seam gas pressure.

1.2 *Gas migration law in coal seam*

According to the previous research on gas flow regularity, the migration law follows Darcy's law, that is, Laminar Flow—(Sun Peide, 1988).

In the actual case, when drilling to expose the seam, affected by factors, such as mechanical operation, the stress around the borehole changes, leading to the instability of the gas flow around the borehole in the seam. After a period of time when stress gets its balance, the gas flow is gradually stabilized in the radial unstable seam, Academician Zhou Shining thinks that the flow of gas in coal seam still obeys Darcy's law—(Zhou Shining & Lin Boquan, 1999).

1.3 *Model of gas flow in manometric borehole*

Coal is a kind of uneven double porous media made up of macro-cracks and micro-pores. Gas in coal seam remains in the macro-cracks and micro-pores in free state and adsorbed state. Once getting pressure relief, gas in coal seam begins to flow along the pores and fractures, while the absorbed gas is desorbed. Gas flow in Coal seam is actually a very complex process affected by many factors. In order to simplify the process, the coal seam gas flow model has the following assumptions—(Wang Xiaoliang, et. al, 2003).

1. The original gas in coal seam has even pressure distribution. As the permeability of the roof and floor of coal seam is much smaller than the coal seam, the rock mass of the roof and floor is, therefore, supposed to be gas-tight layers, completely free from gas;
2. Coal seam permeability and porosity is not affected by the change of gas pressure in coal seam;
3. Gas in coal seam consists of free gas and adsorbed gas, and it conforms to the Langmuir equation;
4. the gas field gas drilling flow can be considered as an ideal gas, and complies with the ideal gas state equation;
5. The gas is ideal. The gas flow in coal seams is laminar permeability in compliance to Darcy law;

With the above assumptions, the coal seam gas dynamic model of two-dimensional flow can be set up as follows:

$$\left(\frac{n}{p_0}+\frac{ab\rho_m k_a dr}{1+(bp)^2}\right)\frac{\partial p}{\partial t}=\frac{k}{2\mu p_0}\left(\frac{\partial^2 p^2}{\partial x^2}+\frac{\partial^2 p^2}{\partial r^2}\right) \quad (1)$$

Boundary conditions: coal wall, $p = p_0$; coal seams within coal wall, $p = p_a$.

The initial conditions: $t = 0$, $p = p_a$

The drill hole helps the discretization of the gas in its flow region in the coal seam. According toformula (1), the differential equation of the gas flow in the coal seam can be derived. Due to the gas pressure gradient around the drill hole, the coal seam gas always flows from where pressure is high to where pressure is low. That is, the gas will flow to the wall of the drill hole from a distance. The amount of gas emission per unit area $q(m^3/(m^3 \cdot s))$ on the wall of the drill hole can be obtained by Darcy Law as follows:

$$q=-\frac{k}{u}\frac{dp}{dx} \quad (2)$$

With the mathematical modeling of coal gas seepage, the discretizating of the gas by numerical method, and the using of FPRTAN language programming, the distribution of gas pressure and the law of gas emission can be calculated with analog equation under certain boundary conditions and initial conditions. Therefore, when the wall of the drill hole is suddenly exposed, the gas emission on the wall will sharply rise to the maximum amount, while with the exposure duration increasing, the gas pressure around the manometric hole decreases, the range of pressure decay enlarged, — the closer the gas pressure gradient to the drill hole wall, the larger the pressure; conversely the farther, the smaller. The longer the exposure duration is, the larger is the range of pressure decay, and the longer time it takes the hole to regain a gas pressure balance after hole sealing.

2 ACTIVE MANOMETRY

2.1 *Principles of active manometry*

The method of active manometry was promoted by academician Zhou Shining in 1980's. Active manometry is to aerate certain amount of air into the drill hole where coal seam is exposed or the manometric room through preinstall devices after having been sealed, so that the measuring time is largely shortened as the time to balance gas pressure is shortened. The compensate gas should be aerated into the drill hole after the drill hole is sealed. The gas out of the relief ring will start to flow toward the drill hole. The pressure relief ring in coal seam will not expand once the hole is drilled. The length of time for measuring the pressure is determined by the amount of gas needed to balance the pressure. If proper amount of gas is aerated into the drill hole in advance, the manometric speed will be accelerated. The compensate gas is used to make up for the gas emitted through the drill hole before it is sealed. Among CH_4, N_2, CO_2 or some other inert gases, according to the result of experiments, CO_2 has the highest adsorbability, CH_4 second, N_2 the lowest. For the sake of safety and the absorbtion-desorbtion performance of coal to gas, N_2 is a preferential choice.

2.2 *Manometric method with grouting hole sealing*

The hole is sealed with grouting. The materials for hole sealing is often cement paste, which expands rather than shrinks. The hole is sealed by compressed air grouting device or mud pump. This manometric method applies to gas pressure measure at any condition in the pit, in particular applies to the measure of gas in close distance coal seams and coal seams groups.

Grouting hole sealing is a widely-used way of hole sealing by now, which is especially adopted when the drill hole is too long. The sealing materials used are usually cement mortar or cement paste. The manometric devices often includes piezometer tube, inspection pipe, injection pipe, grouting pump, wood peg, baffle plate etc. (Fig 1.—Lan Zequan, et. al, 2009). If the execution condition is good enough, the inspection pipe and baffle plate can be omitted. Beside, considering the influence of water onto the gas pressure, the gas pressure value measured may need to be adjusted according to the following formula:

$$p_0 = p \pm 0.011 \times L_1 \sin\theta;$$

P_0: gas pressure in coal seam,
P: measured gas pressure, *MPa*;
L_1: Length of water in the piezometer pipe, *m*
θ: angle of the drill hole, minus sign for upward drilling, plus sign for downward drilling.

2.3 *Analysis of gas pressure balance*

In the gas room of the manometric drill hole, the two ends of the sealed hole bear the same amount of pressure when the gas pressure achieves balance. According to the law of mass conservation, when the gas pressure in the manometric drill hole reaches balance, the amount of compensate gas in the gas room is approximately equal to the amount of axial leakage of the sealed section. As is shown in the following formula:

—(Gao Jianliang & Hou Sanzhong, 2001)

$$2m\lambda_1(p_0 - p_1)G(F) = (2r_0 b + b^2)\lambda_2 \frac{p_1 - p_2}{L} \tag{3}$$

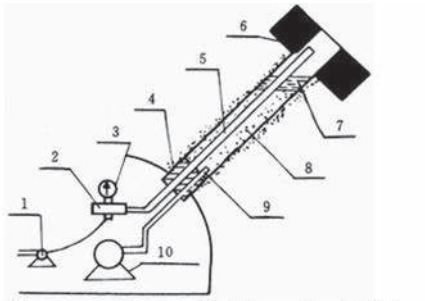


Figure 1. Schematic diagram of grouting hole sealing.

$$B = \frac{b(2r_0 + b)g}{2mLG(F)} \cdot \frac{\lambda_2}{\lambda_1}, \tag{4}$$

$$p_1 = p_a + \frac{p_0 - p_a}{B + 1} \tag{5}$$

B is dimensionless quantity, which can be defined as depressurization effect coefficient. The change of B value can accurately reflects the relations between the measured gas pressure value and the actual gas pressure value. As we can see from Formula (4), When B approaches 0, p_1 is close to the original gas pressure p_0. This is to assume that the hole sealing is fine and air-tight. When B approaches ∞, p_0 is close to the original gas pressure p_a. This is to assume the drill hole is unsealed and open wide.

From the expression of B, the value of B is inversely proportional to the length of sealed hole, the length of gas room m, and the manomentric time function, and in direct proportion to the radius r_0 of Manomentric drill hole r_0, the width b of non-elastic deformation around the drill hole b and the specific value of air permeability coefficient λ_2/λ_1. From what affects the B value, we can see that some of factors are very hard to control, such as λ_1, b. Therefore, the simplest way to accelerate the measuring pressure speed is to increase the length of sealed hole and decrease the capacity of the manomentry gas room.

Table 1.

Letter	Implication	Unit
m	The length of gas room	m
λ_1	The original coal seam gas permeability coefficient	$m^2/(MPa^2 \cdot d)$
p_0	The original gas pressure of coal seam	MPa
r_0	The radius of manometric drill hole	m
b	The inelastic deformation band width around the drill hole	m
p_1	Stable gas pressure value in gas room of manometric drill hole	MPa
$G(F)$	Manometric time function	—
λ_2	The permeability coefficient of the inelastic deformation zone of peripheral coal seam in the sealing section of the pressure hole	$m^2/(MPa^2 \cdot d)$
p_a	The press from the inner end part of manometric drill hole to the sealing part	MPa
L	The distance from the inner end part of manometric drill hole to the sealing part	m

2.4 *The approach to fast and accurate coal gas pressure determination—to shorten the exposure time of the drill hole, and to decrease the volume of the manometric room*

As is analyzed above, the gas flow field on the wall of drill hole can be approximately regarded as a steady one from the time when the hole is drilled to the time when the hole is sealed, in the course of which the gas pressure in the hole is much smaller than that original gas pressure in the coal seam. That is, the distribution curve of coal gas pressure in the drill hole is a logarithmic curve. The farther the distance is to the wall o drill hole, the higher the gas pressure is in the coal seam, which means the gas pressure gradient is large near the wall of drill hole; while the gas pressure gradient is small at the position far away from the hole wall. In the process of drilling, the inner wall of the drill hole in coal seam section is suddenly exposed, due to the increase of gas pressure gradient, the gas in the coal seam will rapidly rush out of the hole. The longer the exposure lasts, the larger amount of gas is emitted. Therefore, the hole should be sealed soon after the drilling work is finished to shorten the exposure time of the hole wall, so that the gas pressure in the gas room can rapidly achieve balance, and the menometric period is largely shortened.

When the manometric hole is sealed, with the accumulation of high pressure gas in the menometric room, the pressure gradient near the hole wall gets lower, the amount of gas emission per unit decreases as well. When the supplementary amount of gas in the menometric room Q_1 equals to the gushing amount of gas in the coal seam hole section Q_2, the gas pressure in the menometric room and in the coal seam stays in balance, and the gas pressure gradient near the hole wall is 0. That is,

$$Q_1 = Q_2 = S \times \int_0^T f(q)dt$$ In it:

Q_1 is the capacity of manometric room, including unsealed hole section and the lumen capacity of piezometer tube;
S refers to the exposed coal wall area of the coal seam hole section in the manometric room;
T stands for the time needed for the manometric hole room to achieve the pressure balance right after the hole is sealed;
$F(q)$ is the amount of gas emission per unit area, a function relating to time. Therefore, the capacity of manometric room should be decreased to on extreme, while the exposed area of the hole wall should be enlarged to the other, so that the manometric period is greatly shortened.

In order to shorten the exposure time of the drill hole wall and decrease the volume of the manometric room, the hole should be sealed right after the drilling work is finished, as long as the hole has pierced the coal seam. The radius of the piezometer tube and the length of the drill hole should both be shortened properly; the hole sealing should be stopped once it reaches the seam (roof) floor, or high pressure gas should be injected into the manometric room after the hole is sealed.

3 CONCLUSION

1. It is a growing trend to use active hole sealing to determine the gas pressure of the coal seam in the future gas pressure measurement.
2. The decrease of exposure time of the manometric hole and the volume of manometric room can help to shorten the manometric period. The manometric drill hole should be right as long as it pieces the coal seam, and the capacity of manometric room (including the radius of piezometer tube) should be decreased as much as possible. The drill hole should be sealed right after the drilling work finished, in order to shorten the exposure time of the hole wall. Or high pressure compensation gas should be injected into the room. The gas pressure in the coal seam can be rapidly determined.
3. The key for manometric accuracy lies on the quality of sealing. With the manometric room and tube ready, to inject cement paste (or other hole sealing materials) into the drill hole can effectively prevent the tiny fractures around and on the inner wall of the hole. Therefore, the densification of the sealed hole section will largely increase the quality of hole sealing and accuracy of manometry.

REFERENCES

Gao Jianliang & Hou Sanzhong. 2007. Dynamic Gas Pressure Distribution and Emission Law on excavating face [J]. Journal of Coal. 32(11):84–87.

Lan Zequan, et al. 2009. Status and Analysis of Coal Seam Gas Pressure Determination by Direct Method. *Safety in Coal Mine.* 2009(4):74–78.

Sun Peide. 1988. Theories of Coal Seam Gas Migration and Its Utilization(C)/China Coal Society 1988 Academic Annual Conference Proceeding. Beijing: Coal Industry Press. 171–177.

Wang Xiaoliang, et al. 2003. Computer Model of Coal Gas Migration [J]. Journal of Taiyuan University of Technology. 34(4):402–405.

Xun Bingxing, et al. 2010. Approaches to Fast and Accurate Coal Gas Determination [J]. Safety in Coal Mine. 2010(5):93–99.

Zhou Shining & Lin Boquan. Theories of Coal Seam Gas Occurrence and Migration [M]. Beijing: Coal Industry Press. 1999: 82–86.

Progress in Mine Safety Science and Engineering II – He et al. (Eds)
© 2014 Taylor & Francis Group, London, ISBN 978-1-138-00122-0

Study on effect of gas adsorptive constant under electro magnetic fields exerted

Li Zhang, Xueqiu He, Jianhua Yue & Enyuan Wang
College of Energy Resource and Earth Science, China University of Mining and Technology, Xuzhou, Jiangsu, China
Research Center of State Administration of Work Safety, Beijing, China

ABSTRACT: Experimental study was done on the effects of electromagnetic fields on gas adsorptive constant a/b of different coal rank. The research results show that the electromagnetic fields almost have no effects on gas adsorptive constant a, but can reduce adsorptive constant b obviously. Adsorptive constant b decreases with voltage and frequency of electromagnetic field exalting. The exerted electromagnetic fields can reduce the capability of coal adsorption to gas and gas adsorptive volume.

1 INSTRUCTIONS

Gas accident is the main disasters of coal mines, and it is also called "the first killer" of coal mines. The direct reason why both gas explosion and outburst of coal and gas accident took place are there is a plenty of adsorbed gas in coal seams, 90 percent of gas in coal seam exists with the adsorbed form. Characteristics of gas adsorption in coal are one of basis for summarizing the law of gas explosion and forecasting and preventing gas accident. Studying on characteristics of coal adsorption to gas is help to expounding mechanism of gas adsorption and emission law. The purpose of the current study is to determine the adsorption properties of different coal by using electromagnetic fields exerted in order to go deep into research mechanism of coal adsorption/ emission to gas. The result of this study will lead to a better understanding of prevention gas accident and hence will be provide a new method to reducing adsorptive gas content.

2 EXPERIMENT

2.1 *Coal samples and experimental methods*

Coal samples are taken from Renlou coal mine and Yangquan coal mine. Coal samples are crashed into particles in the size of 0.25 mm to o.5 mm in diameter. Experiments are carried out by use of adsorption and emission apparatus made by China University of Mining & Technology, and an electromagnetic field generator is used to exert alternative electromagnetic field on coal particles containing gas (Zhang 2002). The setup of the experimental system is show in Fig. 1. The effect of electromagnetic field exerting model on gas adsorptive constant is tested under conditions of different voltage or frequency.

The experiment is composed of four steps, namely, gas pumping, lower pressure gas adsorption, high pressure gas adsorption and gas emission measurement. Experiments are conducted when alternative electromagnetic field is exerted on coal containing gas in the last three steps to study gas adsorptive constant *a*/*b*. The gas used is methane, and coal samples are anthracite and bituminous coal.

The alternative electromagnetic field is exerted on coal particles in the last three steps with fixed parameters which are voltage of 500 to 1200 V, and frequency of 0.54 to 1.58 MHz. When alternative electromagnetic field is exerted in the second step or the third step, it is exerted all the time. When it is applied in adsorptive experiment, the operation are as following: First, the coal samples is pumped to vacuum, then let one atmosphere methane absorb into coal samples until it reach to adsorptive balance, meanwhile record adsorptive amount changing with time. When the measurement of high



Figure 1. Experimental Instrument.

pressure gas adsorption and emission, operation are as following: first, the coal samples is pumped to vacuum, then filled in certain pressure methane until it reach to adsorptive balance, then made the adsorptive pressure fall down to certain pressure several times reaching to the new adsorptive balance until to one atmosphere, meanwhile record every emission amount changing with time. Gas emission experiment must be kept the adsorptive balance pressure same, otherwise it has no comparable. The research work is carried out to study effect of gas adsorptive constant *a*/*b* in which a series of experiment is repeated with electromagnetic field exerted.

2.2 *Experimental results and analysis*

When alternative electromagnetic field is exerted in adsorptive step, typical experimental result is shown in Figure 2, Figure 3, Figure 4 and Figure 5 in which y axis represent gas adsorptive quantity calculated indirectly from every ton of coal adsorptive quantity and x axis represent adsorptive balance pressure. Figure 2 and Figure 3 show the adsorptive results which the volt of alternative electromagnetic is fixed 1000 v, but the frequency is changed. In Fig. 2 coal sample is taken from Yangquan coal mine which the coal is anthracite. In Fig. 3 coal sample is taken from Renlou coal mine which the coal is bituminous coal. Both in Fig. 2 and Fig. 3, curve 1 represent the characteristics curve of gas adsorption without electromagnetic field, and curve 2 is electromagnetic field which voltage is 1000 volt and frequency is 0.54 MHz. Curve 3 is electromagnetic field which voltage is 1000 volt and frequency is 0.73 MHz, Curve 4 is electromagnetic field which voltage is 1000 volt and frequency is 1.11 MHz, curve5 is electromagnetic field which voltage 1000 volt and frequency is 1.58 MHz.

Figure 4 and Figure 5 show the adsorptive results which the frequency of alternative electromagnetic is fixed 0.54 MHz, but the volt is changed. Fig. 4 coal samples is the same one with Fig. 2, and Fig. 5 coal samples is the same one with Fig. 3. Both in Fig. 4 and Fig. 5, curve 1 represent the characteristics curve of gas adsorption without electromagnetic field, and curve 2 is electromagnetic field which voltage is 500 volt and frequency is 0.54 MHz. Curve 3 is electromagnetic field which

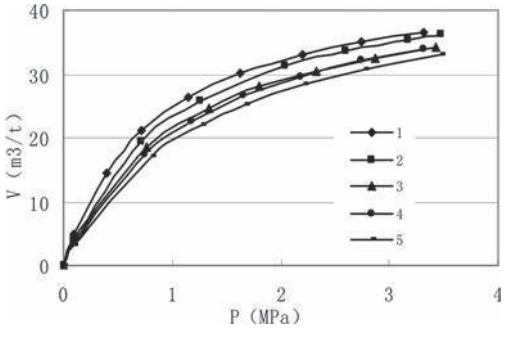


Figure 2. Gas Adsorption frequency Characteristics of Yangquan coal samples.

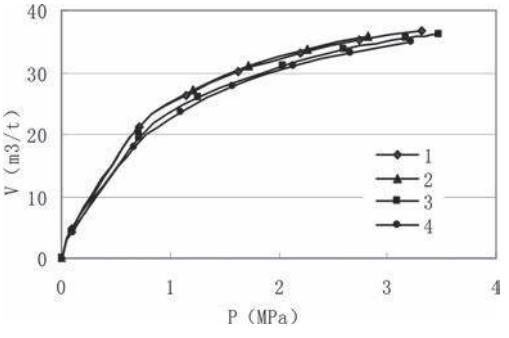


Figure 4. Gas emission voltage Characteristics of Yangquan coal samples.

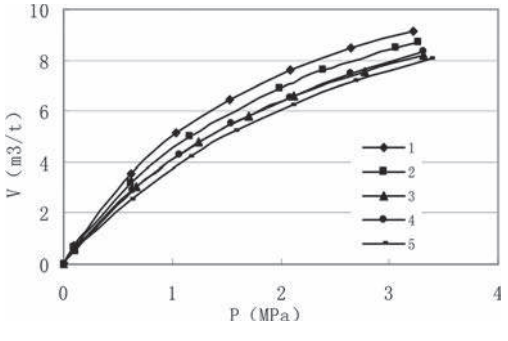


Figure 3. Gas Adsorption frequency Characteristics of Renlou coal samples.

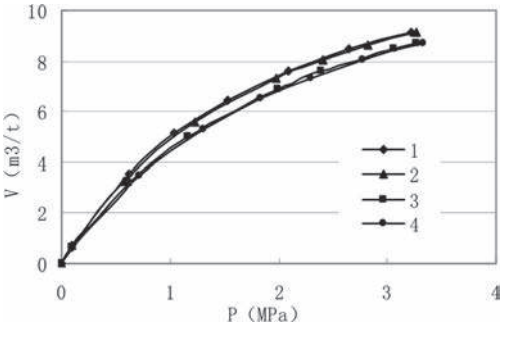


Figure 5. Gas emission frequency Characteristics of Renlou coal samples.

Table 1. Adsorptive constant of experimental coal samples.

Frequency (MHz)	Yangquan coal sample			Renlou coal sample		
	a	*b*	*r*	*a*	*b*	*r*
No exerted	46.1606	1.1596	0.9936	14.7500	0.5100	0.9945
0.54	47.0168	0.9679	0.9975	14.7168	0.4435	0.9959
0.73	45.0000	0.9117	0.9954	14.4301	0.3975	0.9967
1.11	46.2532	0.8213	0.9968	15.1132	0.3665	0.9978
1.58	46.1461	0.7210	0.9949	15.6303	0.3160	0.9947

Table 2. Adsorptive constant of experimental coal samples.

Volt (V)	Yangquan coal sample			Renlou coal sample		
	a	*b*	*r*	*a*	*b*	*r*
No exerted	46.1606	1.1596	0.9936	14.7500	0.5100	0.9945
500	46.8523	1.1367	0.9964	14.9300	0.4875	0.9973
1000	47.0168	0.9679	0.9975	14.7168	0.4435	0.9959
1200	46.1577	0.9582	0.9941	15.0132	0.4165	0.9938

voltage is 1000 volt and frequency is 0.54 MHz, curve4 is electromagnetic field which voltage 1200 volt and frequency is 0.54 MHz.

It can be seen clearly from the above figures that the gas adsorption characteristics curves with electromagnetic field are different from that without electromagnetic field. The main difference is that gas adsorptive quantity is reduced in experiments with electromagnetic field contrasting with that without electromagnetic field. Gas adsorptive amount is abated with both voltage and frequency of electromagnetic field lift. Electromagnetic field effect can slack amount of coal adsorption to gas and increase. Electromagnetic field effect can debase ability of coal adsorption to gas (He & Liu 1995, Zhang 1999, 2000).

2.3 *Adsorptive constant Analysis*

When test temperature is 30 °C, test gas is methane, the two kinds coal samples adsorptive constant is shown in Table 1 and Table 2.

From the above tables can be learn, the electromagnetic field have effect on gas adsorptive constants *a*/*b*, electromagnetic effect of adsorptive constant *a* is inconspicuousness. Adsorptive constant *b* decreases with voltage and frequency of electromagnetic field exalting.

3 MECHANISM ANALYSIS

Coal adsorption to gas is physical adsorption. Under high pressure and at certain temperature it is follow the famous 1 angmuir equation as following (Gu 1994):

$$Q = \frac{abP}{1 + bP} \tag{1}$$

Where: T is temperature, °C; P is adsorptive balance pressure, MPa; Q is adsorptive gas content under P pressure, ml/g or (m^3/t); *a, b* are Langmuir adsorptive constant, *a* is saturation adsorptive content, ml/g or (m^3/t); *b* is adsorptive constant, MPa^{-1}.

A is saturation adsorptive content of coal. It is decided mainly by metamorphic degree of coal, bore rate of coal, and other own characteristics of coal, and it has very little influence with outside. So electromagnetic field can not change constant *a.* Constant *b* is decided by temperature and surface potential well. The higher the temperature is, the less the value *b* is, and the less adsorptive gas content is. On the contrary, the lower the temperature is, the larger the value *b* is, and the more the adsorptive gas content is. For the depth of surface potential well, the deeper the surface potential well is, the more the adsorptive gas content is. On the contrary, the shallower the surface potential well is, the less the adsorptive gas content is. The electromagnetic field can make temperature high and reduce depth of surface potential well, so it can reduce the constant *b*.

4 CONCLUSIONS

Coal adsorption to gas under electromagnetic field is physical adsorption. The gas adsorptive capacity

of coal is abated for the agency of electromagnetic field. When the frequency of electromagnetic field is changeless, the capacity of coal adsorption to gas is reduced with the voltage of electromagnetic field lifted. When voltage of electromagnetic field is changeless, the capacity of coal adsorption to gas is reduced with the frequency of electromagnetic field lifted. An alternative electromagnetic field can reduce the amount of gas adsorptive constant b. Thus it is possible to reduce the elastic potential energy of gas and prevent gas accident.

REFERENCES

Guxiren. Surface chemical. Beijing Science press, 1994, 6.

He Xueqiu, Liu Mingju., Fracture Electro-magnetic Dynamics of Coal or Rock Containing Gas. Xu Zhou: China University of Mining and Technology, 1995, 135–136.

Zhang Li. The Research on Diffusion and Permeation Mechanism of Coal Bed Methane. Tai Yuan: Department of Mining Engineering of Tai Yuan University of Technology, China, 1999.

Zhang Li. Study of The Process of Adsorption of Gas in Coal. India: Oxford & IBH Publishing Co. Pvt. Ltd, New Delhi, 2000, 151–155.

Zhang Li. Study on the Effects of Electromagnetic Fields on Gas Adsorption and Emission and Its Mechanism XuZhou: China University of Mining and Technology, China, 2002.

Progress in Mine Safety Science and Engineering II – He et al. (Eds)
© 2014 Taylor & Francis Group, London, ISBN 978-1-138-00122-0

Hazard prediction and prevention of rock burst in island working face

S.S. Guo
State Key Laboratory of Gas Disaster Monitoring and Emergency Technology, Chongqing, China
Chongqing Research Institute of China Coal Technology Group, Chongqing, China

ABSTRACT: When the mining depth is larger, the stress concentration is at a very high level at the island working face and its surrounding roadways. The risk of rock burst is higher coupled with the influence of the geological tectonics. The article analyzed coal and rock physical and mechanical properties of 2–228 island working face in Liyazhuang coal mine, determined the energy source of rock burst using micro seismic monitoring technology, determined the hazardous area and level of rock burst, formulated the corresponding prevention measures, and to achieve the safety mining of at the island working face. The article provides a beneficial reference for the same conditions of the mine mining area and other similar mine island working face.

1 INTRODUCTION

The rock burst disaster in our country has become increasingly serious with the increase of mining depth. Because of the complexity and instantaneous burst of rock burst, prediction and prevention the rock burst disaster has always been a problem in safety production of coal mine (He Manchao et al. 2005, LI T 2007, Pan Liyou 2006). For high gas coal mine island working face of large mining depth, under the coupling of high ground stress, high gas and geological structure, the mechanism of coal and rock dynamic disaster is more complicated, which is difficult to predict and prevent. According to the actual situation of 2–228 island working face of Liyazhuang coal mine, this article analyzed the mining technical conditions such as coal and rock physical and mechanical characteristics, stress field distribution and gas parameters. Combined with monitoring technology, this article also analyzed the causes of dynamic phenomenon and sources of energy, predicted disaster degree and the range in advance, and taken appropriate control measures to achieve the safety mining of at the island working face.

2 PRODUCTION TECHNOLOGY CONDITIONS OF 2–228 ISLAND WORKING FACE

The 2–228 working face of Liyazhuang coal mine is located in the second mining area on the left, which is an island working face both sides of the section has been worked out (As shown in Fig. 1). The upper side of 2–228 working face is 2–220 goaf, equipped with 20 m pillar; the underside of 2–228 working face is 2–224 goaf, equipped with 20 m pillar. 2–228 working face is about 650 m underground. The strike length of 2–228 working face is about 630 m and tendency length is about 130 m. The thickness of main mining no. 2 coal seam is about 3.16 m on average with 2 layers of dirt band (mainly mudstone, carbonaceous mudstone). The Coefficient of the coal seam is 1.5. The average angle of the coal seam is 6°. The structure of the coal seam is complex. The immediate roof of no. 2 coal seam is sandy mudstone (0–2.87 m), basic roof is medium-fine sandstone (2.1–4 m), direct bottom is siltstone (1.4–3.0), and basic bottom is mudstone (1.5–1.7 m). Affected by factors of high original rock stress, mining stress concentration

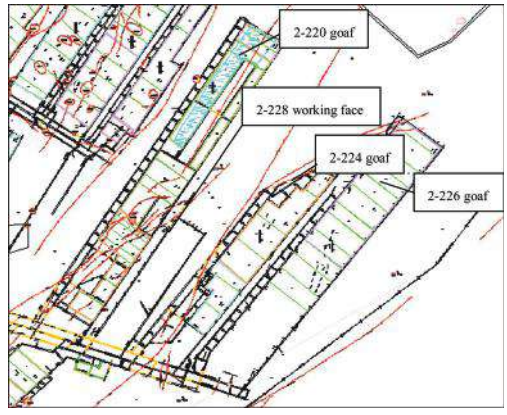


Figure 1. The arrangement plan of 2–228 island coal face.

and gas, the no. 2 coal seam appears rock burst and jet orifice phenomenon, which is a serious threat to safety production.

3 PHYSICAL AND MECHANICAL PARAMETERS, AND THE EVALUATION OF THE ROCK BURST ORIENTATION OF COAL AND ROCK

Over the years, domestic and foreign scholars did lots of experimental study on rock burst, and gained valuable research results (Pan Jienan et al. 2005, Zou Deyun et al. 2004, Zhao Yixin et al. 2007, Pan Jienan 2006, Su Chengdong 2004, Feng Zengchao et al. 2003, Pan Yishan et al. 2003, Li Shulin 2001) They thought there must have two kinds of factors to cause rock burst: (1) Stress conditions. In-situ stress is the basic force mine dynamic phenomena, which belongs to the external factors. (2) Mechanical properties of coal or rock. Mechanical properties of coal or rock are important internal factors caused Rock burst. The relationship between the risk of rock burst and the structure characteristics of coal and rock are very close. The impact tendency of coal and rock characteristics is the inherent properties of coal (Pan Jienan et al. 2005, Zou Deyun et al. 2004). The impact tendency index of coal and rock includes dynamic failure time, elastic strain energy indices, impact energy indicators, brittleness coefficient, and so on.

In order to determine the impact tendency of 2–228 island working face, we took the coal and rock sample in coal seam and roof of 2–228 working face, and measured impact tendency of coal and rock sample according to the standard evaluation method of coal and rock impact tendency.

Processing production of coal sample and physical mechanical parameters test are in strict accordance with the provisions of *Measurement method of coal and rock physical and mechanical properties* (GB/T 23561–2009), and *Measurement method of coal seam impact tendency classification index* (MT/T 866–2000). The experiment determined natural apparent density, compressive strength, consistent coefficient, elastic modulus, deformation modulus, wave velocity, rock burst energy index, elastic energy index, dynamic failure time, and other parameters. The determination results as shown in Table 1.

Known from the analysis of Table 1, compressive strength and elastic modulus of coal samples are medium. According to the comprehensive results analysis of rock burst energy index, elastic energy index and dynamic failure time, no. 2 coal seam of 2–228 island working face has medium impact tendency. Sandstone and medium grained sandstone in coal seam roof have high compressive strength and resistance to deformation ability, coefficient is 12.6 and 19.0 respectively, and belongs to the class hard rock. The thickness of Sandstone is about 4.6 m, which bending strength is 23.42 MPa, modulus of elasticity is 34.5 GPa, is 650 m depth from surface. The bending energy index of sandstone is 7.6 kJ, and elastic energy index UWQ ≤ 10 kJ, which belongs to no impact tendency rock with reference to *the method for determination of the rock impact tendency classification index* (Yang Zhiguo et al. 2009). The compressive strength of sandy mudstone in coal seam roof is medium and coefficient is 5.9, belongs to medium hard rock and no impact tendency rock.

Table 1. Test results summary of coal and rock physical and mechanical parameters.

name of rock / parameters	coal samples		sandstone		medium grained sandstone		sandy mudstone	
	minimum~maximum	mean	minimum~maximum	mean	minimum~maximum	mean	minimum~maximum	mean
natural apparent density/kg.m^{-3}	1328~1350	1338	2941~3075	3043	2630~2742	2701	2621~2632	2627
wave velocity/m.s^{-1}	1387~1945	1751	4340~4644	4468	2255~4650	4213	3071~3992	3431
compressive strength/MPa	1074~21.09	13.23	51.3~187.1	126.3	145~215	190	24.03~94.51	59.3
elastic modulus/GPa	1.62~4.04	2.69	11.6~47.6	34.5	30.4~46.2	39.7	5.69~19.03	12.4
deformation modulus/Gpa	0.91~2.91	1.83	6.52~41.36	28.3	23.5~43.2	35.0	4.05~11.37	7.71
poisson ratio	0.3~0.41	0.35	0.27~0.39	0.32	0.26~0.28	0.27	0.30~0.37	0.34
Protodikonov's hardness coefficient/f	1.1~2.1	1.3	5.1~18.7	12.6	14.5~21.5	19.0	2.4~9.5	5.6
elastic energy index/WT	1.49~7.43	3.89						
rock burst energy index/WN	0.89~3.57	1.70						
dynamic failure time	22~346	196						
Bending strength/ MPa			8.04~29.46	23.42				
bending energy index/kJ				7.6				

4 THE OVERBURDEN STRESS DISTRIBUTION OF 2–228 ISLAND WORKING FACE

We simulated the overburden stress distribution of 2–228 island working face by using numerical simulation software FLAC^{3D}. The simulation range for the 2–228 island working face is: length 600 m, tend to range from 2–220 goaf to 2–224 goaf. The direction of excavation is along with working face advancing direction. The simulation result shown in Fig. 2.

Through the Fig. 2 stress distribution in three-dimensional figure, we can see the pressure on either side goaf of the 2–228 working face have been relieved, and the stress of 2–228 island working face and coal pillar concentrated, especially on both sides coal pillar of working face and near security exit.

We intercepted stress distribution along the X axis section of 2–228 working face, as shown in Fig. 3. The internal stress of 2–228 island working face (vertical in-situ rock stress) is 14 MPa, overburden maximum stress close to 24 MPa, and the abutment pressure in front of the working face stress reached more than 20 MPa. Working stress concentration caused by mining at around double the original vertical stress. As the isolated island working face, the 2–228 working face under the concentration of stress is bigger, near the coal pillar or fault, stress concentration threshold is reduced, it is prone to dynamic disasters.

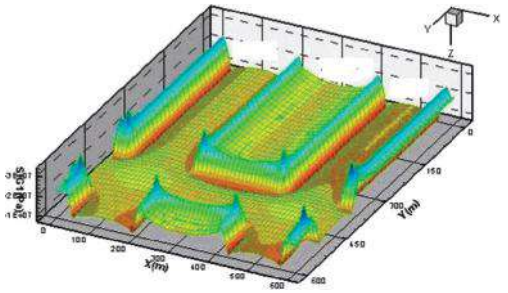


Figure 2. Stress distribution in three-dimensional of 2–228 Island working face.

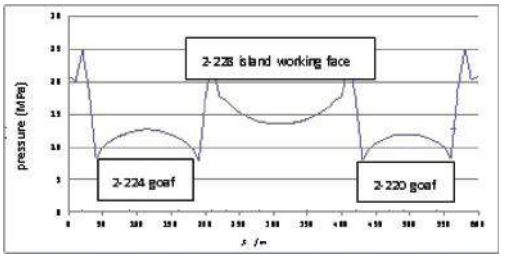


Figure 3. stress distribution along the X axis distribution of 2–228island working face.

5 MICRO SEISMIC MONITORING OF PERCUSSIVE ROCK BURST SOURCES AND ENERGY

The substance of micro seismic events is a form of series of dynamic evolution caused by surrounding rock stress, strain, deformation, rupture and instability and failure. In the process of coal mining stope advance, coal and rock mass in front of the working face are divided into the elastic zone, plastic zone and plastic zone, which corresponds to the original stress zone of mining abutment pressure, peak stress zone and stress reduction zone. In high stress area of coal and rock, under the mining activities of disturbance, coal and rock stress boundary conditions and original rock stress change, stress release caused the fracture of coal and rock fracture micro seismic events. So the micro seismic events can reflect the high stress of coal and rock mass and rock ultimate strength area.

Seismic technology is a kind of monitoring of mine coal and rock dynamic disaster regional prediction method, which can monitor coal and rock seismic activity in real time, continuous and online, and it becomes one of the important means of forecasting rock burst disaster and mechanism research in coal mine (He Manchao et al. 2005, LI T 2007, Pan Liyou 2006, Yang Zhiguo et al. 2009). On the basis of analysis of coal roof and floor rock physical and mechanical properties and stress distribution of 2–228 island working face, we arrangement 11 points in no. 2 mining area of Liyazhuang coal mine and continuous monitor for three months With SOS micro seismic monitoring system. Seismic source localization plan is shown in Fig. 4.

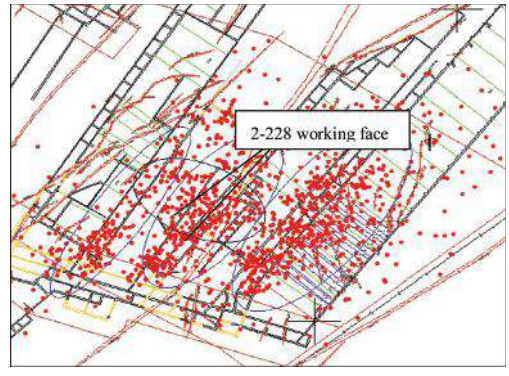
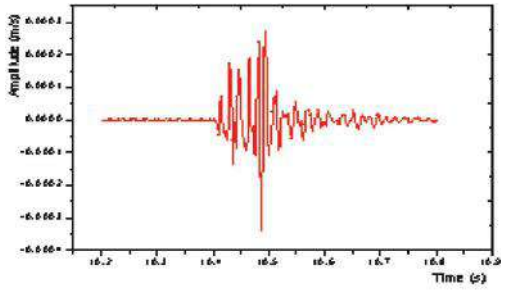


Figure 4. Seismic source localization plan.

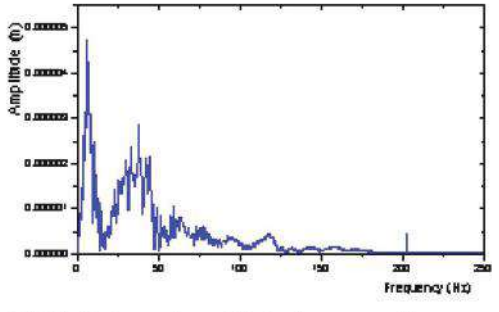
We monitored 1207 times shock in no. 2 mining area within 3 months, as shown in Fig. 4. Micro seismic occurred, which indicated that regional coal pillar and roof and floor of 2–228 working face has burst, the place of surrounding rock in a state of flux. Micro seismic source distribution mainly concentrated in the 2–228 working face, coal pillar between 2–228 working face and 220 goaf, coal pillar between 2–228 working face and 2204 goaf, in the basic between 20 m upper area and 50 m underside of 2–228 working face. This suggested that the area under the condition of high stress by working face mining disturbance, damage and the roof and floor strata occurred in the form of seismic performance.

Micro seismic monitoring system recorded seismic energy of the 2–228 working face is concentrated in between 10^2~10^5 j. The article tried to analyze the relationship between seismic energy and the occurrence of rock burst based on. 9 measuring point laid out in 2–228 conveyance road which detected in more than 10^3 j of energy of seismic waveform and spectrum characteristics, as shown in Fig. 5.

As shown in Fig. 5, the rock burst which vibration energy is greater than 10^3 j, its amplitude of main vibration speed is between 0.2×10^{-4}~5.0×10^{-4} m/s, and duration time of signal is between 600~1800 ms. The attenuation is fast, and the higher the energy, the longer the duration. Look from the frequency spectrum, signal distribution between 0~160 Hz, frequency band is wide, between 10~75 Hz. This from a side show that the 2–228 island working face has the possibility to occur rock burst, fault activation, goaf roof fracture, roof fracture of cutting hole, and other factors are the main cause of micro seismic signals.



(a) No.9 channel amplitude-time figure



(b) No.9 channel amplitude-frequency figure

Figure 5. Part micro seismic events waveform and spectrum graph of energy is greater than 103 j.

6 PREVENTION AND CONTROL OF ROCK BURST

In view of the rock burst occurred in zoning and characteristics in 2–228 island coal face of Liyazhuang coal mine, it shows prevention and control of rock burst should follow the following principles: (1) Try to avoid the high stress area formation or work in high stress area; (2) Ensure maximum in-situ stress direction parallel mining or tunneling; (3) Expand the scope of stress release, in order to reduce the stress concentration and stress release rate; (4) Control conditions of coal seam storage energy; (5) Control of roof sudden release of energy and load; (6) Minimize construction to the effect of percussive ground pressure. According to the fact that 2–228 island working face has been formed, it should take the following measures to prevent and control rock burst:

1. Construct gas drainage unloading borehole in mining-coal bed, and drill before mining. The main purpose of the construction of drainage hole is: On the one hand, using the drilling pressure relief effect. The essence of the borehole pressure relief is under high stress conditions, using of accumulated elastic energy to subvert the borehole in coal seam coal body around, make coal unloading, releasing energy, eliminate risk impact. On the other hand, using gas release of coal seam gas potential, increase the strength, thereby increasing resistance to the potential of percussive ground pressure.

   Drainage unloading borehole can adopt positive parallel or oblique parallel hole drilling way (Fig. 6). Borehole spacing is between 5~7 m and 110 m deep.
2. Coal seam water injection. Coal seam water injection is through increasing the moisture content of coal seam or water saturation in coal seam to change state of coal and rock deformation, make sure the failure does not occur so as to prevent the occurrence of rock burst. Arrangement water injection hole drilling in return airway along the coal seam strike, water injection hole drilled parallel to the working face, and separation distance is 12 m. The diameter of water injection hole is 75 mm, and depth

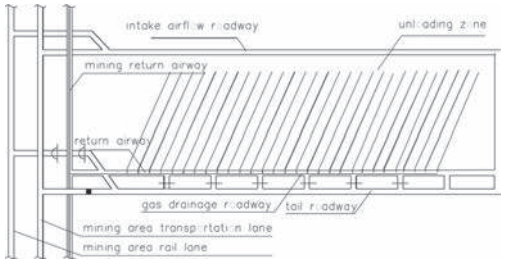


Figure 6. Drainage unloading borehole layout diagram.

is 60 m. Water injection of every single hole is about 3056 t. Injection time should not less than 30 days. Water injection pressure is 6~12 Mpa.

7 CONCLUSIONS

1. Through the measurement of coal and rock physical and mechanical parameters, the no. 2 coal seam of Liyazhuang coal mine has medium impact tendency and no impact on the roof strata. Due to stress concentration, hazard of 2–228 island working face is rock burst risk, and the rock burst hazard degree is weak shock hazard.
2. Through analysis of overlying rock stress distribution, stress concentration regions of 2–228 island working face mainly concentrated on both sides coal pillar of working face and near security exit.
3. Stress concentration, fault activation, goaf roof fracture, goaf roof fracture directly, roof fracture of cutting hole are the main reasons causing weak rock burst hazard of 2–228 Island working face.
4. Through the construction of drainage in the coal seam pressure relief drilling and extraction, and water injection before mining, can effectively reduce the chance of rock burst risk.
5. Liyazhuang coal mine should adjust mining sequence, mining area and layout of the working face, realize coal pillar mining, and avoid formation of stress concentration.

REFERENCES

Brunauer. S, et al. 1938. Adsorption of gases in multimolecular layers. *Journal of the American Chemistry Society*, 60:309–319.

Feng Zengchao, et al. 2003. Correlativity of rock in homogeneity and rock burst trend. *Chinese Journal of Rock Mechanics and Engineering*, 22(11):1863–1865.

GB/T 23561–2009, Measurement method of coal and rock physical and mechanical properties.

He Manchao, et al. 2005. Rock mechanics in deep mining engineering. Chinese Journal of Rock Mechanics and Engineering, 24(16):2803–2813.

LI T, et al. 2007. A review of mining-induced seismicity in China. *International Journal of Rock Mechanics and Mining Sciences*, 44(8):1149–1171.

Li Shulin, 2001. Experimental study of dynamics damage on rock burst tendency. *Journal of Liaoning Technical University (Natural Science Edition)*, 20(4):436–438.

MT/T 174- 2000. Classification and laboratory test method on bursting liability of coal.

MT/T 866–2000. Measurement method of coal seam impact tendency classification index.

Pan Jienan, et al. 2005. Relationship between rock composition and coal bearing formation and its burst texture potential. *Chinese Journal of Rock Mechanics and Engineering*, 22(11):4422–4427.

Pan Jienan, et al. 2006. Relationship between deformation & failure of coal and its burst potential under uniaxial compression. *Safety in Coal Mines*, (8):1–4.

Pan Liyou, et al. 2006. Practical technology of prediction and prevention for rock burst. *China University of Mining and Technology Press*, 1–3.

Pan Yishan, et al. 2003. Distribution, type, mechanism and prevention of rock burst in China. *Chinese Journal of Rock Mechanics and Engineering*, 22(11): 1844–1851.

Su Chengdong. 2004. Experimental study on the effect of crystal size and specimen length on the burst tendency. *Chinese Journal of Rock Mechanics and Engineering*, 23(22):3750–3753.

Yang Zhiguo, et al. 2009. Research of mining based on micro seismic monitoring technology in high-stress area. *Chinese Journal of Rock Mechanics and Engineering*, 28(Supp. 2):3632–3638.

Zhao Yixin, et al. 2007. The relationship between bum p-prone prosperity and micro structure characteristics of coal. *Journal of China Coal Society*, 33(1):64–68.

Zou Deyun, et al. 2004. Research of energy storing and gestation mechanism and forecasting of rock burst in the coal and rock mass. *Journal of China Coal Society*, 29(4):159–163.

This page intentionally left blank

Progress in Mine Safety Science and Engineering II – He et al. (Eds)
© 2014 Taylor & Francis Group, London, ISBN 978-1-138-00122-0

Research on technology of paste-like filling mining under villages

Yu Dong, Yu-Cheng Huang, Lei-Chang Shao, Kai Wang & Zhong-Jie Duan
School of Resources and Safety Engineering, China University of Mining and Technology (Beijing), Beijing, China

ABSTRACT: With the contradiction between resource depletion, environmental disruption and economic development becoming increasingly prominent, mining under buildings, railways and water has drawn more and more attentions. Filling mining which ensures safe production conditions can effectively exploit the coal resources under buildings, railways and water. Mining under villages in Xuecun coalmine is analyzed in this paper, combined with the existing mining under buildings methods, the scheme of mining with paste-like filling under villages was confirmed. The system and process of paste-like filling were studied. The economic and social benefits of mining with paste-like filling under villages were comprehensively analyzed, which could provide guidance for production practice in Xuecun coalmine.

1 INSTRUCTIONS

According to the incomplete statistics of key state-owned coal mines, the amount of coal resources under buildings, railways and water are 13.79 billion tons, with the amount of coal resources under buildings are 8.76 billion tons, that accounts for over 60% of the total amount of "three under" coal resources. At the same time, with the demand of industrial production for coal resources increases and mining area coal resources are drying up, to free coal resources under buildings, railways and water is imperative (Zhang Huaxing 2011).

Based on the specific geological conditions of Xuecun coalmine and actual distribution of surface villages, to put forward a suitable mining method for coal resources under villages in Xuecun coalmine, with economic, efficient and safe mining scheme selected, has important economic value and social significance for coal mining under villages.

2 COAL UNDER THE VILLAGES AND MINING CONDITIONS

2.1 *The village overview and coal pillar situation*

Dashucun villages are located in the border of Xuecun coalmine northern coal field and Dashucun coal field, Dashucun industrial square pillar is in the east, Dongzhuang coal pillar is in the west and in the south is Xuecun coalmine 6th panel. Dashucun village pillar stretches across two coal field in the north and south. The strike length of coal pillar is about 1015 m, the incline length is about 1010 m, and the coal pillar covers an area of 1.025 km^2. The majority of housing constructions is bungalow or brick masonry structure. The ground elevation is about +206.2 m ~ +222.2 m. The mining coal seam is 2# coal seam (big coal) and 4# coal seam (yeqing coal), 2# coal seam belongs to the stable seam, which thickness is about 5.5 m; 4# coal seam belongs to the comparatively stable seam, which thickness is about 1.3 m. The liner distance between ground and 2# coal seam roof is about 426 m~625 m, the layer spacing between 2# and 4# coal seam is 33 m.

2.2 *Mining coal seam reserves*

The minable seam of Dashucun coal pillar are 2# and 4# coal seam, the coal reserves is shown in Table 1. 4# coal seam as the liberation seam would be mined first, which plan with caving mining method had passed the argument. The paper is gong to analyze the mining scheme of 2# coal seam.

Table 1. Mining coal reserves.

	Inclined area	Coal thickness	Recoverable reserve
Coal seam	m^2	m	10^4t
Yeqing coal (4#)	956237	1.3	174
Big coal (2#)	956237	5.5	736.3
Total			910.3

* Coal bulk density is 1.4 t/m^3

3 STUDY ON TECHNOLOGY OF MINING THE VILLAGES PILLAR WITH PASTE-LIKE FILLING

3.1 *Mining methods under buildings*

Mining under buildings has a long history and has much successful experiences. In addition to the village relocation, more typical methods include strip mining method, harmony mining method, overburden rock abscission layer grouting method and goaf filling mining method (Huang Yucheng, et al. 2003).

1. Strip mining method. The method is a kind of effective mining technology for controlling the surface subsidence. The surface subsidence coefficient of strip mining method is small, usually is 0.05~0.2. The main disadvantages of strip mining method are the low recovery rate which generally is 30%~60%, the high tunneling rate, the working face moving frequently and the production efficiency is low.
2. Harmony mining method. Fundamentally, the harmony mining method can also protect the surface building from damage caused by uneven surface subsidence, but it can't control the surface subsidence effectively and has difficulty especially for the mining under a wide range of urban buildings.
3. Overburden rock abscission layer grouting method. From the perspective of the engineering practice result, the overburden rock abscission layer grouting technology can effectively delay the speed of surface subsidence under the condition of certain strata, the surface subsidence can reduce about 30%~70%, but at the moment, the knowledge of temporal and spatial dynamics distribution law of abscission layer is still not enough in-depth and thorough.
4. Goaf filling mining method. By filling method can greatly reduce the surface subsidence and protect the subsidence of surface buildings effectively, at the same time, with the filling mining method, we can improve the coal recovery rate of coal pillar under villages, make full use of the coal gangue waste, and reduce the environment pollution.

3.2 *Determination of filling mining technology*

Based on the following several factors, for Dashucun coal pillar mining confirms to adopt the filling mining method.

1. 4# coal seam of Dashucun coal pillar had determined to adopt caving mining method, the surface deformation caused by mining had a certain impact on the village. In order to reduce the damage and influence of coal mining under the village and produce more coal resources, adopting filling mining method could be more effective.
2. Filling mining technology is comparatively mature, adjacent Xiaotun coalmine had taken advantage of filling mining method to exploit the safety coal pillar under Nanwangcun, the coalmine has been equipped with the appropriate filling mining technology and practical experience.

Nowadays, there are four kinds of filling mining technologies in coalmines: waste rock filling, paste filling, high water filling and paste-like filling.

Paste-like filling slurry concentration is controlled at 75%~79%, the slurry liquidity performs well and is beneficial to roof-contacted filling. Additionally, the slurry quality control and delivery of paste-like filling by pump are more convenient, the probability of blocking pipe incidents is low and the stability and reliability of the system work better. The new pattern of mining with paste-like filling can organically combine with the utilization of industrial solid waste and the control of surface subsidence to realize low degree of surface damage, high utilization rate of resources and less waste products, which shows the connotation and characteristics of resources green mining (Huang Yucheng, et al. 2013). Therefore, the paste-like filling process is selected.

2# coal seam thickness is 5.5 m, given the filling mining technology level, mining 2# coal of Dashucun village pillar should adopt slicing and filling scheme: the higher slice mining thickness is 2.8 m and the lower slice mining thickness is 2.7 m. The mining sequence is that filling mining the higher slice first, then filling mining the lower slice.

Comprehensive consideration about the coal production of filling working face and the existing filling equipment capacity matching, the width of filling mining working face is determined to 80 m, the first mining face of higher slice is filling mining 2#-1 face, subsequently, working faces are seriatim arranged northwards, after the completion of those working faces mining, then new working faces are seriatim arranged southward for mining. Working faces layout is shown in Figure 1.

3.3 *Filling station and filling drill*

Position of filling station: By comprehensive consideration of Dashucun coal pillar and the ground can be used to layout the filling area, the surface filling station is arranged in the south of Dashucun about 200 m faraway, the geographical coordinates of (X, Y) = (23529, 46505), as shown in Figure 1.

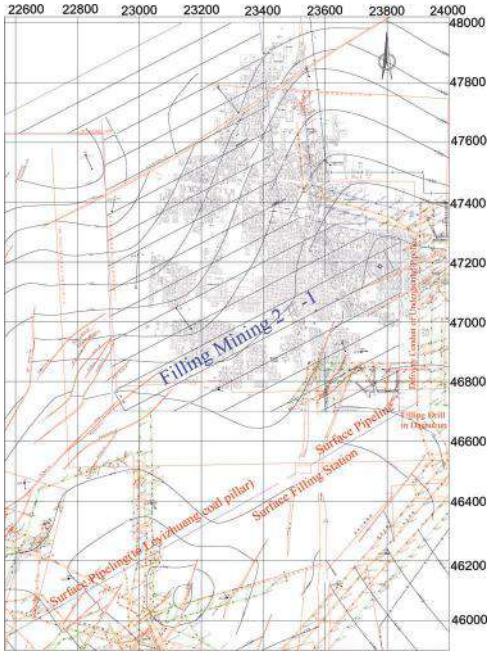


Figure 1. Working faces layout and the surface position of filling station.

Layout of filling drill: Considering the filling station layout and filling pipeline, the filling drill is arranged in the southeast of filling area, above the 8# guideline of northeast roadway, the geographical co-ordinates of (X, Y) = (23898, 46730).

3.4 *Design capabilities of filling system*

Composition of filling materials: As the concentration of the paste-like filling is 78%, the corresponding ratio of slurry includes 6% cementing material, 52% coal gangue, 20% fly ash and 22% water.

Capability of filling system: the capability is mainly considered to the coal production of filling working face and the existing filling equipment capacity matching. To design a single filling working face with an annual coal output of 360000 t/a, an annual working day is 330 days, then the working face production is 1100 t per day. The coal density is 1.4 t/m^3, and the filling volume is 786 m^3 per day. The filling valid time is 6 h per class, and the work capability of filling system needs to be 130 m^3/h. Therefore, the filling capability of filling system is 130 m^3/h and the designed capability is considered 150 m^3/h. With the density of filling slurry for 1900 kg/m^3, the calculation of filling materials consumption is as shown in Table 2.

Table 2. Consumption calculation table of filling materials.

Item		Quantity
Filling quantity	Ability of filling system/m^3/h	150
	Class filling quantity/m^3/class	786
	Class effective fill time/h/class	6
Material ratio	Cementing material/kg/m^3	114
	Coal gangue/kg/m^3	988
	Fly ash/kg/m^3	380
Consumption of filling materials	Water/kg/m^3	418
	Per hour consumption Cementing material/t/h	17.1
	Coal gangue/t/h	148.2
	Fly ash/t/h	57
	Water/m^3/h	62.7
	Per class consumption Cementing material/t/h	89.6
	Coal gangue /t/h	776.6
	Fly ash/t/h	298.7
	Water/m^3/h	328.5

3.5 *System composition of filling preparation station*

There are four kinds of materials used in paste-like filling, which are fragmentized coal gangue, fly ash, special cement and water. The process of filling is as follows (Sun Henghu, et al. 2002):

1. At first, to process the fragmentized coal gangue.
2. In the next place, mixing the coal gangue, fly ash, special cementing material and water in proportion to make into paste-like slurry.
3. Then, through filling pump, the paste-like filling slurry is transported to the underground working face to filling confined space of mined-out area which is formed by hydraulic filling support with secondary isolation measures.

The entire filling process flow is as shown in figure 2, which can be divided in to four basic links as waste rock broken, slurry preparation, pipeline pumping and filling body building.

Therefore, the structure of filling preparation station system mainly includes the subsystems of coal gangue broken, filling slurry preparation, pipeline pumping and the system of measurement and control.

4 GROUND DEFORMATION PREDICTION OF FILLING MINING

4.1 *Design capabilities of filling system*

Ground movement parameters: According to the filling mining technology data of neighboring

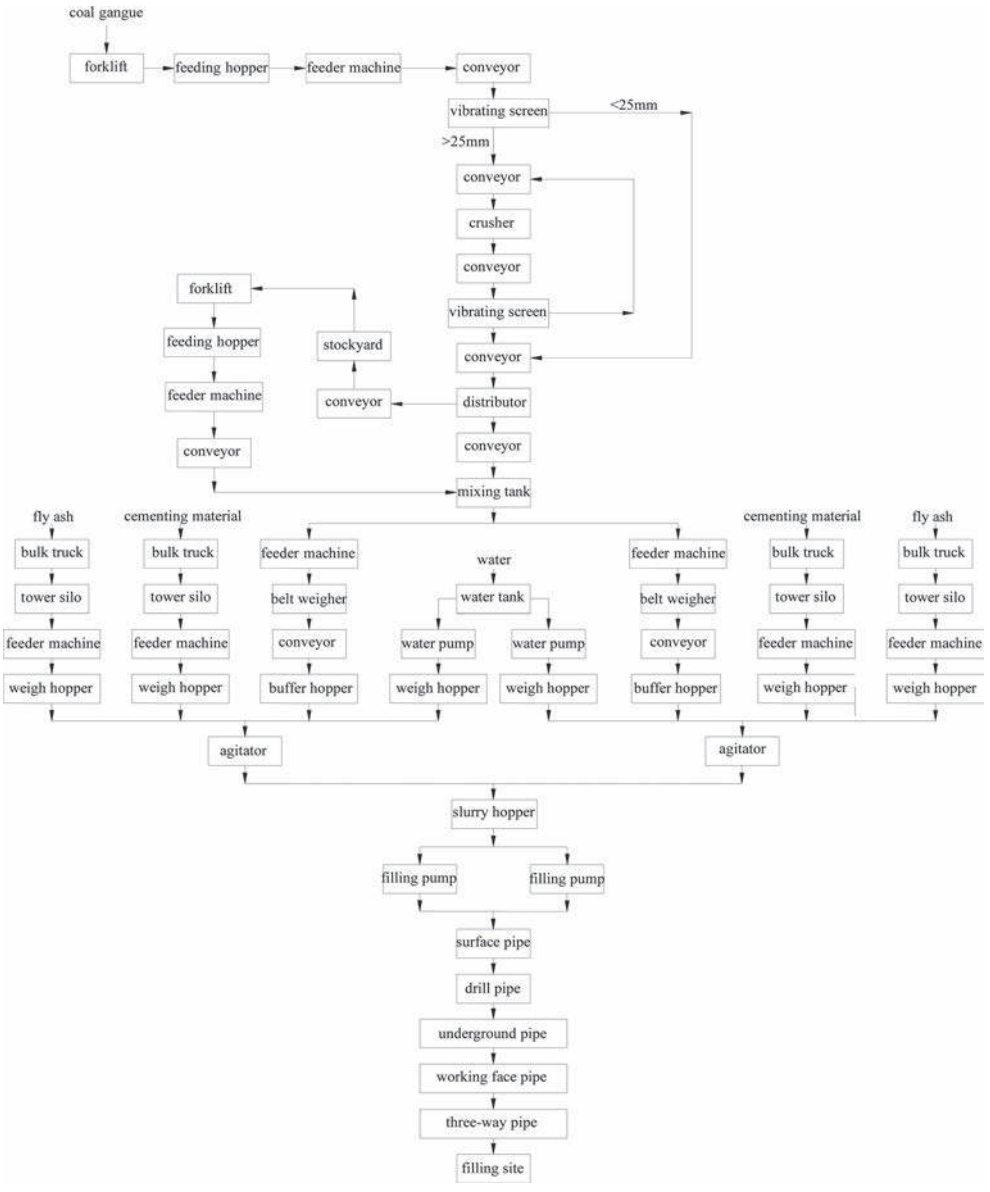


Figure 2. Process flow of paste-like filling system.

Xiaotun coalmine, the filling ratio of slicing and filling method can be 90%, then the surface subsidence co-efficient q will be 0.08, here to take q = 0.1. Determining the basic prediction parameters of surface movement and deformation is as shown in Table 3.

Housing deformation resistance parameters: According to the measurement of surface movement and deformation, housing capability of resistance to compression is stronger than resistance to tension. Considering the sensitivity of mining under villages, in the study of the scheme, the building ability to resist deformation is reduced. Based on computation and building deformation situation analysis, the critical deformation value of the building damage level are as follows:

1. I-level damage, compression deformation ≤2.0 mm/m, tensile deformation ≤1.5 mm/m;
2. II-level damage, compression deformation ≤3.5 mm/m, tensile deformation ≤3.0 mm/m.

Table 3. Basic prediction parameters of surface movement and deformation.

Coal seam	Mining method	q	Coal thickness m	b	k	tgβ	S1	S2	S3	S4
Yeqing coal (4#)	Caving mining	0.8	1.3	0.3	0.6	2.2	0	0	0	0
Big coal (2#)	Filling mining	0.1	5.5	0.3	0.6	2.2	0	0	0	0

*q – subsidence coefficient; b – horizontal movement coefficient; k – coefficient related to lithology; tgβ – tangent of major influence angle; S – deviation of inflection point.

Table 4. Situation of surface maximum deformation and buildings damage.

	Wi/ mm		εs+/ mm/m	εs−/ mm/m		εt+/ mm/m		εt−/ mm/m	
Deformation Value	1560	2.62	2.92	–2.79	–2.73	–2.29	2.31	–2.4	–3.04
Location	West of Dashu-cun	North-east of Dashu-cun	Southeast corner of Dashucun	Southeast of Dashu-cun	West of Dashu-cun	North-east of Dashu-cun	North-east of Dashu-cun	East of Dashu-cun	South of Dashu-cun
Level		II	II	II	II	II	II	II	II
Area/m²		53817	26576	34866	32404	21442	28673	10191	56547
Total/m²									264516

*Wi – maximum subsidence value; εs+ – maximum tensile deformation valve of buildings east-west direction; εs− – maximum compression deformation valve of buildings east-west direction; εt+ – maximum tensile deformation valve of buildings north-south direction; εt− – maximum compression deformation valve of buildings north-south direction;

4.2 *Ground movement and deformation prediction*

The design using the probability integral method for prediction of surface movement and deformation caused by mining is adopted.

The prediction and analysis of filling mining working condition of 4# coal fully mining +2# coal higher slice (2.8 m) +2# coal lower slice (2.7 m) is as shown in Table 4.

From the table, it shows that after 4# coal fully mining and 2# coal filling mining, within the scope of the village deformation, the maximum horizontal deformation value is +2.92/–3.04 (mm/m), the II-level damage area of the village is 264516 m² accounting for 33% of the village with a total area of 784617 m².

5 ANALYSIS OF ECONOMIC BENEFITS AND SOCIAL BENEFITS

5.1 *Economic benefits of filling mining*

In the mining area of Dashucun coal pillar, the recovery rate is calculated at 82%, 4# coal can be produced 1.427 million tons with caving mining method. Coal mining profit is calculated at 100 yuan per ton, then 4# coal total profit can be 142.7 million yuan; 2# coal can be produced 6.038 million tons with filling mining method, coal filling costs 49.17 yuan per ton, then coal filling profit is calculated at 50.83 yuan and 2# coal total profit can be 306.91 million yuan; After coal mining, the total profit of 4# and 2# coal can be 449.61 million yuan. To deduct village compensation fees of 44.61 million yuan, enterprise net profit can be 405 million yuan.

5.2 *Analysis of social benefits*

Paste-like filling mining with remarkable social benefits and environmental benefits has opened up an ideal way for mining under buildings, railways and water and green mining (Liu Zhijun 2010).

1. To protect natural environment. Paste-like filling mining can control surface subsidence effectively, realize mining without villages relocation, protect surface environment, and maintain the balance of groundwater ecosystem.
2. To improve the recovery rate of coal resources. Paste-like filling mining improves coal resources recovery rate significantly, reduces the loss and waste of mineral resources, extends the service life of the coalmine mining, increases employment opportunities and at the same

time, increases the total mining production of the whole mine.
3. To realize green mining. Paste-like filling technology not only considers the needs of the mining process, but also considers the social requirements of comprehensive utilization and disposal of mining wastes, the environmental protection and pollution reduction. The waste such as coal gangue and fly ash are used in the underground backfilling to realize mining with no waste and pollution.

6 CONCLUSION

1. Dashucun village coal pillar mining adopts the paste-like cemented filling process, and for 2# coal mining, slicing and filling method is selected, the higher slice mining thickness is 2.8 m and the lower slice mining thickness is 2.7 m. The designed filling capability of filling system is considered to be 150 m^3/h.
2. In the area of Dashucun coal pillar, after 4# coal was fully mined, 2# coal adopts filling mining method, 2# coal production can be 6.038 million tons with the profit of 306.91 million yuan. The total profit of 2# and 4# coal can be 449.61 million yuan, after deducting village compensation fees, the enterprise net profit will be about 405 million yuan.
3. Paste-like filling mining with remarkable social benefits and environmental benefits has opened up an ideal way for mining under buildings, railways and water and green mining, that is beneficial to protect the natural environment, improve the recovery rate of coal resources and realize green mining.

REFERENCES

Huang Yucheng, Dong Yu, Duan Zhongjie, et al. 2013. Practice of the technology of coal mining with paste-like filling under water. *China Mining Magazine* 22(7):80–82.

Huang Yucheng, Sun Henghu, Shi Zhaobing, et al. 2003. Discussion on Feasibility of Coal Mining under Building Structures with Like Gypsum Material Back Filling. *Coal Science and Technology* 31(10):51–53.

Liu Zhijun. 2010. Research of Paste-like filling mining with coal gangue technology. *Coal Engineering* (3):29–31.

Sun Henghu, Huang Yucheng & Yang Baogui. 2002. *Contemporary Cementation Filling Technology*. Beijing: Press of Metallurgy Industry.

Zhang Huaxing. 2011. On the Technology of Coal Mining under Buildings, Railways and Water-body in Future. *Coal Mining Technology* (1):1–3.

Progress in Mine Safety Science and Engineering II – He et al. (Eds)
© 2014 Taylor & Francis Group, London, ISBN 978-1-138-00122-0

Study of rockbolts nondestructive detecting based on improved immune Danger Theory

Xiaoyun Sun & Yang Zhao
School of Electrical and Electronics Engineering, Shijiazhuang Tiedao University, Shijiazhuang, Hebei Province, China

Jiulong Cheng & Xiaoyun Sun
State Key Laboratory of Coal Resources and Safe Mining, China University of Mining and Technology (Beijing), Beijing, China

ABSTRACT: Owning to terrible environment and sensitive disturbance for rockbolts, it is important and necessary to detect rockbolts quality accurately. A nondestructive detecting method of rockbolts based on immune danger theory is proposed, using acoustic stress reflection technology, a series of danger and abnormal signals are exacted. So the defect type is detected by immune danger theory. Compared with the current artificial immunity algorithm, the result shows that the former diagnose accuracy is higher.

1 INTRODUCTION

Rockbolts as an important part of the support system was used in underground tunnels widely, as well as in slope reinforcement of surrounding rock and supporting. There are important parameters to evaluate the quality of the rockbolts, such as rockbolts length, Anchorage section length, free section length and constructive defects (Such as the imperfect location and grouting saturation in the rockbolts body). But rockbolts construction is concealed work. As the conventional method, pull-out and coring experiment are not only belong to destructive testing methods, but also are difficult to make effective detection. Existing non-destructive testing technology mainly includes electromagnetic method, sonic frequency stress wave method and ultrasonic method. The general information processing technology could not effectively test the quality of rockbolts, because it is difficult to distinguish the bottom reflected signal of rockbolts detection at present. Many scholars at home and abroad have been considerable research on nondestructive testing of rockbolts (Sun & Cheng 2008, Sun et al. 2012, He et al. 2004, Liu & Yue 2006, Xv 2002).

Most of the theory about the Artificial Immune System (AIS) were based on the self-nonself model which was introduced early. People think of that the organism could identify the "self" or "nonself" automatically and make immune response again "nonself". The theory has been widespread application in many fields such as pattern recognition, data processing, network security, optimization study and fault diagnosis (Mo & Zuo 2009). But the system needs identify and process all signal (antigen) which is different with "self" by the detector (antibody). A best complete detector set should be set up to reduce the missed detection probability of system. So the scale of the detector set would exponential increase follow the size of detector room (Zhou & Dasgupta 2007). Therefore, it leads to consume large amounts of resources and time in actual testing.

In 1944, Matzinger, a United States NIH immunology expert, proposed the immune-danger model theory (Matzinger 1994, Matzinger 2001). He considered that the key to specific immune response lies in danger signal rather than "nonself". Under the influence of different impulse force and impulse point, the audio reflected wave would be varying degrees fluctuate in rockbolts detecting. If abnormal signals are distributed at the edge of detectors detection space, the fluctuation would make some data point fall outside the detection space and omit. There must be some noise in the sampled signal. There are also residual even by the signal processing method. So it makes false alarm.

To address the problem, this danger theory for reference by the article, propose the immune danger theory algorithm to test rockbolts. The algorithm overcomes the limitations of the artificial immune system based on "self-nonself" pattern. It only need process the "danger" signal to complete

the rockbolts quality detection, rather than process all "nonself" signals. Reduce the omission and false alarm and enhance the speed and accuracy of rockbolts quality detection.

2 IMMUNE DANGER ALGORITHM

2.1 *Variable radius detector*

Immune algorithm is the detection about "self-nonself". It is a round area which was covered by each detector and without overlaping each other. There must be detecting vulnerability between adjacent detectors. In order to reduce the test loophole we can make the radius of detector as variable, and there is a maximum. It can fill the loophole between detectors and improve the fault coverage rate (Liu 2009).

2.2 *Detector cluster*

As the detector set were generated at random and even distributed, it could distinguish between "self" set and "nonslef" set only, but not the concrete types of "nonself". That is to say, it could only find the abnormal data.

The initial detector set was produced according to the self set, so the detectors were uneven distributed. The maximum detection radius has been defined r in order to make the detectors even distributed. If there are some overlapping areas between the new detector and any detector in the set, the new detector should be abandon until the detector is eligible.

2.3 *Affinity of antigen and antibody*

The known self set 'a' whose count is M and dimension is N in the system can be defined antibody. Its expression can be described as follows (Guo et al. 2012).

$$\mathrm{a} = \{V_{a1}, V_{a2}, \cdots, V_{aM}\} \tag{1}$$

Note:

$$V_{ai} = (V_{ai1}, V_{ai2}, \cdots, V_{aiN}), 0 \le V_{ai} \le 1, i = 1, 2, \cdots M$$

The known nonself set 'b' in the system whose count is M and dimension is N. we can define is antigen. Its expression can be described as follows.

$$\mathrm{b} = \{V_{b1}, V_{b2}, \cdots, V_{bM}\} \tag{2}$$

Note:

$$V_{bi} = (V_{bi1}, V_{bi2}, \cdots, V_{biN}), 0 \le V_{bi} \le 1, i = 1, 2, \cdots M$$

The expression of affinity 'u' between antibody and antigen can be described as follows.

$$u = 1/(1 + \sum_{i=1}^{M} \sqrt{\sum_{j=1}^{N} (V_{aij} - V_{bij})^2}) \tag{3}$$

Note:

$$0 \le V_{ai} \le 1, i = 1, 2, \cdots M, j = 1, 2, \cdots N$$

$$0 \le V_{bi} \le 1, i = 1, 2, \cdots M, j = 1, 2, \cdots N$$

.

We usually define the input data as antigen and defined the detectors as antibody in the immune system.

$$\mathrm{d} = \sqrt{\sum_{j=1}^{N} (V_{aij} - V_{bij})^2} \tag{4}$$

The letter d above is the Euclidean distance between set 'a' and set 'b'. The smaller the distance is, the bigger the affinity 'u' is.

2.4 *Danger detection and abnormal detection*

For the sampled signal, we extract the characteristic of the danger signal and then compare the characteristic value with the danger threshold. If the value is larger than the danger threshold, "danger = 1", otherwise "danger = 0".

Compare the affinity between antigen and each element in self set. If there is affinity which is larger than the given abnormal value, "abnormal = 0", otherwise "abnormal = 1".

Compare the affinity between antigen and each element in self set. If there is affinity which is larger than the given abnormal value, "abnormal = 0", otherwise "abnormal = 1".

Only if the danger signal and abnormal signal are both equal to 1, the immune response would take place and the fault type would be judged automatically.

2.5 *Rockbolts fault diagnosis algorithm based on immune danger theory*

The structure diagram of rockbolts quality diagnosis system based on immune danger theory is shown in Fig. 1.

- The detectors are produced according to self string. Then cluster the detectors according to nonself string and mark each kind of them. So we can get the mature detector set.
- Pretreat the input data and extract the characteristic vectors. Then it would become the antigen by normalizing them.

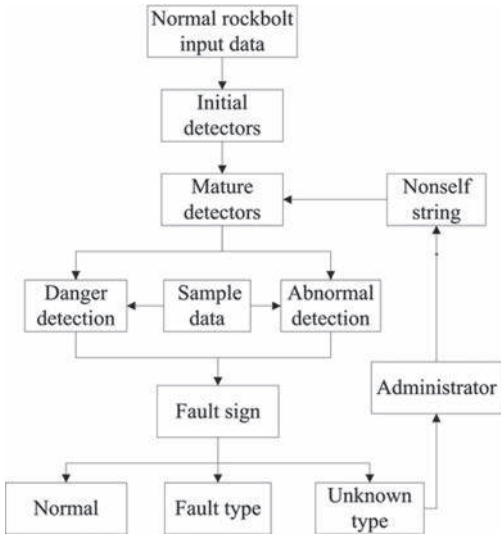


Figure 1. The rockbolts fault diagnosis system based on immune danger theory.

- Calculate the affinity between input antigen and every antibody.
- Compare each affinity with the given abnormal value. Send the abnormal signal which is "abnormal = 1" if the affinity is smaller than the value.
- Send the danger signal "danger = 1" if the danger characteristic value of antigen is larger than the danger value.
- If "danger = 1" and "abnormal = 1" are right, the immune response would be activated.
- We can compare all the sets which the antigen belongs to one by one to judge the type of antigen according to the cluster. Alarm the administrator and let him process the self and nonself sets if it is not in the type which it belongs to.

3 EXPERIMENT ANALYSIS

ANSYS-DYNA has been used to model and simulate for the different kinds of rockbolts in this experiment. The sampling frequency is 20 KHz. Simulate hammer knocking the head of rockbolts, and then get the acceleration waveform curves of the top rockbolts with the sensors at the top of rockbolts collecting the reflected wave. Including 12 groups normal data and 22 groups defects, long and short data. Figure 2–5, respectively, for normal, internal defects, long and short casting models.

3.1 *Data preprocessing*

According to the acceleration waveform curves of the top rockbolts, its vertical amplitude means

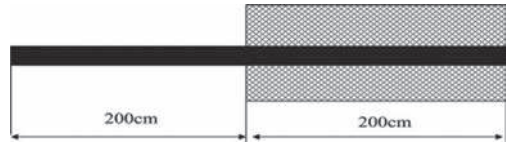


Figure 2. Normal rockbolts casting model diagram.

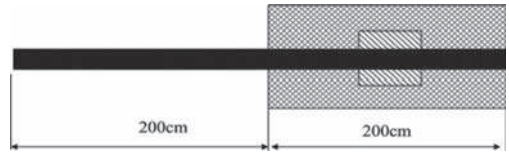


Figure 3. Internal defects rockbolts casting model diagram.

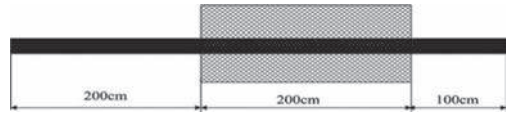


Figure 4. Long rockbolts casting model diagram.

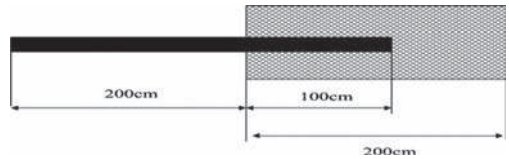


Figure 5. Short rockbolts casting model diagram.

reflected wave energy. The reflection points at the top and bottom of anchorage section could be found out. The data pretreatment includes 2 parts.

- Solve the amplitude of acceleration curves quadratic sum 'E' between the top and the bottom interface of anchorage part.

$$E = \sum y_i^2 \tag{5}$$

Make it normalized.

$$E^* = E/\max E \tag{6}$$

- Solve the maximum amplitude point in the anchorage part and make it normalized.

$$Y^* = Y/\max Y \tag{7}$$

Make up a two-dimensional normalized feature vector with two characteristic values E* and Y*.

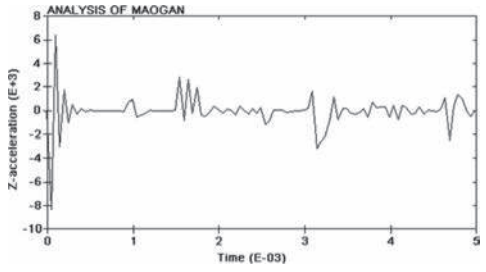


Figure 6. The acceleration waveform curves of the top normal rockbolts.

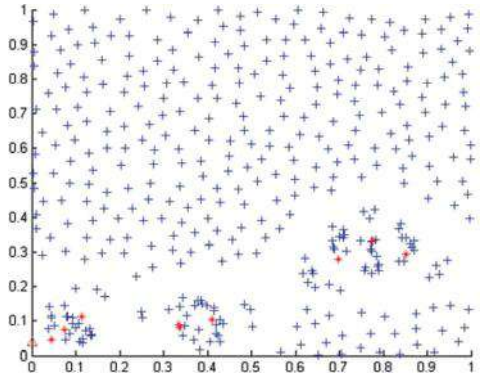


Figure 7. The distribution map of mature detector.

Then use it to research the condition of rockbolts anchorage quality.

3.2 *Numerical simulation and verification*

The acceleration waveform curves of the top rockbolts whose free section and anchorage section both are 2 m, as shown in Fig. 6. Then the feature vector could be got with the method above. Points A and B are the reflection points at the top and bottom of anchorage section.

According to formula (6) and (7), acquire the feature vector of known normal rockbolts and for testing rockbolts. Make the former as self set and the latter as nonself set. Execute the first step of algorithm, the initial detector set has produced with self and nonself sets and cluster them, as shown in Fig. 7. '+' stands for detector, '*' stands for nonself string and 'Δ' stands for self string. It achieved mark the type of rockbolts by cluster operations. The distance from detector to nonself string was more closely, but the detectors are uniform distribution in all the space if the distance is more than the given value.

The data of Table 1 and Table 2 is the experimental result by testing the simulation data of rockbolts.

They are using the detecting algorithm based on danger theory (DT) and traditional artificial

Table 1. Test results of normal rockbolts.

	E*	Y*	Self-nonself model	Danger theory	E*	Y*	Self-nonself model	Danger theory
Normal Rockbolt	0.0012	0.0767	normal	normal	0.0008	0.0489	normal	normal
	0.0007	0.0430	normal	normal	0.0025	0.0246	ovelong	ovelong
	0.0011	0.0810	normal	normal	0.0018	0.1082	normal	normal
	0.0011	0.0864	normal	normal	0.0006	0.0361	defect	normal
	0.0010	0.0694	normal	normal	0.0008	0.0845	normal	normal
	0.0013	0.1115	normal	normal	0.0009	0.0885	normal	normal

Table 2. Test results of abnormal rockbolts.

E*	Y*	Type	Self-nonself model	Danger theory	E*	Y*	Type	Self-nonself mode	Danger theory
0.8527	0.2927	short	short	short	0.3313	0.0826	defect	defect	defect
0.6981	0.2778	short	short	short	0.4103	0.1036	defect	unknow	defect
0.7759	0.3329	short	short	short	0.2976	0.1210	defect	defect	defect
0.7983	0.3156	short	short	short	0.3813	0.1070	defect	defect	defect
0.0448	0.0448	overlong	overlong	overlong	0.2980	0.1070	defect	defect	defect
0.1134	0.1134	overlong	overlong	overlong	0.3364	0.0812	defect	defect	defect
0.0758	0.0758	overlong	overlong	overlong	0.4465	0.2693	defect	unknow	unknow
0.0844	0.0844	overlong	overlong	overlong	0.4076	0.1093	defect	defect	defect
0.3167	0.0957	defect	defect	defect	0.3514	0.0958	defect	defect	defect
0.3069	0.0841	defect	defect	defect	0.3338	0.0878	defect	defect	defect
0.5372	0.1868	defect	unknow	unknow	0.2831	0.0754	defect	defect	defect

immune algorithm based on "self-nonself" model (SNS) respectively. The acceleration waveform curve could be got by modeling and simulating the rockbolts with the software ANSYS-DYNA. So simulation data of rockbolts could be got by sampling and pretreatment the curve.

It is obvious in the tables, the fault diagnosis rate of normal rockbolts is 91.67% and fault diagnosis rate of abnormal rockbolts is 90.91% with the detecting algorithm based on immune danger theory. The fault diagnosis rate of normal rockbolts is 83.33% and fault diagnosis rate of abnormal rockbolts is 86.36% with traditional artificial immune algorithm based on "self-nonself" model.

4 CONCLUSION

This article has presented a new fault diagnosis algorithm based on the danger theory of biological immunology. It judges the fault type of rockbolts through the synergy of danger signal and abnormal signal. It has overcome the limitation of artificial immune system model based on "self-nonself". The experimental results show that the method has higher detection validity and fault coverage than traditional artificial immune algorithm.

ACKNOWLEDGMENT

This work is supported by the National Natural Science Foundation of China (Grant No. 51274144, 50974081) and the Natural Science Foundation of Hebei Province (Grant No. F2012210031, CPRC023) and A Foundation for the Author of National Excellent Doctoral Dissertations of China (No. 200958, No. 2013T60197).

REFERENCES

Guo, Wei et al. 2012. Research of avionics fault diagnosis algorithm based on immune danger theory. *Computer Measurement and Control* 20(4):948–954.

He, Cunfu et al. 2004. The modal acoustic emission source location technique in pipeline using the wavelet transform of dispersive waves. *Journal of Beijing University of Technology* 30(9):96–101.

Liu, Jinmin. 2009. *Research and application of immune algorithm for fault diagnosis (Master degree thesis)*. Taiyuan: Taiyuan University of Technology.

Liu, Minggui & Yue, Xianghong. 2006. Analysis of bolts anchoring quality based on wavelet neural nework, *Chinese Journal of Rock Mechanics and Engineering* 25(1):83–87.

Matzinger, P. 1994. Tolerance danger and the extended family. *Annual reviews of immunology* 12(l):991–1045.

Matzinger, P. 2001. The danger model in its historical context. *Scand journal immunology* 54: 4–9.

Mo, Hongwei & Zuo, Xingquan. 2009. *Artificial immune system*. Beijing: Science press.

Sun, Xiaoyun & Cheng, Jiulong. 2008. Application of Information Processing Technology on Nondestructive Detecting of Rock Bolts, *China Mining Magazine* 11(135):87–90.

Sun, Xiaoyun et al. 2012. Application of Information Processing Technology on Nondestructive Detecting of Rock Bolts, I*nt. J. Modelling, Identification and Control* 16(3):241–245.

Xv, Ming. 2002. *A Study on Nondestructive Detection and Intelligent Diagnosis Technology of Anchorage System Quality (Doctor degree thesis)*. Chongqing: Chongqing University.

Zhou, Jian & Dasgupta, D. 2007. Revisiting negative selection algorithms. *Evolutionary Computation* 15(2): 223–251.

This page intentionally left blank

Progress in Mine Safety Science and Engineering II – He et al. (Eds)
© 2014 Taylor & Francis Group, London, ISBN 978-1-138-00122-0

Experimental study on fireproofing performance of active explosion suppression system

Yong-Yu Wang, Jun-Feng Wang, Yu-Long Zhang, Jian-Ming Wu & Shuo Liu
College of Mining and Technology, Tai Yuan University of Technology, Taiyuan, P.R. China

ABSTRACT: Based on the theory of the system of flame retardant and active explosion suppression used in the South Africa HS mine, three different experiments were conducted to investigate the effects of HS system's explosion suppression. Experimental results show that HS system is of excellent practical effects and reliable safety performance. This system has the ability to cut off chain reactions on gas explosion propagation effectively in a very short time. so as to prevent gas combustion and control gas explosion successfully. Therefore, HS system has tremendous promoting values in China.

1 INTRODUCTION

The accidents of coal mine gas explosion have always been one of the main accidents in coal mines. By the statistics, more than 90% of the coal mines in our country are gaseous mines, nearly half of which belong to high gaseous mines. In order to reduce the mine gas disasters, based on the codes and specifications in our country the equipment and/or facilities, which are insulating and for suppressing explosion, are required to set up in the corresponding position of underworkings in coal mine, such as high gassy mines, coal and gas outburst mines, multi-seam mining mines, and mines easy to spontaneous combustion. Currently water barrier and rock dust barrier are mainly utilized to suppress explosion in mines of China, but these kinds of passive measures do not achieve the desired effectiveness due to ventilation evaporation, rock dust pollution and damp agglomeration (Wang Jun-feng et al. 2010).

The explosion suppression system used in the South Africa HS mine is an active explosion suppression system developed exclusively by Hans in South Africa. It could change traditional passive explosion suppression system to active explosion suppression system and timely block reaction chain of gas explosion effectively. This technology of explosion suppression has been at the international advanced level (Ma Li et al. 2010). In the previous work (Wang Jun-feng et al. 2010), the four basic parameters of this system, i.e., lag time of spraying, time for fogging, duration of effective fog and rate for spraying were systematically measured and calculated. These results shows that the system can effectively restrain the combustion and explosion of gas and dust in coal mine. In this paper, based on the theory of the explosion suppression of HS system, the basic function parameters of HS system were further measured according to the home and abroad regulations and standards (GB/T18154-2000, EN/1127-1, EN/14373). Meanwhile, the effect of active explosion suppression of HS explosion suppression system was further verified by combined with field-tested, data processing and theoretical analysis.

2 THEORY FOR THE HS SYSTEM

HS explosion suppression system is an active suppression system, which theory is shown in Fig. 1. When a methane or dust explosion occurs in the local areas of coal mine, the system can use its optical detector to monitor the accident point, and automatically transmits the signal to the central electronic controller in a few milliseconds. After the signal is checked, the controller will issue a instruction to open the high-pressure vessel, and the explosion suppression materials stored in the high-pressure container are released in a short period time, which enables to form a physical barrier to block extreme pressure and high temperature resulting from explosions. And then the fire could be extinguished simultaneously. Therefore, this system can cut down the scale of this disaster, and reduce the release of harmful gases in the end (Wang Jun-feng et al. 2010, Ma Li et al. 2010).

3 HS SYSTEM TEST FOR ACTIVE EXPLOSION SUPPRESSION AND FLAME RETARDANT

In order to study the HS mine system performance of active suppression and flame retardant, and

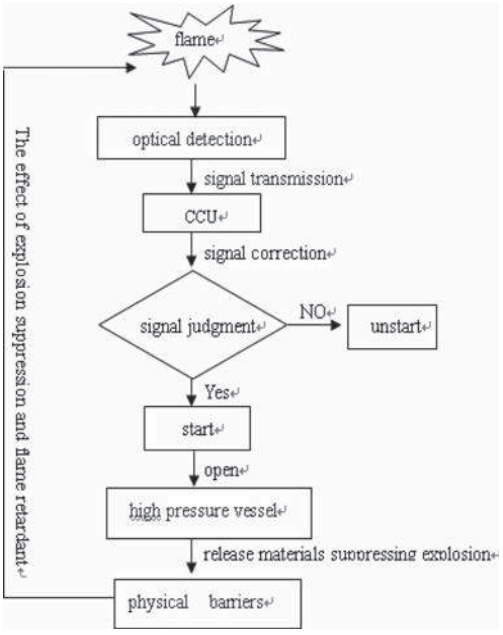


Figure 1. HS system theory for active explosion suppression and flame retardant.

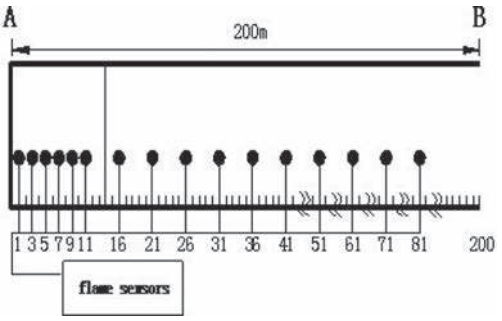


Figure 2. Appearance of testing gallery.



Figure 3. Explosion test without using CH4-2 system.

verify the effectiveness of the system, a group of pipeline tests about gas explosion suppression was conducted, which is similar to our previous studies (Wang Jun-feng et al. 2010), and the process is simply described here.

3.1 *Test procedures*

Comparative tests were carried out to check out the performance of HS active suppression explosion. A cylinder (i.d. 3 m, length 220 m) is formed the testing gallery. The schematic of the testing gallery is shown in Fig. 2, left side (A) of which is closed, the right (B) side of which is open; From side A, 16 flame speed sensors was arranged along the length, with setting one sensor every 2 meters from 1 m to 11 m, every 5 meters from 12 m to 41 m, and every 10 meters from 42 m to 81 m. HS system was equipped with high speed camera (Speed MS50 K), whose spectrum range is 400 nm–1000 nm with 1300000 pixels, and its shutter speeds are 1300 frames/s. A volume of 65 m3 air mixed gas with the 8.5 ± 0.5% (v%) concentration of CH4 was ignited by DDH-I type ignition device, which was installed in the 1.2 m distance from blind end and 1.35 m above testing gallery. At the same time the signals inside roadway were collected.

3.2 *Test results and analysis*

The first experiment was carried out without using the CH4-2 system. In the distance of 12 m from side A, plastic film was used to build an enclosed space, which was evenly filled with 45 m3 of mixed gas including CH4 and air. The high-speed camera was used to take photos of explosion phenomena in the exit of roadway and the system of collection and analyses was applied to analyse and record flame propagation speed passing by sensors when starting ignition device detonated mixed gas in the blind end. The experimental results were shown in Fig. 3 and Fig. 4.

The moment of detonating the mixed gas in the testing gallery without CH4-2 system is shown in Fig. 3. A violent explosion was occurred, which causes the temperature to raise suddenly, generating a large amount of harmful gases including CO, and huge disruptions in the end. From the continuous curve of flame propagation velocity in Fig. 4, it can been seen that the flame propagation speed got faster with the increase of roadway distance and it maintained a great speed within a certain distance in the semi-closed testing gallery. The flame propagation speed was fitted and the reuslt is shown in Fig. 4. It can been see that the fitting curve fits well as a whole in addition to some individual points, and the relationship can be described by the following equation: $y = -4E\text{-}06x^5 + 0.0006x^4 - 0.0303x^3 + 0.2787x^2 + 10.889x - 21.266$. The fitting curve

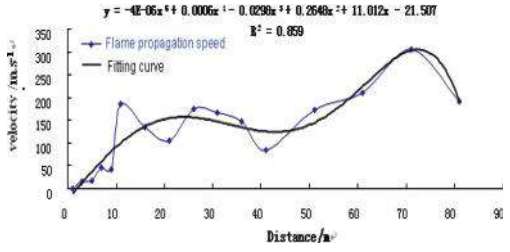


Figure 4. Explosion flame propagation speed without using CH4-2 system.

shows that within a certain distance away from the shot point, the flame propagation speed raised with the increase of the roadway distance and then it began to decrease when it reached the maximum distance at about 72 m from the semi-closed testing gallery. The reason for this trend is that with the combined effect of precursory shock waves and flame front produced by the initial explosion in the explosions, the flame area of combustible gases will be increased and stretched, and the propagation speed of flame wave will be increased continuously, and then reached the peak velocity in the end. At the last stage, due to the reduction of methane involved in the reaction per unit time, the energy generated by the combustion was not sufficient to supply the energy dissipation of shock wave spreading forward, the flame propagation speed decreased continually (Zhang Xiu-hua & Wu Yan-yan 2012, Wang Jun-feng et al. 2011).

In test 2, one CH4-2 machine was introduced into the test, which was set 5 m distance from blind end of testing gallery to check its positive effect of explosion suppression. In the distance of 12 m from blind end, plastic film was used to build an enclosed space, which was evenly filled with 65 m3 of mixed gas including CH_4 and air. Besides, some coal dusts with high explosibility were spread evenly in the 14 m distance from plastic film to demonstrate the explosion suppression effect of CH4–2 machine. A high-speed camera was used to take photos of explosion phenomena in the exit of roadway and a system of collection and analyse was applied to analyse and record the flame propagation passing speed by sensors when a starting ignition device detonated the mixed gas in the blind end. The experimental results are shown in Fig. 5 and Fig. 6.

Compared with Fig. 3 and Fig. 5, it can be found that the smoke produced by explosion was decreased rapidly and the explosive intensity was weakened obviously when one CH4-2 machine was set in the testing roadway. The test result show that its effect of explosion suppression was good. It also can been see from Fig. 6 that the no signal was detected by the sensors outside the 7 m distance



Figure 5. Explosion test with using one CH4-2 machine.

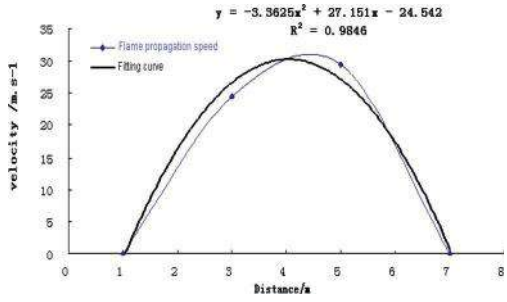


Figure 6. Explosion flame propagation speed with using one CH4-2 machine.

from blind end of testing gallery, which indicates that the explosive flame was controlled absolutely. The explosion flame propagation speed was also fitted, which can be expressed by: $y = -3.3625x^2 + 27.151x - 24.542$. These results show that the flame travel speed of gas explosion was decreased rapidly and then reduced to 0 when the flame propagated to 4 m distance from blind end in the testing gallery because of the flame retardant of CH4-2 machine. Besides, only a small quantity of coal dust was blown out according to analyzing the pictures taken by high-speed camera, which shows that the energy of gas explosion was weakened and its travel speed was decreased and the explosive blast was controlled. Experimental results showed that explosion phenomena was controlled indeed when one CH4-2 machine was set in the testing gallery. As a result, the gas explosion was controlled successfully and the expected effect of explosion suppression and flame retardant was achieved.

To take the further research on the effect of explosion suppression of HS machine, the test 3 was carried out. Two CH4-2 machines were set along the longitudinal of roadway to detect the performance of explosion suppression. One CH4-2 machine was set in the 7 m distance from blind end of testing gallery, while the other was set in the 12 m distance from blind end of testing gallery. In addition, plastic film was used to build an enclosed space in the distance of 12 m from blind end, which was evenly filled with 65 m^3 of mixed gas containing CH_4 and air. Meanwhile,

some explosive coal dusts were evenly spread in the 14 m distance from plastic film to demonstrate the effect of explosion suppression. The high-speed camera was used to take photos of explosion phenomena in the exit of roadway and the system of collection and analyses was applied to analyse and record flame propagation passing speed by sensors when detonating mixed gas was started with a ignition device. The experimental results are shown in Fig. 7 and Fig. 8.

Fig.7 shows the effect of explosion suppression when setting two CH4-2 machines in the testing gallery. Compared with Fig. 3 and Fig. 5, it can be seen that the explosion suppression of two CH4-2 machines performed well, which can be proved by the smoke produced by explosion at the exit of testing gallery was decreased obviously and the explosive intensity is weakened sharply. It also found that the machine set in the 7 m distance from blind end while the other one set at 12 m distance from blind end did not start, and the coal dusts were hardly blown out at the exit of testing gallery, which makes it clear that the spread of explosive flame was stopped at 10 m in the front of the second CH4-2 machine whose the farthest sensing distance is 10 m and it did not start because it did not induct enough signals. The test demonstrates that CH4-2 machine is able to suppress gas explosion absolutely under its normal work. The fitting result is shown in Fig. 8, which is similar to Fig. 4. It can be seen that the flame produced by explosion in the testing gallery was controlled in the 7 m distance from blind end because of flame retardance and explosion suppression of the first machine. Then the flame propagation speed was slowed down quickly and was reduced to 0 before it got to the second machine (in the 12 m distance from blind end), which demonstrates the machine worked well obviously. From the result of test 3, this conclusion can be found that the CH4-2 machine can form explosion suppression barriers with special flame retardant materials and block reaction chain of gas explosion effectively in a remarkably short period of time, and then nip possible gas accident in the bud.



Figure 7. Explosion test with using two CH4-2 machines.

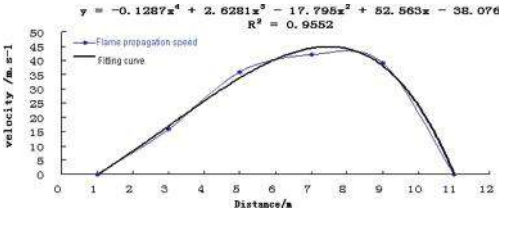


Figure 8. Explosion flame propagation speed with using two CH4-2 machines.

4 CONCLUSION

The South Africa's HS mine suppression system working principle is as follows: it detects and analyses mashgas (coal dust) explosion signal under mining depend on its optical detector; then it completes superspeed behavior of flame retardance and explosion suppression with the electronic controller; it replaces the traditional passive explosion suppression system with a active explosion suppression system. Through groups of experiments with the function of HS mine suppression system, it has been found that HS system indeed has a good practical effect and a reliable safety performance. This system can save workers lives and property as much as possible by blocking reaction chain of gas explosion effectively in a remarkably short period of time and realize the goal of flame retardance and explosion suppression. The South Africa's HS mine suppression system, which is an advanced technique and has very strong vitality, fills the void in terms of active explosion suppression in China. Therefore, it shows great promoting values and wide ranges of potential applications in China.

REFERENCES

EN/1127-1.2007. Explosion prevention and protection in explosive gas environment[S].

EN/14373. 2005. Explosion suppression system [S].

GB/T18154.2000. Technical requirements of monitor type explosion suppression device[S].

Ma Li, Louis, et al. 2010. An experimental research on HS fireproofing technology based on active explosion inhibition in coal mine [J], *China Coal* 9(9): 102–105.

Wang Jun-feng, Wu Jian-ming, Bai Yun-long. 2010. Experimental Research on the Effects of South Africas' HS Suppress ion System [J]. *CSSJ* 20(6):63–68.

Wang Jun-feng. Wu Jian-ming. Yu sheng, Helmuth Spath. 2011. The Experiment Research of the Powder Jetting Performance for the South Africa HS A ctive Explosion Suppression System [J]. *Procedia Engineering*.

Zhang Xiu-hua, Wu Yan-yan.2012. Numerical Analysis of Shock Wave Propagation Law of Internal Gas Explosion [J]. *Applied Mechanics and Materials*:299–302.

Progress in Mine Safety Science and Engineering II – He et al. (Eds)
© 2014 Taylor & Francis Group, London, ISBN 978-1-138-00122-0

Influence of concentration distribution on gas explosion shockwave in tunnels

Jiachen Chen
State Key Laboratory of Explosion Science and Technology, Beijing Institute of Technology, Beijing, China

Lei Pang
Chemical Engineering College, Beijing Institute of Petrochemical Technology, Beijing, China

Qiuju Ma
State Key Laboratory of Explosion Science and Technology, Beijing Institute of Technology, Beijing, China

ABSTRACT: A commercial software package AutoReaGas, was used to carry out the numerical investigation for the distribution difference of shockwave from methane-air explosion in coal laneways under different concentrations of methane. The study verifies that the strongest shockwave is produced under the optimum concentration. The higher the concentration in premixed area, the larger the increasing area of shockwave overpressure, and the larger the distance between the location of shockwave overpressure maximum and the ignition in whole explosion field. The reason is that the propagation of the shockwave promotes the flow and diffusion of the unburned gaseous mixture in front of flame. A change of the methane-air mixing state and the premixed area gives rise to the distribution difference of shockwave on time and space.

1 INTRODUCTION

Gas explosion is one of the main types of accidents in coal mining. Gas explosion is a kind of nonpoint explosion. It is generally deflagration, but it can also reach detonation under specific conditions. There are many researches on the shock wave disasters in gas explosion. Gas explosion is volume explosion, and the disaster effects are greatly influenced by external factors, resulting that the explosion shock wave related researches are mainly focused on the time and space distribution of shock wave intensity, influence factors on shock wave propagation, the damage criterion of shock wave and the disaster effects on human body. Ibrahim (2001) and Valeria (2009) studied the influence of obstacles in roadway on the explosion using experimental and large eddy simulation methods. They pointed out that bigger section blocking rate would bring higher shock wave peak overpressure and shorter time of arrival. Lin et al (2007) conducted gas explosion experiments in a pipe (80 mm × 80 mm in section) with some spiral metal ring inside. They found that the flame speed got higher with the increase of the height of ring. Ye et al (2005) studied the inhibitory effect of water spray on the pipe gas explosion by experiments, and found that the inhibitory effect is proportional to the spray density and length. Jia (2007) and Jing (2008) summarized the change law of the overpressure when shock waves ran through the discontinuity section of the laneway by the means of theoretical analysis.

The characteristics of gas have significant influence on the disaster effects in gas explosion and may complicate the disaster. For example, the peak overpressure of shock wave gets higher as the premixed area increases, and the attenuation of shock wave along the axis gets more slowly (Xu, J.D. & Xu, S.L. 2004). Any flammable gas has its corresponding explosion limit. The explosion limit of methane is about 4.6%−14.3% (Zhao, H.Y. 1996). Outside the range, even a strong ignition source cannot stimulate the explosion. The explosion limits of gas can be influenced by many factors, such as initial temperature, initial pressure, etc. and also it is directly related to the environment and the determination method. As to the flammable gas cloud within the scope of the explosion limit, the explosion parameters display a marked difference when concentrations vary. The optimal concentration often leads to the highest explosion parameters. For instance, the constant volume explosion overpressure of methane/air mixture at a concentration of 10.1% can reach as high as 0.86 MPa, and the highest temperature can reach 2340 K (Zhao, H.Y. 1996).

Obviously, this concentration is slightly higher than the stoichiometric concentration (9.5%) of methane. Therefore, study of the effects of gas concentration on the gas explosion in laneways is of great significance for the understanding gas explosion mechanism and accident prevention. In this work, the different distributions of shock wave in underground gas explosion at different concentrations are researched by CFD code AutoReaGas. The physical mechanism of how gas concentration affects the shock wave disaster is revealed.

2 NUMERICAL METHOD

In this article, the gas explosion process meets mass, momentum, energy and chemical components conservation equations. The k-ε turbulence model is used to model the turbulence which is the key factors in the gas explosion, and the single-step chemical reaction is used to describe the reaction process of gas explosion. AutoReaGas uses following model (AutoReaGas™ Interactive Software Theory Manual. 2002 & AutoReaGas™ Reactive Gas Dynamics and Blast Analysis software User Manual Version 3.1. 2002) to describe the turbulent burning velocity:

$$S_t = 1.8u'^{0.412} \cdot L_t^{0.196} \cdot S_l^{0.784} \cdot \nu^{-0.196} \quad (1)$$

Where, u' is turbulence intensity, L_t the characteristic length scales, S_l the laminar burning velocity, S_t the turbulent burning velocity, and ν is kinematic viscosity.

The coupling problem between the pressure and velocity in transient flow field is numerically solved by the finite volume discrete methods and the improved SIMPLEC algorithm. Rectangular grids are used in the discretization in space. Because of the limitation of computing power, the effect of small scale physical objects on explosion flow field is calculated by sub-grid technique in AutoReaGas (AutoReaGas™ Interactive Software Theory Manual. 2002, AutoReaGas™ Reactive Gas Dynamics and Blast Analysis Software User Manual Version 3.1. 2002, Maremonti, M., Russo, G., Maremonti, E. & Tufano, V. 1999, Tufano, V., Maremonti, M., Salzano, E. & Russo, G. 1988, Salzano, E., Marra, F.S., Russo, G., Lee, J.H.S. 2002 & Bretislav, J., Petr, S., Jan, H.& Lukas, V. 2006).

AutoReaGas is mainly used to simulate gas explosion and its shock effect. It is specifically designed for congestion and restrictions (AutoRea -Gas™ Interactive Software Theory Manual. 2002 & AutoReaGas™ Reactive Gas Dynamics and Blast Analysis software User Manual Version 3.1. 2002). The reliability of AutoReaGas in the field of gas explosion has been verified. The reliability of this software in the numerical simulation on gas explosion have been reported in literature (AutoRea -Gas™ Interactive Software Theory Manual. 2002, AutoReaGas™ Reactive Gas Dynamics and Blast Analysis software User Manual Version 3.1. 2002, Maremonti, M., Russo, G., Maremonti, E. & Tufano, V. 1999, Tufano, V., Maremonti, M., Salzano, E. & Russo, G. 1988, Salzano, E., Marra, F.S., Russo, G., Lee, J.H.S. 2002 & Bretislav, J., Petr, S., Jan, H.& Lukas, V. 2006).

3 NUMERICAL PROCEDURE

The calculation model is a 1000 m straight laneway with a section area of 6 m^2, as shown fig. 1. One end is closed and the other is open. According to the grid feature, the cross section is simplified to a square shape, 2.45 m × 2.45 m. A weak hemispherical ignition source is set near the closed end. At initial moment, the gas is premixed and perfectly still. Kindracki (2007) found that the maximum explosion parameters are obtained when methane concentration in air is higher than 9.5%. So the concentration of 10.1% (Zhao, H.Y. 1996) is chosen in this study. The premixed methane/air mixture is 100 m long. The support system is simplified to rectangular pillars with a section size of 0.1 m × 0.1 m and the space is 1 m. Three different methane concentrations, 7.0%, 10.1% and 13.0% are set for this simulation. The grid size is 0.49 m × 0.49 m in radial direction and 0.50 m in axial direction. The total number of grid and node are 50000 and 72036 respectively.

4 RESULTS AND ANALYSIS

Monitoring points are located in center of the cross section of the roadway. Profiles of peak overpressures along with the axial distance for different gas concentration are shown in Fig. 2. Firstly, in the whole explosion field, the shock wave overpressure under the concentration of 10.1 (1.13 MPa) is higher than that under the concentration of 7.0% (0.63 MPa) and 13.0% (0.44 MPa) which confirmed that the maximum explosion parameters can be obtained at the optimum concentration, while the explosion parameters will decrease when the concentration goes higher or lower than the optimum concentration.

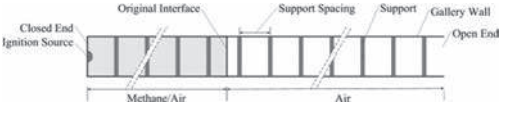
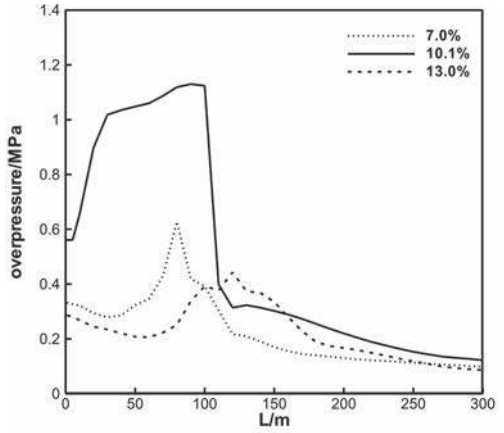
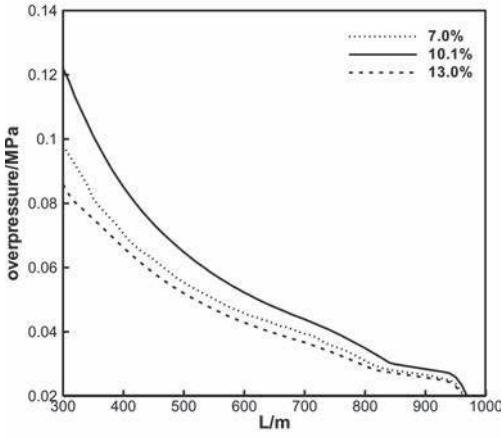


Figure 1. Top view of calculation model.



(a) L<300 m



(b) L>300 m

Figure 2. Peak overpressure vs. axial distance under different concentrations.

In figure 2, the peak overpressures along the axial distance for all three kinds of concentrations firstly increase rapidly, and then turn gradually attenuated. If the overpressure rising area is defined as shock waves near field and the attenuation area as far field, the higher the gas concentration of premixed area is, the larger the shock wave near field range gets. Near field ranges for these three kinds of concentration are 80 m, 100 m and 120 m respectively. It also shows that the peak overpressure in the whole flow field gets farther from the explosion source for higher gas concentration. In addition, according to figure 2(b), the peak overpressure for the optimum concentration is always the highest at the same axial location.

The gas concentration of premixed area also influences the spread of flames. According to the calculation results, the lengths of flame area under these three concentrations (7.0%, 10.1%, and 13.0%) are 110 m, 250 m and 280 m respectively. It suggests that when the gas concentration of premixed area is lower than the optimal concentration and higher than the lower explosion limit, the flame area range is close to the premixed area; when at the optimum concentration, the flame area is longer than the premixed area length; When at a concentration higher than the optimum concentration and lower than the higher explosion limit, the flame area is longer than the premixed area length and also a little longer than the flame area length corresponding to the optimum concentration.

According to the physical mechanism of gas explosion, when the concentration of premixed gas mixture is higher than the optimum concentration and lower than the higher explosion limit, the shock wave overpressure inside the premixed area could not reach the highest value. As the shock wave propagates along the laneway axis, a large amount of unburned gas diffuses and expands forward in the same direction, and reaches the optimum concentration at certain location outside the premixed area, and then the highest overpressure turns up. When the concentration of premixed gas mixture is lower than the optimum concentration and higher than the lower explosion limit, the unburned gas diffuses forward as the shock wave propagates, and the highest overpressure appear at a location after which the gas concentration gets lower. Thus higher overpressure will never appear any more.

5 CONCLUSION

The shock wave diffusion under different premixed gas concentrations are researched by numerical method. It is confirmed that the explosion parameters is the highest under the optimum concentration, while at a concentration higher or lower than the optimum concentration, the explosion parameters will go down. When gas concentration gets higher, the range of overpressure rising area gets larger, and the maximum overpressure in the whole flow field appears farther from the explosion source. This is because that the spread of shock wave make the unburned gas ahead of the flames flow and diffuse, which will change the methane/air mixing state and the range of mixed area and result in the distribution difference of shock wave and flame in time and space. The difference of explosion disaster effect and the diffusion mechanism of unburned gas under different gas concentrations are the based study references

for the accident investigation and prevention, the transition from gas explosion to combustion and the conversion mechanism between explosion and fire hazard.

ACKNOWLEDGMENTS

The authors would like to acknowledge the financial support of Beijing Natural Science Foundation (No. 8132029) for this study.

REFERENCES

AutoReaGas™ Interactive Software Theory Manual. 2002. *Century Dynamics and TNO.*

AutoReaGas™ Reactive Gas Dynamics and Blast Analysis software User Manual Version 3.1. 2002. *Century Dynamics and TNO.*

Bretislav, J., Petr, S., Jan, H. & Lukas, V. 2006. Vented confined explosions in Stramberk experimental mine and AutoReaGas simulation. *Journal of Loss Prevention in the Process Industries* 19: 280–287.

Jia, Z.W. & Jing, G.X. 2007. Study on propagation rules about gas explosion shock wave in the laneway with abrupt change of sectional area. *China Safety Science Journal* 17(12): 92–94.

Jing, G.X. & Jia, Z.W. 2008. A theoretical study on propagation of shock wave of a gas explosion at a section of laneway with sudden change of area. *Science & Technology Review* 26(11): 62–64.

Ibrahim, S.S. & Masri, A.R. 2001. The effects of obstructions on overpressure resulting from premixed flame deflagration. *Journal of Loss Prevention in the Process Industries* 14: 213–221.

Kindracki, J., Kobiera, A., Rarata, G. & Wolanski, P. 2007. Influence of ignition position and obstacles on explosion development in methane-air mixture in closed vessels. *Journal of Loss Prevention in the Process Industries* 20: 551–561.

Lin, B.Q., Jian, C.G. & Mang, H. 2007.Study on influence of conduit support on gas explosion flame propagation. *International Symposium on Mining Science and Safety Technology*.

Maremonti, M., Russo, G., Maremonti, E. & Tufano, V. 1999. Numerical simulation of gas explosions in linked vessels. *Journal of Loss Prevention in the Process Industries* 12: 189–194.

Tufano, V., Maremonti, M., Salzano, E. & Russo, G. 1988. Simulation of VCEs by CFD modelling: An analysis of sensitivity. *Journal of Loss Prevention in the Process Industries* 11: 169–175.

Salzano, E., Marra, F. S., Russo, G., Lee, J. H. S. 2002. Numerical simulation of turbulent gas flames in tubes. *Journal of Hazardous Materials* A95: 233–247.

Valeria, D.S. & Almerinda, D.B. 2009.Gennaro R. Using large eddy simulation for understanding vented gas explosions in the presence of obstacles. *Journal of Hazardous Materials* 169: 435–442.

Xu, J.D. & Xu, S.L. 2004. Experimental study on mine gas explosion diffusion. *Coal Science and Technology* 32(7): 55–57.

Ye, J.F., Chen, Z.H., Fan, B.C. & Xie, B. 2005. Suppression of methane explosions in a field-scale pipe. *Journal of Loss Prevention in the Process Industries* 18: 89–95.

Zhao, H.Y. 1996. Gas and dust explosion theory. Beijing: *Beijing Institute of Technology Press.*

Progress in Mine Safety Science and Engineering II – He et al. (Eds)
© 2014 Taylor & Francis Group, London, ISBN 978-1-138-00122-0

The application of the relaxative operator theory to predict the emission volume of gas in coal mine

Liyun Tan & Yang Xue
The Department of Basic Science, North China Institute of Science and Technology, Beijing, China

Haiyang Ju
School of Safty Engineering, North China Institute of Science and Technology, Beijing, China

ABSTRACT: In order to predict the relative emission volume of mine gas, a model called grey system theory is built by using the relaxative operator theory. To apply this model to forecast the emission volume of mine gas, we create the grey theory depending on the emission volume in coal mine, and then to forecast the grey system of coal mine. It is shown that the grey system model has the first-degree precision by comparing the degrees of precision.

1 INTRODUCTION

With the development of the economy of China, the demand of coal become in a higher tension gradually. During this period, the serious accidents of coalmine consistently happen in the state. Among these accidents, the accidents caused by the explosion of gas are in a high proportion, and it directly leads to the loss of the economy and human's safety. Hence, one measure to prevent such accidents is to accurately forecast the emission of coalmine. There are many geological factors affecting the emission of gas. The nonlinear relation among these factors is very complicated and uncontrolled. So, it's difficult to forecast the volume of emission of gas from coal mine.

The grey system is a totally new traverse science invented by China's notable scholar Prof. Julong Deng at 1982. It's mainly to research the uncertain system which only includes small sample or limited information. By creating, developing and extracting the effective information from the known part, the action of a system can be correctly recognized and effectively controlled. In last 20 years, the Grey System was not only developing in the theoretical field, but in the field of natural science and social science it brought about a series of breakthroughs.

In the paper "The application of the grey system to forecast the emission volume of gas from coal mine" published in the academic journal of coal, No. 5, I notice that the original value of 2003 is 2.675 while the forecasted value is 5.135, so the relative error reaches to 91.9% (Wu A. et al. 2005). Meanwhile, in the precision test, the values of C and P are also improper. Conclusively, the precision is low and couldn't be utilized. However, by the relaxative operator theory to improve, the result is in a high precision and meets the requirement of the first degree precision.

2 THE THEORY AND ANALYSIS OF THE GM(1, 1) MODEL

In the application of Grey System Theory to forecast the emission volume of gas from coal mine, we usually select a grey system theoretical differential equation model called GM(1, 1) which includes a first-order variable. The forecasting process can be split to three steps: grey generation, parameter calculation and precision test.

2.1 *Grey generation*

We define the original series as $X^{(0)} = (x^{(0)}(1), x^{(0)}(2), \ldots, x^{(0)}(n))$, and n is the length of the series. By the process of accumulating and generating, we get the series $X^{(1)} = (x^{(1)}(1), x^{(1)}(2), \ldots, x^{(1)}(n))$, and

$$x_k^{(1)} = \sum_{j=1}^{k} x_j^{(0)}$$

Based on the generated series, we build the grey generation model

$$\frac{dx^{(1)}}{dt} + ax^{(1)} = b \tag{1}$$

(1) is the grey differential equation, noted as *GM* (1, 1), and a, b are the parameters to be identified.

2.2 *Parameters calculation*

The parameters in (1) is obtained by the Least Squares Method $\begin{pmatrix} a \\ b \end{pmatrix} = (B^T B)^{-1} B^T y_n$, and

$$B = \begin{pmatrix} -(x_1^{(1)} + x_2^{(1)})/2 & 1 \\ -(x_2^{(1)} + x_3^{(1)})/2 & 1 \\ \vdots & \vdots \\ -(x_{n-1}^{(1)} + x_n^{(1)})/2 & 1 \end{pmatrix}, \quad y_n = \left(x_2^{(1)}, x_3^{(1)}, \ldots, x_n^{(1)}\right) \tag{2}$$

The discrete time responding variable $\hat{x}_{k+1}^{(1)}$ is determined by the following equation

$$\hat{x}_{k+1}^{(1)} = \left(x_1^{(1)} - \frac{b}{a}\right) e^{-ak} + \frac{b}{a} \tag{3}$$

We then reduce $\hat{x}_{k+1}^{(1)}$ by accumulating, and the estimation of the original data are

$$\hat{x}_{k+1}^{(0)}, \quad \hat{x}_{k+1}^{(0)} = \hat{x}_{k+1}^{(1)} - \hat{x}_k^{(1)} \tag{4}$$

2.3 *Precision test*

We define the original series as $X^{(0)} = (x^{(0)}(1), x^{(0)}(2), \ldots, x^{(0)}(n))$, The simulating series of that model is

$$\hat{X}^{(0)} = \left(\hat{x}^{(0)}(1), \hat{x}^{(0)}(2), \ldots, \hat{x}^{(0)}(n)\right)$$

The residues is

$$\varepsilon^{(0)} = \left(\varepsilon^{(0)}(1), \varepsilon^{(0)}(2), \ldots, \varepsilon^{(0)}(n)\right) = \left(x^{(0)}(1) - \hat{x}^{(0)}(1), \ldots, x^{(0)}(n) - \hat{x}^{(0)}(n)\right)$$

The relative error series is

$$\Delta = \left(\left|\frac{\varepsilon(1)}{x^{(0)}(1)}\right|, \left|\frac{\varepsilon(2)}{x^{(0)}(2)}\right|, \ldots, \left|\frac{\varepsilon(n)}{x^{(0)}(n)}\right|\right) = \{\Delta_k\}_1^n$$

We define $\bar{\Delta} = \frac{1}{n}\Sigma_{k=1}^{n}\Delta_k$ as the average simulating relative error, $1 - \bar{\Delta}$ as average relative precision. When $\bar{\Delta} < \alpha$ and $\Delta_n < \alpha$ (the given $\alpha > 0$), the model is called residuals qualified model.

Defining ε as the absolute relevant degree of $X^{(0)}$ and $\hat{X}^{(0)}$, if $\varepsilon_0 > 0$ is given and $\varepsilon > \varepsilon_0$, we call the model as the relevant degree qualified model.

Defining

$$\bar{x} = \frac{1}{n}\sum_{k=1}^{n} x^{(0)}(k), S_1^2 = \frac{1}{n}\sum_{k=1}^{n}(x^{(0)}(k) - \bar{x})^2,$$

$$\bar{\varepsilon} = \frac{1}{n}\sum_{k=1}^{n}\varepsilon(k), S_2^2 = \frac{1}{n}\sum_{k=1}^{n}(\varepsilon(k) - \bar{\varepsilon})^2$$

Table 1. The degrees of the precision test.

Index Precision Critical value Degree	Relative error α	Relevant degree ε_0	Ave Variance rate c_0	Small Prob errot P_0
1st degree	0.01	0.90	0.35	0.95
2nd degree	0.05	0.80	0.50	0.80
3rd degree	0.10	0.70	0.65	0.70
4th degree	0.20	0.60	0.80	0.60

C = S2/S1 is the average variance ratio, and when C0 > 0 and C < C0, we call the model as the average variance ratio qualified model $P = P(|\varepsilon(k) - \bar{\varepsilon}| < 0.6745 \cdot S_1)$ is called small error probability. When $P_0 > 0$ and $P > P_0$, we call the model as small error probability qualified model.

The four definitions above are the methods to test the model. They all judge the precision by criticizing the residues. To give values to *a, ε, C, P* is to determine the degree of simulating the precision. The commonly used precision degrees can be seen in Table 1.

Generally, the commonly used index is the relative error test.

3 THE RELAXATIVE THEORY

In the grey theory, before modeling, we usually take a relaxative operator to the original series according to the qualitative analysis. It will result to that the disturbance to the series will be weakened, and also result to a desirable effect.

We call an operator as the relaxative operator when it meets three axioms below (Si F. et al. 1999).

Axiom 1 (fixed point axiom): Defining X as the data series of systematic action, D is the series operator, namely XD = (x(1)d, x(2)d, …,x(n)d), so D meets that x(n)d = x(n).

Axiom 2 (information fully used axiom): The data x(k)d, (k = 1, 2…, n) in the data series of systematic action should react with the operator in the whole process.

Axiom 3 (Analysis axiom):Any x(k)d, (k = 1, 2…, n) can be expressed by elemental formula including x(1), x(2), x(3).

We regard the operator meeting the three axioms as the relaxative operator. If the rate or amplitude of the relaxative series is weaker w-hen compared to the original series X, the relaxative operator will be called weakened operator. Otherwise, the relaxative operator will be called strengthened operator. The operator below is a commonly used weakened operator.

We define the original series as X = (x(1), x(2), …, x(n)), and make XD = (x(1)d, x(2)d, …,x(n)d) and

$$x(k)d = \frac{1}{n-k+1} \times \left[x(k)+x(k+1)+\cdots+x(n)\right]; k = 1,2,\ldots,n$$

When X is an increasing series, decreasing or fluctuating series, D is a weakened operator.

$$XD^2 = XDD = (x(1)d^2, x(2)d^2, \cdots, x(n)d^2)$$

And

$$x(k)d^2 = \frac{1}{n-k+1}\left[x(k)d + x(k+1)d + \cdots + x(n)d\right]; \quad k = 1,2,\ldots,n$$

When D^2 is an increasing series, decreasing or fluctuating series, D^2 is a second-order weakened operator.

4 FORECASTING THE EMISSION VOLUME OF GAS FROM COAL MINE BY RELAXATIVE OPERATOR

The emission volume of gas from coal mine is influenced by many factors, the relationship among which is very complicated. So it's obviously a gre-y system. The data of the emission volume of gas in last 10 years at a coal mine are shown in table 2.

4.1 *The original data by a weakened operator weak the influence of the disturbance to the sy-stematic action*

The original series is

$$X^{(0)} = \left(x^{(0)}(1), x^{(0)}(2), x^{(0)}(3), \ldots, x^{(0)}(10)\right) = \left(2.685, 4.095, 2.725, \ldots, 3.053\right)$$

To exert a weakened operator D above mentioned on $X^{(0)}$, we get

$X^{(0)}D$ = (3.7276, 3.8434, 3.8120, 3.9673, 3.8452, 4.0468, 4.0028, 3.7093, 2.864, 3.053)

$X^{(0)}D^2$ = (3.6871, 3.6826, 3.6626, 3.6412, 3.5869, 3.5352, 3.4072, 3.2088, 2.9585, 3.053)

Defining

X = (3.6871, 3.6826, 3.6626, 3.6412, 3.5869, 3.5352, 3.4072, 3.2088, 2.9585, 3.053)

X's 1-AGO is

$X^{(1)}$ = ($x^{(1)}(1)$, $x^{(1)}(2)$, $x^{(1)}(3)$, …, $x^{(1)}(10)$)
= (3.6871, 7.3697, 11.0323, 14.6735, 18.2604, 21.7956, 25.2028, 28.4116, 31.3701, 34.4231)

4.2 *Building the systematic model of forecasting the emission volume of gas*

We get $X^{(1)}$ by accumulating, the built data matrix B, y_N is

$$B = \begin{pmatrix} -5.284 & 1 \\ -9.2210 & 1 \\ \vdots & \vdots \\ -32.8966 & 1 \end{pmatrix},$$

$$y_N = \left(7.3697, 11.0323, 14.6735, \ldots, 34.4231\right)$$

From (3), we get

$$\begin{pmatrix} a \\ b \end{pmatrix} = \begin{pmatrix} 0.0272 \\ 3.9514 \end{pmatrix}, \quad \frac{b}{a} = 145.272$$

The forecasting model is

$$\hat{x}_{k+1}^{(1)} = -141.585e^{-0.0272k} + 145.272$$

The results are in table 3 in next page.

4.3 *Precision test*

By calculations,

$$\bar{\varepsilon} = -0.00075, \bar{x} = 3.4423, \Delta = 0.0208,$$
$$\Delta_n = 0.0011, S_1 = 0.2602, S_2 = 0.0906$$

$$C = \frac{S_2}{S_1} = 0.3482 < .035, 0.6745 \cdot S_1 = 0.1755,$$
$$P = P(|\varepsilon(k) - \bar{\varepsilon}| < 0.6745 \cdot S_1) = 0.90$$

Table 2. Statistic of gas relative emission of 4th ward of some coal mine.

Year	1994	1995	1996	1997	1998	1999	2000	2001	2002	2003
Elative emission volume of gas /$m^3 \cdot (t \cdot d)^{-1}$	2.685	4.095	2.725	4.700	2.837	4.223	4.388	5.400	2.675	3.053

Table 3. Statistic data analysis of gas relative emission.

Year	Rank	x	$x^{(1)}$	Grey forecasting $\hat{x}^{(1)}$	Grey forecasting $\hat{x}$	$\varepsilon^{(0)}$
1994	1	3.6871	3.6871	3.6871	3.6871	0
1995	2	3.6826	7.3697	7.4862	3.7991	–0.1165
1996	3	3.6626	11.0323	11.1835	3.6973	–0.0347
1997	4	3.6412	14.6735	14.7815	3.5980	0.0432
1998	5	3.5869	18.2604	18.2830	3.5015	0.0854
1999	6	3.5352	21.7956	21.6906	3.4076	0.1276
2000	7	3.4072	25.2028	25.0067	3.3161	0.0911
2001	8	3.2088	28.4116	28.2338	3.2271	–0.0183
2002	9	2.9585	31.3701	31.3743	3.1405	–0.182
2003	10	3.053	34.4231	34.4306	3.0563	–0.0033

$$|s| = \left| \sum_{k=2}^{9} (x(k) - x(1)) + \frac{1}{2}(x(10) - x(1)) \right| = 2.1314$$

$$|\hat{s}| = \left| \sum_{k=2}^{9} (\hat{x}(k) - \hat{x}(1)) + \frac{1}{2}(\hat{x}(10) - \hat{x}(1)) \right| = 2.1250$$

$$|\hat{s} - s| = \left| \sum_{k=2}^{9} [(x(k) - x(1)) - (\hat{x}(k) - \hat{x}(1))] + \frac{1}{2}(x(10) - x(1)) - (\hat{x}(10) - \hat{x}(1)) \right| = 0.0064$$

$$\varepsilon = \frac{1 + |s| + |\hat{s}|}{1 + |s| + |\hat{s}| + |\hat{s} - s|} = \frac{5.2564}{5.2564 + 0.0064} = 0.9988 > 0.90$$

From the relative error test to see, the precision is close to the first degree; From the average variance test to see, the precision is in the first degree. From the small probability error test to see, the precision is close to the first degree; From the grey absolute relevant degree to see, the precision is in the first degree.

5 CONCLUSION

As we use the relaxative operator theory, it greatly reduces the influence of the disturbance on the data series of systematic actions. So, the forecasting effect above is more accurate than the original paper.

ACKNOWLEDGEMENTS

The authors gratefully acknowledge foundation by the Higher Education Research Fund Project of NCIST (No:HKJYZD201215)

REFERENCE

Si Feng, et al. 1999. The grey system theory and its application. Beijing:The Science Press (in Chinese).

Wu Aiyou, et al. 2005. Application of the grey system theory for predicting amout of mine gas emission in coal mine, Journal of china coal society, 30(5):589–592 (in Chinese).

Progress in Mine Safety Science and Engineering II – He et al. (Eds)
© 2014 Taylor & Francis Group, London, ISBN 978-1-138-00122-0

Outburst prevention technology and effects of hydraulic flushing with effects of pressure relief and increasing permeability

Wei Meng & Bo Li
College of Safety Science and Engineering, Henan Polytechnic University, Jiaozuo, Henan, China

ABSTRACT: The paper analyzed the advantages and disadvantages of hydraulic outburst prevention and expatiated on the validity of hydraulic flushing technique eliminating working face with outburst hazard. Studies have shown that high pressure water jet of hydraulic flushing technique could break coal body, change stress state of coal, increase preexisting cracks and produce more cracks improving permeability coefficient.

1 INTRODUCTION

Low air permeability coal seam has account for more than 95% of coal seams mined by the high mines and outburst mines, permeability coefficient in coal seam is just 10–3~10–4 mD thus it dreamed big to gas drainage and drainage rate is low. (Yu 1992, Wang 2005, Qin et al. 2008).

Mining protective layer and pre-pumping coal gas could release the crustal stress and gas potential in coal seam and change the properties of the coal itself which lead to eliminate outburst hazard in coal seam. Yet utilizing pressure relief antireflection strengthening pumping discharge is the most significant mean to eliminate outburst in single permeability coal seam which outburst seriously. Waterpower, mechanical force and bursting force are included in the dynamic for antireflection of pressure relief, the disadvantages of mechanical force and bursting force are listed as follows: operating process is difficult, range of pressure relief is limited and that is easy to produce sparks. Outburst prevention measures such as hydraulic extrusion, hydraulic cutting and hydraulic flushing achieved better application effect via experiments. However hydraulic extrusion and hydraulic cutting conducted in front of heading face or working face which belong to measures for eliminating outburst hazard partly, it induced outburst and cannot guarantee the safety in process that achieve little effect on advance eliminating outburst in region.

Hydraulic flushing utilizing rock roadway as safety barrier, adopt high pressure water jet to break up coal and rush out part coal and gas which aroused stress of coal and rock mass around drill decreased, pressure relief and strengthen drainage effective, for the sake of improving quantity of drainage, reducing measures of quantities, shortening the time of measures and eliminating outburst hazard in working face safely and rapidly. (Yu & Wang 2000, Lin & Cui 1992, Li 2006, Yao et al. 1993, Gas group of china mining college 1979) Not eliminate the hazard as jet orifice and outburst bring from drilling in coal roadway, but avoid collapsing hole, sticking to improve drilling hole rate and reduce the construction cost due to taking strata as baffle to drill into coal seam.

2 HYDRAULIC FLUSHING TECHNOLOGY AND ITS BASIC PROCESS

2.1 *Action principle of hydraulic flushing*

Hydraulic flushing is a process that high pressure jet break up coal, release large gas and change the state of stress. The primal damage of coal is that high pressure jet which contain high energy break up coal body, formed holes with smaller diameter, then enlarge holes by breaking coal around broken holes under the effect of coal gas pressure gradient and reflection on jet residual energy.

Several holes with larger diameter were rushed out in outburst dangerous coal seam, released a large number of gas and a certain number of coal and formed a certain pressure relief, gas drainage area in coal body during punching process, prevention of outburst usually have taken in the area. Due to water damp fully coal body which decrease brittleness of coal, increase plasticity, reduce stress concentration within coal body, play its comprehensive outburst prevention role.

2.2 *Hydraulic flushing system*

The system consists of punching nozzle, blow-out preventers, drilling rigs, gas-liquid-solid separator,

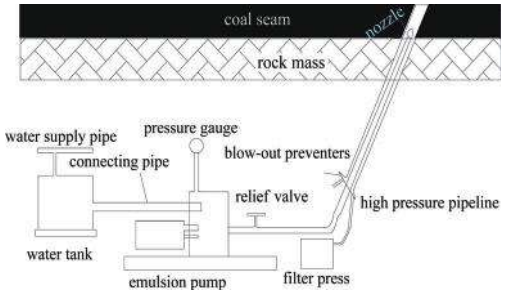


Figure 1. System diagram of hydraulic flushing.

emulsion pump and high-pressure piping. nozzle possess capacity of the secondary crushing, not break coal in the front, but nozzle tail jet is used to remove the pushing coal, control the blocking phenomenon which caused by transient collapsing of coal; the maximum output power, flow and tank capacity of emulsion pump are respectively 31.5 MPa, 200 ml, 1000 L; high-pressure duct with diameter of 31.5 mm was selected as hp piping, system schematic diagram is drawn as Figure 1.

2.3 *Process description*

Hydraulic flushing technology utilizing high pressure water to form a big hole around drill while arouse coal around dirll relieve fully, the gas permeability increased by a large margin, gas within coal seam greatly released, use cement mortar to hole sealing after punching, junction of coal and rock is the depth of sealing hole, finally connect drilling with drainage pipeline to conduct gas drainage for removing outburst.

2.4 *Punching process*

Exit the drill pipe change drill into a special nozzle while change drill pipe into one with smaller diameter which conducive to the discharge cinder, open emulsion pump and drilling machine at the junction of coal and rock, feed drill pipe into drill hole slowly, retrograding drill pipe while punching when reach the max depth, so circulates until ran out of coal and backwater became clear. Then add drill pipe until all coal section rushed out according to such method.

3 ARRANGEMENT OF PUNCHING AND DRILLING

3.1 *Situation of experimental place*

Experimental working face owns a strike length of 370 meters, tendency long is 110 meters, the average coal seam dip angel is 38°, average gas content is 7.89 m^3/t, absolute outflow of gas is 9.2 m^3/min, average pressure of coal seam is 0.82 Mpa. The mine gas pressure is 1.1 times as much as outburst starting condition in case that take 0.74 Ma as outburst starting condition, it became the most serious gas and coal outburst working face. It has to adopt various kinds of gas-prevention measures due to the constantly dynamic phenomenon when drilling on working face. As a result that it appeared orifice, hole collapse, jamming of a drilling tool when carry out bedding drainage drilling on working face, the drill was able to hit the desired depth, the middle of working face appeared empty face between 40 m and 50 m which caused it is hard to realize removing outburst.

3.2 *Drilling hole design*

The test fix up a drill site every 10 meters from south to north in rock concentrated lane, construct strata penetration drilling successively, each drill site owns 4 drills besides No.1 drill site devise 16 drills, the direction, dip and deflection of each drill drilling towards middle working face within the scope of 40 meters until penetrating coal seam as shown in Figure 2.

4 EFFECT INVESTIGATION ANALYSIS OF HYDRAULIC FLUSHING

4.1 *Effect analysis of coal running out*

Complicated geologic structure tectonism not changed combined form of coal seam, but destroyed coal structure of coal itself, which lead coal seam $二_1$ is mellow and fragile, present in powder form. When the hydraulic punching experiment was carried out, the common number drills is 52, the accumulation coal output is 416t, average coal output of each drill is about 8t, calculate

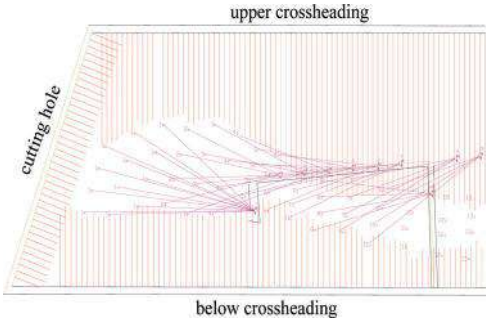


Figure 2. Schematic diagram of strata penetration drilling.

according to discharge of coal, the accumulation punching volume is 301.08 m^3, average punching volume of each drill is about 5.79 m^3, equivalently expand drill with diameter of 75 mm to hole with diameter of 2823 mm, the hole changed stress of coal and release pressure of coal around drill, stress gradient descent, accumulative elastic potential energy released within coal and rock stratum; meanwhile aroused coal seam air permeability increased which make gas within coal discharged and gas expansion accumulatived within coal released (Liu et al. 2005, Jiang & Yu 1996, Liang & Zhang 1997, Xin et al. 2002).

4.2 *Effect analysis of gas reminder quantity and gas pressure*

Determine five covers coal seam original content of gas and proximate analysis (shown in Table 1) before hydraulic flushing, it can be seen from the test results that content of gas is between 5.25 and 7.33 m^3/t, average is 6.29 m^3/t, seen from the data of content of gas by site test that gas occurrence has a tendency to magnify from the shall on to the bottom and travel southward on working face. The coal quality of mine is lean coal, coal seam 二$_1$ belongs to pore development, porosity is between 7.25% and 8.61%, the average is 8.02%, much higher than average porosity of lean coal 4.5%. Namely under the same gas pressure, the bigger coal porosity is, the more free gas amount coal contained (Zhou & Lin 1999), it also explained that low content of gas in coal seam 二$_1$ correspond high gas pressure, so on the basis of preliminary study and combined experiences of other national mining area, used coal seam gas-bearing capacity replaced gas pressure as index for predicting outburst region, set critical value of content of gas as 6 m^3/t through comprehensive analysis. Measured maximum coal seam gas-bearing capacity is 7.33 m^3/t in coal seam 二$_1$ during the test which has beyond critical value for content of gas, this illustrates that eliminating outburst measure is invalid on working face.

Utilizing hydraulic flushing to rush out a certain amount of coal and discharge part of gas which decrease stress of coal around drill, release the stress of coal at different degree that enhanced gas permeability coefficient of gas, increased natural discharge of gas and quantity of drainage, gas emission on working face decreased obviously, it does not appear the phenomenon as jet orifice and sticking after drilling holes along seam on upper and lower roadways of working face, drilling holes along seam can reach desired depth which eliminating empty surface zone with 40–50 m on the middle working face. For verifying effectiveness of this measure, select appropriate location in bottom road, re-determinate of the primary middle blank tape (seen as Table 2). It can be seen from test result that gas pressure of coal seam is less than 0.74 MPa. Coal seam gas-bearing capacity is between 1.88 and 5.93 m^3/t, the average is 3.9 m^3/t, compared with coal seam gas-bearing capacity 6.29 m^3/t without hydraulic flushing, it has decreased by 37.9 percents which below the critical value.

Table 1. Margin settings for A4 size paper and letter size paper.

Sampling location	Buried depth (m)	Mad (%) moisture	Aad (%) ash	Vf (%) volatile	Content of gas of raw coal (m^3/t)	Back calculation of gas pressure (MPa)
Below crossheading cutting hole 5 meters south on working face	360	0.61	11.63	22.19	7.33	1.13
11 meters from cutting hole on working face to below crossheading	355	0.54	9.96	20.04	5.25	0.64
30 meters from open mouth to below crossheading	360	0.53	16.08	21.15	7.31	1.05
20 meters from cutting hole on working face to below crossheading fourth cross-hole	330	0.55	23.72	25.96	5.98	0.98
105 meters from cutting hole to below crossheading	360	0.56	13.1	19.85	6.7	1.45

Table 2. Gas pressure surveyed indirectly of coal seam in the working face after flushing.

Sampling location	Buried depth (m)	Mad (%) moisture	Aad (%) ash	Vf (%) volatile	Content of gas of raw coal (m^3/t)	Back calculation of gas pressure (MPa)
11.5 meters from cutting hole to below crossheading	2.72	0.43	12.07	18.17	30.174	0.328
105 working face concentration roadway 2~3, the middle of drill site	5.93	0.21	10.28	17.83	30.174	0.328
50 meters from cutting hole to below crossheading	4.76	0.44	9.97	19.89	30.174	0.328
105 working face, 4~5 concentration roadway, the middle of drill site	1.88	0.22	37.24	15.39	30.174	0.328

Table 3. Summary table of effect assessment of elimination outburst in the working face.

Evaluation method	Evaluation index	Critical value of index	Index range	Effect of removing outburst
Single-phase index	Destruction type	III~V	II~III	Effective
	ΔP	>10	3.5~6.5	
	f	0.5	0.17~0.57	
	Survival gas pressure (MPa)	>0.74	0.27~0.69	
Comprehensive index	D	>0.25	0	Effective
	K	>15	8.54~35.29	
Survival gas content	Survival gas content (m3/t)	>6.0	1.88~5.93	Effective
Gas drainage rate method	Gas drainage rate (%)	>30	31.2	Effective

5 EFFECT EVALUATION OF HYDRAULIC FLUSHING

Using single-phase index method, comprehensive index method, survival gas content method and gas drainage rate method to evaluate effect of removing outburst. Test the effectiveness of removing outburst on working face by hydraulic flushing, the results of assessment is shown in Table 3, it can be seen that after taking measure of hydraulic flushing each index is below critical value, to sum up that hydraulic flushing is effective for removing outburst on working face.

6 CONCLUSIONS

1. It descends the stress gradient of coal around drill by using hydraulic flushing; caused coal gas permeability increased by a large margin while release stress, the gas released and gas pressure gradient fell sharply, not eliminate the stress and gas condition aroused by outburst, and increase outburst resistance restrained by coal body, playing an increasingly important part in comprehensive antioutburst.
2. During investigate of pressure relief effect, the common number drills is 52, the accumulation coal output is 416t, average coal output of each drill is about 8t, calculate according to discharge of coal, the accumulation punching volume is 301.08 m^3, average punching volume of each drill is about 5.79 m^3, eliminate the pressure around drill which make coal seam obtained pressure relief.
3. It can be seen from the contrast before and after the measures that content of gas has decreased from 6.29 m^3/t to 3.9 m^3/t, dropped below gas critical value, eliminate the phenomenon of gas transfinite which explained that hydraulic flushing is effective to eliminate the hazard of outburst on working face. Not only improve the working environment, but also guarantee the safety production on mining faces, the effect of gas control is obvious.

REFERENCES

Gas group of china mining college. Prevention and Control on Coal and Gas Outburst [M]. Beijing: Coal industry publishing house, 1979.

Jiang Cheng-lin, Yu Qi-xiang. Rules of Energy Dissipation in Coal and Gas Outburst [J]. *Journal of China Coal Society*, 1996, 21(2): 173~178.

Li Jian-ming. Coal and Gas Outburst Prevention and Control Technical Manuals [M]. Xvzhou: China Mining University Press, 2006.

Liang Bing, Zhang Meng-tao. Assumption of the Instable Mechanism of Coal and Gas Outburst from the Consideration of Their Coupling Effect and Instable Fracture of Coal [J]. *China Safety Science Journal*. 1997, 7(1): 6~9.

Lin Bo-quan, Cui Heng-xin. Gray Mine Gas Pumping Discharge Theory and Technology [M]. Xvzhou: China Mining University Press, 1992.

Liu Ming-ju, Kong Liu-an, Hao Fu-chang etc. Application of Hydraulic Flushing Technology in Severe Outburst Coal [J]. *Journal of China Coal Society*, 2005, 30(4): 451–454.

Qin Yue-ping, Yao You-li, Liu Chang-jiu. Technology of surface boreholes for drainage of goaf gases and application in Tiefa Mining area [J]. *Journal of Liaoning Technical University*, 2008, 27(1): 5–8.

Wang Zhao-feng.. Problems on drainage of in coal mine in China and its Countermeasure Discussion [J]. *Safety in Coal Mines*, 2005, 36(3): 29–44.

Xin Xin-ping, Wei Guo-ying, LI Xue-chen etc. Serious outburst prevention technique of excavating in coal seams rapid research identifying information. Jiaozuo: Jiaozuo coal group co., LTD. Research institute of science and technology, 2002.2.10.

Yao Bao-kui, Sun Guang-kui, Yin Dai-xun etc. The regional prediction of coal and gas outburst [M]. Beijing: Science and Technology of China Press, 1993.

Yu Qi-xiang. Gray Mine Gas Pumping Discharge Theory and Technology [M]. Xvzhou: Chian Mining University Press, 1992.

Yu Bu-fan, Wang You-an. Coal mine gas disasters prevention and use of technical manual [M]. Beijing: China coal industry publishing house, 2000.

Zhou Shi-ning, Lin Bo-quan. Coal seam gas occurrence and flow theory [M]. Beijing: China coal industry publishing house, 1999.

This page intentionally left blank

Progress in Mine Safety Science and Engineering II – He et al. (Eds)
© 2014 Taylor & Francis Group, London, ISBN 978-1-138-00122-0

Experimental research on major properties of the sealant to control toxic and harmful gases leakage in coal mine

Ji Li, Fumei Song & Huaiyu Kang
Hebei Province Key Laboratory of Mine Disaster Prevention and Control, North China Institute of Science and Technology, Sanhe, Hebei, China
School of Safety Engineering, North China Institute of Science and Technology, Sanhe, Hebei, China

ABSTRACT: In this paper, exploratory research was done on how polyurethane foam controlled toxic and harmful gases leakage from coalmine. We made 38 groups of experiments by the orthogonal experimental method and single-factor experiment method, which obtained the optimal ingredient ratio. We also prepared polyurethane foam and evaluated its major properties. The results show that sealant can meet the requirements of mechanical properties and high cohesive property under the conditions of coalmines and also has the properties of foaming rapidly, high expansion foaming, dimensional stability, etc. which can be applied well in the prevention and control toxic and harmful gases leakage in coalmine.

1 INTRODUCTION

The working environment of many coalmines is underground, and the conditions are very poor, which have all kinds of toxic and harmful gases and substances, as CO, H_2S, $C0_2$, CH_4, NO_2, SO_2 and coal dust (Shpirt & Goryunova 2009), etc. Some kinds of toxic and harmful gases and substances exist in the coal fissures and pores formed in the production and processing of coal fuels, others exist in the coal seams, roof and floor rock, etc. When the content of these toxic and harmful gases and substances exceeded the critical value, the toxic and harmful gases would be harm to people, and sometimes lead to take place the fire and explosion, which endanger miners' health and safety (Lian 2009).

At present, mining ventilation is the main means to control toxic and harmful gases leakage from coalmines, which discharges the toxic and harmful gases by changing the direction and pressure of the wind, thus the purpose of lowering toxic and harmful gases was achieved (Li & Zhang 2009). Although mining ventilation method has the virtue of controlling toxic and harmful gases exhalation from the mine by wind pressure regulation, it was difficult to meet the requirements of reducing great amount of toxic and harmful gases from the holes with open fractures, cracks, rock wall, mine goaf and the course of blasting for drivage (Li & Shen 2003), etc. In addition, a large number of toxic and harmful gases would be substituted from goaf and hole because of the influence of the ventilation pressure (Xu et al. 2009), even bring out the accidents.

Therefore, in connection with the characteristics of wide areas of toxic and harmful gases leakage, complex rock surface and space condition, and high strength of blasting vibration in coalmines, this paper proposed to use rigid polyurethane foam as sealant and measure the major safety properties of sealant in laboratory. This paper could provide theoretical basis for control toxic and harmful gases leakage in coalmine.

2 THE LABORATORY PREPARATION OF RIGID POLYURETHANE FOAM

2.1 *The composition of experimental materials*

Rigid polyurethane foam is a synthetic material with the characteristics of porosity, low relative density, and high specific tenacity, etc. which is a kind of safety material as sealing material, anchor material in mines, explosion-proof material of fuel tank, filter material (Zhu & Liu 2004), etc.

The polyurethane needs to have some characteristics, as fast frothing, rapid froth coverage, stable froth, high anti-penetrability, antistatic property and low exothermic reaction, etc. for controlling toxic and harmful gases leakage from coalmine. The rigid polyurethane raw material is mainly composed of PAPI (Polyphenylmethane Polyisocyanate), sucrose polyether polyol, foaming agent, catalyst, cross-linking agent, foam stabilizer, frame

retardant (Andrzej et al. 2001, Zhang 2005, Dong et al. 2007), etc.

2.2 *Experimental project*

By orthogonal experiment and single-factor experiment, 38 groups of experimental mix proportion schemes were gotten. According to the proportion schemes, the optimum ratio of experiment was as follows:

PAPI: 50.00% (mass fraction)
Sucrose polyether polyol: 27.82% (mass fraction)
Foaming agent: 7.65% (mass fraction)
Catalyst: 0.49% (mass fraction)
Others: 14.04% (mass fraction)

2.3 *Experimental process*

Mix sucrose polyether polyol, foaming agent, catalyst, cross-linking agent, foam stabilizer, and frame retardant as white material, its appearance was bright yellow viscous liquid.

Mix PAPI and auxiliary material as black material, its appearance was dark brown viscous liquid.

Mix and stir black material and white material rapidly, and then kept them for 40 seconds, the color of reagent began to turn from brown into ivory and began to expand. The foaming time was about 5 minutes (the ambient temperature was: 12.5°C, the humidity was 12.8%).

Measure the foaming volume: it was about 30 times larger than before foaming. The rigid polyurethane shaping material is shown as Figure 1.



Figure 1. Transect of rigid polyurethane foam.

3 THE TEST OF MECHANICAL PROPERTIES OF RIGID POLYURETHANE MATERIAL

The sealant to control toxic and harmful gases leakage needs to have mechanical property of high compressive, tensile and impact force strength, etc. On the one hand, the unconscious damage in the process of operating resulted in large number of toxic and harmful gases leakage, on the other hand, the blasting operations often carried out in coalmines, which can bring out strong vibration force to make a certain pressure on the sealant. If the mechanical strength of rigid polyurethane foam is too low to sustain the pressure, the damage of sealant will lead to great amount of toxic and harmful gases leakage, which can affect the health and safety of workers seriously. Therefore, it is necessary to test the mechanical properties to learn the rigid polyurethane material's compression, tensile and impact force strength, which helps our research on the security during the use of sealant.

3.1 *The test of compressibility*

3.1.1 *Experimental standard and apparatus*

The compressibility test is one of the most important mechanical property indicators of rigid polyurethane foam, which is in according to Test method for compression of rigid cellular plastics (GB 8813-88).

Specimen size: Depth: 50 ± 1 mm; Basal plane: circle, Diameter: 60 mm; Parallelism tolerance of two parallel surface: <1%.

Experimental apparatus: Microcomputer Control Electronic Universal Testing Machine.

Test requirement:

Put each specimen in the center of two flat slabs.

Compress the specimen with 2 mm/min speed rate of the moving slab.

Relative deformation of specimen should reach 10% at most.

3.1.2 *Results*

Specimen description:

Initial specimen: light yellow solid, smooth surface, uniformly distributed pores, not crisp.
Compressed specimen: Surface appeared crimple. The compressed specimen is shown as Figure 2.

When compression began, as the deformation increasing, the initial curve increased significantly, when the relative deformation of specimen reached 10%, the pressure reached the maximum value.

Compression stress when the relative deformation reached 10%.



Figure 2. Compressed specimen.

$$\sigma_{10} = \frac{F_{10}}{S_0} = \frac{2403.8}{2827.44} = 850.2 \text{ kPa} \quad (1)$$

where F_{10} = pressure when to 10% deformation; S_0 = specimen area.

3.2 *The test of tensile strength*

3.2.1 *The test of tensile strength*

The test of tensile strength is according to Test method for tensile properties of rigid cellular plastics (GB 9641-88).

Specimen size: Shape: dumb bell, Total length: 150 ± 0.5 mm, Distance between fixtures: 100 mm, Scale distance (L): 50 ± 0.1 mm, End width: 40 mm, Width of narrow part (l): 25 ± 0.1 mm, Depth (d): 10 ± 0.1 mm.

Experimental apparatus: Microcomputer Control Electronic Universal Testing Machine.

Test requirement:

Clip the specimen to match the specimen axis together with the line of center between upper and lower fixtures.

Use the movable clamp to make the force uniformly distributed on the specimen.

The speed of movable clamp is 5 mm/min.

3.2.2 *Results*

Fracture tensile stress:

$$\sigma_r = \frac{F_r}{d \times l} = \frac{51.5}{10 \times 25} = 206.0 \text{ kPa} \quad (2)$$

where F_r = fracture tensile pressure; d = specimen depth; l = width of narrow part.

Elongation at break:

Put the specimen after break for 3 min, connect the two parts at break, then measure the scale distance.

$$e = \frac{\Delta L}{L} = \frac{0.964}{50} \times 100\% = 1.928\% \quad (3)$$

where ΔL = measurement value minus original value; L = original value.

3.3 *The test of impact strength*

3.3.1 *Experimental standard and apparatus*

Impact strength is an important indicator to measure toughness property of rigid polyurethane material, which is in according to Plastics-Determination of charpy impact strength of rigid materials (GB/T 1043-93).

Specimen size: Length: 120 mm, Width (w): 15 mm, Depth (d): 10 mm, Distance between supporting lines: 70 mm.

Experimental apparatus: XJJ-5 J Type Simple Supported Girder Impact Tester.

Test requirement:

Put the specimen on the plane surface of two supported nipper jaws.

Make the specimen profile near to the blade of supported nipper jaws and the impact line lie in the center of two support pillars.

Choose the pendulum bob with the energy for 1J, then impact the specimen to damage once and read the number of index dial.

3.3.2 *Results*

Impact strength:

$$a = \frac{A}{w \cdot d} = \frac{0.399}{15 \times 10} \times 10^3 = 2.66 \text{ kJ/m}^2 \quad (4)$$

where A = impact energy; w = specimen width; d = specimen depth.

3.4 *The analysis of mechanical properties tests of rigid polyurethane material*

In according to the test of compressive, tensile and impact strength, the relative deformation reached 10%, the compression stress was 850.2 kPa, the tensile strength reached 206.0 kPa and the impact strength reached 2.66 kJ/m^2, as the specimen was collapsing. Thus, the results showed that the sealant could sustain a certain degree of external pressure, tensile and impact force by blasting operations, and meet the mechanical requirements

for the coalmine. Through the visual inspection, we can see that rigid polyurethane foam has a good plasticity, compressed deformation without breaking, regardless of location and constraints, which is a good sealant material to prevent and control toxic and harmful gases leakage in coalmine.

4 THE TEST OF DIMENSION STABILITY

The dimension stability property of rigid polyurethane foam is very important during the process of sealing toxic and harmful gases. In the condition of sealing the gases, if the size of rigid polyurethane foam was volatile, especially contractible trend, it would affect the sealing performance seriously, probably resulting in the toxic and harmful gases leakage again. Therefore, it is very necessary to do the test of dimension stability for rigid polyurethane.

4.1 *Experimental standard and instruments*

The dimension stability test is an indicator of rigid polyurethane foam, which tests according to the test method for Dimensional Stability of Rigid Cellular Plastics (GB 8811–88).

Test method: Keep the specimen for a certain time under the experimental condition, and then measure the change of linear dimension after adjusting the state to standard environment.

Specimen size: Length: 100 mm, Width: 100 mm, Depth: 25 mm.

Experimental apparatus: Temperature Chamber, plastic mould, ruler, vernier caliper, hacksaw, knife.

4.2 *Experimental process*

1. Measure three different locations in each specimen's length (L_1, L_2, L_3), width (W_1, W_2, W_3), and measure the thickness of five different point in each specimen (T_1, T_2, T_3, T_4, T_5). The test location of each specimen is shown as Figure 3.
2. Put the test specimen level on chamber's wire netting, the interval of each at least 25 mm, adjust the temperature to 23~25 °C.
3. After 20 ± 1 hours, remove the specimen from the chamber and place 1 hour.
4. Measure the specimen size after above steps and take a visual inspection.
5. Repeat step (1), (2), (3), (4) for 40 days.

4.3 *Results*

Visual inspection result: Surface condition, shape, and color had no change.

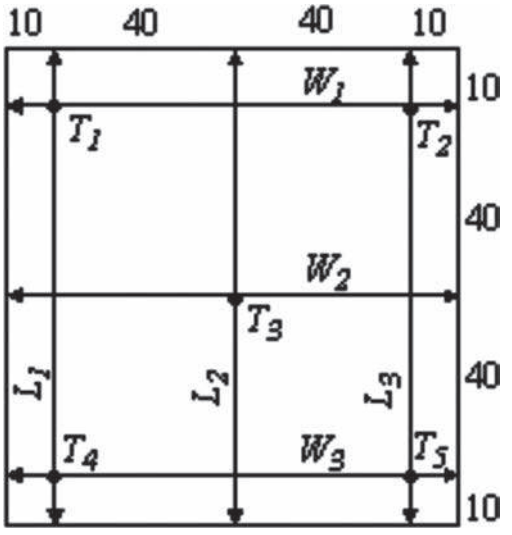


Figure 3. The location of test specimen.

Measure results:

The length, the width and the thickness of specimen had small changes, less than 0.3% for 40 days.

Specimen had a slight inflation trend.

The results show that the rigid polyurethane foam has good dimension stability. Do not worry about the secondary toxic and harmful gases leakage because of the material's good dimension stability.

5 THE TEST OF COHESIVE PROPERTY

As the sealant to control toxic and harmful gases leakage, rigid polyurethane foam should have good gas tightness. If the air tightness was not low enough, it would result in the secondary toxic and harmful gases leakage which would pollute the environment and affect the health and safety of workers seriously. This experiment evaluates the air—sealed of the sealant by measuring the cohesive property between rigid polyurethane foam and coal samples from five different collieries.

5.1 *Experimental test*

Apparatus: Experimental apparatus: Machine for Material Testing (TY8000).

Method:

The test of different kinds of coal samples on identical bonding position: The chosen coal samples come from five high outburst coalmines Pingdingshan Colliery, Zhaogezhuang Colliery,

Tangshan Colliery, Huaibei Luling Colliery, and Xinlong Hongling Colliery. Five coal samples respectively bond with rigid polyurethane foam (the same bonding area), and then measure the maximum compression and shear force of the interface and calculate the bonding strength.

The test of same kind of coal samples on different bonding positions: Select one kind of coal samples with the minimum bonding strength to bond with rigid polyurethane foam on different locations, and then measure the maximum compression and shear force of the interface and calculate the bonding strength.

Specimen size:

Different coal samples test: specimen size: 50 mm × 100 mm × 20 mm, bonding area: 50 mm × 40 mm.

Different locations test: specimen size: 20 mm × 120 mm × 20 mm, bonding length: 10 mm, 20 mm, 30 mm, 40 mm, 50 mm, 60 mm, 70 mm, 80 mm, 90 mm, 100 mm.

5.2 *Results*

Test the bonding level between rigid polyurethane foam and coal samples from five different high outburst collieries. In the case of other environmental conditions are the same, the bonding strength data are shown as Table 1.

The data from Table 1 show that the best bonding level with rigid polyurethane foam is the coal sample from Huaibei Luling Colliery, and the minimum bonding strength is the coal sample from Xinlong Hongling Colliery. The average bonding strength between rigid polyurethane foam and five kinds of coal samples is 427.25 kPa.

Select the coal samples from Xinlong Hongling Colliery to bond with rigid polyurethane foam on different locations (different bonding length, same bonding width as 20 mm), the bonding strength data are shown as Table 2.

The data from Table 2 show that the experimental error is larger on the first location because of the smaller bonding area. The geometric average bonding strength between rigid polyurethane foam and the same coal samples on different boding locations is 387.95 kPa. This data is the average bonding strength between rigid polyurethane foam and high outburst collieries.

The results show that bonding strength is high level between the rigid polyurethane foam and coal samples, which hardly cause the leakage on the bonding location. Therefore, the rigid polyurethane foam has good cohesive property as a sealant to prevent and control toxic and harmful gases leakage in coalmine.

Table 1. Bonding strength test data between rigid polyurethane foam and different coal samples.

Coal samples	Bonding strength (kPa)
Pingdingshan Colliery	421.39
Zhaogezhuang Colliery	415.01
Tangshan Colliery	417.41
Huaibei Luling Colliery	496.33
Xinlong Hongling Colliery	386.15

Table 2. Bonding strength test data between rigid polyurethane foam and same coal samples on different bonding locations.

Bonding locations (mm)	Bonding strength (kPa)
10	594.50
20	419.50
30	401.75
40	389.45
50	398.20

6 CONCLUSIONS

The preparation of rigid polyurethane foam is completed, which can meet the requirements of certain mechanical properties, dilatability, dimension stability and low permeability.

1. The rigid polyurethane foam has some good physical feature, as rapid foaming, high multiple foaming, and well-distributed, compact froth, which can meet the practical requirements of the site.
2. The rigid polyurethane foam can meet the requirement of mechanical properties. As the relative deformation reaches to 10%, its compression strength is about 800.0 kPa, as the specimen was collapsing the tensile strength reached 206.0 kPa and the impact strength reached 2.66 kJ/m^2.
3. The rigid polyurethane foam has good dimensional stability, less than 0.3% of its deformation for 40 days in experimental state.
4. The rigid polyurethane foam has good cohesive property, which the average bonding strength between rigid polyurethane foam and high outburst collieries is 387.95 kPa. Therefore, the rigid polyurethane foam as the sealant can control toxic and harmful gases leakage in coalmine safely and effectively.

REFERENCES

Andrzej, K.B. et al. 2001. Natural-fiberreinforced polyurethane microfoams. *Composites Science and Technology*: 2405–2411.

Dong, J.L. et al. 2007. Preparation of Flame-retardant Rigid Polyurethane Foam. *China Plastics* 21(12): 50–54.

Li, D.B. & Zhang, M. 2009. Discuss the Choice and Safety Measures for Ventilation System in Coalmine. *Management & Technology for SME*: 275–276.

Li, W.J. & Shen, Y.H. 2003. Study on Properties of Polyurethane as Seal Material under Coal Mine. *Coal Conversion* 26(4):76–78.

Lian, G.Z. 2009. Analysis and Prevention on Occupational Hazardous Factors of Coal Enterprises. *Economic Research Guide*: 99–101.

Shpirt, M.Y. & Goryunova, N.P. 2009. Main Methods for Decreasing the Emission of Greenhouse Gases Formed in the Production and Processing of Fossil Fuels. *Solid Fuel Chemistry* 43(6): 378–386.

Xu, X.H. et al. 2009. Analysis the Partial Ventilation in Coalmine. *Shandong Coal Science and Technology*: 163–164.

Zhang, Y.L. 2005. *Plastic Formulations and Component Design Collection.* Beijing: China Machine Press.

Zhu, L.M. & Liu, Y.J. 2004. *Polyurethane Foam Plastic*. Beijing: Chemical Industry Press.

Progress in Mine Safety Science and Engineering II – He et al. (Eds)
© 2014 Taylor & Francis Group, London, ISBN 978-1-138-00122-0

A new borehole arrangement for draining the methane in mining induced fractured zone and the utilization of the drained methane in Yangquan Nanzhuang Coal Mine

Douqun Zhang
School of Resource and Safety Engineering, China University of Mining and Technology (Beijing), Beijing, China
State Development and Investment Corporation, Beijing, China

Jie Zang, Yifeng Jiang & Kai Wang
School of Resource and Safety Engineering, China University of Mining and Technology (Beijing), Beijing, China

ABSTRACT: Field observation has proved that the main methane resources of the 12# mining faces of Nanzhuang Coal Mine came from the upper adjacent coal seams. In order to drain this methane, lots of measurements has been undertaken. However, the drainage efficiency was low and methane emission amount was still large. In this paper, a newly developed borehole arrangement for draining the gas in the fractured zone was described. The core of this arrangement was the cooperation of the high-level and low-level boreholes based on the methane enrichment regularity of the fractured zone. Subsequently, this newly developed arrangement was applied in mining faces of 12# coal seam in Nanzhuang Coal Mine. The field observation demonstrated that this arrangement profoundly enhanced both the drainage efficiency and safety mining. More importantly, with utilizing the drained methane, Nanzhuang Coal Mine obtained substantial economic benefits and did paramount work for the greenhouse gas control.

1 INTRODUCTION

Coal Seam Methane (CSM) or coalbed methane (CBM) is the naturally occurring gas in coal seams, which is normally considered as the cause of coal mine disasters like coal and gas outburst and methane explosion (Wang and Xue, 2008). But recently, the nature of CSM as the clean and efficient energy has been progressively understood (Chen et al., 2012). Besides, as a greenhouse gas, CSM has over 20 times the greenhouse effect and 7 times more harming of the Ozone Layer compared to carbon dioxide (Chen et al., 2012).

CSM drainage and utilization have been conducted all over the world, especially in China. China has abundant CSM resource, which is estimated at 36.8×10^{12} m^3 within the depth of 2000 m (Cheng et al., 2011, Wang et al., 2012a). In order to improve the safety and efficiency in mining and protect the environment, most coal mines in China drained the CSM (Li et al., 2007, Liu et al., 2009a, Liu et al., 2009b, Liu et al., 2010, Lu et al., 2009, Lv et al., 2012, Sang et al., 2010, Wang et al., 2012a, Wang et al., 2008, Zhou, 2012, Zhou et al., 2012), and the early pioneers were the coal mines in Yangquan Mining Area.

Yangquan Mining Area has multiple coal seams and abundant CSM, but the methane was difficult to drain. Therefore, methane emission in coal mines in Yangquan Mining Area was comparatively high. Statistical analysis of methane sources in pairs of coal mines showed that the adjacent coal seams were the main sources of methane emission of mining faces, and whether this part of methane could be appropriately controlled would significantly impact the safety mining. Taken mined faces of 12# coal seam in Nanzhuang Coal Mine for example (Wang et al., 2012b), many years' field observations have demonstrated that the main methane sources of mining faces of 12# coal seam were the working coal seam, overlaying adjacent coal seams and lower adjacent coal seams, while the methane quantity emitting from the overlaying adjacent seams, which was the focus of drainage, accounted for more than 85% methane emission of mining faces of 12# coal seam. For the purpose of draining this part of methane, a single sort of boreholes were arranged in tail roadway terminating at 9# coal seam. However, the drainage efficiency was not very high and methane emission from the fractured zone was still high. In order to reverse this trend, measures like increasing air volume and limiting the mining speed had been carried out. In such a case, however, not only the production efficiency was reduced, did the drainage efficiency be little enhanced. Thus, new technologies for controlling

the gas emitting from overlaying adjacent seams of 12# coal seam must be developed.

In this paper, a new borehole arrangement to drain the gas in mining induced fractured zone was depicted. The essence of this arrangement regime was the cooperation of the high-level boreholes and the low-level ones in terms of the evaluation on the methane enrichment regularity of the fractured zone which is divided into two regions by the thick and stiff Medium Sandstone. Subsequently, this newly developed borehole setting was applied in mining faces of 12# coal seam in Nanzhuang Coal Mine. This borehole arrangement significantly enhanced the drainage efficiency and safety mining of the applying faces. More importantly, with utilizing the drained methane, Nanzhuang Coal Mine obtained substantial economic benefits and did paramount work for the greenhouse gas control.

2 DESCRIPTION OF THE COAL GEOLOGY CONDITION OF NANZHUANG COAL MINE

Nanzhuang Coal Mine is located in southern Yangquan City, Shanxi Province, China, which is 12.59 km^2 in terms of mine area and 200 t/y of approved production capacity. The coal-bearing strata are Shanxi Formation (Lower Permian) and Taiyuan Formation (Upper Carboniferous), and the minable coal seams are 3#, 6#, 12# and 15# coal seams, among which the 3# and 6# coal seams has been mined. The stratigraphic column of Nanzhuang Coal Mine (partial) is shown in Table 1.

Table 1. Stratigraphic column (partial).

Lithology	Thickness (m)
8# Coal Seam	0.31
Medium Sandstone	15.93
9# Coal Seam	0.28
Mudstone	6.71
Medium Sandstone	13.38
10# Coal Seam	0.18
Mudstone	2.86
K_4 Limestone	1.69
11# Coal Seam	0.36
Fine Sandstone	3.80
Sandy Mudstone	3.00
Mudstone	3.00
12# Coal Seam	1.22
Mudstone	1.98
Fine Sandstone	3.33
Mudstone	1.98
K_3 Limestone	3.06
13# Coal Seam	0.31
Sandy Mudstone	3.8
Fine Sandstone	11.37
Sandy Mudstone	6.26
K_2 Limestone	5.3
14# Coal Seam	0.53
Fine Sandstone	5.38
Sandy Mudstone	8.3
15# Coal Seam	5.86

The coal seam addressed in this paper is 12# coal seam, which is 1.22 m high in average and inclines about 6°. Mining faces of 12# coal seam, of which the designed length and mining height were respective 180 m and 1.5 m, applied the complex mechanical strike retreating coal mining technology. The ventilation system of these faces were consisted of three roadways, namely a rail roadway as the return airway, a haulage roadway as the intake airway and a tail roadway as the special gas drainage gateway.

3 PRACTICE OF THE NEW FRACTURED ZONE GAS DRAINAGE TECHNOLOGY IN NANZHUANG COAL MINE

3.1 *Deficiencies of the previous fractured zone drainage setting*

Before 2009, while mining 12# coal seam, the boreholes were drilled in the special gas drainage tunnel of the mining faces to the 9# coal seam, which is in the upper fractured zone and about 35 m upper to 12# coal seam. However, this borehole arrangement could not fully mitigate the methane emission from the upper fractured zone. Taking NO. 4604 mining face as example, with mining proceeding, the methane emission increased from 10 m^3/min to 70 m^3/min while the drained volume was only 36 m^3/min, and the average methane concentrations in mining face, return airway, upper corner, and tail roadway were 0.7%, 1.0%, 1.0%, and 3.0%, respectively, which were apparently beyond the permitted methane concentrations of coal mines in China (Cheng et al., 2011). Due to these high concentrations, which were readily cause methane explosion, Nanzhuang Coal Mine took measures such as enhancing the ventilation volume from 1240 m^3/min to the permitted maximum 1650 m^3/min, reducing the mining speed, and so on. Subsequently, however, the situation was of little improvement.

From field observations, it was found that the methane concentration of the mining face increased substantially after the overlaying strata cracking which could be monitored by the overburden stress

variation. We analyzed that two causes resulted in this phenomenon. One is the closely upper methane occurring zone consisted of 11#, 10# coal seams and the K_4 Lime stone. After mining of the 12# coal seam, this region cracked rapidly and thus the methane spontaneously desorbed and migrated to the mining faces subject to the impact of the negative pressure of ventilation. The other is the inefficiency of the drainage setting. Due to the thick Medium Sandstone and Mudstone under 9# coal seam, the negative pressure of the drainage boreholes terminated in 9# coal seam could hardly affect the region around 10#, 11# coal seams and thus the methane in this area.

3.2 *Development of the new drainage arrangements*

In terms of the interpretations above, we modified the previous drainage setting and proposed a new drainage arrangement, as depicted in Fig. 1.

With the field observations and numerical simulations (Wang et al., 2012b), we concluded that the fractured zone of 12# mining seam was partitioned into two regions by the thick and stiff Medium Sandstone under 9# coal seam, where the upper one consisting of 8# and 9# coal seams was called the high gas enrichment zone and the lower one consisting of 10#, 11# coal seams and K_4 Limestone was called the low gas enrichment zone, as depicted in Fig.1 (a). The influence of gas in the low enrichment zone on the mining face was almost instantaneous after the overlaying seams cracked, while the impact of the gas in high enrichment zone was hysteretic. Based on these understandings, we determined to arrange different sorts of boreholes to drain the gases in these two zones, respectively. As is illustrated in Fig. 1, the high-level boreholes in the tail roadway were maintained, while new low-level boreholes were drilled in the return airway to extract the gas around 10# and 11# coal seams. Besides, in order to properly utilize the negative pressure induced by ventilation, the orientation of low-level boreholes was toward the wind.

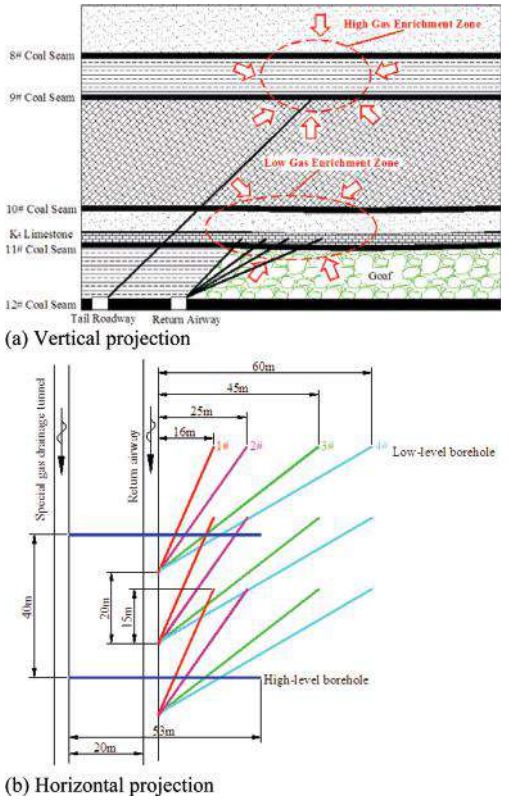


Figure 1. Arrangement of the new drainage boreholes.

3.3 *Application results*

The newly developed borehole arrangement was firstly applied in the NO. 4611 working face, and the paramount implication was the improvement for the safety mining. With this arrangement, the methane concentrations in mining face, return airway, upper corner, and tail roadway decreased to 0.5%, 0.5%, 0.7%, and 1.8%, respectively, which were lower than the permitted concentration of coal mines in China and far lower than the explosion concentration. Besides, through applying this drainage scheme, the drained volume increased to more than 80 m^3/min which accounted for more than 85% of the total methane emission volume.

Another improvement was the increase in coal production. After applying the new cooperative borehole setting, the mining speed increased from 2–2.5 m/d to 4–5 m/d, and the coal production per month enhanced from 20 thousand tons to more than 4o thousand tons.

Besides, Nanzhuang Coal Mine stored the drained methane and then utilized these gases for economic and environmental concerns, and these will be presented in the next section.

4 UTILIZATION OF THE DRAINED METHANE IN NANZHUANG COAL MINE

Due to the multiple overlaying coal seams and their high methane content, the concentration of the drained methane of the 12# coal seam was generally greater than 40% and could be directly applied for power generating. Therefore, Nanzhuang Coal Mine built a set of power generators with capacity

of 10 × 500 kW. From 2009, Nanzhuang Coal Mine has generated electricity about 47 million kW•h, all of which was utilized for self-consumption and nearly 30 million RMB was saved.

Additionally, Nanzhuang Coal Mine utilized these gases for commercial concern, such as selling to the fuel enterprises, and more than 30 million RMB was earned. Besides, China government subsidized the enterprises who utilized coal mine methane or coalbed methane, and with this subsidy, Nanzhuang Mine received 20 million RMB.

Furthermore, the negative impact of methane on environment has attracted more and more attention all over the world recently. It has demonstrated that methane has over 20 times the greenhouse effect and 7 times more harming of the Ozone Layer compared to carbon dioxide (Wang et al., 2012a). Nanzhuang Coal Mine annually utilized about 30 million normal cubic meters methane which were mainly converted to the significantly lower-effective greenhouse gas carbon dioxide and water.

5 CONCLUSIONS

With the field observations and simulation results, it was found that the fractured zone of 12# mining seam was divided into two regions by the thick and stiff Medium Sandstone under 9# coal seam, where the upper one consisting of 8# and 9# coal seams was called the high gas enrichment zone and the lower one consisting of 10#, 11# coal seams and K4 Limestone was called the low gas enrichment zone. The influences of gas these two regions on the mining faces of 12# coal seam are totally different, where the lower one was almost instantaneous after the overlaying seams fell, while the upper one was hysteretic. Based on these understandings, a new borehole arrangement for draining the gas in mining induced fractured zone was developed. The high-level boreholes in the tail roadway were maintained, while new low-level boreholes were drilled in the return airway for extracting the gas around 10# and 11# coal seams. Besides, in order to properly utilize the negative pressure induced by ventilation, the orientation of low-level boreholes was toward the wind.

Through applying the newly developed drainage scheme, two direct positive benefits were obtained, one was the decrease of the methane concentration in mining faces and the related airways, the other was the increase in mining efficiency raising from 2–2.5 m/d to 4–5 m/d. Besides, Nanzhuang Coal Mine developed a series of utilization schemes such power generation, selling as fuel gas, self-consumption as fuel gas and so on. From 2009, Nanzhuang Coal Mine has generated electricity about 47 million kW•h, all of which was utilized for self-consumption and nearly 30 million RMB was saved. By selling outside, more than 30 million RMB was earned. In addition, China government subsidized the enterprises who utilized CSM, and with this subsidy, Nanzhuang Mine received 20 million RMB. Furthermore, utilization of CSM of Nanzhuang Coal Mine implied a profound significance in greenhouse gas control in that methane has over 20 times the greenhouse effect and 7 times more harming of the Ozone Layer compared to carbon dioxide.

ACKNOWLEDGEMENTS

The authors gratefully acknowledge the support of National Natural Science Foundation of China (No. 51174212), the Fundamental Research Funds for Central Universities (2010QZ05 & 2013QZ01), the Special Research Foundation for Doctorate Disciplines in Universities of China (20120023110006), and the Open Funds of State Key Laboratory Cultivation Base for Gas Geology and Gas Control—Henan Polytechnic University (WS2012 A01 & WS2013 A03).

REFERENCES

Chen, Z., Liu, J., Pan, Z., Connell, L.D. & Elsworth, D. (2012) Influence of the effective stress coefficient and sorption-induced strain on the evolution of coal permeability: Model development and analysis. *International Journal of Greenhouse Gas Control,* 8, 101–110.

Cheng, Y.-P., Wang, L. & Zhang, X.-L. (2011) Environmental impact of coal mine methane emissions and responding strategies in China. *International Journal of Greenhouse Gas Control,* 5, 157–166.

Li, Z.-X., Lu, Z.-L., Wu, Q. & Zhang, A.-R. (2007) Numerical Simulation Study of Goaf Methane Drainage and Spontaneous Combustion Coupling. *Journal of China University of Mining and Technology,* 17, 503–507.

Liu, H.-B., Cheng, Y.-P., Song, J.-C., Shang, Z.-J. & Wang, L. (2009a) Pressure relief, gas drainage and deformation effects on an overlying coal seam induced by drilling an extra-thin protective coal seam. *Mining Science and Technology (China),* 19, 724–729.

Liu, H., Cheng, Y., Zhou, H., Wang, F. & Chen, H. (2010) Fissure evolution and evaluation of pressure-relief gas drainage in the exploitation of super-remote protected seams. *Mining Science and Technology (China),* 20, 178–182.

Liu, L., Cheng, Y.-P., Wang, H.-F., Wang, L. & Ma, X.-Q. (2009b) Principle and engineering application of pressure relief gas drainage in low permeability outburst coal seam. *Mining Science and Technology (China),* 19, 342–345.

Lu, T., Yu, H., Zhou, T., Mao, J. & Guo, B. (2009) Improvement of methane drainage in high gassy coal seam using waterjet technique. *International Journal of Coal Geology,* 79, 40–48.

Lv, Y., Tang, D., Xu, H. & Luo, H. (2012) Production characteristics and the key factors in high-rank coalbed methane fields: A case study on the Fanzhuang Block, Southern Qinshui Basin, China. *International Journal of Coal Geology*.

Sang, S., Xu, H., Fang, L., Li, G. & Huang, H. (2010) Stress relief coalbed methane drainage by surface vertical wells in China. *International Journal of Coal Geology,* 82, 196–203.

Wang, F., Ren, T., Tu, S., Hungerford, F. & Aziz, N. (2012a) Implementation of underground longhole directional drilling technology for greenhouse gas mitigation in Chinese coal mines. *International Journal of Greenhouse Gas Control,* 11, 290–303.

Wang, K. & Xue, S. (2008) Gas drainage practices and challenges in coal mines of China. *Coal Operators' Conference.*

Wang, K., Zang, J., Zhou, A. & Gao, H. (2012b) Application study on cooperative drainage technology for mining-affected pressure relief gas in overlaying adjacent seams. *AGH Journal of Mining and Geoengineering Selected full texts,* 36, 385–393.

Wang, L., Cheng, Y.-P., Li, F.-R., Wang, H.-F. & Liu, H.-B. (2008) Fracture evolution and pressure relief gas drainage from distant protected coal seams under an extremely thick key stratum. *Journal of China University of Mining and Technology,* 18, 182–186.

Zhou, F. (2012) History matching and production prediction of a horizontal coalbed methane well. *Journal of Petroleum Science and Engineering,* 96–97, 22–36.

Zhou, F., Allinson, G., Wang, J., Sun, Q., Xiong, D. & Cinar, Y. (2012) Stochastic modelling of coalbed methane resources: A case study in Southeast Qinshui Basin, China. *International Journal of Coal Geology*.

This page intentionally left blank

Progress in Mine Safety Science and Engineering II – He et al. (Eds)
© 2014 Taylor & Francis Group, London, ISBN 978-1-138-00122-0

The empirical analysis of ARIMA multiplicative seasonal model to forecast the total number of coal mine accidents

Lin Liu
The Library of North China Institute of Science and Technology, Beijing, China

Hui Yao
School of Humanities and Social Sciences, North China Institute of Science and Technology, Beijing, China

Liyun Tan
The Department of Basic Science, North China Institute of Science and Technology, Beijing, China

ABSTRACT: This paper is to research an application of the multiplicative seasonal model to forecast the total number of China's coal mine accidents. By the empirical analysis on the data of coal mine accidents from January 2006 to December 2010, an accepted multiplicative seasonal forecasting model ARIMA(4, 1, 1)(1, 1, 1)^{12} is built up after differing the series to be stationary and estimating the order and parameters of the model. Furthermore, the test of this multiplicative seasonal model shows that it has a desirable fitting effect on the data of coal mine accidents. At last, this model is applied to forecast the number of national coal mine accidents from January 2010 to December 2010, and the forecasted values have a high accuracy when compared to the actual data.

1 INTRODUCTION

With a high attention from China's government on the safety production of coal mine, the situation of it turned better gradually. Besides, China has enacted a series of law, rules and technical regulations to promote the development of the safety production of coal mine, which later plays a crucial rule to reduce the number of coal mine accidents. For example, an emergency notice was issued in August 2005 to strictly close down some illegal coal mines which don't meet the requirement of producing safely. And then a series of law was also enacted to strengthen the fundamental safety management of small coal mines and national key coal mines, to strengthen the action of monitoring the status of gas, and to clear the usage of the safety fees which includes a measure that the upper limit of the original standard is changed to be the lower limit of the new standard. The law also allows companies to raise the level of the extraction standard, to strengthen the management of rating agencies and the training of safety production. These measures made the number of coal mine accidents decrease even if the volume of the production of coal has constantly increased since 2006. To research the regulations of the accidents, the paper takes the Seasonal ARIMA model to forecast, and the result shows that the forecasted values are in a high accuracy and this model will guide the future work.

2 THE MULTIPLICATIVE SEASONAL MODEL

2.1 *The introduction of the multiplicative seasonal ARIMA model*

The time series analysis is a statistical method to reveal the dynamic law of a system through dynamic data (Box 2005). Its core idea is that, with the finite number of data in the series, a model could be created to precisely reflect the dynamic relationship hided in the time series, and then to forecast the future.

The model of ARIMA is one of the stochastic time series analysis methods (Xue 2011, Zhang 2005). Stochastic time series includes the stationary time series (its statistical feature does not depend on time) and the nonstationary time series. To the stationary time series, we could analyze it by Autoregressive Processes (AR(p)), Moving Average Processes (MA(q)) and Mixed Autoregressive Moving Average Processes (ARMA(p, q)). Similarly to analyze the nonstationary time series, this series is initially to be computed by the d-th order difference, and then erect the ARMA model, namely the ARIMA(p, d, q) model. Accordingly,

the Multiplicative Seasonal Model is a combination of the stochastic seasonal model and the ARIMA model.

Also, a time series changing seasonally couldn't be modeled by ARMA immediately. Firstly, it should be differed to remove the seasonality of the series, and the length of one difference step is one seasonal cycle. Generally, if the series is processed by a D-th order difference the cycle length of which is s, the seasonality will almost be removed. Furthermore, if the series needs to be turned stationary by a d-th order difference before it's impacted by the seasonal difference, a model called the Multiplicative Seasonal Mod-el ARIMA(p, d, q) $(P, D, Q)^s$ could analyze the original series, and the model is described as below:

$$\phi_p(B)\Phi_P(B^s)\nabla_s^D y_t = \theta_q(B)\Theta_Q(B^s)u_t$$

In the equation, p represents the order of Seasonal Autoregressive Processes, and q represents the order of Seasonal Moving Average Processes. Moreover, $\Phi p(B^s)$ and $\Theta p(B^s)$ respectively represent the operators of the Seasonal AR(p) and MA(q) models.

2.2 *The process to build the multiplicative seasonal model*

The modeling process can be divided into three concrete steps: smoothing the data; identifying a process and estimating the order and parameters; testing the model.

1 Smoothing
This step can be completed by differing or taking the data's logarithm.

2 Identifying and estimating
In the step of identifying, we generally determine the order and estimate the parameters by the Box-Jenkins method. That is to say, we could obtain the results through the analysis of the autocorrelogram and partial-autocor-relogram. And the length of season could also be learned from the background of practical applications.

3 Testing
The methods to judge whether the model is suitable are the goodness of fitting tests, one classical method of which is to make an analysis of the residual series. If the residual series is not the white noise series, it bespeaks that the amount of effective information is still left in the residual series. As a result, the model needs to be improved until the residual series is squeezed to be the white noise series.

3 EMPIRICAL ANALYSIS

3.1 *The sample selected*

The data in this paper show the total number of coal mine accidents happening in China from January 2006 to December 2010. (The data are from "The report of national coal mine accidents analysis in 2010" published by the Department of Accident Investigation at State Administration of Coal Mine Safety). The data processed to model are from January 2006 to December 2009, and the data of 2010 aim to be compared with the forecasted data, see table 1.

As shown in Fig. 1, the original data are drawn as a line graph. The series is non-stationary and has an obvious descending trend, including a seasonal fluctuation the cycle of which has 12 months.

We easy know the original data are drawn as a line graph. The series is non-stationary and has an obvious descending trend, including a seasonal fluctuation the cycle of which has 12 months.

Table 1. The total number of coal mine accidents from 2006 to 2010.

	2006	2007	2008	2009	2010
Jan	143	195	74	94	42
Feb	149	64	152	175	138
Mar	303	194	214	158	143
Apr	290	236	190	153	136
May	277	269	187	149	133
Jun	284	248	187	158	140
Jul	274	259	164	172	123
Aug	274	257	167	115	129
Sep	242	187	179	124	107
Oct	270	178	166	132	99
Nov	247	169	138	125	100
Dec	192	165	61	113	42

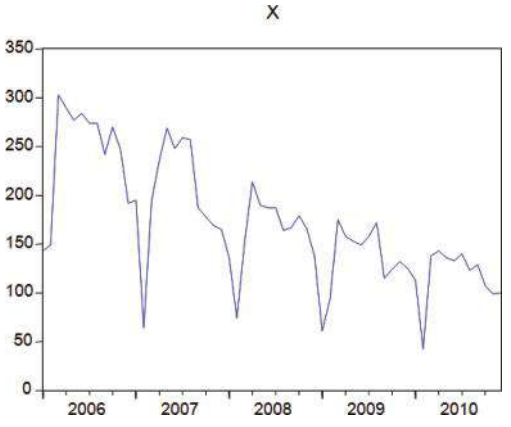


Figure 1. The original series.

3.2 *Processing data*

To remove the trend and alleviate the fluctuation of the original series, the series should be taken by natural logarithm (log(x)) and then differed between the adjacent points (log(x) and log(x(-1))). After calculation, a new series is created, which is noted as ilx, namely ilx = log(x)-log(x(-1)). From the autocorrelogram and partial autocorrelogram of series ilx, the trend in series ilx is almost removed. However, when k is equal to 12, the coefficients of autocorrelation and partial autocorrelation are significantly not equal to 0, which indicates that the seasonality exists in series ilx. So, a seasonal difference should be exerted on the series ilx, which leads to a new series called silx (silx = ilx-ilx(-12)). The result from the autocorrelogram and partial autocorrelogram of series silx shows that the seasonality in series ilx doesn't exist in series silx.

Now the next step is to test whether the hypothesis is accepted that the mean value of the series is equal to 0.

To further test whether the series is stationary, a formal method called unit roots test is provided. The results of unit roots test can be seen in table 2.

3.3 *Identifying a model*

As the trend in the original series log(x) is removed by a first-order difference, the value of d should be equal to 1; And similarly, the seasonality in the series ilx disappears after it's processed by a seasonal difference, so D is also equal to 1 and the ARMIA(p, d, q) $(P, D, Q)^s$ is thereby selected. After observing the autocorrelogram and partial-autocorrelogram of series silx, we prefer to pick q = 1, p = 2 or p = 3. Compared to the non-linear estimation possessed by MA(q) and ARMA(p, q) processes, the AR(p) model as a linear equation is easier to estimate, explain and forecast. Consequently, in the practical process of modeling, we prefer the high order AR(p) processes to the MA(q) and ARMA(p, q) processes. According to the analysis above, the candidate combinations of (p, q) include: (3, 1), (4, 0), (4, 1). When k is 12, the sample's coefficients of autocorrelation and partial-autocorrelation are significantly not equal to 0, so P = Q = 1.

Table 2. The unit root tests of series silx.

Null Hypothesis: SILX has a unit root Exogenous: None Lag Length: 10 (Automatic based on SIC, MAXLAG = 10)			
		t-Statistic	Prob.*
Augmented dickey-fuller test statistic		–2.582438	0.0113
Test critical values:	1% level	–2.630762	
	5% level	–1.950394	
	10% level	–1.611202	

3.4 *Modeling and testing*

By the econometric software Eviews 6.0 (Yi 2011), it can build models immediately and figure out the parameters and coefficients conveniently. For example, in the modeling of ARIMA(4, 1, 1)$(1, 1, 1)^{12,}$ we choose the option of Quick/Estimate Equation in main menu, and open equation definition dialog and enter silx ar(1) ar(2) ar(3) ar(4) ma(1) sar(12) sma(12)

Among the variables above, sar(s) and sma(s) are respectively the variables in the seasonal Autoregressive part and the seasonal Moving Average part.

After calculation, each model meets the conditions of stationary and invertible in the ARMA modeling process. At the same time, the models are reasonably defined and desirably fitting the data. Among these models, the AIC value of the 3rd model is the smallest. Therefore, it is appropriate to choose the 3rd model ARIMA(4, 1, 1)$(1, 1, 1)^{12}$ as the final model to forecast.

The diagnosis of one model is accomplished by the check for of residuals. If the residuals is the white noise series, this model satisfies the requirement that nearly all the effective information in this series has been extracted out. Otherwise, it

Table 3. The coefficients of models.

AR(1)	0.310392	1.31654	0.23576	0.8176
AR(2)	0.043415	0.35988	0.12063	0.9060
AR(3)	–0.03125	0.24198	–0.1291	0.8994
AR(4)	–0.03168	0.13109	–0.2417	0.8131
SAR(12)	–1.03122	0.21763	–4.7383	0.0005
MA(1)	–0.60879	1.35473	–0.4493	0.6612
SMA(12)	–0.97035	0.01944	–49.912	0.0000
R-squared	0.978271	Meandependent var		0.01309
Adjusted R-squared	0.967407	S.D. dependent var		0.34330
S. E. of regression	0.061978	Akaikeinfo criterion		–2.44676
Sum squared resid	0.046095	Schwarz criterion		–2.09881
Log likelihood	30.24426	Hannan-Quinn criter.		–2.38787
Durbin-Watson stat	2.067253			

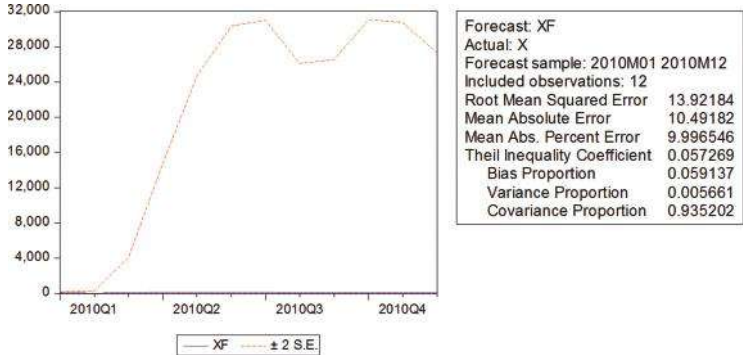


Figure 2. The evaluation of forecasting.

Table 4. The comparison of the forecasted and actual of national coal mine accidents in 2010.

Time	Actual	Forecasted
Jan	113	109.0416099435865
Feb	42	51.93337674685569
Mar	138	109.3236418326786
Apr	143	158.4728579996975
May	136	142.2675432252291
Jun	133	139.1757191951475
Jul	140	138.3757815999062
Aug	123	120.2249550319826
Sep	129	124.1645418845084
Oct	107	131.5449858243743
Nov	99	119.8695586088724
Dec	100	99.23168542329205

needs to be furthermore improved. After the residual analysis on the Multiplicative Seasonal model above, which includes the unit root test taken to the residuals and the analysis of the autocorrelogram and partial-autocorrelogram of the residues, we conclude that the residues is both stationary and totally stochastic, and the model built up well fits the trend of the data in the series.

3.5 *Forecasting*

We apply the ARIMA(4, 1, 1)(1, 1, 1)^{12} model to forecast the number of national coal mine accidents from January 2010 to December 2010. The forecasted value is shown in table 4.

The mean absolute percent error MAPE, which is 9.99 less than 10, indicates that the forecasted values are in a high accuracy. Besides, Thell Inequality Coefficient TIC is 0.057, and Bias Proportion BP 0.059 and Variance Proportion VP 0.005 are relatively small while Covariance Proportion CP 0.935 is relatively large. All these parameters suggest that the result of forecasting is desirable. See the Figure 2.

4 CONCLUSION

Compared to ordinary time series models, the Multiplicative Seasonal Model needs more historical data, and the Multiplicative Seasonal Model can be applied to a wider field because data in daily life always have an obvious trend and seasonal features. Therefore, the Multiplicative Seasonal Model can well solve such problems that involve some issues about forecasting, and as well as reach a high precision. The model in this paper, ARIMA (4, 1, 1)(1, 1, 1)^{12,} well matches the monthly changing number of national coal mine accidents. Moreover, the more historical data, the more accurate the forecasted result is. All above, the Multiplicative Seasonal Model is a practical tool for us to forecast or to apply in many other fields.

ACKNOWLEDGEMENTS

This work (Thesis) was financially supported by the Basic Scientific Research Fund Project of Central Universities (No:3142013104) and the Higher Education Research Fund Project of NCIST (No: HKJYZD201215).

REFERENCES

Box G, et al. 2005. Time series analysis: Forecasting and Control (3rd).Beijing: Posts & Telecom Press (in Chinese).

Xue Li-ming & Hou Yun-bing, 2011. Chinese energy consumption structure prediction by application of ARIMA. *China mining magazine,* 20(4):24–27 (in Chinese).

Yi Danhui, 2011. Data Analysis and the application of Eviews. Beijing: China Renmin University Press (in Chinese).

Zhang hui & Liui Jia-kun, 2005. Modeling and Prediction of Freeway Traffic Flow using seasonal ARIMA modles. *Journal of Tianjin University,* 28(9):838–841 (in Chinese).

Progress in Mine Safety Science and Engineering II – He et al. (Eds)
© 2014 Taylor & Francis Group, London, ISBN 978-1-138-00122-0

Monitor and control node in coal production safety based on LonWorks Fieldbus

Tao Zhang
North China Institute of Science and Technology, Yanjiao, Sanhe, Hebei, China

ABSTRACT: The paper introduces the monitor and control system in coal production safety which basing on LonWorks Field Bus firstly. On the base of the importance of the measure and control node which basing on LonWorks, the paper discusses the design process of the measure and control node which basing on LonWorks technology. The paper proposes the hardware and software block diagram of the measure and control node which basing on LonWorks technology. The designed node has application value on the monitor and control system in coal production safety.

1 INTRODUCTION

Since 2000, in need to continuously improve the national coal mine safety production requirements and the enterprise own development, China's high gas coal mine has equipped with a monitoring system of coal mine safety production.

The monitoring system of coal mine safety production is one of the important guarantees to improve the mine safety production level and production safety management efficiency, is an important way to improve China's coal mine safety, efficient, orderly production, and is the route one must take our coal mine enterprises to modern management.

With the rapid development of electronic technology, computer software and hardware technology, automation technology, and the need of enterprise development, the main domestic research institutes and manufacturers have launched a series of coal mine production safety monitoring system. The coal mine safety production monitoring system including monitoring and control system of coal mine safety production is dominated by a single microcomputer, including the Distributed Control System (DCS) based on the monitoring system of coal mine safety production, and other types of coal mine safety integrated and digital network monitoring and management system.

But DCS system has its inherent shortcomings, mainly DCS systems of different manufacturers with different communication modes, resulting in between DCS and DCS, DCS from different manufacturers and the Intranet/Internet network are difficult to realize network interconnection and information sharing, therefore, from this perspective, DCS system is not open (Li Z.J. 2006).

2 MONITORING AND CONTROL SYSTEM BASED ON FIELDBUS

Fieldbus Control System (FCS) is the intelligent field instrument developed. It was designed by digital communication instead of 4–20 mA analogue transmission technology, but with the integration of fieldbus and intelligent instrument control (instrument calibration, configuration control, diagnosis, alarm, record) development, resulting in a hitherto unknown revolution in control field.

Distributed Control System (DCS) of communication to achieve a closed system with a private network, and the Field bus Control System model (FCS) breaks through the defects caused by DCS, the closed, proprietary solutions become based on open, standardized solution.

FCS can take from different manufacturers and abide by the automation equipment with the same protocol specification, through the field bus network connected into a system, to achieve various functions integrated automation; at the same time, the distributed system structure of traditional DCS combination of concentrated and dispersed, into a new field bus based on distributed structure, in the traditional DCS network under a and then introduce a fieldbus network layer, electronic equipment, a variety of intelligent I/O module underlying intelligence and various kinds of intelligent instruments through the field bus control network layer (Wang C.L. 1999).

In the field bus control system, sensor measurement, compensation calculation, engineering quantity processing and control functions in the field of equipment complete, relying on the field devices to complete the basic functions of automatic control, operation state and can at any time

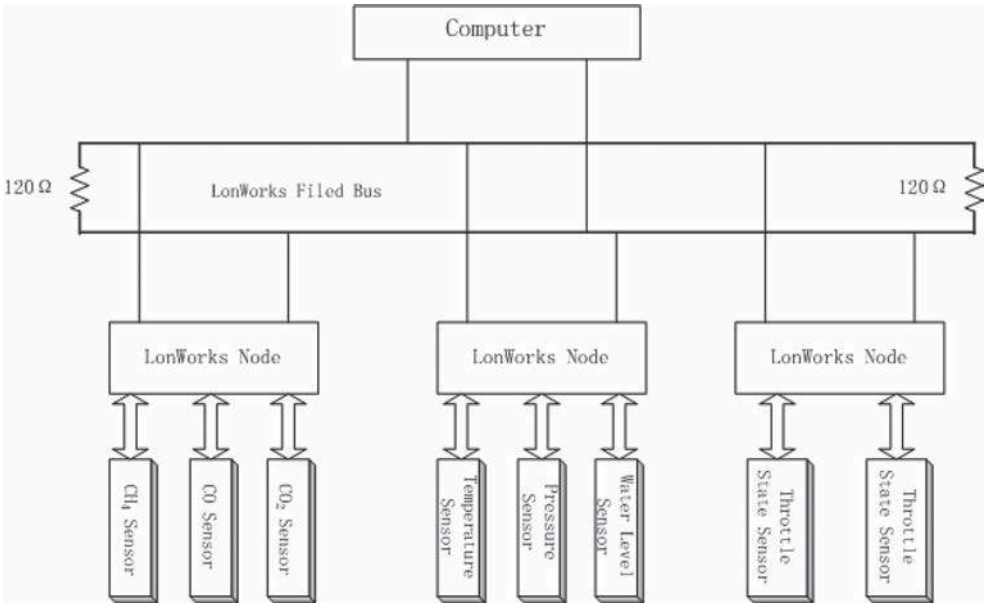


Figure 1. The monitoring and control system of coal mine safety production based on LonWorks filed bus.

diagnostic equipment, complete the implementation of decentralized control.

LonWorks is a local operation network the United States of America Echelon company launched in 1992, all the seven layer model of the communication protocol using LonTalk to support OSI/RM, LonTalk protocol for the management of LON network by hardware and firmware neuron chip.

The application of LonWorks technology using object-oriented design method, through the network variables to simplify the design of network communication for parameter settings, greatly shorten the product development cycle. At present, the LonWorks bus has high reliability, safety, easy to realize and interoperability advantages, make LonWorks products in a very wide range of applications, LonWorks bus has become a field of mature bus.

In this paper, Figure1 shows the monitoring system of coal mine safety production of LonWorks bus (Wang R.L. & Lei B. 2004).

3 INTELLIGENT CONTROL NODE BASED ON LONWORKS FIELD BUS

3.1 *Summary*

LonWorks measurement and control node has two basic functions: one is connected with various sensors in the industrial field, control the working status of a sensor, or read the industrial field measurement data; the two is connected with the upper PC, accept all kinds of the PC's control command, or to the upper PC transfer various industry scene measurement data.

The principle and the working process of LonWorks measurement and control nodes connected to the various sensor is basically the same, according to the LonWorks measurement and control nodes connected with a temperature sensor as an example, the LonWorks control node of temperature measurement (Zhang T. & Jiang J.P. 1999).

3.2 *Hardware design*

Figure 2 shows the hardware structure of LonWorks temperature measurement node (Liu J.H. 1999).

Micro controller selects the neuron chip as the core components of the LQICLON control unit, with 24 bit analog to digital converter ADS1216, uses AD590 as temperature sensor, and comprises an optoelectronic isolator PS2501 unit.

Data acquisition and control module LQICLON to realize the LonWorks technology, it can complete the acquisition and equipment control switch of various industrial standard digital signal, it has 12 digital inputs, 12 digital output, and a light emitting diode display input/output state, has the high reliability, the hardware connection is simple, the software is easy to the advantages of programming.

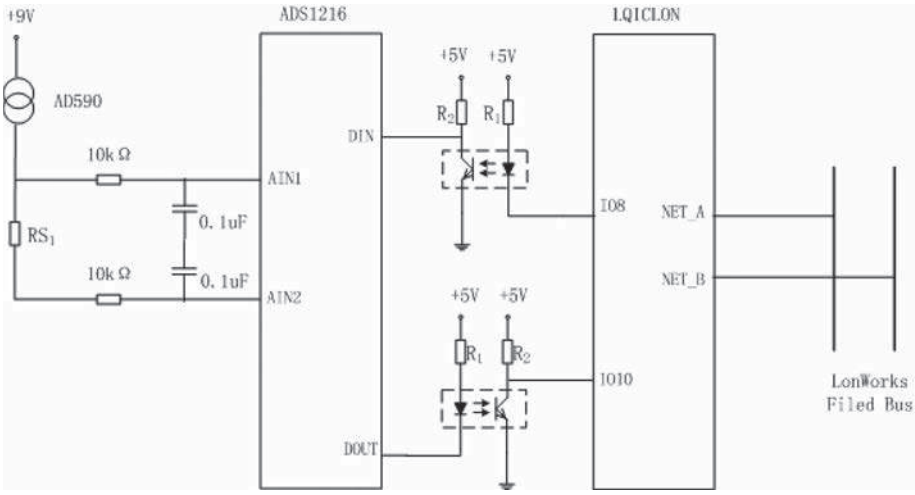


Figure 2. Hardware structure chart of LonWorks temperature measurement node.

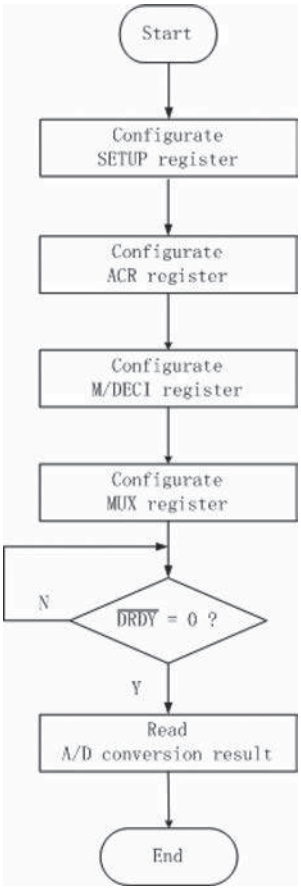


Figure 3. Subroutine structure chart of LonWorks temperature measurement node.

Thermocouple AD590 as the temperature sensor, the need for the cold end temperature compensation.

The connection between AD590 and ADS1216 thermocouple analog-to-digital converter by RC low-pass filter, in order to reduce the impact of temperature simulation of harmonic signal.

24 bit resolution ADC ADS1216 with high conversion accuracy, it has 8 single-ended input channels or 4 channels of differential input channels. This design uses ADS1216 AIN1 and AIN2 to form a differential input channels, to receive the temperature simulation measurement signal (Yang X.H. 1999).

3.3 *Software design*

LonWorks temperature measurement node function is equivalent to the coal mine safety monitoring and control system of underground substation, so the corresponding function it should also have the coal mine substation, and the characteristics of LON fieldbus.

LonWorks temperature measurement node program mainly includes the main program, temperature measurement program, communication program (Yang Y.H. 1999).

In the design of these programs, most of the procedures described in the literatures are, here no longer say. This paper only gives the temperature measurement subroutine, as shown in Figure 3.

4 CONCLUSION

The paper first gives the framework of monitoring system in coal mine safety production using LON

bus, for the temperature control of LonWorks node system is discussed and designed in detail, the design block diagram of hardware circuit and software design of LonWorks temperature measurement and control nodes are given.

The advanced LON bus technology is applied in the intelligent measurement and control system, greatly improve the reliability of the system; the independent development of international standard based on intelligent node MCU, not only saved a lot of money, but also the purchase of similar equipment in general, can save a lot of R & D costs, for coal mine safety production monitoring system based on LON bus based on the practical application value.

REFERENCES

Li Z.J. 2006. *Field bus technology and application.* Beijing: Mechanical Industry Press.

Liu J.H. 1999. *Intelligent sensor system*. Xi'an: Xi'an Electronic and Science University press.

Wang C.L. 1999. Discussion and practice of field bus and DCS. *Automation panorama,* 19 (5):4~7.

Wang R.L. & Lei B. 2004. Present situation and development of industrial Ethernet. *Automation panorama* 20 (4): 63~65.

Yang X.H. 1999. *The field bus technology and its application*. Beijing: Tsinghua University press.

Yang Y.H. 1999. *Technology and application of LON network control.* Xi'an: Xi'an Electronic and Science University press.

Zhang T. & Jiang J.P. 1999. Research on servo system based on neural network. *Journal of China coal society* 24 (5):522–525.

Progress in Mine Safety Science and Engineering II – He et al. (Eds)
© 2014 Taylor & Francis Group, London, ISBN 978-1-138-00122-0

Study on subsidence reducing technique by continuously filling grouts into stope overburden bed-separation along the dip

Xinmin Fan
Xishan Coal Electricity Group Company, Taiyuan, China

Xinmin Fan, Pengfei Wang, Lilin Zhou, Zhiqiang Wang & Jingli Zhao
School of Resource and Safety Engineering, China University of Mining and Technology, Beijing, China

ABSTRACT: The study was conducted based on stope overburden bed-separation grouting along the dip. Adopted two methods, theoretical analysis and indoor analogical simulative experimentation, proposed subsidence reducing technique by continuously filling grouts into stope overburden bed-separation along the dip. Its core was to completely cancel pillar between faces, to realize overburden's sufficient mining before grouting, to maintain continuity of bed separation zone. On the premise of reducing quantity of grouting and drilling works, achieved relatively ideal subsidence reducing effect. In the end, this technology was verified based on practical background, considered that within the application, the technology had a feature that the mining degree was higher, grouting effect was more evident, working section recovery was increased and drilling quantity was reduced. Therefore, considered that this technology had a certain application value.

1 INTRODUCTION

In 1980s, industrial test of overburden bed separation filling technology was first conducted in Lao Hu-tai coal mine, Fushun Mining Bureau and succeeded (Xueli Fan 1998). Then industrial tests of bed separation filling technology were successively conducted in dozens of coal mines such as Datun Xuzhuang, Kailuan Tangshan, Xinwen Huafeng, Yanzhou Dongtan coal mine, etc. And some achievements were made (Yimeng Meng & Zhenxian Lv 1993, Yaping Zhong & Yanfa Gao 2001, Weijia Guo & Guanghan Shen 1995, Dongjian Zhang & Hengqing Guo 1999, Huaxing Zhang, Zunyi Wei 2000).

The fundamentals of reducing surface subsidence by grouting is to make use of space of bed separation in overburden generated during strata movement, inject materials through borehole into space of bed separation to support overburden, thus to slow down spread of strata movement towards surface. The premise of application of the technology was that a relatively large space of bed separation could form in overburden after mining, the rational arrangement of grouting holes was the key of the technology, but dynamic distribution rules of bed separation were not studied thoroughly. Therefore, conditions for generation of bed separation were discussed by many domestic scholars (Yuzhuo Zhang & Liliang Chen 1996, Weijia Guo et al. 1995, Minggao Qian et al. 1996).

In reference 10, based on key stratum theory, bed separation was proved to occur mainly below the key strata by experimental and theoretical researches, and dynamic rules of bed separation were revealed.

In references 11 and 12, an in-depth study was conducted of separation's position and volume, dynamic developmental characteristics as well as affecting factors during strata movement. It turned out that overburden bed separation mainly occurred below the key strata, and the highest bed separation space stopped right below the primary key stratum. The length and the largest volume of separation zone after initial rupture of the key stratum were only 25%–33% of that before initial rupture of the key stratum. Therefore, bed separation filling technique should be applied before initial rupture of the key stratum, and kept the primary key stratum from breaking.

References 16 discussed issues about the space-time laws of the bed separation's development, the method of evaluation of subsidence reducing effect and application of bed separation grouting to reduce subsidence in coal mining under buildings. Considered that under the same conditions, the height of bed separation changed with the size of gob. When the gob size reached sufficient mining, the height of bed separation reached its maximum; Accurate evaluation of grouting effect should base on a comparison between measured volume of subsidence basin after grouting and that didn't

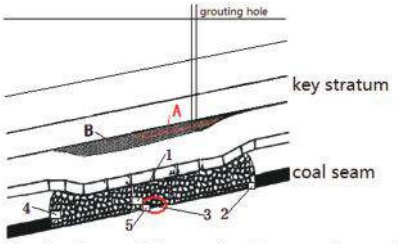
grout in the same mining district. Most lengths of working faces along the dip were between 100 m and 200 m, since mining depths were mostly over 400 m, exploitation range generally couldn't reach sufficient mining size, even extremely insufficient mining, although which along the strike could. In that case, the height of overburden's failure couldn't reach its maximum in sufficient mining conditions, separation gap was not fully developed, maximum separation space could not be obtained, surface subsidence could not reach its maximum. Therefore, this effect should be taken into consideration when evaluating grouting effect.

Combined with the mining situations in our country, bed separations that were available for grouting had occurred in deep mining, and there were multiple grouting positions that were suitable for grouting according to different geological and mining conditions, but due to the limitation of ability of working faces' management, the lengths of face were limited, sufficient mining conditions was difficult to form along the dip, bed separation zone grouting technique was difficult to be implemented smoothly.

2 RESEARCH ON SUBSIDENCE REDUCING TECHNIQUE BY CONTINUOUSLY FILLING GROUTS INTO STOPE OVERBURDEN BED-SEPARATION ALONG THE DIP

The result of study of dynamic developmental characteristics of overburden bed separation indicated that (Minggao Qian at al. 2003, Jialin Xu & Minggao Qian 2000, Jialin Xu & Minggao Qian. 1998, Jialin Xu et al. 2006, Weibing Zhu et al. 2005), grouts should be injected between fissure zone and bending zone, and present results showed that the division of the "Three-Zone" (Zhiqiang Wang et al. 2011) should base on key stratum theory, so should bed separation subsidence reducing mechanism by grouting. Here raised a subsidence reducing technique by continuously filling grouts into stope overburden bed-separation along the dip, see figure 1.

As shown in figure 1, during producing, section intake airway was arranged along roof of coal seam, return airway was arranged along floor of coal seam, during producing of succeeding face, section intake airway was still arranged along roof of coal seam, return airway was arranged under the gob of last section (Jingli Zhao & Jian Wu 1998), pillar could be totally canceled between faces. According to the conclusion of references 29 and 30, concluded that when adopting arrangement as shown in figure 3, the movement of adjacent working face of overburden strata would form



1-intake airway of last section; 2-return airway of last section; 3-triangular shape coal loss pillar between faces; 4-section intake airway of succeeding face; 5-section return airway of succeeding face

Figure 1. Schematic diagram of completely pillarless overlapping overburden bed-separation zone grouting.

one body, reflected the characteristics of single workface, grouting for overburden bed separation zone shown in the figure had the following characteristics:

(1) Mining was sufficient, filling effect was good. Multiple overlapping faces reflected the characteristics of single workface, when succeeding face was producing, the mining effect on overburden along the dip needed to add up all multiple overlapping faces, the method of determining whether overburden along the dip achieved sufficient mining degree borrowed empirical formula (1) (Yonghai Teng et al. 2009):

$$\Sigma L = (1.2 - 1.4)H_0 \tag{1}$$

Where ΣL, cumulative length of faces along the dip, depended on the number of overlapping faces; H0, the height from face to bed separation positionfor grouting.

The evaluation of grouting effect could depend on formula of elastic thin plate theory(2) (Jinhai Liu et al. 2009):

$$\rho = \frac{k a_m^4 b_m^4}{\pi^4 D(a_m^2 + b_m^2)^2 + k a_m^4 b_m^4} \times 100\% \tag{2}$$

Where k is Winkler foundation coefficient, k = (E0/h0)-2; E0, the elasticity modulus of foundation; h0, cushion thickness; D, flexural rigidity, D = Eh3/12(1-μ2); μ, Poisson's ratio; a_m, b_m were limit sizes of rock plate.

$$a_{m=ab_m/b,}b_m = \sqrt{\frac{[\sigma_t]\delta^2}{6\eta q}} \tag{3}$$

a, b were the length of strike and the length of dip; δ, thickness of rock plate; q, the loads acting on rock plate, q = γδ, γ was unit weight; η was shape

coefficient: $\eta = 0.00302(a/b)3 - 0.03567(a/b)2 + 0.13953(a/b) - 0.05859$

Analyzed formula (1) and (2), the longer the length of face and the more sufficient the mining degree, the better the filling effect you would get. As shown in the figure, the increase of the number of overlapping faces was equivalent to the increase of the length of face along the dip. Obviously, mining of overburden was more sufficient, and filling effect was better in this technique.

(2) Connection between mining influence and grouting was more reasonable, as shown in figure 2, during producing of first face, influenced by mining degree and the distance between the key stratum and the face, volume of initial bed separation was very small, even bed separation would not appear; When the number of overlapping faces increased, bed separation began to develop, before it reached sufficient mining, bed separation was in a development stage, continuous grouting could be achieved through grouting holes, keeping bed separation in development stage for a long time, bed separation was always in cycle of initiation—development—grouting—initiation—development—grouting, grouting continued with the mining degree gradually becoming sufficient, making a better filling effect.

(3) Grouting quantity. The position of water-conducting fractured zone rose with the increase of mining range. Therefore, grouting layer was influenced by mining range, thickness of overburden, bulking property, fracture angle, as shown in figure 1, grouting layer in the system rose, grouting quantity declined.

(4) Drilling work quantity. Continuous bed separation formed as pillars were canceled, and grouting quantity declined, the number of grouting holes along the dip was fewer than that in isolated section-grouting system.

3 EQUIVALENT MATERIALS SIMULATION EXPERIMENT STUDY OF OVERBURDEN BED SEPARATION

Experiment was mainly based on prototype of seams and overburden of a certain coal mine, studied situations of overburden bed separations when adopting completely pillarless overlapping faces in inclined and nearly horizontal coal seams. Two-dimensional test bed was used in this experiment, the size of the test bed was length × width × hei ght = 1620 mm × 160 mm × 1300 mm, adopting plane stress model. Set geometric similarity ratio toαL = 100:1, bulk density ratio to $\alpha\gamma$ = 1.5:1, time ratio to αt = 10. The experiments of nearly horizontal and gradually inclined coal seams were conducted respectively in which advance of face was simulated and bed-separation in overburden developed with it. The key stratum rose with the increase of the advancing distance, and with the strata continuously reaching its limited span, the level of bed separation would rise.

3.1 *Mechanical properties of rock used for simulation*

Measured data of physical and mechanical properties of roof and floor of each layer used for simulation were shown in table 1.

3.2 *Analysis of phenomena of experiment*

The distribution of overburden bed separation and arrangement of grouting holes in inclined coal seam were shown in figure 2.

As shown in figure 2, with the pillar canceled between faces, overburden above the first face would form a integral structure with overburden above the succeeding face, which meant that overlapping faces should be taken into consideration when dividing "Three Zone". Concrete contents had been described in paper "Determination of height of "Three Zone" in the stope with stagger position and internal misaligned roadway layout", here only cited the conclusion because of the limit space of the thesis. As multiple faces reflected the characteristics of single face, the position of fissure zone rose with the increase of the number of succeeding faces, but it was continuous above the stope, therefore, continuous grouting for multiple faces can be achieved. The distribution of overburden bed separation of nearly horizontal coal seams was shown in figure 3.

As shown in figure 3, pillar between sections was canceled, overburden formed a integral structure, multiple faces reflected the characteristics of single face, The position of fissure zone rose, continuous separation zone formed in the upper part of the stope, so grouting can be used for continuous separation zone generated by multiple faces.

2.3 *Conclusions of the experiment*

By contrast of feature of overburden's movement without pillar and that with pillar, the results were as follows:

1. With the pillar canceled between faces, overburden above the first face would form a integral structure with overburden above the succeeding face, The position of fissure zone rose, mining was more sufficient;
2. Due to mining of succeeding face, after determining grouting layers, bed separation was continuous, and with the mining of each

Table 1. Thickness of strata and physical and mechanical property of roof and floor of coal seam.

Strata	Thickness (m)	Density (kg/m^3)	Elastic modulus (MPa)	Poisson's ratio	Internal friction (°)	Tensile strength (MPa)	Cohesion (MPa)	Compressive strength (MPa)
medium sandstone	6	2500	23000	0.23	32	6	6.4	66
fine sandstone	6.62	2500	22000	0.22	24	7	5.2	73.6
siltstone	3.4	2570	35000	0.22	35	2.3	2.8	39
fine sandstone	5.4	2500	22000	0.22	24	7	5.2	73.6
siltstone	4	2570	35000	0.22	35	2.3	2.8	39
sand-mudstone	5.5	2300	9120	0.26	34	4	1.2	52.2
siltstone	6	2570	35000	0.22	35	2.3	2.8	39
medium-fine sandstone	7.65	2650	37882	0.19	45	7	2.6	68
siltstone	5.5	2570	35000	0.22	35	2.3	2.8	39
sand-mudstone	2.5	2300	9120	0.26	34	4	1.2	52.2
coal seam	5.5	1450	3100	0.3	35	1.2	0.8	15
siltstone	5	2570	35000	0.22	35	2.3	2.8	39

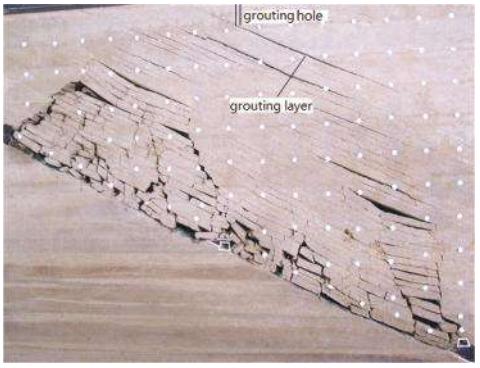


Figure 2. Grouting layer and holes layout completely without pillar in inclined coal seam.

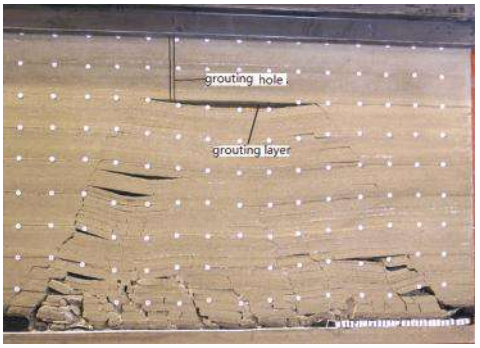


Figure 3. Grouting layer and holes layout completely without pillar in nearly horizontal coal seams condition.

succeeding face, strata below the grouting layer suffered another mining influence, after layout of grouting holes during early stage, with the increase of mining range along the dip and activation of strata below the bed separation for grouting, immediately began to grout when negative pressure appeared at orifice, which meant that grouting work was always performed after activation of strata, subsidence reducing effect was better;

3. Bed separation was continuous in pillarless mining, as a result, efficiency of grouting holes could be made full use of, drilling work quantity was reduced.

4 APPLICATION ANALYSIS

A certain coal mine II_{102} mining district was under village, the length of strike was 2340 m, the length of dip was 700 m, area was 1.6 km^2, the thickness of main mining coal seam was 3 m, average angle was 18°, average depth was 600 m. Ground level was +27 m, the thickness of overburden was 240 m. As the whole mining district had suffered rock magmatic intrusion, igneous rock with huge thickness of 120 m formed 180 m above the coal seam, movement angles of bedrock's rise and dip both were 75°, as shown in figure 4, uniaxial tensile strength of igneous rock was 7.9 MPa, uniaxial compression strength was 96.4 MPa, elastic modulus was 32.4 GPa, Poisson' ratio was 0.256. Determined that first caving span of igneous rock

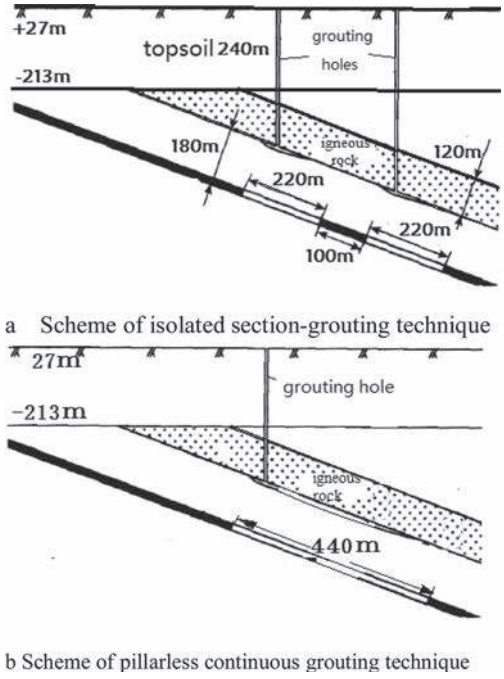


Figure 4. Contrast of schemes of grouting for bed separation.

with huge thickness was 150 m, unidirectional limit size of corresponding face was 245 m.

Isolated section-grouting filling technique was adopted in original scheme. First, determined to adopt 200-meter-long longwall working face for stopping, as shown in figure 4(a), in order to prevent isolated separations below the key stratum from connecting, the width of pillar to be remained was greater than 96.46 m, adopted 100 m. Used combination of 2-millimeter-long refuse and fly ash as aggregate in grouting system, it was carried by water to bed separation of igneous rock with huge thickness through ground drilling holes, water was discharged through drainage holes continuously, and that cycle repeated, until separation was fully filled with refuse and fly ash.

First made judgements about the mining degree and filling effect, with the calculation of formula, found that overburden was in critical state of sufficient mining during producing of single face, subsidence reducing rate was 57%.

What's more, the length of face was 220 m, the length of pillar left was 100 m, after two adjacent sections were mined out, there was still about 140-meter-long coal seam could not be mined, resulting in a waste of about 220-meter-long coal seam.

In order to improving current situation of grouting technique, raised a scheme of completely pillarless continuous grouting technique for the coal mine, as shown in figure 4(b). By calculating, overburden was in insufficient mining stage during producing of succeeding face, subsidence reducing rate was 85.6%.

In the meantime, the length of face was 220 m, after three overlapping face formed, protective coal pillars were preserved for mining district on the border of mining district, thus realized fully recovery of resource of the coal mine. In comparison with the original design, taking advancing distance of the mining district into consideration, nearly 1.74 Mt coal resource can be recycled.

In addition, compared (a) with (b) in figure 4, as grouting holes were arranged over first face, and grouting had begun during producing of first face, after activation of strata and mining influence when succeeding face was producing, immediately began to grout when negative pressure appeared at orifice, could effectively support igneous rock, compared with original scheme, subsidence reducing rate and recovery increased while also quantity of drilling was reduced.

5 CONCLUSION

The study was conducted based on grouting for overburden bed-separation along the dip. Proposed subsidence reducing technique by continuously filling grouts into stope overburden bed-separation along the dip. The biggest difference was that pillar between faces was canceled completely. By theoretical and experimental analysis, concluded that the technology had a feature that the mining degree was higher, the connection of grouting and mining was more reasonable, and on the premise of relatively small quantity of grouting and grouting drilling works, achieved relatively ideal subsidence reducing effect. In the end, this technology was verified based on practical engineering context, considered that the technology had a feature that the mining degree was higher, grouting effect was more evident, mining district arrangement was more reasonable and drilling works quantity reduced and so on. Therefore, considered that this technology had a certain promotional value.

REFERENCES

Desen Zhao. 2000. Study on mining overburden bed-separation distribution law and surface subsidence control. Fuxin: Liaoning technical university, 15.

Dongjian Zhang & Hengqing Guo. 1999. Technology of grouting into overburden bed-separation in Jining mining area. *Mining survey,* (3): 34~36.

Huaxing Zhang & Zunyi Wei. 2000. Practice and cognition of grouting into bed-separation section. *Coal Science and Technology,* 28(9): 11~13.

Jialin Xu & Minggao Qian. 1998. Study on borehole layout for grouting into bed-separation to reduce subsidence. *Journal of China University of Mining & Technology* 27(3): 276~279.

Jialin Xu & Minggao Qian. 1998. Study on experiment of borehole layout for grouting into bed-separation. *Journal of China University of Mining & Technology* 27(3):276~279.

Jialin Xu & Minggao Qian. 2000. Method of judgement of position of overburden key stratum. *Journal of China University of Mining & Technology* 29(5): 463~467.

Jialin Xu & Minggao Qian. 2000. Study on the effect of key stratum motion on the surface movement. *Journal of Coal Science & Engineering* 25(2): 122~126.

Jialin Xu et al. 2004. Study on evolution laws and application of rock strata movement bed-separation. *Chinese Journal of Geotechnical Engineering* 26(5): 632–636.

Jialin Xu et al. 2006. Study on partial fillmining technology for controlling mining subsidence of mine. *Journal of mining and safety engineering* 23(1): 6~11.

Jingli Zhao & Jian Wu. Full-seam mining adopted roadway layout of stagger arrangement in thick coal seam. *China pa tent*: ZL98100544.6, 2002–01–23.

Jinhai Liu et al. 2009. Elasticity sheet method for subsidence reducing effect evaluation of grouting into bedseparation. *Engineering Mechanics* 26(11): 252–256.

Jinzhuang Wang et al. 1999. The mechanism and application discussion of technology of grouting into overburden bed-separation to reduce surface subsidence in coal mine. *Journal of China University of Mining & Technology* 28(4): 331–334.

Lun Yang. 2002. Rediscovery on technology of grouting into mining overburden bed-separation to reduce subsidence. *Journal of Coal Science & Engineering* 27(4): 352–356.

Minggao Qian et al. 1996. Study on the key stratum theory in ground control. *Journal of Coal Science & Engineering* 21(3): 225–230.

Minggao Qian et al. 2003. Theory of key stratum in ground control. *Xuzhou: China University of Mining & Technology Press*.

Weibing Zhu et al. 2005. Experimental study on compressioncharacteristic of coal ash and gangue powder. *China coal* 31(11): 36~38.

Weibing Zhu et al. 2007. Theoretical study on technology of grouting into separated sub-areas of overburden bed-separation to reduce subsidence. *Journal of Coal Science & Engineering* 32(5): 458–462.

Weijia Guo & Guanghan Shen. 1995. Study on movement deformation and control of mining overburden in HuaFeng mine. *Journal of Shandong Mining Institute*. 14(4): 359~364.

Weijia Guo et al. 1995. Study on feature of mining overburden bed-separation and law of bed-separation. *Journal of Coal Science & Engineering* 20(1): 39–44.

Xueli Fan. 1998. Theories and practice of mining damage prevention and control in northeastern mining area of china.

Yaping Zhong & Yanfa Gao. 2001. Engineeringpractice of grouting into overburden to reduce subsidence in Tang Shan mine. *Mine Ground Pressure and Roof Control* (4): 75~76.

Yimeng Meng & Zhenxian Lv. 1993. Application of technology of high-pressure grouting to reduce surface subsidence in Da Tun mining area. *World Coal Technology* (4): 24~26.

Yimeng Meng & Zhenxian Lv. 1993. The application of high-pressure grouting technology to reduce surface subsidence in Da Tun mining area. *World Coal Technology*. (4): 24~26.

Yonghai Teng et al. 2009. Research and Applications of surface subsidence law in fully mechanized top coal caving. *China Coal Industry Publishing House, Beijing*.

Yuzhuo Zhang & Liliang Chen. 1996. Conditions for bed-separation in Long wall mining. *Journal of Coal Science & Engineering* 21(6): 576–581.

Zengzhang Guo. 2000. Study on surface movement design method in Extremely insufficiently mined condition and deep coal pillar mining technology under building. *China university of mining and technology, Xuzhou*.

Zheng Lu et al. 2008. Grouting range determining method of old mined-out areas in longwall mining. *Journal of mining and safety engineering* 25(4): 499–501.

Zhigang Wang. 1995. Preliminary summary of overburden grouting to reduce subsidence in top coal caving face. *Coal Mine Modernization*. (4): 26–27.

Zhiqiang Wang et al. 2008. Stable characters of key stratum in stagger arrangement roadway layout top-coal caving mining. *Journal of China Coal Society* 33(9): 961~965.

Zhiqiang Wang et al. 2011. China Patent: Method for determining the caving height of stope. application number: 201110409969.

Zhiqiang Wang. 2009. Research on strata pressure laws of working face lapped each other of the stagger arrangement roadway layouts in thick coal seams. *China university of mining and technology, Beijing*.

Zhongyu Mao & Xuemin Wang. 1995. Flotation tailings water used for grouting to control surface patchy crack subsidence. *Caol Science and Technology* 2(4): 26–29.

Progress in Mine Safety Science and Engineering II – He et al. (Eds)
© 2014 Taylor & Francis Group, London, ISBN 978-1-138-00122-0

Optimization of roadway layout and its effect analysis for lower protective seam in fully mechanized caving mining

Zhongbao Chang
Xishan Coal Eelectricity Group Company, Taiyuan, China

Qingbo Hui, Yutong Li, Zhiqiang Wang & Jingli Zhao
School of Resource and Safety Engineering, China University of Mining and Technology, Beijing, China

ABSTRACT: The research was conducted based on lower protective seam mining. Practice showed that adopting super-long fully-mechanized caving face for lower protective seam mining has problems of large volume of gas emission, relatively low yield of face, large engineering quantity of roadway and limited released range, etc. In the study, first through measured data obtained parameters of range of overlying coal seams that lower protective seam released. On this basis proposed a technical optimization measures and obtained a series of effects, including: If arranged completely pillarless working faces overlapping each other in protective layer, the adjacent face could increase pressure-released area of No. 1 coal seam by 99,200 square meters compared to the original method. After changing original "U + I" ventilation mode of the protective layer's first mining face to "Y+L" mode, succeeding working face could save engineering quantity by 3238 m. On the basis of increased recovery rate and reduced quantity of roadway engineering, after the optimization, economic benefit could be increased by 95.037 million yuan compared with the original scheme. Combined with daily output, advancing speed and their effect on gas emission, adjusted the length of the original super-long fully-mechanized caving face to 125 m, advanced 4.2 m per day. Finally, tested the releasing effect of protective seam face in fully mechanized caving mining, and considered that overlying coal seam was in full-pressure-released state, proved that optimized measure was reasonable.

1 INTRODUCTION

Coal seams in our country generally have characteristics of high metamorphic grade, low pressure, low permeability and low gas bearing saturation (Jianping Ye et al. 1999, Shining Zhou et al. 2001). Coal Seam mining can cause movement of rock, break as well as "Pressure relief anti reflective" effect of surrounding rock, which means that coal seam permeability will increase from tens to hundreds of times, and that creates conditions for further extraction of gas (Qixiang Yu 1992, Jialin Xu et al. 2004, Minggao Qian et al. 2003, Qianting Hu et al. 2000, Qixiang Yu et al. 2004, Minggao Qian et al. 2003, Jialin Xu & Minggao Qian 2000). In the study of pressure-relief effect of coal mining on overlying coal and rock strata (Xueqiu He et al. 2006), got the following conclusions: when mining depths were the same, effective pressure-relief height was proportional to the length of the working face. For a long time, research had been focused on the pressure releasing effect of the protected seam, ignored that when the length of protective layer mining face was increased, the gas emission would increase, and generated problems of related face's high production and high efficiency and large engineering quantity of roadway, especially in fully-mechanized caving mining face.

The practice also has shown that although the Xinglong Coal mine, Lu'an Wangzhuang mine have successfully applied nearly 300-meter-long experimental mechanized caving face (Shenggen Cao & Xiexing Miao 2001, Bin Ding et al. 2005, Zhiqing Zhao & Yue Zhang 2005), due to threat of gas, face production capacity was difficult to make a further increase (Baozhong Yang 2004).

In summary, on the basis of pressure relief in super-long fully-mechanized caving face in protective layer, for problems that existed in super-long fully-mechanized caving face such as large gas emission, relatively low yield, large roadway projects and the limited releasing range, conducted a research, optimized the corresponding technical measures as well as technique parameters, and the destressing effects were finally validated.

2 ENGINEERING CONTEXT

A certain mine are mainly mining two coal layers, average thickness of the upper coal seam 1# is 1.81 m, its original gas content is 32.41 m^3/t, gas pressure is up to 1.3 Mpa, permeability coefficient of the coal seam is only 0.00037 m/(MPa2.d), belongs to hard drainable coal seam. In production practice, there have been several coal and gas outbursts, which seriously affected production. Average thickness of coal 2# 138.5 meters below the coal 1# is 6.7 m, original gas content is 7.13 M^3/t, gas pressure is 0.2–0.3 MPa, belongs to low-gas coal, average dip angle is 5°.

The mine mined coal 1# in early stage, the length of working face designed was 150 m. Coal and gas outburst happened 30 times during tunneling of return-air roadway and exterior alternate tail roadway, face's advance was less than 100 m when it was forced to halt due to coal and gas outbursts, but fresh air supply was continued for working face, air volume was 660 m^3/min, return air volume was 420 m^3/min, gas concentration was 0.22%; air volume of alternate exterior tail roadway was 240 m^3/min, gas concentration ranged from 0.6% to 0.7%. In order to achieve safe mining of coal 1#, pre-pressure relief and gas extraction were needed, so designed to pre-mine coal 2# as a protective layer which was below coal 1#. Due to the large distance between the two coal beds, research was needed to conduct to determine whether the coal 2# had the function of protective layer. Arranged 250-meter-long fully-mechanized caving face within coal 2#, and the layout orientation of face of upper and lower coal seams were shown as figure 1.

As shown in Figure 1, the protective layer mining face used "U + I" ventilation mode while the protected seam used "U+L" mode. In order to grasp mining effect of coal 2# on destressing effect of coal 1#, measured parameters at the same time. First, obtained parameter changes of gas from protected layer during the producing of protective layer's face, and use it as judge foundation for distressing border along the strike of protected layer. Then during the advancing and producing of protected seam face, obtained parameter changes of gas and used it as distressing border along the dip of protected layer's face.

When coal 2# working face advanced 16 m near alternate exterior tail roadway of coal 1# working face, gas concentration in return airway and tail roadway of coal 1# face was increased to 1.9% and 2.2% respectively. pre-extracted gas in protected seam working face due to serious overranging gas concentration in coal 1# working face with the advancing of coal 2# working face.

From the measured data know that gas gushed out because of the distressing effect on coal 1#. Amount of ventilation air methane increased from 2.6 m^3/min to 13.6 m^3/min before gas extraction; In the range from the beginning of extracting to 110 m past tail roadway coal 2# advanced, the distribution range of the extractable pressure relief gas expanded and the extraction volume increased, and extraction volume increased from 7.2 m^3/min to 27.2 m^3/min. Coal 2# face continued to advance, and during the stage that coal face reached intake airflow roadway of coal 1# and advance 72 m, the extraction volume was always maintained 27 m^3/min on average. After that, the concentration of extractable pressure-relief gas reduced, and reasons were thought to be the re-compaction of coal 1# face, and began to stabilize.

In order to further obtain the released range of coal 2# face along the dip, resume production of coal 1# face while volume of gas extraction of coal 1# face was always maintained at an approximate setting value (the measured data was 11.2 m^3/min), so that determined the released range of the coal 2# along the dip by the measured data of ventilation air methane per ton. Before the coal 1# face advanced 30 m past return airflow roadway of coal 2# face, the range of face ventilation air methane per ton was 11.3~157.8 m^3/t; When the coal 1# face advanced 30 m to 240 m past return airflow roadway of coal 2# face, ventilation air methane per ton reduced to 8.9 m^3/t from 34.4 m^3/t; After advanced 240 m, ventilation air methane per ton rose again, up to 45 m^3/t, 22.3 M^3/t on average.

According to measured data, got the destressing parameters of coal 1# when mining coal 2# in fully-mechanized caving, as shown in figure 2.

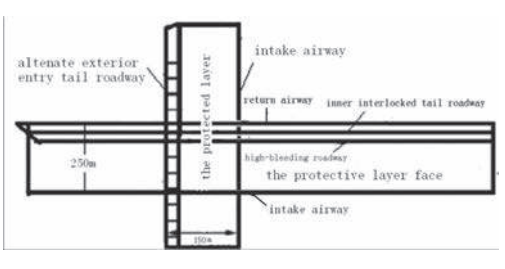


Figure 1. Schematic diagram of faces' layout of the upper and lower coal seams.

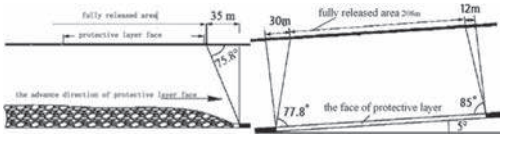


Figure 2. Destressing situation of coal 2# mining for coal 1#.

As can be seen from figure 2, during advancing of the coal 2# face along the strike, coal 1# face began to be in fully distressed area about 35 m behind the coal 2# face, the corresponding pressure-relief angle was 75.8 °. Along the dip of the working face of coal 2#, coal 1# obtained pressure relief from 12 m inner side of the upper end to the 30 m inner side of the lower end. corresponding pressure relief angle were 77.8 ° and 85 °.

3 PROBLEMS

3.1 *Gas emission of working face was large*

During mining of super-long fully-mechanized caving face, due to large thickness, gas emission were large, mainly including gas from coal wall, gas from dropped coal, gas from drawing coal, gas from goaf. Goaf gas came from residual coal in goaf and the released overlying coal. In order to effectively discharge gas and realize safe production, designed alternate interior tail roadway, rear high level suction roadway, high level suction roadway along the. See in figure 3.

Processed data of the super-long fully-mechanized caving face of coal 2# in different mining period, found the following characteristics:

1. Air supply amount of coal 2# super-long fully-mechanized caving face during the early mining period was 2463 m³/min, advanced 2.6 m per day, daily output was 5974 t, did not achieve the anticipated goal of high production and high efficiency of super-long fully-mechanized caving face.
2. After normal stopping, face daily advance distance was 3.35 m, daily output was up to 8699 t, ventilation air methane was 26.9 m³/min, and during the mining process, gas concentration of upper corner in fully-mechanized caving face sometimes exceeded limit.

In summary, super-long fully-mechanized caving face was used for mining as a protective layer, its high productivity and high efficiency advantages were not fully reflected, and the large amount of gas emission threatened the safety of face production.

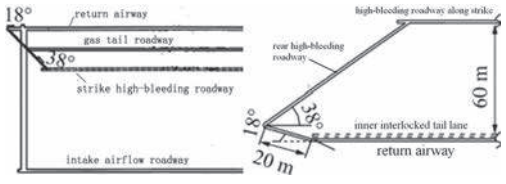


Figure 3. Gas drainage measures of coal 2# super-long fully-mechanized caving face.

2.2 *Large quantity of roadway engineering*

As shown in figure 3, in order to ensure the safe production of coal 2# face, arranged gas tail roadway, strike high level suction roadway, rear high level suction roadway. In accordance with the designed advance distance, the lengths of these roadways were 1600 m, 1530 m and 108 m respectively. It could be seen that the roadway workload of super-long fully-mechanized caving face was very large, increased mine production costs, reduced production efficiency.

As coal 2# belonged to the super-long fully-mechanized caving face, at least 20 m wide coal pillar must be remained between faces. According to the measured destressing parameters, at least a scope of 62 m between two faces along the dip would be in unprotected areas, and affected by coal pillar of protective layer face, unprotected areas of coal 1# belonged to high stress distribution areas. Therefore, riskiness of coal and gas outburst of coal 1# was increased during the mining process.

4 TECHNICAL MEASURES OPTIMIZATION OF PROTECTIVE LAYER FACE

4.1 *Optimization of roadway layout*

In order to achieve the fully pressure-relief of protected layer and reduce the amount of roadway engineering of protective layer, optimized the face layout of protective layer, that is, adopted layout of working face overlapping each other completely without coal pillar between two faces (Jingli Zhao & Jian Wu 2002), as shown in Figure 4.

As shown in Figure 4, arranged the succeeding face's return air roadway below the last face's goaf, during producing of the succeeding face, the overlying strata of the two working face moved, forming a whole, reflected the characteristics of a single face (Zhiqiang Wang 2009). With this feature, used this roadway layout in coal 2# and improved some problems existed in original roadway layout. Including:

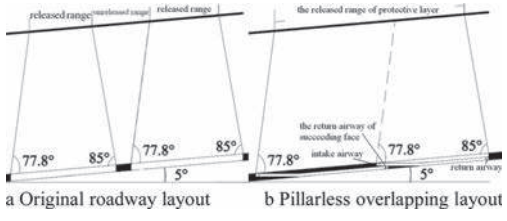


Figure 4. Pressure-relief effect contrast of coal 1# before and after roadway layout optimization.

1 The pressure relief range

As shown in figure 4 was the original layout scheme, since coal pillars existed between super-long mechanized caving face of protective layer, destressed zone and undestressed zone alternately appeared in coal 1#. From the face layout of two seams, saw that this would greatly influence the coal 1#'s face advancing. Figure 4 (b) showed pressure relief situation of coal 1# destressed by working face overlapping each other completely without coal pillar, if a single face was mining, there were no differences with original roadway layout, that is, a pressure relief border existed from both sides towards coal 1#, But after succeeding face was formed, due to the particularity of internal misaligned arrangement, the pressure relief boundary lines at lower end of original face disappeared, only existed on both sides of succeeding face. Thus forming a continuous distressing range in the protected layer, and compared to original roadway layout, adjacent two faces could increase pressure relief range of coal 1# by 99, 200 square meters which brought a positive effect for the safe mining of coal 1#.

2 The amount of roadway engineering

As shown in figure 5, after roadway's optimization, made full use of coal seam's dip and face's overlapping relationship, remained the return airway, tail roadway and the strike high level suction roadwayof the first mining face, Used stope space "O"-ring theory (Minggao Qian & Jialin Xu 1998), after forming internal misaligned overlapping in succeeding face, changed the face's original "U + I" ventilation mode to "Y+L" mode, that is, two roadways of succeeding face were all for air intake, polluted air was discharged through return airway of the first face.

Compared the amount of roadway engineering, due to starting saving excavation of gas tail roadway, strike high level suction roadway and the rear high level suction roadway from succeeding working face, a single working face can save the amount of mine engineering 3238 m.



Figure 5. The arrangement of coal 2# face after optimization of roadway.

3 Technical and economic comparison

What was shown in Figure 6 was overlapping part of face completely without coal pillar. Calculating according to1600 m advance distance of the face, the loss of coal was 114,800 t. If according to design, preset 20 m coal pillar between two faces, the coal loss was 415,400 t. As could be seen, used overlapping completely without pillar, coal resource could be recovered 300,600 t. The economic comparison of optimization technical measures with original program was shown in table 1:

In fact, the table did not reflect the economic evaluation of the pressure relief range after the optimization of technology. Because there is not yet accounting the security investment of protective layer, so temporarily ignore it. However, it can be seen from the table, only consider addition of the recovery rate, the reduction of the roadway excavation and maintenance costs, the optimized technical measures added value of 95.037 million yuan than the original program. Thus, the economy of optimized technical solutions is objective.

4.2 *The optimization of process parameters*

4.2.1 *Working face production effects on gas emission*

Studies showed that production of working face had a greater influence on volume of gas emission, literature (Zhijun Du 2006, Guanglong Dai & Fangjian Chu 2005, Shaolin Lv 1997) indicated that face production wasn't proportional to volume of gas emission. Through analysis, got the



1-Intake airway of the last section; 2-Return airway of the followed face.

Figure 6. Triangle coal loss of working face overlapping each other completely without coal pillar.

Table 1. Economic benefits after technical optimization.

Evaluation index	Total	Gross (ten thousand yuan)
Recovery economy	+300600 t	+9018
Roadway excavation and support	–3238 m	–4857
Total	9503.7 yuan	

Note: + – in table represented the increased economic efficiency and reduced cost respectively. Unit benefit of coal mining was calculated in term of 300 yuan, the drivage and support cost of roadway take 1500/m.

relationship between production of super-long fully-mechanized caving face and volume of ventilation air methane, as shown in figure 7.

The measured data showed that when face production was less than 8000t, the addition of face gas emission approximate linearly increase with the increasing of production capacity; when face production is 8000t-12000t, the gas emission remains in the 26–27 m ³/min, when face production was greater than 12000t, gas emission was in a downward trend with the increase of production.

As shown in the figure, the relationship between amount of ventilation air methane and face production capacity is in negative exponential trend, and the calculation formula is:

$$Q = 10.424te^{(-0.0001t)}$$

3.2.2 *Advance speed influence on volume of gas emission of adjacent layer*

Through calculation of length and advance speed of protective layer face, daily pressure relief area in protective layer could be obtained. During the normal production of the protective layer, measured data of gas emission of adjacent layer and processed data by using liner regression.

As shown in figure 8, face advance speed and volume of gas emission of protection layers exist obvious exponential relationship, and they satisfy the relation:

$$q = 104.08ve^{-0.234v}$$

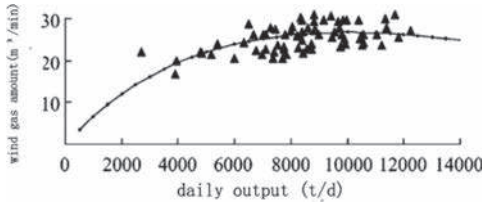


Figure 7. Relationship between super-long fully-mechanized caving face's daily output and volume of gas emission.

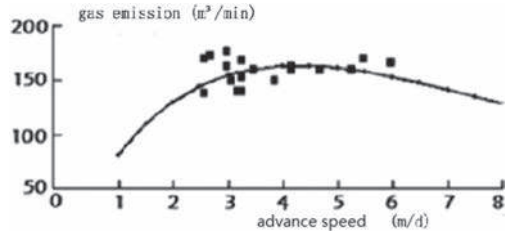


Figure 8. Relationship between face advance speed and volume of gas emission.

Analyzed the formula, and thought that when face advance speed was less than 3.5 m/s, volume of gas emission of protected layer was proportional to face advance speed; When face advance speed was between 3.5~5.5 m/s, volume of gas emission of pressure relief layer mainly remained at 160 to 163 m³/min; When advance speed was greater than 5.5 m, volume of gas emission of pressure relief layer had a downward trend.

In summary, synthesized factors of the optimization measures of roadway layout, volume of gas emission of protected layer and the large amount of gas emission of super-long mechanized face, determine that the length of the face was 125 m, in coal for the, daily cut was 7, the cumulative advance distance was 4.2 m after optimization of roadway layout in coal 2#.

5 EXAMINATION OF DESTRESSING EFFECT AFTER TECHNICAL OPTIMIZATION

In order to ameliorate the problems of lower relative yield and large volume of gas emission existed in original designed super-long fully-mechanized caving face. Optimized the original face length to 125 m, so pressure relief effect of coal 1# caused by the mining of optimized coal 2# needed to be verified. Established numerical simulation model of UDEC^{2D}, according to the actual situation, set the length and width of the model to 544 m and 236 m, added uniform loading of 9 MPa above the model, and left 150 m protective coal pillar at the two boundaries of the model. The focus of the analysis was the pressure relief effect on the protected layer when succeeding face was producing. Due to use of face overlapping each other completely without coal pillar, so triangle coal loss would be left between succeeding face and the first mining face.

The specific physical and mechanical properties of coal and rock were shown in table 2.

Through processed data calculated, obtained the deformation and the vertical stress changes of protected layer when succeeding face was producing, as shown in figure 10.

As shown in figure 10, the effect of coal 2# adopting face overlapping each other completely without coal pillar on protective layer of coal 1# was in area of 75 m away outside the face. And the maximum compression ratio was 0.15%, the maximum stress concentration coefficient was approximately 1.2; Protected layer was released by expansion within the range 5 ~ 75 m of inner side of the protective layer face; the expansion ratio was approximately 0.8%, the stress was about 9% of stress in virgin rock mass. Expansion releasing state of the protected layer in the middle of the two

Table 2. The table of physical and mechanical parameters of coal rock.

Strata	Siltstone	Gritstone	Fine sandstone	Medium sandstone	Coal	Mudstone	Sandy mudstone
Elastic Modulus/GPa	20.2	25	15	35	2.2	2	1.5
Tensile Strength/ MPa	1.3	1.4	1.5	1.5	1	1.2	1.3
Normal stiffness/ $GN \cdot m^{-1}$	16	18	21	20	5	9.6	7.5
shear stiffness/ $GN \cdot m^{-1}$	12	14	16	16	3.5	6.2	4.5
Poisson ratio	0.19	0.19	0.2	0.15	0.28	0.24	0.26

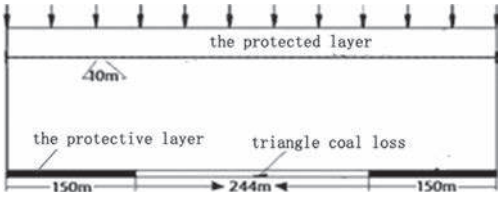


Figure 9. Experimental model.

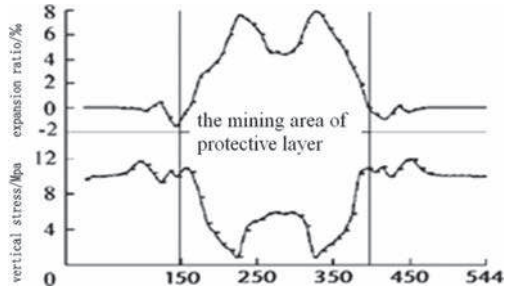


Figure 10. Mining effect of coal 2# completely without coal pillar on deformation and stress of coal 1#.

faces has been restored to some extent; the expansion rate was stable at 0.4%, and the maximum stress recovered to 60.4% of stress in virgin rock mass. Considered through analysis that because of triangle coal loss between two faces, so here was easy to be stable and compacted. More than 3 ‰ of protected layer on both ends of the protected layer was within 195 m range 33 m and 16 m staggered with protective layer face. Showed here was in the state of full pressure relief, and the pressure discharging angles were 77.6 ° and 83.4 °.

6 CONCLUSION

Theory and practice showed that mining using super-long fully-mechanized caving face as lower protective layer had problems of large gas emission, large amount of roadway workload, difficult to achieve high yield and high efficiency of face, and the pressure relief range was limited, etc. On this basis further proposed technical optimization, achievements included: the adjacent face could increase pressure-released area of coal 1# by 99,200 square meters compared to the original method if arranged completely pillarless working faces overlapping each other in protective layer. After changing original "U + I" ventilation mode of the protective layer's first mining face to "Y+L" mode, succeeding working face could save by 3238 m. Compared with the original scheme, after the optimization, economic benefit could be increased by 95.037 million yuan. Combined with daily output, advance speed and their effect on gas emission, adjusted the length of the original super-long fully-mechanized caving face to 125 m, advanced 4.2 m per day.

REFERENCES

Baozhong Yang. 2004. The Problems of the top coal caving technology. Express Information of Mining Industry (8): 25–26.

Bin Din, et al. 2005. Adaptability analysis of the rock pressure law and bracket in super-length fully-mechanized mining face. Ground Pressure and Strata Control 22(4): 99–101.

Guanglong Dai & Fangjian Chu. 2005. Analysis of gas emission law in Fully-Mechanized caving coal face. Safety In Coal Mines 36(8): 55–57.

Jialin Xu & Minggao Qian. 2000. Study on Drainage of Relieved Methane from Overlying Coal Seam Far Away from the Protective Seam by Surface Well. China University of Mining and Technology press 29(1): 78–81.

Jialin Xu et al. 2004. Study on "coal and coal-bed methane simultaneous extraction" technique on the basis of strata movement. Journal of china coal society 29(2): 129–132.

Jianping Ye et al. 1999. Coal reservoir permeability and its controlled factors in china. Journal of China Coal Society 24(2): 118–122.

Jingli Zhao & Jian Wu. Full-seam mining adopted roadway layout of stagger arrangement in thick coal seam [P]. China patent: ZL98100544.6, 2002–01–23.
Minggao Qian & Jialin Xu. 1998. Study on the "O shape" circle distribution characteristics of mining induced factures in the overlaying strata. Journal of China Coal Society 23(5): 465–469.
Minggao Qian et al. 2003. Dominant stratum theory for control of strata movement. China University of Mining and Technology press, Xuzhou.
Minggao Qian et al. 2003. Green Technique in Coal Mining. Journal of China university of mining 32(4): 343–348.
Qianting Hu et al. 2000. Countermeasures for Prevention and Control of Coal and Gas Outburst Hazard in China's Coal Mines. Mining Safety & Environmental Protection 27(1): 1–4.
Qixiang Yu. 1992. The prevention and control of mine gas. China University of Mining and Technology press, Xuzhou.
Qixiang Yu et al. Shining Zhou. 2004. Principles and Applications of Exploitation of Coal and Pressure Relief Gas in Thick and High-Gas Seams. Journal of China university of mining 33(2): 127–131.
Shaolin Lv. 1997. Characteristics of Gas Emission from Two Type High Productive and Efficient Longwall Faces. Coal science and technology 25(4): 21–23.
Shenggen Cao & Xiexing Miao. 2001. Ground pressure controlling on super-length fully-mechanized mining face with top-coal caving. Journal of China Coal Society 26(6): 621–625.
Shining Zhou et al. 2001. Strategic Studies on prevention theory of coal mine gas disaster. China University of Mining and Technology press, Xuzhou.
Xueqiu He et al. 2006. China prevention theory and technology of coal mine gas disaster. China University of Mining and Technology press, Xuzhou.
Zhijun Du. 2006. The discuss of relationship between coal face production capacity and gas emission. China Science and Technology Information (10): 87.
Zhiqiang Wang. 2009. Research on strata pressure laws working face lapped each other of the stagger arrangement roadway layouts in thick coal seams. China university of mining and technology, Beijing, Beijing.
Zhiqing Zhao & Yue Zhang. 2005. Analysis on application effect of 300 m full mechanized mining face in shendong mining area. Coal Mining Technology 20(6): 25–27.

This page intentionally left blank

Progress in Mine Safety Science and Engineering II – He et al. (Eds)
© 2014 Taylor & Francis Group, London, ISBN 978-1-138-00122-0

Safety evaluation model and application for purification device of sour natural gas based on risk

Jun Yi, Meng Zong & Wen-He Wang
Chongqing University of Science and Technology, Chongqing, China

ABSTRACT: By analyzing the hierarchy of safety factors in purification plant of natural gas, they are divided into personnel, equipment, environment and management. After the study of safety index, evaluation methods and fuzzy arithmetic method for each hierarchy, its fuzzy evaluation flow is given. During the evaluation, the weight of the factors and each hierarchy is decided by analytical hierarchical process, and the operational criterion adapts maximum membership degree. And this model is exemplified in purification plant of natural gas. The results show that the second fuzzy evaluation is effective to assess purification plant of natural gas.

1 INTRODUCTION

The security operation of natural gas purification plant relates to the factory and the safety of operators, for there exists flammable, explosive gas in it. Once incidents come out, it will cause casualties and economic loss (CAI & YAO 2008, PENG et al 2009, SHAO et al 2007). Because of the complex production environment of natural gas purification plant, factors causing the risk in the plant are various, most of which are fuzzy. Therefore, adopting the fuzzy comprehensive evaluation model can analyze the possibilities and consequences of all kinds of risks. Using fuzzy language can express the possibilities and consequences of the risks in the plant, and determine the sort of the risk area, so as to guide the safe production (HUANG & J1 ANG 2007).

2 THE CONSTRUCTION OF SAFETY EVALUATION MODEL

2.1 *The construction of evaluation model*

1. The construction of the factors set of evaluation object
   In this article, the evaluation object factors set expressed by U are all factors that cause the danger of the plant. Assume the evaluation factors that influence the final evaluation results of the evaluation object are u_1 u_2 … u_n. Thus, the factors set can be expressed as:

$$U = (u_i)\ i = 1,2\ldots,n \tag{1}$$

   Each factor can be divided into M number of influencing factors, and the grand set can be expressed as:

$$u_i = (u_{i1} \quad u_{i2} \quad \ldots \quad u_{im})\ i = 1,2,\ldots,n \tag{2}$$

2. The determination of the weight coefficient
   In addition to confirm the factors set of evaluation object and each factor's subset, their weights also need to be determined. Factorial weighting set reflects each factor's influence on evaluation object. It can be expressed as:

$$A = (a_i)\ i = 1,2,\ldots,n. \tag{3}$$

   The a_i must satisfy the normalization condition:

$$\sum_{i=1}^{n} a_i = 1, \tag{4}$$

   A corresponding weighting set is constructed in light of each factor in the factors set, which can be expressed as:

$$A_i = (a_{i1} \quad a_{i2} \quad \ldots \quad a_{im})\ i = 1,2,\ldots,n \tag{5}$$

3. The construction of the alternative set
   The alternative set consists of the overall evaluation results that the valuators made on evaluation object. Generally speaking, the assessment of value range and the degree of language are taken as the evaluation object. The alternative set usually can be expressed as:

$$V = (v_1 \quad v_2 \quad \cdots \quad v_k) \tag{6}$$

Assume the alternative sets are divided into 5 grades. It can be expressed by fuzzy language as:

$$V = (\textit{safest safe general dangerous most dangerous}) \tag{7}$$

2.2 *Class A fuzzy comprehensive evaluation*

Class A fuzzy comprehensive evaluation method is also called single factor fuzzy comprehensive evaluation method. It makes evaluation on a single factor through synthesizing the contribution that each grand of one factor makes to the value of evaluation objects (PENG 2002, PENG et al. 2012). Membership function matrix of each factor level is shown as follows:

$$R = \begin{pmatrix} r_{i11} & r_{i12} & \cdots & r_{i1k} \\ r_{i21} & r_{i22} & \cdots & r_{i2k} \\ \vdots & \vdots & \vdots & \vdots \\ r_{in1} & r_{in2} & \cdots & r_{ink} \end{pmatrix} \quad i = 1,2\ldots,n \tag{8}$$

$$B_i = A_i \bullet R_i = \begin{pmatrix} a_{i1} & a_{i2} & a_{i3} & a_{i4} \end{pmatrix} \bullet \begin{pmatrix} r_{i11} & r_{i12} & \cdots & r_{i1k} \\ r_{i21} & r_{i22} & \cdots & r_{i2k} \\ \vdots & \vdots & \vdots & \vdots \\ r_{in1} & r_{in2} & \cdots & r_{ink} \end{pmatrix} \tag{9}$$

The corresponding rank weights are constructed with regard to each factor

$$A_i = \begin{pmatrix} a_{i1} & a_{i2} & a_{i3} & a_{i4} \end{pmatrix} \tag{10}$$

Therefore, class A fuzzy comprehensive evaluation matrix is shown as:

$$R = \begin{pmatrix} A_1 \bullet R_1 \\ A_2 \bullet R_2 \\ \vdots \\ A_n \bullet R_n \end{pmatrix} i = 1,2,\cdots,n \tag{11}$$

$$B = A \bullet R = \begin{pmatrix} b_1, & b_2, & \cdots & b_k \end{pmatrix} \tag{12}$$

2.3 *Secondary fuzzy comprehensive evaluation*

Class A fuzzy comprehensive evaluation just considers the influence of single factor on the evaluation objects but ignores the relation of various factors. Now the risk level of evaluation objects is calculated after the weight of each factor is given (PENG 2002, PENG et al. 2012, TAN et al. 2012, XIN & WANG 2012). The result of fuzzy comprehensive evaluation comes out according to the overall merit of all influencing factors.

$$C = A \circ B = \begin{pmatrix} c_1 & c_2 & \ldots & c_k \end{pmatrix} \tag{13}$$

After normalization, the synthesis appraisal result vector is shown as:

$$C' = \begin{pmatrix} c_1', & c_2', & \ldots & c_k' \end{pmatrix} \tag{14}$$

Adopting the maximum membership degree principle of judgment, safety grade belongs to:

$$r_{i\max} \left(i = 1,2\ldots,m\right) \tag{15}$$

3 PROJECT CASES

3.1 *The construction of evaluation model*

The Security incidents of purification plant are influenced by many factors. However, each factor can just reflect one side of the problem. In order to evaluate the safety level of the purification plant comprehensively, it is necessary to introduce indicators as much as possible in the evaluation model and follow an independent, comprehensive, comparable principle at the same time (SHENG et al. 2012, ZHOU et al. 2012). So this paper uses the Analytic Hierarchy Process (AHP) analysis and forms well-organized recursive node hierarchy structure, as shown in Figure 1.

3.2 *The confirmation of the result of evaluation matrix*

On the basis of investigation and research, in accordance with the method of fuzzy evaluation and the different grades of membership of each factor given through the expert scoring, it is easy to obtain the first-order evaluation matrix. Then the comprehensive evaluation matrix is obtained

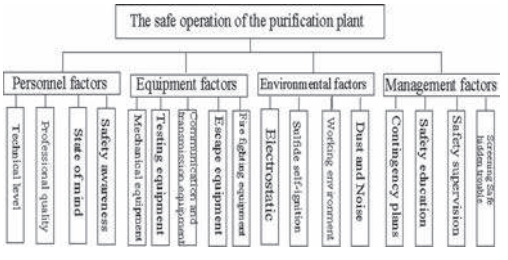


Figure 1. The security hierarchy structure of Purification plant security hierarchy.

Table 1. Fuzzy evaluation results.

evaluation factors			evaluation subfactors				Evaluation situation					$B_i = A_i \circ R_i$	normalization results
V_i	factors	weight allocation	V_{ij}	subitem evaluation content	weight allocation	A_i	R_i	safest	safe	general	dangerous	most dangerous	
V_1	Personnel factors	0.18	V_{11}	Technical level	0.25	$A_1=(0.25\ \ 0.25\ \ 0.1\ \ 0.4)$	R_1	$\begin{pmatrix}0.4&0.3&0.1&0.1&0.1\\0.3&0.4&0.2&0.1&0\\0.2&0.5&0.2&0&0.1\\0.3&0.4&0.1&0.1&0.1\end{pmatrix}$					$B_1=A_1\circ R_1$ $=(0.3\ \ 0.5\ \ 0.2\ \ 0.1\ \ 0.1)$	$(0.25\ \ 0.417\ \ 0.167\ \ 0.083\ \ 0.083)$
			V_{12}	Professional quality	0.25									
			V_{13}	State of mind	0.1									
			V_{14}	Safety awareness	0.4									
V_2	Equipment factors	0.31	V_{21}	mechanical equipment	0.37	$A_2=(0.37\ \ 0.22\ \ 0.12\ \ 0.18\ \ 0.11)$	R_2	$\begin{pmatrix}0.3&0.3&0.2&0.1&0.1\\0.2&0.4&0.2&0.2&0\\0.3&0.4&0.1&0.1&0.1\\0.2&0.3&0.3&0.1&0.1\\0.3&0.4&0.2&0.1&0\end{pmatrix}$					$B_2=A_2\circ R_2$ $=(0.3\ \ 0.3\ \ 0.2\ \ 0.2\ \ 0.1)$	$(0.273\ \ 0.273\ \ 0.182\ \ 0.182\ \ 0.091)$
			V_{22}	Testing equipment	0.22									
			V_{23}	Communication and transmission equipment	0.12									
			V_{24}	escape equipment	0.18									
			V_{25}	Fire fighting equipment	0.11									
V_3	Environmental factors	0.1	V_{31}	electrostatic	0.46	$A_3=(0.46\ \ 0.15\ \ 0.21\ \ 0.18)$	R_3	$\begin{pmatrix}0.2&0.2&0.4&0.1&0.1\\0.3&0.3&0.3&0.1&0\\0.1&0.4&0.3&0.1&0.1\\0.2&0.2&0.4&0.1&0.1\end{pmatrix}$					$B_3=A_3\circ R_3$ $=(0.2\ \ 0.2\ \ 0.4\ \ 0.1\ \ 0.1)$	$(0.2\ \ 0.2\ \ 0.4\ \ 0.1\ \ 0.1)$
			V_{32}	Sulfide self-ignition	0.15									
			V_{33}	Working environment	0.21									
			V_{34}	dust and noise	0.18									
V_4	Management factors	0.41	V_{41}	Contingency plans	0.24	$A_4=(0.24\ \ 0.1\ \ 0.25\ \ 0.41)$	R_4	$\begin{pmatrix}0.5&0.2&0.2&0.1&0\\0.3&0.3&0.2&0.2&0\\0.3&0.4&0.2&0.1&0\\0.3&0.3&0.2&0.1&0.1\end{pmatrix}$					$B_4=A_4\circ R_4$ $=(0.3\ \ 0.3\ \ 0.2\ \ 0.1\ \ 0.1)$	$(0.3\ \ 0.3\ \ 0.2\ \ 0.1\ \ 0.1)$
			V_{42}	Safety education	0.1									
			V_{43}	Safety supervision	0.25									
			V_{44}	screening Safe hidden trouble	0.41									

by allocating and compounding the matrix with corresponding weights of factors. The evaluation results are shown in Table 1.

Obtaining the evaluation matrix from Table 1

$$R=\begin{pmatrix}B_1\\B_2\\B_3\\B_4\end{pmatrix}=\begin{pmatrix}0.25&0.417&0.167&0.083&0.083\\0.273&0.273&0.182&0.182&0.091\\0.2&0.2&0.4&0.1&0.1\\0.3&0.3&0.2&0.1&0.1\end{pmatrix}$$

So the comprehensive fuzzy evaluation matrix is $B' = V \cdot R$ and it is calculated as: $B = (0.3\ \ 0.3\ \ 0.2\ \ 0.182\ \ 0.1)$.

After normalization, it gets $B = (0.277\ \ 0.277\ \ 0.185\ \ 0.168\ \ 0.092)$.

It can judge that the criticality of the plant is "safer" above level by combining the result and maximum membership principle.

4 CONCLUSION

1. Because there exist many risk factors in natural gas purification plant and each factor is complex, it is difficult to form safety evaluation model reasonably with the classical mathematics method, while the membership function in fuzzy mathematics and fuzzy comprehensive evaluation theory can better assess the safety of purification plant.
2. Use expert scoring method to determine the weight of each factor. Therefore, the selection of experts must be extensive, including not only first-line production workers, but also middle supervisors and senior coordinators. This result has universality, for it is discussed in reasonable personnel structure.
3. The overall security situation of the plant is "safer" above level. During calculating it has been found that the proportion of environmental factor is only 0.1. But the fuzzy operation results show that the security situation in the "general" level. Therefore, environmental factors are relatively weak, especially the electrostatic influence. And it is necessary to strengthen the supervision.

REFERENCES

Cai L.Z. & Yao A.L. 2008. Present Situation Analysis on Risk Assessment for City fue1 Gas Pipelines and Expectation. *Natural Gas and Petroleum* 26(6):27–30.

Huang T. & Jiang S.Y. 2007. Applying fuzzy comprehensive evaluation method on road transport system of liquid chlorine. *Journal of Safety Science and technology* 3(3):58–64.

Peng W. et al. 2009. Application Of AHP-fuzzy comprehensive evaluation method in coal-gas station safety status. *Journal of Safety Science and tethnology* 5(2): 93–100.

Peng X.H. et al. 2012. Assessment system of petrochemical enterprises safety production by fuzzy mathematics. *Journal of Safety Science and technology* 8(7): 108–111.

Peng Z.Z. 2002. *Fuzzy Mathematics and Application*. 7–52, 139–186 Wuhan: Wuhan university Press.

Shao H. et al. 2007. Fuzzy mathematical safety evaluation model and application for storage tank district of petrochemical enterprises. *Journal of Safety Science and Technology* 3(6):49–51.

Sheng Y.X. et al. 2012. Index decomposition of dangerous chemical processes risk rank for petroleum chemical enterprise. *Journal of Safety Science and Technology* 8(3):97–101.

Tan Q.L. et al. 2012. A Quantitative Risk Assessment Method for Equipments of High-sulfur Gas Field Gathering Station. *China safety science journal* 22(1):94–98.

Xin C.L. & WANG J.L. 2012. Review on Historical Analysis of Accidents in the Transportation of Hazardous Materials. *China Safety Science Journal* 22(7):89–93.

Zhou Z.Y. et al 2012. Design of a new method for safety assessment on dangerous chemical process. *Journal of Safety Science and Technology* 8(9):118–122.

Progress in Mine Safety Science and Engineering II – He et al. (Eds)
© 2014 Taylor & Francis Group, London, ISBN 978-1-138-00122-0

Coal mine comprehensive safety information management system based on the cloud computing

Shuang-Yue Liu & Tian-Yu Xiong
Civil and Environmental Engineering School, University of Science and Technology Beijing, Beijing, China

ABSTRACT: A Coal Mine Comprehensive Safety Information Management System based on the cloud computing platform which aims at the current shortcomings in the safety of the domestic coal industry management information system were proposed. The system is based on the blue cloud computing platform, integrated coal mine data monitoring, hazard protection and quality assessment of three major subsystems. The introduction of a distributed processing model, aims to integrate existing information platforms solving the problem of heavy hardware construction, light software investments and negligence of service. The goal of scheme is to achieve a smooth transition from the existing information management system and form a set of the integrated cluster security management program.

Keywords: cloud computing, mine safety, safety management

1 INTRODUCTION

The integration of distributed information management system is the development trend of coal mine safety information management in the future. The so-called cloud computing, is relying on the Internet as a service approach, based on the specific needs of computers and related equipment to provide hardware-level-share software resources. With the resources of interconnected networks constructed based pool of computing resources, and the implementation of unified management, according to the actual needs of users to provide services, the emergence of cloud computing technology provides a new way of thinking for research and development of a new generation of distributed Mine Safety Information System (Liu et al. 2012).

2 MINE INFORMATIZATION DEVELOPMENT STATUS AND PROBLEMS

- Uneven development of information technology Although China's coal-mining industry information on the application of information technology has made a certain progress, but low level of development companies and many SMEs, due to lack of funds, technical weakness, lack of awareness and backward management and other reasons, are still in its infancy of the process of information technology (Ma et al. 2010).
- "Information island" restricting the flow of information.

  With the development of information technology, communications and data sharing has become a pressing need. In tradition coal mine enterprise informatization construction lack of unified norms and standards, different mining area in the same item of information management with several subsystems, which lack of the necessary information sharing between systems and equipment, and in a state of "information island" (Zhu & Qi 2012).
- Attaches great importance to the hardware despise software, ignore the service.

  Investigation shows that the coal enterprise information for more focused on the hardware. By 2010, coal mining industry in the aspect of network construction showed that degree of network coverage in more than 90%, large coal mining enterprises network bandwidth in lG more than 70%, computer Internet access rates in more than 90% of companies have over half. But it should be pointed out that, when a lot of coal mines focus on hardware investment in the information construction, they ignore the internal information resources development.

3 CLOUD COMPUTING AND RELATED TECHNOLOGIES

Cloud computing is not a new concept in nature (Leavitt 2009, MELLPP & GRANCE 2011).

As early as in 1961, computing pioneer John McCarthy predicted: "the future of the computing resources can like public facilities (such as water, electricity) is used." (FOSTER et al. 2008) According to the national institute of standards and technology, the core of the cloud computing is to use the network computing resources unified management and scheduling, to constitute a computational resources pool on demand service to users. Providing resources network is known as the "cloud", and service is the nature of cloud (Boss et al. 2007). For this reason, information management system based on cloud computing platform has removed a large number of hardware devices upfront costs troubles (MILOJICIC et al. 2011).

3.1 *The core services of the cloud computing*

Cloud computing core services usually can be divided into three sub layers: Infrastructure as a Service (IaaS), Platform as a Service (PaaS), Software as a Service (SaaS) (WANG et al. 2008). Three sub layers of the relationship can be represented in Figure 1. IaaS provides hardware infrastructure deployment services, demand for the user to provide physical and virtual resources such as computing, storage, and network. PaaS is cloud computing applications running environment, provide the application deployment and management services. With PaaS layer software tools and development language, application developers need to upload the program code and data can use the service, rather than having to focus on the underlying network, storage, management of the operating system problems. SaaS is based on cloud computing platform developed by the application. Enterprise can through rent the SaaS service to solve the problem of enterprise information.

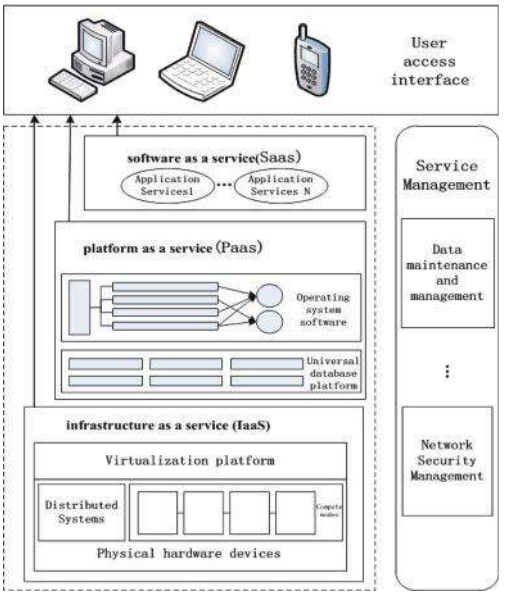


Figure 1. The core service structure of cloud computing.

3.2 *The IBM cloud computing platform*

Currently, Amazon, Google, IBM, Microsoft, Sun, etc., have proposed the cloud computing infrastructure or cloud computing platform (Barroso et al. 2003). "Blue Cloud" infrastructure based on IBM's Almaden research center, used the Xen and PowerVM virtualization software (IBM 2009), Linux operating system images and Hadoop software (Apache 2010). (The Google File System and open source implementations of MapReduce). Compared with the existing network model, the advantages of "Blue Cloud" platform are shown in Table 1.

The important feature of "Blue Cloud" software is the use of virtualization technology (Smith & Nair 2005). Virtualization in "Blue Cloud" has two levels, one is in the level of hardware virtualization, and the other one is by open source virtualization software. Hardware level of server virtuali-

Table 1. "Blue Cloud" computing platform comparison with existing platforms.

	The "Blue Cloud" computing model	Existing models
Application resource allocation	Distribution of virtual resources to applications from the uniform resource pools	Purchase the server for each application deployment server alone
Application runtime environment	Virtualization environment	Physical machine
Application expansion	From the resource pool to increase resources for the application	Purchase of a new server for the application
Application Monitoring	System forms an overall application monitoring system	For each application deployed a monitoring system
OS application deployment and upgrades	Complete automation through self-service interface	Manually
Resource utilization	High	Low

zation can use IBM P series, obtain the hardware logical partitions (LPAR). Logical partitions CPU resources can be managed through IBM Enterprise Workload Manager which reflected the computing platform and upper application cooperation relationship (Nelson M et al. 2005).

4 THE COAL MINE SAFETY INFORMATION MANAGEMENT SYSTEM BASED ON CLOUD COMPUTING

4.1 *The overall system design*

Coal mine safety information management system based on cloud computing, aims to integrate the existing coal enterprises of traditional web information management system, with relying on the powerful data management capabilities to ensure safety production. Cloud Management System (CMS) is mainly composed of three modules, namely: the cloud monitoring data management system, the hidden danger cloud management system, and the evaluation of safety quality standardization cloud management system. void excessive notes and designations.

4.2 *The cloud monitoring data management system*

Under the actual production of coal mine will have a variety of sensors. The sensor data has the characteristics of mass, heterogeneity, and uncertainty. In digital monitoring system of coal mining enterprises which have been built in, to get the data from different sensors are often collected by different monitoring substation, often caused by hardware redundancy. Through the cloud computing platform can realize data mass storage and integration. Sensor data through data collector directly uploaded to the cloud which reduce redundant hardware and realize the software and hardware resources integration. For not construction of the digital monitoring system of coal mining enterprises, build the complete monitoring data management system needs only data sensor and data collector. Data through the cloud management reduce the hardware cost and improve the quality of the software services at the same time.

4.3 *The hidden danger cloud management system*

Digital management of hidden danger mode, in the already built information management platform of coal mine enterprises has been widely used. At present, the underground wireless network communication technology has been mature, relying on the portable digital terminal PDA or PAD as hardware platform, which can realize the real-time digital record of hidden danger and the personnel violate in the pit, totally abandon paper carrier. Compared to traditional computer information management system, based on the cloud platform of mobile intelligent terminal greatly shortens the processing time of the problem. For not building information management platform of coal mine enterprises, set up hidden danger cloud management system, only need a simple terminal hardware support, operating system virtualization of the cloud data resources needed can be automatically configured according to actual condition. Through the SaaS apps in the full life cycle management system application can improve operational efficiency, reduce operational costs.

4.4 *The hidden danger cloud management system*

Currently informatization of safety quality standardization evaluation work is at low level. Quality evaluation management is characterized by the traditional manual approach. Based on a cloud management platform and mobile terminal can be digitized in management of evaluation content. After input assessment data, the system will automatically generate related evaluation results and statistical information with print function. The system also can be added to the policy query and evaluation method study module at the same time, convenient query management personnel evaluation, improving the efficiency and accuracy of the work.

5 CONCLUSION

Mature development of cloud computing and wireless communications technology, provides a new train of thought to develop a new generation of integration of coal mine safety information management system. Safety management platform based on CMS integrated cluster, compared with the existing information management platform, has the following characteristics and advantages:

- Integrated cluster safety management system based on CMS is for the smooth transition of existing information systems. So based on the CMS can speed up the coal mine enterprise's safety informatization construction process, reduce the gap of informationization safety management between SMEs and large enterprise.
- Integrated cluster safety management system based on CMS is a efficient integration of existing information systems. Information management system based on CMS can realize the

maximization of data and information sharing, make the data format between departments to unity, get rid of the existing traditional management way of "information island".

- Integrated cluster safety management system based on CMS is the depth of the use of existing information systems. Cloud computing is the nature of service, based on the three management subsystem, to maximize make full use of existing resources, and to provide complete information chain for coal mining enterprises.

REFERENCES

Apache. 2010. Apache hadoop. http://hndoop.apache.org/core/.

Barroso LA & Dean J, Hölzle U. 2003. Web search for a planet: The Google cluster architecture. IEEE Micro, 23(2):22–28.

Boss G, Malladi P, Quan D, Legregni L & Hall H. 2007. Cloud computing. IBM White Paper. http://download.boulder.ibm.corn/ibmdl/pub/software/dw/wes/hipods/Cloud_computing_wp_final-8Oct.pdf.

Foster I, Yong Z & Raicu I, et al. 2008. Cloud Computing and Grid Computing 360-Degree. Compared..1-10.

IBM. 2009. IBM virtualization. http://www.bm.com/virtualization.

Liu Zhengwei, Wen Zhongiing & Zhang Haitao. 2012. Cloud Computing and Cloud Data Management Technology. Journal of Computer Research and Development, 49(Suppl.):26–31.

Ma Kun, Gao Ding & Bao Hui-ling. 2010. Discussion on coal informatization condition and development. Coal Mine Machinery, 32(03):10–12.

Mellpp & Grance T. 2011. The NIST Definition of Cloud Computing. National Institute of Standards and Technology.

Milojicic D & Wolski R. Eucalyptus. 2011. Delivering a private cloud. Computer. 44(4):102–104.

Neal Leavitt. 2009. Is cloud computing really ready for prime time. IEEE Computer (1):15–20.

Nelson M, Lim BH & Hutchins G. 2005. Fast transparent migration for virtual machines. Proc. of the USENIX 2005 Annual Technical Conf. Berkeley: USENIX Association. 391–394.

Smith JE & Nair R. 2005. Virtual Machines: Versatile Platforms for Systems and Processes. San Francisco:Morgan Kaufmann Publishers.

Wang LI-Zhe, Tao Jie & Kunze M. 2008. Scientific cloud computing: early definition and experience. Proc of 10th IEEE International Conference on High Performance Computing and Communications: 825–830.

Zhu Shuai-hu & Qi Jia-li. 2012. Status and application outlook of mine information network. Coal Engineering, (11):128–130.

Progress in Mine Safety Science and Engineering II – He et al. (Eds)
© 2014 Taylor & Francis Group, London, ISBN 978-1-138-00122-0

Treatment methods of coal mining subsidence area at South Lake in Tangshan city, Hebei province

Chunguang Xu & Ye Chen
China University of Mining and Technology (Beijing), Beijing, China

Zhong Li
Institute of Disaster Prevention, Langfang, Hebei, China

ABSTRACT: The mine environmental problems, such as mining collapse, karst collapse, ground cracks, land subsidence and water pollution, are produced by coal exploitation at the south lake of Tangshan city. Considering the species and distribution characteristics, stable subsidence and unstable subsidence, we'll conduct the geological disaster partition. Adopting scientific principles according to local conditions helps to achieve the purposes of management and protection.

1 INTRODUCTION

It's inevitable to bring about various destructive influences in the process of exploiting the mineral resources. Long-term large-scale and super-strength exploitation of mineral resources causes serious damage to the mine geological environment of our country. It's no time to delay taking the scientific management and treatment for mine geological environment, and there will be one practical significance to the system research of treatment technology of the mine geological environment (WU & CHEN 2010, WU et al. 2005, WU 2003, CHEN 2009). After more than 130 years' exploitation in Kailuan coal mine, the coal mine subsidence area has formed around the urban areas, especially in the south area. The coal mine subsidence area is full of weeds, rubbish everywhere and sewage with waste water, which seriously damages the city's environment and threatens the southern subsidence around the daily lives of residents. Therefore, aiming at the treatment of no less than 3 million square meters of subsidence area and building the center ecological park in the south lake are a beneficial project for people, which can protect the environment and reassure the people (WU 2005, WU et al. 2001).

2 THE BACKGROUND OF GEOLOGICAL ENVIRONMENT

South Lake is located in Tangshan city, Hebei plain, with a total area of 91.4 square kilometers. In general, it is higher in the northeast than southwest from the topography. The landform is alluvial-deluvial plain, which the structure is simple and the type is single, and the rock-soil engineering geological conditions are poor. It is in the meizoseismal region where the active faults distribute. The geological environment is markedly influenced by the exploitation of Tangshan mining branch company. The underground coal field in the south lake of Tangshan is located in the southwest of the northwest wing of Kaiping coal field, whose geological condition is much more complex. The stratums are Quaternary, Permian, Carboniferous and Ordovician from top to bottom. The total thickness of the coal stratum is about 500 meters, having more than ten coal seams. The hydrogeological condition is complex.

3 MAJOR MINE ENVIRONMENTAL PROBLEMS

3.1 *Mining collapse*

With the topography of low-lying of south lake area in Tangshan city, The mine drainage and the precipitation are collected here to form a lake sedimentation (Figure 1). The conditions around the subsidence lake are harsh, such as the slag field, coal gangue and pulverized coal accumulated disorderly. Land subsidence results in the constantly building askew and chapped, Ground fissure and widespread collapse pits. Deformation of the land is intensified by the expansion of the increasing scope mined. Meanwhile, the land appears large volumes of subsidence basin, ground fissure and funnelform collapse pit (WU & CHEN 2003). As



Figure 1. Subsidence lake.

the land is being cracked and rainwater is infiltrating, the original ecological balance has been broken greatly.

3.2 *Karst collapse*

There are a great many karst faults due to the faction of geological structure in this area. Karst morphology dominated by the large gap solution, followed by cave. Generally dissolved in fissures and gaps between layers based on fissures developed from its width 1~5 cm, larger up to 50 cm, and the distribution of it mainly strike NE and NW, partly developed and small. The overlying Quaternary soil structure suffers varying destructions under the influence of exploitation of ground water, "earth hole" collapse is more common. There have been several tubular collapse pits within the bounds of the southern coal mine in the south lake area.

3.3 *Ground fissure*

Directly associated with the Lake District ground fissure zone is generated by the Tangshan earthquake in Tangshan Shengli Road to Wangmatai fracture zone, belonging to the ground fissuers. It has the biggest scale and the highest regularity, with the total length about 11 kilometers. it overall strike NE30°, having multiple-unit fissures around, and the horizontal offset ranges from a few centimeters to hundreds of centimeters (ZHENG et al. 2002).

3.4 *Land subsidence*

With the increasing amount of groundwater, the table drops, forming a cone of depression. And the geotechnical mechanics of stratum is broken, which causes Hangu subsidence and Nanbao-Tanghai subsidence formed nearby Tangshan city (GUO et al. 2004). The south lake is located in the edge of Hangu subsidence and Nanbao-Tanghai subsidence. The cumulative quantity of the land subsidence is less than 300 mm and subsidence rate is less than 15.0 mm/a from 1983 to 2005.

3.5 *Water pollution*

The dirty water poured by residents nearby causes seriously water pollution in the south lake area of Tangshan. Polluted water of Qinglong river flows under Fenghuangtai, passing through Tangxu road into Qingtianjing. The amount of dissolved oxygen at the lake surface nearby Tangxu road is very small, only 0.42 mg/l to 0.62 mg/l, however, with a high value of COD. There are plenty of water blooms at some area of the lake surface. Xixingchi, which is also called the little south lake, dissolved oxygen highly, up to 10 mg/l, and pH is 8.43 to 8.63 (GENNARO & WILLIAM 1986).

4 PRACTICABLE TREATMENT TECHNOLOGY

4.1 *Treatment of subsidence*

4.1.1 *Relocation of residents*

Plenty of shanty towns nearby have been formed because of the constant expansion of subsidence regions. According to the comprehensive plan of the center ecological park construction made by the government, help the residents at coal mining subsidence area move out and take measures to retreat from geological disasters can reach the purpose of the environmental treatment. The immigrant villages at the subsidence area are total 17, that is 6097 families and 17042 persons (SANJEEV 2011, LATIMER 2012).

4.1.2 *Dig the lake and fill it*

28 square kilometers coal mining subsidence area in TangShan city has been planned and treated generally through digging the marsh area and filling the edge zone of subsidence areas. The bottoms of the large subsidence pits are fixed by the clay firstly for preventing from the percolation. After that, filled with cinders and covered soil finally. Generally, the thickness of the soil is 1 meter or more, which lays a foundation for the ecological recovery.

4.2 *Treatment of the land covered by solid waste*

The wastes made by coal mine exploitation form many waste-rock hills over a long time accumulation, including various rock compositions such as the coal gangue, sandstone, mudstone, shale, limestone and so on, and sometimes there are various wastes from the urban people. We adhere to the principle that we should effectively use the solid waste and comprehensively manage it. The

compact and hard waste-rocks are used to build the retaining walls, garden walls and garden plant pools. While the useless are piled with the treatment of slope stepped cutting. All of these lay a foundation for building mountainous of ecological park during the later period.

4.3 *Recover of the landscape*

The parking lot, leisure plaza and plants pool are built on the top of cutted slope of waste-rock so as to make a good use of the fields. The slope of waste-rock are protected by the air brick and the locking structure are made of the concrete, which benefit the growth of herbaceous plant and prevent the dust in the air. Planting large-scale trees in the surrounding of the artificial lake creates a garden landscape. The fences are planted on the both sides of the road instead of protective nets to prevent the tourist from going into the subsidence area and other unsafe fields (Figure 2).

4.4 *Treatment of water pollution*

The drain outlet is stemmed, the sewer network with more than 5300 meters long is embedding, and the waste water of subsidence pits is led into the treatment plant.

Building the waste water sewage sedimentation can achieve the fractional precipitation. Meanwhile, leading the waste water into the north of the pond where cattail, reed and other plants grow may attain the purpose of natural segregation, filtration and absorbing waste water.

We can knock through the disjunctive cesspits so that combine them into a whole big lake, and plant lotus with 5000 square meters, which can purify the lake water and form a special sights for appreciating the flowers.

We might build the lake sights with ornamental value and make use of the dam of the original pond to build a center island with its acreage of 2000 square meters. Building the wharf on the east of the lake makes the visitors can row on the lake (WOLFGANG & CHRISTIANE 1995).



Figure 2. Green belts for the safety protection.

5 EFFECT OF TREATMENT

The subsidence area where the mine geological disasters ever perplexed the people has became a beautiful ecological city park through a reasonable and effective ecological transformation. The original scene, such as the barren land, growing rankly weeds, waste water, coal ash, rubbish and gangue accumulated like a hill, has changed completely. Now it has became an ecological tourist area with a overlapped function including holiday villages, leisure areas, children park and extreme sports ground, so that it satisfies the demands of people's increasing spiritual culture and greatly promotes the development of the tourism in Tangshan city.

6 CONCLUSIONS

1. A series of environmental problems, such as mining collapse, karst collapse, ground fissure, land subsidence and water pollution, are produced by coal exploitation in the subsidence area of the south lake, Tangshan city, which seriously affect the people's daily life and production.
2. Considering the different mine environmental problems of the south lake, the different treatment technology are taken due to the influences for achieving the object of control and protection.
3. The construction of an ecological city at the south lake of Tangshan city can make good use of the characteristics of topography and turn the waste into the treasure. And then achieve the purpose of mine environmental treatment and development plan of building a livable city. The effect of the treatment is noticeable.

ACKNOWLEDGMENT

This study was financially supported by Teachers' Scientific Research Funds of China Earthquake Administration (No. 20110113), which we gratefully acknowledge.

REFERENCES

Gennaro, G.M. & William, G. 1986. Mine subsidencce damage from room and pillar mining in lllinois [J]. *International Journal of Mining and Geological Engineering* 4(2).

Latimer, C. 2012. Mine subsidence damageshomes [J]. *Australian Mining*.

Qi Chen 2009. Research of treatment technology of mine environment and treatment model [D]. *Beijing: China University of Mining & Technology (Beijing)*, (in Chinese).

Qiang Wu 2003. Study of classification of geologic environmental problems in mines in China [J]. *Hydrogeology and Engineering Geology* 14(5):107–111 (in Chinese).

Qiang Wu 2005. New technologies and new methods of comprehensive management of coal mine water disaster [J]. *Beijing: China University of Mining & Technology (Beijing)*:294–296 (in Chinese).

Qiang Wu & DongLin Dong, et al. 2001. Water Environment Problems Due to Mining. *Beijing: China University of Mining & Technology (Beijing)*:182–186 (in Chinese).

Qiang Wu & Fuchang Liu, et al. 2005. Theory and practice of mine environmental research [M]. *Beijing: publisher of geology,* (in Chinese).

Qiang Wu & Peipei Chen 2003. The ground fissures Research and Prospects [J]. *The Chinese Journal ofGeological Hazard and Control* 14(1):22–27 (in Chinese).

Qiang Wu & Qi Chen 2010. An analysis of the mine environmental treatment model and its applicability [J]. *Hydrogeology and Engineering Geology* 37(6):91–96 (in Chinese).

Sanjeev, K. 2011. Potential of Soil and Groundwater Contamination Due to Mine Subsidence Under a Landfill [J]. *Soil and Sediment Contamination: An international Journal* 8(4):441–453.

Wolfgang, A.L. & Christiane, P. 1995. The mechanism of mine-collapse deduced from seismic observations [J]. *Pure and Applied Geophysics PAGEOPH* 147(2).

Xixin Zheng & Qiang Wu, et al. 2002. Urabn land subsidence research progress and trends [J]. *Geology Review* 48(6): 612–618 (in Chinese).

Yonglong Guo & Qiang Wu, et al. 2004. Review of distributed domestic wastewater pollutant sources and methods [J]. *Environmental Science and Technology* 27(1):100–102 (in Chinese).

Progress in Mine Safety Science and Engineering II – He et al. (Eds)
© 2014 Taylor & Francis Group, London, ISBN 978-1-138-00122-0

TBM tunneling in squeezing ground: Problems and solutions

H.S. Ma & J. Wang
CNNC Beijing Research Institute of Uranium Geology, Beijing, China

L.J. Yin
Ecole Polytechnique Federalede Lausanne (EPFL), Lausanne, Switzerland

ABSTRACT: The squeezing ground encountered in Tunnel Boring Machine (TBM) tunneling presents great challenges and may trigger the potential hazards without warning. A detailed understanding of such unfavorable condition is therefore critical to a successful bored tunnel. In this paper, a brief review on the definition and the factors related to squeezing condition is presented. The main problems involved and the corresponding mitigation measurements for the TBM tunnelling under squeezing ground are discussed as well. Finally, further researches to be conducted for better coping with these problems are emphasized.

1 INTRODUCTION

The squeezing ground behaviour experienced during TBM tunnel excavation, has caused great difficulties with major delays in construction schedules and cost overruns (Barla 2001, Ramoni & Anagnostou 2010). There are numerous cases involving squeezing phenomena, including: the Cristina tunnel in Italy, the Gotthard tunnel in Switzerland, the Simplon tunnel crossing the Italian-Swiss border, the Hartebeestfontein Gold Mine project in South Africa, the Uluabat Tunnel in Turkey, the Ghomroud water conveyance tunnel in Iran and so on (Barla 2001, Ramoni & Anagnostou 2010, Malan 2002, Ramoni & Anagnostou 2012, Farrokh & Rostami 2008, Schubert et al. 2006). These cases provide some insight into the ground response during excavation, as well as presenting the main potential difficulties and hazards for TBM tunneling in squeezing condition, with a typical example shown in Figure 1 (Schubert et al. 2006). This paper aims to provide a better understanding of such unfavorable condition by brief introduction of squeezing ground definition and influencing factors, and detailed description of the main problems related to TBM tunneling under squeezing condition. Moreover, the corresponding mitigation measurements are proposed from three categories: i) selection of TBM type and modification of TBM, ii) condition of ground and iii) optimization of TBM operation.



Figure 1. Failure of stiff lining at the Gotthard basis tunnel due to ground squeezing, after Schubert et al. 2006.

2 GENERAL DEFINITIONS OF SQUEEZING GROUND

As proposed by the International Society of Rock Mechanics (ISRM) (Barla 1995), squeezing rock is the time dependent large deformation, which occurs around the tunnel and is essentially associated with creep, caused by exceeding shear stress. Deformation may terminate during construction or continue over a long time period. (Furthermore, many other researchers also gave some different definitions but with common arguments of squeezing, please see the Ref of Barla (2001)).

The term "time dependency" involved in squeezing ground behaviour, is mainly due to the creep caused by exceeding a limiting shear stress creep and consolidation processes taking place around the tunnel (Deere. 1981, Aydan et al. 1993, Anagnostou & Kovari 2005).

3 FACTORS RELATED TO TBM PERFORMANCE IN SQUEEZING CONDITION

As TBM performance is the result of the interaction between rock and TBM machine, both of the rock mass properties and TBM design/operation parameters should be included for this issue. The factors influencing TBM performance in squeezing ground can be briefly summarized as shown in Table 1.

4 PROBLEMS IN SQUEEZING CONDITION FOR TBM TUNNELING

4.1 *Jamming of cutterhead, shield, back-up equipment*

Due to the particular excavation technology of TBM tunneling, the convergences which exceed 5% of the tunnel radius are to be considered problematical (Kovari 1996). When the friction produced by the squeezing ground acting on the cutterhead or shield cannot be counteracted by the available thrust, the TBM becomes jammed (Steiner 1996, Einstein 1989). It is the main challenge for TBM tunneling in squeezing ground due to high pressure by ground and core extrusion. Several factors as follows contribute to this problem.

1. Ground condition
   The squeezing behavior is associated with ground conditions, such as geological conditions, rock properties, the ratio of in-situ stress relative to rock mass strength, the groundwater condition, and so on. As stated by Farrokh et al. (2009), the rock mass in the shield jamming locations usually consists of schist, quartz veins and some soft interbedded graphite schist. In these locations, it is important for occurrence of ground squeezing if the strike of the schistosity is parallel to the tunnel axis.

   The double shield TBM was once jammed in a section of the Connection Works No. 7 tunnel of the Yellow River Diversion Project (YRDP) (D = 4.8 m, L = 13.52 km) in China (Shang et al. 2004). The existence of an interlayer shear zone in the lower part of the anticlinal core, together with local concentration of ground stresses caused a high rate of convergence (20–40 mm/h) of marls in the tunnel wall, which directly brought about TBM jamming and 9 days delay to release the machine.
2. Time-related factors (or advance rate)
   The danger of TBM blockage in a squeezing zone decreases with increasing advance rate. However, nobody can guarantee that high advance rates can be maintained throughout a squeezing zone. Several factors contribute to advance rate under such typical condition.
   i) Standstills: In cases where a TBM is forced to stop for a long period in squeezing ground, the still ongoing displacements then may squeeze the machine, making a restart difficulty (Barla 2001, Barla & Pelizza 2000). Based on the data by Ramoni and Anagnostou (2010), Table 2 gives the summary of standstill causes and the related jamming cases.
   ii) Excavation method and support technique: as stated by Barla and Pelizza (2000), the

Table 1. Factors related to TBM performance in squeezing condition

Ground condition parameters	TBM machine parameters	Operation parameters
Strength and deformability of rock mass; lithologic character; overburden; permeability; groundwater condition; orientation and thickness of discontinuities.	TBM type; length of shield; available thrust and torque; cutterhead design; back-up equipment design.	Advance rate; thrust, torque; standstill; overcutting; support method.

Table 2. Standstill causes and related jamming cases.

Standstill causes	Case	TBM type	Diameter/m	Resulting in…
Maintenance stop	Tunnel 38 of the Yindaruqin Irrigation Project, China	Double shielded TBM	5.54	TBM trapped
High extrusion rate of core	Gil-gel Gibe II Tunnel, Ethiopia	Double shielded TBM	6.98	Shield and segmental lining damaged
Holiday stops	Yacambú–Quibor Tunnel, Venezuela	Gripper TBM	4.80	TBM jamming
	Nuovo Canale Val Viola, Italy	Double shielded TBM	3.60	TBM jamming
Interruption of electric power supply	Evinos–Mornos Tunnel, Greece	Gripper TBM	4.20	Cutterhead jamming

major difficulty for open TBM's advancing in strongly converging and unstable ground derives from the difficulty of placing supports like steel sets, wire mesh and shotcrete, and the inability of these supports to counteract immediately the tendency of the ground to deform and squeeze.

In addition, if the proper backfilling of segmental lining was not achieved, it presents the impossibility of fully utilizing the installed thrust force, leading to TBM trapped, such as that experienced in the Stillwater Tunnel project (Ramoni and Anagnostou 2010) (USA, Double shielded TBM) and Los Rosales Tunnel (Colombia, Double shielded TBM).

iii) Shield length: compared with gripper TBMs, the Shielded TBMs with long shield are highly sensitive to rapid convergences and associated with heavy risk of blockage by converging rocks, if special technical precautions are not taken (Barla & Pelizza 2000).
iv) TBM thrust: high thrust is the prerequisite to maintain advance rate to rapidly pass the squeezing zone.

4.2 *Damage to support*

High pressures on the tunnel lining in the long term can lead to structural or functional failure of these supports. During the construction of water transmission tunnel in Yacambu, Venezuela (Wittke et al. 2005), the two open type TBMs faced extremely unstable ground conditions associated with high and rapid squeezing of the tunnel walls (see Fig. 2).



Figure 2. Water transmission tunnel in squeezing rock, Yacambu (Wittke et al. 2005).

In some occasion it was also necessary to cut down the already erected but deformed steel set due to heave squeezing, re-excavate the tunnel perimeter by hand-mining, and re-install the supports.

At the Faido multifunction station of Gotthard base tunnel project (Ehrbar 2008), the cutterhead had been changed from 8.80 m to 9.40 m in order to obtain more space for deformations and rock support. The deformation behind the cutter head became locally big, and there was a risk that the back-up installation could not pass through the excavated hole. Due to very large radial deformations and an influence of the second tube on the first (eastern) tube, some heavy damage unexpectedly presented in the rock support and lifting of the concrete floor (see Fig. 3).

4.3 *Specifically for different types of TBM*

1. Gripper TBMs: i) difficult to apply thrust due to reduced gripper action for gripper TBM; ii) more time for support installation such as steel sets, wire mesh and shotcrete; iii) the inability of these supports to counteract immediately the tendency of the ground to deform and squeeze; and iv) the reduced performance of the back-up system by squeezing ground behavior (e.g. re-profiling works, twisting of the tracks).
2. Shield TBMs: A higher frictional resistance has to be overcome due to larger area exposed to the squeezing pressure, and consequently, the risk of shield jamming is higher than gripper TBM if all other parameters being equal.

4.4 *Other main problems*

1. Inadmissible convergences of the bored profile, required to re-profile the tunnel if squeezing exceeding the limits.



Figure 3. Deformed steel rib in the floor at the end of yield phase (Ehrbar 2008).

2. Face instability (Barla 2001, Schubert 2000). The instability of the tunnel face is generally not a problem since any squeezing is excavated as part of the cutting process. However in severe squeezing conditions, the face extrusion may become important and it is difficult to control.
3. Difficult to control TBM direction in soft and heterogeneous grounds, e.g. when the machine is heading perpendicularly to the stratification or in case of bed separation and bulking (Barla 2001).

5 SOLUTIONS TO DEAL WITH SQUEEZING GROUND

5.1 *Selection of TBM type and modification of TBM*

1. Selection of TBM type. Based on the advantage and disadvantages of different TBMs listed in Table 3, select the TBM type depending on (Ramoni & Anagnostou 2010): i) how high the bearing capacity of the ground is in the gripper area; ii) how rapidly the convergences or ground pressure develop; iii) how much support had to be installed in the TBM area in order to stabilize the opening and control the deformation.
2. Modification of TBM. In special geological situations, due to the type of rock formation together with the tectonic actions and/or the overburden, immediate squeezing behavior the tunnel can occur and the TBM shall be designed to cope with these grounds. Some suggestions related to effective modification of TBM components are given in Table 4.

Table 3. Advantages and disadvantages of different TBMs (Ramoni & Anagnostou 2010).

TBM type	Advantage	Disadvantage
Gripper TBM	Shorter length greater flexibility of tunnel support	Lower thrust (gripper bracing problem) Lower AR (big support requirement)
Shielded TBM	Highly industrialized tunnel construction some recent technology higher thrust, torque	Longer shield length

5.2 *Condition of ground*

1. Apply proper support
   Two successful cases should be mentioned for this issue.
   i) The water transmission tunnel of the Yacambu project in Venezuela (Wittke et al. 2005). The tunnel is located in so-called squeezing rock (see Fig. 2). This tunnel was excavated by a tunnel boring machine (TBM-G) and supported by steel arches, shotcrete and anchors. However, the stiff support was overloaded because the rock adjacent to the tunnel became plastic due to high overburden. An adequate design would therefore have consisted of a shotcrete membrane with horizontal slots, fixed by yielding rock anchors (see Figs. 5–6). Such a support

Table 4. Modification of TBM components.

TBM component	Modification
Cutterhead	Larger cutterhead to have more space for deformation and rock support (Ehrbar 2008)
Power system	High thrust enough to overcome the resistance between the rock and shield
Cutterhead canopy	Shrinkable (see Fig. 4)
Overboring system	Increase the radial gap between shield/rock from 6–8 to 15–25 cm
Shield (Ramoni & Anagnostou 2010)	As short as possible Slightly conical As smooth as possible Bearing capacity, high enough for the ground pressure Higher deformability of the shield Flexible design of the rear part of the shield reduced rear shield diameter or collapsible rear shield design (Wittke 2005)
Back-up system (Ramoni & Anagnostou 2010)	To make the back-up trailers small enough relatively to boring diameter to gain some space in case of unexpectedly high ground deformations in the back-up area. Considering the intervention limitation in the back-up area when planning a TBM drive for squeezing ground and where necessary requirements must be formulated in the TBM specifications.
Mucking system design	Capacity should be attuned to the TBM advance rate, otherwise, it can cause packing of the muck around shield and then reduce the space available for deformations and may therefore lead to an earlier development of ground pressure upon the shield.
Support	Practically rigid support and yielding supports, for much information see Ref. (Ramoni & Anagnostou 2010)

would have allowed for radial displacements to enable the above cited arching action within the rock mass. After certain displacements combined with the partial closing of the slots, the remaining gaps would have had to be fixed thus creating a stiff support. This process is strongly time-dependent because of the time-dependent plastic behavior of the rock mass.

ii) Yacambú-Quibor tunnel (Schubert et al 2000). The 5 m diameter 23.3 km long Yacambú-Quibor tunnel is designed to carry water through the Andes from the Yacambú dam in the wet tropical Orinoco basin to the semi-arid but fertile Quibor basin, in western Venezuela. Over the 32 years (1976–2008) of construction approximately 30 different support designs were used and, in better rock conditions under moderate stress conditions, many of these designs were successful. However, in the very weak graphitic phyllites at depths of up to 1200 m below surface, squeezing could only be handled effectively by installing yielding support in a circular tunnel profile as shown in Figures 7–8.

2. Pre-treatment of the ground
Pre-treatment of the ground can be performed by grouting, reinforcement or drainage which are carried out basically either before or during the TBM drive (Ramoni & Anagnostou 2010):



Figure 4. Gripper TBM with shrinkable canopy used at Gotthard base tunnel (Herrenknecht 2009).



Figure 5. Shaft Konrad, yielding support in squeezing rock (Wittke et al. 2005).

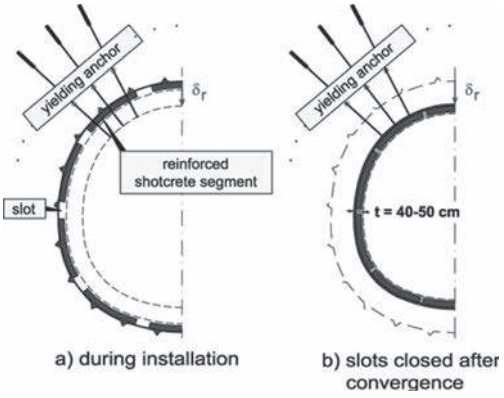


Figure 6. Yielding support, principle (Wittke et al. 2005).

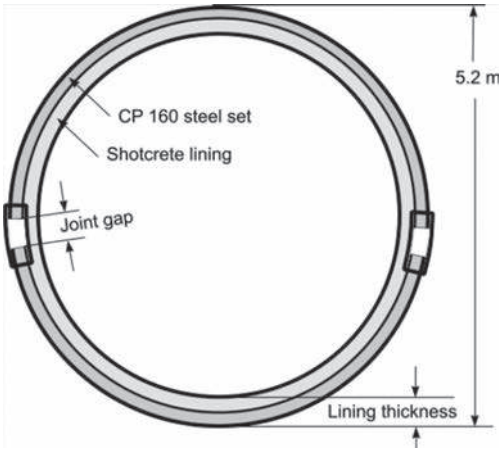


Figure 7. Design details of the yielding support used in the Yacambú-Quibor tunnel (Schubert et al 2000).



Figure 8. Assembled steel set with two sliding joints in the site workshop (Schubert et al 2000).

(i) The solution conducted before TBM drive is of course preferable as improvement work will not interfere with the TBM operation, however, it necessitates in nearly all cases the construction of an intermediate access tunnel or a pilot tunnel, which may also be technically demanding, costly and time-consuming. The pretreatment of the ground from the TBM itself during TBM drive does not require auxiliary structures, but slows down the TBM drive considerably. (ii) The applicability of grouting or drainage depends strongly on the ground characteristics. Squeezing rocks are unfavourable in this respect as they often have a high fraction of fines and, therefore a low permeability.

5.3 *Optimization of TBM operation*

1. Maintaining a high overall advance rate. by operational measures (applied systematically), appropriate construction site organization (necessary logistical precautions), cutting down standstill time as short as possible, also keeping necessary maintenance work, and considering holiday period and even the possibility and frequency of strikes (Ramoni & Anagnostou 2010).
2. Overboring. One of the effective measures to manage squeezing is overboring by overcutters, as shown in Figure 9, which can increase the radial gap between shield/rock from 6–8 to 15–25 cm, but the overboring technology still requires further development.
3. Deal with TBM jamming. Several solutions can be useful to free TBM as follows: providing high thrust, injecting proper lubricants to reduce the friction between outer shield surface and ground, and performing hand-mining (see Fig. 10) from the front shield and near the cutterhead (Barla 2001, Farrokh & Rostami 2009). If these measures still fail to work for a double shielded TBM, it has to perform openings on the telescopic shield at 4–5 m from the face and implement over-cutting through these openings.
4. Finding evidence of squeezing conditions during the excavation. This measure is very important and allowing the operator to prepare for upcoming unfavorable conditions. If known in advance, operators can implement measures to avoid TBM jamming and time-consuming activities of releasing the machine with manual labor. Two actions proposed by Farrokh and Rostami (2009) can be taken to perform squeezing prediction as follows:
   i) Based on TBM operational parameters (TBM thrust, torque) and some composite performance indexes. These parameters can play a very important role in predicting potential problems in ground conditions near the sections with high potential of squeezing. Preliminary findings show that unusual increase in re-gripping pressure, higher thrust than normal level, and sudden decrease in penetration rate are indicative of the upcoming squeezing situations.
   ii) Tunnel wall convergence monitoring method: directly measured by using a scaled instrument in the grout holes inside the segmental lining, or measured by comparing the available annular space around the segmental lining at the end of the tail shield (in vertical direction) and the annular space around the segmental lining in the non-squeezing ground.

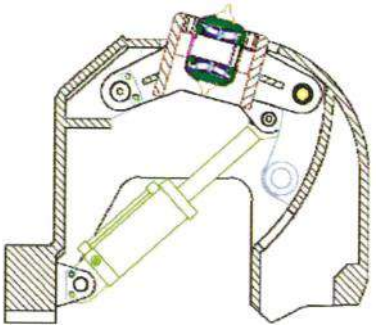


Figure 9. Robbins overcutters (Home 2009).



Figure 10. Hand mining around the front shield and stabilizing by wood timbers (Farrokh & Rostami 2009).

6 CONCLUSION

To better coping with squeezing ground encountered during TBM tunneling, several developments may be required as follows: the improvements of TBM technology for future applications; the fur-

ther study on fundamental theory and mechanism to better understand the rock-machine interaction under squeezing condition; the substantial attention given to prior engineering geological and hydrogeological investigations and analyses, in order to assist the flexible design of TBM tunneling.

REFERENCES

Anagnostou, G. & Kovari, K. 2005. Tunnelling through Geological Fault Zones. *Institute for Geotechnical Engineering,* ETH Zurich.

Aydan, Ö., Akagi, T. & Kawamoto, T. 1993. The Squeezing Potential of Rocks around Tunnels: Theory and Prediction. *Rock Mechanics and Rock Engineering* 26(2):137–163.

Barla, G. 1995. Squeezing rocks in tunnels. *ISRM News Journal* (3/4):44–49.

Barla, G. 2001. Tunnelling under squeezing rock conditions. *In: Euro Summerschool on Tunnelling Mechanics:* 169–268. Innsbruck.

Barla, G. & Pelizza, S. 2000. TBM tunneling in difficult ground conditions. In: GeoEng2000 – An International Conference on Geotechnical & Geological Engineering. Melbourne, Australia.

Deere, D. 1981. Adverse Geology and TBM Tunnelling Problems. *In: Proc. RETS, Society of Mining Engineers* 1:574–586.

Ehrbar, H. 2008. Gotthard base tunnel, Switzerland experiences with different tunneling methods, *International South American Tunnelling.*

Einstein, H.H. 1989. Design and analysis of underground structures in swelling and squeezing rocks. *Underground Structures Design and Instrumentation Developments in Geotechnical Engineering*: 202–262.

Farrokh, E. & Rostami, J. 2008. Correlation of tunnel convergence with TBM operational parameters and chip size in the Ghomroud tunnel, Iran. *Tunnelling and Underground Space Technology* 23:700–710.

Farrokh, E. & Rostami, J. 2009. Effect of adverse geological condition on TBM operation in Ghomroud tunnel conveyance project. *Tunnelling and Underground Space Technology* 24:436–446.

Herrenknecht M, Böckli O, Bäppler K. 2009. Gotthard Base Tunnel, Section Faido previous experience with the use of the TBM. *Proceedings of the Rapid Excavation and Tunnelling Congress, Las Vegas*: 1182–1205. SEM Inc. Littleton.

Home, L. 2009. Improving advances rates of TBMs in adverse ground conditions. *Geomechanics and Tunnelling* 2:157–167.

Kovari, K. 1996. Basic considerations on Tunnelling in Squeezing Rock. *International Journal of Rock Mechanics and Mining Science* 29:203–210.

Malan, D.F. 2002. Simulating the time-dependent Behaviour of Excavations in Hard Rock, *Rock Mechanics and Rock Engineeering* 35(4):225–254.

Ramoni, M & Anagnostou, G. 2010. Tunnel boring machines under squeezing conditions, *Tunnelling and Underground Space Technology* 25:139–157.

Ramoni, J. & Anagnostou, G. 2012. The Interaction Between Shield, Ground and Tunnel Support in TBM Tunnelling Through Squeezing Ground, *Rock Mech Rock Eng* 44(1):37–61.

Schubert, W., Fasching, A. & Goricki, A. 2006. Tunnelling in Fault Zones-State of the Art. In Lee, In-Mo, Yoo, Chungsik & You, Kwang-Ho (eds.), *Safety in Underground Space: Proc. of the ITA-Aites 2006 World Tunnel Congress*: 22–27 April 2006, Seoul: Elsevier; Tunnelling and Underground Space Technology 21 (2006): abstract 376–377.

Schubert, W., Moritz, B. & Sellner, P. 2000. Tunneling methods for squeezing ground, *Rivista Italiana di Geotecnica*:16–21.

Shang, Y.J., Xue, J.H., Wang, S.J. et al. 2004. A case history of Tunnel Boring Machine jamming in an interlayer shear zone at the Yellow River Diversion Project in China, *Engineering Geology* 71:199–211.

Steiner, W. 1996. Tunnelling in squeezing rocks: Case histories. *Rock Mechanics and Engineering* 29(4): 211–246.

Wittke, W., Gattermann, J.H. & Wittke-Gattermann, P. 2005. Some aspects for geotechnical investigations for TBM and NATM tunneling in rock. In Erdem & Solak (eds), *ITA-AITES World Tunnel-Underground Space Use: Analysis of the Past and Lessons for the Future*:693–699. Taylor & Francis Group, London.

This page intentionally left blank

Progress in Mine Safety Science and Engineering II – He et al. (Eds)
© 2014 Taylor & Francis Group, London, ISBN 978-1-138-00122-0

On the best escape route with multiple optimization objectives during mine fire time

W.M. Gai
School of Civil and Environmental Engineering, University of Science and Technology Beijing, Beijing, China
Chinese Academy of Governance, Beijing, China

W.M. Gai & Y.F. Deng
Chinese Academy of Governance, Beijing, China

J. Li
Institute of Public Safety, China Academy of Science and Technology, Beijing, China

Y. Du & B. Cao
School of Civil and Environmental Engineering, University of Science and Technology Beijing, Beijing, China

ABSTRACT: Based on the theories of operations research, a mathematical model for the best escape route during mine fire time is built in this paper, which serves the multi-objective optimization process. An approximate search algorithm with multiple optimization objectives is proposed for the model based on heuristic algorithm, which could find out the shortest escape route from the multiple—weight escape route network by constructing auxiliary functions. Along with the study case of the mine fire emergency rescue system of a coal mine, the algorithm procedures are introduced, the convergence rate of the algorithm are analyzed, and the time complexity and the strengths of the algorithm are discussed. By this algorithm, decision makers can find out the optimum rescue route on the tunnel distribution sketch map of a coal mine, thus realizing the multiple optimizing targets, and providing strong technical support for mine fire rescue under mine.

1 INTRODUCTION

In the event of coal mine fire, there will be a serious threat to the lives and safety of the underground staff, so the mine fire is one of the major threats of the coal mine production safety. The Coal mine underground space is at a premium and the mine tunnel complex Unicom, it will generate a lot of heat, toxic and hazardous fumes in case of fire, and these toxic gases in the mine are more difficult to dissipate. Therefore, the pros and cons of the escape route will affect the degree of injury on the health of persons in accidents. Choose the best relief route and escape routes, however, are a more difficult task. Accidents and heavy casualties are due to the wrong choice of relief and escape routes during mine fire time at home and abroad. In order to assist the relief commander decisions, reduce errors, it is necessary to use the computer to choose the best relief and escape routes (GAO R et al. 2008, WAN D et al. 1994, WANG D M et al.).

The mine fire escape routes discussed in this article sometimes need to consider a number of optimization targets. With the development of computer technology, there have been some studies on the optimization of emergency rescue plan, and the shortest path algorithm is a classical algorithm to solve the optimization problem, such as Dijkstra algorithm, Floyd algorithm (YU G & Yang J 1998, Current J & Marsh M 1993). However, these algorithms are more often than not limited to single-objective optimization (GAO R et al. 2008, YANG H C & SUN B 2011, XIAO G Q et al. 2001). For the optimization of major emergency rescue programs discussed in this paper, multiple optimization goals need to be taken into consideration at the same time, so we need to find a workable compromise between these goals in the solution process. Current has summarized and classified the researches on multiple—objective shortest paths and he pointed out that the usual approach is by linear weighting of different targets or converting one goal into a constraint. However, on one hand, the weight of the first method is very difficult to determine, on the other hand, the constrained shortest path problem has proved to be an NP-complete problem, so sometimes it is not

possible to obtain the solution if we adopt the second method, which is obviously not suitable for the need of fast solution for the emergency evacuation optimization problem (GAO R et al. 2008, CURRENT J et al. 1990, WEI H et al. 2005, HAO G et al. 2007, LIU J et al. 2007).

A multi-objective optimization model of escape route and its algorithm are proposed in this paper, which can meet the need of optimizing the different goals of emergency evacuation at the same time and solving the results quickly. In this algorithm, the Dijkstra algorithm is called by constructing auxiliary function, and some of the optimization goals are converted into a constraint, then the structure weight shortest is iteratively solved to find the minimum value of the main optimization goal.

2 OPTIMIZATION MODEL FOR ESCAPE ROUTE DURING MINE FIRE ACCIDENTS

2.1 *Problem description*

The intricate paths in the vicinity of the roadway underground can be seen as a connecting network from the perspective of graph theory. In the network graph, the paths are equivalent to the edges and the paths' intersections are equivalent to the vertices. When the selection factors of escape route in the undirected network graph are given, the escape route optimization problem in the layout network of the entire roadway underground can be converted into a graph topology optimization problem.

In order to evacuate the affected people to safe areas in time during mine fire emergencies, it is very important to select the best program among the many possible alignments to assist evacuation. There are double impact factors in choosing the escape route for disaster victims: the disaster victims' prevailing time (generally measured by the "equivalent length" (XIAO G Q et al. 2001)), and the impact on the health of persons walking on the roadway (death, injury and so on).

Considering the roadway itself and the catastrophic impact, the influencing factors on human walking speed can be seen as a corresponding coefficient to calculate the equivalent length of the lanes when solving the best relief route (Li G 2000, Fu E J & Tang A D 2006, Li S L et a1. 1999),

$$L_{ij} = k_{\mathrm{h}} k_{\mathrm{t}} k_{\mathrm{g}} k_{\mathrm{v}} \cdot l_{ij} + \sum_{\mathrm{j}=1}^{n_{\mathrm{ob}}} l_{ijm} \tag{1}$$

where, L_{ij}, l_{ij} = equivalent length and actual length of the roadway between node i and j; l_{ijm} = equivalent length of the m-th access obstacles, $1 \le m \le n_{\mathrm{ob}}$; n_{ob} = number of local obstacles of the roadway between node i and j; k_{h}, k_{t}, k_{g}, k_{v} = influence coefficients which depend on the height of the tunnel, the tunnel transport, roadway slope and wind speed on the roadway respectively. The conditional probability p_{ij} of the various consequences (death, injury, etc.) of the personal Walking in the roadway between nodes i, j after mine fire occurs, can be calculated by the corresponding "probability variable" (STRICKLAND J A & FOUREMAN G L 2002, GUTH D J et al. 1997, LEEK K W 2002):

$$p_{ij} = \frac{1}{\sqrt{2\pi}} \int_{-\infty}^{Y-5} \exp\left(-\frac{u^2}{2}\right) du \tag{2}$$

where, Y = random variable, and $Y = k_1 + k_2 \ln(D_{ij})$; k_1, k_2 = risk parameters dependent on the type of the accident; D_{ij} = subjected dose of the thermal radiation or toxic gases when the accident victims walking in the roadway, it can be obtained through the human body the fragile model (ZHOU Y F & LIU M 2011).

As a classic problem of graph theory, the definition of the shortest path is to identify a path with minimum weight between two vertices in a weighted graph. If the equivalent length of the path is taken as the weight of the edge, the optimization goal of choosing the rescue route is to realize the minimization of the total equivalent length of the route between the rescue base and the affected location. And if the impact on the health of persons walking on the roadway is taken as the weight of the edge, the optimization goal is that the average death probability on the route does not exceed the total amount of available oxygen. For the policymakers of escape route optimization program, it is necessary to ensure the efficiency of the rescue work as well as the safety of the affected personnel underground, i.e., to find the shortest path in the network containing two weights.

In summary, in addition to the main goal, there is a secondary optimization objective considered in this paper, i.e. the limiting condition. Based on graph theories and methods, the rescue route optimization problem considered in this paper can be described as: for network G = (V, E) in which $V(G) = \{v_i\}$ is a set of nodes in graph G, any vertex $v_i \in V(G)$ corresponds to point (x_i, y_i) in the plane; $E(G) = \{e \mid e = (v_p, v_q) = (v_p, v_q); v_p, v_q \in V\}$ is the set of edges of graph G, $|E| = n_e$, $|v| = n_v$, $F_1(p)$ represents the total equivalent length of a route from the rescue base to the affected location, i.e., the main optimization objective function, $F_2(p)$ represents the the victimized degree of persons' health, on the route from the affected location to the safe area,

i.e., the secondary optimization objective function, and $F_1(p), F_2(p) \geq 0$. w_1 and w_2 are the corresponding weights of the edges to the primary optimization target and the secondary optimization target. Assign different weights to the edges of the graph G according to the two optimization objectives, and we can get the optimal rescue route from node s to node t. In this way, the isomorphic relationship is established between the optimization of rescue route during gas leak emergencies and a complete graph containing double weights. The shortest route problem is a classic problem in graph theory, but the traditional algorithms can't directly find out the shortest path of double-weighting network graph. So we need to establish a reasonable mathematical model and design a suitable algorithm for the model according to the specific situations in practice.

2.2 *Establishment of optimization model of rescue routes for mine fire emergencies*

In order to get the bi-objective path selection model of the time-varying network, suppose F_1 as the main optimization objective, and F_2 as the secondary optimization objective. P denotes a feasible path (applicable scheme) from node *s* to node *t,* and the bi-objective shortest path model can be expressed as follows:

$$F_1(p^*) = \min F_1(p) \tag{3}$$

$$F_2(p^*) \leq l_t \tag{4}$$

$$F_1(p) = \sum_{(i,j)\in p} w_{1_{ij}} \tag{5}$$

$$F_2(p) = \sum_{(i,j)\in p} w_{2_{ij}} \tag{6}$$

Where, p^* = optimal solution for the model if p^* can satisfy both formula (3) and (4); P = collection of all feasible paths from node *s* to node *t,* $p \in P$; S = collection of the paths that meet equation (4); w_{1ij} = the target weight of the edge (v_i, v_j); w_{2ij} = restriction weight; l_t = maximum permissible value of the secondary optimization objective.

3 ON ALGORITHM FOR THE BEST ESCAPE ROUTES DURING MINE FIRE EMERGENCIES

In 1996, Zhan and Noon tested with actual traffic network 15 of the 17 algorithms previously tested by Cherkassty, and the test results showed that the fastest algorithm to calculate the shortest path is the Dijkstra algorithm. The Dijkstra algorithm is only applicable to solving the shortest path for the network with one weight, and cannot directly solve the shortest path problem of network graph with double weights (CURRNT J et al. 1990). An optimization model of rescue route and its algorithm are proposed in this paper, which can meet the need of optimizing the multiple goals at the same time and solving the problems quickly.

3.1 *Auxiliary functions and their properties*

In order to solve the shortest path problem for the double weighting network, a new weight for graph G is constructed with the target weight w_1 and limit weight w_2 and w_3, which is expressed as $w = \alpha w_1 + (1 - \alpha) w_2$, and $w_2 = (k_1 w_2 + k_2 w_3)$ $(0 \leq \alpha \leq 1)$. If there is a feasible path *p* from the specified source node *s* to the destination node *t,* a function can be established as follows:

$$f(\alpha) = \sum_{e_i \in p} \left[\alpha w_1(e_i) + (1-\alpha) w'_2(e_i) \right] \tag{7}$$

For any $\alpha \in [0, 1]$, p_{st} is the shortest path that satisfies min $f(\alpha)$ by Dijkstra algorithm. According to formula (5), (6), the corresponding target function values $F_1(p_{st})$ and $F_2(p_{st})$ of p_{st} can be obtained respectively. There is also a corresponding value *a* in the interval [0, 1] for each value of $F_1(p_{st})$ (also $F_2(p_{st})$). $F_1(p_{st})$ and $F_2(p_{st})$ are actually functions of the parameter α, respectively referred to as $F_1(p) = f_1(\alpha)$ and $F_2(p) = f_2(\alpha)$, wherein $0 \leq \alpha \leq 1$ and $p \in$ P. These two functions have the following properties:

Property 1: $f_1(\alpha)$ is a decreasing function on [0, 1] with its value minimized when $\alpha = 1$; $f_2(\alpha)$ is an increasing function on [0, 1], with its value minimized when $\alpha = 0$.

Proof Procedure of Property 1: Apply the Dijkstra algorithm and we obtain p_{st1}, p_{st2} that respectively satisfy min $f(\alpha_1)$ and min $f(\alpha_2)$ and $\alpha_1 < \alpha_2$. Based on equation (5) to (7), $\alpha_1 \cdot F_1(p_{st1}) \leq (1 - \alpha_1) \cdot F_2(p_{st1}) \leq \alpha_1 \cdot F_1(p_{st2})$ $(1 - \alpha_1) \cdot F_2(p_{st2})$, $\alpha_2 \cdot F_1(p_{st1}) \geq (1-\alpha_2) \cdot F_2(p_{st1}) \geq \alpha_2 \cdot F_1(p_{st2}) + (1 - \alpha_2) \cdot F_2(p_{st2})$. So $\alpha_1 (F_1(p_{st1}) - F_1(p_{st2})) + (1 - \alpha_1) (F_2(p_{st1}) - F_2(p_{st2})) \leq 0$, $\alpha_2 (F_1(p_{st1}) - F_1(p_{st2})) + (1 - \alpha_2) (F_2(p_{st1}) - F_2(p_{st2})) \geq 0$. Also $0 \leq \alpha_1 < \alpha_2 \leq 1$, so $F_1(p_{st1}) - F_1(p_{st2}) \geq 0$, $F_2(p_{st1}) - F_2(p_{st2}) \leq 0$, i.e., $f_1(\alpha_1) \geq f_1(\alpha_2)$, $f_2(\alpha_1) \leq f_2(\alpha_2)$. So it can be concluded that $f_1(\alpha)$ is a decreasing function, and $f_2(\alpha_1)$ is an increasing function. As $0 \leq \alpha \leq 1$, so $f_2(\alpha)$ has a minimum value when $\alpha = 0$, and $f_1(\alpha)$ has a minimum value when $\alpha = 1$.

Proof Procedure of Property 2: When $\alpha = 0$, $w_3 = w_2$, then min $f(0) =$ min $F_2(p) = f_2(0)$. If $f_2(0) > l_t$, then p^* has no solution. If the path p_{st} that satisfies min $f(\alpha)$ exists and $\alpha = 1$, $w_3 = w_1$, then min $f(1) =$ min $F_1(p) = F_1(p_{st})$ (wherein $p, p_{st} \in$ P). If $f_2(1) \leq l_t$, it can be concluded that $f_2(\alpha) \leq l_t$ is true of all

$\alpha \in [0, 1]$ according to the properties above. And according to formula (1), (2), $p^* = p_{st}$.

If the interval [0, 1] is divided into n subintervals of equal span, $k = 0, 1, 2,\ldots, n - 1$. Assume $\alpha = 0$, and we get the path p_0 that satisfies min $f(\alpha)$: $f_2(0) = l_{t0}$. Assume $\alpha = 0$, and we get the path p_1 that satisfies min $f(\alpha)$: $f_2(1) = l_{t1}$. Based on the above properties of the constructed auxiliary functions, we can deduce the following conclusions:

Conclusion 1: When $\alpha = k$ / n, the path p_{st} that satisfies min $f(\alpha)$ exists, and as $f_2(\alpha) = l_t$, there can be no other path $p \in$ P that satisfies both $p \in$ S and $F_1(p, s, t) < F_1(p_{st})$.

Conclusion 2: If the path p_1 that satisfies min $f(\alpha)$ exists when $\alpha = k/n$, and $f_2(\alpha) < l_t$, and the path p_2 that satisfies min $f(\alpha)$ exists when $\alpha = (k + 1)/n$, and $f_2(\alpha) > l_t$, then according to Property 1 and 2, it can be concluded that there may be another path $p \in$ P that satisfies $F_2(p_1) \le F_2(p) \le l_t$, and $F_1(p_2) \le F_1(p) \le F_1(p_1)$.

Conclusion 3: If we assign to a all the possible of k / n ($k = 0, 1, 2,..., n - 1$), and solve all paths that satisfy min $f(\alpha)$, we can obtain the trend curves of the two objective functions f_1 and f_2. According to f_1 and curve f_2, if the limit of the secondary optimization goal is set differently, then we will obtain different optimal solutions of p^*: if $l_t \ge l_{t1}$, then $p^* = p_1$; if $l_t = l_{t0}$, then $p^* = p_0$; if $l_t \ge l_{t1}$, then p^* has no solution and if $l_{t0} < l_t < l_{t1}$, then a series of sampled values of the optimal solutions that satisfy $f_2(\alpha) \le l_t$ will be obtained in the interval [0, 1] by applying the segmentation method, and the path that satisfies min $f_1(\alpha)$ among these sampled values is the optimal solution p^*.

3.2 *Optimization search algorithm*

Assume that the optimal path p^* from the source node s to the target node t exists, $\alpha \in [u, v]$ (wherein $0 \le u, v \le 1$), from Conclusion 1 and 2 we know that if path p_u and p_v that satisfy min $f(\alpha)$ exist when $\alpha = u$ and $\alpha = v$, and $f_2(u) < l_t$, $f_2(v) > l_t$, then p^* can be determined within interval $[u, v]$ by the previously constructed auxiliary functions. The interval $[u, v]$ is referred to as the approximate range of the optimal path. And path p_u is an approximate solution of the optimal path, referred to as p^{app}. If the path that satisfies min $f(\alpha)$ exists and is obtained when $\alpha = \alpha^*$ i.e., $f_2(\alpha^*) = l_t$, then the path obtained is the optimal solution p^* that we mean to find.

In accordance with the properties and conclusions in the Section 2.1, if the $[u, v]$ is divided into n subintervals of equal span,, $k_i = 1, 2,\ldots, n - 1$, and if there exists an optimal or approximate optimal path, then we can search iteratively for the solution in the current approximation interval $[u, v]$ until the optimal solution is obtained. The path that satisfies min $f(\alpha)$ can be obtained by calling the Dijkstra algorithm. Therefore, steps of the bi-objective optimiFation search-type algorithm can be described as follows:

1. $\alpha \leftarrow 1$, the Dijkstra algorithm is called to seek path p_1 that satisfies min $f(\alpha)$ from the source node s to the destination node t.
2. If $F_2(p_1) \le l_t$, $p^* \leftarrow p_1$, the algorithm ends; else $\alpha \leftarrow 0$, the Dijkstra algorithm is called to seek the path p_0 that satisfies min $f(\alpha)$ from the source node s to the destination node t; else if $F_2(p_0) > l_t$, there is no solution, then the algorithm ends; else if $F_2(p_0) = l_t$, $p^* \leftarrow p_0$, the algorithm ends; else $p^{app} \leftarrow p_0$, $u \leftarrow 0$, $v \leftarrow 1$, $i \leftarrow 1$.
3. $\Delta \leftarrow (v - u) / n$, $k \leftarrow 1$.
4. $\alpha \leftarrow u + k \cdot \Delta$, the Dijkstra algorithm is called to seek the path p_{ik} that satisfies min $f(\alpha)$ from the source node s to the destination node t.
5. If $F_2(p_{ik}) = l_t$, $p^* \leftarrow p_{ik}$, the algorithm ends; else if $F_2(p_{ik}) < l_t$, $p^{app} \leftarrow p_{ik}$, $u \leftarrow \alpha$, if $k = n - 1$, go to step (7); else $v \leftarrow \alpha$, go to step (7).
6. $k \leftarrow k + 1$, go to step (4).
7. $i \leftarrow i + 1$, if $i \le m$, go to step (3).

Take the disaster rescue project of a coal mine in Xuzhou as an example. Selected a site of the accident, and then import the geographic information data of roadway underground. The affected location, node (0, 0), is the source node, and the node (3, 2) is the destination node. The path network between the source node and the destination node is defined as a network diagram, the roadway being the edges of the graph, and the intersections being the nodes of the graph. The number of nodes demonstrates the scale of the graph. According to the optimization objectives, the equivalent

Table 1. Input data of original problem.

Number	Path	Equivalent length m	Death probability
0	(0, 0) – (0, 1)	500	0.078
1	(0, 0) – (1, 0)	333	0.063
2	(0, 1) – (0, 2)	300	0.039
3	(0, 1) – (1, 1)	167	0.052
4	(0, 2) – (1, 2)	100	0.051
5	(1, 0) – (1, 1)	250	0.078
6	(1, 0) – (2, 0)	250	0.090
7	(1, 1) – (1, 2)	200	0.026
9	(1, 2) – (2, 2)	100	0.064
10	(2, 0) – (2, 1)	167	0.051
11	(2, 0) – (3, 0)	200	0.06
12	(2, 1) – (2, 2)	143	0.0199
13	(2, 1) – (3, 1)	125	0.05
14	(2, 2) – (3, 2)	91	0.058
15	(3, 0) – (3, 1)	125	0.02
16	(3, 1) – (3, 2)	111	0.031

Table 2. Simulation results.

Contrast content algorithm		Optimal route	Total equivalent length (m)	Average death probability
Dijkstra Algorithm	The Path of the Shortest Equivalent Length	[(0, 0), (1, 0), (1, 1), (2, 1), (3, 1), (3, 2)]	1135	0.036
	The Path of the Shortest Equivalent Length Health Risk	[(0, 0), (1, 0), (1, 1), (3, 0), (3, 1), (3, 2)]	9600	0.0308
Optimization Research Algorithm		[(0, 0), (1, 0), (2, 0), (2, 1), (3, 1), (3, 2)]	1020	0.032

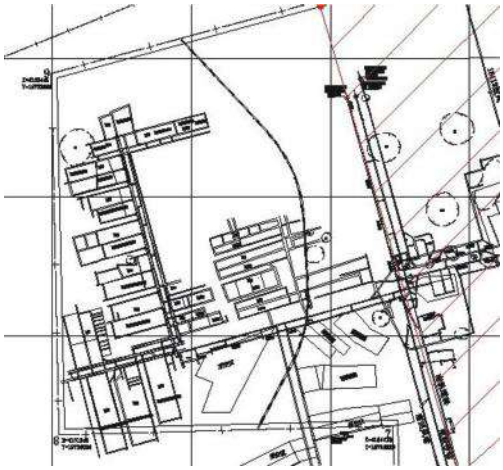


Figure 1. Mine roadway layout diagram.

length of the route and the death probability on the roadway on the path are three different weights of the edges. Assign random weights to each edge of the graph, and compile and run the optimization search algorithm, then we can obtain the best escape route from node (0, 0) to node (3, 2). For the input parameters and the optimization results, see Table 1 and Table 2, where the limit value of total oxygen consumption is 51 ml. Compared with the Dijkstra algorithm, the obtained optimization solution by applying the optimization search algorithm can meet the optimization objectives of the equivalent length and the death probability on the roadway at the same time. Mine roadway layout diagram seen in Figure 1.

The user layer of the bi-objective optimization system is developed in c # language of the. net architecture. The underlying layer is developed by using the NetworkX Library of Python and directly calling the packaged Dijkskra algorithm. The data can be imported from EXCEL or dynamically read from the database (ZHOU Y F & LIU M 2011, ZHOU Y D 2008).

4 PAPER SUBMISSION

In this paper, the mathematical model of the rescue route with multi-objective optimization during mine fire emergencies is built by applying the graph theory and optimization method in operations research, and the optimization search algorithm for the model is proposed. The weight of the path network in multi—objective optimization problems is easily determined by applying this algorithm, the convergence of the algorithm is faster, and the optimal solution obtained is an approximate optimal solution. The model is applicable not only to the rescue route optimization problems, but also to other optimization problems.

The proposed algorithm is not only helpful to the decision makers to solve the problems of emergency evacuation route optimization, but also to propose problems based on the two trend curves of objective functions by applying the algorithm.

ACKNOWLEDGEMENT

This paper is supported by and National Natural Science Foundation of China under Grant 71173198, National Science and Technology Support Program of China under Grant 2012BAK03B05 and 2012BAK20B02.

REFERENCES

Current, J. & Marsh, M. 1993. Multi objective transportation network design and routing problems: taxonomy and annotation. European Journal of Operational Research, 65: 1–6.

Current, J. et al. 1990. An interactive approach to indentify the best compromise solution for two objective Shortest path problems Computer & Ops. Res., 17 (2): 187–192.

Fu, E.J. & Tang, A.D. 2006. Choose the Optimum escape route during mine fire. *Saf Coal Mines,* 383: 32–35.

Gao, R. et al. 2008. Mathematical model and algorithm of a dynamic optimum rescue route during mine fire

time based on Map Object. Journal of University of Science and Technology Beijing, 30(7):705–709.
Guth, D.J. et al. 1997. categorical regression analysis of acute exposure to tetra-chloroethylene. Risk Analysis, 17(3):321–332.
Hao, G. et al. 2007. A Fast Algorithm for Bi-objective Shortest Path. Journal of Highway and Transportation Research and Development, 24(11):96–104.
Leek, K.W. 2002. A methodology for assessing risk from released hydrocarbon in an enclosed area. Journal of Loss Prevention in the Process Industries, (15):11–17.
Li, G. 2000. Study On Mine Safety Monitoring and Production Dispatching System Based on GIS. Xuzhou: China University of Mining & Technology.
Li, S.L. et a1. 1999. The confirmation of the best route for evading accident under the pit. Liaoning Technical University (Natural Science), 18(1): 27–30.
Liu, J. et al. 2007. Maximum constrained capacity path problem in networks with double weights. Journal of Yunnan University, 29 (S1): 1–3.
Pan, X.T. 2008. Analytical model based on the Python controls to achieve. Beijing: China University of Geosciences.
Strickland, J.A. & Foureman, G.L. 2002. US EPA's acute reference exposure methodology for acute inhalation exposure. The Science of the Total Environment, (288):51–63.
Wan, D. et al. 1994. Travel ability of shaft and roadway in a mine fire hazard and selection of optimal rescue and escape routes. Journal of China Coal Society, 19(1):58–64.
Wang, D.M. et al. 1996. Mine Fire Rescue Decision—Making Support System. Beijing: China Coal Industry Press.
Wei, H. et al. 2005. An approach to bi-objective shortest path. Systems Engineering, 23(7):113–117.
Xiao, G.Q. et al. 2001. Shortest Evacuation Route on Toxic Leakage. Journal of Northeastern University (Natural Science), 22(6): 674–679.
Yang, H.C. & SUN, B. 2011. Optimization of evacuation based on PERT and shortest path theory. Fire Science and Technology, 30(2):103–107.
Yu, G. & Yang, J. 1998. On the robust shortest path problem. Computer & Ops. Res., 25: 457–461.
Zhou, Y.D. 2008. A python calculation grid based on service-oriented parallel Computing. Shanghai: Shanghai Jiao Tong University: 19–45.
Zhou, Y.F. & Liu, M. 2011. Risk analysis of major accidents in chemical industry areas. Journal of Disaster Prevention and Mitigation Engineering, 31(1):68–73.

Progress in Mine Safety Science and Engineering II – He et al. (Eds)
© 2014 Taylor & Francis Group, London, ISBN 978-1-138-00122-0

Mine sewage control system using PLC technology

Jing Jiang
North China Institute of Science and Technology, Beijing, China

Xuesong Zhang
National Laboratory of Electro-Optics System Technology, Hebei, China

ABSTRACT: Due to sewage affect on the environment becoming more and more seriously, sewage of mine was needed to treat urgently. In this paper, we have used the Sequencing Batch Reactor Activated Sludge Process to meet the needs of drainage control system, but the method was so complicated. Only automatic control part of this method was realized, strengths of Sequencing Batch Reactor Activated Sludge Process were played. Programmable Logic Controller from Mitsubishi FX2N Series was used in the automatic control system of sewage treatment with stable operation, low cost, good effect and so on.

Keywords: Sequencing Batch Reactor Activated Sludge Process; sewage treatment; Programmable Logic Controller

1 INTRODUCTION

The problem of mine sewage must be urgently resolved due to the increasing sewage problems from coal mine on the surrounding environment. According to different principles of wastewater treatment technologies, wastewater treatment technology was divided into physical method, chemical method and biological method. Among, biological method was defined that organic pollutants from sewage water were converted and absorbed by the degradation roles of microbial biological. In common, biological methods can be divided into activated sludge method, AB method, bio-film method, oxidation ditch method, and so on.

SBR method is the sequencing batch reactor activated sludge process, which is an activated sludge wastewater treatment technology by continuous feeding, intermittent drainage and cycle intermittent aeration. SBR is a predecessor of Fill-and-Draw system by intermittent operation, which is an improvement of activated sludge reactor fully produced by the early twentieth century (Wang Dayu 2001). In 1912, Clark and Gage form the United Kingdom had found that long time aeration of the wastewater will produce sludge, and water quality will be improved. In 1914, Alden and Lockett had found that the aeration of the sewage were static precipitated, the clean water were tossed away and the sludge were leaved in the bottom for the next wastewater treatment. The time used in the waste water treatment was significantly reduced by above method (Li Hai, 2002). However, due to some technology problems could not be solved technical such as cumbersome manual management, monitoring technology backward, aeration equipment blocked etc., we found it difficult to expand the applications at that time. In the early seventies, R. Irvine and other researchers from NaMe Dame University in the United States had proposed that SBR can be used as a better alternative technology in the continuous flow activated sludge process (CFS) by compared and researched the characteristics of SBR and CFS in the experiments (Wang Youle 2002). In the 80s of 20th century, due to the rapid development and application of automation and computer technology in the field of wastewater treatment, the activated sludge wastewater treatment technology had gain significant progress (Zhang Yu 2009). Since mid-90 s, the research and application of SBR technology were begun in our country, but most SBR technology was in the pilot stage or in the application stage of small sewage treatment.

2 SBR PROCESS FLOW

SBR is a biological method, which is an activated sludge wastewater treatment technology under intermittent aeration. Different from the traditional wastewater treatment process, the operation mode of space partitioning was placed by time division technology, steady-state biochemical reactions was placed by non-stable alternative technology; the traditional dynamic precipitation

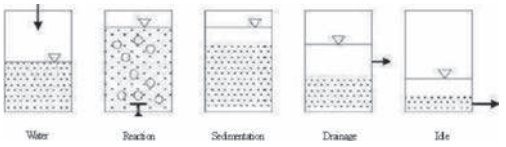


Figure 1. Five processes of SBR.

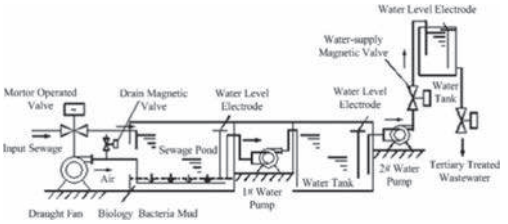


Figure 2. Wastewater treatment system schematic.

was placed by ideal standing precipitation technology in the SBR technology. SBR process technology is an advanced sewage treatment systems, which including the follow steps (Nandalal K D W 2003), that is, regulation, primary sedimentation, aeration, secondary sedimentation and biological nitrogen removal process in one pool. According different time to operate various steps, the whole process were run in a pool again and again, simple process, compact and reasonable.

The above technique can effectively remove BOD5 and Suspended Solids (SS) in the wastewater. Nitrogen compounds were converted to nitrate in the wastewater, and then be converted to ammonia, so the concentration of ammonia (NH_3-N) will be significantly reduced in the output water. SBR was mainly used in small-scale wastewater treatment process. In this paper, the automatic control system of sewage treatment from mine was designed. A partition wall was placed in the SBR reaction tank, which divided reaction tank into two parts, pre-reaction zone and the main reaction zone. There was a connected hole in the bottom of the wall. Water, reaction, sedimentation, drainage and idle five processes (Otterhl R, Grottker M 1997) in the each cycle are carried out in the same pool again and again, shown in Figure 1.

3 DESIGN OF ELECTRICAL CONTROL SYSTEM

SBR technology is a more advanced process technology due that SBR meets the basic needs of sewage treatment of coal mine. However, the typical shortcomings of SBR method is operated complexity, SBR method could play to its strengths after achieve automatic control. Although some sewage treatment plant have automated to some extent, most of the traditional control methods were used, namely, control ineffective. Time process control are mainly based on the pre-set time to implement automatic control from five running phase of SBR, that is, water, reaction, deposition, emissions, idle. However, sewage quality and quantity were varies with time, the sewage treatment process has significant time variation, so the dynamic behavior and operating characteristics must be more considerate. Sometimes, the concentration difference between organic matters were several times, if SBR method was used to control on the same response time, the quality of sewage treatment were constrained due to run water quality fluctuations (Zeeman G, Sanders W 2000). A more effective control method was required to ensure reliable operation of treatment systems in the method of SBR.

3.1 *Technical requirements of SBR wastewater treatment process*

SBR wastewater treatment technology is a highly efficient wastewater reuse technology, which used advantage bacteria technology to treat on life wastewater. The treated water can be used to irrigate green areas, flowers, flush toilets and vehicles, so as to conserve water resources. The program of SBR wastewater treatment system must fully consider narrow features in the life area to make the devices small, stable, less investment purposes. Wastewater treatment efficiency were directly affected by bacterial metabolism due to environmental temperature change in the wastewater treatment process, so a buried structure treatment pond was used to reduce the temperature effect of the wastewater treatment.

Meanwhile, considered SBR parameters change, hardware design and equipment debug complex in the process of wastewater treatment, using advanced PLC control technology can improve the efficiency of SBR wastewater treatment and easy to operate. SBR wastewater treatment system were composed by the sewage treatment pond, clear water tank, water tank, electric control box and pump, Roots blower, electric valves, solenoid valves and other components. Level switches were set to detect the water level of ponds and tanks in the sewage treatment pool, clear pool, water tank. The schematic of SBR wastewater treatment system was shown in figure 2.

3.2 *Power equipment of SBR wastewater treatment system*

Three-phase AC induction motors were used in the power equipment (pump, Roots blower,

electric valves) of SBR wastewater treatment system, waterproof and moisture-proof type of motors and solenoid valve were matched. 1# Clean Water Pump: Vertical Centrifugal LS50–10-A, head 10 M, flow 29 M3/h, 1 kW; 2# clean water pumps: vertical centrifugal pumps LS40-32.1, head 30 M, flow 16 M3/h, 3 kW; aeration Roots Blower: TSA-40, 0.7 M3/Min, 1.1 kW; electric valve: body D97A1X5-10ZB-125 MM, electrical equipment LQ20-1, 380V/60 W (three phase), torque 200 N·M, speed 1r/Min.

Consider of the interference performance, corrosion resistance electrodes were used in the level detection switch of water pool, clear pool, water tank. With PLC own 24 V DC power supply, the power supply capacity were considered when external load. The third grounding was used to improve anti-jamming capability in the PLC ground terminal.

4 HARDWARE DESIGN OF CONTROL SYSTEM

4.1 *Main circuit design*

Define abbreviations and acronyms the first time they are used in the text, even after they have been defined in the abstract. Abbreviations such as IEEE, SI, MKS, CGS, sc, dc, and rms do not have to be defined. Do not use abbreviations in the title or heads unless they are unavoidable.

1# water pump M1, 2# Pump M2, aeration fans M3 were respectively controlled by the main circuit contactor KM1, KM2 and KM3. Electric valve motor M4 was controlled by AC contactor KM4 and KM5 to complete open and close function of valves. The overload protection of Motor M1, M2, M3 and M4 were implemented by thermal relay FR1, FR2, FR3 and FR4. Thermal protection switches with closed were also equipped with electric valve motor M4 to achieve dual protection of valve motor M4. Short-circuit protections of the load circuit were achieved by the Fuse FU1, FU2, FU3 and FU4. The short circuit protection of AC control loop and PLC control loop were respectively realized by FU5 and FU6. The main control circuit figure of SBR wastewater treatment system was shown in figure 3.

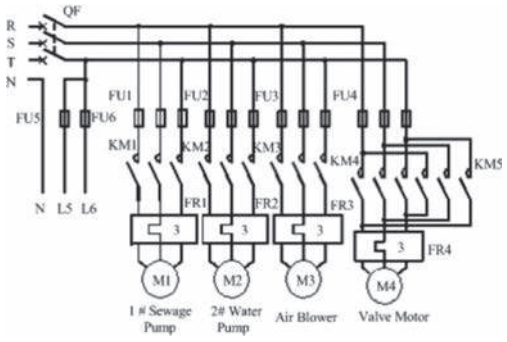


Figure 3. Main electric circuit of SBR wastewater treatment control system.

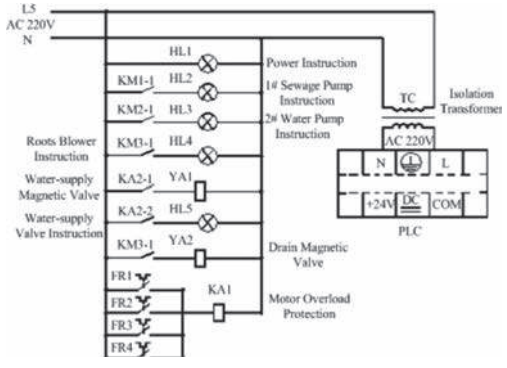


Figure 4. AC control circuit of SBR wastewater treatment system.

4.2 *AC control circuit design*

The isolation transformer TC was used in the PLC power supply circuit to prevent power interference. According to the electricity consumption of PLC, isolation transformer TC was configured with the standard, variable ratio of 1:1, the capacity of 100 VA transformer. The power instruct lights HL were set in the control circuit, that is, 1# clear water pump M1, 2# clear water pump M2, indicating lamps HL1, HL2 and HL3 were also set in the aeration air blower M3. The above instruct lights were controlled auxiliary switch of contact device KM1, KM2 and KM3. The overload protection of M1, M2, M3 and M4 were realized by four thermal relay FR1, FR2, FR3 and FR4. Overload protect was composed by closed-switch of contact KM1 and intermediate relay KA1, KA1 has also played the role of voltage conversion, the 220 V AC signal was converted into DC 24 V signals, which was sent into the PLC to complete overload control.

Water-supply solenoid valve YA1 and indicator lamp HL1, drain valve YA2 were controlled by the contactors of intermediate relay KA2 and KA3. The AC control circuit of SBR wastewater treatment system was shown in figure 4.

4.3 *PLC control circuit design*

The schematic diagram of PLC control circuit in the SBR wastewater treatment system was shown

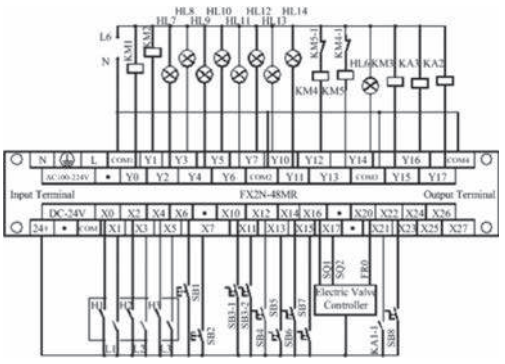


Figure 5. Circuit schematic of SBR wastewater treatment system on PLC.

Table 1. Input interface table of SBR wastewater treatment system based on PLC.

No	Station name	Symbols	Input
1	High Water Level Switch Signal of Sewage Pool	H1	X000
2	Low Water Level Switch Signal of Sewage Pool	L1	X001
3	High Water Level Switch Signal of Clear Pool	H2	X002
4	Low Water Level Switch Signal of Clear Pool	L2	X003
5	High Water Level Switch Signal of Water Tank	H3	X004
6	Low Water Level Switch Signal of Water Tank	L3	X005
7	Start Button (Green)	SB1	X006
8	Stop Button (Red)	SB2	X007
9	Switch (Automatic)	SB3–1	X010
10	Switch (Manual)	SB3–2	X011
11	Manually Switch on Electric Valve	SB4	X012
12	Manually Switch off Electric Valve	SB5	X013
13	Manual Rotary Switch of 1# Clean Water Pump	SB6	X014
14	Manual Rotary Switch of 2# Clean Water Pump	SB7	X015
15	Travel Switch on Electric Valve	SQ1	X016
16	Travel Switch off Electric Valve	SQ2	X017
17	Electric Valve Fault Alarm	FR0	X020
18	Thermal Protection Alarm	KA1	X021
19	Manual Rotary Switch of Aeration Blower	SB8	X022
20	Redundant Input		X023-X027

in figure 5. Among them, L6 was taken as power source of PLC output circuit, which was separately output to load of circuit as power supply. All COM ports were short circuit to access to N port

Table 2. Output interface table of SBR wastewater treatment system based on PLC.

No	Station Name	Symbols	Input
1	1# Clear Water Pump Contactor	KM1	Y000
2	2# Clear Water Pump Contactor	KM2	Y001
3	High Level(red light) of Sewage Pool	HL7	Y002
4	Low Level (green light) of Clear Pool	HL8	Y003
5	High Level (red light) of Clear Pool	HL9	Y004
6	Low Level (green light) of Sewage Pool	HL10	Y005
7	High Level(red light) of Water Tank	HL11	Y006
8	Low Level (green light) of Water Tank	HL12	Y007
9	Electric Valve Opening (green light)	HL13	Y010
10	Electric Valve Closure (yellow light)	HL14	Y011
11	Electric Valve Contactor (open)	KM4	Y012
12	Electric Valve Contactor (close)	KM5	Y013
13	Thermal Protector Alarm (red light)	HL6	Y014
14	Roots Blower Contactor	KM3	Y015
15	Solenoid Valve Relay (empty)	KA3	Y016
16	Solenoid Valve Relay (supply)	KA2	Y017
17	Redundant Output		Y020-Y027

of power source in the output circuit. In the input circuit, the signal power was supplied by 24 V DC power of PLC. With relay output, all COM ports were short circuit to access to positive terminal of DC 24 V power source. The input and output interface functions of PLC in the SBR wastewater treatment system were shown as table 1 and table 2.

5 SOFTWARE PROCESS OF CONTROL SYSTEM

According to operation sequence and restriction relations of each controlled objects, spatial distribution of PLC registers were determined, the functions of special-purpose register were confirmed, so control system were programmed. The flow of wastewater treatment systems was shown in figure 6.

PLC controller from Mitsubishi FX2N series were used in the treatment system of coal mine wastewater control by the blower, water pump, trip

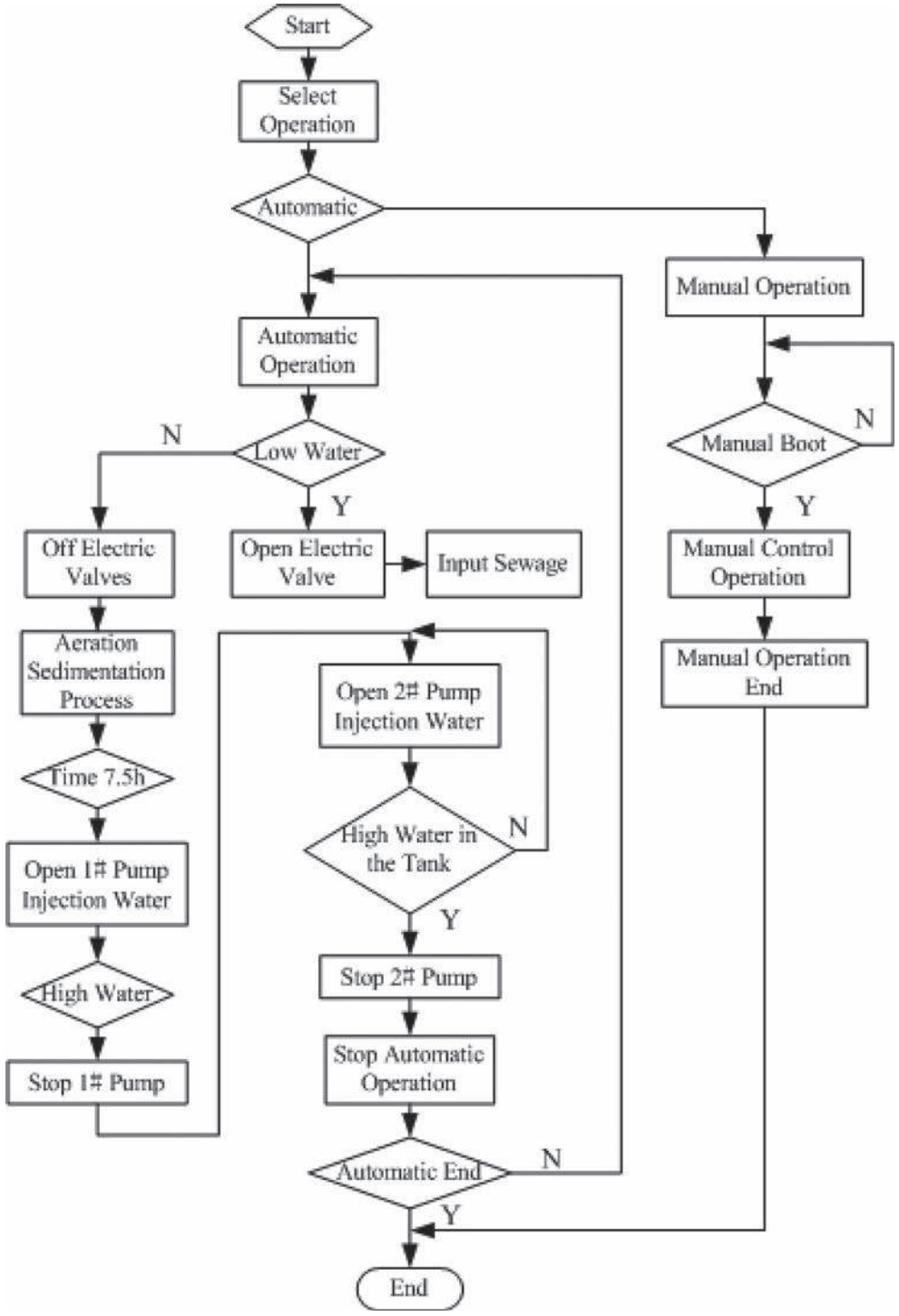


Figure 6. Control flow of SBR wastewater system.

switches, remote input/output switching value and the liquid level, flow and other analog variables to achieve automatic control of wastewater treatment areas. Sewage from mine was treated through the SBR to meet the national emission standards, which stable operation, low cost and good effect. Mine sewage was treated by the SBR method to irrigate plants, clean toilets, etc. Not only were solved of water shortage problem, but also to generate good economic and environmental benefits.

Phosphorus and Nitrogen have not considered removing in the existing activated sludge and biofilm process. Activated sludge oxidation ditch and SBR method were able to play the remove role of nitrogen and phosphorus, but it is ineffective in the small system of sewage treatment. Therefore, the removal functions of nitrogen and phosphorus should be considered to further study in the small wastewater treatment facilities. Meanwhile, with the improvement of environmental requirements and management constraints, assembly series, closed, automation and efficiency will be further development directions in small-scale sewage treatment facilities on mine.

REFERENCES

Li Hai, Sun Ruizheng, Chen zhenxuan. "Municipal Wastewater Treatment Technology and Projects (Version 2)", Chemical Industry Press, 2002.

Nandalal K D W. "Resolving conflicts in water sharing: a systemic approach", Water Resources Research, vol. 39, Dec. 2003, pp. 1–11.

Otterhl R, Grottker M and Lange J. "Sustainable water and waste management in urban area", Wat Sci Tech, vol. 35, 1997, pp.121–133.

Wang Dayu, Lei Lecheng. "Water treatment technology and engineering design", Chemical Industry Press, 2001.

Wang Youle, Zhang Ting, Li Xiaoyan. "Research and application of water resources model on campus" Environment Herald, February, 2002, pp.15–17.

Zhang Yu, et al. "Managing Countermeasures for Source-separated Sewage Treatment and Recycling in Campus", Journal of Anhui Agricultural Sciences, 2009, 23.

Zeeman G, Sanders W and Lettinga G. "Feasibility of the onsite treatment of sewage and swill in large buildings", Wat Sci Tech, vol. 41, 2000, pp. 9–16.

Progress in Mine Safety Science and Engineering II – He et al. (Eds)
© 2014 Taylor & Francis Group, London, ISBN 978-1-138-00122-0

A brief analysis of electromagnetic interference caused by the electrical and electronic equipments in the underground coal mine safety monitoring system

Xingzhi Hu, Jikun Wang, Xuezhe Li & Feiji Ding
North China Institute of Science and Technology, Yanjiao, Beijing-East, China

ABSTRACT: The safety monitoring system is one of the most essential components for the safety protection system in the production process of the coal mine. The number of power electronic equipment such as inverter and other monitoring systems for has risen steadily. This paper introduces the principle of electromagnetic interference and the working principle of the inverter. We summed up the impact of the inverter to the monitoring system, carried out our solution method to the inverter harmonic interference phenomena which may cause side effects to the hardware. In the application field, this paper has also made a certain reference and guidance to the mine safety production.

1 INTRODUCTION

Coal mine safety monitoring system can synchronously transmit the underground circumstances to the monitoring centre up to the ground to detect the coal mine production and production failure.

The introduction of this technology in the field of mine safety can be briefly described as follows:

1. Form a centralized real-time mine production monitoring system from the company to the counties, from the countries to the provincial cities within a certain range by the implementation of computer networking: real-time monitor coal mine production safety situation in the region, especially the underground methane concentration;
2. Take timely operations to disposal emergency cases: immediately make adjustments to the operation mode; instantaneously stop the underground production, rapidly withdrawal underground miners.

According to state regulations, most of the mines have been equipped with a safety monitoring system. For the sake of safe production, we need to create a system which can provides us an intuitive, reliable means to command and control coal disasters, offer us simple and scientific decisions to effectively get rid of the coal mine methane disaster, and curb the accident-prone tendency at the same time.

Currently, the coal mine safety monitoring system is a computer network-based digital surveillance system. Based on the computer networks and computer software, the technology of the coal mine safety monitoring system is a integrated technology which involves with information industry and industrial. It is the result of the development and improvement of modern control technology, digital communication technology and microelectronics.

The base-band transmission and out-of-band transmission are the main communication methods in domestic coal mine safety monitoring system. For the sake of the long-distance, transmission cable in general and underground power cables are arranged in parallel, large-scale mechanical and electrical equipment frequently run, start-up and shutdown will produce a strong electromagnetic interference, so the band transmission (such as FSK, PSK, PFSK MSK etc.) is used frequently in the monitoring system at the mine sites. Theoretical analysis shows that the band transmission using time division baseband transmission (e.g., RS-232C, RS-485, etc.) has obvious advantages. Among all kinds of band transmission methods, FSK the most suitable for coal mine applications because phase mutation will not emerge in this information transmission conversion, it can not only can effectively improve the communication distance of the system, but also have significant anti-jamming capability.

However, with the frequent start mine of information technology, the continuous progress of automation, the use of new high-power electronic devices, high-power electrical equipment and the use of radio frequency equipment, down whole electromagnetic environment is getting worse, causing serious electromagnetic radiated interference. Electromagnetic interference weakens the controlling signal and the detection signal. Severe

damage to the system may leads to a correct detection signal or disorders of the control system. Strong Electromagnetic Interference (EMI) can even cause damage to the system's hardware or microprocessor system program is running out of control, leading to control failure. Consequently, large numbers of false alarms in the safety monitoring system equipment may leads to accidental power failure which means a certainly lowing credibility of the information.

2 THE PRINCIPLE OF THE ELECTROMAGNETIC INTERFERENCE

Electromagnetic interference may result in the degradation in the performance of the device, the transmission channel and the system. On account of the different interference sources, electromagnetic interference can be divided into natural disturbance interference and human disturbance interference. Natural disturbances including cosmic interference, the day electrical interference and lightning impulse; human disturbance including industrial interference, radiation interference, conducted interference, crosstalk, the antenna end of conducted interference, wideband interference, narrowband interference harmful interference, high-power effect and electromagnetic pulse interference. All electromagnetic interference generated by the three basic elements of portfolio: sources of electromagnetic interference, the interference energy-sensitive receiver, the sources of electromagnetic interference transmitted to the receiver medium channel.

The sources of electromagnetic interference issue of electromagnetic energy transmitted through the intermediary channel to the interference energy sensitive receiver, the receiver shall exhibit some form of "response", and the "effect" of interference. (shown in Figure 1)

3 THE WORKING PRINCIPLE OF THE FREQUENCY CONVERTER

Excellent control performance, obvious energy-saving effect, easy to adjust and maintenance, smooth to start, the frequency converter technology is an all-star technique in the safety monitoring system. With variable speed technology matures and the inevitable trend of energy conservation requirements, devices based on inverter technology are increasingly being used in mine production.

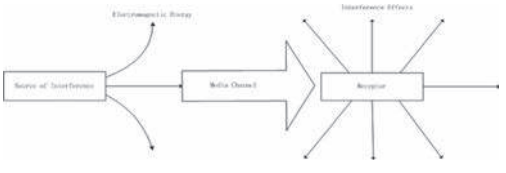


Figure 1. The working principle of electromagnetic interference.

4 HOW DOES THE INVERTER AFFECT THE MONITORING SYSTEM?

The inverter, as a power electronic devices, itself is a source of interference, so the impact of the monitoring system has brought great damage to the underground communications and safety monitoring system.

4.1 *Increase data collection errors*

The signal input channel interference immersed in the measuring unit of the microcomputer system and is superimposed on the useful signal, so that the data acquisition error increase, especially when a weak signal when the sensor output is relatively more intense interference.

4.2 *Failure of the monitoring state*

Usually the control of the microcomputer output signal, and less susceptible to outside interference, but the microcomputer outputs a control signal to the input signal and this signal is often based on the status of certain conditions the logic processing result, if this status of this input signal is subjected to interference introducing false status signal will result in increased output control error or malfunction.

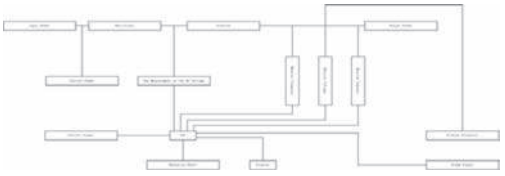


Figure 2. The working principle of the frequency converter.

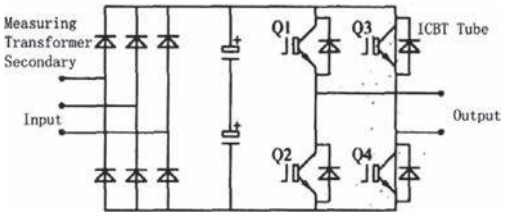


Figure 3. The inverter unit.

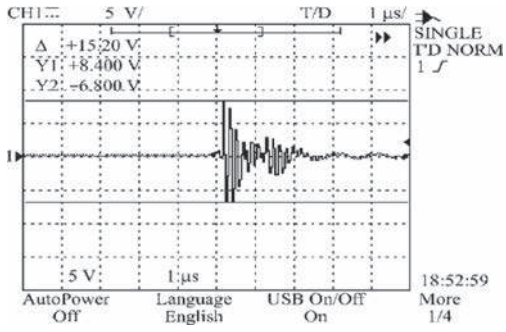


Figure 4. External circuits of the inverter to the motor segment electromagnetic interference test results.

4.3 *Changes of the disturbed data*

RAM memory can be written to the computer system, the interference signal against the lower RAM data can be tampered with, procedures and forms may remain in the program memory EPROM avoid this data is subject to interference and sabotage in the SCM system, But for the on-chip RAM, chip, plug-in RAM data are likely to be interfered change.

4.4 *The spectrum of the electromagnetic interference of the inverter is wide*

Below 1 200 MHz electromagnetic interference, with periodic electromagnetic interference in the 500 MHz bands below the 500 MHz have electromagnetic interference, the maximum frequency of 119 MHz, the value of 31.5 dBmV/m, more than 500 MHz electromagnetic interference is less than a 60 dBmV/m.

Inverter to the motor segments the strong external circuits' induction pulse signal interference. Electromagnetic interference on the line in the winch operation process, the test results is shown in Figure 4.

As can be seen from Figure 2, the drive to the motor segment external circuits induction pulse signal interference intensity of the peak-to-peak value of about 15 V, is a normal level of interference, because in the actual case, the section of cable is short, so the impact will not too large. Filter to the upper the feed switch long section of cable, strong interference.

According to the actual test results, winch drives and pumps, the rig starts to have a greater external circuits induced surge signal the Working Face Wind Tunnel probe by the winch drive and rig power cables, waist Lane probe by the pump start. Among them, the rig starts probe. When inverter and rig at the same time start to generate strong

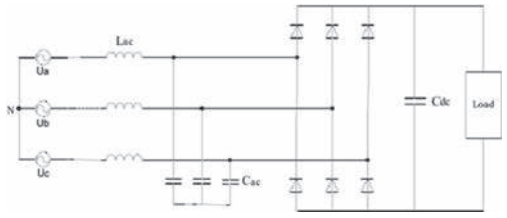


Figure 5. The three-phrase rectifier with LC filter installed in AC side.

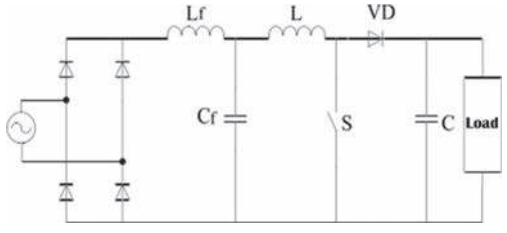


Figure 6. Single-phase PFC circuit based on Boost Convertor.

signal interference, leading to the phenomenon of false alarms in the probe.

Coal mine safety monitoring system alarm status, inspection in accordance with the order of the substation within the transmission channel one by one inspection, the inspection period and the number of sub-station on that channel, sub-stations, the more the longer the inspection cycle.

When the monitoring value is abnormal, the system changes its order of sub-stations inspection by inspection, increase the polling frequency of the sensor where the sub-station is, shorten the inspection period of the sub-station, while the substation inspection remains the same, repeatedly polling the sub-station within the specified time, if the monitored values returned to normal, this alarm is determined as a false alarm. (Shown in Figure 3).

The working process of the software in the coal mine safety monitoring system can be described as follows:

1. Receives sub-station data;
2. Analysis the completion monitoring by distinguishing the value of the alarm status is true or false by detecting the calibration of state, the change status or the duration.

ACKNOWLEDGEMENTS

The research was supported by Fundamental Research Funds for the Central Universities No.

JD1203B V2012 and Fundamental Research Funds for the Central Universities No.3142013099.

REFERENCES

Changxin Fan, Bingxiang Xu, Communication Theory (5th edition) [M) Beijing: National Defense Industry Press, 2001: 230~262. (in Chinese).

Jiping Sun. Coal mine of electromagnetic interference on communication and monitoring system [J]. Mining automation, 200 (2): 23~26. (in Chinese).

Jiping Sun. The Obstacles mine safety monitoring system [M] Beijing: China Coal Industry Labor Protection Science and Technology Institute of Security Monitoring Professional Committee, 2005. (in Chinese).

Wei Zhang, Tianren Yao. The narrow-band interference suppression in DSSS [J]. Communication technology, 2002 (9): 24–26. (in Chinese).

Xingzhi Hu, Jikun Wang. Frequency devices. Electromagnetic interference mechanism of coal mine safety monitoring system [J] Journal of North China Institute of Science and Technology, 2013 (1): 83~85. (in Chinese).

Progress in Mine Safety Science and Engineering II – He et al. (Eds)
© 2014 Taylor & Francis Group, London, ISBN 978-1-138-00122-0

The desorption laws and diffusion model of coal gas in different particle size

Cuixia Wang, Shugang Li & Jikun Liu
School of Energy and Resource, Xi'an University of Science and Technology, Xi'an, China

Yueping Qin
Faculty of Resources and Safety Engineering, China University of Mining and Technology, Beijing, China

Zhuo Shen
National Institute for Occupational Safety, Beijing, China

ABSTRACT: In order to investigate the effect of coal particle size on gas desorption and diffusion law at constant temperature, the constant temperature dynamic coal particle gas adsorption and desorption experiment with different particle sizes was conducted in the coal gas adsorption and desorption experiment system. The results suggest that gas desorption laws of different particle size of coal samples show a good consistency at different pressures, and the cumulative desorption of gas coal particle is linear with time. For the same particle, the higher the initial pressure, the more the maximum gas desorption; the smaller the coal particle is, the more quickly the gas desorption rate is at the same initial pressure. Then, the gas spherical flow mathematical model is built based on Darcy law and is analysed with finite difference method. At last, the gas spherical flow mathematical model is constructed with Visual Basic. The contrast between numerical simulation and experimental results shows that the gas flow in the coal particle internal micropore accords with Darcy's law.

1 INTRODUCTION

In order to reveal the migration and diffusion law of gas in coal and describe the gas desorption and diffusion law accurately, the constant temperature dynamic coal particle gas adsorption and desorption experiment with different particle size was conducted in the coal gas adsorption and desorption experiment system. The gas emission is simulated and calculated with computer program developed by Visual Basic. The simulation results are compared with the experimental results. They provide the basis for the study of coal particle gas diffusion law and supply evidences for the further study of the gas emission law and gas outburst mechanism.

2 COAL GAS DESORPTION EXPERIMENT UNDER DIFFERENT PARTICLE SIZE

The coal gas isothermal adsorption and desorption experiment system mainly includes coal gas adsorption and desorption experiment system, data acquisition system, constant temperature system, weighing system and drying of degassing system. In order to investigate the effect of coal particle size on gas desorption and diffusion law at constant temperature, the coal samples were processed and selected in 4–4.75 mm, 1–1.2 mm, 0.425–0.55 mm and 0.2–0.25 mm, their numbers are $1^{\#}$, $2^{\#}$, $3^{\#}$ and $4^{\#}$. Then, the desorption experiments with the four coal samples were conducted at different pressure. The cumulative desorption amount variation curves of the four coal samples at four different initial pressures were plotted. The experiment data analysis shows that the cumulative desorption reciprocal was linear with time square reciprocal and R^2 was more than 0.99 (Qin Yueping, et al. 2012). The equation can be expressed as:

$$\frac{1}{Q} = \frac{1}{AB} \cdot \frac{1}{\sqrt{t}} + \frac{1}{A} \tag{1}$$

Equation (1) also can be expressed as:

$$Q = \frac{AB\sqrt{t}}{1 + b\sqrt{t}} \tag{2}$$

In the formula, Q is the cumulative desorption of gas (ml/g), T is desorption time (h), A and B are desorption constants.

The analysis suggests that gas desorption laws of different particle size has a good consistency at different pressure. At a given pressure, the gas desorption will increase and desorption rate will decrease with time. When time tends to infinity, desorption rate becomes close to zero. The smaller the coal particle is, the more quickly the gas desorption rate is, and the shorter the complete desorption time is. The analysis shows that desorption constant A depends on the initial pressure: the higher the pressure, the bigger A. B will increase with the decrease of particle size.

Due to space limitation, only the curves of cumulative desorption with time at 0.5 MPa, 1 MPa, 2 MPa and 4 MPa and the relationship curve of the cumulative desorption reciprocal with time square reciprocal are depicted here. They are showed in Fig. 1 and Fig. 2. Gas adsorption constants of the coal samples were obtained by experiment results. a is 26 m^3/t and b is 0.3 MPa^{-1}.

3 DIFFUSION MODEL OF COAL PARTICLES

Coal particle is a kind of porous media, so there are many factors influencing the gas emission in it. Several assumptions were made to simplify the problems and find out several main factors affecting the law of its radiation.

1. As an isotropic porous media, the porosity and permeability coefficient of the coal particle are not affected by the internal gas pressure change of coal particle (Zhou Shining 1957, Li Yunhao, et al. 2007).
2. Adsorption gas in coal grains was mainly considered but the free gas in the micropores in the process of analysis was ignored. Gas content can be expressed as:

$$Q = \frac{abp}{1+bp} \tag{3}$$

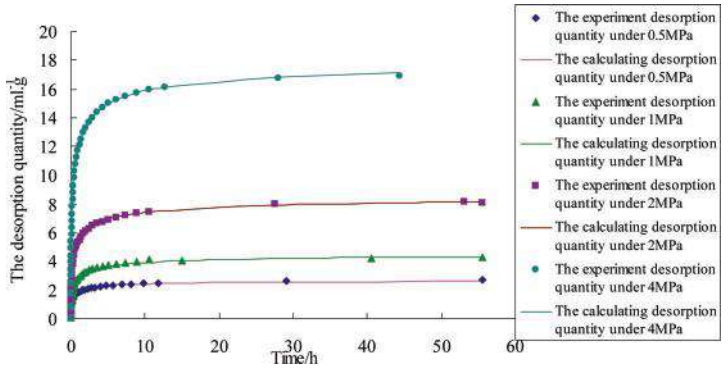


Figure 1. The curves of cumulative desorption with time at different pressure.

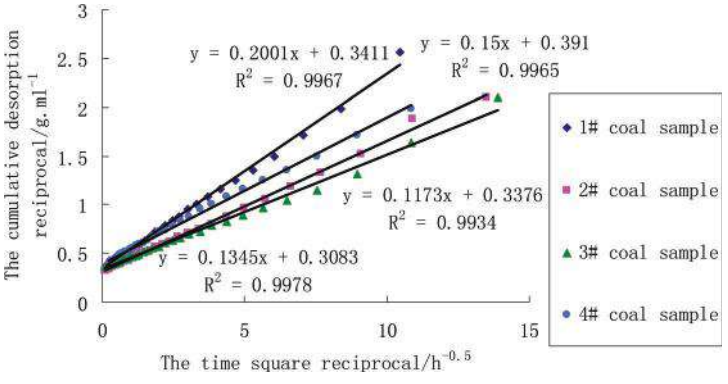


Figure 2. The relationship curve of cumulative desorption reciprocal with time square reciprocal of four coal samples at 0.5 MP.

In the equation, a, b are Langmuir adsorption constant (m^3/t, MPa^{-1}), p is the internal gas pressure of coal particle (MPa), Q is coal particle gas content of unit mass (m^3/t).

3. Temperature keeps invariant in gas diffusion process.
4. Changes of pressure and density of the gas meet the state equation of ideal gas.
5. The gas flow in coal is laminar flow, and in accordance with the Darcy's law (Tian Zhiwei 2010, Li Hongyan 2008, Yi Jun, et al. 2007, Hu Weiyue, et al. 2009, Yang Qingling, et al. 2007).

$$u = -\left(\frac{K_x}{\mu}\frac{\partial p}{\partial x} i + \frac{K_y}{\mu}\frac{\partial p}{\partial y} j + \frac{K_z}{\mu}\frac{\partial p}{\partial z} k \right) \tag{4}$$

In the equation, Kx, Ky, Kz are the coal seam permeability along the x, y, z direction respectively, μ is gas viscosity coefficient.

According to the law of mass conservation, in any control volume unit of the flow field of coal particle, the quality of inflow and outflow of the volume is equal to the increase of gas quality of control volume unit itself in dt (Zhou Shining & Sun Jizheng 1965).

$$\frac{\partial Q}{\partial t} = \nabla\left(\rho_g u\right) \tag{5}$$

In the equation, Q is gas content(m^3/t), t is time (s), ρ_g is gas density (kg/m^3), u is velocity (m/s), ∇ is Hamiltonian operator.

A finite difference method was used to calculate the model. The radius was divided into N segments by each node from the center to the surface, which is showed in figure 3; the node numbers are 0, 1, 2…N. Considering the variation of parameters such as pressure, gas content, seepage velocity and so on in the center of sphere was less than in the spherical near, the node space used equal ratio change and decreased gradually from the center of sphere to spherical. The whole coal briquette can be divided into several spherical shells and one center ball when the middle of the two adjacent nodes seems to be the concentric sphere.

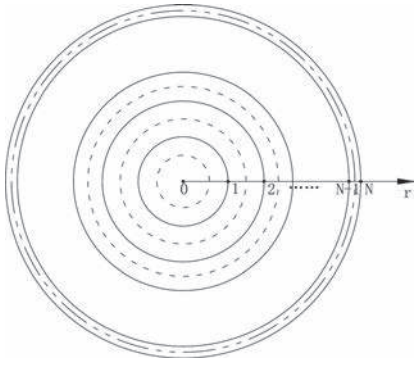


Figure 3. The dividing schematic diagram of pitch points under spherical coordinate system.

The difference equations can be established by changing derivative into difference quotient according to the above differential equation, also it can be built by using the law of mass conservation according to the balance of the quality of the spherical shell as showed in figure 3. Here's a brief analysis of the process of creating difference equation using the law of mass conservation.

In addition to spherical shell of center ball and the node N of outer surface, all interior and exterior surface of spherical shells are the center of the sphere between two nodes. The gas flow velocity and flow rate of each spherical shell surface can be represented by the pressure between two nodes according to Darcy's law.

Spherical shell i contains a node i. The gas quantity lateral flowing into the spherical shell can be expressed in formula (6) (Zhou Shining 1983, Qian Jin, et al. 2010).

$$K\frac{\left(\frac{P_{i-1}^n - P_i^n}{2} + \frac{P_{i-1}^{n-1} - P_i^{n-1}}{2}\right)}{r_i - r_{i-1}} \times 4\pi\left(\frac{r_{i-1} + r_i}{2}\right)^2 \tag{6}$$

The gas quantity flowing out the lateral of spherical shell can be expressed in formula (7).

$$K\frac{\left(\frac{P_i^n - P_{i+1}^n}{2} + \frac{P_i^{n-1} - P_{i+1}^{n-1}}{2}\right)}{r_{i+1} - r_i} \times 4\pi\left(\frac{r_{i+1} + r_i}{2}\right)^2 \tag{7}$$

The gas desorption quantity in spherical shell in unit time can be expressed in formula (8).

$$\frac{4}{3}\pi\left[\left(\frac{r_{i+1} + r_i}{2}\right)^3 - \left(\frac{r_{i-1} + r_i}{2}\right)^3\right] \times \frac{ab\rho}{2\left(1 + b\sqrt{\frac{P_i^n + P_i^{n-1}}{2}}\right)^2\sqrt{\frac{P_i^n + P_i^{n-1}}{2}}} \frac{P_i^n - P_i^{n-1}}{\Delta t} \tag{8}$$

In the equation, subscripts i – 1, i and i + 1 are the node number and the superscripts n-1 and n are the time node number, Δt is the n-th time step. The differential equation of gas unsteady flow in coal globe based on mass conservation is expressed in formula (9).

$$k\frac{\left(\frac{P_i^n-P_{i+1}^n}{2}+\frac{P_i^{n-1}-P_{i+1}^{n-1}}{2}\right)}{r_{i+1}-r_i}\left(\frac{r_{i+1}+r_i}{2}\right)^2 - k\frac{\left(\frac{P_{i-1}^n-P_i^n}{2}+\frac{P_{i-1}^{n-1}-P_i^{n-1}}{2}\right)}{r_i-r_{i-1}}\left(\frac{r_{i-1}+r_i}{2}\right)^2 = \frac{1}{3}\left[\left(\frac{r_{i+1}+r_i}{2}\right)^3-\left(\frac{r_{i-1}+r_i}{2}\right)^3\right] \times \frac{ab\rho}{2\left(1+b\sqrt{\frac{P_i^n+P_i^{n-1}}{2}}\right)^2\sqrt{\frac{P_i^n+P_i^{n-1}}{2}}} \frac{P_i^{n-1}-P_i^n}{\Delta t} \quad (i=1,2,\&,N-1) \tag{9}$$

The partition control body of 0 node is spherule, rather than spherical shell. Its differential equation is expressed in formula (10).

$$k\frac{\frac{P_0^n-P_1^n}{2}+\frac{P_0^{n-1}-P_1^{n-1}}{2}}{r_1}\left(\frac{r_1}{2}\right)^2 = \frac{1}{3}\left(\frac{r_1}{2}\right)^3\frac{ab\rho}{2\left(1+b\sqrt{\frac{P_0^n+P_0^{n-1}}{2}}\right)^2\sqrt{\frac{P_0^n+P_0^{n-1}}{2}}}\frac{P_0^{n-1}-P_0^n}{\Delta t} \tag{10}$$

According to the boundary conditions, when r is equal to R, P is equal to P_w, so the relationship between P_N and P_W is showed in formula (11).

$$P_N = P_w \tag{11}$$

So the complete equation set which makes N node pressure squares of the n moment as unknown quantity is formed by formula (9), formula (10) and formula (11). The pressure of next moment can be calculated when one time step and the pressure of last moment are given. From this the gas pressure in coal globe at any time can be calculated. Considering the gas emission rate will decrease with time, the equal ratio time step is used in the calculations and is increased gradually. In this way, time can be saved while ensuring the accuracy.

On the right-hand side of formula (9) and formula (10) are nonlinear expressions of node pressure squares of the n moment, so iterative method should be used. The number under radical sign should be calculated when $P_i^n = P_i^{n-1}$, was set. In this way quasilinear system of equations and a group of solutions are obtained, then the number under radical sign is calculated with the solution, once again new quasilinear system of equations and a new group of solutions are obtained. The final result will be attained until the relative error of two computing solutions is less than a small value.

The coal desorption gas quality in Δt can be calculated with formula (12) after the gas pressure square is obtained.

$$\Delta Q = k\frac{P_{N-1}^n-P_N^n}{r_N-r_{N-1}}\times 4\pi R^2\Delta t \tag{12}$$

The coal cumulative desorption gas is the sum of desorption quantity at any time-point.

4 PROGRAM DESIGN

In order to avoid conversion between units in the process of operation, several dimensionless numbers are used.

The dimensionless radius:

$$X = \frac{r}{R} \tag{13}$$

The dimensionless pressure:

$$Y = b^2P \tag{14}$$

The dimensionless time:

$$T\frac{tk}{\rho aR^2b^2} \tag{15}$$

The dimensionless desorption dimensionless number:

$$M_L = \frac{Q}{a\rho R^3} \tag{16}$$

Gas flow equation of coal particles dimensionless:

$$\Delta T\frac{Y_i^n-Y_{i+1}^n}{X_{i+1}-X_i}\left(\frac{X_{i+1}+X_i}{2}\right)^2 - \Delta T\frac{Y_{i-1}^n-Y_i^n}{X_i-X_{i-1}}\left(\frac{X_{i-1}+X_i}{2}\right)^2 + \frac{1}{3}\left[\left(\frac{X_{i+1}+X_i}{2}\right)^3-\left(\frac{X_{i-1}+X_i}{2}\right)^3\right] \times \frac{1}{\left(1+\sqrt{\frac{Y_i^n+Y_i^{n-1}}{2}}\right)^2\sqrt{\frac{Y_i^n+Y_i^{n-1}}{2}}}Y_i^n = \frac{1}{3}\left[\left(\frac{X_{i+1}+X_i}{2}\right)^3-\left(\frac{X_{i-1}+X_i}{2}\right)^3\right] \times \frac{1}{\left(1+\sqrt{\frac{Y_i^n+Y_i^{n-1}}{2}}\right)^2\sqrt{\frac{Y_i^n+Y_i^{n-1}}{2}}} - Y_i^{n-1} - \Delta T\frac{Y_i^{n-1}-Y_{i+1}^{n-1}}{X_{i+1}-X_i}\left(\frac{X_{i+1}+X_i}{2}\right)^2 - \Delta T\frac{Y_{i-1}^{n-1}-Y_i^{n-1}}{X_i-X_{i-1}}\left(\frac{X_{i-1}+X_i}{2}\right)^2 \tag{17}$$

The difference equation dimensionless of control volume in 0 node is showed as formula 18.

$$\Delta T \frac{\frac{Y_0^n - Y_1^n}{2} + \frac{Y_0^{n-1} - Y_1^{n-1}}{2}}{X_1} \left(\frac{X_1}{2}\right)^2 = \frac{1}{3}\left(\frac{X_1}{2}\right)^3 \frac{1}{2\left(1+\sqrt{\frac{Y_0^n + Y_0^{n-1}}{2}}\right)^2 \sqrt{\frac{Y_0^n + Y_0^{n-1}}{2}}} \left(Y_0^{n-1} - Y_0^n\right) \tag{18}$$

The boundary condition is $Y_w = b^2 P_w$ when $X = 1$ and $Y_N = Y_w$.

The gas dimensionless desorption in Δt is formulation 19.

$$\Delta M_L = \Delta T \frac{Y_{N-1}^n - Y_N^n}{X_N - X_{N-1}} 4\pi \tag{19}$$

A computer program is developed with Visual Basic based on finite difference calculation model and its corresponding boundary conditions. The program structure diagram is showed in Fig. 4 (Zhou Shining 1983).

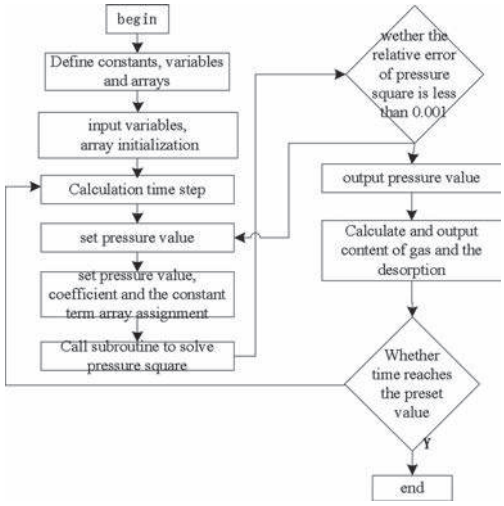


Figure 4. Flowchart of program structure.

5 COMPARATIVE ANALYSIS OF CALCULATION AND EXPERIMENTAL RESULTS

The coal particle radius is 0.27 mm and its permeability coefficient is 1×10^{-5} m^2/(MP^2 · s). Gas adsorption parameters are obtained by analyzing the experimental results. a is 27.32 m^3/t, b is 0.35 MPa^{-1} and the coal density is 1.2 m^3/t. The gas flow equation is calculated with the program designed by VB based on the experimental parameters and the dimensionless cumulative desorption of gas is obtained. Then the dimensionless time and the dimensionless cumulative desorption are translated into dimension time and dimension cumulative desorption.

In order to comparatively analyze the simulation and experimental cumulative desorption, they are transformed into desorption quantity of unit mass of coal. The results are obtained by finely adjusting the permeability coefficient and a of coal particles, as shown in Fig. 5 and Fig. 6.

Fig. 5 shows that simulation by the gas flow equation under spherical coordinates and experimental cumulative desorption has a high fitting degree. Moreover, neither the simulation nor the experimental cumulative desorption confirms that the reciprocal of accumulated desorption quantity and time square has a good linear relationship at external pressure remaining unchanged. This affirms that the gas inside the coal particle flow in the micro pore accords with Darcy's law.

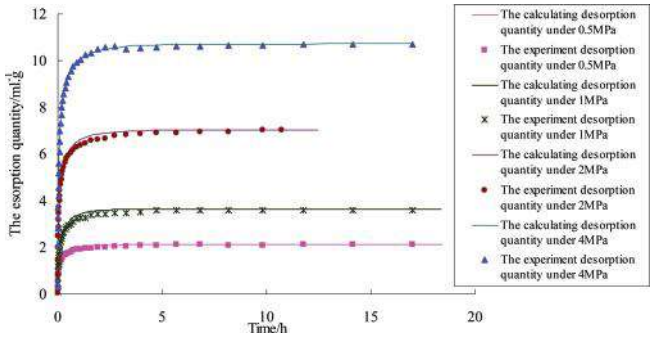


Figure 5. The simulation and experimental desorption of 4# coal sample at different pressure.

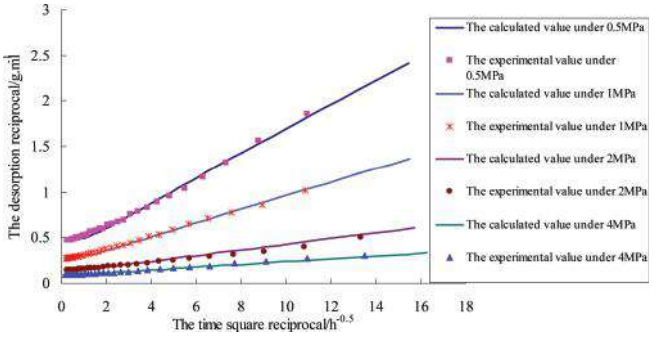


Figure 6. The relationship between desorption quantity reciprocal and time evolution reciprocal of 4# coal sample.

6 CONCLUSION

1. The change curve of cumulative desorption of coal sample at four different initial pressure along with time is obtained by dealing with experiment data of constant temperature desorption. The result shows that the reciprocal of accumulated desorption quantity and time square have a good linear relationship. Empirical formula of gas desorption laws is simulated and the physical meaning of each parameter is analyzed.
2. The radiation model of the radial methane flow in spherical coal grains is established and is calculated with finite difference method based on mass conservation law and Darcy's law and the mathematical model is non-dimensionalized. The coal particle gas diffusion equation is calculated with computer program developed with VB.
3. Simulation computation is performed with the basic parameters of the experimental coal sample. By contrast, the simulation results accord with the experimental very well. It confirms that the gas flow in the coal particle internal micropore accords with Darcy's law.

ACKNOWLEDGMENTS

Financial support for this work provided by the Scientific Planning Project of XinJiang Uighur Autonomous Region (No.201333110) is deeply appreciated.

REFERENCES

Hu Weiyue, et al. 2009, The Flowing and Outburst Mechanism of Gas in Coal-based Pore and Fractured Medium. *Coal Geology & Exploration,* 37(4):6–8.

Li Hongyan 2008, Status-quo and Tendency of Research on Coupling Theory of Mining Stress Field and Gas Seepage Field. *Coal Mining Technology,* 13(3): 4–7.

Li Yunhao, et al. 2007, The Numerical Simulation of Gas Flow in the Coal Seam and its Application to the Coal Wall. Journal of Safety Science and Technology, 3(2):74–77.

Qian Jin, et al. 2010, Anisotropic Numerical Simulation of Coal-bearing Strata with Finite-difference. Coal Geology & Exploration, 38(2):64–66.

Qin Yueping, et al. 2012. Constant Pressure Dynamic Law of Gas Desorption Experiments. Journal of Liaoning Technical University (Natural Science), 31(5):581–586.

Shi Yu, Yang Zhengming, Huang Yanzhang. 2009, Study on Non-linear Seepage Flow Model for Low Permeability Reservoir. *Acta Petrolei Sinica,* 30(5):731–734.

Tian Zhiwei 2010, Research Advances in Coalbed Methane Seepage Mechanics. *Geological Science and Technology Information,* 29(1):61–64.

Xie Quan, et al. 2011, Experimental Investigation on Single-phase Non-linear Flow in Low Permeability Cores. *Chinese Journal of Rock Mechanics and Engineering,* 30(supplement 2):3975–3981.

Xu Jianhong, et al. 2007, A New Method for Calculating Threshold Pressure Gradient in Low Permeability Reservoirs. *Petroleum Exploration and Development,* 34(5):594–602.

Yang Qingling, et al. 2007, Study on GAS Flow Theory in Coal Seam. *Coal Technology,* 26(2):67–69.

Yi Jun, et al. 2007, An Experimental Research on the Characters of Methane Seepage in Stress Field And Temperature Field. *China Mining Magazine,* 16(5):113–116.

Zhou Shining 1957. Coal Seam Gas Movement Theory Analysis. Journal of CUMT International Journal of Mining Science and Technology, 1:36–45.

Zhou Shining 1983, The Application of Electronic Computer in the Study of the Coal-bed Gas Flow Theory. Journal of China Coal Society, 2:29–36.

Zhou Shining & Sun Jizheng 1965, Coal-bed Gas Flow Theory and its Application. Journal of China Coal Society, 2(1):24–37.

Progress in Mine Safety Science and Engineering II – He et al. (Eds)
© 2014 Taylor & Francis Group, London, ISBN 978-1-138-00122-0

Research on heat damage control and combined technology of waste heat utilization

Jie Ma
North China Institute of Science and Technology, Beijing, China

ABSTRACT: This thesis analyzes the heat damage control and researches the combined technology of heat pump and cooling for waste heat utilization based in Zhujixi Coal Mine in Anhui Province. The combined technology is to fully recover waste heat, convert high-level heat damage into heat supply resource for coal mine. Thus it can lower underground cooling load and operating cost, replace boiler heat source with recovered energy and achieve energy conservation and emission reduction.

1 INTRODUCTION

In coal-mining site, huge heat energy consumption is needed for ground building heating, shaft protected from cold and hot water using in worker's bathroom. Traditionally, the heat energy is provided by coal-fired boilers, which leads to serious pollution as well as large consumption of energy.

High temperature damage is one of the top five mine disasters (W Wen et al. 2002). The main sources of heat dissipation include rock high temperature and great air compression heat from in-depth mining, heat release of geothermal water, coal oxidation, machine and lighting equipment, human heat and so on. Heat damage control requires great investments and system operation needs huge energy consumption. Statistics of large mine cooling systems at home and abroad show that energy consumption of the cooling systems accounts for 15%–20% of that from production systems (W Xiujun & H Chunsheng 2007). In addition, drainage and ventilation in high temperature mines have a relatively high temperature and remain constant in all seasons. Such low-level heat energy is greatly stored in the mines and has been released into the atmosphere instead of been applied.

Researches from home and abroad are mainly focused on heat damage control and heat damage utilization separately at present. Although China University of Mining & Technology makes a lot of researches on them, the combination of both are still not available. This thesis presents a combined tech-nology of heat pump and cooling based on Zhujixi Coal Mine in Anhui Province. Heat pump system is used to convert high-level heat damage into heat supply resource for coal mines, which could replace traditional boilers in winter; while in summer the combined technology could help offer hot shower water, cool incoming air flow, and lower underground cooling load. The paper also designs an overall plan for heat damage control and waste heat utilization, which optimizes the systems and takes the facilities, equipment and pipelines into consideration to lower investments and operating costs.

2 UNDERGROUND COOLING AND HEAT BALANCE OF HEAT UTILIZATION

Summer: draw incoming air flow heat through the heat pump and supply it for shower water, while take excessive heat through mine ventilation. After being precooled and dried, the incoming air flow has a relatively low temperature and humidity, as well as strong moisture absorption and cooling ability which could prevent such underground heat damages as heat dissipation from wall rock and hot water. For heat damages that could not be removed through air flow, cooling units are applied in the shaft and the condensation heat is discharged through cooling tower or return air flow. Since the mine air flow has been precooled, it would reduce cooling units load in the shaft and its operating time.

Meanwhile, part of heat pump units draw heat from buildings to be supplied for air-conditioners. The drawl waste heat could be carried away through mine ventilation or drainage. See Figure 1 for heat balance.

Transition seasons: Waste heat recovery system is given priority according to the underground temperature. Recover the waste heat of mine total return air and supply it for hot shower water. When cool energy is needed under the shaft, the heat

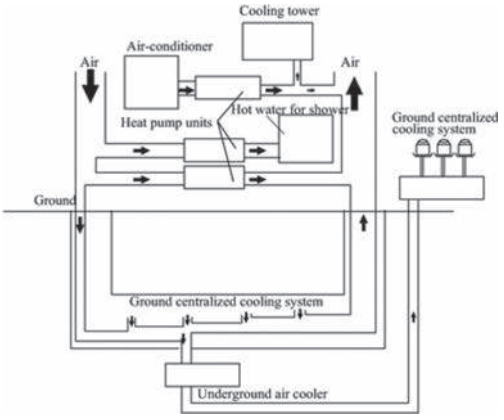


Figure 1. Heat balance in summer.

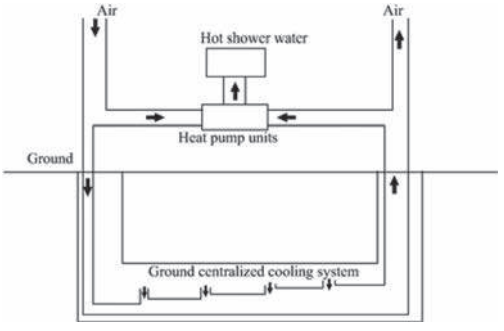


Figure 2. Heat balance in transition seasons.

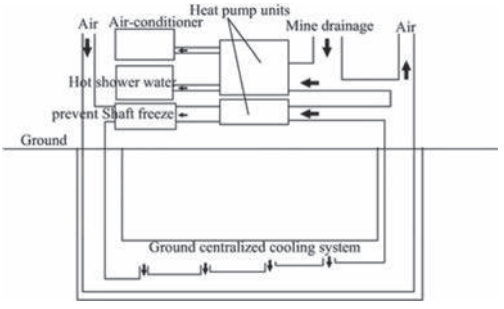


Figure 3. Heat balance in winter.

from mine incoming flow is recovered and then is provided for shower water. See the Figure 2 for the heat balance.

Winter: Since the Zhujixi Coal Mine is of high temperature, huge heat energy is stored in its total return air and mine drainage. In consideration of the relatively large total return air, the plan prefers to apply waste heat system to recover the waste heat of total return air, to provide heat for pithead antifreezing, shower hot water and building heating. See the Figure 3 for the heat balance.

3 CALCULATION OF INLET AIR FLOW COOLING HEAT OF WASTE HEAT UTILIZATION

In summer heat pump systems are used to draw heat from mine incoming air flow for shower water and at the same time air flow is precooled and dried. During the hottest summer days at least four heat pump units run to cool mine incoming air flow in Zhujixi Coal Mine. The cooling capacity provided by these 4 units reaches up to 4400 kW whose influence on the temperature of incoming air flow is calculated.

Incoming air quantity in pithead of auxiliary shaft: 400 m^3/s.

Dry-bulb temperature calculated outside air-conditioning room in summer: 35.6°C.

Wet-bulb temperature calculated outside air-conditioning room in summer: 28.1°C.

The relative humidity of mine incoming air flow in hottest summer days is 57%, and h_1 (the enthalpy of incoming air flow) is 89.81 kJ/kg.

$$Q = \rho V (h_1 - h_2) = (89.81 - h_2) \times 400 \times 1.01 = 4400 \text{ kW}$$

$h_2 = 78.92$ kJ/kg

H_2-the enthalpy of incoming air flow after cooling treatment

Consulting the psychrometric chart with the same relative humidity, it is found that the temperature of incoming air lowers by 3 °C under the condition that the incoming air temperature is 32.8°C and 77% air contains 83.20 kJ/kg of enthalpy. That could effectively reduce the underground heat damage.

4 RECOVERABLE WASTE HEAT CAPABILITY IN HIGH TEMPERATURE MINE WITH HEAT DAMAGE

4.1 *Calculation of mine drainage waste heat*

According to geological exploration data and field survey of Zhujixi Coal Mine, the mine drainage water volume reaches 150 m^3/h. Underground cooling measures are taken in this coal mine and the water temperature is above 32°C. Considering the working capacity of the current heat pump, the recoverable heat quantity could reach 4187 kW.

4.2 *Calculation of waste heat of mine total return air*

The temperature and humidity of mine return air are hardly affected by outdoor air temperature and remain constant all year around. The design air quantity in Zhujixi mine is at least 380 m^3/s. After measurement, the winter ventilation temperature is above 26°C and the relative humidity remains 95% all year around. Considering the technology of current heat pumps, the recoverable heat quantity could reach 26, 193 kW.

4.3 *The total quantity of recoverable waste heat*

The total quantity of recoverable waste heat is 30, 380 kW, equal to that produced by the 43-ton boiler. However, the maximum using heat is up to 15, 514 kW in winter in the mine, which is equal to that produced by the 22-ton boiler. Therefore boiler heat supply could be fully replaced through recovering the waste heat in high temperature mines like Zhujixi.

5 UNDERGROUND COOLING PLAN FOR ZHUJIXI MINE

In the late period of production in Zhujixi, eight tunneling places and two working faces are in operation and the total heat load in the shaft reaches 11, 000 kW. The plan designs the ground centralized cooling system and supplies water with large temperature difference, thus which can not only keep enough space for installed capacity in the shaft but also effectively reduce pipelines and pipe fittings that transmit refrigerants from ground to underground. See the underground cooling plan in Figure 4. In the ground centralized cooling system, the condensation heat goes through closed cycle cooling water and is directly emitted to the air through the cooling tower. Two cooling units are set up on the ground, each going through two-level cooling systems. The cooling unit at the first level is responsible for main cooling load; the design temperature of the incoming refrigerant water is 18°C, while that of the outlet water is 5°C. The cooling unit at the second level is less efficient and is responsible for remaining cooling load; the design temperature of incoming water is 7°C and that of the outlet water is 2.5°C (China Coal Construction Association 2007). The total cooling capacity at these two levels is 6000 kW.

The primary refrigerated water at the temperature of 2.5°C is transmitted to the underground cooling chamber through single circulating pump in the refrigeration room on the ground, then it is converted into secondary refrigerated water at the temperature of 6.5°C through the high and low pressure heat exchanger and is transmitted to each cool using point. At each point, cooling capacity is discharged through underground air cooler. The temperature difference of underground return water is considered to be 12°C.

6 WASTE HEAT UTILIZATION PLAN FOR ZHUJIXI COAL MINE

As showed in Figure 5, return air heat exchanger is installed on the total return air diffusion tower and it transfers huge heat from return air to circulation water by means of spray. As the low-temperature heat source of heat pump system (J Nengzhao 1997), the temperature of circulation water is lowered after the heat of it is drawn by the system. Finally, the circulation water is conveyed to the return air exchanger. The process goes on like that over again and again.

In winter, the recovered heat from return air through this system is supplied to building heating, shaft antifreezing and daily hot water (N Yongsheng & W Jianxue 2012).

In summer, the incoming air is cooled through the shaft antifreezing heat exchanger to lower the underground cooling load and to convert heat damages into heat energy for hot shower water.

In transition seasons, the heat that is recovered from mine return air or incoming air by the heat pump units is supplied to daily hot water.

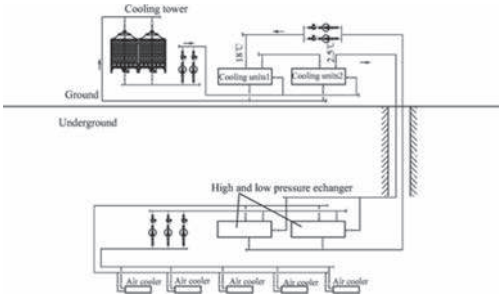


Figure 4. Ground centralized system flowchart.

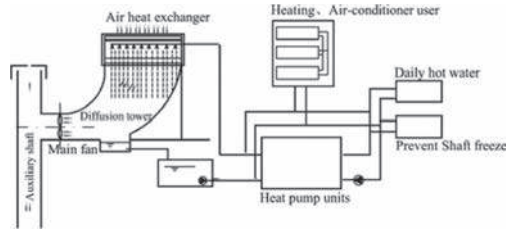


Figure 5. Return air heat exchange schematic diagram.

7 OVERALL PLANS OF UNDERGROUND COOLING AND WASTE HEAT UTILIZATION FOR ZHUJIXI MINE

The plan takes an overall consideration of heat damage control and waste heat utilization in Zhujixi Coal Mine, which optimizes the systems, uses complex facilities, shares the softened water treatment system and gives an overall consideration of cooling tower equipment and pipeline layout.

Complex facility is an integrated unit that combines underground cooling with the recovery and utilization of ventilation heat. The facility has two storeys and one auxiliary storey. It is 66 meters long and 22 meters wide and runs from south to north. In the first floor, there are electric room, underground cooling room and chemical water room from east to west. The height of the first floor is 7 m. In the second floor, there are electric room, heat recovery room and impounding trunk for shower water from east to west. The height of this floor is 5 m. In the auxiliary floor there are staircases and some offices and the height of this floor is 3 m. The second floor roof plane has an elevation of 12.00 m and it is mainly for the cooling tower collecting pool which combines the underground cooling system with mine ventilation heat recovery and utilization system. The mechanical cooling tower is erected upon the collecting pool. The auxiliary floor roof plane has an elevation of 15.00 m and is equipped with water tank on the top.

The production pool, pump room, raw water decontamination plant and other auxiliary production buildings are located in the south of the complex facility; the soften water tank lies in the southwest corner of complex facility. Piping rack is mainly used for erecting refrigerant pipes and it stretches along the road to the gangue shaft and main shaft. Two refrigerant pipes starting from the underground cooling room of the complex facility could easily reach the gangue shaft and the main shaft and extend to the underground. The cold and hot water pipes from the heat pump room of the complex facility could also be laid out along the roads in the mine area.

8 CONCLUSION

1. Present the heat quantity balance pattern in winter and summer for underground cooling and heat utilization.
2. Analyze the influence of waste heat utilization on incoming air cooling capacity and on waste heat capacity of high temperature heat damage.
3. Put forward the overall plan of mine heat damage control and waste heat utilization for Zhujixi Coal Mine, which optimizes the systems and takes the complex facility, equipment and pipelines into consideration.

To sum up, based on the Zhujixi Coal Mine of Anhui Province, this paper combines heat pump technology and underground cooling technology and then converts high temperature heat damages into heat supply so as to lower the underground cooling load as well as to replace traditional boiler heat source with heat recovery and utilization. All achieves the goal of energy conservation, emission reduction and less investment.

REFERENCES

China Coal Construction Association. 2007. *Regulations of Heat Damage Prevention Underground Coal Mine*. Beijing: China Planning Press.

Jiang Nengzhao. 1997. *Heat Pump Technology for Air-conditioner*. Beijing: China Machine Press.

Niu Yongsheng. & Wang Jianxue. 2012. Recycling of Mine Waste Heat in Zhujixi Coal Mine. *Safety in Coal Mine* (9): 195.

Wang Wen et al. 2002. Treatment of Heat Damage Under Mine. *Mining Safety & Environmental Protection* (6): 31–33.

Wei Xiujun. & Hu Chunsheng. 2007. *Theory of Underground Cooling and Engineering Design*. Beijing: Coal Industry Publishing House.

Progress in Mine Safety Science and Engineering II – He et al. (Eds)
© 2014 Taylor & Francis Group, London, ISBN 978-1-138-00122-0

Research on mine refrigeration of large mines with large mining depth

Yongsheng Niu
China University of Mining and Technology, Beijing, China
North China Institute of Science and Technology, Beijing, China

Jianxue Wang
Beijing CUMT Energy Conservation Technology Co., Ltd., Beijing, China

ABSTRACT: Zhujixi coal mine is a typical large mine characterized with large mining depth, high ground temperature, large heat dissipation from electromechanical equipment and serious heat damage. This paper takes Zhujixi coal mine as an example and puts forward ground two-stage refrigeration, large temperature difference to supply cooling as well as the adoption of high-low pressure heat exchanger to overcome high hydrostatic pressure. Those solutions solve the problem of difficult heat removal in high temperature mine and of high hydrostatic pressure in large mining depth mine. In addition, it suggests applying domestic equipment to underground cooling from the point of economic benefits.

1 INTRODUCTION

With the increase of mining depth and the continuous enhancement of mining mechanization, high temperature heat damage of mine in China has become more prominent. According to the ground temperature observation data of our country in coal field, the average rising rate of ground temperature (geothermal gradient) in coal mines is up to 2–4°C/hm (1 hm = 100 m) (W Xiujun. & H Chunsheng 2007). Most high temperature mines (about 90%) are deep mined and the rock temperature is very high there.

In *The Safety Regulations for Coal Mine* it is explicitly stipulated that the air temperature should be no higher than 26°C in mining face or 30°C in electromechanical chamber. Mining must be stopped if the air temperature respectively exceeds 30°C and 34°C in the above-mentioned two places (The State Bureau of Safe Production Supervision and Administration & State Administration of Coal Mine Safety 2011).

Zhujixi coal mine is located in Panji area and the expected production capacity is 4 million tons per year. The horizontal elevation of the coal mine is –960 meters in height, while in the constant-temperature zone its depth is 30 meters, its temperature is 16.8°C, its average geothermal gradient is 2.78°C/hm and the ground temperature in horizontal working face is over 43.49°C. All above demonstrate it a typical high geothermal mine. According to the forecast of underground meteorological environment, there will be a working environment in some parts of working face where the temperature will be over 36°C and the relative humidity will be 97% or more, which far exceeds the rules in *The Safety Regulations for Coal Mine*. Therefore, the underground cooling must be carried on.

In order to reasonably, effectively and economically lower the temperature in the working face and to fully utilize the technology of mining, ventilation and cooling at the same time, artificial refrigeration measures must be taken to improve the underground working environment, to protect miners' health and to improve labor productivity.

2 COOLING LOAD ANALYSIS OF UNDERGROUND REFRIGERATION IN ZHUJIXI COAL MINE

The thermal environment of mine is affected by many factors and dominant factors among them are summarized as follows.

2.1 *Ground atmospheric environment*

Air current of mine is carried from the ground into the underground, so the ground atmospheric environment has a great influence on the meteorological conditions of underground air current. Located in the alluvial plain of the Huaihe River, Zhujixi coal mine belongs to temperate sub-humid monsoon climate, has obviously seasonal characteristics and is extremely hot in summer. According to the meteorological observation statistics of 10 consecutive years from the weather station in Fengtai county nearby, the average temperature

is 19.3°C and the relative humidity is 70.9% and the atmospheric pressure is 101, 160pa in April, while they correspondingly are 31.9°C, 81.8% and 100, 091pa in July when it is hottest among hotter months from June to September. Air inlet from ground is a bit higher both in temperature and in humidity in summer, which leads to underground at a higher temperature and humidity.

2.2 *Geology and geothermal environment*

The observation well data from Jiulonggang of Huainan is recorded that the depth is 30 meters and the temperature is 16.8°C in constant temperature zone. Because its geothermal gradient is 2.44–3.01°C/nm (one single hole) and the average is 2.78°C/hm, the geothermal gradient of temperature hole in Zhujixi coal mine is at the normal geothermal gradient range within which there exists a high-temperature area in the medium-deep part of the zone. The primary high temperature zone (31°C or above) generally lies under –504 to –630 meters and the secondary high temperature zone (37°C or above) under –701 to –880 meters.

2.3 *Production environment of mine*

The production environment of mine during mining has a direct influence on the underground thermal environment from heat sources such as heat from high temperature palisades, heat from electromechanical equipment during operation, heat release in transportation of coal and gangue, compression heat from ventilating air and heat from oxidation in extracting bare rock and coal (W Wen et al. 2002). All makes heat exchange with the mine air current occur and finally causes the underground temperature to rise.

2.3.1 *Heat dissipation from high temperature palisades and rib*

The coal seam of Zhujixi coal mine is deep buried and ground temperature is high, so a lot of terrestrial heat is conveyed to ventilating air underground at the form of radiation and ventilating convection through the high temperature palisades and rib. This is an important factor to cause the high temperature underground.

2.3.2 *Heat dissipation from electromechanical equipment during operation*

Zhujixi coal mine is intensively exploited and it is operated by means of machines in mining, excavating and transporting. Besides, the installed capacity of electromechanical equipment is larger. The production capacity of fully mechanized coal face is 1.0 Mt/a~4.0 Mt/a and its installed capacity is 6000 kW ~ 7000 kW.

The average power of ordinary excavating face is 200 kW and that of fully mechanized coal face is 350 kW in coal roadway.

2.3.3 *Heat release in transportation of coal and gangue*

The temperature of coal and gangue falling from coal face is close to the initial temperature of surrounding rocks. Coal and gangue transfers their own heat to the air current during the process of transporting them to the ground, which causes the rising of temperature of air current.

2.3.4 *Compression heat from air current*

Zhujixi coal mine is deep mined, whose first level elevation is 780 meters and second level elevation is 950 meters, so the air current temperature largely rises out of its own natural compression.

2.3.5 *Heat release from oxidation*

Most coal seams of Zhujixi coal mine is easily self-ignition. Coal and surrounding rock containing coal and sulfur release heat from oxidation so it is also the heat source of local temperature rising.

2.3.6 *Heat from occupants*

There are 25 people in coal roadway, 17 people in rock roadway and 40 people in coal face.

Considering the above factors, the cold load statistics of underground cooling for Zhujixi coal mine is shown in the following table:

It can be clearly known the cooling demand of Zhujixi coal mine from the above table. They are respectively the heading during construction period, one stope face in startup, 2 working faces during production and one heading in production tail. Therefore, the scale of installed equipment for underground cooling is determined by the cooling load demand of production tail.

3 UNDERGROUND COOLING SCHEMES

3.1 *Options of refrigeration*

There are mainly two options to underground cooling among all. One is non-mechanical cooling method, namely strengthening the ventilation of mine, In general, heat damage can be coped with through strengthening ventilation under the circumstance when the ground temperature is 35°C below (H Hanhua 1997). Another is mechanical cooling method that is to condition the air of underground working environment. Target temperature cannot be reached solely by means of ventilating enhancement when the ground temperature reaches 35°C or above, so mechanical cooling method must be adopted. The low temperature of

Zhujixi coal mine reaches 43.49°C or above, which far exceeds the restricted temperature of 35°C, so mechanical cooling is a must.

Owing to different positions of refrigerating machines, there are usually three refrigerating modes such as mobile underground local cooling, underground centralized cooling and ground concentrated cooling.

3.1.1 *Mobile underground local cooling*

If heat damage is not very serious and individual temperature exceeds the limitation, local mechanical cooling measures can be taken to improve the meteorological conditions in coal face (W Wen et al. 2002).

The heat damage in Zhujixi coal mine is serious. The condensing heat is difficult to exhaust if mobile underground cooling is selected. According to recent data of high temperature mine, the return current temperature in mine could be over 32°C. If using return current to refrigerate, the refrigerating capacity of refrigerating machines will badly decline and the expected cooling effect cannot be met at the same time. Therefore, this refrigerating machine cannot be readily chosen for Zhujixi coal mine.

3.1.2 *Underground centralized cooling*

Underground centralized system refers to setting the condensing cooling device-cooling tower on the ground, while what is set up underground are refrigeration host, circulating water pump house, terminal air cooler device and pipe system.

Underground centralized refrigeration equipment is very expensive since this equipment can only be available in abroad markets at present. In spite of this, it needs anti-explosion protection for electrical and control equipments. Therefore, it is not economic to choose this mode. Besides, the total capacity of installable refrigerating units is finite because of the limited installed space in the underground cooling chamber. In all, this scheme is not recommended to adopt.

3.1.3 *Ground concentrated cooling*

This refrigeration method is to set underground refrigeration host and cooling water system & equipments in ground refrigerating station while to allocate cold-exchanging room, circulating water pump house, terminal-device air cooler and piping system underground. Refrigerant water is conveyed to underground through heat-insulted pipes and air current is cooled by air cooler.

Although Zhijixi coal mine is over 900 meters in vertical depth, there must be coupling devices and high-low pressure heat exchanging device for ground central air-conditioning system if the depth of mine is over 600 meters in the base of *Regulations of Mine Design in Coal Industry*. In addition, these devices can be made in China currently.

Ground concentrated cooling, which is not only safe and reliable but also convenient to refrigerate and to install and maintain equipments, can meet the cooling demand requirement of production tail in Zhujixi coal mine. Besides, all related equipments can be purchased in china. This scheme is recommended for the advantage of low unit investment, high efficient system and good underground cooling effect.

3.2 *Refrigerating parameters*

According to *Regulations of Heat Damage Prevention Underground Coal Mine,* the temperature of outlet water from refrigerator should not be higher than 3°C when ground concentrated cooling mode is put into practice.

The determination of refrigerating parameters not only is closely related to also affect the equipment selection. Low outlet water temperature from refrigerator is easy for the primary and secondary system to adopt domestic indirect exchange method at the advantage of reducing the engineering investment and dehumidification underground dehumidification. Big temperature difference from outlet and inlet of refrigerant water can reduce the circulation of refrigerant water in system, the volume of water-transmitting equipment and the operation cost.

Therefore, outlet water temperature is designed to be 2.5°C and return water temperature be 18°C in the ground concentrated refrigerating station.

3.3 *Underground cooling process*

As shown in figure 3.1 of ground concentrated cooling, the condensing heat is directly emitted to the atmosphere by means of the closed circulating cooling water through the cooling tower and on the ground there are two refrigerating units each of which works by two-stage refrigeration. Primary electrical refrigerating units are responsible for the main cooling load, of which the refrigerant water inlet temperature is designed to be 18°C and the outlet temperature is 5°C. Owing to its low-efficient cold working secondary electric refrigerating units deal with the remaining cooling load and the water temperature of inlet and outlet is respectively 7°C and 2.5°C. The total refrigerating capacity of the two stages is 6000 kW.

The primary chilled water of 2.5°C is conveyed to underground cooling chamber through the primary circulating pump in the ground refrigerating machine house and then is exchanged to the secondary chilled water of 6.5°C through high-low pressure heat exchanger. Finally the treated water

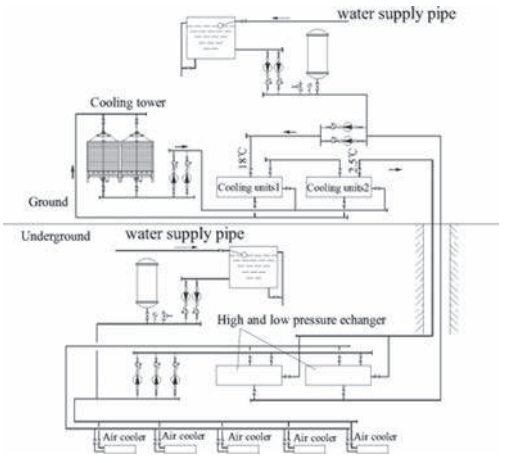


Figure 1. Flow chart of ground concentrated system.

is transported to each cooling spot where water is refrigerated by underground air cooler. The underground backwater temperature difference is designed to be 12°C.

3.4 *Construction of refrigerating machine room*

It is known from the cooling demand of the whole period in Table 1 that the cooling load fluctuation of Zhujixi coal mine during refrigeration is divided into two phases: smaller cooling load in construction period and startup time and larger cooling load in early production and production tail. Therefore, the construction scale of ground refrigerating house can be made by stages. Two 6000 kW refrigerating units are constructed in production tail instead of one unit to meet the cooling demand because the cooling capacity of ground concentrated cooling is required to reach 7650 kW in the early production. This paper suggests constructing two 6000 kW refrigerating units simultaneously and reserving adequate space for expanding one 6000 kW refrigerating unit.

3.5 *Layout of underground cooling chamber*

The layout of underground cooling chamber needs to take high-low pressure heat exchanger and secondary circulating pumps into account. Secondary water is neither constant pressure device nor pump power distribution.

Two sets of high-pressure heat exchanger whose heat transfer ability is up to 10 MW are suggested in order to leave enough room for future expansion in limited space.

Secondary circulating pumps are designed to be controlled by variable frequency and three pumps

Table 1. Cooling load table of underground refrigeration.

No.	Title of cooling face	Refrigerating capacity (kW/face)	Qty of faces (Face (pcs))	Total refrigerating capacity of all faces (kW)
1	Construction period			4500
1.1	Heading	750	6	4500
2	Startup time			5900
2.1	Heading	750	6	4500
2.2	Stope face	1400	1	1400
3	Early production			
3.1	Heading	750	6	4500
3.2	Stope face	1400	2	2800
4	Production tail			
4.1	Heading	750	8	6000
4.2	Stope face	2400	2	4800

like this will be collocated, two of which are put into operation and one for reservation to adapt themselves to the lift out of flow changes of secondary system operation which results from the difference of cooling supply in early production and production tail.

Constant pressure water inlet device and filter device are built up at a time in secondary circulating water system.

3.6 *Design of chilled pipeline system under mine*

Chilled pipelines are installed along the main entry and the cooling pipes are set in the crossheading of sealing tape machine in stope face.

The main pipes of underground chilled ducts are connected by flange and fast connectors are used at the end, which is easy for pipes to be dismounted with the advance of coal mine.

It is necessary to uniformly take the ducts of watering and air-pressing into consideration to determine the installed location of chilled pipelines in roadway. In the principle of convenience for traffic, pedestrians and installation & maintenance, special makers should be periodically made on the pipe so as to easily distinguish and manage pipes.

According to *Regulations of Heat Damage Prevention Underground Coal Mine,* it is appropriate if the flow velocity of chilled pipelines is 1.9–2.5 m/s (China Coal Construction Association 2007) and duct pressure should design to be 4.0 MPa based on which to decide the wall thickness of chilled pipes.

3.7 *Terminal equipments of underground cooling*

3.7.1 *Arrangement of air cooler in the driving face*

Air cooler is advised to be set in a place of driving face where it is less than 100 m far away from inlet tunnel air cooler at the opposite direction. Air cooler moves forward with the advance of heading and it moves once every 100 m advance.

Overcoming the resistance of air cooler should be considered in selecting the type of local driving fan because air cooler is not motivated by itself. Metal hose is adopted to connect air cooler water pipes with main pipe of refrigerant water.

3.7.2 *Arrangement of air cooler in stope face*

Air cooler in stope face is advised to set in the crossheading of belt and it is divided into pre cooling air cooler and face-cooling air cooler based on purpose. Pre cooling air cooler is responsible to eliminate the heat load occurring along the belt crossheading to precool the intake in stope face while face-cooling air cooler is to eliminate the heat load gained along the stope face to cool it.

The paper suggests selecting such an air cooler whose parts can be alternatively used and cooling exchange capacity is up to 400 kW since this device is always moved around.

The face-cooling air cooler is designed to arrange in the crossheading of belt machine where it is less than 100 m away from the coal face. The cooler must move back at intervals with the processing of extraction in coal face.

4 CONCLUSIONS

1. This paper analyses the environment of cooling load in underground cooling and the characteristics of heat damage in Zhujixi coal mine.
2. According to the analysis of common refrigerating methods for underground cooling, this paper recommends to apply ground concentrated cooling method to Zhujixi coal mine based on the characteristics of heat damage and determines the refrigerating parameter for cooling at the same time.
3. This paper puts forward the ground concentrated cooling process in Zhujixi coal mine and confirms the scale of ground refrigerating station, the layout of underground chamber, underground chilled pipelines and terminal cooling equipments.

To sum up, this paper makes a research on the typical high-temperatured Zhujixi coal mine whose depth is more than 900 meters and heat damage is serious. It not only puts forward the adoption of concentrated two-stage refrigeration on the ground and the high-low pressure heat exchanger to solve the problem of high hydrostatic pressure in large mining depth mine, but also suggests using domestic equipments to overcome the underground heat damage of similar mines.

REFERENCES

China Coal Construction Association. 2007. *Regulations of Heat Damage Prevention Underground Coal Mine*. Beijing: China Planning Press.

Hu Hanhua. 1997. Dynamic Research on Ventilation and Cooling in Deep & High Temperature Mine. *Metal Mine* (7): 37–46.

The State Bureau of Safe Production Supervision and Administration. & State Administration of Coal Mine Safety. 2011. *The Safety Regulations for Coal Mine*. Beijing: Coal Industry Publishing House.

Wang Wen et al. 2002. Treatment of Heat Damage Under Mine. *Mining Safety & Environmental Protection* (6): 31–33.

Wei Xiujun. & Hu Chunsheng. 2007. *Theory of Underground Cooling and Engineering Design*. Beijing: Coal Industry Publishing House.

This page intentionally left blank

Progress in Mine Safety Science and Engineering II – He et al. (Eds)
© 2014 Taylor & Francis Group, London, ISBN 978-1-138-00122-0

Application feasibility study of single based station CORS in deformation monitoring of mine slope

Q.B. Wei, W. Li, L.B. Gao & C. Wang
University of Science and Technology Liaoning Civil Engineering Academy, Anshan, Liaoning, China

Q.L. Li
Shenyang Longtian Surveying and Mapping Technology Co., Ltd., Shenyang, Liaoning, China

ABSTRACT: This paper introduce the methods and common characteristics in deformation monitoring of mine slope and the need to establish CORS (Continuous Operational Reference System), which based on the significance of deformation monitoring of mine slope. It validates the feasibility of application in deformation monitoring of mine slope combined with the actual situation of mine slope.

1 THE SIGNIFICANCE OF DEFORMATION MONITORING OF MINE SLOPE

Nowadays, with the rapid development of China's economy, the demand for energy and mineral resources is also a substantial increase. In order to increase yields, all districts make great efforts to expand the scale of production, but the ensuing increase in production at the same time that these project area and operation of the project during the formation of slope safety (deformation) monitoring issues.

In slope engineering construction, through safety monitoring the slope engineering, this can play a role in some of the following:

- We should evaluate the stability during slope construction and use, make such deformation forecasting. For sliding and slid landslide, we should control their evolution, in time to capture the characteristics of collapse and hazard information, such as the correct analysis and evaluation, forecasting and management of slide, landslide and related projects, providing reliable information and scientific evidence.
- To prevent landslides and possible slip and creep, we should provide timely decision support, the boundary conditions of prediction and forecasting landslide, scale, sliding direction, time of occurrence and degree of harm, and to take timely measures to avoid and mitigate disaster losses.
- By monitoring, we can provide the corresponding parameter basis of the parties to departments for decision-making, provide relevant information to develop disaster prevention and relief corresponding countermeasures.
- For the monitoring slid failure and reinforcement landslide, the monitoring results are the scale to evaluate the treatment effect.
- To provide parameters, for carrying out the numerical simulation of displacement back analysis.

2 THE COMMON METHODS AND CHARACTERISTICS OF DEFORMATION MONITORING OF MINE SLOPE

There are three current commonly used methods in mine slope deformation monitoring, namely geodetic method, close-range photogrammetric method and GPS method. Now we compare the characteristics and applicability of these methods, as show in table 1:

3 THE NECESSITY AND SIGNIFICANCE OF CORS ESTABLISHED

- The establishment of the CORS can greatly improve the survey accuracy, speed and efficiency, reduce labor intensity and cost.
- The establishment of the CORS can real, effective, long-term monitor the deformation of construction, fast prediction of disaster.
- CORS will be an important part of the digital mine, and establish the mine's 3d, dynamic, geocentric reference frame, and thus achieve a real digital mine from the real surface of the spatial location information.

Table 1. Compare current commonly used methods.

Common monitoring methods	Monitoring instrument	Characteristics of the method	Applicability of the method
geodetic method	Total Station	Precision, high speed, high degree of automation, easy to operate, saving manpower, track automatically continuous observation and large amount of monitoring information	Adapt to different stages of deformation displacement monitoring; as the limits conditions of the terrain, adapt to larger rate of the horizontal deformation displacement and crag change of landslide cracks monitoring; influenced by climatic conditions
close-range photogrammetric method	Measurement Camera	large amount of monitoring information, saving manpower, putting fast, safe, but relatively low accuracy	adapt to larger rate of the horizontal deformation displacement and crag change of landslide cracks monitoring; influenced by climatic conditions
GPS method	GPS receiver	Precision, putting fast, easy to operate, all-weather observation, terrain and sight unrestricted; high cost but developing promising	adapt to three-dimensional displacement monitoring of Slope body' surface in different deformation stage

4 SINGLE BASED STATION CORS SYSTEM

4.1 *The principle of single based station CORS system*

Single base station CORS is only a continuously operating reference stations. Like RTK of one plus one or one plus N, but the base station consists is instead of a continuously operating reference station. A control software of base station real-time monitor satellite state, store and transmit data, while a server provide differentiated services network and user management.

The principle of the system is as follows:

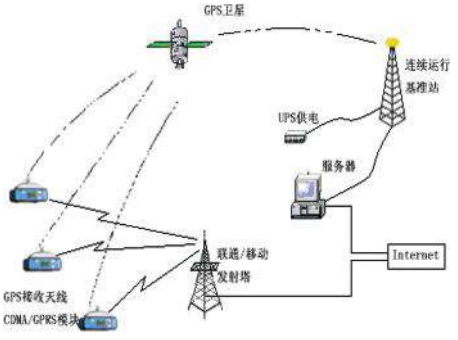


Figure 1. The diagram of the entire system.

4.2 *The advantages of single based station CORS system*

- Less investment;
- You can upgrade and expansion at any time;
- Data reliability, stability, security;
- Wide range of operations;
- Short construction period.

5 FEASIBILITY OF THE APPLICATION EXPERIMENT

5.1 *Monitoring network of slope plane displacement*

Case in a surface mine to study in Anshan. Monitoring points are based on characteristics of the slope to choose. On-site field surveys, we conduct the safety monitoring network optimization, network conduction and initial observation. Considered in the design optimization, we enhanced grid structure, taking into account the situation and development trend of conventional high-precision measuring instruments. There are seven monitoring points, numbered form 01~07, alone the slope of the distribution. The ultimately determine design shown in Figure 2.

5.2 *Comparison and analysis of parameter selection*

5.2.1 *Comparison height cut-off angle*

There are three high cut-off angles of 15°, 20°, 25°, using HDS2003software to solute baselines,

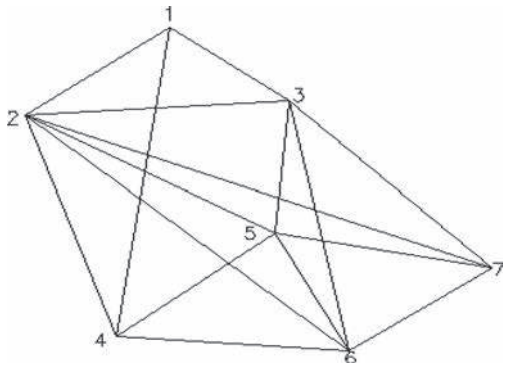


Figure 2. The design figure of monitoring network.

through comparison of the GPS network observations with conventional corner, the choice of cut-off angle 20 ° height works best.

5.2.2 *Comparison session length*

It broken down into 3 hours, 6 hours, 12 hours for observation data of twelve hours and high cut-off angles of 20°.Using HDS2003 software to solute, through the influence of the baseline analysis shows that: 3 hours observation can meet the requirements, six hours and twelve hours of observations were no significant differences observed values.

5.2.3 *The starting point coordinates precision*

The reference point 01 as starting point, using HDS2003 for a sophisticated baseline solver. Through comparison with the results of joint measurement geocentric coordinates and concluded: starting point joint measurement precision geocentric coordinates can be improve the accuracy of baseline solution, its impact on the results of baseline solution that can not be ignored.

5.3 *Four parameters for solving*

We check out the location in the mining area based on the control network results table of the original mine, according to the actual distribution of the control points, select the measurement sequence and walking routes, determine the points for solving four parameters and checking. Obtain the four parameters by using the three of points:

szdCx1 = 153.4178875911,
szdCy1 = –284.0327895976,
szdCa1 = 0.00003869900054746,
szdCk1 = 0.99997218215827788,

The other point to check, ΔX = 0.021 m, ΔY = 0.008 m, ΔH = 0.002 m, Check is successful.

Table 2. Accuracy of calculation in different cut-off elevation angles.

High cut-off angles	RMS MIN (mm)	RMS MAX (mm)	RMS MEAN (mm)	Ratio MIN	Ratio MAX	Ratio MEAN
15°	4	6	5.07	7.3	16.6	5.15
20°	4	5	4.85	6.6	16.7	5.43
25°	4	5	4.78	4.9	16.9	5.51

Table 3. Accuracy of calculation in different session lengths.

High cut-off angles	RMS MIN (mm)	RMS MAX (mm)	RMS MEAN (mm)	Ratio MIN	Ratio MAX	Ratio MEAN
3h	4	13	6.5	7.9	21.4	9.4
6h	3	10	7.3	8.9	64.7	22.4
12h	2	13	6.9	7.6	39.8	15.5

Table 4. Table of the results.

Dot mark	X	Y	Z
1	54066.229	3131.212	141.393
2	54180.099	3121.693	141.787
3	54066.130	2859.219	142.262
4	53757.446	3087.949	141.248
5	53720.976	3198.699	141.268
6	53695.687	3120.941	141.340
7	53768.023	3130.292	141.305
Dot mark	ΔX/m	ΔY/m	ΔH/m
1	–0.017	–0.031	0.007
2	0.026	–0.002	–0.005
3	0.012	0.033	0.001
4	0.021	0.007	–0.003
5	–0.023	0.003	0.023
6	–0.011	–0.025	0.047
7	–0.025	–0.005	0.039

5.4 *Achievement test*

Measuring preserved relatively intact points one by one in the original control network in the mining area, real-time saving each measurement data, transmitting and processing the data after observation. Comparing the results with the results of original control network as follows:

6 CONCLUSION

The experiments in this paper is the use of single based station CORS system to measure the well-preserved known points in the network of the

mine, and to test accuracy, stability and reliability of the single based station CORS system. It proven single based station CORS system stability, simple operation, high precision, constantly monitor, expanding the range of operations, used for mine slope deformation monitoring can greatly save manpower, material and financial resources.

REFERENCES

Bai, L et al. 2005. Research on the Precision and Stability of the Solution of GPS Cors. Journal of Henan polytechnic university (Natural science) 24(4), 15~18.

Liu, J.N. & Liu, H. 2003. Continuous operational reference system-infrastructure of urban spatial data. Wuhan University (Information Science Edition) 2003 (6):259~264.

Liu, J. 2005. The considerations of China development continuously creating reference station system. China surveying and mapping news 4 (6):54~58.

Ling Rui S86 Product Manual.

Li, J et al. 2007. Online Satellite Positioning User Service Based on CORS. Bulletin of surveying and mapping 3 (8): 25~32.

Neilan, R.E et al. 1997. The International GPS Service in 1997:5 Years of Practical Experience; 3 Years of Official IAG Service. In: Proc. of IAG Assembly. RIO.

The introduction of CORS by SOUTH.

Yang, G et al. 2007. Counstruction and application of GZCORS. Geospatial information 5 (3):20~2.

Zhou, L. 2004. The necessity and significance of CORS established. South surveying and mapping news 5 (3):46~51.

Zhang, K. 2003. Development of the Victorian High Precision Permanent GPS Tracking Network with Real time Positioning Capacity. Proceedings of the International Symposium Satellite Navigation Technology and Application Melhoume, Australia, July.

Progress in Mine Safety Science and Engineering II – He et al. (Eds)
© 2014 Taylor & Francis Group, London, ISBN 978-1-138-00122-0

Study on building permanent underground refuge chamber in Dayangquan Coal Mine

Tian Zhang, Longzhe Jin, Na Gao & Xiao Huang
School of Civil and Environment Engineering University of Science and Technology Beijing, Beijing, China

ABSTRACT: By analyzing the conditions of Dayangquan Coal Mine, a permanent refuge chamber was constructed in an abandoned underground. By analyzing the risk factors, the protection functions of the permanent refuge chamber were determined to be heat-resistant, anti-explosion and gas-outburst-prevention. The space was divided into buffer area, emergency area and refuge area. The total length of the chamber was determined to be 33 m, the width to be 4.2 m and the effective area to be 138.6 m^2 according to the size of magazine, people and equipment. According to the per capita air supply volume, the minimum air supply volume of the compressed air supply system was 14.4 m^3/min for 40 persons. The minimum oxygen supply volume of oxygen generation purifier was 24 L/min. The fireproof anti-explosion airtight system was composed of 4 protection doors which was determined. The study provides reference for the building of permanent refuge chambers with similar scales.

1 INSTRUCTION

Coal mines in China are mostly underground mining with characteristics of complicated environment and varied accident types, etc. In recent years, the underground accidents occur frequently in the coal mines in China with mass casualties and property damages which restrict the development of coal industry in the country. According to relevant statistical data, the number of persons who died on the spot with the reasons of explosion and high temperature, etc. only accounts for about 10% of the total casualties. Most casualties are caused by oxygen depletion, asphyxiation from high concentration poisonous and harmful gases, blocking-up of escape route, etc. This paper carries out study on the site selection and building of permanent refuge chamber and the key techniques of various life support systems which have important significance not only to the improvement of emergency rescue capacity of Dayangquan Coal Mine but also to the building of permanent refuge chambers with similar size (Yang 2002).

2 THE GENERAL SITUATION OF DAYANGQUAN COAL MINE

2.1 *The situation of mine distribution*

Dayangquan Coal Mine is located to the south of Xiyuzhang Village, Yijing Town, Yangquan City, with the length of 3.7 km from west to east, and the width of 4.0 km from south to north. Currently, mining is mainly conducted at No. 12 and 15 coal seams. The mine field covers an area of 10.7891 km^2, with a mining elevation of 650–450 m. The stratum of mine is northeast to southwest tilt, with a dip angle of about 10°, and a fault throw of about 20 m. Fully-mechanized excavating and blasting methods are adopted for the mine. The driving face is divided into haulage roadway, rail roadway and return airway, and the stope face is divided into haulage tunnel, return air tunnel and tail roadway. The length of stope face of No. 12 coal seam is 180–200 m, and that of No. 15 coal seam is 150–180 m. The main support patterns are anchor rod anchor cable and anchor mesh.

2.2 *Underground mining conditions*

The conditions underground:

1. Gas conditions: based on an appraisal, the absolute gas emission rate of Dayangquan Coal Mine is 89.5 m^3/min, and the relative gas emission rate is 37.61 m^3/t, so it is a highly gassy mine.
2. Coal dust conditions: the minimum ignition temperature of coal dust cloud for No. 12 coal seam is 900°C, and that of No. 15 coal seam is 920°C. The coal dust in both seams is non-explosive.
3. Water content: the normal water inflow of No. 12 coal seam and No. 15 coal seam is about 45 m^3/h, and 80 m^3/h in maximum. There are mainly water seepage from the roof, the shaft and the goaf, among which the seepage from goaf is the major source of the mine inflow.

4. Geothermal and geostatic pressure: according to coalmine production practices, there have been no abnormal phenomena of geothermal and geostatic pressure found till now.

According to the general situation of Dayangquan Coal Mine, the permanent refuge chamber will be constructed in No. 12 coal seam or No. 15 coal seam, which can resist damages caused by accidents of highly gassy mine, such as fire, explosion and outburst of gas.

3 STUDY ON SITE SELECTION OF THE PERMANENT REFUGE CHAMBER

3.1 *Principles of site selection*

Chamber siting rules:

1. The refuge chamber shall not be arranged at places with potential safety hazards, such as substations, explosive magazines and oil storage facilities (Sun 2010).
2. The refuge chamber shall be constructed in areas with stable surrounding rocks and shall be far away from places such as faults, which are liable to be affected by mining and geological activities (Mickey 2007).
3. Underground hydrogeology and mining area distribution shall be considered for site selection of the refuge chamber, and it is required to be arranged on the mining route for avoiding of disasters (Rick & Graham 1999).
4. The refuge chamber shall be constructed by taking full use of existing chambers which are well supported, so as to reduce the construction cost and construction period (Yu et al. 2010).

3.2 *Determination of site selection*

Mining was mainly conducted in No. 12 coal seam and No. 15 coal seam of Dayangquan Coal Mine. Specifically, it was conducted on working face 2121 of No. 12 coal seam, and working face 8125 of No. 15 coal seam. Based on the distribution of underground mining area, hydrogeology and situations of the existing chambers, the permanent refuge chamber of Dayangquan Coal Mine was finally selected in the abandoned explosive magazine at +630 mining level in No. 12 coal seam (as shown in Fig. 1).

The advantages of the site:

1. The chamber was existing, with a clear height of 2 m, so the dimensions of chamber was close to the requirement of building size so as to reduce the construction period and construction cost.
2. This site was about 600–700 m away from the personnel on working face of No.12 coal seam, thus the specified requirements that the distance from refuge facilities should not exceed 1000 m can be satisfied.
3. The surrounding areas exceed 1000 m were provided with moveable refuge chamber as the refuge space. Its length was enough for 30 mobile personnel in the roadway to avoid dangers.

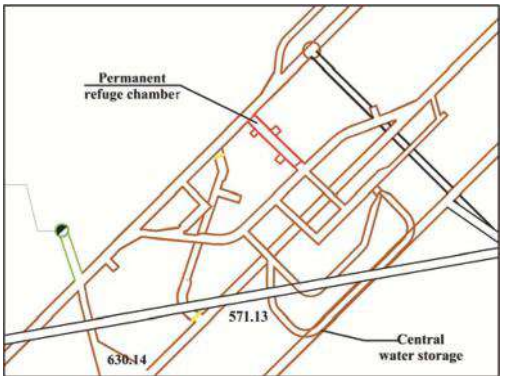


Figure 1. The site of the permanent refuge chamber at +630 mining level in No. 12 coal seam for 40 persons.

4 STUDY ON FUNCTIONAL STRUCTURE AND SCALE OF THE PERMANENT REFUGE CHAMBER

4.1 *Study on basic function and structure of refuge chamber*

4.1.1 *Function of refuge chamber*

Based on the risk factors of Dayangquan Coal Mine, the permanent refuge chamber of No. 12 coal seam has the functions such as high temperature resistance, shock resistance and air-tightness. The protection parameters are shown in Table 1 (Sui 2007).

4.1.2 *Structure of refuge chamber*

Based on relevant specifications and major functions of the chamber, the space of the permanent refuge chamber of Dayangquan Coal Mine was divided into the three areas (as shown in Fig. 2).

1. Buffer area: it prevented the poisonous gas from entering the chamber along with the refuge personnel. There were air curtain isolation system, sanitary fittings and power control system arranged within this area.
2. Refuge area: as the major movement area of refuge personnel, it provided the refuge personnel with oxygen supply system, refrigerating system, purification system, monitoring and controlling system, communication system, food and water, which were necessary for survival.

Table 1. The protection parameters of the permanent refuge chamber of Dayangquan Coal Mine.

Protective performance	Protective parameters
Resistance to instantaneous high temperature	>1000°C
Resistance to explosion shock	>0.5 MPa
Airtight function	CH_4, CO
Oxygen volume	18%~23%
Interior temperature	35°C
Interior humidity	80%
Monitoring	CO, O_2, CH_4, CO_2
Communication and signal transmission	Not less than two methods

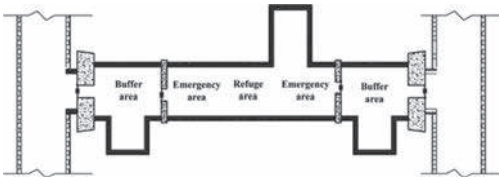


Figure 2. The area distribution of the permanent refuge chamber of Dayangquan Coal Mine.

3. Emergency area: it provided the injured refuge personnel with simple curing. There were simple medical supplies, equipment and stretchers arranged within this area.

4.2 *Building size of the refuge chamber*

4.2.1 *Overall dimensions of the refuge chamber*

The overall dimensions of the permanent refuge chamber of Dayangquan Coal Mine were determined by total receiving capacity, equipment volume, safety factors of spatial size.

1. Effective area of chamber

$$S = (S_1 \times \mathrm{n} + S_2 + S_3) \times R \times K \quad (1)$$

where S = effective area of the chamber; S_1 = the average effective area; n = the rated receiving capacity of the chamber; S_2 = the equipment area of the refuge chamber; S_3 = the area of protecting wall; K = the safety dimension factors of the chamber; and R = impact factor of the spatial environment. The calculated effective area of chamber was 138.6 m^2.

2 Overall dimensions of chamber

① Length:

$$L = A + 2 \times B + 2 \times (C + D) + E \quad (2)$$

where L = the overall length of the chamber; A = the length of the refuge area; B = the length of buffer area; C = the thickness of internal protecting wall; D = the thickness of external protecting wall; and E = the length of the shoring roadway of the chamber. The calculated total length of refuge chamber was 33 m.

② Width:

$$W = \frac{S}{L} \quad (3)$$

where W = the width of chamber; S = the effective area of chamber; and L = the total length of chamber. The calculated effective width of chamber was 4.2 m.

③ Height:

Based on the requirements for equipment, personnel and spatial size, the effective height of main chamber was determined as 3.4 m, and that of the auxiliary chamber was 2.8 m.

Finally, the total length of the permanent refuge chamber of Dayangquan Coal Mine was 33 m, the length of buffer area of the chamber was 6 m, and that of the refuge area was 15 m. The two auxiliary chambers were 3 m in depth (the intermediate chamber was originally owned by the explosive magazine), and main chamber section was 3.4 m in effective height and 4.2 m in effective width; the auxiliary chamber was 2.8 m in effective height and 3.0 m in effective width(as shown in Fig. 3).

4.2.2 *Study on sectional dimensions and supports of the refuge chamber*

According to the theory of loose circle, the permanent refuge chamber of Dayangquan Coal Mine belongs to big broken rock zone, class IV, thus the combination of anchoring, meshing and shotcreting was applied for supporting.

1. Sectional dimensions: according to the theory of loose circle, the sectional dimensions for semicircular arch structure were as follows: the clear width of main chamber was 4.2 m, the diameter of semicircular arch was 2.1 m, and the height of chamber wall (including chamber floor) was 1.6 m; the clear width of auxiliary chamber was 3.0 m, the diameter of semicircular arch was 1.5 m, and the clear height of chamber wall was 1.3 m.
2. Support type: secondary support method was adopted according to the type of wall rock and the experience: the primary support applies anchor, anchor cable, anchor net and shotcreting method, with the specifications of anchor cable being ① $\Phi 21.6 \times 8300$ mm, ② $\Phi 21.6 \times 6300$ mm and the anchoring length being 1000 mm. The secondary arch building support, with the strength being C30, was provided with joist steel of No. 11 and metal mesh(as shown in Fig. 4).

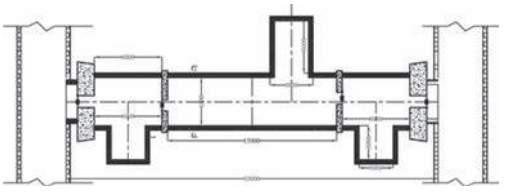


Figure 3. The overall dimensions of the permanent refuge chamber of Dayangquan Coal Mine.

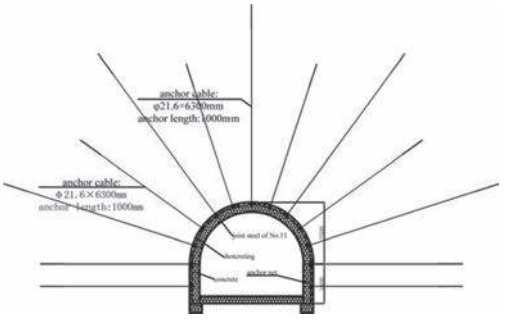


Figure 4. The cross dimensions and supporting pattern of the permanent refuge chamber of Dayangquan Coal Mine.

5 STUDY ON LIFE SUPPORT SYSTEMS OF THE PERMANENT REFUGE CHAMBER

In order to meet living needs of refugees, the refuge chamber of Dayangquan Coal Mine was provided with fireproof anti-explosion system, air curtain isolation system, oxygen supply system, communication system, safety monitoring and control system, refrigeration and dehumidification system and auxiliary system. As the oxygen supply system and fireproof anti-explosion airtight system were used as crucial protection system against fire, high temperature, explosion and gas outburst, they would be studied with emphasis.

5.1 *Study on oxygen supply system*

According to the ground conditions of the permanent refuge chamber of Dayangquan Coal Mine, drilling was inadvisable. Therefore, the mode of "two-stage oxygen supply" was adopted so as to meet oxygen demands of refugees, including mine compressed air oxygen supply system and oxygen generation purifier (Gao et al. 2012).

5.1.1 *Compressed air oxygen supply system*

For the mine compressed air oxygen supply system, fresh air is transferred into the refuge chamber by the ground compressor and compressed air duct, and then released into the space uniformly after depressurization, flow stabilization and noise reduction by the compressed air control system of the refuge chamber. According to the differential pressure principle, contaminated air is vented through return air duct to realize air circulation.

As average air supply per capita shall not be less than 0.3 m^3/min, the total air supply of the refuge chamber should be determined as:

$$Q = Q_1 \times n \times K \tag{4}$$

where Q = total air supply of refuge chamber per unit time; Q_1 = average air supply per capita; n = the capacity of refuge chamber; and K = safety factor. The minimum calculated air supply should be 14.4 m^3/min.

5.1.2 *Oxygen generation purifier*

When external air supply pipes of underground compressed air supply system were damaged or forcing fan was broken down, the oxygen generation purifier must be started. The system was composed of three parts, i.e. conflux system, control system and purification system.

1. Conflux system: oxygen from oxygen bottles was organized uniformly and then conveyed to the control system through pipeline.
2. Control system: input oxygen went through the processes of depressurization, current stabilization and noise reduction. According to actual person number in the refuge chamber, a certain amount of oxygen was sent to the purification system.
3. Purification system: co_2 generated by human body was absorbed and purified and then released into air together with input oxygen so as to meet air supply demands.

Total oxygen storage volume of the oxygen generation purifier system in the permanent refuge chamber of Dayangquan Coal Mine was:

$$Q_y = q \times n \times K \tag{5}$$

where Q_y = total volume of the oxygen generation purifier system; q = average air demand per capita, rated; n = the capacity of refuge chamber; and K = safety factor. The minimum calculated oxygen storage volume of the oxygen generation purifier system of Dayangquan Coal Mine was 24 L/min.

5.2 *Study on fireproof anti-explosion airtight system*

The fireproof anti-explosion airtight system of the refuge chamber was used to protect the chamber

against damages from fire, explosion and gas outburst accidents, which was the first course of protection system of the chamber. The system includes: fireproof anti-explosion airtight door and fireproof anti-explosion airtight wall.

1. Fireproof anti-explosion airtight door

As indicated in the figure 3, the permanent refuge chamber of Dayangquan Coal Mine was provided with 4 fireproof anti-explosion airtight doors on both sides. Two outside protective doors were mainly used to realize anti-explosion, high temperature resistance and airtight functions. The door body should be made of 16Mn steel with yield strength and elasticity modulus respectively as 350 MPa and 206GPa. Two medium protective doors were mainly used to realize airtight function with total weight less than that of outside protective door.

2. Fireproof anti-explosion airtight wall

Fireproof anti-explosion airtight walls of the chamber were similar to the protective doors, with main functions of anti-explosion, high temperature resistance and airtight. In order to guarantee overall performance of the doors and walls, they should be grouted as a whole with concrete of C30.

The system was enough strong to resist instantaneous high temperature of 1000°C, continuous high temperature of 260°C and shock wave greater than 0.5 MPa. Meanwhile, anti-explosion airtight doors were flexible, swift and airtight in manual startup mode (Silvestrini et al. 2008).

5.3 *Study on other systems*

Other systems were set in the refuge chamber for the basic survival needs.

1. Air curtain isolation system

The air curtain isolation system was mounted above the entrance of external protective door of the permanent refuge chamber of Dayangquan Coal Mine. When refugees enter, an air curtain was formed by this system, and it could effectively prevent toxic gas from entering into the refuge chamber with refugees.

2. Safety monitoring and control system

The safety monitoring and control system which was mounted on the inside and outside of the refuge chamber of Dayangquan Coal Mine can monitor temperature, humidity and the changes of CO, CO_2, O_2, CH_4, H_2S and then transfer the data to ground control center so as to facilitate dispatching (Zhang 2005).

3. Refrigeration and dehumidification system

All the persons and equipment would release water and heat during refuge and operation to cause temperature and humidity rise, which would finally bring about suppression in the chest and heatstroke to refugees. In case of serious situation, it would treat to life. Ice generation refrigeration and dehumidification system was adopted in the refuge chamber to maintain indoor temperature not greater than 35°C and humidity not greater than 80% (Luo et al. 2005, Xu & Li 2005).

4. Auxiliary systems

The auxiliary systems of the permanent refuge chamber could meet basic survival needs of refugees, including lighting system, power system, water, food, sanitary installation, armamentarium, fire fighter and self-rescuer.

6 CONCLUSIONS

The following conclusions can be drawn according to the study.

1. Based on the analysis of the mine conditions, it was determined that the permanent refuge chamber would be located in the abandoned plane explosive magazine at +630 mining level of No. 12 coal seam; this option reduced construction period and cost.
2. Based on the analysis of main harmful factors of the mine, it was determined that main functions of the permanent chamber were resistance to high temperature and shock and air-tightness.
3. According to function demands of the refuge chamber, the space was separated into buffer area, emergency area and refuge area.
4. According to per capita area, equipment volume and space dimensions, it was determined that effective area of the refuge chamber was 138.6 m^2 with an overall length of 33 m; for the main refuge chamber, the section should be in arch shape with an effective height of 3.4 m and an effective width of 4.2 m; for auxiliary chambers on both sides, the dimensions were a depth of 3 m, an effective height of 2.8 m and an effective width of 3.0 m. They should be supported in combined methods of grouting, anchorage and arching.
5. According to air supply volume per capita, it was determined that the minimum air supply volume of compressed air oxygen supply system was 14.4 m^3/min and that of oxygen generation purifier was 24 L/min.
6. According to requirements for anti-explosion, high temperature resistance and airtight performance, the fireproof anti-explosion airtight system should be composed of fireproof anti-explosion airtight doors and walls. The doors should be made of 16 Mn steel and the walls should be constructed by C30 concrete.

REFERENCES

Gao, N. et al. 2012. Research and Application of Oxygen Supply System in Changcun Coal Mine Refuge Haven. *Journal of China Coal Society* 37(6):1022–1025.

Luo, M.Z. et al. 2005. Human Body's Thermal Adaptation and Thermal Comfort. *Refrigeration and Air-Conditioning* 1:75–78.

Mickey, D.M. 2007. *Analysis of Underground Coal Mine Refuge Shelters*. Morgantown: West Virginia University.

Rick, B. & Graham, B. 1999. Criteria for The Design of Emergency Refuge Stations for an Underground Metal Mine. *Journal of the AusIMM* 12:1–12.

Silvestrini, M. et al. 2008. Flame Acceleration and DDT Run-up Distance for Smooth and Obstacles Filled Tubes. *Journal of Loss Prevention in the Process Industries* 21(5):555–562.

Sui, P.C. 2007. Self-Rescue of Miners and the Refuge Chamber. *Modern Occupational Safety* 6:82–83.

Sun, J.P. 2010. Effect and Configuration of "Six Systems" for Safety Act of Rescue of Coal Mine Underground. *Industry and Mine Automation* 10:1–4.

Xu, L.X. & Li, B.Z. 2005. Influence of Indoor Thermal Environment on Thermal Comfort of Human Body. *Journal of Chongqing University(Natural Science Edition)* 28(4):102–105.

Yang, D.M. 2002. The Mine Rescue Actuality in Our Country. *Modern Miner* 4:4–11.

Yu, X.Y. et al. 2010. Discussion and Application of Underground Refuge Room in Coal Mine. *Coal Science and Technology Magazine* 2:19.

Zhang, L.Z. 2005. *Dehumidification Technology*. Beijing: Chemical Industry Press.

Progress in Mine Safety Science and Engineering II – He et al. (Eds)
© 2014 Taylor & Francis Group, London, ISBN 978-1-138-00122-0

Study on distribution law of lead abutment pressure in fully mechanized caving face with large mining height

Fu-Lian He, Zhi-Yang Liu, Tong-Da Li, Sheng-Rong Xie, Huan-Kai Wu & Zhen Wei
School of Resource and Safety Engineering, China University of Mining and Technology (Beijing), Beijing, China

ABSTRACT: As the lead abutment pressure in fully mechanized caving face is difficult to be described quantitatively, the front coal mechanical model of mechanized caving face is established. The calculation formula of abutment pressure value and its distribution width is obtained by using elastic-plastic limit equilibrium theory. Furthermore, this paper researches the main factors of limit equilibrium area width and conducts formula derivation of horizontal displacement of the coal in limit equilibrium area. Results shows that: firstly, the lead abutment pressure increases with the increasing distance to working face in mechanized caving face, and arrives at the peak value in elastic-plastic junction. Secondly, the limit equilibrium width increases with the increasing mining height, roof coal thickness, occurrence depth, literal pressure coefficient and attenuation coefficient, and decreases with increasing caving ratio, coal-rock cohesion and internal friction angle; thirdly, the horizontal displacement in plastic area has linear increasing relationship with the plastic area width, Poisson's ratio of coal, and has inverse proportion with elastic modulus of coal. Lastly, the practical example of 8313 fully mechanized caving face of Dongrisheng coal mine of Pingshuo mining area verifies the rationality of mechanical model and calculation formula.

Keywords: lead abutment pressure, fully mechanized face, elastic-plastic limit equilibrium theory, horizontal displacement

1 INTRODUCTION

The lead abutment pressure caused by coal mining is one of essential reasons for dynamic disasters such as rock burst, water inrush and coal and gas outburst. Further research on distribution law of lead abutment pressure has significance of realizing the stability analysis of roadways, determination of fore-support distance and prevention of dynamic disasters (Pu & Liao 2002, Si et al. 2007). Domestic and abroad scholars have been researching the formation mechanism and distribution law of regular mining abutment pressure and thus put forward some mature theory and control techniques. However, in the condition of fully mechanized caving with large mining height, the research is conducted little. Because of stope structure, mining draft, mining height and roof coal, the distribution law of abutment pressure in fully mechanized caving face of thick coal seam performs specially (Liu et al. 2011, Yang et al. 2009, Gao et al. 2010). While, the present abutment pressure research methods focus on sites measurement and physical simulation, which only roughly judges abutment pressure distribution law. From the perspective of mechanical explanation, the research is not mature, and hence the lead abutment pressure is difficult to be described (Xie & Wang 2010, Xia et al. 2011, Jiang & Ma 2002). Therefore, the distribution law feature of fully mechanized caving face needs to be studied with mechanical way.

This paper takes the front coal of fully mechanized caving face with large mining height as research object. With the premise of adequate consideration to geological and production conditions, the lead abutment pressure of fully mechanized caving face is researched by means of elastic-plastic limit equilibrium theory, meanwhile, the nonlinear plastic modulus is introduced to deduct the horizontal displacement formula in plastic area, which provides basis for stope, roadway surrounding rock control and dynamic disasters prevention.

2 THEORETICAL ANALYSIS OF LEAD ABUTMENT PRESSURE IN FULLY MECHANIZED CAVING FACE WITH LARGE MINING HEIGHT

2.1 *Establishment of mechanical model*

Lead abutment pressure means the increasing vertical press of the front coal caused by mining, of which the value is usually 2~4 times than rock stress. In the role of high abutment pressure, the

front coal is easily damaged and enters limit equilibrium state. At the seam time, the abutment pressure transfers to the deep part of coal and even the elastic area. In the dynamic adjustment process of abutment pressure, the width of limit equilibrium area and its abutment pressure also dynamically changes (Zhao et al. 2011, Gong 2006). The coal body in limit equilibrium area is taken as the research object so as to conduct further study of the changing feature of lead abutment pressure. The mechanical model is established as shown in Figure 1.

According to the structure of fully mechanized caving stope and the mechanical characteristics, the assumptions are taken as follows: ① coal is uniform continuous medium and the elastic-plastic coupling influence of front coal is out of consideration in analysis process, and volumetric strain in front plastic area is zero; ② the relationship of horizontal and vertical stress is shown as follows:

$$\sigma_x = \alpha\sigma_y \tag{1}$$

Where, σ_x is horizontal stress, σ_y is vertical stress, α is lateral coefficient;

③ damage and deformation of plastic area meets Moore—Coulomb criterion:

$$\tau_{xy} = \sigma_y \tan\varphi_0 + c_0 \tag{2}$$

Where, τxy, c_0, φ_0 respectively are shear stress, cohesion and internal friction angle in interface.

④ taking the emergence and development defects in the roof deformation process into consideration, the roof coal is regarded as continuum damage body and thus the dynamic change occurs (Xie & Wang 2008, Wang 2011). In the elastic-plastic interface where $x = x_0$, stress boundary conditions are shown as follows:

$$\sigma_y|_{x=x0} = k\gamma H + \eta\gamma_0 M_0 \tag{3}$$

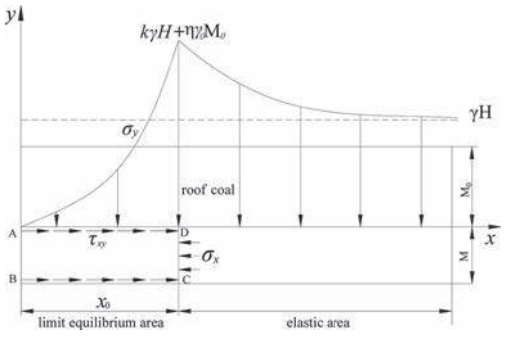


Figure 1. Mechanical model of limit equilibrium area coal.

Where, σ_y is vertical stress; K is stress concentration coefficient; γ is average bulk density of overlying strata; H is occurrence depth; η is attenuation coefficient; M_0 is roof thickness; γ_0 is roof bulk density; x_0 is width of limit equilibrium.

The advancing face direction is choose to x-axis, vertical direction is y-axis. And, the arbitraty unit coal in limit equilibrium area is taken as object, of which the height is M. The mechanical model is established as Figure 2. The unit is in limit equilibrium state and its equilibrium formula is:

$$Md\sigma_x - 2\tau_{xy}dx = 0 \tag{4}$$

2.2 *Deduction calculation of abutment pressure value and its peak position*

Combined with (1), (2) and (4), the followed formula is obtained:

$$\frac{d\sigma_y}{dx} - \frac{2\tan\varphi_0}{M\alpha}\sigma_y - \frac{2c_0}{M\alpha} = 0 \tag{5}$$

Differential Equation is solved as:

$$\sigma_y = \frac{M\alpha}{2\tan\varphi_0} e^{\frac{2\tan\varphi_0}{M\alpha}(x-c)} - \frac{c_0}{\tan\varphi_0} \tag{6}$$

Where, C is unknown constant, when the (6) is brought to (2), the followed formula is obtained:

$$\tau_{xy} = \frac{M\alpha}{2} e^{\frac{2\tan\varphi_0}{M\alpha}(x-c)} \tag{7}$$

Take the ABCD in Fig. 1 as research object, and the equilibrium formula is:

$$M\alpha\sigma_y|_{x=x_0} - 2\int_0^{x_0}\tau_{xy}dx = 0 \tag{8}$$

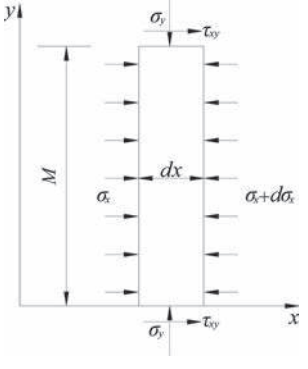


Figure 2. Mechanical model of unit body in limit equilibrium area.

When (8) is substituted by (6), (7), the followed formula is obtained:

$$C = \frac{M\alpha}{2\tan\varphi_0} \ln \frac{M\alpha}{2C_0} \tag{9}$$

When (9) is brought in (1), (6), (7), the following three formulas are obtained:

$$\sigma_y = \frac{c_0}{\tan\varphi_0} e^{\frac{2\tan\varphi_0}{M\alpha}x} - \frac{c_0}{\tan\varphi_0} \tag{10}$$

$$\tau_{xy} = c_0 e^{\frac{2\tan\varphi_0}{M\alpha}x} \tag{11}$$

$$\sigma_x = \frac{\alpha c_0}{\tan\varphi_0} e^{\frac{2\tan\varphi_0}{M\alpha}x} - \frac{\alpha c_0}{\tan\varphi_0} \tag{12}$$

When (10) is substituted by (3), the followed formula is obtained:

$$x_0 = \frac{M\alpha}{2\tan\varphi_0} \ln\left(\frac{k\gamma H + \eta\gamma_0 M_0 + c_0\cot\varphi_0}{c_0\cot\varphi_0}\right) \tag{13}$$

As is known from (10)~(12), σ_x, σ_y and τ_{xy} gradually increase in (0, x_0) and reach the maximum at x_0. According to (13), the width of limit equilibrium is affected by some factors such as mining depth, mechanical property of coal and rock, caving ratio. The following part conducts further study on influencing factors of lead abutment pressure distribution law.

3 INFLUENCING FACTORS ANALYSIS OF LIMIT EQUILIBRIUM AREA IN FULLY MECHANIZED CAVING FACE

3.1 *Occurrence depth*

When the parameters are set by: α = 0.3, c_0 = 0.5 MPa, φ_0 = 15°, k = 2, γ = 27 KN/m^3, γ_0 = 14 KN/m^3, M = 4 m, M_0 = 10 m, η = 0.9, the (13) is substituted as:

$$x_0 = 2.2\ln(1.2 + 0.03H) \tag{14}$$

As is known from the analysis of (14), H has logarithmic function relationship with x_0. When it is in (200, 600), the limit equilibrium width increases as the occurrence depth increases. Also, the expression formula of the width x_0 and H is obtained when the attenuation coefficient η = 0.2 and η = 0.6. The corresponding distribution curve of H—x_0 are shown in Fig. 3 when H is set by the following value 200, 300, 400, 500, 600.

As is known from Fig. 3, in the condition of other given parameters, the limit equilibrium width x_0 grows as H and η gradually increases.

3.2 *Caving ratio*

When the parameters are set by: α = 0.3, c_0 = 0.4 MPa, φ_0 = 20°, k = 2, γ = 27 KN/m^3, γ_0 = 14 KN/m^3, H = 300 m, η = 0.8, the coal seam thickness M_{total} = 14 m and the caving ration fcb: M/M_0, where M_0 = 14–M (3.5 < M < 7.5), then, (13) is substituted by:

$$x_0 = 0.42M\ln(1574 - 0.01M) \tag{15}$$

When $f(M) = M\ln(15.74 - 0.01M)$ (16)

If M is solved by first derivative and second derivative, the followed formula are obtained:

$$f'(M) = \ln(15.74 - 0.01M) - \frac{M}{1574 - M} \tag{17}$$

$$f''(M) = \frac{M - 3148}{(M - 1574)^2} \tag{18}$$

Apparently, f″(M) < 0, so f′(M) is monotonically decreasing function at (3.5, 7.5), and f′(7.5) > 0, and f(M) is monotonically increasing function at (3.5, 7.5), ie, f(M) increases with M increases. Therefore, the compound function related about M and x_0 is increasing function at (3.5, 7.5). Also, the expression formula of x_0 and M is obtained when the coal seam respectively are 12 m, 15 m and 18 m, and so is the corresponding f_{cb}—x_0 curve distribution figure.

As is known from the Fig. 4, if the other parameters are given, the width x_0 decreases with the caving ratio f_{cb} and coal seam thickness increase.

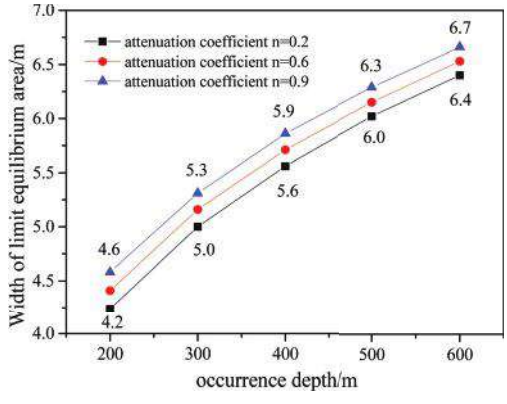


Figure 3. Relationship between limit equilibrium width and roadway occurrence depth.

3.3 *Thickness of roof coal seam*

When the parameters are set by: α = 0.3, c_0 = 0.5 MPa, φ_0 = 20°, k = 2, γ = 27 KN/m^3, γ_0 = 14 KN/m^3, H = 200 m, M = 5 m, η = 0.8 then, (13) is substituted as:

$$f(M_0) = 2.1\ln(8.8 + 0.1M_0) \tag{19}$$

As is known from (19), M_0 has logarithmic function relationship with x_0. The function monotonically increases (10, 40), ie, the limit equilibrium width x_0 grows with the roof coal thickness M_0 increases. The expression formula of x_0 and M_0 is obtained when the lateral coefficient α = 0.35 and α = 0.4. The corresponding distribution curve of M_0—x_0 are shown in Fig. 5 when M_0 is set by the following value 10, 20, 30, 40.

As is known from Fig.5, if the other parameters are given, the limit equilibrium width x_0 gradually increases with roof coal thickness and lateral coefficient.

3.4 *Mining height*

When the parameters are set by: α = 0.3, k = 2, γ = 27 KN/m^3, γ_0 = 14 KN/m^3, M_{total} = 15 m, H = 200 m, η = 0.9, if it is in the condition of less stable surrounding rock, c_0 = 0.5 MPa, φ_0 = 25°, and then (13) is substituted by:

$$x_0 = 0.32M\ln(10.9 + 0.1M_0) \tag{20}$$

Compared with regular fully mechanized caving face, the mining height is usually more than 3.5 m as to the fully mechanized caving face with large mining height. When (20) is substituted with the value of M that are 2 m, 2.5 m, 3 m, 3.5 m, 4 m and 4.5 m, the limit equilibrium width x_0 is obtained, and the variation law is analyzed. And, the corresponding distribution curve figure is drawn.

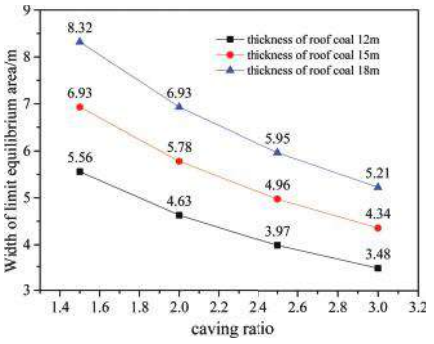


Figure 4. Relationship between limit equilibrium width and caving ratio.

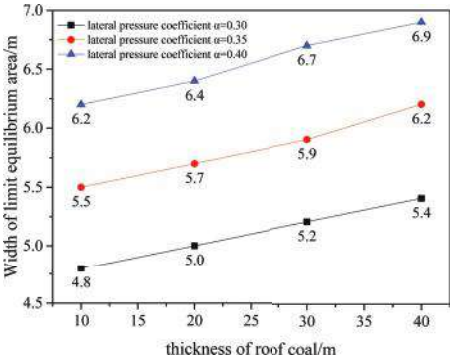


Figure 5. Relationship between limit equilibrium width and roof coal thickness.

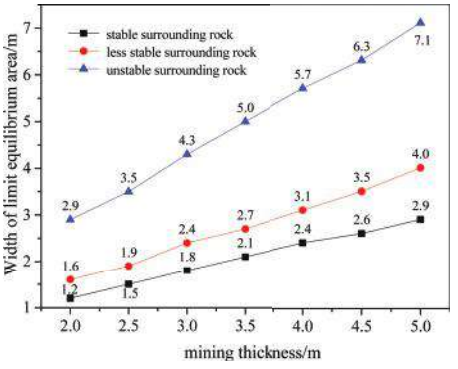


Figure 6. Relationship between limit equilibrium width and caving ratio.

As is known from the Fig. 4, if the other parameters are given, the width x_0 decreases with the caving ratio fcb and coal seam thickness increase.

4 HORIZONTAL DISPLACEMENT DEDUCTION OF PLASTIC AREA COAL IN FULLY MECHANIZED CAVING FACE

The transverse deformation of coal body in fully mechanized caving face is obvious of which the value could be obtained by means of the relationship between average stress and strain multiply the nonlinear plastic modulus.

According to the relationship between average stress σ and average strain ε:

$$\begin{aligned} \sigma &= \frac{1}{3}(\sigma_x + \sigma_y + \sigma_z) \\ \varepsilon &= \frac{1}{3}(\varepsilon_x + \varepsilon_y + \varepsilon_z) \end{aligned} \tag{21}$$

Generalized Hooke's theorem shows:

$$\begin{cases} \varepsilon_x = \frac{1}{E}\left[\sigma_x - \mu\left(\sigma_y + \sigma_z\right)\right] \\ \varepsilon_y = \frac{1}{E}\left[\sigma_y - \mu\left(\sigma_x + \sigma_z\right)\right] \\ \varepsilon_z = \frac{1}{E}\left[\sigma_z - \mu\left(\sigma_x + \sigma_y\right)\right] \end{cases} \tag{22}$$

(21) is further dealt to:

$$\varepsilon = \frac{1-2\mu}{E}\sigma \tag{23}$$

And, $$\varepsilon_x - \varepsilon = \frac{1+\mu}{E}\left(\sigma_x - \sigma\right) \tag{24}$$

Then:

$$\begin{cases} \varepsilon_x = \frac{1+\mu}{E}\left(\sigma_x - \sigma\right) + \varepsilon \\ \varepsilon_y = \frac{1+\mu}{E}\left(\sigma_y - \sigma\right) + \varepsilon \\ \varepsilon_z = \frac{1+\mu}{E}\left(\sigma_z - \sigma\right) + \varepsilon \end{cases} \tag{25}$$

The stress-strain relationship of the front coal body of plastic area and fully mechanized caving face with large mining height could be expressed with the above formula multiplied by plastic modulus Ψ. If the coal body was in elastic state, Ψ = 1. In the formula, E_0 is integrated elastic modulus of coal body in plastic area, and passion's ratio is μ_0. According to the basic assumption (1), ε = 0. According to the plain strain principle: $\varepsilon_z = 0$, $S_z = 0$, $\sigma_z = \sigma$. Combined with the above analysis:

$$\sigma = \frac{1}{2}(\sigma_x + \sigma_y) \tag{26}$$

$$\begin{cases} \varepsilon_x = \frac{\psi(1+\mu_0)}{2E_0}(\sigma_x - \sigma_y) \\ \varepsilon_y = \frac{\psi(1+\mu_0)}{2E_0}(\sigma_y - \sigma_x) \end{cases} \tag{27}$$

As to front coal body in large mining height face, it is extruded in the gob direction in the process of forming plastic area which makes coal body swell. In the situation that is out of swell deformation, the swelled coal area in gob side is equal to the reduced coal area in plastic region. Take the arbitrary point in plastic area as object, and the distance to coal wall is denoted by x. The horizontal displacement is denoted by S_x, and vertical displacement is S_y, then:

$$Mx = (x + S_x)(M - S_y) \tag{28}$$

Then the following formula is solved:

$$S_y = \frac{S_x M}{x + S_x} \tag{29}$$

And $\varepsilon_y = \frac{S_y}{M - S_y} = \frac{S_x}{x}$, this formula is derived by:

$$\frac{d\varepsilon_y}{dx} = -\frac{2\varepsilon_y}{x} \tag{30}$$

The differential equation is solved:

$$\varepsilon_y = \frac{B}{x^2} \tag{31}$$

Where B is constant, substitute (31) to (27):

$$\psi = \frac{2E_0 B}{(1+\mu_0)(\sigma_y - \sigma_x)x^2} \tag{32}$$

Appended with boundary conditions: $x = x_0$; $\Psi = 1$; $\sigma_y - \sigma_x|x = x_0 = (1 - \alpha)k\gamma H + \eta\gamma_0 M_0$:

$$B = \frac{(1+\mu_0)\left[(1-\alpha)k\gamma H + \eta\gamma_0 M_0\right]x_0^2}{2E_0} \tag{33}$$

Ψ is reverse solved when (32) is substituted (33):

$$\psi = \frac{\left[k\gamma H(1-\alpha) + \eta\gamma_0 M_0\right]x_0^2}{(\sigma_y - \sigma_x)x^2} \tag{34}$$

And

$$S_x = x\varepsilon_y \tag{35}$$

The horizontal displacement is obtained when (28) is substituted by (20), (27), $x = x_0$:

$$S_{x_0} = \frac{(1+\mu_0)\left[(1-\alpha)k\gamma H + \eta\gamma_0 M_0\right]x_0}{2E_0} \tag{36}$$

The results concluded from horizontal displacement analysis of (36) in plastic area are: ① horizontal displacement $S\ x_0$ is proportional with limit equilibrium width x_0, and increases with the increasing width; ② horizontal displacement S_{x_0} is reversely proportional with integrated elastic modulus E_0 and has linear increment relationship with passion's ratio of plastic area coal.

5 ENGINEERING APPLICATIONS

The average coal occurrence of 8313 working face of Dongrisheng coal mine of Pingshuo mining area

is 191 m. Coal inclination is 1~3° which belongs to nearly horizontal coal seam. The thickness of coal seam is 12.81~16.95 m of which the average value is 15.11 m. The mining coal seam belongs to thick coal seam and its roof and floor rock strata belong to sandy mudstone and siltstone and have stable structure. The working face is with a large mining height that is M = 4.1 m, the caving height is 11.01 m and the ratio is 1:2.69. Based on the above theory, the abutment pressure is analyzed. The related parameters are:$\alpha = 0.25$, $c_0 = 0.3$ MPa, $\varphi_0 = 15.8°$, $k = 2$, $\gamma = 27$ KN/m^3, $\eta = 0.8$, $\gamma_0 = 14$ KN/m^3, $P_0 = 200$ KPa, $\mu_0 = 0.306$, $E_0 = 3.2$ GPa. When they are substituted in (12):

$$x_0 = \frac{M\alpha}{2\tan\varphi_0}\ln\left\{\frac{k\gamma H + \eta\gamma_0 M_0 + c_0\cot\varphi_0}{c_0\cot\varphi_0 + P_0/\alpha}\right\} = 3.38 \text{ m}$$

$$S_x = \frac{(1+\mu_0)\left[(1-\alpha)k\gamma G + \eta\gamma_0 M_0\right]x_0}{2E_0} = 188 \text{ m}$$

Because of mining, abutment pressure transfers to deep part. Combined with relative study (Xie et al. 2006), disturbance coefficient $\beta = 1.82$, so the limit equilibrium width of front coal in 8313 face $x = \beta x_0 = 6.15$ m.

The average displacement value measured in field is 210 mm when the limit equilibrium width is 6.57 m.

6 CONCLUSIONS

1. Lead abutment pressure increases with the distance to face increases and reaches the maximum in the interface of elastic and plastic, besides, the value and maximum position of abutment pressure are affected by some factors such as mining depth, mechanical property of coal and rock, and caving ratio;
2. The limit equilibrium width increases with the increasing mining height, roof coal thickness, occurrence depth, literal pressure coefficient andattenuation coefficient, and decreases with increasing caving ratio, coal-rock cohesion and internal friction angle;
3. As is known from transverse displacement of coal body in plastic area, the horizontal displacement in plastic area has linear increasing relationship with the plastic area width, Poisson's ratio of coal, and has inverse proportion with elastic modulus of coal;
4. The practical example of 8313 fully mechanized caving face of Dongrisheng coal mine of Pingshuo mining area verifies the rationality of mechanical model and calculation formula which has more extensive applicability.

ACKNOWLEDGEMENT

The Project is Supported by National Natural Science Foundation of China No. 51234005, financially supported by National Basic Research Program of China under Grant No. 2010CB226802, Fundamental Research Funds for the Central Universities (2010YZ02).

REFERENCES

Gao Y. et al. 2010. Study of mining roof abutment pressure distribution law and affecting factors under sea[J]. *Rock and Soil Mechanics*31:1309–13.

Gong P L. 2006. *Surrounding* Rock Control Theory and Application Study of the Coal Face with Greater Mining Height. *Taiyuan, Taiyuan University of Technology*.

Jiang F X & Ma Q H. 2002. Mechanical solution of the maximum point of dynamic abutment pressure under deep long2wall working face[J]. *Journal of China Coal Society*27:273–5.

Liu J H. et al. 2011 Survey on abutment pressure distribution of fully mechanized caving face in extra-thick coal seam of deep shaft[J]. *Journal of China Coal Society*36(supplement 1): 18–22.

Pu H & Liao X X. et al. 2002. Effect of the key strata movement in the mining-*induced* overlying strata on the abutment pressure distribution in surrounding rock[J]. *Journal of Rock Mechanics and Engineering*21(supplement 2):2366–9.

Si R J. et al. 2007 Numerical simulation of abutment pressure *distribution* laws of working faces[J]. *Rock and Soil Mechanics*28:351–4.

Wen Z J. Study on the Key Technologies and Mechanical Model of Gob-*Side* Retaining Entry. *Master thesis of Shandong University of Science and Technology,* 2011.

Xia Y X. et al. 2011. Study of the lead abutment pressure distribution base on microseismic monitoring[J]. *Journal of China Coal Society* 40:868–73.

Xie G X & Wang L. 2008. Effect of mining thickness on abutment pressure of *working* face. *Journal of China Coal Society*33:361–3.

Xie G X & Wang L. 2010. Thickness effects of fracture characteristics of coal seam and surrounding rocks in fully mechanized top-coal caving face[J]. *Journal of China Coal Society*35:177–81.

Xie G X. et al. 2006. Study on distribution laws of stress in inclined coal pillar for fully-mechanized top-coal caving face. *Chinese Journal of Rock Mechanics and Engineering* 25(3): 545–549.

Yang K. et al. 2009. Experimental investigation into mechanical *characteristics* of surrounding rock with different mining thicknesses[J]. *Journal of China Coal Society*4:1446–50.

Zhao P. et al. 2011. Numerical simulation of abutment pressure in coal for non-pillar mining[J]. *Journal of China Coal Society*36:2029–34.

Progress in Mine Safety Science and Engineering II – He et al. (Eds)
© 2014 Taylor & Francis Group, London, ISBN 978-1-138-00122-0

The explosion-proof design of Abandoned Mine Detection Robot

Liwei Lei, Bin Zhu & Ruiqing Jia
School of Mechanical Electronic and Information Engineering of China University of Mining and Technology (Beijing), Beijing, China

ABSTRACT: How to exploit and utilize abolished mine has become a new issue of recycling resources in the world today. The explosion-proof design for coal robots which is used to detect the environment must be adopted. Based on a study of the necessity of the abandoned mine reuse, the wheel mine detection robot which designs for detecting the environment of abandoned mine is introduced. This paper is focus that the explosion-proof designs of the mine detection robots. The reference for the mine detection robots design will be provided in the future.

1 INTRODUCTION

Along with mining activities, abandoned mine is naturally produced as abandoned land. According to the characteristics of different abandoned mine, how to reform and rebuild is a way of "recycling resource" in many mining powers. In the middle of the 20th century, the research of abandoned mine has been begun in the UK, Germany, the United States of America and other developed countries. Meanwhile, a series of solutions have been put forward (Miao & Qian 2009). Mineral resources are very rich in our country who is a mining giant. There are a large number of abandoned mines are formed by several of reasons every year. Based on *the "12th five-year" plan on coal mine safety production* announced by The national security agency, 9535 small coal mines were closed because of unsafe in the "11th five-year plan" period. There are 459 state-owned key coal mines have been abandoned and more than 1100 mine pits that had been or would be shut down in the list released by the SAWS (State Administration of work safety) in 2007. A lot of mine pits would be closed too because of other reasons. The abandoned mine pits will do great harm to the natural environment though it has been closed. Some produce a large number of harmful gas leak in the earth's surface, threatening the normal production and life of human beings (Garden 1983, Thielemann & Welte 2001, Tang et al. 2005). Some turn into the pollution source of groundwater, endangering the human condition (Hu & Yan 2000). Others caused the surface subsidence, damaging the people's life and property safety (He & Qiu 2000). To solve the above problems, some experts and scholars put forward the study of governance the abandoned mine. Some abandoned mines can turn into warehouse, garage, museums and other facilities to save precious land resources. Some can mine the mineral resources again. Others which are useless must carry on the corresponding processing to prevent damaging human being. The recycling of the abandoned mine is very necessary and beneficial, it is not only good for environmental protection but also promote comprehensive utilization of resource (Zheng & Zhao 2003, Meng 2011, Xie & Tang 2010).

In order to draft the treatment measures for the abandoned mines reasonably, the investigation to it inside is necessary. Due to the environment of abandoned mine is complex, the person in the mine pits may be damaged by the explosive gas and other accidents occurring at any time. Thus, the robot needs to be designed for replacing or partly replacing the person into the mine pits. And, the AMDR (Abandoned Mine Detection Robot) must be flexible, reliable and possess good obstacle-surmounting. The logical judgement ability is needed in a poor communications and unknown information environment. Obvious, the most important is still higher safety performance.

2 THE OVERALL FLAME-PROOF DESIGN OF AMDR

The environment of abandoned mine pits is worse than the ordinary ones. The flooded shafts and collapses and other accidents may happen at any time because of the lack of ventilation measures, high temperature, harmful gases, dust, severe hypoxia condition and the underground situation is more complex and changeable.hence, the AMDR safety performance must be much higher than all the other equipments in the mine. Thus, it is necessary

to conduct a comprehensive control of the AMDR safety as a whole.

2.1 *The strategy of flame-proof structure adopted*

The AMDR is equipped with some instruments that are used to detect the surrounding environment and transfer information back to the control centre. The explosion risk is very high when these instruments and equipments in service. So, we should use the intrinsically safe electrical equipment or other special design for the electrical equipment. In principle, the flame-proof equipment is not allowed to use in mine. But the intrinsically safe electrical equipment is very rarely at present, especially the power supply, motor and other key equipments. Therefore, the AMDR adopted the safety strategy of flame-proof after the redundant safety measures drawn up in the case of the basic principles of electric explosion-proof allowed.

2.2 *High performance materials selected*

There is a possibility of explosion because of underground gas and dust accumulation. Static electricity and sparks can't be caused during the AMDR working time. The friction, spark resistance and antistatic properties of the material which used underground are made clear rules by the nation. The AMDR subjected to friction, collision inevitably as working. For this reason, the materials with special properties will be used to avoid explosion by reducing the static electricity and sparks in the working process.

2.3 *Safety communication methods selected*

There is no strict unified limitation about the EM (electromagnetic) equipment working underground. The SAWS made some limits for the use of EM equipment under mine. According to the IEC 60079-0-2007 *Explosive atmospheres–Part 0; Equipment-General requirements,* the transmitted power of EM waves is less than 6 W and the frequency of EM wave was made a certain limitation.

3 THE FLAME-PROOF ENCLOSER DESIGN OF THE AMDR

Flame-proof encloser is a platform to contact walking mechanism and also a shell to protect the internal electrical components. The AMDR should be strong enough to withstand the internal or external explosion of combustible gas. And it must have enough space to accommodate control system, power system, communication system, detection instrument. The interface which contacts flame-proof encloser and walking mechanism is the key part of power output. It must meet the requirements of flame-proof. Finally, flame-proof encloser must be good at heat dissipation to prevent temperature rising that can causing an explosion. To sum up; flame-proof encloser has the very high request in material selection and structure design.

3.1 *The explosion-proof encloser material selected of the AMDR*

The national standards for the coal mine equipment shell material are clear. But the material is not ruled strictly for the mine robot flame-proof enclosure. The cast steel, ordinary mine equipment shell material, couldn't meet the requirements of the AMDR obviously with high precision and high maneuver performance. Light alloy with low density and high intensity is the best choice of the AMDR flame-proof encloser material.

ZL401 cast aluminium alloy could be used for the shell of the coal electric drill which is the only alloy known currently. Compared with cast steel shell, the cast aluminium alloy encloser is less than half of it in weight in the same intensity. However, the cast aluminium alloy encloser need to further friction spark test. There is no special alloy for the mine robot encloser currently. ZL401 aluminium alloy is used as the mine robot flame-proof encloser material temporarily. Now, a lot of measures are taken to reduce the possibility of a collision in the design of mine robot (Zheng 1990, Li et al. 2009).

3.2 *The flame-proof encloser shape design of the AMDR*

Flame-proof encloser demands its volume so smaller that it can go through the narrow space in the tunnel. There also should have enough space to equip electrical components inside and have enough wall thickness to guarantee the strength. Meanwhile, we should consider the heat dissipation problem in the flame-proof encloser shape design of AMDR. For the above problem, the safety of the robot is the most important at all. So, the strength of flame-proof encloser must be considered firstly.

In the explosion process, the explosive mixtures combust and expand around at the same time. The pressure wave transfers to the air in sphere. In the same volume, the explosion pressure is changeable with different encloser shape because of the heat dissipation area and speeds of flame-proof encloser is different. Since there is no any obstacles, pressure waves impact spherical encloser inner wall almost at the same time. The sphere encloser

bears the higher pressure right now. If the pressure wave reaches all parts of inner wall in a longer time lag, inner wall absorb more explosive energy. The impact on the encloser wall is smaller. So, the more complex the shape of encloser will be, the better the isolation effect will be. There are four different shape container internal comparison of explosion pressure in Table 1. As you see, cuboids container is the minimum compression and sphere is the maximum. According to the requirements, cuboids are the best shape of flamer of encloser.

But, the interior space of cylinder is bigger than cuboids in the same surface area. In case of the same quality of material, the internal space of cylindrical encloser is bigger and the intensity of encloser is higher than cuboids. And the internal stress distribution is more uniform. The flame-proof encloser adopted cylindrical shape after having a comprehensive consideration for the robot safety, mobility. The flame-proof encloser is modified at the bottom to improve the robot motion performance.

We built the model of flame-proof encloser and had finite element analysis with Solidworks after its design had been completed. The structure of the flame-proof encloser is optimized based on the results of analysis. Figure 1 shows the stress diagram of cast aluminium encloser. Flame-proof encloser reduced the weight through reducing too much local stress reserve to improve the mobility of the robot after optimization.

Table 1. Under the same volume of different shape of pressure vessel explosion.

Shape	Volume (L)	Pressure ($\times 10^5$Pa) (CH_4 9%–10%)
Sphere	8	7.1
Cube	8	6.1
Cylinder	8	5.5
Cuboids	8	5.1

* From Principle of explosion-proof.

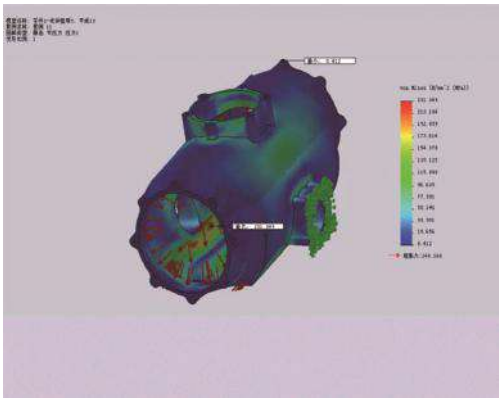


Figure 1. Stress diagram of cast aluminium enclosure.

3.3 *The flame-proof encloser structure design of the AMDR*

There are two kinds of the flame-proof structure encloser design of the AMDR. One is the relative motion of kinematic pair flame-proof structure, and the other one is no relative motion of the tightness of flame-proof structure design.

Figure 2 shows the flame-proof structure of the drive shaft. The drive shaft output drive power outward through the flame-proof encloser. The flame-proof design of the shaft should have two flame-proof joints. One flame-proof joint is formed by the surface of driven shaft and isolation bearing cover inner hole, named a. The other one flame-proof joint is formed by the surface of bearing end cover and encloser, named b. There are sealing between the shaft sleeve and flame-proof encloser, and between the drive shaft and the shaft seat ring to prevent water into the flame-proof encloser.

There are three tightness flame-proof structures. Three flame-proof joints are all combined with the surface of the two fastening together with the bolt as Figure 3, Figure 4 show. The Figure 4 shows windows design that toughened glass with flange clamp is installed in the head. Adopts toughened

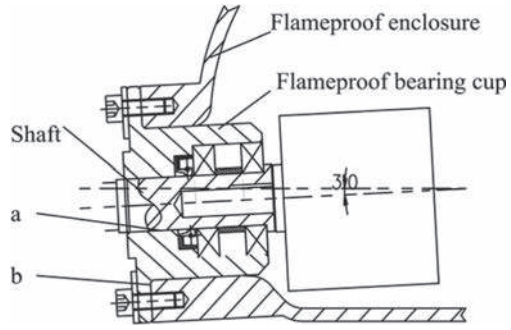


Figure 2. Flame-proof structure of the drive shaft.

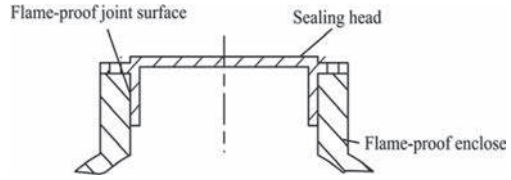


Figure 3. Schematic diagram of sealing head structure.

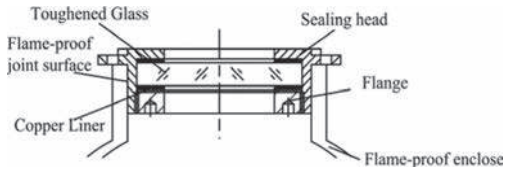


Figure 4. Schematic diagram of sealing head window structure.

glass with explosion-proof standards, add a gasket made of red copper between shell cover and toughened glass to avoid explode.

4 THE WALKING MECHANISM DESIGN OF THE AMDR

The AMDR must be flexible and good at climbing obstacle due to the mine terrain is complex. The wheeled walking mechanism possesses good manoeuvrability, high efficiency and simple structure. The tire grounding area is increased through adopting All-wheel-drive (AWD) models to obtain all terrain adaptation wheel structure (Zhu & Chen 2009). The AMDR adopts six-wheel drive, increasing contact point with the ground, avoiding the phenomenon of the robot drive wheels overhead, increasing the terrain adaptability, also reducing the weight.

4.1 *The drive mechanism design of the AMDR*

As Synchronous belt transmission ratio is accurate which can satisfy the requirement of detecting robot flexible mobility. Robot adopts synchronous belt transmission mode with one power output shaft on each side. Compared with all motor driven, it can reduce motor number and the flame-proof joint number, optimize the stress distribution of flame-proof encloser, increase internal space improve the AMDR's mobility and safety greatly. Synchronous belt is closed in a confined space, avoiding friction sparks produced, improving the safety of the robot.

In order to ensure stability in movement, reduce inertia collision in motion sudden changes, the damping system is joined between walking mechanism and flame-proof encloser shown as Figure 5. Damping system absorbs most of impact energy using polyurethane rubber rods, decreases amplitude of the flame-proof encloser, reduce sparks of collision.

4.2 *The wheel design of the AMDR*

The AMDR's tire and wheel requires explosion-proof capability relative to the ordinary which

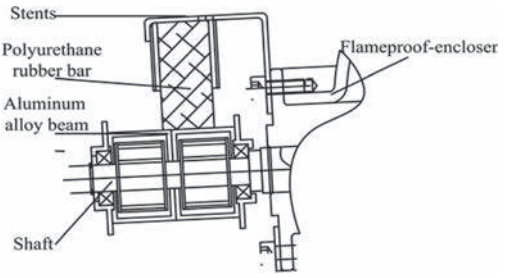


Figure 5. Schematic diagram of damping system.

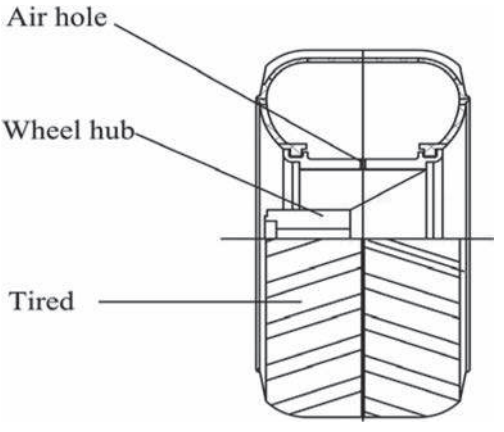


Figure 6. Schematic diagram of wheel structure.

have enough strength and grip, and wear resistance, aging resistance. So, the AMDR tire material chose oil-resistant nitrile butadiene rubber, it owns well elasticity and water resistance, oil resistance, aging resistance and strong load. Wheel hub is made of nylon added flame retardant. Tyres are designed as hollow non-pneumatic, drilling hole through the wheel hub to connect with the atmosphere. When the ground changed suddenly, tire occur deformation for shocking. The air in the tires flows rapidly through holes. Then the tire fills gas again quickly with elastic recovery and as shown Figure 6. This design increases the AMDR damping system, reduces the probability of spark collided with the ground and improves the explosion-proof performance further.

5 THE COMMUNICATION SYSTEM DESIGN OF THE AMDR

The recent studies shows that the key is put on the selection of transmitting frequency and power of radio equipment in the environment with existence of gas to ensure that the temperature is not

higher than 150°C when continuous operating in the environment with a certain mass of coal dust to prevent from fire damp explosion. Therefore, the transmitting frequency of radio equipment should be higher than 450 MHz to guarantee the safe (Yang 2008). The radio transmission is great influenced by the shape of the tunnels. In straight tunnel, if frequency is higher, attenuation rate is smaller, and it is beneficial for EM waves to transmit. In curved tunnels, it decay rapidly, and it is unfavourable for EM waves to transmit. The studies show that 900 MHz is optimal frequency for radio communication in mine tunnel (Sun et al. 2005).

The AMDR is equipped with the single-chip 433/868/915 MHz transceiver nRF905 whose maximum transmitted power is 10 mW. The frequency point needs not to apply for because the stipulation made by State Radio Monitoring Centre is conformed. The requirement of underground radio equipment is met too which is made by the SAWS. It is reliable, small, light, strong anti-jamming capability and low error rate.

6 CONCLUSION

With the development of national economy, there are more and more abandoned mines in various reasons. These abandoned mine will not only cause huge waste of resources, but also do great harm to the environment and society if the management is not properly. The re-exploitation of abandoned mine is imperative. The research of the robots replacing human in abandoned mine has very broad prospects. The research focuses on the explosion-proof performance of the encloser, walking mechanism and communication method under the situation of flooded shafts or collapses. Meanwhile, this paper provides the reference for the safety design of the mine robot in the future.

REFERENCES

Garden, S.G. 1983. A problem of surface methane emission [J]. *Municipal Engineer* 110 (4):133–143.

Hu Weiyue & Yan Lanying. 2000. Characteristics of Groundwater Polution in Abandon Coal Mine and Control Technique. *Coal Mine Environmental Protection* 14(4):37–38. (in Chinese).

He Yueguang & Qiu Bin. 2000. A supervision on surface subsidence of abandoned pit in karstic district and some protective measurements. *Jiangxi Nonferrous Metals* 14(3):1–3, 13.

Li Yunwang, Ge Shirong & Zhu Hua. 2009. Design and Manufacture of Flame-proof Enclosure of Coal Mine Rescue Robot. *Coal Mine Machinery* 30(2):104–106.

Meng Pengfei. 2011. Study on the recycling of the discarded mine resources. *China Mining Magazine* 20(7):62–65.

Miao Xiexing & Qian Minggao. 2009. Research on Green Mining of Coal Resources in China: Current Status and Future Prospects. *Journal of Mining & Safety Engineering* 26(1):1–13. (in Chinese).

Sun Jiping, Li Jisheng & Lei Shuying. 2005. Choice of optimal frequency for radiao communication in mine tunnel. *Journal of Liaoning Technical University* 24(3): 378–380.

Tang Jupeng, Yishan Pan & Zhengguo Liang. 2005. Numerical simulation of leaking gas source concentration from abandoned Beipiao mining area. *Journal of China Coal Society* 30(3):301–304. (in Chinese).

Thielemann, T. & Welte, D.H. 2001. Does coalmining induce methane emissions through the lithosphere/atmosphere boundary in the Ruhr basin, Germany [J]. *Journal of Geochemical Exploration* 113(3):219–231.

Xie Fang & Tang Deshan. 2010. Study on the utilization model of infrastructure in declined mine based on the circular economy. *China Mining Magazine* 19(7):60–63.

Yang Weihua. 2008. Resear on Power Limitation for Radio Operation in Mine. *Radio Engineering of China* 38(1):47–48, 61.

Zheng Lunjin. 1990. The Spark problems of Light-alloy Materials in Mine. *Mining & Processing Equipment* (12):53–56.

Zheng Min & Zhao Junwei. 2003. A New Comprehensive Utilization Way of Abolished Ming Pits. *Conservation and Utilization of Mineral Resources* (2):49–53.

Zhu Leilei & Chen Jun. 2009. A Review of Wheeled Mobile Robots. *Machine Tool & Hydraulics* 37(8): 242–247.

This page intentionally left blank

Progress in Mine Safety Science and Engineering II – He et al. (Eds)
© 2014 Taylor & Francis Group, London, ISBN 978-1-138-00122-0

Study on the regulation of water hazards and prevention work in Yima Coalfield

Song-Ying Li
College of Geoscience and Surveying Engineering, China University of Mining and Technology, Beijing, China
Geological Institute Yima Coal Industry Group Co., Ltd., Yima, Henan, China

Zi-Qiang Ma & Meng-Li Ren
College of Geoscience and Surveying Engineering, China University of Mining and Technology, Beijing, China

Xu-Le Zhang
Yuejing Coal Mine Yima Coal Industry Group Co., Ltd., Yima, Henan, China

ABSTRACT: In order to get the regulation of water hazards and to supply for the future water prevention work in Yima Coalfield, the historic data, geological structure, the distribution of small coal mines, the river region, the main aquifer and aquifuge, mining thickness and the fissures have been analyzed systematically. With small coal mines closure, treatment of fissures and channels, and the deeper mining activities, the main water hazards have changed from precipitation, surface water and kiln water into roof flood. The threat of the roof water mainly happened on the core of syncline with 700 m deep and also happened on the edge of fault and the rich abundance region. Roof water inrush has close relationship with mining thickness and periodic mine pressure. For roof water hazard, "three maps-two predictions" was proposed and applied in evaluation and prediction of water inrush source, channel and intensity. With geophysical prospecting, the suspected water rich area has been obtained and then the drainage work could be done before mining. Besides, other water prevention work which can improve the drainage capacity of the working face also should be carried out.

1 COALFIELD SITUATION

Yima Coalfield is the only Jurassic continental coalfield in Henan with the area of 100 km^2. The coalfield is located on the west poor water area in Henan, across the country of Yima and Mianchi. The whole coalfield is shown as an asymmetric syncline. It starts from the outcrop of coal seam in the north and disappears on the edge of reverse fault F_{16} to the south. Both of the east and west boundaries are missing as sedimentation. The minable seams distribute in the Middle Jurassic Yima Group including 5 layers in 2 groups. Respectively, they are 1–1 seam and 1–2 seam; 2–1 seam, 2–2 seam and 2–3 seam from above to bellow (WANG Yun-quan & MENG Fan-shun 1994, WANG Yun-quan, et al. 1990). The total thickness of coal seam is about 3~40 m. Its rank is long flame coal with 2~1200 m depth. The land surface is hills with south higher than north. The layers which are mainly gravel, sandstone and mudstone with no rich aquifers dip south by east.

There are five coal mines and one opencast coal mine in Yima Coalfield (Fig. 1). The annual production of raw coal is about 1.3×10^7 *t*. The total production of coal is about 2.3×10^8 *t* and the current coal resources are about 4.5×10^8 *t*. After mining for several years, each coal mine has turned to the 2# coal seam where the maximum depth is 1040 m. Rock burst, spontaneous combustion of coal seam and water hazards are the main disasters in Yima Coalfield (XIA Yong-xue, et al. 2011, ZHAO Shan-kun, et al. 2012, PAN Jun-feng, et al. 2012, MU Hong-cai 2005, LI Jian-xin 2006, DU Dong-jian & MA Xian-chao 2012, ZHAI Er-an 2005). Compared with the former, the study on water hazards is shortage.

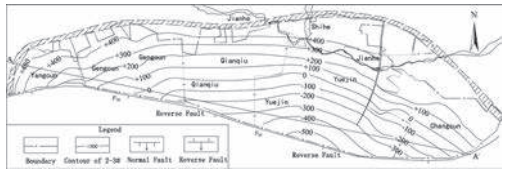


Figure 1. Distribution of coal mine in Yima Coalfield.

2 HYDROGEOLOGICAL CONDITIONS

2.1 *Precipitation and Surface Water*

The local average annual precipitation is about 670 mm with the flood season lasting from July to September. Jianhe and Shihe are seasonal rivers which flow though the east of the coalfield. They cross Qianqiu, Yuejin and Changcun Coal Mines which are the main surface water. Shihe dries up most of the time in the year and the maximum flow is 100 L/s in rainy season. Jianhe sometimes dries up, but its maximum flow had ever reached 1446.5 L/s. Precipitation is the main supplies for each aquifer through the fissures on the ground in shallow coal field. The surface river provides sufficient water by fissures, collapse and artificial channel. As small coal mines closure, treatment of fissures and collapses, and deeper mining activities, the impact of precipitation and surface water become smaller on the coal mines.

2.2 *Main aquifers*

The main aquifers are as followed (Fig. 2).

The Middle Jurassic Sandstone Fractured Confined Aquifer. It is above the coal seam with distance of 4.0~54.0 m. The layer consists of packsand, sandy mudstone and conglomerate with the average thickness of 180 m. The gravels mainly contain quartzite, quartz sandstone and limestone. The water yield property is relatively weak and this aquifer is the direct water bearing strata. The water quality type is HCO_3^-Na·Ca. The permeability coefficient is 0.000405~0.0322 m/d and the specific capacity is about 0.00007~0.00622 L/(s·m). This aquifer doesn't have the identical water level with poor connection. In the shallow parts, it is supplied by precipitation and river. Currently, its discharge form is drainage.

The Upper Jurassic and Cretaceous Gravel Fractured Confined Aquifer. The thickness of the layer is 0~880 m with the average thickness of 467 m. The gravels are mainly quartz sandstone and limestone with poor sorting features. The water yield property is weak for high cementation. In some parts of the aquifer, the water yield property is well for fissures developing. The water quality type is HCO_3^-Ca. The permeability coefficient is 0.2~1.47 m/d and the specific capacity is about 0.0626~0.178 L/(s·m). This aquifer mostly receives water from Neocene layers while the south region receives precipitation. Its discharge form is drainage.

The Neogene Mudstone Confined Aquifer. The thickness is about 0~50.8 m with the average thickness of 10.3 m and water yield property is moderate. The water quality type is HCO_3^-Ca.

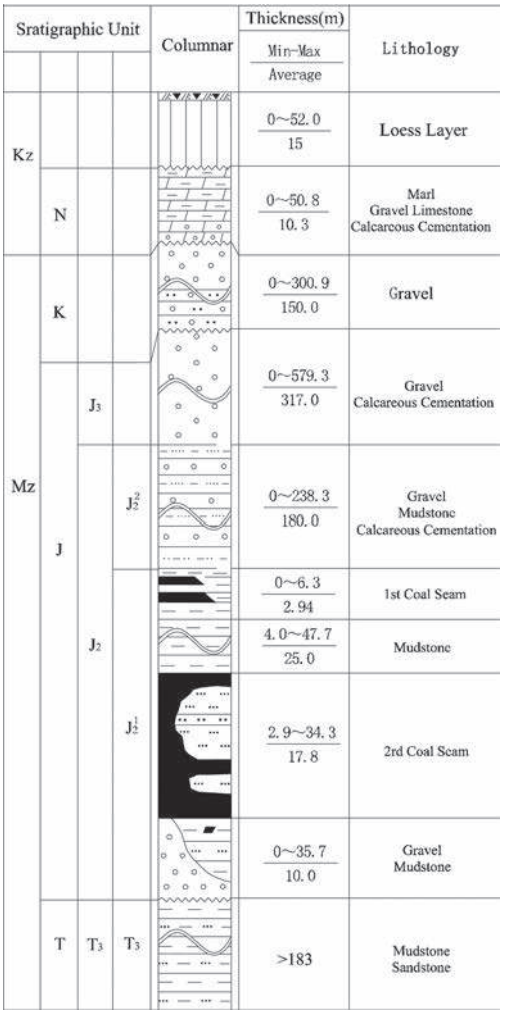


Figure 2. Stratigraphic columnar in Yima Coalfield.

The permeability coefficient is 0.22~206.1 m/d and the specific capacity is about 0.0695~0.455 L/(s·m). This aquifer receives the precipitation and Quaternary phreatic water with big seasonal change. Currently, the pumping is its discharge form.

The Quaternary Gravel Phreatic Aquifer. The thickness is less than 2 m and the water type is HCO_3^-Ca. The permeability coefficient is 0.22~206.1 m/d and the specific capacity is about 0.029~6.71 L/(s·m). This aquifer receives precipitation and river with big seasonal change.

2.3 *Main aquifuge*

The Middle Jurassic mud aquifuge of the 2nd coal seam roof is about 4.0~54.0 m with 28.0 m on

average, which is the direct roof of the 2nd coal seam (Fig. 2). The destruction on surrounding rocks caused by excavating roadway is limited and the layer is able to prevent the water. However, the fissures would access to the overlying aquifer after mining, which lead to the poor prevention of the aquifuge.

3 REGULATION OF WATER HAZARDS

According to the statistics, 79 times water inrush have been happened in Yima Coalfield. According to the source of water, the roof sandy conglomerate water is of 48.1% with 38 times; the goaf water is of 43% with 34 times; the surface water is of 8.9% with 7 times. According to the intensity of water inrush, the outsize inrush and large inrush accidents are each 3 times of 7.6% which water sources are surface water. Others are middle and small intensity which water sources are roof gravel water and goaf water. In the view of time, various types of water inrush accidents had happened before 1997. Nevertheless, the roof conglomerate water inrush is the main type after 1997, which the water bursting water quantity is about 6~450 m^3/h (Table 1).

3.1 *Precipitation and phreatic water*

Precipitation is the main factor of water filling in Tianxin Coal Mine (opencast coal mine). The mining elevation of other coal mines is about 200 m while the depth is less than 300 m in general. After mining, the fissures would extend to the limestone in Neogene, unconsolidated layers in Quaternary and even to the land surface. The precipitation could fill into mines through the fissures. Sometimes, the Neogene and Quaternary phreatic water could also be filled by same channels. The water inflow showed obvious seasonal changes in the late 1990s. As the deeper mining activities and treatment of collapse and fissures in recent years, the effect of precipitation becomes small. Meanwhile, the water inflow didn't show seasonal changes.

3.2 *Surface water*

As for enough waterproof coal pillars, Jianhe and Shihe don't directly supply the coal mines. But with the small coal mines mining along the rivers in 1980s, the waterproof coal pillars have been broken, which made the surface water become the main hazard (LI Song-ying, et al. 2003). During the flood season, the surface water caused lots of flooded accidents (Table 2). The region which was threatened by surface water showed zonal distribution along Jianhe and Shihe. However, Gengcun and Yangcun haven't been affected by surface water. With small coal mines closure and treatment of collapse and fissures, the influence of surface water is limited.

3.3 *Kiln water*

According to the statistics, there are more than 700 kilns in Yima Coalfield within the elevation of 200 m. Before the 1990s, the kiln water was the main factor for water filling of coal mines as each coal mine accessed to the goaf area. With the deeper mining activities and small coal mines closure, the threat of kiln water had been weakened.

Table 1. The table of main roof flood hazards.

Time	Names	Faces	Water inflow (m^3/h)	Total ($\times 10^4$ m^3)	Depth (m)	Thickness (m)	Remarks
2001.11	Yuejin	25030	180	9	900	3	Stop for 35 days
2003.06	Yuejin	25050	300	10	930	3	
2004.05	Qianqiu	21181	180	16	720	20	Flooded
2004.06	Yuejin	25060	70	30	930	3	
2004.09	Yuejin	25070	68	5	960	3	
2005.09	Changcun	21161	180	6	640	10	
2005.11	Yuejin	25080	450	260	960	3	Stop for 15 months
2006.08	Gengcun	2–3#13151	100	1	510	10	Flooded
2007.04	Yuejin	25090	110	18	1000	3	
2009.03	Yuejin	25072	140	10	960	5.8	Thickness contains upper layer
2011.06	Changcun	21132	350	20	640	15	
2011.08	Yuejin	25110	350	90	1030	10	
2011.10	Qianqiu	21172	300	380	720	17	Thickness contains upper layer

Table 2. The main accidents of surface water.

Time	Name	Water-inflow (m^3/h)	Reasons	Degree
1982.07.30	Yuejin	1298	Mining under river	Flooded
1985.03.21	Changcun	2400	Mining under river	Flooded
1985.07.25	Changcun	697	Mining under river	Flooded
1987.09.08	Changcun	2100	Mining under river	Flooded
1988.08.09	Changcun	4166	Mining under river	Flooded
1996.07.11	Qianqiu	1656	Mining under river	Stop for 1 day

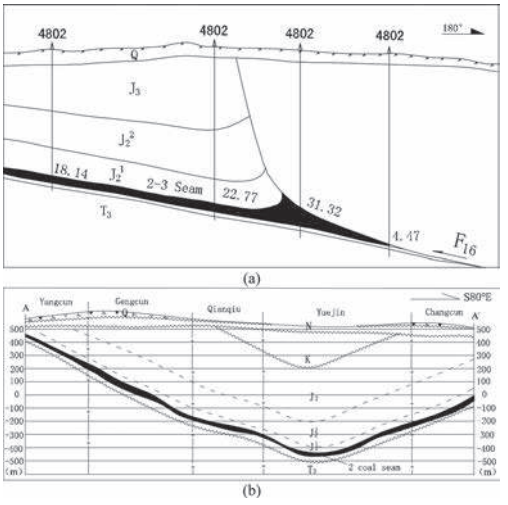


Figure 3. (a) Geological profile of 48 line; (b) Geologic section in deeper trend in Yima Coalfield (AA′).

Because the goaf areas connected to the big coal mines and the channel was clear, the upper goaf areas could not accumulate a lot of water.

3.4 *Roof water*

During the shallow mining, roof water flows into coal mines with trickling or bursting with small intensity, which didn't affect the production. As deeper mining, the frequencies of roof flood and water inflow increased obviously, which severely affected the production and even threatened the working face (Table 2). For example, roof flood had been occurred in the working face 25080 of Yuejin coal mine as it accessed to the F_{2-3}. The normal water inflow was about 10 m^3/h while the max water inflow was about 450 m^3/h. Finally, the inflow dropped to about 150 m^3/h after 100 days and the whole quantity was more than 2.6×10^6 m^3. The working face 21172 of Qianqiu coal mine crossed a fault and the max water inflow was more than 300 m^3/h with a steady quantity of 200~250 m^3/h. By the end of June 2013, the total amount was about 3.8×10^6 m^3.

The regulation of roof water hazards in Yima Coalfield are as followed:

The roof water hazards happened below the elevation of −50 m and mining depth is over 700 m. In this area, the water yield property is much stronger as the area is around the reverse fault 16# and the syncline core (Fig. 3). Besides, the thickness of conglomerate in this area is more than 400 m with strong water capacity. Yuejin coal mine locates in the core of the syncline and has been threatened by roof water. The adjacent domains between Qianqiu and Changcun are also threatened.

The water yield property of roof fractured aquifer is uneven with poor connection. In the fault zone and its tip area, the water yield property is relatively strong which could lead to water hazard (ZHANG Chunguang, et al. 2012). Once water inrush happened in a working face, the adjacent face could also be threatened.

The roof water inrush has close relationship with the periodic weighting of mining.

The roof water inrush also has close relationship with the mining thickness. The max coal thickness is more than 20 m by caving mining, which would destroy the roof seriously. According to the empirical formula, the height of roof fissure could be more than 300 m and may cross the mudstone aquifuge, the Middle Jurassic sandstone aquifer. Finally, it could be reached into the Upper Jurassic and Cretaceous conglomerate aquifer.

In the beginning of roof water inrush, the water quality type is general HCO_3^-Na. After some time, it changes into HCO_3^-Ca (Table 3). According to the change, it can be inferred that the water comes from the Middle Jurassic sandstone aquifer and then turns into the Upper Jurassic and Cretaceous gravelstone aquifer. It can be seen that why the quantity could be steady after water inrush.

4 CONTROL TECHNIQUES

4.1 *Precipitation and surface water*

The shallow part of coalfield, river and its terrace should be patrolled regularly. The collapse and ground fissures should be filled in time.

Table 3. The comparison of water quality before and after water inrush.

	Previous period	mg/l	meq/l	meq%	Later period	mg/l	meq/l	meq%
Cation	K^++ Na^+	184.11	7.36	83.6	K^++ Na^+	20.11	0.80	6.30
	Ca^{2+}	19.64	0.49	11.1	Ca^{2+}	105.81	2.64	41.6
	Mg^{2+}	4.86	0.20	4.60	Mg^{2+}	79.49	3.27	51.6
	NH_4^+	1.00	0.06	0.70	NH_4^+	1.00	0.06	0.50
Anion	Cl^-	35.10	0.99	11.30	Cl^-	44.67	1.26	9.90
	SO_4^{2-}	48.03	0.50	11.40	SO_4^{2-}	56.68	0.59	9.30
	HCO_3^-	392.36	6.43	73.1	HCO_3^-	613.86	10.06	79.4
	CO_3^{2-}	11.35	0.19	4.20	CO_3^{2-}	5.40	0.09	1.4
PH		8.00			PH	7.60		

4.2 *Kiln water*

The small coal mines which were closed should also be patrolled regularly. Once there are unfilled shafts, collapses and fissures, the treatment should be carried out in time.

4.3 *Roof flood*

The treatment of roof flood is the key and difficulties in the future in Yima Coalfield.

The regulation of water yield property and water inrush should be deeply studied for water prevention. Firstly, the distribution of water rich area could be obtained by the method of "three maps-two predictions" and the study of structure. Secondly, the distribution of roof safety area could be got by the thickness of aquifuge, mining thickness and the height of fissures. Finally, the water origin, channel and the intensity of the roof flood could be predicted and evaluated by the comprehensive map (LIU Wu-tao, et al. 2001, WU Qiang, et al. 2013, WU Qiang, et al. 2000, WU Qiang, et al.2010, WU Qiang, et al. 2011, LIU Wei-tao, et al. 2007).

The geological structure and water yield property in working face could be detected by 3-D seismic exploration and transient electromagnetic prospecting. The suspected area could be obtained by analyzing the data of geophysical prospecting (WANG Wei, et al. 2012, YU Jing-cun, et al. 2011, LIU Yunqi, et al. 2009).

Before mining, the suspected water rich area could be drained. It could reduce the affect of roof water during the production.

Before mining, drainage system should be built. The capacity of water drainage in mining area should be improved. Track roadway is the key to waterproof and drainage of working face. It would be tunnelled in positive slope as far as possible with inside high and outside low, which can avoid flooding of roadway or working face after roof flood.

5 CONCLUSIONS

Various types of water hazards exist in Yima Coalfield, including precipitation, surface water, kiln water and roof flood. With small coal mines closure, the treatment of river and ground fissures and deeper mining activities, the main water hazard has changed into roof flood. The treatment of roof flood would be the key and difficulties in the future in Yima Coalfield. For roof flood, the source, channel and the intensity can be predicted and evaluated by "there maps-two predictions" with the study of water yield property. The suspected water rich area could be found by geophysical prospecting and then water drainage could be carried out. The water drainage should be the main work to prevent roof flood, meanwhile, it is also important to improve the capacity of drainage system in working face and enhance the ability of water resisting.

ACKNOWLEDGEMENTS

This article was supported by the National Natural Science Foundation of China (41130419), the Henan Provincial Bureau of foreign experts (20124100081) and the Fundamental Research Funds for the Central Universities (2010YD02).

REFERENCES

Du Dong-Jian, Ma Xian-Chao. 2012. Water hazard features and controlling techniques in Qianqiu Coalmine, Henan. *Coal Geology of China,* 24(10):38–41.

Li Jian-Xin. 2006. Practices on mine fire comprehensive prevention and control technology for mine seam gateway in high stress area and under mine goaf. *Coal Science and Technology,* 34(8):23–25.

Li Song-Ying, Du Yi-Ming, Sun Xiao-Zhen, et al. 2003. The preventing and controlling water hazards in small coal mines in coal fields of Yima Coal Mining (Group)

Co., Ltd. *Journal of Jiaozuo Institute of Technology (Natural Science),* 22(5):184–186.

Liu Wu-Tao, Li Jia-Xiang, Zhang Wen-Liang. 2001. An evaluation of roof water-inrush grade using fuzzy mathematics method. *Journal of China Coal Society,* 26(4):399–403.

Liu Wei-Tao, Wu Qiang, Ji Bao-Jing, et al. 2007. Analysis of deformation & destruction mechanism and stability of F0 fault crush zone in Fangezhuang Coal Mine. *Journal of China Coal Society (China),* 13(3):261–265.

Liu Yunqi, Li Xiaoming, Li Yongjun, et al. 2009. The detection of hydrous quality about roof sandstone by mine transient electromagnetic method. *Journal of North China Institute of Science and Technology,* 6(4):39–42.

Mu Hong-Cai. 2005. Safety sealing and opening for fire disaster of fully mechanized top caving mining face with high gassy and spontaneous combustion. *Coal Science and Technology,* 33(2):33–35.

Pan Jun-Feng, Ning Yu, Du Tao-Tao, et al. 2012. The theory and system for preventing rock burst in large-scale areas. *Journal of China Coal Society,* 37(11):1803–1809.

Wang Yun-Quan & Meng Fan-Shun. 1994. The influence of sedimentary environment of the Yima formation on coal-forming processes in the Yima coal field, Hean. *Sedementary Facies and Palaeogeography,* 14(1):24–33.

Wang Yun-Quan, Yan Xiuzhang, Meng Fan-Shun. 1990. An analysis of factors influencing the thickness of the main workable coal seams in Yima coal field. *Journal of Jiaozuo Mining Institute,* (2):8–20.

Wang Wei, Gao Xing, Li Song-Ying, et al. 2012. Channel wave tomography method and its application in coal mine exploration: an example from henan yima mine area. *Chinese journal of geophysics,* 55(3):1054–1062.

Wu Qiang, Cui Fang-Peng, Zhao Su-Qi, et al. 2013. Type classification and main characteristics of mine water disasters. *Journal of China Coal Society,* 38(4):561–565.

Wu Qiang, Huang Xiao-Ling, Dong Dong-Lin, et al. 2000. "Three maps two predictions" method to evaluate water bursting conditions on coal roof. *Journal of China Coal Society,* 25(1):60–65.

Wu Qiang, Chen Hong, Liu Shou-Qiang. 2010. Methodology and application on size-limited structure predictions with ANN based on loop over-lapping theory: a case study of Lingzi Coal M in e in Zibo. *Journal of China Coal Society,* 35(3):449–453.

Wu Qiang, Zhao Suqi, Li Jinsheng 2011. The preparation background and the main points of Rule of mine prevention and cure water disaster. *Journal of China Coal Society,* 36(1):70–74.

Xia Yong-Xue, Lan Hang, Wei Xiang-Zhi. 2011. Study of comprehensive evaluation technology for rock burst hazard based on microseismic and underground sound monitoring. *Journal of China Coal Society,* 36(s2):358–364.

Yu Jing-Cun, Hu Bin, Liu Zhen-Qing, et al. 2011. The application of transient electromagnetic detection technology. *Geophysical & Geochemical Exploration,* 35(4):532–535.

Zhao Shan-Kun, Liu Jun, Li Gang-Feng. 2012. Research of fault rockburst prediction with multi-parameter. *Journal of Henan Polytechnic University (Natural Science),* 31(2):145–149.

Zhai Er-An. 2005. Cause analysis and countermeasures of water-bursting of 25 mining area in Yuejin coal mine. *Coal Engineering,* (3):41–42.

Zhang Chunguang, Li Songying, Yang Pei, et al. 2012. Structural control mechanism on groundwater in Shanmian coalfield. *Coal Geology and Exploration,* 40(5):42–46.

Progress in Mine Safety Science and Engineering II – He et al. (Eds)
© 2014 Taylor & Francis Group, London, ISBN 978-1-138-00122-0

The safety technology of head rope replacement in large friction hoisting mine

A.T. Balkema & G. Westers
A.A. Balkema Publishers, Rotterdam, The Netherlands

Meng-Juan Dong & Fu-Yin Jia
College of Energy Sources and Safety, China University of Mining and Technology, Xuzhou, Jiangsu, China

ABSTRACT: The head rope exchange work is frequently in friction hoist mine. Due to the backward rope exchange technology and equipment, the work is difficult and time consuming, and has many potential accidents, quite easy to cause casualties. First put forward the rope exchange method of interactive rope exchange vehicle, establishing the statics model of interactive rope exchange system. Determine the mechanical properties of rope exchange system, developed the safety rope exchange vehicle suit for the rope exchange work in mine. And assay its properties. Under the premise that the tension of hoist system head rope unchanged, the equipment can realize the synchronous swaps of the new and old head rope at wellhead, achieve high velocity, safety, and environment adaptive capacity. And is of great significance to protect the safe and efficient production of mine.

Keywords: head rope, replacement, rope exchange vehicles, statics

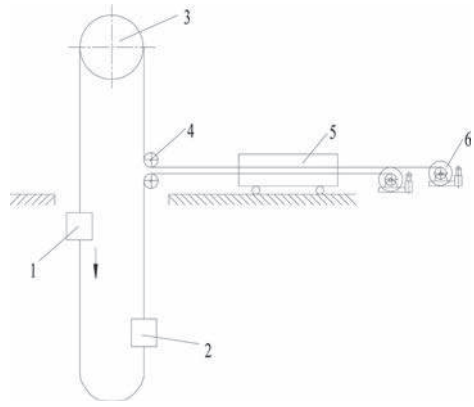
1 OUTLINE

In friction lifting mine, Hoisting System run by the friction between the head rope and the friction wheel, the safety and reliability of the first line directly affect safety. According to "coal mine safety rules", the head rope needs to be replaced every 2 years, if broken wire, corrosion, wear is overrun, rope diameter shrinkage exceed limit, and so on appeared on the head rope, it must be replaced in time, even if less than two years.

At present, the tool used in the head rope replacement in our country is relatively backward, operation time is long, large labor intensity, workers in hazardous area working frequency is high, the probability of an accident is big, and the old and the new head rope connection with card, easy to cause new head rope damage (Jia F Y & Dong M J 2011, Zuo Y Q & Jia F Y 2011, Ma K C & Jia F Y 2011, Ma K C & Jia F Y 2011). This is especially ture in large coal mine, the rope replacement work need 40–50 people, 3–7 days every time. With the increasing of mining depth, mine exceed ten million tons becoming more and more, the diameter of wire rope exceed 60 mm in some mines. If the rope replacement is still using the original method, it takes not only the low efficiency, but also the high risk. Therefore to ensure hoisting safety, study on the head rope replacement is of great significance.

2 METHOD OF EXCHANGING THE NEW AND OLD ROPE

The method of exchanging the new and old rope worked by the rope exchange vehicle. As showed in figure 1, let a cage in the bottom, the other in the wellhead, fixed the bottom cage at wellhead, disassembly the Container tent, head rope and the



1-cage1; 2-cage2; 3- friction wheel; 4- guide wheel; 5- rope exchange vehicle; 6-pull and put rope hoist

Figure 1. . Schematic of replacing ropes.

Wedge wire ring, use messenger lead in the new rope, then connect the cage by Wedge wire ring (Ma K C & Jia F Y 2011). Rope exchange vehicle straining the new and old head rope, draw the cage in bottom to wellhead. Remove the shed, start the winch, release the wellhead cage to bottom. Draw the bottom cage to the wellhead, disassemble the Container tent at wellhead. Lock the new head rope at the other side, remove the head rope of the wellhead cage, relieve the Wedge wire ring, draw the new head rope and assemble the Wedge wire ring and connect the wellhead cage, start the winch, remove the shed after the wellhead cage was drawed, arrive here, rope exchange work is complete.

This method cooperate the rope exchange vehicle can realize the function of sending new rope and drawing old rope automatically. Implements all operations accomplished at wellhead, quick and convenient, the operator and accident potential less than before, achieve high safety and efficiency.

3 STATICS MODEL OF TOWER-TYPE REPLACING ROPE SYSTEM

As Mi for quality of cage; mi for quality of rope; e for napierian base, e = 2.718; μ for friction factor; α f or the circumference angle between wire rope and friction wheel; σ for antislip safe coefficient; Fi for wire rope tension.

1 Static condition

Point c wire rope tension:

$$F_c = m_1 g + M_1 g + m_3 g$$

Point d wire rope tension:

$$F_d = m_5 g + F_a$$

When

$$F_c > F_d$$

The tension difference on both sides of the friction wheel:

$$F_c - F_d$$

The limit friction between rope and the friction wheels:

$$f_{m1} = F_d(e^{\mu_1 \alpha} - 1)$$

The rope and the friction wheel will not occur for sliding conditions:

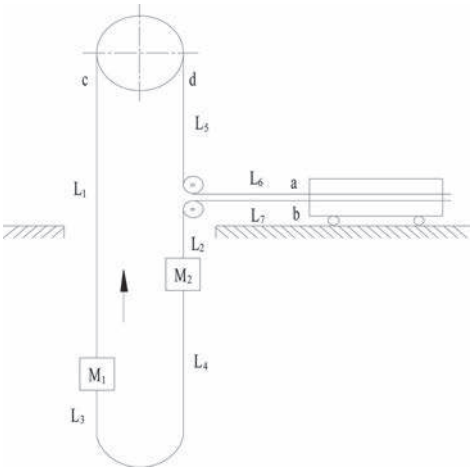


Figure 2. Statics model of tower-type replacing rope system.

$$F_c - F_d < F_d(e^{\mu_1 \alpha} - 1) / \sigma_j$$

Have

$$F_a > (m_1 g + M_1 g + m_3 g) / [(e^{\mu_1 \alpha} - 1) / \sigma_j + 1] - m_5 g \quad (1)$$

When $F_d > F_c$,

$$F_d - F_c < F_c(e^{\mu_1 \alpha} - 1) / \sigma_j \quad (2)$$

$$F_a < (m_1 g + M_1 g + m_3 g)\left[(e^{\mu_1 \alpha} - 1) / \sigma_j + 1\right] - m_5 g \quad (3)$$

Have

$$(m_1 g + M_1 g + m_3 g) / \left[(e^{\mu_1 \alpha} - 1) / \sigma_j + 1\right] - m_5 g < F_a < (m_1 g + M_1 g + m_3 g) \left[(e^{\mu_1 \alpha} - 1) / \sigma_j + 1\right] - m_5 g \quad (4)$$

Point b wire rope of static tension:

$$F_b = M_2 g + m_2 g + m_4 g$$

2 State of uniform acceleration

Set the acceleration to a Point c wire rope tension: $F_c = (m_1 + M_1 + m_3)(g + a) + F_z$, as F_z for Mine hoists resistance;

Point d wire rope tension: $F_d = m_5(g - a) + F_a$

$$\left[(m_1 + M_1 + m_3)(g + a) + F_z\right] / \left[(e^{\mu_1 \alpha} - 1) / \sigma_d + 1\right] - m_5(g - a) < F_a < \left[(m_1 + M_1 + m_3)(g + a) + F_z\right] \times \left[(e^{\mu_1 \alpha} - 1) / \sigma_d + 1\right] - m_5(g - a) \quad (5)$$

Point b wire rope of static tension:

$$F_b = (M_2 + m_2 + m_4)(g - a) - F_z$$

3 Uniform state

Point c wire rope tension:

$$F_c = m_1 g + M_1 g + m_3 g + F_z$$

Point d wire rope tension: $F_d = m_5 g + F_a$

$$\begin{aligned}&(m_1 g + M_1 g + m_3 g + F_z) / \left[(e^{\mu_1 \alpha} - 1) / \sigma_d + 1\right] \\ &- m_5 g < F_a < (m_1 g + M_1 g + m_3 g + F_z) \\ &\times \left[(e^{\mu_1 \alpha} - 1) / \sigma_d + 1\right] - m_5 g \end{aligned} \quad (6)$$

Point b wire rope of static tension:

$$F_b = M_2 g + m_2 g + m_4 g - F_z$$

In a mine for example, parameters are as follows:

head rope: 6.535 kg/m; 840 m; 4 root
tail rope: 9.954 kg/m; 782 m; 2 root
skip: 23.67 T
friction coefficient: backing 0.3
Anti-slip coefficient: 1.75 (static); 1.25 (motion)

When exchange the rope, the hoist started with rope exchange vehicle, The difference tension on both sides of the drum is 0, have

$$F_a = (m_1 + M_1 + m_3)(g + a) - m_5(g - a) + F_z \quad (7)$$

$$F_b = (m_2 + M_2 + m_4)(g - a) - F_z \quad (8)$$

$$F_a = F_b = \frac{105206}{4} = 26301N$$

Table 1. The rope static tension when the left skip at bottom hole.

	F_a	F_b
Static condition	105206	94182
State of acceleration	109819	89741
Uniform state	101726	90702

Table 2. The rope static tension when the left skip at wellhead.

	F_a	F_b
Static condition	94182	105206
Retarded state	97631	102800
Uniform state	97661	101726

So the rope tension release of rope exchange vehicle as long as more than 26301 N.

4 COMPOSITION AND TEST OF ROPE EXCHANGE VEHICLE

4.1 *The composition of rope exchange vehicle*

The rope exchange vehicle is a collection of a pull system, and rope winch, protection system and power system, able to apply all replacement, maximum release speed can reach 0.5 m/s, greatly save the rope release time. When the method of exchange rope in appropriate cases, can exchange rope work done within 12 hours in mine, which 1000 m deep and the head rope more than 40 mm in diameter. And release rope are implemented by high-quality friction liner, old and new head line tolerance status the same as the friction roller, do not damage the head rope. As shown in figure 3.

4.2 *The tensile test of rope exchange vehicle*

The pulling force of rope exchange vehicle is the key to implement the old and new head rope syn-

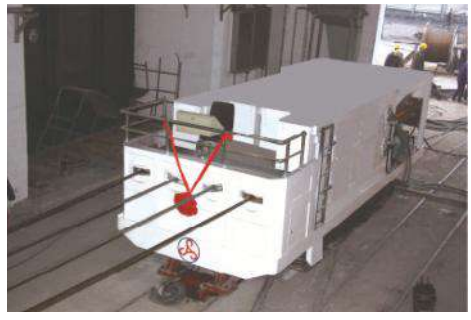
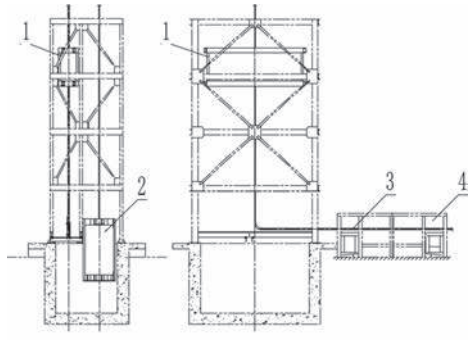


Figure 3. The photo of rope exchange vehicle.



1-balance weight; 2-cage; 3- test rope; 4- test unit

Figure 4. The experiment principle of rope tension release.

Table 3. Test tensile value of rope exchange vehicle.

Clamping cylinder pressure (MPa)		4	5	6	7	8	9	10	11	12
1# unit	Pull rope force (KN)	36	46	52	67	71	84	90	104	118
	Put rope force (KN)	38	48	54	69	75	85	94	104	113
2# unit	Pull rope force (KN)	36	43	50	65	70	87	96	108	116
	Put rope force (KN)	35	44	51	69	78	86	94	101	116
3# unit	Pull rope force (KN)	37	40	50	66	79	83	96	103	112
	Put rope force (KN)	39	45	51	69	77	81	97	106	116
4# unit	Pull rope force (KN)	38	49	52	68	72	88	98	103	112
	Put rope force (KN)	39	48	56	68	75	96	102	109	114

chronous interaction exchange on wellhead, so according to the actual parameters design of mine, the test will determine the pulling force. As shown in figure 4. Connect the test cage and the balance weight, test cage side weight is greater than the balance weight side. Requirements in under the action of no external force, cage rely on gravity to run down. Load the clamping cylinder pressure ceaselessly, stop the pressure when the rope slide in the unit, the force is under different clamping pressure corresponding to the pulling force of rope exchange vehicle. According to table 4, the pulling force of rope exchange vehicle were greater than 26301 N, meet the requirements.

5 PRACTICAL APPLICATION

Under the premise of head rope tension unchanged in hoisting system, the new and old rope interactive rope exchange vehicle rope exchange technique to realize the new and old rope Synchronous swaps wellhead. Solved the problem which previous rope replacement work labor force intensity big, long operation time, risk degree is high, and easy to appear the accident in mine. The pull system of rope exchange vehicle can meet the requirements of mine for the pulling force, and release rope are implemented by high-quality friction liner, do not damage the head rope; The security protection system can effectively avoid the elevator carry overrun, ensure the safety of the elevator running provides guarantee for mine safe and efficient production.

REFERENCES

Chang Y W. 2008. Fault diagnosis of a mine hoist using PCA and SVM techniques. *Journal of China University of Mining and Technology* 18(3):327–331. (In Chinese).

Deng S J. 2004. Method of designing the delayed limit velocity for mine hoist. *Journal of China University of Mining and Technology* 33(6):721–725. (In Chinese).

Dong M J, Jia F Y, Zhu C, Jiang X H, Chu L, Qiu S J & Han X D. 2008. ZHT Cage-supported Damping Swing-deck with Self-driven Changing Floor Used in Mine. *Coal Mine Machinery* 29(6):170–171. (In Chinese).

Jia F Y, Li Z J, Wang Y B & Sun J X. 2008. Analysis on safety and reliable braking of sliding rope on frictional hoist. *Coal Mine Enginering* (5):99–100. (In Chinese).

Jia F Y, Bi J M, Bi S H, Chu L & Wang Y B. 2008. SLT Cage Path Rope Online Detect Automatism Modulate Device. *Coal Mine Machinery* 29(4):117–118. (In Chinese).

Jia F Y, Wang Y B, Chu L & Bi J M. 2008. Analysis and Application of Botton of Well Equalize Hold Theory. *Coal Mine Machinery* 29(5):174–175. (In Chinese).

Jia F Y & Dong M J. 2011. Stabilizing Cage Technology of Deep Shaft Friction Hoist. *Journal of China Coal Society* 36(5):177–180. (In Chinese).

Ma J. 2008. Distribution of wire deformation within strands of wire ropes. *Journal of China University of Mining and Technology* 18(3):475–478. (In Chinese).

Ma K C & Jia F Y. 2011. Replacement Method and Safety Analysis on First Rope of Mine Shaft Hoist. *Coal Science and Technology* 39(9):73–76. (In Chinese).

Ma K C & Jia F Y. 2011. Selection of the method for safety replacing first rope of hoist based on AHP and MEA. *Coal Technology* 32(12):93–95. (In Chinese).

Wang H Y. 2007. Research on Detection Device for Broken Wires of Coal Mine-Hoist Cable. *Journal of China University of Mining and Technology* 17(3):376–381. (In Chinese).

Zuo Y Q & Jia F Y. 2011. Replacing Head Ropes with Rope Belt Rope Method and the Safety Analysis. *Coal Technology* 32(8):178–180. (In Chinese).

Progress in Mine Safety Science and Engineering II – He et al. (Eds)
© 2014 Taylor & Francis Group, London, ISBN 978-1-138-00122-0

Kinetics study on anthracite coal oxidation at low temperature by thermal analysis

Xiao-Xing Zhong & Guo-Lan Dou
School of Safety Engineering, CUMT, Xuzhou, China
Key Laboratory of Gas and Fire Control for Coal Mines, Xuzhou, China

Yun Chen
School of Safety Engineering, CUMT, Xuzhou, China

De-Ming Wang
School of Safety Engineering, CUMT, Xuzhou, China
Key Laboratory of Gas and Fire Control for Coal Mines, Xuzhou, China

ABSTRACT: The oxidation at low temperature (T ≤ 70°C) is the key process on researching the coal spontaneous combustion. Due to the lower oxidizability of anthracite coal than other types of coal, most researches about coal spontaneous combustion were centered on the higher temperature, but few on lower temperature. C80 micro calorimeter was applied to investigate the heat flow of Kabuliang anthracite coal with different temperature rising rates (0.1°C/*min,* 0.2°C/*min* and 0.4°C/*min*) from room temperature to 200°C, it was found that the heat release process of anthracite coal took place before 40°C. Based on Popescu non-model method, the mechanism functions and kinetic parameters were analyzed, the result indicates that oxidation reaction of Kabuliang anthracite coal corresponds to the anti Jander equation controlled by the three-dimensional diffusion model at 40–70°C, the value of activation energy is 72.81(KJ/mol) and the value of pre-exponential factor is 53903.35(s^{-1}).

Keywords: Anthracite coal, Coal oxidation at low-temperature, Popescu method, Kinetics

The anthracite coal with low ash and sulfur is superior coal resources, although it is a kind of high rank coal, it also occurs spontaneous combustion[1]. Spontaneous combustion of coal is a complicated process of the reaction between coal and oxygen, which includes the oxidation process at low temperature (T ≤ 70°C) and accelerated reaction process (T ≥ 70°C), and the oxidation process at low temperature is the key process of the coal spontaneous combustion prevention and the mechanism research[2]. Because of the weaker oxdability of the anthracite coal at the low-temperature oxidation process than other types of coal, most researches about the character of anthracite coal spontaneous combustion is still on accelerated reaction process, but few in low-temperature oxidation process[3–9]. For the research of reaction mechanism function, thermal analysis technique is widely used because of the advantage on test speed and repeatability. However, the common thermal analysis apparatuses such as DSC and DTA are hard to get accurate changes of heat and mass with the small test mass and high temperature heating rate, which has restricted the research on mechanism function of low-temperature oxidation process[10]. In recent years, along with the development of micro calorimeter, it has become an efficient way to investigate the coal low-temperature oxidation process depending on its advantages of larger test mass, lower temperature heating rate and higher test precision[11]. C80 micro calorimeter was used to investigate the low-temperature oxidation mechanism of anthracite coal.

1 EXPERIMENT

1.1 *Sample coal*

Kabuliang (KBL) anthracite coal was used as the test coal sample, it was transported to the laboratory sealed perfectly after collecting from the coal mine. Coal was broken into pieces under the protection of nitrogen, and then, the part of particle

Table 1. Proximate and ultimate analyses of the coal sample.

Coal sample	Proximate analysis (dry basis)				Heat	Ultimate analysis (dry basis)	
	Moisture (%)	Ash (%)	Volatile (%)	Fixed C (%)	Q (KJ/mol)	H (%)	S (%)
KBL anthracite coal	1.12	6.86	11.76	80.26	32.93	3.78	0.23

size ranging from 0.18–0.38 mm were sieved out to be test coal sample. The proximate and ultimate analyses of the coal is shown in Table 1.

1.2 *Experimental apparatus and process*

C80 micro calorimeter produced by Setaram corporation was used as experimental apparatus. The 500 mg coal sample and $\alpha - Al_2O_3$ were put into the reaction cell and reference cell respectively in the experiment. At the beginning of experiment, a 70 ml/min high purity nitrogen was admitted into reaction and reference cell, the coal sample was dried for 10 h in 105°C temperature control stove for getting rid of water. Then, the temperature was cooled down to 26°C under the protection of nitrogen, a 70 ml/min high purity oxygen was admitted into reaction and reference cell after temperature stabilized. The experiments were started with the 200°C as ending temperature at different temperature rising rates (0.1°C/*min,* 0.2°C/*min* and 0.4°C/*min*).

1 EXPERIMENTAL RESULTS AND ANALYSIS

2.1 *Experimental results*

The heat flow curves at different temperature rising rates of anthracite coal were shown in Fig 1, and the initial heat release temperatures at different temperature rising rates were shown in Table 2. From the Fig 1 and Table 2, before 200°C, the oxidation of anthracite coal is a process of slow heat release at lower temperature, then accelerated heat release at higher temperature. The initial temperature is lower than 40°C when using the C80 micro calorimeter, which is lower more than 40°C by using the DSC[12–13]. Thus, the heat release characters at low temperature are more accurate by using C80 micro calorimeter than DSC.

2.2 *Calculation and analysis on mechanism functions of coal spontaneous combustion*

In order to avoid the effect of kinetic compensation effect, the Popescu non-model method based on multiple scanning rates was used to determine the mechanism functions of KBL anthracite coal between 40°C and 70°C. This method not only does not use any approximate calculation of temperature intergral but also does not take any forms $k(T)$ into

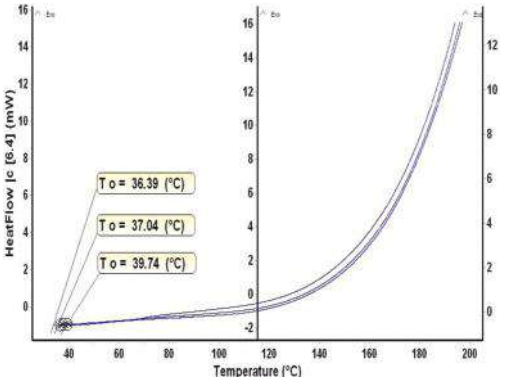


Figure 1. Heat flow curves at different temperature rising rates.

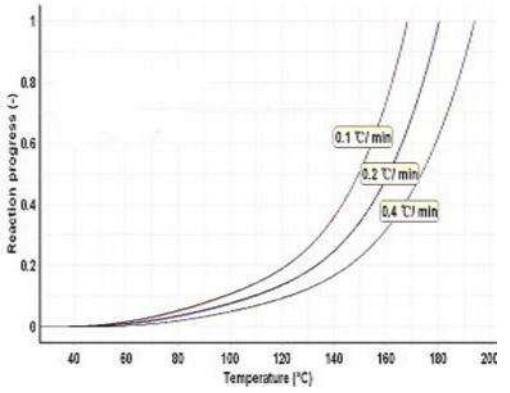


Figure 2. Conversion of KBL coal sample.

Table 2. Initial heat release temperature of KBL coal sample at different temperature rising rates.

Temperature rising rate (°C/min)	0.1	0.2	0.4
Initial heat release temperature T (°C)	36.39	37.04	39.74

consideration, which has been widely used in the research of coal combustion mechanism[14–19].

2.2.1 *Principle of kinetic mechanism obtained by Popescu method*

Popescu is a non-model kinetic analysis method which is based on multiple scanning rates[20], two temperature values $T = T_m$ and $T = T_n$ will determine a pair of values of α on each curve of different heating rate: (α_m1, α_n1)… (α_m3, α_n1), and also three pairs of T at two conversion values $\alpha = \alpha_m$ and $\alpha = \alpha_n$: (T_m1, T_n1)…(T_m3, T_n3). The basic kinetic function:

$$\frac{d\alpha}{dT} = \frac{1}{\beta} f(\alpha)k(T) \tag{1}$$

After taking the rearranging the terms, logarithms and approximate calculation, Eq (1) then becomes

$$G(\alpha)_{mn} = \int_{\alpha_m}^{\alpha_n} \frac{d\alpha}{f(\alpha)} = \frac{A}{\beta}(T_n - T_m)\exp\left(-\frac{E}{RT_\xi}\right) \tag{2}$$

Where α is the conversion; β is the temperature heating rate; $k(T)$ is the reaction rate constant; $f(\alpha)$ is the mechanism function; $G(\alpha)$ is the integral of $f(\alpha)$;

$$T_\xi = \frac{T_m + T_n}{2} \tag{3}$$

The conversion at any temperature T on the heat flow curves

$$\alpha_T = \int_{T_O}^{T} \frac{dH}{dT}dT \Big/ \int_{T_O}^{T_{end}} \frac{dH}{dT}dT = \Delta H_T / \Delta H \tag{4}$$

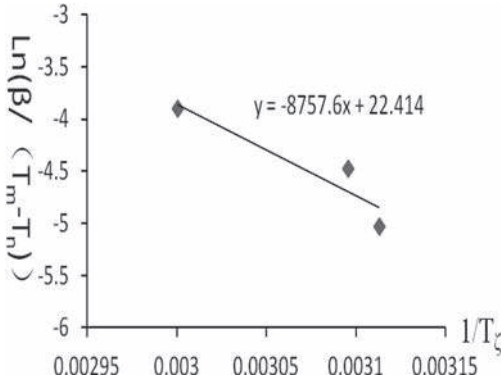


Figure 3. Plots of ln ($\beta/(T_n - T_m)$) versus $1/T_\xi$.

Where T_0 is the initial heat release temperature; T_{end} is the ending temperature; αT is the conversion at the temperature T; ΔH is the output of heat.

From Eq(2), the integral term at certain temperature T is constant, which means the plot of the values of mechanism function $G(\alpha)_{nm}$ versus $1/\beta$ has to lead a straight line with an intercept of zero. Thus, by the calculating the values α on each curve of different heating rate, the mechanism function can be determined by the plot of $G(\alpha)_{nm}$ versus $1/\beta$. If the plot of the values of $G(\alpha)_{nm}$ versus $1/\beta$ is a straight line with an intercept of zero, then the chosen $G(\alpha)$ is the mechanism function of the reaction. This method determines mechanism function with few assumption, and it also does not take the forms of k(T) into consideration, which avoids the effect of kinetic compensation effect, the analysis result has higher credibility.

2.2.1 *Mechanism function at low-temperature reactions*

According to the heat flow curves, the values of conversion α versus temperature T obtained by Eq(4) using AKTS analysis software are shown in Fig 2. Based on the principle of Popescu method, the conversion values α of three different temperature rising rate at 40°C and 70°C were put into 20 typical kinetics mechanism functions in Table 3. The linear regression method was used to analyses the scatter diagrams of $G(\alpha)_{nm}$ versus $1/\beta$. The linear regression results of mechanism functions $G(\alpha)_{nm}$ versus $1/\beta$ between 40°C and 70°C of KBL anthracite coal are shown in Table 3, where R^2 is the linear correlation coefficient which reflects the fitting degree of regression line and r_{SD} is the standard deviation which reflects the deviation between actual value and regression value. The function with maximum R^2 and minimum r_{SD} is the probable mechanism function.

Comparing the linear correlation coefficient and standard deviation for every kinetics mechanism function in Table 3, the NO.19 function is the most probable one. In consequence, the anti Jander equation controlled by the three-dimensional diffusion model is the most probable mechanism function for reaction of KBL anthracite coal between 40°C and 70°C.

2.3 *Activation energy and pre-exponential factor*

Taking logarithms, the Eq (2) becomes

$$\ln\left(\frac{\beta}{T_n - T_m}\right) = \ln\left[\frac{A}{G(\alpha)_{mn}}\right] - \frac{E}{RT_\xi} \tag{5}$$

The data of conversion and temperature were taken into the Eq (5) where $G(\alpha)$ is the function

Table 3. The linear regression results of 20 typical kinetics mechanism functions.

Number	Mechanism	Integral $g(\alpha)$	Correlation coefficient/R^2	Standard deviation/r_{SD}
1	One-dimensional diffusion	α^2	0.971231	0.00008590
2	Two-dimension diffusion, cylindrical symmetry	$\alpha + (1-\alpha)\ln(1-\alpha)$	0.971252	0.00004337
3	Three-dimensional diffusion, spherical symmetry	$[1-(1-\alpha)^{\frac{1}{3}}]^2$	0.466377	0.44723589
4	Three-dimension diffusion, cylindrical symmetry	$1-\frac{2}{3}\alpha-(1-\alpha)^{\frac{2}{3}}$	0.971259	0.00000967
5	Random nucleation and later growth mechanism	$[-\ln(1-\alpha)]^{\frac{1}{3}}$	0.566358	0.08948054
6	Random nucleation and later growth mechanism	$[-\ln(1-\alpha)]^{\frac{1}{2}}$	0.775380	0.03938507
7	Random nucleation and later growth mechanism, one core	$-\ln(1-\alpha)$	0.942557	0.00389771
8	One-dimensional phase boundary reaction	α	0.941002	0.00388895
9	Exponential function law, n = 3/2	α^{3-2}	0.970014	0.00049734
10	Reaction order, n = 1/4	$1-(1-\alpha)^{\frac{1}{4}}$	0.942171	0.00097392
11	Phase boundary reaction, spherical symmetry	$1-(1-\alpha)^{\frac{1}{3}}$	0.942042	0.00129834
12	Phase boundary reaction, cylindrical symmetry	$1-(1-\alpha)^{\frac{1}{2}}$	0.941783	0.00194684
13	Reaction order, n = 2	$1-(1-\alpha)^2$	0.939421	0.00776267
14	Reaction order, n = 4	$1-(1-\alpha)^4$	0.936178	0.01545747
15	Second order, chemical reaction, F_2	$(1-\alpha)^{-1}$	0.944085	0.00390570
16	Reaction order, chemical reaction	$(1-\alpha)^{-1}-1$	0.944085	0.00390569
17	2/3 order, chemical reaction,	$(1-\alpha)^{-1/2}$	0.943324	0.00195086
18	Third order, chemical reaction, F_3	$(1-\alpha)^{-2}$	0.945585	0.00782708
19	Anti Jander function, three-dimensional diffusion	$[(1+\alpha)^{\frac{1}{3}}-1]^2$	0.971185	0.00000936
20	Three-dimensional diffusion	$[(1-\alpha)^{-\frac{1}{3}}-1]^2$	0.971295	0.00000993

of anti Jander equation controlled by the three-dimensional diffusion model, then making the scatter diagram of the $\ln(\beta/T_n - T_m)$ versus $1/T_\xi$, which is shown in Fg 3, the values of activation energy and the pre-exponential factor obtained from slope and intercept are: E = 72.81(KJ/mol), A = 53903.35(s^{-1}).

3 CONCLUSION

The heat release process of KBL anthracite coal takes place before 40°C by the test of C80 micro calorimeter, which is a process of slow heat release at lower temperature then accelerated heat release at higher temperature from the initial heat release temperature to 200°C. Based on Popescu non-model method, the mechanism functions and kinetic parameters were analyzed, the result indicates that oxidation reaction of KBL anthracite coal between 40°C and 70°C corresponds to the anti Jander equation controlled by the three-dimensional diffusion model the value of activation energy is 72.81(KJ/mol) and the value of pre-exponential factor is 53903.35(s^{-1}).

ACKNOWLEDGEMENTS

This work was financially supported by the National Natural Science Foundation of China Youth Science Foundation (Grant No.51004105

and 51204171), Coal Joint Fund (Grant No.511340201).

REFERENCES

[1] Zhan Jian-min et al (2008). Underground coal fire in china: origin, detection, fire-fighting, and prevention. Beijing: China coal industry publishing house; p. 368–370. (In Chinese).

[2] Wang De-Ming (2008). Mine Fires. Xuzhou: China University of Mining and Techology Press; p. 1–4.

[3] Wang Yu-ling, Xia Wen-cheng & Yang Jian-guo et al (2012). Low-temperature oxidation process of anthracite particle surface. *Journal of China University of Mining & Technology*. 41 (4): 578–581. (In Chinese).

[4] Yu Ming-gao, Wang Yu-tian & Lu Ping (2003). Effects of water copperas on spontaneous combustion characteristic of anthracite from No.5 coal mine in Yangquan mining area. *Journal of China University of Mining & Technology*. 32 (2): 157–160. (In Chinese).

[5] Lu Chang & Zheng Yang-min (2009). Research on low-temperature oxidation and pyrolysis of coal by thermal analysis experiment. *Procedia Earth and Planetary Science.* 718–723.

[6] Wang Hai-hui & Bogdan Z (2003). Coal oxidation at low temperatures: oxygen consumption, oxidation products, reaction mechanism and kinetic modeling. *Procedia Earth and Planetary Science.* 29: 584–513.

[7] S. Krishnaswamy, R.D. Gunn & P.K. Agarwal (1996). Low-temperature oxidation of coal. 2. An experimental and modelling investigation using a fixed-bed isothermal flow reactor. *Fuel*. 75: 344–352.

[8] M. Itay, C.R. Hill & D. Glasser (1989). A study of the low temperature oxidation of coal. *Fuel Processing Technology*. 21:81–97.

[9] A.Y. Kam, A.N. Hixson & D.D. Perlmutter (1976). The oxidation of bituminous coal—I Development of a mathematical model. *Chemical Engineering Science*. 31: 815–819.

[10] Va´clav Slova´k· Boleslav Taraba (2010). Effect of experimental conditions on parameters derived from TG-DSC measurements of low-temperature oxidation of coal. *Therm Anal Calorim*; 101: 641–646.

[11] Sun Jin-hua & Ding Hui (2007). Heat risk evaluation on chemical materials, Beijing: Science Press; p. 116–129. (In Chinese).

[12] Zhong Xiao-xing (2008). Research on oxidation kinetics testing method for the propensity of coal to spontaneous combustion. Xuzhou: China University of Mining and Techology; p. 30–31. (In Chinese).

[13] Wang Qing-song, Sun Jin-hua & Guo Song (2008). Spontaneous conbustion identification of stored wet cotton using a C80 calorimeter. *Industrial Crops and Products.* 28: 268–272.

[14] Zhang Bao-sheng, Liu Jian-zhong, Zhou Jian-Hu, et al (2006). Popescu method for combustion kinetic mechanisms of coals. *Proceedings of the CSEE*; 26 (15): 68–72.

[15] Pone J D & Hein K A (2007). The spontaneous combustion of coal and its by-products in the Witbank and Sasolburg coalfields of South Africa. *International Journal of Coal Geology*; 72 (2): 124–140.

[16] Zhang Bao-sheng, Liu Jian-zhong, Zhou Jun-hu & Cen Ke-fa (2007). New model-free method based approach to mechanism of limestone decomposition. *Journal of Chemical Industry and Engineering (China)*; 58 (5): 1204–1209.

[17] Zou Chong, Zhang Sheng-fu, Wen Liang-ying et al (2011). Anthracite combustion kinetics study by thermal analysis. *Journal of China Coal Society*; 36 (8): 1370–1374. (In Chinese).

[18] Liu Jian, Chen Wen-sheng & Qi Qing-jie (2005). Study on the spontaneous combustion tendency of coal based on activation energy index. *Journal of China Coal Society.* 30(1): 67–70. (In Chinese).

[19] Li Xiao-min & Lin Qi-zhao (2012). Maximum probability mechanisms of pyrolysis of corn stalk. *CIESC Journal*. 63(8): 2599–2605. (In Chinese).

[20] C. Popescu (1996). Integral method to analyze the kinetics of heterogeneous reactions under non-isothermal conditions A variant on the Ozawa-Flynn-Wall method. *Thermochimica Acta*; 285 (2): 309–323.

This page intentionally left blank

Progress in Mine Safety Science and Engineering II – He et al. (Eds)
© 2014 Taylor & Francis Group, London, ISBN 978-1-138-00122-0

Research on thermal stability of new-style foamed gel

Shuijun Yu, Hong Zhao & Xiaoli Chen
Henan Province Key Laboratory of Prevention and Curve of Methane and Fires, Henan Polytechnic University, Jiaozuo, Henan, China
School of Safety Science and Engineering, Henan Polytechnic University, Jiaozuo, Henan, China

Guodong Meng
School of Safety Science and Engineering, China University of Mining and Technology, Xuzhou, Jiangsu, China

ABSTRACT: Common fire-prevention materials cannot be filled quickly and are toxic, corrosive and low efficiency. In order to solve the disadvantages of these common materials as well as to improve the efficiency of anti-extinguishing, a better coagulant was selected for developing a new type of environmentally friendly foamed gel. The results show that the dehydration rate of foamed gel accelerated with increasing temperature; The foamed gel in various stages of different temperatures meet different dynamics characters and mainly affected by the surface control and diffusion control; The complete dehydration time formula can be used to estimate complete dehydration time of foamed gel within a specific range; The differences in the physical properties made foamed gel a better evaporation-water loss rate than gel. So the new-style foamed gel is an effective anti-extinguishing material with good thermal stability.

1 INTRODUCTION

The mine fire caused by coal spontaneous combustion is always of great area and concentration. Air leakage is serious because of mining disturbance. All these unfavourable factors bring substantive inconvenience for fire prevention in goaf and threat to safety of mine (Lu & Geng 2009, Shao 2007). The technology of preventive grouting, water injection and spraying inhibitor that are widely used both in China and abroad, even dytory and three-phase foam which rose later, have a certain degree of shortage (Liang & Luo 2008). For example, due to the gravity, it is difficult for water, grouting and inhibitor to deposit high. Nitrogen and inert foam can only absorb limited heat in coal because their gas heat capacity is small and cannot be closed tightly when put out a fire (Wang, et al. 2010).

Gels possess better high-temperature resistance, stability and larger heat capacity that can reduce the temperature quickly and exclude fire source than the material mentioned above (Zhang, et al. 2002). But it still has some insufficient such as the great material consumption, difficulty in underground transportation; inappropriation for large area backfilling due to its tendency to solidify when diffuse certain distance in goaf; contamination to underground environment because of the ammonia of coagulant. Foam fire-fighting technology can make material cover the whole goaf in short time come true due to its fluidity. Foamed gel is the combination of foam and gel so it possesses the fire-fighting characters of both: the foamed gel first fill the coal mined-out area by the character of flow (Bober M, et al. 1997) and then, after the foams burst, it has a better effect in plugging wind by coving the coal evenly where reflects the character of gel (Cao & Tian 2009). Beyond that, foam gel has better material utilization than gel, so it can form larger filling volume with equal quality of material. So far, the foamed gel is widely used in area of oil while merely in coal so the research of it as mine fire-fighting material is deficient. Foamed gels developed till now are ammonia or corrosive to both machines and operators due to the acidic or alkaline coagulant (Yu & Jia 2012). So the new-style foamed gel have obvious advantage and broad application prospects.

The water steam from foamed gel in high temperature reduces the concentration of O_2 and lower environment temperature as well as prevents fire rekindling in the same time (A.M. Tafreshi & M. di Marzo 1999). The effect of steaming makes gel absorb a lot of heat so the inner temperature of gel is not high and its inner structure can stay stable (Sui 2007). Just as some researchers think that the gel is better due to its lower dehydration rate than water in isolating large area fire. But there are bare reports about the evaporation character of these material or related references (Xu, et al. 2003) about character parameters about some of

them so far. In order to make good use of the physicochemical properties of it and offer thermal stability to mine coal-mine fire, the thermal stability (Luo, et al. 2007) of foamed gel is studied and its rule is summarized by implying chemical kinetics (RETUERT, et al. 2004) and heat-transfer characteristic (Tian, et al. 2010).

2 MATERIALS AND METHODS

2.1 *Materials and equipment*

The new-style foamed gel is mainly made up of four parts: base stock, coagulant, foaming agent and water. Among them, the base stock is sodium silicate whose Baume number, modulus and density is 42.16, 3.3 and 1.40 g/cm^3; the water is tap water that is not distilled and filtered considering the practical water-using condition of mine; A, B, C and D are four kinds of ammonia-free coagulant selected roughly. Among them, A and B are Lewis acid containing 3-price cation while C containing 1-price cation. D is a kind of low-corrosive organic acid. Equipment contain digital blast drying oven (GZX-9023MBE), electronic balance (BS2202S), self-assembled foam-making device etc.

2.2 *Methods*

2.2.1 *The selection of coagulant*

Coagulant is very important to foamed gel because parts of the coagulant may output a lot of NH_4 in the chemical process or is corrosive to both workers and equipment due to their own characters such as acidic or alkaline. What is more, coagulants also influence fire prevention, extinguishing and mechanical properties of foamed gel largely.

Four kinds of foamed gel named a, b, c and d respectively containing coagulant A, B, C and D are produced by foam-making device. The results show that foamed gel made by coagulant A and B have worse thermal stability and strength and their structure made by aeration process of machine are easy to loosen and collapse due to the thin foam wall. While the foamed gel made by coagulant C and D possess thicker foam wall, better mechanical properties and stronger strength than the two foamed gel mentioned above. Then set c and d in 10°C for 20 d and weight them every 24 hours and compare their dehydration rate. The dehydration of material is:

$$v = 100\% \times \frac{m_q - m_h}{m_q} \tag{1}$$

where m_q = the original mass of gel, g; m_h = the mass of gel in a certain time, g.

2.2.2 *Influence of temperature on foamed gel*

The dehydration rate of material is one of the most important aspects of fire-fighting because the lower dehydration rate the better early stage fire-fighting property. Foamed gel made by 4% of coagulant D, 9% of sodium silicate and 0.2% of foaming agent in preparation for discovering the influence of temperature on it. The foamed gel is set respectively under the stable condition of 20°C, 40°C, 60°C, 80°C, 100°C and 120°C and calculated the dehydration rate during 15 hours by recording its mass per hour.

2.2.3 *The entire dehydration time under different temperature*

The foamed gel containing more than 90% water absorb pretty much heat due to the large specific heat of water. In order to improve the efficiency and persistence of fire-extinguishing such strategies as pouring water in time should be adopted. Put the foamed gel the same material and percentage mentioned above in steel disk whose height is 25 mm while diameter is 150 mm and set stable temperature of drying oven respectively 20°C, 40°C, 60°C, 80°C, 100°C and 120°C then record the six entire dehydration times under different temperature.

2.2.4 *The comparison of thermal stability b between ammonia-free and ordinary gel*

In order to compare the thermal stability in doors for long time, the same foamed gel and ordinary gel mentioned above is put in stable temperature as low as 10°C and their dehydration rate time during 500 hours is calculated per 50 hours. Put the same two materials mentioned above in higher stable temperature of 40°C, 60°C, 80°C and 100°C respectively to calculate their dehydration rate times during 6 hours.

3 RESULTS AND DISCUSSION

3.1 *The selection of coagulant*

Figure.1 shows the comparison of dehydration of foamed gel c and d. Their trend lines are substantially linear and foamed gel d have lower dehydration rate than c in any time where an obvious advantage of coagulant D than C in making foamed gel is shown. In addition, the dehydration rate of foamed gel c is about double of d where can be seen a better fire-fighting persistence in the practical application of the mine. In conclusion, foamed gel made by coagulant D is more appropriate than C.

3.2 *Influence of temperature to foamed gel*

Figure.2 shows the influence of various temperatures ranging from 20°C to 120°C on foamed

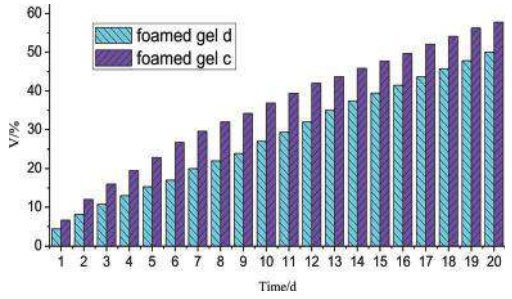


Figure 1. Dehydration rate comparison between foamed gel c and d.

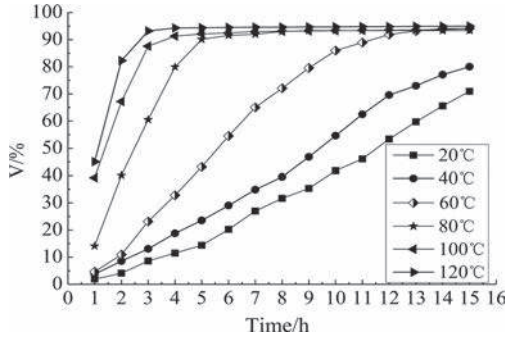


Figure 2. Relationship between dehydration rate of foamed gel d and different temperatures.

gel d. Overall, the dehydration rate of foamed gel increases with increasing temperature. Owing to the larger average energy of the movement of water molecules in high temperature, water -loss rate in high temperature is bigger than that in lower. When the temperature was lower than 60°C, the trend lines of dehydration rate are substantially linear and their own slopes are almost uniform with time; The rate slope is affected by surface control where the surface area is unchangeable when the slope stay invariant and its kinetic equation can be expressed as $v = at + m$. The dehydration rate in 80°C, 100°C and 120°C is bigger than that under 80°C. These three slopes between 0~3 h are almost fixed and is also affected by surface control which fit $v = at + m$; While the lines between 3~6 h are curves and their slopes are affected by diffusion control which fit exponential relationship $v = \alpha \cdot t^{\beta}$ ($\beta < 1$); After 6 hours, their dehydration rates are straight paralleled with x-axis and the slopes are zero when free water vaporize up.

3.3 *The entire dehydration time under different temperature*

As shown in fig. 3, it is concluded that the higher is the temperature, the shorter the complete

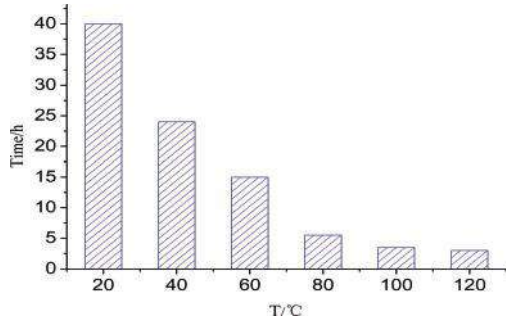


Figure 3. Relationship between complete dehydration time of foamed gel and temperature.

dehydration time. The complete dehydration time above 80°C is much smaller than that below 80°C, and time of 20°C is about ten times than that of 120°C. The main reason of the shorter complete dehydration time is that the steams vaporize fast owing to the accelerated movement of water molecules in high temperature.

The relation between temperature and complete dehydration time is $y = 0.0047x^2 - 1.0198x + 58.2$ with the squared correlation coefficient $R^2 = 0.9959$. Foamed gel filled as fire-fighting material in coal mined-out vaporized gradually, but the loss of water make the effect of absorbing heat and reducing temperature worse. The foamed gel losing some elasticity and strength owing to dehydration also reduces the effect of isolating O_2. The above derived relation may estimate complete dehydration time of foamed gel between 20°C and 120°C. Thus, mined-out will be filled in time to fill mined-out area in time to avoid mine disasters caused by spontaneous combustion.

3.4 *The comparison of thermal stability between ammonia-free and ordinary gel*

To compare the dehydration of foamed gel and ordinary gel for a long time, the dehydration rate of both in 6 hours was compared respectively in the constant temperature, and the condition in 10 °C for 500 hours was observed. The results were shown in figure 4 and figure 5. Results in figure 4 and figure 5 show that dehydration rate of gel is always greater than foamed gel and this trend could remain for a long time. The dehydration rate gap becomes more obvious with time, which proved that foamed gel had better thermal stability than gel under the same conditions. After filling in glue-note area, the free water secreted from gel loses in two ways, which was penetration into the coal seam and evaporation. The dehydration of gel reduced the fire prevention performance. The difference of dehydration measured in experiment is

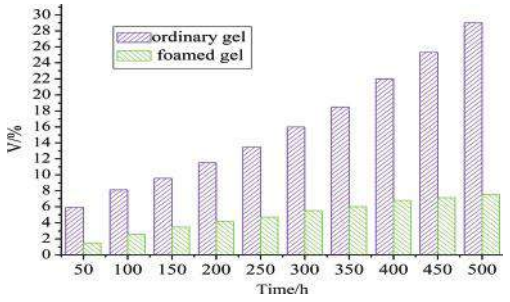


Figure 4. The dehydration rate of ordinary gel and foamed gel at 10°C temperature.

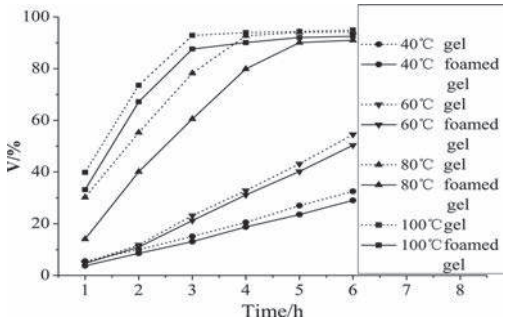


Figure 5. The dehydration rate of ordinary gel and foamed gel at different temperature.

mainly because of the difference in covering performance and physical structure between gel and foamed gel. The structure of the gel is tight and uniform, but foamed gel is different because it is heaped up by foams whose wall is thin and skeleton loose. Those reasons lead to the fact that moisture diffusion in foamed gel is tougher than in gel. And even, the burst of surface foam which then cover over the foamed gel hinder the sublayer foamed gel from water evaporation and diffusion to a certain extent, make the sublayer foamed gel still have plenty of water. For this reason, foamed gel have smaller dehydration rate than gel.

4 CONCLUSION

Foamed gels generated from different coagulants have different states and dehydration rates. Some of these coagulants are appropriate to be gel, but another are not because they are structural soft and collapse easily in mechanical aeration process.

Foamed gel dehydration rate meet different dynamic characteristics in different temperature. When at low temperature process (less than 60°C) and early stage of high temperature process (more than 80°C), the dehydration rate is affected mainly by surface control, fitting the equation $v = at + m$, where the surface area is unchangeable when the slope of curve stay invariant. However, at middle stage of high temperature process, the dehydration rate effected by diffusion, fitting the equation $v = \alpha \cdot t^{\beta}$.

The formula $y = 0.0047x^2 - 1.0198x + 58.2$ is used to describe the relationship between temperature and complete dehydration time of material. Making use of that relation may estimate complete dehydration time of foamed gel between 20°C and 120°C and fill mined-out area in time to avoid mine disasters caused by spontaneous combustion.

Due to lower dehydration rate, which is caused by different covering performance, physical structure and compactness, foamed gel has fire prevention effect in long-term.

ACKNOWLEDGEMENTS

Changjiang Scholars and Innovative Research Team Development Program (IRT0618); The State Administration of Work Safety of Coal Mine Safety Production Technology Development Program (08-149); The basis of Henan Province, and cutting-edge technology research projects (082300463205, 09230041004) Natural Science Foundation of Henan Province Department of Education (2007620004).

REFERENCES

Bober M, Persson H, Persson B *Fire Technol.* 1997:33(4):336–55.

Fuxi Zhang, Jiyong Liu, Xinhai Zhang. *Mining Safety & Environmental Protection,* 2002, 29(5):51–53 (In Chinese).

Guobin Lu, Ming Geng. *Journal of Liaoning Technical University* (Natural Science), 2009, 28(3): 28–30 (In Chinese).

Jingcai Xu, Xinhai Zhang, Hu Wen, etc. 2003 Theory and technology of extinguishing and preventing coal seam spontaneous combustion with gel. Bei Jing: China Coal Industry Publishing House. (In Chinese).

Jun Shao. Coal *Science and Technology,* 2007, 35(5): 1–3 (In Chinese).

Kai Cao, Zhaojun Tian. 2009, New thinking of coal fire control-gel foam coal fire control technology. Science paper Online, (In Chinese).

Retuert J, Martinez Y, Quijada R. Highly porous silica networks derived from gelatin siloxane hybrids prepared starting from sodium metasilicate. *Journal of Non-Crystalline Solids,* 2004, 347 (1–3):273–278.

Shunjun Yu, Boyu Jia. Journal of Shandong University of Science and Technology (Natural Science), 2012, 31(2):42–47 (In Chinese).

Tafreshi A M, di Marzo M, *Fire Safety Journal.* 1999: 33(4):295–305.

Tao Sui, 2007, The application study of fly ash gelatin precautions-extinguisher fire technology in coal mine. Ms D Thesis. Tai Yuan: Taiyuan University of Technology, (In Chinese).
Yuntao Liang, Haizhu Luo. *Journal of China Coal Society,* 2008, 38(2):126–130 (In Chinese).
Zhaojun Tian, Deming Wang, Yongliang Xu, etc. *Journal of China University of Mining & Technology,* 2010, 39 (2):6–10 (In Chinese).
Zhenmin Luo, Jun Deng, Yongbin Yang, etc. *Journal of China University of Mining & Technology,* 2007, 36 (6):748–751 (In Chinese).
Zhihua Wang, Guoguang Wu, Xianliang, etc. *Energy Technology and Management,* 2010(1): 49–51 (In Chinese).

This page intentionally left blank

Progress in Mine Safety Science and Engineering II – He et al. (Eds)
© 2014 Taylor & Francis Group, London, ISBN 978-1-138-00122-0

The application research of K shortest path algorithm in avoiding mine disaster

F. Wang, H.G. Guo & G.J. Lu
College of Mining Engineering, Taiyuan University of Technology, Taiyuan, China

ABSTRACT: The safety situation of coal mine is still not optimistic in China. The mine disasters seriously affect the safety of life and property of the miners. To avoid the danger, the miners should flee to the safety sites in the shortest time at the beginning of the disaster. Thus, we expound, in this paper, a method to get optimum path in the weighted undirected graph based on the Dijkstra algorithm, and propose a new method of calculating K shortest path. Then combining with mine specific examples, using VB programming language, this paper make it possible to get the two routes quickly and accurately.

1 INTRODUCING THE THEORY OF THE OPTIMAL PATH TO AVOID DISASTER

In recent years, the safety situation of coal mine is relative calm, along with the wide attention from all sectors of society on security issues, especially on the safety of coal mine. However, 1201 accidents have still occurred and killed 1973 people in 2011. The safety situation of coal mine is still not optimistic based on the increasing number of coal mine and the growing coal production. The miners should flee to the ground or underground safe places as soon as possible, to effectively reduce casualties and property losses. In this paper, we focus on helping miners find the optimal path to escape during a fire, thereby they can safely flee in time.

The optimal path to avoid disaster is a route spending the least time from a disaster site to a safe place (Li, 2001). However, the optimal path to avoid disaster might be destroyed, or be no longer suitable to escape, due to the special underground environment, the complicated roadways. Therefore, multiple escape routes will usually be elected in order to nip in the bud, which is the so-called K optimal path to avoid disaster.

1.1 *The calculation method of the optimal path*

Currently, the Dijkstra algorithm is the most authoritative one among many algorithms for the optimal path, due to the easily understanding about the computational process and time complexity. The Dijkstra algorithm is generally used to calculate the optimal path of weighted directed graph. But, both the downwind and upwind roadways can be used as an escape route during the underground escape. Thus, the research of this topic is to find the optimal path of the weighted undirected graph.

The following simply introduces the calculation of the optimal path by the Dijkstra algorithm (Wang, 1994; Ji, 2008):

There is a weighted undirected graph G = (V, E, W), of which V stand for nodes, E stand for edges, and W stand for the weight of every edge. V = {v0, v1, v2, v3…vn}, the set of permanent markers S = {v0}, T = V – S. The parent node of v0 is –1, the parent node of the others is 0. The weight Wij = (v i, v j), if there is no side between vi and vj, then Wij = ∞. Dij is the sum of weight from vi to vj. The initial numerical value of Dij is the same with that of Wij.

The method of calculating the optimal path from v0 to vn is shown as following:

1. For random node, vi ∈ T, D0k = min (D0i), then S = {v0, v k}.
2. For random node, vi ∈ T, if D0k + Wk i < D0i, then D0i = D0k + Wk i, and the parent node of vi becomes vk.
3. After repeating these two steps until vn ∈ S, D0n is the weighted sum of the optimal path.

By seeking the parent node backwards until v0, the optimal path from v0 to vn will be found.

1.2 *The calculation method of the K optimal path*

The traditional method to calculate the K optimal path is defringe algorithm. Specifically, firstly the optimal path is calculated by the Dijkstra algorithm. Then the new optimal path is determined after deleting a random edge of the opti-

mal path. Thus the K optimal path is obtained. This method is relatively complicated, and different optimal paths will be obtained by deleting different edges, resulting in that the k optimal path calculated by this method is not the accurate optimal path, but the approximate shortest path. Based on the traditional Dijkstra algorithm, we proposed a new method to calculate the accurate K optimal path in this paper. The detail is introduced as following:

1. A permanent marking point is made according to the Dijkstra algorithm from the source node also called the positive direction, stored in a collection S. Then the adjacent temporary marker point is modified.
2. A permanent marking point is made according to Dijkstra algorithm from the target node also called the opposite direction, stored in a collection E. Then the adjacent temporary marker point is modified.
3. Another permanent marking point is made from the positive direction, stored in the collection S. The adjacent temporary marking points are then modified. If the permanent tag node is already in the collection E, setting the permanent marker as the center, tracing to find an optimal path respectively according to positive direction and reverse direction. If not, going to the next step.
4. Another permanent marking point is made from the opposite direction, stored in collection E, The adjacent temporary marking points are then modified. If the permanent tag node is already in the collection S, setting the permanent marker as the center, tracing to find an optimal path respectively according to positive direction and reverse direction. If not, going to the next step.
5. Going on one step from the positive direction, one step from the opposite direction, repeat the steps (2) and (3), do the loop continuously, until you find the desires of K, the optimal path or the source node and destination node are all permanent marker, the algorithm is end.

2 INTRODUCTION OF THE SPECIFIC SITUATION OF MINE

With regard to mine system, the intersections of roadways can be considered as nodes, and a roadway can be considered as an edge. Then the complicated roadway relations of mine can be reflected in a network planning. How do we formulate the weight of every side? In fact, the length of each roadway are different, leading to the transit time is varied. Theoretically, the longer the roadway is, the more transit time the roadway needs. Thus, the weight of each side can be represented by the length of corresponding roadway. However, even if two roadways have the same length, the transmit time is different because there are many factors affect the transit time. We can use the influence coefficient to reflect the effect of all factors. Therefore, the equivalent length is obtained by multiplying of the actual length of roadway and various coefficients to reflect the transit time.

Namely, $Wij = Kh * Kw * Kp * Kf * Kv * Lij + \sum Lm$

Of which,

Wij – The equivalent length of roadway;
Kh – The influence coefficient of height of roadway;
Kw – The influence coefficient of width of roadway;
Kp – The influence coefficient of gradient of roadway;
Kf – The influence coefficient of muddy degree of roadway;
Kv – The influence coefficient of wind speed of roadway;
Lij – The physical length of roadway;
n – The number of local obstacles;
Lm – The equivalent length of local obstacles.

3 THE SPECIFIC EXAMPLE

The actual data of ventilation system of one mine in Huasheng are used to determine the K optimal path by combining the parameters of the concrete and VB programming language, in order to guide the escape of mine personnel.

3.1 *The ventilation network map*

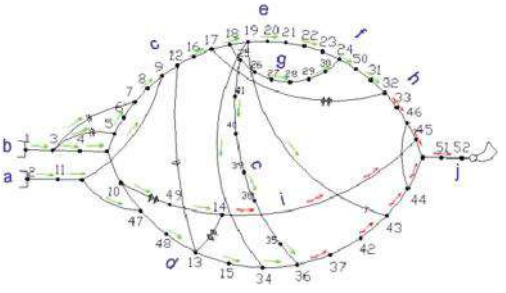


Figure 1. The mine ventilation network diagram of 3101# working face. a, main slope. b, Auxiliary slope. c, auxiliary trading big alley. d, belt transport roadway. e, transportation roadway. f, working face. g, auxiliary transport roadway. h, return airway. i, return air alleys. j, return air shaft.

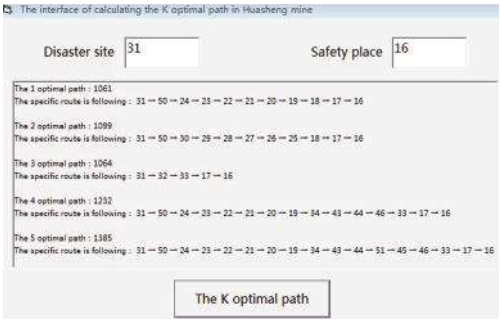


Figure 2. The operation interface.

3.2 *The operation interface of getting the optimal path*

Based on the actual parameters of every roadway, the equivalent length (m) of every roadway can be calculated by the computational formula of equivalent length. Then, the optimal path from any disaster site to the safety place can be obtained by the VB program. The operation interface is showed in Fig. 2.

3.3 *The analyses of the pros and cons of choosing the optimal path*

1. As long as inputting the disaster place and safety place, we can quickly find out the corresponding optimal path and the K optimal path;
2. If the optimal path is broken, we can quickly adjust the escape routes according to the K optimal path;
3. It is the key problem that how to notify the optimal path to disaster personnel timely and accurately. During mine disaster, such as a fire, miners are very panic and difficult to judge the escape direction sanely. So miners should remember expertly the avoiding disaster optimal path. However, during a fire, if the optimal path is changed, we should make use of the communications-equipment to inform miners.

4 CONCLUSION

In this paper, a method of the optimal path in the weighted undirected graph and a new method of calculating the K optimal path are proposed based on the traditional weighted directed graph. The K optimal path is convenient for miner to escape, can also assist in the decision-making of leadership. Further studies should focus on the determination of the changing parameters of the roadway to calculate the optimal path.

REFERENCES

Ji H.F. & Xu A.G. 2008. The design and implementation of Dijkstraalgorithm. *Journal of liaoning engineering technology university (natural science edition)* 27(S1):222–223.

Li X.D. 2001. The determination and application of route for avoiding disaster during a mine. *Coal mine safety* 26(12):20–22.

Wang D.M. & Wang S.S. 1994. The research of the optimal avoiding disaster path during a mine fire by computer [J]. *Journal of China university of mining* 23(3):27–32.

This page intentionally left blank

Progress in Mine Safety Science and Engineering II – He et al. (Eds)
© 2014 Taylor & Francis Group, London, ISBN 978-1-138-00122-0

Study on goaf spontaneous combustion prediction simulation of gas-drainage in spontaneously flammable and thick coal seam

Zhongya Zheng, Qun Zhang & Changfu Xu
Mine Safety Technology Research Institute of China Coal Research Institute, Beijing, China
The State Key Laboratory of High Efficient Mining and Clean Utilization of Coal Resources, Beijing, China

Chao Ma
China Coal Science and Industry Group, Beijing, China

Haifei Yao & Haijun Wu
Mine Safety Technology Research Institute of China Coal Research Institute, Beijing, China
The State Key Laboratory of High Efficient Mining and Clean Utilization of Coal Resources, Beijing, China

ABSTRACT: ZF4403 working face of Xiagou coal mine is the typical thick and spontaneously flammable coal seam fully mechanized caving mining working face under the condition of gas drainage, air leakage in goaf is large, residual coal is thick and coal is broken, the threat of goaf spontaneous combustion is serious during mining face. Combined with the coal seam occurrence condition of ZF4403 working face, seepage model of goaf is established, using the numerical method based on flow field simulation to calculate oxygen concentration and distribution law of air leakage intensity in goaf, and made numerical simulation analysis by Fluent software, combined with the limit parameters of coal spontaneous combustion from experiment, to predict spontaneous combustion dangerous area. The result shows that the reliability of spontaneous combustion prediction simulation data of spontaneously flammable and thick coal seam ZF4403 fully mechanized caving mining working face under the condition of gas drainage is high, boundary values match degree of spontaneous combustion dangerous area is 74.63%~96.78%, width match degree of spontaneous combustion dangerous area is 84.37%~99.78%, simulation data coincided with the measured results on a high level, practicality is good. The range of measured spontaneous combustion dangerous area in goaf where air input is 60.30~174.20 m, the range of that in goaf where air output is 32.60~122.40 m.

1 INSTRUCTIONS

Xiagou coal mine is located in the southern Binchang mining area, easternmost south wing of Dafosi syncline, bordered by Tingkou anticline to the north and Binxian anticline to the south, it is the simple monoclinic structure of north or northwest tilt. Xiagou coal mine is gaseous mine, mainly mining the 4th coal seam, lower Jurassic Yan'an group. The average thickness of the 4th coal seam is 16.80 m, it is low metamorphic humic bituminous coal. 404 mining area is gas abnormal zone, the spontaneous combustion period of 4th coal seam tested by Xi'an University of Science and Technology is 33d, and coal dust is explosive. The fully mechanized mining of spontaneously flammable and thick coal seam under the condition of gas drainage further increased the air leakage in goaf, expanded the scope of spontaneous combustion dangerous area in goaf, increased oxygen concentration in goaf, seepage intensity increased, the oxidation complex reaction time of residual coal and oxygen became longer, greatly improved the possibility of coal spontaneous combustion in goaf. Taking ZF4403 fully mechanized caving mining working face in 404 mining area as an example, seepage model of goaf is established, using the numerical method based on flow field simulation to calculate oxygen concentration and distribution law of air leakage intensity in goaf, and made numerical simulation analysis by FLUENT software, combined with the limit parameters of coal spontaneous combustion from experiment, to predict spontaneous combustion dangerous area. It is greatly significant for building the spontaneous combustion prediction system in goaf of thick and spontaneously flammable coal seam under the condition of gas drainage.

2 PROFILE OF ZF4403 WORKING FACE

The elevation of ZF4403 working face is between +465.35 and +469.28 m, the depth is about 439.70~590.00 m, the upper surface is plateau beam topography cutting by valleys. ZF4403 working face used top coal fully mechanized caving mining technology, roof managed with all caving method. The mining height of working face is 3.10 m, with caving height of 9.30 m and caving ratio 1:3. The strike length of working face is 1800 m, tilt length is 186 m, mining area is 316200 $m^{2,}$ geological reserves is 7.7 million tons, recoverable reserves is 5.37 million tons, recovery rate of 80%, producing 210, 000 tons per month, mineable period is 20.5 months. The geological structure of working face is simple, joints and cracks of coal seam is developed. When driving two lanes and cut, the phenomenon of floor and roof watering gushing locally emerged, mainly for coal seam fracture water. Working face arranged 3 roadways in 4th coal seam, are respectively air return tank, transport trough and draining lane, the average angle of working face is 3°. The air return side is equipped with gas drainage system for goaf gas drainage, spontaneous combustion of residual coal is a very serious problem in the production process.

3 THE INFLUENCE OF GAS DRAINAGE ON COAL SPONTANEOUS COMBUSTION IN ZF4403 GOAF

3.1 *The influence of gas drainage in goaf on air leakage*

The relationship between gas drainage and air leakage in goaf is mainly affected by two aspects (Xu 2002), one is the size of drainage flow; second is the drainage location. Due to the relatively high gas content in ZF4403 working face, a lane of 3.80 m wide and 2.70 m high is arranged as gas drainage tunnel in the coal seam which is 7 m from the roof in the upper part of air return side. The drainage flow is about 444 m3/min, gas concentration from 0.80 to 2.64% with an average of 1.25%. For this high gas drainage roadway that drainage mouth is in close proximity with working face, when drainage flow is less than a critical value, the air leakage of working face gradually reduced with the increase of drainage flow, and turned to increase when the drainage flow exceeded a certain value. When the case of a large flow of gas drainage or diversion of gas, the degree of spontaneous combustion hazard is high. Specific performance is one thing to make spontaneous combustion in the spontaneous combustion dangerous area of original air inlet side intensified, the other is easy to lead local secondary fire area near the mouth of drainage.

3.2 *The dilution effect of gas drainage in goaf on the oxygen concentration in air flow*

The greater the intensity of gas drainage in goaf is, the more the amount of gas emission is, and with the conduct of drainage, the coal gas emission ability becomes greater. Therefore, the gas emission in goaf under the condition of drainage has a dilution effect on the oxygen concentration in goaf. The reduction and uneven distribution of oxygen concentration in goaf is not entirely due to the oxidized consumption of residual coal. Gas distribution and oxygen distribution in goaf is interactive, with the increasing of gas emission intensity, the oxygen gradient becomes greater. From the comparison of air leakage intensity distribution and gas emission intensity in goaf, near the working face, air leakage intensity within the region of goaf is very great, gas concentration is very low, and the impact of gas emission intensity is weak; While in the deep part of goaf, relying on the effect of wind pressure differential across the working face, air leakage from the working face to goaf is extremely weak, and the impact of gas emission is relatively strong.

4 THE MATHEMATICAL MODEL OF LEAKAGE FLOW FIELD IN FULLY MECHANIZED CAVING GOAF

4.1 *The seepage model of goaf*

Fully mechanized caving goaf can be seen as composition of rock and loose coal, As the uneven spatial and temporal distribution of loose coal voids, air leakage source and sink is difficult to determine, leakage flow field is very complex, only considering the average leakage intensity, that is, air leakage through unit area of loose coal. Assuming that the density of air leakage flow in goaf is constant, air adsorption and desorption of loose coal under ambient temperature and pressure achieves balance; then comes to the following balance equation:

$$\frac{\partial \overline{Q_x}}{\partial x} + \frac{\partial \overline{Q_y}}{\partial y} + \frac{\partial \overline{Q_z}}{\partial z} = 0 \tag{1}$$

In the equation, x, y, z respectively represent axis; indicates air leakage intensity (air leakage through unit area of coal).

The gap channel of loose coal in goaf is very irregular, so the staggered and zigzag flow channel makes air flow in loose coal very complex. Statistics

show that even though seepage state in goaf will change in different locations, as the seepage rate in goaf decreases rapidly, goaf seepage state is seen as laminar flow, the seepage momentum equation obeys Darcy's law. It can elicit the goaf seepage model formula (Deng et al. 2004):

$$\frac{\partial}{\partial x}\left(K_x\frac{\partial H}{\partial x}\right)+\frac{\partial}{\partial y}\left(K_y\frac{\partial H}{\partial y}\right)+\frac{\partial}{\partial z}\left(K_z\frac{\partial H}{\partial z}\right)=0 \quad (2)$$

In the formula, x, y, z respectively represent axis; H is total head, Pa; K represents Porous medium permeability coefficient in goaf, Kx = Ky = Kz, According to scene observations and experiments, it can be obtained by the law of permeability influence function of coal spontaneous combustion: voidage f is 0.37, $K = 2.17 \times 10^{-3}$ m^3 · s/kg.

4.2 *Oxygen and gas concentration field model*

The moving process of oxygen in porous media includes diffusion, seepage and mass transfer. Oxygen and gas seepage velocity of loose coal in goaf is generally small, it is seen as laminar flow state. According to the theory of porous mass transfer, the oxygen and gas mass balance equations in loose coal as follow (Deng et al. 2001, Qin et al 2003):

$$\begin{aligned}&\overline{Q}_x\frac{\partial C}{\partial x}+\overline{Q}_y\frac{\partial C}{\partial y}+\overline{Q}_z\frac{\partial C}{\partial z}\\&=D_x\frac{\partial^2 C}{\partial x^2}+D_y\frac{\partial^2 C}{\partial y^2}+D_z\frac{\partial^2 C}{\partial z^2}-V(T)\end{aligned} \quad (3)$$

$$\begin{aligned}&\overline{Q}_x\frac{\partial\left(C_{CH_4}\right)}{\partial x}+\overline{Q}_x\frac{\partial\left(C_{CH_4}\right)}{\partial y}+\overline{Q}_z\frac{\partial\left(C_{CH_4}\right)}{\partial z}\\&=D_{CH_4}\left(\frac{\partial^2 C_{CH_4}}{\partial x^2}+\frac{\partial^2 C_{CH_4}}{\partial y^2}+\frac{\partial^2 C_{CH_4}}{\partial z^2}\right)+S_{CH_4}\end{aligned} \quad (4)$$

In the equations, D represents diffusion coefficient of oxygen in loose coal, it equals to 2.88×10^{-5} m^2/s; V(T) is the oxygen consumption rate of coal in oxygen concentration of C; according to the experiment results, the oxygen consumption rate of Xiagou coal mine 4403 fully mechanized caving mining working face in fresh air flow and under 25°C, it equals to 6.05×10^{11} mol · cm^{-3} · s^{-1}.

4.3 *Definite conditions and boundary conditions*

4.3.1 *Definite conditions*

Assuming that working face pressure is stability, goaf temperature is stability, it is seen as steady-state seepage flow. Namely:

$$\frac{dC}{d\tau}=0 \quad (5)$$

Goaf wall is adiabatic surface. Namely:

$$\overline{Q}=0 \quad (6)$$

4.3.2 *Boundary conditions*

According to the observation data of Xiagou coal mine ZF4403 fully mechanized caving face, comes to the function of oxygen concentration mass fraction of goaf changing with the working surface distance:

Fitting equation of oxygen concentration in air inlet side:

$$C = 0.0000001y^4 - 0.00005y^3 - 0.0024y^2 + 0.0981y + 17.674$$

Fitting equation of oxygen concentration in air return side:

$$C = 0.0000005y^4 - 0.0001y^3 + 0.0124y^2 - 0.4851y + 23.761$$

According to scene observations and experiments, calculated the oxygen consumption rate of Xiagou coal mine 4th loose coal under the oxygen concentration of 21% to be 1.95×10^{-6} kg × m^{-3} · s^{-1}, production rate of CH_4 to be 6.83×10^{-7} kg · m^{-3} · s^{-1}.

5 NUMERICAL SIMULATION OF AIR LEAKAGE FLOW FIELD OF ZF4403 FULLY MECHANIZED CAVING GOAF

5.1 *Physical model of goaf and meshing*

According to the coal seam occurrence and mining conditions of ZF4403 fully mechanized caving face, combining with the dynamic effects of gas drainage system in return corner on goaf spontaneous combustion, using Fluent software, the physical model of ZF4403 fully mechanized caving goaf is established. The model is hexahedron, the length of goaf floor and working face is 195 m, in the places that 200 m deep in goaf, 15 m high to the floor, the energy exchange of wall with the outside world is zero. The thickness of central float coal is 1.77 m, the thickness of float coal in two roadways is 8.86 m.

Taking the intersection of goaf air inlet side and working face as the dynamic origin, the direction to the air return side is x-axis, the direction perpendicular to working face deep into the goaf is y-axis, the direction vertically upwards is z-axis. The mesh step in x-axis and y-axis is 1 m, the grid step of z-axis on the float coal and overburden is 0.20 m. As shown in Figure 1:

Table 1. The quantitative datum of oxygen concentrations simulation in goaf (%).

Depth (m)	18.10	33.10	48.90	64.20	80.50	94.50	107.10	120.60	126.90
Air input side (%)	20.96	20.03	17.74	17.48	17.02	16.45	15.46	13.88	9.87
Air output side (%)	20.97	18.44	16.46	16.33	16.17	10.08	7.45	4.99	4.18

5.2 *Simulation results and analysis*

5.2.1 *Oxygen concentration and gas concentration*

Spontaneous combustion easily happens in the place that oxygen concentration range of 5% to 18%, it is called the spontaneous combustion oxidation heating zone. It can be seen from Figure 2, the 40 m to 180 m deep part of ZF4403 caving face is spontaneous combustion oxidation heating zone. The quantitative datum of oxygen con-centrations of two roadways in goaf calculated by Fluent simulation results is shown in Table 1:

Figure 3 is the gas concentration distribution of the place that is 1 m high to the floor in goaf under the condition of gas drainage. It can be seen from the figure that gas concentration of air return side is higher than that of air inlet side, and converged near the mouth of gas drainage. The gas concentration of two sides both increased with a certain gradient to the deep goaf, in line with the seepage law of goaf. The gas drainage system of air return side makes gas pumped out of goaf, but not enough to pump out all the gas in the deep goaf; it occurs gas accumulation in the deep goaf, but it doesn't pose a threat to working face due to its low oxygen concentration.

5.2.2 *Goaf seepage and relative pressure*

Figure 4 shows the seepage diagram of the place that is 1 m above the floor in goaf. The figure shows the influence of gas drainage system in air return side on goaf seepage. According to Fluent simulation results, The quantitative datum of seepage velocity of two roadways in goaf calculated by Fluent simulation results is shown in Table 2:

Figure 5 is the goaf relative pressure distribution diagram calculated by airflow velocity of air return roadway and air inlet roadway, it can be seen from figure that pressure of goaf air inlet side is larger than air return side for about 20 Pa.

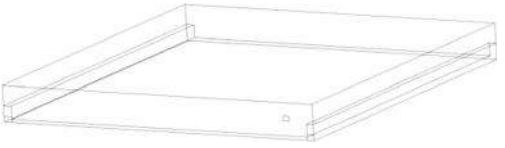


Figure 1. Physical model of ZF4403 mechanized caving goaf.

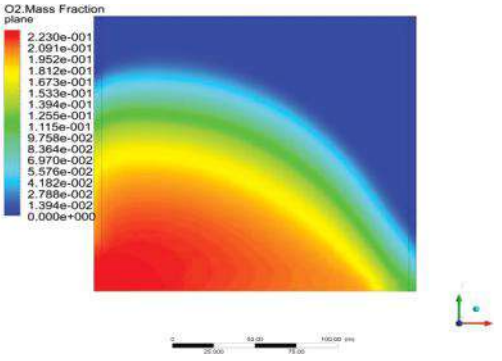


Figure 2. Goaf oxygen concentration distribution.

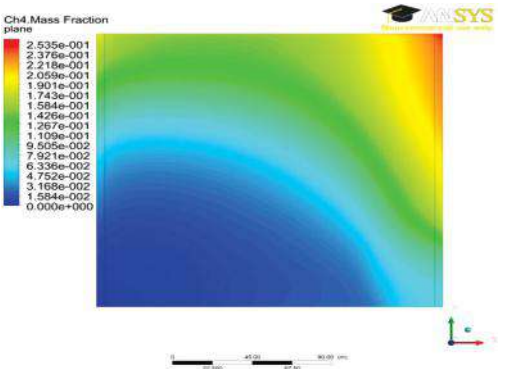


Figure 3. Goaf gas concentration distribution.

6 GOAF DANGEROUS AREA FORECAST AND MATCH DEGREE ANALYSIS

According to the literature, goaf float coal is prone to spontaneous combustion in oxygen concentration of 5% to 18% (Luo et al. 2002, Wang 2005). Numerical simulation results based on Fluent software can be used to calculate the distribution range of spontaneous combustion dangerous area of ZF4403 fully mechanized caving goaf. The measured datum are shown in Table 3, the distribution range of spontaneous combustion dangerous area and match degree analysis are shown in Table 4.

It can be seen from the datum of Table 3 and Table 4 that the width match degree of spontaneous

combustion dangerous area based on Fluent is 84.37% ~ 99.78%; Among the four threshold values of air inlet and return side in goaf spontaneous combustion dangerous area range, except the match degree of cooling zone and oxidation heating zone boundaries with a low degree of 74.63%, the rest are more than 90%. The gas drainage flow in drainage roadway is large, air leakage of inlet side in goaf increases and the distribution gradient of oxygen concentration reduces. Minimum oxygen concentration gradient appears near the working face, the gradient increases towards the goaf direction. It leads to an increasing error of cooling zone and oxidation heating zone boundaries under the condition of a certain error range of oxygen concentration. In summary, the accuracy of Fluent numerical simulation results for forecasting goaf spontaneous combustion dangerous area of Xiagou coal mine ZF4403 working face is worthy of recognition.

7 CONCLUSION

Chose Xiagou coal mine ZF4403 fully mechanized caving mining working face in 404 mining area to research, seepage model of goaf is established, using the numerical method based on flow field simulation to calculate oxygen concentration and distribution law of air leakage intensity in goaf, and made numerical simulation analysis by FLUENT software, combined with the limit parameters of coal spontaneous combustion from experiment, to predict spontaneous combustion dangerous area, come to the following conclusions:

1. Air leakage distribution in goaf is complex under the condition of gas drainage. Air leakage of air inlet side is the largest, air leakage of gas drainage mouth and return air corner comes second. Air leakage in middle goaf reduces with a certain gradient from air inlet side to air return side, the spontaneous combustion range

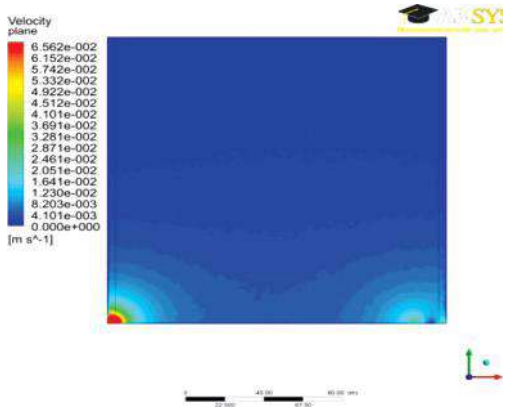


Figure 4. Diagram of goaf seepage velocity.

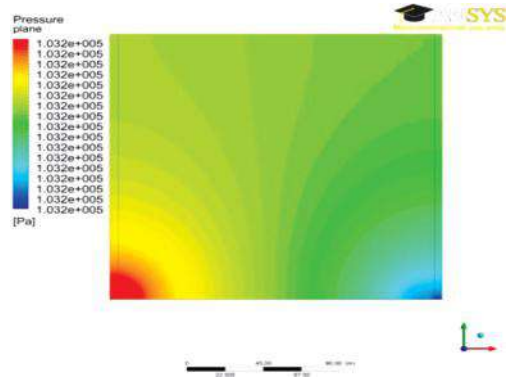


Figure 5. Diagram of goaf relative pressure.

Table 2. The quantitative datum of seepage velocity simulation in goaf (cm/s).

Depth (m)	18.10	33.10	48.90	64.20	80.50	94.50	107.10	120.60	126.90
Air input side (%)	2.01	0.50	0.26	0.23	0.18	0.15	0.12	0.09	0.07
Air output side (%)	0.72	0.31	0.18	0.11	0.05	0.03	0.03	0.02	0.02

Table 3. The observed oxygen concentration of air inlet and return roadway in goaf ZF4403 (%).

Depth (m)	18.10	33.10	48.90	80.50	107.10	120.60	143.60	162.10	173.30
Air input side (%)	21.02	19.97	18.2	17.65	14.32	12.45	8.37	6.24	5.01
Air output side (%)	20.83	17.9	15.35	11.17	7.45	5.3	3.98	2.56	2.01

Table 4. The distribution range of spontaneous combustion dangerous area and match degree analysis.

Division method		Distribution range of spontaneous combustion dangerous area (m)	Width of spontaneous combustion dangerous area (m)
Numerical simulation results	Air output side (%)	30.00~120.00	90.00
	Air input side (%)	45.00~180.00	135.00
Measured results	Air output side (%)	32.60~122.40	89.80
	Air input side (%)	60.30~174.20	113.90
Match degree (%)	Air output side (%)	92.02/98.04	99.78
	Air input side (%)	74.63/96.78	84.37

of middle float coal and air leakage distribution decreases linearly.

2. The goaf gas converged near the mouth of gas drainage, the gas concentration of two sides both increased with a certain gradient to the deep goaf. It occurs gas accumulation in the deep goaf, especially in the deep goaf of air return side, and it is not enough to pump out all the goaf gas, but it doesn't pose a threat to working face due to its low oxygen concentration.
3. The numerical simulation analysis made by Fluent software shows that, boundary values match degree of spontaneous combustion dangerous area is 74.63% ~ 96.78%, width match degree of spontaneous combustion dangerous area degree is 84.37% ~ 99.78%, simulation data coincided with the measured results on a high level, practicality is good. The range of measured spontaneous combustion dangerous area in goaf where air input is 60.30 ~ 174.20 m, the range of that in goaf where air output is 32.60 ~ 122.40 m.

REFERENCES

Deng, J. Xu, J.C & Wen H. et al 2001. Study of the predic-tion model of coal spontaneous combustion in the gate close to gob of fully mechanized longwall top-coal caving face [J]. Journal of China Coal Society, 26(1):62–66. (in Chinese).

Deng, J. & Zhang Y.N. et al 2004. Study on prediction model of coal spontaneous combustion stage [J]. Journal of China coal society, 29(5): 568–571. (in Chinese).

Luo, H.Z. & Liang Y.T. et al 2002. Technology of spontaneous combustion control for fully mechanized caving mining in high gassy combustible thick seam [J]. Coal Science and Technology, 30(9):1–4. (in Chinese).

Qin, Y.P. & Zhu, J.F et al 2003. Simulation test and research on gas migration law in goaf of fully mechanized coal cav-ing mining face [J]. Coal Science and Technology, 31(11):13–16. (in Chinese).

Wang, D.M. 2005. Mine ventilation and safety. Xuzhou: China University of Mining and Technology Press.

Xu, J.C 2002. Decision theory on dangerous area of coal spontaneous combustion [M].Beijing: Coal Industry Press (in Chinese).

Progress in Mine Safety Science and Engineering II – He et al. (Eds)
© 2014 Taylor & Francis Group, London, ISBN 978-1-138-00122-0

A study of GM (1, 1) residual correction model in gas concentration prediction of heading face

Bing Wu, Zhanyu Liu, Yao Zhou & Peng Lou
Faculty of Resources and Safety Engineering, China University of Mining and Technology (Beijing), Beijing, China

ABSTRACT: In order to fully utilize the existing monitoring data to predict gas emission in coal mine so as to early-warn the gas overrun and guide gas controlling, a mathematical forecasting model is established for dynamically predicting the gas concentration. As the change of gas concentration in coal mine heading face is subjected to many uncertain factors, it is difficult to determine the variation rule of gas concentration. Therefore, the gray theory is used to establish the corresponding dynamic prediction analysis model of gas concentration in which the model modifies the original GM (1, 1) prediction model by using ARMA residual error predictive model, then a modified GM (1, 1) model is established. The modified GM (1, 1) model is applied to gas prediction in the 15, 101 heading face of Xinshun mine. It turns out that the results of gas concentration prediction based on GM residual correction model coincide well with the actual situation. Compared with the situation in which only GM (1, 1) model is used, the prediction accuracy has been greatly improved.

1 INTRODUCTION

Currently, coal mine gas monitoring system is merely used in concentration monitoring and alarm limit, and gas concentration alarm is only about evaluation of the current state rather than possible futural early warning of hazardous conditions. Since the simple real-time data monitoring has been unable to meet modern coal mining on the monitoring requirements, it plays an important role in preventing the gas overrun and guiding gas controlling to learn about how to make full use of existing monitoring data for gas forecast (Wang, 2010, Yan, 2012).

In terms of gas concentration prediction, Zhou Changchun et al. (Zhou & Huang, 1995) have established a fuzzy time series forecasting model to achieve a gas concentration of long-term full-state forecasting; Zhu Yu (Zhu, 2010)have constructed a gas prediction model by using structural neural network learning method; Dong Dingwen et al. (Dong et al., 2011) have achieved gas concentration prediction by using the HHT method to get the instantaneous characteristics of gas concentration time series and combining with three kinds of forecasting model such as autoregressive (AR), radial neural networks and support vector machine; Li gang (Li, 2009) improved the traditional chaotic forecasting methodand put forward the improved algorithm of gas concentration of chaotic time series prediction; TaoYunji (Tao, 2007) have used the improved grey markov model to forecast the gas concentration in working face of stope.

Because of many factors influencing coal mine gas emission (Guo et al., 2009, He et al., 2008, Zhu et al., 2007), such as natural factors (including geological structure, coal thickness, coal structure, buried depth, etc.), mining technology and various combination of factors, it is difficult to determine relationship of factors which are often of non-linear characteristics.

Therefore, coal mine gas emission is a typical grey system (Tao et al., 2007, Wu et al., 2005); gray prediction model can be used to predict the gas concentration.

2 ANALYSIS OF PREDICTION MODEL

The grey system theory is created by a Chinese scholar professor Deng Julong (Deng, 2002), it treats the "small sample, poor information" uncertainty system of "part of the information is known, some information is unknown "as the research object (Deng, 1987). The basic guiding principle of grey prediction GM (1, 1) is transfering the ruleless original data sequence to new regular data sequence through the successive accumulation, weakening the original sequence randomness and on the basis of the new data sequence using the

exponential function curve to get approximation. The advantage is that the modeling process is simple with less sample data and simpler calculation.

Because the gray prediction is a "small sample" prediction based on GM (1, 1) model, and the solution for the GM (1, 1) model is exponential curve, too many sample data lead to a poor accuracy, gas concentration is greatly influenced by mining activity. With the changes of mining and underground environment, old data are gradually diminished and new data's significance will gradually increase, therefore, to make use of gas monitoring data for real-time forecasting of gas concentration, metabolic gray prediction model needs establishing which continuously adds in new data at the same time removing old data to predict the gas concentration (Wei, 2012).

Different ways of prediction would provide us with different useful information, different accuracy of prediction as well (Bates & Granger, 1969, Holden & Peel, 1989, Liu, 2005). Sometimes, to make use of the advantage of each prediction model, different ways are combined to form a prediction group to upgrade the accuracy. There is a relatively big inaccuracy of data prediction in gray prediction model, so we often correct the residual error to improve the accuracy of GM (1, 1) model. In gray theory, setting a GM (1, 1) model with residual error and correcting the original model is used as a way of correcting error (Liu, 2010), however, this method would result in losing information and then influencing the accuracy. Therefore, ARIMA model is needed to be added in grey theory.

3 ESTABLISH OF CORRECTED MODEL BASED ON GM (1, 1) RESIDUAL ERROR

3.1 *Metabolic gray prediction model*

Step one, to select former 10 data from original data:

$$x^{(0)} = \left\{x^{(0)}(1), x^{(0)}(2), ..., x^{(0)}(10)\right\} \tag{1}$$

Since the original data are more likely to be random and irregular, we shall adduct in the whole data and predict with new data array (while 10 data are all constant, the prediction number would be a constant, no need using the below format).

Step two, to smooth the original data with natural logarithm:

$$x^{(0)}(t) = \log(y(t)), t = 1,2,...,10; \tag{2}$$

Step three, adduct in the processed data:

$$x^{(1)} = \left\{x^{(1)}(1), x^{(1)}(2), ..., x^{(1)}(10)\right\} \tag{3}$$

Among them,

$$x^{(1)}(t) = \sum_{i=1}^{t} x^{(0)}(i), t = 1,2,...,10 \tag{4}$$

Step four, to design an accumulation matrix B and constant vector:

$$B = \begin{bmatrix} -\frac{1}{2}(x^{(1)}(1) + x^{(1)}(2)) & 1 \\ -\frac{1}{2}(x^{(1)}(2) + x^{(1)}(3)) & 1 \\ \cdots & \cdots \\ -\frac{1}{2}(x^{(1)}(N-1) + x^{(1)}(10)) & 1 \end{bmatrix} \tag{5}$$

$$Y_N = \left[x_1^{(0)}(1), x_1^{(0)}(2), ..., x_1^{(0)}(10)\right]^T \tag{6}$$

Step five, use method of least squares to solve gray parameter $\hat{a}$:

$$\hat{a} = \begin{bmatrix} a \\ u \end{bmatrix} = (B^T B)^{-1} B^T Y_{10} \tag{7}$$

Step six, to compute the fitting sequence of clustering sequence $\left\{\hat{X}^{(1)}(t)\right\}, t = 1,2,...,10$ and then compute the first-step prediction value.

Step seven, return the fitting model of accumulation sequence to fitting sequence of transformed data sequence $\left\{\hat{x}^{(0)}(t)\right\}, t = 1,2,...,10$ and calculate the latter four values.

Step eight, replace the first data of $y(t)$ sequence with the newly produced data in metabolic way and repeat from step one to eight, and fitting sequence of GM (1, 1) is solved.

3.2 *Residual error correcting model*

ARIMA model is used to correct GM (1, 1) model in order to improve accuracy. In the meantime of verifying the prediction with historical data, we also obtain an error sequence between true values and prediction, and regard it as a random sequence to establish its prediction model, and then correct the GM (1, 1) model with it. The process of establishing ARIMA model is: test the smoothness of residual error, if it is smooth, then establish ARIMA model; if not, smooth it after several times of difference operation and then establish ARIMA model.

After being modified, the GM (1, 1) model is accurate enough to predict the change of gas concentration in 15 minutes, and the error becomes bigger along with the prediction time.

4 MINING FACE APPLICATION EXAMPLE

Xinshun mine is a high-gas one with absolute gas emission of 13.941 m3/min and relative emission of 33.669 m3/t, designed production of 1.8 million t/a as well. As the low permeability of coal seam leads to poor gas pre-drainage efficiency, gas concentration is higher at coal lane tunneling and frequently exceeds the limits. When tunneling stopped, the concentration decreased quickly due to the large gas attenuation coefficient (borehole gas flow attenuation coefficient is 0.1393d-1).

4.1 *Establishment of the gas concentration predict-ion*

The gas concentration monitoring data is selected for analysis which is from 10: 00 to 11:57 on March 2, 2012 in the return air duct heading face, as is shown in Table 1.

GM (1, 1) of grey prediction model is used to fit the above 35 data, the last 5 data for prediction and verifying the forecast results, the results are shown in Table 2.

By comparing the predictive values with the true values, it turns out that simply using GM model prediction leads to large gas concentration error(as shown in table 3).

4.2 *The residual modification of GM model by ARIMA*

4.2.1 *Stationary test of the residual sequence*

Before modeling on the residual sequence, use Eviews6.0 software to check whether the residual sequence is smooth or not, if so, directly establish ARMA model, if not, it has to be taken some steps of difference. After it's smooth, use the ARMA model and establish ARIMA model. Residual sequence is tested on the unit root test, the results are shown in Figure 1:

The Figure 1 shows that the values of t-statistic are less than the critical values of significance level, it means sequence is smooth. So do not use the difference, but ARMA sequence fitting. Consider to use ARMA model, Select the ARMA (2, 2) model as a predictive model. Parameter estimation results are shown in Table 4.

4.2.2 *To test the established model*

The above established ARIMA (2, 0, 2) model is used to fit residual error sequence and obtain the residual sequence of residuals, and its autocorre-

Table 1. The gas concentration monitoring data of the return air duct heading face.

Time	Concentration	Time	Concentration	Time	Concentration	Time	Concentration
10:00	0.36	10:30	0.35	11:00	0.31	11:30	0.3
10:03	0.35	10:33	0.38	11:03	0.34	11:33	0.33
10:06	0.31	10:36	0.43	11:06	0.36	11:36	0.32
10:09	0.31	10:39	0.41	11:09	0.36	11:39	0.29
10:12	0.59	10:42	0.4	11:12	0.33	11:42	0.35
10:15	0.44	10:45	0.35	11:15	0.34	11:45	0.46
10:18	0.39	10:48	0.45	11:18	0.32	11:48	0.51
10:21	0.33	10:51	0.46	11:21	0.36	11:51	0.41
10:24	0.35	10:54	0.42	11:24	0.31	11:54	0.37
10:27	0.34	10:57	0.37	11:27	0.37	11:57	0.35

Table 2. The results of fitting and prediction.

Time	Fitted value	Time	Fitted value	Time	Fitted value	Time	Fitted value
10:00	0.3600	10:30	0.3502	11:00	0.3087	11:30	0.2920
10:03	0.2946	10:33	0.3698	11:03	0.3143	11:33	0.3182
10:06	0.3443	10:36	0.4222	11:06	0.3452	11:36	0.3245
10:09	0.4053	10:39	0.4301	11:09	0.3684	11:39	0.3040
10:12	0.4807	10:42	0.4116	11:12	0.3425	11:42	0.3257
10:15	0.5185	10:45	0.3559	11:15	0.3342	11:45	0.4214
10:18	0.4488	10:48	0.4122	11:18	0.3213	11:48	0.5315
10:21	0.3123	10:51	0.4629	11:21	0.3476	11:51	0.4699
10:24	0.3240	10:54	0.4594	11:24	0.3240	11:54	0.3734
10:27	0.3328	10:57	0.3770	11:27	0.3063	11:57	0.3276

lation and partial autocorrelation coefficient diagram is shown in Figure 2.

From the above figure, the residuals obtained after fitting are white noise sequence which means the selected model is appropriate. Therefore it can be used to predict.

Table 3. Comparison of prediction results.

Time	True value	Predicted value	Relative error%
11:45	0.46	0.4214	8.39
11:48	0.51	0.5315	–4.22
11:51	0.41	0.4699	–14.61
11:54	0.37	0.3734	–0.92
11:57	0.35	0.3276	6.41

Null Hypothesis: Y has a unit root
Exogenous: Constant
Lag Length: 1 (Automatic based on SIC, MAXLAG=9)

		t-Statistic
Elliott-Rothenberg-Stock DF-GLS test statistic		-8.164292
Test critical values:	1% level	-2.627238
	5% level	-1.949856
	10% level	-1.611469

Figure 1. The unit root test of residuals.

4.2.3 *Prediction and error*

The gas concentration for five steps in metabolic GM (1, 1) model and the residuals in the ARIMA model of the residual sequence are predicted and the final prediction and error is shown in Table 5:

Comparing the relative error in Table 5 with Table 3, it can be seen that the corrected model has narrowed prediction errors of simply using GM (1, 1). Therefore, using the ARIMA model residuals modeling program for secondary modeling, re-correcting the main model has a good effect for forecasting the gas concentration change trend. But if mine technician discover abnormal gas emission and artificially take measures to control the gas concentration, it will lead to a decline in gas concentration prediction accuracy.

5 CONCLUSION

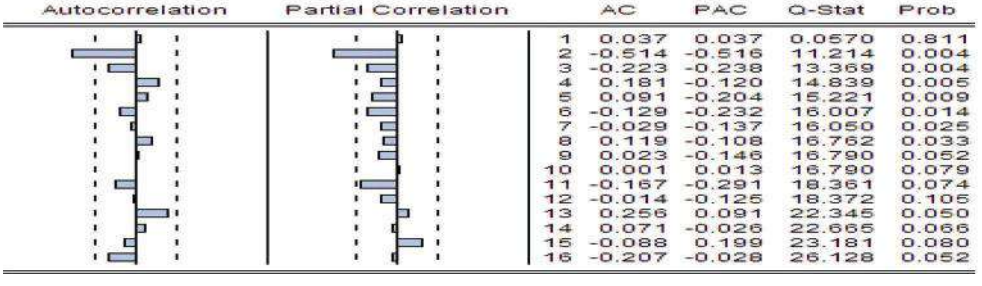
GM (1, 1) model based on ARIMA residual error correction is established and the combined model takes advantages of the two kinds of mathematical model, gray forecast model and ARIMA model. Compared with simply using the grey forecasting model, it could improve the prediction accuracy of gas concentration and reduce the relative prediction error.

By adopting the metabolism model (that is, the prediction model automatically weeds out the

Table 4. Parameter estimates table.

Time		GM Predictive value	The error predictive value	The final predictive value	T statistic
Non-Seasonal Models	AR1		–0.676499	0.068000	–9.948555
	AR2		–0.505430	0.071010	–7.117764
	MA1		0.881094	0.026460	33.29885
	MA2		0.958774	0.013046	73.49034
constant			6.6×10^{-5}	0.004747	0.013912

Date: 03/29/13 Time: 16:31
Sample: 1 40
Included observations: 38



	AC	PAC	Q-Stat	Prob
1	0.037	0.037	0.0570	0.811
2	-0.514	-0.516	11.214	0.004
3	-0.223	-0.238	13.369	0.004
4	0.181	-0.120	14.839	0.005
5	0.091	-0.204	15.221	0.009
6	-0.129	-0.232	16.007	0.014
7	-0.029	-0.137	16.050	0.025
8	0.119	-0.108	16.762	0.033
9	0.023	-0.146	16.790	0.052
10	0.001	0.013	16.790	0.079
11	-0.167	-0.291	18.361	0.074
12	-0.014	-0.125	18.372	0.105
13	0.256	0.091	22.345	0.050
14	0.071	-0.026	22.665	0.066
15	-0.088	0.199	23.181	0.080
16	-0.207	-0.028	26.128	0.052

Figure 2. Residual correlation function figure of the residual sequence.

Table 5. Prediction and error.

Time	GM Predictive value	The error predictive value	The final predictive value	True value	Absolute error	Relative error%
11:45	0.4214	0.0119	0.4413	0.46	0.0187	4.06
11:48	0.5315	0.0222	0.5537	0.51	–0.0437	–8.56
11:51	0.4699	–0.0178	0.4521	0.41	–0.0421	–10.25
11:54	0.3734	–0.0027	0.3707	0.37	–0.0007	–0.19
11:57	0.3276	0.0136	0.3412	0.35	0.0088	2.51

old data and makes use of the new data) on the dynamic prediction of gas concentration, we can alarm the gas overrun in advance.

Through the practical application it is concluded that the model can effectively predict the change of gas concentration within 15 min (every 3 min a measurement data), however, in a longer period the predicted results are of large errors.

REFERENCES

Bates, J.M. & Granger, C.W.J. 1969. The combination of forecasts. *Operations Research Quarterly* 20(4): 451–468.

Dong D.W. et al. 2011. The Mine Gas volume fraction Prediction based on HHT method. *China Safety Science Journal* 9:100–105.

Deng, J.L. 1987. *The basic methodology gray system.* Wu han: Huazhong university of science press.

Deng, J.L. 2002. *Grey prediction and grey decision*. Wu Han: Huazhong University of Science and Technology press.

Guo, D.Y. et al. 2009. Stepwise regression method for predicting gas emission from coal faces. *Journal of University of Science and Technology Beijing* 31(9): 1095–1099.

Holden, K. & Peel, D.A. 1989. Unbiasedness efficiency and the combination of economic forecasts, *Journal of forecasting* 8(3): 175–188.

He, L.W. et al. 2008. Complexity and measurement of complex degree of gas gush in heading faces of coal mine. *Journal of China Coal Society* 38(5): 547–550.

Li, G. 2009. Study on fractal analysis of gas concentration and chaotic prediction model. Master dissertation. China University Of Mining And Technology, Beijing.

Liu, S.F. 2010. *The grey system theory and its application*. Bei Jing: Science Press.

Liu W.S. 2005. The study of Shanghai stock price index based on Grey Theory and Autiregressive integrated moving average models. Master dissertation. HoHai University, Nan Jing.

Tao, Y.Q. et al. 2007. Grey prediction on gas emission quantity. *Journal of Chongqing University(Natural Science Edition)* 30(6):121–124.

Tao Y.Q. et al. 2007. Predict gas emissing quantity of mining coal face with improved GreyMarkov model. Journal of China Coal Society 32(4): 391–395.

Wu, A.Y. et al. 2005. Application of the grey system theory for predicting the amount of mine gas emission in coal mine. *Journal of China Coal Society* 30(5): 589–592.

Wei, C.R et al. 2012. Based on the grey metabolism model to forecast the gas emission coal mine. *Journal of Hunan University of Science & Technology (Natural Science Edition)* 27(3):16–21.

Wang, X.L. 2010. Intelligent Forecasting Approaches of Development Trends of Coal Gas Monitoring Data. Doctoral dissertation, Xi'an University of Science and Technology, Xi'an.

Yan, D.H. 2012. Research on Prediction Model of Gas Concentration of Driving Ventilation in High Gas Coal Mine Based on Neural Network. Master dissertation, Xi'an University of Science and Technology, Xi'an.

Zhou, C.C. & Huang, Y.P. 1995. Coal mine gas concentration in the work environment full state prediction. *Journal of Xi'an University of Science & Technology* 04:315–319.

Zhu H.Q. et al. 2007. Differen-tsource gas em ission prediction model of working face based on BP artificial neural netw ork and its application. *Journal of China Coal Society* 32(5): 504–508.

Zhu, Y. 2010. Constructive Neural Networks in Time Series Prediction Gas Applications. Master dissertation. Taiyuan University of Technology.

This page intentionally left blank

Progress in Mine Safety Science and Engineering II – He et al. (Eds)
© 2014 Taylor & Francis Group, London, ISBN 978-1-138-00122-0

Study on barrier door of gas explosion with foam ceramics as the main body

Jian-Hua Sun, Zheng Qu, Hong-Yu Fan & Chun-Rong Wei
Heilongjiang University of Science and Technology, Harbin, Heilongjiang, China

ABSTRACT: Based on the studying on barrier device of gas explosion, an optimized design scheme of gas explosion barrier door with foam ceramics as the main body is proposed. The author uses ANSYS software and finite element method to simulate and compare the main performances of four typical doors in thickness, such as uniform thickness, thick in the upper and thin in the lower, thin in the upper and thick in the lower, secant circular. Results of simulation reveal that the moistest stability and good withstand voltage in structure dose the secant circular door have, describe optimization in detail and provide a feasible optimization of barrier device of gas explosion.

Keyword: barrier device of gas explosion, foam ceramics, secant circular door, optimization design

1 INTRODUCTION

The safety production is always threatened by the gas explosion in coal mine. Due to the participation of coal dust, gas explosion will be endowed with a new ability called continuity. The first explosion maybe flowed by secondary explosion or repeated explosion, so that the region of disaster and damage will been enlarged greatly. Therefore, It is necessary and urgent to develop an effective barrier device to avoid secondary and repeated gas explosion.

The barrier device of gas explosion mostly used in coal mine of China are water bag and rock powder shed which can be used to separate different regions. Though having achieved certain results over the past, the lag or advance of working time will influence its barrier explosion effect, such as the water tent and the rock powder tent etc. A new design of partition gas explosion barrier door with foam ceramics as the main body is proposed based on the study of Nie Baisheng, He Xueqiu and Zhang Jinfeng—on effect of foam ceramics upon gas explosion flame propagation. The author plan to set several devices in return airway of working face and crossheading between mining areas to barrier or reduce flame and shock waves propagation of gas explosion, so that the range of propagation will be controlled, the damage degree will be reduced, and the secondary or repeated explosion will be avoided.

2 DESIGN OF BARRIER DOOR

The barrier device consist of three layers—porous metal plate and foam ceramics and porous metal plate, which is similar to the sandwich, as the fig 1 shown. The holes in the two porous metal plate have different center and diameter, and each hole facing the polluted air is filled by a hollow metal spheres to avoid mixing of fresh air and polluted air. As fig 2(a) and fig 2(b) shown, the fig 2(a) is the closed barrier door and the other is open.

After gas explosion, shock waves will break the hollow metal spheres outside the first layer of symmetric porous metal material 2 and arrive at internal material. The special structure of the foam ceramics would reduce the pressure from gas explosion and block it, at the same time, decrease temperature of flame and speed of propagation. If the door can not bear the impact, the more barrier doors we need to set. As a result, the shock resistance of the first barrier door should be regarded as the important parameters, and it will be seriously influenced by the shape of barrier door. To find out most stable door, More analyses and researches on different shapes of doors s necessary.

Using ANSYS software and finite element method to simulate and compare the main performances of four typical shapes of doors, such as shapes of doors uniform thickness, thick in the upper and thin in the lower, thin in the upper and thick in the lower, secant circular.

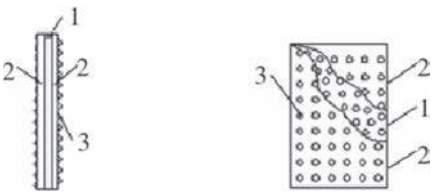


Figure 1. Schematic diagram of material composition of barrier air door of gas explosion (1- ceramic foam, 2- asymmetric porous metal material, 3- asymmetric porous metal material with hollow metal spheres).

3 SIMULATION ANALYSIS OF DIFFERENT MORPHOLOGY OF BARRIER DOOR IN COAL-MINE

The designed barrier door is 200 cm long and 200 cm high and 6 cm thick, and consists of three layers—porous metal plate and foam ceramics and porous metal plate. According to the natural and fixed attribute of material itself, elastic modulus is 72Gpa and Poisson Ratio is 0.226. The elastic modulus and Poisson Ratio of metal plate is 206Gpa and 0.3, which is close to steel.

The optimum item is structural analysis, and element type is Solid, brick 8 node 185.

The first step is to mesh generation;

Displacement constraints: barrier door is fixed by over 5 cm door case and over 30 cm door bank and multi-group high strength hinge, so as to constraint the degrees of freedom of fixed part.

Load constraints: According to the maximum pressure of gas explosion which is 1 to 2 Mpa, the selection of the maximum pressure is 2 Mpa. Using the chosen pressure and constraints on the barrier door to simulate.

After the analysis of ANSYS, the compression situation of four different doors is shown as the fig underside.

3.1 *Uniform thickness*

As the graphs show, the maximum force is 2.35 Mpa on z axis, and the minimum is 1.88 Mpa, the force in the middle of the door and stress in the hinge is larger; the maximum Mises stress is 2.09 Mpa, the minimum is 1.39 Mpa; the maximum displacement on z axis is 0.795×10^{-6} m, the minimum is 0.748×10^{-6} m.

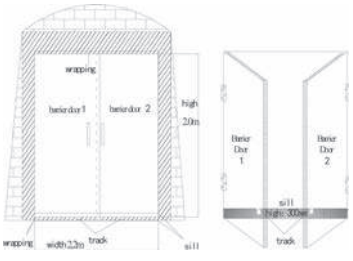


Figure 2. (a) barrier door closed; (b) barrier door open.

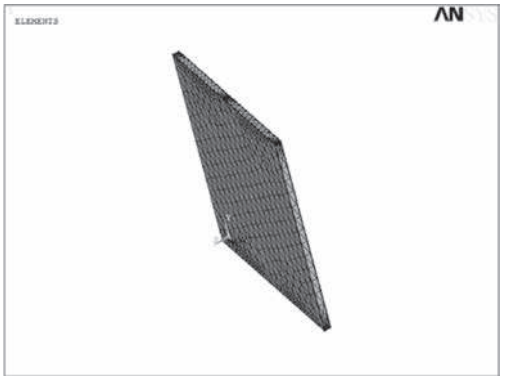


Figure 3. (a) Free mesh generation of uniform thickness.

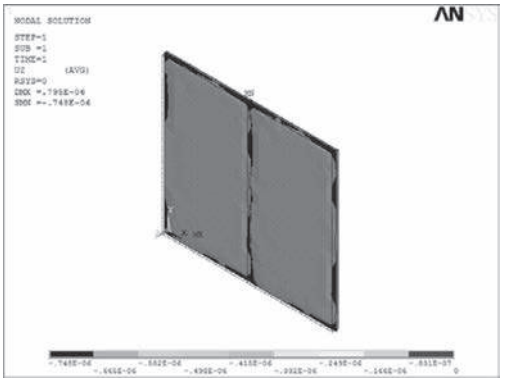


Figure 3. (b) Contour band of displacement on z axis.

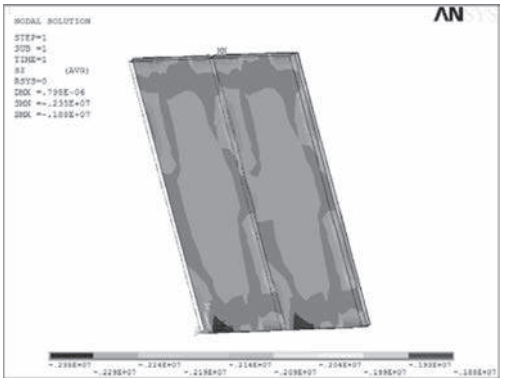


Figure 3. (c) Contour band of force on z axis.

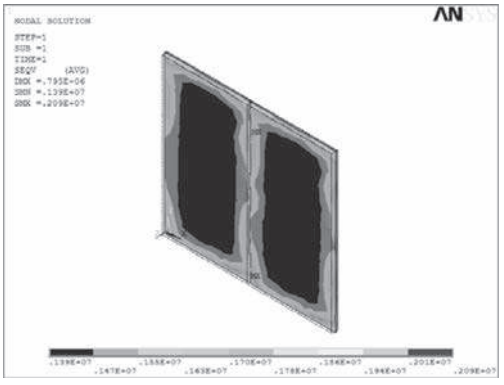


Figure 3. (d) Contour band of Von Mises.

3.2 *Secant circular*

As is shown from the graphs, the maximum force is 5.24Mpa on z axis, and the minimum is 2.77Mpa, the force in the middle of the door is larger than around; the maximum Mises stress is 4.44Mpa, the minimum is 0.687224Mpa; the maximum displacement on z axis is $0.749 \times 10–^{4}$ m, the minimum is 0.301×10^{-5} m.

3.3 *Thick in the upper and thin in the lower*

As the graphs shown, the maximum force is 2.55Mpa on z axis, and the minimum is 1.86Mpa, the force in the upper of the door is larger than around; the maximum Mises stress is 2.25Mpa, the minimum is 1.4Mpa; the maximum displacement on z axis is 0.131×10^{-5} m, the minimum is 0.119×10^{-5} m.

3.4 *Thin in the upper and thick in the lower*

As the graphs show, the maximum force is 2.55Mpa on z axis, and the minimum is 1.86Mpa, the force in the lower of the door is larger than around; the maximum Mises stress is 2.24Mpa, the minimum is 1.4Mpa; the maximum displacement on z axis is 0.131×10^{-5} m, the minimum is 0.119×10^{-5} m m.

4 CONCLUSION

1. The pressure distribution of different foam ceramics on each axis is shown as fig. 7(a), the shock wave pressure spread regularly and change greatly on Z axis; secant circular door can sustain the maximum pressure of 24Mpa, which is 2.5 time than others.
2. As the fig. 7(b) show us, the uniform thickness door, thin in the upper and thick in the lower door and thick in the upper and thin in

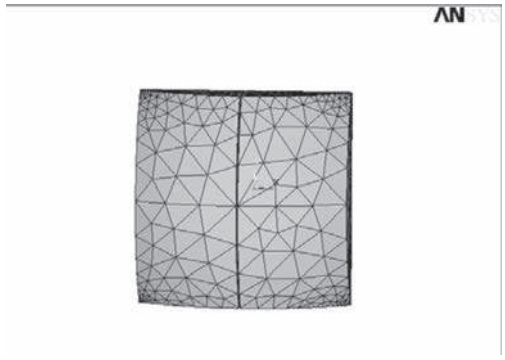


Figure 4. (a). Free mesh generation of uniform thickness.

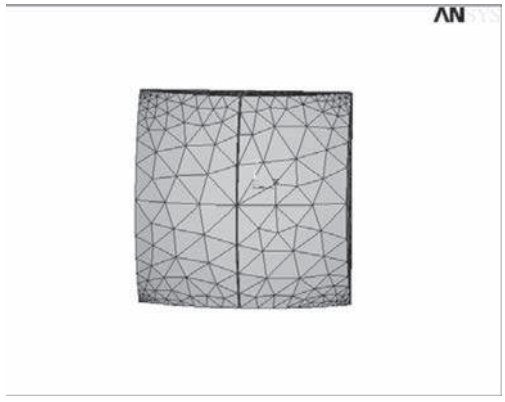


Figure 4. (b) Contour band of displacement on z axis.

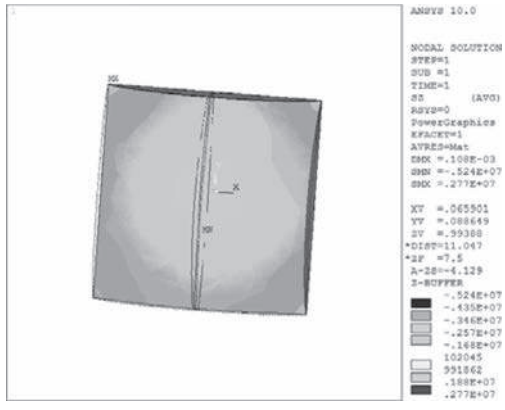


Figure 4. (c) Contour band of force on z axis.

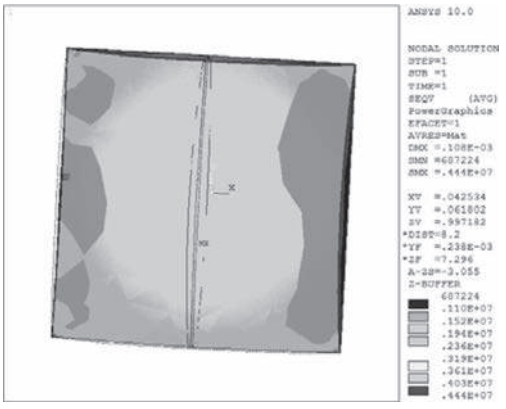


Figure 4. (d) Contour band of Von Mises.

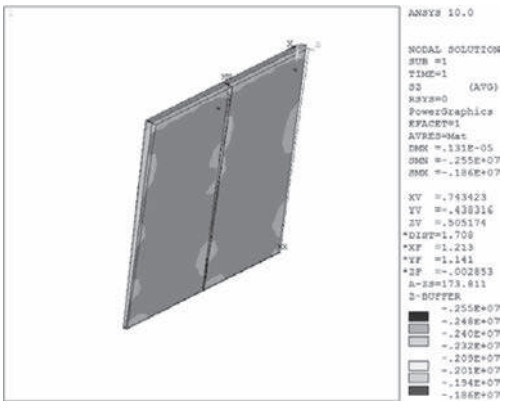


Figure 5. (c) Contour band of force on z axis.

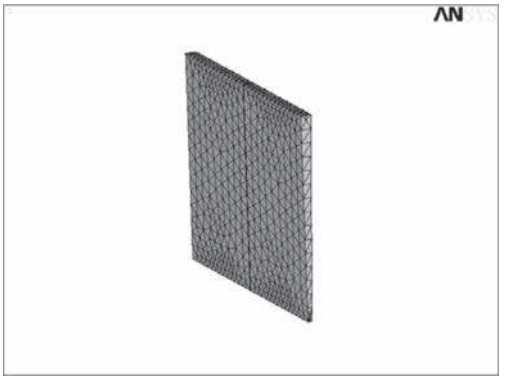


Figure 5. (a) Free mesh generation of uniform thickness.

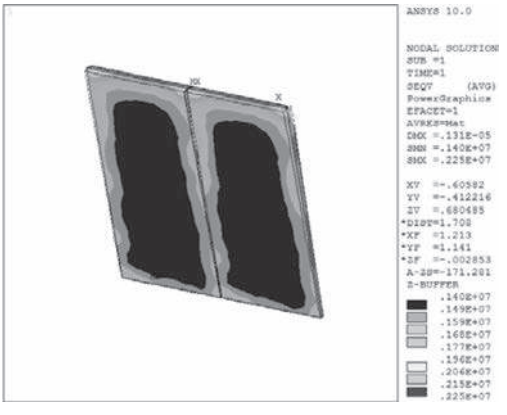


Figure 5. (d) Contour band of Von Mises.

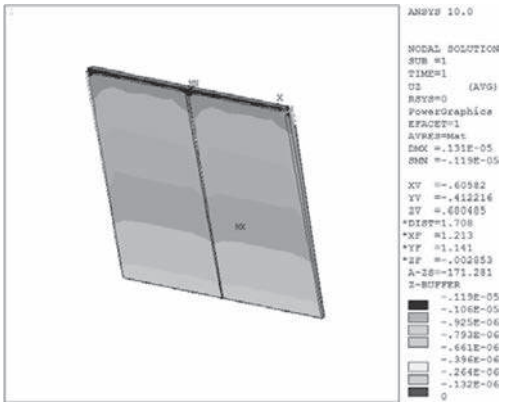


Figure 5. (b) Contour band of displacement on z axis.

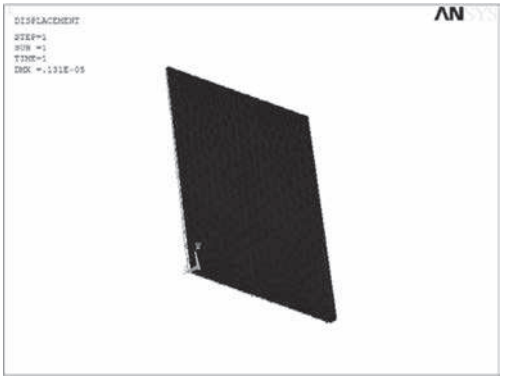


Figure 6. (a) Free mesh generation of uniform thickness.

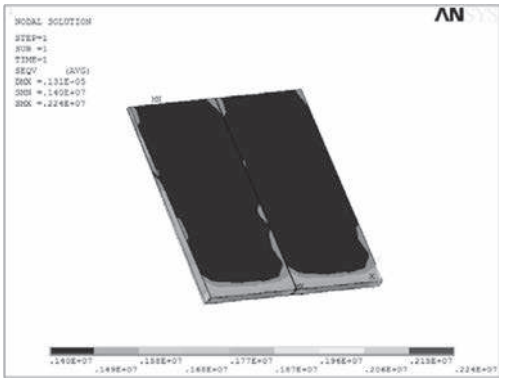


Figure 6. (b) Contour band of displacement on z axis.

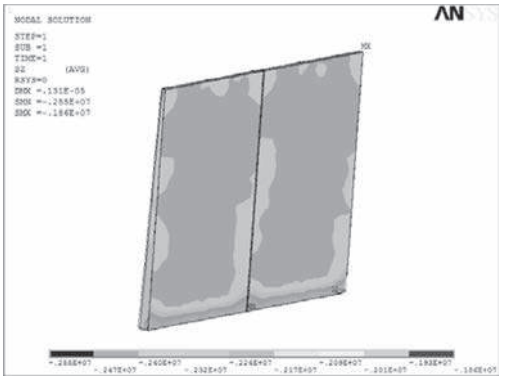


Figure 6. (c) Contour band of force on z axis.

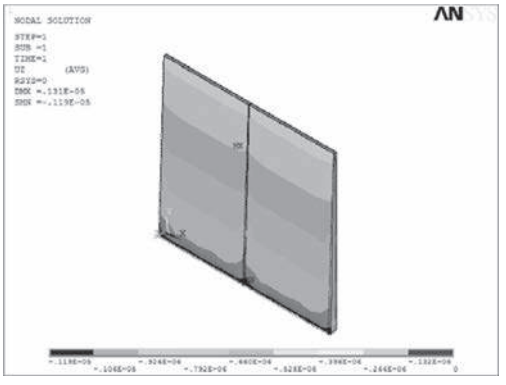


Figure 6. (d) Contour band of Von Mises.

the lower door have the same displacement on X axis dose, thick in the upper and thin in the lower door has less displacement on Y axis dose, uniform thickness door has less displacement on Z axis dose; the maximum displacement

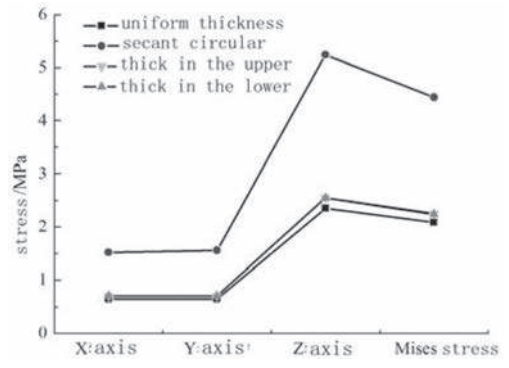


Figure 7. (a) Comparison of axial stress in different form barrier doors.

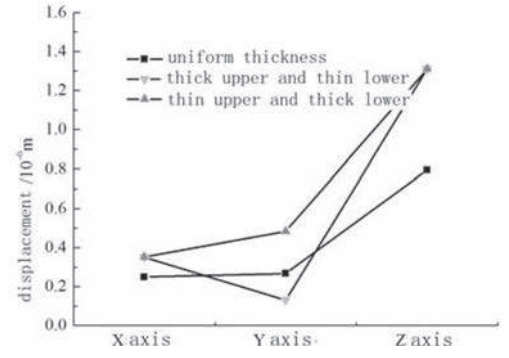


Figure 7. (b) Comparison of displacement in different form barrier doors.

0.108×10^{-3} m which is 30 times higher than the other three, which is not easy to display in the graph, occurred in the simulation of secant circular door; however, the actual displacement is about 1.1 mm. The author believes that the geometry of circle should be considered, and the steadiness of circle results from its distribution under the stress conduction, and the circle can be quickly restored to the original strength after the reversible deformation;

3. The force of secant circular door was shown as vertical band, and the forces in the middle or on the whole device is larger, and the largest force would be found in the middle of the door and docking part; stress concentration always occurs in the geometric center of the door. Strengthening the outer plate and oversizing strength and density of the host materials would solve the problem.
4. The docking part is the thickest part of the door, and the thick dose of door will cause the increasing of blocking probability and sharp increasing of stress. In order to avoid that, the

porosity of this part would be increased, so that shock wave can pass through freely; as a result, sharp increasing of stress would not occur.

REFERENCES

Baisheng Nie. The roles of foam ceramics in suppression of gas explosion overpressure and quenching of flame propagation. Journal of Hazardous Materials, 2011, 192 (2): 741–747.

Chumakov Y A, Knyazeva A G. Thermal Explosion of a Gas Mixturein a Porous Hollow Cylinder[J]. Combustion, Explosion, and Shock Waves, 2010, 5 (1):507–514.

Catlin C A, Fairweather M, Ibraiim S S. Predictions of turbulent, premixed flame propagation in explosion tubes[J]. Combustion and Flame, 1995, (102):115–128.

Dal J P, Young S L, Anthony R G. Prediction for vented explosions in chambers with multiple obstacles[J]. Journal of Hazardous Materials, 2008, 155: 183–192.

Eder A, Brehmn, Analytical and experimental insights into fast deflagrations, detonations and deflagration-to detonation transition process[J]. Heat and Mass Transfer, 2001, 37: 543–548.

Ferrara G, Willacy S K, Phylaktou H N, et al. Venting of gas explosion through relief ducts: Interaction between internal and external explosions[J]. Journal of Hazardous Materials, 2008, 155: 358–368.

Furukawa J. Flame front configuration of turbulent premixed flames[J]. Combustion and Flame, 1998, (112): 293–301.

Gulder O L.Flame front surface characteristics in turbulent premixedpropance /air combustion[J]. Combustion and Flame, 2000, 120: 407–416.

Ibrahim S S, Masri A R. The effects of obstructions on overpressure resulting from premixed flame deflagration[J]. Journal of Loss Process Industries, 2001, 14: 213–221.

Kasmani R M, Andrews G E, Phylaktou H N. The Influence of Vessel Volume and Equivalence Ratio in Vented Gas Explosions[J]. Chemical Engineering Transactions, 2010, 19: 463–468.

NIE Baisheng, Effect of Foam Ceramics Upon Gas Explosion Flame Propagation. Transactions of Beijing Institute of Technology. 2008, 28(7).

Nie Baisheng. The effect of foam ceramics on gas explosion flame propagation[J]. Journal of Beijing Institute of Technology, 2008, 28(7): 573–576. (In Chinese).

NIE Bai-sheng. The experiments and mechanism of foam ceramics affecting gas explosion process. Journal of

Nishimura I, Mogi T, Dobashi R.Simple method for predicting pressure behavior during gas explosions in confined spaces considering flame instabilities[J]. Journal of Loss Prevention in the Process Industries xxx, 2011: 1–4.

Paris L, Christophe C, Iddir O. Innovative design of an LDPE reactor bay against gas explosion usinga risk-based approach coupled with high fidelity computer tools[J]. Journal of Loss Prevention in the Process Industries, 2010, (23): 561–573.

Pang Lei. Hazard Characteristics from Gas Explosion in Underground Constructions[J]. Procedia Engineering, 2012, 43: 293–296.

Starke R, Roth P. An Experimental Investigation of Flame Behavior During Explosions in Cylindrical Enclosures with Obstacles[J]. Combustion and Flame, 1989, (75): 111–118.

Sun Jianhua, The porous-leak-pressure barrier explosion of the automatic air-door that is used in the mine, China Mining Magazine, 2011.20(3):105–106; China Coal Society, 2008, 33(8):903–907(In Chinese).

Ulrich Bielert, Martin Sichel. Numerical simulation of premixed combustion processes in closed tubes[J]. Combustion and Flame, 1998, (114): 397–419.

Valeria D S, Almerinda D B, Gennaro R.Using Large Eddy Simulation for understanding vented gas explosions in the presence of obstacles[J]. Journal of Hazardous Materials, 2009, 169: 435–442.

Zhang Fan. properties of materials. Shanghai Jiao Tong University Press Co. Ltd. 43–59.

Zhang Hongcai. finite element analysis: ANSYS 13.0 from introduction to actual combat. China Machine Press. 27–33.

Zhang Jiuling. Numerical Simulation on Inert Gas Injection Applied to Sealed Fire Area[J]. International Conference on Information Computing and Applications, 2010, (105): 347–353.

Progress in Mine Safety Science and Engineering II – He et al. (Eds)
© 2014 Taylor & Francis Group, London, ISBN 978-1-138-00122-0

Prediction of coal and gas outbursts with random forests

Yong Lin, Xingjia Lu & Jianbo Fan
College of Science, Ningbo University of Technology, Ningbo, Zhejiang, China

ABSTRACT: Coal and gas outbursts are one of the most serious and devastating risk factors accompanying mining industry. In order to reduce the possibility of outbursts, it will be helpful to find out perfectly suitable classification algorithms, for the prediction of coal and gas outbursts. Ensemble classification algorithms predict class label of unknown records by aggregating predictions made by multiple classifiers and they are proved to be robust and precise in supervised learning technology. Based on our experiments, we found that the random forest algorithm demonstrate better performance compared with other ensemble methods, such as Bagging and Boosting. Another, the random forest algorithm is more stable than decision tree classifiers, and the experiments demonstrate that it is a good candidate for the prediction of coal and gas outbursts. We also explore the issue about how to configure a preferable profile for the random forest algorithm for the prediction of the outbursts.

1 INTRODUCTION

Gas is released often during coal mining process when the subsequent pressure release in the surrounding strata. At certain concentrations and volumes, gas may cause major risks of explosions and asphyxiation (Imgrund & Thomas 2013). On certain conditions, gas is released suddenly from coal mine, known as a coal and gas outburst (or gas outburst). This phenomenon has occurred in most coal producing countries and catches attentions from different nations accordingly in the history. With the recent development of the technical and political conditions, coal and gas outbursts only take place in a few countries. A lot of experience gained in the past has disappeared. Today apart from Australia, gas outbursts are a significant problem in China, Kazakhstan, Ukraine, Germany, Turkey and Mexico.

The prediction of coal and gas outbursts becomes a hot topic in recent years. An accurate predictor will be helpful for coal mine to take corresponding policy to reduce the possibility of disasters and save life from dangers. Researchers attempted various approaches, including neural network, grey correlation, SVM, etc. (Wangsheng et al. 2003). Using the neural network approach, the predicted weight sometimes turns out to have unreasonable distribution (Shiliang & Aiyou 2009). By grey correlation, the accuracy of the prediction may become worse unless the training data has a large amount (Hua et al. 2009). Although the SVM algorithm has been applied to the prediction of coal and gas outbursts, an appropriate kernel function needs to be carefully designed and verified. While the machine learning technology provides us a great deal of classification algorithms. In this paper, we focus on the feasibility and usability of decision tree algorithms and ensemble learning (Dietterich 2000) algorithms for the prediction of gas outbursts.

Since we get enough measuring parameters from historical coal and gas outburst events, which can be used as features of the coal mine and gas condition for the outbursts. Then for any other coal mines, it will be naturally to rely on supervised learning to predict the possibility of their future outburst given the historical feature data of outbursts. The ensemble methods have been proved to be very successful supervised learning. Ensembles combine multiple hypotheses to form a better hypothesis. In other words, an ensemble is a technique for combining many weak learners in an attempt to produce a strong learner. The term ensemble is usually reserved for methods that generate multiple hypotheses using the same base learner. The broader term of multiple classifier systems also covers hybridization of hypotheses that are not induced by the same base learner. Evaluating the prediction of an ensemble typically requires more computation than evaluating the prediction of a single model, so ensembles may be thought of as a way to compensate for poor learning algorithms by performing a lot of extra computation. Fast algorithms such as decision trees are commonly used with ensembles and served as random forests, which will be more stable and robust for the prediction.

2 RANDOM FOREST

2.1 *Tree classifiers and ensemble learning*

Tree classifiers are unstable due to unexpected distribution of the real data (Leistner et al. 2009). An ensemble is a supervised learning algorithm, since it is trained first and then used to make predictions. The trained ensemble represents a single hypothesis. Empirically, ensembles tend to yield better results when there is significant diversity among the models (Kuncheva & Whitaker 2003). Therefore, ensemble methods are normally designed to promote diversity among the models in their combination.

Random Forests (RFs) are a combination of the weak classifiers of tree, and this can be used as ensemble to produce a strong learner. Each tree depends on the values of a random vector sampled independently and with the same distribution for all trees in the forest. The generalization error of a forest of tree classifiers depends on the strength of the individual trees in the forest and the correlation between them. Using randomly selected features to split each node will yield error rates that compare favorably to Adaboost, therefore RFs are expected to be more robust with respect to noise (Kotsiantis 2007).

At each internal tree node, a decision forest randomly can select F feature attributes, and evaluate just those attributes to choose the partitioning attribute. They tend to produce trees larger than trees where all attributes are considered for selection at each node, but different classes will be eventually assigned to different leaf nodes. At each internal tree node, RFs evaluate the quality of all possible partitioning attributes, but randomly select one of the F best attributes to label that node based on information gain, etc. RFs are an effective tool in prediction compared with boosting and adaptive bagging.

Bagging alone utilizes the same full set of predictors to determine each split. However the RF algorithm applies another judicious injection of randomness: namely by selecting a random subset of the predictors for each split (Breiman 2001). The number of predictors to try at each split is known as m_{try}. While this becomes new parameter, typically (classification) or (regression) works quite well. RFs are not overly sensitive to m_{try}. While Bagging is a special case of random forest where $m_{try} = k$.

2.2 *Random forest classifier*

A random forest is an ensemble of decision trees. Each tree in the forest is built and tested independently from other trees; hence the overall training and testing procedures can be performed in parallel. During the training, each tree receives a new bootstrapped training set generated from the original training set by subsampling with replacement. We refer to those samples which are not included during the training of a tree as the out-of-bag samples of that tree (Leistner et al. 2009). These samples can be used to compute the out-of-bag-error of the tree as well as for the ensemble which is an unbiased estimate of the generalization error.

During training, each decision node of the tree creates a set of random tests and then selects the best according to quality measurement such as information gain or Gini index. The trees are usually grown to their full size without pruning. We denote the nth tree of the ensemble as

$$f_n(x) = f(x, \theta_n) : \mathrm{X} \rightarrow \mathrm{Y} \tag{1}$$

where θ_n is a random vector capturing the various stochastic elements of the tree (such as the randomly subsample training set or selected random tests at its decision nodes). We denote the entire forest as $F = \{f_1, \ldots, f_N\}$, where N is the number of trees in the forest. We can write the estimated probability for predicting class k for a sample as

$$p(k \mid x) = \frac{1}{N} \sum_{n=1}^{N} p_n(k \mid x) \tag{2}$$

where $p_n(k|x)$ is the estimated density of class labels of the leaf of the nth tree. The final multi-class decision function of the forest is defined as

$$C(x) = \arg\max_{k \in Y} p(k \mid x) \tag{3}$$

Breiman (2001) defined the classification margin of a labeled sample (x, y) as

$$m_l(x, y) = p(y \mid x) - \max_{\substack{k \in Y \\ k \neq y}} p(k \mid x) \tag{4}$$

It is obvious that for a correct classification, $m_l(x,y) > 0$ should hold. Therefore, the generalization error is given by

$$GE = E_{(X,Y)}(m(x, y) < 0) \tag{5}$$

where the expectation is measured over the entire distribution of (x, y), and the error has an upper bound in form of

$$GE \leq \bar{\rho} \frac{1 - s^2}{s^2} \tag{6}$$

where $\bar{\rho}$ is the mean correlation between pairs of trees in the forest 1 and s is the strength of the

ensemble (i.e., the expected value of the margin over the entire distribution).

3 EXPERIMENTS

3.1 *Data preparation*

Experiments are taken to verify the performance of different algorithms for classifying coal and gas outbursts. Four indexes are chosen as features of coal and gas outbursts: drill cuttings analysis index (K_1), the maximum amount of drilling (S), drilling gas inrush initial velocity (q_0), coals solidity coefficient (f) (Xuchao & Dongling 2011, Chenggong & Youan 2004). The experiments are implemented with multiple classes of outbursts, representing outburst tendency (tendency), outburst, and no outburst (normal). We use a set of data from the outbursts of several coal mines in China (Yu-feng & Zhong-cai 2010, Tao & Tianwei 2011). Of the total 40 records, 66% are used for training and others for testing. Table 1 presents some sampling data for the features of coal and gas outbursts.

3.2 *Statistical metrics of predictive results*

The experiments are taken with Weka machine learning package, and the results are evaluated by several statistical metrics. We provide an explanation of these parameters in the following parts. The statistical metrics of the predictive results are evaluated by accuracy, Kappa statistics, mean absolute error, root mean squared error, and relative absolute error. For the prediction performance, we normally refer to accuracy, which is the number of correctly classified instances versus the number of total instances, known as percent agreement calculation. The Kappa statistics, also called Cohen's kappa coefficient (Kappa), is a statistical measure of inter-rater agreement for categorical items (Carletta 1996). It is generally thought to be a more robust parameter than simple percent agreement calculation, since Kappa takes into account the agreement occurring by chance.

Table 1. Features for coal and gas outbursts.

No.	K_1	S	q_0	f	Outburst
1	1.46	2.79	3.29	1.63	Tendency
2	2.18	4.03	4.55	0.29	Outburst
3	1.48	3.10	2.78	1.88	Tendency
4	2.22	4.13	5.11	0.36	Outburst
5	0.57	1.92	4.03	2.27	Tendency
6	1.17	2.03	0.97	2.48	Outburst
7	2.24	1.98	3.21	0.29	Normal
8	2.19	4.38	5.23	0.34	Outburst
9	0.77	2.52	2.34	2.16	Normal
10	2.23	4.31	5.09	0.31	Outburst
11	1.46	2.61	4.15	1.75	Tendency
12	2.21	3.98	4.59	0.35	Outburst
13	0.72	2.35	2.55	2.15	Normal
14	0.68	2.58	2.79	2.43	Normal
15	2.19	4.13	5.22	0.36	Outburst
16	1.40	3.01	4.09	1.75	Tendency
17	0.89	3.45	4.34	2.78	Tendency

$$Kappa = \frac{\Pr(a) - \Pr(e)}{1 - \Pr(e)} \tag{7}$$

where Pr(a) is the relative observed agreement among raters, and Pr(e) is the hypothetical probability of chance agreement, using the observed data to calculate the probabilities of each observer randomly saying each category. If the raters are in complete agreement then $Kappa = 1$. If there is no agreement among the raters other than what would be expected by chance, $Kappa = 0$.

In statistics, the Mean Absolute Error (MAE) is a quantity used to measure how close forecasts or predictions are to the eventual outcomes, which is an average of the absolute errors $e_i = |\hat{x}_i - x_i|$. The mean absolute error is given by

$$MAE = \frac{1}{n}\sum_{i=1}^{n} |\hat{x}_i - x_i| \tag{8}$$

The Root Mean Squared Error (RMSE) of predicted values $\hat{x}_t$ for times t of a regression's dependent variable x_t is computed for n different predictions as the square root of the mean of the squares of the deviations:

$$RMSE = \sqrt{\frac{\sum_{t=1}^{n} (\hat{x}_t - x_t)^2}{n}} \tag{9}$$

Mathematically, the Relative Absolute Error (RAE) of an individual program is evaluated by the equation:

$$RAE = \frac{\sum_{i=1}^{n} |\hat{x}_i - x_i|}{\sum_{i=1}^{n} |x_i - \bar{x}|} \tag{10}$$

where $\bar{x} = \frac{1}{n}\sum_{i=1}^{n} x_i$ is the average value of the samplings.

The Root Relative Squared Error (RRSE) is computed by dividing the RMSE by the RMSE obtained by just predicting the mean of target values (and then multiplying by 100). Therefore, smaller values are better, and the values >100%

indicate that the scheme is doing worse than just predicting the mean. The root relative squared error of an individual program *i* is evaluated by the equation:

$$RRSE = \sqrt{\frac{\sum_{i=1}^{n} (\hat{x}_i - x_i)^2}{\sum_{i=1}^{n} (x_i - \overline{x})^2}} \tag{11}$$

3.3 *Experimental results*

Experiments are taken for random forest and other tree classification algorithms, as well as several ensemble algorithms. For comparison with the tree classification algorithms, we choose several tree like classification algorithms, including Best-First decision Tree (BFTree), decision stump, Functional Tree Algorithm (FT), J48 decision tree-inducing algorithm, Logical Analysis of data Decision tree (LAD), Naive Bayesian decision Tree (NBTree), random tree, Reduced Error Pruning Tree algorithm (REPTree).

For ensemble algorithms, we consider AdaBoost as well as Bagging. The weak classifier for AdaBoost is the DecisionStump algorithm. The experimental results for coal and gas outbursts are given in Table 2.

The results indicate that RF has an accuracy of 85.71%, which is better than BFTree, DecisionStump, FT, J48, LADTree, NBTree, RandomTree, REPTree. Also, compared with the ensemble algorithms of AdaBoost and Bagging, the accuracy of RF is also better for nearly 15%.

For Kappa statistics, the RF algorithm has a value of 0.77, which is higher than all other algorithms. This indicates that the raters have greater chance of agreement than other algorithms. For the Mean Absolute Error (MAE), random forest is also better than other algorithms except for the RF algorithm, which indicates that although the MAE is useful to represent the absolute errors, its value is not enough to represent the quality of prediction yet. While the Root Mean Squared Error (RMSE) provides more precise statistics of the prediction error, and the RMSE value of random forest is lower than other algorithms accordingly. As for the Relative Absolute Error (RAE) and the Root Relative Squared Error (RRSE), the results demonstrate similar performance as for MAE and RMSE. Also, for RRSE, if the values are greater than 100%, it indicates the algorithms are rather worse for the computing. From the results, we can come to a conclusion that the algorithms of BFTree, DecisionStump, FT, J48, LADTree, REPTree are not suitable for the prediction of outburst, at least for the case when we refer to K_1, S, q_0 and f.

Next, we take experiments to verify the performance of different forests for the computing. The number of trees ranges from one to ten, then the time spent for the prediction of coal and gas outbursts changes a little bit from 0.002 seconds to 0.01 seconds (Figure 1), which indicates that the RF algorithm is fast enough for the computing of outbursts in real engineering.

In order to figure out how many trees are suitable for the random forest, we further refer to the statistical parameters. From Figure 2, when there is only 1 tree, the Kapa statistics is 0.65, while it increases to 0.77 when the tree number is 7 or above. The measurement of error also becomes tolerable when the number of trees increases, and as is shown in Table 2, the MAE is 0.21 and the RMSE is 0.31 when the number of trees is 10. Although the RMSE is 0.13 when the number of trees is 1, the MAE has a value of 0.38 and this is higher than the value of other number of trees. These results indicate, if we only refer to the RMSE, we still cannot evaluate the error precisely. While it is similar for the RAE, it is only 33% when the

Table 2. Comparison of Random Forest with Other Algorithms.

Algorithm	Accuracy (%)	Kappa	MAE	RMSE	RAE (%)	RRSE (%)
BFTree	57.14	0.26	0.34	0.48	78.58	102.78
DecisionStump	57.14	0.15	0.38	0.47	88.53	102.10
FT	57.14	0	0.29	0.53	65.91	115.14
J48	57.14	0.26	0.34	0.48	78.58	102.78
LAD Tree	57.14	0.15	0.27	0.48	62.80	104.24
NBTree	71.42	0.46	0.30	0.39	70.11	83.05
RandomTree	78.57	0.66	0.14	0.38	32.95	81.42
REPTree	57.14	0.15	0.38	0.47	88.53	102.10
RandomForest*	85.71	0.77	0.21	0.31	48.33	66.64
Ada Boost	71.43	0.49	0.35	0.39	81.08	84.89
Bagging	64.29	0.44	0.33	0.38	76.14	81.91

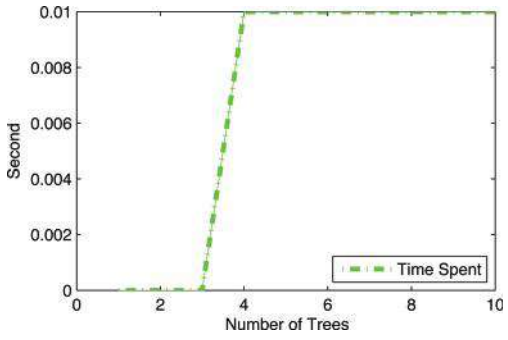


Figure 1. Time spent for the computing of random forests.

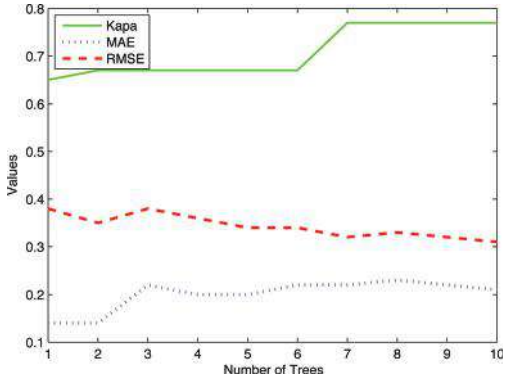


Figure 2. Variation of Kapa Statistics, MAE, RMSE in Random Forests.

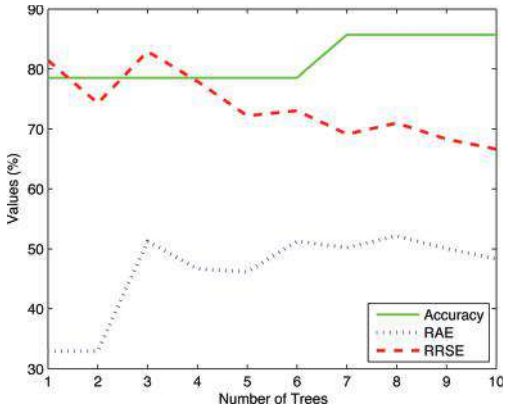


Figure 3. Variation of accuracy, RAE, RRSE in random forests.

number of trees is 1 (Figure 3), much lower than that of other number of trees. But the RRSE is 82% when the number of trees is 1, which means the root relative squared error is rather high. The accuracy for 7–10 number of trees also becomes 82% when the number of trees is 7 or above, and the errors of MAE and RMSE is about 0.35 and 0.2 respectively. Therefore, ideally the number of trees in the RF algorithm will be 7 or above.

4 CONCLUSIONS

Coal and gas outbursts are serious risk factors for the mining industry, but the machine learning technology provides useful methods to predict this phenomenon. By analysis of four parameters from historical outbursts, K_1, S, q_{10}, and f, we evaluate the effectiveness of different machine learning algorithms. We provide a comparison of the decision tree algorithms and ensemble algorithms, and find out that the ensemble decision tree—random forest, demonstrate good performance for the outburst prediction. When the number of trees goes to 7 or above, the prediction accuracy reaches expected level and the error rate is tolerable, which is acceptable for the outburst prediction. Correspondingly, some decision tree algorithms exhibits worse error rate and are not expected to be used directly for the prediction.

ACKNOWLEDGEMENTS

This work was supported by Ningbo Nature Science Foundation Funding (No.2012A610020) and Zhejiang Province Department of Education Foundation Funding (No.Y201225208).

REFERENCES

Breiman, L., Random forests, *Mach. Learn.* 45(1) (2001) 5–32.

Carletta, J., Assessing agreement on classification tasks: the kappa statistic, *Comput. Linguist.* 22(2) (1996) 249–254.

Chenggong, C. & W. Youan, Qualitative and Quantitative Analysis of General Regularity of Coal and Gas Out burst, *China Safety Science Journal* 14(6) (2004) 109–112.

Dietterich, T.G., Ensemble methods in machine learning, in: Proceedings of the First International *Workshop on Multiple Classifier Systems, MCS'00,* Springer-Verlag, London, UK, UK, 2000, pp. 1–15.

Hua, D., W. Jian & W. Bin, Coal and gas outburst forecast based on ANN and grey correlation, *Journal of Xian University of Science and Technology* 29(2) (2009) 136–139.

Imgrund, T. & R. Thomas, International experience of gas emission and gas outburst prevention in underground coal mines, in*: Coal Operators' Conference,* Research Online, 2013, pp. 331–338.

Kotsiantis, S.B., Supervised machine learning: A review of classification techniques, in: *Proceedings of the*

2007 conference on Emerging Artificial Intelligence Applications in Computer Engineering: Real Word AI Systems with Applications ineHealth, HCI, Information Retrieval and Pervasive Technologies, IOS Press, Amsterdam, The Netherlands, The Netherlands, 2007, pp. 3–24.

Kuncheva, L.I. & C.J. Whitaker, Measures of diversity in classifier ensembles and their relationship with the ensemble accuracy, *Machine Learning* 51(2) (2003) 181–207.

Leistner, C., A. Saffari, J. Santner & H. Bischof, Semi-supervised random forests, in: *IEEE 12th International Conference on Computer Vision,* 2009, pp. 506–513.

Shiliang, S. & W. Aiyou, Study on area forecast of coal and gas outburst based on coupling of neural network and genetic algorithm, *Engineering Sciences* 11(9) (2009) 91–95.

Tao, L. & L. Tianwei, The Research on Distribution of Coal and Gas Outburst of Xieyi Mine in Huainan Mining Area, *Highlights of Sciencepaper Online* 4(6) (2011) 559–563.

Wangsheng, Q., L. Biaocan & C. Sijing, Developing trend and perspective in the research of predicting the coal and gas outburst, *China Safety Science Journal* 13(12) (2003) 1–4.

Xuchao, H. & S. Dongling, Study on coal and gas out burst status and early warning technology in china coal mine, *Coal Science and Technology* 39(7) (2011) 61–63, 69.

Yu-feng, S. & L. Zhong-cai, Application Study of SVM in Analysis of Coal and Gas Outburst, *China Safety Science Journal* 20(1) (2010) 25–30.

Progress in Mine Safety Science and Engineering II – He et al. (Eds)
© 2014 Taylor & Francis Group, London, ISBN 978-1-138-00122-0

Goaf frictional ignition and its control measures in underground coal mines

G.F. Wang, T.X. Ren & C. Cook
Faculty of Engineering and Information Sciences, University of Wollongong, New South Wales, Australia

ABSTRACT: Goaf Frictional Ignition (GFI) poses a serious threat to the safety of underground coal mines, and has caused many underground fires and catastrophic explosions. This paper examined occurrences of GFI incidents and the underlying mechanisms of ignition source and environment. Most of these incidents were attributed to rock on rock frictional ignition. The eventuation of frictional ignition relies on the presence of hot spots with enough incendive ignition energy, which requires a minimum threshold sliding distance and sliding velocity. The incendivity of the environment can be enhanced by the presence of liquid carbon hydrogen, the increase of virgin rock temperature, and the presence of hydrocarbon gases from thermal decomposition product of coal volatile. The paper discussed the newly proposed concerns on the varying incendivity of environment; finally it summarized the GFI engineering controls and discussed their applicability.

1 INTRODUCTION

Goaf Frictional Ignition (GFI) refers to the ignition of flammable gas mixture by friction in the goaf area. It poses great threats to the underground coal mine safety. Goaf fires and explosions emanating from it have caused substantial property losses and casualties all around the world. On July 16th, 1986, 12 people were killed by an explosion in Moura No. 4 Underground Mine in Central Queensland, and GFI was suspected as one of the two possible ignition sources (Lynn et al. 1986). In USA 1997, an explosion occurred in Upper Big Branch underground coal mine and caused considerable property loss, which was surely induced by GFI (Page et al. 2010). A fatal explosion happened in Sago Mine, West Virginia, USA, where 12 men were killed on January 2nd, 2006, and GFI was not ruled out as a possible cause (Gates et al. 2007). In New Zealand, the Pike River coal mine explosion disaster on November 19th 2010 killed 29 out of the total 31 underground workers at that time. As no one has been able to reenter the coal mine after the explosion, the ignition source of the first explosion has not been determined by scene inspection and GFI remains a possible ignition source (Royal Commission on the Pike River Coal Mine Tragedy 2012). The mine geology, mining conditions and the incidents history at Pike River indicate a high possibility of frictional ignition in the goaf; It is a gassy mine, over a five-day period in October 2010 there were six over 5% methane overrun panel; sandstone, which has high incendivity, directly overlies the active coal seam with the thickness of over 30 meters; and the incendivity of the sandstone was substantiated by the frictional ignition incidents in the mine's tunnel development phase; it adopted free-standing goaf management strategy, and the coal extraction height was in 10–13 meters range, which can yield friction velocity from 14 to 16 m/s, and this velocity range has been proven to be readily to cause frictional ignition; The width of the panel was 31 meters, which was capable to yield plate like rock falling, and this has been proven by the platelike roof falling with windblast on 30th October 2010, while the plate-like roof falling blocks can provide friction platform with sufficient sliding distance for the overlain falling rocks (Royal Commission on the Pike River Coal Mine Tragedy 2012).

The incidences of GFI have been reported even more in China. China extracts about half of the world's total coal production, and over 90% of that is from underground coal mines. On 14th February 1999, at Xinjian coal mine Qitaihe city of Heilongjiang Province, methane accumulated in an abandoned conveyor roadway which connected to a high gassy coal seam. The impact and friction associated with the cave-in of the rich quartz sandstone roof ignited the firedamp, and caused an explosion which killed 49 men (Yang & Gu 2010); On 5th November 1999, at Yinan coal mine of Handan City in Hebei Province, methane built-up under the massive free-standing roof in the goaf, the friction and impact during the caving of the roof ignited the firedamp, caused an explo-

sion which killed 33 men (Yang & Gu 2010). At Meiyukou and Xinzhouyao coal mines of Datong Mining Group, goaf methane ignitions have been reported times, and the fires were called 'ghost fires' by underground coal miners. On 3rd December 2005, at 8317 fully mechanized longwall face in Xinzhouyao coal mine, during the goaf roof caving, a stream of flame came out of the goaf, which caused face stop for nearly 1 week. After analyzing and investigating the accident causes, open flame, blasting explosives and electrical charges were ruled out, and rock on rock frictional ignition was considered to be the most possible cause (Yang & Gu 2010). A total of 26 goaf methane explosion (fire) incidents were reported in the counties of Yang Cheng and Qinshui in China. After ruling out the possibilities of open flame, blasting explosive, detonators, electrical arc and contrabands, these incidents were attributed to rock on rock frictional ignition (Qin 2005).

2 MECHANISMS OF GFI

The eventuation of frictional ignition relies on the co-presence of both incendive ignition source and incendive environment. Systematic and comprehensive investigations were conducted on the ignition source, and the corresponding mechanisms were proposed, developed and substantiated by laboratory experiments and field observations. The study on incendivity of ignition environment mainly focused on the methane concentration of methane-air mixture. Some new factors which affect the incendivity of the environment have been identified by researchers and preliminarily probes have been conducted on these concerns. This section critically examines the ignition source mechanisms and their supporting laboratory tests, and distilled the core of research outcomes from the perspective of industrial engineering controls. This section also summarizes the new concerns on the incendivity of the environment and the ongoing research outcomes.

2.1 *Ignition source mechanisms*

From the perspective of ignition sources, frictional ignition can be broadly divided into three categories: rock on rock, metal on rock, metal on metal. As in the goaf area, the presence of metal is rare, so GFI can be classified as the rock on rock, which has been proven to be incendive enough to ignite explosive range methane-air admixture theoretically and experimentally. Insights into the corresponding mechanisms have gone through different phases and gradually matured (Burgess & Wheeler 1928, Nagy & Kawenski 1960, Page 2010, Rowell 1969, Powell & Billinge 2001, Qin 2003, Qin 2005, Rae 1964, Ramsay et al. 1965, Ward et al. 2001, Wynn & Britain 1952).

Although it was the sparks generated from the impacts and friction that raised the concern of frictional ignition, it has been proven that most of the frictional ignitions were not caused by sparks, provided that the sparking particles are not pyrite, which can burn in the air. Burgess and Wheeler from UK SMRE (Safety in Mines Research Establishment) found in the laboratory that it was very difficult to ignite admixtures of methane and air with sparks (Burgess & Wheeler 1929), and Blickensderfer et al. from U.S. Bureau of Mines confirmed the above finding (Blickensderfer et al. 1972). Researchers revealed that methane ignition requires a high temperature (no less than 650 °C) associated with adequate heating area and induction time, while sparks do not usually possess the adequate combination of life time, temperature, and surface area (Trueman 1985). Australian researchers Ward et al. observed the ignitions associated with the presence of sparks, and found that ignitions mostly developed from the contact points of friction rather than sparks (Ward et al. 2001). Pyrite sparking particles are another story, because they can react with oxygen, generate more heat and keep the temperature going higher, and then prolong the lifetime above the incendive temperature (Ward et al. 2001, Allsop 1939). In conclusion, previous research conducted inlaboratory illustrated that normal sparks which just hold the frictional heat are not capable of being the ignition source in most frictional ignition cases.

Hot spots consisting of molten minerals from sliding rocks, which appear at the contact point of sliding rocks and its trail, are the major contributor to frictional ignitions. Hot spots mechanism was firstly proposed in 1929, when Burgess and Wheeler argued that a stationary spark at the contact between cutting pick and the rock might be ignition source, which is equal to the hot spot (Burgess & Wheeler1929). Powell from UK SMRE reported that in a set of rubbing tests with rock sample cube rubbing against sandstone wheel enclosed in a 7% methane-air mixture, when ignitions occurred, the subsequent examination always revealed patches of glassy, fused quartz on the rubbed surface of the rock sample cube, which were the chilled hot spots (Powell & Billinge 1975). The high-speed cine-film, which recorded on another set of tests, also confirmed the presence of hot spots at the friction trace (Powell & Billinge 1975, Powell et al. 1975). Ward et al. observed the frictional ignitions in his tests, and found that ignitions originated from the hot spots at the close trail of the contact point of friction (Ward et al. 2001). All the above laboratory findings underpin the hot

spots mechanism, and theoretical interpretations were proposed as well.

Quantitative research was conducted, based on the appreciation of incendivity of rock on rock friction, aiming to provide data which engineering controls can be based upon and developed. Rae from UK SMRE conducted systematic research on the criteria of rock on rock frictional ignition by making use of highly incendive sandstone (Darley Dalesandstone) with the outcomes, as shown in Figure 1. (Rae 1964).

Figure 1 shows that the mean sliding distance prior to ignition is in inverse relationship with the momentum of the sliding, the larger the momentum the shorter the sliding distance is needed; while the most highlighted feature in Figure 1 is the existence of the threshold mean sliding distance prior to ignition, which in this specific case is 5.44 m (1/0.1838). The existence of threshold friction distance prior to ignition is also demonstrated by the outcomes of the experiments conducted by Ward and Xu, as shown in Table 1 and Table 2 respectively.

Table 1 shows that, under Ward's experimental environment, the sliding distance prior to the frictional ignition decreases substantially with the increase of sliding speed and momentum; and even with the most incendive speed in the experiments, which was 5.1 m/s, the sliding distance prior to the frictional ignition was no less than 10.2 m (Ward et al. 2001). Table 2 shows that the dry conglomerate gave the highest incendivity; while even with the conglomerate against conglomerate under the contact pressure of 171–228 N, the minimum sliding distance before frictional ignition was 20 m (which is worked out with 10 m/s × 2 s) (Xu et al. 2007). The discrepancy of the minimum sliding distance prior to frictional ignition among the research outcomes of Rae, Ward and Xu, was due to the different contact loads and rocks adopted in their experiments. The maximum contact loads adopted in Rae's experiments were much higher than those adopted by the other two researchers, and were more approximate to the realistic adverse underground environment. Nevertheless, all these

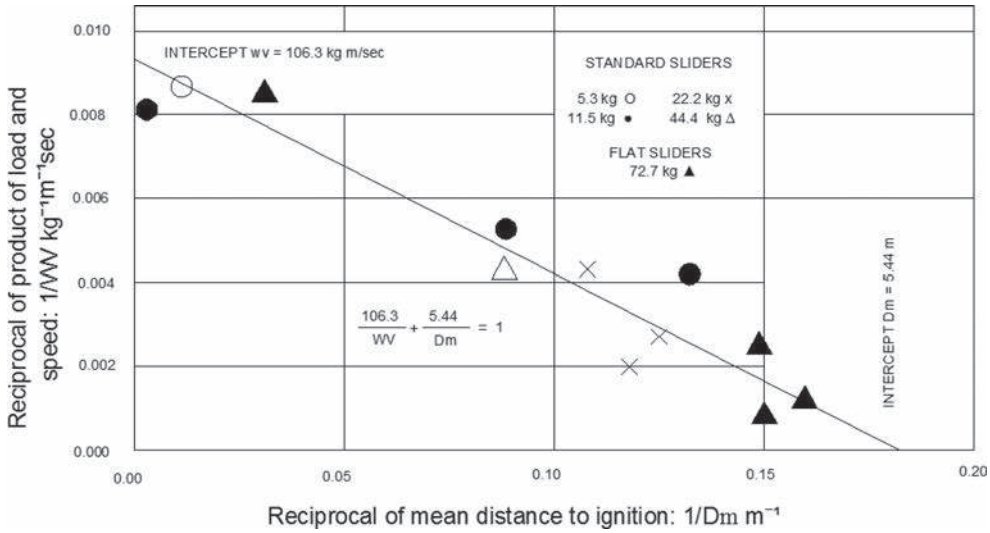


Figure 1. Tests outcomes from UK SMRE (Rae 1964).

Table 1. Sliding time and distance prior to ignition for different rock sliders using sandstone wheel from Appin Colliery (Sample A1) (Ward et al. 2001).

Wheel speed (rpm)	Wheel speed (m/s)	Time to ignition for different rock samples used as sliders (s)/distance prior to ignition (m)			
		M1 Claystone	A1 Sandstone	FB1 Quartzite	SB10 Siliceous coal
700	5.1	No ignition	12/61.2	2/10.2	2/10.2
500	3.7	No ignition	28/103.6	15/55.5	11/40.7
300	2.2	No ignition	No ignition	35/77	30/66

Table 2. Data from Xu's gas explosion induced by the rock friction experiments (Xu et al. 2007).

Rock type	CH4 concentration (%)	Contact normal force (N)	Sliding speed ($m \times s^{-1}$)	Sliding time (s)	Number of tests	Number of explosion
Gritstone on Gritstone	5~16	120~150	3	10~998	10	0
Conglomerate on Conglomerate	5~16	120~150	3	10~998	10	0
Mudstone on Conglomerate	5~16	171~228	10	9~60	10	0
Mudstone on Gritstone	5~16	171~228	10	9~60	10	0
Gritstone on Gritstone	5~16	171~228	10	6~32	10	7
Conglomerate on Gritstone	5~16	171~228	10	6~32	10	8
Conglomerate on Conglomerate	5~16	171~228	10	2~32	10	8

research outcomes support that threshold sliding distances would be needed to yield incendive enough ignition sources.

The threshold sliding distance is backed by the heat requirement to yield incendive enough hot spots under the given experimental environment. According to the frictional heat accumulation theory, heat generated in the sliding process equals the normal stress load at the contact multiplies the dynamic friction coefficient and the sliding distance, as shown in Equation 1. The normal stress load at the contact cannot be infinite but limited by the rock strength and hardness, i.e. the force applied at the contact cannot exceed the strength of the sliding bodies; combining with the given heat requirement and the fixed range of dynamic friction coefficient in the defined environment, the minimum threshold sliding distance can be estimated with the following equation, in which the cooling procedure associated with the sliding is ignored.

$$Q = F \times C \times L \quad (1)$$

Where Q = the heat generated in the friction process; F = applied normal force at the contact; C = the dynamic frictional coefficient at the contact point; and L = sliding distance prior to the frictional ignition.

Besides the threshold sliding distance, the threshold sliding velocity is another decisive factor to yield incendive enough ignition sources. In the tests conducted by Rae from UK SMRE, the sliding speeds of 21.3 m/s, 10.6 m/s, 5.3 m/s, 5.3 m/s, and 1.6 m/s were found to be the minimum speeds under the contact loads of 5.3 kg, 11.5 kg, 22.2 kg, 44.4 kg and 72.7 kg respectively (Rae 1964). Ward's research also confirmed that the incendive rock on rock sliding under higher speed, which was 5.1 m/s, may lose its incendivity under lower speeds, which were 2.2 m/s and 3.7 m/s (Ward et al. 2001). Qin et al. conducted FI tests under two sets of sliding speed, which were 4.2 m/s and 7.43 m/s with the same experimental environment, and found that 4.2 m/s did not yield any frictional ignition while the speed of 7.43 m/s yielded 13 frictional ignitions out of the 29 experiments (Qin et al. 2005). In the tests conducted by Xu et al., the 3 m/s sliding speed did not yield frictional ignitions while 10 m/s sliding speed yielded frictional ignitions, as shown in Table 2. (Xu et al. 2007).

Cooling process associated with the frictional heating up is the underlying rational of the threshold sliding speed requirement. Blickensderfer conducted research on the cooling process of the trail of the sliding; and a cooling model was proposed and validated based on the research outcomes of the laboratory experiments; a typical cooling curve of the sliding trail based on the theory is shown in Figure 2 (Blickensderfer 1975). The theoretical model revealed that the lifetime of hot streaks on the trail of the contact point over the minimum ignition temperature of methane-air admixture stays within very short time, which is less than10 milliseconds; combining with the finding that a threshold area of hot spot is needed to ignite methane-air mixture under the given temperature (Powell 1969, Rae et al. 1964), and sliding width is fixed under a specific friction, then the area of the hot streaks with temperature over the minimum ignition temperature is indirect proportion with the sliding speed (Blickensderfer 1975). So, a threshold sliding speed is needed to reach or overtake the threshold hot spot area to yield an incendive ignition source.

In conclusion, apart from the frictional ignitions originating from pyrite sparks, which can burn in the air; in given environment, the eventuation of frictional ignition relies on the presence of

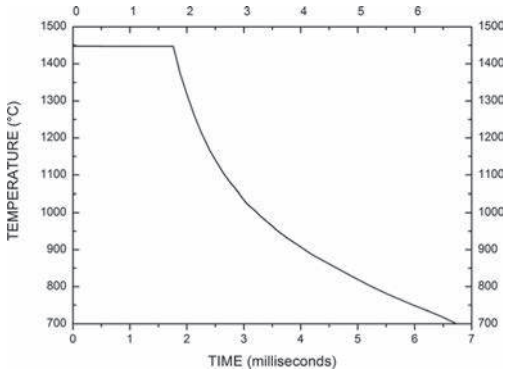


Figure 2. Calculated cooling curve of a narrow zone in the hot-streak trail (Blickensderfer 1975).

hot spots with enough incendivity. The presence of the incendive frictional ignition sources requires minimum threshold friction distance and friction speed.

2.2 *Ignition environment mechanisms*

From the perspective of ignition environment, even though it has been well established that the ignitable range of methane concentration is from 5% to 15%, the ignitable oxygen concentration is no less than12%, and the methane concentration of 7% has the highest incendivity (Ramsay et al. 1965, Rae et al. 1964, Cutler 1974); new concerns in this regard have arisen from the industry. One notable concern is the presence of liquid hydrocarbon; an underground coal mine in Utah, USA came across some liquid hydrocarbon in the coal measures strata, and U.S. NIOSH (National Institute for Occupational Safety and Health) laboratory experiments have confirmed that with the presence of the liquid hydrocarbon, the frictional ignitions are much easier to be triggered (Cash dollar 2008). Not only in USA, but somemines around other parts of the world are facing the presence of liquid hydrocarbons. Armstrong reported that oil occurrence has been observed in the three strata overlying the major active Bulli coal seam, among which, coal cliff sandstone directly overlaid on the coal seam, while Scarborough sandstone and Bulgo sandstone are the third and fifth overlying strata respectively (Armstrong et al. 2006). Although it has not been recorded in accessible literature, the presence of liquid carbon hydrogen in underground coal mines is not rare in China as well.

The incendivity of the environment can also be boosted by the increase of Virgin Rock Temperature (VRT). Theoretically, it has been supported by the frictional ignition predicting model developed by Blickensderfer, in which higher temperatures of the sliding bodies boost the frictional heating up and ease cooling speed as well as intensity of the trail (Blickensderfer 1975). The studies conducted by China Coal Research Institute show that the increasing of environmental temperature will significantly boost the incendivity of the rock friction (Qin et al. 2005); Qin et al. conducted rock on rock frictional ignition experiments under different environment temperatures (which were also the initial rock temperature) with the same other parameters, and found that clusters of sparks were seen with temperature reaching 10 °C while no sparks were seen under 5 °C (Qin et al. 2005). Even though the model developed by Blickensderfer included the temperature as a variable, no verifying experiments have been done by taking it as the independent variable, which can be done in further study.

Another concern on frictional ignition environment is the presence of higher incendive gas content in the methane-air admixture at some local areas, especially in the areas of oxidation and temperature rising zone in the goaf, where thermal decomposition gas product of coal volatile can be expected. The presence of these contents would increase the incendivity of the local gas environment (Li et al. 2012). This concern is backed by the research outcomes of methane, oxygen, and spontaneous combustion danger area distribution pattern in the goaf area. Chinese researchers conducted methane and oxygen concentration monitoring in the goaf area of U shape ventilation Longwall panel, and obtained methane distribution in the goaf area as shown in Figure 3 (Yang & Gu 2010).

Figure 3 shows that the explosive range of methane exists between 10 to 76 meters in by the goaf. Combining with previous research outcomes of the oxygen distribution pattern in the goaf under the spontaneous combustion research, which is that the heat elimination through ventilation zone is between 0 and 25 meters with oxygen concentration of 20 to 16 per cent, the oxidation and temperature raising zone is between 25 and 60 meters with oxygen concentration of 16 to 7 per cent, and asphyxiation zone with oxygen concentration of less than 7 per cent; it is highly probable that there are overlapping areas with explosive mixture of oxygen, methane and presence of gas products from thermal decomposition of coal volatile. It would be meaningful to further investigate the gas make of the product of thermal decomposition of coal volatile and its enhancing effect of the incendivity of the methane-air admixture gas body.

In summary, the presence of incendive ignition source relies on presence of threshold sliding distance and sliding speed for the incendive rocks; the incendivity of the environment can be boosted by the presence of liquid carbon hydrogen, the increase of virgin rock temperature, and the presence of the gas product of the thermal decomposition prod-

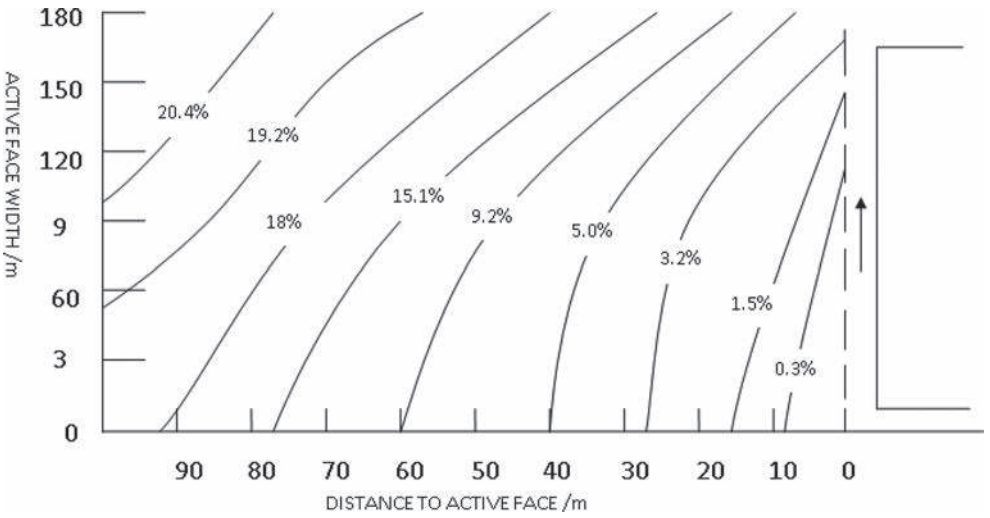


Figure 3. Methane distribution pattern in the goaf of a Longwall panel in China (Yang & Gu 2010).

uct of coal volatile. Although the mechanisms of ignition source have been systematically studied, the new concerns regarding the incendivity of the environment have just been preliminarily probed.

3 GFI CONTROLS

GFI controls are divided into two categories: frictional ignition source controls and frictional ignition environment controls. The rational underlying ignition source controls is to avoid the presence of the threshold values of the friction momentum, speed and distance. Frictional ignition environment controls rely on avoidance of the presence of methane air mixture in explosive range and the presence of the higher incendive thermal decomposition gas product of coal volatiles in the areas where incendive ignition sources are likely present.

3.1 *GFI source controls*

Forced or induced roof caving, goaf backfilling and partial extraction can all limit the possible friction speed between the rocks by controlling the freestanding height of the overhang roof, according to the terminal speed of free falling theory.

$$V = \sqrt{2gh} = 4.43\sqrt{h} \tag{2}$$

Where V = the terminal speed of falling rocks; h = the free-standing height of the overhang roof. Among these three control measures, forced roof caving is the most economical and practical one and has been adopted widely to tackle this issue (Yang & Gu 2010, Qin et al. 2003). Goaf backfilling and partial extraction have been adopted in some underground coal mines for surface subsidence control or resource recovery reasons, and are helpful for GFI control. The required forced caving height can be worked out with the following formula:

$$h_e - h_f(k-1) = H_{threshold} \tag{3}$$

Where h_e = coal extracting height; h_f = forced caving height; k = swell factor of the forced caving rocks; $H_{threshold}$ = the threshold free-standing height which can yield the threshold terminal speed.

Forced roof caving can avoid the presence of massive friction contact load by avoiding the weighting associated with the falling of massive volume of free standing roof. The presence of large areas (even up to hundreds of thousands of square meters) of free standing overhang hard conglomerate or sandstone roof has been reported in underground coal mines. The fall of such large area of rock would incur massive load at the contact point of friction, which would be very highly incendive. Forced roof caving with designed increment value will keep the falling rock mass within the designated range, which will significantly alleviate the load at the friction contact.

Forced roof caving can also avoid the presence of incendive sliding distance. By implementing forced roof caving with reasonable increment, the formation of rock blocks with large surface, especially plate-like falling of roof strata, which can provide incendive sliding distance, is avoided. In conclusion, the forced or induced roof caving can limit the possible friction speed between the rocks,

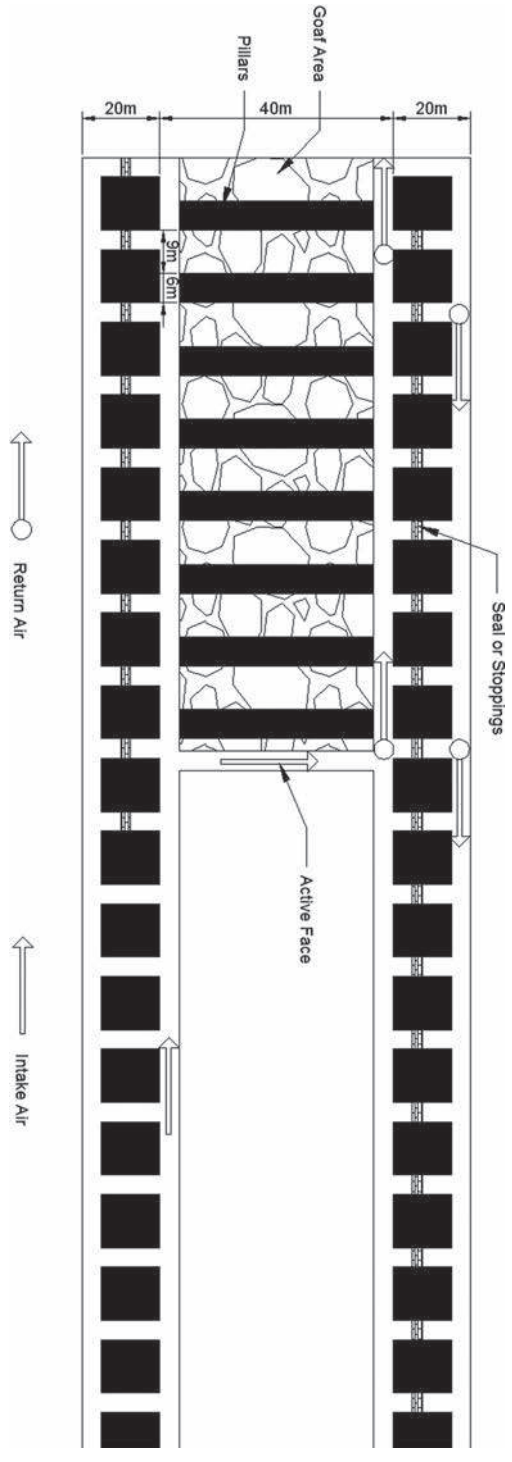


Figure 4. The use of a bleeder system to keep the methane concentration below the explosive range at a room and pillar panel (Qin et al. 2003).

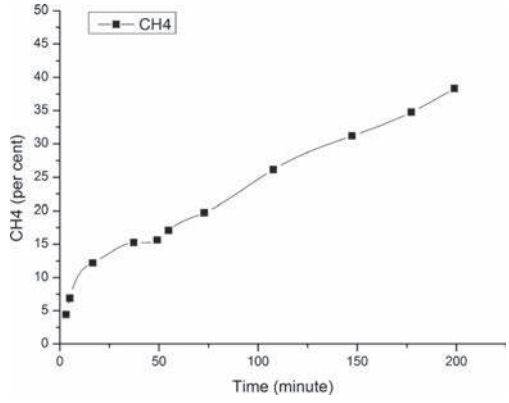


Figure 5. Methane concentration variation after rapid goaf sealing (Qin et al. 2003).

limit friction load at the contact, and avoid the presence of rock surface which can provide long enough sliding distance.

3.2 GFI ENVIRONMENT CONTROLS

Keeping the methane concentration beyond the explosive range is the most effective and preferable approach on this issue. To control the methane level below the explosive fringe under a particular panel ventilation system is mainly achieved by removing methane emissions from the goaf. Bleeder system has been widely adopted by the industry to achieve this; the bleeder system can take away the methane emission from the goaf or adjacent methane bearing strata, as shown in Figure 4.

Figure 4 shows the use of a bleeder system. The on-site monitoring results showed that the outcome was very satisfactory; the methane concentration of the general gas body was kept below 3% after the coal face had passed over 80 meters (Qin et al. 2003). However the bleeder system should not be adopted in coal faces with a high risk of spontaneous combustion.

Rapid goaf sealing technology is another practical approach to keep methane concentration beyond the explosive range. If the goaf can be sealed tightly within short time, methane emission from the goaf can be isolated, which would promptly raise the methane concentration in the goaf and simultaneously reduce the oxygen concentration to below the lean flammability limit; thereby the risk of frictional ignition can be eliminated (Qin et al. 2003). In June 2001, an industrial trial was conducted in an underground coal mine in China with a rapid goaf sealing method; the goaf was sealed with around 30 minutes. After the sealing, tube bundle was used to monitor the gas

content on the goaf side of the seal, and the results are shown as in Figure 5 (Qin et al. 2003).

Figure 5 shows that within around an hour after goaf sealed off, the methane concentration of the general gas body on the goaf side of the seal passed the explosive range. The rapid goaf sealing technology is not universally adoptable; it cannot be applicable in active Longwall panel but is very effective in room and pillar or hydro mining panel as shown in Figure 4, especially after a large scale plate-like roof fall, which might create a very favorable condition for the incendive rock on rock friction.

4 CONCLUSION

GFIs in underground coal mines pose a serious safety threat that may potentially lead to major gas explosions or fires. This paper provided an examination of GFI incidents and their underlying mechanisms. The eventuation of frictional ignition incidents relies on co-presence of both incendive ignition source and incendive environment. The presence of incendive ignition source depends on two critical and decisive parameters, i.e. the friction distance and friction speed. The incendivity of the environment is generally determined by the methane, oxygen concentrations, and can be boosted by the presence of liquid hydrocarbon, the increase of virgin rock temperature, and the presence of hydrocarbon gases from thermal decomposition product of coal volatile. Effective control measures can be developed to limit the friction distance and friction speed associated with rock falls in the goaf, therefore avoid the development of an incendive ignition source; they can also be developed by keeping the methane-air admixture beyond the explosive range. These control measures include forced or induced roof caving, bleeder ventilation system and rapid goaf seal-off.

5 ACKNOWLEDGEMENTS

This work is sponsored by a scholarship from the University of Wollongong and the China Scholarship Council.

REFERENCES

Allsop, G. & Wheeler, R.V. 1939. The ignition of firedamp by pyrites during coal cutting. *Transactions of the Institution of Mining Engineers 1938–39, XCVI.*

Armstrong, M. et al. 2006. Determining the controls for strata gas and oil distribution within sandstone reservoirs overlying the bulli seam. *Proceedings of Coal Operators' Conference, University of Wollongong, Wollongong, NSW, Australia*.

Blickensderfer, R. 1975. Methane Ignition by Frictional Impact Heating. *Combustion and Flame*, 25: p. 10.

Blickensderfer, R. et al. 1972. *Testing of coal cutter materials for incendivity and radiance of sparks.* U.S. Bureau of Mines, Report RI 7713.

Burgess, M.J. & Wheeler, R.V. 1928. The ignition of firedamp by the heat of impact of rocks. *[Gt. Brit.] Mines department, Safety in mines research board.*

Burgess, M.J. & Wheeler, R.V. 1929. *The Ignition of Firedamp by the Heat of Impact of Metal Against Rock*. UK Safety in Mines Research Board: Sheffield.

Cashdollar, K.L. 2008. *Frictional Ignition of Methane-Air in the Presence of Liquid Hydrocarbons.* Department of health and human services, National Institute for Occupational Safety and Health, DHHS (NIOSH) Publication No. 2008-124.

Cutler, D.P. 1974. The ignition of gases by rapidly heated surfaces. *Combustion Flame*, 22: p. 105–109.

Gates, R.A. et al. 2007. *Report of investigation, fatal underground coal mine explosion, January 2, 2006, Sago Mine, Wolf Run Mining Company, Tallmansville, Upshur County, West Virginia, ID No. 46–08791.* United States department of labor, Mine safety and health administration, Coal mine safety and health.

Li, G. et al. 2012. Influence of coal particles on methane/air mixture ignition in a heated environment. *Journal of Loss Prevention in the Process Industries*, 1(5).

Lynn, K.P. et al. 1986. *Report on an accident at Moura No.4 underground mine, Warden's Inquiry.* Department of natural resources and mines, Queensland Government.

Nagy, J. & Kawenski, E.M. 1960. *Frictional ignition of gas during a roof fall. U.S. Bureau of Mines*. Report of investigations 5548, Washington.

Page, N.G. et al. 2010. *Report of investigation, fatal underground mine explosion, April 5, 2010, Upper Big Branch Mine-South, Performance Coal Company, Montcoal, Raleigh County, West Virginia, ID No. 4608436.* United States department of labor, Mine safety and health administration, Coal mine safety and health.

Powell, F. & Billinge, K. 1975. The frictional ignition hazard associated with colliery rock. *The Mining Engineer*, 134: p. 8.

Powell, F. et al. 1975. The ignition of methane-air by machine picks cutting into rock. *16th International Conference on Coal Mine Safety Research, Washington D.C.*.

Powell, F. 1969. Ignition of gases and vapors—Review of ignition of flammable gases and vapors by friction and impact. *Industrial & Engineering Chemistry*, 61(12): p. 9.

Qin, Y.J. et al. 2003. Comprehensive prevention and control technologies on goaf gas explosions (fires). *Safety In Coal Mines*, 34(2). Journal ISSN:1003-496X. Paper Accession Number:1003–496X(2003)11-0006-02.

Qin, Y.J. et al. 2005. The determination of ignition sources of goaf gas explosions (fires). *Safety In Coal Mines*, 36(7). Journal ISSN:1003–496X. Paper Accession Number:1003496X(2005)07-0035-03.

Rae, D. 1964. *The role of quartz in the ignition of methane by the friction of rocks. Safety in Mines Research Establishment*, Research report No.223, Minstry of Power.

Rae, D. et al. 1964. *The size and temperature of a hot square in a cold plane surface necessary for the ignition of methane.* Safety in Mines Research Establishment, Research report No.224, Minstry of Power.

Ramsay, H.T. et al. 1965. A summary account of the manner and the frequency of ignition of firedamp in British Coal Mines. *The Mining Engineer,* Vol.124.

Royal Commission on the Pike River Coal Mine Tragedy Report. 2012. *Royal Commission on the Pike River Coal Mine Tragedy*. Wellington, New Zealand.

Trueman, R. 1985. A literature review of the ignition of methane-air mixtures by coal-cutting picks. *Journal of the South African Institute of Mining and Metallurgy,* 85(7): p. 7.

Ward, C.R. et al. 2001. Identification of potential for methane ignition by rock friction in Australian coal mines. *International Journal of coal geology*, 45: p. 13.

Wynn, A.H.A. & Britain, G. 1952. *The ignition of firedamp by friction.* UK Safety in Mines Research Establishment, Ministry of Fuel and Power, Research report 42.

Xu, J.L. et al. 2007. Study on Gas Explosion Induced by Impact-Friction Sparks During Roof Collapse with Fully-Mechanized Top-Coal Caving Mining. *Journal of China University of Mining & Technology*, 36(1). Paper Accession Number:1000–1964(2007)01-0012-05.

Yang, T.B. & Gu, J.J. 2010. Prelinary probe into goaf area rock on rock frictional ignition and the induced gas explosion. *Safety In Coal Mines*, Journal ISSN:1003–496X. Paper Accession Number:1003–496X(2010)08-0111-03.

This page intentionally left blank

Progress in Mine Safety Science and Engineering II – He et al. (Eds)
© 2014 Taylor & Francis Group, London, ISBN 978-1-138-00122-0

The water hazards caused by burst of overburden strata separation and the control strategies

Jing-Ming Wang & Hao Huang
North China Institute of Science and Technology, Beijing, China

ABSTRACT: Hazards due to stratum separation are a type of roof water hazards that unexpectedly happen even without any water reservoir. However, the hazard origins have not been understood or explained, resulting in great difficulties in control of water hazards in coal mines. To solve the problem, Haizi Coal Mine is taken as a case study. The hydrogeological, geotechnical and mining conditions are analyzed in a case study in Haizi Coal Mine. The roof stratum failure and displacement are analogized physically and simulated numerically. A new type of water hazards is found finally, and a new theory for the mine hazards, i.e. water hazards caused by burst of water cells formed by overburden stratum separation, is put forward. The drilling and borehole camera scanning have verified the above theory. According to the theory, the dynamic draining measures are proposed and used successfully in the control of the water hazard. The research achievements are applied to other working faces with the similar hydrogeological conditions for coal mining safety. The investigation on the hazards by simulations not only theoretically fills the gap of water hazard classification for coal mines, but also finds a way for the control of water hazards in coal mines.

1 INTRODUCTION

Roof water hazards under simple hydrogeological-condition at some coal mine occurred at China's Yili in Xinjiang province, Huanglong in Shanxi, Hongliu of Shendong mining area, Zaozhuang in Shandong, Laohutai in Liaoning, Wanbei in Anhui and so on in recent years. Water hazards from roof at working face 745 in Haizi coalmine of Huaibei Mining Group Corporation with the capacity of 3887 m^3/h resulted in five workers' death in 2006; Roof water inrush with rock happened in Yili and resulted in 16 workers' death in 2002; The same kind of hazard happened in Laohutai coalmine in Inner Mongolia, causing 19 workers' death in 2004. Several inrushes took place in Hongliu coalmine, Shendong mining area. However, this type of hazards had not been controlled, and its origins had puzzled scientific and technical personnel in water hazards prevention and control. The author conducted a series of investigations in this type of hazards, mechanical model derivation, analog experiments, numerical simulation, and finally find that the water reservoir is due to roof stratum separation—a new type of water hazards. The conclusion is drawn that the burst of water cells formed due to overburden stratum separation (Meng 2007, Wang 2003, Mining Institute 1981) happened under the action of impact pressure by means of hard roof-caving.

Roof separation is a common phenomenon in overburden during coal mining. Some specialized researches (Su, et al 2002) on formation mechanism of roof caving and mechanicalmodelling about roof caving had been done by some scholars before, including analog experiments, numerical simulations, such as simulations in the discrete element method (Xu, et al 2004, Cao, et al 2000), in finite element method (Su, et al 2003), in contact element method (Zhang, et al 2008) and in finite difference method (Chen & Wang 2008). Roof stratum impact also has been deeply researched in our country, involving the stratum structure (Meng 1997, Pan 2005), the key strata analysis method (Qian, et al 2003) and fuzzy mathematics method (Liu, et al 2006). It is generally believed that roof impact bias is related tothe lithologic structure of the roof, and the formation of impact pressure is the process of the accumulation and rapid release of energy before and after the failure of tight roof. However, water hazards due to overburden stratum separation under the action of impact pressure have never been reported before. Therefore, this is a new type of water hazards. It is significant in theory and in practice for researches this type of water hazards in order to enrich the classification of water disasters, identify the hazard causes, and finally develop control measures

2 THE HYDROGEOLOGYCAL ANALYSIS OF HAZARD ORIGINS DUE TO STRATUM SEPARATION

2.1 *Hydrogeologic condition of haizi coalmine*

Haizi Coalmine is located in Linhuan mine area, Huaibei coalfield, North China coal basin. The mine strata dip overall to the north with angle of 10° to 30°. Working face 745 is located in the east wing of mining district 84. The parameters of the face are: 403 m. of the average overburden of coal seam, 350 m in length, 70~120 m in tilted width, s18° in dip angle, 0.2~3.2 min coal thickness. The comprehensive mechanized mining method was applied. Natural collapse method was used to manage roof. The strata from the roof are followed by argillite, siltstone and fine argillite, sandstone and dioritic porphyrite. The main aquifer of the mine field includes sand-gravel layer at the bottom of quaternarysystem, the sandstone aquifer in the overburden of the seam, the limestone aquifers of Taiyuan group and Ordovician limestone aquifer. The quaternary system aquifer is too far away from the working face 745 to cause any hazards to the working face. Ordovician limestone aquifer lying 150 m under the coal floor is too far to cause any hazards either. The sandstone aquifer in the overburden is the only aquifer to have some effect on mining with small amount of water flow. 16 water inrushes happened in 4 working faces in mining district 84 when coal 7# was mined since August in 1998. In the inrushes, 4 was less than 50 m^3/h of water flow, 7 is less than 100 m^3/h, 4 is less than 150 m^3/h, 1 is 211 m^3/h. These water inrushes all happened in the mined areas and never caused any disasters.

However, roof water hazards at this working face happened at in May 21, 2006, with 3887 m^3/h of flow, nearly 500 m^3 of waste rock and caused 5 lives loss.

2.2 *The hydrogeological analysis of hazard origins due to stratum separation*

According to the mining theory, the caving-in zone, permeable fractured zone, flexural-subsidence zoneformed after mining. Under normal circumstances, flexural-subsidence zone is gradient with permeable fractured zone, and gradually develops to the surface, resulting in surface subsidence. Flexural-subsidence zone reach the surface rapidly if top part of the overburden is sand (Dong & Wang 2007), while the subsidence caused by the hard roof failure occurs slowly. Through the analysis of the borehole histograms, 80 m of intrusion rock in thickness is 50–60 m above the roof of coal 7 in Haizi Coalmine. According to the key stratum theory, the hard roof is the key stratum to bear gravity. The hard rock over the roof would not bend synchronously with the underlying soft rock because its inflexibility is larger than the lower one so as to form separations between strata in the overburden. Because the bottom layer of separation is aquiclude, a big water cell forms by the recharge from sandstone aquifer. When the space of overburden stratum separation is too large, the key stratum in the roof of the separation will break, and then the cells burst because of huge impact stress, and so that the water hazards occurred, as shown in Fig 1. According to statistics, many coal mines with similar hydrogeological conditions suffered from roof water inrush as heavy as Haizi coal mine. The specific conditions is shown in Table 1. The common characteristics of the hazards are momentary, swift and violent process with debris.

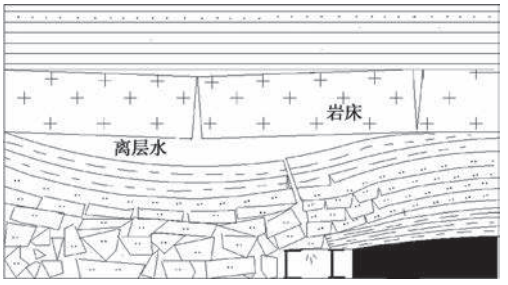


Figure 1. Secondary abscission layer formation water disasters.

Table 1. Hdrogeological conditions to cause water hazards due to stratum separation.

Coalmine	Mining height/m	Hard roof thickness/m	Distance to coal/m	Hazards
Haizi	2.6	70	50–60	5's death
Yili	3.3	30	41	16's death
Huang. lin	0.8–6.75	71.19	>25	9's death
Hongliu	5.3	40.6	51.2	Major danger
Laohu. tai	18–25	30	75	19's death

3 THE ORIGINS OF WATER HAZARDS DUE TO ROOF STRATUM SEPARATION

3.1 *Mechanicalmodel*

The strata above the working face can be simplified as a beam fixed at both ends. It is assume that there are n strata named 1, 2, 3… n in turn above the coal seam. Based on the knowledge of material mechanics, when the beam fixed at both ends

bends, the maximum curvature and deflection are as follows:

$$\rho_{\max}(i)=\frac{\gamma_i L_j^2}{2E_I m_i^2} \quad and \quad \varpi_{\max}(i)=\frac{\gamma_i L_i^4}{32Eim_i^2} \tag{1}$$

In the formula, γ_i: the bulk density of No. i stratum, *Li*: the span of No. i stratum; *Ei*: the elastic modulus of Mo. i stratum; mi: the thickness of No. i stratum. If the curvature and deflection of the adjacent stratum satisfy the followings:

$$\begin{aligned}\rho_{\max}(i)\geq\rho_{\max}(i-1)\\ \varpi_{\max}(i)\geq\varpi_{\max}(i-1)\end{aligned} \tag{2}$$

the strata will bend synchronously, othervice the strata will bend separately, as shown in Figure 2. Based on the knowledge of material mechanics, the stresses in curvature center and deflections are maximum when the beam is fixed at both ends. Therefore, the working face where people work is the most dangerous place because of water inrush.

3.2 *The analog experiment*

In order to verify the view that water hazards due to stratum separation, the experiments with similar materials have been done on basis of mining conditions, roof lithologic characters and boundary conditions at working face 745. According to the three laws of analog simulation, the parameters of the materials is shown as Table 2.

The analog experiments were conducted on a plane stress model and a 3-dimensional model. The plane model is 1 m high, 3 m long, and 0.3 m wide. 55 observation points were fixed in the model, including 39 pressure points and 16 displacement points.

Through the observation, the movement of overlying strata is in layer way or in group way. The weak strata's movement is attached to the strong and thick strata's movement, as shown in Figure 3. Observation points 40#, 44#, 48#, and 52# were 17.5, 17.5, 43.3, 52.3 cm above coal roof, and the last two are located in igneous rock bed. From Figure 3 we can see that: ①The displacements of roof strata is divided into two groups by the bottom of igneousrock (the gray rock in Figure 3). The vertical displacements of two points (No. 40#, 44#) in coal strata under igneousrock bed is much larger than those of two points (No. 48#, 52#) in igneous rock bed, resulting in strata separation. The two points in coal measure strata start to move at the same time, and the difference beteen the movements is obvious, while thetwo points in igneousrock began to move consistently, but difference two displacements. is little. ② Closer the strata

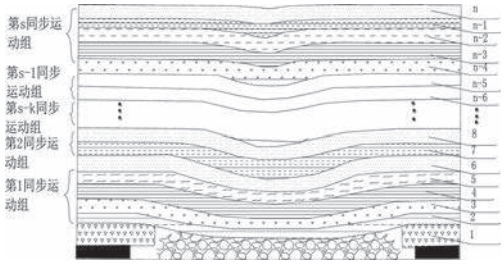


Figure 2. the strata bend synchronously and separately.

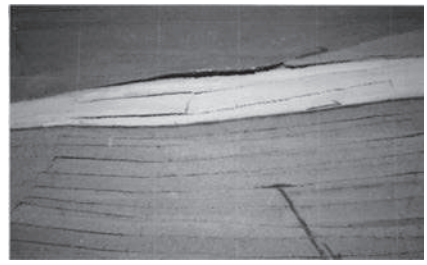


Figure 3. Stratum separation shown by physical analogue.

Table 2. Parameters for physical analogue for working face 745.

Rock	ρ/ (t·m^{-3})	σ_c/ MPa	σ_t/ MPa	ρ/ (t·m^{-3})	Model σ_c/ MPa	Material Ratio	Cohesion/ MPa	Friction Angle/(°)	Elastic Modulus E/(10^4 MPa)	Poisson Ratio μ
Argillite 1	2.73	53.40	2.30	1.50	0.294	8:0.9:0.1	2.04	46.3	5.8	0.35
Sandstone	2.97	110.40	8.55	1.63	0.479	9:0.9:0.1	4.50	34.6	7.7	0.32
Siltstone	2.73	61.91	12.9	1.50	0.276	10:1:0	4.40	34.2	7.3	0.38
Argillite 2	2.73	31.91	1.13	1.50	0.176	10:1:0	2.14	37.2	5.9	0.37
Sandy shale	2.73	31.91	0.40	1.50	0.176	10:1:0	2.04	42.0	5.5	0.40
Porphyrite	2.76	131.50	12.8	1.59	0.570	9:0.9:0.1	4.48	48.1	8.2	0.32

Note: MaterialRatio: sand: calciumcarbonate: gypsum = 1:1:1

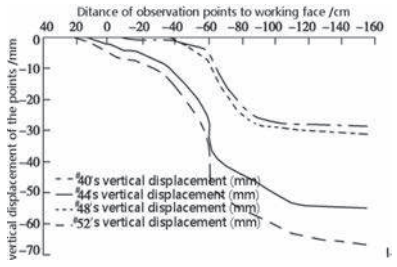


Figure 4. Vertical displacement curves at different positions in line 2 in overburden strata.

to the coal roof is, larger is the displacement. The displacement of point 40 > point 44 > point 48 > point 52. Closer the roof strata to the coal is, the less is the displacement of the stratum separation, but they fractured obviously. The strata (the white layers in Figure 3) close to the igneousrock separate obviously, as shown in Fig 4, but they did not fracture obviously—bending was the main deformation. This means that the surroundingrock of the stratum separation is characterized by impermeability and is favorable to form a water sell.

2.3 *The numerical simulation of FLAC3D*

Advance support stress zone of the coal wall is 10–14 m wide through the observation in Haizi Coalmine before, and the compacted zone is 60–75 m in the goaf after mining. The height of fractured zone is 8–10 times of the mining height, while the failure depth of floor is 10–12 m. According to the conditions of the working surface, the scope of the numerical simulation is 200 m long (60 m before and after the wall, 80 m of the mined area), 520 m wide (150 m upper and lower from roadway), 238 m high (55 m of floor in average, 169 m of roof). The floor elevation of the model is –395 m, while the roof is –157 m. The mechanical parameters are shown in Table 2.

With the same geometry with physical simulation, the model is divided into 68640 grids, 73677 nodes. Both the lateral sides and bottom are constrained by simply-supported structure, and the lateral sides are fixed for horizontal displacement, while the longitudinal displacement is allowed. Longitudinal displacement of the bottom is fixed, while the horizontal displacement is allowed.

Failure criterion is based on Coulomb Mohr Strength Theory. The results of the simulation is shown in Figure 5 and 6. As can be seen in Figure 5, just above the working face, the stress of igneousrock is $-0.15 \times 10-6 \sim 0.0$ Mpa, and the stress of coal measure strata is $-5.5 \times 10 \sim -5.0 \times 106$ MPa. The simulation also shows that stress gradient changes suddenly at the interface of strata separate obviously.

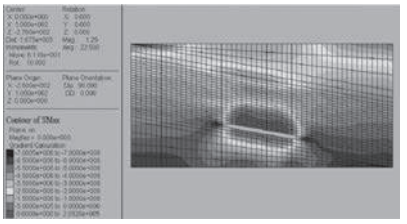


Figure 5. The maximum principal stress contours of surrounding rock.

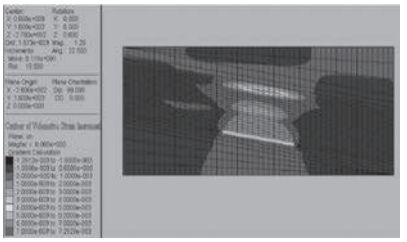


Figure 6. Contours of volumetric strain increment of surrounding rocks when working face advances 40 m.

The strain gradient change suddenly too in the interface of igneous rock and its covered layers, when working face advances 40 m as shown in Fig. 6. There is some difference between the results of the FLAC simulation and RFPA simulation used by literature[7], due to the difference of the structure of stratum and layout of excavating. As is shown in Figure 6, when the advance distance of mining working face is 40 m, volumetricstrain concentration behavior of the stratum under igneousrock occurred, and the stratum separation is obvious.

2.4 *Numerical simulation of distinct element code*

The two-dimensionalmodel is 200 m long, 138 m at vertical direction, 2.5 m of miningheight, and the grid partition is shown in Figure 7. The caving pace of main roof is 10 m. The load of upper boundary is applied by 300 m deep rock's weight, and the lower boundary is fixed in vertical direction. The left and right bordarys are fixed inhorizontal direction. The mechanicalparameters are shown in Table 2. Uatural caving method to manage the roof during mining.

The numerical simulation shows that the stratum separation under igneous rock is not obvious when the working face advanced for 200 m. The Figure 8 shows that stratum separation between igneous rock and its covered layers is obvious when the working face advanced for 250 m and 300 m, as seen in Figure 9 and Figure 10. The space of stratum separation becomes obviously bigger and bigger with the advance of working face.

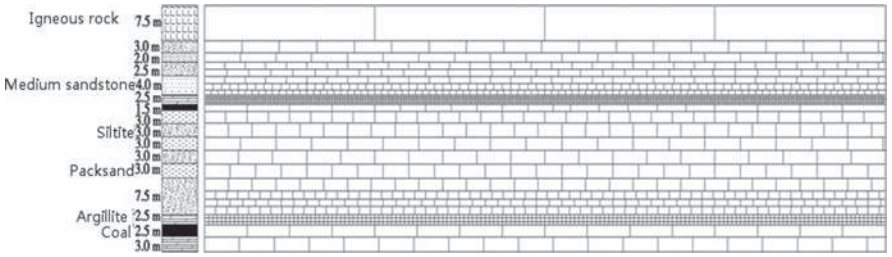


Figure 7. Roof stratum column and discrete elements for working face 745.

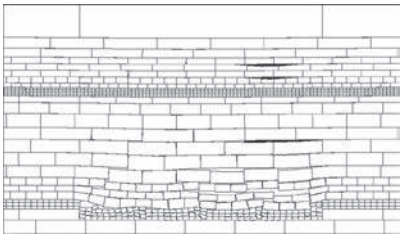


Figure 8. Roof stratum separation when working face advances 200 m according to discrete element simulation.

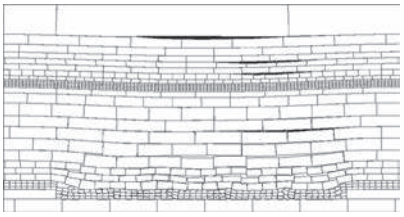


Figure 9. Roof stratum separation when working face advances 250 m according to discrete element simulation.

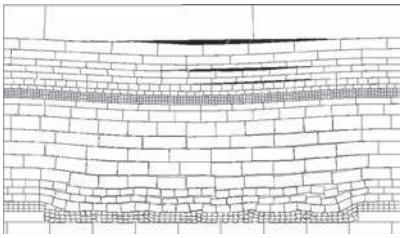


Figure 10. Roof stratum separation when working face advances 300 m according to discrete element simulation.

The results of UDEC simulation are accord with the key stratum theory (12). From the lithology we can see that there are four sub-key strata (three fine sandstone strata of 3 m thick and one medium sandstone of 5 m) and one main key stratum (thick igneous rock) in the roof of working face 745. The stratum separation formed in the bottom of sub-key stratum at first. When the first key stratum broke, the stratum separation occurred in the second key stratum. Then it developed to the third key stratum, and it ended in the main key stratum.

4 THE PREDICTION AND CONTROL OF THE WATER HAZARDS DUE TO STRATUM SEPARATION

Targeted measures was taken to control the water hazards according to the knowledge of stratum separation origins, that is to drill borehole to the water cells in the upper and lower roadways in the direction against advancing to drain as shown in Figure 11. In order to ensure that the bore would not be plugged due to the roof failure ahead of working face, water-pervious drivepipes were embedded in the bores.

This technology of mining-drainage obtains good results in application in the 1 st working face at Shendong Coalmine, in which average mining height is 5.3 m, and the roof strata consist of sandstone and argillite with 51 m in thickness. The water inrush started in the goaf when the working face advanced for 39 m, and water flow increased from 15 m^3/h to 212 m^3/h. The water inrush happened again with flow 1817 m^3/h when the face advanced for 55 m, seriously threatened the safety. The hazards were caused by quick-release of water from roof stratum separation. In order to prevent the hazards from happening again, six stages water drainage engineering were exercised anticipative goal was reached. 16865 m^3 of water were drained out within 20 days in the first stage of engineering. The waterinflow boreholes is shown in Table 3. Playing the same effect with the first one, the other 5 stages of drainage engineering are omitted here.

5 CONCLUSIONS

According to the analysis of hydrogeological conditions, mechanical model of the roof caving and bending, analog experiments, distinct element

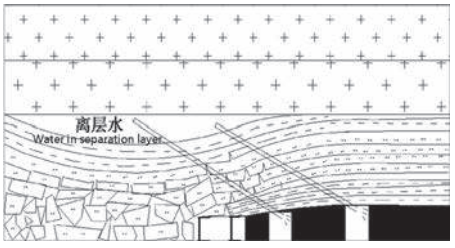


Figure 11. Layout of boreholes for roof cell water draining.

Table 3. The water quantity of drilling in the first drainage test at working face.

Borehole	aqf above coal m	Initial flow m^3/h	Max flow m^3/h	Average flow m^3/h	Total water value m^3
T2–3	44.84	10	40	15.71	6156.7
T2–2	55.05	8	60	0.26	83.9
T2–1	58.17	4	10	4.45	926.6
T3–3	60.49	27	85	38.06	6393.9
T1–2	58.82	9	90	45.89	3304.0

simulations and site observation at working face. The conclusions are drawn as follows:

1. The necessary condition to form a water cell is the combination of hard stratum and weak aquiclude below. The thicker hard stratum is, the bigger separation space will be. The more groups of strong—weak strata combination, the more separation cells will be.
2. The mining analog experiment demonstrated that the vertical displacement of hard rock stratum is much less than that of weak rock stratum in the same vertical line and obvious separation space occurred between hard and weak rocks in the mining process. The experiments confirm the results with th numerical simulation and key stratum theory.
3. The upper hard layer impact failure is cause of water cell break or water hazard.
4. The drilling through the water cell in the direction against advance to drain is the effective method to control the water hazard caused by water cell burst.

REFERENCES

Cao Sheng-gen, et al. 2000 Numerical simulation study on roof stability of face area in fully mechanized mining with top coal caving. *Chinese Journal of Rock Mechanics and Engineering,* 19(7): 632–636. (in Chinese).

Chen Xin-ming & Wang Jing-ming. 2008. Investigation on water hazards caused by burst of the water cell formed by overburden strata separation and its control in Haizi Coal Mine. *Journal of Hebei University Engineering (Nature Science Edition),* (1): 35–37. (in Chinese).

Dong Shu-ning & HU Wei-yue. 2007. The types of water hazards of coal mines in China and their control factors. *Coal Geology and Exploration,* (5): 34–37. (in Chinese).

Li Xin-yuan, et al. 2007. Storage and release regular of elastic energy distribution in tight roof fracture. *Chinese Journal of Rock Mechanics and Engineering,* 26(1): 2786–2793. (in Chinese).

Liu Hai-yan, et al. 2006. Study on stability characteristics of main seam roof in Yanzhou Coalfield. *Chinese Journal of Rock Mechanics and Engineering,* 25(7): 1450–1456. (in Chinese).

Meng Fan-long. 2007 Roof control technology for high coal mining face in "two hard" seam. *Coal Engineering*:7–9. (in Chinese).

Meng Zhao-ping.1999. Influence of sedimentary characters on stability of roof of coal seams (D). Beijing: Beijing China University of Mining and Technology, (in Chinese).

Mining Institute, 1981 China Coal Research Institute. The law of ground movement and overburden failure in coal mines. Beijing: China Coal Industry Publishing House, (in Chinese).

Pan Jie-nan, et al. 2005. Relationship between rock composition and texture of coal-bearing formation and its burst potential. *Chinese Journal of Rock Mechanics and Engineering,* 24(24): 4422–4427. (in Chinese).

Pan Jun-feng, et al. 2007. Study on movement and stress evolutionary process of impacted roof with 3DEC. *Chinese Journal of Rock Mechanics and Engineering,,* 26(1): 2546–2552. (in Chinese).

Qian Ming-gao, etal. 2003. The theory of key strata on ground control. Xuzhou: China University of Mining Technology Press, (in Chinese).

Su Zhong-jie, et al. 2003. Numerical simulation on mechanism of deformation of separated strata in overburden. *Chinese Journal of Rock Mechanics and Engineering,* 22(8): 1287–1290. (in Chinese).

Su Zhong-jie, et al. 2002 Application of mechanical model to deformation of covered rock separation strata. *Chinese Journal of Geotechnical Engineering,* (6): 778–781. (in Chinese).

Wang Jing-ming, et al. 1999. The height determination of the conductive fracture induced by high-face mining under desert. *Coal Geology & Exploration,* 27(1): 45–48 (in Chinese) t due to stratum separation.

Wang Jin-hua. 2003 The state in art for high rag effective mining technology in China. *Coal Science and Technology,* 31(1): 5–8. (in Chinese).

Xu Jia-lin, et al. 2004 Study and application of separation distribution and development in the process strata movement. *Chinese Journal of Geotechnical Engineering,,* 26(5): 632–636. (in Chinese).

Zhang Bai-sheng, et al. 2008 Application of contact element method in analyzing separation and deformation of the stratified roof. Journal of Coal Society, (4): 387–390. (in Chinese).

Progress in Mine Safety Science and Engineering II – He et al. (Eds)
© 2014 Taylor & Francis Group, London, ISBN 978-1-138-00122-0

Research on multivariate hierarchical analysis and evaluation on rock burst hazard

Zhengxing Yu
China Academy of Safety Science and Technology, Beijing, China

Fuxing Jiang & Quanjie Zhu
School of Civil and Environment Engineering, University of Science and Technology Beijing, Beijing, China

Jiajie Li
Norman B. Keevil Institute of Mining Engineering, University of British Columbia, Vancouver, BC Canada

ABSTRACT: In order to effective pre-assessment on the potential danger of the rock burst to the coal working face, a multivariate Analytic Hierarchy Process (AHP) is proposed based on the hazard zone and the hazard extents. The influencing factors of rock burst can divided to five sections, including mining depths, coal and rock structure, geological structures, overlying strata spatial structure and pillar induce. In this paper, a model was established using AHP. To define the single factor, a judgment matrix was constructed. To evaluate the single factor on a specific working face several methods were adopted, for example the theory of mining pressure and strata control, the project analogy method and the numerical simulation analysis. First, through the evaluation of single factor using a proper method, the hazard zone formed by a single factor was defined. Then, the interaction relationships among these impact factors in inducing rock burst were comprehensive analyzed. When a zone was simultaneously affected by several factors, the multi-factor coupling evaluation method was used to assess the hazard zones and the hazard extents. The proposed model was applied to evaluate the risk of rock burst, using the No.5305 working face in Jisan Coal Mine as a case study. The hazardous zones with different extents were confirmed. The prevention and control measures were used in advance and received a good effect. The feasibility and validity of the model for hazardous zones and hazard extents of rock burst was tested and verified.

1 INTRODUCTION

With the increment of exploiting depth, more and more coal mines are threatened by rock burst which occurs more and more frequently. It leads to seriously properties losing and casualties. Poland government ruled that coal mines must submit an evaluation report of rock burst risk before working face mining, and prevention and control measures should be formulated simultaneously, then the report and these measures were to be checked and modified strictly. This received a good effect (Ji Z, Sun C & Jiang F. 2008). Therefore, it's necessary to conduct a previous evaluation in the longwall mining working face under the condition of potential rock burst risk.

In terms of hazard evaluation of rock burst, many researchers have presented different evaluation methods. AE method of evaluating the danger of rock burst is presented (Dou L, He X & Bernard D. 2000).Weight-variable identification model of comprehensive evaluation on burst liability of coal and rock is built (Zhang K. & Xia J. 2004). By means of the in-situ stress measurement and calculation of stresses by non-linear finite element method, the effect of in-situ stress on rock burst was analyzed; a criterion is set up, based on the strength testing of coal; the criterion of energy is put forward to evaluate the risk of rock burst in the light of engineering practice (Yin, et al. 1997). Model of set pair analysis for evaluating rock burst risk is established in coal mines (Zhang, et al. 2011).Evaluation model of rock burst risk in mining based on blind data theory is presented (GAO, et al. 2010). Model of fuzzy comprehensive evaluation on rock burst danger in coal mine is presented (Yi, et al. 2011). Research of prediction model of rock burst in coal seam based on fuzzy neural network is presented (Liu X. 2008). Prediction and control of rock burst is conducted by evaluating rock mass stress (Chen X, Sun S. & Zhang B. 2002). Macro-evaluation method of rock burst risk in an "Isolated Island" working face is presented (Yu Z, Jiang F & Gui B. 2011).

Bayesian discriminant analysis is used for predicting coal and gas outbursts (Wang, et al. 2010). A coupled artificial neural network and fault tree analysis model to predict coal and gas outbursts is presented (Zhang R L & Lowndes I S. 2010). The catastrophe progression method in predicting coal and gas outburst is presented (Zhang, et al. 2009). A finite element perturbation method for the prediction of rock burst is presented (Sharan 2007). Fractal character and mechanism of rock bursts is presented (Xie & Pariseau. 1993). The Seismic Moment Method was applied to predict coal face rockbursts and microseismicity in deep longwall coal mining (Fujii Y, Ishijima Y & Deguchi G. 1997). The prediction method of rock-burst based on overlying multi-strata spatial structure theory is presented (Wang, et al. 2009).

Methods aforementioned all have received better effects, nevertheless it is difficult to evaluate rock burst hazard effectively by the presented evaluation methods with increasing of exploitation depth. the major performances are as follows: (1) it feels overtheoretical, not-easy to learn, and inconvenient to apply in site; (2) Most of these methods are used for macro evaluating for a whole working face or a mining area, while rock burst risk level in different zones of a certain working face is different; (3) the evaluation is implemented incompletely, only aiming at one or few influence factors. (4) More static evaluation methods are presented, lack of dynamic simulation evaluation with the process of face mining.

On the basis of engineering practice and theoretical research of rock burst prevention and controlling, overlying multi-strata spatial structure theory is applied to simulate longwall mining, and then multi-factor analytical hierarchy process evaluation method of rock burst risk is presented, based on geological, mining, and mining boundary conditions of longwall mining working face. The purpose is to investigate a practical, targeted and operable method, which can be applied to beforehand evaluate the potential dangerous areas and criticality, in order to meet the engineering requirements in site.

2 FACTORS INFLUENCING ROCK BURST AND CORRESPONDING EVALUATION METHODS

There are plenty of influence factors on rock burst, and the mechanism is complicated. For customized evaluation of rock burst risk, influence factors induced rock burst need to be analyzed by selecting appropriate evaluation methods, with the condition of specific zone and mining conditions.

2.1 *Factors influencing rock burst*

Whether rock burst occurs in bursting liability of coal seam which had been tested, the dominating influence factors are as follows:

(1) Exploitation depth

The pre-mining status of stress can be described by vertical stress and horizontal stress. The vertical stress and horizontal stress are both compressive stress, and the horizontal stress is the force derived from the vertical stress. Vertical stress increases in direct proportion with the increasing depth, but the horizontal stress, exceeding a certain value of depth, is non-linear with increasing depth. Increasing extent is different along with properties of the surrounding rock, and the basic variation is that the increasing proportion along with mining depth is expanded gradually. Consequently, the deeper mining depth and the higher stress level are more liability to burst. It is generally acknowledged that the critical depth of bursting is 500–600 m in a single gravity stress field.

Different depth ranges, due to the influence on mining depth, are classified as an interval of 100 m.

(2) Coal and rock structure

Coal and rock structure refers to coal and rock strata, rock set and key strata, which may induce rock burst, also be called bursting strata. Bursting strata are divided into the single stratum and combined strata, therefore, the motion effects of a single bursting stratum and the spatial structure of combined strata need to be investigated. Single stratum includes hard roof, hard coal seam, hard floor and key strata; combined strata refer to the combination of the single stratum aforementioned.

According to transferring strata beam theory (Song 1989), abutment pressure distribution along the strike and dip in longwall face is related to strength and motion evolution of rock beams themselves. The lower coal strength, the higher strength of rock beam, the extent of abutment pressure will be larger, consequently the coefficient of stress concentration becomes small and the risk of bursting will be diminished. Conversely, the higher coal strength, the lower rock beam strength is lower, so the extent of the abutment pressure will be greater and the stress concentration coefficient becomes large, the risk of bursting is higher. According to the theory of key strata (Qian, et al. 2003), mine earthquake or rock burst is to be induced by key strata instability.

The factors of coal and rock structure for rockburst risk are included hard roof (main roof), hard coal, hard floor and key strata et al. Different combinations represent distinct dangerous levels. For example, Huafeng Coal Mine, which the characteristics of coal and rock structure are hard main

roof, hard coal seam, hard floor and huge thick conglomerate overlying, is one of most bursting threatened mines in China. Additionally, there are other types of coal and rock structure.

(3) Geological structure

Practice has proved that the tectonic stress resulting in rock-burst mines is relatively greater in the zone near geological structures where coal seams get thinner or have changing inclination, where tectonic stress appears, and where stress occurs in faults, folds, coal seams and strata. As a principal factor inducing rock burst, the tectonic stress generated from fault activation and anticline has a significant influence on producing rock burst. Stress largely concentrates on the shaft and fault of anticlines, so the rock bursts and mine earthquakes occurring in adjacent working faces or mines have close ties to the faults and structures of the anticline. When a working face is close to these structures, it will suffer from a significantly increased and intensified rock burst.

Around the zone where coal seams get thinner and where faults, folds and other geological structures occur, the tectonic stress resulting in rock-burst mines is relatively greater. As a principal factor inducing rock burst, the tectonic stress generated from fault activation and anticline has a significant influence on producing rock burst. Stress largely concentrates on the shaft and fault of anticlines, so the rock bursts and mine earthquakes occurring in adjacent working faces or mines have close ties to the anticlinal structure and faults. When a working face is close to these structures, it must get work prepared for pressure relief and prevention in advance. In this paper, the microseismic monitoring approach is used to study the classification of structure-controlled bursts and how to make an early warning, and it is proposed to divide the structure-controlled bursts into 2 types, i.e., pressurization and decompression.

(4) Spatial structure of overlying strata

Jiang has proposed a theory on the spatial structure of overlying strata (Jiang 2006), which refers to the three-dimensional structure formed after the rupture of overlying strata, including macroscopic hinged structures in the rupture zone and mesoscopic fractures at the edge of rupture zone, namely, the "θ" type of island mining face with four-side goaf and a support in the center, the "O" type spatial structure of mining face with one-side goaf but without a support in the center, the "S" type spatial structure of mining face with double-side goaf, and the "C" type spatial structure of island mining face with three-side goaf. As the spatial structure of overlying strata forms, the rupture and high stress field of the roof and floor are transferred and thus rock bursts may be induced.

The spatial structure of overlying strata mainly affects the following phases in push-mining of working faces, namely, the phase when the basic roof fractures for the first time, the phase in the square of working faces, the phase in the square of double working faces, the phase in the square of tree working faces, and the phase in periodic weighting of main roofs. Based on the above phases, we can differentiate the risk zones of rock burst, which are affected by the spatial structure of overlying strata.

(5) Induced by coal pillar

Coal pillar is an isolated body during exploitation. Since the presence of residual coal pillar, the stress field of coal pillar is different from that of other areas. Island-shaped or peninsula-shaped pillar may sustain the bearing pressure caused by multiple goaf directions. Not only the pillar itself is prone to burst, but also the upper pillar will pass concentrated stress to the lower pillar, which is consequently easier to suffer from rock burst.

Supported by the remaining pillar, the upper rock did not break or subside, while the surrounding rock above the goaf has broken and subsided, so there definitely exists high stress above the goaf area around the coal pillar. Taking the coal pillar as a center, there are pressure zone and strong shear zone extending outward. The following two theories can explain how rock burst occurs in coal pillar area: ① the theory on the burst of high-risk areas far from the coal pillar. It means that the high stress difference generates a strong shear force, resulting in fracture and release of rock burst induced by elastic energy; ② the theory on the burst of high-risk areas close to the coal pillar. It refers that the coal pillar itself loses stability under strong shear force and thus induces rock burst. Therefore, the strong shear is the root cause to induce rock burst.

The hazard of rock burst, which is affected by coal pillar, can be evaluated by calculating the stress concentration factor of coal body, and a quantitative analysis on different stress concentration factors is possible when dividing those factors into several levels: 1.5 ~ 2, 2 ~ 2.5, 2.5 ~ 3 and >3.

2.2 *Evaluation methods of rock burst risk*

Different evaluation methods based on various factors, the main evaluation methods are underground pressure and strata control analysis method, engineering analogy method and numerical simulation analysis method.

(1) underground pressure and strata control analysis method

Underground pressure and strata control analysis methods mainly contain that whether the stress

induced by mining reaches to the stress level of bursting, whether the difference of high stress would be generated by strata motion, how much is the high stress magnitude of the difference, and the dynamic distribution of mining stress field. Instability of the key strata, of which the characteristics and the influence of mining need to be analyzed, would induced rock burst or mine earthquake. The dangerous zones can be determined by stress level and status of coal and rock.

(2) engineering analogy method
Through similar conditions, there is something in commonality and differentia of bursting. The longwall face to be evaluated is analogy with the ones adjacent or other mines burst, to identify commonalities and determine the dangerous zones and magnitudes.

(3) Numerical simulation analysis method
Numerical simulation analysis method is an approximate method, such as boundary element method, finite element method, discrete element method and discontinuous deformation method (DDA) etc. It is assumed that the coal and rock mass is homogeneous and isotropic, and can simulate the stress distribution and concentration in certain mining areas, sequentially analyze the magnitudes of bursting risk. Investigations on rock burst are presented using numerical simulation analysis method, which has become a powerful tool for rock mechanics and rock engineering.

2.3 *Multivariate hierarchical evaluation*

The multivariate hierarchical analysis and evaluation on rock burst hazard refers to the process of determining the risk zone through univariate evaluation by applying mining pressure theory and approaches like engineering analogy and numerical simulation. Such process is based on the conditions such mining depth of specific faces, coal structure, geological structure, spatial structure of overlying strata and mining boundaries. The factors inducing rock burst may act individually or work together, and the same region may be influenced by several different factors, which will lead to local stress concentration. Make a comprehensive analysis on the act of these factors in inducing rock burst, adopt multivariate hierarchical analysis, build a judgment matrix, calculate the feature vector and the maximum eigenvalue and check their consistency, comprehensively analyze the weight of various factors on inducing rock burst, and evaluate the risk factors when the same area is influenced by several factors at the same time. The higher the burst risk factor, the greater the risk degree. The evaluation results serve as a basis to determine the three levels of areas with varying risk degrees: general risk zone, moderate risk zone and high-risk zone.

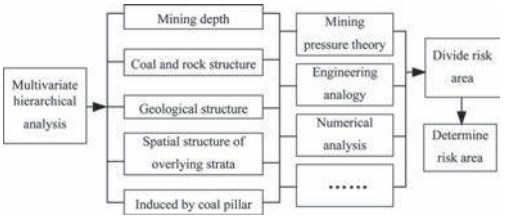


Figure 1. Roadmap of evaluation technologies.

Fig. 1 is the technological roadmap of evaluating the rock burst hazard of working faces through multivariate hierarchical analysis.

3 METHODS ESTABLISHMENT OF EVALUATION MODEL

Analytic hierarchy is an approach proposed by the American professor Saaty for a hierarchical analysis on decision weights (Saaty & Alexander. 1989). The approach makes a combination between quantitative analysis and qualitative analysis, applies the experience of decision-makers in determining the relative importance of criteria measuring whether goals can be achieved, gives a reasonable weight to each criterion of all decisions, and obtains the priorities of those decisions by the weights, thus effectively applying to those projects difficult to be resolved by quantitative methods.

Based on the nature of issues and the overall objective to be achieved, analytical hierarchy process decomposes the issue into different constituent factors, and arranges the factors at different levels in accordance with their correlation and affiliation to form a multi-leveled analytical structure model, which ultimately boils the issue down to how to determine the relative important weights or priorities at the lowest level relative to the highest level.

(1) Establishment of hierarchical model
Complex issues are divided into so-called elements, which are divided into several groups according to their different properties and has formed different levels. Elements at the same level are taken as criteria to dominate certain elements at the next level. At the same time, they are dominated by elements at the previous level. The dominance between levels is not necessarily absolute. Namely, there can be such element that doesn't dominate all elements at the next level. The number of levels and complexity of issues have a relation to how detailed the analysis requires to be. There cannot be more than nine

factors at each level. A good hierarchical structure is extremely important for solving an issue.

Divide the goals of decision, considerations (decision criteria) and decision-making objects into top level, middle level and lowest level according to their relations, and draw a hierarchy chart.

Top level: the purpose of decision-making; issues to be solved.

Lowest level: decision alternatives.

Middle level: considerations; decision-making criteria.

For neighboring levels, the top one is called target level, and the lower one is called level of factors.

(2) Pairwise comparison constructed for judging matrix

After the establishment of the hierarchy, the affiliation is be determined between elements of upper and lower levels. Take an upper-level element A_k as a criterion, which dominates the next level's elements $B_1, B_2, \ldots, B_n$. Our aim is to give corresponding weights to $B_1, B_2, \ldots, B_n$ based on their relative importance under the criterion A_k.

If there are only qualitative results when determining the weights between factors at all levels, usually it is not easy to be accepted by others. Therefore, Saaty, et al. proposed the method of consistent matrix:

① Avoid putting all factors together and adopt the method of pairwise comparison.

② In order to improve accuracy, relative scale is used at this time to minimize the difficulty when factors of different nature are mutually compared.

Suppose there are n factors $x_1, x_2, x_3, \ldots, x_n$, whose importance to the decision-making (weights) are $v_1, v_2, v_3, \ldots, v_n$. Make a pairwise comparison between the importance of all factors, and their mutual relation can be represented by the following matrix:

$$\begin{bmatrix} v_1/v_1 & v_1/v_2 & v_1/v_n \\ v_2/v_1 & v_2/v_2 & v_2/v_n \\ v_n/v_1 & v_n/v_2 & v_n/v_n \end{bmatrix}$$

The matrix is called judgment matrix. It makes a pairwise comparison for the importance of certain factors at the same level (single hierarchical arrangement), and quantizes the relative importance of all factors through the approach of scaling.

Judgment matrix presents the relative importance of all factors at this level in comparison with a certain factor at the above level. For criterion A_k, which element is more important, B_i or B_j? How much more important? A certain value is required to be given to differentiate the importance. The element a_{ij} of judgment matrix is given by Saaty's approach of 1–9 scaling, which is a good way to quantize the judgment of thinking. When making a differentiation, people always use words like "the same", "greater", "much greater", "extremely greater". If further subdividing these levels, compromise wording can be inserted in two adjacent levels, so for most decision-makings, 1–9 scaling is adaptive, as shown in Table 1. As the scaling primarily reflects the quantitative value of interrelationship between qualitative indexes, its size of value is not important. The key point is whether the interrelationship of its values can accurately reflect people's judgment on the qualitative importance.

Table 1. Meaning of 1–9 scaling.

Scaling	Meaning
1	It represents that two factors have the same importance in comparison
3	It represents that one factor is a little more important compared to another factor
5	It represents that one factor is obviously more important compared to another factor
7	It represents that one factor is a highly more important compared to another factor
9	It represents that one factor is extremely more important compared to another factor

2, 4, 6 and 8 represents the median value of the above determination.

(3) Calculate relative weights of elements under single criterion

This step is to calculate the ranking weights of element $B_1, B_2, \ldots, B_n$ under the criterion A_k, and to check their consistency. For $B_1, B_2, \ldots, B_n$, judgment matrix X is obtained through pairwise comparison to solve the eigenvalue.

$XW = \lambda_{max} W$. By calculating the largest eigenvalue λ_{max} of judgment matrix, the obtained W adopts ranking weight under criterion C_k after normalized as element $B_1, B_2, \ldots, B_n$, where W is the corresponding feature vector, that is the importance (weight) vector $W = [w_1, w_2, w_3, \ldots w_n]^T$. This method is called as eigenvalue approach for calculating ranking weights. λ_{max} exists with uniqueness, and W may be composed of positive components. Except a lack of constant multiple, W is unique. The calculation of λ_{max} and W generally adopts the power method. If precision is not highly demanded, we can calculate λ_{max} and W through approximation methods, which mainly include sum method and root method. This paper applied the root method for calculation with main steps as follows: first, normalize the elements of X by the column; second, add the elements of A by the row; third, normalize the resulting rows and vectors to

obtain the ranking weight vector W; fourth, calculate λ_{max} in accordance with formula (1):

$$\lambda_{max}=\sum_{i=1}^{n}\frac{(XW)_i}{nW_i} \tag{1}$$

The $(XW)_i$ in Formula (1) represents the ith element of XW.

Eigenvalue method is the earliest approach proposed in *AHP* to calculate ranking weight vectors in wide use. When judging the matrix structure, consistency is not required due to the complexity of objects and the diversity of people's knowledge. But it's reasonable to require a general consistency in the judgment, so it normally violates our common sense if a case goes as: A is extremely more important than B, B is extremely more important than C, and C is extremely more important than A. Moreover, when the judgment deviates too much from consistency, there will be a problem if decisions are made on the calculation results of ranking weight vectors. So a consistency test is required after getting the λ_{max} by steps as follows:

$$C.I.=\frac{\lambda_{max}\text{-n}}{\text{n-1}} \tag{2}$$

Where n is the order of judgment matrix.

① Average random index $R.I.$ of consistency

Average random index of consistency is obtained by taking the arithmetic mean from repeated (500 times) calculation of random judgment matrix eigenvalues. Saaty's average random indexes of consistency are shown in Table 2.

② Calculate the consistency ratio $C.R.$

$$C.R.=\frac{C.I.}{R.I.} \tag{3}$$

When $C.R.$ <0.1, it is generally considered that the consistency of judgment matrix is acceptable.

(4) Calculate the combination weight of elements at all levels

In order to obtain the relative weight of all elements at each level in the hierarchy compared to the overall objective, we need to appropriately combine the results of the third step, and check the general consistency of the determination. This process is carried out in turn from the highest level to the lowest level. The end results involve the lowest level elements, the relative weight of decision priorities and the consistency checking on the judgment of the entire hierarchical model.

AHP's final result is the weight of decision priorities relative to the overall objective, and gives the overall consistency index of all judgments in the entire hierarchy, which is the foundation of the combination's ranking weight, and decisions can be made accordingly.

Table 2. Average random index of consistency.

Order n	1	2	3	4	5	6	7	8	9
R.I	0	0	0.58	0.90	1.12	1.24	1.32	1.41	1.45

3.1 *Hierarchical model of risk evaluation*

The factors inducing rock burst may act individually or work together, and the same region may be influenced by several different factors, which greatly increases the risk of rock burst in the region.

Establish a hierarchical model of evaluation system for rock burst hazards. For the problems concerning multivariate hierarchical analysis and evaluation on rock burst hazard, divide them into 5 levels, i.e., mining depth, coal structure, geological structure, spatial structure of overlying strata and that induced by coal pillar. Different properties are channeled to different groups at different levels, as shown in Fig. 2, and determine the

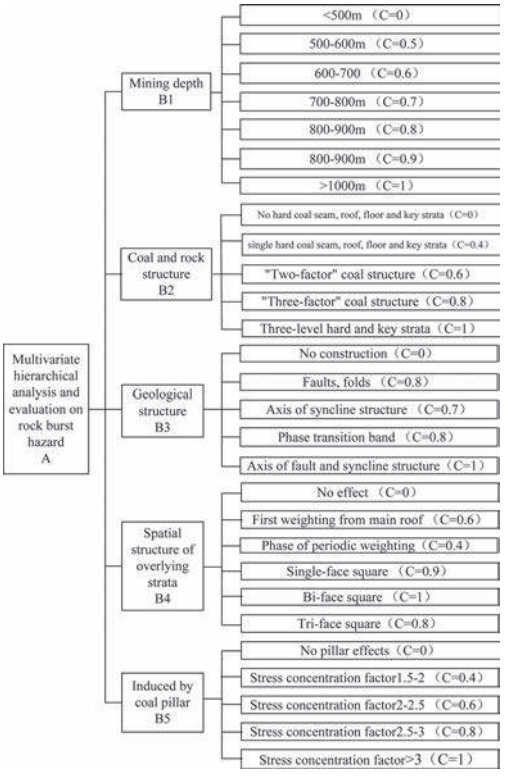


Figure 2. Rock burst hazard multivariate hierarchical model.

evaluation index. After getting the corresponding weight of evaluation indexes, calculate the risk index of burst hazard and determine the degree of risk. The region's risk index of rock burst hazard is the overall objective A. B_1, B_2, B_3, B_4 and B_5 respectively represent the mining depth, coal structure, geological structure, spatial structure of overlying strata and the quantized value of inducing factors of coal pillar. K_1, K_2, K_3, K_4 and K_5 respectively represent the mining depth, coal structure, geological structure, spatial structure of overlying strata and the weight of inducing factors of coal pillar. The relation between the overall objective A and B-level elements can be expressed by formula (4).

$$A = K_1B_1 + K_2B_2 + K_3B_3 + K_4B_4 + K_5B_5 \quad (4)$$

Based on the analysis on causes to rock burst hazards, the author made a thorough study in various factors, in order to give an empirical relationship for guiding on-site production.

(1) Construct a judgment matrix

Make a pairwise comparison for the above five levels of factors, construct a judgment matrix according to the 1–9 scaling, and the matrix is as follows:

$$\begin{bmatrix} 1 & 1/2 & 1/3 & 1/3 & 1/2 \\ 2 & 1 & 2 & 1/2 & 2 \\ 3 & 1/2 & 1 & 2 & 1/2 \\ 3 & 2 & 1/2 & 1 & 1/2 \\ 2 & 1/2 & 2 & 2 & 1 \end{bmatrix}$$

(2) Calculate the maximum eigenvalue and eigenvector

After calculation, the eigenvector of judgment matrix is W = [0.0844, 0.2543, 0.2022, 0.2140, 0.2451]^T, and the largest eigenvalue is $\lambda_{max} = 5.6035$.

(3) Consistency check

$C.R.$ = 0.065 <0.1, so the consistency of judgment matrix can be accepted.

The multivariate analytic hierarchy relationship of rock burst hazard is as follows:

$$A = 0.0844B_1 + 0.2543B_2 + 0.2022B_3 + 0.214B_4 + 0.2451B_5.$$

Finally, determine the degree of risk in a given region through Table 3.

Considering the complexity of rock burst, the above formula of general experience can basically be applied to most mining cases, but in specific conditions, it should be analyzed based on the actual situation, in order to re-construct the judgment matrix and have a consistency checking and determine the multivariate hierarchical relationship of rock burst hazard.

Table 3. Comparison table for risk factors and the degree of risk.

Risk factor	$A < 0.33$	$0.33 \le A < 0.66$	$A \ge 0.66$
Degree of risk	General risk area	Moderate risk area	High-risk area

4 ENGINEERING APPLICATIONS

Since 2003, several serious rock bursts have occurred in Jisan Coal Mine during extraction. Hundreds of meters of roadway were destroyed, and dozens of single props were damaged, posing a big threat to mining safety.

Working Face No. 5305 is Shanxi formation coal seam No. 3 with thickness of 1.2 ~ 3.6 m. The working face is westward adjacent to the goaf of working Face 5306, and eastward adjacent to the goaf of Face No.5304. It belongs to island face, with a mining depth of 615 ~ 702 m but without immediate roof. The main roof is in fine sandstone and siltstone, strong and stable, with a thickness of 13.57 ~ 25.49 m. The overall trend of the coal bed shows a relived syncline, which is high in the north and south and low in the middle. Most faults are developed in the south wing of the syncline, with a main of direction of SE or SEE. Revealing faults according to the actual situation, it is expected to expose 15 faults with a fall of 1.3 ~ 4.6 m. Working Face No.5304 is a skip-mining face, and a coal pillar of 200 m long is left in the centre of face. The tendency of coal seam No.3 and rock burst is identified as weak shock. For "island" faces with complex mining environment, an evaluation on rock burst hazard before mining is needed in order to take preventive measures in advance.

4.1 *Analysis on influencing factors*

First, apply the theory of strata movement and underground pressure, combine with the mining conditions of Face No. 5305, and determine the influencing factors of rock burst. Second, adopt methods such stress analysis, evaluation on rock pressure and geological structure and engineering analogy to assess potential risk zones.

(1) Evaluation on the relation between mining depth and rock burst hazard

Working Face No. 5305 has an average mining depth of 658 m, which exceeds the critical depth of incurring a rock burst, so its depth meets the condition.

(2) Evaluation on the relation between coal structure and rock burst hazard

Make an analysis on the distribution of critical rock stratum that induces burst hazard and its relationship with the location of coal seam: About 20 m above the main roof of coal seam, there is fine sand strata with a thickness of 9.76 ~ 21.65 m. The presence of this hard roof will aggravate the stress concentration of working face, crossheading and area near the pillar. It is a crucial stratum for inducing rock burst.

There is extremely thick and hard stratum of red medium-sand, 132.2 ~ 186.3 m away from the roof of coal seam No.3. The key stratum may induce mine earthquake if disturbed. Since the stratum is far from the earth's surface (about 340 m), there won't be direct impact on the earth's surface during a mine earthquake. This stratum is also critical for inducing rock burst.

(3) Evaluation of engineering analogy on the relation between geological structure and rock burst

Geological structure is one of the factors inducing rock burst. Stress can locally concentrate in the axis of the syncline and in the vicinity of faults, thereby inducing rock burst.

The coal stratum of Face No.5305 has an overall trend of a relived syncline, which is high in the north and south and low in the middle, and there is large tectonic stress near the axis. The fault is in the vicinity of synclinal axis, indicating that the tectonic stress is strong in the premise, so the geological structure (relived syncline and fault) has a possibility of inducing rock burst.

The rock burst happened in the mine's working Face No.6303 and No.6304 was caused by geological structure. See Table 4 for an engineering analogy on the geological structure of three faces.

According to the engineering analogy of geological structure, it is determined that rock burst may occur in the working face, which is a risk zone to induce rock burst since it is affected by geological structure, see Fig. 3 (a).

Table 4. Engineering analogy for rock burst induced by geological structure.

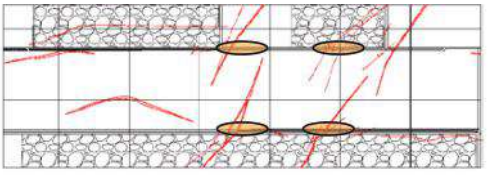
Working face	Syncline	Axis fault	Oblique fault, goaf	Extent of burst
6303	Yes	Yes	No	Rock burst occurs.
6304	No	No	Yes	Strong vibration in coal wall and roof, stop mining to deal with it.
5305	Yes	Yes	Yes	Ground pressure may occur.

(4) Evaluation on the relationship between the movement of the spatial structure of overlying strata and dynamic disasters (rock burst and mine earthquake)

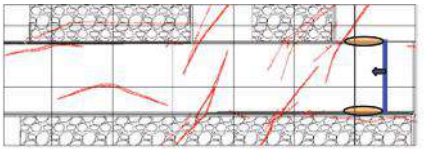
With the advance of working face, the spatial structure of overlying strata will gradually form the shape of "S" and "C". If stress is aggregated to a concentration, it may induce rock dynamic disasters (rock burst and mine earthquake).

① Initial fracture of main roof

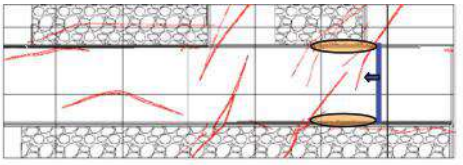
With the recovery of working face, the first weighting step of main roof is about 60 m according to mining experience of the mine. Taking a comprehensive



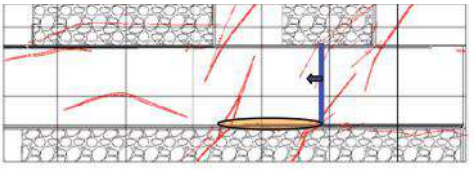
(a) Geological structure and risk zone of rock burst



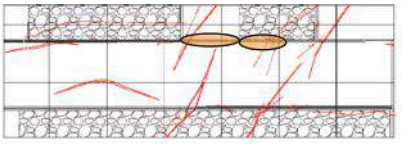
(b) First weighting of main roof and risk zone of rock burst



(c) Square of working face and risk zone of rock burst



(d) Square of double face and risk zone of rock burst



(f) Hazardous zone of rock burst affected by C-shape structure of overlying strata

Figure 3. Multi-factor-induced burst danger zone.

consideration on the impact of faults, the risk zone is identified as shown in Fig 2 (b).

② Square of working face

When the recovery of working face reaches about 220 m with a range of 200 ~ 230 m, it goes into the phase of face square. Taking a comprehensive consideration on the impact of two faults nearby, the risk zone is identified as shown in Fig 2 (c).

③ Square of double face and impact of three faces

There is extremely thick and hard stratum of reddish-brown fine-grained sandstone above the coal seam, and it is a critical stratum affecting the recovery of working face. When face recovery reaches from 200 m to 450 m and forms double-face square with Face 5306, the act of mining may have an impact on the upper hard-thick strata.

In the process of mining, evaluation of numerical simulation is adopted in order to study the changes of stress, the fracture damage, and the possibility of inducing mining earthquake or rock burst. Establish a three-dimensional numerical model, the top of which is 331 m vertically away from the ground. Through simulation, the hard roof might have certain impact on the coal wall of working face in the process of recovery. The thick and hard critical stratum may be disturbed, and the hard-thick strata in the overlying stratum of coal seam may suffer from a fracture, so there is a possibility of instability, which induces mining earthquake. A large amount of elastic energy will be released in the process of rock fracture, and it can easily lead to mining earthquake or rock burst. As it is far away from the ground, there won't be an impact on the earth's surface, but there is a possibility of mining earthquake inducing rock burst in front of the working face. According to the numerical simulation results, the scope affected by the fracture of thick and hard critical stratum and main roof ranges 350 ~ 435 m from the open-off cut, and the risk zone in this phase is identified as shown in Fig. 3 (d).

(4) Phase of periodic weighting

After the periodic weighting of main roof, risk will rise in the hazardous zone within a scope of 70 ~ 100 m in front of the working face. When working face pushes through the area of coal pillar, the risk of burst for the face is mainly affected by the structure of "C"-shape overlying stratum. According to the movement of "C"-shape overlying strata, the risk zone is identified as shown in Fig. 3 (e).

(5) Evaluation on rock burst induced by coal pillar

The coal pillar left in the centre of adjacent skip-mining Face No. 5304 may lead to local stress concentration and an accumulation of a large amount of elastic energy, so there is a risk of rock burst.

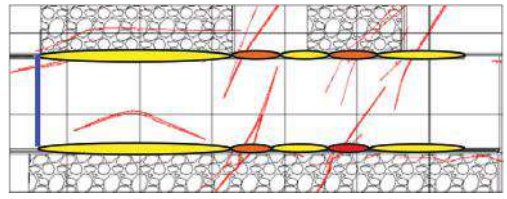


Figure 5. Risk zone of burst determined by multivariate analytic hierarchical evaluation.

Evaluate the risk of rock burst induced by coal pillar though engineering analogy. In Sep. 9, 2006, the boring head of Face No. 1410 in Huafeng Coal Mine induced rock burst and caused great damages and casualties. Microseismic monitoring displayed a mine earthquake magnitude of 2.0 and energy of 2.2×10^7 J.

In a range of 380 ~ 730 m from the open-off cut, Face No. 5305 is threatened by the rock burst which may be induced by coal pillar. Based on the above analysis, the mining height of Face No. 5305 is small, and there is fully mechanized coal mining on one side of full-height at a time. It is unlikely to have burst of high intensity, but there is still a possibility. Face No. 5305 has strong shear zone in both sides of the coal pillar, and the risk zone is shown in Fig. 3(f).

(6) Multivariate analytic hierarchical evaluation on the risk of rock burst and the determination of risk zones

According to the multivariate evaluation on the risk of rock burst, these areas are divide into three categories: 6 general risk zones (yellow), 3 moderate risk zones (orange), 1 high-risk zone (red), as shown in Fig. 5.

5 CONCLUSIONS

1. Areas with different degrees of risk are determined according to the multivariate hierarchical evaluation on the risk of rock burst in working face. The method focuses on specific conditions and has a dynamic and integrated feature. Since some of the indexes depend on experience, it belongs to semi-quantitative evaluation method that can more accurately determine the risk of hazardous area.
2. By means of numerical simulation, in double face square, the hard-thick strata above the coal seam may be affected by the mining area and have mining earthquake induced by the hard-thick strata. It won't produce disastrous effects to the ground, but may lead to a sharp concentration of coal seam stress, which may induce burst.

3. Based on the evaluation results, take the principle of "pressure relief before mining" for risk zones in advance. Design for pressure relief according to the degree of risk during construction while checking the stress in process of mining to ensure that measures are in place for getting rid of danger and playing a relief effect.

ACKNOWLEDGEMENTS

The research presented in this paper was supported by National Key Basic Research Development Plan (973 Program) (2010CB226803), and State Science and Technology Projects (2011ZX05040–001).

REFERENCES

Chen X, Sun S. & Zhang B. 2002. Prediction and control of rock burst by evaluating rock mass stress. *Journal of Liaoning Technical University* 21(4): 443–445.

Dou L, He X & Bernard D. 2000. Ae method of evaluating the danger of rock burst. *Journal of China University of Mining & Technology* 29(1): 85–88.

Fujii Y, Ishijima Y, Deguchi G. 1997. Prediction of coal face rockbursts and microseismicity in deep longwall coal mining. *International Journal of Rock Mechanics and Mining Sciences* 34(1): 85–96.

Gao F, Zhang Z, Gao Y, et al. 2010. Evaluation model of rock burst risk in mining based on blind data theory. *Journal of China Coal Society* 35(S): 28–32.

Jiang F. 2006. View point of spatial structures of overlying strata and its application in coal mine. *Journal of Mining & Safety Engineering* 23(1): 30–33.

Ji Z, Sun C & Jiang F. 2008. Present status and analysis on rock burst prevention and control technology in Poland. *Coal Science and Technology* 36(1): 11–14.

Liu X. 2008. Research of prediction model of bumping pressure in coal layers based on fuzzy neural network. *Industry and Mine Automation* (1): 8–12.

Qian M, Miao X, Xu J, et al. 2003. *The theory of key strata in ground control*. Xuzhou: China Mining University Press.

Saaty, T & Alexander, J. 1989. *Conflict Resolution: The Analytic Hierarchy Process*. New York, New York: Praeger.

Sharan S K. 2007. A finite element perturbation method for the prediction of rockburst. *Computers & Structures* 85(17–18): 1 304–1 309.

Song Z. 1989. *Practical mining pressure control*. Xuzhou: China Mining University Press.

Wang C, Jiang F, Sun Q, et al. 2009. The forecasting method of rock-burst and the application based on overlying multi-strata spatial structure theory. *Journal of China Coal Society* (2): 150–155.

Wang C, Wang E, Xu J, et al. 2010. Bayesian discriminant analysis for prediction of coal and gas outbursts and application. *Mining Science and Technology* (*China*) 20(4): 520–523.

Xie H P, Pariseau W G. 1993. Fractal character and mechanism of rock bursts. *International Journal of Rock Mechanics and Mining Sciences & Geomechanics Abstract* 30(4): 343–350.

Yi E, Mou Z, Dou L, et al. 2011. Study on fuzzy comprehensive evaluation on mine pressure bumping dangers. *Coal Engineering* (6): 70–73.

Yin G, Xian X, Jin L, et al. 1997. The effect of crustal stresses on rock burst and evaluation of zone prone to rock burst. *Journal of China Coal Society* 22(2): 22–27.

Yu Z, Jiang F & Gui B. 2011. Application of macro- evaluation method of rock burst hazard in an "Isolated Island" face. *Mining Safety & Environmental Protection* 38(5): 30–32.

Zhang K. & Xia J. 2004 Weight-variable identification model of comprehensive evaluation on burst liability of coal. *Chinese Journal of Rock Mechanics and Engineering* 23(20): 3 480–3 483.

Zhang R L & Lowndes I S. 2010. The application of a coupled artificial neural network and fault tree analysis model to predict coal and gas outbursts. *International Journal of Coal Geology*. 2010, 84: 141–152.

Zhang T J, Ren S X, Li S G, et al. 2009. Application of the catastrophe progression method in predicting coal and gas outburst. *Mining Science and Technology* (*China*), 2009, 19(4): 430–434.

Zhang Z, Gao F, Xu A, et al. 2011. Model for estimating rock burst risk in a coal mine based on set pair analysis. *Journal of China University of Mining & Technology* 40(3): 379–384.

Progress in Mine Safety Science and Engineering II – He et al. (Eds)
© 2014 Taylor & Francis Group, London, ISBN 978-1-138-00122-0

Study on stability of thick-hard key stratum based on numerical simulation in longwall mining

Zhengxing Yu
China Academy of Safety Science and Technology, Beijing, China
School of Resources and Safety Engineering, China University of Mining and Technology (Beijing), Beijing, China

Fuxing Jiang, Quanjie Zhu & Sitao Zhu
School of Civil and Environment Engineering, University of Science and Technology Beijing, Beijing, China

ABSTRACT: To study the dangerous of rock burst induced by instability of key strata overlying, the stability of longwall mining face need to be investigated before mining. Taking thick-hard key strata of overlying mining face No. 5305 in Jinsan Coal Mine for example, the stability of numerical simulation for mining was performed. The results showed that the height of roof strata rupture to the key strata beneath when the face advancing 350 m; distribution of plastic zone along strike and dip direction indicated key strata failure, when face advancing 435 m, the dangerous distance of rock burst impacted by failure of key strata is 350 ~ 435 m away from open-off cut. It is practiced that, while the face advancing to this area, mine earthquake was reduced by the thick key strata failure, so there is no induced burst, due to take stress relief in advance. Prevention goal of mine earthquake without disaster is realized.

1 INTRODUCTION

Rock burst is one of the serious disasters in coal mine exploiting. With the increment of exploiting depth in China, more and more coal mines are threatened by rock burst and mine earthquake which occur more and more frequently. It leads to seriously properties losing and casualties. Key Strata Theory (Qian M, et al. 1996), which is better application for gas extraction, surface subsidence, water inrush, underground pressure control and rock burst prevention (Xu J & Qian M. 2000; Qu Q, Xu J & Qian M. 2007; Zhu W, et al. 2009; Xu J & Ju J. 2011; Xu J, Chen J, Jiang K. 2007; Cheng Y, et al. 2006), was presented by Qian. The instability of key strata is one of the main factors induced rock burst, and there is a close relationship between the instability of key strata and rock burst. Therefore, the possibility of rock burst induced by the instability of key strata should be investigated before mining to take stress relief measures in advance. In terms of risk evaluation of rock burst, many researchers have presented different evaluation methods. Bayesian discriminant analysis is used for predicting coal and gas outbursts (WANG C, et al. 2010). A coupled artificial neural network and fault tree analysis model to predict coal and gas outbursts is presented (Zhang R L & LOWNDES I S. 2010). The catastrophe progression method in predicting coal and gas outburst is presented (Zhang T J, et al. 2009).

This paper is based on the numerical simulation, to study the stability of thick-hard key stratum.

2 BACKGROUND

Jinsan Coal Mine is one of China's oversize mines. Since 2003, serious coal rock behavior is occurred repeatedly during the mining period, hundreds of meters tunnel is destroyed, and dozens of props are damaged. A great threat is brought to the coal mine production safety.

Working Face No. 5305 is Shanxi formation coal 3 with seam thickness of 1.2 ~ 3.6 m. The working face is westward adjacent to the goaf of working Face No. 5306, and eastward adjacent to the goaf of Face No. 5304. It belongs to island face, with a mining depth of 615 ~ 702 m but without immediate roof. The main roof is in fine sandstone and siltstone, strong and stable, with a thickness of 13.57 ~ 25.49 m. The overall trend of the coal bed shows a relived syncline, which is high in the north and south and low in the middle. Most faults are developed in the south wing of the syncline, with a main of direction of SE or SEE. Revealing faults according to the actual situation, it is expected to expose 15 faults with a fall of 1.3 ~ 4.6 m. Work-

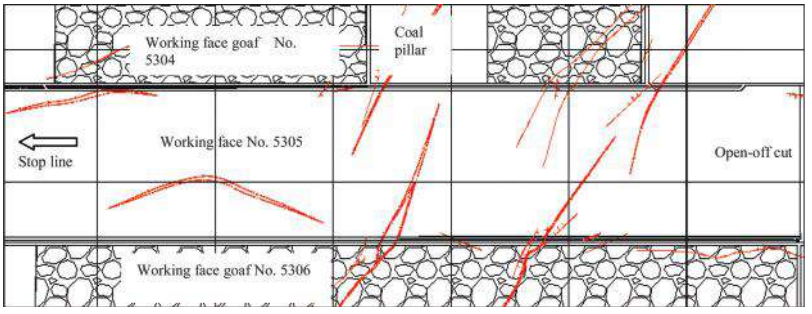


Figure 1. The plan view of the working face No. 5305.

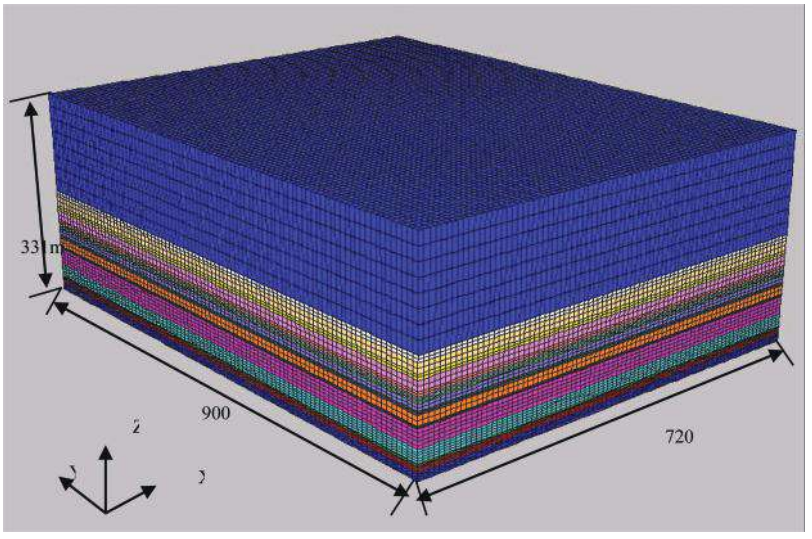


Figure 2. 3-Dimensionalnumerical model.

ing Face No. 5304 is a skip-mining face, and a coal pillar of 200 m long is left in the center of face. The tendency of 3 coal and rock burst is identified as weak shock. For "island" faces with complex mining environment, an evaluation on rock burst induced by key stratum instability before mining is needed in order to take preventive measures in advance.

3 NUMERICAL MODELING AND ANALYSIS OF RESULTS

3.1 *Setting up of the numerical model*

In this paper, FLAC^{3D} has been used to simulate the stability of the hard-thick key stratum. Fig. 2 shows the three-dimensional numerical model established, and the top boundary of the model is located approximately at a depth of 330 m. The dimension of the model is 720 m × 900 m × 331 m. Roller boundaries are placed at four boundaries of the model except at the top and bottom boundary. The boundaries are "fixed" only in a specified direction (i.e., no displacement or velocity is allowed). Lateral boundaries cannot move in the horizontal direction. The fixed bottom boundary cannot move in the vertical direction. A vertical stress of 8.2 MPa (*zz*-stress) was applied at the top boundary of the model. Fig. 3 shows the boundary conditions of the numerical model.

3.2 *failure criterion*

FLAC has several built-in material behavior models. The failure of rock material is assumed to follow the Mohr–Coulomb criterion as illustrated in Fig. 4 which is used for materials that yield when

subjected to shear loading, but the yield stress depends on the major and minor principal stresses only; the inter mediate principal stress is assumed to have no effect on yield.

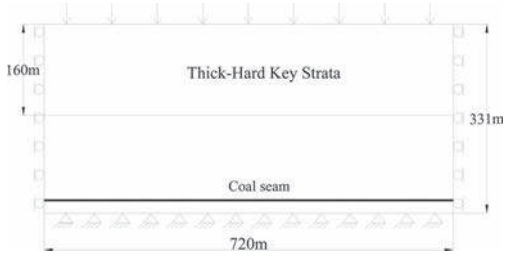


Figure 3. Boundary conditions of the numerical model.

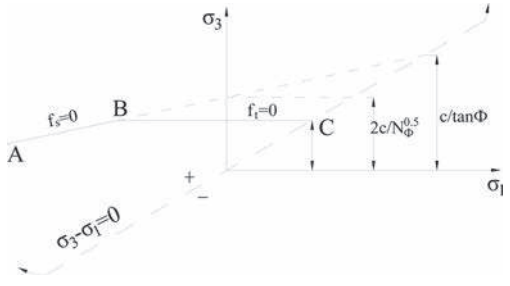


Figure 4. Mohr-Coulomb failure criterion (FLAC3D 2002).

The failure envelope $f(\sigma_1, \sigma_3) = 0$ is defined from point *A* to *B* by the Mohr-Coulomb failure criterion $f_s = 0$ with

$$f_s = \sigma_1 - \sigma_3 N_\varphi + 2c\sqrt{N_\varphi} \quad (1)$$

and from B to C by a tension failure criterion of the form $f_t = 0$ with

$$f_t = \sigma_3 - \sigma_t \quad (2)$$

Where ϕ is the friction angle, *c,* the cohesion, σ_t the tensile strength, and

$$N_\varphi = \frac{1+\sin\varphi}{1-\sin\phi} \quad (3)$$

3.3 *Physical and mechanical properties of coal and rock*

The layer sequence and the thickness of each layer used in the model are given in Table 1. Physical and mechanical properties selected to represent the coal and rock masses and to perform stress-deformation analysis are also shown in Table 1. The values selected to represent Young's Modulus, cohesion and tensile strength is about 30% less than the intact rock values. The value used to represent Poisson's ratio is about 20% higher than the intact rock value. Therefore, the selected mechanical property values represent the equivalent continuum properties of each rock mass.

Table 1. Physical and mechanical property values used for rock and coal masses in the numerical model.

Layer sequence from top to bottom	Thickness (m)	Density (kg/m^3)	Bulk modulus (GPa)	Shear modulus (GPa)	Cohesion (MPa)	Internal friction angle (°)	Tensile strength (MPa)
Fine Sandstone	160	2700	16.667	10	5	35	5
Mudstone	10	2400	10.9	6.85	2.6	32	2
Siltstone	15	2550	16.05	10.57	3	34	4
Coarse Sandstone	8.5	2680	17.95	11.3	3	36	4.5
Mudstone	15	2400	10.9	6.85	2.6	32	2
Fine Sandstone	7	2700	16.667	10	5	35	5
Mudstone	5	2400	10.9	6.85	2.6	32	2
Siltstone	4.5	2550	16.05	10.57	3	34	4
Fine Sandstone	10	2700	16.667	10	5	35	5
Coarse Sandstone	5.5	2680	17.95	11.3	3	36	4.5
Fine Sandstone	14.5	2700	16.667	10	5	35	5
Siltstone	4	2550	16.05	10.57	3	34	4
Medium Sandstone	28	2700	17.9	12.3	6	36	4.8
Fine Sandstone	19.5	2700	16.667	10	5	35	5
Coal No. 3	3.5	1400	1.667	0.77	1	25	1
Siltstone	4	2550	16.05	10.57	3	34	4
Fine Sandstone	5	2700	16.667	10	5	35	5
Siltstone	12	2550	16.05	10.57	3	34	4

4 ANALYSIS OF RESULTS

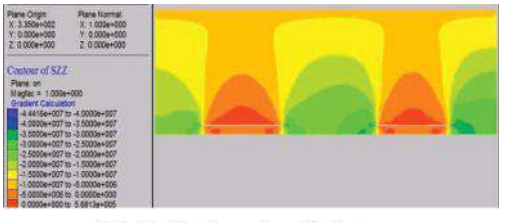
The model built was calculated to equilibrium, and the stress status of the key stratum was initialed. Then stoping the working face No. 5304 and No. 5306, respectively, the stress status of the key stratum was monitored to determine the disturbed situation of the key stratum. Finally, the stoping of working face No. 5305 was simulated to analyze the instability of key stratum and the possibility of mining earthquake.

After the longwall face No. 5304 and No. 5306 were mined out, the distribution of vertical stress is illustrated in Fig 5(a), the stress status of the key stratum is changed a little and the scale of stress value is 5–15 MPa; the distribution of plastic zones is illustrated in Fig 5(b), and the statue of the key stratum is intact. Therefore, the key stratum is stable judged by the distribution of vertical stress and plastic zones.

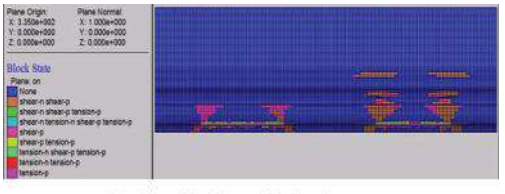
When the 5305 face was advancing 250 m, 300 m, 350 m, 400 m respectively, the failure height of the overburden strata above coal seam is increasing, according to the distributions of plastic zones shown in Fig. 6. When the face was advancing 350 m, the failure height of the overburden strata reaches to the underneath of the key stratum. When the face was advancing 400 m, the key stratum is starting to fracture, as shown in Fig. 6(d) and Fig. 7. At this point, there is the risk of rock burst induced by mine earthquake, if the key stratum is fractured. While the face was advancing 435 m, the key stratum has fractured mainly, as shown in Fig. 8; the risk of rock burst induced by mine earthquake is reduced. Consequently, the most dangerous area is the scope of 400 m~435 m away from open-off cut.

According to the numerical simulation results, the scope affected by the fracture of thick and hard critical stratum and main roof ranges 350 ~ 435 m from the open-off cut.

When the longwall mining face was advanced at the distance 410 m from open-off cut, the hard-

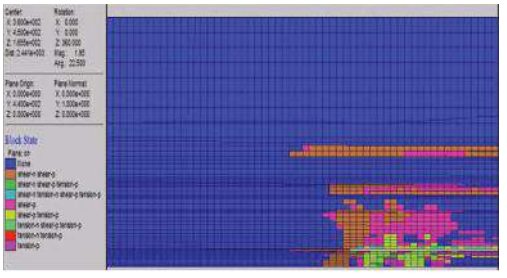


(a) distribution of vertical stress

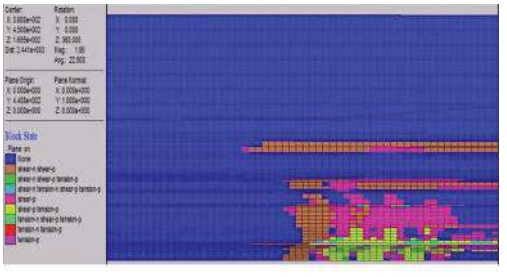


(b) distribution of plastic zones

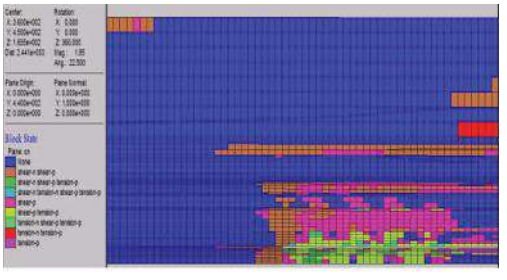
Figure 5. Pre-mining state stress of the key stratum.



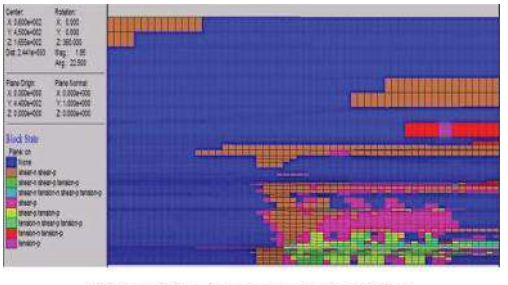
(a) working face advancing 250m



(b) working face advancing 300m



(c) working face advancing 350m

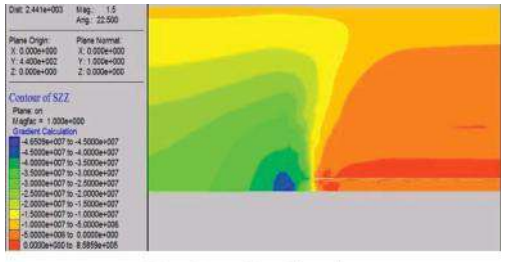


(d) working face advancing 400m

Figure 6. distribution of plastic zones.

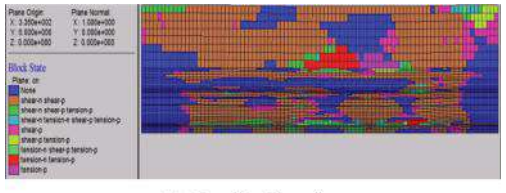


(a) the dip direction

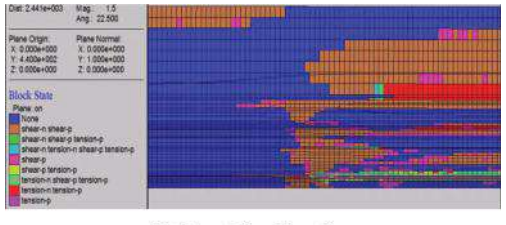


(b) the strike direction

Figure 7. Distribution of vertical stress when the face was advancing 400 m.



(a) the dip direction



(b) the strike direction

Figure 8. Distribution of plastic zones when the face was advancing 435 m.

thick key stratum was fractured and induced mine earthquake. The prevention measures of stress relief were applied in advance, simultaneously, the monitoring and pre-warming methods was used. Finally, there is no rock burst induced in this working face.

5 CONCLUSIONS

It is practiced that, when the longwall mining face was advanced at the distance 410 m from open-off cut, the hard-thick key stratum was fractured and induced mine earthquake. Due to the prevention measures of stress relief in this area underneath the key stratum in advance, there is no coal burst in the working face. The method of numerical simulation is suitable for investigating the possibility and influenced zones of rock burst and mine earthquake induced by the instability of the key strata.

ACKNOWLEDGEMENTS

The research presented in this paper was supported by National Key Basic Research Development Plan (973 Program) (2010CB226803), and State Science and Technology Projects (2011ZX05040–001).

REFERENCES

Cheng Y, Jiang F, Cheng J, et al. 2006. The primary study on microseismic locating and monitoring technology of shock bump caused by key stratum movement. *Journal of China Coal Society* 31(3): 273–277.

Flac3d (*Fast Lagrangian Analysis Continua in 3dimensions*) (2002) Version 2.1, Itasca Consulting Group, Minneapolis.

Qian M, Miao X, Xu J. 1996. Theoretical study of key stratum in ground control. *Journal of China Coal Society,* 21(3): 225–230.

Qu Q, Xu J, Qian M. 2007. Study on influence of key strata movement on gas emissions of adjacent layers. *Chinese Journal of Rock Mechanics and Engineering* 26(7): 1478–1484.

Wang C, Wang E Y, Xu J K, et al. 2010. Bayesian discriminant analysis for prediction of coal and gas outbursts and application. *Mining Science and Technology* (*China*) 20(4): 520–523.

Xu J, Chen J, Jiang K. 2007. Effect of load transfer of unconsolidated confined aquifer on compound breakage of key strata. *Chinese Journal of Rock Mechanics and Engineering* 26(4): 699–704.

Xu J & Ju J. 2011. Structural morphology of key stratum and its influence of strata behavious in fully-mechanized face with super-large mining height. *Chinese Journal of Rock Mechanics and Engineering* 30(8): 1547–1556.

Xu J & Qian M. 2000. Method to distinguish key strata in overburden. *Journal of China University of Mining & Technology* 29(5): 463–467.

Zhang R L, Lowndes I S. 2010. The application of a coupled artificial neural network and fault tree analysis model to predict coal and gas outbursts. *International Journal of Coal Geology* 84(2): 141–152.

Zhang T J, Ren S X, Li S G, et al. 2009. Application of the catastrophe progression method in predicting coal and gas outburst. *Mining Science and Technology* (*China*) 19(4): 430–434.

Zhu W, Xu J, Shi X, et al. 2009. Research on influence of overburden primary key stratum movement on surface subsidence with in-situ drilling test. *Chinese Journal of Rock Mechanics and Engineering* 28(2): 403–409.

This page intentionally left blank

Progress in Mine Safety Science and Engineering II – He et al. (Eds)
© 2014 Taylor & Francis Group, London, ISBN 978-1-138-00122-0

Research on the free radical affecting methane outburst within coal under the electromagnetic radiation

M. Shang-Quan & F. Jing
North China Institute of Science and Technology, Beijing, China

ABSTRACT: Currently coal and methane outburst disasters still remain seriously. This article aims at looking for the source of methane from the microscopic molecular structure of coal. chemical changes and particle interactions in chemical changes of coal and methane outburst during the impact are theoretically analyzed and a set of electromagnetic radiation experimental scheme is set to research the possibility of fracture and bond of CH_3–, CH_2 = CH– and H– and creating new methane. The basic theory of seam methane disaster prevention through the experiment is innovated.

1 INTRODUCTION

In China, there are more than 55% of key state-owned coal mines with high methane outburst. Although in recent years, coal mine methane has been effectively controlled, the major methane outburst accidents still occurred now and then. The complex process mechanism of coal and rock dynamic disasters has not yet been fundamentally solved and the prevention is a worldwide problem. For a long time, lots of researches using mechanics approach from a macro perspective on mine coal and methane outburst mechanism have been done. Most researchers believe that the outburst phenomenon is caused by the combination of three factors, which are stress, methane pressure and structural properties of coal, and also the high-speed release is caused by the potential of coal body, including of elastic energy, methane potential in the surrounding rock and coal. The mechanism of explanation about the role of the organic macromolecular structure of coal and chemical properties of free radicals is not generally accepted. My experiment shows that a radical change in the coal has played an important role in the process of methane outburst, which should be experimented.

2 RESEARCH STATUS

The observations and researches of rock fracture electromagnetic radiation (EME) were carried out earlier in China and the former Soviet Union. In 1953 Guevara Pavlovic, Pal Mainbranch(GUEVARA 1954) experimentally recorded and studied granite, gneiss and quartz piezoelectric phenomenon and the light emission. American scholar Nitson(NITSON 1977) and Chinese scholar Xu Weimin(XU 1985) also reported laboratory findings of the piezoelectric effect of rock. Shefrin Zoff(SHEFRIN 1975) studied the effect of feldspar stepanov, experimentally found that under a uniaxial deformation with the speed of 0.2 mm/s, the surface density of the sample was 10^{-5}~10^{-9}C/m^2 charge. Sun Zhengjiang(SUN 1985) recorded electromagnetic radiation signal when loaded on diorite, marble, limestone, and when the main rupture happened, according to the magnetic field strength, he calculated the fracture surface charge was 5.2×10^{-4}C, the surface charge density is 1.4×10^{-2}C/m^2. He Xueqiu and Liu Mingju's studies have shown(HE 1995) that, for the first time through experiment, there are electromagnetic radiation generating during the process of deformation and failure of coal. Wang Enyuan, He Xueqiu, Nie Baisheng(WANG 2005, WANG 2003) studied the spectrum of electromagnetic radiation and variation of coal and rock containing methane, found out that the deformation and fracture of coal and rock and electromagnetic radiation are closely related. Coal contains large amounts of free radicals, Feng Shian(FENG 1998) found that tectonic coal and its adjacent non-deformed coal compared to radical concentration is not the same, radical concentration is regarded as coal methane outburst dangerous area predictors. Tang Xiuyi(ZHANG 1997) measured radical concentration in coal mines in Huainan, Huaibei outburst and non-outburst, the former was doubled more than the latter. Guo Deyong(GUO 1999), after the study of tectonic coal ESR spectra, also supported the use of radical concentration as coal and methane outburst prediction of a zoning indicator.

On the whole, the study on mechanism of coal and methane outburst has made significant progress in china and abroad. However, owing to the physical and mechanical properties of coal nonlinear, rock damage in the form of methane occurrence and migration diversity and complexity of the process, the cause is not very clear. Thus, a theoretical and experimental theoretical system has not been formed and no definite experimental result can reveal the mechanism of coal and methane outburst.

3 COAL STRUCTURE AND RADICAL RESEARCH

The main structure of coal is amorphous polymers. Each coal molecule is composed of a number of the basic structural unit with similar but not exactly the same structure (HALL 1994). The basic structural unit of the core is mainly condensed aromatic ring, and a few hydrogenated aromatic, alicyclic and heterocyclic. The complete molecular structure of the coal comprises two parts: more stable performance, with a solid, not a chemical reaction of the core (aromatic nucleus) and surrounding the nucleus and a variety of side chain functional groups. Oxygen-containing functional groups are the major part of the functional group, including light phenol group, a carboxyl group, a methoxy group, and the carbon group, and also a small number of sulfur-containing functional group and nitrogen-containing functional groups. The basic structure units are connected with each other via a bridge to form the coal macromolecule. Coal molecules can form different three-dimensional structure through intermolecular cross-linking and wound around the space.

Because of amorphous, highly complex and heteroge-neous structures of coal, it is still controversial about the chemical structure of the coal. Nevertheless, some of the structural model has been widespread concerned, such as Fuchs Model, Given Model, Wiser Model, Honda Model, Shinn Model etc. Wiser Model is considered to be more comprehensive reasonable model, shown in Figure 1.

It is not definite about how big the coal Molecules is. The basic structural units can be considered broadly in the range of 200 to 400, and the relative molecular weight is in the range of thousands (YE 2008). In the coal polymer structure is also more evenly distributed small amounts of small molecules (≤500amu). Zhang Yugui (ZHANG 2003) thinks the small molecule compounds in coal, although the number is not much, has a great influence on the nature of the coal. Hydrocarbons in the coal are mainly n-alkanes. Hydrocarbon

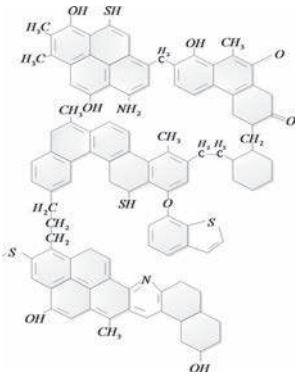


Figure 1. Wiser Model (YE 2008).

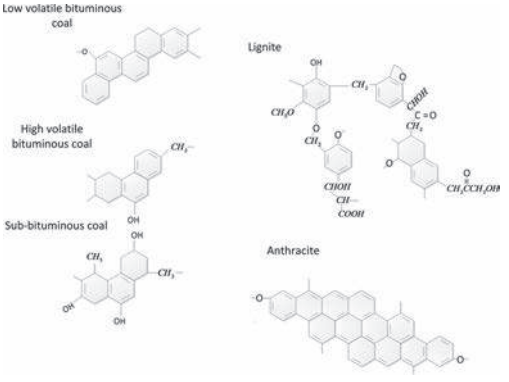


Figure 2. The basic structural unit of five kinds of coal diagram (TAO 1984).

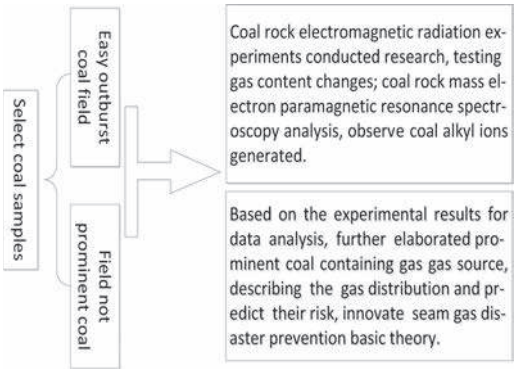
distribution is very wide, from the above C_1-C_3, and C_7 even found in reports(FANG 1996, FANG 1997), in addition to a small number of cycloalkanes, long chain olefins and 1–6 ring aromatic hydrocarbons (with 1–2 ring based) and so on. Between the C_{23}-C_{33}, coal intermolecular forces, charge transfer forces, π-π interactions, hydrogen bonding, van der Waals forces etc exist between ions. The bridge bond is quite common in the low rank coals which consists mainly of three kinds which are methylenebond(-CH_2-, -CH_2-CH_2-, -CH_2-CH_2-CH_2-, etc.), thioether bond, an ether bond (-0-, -S-, -SS-, etc.) and methylene ether bond (-CH_2-O-, -CH_2-S-, etc.), especially methylene ether bond. Moderate degree of coalification has the minimum number of coal bridges, mainly in the form-CH_2-and-O-, and to anthracite phase bridges increased again, primarily Car-Car, Figure 2.

Prediction: facing the problems of inconsistency during the process of the release of excess methane, methane composition and coal seam methane, could we find the source of the methane by taking it from projecting the microscopic molecular

structure of coal? Under the action of electromagnetic radiation, coal macromolecular structure has changed, part alkyl (CH_3-, CH_2 = CH-) and hydrogen (H-) molecules fractured from the coal. The reaction forms a new methane (CH_4) or methane and let the methane-containing coal and rock along with the stress gradient to rupture.

4 SUMMARY OF THE EXPERIMENTAL PROGRAM PREDICTION

A. Experimental General Idea



B. Experimental Methods

Subjects: The original state coal (block), crushing coal, after pumping through the methane exhaust methane of the coal.

Experimental environment: Keep coal in the underground with ambient pressure and temperature environments.

Experimental apparatus: Electromagnetic emission source, electromagnetic energy meter (tesla), high frequency mechanical wave recorder, coal and rock strain recorder, methane, ethane, carbon monoxide sensors, data logger.

Experimental principle: Figure 3

a. electromagnetic excitation b. gauge c. methane receiving container (sealed) d. methane test container (built methane, ethane, carbon monoxide sensors, not sealed) e. sealed container f. valve g. grating strain sensors h. Light vibration receiver i. data logger

Experiment: Excitation of electromagnetic waves, while recording non-excited state and the excited state changes of various physical quantities of data and curves.

(1)Fixed electromagnetic energy, and change the frequency of the electromagnetic wave. The Experiment tests the electromagnetic frequency characteristics of coal and rock.

(2)Fixed frequency of electromagnetic wave, and change the electromagnetic energy. The experiment

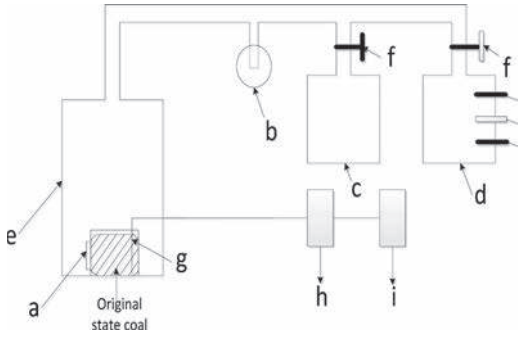


Figure 3. Electromagnetic waves schematics coal testing laboratory.

tests coal and rock under the action of the electromagnetic energy characteristics

Note: The experiment can be divided into two parts: The first step is to collect the methane, open the methane container valve, close the test container valve, store methane samples and analyze methane components with a spectrum analyzer. The second step is to close and collect the methane container valve, open the container valve inspection, inspect methane under the action of the electromagnetic state of change.

C. Experimental Targets:

1) According to the analysis of coal methane source from coal rocks, except coal and adsorption of free methane, is there a source of methane or methane product?

2) According to the theoretical analysis of coal different methane outburst effect, the methane outburst prevention theory and technology are innovated.

5 CONCLUSIONS

In summary, under the action of the external environment, coal containing methane has many effects, including optical radiation of electronic band mechanism, friction effect, piezoelectric effect, electromagnetic effect and so on. These experiments can test whether the expected effects make the coal macromolecular structure changed or not, such as Part alkyl (CH_3-, CH_2 = CH-) and hydrogen (H-) from the coal macromolecular fracture and whether form a new methane (CH_4) or methane. This experiment can provide strong arguments to analyze the different impact of methane during the process of coal containing methane. Under the premise of further exploring different methane outburst source, the prevention technology can be developed.

ACKNOWLEDGEMENT

This research was funded by Central college scientific research fund fees.3142013111

REFERENCES

Fang Pr, Zhou X-J, Tao R-Z et al. Fullerenes Discovered in Coal Mines of Yunnan, China. *Materials Research Innovation,* 1996, 1(2):129–134.

Fang Ph, Wong R. Evidence for Fullerene in a Coal of Yunnan, Southwestern China. *Materials Research Innovation,* 1997, l(l):130–132.

Feng Shian, Tang Xiuyi. Has Methane Outburst Coal Structure and Its Significance [J]. *Coal Geology of China,* 1998, 10 (1):24–26.

Guevara Pavlovic, Pal Mainbranch. the Piezoelectric Effection of Rock. *USSR Academy of Sciences report,* 1954, 99(2):239.

Guo De Yong, Han Dexin. Tectonic Coal EPR Experimental Study[J]. *China University of Mining,* 1999, 28 (1):94–97.

Hall F E, Chun-He Zhou, Methaneen Kam, et al. Adsorption of Pure Methane, Nitrogen, and Carbon Dioxide and Their Binary Mixtures on Wet Fuitland Coal[C].*SPE* 29194, 1994.

He Xueqiu. Coal Containing Methane flow Dynamics [M]. Xuzhou: *China University of Mining Press,* 1995.

He Xueqiu, Liu Mingju. Coal Containing Methane Destruction Electromagnetic Dynamics[M].Xuzhou: *China University of Mining Press,* 1995.

Nitson U. Electromagnetic Emission Accompanying Fracture of Quartz-bearing Rocks[J]. Geophys. Res. letter1977, 4: 333–336.

Shefrin Zoff, Micoud Ivanov. in the Process of Deformation and Failure of the Left Outer Groove Plane Electrochemical. *USSR Academy of Sciences report,* 1975, 225(2):313–315.

Sun Zhengjiang, Wang Lihua, Gao Hong. Rock Specimen Rupture of Electromagnetic Radiation and Light Emission [J]. *Geophysics,* 1986, 29 (5):491–495.

Tao Zhu. Coal Chemistry [M]. Beijing: *Metallurgical Industry Press,* 1984.

Wang Enyuan, He Xueqiu, Dou Linming, etc. During Coal Mining Coal Rock Electromagnetic Radiation Characteristics and Application [J].2005, 48 (1):216–221.

Wang Enyuan, He Xueqiu. Deformation and Fracture of Coal or Rock Electromagnetic Radiation Experimental Study [J]. *Geophysics,* 2000, 43 (1):131–137.

Xu Weimin, Tong Wusheng. Rock Burst of Electromagnetic Radiation during the Experimental Study [J]. *Geophysics,* 1985, 28 (2):67–76.

Ye Cuiping, Xie Kechang, Coal Macromolecular Structure Determination of Compounds and Model[D], *Taiyuan University of Technology,* 2008, Taiyuan.

Zhang Yugui, Cao Yunxing, Li Kaiqi. Paramagnetic Resonance Characteristics of Tectonic Coal Exploration [J]. *Jiaozuo Institute of Technology,* 1997, 16 (2):37–40.

Zhang Yugui, Wang Baojun, Tian Yajun, etc. Fushun Coal and Resin Lens Coal CS: Solubles Clan Composition and Extraction [J], *China University of Mining,* 2003, 32 (3), 267–273.

Progress in Mine Safety Science and Engineering II – He et al. (Eds)
© 2014 Taylor & Francis Group, London, ISBN 978-1-138-00122-0

Study on safety monitoring system of mine machine

Wu Zhao
School of Mining Engineering, Jiangsu Jianzhu Institute, Xuzhou, China

Shu-Ming Wang
Jinling Institute of Technology, Nanjing, China

Shu-Yun Qiao
Xuzhou Institute of Technology, Xuzhou, China

ABSTRACT: This paper studies on machine safety monitoring system of coal mine to tackle the problem of prevention of mechanical hazards protection, electrical safety and warning, Transport protection and so on. The system overall design includes three layers of controlling, information and equipment (Qiao et al. 2008). With the actual situation of a coal mine electrical and mechanical equipment monitoring and protection, respectively on the key technology of CAN-BUS, digital signal processing, distributed computing, database selection of in-depth research, after several trials in the north wing of central substation and a mine central pump house, the system run effect obviously in the aspect of safety, reliability and compatibility.

1 INTRODUCTION

Along with the construction of mechanization, coal mine production scale, large power equipment put into use, put forward new requirements for safe operation of coal mine power grid (Zhao 2011). After investigation, found that domestic coal transportation, ventilation general aimed to enhance the water supply equipment safety protection; electrical power equipment, leakage protection, short-circuit and overload has done a lot of work, but the machine protection each orphan, fault in coal mine power grid has randomicity and contingency, is not conducive to the power grid state (Mu et al. 2008), the mechanical operation of remote monitoring. To solve this problem, combined with the status of a mine safety system, early warning and protection system design, reasonable selection of new technology, perfect function, reduce the machine maintenance, improve the fault judgment, to ensure that the location and the cause of the accident to understand, identify signs of measures, reduce the failure effect, improve the safety production of the coal mine electrical and mechanical equipment the level of safety management.

2 SYSTEM DESIGN

The overall design of the system is divided into three layers, including the control layer, the information layer and the equipment layer:

1. The control layer: through the core switch and the ground control center with Ethernet interface CAN-LAN substation and industrial Ethernet switching device is connected, through the establishment of underground double fiber ring of high-speed information channel (Qiao et al. 2008) (using the TCP/UDP protocol, 100Mbps/10 Mbps adaptive transmission rate, transmission distance is less than 40(km), BER < 10–80).
   Ground center station by two Gigabit redundant Ring net switches, the two database server, a communication server, consisting of three industrial computers and other equipment, guarantee the safety of data transmission, stability. And equipped with display system, display the monitoring of network information. Equipped with UP uninterruptible power supply and redundant power supply, ensure the acquisition data of underground monitoring node of 24 hours of uninterrupted.
2. Information layer: the information of monitoring data processing, transfer, backup and analysis, discarding unnecessary data. Release function through data, all the monitoring node data released to bureau-level LAN (Deng & Wei 2007), in the LAN users authorized permission, real-time status monitoring nodes, view the real-time data, the query of historical data, alarm record monitoring.
3. Equipment layer: it is divided into the ground monitoring network and the underground

monitoring network. The ground monitoring network is mainly used for industrial bus, through the monitoring device, high-low voltage switch tank Protection Device. And the output of various kinds of report information. Cabinet protection device will ground information through the network access server industrial Gigabit self-healing ring network switch. The underground monitoring network mainly uses CAN bus, data acquisition device is connected with the CAN-BUS field bus and underground communication station.

3 KEY TECHNOLOGY

3.1 *Data bus technology*

Data bus technology CAN (Controller Area Network) is the most widely used, which is characterized by (1) Constitute a host system, CAN uses the main competitive bus structure, with multiple master operation and serial bus distributed arbitration and broadcast communication features. The network can take the initiative to send messages to other nodes on the bus nodes. (2) Stronger anti-interference ability. Only 2 wires connected with external and internal integration, error detection and management module, when the error occurs when a node of CAN bus, automatically close the node output function, and cut off the connection between nodes, so that other nodes are not affected. (3) Adopt non-destroyed bus arbitration technique. When multiple nodes initiate communication at the same time, avoid priority low priority high, while the node with the highest priority can be not affected continue to transmit data, save the bus conflict arbitration time. (4) Data transmitting with low bit errors ratio, CRC checksum test measures. Using CAN bus short frame structure, each frame of information containing 8B, short transmission time.

3.2 *Digital signal processing*

Technology of DSP digital signal processing (The digital signal process) has strong flexibility (Li et al. 2007). Its characteristics are

1. High degree of integration, integration of the chip is tens of millions of orders of magnitude.
2. High speed, its chip processing speed reached hundreds of megabytes of magnitude.
3. High current and low voltage, high speed signal processing chip current above 1 A. In order to reduce the power consumption of the system adopts low voltage.
4. Using a variety of parallel architectures. Because the digital circuit adopts two value logic, as long as the change of environmental temperature, circuit noise does not cause the circuit logic inversion, digital circuits are not affected by complete. Therefore, the application of digital signal processing technology has good stability.

3.3 *Distributed computing technology*

Application of distributed computing technology (DC:Distributed Computation), the system is divided into the main computer system and monitoring station computer system control center. It is characterized by distributed computing can load calculation on multiple computers balance. The program, the data processed by the program and the actual computation tasks are distributed in the network, processing ability to regulate multiple computers, characteristics and application is composed of different modules (Shao et al. 2007).

3.4 *Real-time database technology*

Real-time database RTDB (Real-Time Database) is the combination of database and real-time technology (Liu & Yao 2005). Is characterized by:

1. Collection, processing, storage and real-time data in the whole system,
2. It is responsible for the history data statistics, analysis, alarm, query and other requirements.
3. It is responsible for the underground monitoring collected data processing and storage, communication between the database and server.
4. It is responsible for the data processing and analysis by the network is displayed to the user, so the real-time database and provide basic data and basic information for monitoring system, is the foundation of realizing the whole safety coal mine electrical network real-time monitoring and warning function.

4 SYSTEM FEATURES

4.1 *System function*

Monitoring system of coal mine electromechanical equipment and high and low voltage power grid real-time data acquisition, transmission of information, record data, online monitoring. The technique involves industrial Ethernet, field bus, embedded software, digital signal processing, distributed computing, real-time database, configuration software, network integration technology (Liu & Yao 2005, Deng & Wei 2007).

The monitoring system, the database server is first transferred to the system hardware configuration table and data dictionary, loading hardware

drivers, generating equipment monitoring and real-time database, and according to the timing acquisition hardware configuration data; when the monitoring workstations are identified, through the database server load monitoring interface configuration file generation monitoring interface of the control system, and generates a mapping system all real-time monitoring data, and then the server and workstation continuous exchange of real-time data (Li et al. 2007), realize the process of monitoring system.

4.2 *System structure*

System between the high-speed transmission data through the real-time database, network and the seamless connection. The system has real-time monitoring, electrical protection, fault warning, integrated query and system management function.

The system structure as shown in Figure1.

4.3 *System performance*

Resource sharing: system provides the connection open data, avoid coal mine power network subsystems independent operation monitoring island formation.

Safety: the system CAN bus for data transmission and automatic control between the underground monitoring equipment (Mu et al. 2008), realize the connection between the field bus and the ground control center by downhole LAN.

System compatibility: the implementation of international standards, is open, convenient for other systems connected; to consider the use of domestic main stream equipment, use of existing equipment, saving investment.

Scalability: the underground monitoring equipment and communication equipment using the embedded system software and communication software, flexible configuration, convenient installation, so as to the future of the system expansion and upgrade.

5 EFFECT OF PRACTICE

5.1 *Operation practice*

This system is put into use in a certain mine north wing of central substation and a central pump house, and achieved good effect and economic benefit of society. Practice shows that the system design is reasonable, stable and reliable operation, and the operation is simple and convenient. The system is able to achieve accurate monitoring, equipment operation data, provide the basis.

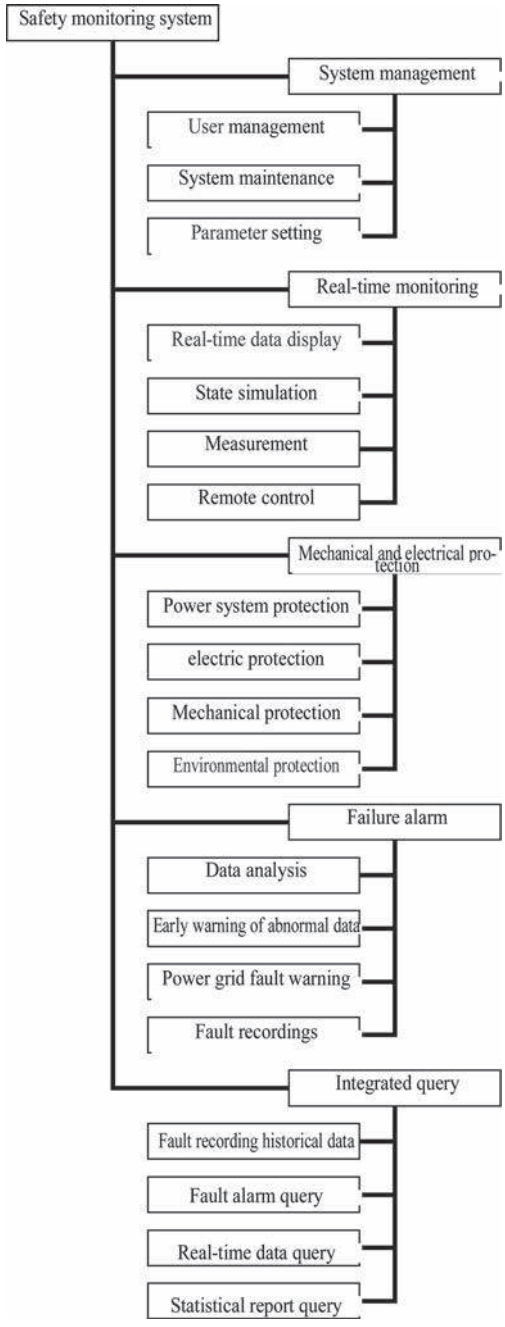


Figure 1. Mine machine safety monitoring system.

5.2 *System features*

1. Through the implementation of protection of underground electrical facilities and all kinds of fault detection, improve safety, stability operation of coal mine equipment.

2. System provides WEB data (Deng & Wei 2007) query function: users can query real-time underground monitoring equipment on the Internet, to facilitate the timely understanding of the operation situation of the underground system.
3. Some operating parameters reflect the real-time system on power system equipment, the user through the operation can observe real-time parameters of equipment.
4. system to achieve human-computer intelligent interaction in general, remote 24 hours of coal mine electromechanical equipment condition monitoring, provide a variety of information visualization of query tools, improve the management level, enhance the mine disaster and safety production capacity.

REFERENCES

Deng, Q.G. & Wei, J.P. 2007. Coal mine safety monitoring system based on network technology. *Journal of Henan Polytechnic university (Natural Science),* 2007(3):241–244.

Liu, Z.H. & Yao, M. 2005. Implementation of Real-time Monitoring and Control Information System for Coal Mine Safety. *Industry and Mine Automation,* 2005(2):4–6.

Li, Y.Q. et al. 2007. The Colliery Safety Real-Time Monitoring System Based on Web. *Shandong Science,* (2):59–63.

Mu, R. et al. 2008. Study on Forewarning and Monitoring Information System for Coal Mine. *Technology and Innovation management,* 2008(2):203–205.

Qiao, S.Y. et al. 2008. Design of Monitoring and Early Warning System for Coal Mine Grid Disaster and Its Implementation. *Computer Engineering and Design,* 2008(12):52–55.

Shao, C.G. et al. 2007. Study on Construction of Early Warning System of Mine Safety. *Coal Technology,* 2007(5):63–65.

Zhao, W. 2011. Based on the mine hoist fault diagnosis of vibration test. *manufacturing automation,* 2011 (3): 49–52.

2 *Metal and nonmetal mine safety*

This page intentionally left blank

Progress in Mine Safety Science and Engineering II – He et al. (Eds)
© 2014 Taylor & Francis Group, London, ISBN 978-1-138-00122-0

Numerical investigation of three-point bending fracture test on granite

H.J. Wang, D.A. Liu, J.R. Niu & Z.D. Cui
Key Laboratory for Geomechanics, Institute of Geology and Geophysics, Chinese Academy of Sciences, Beijing, China

F. Zhao
State Key Laboratory for Geomechanics and Deep Underground Engineering, China University of Mining and Technology, Beijing, China

ABSTRACT Three-point bending tests on specimens with different offset notches are widely used to study the propagation of mixed cracks. This paper adopts the experimental scheme that makes the loading direction perpendicular to the existing crack to investigate the I-III mixed cracks. Load-displacement curves of different offset notch positions (L = 20 mm, 30 mm) and photos of crack development can be obtained. This paper presents the numerical investigations using finite element program to obtain the stress-strain nephogram and crack trend graph. These results agree well with the experimental results. The results show that the crack nonlinear extended not only at the specimen surface but also along the thickness direction. On the other hand, the stress-strain curves and failure characteristics for specimens with different offset amounts were comparative analyzed. It can be noted that different offset amounts have great influence on the rock fracture modes.

1 INTRODUCTION

With the greater depth of the underground projects, numerous research have continually entered into underground space such as deep tunnel, coal mining, underground storage of nuclear waste and geological storage of carbon dioxide as well as shale gas exploitation (Cai M et al. 2004, Molli G et al. 2010, Jordan K. Eccles et al. 2012). Thus, the investigation of underground space is of vital importance. Due to the simple underground environment and low field stress of tens of meters under the ground, geological investigation and exploration are enough for the well run of the underground engineering. However, the underground environment will be more complicated as the human being development going into thousands of meters depth of underground space. Deep rock mass or human engineering is violently affected by the complicated mechanical environment including high stress, high temperature, high karsts water pressure and intense exploitation disturbance (He et al. 2012, K. Khan et al. 2000).

Three-point bending fracture tests on rock which can obtain the macro-micro failure mechanism have become effective mean for research (G.S. XIEDAKIS et al. 1996, G.S. XIEDAKIS et al. 1997). Some foreign researchers suggested that specimen diameter and the shape of the existing crack have great influence on the rock fracture toughness. However, the effects of loading rate, crack dimension and specimen thickness can be ignored (M.R. Ayatollahi et al. 2011, MANHANTY D K et al. 1992, Smith DJ et al. 2001, Akos Rechtorisz et al 1998). And existing crack length and offset amount can affect the specimen failure mechanism greatly by the study of mixed crack development modes in marble three-point bending test (F. Dai et al. 2011, Levent Tutluoglu et al. 2011). The double-K fracture parameters can be simply determined by three-point bending test (XU et al. 2000, XU et al. 1999). Meanwhile, the unstable crack growth trajectory can be captured by the I-III mixed loading on marble rectangular beam (Yang et al. 2011, M.R.M. Aliha et al. 2013, Tae Young Ko et al. 2013).

There are large amount of random cracks in engineering rock. And the load acted position may be apart some distance from crack location and not act along the crack propagation direction (Pan et al. 2012). Thus, this paper used the Mechanical Testing Simulation system to perform granite three-point bending test with different offset notches for the in-situ observation. The study has investigated the failure characteristics and crack development mechanism as well as different crack offset distances influence on fracture property. In addition, comparing to the experimental methods proposed by many domestic and foreign scholars, this paper has conducted the test making the existing crack

perpendicular to the loading direction. That is to say, the notch direction is set to be horizontal for the study of the I-III mixed cracks propagation. It will provide great help for the material collection of failure and stability evaluation of deep fractured surrounding rock.

2 EXPERIMENTAL PROCEDURE AND ANALYSIS

2.1 *Equipment and tested samples*

The testing equipment used in this study is Mechanical Testing Simulation system monitored by computer. The loading capacity of this testing system is 100 KN. And the main machine composes of two ball screws, a moving beam, one bottom supporting structure, four support light bars, one upper beam and four aluminum side cowlings, as shown in Fig. 1. Fixed on the experimental set, the specimen can be applied tension or compression strength through the movement of moving beam driven by ball screws.

The granite samples for these tests were cored from Laizhou, Shandong province, at the depth of 400 m. The specimen dimensions are 140 mm × 60 mm × 30 mm with the density of 2.62 g/cm3. These granite samples consisted of 38.6% quartz, 31.9% K-feldspar, 22.7% plagioclase, and 6.8% clay minerals by the analysis of X-ray diffraction. It was observed that the samples were white and intact with few native cracks.

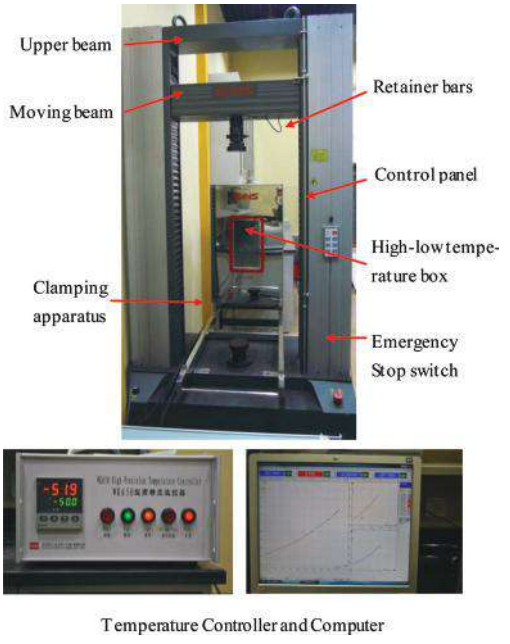


Figure 1. Photos of the experimental.

2.2 *Experimental procedure*

In these fracture tests, the rectangular granite specimens were used for study. To date, arranging the notch downwards in three-point bending test was popular in most research (Huang et al. 2013, Aliha et al. 2011, Ali Fakhimi et al. 2013). The new method, unlike conventional approaches, was applied in three-point bending test to observe the fracture features of granite. The distance from the media axis was determined as L and the notch depth represented was 2.5 cm. Meanwhile, the notch should be kept perpendicular to the specimen edge, shown in Fig. 2.

2.3 *Analysis of test results*

In these two tests, the notch distance from media axis L were designed as 20 mm and 30 mm respectively and the stress-strain evolution were plotted in Fig. 3.

It can be noted that the granite failure is actually the brittle fracture from the stress-strain curve. At the initial stage of the tests, both the specimens have the relatively flat development in the stress-strain curve and then the slope of the curve increase with the increasing of the strain. These can be interpreted by the appearance of the initial cracks in weak region of the specimen after being loaded. But these cracks didn't coalesce longitudinally and these micro cracks finished cracking with the increasing of the stress. Due to the system limitation for the formation of overall fracture surface, the curves enter into the second stage. The slope of the curves retain at the constant value approximately at the second stage which can be named as elastic stage. The elastic deformation belongs to the rock material properties. The strain energy is accumulated in this stage where the work

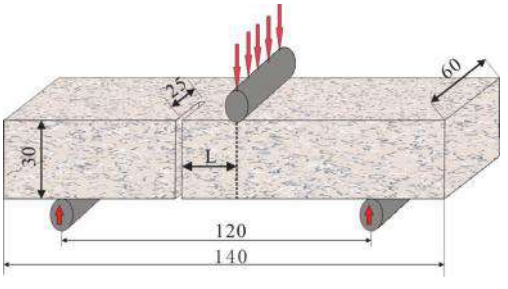
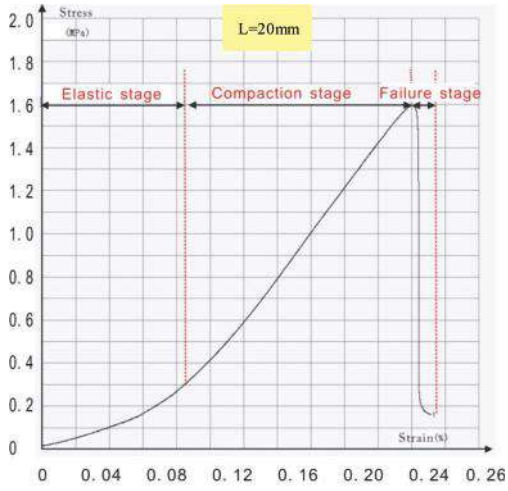
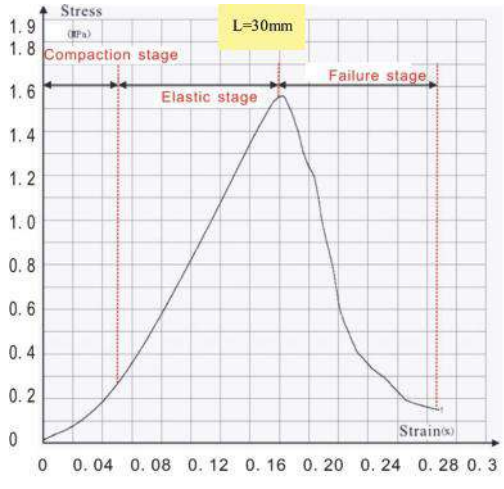


Figure 2. Specimen geometry and the three point loading configuration of the beam.



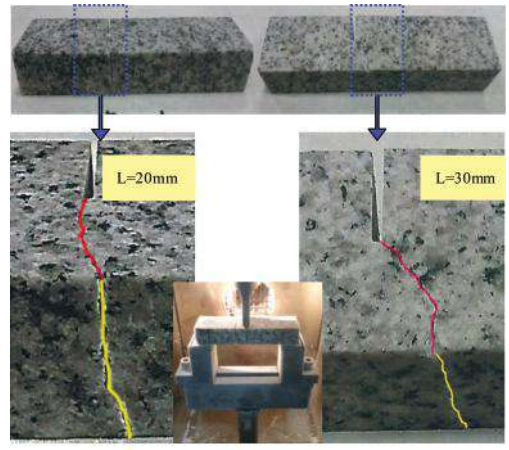
(a) Notch distance from media axis is 20mm



(b) Notch distance from media axis is 30mm

Figure 3. Stress-strain evolution for the two granite specimens.

was done from outside without making the micro cracks instability. At the third stage which is called as nonlinear failure stage, the slope of the curves decreases rapidly. The amount of the micro cracks with instable development gradually increases causing total fracture surface formation. It can be observed that the maximum failure loads for these two specimens with two notch distance values are nearly equal and there are big differences in the curves after peak value from the analysis on the stress-strain curves. The specimen with notch



(a) Notch amount L=20mm (b) Notch amount L=30mm

Figure 4. Fracture photos of the two specimens with different offset notches.

distance L of 20 mm had the brittle fracture and experienced instant destruction without any residual stress. However, the failure mode of specimen with L of 30 mm belonged to the quasi-brittle fracture. After the peak value, the stress is decreasing gradually indicating that the fracture mode is more complex.

Comparing the failure characteristics of these two specimens after the fracture, the cracks development is quite different. In Fig. 4, the red curve represents the transverse crack propagation and the yellow curve describes the longitudinal crack trend. According to the experimental field notes and images analysis, the fracture mode of the specimen with L of 20 mm is Mixed Mode I-III fracture. From the enlarged view of the crack, the form of the crack development is mainly the Mode-I fracture near the notch tip. After the Mode-I fracture (tension, opening) propagation length of 10 mm, the specimen has the Mode-III crack (anti-plane shear) propagating forward until the total fracture destruction, as shown in Fig. 4a. In the case of L = 30 mm, the crack propagation is mainly Mode-III fracture. It can be noted that two thirds of the whole crack length are shear failure from the initial cracking point at the notch tip. At about 10 mm distance from the specimen edge, the tension crack failure begin to occur which can be clearly observed from Fig. 4b.

3 NUMERICAL INVESTIGATION

This paper applied the nonlinear finite element method (Automatic dynamic incremental nonlinear

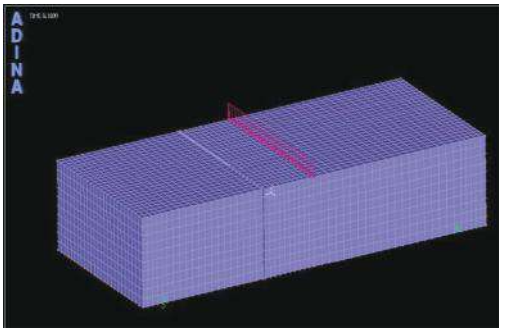


Figure 5. Mesh distribution of finite element mode.

analysis) to perform the numerical simulation [11]. Fig. 5 shows the model and the grid partition. There are a total number of 12000 units through the mesh refinement at the offset notch location. The parameters used for the numerical simulation include elastic modulus E of 53GPa, Poisson's ration γ of 0.167, density of 2.615 g/m3, the maximum tension strength of 2.6 MPa and the maximum uniaxial compressive strength of 75 MPa as well as the maximum strain of 0.22% etc. All these parameters were obtained by the conventional mechanical tests.

With the offset amount of 20 mm, the load controlled by displacement was gradually acted on the specimen. Fig. 6a shows that crack first appears at the tip of the notch and then large amount micro cracks generate inside the notch. As the load increasing, the amount of open cracks at the internal notch increase continually and the open crack at the notch tip also extends o the central region, as shown in Fig. 6b. There are many cracks appearing at the central part of the specimen where the load acted. It can be observed that a great number of closed cracks generated at the central of the specimen. Meanwhile, the red line represents the open crack and the gray line for the closed crack. According to the previous study and experimental experience, the location where large opening displacement and coalescence occur is most prone to fracture. Thus, it is consistent with the experiment result that the specimen experienced the tensile fracture at the notch finally.

As for the other case of L = 30 mm, the stress nephogram obtained by numerical results is shown in Fig. 7. Fig. 7a describes the stage of initial loading process and Fig. 7b shows the last failure process. At the initial loading stage, it can be observed that the stress concentration appear at the crack tip. The micro cracks generate at the crack tip and then develop to the lower right. With the increasing of load, the area of the stress concentration has an ascent trend, develops to the lower right

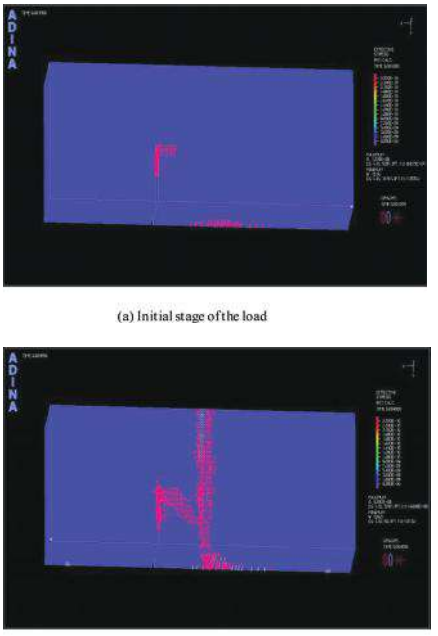


Figure 6. Numerical graphs of specimen failure process with L=20 mm.

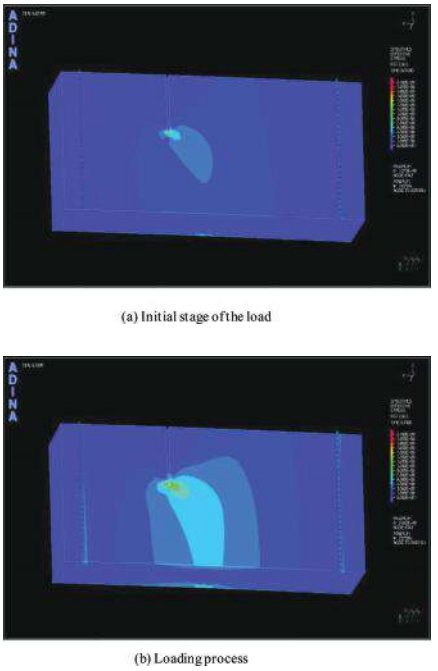


Figure 7. Numerical graphs of specimen failure process with L =3 0 mm.

gradually until propagates to the specimen edge and coalesces to failure finally. It can be noted that the failure mode of the case of L = 30 mm is mainly anti-plane shear failure from the crack formation, propagation until coalescence and equivalent stress direction. Corresponding to the tested specimen photos, these results are well agreed with the test results in Fig. 4b.

4 CONCLUSION

Basing on the new experimental method, this paper has presented the experimental and numerical investigation of the granite specimens' failure properties with different offset notches using three-point bending test. Thus, the overall conclusions of this study are hence thresholds:

1. Arranging the notch perpendicular to the loading direction, this three-point bending test can simulate the failure mode of the case that the crack propagation of the underground engineering rock mass is perpendicular to the acted loading direction.
2. The experimental procedure can be split into three stages: compaction stage for the micro cracks generation, elastic stage for strain energy accumulation of crack development and nonlinear failure stage.
3. It can be clearly observed that the failure modes for the specimens with different offset amounts are quite different by the experimental and numerical results. The specimen with L = 20 mm mainly experienced the tensile failure process whereas the I-III mixed mode (mainly anti-plane shear) for the case of L = 30 mm.

REFERENCES

Akos Rechtorisz, Imre Bojtar, Miklos Galos. 1998. Determination of Stress Intensity Factors on Rock Specimens. *2nd Int. PhD Symposium in Civil Engineering*, *Budapest*.

Aliha, M.R.M., Ayatollahi, M.R. 2011. Mixed mode I/II brittle fracture evaluation of marble using SCB specimen. *Procedia Engineering*, (10): 311–318.

Aliha M.R.M., Ayatollahi M.R. 2013. Two-parameter fracture analysis of SCB rock specimen under mixed mode loading. *Engineering Fracture Mechanics,*. (103):115–123.

Ali Fakhimi, Ali Tarokh. 2013. Process zone and size effect in fracture testing of rock. *International Journal of Rock Mechanics & Mining Sciences,* (60):95–102.

Ayatollahi M.R., Aliha M.R.M., Saghafi H. 2011. An improved semi-circular bend specimen for investigating mixed mode brittle fracture. *Engineering Fracture Mechanics*, (78): 110–123.

Baoshan Huang, Xiang Shu, Gang Zuo.2013. Using notched semi circular bending fatigue test to characterize fracture resistance of asphalt mixtures. *Engineering Fracture Mechanics,* (109): 78–88.

Cai M, Kaiser PK, Tasaka Y, Maejima T, Morioka H, Minami M. 2004. Generalized crack initiation and crack damage stress thresholds of brittle rock masses near underground excavations. *Int. J. Rock Mech. Min. Sci*, (41): 833–847.

Dai F., Xia K., Zheng H., Wang, Y.X. 2011. Determination of dynamic rock Mode-I fracture parameters using cracked chevron notched semi-circular bend specimen. *Engineering Fracture Mechanics*, (78): 2633–2644.

Jordan K., Eccles, Lincoln Pratson, 2012. Richard G. Newell, Robert B. Jackson. The impact of geologic variability on capacity and cost estimates for storing CO2 in deep-saline aquifers. *Energy Economics*, (34):1569–1579.

Khan K., Al-Shayea N.A. 2000. Effect of Specimen Geometry and Testing Method on Mixed Mode I-II Fracture Toughness of a Limestone Rock from Saudi Arabia. *Rock Mech. Rock Engng*, 33 (3):179–206.

Levent Tutluoglu, Cigdem Keles. 2011. Mode I fracture toughness determination with straight notched disk bending method. *International Journal of Rock Mechanics & Mining Sciences*, (48):1248–1261.

Manchao He, Xuena Jia, M. Coli, E. Livi, Lui's Sousa. 2012. Experimental study of rockbursts in underground quarrying of Carrara marble. *International Journal of Rock Mechanics & Mining Sciences*, (52): 1–8.

Manhanty D.K., Savent G.Y. 1992. Experimental investigations on stable crack growth in three-point bend specimens under mode I and mixed mode (I and II) loading[J]. *Engineering Fracture Mechanics*, (43): 41–53.

Molli G, Cortecci G, Vaselli L, Ottria G, Cortopassi A, Dinelli E, Mussi M, Barbieri M. 2010. Fault zone structure and fluid-rock interaction of a high angle normal fault in Carrara marble (NW Tuscany, Italy). *J. Struct. Geol,* (32):1334–8.

Peng-Zhi Pan, Fei Yan, Xia-Ting Feng. 2012. Modeling the cracking process of rocks from continuity to discontinuity using a cellular automaton. *Computers & Geosciences*, (42):87–99.

Smith DJ, Ayatollahi MR, Pavier MJ. 2001. The role of T-stress in brittle fracture for linear elastic materials under mixed mode loading. *Fatig Fract Engng Mater Struct*, (24):137–50.

Shilang Xu, H.W. Reinhardt. 2000. A simplified method for determining double-K fracture parameters for three-point bending tests. *International Journal of Fracture* (104): 181–209.

Shilang Xu, H.W. Reinhardt. 1999. Determination of double-K criterion for crack propagation in quasi-brittle fracture, Part II: Analytical evaluating and practical measuring methods for three-point bending notched beams. *International Journal of Fracture*. (98): 151–177.

Tae Young Ko, John Kemeny. 2013. Determination of the subcritical crack growth parameters in rocks using the constant stress-rate test. *International Journal of Rock Mechanics & Mining Sciences,* (59):166–178.

Xiedakis G.S. Samras I.S., Zacharopoulos, D.A. 1996. Crack growth in a mixed-mode loading on marble beams under three point bending. *International Journal of Fracture*, (79):197–208.

Xeidakis G.S., Samaras I.S., Zacharopoulos D.A., Papakaliatakis G.E. 1997. Trajectories of Unstably Growing Cracks in Mixed Mode I-III Loading of Marble Beams. *Rock Mechanics and Rock Engineering*, 30(1): 19–33.

Yang S.T., Hu X.Z., Wu Z.M. 2011. Influence of local fracture energy distribution on maximum fracture load of three-point-bending notched concrete beams. *Engineering Fracture Mechanics*, (78): 3289–3299.

Progress in Mine Safety Science and Engineering II – He et al. (Eds)
© 2014 Taylor & Francis Group, London, ISBN 978-1-138-00122-0

Potash exploration overview and safety considerations in Canada

J. Han
School of Management, China University of Mining and Technology (Beijing), Beijing, P.R. China

L. Piché & P. Geo
North Rim Exploration, Ltd., Saskatoon, Saskatchewan, Canada

ABSTRACT: In order to help a junior potash company undertake a successful exploration in Saskatchewan, Canada, geological information and data for the area must first be collected and analyzed. Exploration drilling is a high risk endeavor and every effort should be made to minimize risks. For illustration of exploration process and safety considerations, a drilling incident example is provided to show the importance of careful planning, proper training and clear communication. The exploration procedures and safety considerations successfully applied in Saskatchewan will benefit junior company in the development of his potash greenfield project.

1 INTRODUCTION

Potassium from potash is an important nutrient for plants and crops. As the world's population continues to increase, farmers will need to produce higher yields from less land, which supports potash demand growth of 2%-3% per year. Unfortunately, China is a country that has a shortage of potash, with 2.2% of global potash resources and 20% of the world's potash demand. Over 50% of Chinese potash consumption relies on the importation from foreign countries; meanwhile, the potash deposits in Canada are the world's single-largest source of mineable potash, comprising almost 50% of the global known potash reserves. Presently, there is great interest in exploring and developing potash deposits worldwide.

Yanzhou Coal, purchased 19 potash permits in Saskatchewan, Canada after a seven month due diligence process. The deal worth USD 260 million was inked in July 2011 and the potash property was transferred in September of 2011. Yanzhou Coal's team arrived in Saskatchewan in late 2011 to begin potash exploration and development of their properties. To date 2D seismic programs and nine drillholes have been completed. The estimated potash resources for only two of their 19 potash permits is 4.73 billion tonnes (Indicated plus Inferred resources) (Piche & Mackintosh, 2013), which is equivalent to nine times the total domestic potash resources in China.

This paper presents a summary of potash exploration and development in Saskatchewan, Canada, and provides general geological information on Saskatchewan's Prairie Evaporite Formation and safety considerations for field drilling activities.

2 GENERAL INFORMATION-YANZHOU COAL AND POTASH IN CANADA

2.1 *Yanzhou Coal*

Yanzhou Coal is an international public mining company and one of the leading producers of fertilizers and coal-based chemicals. In the mineral business, Yanzhou Coal is a leading supplier with sites in China as well as Australia and Canada. Yanzhou Coal has been listed on the Stock Exchanges of New York, Shanghai and Hong Kong respectively since 1998 and on the Australian Securities Exchange after its merger with Gloucester Coal Limited in 2012. Yanzhou Coal employs more than 100,000 people.

Yanzhou Coal aims to become a comprehensive provider of energy and fertilizer through healthy, sustainable and environmental-friendly growth, which benefits its shareholders, customers and employees. Thanks to its diversified business segments and innovative technologies, Yanzhou Coal has developed into a growth-oriented supplier of coal, coke, methanol, fertilizer and aluminium products, with the acquisition of Australian Felix Resources in 2009 and the Potash Properties in Canada.

2.2 *Potash properties in Canada*

In September 2011, Yanzhou Coal purchased 19 Potash Permits (KPs) in Saskatchewan, Canada and formed a new subsidiary—Yancoal Canada Resources Co., Ltd. ("Yancoal Canada"). Yancoal Canada owns 100% of more than 1,325,388 acres

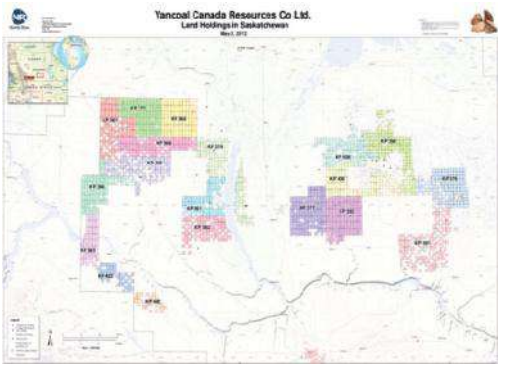


Figure 1. The location of Yancoal Canada's 19 Potash Permits.

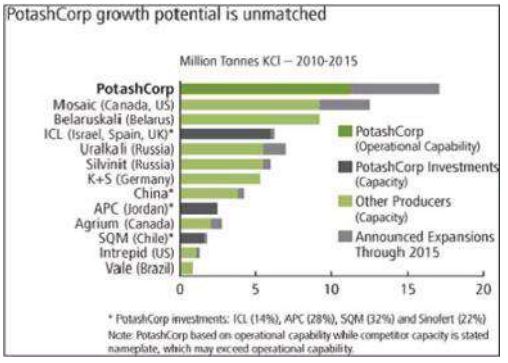


Figure 2. The World's Major Potash Producer's Capacity (From SMA Source).

(5,363.84 km2) of Potash Subsurface Exploration Permits, ranking the 3rd in position (by total acres) in Canada, after BHP Billiton and Canada Potash Corporation.

Yancoal Canada's potash property is situated in central and southern Saskatchewan, between the cities of Saskatoon and Regina (shown in Figure-1). Topography is relatively flat with gently rolling cleared farmland/pasture mixed with local poplar/aspen bluffs. The property has several positive features with regards to infrastructures. There is reasonable access to transportation facilities, natural gas pipelines, major power transmission lines, labor force and services. Water supply sources such as local underground reservoirs and natural surface water sources are currently being evaluated by Golder Associates.

Integrated with its professional mining experience, advanced mining technology and fertilizer produce and sale network, Yancoal Canada plans to become a real potash producer in Canada. Yancoal Canada is committed to local economic development while protecting environment, as they explore and develop their 19 potash permits phase by phase. Yancoal Canada began their potash exploration program and exploration activities in late 2011. The targeted plant production for Yancoal Phase-1 Project is 2.8 million tonnes per year, including production from both primary and secondary solution mining, with anticipated operation by late 2018.

3 POTASH IN SASKATCHEWAN

3.1 *Potash mining*

In general, potash deposits located at depths less than 1100 m below surface are exploited by conventional mining method. Solution mining methods are typically used for those deposits, which are deeper than 1100 m (Rubiolo, 2010).

The present time, there are three operating potash companies in Saskatchewan; Potash Corporation of Saskatchewan ("PCS"), Mosaic Potash and Agrium Inc. In 2011, the three potash producers combined produced approximately 17 million tons of KCL and had cumulative values totalling $ 6.85 billion. (MOE, 2012). Figure 2 shows the world major potash producer's capacities.

The last several decades have seen many cycles of world potash demand, the effects of which directly impact potash exploration in Saskatchewan. Saskatchewan's potash industry is currently undergoing a boom with current demand significantly increasing expansion and exploration within the province. Potash activity is presently being undertaken from existing potash producers (as Greenfield and Brownfield Projects) and junior exploration companies (as Greenfield Projects).

3.2 *Saskatchewan Potash Deposit and Geological Anomalies*

The potash deposits within Canada are the world's single-largest source of mineable potash, comprising almost 50% of the world's known potash reserve. Saskatchewan's potash resources occur within Middle Devonian Elk Point Group strata as relatively flat-lying and laterally extensive bedded deposits comprised predominantly of bedded halite (NaCl), sylvite (KCl), carnallite (KCl. $MgC_{12}.6H_2O$) and clays or insolubles. The Prairie Evaporite Formation extends from the southern extremities in North Dakota and north-eastern Montana up through southern and central Saskatchewan and into north-eastern Alberta (shown as Figure-3). The potash beds occur within the uppermost strata of a relatively thick evaporite succession known as the "Prairie Evaporite



Figure 3. Potash Deposit in Saskatchewan (From Saskatchewan Energy and Resources (SER) Website).

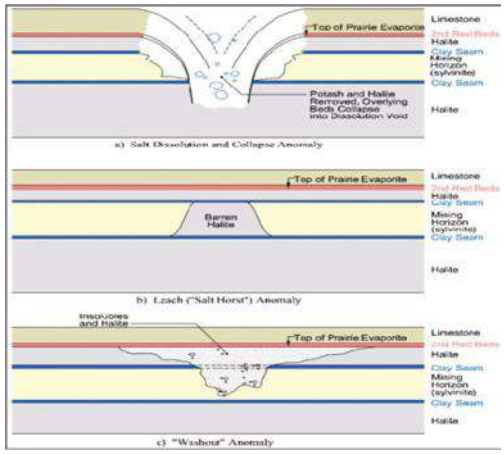


Figure 4. Anomalies Affecting Potash-bearing Bed Geology.

Formation", which essentially is comprised of a broadly distributed salt deposit with anhydrite interbeds. Three potash units may be present including (from the base to uppermost) the Esterhazy, Belle Plaine, and Patience Lake Members (Holter, 1969).

The potash-bearing beds may be affected by three general types of anomalies, a) Salt dissolution and collapse, b) Leach anomalies, and c) Washout anomalies. In general, a disturbance that affects the normal character of the sylvinite-bearing beds is considered an "anomaly" and, thus, represents an area which is not suitable for mining. The impact of these types of anomalies on mining operations is that the grade of the potash ore being sent to the mill drops as mining cuts through anomalous ground, or that a portion of the potash ore reserve is left in the ground as mining operations abandon the anomalous ground as a safety pillar surrounding it. Figure 4 illustrates the types of disturbances that created anomalous altered zones within the main sylvinite-bearing beds as is typical for Saskatchewan potash mining properties (Halabura & Hardy, 2007).

4 POTASH EXPLORATION

The two main methods of data acquisition used for determining the geology and delineation of a potash Mineral Resource are seismic programs (either 2D or 3D) and drilling with core retrieval.

Seismic: Reflection seismic methods can be used to create images of the geologic changes and some of the above discussed anomalies. 2D and 3D seismic surveys are highly effective subsurface analytical tools for potash exploration used in the identification and estimation of the degree of salt loss, salt dissolution-induced collapse structures, and the identification of other geological elements. These seismic programs can help complete a picture of the subsurface that should enhance the ability of the exploration team to successfully select well locations.

Drilling: Holes or wells are drilled in areas where the 2D and 3D seismic survey indicated as favorable for potash mineralization or for investigation of geological structures. Drilling further defines the extent, grade and type of potash mineralization present on the property and provides further calibration for interpretation of seismic data. Holes are drilled vertically targeting the Prairie Evaporite formation, which are conventionally cored using invert or brine drilling fluids so as not to dissolve the salt and potash sequences. Samples are collected from the potash sequence for observation and assay analysis, and each hole is logged using industry-standard down-hole geophysical logging techniques.

5 SAFETY CONSIDERATION

Mineral exploration, by nature is a high risk activity. The safety consideration, risk assessment and risk mitigation plans are paramount for successful exploration portfolio management. Some of the key factors and consideration for safe and smooth drilling activity are the following:

- Select a reputable exploration management company with relevant experience in the potash sector;
- Collect and analyze all historical and existing data and information on the targeted area;
- Complete seismic programs prior to drilling to help locate well;
- Combine the experience and talent of the seismic team and the exploration team during selection of the well location to minimize risks of encountering anomalies;

- Select suppliers and field operators with strong safety records and training;
- Have in place a well-arranged schedule and emergency plan for potential incidents and risks;
- Plan at all times for prompt and effective communication between operator, field team and local government.

In the following, one the Saskatchewan potash exploration wells completed by a Junior company is provided as an example of how risk was mitigated and managed using the above considerations. During the drilling of an exploration well, while coring the Prairie Evaporite Formation, fluids (brine) were encountered with unusually high pressures. The blow-out preventers (BOP's) were immediately shut to ensure a blow-out would not occur. Following the initial pressure kick the drilling fluid (or mud) was continually "weighted up" (addition of barite to the drilling fluid in an effort to push pressurized fluids back into the formation) and circulated in the hole in an attempt to secure the well until the well was cemented in and abandoned.

Prior to the drilling of the well all geological data, including the seismic was thoroughly reviewed and analyzed. From the data at hand there was no reason to expect an influx of fluid during the second core run in the Prairie Evaporite Formation. Not only is it unusual to encounter fluids in the middle of the salt bed, the pressures encountered in this well are abnormally high for the potash exploration industry. The zero casing and drill pipe pressure was achieved when the fluid column was at 2000 kg/m3. This equates to a bottom-hole pressure of approximately 30 MPa which is hydrostatically over-pressured by about 15 MPa.

Although this incident was an unfortunate situation to encounter while drilling, all parties involved were diligent and responsible when determining the correct solution to implement. Due to safeguards put in place prior to the start of drilling and the incident of pressurized brine, this well did not experience a blow-out and there were no injuries to field personnel or to the environment. The following success factors attributed to preventing a blow-out.

1. Blow-Out Preventers (BOPs):
   - Proper sized BOPs were used in the drilling operations to counteract the pressures experienced in the wellbore.
   - The BOPs were inspected and tested regularly as per government regulations.
2. Casing Installation:
   - Casing was installed from surface to core point which contained the fluid/pressure in the wellbore (including surface and intermediate casing). This intermediate casing is not installed in all potash wells in Saskatchewan.
   - Casing was cemented from surface to core point which prevented casing from bursting under pressure. Some Saskatchewan potash wells only "tack" the intermediate casing in. There is speculation that the high pressures in this well may have dislodged the intermediate casing if it had only been tacked in place.
3. Operations:
   - Casing and BOPs were pressure tested prior to drilling out casing shoe.
   - Drillers and well supervisors had proper training and certificates in "First Line Supervisor's Blowout Prevention" and "Second Line Supervisor's Well Control", respectively. They not only had the training, but were prompt and accurate with implementation protocols outlined in these training and certificate programs.

6 CONCLUSION AND RECOMMENDATIONS

Presently, the potash sector in Saskatchewan, Canada is booming. Yancoal Canada is progressing with the development of their Saskatchewan potash properties using the methodology that an effective and well-organized exploration program is the key factor for junior potash exploration companies and their Greenfield Project. For illustration of exploration process and safety considerations, a drill incident example is provided to show the importance of careful planning, proper training and open, clear communication.

In undertaking a potash exploration and development project, the first priority task is to estimate the amount and quality of potash contained within the targeted potash permit area. This paper demonstrates the importance of collecting and analyzing existing geological data prior to completing drilling programs in order to minimize risks from geology anomalies. Outside of geology knowledge, safety considerations, risk assessment and risk mitigation plans are paramount for successful exploration portfolio management. Some of the key factors and consideration for safe and smooth drilling activity are the following:

- Select a reputable exploration management company with relevant experience in the potash sector;
- Collect and analyze all historical and existing data and information on the targeted area;
- Complete seismic programs prior to drilling to help locate well;

- Combine the experience and talent of the seismic team and the exploration team during selection of the well location to minimize risks of encountering geological anomalies;
- Select suppliers and field operators with strong safety records and training;
- Have in place a well-arranged schedule and emergency plan for potential incidents and risks;
- Plan at all times for prompt and effective communication between operator, field team and local government.

ACKNOWLEDGEMENTS

The authors gratefully acknowledge: RPS Energy for their assistance with Seismic Interpretation; The North Rim project team for their execution of the drilling program and their contribution to the NI 43–101 Technical Report of the targeted area; Mr. Dave Mackintosh, P. Geo. for his contribution to Yancoal Potash Project.

REFERENCES

Fuzesy, A. 1982. Potash in Saskatchewan, *Saskatchewewan Industry and Resources Report*, P 44.

Halabura S.P & Hardy M. 2007. An overview of the geology of solution mining of potash in Saskatchewan, P 3, 10 and 13.

Holter, M.E. 1969. The middle Devonian Prairie evaporite of Saskatchewan, *Saskatchewan Department of Mineral Resources,* Report No. 123.

Piché. L & Mackintosh D. 2013. *NI 43- 101 Technical Summary Report,* an unpublished report prepared for Yancoal Canada Resource Co., Ltd., P8, 32.

Potash: Tonnes of Interest, 2012. *The official Publication of the Saskatchewan Mining Association*, P 16.

Rubiolo, D. 2010. Potash exploration in north and south America", *GEONOMOS* 18 (1): P.41–42.

This page intentionally left blank

Progress in Mine Safety Science and Engineering II – He et al. (Eds)
© 2014 Taylor & Francis Group, London, ISBN 978-1-138-00122-0

Experimental study on high temperature shear strength parameter of salt rock

Kun Fang, Yun-Peng Li, Wei-Wei Bi & Jin-Peng Wu
College of Mechanical and Transportation Engineering, China University of Petroleum, Beijing, China

ABSTRACT: In order to research the thermal effect's law of shear strength parameters of rock salt under high temperature condition, the triaxial compression tests of two place's salt rock under different high temperatures and different confining pressure are carried out. Salt rock thermal damage variable is defined, exported shear strength parameters under the condition of the different high temperature and its thermal damage relationship. The research indicated that with the increase of temperature, salt rock thermal damage also increases, the shear strength parameters of rock salt deteriorated significantly, shear strength and triaxial compressive strength is gradually attenuation trend. Two area's salt rock shear strength parameter and intensity values different, but have the same attenuation trend. this analysis method can be used for salt cavern stability evaluation analysis reference.

1 INTRODUCTION

Salt rock is a soft rock with low intensity, large deformation. Because of the very low permeability, good creep, injury healing, and other characteristics, salt rock is widely used as energy storage medium. Mechanical properties of rock salt in the Underground Storage will be affected by temperature, the impact of temperature on rock salt is mainly reflected in the mechanical properties (strength, deformation) and thermal characteristics (linear expansion, thermal conductivity, specific heat, temperature, conductivity) etc. Therefore, scholars have undertaken extensive research on the thermodynamic properties of rock salt. As in literature 1, through a series of tests for heated salt rock at different temperatures, Obtains the relationship between compressive strength and axial strain along with temperature change under the high temperature function. As in literature 2, testing studies is made on the mechanical properties of rock salt after undergoing different high temperatures, The mechanical properties include stress—strain curve, peak stress, peak strain, modulus of elasticity. There are other scholars on these issues were also made by the appropriate research and obtain valuable results, as in literature 3–7. Nevertheless, due to the particularity of rock salt and its engineering use, the thermal effect of the salt rock is still much widespread concern. According to the salt rock triaxial compression under different temperature conditions in this article, it analyses the change rules of shear strength parameters of rock salt in different confining pressure, different temperature conditions. Introduction of heat damage variable, establish the high temperature shear strength parameters of rock salt, rock salt triaxial compressive strength and thermal damage factor with temperature changes in relationship, and the corresponding thermal effects of the law is discussed.

2 RELATIONSHIP BETWEEN HIGH TEMPERATURE SHEAR STRENGTH PARAMETERS AND TEMPERATURE

As the temperatures rising, salt rock's internal moisture evaporation and drying increases, molecular thermal motion increased, weakening its grain and the cohesive force between the particles. In addition, as the temperature increase, the internal crack source of rock salt growth and micro-cracks probability increases. It caused the salt rock's skeleton mineral particles and the structure of the fine view changed, which is damage. With the continued accumulation of this damage, resulting in the continuous degradation of shear capacity of the salt rock and reduce. This strength deterioration could embody in the damage characteristics of the shear strength parameters of rock salt. High temperature conditions, the shear strength of rock salt are not only related to temperature changes, and also have a certain relationship with the micro-damage of the rock salt's structure.

As in literature [8], Mohr-coulomb strength conditions considering temperature effects can be expressed as follow.

$$\sigma_1(T,\sigma_3) = m(T)\sigma_3 + b(T) \tag{1}$$

m(T), b(T) is triaxial compressive strength parameters.

$$\left.\begin{aligned} m(T) &= \frac{1+\sin\varphi(T)}{1-\sin\varphi(T)} \\ b(T) &= \frac{2C(T)\cos\varphi(T)}{1-\sin\varphi(T)} \end{aligned}\right\} \tag{2}$$

According to the Mohr—Coulomb strength conditions and salt rock shear strength thermal damage, thermal damage factor as (3).

$$\left.\begin{aligned} \varphi(T) &= \arcsin\left[\frac{m(T)-1}{m(T)+1}\right] \\ c(T) &= \frac{b(T)[1-\sin\varphi(T)]}{2\cos\varphi(T)} \end{aligned}\right\} \tag{3}$$

C(T), φ(T) is salt rock cohesion and the angle of internal friction when temperature is T.

Define thermal damage factor as follow.

$$\left.\begin{aligned} D_C(T) &= 1-\frac{C(T)}{C(T_0)} \\ D_\varphi(T) &= 1-\frac{\varphi(T)}{\varphi(T_0)} \end{aligned}\right\} \tag{4}$$

$C(T_0)$ is the cohesive force of room temperature; $\varphi(T_0)$ is the internal friction angle of room temperature; $D_C(T)$, $D_\varphi(T)$ respectively be the damage factor when temperature is T. (4) is organized as follow.

$$\left.\begin{aligned} C(T) &= C(T_0)(1-D_C(T)) \\ \varphi(T) &= \varphi(T_0)(1-D_\varphi(T)) \end{aligned}\right\} \tag{5}$$

The above equation is the shear strength parameters of rock salt with temperature relationship which represented by the thermal damage factor. Thus, once the salt rock thermal damage factor variation with temperature is obtained, it can get different salt rock under high temperature shear strength parameter values as long as known salt rock strength parameters.

Take (5) and (2) into (1) to obtain the relationship between three axial compressive strength and thermal damage factor for salt rock, as (6).

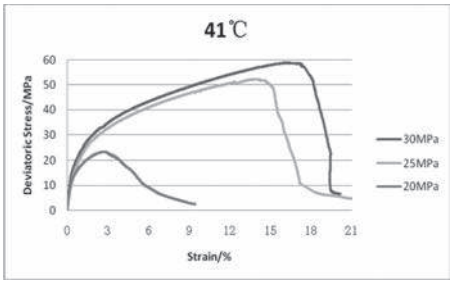
$$\begin{aligned} \sigma_1(T,\sigma_3) = {} & \frac{1+\sin\left(\varphi(T_0)(1-D_\varphi(T))\right)}{1-\sin\left(\varphi(T_0)(1-D_\varphi(T))\right)}\sigma_3 \\ & + \frac{2\left(C(T_0)(1-D_C(T))\right)\cos\left(\varphi(T_0)(1-D_\varphi(T))\right)}{1-\sin\left(\varphi(T_0)(1-D_\varphi(T))\right)} \end{aligned} \tag{6}$$

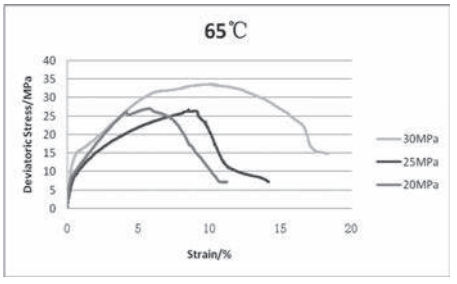
3 HIGH-TEMPERATURE STRENGTH PARAMETERS OF ROCK SALT TEST

3.1 *High temperature triaxial tests of rock salt*

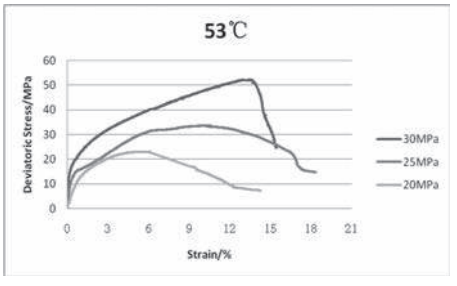
Sample using rock salt core which at different depths of two reservoirs, salt rock is white or grey, it is diameter 50 mm, height 100 mm standard cylinder. The test is divided into at room temperature, 41°C, 53°C, 65°C, each temperature is divided 20 MPa, 25 MPa, 30 MPa. Some of the test curve as shown in figure 1.

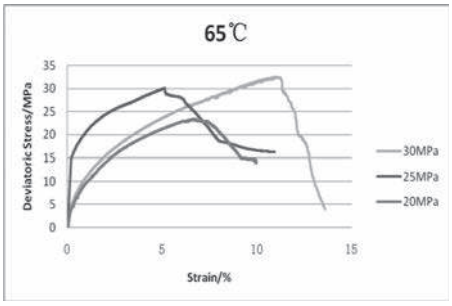
Using the pressure of the triaxis compression curves under same temperature, obtain triaxial compressive strength parameters m and b values of rock salt in each temperature. Through (3), get the shear strength parameters of rock salt is different under high temperature condition, namely the cohesion and internal friction angle, are listed in table 1. From table 1, it can be seen at high temperatures, parameters m and b decrease with the increasing temperature, the cohesion and friction angle have the same regularity. The shear strength parameters under two areas have significant differences.





(a) Triaxial compression curves at two temperatures in reservoir A





(b) Triaxial compression curves at two temperatures in reservoir B

Figure 1. Rock salt high temperature triaxial compression test curve.

Table 1. Cohesion and internal friction angle in different temperature.

Storage cavern	Temp °C	m	b	C/Mpa	φ/(°)
1	29	3.024	9.024	2.82	30.2
	41	2.673	8.731	2.67	27.1
	53	1.904	6.319	2.29	18.13
	65	1.907	6.058	2.19	18.18
2	29	3.679	4.931	1.29	34.93
	53	2.657	2.983	0.92	26.94
	65	2.053	2.063	0.72	20.17

3.2 *Salt rock strength thermal damage effect*

The damage factor of the salt rock which using table 1 and the (4) at different temperatures are listed in table 2. The change law of the thermal damage factor with temperature as shown in figure 2. From table 2 and figure 2 can be seen, as the increasing temperature, the damage value also increased, two area rock salt thermal damage factor was increased with increasing temperature. The two rock salt thermal damage factor in one reservoir consistent trends, reservoir 1, after the temperature reaches 53°C it has slowdown trend.

The change law's approximation fitting equation of two reservoir thermal damage dependence of temperature as follow.

$$\left.\begin{aligned} D_{c1}(T) &= -0.848e^{-0.01741T} + 0.52 \\ D_{\varphi 1}(T) &= -1.659e^{-0.03924T} + 0.51 \end{aligned}\right\} \tag{7}$$

$$\left.\begin{aligned} D_{C2}(T) &= -1.819e^{-0.04424T} + 0.50 \\ D_{\varphi 2}(T) &= -2.266e^{-0.03977T} + 0.71 \end{aligned}\right\} \tag{8}$$

The two reservoir's relationship between shear strength parameters and temperature as follow.

$$\left.\begin{aligned} C_1(T) &= C_1(T_0)(1 + 0.848e^{-0.01741T} - 0.52) \\ \varphi_1(T) &= \varphi_1(T_0)(1 + 1.659e^{-0.03924T} - 0.51) \end{aligned}\right\} \tag{9}$$

Table 2. Thermal damage to the value of rock salt at different temperatures.

Storage cavern	Temp °C	29	41	53	65
1	$D_{C1}(T)$	0	0.053191	0.187943	0.222163
	$D_{\varphi 1}(T)$	0	0.109814	0.355735	0.382339
2	$D_{C2}(T)$	0	0.144064	0.288137	0.439907
	$D_{\varphi 2}(T)$	0	0.269954	0.439907	0.581659

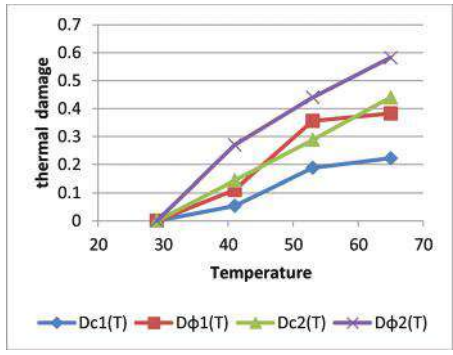


Figure 2. Rock salt thermal damage factor and temperature curves.

$$\left.\begin{aligned} C_2(T) &= C_2(T_0)(1 + 1.819e^{-0.04424T} - 0.50) \\ \varphi_2(T) &= \varphi_2(T_0)(1 + 2.266e^{-0.03977T} - 0.71) \end{aligned}\right\} \tag{10}$$

Take (7) and (8) into (6) type, obtained two change laws of rock salt triaxial compressive strength as the change of temperature.

Take 53°C , 65°C as the example, salt rock shear intensity parameter as shown in table 3 which using (9) and (10). Combine Table 3 and (1) can obtain the salt rock triaxial compressive strength under different temperature (20 MPa confining pressure as example) as Table 4. From Table 3 and Table 4, it can be seen that the salt rock shear strength increased with the temperature decrease, mean the salt rock strength degradation with the temperature increased, and salt rock shear strength parameters of two reservoirs have the same regularity. Through this Table or analysis method can be conveniently obtained the thermal damage or attenuation coefficient of salt rock shear strength. By (9), (10), (11) and (12) clearly visible, if the salt rock thermal damage factor with temperature variation was obtained by the test, it can convenient obtain the salt rock shear strength parameters thermal damage equation only by the normal temperature test, which can be used as a salt cavern gas storage security and stability evaluation of mining operation in the note reference.

$$\sigma_1(T,\sigma_3)\big|_{K1} = \frac{1+\sin\left(\varphi(T_0)(1+1.659e^{-0.03924T}-0.51)\right)}{1-\sin\left(\varphi(T_0)(1+1.659e^{-0.03924T}-0.51)\right)}\sigma_3 + \frac{2\left(C(T_0)(1+0.848e^{-0.01741T}-0.52)\right)\cos\left(\varphi(T_0)(1+1.659e^{-0.03924T}-0.51)\right)}{1-\sin\left(\varphi(T_0)(1+1.659e^{-0.03924T}-0.51)\right)} \quad (11)$$

$$\sigma_1(T,\sigma_3)\big|_{K2} = \frac{1+\sin\left(\varphi(T_0)(1+2.266e^{-0.03977T}-0.71)\right)}{1-\sin\left(\varphi(T_0)(1+2.266e^{-0.03977T}-0.71)\right)}\sigma_3 + \frac{2\left(C(T_0)(1+1.819e^{-0.04424T}-0.50)\right)\cos\left(\varphi(T_0)(1+2.266e^{-0.03977T}-0.71)\right)}{1-\sin\left(\varphi(T_0)(1+2.266e^{-0.03977T}-0.71)\right)} \quad (12)$$

4 CONCLUSION

A: Use the salt rock shear strength parameters for the thermal damage variable, it defines the thermal damage factor of rock salt shear strength, and derived the variation of salt rock strength and thermal damage factor under the condition of high temperature, which can describe the influence of high temperature environment for effective change of salt rock strength regularity.

B: With increasing temperature, salt rock strength and shear strength parameters deteriorated significantly damage, manifested as the shear strength parameters of rock salt decreases, compressive and shear strength showed a significant attenuation of the trend. Rock salt of two reservoirs shear strength parameter values, although some differences, but it has the same regularity.

Table 3. Different regions of the salt rock shear strength parameter compared with the temperature variation.

Storage cavern	Temp °C	Test data		Damage effects	
		C/MPa	φ/(°)	C/MPa	φ/(°)
1	53	2.29	18.13	2.33	21.06
	65	2.19	18.18	2.15	18.71
2	53	0.92	26.94	0.87	19.75
	65	0.72	20.17	0.99	16.10

Table 4. Triaxial compressive strength of rock salt at different temperatures compared (confining pressure is 20MPa).

Storage cavern	Temp °C	Test data	Damage effects
1	53	44.37480	49.21047
	65	44.17439	44.87736
2	53	56.10366	42.86848
	65	43.09773	37.95315

C: With rock salt temperature test, using thermal damage factor analysis method, can easily get high triaxial compressive strength of rock salt with temperature-dependent thermal effect equation, and the shear strength parameters of rock salt thermal damage formula, which are for salt cavern gas storage injection and production operations evaluation and analysis of the security and stability of reference.

REFERENCES

1. Liang Wei-guo, Zhao Yang-sheng. Testing study on physiccal and mechanical properties of heated salt rock with 240°C, Chinese Journal of Rock Mechanics and Engineering, 23(14), 2365 (2004).
2. Gao Xiao-ping, Yang Chun-he. Experimental studies on temperature effect of mechanical properties of rock salt, Rock and Soil Mechanics, 26(11), 1775 (2005).
3. Alm O, Jaktlund L L. The influence of microcrack density on the elastic and fracture mechanical properties of Stripa granite[J]. Physics of the Earth and Planetary Interiors, 40(3), 161 (1985).
4. Udo Hunsche, Otto Schulze. Effect of humidity and confining pressure on creep of rock salt[A]. The-Mechanical Behavior of Salt, Proceedings of the ThirdConference[C] Edited by M. Ghoreychi. P. B 6rest and H. Reginald Hardy,Jr. Germany: Tans Tech Publication, 237 (1997).
5. Du Shou-ji, Liu Hua, Zhi Hong-tao. Testing study on mechanical properties of post-high-temperature granite[J]. Chinese Journal of Rock Mechanics and Engineering, 23(14), 2359 (2004).
6. Chen Jian-wen, Yang Chun-he, Gao Xiao-ping. Study on the coupled damage of temperature and mechanics for salt rock[J]. Chinese Journal of RockMechanics and Engineering, 24(11), 1986 (2005).
7. Hartmut Kern, Jorg H. Fanke. The effect of temperature on the chemical and mechanical behavior of camallite_halite rock[A]. The Mechanical Behavior of Salt, Proceedings of the First Conference[C]. Edited by H.Reginald Hardy, Jr. Germany:Trans Tech Publication, 180 (1981).
8. You ming-qing. Mechanical properties of rock[M], Beijing: Geological Publishing House.

3 *Mine product testing technology and safety symbol management*

This page intentionally left blank

Progress in Mine Safety Science and Engineering II – He et al. (Eds)
© 2014 Taylor & Francis Group, London, ISBN 978-1-138-00122-0

Fast verification method of mining mechanical anemometers based on wind speed equivalent weight

Wen-Yao Ni
Key Laboratory of Hebei Province for Mine Disaster Prevention, Safety Engineering School, North China Institute of Science and Technology, Yanjiao, Beijing-East, China

Wen-Mei Gai
Civil and Environmental Engineering School, University of Science and Technology Beijing, Beijing, China

ABSTRACT: The problems in the current domestic use of the pitot tube combining micro-manometer to verify the mining mechanical anemometers were analyzed. Based on the structure principle of hydrodynamics, under the premise of the test with no violation of the orders anemometer verification, a new method based on wind speed equivalent weight to verify the anemometer was introduced. And the field test in the scene of the Key Laboratory of Hebei Province for Mine Disaster Prevention demonstrates that this method is a simple, fast, and accurate method to verify the mining mechanical anemometers within the expiration date of the wind tunnel.

Keywords: Machinery anemometer, pitot tube & micro-manometer method, air velocity equivalent weight metho, verification

1 INTRODUCTION

"Coal Mine Safety Regulations" provides in No.106 issue for that: "Mine must have a sufficient number of ventilation safety testing instruments, meters must be authorized by the National Safety Instrumented measurement units qualified to carry out inspection."

In the early 1960s, came the domestic application of anemometer verification with low-speed wind tunnel. The current mining anemometer verification adopts "Orders of Mining Anemometer Verification" (JJG01–96) promulgated by the original Coal Industry of China in 1996, which provided that the period of anemometer verification is six months. In this verifying method, the dynamic pressure of air current is measured by the pitot tube & micro-manometer, which is converted into the actual air velocity, and then drawn into a calibration curve with the anemometer readings, used together with the anemometer.

At present, for the resolution ratio in reading the compensated micro-manometer currently used in china is 0.1 pa, errors comes easily in reading the micro-manometer when measured at low air speed (to lower dynamic pressure). In the meantime, the micro-manometer adjustment process before reading is more time-consuming, particularly for the fine-tuning reading. Therefore it is necessary to improve the method of anemometer verification. Under the premise of according with the orders of anemometer verification, a fast method of anemometer verification was introduced in the text.

2 FAST VERIFYING METHOD OF ANEMOMETER—AIR VELOCITY EQUIVALENT WEIGHT METHOD

According to the Proportion Law of ventilator in hydrodynamics, the air flow in the wind tunnel and the ventilator speed is in direct proportion, so is the air speed of any point and the wind speed, for the cross-section of any point in the wind tunnel is constant. And the Verification of speed can be fast and accurate. Whereas the above analysis, the corresponding relation equation of them can be built up with determination of the air speeds to different ventilator speeds, improving the pitot tube & micro-manometer method, which is process-complicated and time-consuming with greater error in lower air velocity, into a method of calculating air velocity with determination of the ventilator speed, called the air velocity Equivalent weight method.

2.1 *The determination arrangement*

Fig. 1 is the sketch map of technical determination arrangement for correcting anemometer. After

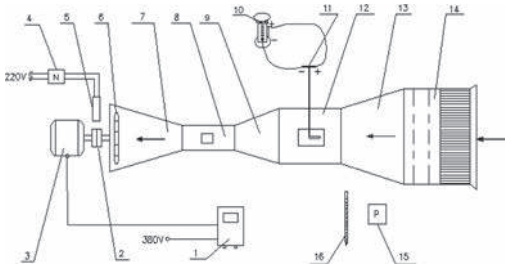


Figure 1. Sketch Map Of Technical Determination Arrangement.
1-Electronic control box, 2-Axle connecting machine, 3-DC motor, 4-Digital Speed Display, 5-Photoelectric speed sensor, 6-Air impeller 7-the proliferation segment, 8-High-speed segment, 9- the second contraction segment, 10-the compensated tasimeter, 11-Pitot tube, 12-Medium-speed segment, 13-the first contraction segment, 14-Rrectification segment, 15-Barometer, 16-Thermometer.

Axial-flow exhaust fan is activated by the speed control DC motor, then the air current enters into the XRS-type testing wind tunnel when it is rectified, with airflow speed changed through a second contraction and once diffusion in the wind tunnel. When to its maximum permissible speed of 2800 rpm, wind speeds to three experimental segments in the wind tunnel are 2.61 m/s, 15.44 m/s and 48.67 m/s. Select corresponding experiment segment to correct according to the measuring range of the mining anemometer when verification.

The silicon controlled rectification automatic speed-control system was adopted in the adjustment of the ventilator speed. There are two: First, the "stepless speed regulation" is the adjustment in the largest range of biggest ventilator speed fan in any way; second, the "fixed speed" is, for each test segment, setting up multiple sets of fine-tuning potentiometer, and setting the value of many groups under the required speed.

2.2 *Parameter measurement*

2.2.1 *Parameter measurement of ventilator speed*

To measure the ventilator speed by the digital speed display combined with the photoelectric speed sensor,

$$n = \frac{60z}{H \cdot t} \tag{1}$$

where: n indicates actual fan speed, rpm, z is signal number showed by Speed Display, H indicates signal number given by the ventilator in a cycle, t is measurement time, s.

2.2.2 *Actual air velocity measurement in the experimental segment*

To measure the air velocity by pitot tube combined with the compensated micro-manometer.

$$v = \left(\frac{2\xi h_v}{\rho} \right)^{0.5} \tag{2}$$

where: v is the actual air speed, m/s, ξ is current coefficient of pitot tube, authenticated that ξ = 1.004, ρ indicates the density of humid air, kg/m^3, h_v indicates airflow pressure, pa.

$$\rho = \frac{C \cdot P}{T} \tag{3}$$

where: P is the actual atmospheric pressure of measurement location, hpa, C is coefficient without calculating partial pressure of saturated steam, ks^2/m^2, P is actual atmospheric pressure in the location, hpa, considered common conditions and the actual situation in underground coal mines of anemometer verification, t generally between 10~30 °C, when C = 0.346, T is the thermodynamic temperature of the air in the location, K.

$$T = 273.15 + t \tag{4}$$

where: t – temperature of the dry air in the location, °C.

$$h_v = \rho_t \cdot g \cdot h \tag{5}$$

Where: ρ_t is the density of pure water at temperature t, kg/m^3, in the experimental test conditions, its value varies at 0.99673~0.99715, approximate values for the 1.0. g is the gravity acceleration of the location, Xuzhou region as 9.81 m/s^2, h is height of the water column of the compensated tasimeter, mm.

Return Eqn. (3), (4), and (5) also parameter values of ξ, C, and ρ_t etc. into Eqn. (2) and get the computational formula of actual air speed as:

$$v = \left[56.932h \frac{(273.15+t)}{P} \right]^{0.5} \tag{6}$$

2.2.3 *Test result*

The authors have tested the mining mechanical anemometers in the scene of the Key Laboratory of Hebei Province for Mine Disaster Prevention based on the air velocity Equivalent weight method. The anemometers were verified in the medium-speed segment of the wind tunnel with the above-mentioned arrangements and

Table 1. Datum of speed and air velocity determined of the XRS-type wind tunnel.

Serial Number	P/hpa	t/°C	ρ/kg·m^{-3}	h/mm	n/rpm	v/m·s^{-1}
1	1003	24.8	1.1648	0.034	168.1	0.76
2	1003	24.8	1.1648	0.061	230.1	1.01
3	1003	24.6	1.1655	0.245	408.1	2.03
4	1003	24.7	1.1651	0.551	615.0	3.05
5	1003	24.8	1.1648	0.980	819.9	4.06
6	1003	24.9	1.1644	1.532	1017.3	5.08
7	1003	25.1	1.1636	2.205	1218.9	6.10
8	1003	25.3	1.1628	3.921	1615.3	8.14
9	1003	25.7	1.1612	6.127	2027.7	10.18
10	1003	25.9	1.1605	8.823	2428.6	12.22
11	1003	26.2	1.1593	12.01	2835.5	14.26

computational formula. The measured results can be seen in Table 1.

The relational equation between the n and v was obtained by data regression of them showed in Table 1 as:

$$v = 0.0051n - 0.0847 \quad (7)$$

Its dispersion is $R^2 = 1$, which shows that the proportional liner relationship between the n and v is more obvious. Similarly, the corresponding segment in the high-speed wind tunnel, the above-mentioned methods can also be used to draw the equivalent relationship between n and v, and not to recount it here.

2.3 *Example analysis of anemometer correction*

For example of medium-speed anemometer verification, dismantle the pitot tube and the compensated micro-manometer showed in Fig. 1, have the anemometer to be verified installed in the axis of the medium-speed segment in the wind tunnel with other arrangements remained.

Verify air velocity by 6 points (maximum speed of not more than anemometer range) With "fixed-point" approach from low-speed to high-speed from low speed to high speed, read the n and the x to the ventilator speed and the anemometer at each measuring point. For the atmosphere condition when verifying the anemometer was near to that of the actual velocity determination in the air velocity Equivalent weight method (the relevant parameters seen in the Table 2), so the air density correction is omissible. So that the actual air velocity v to each measuring point can be worked out with the ventilator speed v substituted into Eqn. (7) directly. Finally, draw the corrective curve of the anemometer with v and x (see Fig. 2), obtaining the fitted equation (also called corrective formula

Table 2. Verifyed data of medium-speed anemometer Anemometer number:2132.

Serial Number	P(hpa)	T(°C)	N(rpm)	V(m·s^{-1})	X(case·min^{-1})
1	1004	25.2	153.7	0.69917	26.5
2	1004	25.2	465.2	2.28782	138.6
3	1004	25.1	863.7	4.32017	281.7
4	1004	25.1	1261.9	6.35099	413.8
5	1004	25.1	1657.4	8.36804	555.6
6	1004	24.9	2011.9	10.17599	678.0

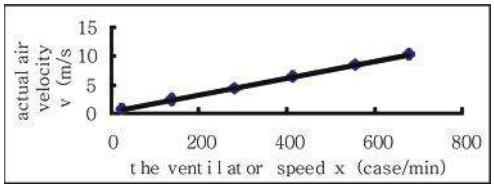


Figure 2. Corrective curve of the anemometer.

of anemometer) of the relationship between them from the curve as well, as:

$$v = 0.0146x + 0.2781 \quad (8)$$

The regression dispersion of the equation is $R^2 = 0.9999$, much approaching to 1, so the curve fits well.

Up to this point, the anemometer on the finish of the fast and accurate verification could be attached to anemometer calibration box with the above-mentioned corrective curve anemometer and the formula, to be used together with the anemometer in the normal usage period until the next correction.

3 CONCLUSIONS

1. Based on the Proportion Law of hydro-mobility of hydrodynamics, with the standard wind tunnel, measured with the standard calibration of the Department, the relationship equation between the actual ventilator speed and the actual air velocity inside the wind tunnel was set up. It can be corrected traditionally with the anemometer readings and the actually tested air velocities for comparison, which has been improved to be the correction method of anemometer readings compared with the ventilator speeds, which is the equivalent wind speed law.
2. The method of equivalent air velocity to verify the anemometer, only needs to standardize the relationship between the ventilator speed and the actual air velocity once, simply in the pitot

tube and micro-manometer method of ministerial orders, Then the anemometer can be verified fast and accurately by determination of the ventilator speed. It has overcome the defects of time-consuming and easy with reading errors etc. brought about by the pitot tube and micromanometer installment during traditional correction of anemometer each time.

3. Whether the equivalent velocity method or the traditional one, only can be used in the valid period of the standard wind tunnel. To the standard wind tunnel itself, it must also be periodically corrected in accordance with the relevant standards. If there is damage in the use of its period, in the absence of rehabilitation and correction by the former, it shouldn't be used for the job of the anemometer calibration.
4. Under normal circumstances, for the year-round change of air density in the mine area is very small, the anemometer can be corrected directly in the method introduced in the text. However, when the anemometer calibration and the test of equivalent velocity, or the usage and the correction of anemometer, are to the large difference in atmospheric conditions (such as the anemometer corrected in the plains used in high altitude), air density must be corrected accordingly in the use of the air velocity Equivalent weight method to verify the anemometer.

ACKNOWLEDGEMENTS

The authors gratefully acknowledge foundation by the China National Key Basic Research Development Project Program (2011CB201202 and 2012CB724206).

REFERENCES

Gu Xiu-Gen, Ni Wen-Yao. 2004. Research of adjustion to the operating point quickly in the function authentication of mine fan. Coal Engineering, 9:0–029 (in Chinese).

Guo Jing-Fa 2012. Mining anemometer automatic verification research and application processing system. Shandong Coal Science and Technology, 2:30–39 (in Chinese).

JJG01-96. 1997. VR of Mine anemometer (JJG01-96). Beijing: Standards Press of China, 107–110 (in Chinese).

Ni WY, Meng ZZ. 2013. Study on Using Independently Developed Equipment for Mine's Axial-Flow Main Ventilator Performance Test. Advanced Materials Research, 619:56–61 (in Chinese).

State Administration of Coal Mine Safety Supervision Bureau 2011. Coal Mine Safety Regulations. Beijing: Coal Industry Press, 127–130 (in Chinese).

Zhu Jin-Bo 2011. Engineering Fluid Mechanics. China University of Mining and Technology Press, 127–130 (in Chinese).

Progress in Mine Safety Science and Engineering II – He et al. (Eds)
© 2014 Taylor & Francis Group, London, ISBN 978-1-138-00122-0

Development of a new kind of safety helmet of underground miner for emergent hedge

Xiao-Ming Liu, Yu-Kun Gao, Zhi-An Huang, Ying-Hua Zhang, Yan-Feng Zhang & Qian Zhao
State Key Laboratory of High-Efficient Mining and Safety of Metal Mines, University of Science and Technology Beijing, Ministry of Education, Beijing, China

ABSTRACT: According to fact that traditional safety helmet can only protect head of wearer, on the basis of traditional helmet, by using computer-assisted method, a new kind of safety helmet of underground miner for emergent hedge was developed. In case of danger, through releasing adiabatic protective material beneath brim of the helmet, a confined space can be formed at head position of wearer as eye vision of wearer can be assured. Experimental results show that as temperature rises over time, order of temperature from highest to lowest is temperature at the face position, temperature at the front of head, temperature at the back of head and temperature over head. Through comprehensive analysis of experimental results, conclusions can be drawn as follows: the optimal oxygen supplying method is supplying oxygen vertically at the front of head and making air flow out from the bottom, and the optimal oxygen supplying speed is 0.1 m/s, moreover, inlet air temperature should stay at about 300 k. The research result can supply new program of emergent hedge for underground miner.

1 INTRODUCTION

Many kinds of accidents would happen during process of coal production, such as fire, gas explosion, sudden gush out of harmful gases and so forth. A safety helmet is one of the protective equipments which underground miners have to wear.

Traditional mine safety helmets can only defend impacts coming from space above head. When mine disaster such as mine fire or gas explosion happens, miners' faces often completely expose to harm such as sudden gush out of flue gas, toxic or harmful gases and so on, but there are often no proper device or equipment to offer protection. Although some innovations and improvements of traditional mine safety helmets have been made both at home and abroad, few of them can completely meet the need of protecting miner in above imminently hazardous situations. Therefore, it is extremely important and urgent to design a new type of mine safety helmet (Huang H R 2000, Jiang X R 2010).

On the bases of original mine safety helmet and against imminently hazardous situations that threaten head and face of miners, through theoretical calculation and material selection, designing system of a kind of airtight oxygen supplying safety helmet for mine emergent hedge was put forward (Jin P L 2001). Through actual experiment, anthropometric indicators were got when the safety helmet was worn, and characteristics of the safety helmet were known. Through simulating oxygen supplying methods by adopting FLUENT, the optimal oxygen supplying method of the safety helmet was finally designed out. This research can provide idea and reference for other relating researches, and can offer certain technical support for safe development of mines.

2 CHARACTERISTICS OF TRADITIONAL SAFETY HELMETS

As a tool to protect head, a safety helmet shall meet the following conditions in respects of design and structure:

1. Weight: the material adopted to make the helmet should be as light as possible and has enough strength so that it can stand assault of falling objects. Weights of helmets of small-size edge, medium-size edge and roll edge should not exceed 430 g, weight of a large-size helmet should not exceed 460 g, and weight of a cold-proof helmet should not exceed 690 g (weight requirements above do not include additional components).
2. Comfort: the helmet should be comfortable to wear, ensuring that wearers don't feel muggy even under sunshine.
3. Vertical spacing: vertical spacing is the axial distance between the highest point of head top and the inner surface of cap shell when the helmet is worn. Proper vertical distance should be 25~50 mm.
4. Horizontal spacing: when the helmet is worn, the horizontal spacing between cap hoop and each surface of cap shell should be 5~2 mm.

5. Wear height: when the helmet is worn, the axial distance between bottom edge of cap hoop and the highest point of head top should be 80~90 mm.
6. Size of cap hoop: size of cap hoop should be in either one of three ranges which are respectively 51~56 mm, 57~60 mm and 61~66 mm.
7. Size of brim: the minimum size of brim is 0 mm, and the maximum size of brim is 70 mm. Inclination of brim should be 0°~60°.
8. Size of visor: the minimum size of visor is 10 mm, and the maximum size of visor is 70 mm.

There are two current standards of safety helmet in our country which are GB2811-2007 *safety helmet* and GB/T2812-2006 *safety helmet test method*.

There are relevant standards about safety helmet around the world, such as USA ANSIY89. 1-1997, Canada CAN/CZA-Z94.1 and so forth (Sheng H T 2011).

3 THE DESIGN OF SAFETY HELMET FOR MINE EMERGENCY HEDGE

On the original basis, a protective cover was added beneath brim of the helmet so that in case of danger, through releasing it, a confined space could be formed at head position of wearer and eye vision of wearer could be assured as the protective cover was made of transparent adiabatic material, and at the same time, oxygen could be automatically produced in internal space for a while.

Requirements of choosing material to make safety helmet for mine emergency hedge are as follows: firstly, a confined space can be formed to protect wearer's face; secondly, eye vision of wearer can be ensured and wearer's eyes also can be protected. Therefore, aluminium foil coated flame-retardant cotton cloth material was chosen against the first requirement, PVC (Polyvinyl Chloride) was chosen against the second requirement.

This safety helmet for mine emergency hedge can supply oxygen by an oxygen candle which is activated by a fire cap. Schematic diagram of the oxygen candle structure is shown in Fig. 1 (Zhang Z H 1995, Zhang G P 1991):

The appearance and structure of the safety helmet are shown in Fig. 2–Fig. 4.

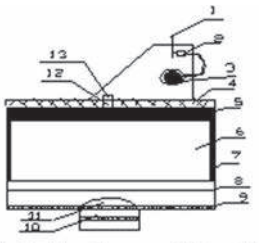
4 PERFORMANCE EXPERIMENTS OF THE SAFETY HELMET FOR EMERGENCY HEDGE

4.1 *Experimental purposes*

Through carrying out anthropometric indicator experiments on the designed helmet, temperature, pulse, carbon dioxide concentration and some other parameters were measured when the helmet was worn so that theoretical basis can be provided for follow-up research on oxygen supplying method.

4.2 *Experimental apparatus and methods*

Main experimental apparatus include safety helmet, safety cover, dry bulb thermometer, wet bulb thermometer, thermocouple thermometer, stopwatch, gas chromatograph and so on.



1—trigging bezel; 2—blow hammer (firing pin); 3—spring; 4—adiabatic board; 5—trigger drugs; 6—oxygen candle;

Figure 1. Schematic diagram of the oxygen candle structure.



Figure 2. The 3D effect graph.

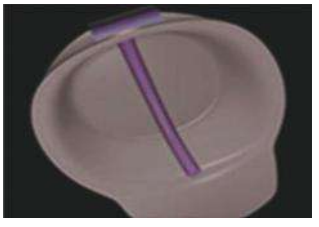


Figure 3. Arrangement of oxygen candle and vessel.

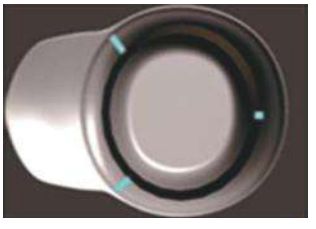


Figure 4. Fixed mode of down part of the helmet.

Experimental methods are as follows: a few 25-year-old healthy men were chosen to wear the helmet, and four measuring points respectively numbered T1, T2, T3 and T4 were respectively arranged at top of head, the front of head, the back of head and face position. As outside temperature was kept steady, parameters such as temperature, pulse frequency, carbon dioxide concentration and some others were measured at the four measuring points respectively within 5 minutes in the following three circumstances: stillness, walking and running.

4.3 *Experimental results and analysis*

1. Temperature variations of measuring points in the three circumstances
   Temperature variations of measuring points in the three circumstances are respectively shown in Fig. 5–Fig. 7.

   As shown in Fig. 5, under condition of stillness, temperature at each measuring point rises gradually and changes relatively fast from the first to second minute, but becomes steady from the third to fifth minute. Temperature at T4 keeps the highest and rises fastest, because T4 is measuring point at the face position inside the helmet where heat produced by breathing gathers. Temperatures at T1, T2 and T3 are similar.

   As shown in Fig. 6, under condition of walking, temperature at each measuring point rises gradually, and temperatures at T1, T2 and T4 change relatively fast from the first to second minute. From the third to fifth minute, temperature at T1 becomes steady, but temperatures at T2 and T4 keep on rising. Temperature at T3 stays at about 31.7 °C. Temperature at T4 keeps the highest because more heat can be produced by breathing under condition of walking. Temperature at T2 keeps the second highest because certain amount of heat can be diffused by the head under condition of walking.

   As shown in Fig. 7, under condition of running, temperature at each measuring point rises gradually, and temperatures at T2 and T4 rise fastest up to 39.1 °C, because more heat can be diffused by the head and much more heat can be produced by breathing under condition of running. Temperature at T1 rises to 35.4 °C within the first minute and becomes steady from the second to fifth minute. Temperature at T3 stays at about 35.5 °C.
2. Pulse frequency in the three circumstances
   As shown in Fig. 8, wearers can keep a normal heart rate for 5 minutes without extra oxygen supply in the three circumstances.
3. Concentration of CO_2 in the three circumstances
   As shown in Fig. 9, in the three circumstances, concentration of CO_2 produced by human is proportional to time. The maximum permissible concentration of CO_2 in air is 25000 PPM. Therefore, oxygen should be supplied in the helmet within 2 minutes.
4. Temperature variation at each measuring point
   As shown in Fig. 10, temperatures at T2 and T4 rise faster than that at T1 and T3. At T1, T2 and T3, differences of temperatures under condition

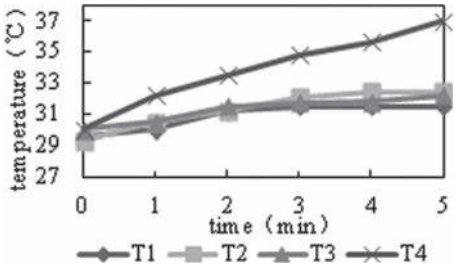


Figure 5. Temperature variation under condition of stillness.

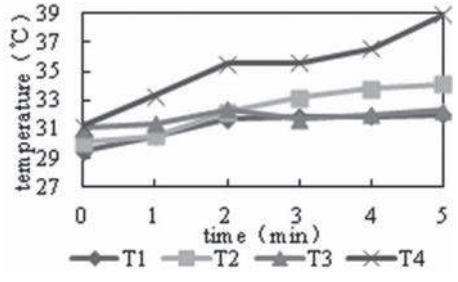


Figure 6. Temperature variation under condition of walking.

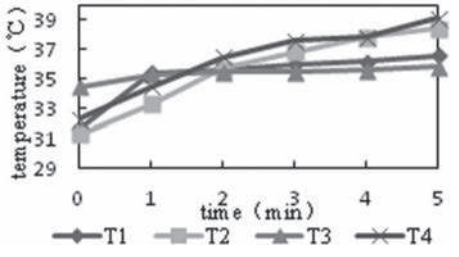


Figure 7. Temperature variation under condition of running.

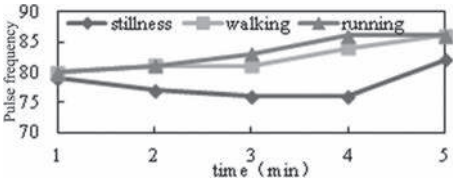


Figure 8. Pulse frequency in the three circumstances.

of stillness and walking are commonly less than 1 °C, but temperatures under condition of running are commonly more than 3 °C higher than temperatures under condition of stillness at these three measuring points. Temperature at T4 rises fastest in the three circumstances, because T4 is measuring point at the face position inside the helmet where more heat can be produced as breathing amount increases.

5 DESIGN OF OXYGEN SUPPLYING METHOD OF THE SAFETY HELMET FOR EMERGENCY HEDGE

5.1 *3D model of the safety helmet for emergency hedge*

The helmet was seen as a sphere with radius 10 cm, the hood was seen as a cylinder with height 10 cm and mask radius 10 cm. According to anatomical structure of head, thickness of head tissue and thermal influence, head was seen as a cylinder with radius 4 cm and height 10 cm, and windpipe was seen as a cylinder with radius 1 cm. After comprehensively considering heat generated by the safety helmet during experiment and possibilities of setting up oxygen supplying air-duct, three designing programs of air-duct were put forward as shown in Fig. 11 (Han Z Z et al. 2004).

Based on oxygen supplying flow being 1 L/min, radius of import tube being 1 cm and oxygen supplying speed being 10 cm/s, three models were respectively designed as follows: (a) supplying oxygen downward at top of head and making air flow out from the bottom; (b) supplying oxygen vertically at the front of head and making air flow out from the bottom; (c) supplying oxygen horizontally at the front of head and making air flow out from the bottom.

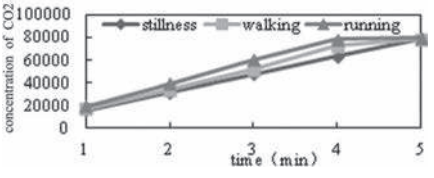


Figure 9. Concentration of CO_2 at T4 in the three circumstances.

5.2 *Design of oxygen supplying air-duct of the safety helmet for emergency hedge*

Through numerical simulation with FLUENT, wind speed at air inlet was set to be 10 cm/s, and environmental temperature and inlet air temperature were all set to be 298k. The bottom was set as pressure outlet and pressure was set as the

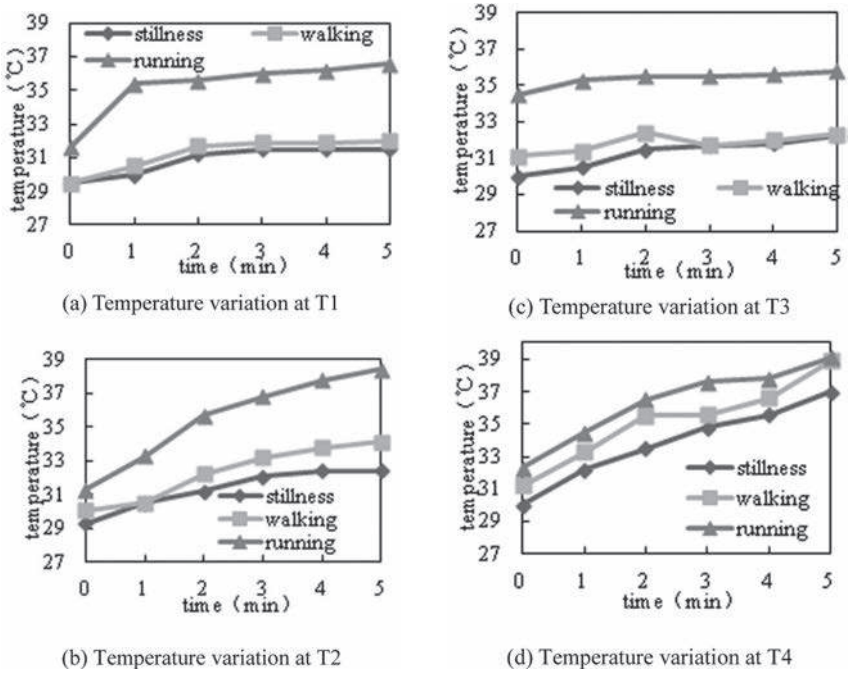


Figure 10. Temperature variation at each measuring point.

standard atmospheric pressure. Without considering influence of time, steady flow was adopted to simulate the three oxygen supplying methods above. Results of numerical simulation are shown in Fig. 12–Fig. 14.

What can be known from Fig. 12– Fig. 14 is that through supplying oxygen vertically at the front of head and making air flow out from the bottom, temperature rises slowest in the mask, and oxygen fully gathers at the face position, meeting the requirement. Therefore, this kind of oxygen supplying method should be chosen when designing oxygen supplying air-duct of the helmet.

5.3 *Design of oxygen supplying speed of the safety helmet*

Although it had been known that the best ventilation—cooling effect can be got by supplying oxygen vertically at the front of head and making air flow out from the bottom, the optimal oxygen supplying speed still needed to be further studied.

As temperature at air inlet was fixed to 298k, temperature distributions of the helmet when oxygen supplying speed was respectively 8 cm/s, 10 cm/s and 30 cm/s were got and shown in Fig. 15~Fig. 17.



(a) Supplying oxygen downward at top of head



(b) Supplying oxygen vertically at the front of head



(c) Supplying oxygen horizontally at the front of head

Figure 11. Three methods of air supply.

As shown in Fig. 15~Fig. 17, when oxygen supplying speed increases from 8 m/s to 10 m/s, temperature drops from 308k to 302k significantly; however, when oxygen supplying speed increases from 10 cm/s to 30 m/s, there is no obvious temperature change.

As temperature at air inlet was fixed to 298k, wind speeds at the face position in the helmet when oxygen supplying speed was respectively 8 cm/s, 10 cm/s, 30 cm/s and 50 cm/s were got and shown in table 1.

From Table 1, it can be seen that when oxygen supplying speed is 10 cm/s, wind speed is 0.0361 m/s. As oxygen supplying speed continues to increase, wind speed at the face position turns higher and higher. When oxygen supplying speed is in range of 10 cm/s~30 cm/s, effect of temperature dropping is not obvious, and high oxygen supplying speed makes wearer feel uncomfortable, moreover, amount of oxygen candle increases with oxygen supplying speed increasing, therefore, oxygen supplying speed of the safety helmet should



Figure 12. Temperature distribution while supplying oxygen downward at top of head.



Figure 13. Temperature distribution while supplying oxygen vertically at the front of head.



Figure 14. Temperature distribution while supplying oxygen horizontally at the front of head.



Figure 15. Temperature distribution when oxygen supplying speed is 8 cm/s.



Figure 16. Temperature distribution when oxygen supplying speed is 10 cm/s.



Figure 17. Temperature distribution when oxygen supplying speed is 30 cm/s.

be controlled at about 10 cm/s which can meet the need of supplying oxygen and dropping temperature at the same time.

6 CONCLUSIONS

1. A new kind of safety helmet for mine emergency hedge has been designed based on original miner's helmet. On the one hand, appearance and structure of the safety helmet has been designed to achieve the purpose of protecting wearer's face in case of danger; on the other hand, oxygen candle has been selected to provide oxygen, guaranteeing wearer's breath and safety.

Table 1. Wind speeds at the face position.

	8 cm/s	10 cm/s	30 cm/s	50 cm/s
Wind speed at the face position (m/s)	0	0.0361	0.1	0.2

2. The regularity of temperature changing inside the helmet has been got. As time develops, order of temperature from largest to smallest is temperature at the face position, temperature at the front of head, temperature at the back of head and temperature over the head. The highest temperature at the face position is 39.1 °C, and pulse frequency of wearer keeps at 77 times/min. Concentration of CO_2 inside the helmet reaches the critical value of 25000 PPM within 2 minutes under condition of no oxygen supply, which shows that the helmet can only ensure safety of wearer for 2 minutes.
3. The optimal oxygen supplying method has been optimized by numerical simulation. The best ventilation-cooling effect can be got by supplying oxygen vertically at the front of head and making air flow out from the bottom. And the optimal oxygen supplying speed is got to be 10 cm/s which can meet need of supplying oxygen for wearer and reducing weight of oxygen candle at the same time.

REFERENCES

Han Z Z. Wang J, Lan X P. The calculation and employing of FLUENT. Beijing Institute of Technology press, 2004.

Huang H R. The statue and analysis of safety helmet in home and aboard. *China labor protection supplies*, 2000, (1):30–34.

Jiang X R. Briefly explore about domestic and international safety helmet technology: China university of mining and technology. *China Personal Protective Equipment*, 2010, (4):31–34.

Jin P L. The development research of the new safety helmet. *China Personal Protective Equipment*, 2001, (3):16.

Sheng H T. The implement and product control of the standards of safety helmet. *Safety*, 2011, (8):48–50.

Zhang Z H. The oxygen candle starter of self-rescuer, *Mine Safety*, 1995, (11):29–36.

Zhang G P. The selection of oxygen candle and the effect to the oxygen candle of the fuel and catalyst. *Ship science and Technology*, 1991, 13(5):46.

Progress in Mine Safety Science and Engineering II – He et al. (Eds)
© 2014 Taylor & Francis Group, London, ISBN 978-1-138-00122-0

The research of dynamometer for anchor cable in mine tunnel based on the industrial Ethernet

Xuezhe Li, Xiaoping Li, Haimei Feng & Junming Liu
North China Institute of Science and Technology, Beijing, China

ABSTRACT: The traditional dynamometer for anchor cable has disadvantages of low precision, poor anti-interference ability, measurement results cannot be uploaded automatically, the comprehensive analysis of measurement results is difficult. In the paper, a dynamometer for anchor cable based on industrial Ethernet is proposed. The paper also introduces the principle and implementation of system project. It has the core of STC12C5A single-chip microcomputer, and realizes the accurate measurement of anchor stress condition by using fine torque measurement module, and realizes the data communication and sharing by using RTL8019AS Ethernet control chip. The sensor can monitor the status of anchor stress condition real-time and also can make pre-caution to the possible production accident.

1 INTRODUCTION

The analysis of anchor cable stress condition in mine tunnel is an important content of tunnel monitoring. Dynamic observation of anchor cable stress state is significant to the verification of roadway supporting effect, the monitoring of mine pressure regularity, and guarantee the safety of mine production (Wu 2007). At present, some dynamometers for anchor cable based on different principles have been developed at home and abroad. These instruments solves the problem of the coal mine pressure monitoring in a certain extent, but they generally also have some disadvantages of high cost, low precision, poor anti-interference ability, inconvenient installation and maintenance, these deficiencies limit their further development in the area of coal mine. In recent years, the technology of industrial Ethernet is developed rapidly, and has been widely used in coal mine area (Li 2010). In view of the characteristics of industrial Ethernet technology and the current situation of roadway cable force measurement technology, a dynamometer for anchor cable based on industrial Ethernet technology is designed in the paper. The sensor is designed by STC12C5A single-chip microcomputer and RTL8019AS Ethernet control chip. It realizes the monitoring of anchor stress condition real-time and reliably. And then through the Ethernet interface, the measurement results will be automatically uploaded to underground fiber ring network. The monitoring computer can directly receive the results and achieve storage, computation and analysis of the data. It greatly improves the precision and efficiency of detection.

2 PRINCIPLE AND SCHEME OF THE SENSOR

2.1 *The operation principle of the sensor*

The dynamometer for anchor cable is mainly composed of a torque measurement module and an instrument body. When measuring, the torque module is installed between the anchor plate and the fastening nut, and the nut is screwed by the spanner. Then the stress value of anchor cable is converted to a 0~5V voltage signal through the torque measurement module, according to the sampling voltage value, the instrument body achieves the analysis and calculation of anchor cable stress condition. Finally, the ground monitoring computer analyses the calculation results, which are uploaded through the Ethernet communication circuit. The installation diagram of dynamometer for anchor cable is shown in Figure 1.

2.2 *The technical scheme of the sensor*

The dynamometer for anchor cable designed in this paper composes of power supply circuit, CPU

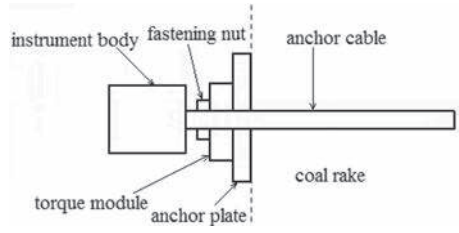


Figure 1. The installation diagram of sensor.

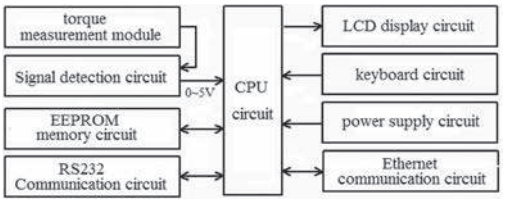


Figure 2. Structure diagram of dynamometer for anchor cable.

circuit, Ethernet communication circuit, signal detection circuit, LCD display module, keyboard module and torque measurement module. System structure diagram shows as Figure 2. Single chip microcomputer is designed by STC12C5A, which implementates functions of keyboard input, LCD display, anchor cable stress value detection, Ethernet communication chip control etc. STC12C5A60S2 is a high efficiency controller, which has advantages as follow, the technology is mature and reliable, the speed and precision of ADC is high, the price is low, its hardware and software resources can meet the design requirements (Chen 2010). The detection of anchor stress condition is achieved by fine torque measurement module, with the corresponding amplification and adjustment circuit. The module has the advantages of high precision, stable and reliable performance, compact structure, waterproof and dustproof, easy to use. Ethernet control chip is designed by RTL8019AS, which is a mature technology and widely used network control chip produced by Realtek Corporation. In addition, the sensor is also designed with the keyboard, LCD display, EEPROM memory circuit, which accomplish functions of sensor calibration and parameter display.

3 HARDWARE CIRCUIT DESIGN

3.1 *The design of CPU circuit*

CPU circuit consists of power module, CPU, reset circuit, clock circuit and program debugging download circuit. In this system, CPU is designed by STC12C5A60S2, whose main role is to execute AD conversion, process and display the sampling results, control Ethernet communication chip etc. The CPU circuit diagram is shown as Figure 3. The emphasis of CPU circuit design is pin function definition. In this system, P0 is used as the data interface, which is connected with the 8 bit data bus of RTL8019AS. P2 is responsible for data bus simulation of LCD screen; P1 achieves functions of LCD control, keyboard input and AD sampling, wherein WY1 is used for detecting of anchor cable stress value; P3 and P4 are responsible

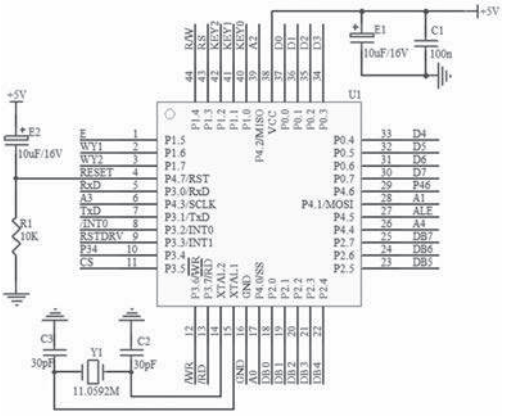


Figure 3. CPU circuit schematic diagram.

for the simulation of RTL8019AS control signals and address signals.

3.2 *The design of anchor cable stress detection circuit*

In the system, the detection of anchor stress condition is achieved by fine torque measurement module, with the corresponding amplification and adjustment circuit., the circuit schematic diagram shows as Figure 4. The detection circuit is based on full bridge strain acquisition circuit and high accuracy, low drift operational amplifier of AD620, which not only eliminates the temperature drift and nonlinear error of strain gauge, but also can obtain higher sensitivity and accuracy. The transfer function of the signal detection circuit is: $Q_P = K \times \Delta U_1 + B_0$, wherein Q_P is the anchor force value, K is the proportional coefficient, B_0 is the compensation constant (Shi 2000). These constants can be determined by calibration method. SCM can easily calculate the cable force according to the sampling voltage and the transfer function.

3.3 *The design of Ethernet interface circuit*

In the system, the network control chip adopts RTL8019AS, which is produced by Realtek company. The connection of key signal in the circuit is designed as follows:

1. Data bus mode setting: 8019AS has 8 bit and 16 bit two data bus mode, which is selected by pin of IOCS16B (96 pin). In the system, we set the mode of 8 bit data bus by connecting IOCS16B to ground through a 27 K resistor.
2. I/O base address settings: I/O base address of 8019AS chip is setted by pins of IOS0~ IOS3 (pins 81, 82, 84, 85). In the circuit, we set the address of 300H by connecting IOS0~IOS3 to ground.

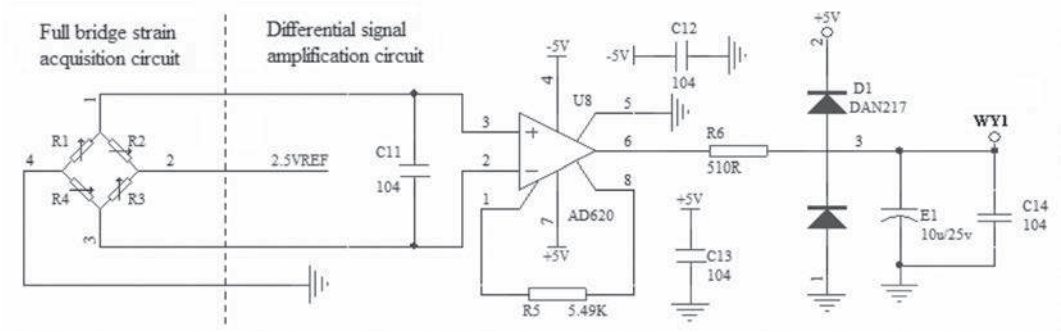


Figure 4. Anchor cable stress detection circuit schematic diagram.

3. Hardware configuration setting: In the design, pin of JP (65 pin) is connected to power 5V, which set the hardware configuration mode for the jumper mode. The jumper mode, when 8019AS chip resets, CPU will read the state of each jumper pin, and save as the initial configuration of the system default.
4. 8019AS reset design: we control the RTL8019AS chip reset by MCU P3.3, which is connected with reset pin of RSTDRV.
5. Data and address bus design: In 8 bit data bus mode, P0 of MCU is used as the data interface, which is directly connected with 8 bit data bus SD0~SD7 of RTL8019AS; The address range of internal registers and memory of 8019AS is 00H~1FH, the I/O base address has been setted to 300H, thus addressing range of address bus is 300H~31FH. In the system, the low 5 address bits SA0~SA4 of 8019AS are directly connected to low 5 bits of P4 of MCU, SA8 and SA9 are controlled by the chip select signal CS.

3.4 *The design of user interface*

In order to facilitate the users, achieve the calibration and display of parameters, system is designed with keyboard and display module. Using the general matrix keyboard with interface circuit, we can conveniently select the function and input parameters. Using LCD screen, we can display cable force real time. The key interface is designed by 74HC148, and the LCD screen is designed by LCD1602.

4 SOFTWARE DESIGN

4.1 *Software overview*

The software of the dynamometer is designed by C language, we use the KeilC51 platform to complete the establishment of project, compile, program download. Software includes: main program module, keyboard input module, LCD display module, parameter calibration module, cable force measurement module and Ethernet communication module etc. SCM first display the boot information on the LCD screen, then according to the hardware settings, respectively, into the "calibration" and "measurement" mode. In "calibration" mode, SCM acquires calibration curve under the control of keyboard, which provides reference data for the precise measurement of cable force; In "measurement" mode, SCM collects, calculates and displays the measurement results, meanwhile uploads the results to fiber ring network through the Ethernet interface, then the monitoring computer achieves further analysis and processing. System software main program flow diagram is shown as Figure 5.

4.2 *The design of Ethernet communication software*

The design of Ethernet communication software is very important in system software design. Following is a brief description of the key software modules.

1. Design of RTL8019AS initialization modules: RTL8019AS initialization involves registers CR, PSTART, PSTOP, TPSR, BNRY, CURR etc (Zhou 2003). The initialization process is shown in Figure 6.
2. Design of data transmission module: When transmitting data packets, SCM writes data in the specified format into the chip and starts sending commands, then RTL8019AS automatically converts data into physical frame format for transmission on the physical channel.
3. Design of data receiving module: When receiving data packets, RTL8019AS automatically restores the physical signal received to the data, and stores the data in the specified format in

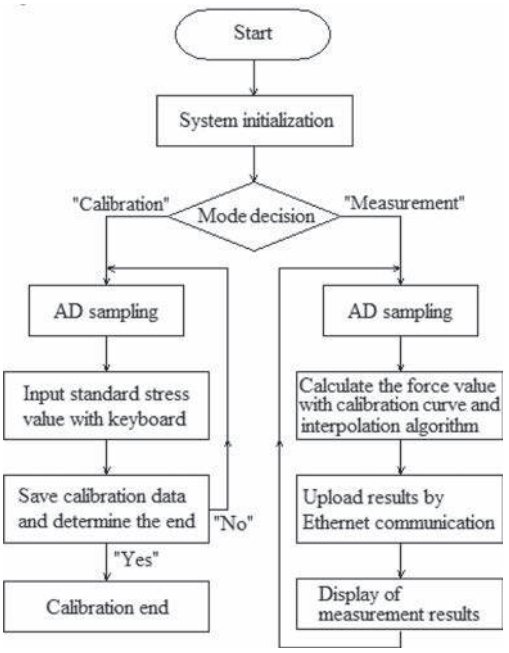


Figure 5. System software main program flow diagram.

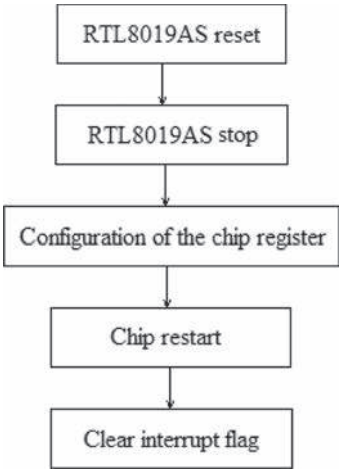


Figure 6. RTL8019AS initialization flow diagram.

RAM, then SCM can read data from RAM and complete the corresponding function.

4. Design of register read-write module: SCM realizes the chip initialization, physical address setting, data packets receiving and transmitting by controlling the RTL8019AS internal registers and DMA port, these functions are achieved through the register read-write module.

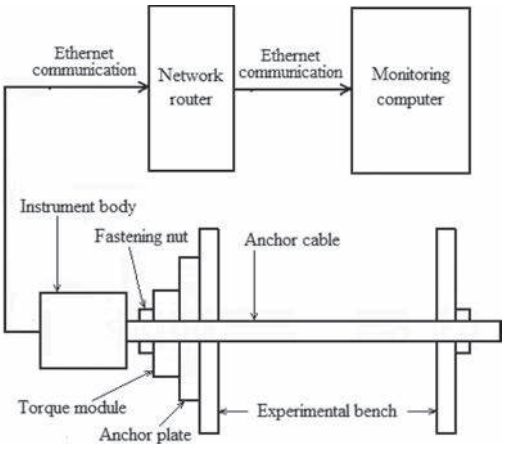


Figure 7. Experimental diagram of the dynamometer.

Table 1. Experimental result of the dynamometer.

Index	Standard tension (KN)	Sampling voltage (V)	Measurement tension (KN)	Error (KN)
1	10	0.48	9.9	0.1
2	20	0.72	19.8	0.2
3	50	1.51	48.8	1.2
4	100	2.79	98.1	1.9
5	150	4.15	147.2	2.8

5 EXPERIMENT AND ANALYSIS

Aiming at the dynamometer for anchor cable designed, we do the experiment on WDW-300 microcomputer control electronic universal testing machine, the experiment is schematically shown in Figure 7. The testing machine provides standard stress signal in fixed step of 10 KN; SCM records the voltage value corresponding with each stress point automatically, then calculates the actual stress value of anchor cable; The computer obtains the measurement results from the dynamometer through Ethernet interface. The experimental data are shown in Table 1. Experimental results show that the dynamometer designed in the paper can achieve precision measurement of anchor cable stress value, the error is limited within ± 2.5%; The sensor can upload the measurement results flexibly through Ethernet communication, can meet the requirements.

6 CONCLUSION

In this paper, a dynamometer for anchor cable based on industrial Ethernet is proposed, which

involves the computer control technology, modern sensor technology, Ethernet technology, and has advantages of high precision, high efficiency, low cost and flexible control. Innovation of this paper is fully integrated hardware and software advantages, design and implement a high precision, full-automation dynamometer for anchor cable, which provides a new technical means for ensuring safety production of coal mine.

ACKNOWLEDGEMENT

The research has been funded by Central College Fundamental Research Funds. Fund project number is 3142013099.

REFERENCES

Chen, Guiyou. 2010. *Enhanced 8051 practical development technology [M]*. Beijing: Beihang University press.

Li, Manchang. 2010. The design of high-speed data acquisition system based on Ethernet [J]. *Engineering and test,* 2010(2):50–52.

Shi, Chengping. 2000. A new portable bolt dynamometer [J]. *Coal science and technology*, 2000(7):50–51.

Wu, Zhigang. 2007. Research and application of new dynamometer for anchor or bolt [J]. *Coal science and technology*, 2007(11):36–38.

Zhou, Ligong. 2003. *The application technology of MCU and TCP/IP*. Guangzhou zlg mcu Development Co., Ltd.

This page intentionally left blank

Progress in Mine Safety Science and Engineering II – He et al. (Eds)
© 2014 Taylor & Francis Group, London, ISBN 978-1-138-00122-0

Research on safety lead-acid battery charger in coal mine

Quan-Zhu Zhang
North China Institute of Science and Technology, Sanhe, Hebei, China

Ming-Yan Xu
Anhui University of Science and Technology, Huainan, Anhui, China

ABSTRACT: Around global development goals and needs of the coal mine safety production in our country, and solving the key scientific and technological problems about security of mining safety electrical equipments to strengthen the management of mine power supply equipments and establish safe and reliable power supply system. Charging unit is the important electrical equipment matched with lead-acid storage battery in coal mine, its good or bad performance directly affects the running reliability of lead-acid battery. This paper designed a set of mine safety intelligent lead-acid battery charger, it not only solved the problems of common battery charger and also provide effective protection for charging process. So it can meet the needs of actual production.

1 INTRODUCTION

Safety is the eternal theme in coal mine production, is the important guarantee for realizing safety production, the core of coal mine production is to realize high production and high efficiency on the basis of safety. Practical experience tells us: only setting up the concept that coal mine safety is the highest efficiency of business, it can be advantageous to realize the organic unity of both efficiency and security. Safe production is the important guarantee for sustainable, stable and healthy development of our country mining industry, with the development of social economy, safe production more and more highlights its important position and role. Mine battery electric locomotive (Bai, et al 2007) is a major transport device for coal mine production, mainly driven by DC motor at present. Aiming at common faults of lead-acid storage battery in mine battery locomotive, the paper introduced a set of mine safety intelligent charger (Liang & Zhang 2006), it used advanced switching power supply technology and intelligent control technology, not only improve charging efficiency, but enhance charging reliability and not producing any harmful gases in the charging process. The charger has characteristics such as light weight, small volume, high efficiency, good control performance, and protection functions for over-voltage, under-voltage, over current, overload, battery voltage detection and polarity, at the same time it achieves the whole process of tracking management and health diagnosis for equipment use and maintenance to provide quick and efficient material guarantee for coal mine safety production.

2 STRUCTURE OF THE SAFETY CHARGER

The security smart charger (Li 2009) has only one cavity including main circuit, control circuit, detection circuit and drive circuit, the structure diagram is shown in Figure 1, the back of control device is equipped with external radiator system mainly for power device (Su 2009) heat leak. In order to realize high efficient and safety charging for lead-acid storage battery, the charger used the charging way of constant current in early stage and constant voltage in later stage to avoid large charging current for constant voltage charging in early stage and over-charging phenomenon for constant current charging in later charging, on the basis of the monitoring,

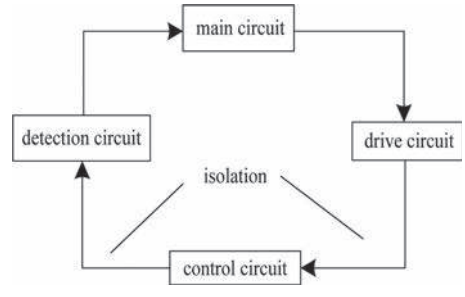


Figure 1. The installation diagram of sensor.

it carried on the management and control for storage battery, more conducive for the maintenance of battery and prolong the battery life. Battery charger charges for storage battery on the one hand and completes the management for the battery on the other hand. Control circuit provides the real-time detection for charging voltage and current and gives alarm indication for abnormal situation, stops output to protect the battery at the same time. Battery charger provides battery condition monitoring unit that provides real-time acquisition, storage and records for single battery in the process of charging, then implements the functions of information ground transmission through the USB interface, with mating battery ground software analysis system for analyzing storage batteries including working condition of all single batteries and judging timely the poor section of single battery to remind the maintenance staff to timely replacement of batteries. In addition, it uses output contactor and detection control to realize the battery polarity protection. The design of charging system adopted high frequency switching power supply technology, the main circuit consists of three-phase bridge rectifier circuit, IGBT single-phase high-frequency inverter circuit, high frequency transformer, single-phase full bridge high frequency rectifier circuit and filter circuit. Main circuit used IGBT as the power device master, continuous adjustment of output voltage and output current is achieved by IGBT single-phase inverter, it adopts the PWM control mode.

2.1 *Control circuit design*

Control system of the charger (Wang 2006) is mainly composed of control signal generating part, signal acquisition part, drive part, system protection part, function setting part and status display parts, they real-time exchange data and information among them through the CAN bus, the system block diagram is shown in Figure 2, each component has a reasonable allocation fully guaranteeing the accuracy and reliability of the system control. The control system design combined with the advantages of good steady state performance for voltage loop control and the advantages of improvement for current loop control system dynamic performance, the control object is output voltage and output filtering inductance current. Control circuit used the digital integrated circuit device, highly integrated to the control circuit of the machine. Control system used single chip processor as the core, through the acquisition of status information, such as battery terminal voltage, temperature, and charging current, after modulus conversion in sampling circuit, these signals are sent into the single chip microcomputer for proceeding analyzing and processing to generate corresponding control signals for switching device IGBT in main circuit and the charge and the discharge circuit. It finally realized intelligent charging by adjusting output voltage and current through double loop ratio control, at the same time the control system monitored various parts of the main circuit and temperature of IGBT to play a very good protection effect for charging system and realize the battery quick green and charging. The charging device (Zhang 2009) has a good human-machine interface, charging parameters and state can be displayed on digital tubes, operates conveniently and has a good reliability.

2.2 *Fault detection of the charger*

IGBT inverter bridge consisting of power electronics device works in the switch state, and susceptible to instantaneous peak voltage, short

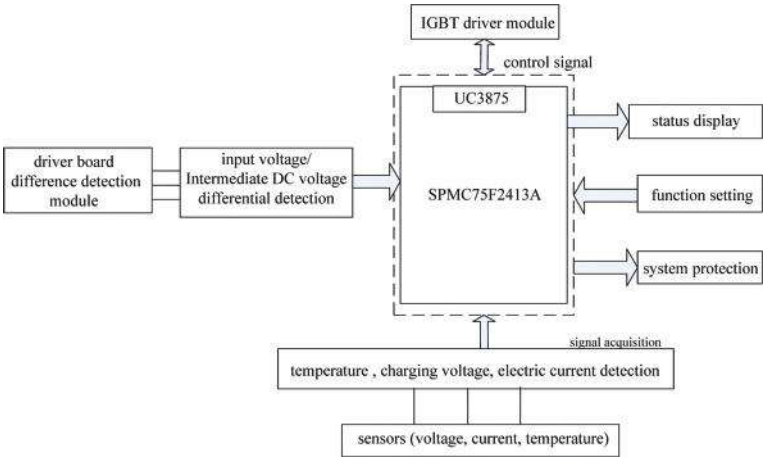


Figure 2. Control system diagram of the charger.

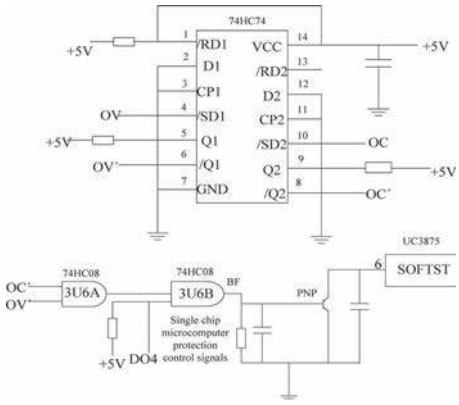


Figure 3. Protection circuit diagram.

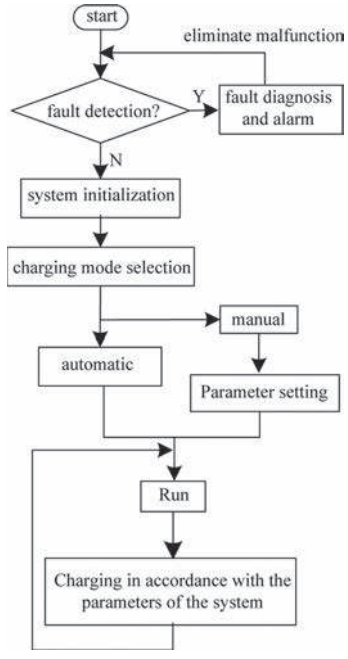


Figure 4. Main program flow chart of charging.

circuit current, instantaneous direct connection and overload for the arm up switch tube and down switch tube caused by instantaneous phase PWM signal chaos, it often leads to abnormal operation of the circuit and burns semiconductor devices of the bridge arm. So, the device joined the corresponding protection circuit to guarantee that switch components will not be damaged due to the circuit fault, and improve the safety and reliability of the device. UC3875 offers the input signal for SOFT-START, it is used to conveniently realize all kinds of protection function of inverter system. Concrete implementation block diagram is shown in Fig. 4. Output of fault signal through 74HC74 latch does comprehensive setting by gate 74 HC08, then connected to a foot of UC3875 (Zhu 2010) soft start through PNP triode. The use of latch prevents the misoperation caused by interference signal and makes the protection action more reliable.

3 SOFTWARE DESIGN OF CONTROL SYSTEM

A charger with a superior performance should not only have good hardware system but have a good software system. The design idea of the main program for charging is that charging scheme of the design is constant current charging and constant voltage charging, it implements automatic conversion for different charging stages and real-time shows charging status and alarm function for achieving the purpose of quick charging and prolonging storage battery recycling. The software of charger adopts the modularized program design method, charging flow chart is shown in Figure 4. The charger did a fault detection in internal after power on, if found abnormity, it displayed fault type and location and eliminated the fault to identify the system is normal, only then can the system initialize. System initialization procedures included the I/O port initialization, event initialization, ADC initialization, timer initialization, etc. Charging mod selection is mainly made users select of charge mode according to the state of storage battery including automatic charging and manual charging. Manual charging does real-time operation according to the characteristics of the storage battery. Parameter setting is mainly used for a variety of charging parameters including starting current, stop charging pressure, park voltage. Battery started charging when not pressing the pause key. Program flow char of external fault interruption is shown in Figure 5, if found defective signals during the process of charging, they will real-time display, at the same time, the system immediately clear the fault signals in order to ensure the charger to work normally.

Battery voltage, current and temperature did real-time monitoring throughout the charging, detective signals sent to single chip microcomputer for processing to control open and shut off of IGBT to achieve the fast charging strategy.

4 RESULTS AND DISCUSSION

The collected voltage waveform of the safety mine lead-acid battery charger is shown in Figure 6 and

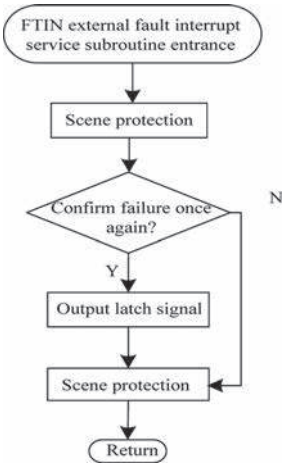


Figure 5. External fault interrupt program flow chart.



Figure 6. The collected voltage waveform of the charger.



Figure 7. The collected voltage waveform of the charger.

Figure 7, the waveform is basic consistent with theory waveform but existing some high frequency interference, considering the influence of high frequency transformer used in the charger, and the interference is within acceptable range.

5 CONCLUSION

Technological innovation is to promote the progress of enterprise technology and the development of enterprises, Coal technology innovation to really play to the role of the first productivity, while safety is the stability of coal industry, the fundamental guarantee of sustainable, rapid development, is the relationship between coal mine worker's life safety and physical and mental health, relationships, loss to the state and collective property from a top priority. Coal technology innovation should really play the role of the first productivity, and security is the fundamental guarantee for stability, sustainable and rapid development of coal industry, is a top priority about the relationship between coal mine worker's life safety and physical and mental health, not loss of national and collective property. So Coal mining technology innovation must conscientiously implement the Party's production policy of "safety first". With the development of China's coal and the requirements of safety situation, use information technology to transform traditional coal industry, rely on advanced management concept and use a variety of modern information and automation technology. Design aim of the Mine safe intelligent charger is to provide comprehensive and systematic theory and technical support and is of great significance to promote coal mine safety production.

ACKNOWLEDGEMENT

The research has been funded by Central College Fundamental Research Funds. Fund project number is 3142013101, A07001.

REFERENCES

Bai Xibin, et al 2007. Study of circuit structure of locomotive battery chargers [J]. *Practical World*.

Li Jun 2009. Study on fast-charging technology for lead-acid batteries [D]. *Sichuang: Southwest Jiaotong Universtry*.

Liang Cuifeng & Zhang Lei 2006. The present situation of lead acid battery and its development directon [J]. *Guangdong Chemical Industry*.

Su Yun 2009. Research of mine-used lead-acid battery fast-charging device [D]. Anhui University *of Science & Technology*.

Wang Zhegong 2006. Operation and maintenance of lead-acid batteries [M]. Beijing: *Water conservancy electric power press.*

Zhang Quanzhu, et al 2009. Study on intelligent lead-acid battery charger of mining electric locomotive [J]. *Industry and mine automation*.

Zhu Huibo & Qin Yulong 2010. Design of motor vehicle charging power supply based on the UC3875 [J]. *Telecom Power Technology*.

Progress in Mine Safety Science and Engineering II – He et al. (Eds)
© 2014 Taylor & Francis Group, London, ISBN 978-1-138-00122-0

Studies on the large capacity mine lithium ion battery intelligent charger

Z. Quan-Zhu, S. Xiao-Lei, D. Yong-Hong & M. Hong-Mei
Information and Control Technology Institute, North China Institute of Science and Technology, Beijing, China

ABSTRACT: Combined with the security problem of the charging of mine large-capacity lithium ion battery, the author puts forward a reliable scheme of the lithium-ion battery charger. In this paper, the key structure and function of the charger are introduced and analyzed, the parameter of the phase-shifting chip UCC3895 are designed and optimized, the authors also introduces the MAX11068 battery management chip's application in the charger, which can quickly and safely complete the charging process of the large capacity lithium ion batteries. The promotion and application of the large-capacity lithium ion battery is of great significance in the coal mine security production.

1 INTRODUCTION

Different from the past lithium ion battery, the large-capacity lithium ion battery is over 3 Ah generally. To reach high battery capacity and voltage for the device, the lithium ion batteries should be connected in series and parallel in practical applications. At present, the application of the large-capacity lithium ion battery in some place and equipment such as movable life-saving cabin, refuge chamber, mining electric locomotive and dust vehicle is already in research phase. The popularization and application of the large-capacity lithium ion battery in coal mine production at home and abroad is seriously constrained by the battery's security. Due to the drive of the national "863" major projects and electric vehicle market, the study of large-capacity lithium ion battery in green electric vehicle power has began (BI 2008), however, its application as power in the mine electrical equipment or other mining equipment is almost blank because of the lack of corresponding standards, security charging and BMS technology. Now the lead-acid batteries, small capacity, short lifetime and against environment protecting, are most commonly used in production of coal mine. If they can be replaced by the large-capacity lithium ion batteries, this will greatly save the production costs and improve coal mine production environment. Large-capacity lithium ion battery should be charged in cycle constantly in applications, then to design a safe charging scheme is of great significance to the popularization and application of large-capacity lithium ion battery in coal mine safety production. Combining security features of the large-capacity lithium ion battery with former scholar' research, the authors puts forward a safe charger scheme of the large-capacity lithium ion battery.

2 SECURITY PRECAUTIONS OF LITHIUM ION BATTERY CHARGING PROCESS

Lithium ion battery is strict with voltage, current and temperature whether in charging or discharging, which should be controlled strictly in the process of charing (WANG 2005). Some primary notices as follows:

3 LITHIUM ION BATTERY CHARGING PROCESS

Lithium ion battery charging process is divided into two stages: constant current fast charging and constant voltage slow charging. In the first stage, the voltage of the battery rises all the time, immediately transferred to the second stage as soon as the voltage reaches the settings. Current weakens to the settings gradually along with the battery rising to finish charging. To the first charging of the battery, the time should be as long as possible (generally three or four hours), so that the electrode oxidize as completely as possible. The initial charge mode run once every so often, in order to achieve maximum releasing of the battery's capacity.

The scheme selects eight strings battery pack SE60AHA (monomer's nominal voltage is 3.2 V). At first we should charge the battery fast in constant current mode (≤1CA), then start slow charging when it reaches to constant 24 V (plus or minus 50 mv less). Stop charging until the battery is full or start tiny current charge according to the actual situation. This constant current mode followed by constant voltage should take about two hours to charge the battery fully.

4 FUNCTION REALIZATION AND RESEARCH PRIORITIES

Shown in Figure 2, the intelligent charger mainly consists of four parts: AC/DC main circuit, DSP control part, the output sampling part and lithium ion batteries management. Work as follows: input mine voltage AC 380V/50 Hz or AC660V/50 Hz, after inverter, rectifier, inverter and filtering, output controllable DC voltage and current to the batteries by controlling the IGBT off and on. In this process, the IGBT's temperature, the output and input value of the voltage and current are transformed to the controller DSP by the sampling circuit to complete the closed-loop control and protection (ZHANG 2009). Lithium ion battery's equalization control, collection and protection of voltage and temperature are completed by the BMS chip MAX11068. The emphasis of this scheme include IGBT inverter control technology, voltage and current double closed-loop and BMS technology.

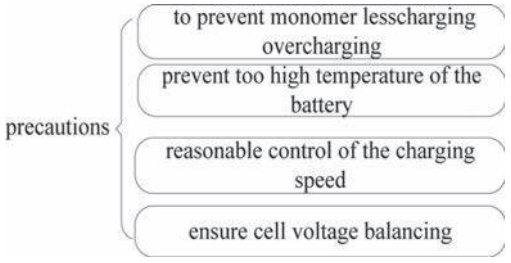


Figure 1. Rechargeable lithium-ion battery pack precautions.

4.1 *Setting of IGBT inverter PWM signal parameter and the output of experimental waveform*

The achievement of the output of the voltage and current double closed-loop control are completed mainly by adjusting the PWM pulse signal, which could control the IGBT's off and on, generated by the chip UCC3895. On the basis of theoretical analysis and experimental verification, the parameters of the chip are optimized and adjusted. Shown in Figure 3, UCC3895 uses average current control mod, which has high noise inhibiting ability, no slope compensation, and widely used in the PWM control circuit (Mihail 2012). Then the input of the error amplifier noninverting is voltage control signal V_+, the input of the inverting is the inductor current signal V_- in the end. Output of the Error amplifier tracks error signal, the signal is compared with the saw tooth signal of the RAMP pin to obtain PWM, as the IGBT's driving control signal. The CS pin is overcurrent end, whose turn-off voltage is 2.5 V and its input signal is inductor current signal. When an overcurrent or short-circuit occur, it can immediately turn off the PWM output, the large-capacity lithium ion battery can be well protected against overcurrent and damage when charging. The SS pin to the ground through a capacitor can achieve soft-start function, the experimental output waveform shown in Figure 5.

The setting of Frequency: $f_{out} = f_{in}/2$. f_{out} is the frequency of the four outputs, f_{in} is the internal clock frequency of the chip, then the t_{osc} can be calculated. In order to get the output frequency of 20 kHz, f_{in} = 40 kHz, C_T = 100 pf, which can be calculated by the chip clock cycle:

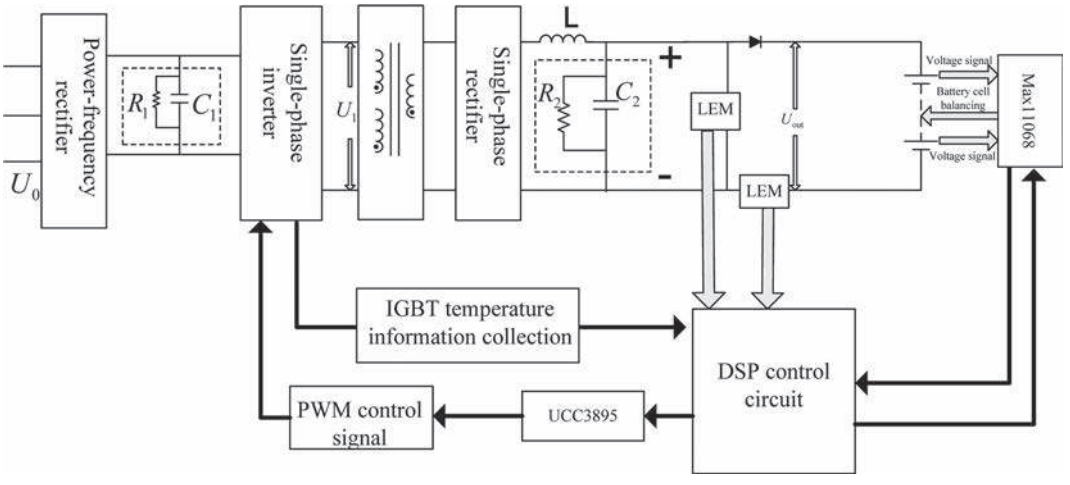


Figure 2. Lithium-ion battery smart charger main circuit topology.

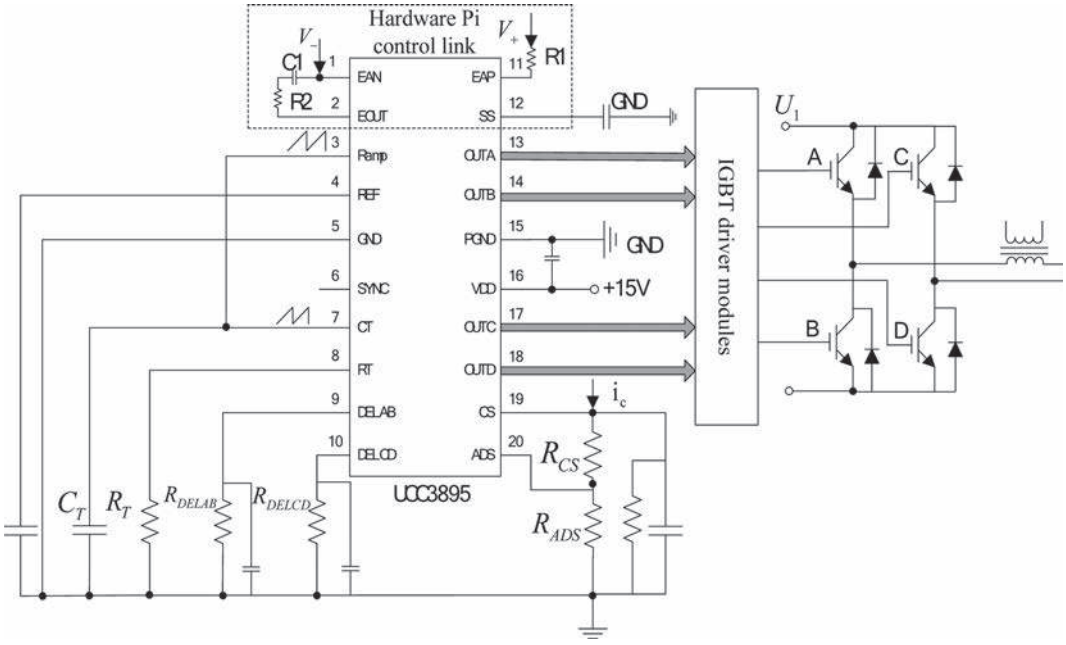


Figure 3. UCC3895 drive the IGBT topology.

$$t_{osc} = \frac{5R_T C_T}{48} + 120ns \quad (1)$$

The setting of the delay time $T_{DELAY:}$

$$t_{DELAY} = \frac{25\times10^{-12} R_{DEL}}{V_{DEL}} + 25ns \quad (2)$$

The output delay time, the voltage V_{DEL} across the DELAB and DELCD meet:

$$V_{DEL} = 0.75\times(V_{CS} - V_{ADS}) + 0.5\text{v} \quad (3)$$

The range of the '$V_{CS} - V_{ADS}$' is 0V ~ 2.5V. The range of the V_{DEL} is 0.5V to 2.375V, the output current size must meet:

$$I_{DEL} = \frac{V_{DEL}}{R_{DEL}} \le 1mA \quad (4)$$

Selected the R_{DELAB} = R_{DELCD} = 109 kΩ, R_{CS} = 200 kΩ, R_{ADS} = 100 kΩ, in this case:

I_{DEL} = 0.016 mA < 1 mA.The range of dead time T_{DELAY} is 1.15us ~ 5.45 us.

4.2 *The double close-loop control*

The control of the charger output choose the double close-loop control mode: outer voltage loop, inner current loop. The output waveform can be well fitted for the lithium-ion battery charging wave form (the maximum error is 50 mV), as shown in Figure.6, which plays a very large role in improving the efficiency of the battery and extending its life. Inner current loop is set by software, the outer by UCC3895. peripheral circuit shown in Figure 5 hardware PI modulation link.

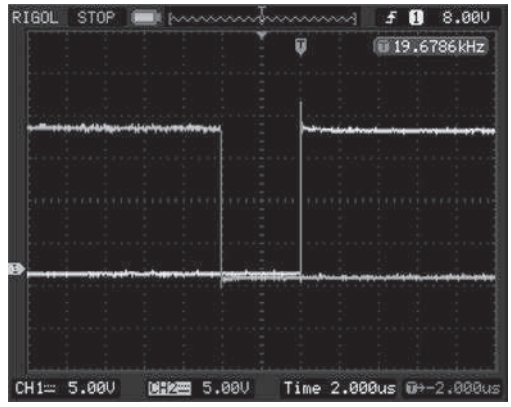


Figure 4. OUTA and OUTB output waveform, T_{DELAY} = 4 us.

Initial charging began with the constant-current mode outputting, K1 is off, K2 is closed to the b side, the internal error comparator of the UCC3895

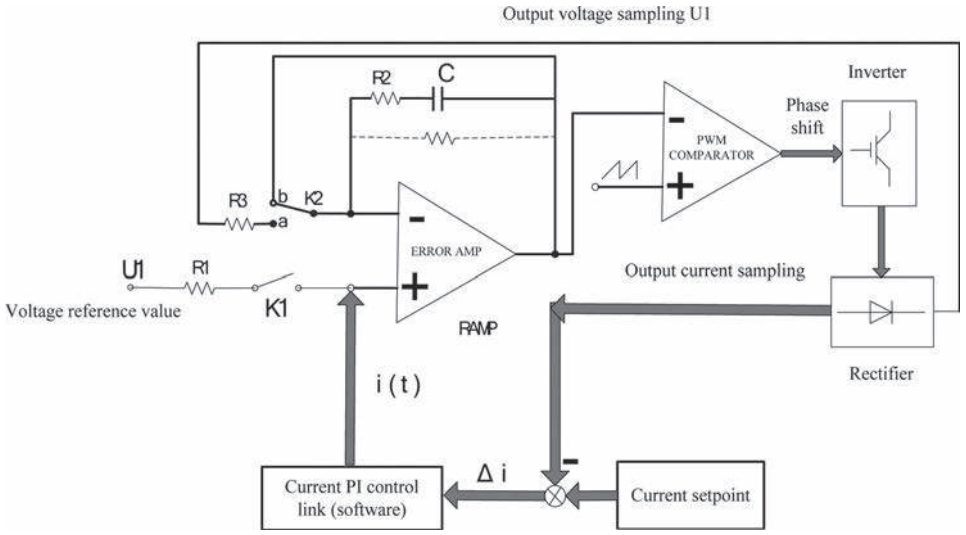


Figure 5. Voltage and current structure diagram.

is wired as follower, enter the current closed loop control mode, the K_I, K_P of the current loop is set by software. The relation ship between the input and output is:

$$i(t) = K_P \Delta i(t) + K_I \int_0^t \Delta i(t) dt \tag{5}$$

In constant current mode, the voltage of the battery will continue to rise with the conduct of the charging process. In the current loop, in order to maintain the constant current, the output voltage of the charger will continue to rise, and always maintains a certain pressure difference. Immediately transfer to the voltage closed-loop control in constant voltage mode, when the charger output voltage rise to the reference value U1, K1 is opened and K2 is closed to the a side, R1 is equal to R3 in it. The input-output relationship:

$$u(t) = -\frac{R_2}{R_3} e(t) - \frac{1}{R_3 C} \int e(t) dt \tag{6}$$

$$e(t) = U_1(t) - U_2(t) \tag{7}$$

With the decreasing of the pressure difference in the constant voltage mode, the output current continue to decrease to certain rules when the current is reduced to 0, then the battery is fully charged, the charger stop charging or continue to trickle mode charge (WANG 2004).

4.3 *BMS of large capacity lithium ion battery*

Because the majority BMS of the lithium ion battery at home has complicated control strategy,

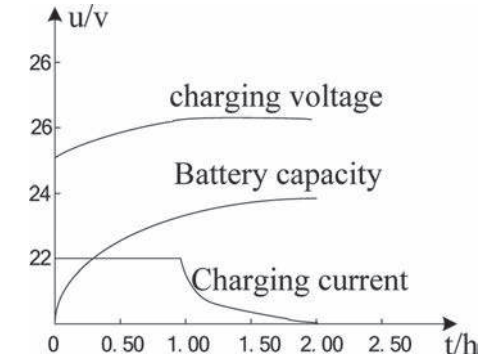


Figure 6. Rechargeable lithium-ion battery pack equalization waveform.

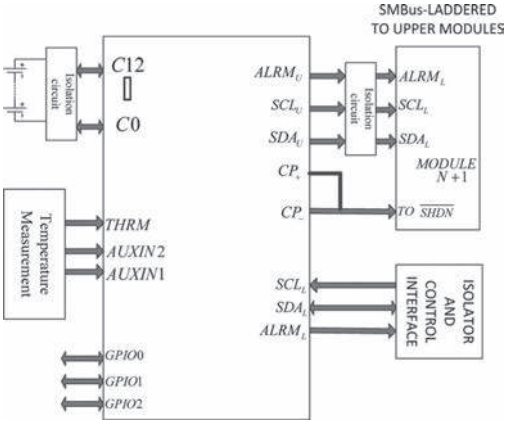


Figure 7. MAX11068 work topology.

large volume and high cost, it can't be applicated in the mine (LEI 2010). The MAX11068, BMS IC produced by TI solve these problems very well. It have great temperature detection, overvoltage and undervoltage alarm function, and can make active voltage balance.

5 CONCLUSIONS

The mine charger of the large-capacity lithium-ion battery put forward by the author can use AC 380 V 50 Hz or AC 660 V 50 Hz to charge the battery fast and safely. Inversion use the IGBT power modules, which has fast responsetime, 25 kHz inverter frequency. The PWM control pulse signal is formed by UCC3895. The chip has excellent over-current protection and soft start function which can protect the circuit so well though the whole charging process, the double closed-loop control is also completed by this IC. In addition, the BMS use the latest BMS IC, MAX11068, which can save cost and improve the security in using the lithium ion battery. Based on the demand and problem in the high-capacity lithium battery charging, the author put forward a reasoned and safe charger design of the large-capacity lithium-ion battery.

ACKNOWLEDGEMENT

This research was funded by Central college scientific research fund fees. 3142013101, 3142013121.

REFERENCES

Bi Dao-zhi. Research progress of high capacity and high power Li-ion batteries [J]. *Chinese Battery Industry,*2008. 4 (2):114–119.

Lei Jing-jing, et al. Power Lithium-ion Battery Management System Research Progress [J]. *Chinese Journal of Power Sources*, 2010. 11(10):1192–1195.

Mihail Octavian Cernaianu, et al. Battery Charger System Employing Average Current Control [C]. Lecture Notes in Information Technology—Proceedings of 2012 International Conference on Power and Energy Systems (ICPES2012), China Hongkong: Information Engineering Research Institute, USA, 2012–04 (2):22–30.

Wang Qing-song, et al. Lithium-ion Battery Safety Features and Thermal Model [J]. *The China Security Science and Technology*, 2005. 6 (3):19–21.

Wang Zhen-po & Sun Feng-chun. Study on the characteristics of large capacity lithium ion battery [J]. *Journal of Beijing Institute of Technology*, 2004. 12 (12):19–21.

Zhang Quan-zhu, et al. Mine Electric Locomotive Lead-acid Battery Smart Charger [J]. *Industry and Mine Automation*, 2009.10 (10):8–11.

This page intentionally left blank

Progress in Mine Safety Science and Engineering II – He et al. (Eds)
© 2014 Taylor & Francis Group, London, ISBN 978-1-138-00122-0

The structural optimization and numerical simulation of wet centrifugal precipitator in fully mechanized heading face

Hai-Fei Yao
Mine Safety Technology Branch, China Coal Research Institute, Beijing, China
State Key Laboratory of Coal Mining and Clean Utilization, China Coal Research Institute, Beijing, China

Ping-Jun Hu
Henan Dayou Energy Co., Ltd., Yima, Henan, China

ABSTRACT: For the characteristics of driving working face of chinese coal mine, designing three types of structural model of wet centrifugal precipitator. In order to optimize their internal structure efficiently, three types of structural physical model are established and meshed by Gambit 2.2. Solving containing dust airflow three-dimensional velocity distribution in the precipitator, static pressure field distribution, the characteristics of turbulent flow field; the move track of different size of dust in the precipitator by Fluent 6.2. Simulation results showed that shunt plate plays an important role in separating airflow. It can make the movement of vortex steady, besides, maintaining the continuity and stability of high-speed airflow, the symmetry of static pressure distribution, the regular change of turbulent kinetic energy; steady flow field and high speed centrifugation are critical to remove respirable dust. The precipitator which contains shunt plates and two rows of baffle in the middle (Model three) have advantage in maintaining air flow velocity and the changement of turbulent kinetic energy compared with the one which contains shunt plates and three rows of baffle in the middle (Model one), however, two die areas take place in the front of the first baffle, which reduce the collection efficiency. Through the above-mentioned aspects of the general comparison, choosing the structure of model one as the production model of precipitator.

1 PREFACE

As pre-open working face of mechanized mining, mechanized heading face produce large amount of dust, which is only less than mechanized mining. Because of the characteristic of multi-process, dust dispersion and high degree of dust dispersion, mechanized heading face become the focus of dustproof (Jin et al. 2001, Wang, X.Z et al. 2001).

At present, the dust control measures in mechanized heading face mainly is inside and outside the spray of boring machine, air curtain, wet dust, spray in reproduced point, water curtain in roadway, etc. However, some disadvantages may take place in practice: first, we usually apply the ventilation mode of active pressure wind and passive wind, spray in mechanized heading face, transform face airflow into air mist easily, which may affect the sight of the worker and bring a serious hidden danger; second, The above measures don't control the airflow, therefore, collection efficiency is relatively low (Jin 2001). Precipitators are used widely in Some of the major coal-producing countries, but dust equipment abroad generally large in size and didn't apply in our country's roadway (Dong et al. 2006), therefore, it's important and significant to develop precipitator which is suited to China's coal mines.

We will establish three internal structure physical models of wet centrifugal collector by Gambit 2.2 in this article, and then meshing. Solving three-dimensional velocity distribution, static pressure field distribution, turbulence characteristics of flow field of dust-laden air, the move track of different size of dust in the precipitator by Fluent 6.2. So as to choose optimal model.

2 MATHEMATICAL MODE

2.1 *Gas equations*

Gas flow in flow field can be described by Navier-Stokes equations, and then close equations by revised turbulent fluctuation RNG k-ε two-way model, dealing with wall flow by wall function method (Wang et al. 2004). The model reflect the impact of small-scale through viscosity which is got after large-scale motion and amendments, remove small-scale movement systematically from

equations. k equation and ε equation is similarly to the standard k-ε model.

$$\frac{\partial(\rho k)}{\partial t}+\frac{\partial(\mu k u_i)}{\partial x_i}=\frac{\partial}{\partial x_j}[\alpha_k \mu_{eff}\frac{\partial k}{\partial x_j}]+G_k-\rho\varepsilon \quad (1)$$

$$\frac{\partial(\rho\varepsilon)}{\partial t}+\frac{\partial(\mu\varepsilon u_i)}{\partial x_i}=\frac{\partial}{\partial x_j}\left[\alpha_k \mu_{eff}\frac{\partial \varepsilon}{\partial x_j}\right]+\frac{C_{1\varepsilon}^{*}\varepsilon}{k}G_k-C_{2\varepsilon}\rho\frac{\varepsilon^2}{k} \quad (2)$$

Where, k and ε are unknown quantity, ρ is density of fluid (kg/m^3), μ is fluid dynamic viscosity coefficient, $\alpha_k = \alpha_\varepsilon = 1.39$, G_k is item of turbulent kinetic energy k which was produced by average gradient, u_i is time-averaged velocity (m/s), $C_{1\varepsilon}^{*}$, $C_{2\varepsilon}$ are empirical constants.

Compared with standard k-ε model, the main change of RNG k-ε model is (Shih, T.H et al. 1995): First, through revising turbulent viscosity, consider rotation and swirling flow during the average flow; Second, adding one item up to ε equation, reflect average strain rate of mainstream E_{ij}, so the produce items of RNG k-ε model not relevant to the situation of flow, but a function of space coordinates in the same question. Therefore, RNG k-ε model can deal with high strain rate and large streamline curvature of flow (Pan, X.Q & Yuan, J. 2004).

2.2 *Discrete phase model*

Solving discrete phase particle track under particle effect balance equation of lagrangian coordinates. The form of particle effect balance equation under cartesian coordinate system (x direction) is (Morsi, S.A. & Alexander, A.J. 1972):

$$\frac{du_p}{dt}=F_D(u-u_d)+\frac{g(\rho_p-\rho)}{\rho_p}+F_x\mu \quad (3)$$

Where, u_p is particle velocity (m/s), FD $(u - u_d)$ is quality drag force of particle (N/Kg), u is fluid phase velocity (m/s), μ is fluid dynamic viscosity coefficient, ρ_p is particle density (kg/m^3), F_x is other forces in x direction.

3 PHYSICAL MODEL AND BOUNDARY CONDITION

3.1 *Set up physical model*

The whole model is divided into nine sub-block by GAMBIT software, then meshing, physical model and mesh division are showed in Fig. 1. considering

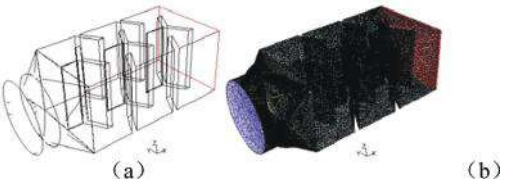


Figure 1. The physical model and mesh of precipitator. (a) The physical model of precipitator; (b) Meshing of precipitator.

Table 1. The set of various types of value.

Boundary conditions		Define
Inlet Velocity Magnitude		23.6 m/s
Hydraulic Diameter		0.6 m
Turbulence Intensity		2.87%
Outlet Boundary Type		Outflow
Wall	DPM Condition	Trap
	Shear Condition	No Slip

calculation and simulation of numerical simulation, this article simplify model from the following aspects: gas is incompressible; parameters of gas flow change little as time, so consider gas flow as unsteady flow; consider the gas-solid flows, replace effect of liquid film sticky with simplify trap boundary condition; Suppose wall of precipitator insulation, ignore heat transfer between the gas-particle and the wall.

3.2 *Set boundary condition*

The set of various types of value are showed in table 1.

In the process of calculation, determine flow field whether arrive at convergence according turbulent kinetic energy, turbulence dissipation rate, velocity and residual of continuity equation (Han, Z.Z et al. 2004, Fan, J.R et al. 2001). Suppose residual of the above physical quantity is 1.0×10^{-3}, flow field arrive at convergence in this numerical simulation.

4 SIMULATION RESULTS AND ANALYSIS

4.1 *Simulation and analysis of airflow field in precipitator*

To choose the best model, this article will study the velocity, pressure field, distribution law of turbulent kinetic energy among the precipitator which contains shunt plates and three rows of baffle in the middle (Model one), the one contains no shunt plate and three rows of baffle in the middle (Model

two), the one contains shunt plates and two rows of baffle in the middle (Model three), As shown in Fig. 2.

4.1.1 *Simulation and comparison of the speed variation*

Z = 0 axial cross section velocity vector of three models of precipitator are shown in Fig. 3.

As can be seen from fig. 3, in the course of removing dust, the velocity of air flow become higher and higher, the maximum speed mainly take place near baffle, especially on the edge of baffle, the minimum speed take place in the export. the velocity of air flow get smaller first and then progressively larger from entrance to export, which caused by the change of x axis cross-sectional area of precipitator, Because the airflow which was sucked in precipitator is steay, when it comes to the edge of baffle, area suddenly reduced, the velocity of air flow increase. Except for high-velocity zone in precipitator, there are 10 main vortexs which lies behind vertical filter, the two adjacent vortex form vortex pairs at the same time.

The feature line which is formed by linking point (0, 0.25, 0.2) and point (1.8, 0.25, 0.2) is shown in Fig. 4, the change of velocity of three models in feature line is shown in Fig. 5.

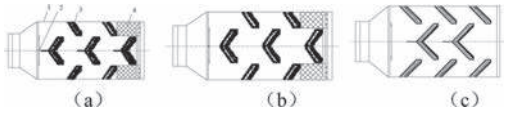


Figure 2. Vertical view of wet centrifugal precipitator. 1—the body of precipitator; 2—nozzle; 3—vertical gas-liquid filter; 4—flat gas-liquid filter; (a) model one; (b) model two; (c) model three.

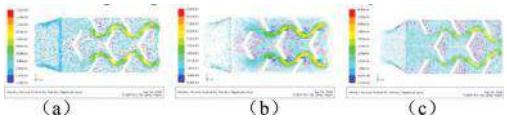


Figure 3. Velocity vector of z = 0 axial cross section. (a) model one; (b) model two; (c) model three.

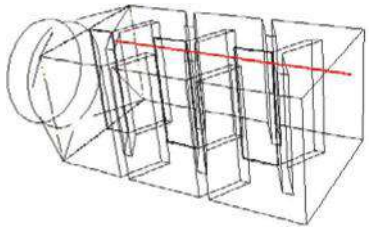


Figure 4. The location of feature line.

Compared with model one, because of lack of shunt plate, movement of vortex pairs of model two is very unsteady, which will influence the continuity and stability of high-speed airflow, through velocity is swifter; because of the change of filter layout, the distance between the first filter and entrance extended segment become small, the vortex make the first filter nearly useless, which cause the velocity of air flow reduce about 1/3.

4.1.2 *Simulation and comparison of static pressure distribution*

Z = 0 axial cross section static pressure distribution nephogram of three models of precipitator under rated operating conditions are shown in Fig. 6.

As can be seen from fig. 6, Local high-pressure zone exists both sides of the shunt plates, which is beneficial to form a stable, continuous high-velocity zone, so compared with figure (a), the symmetry of pressure distribution in figure (b) (c) is poorer. The three models' static pressure drop in feature line are shown in fig. 7, The static pressure

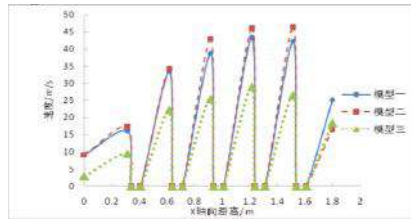


Figure 5. The velocity distribution of three models in feature line.

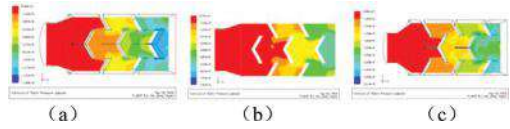


Figure 6. Static pressure distribution nephogram of z = 0 axial cross section under rated operating conditions. (a) model one; (b) model two; (c) model three.

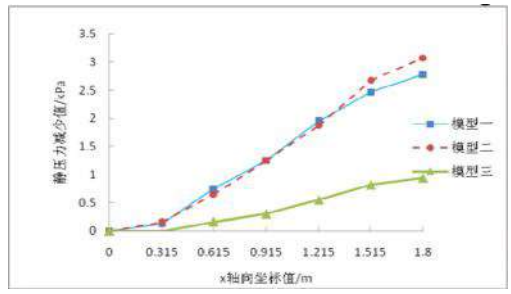


Figure 7. Static pressure distribution of three models in feature line.

drop of model three is significantly lower, It can be seen that the filter layout way is the main factor that affects the flow field. After the comparison between speed change and the symmetry of static pressure distribution, from the aspect of maintaining flow stability and static pressure distribution symmetry, model two is poorer than model one and three, so we can give up model two and only analysis model one and three in the following article.

4.1.3 *Simulation and comparison of turbulent kinetic energy distribution*

Z = 0 axial cross section turbulent kinetic energy of precipitator under rated operating conditions are shown in Fig. 8.

As can be seen from fig. 8, turbulent kinetic energy contour change from thin to dense, reach maximum in the tail of precipitator. Because of viscidity on the wall of precipitator, which will create velocity gradient and eddy, turbulent kinetic energy is bigger on the wall and the baffle. The vortex on outer wall boundary layer move fast, driving movement of the inner vortex, receiving the energy of turbulent vortex from the mainstream (Xu J. & Ge M.C. 1998, Wang, H.G et al. 2004, Zhou, G.J. & Yan, Z.Y. 1992). Comparing Figure a and Figure b we can see that Z = 0 axial cross section turbulent kinetic energy of model three is disorder and random. This shows that the change of turbulent kinetic energy is unstable, which will cause air speed and air resistance impermanence, it isn't beneficial to remove dust stable and efficient and the safe of mechanized heading face.

4.2 *Simulation and comparison of dust trajectories in precipitator*

To choose better model from model one and three, this article make dust trajectories numerical simulation by the method of single-phase coupling, studing the move track of different size of dust under rated operating conditions. The direction of incident velocity plumb imported face of velocity, incidence velocity is same as inlet velocity, solid mass flow rate is zero, in order to observed trajectory, set source of jet is single-size dust, distributing

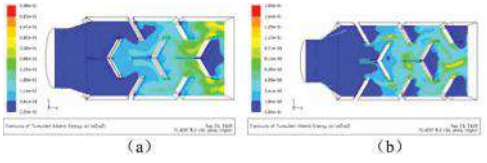


Figure 8. Turbulent kinetic energy of z = 0 axial cross section under rated operating conditions. (a) model one; (b) model two.

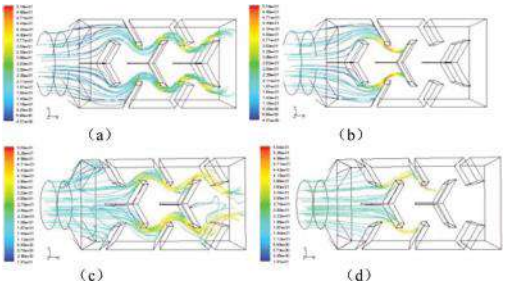


Figure 9. Dust trajectories in the precipitator. (a) Model one and dust particle is 7.07 μm;(b) Model one and dust particle is 30 μm; (c) Model three and dust particle is 7.07 μm; (d) Model three and dust particle is 30 μm

uniform in entrance section. This article only set 7.07 μm and 30 μm representative size for example. The dust trajectories of model one and model three are shown in Fig. 9.

As can be seen from fig. 9, incidence dust was divided into two parts uniformly and continue to move with air flow at the first shunt plate, trajectories is similar to "zhi"-shaped curve, incidence dust in the left of speed entrance turn left, incidence dust in the right of speed entrance turn right, all of these are due to the guide of airflow field.

Compared with (a) and (c) in Fig. 9, adding two low-speed zones in the front of the first baffle, which is called "dead zone" in engineering, "dead zone" isn't beneficial to separate gas and solid (Jones, W.P. & Launder, B.C. 1972), can't use space of precipitator effectively, reduce the efficiency of collection. Compared with (b) and (d), "dead zone" affect the dust size of 30 μm little, dust was trapped fully after the third baffle. in general, part dust in model three move disorder, but dust in model one move regularly.

Based on the above simulation and analysis, choosing model one as the last model of precipitator.

5 CONCLUSION

Through setting geometrical model and boundary condition, this article do gas-solid flow numerical simulation for wet centrifugal precipitator, analysis and compare the distribution law of velocity, pressure, turbulent kinetic energy of airflow field in three different precipitator, the dust move law of different sizes of dust under rated operating conditions, The results showed that:

1. Except for high-velocity zone in precipitator, there are 10 main vortex which lies behind vertical filter, the two adjacent vortex form vortex

pairs at the same time. There are local high-pressure zones on both sides of shunt plate, which is beneficial to form stable and continuous high-velocity zone, Compared with model one, the symmetry of pressure distribution in model two is poorer. There is high pressure zone before the first filter, the distrance between baffle and wall of precipitator is smaller, all of these may hinder the formation of vortex and cause the asymmetric of pressure distribution in the whole flow field.

2. Turbulent kinetic energy contour change from thin to dense, reach maximum in the tail of precipitator, Z = 0 axial cross section turbulent kinetic energy distribution of precipitator under rated operating conditions is very disorder, which isn't beneficial to remove dust stable and efficient and the safe of mechanized heading face.
3. Adding "dead zone" in the front of the first baffle in model three, "dead zone" isn't beneficial to separate gas and solid, can't use space of precipitator effectively, reduce the efficiency of collection. Based on the above simulation and contrast, choosing the precipitator which contains shunt plates and three rows of baffle in the middle (Model one) as the last model of precipitator.

REFERENCES

Dong, F. & Li, J. & Zhai, M. et al. 2006. Analysis on the Problems of Wet Dust Catchers in Operation. *Poer System Engineering*, 22(4):57–59.

Fan, J.R. & Yao, J. Zhang, X.Y. et al. 2001. Modeling particle-to-particle interaction in gas-solid flows. *Journal of Engineering Thermophysics*, 22(5):35–39.

Han, Z.Z. & Wang, J. & Lan, X.P. 2004. *Fluent simulation of fluid engineering examples and applications.* Beijing: Beijing University of Technology Press.

Jin, L.Z. 1993. *Control Coal Mine Dust*. Beijing: Coal Industry Press.

Jin, L.Z. & Jiang, Z.A. & Pan D.Y. et al. 2001. Study on the law of dust distribution in diving roadway. *Coal Science and Technology*, 29(3):43–44.

Jones, W.P. & Launder, B.C. 1972. The Prediction of laminarization with a two-equation model of turbulence. *Int. J. Heat and mass transfer*, (15):301–314.

Morsi, S.A. & Alexander, A.J. 1972. An investigation of the particle trajectories in two-phase flow systems. *J. Fluid Mech,* 55(2):193–208.

Pan, X.Q. & Yuan, J. 2004. Numerical Simulation of Engineering Fluid by Using CFD Software. *Journal of Nanjing Institute of Technology (Natural Science Edition,* 2(1):62–65.

Shih, T.H. & Liou, W.W. & Shabbir, A. & Yang, Z.G. et al. 1995. A new k-ε eddy viscosity model for high Reynolds number turbulent flows. *Comput Fluid*, 24(3):227–238.

Wang, F.J. 2004. *Analysis of Computational Fluid Dynamics*. Beijing: Tsinghua University Press.

Wang, H.G. & Liu, S.J. & Fan, S. 2004. Numerical Simulation of Reynolds Stresses of Gas-solid Two-phase Flows in an Inertial Separator. *Journal of Engineering for thermal Energy and Power*, 19(4):380–382.

Wang, X.Z. & Jiang, Z.A. & Wang S.W. et al. 2007. Numerical simulation of distribution regularities of dust concentration during the ventilation process of coal roadway driving. *Journal of China Coal Society*, 32(4):386–387.

Xu J. & Ge M.C. 1998. Numerical of Gas-solid flow. *Journal of Engineering Thermophysics,* 49(2):110–112.

Zhou, G.J. & Yan, Z.Y. 1992. *Hydrodynamics*. Beijing: Higher Education Press.

This page intentionally left blank

Progress in Mine Safety Science and Engineering II – He et al. (Eds)
© 2014 Taylor & Francis Group, London, ISBN 978-1-138-00122-0

Literature-based study of warning sign and of its effectiveness

Chixiang Ma
School of Resources and Safety Engineering, China University of Mining and Technology (Beijing), Beijing, China
School of Municipal and Environmental Engineering, Jilin Jianzhu Univesity, Changchun, China

Shuaidong Jia & Yanan Zhang
School of Resources and Safety Engineering, China University of Mining and Technology (Beijing), Beijing, China

ABSTRACT: The term warning sign which is clarified as it is typically applied to organization, to product, and particularly to workplace safety, is intended to alert persons to potential dangers in the environment and/or in the product. Warnings have become an important part of our modern lives not only because they provide essential information, but also because of constantly increasing regulations that require warnings to be present almost everywhere. During the past three decades, the body of empirical research on warning design and evaluation has grown in Europe and America. However, little research in this area has been delved in China. This paper reviews the literature on warning sign (safety/warning label included) and its effectiveness to support a reasonable, effective and cost-efficient approach to the design of warnings in China, especially in coal mine. There are now basic principles and guidelines for warning sign design and placement (using system approaches). Similarly, effectiveness evaluation (behavioral intention and behavioral compliance) have been developed. And, a series of researches and literatures have investigated several factors that determine safety sign compliance, including sign characteristics (salience, wording, size, layout and placement, pictorial symbols), personal factors (age, culture/ethnicity, gender, length of service, individual experience), situational factors (familiarity and training, risk perception, rewards and punishment, cost of compliance), organizational safety climate, (organizational environment, personal communication, administrative situations).

1 INTRODUCTION

Safety issue has been always the accompaniment during people using and maintaining a product or environment. Warnings are part of the interface between people and the surrounding (product and environment), which are intended to alert persons to potential dangers. Warning sign has been in applied in products and environments, including almost all industries. Warning signs are given in so many fundamentally different situations that the ways in which they are administered are very different as well.

During the past three decades, there has been a substantial, and increasing, amount of research on risk (safety) communications, more specifically, warning sign. The purpose of this article is to provide a review of the guidelines for warning design and evaluation based on empirical research and theory analysis in different industries. Through the review of the achievement, the warning sign design and evaluation can catch the scientific idea and method in China, especially in coal mine.

The design and evaluation of safety sign has received considerable attention by human factors/ergonomics researchers. These researches have encompassed both theoretical issues as well as application concerns, including a number of reviews and collections of the safety sign research literature. Two are collections of research articles from the Human Factors and Ergonomics Society (Laughery et al., 1994; Wogalter et al., 2001) (Laughery K. R., 1994; Wogalter and Young, 2001). A book by Edworthy and Adams (1996) (Edworthy and A, 1996) contained a general review of visual and auditory warnings. Other reviews published in the 1990s include Wogalter et al. (1995) (Wogalter and Barlow et al., 1995), Wogalter et al. (1999) (Wogalter and Young, 1999). More recent reviews are reported in Wogalter M.S. et al. (2002) (Wogalter and Conzola et al., 2002), Laughery K. R. and Wogalter M.S. (2011) (R. and S, 2011). Also, a substantial handbook that reviews the warnings literature has been published (Laughery, 1993; Wogalter et al., 2006; Wogalter, 2006) (Laughery and Wogalter et al., 1993; Wogalter, 2006; Wogalter and Silver et al., 2006).

Besides, there are lots of literatures about the specific application and research of warning sign in different industries, transportation, agriculture and medicine etc.. Among them is, such as Elliott M.A, et.al. (2003) (Elliott and Armitage et al., 2003) about warning sign of speed limits, Waterson, P. et al. (2012) (Waterson and Pilcher et al., 2012) about safety signs for children on board trains, Clack, Z.A et al. (Clack and Pitts et al., 2000) about warning sign of safety-belt using in transportation, Rother H.(2005)(Rother, 2005) about pesticide warning labels in agriculture, Huddle J.R et.al. (1991) (Huddle and Vanhoy et al., 1991) about warning sign for nuclear instruments in nuclear safety.

In this paper, the review and discuss of warning sign encompasses visual safety management, therefore, is limited to warning signs presented to the visual sense. However, during the safety communication process, there are common processing systems independent of the receiving modality, in other words, after the sensation experience, the later ones (the knowledge and compliance stages) are applicable regardless of the sensory modality that initiated it.

2 THE FUNCTION PRINCIPLE OF WARNING SIGN

Based on the relevant theory of safety field, the research detail and basic organization of the paper are explained.

2.1 *Relevant basic theory*

In the fields of safety, as well as in human factors and ergonomics, there is a basic set of strategies to prevent hazards from injuring people and damaging property, called the safety hierarchy or hazard control hierarchy (Sanders and McCormick, 1993). In the hierarchy, the priorities for dealing product or environmental hazards are: first is to design them out, second is to guard against them, and third is to warn.

The first and preferable approach to dealing with hazards is to eliminate them through an alternative design (such as substitution etc.). However, it is not always technologically and/or economically feasible to design out hazards. Guarding, the second priority, can be viewed as a means of preventing people from the hazard through time and/or space partition (such as installing interlocking device, reducing duration of exposure etc.). However, like the alternative design issues, guarding is not always practical or effective. A third technique of control hazards is to warn. As already referred, warning sign are intended to provide information to alert persons to potential dangers in the environment and/or in the product.

2.1.1 *Hazard and accident-causation theory*

It has been universally accepted that, hazard is the cause (root) of accident, that is to say, effective hazard control can prevent accident from occurring. According to GB13861-2009, hazard is categorized into four types: human, thing, environment, and management factors.

According to the modern accident-causation (G. and B. et al., 2005), from the point of individual behavior-safety control, hazard is embodied unsafe act (behavior) and unsafe condition; meanwhile, under certain situation, unsafe act (behavior) can transform and result in unsafe condition. The unsafe act and unsafe condition is the direct cause of accident, deeper analysis comes to the indirect (common) cause, which include three elements: inadequate safety knowledge, inadequate safety awareness, and inadequate safety habit.

It has been general agreement among researchers, and industry that individual (staff) unsafe behavior (act) is the elementary level in event (accident)-chain modeling, no matter in a simple system or in a sophisticated socio-technical system (Leveson, 2004). Thus, study on behavior safety is worthwhile. The accident-cause analysis is ranged in individual scope, i.e. not go further to organizational cause, which is addressed as the common cause of accident (see Fig. 1).

2.1.2 *Purpose of warning sign*

Warning sign is safety communication, and it is intended to communicate information about safety issues or problems. Its purposes can be referred to as safer world, provide information, influence behavior, and reminder, among which, the behavior influence is the effect issue, and that is to say, compliance behavior is the result of warning.

As the paper is a behavior-based study, it is focused on the issue of influence behavior. From this point of view, warning can be regarded as an effort to influence or control behavior, which concentrates on whether the behavioral intent of the warning is achieved. If the compliance behavior is

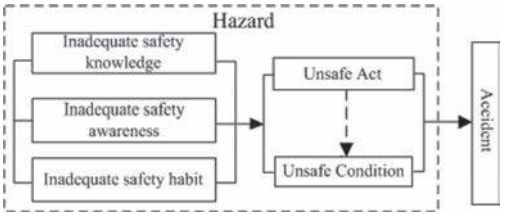


Figure 1. The common cause of accident.

achieved, the safe act is achieved to a large degree, and meanwhile, the unsafe act (unsafe condition) falls.

In the last analysis, the purpose of warnings is to make the world a safer place. In other words, reduced accidents and losses (injuries and damages) and improved safety and health would be goal for evaluating the effectiveness of warnings at this level.

2.2 *The function principle of warning sign*

Warnings and safety signs have three main purposes (Wogalter, 2006): firstly, to communicate safety related information so that people can make better, more informed decisions regarding safety issues; secondly, to persuade people to behave safely in order that their behavior helps to reduce or to prevent injury and health problems; and, thirdly, to remind individuals who may already know the hazards but may not be consciously aware of them at the time that knowledge is necessary (i.e., warning can recall pre-existing knowledge).

2.2.1 *The principle of warning sign to prevent accident*

From the engineering viewpoint, the primary reason to provide a warning is to reduce accidents (Lehto and Papastavrou, 1998). As effective warning sign is an important method to control hazard, and the elimination and reduction of hazard can prevent accident from occurring, the principle of warning sign to control to prevent accident is logical. To be specific, warning sign is set according to hazard identification (unsafe act and unsafe condition); and meanwhile, reasonable warning sign can eliminate and reduce hazard, and further prevent and reduce accident and loss. The principle of warning sign to prevent accident is shown in Fig. 2, which is also illustrative diagram of warning sign design, after all, the design of warning sign is aimed at accident-prevention and loss-reduction.

2.2.2 *The function principle of warning sign's effectiveness*

Warnings, like the other strategies can also be limited in effectiveness. As the visual warning sign,

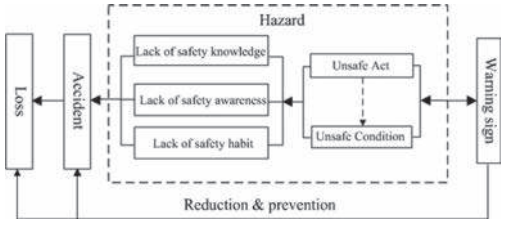


Figure 2. The principle of warning sign to prevent accident.

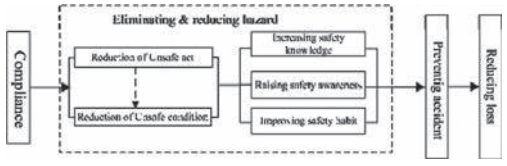


Figure 3. The function principle of warning sign's effectiveness.

people may not see, and/or they may not understand it, or they may not be sufficiently motivated to comply with it. Although these limits exist, far from not setting the warning signs where it is proper and required, these limitations mean warning sign deserve more attention to achieve better effect (Laughery, 2006). That is to say, it should be designed more attentively so that it is more likely to be effective. The parameters and elements needed during design will be explained later in the paper.

Then, the critical question arises, "Does warning work and how to evaluate whether it effect?"

That is issue of the effectiveness evaluation. As mentioned above, the compliance behavior (and/ or intent) is defined as the chief indicator to evaluate the effectiveness of warning sign in the article. The effectiveness is attributed to compliance behavior, because the compliance is in conformity with the idea of behavior control and behavior safety science, in which unsafe behavior contributes to almost all accident. That means, if people behave according to the correct directives and rules (warning sign), accident and loss can be prevented and reduced to a large degree. The function process of compliance is shown in Fig.3.

As safety communication, the effect of warning sign follows the information processing procedure. Therefore, this indicator (compliance) is a later stage in the communication procedure. A further discussion about other evaluating criteria and indicators and influencing factors will be made in the following paragraph based on literature-review.

3 DESIGN OF WARNING SIGN

As mentioned above in the article, from the engineering viewpoint, the primary reason to provide a warning is to reduce accidents. However, from a decision-making perspective, warnings may be ignored if they seem to be irrelevant to task performance. Another concern is that excessive warnings may result in information overload. Therefore, scientific design is significant for more intelligent and considerably more effective warning signs. So whether the regulatory requirements concerning warnings are satisfied by warnings is enough for a warning sign design, obviously no.

For example, most regulatory requirements very limited amounts of risk and emergency information, but, it is found that the effectiveness of warnings can be improved significantly by providing more information about the likelihood of the occurrence of the stimulus. It needs more thorough research to meet the demand of warning design.

The design is based on two typical theories or models, communications theory and human information processing theory. The typical, basic communication model has four components: the source, the medium, the message and the receiver (see Fig. 4).

The human-information processing framework is a stages model, consisting of stages through which warning information flows (see Fig. 5).

Generally speaking, in warning sign design, two aspects should be considered, design parameters of the warning sign, and characteristics of the target user (i.e. receiver) and situation. Design parameters include format factors such as wording, pictorial symbols, color/contrast, size, layout and placement, and content factors that should be expected to matter are explicit information considering hazards, consequences and conductions.

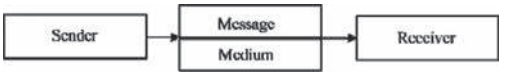


Figure 4. Basic communication model.

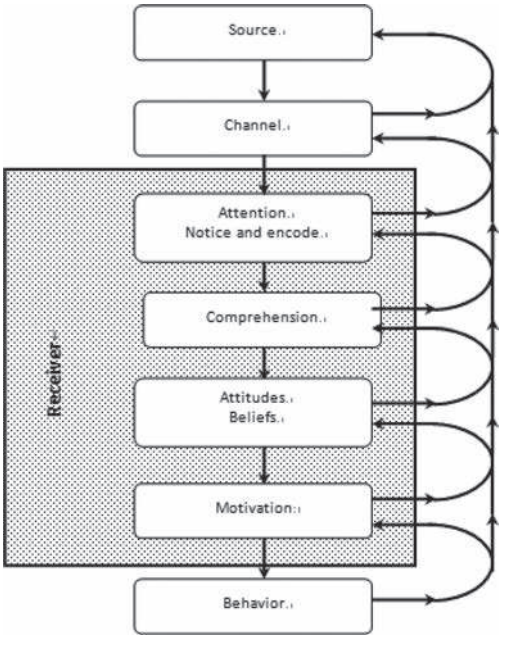


Figure 5. The C-HIP model.

3.1 *Salience*

Existing research indicates warning labels are generally ineffective due to users ignoring them(Rodriguez, 1991). And it has been found that salient warning sign increase the likelihood of reading, comprehension, recall and compliance (Braun and Mine et al., 1995; Glover and Wogalter, 1997; Hopkins and Parseghian et al., 1997).

Traditional researches focus the features of salience on size of the label, location, bold print, and pictorial symbols (Hussain and Arens et al., 1991; Kline and Braun et al., 1993; Braun and Mine et al., 1995) etc. Michael A. Rodriguez (Rodriguez, 1991) studied the combined effect of color, shape. Laughery, K.R (Laughery and Young, 1991) studied the principle of searching warning messages through eye tracking procedures.

3.2 *Design parameters and elements of warning sign*

3.2.1 *Wording*

Standards, guidelines, and research findings suggest that an effective warning sign should generally include four message components, signal word, hazard, consequence, and instruction statements (Young and Wogalter et al., 1995). It has a practical implication that word is the main form of expression message. For the first component, the most common used signal words are DANGER, WARNING, CAUTION, and NOTICE, successively connotes the degree of hazard from the greatest to the least. It is found that the presence of a signal word in warning sign increases its effectiveness and the level of perceived hazard(Wogalter and Jarrard et al., 1992; Wogalter and Brelsford, 1994; Young and Wogalter et al., 1995).

Secondly, warning sign should describe the potential hazard present in the situation. The hazard description should be specific and complete so that people can catch up the nature of hazard. It needs to notice that brevity should be considered as well as completeness.

Third, description of the possible consequences of non-compliance should be included. It has been cognizant of the importance of consequences information of warning sign in China. More explicit consequence description have been associated with greater levels of perceived dangerousness, hazard understanding, perceived injury severity, intent to act cautiously and protective equipment use (Dingus and Wreggit et al., 1993; Laughery and Vaubel et al., 1993; Braun and Silver, 1995; Ayres and Wood et al., 1998; Al-Madani, 2000; Clack and Pitts et al., 2000).

Finally, the warning sign should offer directives or instruction on how to avoid the hazard and how

to deal with the conceivable consequence when an abnormal incident occurs. In fact, instruction is hazard avoidance directives, which should describe specific actions that need to be taken (or avoided) by the warning recipient for safe behavior (act).

In a word, explicit information for all three warning content categories: hazard, consequences and instructions is of great importance. Explicit and overall information play a significant role in compliance (Laughery Sr and Paige Smith, 2006).



Figure 6. Representative warning designs used in China.

3.2.2 *Pictorial symbols*

Usually, the majority of people notice pictorial symbols at first glance at a warning sign. So it is not surprising that including pictorial symbols in warning sign increases their salience and likelihood of being noticed. An important function of pictorials is to facilitate warning comprehension. Comprehension is the degree to which the recipient understands the warning, based upon the intended meaning the warning is designed to convey.

A warning must first be legible (early stage of information processing) before it can be comprehended (later stage of information processing). However, it has been demonstrated that many warning symbols currently in use are poorly understood. To answer this issue, the American National Standards Institute (1998) standard ANSI-Z535.3 Criteria for Safety Symbols recommends the use of training to improve comprehension. Mary F. Lesch (2003; 2008) (Lesch, 2003; Lesch, 2008) has studied age-related differences and impact of training, and different training methods for improving warning symbol comprehension. It was found that training should be used to improve warning symbol comprehension since failures to adequately understand warning information may lead to injury or death, and relatively simple training conditions can dramatically improve accuracy and speed of responding to warning symbols.

An important function of pictorials is to facilitate warning comprehension. Comprehension is the degree to which the recipient understands the warning, based upon the intended meaning the warning is designed to convey. Both the ISO 3641-1 Standard and the ANSI Z535 Standard have established minimum acceptable levels of comprehension by the general population (67% and 85%, respectively). But in China, the relevant standard has not referred to acceptable levels of comprehension. Below (see Fig. 6) are three examples of a warning format recommended in design guidelines in GB2894-2008.

3.2.3 *Placement and layout*

Placement or location relates to where the warning will be embedded within a context of use. Warnings are most effective when they are presented proximate (in time and space) to the hazard (Wogalter and Conzola et al., 2002). The placement of warning signs is not a transparent process, Krisp, J.M. et al. applies a well-documented computational method to identify the wildlife warning sign placement in southern Finland (Krisp and Durot, 2007). Frantz has studied the placement of warning, and using task-analytic approach to generate alternative warning locations (Frantz, 1993; Frantz and Rhoades, 1993; Frantz and Rhoades et al., 2000).

Researchers find that warning layout (spatial structure) and organization (semantic structure) can also influences effectiveness. It can affect the readability and memorability of warning information. Some results may be as references for placement design, such as: warning in outline form is regarded as more appealing, easier to process, and more effective than other layouts.

3.2.4 *Other parameters*

Besides these parameters mentioned above, color, shape, size, auditory warning and receivers' characteristics are also the necessary factors considered in warning design. In practice, color is usually coordinated with shape and light (Easterby and Hakiel, 1980; Hussain and Arens et al., 1991), and the applications of color can facilitate comprehension and perceptions (Kline and Braun et al., 1993; Braun and Mine et al., 1995; McDougald and Wogalter, 2013). Generally speaking, larger size means more salient; another aspect of size is the signal word-text size, the difference of size affects readability of the warning (Silver and Braun, 1993). Auditory warning may be used when the visual environment is unavailable and when the message is relatively short and simple. Visual with auditory warning have been widely applied in transportation and many industrial systems, a proper type of auditory alarm is effective for eliciting perception of hazards (Chan and Ng, 2009).

As for receivers' characteristics, these contain demographic variables such as gender, age, work seniority, cultural and educational background, product or task familiarity and training, and individual differences. The researches on individual issue focus on the Need for Cognition measured

through NFC (Need for Cognition Scale), which is regarded as an important cognition factor influence of hazard perception and further of rules and warnings compliance (Gramann and Bonifield, 1995). More specific of warning's participant, more effective for behavior obeying. It was found that warning containing a direct reference to the individual led to higher compliance compared to a warning containing no reference to the individual (Wogalter and Brelsford, 1994; Wogalter and Young, 1994). These issues will be further discussed below in part of influencing factors.

4 EFFECTIVENESS OF WARNING

Guidelines for warning sign design and measures of the effectiveness should be compatible. In fact, due to ethical constraints and measurement method, very few warning sign have actually been evaluated or tested for efficacy.

4.1 *Evaluation processes and methods*

As referred above in the article, warning sign is a safety (risk) communication, with the intent of evoking the safety behavior (act). To determine whether a warning is effective, a systematic evaluation process (method) is indispensable. Evaluation processes fall into two main categories, formative and summative evaluation, which successively occurs while the warning is being designed, and after all design activities have been completed (Ballantyne and Hughes, 2006).

Formative evaluation means diagnostic use of assessment to provide feedback to participants over the process of design, which supports iterative design of warning sign, so that the warning can be changed repeatedly throughout the process, until a final iteration is agreed upon. As in education field, efforts to strengthen formative evaluation can produce significant learning gains in the test scores of the students (Black and Wiliam, 1998), so does the warning design. It means the ease of identifying problems early in the design cycle, and is a beneficial method.

After all, not all the factors can be identified in the design cycle, so summative evaluation is needed, which is a basis for actual result and for warning improvement. Summative evaluation can be the sole approach to evaluation, or it can be combined with formative evaluation. In summative evaluation, the final product (warning sign) must be "released" into the context of use, and then criterion measures can be gathered from participants over a period of time.

Recognition Test and Recall Test (Cairney and Sless, 1982), sample questionnaire survey (TAY and DE BARROS, 2010), digital questionnaire interview (Vardavas and Connolly et al., 2009), face-to-face interview(Rother, 2005), literature searches and expert selection, hybrid communication/human information processing model analysis, stimulus, laboratory experiments are the evaluation methods employed by researchers.

4.2 *Evaluation criteria and indicators*

To gain evaluation result, criteria and indicators used must be careful selected. In terms of communication theory, measures of noticeability, comprehension, legibility, understandability, recall, reaction time, compliance and search time have been used to assess effectiveness. Besides, subjective ratings of hazardousness, risk, as well as likelihood of injury, likelihood of compliance are often used. In addition, measures of the intermediate processes concerned with the stages of the information-processing model (e.g., attention), which occur prior to behavioral compliance. Other methods to gain subjective report can include paired comparisons of design alternatives followed by ratings of various dimensions such as likelihood of compliance, and these indicators are commonly employed in formative evaluation.

Recall (recall accuracy) is in common use in warnings evaluations as the objective measure indicator. Incidental recall accuracy can reflect the extent to which the warning communicated the risk information and simulated real-world exposure scenarios.

4.3 *Evaluation considerations and influencing factors*

Whether a warning sign is effective depends on many aspects, which can be categorized as internal factors and external factors, from the viewpoint of warning sign. So-called internal factors refer to the warning sign itself. So it is coincidence with design parameters, which means good design is an important element in effectiveness. The specific factors can be discovered above.

The external influencing factors which are commonly employed contain demographic variables, emotion, training and familiarity, situational, safety climate. Demographic variables refer to age, culture/ethnicity, gender, length of service, individual experience, etc.. For example, it is usually a consensus that older individuals have greater difficulty in understanding warning.

Situational factors include many elements, such as familiarity and training, risk perception, rewards and punishment, cost of compliance which is regarded as a critical factor to compliance intent and behavior. Safety climate belongs to organizational element which is made up of

personal communication, administrative situations, and work environment.

5 GENERAL DISCUSSION AND CONCLUSION

During the past 30 years, warning research has made substantial progress in design and effectiveness issues in Europe and America, which can and should be guideline for more effective warnings and for more scientific standards and regulations in China. In terms of the severe reality, there is golden opportunity as well as great challenge for warning research, it answers very well for coal mine.

Warnings sign should be designed to be noticed and encoded and to provide enough information to evoke compliance and safe behavior. The factors that should be considered include two aspects, design parameters of the warning sign, and characteristics of the target user and situation. Design parameters include format factors such as wording, color/contrast, pictorial symbols, size, layout and placement, and content factor that should be expected to matter is explicit information considering hazards, consequences and introduction.

About effectiveness, the evaluation process can be classified informative and summative evaluation which successively occurs while the warning is being designed, and after all design activities have been completed. And the measure methods contain subjective and objective measures, of which subjective measure is more applicability. Different indicators of subjective measures, including behavioral intent, usability, noticeability, guessability, comprehension, reaction time, etc. converge on the same or similar results: behavioral compliance, while recall(such as incidental recall accuracy) and attention are usually the indicators measured in objective assessment. The influencing factors often be used contains demographic variables, emotion, training and familiarity, situational, organizational safety climate.

In conclusion, these parameters and factors above-mentioned should be considered in the future enacting and revise of standards and in the future design of warning sign. And these front researches could and should support a cost-efficient, user-oriented technique to the design of warning sign, and further result in more effective warning system that in turn contribute to product and environmental safety.

ACKNOWLEDGEMENTS

Great thanks for National Natural Science Foundation of China (NO.51074167), The Special Research Foundation on Doctoral Program in University in the Year 2010 (NO.20100023110005) and Special Funds for Fundamental Research in Central Universities.

REFERENCES

Al-Madani, H. (2000). Influence of drivers' comprehension of posted signs on their safety related characteristics. *Accident Analysis & Prevention* 32 (4): 575–581.

Ayres, T. and C.T. Wood, et al. (1998). Effectiveness of warning labels and signs: An update on compliance research. *Proceedings of the Silicon Valley Ergonomics Conference & Exposition.*

Ballantyne, R. and K. Hughes (2006). Using front-end and formative evaluation to design and test persuasive bird feeding warning signs. *Tourism Management* 27 (2): 235–246.

Black, P. and D. Wiliam (1998). Assessment and classroom learning. *Assessment in education* 5 (1): 7–74.

Braun, C.C. and N.C. Silver (1995). Interaction of signal word and colour on warning labels: differences in perceived hazard and behavioural compliance. *Ergonomics* 38 (11): 2207–2220.

Braun, C.C. and P.B. Mine, et al. (1995). The influence of color on warning label perceptions. *International Journal of Industrial Ergonomics* 15 (3): 179–187.

Cairney, P. and D. Sless (1982). Communication effectiveness of symbolic safety signs with different user groups. *Applied Ergonomics* 13 (2): 91–97.

Chan, A.H.S. and A.W.Y. Ng (2009). Perceptions of implied hazard for visual and auditory alerting signals. *Safety Science* 47 (3): 346–352.

Clack, Z.A. and S.R. Pitts, et al. (2000). Do reminder signs promote use of safety belts. *Annals of Emergency Medicine* 36 (6): 597–601.

Dingus, T.A. and S.S. Wreggit, et al. (1993). Warning variables affecting personal protective equipment use. *Safety Science* 16 (5–6): 655–673.

Easterby, R.S. and S.R. Hakiel (1980). Safety labelling of consumer products: Shape and colour code stereotypes in the design of signs: TRC Repost No T79–8008; University of Aston, Applied Psychology Department, Birmingham, Report No AP-REP-75, Dec 1977, 49 pp, abstr in: R and D Abstracts. *Applied Ergonomics* 11 (1): 50.

Edworthy, J. and A. A, Eds. (1996). *Warning Design: A Research Prospective.* London, Taylor & Francis.

Elliott, M.A. and C.J. Armitage, et al. (2003). Drivers' compliance with speed limits: An application of the theory of planned behavior. *Journal of Applied Psychology* 88: 964–72.

Frantz, J.P. (1993). Effect of location and presentation format on attention to and compliance with product warnings and instructions. *Journal of safety research* 24 (3): 131–154.

Frantz, J.P. and T.P. Rhoades (1993). A task-analytic approach to the temporal and spatial placement of product warnings. *Human Factors: The Journal of the Human Factors and Ergonomics Society* 35 (4): 719–730.

Frantz, J.P. and T.P. Rhoades, et al. (2000). Assessing the effects of adding messages to warning labels. *Proceed-*

ings of the Human Factors and Ergonomics Society Annual Meeting, SAGE Publications.
G., F. and L.B., et al. (2005). Behavior Based Model for Organizational Safety Management. *China Safety Science Journal*(15): 21–7.
Glover, B.L. and M.S. Wogalter (1997). Using a Computer Simulated World to Study Behavioral Compliance with Warnings: Effects of Salience and Gender. *Proceedings of the Human Factors and Ergonomics Society Annual Meeting*: 1283–1287.
Gramann, J.H. and R.L. Bonifield (1995). Effect of personality and situational factors on intentions to obey rules in outdoor recreation areas. *Journal of Leisure Research* 27 (4): 326–343.
Hopkins, J. and Z. Parseghian, et al. (1997). A Driving Simulator Evaluation of Active Warning Signs. *Proceedings of the Human Factors and Ergonomics Society Annual Meeting* 41 (2): 921–925.
Huddle, J.R. and J.R. Vanhoy, et al. (1991). A warning-sign and safety-interlock system for an NEC 5SDH accelerator. *Nuclear Instruments and Methods in Physics Research Section B: Beam Interactions with Materials and Atoms 56–57, Part 2* (0): 1173–1175.
Hussain, S.G. and J.B. Arens, et al. (1991). Effect of light sources on highway sign color recognition. *Applied Ergonomics* 22 (2): 27–34.
Kline, P.B. and C.C. Braun, et al. (1993). The Impact of Color on Warnings Research. *Proceedings of the Human Factors and Ergonomics Society Annual Meeting* 37 (14): 940–944.
Krisp, J.M. and S. Durot (2007). Segmentation of lines based on point densities—An optimisation of wildlife warning sign placement in southern Finland. *Accident Analysis & Prevention* 39 (1): 38–46.
Laughery K.R., Ed. (1994). *Human factors perspectives on warnings.* Santa Monica, CA, Human Factors and Ergonomics Society.
Laughery Sr, K.R. and D. Paige Smith (2006). Explicit information in warnings. *Handbook of warnings*: 419–428.
Laughery, K.R. (2006). Safety communications: Warnings. *Applied Ergonomics* 37 (4): 467–478.
Laughery, K.R. and K.P. Vaubel, et al. (1993). Explicitness of consequence information in warnings. *Safety Science* 16 (5–6): 597–613.
Laughery, K.R. and M.S. Wogalter, et al. (1993). Human factors perspectives on warnings: *selections from Human Factors and Ergonomics Society Annual Meetings,* 1980–1993, The Society.
Laughery, K.R. and S.L. Young (1991). An Eye Scan Analysis of Accessing Product Warning Information. *Proceedings of the Human Factors and Ergonomics Society Annual Meeting* 35 (9): 585–589.
Lehto, M.R. and J.D. Papastavrou (1998). A signal-detection theory based perspective on design of warning. *Perceptual and Motor Skills* 86 (2): 720–722.
Lesch, M.F. (2003). Comprehension and memory for warning symbols: Age-related differences and impact of training. *Journal of Safety Research* 34 (5): 495–505.
Lesch, M.F. (2008). A comparison of two training methods for improving warning symbol comprehension. *Applied Ergonomics* 39 (2): 135–143.
Leveson, N. (2004). A new accident model for engineering safer systems. *Safety Science*(42): 237–70.
McDougald, B.R. and M.S. Wogalter (2013). Facilitating pictorial comprehension with color highlighting. *Applied Ergonomics(Available online 4 June 2013)*.
R., L.K. and W.M. S (2011). A three-stage model summarizes product warning and environmental sign research. *Safety Science*.
Rodriguez, M.A. (1991). What Makes a Warning Label Salient. *Proceedings of the Human Factors and Ergonomics Society Annual Meeting* 35 (15): 1029–1033.
Rother, H. (2005). Risk perception, risk communication, and the effectiveness of pesticide labels in communicating hazards to South African farm workers. Michigan, United States, Michigan State University. 3189735: 457–457 p.
Sanders, M.S. and E.J. McCormick, Eds. (1993). *Human Factors in Engineering and Design, 7th. ed.* New York, McGraw-Hill.
Silver, N.C. and C.C. Braun (1993). Perceived readability of warning labels with varied font sizes and styles. *Safety Science* 16 (5–6): 615–625.
Tay, R. And A. De Barros (2010). Effectiveness of Road Safety Messages on Variable Message Signs. *Journal of Transportation Systems Engineering and Information Technology* 10 (3): 18–23.
Vardavas, C.I. and G. Connolly, et al. (2009). Adolescents perceived effectiveness of the proposed European graphic tobacco warning labels. *The European Journal of Public Health* 19 (2): 212–217.
Waterson, P. and C. Pilcher, et al. (2012). Developing safety signs for children on board trains. *Applied Ergonomics* 43 (1): 254–265.
Wogalter, M.S., Ed. (2006). *The Handbook of Warnings*. Mahwah, NJ, Erlbaum.
Wogalter, M.S. and J.W. Brelsford (1994). Incidental Exposure to Rotating Warnings on Alcoholic Beverage Labels. *Proceedings of the Human Factors and Ergonomics Society Annual Meeting* 38 (5): 374–378.
Wogalter, M.S. and N.C. Silver, et al. (2006). Warning symbols. In: Wogalter, M.S. (Ed.). *Handbook of Warnings*. Mahwah, NJ, Lawrence Erlbaum Associates: 159–76.
Wogalter, M.S. and S.L. Young (1994). Enhancing warning compliance through alternative product label designs. *Appl. Ergonomics* 25: 53–7.
Wogalter, M.S. and S.L. Young (1999). The relative contribution of injury severity and likelihood information on hazard-risk judgments and warning compliance. *Journal of Safety Research* 30: 151–62.
Wogalter, M.S. and S.L. Young, Eds. (2001). Human Factors Perspectives on Warnings, vol. 2. *Selections from Human Factors and Ergonomics Society Annual Meetings* 1993–2000. Santa Monica, CA., The Society.
Wogalter, M.S. and S.W. Jarrard, et al. (1992). Effects of Warning Signal Words on Consumer-Product Hazard Perceptions. *Proceedings of the Human Factors and Ergonomics Society Annual Meeting* 36 (13): 935–939.
Wogalter, M.S. and T. Barlow, et al. (1995). Compliance to owner's manual warnings: influence of familiarity and the placement of a supplemental directive. *Ergonomics* 38 (6): 1081–1091.
Wogalter, M.S. and V.C. Conzola, et al. (2002). Research-based guidelines for warning design and evaluation. *Applied Ergonomics* 33 (3): 219–230.
Young, S.L. and M.S. Wogalter, et al. (1995). Relative Order and Space Allocation of Message Components in Hazard Warning Signs. *Proceedings of the Human Factors and Ergonomics Society Annual Meeting* 39 (15): 969–973.

Progress in Mine Safety Science and Engineering II – He et al. (Eds)
© 2014 Taylor & Francis Group, London, ISBN 978-1-138-00122-0

Study on special protective clothing of coal mine

Jian Yao & Dongmei Tian
North China Institute of Science and Technology Safety Engineering, Beijing, China
Key Laboratory of Mine Disaster Prevention and Control, Hebei Province, Beijing, China

ABSTRACT: The coal miner's work first of all to ensure the safety and health at work, which is one of the most basic premises, is also a manifestation of social progress. Miners protective excellent performance clothing to protect miners' in the daily work of health, ensure safety in production. Based on the analysis of the underground environment of coal mining and the future trend, describes in detail the specific requirements of coal mine occupation safety of miners protective clothing, so as to meet the requirements of modern coal mine production safety, build a solid and reliable safety for coal mine workers.

1 INTRODUCTION

China is one of the main coal-producing countries in the world, the coal industry production value, profit and contribution to GDP growth in the display industry and future development potential. However, due to coal mining investment in safety facilities and guarantee ability is insufficient, safety consciousness, the coal mine production safety accidents occur frequently. At present, the miners in personal protective equipment including safety helmet, miner's lamp, overalls, gloves, wading boots, self-rescuer, etc (Cheng 2010). Which overalls belong to basic labor insurance supplies, just play a basic role, such as clothing, wear-resisting, resistance to hook for mine risk factors existing in the basic no protective functions, reach the purpose of security miner life safety and body health.

Is the purpose of this paper is discussed in the process of production in coal mine to the specific requirements of the occupational safety and protection for miners and mining protective clothing fabric requirements and the latest design concept and its development prospect, for the safety of the miners.

Modern coal mines work clothes is protective clothing with special function, can adapt to the coal mine complex work environment, to better protect miners' life safety and health. Based on the important role of mining protective clothing in coal mine production, both at home and abroad in the mining design of protective clothing are of different levels of study.

Check related data; we have a standardized research on protective clothing at home and abroad comparison:

First of all, the research on the standardization of protective clothing in China started relatively late, and abroad, especially in western developed countries, industrial revolution earlier, in the process of production workers may face the dangers of understanding more deep, so early in the standardization of protective clothing research development.

Secondly, the imperfect protective clothing standardization system in our country, and the western countries to produce all kinds of protective clothing, protective clothing performance test method standard is also very complete, high standardization degree, has formed a relatively perfect standardization system. EN standards system such as the European Union, the United States ANSI standard system, Japanese JIS standards system, German DIN standard system and the British BSI standards system. The most perfect is the international organization for standardization system of ISO standards.

In addition, our country at present the standardization study of protective clothing has many problems. Protective clothing, for example, the standard system framework is not comprehensive, protective garment production enterprises to participate in the extent of the standards is not enough, all kinds of protective clothing performance testing standards of research funding shortage, for real life safety is related to specific workers in protective clothing is equipped with and using less standard.

Through the above comparison, we can see that with the west in our country at present stage in the standardization of protective clothing research has the very big difference; a lot of research is worth us to draw lessons from abroad. We should intensify efforts to research the suitable protective clothing in coal mine.

2 THE COAL MINE OF PROTECTIVE CLOTHING FABRICS

Coal mines in China are widely distributed, protective clothing for the protection of the coal mine is very important for the safety and health practitioners, the current in coal mine special protective clothing in the process of the management and use, the state-owned key coal mine, local state-owned coal mine and the villages and towns coal mine there are some problems, enterprise to issue some of the protective clothing comfort is poorer, is uncomfortable to wear, or even influence work, cause the employees don't want to use the protective clothing, must cause we attach great importance to these problems.

In order to adapt to the environment underground, mining protective clothing in the fabric design must meet certain requirements. Here first on the market at present the main several requirements of protective clothing fabrics.

2.1 *Functional requirements*

1. Anti-static
   The cause of the underground coal mine gas explosion, one is electric leakage caused sparks gas explosion (Chen et al. 2010). Second is human body electrostatic sparks caused by gas explosion. Spark damage is the most common form of coal mine electric injury. Therefore in coal mine safety in production, we should seriously consider workers clothing, avoid clothing friction caused by static electricity, and reduce the gas explosion accidents.

   Considering the downhole complex natural conditions, humidity is also different, to the miners equipped with anti-static properties of the pure cotton fabric clothing, is the current coal mine production safety have to implement the most basic work.
2. Flame retardant
   Coal mine working environment cause the hidden trouble of the combustion is more, and mean to operate near the melted metal (Gao et al. 2011). In addition, there are many flammable and explosive substances, in a flash fire accident in which has the function of flame retardant protective clothing, can protect the body from damage within a certain amount of time.

   Miners protective clothing usually adopt natural fiber fabric, internationally commonly used natural fiber methods mainly include Proban flame retardant finishing of fabrics and Pyrovatex CP method of two types (Hu & Xing 2008): the former flame retardant, good resistance to wash fabric strength loss is small, but the feel of the treated fabric softness, color change is bigger, but also need special ammonia fumigation equipment; Have little impact on the latter for fabric color, feel is soft, without special equipment, is currently the most rapidly growing finishing methods.
3. Dust proof
   At present our country is still more than most of the coal mining face dust concentration national occupational health standards, a serious threat to the miners' health. Dust is mainly through the respiratory tract and skin penetration into the body, pneumoconiosis disease of coal miners as occupational diseases.

   According to the characteristics of the large underground work dust concentration, should according to the nature of the miners working with from the suction filter type dust respirator, at the same time requires protective clothing work closely with the miners. Openings in the neckline, cuffs, and hem parts for dustproof design, fabric should also have good dustproof performance, in order to ensure the occupational health of the miners.
4. Waterproof and oil-repellent
   Miners in the labor operation will often come into contact with water or the liquid medium such as oil, this kind of medium can clothes, skin contact, cause human body contamination infection or causes rheumatism disease, so the miner's protection should have the function of waterproof and oil-repellent.

   Antistatic, flame retardant and waterproof oil-repellent is contradictory, normally because of anti-static and waterproof oil agent, such as organic silicone, static acid derivatives are combustible materials (Li & Li et al. 2009), they Shared with flame retardant, on the one hand can make the per unit area of fabric with flame retardant agent on the relative reduction; On the other hand, antistatic agent, waterproof and oil agent more attached to the surface of fiber, the fabric on the surface of the combustion increase (Li 2011). Use of organic conductive fiber, phosphate flame retardants and fluoride compound waterproof and oil agent compatible technology can make the fabric fabric with antistatic, flame retardant and waterproof and oil properties (Lian 2009).
5. Warning
   Protective clothing to stain resistant generally large area USES brunet, this stone color approximation with downhole, underground work in the car and are relatively dense, heavy car and driving the driver's vision "blind area", it is easy to happen accident (Miao 2010). So,

in the homework in dangerous environment and protective clothing should be local miners using high luminosity of the material, in the clothing of the chest, back, waist, thigh, knee, setting up reasonable reflective article, in order to play a warning role. In addition, in the process of rescue, high luminosity of the material is easy to identify, to accurately position the miners' life safety to ensure the miners.

2.2 *The technical requirements*

Our country is one of the earliest productions of protective clothing in the world. With time development, the design of the protective clothing differentiation, set all kinds of protective clothing in China national standard, put forward the "safe, applicable, beautiful, generous" (Wang 2009), the general requirements of, for protective clothing design, management, research, and the system elements such as bidding and using make procedural management specification.

Aimed at the particularity of the miners, the state introduced a coal industry standard MT/T 843-843 "the miner's ordinary work clothes" (Wang 2012). This standard is mainly applied to pure cotton fabric, the principles of design, fabric selection, technical requirements, test methods were compared for specific provision, the main protection in the underground work normal damage and dirt. Moreover, GB 12014-2009 "antistatic clothing and GB17956-2000 standard" dusters "and so on is that of has a dustproof and function of anti-static work clothes quality requirements, performance index and test method to make the provisions of the (Wu 2012). Along with our country to the safety of the coal industry are becoming more and more attention, the miners protective clothing required technical requirements also more and more, and our country about the miners' protective clothing standards are not perfect, need to related department to improve as soon as possible.

2.3 *Comfort requirements*

Underground work has its particularity, the labor intensity is big. Under bending, stretching knee, clothing must apply the principle of ergonomics in the design of the structure, the underground work environment of the human—clothing—environment system characteristic (Xie et al. 2011), establish reasonable clothing "environment". As the second skin of human body, underground work should consider more the comfort level of the underground work requirements.

2.4 *Aesthetic requirements*

Research has shown that underground work should not only attach importance to protection, soft protection should also be fully appreciated. Some experts put forward soft protection is to point to by color, style and so on to the operators' psychological protection; and hard protection is to point to by material, design, physiological protection structure for the operators. Underground work clothing color and style design to influence the psychological safety of the miners, it is also one of mine occupational safety factors to consider.

2.5 *Hygiene requirements*

Complicated in the underground work environment, change of temperature and humidity, and downhole operation work and job level have different features, human-computer interaction, miners' protective clothing should meet the demand of different category assignments of hygiene.

According to each part of the human body movement during operation conditions and needs, the miners should be considered the performance of protective clothing fabrics is not unity (Xiong & Chen 2008). Due to large underground work exercise, for example, often under the environment of high temperature operation, under his arm, shoulder and other areas with preferable fabric moisture absorption moisture splicing; In protective clothing of miners neckline appropriate USES cotton knitted fabrics in order to improve the touch with his collar and neck, and in the operation to contain larger body parts with elastic fabric design.

The requirements of the protective clothing fabrics plays an important role in the actual downhole operation, however, is the current research situation in our country, most of protective clothing is still cannot achieve the required level, can maximum limit protect miners' health and safety.

Relevant data show that water is a major cause of underground personnel casualties occur, so, functional ways, from the homework take increase in permeable accident rescue function should bear the brunt. Miners' protective clothing with a life-saving device is in the fabric and material between joining a controlled balloon, the balloon light weight, wear comfortable, in does not affect the normal work at ordinary times (Yang et al. 2010). Man dressed in flooded when the initiative can be inflated, upper body form the airbag cover, effectively prevent the workers suffered from impact damage, and effectively protect the main parts of the body from strong impact and damage.

3 NEW COAL MINE WORKERS OF PROTECTIVE CLOTHING FABRICS DESIGN TRAIN OF THOUGHT

From what has been discussed above, protective clothing fabrics design scheme can have the following kinds.

1. The cotton fabric finishing, antistatic, flame retardant effect and so on in order to achieve (Yang & Qing 2011), but don't last, it concludes that the fabrics of various performance with the increase gradually reduce the number of washing, and pure cotton after finishing, the fabric strength will be greatly reduced, the feel is rough and hard, this is the technology cannot be improved.
2. Inflaming retarding t and electrostatic prevention were used in the fabric (Yu et al. 2010). A layer of cover membrane which has Inflame retarding t and electrostatic prevention formed on the surface of the fabric evenly. This method to a certain extent, improve the durability of the fabric with double proof, intensity is also improved. But the coating aging flame-retardant antistatic performance is poor, feel is also poor.
3. Make conductive fiber filament embedded in pure cotton fabric, flame retardant finishing on fabric (Zhang et al. 2011). This method can obtain good flame-retardant antistatic performance, but the washing resistance is poorer, flame retardant fabric strength is low, shooting style is still thick and hard.
4. According to the requirements of the coal mine with fabric performance analysis, and flame retardant cotton fiber blended yarn, or directly with pure cotton flame retardant fiber yarn, add conductive fiber to the water in the process of weaving filament, thus give essentially the antistatic flame-retardant dual function, and then carries on the simple finishing, finishing here focus on three, since the strength of flame retardant fiber and conductive fiber filament is much bigger than cotton, fabric ultimate strength, abrasion resistance and so on have been improved.

The main points of the four kinds of solutions together require protective clothing is to flame retardant and antistatic, from the aspects of comprehensive consideration, the fourth design ideal, also is we agreed.

Underground in addition, some working noise is very large, and the environment temperature is high, if you can in the fourth kind of design scheme, on the basis of plus noise proof and heat insulation function to design of protective clothing, coupled with dustproof, waterproof and oil-repellent, can design a set of comprehensive protection ability stronger mining protective clothing.

Protective clothing research, according to the present coal mine has fire retardant anti-static performance very bullish on the prospect of development of protective clothing. First of all, the development of textile flame retardant standard currently has the following three aspects: internationalization and standardization, the performance requirements of comprehensive and multiplicity and the standard quantity and type of increase. Secondly, from the development strategy of flame retardant protective clothing, protective obey such fibers, improve performance, reduce costs; Make full use of domestic conditions, development of flame retardant finishing process (Zhang et al. 2011); Strengthening research of fabric structure, can satisfy the protection performance of flame retardant protective clothing and performance, and can well satisfy the comfort; Strengthen cooperation development, to strengthen coordination and cooperation between various departments, to produce one performance good protective clothing. Finally, in terms of environmental protection, the protective clothes is made of fabric environmental protection, harmless to human health of chemical agent, pigment, and control the harmful substances, in order to realize the virtuous cycle of nature and humanity, technology (Zhu 2011), and achieved very good environmental benefits.

4 CONCLUSIONS

Coal enterprises in our country's achievement of continuous case, the coal mine production safety situation is still not optimistic, coal mine safety accidents have occurred. We must develop a strong protective function of protective clothing, to protect the life safety of mine workers. Based on the existing mining coal mine is expounded on the basis of special protective clothing research requires protective clothing fabrics, including dust, anti-static, waterproof and oil proof, flame retardant, such as performance, technical and protective clothing, comfort, aesthetics and occupational health and to the specific requirements of the special protective clothing miners.

According to new research, made protective clothing fabrics and flame retardant fiber, flame retardant and antistatic properties are very good, has the broad prospects for development, the study on people's life and property security, promote the sustained and steady development of the coal industry in China, speed up the process of our socialist modernization construction has the very vital significance. Hope this paper the uniform national standards and industry stand-

ards for miners' modification and redesign play a role in promoting, further to the coal industry in our country to provide a solid guarantee of safety production.

REFERENCES

Cheng Deliang. 2010. Involved in the protective clothing acid-base classes of chemical protective clothing drafting national standards introduced [J]. *Chinese standardization,* 10 (9):67–72.

Chen Lei, et al. 2010. Flame retardant protective clothing test standard of comparison analysis [J]. *Journal of textile science and technology progress,* 10(04):33–38.

Gao Zhifeng, et al. 2011. The antistatic performance of conductive fiber and its fabric is introduced [J]. *China fiber inspection,* 11(02):44–47.

Hu Fujing & Xing Juanjuan. 2008. GB/T20097–2006 general requirements of the protective clothing introduction [J]. *Journal of Chinese individual protective equipment,* 08 (01):76–79.

Li Lijun & Li Feng. 2009. High temperature resistant flame retardant protective clothing research progress [J]. *Journal of fire control technology and product information,* 09(04):88–91.

Li Qiu yu, et al. 2011. Carbon black conductive fiber in the application of blended wool fabric [J]. *Journal of wool spinning technology,* 11(10):103–106.

Lian Zhijun. 2009. Coal mine accident emergency rescue protective clothing performance requirements and selection [J]. *Journal of coal mine safety,* 09(12):106–110.

Miao Yong. Common labor protection clothing new material application [J]. *Science and technology,* 07(20):309–344.

Wang Laili. 2009. Development present situation and prospect of high-performance protective clothing [J]. *Journal of Chinese individual protective equipment,* 09(03):31–35.

Wang Wanqi. 2012. special protective clothing roundup [J]. *Journal of labor protection,* 12(12):56–59.

Wu Xiangji. 2012. New antistatic fabric material in the design and research [J]. *Journal of Shanghai textile science and technology,* 12(02):66–70.

Xie Jia xiang, et al. 2011. Antistatic textile design and development [J]. *Modern textile technology,* 11(6):88–92.

Xiong Lihong & Chen Yan. 2008. Coal mine homework personnel protective clothing design research [J]. *Journal of Chinese individual protective suits,* 08(4):12–15.

Yang Wenfen, et al. 2010. Standard for protective clothing acid-base classes of chemical protective clothing read [J]. *Journal of labor protection,* 10(10):125–130.

Yang Zhen & Qing Ning. 2011. Insulation materials research and development [J]. *Chemical industry new materials,* 11(05):91–93.

Yu Lili, et al. 2010. Assembly and chemical defense research institute [J]. *modern occupational safety,* 10(12):32–35.

Zhang Xinyuan, et al. 2011. The performance of high performance carbon fiber and its application [J]. *Cotton textile technology,* 11(04):46–50.

Zhang Zhongbin, et al. 2011. Protective clothing commonly used high and low temperature heat insulation performance study [J]. *China safety science and technology,* 11(8):56–60.

Zhu Fanglong. 2011. Additional heat transfer numerical simulation of phase change material layer thermal protective clothing [J]. *Journal of applied basic and engineering sciences,* 11(04):79–85.

This page intentionally left blank

4 *Mine rescue tools and techniques*

This page intentionally left blank

Progress in Mine Safety Science and Engineering II – He et al. (Eds)
© 2014 Taylor & Francis Group, London, ISBN 978-1-138-00122-0

How to improve the psychological quality of mine rescue commanders and fighters

Qi-Zhong Li
North China Institute of Science and Technology, Beijing, China

ABSTRACT: Qualified mine rescue commanders and fighters must have good psychological quality, and good psychological quality of the mine rescue commanders and fighters is a can not be ignored factor for a successful rescue of coal mine accidents. The mine rescue commanders and fighters should strengthen the training of technical and theoretical, at the same time, they should improve psychological quality in usually. The paper discusses an effective way to improve the psychological quality of mine rescue commanders and fighters.

1 INTRODUCTION

A person's psychological quality which based on the innate quality is gradually formed by the influence of acquired environment and education. Psychological quality includes the human ability of cognition, emotion and emotion quality, character, temperament, personality and so on.

Good psychological quality is an important component ability of a rescue commanders and fighters. Mine rescue team is specialized staffs who handle and rescue disaster of mine fire, flood, mine gas and coal dust explosion, gas outburst, etc. In terms of job nature, the rescue commanders and fighters must be facing the bad, dangerous working environment, sometimes endangers their personal safety. So they must have the good psychological quality in the handling of disaster, which directly affect the rescue to be successful or not.

2 UNFAVORABLE FACTORS INFLUENCING THE PSYCHOLOGICAL QUALITY OF THE RESCUE COMMANDERS AND FIGHTERS WHILE THEY ARE WORKING

Some unfavorable factors such as fear, emotion, fluky psychology, psychological dependence and the paralysis of thought often appear in the disaster relief, which influence the psychological quality of the rescue commanders and fighters Because of these factors will lead to adverse psychological state of the rescue commanders and fighters, some mistakes will be making in the rescue process, and it will cause the failure of rescue work.

2.1 *Fear in harsh environment*

Fear is a strong and depressed emotional state which individuals or groups felt deeply in danger of real or imagined. It often manifests as nervous, fear, inability to concentrate, mind going blank, and inability to correctly judge or control behavior. Fear is an innate emotional response of all animal including human. Fear is emotional reaction to an expected to be hurt or unpleasant when face stressors, which usually cause avoidance behavior.

2.2 *The emotional psychology in stress state*

Study on physiological psychology shows that, when face major emergencies, people will produce a stress state. Stress refers to the adaptive responses of people to some unexpected environmental stimuli. When people encounter some unexpected danger or face some unexpected events, people's body and mind are in high tension, this high tension is called the stress state. "Stress" can be simply described as "great confusion of psychology", which will produce the general excitement, cause the scope of attention and perception to be narrowing, cause the speech is not standardized and incoherent, cause behavior disorders. In the mine accident rescue, if mishandled, they will cause their casualties.

2.3 *Fluky psychology caused by empiricism*

Fluky psychology is the illusion of human's cognition and thinking, when they gain success or removed from the disaster by accidental. Some rescue commanders and fighters think that it no problem to do so the past or they often do it by this

way but nothing happens, they clearly know it is illegal operation, but they still insist on doing.

2.4 *Anaclisis and paralysis of the mind*

Anaclisis is a kind of state of mind without resolution or autonomous when people deal with problems. For example, in the treatment of an accident, the new commanders and fighters blindly follow the elder without according to procedures. Paralysis of thought manifest as free riding, and inobservance for the rules of operation.

3 EFFICIENT WAY TO CULTIVATE THE GOOD PSYCHOLOGICAL QUALITY OF RESCUE COMMANDERS AND FIGHTERS

The cultivation of rescue commanders and fighters' psychological quality, is a gradual process of constantly overcoming congenital mental deficiency, constantly honing mind, gradually enhance psychological adaptability and gradually improve the psychology bearing capacity. It will not complete in a short time, and it is not only have relationship with their internal factors such as psychological temperament, character, volitional quality, control ability and so on, but also cannot separate from subjective efforts such as personal learning, experience accumulation and good at summarizing. Therefore, the cultivation of the psychological quality mainly depends on the ability of the self psychological transformation and cognition. Their deficiencies in temperament, character and will can be gradually overcome and consummated through practice.

3.1 *Attaching importance to accumulation of actual combat*

The battlefield is the best training ground. The experience accumulation of rescue commanders and fighters officers are from the mine rescue actual combat, which is an important way to improve the psychological quality. Every rescue operation is a time of baptism and challenge of mind. The so-called unruffled senior general demeanor come from their own knowledge and combat experience. Through the actual combat, they will increase their own knowledge and accumulate experience.

3.2 *Attaching importance to summary of actual combat*

There will have successful experience in every mine accident rescue and must have space to summarize. Be good at summing up experience, taking lessons bravely, it is an important measure to improve their own quality and command ability for all level rescue commanders and fighters. Therefore, they must sum up experience, analyze problems and learn the lesson in order to promote their command ability.

3.3 *Attaching importance to theory and case learning*

The on-the-spot psychological quality of rescue commanders and fighters closely related to their cultural background and professional theoretical level which make their adaptation to the disposal of gusty mine accident will be stronger, psychological quality can be better reflected in the disaster. The theoretical study includes the basic theory of rescue, mine rescue skills and tactics, psychological knowledge and common sense, typical mine rescue case etc. Because they are difficult to experience various types of disasters and accidents, so it is particularly important to strengthen the research and analysis of the case. They should constantly acquire knowledge from heavier, large mine accident rescue case, once encounter similar accident, they will have certain psychological preparation, well-thought-out plan, calm response and scientific disposal method.

3.4 *Attaching importance to random drilling*

Random drilling is an effective way to improve psychological quality and practice ability of organization, which can make the on-the-spot reaction, insight, associative memory and will get testing and training in full. It test the rapid response capability and the ability to adapt changing circumstances of rescue commanders and fighters, and it is a good chance to check out whether a rescue commanders and fighters have good psychological quality and solid comprehensive service quality or not.

3.5 *Attaching importance to psychological adjustment*

Mine rescue teams struggle with the mine disaster for a long time, their members are always in a state of readiness, especially in the mine accident rescue process, they are always in a tense and busy fighting. So tension, fear and other bad state can hardly be avoided, once these psychological problems cannot be solved effectively, the psychological pressure cannot discharge timely, it may lead to psychological illness, lead to excessive tension and fault in decision-making in rescue. In recent years, the psychological adjustment ability of the mine rescue team is incorporated into the routine training. The method includes self mental relaxation, image reproducing, hint, transfer and the

conversation to firm confidence. Some of the rescue team has also opened up a mental health Web site, the psychological consultation room, catharsis room and comprehensive psychological training field, hired or fostered qualified counselors, to further strengthen the psychological health education and psychological counseling for the members. They focus on improving the self-control ability, the self-adjustment ability to ease the pressure, enhance the adaptability, improve the comprehensive psychological quality and command level.

3.6 *Fostering stable emotional state*

In the intense process of rapid transformation of rescue success and failure, the emotion of rescue commanders and fighters will have some drastic changes which will have positive or negative influence on action effect of the rescue team and their ability of body. A high degree of political awareness, responsibility and sense of honor is the important aspect of fostering emotional stability. Therefore, they should pay more attention to it in peacetime.

4 CONCLUSION

Mine rescue is a very sacred, very dangerous and very hard work. Their mission is walk along the reverse route of escape direction. Whether mine rescue is successful or not is determined by the interaction of inside conditions which is formed by the combination of the body, technology, tactics, psychology, conducting art, missions and other factors. But the psychological factor is one of the most important factors. Many failed rescue case shows that bad psychological quality is an important cause of its casualties and failure of rescue. It can be said that bad psychological factors are significant potential safety hazard of mine rescue. Therefore, we must pay special attention to improve the psychological quality of rescue commanders and fighters.

ACKNOWLEDGMENTS

A lot of thanks to the fundamental research funds for the Central Universities Fund (DX2013B01).

REFERENCES

Carlos Castro. 2001. An Elementary Derivation of the Black Hole Entropy in any Dimension Entropy. Entropy:107–110.

Chen Xiju. 2009. Existence of mine rescue work in China and the problems and solutions [J]. *Coal mine safety*:65–68 (in Chinese).

Gong Jing. 2008. Fire commanders and training ways of psychological quality model [A]. *Proceedings of the tenth annual meeting of China Association for Science Papers (a)* [C]:73–76 (in Chinese).

Luo Yunguo. 2008. Management of mine rescue team [J]. *Heilongjiang science and technology information* (12):134–138 (in Chinese).

O'Brien G.UK. 2006. Emergency Preparedness:A Step in The Right Direction? Journal of International Affairs: 65–69.

Shi Xianji. 2005. To strengthen the psychological education training to improve their psychological [J]. *Army political work theory research* (06):34–38 (in Chinese).

Uffink J. 1996. The Constraint Rule of the Maximum Entropy Principle. Studies in History and Philosophy of Modern Physics: 62–66.

Yang Daming. 2002. Current situation of China mine rescue [J]. *Contemporary miners* (04):165–169 (in Chinese).

Zhao Yueyue. 2009. How to improve the mine rescue team emergency rescue ability [J]. *Technology and development of economy* (08):57–63 (in Chinese).

This page intentionally left blank

Progress in Mine Safety Science and Engineering II – He et al. (Eds)
© 2014 Taylor & Francis Group, London, ISBN 978-1-138-00122-0

Assessment of Emergency Preparedness Effects of work safety in Xinjiang autonomous region of China based on weighted Rank Sum Ratio

Wenxun Zhang & Fanqi Kong
Xinjiang Academy of Safety Science and Technology, Urumqi, China

Tianhan Jiang
China Academy of Safety Science and Technology, Beijing, China

ABSTRACT: Emergency readiness assessment of work safety in Xinjiang autonomous region, China, is carried out to provide evidence for constructing Xinjiang's work safety emergency ability. Four work safety indicators are selected as assessment indices. The weighted Rank Sum Ratio (RSR) method is used to assessment the effects of work safety emergency management of 15 areas in Xinjiang. The results show that the emergency preparedness of work safety in the above areas is generally fine. And the work safe risk in Xinjiang has declined in the past years.

1 INTRODUCTION

There are many factors such as safety strategy, control target for work safety, safety regulation, safety management structure, etc., affecting regional work safety risk. And it is difficult to evaluate the control level of regional work safety risk. Emergency preparedness is known as the disaster preparedness, used to be a part of the four stages of emergency management "reduction, preparedness, response, recovery" (Sutton J & Tierney K 2006). It is defined as "The cycle of United States emergency preparation includes planning, organization, equipment and training, assessment and improvement of key link, to be enhanced the whole process of action "prevention, protection, response, recovery" (U.S. Department o f Home land Security 2009). Recently, Jiang & Deng (Tianhan Jiang & Yunfeng Deng 2012) presented a novel assessment method of regional Emergency Preparedness Effect (EPE). Quantitative indices of fatalities and economic loss are selected from natural disasters, accidents, social events, and public health events. The results showed that the EPE in China is getting better, while the overall levels of emergency inherent risk have dropped down in recent years. The assessment framework of regional emergency preparedness is effective, and the method is feasible. In this paper, we improved the above method to assessment the effects of work safety emergency management of 15 areas in Xinjiang autonomous region, China.

2 METHOD

2.1 *Assessment index*

A comprehensive national control indicators of relative index are selected as the basis of risk indicators in this paper (Xianzheng Wang 2004). Different weights are assigned to those indices, including Mortality of one Hundred Million Yuan (MHMY, 30%), Mortality of one Hundred Thousand Workers (MHTW, 40%), Mortality of Ten Thousand Vehicles (MTTV, 25%) and Mortality of Million Tons in Coal Mine (MMTCM, 5%). MHTW is most important, which can reflect the risk level of mining and trading industry. The second is MHMY, and the third is MTTV. Considering the Xinjiang coal mine accidents are severe, relatively large impact on mortality, MMTCM is included in this paper.

2.2 *Assessment method*

The weighted Rank Sum Ratio (RSR) method (Shaojiang Yang 1994) is used to assessment the work safety risk of 15 areas in Xinjiang as follows.

$$PSRI_j = \frac{\sum_{J=1}^{K} R_{ij} W_j}{N \times \sum_{J=1}^{K} W_j} \tag{1}$$

where, $PSRI_j$ (j = 1, 2,...,N) is the rank sum ratio of the ith City. N is the total number of cities to be

assessmented. R_{ij} is the rank of the jth index in the ith city. W is the weight coefficient of each index, here, $W_1 = 30$, $W_2 = 40$, $W_3 = 25$, $W_4 = 5$. Results are shown in Table 1.

Then Emergency Preparation Effect Risk Index (EPERI) of local work safety can be calculated according to the literature (Tianhan Jiang & Yunfeng Deng 2012).

$$EPERI = \frac{PSRI_i - \overline{PSRI_{i-1}}}{\overline{PSRI_{i-1}}} \times 100\% \quad (2)$$

3 RESULTS

The data from 2007 to 2011 used in this paper of work safety risk were obtained from Xinjiang work safety supervision and Management Bureau dispatch statistical information center (4 relative indices). The results were shown in Figure 1.

Figure 1 shows the work safety risk changes in different regions of Xinjiang from 2007 to 2011. Overall, the safety risk is roughly identically distributed in each year. High risk value may be followed by high risk value in next years. These results showed that the risk level of work safety can reflect the inherent risks of work safety of a city. And Kezhou's work safety risk is significantly higher than average risk of work safety in Xinjiang, China.

EPERI from 2007 to 2011 of 15 areas of Xinjiang is also calculated. The results are shown in Table 1 and Figure 2.

As is shown in Figure 2, Xinjiang work safety risk level is declining from 2007 to 2011, which reflects the work safety emergency preparedness effect gradually improve. The emergency preparedness effect was poor in Tacheng; The safety risk level didn't change in Hetian, and its emergency preparation effect was not obvious. The remaining 13 areas decreased, especially Hami, Kashi, and Changji Zhou was obvious, and emergency preparedness were better.

The work safety risks changed in Xinjiang from 2007 to 2011 are shown in Figure 3. From Figure 3, MMTCM, MTTV and MHMY decreased year by year, MHTW showed a downward trend, in addition to rebound in 2010. By comparing the results in Figure 2 and Figure 3, the declining trend is same. It indicates that the overall work safety risk decrease, and the emergency preparedness effects are fine in Xinjiang, China.

Bazhou, Hotan, and Tacheng is selected for analyzing the emergency preparation effect of work safety, among which, Bazhou can represent the regions with better emergency preparation effects.

Table 1. The work safety risk index and emergency preparedness effects in Xinjiang, China.

	2007	2008	2009	2010	2011	EPERI
Urumqi city	0.32	0.4	0.3	0.32	0.21	–18.87%
Changji zhou	0.86	0.52	0.44	0.24	0.32	–33.98%
Bazhou	0.59	0.45	0.44	0.27	0.28	–24.72%
Kashi	0.79	0.46	0.3	0.21	0.23	–41.55%
Yilizhou	0.41	0.36	0.28	0.22	0.27	–19.93%
Turpan	0.57	0.66	0.55	0.39	0.39	–21.44%
Hami	0.58	0.42	0.36	0.51	0.4	–41.89%
Bozhou	0.48	0.28	0.26	0.24	0.16	–26.93%
Aksu	0.61	0.83	0.57	0.61	0.45	–18.90%
Kezhou	2.16	3.6	0.73	1.24	0.31	–62.11%
Hetan	0.2	0.11	0.26	0.16	0.13	0.19%
Tacheng	0.41	0.28	0.32	0.56	0.3	9.07%
Altany	0.21	0.22	0.15	0.17	0.12	–22.13%
Karmay city	0.16	0.18	0.19	0.15	0.16	–5.02%
Shihezi city	0.19	0.17	0.14	0.17	0.12	–11.13%

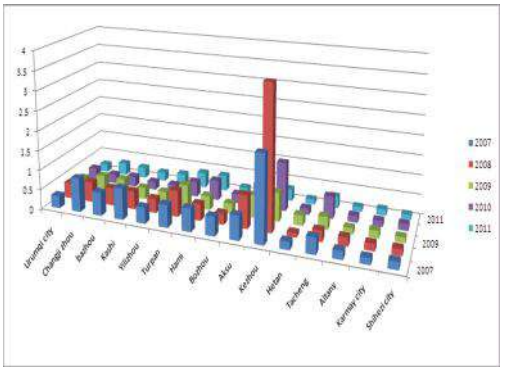


Figure 1. Changes of work safety risk in Xinjiang regions from 2007 to 2011.

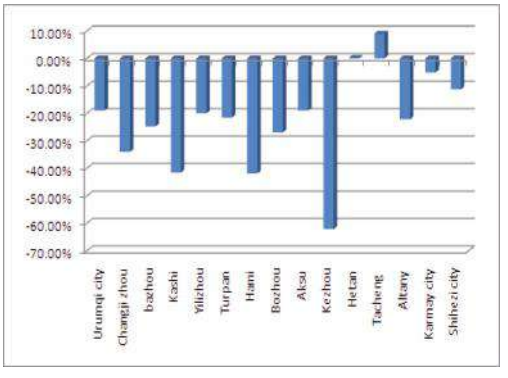


Figure 2. Emergency preparedness effect risk index of Work safety in Xinjiang regions.

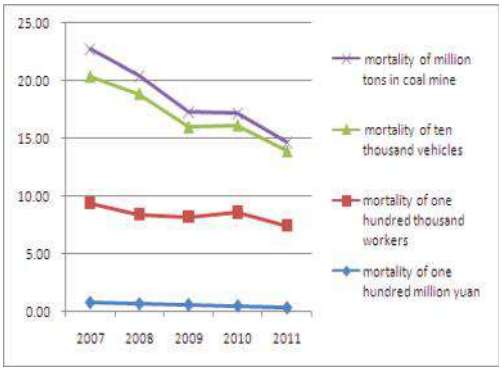


Figure 3. Xinjiang safety production 4 single safety risk (safety relative index) annual variation.

Hotan represents the regions with the general emergency preparedness effects. Tacheng area is less effective in work safety emergency management.

MHMY and MTTV in Bazhou decreased year by year; MHTW and MMTCM from 2008 to 2011. Overall, the work safety risk in Bazhou decreases, and emergency preparedness effects are fine.

MHTW and MMTCM in Hetian changed from high to low, and from low to high again; MHMY and MTTV has declined, but it was not obvious.

MMTCM and MHTW in Tacheng changed from high to low, and from low to high again; MHMY and MTTV has declined, but the decline is not obvious. Overall, the work safety risk is high in Tacheng, and emergency preparedness effect is poor.

4 CONCLUSION

The emergency preparedness of work safety in Xinjiang is generally fine. And the work safe risk in Xinjiang has declined in the past years, except Tacheng and Hotan.

ACKNOWLEDGEMENTS

We would like to thank the Xinjiang Administration of Work Safety for the survey data provision.

REFERENCES

Shaojiang Yang. Application of weighted RSR in comprehensive evaluation of economic benefit. *Statistics and Forecast (in Chinese)*. 1994; 02:38–41.

Sutton J, Tierney K. Disaster Preparedness: Concepts, Guidance and Research. *Report prepared for the Fritz Institute Assessing Disaster Preparedness Conference*; 2006.

Tianhan Jiang, Yunfeng Deng. Effect Evaluation Method of Regional Emergency Preparedness Based on the Rank Sum Ratio. *Proceedings of the 5th annual meeting of Risk Ananlysis Council of China Association for Disaster Prevention, Nanjing, China*, 2012; 670–674.

Xianzheng Wang. On the establishment of index system of safe production control. *Labour Protection (in Chinese)*, 2004; 3:68–69.

This page intentionally left blank

Progress in Mine Safety Science and Engineering II – He et al. (Eds)
© 2014 Taylor & Francis Group, London, ISBN 978-1-138-00122-0

Application of reverse circulation DTH hammer in mine rescue drilling

Fanqi Kong & Xiaolin Lai
Xinjiang Academy of Safety Science and Technology, Urumqi, Xinjiang, China

ABSTRACT: When accidents such as water permeation, mine fire, roof fall occurred under the coal mines, it was important to get through the blocked layer and rescue the persons rapidly, which could reduce accident casualties and economic loss. Conventional DTH hammer drilling technology was often used in mine rescue drilling, and there were many successful examples. Because of many difficulties such as broken formation, rich fractures, and complex downhole condition, such technology brought out many problems such as low speed, low efficiency, and more accidents. In order to solve the problems, this paper introduced the reverse circulation DTH hammer drilling technology, which had outstanding advantages in complex formation drilling such as fast drilling speed, low air requirement, and not being affected by the formation condition etc. The applicability of reverse circulation DTH hammer drilling technology used in mine rescue drilling was also discussed.

1 THE IMPORTANCE OF MINE RESCUE DRILLING

Data from State Administration of Work Safety of China showed that 779 accidents occurred in coal mines across the country in 2012, and caused 1,384 people's death and amazing property losses. According to incomplete statistics, people killed directly by explosion, collapse, shock and other injuries in coal mine accidents only accounted for 10 percent of the total casualties, while 90 percent of them died due to oxygen depletion, toxic and harmful gases with high concentrations, escape routes which couldn't lead to a safe area (Xinda Zhao et al. 2012).

Once the escape routes were blocked, we used to dig through the routes directly or dig a new route for rescue. Such a method usually suffered many unexpected factors, and was difficult to rescue the trapped people before they died (Yuanming Song et al. 2004). For example, 'Qiyi' coal mine in Lianyuan city of Hunan province happened water inrushing in 2003, the exits were blocked by water and mudstones, seventeen miners were trapped in the downhole. Rescue was immediately organized by digging through directly and around the route, six days later, the route got through by digging a new hole, and found that the trapped men died of suffocation.

If we can get through the blocked layer quickly, provide the trapped men air, water, milk and foods to make sure that they can live in the downhole. We can also build up communication with them to calm down their stress feelings, tell them that they were safe and could be rescued. Then, we could dig through the blocked layer to bring them out, as shown in Fig. 1. Such a method could greatly reduce the person casualties and economic losses.

This method was proved effective and feasible by some successful rescues. One of them was the rescue of Chile copper mine in San Jose, collapse happened in the hole of 510 meters from the earth in 2010, 33 miners were trapped. After the accident happened, three holes were drilled to fix the miners' position and supply them water, foods and some other necessities. Sixty-nine days later, the trapped men were rescued by a broadened hole drilled into the earth. The successful rescue

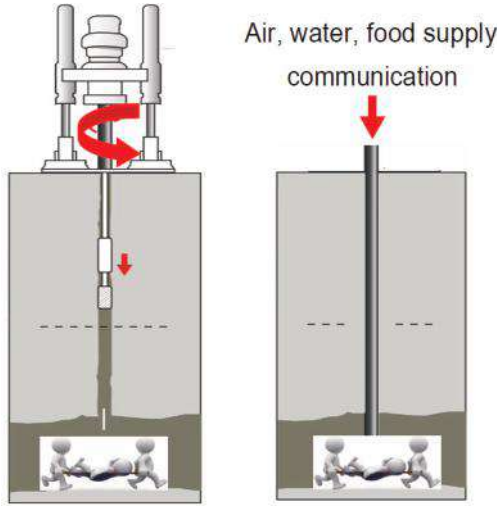


Figure 1. Mine rescue drilling and air, water, food supply.

of Chile copper mine brought great inspiration to the leader of National Workplace Emergency Management Center of China, Zhijian Wang, the executive deputy director, said that we should pay more attention to the study of mine rescue drilling technologies (Zhijian Wang 2011).

2 APPLICATION OF REVERSE CIRCULATION DTH HAMMER IN MINE RESCUE DRILLING

Conventional DTH (drill-the-hold) hammer drilling technology (Fig. 2) often used in mine rescue drilling, and there were many successful examples, such as Chile copper rescue previously mentioned, but there were also many difficulties such as broken formation, rich fractures, and downhole condition complex, using conventional DTH hammer drilling technology had many problems such as low speed, low efficiency, and more accidents. For example, Luotuo Shan coal mine in China happened water permeation accident in 2010, the No. 3 rescue drilling deflected for the complex formation condition, had to reselect the drilling point, and wasted the precious rescue time.

In order to solve this problem, I am glad to introduce the reverse circulation DTH hammer drilling technology (Fig. 2), which had outstanding advantages in complex formation drilling. It had fast drilling speed, low air requirement, and not be affected by the formation condition etc.

2.1 *What is reverse circulation DTH hammer drilling technology?*

The reverse circulation DTH hammer drilling technique is an important constituent part of the Multi-Tech air drilling technology, and more importantly, it is a major breakthrough of air drilling technology. It is combined with DTH impacting breaking rock, flushing medium reverse circulation and continuous coring three advanced drilling techniques into one system, and naturally it has become an integrated high-tech drilling techniques. The hollow-through DTH, reverse circulation bit, and dual-wall drill pipe are constituted the center channel, then the flushing medium along with the center channel forms the reverse circulation, and so the core transportation in the process of drilling is realized and it effectively solved the problem of the orifice dust pollution. At present, this drilling technology is developing rapidly as the application filed which is gradually expanded, and it has got good applications in drilling engineering filed such as geological core exploration, water well drilling and foundation engineering (Kun Yin 1996, Liexiang Han 2008).

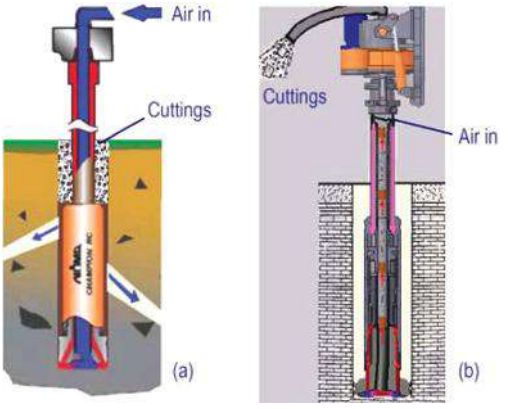


Figure 2. (a) conventional DTH hammer drilling; (b) reverse circulation DTH hammer drilling.

2.2 *What is the difference?*

The essential difference between reverse circulation DTH hammer drilling and conventional DTH hammer drilling is the air circulation mechanism, as shown in Fig. 3.

The compressed air of conventional DTH hammer drilling gets into the drilling system from the centre of drill pipe, transports cuttings from the bottomhole between the hammer casing and the hole wall to the collector sub. The circulation is built on the drilling system and the hole wall. When it encounters broken or rich fractures formation, the air is leak into the formation, and the circulation is hard to build up. While during the reverse circulation DTH hammer drilling, the compressed air gets into the drilling system from the interlayer of dual-wall drill pipe, transports cuttings from the bottomhole in the center of the dual-wall drill pipe to the collector sub. As shown in Fig. 3. Its circulation is built up in the drilling system only, which will not be or less affected by the formation condition. As the cross-sectional area of the pipe center is much smaller than the cross-sectional area of the annulus, with the condition of same amount air supply, the air flow transport with cuttings in reverse circulation DTH hammer drilling is much faster than the air flow in conventional DTH hammer drilling, and so the effect of transporting cuttings is much better, without the repeat break of cuttings, and the drilling speed could be substantially increased (Kun Bo, 2011).

The advantage of reverse circulation DTH hammer could be summarized as follows:

1. Need only one fifth of air supply of conventional DTH hammer drilling.
2. Good in transporting cuttings.

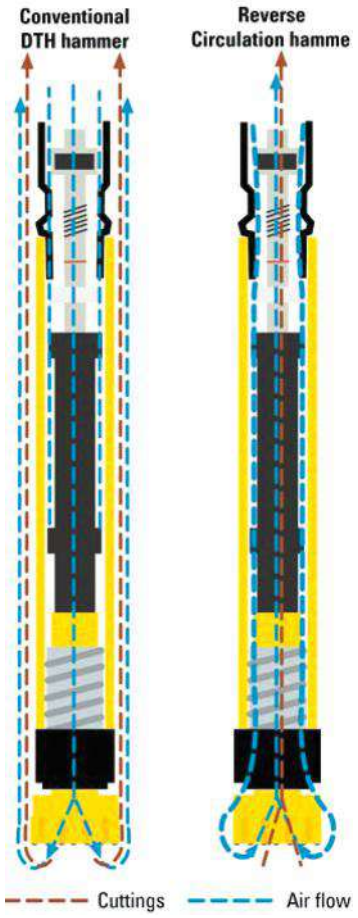


Figure 3. Air circulation of conventional DTH hammer drilling & reverse circulation DTH hammer drilling.

3. Drilling speed is 3–4 times of conventional drilling.
4. Few affection to the hole wall, and less be affected by the formation condition (William C. 2009).
5. Could be used in broken and rich fracture formation without leakage.

2.3 *Applicability in mine rescue drilling*

Before we discuss the applicability of reverse circulation DTH hammer in mine rescue drilling, we should know what is the feature of mine rescue drilling; and what difficulties we would encounter. The features and difficulties of mine rescue drilling are summered as follows:

1. First, the position of trapped miners should be exactly fixed, and then the drilling point be fixed.
2. Drilling speed should be really fast to make sure that the isolated area could be drilled through timely.
3. Maybe encounter broken formation, fracture rich formation, mined-out regions, the drilling mud or air would get lost into the formation.
4. The drilling hole should be big enough to transport air, water, food, and build up communication between the trapped miners and outside people. The drilled hole could be expanded by drilling once again to a larger diameter to get out the miners through the hole.

The reverse circulation DTH hammer drilling technology has lots of advantages as previously mentioned, for example the drilling speed is fast, less be affected by the formation geography, the drill bit diameter range could be 100–200 mm or even bigger, which could meet the requirements of mine rescue drilling.

ACKNOWLEDGEMENTS

The authors would like to thank Dr. Pinlu Cao for his help in preparing the draft, and thank to the financial support of Xinjiang Science and Technology Agency in China.

REFERENCES

Kun Bo. Kun Ying, Jianming Peng. Reverse circulation DTH hammer drilling technique. *Global Geology* 2011; 14:259–264.

Kun Yin. Reverse circulation DTH hammer drilling technique and its application. *Exploration Engineering (Rock & Soil Drilling and Tunneling)* 1996; 5:13–15.

Liexiang Han, Haifang Sun. Status and development of reverse circulation air-drilling technology. *Drilling & Production Technology* 2008; 31:1–5.

William C., Lyons BG, Reuben L. et al. *Air and gas drilling manual*: Applications for oil and gas recovery wells and geothermal fluids recovery wells. 3rd Ed. Gulf Professional Publishing; 2009.

Xinda Zhao, Huanran Zhu, Dechun Liu. Coal mine safety risk six big systems model of mine construction practice. *Shandong Coal Science and Technology* 2012; 5:246–247.

Yuanming Song, Zhijun Liu, Wansheng Wang. Practice of quick drill in coal mine emergency rescue. *China Safety Science Journal* 2004; 14:63–65.

Zhijian Wang. Considering and researching of drilling technology in mine rescue. *Journal of Safety Science and Technolog* 2011;7: 5–9.

This page intentionally left blank

Progress in Mine Safety Science and Engineering II – He et al. (Eds)
© 2014 Taylor & Francis Group, London, ISBN 978-1-138-00122-0

Study on chemical oxygen source in underground emergency refuge system

Shu Wang, Longzhe Jin, Shuci Liu & Zheng Zhang
Civil and Environment Engineering School, University of Science and Technology Beijing, Beijing, China

ABSTRACT: A series tests were carried out to test chemical oxygen, including chlorate Oxygen Candle (OC) and potassium superoxide Oxygen Regeneration Plate (ORP), with respect to the Oxygen Generation Rate (OGR), surface temperature, toxic/harmful gas production, noise level, and monitor the influence on internal environmental parameters of a sealed mine refuge space, analyze and discuss characteristics of both chemical oxygen sources and things to be paid attention in application. Then it is proposed that chemical oxygen can be effectively used as emergency oxygen source in underground emergency refuge space, especially for high temperature and deep non-coal mines. In this way, additional heat from long-time use of chemical oxygen can be avoided. Meanwhile the safety and reliability of the oxygen supply system can be further increased, and the duration of life-support capabilities in emergency refuge facilities are improved.

1 INTRODUCTION

In underground mining in china, the oxygen supply system is conventionally dependent on a forced air, with compressed oxygen for underground emergency refuge system (Gao et al. 2012). The forced air supply has to be connected with aboveground boreholes through pipelines, thus having poor independence, as it will not be able to supply oxygen once the pipelines are destroyed in mine accidents. The compressed oxygen cylinders need regular maintenance and are prone to quick discharge or explosion due to increased internal pressure if long exposed to high-temperature or fire.

Chemical oxygen, a solid source to provide oxygen by decomposing rich oxides (Qin & Zhang 2009), is typically divided into two categories: one is called chlorate "Oxygen Candle" (OC), made generally by molding or casting mixture of the base metal chlorate, a certain amount of catalyst, chlorine inhibitor, fuel, and binder (Shafirovich et al. 2002, Shafirovich et al. 2003); the other one is the peroxides or superoxides of alkali metals, such as potassium/sodium superoxide and calcium peroxide (Wang et al. 2010). Chemical oxygen has the advantages of being highly independent, providing higher oxygen storage in small volume than conventional underground oxygen supply methods do. Thus it is possible for chemical oxygen generator to be used as oxygen source in underground emergency refuge facilities (including refuge stations and refuge chambers).

However, the underground emergency refuge facilities impose very stringent requirement on its internal survival environment. Therefore, considering the fact that chemical oxygen may have some potential hazards or other problems, for instance, producing toxic/harmful gases or having influence on thermal environment, a series tests on the chlorate Oxygen Candle (OC) and potassium superoxide Oxygen Regeneration Plate (ORP) were carried out to determine their Oxygen Generation Rate (OGR), the surface temperature, toxic/harmful gas production, noise level; the influence on environmental parameters in a sealed refuge chamber was also monitored; then characteristics of both chemical oxygen sources and things to be paid attention in application were analyzed and discussed. This study provides important information to expand the application of chemical oxygen in the non-coal-mine emergency refuge space.

2 EXPERIMENTAL

2.1 *Test platform used in the experiment*

The test platform was comprised of a refuge chamber (Figure 1) with an internal net volume of 6.84 m^3, an air purifier (24V, 30 W) as shown in Figure 2, and a KJ70 coal-mine safe-production monitoring system, which is used to monitor concentrations of such environmental parameters as O_2, CO, CO_2, CH_4, H_2S, temperature, and relative humidity inside in real time.



Figure 1. Refuge chamber.



Figure 2. Air purifier.



Figure 3. Oxygen Candle (OC).

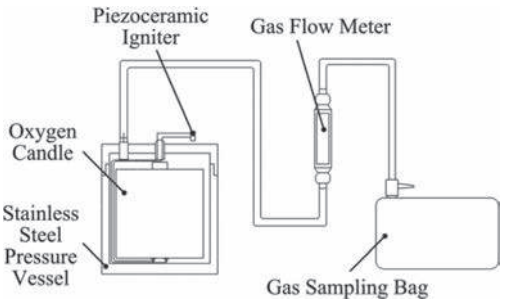


Figure 4. The OC oxygen-producing performance test process.



Figure 5. Potassium superoxide Oxygen Regeneration Plate (ORP).

2.2 *OC oxygen supply performance test*

The tested OC, as shown in Figure 3, was 150 mm in diameter, 180 mm in height, 2.8 Kg in gross weight, produced approximately 300 L oxygen theoretically, and was started with a piezoceramic igniter.

2.2.1 *OC performance test*

1 Oxygen generation characteristics

Here the Oxygen Generation Rate (OGR), oxygen generation capacity, and oxygen purity were monitored. As shown in Figure 4, the OC was placed into a sealed stainless steel pressure vessel, with a piezoceramic igniter and gas pipes connected on the top; the sealed stainless steel pressure vessel was connected with a gas flow meter and a gas sampling bag through pipelines. The OGR of OC was recorded every 30s. And a gas chromatograph-mass spectrograph (Trace DSQ and Trace GC2000) was applied to analyze sample composition.

2 Surface temperature and the Noise Pressure Level (NPL)

The surface temperature was monitored by Pt100 temperature sensors, which were fixed respectively at the bottom, the side wall, the top, and the gas outlet of OC. The Noise Pressure Level (NPL) was monitored by noise analyzer (AWA6270+).

2.2.2 *OC oxygen supply performance test*

The oxygen supply simulation test was carried out to monitor OC's effect on internal environment of the simulated chamber. Five environmental parameters (oxygen content, carbon dioxide content, carbon monoxide content, temperature, and relative humidity) inside the sealed refuge chamber were monitored during one OC's combustion.

2.3 *ORP oxygen supply performance test*

The tested ORP (Figure 5) was composed of 95% KO_2 and 5% asbestos, had an oxygen generation capacity of 203 L/Kg, and CO_2 absorbing capacity of 152 L/Kg. A single plate was 315 mm long, 220 mm wide, 6 mm thick, and 390 g in weight.

2.3.1 *ORP performance test*

In the test, 2 pieces of ORPs were fixed vertically on the reagent bed of the air purifier; keep the purifier running during the test to make surrounding air circulate through ORP at the speed of 5 m/s; CO_2 was forced into the chamber through a pipe at the rate of 1.6 L/min (equal to the CO_2 amount produced by 4 people (Li et al. 2010)). The whole test duration was 90 min, and the environmental changes inside the chamber were obtained

with KJ70 coal-mine safe-production monitoring system.

2.3.2 *ORP-soda lime combined oxygen supply performance test*

The soda lime used in the test has an actual CO_2 absorbing capacity of 97 L/Kg. During testing, soda lime (1.5 kg) was evenly distributed over the bottom of the reagent bed and then ORP was placed vertically. Other test conditions were the same as mentioned in 2.3.1.

3 RESULTS AND ANALYSIS

3.1 *OC oxygen supply performance test*

3.1.1 *OC performance test*

The OGR curve of OC is shown in Figure 6. The OC completed the combustion process within 15 min. The OGR was undulating, with the rate peaks appearing at 0.5 min, 5.5 min, 7.5 min and 10 min, and the rate at 10 min is the maximal, 41.67 L/min. The OC produced a total of 241 L oxygen, mean OGR was 15.38 L/min, and OC's utilization rate was 80.33%.

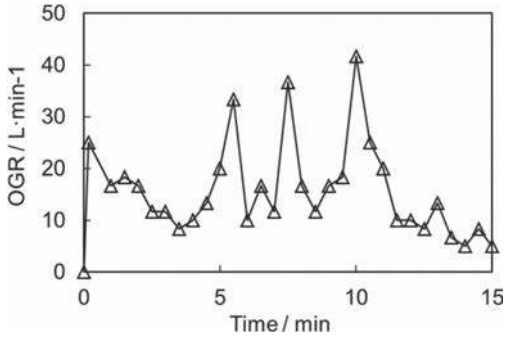


Figure 6. The changing curve of oxygen flow rate.

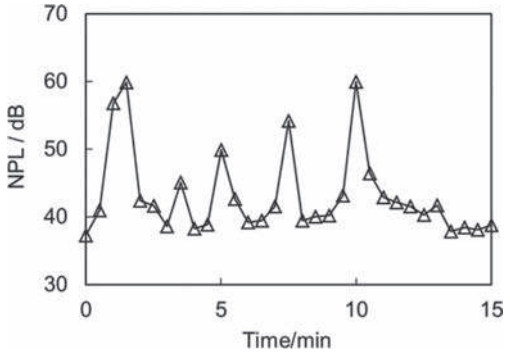


Figure 7. The changing curve of noise value.

Data about noise monitoring during OC burning is shown in Figure 7. At the very beginning, NPL reach the maximum value (59.9 dB) due to intensive reaction of the ignition charge; overall NPL from reaction of the core was lower but increased gradually with ongoing reaction, because continually accumulated heat inside the unit made the decomposition of sodium chlorate more violent.

The observed phenomena indicate that, insulation material of OC cannot be selected based on thermal insulation only. Though good insulation coefficient may contribute to lowering temperature of OC surface, heat accumulated inside the unit may cause OC core's temperature to rise higher, leading to more violent decomposition reaction, increased undulation of the OGR, bigger noise, and also directing the decomposing reaction of potassium chlorate towards producing more chlorine (Sun 1997), increasing possibility to generate toxic/harmful gases such as Cl_2 and CO.

The gas composition of the samples, which were taken respectively during 0~5 min and 5~10 min, is shown in Table 1.

It is observed from the result that, CO was generated mostly at the initial stage due to the incomplete combustion of the ignition charge, for the 1st gas sample contained a little more CO than the 2nd sample do; chlorine was not detected, with oxygen purity up to 97.06% and that was 233.91 L available oxygen. Assuming oxygen consumption rate is 0.5 mL/min per head, the tested OC can produce oxygen for 2 h consumption by 4 persons.

The temperature—time curves at the gas outlet, the bottom, the side wall and the top of OC are shown in Fig. 8. After being started, the OC core

Table 1. The gas composition of samples.

Number	O_2 (%)	Cl_2 (%)	CO (ppm)
1	96.32	0	6
2	97.81	0	2

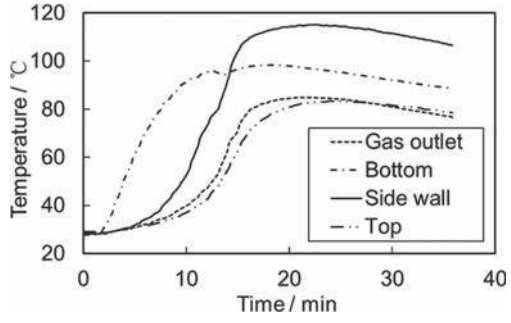


Figure 8. The changing curve of temperature.

was reacting from bottom to top, as a result the temperature at the bottom rose fast, at the rate of about 10°C/min; 10 min later, the temperature of the whole unit rose sharply, and quickly reached the top, which were 115.1 °C at the side wall, 98.3 °C at the bottom, 85.0 °C at the gas outlet, and 83.5 °C at the top; 20 min after OC reaction stopped, the surface was still at relatively higher temperature as the massive heat accumulated inside the insulation was released slowly. In general, the surface temperature met the requirements in national standard Electric Devices in Explosive Gas Atmosphere (GB 3836.1–2000).

3.1.2 *OC oxygen supply performance test*

The values of environmental parameters inside the chamber before and after the test are shown in Table 2. After the test, the oxygen concentration rose from 21% to 24%, slightly higher than the standard level, but this would not happen if there were refugees inside the chamber consuming oxygen constantly; trace amount of CO_2 was generated, negligible; CO was mainly produced at the initial stage of combustion, much lower than the safe limit of 24 ppm; the inside temperature rose by 0.63 °C and RH by 7%, all within acceptable ranges.

3.2 *ORP oxygen supply performance test*

3.2.1 *ORP performance test*

Table 3 shows the changes of environmental parameters inside the chamber before and after the test when using ORPs alone. Theoretically, two pieces of ORPs (weighing 780 g in total) can produce 158.34 L oxygen, which could be consumed by 4 persons for 80 min (assuming average oxygen consumption at 0.5 L/min per head). However the test results showed that, after 90 min, the O_2 concentration inside the chamber rose merely by 0.3%, i.e. 20.52 L oxygen produced at the average OGR of 0.23 L/min; and the average CO_2 absorbing rate was 0.31 L/min; the temperature inside the chamber rose slightly while RH reduced to 31%.

In general, when using ORP alone, both OGR and CO_2 absorbing rate can hardly meet the refugees' respiratory demands, and this mainly resulted from two reasons:

1. The KO_2 on the plate surface reacted with water to generate KOH which then reacted with CO_2 to generate pasty K_2CO_3 and $KHCO_3$, and these pasty substances accumulated gradually on the surface to impede further reaction of steam and CO_2 with KO_2 covered, leading to incomplete reaction of ORP and thus lowering reaction efficiency;
2. Water needed for ORP reaction, which could only come from moisture in air in the test, was limited in the sealed chamber, leading to the low OGR. In the actual usage, massive moisture from refugees may help to increase the OGR to some extent, though the effect not so significant.

3.2.2 *ORP-soda lime combined oxygen supply performance test*

The changes of the environmental parameters before and after the test were presented in Table 4.

After 90 min actions of ORPs (2 pieces) with soda lime (1.5 kg), the O_2 concentration inside the chamber rose to 22.1%, the average OGR increased to 1.14 L/min, which indicating that addition of soda lime contributed to increasing ORP's reaction efficiency, because water and heat generated by soda lime provided favorable conditions for ORP's reaction; with soda lime, CO_2 concentration inside the chamber was under control, and the average CO_2 absorbing rate rose to 2.01 L/min; meanwhile,

Table 2. Changes of internal environmental parameters during oxygen supply performance test of oxygen candle.

	O_2 (%)	CO_2 (%)	CO (ppm)	Temperature (°C)	Relative Humidity (%)
Before	21.00	0.05	1.00	31.88	23.00
After	24.00	0.11	4.00	32.50	30.00

Table 3. Changes of internal environmental parameters during oxygen regeneration plate performance test.

	O_2 (%)	CO_2 (%)	Temperature (°C)	Relative Humidity (%)
Before	20.7	0.03	22.2	45
After	21	1.73	22.8	31

Table 4. Changes of internal environmental parameters during oxygen regeneration plate-soda lime combined oxygen supply performance test.

ORP pieces		O_2 (%)	CO_2 (%)	Temperature (°C)	Relative Humidity (%)
2	Before	20.6	0.07	22.4	62
	After	22.1	0.61	24.1	87
4	Before	20.6	0.04	25.0	60
	After	23.2	0.60	28.5	91

both the temperature and RH rose considerably, but not to the extent endangering human health.

In the case of four ORPs and 1.5 kg soda lime used, 177.84 L oxygen was produced within 90 min, at the average OGR of 1.98 L/min, sufficient for 4 persons' oxygen demand. As the increased quantity of ORPs created a considerable press drop of air passing through reagent bed, which reduced the efficiency of air purifier, thus it was not a simple linear relation between the average OGR and the quantity of ORPs. Additionally, with joint action of ORPs and soda lime, the temperature and RH inside the chamber rose faster, respectively at 28.5°C and 91% RH after the test. In such a hot and humid environment refugees may feel discomforted, even suffering heatstroke, so measures to reduce temperature and humidity have to be taken.

3.3 *Comparison of application characteristics of OC and ORP*

Based on previously tested results, it is concluded that the two chemical oxygen sources, chlorate OC and potassium superoxide ORP have different characteristics in OGR, starting method and reaction conditions et al.

1. Oxygen generation rate

OC produces O_2 quickly (241 L oxygen within 15 min in the test), reacts completely, and the action process is not affected by any external environmental conditions.

ORP is not easy to react completely due to the pasty reaction products accumulated on the surface; its OGR is heavily influenced by external temperature, humidity, air flow speed. When using ORP alone, it can hardly meet the respiratory requirement of underground emergency refuge space due to its relatively low OGR and CO_2 absorbing rate; when used with soda lime, the OGR of each ORP (390 g) rose to 0.5 L/min, meeting O_2 demand of one person.

2. Starting method

For OC, the ignition charge has to be ignited with a mechanical firing pin or an electronic igniter before starting reaction of the OC column, and the reaction, once started, cannot be interrupted. Except the case of too low humidity of the air flow, ORP can start reaction whenever exposed to air, with the reacting rate affected by external environmental conditions.

3. Heat production

Though OC and ORP both release massive heat during usage, there are slight differences between them. As the quick reaction of OC, heat accumulated inside the housing insulation can be isolated from the refuge space if properly treated.

ORP needs to be exposed to air, thus the heat is released to the surrounding environment throughout the whole reaction. In the case of long-time use, the accumulative effect of heat cannot be overlooked because this will necessitate a temperature and humidity control system of higher quality.

4. Safety

Due to the quite intense reaction, OC's surface temperature is relatively high (the measured max. is 115.1°C). Though meeting the requirement in the national standard, necessary safety measures have to be taken to avoid scalding injury.

The trace CO produced by OC is much lower than the safety limit, and can be eliminated by the air purifier in practical application; while ORP would emit trace alkaline dust which would pollute air inside the refuge space with no measure to take.

In addition, OC have no changes for its shape after reaction, and is relatively easy to be treated. In contrast, the products from ORP reaction are possibly pasty due to fusion problem. Furthermore, the ORP that is not reacted completely will, whenever in contact with water, generate KOH, a strong alkali, which is caustic. Therefore, the products from ORP reaction have to avoid contact with water or other organics, making it harder to treat.

4 CONCLUSIONS

In the present study, we evaluated the oxygen supply performance of both chlorate OC and potassium superoxide ORP, and their influence on the internal environment of a sealed refuge chamber. The differences between these two chemical oxygen sources and things to be paid attention in application were also discussed.

OC, once started, reacts quickly and completely, not affected by any external environmental conditions. After reaction in the sealed refuge chamber, the changes of environmental parameters are within acceptable range. Attentions shall be paid to in use of chlorate OC is as follows: firstly, to avoid O_2 concentration exceeding the standard, OC size is to be selected depending on the number of refugees and the volume of the refuge space; secondly, necessary safety measures shall be taken to avoid scalding injury during usage.

ORP is not easy to react completely due to the pasty reaction products accumulated on the surface; its OGR is heavily influenced by external temperature, humidity, air flow speed. When using alone, it can hardly meet the respiratory requirement of refugees due to its relatively low OGR and CO_2 absorbing rate; when used with soda lime,

the OGR of each ORP (390 g) rose to 0.5 L/min, meeting O_2 demand of one person. The following attentions shall be paid to in use of potassium superoxide ORP: firstly necessary measures shall be taken to control alkaline dust and massive heat in condition of long time use; secondly the products from ORP reaction have to avoid contact with water in order to prevent generation of KOH which is strongly caustic.

In general, chemical oxygen, with high oxygen density and good independence, can be effectively used as emergency oxygen source for deployment in underground emergency refuge space, especially for high temperature and deep non-coal mines. In this way, additional heat from long-time use of chemical oxygen can be avoided. Meanwhile the safety and reliability of the oxygen supply system can be further increased, and the duration of life-support capabilities in emergency refuge facilities are improved.

ACKNOWLEDGEMENTS

This work is supported by the National Key Technology R & D Program of China under Grant No. 2012BAK09B07.

REFERENCES

Gao, N., Jin, L., Wang, L. & You, F. 2012. Research and application of oxygen supply system in Changcun Coal Mine refuge haven. *Journal of China Coal Society (in Chinese),* 37, 1021–1025.

Li, J., Jin, L. Z., Wang, S. & Zhu, J. 2010. Respiratory quotient calculation of the human body at a confined space in coal mines. *Journal of University of Science and Technology Beijing,* 32, 963–967.

Qin, A. & Zhang, S. 2009. The status of development of oxygen-making technology. *Contamination Control & Air-conditioning Technology,* 32–37.

Shafirovich, E., Mukasyan, A., Varma, A., Kshirsagar, G., Zhang, Y. & Cannon, J. 2002. Mechanism of combustion in low-exothermic mixtures of sodium chlorate and metal fuel. *Combustion and flame,* 128, 133–144.

Shafirovich, E., Zhou, C., Mukasyan, A., Varma, A., Kshirsagar, G., Zhang, Y. & Cannon, J. 2003. Combustion fluctuations in low-exothermic condensed systems for emergency oxygen generation. *Combustion and flame,* 135, 557–561.

Sun, G. 1997. Study on oxygen generation by chemical methods. *Low Temperature and Specialty Gases,* 56–60.

Wang, B., Wang, Y. & Ma, L. 2010. Two oxygen-generating techniques by chemical method in closed environment. *Chemical Defence on Ships,* 10–14.

Progress in Mine Safety Science and Engineering II – He et al. (Eds)
© 2014 Taylor & Francis Group, London, ISBN 978-1-138-00122-0

A probe into the working procedures of crisis public relations in mine disasters

Xiaoming Shao, Huafeng Xu & Jingru Tang
North China Institute of Science and Technology, Beijing, P.R. China

ABSTRACT: By adopting document survey, questionnaire investigation and sampling survey, etc, this paper analyses and studies enterprises' crisis public relations in mine disasters, and puts forward the designs for both the related organizations and models of working procedures, thus offering some reference proposals and bringing some practical application value.

1 INTRODUCTION

In recent years China has launched a series of policies and measures to reinforce the supervision and management of coal industry. But according to the latest statistics from State Administration of Coal Mine Safety of China, in 2010 there were 970 disasters in small coal mines with 1, 700 deaths around the country, and in 2011, there were 1, 201 coal mine disasters with 1973 deaths throughout the country. This indicates that the current situation of coal mine safety production remains severe. Because coal mining belongs to underground operation, its process of production is complicated and dangerous. Thus, serious crisis like coal mine disasters often arise in the production. Correspondingly, the ability of crisis PR (abbreviated for Public Relations hereafter) of mining enterprises has encountered an acid test. However, the awareness of crisis PR of mining enterprises in China remains backward and the PR ability and level reflected in some emergencies like mine disasters is also quite undesirable. By far, in terms of the approaches adopted by some enterprises in the face of coal disasters, the author of this paper has conducted a survey, which reveals the outsiders' degree of satisfaction as Fig. 1.

A considerate number of collected documents have also revealed the similar results, which clearly warn that in China the crisis PR ability of the mining enterprises in the face of mine disasters need to be further improved.

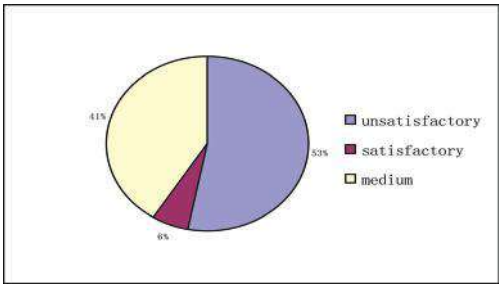


Figure 1. Questionnaire on the outsiders' degree of satisfaction.

2 CRISIS AND CRISIS PR

What is crisis? In the general sense, crisis refers to some emergent or disastrous accidents or events which endanger the welfare, the image or the survival of social organizations. And crisis is principally characterized by its urgency in time, severity of threat and the uncertainty of its further development.

Among the theorists, crisis PR can be divided into two types (LU 2002). In the narrow sense, crisis PR mainly refers to what has to be done to retrieve social understanding and good reputation through a series of PR campaigns when an enterprise is encountered with trust crisis, image crisis or work faults. But in the broad sense, crisis PR refers to the prevention, control and processing of crisis from the perspective of PR, which renders the crisis PR more thorough and integrated (LIU 2006).

3 CHARACTERISTICS OF MINE DISASTER CRISIS

3.1 *Burstiness*

Whether it is natural factors or human factors, one of the characteristics of mine disaster is its burstiness.

3.2 *Destructiveness*

Mine disaster is extremely destructive. It can lead to irreversible damage not only to the life and property of thousands of miners, but also to coal industry and the environment in China.

3.3 *Urgency*

On account of the unexpected burstiness and the severe destructiveness of mine disasters, rescue and relief work is very urgent and pressing. The action of crisis response and handling is quite time-conscious.

3.4 *Concern from media*

Mine disaster crisis often become the focus of social and media concern and the hot topics, thus becoming the content of news report and triggering different social response of the mine disaster (WANG 2009).

4 THE WORKING PROCEDURES OF MINE DISASTER CRISIS PR

4.1 *Design of organizational system*

A coal mining enterprise is expected to establish and improve crisis management institute. One is to establish a standing crisis management institute and make full preparation beforehand; the other is to establish an on-the-spot emergency team.

(1) Design of the framework of crisis management organization

A. Three-hierarchy organization and management model.

In terms of the form of the framework of crisis management organization in the mining enterprise, for any individual enterprise, it doesn't matter which one is the best option, but the top priority lies in the exploration of the most suitable one. In the general sense, the design of the framework of crisis management organization can adopt three-hierarchy organization and management model (See Fig. 2 below).

The first hierarchy is Crisis Management Committee, a decision-making organ made up of senior-/medium-level leaders, is a part-time matrix organization whose principal responsibilities include the formulation of crisis management policies, the making of Crisis Management Manual, the allocation of staff in Crisis Management Office, the inspection and supervision of the regular crisis management work, presiding over the regular crisis management meeting and being responsible for the resolution of some major crisis events, etc.

The second hierarchy is Crisis Management Office, a standing executive institution made up of full-time staff. As a standing institute, its routine responsibilities can be undertaken by the department of PR or the related offices. Its principal responsibilities include the implementation of all the work concerning crisis management, information collection, supervision of market, training work for the part-time staff, the resolution of some common crisis events and reporting works to Crisis Management Committee.

The third hierarchy is Crisis Management Working Group, which is a grass-root operational institution or on-the-spot operational institution for some organization, is also a matrix organization. While at ordinary times some part-time staffs are responsible for keeping in contact with Crisis Management Office (WANG, 2005).

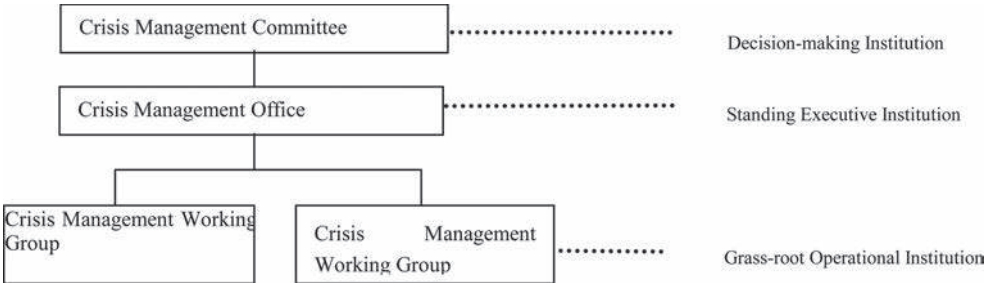


Figure 2. Three-hierarchy organization and management model.

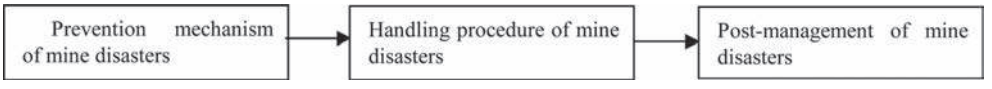


Figure 3. Procedure models of mine disaster crisis PR.

B. The allocation of crisis management staff

Crisis management staff have to possess crisis PR ability, which usually includes four qualities as follows: ① being sensitive enough to perceive the crisis in the budding stage; ② being able to apply appropriate means to resolve the crisis on the spot; ③ having a relatively strong reaction capability; ④ possessing the quality of transpositional consideration and showing adequate concern for the public.

C. The establishment of the system of "spokesman".

At the initial stage of crisis event, rumors spread and news concerned are in chaos. Crisis Management Committee has to establish the system of "spokesman", guide the public opinion initiatively and take the initiative in the solution of the crisis.

(2) Emergency organizations and institutions (take state-owned mines for instance)

The leadership organizational system for safety production accident is made up of all the leadership members of a mining enterprise, professional coordinating and directing institution, every safety production department, every profession, every emergency supporting department, every emergency rescue and relief team and grass-root unit affiliated with relevant mining enterprise. Emergency rescue and relief team mainly consists of first-aid team, armed protection section, emergency rescue staff in every grass-root unit, social force and volunteer group.

Emergency rescue and relief headquarter for the major safety accidents should be established to be in charge of organizing and directing the mission of emergency rescue and relief. It can be designed as follows:

General Director: mine director

Deputy General Directors: deputy mine director in charge of production, section chief in charge of safety supervision, chief engineer, deputy mine director in charge of logistics, chairman of the labor union, etc.

Membership: every deputy chief engineer and the major principals from safety supervision section, technical section, tunnel work section, mechanical transportation work section, first-aid team, armed protection section, supply section, operation and management department, logistics station, and hospital, etc.

The headquarter consists of the following ten professional teams of rescue and relief:

1. On-the-spot rescue team: located at the safe site near the disaster area, it is made up of the staff from first-aid team, tunnel work section and mechanical transportation work section. And the first-aid team leader acts as the captain of the team.
2. Technical team for rescue work: designed in the mine's meeting room for dispatching work, it consists of the staff and experts from technical section, safety supervision section, tunnel work section and mechanical transportation work section. And the chief engineer acts as the captain of the team.
3. Dispatching team for rescue work: designed in the dispatching room, it is made up of the relevant staff from technical section, safety supervision section, tunnel work section and mechanical transportation work section, etc. And the deputy mine director acts as the captain of the team.
4. Safety supervision team: it is made up of the relevant members from safety supervision section and supervision and inspection office. And the section chief of safety supervision section acts as the captain.
5. Supply team: it is made up of the relevant members from operation and management department, supply center, tunnel work section and mechanical transportation work section, etc. And the mine director of logistics acts as the captain.
6. Medical aid team: In accordance with the signed agreement, it is made up of the medical staff from the designated hospital. And the hospital president acts as the captain of the team.
7. Security and protection team: it consists of the members from armed protection section, and the deputy mine director acts as the captain of the team.
8. Disaster investigation team: it is made up of the relevant members from safety supervision section, technical section, operation and management department, etc. And the section chief of safety inspection plays the role of the captain.
9. Media liaison team: it is made up of the relevant personnels from the section of party work belonging to operation and management department (or PR department) with the deputy mine director as the captain. It is the spokesman who unifies the voices in the face of press circles, answers the questions from the reporters and introduces the efforts that this organization is exerting.
10. Post-disaster handling team: it is made up of the relevant personnels from the labor union and the operation and management department with the chairman of the labor union as the captain.

4.2 *Procedure designing models of mine disaster crisis PR*

The procedures of mine disaster crisis PR consist of three parts in accordance with the chronological sequence of the crisis: prior to the crisis, in the crisis and after the crisis (See Fig. 3).

(1) The perfection of the prevention mechanism of crisis PR

The prevention of crisis PR refers to the activities involved in the supervision of potential dangers and the management of pro-control crisis.

A. To establish crisis awareness at all levels in the mining enterprise.

In the crisis management, to establish a notion of "crisis" should be the first priority. It is essential for all the staff to receive regular crisis-related education and training. This survey also reveals that 14% of the staff from the state-owned enterprises can do well in "crisis-related education and leaning" and study "very often or regularly", and among them 8% are technical peronnels and 6% are front-line workers. But 86% of the surveyed staff can study only "occasionally". Obviously, the state-owned enterprises can realize the importance of crisis management training, but it leaves much to be desired. Thus, further steps should be taken to strengthen the relevant education and training.

B. To improve the construction of the ability of decision-making system

Decision-making system is the core of crisis management; its principal responsibility lies in how to make decision in the face of crisis. To improve the decision-making ability in crisis management, the application of basic facilities should be placed in the first place. That means making full use of schools, training institutions, research labs, tele-communication network, library, database and so forth, perfecting the scientific approaches in the research of decision-making. Second, information technology has to be fully applied. The decision-makers in the crisis are expected to make use of high technology to improve the overall level of standardization, scientization and efficiency in decision-making in the face of crisis. (JU 2001)

C. To evaluate the potential crisis

Crisis-triggering accidents eventually lead to crisis on account of the gradual accumulation of some hidden dangers. With the application of certain means of detection, mining enterprises can detect the hidden dangers, evaluate the potential crisis, and predict the possible worst situation.

D. To improve the pre-warning system of crisis management

A scientific and sensible crisis plan should be formulated and a perfect set of crisis pre-warning system should be established as well. In the past years, China has strengthened the management of coal mine crisis. Therefore, the state-owned mining enterprises in China have attached sufficient importance to the crisis plan. Every mining enterprise in this survey has certain plan for crisis management. Meanwhile, coal mine enterprises are expected to conduct regular mock training for the plan of crisis handling so as to make the leaders and other staffs in the enterprises understand and know enough about the crisis, and to familiarize themselves with their own missions and roles in the crisis. In addition, along with the changing of condition and environment, the coal mine enterprises can make timely amendment, supplement and improvement on the plan so as to meet the practical demand all the time.

(2) The procedures of mine disaster crisis handling

A. The establishment of crisis handling team

The members of crisis team include the leaders and relevant persons in charge in addition to PR personnels. In the major mine disasters, the leaders must attend to the matter personally. More exactly, the leaders are supposed to call a panel meeting and start the emergency plan.

B. Doing field visit to the site of disaster and keeping the damage under control

Crisis team is expected to arrive on the scene at the first time to know the overall situation of the disaster. And then it should conduct the task of disaster investigation and find out the situation as soon as possible so as to assemble messages about the crisis, including the time, the site, the casualties, etc, and then form an initial investigation report.

C. Making an analysis of the situation and establishing the countermeasures

The situation should be analyzed, emergency plan should be carried out immediately, and the effective solutions to keeping the crisis under control are also expected to be worked out. The crisis is expected to be handled timely and reasonably so as to minimize the damage deriving from the crisis. Along with the investigation of the disaster,

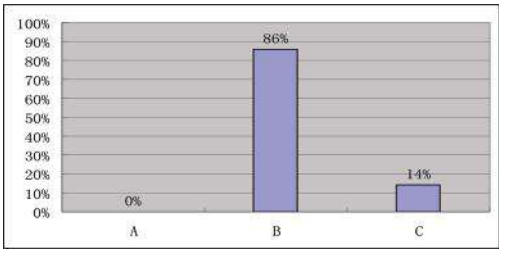


Figure 4. The Situation of crisis-related education and training (Notes 1 A: Never B: Occasionally C: Often or regularly).

rescue and relief work should be well organized to restrain the further worsening.

D. Consoling the victims and alleviating the confrontation

This is a key step. Regardless of various reasons, the top priority is to console the victimized public from the bottom of their hearts. Only in this way is the crisis likely to be resolved smoothly.

(3) Later management of mine disaster crisis

A. An objective evaluation of crisis

After handling the crisis event, the emphasis should be put on the evaluation and amendment of crisis handling procedures and on the perfection of pre-warning plan of crisis management so as to render it more complete and perfect. Meanwhile, a summary report is to summarize the existing problems and the related experience in the process of handling crisis.

B. Rapid recovery and rebuilding of good image

First, to establish a strong awareness of rebuilding the good image of the organization. The organization concerned is to establish a strong awareness of rebuilding a good PR image. Only when the PR image of the organization is rebuilt can it be in a good state in terms of PR.

Second, the objectives of rebuilding the enterprise image. The objectives of rebuilding the enterprise image can be classified into four aspects as follows: first, to make the victims or their family members enjoy the maximum amount of consolation; second, to make the benefit losers regain confidence; third, to make those passive and hesitant observers become sincere partners in cooperation; fourth, to win more new caregivers and supporters for the career. (SHAO 2009)

Third, to adopt effective measures to build a good image. After establishing the objectives of rebuilding image, the key lies in how to take effective measures to carry it out. These measures consist of internal factors and external ones. Inside the enterprise, various communication activities should be arranged in an honest and frank attitude so as to achieve a very interactive two-way communication between the enterprise authorities and its staff and ensure an impeded communication of message, thus further improving the degree of transparency of enterprise's management and staff's trust in the organization. Outside the enterprise, first, it is quite essential to keep in contact with the public who are closely related with the enterprise, and inform them of the new situation and development after the crisis; second, considering the degree of damage of PR image of the enterprise, importance should be attached to launching some PR campaigns which help make up the damage in image and achieve overall communication with the public; third, solutions to improving the reputation of the enterprise are expected to be found so as to change the public's negative impression on the organization concerned.

5 CONCLUSIONS

Based on the advanced PR theory at home and abroad, and with the combination of actual investigation and research among both the internal and external public, this paper makes a systematic probe into the procedures of crisis PR in the face of handling mine disasters, including the design of organizational system, the prevention mechanism of crisis PR in the mine disasters, handling procedures, later management. This research is of practical application value to the management of coal mine crisis PR, so it is worth learning and promotion for coal mine enterprises and other departments concerned.

ACKNOWLEDGEMENTS

This paper is one of the achievements of the project "A Research into Enterprise's Crisis PR Strategies Based on Handling Mine Disaster" (Project No.: B0831) funded by North China Institute of Science & Technology. Gratitude is conveyed to all the project members who have given tremendous support.

REFERENCES

Lu Wei-xia. Public Relations Based on Case Study. University of International Business and Economics Press. 2002.

Liu Jun. A Study of Public Relations. *China Machine Press*. 2006.

Ju Yan'an. A Study of Public Relations. 2nd ed. Shanghai: *Fudan University Press*; 2001.

Wang Jun-cai. A Research into the Management Models of Safety Production Aimed at Crisis Management in the Coal Mines—Take Gaozhuang Coal Mine (affiliated with Zaozhuang Mining Group Co., Ltd) for Instance. *Tianjin University*. 2009.

Wang Xiu-ling. On the Functions of Supervision and Guidance by Public Opinions from Meida in the News Report of Mine Disasters. *Journal of North China Institute of Science & Technology*. 2005 (2): 115–118.

Shao Xiaoming. An Exploration into the Public's Countermeasures in Mine Disaster Crisis PR. *Chinese Mining Industry.* 2009 (03): 49–51.

This page intentionally left blank

Progress in Mine Safety Science and Engineering II – He et al. (Eds)
© 2014 Taylor & Francis Group, London, ISBN 978-1-138-00122-0

Mine rescue training programs and research

H. Xie
Key Laboratory of Mine Disaster Prevention and Control, Hebei, China
North China Institute of Science and Technology, Hebei, China

T. Yan
North China Institute of Science and Technology, Hebei, China

ABSTRACT: This article studies the basic principle of mine rescue training, and carries on system analysis from the aspects of physical indicators, physical index standards, exercise prescriptions, physical indicators quantitative scheme and so on. For the requirements of a certain rescue team members' body function, flexibility quality and endurance quality, the writer designs training programs and empirical analysis.

1 INTRODUCTION

Mine rescue team is one of the important guarantee for safety in mine, it can control the situation effectively, protect the safety of life and property when the accident occurred. However, the working environment of Mine rescue team members is facing adverse factors such as high temperature, high humidity, high concentration of toxic, harmful gases, serious explosive threat and narrow spaces (Wang, J. & Deng S. 2003). In such an environment, energy consumption of per unit time can be enormous and it is not conducive to dealing with all kinds of risk factors. Therefore, it is very necessary to carry out rescue team training programs and research scientifically and reasonably.

2 BASIC PRINCIPLE OF PHYSICAL TRAINING

2.1 *Basic concepts*

Physical training refers to the physical quality training, and it is the important foundation of technical, tactical training and successfully completed mine accident rescue mission (Chen, R. Wang, J. & Huang, B. 2005). Physical training includes: strength training, endurance training, agility training, flexibility training, coordination training and recovery training (Chen, D.L. Xu, N.Q. & Zhang, L.M. 2004).

2.2 *Basic principles*

Biological stress theory, adaptive theory, ultravolume recovery laws are the important theoretical basis of mine rescue training.

Biological stress theory. The body has two biological characteristics of stability and adaptability, and stability refers to with the change of external environment, such as temperature and humidity, the body fluids and body temperature can maintain fluctuations within a certain range of physiology. Body has suffered external changes in the environment for a long time and stimulate it's patterns and features to adapt the environment, the special function response is called adaptive. One purpose of mine rescue training is forming long-term adaptation to the rescue environment.

Adaptive theory. At the initial of general basic training and a training cycle, we usually increase the load of the body to adapt to the process step-by-step. In the special stage of training, the training is to improve load strength stimulus to enhance human's adaptation. The other purpose of mine rescue training is forming the heavy-duty, high-intensity training for the long-term adaptation.

Over-recovery laws. The objective existence of over-recovery offers very important biological basis for how to improve performance, how to enhance quality and how to arrange reasonable training. The last purpose of mine rescue training is improving the ability of recovery.

3 OVERALL PROGRAM OF MINE RESCUE TRAINING

Overall program includes four parts: physical indicators, physical standards, exercise prescriptions, quantitative program of physical indicators.

3.1 *Physical indicators and standards*

In order to complete the training tasks successfully and reach the physical reserves need for mine rescue, the author chooses lead-up, weightlifting, double-leg squat stand, long jump, 100 M, 5000 M, 5 km armed off-road, back-up sandbags, place the front leading and combined exercises as physical indicators, and develops physical standards (see Table 1).

3.2 *Exercise prescriptions library*

3.2.1 *Prescription library project*

Prescription library items were divided into two broad categories: the collective and humanity. Collective classes include power quality training, endurance quality training, flexibility quality training, anti-seasickness training, responsive quality training, and so on. Humanity classes are richer and more targeted.

3.2.2 *Examples of training project details (Power Quality)*

1. Preparation section (10 minutes)
   - ① jogging: (depending on the topography, the environment, and the interests).
   - ② two-person gymnastics (per section 2X8 beat): pressure shoulder; side movement; enlarge chest (lunge); turn body movement; activity knee, wrist, shoulder, neck joints.
2. Basic part (40 minutes)
   - ① pass grenade or solid ball exercises: pairs back to stand, half a meter apart. pass grenade or solid ball from left hand to right hand, then from right hand to left hand; pass grenade or solid ball up and on. Each method for a group of 10 times, each direction can be exchanged.
   - ② two people throw grenades or solid ball face to face: 15 times, distance between two people depends on the situation.
   - ③ two people throw grenades or solid ball back to back: 15 times, distance between two people depends on the situation.
   - ④ tuck jump in situ: men 20 times X 2, women 15 times X 2.
   - ⑤ triple jump: men 20 times X 2, women 15 times X 2.
   - ⑥ one foot jump 20 meters and relay 2 times (1 time for left foot and 1 time for the other).
   - ⑦ do push-ups to fatigue, rest around 3 minutes, and then do sit-ups to fatigue.
3. End of the Section (10 minutes)
   - ① breathing exercises.
   - ② stretching.
   - ③ muscle relaxation exercises.
   - ④ double opioid antagonist activity.

3.3 *Physical indicators quantitative scheme*

To achieve physical test quantitatively purpose, writer has developed a SKDL-II mine rescue team members physical test system. System consists of hardware and software two parts.

3.3.1 *Hardware*

Hardware, the acquisition sub-system, is divided into: body shape test unit, physical test unit, as well as a total of 11 instruments (height measuring apparatus, weight measuring apparatus, lung capacity scanner,

Table 1. Physical standards for mine rescue team members.

	Age				
	Standard				
Project	Below the age of 25	25–29 years old	30–34 years old	35–39 years old	40–44 years old
Pin-up (time)	8	7	5	4	3
Weightlifting (time)	30	25	20	15	10
Double Leg Squat stand (time)	90	85	80	70	60
Long Jump (m)	4.3	4.1	3.9	3.7	3.5
100 M (seconds)	15″	15′3″	15′5″	16″	16′5″
5000 M (minutes, seconds)	23 engaged	23’30”	24 engaged	25 engaged	
5 km armed off-road (minutes, seconds)	26 engaged	26′30″	27 engaged	28 engaged	
The sandbag run (sub-)	7 engaged	8 engaged			
Place the front Leading (seconds)	Double-boxing (double-palm) at the same time touch and hold for 3 seconds			Both hands (fists) at the same time touching the ground for 3 seconds	
Combined exercise (minutes, seconds)	1 engaged	1′20″	1′40″	1′50″	2 engaged

response tester, close eyes stand tester, vertical jump tester, sit-ups tester, one minute sit-ups tester, gripping power analyzer, seated in front leading tester, step test scanner) to complete 11 of the test.

3.3.2 *Software*

Software, the information management system, includes data analysis unit and experts training unit.

The test system is designed for mine rescue team specially, generally apply to armed police fire, dangerous chemicals, rescue personnel, earthquake rescue's physical test. It has many information management functions such as collection, analysis, evaluation, diagnosis, and so on. Main features includes:

1. Monitoring and evaluating health condition to mine rescue team members regularly;
2. For the purposes of scientific training arrangement, it can provide the basis;
3. Intelligent evaluation for mine rescue team member's physical training effects;
4. Providing safety and scientific physical programs for mine rescue team member;
5. Establishing the database for mine rescue team member's result of physical test;
6. Providing monitoring reports to the brigade regularly.

4 MINE RESCUE TRAINING EMPIRICAL ANALYSIS

4.1 *A mine rescue team formed*

The battalion has 1 commander, 2 deputy team leader, 1 chief engineer. The squadron has 1 squadron, 2 deputy commander, 1 engineering technician. Each battalion consists of 3 squadrons and each squadron consists of 3 teams. There are 9 teams and each team 9 to 10 people, totally 87 members.

4.2 *Physical test situations*

In accordance with the indicators to quantify the 87 members for the first test, the results of the test are in Table 2.

As Table 2 shows, the members' physical strength, flexibility, and cardio endurance quality are in poor condition. In response to this situation, the author calls in endurance quality, flexibility quality, and responsive quality training programs from the prescription library to conduct a 3-month training.

4.3 *Physical training results*

After 3 months of training, we have done second test for the 87 members and the results are in Table 3.

Comparing the test results before and after physical training, we found that the members' fitness had become larger ascension.

Table 2. First test results of mine rescue team.

Sample volume	87		
Total eligible rate (%)	17.24	Anti-vertigo is not qualified rate%	22.84
Best rate%	0	Power is to be found not qualified rate%	11.63
Good rate%	0	Body does not pass rate%	81.93
Excess rate%	23.75	Flexible quality is not qualified rate%	100
A hasty one percent	18.75	Aerobic endurance is not eligible rate (%)	70.24

Table 3. Second test results of mine rescue team.

Sample volume	87		
Total eligible rate (%)	66.66	Anti-vertigo is not qualified rate%	20.24
Best rate%	21.43	Power is to be found not qualified rate%	10.71
Good rate%	45.24	Body does not pass rate%	15.48
Excess rate%	17.86	Flexible quality is not qualified rate%	27.38
A hasty one percent	11.90	Aerobic endurance is not eligible rate (%)	7.14

5 CONCLUSION

There are many problems in mine rescue physical training, and the no-depth study leads to extensive training method. There are some progresses which are as follows:

1. This article has studied system for mine rescue physical training by focusing on means and methods of sports science;
2. By the development of SKDL–II mine rescue team test system, physical test has developed from manual operation to information. The system has laid the information base of physical training;
3. With the in-depth, improve and promotion of «The Mine Rescue Commander Physical Standards», the standards will standardize mine rescue physical training and improve the fighting capacity.

ABOUT THE AUTHOR

Xie hong, male (1965-), PhD, professor-level senior engineer, and is now working in North China Institute of Science and Technology, has won the Sun yueqi Youth Science and Technology award. The 4th national safety expert.

NOTE

The central university basic research and operational costs funded.

REFERENCES

Chen, R. Wang, J. & Huang, B. *Three kinds of cardiorespiratory exercise load test evaluation of validity of the research* [J]. Sports Science, 2005, 25 (6):52–54.

Chen, D.L. Xu, N.Q. & Zhang, L.M. *Male and female college students at harvard to run step test index and evaluation criterion of comparative experiments* [J]. Sports Science, 2004, 24 (1):28–29.

Wang, Z.J. & Xie, H. *The Mine Rescue Commander*. Beijing Coal Industry Publishing, 2007.

Wang, J. & Deng S. *Level pilot question* [J]. China Sports Science and Technology, 2003, 39 (2):61–64.

Zhou, Y.P. & Sheng, G.Q. *Different height of the steps after test the heart rate response, heart rate decreased slope and VO2 max, 12 min, the relationship between the step index of experimental research* [J]. Sports Science, 2005, 25 (1):38–41.

Progress in Mine Safety Science and Engineering II – He et al. (Eds)
© 2014 Taylor & Francis Group, London, ISBN 978-1-138-00122-0

An completeness evaluation method of community emergency response plan

Guoyou Ren
China Institute of Industrial Relations, Beijing, China

ABSTRACT: The community emergency response plan is necessary part of the national emergency plan system, which plays an important role in emergency response. Whether the plan can be implemented effectively depends on its integrity. Through the comprehensive analysis on the defects and inadequacy of China's current emergency system, we gave the main factors and causes that restricted the current emergency system. Using the Fault Tree Analysis (FTA), we established a community emergency response plan completeness evaluation method, and take one community emergency response plan for earthquake for example, the community emergency incompleteness degree was evaluated. The method provides a scientific basis for the development or revision of the community emergency response plan.

1 INTRODUCTION

Throughout all the domestic and overseas emergency rescue models (XU Ruo-que 2012) and practice, the emergency rescue methods that based on the community level are widely approved in both theoretical and practical ways, however, that based on China's actual conditions is urgent to conduct now. Since the SARS broke out in 2003, China's government has established an emergency management model with the core of "one-case-three-system" policy. Although the achievement of "one-case-three-system" policy in China is remarkable in recent years (XIA Bao-cheng et al. 2012), the existing response plans are mainly around the empirical emergency response technology and the research of the emergency management based on the community level is relatively insufficient. Reflecting the "5•12" China Wenchuan quake (DANG Qing-hua 2009) and the "4•14" China Yushu quake (DENG Fang & LIU Ji-fu 2012), etc., we found that the complete-ness of the community emergency response plan was one of the key factors that influenced the result of emergency rescue and integrity is directly related to whether the plan is practical and effective. But the research achievement on how to evaluate the completeness of community emergency response plan has been rarely reported. In this article, the factors that influence the completeness of community emergency are explored, and its evaluation method is put forward using the fault tree analysis.

2 THE DEFECTS AND INADEQUACY OF THE CURRENT EMERGENCY RESPONSE PLAN SYSTEM

2.1 *The defects of the current emergency response plan system*

2.1.1 *The formation of current emergency response plan system*

Since 1949, China's emergency response plan has experienced the transformation from single plans to comprehensive plans. The plans mainly consisted of 3 levels, including national level, local level (province, city/district, county) and community level (mainly refers to streets). Among the 3 levels, the community level was the weakest one (dashed box in Fig. 1). After the national government promulgated the Overall Response Plan of National Public Emergencies in 2006, although the fundamental position of the emergency response plan system was strengthened in our national emergency management system, which played an important role in various levels and kinds of emergency rescue tasks, the defects of current emergency response plan system were also exposed gradually.

2.1.2 *The inherent defects existed in the response plans*

The defects mainly include the content incompleteness; the non-standard generation process of the response plans; the insufficiency of systematic planning and coordination between significant response plans; the lackness of operability in the

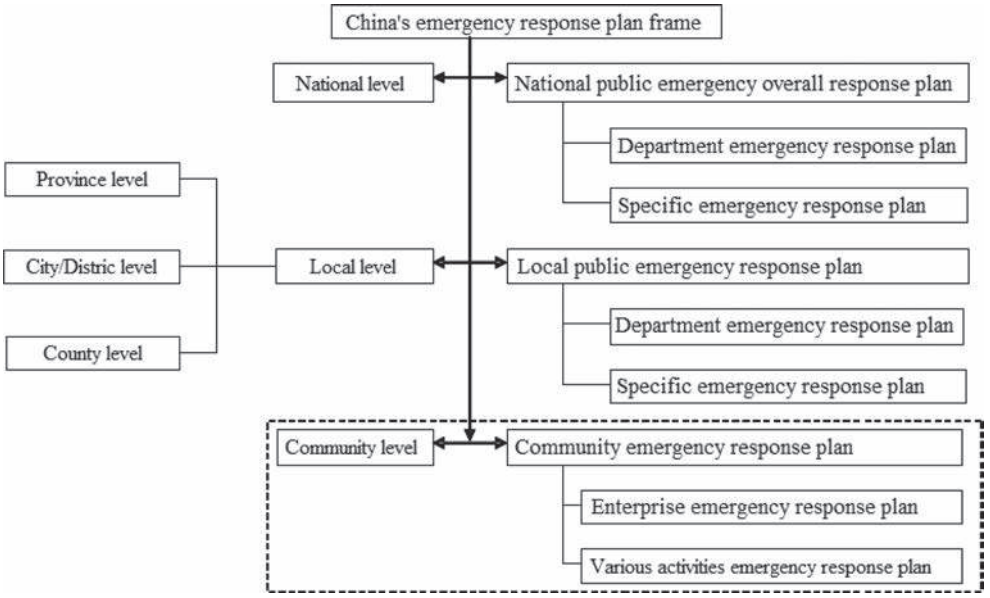


Figure 1. China's current emergency response plan system and its structure.

bottom level (that is community level) response plans.

2.1.3 *The acquired inadequacy during the plan executing process*

The inadequacy mainly included the absence of the qualified "emergency management specialists"; the insufficiency of functional identification and analysis methods for the risk resource on risk evaluation basis. It led to defect that the form matters outweigh content and the plan executers are incapable of indentifying all the potential risks; the lackness of comprehensive measures to cope with unknown risks; inadequate drill and skill training for the first line administrative staff, which causes the extreme shortage of practical experience.

2.2 *The factors that influence the completeness of emergency response plans*

Whether the emergency response plans are complete or not is an important symbol embodying how perfect the national emergency management system is and also a reference to indicate if the governments at all levels perform their emergency rescue duties. Actually, before the 1950s, the emergency rescue was considered as a moral obligation of the neighbors of the victims, religion organizations and community residents, other than the government (CHEN An et al. 2009). With the transformation of the government function, the establishment of emergency response plans, their executing effect and the scientific evaluation of their completeness have become the basic issues the government emergency managers should pay close attention to. The factors that influence the completeness and effectiveness of the emergency response plans need analyze from 4 stages in emergency management (prevention and emergency preparation, monitoring and pre-warning, emergency response, post-processing).

2.2.1 *The emergency prevention and preparation stage*

In the emergency prevention and preparation stage, influencing factors mainly include emergency plan development and review, emergency drills, emergency source guarantee, establishment of emergency response organizations, carry out supervision and inspection.

2.2.2 *The forecast and early warning stage*

In the forecast and early warning stage, influencing factors mainly include warning, action to build community monitoring and early-warning system and the community risk assessment.

2.2.3 *The emergency response stage*

In the emergency response stage, mainly include response to classification, command and control, the mobilization of social assistance, emergency handling and rescue, information release, on-site monitoring and evaluation.

2.2.4 *The post-processing*

In the post-processing, influencing factors mainly include dealing with the aftermath, investigation, and the accident evaluation summarizing.

3 THE RESPONSE PLANS' STANDARD FAULT TREE ANALYSIS AND ITS BUILDING PROCESS

The building of the fault tree is a fundamental task of using FTA to analyze the completeness of the emergency response plans, with the aim to analyze the completeness issue of general community emergency response plans. There are 4 key steps in building fault tree.

3.1 *Analyze the top event*

In the fault tree, the top event is not expected to occur. We use it to analyze the loss and frequency of the system accidents, and find out the accident that has serious consequences, and usually that is liable to occur is referred as the top event of the analysis, In this research, for the incompleteness of emergency response plan is not hoped to occur, we determined the incompleteness of emergency response plan as the top event.

3.2 *Subdivide the events and the relationship between different levels*

Considering the reality of the establishing and using of the emergency response plans and the emergency rescue practice in our country, we divided the events on the standard fault tree into the top event and basic events. In this way, we defined the events on the fault tree normatively and clearly. In the process of defining the events we take into whether the events happen account regardless of the correctness. Meanwhile, in order to make the standard fault tree have the wide adaptation to general accident emergency response plans, we consider the balance between the refining degree and the generality during the process of subdividing the events to basic events.

3.3 *Build the community response plans' standard fault tree*

The fault tree is built on basis of expressing the cause of the events and the level relation of their logic relationship. It indicates clearly the logical relationship between the basic events, with the logical relation symbol, thus, the standard fault tree of the general emergency response plan system can be generated. In this fault tree, once any of the 4 level of sub-events happened, such as "no emergency prevention or preparation" "no forecast and early warning" "no emergency response" "no post-processing", the top event "incomplete emergency response plans" was certain to happen. Therefore, the 4 sub-events were connected by the logic symbol "or". By analogy, we made sure all logical relationship between the basic events, thus the built standard fault tree shown in Fig 2.

3.4 *Determine the weight of basic events*

As a relative concept, weight is given according to a certain index, referring to the extent of the relative importance of this index in the overall evaluation. Therefore, the weight reflects the degree to which evaluating subject lays emphasis on the objective things. Namely it function to quantitatively distribute the importance degree of different aspects of the evaluating objects, and treat the effect of each evaluating factor in the overall evaluation differently. In order to realize the progress from qualitative explanation to quantitative calculation, the determination of the weight is a quite important link. Since the weight is crucial in the process of evaluation and decision, it reflects the status and the effect of each factor in the evaluation and decision-making process. Usually there are many theoretic methods to define the weight, like the subjective methods as the subjective experience method, the arrangement and classification for primary and secondary indexes method, the expert investigation method and so on, and the systematic method (CAO Xiu-ying & LIANG Jing-guo 2002; SUN Bin & WANG Li-jie 2006; Wang Hong-kai et al. 2003; BAO Xin-zhong et al. 2009; ZHONG Jia-ming & LI Ding-fang 2008; CHEN Xiao-hong & LIU Yi-fan 2010; Wu Zong-zhi & Liu Mao 2003) to determine the weight based on the Rough Set (Pawlak 1982).The contribution each basic event makes to the top event is different in the standard fault tree, i.e., the weight is different. Normally, the weight of basic events can be deter-mined by the probability or the fault tree structure. At present, because of the lack of the analysis data after the launch and the execution of the emergency response plans, it's not feasible to determine the weight of basic events from in the probability way.

Therefore, we determined the weight of events according to the formula (1) from the structure of the fault tree, and calculated from the top event level by level, until the weight of all events had been calculated (the results are in Table 1).

$$p(e_i)=\begin{cases}1, & e_i \text{ is the top event}\\ p(e_i), & e_i \text{ is not the top event, logical relation is "or"}\\ \dfrac{p(e_j)}{t}, & e_j \text{ is not the top event, logical relation is "and"}\end{cases} \quad (1)$$

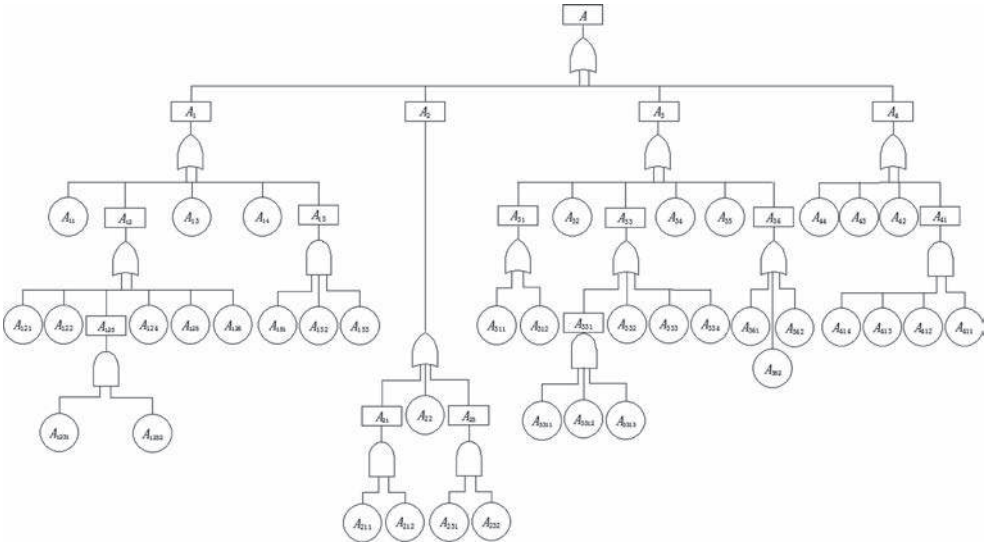


Figure 2. The standard fault tree of community emergency response plans.

Table 1. Weight table of basic events.

Sequence number	Basic events	Weight
1	A11, A13, A14, A22, A32, A34, A35, A41, A42, A43, A121, A122, A124, A125, A126, A332, A333, A334, A361, A362, A363	1
2	A1231, A1232, A211, A212, A231, A232	0.50
3	A151, A152, A153, A3311, A3312, A3313	0.33
4	A411, A412, A413, A414	0.25

In the formula, $p(e_i)$ is the weight of event of e_i; event e_j is the immediate father event of event e_i; t is the number of the immediate son events of event e_j.

Based on the formula (1), A_{11} is one of the basic events, so its weight is 1. Similarly, the weight of A_{13} is 1. The other is and so on. Other weight values are calculated, the results are in table 1.

4 THE EXAMPLE ANALYSIS OF COMMUNITY EMERGENCY RESPONSE PLANS

4.1 *The calculation of the community emergency response plan completeness degree*

Through the features of community emergency response plan we can see that community emergency response plan requires not only the plan project itself be simple, fast and practical, and what' more is it's related to the safety and culture quality of the managers and the residents in the community. Therefore, establishing the calculation methods of community emergency response plan completeness based on the community's actual conditions is one of effective ways to solve the problem of community emergency response plan completeness evaluation. In order to get the completeness degree of the emergency rescue plan to evaluate more intuitively, we used the number of minimum cut sets in the standard fault tree (LIU Jiefu et al. 2008) to normalize the evaluation result:

$$p = \left(1 - \sum_{i=1}^{n} \frac{p(e_i)}{m}\right) \times 100\% \tag{2}$$

Where p is the complete rate of the plans, %; m is the number of minimum cut sets in the standard fault tree; n is the number of lost basic events of the plans to evaluate; $p(e_i)$ is the weight of basic event e_i.

4.2 *An example analysis of community earthquake emergency response plan*

4.2.1 *The statistics of the content missing condition in the emergency response plan*

Through sorting the quake emergency response plan in a certain community (Club.china 2010), according to table 1 and table 1, we found out 12 lost basic events in the emergency response plan

and determined their weight, the relevant result is shown in table 2.

4.2.2 *The calculation of the emergency response plan completeness degree*

According to the table 2, the plan lost 12 basic events, and at the same time we acquired the weight of the lost basic events in the emergency response plans from the standard fault tree. According to formula (2), the emergency response plan completeness degree is:

$$p = \left(1 - \sum_{i=1}^{n} \frac{p(e_i)}{m}\right) \times 100\% = \left(1 - \frac{9.75}{36}\right) \times 100\% = 72.92\%$$

That is, the emergency response plan completeness degree in a certain community calculated with this method is 72.92%.

4.2.3 *The revision and improvement suggestions for the emergency response plan*

The above results show that the level for establishment of the community emergency response plan is still low. It does not meet the demand for strengthening the community-centered sophisticated social management. Therefore we put forward the specific suggestions of improving the emergency response plan as follows:

1. Enhance the application of emergency evaluation technology in the community. As the emergency evaluation and forecast and oil region pre-warning technology is concerned, the plans in the communities level in our country need to promote, especially for some severe nature disasters as earthquake. It is badly in need to improve the completeness of the earthquake scene set, enhance the deep level comprehension of the earthquake emergency, and strengthen the foresight of the emergency rescue plan.
2. Improve emergency preparation ability gradually. For the community, we should use a variety of ways and approaches to carry out the earthquake emergency drill, popularize the idea and practice of building the safe communities, and create the fundamental effect of building the safe communities practically.
3. Strengthen the construction work of the post-disaster recovery ability. Strengthen the post-disaster summary and evaluation work further in communities. Particularly, the managers need finish the post-disaster compensation work for the victims perfectly, in addition, build the disaster monitoring network that is suitable for community reality. Furthermore, it is also very important to make people play part in earthquake relief work.

Table 2. The lost basic events in the earthquake emergency response plan in a certain community.

Sequence number	Basic events	Symbols	Weight
1	No emergency training or rehearsal	A_{13}	1
2	No community risks evaluation	A_{22}	1
3	No monitoring examination	A_{14}	1
4	Not declaring the emergency response consequence	A_{43}	1
5	No insurance compensation	A_{414}	0.25
6	Not evaluating the accident	A_{42}	1
7	Not building monitoring network	A_{231}	0.50
8	Not monitoring event information	A_{211}	0.50
9	Not identifying or classifying the accident	A_{212}	0.50
10	Not analyzing the development trend of the accident	A_{363}	1
11	No site monitoring	A_{361}	1
12	No assessment of loss	A_{362}	1

5 CONCLUSIONS

1. The community emergency response plan's completeness evaluation method is easy to find the deficiency of the emergency rescue plan effectively.
2. The completeness of emergency response plan is influenced mostly by emergence practice. With the development of the emergency response practice and the establishing process of the plan, the standard fault trees need improved and promoted continuously that should be paid attention when using.
3. The calculation method of emergency completeness degree provide the reliable base for improvement and modification of the emergency response plan.
4. The example analysis shows that the completeness evaluation method of emergency response plan are scientific and practical and is helpful to distinguish the completeness of the emergency response plan quickly, thus improves

the operational efficiency of the emergency response plan rapidly.

ACKNOWLEDGEMENTS

This paper is Supported by Beijing Natural Science Foundation(8123044).

REFERENCES

Bao Xin-Zhong, Zhang Jian-Bin, Liu Cheng, 2009. A New Method of Ascertaining Attribute Weight Based on Rough Sets Conditional Information Entropy. *Chinese Journal of Management Science,* 6(3):131–135.

Chen An, Chen Ning, Ni Hui-Hui, etc. 2009. *Modern emergency management theory and method.* Beijing: Science Press.

Cao Xiu-Ying, Liang Jing-Guo, 2002. The Method of Ascertaining Attribute Weight Based on Rough Sets Theory. *Chinese Journal of Management Science,* 10(5):9–10.

Chen Xiao-Hong, Liu Yi-Fan, 2010. Expert weights determination method and realization algorithm based on interval numbers group decision matrices. *Systems Engineering and Electronics,* 10(10):2128–2131.

Club. china. The community of earthquake emergency plan (Reference Version).http://club.china.com/data/thread/1011/2720/15/16/8_1. Html.

Dang Qing-Hua, 2009. From the perspective of Wenchuan earthquake "safe community" building. *China Emergency Rescue,* 5:62–65.

Deng Fang Liu Ji-Fu, 2012. Modeling Research on Synergetic Emergency Response to Plateau Earthquake—Case Study into Yushu Earthquake. *China Safety Science Journal,* 22(3):171–176.

Liu Jiefu, Zhang Panjuan, Chen Zhifen, Chen Jin, 2008. Study on evaluation method of natural disaster emergency plan in China (Part I): completeness evaluation. *China Safety Science Journal,* 18(2):5–11.

Pawlak Z, 1982. Rough sets. International *Journal of Information and Computer Science,* 11(5):341–356.

Sun Bin, Wang Li-Jie, 2006. Study of the Method for Determining Weight Based on Rough Set Theory. *Computer Engineering and Applications,* 29:216–217.

Wu Zong-zhi, Liu Mao, 2003. Gradation and Categorization System of Emergency Plan for Major Accidents and Their Main Contents. *China Safety Science Journal,* 13(1):15–18.

Wang Hong-kai Yao Bing-xue Hu Hai-qing, 2003. The Method of Ascertaining Weight Based on Rough Sets Theory. *Computer Engineering and Applications,* 39(36):20–21.

Xu Ruo-Que. Study of the earthquake emergency rescue mode of the minority area of Southwest China. *The Journal of Yunnan Administration College,* 2012(4):49–54.

Xia Bao-Cheng, Niu Shuai-Yin, Zhang Yong-Ling, Wu Xiao-Tao, 2012. Study on completeness evaluation index and method of China special emergency plan. *Journal of Henan Polytechnic University(Natural Science),* 31(1):19–24.

Zhong Jia-Ming, Li Ding-Fang, 2008. Research on optimization method of attribute weight determining based on rough set theory. *Computer Engineering and Applications,* 44(20):51–53.

Progress in Mine Safety Science and Engineering II – He et al. (Eds)
© 2014 Taylor & Francis Group, London, ISBN 978-1-138-00122-0

Analytical and improvement research on emergent evacuation system of terminals based on behavioral mode characteristics

Hong-Xun Hao
China University of Mining and Technology (Beijing), Beijing, China

ABSTRACT: Theoretically guided by Thurley model, beginning with the research outcomes on the psychological bias and irrational behavioral decision in emergencies of an individual, and by combining with the characteristics of current emergent evacuation of terminal, this paper divides the disposal by individuals of the information on safe evacuation in emergencies into three stages: perception, response and action; and performs analysis for influence on the relevant portion of the emergent safety system of terminal by individual behavioral characteristics at different stages. Based on this, some suggestions for improvement of emergent safety system of terminal in case of sudden events are put forward, which provide valuable reference to enhancing occupant evacuation efficiency, lowering evacuation risk in case of sudden event in terminal and strengthening operational safety of civil aviation.

1 INTRODUCTION

Emergent evacuation of occupants is an important component of social public safety, while terminal is one of the areas in airport operation where occupants are relatively concentrated and accident consequence influence is serious. Its safety problem has been attracting extensive concern. For example, on January 24, 2011, suicide bomb explosion swept the arrival hall of Moscow Domodedovo International Airport in Russia, causing about 40 deaths and more than 180 injuries. The rescue team evacuated all of the injured in two hours. On April 7, 2011, due to safety violations, the domestic terminal of Melbourne Airport of Australia Airlines was thrown into mess, and 6, 000 occupants were evacuated.

With speedy development of civil aviation industry, the terminal has gradually evolved into a multi-purpose and super spacious building complex. Modern airport terminal is characterized by vast building space. At one side of its main entrance, single large roof structure is largely used. Due to operation function need, the large space area in the building is hard to be split, and several-storeyed space is interconnected from time to time. The functions and characteristics of terminal building contribute to its complex occupant structure, high concentration of occupants at entrance and exit of arrival and departure hall etc., and unfamiliarity by passengers of exit, evacuation route and fire fighting facilities[1]. High occupant loads lead to long evacuation distance and small evacuation width. In the event of emergency, punctual evacuation is the prime issue of securing safety.

Intending to begin with the research outcomes on the psychological bias and irrational behavioral decision of individuals in emergencies, this paper researches and discusses the influence of different response modes on the emergent evacuation system of terminal in case of sudden event from three stages—event occurrence to occupant perception, perception to decision, evacuation beginning to evacuation completion, and according to the physiological and psychological features of occupants and the building design characteristics of terminal. And based on this, assessment and improvement strategies for the emergent evacuation system of terminal in case of sudden event are put forward, which provide valuable reference to strengthening the operation safety of civil aviation.

2 EMERGENT EVACUATION SYSTEM OF TERMINAL AND THURLEY MODEL

The hardware facilities in the emergent evacuation system of terminal mainly consist of evacuation facilities, guiding system and evacuation route. The evacuation facilities mainly take into account the width, quantity, interval and setting rationality of such facilities as exit, evacuation staircase and evacuation passageway. For the emergent lighting, indicating mark and emergent broadcasting in the guiding system, main consideration is taken into the influence of mark visibility, location rationality

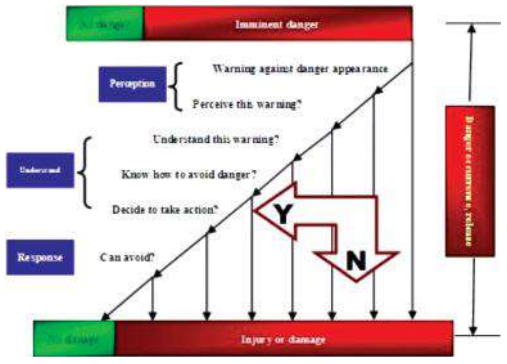


Figure 1. Thurley model.

and system availability. For the evacuation routes, main account is taken into the flexibility, neatness and visibility of the evacuation routes[2].

When it comes to management measures, daily management is the priority: inspection and maintenance of evacuation facilities, rehearsal and education of evacuation pre-plan, duty allocation of evacuation training, reasonable adjustment of plan.

The model divides the accident occurrence into danger occurrence and danger release, and matches the perception, cognition and behavioral response (the process where a person disposes of danger information) with danger process. Danger occurrence corresponds to the normal operation of potential peril, and danger release corresponds to the emergent evacuation of terminal in case of sudden event. The danger occurrence and release stage includes three parts—perception, cognition and behavioral response, and six problems, as shown in Fig. 2.1.

Starting from the perspective on whether personal properties match and coordinate with machine performance and environmental situation, Thurley model thinks that the information on machinery and environment is continuously reflected to men's brain through their sensory organs; if men can correctly get to know, understand, judge, make proper decision and give appropriate action, accident occurrence or injury to themselves or others by accident can be avoided.

3 ANALYSIS OF INFLUENCE OF BEHAVIORAL MODE ON EMERGENT EVACUATION SYSTEM OF TERMINAL

In this section, the following three problems are analyzed: (1) how men collect information and perceive fire accident to happen; (2) after perceiving fire, how men judge and confirm the imminent disaster danger, and choose escape route and leave dangerous place according to environmental factors; (3) how men behave influenced by mass when they take action according to their decision. So, human behaviors are divided into three stages for discussion: perception stage, response stage and action stage.

(1) In perception stage: cognition psychology considers human information processing system consists of Perception, Judgment and Behavior. Consciousness is between the first and second stage of the system. If perception process, i.e., information input process, is faulty, and if no seeing, seeing by mistake, no hearing or hearing by mistake, will lead to mis-judgment, thus delaying evacuation opportunity. The reasons that cause faults in the perception process include inadequate signal induction, cognition lagging, misjudgment, perceptual ability defect, information selection, distortion and misconception.

Based on the basic characteristics of perception, the factors that influence passengers to perceive correct perception of the information of sudden event warning: ability of signals attracting attention; time length of signal emergence; rolling speed; features of signal contents; size and variety of information volume; perceiving ability, concept, expectation and experience of individuals and external environment, etc. Specific behavioral characteristics and influential factors in this stage are shown in Table 31.

(2) In response stage: when men find by relying on their limited cognitive ability and decision resource they are hard to obtain sense of safety, they will seek help from their own experience and intuitive sense and get balance and eliminate unease. Owing to the important position of experience and intuitive sense, they behaviors will be controlled by some inherent behavioral modes, and thus perceptual bias appears. The bias is not necessarily a worry. What concerns us is lack of understanding of the bias, and stiff insisting on the irrational behaviors brought by it. Below, specific psychological and behavioral manifestations brought forth from external environmental factors and individual perception bias influence, for example, excessive confidence, over-response, under-response, regret aversion, ambiguity aversion, prime/immediate effect, halo effect, disjunction effect, etc.

Psychological bias will be affected by various factors, including subjective factors like characters, emotion and experiences, and external environment factors like physical environment, information expression method and the behavioral manifestations of the persons around. These factors will lead the people to all kinds of cognitive bias. In particular, in case of unforeseeable or

Table 1 Factors affecting cognitive effects.

Influential factors			Perception stage
Human factors	Individual factors	Vision	Main source of receiving warning information
		Hearing	Auxiliary source of receiving warning information, easily interfered by noise
		Psychological capability	The stronger capability, the more complete and clear the information received.
		Experimence on disaster	Experimenced persons are more sensitive to perceive danger.
Environmental factors	Warning information	Visual information	Stimulate intuition
		Audio information	Auxiliary stimulus
		Communication equipment	Rapid, highly reliable
		From the persons around	Rapid, large scope, easily causing panic
	Disaster factors	Smoke	Attentive
		Flare	Stimulate intuition, rapid
		Temperature	Lack of features, soft stimulus
		Noise	Abnormal noise can attract the attenion of men.

uncertain sudden incidents, these biases will be more obvious. Specific behavioral characteristics and influential factors in this stage are shown in Table 3.2.

(3) In action stage: In sudden incidents, individuals mainly manifest adaptive and non-adaptive behavior. Adaptive behavior means in emergency, the people give prompt response, which is the action helping to control the situation, such as helping others to escape, putting up fire, notifying others or sending alarm. On the contrary, if a behavior leads fire to develop towards adverse situation or is disadvantageous to others' safety, for example, push against each other, knock down and tread others, which are non-adaptive behaviors, mainly including stiff behavior, homing (back off) behavior, phototaxis behavior and returning behavior. The crowd in sudden event will give irrational behaviors such as going with the crowd, role expectation, family love (small group), competition and nonverbal communication.

In public places like terminal, for most of the people in fire accident, the measure at their first response is to escape from the building or run away after giving warning, instead of helping to fight fire, because they think full-time security guards and staff will be responsible. In choosing exit, most of the people at different ages and in unfamiliar environment will look for the exit according to evacuation mark; without obvious mark, they tend to turn back or look for their familiar places. It is worth noting that there is a relatively high proportion among the people at 18–30 years old that tend to take drastic actions in emergencies. A small proportion of them follow the crowd to queue and walk out, rather, they desperately run forward to leave and look for other exits as soon as possible, with the proportion higher than youngsters and the middle-aged and the old[3].

As described in literature[4], in case of danger, the people in panic will have some common actions to escape in order to seek their own safety. For example, in case of fire, their fleeing action is characterized by: choosing the distance shortest to the emergent exit; flee to the direction away from smoke and fire; choosing the route without least obstacles; choosing habitual and experienced road and exit; returning from the entering direction; going forward by phototaxis; moving along the wall; following the crowd, and so on. Specific behavioral characteristics and influential factors in this stage are shown in Table 3.3.

Table 2. Main factors affecting response decision.

Influential factors			Response stage
Human factors	Individual factor	Extent of understand event	The higher extent of understanding, the larger the possibility of objective evacuation and rational response, the lower the sense of panic; effectively resist the nervous atmosphere brought by mass panic.
		Psychology	The stronger psychological capability, the stronger the ability to resist psychological stress caused by adverse situation and adjust negative emotion, including tolerance and adaptive capacity, etc.
		Experience on disaster	Experiences help men weaken panic and make rational and confident decision.
		Extent of familiarity	Men familiar with the environment are calm-minded on the whole.
	Group factor	Small group	Means relatives, friends and acquaince manage to gather to support each other and add sense of safety.
		Large group	Means the strange group where time and space just converge, easily influenced by the emotion and behaviors of the men around.
Environmental factors	Evacuation guiding information	Visual information	Helps passengers understand the meaning and danger extent of warning, prompt peoples how to avoid danger.
		Audio information	Auxiliary and supplement to visual information
		Exit distance	Key factor that decides whether passengers take action
		Evacuation passageway	Key factor that decides whether passengers take action

4 SUGGESTIONS ON OPTIMIZATION OF EMERGENT EVACUATION SYSTEM OF TERMINAL

For perception stage: the revelation brought by the first problem "do danger constitution and manifestation have warning" is to allow the non-obvious dangerous state to be fully manifested. The revelation brought by the second problem "whether to feel warning" is that different persons have different perceiving ability, individuals' perceiving ability and anti-interference ability can be improved by counting on experiences and training. In the scenario where interference is serious, we manage to enhance signal intensity. For the entire warning and indication system, clear and unified indication, correct and complete settings should be taken into account. On the part of application, stress on striking color and clear and neat patterns. Marks should be highly identified. It is then suggested that:

a. At the conspicuous location in the terminal building, put on the warning marks in danger occurrence stage, including the warnings on individuals' unsafe behavior and fire safety;
b. In the place where interference is serious, warning type that can avoid interference is adopted, for example, use light signal or sound signal significantly differing with noise frequency, or increase signal intensity;
c. Adopt new indication and guiding marks, based on evacuation lighting function, add remotely controlled sound function to correctly guide the crowd to evacuate;
d. Provide various auxiliary facilities, such as public emergent telephone, emergent mask storage cabinet (attached with clear prompt mark and detailed instructions of use), etc.;
e. Timely inspect and maintain various facilities and equipments, to ensure the availability and integrity of the equipments.

Table 3. Factors affecting the evacuation effects in action stage.

Influential factors			Action stage
Human factors	Individual factor	Stiff, evade	Do no good to prompt evacuation action, and affect evacuation speed.
		Physiology	Embodied in physical strength and action, etc.
		Experience	Those experienced can act quickly.
		Extent of familiarity	Those familiar with the environment lead to high evacuation efficiency, avoiding blindly dashing.
	Group factor	Following the crowd	Blindly following the crowd makes evacuation in order and direction-oriented; blindly following the crowd causes lowered exit usage rate and route blockage.
		Small group	Delay evacuation chance due to looking for relatives and friends, disturb the order on the site, or even return to the dangerous zone.
		Expectation	Queue, mutual help
		Competition	Fall over each other to the exit, push or even tread.
Environmental factors	Evacuation indication information	Visual information	Main information source in evacuation action.
		Audio information	Auxiliary and supplementary information source in evacuation action.
		Light	In smoke, people will give up the original route and run towards the bright places.
		Exit distance	The shorter the distance, the higher the efficiency.
		Exit width	Related to people flow, guaranteeing width to avoid blockage at the door.
		Evacuation passageway	More passageways are good to disperse stream of people, lessen evacuation pressure.

For response stage: The revelation brought by the third, fourth and fifth problem is, through education and training, to allow individuals can correctly understand its meaning after perceiving warning, know how to avoid danger or control the severity of the consequence, and can correctly make decisions, influenced by the factors in all aspects. So, it is suggested that:

a. Through strict examination system, ensure each staffer can correctly respond, and rapidly act and do their work well in danger occurrence and release;
b. Regularly organize evacuation rehearsal, and enhance the safety consciousness of the whole people in the society on the whole, and popularize evacuation knowledge;
c. The terminal must keep the mass informed of the severity of the situation at the first time.

For action stage: The revelation brought by the sixth problem is, after the decision is made, enough time should be left for taking action, and the people be allowed to rapidly and correctly act as far as possible. So, it is suggested that:

a. Strengthen site management, designate authoritative guiding persons. Ensure the site controllability, correctly guide the people to rationally understand the ongoing matter, and how to adjust their emotion to cope with some possible threats;
b. Evacuate in stages. At first, evacuate the zone directly affected. If a trend out of control appears, the whole building is evacuated in order according to the available emergent rescue measures;
c. Set up refugee and safety zone in the terminal. Adopt fire separation zone, fire wall or fire prevention roll curtain to form relatively independent space, which can also serve as the place where the people await rescue.

5 CONCLUSION

This paper at first describes the behavioral mode characteristics of individuals in emergent evacuation process. By combining with Thurley model, analysis is conducted for its influence on evacuation effects in stages. Based on this, corresponding suggestions and measures are put forward. The suggestions provide valuable reference to enhance evacuation efficiency, lower evacuation risk in

sudden event met by the terminal and improve the operational safety of civil aviation. What is not enough is lack of specific data on terminal rehearsal or actual evacuation. Hence, it is inadequate in assessment of present situation.

REFERENCES

Bryan. Human J.L. 1998. Behavior and Fire. The Development Maturity of a Scholarly Study Area. Proceedings the First International Symposium Human Behavior in Fire, University of Ulster, P. Brennan1997. Timing Human Response in Real Fire. Proceeedings of the 5th International Symposium of Fire Safety Science, Melbourne, Australia.

Cheng Hu, Chuansheng Jiang, et al. 2005. Studies On Human Behavior In Fires In China, International Journal on Architectural Science, 6(3): 133–143.

Gwynne S, Galea E. R. A review of the methodologies and critical appraisal of computer models used in the simulation of evacuation from the built environment. Fire Safety Engineering Group, University of Greenwich, London SE18 6PF, UK.

Shao Hui, Wang Kaiquan 2008. *Safety Psychology,* Beijing: Chemical Industry Press.

Shields T.J., Proulx G. 1999. The Science of Human Behavior, *Past Research Endeavour, Current Developments And Fashioning a Research Agenda.* Invited Paper6 International Symposium of Fire Safety Science, Poitiers, France.

Thompdon P A, Marchant E. W. 1995. A computer model for the evacuation of large building populations. *Fire safety journal,* 24:131–148.

Xia Lingcao, Zhu Jiang, Liu Wenli 2010, *Ideas and Practices of* Buildings Fire Design for the Large Terminal Airport, Building Science, 26(11):95–99.

Yuan Baoping, Wu Tao et al 2005. Fire protection design and safe evacuation of airport buildings, *Fire Science and Technology,* 24(4):440–442.

Zhao Daoliang, Liu Xueying 2008. Influence of psychology going with the crowd on occupant evacuation in emergencies, 2008 (Shenyang) International Colloquium on Safety Science and Technology, Shenyang, 789–792.

5 *Mine safety management and standardization*

This page intentionally left blank

Progress in Mine Safety Science and Engineering II – He et al. (Eds)
© 2014 Taylor & Francis Group, London, ISBN 978-1-138-00122-0

Forecasting of coal mine CBM productivity based on wavelet transform

H.Q. Zhou & B. Cheng
National Key Laboratory of Gas Disaster Detecting, Preventing and Emergency Controlling, Chongqing, China
Chongqing Research Institute, China Coal Technology and Engineering Group, Chongqing, China

ABSTRACT: According to the difficult question how to calculate the productivity of CBM wavelet analysis method was introduced. By the use of wavelet transform method, time series of CBM productivity was decomposed to different levels in accordance with three-time scales, and series at different levels were calculated by the use of appropriate autoregressive model, then prediction results of original time series could be gotten through the series reconstruction. Using the monitoring CBM productivity data of No.35 drilling field in No.7 coal seam at Yuyang coal mine as a practical prediction case compared with the predicted result of autoregressive model of original time series, the results showed that the wavelet analysis-based forecasting model improved the forecast accuracy significantly, it had been important guiding value for CBM extraction engineering of deployment and mine gas management.

1 INTRODUCTION

According to the *The Five-Year Plan of CBM Development and Utilization for 2011 through 2015* published by National Energy Administration in 2011: the newly added geological reserves of CBM is projected to reach 8500 billion cubic meters, the ground CBM productivity is projected to reach 90~110 billion cubic meters and the underground CBM productivity is projected to reach 125 billion cubic meters by 2015 (National Energy Administration 2011). Thus it can be seen that: the commercial CBM development continues to be underground productivity based. The coal mine CBM productivity prediction is the important basis of the CBM economic evaluation and development plan (Zhang Peihe 2007). The reservoir numerical simulation is a common method at present. This method creates the continuous partial differential equations of gas, water, oil and other fluids based on the Fick law that gas diffusion in reservoir matrix followed and the Darcy law that gas seepage in cleat-fracture followed. The more famous reservoir simulation software are COMET and COMET3-D of ARI, COALGAS of Holdi tch and so on (Tang Xiuyi 1996). The mathematical models using by reservoir numerical simulation are determinate type equations, so it requires high precision input parameters or else the simulation results can't reflect the actual situation. The CBM productivity prediction is affected by multiple factors because the CBM development is a complicated system process. More and More field practice showed that the CBM productivity prediction presents a certain regularity fluctuation.

The wavelet transform is a new applied mathematical branch developed since 1980s' and has a comparative theoretical framework. The wavelet transform can decompose intertwined mixed signal composed of different frequencies into different block-signal. The transform has a good "microscope" function in time and frequency domain. The original signal is decomposed into different frequency channel. The decomposed signal is more single and smooth than the original signal, so the decomposed signal has a better stability than the original one and an obvious advantage for information analysis (Xu Ke et al. 2001).

2 THE BASIC THEORY OF WAVELET ANALYSIS

The essence of wavelet transform is that a series of derived wavelet are produced by means of displacement, constrained scaling in time shaft and scope change by using a suitable mother-wavelet, a series of wavelets is used to compare with the analysis signal in the time axis, then the wavelet coefficient which is used to characterize the similarity degree of signal and wavelet can be gotten. Because derived wavelet can achieve the arbitrarily small regulation accuracy and accurately measure the finite long signal, so the regional information of local time can be gained which Fourier analysis cannot obtain (Gu Jie 2003).

Multi-resolution analysis set out from a subspace at first, and then a basement is established in this subspace. After that using this basement and its corresponding transformation expand it into

the space L_2, in that way its whole space L_2 can be gotten. Let $\{\varphi k,n\}k$, $n \in Z$ be the orthogonal wavelet basis of the space L_2, arbitrary $f \in L_2$, $f(x)$ can expand as follows,

$$f(x) = \sum_{k,n \in Z} d_{kn} \varphi_{kn}(x) \tag{1}$$

$d_{kn} = <f, \varphi k,n>k$, k, $n \in Z$ in the formula (1).

Stephaney G Mallat utilized the thought of multi-resolution analysis and based on its structure, unified structure of wavelet function and put forward the pyramid algorithm that the discrete signal decomposed and reconstructed in accordance with wavelet transform (Stephane G Mallat 1989). The original signal X could be decomposed to d_1, d_2, …, d_J and c_J by the wavelet decomposition (among them J was the maximum number of plies of decomposition), c_J and d_J respectively called the approximation signal and detail signal under the original signal in the resolution 2-j, the detail signal and approximation signal of each layer were the composition of the original signal X in neighboring and different frequency ranges. Using Stephaney G Mallat algorithm for wavelet decomposition, the signal points of the details signal and approximation signal which got in every time after decomposition reduced a times before than decomposition, but the signal points could be increased by reconstructing the signal of wavelet decomposition. Respectively, D_1, D_2, …, D_J and C_J could be gotten by reconstructing d_1, d_2, …, d_J and c_J, and they had the same number of points than the original signal (Yang Shuzi et al. 1991).

3 THE WAVELET PREDICTION METHOD

Set $X = \{x_1, x_2, \ldots\}$ as the original time series, and decomposed it by the method of wavelet, and reconstructed each layer of time series what could be get was

$$X = G_1 + G_2 + \cdots + G_N + X_N \tag{2}$$

In this formula, respectively, $G_1 = \{g_{1,1}, g_{1,2}, \ldots\}$, $G_2 = \{g_{2,1}, g_{2,2}, \ldots\}$, …, $G_N = \{g_{N,1}, g_{N,2}, \ldots\}$ were reconstruction results of detail signal of the first layer, the second floor, …, the *Nth* layer, $X_N = \{X_{N,1}, X_{N,2}, \ldots\}$ was the reconstruction result of approximation signal of the *Nth* layer, N was the biggest number of decomposition layers, therefore,

$$x_i = g_{1,i} + g_{2,i} + \cdots g_{N,i} + X_{N,i} \tag{3}$$

The value x_i of the moment $\{t_i | i \le M\}$ was known and the status value of the step k was needed to predict, namely needed to calculate x_{M+k}. From the formula (3) can get

$$x_{M+k} = g_{1,M+k} + g_{2,M+k} + \ldots g_{N,M+k} + x_{N,M+k} \tag{4}$$

Prediction methods and steps of $g_{1,M+k}$, $g_{1,M+k}$, …, $g_{N,M+k}$ and $x_{N,M+k}$ were as follows.

1. The model of $AR(n)$ was established for $G_j (1 \le j \le N)$ and the known formula $g_{j,i} (i \le M)$ was used to estimate the parameter of the model.
2. The applicability detection for $AR(n)$ which established in step (1) was tested.
3. The predicted value $\hat{g}_{j,M+k}$ could be obtained according to the appropriate model of $AR(n)$ to predict $g_{j,M+k}$,. Set predicted values of $g_{1,M+k}$, $g_{2,M+k}$, …, $g_{N,M+k}$ and $x_{N,M+k}$ as $\hat{g}_{1,M+k}$, $\hat{g}_{2,M+k}$, …, $\hat{g}_{N,M+k}$ and $\hat{x}_{N,M+k}$, the predicted value of the original time series X could be got by the formula (3).

$$\hat{x}_{M+k} = g_{1,M+k} + g_{2,M+k} + \ldots + g_{N,M+k} + \hat{x}_{N,M+k} \tag{5}$$

4 THE EXAMPLE ANALYSIS OF MODEL PREDICTION

The original data which this paper used to research was time series $(Si)(t)$ of CBM productivity of Yuyang coal mine. The method of wavelet prediction and the AR model of time series were separately used for different samples to forecast, and forecast results were compared and analyzed.

The comparison result in Fig. 1 intuitively showed that the wavelet transform forecasting model can predict the underground CBM productivity accurately. The model can provide guidance for CBM drainage engineering design and "Drainage—mining—Tunneling" deployment of coal mine.

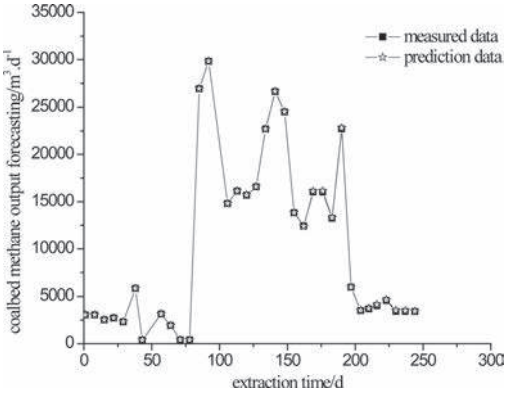


Figure 1. The prediction and measured data.

5 CONCLUSIONS

Wavelet analysis-based forecasting model used wavelet transform and projected the original time series (Si) (t) to different scales, and forecasted the sequence of multiple scales by using the model which was appropriate for AR, finally, complete prediction results could be got by the sequence reconstruction. The biggest advantage of Wavelet analysis was that time series could be decomposed into different levels according to the different scale, signals on the all levels were more stable than the original, in this case the problem became easy to analysis and forecast, meanwhile, the method of wavelet analysis had good localization property in time domain and frequency domain at the same time, because the step length of analysis was used for the component of high frequency in time domain and rough analysis was utilized for the component of low frequency, therefore some of the adaptive ability could be shown for the data, compared with the original method of AR forecasting model, the method of wavelet analysis had better fitting degree.

ACKNOWLEDGEMENTS

This work was financially supported by the National Science and Technology Major Project (ID: 2011ZX05040-003-003).

REFERENCES

Gu Jie 2003. Application of wavelet analysis to short-term forecasting of power system, *Proceedings of The Csu-epsa*, 15(2):40–44 (in Chinese).

National Energy Administration 2011. Coal-bed methane (coal gas) development and utilization of "Twelfth Five-Year" Plan (Beijing) (in Chinese).

Stephane G Mallat 1989. A Theory for Multiresolution Signal Decomposition: The Wavelet Repre--sentation. *IEEE Transaetions on Pattern Analysis and Machine Intelligence (New York)*, 11(7):674–693.

Tang Xiuyi 1996. A few basic awareness of the problem about CBM, *Coal Geology & Exploration (Xi'an)*, 24(3):20–26 (in Chinese).

Xu Ke, Xu Jinwu, BAN Xiaojuan 2001, Forecasting of Some Non-Stationary Time Series Based on Wavelet Decomposition. *Acta Electronica Sinica (Beijing)*, 29(4):566–568 (in Chinese).

Yang Shuzi, Wu Ya 1991. Engineering. application of time series analysis. Wuhan: Huazhong University of Science and Technology press (in Chinese).

Zhang Peihe 2007. Study on CBM Well Capacity Grading Scheme, *China Coalbed Methane (Beijing)*, 4(1): 28–30 (in Chinese).

This page intentionally left blank

Progress in Mine Safety Science and Engineering II – He et al. (Eds)
© 2014 Taylor & Francis Group, London, ISBN 978-1-138-00122-0

Discuss on safety training of coal enterprises

Qijun Du
Institute of Higher Education, North China Institute of Science and Technology, Beijing, China

Bingjun Kou
Institute of Foreign Languages, North China Institute of Science and Technology, Beijing, China

ABSTRACT: With the establishment of modern enterprise system and its huge benefits, the establishment of a modern enterprise has become the only way for coal enterprise to make sustainable development. Only improving the current coal enterprise safety education, constantly strengthening staff training, and improving the overall safety of the workers quality, can we ensure the competitive advantage of enterprise itself, and keep an impregnable position in the market competition. As a result, the coal enterprise safety education is an effective way to enhance their awareness of the importance of enterprise staff safety, and it is a main method of improving the quality of company worker safety, and it is also the important guarantee to realize safety in production.

1 INTRODUCTION

With the establishment of modern enterprise system and its huge benefits, the establishment of a modern enterprise has become the only way for coal enterprise to make sustainable development. Nationally, many coal enterprises carry out the safe production work, and the worker's safety production overall qualities has become the core of the safe production work. Only the improvement of worker's safety comprehensive quality, can it make great progress in the level of enterprise safety production, which can truly establish a kind of modern safe company guided by the scientific concept of development. Therefore, it's very important to strengthen the safety education and training to coal enterprise's worker.

2 THE MEANING OF THE SAFETY EDUCATION AND TRAINING TO COAL ENTERPRISE'S WORKER

2.1 *It's an important reflection of "people-centered" scientific concept of development to do well in safety education and training*

For coal enterprises, the adherement to the people-oriented often takes safe production as a starting point and foothold of all the work, determines the worker's personal safety and production safety, ensures the worker rights and interests, makes the worker in a safe environment, gives full play to the initiative, so as to improve enterprise production benefit. Safety education and training is to be in accordance with the requirements of the coal industry safety in production, through the improvement of the workforce, and the initiative to implement the rules and regulations, which can be effectively to arouse the enthusiasm of worker safe production, realize production safety, so as to prevent accidents, reduce damage and protect workers' health and safety.

2.2 *It's a social need to realize safe production to do well in safety education and training*

To ensure safety in production is the basic reflect respect for life, and the basic needs of worker. For coal enterprises, safety is the bottom line, only to do well in safety education and training, can it make the enhancement of safety production for workers, who can attach importance to technical requirements, rules and regulations and operating procedures in the production practice, and keep in mind the importance of safety production to enterprise and themselves. It has been proved that despite of the advanced work equipment, as long as the user don't operate according to regulations, it may be possible to cause accident. Otherwise, even if the equipment is not the most advanced, as long as strengthening maintenance to ensure the equipment in good condition, it also can prevent major accidents. In addition, the worker's safety awareness, responsibility, labor discipline, the technical operation standard, group and the control in the process of production, mutual control, depend on people's ability to control. Therefore, safety

education and training is necessary to safe production work.

2.3 *It's internal needs of the company's development to do well in safety education and training*

Worker safety education is the key to assure the safety production in coal enterprise, only the staff realize the importance of safety work, can it grasp the production safety. In order to do well in safety education, it should begin with the worker thought, analyzing the dynamic of the worker thought. Try to predict the possibility of accident, master accident rule, make a qualitative and quantitative analysis and evaluation, and put forward corresponding measures according to the evaluation results, to prevent and eliminate accidents and ensure safety in production. Only to do well in safety education, raise the level of worker safety management, make the worker in the production process, strict with operating procedures, can it ensure safety.

3 THE PROBLEMS OF COAL ENTERPRISES IN SAFETY EDUCATION TRAINING WORK

3.1 *The notion of coal enterprises to carry out safety education training is not strong*

At present, some coal enterprises pay less attention to safety education training work for workers, which mainly embodied in the less of training institution, the discontinuity of training. In order to reduce operating costs, some enterprises slash the funds on safety education training, even cancel safety education training for the workers. And although some coal enterprise, carry out safety education training work, due to the holding time, the related compensation policy and treatment is not clear, which have a side effect on workers to participate in the safety education training. In addition, in specific training, due to the lack of pertinence and features, it also affects workers' the initiative to learn.

3.2 *The coal enterprise safety education training work is not adapted to sustainable development*

For safety education training, the main purpose is to improve workers safety awareness and labor quality, and meet the needs of the enterprise sustainable development. But some coal enterprise leaders think safety education training, only needs to tell the current practical technology, without consideration for further development of the enterprise. In addition, some coal enterprises do not put safety education training in the height of the development strategy, and often cut funds for training, thereby greatly influence the enterprise safety education training. It can't keep up with the pace of enterprise development.

3.3 *The lack of teachers in safety education training*

At present, from the perspective of national coal industry, the shortage of faculty is still a key issue. The training teachers are mostly masters with practical experience in the enterprise, but congenital deficiency in the theory and teaching methods; And the external security education training teachers, although have deep theoretical knowledge, they often lack practical experience, which makes the boundary between coal enterprise safety education training and knowledge education field not clear, low efficiency of the employees to learn and master the knowledge and skills.

3.4 *The coal enterprise safety education training course is not reasonable*

At present, coal enterprises are basically not out of the teaching model in safety education training courses. The curriculum content is too old and stiff, which can't keep up with the renewal speed of professional knowledge and skills. At the same time, the coal enterprise often exist many problems, such as more theoretical knowledge, less practical skills, which has make seriously effects on safety education training to the workers.

3.5 *The form of coal enterprise safety education training is too simple*

In the form of safety education training, many coal enterprises still adopt the traditional pattern of classroom teaching, some enterprises adopt the meeting way of "trainer teaches above, worker sit here to listen", and some companies take the form of lounge training, and the training contents are the same, few practical things. These kind of training content and form makes trained workers the loss of interest, and the result of these safety education training modes make less sense.

4 THE IMPROVEMENT MEASURES ON SAFETY EDUCATION TRAINING EDUCATION WORK

4.1 *Completely change the concept of safety education and training*

Coal enterprise leaders must first thoroughly change the concept of safety education training, pay attention to the cultivation of technical talents. For

enterprise safety education training worker, it should give support on worker, money, material, so as to make enterprises into a learning organization, and improve enterprise comprehensive quality, which can make a rapid development of the coal enterprise.

4.2 *Make a reasonable arrangement on safety education and training according to the coal enterprises need*

According to the need to make reasonable arrangement of safety education training, that is what workers should do and what they learn in enterprise. The training should have a purpose. Enterprise training should not be too simple, it needs to put what they learn into practice.

Specifically, for front line workers, it should improve their practical skills through the study of theoretical knowledge and knowledge of site operation; For professional and technical personnel, it should to improve their professional skills through innovation and collaboration ability and professional knowledge update; For the grassroots management personnel, it should improve their management level through the development of management wisdom.

In the training, we should pay special attention to avoid empty content about all kinds of knowledge and technology, and integrate theory with practice, training with practice, through practice operation training, simulation exercises to improve job skills. Worker safety education needs to be more vivid, imagery, easily to remember the profound content, to be able to tightly close to the coal production, life, human feelings, hit the worker's heart of hearts, which can be effective.

4.3 *The coal enterprises specifically write training materials*

Coal enterprises should adhere to the principle of interest, practicality and clearness, and specifically write training materials. In the process of training materials, the illustration of the theory must be concise, and should pay attention to the combination of actual case and theory, improve the practicability of training materials. At the same time, with the continuous development of coal enterprises, and the rapidly update of all kinds of knowledge, the training materials will enrich timely, which can make the workers be able to acquire new technology and new knowledge in every training.

4.4 *Taking a variety of forms in training process*

In safety education training work, coal enterprises should take a variety of safety education training forms to get better effect. For example, it can take on-the-job training, short-term off-job training and internal job rotation training, etc. On-the-job training is on-the-job training to all staff, so that they can grasp their own work practice standards, to realize the goal of jobs, positions; Short-term off-job training is for elite technical backbone, personnel. It can hold business seminars, technical BBS to make a short-term off-job training, by hiring a professional to guide and launching the discussion; Internal job rotation training is for new highly educated workers, adopts the way of job rotation to train, which can strengthen their understanding of many aspects of this enterprise and cultivate inter-disciplinary talents.

In addition, writing safety advise, epigram, security ballads, organizing employees to undertake safety, safe and funny activity, entertainment performance and so on, are also a good way of education and training.

Along with the development of economy and society, the mode of safety education training should also be continuous innovation, constantly broaden the channels. Safety accident case analysis, image display, security debate, and other forms of education should be applied in safety training. In safety education training work, coal enterprises should take a variety of safety education training forms to get better effect. For example, it can take on-the-job training, short-term off-job training and internal job rotation training, etc. On-the-job training is on-the-job training to all staff, so that they can grasp their own work practice standards, to realize the goal of jobs, positions; Short-term off-job training is for elite technical backbone, personnel. It can hold business seminars, technical BBS to make a short-term off-job training, by hiring a professional to guide and launching the discussion; Internal job rotation training is for new highly educated workers, adopts the way of job rotation to train, which can strengthen their understanding of many aspects of this enterprise and cultivate inter-disciplinary talents.

In addition, writing safety advise, epigram, security ballads, organizing employees to undertake safety, safe and funny activity, entertainment performance and so on, are also a good way of education and training.

Along with the development of economy and society, the mode of safety education training should also be continuous innovation, constantly broaden the channels. Safety accident case analysis, image display, security debate, and other forms of education should be applied in safety training.

4.5 *The safety education training should be pragmatic*

Safety education training must solve these problems, such as formalization, labor inspection, less

attention to the actual effect of training. Safety education and training must be pragmatic, truly enhance employee safety awareness, business skills, professional ethics, improve the purpose of the comprehensive security quality, so as to enables workers master the actual knowledge to promote safety production. It needs to play staff initiative, steadfast, and take serious training. Besides, it also need to take hard actions, have a clear plan, staging layered implementation, not only pay attention to the theoretical training, but also attach more importance on the practical work of training, so as to build a cultural, knowledgeable worker team.

In the concrete operational level, firstly, it is need to establish and improve the safety education training mechanism, make the workers really learn the knowledge and skills; Secondly, it is to intensify supervision and examination of the enterprise safety education training, rewards and punishment; Thirdly, it is to build a new track of safety education training learning effect evaluation mechanism, to master workers' actual situation, commendation first, spur behind.

In view of the viewpoint of discipline is weak tendency, it needs to carry out the "ideas" education. It should educate workers to learn disciplines, abide by the rules, operate according to procedures, consciously obey discipline of good habits; For the relaxed thought, it should carry out the education concept of "warning", wake-up call; For the thought about no progress, only no fault, it needs to carry out the education concept of "incentive", and accomplish responsibilities clearly, study human psychology and behavior regularity.

4.6 *Coal enterprises should enhance the high quality and professional teachers*

Coal enterprises should implement training teachers' qualification authentication system, gradually change use measures for the administration of coal mine enterprise part-time training teachers, part-time teacher training and solve business from the shortcomings of both ends. In addition, taking the teachers' professional knowledge, the degree of familiarity of teachers to operate equipment and technological process, teachers professional dedication as the investigation of the main factors on the quality of the teachers' training, and forming a training team with high knowledge of professional teachers as the priority to improve training quality.

5 THE INNOVATION OF SAFETY EDUCATION TRAINING METHODS

In the practice of safety education training work, there are many methods, such as: teaching method, question and answer method, discussion method, demonstration method, operation video, experimental method, case analysis, slideshow image method, multimedia teaching method and visiting method, on-the-spot guidance, job training and so on. But in the actual process of education and training, what kind of teaching method should be adopted is determined by the purpose of training.

5.1 *Class teaching methods of safety education training*

1. The teaching method. In safety education training, the teaching is the most commonly used method, which is to train teachers by concise and vivid oral language interpretation, safety knowledge training to the staff training. During teaching, teachers should pay attention to language arts, to use vivid, clear, accurate and easy to understand language from the beginning to end.
2. Question and answer method. Question and answer method of safety education training that is on the basis of original knowledge and experience training teachers inspire question-and-answer method of conversation, lead staff to positive thinking, and thus acquire a learning method of safety knowledge.
3. Discussion method. Safety education training discussion method that is under the guidance of teachers, the worker will study the problems encountered in the training, on the basis of carefully prepared to discuss and exchange views, in order to achieve the goal of complement each other, put our heads together and improve together.
4. Operation demonstration method. Safety education training operation demonstration method, that is to train teachers with teaching, and teaching methods, such as to show physical training worker, courseware and teaching demonstration, make employees get visual perceptual knowledge. This way can change the teaching from static to dynamic, the teaching theory from abstract to concrete, which stimulate the learning interest, so as to improve learning result.
5. The experimental method. Experimental method of safety education and training, that is under the guidance of teachers, the workers use certain equipment for independent operation. This method helps to obtain direct safety knowledge and experience, combine actions with brain, which can deepen our understanding to the knowledge.

5.2 *Scene teaching method of safety education training*

Safety education training teaching, that is, according to the training of teaching content and purpose,

it is in the enterprise production site, workshop or production jobs, job site for the classroom, the scene of the equipment, the facility as a training on intuitive teaching AIDS in teaching.

1. The method of observation. Safety education training visit teaching method, is based on training objectives, organize staff to visit the enterprise production in factory, through the observation and summarizes the advanced experience of production and work, it can draw on lessons l, so as to gain new knowledge of safety.
2. Practice method. Safety education training practice teaching method, is training the workers to do the job rotation internship. Under the guidance of experienced teachers, they are engaged in the actual work for a long period, so as to master certain skills, increase the perceptual knowledge. This kind of teaching method is a common way for new employees.
3. Post training method. Safety education training post training method, is a way to teach on the spot, and it's also a kind of activity to put what they learned into practice. It mainly make a comprehensive training on different views and levels according to the requirement of the job procedures. In many cases, it lets skillful workers teach the new workers on the spot. The new workers operate by themselves, so as to meet the standard and start to work after practice.

6 CONCLUSIONS

All of above, with the development of the modern enterprise, the enhancement of workers' awareness in safe production has become an important part of the healthy development of the modern enterprise. Safety education training work is the key to ensure safe production in coal enterprise, strengthen the safety management. To this end, we need to change the present situation of the safety education training, feet on the ground, and try to explore new methods of training teaching. Based on reality, it needs to look into the future, and make efforts to create a new situation of safety production for coal enterprises.

REFERENCES

GaoMing. 2012. Thinking of effective patterns and ways of training of staff education [J]. Occupation.

He Tantan. 2012. Research on the Situation and Development Strategy of Education Training Market in China.

Jia Wenlan. 2009. On the strengthening of coal mine safety training to improve training quality [J]. Intelligence.

Liuling. 2012. Reflections on strengthening safety training work of coal mines [J]. Staff and Worker's Education of China.

Pan Yuefei, Lu Yongbo, etc. 2010. Innovation research on coal industry management system based on regional diversity [J]. Business Research.

This page intentionally left blank

Progress in Mine Safety Science and Engineering II – He et al. (Eds)
© 2014 Taylor & Francis Group, London, ISBN 978-1-138-00122-0

Study on problems of safety culture construction in coal mine and the countermeasures

Ying Zhao & Yongzhi Wang
College of Humanities and Social Sciences, North China Institute of Science and Technology Sanhe, Hebei province

ABSTRACT: At present, coal mine safety culture construction in China has made great progress, but there are also some problems, such as the construction of safety culture in the form of floating, generally weak safety concept, having not formed the evaluation measurement system effectively and having deviated from the essence of people-oriented. Therefore, we should pay attention to safety technology training, create an atmosphere of safety production, develop evaluation and measurement system, and learn the relevant legal system. By doing that, we will promote the function of safety culture and push forward the healthy development of the construction of safety culture.

Keywords: coal mine safety culture construction; problems; countermeasures

Cherishing life, preventing disaster, protecting the physical and mental health and safety of people is the key to promote economic development, social security and national stability. The core and the basic requirements of *scientific development concept* determine that the "people-oriented" takes human life first. In coal mine, as a high-risk industry, it is required to use more "safe development" to build consensus, strengthen the construction of safety culture, and enhance initiative and effectiveness.

1 FOREWORD

Coal mine safety culture is the sum of material wealth and spiritual wealth created in long-term coal mining activities to ensure the safety and health in various activities, including the protection of miners in the production in body and mind, healthy, harmless, no wound and no dead working environment, and safety awareness, values and behavior norms of coal mine workers. It plays very important roles in leading leaders and workers to enhance safety consciousness, cultivate the safety concept, control unsafe state of material, constrain unsafe human behavior, actively investigate all kinds of accident hidden danger, avoid personal or impersonal safety accidents and so on. In recent years, China's coal enterprises have made some positive exploration in the field of safety culture construction, and got some achievements. Because our coal mine enterprises enter the market in very short time, it is still in the initial stage to treat the safety as a culture for research and construction.

2 COAL MINE SAFETY CULTURE CONSTRUCTION PROBLEMS

At present, in the atmosphere of all industries strongly advocating the building of safety culture, safety culture construction of coal enterprise has made some progress, but in the specific implementation process, there are also some problems that can not be ignored and should be further improved and deepened.

2.1 *Floating in the form of safety culture construction*

With the development of reform and opening-up and social economy, most enterprises have carried out the construction of enterprise culture. The importance of safety culture construction is spoken in various meetings and documents, which forms the "cultural fever". However, from the view of specific execution situation of coal mine safety culture construction, there is widespread formalism phenomenon.

In reality, some enterprises consider safety culture as a carrier of the ideological and political work, only emphasizing its political function, not paying attention to its business function. They draw an equal sign between the safety culture construction and ideological and political work of coal mine. In the actual operation, they emphasize political study and ignore the construction of safety in other aspects. So the safety culture construction has strong political color, and is not into merged in the whole process of production

and management. (Wang Dan 2009) In a word, safety cultural construction is performed not in order to improve the production performance, but only for the sake of safety culture. Production did not give support to the safety culture and it also greatly reduced the effectiveness of safety culture construction.

2.2 *Weak safety concept*

The culture, formation and development of safety culture idea directly affect the process of safety production and relate the survival and development of enterprises. Therefore, in the process of coal production, to establish the safety concept is the first. Only the formation of safety concept correctly, can effectively promote the safety production of enterprises.

Restricted by the level of economic development and staff own quality, the safety concept of miners is generally weak at present. It is in the dependent and passive position basically. They abide by the rules and regulations only because they are afraid of being punished. The so-called "safety first" and "safety discipline" consciousness is fuzzy. In addition, various safety regulations in some enterprises are to some extent on paper or verbal, not into a habit and behavior criterion of all employees, which is not enough to let them consciously accept and promote coal mine safety culture.

2.3 *No effective evaluation measurement system*

The establishment of evaluation index system of safety culture is an arduous and complex task, including the establishment of safety culture evaluation index, determination of evaluation method, measurement of evaluation results and so on. At present, domestic research in this area is still not perfect.

Compared with foreign countries, China has not formed a set of effective model and index system of the evaluation and measurement on safety culture, which resulted in the current coal industry security standards obsolete, lack of pertinence and maneuverability. Enterprises, as responsible body and the implementation main body for safety production, are less or passively involved in the standardization construction. Some leaders of the larger coal mines think that the enterprise has passed ISO quality management system and HSE management system certification, and safety standardization has little difference with safety management and safety standards, so they do no need to carry out safety standardization construction. Some leaders of coal mines are lack of awareness of the importance to carry out safety standardization, and lack of management, enthusiasm. They implement standards not strictly, and are not willing to invest in safety standardization of equipment.

2.4 *Deviation from the essence of people-oriented*

Nature of safety culture is people-oriented, which penetrates in people's production process and life, and with tangible or intangible transfer channels, formal or informal way to every member, affect everyone's life and work quality. At present, the phenomenon is serious that many coal enterprises pay more attention to production than safety, especially some local small coal mines, basically there is no safety culture consciousness, even though they are mostly embodied in the system, preaching and slogans, not really reflect the essence of people-oriented. (Dong Xiaobo et al. 2010).

Safety is the first for coal mining enterprises and no security is no benefit, no development. The mine enterprise employees, especially those underground workers, work in a difficult and hostile environment, and may suffer from water, fire, gas and other accidents and occupation disease harm, and should get social recognition and respect from people. Safety culture construction of coal enterprise should really reflect on life and health care, mobilizing the enthusiasm of staff fully. The idea of "respecting people, caring for people, paying attention to the people" should be established through the coal mine safety culture construction.

3 COUNTERMEASURES

To solve the problems in China coal mine safety cultural construction, the following measures should be taken, so as to promote the safety culture function, and promote the healthy development of the construction of safety culture.

3.1 *Pay attention to the safety and technical training*

In recent years, many coal mines are performing continually staff full-time and amateur training. There are a large number of participants, but the effect is not satisfactory. There are main three reasons: the first is that farmers rotate workers who are engaged in the mining front-line work are mostly used in coalmines, liquidity is very strong; the second is that coal mines perform the training and contests, only to complete the training mission, to cope with the safety supervision department supervision; the third is that the training content for the general staff training, is limited to post content, lack of coal mine safety comprehensive knowledge systems.

The importance of safety technology training is self-evident. Employees' safety behavior should be regulated through various forms of training. Improve the skills of workers, and gradually improve the quality of safety culture of employees, to realize the need of coal mine safety culture construction. Therefore, systematic training, namely off-the-job training, systematic explanation, special counseling and other forms of organization, should be performed. Organize staff to systematic study, training and examination about system of standard to make the worker to memorize the safety concept, know behavior taboos and code of conduct, and master the operation standard. Select excellent site class leader, technician as "coach", carries on the training to the team of workers. At the same time take the scene to observe the form, organizing staff to site visit and study to the region and posts which implement better in standardized management, standard operation, and practical demonstration site key steps and key link of operation. In addition, carry out athletic contest, which is in accordance with the different work process standardization requirements, hierarchical organizations conduct athletic contest, select and recognition of norms of behavior model, to motivate staff as soon as possible to develop the norms of behavior.

3.2 *Build safe production atmosphere*

People's unsafe behavior and unsafe state of object is the direct cause of accident, in which the unsafe behavior of the people is the most important reason, because most of the accidents are caused by human error. The key to create a safe atmosphere is to manage people, educate people, inspire people, and let the staff form strong safety awareness in the influence by environment, to achieve fundamental change from "want me to be safe" to "I want security."

Grasp the construction of safety culture and perform safety culture education is the important way to create a safe atmosphere and firmly establish the ideological line. Therefore, through the safety publicity and education, build safety culture atmosphere, arouse the enterprise staff concerned about safety work. Through radio, television, audio-visual products, newspapers, posters, banners, books, carry out various forms such as knowledge contest, speech contest, theatrical performances and other activities, strengthen the construction of cultural security propaganda, to create a "everyone concerned about the security" safety culture, improve staff safety consciousness consciously. Constantly during work, enrich the contents and forms of safety culture construction. For example, use family education to promote the construction of safety culture. (Yang Shuqian 2010).

3.3 *Develop evaluation and measurement system*

Through evaluation of safety culture level and measurements of atmosphere, it can make the enterprise know the situation of safety culture of enterprise development, understand the weak part of safety culture construction work, determine the direction and goal of safety culture improvement. The key of evaluation and measurement is to construct the index system and select method. In construction of evaluation model, mature evaluation model should be referenced, and successful foreign experiences and practices should be learned from and modification and innovation should be made, in order to adapt to the situation in the construction of safety culture in coal mine in China, and to achieve the scientific, rational and efficient purpose.

There are some preliminary research results about the evaluation of enterprise safety culture. Some experts and scholars study and establish the evaluation model. Some coal enterprises establish a safety culture evaluation system, and discuss the theory and practice. Shenhua Group, Datong Coal Mine Group, Yanzhou Group, Yang Coal Group and other large-scale coal enterprises all have a similar representative practice and system on safety culture construction and evaluation. These groups themselves have a certain influence and competitiveness in the international coal industry, research on these large groups has a broad field. However, from the literature, a part of safety evaluation method from the coal mine enterprises don't pay too much attention to the research method, the test research process and the experiential of conclusion. Another part comes from universities, colleges and research institutes, paying attention to the research of coal mine safety culture evaluation system by the method of mathematics and science, but there are gaps in variable selection, model building from reality. Therefore, it is the trend to perform normative study on coal mine safety culture evaluation, and keep close to the actual coal mine safety management.

3.4 *Learn relative legal system*

Perfect safety legal system and improvement of enforcement environment of safety legal system are the foundation of safety culture safeguard. Good safety production legal environment can regulate safety production norms and behavior of coal enterprises and employees, and regulate safety cultural construction model and overcome formalism. Therefore, safety production laws and regulations

system should be established and "production safety law" related laws should be improved, the production safety and technical specifications, standards and revision should be developed to improve the law enforcement strength, ensure the safety production laws and regulations to implement, to provide a good legal environment for the safe production of coal mine safety culture construction.

In the work, according to the needs of coal mine safety management, focus on the organization of cadres and workers to learn "production safety law" and the "Mine Safety Law", so that the majority of workers are fully aware of the post legal responsibility, behavior standard and working standard, the personal behavior itself into the legal responsibilities of the society. By organizing knowledge contest or activities such as discussion about "violation the regulation" is the "illegal", "security and law", let the employees be infected in the activity. And then they resolve doubts, master knowledge of relevant laws and regulations, especially analyze the positive and negative examples in terms of security, to clarify the relationship of violation and illegal, a legal concept, improve the awareness of law-abiding. In addition, investigation of all kinds of accident should be performed thoroughly, and treat in serious, and the results should be widely advertised, making the workers understand the importance of safety in production.

4 CONCLUSION

Today, enterprise management of "people-oriented" has got much attention increasingly. Safety culture is an invisible hand. The enterprise safety culture is the must route for coal mines with labor intensive and high risk to achieve long-term effective mechanism of safety. Therefore, we should strengthen the coal mine safety culture construction, and improve the safety management level of enterprises to provide security for coal mine safety production.

REFERENCES

Dong Xiaobo, Zhang Tongjian, Tan Zhanglu. Construction of a new type of safety culture in coal mine [J]. China mining, 2010 (4).

Wang Dan, Discussion on China coal mine safety cultural construction [J]. Safety, 2009 (8).

Yang Shuqian, discussion on coal mine safety culture construction elements [J]. China coal, 2010 (5).

Progress in Mine Safety Science and Engineering II – He et al. (Eds)
© 2014 Taylor & Francis Group, London, ISBN 978-1-138-00122-0

Game model and analysis of market-based refined safety management in a coal mine enterprise

Yifei Weng
North China Institute of Science and Technology, Beijing, P.R. China

ABSTRACT: In this thesis, first of all the concept and basic connotation of market-based refined safety management is described. Then in view of short-term, static game analysis of market-based refined safety management is made, as well as long-term Dynamic game analysis of market-based refined safety management. Finally conclusions can be drawn that, as for the static state in a short-term, the market-based refined safety management will influence the profit of divisions; but from a long-term dynamic state, it is best for the whole benefit of an enterprise.

1 BASIC CONNOTATION OF MARKET-BASED REFINED SAFETY MANAGEMENT

Market-based refined safety management of a coalmine enterprise is a mode or system of safety management that coal mining enterprises implement, which adopts the method of internal marketization, the safe hidden trouble that has been priced beforehand will be considered as commodity to trade in the market through the operation of the "invisible hand"- market mechanism in coal mine enterprise. It is a process of searching field, processing, selling hidden trouble, providing safety services of a safety manager, and the process of the acquisition of hidden dangers by the units and personnel. This management mode can scientifically configurate the safety-related resources such as people, money, material, information through benefits and costs of internal marketization mechanism, regulate and control process of production and management, to act on human, machine, ring and other safety factors. It will eventually drive safety of fine management in place, to realize the purpose of constructing an intrinsically safe mine.

2 SHORT-TERM STATIC GAME ANALYSIS OF MARKET-BASED REFINED SAFETY MANAGEMENT

Market-based refined safety management characterized by the safety services market or a division within the enterprise provides safety services to another part, in accordance with the market price to charge (services), so as to promote the safety in productive divisions to strengthen safety management, improve the level of safety, reduce objective safety requirements, thereby reducing safety service and safety service.

With a simple form below to demonstrate the process of game analysis in safety service and its charging. Assuming there are only three divisions in enterprise's internal safety market, among them, there are two equivalence that are in the same level of production (such as two area teams or a team), the safety level needs to be under a certain environment to ensure production run smoothly (expressed as division 1 and division 2); another is safety services division (division 3), which provide safety services for division 1 and 2, and charge service fee. These three divisions are willing to establish safe work environment, and pursue the purpose of safe production. This is because productive divisions in a safe environment can maximize output, thereby profits and interests of division and its personnel. And by providing services, the safety service division can achieve safety in production, thereby the aim of this division. Its subjective aim is to obtain the most safety service fee; objectively it can ensure entire enterprise meet least hidden dangers and highest safety level. The two productive divisions also face with two choices: whether to implement market-based refined safety management or not. Economic resources of the two productive divisions are limited, so when the money for purchasing safety services is increased, the money used to pay or produce will be reduced; and the two divisions decide to buy safety services respectively but they don't know, this is a static Nash equilibrium. So there are four combinations.

If both productive divisions (teams or sub-teams) choose market-based refined safety management in short term, the money for buying safety services

will be increased, meanwhile the time for improving the level of safety also increased, and money for salary and the productive time will be reduced, therefore the output and profits will decline in short term. Because of the concerns about the output would be less than the other or the temptation of productive profits, there will be a different situation. Assuming no external constraints and both productive divisions decide independently, they will not choose the market-based refined safety management, because if they do so, there will reduce the money for purchasing safety service and the time for improving the level of safety; while they will also increase salary, productive time, the output and profits in the short term. The reasons are: if Productive Division II implements the market-based refined safety management to meet or improve safety standards, Productive Division I, without implementing resulting in low level of safety (to purchase safety services inadequate or resist internal marketization), then reflects a short-term profit superficially. If the Productive Division II does not choose the market-based refined safety management, Productive Division I must follow it and also won't choose, even if the result is low level of safety (to purchase safety services inadequate or resist internal marketization), if not, Productive Division I would be at a competitive disadvantage. In other words, in short term, regardless of choice of the Productive Division II, from the interests of Productive Division I, it won't choose, and thus the result is a low level of safety. In the same way, the productive Division II also won't choose, and the result is a low level of safety. Due to competitive pressure of production or profits, there will be the result that both Productive divisions do not choose the mode, which results in low safe levels. Actually if it is not forced, the internal productive division won't take the refined management initiatively which will affect the short-term interest; in other words, the short-term safety may give way to production and profits, even if safety is good for every division.

Actually a coal mining enterprise usually has not only two divisions, such as productive and supportive divisions, in levels of team and subteam. Based on the above short-term game analysis, without unified arrangement of market-based refined safety management by the whole enterprise, cooperative agreement among divisions won't be reached. Therefore, it is suggested that in internal divisions of coalmine enterprise, introducing the market-based refined safety management is very difficult, and it needs whole mine's coordinate linkage, leader' imposing, and all kinds of incentives and punishment.

Here we begin the quantitative analysis of the short-term game process. Neither productive division implements the market-based refined safety management, but their safety costs per unit of production is different, supposing Division I as C_1, Division II as C_2, the total market quantity as $Q = q_1 + q_2$. Here P is market clearing price (the price of all products can be sold), which is a function of total market output:

$$p = p(Q) = 320 - Q \tag{1}$$

Supposing two divisions' fixed costs are equal or not to be considered, and in accordance with the safety standards to determine the unit safety costs equal, set $c_1 = c_2$ 80, and their total safety cost should be $80q_1$ and $80q_1$. Finally, emphasizing that the two productive divisions decide their respective production at the same time, but they don't know each other's production before decision. These questions constitute a game. Two parties are Division I and Division II, and their decision-making space is infinite variety of optional strategy. Each division's profit is that revenue minus cost. According to the given situation, the benefit of two divisions respectively is

$$u_1 = q_1 p(Q) - c_1 q_1 = q_1[320 - (q_1 + q_2)] - 80q_1 \tag{2}$$

Namely:

$$u_1 = 240q_1 - q_1 q_2 - q_1^2 \tag{3}$$

Correspondingly,

$$u_2 = 240q_2 - q_1 q_2 - q_2^2 \tag{4}$$

Each party's benefit depends on the strategies (output) they choose.

If (q_1, q_2) is the sole Nash Equilibrium, the necessary and sufficient condition of (q_1, q_2) as the answer of Nash Equilibrium is the problem of maximum of q_1^*, q_2^*:

$$\begin{cases} \max\limits_{q_1}(240q_1 + q_1 q_2^* - q_1^2) \\ \max\limits_{q_2}(240q_2 + q_1 q_2^* - q_2^2) \end{cases} \tag{5}$$

To test the max values, only making the derivative of (q_1, q_2) be zero respectively in the above formula, can get their max values.

$$\begin{cases} 240 - q_2^* - 2q_1^* = 0 \\ 240 - q_1^* - 2q_2^* = 0 \end{cases} \tag{6}$$

From the above formula, we can get the answer in the game: $q_1^* = q_2^* = 80$, in other word, (80, 80) is the only assembly in the Nash Equilibrium strategies. Both get benefit $80 \times (320–160) - 80 \times 80 = 6400$,

total output is 160, market price 320–160 = 160, and profit of the both sums up to 12800. This outcome results from the situation that both divisions do not carry out the market-based refined safety management, but they make the strategies at the same time according to their own upmost benefit. From the analysis, neither division maximizes its value.

If they both conduct the market-based refined safety management, we will regard the total benefit as the target to consider the best output in the market. First of all, calculating the total output (Q) which can achieve the best benefit based on the market conditions. Total benefit is:

$$U = QP(Q) - cQ - Q(320 - Q) - 80Q = 240Q - Q^2 \quad (7)$$

We can get $Q^* = 120$, then total benefit is $U^* = 14{,}400$. Comparing this result with the outcome based on their own benefit, the total output is less (25%), but profit is more (12.5%). Therefore, if both productive divisions do not compete in the aspect of output or profit, carry out the market-based refined safety management, join together, and produce what they should do respectively, their working focus is not on the output or profit, but on how to scientifically establish the market-based refined safety management within an enterprise. Figure out the output which can get the most profit, then each produces the half (60), they will get more benefit than before (7200 > 6400). However, it is hard to maintain the balance because of the lack of control in the independent decision-making. The main reason for it is that this strategic assembly (60, 60) of the upmost output is not a Nash Equilibrium, namely, in this output assembly, each division can get more profit by enhancing their own output, they have the impulse to opposite or abandon the market-based refined safety management, under the restriction of agreement which is lack of enough force, this kind of management dooms to be fail due to the impulse. As a result, no one carry out this management, which is not the best in short-term.

3 LONG-TERM DYNAMIC GAME ANALYSIS OF MARKET-BASED REFINED SAFETY MANAGEMENT

We still assume that there are three divisions in a company's safety market, two are productive divisions and the rest is a safety service division. They are willing to establish a safe working environment. These two productive divisions also encounter with two options: to carry out the market-based refined safety management or not. Their finance resource is limited, which means the more money is used in safety, the less used in production. In the long run, one productive division can see the other whether conduct the market-based refined safety management, which is a dynamic Nash Equilibrium, see Table 1.

Situation one: the strategy of Productive Division I: no market-based refined safety management within 10 years; the strategy of Productive Division II: no market-based refined safety management within 10 years. Then the total benefit of Productive division I is 640 units as the same as Productive Division II. The total benefit of the two divisions is 1280 units.

Situation two: the strategy of Productive Division I: conducting market-based refined safety management within 10 years; the strategy of Productive Division II: conducting market-based refined safety management within 10 years. Then the total benefit of Productive Division I is 720 units as the same as Productive Division II. The total benefit of the two divisions is 1440 units.

Situation three: the strategy of Productive Division I: conducting market-based refined safety management; the strategy of Productive Division II: conducting market-based refined safety management only in the first year. Then the total benefit of Productive Division I is 653 units, and Productive Division II is 636 units. The total benefit of the two divisions is 1292 units.

Situation four: similar to situation three, the strategy of Productive Division I: conducting market-based refined safety management only in the first year; the strategy of Productive Division II: conducting market-based refined safety management. Then the total benefit of Productive Division I is 636 units, and Productive Division II is 653 units. The total benefit of the two divisions is 1292 units.

Situation five: the strategy of Productive Division II: conducting market-based refined safety management only in the first year, then from the second year that are similar to the first-year strategy of Productive Division I. the strategy of Productive Division I: no market-based refined safety management in the first year, then conducting market-based refined safety management in the third year to expect that Division II would carry out this management in the fourth year, after knowing and making sure that the Productive Division II imitated their first-year's method at the beginning of the third year. Then the total benefit of Productive Division I is 708 units as the same as Productive Division. The total benefit of the two divisions is 1416 units.

Situation six is opposite to the situation five.

The optimal solution: comparing such six situations, in long-term repeated game, the total revenues

Table 1. Long-term dynamic game analysis of market-based refined safety management (unit: million).

	Strategy	1	2	3	4	5	6	7	8	9	10	Sum	General Sum
Situation one	Productive Division I: no conduction in 10 years	64	64	64	64	64	64	64	64	64	64	640	1280
	Productive Division II: no conduction in 10 years	64	64	64	64	64	64	64	64	64	64	640	
Situation two	Productive Division I: conduction in 10 years	72	72	72	72	72	72	72	72	72	72	720	1440
	Productive Division II: conduction in 10 years	72	72	72	72	72	72	72	72	72	72	720	
Situation three	Productive Division I: no conduction in 10 years	80	64	64	64	64	64	64	64	64	64	656	1292
	Productive Division II: conduction in the first years	60	64	64	64	64	64	64	64	64	64	636	
Situation four	Productive Division I: conduction in the first years	60	64	64	64	64	64	64	64	64	64	636	1292
	Productive Division II: no conduction in 10 years	80	64	64	64	64	64	64	64	64	64	656	
Situation five	Productive Division I: no conduction in first two years	80	64	60	72	72	72	72	72	72	72	708	1416
	Productive Division II: no conduction in second, third years	60	64	80	72	72	72	72	72	72	72	708	
Situation six	Productive Division I: no conduction in second, third years	60	64	80	72	72	72	72	72	72	72	708	1416
	Productive Division II: no conduction in first two years	80	64	60	72	72	72	72	72	72	72	708	

are maximized as well as each division's revenue in Situation two, that is both divisions implement market-based refined safety management.

The second optimal solution: the situation five and situation six. One of the productive divisions (the rational one) conducts the market-based refined safety management in the first year, but the other one (the irrational one) does not; from the second year, the rational one conducts the first-year's strategy of the irrational one, then the irrational division adjusts its strategy to conduct market-based refined safety management in the third year for a long-term benefit.

What worth stating is that if the two divisions are both sensible, namely they both conduct market-based refined safety management in the first year, then the second optimal solution will turn to the optimal one.

4 CONCLUSIONS

In conclusion, the degree of market-based refined safety management within a coalmine enterprise has a direct ratio with the level of safety, and also relates to the benefit of an enterprise and divisions. At the beginning of market-based refined safety management, difficulty and resistance are huge because of the under-level Nash Equilibrium. Actually, the level of safety of divisions and economic benefit maintain at a lower level. After the compulsory execution, divisions will find that output is a little less, while benefit is more, which make a high-level balance come true. As for the static state in a short-term, it will influence the profit of divisions, but from a long-term dynamic state, it is best for the whole benefit of an enterprise.

ACKNOWLEDGEMENTS

This work was financially supported by the Basic Scientific Research Fund Project of Central Universities (No.: 3142013104). Meanwhile I appreciate Prof. Yan Ye, Prof. Liuwei and Prof. Wang Dan's help for this paper.

REFERENCES

Nash, John. Essays on Game Theory [M]. *Capital University of Economics and Trade Press*. 2000.

Weng, Yifei. Research on the Complexity of System Safety Management [J]. *Safety and Environmental Protection of Mining Industry*. Vol 35. 2 (2008): p. 78–80.

Progress in Mine Safety Science and Engineering II – He et al. (Eds)
© 2014 Taylor & Francis Group, London, ISBN 978-1-138-00122-0

Analysis on the factors' characteristics of coal miners' safety behavior based on trajectory crossing

Rong Ni
Jiangsu Jianzhu Institute, Xuzhou, Jiangsu, China

ABSTRACT: Miners unsafe behavior is due to human unsafe behavior and interaction of matter produced unsafe behavior. In this paper, the assignment method for column joint analysis of the questionnaire drawn: the safety of workers and trade unions act age, educational level, personality traits, work experience and their sense of safety has correlation with the risk of the work environment to develop codes of conduct and corporate science-related, propose appropriate measures to tackle the problem.

China's coal output in 2000 from 12.25 tons in 2012 increased to 36.5 tons, the annual coal output growth of 15.78%. But the coal output growth caused casualties occur frequently, the total coal production accounted for the world total 1/4, while the number of casualties is higher than the sum of the coal mine accident casualties other coal-producing country, the main reason is that human error.

Work has its special properties in coal mine production line workers, the subject they are productive activity, and is the main excitation accident. Personnel errors has become an important source of danger of accidents, on the one hand, it lies in internal factors, such as age, physical, physiological, psychological, their safety awareness effect; on the other hand it lies in the external factors of workers in the work, such as the environment, enterprises of staff supervision, the completeness of machinery and equipment effects of the above factors, induced to have accidents tend to internal factors, external factors, individual, forming a human behavior set beam. Therefore, prevention and reduction caused by "human" factors of accidents has become an important issue to be solved in coal mine enterprise.

1 LITERATURE REVIEW

Safety behavior science as applied branch of behavioral science, which is based on sociology, psychology, physiology and other disciplines. Through the analysis, pattern recognition, study on the influence of human factors and safety behavior, control human's behavior rule, application of discipline to achieve incentive safety behavior and inhibition of unsafe behavior (Li Jizu 2009). In recent years, research on safety behavior at home and abroad can be divided into 2 categories: one is from the theoretical research, mainly has: safety behavior of safety culture and management mode; unsafe behavior causes and prevention and control; correlation between safety psychology and safety behavior, and safety attitude, safety awareness, safety consciousness, safety climate on safety behavior; safety behavior model, intervention, evaluation, incentive, simulation(Tan Bo 2000–2010). On the other hand is the empirical study, the safety behavior science used in mine, reveal the unsafe behaviors and by correcting unsafe behaviors reduce the security accident way. These two kinds of research is mainly based on qualitative analysis, quantitative analysis of the lack of necessary connection between behavior and accidents, most of the literature belongs to nature.

2 THEORETICAL BASIS AND DATA ACQUISITION

2.1 *Theoretical basis*

Theoretical study leading causes of casualties have been one hundred years of history. With the development of productive forces, changes in production methods, production relations, as reflected in the existence of differences in security perceptions. More research scholars tend to study the accident causation studies, the occurrence of the accident was due to human factors and physical factors trajectory of the intersection of the accident is the intersection of time and space. Meanwhile, track crossover theory as accident causation theory, emphasizing the human factor and physical factors occupy the same important position. So, in order to effectively prevent accidents, people must also take measures to eliminate unsafe behaviors and material insecurity.

On the tracks cross the basic idea is (Huang Xinwen 2009): damage accident was caused by

interrelated events occurring in a certain order, these events took place two developments by people and objects series result of the formation. When a person's unsafe behavior and material insecurity in their development process (tracks), at a certain time and space had contact with (cross), the energy "upstream" in the body when injuries occur (Sergio Ley Lopez, et al. 2009).

This paper focuses on the study of human security awareness, self-control and other aspects of human behavior trajectory, from the work environment, the external aspects of the analyze disturbed behavior trajectories to analyze the most accident-prone populations.

2.2 *Data acquisition*

The main object of this research for the coal mine workers. This research adopts the overall sampling technology, drawing on the results and data of other industry, combining the characteristics of the coal mine production, through the questionnaire survey method, a more comprehensive survey from the aspects of respondents age, culture degree, underground work life, personality traits. Selection the sample can effectively reflect the overall situation. The statistical analysis method uses contingency analysis method to analyze the questionnaire results by using SPSS software.

3 ANALYSIS OF INTERNAL FACTORS OF COAL MINE WORKER SAFETY BEHAVIOR

Internal factors affecting the safety of workers and staff are reflected in the underground illegal behavior. It is a concrete manifestation of coal mine workers' self-management. As you can see from Figure 1, the incidence of unsafe behavior of most of the employees think it is deliberately risk-taking unconscious behavior and convenience.

Figure 3 describes the staff awareness of safety responsibility system and accept the safe education training. Nearly half of the people who think that they are equivalent in the management and improve the overall level of safety enterprise burden of responsibility, but also more than 1/4 employees that their responsibility is greater than managers, it has a strong sense of ownership of employees in the responsibility for security issues In the safety education and training, more than half of the people reflected to receive the accumulated 8 hours of safety education and training in a quarter, but there are also more than 1/3 of people reflect the cumulative received 8 hours of safety education and training needs 1 years or even 1 years, in the coal mine such high-risk industries,

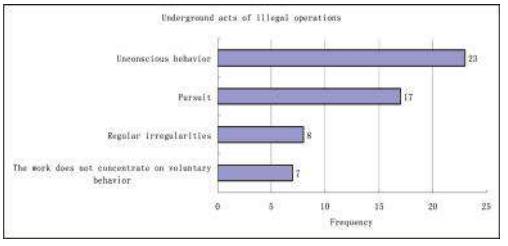


Figure 1. Workers underground illegal operation behavior distribution.

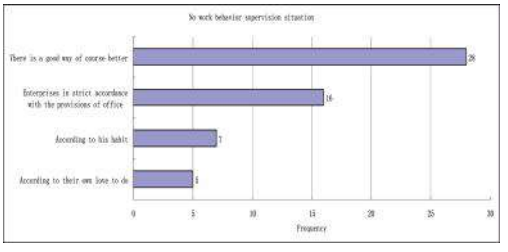
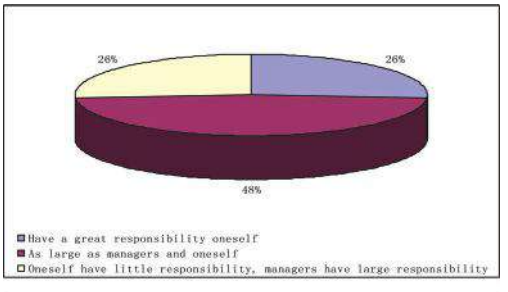


Figure 2. Does not work when the distribution behavior supervision.



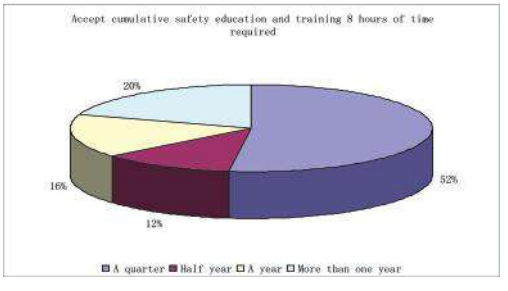


Figure 3. Security responsibility to the employee's safety education training intensity.

safety education activities should be incorporated into the normal management, from time to time, safety education and training, from the point of safety education and enhance the strength of the space.

4 ANALYSIS OF FACTORS INFLUENCING THE UNSAFE BEHAVIOR OF COAL MINE STAFF OUTSIDE

4.1 *Analysis of the influence of environmental factors on the workers' safety*

Different people in the same environment, the same people in different environments may have different responses to environmental factors, work method of this external from the working environment, the working state of the equipment, working effect, other leaders. These factors are the mine operators to produce certain effect, because of the existence of individual differences between man and man; different people face environment will respond differently, thus forms the operator behavior of coal mine underground uncertainty.

Figure 4 shows the results can be concluded, in the past 1 years underground workers is not a safe working environment for 44%, especially in number more than 5 accounted for 10%,. The proportion is not optimistic for the coal mine safety production and reflects the production process safety hidden large. Most of the staff that external factors affecting employee safety focus on the environment and the machine equipment, especially the environmental factors of insecurity, especially in underground work, working under the state of emergency, often appear abnormal psychology, wrong judgment is the main factor of safety accidents caused by the habitual unsafe behavior and speculative behavior.

4.2 *Analysis of outer interference of human factors on coal mine safety act*

It can be seen from Figure 5, when colleagues are illegal operations, no employees would have to pay no heed even associate oneself with undesirable elements, but to take certain measures to stop, take the initiative to stop a large proportion, which shows a security alert staff is very high, can take the initiative to avoid side safety hidden danger.

4.3 *Analysis of external factors on the relationship between coal mine worker safety behavior*

Questionnaire was designed in the 13 kinds of external environment and the safety of the coal mine worker behavior factors of respondents according to their own understanding on safety behavior factors influence extent size to choose, as shown in Table 1.

The degree of impact to judge according to the production staff safety behavior of external factors, to sort the influencing factors of the assignment scoring method. Greater influence gains 5 points.

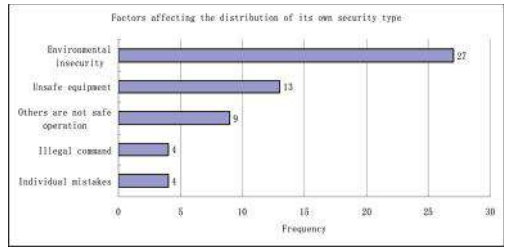


Figure 4. Effects of external factors on the distribution of worker safety.

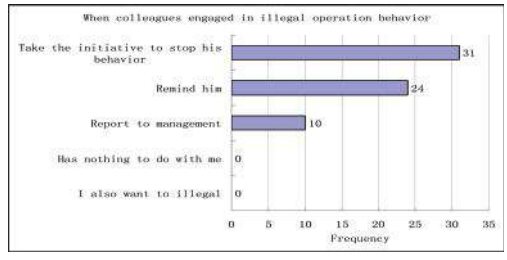


Figure 5. Colleagues violations of the distribution.

Great influence gains 4 points. Influence gains 3 points. A little effect gains 2 points. No effect gains 1 points, calculating the effect of comprehensive scoring average factor ranking as shown in the following Table 2.

In the sorted result, however, the risk of employee security awareness is most affected by work environment size, ventilation, lighting, temperature, noise and dust environmental indicators, such as enterprise behavior standards set by the three factors such as scientific, impact on the safety consciousness is the smallest safety publicity logo, family, neighborhood relations, managers of praise, praise three colleagues. Taken together, the dangers of working and environmental comfort will have great influence on the safety of the employees behavior, more focus in terms of working environment.

5 COUNTER MEASURES

5.1 *Improve the working environment and improve employee safety and reliability*

The coal mine environment, is the object and scope of employee activities. Staff not only is limited by space, lighting, air, etc, but also moments by coal dust, roof, gas, water and fire threat. Because

Table 1. The external environment influence factors on safety behavior survey results statistical table.

Influence factors	Greater influence	Great influence	Influence	Little influence	No influence
1) Good ventilation, lighting, temperature and suitable noise and dust pollution, the working environment.	35	6	4	3	2
2) Family, children education employment smoothly, no neighborhood disputes.	17	16	7	5	5
3) Safety posters, blackboard newspaper, security identification etc.	11	12	19	8	0
4) Punishment behavior incentive, safety violations.	21	18	8	2	1
5) Managers praise, colleagues admired	14	15	15	6	0
6) Whether the mutual love between colleagues, subordinates whether mutual trust.	19	21	5	3	2
7) All occur in the working process to inform.	27	12	8	3	0
8) Distribution of the enterprise production tasks is reasonable.	18	26	4	1	1
9) Norms enterprises to formulate reasonable.	25	17	6	2	0
10) Accepted the safety education and training.	18	21	7	4	0
11) Risk the size of the work environment.	30	13	7	0	0
12) Wage income level.	22	18	8	2	0
13) Before the class safety education and meeting	16	20	9	4	1

* Assignment according to the fuzzy evaluation method of the data in the table.

Table 2. Safety behavior influence factor score and sorting.

Influence factors	Composite scores
11) Risk the size of the work environment	4.46
1) Good ventilation, lighting, temperature and suitable noise and dust pollution, the working environment.	4.38
9) Norms enterprises to formulate	4.30
7) All occur in the working process to inform the 27.	4.26
12) Wage income level.	4.20
8) Distribution of the enterprise production tasks is reasonable.	4.18
4) Punishment behavior incentive, safety violations.	4.12
10) Accepted the safety education and training.	4.06
6) Whether the mutual love between colleagues, subordinates whether mutual trust.	4.04
13) Before the class safety education and meeting	3.92
5) Managers praise, colleagues admired	3.74
2) Family, children education employment smoothly, no neighborhood disputes.	3.70
3) Safety posters, blackboard newspaper, security identification etc.	3.52

* Assignment according to the fuzzy evaluation method of the data in the table.

modern technology methods are limited, it is not the change of the natural environment condition of accurately predict and control. Coal mining enterprises must strive to improve the working environment, constantly relying on scientific and technological progress, technical innovation, management innovation and system innovation, take the technological transformation of mine, ensure equipment, upgrade equipment, facilities, improve the reliability of production system, trying to eliminate and reduce the adverse incentives.

5.2 *Strengthen the humanistic care, create a harmonious working environment and reduce the accident rate*

Although employee security awareness in the family, neighborhood, and managers correlation is less

than other factors, however, from the aspects of the humanized management, content and methods to improve ideological and political work, adhere to heuristic education, starting from the care, love, respect for employees, that the violations may give oneself, the damage to others, family, enterprise, enhance the worker's ego to protect consciousness.

5.3 *Analysis of worker characteristics, targeted psychological counseling*

There are personality differences between person and person. Different people on the same kind of work have different adaptability, different work requires people with different personality traits. A character is careless person engaged in complex, delicate work, he will feel overwhelmed, making it feel mental fatigue; and let a person personality is composed of flexible in a monotonous, simple work, he may tell mood is low, and even produce rebellious attitude. In both cases, are prone to misuse, the lively, active, aggressive, careless of workers is not suitable for high risk work. Characteristics analysis is advantageous to the enterprise to the worker at the time of recruitment hiring employees as reference.

5.2 *Strengthen the site safety supervision, eliminate safety hidden trouble*

Miners working in underground coal mines safety supervision is an indispensable part of daily work, is also an important link to ensure safety in production. Therefore, the in mine safety supervision work must be done. Supervisory personnel deal with s in mine on danger signals in a timely manner, and monitor the miners' operation behavior, prevent the happening of the phenomenon of illegal operation.

REFERENCES

Huang Xinwen 2009. Based on theoretical analysis and cross-track interference. *Fall Accidents Security,* (2):45–47.

Li Jizu 2009. Safety behavior. *mechanical industry press*:1–5 (Beijing).

Sergio Ley Lopez, et al. 2009. From the "track crossover theory" coal mine safety accident causation and prevention. *Shan xi Coking Coal Science and Technology,* (1):71–73.

Tan Bo 2000–2010. Research progress and its safety behavior analysis. *China safety science journal* (Beijing).

This page intentionally left blank

Progress in Mine Safety Science and Engineering II – He et al. (Eds)
© 2014 Taylor & Francis Group, London, ISBN 978-1-138-00122-0

Human behavior classification and application in the field of work safety

Yuebing Zhang & Li Pan
North China Institute of Science and Technology, East Yanjiao, China

ABSTRACT: In order to address the inadequate understanding of safety behavior science research object—human behavior in the field of work safety, an in-depth analysis of the differences between safety behavior science and behavior science, and human error and human unsafe behavior is performed, which classifies the human behavior from initiative and passivity, the different stages and the depth of the behavior sense. The results show that, the control measures of different kinds of behavior in work safety production are different. The situated behavior should be stimulated or suppressed by the links between behavior and need. The lack of the knowledge-type unsafe behavior should be prevented through education and training. The decision-making unsafe behavior of incomplete information should be controlled through science and technology and effective means of information collection. The theoretical research has certain guiding significance to enterprises in their safety behavior management.

1 PREFACE

Human behavior is mainly the initial trigger hazard in work safety accidents (Zhang Yuebing 2011). Statistics show that, more than 80% of the accidents are caused by unsafe human behavior. At the same time, the employees behavior of actively participation in safety activities can effectively enhance the level of enterprise's safety culture (Cooper & Phillips 2004), therefore, research on work safety human behavior remains hot in safety management. Safety behavior science is the reflection of the main achievements of these studies, which has become a new subject in the field of safety science and technology. It not only absorbs and refers to the theories and methods of behavior science, but also inherits and carries forward the early research of safety behavior science. It also enriches the content and enlarges the connotation of behavior science (Luo Yun 2012). Safety behavior science is the science of analysis, forecast and control human behavior theory and method from the perspective of safety to study human and safety issues by using scientific methods, to reveal the principal of human behavior in a production environment (Liang Li 1997).

From the former researches, many theories of safety behavior science copy the knowledge and theory system of behavior science, lack deeper understanding of human behavior in work safety. Therefore, this paper will deeply study the differences between behavior science and safety behavior science, and through behavior classification, more deeply understand the research object of safety behavior science, namely, the human behavior in work safety.

2 SUMMARY OF BEHAVIOR SCIENCE AND SAFETY BEHAVIOR SCIENCE

Safety behavior science is an important branch of behavior science, which is the application of behavior science in the field of work safety, and is an applied science which is based on the science of physiology, psychology and sociology. It analyzes, recognizes and studies the factors and mode of influence in human safety behaviors, masters the rules of human behavior, and realizes driving safety behavior and restraining unsafe behavior. The theory of behavior science can be directly applied to the safety behavior science. It however has significant difference.

Generally, the Hawthorne experiment plays a foundational role in behavior science. The behavior science focuses on individual behavior, group behavior and organizational behavior. The dominant theory of the individual behavior needs theory, two-factor theory, expectancy theory, the mature theory and frustration theory. The group behavior theory is mainly group classification theory (the theory of how to establish the relation between persons), group conflict theory (the theory of causes and solution of conflict between peoples), as well as group pressure, group norm, group cohesion, group morale, group interpersonal

relationships and information communication. Dominant organizational behavior theory is leadership effectiveness theory. At present, the overseas study range of behavior science is very wide, including many social problems, such as the support of the elderly, socialization and crime of young people; the medium-sized enterprises and organization behavior problems, such as enterprise work safety problems, organization culture and so on; microcosmic personal behavior problems, such as drug addiction, the reason of the formation of chronic illness, the education and so on. Although the thinking and research of human from philosophical, historical, political, religious, legal aspects has long history, while the human behavior emerged only in the late nineteenth century and early twentieth century.

Unsafe behaviors in work safety have long been noted. The earliest research of unsafe behavior can be traced back to the 1919's Greenwood and Woods' accident proneness theory. Late on, the accident causation theories, such as Heinrich causal chain theory, Boulder causal chain theory, Surry's model and etc. are all associated with unsafe behaviors. But it is generally believed that the earliest proposed and the systematic study of the safety behavior science is British Gene Earnest and Jim Palmer, which in 1979 proposed the name Behavior Based Safety (BBS) (John Austin 2003). But in the subsequent developments, safety behavior science continued to absorb and learn from the theoretical achievements of other subjects, and made this subject richer. For example, the achievements of Human Reliability and Human Error of man-machine engineering and ergonomics, proposed behavior theory and countermeasure of controlling human error (Zhang Tong & Zhang Lichen 2003, Zhang Jingjing et al. 2003). From anthropology and sociology point of view, study on influence of social culture, enterprise culture on people's safety consciousness and behavior were conducted (Liu Feng et al. 2007, Liu Ying et al. 2008, Pousette et al. 2008, Wills et al. 2006, Quan Zhou et al. 2008). Based on system theory, all kinds of influence factors of safety behavior were considered, which referred to the research achievements of psychology, behavior science, the man-machine engineering and ergonomics, sociology, anthropology, physiology and etc., to study the performance shaping factor (PSF) of human safe behavior and unsafe behavior to determine what are the influence factors of safety behavior, and what are the impact of these factors on human behaviors (Jiang Yingjie et al. 2011, Sun Zhijiang et al. 2008). Generation of safety behavior science not only is the need of social practice, but also is the inevitable trend for the modern science to the integrated one (LI Jizu 2008).

As can be seen, the behavior science is general, while safety behavior science research in specific areas is specific.

3 HUMAN UNSAFE BEHAVIOR AND HUMAN ERROR

Human unsafe behavior was proposed in production practices. In the "enterprise employee casualties classification" (GB6446–1986), human unsafe behavior is defined as human error caused accidents. From the definition, firstly unsafe behavior is the human error, that is not in the correct and scientific methods to work; secondly has the possibility of leading to accidents. According to this definition, first of all, unsafe behavior aims at specific dangerous work environment and the direct hazards in it, otherwise there is no significance. For example, smoking in the environment with a flammable and explosive substances is unsafe behavior, while in an environment surrounded by cement, steel, and with good ventilation, smoking is not unsafe behavior; secondly, the unsafe behavior determination is restricted by the level of understanding. To be sure, there are a lot of human unsafe behaviors that are not recognized; finally, human unsafe behavior also has a relationship with the actor ability and the loss acceptable level of the accident. For example, for an old people skating is unsafe behavior, but for a young man is safe behavior. In short, unsafe behavior is a relative concept, which is the problem of understanding. It has no significance to talk about whether or not the behavior is the unsafe behavior without specific situation. Employees should try to reach an agreement in the scope definition of unsafe behavior.

In actual operation, the "three violation" behavior is often defines as unsafe behavior, namely, the relevant rules and regulations are the measure standards of whether or not a behavior is safe behavior, which requires reasonable enterprise rules and regulations. But in fact, restricted with the level of knowledge and experience, management system is difficult to be scientific, and even some scientific management system cannot work. Various rules and regulations can only ensure order optimization within the acceptable scope of the enterprise. It doesn't ensure that there is no accident when all employees act in accordance with the enterprise management system, but only can ensure the possibility of accidents dropping as low as possible. For example, in accordance with the rules high-altitude operation must fasten the safety belt, but the moving safety belt may fall.

Human reliability (HR) and human error (HE) are positive and negative name. The concept of human reliability is drawn from the product

reliability study, which considers that human behavior reliability exists as mechanical apparatus, i.e. it has statistic rules on weather a behavior can reach the target. While the human error is defined as the behavior occurring out of a predetermined range, or that human behavior results deviate from the prescribed target, and has a bad effect being human error. Therefore, we can name the possibility of human behavior without error as human reliability (ZHANG Jingjing et al. 2011).

Human unsafe behavior is a special term in the field of work safety, while human error is a term which has a certain relationship with work safety in the behavior science study. Some scholars equate them, but they have significant differences. Human error is a behavior which can't reach the fixed goal, but not always leads to accident. Only when the goal is a safety goal can human error draw equal sign with unsafe behavior. For example, when safety goal is avoiding collision, need to step on the brake and human error occurs, even step on the accelerator, and leads to accident. There are three kinds of goals in human behavior: safety goal, accident goal and non safety goal. Safety and accident goals are both closely related to work safety. Safety goal behaviors are actions taken to prevent some accidents. Accident goal behavior usually refers to the deliberate violation behavior, which is mainly due to the actor's lack of work safety knowledge or the information obtained is insufficient, which causes the actor not clear about the results of the action. No one is subjectively willing that the accident to take place. Non safety goal means that it has no matter with accident. For example, shooting behavior during the football match, whether the ball is shot into the goal, an accident will not happen.

4 HUMAN BEHAVIOR CLASSIFICATION IN WORK SAFETY

In work safety, human behaviors vary. Different kinds of behavior follow different mechanism. Different behavior also has large different effect on work safety. Therefore, it is necessary to study deeply and classify various behaviors.

4.1 *Classification according to the initiative and passivity of behavior*

Motowidlo and Scotter (Motow & Scotter 1994) proposed in 1994 that individual behavior was composed of task behavior and situational behavior, where task behavior emphasizes the passivity, that is, the individual must follow the conduct in the work, such as safety rules and safety operation procedures; situational behavior emphasizes the initiative, that is, the individual in the work is aware of participation, such as safety communication and discussion. In view of this, Cheyne et al. (Cheyne & Cox 1998) used 2 indexes of structural safety behavior and interaction safety behavior to express. Neal dan Griffin (Neal et al. 2000) further used 2 indexes of safety compliance and safety participation behavior to reveal the behavior safety performance of employees, that is, safety compliance behavior is the behavior where employees strictly abide by the rules and regulations, proceed in accordance with safety procedures, while safety participation behavior is the behavior where employees actively participate in safety at work, such as helping and supervising colleagues, putting forward safety views and suggestions to leadership, although it did not make a direct contribution to safety performance, but could promote the formation of good safety climate, which influences the safety consciousness and behavior motivation of individual.

The safety behavior classification mentioned above is distinguished from passivity and initiative of behavior. The author agrees with the classification name of task behavior and situational behavior more, but from Motowidlo and Scotter's explanation of these two kinds of behavior, this classification method is more suitable for the management and executive behavior, and decision-making behavior basically is the situational behavior. The author thinks that the task behavior is a series of action in order to accomplish the objectives of the organization, which is distributed by supervising authority and performed by subordinate agencies or personnel according to authority-responsibility relationship of organizational structure. These actions have direct relation with actor's wages and rewards, which can satisfy the human physiological needs. Situational behaviors are those that are not assigned by organization. The author thinks this also can be divided into two categories: one is the organization unwanted behavior, such as all kinds of illegal behavior, the behavior motivation is not from the needs of the individual to get paid to meet survival, but from the other physiological and psychological needs, such as laziness, fondness of the limelight, adventures, strong curiosity to save time or other subconscious behavior. We can call this situational behavior as negative situational behavior. The other one is the organization wanted behavior but fails to consider or can't require specifically, such as the scene disposal of some emergency, actively participating safety production behavior, safety recommendations, helping and supervising colleagues and so on, which are called positive situational behavior.

Constraining situational behavior is beyond the scope of enterprise management. Enterprises

should take corresponding measures to inhibit negative situation, to promote the positive scenario behavior according to the actor's need, such as constructing the concept of illegal is shameful, safety is a kind of ability.

4.2 *Classification according to the behavior stage*

According to the behavior stage, behavior can be divided into decision-making and execution behavior. Individuals are affected by physiological factors and surrounding environments, and produce different levels need. These needs produce motivation of the behavior which may meet the needs, after the treatment (the brain needs to extract the past experience and knowledge information) of different structure and function brain (according to the material, it determines consciousness, structure determines function, and individual psychology is outward manifestation of different brain structures). Need converting into motivation is an individual decision-making process, that is, the individual according to their knowledge, experience, ideas decide what behavior can meet the need, and then judge which of them is feasible according to the actual ambient situation and own ability, finally the individual behavior motivation is obtained. For example, for a task behavior of driving from A to B, firstly the actor is clear that finishing this task can meet the individual physiological, psychological needs. He knows it will meet the need to be respected that drive in the right in line with China's traffic rules, which also is driver's behavior rule.

In production, the accident is caused by the human execution behavior, which is caused by the existence of triggering energy and complete accident triggering chain (ZHANG Yuebing 2011). Therefore, most research on unsafe behavior is all about execution behavior. However, the decision-making behavior plays an essential role, namely, it decides the accident is inevitable due to the occurrence of decision error. The decision-making behavior here includes the decision-making behavior of the decision-making layer, management layer and execution layer, namely, some decision-making and execution behaviors are done by the same person. Work safety accidents often occur contrary to people's willingness, therefore, the main causes of unsafe behavior have only two: one is the lack of knowledge needed in decision making. Despite the safety needs, we do not know what kind of behavior can meet the safety needs, or do not know what kind of behavior can cause accidents. For example, in June 30, 2011, an arts and crafts plastic cork factory exploded in Yongqing Village Xingdong Town Tongzhou District, Nantong in Jiangsu Province, resulting in 4 deaths 11 injuries. The cause of the accident is the factory used a glue solvent evaporating a flammable and explosive gas, at the same time, the workshop was ventilated poorly, resulting in flammable and explosive gas thickness reaching the explosion limit, finally in case of fire explosion accident occurring, the accident was due to the lack of knowledge; the other is the decision-based information was incomplete. Because the information is not complete, therefore, whether a behavior will lead to accidents has a great chance and uncertainty, especially when a certain income appears. The decision-makers choose between the possible losses and certain income, and tend to choose the certain income. It must be pointed out that the certain income here is very relevant to the human concept. For example, if the enterprises set up the concept of adventure shameful, safety glorious, then safety behavior can be respected by other enterprise personnel, and risky operation will be spurned and looked down upon, so the respect after the safety operation is the certain income. Most of the time the workers' violation is intentional, and they also know the violation has risk, but still to do so, because lazy physiological need is the certain income. Therefore, unsafe decision-making behavior can be divided into lack of knowledge type of unsafe decision-making behavior and incomplete information type of decision-making unsafe behavior. In contrast, the lack of knowledge type of unsafe decision-making behavior is more harmful, because although in the incomplete information type of decision-making unsafe behavior the information is not complete, but the decision-makers know what accident may happen, and preliminary estimate the possibility. Strictly speaking, human decision-making behavior all are incomplete information decision-making behavior, only their degrees of incompleteness are different.

Execution behavior refers to the actor completing a variety of actions in accordance with certain procedures after the decision was made. These actions are the initial accident trigger energy (ZHANG Yuebing 2011). Accident is caused by execution behavior mainly because of human error, which has many causes, such as the brightness of light, whether the operation is consistent with the habits and so on. Especially for complex operation system, the possibility of human error is greater. A large amount of research in this has been done in ergonomics and man-machine engineering field.

4.3 *Classification according to the sense depth of behavior*

Not every behavior is deliberate as some behaviors may be carefully considered in brain, and some will consider less, even don't go through the brain, therefore, the safety behavior can be divided into

conscious behavior, subconscious behavior and unconscious behavior.

The actor's consciousness should be increased in the enterprises production, considering this behavior will have any risk before implementing it, how to avoid the risk, how serious the risk should be, and whether there is any remedy measures and so on, that is, to enhance safety consciousness of the enterprise employees. For example, workers with bad safety consciousness would put the broken glass replaced on the trash, but a strong safety consciousness worker will consider whether it will cut others.

The famous British psychologist Reason in his book "Human Error" (Reason 1990) thought that most of the human error is unintended, namely, caused by the negligence; some mistakes are intentional, which means the actor solves the problem according to a set of incorrect operation plan, but he believes that this is correct or is the better method. The vandalism is not considered. As can be seen, the former human error is because the people's attention resources are not concentrated on the behavior, the later is due to the actor's knowledge and experience or information obtained being not sufficient.

At the same time, we should see, human attention resources are limited, it is neither possible nor realistic to think about everything carefully. Therefore, enterprises should identify the various behaviors which often occur, especially dangerous behaviors, and then carefully research on these behaviors, formulate standard actions, and let everyone develop safety behavior habits as far as possible to save the attention resource, and focus on other actions. In addition, a large number of accidents in the same industry can be explained and publicized, in order to reduce mental labor of consciousness behavior. The thorough reason of deliberate violation behavior should be found out to effectively prevent it.

In addition to the above three kinds of classification methods, Rasmussen (1983) classified human behaviors into three types: skilled behavior, rule behavior and knowledge behavior. Skilled behavior only requires the operator to response subconsciously to system information; rule behavior is controlled by a set of rules or procedures, which needs the understanding on rules and procedures and the support of corresponding empirical; knowledge behavior occurs in the situation who is not clear of the present symptoms, target state conflict or fresh scene environment completely not encountered, the operator must carry on analysis and decision relying on their own knowledge and experience.

In addition, other scholars classify the human error types related to the safety production. The earliest was used in the THERP method, which divided into Commission and Omission. The former refers to tasks not completed, and the latter refers to tasks or steps omitted.

5 CONCLUSION

1. In recent years, safety behavior science has gradually become a hot topic in safety science research. Safety behavior science learned from many theories' achievements of behavior science. At the same time, safety behavior science researches on special field, that is, human behavior in the work safety field is more in favor of understanding of safety behavior science.
2. By studying the human behavior in safety production field, we can see that enterprise can do these to control human unsafe behavior: ① Incentive positive situational behavior and suppress negative situational behavior according to the human needs; ② Enhance the safety consciousness of all the people in the enterprise, for all kinds of behavior, consider more about what kind of danger exists, which accident might occur, how to prevent it and how to control and rescue after the accident occur and so on; ③ For consciousness behavior, establish the connection between safety behavior and esteem needs, social intercourse needs, and through publicizing and other means to strengthen this kind of needs; ④ Study those high risk, often occurring behavior, standardize these behavior, and through training, so that all the enterprise employees develop the right habits, or preach, analyze typical accident cases in the same industry, thus saving the attention resources in work safety; ⑤ Enhance scientificalness of decision behavior, strengthen learning and training of safety knowledge, strengthen the collection, management and use of safety information; ⑥ Improve the reliability of the execution behavior from human engineering and ergonomics; ⑦ Strengthen exercise of the skill behavior, improve the understanding of the rules behavior, and improve learning of knowledge behavior.

REFERENCES

Cheyne A, & Cox S 1998. Modeling safety climate in the prediction of levels of safety activity. Work and Stress, 12(3):255–271.

Cooper M.D., & Phillips R.A. 2004. Exploratory analysis of the safety climate and safety behavior relationship. Journal of Safety Research 35: 497–512.

Jiang Ying-jie, et al. 2011. Review of performance shaping factor analysis methods. China Safety Science Journal 7(1): 66–72.

John Austin 2006. An introduction to behavior-based safety. Stone, Sand & Gravel Review (2): 38–39.

Liang Li 1997. An approach to safety behavior science. China Safety Science Journal 7(2): 10–13.
Li Ji-zu 2009. Safety Behavior. Beijing: Mechanical Industry Press: 1–5
Liu Feng et al. 2007. The dynamical exploration on the organizing of safety culture——behavior based safety. Industrial Safety and Environmental Protection 33(4): 53–56.
Liu Ying et al. 2008. Construction mode for coalmine safety culture based on behavioral science. China Safety Science Journal(Cssj) 18(8): 62–67.
Luo Yun 2012. Safety Behavior Science. Beijing: BEHANG University Press: 3.
Motow S J, & Scotter J T 1994. Evidence that task performance should be distinguished from contextual performance. Journal of Applied Psychology 79(4):475–480.
Neal A, et al. 2000. The impact of organizational climate on safety climate and individual behavior. Safety Science, 34(1–3):99–109.
Pousette A, et al. 2008. Safety climate cross-validation, strength and prediction of safety behavior[Z]: 398–404.
Quan Zhou, et al. 2008. A method to identify strategies for the improvement of human safety behavior by considering safety climate and personal experience[Z]: 1406–1419.
Reason J 1990. Human Error. Cambridge: Cambridge University Press.
Sun Zhi-jiang, et al. 2008. Study on causation analysis method for human errors. China Safety Science Journal(Cssj) 18(6): 21–27.
Wills R A, et al. 2006. Comparing safety climate factors as predictors of work-related driving behavior. Journal of Safety Research 37: 375–383.
Zhang Jing-jing, et al. 2011. Analysis and study on human reliability. Journal of Safety Science and Technology 7(1): 76–81.
Zhang Tong, & Zhang Li-chen 2003. People S reliability and Man-made errors. Journal of Liaoning Institute of Technology on Social Science 5(3): 53–54.
Zhang Yue-bing et al. 2011. Theoretical research on hazards and it's application in accident prevention. China Safety Science Journal, 21(6): 10–16.

Progress in Mine Safety Science and Engineering II – He et al. (Eds)
© 2014 Taylor & Francis Group, London, ISBN 978-1-138-00122-0

Study on coal mine hazard information management system based on PDCA

Xiangwei Zou, Haihe Guan, Zhenjiang Yu, Zhiguo Guo & Zhiyan Zhao
School of Resources and Safety engineering, China University of Mining and Technology, Beijing, China

ABSTRACT: This article analyses the current status of safety production and hazard management in coal mine and also makes a lot of analysis on the advanced and effective management model at home and abroad from the perspective of the accident risk control. Therefore, combining with the concept of PDCA management model, it is reasonable to design a coal mine hazard closed-loop management system based on risk control management model. The system uses hazard information closed-loop management model as the main technical route. The process can be showed as "investigation—audit—rectification—review (feedback)—assessment". It does make mine hazard information management more systematic and standardized.

1 INTRODUCTION

With the rapid development of China's economy and the increasing demands for energy, the coal industry, which is mainly energy enterprise, occurs accidents frequently [Chen 2010]. It not only causes irreparable heavy casualties and economic losses, also makes more and more people pay attentions to its negative effects [Tan et al 2011]. Due to defects of the poor work conditions of coal mine underground, weak safety consciousness of staff, long production period and so on, it makes that the mine hazard information cannot be timely and accurately investigated and handled [Yang & Yu 2003]. A lot of researches suggest that the fundamental cause of frequent accidents in coal mine is "extensive" management of coal mine hazard information. Due to staff's negligence, weak security awareness, poor binding management and other reasons, this management model easily leads to an untimely and ineffective treatment of some important risk information, eventually resulting in an accident. Therefore, in order to improve this neglect and passive management mode and strengthen automation, accuracy and celerity of the hazard information management to achieve purposes of coal mine production safety risk control [Cai & Ma 2004]. It is necessary to establish a hazard information closed-loop management system with the function of convenience, practicality, security, scalability and advancement to achieve the transformation from "extensive" management to "information" management model [Yao et al 2011].

2 THE MANAGEMENT PROCESS OF PDCA MODEL

The PDCA circulation method is firstly put forward by Deming, a American management expert. It is a currently widely used management model in the implementation of safety management process in the industries [Zhang & Cui 2002]. Its management model is showed in Figure 1.

3 DESIGN OF INFORMATION MANAGEMENT SYSTEM

3.1 *Objectives and functions of information management systems*

The design of system treats the risk control as the core, using the PDCA management model to establish a more perfect and more specific hazard closed-loop information management system. It implements closed-loop management to different operating processes. The main function of the system is to achieve a unified process management to the unsafe behaviors and unsafe states and environmental factors in the production through the software platform after the reclassified of traditional hazard category division.

3.2 *Database design*

The main functions that the whole system needs have been defined through a lot of demand analy-

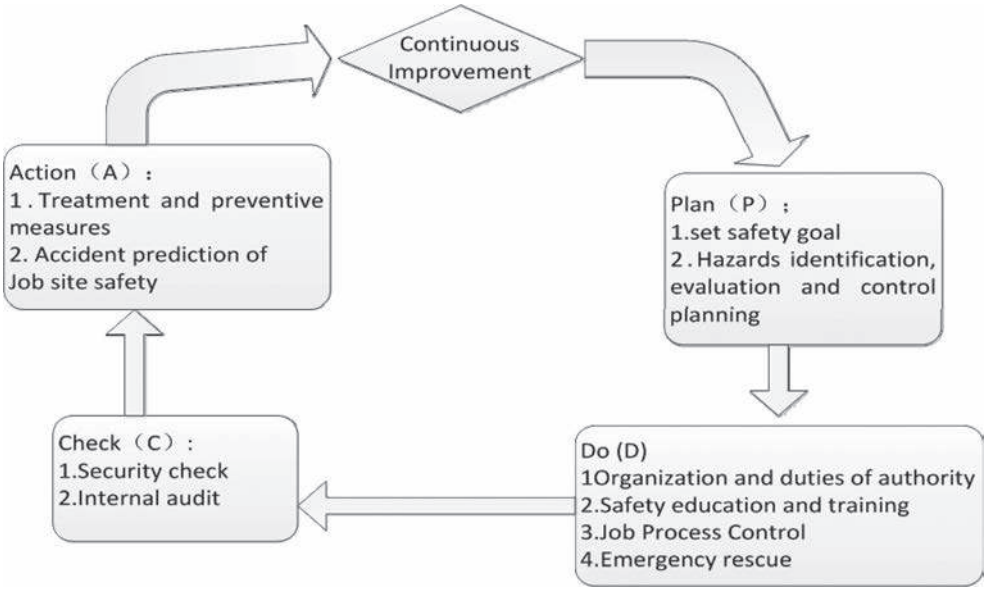


Figure 1. PDCA model management process [Wang 2012].

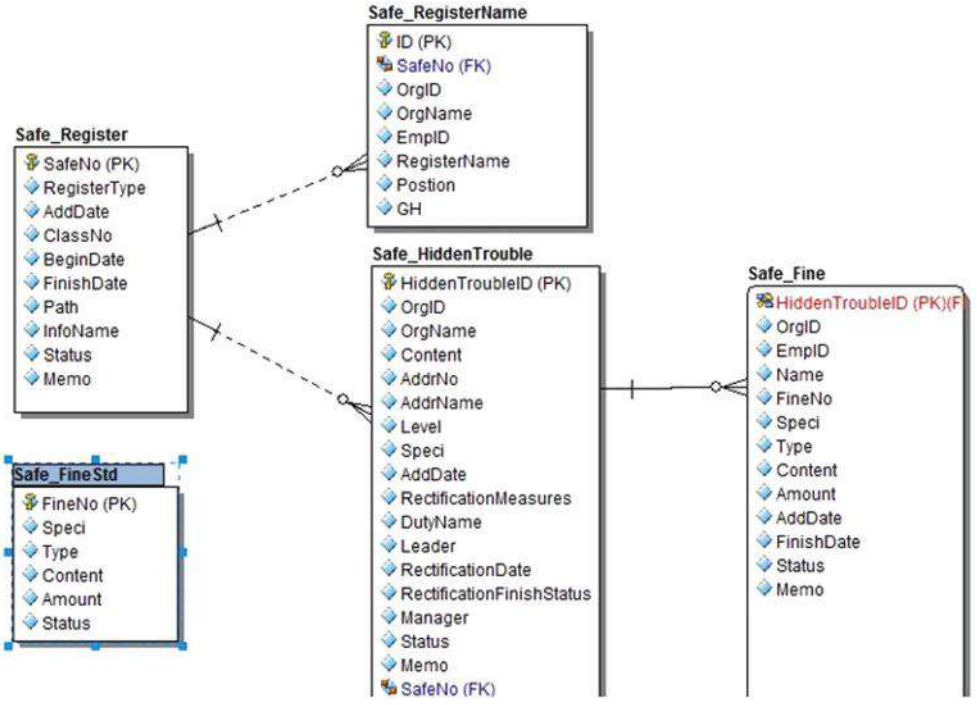


Figure 2. Data table logical chart.

sis. Then database of the information system need to be designed carefully. The system chooses SQL Server 2008 enterprise with the best integrated performance on the. net platform to design database. The main data tables and their logical relationship are shown in Figure 2.

4 DESIGN AND DEVELOPMENT OF THE CLOSED-LOOP HAZARD MANAGEMENT PROCESS

4.1 *Design of the whole structure*

After the analysis of the existing problems of hazard governance processes in apricot Mine of Jixi Mining Bureau, it constructs a hazard information closed-loop management structure, and this structure is mainly composed by hazard investigation processes, hazard rectification process and the audit process. Each of these processes implements the hazard information closed-loop management in accordance with the PDCA management model, just like 'plan—implementation—audit—feedback (processing)'. It makes each process nose to tail, realizing the PDCA closed-loop process management to the hazard information of the whole system. The overall structure design of the system is shown in Figure 3.

4.2 *The implement of the main functions*

4.2.1 *Hazard information input*

The closed-loop management process of inputting hazard information is showed in Figure 4. Among them, the all underground staff can report the specific hazard information to the information station. Then the information station centralizes and records the hazard information which will be audited by the safety supervision department. The audit mainly includes hazard content, responsibility, the responsible units, the amount of fines, etc.

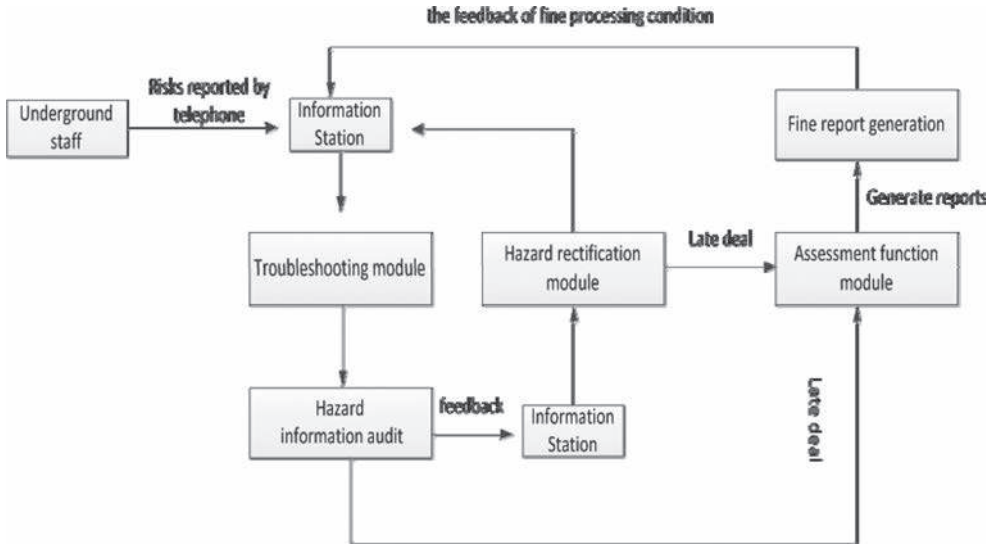


Figure 3. The process of the whole structure.

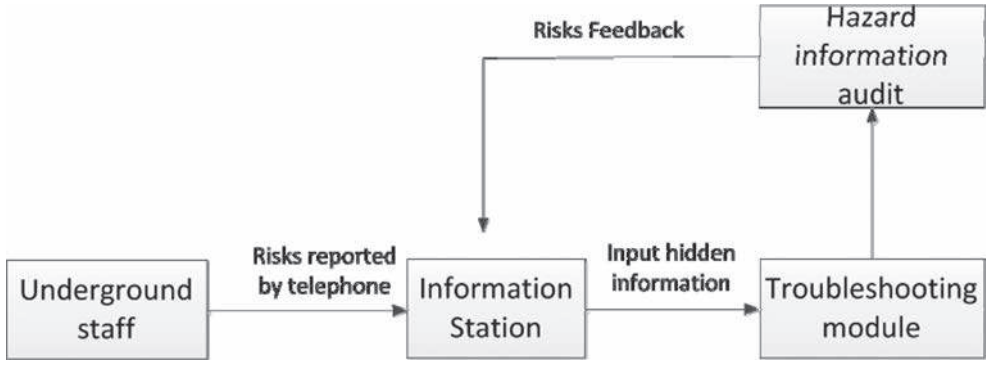


Figure 4. The process of the hazard information input.

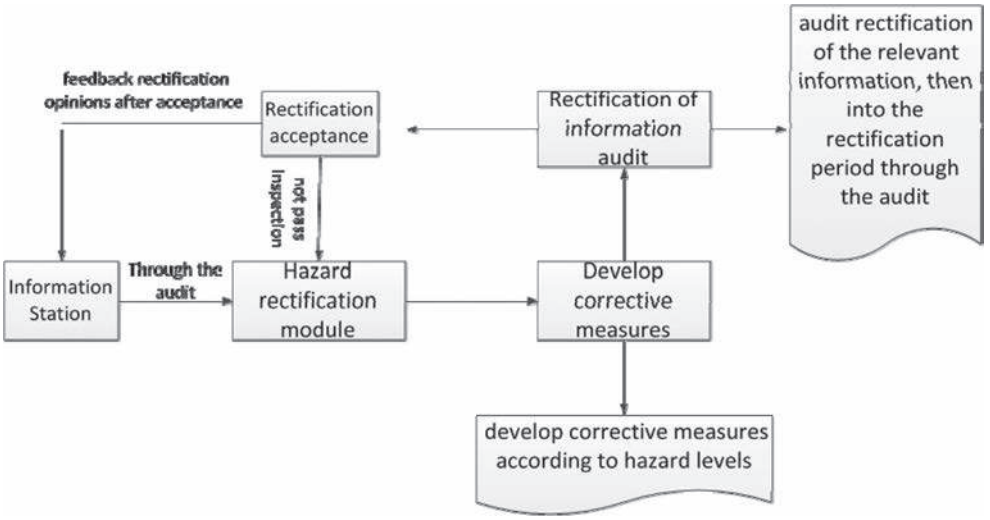


Figure 5. The process of the hazard rectification.

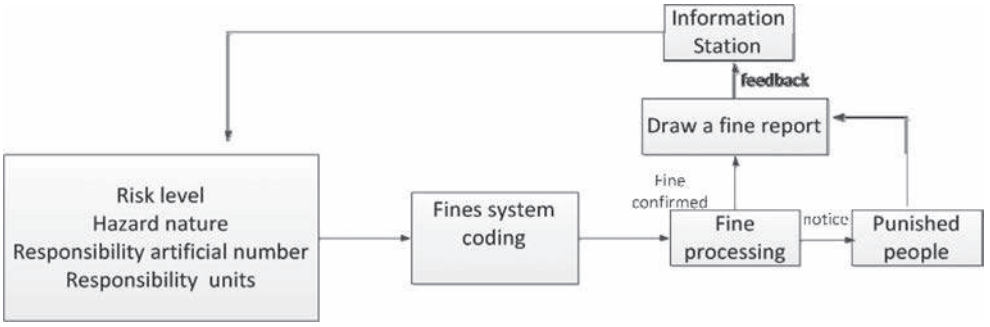


Figure 6. The process of the assessment.

The results will be feedback to the information station after the audit.

4.2.2 *Hazard rectification*

The hazard information will enter the closed-loop management of the hazard rectification, which is showed in Figure 5 after passing the audit. The man in charge of the hazard needs to take corrective actions according to the hazard levels. A and B grade need to be audited by mine or more senior leaderships. After passing the audit, the rectification should be completed within the deadline, and be applied for acceptance. Hazard is required to continue to reform unless the hazard rectification passes the acceptance.

4.2.3 *Assessment*

Once hazard information is input completely, it has already identified the amount of the fines, the responsibility, responsibility units and so on. The status without rectifications in limit time will enter the assess process, namely the fine process. The process of the assessment is showed in Figure 6

5 CONCLUSION

The PDCA management model is applied to coal mine hazard information closed-loop management system. It will implement the closed-loop hazard information management according to the science program of plan-do—check-action, in the meanwhile, it increases the work of information audit and feedback about the hazard information input, the hazard rectification, assessment and other information. It makes various processes closely linked and hazard information timely and effective

controlled, which can reduce the incidence of the accident.

REFERENCES

Cai, W & Ma, S.Q. 2004. Present situation and Countermeasures of the Coal Safety Management in our Country. *Coal Science and Technology*, 32(12):74–76. (In Chinese).

Chen, X.L. 2010. Research of Quantization Management Information of Hidden Danger of Coal Mine. *Industry and Mine Automation*, (12) (In Chinese).

Tan, B, et al. 2011. Establishment and Operation of Detection and Control Closed Loop Model for Mine Hidden Dangers. *Coal Engineering*, (1) (In Chinese).

Wang, Y.R. 2012. Study on Coal Mine Safety Management Information System Based on Risk Control. *Electrical and automation technology*, (In Chinese).

Yang, D.M & Yu, B. 2003. Study on State and characteristics of the State-owned Coal Mine Safety Production. *Coal Science and Technology*, 31(9):38–39. (In Chinese).

Yao, Y, et al. 2011. Design and Implementation of Mine Safety Hazard Information Management System. *Information Technology*, (6):217–218.(In Chinese).

Zhang, J.L & Cui, G.Z. 2002. *Safety System Engineering*. Beijing: China Coal Industry Publishing House, (In Chinese).

This page intentionally left blank

Progress in Mine Safety Science and Engineering II – He et al. (Eds)
© 2014 Taylor & Francis Group, London, ISBN 978-1-138-00122-0

Application of optimized decision-making system in coal mine hidden dangers information management

Shuang-Yue Liu, Ming Zhu & Li Peng
Civil and Environmental Engineering School, University of Science and Technology Beijing, Beijing, China

ABSTRACT: Hidden danger is the main reason for the coal mine accidents. Dealing with hidden information effectively is the key to safety. After analyzing 3 years' hidden danger data of one coal mine in China, I propose three optimization scheme—"control the cooperative hidden dangers", "person liable will be held accountable when frequently hidden dangers or serious hidden dangers are checked out", "establish the standard hidden danger table"—based on the existing management information system. Establishing decision-making system based on knowledge base and database, with the three optimization scheme, the system has made significant effect in practical work.

Keywords: hidden danger; MIS; optimized decision-making system

1 INTRODUCTION

With the in-depth understanding of the hidden danger and the expansion of the mining region, the measures which just change paper records to system information can no longer suit the coal mines' need. So, it is necessary to establish an optimized decision-making system by collecting and analyzing the historical information on the basis of traditional MIS (Shi et al. 2005).

2 MAIN RESEARCH CONTENTS

2.1 *Classification and categorization of hidden danger information*

Hidden danger can be classified according to seven types of work: coal mining, coal digging, rock excavation, electromechanical, transportation, ventilation and prevention and control of water. Though different coal mining enterprises classify the level of hidden dangers in different ways (Wu 2003, Liu 2008, Zhao et al. 2012), we can divide hidden danger into two categories—general danger and serious danger—according to the corrective ability of coal mine and the consequences of the hidden danger. In principle, general hidden danger should be treated by section itself; when a great hidden danger checked out, it should be reported to company level security department quickly, defined person liable and formulated rectification measures by mine grade leadership. The company safety supervision department is responsible for the inspection, and report to the governance about the situation at last (Hu & Zhang 2013, Chen 2012).

2.2 *Analysis on cooperative hidden danger information*

Based on the analysis of coal mine accidents in recent years, I find a situation that there were always two or more than two hidden dangers cooperated to cause each accident which should pay more attention in daily Investigation work (Liu 2005). When hidden danger information is found and reported, we should consider whether there are any other hidden danger exist to cooperate with the former one to make accident happen.

Therefore, based on the historical accident, I build the initial cooperative hidden danger table, and fit into the process of the hidden danger management. The main building steps are as follows:

Preliminary analysis and information classification: according to the coal mine accidents in China, summarize and classify the historical information, establish reasonable headers in the table, do matting for next step;

Establish the initial table according to the actual situation: To search and analyze related domestic cases depending on the own geographical location, the ways of mining, environment, etc factors, establish suitable table supported by those data.

Long-term accumulate and enrich the table: the cooperative hidden danger table shouldn't be static, it's item will be deleted, revised and supplied with the change of system, laws and regulations, facilities, technology and other factors.

2.3 *Standard hidden danger table*

Standard hidden danger table is of important guiding significance to the activity of removing the hidden dangers in coal mine. it is one of the core table of the knowledge database, can greatly reduces the input personnel's input time, provides re-commending measures for each kind of person liable, and so on (Xie & Lu 2009).

Before establishing the data table, we should collect the following data:

Domestic and foreign related laws, regulations, rules, norms, standards and other requirements
Other professional disciplines, superior instructions, and other rules
The enterprise internal rules and regulations, operation procedures, safety technical measures and other related information
Enterprise notice of the hidden danger in the past three years
Other relevant information

The specific method to establish the standard database is to set clear objectives about which kind of information is necessary and make the information collection table first. And then according to China's coal mine relevant laws, rules and mining company's internal rules, organizing experts to read and split the laws and rules, list the hidden danger information involved and make accurate descriptions, after that step, Summarize the information and merger similar items and increase or decrease the head of table according to the need.

2.4 *Educational punish when two kinds of information occur*

After sorting and analyzing the hidden danger information from 2010 to 2012, I find the information can be divided into three kinds (Wang et al. 2010): accidental general hidden danger (A); frequent hidden danger (B); serious hidden dangers (C).

According to the distribution of hidden danger information, I give the following definition to that three kinds: A refers to the hidden dangers which were checked out no more than 3 times in 1 years; B refers to the hidden dangers which were checked out more than 3 times at the same area or equipment in 1 years; C refers to the hidden dangers which may result in serious personal casualty accidents or major economic damage.

After sorting out the three years' information, I found that A accounted for the largest proportion, B and C are rarely. But we must not only timely govern the two kinds of hidden danger but also call three kinds of people (Li et al. 2012) liable to account for the dangers' occurrence because of the serious consequences the danger may lead to. The specific process of three kinds of person liable is as shown in Figure 1.

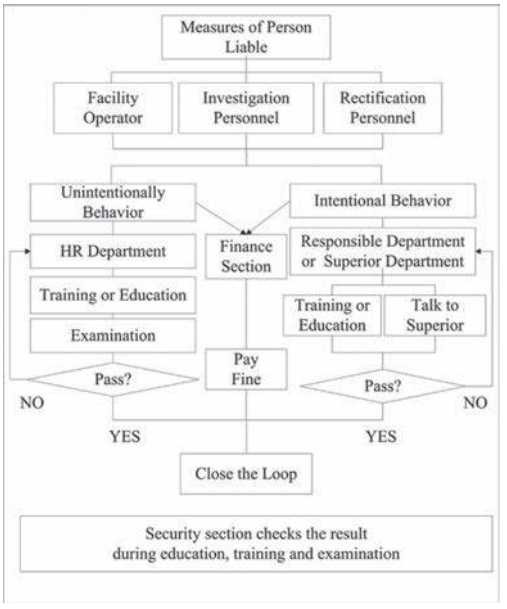


Figure 1. Accountability process for frequent hidden danger or serious hidden dangers.

3 DATABASE'S ESTABLISHMENT AND THE APPLICATION OF THE SYSTEM IN PRACTICAL WORK

3.1 *Database's establishment*

According to the research contents above, establish the decision-making database, the membership tables and their functions are as follows:

Personnel information table: records basic information, responsible region and responsible facility of personnel, the table is a convenience to manage staff permissions and do the accountability processing
Eliminated hidden danger table: records the historical eliminated information and could be used to judge whether the hidden danger belongs to "frequent hidden danger".
Cooperative hidden danger table: Records the cooperative hidden dangers which caused accident through cooperation in the past.
Standard hidden danger table: Records the hidden dangers' related information, standardizes descriptions. Standard information would be provided in the hidden danger management process.

Other tables: such as department table, Laws and regulations table and so on, these tables are used to maintenance the other membership in the decision-making database and convenient for human-machine interaction.

3.2 *System flow and its description*

As shown in the Figure 2, decision-making database participates in the whole process of hidden danger management, system is mainly divided into four modules (Li et al. 2010) on the basis of hidden danger's Closed-Loop management: Information input, rectification, acceptance check, information elimination (Tan et al. 2010).

According to above research result, I designed the system flow chart, realize the closed-loop management from "information reported" to "information eliminated".

Information input: When a hidden danger is found, input person should check whether there is a standard information which has been recorded already by comparing the information with the "standard hidden danger table", if "yes", system will insert the standard information into rectification notices itself; if "no", input person should entry the relevant information manually. Then judge whether there are any hidden dangers may exist to cooperate with the reported one to cause accidents by comparing with the key word in the "cooperative hidden danger table", if "yes", related department should organize targeted investigation, if the cooperated danger is checked up, the level of related hidden danger information rises to "serious hidden danger". Since then, this step finishes, system sends the relative information to the specified rectification people via SMS, email and system platform (Zhao et al. 2010).

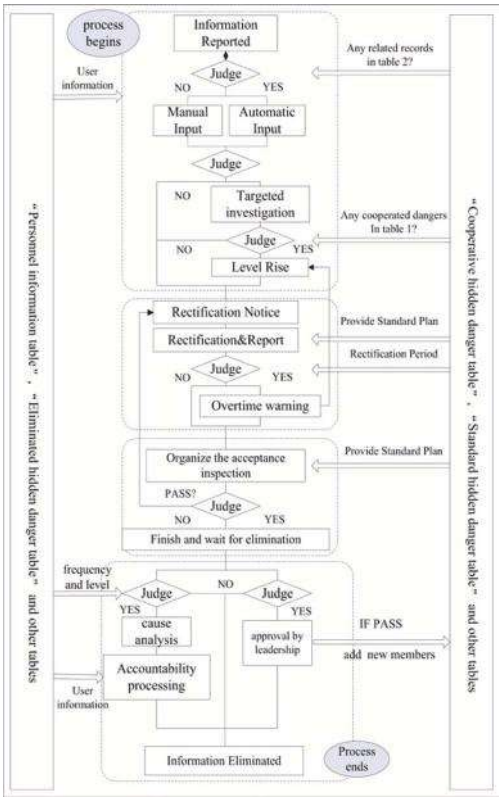


Figure 2. Main workflow of optimized decision-making system.
Notes: "Table 1" is the "cooperative hidden danger table"; "Table 2" is the "standard hidden danger table".

Rectification: When specified rectification people receive the information, they can work by the guidance of "standard hidden danger table" which can provide them standard plan and other information. Rectification people shall submit an application for acceptance check within the specified time, if the difficulty is too much for specified rectification people, they should report it to the high level department for processing.

Acceptance check: similarly, "standard hidden danger table"—if there are any relative records in it—provides inspection standards for factor checkers. The danger information will be submitted and wait to be eliminated if the rectification result is qualified, or it would be returned for a second time rectification.

Information elimination: Firstly, eliminate personnel judge whether the information belong to "frequent hidden danger" or "serious hidden dangers", if so, the relevant departments need to give educational punishments to the person liable according to the flow chart. Secondly, they should judge whether the information could be inserted into the "standard hidden danger table" or "cooperate hidden danger table", if so and approved by mine grade leadership, elimination personnel should add that information to the table(s). Finally, hidden danger information is eliminated and added to the "elimination hidden danger information table", the whole process ends.

4 CONCLUSION

The optimized decision-making system is established on the basis of the research above, and it makes great achievement in practice work:

Hidden danger information can be transferred to the responsibility accurately and timely.
Introduce optimized educational punishment which enhance personnel's safety awareness

Greatly reduce the time of information input, rectification information report and other human-computer interaction with the growth of decision-making database.

Provide standard information which can enhance the efficiency of hidden danger management.

REFERENCES

Chen Xin. 2012. Study on the interactive cultural support system of harmony and integrityculture of Shandong province tianchen coal mine. Shangdong: Shandong University of Science and Technology.

Hu Zhen-feng & Zhang Rui-xin. 2013. Research and Realization of Coal Mine Hidden Danger Management Information System. *Coal Engineering* 2013(2):132–134.

Liu Dong-dong. 2008 Research on the Standard of Management System of Hidden Safety Danger in Production in Our Country Industrial Enterprise. Harbin: Harbin Engineering University.

Liu Guan-xue. 2005. Case Analysis of Gas Meter Explosion. *Mining Safety & Environmental Protection* 34(4):78–82.

Li Xian-gong, Song Xue-feng & Meng Xian-fei. 2010. Study on Prevention and Control of Coal Mine Safety Risk and Design of Hidden Danger Closing Management Information System. *China. Safety Science Journal* 20(7):89–95.

Li Xin, Liu Shuang-yue & Liang Yu-xia, et al. 2012. *Journal of Safety Science and Technology* 8(5):188–193.

Tan Bin, Fu Yu-lu & Cao Qing-ren. 2011 Establishment and Operation of Detection and Control Closed Loop Model for Mine Hidden Dangers. *Coal Engineering* (1):126–128.

Shi Jian-jiang, Wang Li-juan & Zhangmudi, et al. 2005. Design and Realization of the Safety Management Information System in Huaibei Mining Group. *Industry and Mine Automation* z1:166–168.

Wang Yi—gong, Cao Qing-gui & Zhang Hua, et al. 2010 Study on Dynamic Control Technology in the Safe Objectives Management of Coal Mine. *China Mining Magazine* 19(9):46–49.

Wu Chang-jun. 2003. Contemporary Safety Management Methods in Coal Enterprise. *Safety in Coal Mines* 34(9):51–53.

Xie Xue & Lu Pin. 2009. Application of Feedback Control Theory in Safety Risk Management. *Industrial Safety And Environmental Protection* 35(10):58–59.

Zhao Dong, Shen Yu-qi & Zhao Zhi-qiang, et al. 2012. Risk Classification Method for Accident Potential Based on Development and Control Measures of Accident. *China Safety Science Journal* 22(4):71–76.

Zhao Zuopeng, Yin Zhi-min & Chen Jin-cui, et al. 2010. Application of Cooperation Software Technology to Mine Hidden Danger Prevent and Prediction System. *Coal Engineering* (5):115–117.

Progress in Mine Safety Science and Engineering II – He et al. (Eds)
© 2014 Taylor & Francis Group, London, ISBN 978-1-138-00122-0

Systems thinking theory in the safety production management system construction

Hao Liu & Xin-Ling Wang
School of Management, North China Institute of Science and Technology, Beijing, China

ABSTRACT: In recent years, China's coalmines have stably improved safety production, but coalmines safety production has not been fundamentally improved. One of the most important and direct reason for this problem is that the current coalmines safety production management system was not designed and optimized from the point of view of systems thinking so that coalmines safety production management system has large defect. The coalmines safety production management system based on systems thinking theory, as the starting point to the safety objectives, is broken down into five subsystems according to the entire process of safety production management. The five subsystems include safety objectives subsystem, safety support subsystem, safeguard subsystem, safety prevention and control subsystem and safety operation subsystem. The five sub-systems, both inter-conditional upon each other and support each other, and then together form an organic whole. This system can improve the safety production management of systematic, standardized and scientific level.

1 INTRODUCTION

The development of coalmines safety, no coalmines safety production accidents related to comprehensively implement the scientific outlook on development, related to the building of a harmonious society, related to the health of the coal industry in sustainable development and energy security of the country. In recent years, governments at all levels and enterprises attached great importance to the coal mine production safety work, took a variety of substantive initiatives, such as strengthened the coal mine production safety external supervision, increased coal mine safety production inputs, implemented a variety of safety production management, and so on. Needless to say, (Lewis MS & Alford JR. 1980) these measures promoted the steady improvement of the national coal mine safety production, all types of accidents had been some control, one million tons mortality showed a downward trend. However, China's coal mine safety production situation is still grim, did not fundamentally curb coal mine accident-prone momentum. This was reflected in: first, the total coal mine accidents is relatively large; second, one million tons mortality is relatively high compared with developed countries; third, major accident of the mine has not been fully effective containment. The reasons for this are many, one of the most important, the most direct cause is that coal mine safety production management system there are significant shortcomings.

2 THE MAIN PROBLEMS OF THE COAL MINE SAFETY PRODUCTION MANAGEMENT SYSTEM

2.1 *Less comprehensive*

Existing coal mine safety production management system did not look at the coal mine safety production management issues from a global perspective, (Liu ZX et al. 2007) the work and activities related to production safety have not been able to organically linked, not put forward a comprehensive system of coal mine safety production management solutions.

2.2 *One poor*

Existing coal mine safety production management system on security issues to talk about security, not out of the management of production safety, (Zhang SD & Yu CW. 2008) safety production management was not with the production process, management processes organically integrated.

2.3 *Poor operability*

Existing coal mine safety production management system focused on a theoretical level, (Andrew Hopkins 1999) focused on the structures of the framework, the lack of safety production management system implemented in the production process, every aspect of the management process, methods, procedures, initiatives.

Therefore, in the coal mining enterprises to establish a systematic safety management system is an important guarantee for improving coal mine safety production management level and coal mine safety production of sustainable development.

3 SYSTEMS THINKING THEORY GUIDANCE FOR THE CONSTRUCTION OF COAL MINE SAFETY PRODUCTION MANAGEMENT SYSTEM

The reason why the majority of our coal mine safety production management system is a fragmented, incomplete system, the most fundamental reason is the American management expert Peter M. Senge said, is that there is no way of systems thinking, instead of using way of fragment and the local thinking.

(Forrester, J.W. 1994) Peter M. Senge, human society entered the industrial revolution, the deepening of the degree of specialization, intensification of social differentiation, contributed to the fragmentation of the human thinking way.

When we are faced with a complex problem, always used to be divided into pieces that can simply to think, and then be integrated. This first division then combined way of thinking is the mainstream of modern human way of thinking, this way of thinking for many complex tasks is very appropriate, because it can complete a complex task.

Yet on the other hand, divided thinking artificially divided the overall system into many parts, and to focus too much attention to every part of them, ignored the overall thinking, lost the overall sense of unity, the loss of insight into the formation of the system of interaction between the elements and the formation of complex phenomena.

(Senge, P.M. 1990) The divided thinking would be tempted to an individual or organization forest for the trees and evasive, and even strive to manufacture even more erroneous results. The divided thinking r often makes people to unable to explore the enormous power of system structure functioning in the deep and behind the problem, while this forces will destroy the people's efforts. Based on divided thinking hazards, Peter M. Senge proposed the systems thinking theory.

Excellence of the systems thinking is that it has always focused on exploring the overall and long-term solutions of the complex issues. Systems thinking is that looks at the essence of the problem, looks at the cyclic causal interaction of whole system, rather than a linear causal relationship, breaking the linear thinking and its reactive derivative action.

Systems thinking theory is that all factors of the system, though not the same and seemingly independent, but in fact they are closely related to each factor, links and interacting, but these effects are usually hidden and not easily perceived. Only the system as a whole, rather than any single part of the system, to think deeply, we can be able to understand the whole system.

Systems thinking allows us to see the interrelated factors rather than a single, see the situation gradually changes rather than the immediate short term, can help us understand the whole changing shape, learn how to effectively grasp the changes, made countermeasures. Systematic thinking is "see the whole" of a Discipline.

Coal mine safety production management system is a system, each factor and link in the system are also closely related to each other, implicated interact with each other, of course, the effect of some factors often after several months and years before completely reveal.

Currently the design of coal mine safety production management system are mostly carried out from different sides, (Lee T.R. 1996) that is the complete system was artificially divided, but divided thinking was used to some parts of the system, which would bring the pieces reflect on the serious consequences, although some consequences would not be immediately apparent, but once obviously apparent, the consequences of the problem was often serious, irreversible. Therefore, coal mine safety production management system must be theoretical guidance for the use of systems thinking to establish a scientific and systematic coal mine safety production management system.

4 DESIGN AND OPTIMIZATION OF FRAMEWORK FOR COAL MINE SAFETY PRODUCTION MANAGEMENT SYSTEM BASED ON SYSTEMS THINKING

The traditional coal mine safety production management system defects in systems thinking theory as a guide, a comprehensive summary analysis, extensive research, based on the characteristics of coal mine safety production management, combined with the status of coal mine safety production management and business practice, I believe that, coal mine production safety management system should be five aspects of the design and optimization.

4.1 *General structure of coal mine safety production management system*

The starting point of departure of coal mine safety production management system design point of departure should be to establish a science

safety objectives subsystem. As the starting point to the safety objectives subsystem, the coal mine safety production management system includes safety objectives subsystem, safety support subsystem, safeguard subsystem, safety prevention and control subsystem and safety operation subsystem according to the entire process of safety production management. (Liu YJ et al. 2007) The five subsystems in the coal mine safety production management system, both inter-conditional and support each other, and thus together form an organic whole, constitute the general structure of total safety production management system, shown in Figure 1.

The five subsystems of coal mine safety production management system, each subsystem includes the related elements, the various elements of each subsystem mutual support, mutual cooperation, together form a relatively independent subsystems structure.

4.2 *The specific content of five sub-systems*

4.2.1 *The safety objectives subsystem*

The safety objectives are both a sub-system, but also is an independent factor. The safety objectives are to guide safety production management system and the end result. The main contents include safety objectives system, safety objectives management operation mechanism, the safety objectives system assessment mechanism.

4.2.2 *The safety support subsystem*

The safety support subsystem is the basis of safety production management system. Its content includes safety theory, safety culture, safety qualities, safety responsibilities, safety rules five elements. The main contents of safety theory include: safety theory study mechanisms, safety theory research mechanisms, safety theory application platform. The main contents of Safety culture include: safety objectives vision, safety concept, safety rules, safety environment and safety behavior. The main contents of safety qualities include: the safety qualities of education and training of staff, the safety qualities safeguard of education and training of staff, the safety qualities incentives of education and training of staff, innovation of safety education and training methods and means, rules of safety qualities and other aspects of the safety qualities subsystem. The main contents of the safety responsibilities are: job safety accountability, promotion and implementation of safety responsibilities and safety accountability assessment. The main contents of safety rules include: the preparation of safety rules and improvement of safety rules system.

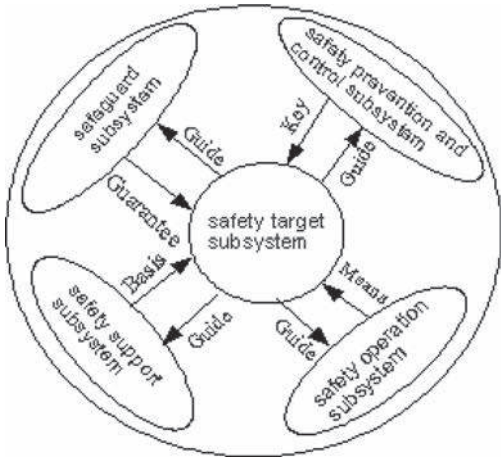


Figure 1. General structure of coal mine production safety management system.

4.2.3 *The safeguard subsystem*

The safeguard subsystem is a guarantee of safety production management systems. It consists of safety technology, safety investment, safety environment, safety oversight four basic elements. The safety technology main contents include: safety technology management organization, safety technology management processes, safety technology management methods and measures, safety production technology research, science and technology talent team construction, safety technology investment guarantee mechanism, protection of safety intellectual property. The safety investment main contents include: safety investment guarantee mechanism, safety investment management mechanism, safety investment oversight and assessment mechanism. The safety environment main contents include: safety quality standardization creation, ground safety environment to refresh and develop and employees civilized behavior. The safety oversight main contents include: safety oversight systems, safety monitoring focus and business management.

4.2.4 *The safety prevention and control subsystem*

The safety prevention and control subsystem is the key to safety production management system. It consists of accident prevention, hidden danger investigation, "three violations" rectification three basic elements. The establishment of safety prevention and control subsystem reflects the before, during and after the three aspects of safety prevention and control. The main contents of accident prevention include: risk control management in advance and emergency rescue plan two aspects. The main contents of hidden danger

investigation include: hidden danger investigation working mechanism, the closed-loop management system of hidden danger investigation, hidden danger investigation governance mechanism, hidden employees investigation and admonishing mechanism, pointed out by hand and speak with the mouth safety confirmation method. (Reason J et al. 1998) The "three violations" rectification main contents include: "three violations" prevention, "three violations" investigation, "three violations" helpers and behavior modification, "three violations" rectification protection mechanism.

4.2.5 *The safety operation subsystem*

The safety operation subsystem includes self-management and site management two elements. The main contents of self-management include: group management and control, mine and plant (office, subsidiary) self-control, branch and area (workshop) self-governance, team self-management, employee self-discipline. The main contents of site management include: job fine management, team on-site management, job sporadic operations personnel management, site-specific sudden exceptions emergency treatment, (William Graebner. 1973) hidden danger investigation and remediation closure grading management act, coding, fixed location, identification, Kanban management.

5 THE FEATURES OF THE SAFETY PRODUCTION MANAGEMENT SYSTEM IN COALMINES BASED ON SYSTEMS THINKING THEORY

The safety production management system in coalmines based on systems thinking theory is the height from the system to systematically summarize to form a complete set of safety production management mode by regulating the various elements of safety production, with the current existing safety production management models and methods at home and abroad, the system has four distinct characteristics.

5.1 *Systemic*

The safety production management system in coalmines based on systems thinking theory uses systems thinking theory to systematically think the production process, managing all aspects of the process of the potential safety risks, analyzes mining production processes, management processes, from the system to find deep-seated safety problems, serious solve the problem of safety objectives, safety support, safeguard, safety prevention and control and safety operation and other aspects, and thus improve the system, flexibility to change mechanism, improve rules, strengthen management, implement responsibility, truly lay the basis of safety production management, systematically analyze the complex, messy, diverse, safe work to form a sound, comprehensive, scientific safety production system.

Traditional safety production management system divided the system into simple pieces to deal with, focused too much attention to every part of them and ignored the whole system thinking to the safety production management system.

5.2 *Normative*

No rules, no standards. The safety production management focuses on implementation, and to effectively implement, we must first establish a standard. The safety production management system in coalmines based on systems thinking theory has established appropriate standards, regulations, systems, procedures, etc. of the production process, every aspect of the management process, each step, each of the posts, to establish a strong order to regulate the management, normatively solve the various elements of safety management longstanding issues, gaps and deficiencies, the safety production management more standardized.

5.3 *Completeness*

The safety production management system in coalmines based on systems thinking theory covers all safety-related factors, the safety aspects involved in safety production system, especially those closely related factors are accommodated without omission, to build safety production management defense from the organization, thinking, behavior, system, supervision and other aspects, to achieve safe production management vertical in the end, lateral to the edge.

The safety production management system in coalmines based on systems thinking theory focuses on safety production management level, system, process comprehensiveness. The safety production management system level covers group, mines (office, subsidiary), branch and area (workshop), team and staff. The rules system of safety production management covers safety production management rules, accountability rules, supervision rules, reward and punishment rules. The safety production management process covers the production and management of the entire process. The site management as a core of the fine management positions, covering the entire job process including pre-operation, operation and after operation and all operations personnel management including sporadic operations personnel.

5.4 *Long-term nature*

The safety production management system is the only scientific way to achieve controlled and orderly, long-term stability safety production management. The safety production management system in coalmines based on systems thinking theory bases on current and long, from the systems and mechanisms, measures levels to build long-term mechanism of safety production, concerns the daily management, focuses on daily behavior of workers to develop, promotes normalization of safety production management, integrates the safety production measures into the daily production, management process, both catch every post production and control safety, safety production management to maintain sustained and unremittingly work situation, in order to achieve long-term rather than short-term safety production of effect, efficiency.

6 THE EFFECTS OF THE SAFETY PRODUCTION MANAGEMENT SYSTEM IN COALMINES BASED ON SYSTEMS THINKING THEORY

Accordance with the "system is complete, clear responsibilities, focused, scientific management" requirements, the coal mine company's existing regulations and accountability comprehensive sort, erected safety production management system can effectively improve coal mine safety production management in a scientific, institutionalized and standardized level. The system implemented in Huaibei Mining Group five years, and achieved good results.

6.1 *Cultivate an advanced safety concept*

In the safety production management system construction and implementation stage, through various forms of publicity and education, formed advanced safety production management philosophy, enhanced employee safety ideology, improved the safety production management personnel perform their duties sense of responsibility, developed a staff safe and civilized behavior, effectively reduced the person's unsafe behavior.

6.2 *To achieve a fundamental change in safety production management*

Through the implementation of safety production management system, achieved safe production from the employee passive acceptance to active self-management of safety production management changes; realized from centralized to carry out safety special rectification to the normalization of safety production management changes; realized from the rule of man to the rule of law of safety production management changes; realized from the experience to the scientific, standardized and systematic safety production management changes; implemented in full after the investigation to prevent changes.

6.3 *Enhance security capabilities*

Through the building of the safety production management system, further clarified the safety goals, improved employee safety qualities, improve various rules and regulations, improved the safety production environment, and strengthened safety supervision, further implemented at all levels of safety responsibility to improve the safety prevention and control capabilities, greatly enhanced the safety infrastructure management, safety capabilities have been further enhanced.

Effectively curb the larger and more accidents

The safety production management system in coalmines based on systems thinking theory in Huaibei Mining Group implemented five years, one million tons mortality rates declining, the whole group of companies to eliminate a larger and more accidents, there are 16 on the production and infrastructure mine to achieve the safe production. Huaibei Mining Group achieved the best safety results since the establishment.

6.4 *Effectively curb the larger and more accidents*

The safety production management system in coalmines based on systems thinking theory in Huaibei Mining Group implemented five years, one million tons mortality rates declining, the whole group of companies to eliminate a larger and more accidents, there are 16 on the production and infrastructure mine to achieve the safe production. Huaibei Mining Group achieved the best safety results since the establishment.

7 CONCLUSION

The safety production management system in coalmines based on systems thinking theory, can be established risk control management system from group company, the grassroots mines, branch and area, team to every post, can be achieved without defect management from the design to the production process, from the device to the environment, can be further clarified the responsibility of all levels of management, and standardized management decision-making and the production process, improved rules and regulations, refined job

working standards, been strict with assessment of accountability to ensure that all levels of production management, various positions responsibility, management in place, assessment in place, accountability place.

The safety production management system in coalmines based on systems thinking theory is the law of coal mining enterprises to explore safe development. It is the foundation to consolidate safety production, is the important initiatives to build long-term mechanism of safety production and improve the management of production safety systematic, standardized and scientific level.

REFERENCES

Andrew Hopkins. 1999. For whom does safety pay? The case of major accidents. *Safety Science*. (32):143–153.

Forrester, J.W. 1994. System Dynamics, System Thinking, and Soft OR,. *System Dynamics Review*. Summer, vol. 10, No. 2.

Lee T R. 1996. Perceptions, attitudes and behavior: the vital elements of a safety culture. *Health and Safety,* (10): 1–15.

Lewis MS & Alford JR. 1980. Can government regulate safety? Theoretical mine example. America. *Political Science Review,* (74): 745–756.

Liu YJ et al. 2007. Study of a comprehensive assessment method for coalmine safety based on hierarchy grey analysis. *Journal of China University of Mining & Technology,* 17(l):6–1.

Liu ZX et al. 2007. Market oriented management method of coal mine accident hidden dangers. *Journal of Coal Science & Engineering,* 13(3): 355–358.

Reason J et al. 1998. Organizational control and safety: the varieties of rule based behavior. *Journal of Occupational and Organizational Psychology,* 71: 28–34.

Senge, P.M. 1990. The Fifth Discipline: The Art and Practice of the Learning Organization. New York, NY: Doubleday.

William Graebner. 1973. The coal mine operator and safety: A Study of Business Reform in the Progressive Period, *Labor History,* 14(4): 483.

Zhang SD & Yu CW. 2008. Management present situation and countermeasures of coalmines safety production. *Journal of Coal Science & Engineering,* 14(2): 326–328.

Progress in Mine Safety Science and Engineering II – He et al. (Eds)
© 2014 Taylor & Francis Group, London, ISBN 978-1-138-00122-0

Research on the safety prevention measures of mine water disaster in Shaqu coal mine of Liulin region

X.H. Wang, Y.B. Wang, J.H. Cheng, J.J. Fan, H.J. Xu, X. Zhang & Z.W. Liu
College of Geoscience and Surveying Engineering, China University of Mining and Technology (Beijing), Beijing, China

ABSTRACT: Based on the hydrogeological data of Shaqu coal mine, the paper analyzes the influencing factors of mine water disaster from three aspects: mine water filling factors, aquifer influences of the mine water filling and analysis of water inrush. The results indicate that the main factor of the mine water disaster is the water of old kiln in the east of coal mine field. The gob area of 4# coal is 17680 m^2 and the volume of accumulated water is 21900 m^3 while they are 4727 m^2 and 5300 m^3 individually in the 5# coal. The exploiting sticks to the principle "exploring where there is a doubt and exploring goes ahead of digging". The height of water-conducting crack zones of 3#, 4#, 5#, 6#, 7#, 8#, 9# and 10# coal seams can conduct the water in the upper coal gob area and the maximum water inrush coefficient is greater than critical water inrush coefficient (0.06 MPa/m). Ordovician limestone karst water is dangerous to the tectonic broken coal seams in the mine field. Based on this situation, the paper puts forward water disaster safety prevention and control measures in the study area from seven aspects.

1 INTRODUCTION

Mine water disaster is one of the most serious geological disasters during mining. It threatens the mine production and the life safety of the workers. In the process of coal mine construction and production, prevention of mine water inrush is the important work to ensure coal mine safety production and reasonable recovery of coal resources, it improves the economic benefits as well (Jia Shu 2011). Many scholars analyze the factors of mine water inrush and measures of prevention (Jin Dewu et al. 2013, Xiao Youcai et al. 2008, Cheng Pingrong 2007, Tang Jingzhong 2009, Wang Jianhe et al. 2009, Shi Yicheng et al. 2006, Mao Zhenxi 2007). This study puts forward water disaster safety prevention measures by analyzing water filing factors, the influence of aquifer and the water inrush character of Shaqu coal mine.

2 STRUCTURE CHARACTERISTICS OF THE STUDY AREA

Mine field locates in the west of Liliu mine area and the south central of Sanjiao-Liulin monoclinic coal-bearing region. It is a slowly-inclined monoclinic structure. From north to south, the strata makes for south-north to north-west direction, leans from west to south-west, the dip most 3–7° and 3–15°on the surface, local area dip 18–23° affected by small folds and faults. The main structures of the mine field are wide flat and small fold structures. There are few faults with short extending and small fault throw. The only Graben

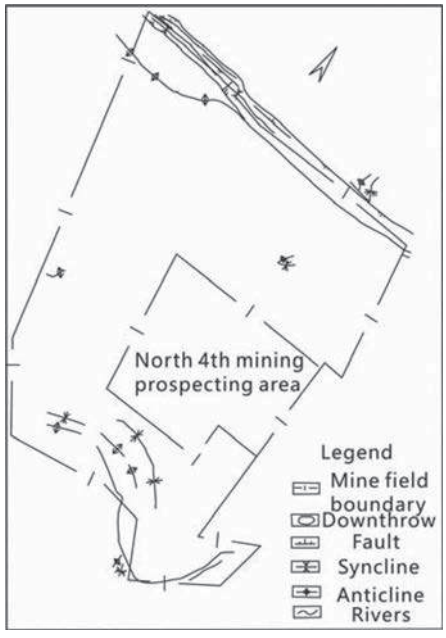


Figure 1. Structural map of Shaqu coal mine field.

type fault is in Jucaita fault on the column on the surface and 4 drillings expose structure near Sanchuan River. There are more than 30 small faults (fault drop is less than 10 m) and more than 40 collapse columns. Figure. 1 shows the structures such as faults, folds and collapse columns within the scope of Shaqu1# mine. There are no igneous activities, the mine filed structure is simple. Main mining coal seams in the study area are 4# and 5#, secondly are 8#, 9# and 10#, individual mining 3# and 6# coal seams.

3 MINE WATER FILLING FACTORS AND ANALYSIS OF WATER INRUSH IN THE STUDY AREA

3.1 *Mine water filling factors*

1 Surface water and atmospheric precipitation

In the Shaqu coal mine field, there exist Cenozoic thick layers of loess, silty clay, sandy clay and impermeable layer of clay. Moreover, the buried depth of coal seam is relatively great, thus, the crannies caused by mining has not yet spread to the surface. Rivers and creeks are relatively far from coal seams and there are thick layers of Shale rock between them and no room for channels between them. Shaqu coal mine is mining 4# coal seam (the upper group) of Shanxi Formation of Permian. Annual precipitation and precipitation seasonal changes have little influence on water inflow by analyzing the monthly average water inflow change law with season. Surface water and atmospheric precipitation has no influence on coal seam mining in the area.

2 The water of old kiln

Shaqu coal mine is a new mine and the range of its goaf and water area is limited. There are more than 40 local small coal mines on the eastern edge, including nine adjacent local coal mines. Two coal mines (Liulin coal mine and Jinjiazhuang coal mine) are located in the mine field, 4 # coal seam is the main coal seam; the small mines have hundred years history near outcrop of coal seam of east 2~3 km outside mine field, forming a large number of old empty hydrops area, and it has a potential threat to coal mine although it is far apart from mine. Table 1 and Table 2 show the water accumulating volume of goaf by calculating.

3 Aquifer

K_4 sandstone aquifer is the roof of 2# coal seam and the direct aquifer of the upper group coal, it has a certain influence on mine production because of the weak-medium watery. According to the height formula of hard rock water flowing fractured zone in “three under” mining procedures, the height

Table 1. Goaf water summary table of the 4# coal seam in mining field.

Location	Water area number	Coal seam thickness (m)	Area of goaf (m^2)	Water accumulating volume of goaf (m^3)
Southeast	JS-1	2.70	4767	3900
Southeast	JS-2	4.60	12913	18000
Total			17680	21900

Table 2. Goaf water summary table of the 5# coal seam in the mining field.

Location	Water area number	Coal seam thickness (m)	Area of goaf (m^2)	Water accumulating volume of goaf (m^3)
East	JS-1	3.70	4727	5300
Total			4727	5300

$H_1 = 20\sqrt{\sum M} + 10$, calculating the 2#, 3#, 4# and 5# coal seams water flowing fractured zone height (both maximum value), 2# coal seam water flowing fractured zone height $H_1 = 20\sqrt{1.68} + 10 = 36$ m, 3# coal seam water flowing fractured zone height $H_1 = 20\sqrt{2.00} + 10 = 38$ m, 4# coal seam water flowing fractured zone height $H_1 = 20\sqrt{6.50} + 10 = 61$ m, 5# coal seam water flowing fractured zone height $H_1 = 20\sqrt{5.04} + 10 = 55$ m. 3#, 4#, and 5# coal seams water flowing fractured zone are conducting the upper coal seam goaf water, so when we mining these coal seams, upper goaf water should be drained and strengthen drain work which can prevent water disasters accident. In the shallow buried zone, it is easy to accept the surface atmospheric precipitation replenishment, adding to the weathering fracture development, the atmospheric precipitation and surface water will affect mine production.

L_5 limestone aquifer is the direct water filling aquifer of the 6# coal seam roof and the average thickness is 4.65 m. L_1 limestone aquifer is the direct water filling aquifer of the 8#, 9# and 10# coal seams roof, and the average thickness is 6.02 m. According to the height formula hard rock water flowing fractured zone in "three under" mining procedures, the height $H = 30\sqrt{\sum M} + 10$, calculating the 6#, 8#, 9# and 10# coal seams water flowing fractured zone height (both maximum value), 6# coal seam water flowing fractured zone height $H = 30\sqrt{1.60} + 10 = 48$ m, 8# coal seam water flowing fractured zone $H = 30\sqrt{9.33} + 10 = 102$ m, 9# coal seam water flowing fractured zone height

$H = 30\sqrt{2.10} + 10 = 53$ m, 10# coal seam water flowing fractured zone height $H = 30\sqrt{3.99} + 10 = 70$ m. 6#, 8#, 9# and 10# coal seams water flowing fractured zone are conducting the upper coal seam goaf water, so when we mining 6#, 8#, 9# and 10# coal seams, the upper goaf water should be drained and strengthen drain work which can prevent water disasters accident.

3.2 *Analysis of water inrush*

The direct water filling aquifer of upper coal seam is the lower Shihezi Formation sandstone fracture aquifer, the indirect filling aquifers are mainly the upper Shihezi Formation sandstone fracture aquifer, Taiyuan Formation karst fractured aquifer, Ordovician middle limestone and karst fractured aquifer. The direct water filling aquifer of lower coal seam is the Taiyuan Formation karst fractured aquifer, the indirect water filling aquifers are mainly the lower Shihezi Formation sandstone fracture aquifer and Ordovician limestone karst fractured aquifer.

All mineable coal seams are located under the Ordovician limestone karst fracture aquifer which water level is 801.47 m (the pumping data of the 14 # drilling). We can analyse the influences of the Ordovician limestone karst water to all mineable coal seams according to the coefficient of water inrush.

The calculation formula of coefficient of water inrush is:

$$Ts = P/M \; P = (H_0 - H_1 + M) \times 0.0098 \qquad (1)$$

Table 3. The calculation results of coefficient of water inrush.

Coal seam	The lowest elevation height of coal seam floor (m)	The thickness of water-resisting (m)	Water head pressure (MPa)	The biggest coefficient of water inrush (MPa/m)
2	100	141	8.2562	0.0586
3	60	125	8.491	0.0679
4	60	121	8.4522	0.0699
5	60	116	8.4032	0.0724
6	40	100	8.4420	0.0844
8	0	72	8.5600	0.1189
9	160	69	6.9724	0.0996
10	0	55	8.3930	0.1526

Where T = the coefficient of water inrush, MPa/m; P = the bearing waterhead pressure of water-resisting floor, Mpa; M = the thickness of water-resisting floor, m; H_1 = the lowest elevation height of coal seam floor; H_0 = the water level elevation height of the Ordovician limestone karst water.

The water level elevation height of the Ordovician limestone karst water (H_0) is 801.47 m.

Table. 3 shows the biggest coefficient of water inrush of all coal seams.

4 THE SAFETY PREVENTION MEASURES OF MINE WATER DISASTER IN THE STUDY AREA

Through analyzing the mine water filling factors, aquifer influences of the mine water filling and the analysis of water inrush characters in the Shaqu coal mine, the paper puts forward the prevention measures of mine water disaster.

1. Improve the hydrogeology observation system
The hydrogeology observation system is a window to understand the dynamic change of groundwater under the action of natural and human factors. The coal mine has set up the hydrogeology observation system, but there are only two limestone boreholes of Taiyuan Formation. More observation boreholes should be set in the development district.

2. Prevention measures of roof water disaster
Deal with the water filling of roof we should reference the partition map of roof water inrush risk evaluation, finding out the reason and deciding to take drainage method or directly drain the mine on the basic of actual situation of the mine. To prevent the water of coal seam roof of sandstone and the thin layer of limestone, drainage method can be taken because of the limited static reserves. But when the hydrogeology condition is complicated and the water volume is large, plus the permeable structure can connect the Ordovician limestone aquifer, waterproofing measures to the permeable structure such as grouting reinforcement or setting the waterproof coal pillars should be taken first.

3. Prevention measures of floor water disaster
Design mining under pressure we should reference the hydrogeology supplement exploration reports which aim at preventing the water filling of lower coal seam floor. In accordance with the mine actual production situation, we should design the mining with some technologies such as mining under pressure or draining water to reduce pressure and divisional isolation, routes to avoid disaster, a certain

ability to prevent disaster through drainage, unobstructed communication, beforehand grout reinforcement of floor.

4. Old kiln flood control

The exploration and drainage of old kiln water we must stick to the principle "exploring where there is a doubt and exploring always go ahead of digging". Meanwhile, we design the exploration and drainage project should according to the requirements of the prevention and control of coal mine water. A great quantity of goaf water in the east of mine field would pose a threat to the mine production. Therefore, to avoid accidents, strengthen the exploration and drainage work during mining is necessary.

5. Prevention of water disaster caused by faults of collapse columns

The geological condition is simple in Shaqu mine area, but the water inrush accident caused by faults occupies a big proportion. There are problems which aim at finding water-conducted fracture structures that present at mining and tunneling face in almost every mine. The method which combines geophysical and drilling is the main one of faults exploration. In addition, the underground drainage tests can probably control the development area, so it can be the basis for exploration and drainage work.

6. Close poor drillings

Abandoned drillings that closed poor in history tend to become water guide channel of underlying aquifer. There are some exploration holes constructed around and in the mine field in the 1950s. Because of historical reasons and technical reasons, the drilling or sealing quality is bad, even with no data. These drillings are likely to be the hydraulic connection channel of various aquifers, which would cause a water inrush accident once revealed in mining process. Thus, to avoid water inrush accident, the closed poor holes should be paid high attention to.

7. Mine daily technical and management work

Mine daily technical management is the most important part of the water prevention work. It's important for reducing mine water disaster to do the daily technical management. This work not only discover hidden signs, but also accumulate the information of mine water prevention work, which is significant for analyzing water disaster factors and taking water prevention and control measures accurately and timely.

5 CONCLUSIONS

The results can be got by analyzing the water disaster factors and prevention measures of mine water disaster.

1. The factor of the filling water of the mine is mainly the goaf water of old kiln in the east of mine. The gob area of 4# coal is 17680 m^2 and the volume of accumulated water is 21900 m^3 while they are 4727 m^2 and 5300 m^3 individually in the 5# coal. Therefore, the principle "exploring where there is a doubt and exploring always go ahead of digging" of the water exploration of old kiln must be sticked to, meanwhile, it should strengthen the work of exploration to prevent the accident.
2. Calculating the height of water flowing fractured zone and the water inrush coefficient of 3#, 4#, 5#, 6#, 8#, 9#, 10# coal seams respectively. The coal seam height of water flowing fractured zone is greater than its upper seams interval, thus, it's easy to form the connection channel to the upper seam gob area. Therefore, it should drain the water in the upper seam gob area while mining. Meanwhile, the maximum inrush coefficient is greater than the critical water inrush coefficient (0.06 MPa/m), so Ordovician limestone karst water is dangerous to the tectonic broken coal seams in the mine field.
3. Combined with several aspects such as the factors of the mine water filling, the influences of aquifer to the mine water filling and analysis of inrush water, the prevention measures of mine water disaster are raised from seven aspects, which provide theoretical support for the mine safety production.

ACKNOWLEDGEMENTS

This research is supported by two "Twelfth Five-Year plan national special science and Technology Majors". They are "Dynamic evaluation model and software system of coal reservoirs development" (No. 2011ZX05034-005) and "Research on technique and equipment of replacing methane by injecting CO_2 in deep coal seams" (No. 2011ZX05042-003).

REFERENCES

Cheng Pingrong, 2007. Yaoqiao Coalmine Hydrogeological Characters and Mine Flooding Controlling Measures. *Coal Geology of China* 19(4): 51–53.

Jia Shu, 2011. Mine Water Analysis and Prevention of Disaster. *Shanxi Coking Coal Science & Technology* 2:47–49.

Jin Dewu, Liu Yingfeng, Liu Zaibin, et al., 2013. New Progress of Study on Major Water Inrush Disaster Prevention and Control Technology in Coal Mine. *Coal Science and Technology* 41(1): 25–29.

Mao Zhenxi, 2007. Talking about the Hydrogeological Condition of the Coalfields in Shanxi Province and

the Formation Cause of Mine Water Disaster. *Sci-Tech Information Development & Economy* 17(31): 141–143.

Shi Yicheng, Yang Guihua, Zeng Zhifang, 2006. Hydrogeological Condition and Prevention-Cure of Mine Water Hazards in Enkou Coal Area. Coal Technology 25(6): 89–91.

Tang Jingzhong, 2009. Discussion on Coalmine Water Disaster Control in Heshan Coalfield. *Coal Geology of China* 21(2): 34–38.

Wang Jianhe, Ren Fengwei, Chen Yanzhao, et al., 2009. Hydrogeological Analysis and Groundwater Prevention Measures for Quandian Coal Mine. *Zhongzhou Coal* 6:91–93.

Xiao Youcai, Ma Zhe, Yang Lanhe, 2008. Mine water disasters in Pingdingshan coal mining area: types of disasters and preventive/control measures. *China Coal* 34(5): 44–47.

This page intentionally left blank

Progress in Mine Safety Science and Engineering II – He et al. (Eds)
© 2014 Taylor & Francis Group, London, ISBN 978-1-138-00122-0

Application of the combination forecasting method in coal mine accidents forecasting

Jinsan Li & Yuncai Ning
School of Management of China University of Mining and Technology (Beijing), Beijing, China

ABSTRACT: Coal mine accidents have a huge impact on the personal safety and the production of coal mining enterprises, and also will cause significant loss in economy. Therefore, the prediction of coal mine accidents is particularly necessary. According to the statistical data aiming at our country's coal mine accidents from the year 2000 to 2011, this paper uses combination forecasting method of coal mine accidents to provide determinative basis for safety management of coal enterprise, so as to reducing coal mine accidents in the maximum extent.

1 INTRODUCTION

In recent years, the death toll of coal mine accidents in China has shown a downward trend. But the total amount and the number of coal mine accidents are still far higher than that of developed countries. The problem about safety in production which is worried about all the time (Liu 2002, Wang 2006, Zhu & Hao 2012). It is the fact that our country's energy consumption structure is dominated by coal without any changes in a long time. Therefore, the prediction research of coal mine accidents has a certain practical significance.

Coal mine accidents prediction is an important content in the research of coal mine safety by which can grasp the future development trend of coal mine accidents, so as to taking corresponding measures in time, and providing the basis for safety management (A.P. Squelch 2001, Hu & Li 2009, Yu & Jin 2001). This paper combines the secondary moving average method, cubic exponential smoothing method and grey prediction method. Each method plays a role in establishing combination forecasting method, so as to forecasting the coal mine accidents.

2 SINGLE FORECASTING METHOD

2.1 *Secondary moving average method*

The secondary moving average method is a simple forecasting technique. Its basic idea is based on the time sequence information, itemized passage of time, and sequentially calculates the chronological average which contains a certain number, so as to reflecting the trend of the data sequence (Liu & Xiong 2007, Kathleen & Kowalski 2003). This article mainly analyses the secondary moving average method. The basic formula is as follow:

$$\hat{y}_{t+T} = a_t + b_t \bullet T \tag{1}$$

$$a_t = 2M_t^{(1)} - M_t^{(2)}, b_t = \frac{2}{N-1}(M_t^{(1)} - M_t^{(2)}) \tag{2}$$

$$M_t^{(2)} = M_{t-1}^{(2)} + \frac{M_t^{(1)} - M_{t-N}^{(1)}}{N}, t \geq N \tag{3}$$

$$M_t^{(1)} = \frac{y_t + y_{t-1} + \cdots y_{t-N-1}}{N} = M_{t-1}^{(1)} + \frac{y_t - y_{t-N}}{N}, t \geq N \tag{4}$$

Where $M_t^{(1)}$ = the first moving average in the t cycle; $\hat{y}_{t+T}$ = the predictive value in the t+T cycle; N = the item of average numbers.

2.2 *Cubic exponential smoothing method*

The exponential smoothing is a very effective short-term forecasting method. This method is very simple, as long as getting few the amounts of data that can be continuous used (Cheng 2007, Liu & Ma 2007, Yu & Xie 2007, Zhang & Li 2002). It includes the first exponential smoothing method and the secondary exponential smoothing method and the multiple exponential smoothing methods. This article mainly analyses the cubic exponential smoothing method. The basic formula is as follow:

$$F_{t+T} = a_t + b_t \bullet T + c_t \bullet T^2 \tag{5}$$

$$a_t = 3S_t^{(1)} - 3S_t^{(2)} + S_t^{(3)} \tag{6}$$

$$b_t = \frac{\alpha}{2(1-\alpha)} [(6-5\alpha)S_t^{(1)} - 2(5-4\alpha)S_t^{(2)} + (4-3\alpha)S_t^{(3)}] \tag{7}$$

$$c_t = \frac{\alpha^2}{2(1-\alpha)^2}[S_t^{(1)} - 2S_t^{(2)} + S_t^{(3)}] \quad (8)$$

$$S_t^{(1)} = \alpha Y_t + (1-\alpha)S_{t-1}^{(1)} \quad (9)$$

$$S_t^{(2)} = \alpha S_t^{(1)} + (1-\alpha)S_{t-1}^{(2)} \quad (10)$$

$$S_t^{(3)} = \alpha S_t^{(2)} + (1-\alpha)S_{t-1}^{(3)} \quad (11)$$

Where α = an exponential smoothing coefficient, $0 < \alpha < 1$; F_{t+1} = the predictive value of the cubic exponential smoothing method in the t + T cycle.

2.3 *Grey prediction method*

Grey prediction method is based on the grey modules, and using differential fitting method to establish the accumulation model. It is mainly used in forecasting of single variable time series (Hu 2007, Liu et al. 2007). The GM (1, 1) model is a concrete application of the grey prediction method; its basic formula is as follow:

$$\hat{x}^{(1)}(k+1) = (x^{(1)}(1) - \frac{u}{a})e^{-ak} + \frac{u}{a} \quad (12)$$

$$\hat{x}^{(0)}(k+1) = \hat{x}^{(1)}(k+1) - \hat{x}^{(1)}(k) \quad (13)$$

$$x^{(1)}(i) = \sum_{k=1}^{i} x^{(0)}(k) \quad (14)$$

$$\begin{pmatrix} a \\ u \end{pmatrix} = (B^T B)^{-1} B^T Y_n \quad (15)$$

$$B = \begin{pmatrix} -\frac{1}{2}[x^{(1)}(1) + x^{(1)}(2)] & 1 \\ -\frac{1}{2}[x^{(1)}(2) + x^{(1)}(3)] & 1 \\ -\frac{1}{2}[x^{(1)}(3) + x^{(1)}(4)] & 1 \\ \cdots\cdots & \\ -\frac{1}{2}[x^{(1)}(n-1) + x^{(1)}(n)] & 1 \end{pmatrix} \quad (16)$$

$$Y_n = [x^{(0)}(2), x^{(0)}(3), x^{(0)}(4), \ldots, x^{(0)}(n)]^T \quad (17)$$

Where $x^{(0)}(i)$ = the original data.

3 THE EFFECTIVENESS OF THREE PREDICTION METHODS

The following table shows China's coal mine death toll in the 2000–2011 years, according to the data of 2000–2008, using three methods to predict the coal mine death toll in 2009, and then compared with the actual value of 2009. Data in the table derived from the state administration of production safety supervision and management of the calendar year issued.

3.1 *The predictive results of secondary moving average method*

According to the experience, choose N = 2, then using formula (1) to forecasting the death toll, the results are shown in the table 2.

3.2 *The predictive results of cubic exponential smoothing method*

Due to the original data changes greatly, so the smooth index should be selected a larger value, so that the recent trends can be fully considered. After many repeated calculation, choose = 0.45. Then take the average value of three years from 2000 to 2002 as the initial value. The initial value is 6547.67, and the predictive results are shown in the table 3.

Table 1. China's coal mine death tolls in the 2000–2011 years.

Year	Death toll	Year	Death toll	Year	Death toll
2000	5798	2004	6027	2008	3215
2001	6850	2005	5986	2009	2630
2002	6995	2006	5770	2010	2433
2003	6683	2007	3758	2011	1973

Table 2. The predictive results of the secondary moving average method.

Year	Death toll	$M_t^{(1)}$	$M_t^{(2)}$	Predicted results (integer)
2000	5798			
2001	6850			
2002	6995	6324		
2003	6683	6922.5	6623.25	
2004	6027	6839	6880.75	
2005	5986	6355	6597	
2006	5770	6006.5	6180.75	
2007	3758	5878	5942.25	
2008	3215	4764	5231	
2009	2630	3486.5	4035.25	1840
2010	2433	2922.5	3114.5	2347
2011	1973	2531	2636.75	2214
2012		2202.5	2276.75	1980
2013				1831
2014				1683

Table 3. The predictive results of cubic exponential smoothing method.

Year	Death toll	$S_t^{(1)}$	$S_t^{(2)}$	$S_t^{(3)}$	Predicted results (integer)
2000	5798	6210.32	6395.87	6479.36	
2001	6850	6498.18	6441.91	6462.51	
2002	6995	6721.75	6567.84	6509.91	
2003	6683	6704.31	6629.25	6563.61	
2004	6027	6399.52	6525.87	6546.63	
2005	5986	6213.44	6385.27	6474.02	
2006	5770	6013.89	6218.15	6358.87	
2007	3758	4998.74	5669.42	6048.62	
2008	3215	4196.06	5006.41	5579.62	
2009	2630	3491.33	4324.63	5014.88	2448
2010	2433	3015.08	3735.33	4439.08	2254
2011	1973	2546.14	3200.2	3881.58	1845
2012					1664
2013					1427
2014					1208

3.3 *The predictive results of grey prediction method*

According to the formula (12) and formula (13), get $a = 0.08663$, $u = 8364.7$. The predicted results are as follow:

The predictive result of 2009:

$$\hat{x}^{(0)}(10) = \hat{x}^{(1)}(10) - \hat{x}^{(1)}(9) \approx 3766$$

The predictive result of 2010:

$$\hat{x}^{(0)}(11) = \hat{x}^{(1)}(11) - \hat{x}^{(1)}(10) \approx 3454$$

The predictive result of 2011:

$$\hat{x}^{(0)}(12) = \hat{x}^{(1)}(12) - \hat{x}^{(1)}(11) \approx 3167$$

The predictive result of 2012:

$$\hat{x}^{(0)}(13) = \hat{x}^{(1)}(13) - \hat{x}^{(1)}(12) \approx 2904$$

The predictive result of 2013:

$$\hat{x}^{(0)}(14) = \hat{x}^{(1)}(14) - \hat{x}^{(1)}(13) \approx 2663$$

The predictive result of 2014:

$$\hat{x}^{(0)}(15) = \hat{x}^{(1)}(15) - \hat{x}^{(1)}(14) \approx 2442$$

According to the data above, three methods of forecast results are as follows:

Table 4. The comparison result of the three prediction methods.

Method	The predictive value of 2009	The actual value of 2009	The relative error
Secondary moving average method	1840	2630	0.3
Cubic exponential smoothing method	2448	2630	0.07
Grey prediction method	3766	2630	0.43

3.4 *Briefly discussion of three methods*

From the above three kinds of effective method for predicting degree, it can be seen that the Cubic exponential smoothing method has the highest prediction accuracy, the next is the secondary moving average method, and the last is the grey prediction method. The grey prediction method can use some grey information to make prediction, and it can predict more accurate results in the short-term, but in the long-term forecast results are prone to error (He 2008); the secondary moving average method is rely too much on the average of last time, so the predictive value often has a great deal of uncertainty. The smoothing coefficient of cubic exponential smoothing method has a lot of subjectivity, so the selection of it also has a great impact of the predictive results.

4 THE ESTABLISHMENT OF COMBINATION FORECASTING METHOD

In the 1960s, Bates and Granger presented combination forecasting theory for the first time. They combined two or more methods with weights (BATES & GRANGER 2004) in recent years; the combination forecasting method is widely used in various fields (Chu et al. 2004, Wang et al.2007, Li & Zhou 2010). Its basic formula is as follow:

$$Y = \sum_{i=1}^{n} w_i y_i \tag{18}$$

Where, Y = the final predicted value; w_i = the weight of the corresponding single forecasting method, and $\sum_{i=1}^{n} w_i = 1$; y_i = the predictive result of single method.

The weight of each forecasting method can be seen in the following table.

Then the final weights of combination forecasting method are: $\omega_1 = 0.167$, $\omega_2 = 0.716$, $\omega_3 = 0.117$.

Table 5. The weight of each forecasting method.

Method	(1) The relative error	(2) The proportion of total error	(3) The reciprocal of the proportion	(4) Weight
Secondary moving average method	0.3	37.5%	2.667	0.167
Cubic exponential smoothing method	0.07	8.75%	11.429	0.716
Grey prediction method	0.43	53.75%	1.86	0.117
Total	0.8	100%	15.956	1.000

Table 6. The prediction effectiveness of combination forecasting method.

Year	Predictive value	Actual value	The relative error
2010	2410	2433	0.95%
2011	2061	1973	4.5%

It can be seen from the data in Tab. 6, the combination prediction method for the relative error of the predicted value and the actual value is controlled within 4.5%, therefore, it can be considered that the combination forecasting method is fit for the validly test. It can get the predictive results of three years which is from 2012 to 2014 by using the combination forecasting method.

$$Y_{2012} = 0.167 \times 1980 + 0.716 \times 1664 + 0.117 \times 2904 \approx 1861$$

$$Y_{2013} = 0.167 \times 1831 + 0.716 \times 1427 + 0.117 \times 2663 \approx 1639$$

$$Y_{2014} = 0.167 \times 1683 + 0.716 \times 1208 + 0.117 \times 2442 \approx 1432$$

5 CONCLUSIONS

According to the coal mine accident statistics in recent 10 years in our country, this paper uses the combined forecasting method to forecast the future of the coal mine accidents in China. Compared with single forecasting method, the weight distribution method of the combination forecast greatly improve the forecast accuracy of the coal mine accidents, and it has certain applicability for guiding the safety work of coal mine accidents in China.

From the predictive results of 2012, 2013 and 2014, it can be seen that the death toll of coal mine accidents will continue to show a downward trend, but the absolute numbers are still too large, the situation remains grim. Therefore, it is necessary to take various security measures to reduce the loss as possible as they can for the government and enterprises. And make sure of the safety production of coal mine.

The forecast model in this paper can also be used as the indicators of other accidents in coal mines, so as to providing reliable scientific basis for coal mine safety measures and decisions.

REFERENCES

Bates & Granger.1969. Combination of forecasts. *Operations Research Quarterly*20 (4):451–468.

Cheng Liangping.2007. Development analysis on information management system of casualty accident statistics. *Industrial Safety and Environmental Protection*33 (3): 56–57.

Chu Liangyong, Tian Zhiguang & Xie Xinlian. 2004. Application of the combination forecast model in the logistics demand forecasting. *Joural of Dalian Maritime University* (4):43–45.

He Guohua. 2008. Forecast of regional logistics requirements and application of grey Prediction Model. *Jourrnal of Beijing. Jiaotong University (Social Sciences Edition)*:36–37.

Hu Jinhang. 2007. The application of grey system theory in mathematical modeling. *Science and Technology Consulting Herald* (8): 94–95

Hu Shuangqi & Li Yong. 2009. Prediction of coal mine accidents based on gray Elman neural networks. Journal of Safety Science and Technology (4):106–108.

Kathleen. M & Kowalski-Trakofler. 2003. The concept of degraded images applied to hazard recognition training in mining for reduce of lost-time injuries. *Journal of Safety Research* (34): 515–525.

Liu Jianyu & Xiong Yunfa. 2007. Application of moving average method in the public security intelligence analysis. *Joural of Chinese People's Public Security University (Science and Technology)* (4):54–55.

Li Junjun & Zhou Limei. 2010. Study on the application of the combination forecast method in the comprehensive competitiveness of provincial economy. *Comprehensive Competitiveness* (2):29–31.

Liu Sifeng, Dang Yaoguo & Fang Zhigeng. 2007. The grey system theory and its application. Beijing. *Science Press*: 126–134.

Liu Yang & Ma Fenghai. 2007. Application of cubic exponential smoothing method to city underground deformation prediction. *Technology&Economy in Areas of Communications* (5):62–70.

Liu Yu. 2002. The Study on Our Country's Coalmine Accident Causing Theory and Prevention Countermeasure. *Shaanxi Coal* (2): 53–55.

Squelch. A.P. 2001. Virtual reality for mine safety training in South Africa. J*ournal South African Institute of mining and metallurgy*101 (4): 209–216.

Wang Yumei, Shang Jincheng & Ding Junxin. Application of the combination forecast model in the strategic environmental assessment. *Environmental Science and Technology* (8):66–68.

Wang Xuefeng. 2006. Discussion on coal mine safety in China. *Coal Geology of China* (18): 16–18.

Yu Zhifeng & Xie Zhengwen. 2007. Improved grey model by exponential smoothing for settlement predication and its application. *Central South Highway Engineering* (3):120–122.

Yu Baoquan & Jin Yufei. 2001. Probe into the Intrinsic Causes of Coal Mine Accidents. *Inner Mongolia Coal Economics* (5): 5–6.

Zhu Qingming & Hao Zhang. 2012. Study on the application of cubic exponential smoothing method in coal mine accidents forecasting. *Joural of Safety Science and Technology* (4):105–107.

Zhang Weihong & Li liu. 2008. Application of exponential smoothing method in the sales budget. *China Management Information* (2):85–86.

This page intentionally left blank

Progress in Mine Safety Science and Engineering II – He et al. (Eds)
© 2014 Taylor & Francis Group, London, ISBN 978-1-138-00122-0

A statistical analysis of coal gas explosion accidents in China

Yongguo Cui, Beijing Xie, Jialin Cao & Chuan Wang
Faculty of Resources and Safety Engineering, China University of Mining and Technology, Beijing, China

ABSTRACT: Four hundred and sixty seven coal gas explosion accidents that occurred in China between the years of 1950 and 2000 were investigated through statistical methods so as to review the overall situation and provide quantitative information on coal gas explosion accidents. Statistical characteristics about accident-related factors such as space, time, gas accumulation reasons, gas grade, ignition sources, accidents categories, and accident economic loss were analyzed. Some special conclusions have been achieved. For example, most gas explosion accidents were found to have concentricity on the space-time and hazard characteristics. Such results may be helpful to prevent coal gas explosion accidents. Moreover, comments were made on APS (Accident Prevention System) and safety culture. In conclusion, countermeasures were proposed in accordance with the results of statistical studies, including the change of safety check time.

1 INTRODUCTION

The coal industry is one of the most important parts to worldwide energy supply, especially to that of China. However, there are always some safety problems to be solved urgently, such as coal gas explosion accidents. With the mining depth rapidly increasing, the gas explosion accidents severity grows at the same time (Heping Xie et al. 2012a Research …). These accidents do harm to coal production itself and miners, lives and health. What's more, this accident was one of the most severe accidents in which more than 100 employees were lost their lives.

Coal gas explosions are not only featured by the severe consequences, but also by the high occurrence probability for mining enterprises. Scientists all over the world have already paid much attention to coal gas explosions and obtained some knowledge about it. At the accidents basic features, coal mining safety characteristics and future tasks in China, the probability of occurrence causes of extraordinarily serious gas explosion accidents were studied, and so on (Xueqiu He & Li Song 2012, Hong Chen et al. 2013, Xinquan Zhou & Guoxin Chen 2008). Some expert have paid more attention to the accidents occurred models, for example, gas accident modeling and calculation in coal mine; and the mine gas explosibility determined methods were obtained, etc (Wenchao Wang & Boquan Lin 2006, Joseph H.S. & Amy M.C. 2011, Jianwei Cheng et al. 2012, Maiti J. et al. 2009, Hawksley J.L. 1999). It is without doubt that some useful ways to prevent gas explosion accidents have been worked out and applied (Page K. 2009, Chengwu Li 2005).

Unfortunately, few efforts involving macroscopically statistical study on coal gas explosions have been made. Only a few scientists have recently focused on the statistical features of such accidents. We believe that safety issues of any kind should be of systematic problems and so that the coal gas explosion accidents that occurred in coal mines.

A good knowledge of statistical features of certain accidents, therefore, is the basic requirement to implement APS. In other words, major hazard identification must be performed. Statistical study on accident cases would be a powerful tool to meet this requirement. For this purpose, we collected all the related coal gas explosion accidents that analyzed in China's Coal Mine Accident and Expert Comments Set from the years of 1950–2000 (Jiefan Wang & Wenjun Li 2001). The research focused on statistical features such as space, time and gas accumulation reasons, gas grade, ignition sources, accidents categories, and accident economic loss. Through this research, certain model and representativeness results will be drawn.

2 STATISTICAL FEATURES OF SPACE

Space features were analyzed from two levels: the provincial level and working face level (a roadway in the coal mine).

2.1 *Statistical features of space at the provincial level*

In total, there are 25 provinces in China suffering from coal gas explosion accidents. Statistical data are shown in Tab. 1. Coal gas explosions include two

Table 1. Statistical features of accidents at the provincial level.

Provinces	Times[a]	Deaths[a]	Times[b]	Deaths[b]	Times[c]	Deaths[c]
Shanxi	4	322	81	1428	85	1750
Heilongjiang	10	322	66	1007	76	1329
Liaoning	3	52	60	919	63	971
Henan	6	560	33	944	39	1504
Inner Mongolia	4	156	22	206	26	362
Hebei	6	155	14	250	20	405
Hunan	2	79	18	214	20	293
Guizhou	2	246	17	321	19	567
Jilin	3	128	16	180	19	308
Yunnan	0	0	17	240	17	240
Jiangxi	0	0	16	397	16	397
Anhui	0	0	13	344	13	344
Sichuan	1	124	8	125	9	249
Xinjiang	1	12	8	111	9	123
Guangxi	0	0	7	118	7	118
Hubei	1	30	4	30	5	60
Jiangsu	0	0	5	91	5	91
Shaanxi	1	101	4	97	5	198
Chongqing	0	0	4	43	4	43
Shandong	2	81	1	13	3	94
Gansu	0	0	2	112	2	112
Guangdong	0	0	2	32	2	32
Zhejiang	0	0	2	15	2	15
Qinghai	0	0	1	15	1	15
Total	46	2368	421	7252	467	9620

* Note: Superscripts a, b and c refer to explosion with dust, without dust and the sum the two types, respectively.

Table 2. Statistical features of accidents at the working face level.

Working faces	Times[a]	Deaths[a]	Times[b]	Deaths[b]	Times[c]	Deaths[c]
Heading face	24	1234	249	3999	273	5233
Mining face	15	828	121	2332	136	3160
Other roadway	7	306	51	921	58	1227
Total	46	2368	421	7252	467	9620

* Note: Superscripts a, b and c refer to explosion with dust, without dust and the sum the two types, respectively.

types: explosion with dust and explosion without dust. Both accident occurrence times and casualties were listed for the two kinds of explosions. Risk of a coal gas explosion can be assessed by comparing accident occurrence times or casualties.

2.2 *Statistical features of space at the working faces level*

Statistical characteristics of coal gas explosions at the provincial level are provided in Section 2.1, but those are not enough to constitute space-oriented major hazard identification. More detailed information is also needed, because different working faces have different conditions that may cause coal gas explosions even in the same coal mine. For example, statistical features of explosion accidents in different working faces are shown in Tab. 2.

In Shandong Province, only three coal gas explosion accidents happened, but dust participated in nearly all the coal gas explosions. Whereas, in Yunnan, Jiangxi, Anhui, Guangxi, Jiangsu, Chongqing, Gansu and Qinghai Province, most of the explosion accidents happened without dust.

3 STATISTICAL FEATURES OF TIME

Time statistical analyses were given at two levels: month and hour levels. Time statistical features are

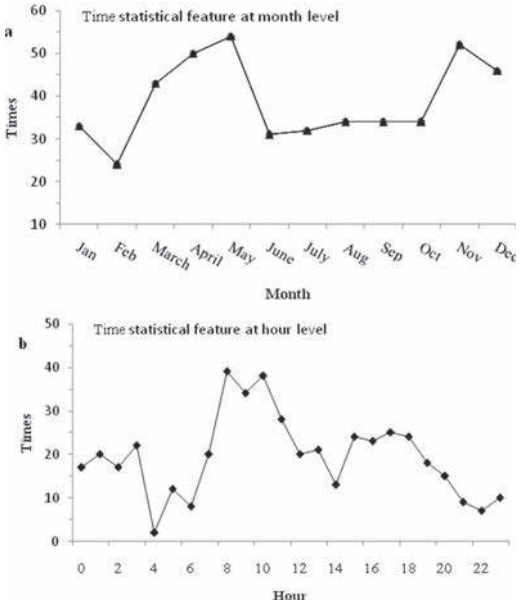


Figure 1. Statistical features of time.

shown in Fig. 1 in terms of statistics of accident cases: Fig. 1a—month level, and Fig. 1b—hour level. Note that y axis in Fig. 1 represents occurrence times of accidents.

4 STATISTICAL FEATURES OF INFLUENCING FACTORS FOR COAL GAS EXPLOSION

Influencing factors for coal gas explosion include quite extensive contents such as concentration of oxygen and granularity of coal gas. However, influencing factors in our study just referred to gas accumulation reasons and ignition sources because of the lack of enough related statistical data.

4.1 *Statistical features of gas accumulation reasons*

According to case statistics, the maximum gas accumulation reasons in the past accidents were Local fan blowing. Existing gas accumulation reasons were classified into eleven groups so as to clarify statistical characteristics. They are as shown in Tab. 3.

4.2 *Statistical features of ignition sources*

Ignition sources in past accidents were divided into 5 types as follows: electrical sparks, flame of blasting, open flames, sparks of strike, and coal self-ignition. Detailed statistical features of ignition sources are shown in Tab. 4.

5 OTHER STATISTICAL FEATURES

5.1 *Statistical features of casualty scales of accidents*

Casualty scales in this study referred to the death toll of employees in a certain accident. Casualty scales are usually divided into four bands according to safety management convention in China. Band I, Band II, Band III, Band IV and Band V indicate that there are 0–3, 3–10, 10–30 and more than 30 casualties in an accident, respectively. The concrete statistical features related to casualty scale are shown in Tab. 5.

5.2 *Statistical features of accidents economic loss*

Accident economic loss referred to the general loss which caused by the coal gas explosion accident. Concrete statistical features of accident economic loss are as follows: in the 467 accidents, 365 accidents provided the economic loss, these accidents caused 7585 employees death and 212.867 million, and the average economic loss is 583000.

6 ANALYSIS AND DISCUSSION

1) According to the space analysis at the provincial level (Tab. 1), Shanxi, Heilongjiang, Liaoning, Henan, Inner Mongolia, Hebei, Hunan, Guizhou and Jilin provinces risk the heaviest casualties caused by coal gas explosions. One of the most important reasons which causes this phenomenon is coal-mine safe production conception have not been developed and implemented in some provinces. Scientific and correct ideas are the foundation of the coal mine safety production (Jiping Sun 2011, Heping Xie et al. 2012. New…, Hovden J. 2012). So these district regions should re-planning coal industry and resolutely implement the safety policy.

Accident cases also showed that heading face and mining face were the two sites where most coal gas explosions took place when more microcosmic space levels were considered.

2) Coal gas explosion accidents ascend sharply from November of the previous year to February of the following year at the monthly level in Fig. 2a. On the contrary, accidents descend rapidly from March to May. This phenomenon may have something to do with the seasonal change, but the authors believe output change plays a much more

Table 3. Statistical features of gas accumulation reasons.

Gas accumulation reasons	Occurrence times	Casualty number	Proportion of times/%	Proportion of casualties/%
Local fan blowing down	109	1983	23.34	20.61
Lack of air supply	70	1309	14.99	13.61
Roadway local calm	57	1190	12.21	12.37
Circulation wind	54	979	11.56	10.18
Unreasonable ventilation system	48	1106	10.28	11.50
Gas accumulation in goaf	46	879	9.85	9.14
Illegal discharge gas	29	879	6.21	9.14
Complex geological conditions	23	531	4.93	5.52
Gas accumulation in blind line	14	514	3.00	5.34
Blasting	4	68	0.86	0.71
Other reasons	13	182	2.77	1.89

Table 4. Statistical features of ignition sources.

Ignition source	Occurrence times	Casualty number	Proportion of times/%	Proportion of casualties/%
Electrical sparks	231	4732	49.46	49.19
Flame of blasting	121	2627	25.91	27.31
Open flames	54	893	11.56	9.28
Sparks of strike	39	792	8.35	8.23
Coal self-ignition	16	488	3.43	5.07
Other ignition	6	88	1.28	0.92

Table 5. Statistical features of casualty scales.

Scales	Occurrence times	Casualty number	Proportion/%	
			Times	Casualties
I	6	5	1.28	0.05
II	115	641	24.63	6.66
III	267	4240	57.17	44.07
IV	79	4734	16.92	49.22

important role than does moisture content change. Generally, ground moisture content of the air in winter is relatively lower than that in other seasons, and lower moisture content is good for coal gas explosibility. Coal is the key energy in China and occupies more than 70% in energy consumption. What's more, more than 60% of coal output is used to generate electricity. In winter, more coal output is needed because waterpower decreases sharply in China while the country's heating demand reaches a peak. Many coal companies usually tend to increase output regardless of safety issues. There are four spans when most accidents occur in a single day in Fig. 2b:7–12 a.m., 15–18 p.m. and 0–4 a.m. Note that the three spans correspond with shift time in most coal mines in China.

3) Local fan blowing down was the mayor gas accumulation reason, and 23.34% of the explosions were induced by it. The second important gas accumulation reason was lack of air supply, and nearly 15% of explosions were caused by it. The third important gas accumulation reason was roadway local calm and nearly 13% of explosions was caused by it.

Overall, local fan blowing down, lack of air supply, roadway local calm, circulation wind, circulation wind and unreasonable ventilation system played the part of 72.38%. These may result from the fact that a large number of coal mines in China have mined for a long time. From the point view of methane, methane is easier to be ignited than coal dust under the same condition. Statistical data showed that dust was usually involved in big coal gas explosion accidents. Obviously, coal dust itself can be part of the fuel in the whole explosion of coal gas. What's worse, flames of dust may become powerful ignition sources for coal gas clouds. So prevention of accumulation and ignition of dust would also be very important to prevent coal gas explosions. According the previous research results, by governing the common causes we can avoid gas accumulation at a great extent (Gui Fu et al. 2005). In other word, coal mine must achieve the safe and reliable ventilation system.

4) Electrical sparks was the mayor ignition source, and nearly half of the explosions were induced by it. The second important ignition source was flame of blasting, and 25.91% of explosions were caused by it. These may result from the fact that a large number of coal mines in China usually use blasting methods rather than automatic machineries to excavate coal.

5) Accidents of Band III took a proportion of 57.17% from the point of view of occurrence times of accidents. And the total proportion would reach 81.8% if occurrence times of accidents of Band II were included. Detailed information is presented in Table 5. Statistical data suggested that conse-

quences of most coal gas explosion accidents are disastrous: a large number of lives would be lost once a coal dust explosion happens.

7 CONCLUSIONS

Coal gas explosion accidents are not rare in China and have caused great loss to both China's international image and coal enterprises, especially to coal miners' lives and health. However, such accidents are not inevitable because most of them are induced by out of duty. Fortunately, some statistical conclusions useful for preventing gas explosions have been presented in our statistical research.

Because casualties caused by coal gas explosions are highest in Shanxi, Heilongjiang, Liaoning, Henan, Inner Mongolia, Hebei, Hunan, Guizhou and Jilin, much more importance should be attached to these nine provinces regarding the prevention of explosions. The whole safety situation related to coal gas explosions would get much better once coal gas accidents in these provinces were reduced. Similarly, the whole safety condition would change for the better if coal gas explosions in heading face were under effective control.

Special safety checks for preventing coal gas explosions should be practiced in the previous year's last 2 months and the following year's March, April, May. Meanwhile, check procedures should be performed especially strictly during these 5 months. Likewise, it is recommended that daily safety patrols of coal mines be arranged around shift times.

To sum up, APS and safety culture badly need to be put into practice to prevent coal mines from being hit by coal gas explosions. APS (including management of technical affairs) is hardware of safety guarantee, and safety culture is software. The two countermeasures should work together rather than be used separately. Recruit more quality employees to work in coal mines is an important way to achieve the goal. The last point worth comprehending is that we should invest enough time and more experts in staff training. In this way, coal mining enterprises must invest time, money and employees in safety training and implement a system of rewards and punishments for safe behaviour. In this way, the gas explosion accidents will be reduced largely.

ACKNOWLEDGEMENTS

The authors gratefully acknowledge foundation by National Natural Science Foundation Project of China (51274206) and the Fundamental Research Funds for the Central Universities (2010YZ05).

REFERENCES

Chengwu, Li 2005. Comprehensive control technology for mine gas uneven area in lower gassy mine. *Science and Technology of Coal Mine (China)* 33(3):1–5.

Gui, Fu. et al. 2005. Common factors leading to accidents and behavior type research based on prevention accident prevention. *Journal of Safety and Environment (China)* 5(2):80–83.

Hawksley, J.L. 1999. Developing a major accident prevention policy. *Journal of hazardous materials* 65:109–121.

Heping, Xie, et al. 2012a. Research and consideration on deep coal mining and critical mining depth. *Journal of China Coal Society* 37(4):535–542.

Heping, Xie, et al. 2012b. New idea of coal mining: scientific mining and sustainable mining capacity. *Journal of China Coal Society* 37(4):535–542.

Hong, Chen, et al. 2013. Characteristics of direct causes and human factors in major gas explosion accidents in Chinese coal mines: Case study spanning the years 1980–2010. *Journal of Loss Prevention in the Process Industries* 26:38–44.

Hovden J. et al. 2010. Is there a need for new theories, models and approaches to occupational accident prevention? *Safety Science* 48:950–956.

Jianwei, Cheng. et al. 2012. Methods to determine the mine gas explosibility—An overview. *Journal of Loss Prevention in the Process Industries* 25:425–435.

Jiefan, Wang & Wenjun, Li 2001. China's coal mine accidents and comments of safety specialists. *Coal Industry Press*. Beijing: Chaoyang

Jiping, Sun. 2011. Research on coal-mine safe production conception. *Journal of China Coal Society* 36(2):313–316.

Joseph H. Saleh & Amy M. Cummings. 2011. Safety in the mining industry and the unfinished legacy of mining accidents: Safety levers and defense-in-depth for addressing mining hazards. *Safety Science* 49:764–777.

Maiti, J. et al. 2009. Severity analysis of Indian coal mine accidents—A retrospective study for 100 years. *Safety Science* 47:1033–1042.

Page, K. 2009. Blood on the coal: The effect of organizational size and differentiation on coal mine accidents. *Journal of Safety Research;* 40: 85–95.

Wenchao, Wang & Boquan, Lin. 2006. Modeling and calculation of gas accident in coal mine. *Mining safety and environmental protection (China)* 33(4):30–32.

Xinquan, Zhou & Guoxin, Chen. 2008. The probability analysis of occurrence causes of extraordinarily serious gas explosion accidences and its revelation. *Journal of China Coal Society* 33(1):42–46.

Xueqiu, He & Li, Song. 2012. Status and future tasks of coal mining safety in China. *Safety Science* 50:894–898.

This page intentionally left blank

Progress in Mine Safety Science and Engineering II – He et al. (Eds)
© 2014 Taylor & Francis Group, London, ISBN 978-1-138-00122-0

Construction way on the team safety culture in coal mine

Dongmei Tian, Jian Yao & Hui Xu
North China Institute of Science and Technology Safety Engineering, Beijing, China
Key Laboratory of Mine Disaster Prevention and Control, Hebei Province, Beijing, China

ABSTRACT: The safety culture is the soul of the security work in enterprise, which is a safe long-term stability of the strong support and maintain normal production and business environment. Strengthen the construction of a safety culture is an important prerequisite to ensure the coordinated development of corporate safety culture construction and foundation. The team is the most basic unit in the entire coal mining enterprises, is the starting point and goal of all of the safety management, but also gave birth to the corporate safety culture cells. It also shows why the coal mine safety culture in construction from the team grabbed. Team safety culture in the construction of a direct impact on production and operation and healthy development of coal mining enterprises, only strengthen the team safety culture in construction, in order for the front-line workers to create a good working environment, to stimulate the enthusiasm and creativity of their work.

1 INTRODUCTION

Team safety culture is relying on the team, combined business with the District team in the activities of team safety concept, safety management system, security, operational measures, safe working environment and the formation of the security features of this team the concept of thinking and safe behavior the way, is the team members put into practice the common security system of values (Fan 2007). Team safety culture through a variety of carriers, means, or an effective form of advanced safety management, safety management system, security, behavior norms, integration or penetrate into the idea of the team members of the team of workers to establish a correct and solid safety awareness, safety values, and create a production safety team safety culture.

Although the party and the state has established a "safety first, prevention first, comprehensive management of safe production approach to the development of the Mine Safety Act, "(Lin 2008) Coal Act, Coal Mine Safety Supervision Ordinance until a series of policies, laws, management departments and business units have done a lot of practical work, have a lot to improve and enhance China's labor protection and production conditions, in order to protect the safety and health of workers in production and construction, safety culture theory, and promoting social 'production and construction development. However, China's coal enterprises 'overall understanding of safety culture and the arts and corporate safety culture in construction due to inadequate attention to workers' safety awareness and safety culture in the low quality of the letter to be improved, so the safety culture of China's coal enterprises exist some general issues mainly reflected in the following areas.

Although the party and the state has established a "safety first, prevention first, comprehensive management of safe production approach to the development of the Mine Safety Act, "(Fan 2007, Luo & Lin 2010)Coal Act, Coal Mine Safety Supervision Ordinance until a series of policies, laws, management departments and business units have done a lot of practical work, have a lot to improve and enhance China's labor protection and production conditions, in order to protect the safety and health of workers in production and construction, safety culture theory, and promoting social 'production and construction development. However, China's coal enterprises 'overall understanding of safety culture and the arts and corporate safety culture in construction due to inadequate attention to workers' safety awareness and safety culture in the low quality of the letter to be improved, so the safety culture of China's coal enterprises exist some general issues mainly reflected in the following areas.

Coal mining enterprises not pay enough attention to the safety culture in construction, light on the surface. (2) Safety culture in construction research emphasis on theory and the theory cannot be combined with practice. (3) Coal employees there is a widespread misunderstanding of the safety culture in construction, compared with weak safety awareness. (4) Scientific, reasonable and effective evaluation of the measurement system is not perfect.

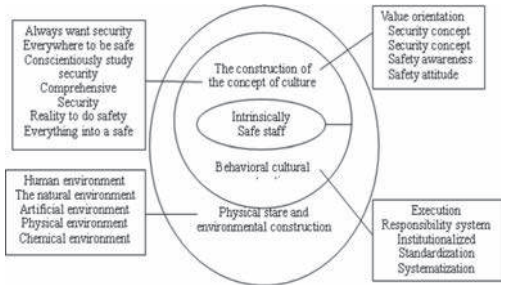


Figure 1. Safety culture in the construction of "Human Security Principles".

2 SAFETY CULTURE IN CONSTRUCTION THEORY

The theory of the safety culture in construction enterprises to build the foundation and guidance; safety culture construction method is the corporate safety culture in construction practice methodology and the way the wizard and guidance (Luo et al 2008, Song & Gao 2012).

2.1 *Safety culture in the construction of "human security principle"*

The intrinsic safety of the produce of enterprise security, safety of human nature, "the people" and "objects" and the combination, in order to build a production safety accident defenses. Safety Culture "human security principles"(Luo & Lin 2010) in enterprise is indicated in Figure 1. Objective of the safety culture in construction is to create the "intrinsically safe" standard of the intrinsically safe: always wanted to secure safety awareness, everywhere you want to secure the safety attitude, conscientiously study the safety of security awareness, comprehensive security capabilities reality do to secure the safety of operations, everything into the safety security purposes.

Shape and develop intrinsically safe, you need to start from the concept of security culture and safety behaviors and cultural need to create a favorable security of state of environment.

2.2 *Safety culture in the construction sphere slopes principles of mechanics*

Safety culture in the construction sphere slopes principles of mechanics (Gan & Lin 2009, Xu & Qiu 2009) can be used in Figure 2 indicate.

The meaning of this principle is: the fire safety status as a "ball stopped on the slope, the inherent safety of the matter, the scene of the fire-fighting facilities and fire equipment, as well as units and

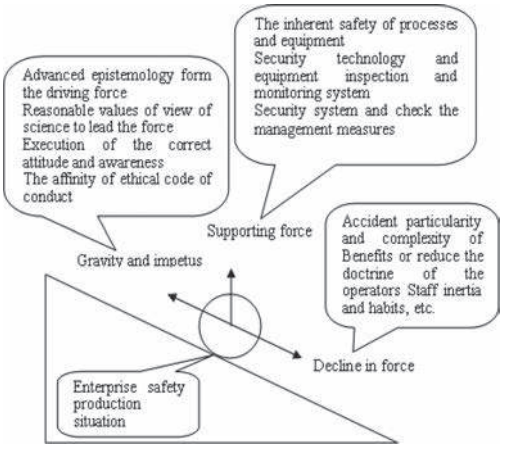


Figure 2. Safety culture in the construction sphere slopes principles of mechanics.

social Fire system and management, "ball "basic" support force ", play a basic role in the assurance of fire safety. Only this support force is not able to fire safety in the "ball" stability and maintain the standards and level, this is because there is a decline in force in the social system "is caused due to following reasons.: First, fire the particularity and complexity, such as the chance of fire, sudden, illegal is not necessarily the objective factors such as fire; the benefits or reduce the doctrine, that security needs to invest, increase costs, and vice versa can be said that the security cost variable formed for profit; the inertia and habit, the formation of the early "masters" under the guidance of habitual illegal, long-term "opportunistic" behaviors. This adverse inertia and habits lead to safety norms need to pay the effort and time, and violation may bring temporary comfort and short-term "interest".

To overcome this decline in force "need" cultural power "to" counterproductive "(Pan & Gao 2007). This "cultural force" is the driving force of the correct epistemology, values and view of science to lead the force. Culture decides ideas, and thinking decides future, and cultural forces decide competitive power.

3 TEAM SAFETY CULTURE CONSTRUCTIONS

3.1 *Strengthen the legal system to create a cultural platform*

Team safety culture construction must have a team safety values as the basis and premise. The safety

concept corrects safety awareness and correcting safety behaviors, safety awareness and safe behaviors to ensure safe production. If the teams haven't the correct security concept which let the workers recognized, the team's safety culture will be difficult to build. Therefore, to create a good atmosphere, the imperative to build a safety culture in construction platform. (1) Create the concept of penetration of the platform. The idea is to recognize the high degree of sublimation. The safety concept decided the attitude of people towards work safety, and guide people's safety behavior. To take full advantage of the media and positions, to further increase public awareness and education efforts, the piecemeal accident prevention and other safety philosophy is rooted in the brain, and internalized in the heart (Mao 2009). (2) To create the responsibility to implement platform. Establish and improve the safe production responsibility system, clearly defined the specific responsibilities of the team members of the security work, specific tasks, and strive to do a Kong accountability, and strive to do the security work was tubes, the team members of the mutual supervision, from top to bottom to form a closed-loop management of the chain of responsibility. (3) Build a behavior specification platform. Any development must have the protection of the policy, correct and effective policies and can promote the carrying out of work and career development. Corporate safety culture as a new career, you need the right policies for guidance in order to promote the corporate safety culture, the smooth construction.

3.2 *Specification employees' safety behavior*

Practice has proved that only continue to improve the quality of decision-making, management and safety culture of the first-line employees, in order to enhance the overall safety quality. The key to improving the quality of employee safety is an update of the concept. Encourage people to establish a correct concept of security, the most basic, and the most effective means of various forms of publicity and education and training.

3.3 *Actively to create a strong corporate safety culture*

Employees in a strong safety culture, their behavior will naturally regulate the rules of this security values and safe behavior. To create a corporate safety culture, the following activities are feasible.

a organization and conduct safety culture, cultural and recreational activities, organized by the security and variety show, to carry out safety knowledge contest, the organization's security literary creation, editing and publishing the case of the accident, and collecting security proverbs, aphorisms to carry out the basketball competition, "safety glass" calligraphy competition(Xu 1994, Xu & Qiu 2011), cultural activities, efforts to create a strong safety culture.

b. of the party, government, workers, groups, women's organizations in accordance with their respective characteristics, focus on safety culture in a creative way to work, such as the "Pioneer Cup" safety contest, security assistance and education of the families of employees, security persuasion activities, pupils written proposal to send security and other activities, the formation of production safety is everyone's responsibility, a good situation for everyone concerned about the safety in production.

c. active use of the comics, posters, newspapers, posters, radio and television and other means of publicity, solid and effective to carry out safety publicity.

d. in the workplace, important positions in key places to set the security warning message, and safety signs.

3.4 *Rational use of management tools*

Security Management is a comprehensive people-centered scientific management, is an important part of the coal business management, it reflects the level of quality of the integrated system of the entire coal. Coal mine safety depends on human security behavior and material in which the security environment, human security is closely related to behavior and safety of persons psychological. Among them, the management is the core. Because the human factor is the dominant management factors are the key factors of the matter is the foundation, and environmental factors are conditions. In the management of production safety should be after tracing the main changes in advance prevention-based, developed in accordance with the law of human psychology and the objective laws of the safety precautions, the introduction and application of psychological science this means better for coal mine safety management services, On this basis, to establish a new security management system, scientific, rational, feasible safety management system is to achieve the security necessary to protect. (1) The team safety production incentives. Team leader in process safety management team to do just take the lead, when well set an example is not enough to lead the team members work together to implementation of the team's safety production targets, it is necessary to know how to stimulate and inspire the morale of the team members of the. This requires that the group leaders know how to use team production

safety incentives. It can be said that the team leader on the team production safety incentives to use the good or bad, to some extent, the success or failure of the team of production safety. (2) The timely education of affection infection. Infection of family education in theory is to promote staff to establish the correct safety awareness, its most basic, the most effective means of publicity and education. The publicity and education of safety production adapt to the internal needs of the knowledge of production safety of the workers, the workers will to accept from a subjective perspective. But previous safety education mostly, "I said you listen to" (Qiu 2010) chalk and talk, not the big deal is paternalistic scolding. Through study and practice the scientific concept of development, deeply appreciate the boy are exaggerated "a very simple philosophy of reason, to solve the problem of safety education into the heart into the brain, must pay attention to the emotional investment in family education can be used France. (3) To build a good working attitude. Mentality will have a direct impact on the daily work behavior of workers, and thus the work of the psychological state has a very important role in the safe production, good workers mentality, not only can guarantee the personal safety of the workers, but also to ensure that the equipment repair, maintenance and tests quality, safe production and will have to protect. If the workers state of mind, love and dedication spirit and dedication, the work is not strong sense of responsibility, it is easy to form a workers safety consciousness, dry work when security measures are inadequate and imperfect probability of the accident will increase. Production safety cannot be guaranteed. Deal with workers attitude change caused by a high degree of vigilance and attention, and to take effective measures to be guided.

4 CONCLUSION

In this paper the current situation and existing problems of China's coal mines on the construction of a safety culture, based on "human security principle" and "sphere slope principles of mechanics, a number of specific solutions for existing problems, such as the introduction of new equipment regulations, new technologies, new processes; improve and deepen the concept of, regulate employee behavior; development of cultural construction was about to; incentive and restraint mechanisms; organizations safety culture, cultural and recreational activities; in the workplace, it is important positions, key places to set the security warning message. Safety signs are affection infection education in a timely manner, and so on. From the everyday little things start to carry forward the spirit of the white weeks comrades. Safety is the eternal theme of the coal mines; miners survive the most basic needs and the necessary conditions, a necessary condition for human development and social progress. Coal mining enterprises and the whole of the coal industry to maintain a stable and sustainable development, to protect the lives and safety and physical and mental health, to make safety culture building as a long-term task, step by step, consistently and unremittingly.

REFERENCES

Fan Weitang. 2007. Safety Production Situation, Differences and Countermeasures in China. Beijing: *Coal Industry Press*: 106–112.

Gan Xinmeng & Lin Hongyuan. 2009. Introduction to safety culture [D]. Sichuan: *Science and Technology Press*: 23–25.

Gan Xinmeng. 2010. Constructing the Corporate Safety Culture and its Activity Patterns. Beijing: *China Safety Science Journal*: 46–49.

Lin Hongyuan. 2008. Safety engineering technology industry is the material basis of the safety culture in construction. *labor safety and health magazine*: 41–44.

Luo Yun, et al. 2008. Safety culture one hundred asking and one hundred answers[D]. *Beijing Institute of Technology Press*: 133–145.

Luo Changhai & Lin Xian. 2010. Enterprise Culture Essence. Beijing: *Tsinghua University Press*: 52–58.

Mao Haifeng. 2009. Discuss the safety culture and its construction. Policy and Regulation Department of State Administration of work safety. Paper compilation of safety culture. Beijing: *China Workers' Press*.9(3): 85–92.

Pan Jian & Cao Weyu. 2007. The application with behavioral science theory on constructing safety culture in the enterprise of "zero harm" [J]. *China Association of Occupational Health and Safety:* 20–23.

Qiu Cheng. 2010. Seeking the source of safety culture[J]. *the alarm bells ringing reported(bound volumes)*: 4.

Song Fufa & Gao Fangfang. 2012. Production Safety Law[D]. Beijing: *China Social Press,* 12(6):79–84.

Xu Deshu. 1994. Construction of safety culture in China—Research and Exploration [X]. Sichuan: *Sichuan Science and Technology Press*: 36–41.

Xu Deshu & Qiu Cheng. 2009. Enterprise Security Culture [X]. Beijing: *Chemical Industry Press Safety Science and Engineering Publishing Center*: 44–47.

Xu Deshu & Qiu Cheng. 2011. General Theory of the Safety Culture. Beijing: *Chemical Industry Press*: 115–120.

Progress in Mine Safety Science and Engineering II – He et al. (Eds)
© 2014 Taylor & Francis Group, London, ISBN 978-1-138-00122-0

Research of distributed monitoring and management system of mine ventilation

Xin-Lei Liu, Bin Shen, Liu-Hui Li, Si-Wei Ren, Lin Zhang, Ke-Qiao Cheng & Xian-Zhen Xu
Department of Safety Engineering, Heilongjiang University of Science and Technology, Harbin, Heilongjiang, China

ABSTRACT: According to problems of less wind speed probes in current mine ventilation monitoring system, and Missing check points, out of work and short of real-time data transmission exited in the work of air volume inspection by miners, this paper provided a Distributed Monitoring and Management System of Mine Ventilation based on micro-power wireless transmission technology. The system structure and its networking mode were studied. After the introduction of mechanical wireless intelligent anemometer and ultrasonic wireless anemometer, the underground wireless monitoring subnet composed of wireless relay stations and wireless gateway was designed in detail, including the specific hardware architecture, working principle, wireless communication process and its key technologies. The application of this system will help to build real-time monitoring of mine ventilation, make effective management of air volume inspection work, is of great significance to ensure coal mine safety production.

1 INTRODUCTION

Mine ventilation monitoring system is an important part of coal mine safety monitoring system which plays an very important role in coal mine safety production (YAN Fei 2009, SUN Jiping 2010). Because of the mine gas accidents are often caused by the stopping or inadequate of air flow in the local area or roadway, so real-timely controlling of air flow condition of the underground main areas is the key of ventilation management. But the current mine ventilation monitoring system is mainly in view of monitoring of the main ventilator working conditions, lacking of underground monitoring stations. And there are also problems of missing check points, out of work and short of real-time data transmission exited in the work of air volume inspection by miners. So, in order to solve the problems above, this paper provides a Distributed Monitoring and Management System of Mine Ventilation based on micro-power wireless transmission technology. This system is a beneficial supplement to the current ventilation monitoring system and will improve the management level of mine ventilation.

2 SYSTEM COMPOSITION AND WORK PRINCIPLE

The structure of the distributed monitoring and management system of mine ventilation includes monitoring terminals (such as mechanical wireless intelligent anemometer and ultrasonic wireless anemometer), wireless wind speed monitoring subnet, CAN bus transmission network and ground monitoring center. The wireless wind speed monitoring subnet composed of several wireless relay stations, locating relay station and a wireless substation is mainly arranged in mining areas and transmits the air volume data to the monitoring center. Wireless substation which is the interface of wireless monitoring subnet and cable transmission network receives wireless monitoring data and sends data to the cable transmission. Cable transmission network can share the existing monitoring system communication network. The monitoring center decodes monitoring data and determines air volume of the specific location. The system overall structure is shown in figure 1.

When used in roadway area, the system can increase or decrease the number of wireless relay station to adapt the detection distance.

3 INTRODUCING OF INTELLIGENT WIRELESS MONITORING TERMINALS

Intelligent wireless monitoring terminal equipments mainly include mechanical wireless intelligent anemometer (WU Qiang et al. 2009) and ultrasonic wireless anemometer (QIN Xianli et al. 2011). The former which can be carried by airflow inspection technician is a mobile airflow monitoring equipment which mainly consists of airflow speed detecting unit, the wireless transmission

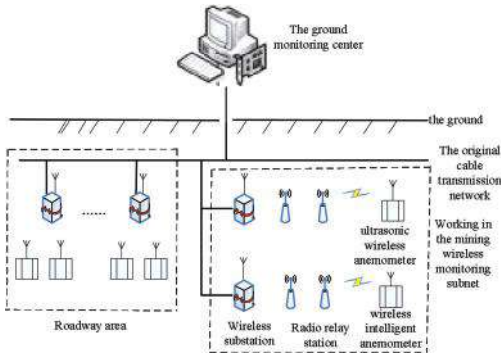


Figure 1. Whole structure of system.

unit, MCU control unit, clock circuit, the function keys and power supplying, etc. It has functions of airflow speed detecting, roadway area inputting, air volume calculation and correction, air volume display and wireless transmission. Airflow speed detecting unit consisting of the impeller and photoelectric encoder can measure the impeller rotating speed within a set time (default 1 min) cooperating with the clock control. Then, according to the calibration curve, it can calculate the airflow speed. The date of air volume used to transmission every time will be automatically saved. Ultrasonic wireless anemometer, the overall structure of which is like the ultrasonic wireless anemometer, has difference in the airflow speed measured by the ultrasonic sensor. And it is the airflow speed sensor of the system, fixed installation and longtime working in underground with no mechanical grinding loss and extension of the calibration cycle by using ultrasonic technology. Wireless communication uses Gaussian Frequency Shift Keying modulation (GFSK), and data of Manchester encoding and decoding is completed automatically in the internal of the chip.

4 WIRELESS MONITORING SUBNET DESIGN

Underground wireless communication is restricted by the roadway environment, and wireless communication distance is limited too. Each of the wireless communication base station's signal coverage is limited, and the cost will no doubt greatly increase if we decorate the whole mine wireless communication systems. So we take the theory of sensors' layout has no blind area to monitor the key regional of underground, to achieve the effective monitoring of goal.

4.1 *A master control chip and wireless communication chip selection*

Macro Chip Company's new generation of high speed and low power SCM STC12C5412AD is chose as the master control chips of wireless substations and wireless relay stations. The SCM use a single clock/machine cycle (1t), 12 times faster than normal 8051 SCM; Integrated 8 channels and 10 bit ADC ports, and save the AD conversion module for the system; with a high speed SPI port that can satisfy the wireless communication with high speed data transmission.

Nodic Company's monolithic RF transceiver chip nRF905 is chose as the wireless communication chip which work in 433/868/915 MHz (SUN Peng 2008), and the transition time between channels is less than 650 μs. It works with 4 modes, and the Shock Burst mode can automatically produce lead code and CRC check code. Current consumption is very low, when transmission power is −10 dBm and the emission current is about 11 mA and receiving current is 12.5 mA. Single-ended whip antenna can be used and the maximum transmission power is 10dBm. In the open area, the furthest transmission distance can reach more than 1 km.

4.2 *Design of hardware*

Wireless substation is mainly composed of wireless data transceiver module and the control unit and 232-CAN conversion module and power supply, and hardware principle as shown in figure 2. After wireless substations receive the testing data, the main control chip (microprocessor) immediately receives the data that read from the nRF905 by SPI interface and decrypt the data and add the address of wireless substation, processed data will be sent to communication interface of cable hardware in the form of packaged (figure 2 takes CAN interface as example), and by which the communication with the ground monitoring center has been finished. Substation is supplied by AC-DC isolation type power. When the power is outage, the power supply control module starts the standby dc power supply, and the DC power should supply no less than two hours.

Wireless relay station is the signal receiving and transfer equipment of the wireless monitoring network. It is composed of wireless data transceiver module, the control unit and the DC power supply. Where it is set and the degree of density of it is determined by the actual situation of the coal mining area, and it has the function of multi-hop routing that can effectively increase wireless signal coverage of the monitoring subnet.

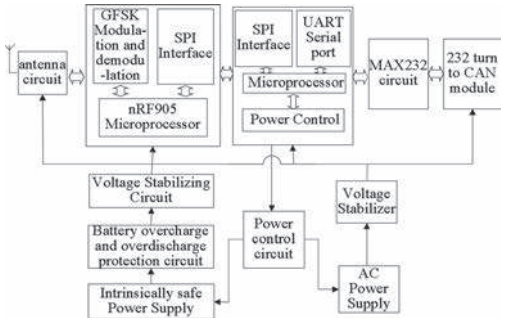
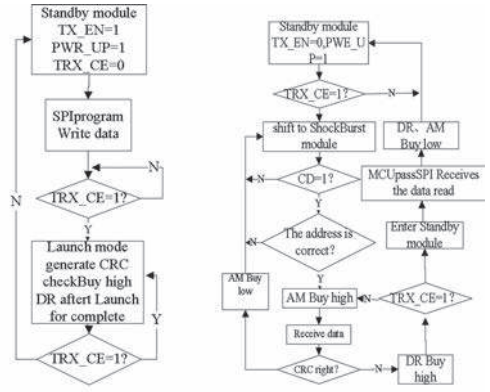


Figure 2. Principle of wireless substation.



(a) flow chart of transmitting (b) flow chart of receiving

Figure 3. Wireless communication flow chart.

4.3 *Communication design of wireless monitoring subnet*

4.3.1 *Wireless communication protocol*

The wireless communication protocol of this system is half duplex mode, and the specific format is as follows:

[Lead code][Wireless substations address code] [Relay station address code] [Superior relay station address code] [Air-flow meter code][Air volume] [CRC check code]

Lead code and CRC check code are automatically added by nRF905, wireless substation address code is 2 bytes which is the primary address location when distinguish the working area and the wind speed is abnormal; Air-flow meter code is 4 bytes, and it is only corresponding to the number of the wind member, and it can ensure the source of the air monitoring data; The superior relay station address code is used to control process that data transfers in wireless communication subnet. Air volume is defined as an integer that is 3 bytes, and the second byte is decimal point.

In the process of wireless communication, it is needed to determine the superior relay station address code at first. If the site address code the same as superior relay station address code, it means that the data were sent by local address; If they are not same and not empty, transmit directly, if they are not same and empty, just add this site address and sent. This way can ensure that data continues to uplink, finally reached wireless substation. Monitoring data can be transmitted by many relay stations, finally reached the wireless substations. The wireless substations will remove the "superior relay station address code" and add wireless substation code after wireless substation having received the data and then sent the packaged data to the monitoring center.

4.3.2 *A single wireless transmission process*

To make nRF905 as a communication interface between intelligent wireless monitoring terminal and wireless monitoring subnet, half-duplex mode is used for communicating (QIN Xianli et al. 2011). The software flow chart of single wireless transmission process is shown in figure 3.

nRF905 uses carrier detection protocol which will have a interception before transmission, namely nRF905 will turn into receive mode to detect whether the CD pin is low before sending date, if it's low (the current frequency channel is unoccupied) then nRF905 will turn into transmit mode to send data. Before receiving data, nRF905 detects carrier information (CD pin) and address matching information (AM pin) firstly, only the carrier is present and sending address is high (right), it receives packets. nRF905 is always working in the standby mode, selecting to transmit or receive data model after receives a command of control system through SPI interface. In wireless communication, after transmitted or received the effective data packet, the data ready DR pin is set in high, MCU detects the DR is high, it turns the nRF905 into a low-power standby mode, and the MCU can read out the effective data received by nRF905 through the SPI port, and the received data will be dealing for further processing according to communication protocol set by MCU.

4.4 *Anti-collision design of wireless communication*

Due to the control channel is shared for all wireless anemometer and other wireless sensors, the anti-collision protocol must be used, this paper adopts the CS-MA/CA mechanism of IEE802.11b, namely that sending data at one time when the channel is free, and using the "binary exponential back off algorithm "(WU Haitao et al. 2002)" delay some time randomly, when delay time is over and then

send the data. Specific ways: when a anemometer needs to launch air signal, it first turns into monitor mode to determine whether received carrier (channel occupied), if not then switch to transmit mode and transmit signal, otherwise it will delay and wait until not detect the carrier.

4.5 *Efficient data reception technology*

4.5.1 *Carrier detect*

When nRF905 work in receive mode, in order to avoid data collision of different transmitter working in the same frequency, carrier detect (CD) PIN will set high, if it appears the same received frequency of carrier as nRF905. When nRF905 get ready to launch data, in order to determine whether the preset channel could output the data, it should enter the receive pattern first.

4.5.2 *Address match*

When nRF905 work in work mode, address match's (AM) PIN will set up high, if introduction data packet's address is the same as nF905's own address. The use of the PIN prompt happens before the data is ready and the signal reset high, when nRF905 is receiving the data. If the data is ready but without the signal's setting high, for example, when CRC checksum is wrong, address match's (AM) PIN will reset low at the end of data packets reception.

4.5.3 *Automatic resending*

In the noisy environment, one way to improve system reliability is launching the same data pocket with several times. nRF905 has the characteristic of automatic resending. By turning up AUTO_RETRAN bit of configuration register, circuit will send the same data in a row once TRX and TXEN keep high. When TRX is in low, nRF905 will be turned to standby mode when it finished current transmitting data packets.

5 THE EXPERIMENT

Underground communication test has been done. The main transport roadway of Dongrong coal mine of Shuang Yashan Mining Group was chosen as test place. With transmission power 10 dBm and communication frequency 433.6 MHz, the effective communication distance can reach 80 m between intelligent wireless monitoring terminal and the station in the straight roadway. But if with 500 dBm and 433.6 MHz, it will be 250 m.

6 CONCLUSIONS

The realization of distributional mine ventilation monitoring and management system based on wireless intelligent anemometer will help to achieve real-time monitoring airflow of mine's critical areas. The system can also realize the supervision of airflow inspection technician's underground work, and will effectively improve the level of safety management of mine ventilation.

ACKNOWLEDGEMENTS

This work was financially supported by Scientic Research Fund of Heilongjiang Provincial Education Department(12513079).

REFERENCES

Macro crystal science and technology. Manual of STC12C5412 AD series MCU device. China. *www.MCU-memory.com*.2006:7–8.

Qin Xianli, Fu Mingchao, Coal mine wireless intelligence portable anemometer based on Zigbee technology. *Industrial Instrumentation & Automation,* 2011(03):15–17.

Qin Xianli, Shen Bin, Liu Xinlei. Research of overrun gas-data wireless transmission system based on nRF905. *Progress in Safety Science and Technology*. 2008:390–393.

Sun Jiping. Coal mine safety production monitoring and communication technology [J].*Journal of China Coal Society,* 2010, 35(11):1925–1929.

Sun Peng, The principle and application of the single-chip RF transceiver nRF905[J].*Practical Electronics,* 2008(2).

Wu Qiang, Shen Bin, Liu Xinlei. The technology of radio frequency gas sensor. *Safety in Coal Mines,* 2009, 40(5): 74–77.

Wu Haitao, Cheng Shiduan. IEEE 802.11 Distributed Coordination Function: Enhancement and Analysis, *Journal of Computer Science and Technology,* 2002, 18, (5):113~116.

Yan Fei. Substation's research and the realization of communication of coal mine monitoring system based on CAN bus[D]. *Xi'an: Xi'an University of Science and Technology,* 2009:1–12.

Progress in Mine Safety Science and Engineering II – He et al. (Eds)
© 2014 Taylor & Francis Group, London, ISBN 978-1-138-00122-0

Selection of coal mine accident cases for training

Wenwang Yang
School of Resource and Safety Engineering, China University of Mining and Technology (Beijing), Beijing, China
School of Mining and Safety Engineering, Anhui University of Science and Technology, Huainan, Anhui, China

Kai Zhu
School of Resource and Safety Engineering, China University of Mining and Technology (Beijing), Beijing, China

Sanlin He
School of Management, China University of Mining and Technology (Beijing), Beijing, China

Yanan Zhang & Shangfei Gao
School of Resource and Safety Engineering, China University of Mining and Technology (Beijing), Beijing, China

ABSTRACT: The previous methods of accident cases selection in the past were unsystematic, incomplete and were only limited to qualitative selection. In this article, a large number of accident cases are analyzed, and then the influence factors of high degree of recognition are got as the factors for the selection of coal mine accident cases by filtering the questionnaires. AHP is used to determine the weight of each factor. Finally, a set of quantitative selection method of accident cases is worked out which is used to select cases for training a certain kind of unsafe act.

1 INTRODUCTION

People's unsafe acts are the main direct causes of the accidents (Fu & Zhang 2013). Limited by the condition of automation, informationization and mechanization of coal mines, unmanned mining underground is impossible (Sun 2011). So only to eliminate people's unsafe acts can the coal mine accidents be reduced. Based on the unsafe acts (Wu et al. 2011, Chen et al. 2012, Zhao & Nie 2011), a set of factors influencing selection will be got. The research method of questionnaire is adopted to study the influence factors, and then a set of quantitative selection system is obtained combining with the mathematical methods such as statistical methods and Analytic Hierarchy Process (AHP), aiming to improve the level of the safety education and training in the coal mine enterprises, the goal of this article as well.

1 ANALYSIS OF THE QUESTIONNAIRE

1.1 *Design of the questionnaire*

This article finds some common indicator elements in those accidents written reports in "China Coal Mine Accidents and Expert Comments Collection"with a statistical analysis. Through analysis and summary, ten component elements which have impacts on the selection of coal mine accident cases are resulted. These elements are numbered from A to J recorded in the Table 1.

Table 1. Statistical data of elements affecting on the selection of coal mine accident cases.

No.	Element number	Element content
1	A	Unsafe acts
2	B	Mine site
3	C	Occurrence time
4	D	Shaft building time
5	E	Mine area
6	F	Gas levels
7	G	Accident loss
8	H	Specific location
9	I	Production capacity
10	J	Ownership

The questions on the questionnaires are about the ten elements above. Five Points Scale designed by Likert who is an American social psychologist is used. Scores of all those tested will be input into the SPASS for processing and then statistical results will be obtained. The survey was carried out among students and teachers in School of Resource & Safety Engineering in China University of Mining & Technology, Beijing, adopting the way of the online questionnaire. 129 questionnaires were given out among which 118 effective questionnaires were recycled. The recovery percent

was 95.6 and the effective recovery percent was 87.4.

1.2 *Questionnaire test*

Before using the questionnaire for coal mine accident cases selection and evaluation, the reliability and validity of the questionnaire must be tested in order to ensure the reliability and rationality of the questionnaire (Zeng & Huang 2005).

1 Reliability test

In Attitude Scaling, the coefficient α created by L.J.Cronbach is commonly used to test the reliability (Wen & Ye 2011). The reliability is acceptable with its internal consistency reliability coefficient α is above 0.50. The internal consistency coefficient between each factor and indicator is calculated (Table 2) and the results show that most elements' internal consistency coefficient exceed 0.6, indicating the reliability is acceptable. The α coefficient of both accident loss and the specific location exceed 0.8. The coefficients of the place of accidents and the gas levels are 0.5 which need optimizing on the expression of statements though it can be accepted.

2 Validity test

Validity Test is to measure the accuracy of the variables using the method of measurement, that is to say the exactitude or the correctness. The method of factor analysis is introduced to test the construct validity of the questionnaire in this article.

Kaiser, a statistician, had given a KMO standard, and the closer to 1 the value of KMO is, the more suitable for factor analysis. It is generally believed that factor analysis is not proper when the value of KMO is less than 0.7 (Wu 2010).

Table 2. Internal consistency coefficient of each index.

	Elements	Number of the observed	α
Total	All the elements	10	0.631
	place of the accidents	4	0.495
	Occurrence time of the accidents	4	0.642
	Gas levels of the mines	3	0.575
	Accident loss	15	0.894
Partial	Specific location of the accidents	8	0.864
	Shaft building time of the mines	4	0.545
	Mine area	4	0.625
	Ownership of mines	4	0.569
	Production capacity of mines	4	0.723

KMO and Bartlett's tests of the questionnaire show that the value of KMO of the questionnaire is 0.701, more than 0.70, and the Bartlett sphere test shows the value of χ^2 is 4601.317, degree of freedom is 1770, the significance probability P equals to 0.00, less than 0.05, rejecting null hypothesis, suggesting the existence of a common factor in overall correlation matrix. Factor analysis is suitable.

For all the questions, principal component analysis is used to take the principal components and the rotation method adopts the maximum variation of rectangular axis. As the SPSS set value uses the standard that Eigenvalues is greater than 1 to retain principal component, seventeen in total are got with Eigenvalues is greater than 1 which also serve as the common factors taken from the factor analysis. They can explain a percentage of 75.206 of the total variance. The factor loading of 53 questions is greater than 0.5 (7 questions, less than 0.5). Every question has a high load to common factors which it belongs to. From the above analysis, it can be concluded that the construct validity of the questionnaire meets the basic design requirements.

2 DETERMINATION OF INFLUENCE FACTORS OF THE SELECTION OF COAL MINE ACCIDENT CASES IN THE TRAINING

Input the contents of the questionnaire into SPSS18.0. Through analyzing the degree of recognition of the factors influencing the accident case selection (Table 3), it turns out to be that the coal mine workers focus their attention on the following factors in turn while they study the accident cases: unsafe acts, accident loss, specific location of accidents underground, mine site, occurrence time, gas levels, ownership, shaft building time, production capacity, mine area. 83% employees think that the more unsafe acts in accident cases, the better training effect. So is the accident loss as 81.4% employees think. Compared with other items, the results of the questionnaire show that the number of people who are for those factors (score 4&5) such as short shaft building time (39%), large production capacity (35.6%), large field area (32.2%) and the typical ownership (49.1%) are all less than a half, indicating that more than a half of the interviewees don't think that the four factors are suitable for being as indicative factors. Those four factors are all about the basic situation of the mine and have no direct relationship with the happening of the accidents. So they are eliminated, getting the final factors that influence accident case selection. They are marked again as follows in Table 4.

Table 3. Statistical results of the factors affecting on coal mine accident case selection.

Factors	Unsafe act	Mine site	Occurrence time	Shaft building time	Mine area
Sum	118	118	118	118	118
Mean	4.1610	3.9237	3.8305	3.3390	3.1356
Proportion of strong agreement (Score 5)	39.8%	28.0%	20.3%	11.0%	7.6%
Proportion of agreement (Score 4&5)	83. 0%	71.2%	67.8%	39.0%	32.2%
Factors	Gas level	Accident loss	Specific location	Production capacity	Ownership
Sum	118	118	118	118	118
Mean	3.5424	4.4153	4.1356	3.1780	3.5000
Proportion of strong agreement (Score 5)	13.6%	37.3%	37.3%	5.9%	16.9%
Proportion of agreement (Score 4&5)	51.7%	81.4%	78.8%	35.6%	49.1%

Table 4. Statistical data of the factors affecting on coal mine accident case selection.

Sequence number	Element label	Element content
1	A	Unsafe acts
2	B	Mine site
3	C	Occurrence time
4	D	Gas levels
5	E	Accident loss
6	F	Specific location

3 DETERMINATION OF METHODS FOR ACCIDENT CASE SELECTION

3.1 *Method of assignment of factors affecting on accident case selection*

There are four or five standards for every influence factors in the questionnaire. Every standard is of different importance to both the influence factors and the whole selection methods. According to the different degrees of recognition for every standard in the questionnaire, proportion of agreement (score 4 & 5) is used as the main indicators supplemented by average value, assigning from large number namely 4 points for the highest identity to small number namely 1 point for the lowest.

In order to explain the assignment method, assignment is conducted among the standards of the gas levels. The coal mines are divided into highly gassy mines, low gaseous mines and coal and gas outburst mines. Based on the statistical results in Table 5, the number 3 is assigned to the highly gassy mines, 2 to the low gaseous mines and 1 the coal and gas outburst mines. Following such assignment method, assignment of standards of every influence factor is obtained (Table 9).

Table 5. Statistical results of receiving the gas levels as the selection criteria.

Items	Highly gassy mines	Low gaseous mines	coal and gas outburst mines
Total number	118	118	118
mean	4.0932	3.7881	3.9153
SD	0.7278	0.8559	0.8631
The proportion of strong agreement (score 5)	30.5%	20.3%	27.1%
The proportion of agreement (score 5 & 4)	79.7%	65.2%	69.5%

3.2 *Calculation of weight of factors affecting on the accident case selection*

The vertical sorting of each factor is determined by assigning the standards of each influence factors. Then a horizontal weight calculation of the effects among every influence factors is done.

The method of AHP (Guo et al. 2008) is adopted to determine the weight. The total weight of the 6 factors is 1. The weight of each influence factors is determined by AHP according to the statistical results of the questionnaire.

1. Establishing hierarchical structure
2. Constructing judgment matrix and assigning The importance of the two elements in this case is compared according to the proportion of agreement (score 5&4) in Table 3. For example, B1:B2 = 83%: 71.2% shows that B1 is more important than B2 by 83/71.2. So do the other elements.

3. Single hierarchical sort (weight vector calculation) and inspection.
   Weight vector is got by adding the column vectors in matrix A:W_A = (15.7635, 13.5503, 12.9033, 9.8392, 15.4915, 14.9967) ^{T}. To solve $AW_A = n'_A W_A$ and $n'_A = 10.0200$ is obtained.
   So weight vector of B5 is got with the same method. W_{B5} = (3.9284, 3.1394, 2.3424) ^{T}. To solve $B_5 W_{B_5} = n'_{B_5} W_{B_5}$ and $n'_{B_5} = 3.00$ is obtained.
4. The consistency check
   Define $CI = (n'-n)/(n-1)$ as the coincidence indicator. When CI equals to 0, pairwise comparison matrix A is completely consistent. When CR = CI/RI < 0.1, the inconsistency can be accepted and it will not affect the sorted qualitative results. The value of RI is shown in the following table.
   It can be got that CRA = 0.0015 < 0.1, indicating the integral consistency of matrix A is acceptable. The value of CRB5 equals to 0, indicating that the integral consistency of judgment matrix B7 is acceptable.
5. The weight of every standard (normalization)

4 CASE ANALYSIS

An unsafe act is randomly selected from the "China Coal Mine Accidents and Expert Comments Collection". For example, the blasters do not use the safety explosive. There are 6 cases that contain this kind of unsafe act. The above scoring system will be used for the 6 cases and the results will be filled into Table 10 to choose the suitable accident cases for current training in Beijing.

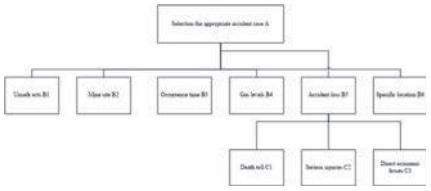


Figure 1. Hierarchy structure chart.

Table 6. Judgment matrix A.

A	B1	B2	B3	B4	B5	B6
B1	1	83/71.2	83/67.8	83/51.7	83/81.4	83/78.8
B2	71.2/83	1	71.2/67.8	71.2/51.7	71.2/81.4	71.2/78.8
B3	67.8/83	67.8/71.2	1	67.8/51.7	67.8/81.4	67.8/78.8
B4	51.7/83	51.7/71.2	51.7/67.8	1	51.7/81.4	51.7/78.8
B5	81.4/83	81.4/71.2	81.4/67.8	81.4/51.7	1	81.4/78.8
B6	78.8/83	78.8/71.2	78.8/67.8	78.8/51.7	78.8/81.4	1

As shown in Table 10, the scores of each case are put as follows D > C > F > E > A > B according to the standard. So the accident case D should be chose to train the blasters to use safety explosive. It can be found that accident D happened recently and it is the most serious accident. This choice is consistent with people's subjective feeling. Therefore, this paper provides a quantitative method when picking out some cases for training some certain unsafe acts from a lot of accident cases.

5 RESEARCH CONCLUSIONS

1. Through the statistical study of accident cases in "China Coal Mine Accidents and Expert Comments Collection", 10 influence factors are resulted for accident case selection, namely unsafe acts, mine site, occurrence time, shaft building time, mine area, gas levels, accident loss, specific location, mine location, production capacity and ownership.
2. The questionnaires are analyzed with SPSS. Results show that employees care more about unsafe acts, accident loss, the specific location of accidents underground and the mine site. While they pay less attention to such factors as

Table 7. Average random consistency index RI.

n	1	2	3	4	5
RI	0	0	0.52	0.89	1.12
n	6	7	8	9	10
RI	1.26	1.36	1.41	1.46	1.49

Table 8. Weight of the standard.

Standard	Unsafe acts	Mine site	Occurrence time	Gas levels
Weight	0.1910	0.1642	0.1563	0.1192
Standard	Death toll	Serious injuries	direct economic losses	accident location
Weight	0.0758	0.0606	0.0453	0.1817

Table 9. Assignment of the standards and the weight.

Factors		Weight	Assignment 4	3	2	1	Score
Unsafe acts		0.1910	≥4	3	2	1	
accident loss	Death toll	1.0758	≥30	10~29	3~9	≤3	
	Serious injuries	0.0606	≥100	50~99	10~49	≤10	
	direct economic losses (RMB)	0.0453	≥100, 000, 000	50, 000, 000~100, 000, 000	10, 000, 000~50, 000, 000	≤10, 000, 000	
Specific location		0.1817	coal face	driving face	goaf	The others	
Mine site		0.1642	The same group co. Ltd	The local cities and counties	The same province	Neighboring provinces	
Occurrence time		0.1563	In recent 5 years	In recent 5~10years	In recent 10~20years	More than 20 years	
Gas levels		0.1192	Gassy mines and coal and gas outburst mines	Highly gassy mines	coal and gas outburst mines	Low gaseous mines	
total		1					

Table 10. Accident case selection for training unsafe acts.

Names of the accidents	Weight/assignment Unsafe acts	Death toll	Serious injuries	Direct economic losses	Specific location	Mine site	Occurrence time	Gas levels	Total Score
	0.1405	0.0576	0.0461	0.0344	0.1336	0.1208	0.115	0.0877	1
A	1	4	2	1	0	1	1	1	0.821
B	1	4	2	0	0	1	1	1	0.7866
C	1	4	1	1	4	1	2	1	1.5076
D	2	4	3	2	3	1	3	1	2.1355
E	1	4	2	1	0	1	2	1	0.936
F	1	4	0	1	0	1	3	1	0.9588

Note: The true names of the units where accidents happened are hidden in this table.

shaft building time, production capability and mine area and so on.

3. This paper gives horizontal hierarchy analysis and longitudinal assignment of the influence factors. A scoring system for accident case selection is obtained and applied. The cases that the blasters do not use the safety explosive for the common unsafe act training are selected successfully.

REFERENCES

Chen Hong, Qi Hui, Long Ruyin. Research on 10-year Tendency of China Coal Mine Accidents and the Characteristics of Human Factors. *Safety Science,* Volume 50, Issue 4, April 2012, Pages 745–750.

Fu Gui, Zhang Su. Discussion of the Theoretical Essence and Application Effect of Behavior Safety [J]. *China Safety Science Journal,* 2013, 23 (3):1–5.

Guo Jin-Yu, Zhang Zhong-Bin, Sun Qing-Yun. Study and Applications of Analytic Hierarchy Process[J]. *China Safety Science Journal,* 2008, 18(5):148–153.

Sun Ji-Ping. Research on the Concept of Safety Production in Coal Mines [J]. *Journal of China Coal Society,* 2011, 36(02): 313–316.

Wen Zhong-Ling, Ye Bao-juan. Test Reliability Estimation: from the α Coefficient to the Internal Consistency Reliability [J]. *Journal of Psychology,* 2011, 43(7):821–829.

Wu Lirong, Jiang Zhongan, Cheng Weimin. Major Accident Analysis and Prevention of Coal Mines in China from the Year of 1949 to 2009. *Mining Science and Technology (China),* Volume 21, Issue 5, September 2011, Pages 693–699.

Wu Ming-Long. Statistical Analysis of the Questionnaire and Practice—SPSS Operation and Application [M]. *Chongqing: Chongqing University Press,* 2010, 5:194–195.

Zeng Wu-Yi, Huang Bing-Yi. Analysis of the Reliability and Validity of the Questionnaire[J]. *Statistics and Information Forum,* 2005, 20(6):11–15.

Zhao Dai-Ying, Nie Bai-Sheng. Statistical Analysis of China's Coal Mine Particularly Serious Accidents. *Procedia Engineering,* Volume 26, 2011, Pages 2213–2221.

Progress in Mine Safety Science and Engineering II – He et al. (Eds)
© 2014 Taylor & Francis Group, London, ISBN 978-1-138-00122-0

Research on relationship between coal mine safety input and safety performance based on system dynamics

Bing Wu
College of Resources and Safety Engineering, China University of Mining and Technology, Beijing, China

Zhen-Feng Liu
College of Resources and Safety Engineering, China University of Mining and Technology, Beijing, China
Henan Rescuing Center for Mineral Disaster, Zhengzhou, Henan Province, China

ABSTRACT: At present, researches on the relationship between coal mine safety input and safety performance focus on the static description. Results of the assessment on these studies lack in follow-up and dynamic management. In this paper, based on the analysis of factors that have impacts on coal mine safety performance in the process of coal production, one model about the relationship between coal mine safety input and safety performance is established using a system dynamics approach. In the process of computer simulation, coal mine safety performance is dynamically forecast by changing the initial safety level value and safety input increase rate of factors which affect system safety performance. The results show that the safety level of coal mine enterprises in the early period influences the coal mine expectant safety performance. The safety level of human factors and management factors in the coal mine enterprises is a positive correlation of coal mine safety performance. These provide a theoretical basis for management decision-making.

1 INTRODUCTION

Coal mine is a multi-process, multi-link and comprehensive industry, its production process involve people, geography, economy, the mining scheme, technical equipment, policy, management, and many other factors. In our country, for a long time, coal mine safety production has become focus of the parties because of more accidents, heavy casualties, and big economic loss. Increasing safety input and improving the level of security are a forceful guarantee for coal mine safety production. Chinese scholars have conducted a lot of research on it. Such as Liu Z.Y. et al. (2003), who has use least squares method to make regression analysis of the relation between safety input and safety level, and also discussed safety input lag. Qian Y.K. et al. (2004) study and put forward the mathematical model of the relationship between safety input and economic benefit from the perspective of township coal mines. Some scholars evaluated the effectiveness of coal mine safety input by using data envelopment analysis (Tong L. & Ding R.J. 2008). From the current study, the research on the relationship between the coal mine safety input and safety performance are mainly concentrated on the static description, be confined to purely mathematical model, be lack of a system demonstration analysis, be short of tracking and dynamic management of evaluation results.

Based on the analysis of coal mine safety production system, this paper will establish the system dynamic model of covering coal mine safety production factors, safety input and safety performance by using the system dynamics principle. The software (Vensim_PLE_v5. 6a) will be used to dynamically evaluate and quantitatively predict system safety performance.

2 THE SYSTEM DYNAMICS MODELING OF COAL MINE SAFETY INPUT AND SAFETY PERFORMANCE

System dynamics steps to solve the problem (Wu J.Z. et al. 1985) is: (1) to identify the problem: how the coal mine safety input influence factors of coal mine production, which in turn affect coal mine safety performance; (2) to determine the system boundary: safety production system in coal mine; (3) to determine causal graph and define the variable: draw causal graph of coal mine safety production system and define the model variable; (4) to establish equations, models and analyze the simulation model.

2.1 *To determine boundary of safety production system in coal mine*

According to the theory of system engineering, the influence factors of coal mine safety production are roughly divided into five parts: human factors, equipment factors, operation factors, environment factors and management factors (Qiu L. & Zhu M. 2005). Human factors refer to the quality and ability of miner. Equipment factor refers to the machinery and equipment level of coal mine production. Operation factors refer to the miner's operation process and mining scheme. Environment factors refer to geology, meteorology, etc.. Management factors refer to organizations, rules and enterprise culture. In this paper, the identified system model is shown in Fig. 1.

2.2 *Causality diagram of coal mine safety production system and the variable definitions*

Safety level of coal mine production factors is affected by safety input which includes staff, funding, technology equipment, etc.. The more investment in safety, the higher level of safety factor and the safety performance make better. When safety performance is close to the expected, the safety investment is reduction. The causality diagram is shown in Fig. 2.

Considering the established flow diagram and system dynamics equation, we define the following variables: state variables and rate variables, auxiliary variables and constants, such as Table 1.

2.3 *Flow diagrams of safety production system in coal mine and equations*

The system dynamics flow diagram of coal mine safety production is established based on the analysis of causality diagram coal mine safety production, as shown in Fig. 3.

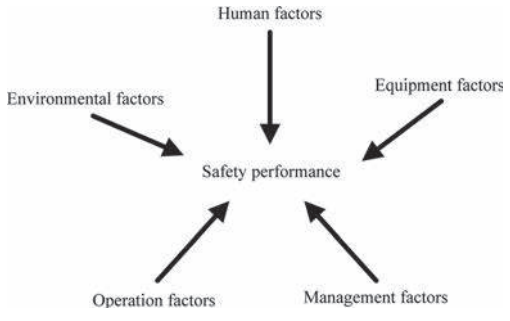


Figure 1. Chart of model of coal mine safety production.

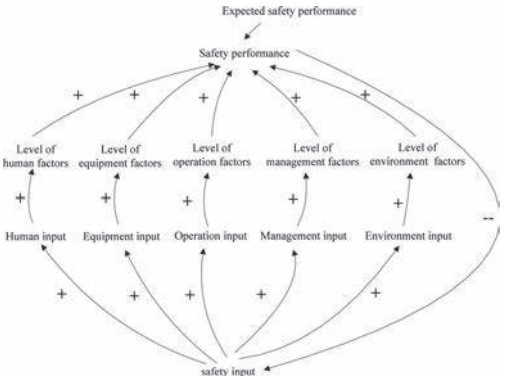


Figure 2. Causality diagram of coal mine safety production.

1. Data sources from domestic and foreign scholars' research.

1. The contribution rate of each factor to system safety performance is summed up to 1, and is obtained by the expert scoring method (Liu Y.J. et al. 2007).
2. The influence coefficient of each factor refers to input-output complete consumption coefficient table in China (Henan Provincial Bureau of Statistics, 2005). According to the formula:

$$f_j = \frac{\sum_{j=1}^{n} a_{ij}}{\frac{1}{n}\sum_{j=1}^{n}\sum_{i=1}^{n} a_{ij}} \quad (1)$$

where f_j = influence coefficient; a_{ij} = complete consumption coefficients; i = line elements; and j = column elements.

3. Equipment factors decline rate is equal to the fixed assets depreciation rate (Institute of Industrial Economics of CASS, 2006). The operation factors decline rate and environment factors decline rate are the same as Equipment factors. Assuming that the personnel quality remains unchanged at a certain stage, human factors decline rate and management factors decline rate are 0.
4. Generally, 90 is optimum standard for enterprise's safety performance. It's assumed that the expected safety performance is 90 in coal mine enterprise.
5. The given initial of safety level refers to safety input and accident losses during 10 years in a certain coal enterprise (Tang X.J. et al. 2007). There into, the investment ratio of enterprise in technology (operation), industrial hygiene

Table 1. Table of model variables.

Variable	Name	Describe
State variables	hflp	safety level of human factors
	eqflp	safety level of equipment factors
	oflp	safety level of operation factors
	mflp	safety level of management factors
	enflp	safety level of environment factors
	puth	safety input level of human factors
	puteq	safety input level of equipment factors
	puto	safety input level of operation factors
	putm	safety input level of management factors
	puten	safety input level of environment factors
Rate variables	ah	affecting rate of human factors
	aeq	affecting rate of equipment factors
	ao	affecting rate of operation factors
	am	affecting rate of management factors
	aen	affecting rate of environment factors
Auxiliary variable	ssp	system safety performance indicators
Costants	rh	the contribution rate of human factors on system safety performance
	req	the contribution rate of equipment factors on system safety performance
	ro	the contribution rate of operation factors on system safety performance
	rm	the contribution rate of management factors on system safety performance
	ren	the contribution of environment factors on system safety performance
	ch	influence coefficient of human factors
	ceq	influence coefficient of equipment factors
	co	influence coefficient of operation factors
	cm	influence coefficient of management factors
	cen	influence coefficient of environment factors
	dh	decline rate of human factors
	deq	decline rate of equipment factors
	do	decline rate of operation factors
	dm	decline rate of management factors
	den	decline rate of environment factors
	ih	increasing rate of human factors safety input
	ieq	increasing rate of equipment factors safety input
	io	increasing rate of operation factors safety input
	im	increasing rate of management factors safety input
	ien	increasing rate of environment factors safety input

(management, environment), auxiliary facilities (equipment), propaganda and education (management, personnel) is 1.746:1.905:1.852:1.458. On the basis of the expected safety performance, the existing equipment factors safety level is 75, then the operation factors safety level is 75*1.746/1.852 = 70, human factors level is 60, management factors level is 65, environment factors level is 80. The above are given initial of each factor safety level.

6. When t = 0, the safety input level of each factor is zero.
7. The safety input increasing rate of each factor is 0.4, then adjust to 0.7 after each simulation.

2. Model equations are established according to the flow diagram:

1. State equations:
   Lhflp. K = hflp. J + DT × (ah. JK-dh. JK); eqflp. K = eqflp. J + DT × (aeq. JK-deq. JK); oflp. K = oflp. J +DT × (ao. JK-do. JK); mflp. K = mflp. J + DT × (am. JK-dm. JK); enflp. K = enflp. J + DT × (aen. JK-den. JK); puth. K = puth. J + DT × ih. JK × 90/ssp. K; puteq.

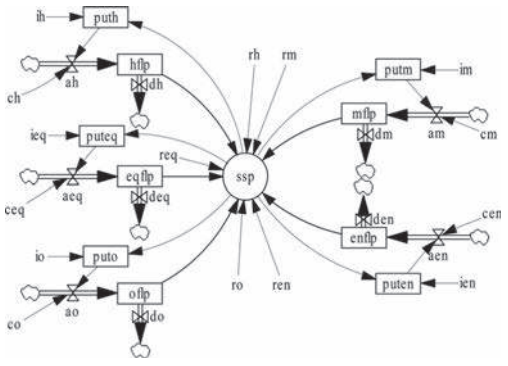


Figure 3. The system dynamics flow diagram of coal mine safety production.

K = puteq. J+DT × ieq. JK × 90/ssp. K; puto. K = puto. J+DT × io. JK × 90/ssp. K; putm. K = putm. J+DT × im. JK × 90/ssp. K; puten. K = puten. J+DT × ien. JK × 90/ssp. K

2. Rate equations:
   Rah.
   KL = ch × puth. K; aeq. KL = ceq × puteq. K; ao. KL = co × puto. K; am. KL = cm × putm. K; aen. KL = cen × puten. K
3. Auxiliary equation:
   A
   ssp. K = rh × hflp. K+req × eqflp. K+ro × oflp. K+rm × mflp. K+ren × enflp
4. Constants:
   C
   rh = 0.4, req = 0.1, ro = 0.1, rm = 0.3, ren = 0.1; ch = 0.08, ceq = 0.06, co = 0.05, cm = 0.07, cen = 0.05; dh = 0, deq = 0.01, do = 0.01, dm = 0, den = 0.01; ih = ieq = io = im = ien = 0.4;
5. Given initial:
   N
   puth = puteq = puto = putm = puten = 0 ; hflp = 60, eqflp = 75, oflp = 70, mflp = 65, enflp = 80;
6. Expected safety performance = 90;
7. Step = 1 month;

3 SYSTEM DYNAMICS SIMULATION OF COAL MINE SAFETY INPUT AND SAFETY PERFORMANCE

In this paper, the system dynamics simulation software being adopted is Vensim_PLE_v5. 6a. The simulation time are more than 4 years (48 months).

3.1 *Simulation*

1. The impact of safety level to safety performance To represent impact of safety level initial value to safety performance in the coal mine safety production, it conducts two simulations. For the first time, the model is simulated according to 50% of the initial level. For the second time, it is simulated according to the above initial level of each factor. The trend graph of safety performance with time is shown in Fig. 4. In the figure, the abscissa represents time (unit: month), and the ordinate (dimensionless: SSP) represents the safety performance.
2. The impact of different safety investment increasing rate of factors to safety performance To illustrate the impact of different safety investment increasing rate of five factors to safety performance, it conducts six simulations. For the first simulation, the safety investment increasing rate of each factor is 0.4. For the second simulation, ih = 0.7, other parameters are unchanged. Then, it successively adjusts ieq, io, im and ien to 0.7. The trend graph of safety performance with time is shown in Fig. 5.

3.2 *Analysis of simulation results*

This paper establishes one model about the relationship between coal mine safety input and safety

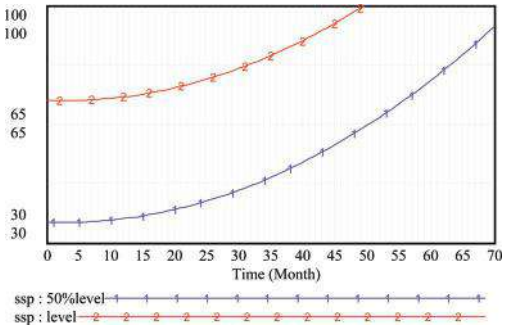


Figure 4. The impact of safety level to safety performance.

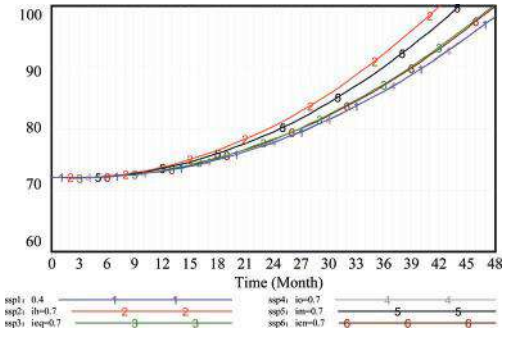


Figure 5. The impact of different safety investment increasing rate of factors to safety performance.

performance on the basis of the key factors which have important influence to the safety performance of coal mine enterprise. It's dynamically simulated the impact of safety initial level and different safety investment increasing rate of factors to safety performance. Expected safety performance is 90 in coal mine enterprise.

1. From the Fig. 4, it's shown that the time to achieve expected safety performance is affected by safety initial level of each factor. The higher the initial safety level is, the less time is used to an expected safety performance after increasing safety input of each factor.
2. As can be seen from Fig. 5, the first simulation shows that safety level and safety performance of the various factors continue to increase after that coal mine enterprises increase safety input. But improving safety performance is a long-term process. Safety performance incensement is relatively small in the first 1–2 years, but the late growth increases significantly. This is because, in the initial production process, the impact of safety input, especially human resources or management involving in training and staff education, on safety level has certain hysteresis.
3. As can be seen from Fig. 5, in the second ~ sixth simulation, the impact of human factors on safety performance whose time cut down more than six months to achieve an expected safety performance is the most obvious. The next impact is management factors. The adjustment of other three factors is no significant difference. The impact of human and management factors on safety performance become more and more strong. Because staff's increased safety awareness can build safety culture, which can't be matched by other physical factors.

4 CONCLUSION

In systems engineering perspective, this paper constructs a system dynamics model of safety input and safety performance in coal mine production. It's dynamically simulated the impact of safety initial level and different safety investment increasing rate of factors to safety performance. It provides a theoretical basis for decisions of safety input in coal mine enterprise. Simulation results show that the higher the safety level is, the faster the expected safety performance achieve. In the long run, increasing safety input has obvious promoting effect for coal mine enterprise's safety performance. Increasing safety input human and management factors will produce obvious effect on the coal mine enterprise's safety performance. That is often ignored when coal mine enterprises increase safety input, instead of blindly improving the level of technical equipment.

REFERENCES

Henan Provincial Bureau of Statistics 2005. Statistical Yearbook of Henan Province: 2~29. Peking: China's Statistics Press.

Institute of Industrial Economics of CASS 2006. China's Industrial Development Report: 197–207. Peking: Economic Management Press.

Liu Y.J. et al. 2007. Comprehensive Safety Evaluation of Coal-mine Based on Analytic Hierarchy Process. *Mining R&D* 27(2): 82~84.

Liu Z.Y. et al. 2003. Relation between Safety Cost and Safety Conditions. *Journal of China University of Mining & Technology* 32(4): 447~451.

Qian Y.K. et al. 2004. Relation between Safety Input and Economic Benefits and as an Example of Coal Mines in China's Town. *The Journal of Quantitative & Technical Economics* (8): 40~45.

Qiu L. & Zhu Ming 2005. Preliminary Discussion on System Dynamics of Mine Safety Production. *Express Information of Mining Industry* (2): 23~25.

Tang X.J. et al. 2007. The Qualitative Analysis on Investment in Safety and Profits. *Industrial Safety and Environmental Protection,* 33(2): 57~59.

Tong L. & Ding R.J. 2008. Efficiency assessment of coal mine safety input by data envelopment analysis. *The Journal of China University of Mining & Technology* (18): 0088–0092.

Wu J.Z. et al. 1985. System Dynamics Modeling. *Systems Engineering* 3(2): 38~48.

This page intentionally left blank

Progress in Mine Safety Science and Engineering II – He et al. (Eds)
© 2014 Taylor & Francis Group, London, ISBN 978-1-138-00122-0

Study on information disclosure of especially serious accident

Bing Wu & Zhonghan Chen
Faculty of Resources and Safety Engineering, China University of Mining and Technology (Beijing), Beijing, China

ABSTRACT: This paper focused on the "7.23" Yong-Wen line especially serious transportation accident, analyzed the problems existing in the information disclosure through the incident information disclosed by media and relevant public opinion reflection, and depicted the fishbone diagram of the causal relationship in chronological order. According to the analysis, there existed disorganized public opinion, inaccurate information, passivity and delaying, and other problems in the information disclosure of "Yong-Wen line accident". Besides, this study also submitted relevant principles and suggestions on the information disclosure in especially serious accident of safety production.

1 INTRODUCTION

The safety production was concerned with the safety of people's lives and properties, and the information disclosure of safety production was concerned with public right to know, right to participate, and supervision right. The China's "Emergency Response Law" in 2007 defined four kinds of emergencies: accidents and disasters, natural disasters, public health events, and social security, and It regulated that emergency measures should be taken to deal with the emergencies. The "Safety Production Law" in 2002 regulated the reporting system of safety production accident, in which departments and relevant local governments responsible for supervision and management on safety production, should never conceal, misstate, or delay to report the accident situation. The important content of deepening openness of government affairs and strengthening service in government affairs consists of making a great effort on disclosure of serious emergencies and hot issues concerned by public, objectively announcing the incident progress, government measures, public preventive measures and investigation results, answering the public concerns timely, and guiding the public opinions in a right way (The General Office of the CPC Central Committee & General Office of the State Council 2011). This paper will research on the information disclosure of emergency rescuing and accident investigation in the "7.23 Yong-Wen line major transportation accident".

2 BASIC INFORMATION OF ACCIDENT SAMPLE

2.1 *The principles of accident sample selection*

Based on the casualties or direct economic losses caused by the accidents, the "Safety Production Accident Reporting and Investigation Disposal Ordinance" in 2007 divided the accidents into four ranks, in which over 30 people dead, or over 100 people injured seriously, or over 100 million direct economic losses, was called especially serious accident. In this paper, the reasons for selecting the especially serious accident as the research sample are that, rescuing and investigating were organized by high official level departments, the research analysis had representativeness, the high extent of public concern and information disclosure, and ensuring the authenticity and accuracy of the obtained information.

2.2 *Summary of accident sample*

"7.23 Yong-Wen line major transportation accident": At 20:30 on July 23rd 2011, on the "Yong-Wen line" in the Wenzhou city, Zhejiang Province, D301 train from Beijing South Rail Station to Fuzhou Rail Station, rail-ended the D3115 train from Hangzhou Rail Station to Fuzhou South Rail Station, which caused 40 people dead, 172 people injured, the line was suspended for 32 hours and 35 minutes, and 193.37165 million RMB direct economic losses (The State Council "7.23" Yong wen



Figure 1. The time nodes graph of Information disclosure of "7.23" high-speed rail accident and public opinion reaction.

line especially serious railway transportation accident investigation team 2011).

2.3 *Resource of information disclosure of the accident sample*

All the information of the accident sample was from the internet, in which the information of laws and regulations, policy files, and investigation reports were all from official websites, and the information of reports related to the accidents were all from Xinhua Net, People's Net, CCTV and other mainstream media.

3 ANALYSIS ON INFORMATION DISCLOSURE AND SITUATION OF PUBLIC OPINION ANSWERING IN THE SAMPLE ACCIDENT

Taking the time when the rail-end accident happened, 18:30 on July 23rd, as the starting point, and when the investigation approved by the State Council as the ending point, this paper will put the important incidents progress information in a time order into the fishbone diagram (See figure 1). In the diagram, the centerline represents the time series: above the centerline, the disclosed incidents information is depicted at different time points; under the centerline, the relevant reflection to the incidents information by the media and public are described (CHEN Jiaxing 2011, The People's Daily editorial 2011, WANG Ganwu 2011, LIU Tiemin 2011). With comparison and analysis, it can be found that the following incidents information constitute the central issue of reflection of public opinion and evolve into the questioning from the public.

3.1 *The information conflict between the announcement of rescuing work almost finished and little Yiyi rescued*

In the CCTV (China Central Television), one of the leading officials responsible for the rescuing said, "Human rescuing was almost done, and 5 or 6 times of rescuing were executed till the life detector cannot find any signs of life…" The media condemned that, after believing that there's no sign of life, special policeman found a 2-year-old girl in the 16th coach of D3115 train before hoisting the train, and after hoisting it, several dead bodies were also found in the train. At the following press conference, the statement of "miracle of life" triggered the media's commotion, which caused the serious questioning on rescuing work and its information disclosure. According to the investigation report's conclusion, there're two parts of rescuing work, on

the bridge, and under the bridge. The above statement by relevant leading official only described the situation of rescuing work under the bridge, but not all the work, and the rescuing on the bridge was still executed without any orders to stop. It reflected that during the information disclosure of rescuing, we only focused on the timeliness of the information disclosure, but neglected the comprehensiveness and accuracy, and the disclosure was disorganized with incomprehensive channel and inaccurate content, which caused public misunderstanding.

3.2 *Ministry of railways expressed 2 pieces of information: "Strive to open the rail by 18:00." And "the condition to open to traffic was met"*

After the accident occurred, relevant department always took the "reopen to traffic" as one of important information to disclose. Although the specific timeline was delayed several times, the reopen to traffic was always emphasized as the goal and task. As for this, the media and public questioned generally: first, under the circumstance of rescuing unfinished, which was more important, life or reopen to traffic; second, whether the condition to reopen to traffic needed careful consideration; third, whether the safety of reopen to traffic was assured with the accident cause wasn't found out yet (LIU Tiemin 2011). The "Accident Investigation Report" confirmed that, the accident caused the train was suspended for 32 hours and 35 minutes, and pointed out that after the cleaning, checking, repairing, re-laying, expert checking and other steps of preparation for reopen to traffic, the train was finally energized and reopened. Indeed, the reopen to traffic should obey the situation of rescuing work and the condition of rail lines (LIU Zhexin 2011). At the beginning of rescuing, the information disclosure should focus on the rescuing situation, and the frequent disclosure on the timeline of reopen to traffic was not convincing from the analysis on the opportunity and motive. Therefore, the direct deviation of guiding public opinion and information disclosure by relevant department caused broad questioning and criticizing by the public.

3.3 *The information of digging and burying the headstock under the bridge and relevant analysis on accident cause*

With the scenes of digging and burying the headstock were shown frequently in the TV, the statement of the train accident caused by unexpected shot by thunder" was generally questioned by the public. The "Accident Investigation Report" confirmed digging and burying the broken headstock and its scattered parts were organized, and revealed the truth that it's stopped by relevant leading officials. Meanwhile, the Report defined the accident as responsibility accident caused by "devices with serious design defects, application and examination without strict checking, incompetent emergencies measures after the shot by thunder" (The State Council "7.23" Yong wen line especially serious railway transportation accident investigation team 2011). The measure of burying the headstock was inappropriately executed, and relevant department should disclose the information through the media in time, and took the blame and the responsibility. The superimposed effect consisting of the influence caused by burying the headstock and the statement of "accident caused by unexpected thunder" seriously influenced the justice and prestige of government, which reflected that the serious mistake on the judgment of public opinion and guidance in the information disclosure.

3.4 *Two views of "burying the headstock was easy to rescuing work" and "it's miracle of life" in the press conference*

It's an important opportunity for the press conference within 24 hours after the accident happened to communicate the information and eliminate the public's suspicion. Unfortunately, the content of the information disclosure and the performance of spokesman caused huge waves. The statements of "miracle of life" and the explanation of "burying the headstock was easy to rescuing work" thoroughly destroyed the expectation and trust of the public to the government dealing with the incident justly and openly, which reflected that the inadequate openness and transparency of communication between the government and the media and the public (DAI Jitao 2012).The government didn't fulfill their responsibility and obligation to disclose the information.

3.5 *The incomprehensive and inaccurate information disclosed in the "accident investigation report"*

After the accident investigation team was established and the members list was announced by the State Council, the media questioned the equity of the investigation team in which the leading official in the Ministry of Railways participated. On August 10th 2011, the State Council changed and enriched the investigation team. Meanwhile, the media continued to focus on the situation of accident investigation report. The predicted submission expiration of accident investigation report, revealed by relevant spokesman was delayed con-

tinually, and the reason for delay involved the technical appraisal (HUANG Yi 2011). At the end of December, the report time of investigation report announced in the State Administration of Work Safety was December 25th, 2011 (The State Council "7.23" Yong wen line especially serious railway transportation accident investigation team 2011). Combined with the research investigation report of the "Safety Production Accident Reporting and Investigation Disposal Ordinance", it can be revealed that, the time technical appraisal was indentified in the report which was expired over the longest timeline of 120 days; whether the report was submitted in the statutory timeline couldn't be ascertained. Meanwhile, the accident rank was divided through three standards: numbers of death, numbers of seriously injured, and the direct economic loss, but the expression of "172 people injured" in the investigation report didn't revealed the numbers of seriously injured, which meant that the information disclosed was inaccurate. In a word, the information disclosure during the accident investigation should follow the statutory procedure, achieve the adequate information disclosure according to the law, and answer the public questioning actively.

On the above, this paper analyzed the problems of information disclosure in high-speed train accident rescuing and investigation phase, and pointed out that the untimely, inaccurate, non-transparent, inactive information disclosure and misjudgment of public opinion, failure of public opinion guidance, delay of answering the public opinion and other problems, which also reflected that the important status of information disclosure in the especially serious accident (DAI Jitao 2012). Therefore, the information disclosure should follow the principles of timeliness, reality, activeness and comprehensiveness, guarantee the people and social organizations' right to know, and make it a positive energy to push forward the accident rescuing and investigation.

4 CONCLUSIONS

1. In the rescuing and investigation of especially serious accident, the information disclosure is the responsibility and obligation of the government, which is concerned with the public right to right to know, right to participate, and supervision right. The government should establish the idea of disclosing the information actively, prompt the rescuing and investigating work, and accept the supervision by the public.
2. In the rescuing and investigation of especially serious accident, the government should highly pay attention to and exert the role of media, predict the public opinion as early as possible, answer the public opinion in time, guide the public opinion timely, report the major events thoroughly and rapidly, and exert the information leading function of the government websites and the mainstream media.
3. The government should strengthen the standardization, institutionalization, legalization of the information disclosure in the especially serious accident. Meanwhile, the government should standardize the job behaviors of the spokesman, the content and procedure of the information disclosure, and establish the accountability system in the information disclosure.

REFERENCES

Chen Jiaxing 2011. We do not need the development lack of safety, http://opinion.people.com.cn/GB/15232304.html

Dai Jitao 2012. Theory of constitutional protection of citizens' right to know—based on "7.23" Yongwen railway accident investigation, *Journal of Jianghan University (Social Science Edition)* 2012(29) l:P56–61 (in Chinese).

Huang Yi 2011. "7.23" Yongwen railway accident investigation report would be submitted in September. http://news.xinhuanet.com/politics/201108/22/c_121894023.htm

Liu Tiemin 2011. Standardization of emergency response is imperative, reflection on the emergency response of the "7.23" Yongwen railway accident, *Journal of Safely Science and Technology* 7(9):5–9 (in Chinese).

Liu Zhexin 2011. Legal Thoughts about "7.23" Yongwen railway accident emergency processing, *Legal Science Monthly,* No. 8:10–16 (in Chinese).

The General Office of the CPC Central Committee & General Office of the State Council 2011. "Opinions Concerning the Deepening of Openness of Government Affairs and Strengthening Service in Government Affairs". http://www.gov.cn/jrzg/2011-08/02/content_1918496.htm)

The People's Daily editorial 2011, the safety belt should be fastening upon especially during high speed period. http://news.xinhuanet.com/comments/201107/25/c_121713928.htm

The State Council "7.23" Yong wen line especially serious railway transportation accident investigation team 2011 Investigation report on "7.23" Yong wen line especially serious railway transportation accident, http://www.chinasafety.gov.cn/newpage/Contents/Channel_5498/2011/1228/160577/content_160577.htm

Wang Ganwu 2011. Safety accidents warned that life is above all. http://news.xinhuanet.com/comments/2011–07/25/c_121714475.htm

Progress in Mine Safety Science and Engineering II – He et al. (Eds)
© 2014 Taylor & Francis Group, London, ISBN 978-1-138-00122-0

Analysis of regularity and occurrence causes of coal-gas dynamic disasters accidents

Wu Sheng
The Key Laboratory Being Built by Anhui Province and Ministry of Education for Coal Mine Safety and Efficient Exploitation, Anhui University of Science and Technology, Huainan, China

Zhiyu Sheng
School of Mechanical and Information Engineering, China University of Mining and Technology (Beijing), Beijgin, China

Mingzhong Gao & Li Yang
School of Energy and Safety, Anhui University of Science and Technology, Huainan, China

ABSTRACT: By statistical analysis of the data of china coal-gas dynamic disasters accidents in the latest 12 years, basic characteristics and regularity in these accidents were shown, such as the decreasing fluctuate tendency of the number of total accidents and deaths, the increasing proportion of occurrence and deaths in the larger accident and the above, and the increasing number of deaths in single accident. Based on the investigation report of major accident and the above in coal-gas dynamics disasters during 2010–2012, and on the analysis of the gas explosion case for direct occurrence causes of the ignition source, the regularity of which electromechanical occurrence factors account for 57.14% was found. The incentive control of electromechanical occurrence factors of the ignition source is the effective way to curb coal-gas dynamic disasters accidents and to prevent accidents to expand.

1 INTRODUCTION

The prevention of coal-gas dynamic disasters in coal mines is the worldwide problem (He 2010), and threat seriously the safety of the underground lives of mine workers and high production efficiency. Coal-gas dynamic disasters include coal and gas outburst, gas (and coal dust) explosion, rock burst and larger roof fall, etc, and affected by coal distribution, minefield layout, mining technology and other factors.

As known, up to 95% of underground mining in China coal and the increasing output year by year since 2001 and development at the pace of 10–25 m/a mining depth, new changes have taken place in coal-gas dynamic disasters (Zhou 2008 & Hu 2012) and become a bottleneck in the safety development of coal mine. Document No. 23[2010] released by China government required that all coal mines should install safety refuge "six systems" and announce investigation reports of safety accidents, provide new basis for the prevention of disasters and case analysis for accident causation, provide new basis for the prevention of disasters and case analysis for accident causation.

By the multidisciplinary theory and method of statistical analysis and case analysis, basic characteristics and rule of coal-gas dynamic disasters accidents in coal mines during 2001–2012 period were studied and the incentive control on ignition source of direct causes of gas explosion accidents were analyzed, so as to explore the approaches from the control of ignition sources for governance coal-gas dynamic disasters.

2 REGULARITY OF COAL-GAS DYNAMICS DISASTERS ACCIDENTS DURING 2001–2012

2.1 *Variation tendency of the total quantity of disasters accidents and deaths*

During 2001–2012 periods, the output increased at proportion of 2.09 one hundred million per year, and the number of total accidents and deaths decreased fluctuant, in the same time, the death rate per million tons dropped year by year. Death rate of township coal mines dropped to 0.754 and it was the first time for the figure down below 1 while nation 0.5 in 2012, but still 22 times of US (SAWS 2013 & MSHA 2012, 2013). The number

of gas accidents declined by 48.58 accidents in average per year, the number of death peaked at 2005 and then decreased. The number of fall drop accidents and death increased from 2001 to 2002, and then dropped during 2002–2012 period. Overall, the tendency of coal-gas disasters displays fluctuating downward in total quantity, as shown in Table 1 and Figure1–3.

2.2 *Characteristics of disasters accidents' proportion based on the accident grade*

There were 2648 cases of the lager accidents and the above from 2001 to 2012, in which, gas explosion and coal and gas outburst accidents together accounted for 48.15%. As Figure 4–5 shown, the number of accidents and deaths in the sort of gas accident and roof fall accident accounted for 60% and increased in the latest 5 year, especially the increasing proportion of the magic accident and the above. Maybe this concerned extension of mining depth and increasing difficulty of dynamics disasters prevention. For example, 91 cases of

Table1. Total output, accidents, deaths, death rate per million tons of China and U.S.A. from 2001 to 2012.

	Output			Death rate per million tons	
Year	One hundred million tons	Accidents	Deaths	China	USA
2001	9.99	3082	5670	5.07	0.04
2002	11.00	4344	6995	4.94	0.027
2003	14.15	4144	6434	3.705	0.03
2004	16.67	3639	6027	3.081	0.028
2005	19.56	3341	5986	2.811	0.02
2006	21.10	2945	4746	2.041	0.044
2007	23.25	2421	3786	1.485	0.033
2008	25.23	1954	3215	1.182	0.028
2009	27.16	1616	2631	0.892	0.018
2010	29.60	1403	2433	0.749	0.049
2011	32.50	1201	1973	0.564	0.019
2012	35.00	779	1384	0.374	0.017

* The data of china are from the website of Sate Administration of Coal Mine Safety and 2012's from SAWS control target, data in America derived from MSHA.

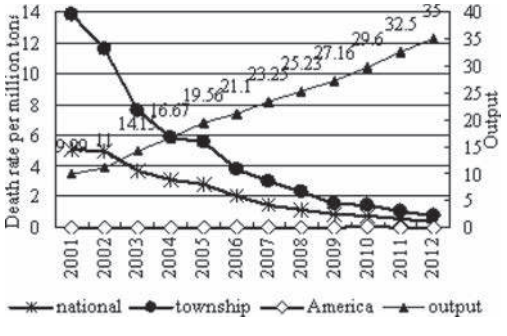


Figure 1. Comparison of tendency based on coal output and death rate.

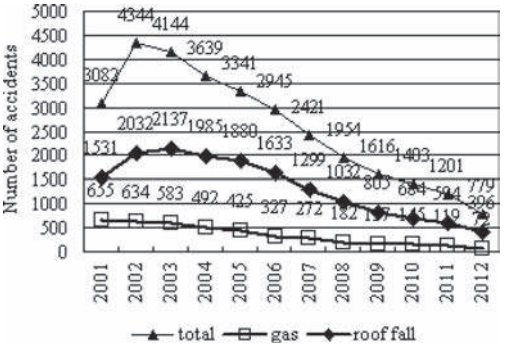


Figure 2. Comparison of tendency based on number of accidents.

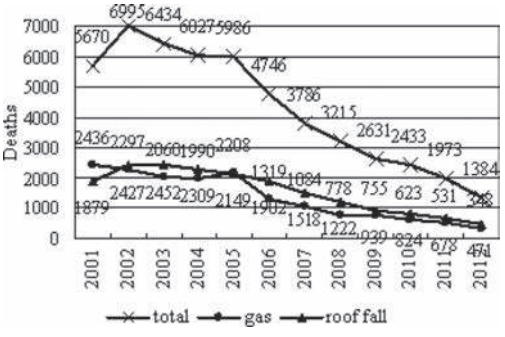


Figure 3. Comparison of tendency based on deaths of accidents.

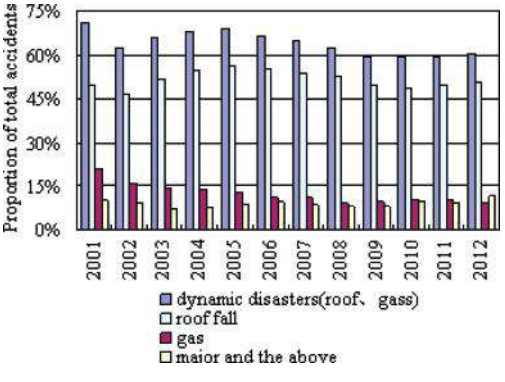


Figure 4. Proportion of the total based on accident types and deaths grade.

magic accidents and the above occurred in 2012, and in which there were 15 cases of gas explosion accidents and 14 cases of coal and gas outburst accidents, both of them together accounted for 31.87%, and outburst accident become the main incentive that could evoke major gas explosion accidents. So the feature that the proportion of accidents and deaths in major accidents and the above increased in last 12 years could be gotten.

2.3 *Feature of the number variation of deaths in an accident*

The number of deaths in a gas accident increased from 3.72 in average per case to 4.83 averages per case during 2001–2012 periods, while the number of roof fall accidents was 1.17 in average per case and 1.66 in national. As Figure 6 shown, the figure of fatal accidents per case of the larger accidents and the above increased from 4.76 in average per case in 2001 up to 6.99 in 2012, and the number peaked 12.85 at 2005. It is obvious that, the death number in average in each fatal accident is increasing, therefore, the prevention and control for coal-gas dynamic disasters of the larger and the above become emphases in mine accidents management.

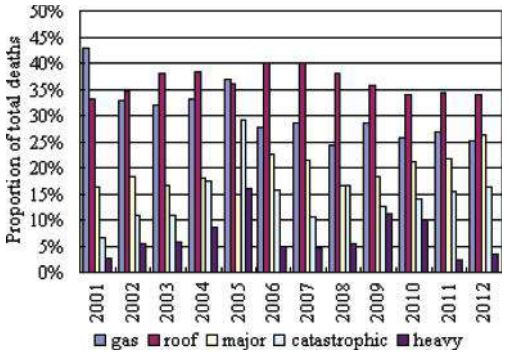


Figure 5. Proportion of the total deaths based on accident types and deaths grades.

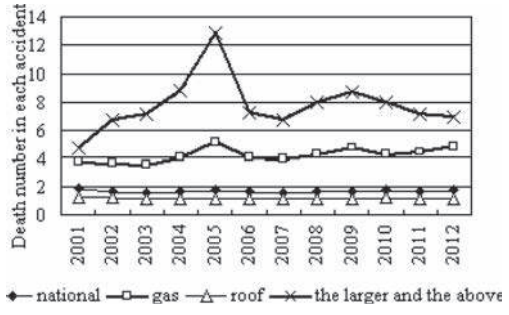


Figure 6. Tendency of death number variation in an accident.

3 ANALYSIS OF DIRECT CAUSES OF THE LARGER AND THE ABOVE DYNAMIC DISASTERS ACCIDENTS

3.1 *Selection of accidents case sample*

The national No. 23[2010] required that all investigation reports of safety accidents in coal mines should make public, and therefore provided basic data of case analysis for accident causation. In the selected 221 cases sample investigation reports of the larger coal accidents and the above during 2010–2012, the sample case percentage of 2012, 2011 and 2010 accounted for 28.5%, 34.4% and 37.1% respectively, in which, there were 70 cases of gas explosion accidents and 65 cases of coal and gas outburst accidents, therefore, the direct causes of ignition source for gas explosion could be studied by these, and the constitute of all sort of the direct incentive were gotten and shown as in Figure 7.

3.2 *Direct causes of the ignition source*

It is shown clearly in Figure 7 that, in the direct causes of different type ignition source of gas explosion accidents sample cases, the percentage of cables short-circuits, illegal blasting, repairs with power on and explosives spontaneous occupied sequentially the top forth. In the samples, the direct causes of 15 gas explosion accidents ignition sources were caused by illegal blasting with 21.43%, 10 cases of coal Seam Spontaneous and explosives spontaneous accounted for 14.29%, and 38 cases of explosion accidents were caused by cable short-circuit, mine lamp, repair with power and electrical cabinet sparks altogether and accounted for 54.29% with the highest proportion in all the ignition sources causes. The direct incentive in electrical control and mechanical together accounted for

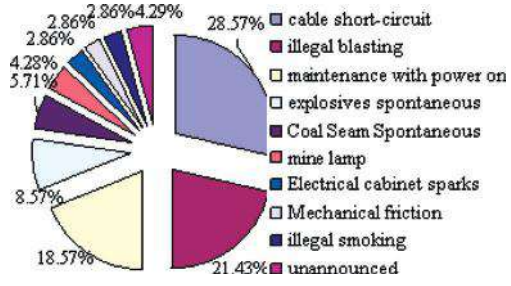


Figure 7. Constitute percentage of different type ignition source.

57.14%, and more than half of direct causes of gas explosion accidents were evoked by the mechanical and electrical equipment and instruments. So it is easily to predict that, with the increasing degree of coal mining mechanization, the proportion of the electrical and mechanical incentive of ignition sources causes will be increased.

3.3 *Analysis of example case*

For example of gas explosion accidents as Xiao Jia Wan coal mine in SiChuan province. On august 29, 2012, in SiChuan, a gas explosion accident occurred in Xiao Jia Wan coal mine, which resulting 48 deaths and 54 injured and 49.8 million Yuan in direct economic losses. The process of the gas explosion were announced as followed, Xiao Jia Wan coal mine made illegal production, and in the condition of no wind or lack of wind, accumulation of gas reached explosive concentration in working places of the No. 10 coal seam lift downhill also the No. 8 and No. 9 coal seam down +1220 miter level roadways. Signal devices of hoist at No. 10 coal seam working points sparked and detonated gas while operating. Under the high temperature and blasting, accumulated gas explored secondary at the No. 8 and No. 9 coal seam lower +1220 miter level roadways, which resulting in 48 deaths and 54 injured also 49.8 million Yuan of the direct economic loss.

In the case, the direct reason of accident causation was electric spark, which caused by the signal control cabinet of hoist and became the direct incentive of ignition source. The causation chains of gas explosion accidents would be cut off if the direct incentives of signal control cabinet spark were controlled.

4 CONCLUSIONS

Based on the above analysis, the following conclusions were gotten:

- From 2001 to 2012 year, basic characteristics and regularity of coal–gas dynamic disasters accidents were that, the number of accidents and deaths decreased fluctuate, the proportion of the larger accidents and the above and the death toll increased, and also the figure of a case accident.
- Electromechanical incentive factors for the ignition source of direct occurrence causes of gas explosion accidents accounted for 57.14%, and the percentage would rise with the increasing of the mining depth and mechanization.
- The governance of coal-gas dynamic disasters accidents of the larger and the above should still be the key focus of the safety protection, and improving the safety and reliability of the electrical control equipment is an efficient way to curb the happen and cut off expand of disasters.

ACKNOWLEDGEMENTS

The paper are founded by national natural science foundation of china (51104003 & 71071003), Anhui provincial natural science foundation of planning project (1308085MG107) and Anhui provincial university natural science research of key project (KJ2011 A090).

REFERENCES

He Xueqiu 2011. Monitoring and Forecasting technological progress of coal dynamic disasters in coal mines. *Science Times,* A3 ed, 31 October 2011.

Hu Qianting & Zhao Xusheng 2012. Present situation of coal and gas outburst accidents in chins coal mines and countermeasures and suggestions for their prevention. *Mining safety & environmental protection* 39(5):1–7.

MSHA 2012. Mining Industry Accident, Injuries, Employment, and Production Statistics, Historical Data Tables for 1978–2008. <http://www.msha.gov/ACCINJ/BOTHCL.HTM.>.

MSHA 2013. Mining Industry Accident, Injuries, Employment, and Production Statistics and Reports. <http://www.msha.gov/ACCINJ/accinj.htm.>.

State Administration of Work Safety (SAWS) 2012.situation of completion in control targets at 2012. <http://www.chinasafety.gov.cn.2013.04>.

Zhou Xinquan & Chen Guoxin 2008. The probability analysis of occurrence causes of extraordinarily serious gas explosion accidences and its revelation. *Journal of china coal society* 33(1):42–47.

Progress in Mine Safety Science and Engineering II – He et al. (Eds)
© 2014 Taylor & Francis Group, London, ISBN 978-1-138-00122-0

Comparative study on the investigation mechanisms for coal mine work safety accidents in China and USA

Guodong Mei
China Academy of Safety Science and Technology, Chaoyang, Beijing, China

Lu Liu
China Coal Information Institute, Chaoyang, Beijing, China

ABSTRACT: While probing into the investigation mechanism for the accidents occurring in American coalmines, the differences of the enforcement basis and mechanisms on the coalmine accidents between China and USA are compared and analyzed. Furthermore, the problems of China in the accident investigation mechanism are reviewed in a scientific, independent and systematic approach. Then, the author suggests the American advanced experiences and operations should be learnt, and subsequently comes up with the countermeasures for improving the investigation mechanism of China.

1 INTRODUCTION

A high risk industry, the coalmines of China cause several thousand deaths every year. Being an important component of work safety in coalmines, the work safety accident investigation mechanism is the essential prerequisite for effectively fulfilling work safety liability, and preventing and reducing accidents. The CPC central government and the State Council attach importance to the investigations for the work safety accidents in coalmines by promulgating a range of laws and regulations in succession. The purpose is to steer and standardize the behaviors of investigation of coalmine accidents. Especially, Decree No.493 Regulations on Reporting, Investigation and Handling of Work Safety Accidents promulgated by the State Council in 2006, and Regulations on Reporting, Investigation and Handling of Work Safety Accidents in Coalmines jointly promulgated by the SAWS and SACMS in 2008 further improved and standardized the mechanisms on reporting and investigation of coalmine accidents in China. In practice, however, some problems are still exposed in the China's investigation mechanisms in coalmines. For instance, accident investigation is of inadequate neutrality, and technical investigation is crossed with liability identification responsibility. Therefore, beginning with the American coalmine safety situation, supervisory system and accident investigation mechanism, this paper expects to provide a direction and some strategies for improvement of the investigation mechanism in coalmine accidents of China through comparative study of American mechanism.

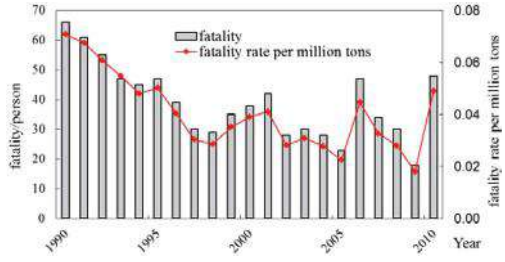


Figure 1. Changes of work safety indicators in American coalmines in 1990–2011.

2 STATUS QUO OF THE WORK SAFETY IN AMERICAN COALMINES

There are more than 2,000 coalmines across USA, which employ about 140,000 coalminers. In 2009–2011, the nation produced separately 975.2 million, 983.7 million and 992.8 million tons annually, and the death toll in the coalmines was 18, 48 and 21 respectively. The death was only 18 in 2009, set a minimum historical record [LI Xinjuan 2011], as shown in Figure 1.

3 GETTING STARTED

3.1 *Legal system on mine safety*

1977 Federal Mine Safety and Health Act ("the Mine Act") is the supreme law enforcing supervision and management of the mines across USA by the federal government. In addition, Federal Code

Vol. 30 Mineral Resources (1998) is the rules for implementation stipulated in accordance with the Mine Act. Also, statutory standard on mine safety and health can be proposed and revised as needed every year. Other coalmine safety-related regulations include Coal General Inspection Procedures Handbook and Inspection Tracking System and 1970 Occupational Safety and Health Act, etc. Systematic, complete and strict legal system in American mine safety has become the first requisite for the country to ensure its accident investigation to be scientific and reasonable [ZHAO Jun et al. 2008, ZHANG Chuanbao & JIA Xiuhua 2011].

3.2 *Mine safety supervision system*

In the meantime, USA in its mining industry possesses rigorous safety supervision and law enforcement system. The key of its success is represented in up-to-down coalmine safety supervision framework, rotational supervision personnel system, thunder-patterned supervision and law enforcement force. Furthermore, in the structure of the mechanism, a community of interest including the supervisors, mine operators and local governments is avoided.

Mine Safety and Health Administration (MSHA) is a functional unit subordinate to the Labor Department of the federal government. MSHA consists of eight departments, responsible for occupational safety and health supervision over the coalmines, metal and non-metal mines throughout USA. Among them, Coalmine Safety and Health Department is in charge of supervision over more than 2,000 coalmines in 27 states [WANG Xianzheng 2001].

The USA mine supervision system attaches particular importance to independence. Across USA, MSHA sets up 12 regional inspectorates in the coal-producing regions, which lead 45 field offices. The regional inspectorates and field offices administer their separate regions, as shown in Figure 2.



Figure 2. Locations of coalmine safety and health regional inspectorates in American.

These field offices have no relation of interest with the mine operators, or with the state and county government. The federal safety supervisions must exchange their posts in rotation every two years. If a coalmine accident involves three or more deaths, the local safety supervisors are disqualified from participating in the accident investigation. Instead, the federal office will dispatch safety supervisors in other regions to do so. These measures ensure objective and impartial supervision and accident investigation.

4 MECHANISM ON INVESTIGATION OF MINE ACCIDENTS IN USA

4.1 *Reporting mechanism on accidents*

1. Time limit of reporting

If an accident occurs, as defined in Clause 50.2 (h) in the Mineral Resource of the Federal Code, the mine operator must, within 15 minutes, report to the regional inspectorate or its field office. If he has no means to immediately get in contact with the authorities, the operator may directly call MSHA. After the situation is roughly made clear, the operator must submit written documents [PENG Cheng 2001].

2. Reporting mechanism

Immediately after receiving the report of the accident or getting to know the accident, the regional inspectorate must as soon as possible report to MSHA all the details of the accident.

4.2 *Accident investigation mechanisms*

1. Types of accident investigation

MSHA organizes accident investigation in three types:

The first is investigation of general accident causes, which aims to figuring out the accident causes, so as to prevent and avoid similar reoccurrence.

The second is special investigation of serious fatality accidents, which aims to ascertaining the operator's management responsibility, so as to provide factual grounds for criminal defense and charges.

The third is investigation of the mine safety supervisor involved in the accident investigation, or internal investigation, which aims to preventing the negligence or other problems of investigators in their work.

2. Composition of the accident investigation team

The accident investigation team of USA generally is composed of three relatively independent investi-

gation teams from the federal government, state government and trade union. Each such investigation team is composed of different members, and the team can engage experts in the investigation.

3. Graded investigation and authority

For a coalmine accident causing three deaths or more, the accident investigation is organized by the head of Coalmine Safety and Health Department.

For a coalmine accident causing less than three deaths, the accident investigation is organized by the chief of regional inspectorate. Immediately upon receipt of the accident report, the chief shall select appropriate members to form a capable accident investigation team, and appoint a team. The team shall as soon as practical collect and fill out a brief initial report of the accident, and within 72 hours report to the head of Coalmine Safety and Health Department [PENG Cheng 2001].

5 COMPARISON OF THE COALMINE ACCIDENT INVESTIGATION MECHANISMS IN CHINA AND USA

For the investigation of a coalmine accident, there are somewhat differences in China and USA in respect of law enforcement grounds, investigation philosophy, accident reporting, members of the investigation team, graded investigation and authority, accident report approval, penalties and investigation duration. The comparative analysis is listed in Table 1.

6 PROBLEMS IN CHINA'S MECHANISM ON COALMINE ACCIDENT INVESTIGATION

1. Orientation of accident investigation philosophy

Article 25 of Regulations on Investigation, Report and Handling of Work Safety Accidents sets forth the duties of the accident investigation team. Its core includes investigation and rectification of the accident causes, and identification of the accident responsibilities and accountability. In practice, however, it can be seen from the accident investigation reports in recent years that, the accountability of the relevant responsible persons and corresponding party and administrative disciplinary sanctions account for a majority proportion, while the descriptions of the direct and indirect causes of the accidents are largely ambiguous and simple, and fall short of in-depth exploration of the radical causes of the accidents.

2. Independence of the compositions of the accident investigation team

An independent accident investigation team can, to the maximal extent, safeguard the public interests, conduct a thorough and objective investigation into the accident, find out the true causes and learn the experiences accordingly. It not only investigates the work safety responsible unit involved in the accident, but investigates the competent industry department. This guarantees the impartiality and thoroughness of the investigation, and does good to objectively evaluate the work safety. In China, the investigation team lacks a strict interest avoidance system since the accident investigation team is generally composed of all-level governments and the relevant departments representing different stakeholders. Such practice is hard to warrant the objectivity and neutrality of the investigation results.

In addition, an independent fund can solve the investigators' worries behind, and is in favor of adopting state-of-the-art technologies and equipment to probe into the accident causes. Hence, it can warrant the accident investigation conclusions to be objective and scientific. In China, the funds of the accident investigation team cannot be independent, and conducting of investigation falls short of financial security. The present laws do not stipulate clearly who will pay the technical appraisal fee. Many necessary technical inspection and appraisal items are even inspected under the entrustment of the accident unit which pays the fee. The public trust of the appraisal results is hardly warranted [ZHANG Ling & CHEN Guohua 2009].

3. Duties of technical and judicial investigation

Technical investigation is generally organized by the accident investigation organ, the purpose of which is to find out the accident causes and adopt preventive measures. Judicial investigation is generally organized by the judicial organ, the purpose of which is to ascertain the responsibilities taken by the organization or individual in relation to the accident, and impose appropriate sanctions on them in accordance with relevant laws and regulations. In China, technical investigation is merged with judicial investigation. Interfered by a lot of human factors, thorough and complete investigation is often hindered, the truth of the accident is covered, and the ultimate intention of accident prevention cannot function.

4. Scientificalness of the operating mechanism on accident investigation

In China, the accident investigation team also includes the administrative officers of relevant departments. This operating mechanism may produce adverse effect on the scientificalness and impartiality of the investigation. In view of the interests of the departments, the administrative officers often concern more the belonging of the accident responsibilities, but pay less attention to

Table 1. Comparison of the coalmine accident investigation mechanism in China and USA.

	China	USA
Law enforcement grounds	1. Regulations on Supervision of Coalmine Safety; 2. Regulations on Reporting, Investigation and Handling of Work Safety Accidents; 3. Regulations on Reporting, Investigation and Handling of Work Safety Accidents in Coalmines	1. 1997 Federal Mine Safety and Health Act; 2. Federal Code, Mineral Resource Volume; 3. Coal General Inspection Procedures Handbook and Inspection Tracking System, etc.
Investigation philosophy	Identification of responsibilities and accountability	Analyze radical causes of the accident and learn experiences and lessons
Accident reporting	1. Once a coalmine accident occurs, relevant person on the scene shall immediately report to the coalmine operator. The operator shall within one hour report to the safety supervision department, coalmine safety supervision department above county level and the residing coalmine safety supervision office. In emergency, relevant person on the scene may directly report to the above organizations; 2. Once the coalmine safety supervision sub-bureau receives an accident report, it shall within 2 hours report to the provincial-level coalmine safety supervision authority; 3. Once the provincial-level coalmine safety supervision authority receives the report of a more serious accident, it shall within 2 hours report to the State Administration of Work Safety (SAWS), and State Administration of Coal Mine Safety (SACMS); 4. Once SAWS and SACMS receive the report of special serious accident and serious accident, they shall within 2 hours treport to the State Council.	1. If an accident occurs, as defined in Clause 50.2(h) in the Mineral Resource of the Federal Code, the mine operator must, within 15 minutes, report to the regional inspectorate or its field office. If he has no means to immediately get in contact with the authorities, the operator may directly call MSHA. After the situation is roughly made clear, the operator must submit written documents; 2. Immediately after receiving the report of the accident or getting to know the accident, the regional inspectorate must as soon as possible report to MSHA all the details of the accident.
Investigation team members	1. The accident investigation team is generally led by the coalmine safety supervision authority and participated by the relevant local people's government, work safety supervision and management department, the department in charge of coalmine safety supervision, inspection authority, the public organ and trade union, and the people's procuratorate is invited; 2. The investigation team consists of technical team, management team and comprehensive team. Relevant experts may be engaged in the investigation.	1. The accident investigation team generally consist s of three relatively independent investigation teams: the federal government, state government and trade union. Each investigation team has different members; 2. The investigation team may engage experts in the investigation.
Graded investigation and authority	1. For special serious accidents, the State Council or the State Council will authorize SAWS to investigate; 2. Serious accidents are investigated by the provincial-level coalmine safety supervision authority; 3. Major accidents are investigated by the coalmine safety inspection sub-bureau; 4. Ordinary accidents are investigated by the coalmine safety inspection sub-bureau.	1. For a coalmine accident causing three deaths or more, the accident investigation is organized by the head of Coalmine Safety and Health Department. 2. For a coalmine accident causing less than three deaths, the accident investigation is organized by the chief of regional inspectorate.
Investigation duration	The accident investigation report shall be submitted within 60 days after occurrence of the accident.	No strict investigation duration is stipulated.

the accident causes. The report pays more emphasis on the identification of the accident responsibilities and accountability.

Besides, determination of the accident investigation procedures is more scientific generally according to the characteristics of an individual accident. In China, it is stipulated that the accident investigation report shall be submitted within 60 days after the accident. Compared with the American practice, this requirement is too rigorous. Limitation of the investigation duration will inevitably affect the quality of the investigation, and in the end affect the scientificalness of the investigation results. USA does not set strict time limit on the investigation of serious accidents. Some mine accident investigation and approval even takes a couple of years [GAO Yanqiu & FU Yaping 2006, LIU Zijun 2011, HE Dean & DING Jintian 2002].

7 CONCLUDING REMARKS

Investigation of work safety accidents is a systematic engineering. The composition of the accident investigation team and its mechanism will all influence the efficiency and quality of the investigation. In the social environment where accidents frequently occur in China in the transition period, the author brings forward the following suggestions by learning from USA's accident investigation mechanism and experiences:

1. Improve the accident investigation philosophy

The philosophy and aim orientation of the accident investigation shall focus on improvement of safety and avoidance of accidents, analysis of the radical causes of the accidents, and learning of experiences and lessons. These measures serve as the important grounds for relevant department, industry and enterprise to formulate standards. Their implementation is supervised and tracked, so as to avoid reoccurrence of similar accidents.

2. Define the division of the investigation team's duties

Division of the duties charged by the coalmine safety inspection body, local government and all other departments is defined in the accident investigation. In the accident investigation team, enterprise and staff representatives are added. For the highly focused accident by the public, several reputed social watchers can be arranged in the investigation team who supervise the investigation process. For special serious accident, the division of work within the investigation team should be more meticulous and technical investigation teams of different disciplines are set up so as to enhance the professionalism and impartiality of the investigation.

3. Apply advanced accident investigation technical means and measures

Advanced investigation methods adopted by USA in accident investigation, such as systematic analysis of causes and accident roadmap, are learnt, field detection, computer simulation and all kinds of modern test techniques are comprehensively utilized the scientificalness and correctness of the investigation results.

4. Establish internal investigation mechanism for inspectors

In the investigation of the coalmine accident, if the responsibilities of the coalmine safety inspection organ and inspectors in the administered region are involved, the author suggests the higher coalmine safety inspection organ organize internal investigation. If finds such problems as dereliction of duty, the organ shall deliver to the inspection department for disposition.

5. Conduct scientific grading and management of accident investigation

The author suggests the investigation work and announcement of the results be made in two stages: the first stage is preliminary investigation, which focuses on investigation of the direct technical and management causes of the accident, announcement of the periodic results as early as possible, and urging relevant departments for a timely correction. The second stage is thorough investigation stage, which concentrates on a more systematic analysis of the underlying causes of the accident, analysis and evaluation of the emergency rescue disposal process of the accident, not setting a limit on the work duration of the investigation team, formulating the schedule of staged accident investigation work, and trying to release a detailed report. In this way, the investigation team can more deeply analyze all kinds of causes of the accident, and respond to the doubts questioned by all the social circles in respect of the mechanism behind the accident and the disposal process.

6. Place emphasis on adoption and application of the accident investigation experiences and lessons

After the accident investigation department submits the conclusions of the investigation report and specific suggestions, the author suggests the relevant competent or supervisory government department play a role on examination and urging of the enterprises or organizations in the relevant field to ensure complete implementation of the suggestions. Only in this way can the losses and

lessons of the accident be transformed into the knowledge and impetus of social progress [JIANG Hong 2009].

ACKNOWLEDGEMENTS

This research was funded by National Project of Scientific and Technical Supporting Programs Funded by Ministry of Science and Technology of China (2012BAK09B01).

REFERENCES

Gao Yanqiu & Fu Yaping. 2006. Problems in investigation and handling of coalmine casualty accidents and solutions. *Safety in Coal Mines* 37(5): 56–59.

He De'an & Ding Jintian. 2002. Probe into some problems in investigation and handling of coalmine accidents. *Safety in Coal Mines* 33(4): 39–41.

Jiang Hong. 2009. American coal mine safety management lessons. *Theories & Practice* 11(3): 50–52.

Li Xinjuan. 2011. Research and analysis of safety management development of American coal mines. *China Safety Science Journal* 21 (10): 162–169.

Liu Zijun. 2011. Some thoughts about investigation and handling of coalmine accidents. *Energy and Environment* 105(2): 103.

Peng Cheng. 2001. Coalmine accident investigation and handling procedures in USA. *China Coal* 27(3): 45–48.

Wang Xianzheng. 2001. *American Coal Mines Safety Supervision System* 7–23. Beijing: Coal Industry Publishing House.

Zhang Chuanbao & Jia Xiuhua. 2011. Comparative study on the law system on coalmine safety in China and USA. *Coal Economic Research* 31(7): 87–90.

Zhang Ling, Chen Guohua. 2009. Revelations from overseas independent investigation mechanisms for work safety accidents. *Journal of Safety Science and Technology* 5(1): 84–89.

Zhao Jun et al. 2008. Comparative study on the law system on coalmine work safety in China and USA. *Journal of Safety Science and Technology* 4(2): 82–85.

Progress in Mine Safety Science and Engineering II – He et al. (Eds)
© 2014 Taylor & Francis Group, London, ISBN 978-1-138-00122-0

Implementation of Kaizen in enterprise HSE management

Xudong Niu, Peng Yang & Ming Qu
Greatwall Drilling Company, CNPC, Beijing, China

ABSTRACT: According to Chinese Philosophy, Tao is the rational basis of human conduct, even though all things on earth are unaware of its existence. What is the Tao of Enterprise HSE Management? After studying the Japanese modern management theories, which has the similar cultural background, we could find a classical thought advocated by western countries: Kaizen. After learning widely from other masters' theories, Dr. Imai, Masaaki formulated the theory of Kaizen, in 1986. This article explains Kaizen's reference value for HSE management and makes suggestions for implementation of Kaizen on basis of author's management practices.

1 INTRODUCTION

In recent years, enterprise's HSE performance has been improved significantly since government continuously increased the investment into HSE management. Enterprise's attention is switching from safety in production to sustainable development, meanwhile, the connotation and denotation of HSE management is also developed further. Under the framework of National HSE Development Strategy, enterprises also formulate their long-term programs for HSE development. In order to make great progress in HSE management, enterprises attempt to induce creative safety concepts, purchase advanced equipments, apply new management methods, establish sound HSE management system and cultivate active safety culture. These management practices strengthen the enterprise's capability of risk management which gradually becomes a core-competitiveness of enterprise.

On the way to achieve sustainable development, many enterprises fell into misunderstanding or encountered the bottleneck of development. Diversification of HSE management practices has confused the managers at all levels. In this situation, enterprise is hard to form a widely accepted guideline on HSE management so as to hinder the sustainable, sound development of HSE management.

To make a comprehensive survey of our neighboring country, Japan. Kaizen has been extensively used on each aspects of HSE management. Kaizen is not only to increase the qualities of products but also to extremely decrease the numbers of HSE accidents. Research and analysis of Kaizen are benefit to direct the enterprise's HSE management.

2 UNDERSTANDING ABOUT KAIZEN

After the Second World War, Japan Government vigorously pursued "Personal enhancement campaign" and "Lean manufacturing campaign" so as to make a good social environment and business environment for creating excellent management theory. In 1960s, with an open mind, Japanese enterprises accepted the advanced Western sciences and technologies as well as management theory. Simultaneously, enterprises also absorbed the Oriental tradition of humanistic spirit. In the end, scholars brought together all kinds of thinking into Kaizen. Nowadays, Kaizen has been applied into many fields, and it has been regarded as the religion of management practices.

The so-called kaizen is to change the current situation slightly in order to reach certain degree of a better and higher level. After studying, Dr. Imai, Masaaki gave Kaizen a new connotation (Imai, Masaaki 2010a):

a. Kaizen is a kind of thought
   Kaizen is a spirit source of sustainable development. Enterprise constantly questions its own cognitive level. In other words, enterprise constantly evaluates the current situation and denies it on the basis of facts observed on site, in order to realize the improvement of current situation.
b. Kaizen is a kind of culture
   When employees reach a consensus and regard Kaizen as a personal core value, enterprise will have the power of culture. By taking full advantages of culture's effectiveness, e.g. guiding effectiveness, coagulation effectiveness, incentive effectiveness, radiation effectiveness,

assimilation effectiveness. So enterprise could create a working atmosphere full of vigor by applying Kaizen, and lay a solid foundation for its future development.

c. Kaizen is a habit of success
Kaizen makes employees have ability and acumen to find, think and solve various problems.

d. Kaizen is a means of self-improvement
The value of life is to continuously improve the quality of individual by learning and practice. Enterprises have recognized that Kaizen could help employees improve their HSE performance. Kaizen emphasizes three key points: firstly, employees must take current place, current thing and current time in to account. Secondly, employees must adhere to principle. Thirdly, employees must embrace team spirit.

3 KAIZEN'S REFERENCE VALUE FOR HSE MANAGEMENT

Dr. W. Edwards. Deming is the first one suggests the idea of the Continuous Improvement, which is the core idea of safety management theory. Japanese researchers evolved and refined this thought according to their management practices, eventually, formulated a school of thought called as Kaizen. How to convert the concept of Continuous Improvement into management practice requires a complicated systematic procedure. Through the study of Kaizen, enterprise would understand how to improve its HSE performance better.

3.1 *The relationship between Kaizen and innovation*

Nowadays, the faster innovation speed in production, technology and knowledge etc. makes enterprise survive more difficultly. Therefore, the sustainability of development is more important than management efficiency. As we known, the sustainable development of enterprise stems from continuous improvement on management. Furthermore, there are two very different ways to enhance the management. The first one is a gradual change characterized by uninterrupted succession, the other one is a radical change characterized by periodical occurence. The former is Kaizen, the latter is innovation. Both of them have the same importance to enterprise's sustainable development. Understanding the relationship between Kaizen and innovation is benefit to lay a firm basis for the long-term development in line with the rules of management.

As shown in fig. 1 (Imai, Masaaki 2010b), the ideal model of development. When the duration of innovation is certain short, this model could be

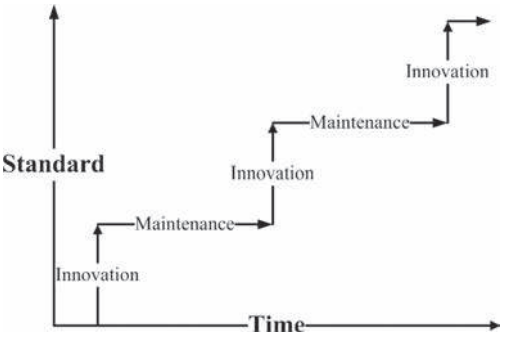


Figure 1. The ideal model of development.

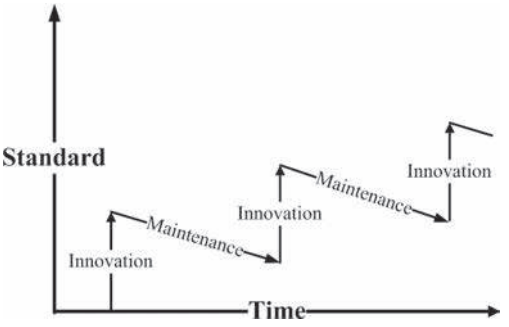


Figure 2. The actual model of development.

realized in reality, for instance, the high-tech enterprise. Nevertheless, this model is very difficult to maintain.

As shown in fig.2 (Imai, Masaaki 2010b), the actual model of development. Many enterprises overwhelmingly emphasize the importance of innovation, and neglect the functions of Kaizen, management performance indicators always oscillate up and down. So enterprise is very hard to remain the steady growth.

As shown in fig. 3 (Imai, Masaaki 2010b), the improved model of development. This model accentuates the advantages of Kaizen. In the process of improving, multiple factors could adapt mutually and fully, such as people, machine, regulation, environment, so as to HSE management system is in good shape.

By comparing with the three models, we can get a better understanding of the divergences between Innovation and Kaizen, and draw conclusions as follow: Firstly, Innovation is an abrupt and discontinuous process, yet Kaizen is a gradual and continuous process. Secondly, Innovation is an activity which the minority of employees participate in, yet Kaizen is an activity which the majority of employees participate in. Thirdly, Innovation

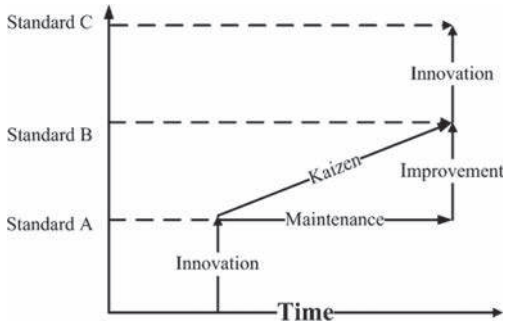


Figure 3. The improved model of development.

requires exterior force to drive, yet Kaizen requires interior incentive to drive. Fourthly, Innovation aims at short-term goals, yet Kaizen aims at long-term goals. Fifthly, the impacts of Innovation are ephemeral, yet the impacts of Kaizen are durable. Sixthly, Kaizen consists of two parts, improvement and maintenance. Seventhly, the evaluation criteria of Kaizen are standards. Eighthly, employees could find possibilities of Kaizen at anytime. Under ideal conditions, enterprise could not start an innovation until Kaizen has been enumerated completely. Kaizen could not replace the Innovation, or hinder the development of innovation, furthermore, both of them are always mutually complementary. Parkinson's Law argues that it is at the time of accomplishment that an organ begins to fall into decay. Therefore, enterprise must take a series of measures to maintain and improve the periodical achievements.

Recently, foreign HSE management consulting services is prosperous. This situation promotes the development of theories, concepts and methodologies concerning HSE management. Many domestic enterprises attempt to get a consultation on HSE management. These enterprises expected that new concepts and management styles could improve their HSE performance promptly. But, the management practices clearly proved that this improvement is a short-term effect. Therefore, enterprise should focus on the process of amalgamation and consolidation of multiple factors by means of Kaizen, as well as the achievement of innovation. Without short cut on enterprise's safety development, enterprise must confront with any difficulties of HSE management, and reconcile the need for innovation with concern for Kaizen.

3.2 *The relationship between Kaizen and standard*

Standard is a specification for repetitive things and concepts in certain range. Standard is also a criteria to measure things, which indicates the cognitive level of regularity in reality. Kaizen argues that the PDCA Cycle interacts orderly with the SDCA Cycle in the process of Kaizen. It is just like a pair of indispensable wheels which make enterprise advance.

As figure 4 shown (Imai, Masaaki 2010a), by zooming in the triangle area of Kaizen, it shows the divergences between PDCA Cycle and SDCA Cycle. The improvement requires PDCA Cycle to constantly ascend in a vertical direction, and the maintenance requires SDCA Cycle to constantly retain in a horizontal direction. In the analysis of figure 4, the following conclusions can be drawn: Firstly, Kaizen consists of many alternate processes of PDCA Cycle and SDCA Cycle. Secondly, PDCA Cycle drives SDCA Cycle. Lastly but not the least, the next PDCA Cycle will not start until all of periodical accomplishments are converted into standards.

Table 1 illustrates the different functions of two cycles in detail. Standard plays an important role in enterprise sustainable development. On one hand, enterprise needs the implementation of standardization. On the other hand, enterprise must protect the authority of existing standards. Only by introducing the discipline and maintaining the standards constantly, could standards present its existence value. Otherwise, standards do not have any practical value.

The National HSE legal system is divided into two parts, the behavior specifications and technical specifications. Accordingly, enterprise HSE regulation system should be comprised of regulations, standards and specifications. HSE standards are classified into four main categories: basic standard, management standard, methodology standard and product standard. According to Kaizen, standard is a general concept. It could be a national standard, an occupation standard, a specialized standard, even a checklist of equipment and so on. In one words, any repeated actions are worth writing a specification so as to normalize it.

HSE standards have the direct effects of regulation, punishment and precaution. Moreover, they have the indirect effects of consolidation, inherit-

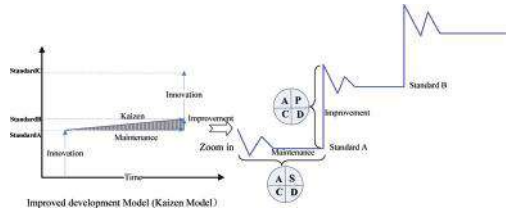


Figure 4. The relationship between PDCA Cycle and SDCA Cycle in Kaizen Model.

Table 1. Comparison of PDCA Cycle and SDCA Cycle.

PDCA Cycle		SDCA Cycle	
Plan	To make plans of improvement	Standardize	To establish standards
Do	To carry out the plans	Do	To maintain standards
Check	To check out the consistency in actions	Check	To verify the effectiveness and correctness of standards
Action	To adjust the goals and measures	Action	To amend the existing standards
Objectives	Never satisfied with current conditions, encourage employees to improve constantly	Objectives	To make current conditions stable, standardize the HSE management

ance and self-discipline. Standard's indirect effects are reflected in the following aspects:

a. To consolidate the periodical achievement of innovation
   The achievement of innovation should be consolidated by building a series of HSE standards, otherwise, HSE performance is hard to be held on a favorable level.
b. To accumulate personal experience and knowledge
   Personal experience and knowledge are materials used to amend existing HSE standards as well as enterprise's valuable treasures. When enterprise investigates the cause of accident, incident and hidden danger, enterprise should carry out a benchmarking against the HSE standards rather than only analyzing the statistics. Only by continuously amending HSE standards could enterprise prevent accidents from occurring repeatedly. In order to ensure its sustainable development, enterprise should take full advantages of HSE standards to amass personal intelligence and inherit valuable information from individuals.
c. To strengthen the awareness of self-discipline
   By learning and obeying HSE standards, employees could strengthen the awareness of self-discipline. By formulating and carrying out HSE standards, top managers could fulfill their HSE commitment. All of these practices are benefit to cultivate an active safety culture.

3.3 *The relationship between Kaizen and New Leadership*

Kaizen requires a new leadership which derived from personal experience and belief rather than authority rank and age. Traditional theory of management divides personal responsibility into two categories, including maintenance and innovation. Nevertheless, the theory of Kaizen divides personal responsibility into three categories, including maintenance, improvement and innovation.

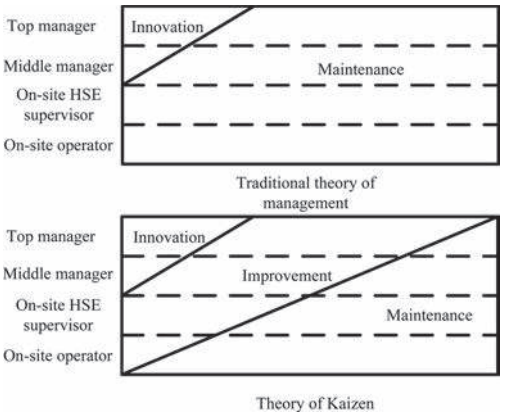


Figure 5. Two kinds of responsibility models.

As shown in Figure 5 (Imai, Masaaki 2010a), manger would take different responsibilities according to their level. The classified responsibility benefits to realize the Delicacy Management. If enterprise wants to achieve outstanding HSE performance, the prerequisite is implementation of Safety Production Responsibility System. Enterprise should clearly define manger's responsibility, rights and accountability at all levels in advance so that everyone knows what he should do or no do. New leadership ensures that entire safety management system works smoothly and efficiently. The management cooperation across all level is more orderly and harmonious.

Managers at different levels have different responsibilities. Table 2 illustrates following conclusions: Firstly, the primary task of on-site operator is to apply the standards and obey the principles. Secondly, on-site HSE supervisor plays a key role in HSE management, as he is a connecting link between the on-site operator and the middle manager. Enterprise's HSE performance depends on the management capacity of on-site HSE supervisor. Thirdly, except for On-site supervision, the middle manager should focus on formulating and

Table 2. The matrix of HSE responsibility.

Vigor	Top manager	Middle manager	On-site HSE supervisor	On-site operator
10 %	Planning the direction of Innovation Management Establishing an Innovation Management System	Carrying out the plan of innovation management	Improving their own works	Through the "Issue System" to participate in the on-site improvement
20 %			Maintaining morale of operators	To constantly improve themselves, become better problem solvers
30 %	Introducing new technologies,equipments	Improving their own works	Making plans and coach operators	Improving professional skills through a variety of training
40 %		Setting and amending standards	Providing superior with proposals	
50 %	Propagating the thought of Kaizen firmly	Convincing employee of Kaizen	Supporting the Issue System	
60 %	Constructing a management infrastructure which is benefit to improve HSE performance	Teaching employee tools of Kaizen	Carrying out TWI and obeying the discipline	Following the rules ,e.g. HSE regulation, Standard Operating Procedure (SOP)
70 %				
80 %	Allocating resources for Kaizen	Supervising the on-site HSE conditions		
90 %				
100%	Changing proposal into management decision.	Carrying out audit of HSE management		

*Note

Maintenance Improvement Innovation

amending standards in order to provide employees with behavior specifications. Fourthly, top managers' priority is to organize the systematic improvement. Therefore, top managers should pay more attention to improving the infrastructure of HSE management, giving the fully support to HSE management system and solving the critical problems.

3.4 *The relationship between Kaizen and issue*

According to the theory of safety management, issue stands for the deviation between reality and expectation, e.g. deviation of human action, deviation of object status and deviation of management system etc. In recent years, enterprises advocated the thought of Preventive Management. Therefore, they should focus on the process of problem solving rather than the result. Kaizen argues that finding issues is just a beginning but analyzing and solving issues are the key point. Management practices have proven that there will not be possibility of improvement without existence of issues. So, every member of enterprise should consider the issues from positive perspective, and make great efforts to create value.

During on-site safety inspection, supervisors usually find various issues. If a company carries out a result-oriented management, issue means failure and punishment. The way of thinking issues makes employee have a negative attitude, which is adverse to solve problems fundamentally. As we known, Kaizen roots in oriental culture with Humanism. So, Kaizen weakens the contradiction of problems, and make people concentrate on process of solving problems rather than on dealing with confliction of interpersonal relationship. In brief, Kaizen could enhance the efficiency and quality on problems solving.

4 PROPOSALS FOR IMPROVING ENTERPRISE'S HSE PERFORMANCE

a. To Introduce Training Within Industry (TWI) improves the on-site HSE performance
   On-site HSE supervisors play a key role in the operation of safety management system. Their main responsibilities should be consultation, training, supervision, guidance, propagation rather than a simple punishment so as to encourage lower-level employees to improve their HSE performance. TWI is seen as a useful approach to cultivate compound high-quality management personnel, and it can significantly enhance the effectiveness of training plan (Patrick. Graup et al. 2009).
b. To Establish a process-oriented reward system promotes the construction of humanistic culture
   The connotation of Kaizen is that improving the results must improve the process at first.

During the running of safety management, manager should focus on leading indicators rather than lagging indicators. Meanwhile manager should increase HSE investment in process control of risk. Neither failure nor success is the criterion for reward. Manager should acknowledge everyone's contribution, even if the result is unsatisfied.

c. To Establish an issue system enhances the communication efficiency

In order to improve the HSE performance continuously, enterprise should establish an issue system to tackle all kinds of HSE information. This issue system has three obvious advantages: firstly, it shortens the time to exchange HSE information so as to enhance the efficiency of solving problem. Secondly, it fully reveals the potential problems so as to arise the manager's attention. Thirdly, it accumulates plenty of valuable information about HSE statistics so as to enhance the rationality of decisions made by top manager.

5 CONCLUSIONS AND RESEARCH PROSPECT

The core connotation of Kaizen seems simple, it comprehensively contains the key elements of safety management system (China Academy of safety science 2011). Firstly, it embodies HSE policies of Full Participation and Continuous Improvement. Secondly, it embodies the spirit of humanity, respects the value of human. Thirdly, it is been used as enterprise's core value. Fourthly, it emphasizes the fact that safety standard is the basis of safety management system. Fifthly, it focuses on the process control of the safety management. Sixthly, it requires enterprise to establish a rated and classified responsibility system concerning safety management. Seventhly, it also requires enterprise to establish a HSE performance evaluation system focusing on leading indicators. Eighthly, it ensures the compliance of safety management system by enforcement of supervision. Ninthly, it carries out the training effect appraise and feedback by implementation of the TWI. Tenthly, it constructs a convenient communication environment served to the efficient operation of safety management system. Lastly, it focuses on the correction and prevention of risk. Management practice has proved that Kaizen could improve enterprise's HSE performance.

In recent years, the theory of Safety Culture has been well developed gradually. This tendency implies the advent of a new creative phase in the safety management. In early 2013, State Administration of Work Safety published a National Strategy for the development of safety culture, as to promote enterprise's safety culture construction. With the development of theory of Safety Culture, scholars began to make further and comprehensive studies on Kaizen (F.W. Guldenmund 2000, RaWq M. Choudhry et al. 2007). Latest research results show that an active safety culture bears four obvious characters: Firstly, employees have the intrinsic motivation to participate in the HSE events. Secondly, enterprise cultivates a Just Culture and develops an effective reward system. Thirdly, employees have the competence in self-learning and self-improvement from issues. Fourthly, enterprise creates a communication platform to exchange information between human and safety management system. Some latest researches prove that continuous enforcement and improvement of Kaizen in safety management can facilitate the transition from HSE system management to HSE culture management. In brief, Kaizen is a long-term research project, and its value will be gradually explored.

REFERENCES

China Academy of safety science (ed.) 2011. *The theory of safety management*. Beijing: Encyclopedia of China Publishing House.

F.W. Guldenmund 2000. The nature of safety culture: a review of theory and research. *Safety Science* (34): 215–257.

Imai, Masaaki 2010a. Gemba Kaizen: A Commonsense, Low-cost Approach to Management: 4–49. Beijing: Machinery Industry Press.

Imai, Masaaki 2010b. *Kaizen: The key to Japan's Competitive Success*: 21–27. Beijing: Machinery Industry Press.

Patrick. Graup et al. 2009. *TWI: training manual of on-site management*. Guangzhou: Guangdong Economic Publishing House.

RaWq M. Choudhry et al. 2007. The nature of safety culture: A survey of the state-of-the-art. *Safety Science* (45):1993–1012.

Progress in Mine Safety Science and Engineering II – He et al. (Eds)
© 2014 Taylor & Francis Group, London, ISBN 978-1-138-00122-0

Analysis on the reasons and response measures for accidents of dangerous chemicals transport

Quanmin Bu
Public Security and Management Department, Jiangsu Police Institute, Nanjing, China
School of Government, Nanjing University, Nanjing, China
Center of Risk and Crisis Management, Nanjing University, Nanjing, China

Jun He
Public Security and Management Department, Jiangsu Police Institute, Nanjing, China

Xing Tong
School of Government, Nanjing University, Nanjing, China
Center of Risk and Crisis Management, Nanjing University, Nanjing, China

ABSTRACT: Over the past 10 years, the number of China's accidents of dangerous chemicals transport constantly rises, these accidents caused car crash and people' death, combustion, explosion, poison, corrosion and other serious results, people's lives and property safety are also seriously affected, therefore, reasons for accidents of dangerous chemicals transport get more attention in the society. Based on analysis of reasons for transport accidents, the author studies corresponding measures so as to avoid accidents of dangerous chemicals transport or reduce resulting loss.

1 INTRODUCTION

In recent years, with an increasing number of dangerous chemicals transportation volume, more and more dangerous chemicals transporters, transportation vehicles and practitioners appear, with small operation scale, old transportation vehicles and facilities, management confusion, lack of safety investment and poor production conditions, many hidden dangers exist in road transportation of dangerous chemicals, which may easily cause disastrous accidents (Zou Zongfeng, et al. 2011). With the rapid development of Chinese industry, the use and application of dangerous chemicals become more and more widespread, which leads to larger road transport volume of dangerous chemicals. The transport of a large number of dangerous chemicals causes a moving source of hazard, transportation security administration becomes increasingly difficult, and transport accident of dangerous chemicals occurs frequently.

2 ANALYSIS ON REASONS OF DANGEROUS CHEMICALS TRANSPORTATION ACCIDENTS

Transport process is needed in production, storage and use of dangerous chemicals. If dangerous chemicals experience accidents or leakage in transport process, death and casualties accidents may occur, it may also cause combustion, explosion, corrosion, toxicity and other serious accidents, which can causes threat to the safety of people's life and property, as well as environmental pollution (Rao Dongsheng 2011). The main causes of transportation accidents are as follows.

2.1 *Dangerous features of dangerous chemicals*

Generally, dangerous chemicals have certain hazards. Different dangerous chemicals vary in terms of hazards. Irritating and toxic harmful dangerous chemicals, such as chlorine, ammonia, sulfur dioxide can stimulate or burn skin, respiratory tract and eyes. Asphyxiate and harmful dangerous chemicals, such as carbon monoxide, asphyxia: cyanide and sulfide can cause human tissue hypoxia. Nerve toxic dangerous chemicals, such as: benzene and benzene derivatives, ally chloride, carbon dioxide, organic phosphorus pesticide have paralytic effect on cans (Mi Yongpeng 2012).

2.2 *Small scale and low degree of specialization*

Although those transportation enterprises of dangerous chemicals have met the relevant requirements set by the Ministry of Transport, many

affiliated businesses can be found in the market, few of them can handle a large number and variety of dangerous chemicals (He Li, et al. 2009). At present, many enterprises handle the transport of their own dangerous chemicals, this lead to low degree of specialization.

2.3 *Quality of practioners*

Many dangerous chemicals practitioners, such as driver, supercargo, loading and unloading managers are poor in knowledge of laws and regulations related to dangerous chemicals, they may even commit illegal transportation. They have little understanding of hazards of dangerous chemicals. As a result, they fail to take timely and effective measures to put the situation under control when dangerous chemicals transportation accidents happen (P. Leonelli, et al. 2010). Some drivers and supercargo have weak responsibility and safety protection consciousness, and have little mastering of provisions related to the safety of dangerous chemicals transportation. Fatigue driving, speed driving, drunk driving and other illegal behaviors are common. These can easily lead to crash and other accidents. And some handling personnel violate relevant operation rules, which can cause accidents and disasters.

2.4 *Condition of vehicles*

Safety condition of dangerous chemicals transport vehicles is one of the important factors, it is the basis for safe transport of dangerous chemicals, poor vehicle condition influences driving safety and cause the accidents. According to provisions in "Road Traffic Safety Law of The people's Republic of China", "Dangerous Chemical Safety Management Regulations" and "Management Approaches on Highly Toxic Chemicals Purchase and Road Transport License" and other relevant laws and regulations, transport vehicles of dangerous chemicals must meet relevant standards of safety technical performance. However, in fact, some transport vehicles of dangerous chemicals fail to meet corresponding safety technical standards and have many hidden dangers.

2.5 *Loading conditions*

Loading conditions in transportation of dangerous chemicals, such as: packaging, loading stuff and factors also have impact on the transport accident. Packing of dangerous chemicals is important to prevent the change of quality and sufficient quantity (Cao Yaoren 2009). It is also an important measure to avoid fire, corrosion and other accidents in the transport process.

But in practical work, because of weak packing container and improper selection of packaging materials, breakage of package, chemical material leakage or other accidents may occur. In loading of objects, some dangerous chemicals with conflicting nature, fire fighting methods or rescue measures are loaded in the same vehicle, which can causes great disaster.

2.6 *Unsound supervision and management by the government and other relevant departments*

1. Laws and regulations concerning highway transportation management of dangerous chemicals is not perfect

Although the central government and relevant departments have issued some provisions and regulations about road transportation of dangerous chemicals, the penalties for illegal behaviors are not serious, as a result, some enterprises and individuals without necessary qualifications risk carrying dangerous chemicals due to their blind pursuit of economic interests.

2. Week review and supervision on qualifications of relevant transport enterprises and individuals

Industry management departments should ensure strict management on qualification of transport operators, technical conditions of transport vehicles and qualifications of practitioners. Business qualification is operating permit for road transport of dangerous chemicals, it is the step for ensuring safe road transportation of dangerous chemicals, while personnel management is also the key to safe road transportation (Phani K. Raj, et al. 2010).

3. Rescue personnel's ability of dealing dangerous chemical accident is not good

Although in recent years, fire and traffic police forces have enhanced their abilities significantly, current emergency disposal mechanism is not scientific and professional. Generally, after the accident, security police forces firstly arrive to control the situation, but they have a poor understanding of dangerous chemicals and their chemical properties, so their countermeasures fail to reduce damage (Liu Qiang 2008).

4. Exchange and cooperation between different government departments are not smooth, the division of responsibilities is not clear.

Up to now, there is no a national regulatory agency of road transportation of dangerous chemicals in China, there are many relevant government departments, overlapping responsibilities and unclear division of responsibilities are serious issues.

2.7 *Supervision and management of transport enterprises*

1. Weak safety consciousness and emphasis on economic interests

Because road transportation of dangerous chemicals is expensive, in order to purse economic benefits, many transport enterprises without necessary permits still risk carrying out dangerous chemicals, overloading is common, which increase the possibility of accident in highway transportation of dangerous chemicals.

2. Backward safety management methods, lack of staff education, supervision and punishment mechanism

Many transport enterprises pay little attention to ex ante safety education, and training of accident prevention and emergency rescue knowledge. They are in lack of professional management personnel, effective organizational structure and management system, as well as corresponding operating procedures (Alev Taskin Gumus 2009). At present, the majority of driver, escort personnel, handling personnel and other employees in the field generally have low academic level and cultural level, they get little relevant training, together with the lack of a supervision and punishment mechanism, reactionary's technical quality and safety awareness are poor.

3. Lack of source management and dynamic supervision on technical condition of transport vehicles

Many dangerous chemicals transporters are not able to monitor technical condition of vehicles, and ensure strict maintenance and inspection (Liao Pengyu, et al. 2008). Their operational conditions, handling equipments and safety facilities are terrible. Some of them conduct illegal modification on dangerous chemical container or transport vehicles, and use unqualified containers or vehicles. This greatly increases the possibility of dangerous chemicals leakage.

2.8 *Road conditions*

The occurrence of traffic accidents is often directly or indirectly related with a number of objective factors, on uneven roads, car can encounter severe vibration and damage on car parts. While on muddy road or hill road, sideslip accident can easily happen.

2.9 *Weather condition*

Weather condition directly affects safe transport of dangerous chemical, for example, rain, fog, snow or ice can cause collision or roll-over accident.

3 COUNTERMEASURES FOR DANGEROUS CHEMICALS ACCIDENTS

According to the causes of transportation accidents of dangerous chemicals, and relevant measures and experience from home and abroad, the author proposes the following measures. At present, monitoring and management on road transport of dangerous chemicals in the United States, Canada, Germany and other developed countries, and relevant laws and regulations and intelligent information technology are relatively mature. Based on actual conditions in China's road transport of dangerous chemicals, and advanced technology and management experience from developed countries, countermeasures are proposed as follows.

3.1 *Rectification on dangerous chemicals transporter*

Dangerous chemicals transporter are directly responsible for the transportation of dangerous chemicals, public security, traffic, safety supervision, industry and commerce departments in all regions need to carry out special inspection on these transporter which carry toxic, explosive dangerous chemicals, and ensure that those dangerous chemicals transporter have sound internal security management system. Those which fail to meet corresponding safety requirements need to carry out rectification before deadline. If they fail to do so, the regulators need to revoke their business licenses of dangerous chemicals transport, cancel their registration, or make alteration in their business licenses (A. Oggero, et al. 2011). To further strengthen responsibilities' dangerous chemicals transporter, strengthen the management of affiliated business management, transporters need to inspect on conditions of dangerous chemicals vehicles, quality and effectiveness of tire wear and brake system, the operation of unqualified vehicles should be discontinued. New highway transportation units should be approved according "Road Transport Management Regulations" and relevant provisions.

3.2 *Rectification on dangerous chemicals transporter*

Transport vehicles of dangerous chemicals are media of carrying dangerous chemicals, public security, traffic, safety supervision, industry and commerce departments should carry out special inspection on highway transportation enterprises. As for unqualified transport vehicles, transport regulator shall revoke corresponding licenses for dangerous chemicals transport. For illegally modified vehicles and tankers, public security depart-

ment should require restoration or removal. In case of insistence between actual volume and the maximum volume, replace of tankers or change of driving license is necessary. And those vehicles which reach standards of dumping, mandatory dumping is needed (Sima Chervin, et al. 2010). Transport department should require dangerous chemicals transporters to be equipped with communication tools and bring the "Safety Card of Dangerous Goods Transport".

Safety, traffic, public security departments should jointly order transport units to be equipped with personnel protection and rescue equipments, running recorder and "GPS" satellite positioning system, and have notice boards which indicate name and type of dangerous chemicals, maximum load, rescue methods, business telephone no. at the back of dangerous chemicals transport vehicles. Reflective tapes need to be pasted at the back and both sides of the vehicles or tanker. Vehicles or tankers' contour should also be marked.

Public security departments should strictly manage the registration of new transport vehicles, and inspect on warning sign, text, GPS locator or running recorder. Quality inspection departments need to strengthen supervision and inspection on dangerous chemicals tankers and other containers, timely rectification is needed for any violation.

3.3 *Regulation on practitioners of dangerous chemicals transportation*

The quality of transport personnel is the key factor to the transportation of dangerous chemicals. Traffic departments in all regions need to carry out a training concerning safety management laws, regulations of dangerous chemicals transport on legal representative, management personnel and other relevant personnel. Qualifications of drivers, loading and unloading managers and escort personnel need strict review. All legal requirements on practitioners should be fulfilled, toxic, explosive and similar dangerous chemicals vehicles need high quality driver and escort personnel, the arrangement of personnel and vehicles should be relatively fixed. Those drivers who have records of overloading, over speeding or others for more than 2 times should be fired. All practitioners need safety education and training about the use of dangerous chemicals container, loading, transport, travel speed and disposal measures after the accident.

3.4 *Strict implementation of licensing system of dangerous chemical road transportation*

Unified application methods for toxic chemicals purchase proof, purchase permit road transport permit should be implemented. Public security departments should report handling conditions of dangerous chemicals road transportation permit to traffic departments of the same level. All transporters of highly toxic chemicals and civil explosives need to apply to corresponding public security organ of county (city or district) level for transport permits, and submit detailed route map and schedule to public security organs. Before each shipment, shipper (or agent) must complete endorsement procedures with licenses and transport permits of shipper, carrier, transport vehicle, escort personnel and drivers in the public security organ. The public security organ which undertakes the endorsement procedure must review the qualifications, transport routes, loading weight and departure time on site and give endorsement opinions transport permit. It also needs to conduct safety education on drivers and attendants of toxic dangerous chemicals and explosives who must master knowledge about highly toxic, dangerous chemicals and civilian explosives, emergency disposal principles and defense self-help methods (Robert Emery 2013). After the endorsement, the approved dangerous chemicals transportation routes and schedules should be send to relevant public security organs. After the completion of the transport process, the shipper (or agent) needs to submit the transport permit to the original issuing authority.

3.5 *Strengthening inspections and penalties road transport of dangerous chemicals*

Public security departments in all regions need to strengthen inspection on transport vehicles of dangerous chemicals, especially on tankers, serious punishment should be imposed for speeding, and violations of relevant traffic regulations. All transport vehicles of dangerous chemicals without corresponding certificates have to be detained. Those vehicles with issues of overloading, poor lighting, mechanical failure or others should be detained in safe place. As for highly toxic and explosive dangerous chemicals, local police station needs to be informed for supervision. In case of undocumented transport of toxic dangerous chemicals or transport of dangerous chemicals in prohibited area, or violations in transport time, routes and driving speed, the vehicle should be detained, and relevant personnel need to be punished according to "Road Traffic Safety Law", "Dangerous Chemicals Management Ordinance" and other relevant laws, regulations and provisions. Public security, transportation, safety supervision and other departments need to jointly carry out inspection on key routes and periods. Public security departments should inform traffic departments about violations of transport vehicle of dangerous chemicals.

3.6 *Delimiting prohibited area, improving road traffic signs and markings*

Public security departments at all regions need to designate highway area and mountainous road, including party and government organs, population settlements area, CBD, commercial areas and schools, water source, communication, military facilities and other regions in which transport of dangerous chemical is not allowed according to conditions of local highway network and traffic. It is necessary to inspect on signs and markings of prohibiting the transport of dangerous chemicals and make further improvement according to "Guide for Setting of City Road Traffic Signs and Markings" and "Recommended Types of Road Traffic Signs and Markings", and inform media about the prohibited area.

3.7 *Establishing and improving transport emergency mechanism*

Suitable locations can be chosen for the establishment of unload of dangerous chemicals according to actual situation. Emergency plan for road transportation accident of dangerous chemicals shall also be in place, emergency rescue technology and information support system further need improvement, high-quality team of emergency rescue and emergency rescue mechanism of rapid response are also necessary to improve the ability of crisis management and reduce loss caused by road transportation accidents of dangerous chemicals, as well as protect people's life and property to largest degree.

3.8 *Establish a unified management mechanism, clarifying scope of responsibilities of various departments, strengthen communication, coordination and cooperation*

The government shall set up a special organization for unified management of road transportation of dangerous chemicals. In many western countries, there are specialized institutions for management of road transportation of dangerous chemicals. For example, the highway transportation management institution in Germany is a semi-official association, as a national industry management organizatio in Germany, it is composed of Germany transporters and employers. Any enterprises which want to be engaged in transport of dangerous chemicals need to become a the members of the organization so as to obtain transport qualification. Through this system, all German transporters of dangerous chemicals are under the unified management system. In the UK, the transport department is responsible for vehicle management and management of drivers, the police are only responsible for highway safety enforcement. Our country is vast in territory, with great demand for dangerous chemicals transportation and complex transport lines, various functional departments should strengthen coordination and cooperation, enhance the linkage and unified management.

3.9 *Improving the ability to disposing of transportation accidents of dangerous chemicals*

Further improvement in on-site rescue emergency command mechanism for dangerous chemicals accidents and accident emergency rescue preplan based on local conditions is also necessary to effectively improve the ability of dealing with dangerous chemical accident. The establishment of social rescue supplies, rescue materials and equipment, professional chemical unit and experts and information database, as well as rescue supplies and equipment storage warehouse is also needed. A sound dangerous chemicals alarm and disposal network needs to be built, the phone number for dangerous chemicals accident alarm is to be published widely.

In case of traffic accident of highly toxic and explosive, dangerous chemicals, public security department should report to the local government immediately. Safety supervision, public security, transportation, environmental protection, health and other related departments have to carry out on-site disposal and accident emergency rescue work in accordance with disposal plan.

4 CONCLUSIONS

In order to avoid transportation accident of dangerous chemicals, on the one hand, government departments have to further strengthen the management of dangerous chemicals transport qualifications, ensure strict vehicle management and inspection, and implement whole-process and complete control in road transport of dangerous chemicals. On the other hand, enterprises should strictly implement national laws and regulations and relevant provisions, improve rules and regulations concerning dangerous chemicals transport, develop targeted measures in order to form a sound accident prevention system for dangerous chemicals transport. At present, some of monitoring networks have not been established; some of them can only monitor local vehicles. According to analysis on previous accidents, as for a regional network, when vehicles coming from other areas encounter accidents, it is difficult to inform local emergency department for treatment, no matter whether GPS has been established. Therefore, the

establishment of a national logistic management information platform can ensure effective protection and timely emergency treatment to minimizing the loss.

ACKNOWLEDGEMENTS

The authors gratefully acknowledge foundation by the Jiangsu Science and Technology Support Program (BE2010738); Jiangsu Colleges and Universities Natural Science Foundation (08 KJB620001); Outstanding Young Teachers of Jiangsu Higher Education Institutions Overseas Training Scheme Funded; Qing Lan Project; Public Security Technical Disciplines and PAPD.

REFERENCES

A. Oggero, et al. 2011. A survey of accidents occurring during the transport of hazardous substances by road. *Journal of Hazardous Materials,* 133 (2):1–7.

Alev Taskin Gumus 2009. Evaluation of hazardous waste transportation firms by using a two step fuzzy-AHP and TOPSIS methodology. *Expert Systems with Applications,* 36(2): 4067–4074.

Cao Yaoren 2009. A Discussion on Establishing the Mechanism of Handling Leaking Accident in Transporting Dangerous chemicals on Highways. *Journal of Hunan Public Security College,* 21(2):35–37.

He Li, et al. 2009. The Problems Existing in Transporting Dangerous chemicals on Highway and Their Countermeasures. *Logistics Science and Technology,* 6:33–35 (in Chinese).

Liao Pengyu, et al. 2008. Causal analysis on traffic accident of dangerous chemicals transportation and Preventive countermeasures in Beijing. *Highway Traffic and Safety,* 8(6):50–53.

Liu Qiang 2008. Safety supervision of the road transport of dangerous chemicals. *Safety, Health and Environment,* 8(10):97–103.

Mi Yongpeng 2012. Treatment Countermeasures of Hazardous Chemical Accidents of Expressway Tunnel. *China Emergency Rescue,* 3:34–37 (in Chinese).

P. Leonelli, et al. 2010. Hazardous materials transportation: a risk-analysis-based routing methodology. *Journal of Hazardous Materials,* 71(1):283–300.

Phani K. Raj, et al. 2010. Pritchard. Hazardous materials transportation on U.S. railroads: application of risk analysis methods to decision making in development of regulations. *Journal of the Transportation Research Board,* 17(7):22–26.

Rao Dongsheng 2011. Study on the Problems and Solutions in Transport of Dangerous Chemicals in China. *Journal of Yangtze University (Natural Science Edit),* 8(8):76–78 (in Chinese).

Robert Emery 2013. A mechanism for providing institutional assurance for the safe handling of acutely toxic or physically dangerous chemicals in research laboratories. *Journal of Chemical Health and Safety,* 20(1):18–22.

Sima Chervin, et al. 2010. Testing strategy for classifying self-heating substances for transport of dangerous goods. *Journal of Hazardous Materials,* 115(3):107–110.

Zou Zongfeng, et al. 2011. Research Status and Development Trend of Hazardous Materials Transportation Safety Management. *China Safety Science Journal,* 21(6):129–135 (in Chinese).

Progress in Mine Safety Science and Engineering II – He et al. (Eds)
© 2014 Taylor & Francis Group, London, ISBN 978-1-138-00122-0

Coal mine accident human error model construction and team safety management mode analysis

Jing Chen, Qinggui Cao & Yongjie Yang
National Key Laboratory of Mine Disaster Prevention and Control, Shandong University of Science and Technology, Qingdao, Shandong Province, China

ABSTRACT: In recent years, coal mine accident happened frequently in our country. Based on the statistics about coal mine accident and accident mechanism analysis, the paper find out the main reason that lead to coal mine accident happened frequently in our country. Based on the existing accident model, it put forward coal mine accident human error model. And make detailed factor analysis and effective analysis for the model. Then, from the angle of team, the paper put forward team safety management mode for coal mine enterprises and the corresponding safety control measures. It is a new safe management thought for China's coal mine industry.

1 INTRODUCTION

Coal is the basic energy and important raw material in our country. it plays an important strategic position in national economy. In the past and the foreseeable future decades, coal is still major energy. Coal industry is the high-risk industry. In recent years, Party and government pay more attention to the coal industry. Under the Joint efforts, the number of coal accident, death rate per million tons is annual decline. Coal mine safety situation is generally stable and tends to improve, but the coal mine safety situation is still severe. China has big gap compared with the advanced world level, death rate per Million tons is about 15 times higher than that of South Africa, 8 times Poland, 6 times Russia and India (Ye Qishen 2009). Coal mine accident not only threaten people's lives and health seriously, but also affect social stability, harmony and international image. So, it is very necessary to find out the root causes of coal mine accidents in our country and construct the corresponding coal mine accident mechanism theory.

For accident mechanism theory, many domestic and foreign scholars and experts have done much research and put forward a lot of typical accident theory. Such as Domino accident model theory proposed by Heinrich in 1936, Energy transfer accident theory proposed by Gibson in 1961, then derived by Haddon in 1966, Gold mine accident model proposed by Lawrence in 1974, and so on. In domestic, Chen Baozhi put forward the two class of hazard point in 1995, Zhang Li put forward Human error accident model in Complex man-machine system in 1996, He Xueqiu put forward rheology and mutation theory and so on (He Xueqiu 2008). All of them reveal some accident mechanism, but still not perfect, especially there are little accident model for coal mine system.

Therefore, based on the analysis of coal mine accident in our country, the paper find out the main reason that lead to coal mine accident happened frequently in our country, construct the accident mechanism model, and provide a new thought for the coal safe management. And as a basis of the model, it find the main reason of coal mine accident happened frequently in our country, and put forward coal mine safety control measures that conform to our national conditions and the safety production status. It provides the basis for our country's coal mine safety management.

2 COAL INDUSTRY SAFETY CURRENT SITUATION ANALYSIS IN OUR COUNTRY

2.1 *Coal mine safety current situation*

With the economy and the coal industry rapid development, the government pay great attention to coal mine safety, But in recent years, coal industry still has many major accidents, According to statistics, during 2001–2004, only extra serious accident that a total of more than 10 persons dead occurred in China more than 188; Since 2004, major coal accidents that a total of more than 30 persons dead occurred more than 20(see Figure1). According to the U.S. expert Heinrich's "1:29:300" accident law[2], we can imagine that although China's coal industry safety standards has been made

Table 1. Coal mine disaster statistics in China during 2004–2010.

No.	Time	Place	Accident type	Death toll
1	2004.12	Tongchuan, Shanxi	gas burst	166
2	2005.02	Sunjiawan, Liaoning	gas burst	214
3	2005.08	Meizhou, Guangdong	coal flood	121
4	2005.11	Qitaihe, Heilongjiang	coal dust explosion	171
5	2006.11	Lingshi, Shanxi	coal mine fire	34
6	2007.08	Xinwen, Shandong	Coal mine flood	181
7	2007.12	Hongdong, Shanxi	coal dust explosion	105
8	2008.07	Weixian, Hebei	coal gas explosion	35
9	2008.07	Nadu, Guangxi	coal mine flood	36
10	2008.09	Xiangfen, Shanxi	coal accident	276
11	2008.09	Wendeng, Henan	coal gas burst	37
12	2008.11	Chengcheng, Shanxi	coal gas explosion	29
13	2008.12	Shanyin, Shanxi	coal mine flood	30
14	2009.02	Tunlan, Shanxi	coal gas explosion	78
15	2009.05	Mujiang, Chongqing	coal gas explosion	30
16	2009.09	Pingdingshan, Henan	coal accident	54
17	2009.11	Xinxing, Heilongjiang	coal gas explosion	108
18	2010.01	Lisheng, Hunan	coal fire accident	34
19	2010.03	Tuoluoshan, Neimeng	coal mine flood	31
20	2010.03	Wangjialing, Shanxi	coal mine flood	38

great progress, there are still a lot of insecurity. The whole safety situation is still serious.

2.2 *Accident reason analysis*

The article select 100 coal mine accident cases from all the accidents happened in 2001–2009 according to the reason type of coal mine accidents, including mine roof accident, gas accident, water disaster accident, transportation accident, mechanical and electrical accident, explosion accident, fire accident and other accidents. Though analysis the accidents process, acquainting accident investigation and handling, the accident reasons were found out. The reason of coal mine accidents in our country mainly includes the following four areas:

(1) Technology and equipment is not inherent safety

As surveyed, the input into security of China coal industry is seriously inadequate. According to the investigation of National Coal Mine Safety Supervision Bureau, the debt of safety facilities, safety equipment, safety engineering of state-owned key coal mines is about 50 billion yuan. Because of inadequate investment in security technology, the equipment renewal is slow. There are many aging and extended service of production facilities in about one third of the state-owned coal mine. The development of new technology and new equipment is lagging of the major systems including mining, excavation, machine, transportation and ventilation (Cao Qinggui 2005). Most of new technologies and new equipment are at the exploratory stage. The mechanization degree of the national coal mining is only about 45%. In most coal mines, the level of production and technology is relative low and the equipment is poor, especially in township coal mines, non-mechanized hand-mining is common and it increases the potential risk for safety production.

(2) Lack of professional and technical personnel, low quality of employees

As the coal industry is tough and more accidents happened, the technical talent import is difficult to some extent and there is a serious lack of professional technical personnel. According to the survey of Coal Mine Safety Research Center, the workers account of technical personnels in the state-owned coal mines who having junior or middle colleges is only about 23%, while in developed country the figure is above 60%. The shortage of talents affects the safety production directly. Meanwhile, rural labor force is surplus. Underground workers works mainly for earning money, and many workers go to work without serious training. Heavy production, light quality, Heavy efficiency, light security, poor safety awareness, poor self-protection, illegal work seriously, all of them buried great hidden dangers for safety production.

(3) Safety training and education is not enough

In our country, the education and training about coal mine safety production knowledge, skills and

others is merely a formality. Training time is too short, the training mode is single. Training effect can not achieve national requirements (Chen Hong 2006).There are many students muddle, some even buy a license for employment, and it also add the difficulty of coal mine safety.

(4) Inadequate safety supervision
Because of the lax enforcement of local safety supervision department, a number of illegal coal mines in the pursuit of profit was not closed or stopped even they should be, resulting that many coal mine enterprises turn a blind eye on a series of national security law. Because of paying no attention to safety propaganda and education, coal accidents happened frequently. The corporation supervision is not enough. Some managers are not sturdy, having no strong safety responsibility sense, can not keep abreast of the working environment and security situation, can not enforce safety regulations strictly. All of these fact lead to lax labor discipline and provide conditions for accidents.

In summary, the accidents main reason is closely related to human behavior. From macro-viewpoint, if the behaviors of corporate decision-making layer, management layer, operate layer are correct; if equipments, machines and tools can achieve inherent safety through the scientific and technical personnel research and safety technical personnel operate standard; if environment conforms to safety standards, the accident would not have happened. So, coal mine accidents human error mechanism model is established, human error is the primary reason for coal mine incidents.

3 COAL MINE ACCIDENT HUMAN ERROR MODEL

3.1 *Coal mine accident human error model building*

By reason analysis for coal mine accident Occurred in our country in recent years, relying on the error theory, based on the accident mechanism that predecessors had established (Li Zhicheng, et al. 2005), the paper constructed "coal mine accidents human error model", as shown in Figure 1.

3.2 *Model factor analysis*

Human error: it means that the person can not complete or fail to complete the required functions under prescriptive conditions, So that persons, objects, environment in the system are affected to certain extent; Person include decider, manager, operator.

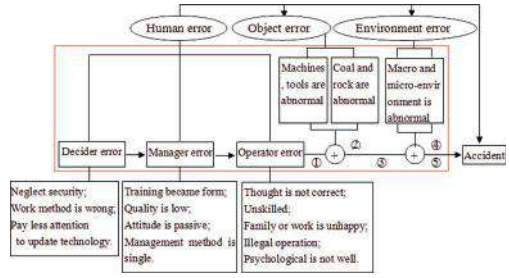


Figure 1. Coal mine accident human error model.

Object error: it means that object is in an abnormal state. Object in this paper include machines, tools and coal.

Environment error: it means that environment is in an abnormal state. Environment in this paper mainly refers to the macro-environment and micro-environment.

Decider error: it means that enterprise leaders and mainly responsible officers have mistakes in work. It includes 3 kinds of types, That is, Neglect the security; false work method; pay less attention to technology import.

Manager error: it means manager and engineering technical personnel's mistake. It includes 4 kinds of types, That is, Training is not in place; Manager's quality is low; the attitude is not correct; Management method is not proper.

Operator error: it means that the person who actual contacted with objects, including the front-line workers, all machine operators, maintenance persons have mistake. It includes 6 kinds of types, That is, thought is not correct; unskilled; unhappy family or work; trusting to luck; illegal operation; psychological is not well.

Macro-environment: it refers to social environment, the enterprise environment such as corporate culture, etc.

Micro-environment: it refers to the actual work environment, Such as light, ventilation, etc.

3.3 *Model effective analysis*

That the theory "coal mine accidents human error model" proposed in the paper mainly reflects that human error is the ultimate reason lead to accident. The model contains two parts, that is, inside and out the red line region. Part of outside red line region embodies the relationship from the macroscopic among human error, object misconduct and environmental degradation, and the accident mechanism and consequences; Part of inside red region describes the different accident processes from the microscopic. As shown in the model diagram, object misconduct and environmental degradation are

caused by human errors, Red area inside is refinement, That is, take coal industry as the research object, person is divided into decider, manager, operator; The object is divided into machine, tools and coal; Environment degradation is considered from macro and micro aspects. According to the arrow direction shown in the red area region, it concluded that there are only 4 processes, as follows:

① → ③ → ⑤ → Accident; That is, accident is directly caused by human error, called "A" class accident. In such accidents, object and environment are in normal state;.

① + ② → ③ → ⑤ → Accident; That is, accident is caused by human error and object misconduct, called "B" class accident. In such accidents, environment is in normal state;

① → ③ + ④ → ⑤ → Accident; That is, accident is caused by human error and environment degradation, called "C" class accident. In such accidents, object is in normal state;

① + ② → ③ + ④ → ⑤ → Accident; That is, accident is caused by human error, object misconduct, environment degradation in the same time, called "D" class accident.

Based on the above analysis, the paper give a new definition for accidents category, that is, All coal mine accidents can be divided into 4 categories, that is, accident is directly caused by human error, we called it "A" class accident; accident is caused by human error and object misconduct, we called it "B" class accident; accident is caused by human error and environment degradation, we called it "C" class accident; accident is caused by human error, object misconduct, environment degradation in the same time, we called it "D" class accident. So, we can say, human error is the ultimate reason of all accidents, and it is the essence of coal mine accident human error model.

Moreover, "management factor" is not mentioned in the model, it does not mean that management is not important. The reason not mention "management factor" is that management is a dynamic process, it can be reflected by the role that people play on object and environment. In fact, the model itself is management process.

4 TEAM CONSTRUCTION SAFETY MANAGEMENT MODE

According to the coal mine accident human error model and coal mine accident main reason in our country, the paper raises the method to improve enterprise safety management level by constructing excellent team management mode, shown in Figure 2.

According to the safety management team construction mode, making the concrete safety management Countermeasure as follows:

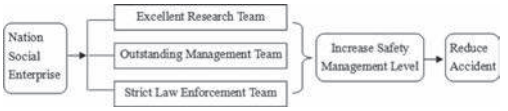


Figure 2. Coal mine safety management team construction mode.

(1) Organize excellent research team, Improve technical support

Pay special attention to construct research team, and concentrate the preponderant scientific manpower on tackling safety issues or to improve the safety technology and equipment performance by referencing the experience of international coal mine advanced science and technology. The nation should take active measures to encourage coal mine enterprises to adopt advanced technology and methods, take particular emphasis on basic research of mine gas disaster prevention to control vital coal mine disasters effectively. Increase safety input, ensure special fund for special use and improve the level of technical equipment to enhance the coal mine safety production level.

(2) Cultivate outstanding management team, Strengthen safety education and training

All enterprises should pay more attention to cultivate an excellent management team for safety education and training, and take great effort to train technicians and managers. The operator who have special work must be special trained before going to work, mine workers must have junior or higher educational level. Workers must be certificated strictly. We should improve the overall quality of coal miners, and meanwhile, we also must train safety inspectors regularly to improve the quality of coal mine safety inspectors.

(3) Create strict law enforcement team, Strengthen safety supervision and law enforcement

Safety laws and regulations in our country have been established basically, but it still needs to strengthen supervision. So, we must establish a strict law enforcement team, and strictly implement coal mines safety production responsibility system. Coal mines should establish various rules and regulations and safety accountability that corporate deciders, managers, operators must be abided; According to the law, we must strengthen accident investigation and punishment, implement accountability strictly, not only prosecute persons responsible for the accident, but also the system should be investigated for responsibility.

5 CONCLUSION

Through made investigation for coal mine enterprises, the paper made research and analysis about the numerous coal mine accident mechanism. Based on the existing accident model, put forward coal mine accident human error model and from the angle of team management, then put forward "safety management team building" mode for coal mining enterprises. It provides a new idea for the coal mine safety management. In the paper, the main research results are as follows:

1. From the perspective of the coal industry, through making analysis about many coal mine accidents, it established the coal mine accident human error model by observation and interpretation on the coal mine accidents mechanism from a new angle, and provided the reference for coal mine accident prevention business.
2. According to the coal mine accident human error model and coal mine accident main reason in our country, it raised safety management team construction mode from the point of team management perspective, and made the corresponding safety management control measures. It provides a new idea for coal mine safety management.

REFERENCES

Cao Qinggui 2005. Study of the enterprise Risk Monitor *and Safety Management Early-warning Technique*. Shandong University of Science and Technology: Qingdao.

Chen Hong 2006. The study on unsafe behavior in China's *major coal mine accidents*. Beijing: Science Press.

He Xueqiu 2008. *Safety Science and Technology.* Xuzhou: The China University of Mining and Technology Press.

Li Zhicheng, et al. 2005. Management system theory and application of qualitative simulation. Beijing: Science Press.

Ye Qishen 2009. Frequent coal mine accidents and control measures. *Mine safety*.32 (5):116–119.

This page intentionally left blank

Progress in Mine Safety Science and Engineering II – He et al. (Eds)
© 2014 Taylor & Francis Group, London, ISBN 978-1-138-00122-0

Analysis on ERP implement in coal enterprises based on management mechanism innovation

Youli Wang
School of Business, North China Institute of Science and Technology, East Yanjiao, Beijing, P.R. China

Jianghui Wang
Beijing Energy Conservation and Environmental Protection Center, Beijing, P.R. China

Shan Shao
China University of Mining and Technology, Beijing, P.R. China

ABSTRACT: ERP, the advanced management and corresponding software can make coal enterprise arrange resource reasonably and effectively. According to the feature of coal enterprises, the paper analyses ERP implement situation in cola enterprises. It is believed that lacking management innovation is the main resistance reason for ERP implement in coal enterprises. The paper put forward the solutions as following: Recreating standardization and normalization of productivity and operating process in coal enterprises; innovating and reform management organization structure.

1 INTRODUCTION OF CONCEPT OF ERP

ERP (Enterprise Resource Planning) is based on the information system of enterprise resource planning and management. On the basis of MRP (Material Requirement Planning), ERP combines the customers' requirements, enterprise's activities and the supplier's producing resource together (Kyung-Kwon 2002). It is a new management pattern of function network structure, which reflects a supply chain management idea for total user's requirement production.

"ERP" was firstly put forward by Garter Group Company in the early 1990s. Its main idea is to face management of the whole supply chain (Stanley 2002). It developed from conservative MRP to MRPII and then to ERP. It is also regarded as a progress of combination of the modern management concept and then applied to the management practice in enterprise. As an advanced management idea, ERP software is widely used in the world. It has been proved to be the management method which can connect the separate department, strengthen the coordination between them, improve the total output and strengthen the enterprise's competition.

ERP is regarded as an effective tool which improves enterprise's business productivity. ERP is the combination of information technology and advanced management concepts. The comprehensive optimized management was realized by the organization of enterprise's plans, production, marketing and financial systems.

According to APICS's statistics, only one ERP system can bring the enterprise the following economic profits: (1) Productivity can be increased by 10%–15%; (2) Stock can be decreased by 30%–50%; (3) Productive cost can be decreased by 12%; (4) The wait time for materials can be decreased by 60%. It has been 20 years since ERP management concept flourished and applied in Chinese enterprise when the implement of ERP is not optimistic in Chinese enterprise, especially in coal enterprise.

2 PRESENT CONDITIONS OF ERP IMPLEMENT IN COAL ENTERPRISE

2.1 *The features of coal enterprise and necessity of ERP implement*

Coal enterprises have some features: mineral resources are limited and non-renewable resources; geological conditions change consistently under the shaft; investment scale is enormous; workers of coal mine mainly work under the ground; the circumstance of work is relatively odious and so on. For coal enterprises, the process of coal productivity is their important activity, which is the decisive factor in the process of producing coal product's value. In general, cost of the process will be 70% of the total cost. The process of coal productivity is

greatly influenced by natural conditions and natural geography. There objectively exist some harmful factors, such as water, fire, gas, roof and so on. They exist in the coal mines under the ground, and these harmful factors, in fact, are opposite effect reflected by workers and environment. The kinds of coal products are relatively single, but the process of producing is very complex. Besides, the process of coal-mining and mine-digging include short-drilling, exploding, transporting, supporting, ventilating, dewatering, power-supplying, blowing, lighting, communicating, and so on. The unsuitable combination of these process and links, the in effectiveness of function and the unbalance of the inner system will lead to malfunction and imperil the safety and health of workers.

So the mine management should control every process of scene-producing and make up standards for every process and make the result of every process conform to the demanded standards. The productive features and process management are suitable to adopt the advanced of ERP, which is in centre of standardized, specialized, and in purpose of systemize, make the mine management strict and synthetic management modernize. The advanced management and corresponding software can make coal enterprise arrange resource reasonably and effectively, the most enormous output and pursue for the biggest increment and profit of coal resource at the least of cost can be realized. Therefore, the management systems of coal enterprises should be innovated and optimized. It gets rid of ineffective process, and cancels competitive and ineffective professional work processes so as to make every process united, unit statement and integrate data. So we can meet the demand of information and built the informative model to make sure that coal enterprises have a scientific and professional process and management. The innovation of management systems will change the administrative levels and working style which are organized and called bureaucracies, It incredibly involve in re-dividing department function, adjusting post function, rearranging power and interest and so on. Therefore, It have great difficulties in practical work in coal enterprises and we must find a suitable method to solve the problems.

2.2 *Present condition of ERP implement in coal enterprises*

The ERP implement of excavating fields is still at the stage of exploration. At present, China and foreign countries have less research about concepts, methods and implement of ERP in coal enterprises especially. At the same time, the concepts, methods and implement are very plain. In the course of practical implement of coal enterprises, ERP is still at the experimental stage, only some big companies try to introduce EPR, For example, Luan Kuang Company bought ERP software of SAP from An Da Xin Company to implement the three subsystems, such as finance, stock and purchase, and marketing management of ERP; Shen Hua Company uses ERP software of Yong You Company, trying to expand other function in center of finance. In the above examples, the companies are all short of main productive project function in which market is the pioneer. But the main productive project is the logical beginning of ERP. Strictly speaking, the ERP system without main productive project is not the real ERP.

According to statistics, among coal enterprises who implement ERP system, 10% –20% coal enterprises can realize system integration on time and budget successfully in general; about 30%–40% of them can not realize system integration or partly realize it; about 50% items failed. While among the 10%–20% of items, the items which take effect are less. The fitness between ERP system and assign enterprises is not as good as Europe and America countries because the designation and development of our ERP-system are deeply influenced by European and America enterprises and most mainly because ERP system is based on procedure rather than function, while our management of coal enterprise are just based on function.

3 MANAGEMENT MECHANISM INNOVATION TO PROMOTE THE SPECIFIC ERP SCHEME IN COAL ENTERPRISES

3.1 *The notion and function of Management mechanism innovation*

The notion of management mechanism is widely used in all fields of modern society. The word "mechanism" was originated in the field of machine-designing and making. And then it was introduced in biological and medical fields (Hipkin 2000). It was in the 1980s when state-owned enterprises are highly encouraged to reform after "reform and opening up" policy was advocated in China. It is significant for coal enterprises to promote ERP management mechanism.

The management mechanism innovation is under the certain technique conditions, the improvement and upgrade of management mechanism which will make full and reasonable use of each kind of resource can make the coal enterprises more harmonious, efficient and productive. It mainly includes the following four aspects (Jaideep Motwani 2002): (1) reforming the standardized and normalize process for production and operation; (2) establishing standard criteria of management information system; (3) innovating the management organization structure; (4) creating the study

organization and encourage staff to learn and improve their operational ability.

Reviewing the world's top 500 enterprises into consideration, we can find that most of them are modern enterprises with good management mechanism. But in the view of Chinese enterprises situation, it is the weakest part. There are many enterprises which can't organize well in their management mechanism. So there is no doubt that whether we can do well with management mechanism innovation in enterprise is the critical element for enterprise's development and competition-promoting. Based on the basic case of poor condition, it is much harder for coal enterprises at this respect.

3.2 *The root of the prevention in EPR implement in coal enterprises*

Both the Chinese and foreign scholars have recognized that the management mechanism innovation is the premise of conducting ERP successfully (Vincent 2003). While the resistance elements of push on Chinese coal enterprise are short of management mechanism innovation. We must implement the informative in those enterprises. Different from the western countries, information keeps the same pace with industry informative in China. Compared with western countries who promote the informative after the mature industry development, China does that in the same time. So it seems much more complicated and difficult.

Enterprise formativeness is mainly divided into two lines: one is mainly depended on the application of computer. This aspect has already matured at present. The main problem is shortage of investment in coal enterprise; the other line is management line which mainly involves the material resource, finance, resource and information resource. Problems in this aspect are more serious. The critical matter is management problem, no matter the size of enterprise is taken into consideration. Management information not only refers to information standard, but also relate to the management chemise. What's more, it signifies the reallocating authority and interests. Therefore, the leader mechanism, management style and the old management concept did all prevent the progress of information. However, coal enterprises do not take it seriously and resolve these problems the implement of ERP failed at last.

The complicated software-- installment is only the tip of the icebergs. The real iceberg is the adjustment of management mechanism and ERP system in coal enterprise. Not only the complicated software and advanced computer technique is involved, but also the adoption of the management concept is very important, although ERP software is very smart. We must admit that there are many reasons which will lead to the failure of ERP. For example; Coal enterprises can not see ERP clearly and confuse the notion of ERP and ERP system. Or they do not recognize their traditional practice procedure, but the basic reason lies in the old system can not adjust to the new one. We can establish the information management mechanism only by canceling the unnecessary link and unity each link and data. As traditional and labor-intensive industry, coal enterprises are lacked in the high qualified modern concept and training courses, those will become the biggest prevention in put into use of ERP system.

3.3 *ERP implement solutions method based on management system innovation in coal enterprises*

According to above analysis we can sum up some ideas as follow: as long as we consider coal enterprises management system innovation as a basic issue in coal enterprises, we can make ERP grow and develop into coal enterprises. By the way of this opportunity of coal enterprise management system innovation, coal enterprises should emphasis on the implement of innovation for standardizing, normalizing the whole management system and push the ERP implement forward.

First, Recreate standardization and normalization of productivity and operating process in coal enterprises. Coal reservation of China is 1/3 of the whole world, but the coal export is only about 5%. As China has joined WTO, coal market becomes internationalized, which is greatly beneficial to our coal export. While facing this opportunity, the price of coal is a serious obstacle. The price of coal is relatively high, which is greatly related to our poor coal management and high coal cost. Therefore, decreasing costs of coal production is the systematic important factor throughout the whole process of coal production. Marketing, stocking, consuming, storing, recycling sales of coal products will influence the coal costs. Integrating the whole supply chain including purchasing transporting, stocking and recycling can decrease cola cost. So any management problems can be found in the supply chain and arrive to the purpose of decreasing costs. Obviously, this will involve in a problem of supply chain management. However, supply chain management is just the center idea of ERP concept. According to the material requirement, the purchase department must offer the product of the exact material they need. The supplier management is very important to ensure the cute offering material of high quality material timely. It has become an important part to establish a good relationship with suppliers. Purchasers should be familiar with the purchasing plan, finance plan, price and supplier's information, external and supplier-choosing and order form marketing. To the key materials

store model should be exactly established to ensure normal production.

Second, Establish normalized management standard system. At present, the level of production and management in coal enterprise are backward. Many unreasonable elements exist in business procedure. The advanced management concept and computer technology are needed in implementing ERP to change the present management mechanism and method. In detail, the outside supply chain can be normalized by the inner supply chain and reorganized procedure. Market requirement, purchasing offer, coal production, products-making, products-sending and services after selling are the complete working chain. According to the flatten and dumb-belled requirement of the modern enterprise reorganize structure of coal enterprise realize organization structure adjustment by modern information technology and modern management technology. Coal production is conducted about hundreds or ever thousands meters below the earth, which needs the workers struggle against the terrible nature conditions, such as slip, rock, work, mash gas, earth temperature and so on. And the production place is always on the move. so it is hard to plan well for coal enterprise. Then ERP is needed to ensure the timely and exact plan. Modern management is totally depends on plans, which is the key point of management. For the management of coal enterprise, department plans should be timely adjusted according to the changeable conditions (production plan, material requirement plan, purchasing plan, finance budget plan), to ensure supply, purchase, store, finance and sales are all on their right places. While all aspects of resource are well bended, controlled and balanced, and ensure that all the departments are well-planed and communicated, this is the aim of ERP.

Thirdly, Innovate and reform management organization structure. ERP is needed when organization structure flatten is becoming a trend and business procedure to be reorganized. The stepped bursiform management organized structure has come into being for a long time. This is a structure with low efficiency and dull reflection which may turn on important information useless because it takes a long time to pass important information to the managerial person. The efficient is very low because of the department's single function and complicated procedures. The present organized structure must be replaced by the flatten one and the business procedure must be reorganized. This is the very concept of ERP. The ERP conduct is needed to re-organize the business procedure, and only with it, the procedure can function well.

Finally, Establish learning organization and encourage staff to learn and improve their operational ability. The basic aim of establishing learning organization is impelled the enterprise's development. The function of enterprise's sustainable development is to improve its total competitive advantages and its competition. The real enterprise in the future is the organization with all the staff who are good at study and absorbed in study. This is the learning organization. By establishing the work environment and enterprise's culture of study organization and leading them to study, to progress and to adjust the new concept, the enterprise can live longer. Coal enterprises should take this kind of organization seriously. Reform the enterprise, transforming the business management concept, strengthening management level and promoting its capabilities of study, competition and creativity.

4 CONCLUSIONS

As China has been a member of WTO, market range is internationalized and the market requirement is changing rapidly. In order to adjust the changes and keep its competition, enterprises have to be dedicated to reforming organization and reorganizing procedure. The implement of ERP is a hard task. It is essential that find out the suitable strategies according to coal enterprise's features. The application of ERP in enterprise can change enterprise's former management organization structure, management style, and management method and management efficiency. It is helpful to optimize enterprise's organization structure and business procedure. It will also raise enterprises competition.

REFERENCES

Hipkin I.B., De Cock. C. Tom and BPR: Lessons for maintenance management. *J. The International of Management Science Omege*. 2000;28:277–292.

Jaideep Motwani, Dinesh Mirchandani, Manu Madan, A. Gunasekaran. Successful implementation of ERP project: Evidence from two case studies. *Int. J. Production Economics.* 2002; 75:83–96.

Kyung-Kwon Hong, Young-Gul Kim. The critical success factors for ERP implementation: on organizational fit perspective. *J. Information & Management.* 2002;40:25–40.

Stanley C. Gardinerm, Joe B. Hanna, Michael S. Latour. ERP and the reengineering of industrial marketing processes, A prescriptive overview for the new-age marketing manager. *J. Industrial Marketing Management.* 2002; 31:357–365.

Vincent A. Mabert, Ashok Soni, M.A. Venkataramanan. The impact of organization size on enterprise resources planning (ERP) implementations. The US manufacturing sector. *J. The international of Management Science Omege*. 2003;31:235–246.

Progress in Mine Safety Science and Engineering II – He et al. (Eds)
© 2014 Taylor & Francis Group, London, ISBN 978-1-138-00122-0

Application of fuzzy comprehensive evaluation for mining idlers' performance

Yunfeng Xing
China University of Mining and Technology (Beijing), Beijing, China
Beijing Materials Handling Research Institute, Beijing, China

ABSTRACT: As all known, the idler's performance affects the overall performance of the underground belt conveyor. In view of the main influence of the idler's performance, a multi-level fuzzy comprehensive evaluation model has been developed based on fuzzy mathematics theory with component quality, manufacturing process and key performance of the idler. A successful application has been proposed to evaluate the overall performance of the idler, which indicates that the model is meaningful for the idler's evaluation and selection.

1 INTRODUCTION

The idler which has various kinds and large quantity has been considered as an important component in belt conveyor system. Because it accounts for approximately 35% of the conveyor cost and bears over 70% resistance (Miao 2012). In view of the poor working conditions underground, the idler's performance, as a key factor (Hou et al. 2012) directly affects the overall performance of the belt conveyor. However, the quality among varieties of products is different and the influencing factors are difficult to be quantified. A reasonable idler's performance evaluation method is particularly critical. The current research interests are mechanical equipment performance evaluation based on technical, economic, social indicators (Xu 2007), the idler's performance qualitative evaluation and selection studies (Huang 2000) and so on. Therefore, the performance evaluation model of the mine idler is important for its grading and selecting. Furthermore, it improves the safe and efficient operation of the belt conveyor.

2 FACTORS ANALYSIS

The mine idler's failure work presents by inflexibility or stuck. The practical experience requires a good performance of idler's life, reliability, rotational resistance, sealing performance, as well as noise and vibration. To address these requirements, one must control strictly various aspects as the design, material selection, manufacturing, assembly, testing and working environment. However, the users usually determine the idler's performance from the manufactured product and the inspecting result, which reflects in appearance, structure, radial runout, axial movement, rotational resistance, waterproof and other testing projects. From another word, one can analyze the idler's performance through component quality, manufacture level and key performance in the product manufacturing process.

2.1 *Component quality*

The idler is composed of idler body, shaft, bearings, seal rings, retaining rings and so on. Specially idler body, bearings and shaft play decisive roles upon the overall performance. Some researches have found that bearings' life determines the idler's life. Bearings' life depends mainly on its quality, load and lubrication condition. KA series bearings and deep groove ball bearings are used widely. Idler body quality directly impacts on the radial runout performance which affects vibration and noise of the belt conveyor. Welded steel pipes are more expensive but widely used due to their good radial runout performance. As stiffness of the idler shaft is mainly considered, stepped shafts are often adopted because less bending deformation can improve the bearing stress state.

2.2 *Manufacturing process*

The manufacturing process level is a comprehensive reflection to technology, equipments, management and service of the enterprise. There are a lot of differences among different manufacturers'

products under the same design or drawing. For finished idler, its performance is mainly manifested by the appearance, structure and assembly quality, which are assessed through spraying quality, welding quality, runout, axial runout, axial load, rotational resistance data.

2.3 *Key performance*

Rotational resistance and sealing performance are the direct embodiment of the idler's performance. They are inversed correspondence. The smaller the resistance is, the worse the sealing performance is and vice versa. The indexes of seal form, seals quality, concentricity and rotational resistance values are used to reflect those performances. Bearing failure is caused by pitting and peeling spots resulting from water and dust ingress and lubrication decrease. It can be examined by waterproof and dustproof test.

3 FUZZY COMPREHENSIVE EVALUATION MODEL

Fuzzy comprehensive evaluation uses fuzzy set theory and fuzzy relation composite theory and gives a comprehensive evaluation from several factors on the situation in subjection grade (Gupta & Qi 1991). The main idea is to make quantitative evaluation by simulating initiation and fuzziness of human thinking and assessing amounts of uncertain factors through fuzzy mathematical knowledge (Qin et al. 2003).

3.1 *Factor sets*

The idler performance is a fuzzy concept which follows fuzzy comprehensive evaluation method and the performance level factor set can be established. Factor sets are composed by the elements which affect the values of the variable factors. Components quality, manufacturing process and key performance are three factors which are selected for evaluation system of idler performance level.

Therefore, idler performance level factor set can be given:

$$U = \{u_1, u_2, u_3\} \tag{1}$$

Where u_1 is components quality, u_2 is manufacturing process, u_3 is key performance.

3.2 *Evaluation sets*

The evaluation sets classify each factor into several grades by different levels of indicators. The level of the indicators is judged by experts and it is on line with the judgment of human experiences. The idler performance levels are classified into four.

The evaluation set V is

$$V = \{v_1, v_2, v_3, v_4\} \tag{2}$$

Where v_1 indicates the performance as "excellent", v_2 represents "good", v_3 is " average ", v_4 is "poor".

3.3 *Single factor evaluation*

The single element u_i $(i = 1\sim3)$ from set U can determine its membership degree γ_{ij} for evaluation level set v_j $(j = 1\sim4)$ the *ith* single element. Evaluation set can be given,

$$\gamma_i = \{\gamma_{i1}, \gamma_{i2}, \gamma_{i3}, \gamma_{i3}, \gamma_{i4}\} \tag{3}$$

$\gamma_{ij} = u_R(u_i, v_j)$ indicates the membership degree of u_i for v_j. f is the fuzzy mapping from U to V, namely, f: U $\rightarrow$F(U)

$$u_R \rightarrow f(u_i) = (\gamma_{i1}, \gamma_{i2}, \ldots, \gamma_{ij}, \ldots, \gamma_{im}) \in F(U).$$

A fuzzy relationship matrix from set U to evaluation set V can be given,

$$R = \begin{pmatrix} \gamma_{11} & \gamma_{12} & \cdots & \gamma_{1m} \\ \gamma_{21} & \gamma_{22} & \cdots & \gamma_{2m} \\ \cdots & \cdots & \cdots & \cdots \\ \gamma_{n1} & \gamma_{n2} & \cdots & \gamma_{nm} \end{pmatrix} \tag{4}$$

R is the fuzzy mapping from set U to set V.

3.4 *Weight sets*

In multi-factor comprehensive evaluation, various factors and grades have different influence on variables. The weight of each factor u_i is decided according to its importance to the variable. Then a weight set can be obtained,

$$A = \{a_1, a_2, ..., a_i, ..., a_n\} \tag{5}$$

Where a_i is the weight value. It follows the normalization and non-negativity conditions,

$$\sum_{i=1}^{n} a_i = 1 (0 \le a_i \le 1) \tag{6}$$

A is a fuzzy set of importance of factor U. a_i is the importance coefficient of u_i. a_i selection is the key point of fuzzy comprehensive evaluation which would directly effect on the evaluation results.

3.5 *Fuzzy comprehensive evaluation*

In multi-factor comprehensive evaluation, various factors and grades have different influence on variables. The weight of each factor ui is decided according to its importance to the variable. Then a weight set can be obtained.

$B = (b_1\, b_2 \ldots\, b_i\, b_m)$ denotes subset of the evaluation set. b_j reflects the position of *jth* evaluation in overall V. R is the fuzzy mapping from set U to set V. According to the fuzzy mathematics theory, R would determine the fuzzy mapping. It makes a fuzzy subset A of U map to a fuzzy subset B of V. Triad (U, V, R) constitutes a comprehensive evaluation model.

A fuzzy comprehensive evaluation will be obtained.

$$B = A \cdot R = (b_1, b_2, \ldots, b_j, b_m)$$

$$B = A \cdot R = (a_1, a_2, a_3) \cdot \begin{pmatrix} \gamma_{11} & \gamma_{12} & \gamma_{13} & \gamma_{14} \\ \gamma_{21} & \gamma_{22} & \gamma_{23} & \gamma_{24} \\ \gamma_{31} & \gamma_{32} & \gamma_{33} & \gamma_{34} \\ \gamma_{41} & \gamma_{42} & \gamma_{44} & \gamma_{44} \end{pmatrix} = (b_1, b_2, b_3, b_4) \quad (7)$$

In the formula, b_j indicates the membership degree of idler performance level in the *j-th* level.

If

$$b_{O'} = max\{b_1, b_2, b_3, b_4\} \quad (8)$$

We can assess performance level by principle of the maximum of degrees.

4 APPLICATION EXAMPLES

4.1 *Establishment of evaluation system*

Choosing component quality, manufacturing process and key performance as the main idler performance evaluation indicators, then a multi-level evaluation system can be established, which is shown in Figure 1. The performance of an ordinary metal idler is evaluated.

4.2 *Evaluation process*

Considering the complexity of the affecting factors of idler's performance, the values given by the questionnaires from experts are used to determine weighted coefficients corresponding to each evaluation indicator. The membership degrees are adjusted according to practical experiences. The actual results of the evaluation are shown in Table 1and Table 2.

Thus we can obtain the fuzzy comprehensive evaluation matrix of the second-level single factor.

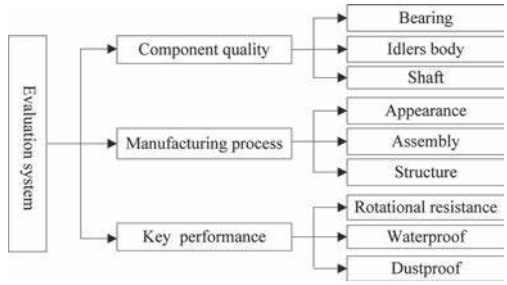


Figure 1. Idler performance evaluation system.

Table 1. Statistics of weights results.

Level-1 indicators	Weights	Level-2 indicators	Weights
Component quality	0.28	Bearing	0.45
		Idler body	0.30
		Shaft	0.25
Manufacturing process	0.40	Appearance	0.16
		Assembly	0.52
		Structure	0.32
Key performance	0.32	Rotational resistance	0.30
		Waterproof	0.34
		Dustproof	0.36

Table 2. Statistics of evaluation results.

	Evaluation sets			
Level-2 indicators	Excellent	Good	Average	Bad
Bearing	0.28	0.75	0.32	0
Idler body	0.65	0.20	0.15	0
Shaft	0.08	0.72	0.15	0.05
Appearance	0.12	0.80	0.08	0
Assembly	0.20	0.68	0.10	0.02
Structure	0.10	0.54	0.35	0.01
Rotational resistance	0.13	0.38	0.34	0.15
Waterproof	0.08	0.42	0.37	0.13
Dustproof	0.05	0.42	0.43	0.10

$$R_1 = \begin{bmatrix} 0.28 & 0.75 & 0.32 & 0 \\ 0.65 & 0.20 & 0.15 & 0 \\ 0.08 & 0.72 & 0.15 & 0.05 \end{bmatrix}$$

$$R_2 = \begin{bmatrix} 0.13 & 0.38 & 0.34 & 0.15 \\ 0.08 & 0.42 & 0.37 & 0.13 \\ 0.05 & 0.42 & 0.43 & 0.10 \end{bmatrix}$$

$$R_3 = \begin{bmatrix} 0.13 & 0.38 & 0.34 & 0.15 \\ 0.08 & 0.42 & 0.37 & 0.13 \\ 0.05 & 0.42 & 0.43 & 0.10 \end{bmatrix} \quad (9)$$

The rows of R_i indicate the membership degrees of fuzzy subset by single factor of first order indicators, To multiply row R_i by the fuzzy weight vector $W_{2i,}$ the membership degree of each subset can be obtained, namely the result of the fuzzy comprehensive evaluation.

The result of the fuzzy comprehensive evaluation of first-level indicators is as follows,

$$B_1 = W_{21} \bullet R_1 = (0.341, 0.5775, 0.2265, 0.0125)$$

It shows that the component quality of the idler rating of "good" and its membership degree is 57.75%.

$$B_2 = W_{22} \bullet R_2 = (0.1552, 0.6544, 0.1768, 0.0136)$$

It shows that the manufacturing process level as "good" and its membership degree is 65.44%.

$$B_3 = W_{23} \bullet R_3 = (0.0842, 0.4080, 0.3826, 0.1252)$$

It can be seen that the main performance of the idler as "good" and its membership degree is 40.80%.

According to the second-level evaluation results, we can obtain a fuzzy comprehensive performance evaluation matrix.

$$R_1 = \begin{bmatrix} 0.341 & 0.5775 & 0.2265 & 0.0125 \\ 0.1552 & 0.6544 & 0.1768 & 0.0136 \\ 0.0842 & 0.4\!08 & 0.3826 & 0.1252 \end{bmatrix} \quad (10)$$

The first-level evaluation result can be obtained by the weighted vector W.

$$B = W \bullet R = (0.1845, 0.554, 0.2566, 0.049)$$

According to the highest degree of membership principle, we can determine the level of idler comprehensive performance evaluation as "good", the membership degree is 55.4%.

4.3 *Analysis*

By comparing the laboratory tests on certain series of idlers, we can find that the evaluation result is reasonable and can reflect the overall performance of idler accurately. For grading the same sort, integration of one and higher level of membership degrees can be considered. The weight of indicator can be adjusted in reason further against particular working conditions.

5 CONCLUSION

Selecting the component quality, the manufacturing process, the key performance as evaluation indicators, a fuzzy comprehensive evaluation model has been established to assess the overall performance of the idler. The result of evaluation is consistent with the practical experience. The evaluation method also can be a reference for idler's grading and selection.

ACKNOWLEDGEMENTS

The authors would like to thank all the reviewers for providing several constructive comments, and also, the authors acknowledge the patience and time of the editors for processing this manuscript. This research is supported by the Fundamental Research Funds for the Central Universities of Ministry of Education of China with No. of 2010YZ05 and the National Natural Science Foundation of China with No. of 51274206.

REFERENCES

Hou Hui & Wang Yun. Factors Affecting the Service Life of Belt Conveyor Idlers. *Journal of Jiangsu Vocational and Technical Institute of Economics and Commerce,* 2:61–63 (in Chinese).

Huang Yuzhi 2000. Belt Conveyor Idler Performance Evaluation and Selection. *Coal Science and Technology,* 4:13–16 (in Chinese).

M.M. Gupta & J. Qi 1991. Theory of T-norms and fuzzy inference methods, *Fuzzy Sets and Systems,* 40:431–450.

Miao Cai 2012. Belt conveyor idler process design and improvement. *Hoisting and Conveying Machinery,* 12: 99–101 (in Chinese).

Qin Baorong, et al. 2003. Fuzzy Comprehensive Evaluation of machine selection hierarchical decision. *China Mechanical Engineering,* 14(3): 216–219 (in Chinese).

Xu Jing 2007. Mechanical equipment performance Fuzzy Comprehensive Evaluation, *Machinery,* 1:24–26 (in Chinese).

Progress in Mine Safety Science and Engineering II – He et al. (Eds)
© 2014 Taylor & Francis Group, London, ISBN 978-1-138-00122-0

Function principle and empirical research of "zero accident" concept

Z.M. Liu & G. Fu
School of Resource and Safety Engineering, China University of Mining and Technology (Beijing), Beijing, China

H.B. Pei
International Engineering Company, China Huadian Engineering Co., Ltd., Beijing, China

ABSTRACT: In this paper, we shall first confirm that "zero accident" can be achieved by statistical results of many accident reasons. And then, the function principle of "zero accident" concept is expounded through the function principle of safety culture, the principle of attitude and behavior and the principle of accident triangle together. Action principle diagram is also plotted. Finally, through the empirical study towards DuPont, Fluor, Alcoa and Shell, the results show that "zero accident" concept is very important to help enterprise to realize "zero accident" objective. If all staff of enterprise could recognize the importance of "zero accident" concept, they will do every detailed work related to safety well. Thus accident rate will reduce greatly, and then we can obtain good safety performance.

1 INTRODUCTION

In 1960's, zero plans appeared in the business world as a management ideology. In 1962, zero defect management, also known as zero shortcomings, was first used in Orlando division of Martin Marita Company in United States. The next year, the U.S. General Electric Company implemented zero defect program in a company-wide scale and increased an important content that is the proposal to eliminate the cause of error, which made the no defect plan more perfect (Zheng 2008). In May 1965, Japanese Electrical Stock Company first launched the zero defect management in Japan, known as zero-defect campaign. National Security Council launched "Zero in on safety" activity, which applied "Zero Defect Program" to the safety management. Japan Industrial Safety and Health Association absorbed the "Zero in on safety" concept of U.S. and launched Zero Incident Campaign under the support of the former Labor Ministry in 1973, also known as "Zero Defect Campaign" or "Zero Accident Campaign" (Nanbao 2008). On October 28, 2006, China and Japan two governments signed the cooperative project for the plan to strengthen China safety science and technology ability in production, and introduced Japan "Zero Accident Campaign" in the demonstration area (Liu 2008). GE and Boeing of United States, NEC of Japan and some other enterprises are the earliest of the world's top 500 enterprises to carry out "Zero Defect Plan" and "Zero Accident Campaign".

In recent years, from investigation on a large number of enterprises, more and more enterprises are starting to make "zero accident" concept as one of their safety management concepts, and establish a "zero accident" objective as their highest safety objective, such as: DuPont, Fluor, Alcoa, Dow, Intel, Motorola, Lonza (Guangzhou), the Rainbow Group, Australian Coal Association and so on. The safety performance of these enterprises is well known, however, the relationship between achieved safety performance and "zero accident" concept has not been studied in depth, and this paper will carry on theoretical and empirical research on this issue.

2 REALIZATILITY OF "ZERO ACCIDENT" CONCEPT

"Zero accident" concept sets zero accident, zero potential hazard as its ultimate objective, dealing with the hazards and problems of post through full participation and safety prediction, making workplace safety, healthy and comfortable, and then creates a bright, lively safety climate (Zheng 2008). The threshold of playing a role for "zero accident" concept is to turn safety concept to "zero", or to recognize that "zero accident" can be realized. "zero" is the wish of all employees. The process is essential that full staff strive and cooperate forward to the "zero" step by step and steady.

Heinrich summed up an important conclusion that "the direct causes of accident are the

Table 1. Statistical results of accident cause.

Statistical parties	Caused by unsafe behavior of people	Caused by unsafe condition of objects
Heinrich	88%	10%
DuPont	96%	4%
National Security Council	90%	10%
China	85%	15%

unsafe behavior of people and the unsafe condition of objects, and the unsafe behavior of people is the main cause" in his book industrial accident prevention in 1931. 50 years of the 20th century United States figured out that only 2% casualties was caused by natural disasters in 75,000, or 98% incidents could be prevented within the capacity of people (State Administration of Coal Mine Safety Personnel Training Department 2002). As Table 1 showing, this inference is confirmed further by several parties' statistics of accident cause today.

The above data shows that accidents are mainly caused by the unsafe acts of people. Meanwhile, other factors related to objects, such as machinery and equipment are designed, manufactured, maintenance and operated by people, and environmental conditions can be also created and improved by people (Hu & Zhou 2001). Therefore, we can control most accidents as long as we control people's behavior (Fu et al. 2005), and "zero accident" can be achieved.

3 FUNCTION PRINCIPAL OF "ZERO ACCIDENT" CONCEPT

Recognizing the reliability of the "zero accident", we must take measures to achieve "zero accident" objective. The function principal of the "zero accident" will lay a solid foundation and provide an effective way for the achievement of "zero accidents" objective.

3.1 *The function principal of safety culture*

Literature (Fu & Li 2009) proposes that safety culture is the core idea needed for enterprise safety management. According to the author's safety management experience and the academic research accumulation, Literature (Stewart 2002) proposes that the safety performance of enterprise is mainly the view of their managers and employees, which means that the enterprise safety performance depends on people's thoughts, ideas and their understanding and implementation of the main

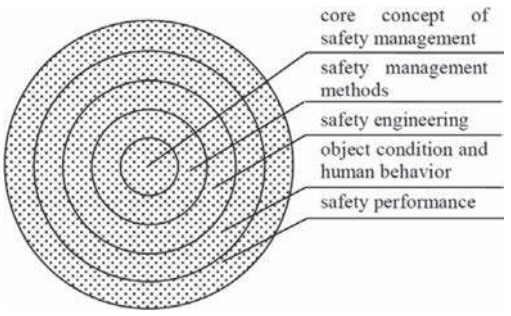


Figure 1. The definition of safety culture.

factors influencing the safety performance. Actually the core ideas of the safety management determine the safety performance of one enterprise. The important point can be used together with Heinrich's theory of accident causation (Heinrich et al. 1980) as shown in Figure 1. The center is the thought of the mind, which are the core ideas needed by safety management. Under its guidance, enterprise establishes a safety management approach including management system, management measures, etc, and then implements safety engineering technology, equipment, facilities and so on. According to the management method, which aims at improving enterprise's unsafe condition of object and unsafe behaviors of human and creating the safety performance.

According to the view of literature (Stewart 2002), the core idea of the safety management is the most important for to enterprise safety, as shown in Figure 1. It is a guidance and support to implement safety management approaches and safety technical measures. As one of the most important key element of safety management, "zero accident" concept plays a role in three aspects, which are safety management, accident prevention and reducing the accident rate according to the function principle of safety culture.

3.2 *Behavior based on attitude principle*

Psychology holds the view that attitude is the individual's relatively durable emotion, cognitive and behavioral intentions towards a concrete object. Attitude is one of the essential psychological factors (Mao 2004) influencing the behavior of individual. Many models about the view act depend on the attitude, such as theory of reasoned action (TRA), technology acceptance model (TAM), theory of planned behavior (TPB) and so on, were proposed in academia to expand research and discussion (Ajzen & Fishbein 1980, Davis et al. 1989, Davis 1986, Davis 1989). At present, TPB has been widely used in the field of behavior

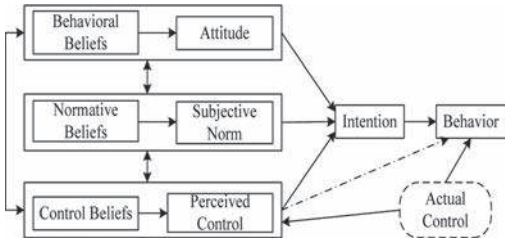


Figure 2. Schematic diagram of TPB model.



Figure 3. Accident triangle.

and correction. The model builds a theoretical framework to study the relationship between attitude and behavior, which regards attitude as the predictive value of behavior (Icek 1991). In this theory, people's attitude towards behavior, subjective criteria and controllability of perceived behavior can guide and control behavior through intermediary role of behavioral intention as shown in Figure 2.

3.3 *Principle of accident triangle*

W. H. Heinrich from America had attempted a more in-depth study on near miss. He investigated more than 5,000 injuries and found that in 330 similar accidents 300 accidents caused no injuries, 29 cases caused minor injuries along with 1 caused serious injury. That is to say, serious injury, minor injury and no injury accident number ratio is 1:29:300, which is the famous Heinrich law, called the accident triangle, as shown in Figure 3.

Heinrich law reflects a general rule between the frequency and the severity of accident, and also illustrates the randomness of accident severity or the severity lying on chance factors. Therefore, it's very difficult to control accident severity. In order to prevent major accidents, we should go all out to prevent accident occurrence, especially, attach great importance to near misses and other "small accident" records and reports (Wu & Xu 2002). Because of "small accident" causing little loss, it is often easily overlooked, but it is actually a favorable indicator of the safety performance (Yu & Wang 2004), which can provide comprehensive and timely feedback for safety management.

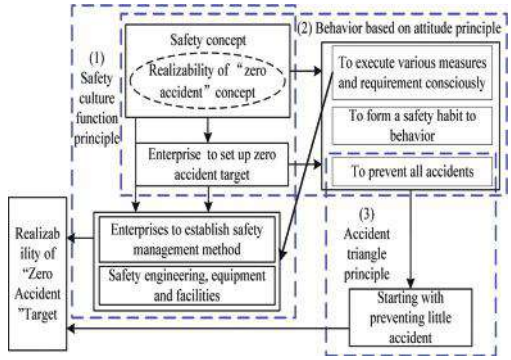


Figure 4. How the "zero accident" concept to play roles.

The safety culture action principle, behavior based attitudes theory and accident triangle principles work together to promote the change of "zero accidents" concept to "zero accidents" objective from three indispensable aspects of "idea", "action" and "methods", as is shown in Figure 4. Three principles commonly guide "zero accidents" concept, which is one of the key elements of safety culture, to strengthen enterprise safety management, prevent accidents and lessen accident rate, as follows:

1. Enterprise should set a "zero accident" objective, hire qualified personnel on safety, establish a perfect safety management system including procedures, regulations, operating instructions, etc, monitor its implementation, and carry out staff training throughout the organization.
2. Enterprise should strengthen safety check, correct employees' unsafe behaviors promptly. Every employee performs his own functions and regards safety as his own problem, implements the measures and requirements consciously, solves problems existing in work initiatively, form safe habits through preventive management.
3. Enterprise should pay attention to near misses or "little accident" records and reports, execute every procedure strictly to prevent the occurrence of accidents or injuries.

4 EMPIRICAL RESEARCH ON THE EFFECTIVENESS OF "ZERO ACCIDENT" CONCEPT

DuPont, Fluor, Alcoa, Shell are in the top 500 companies and their safety performance is well known. These companies have been insisting on the concept of "zero accidents", which is the highest objective of safety in these companies. This paper conducts a statistical study on the concept of "zero accidents" statements, the safety management and

Table 2. Enterprise concept of "zero accident" statements and safety management.

Company	"Zero accidents" objective statements	Safety management
DuPont	Zero injuries, zero occupational diseases and zero accidents. All accidents are preventable (The DuPont Commitment 2008).	1. The idea of prevention first: if not sure a job is safe, do not do it (Wang 2004). 2. Ten safety belief is the soul of DuPont (Dupont China Group Co., LTD 2003). 3. Safety training: first condition of every employee access into DuPont's is to go through safety training, and these safety training not only for new employees, but employees throughout each production processes. 4. Safety training observation program,STOPTM.
Fluor	Health, safety and environmental issues can be systematically identified and managed. "Zero IncidentsSM" is an attainable objective (Health, Safety & Environmental 2008).	1. zero accident plan. 2. Managing Safety to Zero. 3. Safety management system, which aims to HSE management practices into a program, including the project or activity from the beginning to the end of the process, and getting a consistent approach throughout the company.
Alcoa	"Work hard to prevent all accident" (Health & Safety Overview 2008).	1. HSE rules and criterion. 2. Believe that safety is primarily about cultural change, the ultimate objective is to institutionalize effective safety management. 3. Safety plan and behavior. 4. Indoctrinating culture of zero injuries and illnesses.
Shell	To achieve zero-death accident and to prevent possible accidents creating injuries or endanger neighbors or facility.	1. Truly rooted the safety awareness in the heart (Royal Dutch Shell 2007 plc Annual Reports 2008). 2. Heart and brain plan and behavioral change programs. 3. Improve the safety system. 4. Handling of the emergencies in the production. 5. Management system ensure safe production.

the safety performance of these companies with references studying, and the results are shown in Table 2 and Figure 5 (Progress Report Data Summary 2008, HSE Performance 2008, Safety Performance Data 2008, Royal Dutch Shell plc Annual Review and summary financial statements 2008, delivery & growth report 2009).

Through this research on these enterprise, we can get that all employees of enterprises will be dedicated to make every effort to make the details of every safety-related work if companies set a "zero accident" objective from Table 2 and Figure 5 (Progress Report Data Summary 2008, HSE Performance 2008, Safety Performance Data 2008, United States Department of Labor Bureau of Labor Statistics 2008). The management promotes the staff safety behavior through their attitudes and behavior directly, and through the development of safety management systems indirectly. The support of management is the most important factor, and management commitment and leadership are key elements for success. The management's participation is the basis of safety, but all of the employees should participate safety at last, for them inducing safe or unsafe behavior, operating and managing

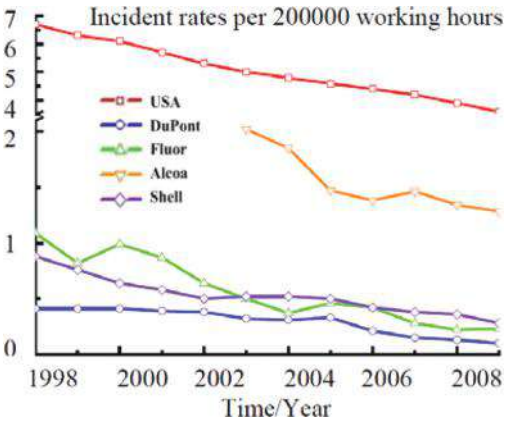


Figure 5. The safety performance comparison between DuPont, Fluor, Alcoa, Shell and all American industries.

equipment directly in operating environment. Employees' participation and management's commitment are like two meshing gears and the gear of the management promises will drive the gear of employees' participation to the rapid rotation if

increasing motor power. Increasing motor power is to do well with safety investments, including funding, taking time to train and effort and then achieving a significant reduction of accident rates and a better safety performance objective.

5 CONCLUSION

Firstly, this paper describes the achievable of "zero accidents" theoretically, and then elaborates action principles of "zero accident" and draws the graphics using the action principle of safety culture, principle of attitude and behavior and accident triangle principle. At last, this paper makes an empirical study on safety objectives, safety management, and safety performance of DuPont, Fluor, Alcoa, Shell, getting the following conclusions:

Accidents are mainly caused by the unsafe acts of people and people can create and improve environmental conditions. Controlling of human behavior could control most of the accidents. "zero accidents" can be achieved.

The action principle of safety culture, principle of attitude and behavior and accident triangle principle can explain the action principle "zero accident". Improving the safety management system, correcting people's unsafe behavior, controlling near misses and other small incidents are the effective way to achieve "zero accidents" objective for enterprise.

"Zero accidents" concept is very important for an enterprise to achieve "zero accident" objective and good safety performance. If all employees realize the importance of "zero accidents" concept, they will do well with every detail safety-related work, thus greatly reducing the accident rate to obtain better safety performance.

REFERENCES

Ajzen I & FishbeinM 1980. Understanding Attitudes and Predicting Social Behaviour [M]. *Englewood Cliffs,NJ: Prentice—Hall*.

Davis FD, Bagozzi RP & Warshaw PR 1989. User Acceptance of Computer Technology: A comparison of Two Theoretical Models [J]. *Management Science*, 1989(35):982–1003.

Davis FD 1986. A Technology Acceptance Model for Empirically Testing New End—User Information Systems: Theory and Results [D]. *Cambridge,MA:MIT Sloan School of Management*.

Davis FD 1989. Perceived Usefulness, Perceived Ease of Use, and User Acceptance of Information Technology [J]. *M IS Quarterly*, 1989(13):319–340.

Dupont China Group Co., Ltd. 2003. Public Department, Dupont Equals to Safety [J], *China COSCO*, 3:76–77.

Fu Gui & Li Changxiu 2009. The Effect of Enterprise Safety Culture And The Discussion of Quantitative Measurement [J]. *China Safety Science Journal*, 19(1):86–92.

Fu Gui, Li Xuandong & Li Jun 2005. Common Causes of AccidentsAnd Prevention Strategies Based in Bahavior [J]. *Journal of Safety and Environment*, 5(1):80–83.

Health & Safety Overview [EB/OL]. [2008-11-1] http//www.alcoa.com/global/en/about_alcoa/sustainability/health_overview.asp.

Health, Safety & Environmental (HSE) [EB/OL]. [2008-9-10] http://www.fluor.com/sustainability/health_safety_environmental/Pages/default.aspx.

Heinrich WH, Peterson D & Roos N 1980. *Industrial Accident Prevention* [M]. New York: McGraw-Hill Book Company (5th).

HSE Performance [EB/OL]. [2008-9-10] http://www.fluor.com/sustainability/health_safety_environmental/Pages/hse_performance.aspx.

Hu Yiben & Zhou Ping 2001. *Accident Prevention Psychology* [M]. Bei Jing: People's Education Press.

Icek Ajzen 1991. Theory of Planned Behavior [J]. *Organizational Behavior and Human Decision Processes*, 50:179–211.

Liu Baolong 2008. The Understanding of "Zero Accidents Activities". *Labor Protection* [J], 2008, (3):12–14.

Mao Haifeng 2004. *Safety Management Psychology* [M]. Bei Jing: Chemical Industry Press, 2004, 3:80.

Nanbao Changxiao 2008. Japanese "Zero Accidents Activities". *Labor Protection* [J], 2008, (3):15–17.

Progress Report Data Summary [EB/OL]. [2008-8-20] http://www2.dupont.com/Sustainability/en_US/Performance_Reporting/data_summary.html#1.

Royal Dutch Shell plc Annual Review and Summary Financial Statements 2008 Delivery & Growth Report [EB/OL] [2009-03-02] http://www.annualreview.shell.com/2008/servicepages/downloads/files/download.php?file=entire_shell_review_08.pdf

Royal Dutch Shell 2007 plc Annual Reports [EB/OL] [2008-11-15] http://www.shell.com/home/content/investor/financial_information/annual_reports/2008/archive_reports_2007.html.

Safety Performance Data [EB/OL] [20080-11-1] http://www.alcoa.com/global/en/about_alcoa/sustainability/health_safe_perform.asp.

State Administration of Coal Mine Safety Personnel Training Department 2002. *Coalmine Safety Management* [M]. Xu Zhou: China Mining University Press, 128–129.

Stewart, JM 2002. *Managing for World Class Safety* [M]. A Wiley Inter science Publication, 2002. 1–31.

The DuPont Commitment [EB/OL]. [2008-8-20] http://www2.dupont.com/Sustainability/en_US/Performance_Reporting/commitment.html.

United States Department of Labor Bureau of Labor Statistics News Washington, D.C. [2008-8-20] http://www.bls.gov/iif/oshwc/osh/os/osnr0030.pdf.

Wang Zhiping 2004. The Safety Belief And Management Practice of Dupont [J], *Foreign Economies and Management*, 26(4):20–24.

Wu Qiong & Xu Kaili 2002. *Safety Managerialics* [M]. Bei Jing: Coal Industry Press, 16.

Yu Guangtao & Wang Erping 2004. The Content, Influence Factors, and Mechanism of Safety Culture [J]. *Advances in Psychological Science*, 12(1):87–95.

Zheng Shuangzhong 2008. To Study Japanese "Zero Accidents Activities". *Labour Protection* [J], 2008, (3):18–19.

This page intentionally left blank

Progress in Mine Safety Science and Engineering II – He et al. (Eds)
© 2014 Taylor & Francis Group, London, ISBN 978-1-138-00122-0

Analysis and statistics of workers' unsafe acts in coal mine gas explosion

Wentao Yin, Gui Fu, Ping Gao & Chun Yang
Faculty of Resources and Safety Engineering, China University of Mining and Technology (Beijing), Beijing, China

ABSTRACT: The literature demonstrates that nearly all of the gas explosion accidents are liability accidents. In order to get the regularity of direct causes of gas explosion, a meticulous analysis of 194 major gas explosion cases have done, and results show that there are 15 kinds of generic unsafe acts can lead to gas accumulation and can divided into 4 categories. In terms of ignition sources, we get 10 kinds of generic acts and separate into 2 categories. Statistical distribution of various generic unsafe acts are also gained: start/stop auxiliary fan optionally (19.10%) and use wrong gas emission measures (12.36%) are the 2 main generic acts lead to gas accumulation. Incorrect blasting operation process (36.72%) and hotline work (10.17%) are the 2 main generic acts that can lead to the emergence of spark.

1 INTRODUCTION

In all types of coalmine accidents, gas explosion occupied the largest share of the major accidents (Coal Mine Safety Supervision Bureau of the State 2012). Except by using engineering technology such as technical equipment or skills to prevent the gas explosion, understanding the law of the accident can also help the people to avoid repetitive accidents. Accident analysis results showed that nearly 100% of gas explosions are liability accidents, and the direct cause is unsafe act.

Behavior-based accident causation model showed in Figure 1 (Fu 2005), which has proposed by national safety scientist Fu Gui, revealed the behavioral science theory that "safety culture influence organizational behavior, organizational behavior will shape individual behavior, and individual behavior can be represented by individual acts" (Fu et al. 2013), is the research's theory basis. The model pointed out that the most effective way to prevent accidents is the avoidance of the unsafe act in operation process. In order to get the specific unsafe acts in gas explosions, the paper discuss the worker's act based on a large number of accident cases, and extract the unsafe acts which lead to the gas explosion directly, then conclude these acts by using of statistics method and get some universal rules. The results can help the coalmine to improve its organizational behavior and can be used for its safety training.

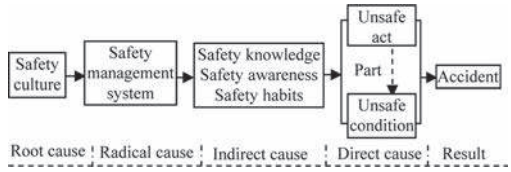


Figure 1. Behavior-based accident causation "2–4" model.

2 BASIC INFORMATION OF CASE SAMPLE

2.1 *Scope of accident cases*

According to the Coalmine Production Safety Accident Reporting and Investigation Regulations (State Administration of Work Safety 2007), coal mine accident can be divided into four levels by death toll such as follow:

1. Extraordinarily serious accident: more than 30 people died in 1 accident.
2. Serious accident: more than 10 and less than 30 people died in 1 accident.
3. Larger accident: more than 3 people and less than 10 people died in 1 accident.
4. Ordinary accident: less than 3 people died in 1 accident.

Based on this principle of classification, author chooses national major gas explosion accidents in coal mine from year 2000 to year 2009 as a research sample.

2.2 *Sources of statistical data*

Publications such as Typical coal mine accident case analysis (Liu & Li 2011), compilation of coal mine accidents cases (more than 100 people) (Coal Mine Safety Supervision Bureau of the State 2007), and so on. A large amount of accident case analysis literatures (Sun 2010, Liu 2004) and some other informations from the Internet.

Table 1. Statistics of national major gas explosion.

Year	Statistics type	
	Case number	Death toll
2000	31	761
2001	27	488
2002	29	704
2003	12	377
2004	21	696
2005	33	940
2006	16	355
2007	14	322
2008	5	105
2009	6	205
Sum	194	4953

2.3 *Sample statistics*

According to the description of accident case from year 2000 to 2009, a total of 194 major gas explosion accidents have been chosen, there are 4,953 people in total deaths, 19.4 cases and 495.3 people per year on average, each accident caused 25.5 deaths. Specific statistics are described in the Table 1.

3 UNSAFE ACT ANALYSIS OF GAS EXPLOSION

Gas explosion occurred when a workplace meet the 3 conditions at the same time: (1) explosive limit methane ($\varphi(CH_4)$ = 5%–16%), (2) source of ignition, (3) enough oxygen ($\varphi(O_2) \geq 12\%$), Because the breathable air is available in working place, therefore, analysis of gas and ignition sources is the core issue of gas explosion analysis, and the direct causes(unsafe act) include emergence of gas accumulation and occurrence of spark are the main content in this part. In addition, through form and object of various kinds of unsafe acts, common types of unsafe act named "generic unsafe act" can be got, and called "generic act" for short.

3.1 *Unsafe act analysis of gas accumulation*

Superficially, gas accumulation is an unsafe condition and formed by a period of time. But a large number of accidents showed that in the production process of underground coalmine, except the gas explosions which are explode in the gob, gas accumulation in other workplace is usually caused by people's unsafe act.

The paper discusses the causes of gas accumulation of these 194 cases of accident through form and object in the process of operation, and gets a total of 4 major categories which include 15 kinds of generic acts concretely. The first category is misusage of ventilation facilities, including 5 kinds of generic acts: misusage of ventilation door, not clear up plugged underground tunnels, not install enough length of air pipes, not qualified construct hermetic wall, take apart the ventilation equipment and installation optionally. The second category is misusage of ventilation devices, including 4 kinds of generic acts: start/stop auxiliary fan optionally, not install auxiliary fan, install auxiliary fan in the wrong place, recirculation ventilation of auxiliary fan. The third category is misusage of ventilation measures, including 4 kinds of generic acts: use series ventilation, use wrong gas emission measure, not blow blasting smoke timely, not adjust the ventilation system timely. The fourth category is misusage of mining operation measures, including 2 kinds of generic acts: mining without gas drainage, blasting without enough minimum resistance and connect the gob. According to the frequency of these acts showing in the accidents, statistical regularity has been got and the result are shown in Table 2.

The extraction of generic unsafe acts are all based on accident cases and combined with the thought of the behavior-based accident causation "2–4" model. Take "Misusage of ventilation door" for example, others are similar. For the sake of improving the quality of ventilation, ventilation door is widely used in the underground coalmine. Currently, most of the small coalmines are using the ventilation door which is made by two pieces of thick staggered planks. This situation can't be changed in a short period of time. Because this is a manpower type door, if workers passed through the door without closing it, it's can lead to air short circuit and then lead to gas accumulation. There have 3 behavioral expression of this unsafe condition, (1) forget to close, (2) close not timely, (3) open intentionally. If people don't have enough safety knowledge and good safety habit, these 3 unsafe acts can occur easily.

From the Table 2, gas accumulation generic unsafe acts are mainly contained in category I, II, III, based on the proportion of these generic acts from high to low, the first 9 generic acts are arranged as follow: start/stop auxiliary fan optionally (34, 19.10%), use wrong gas emission measure (22, 12.36%), recirculation ventilation of auxiliary fan (21, 11.80%), not install auxiliary fan (19, 10.67%), not install enough length of air pipes (18, 10.11%), use series ventilation (13, 7.30%), misusage of ventilation door (10, 5.62%), not qualified construct hermetic wall (10, 5.62%), take apart the ventilation installation optionally (9, 5.06). These 9 generic acts grow into gas accumulation mostly

Table 2. Statistics of national major gas explosion.

Category	Generic act	Case	Proportion
Misusage of ventilation facilities	Misusage of ventilation door	10	5.62%
	Not clear up plugged tunnels	6	3.37%
	Not install enough length air pipes	18	10.11%
	Not qualified construct hermetic wall	10	5.62%
	Remove the ventilation installation at will	9	5.06%
Misusage of ventilation devices	Start/stop auxiliary fan optionally	34	19.10%
	Not install auxiliary fan	19	10.67%
	Install auxiliary fan in the wrong place	3	1.69%
	Recirculation ventilation of auxiliary fan	21	11.80%
Misusage of ventilation measures	Use series ventilation	13	7.30%
	Use wrong gas emission measure	22	12.36%
	Not blow blasting smoke timely	2	1.12%
	Not adjust the ventilation system timely	3	1.69%
Misusage of mining operation measures	Mining without gas drainage	3	1.69%
	Blasting less than minimum resistance line	5	2.81%

lead to a total percentage of 87.64% are most likely to occur in workers.

3.2 *Unsafe act analysis of ignition sources*

According to the appearance characteristics of ignition source in the gas explosion, they can be divided into 3 types: internal-cause ignition sources, external-cause ignition sources, and other ignition sources. Internal-cause ignition sources are mainly due to the spontaneous combustion of coal or explosives, other ignition sources are caused by the shifting of rocks along with stratum and striking, besides of this two types of ignition sources, other ignition sources can be called external-cause ignition sources and the features is the fire/spark can be avoid by means of strengthen the management of workers' behavior. Due to the internal-causes of ignition sources and other ignition sources are happened by chance, the paper mainly analyzes the unsafe acts of the production process of external-cause ignition sources.

Direct causes of external-cause ignition sources mainly include unsafe acts of worker as well as unsafe condition of electrical equipments, here we called them "operating fire" and "electrical fire". Electrical fire is shown as an unsafe condition, because of lack of safety knowledge workers or managers are not redress the dangerous equipment so we can demonstrate the unsafe acts through the administrative vulnerability of electrical equipment. Operating fire is the fire/spark that generated during the production process, intentionally or not. Both of two aspects can be prevented by strengthening the safety training of workers' operating process and inspection, improving the management system and electrical equipment.

Through analysis of 194 cases of gas explosion, a total of 177 cases of accidents that caused 4,449 people die are caused by external-cause ignition sources, accounted for 91.24% of all accident cases and 89.83% of the total deaths. Among them, 118 (66.67%) cases are the operating fire, 59 (33.33%) cases are the electrical fire. And the operating fire occupies the most proportion of accidents, both cases and deaths. So, to avoid operating fire is of great significance for preventing gas explosion. Generic act and its distribution of external-cause ignition sources are shown in Table 3.

From the Table 3, we get 7 kinds of generic acts of "operating fire", and the first four kinds are arranged as follow via proportion from high to low: incorrect blasting operate process (65, 36.72%), hot-line work (18, 10.17%), disassembling the miner's lamp without permission (13, 7.34%), deliberately created open flame (10, 5.65%). Actually, these 4 generic acts occupy a total percentage of 89.83% of the 7 generic acts that can lead to "operating fire". In addition, through our study, a phenomenon should be pointed out particularly that "incorrect blasting operate process" is an exclusive act only happens in blasters whom is one special type of coalmine workers, and this is only a name refer to all of unsafe act respectively in the process of blasting operation collectively, there's not space to cover them in depth here and author will discuss them in another paper. Emergence of these generic acts usually relate to insufficient safety knowledge of workers. Due to the low educational level, front-line workers don't understand the risk of these acts, even don't know he will produce fire/sparks.

Table 3. Types of generic act caused external-cause ignition sources.

Category	Generic act	Case	Proportion
Electrical fire	Electrical equipment lost its explosion-proof ability	26	14.69%
	Not use explosion-proof electric equipment	12	6.78%
	Short circuit of the electric cable	21	11.86%
Operating fire	Metal collision sparks(tools, etc)	5	2.82%
	Deliberately created open flame(light a fire, smoking, etc)	10	5.65%
	Incorrect blasting operate process	65	36.72%
	Disassembling the miner's lamp without permission	13	7.34%
	Hot-line work(cable bond, equipment maintenance)	18	10.17%
	Friction impact between metal tools and rocks	5	2.82%
	Others	2	1.13%

Therefore, coalmine enterprise needs to strengthen the training of its workers, and they will understand the dangers of unsafe acts when they have enough safety knowledge of gas explosion, finally they will avoid these unsafe acts actively. 3 types of generic acts are included in "Electrical fire": Electrical equipment lost its explosion-proof ability (26, 14.69%), not use explosion-proof electric equipment (12, 6.78%), short circuit fault of the electric cable (21, 11.86%). Among them, "electrical equipment lost its explosion-proof ability" share the largest proportion, accounting for about 14.69%.

At present, measures such as replace the general electrical equipment and damaged cables can be used to solve "not use explosion-proof electric equipment" and "short circuit fault of the electric cable" thoroughly. But now there is no way to completely solve the problem of electrical equipment lost its explosion-proof ability, and the most common method used in coalmine is intensive inspection. The types of electrical equipment that lost its explosion-proof ability showed in accident cases have been collected, and got 5 common types of electrical equipments/devices, these 5 types are electrical switches, miner's lamp, exploder, electric coal drill, junction box, and specific distribution is shown in Figure 2. From the figure, we can know electrical switches, miner's lamp and junction box are the 3 main types of equipments/devices that prone to lose its explosion-proof ability, accounted for about 76.93% in total.

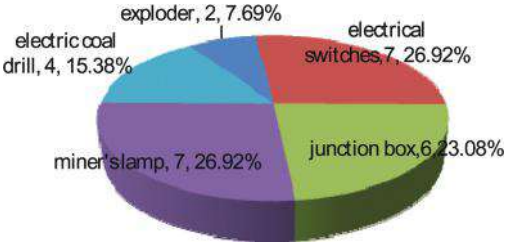


Figure 2. Types of electrical equipment lose explosion-proof ability.

3.3 *Discussion of analysis result*

From the analysis result above, a total of 25 kinds of generic unsafe acts are gotten. All of these acts can happen easily in coalmine, some of them are shared to all of the workers, such as misusage of ventilation door, cause metal collision sparks, and some of them are shared only to a particular type of worker, such as use wrong gas emission measure, incorrect blasting operate process. Overall, the safety pattern of these acts does not have very high technical requirements, but need to understand a certain of safety knowledge, make them aware of their safety responsibilities and comply with the operation standard [9]. Therefore, in order to prevent the major gas explosion, we should focus on acts and incident in our daily work. If every worker in coalmine can improve their behavior pattern and avoid unsafe acts, then, gas explosion accidents can be prevented essentially.

4 CONCLUSIONS

This paper aimed to find the regularity of the direct cause of gas explosion, through the study of analysis of the generic unsafe act in the coalmine major gas explosion accidents based on the behavior based safety model, the following conclusions can be drawn:

1. There are a total of 4 categories and 15 kinds of generic unsafe act that can lead to gas accumulation, and 9 kinds happened frequently, such as start/stop auxiliary fan optionally, use wrong gas emission measure, etc, accounted for 87.64%.

2. Divided the external-cause ignition sources into electrical fire and operating fire. 3 types of generic acts are included in "Electrical fire": electrical equipment lost its explosion-proof ability, not use explosion-proof electric equipment, short circuit fault of the electric cable. Electrical switches, miner's lamp and junction box are the 3 main types of equipments/devices that prone to lose its explosion-proof ability, accounted for about 76.93% in total.
3. There are 7 kinds of generic acts of "operating fire", and the first four kinds are: incorrect blasting operate process, hot-line work, disassembling the miner's lamp, deliberately created open flame, and accounted for 89.83% of the accident ignition sources.
4. The safety way of unsafe acts do not have very high technical requirements. Gas explosion can be prevented as long as coalmine workers can improve their behavior pattern, and avoid the unsafe acts.

ACKNOWLEDGEMENTS

This work was sponsored by the National Natural Science Foundation of China (No. 51074167).

REFERENCES

Coal Mine Safety Supervision Bureau of the State 2007. *Compilation of Coal Mine Accidents Cases (More Than 100 People)*. Xuzhou: China University of Ming and Technology Press.

Coal Mine Safety Supervision Bureau of the State 2012. *The National Coal Mine Accident Analysis Report (2011)*.

Fu Gui 2005. Behavior Based Model for Organizational Safety Management, *China Safety Science Journal*, 15(9):21–27.

Fu Gui, et al. 2013. Discussions on theoretical understanding and effects of behavior based safety, *China Safety Science Journal*, 23(3):150–154.

Liu Jianmin & Li Baotang 2011. *Typical Coal Mine Accident Case Analysis*, Beijing: China Coal Industry Publishing House.

Liu Qingfeng 2004. Causes of four major gas explosion accidents. *Labour Protection,* (7):66–68.

Petersen D 1994. Integrating safety into total quality management. *Professional Safety*, 39(6):28–30.

State Administration of Work Safety 2007. Coalmine Production Safety Accident Reporting and Investigation Regulations.

Sun Jiping 2010. The causes and lessons of "2.22"gas explosion disaster at Tunlan Coal Mine. *Journal of China coal society*, 35(1):72–75.

This page intentionally left blank

Progress in Mine Safety Science and Engineering II – He et al. (Eds)
© 2014 Taylor & Francis Group, London, ISBN 978-1-138-00122-0

Study on STOP applied to safety management of coal mine

Youli Yao
School of Technology, Shanxi Datong University, Datong City, Shanxi Province, China

ABSTRACT: Experience of developed countries and practice of Chinese safety production have both shown that human unsafe behavior is main cause factor of accidents. So, decreasing human mistake and clearing up human unsafe behavior are important for prevention accidents. Safety management is transferring into human as center from thing as center. SAFETY TRAINING OBSERVATION PROGRAMME (STOP) is a new behavior management method. It is also a new safety training method. By STOP card, unsafe behavior is rectified and safe behavior is enforced. STOP is applied to coal mine safety management. In the view of cognitive course of miner and behavior control, it can get miner to consciously control their behavior and gradually form safety behavior habit.

1 INTRODUCTION

According to Chinese coal mine accidents and specialist comment (Wan Jiefan & Li Wenjun 2002), human unsafe behavior occupied 97.67 percent of all immediate cause resulting in heavy accidents in China. Experience of developed countries has also shown this. Research result of American mine specialists showed that accidents resulted from human unsafe behavior occupied 85 percent of all mine accidents. Ten years statistical accidents of American DuPont Company showed that 96 percent accidents are resulted from human unsafe behavior. Japanese data also showed that 96 percent accidents are resulted from human unsafe behavior. Williamson researched on Australian accidents of from 1982 to 1984. He found that 91 percent accidents are resulted from human factor (Zhou Gang & Cheng Weiming 2008, Chao Qingren, et al. 2007, Wang Hanfeng & Zhang Bing 2008, Lu Diankun, et al. 2009). So, decreasing human mistake and clearing up human unsafe behavior are important for prevention accidents. Safety behavior theory supplies method to control human mistake and to clearing up human unsafe behavior. Traditional safety management emphasizes on human duty; whereas behavior science emphasizes human activity. Safety management is transferring human as center from thing as center. In the view of cognitive course of miner and behavior control, it can get miner to consciously control their behavior and gradually form safety behavior habit.

STOP is a new behavior management mode. It is firstly put forward by American DuPont Company (Yang Lei & Zhang Shuang 2010, Jiang Xiufeng 2010). It is also a new safety training method. It is applied to lots of oil companies in the world. By STOP card, unsafe behavior is rectified and safe behavior is enforced.

2 STOP

2.1 *STOP introduction*

STOP is composed of initials of four words, SAFETY, TRAINING, OBSERVATION and PROGRAMME. STOP is a sort of observation program. Observation human behavior and communicating with coal mine worker get unsafe behavior to be controlled. STOP can help personnel to change unsafe behavior and to enhance observation and communication skill to prevent accidents. It is STOP logos that all injuries and occupational disease can be prevented. STOP is applied to coal mine safety management. In the paper STOP application steps is introduced. STOP is not punitive and must be parted from organization discipline.

2.2 *Distinction between STOP and safety check*

Target of STOP is human, whereas safety check includes human, thing etc. STOP emphasizes on two ways communication. Personnel are active. Whereas in safety check personnel checked is passive. For STOP, all personnel can be observation men, whereas for safety check only specialist and managerial personnel can be observation men. STOP both affirm safe behaviors and rectify unsafe behaviors; safety check only aims to thing unsafe situation and human unsafe behavior.

STOP is a no penalty safety program and is parted from organization discipline. STOP allows personnel to discuss their behaviors; up to they wake

to why their behaviors must be changed. All along, it is regarded that only by rectifying unsafe behavior can improve safety level, but STOP thinks that strengthening safe behavior is equally important. Only observation is not enough. Communication is still needed to strengthen their safe behavior and rectify their unsafe behavior. While you are actively looking for safe behavior and unsafe behavior, you give a signal to your environmental other persons that your safety criterion is high. In contrast, if you neglect safe behavior or unsafe behavior, your personnel may think that you don't regard safety and their safety performance will become worsen.

3 STOP STEPS

STOP includes five steps, especially, decide, cease, observe, act and report. Firstly, observation time and point is decided. Secondly, stop near personnel observed. Thirdly, it is observation. Observation content includes stuff reaction, stuff position, personal protective device, tools and equipment, program and order. Fourthly, communication with stuff observed. It is pay special attention to whether they know working routine and working order no blame. Finally, report. By STOP card report are finished.

4 STOP APPLICATION TO SAFETY MANAGEMENT OF COAL MINE

Before application lots of preparation work must be done. It includes establishing organization and work scheme, setting down observation Rota, organizing safety training class and compiling STOP courseware.

4.1 *STOP training*

All participants must know observation content, steps, how to observe and communicate and how to write STOP card. Person observed includes safety miner manager, safety management personnel, safety check personnel, technologists, party chief and personnel agent. Training content includes STOP introduction, behavior method, STOP importance, unsafe behavior rectifying, ABC method, how to observe and fill out a form. Owing to coal mine work time feature, by many times to train, all training content are handed in correlation department and persons to get them perfectly to comprehend STOP method.

4.2 *STOP being put into practice in coal mine*

Group header carries STOP card. Group header observes his personnel while they are going production. In order to preferably observe, at a time observation content is not exceeding 30 items (M. Fleming & R. Lardner 2002, E. Scott Geller 2001, Dominic Cooper 1994). For unsafe behaviors observed, observation man should communicate with personnel observed and obtain their safety acceptance. In order to enhance STOP effect, safety mine manager and all group headers go STOP.

4.3 *Data statistic and analysis for STOP*

Aiming to behavior of infringement of regulations, traditional safety management in coal mine takes punishment measure; but STOP is not punitive. Before taking STOP, we must arrive at a agreement with safety mine manager, safety management department and group headers. STOP observation result don't be treated as three disobey. It couldn't be gist of punishment. At the same time group header and other observer observe same personnel. Observation result is contrasted and observation warp is rectified. All observers fill STOP card. Observation result must be analyzed synthetically. Main problem must be found in production. Aiming to problems found, correlative measures must be taken to improve safety level.

4.4 *Standardizing STOP card*

STOP card is a tool of STOP showed in Table 1. STOP card faithfully memorizes unsafe behaviors and safe situation. By card information, safety problem can be found and be rectified. Periodically, normative card is shared with everybody. Written normalization can be enhanced.

4.5 *STOP effect is verified*

STOP was applied in Tongliang Coalmine for one year; then we verified its effect. Correlation index of before of application STOP and after it is contrasted and analyzed. From June to December

Table 1. STOP card.

Site:	Date:	Time:
Observation information	Personnel reaction Personnel position Personal protective device Tool and equipment program Human engineering environment result from unsafe behavior	
Cause of unsafe behavior and communication result		
Corrective measure and suggest		
Observer:		

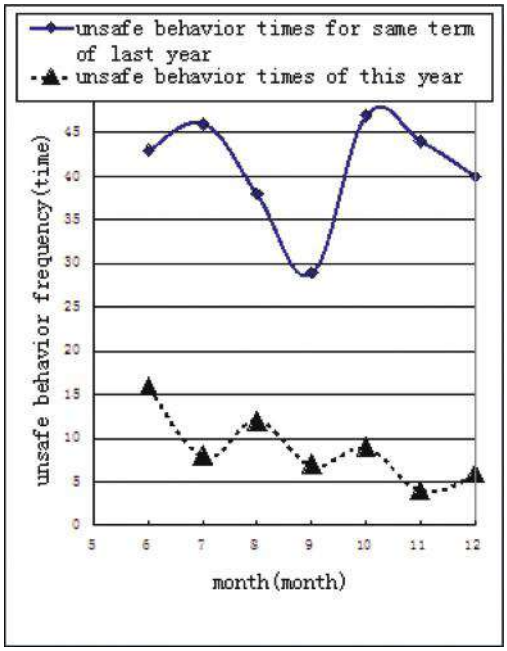


Figure 1. Contrasting before and after STOP applied.

during STOP being applied, total of penalty for accidents is 14350 yuan and same term of last year was 19760 yuan. It is reduced by 27.3%. From June to December during STOP being applied, accidents are four times and same term of last year was seven times. Decrease of unsafe behavior frequency is most visible. From June to December during STOP being applied, unsafe behavior times is 62 and same term of last year is 287. It is 0.216 times of last year. It is showed in Fig. 1.

5 OPEN QUESTIONS AND CORRECTIVE MEASURES OF STOP APPLICATION TO SAFETY MANAGEMENT OF COAL MINE

5.1 *Problems*

1. STOP is not enough regarded. Some people think that it is insignificant. These can result in observation result apart from practice. Some false information is supplied for analysis to mislead safety management of coal mine.
2. STOP is not used masterly. Some people don't know how to use STOP. STOP card written is not standard.
3. Communication skill is wanting. Kernel of STOP is communication. While observer meets to unsafe behaviors, some people are accustomed to criticize. Observer couldn't effectively communicate with personnel observed.

5.2 *Corrective measures*

a) Propaganda force for STOP must be increased. Advanced DuPont Company safety culture and STOP are propagandized to all personnel. This can get personnel to learn that STOP can reduce unsafe behaviors in work.
b) Strengthening training. Periodically, skilled STOP workers train other personnel by scene practice of STOP to enhance training effect. All management staffs and group heads discuss observation techniques and communication skill.
c) Communication skill should be paid attention to. Psychologist thinks that strengthening safe behavior is more important than punishing unsafe behavior. STOP is not punitive. In order to avoid happening once again, during observation, group head must communicate with personnel to get them to know why their behaviors are unsafe and how to work. Communication can not only rectify unsafe behaviors but also encourage safe behaviors. Communication can intensify safe behavior and can ensure to go on. STOP discussing meeting should be convened to emphasize on communication and to enhance communication skill.

6 CONCLUSION

STOP can get personnel to learn that back of safe or unsafe situation substantively means human behavior. Safe behavior can bring up safety situation, in the converse, unsafe behavior can bring up unsafe situation. STOP can not only observe own unsafe behaviors but also observe others unsafe behavior. Safety knowledge and experience are shared each other. After STOP applied in safety management in coal mine, unsafe behavior clearly decrease. Safety consciousness of personnel evidently enhanced.

ACKNOWLEDGEMENT

The work was financially supported by Shanxi Science and Technology Department Foundation (No. 2013041018-01) and Shanxi Datong University doctor foundation (2008B22).

REFERENCES

Chao Qingren, et al. 2007. Study on unsafe behavior of miner [J]. *China Safety Science Journal* 17(12):19–25.
Dominic Cooper 1994. Implementing the behavior-based approach: a practical guide [J]. *The safety and Health Practitioner* 15(3):26–32.

E. Scott Geller 2001. *The Psycholoby of Safety Handbook* [M]. 2nd ed. Florida: CRC Press LLC.

Jiang Xiufeng 2010. STOP applying to oil refinery company [J]. *Security Health and Environment* 10(10):11–12.

Lu Diankun, et al. 2009. Research on human safe behavior[J]. *Coal Mine Modernization* 63(6):82–83.

M Fleming & R Lardner 2002. *Strategies to promote safe behavior as part of a health and safety management system* [M]. Edinburgh: the Keil Centre.

Wang Hanfeng & Zhang Bing 2008. Based on behavior control safety management of coal mine[J]. *Coal Science and Technology* 3(4):61–64.

Wan Jiefan & Li Wenjun 2002. *Coal Mine Accidents and Specialists Comment*. Beijing: China Coal Industry Publishing House.

Yang Lei & Zhang Shuang 2010. Behavior safety observation and communication applying to oil company [J]. *Secruity Health and Environment* 10(10):13–15.

Zhou Gang & Cheng Weiming 2008. Analysis on human mistake and human unsafe behavior. *China Safety Science Journal* 18(3):10–14.

Progress in Mine Safety Science and Engineering II – He et al. (Eds)
© 2014 Taylor & Francis Group, London, ISBN 978-1-138-00122-0

The implications of behavior-based accident causation "2-4 model" in the prevention of coal mine roof accident

P. Gao, G. Fu & W.T. Yin
China University of Mining and Technology (Beijing), Beijing, China

ABSTRACT: In recent years, the number of accounts for the proportion of China's coal mine roof accident is still large in the total coal mine accident and the roof accident prevention is still the focus of China's coal mine safety management. In order to propose an effective method for the prevention of coal mine roof accident, we studied according to behavioral safety "2-4" model of mine roof accident. Through statistical analyzing the unsafe acts of 10 roof accidents, we got the personal habits cause, organizational behavior cause, and organizational cultural reasons of the accident and draw a conclusion that organizational behavior error is the leading cause of the accident. Finally, we put forward three aspects of accident prevention measures which are improving the level of awareness of safety culture, sounding and effectively implying the safety procedures and training safe acts habits.

1 INTRODUCTION

In 2011, the roof accidents held the most proportion of the whole coalmine accident cases and caused the highest death toll, account for 47.2% of the total accidents and 33.7% of the all death toll (State Administration of Coal Mine Safety 2012), the proportion are more than 1/3. Apparently, roof accident should be regarded as the main object of coalmine safety management.

The behavior-based accident causation "2-4 model" is the scientific principle of this paper (FU GUI et al. 2013). According to the two levels, four stages of behavior the model described the unsafe acts of a typical coal mine roof accident is analyzed firstly, then, a statistical analysis of common unsafe acts of 40 coal mine roof accidents from year 2007 to 2010 are given. Through the unsafe acts we analysis the personal habits cause, organizational behavior cause, and organizational cultural reasons of the accident and ultimately arrive at organizational behavior error is the leading cause of the accident. Finally, the behavior prevention and control measures of the coal mine roof accident are given.

2 ANALYSIS OF UNSAFE ACTS OF ROOF ACCIDENTS

2.1 *Analysis of unsafe acts of 1 roof accident*

1. Description.
   12:00 Zhang with workers Zhong and Deng went to 3210 caving coal face. Zhang felt tired when he put the top to carry a child at 16, then he arranged Deng to caving stood behind Deng observing the roof. Deng used an ax to cut off the 18 pillars of thick stick, suddenly shed beams fell and waste rock caving, Deng buried. After Zhang and Zhong rescued 10 minutes Zhong put forward to bell inform the dispatch room.
2. Analysis of unsafe acts.

Table 1. Unsafe acts in the roof accident case.

Category	Actor	Unsafe acts
Direct actor	Deng (Prop caving worker)	1. Using backward hammering ax knock caving method. 2. Standing in an unsafe location. 3. Continue to work without rest, lack of concentration.
Indirect actor	Zhang (Team leader)	1. Not estimated the total amount of work. 2. Arrange the tired Deng continue to work. 3. Not attentively observe the roof, not recognizing the danger. 4. Failed to stop the backward caving method. 5. Did not immediately report the mine rescue team to save lives.
	Zhong (Prop caving worker)	Rescuing alone.

2.2 *Analysis of common unsafe acts of roof accidents*

Table 2. Unsafe acts of coal mine roof accidents.

No.	Unsafe act	Frequency	Proportion
1	Not examine the environment.	6	15%
2	Not prevent unsafe acts of others.	7	17.5%
3	Nobody observe roof while working.	5	12.5%
4	Not reinforce the broken beams.	3	7.5%
5	Not choose the right work methods.	8	20%
6	Stay in the dangerous area.	4	10%
7	Work alone.	4	10%
8	Not evacuate when facing hazards.	1	2.5%
9	Not reject dangerous work.	1	2.5%
10	Work unplanned and with fatigue.	1	2.5%

3 ANALYSIS OF PERSONAL HABITS CAUSE OF ROOF ACCIDENTS

Habits cause is the indirect reasons of roof accidents including lack of personal safety knowledge, safety awareness and poor security practice. These three aspects is the days and months multiplying results and the principle is that accustomed produce unsafe acts and physical state and unsafe acts lead to the accidents. Workers do not operate according to the operating procedures during the operation due to the lack of safety knowledge, safety awareness is not high and do not realize the risk of taking error practices. Continuous use of the wrong acts in the previous operation did not result in the occurrence of safety accidents which prompted the workers formed a habit of unsafe acts.

For example, "Not examine the environment" in Table 2 due to the workers lack of safety knowledge and do not ensure themselves in a safe place during working and not aware that a dangerous work environment may lead to fatalities. The issue of unsafe act "Not choose the right work methods" is workers, but may also be management personnel. The prop caving worker used backward working method in Table 1 may be either due to the coal mine workers do not know other advanced operation mode or due to the managers of the coal mine do not equipped with a state-of-the-art operating equipment. The reason is that the safety knowledge of the workers and the management is not sufficient and they do not know there are other safe practices. Or they may know the security practices but did not taking, which because their safety awareness is not high.

4 ANALYSIS OF ORGANIZATIONAL BEHAVIOR CAUSE OF ROOF ACCIDENTS

Organizational behavior is the quality of the safety management system, namely, system files and their implementation status which run a direct result of habitual behavior of the members of the organization. The run behavior of organizational behavior is the root cause of the accident. From the point of view of the coal mine roof accident, organizational behavior errors include two aspects, one is roof safety procedures are not perfect, the other is a point of order problems in the implementation process.

Point of order is not perfect because the coal mine itself do not have the roof safety procedures or may also be verbal specified operating procedures do not form documented for all types of employees learning, in addition, it may also be due to the rules and there are errors loopholes. Unsound operating procedures cannot correctly guide the employees to form good safety habits, and thus cause unsafe acts. For example, for the unsafe act 2 "Not prevent unsafe acts of others" in Table 2 we reviewed the 2011 coal mine safety procedures and do not found the correct mode of operation involved in such unsafe acts (State Administration of Work Safety 2011).

The implementation of the statutes problems may be because staff training is not in place and there are problems in the supervision and assessment of the regulations implementation. For example, for the unsafe act 4 "Not reinforce the broken beams" it is clearly pointed out that "You must first repair and reinforce the broken beams and columns before continuing" in "Article 8 of the coal shovel work, article 5 of the picks work, Coal Mining, The First Part, <The security technical operation of coal miners Guide>" (China Coal Industry Labor Protection Institute of Science and Technology Organization 2007). When the workers found that the presence of such a danger but do not take measures in rules of the order to eliminate will form potential problems to the accidents. Of course, accidents will not occur 100%. The presence of structural instability beams and columns may be because the safety inspectors do not find such hidden dangers. Security check is not in place is also caused by adverse operation of the procedures.

5 ANALYSIS OF ORGANIZATIONAL CULTURAL REASONS OF ROOF ACCIDENTS

Safety culture refers to the safety concept which is the guiding ideology of the organization's overall security business (work) jointly owned by the members of the organization and it is the guide behavior of organizational behavior. Safety culture in the modern organization performs for the purpose of organizational security, safety vision, safety values and safety faith (FU GUI et al. 2007). Safety culture in the practical process can be expressed as safety culture elements, such as "The relative degree of importance of the safety", "Safety creates economic benefits", "The awareness of safety investment" and so on (Safety Management Research Centre 2013). Coal mine management personnel lack of the knowledge of safety the safety investment results there is no state-of-the-art production equipment in the coal mine and the workers still use more dangerous practices. It is this wrong understanding makes the time of the workers in dangerous operating environment and the roof accident occurred ultimately. Whether the coal mine management has a deep understanding of safety culture elements determines the degree of perfection and the status of implementation of coal mine safety management system file. The level of awareness of safety culture elements is a true portrayal of the level of safety culture construction. Because the employees do not understand or recognize the elements of safety culture and have lower safety awareness having the presence of luck and think that accident probability is very low even if the accident does not necessarily happen to them results in the course of their work on the regulations do not strict, and thus the forming an accident.

6 PREVENTION MEASURES

According to the "safety culture—oriented organizational behavior, organizational behavior determine individual behavior", the measures should be taken from level of awareness of the safety culture (root cause), the improvement and enforcement of safety rules habits (primary cause) and the training of security acts habits (indirect cause).

6.1 *Improve the level of awareness of safety culture*

Under the guidance of a good safety culture coal mines can establish a good safety management system, and thus encourage their employees to have sufficient security knowledge, a high level of safety awareness and good security habits which could greatly reduce the number of occurrences of the employees unsafe acts, and ultimately avoid accidents. By strengthening the safety concept and implying effective management behavior unsafe behavior motivation will be significant constrained thereby weakening the employee's unsafe behavior intention (LIANG Zhen-dong 2012). Thus, improving the level of safety culture could prevent the causes of accidents radically. Ways to improve the safety culture construction is to take all measures, especially quantitative tracking measurement (Online analysis system of corporate safety culture), strengthening safety culture construction, improve cultural guide behavior, improve staff's understanding of the elements of safety culture and lay the foundation for the construction of the safety management system.

6.2 *Sound and effective implementation of safety procedures*

Sound safety procedures is the premise of coal mine roof accident prevention, the effective implementation of the procedures ensures accident prevention. For coal mine roof accident prevention the coal mine should not only establish and improve the procedures for the safe operation of roof but also strengthen the implementation of the procedures. The implementations of procedures rely on consciousness and supervision. The coal mine should to deal with all kinds of employees to carry out effective safety training. The training content is the roof safe work practices and makes the employees consciously observe the order and act according to the rules effectively preventing accidents. Strengthen supervision and punishment of violations is effective measure to intervene unsafe behavior (FU GUI et al. 2005). Coal mines should set up a professional safety oversight personnel to correct personnel violation of operating procedures timely, strengthen education and even take penalties. In addition to professional security officer, we can also set up staff security supervisor of the masses improving safety oversight consciousness and the sense of security between the staff.

6.3 *The training of safe acts habit*

The direct cause of the accident is unsafe acts. Therefore, preventing unsafe acts of employees and making them to complete the task by safe acts is particularly important. Mentioning unsafe behavior study and solutions BBS (Behavior-Based Safety) is mainly used abroad (LI Nai-wen & JI Da-jiang 2011). The application of BBS method requires a longer time to build a safety culture

which is a long process. Thus, this method cannot achieve quick accidents prevention in our country.

The most direct way to training is "Make the employees know how the accident occurred" (FU GUI 2013), which is the accident case training method. Accident cases here can be a real case and it also can be a speculated case according to science information. In training specific unsafe acts in the roof accidents are teached and safe acts are inform to employees, if necessary, simulated training can be used to develop safe operation habits and achieve the purpose of the prevention of accidents.

7 CONCLUSION

Behavioral safety "2-4" model is applied to the coal mine roof accident analysis drawing the following conclusions.

1. There are totally 10 categories unsafe acts in roof accidents. Four kinds of frequency unsafe acts are:
   Not examine the environment.
   Not choose the right work methods.
   Not prevent unsafe acts of others.
   Nobody observe roof while working.
2. The organizational behavior errors play a leading role in the roof accidents.
3. 3 coal mine roof accident prevention measures:
   Improve the level of awareness of safety culture.
   Sound and effective implementation of safety procedures.
   Training the staff's safe act habits.

REFERENCES

China Coal Industry Labor Protection Institute of Science and Technology Organization. The security technical operation of coal miners Guide (bound volumes). Beijing: Coal Industry Press; 2007.

FU Gui, Zhang Su, Dong Ji-ye, et al. Discussions on the theoretical understanding and effects of behavioral safety. China Safety Science Journal; 2013; 23(3).

FU Gui, LU Bai, Chen Xiu-zhen. Behavior Based Model for Organizational Safety Management. China Safety Science Journal; 2005(9); 21–27.

FU Gui. The first means of accident prevention: Know the cause of the accident. http://blog.sciencenet.cn/blog-603730-673606.html; 2013-04-28.

Liang Zhen-dong. SEM-based study on effects of organizational and environmental factors on worker's unsafe behavior. China Safety Science Journal; 2012; 22(11):16–22.

LI Nai-wen, JI Da-jiang. Application Study on Behavior-based Safety in Coal Mine Behavior Management. China Safety Science Journal; 2011; (12):115–121.

Online analysis system of corporate safety culture. http://www.koolsquare.cn/survey/.

State Administration of Coal Mine Safety. 2011 National Coal Mine Accident Analysis Report; 2012.

State Administration of Work Safety. State Administration of Coal Mine Safety. Coal Mine Safety Regulations; 2011.

Safety Management Research Centre. Safety Culture Measurement. http://www.safetyscience.cn/page/aqwhcl/122.php, 2013-02-24/2013-2–28.

Progress in Mine Safety Science and Engineering II – He et al. (Eds)
© 2014 Taylor & Francis Group, London, ISBN 978-1-138-00122-0

Research on safety management capability of coal enterprises of strategic orientation

Hong-Liang Qi
School of Management, China University of Mining and Technology (Beijing), Beijing, China
School of Management, Heilongjiang University of Science and Technology, Harbin, Heilongjiang, China

Yun-Cai Ning
School of Management, China University of Mining and Technology (Beijing), Beijing, China

ABSTRACT: This paper focuses on the coal enterprise safety management ability, in order to achieve "safety, efficient, green, economic and social sustainable" this comprehensive goal, chiefly researches five elements including strategy, institution, personnel, external environment and internal resources, constructs the coal enterprise safety management ability evaluation model.

1 INSTRUCTION

The coal industry, which contributes to two thirds of our general energy consumption, is a pillar industry of our country. For a long time, while supporting fast growth of national economy, coal industry's extensive development also leaves us with heavy prices like incidents causing great number of casualties and serious ecological environment destruction. (Chen ZhiHua 2004). Increasingly prominent security problem and frequent accidents because of the increase of coal mines, as well as the special working environment of coal production all mean that coal production process is facing greater dangers and unsafe factors than general industries. In that case, the stable operation of coal mine production is being severely affected. All the factors above warn us of the serious condition of coal mine safety production, and we must strive to enhance safety management in coal mines, which is extremely significant to the development of coal mines or even the gross economy.

2 LITERATURE REVIEW

At present, the academia tend to study security management from various aspects like coal mine external environment governance, security management mode, security management assessment, security culture and so on. Researches targeted at strategic oriented—security management capability are comparatively rare. Sun JiPing (Sun JiPing 2011) proposed that coal mine safety production needs right ideas, reasonable planning, reliable equipments, practical techniques, qualified personnel, scientific standards, strict rules, fine management, effective rescue, etc. We should meet the demands of normative behaviors, reliable equipments, standardized environment, effective disposal, well—designed institutions and perfect system. Among all the factors above, right ideas are the basis and key of coal mine safety production. Liu TieZhong (Liu TieZhong 2009) claimed that coal mine safety management is the core controlling technique of safety production system consisting of personnel, equipment, environment, system, etc. Its essence is the adverse influence generated by personnel's unsafe behaviors, equipment's unsafe conditions, unsafe environment and unsafe system becoming the affecting factors of coal mine security management capability. Han NingBo. (Han NingBo 2012) summarized and analyzed American experience in mine disaster governance: first is to establish perfect security legal system; second is to build independent system of strict supervision and identification of parties responsible for the accidents; third is to found thorough qualification training; forth is to set up investment system in security technology. But researches home and abroad above are only based on the surface of enterprise management and don't involve deeper strategic construction. These researches might be misleading because on one hand they underestimate strategy's vital influence on security management, and on the other hand they are inclined to induce enterprise's short—term behaviors which are not beneficial for its chronic development.

Enterprise strategic management activities define its overall development direction and key areas of business activities. Strategic management theories' guidance for enterprise management

is particularly important. Theoretical strategic researches focus on the study of strategic process, contents and environment. Among them, strategic process study primarily describes the formation and implementation process of corporate strategy; strategic content study mainly analyzes strategic decision and characteristics of each strategic stage; strategic environment study puts particular emphasis on various realities enterprise is facing.

The researches based on enterprise strategic security management capability, the core elements that need our attention and core ideas embodied should all be in accordance with enterprise strategy. By putting human capital, information capital, organization capital and other intangible assets into use, and applying professional strategic execution management framework, enterprise should implement security management strategic execution into each management group and individual employee in order to make strategic execution more scientific, reasonable, and employees more motivated.

3 CONNOTATION AND ELEMENTS OF STRATEGIC—ORIENTED SECURITY MANAGEMENT CAPABILITY LAYOUT OF TEXT

With reference to previous research results, we can define coal mine security management capability as follows: coal mine security management capability system under strategic orientation consists of five elements which are strategy, system, personnel, internal resources and external environment. Coal mine security management capability is the management capability within the enterprise that results from the interaction between those five elements.

3.1 *Element of strategy*

Coal development and utilization must adhere to the scientific outlook on development in order to achieve safety, efficiency, greenness, economy, society coordination and sustainable exploitation. (Xie HePing, et al.2012) Strategic objectives should reflect the following five points: first is the innovation model of coal development and utilization which stresses quality and benefit; second is the extension of downstream industry chain to enhance coal's value, promote the transformation of coal's deep processing and increase economic added value; third is the increase in studies on coal's basic theories and technology so as to achieve "safe, efficient and clean" digital mine; forth is the realization of comprehensive occupational protection which attached importance to occupational health insurance despite the controlling of casually accidents; fifth is the insistence on the ideas of circular economy development to achieve energy conservation and emission reduction, and to reduce the destruction on ecological environment and build a balanced ecological mechanism.

3.2 *Element of system*

System is the guarantee of enterprise security management. It is the normative documents drafted in the name of the coal mine according to state regulations, laws and industry standards combined with the practical safety production condition of the coal mine. (Ding KeFang & Zhang HongBin. 2009) System construction should be specific, applicable and make authorities and responsibilities clear. In addition to set the bottom line of casualties per ten thousand tons per year and the standard of workers' security knowledge, we should at the same time purposefully establish coal mine safety management system according to strategic objectives. More importantly, enterprise should set up detailed safety system including production equipment updates, accident early warning, early control, emergency rescue system, safety production supervision, miners' safety production training scheme and social goals—related enterprise management assessment based on its own strategy.

3.3 *Element of personnel*

Condition of the coal mine production is complexity, uncertainty and variability, and miner's life safety is directly related to his personal security quality. Modern coal mine security management should be people oriented, and it is the premise of assuring coal mine safety production. Personal safety quality can be divided into two levels: the first level is the basic safety quality including security knowledge and security technique; the second level is the deeper safety quality including: security awareness, perception and attitudes. The first level of safety quality can be ensured and improved by daily safety education while the second level demands the spread of security perception to cultivate employee's safety values and group security awareness to form enduring security constraints, thus effectively controlling personnel work behavior.

3.4 *Element of external environments*

External environment embodies in working environment, capital investment, social culture and other aspects, and among them working environment is extremely important to coal mine security

management. (Chen ZhiHua 2004) First is the gas condition, over half of domestic coal mines are high gassy or gas outburst; second is the roof condition; third is water damage; forth is coal dust explosion; fifth is coal seam spontaneous combustion which can produce toxic or harmful gases that may lead to miner's death from suffocation or gas or coal dust explosion.

3.5 *Element of internal resources*

Making effective use of equipment and taking effective technical measures to ensure the safety of equipment has become the priority of coal mine security management. Coal mine internal resources mainly embody in equipment condition. One condition is the degree of coal mine production mechanization. The lower degree of mechanization, the more tense populated, the greater factors of uncertainty and greater possibility of casualty accidents. We can enhance security management capability by using various advanced machineries and introducing informative and intelligent management system. The other condition is security monitoring equipment which is an effective measure to prevent accidents in coal mine security management system. By adopting up to advanced security technique, monitoring and management method, security management of low accident rate, low incidence of occupational diseases, well—guaranteed occupational security and health can be realized. Regulators can also use information management system to trace, tackle and correct safety condition.

4 CONSTRUCTION AND ANALYSIS OF MODEL

According to the elements of coal mine security management capability determined by previous analysis, we put forward the assessment and analysis model of coal mine security management capability, as shown in Fig. 1.

We divide coal mine security management capability into five levels, the number from 1 to 5 stands for the weakest to the strongest respectively. Experts are organized to score on the elements of coal mine security management capability in recent years, then data are entered into the database. After building historical database, we can apply Bayes Method to calculate the probability that security management capability takes different values.

We set system as I, personnel as C, environment as E and resources as R

$$I = i_0, \quad C = c_0, \quad E = e_0,$$
$$R = r_0, \quad 1 \le i_0, \quad c_0, e_0, \quad r_0 \le 5 \; S = s_0$$

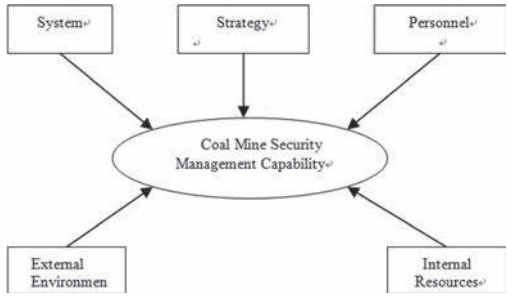


Figure 1. Assessment and analysis model of coal mine security management capability.

Table 1. Probability distribution of coal mine security management S.

S	1	2	3	4	5
P	p1	p2	p3	p4	p5

The probability that

$$P(S = s_0 \mid I = i_0, C = c_0, E = e_0, R = r_0) = \frac{P(S = s_0) \times P(I = i_0, C = c_0, E = e_0, R = r_0 \mid S = s_0)}{P(I = i_0, C = c_0, E = e_0, R = r_0)} \quad (1)$$

We use S for coal mine security management capability, then we can reach the probability distribution shown in Table 1.

5 CONCLUSION

Under the background of rapid development of coal industry, it is of vital importance to explore coal mine security management issues, clarify interaction system between elements of security management, and reveal the law of security management centered in improving security capability. We will carry out further analysis in future empirical studies to further validate the applicability of the model.

REFERENCES

Chen Zhi-Hua. Analysis on Coal Mine Safety Production System Arrangement [J]. Joural of Shandong Economic and Management Cadre Institute, 2004, (6): 81–82.

Ding Ke-Fang, Zhang Hong-Bin. Coal Mine Underground Environment's Important Position in Human—Machine—Environment System [J]. Journal of Coal Safety, 2009 (8): 120–121.

Han Ning-Bo, Zhang Ju. Enlightenment on Advanced American Coal Mine Management Experience [J]. Journal of Jilin Labor Protection, 2011(5): 90–92.
Liu Tie-Zhong, Li Zhi-Xiang. Enterprise Safety Management Theory Review [J]. Science and Technology Management Research, 2009(2): 150–15.
Sun Ji-Ping. Coal Mine Safety Production Concept Research [J]. Journal of Coal, 2012 (2): 314–316.
Xie He-Ping, Qian Gao-Ming, Peng Su-Ping. China's Coal Production Capacity and Scientific Development Strategy Research [A], Science and Technology Innovation to Promote China's Energy Sustainable Development [C]. Beijing: Chemical Industry Press, 2010: 26–31.
Xie He-Ping, Wang Jin-Hua, Shen Bao-Hong. New Ideas on Coal Mining—Scientific Production and Scientific Capacity [J], Journal of Coal, 2012(7): 1070–1071.

Progress in Mine Safety Science and Engineering II – He et al. (Eds)
© 2014 Taylor & Francis Group, London, ISBN 978-1-138-00122-0

Influence of underground noise to people's unsafe behavior in coal mines

G.Y. Cheng
Key Laboratory of Mine Disaster Prevention and Control, Hebei, China
Science and Technology Division of North China Institute of Science and Technology, Beijing, China

S.J. Chen
Key Laboratory of Mine Disaster Prevention and Control, Hebei, China
Safety Engineering College of North China Institute of Science and Technology, Beijing, China

J.L. Qi
Key Laboratory of Mine Disaster Prevention and Control, Hebei, China
Science and Technology Division of North China Institute of Science and Technology, Beijing, China

Y. Cheng
Key Laboratory of Mine Disaster Prevention and Control, Hebei, China
Safety Engineering College of North China Institute of Science and Technology, Beijing, China

ABSTRACT: Noise threatening the workers' life safety and properties virtually. Work and life in the very noisy (above 80 dB) environment may lead to hearing loss, or even permanent hearing loss. Some people may have dizziness, headaches, irritable mood reaction, and even get neurasthenia, indigestion, decreased metabolism, increased blood pressure. From the perspective of psychology and physiology and human behavior, this paper mainly makes an analysis of the influence of underground noise of the coal mine on the unsafe behavior of people. Long-term exposure to noise has a bad effect on people's central nervous system, especially on their learning, memory and work efficiency, which may lead to the decrease in their work, learning efficiency, health standard and quality of life, and even reduce the reliability of workers, as well as unsafe behavior that may result in accidents.

1 INTRODUCTION

Sound is an important aspect of work environment, but those unnecessary sound forms noise that is harmful to workers' physical and mental health. Particularly with the development of modern industry, and the advancement of science and technology, more and more high-power and high-speed mechanical equipments are used for coal production, and the noise pollution becomes increasingly serious in coal mines, thereby the influence of noise on people has become an important social issue (Cheng & Zhu 1998, Shao & Wang 2004, Shao & Wang 2008).

2 THE CONCEPT OF NOISE AND NOISE POLLUTION SITUATION IN COAL MINES IN CHINA

2.1 *The concept of noise*

From the subjective perspective, all sound of disturbance can be called noise; from the physical characteristics, noise is erratically mixture of all sorts of sound waves which have different frequency and intensity. In the production process, all generated sounds can be regarded as productive noises, such as noises from mechanical operation, friction, and striking in the process, and from fans, sirens, pumps and transformers, etc.

2.2 *Noise pollution situation in China's coal mines*

In coal mine system, major noises come from main fans, coal winning machines, transport machines, road-headers, air hammers, electric drills, trolleys, cages, air compressors and auxiliary fans, etc. Because underground working space is small and closed in coal mines, it is difficult for the sound to spread; and due to hard walls around tunnel, sound-absorbing ability is not obvious, which makes the underground noise pollution more serious in coal mines (Ye 2005). Statistics show that noise intensity among many coal mines reach and even exceed the national occupational health standards (Xu & Liu 2008).

The Institute of labor hygiene of Fushun Mining Bureau conducts the survey on workers exposed to noise in Longing coal mine, and the survey indicates that among 248 operational locations, a total number exposed to noise is 5951, which accounts for 44% of current members and 59% of production workers; and workers who are exposed to the noise above 90 dB (A) account for the total number of 76%, and constitute 33% of current members, while the current numbers 24% in the environment where the noise is above 100 dB (A).

Medical examination is made for 120 workers who are exposed to noise, and the number of noise-induced hearing loss accounts for 3.8%. In addition, the alarm signal releases due to noise interference that bring obstacle to communication and contact, thereby the situation of life casualties occurs from time to time. According to statistics of the decade (1974–1983) in Fuxin Mine area, 9 accidents are caused by noise among 88 fatal accidents, which account for 10.2%. In another accident statistics, there are eight accidents which are related to noise, accounting for 10.8%. Therefore it can be seen that the effect of noise on safety and people must not be neglected.

3 INFLUENCE OF NOISE ON HUMAN PHYSIOLOGY AND PSYCHOLOGY

The influence of noise on people is multi-faceted, and the noise not only causes injury to hearing organ, but also does harm to mental and physical health (Tu & Huang 2010). In order to truly understand the influence situation of underground noise on human body, then from the practical point of view, relevant researches about harms of noise on human body are carried out. By considering two respects that is psychology and physiology, according to the relevant theoretical knowledge that have been mastered, we design health questionnaire for employees who work at underground noise resource. For a real conclusion we explore the influence of underground noise on people's psychology and physiology in practice. We conduct the questionnaire survey among five areas which are mine transportation area (JY), ventilation area (TF), mining area (CM), wind and electricity area (FD), tunneling area (JJ). Each work area extracts 20 mine underground workers immediately to answer the questionnaire, finally the questionnaire amounts to 100.

Through this questionnaire survey as well as an analysis of the questionnaire, it comes to the conclusion that by no means the older the age, the more serious influence is caused by noise, and it also has something to do with the age of work that have been made out. The influence of noise also varies depending on the working areas. For example, even in the same age period, due to work in different working regions, the influence on workers is not the same. The influence of underground noise on working personnel is a result of the combined effects of age, length of service, and work areas, and by no means the older the age and the longer age of work, the more serious influence is caused by noise. Moreover, it is not perfect that take into account upon the influence on underground personnel according to only one single factor.

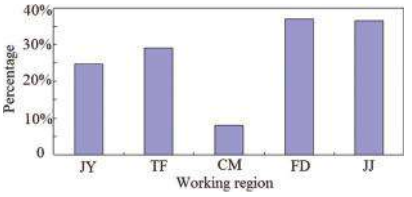


Figure 1. Influence of underground noise on personnel psychology of working region in different age.

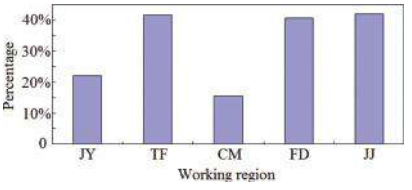


Figure 2. Influence of underground noise on personnel physiology of working region in different age.

The influence of noise on human psychology is annoyance, agitation, irritability, and even irrationalness. The impact on hearing organs is the most significant influence of noise on human physiology, for example, masking effect can be caused by noise, and then noise-induced hearing loss is brought about.

Noise is a vicious stimulus, when people are exposed to noise for a long time, the noise may stimulate the central nervous system, cause autonomic nervous system dysfunction; and with the excitement and inhibition of cerebral cortex out of balance and reflex abnormalities, some symptoms appear, such as dizziness, headache, tinnitus, dreamy, insomnia, nervousness, memory loss, distraction, and even mental disorder appears in severe cases (Tian & Zhou 2010, Liu 1999).

4 AN ANALYSIS OF THE INFLUENCE OF UNDERGROUND NOISE UPON PEOPLE'S UNSAFE BEHAVIOR IN COAL MINE

The investigation and statistical study of many coal mine accidents shows that more than 80% accidents

in our coal mines are caused by unsafe behavior of coal mine workers directly or indirectly. Unsafe behavior of coal mine workers is always blamed as the most important cause of accidents in our coal mines (Xiao 2001). However, some staffs' unsafe behavior results from barriers in their physiology and psychology, and noise is one of the important factors. It is well known that a variety of factors is an interlocking system, and even due to the slightest carelessness accidents may take place. We have discussed that a person's behavior is affected by various factors, and though noise can not affect people's unsafe behavior directly, it has a significantly adverse effect on people's behavior and affect human physical and psychological health (Liu 1999).

Human is a huge changing complex system, and it is not only limited by multi-dimensional factors but also constricted and impacted by a variety of external environment. The noise plays an active role in the completion of simple tasks in a short time, but when people just finishes complicated work that has complex clues and require sustained concentration and higher memory ability, the capacity of the organism will be easily influenced due to the negative effects of noise on cognitive function. In 1998, according to the animal experiments conducted by Yu Sufang etc., the continuous exposure to high intensity noise can bring about the behavioral learning function of the rat's motor nerve and even cause the change of the nerve muscle activity ability and tolerance persistence. In 2000, the results of tests carried on by Cheng Jinxia etc. to the workers exposed to the mechanical noise show that there are significant differences in the reaction time, digit symbol, target tracking and visual retention between the noise group and the control group; and along with the increase of noise intensity and the extension of working years, the error rate increased. This test results indicate that the noise have some adverse effects on workers.

According to statistics, there are all kinds of noises in the underground coal mines and the noise levels are far more than workplace noise standards in the national express provision (Niu 2006). We just analyze the influence of noise on people's unsafe behavior from the angle of the mechanism of unsafe behavior occurrence:

4.1 *The occurrence of unsafe behavior in the process of information receiving and processing*

Unsafe behavior often occurs in the process of information processing, the essence of which is due to receiving wrong information, information processing errors and mistakes in response to the external stimuli (information). Wiggleworth pointed out that all types of injuries and accidents depend upon the human unsafe behavior, and he defines human unsafe behavior as "false or improper response to the external stimuli". Noise is one factor that has an effect on information receiving and processing, for example, noise has a masking effect on human hearing threshold and so-called masking effect is that one sound is disturbed by other sounds, which makes hearing is so difficult. When the noise intensity reaches a certain limit value, it will create masking effect to human hearing, which makes people difficult to receive the information properly, say, others' loud caution or instructions. Worker's reaction time can be also affected by noise, and the reaction time refers to the interval from the time of exposing to external stimuli to the time of starting actions. Generally speaking, the reaction time is normally between 0.1 and 0.5 seconds, but studies show that the reaction time for the complex selections is between 1 and 3 seconds, but in a noisy environment there is also 1 second delayed on average. This influential process can be expressed as the following model:

So when people make false contact and judgment to the external stimuli or the response on external stimulation is delayed, the unsafe behavior often occurs.

4.2 *Unsafe behavior occurs in the case of the function psychological tension*

A certain degree of psychological stress would be happen with the requirement of a certain practical environment. Psychological stress is one individual subjective experience, and is also one kind of complex psychological phenomena generated by the interaction between the objective environment and the workers themselves. According to the psychological research findings, the situation that causes people to perceive something unpleasant

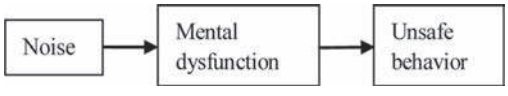


Figure 3. Model 1.

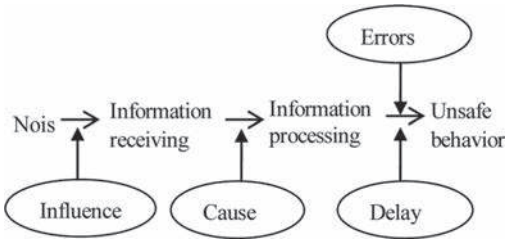


Figure 4. Model 2.

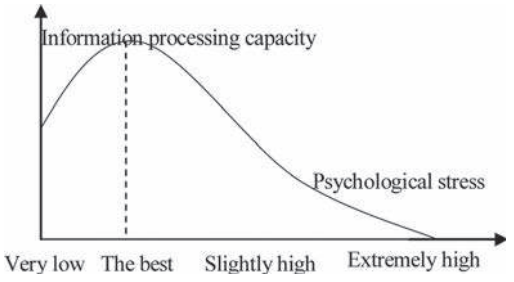


Figure 5. Information processing capacity and tensity.

in the objective environment is called "a tension situation". The noise is a major contextual factor that has an effect on the staff psychological stress. The level of the human brain consciousness and psychological stress are closely related, and accordingly, the human information-processing ability and psychological stress also have a close relationship (Figure). When a person's psychological stress increases, the decrease of the information-processing capacity characterizes some unusual performance in information processing, resulting in unsafe behavior.

5 CONCLUSION

In coal mine system, there are a lot of sources of noise, and according to different locations, noise sources can be divided into mine ground noise sources and underground noise sources. Ground noise come from mine fans, air compressors, boiler rooms, main auxiliary shaft winch rooms, coal machines, etc. Underground noise mainly come from the local fans, drilling machines, blasting, coal mining machines, coal drift machines, local fans and so on.

Environmental noise has a far-reaching impact, and it can have an adverse effect on people's psychology and physiology: the noise can damage hearing and cause deafness; noise can cause the body stress reaction, adrenaline increase, along with the changes in heart rate and the rise in blood pressure; noise may cause insomnia, fatigue, dizziness, headache, memory loss and other various symptoms; noise will also cause restlessness, irritability, and even irrationalness.

A person's behavior is affected by various factors, and though noise can not affect people's unsafe behavior directly, it has a significantly adverse effect on people's behavior: noise has a masking effect on hearing threshold of human hearing, and it can also affect people's reaction time in noisy environments, and the average interval delays about 1 second; and when the inappropriate contact and judgment about external stimuli or the response to external stimulation has been delayed, the unsafe behavior will happen. Noise may also engender psychological stress, and when the psychological tension increases, the decrease of information-processing capacity characterizes some unusual performance in information processing, resulting in unsafe behavior.

ACKNOWLEDGEMENTS

Thanks to the supporter. This work was supported by the National Natural Science Foundation of China (50974061); Natural Science Foundation of Hebei, China (E2009001420).

REFERENCES

Cheng G. & Zhu, K. 1998. Energy-saving and Noise Reduction of the Major Mine Fan [M]. Coal Industry press.

Liu, W. 1999. On the main mine fan noise hazards and prevention of Mine Security [J]. *Sense of safety in coal mine*, 1999.(9):23–24.

Liu, Z. 1999. *The unsafe behavior analysis* [M]. Zhongnan Institute of Technology.

Niu, G. 2004. Mine and control of noise [J]. *Safety and Health*, 2006.(6):40–41.

Shao, H. & Wang, K.J. 2008. *Safety Behavior Management* [M]. Chemical Industry Press.

Shao, H. & Wang, K.Q. 2004. *Safety Psychology* [M]. Chemical Industry Press.

Tian, S. & Zhou, T. 2010. Analysis of human unsafe acts coal production [J]. *Shanxi coal,* 2010. (2): 9–10, 6

Tu, C. & Huang, W. 2010. Unsafe coal mine accidents of human behavior analysis [J]. *Shanxi coal*, 2010. (6):59–61

Xiao, D. 2001. Function of noise on human behavior and the impact of fatigue [J]. *Huaihua Teachers College Journal*, 2001.20(5):55–56

Xu, X. Liu, Q. 2008. From a psychological point of view of the unsafe behavior [J]. *Forestry labor safety,* 2008.21(4): 34–41

Ye, L. 2005. *Safety Behavior* [M]. Tsinghua University Press.

Progress in Mine Safety Science and Engineering II – He et al. (Eds)
© 2014 Taylor & Francis Group, London, ISBN 978-1-138-00122-0

A brief analysis on Chinese classical philosophical thoughts and the idea of safety

Guofeng Xu
China University of Mining Technology, Beijing, China

Guohui Xu
China Ordnance Institute, Ningbo Branch, China

ABSTRACT: Scientific research cannot be carried out without the guidance of philosophical thoughts. In this paper, I make a brief analysis on Chinese classical philosophical thoughts and the idea of safety, and attempt to study safety from the Chinese classical philosophy perspective, so that we can see through the appearance to the essence and provide a theoretical basis for safety prediction and safety management.

1 INTRODUCTION

While our research on safety science is to reveal the objective rules of safety, and to provide safety-discipline theory, application theory and specialized theory, so that our lives and health can be safeguarded during the process of production and livelihood, and our mind and body, related equipments, properties, objects etc. be avoid damage (Chao Wu 2011, Shuangqi Hu 2003).

Chinese classical philosophy, a wonder in the treasure house of world ideological culture, is imbued with profound and sagacious thoughts, which to this day continues to play an important role in our society, work and daily life (Wei Wang 2004).

Scientific research cannot be carried out without the guidance of philosophical thoughts. In this paper, I make a brief analysis on Chinese classical philosophical thoughts and the idea of safety, and attempt to study safety from the Chinese classical philosophy perspective, so that we can see through the appearance to the essence and provide a theoretical basis for safety prediction and safety management.

2 CHINESE CLASSICAL PHILOSOPHICAL THOUGHTS AND THE IDEA OF SAFETY

The I Ching (also known as the Book of Changes) is a representative work on Chinese classical philosophy, which is regarded as one of the most far-reaching classics influences Chinese culture. Since Han Dynasty, I Ching has been revered as the First of all classics, which contains fruits of Chinese wisdom and culture precipitated for more than five thousand years. The basic symbols in I Ching are an unbroken line (—) to represent Yang Yao, and a broken line (--) to represent Yin Yao. While the basic figures in I Ching is 64 sets of six lines each called hexagrams (gua) which are combined by any two of the eight possible trigrams. I Ching use those lines and figures to explain all phenomena of the universe, and to inspire the changing rules of Heaven, Humanity and Earth, that is to say, the integration and consistency of Tao of Heaven, Humanity and Earth. The unity of Heaven and Humanity is the mode of thinking of the universe in I Ching, which created for us a whole entire universal world including Heaven, Earth, Human beings, Things, etc. This mode of thinking tends to understand and grasp the world from a holistic perspective, and to regard human and nature as an organic whole of mutual induction (Jingfang Jin & Shaogang Lv 2005).

I Ching expresses its unique safety consciousness, safety margin, safety principles and safety thoughts, and is the first theoretical classic fully reflects Chinese traditional safety thoughts.

3 THE THOUGHTS OF YIN, YANG AND SAFETY

According to I Ching, everything in the nature has two aspects of Yin and Yang in opposition to each other, while the confrontation between the two sides is mutual unity. The movements of opposition and unity of Yin and Yang is the fundamental reason that things appear, develop, change and disappear in the natural world.

Safety science is to study the nature of safety and movement rules, while the safety status of things is in constant change, the safety is relative. The change of the safety status of things follows the rules of "from quantitative change to qualitative

change". Thus a series of failed to get timely detection and timely treatment of the hidden dangers of accidents continue to accumulate, with all procedures linked with each other. Many a little makes a miracle, the probability of accidents rose quietly in the imperceptibly, and when the risks accumulated to a considerable extent, disaster struck (Xueqiu He 2008).

As Robert Ornstein, the psychologist, and Paul Ehrlich, the biologist put out, many risks we face are like what the boiling frog syndrome shows (Jizu Li 2007, Hui Shao2011). If you put a frog in a kettle that is filled with water that is cool and pleasant, and then you gradually heat the kettle until it starts boiling, the frog will not become aware of the threat until it is too late.

On Feb. 22, 2009, an especially serious gas explosion accident happened in Tunlan Coal Mine of Xishan Coal and Electricity Powder Co., Ltd., Shanxi Coking Coal Group Co. Ltd., with 78 miners died, and 114 injured in this accident, and caused a direct economic losses of 23.68 million yuan. This is a severe liability accident, with loopholes in the accident unit of production safety management, specters investigation and management not in place, illegal command, illegal operations, in violation of operation rules, and lacking of supervision in the relevant government functional departments as the causes of the accident.

These lessens paid for with blood make clear that safety and danger are two opposite parts in the same things in motion, and one's existence depends on the other. While the coexistence of safety and danger is not equivalent, and still they cannot get along with each other peacefully either. Given the motion and variation nature of things, safety and danger change at all times, and in a reciprocal transformation.

4 THREE UNIVERSAL ELEMENTS AND SAFETY

I Ching is the first great theory to put forward the idea of three universal elements---Tao of Heaven, Humanity and Earth, whose clarity, systematicness and profoundness is far beyond other theories. I Ching makes a systematic study on the three universal elements---Heaven, Humanity and Earth, thus made its contents extensive and comprehensive, broad and profound. In addition, I Ching is also an important tool for human beings to understand and thus transform nature. It emphasizes the necessity and importance of a harmonious world, and believes that only on the harmonious basis of the three universal elements---Heaven, Humanity and Earth, can we make man-made things come very naturally. Standing between Heaven and Earth, what we can do is to comply with the natural rules and to make full use of the current situation to pursue good fortune and avoid disaster.

We know that the Safety Ergonomics is to use the theories and methods of ergonomics to study the system of man-machine-environment, that is to say, the research is about the interaction between human being and machine, environment, and about how to combine the three elements reasonably, in order that the machinery and environmental system agree with the physiological and psychological characteristics of human beings, thus to achieve the goal of improving efficiency and safety in production (Baoguo Wang 2007, Christopher D. Wickens 2007).

Therefore, we can make the following conclusions:

Heaven: the specific working conditions and environment for the co-existence of human being and machine, like temperature, noise, etc. which also means the Environment in the system of human being-machine-environment.

Humanity: the main body of work, for instance the operators, or decision-makers.

Earth: any object that men can manipulate, for instance tools, equipments, which is also the element of Machine in this system.

The element of heaven changes constantly. In coal production, gas, flood and fire are regarded as "the big three killers" (Qiong Wu & Kaili Xu 2002). They are the enemies of the miners. However, "the three killers" might simply only be a paper tiger that disasters or the risks of disasters caused by gas, flood and fire can actually be con-



Figure 1. Three universal elements.



Figure 2. System of human being-machine-environment.

trolled and prevented beforehand, and be handled afterwards, while they might also turned into a real tiger that really kills human lives. Head-on clash with a fighting spirit can only bring lessons written in blood with an accumulated cost of lives. The correct practices would be to predict and avoid any hidden accidents through instruments, and when accident happens, miners should know where to evacuate and how to protect themselves, all of those need supports from appropriate regulations, actual sensations, rich experiences and relevant instruments.

Nature has its own rules, as well as earth. When people put the most toxic pollutants into the soil, the earth does not protest for itself. So we can say Earth is the most rule-abiding element, with the highest degree of endurance. In our point of view, Earth can be the most solid foundation in the universe, whereas when it shakes, it can also be the most terrible thing in the universe. Safety production cannot be carried out without equipments, so equipment is the primary carrier for safety. That is to say, equipment is both the target of safety management and the tool for safety management. Some of the equipments are designed for safeguarding other equipments to operate safely. The more advanced the equipments are, the higher the operational reliability it will have, and with which it can alleviate the responsibility and pressure of the equipment operators. Therefore, we should first of all analyze from a scientific view the different characteristics between the elements of human being and machine, then to make best use of the advantages and bypass the disadvantages, to give full play to the advantages of both human beings and machines. That is to say, we should keep our workers from the unsafe behaviors of human beings and the unsafe conditions of machines from the designing stage, in order to ensure that the system is safe in its essence.

Safety is a complicated management system, among which human being, equipment/machine and environment interacts with each other and formed a dynamic safety system. Across various kinds of safety issues appeared nowadays, none of which are not caused by an imbalanced development of the three universal elements---Heaven, Earth and Humanity for lacking guidance from a systematic thoughts. The idea of harmonious coexistence and joint development proposed in the thoughts of the three universal elements in Chinese traditional culture can not only be regarded as a guiding ideology for the development of contemporary society to refer to, it can also provide a new perspective or horizon for safety science research work which currently is under exploration.

5 WU XING (ALSO KNOWN AS FIVE ELEMENTS) AND SAFETY

Yin and Yang are intangible cosmic dynamics. It is because of the two intangible powers, the universe generates the following five elements, which are Metal (jin), Wood (mu), Water (shui), Fire (huo) and Earth (tu). It is believed in Chinese classical philosophy that everything in the universe is composed of the above five basic elements. Wu Xing Theory (or Five Elements Theory) believes that there must be a certain relationship between things, while the internal connection can promote the developments and changes for things. The five elements themselves have the rules of "mutual generation" (also can be known as "mutual conquest") or "mutual overcoming" among themselves, which is also the inexorable law of nature.

Safety itself means a complicated system, and how to describe the composition and operation

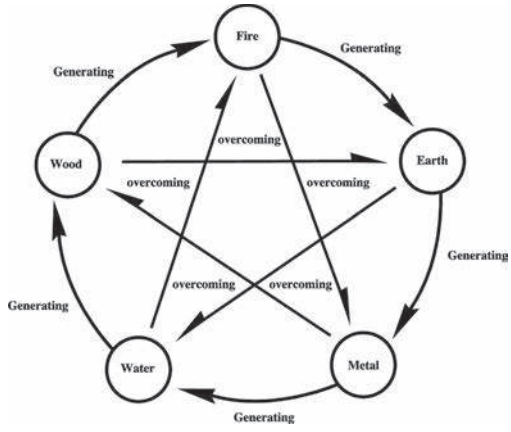


Figure 3. Wu xing.

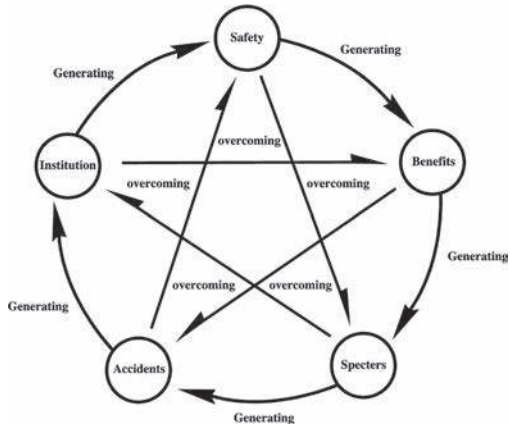


Figure 4. Five elements of safety.

mechanism of this system is vital to safety management (Terry E. McSween 2011). Concerning the safety issues of coalmine production, it also bears the above five basic elements, which are safety, benefits, specters, accidents and institution. The five basic elements themselves and the "mutual conquest" and "mutual overcoming" relationship among them reveal the operation mechanism of safety.

The five elements are "mutual conquest", which means "Wood feeds Fire, Fire creates Earth, Earth bears Metal, Metal enriches Water, and Water nourishes Wood". Thus it is also true that safety "feeds" benefits, benefits "create" specters, specters "bear" accidents, accidents "enrich" institution, and institution "nourishes" safety in the context of coalmine production. The five elements are "mutual overcoming", which means "Wood parts Earth, Earth dams Water, Water extinguishes Fire, Fire melts Metal, Metal chops Wood". Thus it is also true that safety "parts" specters, specters "dam" institution, institution "extinguishes" benefits, benefits "melt" accidents, and accidents "chop" safety in the context of coal mine production.

Safety "feeds" benefits: Coalmine production is a high risk industry, which bears especially high safety pressure. Once accidents happen, both units and individuals would suffer direct or indirect economic losses.

Benefits "create" specters: Units carry out operations without rest, and individuals work day in and day out, the goal of which are pursuing the maximization of benefits. Thus a series of problems would emerge in this process, specters is one of them.

Specters "bear" accidents: A philosopher once said, "All the possible things will happen". Therefore, if specters are not eliminated in time, the accidents will happen.

Accidents "enrich" institution: Accidents bring huge losses to production units. In order to avoid similar accidents, administrators will formulate relevant institution and lay down solutions. Most of the safety regulations, institutions and rules we abide now are established after accidents, on the basis of the causes we find out.

Institution "nourishes" safety: We might not know the origin of many regulations and measures, or might not know where on earth the danger lies in when breaking rules, however, we only just need to simply implement those regulations and rules in a strict way, the safety can still be guaranteed.

Safety "parts" specters: What we call specters are those that we do not know because it is hidden, and are those that have not happened yet. Since it has not happened, it is safe. That is to say, to be safe, you need to kill the hidden danger in the bud.

Specters "dam" institution: Specters appear when those safety regulations, institutions and rules are not obeyed.

Institution "extinguishes" benefits: We leave sufficient room for safety when establishing the framework of relevant regulations and institutions, which have a hold on the maximization of benefits at all times.

Benefits "melt" accidents: Economic losses brought by coalmine safety accidents usually will not be a small number of amounts. In order to pursue the maximum benefits, the frequency of accidents happened needs to be reduced.

Accidents "chop" safety: When accidents happened, there means no safety of course.

6 THE EIGHT DIAGRAMS AND SAFETY

Ancient Chinese philosophers use the Eight Diagrams to represent eight different phenomena in the universe. Seeing through the appearance to perceive the essence is the ultimate significance for our study on the Eight Diagrams.

Safety lies in production itself, and at the same time plays the role of promoting and safeguarding production. We use "—" to stand for safety, and "--" to stand for risks.

In the case of a harmonious development of the Man-Machine-Environment system, safety supervisors should keep in mind the awareness of danger, and should not slack in this respect. If we can keep self-alertness, repercussions will not happen.

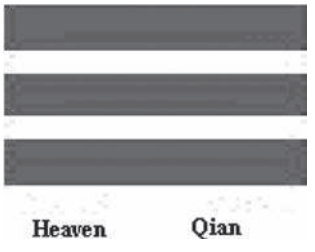


Figure 5. Diagram of qian.

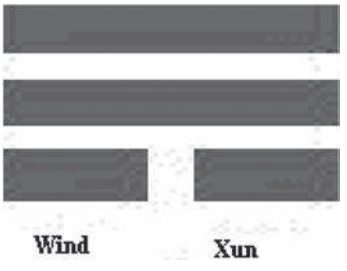


Figure 6. Diagram of xun.

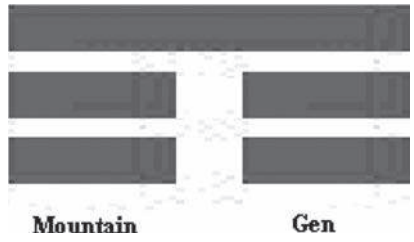


Figure 7. Diagram of Gen.

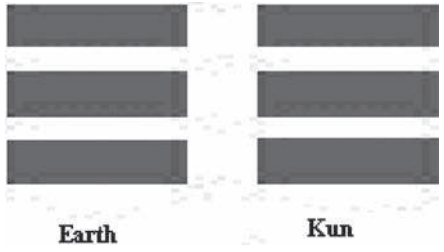


Figure 8. Diagram of kun.

In that case, when enterprises production behaviors have gained safety guarantees, their developments will be sustained in a steady condition. However, lacking of education or guidance in this regard would bring out some unsafe indications.

When unsafe factors appear in mechanical equipments, safety supervisors should notice the indications of disturbance or trouble, and handle the problem of "machine" in time. In designing and using "machines", we should not ignore the characteristics and requirements of men, and should not ignore the characteristics and requirements of environment either, so as not to affect the performance of the machine itself, and further not to threat men's lives, work and his survival. If at this time, the safety management system still does not work efficiently, then

When unsafe factors appear in both the elements of Man and Machine, it is time for us to make some adjustments. At this time, we should first correct our understanding on the unsafe factors appeared in production, and then correct our attitude to eliminate unsafe factors as well. In addition, we should select an appropriate time for eliminating those unsafe factors. When arranging or assigning production tasks, the best solution is to take measures to eliminate those unsafe factors that might appeared in the process of production. Otherwise,

That is to say, if the position of Heaven and Earth be ectopic, the system of man-machine-environment will collapse thoroughly. Thus accidents can hardly be avoided.

7 CONCLUSIONS

I Ching is a representative work on Chinese classical philosophical thoughts. It describes the basic rules followed by everything in the universe, and we can also regard it as the general rules of all things. The things and its motion in the universe cannot be carried out without the domination and restriction of those rules. In this regard, people's life and work cannot do either, if without the domination and restriction of the rules. In the study of safety science, we should keep the philosophical thinking of changes and developments in mind, to improve users' satisfaction through a more efficient work performance, and to reduce safety accidents and losses thereof through a cut-down of human errors, thus to provide a totally new perspective for the study of safety science in the end.

REFERENCES

Baoguo Wang. 2007. *Safety ergonomics*. Beijing, Mechanical Industry Press.

Chao Wu. 2011. *Safety science methodology*, Beijing: China Labor and Social Security Publishing House.

Christopher D. Wickens. 2007. *An introduction to human factors engineering*. Shanghai: East China Normal University Publishing House.

Hui Shao. 2011. *Safety psychology and behavior management*. Beijing: Chemical Industry Press.

Jingfang Jin & Shaogang Lv. 2005. *Full translation of Zhou Yi*. Shanghai: Shanghai Ancient Books Press

Jizu Li. 2007. *Safety psychology*. Beijing: China Labor and Social Security Publishing House.

Qiong Wu & Kaili Xu. 2002. *Safety managerialics*. Beijing: China Coal Industry Publishing House.

Shuangqi Hu. 2003. Research methodology of Safety Science. *China Safety Science Journal* (9):1–4.

Terry E. McSween. 2011. *The values-based safety process: improving your safety*. Beijing: Electronics industry Press.

Wei Wang. 2004. *Studies in philosophy of Science*. Beijing: Tsinghua university press.

Xueqiu He. 2008. *Safety science and Engineering*. Xuzhou: China University of Mining and Technology press.

This page intentionally left blank

Progress in Mine Safety Science and Engineering II – He et al. (Eds)
© 2014 Taylor & Francis Group, London, ISBN 978-1-138-00122-0

Social structural analysis of mine accident

Fanghua Lu & Ye Yan
North China Institute of Science and Technology, Beijing, China

ABSTRACT: Every of work system is a subsystem of holistic social system, which is made up of different social structures and elements. Emergence of mine accidents can not be only ascribed to technology, management or regulations, moreover, it should be seen as a social structural issue. From this, its natural cause should be structural and systematic, involving the relational structure of government-market-society, power-capital-labor, along with the changes in population, job placement, organization, urban-rural split, consumption, interest distribution and stratum structure. Therefore, the ideas of safety structure and safety building have been proposed. Research indicates that in the period of social transformation, the essential approach of controlling mine accidents should be adjusting safety structure, the foundation of this is strengthening safety infrastructure building, and the emphasis should be on safety justice, safety rule by law and safety democracy.

1 INTRODUCTION

Emergence of mine accidents involves the situation of technology, management, regulation, philosophy, society, culture and so on. From the lens of sociology, the reason should be structural and systematic. Class analysis from Marxism and Max Weber's three-in-one social strata theory are classic methodology in conducting analysis on safe production. To radically address the problem of safe production, we need start with adjusting social structure and strengthening safety building to enhance safety development (Yan Ye 2012).

2 MINE ACCIDENT: A SOCIAL STRUCTURAL ISSUE

Every of work system is a subsystem of holistic social system, which is made up of different social structures and elements. Sociologically, social structure can be subject to the following 4 explanations: "Theory of Social Elementary" (Lu Xueyi 1991), "Social Strength Theory" (Sun Liping et al. 1998), "Resource and Opportunity" (Lu Xueyi 2010) and "Proportion Theory". These four theories are correlated: subject of social elementary is social strength, the foundation of social strength is the possession of resources and opportunities, the manifestation of resources and opportunities will be ratio relation, which all consist of social structure. According to the definition of interest structure—the possession of and contrasting relationship in resources and opportunities, social members are put in different social stratum by the possession of resources and opportunities; meanwhile, due to the differences in resources and opportunities of both income and consumption, as well as the vast divergence in organization, identity and region, the social structure has created the substructure, such as family and organization structure, income distribution and consumption structure, Urban-rural split structure and stratum structure.

Social structures, such as population structure, employment structure, organization structure, urban and rural structure, region structure, consumption structure, beneficial distribution structure, stratum structure, have comparatively great effect on the work safety of mine exploiting and other work fields. The social structure of work safety is also called safety structure, which refers to the constitution and relationship of members who occupy certain amounts of resources and opportunities in work safety. For example, population structure is influenced by the number, age and quality of the staff. In job placement, employment security is related to employment structure and employment security in the mining system. Organizational structure involves security management, organizational maintenance and rights protection. Interest distributional structure is also relevant with the divergent distribution of resources among and inside enterprises. Binary structure of city and rural areas leads an influx of migrant workers to industrial enterprises. Consumption structure is related to the external resource consumption structure and the internal difference of consumption between the upper and lower class. Regional structure is pertinent with gross product, internal income

distributions of enterprises, distribution of enterprises and status of accidents. Stratum structure is also related to the relationship between different social strata, involving power, capital, knowledge and labor, which is the core and agglomeration of these substructures, being profoundly associated with the issue of social justice.

In general, a period of rapid social transformation is the period of various of security incidents occurring frequently. Social transformation is the change of social structure itself. Social structure dramatically changes will inevitably lead to conflict and tradition, inevitably leading to "vacuum system", which will inevitably lead to the readjustment of the social interests and the contradictions, thus the possible of higher security incidents will last. It means that the reason is imbalance of social structure and imbalance of resource opportunities possession among social members. That is, a small number of the upper possess the majority of fortune, by contrast, most people enjoy only a small part of the benefit. The consequence of these actions is that those major lower class must work in the risk of their own life, so mine accident itself is a social structural problems.

3 THE ESSENCE AND FOUNDATION OF MINE ACCIDENT GOVERNANCE: OPTIMIZING SAFETY STRUCTURE AND STRENGTHENING SAFETY BIULDING

Mine accident management needs systematic thinking. In the period of fast transformation, the systematic regulation is more important than the technology and internal management under some situations. From a long term perspective, structural adjustment and balanced transition are critical for the long-term mechanism of work safety. "Safety Development" was put forward in the National Eleventh Five-year Plan. In 2012, Premier pointed out the concept of "safety development strategy" in the government report and the eighteenth National Congress of the CPC put forward to "strengthening infrastructure building of public security and enterprises' work safety". Based on the study and analysis, we propose "adjusting safety structure and strengthening safety building" to implement the strategy of "safety development", which is not limited to the field of work safety. Meanwhile, this needs to be pushed forward by both the "visible hand" of the government and social forces. In other words, we have to think beyond the traditional safety governance. Sociologically, "safety structure", equivalent to the "social structure", is the essence; "safety building", equivalent to "society's building", is the basement; "safety development", equivalent to "social development", is an end for the advanced phase. In practice, safety building includes material infrastructures and economic investments, but mainly refers to the establishment of work safety system, especially safety rule by law, safety justice, safety democracy and organization (protecting legal rights). These are the real intentions of safety regulation for governments. Let's focus on the following several aspects.

3.1 *Strengthening the building of "safety justice"*

Safety justice derives from social justice which is to ensure social members get their due rewards or punishment, and to ensure the basic rights of social members (the right to survival and development). The primary value of "equalization of safety" in the whole work safety field is to safeguard mine workers' life safety. From a macro perspective, it involves the issues of structural balance and equality, ie. resources and opportunities justly deployed for mine workers.

The injustices in the mine field mainly involve the following issues:

Urban-rural dual structure and in-system and outside-system split result in injustices in resources and profit allocation. High-risk and high-income occupations "attract" large numbers of the lower workforces from rural (university graduates seldom choose such industries as mining). Such irrational employment structure is one result of this "double-dual-structure".

Irrational income allocation structures exist. The lower workforces engaging in primitive work are not receiving the treatment, protect, higher income and insurances they're deserved.

The main issues are irrational stratum structure and organizational structure, being manifested mainly in: strong top vs. weak bottom, strong capital vs. weak labor, and lack of a middle class in the employment with some industrial businesses; the organized topper is stronger than the unorganized lower workforce who do not have own organizations, thus their security rights are not well guarded.

Therefore, assignments should be done in the following aspects:

Adjustment policies about urban-rural split structure must be impended, so that the lower workforce could enjoy freer employment.

For the lower workforce, employment standards, salary standards, welfare standards, safety awareness improvement (uniform training and certification), injury costs, etc. all call for stronger systems and mechanisms.

The "targeted recruitment" policies for related higher education institutions in high-risk industries are to be gone on and reinforced, so that there

could be an increase in the ratio of mid-class staff in manufacturing businesses.

Organizational work shall be strengthened. In particular, workers' unions need to play their part.

We should make the legal system, democratic institution and social atmosphere to ensure safety justice. Therefore, we discuss safety rule by law and safety democracy in detail.

3.2 *Strengthening the building of "safety rule by law"*

The core of the safety supervision is the "safety rule by law". From this point of view, the government should think the following several aspects further.

It must come to the attention of the authorities that the construction of work safety systems and mechanisms should be strengthened. E.g. a Public Security Commission (which will include a work safety branch) could be set up in the National People's Congress, so that safety legislative and law enforcement can be secured.

The Work Safety Law, the Mine Safety Law and other relative laws and regulations should be amended based on the rights and duties of the workers that actually work in mines rather than from the perspective of a regulator or merely focusing on the property. Meanwhile, the coordination between the labor administrations and the safety authorities should be taken into consideration.

The safety administration need to optimize the structure of their safety supervision team with a broader source covering the officials, scholars, technicians and miners while the association in enforcement should be widely applied. Institutions at the grassroots level should be equipped with enough staff and the salary, other basic interests of their staff should be ensured. The closure and rectification of those violating the laws and regulations must be strictly in line with the legitimate procedure with no chance left for any "underlying rules".

The Labor Contract Law was enacted by National People's Congress in 2007 and put into force in 2008, subject to which rules need be established on the labor contract for mine companies to regulate the labor employment of mine operating enterprises. The registration system needs to be reinforced to restrain the subcontract of the employees and guide the practices of short-term employment. Further, it is necessary to include the training of the workers into a mandatory rule. A certificate will be granted to a worker only after certain standardized training courses.

An emergency rescue system and mechanism with guided-by-science, well-trained, well-equipped, capable of quick response and effective rescue will be built. In addition, basic text data of the mining system should be well maintained.

3.3 *Strengthening the building of "safety Democracy"*

Equalization and legalization of safety will be guaranteed ultimately by the democratic system and realized by the democratic mechanism. As far as safety democracy is concerned, its key element means that the related social members inside and outside the work safety system have the adequate right to know, to participate, to express and to supervise everything with respect to safety and have the beneficial power of safety; and right culture of safety, but not the former power culture of safety, needs to be cultivated and generated within the industry field; construction of democratic organization, democratic system, democracy mechanism (negotiation of salary and security conditions, etc.) for work safety needs to be strengthened etc. The purpose of strengthening democratization of safety is to carry out safety supervision by getting out of the government and to realize the safety supervision throughout the whole society. If the democratic rights and mechanisms are not built up in the grass roots, the structural strength for protecting safety rights will be not balanced.

Within enterprise, democratization of safety can be implemented in the form of trade unions, communist youth league, woman's organizations and vigilantes etc., including the working team's meeting of democratic life. It has been carried out in some enterprises. However, it is not really effective and needs to be further strengthened.

In addition, some useful approaches are suggested and should be implemented as follows. To begin with, in order to pay much attention to the lower practitioners, different kinds of news media should be made full use of and the public attention should also be aroused to concern about security of these practitioners. Next, the basic rights including informing, reporting, and complaining of social members especially the practitioners ought to be fully protected. Besides, the delict of safety law enforcement by governors and security infringement by entrepreneurs ought to be severely boycotted. Furthermore, it is urge that various Rights Agencies should be established to safeguard people's legal rights such as Law Offices, Rights Websites, Safety Technology Enterprises, Safety Training Institutions, Academic Institutions, Safety Evaluation Institutions, etc. Finally, community members should be appealed to participate in the process of the safety supervision so as to make up for the deficiency of the government. In the meantime, reform of the existing political structure should be promoted to limit the power

of government officials, especially top leaders, via checks and balances, system restrictions and democratic management.

We strongly believe that speaking of safeguarding rights for the lower practitioners, a powerful citizen society is desperately needed. Otherwise, the real democracy will not be fully realized. Therefore, miners can not merely depend on the Hometown Association of Chinese Characteristics but are supposed to build their own legal trade union to safeguard their legal rights.

As a matter of fact, the decline of mine accident in 1960s and 1970s in US, can be superficially ascribe to legal regulation and safety legislation, but the essence behind the scene should be the "Iron Triangle"-government, enterprise, union, which execute the sustenance of safety rights, supervision of work safety, promotion of technology and improving of conditions. Therefore, unions of private mines or local unions are encouraged to be established, including state-owned mines. The safety and right-safeguarding role of the labor union should be enhanced. The chairman of the union should be selected from those miners with higher cultural quality and stronger awareness of safeguarding rights. It is of special importance to push forward the establishment of safety inspection and safety right-safeguarding organizations comprising of representatives from the government, enterprises and miners (labor union). If necessary, a unified national miners' union could be set up within the mining industry.

4 CONCLUSION

Mine safety is a project of the social system. It concerns not only natural technology, management and system, but also social structure. Function relies heavily on the structures. Without a proper structure, the function will inevitably be in a mess and it will not be surprised to see a high frequency of accidents in the mining areas. The underlying reason, which is both structural and institutional, involves the hierarchy of the government, market and society, the relative positions between the government authorities, capital and labor, and the structures of population, employment, organization, urban-rural governance, geographic development, consumption, benefit distribution and social classes and their respective changes as well.

ACKNOWLEDGEMENTS

The authors gratefully acknowledge foundation by the Basic Scientific Research Fund Project of Central Universities (3142013104).

REFERENCES

Lu Xueyi 1991. *Sociology*. Beijing: Knowledge Press, 559–560 (in Chinese).

Lu Xueyi 2010. *Social structure of contemporary China*. Beijing: Social science academic Press, 11–12 (in Chinese).

Sun Liping et al. 1998. Social structural transformation of China in the recent trends and risks. *Strategy and Management, 30*(5):1–17 (in Chinese).

Yan Ye 2012 *Social structure of China coal mine accident*. Beijing: Social Science Academic Press, 243–244 (in Chinese).

Progress in Mine Safety Science and Engineering II – He et al. (Eds)
© 2014 Taylor & Francis Group, London, ISBN 978-1-138-00122-0

Discussion on the management system innovation about safe development of China coal mining industry

Jun Zhang
China University of Mining Technology, Beijing, China
North China Institute of Science and Technology, Beijing, China

ABSTRACT: On the background of macroeconomic continuous decrease, the paper ananlyzes the status of coal production and reserves and the cause of zero or negative increase difficult situation, and then proposes the coal industry should catch the right chance to bring about a reform, straighten out various relations in the coal industry management system, and promote coal industry sustainable and stable development. The two types of management systems of state-owned large coal group based on administrative-oriented and private-owned coal group based on market-oriented are designed. The main purpose of this paper is to improve coal industry production concentrated degree, to give government full play for managing, coordinating and adjusting coal group's business behavior and economic benefit, to activate independent business vigor of large coal group, to supplement and perfect resource allocation by private-owned coal group, and to realize resource safety, safe, high, efficient, environment-friendly and harmonious production.

1 INTRODUCTION

Safe development includes coal industry sustainable development, resource safe and safe production in this paper.

In recent years, the situation of national coal mine safety production shows the properties of "three sharp decreases and one obvious promotion": one is a sharp decrease of the total accidents amount, and the accident amount and fatalities decrease 60.1 percent and 56.9 percent respectively; the second is a sharp decrease of major and serious accidents, and the major accident amount and fatalities decrease 42.9 percent and 46.1 percent respectively, and the serious accident 75 percent and 65.5 percent respectively; the third is million-ton death rate decreases 75 percent in coal mines; the forth is that the overall level of safe production improves obviously (Zhang Dejiang 2013). Since the year 2012, the coal demand has appeared zero or negative increase situation caused by macroeconomic. Coal, as the disposable resource accounting for about 70% of energy consumption, has appeared the situation that whole varieties falling in price, and Chinese coal industry got into the period of serious difficulties. The whole national coal enterprises are confronting with multiple difficult situations, such as dispatch and transportation difficulties, price falling, debt increasing and profit decreasing (Wang Liangyan 2012). The cause of these problems created simultaneously is related directly to the current coal management system which does not adapt to the demand of coal industry health development. The main problems of coal management system are the subject functions offside and vacancy coexisting, management system unsoundness, function crossover, and mode backward, etc. And the unscientific management system inevitably open the choice of the coal industry problems. At present, coal management system is still in the course of adjusting, and the constant changing system reform brought disorder to the coal industry. Although experts and scholars study the management system in many aspects, most of which aims only at the system evolution hackling, situation describing and blueprint conception. Therefore, to provide the operable basis, standards and methods become the urgent affairs (Pan Yuefei, et al. 2010). According to the three dimensions score values of coal industry production scale possessing national share, industry output possessing regional economy share and regional coal enterprise average yield, the coal industry management system can be divided into three types of administrative-centralized, administrative-dispersed and enterprise-leading, and this management system have best scientific and practicable in theory, but it is difficult in practice for the more complicated calculating method.

By analyzing coal industry status and contributions to national economy and national energy

structure characteristics and development trend we can draw a conclusion that the construction of large base and group based on administrative-oriented is very necessary for safe development of chinese coal industry. This paper's main innovations are as follows:

1. Improve the proportion of administration-owned large coal bases and groups in coal industry, keep the balance between coal providing and demanding, and ensure the industry develop sustainably.
2. Build the coal industry's rest or cash deposit institution, ensure long-term stabilization and sustainable development of coal industry's economy benefits.

2 SITUATION OF THE CHINESE COAL INDUSTRY

2.1 *Situation of the chinese coal resource and production*

2.1.1 *The situation of production*

Chinese coal production and consumption situation as Table 1 shows. From the year 2008 to 2012 the production and consumption increased continuously, and coal production possessed more than 75% of national total energy, coal consumption scale more than 70%; due to the influence of macro-economy, the coal consumption scale decreased to 66.5% in 2012, but the coal annual production capacity will be raised to 4,100 million tons in 2015; from the data of coal production and consumption and the "Twelfth Five-year" energy plan demonstrated that coal (as the disposable resource) demand will appear to be zero or negative increase situation, but the annual production capacity will be increased continuously. So the conclusion can be drawn that the contradiction between coal supply and demand will obviously appear and the economy situation not sound.

Table 1. The situation of Chinese coal production and consumption.

	Coal production		Coal consumption	
Year	Mt	%	Mt	%
2008	2716	76.8	2740	70.3
2009	3050	77.3	3000	70.4
2010	3240	76.6	3200	70.5
2011	3520	78.6	3570	72.5
2012	3650		3620	66.5
2015	3900			63.0

*Table1 data from National Bureau of Statistics of China.

2.1.2 *Chinese coal reserve compared to the world main coal production nations*

According to the energy data of BP, demonstrated reserves in the world as Table 2 shows. The ratio of reserve and production (R/P) is lower than 50 in China, and that of world average value is 200, and the contradiction of reserve and consumption is getting more obvious especially in the field of coal for power generation and high-quality coking. So the conclusion can be drawn that the coal mining prospect is very bleak and the energy safe situation is not optimistic.

2.1.3 *Regional difference of coal reserve and consumption*

The main distributive regions of Chinese coal are Shanxi, Inner Mongolia, Shanxi, Xinjiang, Guizhou and Ningxia six provinces which possess gross coal reserves 4.19 billion tons and account for about country's 82.6%, which shows the characteristic of rich north and poor south, more west and little east; the main consumption regions are Beijing, Tianjin, Heibei, Liaoning, Shandong, Jiangsu, Shanghai, Zhejiang, Fujian, Taiwan, Guangdong, Hainan, Hongkong and Guilin etc. And fourteen southeast coast provinces (city and region) possess gross coal reserves 0.27 billion tons and only account for about country's 5.3%.

So according to national situation of coal reserve distribution and consumption, it is necessary to construct the five national comprehensive energy bases, such as Shanxi, Erdos Basin, East region of Inner Mongolia, Southwest region and Xinjiang so as to improve the transportation capacity of railway, to decrease the cost of coal transportation,

Table 2. Proved coal reserves in the world at the end of 2012.

Ranking	State	Proved reserves (Mt)	Possess share (%)	R/P
1	U.S.A.	237,295	27.6	257
2	Russia	157,010	18.2	443
3	China	114,500	13.3	31
4	Australia	76,400	8.9	177
5	India	60,600	7.0	100
6	Ukraine	33,873	3.9	384
7	Kazakhstan	33,600	3.9	289
8	S. Africa	30,156	3.5	116
9	Poland	5,709	0.7	40
10	Brazil	4,557	0.5	More than 500

*Table 2 data from BP Statistical Review of World Energy June 2013.

and to satisfy the coal demand of national economy development.

2.2 *The main issues*

The main issues have been highlighted obviously in Chinese coal industry. The first is that the safe production situation is still serious, especially the major and severe accidents have occurred from time to time, as Figure 1 and 2 shows; the second is large fluctuations in the coal market which was gone against the scientific and technological progress, personnel training, safe production and social harmony and stability; the third is that extraction efficiency is lower and environment pollution is serious; the forth is the ratio of coal mining to reserve lower and has to alert the resource safety; the fifth is that the coal production capacity is surplus and supply is more larger than demand.

2.3 *The main constraints to safe development*

Thorough an analysis of the situation of Chinese coal production and reserve, macro-economy and safe production, the main constrains of coal

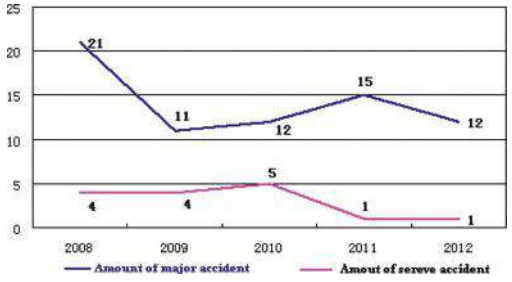


*Figure 1 data from accident inquiry in the net of state administration of work safety.

Figure 1. 2008–2012 the trend of coal major and sereve accident amount changed.

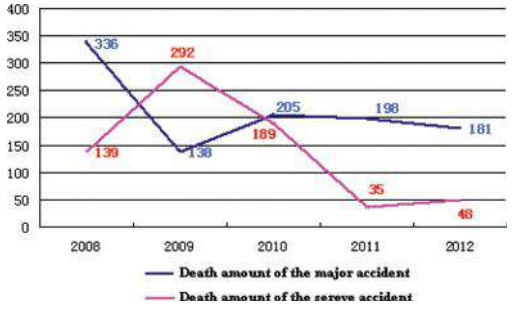


*Figure 2 data from accident inquiry in the net of state administration of work safety.

Figure 2. 2008–2012 the trend of coal major and severe fatality amount changed.

industry sustainable development can be seen as follows:

1. Coal reserves. From the demonstrated coal reserves in the world, the ratio of Chinese coal production to reserve is 50 based on the annual production of 2006, which is no more than 25% that of world average value. Recently, due to the larger increasing of coal production, it is not possible to solve the poor ratio of production to reserve by increasing prospective reserves by means of high accurate geological exploration technology. The mining difficulty of prospective demonstrated reserve will bring a greater challenge to the reserve safe.
2. Environment pollution. At the end of the year 2012, the seriousness of air pollution and the extreme increase haze weather days were directly related to the large scale of coal consumption and bad control of pollution; the environmental pollution problems, such as vegetation destroy and degradation, the effective area of cultivated land decreasing continuously, reclamation difficulty larging, surface water running off and groundwater pollution, have been created by more and more serious coal over-exploitation.
3. Coal industry management system. With the construction of coal exploitation and utility system we should make full use of America, Russia etc. with successful management experience and business system of coal industry for long-term strategic planning and system reforming together with the situation of our country.
4. The coal structure is not coordinated, and regional imbalance is still obvious. The amount of low production capacity in small coal mines still shares more than 80% of the total national coal mines, and the production capacity only shares 34.6% of the total, but the number of accidents and death shares 65.0% and 69.7% of the whole respectively.

2.4 *The main causes of coal industry fall into predicament*

1. Coal industry planning is not reasonable, management system is not scientific, examine and approve power overlapping, and the programme chaos. The main problems include present production excess, price decreasing, low economic benefits, or over capacity production which the management, technology, equipment and personnel quality are not adapted to the demand of safe production, so the accidents frequently happened.
2. Coal industry production concentrated degree lowers the whole capacity of adjusting the balance of improving and demanding or resisting

risk of large market economy fluctuation (Pan Yuefei, et al. 2010).
3. The total coal demand is decreasing because of the drop of manufacturing and heavy industry, and the adjustment of energy structure and the development of new energy.
4. Coal import increases for the coal price drop in international coal market, production capacity excess and serious coal overstocking.

3 THE MANAGEMENT SYSTEM INNOVATION ABOUT SAFE DEVELOPMENT OF CHINA COAL MINING INDUSTRY

Energy security is the base of national, energy sustainable development and the lifeline of national economy development, so reasonable and efficient development or utilization of energy is the strategic demand of the country's great rejuvenation. in the view of global economy decline and the demand decrease of all various coal, it is a good time to take the reforming of coal industry management system and construct large coal bases and groups based on administrative-oriented; it is necessary to transform the government functions that should be changed from supervision and enforcer of law and policy to the founder of industry health development. The government should act as safeguarding and serving roles for safe production, the balance of supply and demand and the safe development by consummates the relevant law, institution, management system and the market operating mechanism (Wang Bingwen, Li Wenxing 2012).

In this paper, the coal industry management system should be reformed according to Figure 3 shows.

According to coal resource property right, the exploitation of coal resource can be divided into two types of state-owned and private-owned, and the coal mines business rights can be divided into state-owned and private-owned large coal groups; the advantages of state-owned large coal group are to keep the balance of supply and demand and price stability (Mengtie 2010), and the advantages of private-owned large coal group is to improve the coal resource market allocation.

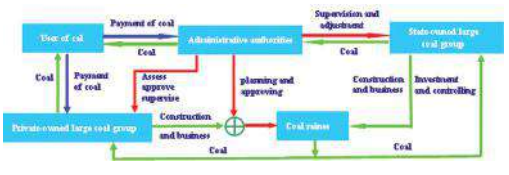


Figure 3. Coal industry management system reformed model.

3.1 *Policy and legal protection*

It is necessary to improve relevant policies, rules and laws for the construction of coal industry management system based on administrative-owned large coal base and group.

1. The laws and regulations of coal industry that adapted to socialist market economy system should be established soundly.
2. To simplify examination and approval procedures, perfect mine's verifying institution, and advance the access threshold of coal market.
3. To enhance the law enforcement team construction, and specifing the order of coal market by law.
4. To keep in step with the coal market quotation, and making the policy of reducg internal coal production and increasing coal import

3.2 *Designing of management system*

3.2.1 *Management systems of state-owned large coal group based on administrative-oriented*

1) The construction of management system

1. To establish a powerful government departments, integrate large state-owned coal group's management functions as a whole to enhance its authority and management efficiency. Do well in supervision, regulation and economic regulation affairs to minimize permit, approval and interference of the production activities and general project.
2. The government department will plan or approve the establishment and construction of large coal groups and mines in the long term so as to improve administrative-oriented large state-owned coal industry concentration.
3. Efficient administration will manage to create coal supply channels and amounts of large state-owned group.
4. Try to give full play of production and management autonomy to large state-owned coal groups in condition of coal resource security and safe production.
5. The government department regulates the macro-economic benefits of large state-owned coal groups by means of the reserve or tax measures.

2) Give full play of management advantages of large state-owned coal groups

1. The Government exploits or plans coal resources by combining the national energy strategy planning, reserves and distribution of coal reserves in the long term, so as to avoid over-capacity and the waste of resources.
2. Improve administrative-oriented large state-owned coal industry concentration, to maintain

balance between supply and demand, and to enhance the ability to withstand market fluctuations.
3. Government departments orient coal selling channels, quantity and price, and maintain the interests of both coal companies and users in order to avoid damaging the whole national interests due to market-oriented discourse power imbalance in the process of enterprises game.
4. According to the global and domestic economy and coal industry situation, the government department adjusts the industry production, coal import or export policies etc, and plays the value of foreign exchange reserves in addition to the protection of the domestic coal resources.
5. Take economic measures (e.g. to establish reserve funds or the coal industry development funds) to adjust the economic benefits of the coal industry, to avoid the coal industry huge economic benefits fluctuations, which is beneficial to protect coal resource, develop industry technology, and train personnel and ensure safe production and keep sustainable development.
6. Separate the enterprise and politic under administrative leading, make full use of large state-owned coal group autonomy in production and management, to avoid the planned economy era management mode reversion, and consciously safeguard the interests of enterprises, and production and operational autonomy. The state supervises and manages the matters that are related to the coal mine's safe production and state-owned assets disposal or other importance in accordance with relevant state policies, laws and regulations.

3.2.2 *Market-oriented private coal group*

1) Building management system

1. Exploiting coal resources to implement a buyout, and the ownership of coal resource property rights belongs to private coal group in a long-term.
2. Strictly executing examination and approval procedures, strengthening index requirements, safety and environment indicators should be of a veto.
3. Guiding the private coal groups to develop soundly by taxation, and funding and policy supporting measures.
4. Improving safety accidents investigation and punishment degree.

2) Private-owned coal group management advantages

1. The private-owned coal group's exploiting qualification should be examined strictly by state, and set the barriers to entry in the hands of economy, talents and management level which can be carried out in practice as a mandatory indicators; so the private coal enterprises have to build the powerful for realizing safe, environment-friendly and efficient exploiting according to the entry barriers.
2. The private coal groups have stable property on coal resources, which can ensure the high efficient investment and coal resource development, and taking initiative measures for guaranteeing the coal mine's safe production (Bai Chongen, et al. 2011).
3. The approving and examining procedures of coal resources has been simplified, and the simplification of procedures and one-time buyout of coal resources will be helpful for the private coal enterprises to compete in the coal market according to the market conditions and financial strength and make the market more perfect; the coal enterprises will initiatively improve the extraction ratio by taking the measures in mining process, technology and management.
4. The modern company operation and variety business models of private coal group will be helpful to ensure coal industry's sustainable development and stability.

4 CONCLUSIONS

This paper is based on the analysis of China's coal industry production, consumption and reserves situation. Considering the influence of the current international and domestic economic situation to coal industry, coal status in China's energy structure, and the twelfth five-year guideline of state energy development, this paper concludes that China's coal industry needs to increase coal production concentration, strengthen the government's administration-oriented force, take economic regulation and other means to keep the balance of coal supply and demand, enhance the capacity of withstanding the risk of coal market fluctuations, ensure the stability of whole coal industry economy, and improve the ability to safe develop sustainably. According to the degree of administrative intervention and the difference of business and management system, we can design two types of management system of state-owned large coal groups based on administrative-oriented and private-owned coal group based on market-oriented, list the specific building methods of two types of management system and respective advantages, so this study will provide helpful reference to the coal industry safe development.

ACKNOWLEDGEMENTS

1. Funds projects: This work was financially supported by the Natural Science Foundation of Hebei Province (E2012508002), the National Natural Science Foundation (51044009), and the Fundamental Research Funds for the Central Universities (3142013100).
2. Author introduction: ZhangJun, male, born in HuaDer, Inner Mongolia in April 1974, vice professor, doctor; now working at North China Institute of Science and Technology, in the post-doctoral stations of China University of Mining Technology Beijing, mainly engaged in the researching and teaching of coal mine's safe production theory, technology, coal mining and roadway support.
3. Tel:13381035808, 010-61591452-602.
4. Email:996946730@qq.com

REFERENCES

Bai Chongen, et al. 2011. Regulation and Property Right: Effect of China's Coalmine Shutdown Policy on Work Safety. *China Soft Science* (10):12–26.

Mengtie 2010. Problem Analysis on the International Coal Market Quotation Formation. *The National Conditions of China* (6):35–37.

Pan Yuefei, et al. 2010. Innovation Research on Coal Industry Management System Based on Regional Diversity. *Productivity Research* (2):192–194.

Wang Bingwen, Li Wenxing 2012. Research on the Policy of Improving China Coal Industry Competitive Power. *Productivity Research* (6):157–160.

Wang Liangyan 2012. Severe Difficulties Test the Enterprise Basic Training. *Business Management* (12):66–68.

Zhang Dejiang 2013. Speech in National Television and Telephone Conference on Safe Production. *Journal of China Safe Production* 25 January.

Progress in Mine Safety Science and Engineering II – He et al. (Eds)
© 2014 Taylor & Francis Group, London, ISBN 978-1-138-00122-0

Grey system theory-based overseas investment risk assessment for mining enterprises

J. Han
School of Management, China University of Mining and Technology (Beijing), Beijing, P.R. China

ABSTRACT: In this paper, based on the grey system theory and combined with AHP weighing & fuzzy comprehensive assessment method, the overseas investment risk assessment model was established. An applied analysis study was conducted by taking the investment risk of Yankuang's potash project in Canada as an example. The result showed that the investment risk of Yankuang was a general risk. By virtue of risk control, it had become a successful overseas investment case. At the same time, findings verified the effectiveness of the assessment model and showed that the established assessment model has an important guiding significance to the study on overseas investment risk assessment for Mining enterprises.

1 INTRODUCTION

With a rapid growth of overseas investment of Chinese mining enterprises, studies on the overseas investment risk assessment is emerging as well. Although there are a lot of research findings in this regard home and abroad, the fuzzy comprehensive assessment method is adopted in most quantitative assessment studies. For instance, the analytic hierarchy process method and fuzzy comprehensive assessment method has been adopted to establish a project risk assessment model for the investment risk of overseas oil-gas exploration and development project (Han et al. 2010). Similarly, an investment risk study of an iron ore project in Australia has been conducted in combination of the analytic hierarchy process method and fuzzy comprehensive assessment method (Hou et al. 2010). A fuzzy comprehensive assessment method has ever been established for the overseas investment risk of Chinese mining enterprises from the aspect of natural risk, political risk, economic risk, social risk, technical risk and financial risk (Xiao et al. 2011). Various risks, such as political risk, foreign exchange risk, business risk and management risk have been analyzed and used to build a multi-level comprehensive assessment method for the overseas investment (Lin 2012). An application of the multi-factor fuzzy comprehensive assessment model on Chinese oil enterprise's overseas investment was demonstrated in an academic paper (Liu 2012). The overseas investment risk assessment model has been set up for an energy company by using the analytic hierarchy process method and fuzzy comprehensive assessment method, so as to assess its overseas investment risk in a power generation project (Liang 2012).

All literatures said above use the fuzzy comprehensive assessment method, but the overall index score is given directly and subjectively, is frequently influenced by subjective factors. In this paper, the grey system theory will be utilized to solve the subjective valuation issue. Meanwhile, in this paper, given the national condition of China and international economic climate, a risk index system for overseas investment of mining enterprises is established by analyzing and summarizing the current situation of Chinese mining enterprises, and the overseas investment, significance and characteristics of M & A of mining enterprises, as well as various risks existing in the M & A process, and an overseas investment risk assessment model for the mining enterprise is set up based on the grey system theory and in combination of AHP weighing and fuzzy comprehensive assessment method, for the purpose of providing an effective method for the safety & risk assessment on the overseas investment and/or M & A by mining enterprises.

2 OVERSEAS INVESTMENT RISK ASSESSMENT MODEL FOR MINING ENTERPRISE ON THE BASIS OF THE GREY THEORY SYSTEM

On the basis of grey system theory and fuzzy comprehensive assessment method, an overseas investment risk assessment model that is suitable for Chinese mining enterprises is to be established by adopting the AHP index weighing. The contents

of the risk assessment model are as shown in the following:

(1) To establish an overseas investment risk assessment index system for mining enterprises.

With analysis and summary of the significance and characteristics of Chinese mining enterprise's overseas investment, various risks existing in his multinational M & A process, an overseas investment risk system for mining enterprises is established. Its criteria consists of risks in three aspects, that is, risks at preparation period, risks at transaction and risks at deal implementation, while the detailed index consists of 15 secondary indexes. Specifically, the index system is shown as following:

Risk at preparation period: the 3 secondary assessment indexes include the assessment risk of investing (M & A) strength, selection risk of investment (M & A) target, assessment and review risk of investment (M & A) target, which are marked as (X_1, X_2…,X_3), respectively;

Risk during transaction: the 7 secondary assessment indexes include political and regulation risk, social and cultural risk, policy risk, investment (M & A) negotiation risk, selection risk of investment (M & A) payment, financing risk, anti-M & A and passive M & A risk, which are marked as (X_4, X_5…,X_{10}), respectively;

Risk at deal implementation: the 5 secondary assessment indexes include the environmental protection risk, aboriginal people's interest risk, M & A integration risk, corporate cultural difference risk and international management risk, which are marked as (X_{11}, X_{12}…,X_{15}), respectively;

(2) To build an assessment matrix and its score collection

In order to ensure the effectiveness of the assessment, overseas investment experts (with overseas investment experience) in this field are invited to score the secondary assessment indexes. For the sake of avoiding the subjective influence of various experts on the assessment result, it is required that the number of assessment experts should not be too less. It is assumed that the number of invited senior experts for overseas investment management is m and $m \geq 6$.

The assessment matrix of secondary index is assumed as

$$X = \begin{bmatrix} x_{11} & x_{12} & \cdots & x_{1,15} \\ x_{21} & x_{22} & \cdots & x_{2,15} \\ \cdots & \cdots & \cdots & \cdots \\ x_{m1} & x_{m2} & \cdots & x_{m,15} \end{bmatrix} \quad (1)$$

Where, x_{ij} refers to the risk assessment score of the jth index as given by the ith expert.

(3) To establish the Grey Scale, Grey Number and Whitening Weight Function of the Risk Assessment

1) To determine the grey scale e and grey number D of the risk assessment

Form the grey ordinal number of risk assessment

$$E = (1,2,\ldots,e),$$

Its corresponding assessment rating is united as

$$S = \{S_1, S_2, ..., S_e\},$$

and form the corresponding number set interval

$$D = \{d_1, d_2, ..., d_e\}$$

Where, e is the risk assessment class number $d_i (1 \leq i \leq e)$ is the grey number and they are in the same number set interval, marked as $\otimes$.

2) Form the whitening weight function

According to the class number e and grey number D as determined in the above, establish the whitening weight function $f_E(\cdot)$, saying the whitening weight function,

$$f_{E_k}(X) \to R$$

Where, $E_k \in E = (1, 2,\ldots, e)$ and $f_E(x_{ij})$ means that $x_{ij}(x_{ij} \in X)$ belongs to the weight of assessment standard of the $E_k(E_k \in E)$ grey class.

(4) To determine the risk assessment index weighing

In this paper, the AHP analytic hierarchy process method [7] is used to determine the weighting of risk assessment index. Due to the limited paper length, the calculation method for AHP weighing is omitted. Here, it is assumed that the AHP weighing is

$$W = (w_1, w_2, ...w_{15}) \quad (2)$$

Where, $\sum_i w_i = 1, w_i \in (0,1)$ refers to the weight of secondary assessment index i.

(5) To determine a comprehensive assessment result

Sort out the whitening weight function of each expert. It is assumed that the whitening weight function of grey number is

$$T_{iE} = \sum_1^m f(x_{mi}) \quad (3)$$

Count the comprehensive values of whitening weight functions of different grey classes. If the statistical gray number of the assessment matrix is set as

$$T_i = \sum_{E=1}^{e} T_{iE} \tag{4}$$

The assessment ratio of the ith risk assessment index is

$$T_{iE} = \frac{T_{iE}}{T_i} \tag{5}$$

The obtained single-factor grey assessment matrix of risk assessment index is

$$R = \begin{bmatrix} r_{11} & r_{12} & \cdots & r_{1e} \\ r_{21} & r_{22} & \cdots & r_{2e} \\ \cdots & \cdots & \cdots & \cdots \\ r_{15,1} & r_{15,2} & \cdots & r_{15,e} \end{bmatrix} \tag{6}$$

The fuzzy comprehensive assessment method is adopted to integrate the index weighing formula (2) and single-factor grey assessment matrix formula. (6). It is assumed that the whitened fuzzy comprehensive assessment matrix is

$$\begin{aligned} Z &= W * R \\ &= \left[w_1, w_2, \ldots, w_{15} \right] * \begin{bmatrix} r_{11} & r_{12} & \cdots & r_{1e} \\ r_{21} & r_{22} & \cdots & r_{2e} \\ \cdots & \cdots & \cdots & \cdots \\ r_{15,1} & r_{15,2} & \cdots & r_{15,e} \end{bmatrix} \end{aligned} \tag{7}$$

It is assumed the rating formula of the risk assessment is

$$Y = \min_{1 \le i \le e} \{ \left| Z \times S - S_i \right| \} \tag{8}$$

Where, $S = \{S_1, S_2, \ldots, S_e\}$ is the value of assessment rating and $Z \times S$ is called as the comprehensive risk score. If the optimum Y is obtained from S_i, the ith grey class is taken as the final assessment risk rating.

3 APPLICATION STUDY

Taking the potash project in Canada invested by Yankuang Group as the object of risk assessment, an applied analysis for the case is carried out by utilizing the risk assessment model put forward in this paper. Yankuang Group, founded in 1976, is a comprehensive and international energy & mining company. Its main businesses involve in coal mining and sales, coal-based chemicals, bauxite and aluminum manufacture, machine manufacturing and other fields. In recent years, Yankuang Group actively carries out the "Go global" strategy and makes investment in the mining sector in Australia and Canada with stable politics and rich resources in pursuit of the internationalized development. Yanzhou Coal Mining Co., Ltd., a subsidiary of Yankuang Group, accessed to Australia in 2004 and purchased Australian Felix Resource Co. in 2009 and became a solely Chinese mining company that has been listed in New York, Sydney, Hong Kong and Shanghai Stock exchange markets respectively since 1998.

The potash is a kind of scarce resource in China. More than 50% potash is imported from other countries. In order to exert its advantages in the mining technology, fertilizer production and sale network, as well as its international operation experience, Yankuang Group engaged professional institutes and experts, set up a professional team to conduct the Due diligence and risk assessment for 19 potash permits in Saskatchewan, Canada. In September of 2011, the approval from relevant governmental departments of China and Canada was obtained. On September 29, the transfer of the potash property was accomplished. At present, the exploration and development of Phase-I Potash project with capacity of 2.8 million tons per year is proceeding smoothly. Specific assessment for the Potash project is shown in the following:

(1) Assessment Matrix Scoring

Eight risk investment assessment experts are invited to score 15 secondary assessment indexes, using matrix formulas (1) as established in the above. At the same time, for the convenience of experts' description on risks, it is specified that the score for the index ranges in 1–10. The numerical value represents the risk degree of the investment index. According to the practical situation of the investment in the potash project of Yankuang Group in Canada, experts score 15 secondary assessment indexes. Then, the experts' assessment scoring matrix is obtained.

$$X = \begin{bmatrix} 1 & 3 & 4 & 3 & 2 & 3 & 5 & 2 & 2 & 2 & 7 & 4 & 4 & 5 & 5 \\ 0 & 1 & 2 & 2 & 1 & 3 & 3 & 3 & 1 & 1 & 4 & 3 & 3 & 4 & 3 \\ 0 & 4 & 4 & 5 & 1 & 4 & 6 & 4 & 3 & 1 & 6 & 2 & 4 & 2 & 3 \\ 2 & 3 & 2 & 3 & 2 & 2 & 4 & 2 & 2 & 3 & 4 & \mathbf{4} & 3 & 4 & 6 \\ 1 & 1 & 1 & 2 & 1 & 3 & 2 & 1 & 1 & 1 & 3 & 2 & 4 & 5 & 4 \\ 1 & 1 & 2 & 2 & 1 & 2 & 3 & 1 & 1 & 1 & 2 & 4 & 2 & 2 & 3 \\ 2 & 2 & 3 & 1 & 2 & 2 & 4 & 3 & 2 & 2 & 4 & 2 & 3 & 3 & 2 \\ 2 & 1 & 2 & 1 & 2 & 2 & 2 & 2 & \mathbf{3} & 1 & 3 & 3 & 3 & 3 & 3 \end{bmatrix} \tag{9}$$

(2) Setting up a Grey Class and Establishment of a Whitening Function

The investment risk in this paper is divided into four levels, saying 4 grey classes (e = 4), "extremely high", "relatively high", "average" and "low", Where, the "extremely high" level means the risk is very high and it is unsuitable to carry out the investment; the "relatively high" level means the risk is high and the investment needs to be implemented prudently; the "average" level means the risk is moderate and investment can be made if there are effective precautions available; and the "low" level means the risk is relatively low and the investment condition is good.

Moreover, if the assessment rating set of 4 grey classes is set as $S = \{S_1, S_2, S_3, S_4\} = \{9, 7, 5, 3\}$, the grey number of each grey class and the whitening function are shown in the following:

Class 1 "extremely high": if $E_k = 1$ and the grey number is $\otimes \in [0,9,10]$, the whitening function is:

$$f_1(x_{ij}) = \begin{cases} x_{ij}/9, x_{ij} \in [0,9] \\ 1, x_{ij} \in [9,10] \\ 0, other \end{cases} \tag{10}$$

Class 2 ("relatively high"): if $E_k = 1$ and the grey number is $\otimes \in [1,7,10]$, the whitening function is:

$$f_2(x_{ij}) = \begin{cases} x_{ij}/7, x_{ij} \in [1,7] \\ \frac{1}{3}(10 - x_{ij}), x_{ij} \in [7,10] \\ 0, other \end{cases} \tag{11}$$

Class 3 ("average"): if $E_k = 3$ and the grey number is $\otimes \in [0,5,7]$, the whitening function is:

$$f_3(x_{ij}) = \begin{cases} x_{ij}/5, x_{ij} \in [0,5] \\ \frac{1}{2}(7 - x_{ij}), x_{ij} \in [5,7] \\ 0, other \end{cases} \tag{12}$$

Class 4 ("low"): if $E_k = 4$ and the grey number is $\otimes \in [0,3,5]$, the whitening function is:

$$f_4(d_{ij}) = \begin{cases} 1, d_{ij} \in [0,3] \\ \frac{1}{2}(5 - d_{ij}), d_{ij} \in [5,7] \\ 0, other \end{cases} \tag{13}$$

(3) Calculation of single-factor grey assessment matrix

Put the expert's assessment scoring matrix formula (9) into the foregoing whitening function and calculate the single-factor grey assessment matrix of assessed indexes according to formulas (3) –(6).

$$R = \begin{bmatrix} 0.0827 & 0.1064 & 0.1489 & 0.6619 \\ 0.1204 & 0.1548 & 0.2168 & 0.5080 \\ 0.1382 & 0.1777 & 0.2488 & 0.4353 \\ 0.1351 & 0.1737 & 0.2432 & 0.4480 \\ 0.0992 & 0.1275 & 0.1785 & 0.5949 \\ 0.1370 & 0.1761 & 0.2466 & 0.4403 \\ 0.1845 & 0.2372 & 0.2920 & 0.2863 \\ 0.1276 & 0.1641 & 0.2297 & 0.4786 \\ 0.1125 & 0.1447 & 0.2026 & 0.5402 \\ 0.0992 & 0.1275 & 0.1785 & 0.5949 \\ 0.2110. & 0.2712 & 0.2589 & 0.2589 \\ 0.1533 & 0.1971 & 0.2759 & 0.3737 \\ 0.1578 & 0.2029 & 0.2841 & 0.3551 \\ 0.1757 & 0.2258 & 0.3162 & 0.2823 \\ 0.1794 & 0.2306 & 0.2839 & 0.3061 \end{bmatrix}$$

(4) Calculation of Index Weighing

Based on the AHP weighing determination methods, the said eight experts will compare and score the inter-index importance. The weighting is as shown in the following:

$W = (w_1,...,w_{15}) = (0.1150, 0.0750, 0.0750, 0.0855, 0.0570, 0.1140, 0.0360, 0.0465, 0.0570, 0.0285, 0.0855, 0.0676, 0.0581, 0.0381, 0. 0613)$

(5) Calculation of Fuzzy Comprehensive Assessment Results.

According to the formula (7), the comprehensive fuzzy assessment matrix for the whitening can be obtained.

$$Z = W * R = (0.1388, 0.1784, 0.2357, 0.4471)$$

According to the formula (7), the comprehensive score of the risk is:

$$Z \times S = (0.1388, 0.1784, 0.2357, 0.4471) \times (9,7,5,3)^T = 5.0178$$

The rating formula for the risk assessment

$$Y = \min_{1 \le i \le e} \{| Z \times S - S_i |\} = Z \times S - S_3 = 0.0178$$

To sum up, the final risk assessment for the Potash project in Canada invested by Yankuang Group is "average", namely, the risk is moderate. Although risks exist to some extent, the investment could be successful though the effective risk controlling and handling. From the perspective of current

progress of this investment project, Yankuang Group has effectively prevented and controlled the investment risk and his potash project in Canada is successfully progressing. At present, the geological exploration and the scoping study have been accomplished; the environmental assessment of the project has been started; and other development preparation is being implemented. Yankuang Group's potash project in Canada has become a successful investment case, which indicates the risk assessment model that is established in this paper is in accordance with practical situation.

4 CONCLUSION

In this paper, based on the grey system theory, a fuzzy comprehensive assessment model is established for overseas investment risk of mining enterprises, which provides a quantitative method of the assessment and study for the overseas investment risk of mining enterprises. This model can deal with the greyness and fuzziness properly in the assessment process and reduce the impact of human factors on the assessment results. At the same time, from the applied analysis on risks of Potash project in Canada invested by Yankuang Group, the feasibility of the method is further demonstrated. Moreover, a significant guidance and reference are provided for other companies and institutes who intends to make oversea investments in mining sector.

REFERENCES

Han, E. et al.2010. Overseas investment risk assessment of Chinese oil enterprises on the basis of Fuzzy-AHP [J], *Henan Science,* Vol.28, No.2: 235–239.

Hou, Y. et al. 2010. Overseas investment risk analysis for Iron ore on the basis of Fuzzy comprehensive assessment [J], *China Mining,* Vol 119, No 12: 61–63.

Liang, N. 2012. Study on assessment and precaution for overseas investment risk of electric power project [D], *Master's Thesis of Beijing Jiaotong University*.

Lin, F. 2012. Multi-level comprehensive assessment method for overseas investment risk [J], *China Investment,* 10: 98–99.

Liu, G. 2012. Study on overseas investment risk of Chinese oil enterprises [D], *Master's Thesis of China University of Geosciences (Beijing)*.

Saaty, T.L. 1980. The analytical hierarchy process, *McGraw Hill,* New York, USA.

Xiao, H. & Xiong Y. 2011. Overseas investment risk assessment of Chinese mining enterprise [J], *Chinese Contemporary Economy,* August: 48–50.

This page intentionally left blank

Progress in Mine Safety Science and Engineering II – He et al. (Eds)
© 2014 Taylor & Francis Group, London, ISBN 978-1-138-00122-0

Cause analysis of behavior of the secondary accidents in coal mines and the prevention

Su Zhang, Gui Fu & Shang-Hong Shi
School of Resources and Safety Engineering, China University of Mining and Technology (Beijing), Beijing, China

ABSTRACT: Expansion of the accidents is common in the process of disaster relief due to improper rescue. Twenty-eight accidents occurred during rescue are obtained statistically through analyzing serious and particularly serious accidents of national coal mines from 2000 to 2009. Statistics show that the number of casualties caused by the secondary accidents account for 19.6% of the total number of casualties in all accidents and the death toll of non-professional rescue workers (miners) account for the most which is followed by the death toll of coal mine managers which account for 65.91% and18.18% of the total deaths respectively. It also shows that casualties caused by blind rescue of coal mine managers account for 52.7% of the total number of casualties in the secondary accidents. So it is essential to strengthen emergency rescue training for the management to prevent the secondary accidents. The direct causes include coal mine managers' illegal rescue, non-professional rescue workers' blind rescue and rescue team members' improper response to the emergency. A further analysis reveals that imperfect emergency rescue management system is the radical cause. Countermeasures and suggestions are proposed according to the analysis, namely to improve the emergency rescue management system, to attach importance to the emergency rescue training of coal mine managers and employees and to strengthen training and readiness training of the mine rescue teams.

1 GENERAL INSTRUCTIONS

Emergency rescue of coal mine accidents is an important part of the coal mine safety work (WANG & FAN 2008). Effective emergency rescue can avoid or reduce casualties and reduce accident ranks, which is the last line of defense to reduce casualties and losses (TIAN & WANG 2012). Emergency rescue of coal mine accidents is carried out under the premise of protecting the lives and guaranteeing safety of the rescue workers. However expansion of the accidents is common in the process of disaster relief due to improper rescue because of relatively weak implementation of the related specific procedures and regulations (ZHOU & ZHU 2005). Twenty-eight accidents occurred during emergency rescue are obtained statistically through analyzing serious and particularly serious accidents of national coal mines from 2000 to 2009. Statistics show that the number of casualties caused by the secondary accidents account for 19.6% of the total number of casualties. The types of secondary accidents, types of casualties and accidents causes are obtained with further analysis and preventative measures are proposed on that basis in order to improve emergency rescue capabilities and prevent or reduce the secondary accidents.

Secondary accidents refer to the accidents caused by natural irresistible factors, the rescue party's negligence or the wrong operation of the persons concerned on the basis of the original medical malpractice, coal mine accidents, and traffic accidents and so on. The secondary accidents mentioned in this paper refer to the accidents caused by improper rescue during the process of emergency rescue in coal mines.

2 ANALYSIS OF CASUALTIES OF THE SECONDARY ACCIDENTS

2.1 *Source of accident samples*

Twenty-eight accidents occurred during emergency rescue are got through reading compilation of serious and particularly serious accidents of Chinese coal mines from 2000 to 2009 compiled by State Administration of Coal Mine Safety (China Administration of Coal Mine Safety 2000–2009). Statistical results show that 88 people were dead and 60 people were injured in the secondary accidents which together account for 19.6% of the total

Table 1. Statistic of the types of the secondary accidents and the casualties.

The type of secondary accidents	Number of the accidents	Percentage of every type of the secondary accidents (%)	The death toll	The number of the injured	Sum of the casualties	Percentage of the death toll of every type of the secondary accidents (%)	Percentage of the casualties of every type of the secondary accidents (%)
Gas poisoning	17	58.62	50	26	76	56.82	51.35
Lack of oxygen	2	6.90	1	1	2	1.14	1.35
Roof caving	5	17.24	22	3	25	25.00	16.89
The second gas explosion	2	6.90	10	27	37	11.36	25.00
Unknown reasons	3	10.34	5	3	8	5.68	5.41
Total	29	100.00	88	60	148	100	100.00

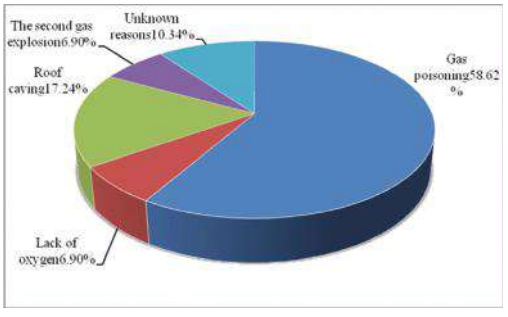


Figure 1. Percentage of every type of the secondary accidents during 2000–2009.

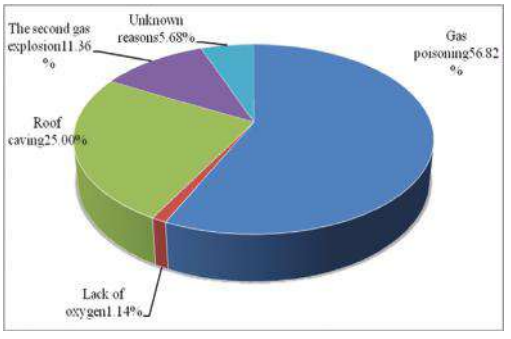


Figure 2. Percentage of the death toll of every type of the secondary accidents during 2000–2009.

number of casualties. Clearly attention should be paid to the secondary accidents to study and prevent which is of substantive significance.

2.2 *Analysis of secondary accidents types*

The secondary accidents mainly include gas poisoning, roof caving, the second gas explosion and lack of oxygen (Table 1).

Remarks: Gas poisoning and roof caving happened simultaneously during the rescue process of the serious gas explosion accident which happened on Nov.30th, 2008 in Changlong Coal Mine, Xinxing District, Qitaihe, Heilongjiang. For convenience of explanation, here the accident is counted as two accidents, so there are twenty-nine accidents in total.

Among them, gas poisoning and lack of oxygen are caused by blind rescue of rescue workers without taking self-rescuers during the emergency rescue process, which in particular require more attention to be prevented for that the number of them account for about 60% of the total number of the secondary accidents and so is the death toll caused by them. The accidents caused by roof caving account for 17.24% of the total secondary accidents (Fig. 1). The death toll caused by roof caving account for 25% of the total number of death and the second gas explosion 11.36% (Fig. 2).

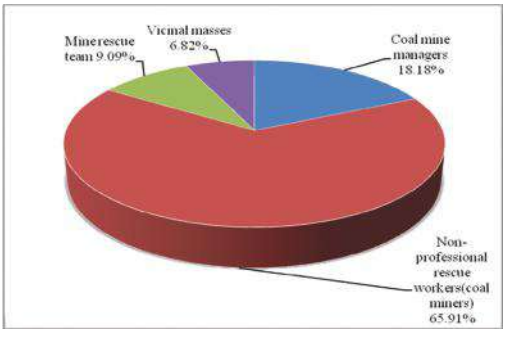


Figure 3. Percentage of the death toll of every kind of people in the secondary accidents during 2000–2009.

2.3 *Analysis of the types of casualties of the secondary accidents*

Casualties of the secondary accidents include four kinds of people, namely coal mine managers, non-professional rescue workers (coal miners), mine rescue team and the vicinal masses (Fig. 3).

Table 2. Statistic of the casualty categories and the casualties of the secondary accidents.

Casualty categories of the secondary accidents	Number of the involved accidents	The death toll	The number of the injured	Sum of casualties	Percentage of the casualties of every kind of people (%)	Percentage of the death toll of every kind of people (%)
Coal mine managers	14	16	5	21	14.19	18.18
Non-professional rescue workers (coal miners)	19	58	28	86	58.11	65.91
Mine rescue team	4	8	27	35	23.65	9.09
Vicinal masses	2	6	0	6	4.05	6.82
Total	…	88	60	148	100.00	100.00

The death toll of non-professional rescue workers (coal miners) account for the most part which is followed by the death toll of coal mine managers which account for 65.91% and 18.18% of the total deaths respectively and 84% together. The death toll of the mine rescue team members account for 9.09% (Table 2). The casualties of vicinal masses are less which cannot be ignored either.

3 CAUSE ANALYSIS OF BEHAVIOR OF THE SECONDARY ACCIDENTS

The direct causes of the secondary accidents include coal mine managers' illegal rescue, non-professional rescue workers' blind rescue and rescue team members' improper response to the emergency and the radical cause is imperfect emergency rescue management system. According to the principle of behavioral science that individual behaviors are determined by organization behaviors (FU 2013), coal mine managers, non-professional rescue workers and mine rescue team lack of the proper training and emergency drill in daily life due to imperfect emergency rescue management system. They usually implement illegal rescue or cope with the emergency improperly when accidents take place which result in the secondary accidents finally.

3.1 *Illegal rescue of coal mine managers*

- First point
  Blind rescue is the main cause of the secondary accidents as the coal mine managers are anxious to save the people and the mine. Due to the lower probability of a serious accident in coal mines, the vast majority of coal mine managers face such a serious disaster for the first time when it happens while they must act as the leaders to make decisions and direct disaster relief the very first time. Because of lacking of daily training of emergency rescue techniques, tactics and skills, they are easily confounded and organize rescue blindly when accidents take place. This will lead to the secondary accidents and make the accidents further expand. Seventeen out of the twenty-eight secondary accidents were caused by blind rescue of coal mine managers whose casualties accounted for 52.7 percent of the total casualties of the secondary accidents (the serial number one, two and three in Table 3). Not only were the managers themselves dead or injured due to blind rescue of managers, but also the non-professional rescue workers (coal miners) suffered the same. Thirty-three non-professional rescue workers were dead and twenty-five were injured owing to managers' blind rescue which together accounted for sixty-seven percent of all the casualties of them in secondary accidents.

  Ten out of fourteen secondary accidents that led to managers' casualties resulted from gas poisoning and one among those fourteen led to injury for lack of oxygen. The casualties caused by gas poisoning and lack of oxygen accounted for more than eighty-five percent of the total casualties of managers. During the rescue, managers got into the wells blindly without taking personal protection equipment and gas detection monitoring equipment such as self-rescuers, gas masks and so on.
- Second point
  Non-professional rescue workers were organized to get into the wells without connecting with the mine rescue teams for the purpose of hiding the accidents. The particular serious explosive combustion accident happened on Jun. 14th, 2008 in Lijiawa Coal Mine, Yuxian, Zhangjiakou, Hebei province. Non-professional rescue workers of Songxi Coal Mine and other coal mines were directed to do the rescue rather than the professional rescue teams. This brought about the death of one rescue worker during the rescue process.
- Third point
  The untruthful situation underground was provided and it led to rescue workers' misjudgment. The serious accident of roof caving and water

Table 3. Statistic of unsafe acts and the casualties of the secondary accidents.

Numbers	Actors	Types of unsafe acts	Casualty categories of the secondary accidents	Number of accidents	The death toll	Number of the injured	Sum of casualties	Percentage of every casualty categories (%)	Percentage of every casualty categories (%)
1	Coal mine managers	Managers led the coal miners into the ells blindly to do rescue	Managers, non-professional rescue workers (coal miners)	8	28	16	44	29.73	65.54
2		Managers organized coal miners to rescue blindly	Non-professional rescue workers (coal miners)	4	15	10	25	16.89	
3		The management blindly rescued without wearing self-rescuers	Managers	5	6	3	9	6.08	
4		Managers hurt themselves during the rescue with wrong judgment of environment	Managers	1	0	1	1	0.68	
5		Managers assigned the non-professional rescue workers task so as to hide accidents.	Non-professional rescue workers (coal miners)	1	1	0	1	0.68	
6		Managers provided untruthful information which led to misjudgment of rescuers.	Non-professional rescue workers (coal miners), mine rescue workers	1	16	1	17	11.49	
7	Non-professional rescue workers (coal miners)	Non-professional rescue workers (coal miners) got into the wells blindly without protection measures.	Non-professional rescue workers (coal miners)	3	8	2	10	6.76	9.46
8		Non-professional rescue workers (coal miners) transported large driving pump inappropriately which hit the wall and caused roof caving.	Non-professional rescue workers (coal miners)	1	2	1	3	2.03	
9		Non-professional rescue workers (coal miners) piled the slag stone improperly which caused roof caving and injuries.	Non-professional rescue workers (coal miners)	1	1	0	1	0.68	
10	Mine rescue team	Mine rescue team coped with the emergency improperly.	Mine rescue team	2	5	11	16	10.81	10.81
11	Vicinal masses	The masses got into the well blindly to save people without organization and protection measures.	Vicinal masses	2	6	0	6	4.05	4.05
12	General headquarters	General headquarters made the wrong rescue plans.	Mine rescue team	1	0	15	15	10.14	10.14
Total					88	60	148	100.00	100.00

bursting happened on Jun. 1st, 2001 in Daoqing Coal Mine, Shebao Company, Baishan, Jilin province. During the rescue, sixteen rescue workers were buried in the auxiliary shaft for the coal mine managers provided untruthful information and the rescue workers entered the struck areas with misjudgment. In this induced accident, coal mine managers violated the regulation in Mine Rescue Procedures that the accident unit must provide comprehensive real technical information and accident conditions to rescue headquarters.

3.2 *Blind rescue of non-professional rescue workers*

The casualties of non-professional rescue workers (coal miners) accounted for more than fifty percent of the total casualties of the secondary accidents (Table 2). The coal miners lacked of awareness of self-protection and had no knowledge of basic methods to handle disasters and rescue, so they obeyed the emergency rescue command of the coal mine managers blindly. Consequently thirty-three people were dead and twenty-five were hurt which together accounted for sixty-seven percent of all the casualties of them in secondary accidents. Three accidents were caused by coal miners who were desperate to save lives without identifying the reasons and basic protection measures. In addition, two accidents were caused by inappropriate measures during the rescue process which resulted in roof caving.

Further analysis shows that the number of non-professional rescue workers (coal miners) died of gas poisoning and lack of oxygen without taking self-rescuers accounted for about fifty percent of the total casualties of them (Table 4). Additionally, casualties caused by the second explosion of methane accounted for 23.26% as they followed the management into the well blindly. Casualties caused by roof caving that resulted from improper measures accounted for 19.77% during the rescue. So it is of great significance to strengthen the knowledge education of emergency rescue for non-professional rescue workers (coal miners) which will enable them to rescue scientifically and orderly so as to prevent the secondary accidents caused by blind rescue.

3.3 *Improper response to emergency of mine rescue teams*

Mine rescue teams are the professional teams to cope with the accidents which are occupational, technical and adopt militarization management. The team members have more self-protection awareness and rescue knowledge than the management and non-professional rescue workers (coal miners) during the rescue process. So they take an obviously low percentage of the total casualties in secondary accidents, namely 9.09% (Table 2). But it cannot be ignored that the total number of casualties of them is large relatively, accounting for 23.65% of the total deaths in the secondary accidents.

The reasons for the casualties of mine rescue teams mainly include that the general headquarters made the wrong rescue plans and that the team members coped with the emergency improperly. Therefore, the general headquarters should take adequate advice of the experts and make scientific rescue plans. The mine rescue teams should increase training and readiness training in daily life and improve their capabilities to prevent and handle the emergency comprehensively.

3.4 *Imperfect emergency rescue management system*

Among the enterprises involved in the twenty-eight secondary accidents, except that some individual coal mines did not make emergency plans for safety production, most of them did have emergency plans which cannot effectively guide the emergency work for lack of pertinence and nor did

Table 4. Statistic of casualties of non-professional rescue workers.

Accident type	The death toll	The number of injured	Sum of casualties	Percentage of the total number of casualties of non-professional rescue workers (%)
Gas poisoning	29	12	41	47.67%
Lack of oxygen	1	0	1	1.16%
The second explosion of methane	8	12	20	23.26%
Roof caving	16	1	17	19.77%
Unknown reasons	4	3	7	8.14%
Total	58	28	86	100.00%

they ever organize drill. The rescue of accidents was unsystematic and illegal rescue appeared.

- First point
  For lack of propaganda, education and training of emergency plans, the operators even the managers did not understand the basic methods to deal with the accidents and implement rescue. They had weak safety awareness and severely lacked of safety awareness and basic general knowledge of emergency. More than a half of the casualties were caused by blind rescue without adopting any technical safety measures.
- Second point
  Some mining enterprises violated the regulation in the Mine Rescue Procedures that the development of emergency rescue must be contained in the development plans of construction and safety technology and so on prepared by mining enterprises. Professional rescue force in some enterprises is weak. Professional rescue teams were not established or rescue agreements were not signed with professional rescue teams. Neither were the enterprises equipped with part-time rescue workers, nor did they have enough necessary emergency rescue equipment. All above mentioned brought on an imperfect rescue work.
- Third point
  The accident rescue site was disordered. Two gas poisoning accidents were caused by blind rescue of the masses nearby who knew the accidents without any protection measures. Although the casualties accounted for a lower percentage, namely 4.05%, it still cannot be neglected.

4 COUNTERMEASURES AND SUGGESTIONS TO PREVENT THE SECONDARY ACCIDENTS

4.1 *To improve the emergency rescue management system*

- First point
  Set up emergency rescue agencies. The mining enterprises should set up emergency rescue agencies and ensure that the emergency rescue is under the charge of the professionals of specialized agencies and the responsibilities of the commanders in chief and the deputy commanders of the emergency rescue agencies and the member units is clear and the full-time or part-time emergency rescue teams that are consisted of the employees within the units are established (LAW Order No. 69, 2007).
- Second point
  Develop emergency rescue plans and organize regular drills. The mining enterprises should develop emergency rescue plans in combination with the state of the hazards, risk analysis and the potential accident risks. In the rescue plans, the scenes of the accidents cannot be set too simple and the possibility that the accidents may lead to secondary disasters must be taken into consideration and emergency rescue capability should be strengthened under complex conditions (HOU & BI 2006). On the basis of the emergency rescue plans, propaganda and training of them should be started and the comprehensive or special emergency drills should be organized at least once a year and the on-site disposal drills should be organized at least once a half year so as to improve emergency awareness (State Administration of Work Safety 2000–2009).
- Third point
  Reinforce the punishment of concealing the accidents. The relevant regulations of reporting the accidents causing coal mine workers' casualties should be implemented strictly. Persons at the accident site must immediately report to the local government or the departments in charge when the accidents happen. Concealing or giving false information of the accidents must be avoided. Responsible persons of the mining enterprises may take chances that concealing the accidents may not be found for the punishment corresponds with the accidents. Therefore, the punishment for responsible persons who hide the accidents must be reinforced, so that the cost for concealing the accidents exceeds the cost for reporting the accidents.
- Fourth point
  To make clear the emergency rescue process and draw up scientific rescue plans. The leaders of the mining enterprises must start the emergency plans at the first time when the accidents take place and establish rescue headquarters and organize rescue as soon as possible. When the government and the relevant personnel reach the accident sites, the rescue headquarters established by the government will act as the supreme headquarters which are responsible for the unified implementation of the rescue work (TIAN & WANG 2012). In order to draw up scientific rescue plans and avoid the secondary accidents caused by the blind rescue, professional and technical personnel of the accident units and the experts who are familiar with the similar accidents and have practical rescue experience should give full play to their roles (State Administration of Work Safety 2012). Besides, the workers who are responsible for handling emergencies in the government and the relevant departments should be trained regularly in the daily prevention and emergency preparedness to raise the level of commanding emergency rescue.

- Fifth point
  To standardize management of the accident sites and delimit the appropriate isolation boundary and prevent the vicinal masses from taking adventures of getting into the wells casually under which circumstances accidents may further expand.

4.2 *To strengthen emergency rescue training of coal mine managers and coal miners*

- First point
  To strengthen emergency rescue training of coal mine managers. The casualties caused by blind rescue of managers without taking self-rescuers account for more than 85% of their total casualties. In fact, the risk of gas poisoning do exist in gas combustion accidents, fire accidents, gas explosion and water accidents and so on. Mine Rescue Procedures provides that the oxygen respirators must be in use before getting into the pits if it cannot be confirmed whether poisonous and harmful gas exist in the shaft and pit bottom. Rescue teams without oxygen respirators are forbidden to get into the pits under no circumstances (Mine rescue regulations AQ1008–2007). So when training the coal mine managers, priority should be given to the accidents caused by gas poisoning during the rescue process and how to use the self-rescuers should be trained as well. As the casualties caused by blind rescue organized by coal mine managers account for more than a half of the total casualties of the secondary accidents, emergency rescue process of their own organizations should be trained and emergency rescue drills should be organized once a year to raise the level of commanding emergency rescue and avoid blind rescue.
- Second point
  Strengthen emergency rescue training of coal miners. The accidents caused by improper rescue of coal miners are mainly gas poisoning and roof caving, so emphasis should be put on the training of preventative measures of those two kinds of accidents when training the knowledge of accidents relief work. Oxygen respirators should be worn correctly to rescue accidents when it cannot be confirmed whether poisonous and harmful gases exist underground. Roof caving can be caused by gas explosion and water accidents. To observe the underground environment when getting into the pits to rescue the accidents and to evacuate the danger zone immediately once the omen of roof caving such as the dregs, roof cracks, leaky roofs etc. are found. Through training, the staff can have knowledge of the contents of emergency plans, emergency process and emergency disposal plans and their safety awareness and emergency disposal skills will be improved. Besides, the secondary accidents can be used to train the staff. The staff will be warned with the past bitter lesson that to blind rescue should be stopped when the information underground is unknown and the rescue without any protection measures should be prohibited.

4.3 *To enhance the capability to cope with the emergency*

To strengthen the training and readiness training of the mine rescue teams and enhance the capability to prevent and cope with the emergency comprehensively. Accidents lead to the team members' own casualties tend to happen more frequently, which result from poor physical quality and psychology bearing capacity and panic and tension when handling emergencies. So the training of physical quality and psychology quality should be stressed in routine training. Moreover, strict and meticulous work style and good work habits should be cultivated and operation ability of all kinds of instruments and equipment should be improved in daily training and practical exercises.

5 CONCLUSIONS

Conclusions are drawn as following through statistically analyzing twenty-eight accidents occurred during emergency rescue in the compilation of serious and particularly serious accidents of national coal mines during 2000–2009 compiled by State Administration of Coal Mine Safety.

- First point
  The secondary accidents mainly include four types, namely gas poisoning, roof caving, the second gas explosion and lack of oxygen. Prevention of gas poisoning and lack of oxygen in particular require more attention for that the number of them account for about 60% of the total number of the secondary accidents and so is the death toll caused by them.
- Second point
  Casualties of the secondary accidents include four kinds of people, namely coal mine managers, non-professional rescue workers (coal miners), mine rescue teams and the vicinal masses. The death toll of non-professional rescue workers (coal miners) account for the most part which is followed by the death toll of coal mine managers which account for 65.91% and 18.18% of the total deaths respectively.
- Third point
  Casualties caused by blind rescue of coal mine managers account for 52.7% of the total number of casualties in the secondary accidents. Not only

are the managers themselves dead or injured due to their blind rescue, but also do the non-professional rescue workers (coal miners) suffer the same. Casualties of the non-professional rescue workers (coal miners) caused by managers' blind rescue account for sixty-seven percent of all the casualties of them in secondary accidents. So it is essential to strengthen emergency rescue training for the management to prevent the secondary accidents.

- Fourth point
  The radical cause of the secondary accidents is imperfect emergency rescue management system. Coal mine managers, non-professional rescue workers and mine rescue teams lack of the proper training and emergency drills in daily life due to imperfect emergency rescue management system. Implementation of illegal rescue of managers, blind rescue of non-professional rescue workers and improper response to emergency of mine rescue team tend to appear when accidents take place which result in the secondary accidents finally.
- Fifth point
  Emergency rescue management system should be improved firstly to prevent the secondary accidents. On that basis, to lay stress on the emergency rescue training of coal mine managers and workers and to strengthen the training and readiness training of the mine rescue team, so that the capability to cope with the emergency can be enhanced.

REFERENCES

AQ1008–2007. Mine rescue regulations.

China Administration of Coal Mine Safety. *Compilation of Serious and Particularly Serious Accidents of National Coal Mines during* 2000–2002. 2011.

China Administration of Coal Mine Safety. *Compilation of Serious and Particularly Serious Accidents of National Coal Mines during* 2003–2005. 2007.

China Administration of Coal Mine Safety. *Compilation of Serious and Particularly Serious Accidents of National Coal Mines during* 2006–2009. 2011.

Fu Gui, et al.. Discussions on the theoretical understanding and effects of behavioral safety. *China Safety Science Journal*; 2013;23(3).

Hou Jin-Ling & Bi Yong-hua. Research progress of and suggestions on coal mine emergency rescue in China. *Coal Economic Research*; 2009(11):86–88.

Order of the President of the People's Republic of China. *the Emergency Response Law of the People's Republic of China*. Order No. 69, 2007.

State Administration of Work Safety. Administrative measures on production safety accident emergency plans. *Order No. 17 of State Administration of Work Safety,* 2009.

State Administration of Work Safety. Guidance on the strengthening scientific rescue and improving emergency rescue of production safety accidents. *Order No.147 of Emergency Management and Emergency Rescue Research Center of State Administration of Work Safety,* 2012.

State Administration of Work Safety. Gas explosion accidents happened on Mar. 29th and Apr. 1st sequentially in Babao Coal mine, Jilin. *http://www.chinasafety.gov.cn/newpage/Contents/Channel_4314/2013/0412/201541/content_201541.html*, 2013-04-12/2013-05-01.

Tian De-yu & WANG Yu-qing. Analusis on responsibility assignment of accident rescue in colliery production. *China Coal*; 2012; 38(2):113–115.

Wang Zhi-Dong & Fan Gong-qin. Coal mine production safety emergency rescue command system. *China Mining Magazine*; 2008; 17(7):16–18.

Xinhua Net.com. Rescue of gas explosion accident was being conducted in Dahuang Coal Mine in Dengta, Liaoning. *http://news.xinhuanet.com/energy/2012-03/23/c_122870901.html*, 2012-03-23/2013-05-01.

Zhou Xin-Quan & Zhu Hong-qing. Discussion on decision making for mine emergent rescue with dilemma in decision making. *Coal Science and Technology*; 2005; 33(1):1–3.

Progress in Mine Safety Science and Engineering II – He et al. (Eds)
© 2014 Taylor & Francis Group, London, ISBN 978-1-138-00122-0

Analysis on relationship of construction accident probability and safety training

Z.M. Liu & G. Fu
School of Resource and Safety Engineering, China University of Mining and Technology (Beijing), Beijing, China

H.B. Pei
International Engineering Company, China Huadian Engineering Co., Ltd., Beijing, China

ABSTRACT: In this paper, from several statistical analyses of construction project management and accident safety performance data, the current construction industry presentative safety performance scores and the number of accidents is not simply a decreasing function of the law. Through both unconventional function of a single correlation curve analysis, the safety training is the critical factor for the number of accidents. With safety psychology, safety rheology and mutation theory, hazard identification and evaluation, safety training theory explains unconventional curves generated scores on the role of factors. Through case studies, this paper indicates that absence of safety training play an effective role in unsafe behavior of employees, and gives solution initiatives.

1 INTRODUCTION

In construction project safety management, there is a seemingly irrational phenomenon: the construction enterprise with good presentative safety performance gets higher probability of accidents than the one which has lower presentative safety performance scores; One construction enterprise, in the presentative safety performance relatively high stage, the probability of accidents increases. To explain this seemingly irrational phenomenon, this paper selected a large hydropower project, which is sponsored by China Huadian Corporation in Cambodia, as a typical case study. Through statistical analysis of all construction enterprises in the project, indicating the data of proportion and range occurred in the "irrational" phenomenon, with safety psychology, safety rheology and mutation theory, the paper gives the phenomenon of scientific analysis and reasonable explanation.

2 RELATIONSHIP BETWEEN PREVENTATIVE SAFETY PERFORMANCE AND THE NUMBER OF ACCIDENTS

In this article, the authors define the presentative safety performance, according to the preparation of the "monthly safety checklist" as the standard through which the construction enterprises are checked by scores. "Monthly Safety Checklist" includes safety organization, safety training, safety measures, safety inspection, and rectification closed-loop rate etc. Accident is defined to the case, resulting in the loss which people do not expect to occur, including statistical accident.

China Huadian lower stung hydropower project (Cambodia) started in April 2010, ended in April 2013. During the period, there have been 12 construction enterprises joined the construction project. Author collected statistics from April 2010 to April 2013, about monthly presentative safety performance and the number of accidents in all construction enterprises, as shown in Figure 1.

Some notes about Figure 1:

1. The monthly safety checks at the beginning of each month through all the construction period of the project;
2. Within the same enterprise, the figure took the average sum of the number of accidents in the same safety checklist score;
3. The safety checklist total score was 100 points. In order to simplify statistical data, safety checklist score T in (T, T +4) was the values T, T is a number divisible by 5;
4. Starting point of the increasing curve as T1, end of the curve positioning T2.

As can be seen from Figure 1, the safety check scores: 16.7% curves increasing when $T \in (60,65)$; 33.3% curves increasing when $T \in (65,70)$; 45.5%

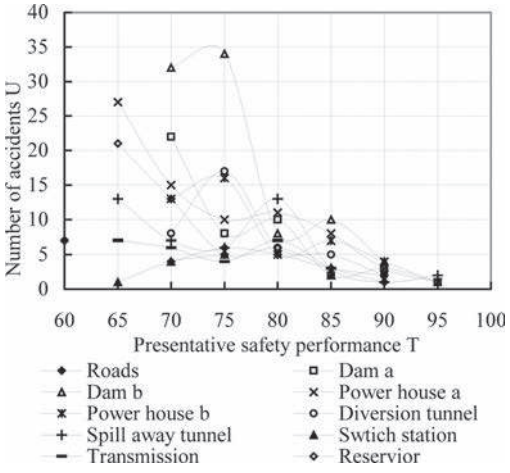


Figure 1. Construction safety checklist scores and accidents data analysis.

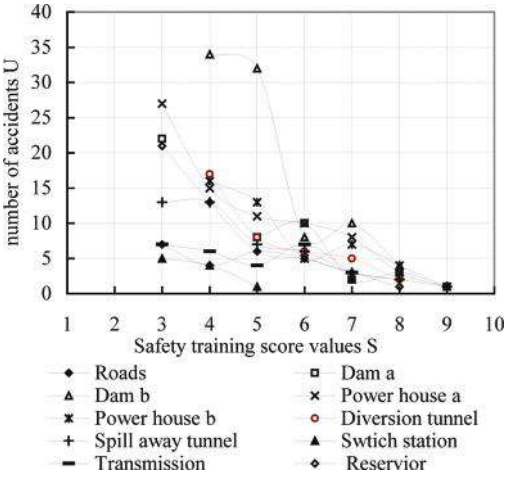


Figure 2. Construction safety training scores and accidents data analysis.

curves increasing when T ∈ (70,75); 27.3% curves increasing when T ∈ (75,80); 11.1% curves increasing when T ∈ (80,85); The number of accidents occurring was too small when T ∈ (90,100), there was no value to the date studying, this paper didn't analysis the dates in the period.

Data analysis and statistics reach the following information:

1. The number of accidents occurring U trend becomes smaller when presentative safety performance score value of T grow;
2. In all T values, the U-values are not all show in downward state. When T ∈ (65, 80), It showed a considerable part of the U-value rising.

3 SAFETY TRAINING AND PRESENTATIVE SAFETY PERFORMANCE RELATIONSHIP RESEARCH

3.1 *Correlation analysis on safety training factor to unconventional curve*

Focusing on range of T values, in which the emergence of proportion of abnormal curves got relatively high, T_2 values were analyzed when T ∈ (65,80), analyzing the common cause of each item marked of the safety checklist. Checking and correlation analyzing safety engineer, safety training, safety inspections loop rate, site safety precautions, safety warning signs, etc of the safety checklist one by one (Xue 2008, Anderson & Rubin 2003, Jöreskog 2003), in all individual correlation analysis, the number of accidents and safety training score value relationship shown in Figure 2.

Making statistics safety training score in each presentative safety performance scores in Figure 1, and verifying the safety training score corresponding to the different number of accidents. As can be seen from Figure 2: 85.7% of the curve showing increasing state when safety training scores S ∈ (3,4); 90% of the curve showing increasing state when safety training scores S ∈ (4,5); 80% of the curve showing increasing state when safety training scores S ∈ (5,6); 80% of the curve showing increasing state when safety training scores S ∈ (6,7); 88.9% of the curve showing increasing state when safety training scores S ∈ (7,8); 88.9% of the curve showing increasing state when safety training scores S ∈ (8,9); The number of accidents occurring was too small when T ∈ (90,100), there was no value to the date studying, this paper didn't analysis the dates in the period.

Data analysis and statistics reach the following information:

1. The safety training scores S value greater, the number of accidents occurring U trend becomes smaller;
2. In all the range of U-value statistics, S values impact on the U-value greater, basically showing decreasing relationship;
3. After changing the abscissa to safety training scores S, most of the curve creasing in figure 1 showing a decrease state. Making the definition of S = S2 when T = T1; S = S1 when T = T2.

3.2 *Safety psychological analysis*

According to some references, the most important cause accident is human physiological and

psychological factor (Sui et al. 2005, Li & Lu 2006, Mao 2004). Most accidents were caused by the deviation of human consciousness, mental status, behavior norms to the surrounding environment, security status, and safety regulations. Human behavior will constitute a new construction safety hazard, and may deduce accidents with human consciousness (Sun 2008).

From safety psychology, mind-set and perceptual constancy made a negative impact to employees who did not receive effective safety training (Wang 2008), prolonged labor load and undiscovered danger paralyzed employee's ability to identify the danger (Rouse et al. 1993, O'Donnell & Eggemeier 1986, Young & Stanton 2001).

Mind-set, that mental state of readiness. Once the objective conditions change, it will make the original needs change, which are sure to satisfy. People of different psychology will produce different reactions mind including constructive reactions and destructive reactions. S = S1, employees did not receive effective safety training, psychological expectations of the construction workers and construction site safety conditions existing danger produced a significant bias, most of the workers on the construction site cannot identify and evaluate the danger completely and truly.

Perceptual constancy negative effect. When the perception of the objective conditions within a certain range is changed, our perceptual image in a considerable extent, still maintains its stability, which is called perceived constancy. When S = S2, employees were often considered to have received safety training, site installation of protective measures have safety supervision, etc., but they did not play it safe management of intrinsically safe state, changing the employees on the construction site safety conditions, the safety perception of employees in the construction has maintained a considerable degree of safe and stability. Safety conditions and employee safety perception deviating, which make negative psychological effect to employees and this kind of danger was more subtle and difficult to identify.

3.3 *Safety rheology and mutation principles analysis*

Construction accidents were caused by human, machine, material, method, environment together accidents showed orderly process and development, through rheological and mutation process (He 2001), as shown in Figure 3. Accidents made the construction process stopped or disturbed, but making construction often stopped or disturbed was a series of orderly construction work, so accidents essence is an ordered set of events. Ordered event is reflected in the incident event and continuous events (Zheng & Zheng 2004).

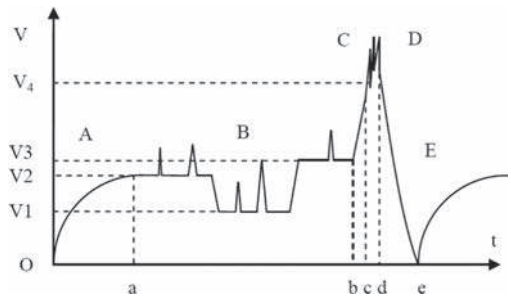


Figure 3. Safety rheology and mutation schematic.

Using safety rheology and mutation principle analysis Figure 1 and Figure 2, and got information blew:

1. During the process beginning OA, when T = T1, the collection of danger made the degree V was significantly higher than when T = T2.
2. Shock stage AB, when T = T2, the oscillation frequency and amplitude ratio of V was more notable than V when T = T1.

The unsafe event ordering more completely when T = T2 than T = T1 was the reason. One accident causing another incident occurred, or both accidents occur simultaneously, forming sequences. Sequence length depends on the presence of unsafe; when an incident occurs, the process does not cause another accident, or not enough to cause another accident occurs, the sequence is stopped, otherwise continue to occur. The risk of work activities degree greater, making probability of a complete sequence of accident greater (Zhang 2006). Behavioral safety made the impact to the accident and its sequence of occurrence and development through employees receiving safety training, and the safety training depth and breadth made impact to employees identify, limit the safety collection. Strengthen the operation process safety management, can reduce the risk of job activity level V, thereby enabling the E (h) value becoming declining, dt expectations becoming promoting, showing the accidents and their sequence and integrity reduced. When T = T1, employees expectation of safe conditions on the construction site reduce and they operate with cautious, illegal operations rate is reduced, impacting of unsafe event series development. That is, the effect of safety training directly affects the orderly arrangement of unsafe events, shocks amplitude and oscillation frequency.

4 CASE STUDY

According to reference (Zhang et al. 2009, Cheng et al. 2009, Fu 2009), safety training plays a crucial role for staff safety psychology and safety behavior.

Table 1. Unsafe behavior on scaffolding platform-A.

Objects	Workers on scaffolding	Workers through a safety channel
safety Status	Scaffolding and safety channels have safety measures, but not in a completely effective protection status.	Staff not receiving effective safety training.
Psychological safety	Scaffolding and safe channels and protection measures, falling objects will not endanger staff below, staff has unsafe awareness.	Safe channel and scaffolding has protection measures and he thought he wear a helmet, and could pass safely.
Unsafe behavior	Directly throwing tools, materials down the side. Random walk on the scaffolding.	Do not look risks around, directly through the scaffolding below.
Unsafe events arranged	Safety measures fail—staff above throwing tools and materials—staff below passing through; safety precautions failure—Random walk on the scaffolding.	

Table 2. Unsafe behavior on scaffolding platform-B.

Objects	Workers on scaffolding	Workers through a safety channel
safety Status	Scaffolding and safe channel has no protective measures, protection is not in a safe state.	Staff receiving effective safety training.
Psychological safety	Without any safety measures, staff keep highly vigilant.	Without any safety measures, staff felt danger.
Unsafe behavior	Throwing items down the side with cautious. Altitude walks with cautious.	Rapid pass.
Unsafe events arranged	Safety measures fail—staff above not throwing items—unsafe events terminated; safety precautions fail—staff below taking measures to pass safety channels.	

Author visited two typical project constructions about safety conditions, staff safety psychology, unsafe behavior and their relationship, as shown in Table 1 and Table 2.

If employees received safety training, but did not really improve their safety awareness, changing its danger assessment on the surrounding perceptual awareness, as they thought the construction site has safety measures. Based on simple danger perception, it will lead directly to the construction process danger behavior, the frequency and style of unsafe behavior increasing significantly. Increasing the accident sequence integrity, unsafe behavior has negative impact on recognition and restrictions to unsafe factors set.

If employees received safety training, without any protective measures at the construction site, major hazards presented or exposed in front of employees directly, resulting in safe environment sensitivity to the staff, and they are always careful. When unsafe behavior occurs, staff will take into account the possible consequences without safety measures subconsciously, and the number and types of unsafe behavior will be relatively reduced.

Through theoretical and case studies, safety management did not meet the specific issues, such as ineffective safety training, invalid safety measures, safety check just in form etc. which bring danger factors. The hidden danger factors in the construction will aggravate unsafe awareness and behavior. It can be seen in construction safety management, we should strengthen the safety training to improve employee safety awareness, virtually eliminating employees' unsafe behavior. The safety checklist should be detailed on check items, safety training total score should be increased to show the true safety management performance.

5 CONCLUSION

Main conclusions:

This article firstly pointed that from the current construction there is a decreasing function of non-normal law between presentative safety performance scores and the corresponding number of accidents, and analyzing safety checklist scores and the corresponding number of accidents statistically in one project. The number of accidents showed a decreasing trend as the presentative safety performance scores increasing, but it did not really reflect the safety performance of construction projects.

Though the analysis on the number of accidents and safety checklist for each individual correlation, the presentative safety performance and safety training showed a significant decreasing function relationship. And it explained the safety training impact on the number of accidents with safety

psychology, safety rheology and mutation theory, hazard identification and evaluation theory.

Through a case study, we can see that ineffective safety management has their own hidden danger factors, which aggravate staff unsafe awareness and unsafe behavior. In safety management, safety training should be strengthen, increasing the safety training ratio in safety performance appraisal, strengthen employee safety awareness, it could virtually eliminate employees unsafe behavior.

REFERENCES

Anderson, TW & Rubin, H 2003. Statistical inference in factor analysis. *Proceedings of the third Berkeley symposium for mathematical statistics and probability*. Berkeley: University of Califorina Press, 5:111–150.

Cheng Weimin, Zhou Gang & Wang Gang, etc 2009. unsafe acts of people's psychological measurement and analysis [J]. *China Safety Science Journal*, 6:29–34.

Gui Fu, Chang-repair 2009. Corporate safety culture and its quantitative measurement study [J]. *China Safety Science*, 1:86–92.

He Xueqiu 2001. Security rheology theory and its application in accidents in mines [J]. *China Safety Science*, 11(1): 6–11.

Jöreskog, KG 2003. A general approach to confirmatory maximum likelihood factor analysis. *Psychometrika*, 34:183–202.

Li Hongjie & Lushun Qing 2006. *Safety Ergonomics* [M]. China University of Geosciences Press.

Mao Haifeng 2004. *Security Management Psychology* [M]. Chemical Industry Press.

O'Donnell RD & Eggemeier FT 1986. Workload assessment methodology [J]. *In Boff KR, Kaufman L & Thomas JP (Eds.), Handbook of perception and human performance*. New York: Wiley, 2:42–49.

Rouse WB, Edwards SL & Hammer JM 1993. Modeling the dynamics of mental workload, and human performance in complex systems [J]. *IEEE transactions on systems, man, and cybernetics*, 23:1662–1671.

Sui Pengcheng, Chen Baozhi & Sui Xu 2005. *Safety principles* [M]. Chemical Industry Press.

Sun Liying 2008. Building Construction Safety Psychology [J]. *Safety and health*, 2:46–47.

Wang Zhigang 2008. Produce unsafe behavior psychological system analysis [J]. *Management innovation*, 6:52.

Xue Wei 2008. *SPSS statistical analysis methods and application*. Beijing: Electronic Industry Press, 326–348.

Young MS & Stanton NA 2001. Mental workload: theory, measurement, and application [J]. *In W Karwowski (ed.), International Encyclopedia of Ergonomics and Human Factors*. London: Taylor & Francis, 1:507–509.

Zhang Jianshi, Gui Fu & Liu Chaojie etc 2009. Safety awareness and Behavior Research [J]. *Hunan University (Natural Science)* (02):15–18.

Zhang Shoujian 2006. Engineering construction safety behavior [D]. PhD thesis. 2006:36.

Zheng Xiazhong & Zheng Gen Paul 2004. Building construction safety accident prediction methods applied research [J]. *People Yangtze*, 35(1):52–55.

This page intentionally left blank

6 *Mine safety science and theory*

This page intentionally left blank

Progress in Mine Safety Science and Engineering II – He et al. (Eds)
© 2014 Taylor & Francis Group, London, ISBN 978-1-138-00122-0

Analysis of mine pressure factor of dynamic disasters to coal seam with large dip angle

Guo Qiang Hao
China University of Mining and Technology (Beijing), Beijing, China

Chen Li
Hebei University of Engineering, Handan, Hebei, China

ABSTRACT: In terms of Working Face 3237 in Mine Zhaogezhuang and by means of using the numerical simulation method, this paper analyzes the distribution rules of the abutment pressure of coal seams with large dip angles. And on the basis further probe into the influence from the abutment pressure of coal seams with large dip angles to the dynamic disasters of coal and gas outburst. The results show that the accumulated elastic energy is of the least when the coal seam dip angle reaching the large dip angle of 55°, the accumulated elastic energy on the upper part shall be less than that of in the middle and lower part of the working face, and all of these are conducive to gas release, thus the possibility of the occurrence of the dynamic disasters of coal and gas outburst is reduced accordingly.

1 INTRODUCTION

After exploiting the coal seam and within the redistribution scope of enclosing rock stress, the vertical stress acting on the coal seam, rock stratum and gangue is called "abutment pressure" (Qian & Shi 2003). The essence of the occurrence of dynamic disasters of coal and gas outburst is because the energy stored inside the coal lithosome is more than its borne ultimate capacity and further sudden breakage is caused accordingly. Both the energy amount stored inside the coal lithosome and the resistance capacity against breakage of the coal seam has a close relationship with the distribution of abutment pressure (Xie et al. 2006, Wang et al. 2010, Wang et al. 2011). Therefore, in order to further discuss the essence of the occurrence of dynamic disasters of coal and gas outburst in coal seams with large dip angles, it is possible to set about from studying distribution laws of the abutment pressure.

Normally divide dip angles of the coal seam into four types: slightly inclined coal seams ranging from 0° to 25°, inclined coal seams ranging from >25° to <35°, largely inclined coal seams ranging from 35° to 55°, while steeply inclined coal seams ranging from >55° to 90° (Meng et al. 2007). According to the above division method and in view of Working Face 3237 of Mine Zhaogezhuang, the author established a four-numerical-value calculation model with the respective coal seam dip angles of 15°, 35°, 55° and 75° in order to probe into the distribution characteristics of the abutment pressure of coal seams with large dip angles as well as its influence to the dynamic disasters of coal and gas outburst.

2 OVERVIEW OF WORKING FACE

The Working Face 3237 of Mine Zhaogezhuang is located in No. 2 cross drift in the west of Level 13, with the coal seam dip angle ranging from 26° to 43° while the average of 35°, and the coal seam protodyaknove's number $f = 0.7–1.0$, the Face seems a monoclinic formation and its occurrence is slightly stable. Relative gas gush amount of the Mine is of 11.64 m^3/t, which belongs to a mine with high gas. The Face has a design trend between 307 and 326 m, an average length of 325 m, a dip length of 96 m and an area of 32500 m^2.

3 MODEL CONSTRUCTION

3.1 *Numerical calculation model*

The numerical model adopts FLAC3D numerical simulation software developed by American Itasca Company. The model has a embedded depth of 1100 m, and its length × width × height is equal to 200 m × 120 m × 150 m. The coal seam dip angle has four circumstances covering 15°, 35°, 55° and 75°. Figure 1 is the numerical calculation model with the coal seam dip angle of 35°, and the model

Table 1. Mechanical parameters of rock strata in working face.

Type	Name of coal lithosome	Volume weight/ ($Kg \cdot m^{-3}$)	Bulk modulus/ Gpa	Shear modulus/ GPa	Tensile strength/ MPa	Internal frictional angle/(°)	Cohesion/ MPa
Overlying rock	Fine sandstone	2600	12.6	6.8	2.55	37.37	10.5
Upper roof	Siltstone	2649	13	7	2.93	38.54	11.6
Immediate roof	Clay stone	2533	8	4.5	1.79	37.49	5.1
Coal seam	Coal	1410	0.89	0.65	0.4	30	1.05
Immediate base	Siltstone	2649	13	7	2.93	38.54	11.6
Lower base	Fine sandstone	2618	7	9	4.13	32.03	14.5
Basal bed	Siltstone	2600	6.8	8.43	4.02	31.33	13.89
Gob area	Gangue	1560	0.33	0.15	0	25	0.01

is totally divided into 234240 units and 243324 nodes. The working face has a dip length of 96 m and the total propulsion of 120 m, and the gob area shall be filled in by dribbling gangue. The side of the model shall restrict the horizontal movement, the bottom shall restrict vertical movement, and the upside shall be exerted with vertical loading for simulating the gravity of overlying rock.

3.2 *Parameters and failure criteria of rock mechanics*

The model calculation adopts the criterion of Mohr-Coulomb, and this yield criterion can be expressed as:

$$f_s = \sigma_3 - \sigma_1 N_\varphi + 2c(N_\varphi)^{1-2} \quad (1)$$

$$f_t = \sigma_t - \sigma_1 \quad (2)$$

where σ_1 is respectively of the maximum and minimum principal stress; φ is of internal frictional angle; c is of cohesion; σ_t is of tensile strength; and N_φ is the parameter related to the internal frictional angle of φ.

4 DISTRIBUTION CHARACTERISTICS OF ABUTMENT PRESSURE

Figure1 refers to when the propulsion of the working face is of 60 m, the distribution characteristics of the abutment pressure along with the working face in the middle and the trend along the coal seam. When the coal seam dip angle is of 15°, the abutment pressure peak value is of 43.14 MPa, the stress rising coefficient is of 1.66, and the distance between the peak value position and the coal wall is of 12.5 m; when the coal seam dip angle is of 35°, the abutment pressure peak value is of 39.22 MPa, the stress rising coefficient is of 1.51, and the distance between the peak value position and the coal wall is of 12.5 m; when the coal seam dip angle is of 55°, the abutment pressure peak value is of 30.71 MPa, the stress rising coefficient is of 1.18, and the distance between the peak value position and the coal wall is of 20 m; and when the coal seam dip angle is of 75°, the abutment pressure peak value is of 35.31 MPa, the stress rising coefficient is of 1.36, and the distance between the peak value position and the coal wall is of 15 m. It can clearly be seen that along with the rise of coal seam dip angle, the abutment pressure peak value and the stress rising coefficient shall decrease firstly before increasing afterwards while go to its minimum when the coal seam dip angle is of 55°; the distance between the peak value position and the coal wall shall increase firstly before decreasing afterwards while go to its maximum when the coal seam dip angle is of 55°. Thus judging from the above analysis, during the process of coal seam dip angles changing from a slight dip to an increased dip and a large dip angle, the abutment pressure peak value and the stress rising coefficient shall decrease while the distance between the peak value position and the coal wall shall increase accordingly; but during the process of increasing from a large dip angle to a steep dip, the abutment pressure peak value and the stress rising coefficient shall increase while the distance between the peak value position and the coal wall shall decrease accordingly.

Figure 2 refers to when the propulsion of the working face is of 60 m, the distribution characteristics of the abutment pressure along with the position of 13 m in front of the coal wall and the dip along the coal seam. It can be seen that the abutment pressure distribution along the dip of non-level coal seams appears asymmetry, and the asymmetry shall intensify along with the coal seam dip angle changing from a slight dip to an increased dip and a large dip angle; while the asymmetry shall weaken along with the change from the increase of a large dip angle to a steep dip. When the coal seam dip angle reaches the upper limit of 55° of the large dip angle, the abutment pressure

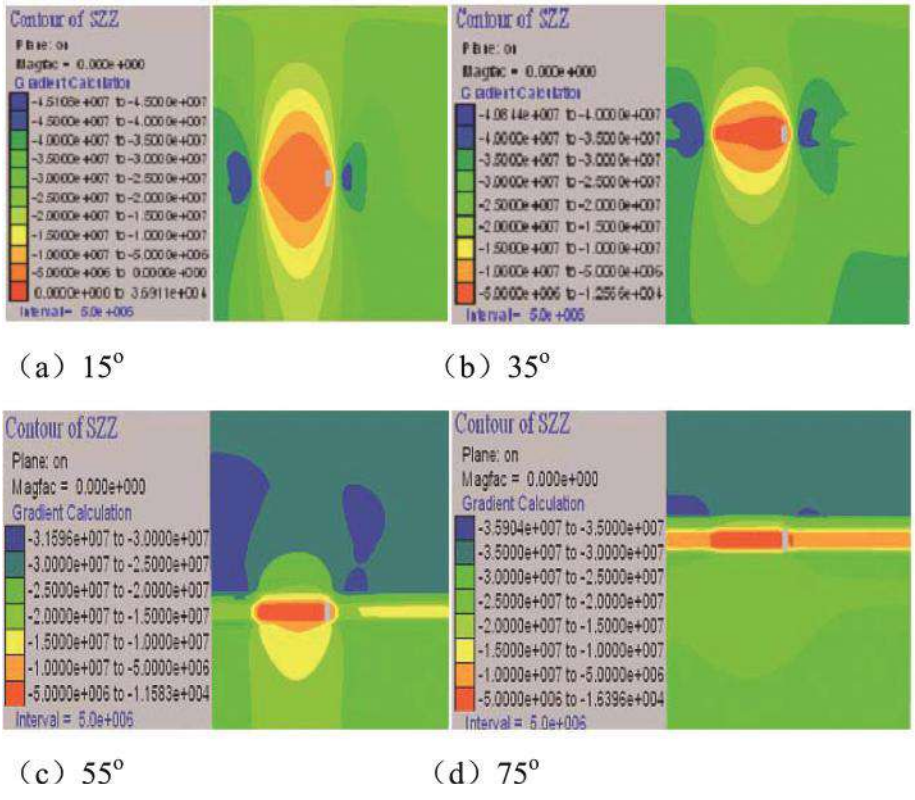


Figure 1. Distribution characteristics of abutment pressure along coal seam trend.

shall all almost be distributed in the middle and lower part to the coal seam dip direction.

5 INFLUENCE FROM ABUTMENT PRESSURE TO DYNAMIC DISASTERS OF COAL AND GAS OUTBURST

The dominant factor causing coal and gas outburst is the elastic energy and high gas energy stored inside the coal lithosome. The coal body shall be compressed within the abutment pressure peak value area, where holes and cracks of the coal body is compressed and closed up, the elastic deformation energy shall be accumulated inside the coal body, but because the coal body inside the peak value area has been under its elastic-plastic state, and thus gas inside holes can not flow easily, which cause gas inside the abutment pressure peak value area can not be released and further become the main power source of coal and gas outburst. Results of the numerical simulation show: along with the increase of the coal seam dip angle, the abutment pressure peak value shall firstly decrease before increasing and reach its minimum when reaching the upper limit of 55° of the large dip angle; and at this time, the abutment pressure shall all almost be distributed in the middle and lower part to the coal seam dip direction. It can be seen that the accumulated elastic energy is of the least when the coal seam dip angle reaching the large dip angle of 55°, the accumulated elastic energy on the upper part shall be less than that of in the middle and lower part, and all of these are conducive to gas release, thus the possibility of the occurrence of the dynamic disasters of coal and gas outburst is reduced accordingly.

6 CONCLUSIONS

By following the coal seam trend and along with the rise of coal seam dip angle, the abutment pressure peak value and the stress rising coefficient shall decrease firstly before increasing afterwards while go to its minimum when the coal seam dip angle is of 55°; the distance between the peak value position and the coal wall shall increase firstly before decreasing afterwards while go to its maximum when the coal seam dip angle is of 55°.

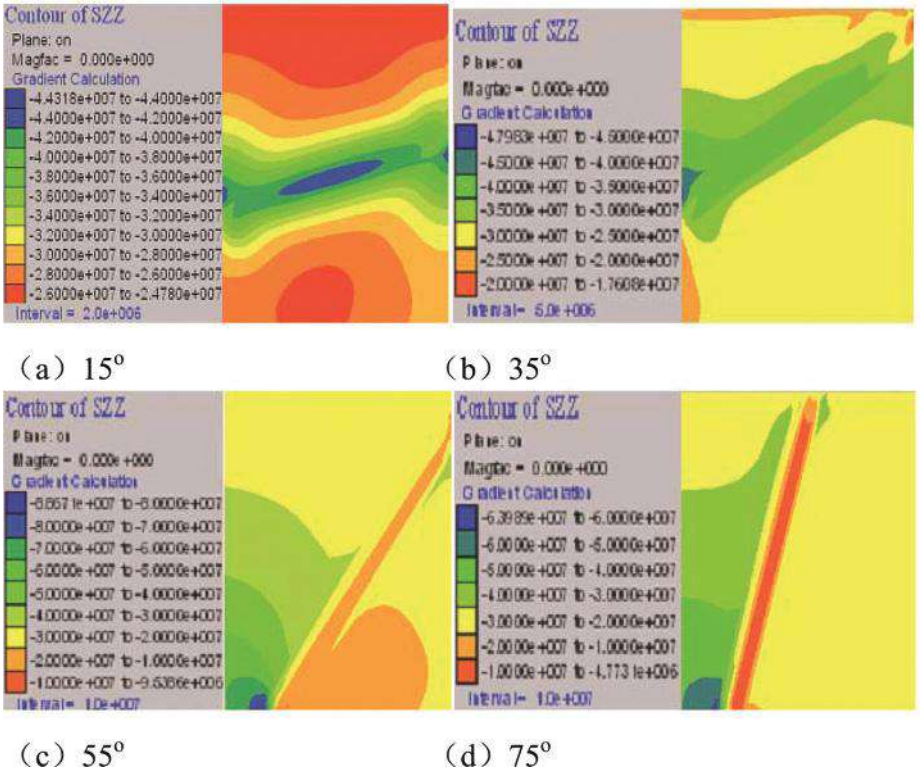


Figure 2. Distribution characteristics of abutment pressure along coal seam dip.

By following the coal seam dip and when the coal seam dip angle reaches the upper limit of 55° of the large dip angle, the abutment pressure shall all almost be distributed in the middle and lower part to the coal seam dip direction.

Too much accumulated elastic energy of the coal body within the abutment pressure peak value area along with the uneasy flow of gas become the main power source of coal and gas outburst.

The accumulated elastic energy is of the least when the coal seam dip angle reaching the large dip angle of 55°, the accumulated elastic energy on the upper part shall be less than that of in the middle and lower part of the working face, and all of these are conducive to gas release, thus the possibility of the occurrence of the dynamic disasters of coal and gas outburst is reduced accordingly.

REFERENCES

Meng, X.R. et al. 2007. Field Research to Mining Pressure Appearance of Coal Seam Fully mechanized Stope with Large Dip Angle and Certain Thousand Meters of Deep Well. Coal *Science and Technology*, 35(11):14–21.

Qian, M.G. & Shi, P.W. 2003. *Mine Pressure and Rock Strata.Control*, Xu Zhou: Press of China University of Mining and Technology.

Wang, Y.G. et al. 2010. Mechanism Analysis and Control of Dynamic Disasters of Coal Lithosome. *Mining Safety and Environmental Protection*, 37(2):17–19.

Wang Z. et al. 2011. Distribution Characteristics of Mining Stress Field and Control Function of Dynamic Disasters of Coal Lithosome Gas. *Journal of Coal*, 436(4):623–627.

Xie G.X. et al. 2006. Abutment Pressure Distribution of Fully mechanized Stope Enclosing Rock and Stratum Thickness Effect of Dynamic Disasters. *Journal of Coal*, 31(6):731–735.

Progress in Mine Safety Science and Engineering II – He et al. (Eds)
© 2014 Taylor & Francis Group, London, ISBN 978-1-138-00122-0

Mechanical mechanism analysis of forming grouting seepage channel in clay sand medium

Haoyu Shi & Duo Tian
North China Institute of Science and Technology, Beijing, China

ABSTRACT: In order to research the forming mechanism of grouting seepage channel in the clay sand medium, designed the grouting experiment system; And knowing the chemical grouting seepage in the clay sand medium mainly have two main forms that cylindricality seepage and surface shape seepage by the experimental result; On the basis of Griffith criterion, deduced the minimum grouting pressure P_{min} that forming the chemical grouting seepage channel, analysis the pressure loss of the chemical grouting seepage in the medium on the basis of percolation mechanics, obtained grouting pressure P_1 that in the different positions of the seepage channel; when $p_1 > p_{min}$, chemical grout will split the medium that forming new seepage channel; when $p_1 < p_{min}$, chemical grout will stop split, the channel is closed.

1 INTRODUCTION

Sand inrush or water sand is a kind of properties and casualties mine geology hazard when excavating nearly at unconsolidated layers sand content of high water sand mixed fluid in the mining face (Sui, et al. 2008). Since 1987, Yanzhou, Jining and Xuhuai areas and so on, more than 100 shafts suffered serious rupture deformation and water bursting tu sand disasters, causing billions of great economic losses, and forming a major security hidden danger (Guo 2010, Su, et al. 2010). Grouting Water-tight and bottom strengthening technology are effective means to control formation broken shaft lining and sand inrush disasters.

Grouting technology in theory and in the actual application has made great progress, but there are still a lot of problems to research and solve. Current, people in face of the structure research of slurry flowing and penetration in the pore diffusion are simplified the grout, and this made in the process are far of grouting theoretical calculation and practical (Zhang, et al. 2005, Feng 2007).

2 PROJECT OVERVIEW

Pingshuo Coal Industry Company No. 1 Coal Mine was founded in 2003, now major mining district is TaiXi 4# seam. Now 4106\4107\4108 production face are all arranged in the TaiXi district. Because of the collapse columns X_7 existed in front of the 4107 working face as well as the collapse columns X_5 existed in front of the 4108 working face. The 4107\4108 working face mining were all affected by the collapse columns to some degree, also it will disrupt production layout as well as increase the the entry excavation amount of coal loss reserves, which lead the face prone to roof fall collapse of sand into a bracket the backplane or even water inrush accident.

In order to through the collapse columns safely and efficiently, We intends to reinforce the roof and floor of the working face by grouting, the experimental study of the sediment medium for filling grouting penetrating through channels formed mechanical mechanism.

3 GROUTING EXPERIMENTAL ANALYSIS

3.1 *Grouting experiment design*

In order to simulate an actual mine geological environment, the design should have a certain strength, it could be able to withstand the great pressure of iron barrel which is act as grouting container. We named the reserved grouting port cap of 5 cm diameter, a diameter of 50 cm, height 50 cm container, the bottom of the active type, the center, Integrated as the "ST-50 type grouting test rig" shown in Fig. 1.

The movement of the slurry and the water in the pores during the grouting process, is the results of the slurry and water (two fluid) which are reflected under the force of the inertial force and pressure as well as the viscous force, gravity and other consolidated. Direct impact on the flow of force is the inertia force, the inertial force and the active force interaction mutual constraints

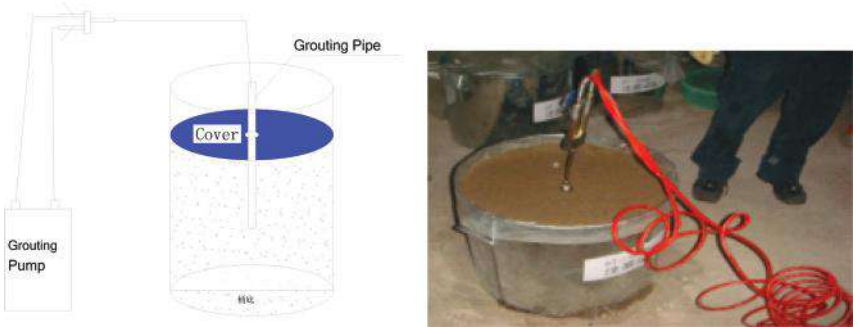


Figure 1. ST-50-type grouting test bench.

lead to the flow changing, This condition applies to the Renault criteria, That means the inertial force and the viscous force is proportional to flow requirements both on models and prototypes, Reynolds number equal, indicating the similarity of the viscous force. Where the flow similar to the flow, It must be geometrically similar, movement similar flow and power. Geometric similarity is the premise and basis of movement similar power. To determine the geometric similarity constant a_L = 10. According to variable head water penetration test result, an underground mine in situ rock mass permeability coefficient is 0.98E-5 cm/s ~ 2.78E-5 cm/s, an average of 1.88 E-5 cm/s, permeability similar constant as 1. Injected medium in accordance with the particle composition of the experimental results, the choice of using loess, sand, gravel, water, etc. are mixed with a certain proportion (Shimada H., et al. 2003), as shown in Table 1.

Table 1. Particle composition.

Granule	Gravel		Sand			Powder
Particle size/mm	20–60	2–20	0.5–2	0.075–0.5	0.05–0.075	0.005–0.05
Percentage/%	18.89	14.37	9.24	24.18	4.45	28.88

2.2 *Groutng experimental results analysis*

Fig. 2 is cutaway model after grouting, seen from Fig. 2 sediment medium, the penetration of the slurry mainly include the formation of the seepage channel while the channel surrounding the pore penetration. The process of Slurry infiltration is actually a process of looking for a seepage channel, the slurry is constantly looking for or manufacture a seepage channel at first and then from the channel or path continued penetration into the surrounding sand, when a channel can't penetrated, By increasing injection pressure, we will find or create another channel.

There are mainly two types of Slurry seepage paths named cylindrical and surface-shaped, during the slurry diffusion process, cylindrical diffusion refers to slurry along the approximate space of the cylinder movement. The planar diffusion "model of the slurry, is refers to the slurry along the approximate plane of the spatial movement

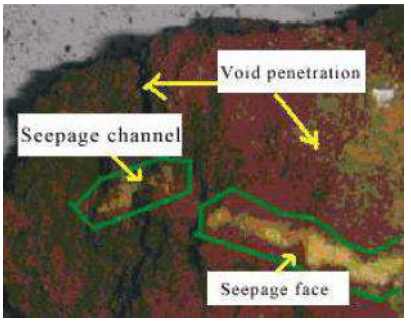


Figure 2. Slurry seepage experimental analysis.

(Feng 2007). This article is only for in-depth study of the formation mechanism of the cylindrical seepage channel.

3 CHANNEL FORMATION MECHANISM ANALYSIS

There are many internal cracks existed in the brittle material, Under the external force, the tip of the micro-cracks generated in the vicinity to a large stress concentration, when the aggregation energy reaches a certain value, crack will start to expand, Griffith strength theory considering only rock cracking non-macroeconomic destruction. Collapse columns are brittle media with sand media-based fillings, according to the process of test restraint grouting is a constantly looking for

or manufacturing channels, when the formation of the seepage channel is the sand media splitting failure process, so the process application conditions meet the Griffith theory, according to Griffith strength theory for judgment:

$$\begin{cases} \dfrac{(\sigma_1-\sigma_3)^2}{\sigma_1+\sigma_3}=8\sigma_1, \sigma_1+3\sigma_3\geq 0 \\ \sigma_3=-\sigma_1, +\sigma_1+3\sigma_3<0 \end{cases} \tag{1}$$

When grouting pressure exist in the seepage channel, the role of stress in micro cracks shown in Fig 3, the slurry pressure at the end face of the channel into the formula (1) can be obtained:

$$\begin{cases} \dfrac{(\sigma_1-\sigma_3)^2}{\sigma_1+\sigma_3-2\mathrm{P}}=8\sigma_1, \\ \qquad when\ \ \sigma_1+\sigma_3-2\mathrm{P}\geq 0 \\ \sigma_3-\mathrm{P}=-\sigma_t, \\ \qquad when\ \ \sigma_1+\sigma_3-2\mathrm{P}<0 \end{cases} \tag{2}$$

Where: σ_1—grouting position Note maximum principal stress, MPa; σ_3—the grouting position at Note body minimum principal stress, MPa; σ_t—grouting position Note body tensile strength, MPa; P—slurry at the end face of stress. By formula (2) can be obtained:

$$\begin{cases} p_{\min}=\dfrac{(\sigma_1-\sigma_3)^2+8\sigma_t(\sigma_1+\sigma_3)}{16\sigma_t}, \\ \qquad when\ \ \sigma_1+\sigma_3-2\mathrm{P}\geq 0 \\ p_{\min}=\sigma_3-\sigma_t, \\ \qquad when\ \ \sigma_1+\sigma_3-2\mathrm{P}<0 \end{cases} \tag{3}$$

Formula (3) is the basic conditions that the slurry of the body to be injection forming a seepage splitting channel, since grouting fluid viscosity, the slurry within the seepage channel stress gradient exists, when the slurry pressure P does not comply with the above formula conditions, the seepage channel is closed, the slurry began to find or create new seepage paths. The slurry seepage distance is the maximum percolation radius.

4 CHANNEL SLURRY STRESS LOSS

According to the fluid dynamics, we can see that horizontally straight tube fluid for steady laminar flow (Zhai 2009). The tiny cylindrical fluid removed from an axis coincident with the tube axis, analysis the force in the horizontal direction (x direction) is shown in Fig. 4.

Actually, grouting pressure generally is greater than 3 MPa, much larger than Grouting liquid weight, so ignored gravity, the friction of the

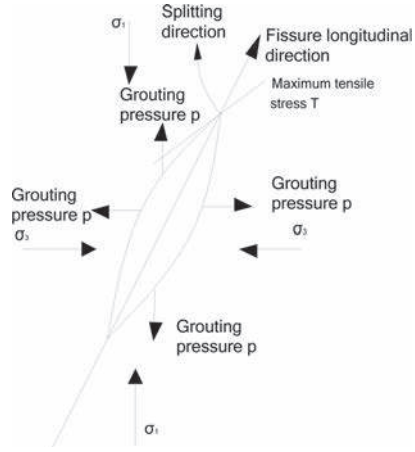


Figure 3. Grouting splitting form a seepage channel computing model diagram.

pressure difference and the cylinder surface at both ends on the side surface stickiness equal (Xie & Su 2004, Wang, et al. 2004), then:

$$(p_1-p_2)\pi r^2=-2\pi rl\mu\frac{dv}{dr} \tag{4}$$

The slurry flow rate is:

$$v=\frac{(p_1-p_2)(R^2-r^2)}{4\mu l} \tag{5}$$

Where: v—the slurry over the flow rate of the interrupter surface, p_1—the pressure of the slurry starting sections, p_2—the pressure of the slurry starting sectional, R—flow into the radius of the circular tube surface, r—remove the minor radius of the cylindrical fluid, μ—the viscosity of the slurry, l—the slurry flow through the length. It can be obtained by the equation (5) flow is:

$$q=\int_A vdA=\int_A^R\frac{(p_1-p_2)(R^2-r^2)2\pi rdr}{4\mu l} =\frac{\pi R^4(p_1-p_2)}{8\mu l} \tag{6}$$

$$p_1-p_2=pl=\frac{128\mu lq}{\pi d^4} \tag{7}$$

The above formula reflects the relationship between the flow Δp, pressure differential q, and the tube diameter d. The slurry flow with seepage channel diameter larger increases with increasing hydrostatic pressure the difference of the injection pressure and medium increases with the viscosity of the slurry decreases.

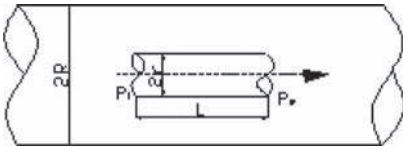


Figure 4. Slurry mechanical analysis diagram in cylindrical channel.

The cylindrical the seepage channel pressure pressure loss (Yu 2009) is:

$$\Delta p_l = \lambda \frac{l}{d} \frac{\rho v^2}{2} \tag{8}$$

$\lambda = f(\mathrm{Re}, \Delta/d)$ is Coefficient of resistance along the way, laminar flow $\lambda = 64/\mathrm{Re}$, Δ/d for wall relative roughness, Re is Reynolds number, into the simultaneous availability of equation (7) and (8), we can see:

$$\Delta p_1 = \frac{128 \mu l q}{\pi d^4} = \frac{64}{\mathrm{Re}} \frac{l}{d} \frac{\rho v^2}{2} \tag{9}$$

From the formula (9) can be seen, when the injection pressure is p_e, the pressure of the slurry is:

$$p_1 = p_e - \Delta p = p_e - \frac{64}{\mathrm{Re}} \frac{l}{d} \frac{\rho v^2}{2} \tag{10}$$

By the formula (10) can be seen, with the growth of the slurry seepage path, the flow velocity is increased, the slurry reduced in seepage channel pressure grouting, the seepage channel aperture increases, the Reynolds number, is conducive to the slurry seepage expansion (Tian, et al. 2012).

5 CONCLUSION

1. According to the occurrence characteristics of the collapse columns, grouting experimental program is designed by the experiment that the slurry of sediment medium the percolation mechanism slurry grouting pressure fracturing in the medium to form a seepage channel.
2. This article is based on Griffith criterion, considering the slurry pressure, the conditions for the formation of the slurry seepage channel is derived, which is primarily related to the earth stress, medium tensile strength as well as grouting pressure.
3. When $p_1 > p_{\min}$ (seepage channel is formed to the minimum required injection pressure), the slurry will continue to be in a cleavage is injection medium to form a new seepage channel; when $p_1 < p_{\min}$ slurry will stop splitting be injection medium.
4. Through the analysis of the pressure loss of the slurry in the medium that: With the growth of the slurry seepage path, the flow velocity is increased, the slurry is reduced pressure grouting of the seepage channel, while the pore diameter of the seepage channels increases, the Reynolds number, conducive to the serous seepage expansion.

ABOUT THE AUTHOR

HaoYu-Shi (1979-), male, Inner-Mongolia Wulanchabu, lecturer, Master, research direction are roadway support and grouting technology. E-mail: shihaoyu2000@163.com National Natural Science Foundation-funded project "based on the nonlinear theory of coal mine deep well prepared to the roadway deformation mechanism study", Grant No.: 51044009; North China Institute of Science and Technology Foundation of grouting technology in geological formations with the reinforcement mechanism and applied research, "Grant No.: JWC2013B.

REFERENCES

Feng Zhiqiang 2007. Material development and research of osmosis and diffusion on chemical grouting for extraordinary cracked coal and rockmass. *China Coal Research Institute.*

Guo Miwen 2010. Experimental Investigation of Propagation Mecha-nism of Chemical Grout Injection into Porous Mediaunder a High Pressure and Closed Environment. *China University of Mining & Technology.*

Shimada H., et al. 2003. The Application of Flyash Cement in Mining Backfill Material. *Australasian Institute of Mining and Metallurgy Publication Series.*

Su Bao-yu, et al. 2010. Study of permeability in single fracture under effects of coupled fluid flow and chemical dissolution. *Rock and Soil Mechanics.*

Sui Wanghua, et al. 2008. Mining inrush of sand mechanism and prevention. Beijing: *Geological Publishing House.*

Tian Duo, et al. 2012. Study on Chemical Grout Permeation Mechanism Based on Experiment of Mud and Sand Medium. *Progress in Renewable and Sustainable Energy.*

Wang Haiming, et al. 2004. Constitutive Relations of Unsaturated Seepage Flow in Fractured Rock Masses. *Chinese Journal of Rock Mechanics and Engineering.*

Xie Xinghua & Su Baoyu 2004. A review of fracture rock hydraulic fracturing research. *Rock and Soil Mechanics.*

Yu Huaqian 2009. Fluid Mechanics Short Course. *Tianjin University Press.*

Zhai Yunfang 2009. Seepage Mechanics. *Petroleum Industry Press.*

Zhang Wenjie, et al. 2005. Research progress of experimental study on seepage characteristic of fractured rock masses. *Rock and Soil Mechanics.*

Progress in Mine Safety Science and Engineering II – He et al. (Eds)
© 2014 Taylor & Francis Group, London, ISBN 978-1-138-00122-0

Mechanism study on gas diffusion through coal particles base on mass transmission fundamental

Zhiliang Wang
Key Laboratory of Mine Disaster Prevention and Control of Hebei province, Yanjiao, Beijing-East, China
Safety Engineering College, North China Institute of Science and Technology, Yanjiao, Beijing-East, China

ABSTRACT: With the increase of mine exploitation depth and appliance widely of large-scale full-mechanized equipment, coal block gas emission has been one of the most gas effusion source. Base on unsteady diffusion theory and mass transmission fundamental, the mathematical and physical model of gas diffusion through coal particles with third type boundary condition was founded and its analytical solution was obtained by separate variableness method. The characteristics of gas through coal particles was analyzed according as mass transmission theory of porous material. The results show that the Biot's criterion of mass transmission can reflect the resistance characteristic of gas diffusion and the Fourier's criterion of mass transmission can represent the dynamic feature of diffusion field varying with time.

1 INTRODUCTION

Mine gas is the primary factor which restricts high yield, efficiency and safety condition in coal mine and the gas emission from shearing fall coal particles is one of the most sources. The process of gas transfer in coal bed can be divided into three stages: the first phase is gas molecules desorption from the inner surface of coal matrix, changing the state from adsorption to dissociation; the second phase is gas molecules entering into external cranny system through millipores, namely it effuses from coaly small soluble cases to coal-bed cranny system (coal-bed diaclases, cleat system) under the influence of concentration gradient, so the process is a diffusion coutse; The third phase is the gas transferring within coal-bed diaclases and cleat system under the pressure gradient, so it is a penetration process. These three phases are combined and interacted mutually, thereinto the gaseous migration speed depends on the slowest one. Abundant research results show that gas migration accord with seepage regulation in biggish pores system and diffuse law in lesser pore system respectively. In the past, the research for coal particles gaseous spread was based on the first type boundary condition, ignoring the gaseous mass transfer from coal particles boundary to cranny. In this paper, taking into account the gaseous mass transfer from coal particles boundary to cranny, the mathematical and physical model of gas diffusion through coal particles with third type boundary condition was founded and its analytical solution was obtained by separate variableness method. The research conclusion will provide theory basis for gas prevention and control in working field, furthermore prefect more theory system on coal particle gas diffusion.

2 MATHEMSATICAL MODEL ON COAL PARTICLE GAS DIFFUSION

The testing study in laboratory on coal particle gas diffusion indicates, when coal particle measurement is less than ultimate granularity, gas migration accord with diffusion law, then coal particle is made up of pore structure basically. the ultimate granularity varies alone with coal quality which is generally from 0.5 to 10 mm. When coal particle is more than ultimate granularity, it can be regarded as a aggregation consisting of ultimate granularity, then its speed of gas diffusion holds the line. Thereout, the shearing fall coal particles can be regarded as a aggregation which is made up of epigranular and nearly spherical coal particles containing mass micropore.

Coal particle intramural gas migration accords with nonsteady diffusion law in spherical coordinate frame. In the original condition, coal particle gas adsorption has been a balanced state. when external stress changing, gas will transform from adsorbed state to unbound state, and adsorbent gas will diffuse from coal particle core to surface following both mass conservation and continuity principle. In the coal particle core, adsorbent gas concentration abides by Langmuir law; In the coal particle surface, the mass transfer between adsorbent gas and dissociate gas abide

by convection quality commutative law. thus the mathematical model is as below that is made up of global unsteady-state diffusion mathematical equation, starting conditions and boundary conditions.

$$\begin{cases} \dfrac{\partial C}{\partial t} = D\left(\dfrac{\partial^2 C}{\partial r^2} + \dfrac{2}{r}\dfrac{\partial C}{\partial r}\right) \\ C = C_0,\ 0 < r < r_0,\ t = 0 \\ \dfrac{\partial C}{\partial r} = 0,\ t > 0,\ r = 0 \\ -D\dfrac{\partial C}{\partial r} = \alpha(C - C_p),\ t > 0,\ r = r_0 \end{cases} \tag{1}$$

Wherein: C is coal particle gas absorbing concentration where diffusion radius is r, kg/m^3; C_0 is coal particle gas absorbing concentration with equilibrium state, kg/m^3; C_p is the dissociate gas concentration within coal particle cranny, kg/m^3; D is the diffusion coefficient of adsorbing gas, m^2/s; α is mass exchange coefficient at coal particle surface between adsorb gas to dissociate gas, m/s; r_0 is the radius of coal particle, m.

3 ANALYTIC SOLUTIONS OF COAL PARTICLE GAS DIFFUSING MATHEMATICAL EQUATION

3.1 *Variables separation differential equation*

To solve diffusion equation, that is set up and dragged into formula (1), then the coal particle gas diffusion mathematical model can be turned as follows:

$$\begin{cases} \dfrac{\partial U}{\partial t} = D\dfrac{\partial^2 U}{\partial r^2} \\ U = (C_0 - C_p)r,\ 0 < r < r_0,\ t = 0 \\ U = 0,\ t > 0,\ r = 0 \\ -D\dfrac{\partial U}{\partial r} = (\alpha - \dfrac{D}{r})U,\ t > 0,\ r = r_0 \end{cases} \tag{2}$$

Because of formula (2) is second-degree parabola mathematical equation, so we can use separation of variables to solve it [9]. We suppose the diffusion equation have variable separate format nonzero special solution, setting:

$$U(r,t) = R(r)T(t) \tag{3}$$

dragging formula (3) into the first one item of formula (2), then we get out:

$$\frac{T'(t)}{DT(t)} = \frac{R''(R)}{R(r)} \tag{4}$$

The left nearside of formula (4) is simply a function for t and right nearside is r. Because t and r are two unattached variable, only when both sides are the same constant, the equation can be established. We set the constant is $-\lambda$, then two differential equations be educed as below

$$T'(t) + \lambda DT(t) = 0 \tag{5}$$

$$R''(r) + \lambda R(r) = 0 \tag{6}$$

dragging formula (3) into the third and the fourth item of formula (2), then the boundary conditions can be get out which suit for ordinary differential equation:

$$R(0) = 0 \tag{7}$$

$$-D\frac{\partial R}{\partial r}\Big|_{r=r_0} = (\alpha - \frac{D}{r_0})R(r_0) \tag{8}$$

3.2 *The solution of differential equation*

Firstly we solve the equation (6) to get its eigenfunction, then we discuss it separately according to the span of λ:

1. When $\lambda < 0$, $R(r)$ does not have a untrivial solution.
2. When $\lambda = 0$, the general also dose not have a untrivial solution.
3. When $\lambda > 0$, we can get the gas density in coal particle anywhere at any time.

3.3 *Analysis on coal particle gas diffusing capacity*

1. Coal particle gas cumulation diffusing capacity at any time can be get out.
2. Coal particle gas terminal diffusing capacity can be get out.
3. The percent of coal particle gas cumulation diffusing capacity at any time to terminal diffusing capacity is deduced.

4 COAL PARTICLE GAS DIFFUSION PROPERTY

4.1 *The criterion of mass transmission*

The smaller of B_i value, the less diffusion resistance and the more powerful diffusivity of coal particle is, which means gas density is basically coherent in the coal particle inside; When $B_i \to 0$, it means that gas diffusion carry out instantly in coal particle interior. Then the mass transmission rate mainly depends on coal particle exterior mass transmission resistance. The more greater of B_i value, the lower

convection mass transmission resistance is, which means gas density is basically coherent on the coal particle exterior; When $B_i \to \infty$, coal particle gas diffusion accords with the first type boundary condition, namely exterior mass transmission resistance is tiny quiet so as to be ignored, then coal particle exterior gas density is equal to dissociated gas density, so gas diffusion rate mainly depends on coal particle internal resistance. When $0 < B_i < \infty$, both coal particle internal and outside mass transmission resistance can not be ignored that are determinant factors for mass transmission rate of coal particle.

4.2 *The Fourier's criterion of mass transmission*

The density distribution of coal particle gas diffusion is indicated. It can be made out from formula (28), the physical significance of F_0 is the ratio of gas diffusion field affecting depth $t \cdot \frac{D}{n_0}$ and coal particle measurement r_0. The bigger of F_0 value, the deeper of affecting depth is for coal particle diffusion field, diffusion time is longer, coefficient of diffusion is bigger with same size coal particle. The smaller of F_0 value, the shallower of affecting depth is.

5 CONCLUSIONS

1. Coal particle gas diffusion mathematical model was set up basing on the third boundary condition and taking into account gas mass transmission characteristics on borderline. The applying scope includes gas diffusion model under the first boundary condition, thus it is not only more scientific and reasonable, but also is provided with application more widely.
2. The analytical solution of coal particle gas diffusion mathematical model was obtained by separate variableness method. The result indicate that we can get out coal particle gas concentration, gas cumulation diffusing capacity at any time and terminal diffusing capacity when $t \to \infty$. So, more research on shearing fall coal particles of working face can be carried out thoroughly and the research conclusion will provide theory basis for gas prevention and control.
3. The Biot's criterion of mass transmission can reflect the resistance characteristic of gas diffusion field, that is the relative size between coal particle internal resistance and exterior convection mass transmission resistance, which is showed as attenuation coefficient on exterior the Fourier's criterion of mass transmission can represent the dynamic feature of gas diffusion field, that is the depth and scope of coal particle gas diffusion field varying with time, which is showed as gas initialization diffusion intensity of shearing fall coal particles on exterior.

REFERENCES

Ding LJ, Chen QY. Numerical Value solution methods. Beijing: Beijing Institute of Technology Press, 2005. (in Chinese).

Hu DM, Lin BQ. Occurrence Regularity and Control Technology of Coalbed Gas. Xuzhou: China University of Mining and Technology Press, 2006. (in Chinese).

Liang B, Sun KM. Theory and Application on Low Permeability Coalbed Methane Exploitation. Beijing: Science Press, 2006. (in Chinese).

Liu W, Fan AW, Huang XM. Heat and Mass Transfer Theory and Application on Porous medium. Beijing: Science Press, 2006. (in Chinese).

Su XB. Pore Characteristic of Coalbed Methane Reservoir. *Journal of Jiaozuo Institute of Technology,* 1998, 17(1):6–11. (in Chinese).

Yang QL, Wang YN. Gas Diffusion Theory and Its Application of Coal Dust. *Journal of China Coal Society,* 1986, 11(3):87–93. (in Chinese).

Yang QL. Experimental Study on Coal Dust Gas Diffusion Law. *Safety in Coal Mines,* 1987, 18(3):9–16. (in Chinese).

Zhang L, Tian JS. Study on Coalbed Methane Desorption Characteristics of Coal Seam 3# in Yangquan Mining Area. *Coal Geology & Exploration,* 2002, 30(1):25–27. (in Chinese).

Zhang LH. The Basic Principle of Numerical Simulation on Oil and Gas Reservoir. Beijing: Petroleum Industry Press, 2005. (in Chinese).

Zhou SN, Lin BQ. Theory of Gas Flow and Storage in Coal Seam. Beijing: China Coal Industry Publishing House, 1999. (in Chinese).

This page intentionally left blank

Progress in Mine Safety Science and Engineering II – He et al. (Eds)
© 2014 Taylor & Francis Group, London, ISBN 978-1-138-00122-0

Cooling parameters fitting analysis in long distance excavation roadway

Zhaoxiang Chu, Xijun Zhang, Jianhu Ji & Yang Zhang
National Key Laboratory of Gas Disaster Detecting, Preventing and Emergency Controlling, Chongqing, China
Chongqing Research Institute of China Coal Technology and Engineering Group, Corporation, Chongqing, China

Wang Baoqi
Zhaolou Coal Mine, Heze Energy and Chemical Co., Ltd., Yanzhou Mining Group, Heze, Shandong, China

ABSTRACT: In order to get the cooling parameters changing law in long distance excavation roadway, some measure points' airflow temperatures were obtained through field investigation when the mine cooling system operated in a long distance excavation roadway where high temperature phenomenon exit. And the quantitative relationships between some parameters were fitted correctly. The results show that the dry-bulb & wet-bulb temperature of the heading face after cooling have a linear relationship to the dry-bulb & wet bulb temperature at exit of the air duct. Besides, the dry-bulb temperature of the heading face after cooling has a second parabolic relationship to the dry-bulb temperature at certain scope in the air duct behind the air cooler. In addition, the wet bulb temperature difference near the heading face was high and could be 5~7 °C in maximum. There was a high moisture exchange occurred in air flow retuning process and thus a retuning hot phenomenon would be occurred and enlarged.

1 INTRODUCTION

In recent years, with the exhaustion of coal resources in shallow mining area, in order to ensure the supply of coal resources, more and more coal mines in east China had reached deep mining. In the deep mining, in addition to some accidental coal and gas outburst, rock burst, water burst and some other disasters in some local areas, the high temperature and heat disaster is the most common puzzling problem (Man-chao He et al., 2010). The thermal and humidity working environments of mine that would affect human health, reduce labor productivity and endanger production safety are collectively called colliery thermal hazard (disaster) by National Standard of China GB 50418–2007 (China National Coal Construction Association, 2007). In order to improve working environment, it becomes necessary to adopt the mechanical refrigeration system in mine (He Manchao, 2009, He Guo-jia et al., 2011, Webber, R.C.W, 2006). However, it is a complex work to prevent the heat damage. In theory, the heat and humidity exchange calculations of the thermal parameters of the underground air flow is necessary, but theoretical calculation often do not go with the real situation because the condition in underground is complex. So it needs to analyse the data from the actual application, ask for the pragmatic data and look for the laws to make up the shortage of theoretical calculation (Yang Shengqiang, 1997, I.S. Lowndes et al., 2006). Taking the long distance excavation roadway of Zhaolou coal mine as example, this article gets some quantitative relationship between cooling parameters, and the analytical conclusion could be used to apply cooling system into normal operation on heading face.

2 MINE HEAT DISASTER PREVENTION

2.1 *General situation of mine*

Zhaolou coal mine locates in the middle part of Juye Coalfield in Shandong province of China. Its designed annual production is over 3 million tons and the length of service is 60 years. Mine coal-bearing strata are Shanxi Group and Taiyuan Formation. The primary mineable coal bed is the 3rd strata, and 700–1200 m in buried depth. The average thickness of coal seam is 6.19 m, with the 2~18° coal seam dip angle. The mine adopts the single level development way and the mechanized top coal caving mining technology.

2.2 *Mine heat disaster prevention technology*

Juye Coalfield's constant temperature zone has a 50–55 m depth, 18.2 °C temperature, and 2.2 °C/100 m average geothermal gradient. The first mining shaft is 900 m deep. The original (coal) rock temperature of most mining areas is 40~45 °C,

and it belongs to the second grade hot temperature zone. According to the theory of airflow temperature forecast, the airflow's dry-bulb temperature in summer of the heading face can reach 33~35 °C. It is far beyond the regulations of "coal mine safety regulation" (China). The phenomenon of the heat damage is so serious that it needs to adopt the mechanical refrigeration cooling measures to lower the extracting coal face's temperature.

In order to thoroughly resolve the problem of heat disaster, Zhaolou coal mine put the underground centralized mechanical chilled water cooling system into use as the whole mine's refrigeration cooling system. And the KM3000 underground centralized cold water cooling system from Germany's WAT Company is the first system in China, and also the first refrigeration unit which has the largest refrigerating capacity single (Chu Zhaoxiang, 2009).

3 COOLING MODE IN HEADING FACE

Currently, heading faces which have adopted cooling measures are mainly supplied cold air by local fan and air duct. Normally speaking, alone excavating head in tunneling also need independent ventilation system, it is to say there will be no influence on the normal ventilation system and equipment. So cooling modes in heading faces are relatively simple and be used to identify the mounting position of the end of the air cooling equipment.

The mounting positions of the end of air cooling equipment are as follows (Gao Xuekui, 2008):

1. Air coolers are installed at the end of the local fans. This way will not alter the air supply amount of the faces but guarantees the demand of the head. Temperature in the roadway will be dramatically reduced for it is very low in fan drum. But if the distance of the roadway is too long, it will have a very large energy loss in the middle of the excavation roadway, and the energy of cooling for the head could not be enough.
2. Air coolers are installed in the middle of the air supply fan drums. The advantage is they can reduce the temperature in the middle of the long distance excavation roadway, while the disadvantage is the resistance inside will be very high. Besides, this way could not ensure the air supplying of the heading face.
3. Air coolers are installed at the end of the fan drums and pushed forward with the working face's development. This method can overcome the shortage that the temperature in the head is low, but comes that heat could not be easily eliminated as the roadway are too long. However, even cooling measures are adopted to reduce the temperature in the head; most of the air current in the roadway areas is still keeping at a high temperature.

Zhaolou coal mine adopts the first method to cool the work faces' air flow temperature of the long distance excavation roadway.

4 TESTING AND ANALYSIS ON COOLING PARAMETERS OF THE EXCAVATION ROADWAY

When the mine cooling system running, the cold air from the air coolers is delivered to the heading faces by the air duct, and comes to the temperature's decrease of the air current. Because of the long ventilation distance and the high temperature difference between the air duct and the environment, the temperature inside the air duct will be also rising. The temperature rising degree depends on the surface area of the air duct, convective heat transfer coefficient between air flow and surface area of air duct, air volume, air flow temperature, degree of the air inside the air duct, temperature of the air in the roadway and other parameters. Here, the 1302 tail entry in excavation roadway of Zhaolou coal mine in summer 2008 was a study subject. Layout in which thermal parameters' measure points were set can be clearly seen in Figure 1. The equipment used during field investigation is aspiration psychrometer, as shown in Figure 2.

4.1 *Temperature relationship between the outlet of air duct and tunneling face*

The dry and wet bulb temperature on measure point 2 which is the outlet of the air duct and point 3 which is the air return side of the air flow on the working face were measured. According to the dating results, the regression analysis relationships were got as Figure 3 and Figure 4.

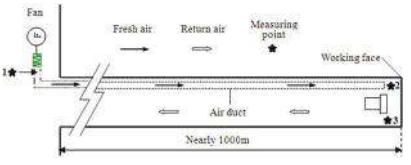


Figure 1. Layout of measuring points in excavation roadway.



Figure 2. Aspiration psychrometer used during investigation.

Figure 3 reveals the relationship of dry-bulb temperature between air duct outlet and working face. After a long distance transportation, the rise of dry-bulb temperature of air in the duct is larger. The cold air's dry-bulb temperature has no large change or even partly decreases in the tunneling face. It is because it makes a heat and moisture exchange with the new excavation rock, but the time is very short. The reason for that is mainly concern to the air flow's relative humidity. The relationship of dry-bulb temperature between air duct outlet and working face is as follow:

$$T_{YG} = 0.6T_{FG} + 10.9 \quad (1)$$

In Equation (1), T_{YG} is the dry-bulb temperature in working face, °C; while T_{FG} is the dry-bulb temperature at the exit of air duct, °C. Formula 1 shows that the two parameters are approximately having linear relationship. At some extend, the dry-bulb temperature of the working face is rising with that of the air duct outlet (about 27~30 °C). Analysis result demonstrates that as long as we can control the dry-bulb temperature of the air duct outlet under 30 °C, the environment of the working face can be maintained within acceptable limits.

Figure 4 reveals the relationship of wet-bulb temperature between air duct outlet and working face. The relationship among them is as follow:

$$T_{YS} = T_{FS} + 2 \quad (2)$$

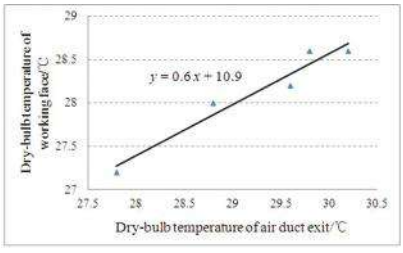


Figure 3. Relationship of dry-bulb temperature between air duct outlet and working face.

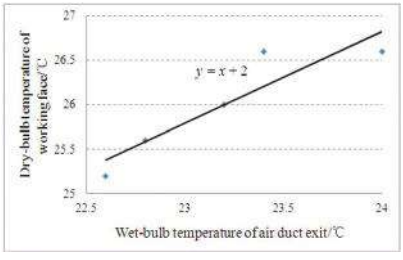


Figure 4. Relationship of wet-bulb temperature between air duct outlet and working face.

In Equation (2), T_{YS} is the wet-bulb temperature in working face, °C; while T_{FS} is the wet-bulb temperature at the exit of air duct, °C. The fitting relationship shows that wet-bulb temperature at working face is higher than that of the air duct outlet, and the difference is about 2 °C. Air flow at working face has an obvious moisture adsorption process, as a result, the relative humidity increases. Employees can stay in a comfortable environment because the relative humidity is still very low. Both the dry and wet-bulbs temperature will increase during the process during which the air flow is returned, thus it is very easy to create an enlarged retuning hot phenomenon.

4.2 *Temperature relationship between behind air cooler and tunneling face*

The temperature of air flow in the air duct lies on the cold contained medium, iced water, after it goes along with the air cooler. And the temperature of air flow after air cooler stands for the variation of the cold contained medium. And then reflect the system's variation of running status. So we fixed up 2 measure points both in the air duct after air cooler and working face (as point 1 and point 3 in Figure 1) to get the dry-bulb temperature. Fig. 5 and Equation (3) show the relationship among them as follow:

$$T_{YG} = 0.2T_K^2 + 5.7T_K + 77.5 \quad (3)$$

In Equation (4), T_{YG} is the dry-bulb temperature in working face, °C; while T_K is the dry-bulb temperature in air duct after air cooler, °C. The fitting result declares that at some extent, the two parameters have a second parabolic relationship. Taking 28.5 °C as a standard, a line can be drawn to intersect the quadratic parabola at two points. The admission fluctuation interval for the air flow after the air cooler is 15.5~19 °C. Otherwise, the cooling system may be abnormal, and will have huge influence to the cooling effect of the working face.

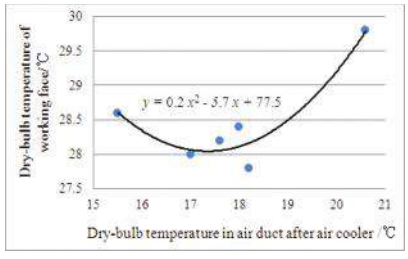


Figure 5. Layout of measuring points in excavation roadway.

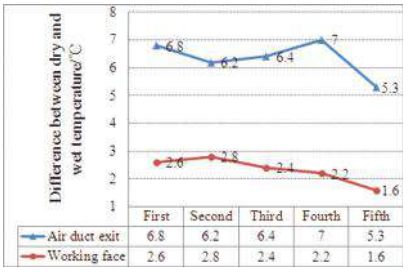


Figure 6. The depression of wet-bulb temperature between air duct outlet and working face.

4.3 *Dry and wet temperature difference analysis in tunneling face*

Mine high temperature excavation roadway uses the air duct to transport cold air. The humidity in the air flow does not increase during the transportation. But at the same time cold air has a big temperature rise. The air duct has the function to avoid humidity and it makes the air flow's temperature rising up but maintains its humidity. As a result, relative humidity of the air flow at exit down to 50~60%, it is relatively low. But the dry-bulbs temperature difference is obvious, about 5~7 °C, as Figure 6. Near the tunneling face, because of the effect of mine water burst and dust suppression by spraying, the air flow has a great moisture transfer with surrounding environment. The air flow dry-bulb temperature rises up while the wet-bulb temperature drops down because of water's evaporation and cooling effect.

It's important to note that returning hot is a universal phenomenon in long distance excavation roadway. It exists even no cooling measures are used, and it is also a universal phenomenon that there is a temperature difference between the outlet of the air duct and working face (Chu Zhaoxiang et al., 2009). After cooling measures are applied into practice it is magnified. In this situation the returning hot phenomenon will become more obvious.

5 CONCLUSIONS

Through field measurement and data analysis, some quantitative relationships about the cooling parameters in long distance excavation roadway (nearly 1000 m) and working face of Zhaolou coal mine were got.

1. The dry-bulb & wet-bulb temperature of the heading face after cooling have a linear relationship to the dry-bulb & wet bulb temperature at exit of the air duct.
2. The dry-bulb temperature of the heading face after cooling have a second parabolic relationship to the dry-bulb temperature at a certain scope in the air duct behind the air cooler.
3. The wet-bulb temperature difference near the heading face in long distance excavation roadway was high and the biggest up to 5~7 °C. There was a high moisture exchange occurred in air flow retuning process and thus a retuning hot phenomenon would be occurred and enlarged.

Finally, the conclusion of this paper is based on concrete cooling technology conditions of Zhaolou coal mine, more general conclusion needs a large number of experimental test and theoretical analysis.

ACKNOWLEDGEMENTS

This work has been supported by National Key Technology Research and Development Program of the Ministry of Science and Technology of China (2012BAK04B02), Major Program of Innovation Foundation of China Coal Technology & Engineering Group (2011ZD001). The author thanks for these financial supports.

REFERENCES

China National Coal Construction Association, 2007. GB 50418–2007, Code for Design of Prevention and Elimination of Thermal Disaster in Coal Mines.

Chu Zhaoxiang & Xin Song & Wang Wei, et al, 2009. Analysis of Partial Heat-harm Phenomenon in Zhaolou Mine, *Modern Mining* 477:110–112.

Chu Zhaoxiang & Xin Song & Wang Wei, et al, 2009. Refrigeration and Cooling Technology in Zhaolou Coal Mine, *Safety in Coal Mines* 40(10):34–36.

Gao Xuekui, 2008. Cooling Research and Application on Large Section Area and Long Distance Tunneling Face, *Coal Mine Modernization* 83:79.

He Guo-jia, Ruan Guo-qiang & Yang Zhuang, 2011. Research and Application on Preventive Measures Against Heat Disaster in Zhaolou Coal Mine, *Journal of China Coal Society* 36(1):101–104.

He Manchao, 2009. Application of the HEMS Cooling Technology in Deep Mine Heat Hazard Control, *Mining Science and Technology* 19:269–275.

Lowndes I.S., Yang Z.Y. & Jobling S., et al, 2006. A Parametric Analysis of a Tunnel Climatic Prediction and Planning Model, *Tunneling and Underground Space Technology* 21:520–532.

Man-chao He, Xiu-ling Cao & Qiao Xie, 2010. Principle and Technology for Stepwise Utilization of Resources for Mitigating Deep Mine Heat Hazard, *Mining Science and Technology* 20:20–25.

Webber R.C.W., 2006. Fundamentals of Planning for Deep Mine Ventilation and Cooling Systems, *Journal of the Mine Ventilation Society of South Africa* 11:13–17.

Yang Shengqiang, 1997. Study on Change Law of Thermal Dynamic of Air Flow and Thermal Resistance in High Temperature and High Humidity Mine, *Journal of China Coal Society* 22(6):627–630.

Progress in Mine Safety Science and Engineering II – He et al. (Eds)
© 2014 Taylor & Francis Group, London, ISBN 978-1-138-00122-0

Study on acoustic emission and damage during the failure of coal rock

Yuliang Wu & Huan Liu
Sichuan Academy of Safety Science and Technology, Chengdu, China

Senmao Zeng
Sichuan Coal Industry Group Limited Liability Company, Chengdu, China

ABSTRACT: Through the linear elasticity character of the rock stress–strain curve under the uniaxial compression test, the paper analyzes the elastic plastic behavior and the damage evolution equation of the ingredient, it shows that the stress is power function of the elastic strain in the process of loading and the stress relief, the ingredient is nonlinear elasticity. It focuses on the relationship among the elastic model, the plastic strain and the damage, then it draws a clear conclusion that there is correlation between the elasticity coefficient and the damage consume energy as well as the power function relationship between the plastic strain and the damage existence, the mechanical energy of the ingredient is obtained in the loading cycle accompany with hysteresis which is caused by interior friction. Finally established the damage evolution equation of non-linear module and the constitutive equation, the mathematical relationship of the elastic modulus and damage is built too.

1 ANALYSIS OF COAL ROCK UNIAXIAL COMPRESSION DAMAGE

The large number of studies have shown that the rock pores and fractures have fractal characteristics, when the pressure is small, large cracks closed firstly, a greater number of small cracks then closed with the stress increases. Original pores would also be deformed with the stress increased, and the compressed pores also getting smaller and smaller with more and more numbers. Therefore, the material characteristic of rock may be nonlinear elasticity. If the material is not damaged, the slope of the stress-strain curve will increase. If damage, the effective bearing area on the effective stress and strain of the slope of the curve should also be increased. Actually, rock would be damaged by one-way stress (Peng, 2007). Assumed the relationship between coal rock the stress and strain damage is:

$$\sigma = C_1 \cdot (1 - D) \cdot \varepsilon_e^n \tag{1}$$

Where C_1, n = material constants; ε_e = the elastic strain of the rock; D = Damage variable; $D = 0$ corresponds to the completely non-destructive state. $D = 1$ corresponds to a state of complete loss of carrying capacity.

There is no plastic strain when no damage exist, but the greater damage, the greater plastic strain deformation, Assumed the relationship between total strain ε and elastic strain ε_e is:

$$\varepsilon_e = C_2 \cdot (1 - D)^m \cdot \varepsilon \tag{2}$$

Where C_2, n = material constants;

Assumed that the damage and the outside elastic power is proportional:

$$Y \,\mathrm{d}\, D = \sigma \,\mathrm{d}\, \varepsilon_e \tag{3}$$

With formula (1) and formula (2) get formula (3):

$$Y \,\mathrm{d}\, D = C_1 \cdot C_2 \cdot (1 - D)^{mn+1} \varepsilon^n \,\mathrm{d}\, \varepsilon = C(1 - D)^l \varepsilon^n \,\mathrm{d}\, \varepsilon \tag{4}$$

Where $C = C_1 C_2$, $1 = mn + 1$ is material constants; Taking into account the initial conditions: $e = 0$, $D = 0$, the damage evolution equation can be solved:

$$D = 1 - \left[1 - \frac{C(l-1)}{Y(n+1)} \varepsilon^{n+1} \right]^{\frac{1}{1-l}} \tag{5}$$

With formula (2) and formula (5) get new formula (6):

$$\sigma = C \cdot \left[1 - \frac{C(l-1)}{Y(n+1)} \varepsilon^{n+1} \right]^{\frac{l}{1-l}} \varepsilon^n \tag{6}$$

The formula (5) and (6) is damage evolution equation and properties of equations respectively, they are subject to the constraints of the four constants, namely, C, Y, n, l.

If:

$$K = \frac{C(l-1)}{Y(n+1)} \tag{7}$$

Then formula (5) and (6) may be abbreviated as:

$$D = 1 - \left[1 - K \cdot \varepsilon^{n+1}\right]^{\frac{1}{1-l}} \tag{8}$$

According to the formula (8) to calculate the damage variable of coal rock under uniaxial compression during whole process, when under these conditions, $n = 3$, $Y = 1$, $l = 2$, $C = 1 \times 10^9$, the coal rock damage—stress curve shown in Figure 1.

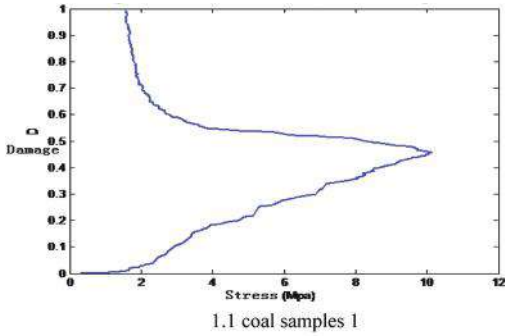
Coal rock damage evolution in the state of uniaxial compression can be broadly divided into four stages:

The first stage is the initial pressurized to 0.3~1.2 MPa, damage variable is close to 0, as lossless stage. This is mainly because the coal rock is in the elastic deformation stage, the geometric dimensions of the initial micro-cracks and micro-holes are not changed, at the same time, there are no new ones generate.

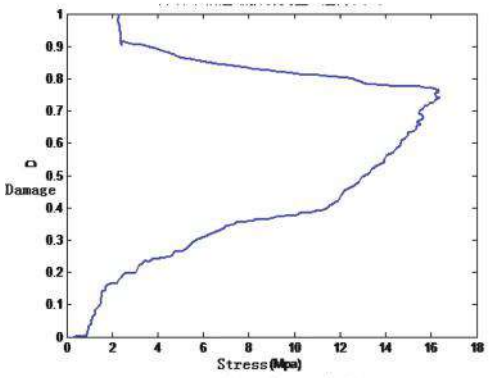
The second stage is from 0.3~1.2 to 5~8 MPa, damage variable increases. From 0.3 to 1.2 MPa, external load across the elastic limit of the coal rock to enter the stage of plastic deformation, micro-cracks or micro-holes began to expand and new micro-cracks or micro-holes in the specimen begins to generate, the change of damage is continuous and stable.

The third stage is from 5~8 MPa to the peak point. Micro-cracks and micro-holes in the specimen closer to the peak point of the rapid expansion of convergence, the specimen appeared macro damage.

The fourth is the post-peak stage, the damage variable rises to 1. The development of the damage in this stage is unstable, part capacity decreased rapidly. The coal rock secondary damage continuous load. It also further explained the coal rock deformation to failure can be regarded as a gradual process: from initial evolution of deformation and damage to the emergence of a macro micro-crack, until to the destruction of the whole process. This shows that the formation of coal rock has dynamic disasters effect.



1.1 coal samples 1



1.2 coal samples 2

Figure 1. Unixal depressing damage—stress curve of coal rock sample.

2 DAMAGE VARIABLE AND ACOUSTIC EMISSION

Coal rock acoustic emission is the micro-seismic pulses generated in the process of coal rock destruction, there is a direct relationship with the inside micro-cracks or defects (Yin, 2005). Damage is the result of the growth and expansion of coal rock micro-cracks or defects, thus the internal defects of the coal rock evolution and growth is directly related. Therefore, there is a causal relationship between the damage and the acoustic emission. Because the acoustic emission distribution which monitored is a statistical distribution l, the relationship between damage and acoustic emission can be established

Assumed η is acoustic emission rate of unit area destroyed infinitesimal, the number of acoustic emission events per unit area is dA:

$$d\Omega = \eta dA \tag{9}$$

Assumed the destroyed acoustic emission cumulative amount of entire cross-section A_0 I is Ω_0, η can be expressed as:

$$\eta = \frac{\Omega_0}{A_0} \tag{10}$$

Expressed dA as:

$$dA = A_0\phi(\varepsilon)d\varepsilon \tag{11}$$

Where $\phi(\varepsilon)$ = is infinitesimal strength statistical distribution function, taking the form of Weibull distribution, namely:

$$\phi(\varepsilon) = \frac{m}{\alpha}\varepsilon^{m-1}\exp\left(-\frac{\varepsilon^m}{\alpha}\right) \tag{12}$$

Where in: m and α are constants. With formula (10), (11), (12), (9) get new formula (13)

$$\frac{\Omega}{\Omega_0} = \frac{m}{\alpha}\int\left[\varepsilon^{m-1}\exp\left[-\frac{\varepsilon^m}{\alpha}\right]\right]d\varepsilon = 1 - e^{-(\frac{\varepsilon}{\alpha})} = D \tag{13}$$

The acoustic emission waveform parameters can be measured using acoustic emission device, formula (13) can be quantitatively given the specimen quantitative value of the damage variable in the process of loading any time.

3 MODEL OF THE ACOUSTIC EMISSION COAL ROCK DAMAGE

Many studies shown (Hao, 2007) that, coal rock compressive failure of substance is inherent defects (such as small holes and cracks, etc.) are stretched and expanded, at last, they blended together. Tensile damage and failure characteristics is the performance of microscopic fracture morphology.

According to formula (13), when $D = 0$, corresponding to the coal rock with intact state, this is just a reference state. when $D = 1$ corresponds to the the complete injury status of coal and rock, the coal the rock completely lost withstand any pull the ability of the stress. Represents an intermediate value between 0 and 1 are not completely broken.

Actual coal rock generally have initial damage named D0 which determined by the modulus E. E is smaller than the inherent elasticity of the material modulus or the initial elastic modulus E_0 is a fracture damage material timely modulus which has been reduced, namely, $E = E_0$ (1–D) thus, the stored elastic energy under the action of external stress is:

$$U = E(1-D)\varepsilon^2/2 \tag{14}$$

Where ε = strain; D = acoustic emission damage variable D can be regarded as the state variables to characterize the level of damage fracture transient when material starts to rupture.

According to the thermodynamic relations, acoustic emission cumulative value of the coal rock damage expression can be obtained:

$$\left(\frac{\partial U}{\partial \varepsilon}\right)_D = E(1-D)\varepsilon = E\varepsilon(1-\frac{\Omega}{\Omega_0}) = \sigma \tag{15}$$

Formula (15) shows that the acoustic emission accumulated is a direct reflection of the degree of damage of coal rock, which can be monitored by inferring the type of coal rock damage evolution. For an established rock system, the level of acoustic emission energy and its variation often correspond to different types damage of the surrounding rock (Li, 2006). Through monitoring the acoustic emission energy changes can infer or analysis the coal type and gas outburst.

For the micro unit which contains defects, when the stress exceeds the ultimate failure strength, defects can be activated, causing damage failure or defect evolution, while releasing the strain elastic energy, exciting acoustic emission. The distribution of coal rock material defects often use two-parameter Weibull distribution.

$$n(\varepsilon) = k\varepsilon^m \tag{16}$$

$$n'(\varepsilon) = km\varepsilon^{m-1} \tag{17}$$

Where $n(\varepsilon)$ = Tensile strain is less than or equal to the number of defects ε which can be activated; K, m = The material properties of the fault activity, constant; $n'(\varepsilon)$ = The change rate between defects and stain.

$$dn = n'(\varepsilon)d\varepsilon \tag{18}$$

Stress has been released because the past damage, therefore the actual number of defects that included in activation will be reduced by a factor (1–D). Assumed that a defect activated damage and failure count corresponding to an acoustic emission, the corresponding acoustic emission count is:

$$dN = (1-D)n'(\varepsilon)d\varepsilon \tag{19}$$

With formula (17) and formula (19) get new formula (20):

$$dN = km(1-D)\varepsilon^{m-1}d\varepsilon \tag{20}$$

Considering to the material defect distribution, activation of randomness and a variety of random factors, random factor r epsilon (e) by the formula (20) can be derived cumulative acoustic emission

count N is:

$$N = r(\varepsilon)\int_{\varepsilon_0}^{\varepsilon} km(1-D)\varepsilon^{m-1}d\varepsilon \tag{21}$$

Where ε_0 = Initial damage strain of the material; $r(\varepsilon)$ = (0, 1) random number in the interval.

$$N'(t) = \frac{dN}{dt} = r(\varepsilon)km(1-D)\varepsilon^{m-1}\frac{d\varepsilon}{dt} \tag{22}$$

Formula (21) and (22) is the theoretical model of the acoustic emission of coal rock material in the destruction process. The Model described that acoustic emission count and rate of change mainly depends on the damage factor, transient strain, strain rate, and the material properties (the total number of inherent defects, materials scale, materials homogeneity, etc.).

4 CONCLUSION

Destructive test and field test of coal rock work is often restricted with problems, the coupling of methane gas and coal rock solid during the coal rock rupture process is still difficult to resolve now. In this paper, acoustic emission and coal rock damage are combined to do some research based on the analysis of laboratory data, the following conclusions may be get:

1. Damage is the result of the growth and expansion of coal rock micro-cracks or defects, thus the internal defects of the coal rock evolution and growth is directly related. Therefore, there is a causal relationship between the damage and the acoustic emission. Because the acoustic emission distribution which monitored is a statistical distribution l, the relationship between damage and acoustic emission can be established
2. The acoustic emission accumulated is a direct reflection of the degree of damage of coal rock, which can be monitored by inferring the type of coal rock damage evolution, which can help to infer or analysis the coal type and gas outburst.
3. Theoretical model of coal rock damage acoustic emission based on determined by e acoustic emission count and acoustic emission change rate was obtained. The Model described that acoustic emission count and rate of change mainly depends on the damage factor, transient strain, strain rate, and the material properties (the total number of inherent defects, materials scale, materials homogeneity, etc.).

REFERENCES

Bear J. 1983. Porous media fluid dynamics [M]. Li Jingsheng, CHEN Chong-xi translation. Beijing: China Building Industry Press.

Beck DA, Brady BHG. 2002. Evaluation and application of controlling parameters for seismic events in hard-rockmines [J]. International Journal of Rock Mechanics and Mining Sciences, 39(5):633–642.

Eng-Teik Ng. 2000. Wavelet-Based Acoustic Emission Analysis of Material Fatigue Bahavior: Bone Cement [D]. USA. The University of Memphis.

Hao YN. 2007. Application research on acoustic emission signal processing based on wavelet theory and DSP technology [D]. Nanning: Guangxi University,

Jose F. Lbauz, Saar Cattaneo, Li Hsien Chen. 2001 Acoustie emission at failure inquasi-brittle materials [J]. Constiuction and Building Materials, 15:225–233.

Li HY, Jiang XF, Yang SH. 2006. Research and application of microseismic monitoring location of strata fracturing based on Matlab [J]. Journal of China Coal Society, l31(2):154–158.

Liu JX. 2002. Experimental Study of AE in Rocks [D]. Beijing: China Earthquake Administration, Geophysical Institute.

Peng RD, Liu HB, Wang JQ. 2007. Developments in rock damage detection techniques [J]. Rock and Mineral Analysis, 26(1):61–66.

Wang N. 2003. Application of the Rock Mass Acoustic Emission Testing Technology in Safety Classification of Stope Roof [J]. Journal of SWUST, (2):104–106.

Yin ZG. 2005. Experimental study on acoustic emission and damage during the failure of rock [D]. Changsha: Central South University.

Zou YH, Wen GC, Hu QT. 2004. Theory analysis and experimental study of spread and attenuation of acoustic emission in rock body [J]. Journal of China Coal Society, 29(6):663–667.

Progress in Mine Safety Science and Engineering II – He et al. (Eds)
© 2014 Taylor & Francis Group, London, ISBN 978-1-138-00122-0

Study on numerical simulation for the fracture law of gob-side entry retaining roof

J.J. Shi, H.Y. Shi & J.Zh. Guo
Key Laboratory of Mine Disaster Prevention and Control, Sanhe, Hebei, China
Safety Engineering College, North China University of Science and Technology, Sanhe, Hebei, China

ABSTRACT: The geological conditions of haulage roadway of the working face 1528 in GeQuan Coal Mine, which belongs to the JiZhong Energy Group Co., Ltd., and the research findings of Key Stratum Theory was taken into consideration, based on which established a mechanical model could reflect the basic features of rock stratum and made a profound investigation on the form and conditions of the fractures on main roofs. A systematic study on the stress, deformation, and damage characters of fractures on main roofs beyond a retained entry has been made by the numerical simulation. The simulation shows that the deeper the fracture is in the rib, the greater the differences between dimension of compression and deformation will likely be, and the greater the influences on the stability of surrounding rock will it has. At the same time, smaller is the overhanging beam in mined-out area, more beneficial to roadway maintenance. On a certain deformation of main roof, it creates subsidence that is great difference in different position of a roadway. The subsidence near those mined-out areas is much more than those near the ribs. The application of a strong and effective measure could help cut the roof out and assure its stability.

1 INTRODUCTION

The deformation damage on main roof in a retained gob-side entry is manifested by the deformation and severe subsidence of the roadway. The reason for this is that the overburden strata gyrate axis-wise towards the mined-out side. In order to suit the deformation character of the main roof, the lane offshoot care we applied should be characterized by great supporting strength at an early stage, quickly growing resistance force, and appropriate supporting pressure; what's more, we need reducible quantity to adapt to the deformation. Along with the support inside the roadway, these two measures we applied could take good care of the immediate roof beyond a roadway, prevent it from dissociate with the covering main roof, assure its entirety, and cut-out both immediate and main roof on the mined-out side (Sun et al. 1993, Zhang 2005, Xie et al. 2004, Zhu et al. 2006).

2 NUMERICAL SIMULATION TEST DESIGN

Test research aims to fully mechanize working face in GeQuan coal mine geological conditions as the background, through the similar simulation, analysis the main roof (key layer) fracture position, and the effect on the stability of the roof.

The test using gypsum and cement for cement based on geological conditions of 1528 working face haulway. The coal seam thickness for an average of 2.35 m, 2.8 m, 2 # coal seam for organized structure, bedding is more apparent, coal seam angle average 15°, and coal seam occurrence situation basically stable. The upper part is more than 5 m thick argillaceous siltstone. The main roof is the thick 10 m of sandstone, immediate roof is argillaceous siltstone block, structure level bedding, argillaceous cementation.

The rock physical and mechanical properties of working face roof and floor show in Table 1.

3 THE MAIN ROOF FRACTURE POSITION NUMERICAL SIMULATION

3.1 *Model established*

The characteristics of the coal seam roof and floor of roadway shown in Table 1.

The calculation model of two-dimensional model, considering the angle of coal seam, set up as shown in Figure 1 and trapezoidal model, a total of 2800 mesh, 5858 nodes. The stress boundary condition, the model surface applied uniform vertical compressive stress, the model under the surface of the vertical displacement fixed. The calculation of the model using Mohr—coulomb criterion is used as a rock mass failure criterion (Qian et al. 1991, Li et al. 2000).

Table 1. Physical-mechanical properties of the rock mass.

Rock name	Average thickness/ (m)	Elastic modulus/ (MPa)	Compressive strength/ (MPa)	Tensile strength/ (MPa)	Poisson's ratio/ (μ)
Powder sandstone	4.60	9198	39.93	2.51	0.25
In sandstone	3.40	13662	62.73	4.23	0.23
Fine sandstone	2.10	15372	83.96	5.50	0.35
Argillaceous siltstone	5.00	8620	24.62	0.76	0.30
Coal seam	2.35	6000	7.00	0.63	0.20
Argillaceous siltstone	5.00	8230	26.37	0.79	0.30

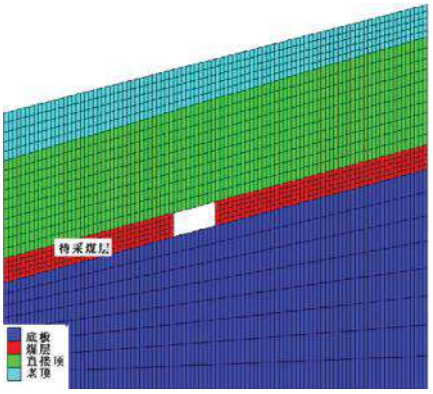


Figure 1. Two-dimensional model.

3.2 *Method and program of the simulation*

Affect main roof rock fracture location factor is more, so choose application standard orthogonal table to optimizing the reasonable arrangement of multi-factor part test.

Considering the practice and simulation design possible, each factor takes three levels. Test two indicators are: (1) the main roof produce the plastic damage position; (2) the main roof maximum shear stress position; Seven factors and three levels; Choose L9 (37) design orthogonal table as shown in Table 2.

Using Orthogonal experiment design (Orthogonal experimental design) simulation scheme is shown in Table 3.

3.3 *The plastic damage simulation results analysis*

Simulation roof plastic state is shown in Figure 2 and Figure 3.

Can be seen from the Figure 2 and Figure 3 (plan1 and 2), plan 1 coal rib outside 5.5 m place main roof started to plastic damage, fracture line to mined-out area outspread; Scheme 2 to shear failure is given priority to, the fracture position main roof in coal rib inside 2.4 m place, fracture line to mined-out area outspread; Plan 3 fracture position in the coal rib inside 1.8 m place, fracture line above the backward outspread; Scheme and main roof without obvious plastic destruction; Plan 5 due to the initial stress is bigger, coal body basic have been occurred shear failure, the fracture position main roof in coal rib outside 6 m place, fracture line to the outspread; Scheme and the fracture position main roof in coal rib inside 1 m place; Plan and no obvious plastic destruction; Plan 8 main roof fracture position in the coal wall outside 7.8 m place, fracture line backward coal body outspread; Scheme and main roof coal fracture position in the coal wall outside 6 m place, fracture line to the coal body extension.

The above plan main roof's destruction mainly shear failure is given priority to, plan 4 and scheme and plastic state diagram no obvious fracture damage, can through the maximum shear stress location estimation, maximum shear stress position is the main roof possible fracture position.

3.4 *Maximum shear stress damage simulation results analysis*

Simulation roof shear stress state is shown in Figure 4 and Figure 5 (plan 1 and 2)

Based on the analysis of the nine shear stress that: plan 1 maximum shear stress in coal rib outside 6.4 m place, maximum shear stress is 26.01 MPa; Scheme 2 maximum shear stress in coal rib inside 2.4 m place, maximum shear stress is 25 MPa; Plan 3 maximum shear stress in coal rib inside 4.2 m place, maximum shear stress is 23.83 MPa; Plan and maximum shear stress in coal rib inside 3 m place, maximum shear stress is 12.17 MPa; Plan 5 maximum shear stress in coal rib outside 5.4 m place, maximum shear stress is 34.46 MPa; Plan and maximum shear stress in coal rib inside 2.8 m place, maximum shear stress is 27.96 MPa; Plan and maximum shear stress in coal rib inside 3.2 m place, maximum shear stress is 15.28 MPa; Eight maximum shear stress in coal rib outside 2.8 m place, maximum shear stress is 35.0 MPa; Plan and maximum shear stress in coal

Table 2. The design of the simulation.

Level	Angle/(°)	The original rock stress state/(m)	Immediate roof and the ratio of mining height are broken/(k)	Coal properties/ (MPa)	Immediate top properties/ (MPa)	Main roof thickness/ (m)	Nature of main roof/ (MPa)
1	15	300	2	8	30	4	4
2	25	500	3	16	40	8	6
3	35	700	4	24	60	12	8

Table 3. The L9(37) design of the orthogonal experimental.

Test number	A	B	C	D	E	F	G
1	1	1	3	2	2	1	2
2	1	2	1	1	1	2	1
3	1	3	2	3	3	3	3
4	2	1	2	1	2	3	1
5	2	2	3	3	1	1	3
6	2	3	1	2	3	2	2
7	3	1	1	3	1	3	2
8	3	2	2	2	3	1	1
9	3	3	3	1	2	2	3

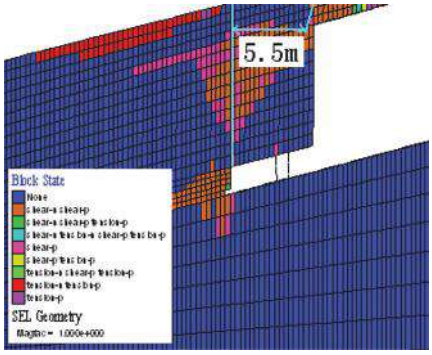


Figure 2. The roof failure in schemes 1.

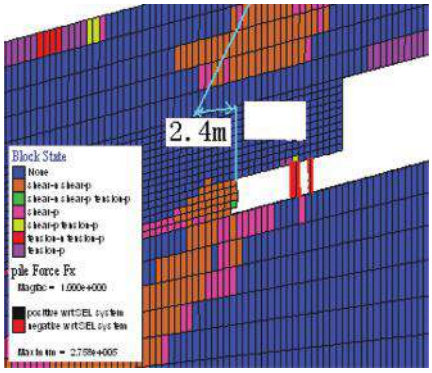


Figure 3. The roof failure in schemes 2.

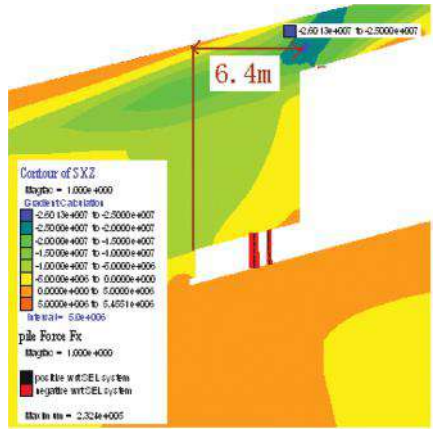


Figure 4. The roof shear stress in schemes 1.

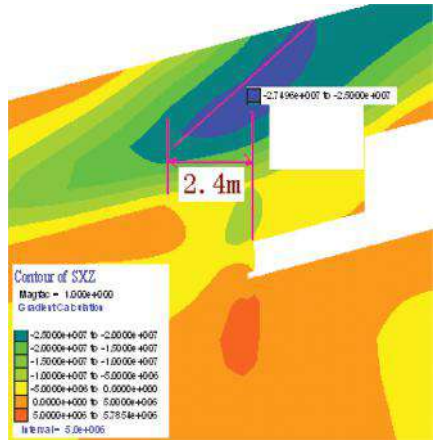


Figure 5. The roof shear stress in schemes 2.

rib outside 6.4 m place, maximum shear stress is 39.75 MPa.

3.5 *The simulation results analysis*

The summary of above results such as Table 4.

Table 4 roof fracture position within the coal rib is, coal wall outside is negative; K_{ij} is factor j first

Table 4. The L9(37) of the orthogonal experimental design and the experimental result.

Test number	Angle/ (°)	O.R.S.S./ (m)*	I.R.R.M.H./ (k)*	C.P./ (MPa)*	I.T.P./ (MPa)*	M.R.T./ (m)*	N.M.R./ (MPa)*	P.S.P./ (m)*	M.S.S.P./ (m)*	Average/ (m
1	1(15)	1(300)	3(4)	2(16)	2(40)	1(4)	2(60)	–5.5	–5.5	–5.95
2	1	2(500)	1(2)	1(8)	1(20)	2(8)	1(40)	2.4	2.4	2.4
3	1	3(700)	2(3)	3(24)	3(60)	3(12)	3(80)	1.8	4.2	3
4	2(25)	1	2	1	2	3	1	3	3	3
5	2	2	3	3	1	1	3	–6	–5.4	–5.7
6	2	3	1	2	3	2	2	1	2.8	1.9
7	3(35)	1	1	3	1	3	2	3.2	3.2	3.2
8	3	2	2	2	3	1	1	–7.8	–2.8	–5.3
9	3	3	3	1	2	2	3	–6	–6.4	–6.2
K_{1j}	–0.55	–0.45	7.5	–0.8	–0.1	–16.95	0.1			
K_{2j}	0.4	–8.6	0.7	–9.35	–9.15	–1.9	–0.85	$K_{1j} + K_{2j} + K_{3j} = -10.75$		
K3 j	–10.6	–1.3	–16.85	0.5	–0.4	9.2	–2.4			
Rj	11	8.15	24.35	9.85	9.05	26.15	2.5			

*O.R.S.S. = The original rock stress state, I.R.R.M.H. = Immediate roof and the ratio of mining height are broken, C.P. = Coal properties, I.T.P. = Immediate top properties, M.R.T. = Main roof thickness, N.M.R. = Nature of main roof, P.S.P. = Plastic state position, M.S.S.P. = Maximum shear stress position.

I level is the sum of the test value (j = 1,2,3,4,5,6,7; on behalf of A, B, C, D, E, F, G, seven factors; I = 1, 2, 3 represents 3 level), R_j represent the first j column every test index range, R_j = Max (k_{1j} k_{2j} k_{3j}) – min (k_{1j} k_{2j} k_{3j}) orthogonal experimental factor analysis based on less experimental condition can infer the influence degree of various factors. The table above shows, through the above 9 simulation results analysis, the roof fracture position in the coal rib in the largest 3.2 m place, minimum in the coal rib outside 6.2 m, the average fracture position for coal rib inside – 10.75/9 = 1.19 m; That is the average fracture position in the upper part of the roadway. Study on roof fracture position of the main influence factors including angle, coal property, the immediate roof thickness and the nature, the main roof thickness and properties as well as the original rock stress state, etc. According to the range analysis.

$$R_6 = 26.15 > R_3 = 24.35 > R_1 = 11 > R_4 = 9.85 > R_5 = 9.0$$

So that the influence of roof fracture is in order.

Main roof thickness > Immediate roof and the ratio of mining height are broken > Angle > Coal properties > Immediate roof properties > Original rock stress state > The properties of main roof.

4 SUMMARY

According to the overlying rock breaking process and failure pattern of the fully mechanized gob-side entry retaining, numerical simulation concluded Through the orthogonal test method to the main roof fracture factors influence, a numerical simulation to get the order: main roof thickness > immediate roof and mining height are broken ratio > Angle > > properties of coal seam, the immediate roof of nature > the original rock stress state > main roof properties.

ACKNOWLEDGEMENTS

This work was financially supported by the Fundamental Research Funds for the Central Universities (3142013100); the Fundamental Research Funds for the Central Universities (AQ1202B); the National Natural Science Foundation (51044009); the Natural Science Foundation of Hebei Province (E2012508002); the Fundamental Research Funds for the Central Universities (3142013035).

REFERENCES

Li H.M. 2000. Control design of roof rocks for gob side entry. *Chinese Journal of Rock Mechanics and Engineering*. 19(5):651–654.

Qian M.G. & Liu T.CH. 1991. *Mine pressure and Control*. Beijing: China Coal Industry Press.

Sun H.H. & Zhao B.L. 1993. *Theory and Practice of Gob*. Beijing: China Coal Industry Press.

Xie W.B. et al. 2004. The key problem study about gob-side entry retaining in top-coal caving mining face. *Journal of China Coal Society* 24(2):46–149.

Zhang G.H. 2005. Roof cracking reason analysis about gob-side entry retaining under initiative support. *Journal of China Coal Society* 30(4):429–432.

Zhu CH.Q. et al. 2006. Reliability analysis on support structure of gob-side entry retaining in fully-mechanized caving face. *Journal of China Coal Society* 31(2):141–144.

Progress in Mine Safety Science and Engineering II – He et al. (Eds)
© 2014 Taylor & Francis Group, London, ISBN 978-1-138-00122-0

Numerical simulating research on changing law of humidity in refuge chamber

Ying-Hua Zhang, Qian Zhao, Zhi-An Huang, Yan-Feng Zhang, Yuan Tian & Yu-Kun Gao
State Key Laboratory of High-Efficient Mining and Safety of Metal Mines, University of Science and Technology Beijing, Ministry of Education, Beijing, China

ABSTRACT: In order to improve the ambient humidity in refuge chamber, affecting factors of humidity in refuge chamber were all analyzed and studied, and PHOENICS software was adopted to simulate changing process of humidity in refuge chamber under different conditions of ventilation. Results show that humidity in refuge chamber can reach 100% within one hour with no ventilation; when air supplying rate is 0.3 m^3/min per person in summer, humidity in refuge chamber maintains at about 80% and people feel cool, which is indicated by two comfort indexes: PMV and PPD; however, when air supplying rate is 0.3 m^3/min per person in winter, humidity in refuge chamber maintains at around 73% and people feel comfortable. A conclusion is finally drawn that ventilation condition has certain influence on humidity in refuge chamber. The research result is beneficial for optimizing design of environmental condition in refuge chamber.

1 INTRODUCTION

The refuge chamber is a kind of closed emergency hedging facility which can provide basic living conditions for people who cannot withdraw to ground timely and safely, playing great role in ensuring safety of people and acquiring rescuing time, but due to its limited volume and underground large-scale crew, changing process of humidity in it is always complex (Sun J P 2011, Zhang E Q et al. 2009, Wang T et al. 2011, Sun J P 2011).

At present, common air conditioning is adopted for controlling humidity in refuge chamber, but this mode has problems in aspects of maintenance, cost and safety. Aiming at this situation, affecting factors of humidity in refuge chamber were all analyzed and studied, and PHOENICS software was adopted to simulate changing process of humidity in refuge chamber under different conditions of ventilation, so that influence of ventilation condition on humidity in refuge chamber can be explored and basis can be provided for controlling and improving humidity condition in refuge chamber.

2 ESTABLISHMENT OF MATHEMATICAL MODELS

Accuracy of software depends on accuracy and genuineness of models established by it. PHOENICS is a kind of general-purpose CFD software for simulation of flow, heat-transferring, reaction and combustion (Wang D 2012). It has many advantages such as good interaction with programmer, wide using range, convenient mesh division, good calculating convergence and powerful post-processing function (Fang K 2006, Xiao K 2010). Its program is mainly composed of three modules: pre-processor (definition and presentation of problem), solver (numerical simulation and calculation) and post-processor (display of calculation results) (Hao W J 2005).The controlling equation of PHOENICS has many advantages such as closing, uniform style, coupling, nonlinearity and so on (Zhang S Q et al. 2010). All these provide prerequisites for accurate establishment of models.

2.1 *Establishment of physical model of refuge chamber*

Model of refuge chamber is shown in Fig. 1. Length in X direction is 37 m, and thickness of wall at entrance is 1 m. Length and thickness of wall in Y direction are respectively 3 m and 0.4 m. Section in Z direction is arched wall, as height of straight wall, radius of circle part and thickness of wall are respectively 1.2 m, 1.5 m and 0.4 m.

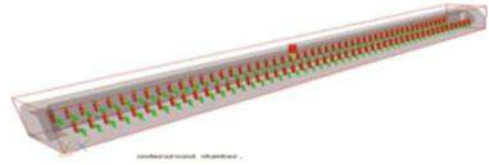


Figure 1. Model of refuge chamber.

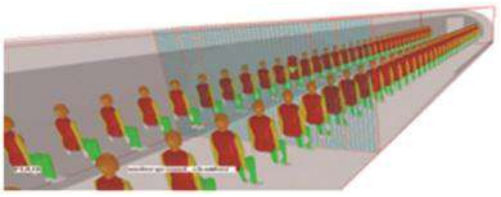


Figure 2. Mesh division of model of refuge chamber.

100 people-models were symmetrically arranged at positions 1 m away from sidewalls of refuge chamber. Three-dimensional parameters of either one model was set to be (0.4 m, 0.5 m, 1.44 m), and spacing between adjacent models was set to be 0.7 m. Heat production, temperature, wet dissipating volume and clothes index were respectively set to be 100 W, 37 °C, 1.667 × 10 – 5 Kg/s and 0.8. Metabolic intensity was set to be metabolism in silent seated status.

Following assumptions were made:

1. The same material was adopted in envelope structure.
2. Air in refuge chamber was ideal incompressible air.
3. Envelope structure and surrounding rock fitted closely, and humidity field was consecutive.

2.2 *Mesh division of model of refuge chamber*

Coordinate origin was fixed at the lower left corner of refuge chamber's model. People-models were toward positive direction of X-axis. Then the models were divided with total 800000 hexahedral grids, as shown in Fig. 2. Adopted dividing principles are as follows:

1. Based on uniform division of the whole model, grids should be refined at positions around human body where temperature gradient was relatively large.
2. Inclination of grid cell should be as little as possible.

3 INTRODUCTION OF EVALUATING INDICATORS OF HEAT COMFORT

Heat comfort is affected by six factors which are four environmental parameters including dry bulb temperature, relative humidity of air, wind velocity and average radiant temperature, and two anthropometric parameters including activity intensity of human body and heat-resistance of clothes, which has been proved by lots of researches (Fanger P O et al. 1974, Zeng G et al. 2007, Wang S G et al. 2010).

Table 1. PMV-PPD grading scale.

Heat comfort	Cool	Slightly cool	Moderate and comfortable			Slightly hot	Slightly hot	Very Hot
PMV	–2	–1	–0.5	0	0.5	+1	+2	+3
PPD	75%	25%	10%	5%	10%	25%	75%	90%

In 1970, Danish scholar Fanger summed up the two widely used evaluating indicators of heat comfort which are PMV (Predicted Mean Vote) and PPD (Predicted Percentage of Dissatisfied) (Bo S S et al. 2011). These two indicators combine six factors which are air temperature, average radiant temperature, air velocity, air humidity, human body metabolism and heat-resistance of clothes, so they are the most comprehensive evaluating indicators of heat environment until now and have been compiled into international standard ISO7730.

PMV represents expected reaction of most people to the same environment, and environmental heat-effect can be scored according to its calculating result. PPD represents percentage of people unsatisfied with heat environment in crowd. PMV—PPD grading scale is shown in Table 1.

The mathematical analysis formula while using PMV as scale plate of human body's heat sensation is as follow:

$$\begin{aligned} PMV = &\left[0.303\exp\left(0.36M\right)+0.028\right] \\ &\{M-W-3.05\times10^{-3} \\ &\left[5733-6.99\left(M-W\right)-P_a\right] \\ &-0.42\left[\left(M-W\right)-58.15\right] \\ &-1.7\times10^{-5}M\left(5867-P_a\right)-0.0014M \\ &\left(34-t_a\right)-3.96\times10^{-8}f_{cl}\left[\left(t_{cl}+273\right)^4\right] \\ &-\left(t_r+273\right)^4\}-f_{cl}h_c\left(t_{cl}-t_a\right) \end{aligned} \tag{1}$$

In the formula, M—metabolism rate of human body, W/m^2; W—mechanical power produced by human body, W/m^2; Pa—partial pressure of water vapor in air around human body, Pa; t_a— temperature o air around human body, °C; f_{cl}—ratio between actual surface area of dressed human body and naked human body; t_c—temperature of outer surface of clothes, °C;t_r—average radiant temperature in room, °C; h_c—convective heat-transferring coefficient, W/m^2°C.

Relationship of PMV and PPD is as follow:

$$PPD = 100-95\exp[-(0.03353PMV^4 + 0.2179PMV^2)] \tag{2}$$

4 ANALYSIS OF NUMERICAL SIMULATION RESULTS

4.1 *Numerical simulation of humidity changing within 96 hours under natural condition (no ventilation)*

Under natural condition (no ventilation), thickness of envelope structure, initial air humidity, solver of software, time step, ending time and iteration frequency were respectively set as 1 m, 80%, transient solver, 3600s, 345600s and 20, and then numerical simulation of humidity in refuge chamber changing within 96 hours under natural condition (no ventilation) was carried out. Simulation results are show in Fig. 3, corresponding PMV and PPD distributions are respectively shown in Fig. 4 and Fig. 5.

As shown in Fig. 3, humidity in refuge chamber can reach 100% within less than one hour. In fact, when humidity is over 80%, people feel very uncomfortable, being unable to perspire and adjust self-temperature smoothly, as a result, their lives suffer from danger.

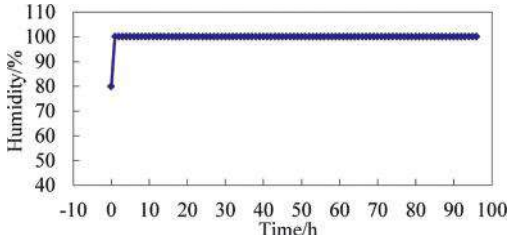


Figure 3. Humidity change under no ventilation condition.

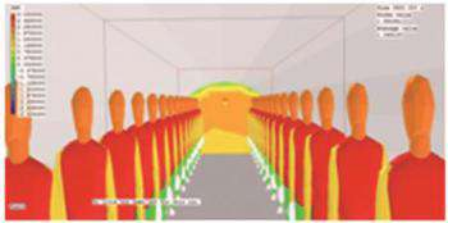


Figure 4. PMV distribution under no ventilation condition.

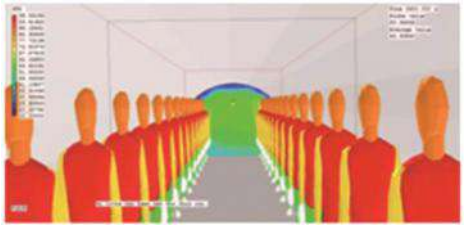


Figure 5. PPD distribution under no ventilation condition.

As shown in Fig. 4, PMV values at middle of cross-section of refuge chamber is only 1.5 as people feel slightly hot, while PMV values near people and wall deviate from zero largely as people feel very hot and uncomfortable.

As shown in Fig. 5, PPD distribution is similar to PMV distribution. All PPD values exceed 50% and values near people are larger, which show that condition in refuge chamber is relatively bad and people feel relatively unsatisfied.

4.2 *Numerical simulation of humidity changing within the first hour under natural condition (no ventilation)*

Change of humidity in refuge chamber mainly focuses in the first hour. In order to get more accurate simulation results, solver of software, time step and ending time were respectively set to be transient solver, 60s and 3600s, and then numerical simulation of humidity in refuge chamber changing within the first hour under natural condition was carried out. Simulation results are show in Fig. 6, corresponding PMV and PPD distributions are respectively shown in Fig. 7 and Fig. 8.

As shown in Fig. 6, humidity in refuge chamber reaches nearly 100% at the 42th minute.

As shown in Fig. 7, PMV values at middle of cross-section of refuge chamber is only 1.7 as people feel slightly hot, while PMV values near people and wall deviate from zero largely as people feel very hot and uncomfortable.

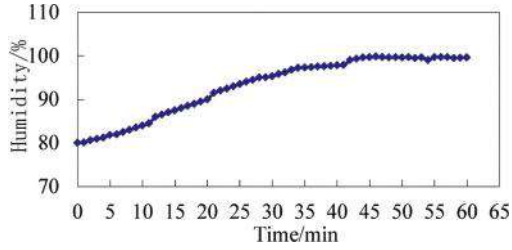


Figure 6. Humidity change within the first hour.

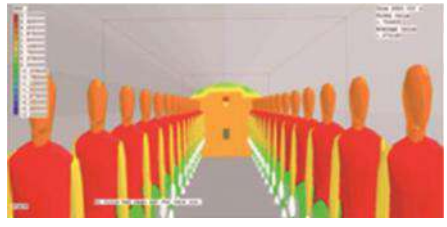


Figure 7. PMV distribution within the first hour.

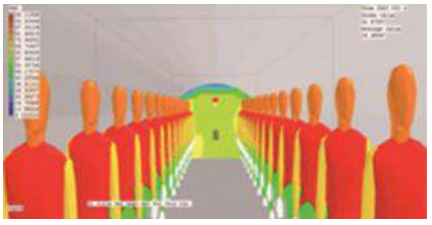


Figure 8. PPD distribution within the first hour.

As shown in Fig. 8, PPD distribution is similar to PMV distribution. All PPD values exceed 50% and values near people are larger, which show that condition in refuge chamber is relatively bad and people feel relatively unsatisfied.

4.3 *Numerical simulation of humidity changing under ventilation respectively in summer and winter*

In order to analyze influence of air humidity in different season son humidity in refuge chamber, numerical simulations of humidity in refuge chamber changing within 96 hours under ventilation in summer and winter were respectively carried out. Thickness of envelope structure, initial air humidity and air supplying volume were respectively set to be 1 m, 80% and 0.3 m³/min per person. Simulation results under ventilation in summer are shown in Fig. 9 and Fig. 10, corresponding PMV and PPD distributions are respectively shown in Fig. 11 and Fig. 12; simulation results under ventilation in winter are shown in Fig. 13 and Fig. 14, corresponding PMV and PPD distributions are respectively shown in Fig. 15 and Fig. 16.

As shown in Fig. 9, under ventilation in summer, humidity of refuge chamber basically maintains at about 80%. As shown in Fig. 10, there are some high-humidity points with humidity over 85% near people and wall.

As shown in Fig. 11 and Fig. 12, PMV values are generally over –1.3 and values around human body reach 0.3. PPD values are all over 40% and values around human body reach 30%. According to Table 1, what can be known is that people feel slightly cold and relatively uncomfortable.

As shown in Fig. 13, under ventilation in winter, humidity of refuge chamber basically maintains at about 73%. As shown in Fig. 14, there are some high-humidity points with humidity over 90% near wall, and humidity of people position and other places basically maintains at about 70%.

As shown in Fig. 15 and Fig. 16, refuge chamber is relatively comfortable, people feel relatively sat-

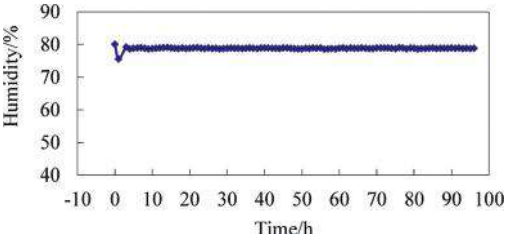


Figure 9. Humidity change under ventilation in summer.

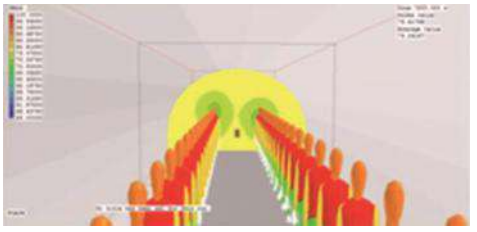


Figure 10. Humidity distribution under ventilation in summer.

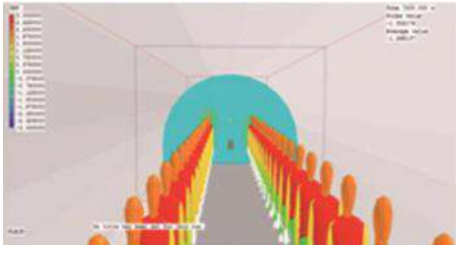


Figure 11. PMV distribution under ventilation in summer.

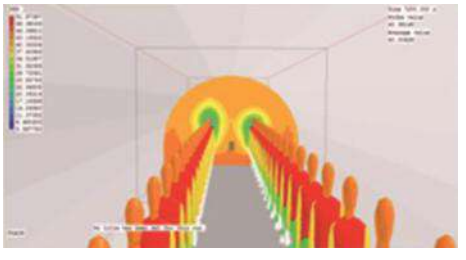


Figure 12. PPD distribution under ventilation in summer.

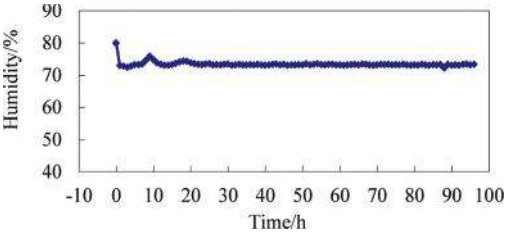


Figure 13. Humidity change under ventilation in winter.

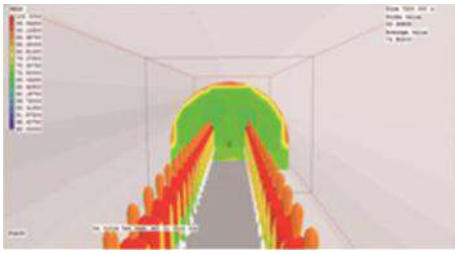


Figure 14. Humidity distribution under ventilation in winter.

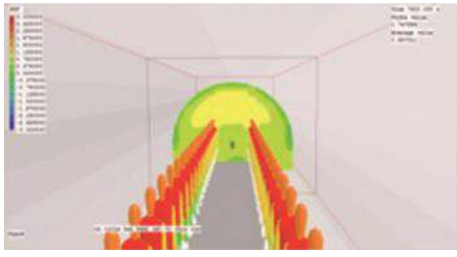


Figure 15. PMV distribution under ventilation in winter.

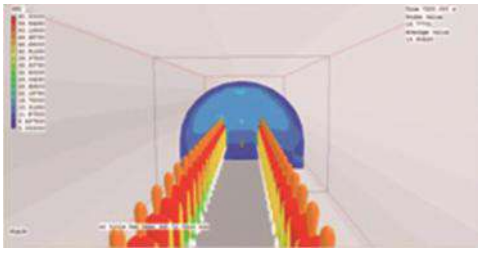


Figure 16. PPD distribution under ventilation in winter.

isfied. So condition under ventilation in winter is better than that under ventilation in summer.

5 CONCLUSIONS

1. Without ventilation, humidity in refuge chamber can reach 100% within one hour and reach the highest value at the 42nd minute.
2. As PMV and PPD distributions show, middle and upside of cross-section of refuge chamber is comfortable. However, it is uncomfortable at positions near people and wall. The reason is that environmental heat can't be uniform without ventilation. Ventilation facilities can be added in actual design so that comfort can be further improved.
3. When air supplying volume is 0.3 m^3/min per person, humidity generally maintains at about 80%. PMV and PPD distributions show that people feel slightly cold.
4. Air humidity in different seasons can lead to a little difference of humidity in refuge chamber. When air humidity is relatively large, humidity in refuge chamber is also relatively large and people feel relatively uncomfortable.

REFERENCES

Bo S S, Wu J W, Liu H M. Review of Heat Comfort Based on PMV/PPD in Cabins of Vessels. *Contamination Control & Air-Conditioning Technology*, 2011, (3):44.

Fang K. Several Kinds in Common Use Software of Computational Fluid Dynamics. *Coal Technology*, 2006, (12):124.

Fanger P O, Östberg O, Nicholl A, et al. Heat comfort conditions during day and night. *European Journal of Applied Physiology and Occupational Physiology*, 1974, (4):120.

Hao W J. *Numerical Simulation of Temperature and Velocity Fields in Vessel Engine Room*. Dalian: Dalian Maritime University, 2005.

Sun J P. Research on key technologies of emergency refuge system in underground coal mine. *Journal of Coal Science*, 2011, 36(11):1890–1894.

Sun J P. The key technologies of the refuge chamber and rescue capsule in the underground coal mine. *Journal of Coal Science*, 2011, 36(5):713–717.

Wang D. Fluid mechanics analysis software and its application. E*lectric Tool*, 2012, (1):12–14.

Wang S G, Xu Z, Zhang T F, et al. Human Heat comfort for mine environment. *Journal of Coal Science*, 2010, (1):97–100.

Wang T, Zhao Y X, Jiang Y D, et al. Design and Application of Underground Refuge Cave in Mine. *Coal mining Technology*, 2011, (4):33–36.

Xiao K.Computational fluid dynamics technology and common software. *Technology Trend*, 2010, (15):288.

Zhang E Q, Wang L, Liu M Y, et al. Explore the application of the refuge chamber in the underground coal mine. *Coal mine Safety*, 2009, (7):90–92.

Zhang S Q, Huang L, Zhang T, et al. Based on PHOENICS fluid simulation software for analysis of natural convection. *China High-tech Enterprises*, 2010, (9):19.

ZengG, Tian Y Z, Zhao H, et al. Analysis on the Environment and Synthesis Factors Affecting the PMV Index. *Construction Conserves Energy*, 2007, (3):11.

This page intentionally left blank

Progress in Mine Safety Science and Engineering II – He et al. (Eds)
© 2014 Taylor & Francis Group, London, ISBN 978-1-138-00122-0

Medium characteristics and water transmissibility of carbonate strata on Ordovician top in Pingshuo, China

Y.M. Qi & H.B. Bai
School of Resources and Earth Sciences, China University of Mining and Technology, Xuzhou, Jiangsu, China
State Key Laboratory of Geomechanics and Deep Underground Engineering,
China University of Mining and Technology, Xuzhou, Jiangsu, China

X.E. Zhao & B. Luo
School of Resources and Earth Sciences, China University of Mining and Technology, Xuzhou, Jiangsu, China

ABSTRACT: The carbonate strata, at the top of Ordovician in Pingshou, characters as the Xiamagou formation. The buried depth is nearly to 200 meters and the lithologic structure consists by a set of dolomitic limestone, limestone containing dolostone and calcite dolostone etc. Within the top 100 meters, additionally, the dolomite component increase and the interbedded limestone and dolostone emerge with the depth. Mercury injection experiments show that the main part of complete core porosities is microporosities which the porosities are small and the joint fissures are immature. Analysis based on drilling and roadway disclosure shows that the unit well inflow of Ordovician top strata changes from 0.006 to 4.76 l/s · m. The drilling water fluid is from 0.1 to 1.5 m^3/h and the permeability coefficient is in the range of 0.0029 to 10.71 m/d. Furthermore, the water transmissibility shows zoning characteristics from top to bottom—weak, strong, moderate, weak. It depends on many factors: the internal one is medium characteristics; others, such as geological structure, buried depth, karstification and filling status etc., are the external reasons. The researches serve as the scientific basis in the course of selecting the target strata of grouting, determining and restructuring the impermeable key layer of Ordovician carbonate groundwater, and will also benefit for its exploration and protection.

1 INTRODUCTION

As the important source of water supply and the control object of mining water hazard, carbonate karstic groundwater of Ordovician has got a lot of attention as the research focus since the sixties of the last century in China (Wu Q. et al. 2011, Qin S.L. & Li Z.S 2008, Hu Z.X. et al. 2009, Huang H.F. et al. 2012). Due to different geographical regions and forming environment, the territorial carbonate strata of Ordovician potentially shows different characteristics in the aspects of rock composition, thickness, karst development degree, burial conditions, and water abundance etc. Depending on these differences, the way of exploiting the aquifer water or the manner of preventing and controlling mine water disaster are selected directly.

Pingshuo is located in northern end of Ningwu coalfield surrounded by mountains on three sides—east Hongtao Hill in the east, Camel Hill in the north and Black Camel Hill in the west. In the south area, the Danshuigou fault is adjacent to the Shuonan reconnaissance area, belonging to the hydrogeological units of Shentou spring area and the loess landform mine with criss-cross ravines. On the one hand, after the exploitation of mineral resources in decades, lacking of effective protection, soil erosion deteriorates seriously. On the other hand, there is a stratum of Ordovician carbonate underground, containing an abundant groundwater in its several hundred meters' thickness.

In recent years, due to water shortage and the polluted environment, people have to exploit water resources from Ordovician carbonate karst groundwater instead of shallow groundwater. At the mine, Ordovician carbonate karst groundwater previously judged as the main water disaster for its water level inundating the main Carboniferous coal seam (Li L.C. et al. 2011, Bai H.B. et al. 2009). Although have been known more than twenty years, its top have not been research thoroughly in Pingshuo mining area. Without the sufficient understandment of this area, it is difficult to find the aim position to exploit or control. To solve this problem, the authors focuses on the medium characteristics and the law of water transmissibility of Ordovician carbonate strata in Pingshuo, and proposes the accurate target area aiming for grouting to preventing water or developing water resources

on Ordovician top strata. This will help to provide scientific basis for mine production and construction, also for the development of water resources.

2 MEDIUM CHARACTERISTRICS

2.1 *Lithology characteristics*

The Ordovician strata in this area are buried stratum with more than 200 meters' depth. The Ordovician top strata are a set of carbonate strata consisted by dolomitic limestone, limestone containing dolostone and limy dolostone etc. From the top to 100 metres depth, the content of dolomite increases, and its accounts for 66.4%. The lithology gradually transform to limy dolostone. Then, the dolomitic limestones appear. They are interbedded. Through the component analysis of some samples, we can know that calcite content of dolomitic limestone is 71.6% and dolomitic limestone is 26.8%. In fine silt crystal limy dolostone, the percentages of dolomite, calcite and quartz are 66.4%, 31.2% and 4%, respectively. Regional geological data indicates that terrain elevated after the Caledonian movement, and then was subjected to weathering eroding in the long period (Dong S.N. & Liu Q.S. 2009) As a result, the Fengfeng formation, the upper Majiagou formation and the lower Majiagou formation of Ordovician are partly eroded, therefore the existing Ordovician top interface is an ancient peel-off strip. Thus, analysis based on the lithology and regional geological data shows that Ordovician top strata is belonged to the lower Majiagou formation the region.

2.2 *Pores characteristics*

Pores in carbonate strata of Ordovician are the main space for occurrence water. The pores with larger diameter play decisive roles in groundwater storage and transport. But the water in the pores with smaller diameter does not follow the same way. It is difficult to drive the groundwater out of them due to molecular forces taking effect, the resistance of moving (between water and the pore wall) increasing and the lower hydraulic gradient. Usually when the diameter of pores is less than 10 μm, the pores no longer work on the migration of groundwater. Through pressure mercury testing and microscopic observation of the core in the region, the pores characteristics of Ordovician top strata are shown in Table 1. The pores are mainly composed by micro pores (10 to 0.1 μm) and ultrafine pores (<0.1 μm). The effective porosity of strata decreases with the depth increasing. The permeability is few mDarcy. The effective porosity of limy dolostone is larger than dolomitic limestone's. But the pores (porosity larger than 10 μm) which contribute to the groundwater transport account for smaller proportion of all with only few percentages. Additionally, the pores with porosity larger than 10 μm account for larger proportion in limestone. This shows that hydraulic conductivity of limestone is usually better than that of dolostone under natural flow conditions.

2.3 *Structural characteristics*

The surface structural characteristics of carbonate strata at the top of Ordovician are observed and analyzed by using scanning electron microscopy by the thin section of sampling rock. Figure 1 (a, b, c, d) show the results of thin sections after zooming 1500 times by using electron microscope. The representatives of rock crystal and cleavages of carbonate strata in the top of Ordovician are distinct in Figure 1. The crystals of dolostone in Figure 1-a are coarse and brecciform with large intergranular porosity and the cleavage develops to facilitate the dissolution. In this case, intergranular and intragranular dissolution can occur simultaneously to form slightly soluble hole, which the

Table 1. The characteristics of pores in Ordovician top strata.

No of Sample	Name of rock	Depth below Ordovician interface (m)	Total amount of mercury (mL/g)	Permeability coefficient (mDa)	Average diameter of pores (μm)	Effective porosity (%)	Proportion of the pores with porosity above 10 μm (%)
35	Limy dolostone	6	0.0553	6.2324	0.1062	11.3242	3
42	Limestone containing dolostone	22	0.0318	3.9546	0.0711	6.9036	2
55	Dolomitic limestone	39	0.0037	2.7875	0.0217	0.8409	27
71	Limy dolostone	91	0.0323	5.347	0.0985	9.569	4

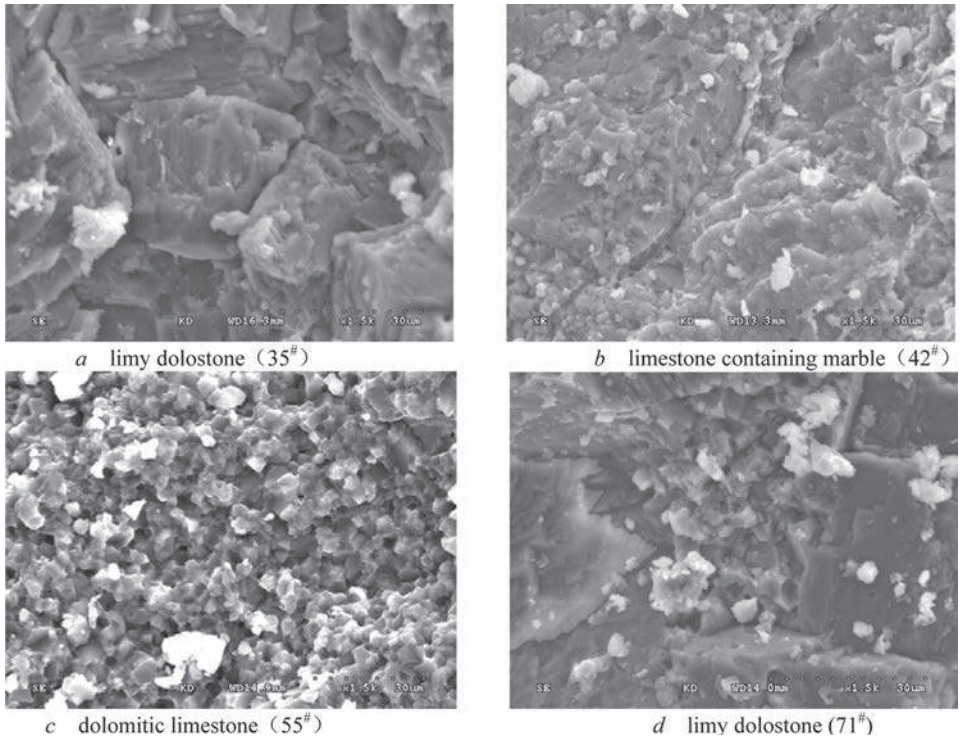


Figure 1. The part SEM figure of carbonate strata in the top of Ordovician.

dissolution rate becomes faster. The lithology in Figure 1-b and Figure 1-c are all micrite. The fine-grained crystal presents granular in Figure 1-c with immature micro-cracks. In Figure 1-b, the shape of crystal is not good and the internal cleavage does not develop, which mostly formed under the conditions of rapid accumulation. Consequently, when along grain boundary subjects to water erosion, its main behaviors are percolation and dissolution. Figure 1-d shows limy dolostone with the shape of leopard skin. It is micritic and fine-grained crystalline. Crystal in Figure 1-d is smaller than that in Figure 1-a. The crystal gap developed but it is less than 5 μm, the dissolution is also mainly along grain boundary.

3 WATER TRANSMISSIBILITY OF TOP STRATA

3.1 *Pumping test*

According to the pumping test results of five representative hydrological holes in Pingshuo mining area (Table 2), we can see that the permeability coefficient of Ordovician top strata changes within the scope of 0.0029 ~ 10.71 m/d. The unit inflow q changes in the range of 0.006 ~ 2.93 l / s • m. In these holes, the holes—K_{16}, K_{18}—are with higher permeability coefficient and unit inflow; K_1, K_2 and k_{17} holes are with lower value. The comprehensive water abundance capability of strata is from weak to moderate and the water conductivity is from weak transmissibility to moderate transmissibility. This reflects the average degree of water transmissibility based on the macroscopical pumping test in the entire expose thickness. It is worth noting that water transmissibility of Ordovician top strata is influenced by structural development greatly, in the region of developed structure, water abounds significantly larger and has the tremendous heterogeneity. For example, K_{16} hole is near the water-conducted fault F_{B26} and K_{18} is located in east wing of Luzigou anticline, near the F_{12} fault.

3.2 *Consumption rate of drilling water fluid*

Influenced by various factors, the water transmissibility of Ordovician top strata may be different along with depth. To prove the viewpoint, the results of lithological changes, footage speed and drilling water fluid consumption in the process of drilling illustrate the difference sufficiently.

Table 2. Pumping test results of Ordovician carbonate strata in Pingshuo minging area.

No of hole	Types of pumping	Test layer	Draw-down No	Still water level (m)	Draw-down (m)	Flow (L/s)	Drilling thickness of acquifers (m)	Stability time (h)	Unit flow (l/s · m)	Permeability coefficient (m/d)	Radius of influence (m)
K_1	Single hole	O_{2x}	1	1059.10	75.73	4.21	179.75	24	0.056	2.37	1167.03
			2		49.93	3.13		24	0.063	2.68	816.73
			3		25.00	1.82		19	0.073	3.11	440.87
K_2	Group holes	O_{2x}	1	1059.20	81.70	3.78	239.15	24.5	0.046	2.51	1294.53
			2		52.45	2.78		24.5	0.053	2.88	889.50
			3		28.20	1.88		24.5	0.067	3.62	536.36
K_{16}	Single hole	O_{2x}	1	1059.40	2.40	5.62	23.00	24	2.34	10.12	76.34
			2		1.54	3.99		9	2.59	10.54	49.99
			3		0.76	2.23		9	2.93	10.71	24.88
K_{17}	Single hole	O_{2x}	1	1061.20	69.25	0.45	190.89	26	0.0060	0.0029	37.27
K_{18}	Single hole	O_{2x}	1	1057.30	1.32	6.28	172.10	23	4.76	2.09	19.12

Table 3. Zoning of the water transmissibility property in Ordovician top strata in study area.

Depth below Ordovician interface(m)	Geological characteristics	Drilling water fluid consumption	Zoning name	Photos of lithology
<10~12	Lithology is more complex. There are brecciated limestone, limestone and dolostone, mostly mud-filled.	0.2~0.4 m^3/h	(*I* zone) zone with weak water transmissibility	
12~42	Lithology is micrite and limy dolostone. Sometimes there is air drilling in the main leakage segment.	1.2~1.5m^3/h, even bigger	(*II* zone) zone with strong water transmissibility	
42~80	Lithology is micrite, dolostone and brecciated limestone etc.	0.5~0.7m^3/h	(*III* zone) zone with water moderate transmissibility	
>80	Lithology is limy dolostone, dolomitic and argilliferous limestone, and drilling is difficult.	0.1 m^3/h or so	(*IV* zone) zone with weak water transmissibility	

In Table 3, the data of drilling in the Ordovician top strata are listed, including the statistic change of lithology, geological characteristics and drilling water fluid with depth. According to the analysis of data, the water transmissibility property of Ordovician top strata in the study area can be zoned in vertical.

4 FACTORS OF AFFECTING WATER TRANSMISSIBILITY

Through above analysis, some factors of affecting water transmissibility are involved. Firstly the different medium conditions affect the water transmissibility of top strata. In general, the water transmissibility of limestone is better than that of dolostone. The larger the effective porosity is and the better the water transmissibility is. The medium characteristics are internal factor of determining the water transmissibility capacity in Ordovician top strata. Geological structure, buried depth, karstification, filling status and cementation are the main external factors affecting the water transmissibility of top strata. Generally, the water transmissibility capacity is better near extension structure than pressure-shear structure. The water transmissibility of strata buried

in shallow is better than the one buried in deep. The more the karst developed, the better the water transmissibility is. The denser the filling is, the worse the water transmissibility is. Overall, the more the extension structure developed, the shallower the burial depth is and the more developed the karstification has, the less compacted filling and cementation appears and the better water transmissibility exists.

Photographs should be with good contrast and preferably in TIFF or EPS format (see Artwork document). Photographic reproductions cut from books or journals, photocopies of photographs and screened photographs are unacceptable. The proceedings will be printed in black only. For this reason avoid the use of colour in figures and photographs. Colour is also nearly always unnecessary for scientific work.

5 APPLICTION ABOUT WATER TRANSMISSIBILITY

The characteristics of carbonate strata in the top of Ordovician, such as medium characteristics and water transmissibility laws, are very useful in practices. For example, in order to prevent the high pressure water disasters in carbonate strata of Ordovician (Bai H.B. et al. 2010), lots of work are getting easy to deal with carbonate strata of Ordovician. For example, because of zone *I* is weak in water transmissibility, it can be used as impermeable layer based on the theory of Key Impermeable Layer (Miao X.X. et al. 2008). In some places, if impermeable layer has defects, it can be transformed and repaired by grouting, then the slurry dehydrates, consolidates or gels in voids or channels occupied by water formerly under the influence of pressure and time. The whole piece of water-resisting rock can be formed by stone body and gel with the surrounding rock. It can repair the defects of impermeable layer and create a advantageous hydrogeological condition to mining. Thereby, if the protection thickness of impermeable layers, including the impermeable layers in zone *I* and others which are under the Carboniferous primary mineable coal seam, are still not enough, then making a new impermeable layer by grouting II and III zone together will be considered. Until the added thickness of key water-resisting strata can prevent the carbonate aquifer groundwater into mine space. For water exploitation and conservation, zone *II* and *III* with abundance water and high water transmissibility are paid more attentions. Usually, in order to get the stable amount of water supply, the wells have to be drilled into zone *II* and *III*.

6 CONCLUSIONS

1. In Pingshuo mining area, strata lithology is a set of carbonate strata within 100 meters depth from the top of Ordovician. It consists of interbedded dolomitic limestone, limestone containing dolostone and limy dolostone etc. The strata belong to the lower Majiagou formation. Some carbonate strata have the larger karst cave. Micro-strucure tests on the more complete core of carbonate strata show that the surface is micro-fractured and karst holes are small, and the strata pores are consist of microporosity and ultramicrovoid.
2. From shallow to deep within 100 metres, Ordovician top strata can be divided into four zones based on water transmissibility. They are weak zone *I*, strong zone *II*, moderate zone *III* and weak zone *IV*. Usually Zone *I*, with the shortest distance to the Carboniferous primary mineable coal seam, can be used as the key impermeable layer. Furthermore, zone *II* and *III* can be used as a goal target for preventing water disaster, also for developing and utilizing the water resources.
3. The developing law of water transmissibility is affected by many factors. The medium characteristics are internal factors influencing the water transmissibility of Ordovician top strata. However, geological structure, buried depth, karstification, filling and cementation are the main external factors influencing the water transmissibility of top strata. If there are the undeveloped structure texture, weak karstification and dense filling, Ordovician top strata can be considered as impermeable key layer.

ACKNOWLEDGEMENTS

The authors thank for the financial support from the 973 (2013CB227900) Foundation, National Natural Science Foundation (41002087), Postdoctor Science Foundation of Jiangsu Province (1001046C) and A Project Funded by the Priority Academic Program Development of Jiangsu Higher Education Institutions.

REFERENCES

Bai H.B., Mao X.B., WU Y., et al. 2009. Research on water-reserved mining with high water pressure under large-scale thrust-fault in Ordovician karst. Chinese Journal of Rock Mechanics and Engineering 28(2): 246–252. [in Chinese].

Bai H.B., Yang J.L., Wang C.S. 2010. Research on limestone aquifuge in top Ordovician and its application in roadway excavated through graben faults. *Journal*

of Mining & Safety Engineering 27(3): 322–329. [in Chinese].
Dong S.N., Liu Q.S. 2009. Study on relative aguiclude existed inm id-Ordovician limestone top in North China coal field. Journal of China Coal Society 34(3): 289–292.
Hu Z.X., Xu J.P., Zheng S.S. 2009. Study on Ordovician limestone water bursting characteristics and controlling countermeasures in north China coalmines. Coal Geology of China 21(10): 34–36. [in Chinese].
Huang H.F., Wang C.S., Bai H.B., et al. 2012. Water protection in the western semiarid coal mining regions of China: A case study. International Journal of Mining Science and Technology 22: 719–723.
Li L.C., Yang T.H., Liang Z.Z., et al. 2011. Numerical investigation of groundwater outbursts near faults in underground coal mines. International Journal of Coal Geology 85: 276–288.
Miao X.X., Pu H., Bai H.B. 2008. Principle of water-resisting key strata and its application to water-preserved mining. Journal of China University of Mining & Technology 37(1): 1–4. [in Chinese].
Qin S.L., Li Z.S. 2008. Determination of karstic water rich zone by the use of hydro-chemical method. Coal Geology of China 20(2): 27–28, 52. [in Chinese].
Wu Q., FAN Z.L., LIU S.Q., et al. 2011. Water-richness evaluation method of water-filled aquifer based on the principle of information fusion with GIS: Water-richness index method. Journal of China Coal Society 36(7): 1124–1128.

Progress in Mine Safety Science and Engineering II – He et al. (Eds)
© 2014 Taylor & Francis Group, London, ISBN 978-1-138-00122-0

The abutment pressure distribution of extremely thick seam top coal caving longwall panel: A case study

Hua Nan
Hami Occupation Technical School, Hami, China
Henan Polytechnic University, Jiaozuo, China

ABSTRACT: Top coal caving mining method is for thick seams of more than 5.0 m. Nowadays, more and more coal mines are employing this mining method in China. To make this method safer and more productive, an extremely thick coal seam mined in Panel 21121 of Qianqiu Mine employing the fully mechanized top coal caving longwall mining was studied in detail. The results showed that the front abutment zone of panel 21121 was wider, up to 90 m with distinct zone features. Based on the characteristics of the abutment pressure trends, it can be divided into the following four zones: initial compression and plastic deformation zone, intensive compression and damage zone, roof rotation zone, and shield support action zone.

1 GENERAL INSTRUCTIONS

Top coal caving longwall mining method is one of the mining methods employed for extracting coal seams more than 5 m thick (Fig. 1). The shield supports in top coal caving mining contains two chain conveyors (AFC's). The front AFC is used to transport coal cut by the shearer. After the bottom coal is mined by the shearer and dumped into the front AFC, the top coal above the shield supports will be broken due the combined pressures from the shield supports and the overlying strata. When the tail beam is lowered and rotated toward the rear AFC, the broken top coal fragments will flow into the rear AFC as shown in Figure 1. For more detailed description of the mining method, please refer to the textbook by Zhou (2006).

The top coal caving longwall mining is widely used in China, and the coal seams to which it has been applied are getting thicker and thicker. However, as the coal seam becomes thicker, the top coal will not be fully broken and fall onto the rear AFC, rather it falls into the gob. In order to solve this problem, the first step is to understand how the front abutment pressure is distributed and how the top coal is fractured in the mining process.

Using both field measurement and theoretical analysis, this paper aims to study the nature of abutment pressure distribution and failure and migration process of the top coal in extra-thick coal seam top coal caving longwall mining.

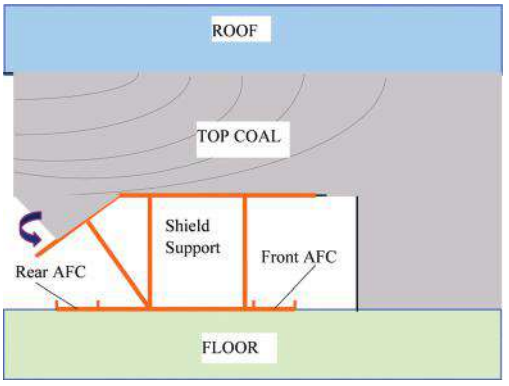


Figure 1. Schematics of the top coal caving longwall mining method.

2 BRIEF DESCRIPTION OF 21121 LONGWALL PANEL

Qianqiu Coal Mine, located at the center of Yima Coalfield, was developed in 1956 and went into production in 1958. The 21121 longwall panel was designed to employ the fully mechanized top coal caving mining method. Mining depth ranged from 616.5 to 702.5 m with an average of 659.5 m. Coal seam, averaging 11.80 m thick, was uniform. In this panel, the cutting height of the shearer at the bottom of the seam was 3.0 m, and the remaining top coal was caused to cave by self-weight.

The coal was blocky or pulverized, and prone to spontaneous combustion. The immediate roof was a dark gray and tightly-cemented mudstone, from 18.23 to 29.05 m thick, and uniformly distributed. It was brittle and broke easily forming smooth surfaces. The main roof, being very thick, was Jurassic-colored bedded conglomerate, sandstone, and powdered sandstone. The immediate floor was dark gray conglomerate with localized floor containing coarse clay layers.

3 RESULTS OF FIELD MEASUREMENTS

In order to understand the abutment pressure distribution and its effects on the failure of extremely thick coal seam, underground measurements using pressure sensors and multi-position borehole extensometers were performed. The results are shown in Figures 2 and 3.

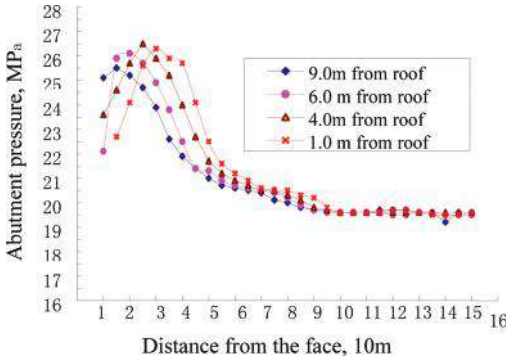


Figure 2. Distribution of the front abutment pressure at different elevations of the coal seam.

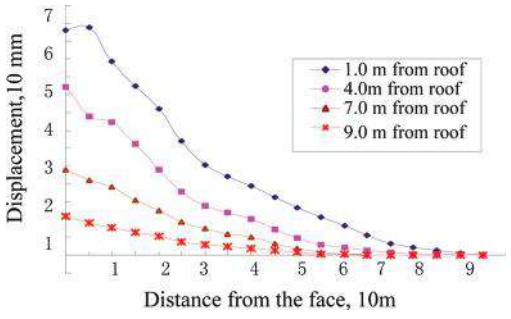


Figure 3. Distribution of coal seam displacement at different elevations.

4 THEORETICAL ANALYSIS

Analysis of the results of field measurements showed that top coal deformation and fragmentation are actually the results of the continuing development of micro-fractures in the coal, and initiation, propagation, and coalescence of fractures. Based on the results of field measurements, under normal rates of face advance, the process of damage, fragmentation, and dropping-down of the top coal requires a maximum distance of 90 m to complete. Various fragmentation processes and their applicable zones are described as follows:

1. The initial compression and plastic deformation zone. This zone begins about 90 m in front of the face. As the face advances, the top coal undergoes vertical compression and deformation under the influence of the initial coal mining operation. The deformation is derived mainly from the compression of the inherent horizontal fractures in the coal seam. As the face continues to advance, the front abutment pressure also continues to increase, plastic deformation and lateral deformation begin to occur in the top coal. This process produces micro-cracks in the coal. Field measurements showed that there are no bed separations between the immediate roof and top coal, and within the top coal.
2. The intensive compression and damage zone. This zone, approximately from 20 m to 40 m in front of the face, is located within the peak pressure area of the front abutment pressure. Due to the increasing roof pressure, the inherent fractures in the coal open up further. So are the microcracks induced in the initial compression and plastic zone. Many new fractures are also produced and developed to the full extent. As a result, top coal is damaged gradually. Field measurements showed that bed separations in this zone are well-developed between the immediate roof and top coal, and within the top coal.
3. The roof rotation zone. This zone occurs approximately from 0 m to 20 m in front of the face. In this zone the magnitude and rate of lateral movement of the top coal toward the gob increase rapidly under the pressure of the broken overhung immediate roof. Constraints from the gob side reduce greatly, allowing the fractures in the top coal to expand freely. In this zone, the fractures expand further, and top coal loses stability and begins to fall down.
4. Shield supports action zone. In this zone, the top coal near the gob edge has entered into a state of flowing and drawing of bulk materials. The special feature in this zone is that top coal, under the pressure of the caved overhung

immediate roof, becomes basically a loose bulk material. The broken coal blocks have lost their orderly arrangement and interlocking condition and slide toward the opening of drawing. However, since the top coal is very thick, the middle part of the top coal often does not break fully and acts like short beams. As a result, the lower and middle portions of the top coal are difficult to draw. Even if remedial measures are taken to break them loose, arches are easily form across the opening of drawing, resulting in a large quantity of top coal being left behind in the gob. Therefore, shied support plays an important role. The repeated lowering and resetting of support legs and forward movement of shield can increase the facture intensity of the lower portion of the top coal, thereby resulting in drastic reduction of the formation of arch structure across the opening of drawing.

5 CONCLUSIONS

Based on the field measurements and theoretical analyses, the following conclusions can be made:

1. With thicker top coal, the advancing front abutment zone of the top coal caving longwall face in panel 21121 was wider, up to 90 m.
2. With thicker top coal, there exit distinct layers, and stress distribution and deformation for each layer are different in the top coal.
3. The front abutment zone of the top coal in panel 21121 could be divided into four zones: Initial compression and plastic deformation zone, intensive compression and damage zone, roof rotation action zone, and shield supports action zone.

ACKNOWLEDGMENT

This research was funded by Technology support project of Xinjiang Autonomous Region (2013911038) and International program of Henna Province (104300510033).

REFERENCES

Kang Tianhe & Jin Zhongming 1999. Laws of coal-rock movement and derived support parameters for a fully mechanized sub-level caving face in a gently inclined seam. International Mining & Minerals, 255–286.

Wang Jiachen 2005. Fully mechanized longwall top coal caving technology in China and discussion on issues of further development. *Coal Science and Technology*, 14–18.

Wu Jian 1999. Fifteen years of mechanized top caving technology in China. *China Coal*, 9–13.

Zhang Dongsheng & Xu Jinhai 2003. The mining model of high production and high efficiency new technique, *China University of Mining & Technology*, 18–112.

Zhang Mengtao 1987. The instability theory of rock bursts and its numerical simulation. *Journal of Rock Mechanics and Engineering*, 97–200.

Zhou Ying 2006. Introduction of Coal Mining, Coal industry publisher, 1–36.

This page intentionally left blank

Progress in Mine Safety Science and Engineering II – He et al. (Eds)
© 2014 Taylor & Francis Group, London, ISBN 978-1-138-00122-0

Research on the fractal characteristics of pore structure of coal particles based on low temperature nitrogen adsorption method

L.C. Dai
National Key Laboratory of Gas Disaster Detecting, Preventing and Emergency Controlling, Chongqing, China
Chongqing Research Institute, China Coal Technology and Engineering Group, Chongqing, China

B.S. Nie & L. Li
School of Resource and Safety Engineering, China University of Mining and Technology (Beijing), Beijing, China

ABSTRACT: Based on low-temperature nitrogen adsorption principle, the pore structure of coal particles is tested and adsorption isotherms of coal particles with different size are obtained by Quantachrome Autosorb-iQ automatic specific surface area and pore size distribution analyzer. Then, microstructure characteristic parameters such as specific surface area, pore volume and average pore size of coal particles are calculated. Besides, fractal dimension of the internal surface of coal particles is calculated with FHH fractal theory. The relationship between fractal dimension and pore structure parameters together with the adsorption capacity of coal particles is analyzed. Studies show that: fractal dimension can characterize the variation of characteristic parameters such as specific surface area and total pore volume of coal particles. In addition, with the increase of fractal dimension, the surface heterogeneity of pore structure is strengthened and so is adsorption capacity. The findings can provide a certain theoretical foundation for mechanism study on coal gas adsorption, desorption and seepage.

1 INTRODUCTION

Coal is a typical double porous media containing both pores and fractures (Yu Bufan 2000).The porosity of coal is determined by its structural characteristics. At the same time, the pore characteristics of coal largely determine its properties such as gas adsorption ability, permeability and intensity (Liu Fangbing 2008). It is confirmed by studies that coal porosity is a system composed of pores with different magnitude. The diameter of these pores range from 0.5 nm to 100000 nm. And there is extremely developed micro-pore within the coal. Specific surface area, pore volume, pore model and pore size distribution can be used to characterize the characteristics of pore structure. It is very important to study the micro-pore structure of coal. For these studies can provide theoretical basis for the mechanism research of coal gas adsorption, desorption and seepage. In recent years, scholars at home and abroad have done a lot of researches on pore characteristics of coal sample by taking advantage of low-temperature nitrogen adsorption method and mercury intrusion method and certain achievements have been acquired (Li Guoxi 2006, Xing Deshan 2007, Jiang Wenping 2011, Qi Lingling 2012).

The pore structure heterogeneity of coal is large, so pore size distribution is difficult to be described by traditional Euclidean geometry theory. With the formulation and development of fractal theory, it is applied to the complex pore structure characteristics research of coal. Tong Hongshu, et al. 2004 calculated the fractal dimension of pore volume and specific surface area of coal and discussed the relationship between gas adsorption capacity of coal reservoir and pore fractal dimension. Zhang Yutao, et al. 2007 carried out quantitative description and research on the pore structure of coal with fractal theory. Song Xiaoxia, et al. 2013 collected nine representative coal samples from zhongliangshan south mine for low temperature nitrogen adsorption experiment and analyzed the relationship between the adsorption pore's fractal characteristics and fractal dimension of tectonic coal and its gas adsorption capacity. Therefore, based on the previous studies, the pore structure of coal particles is tested by Quantachrome Autosorb-iQ automatic specific surface area and pore size distribution analyzer and the microstructure characteristic parameters of coal particles are calculated. Besides, quantitative research is carried out on the pore structure of coal with fractal theory.

2 EXPERIMENTAL PRINCIPLES AND METHODS

2.1 *Experimental equipment*

The equipment used in experiments is Quantachrome Autosorb-iQ automatic specific surface area and pore size distribution analyzer, as shown in Fig.1. The working principle of the equipment is static volumetric method based on isothermal physical adsorption. There are two out-gassing stations on Autosorb-iQ and depuration of two samples can be performed simultaneously. What's more, we can carry on testing and calculation of many physical parameters by taking advantage of this equipment. Physical parameters that can be tested and calculated include Langmuir specific surface area, single-point and multi-point BET specific surface area, DH pore size distribution, BJH pore size distribution, DR microporous surface area, average pore diameter, total pore volume and so on.

2.2 *Production of coal samples*

Coal samples of 9# seam of fenghuang mine in shanxi province were collected. And the samples were prepared into coal particles with five different mesh in the laboratory, 10–20 mesh, 20–40 mesh, 40–60 mesh, 60–80 mesh and 80–100 mesh were included, as specified in Table1 and Table2.

2.3 *Experimental procedures*

BET testing was adopted in the experiment. Besides, N_2 of high purity was taken as adsorbate and adsorption volume of N_2 under different pressures was tested in the case of 77.2 k, which is the boiling temperature of liquid nitrogen. The experimental relative pressure ranges from 0 to1.



Figure 1. Quantachrome Autosorb-iQ.

Table 1. Experimental coal sample industrial analysis.

Sample	Water content (%)	Volatile components (%)	Ash (%)	Fixed carbon (%)
9#	3.17	7.09	8.32	81.42

Table 2. Situation of coal sample preparation.

No.	Coal particles (Mesh)	Particle size (um)	Average size (mm)
1	10–20	840–2000	1.42
2	20–40	420–840	0.63
3	40–60	250–420	0.335
4	60–80	178–250	0.214
5	80–100	150–178	0.164

Experimental procedures are as follows: (1) Determination of gross weight of the sample tube. Weigh the clean empty sample tube using balance with accuracy of 0.1 mg, and record its value; (2) Sample out-gassing. Load coal sample into the empty sample tube that has been weighed, put sample tube into the heating mantle, and then install sample tube on the outgas station. Afterwards, deal with the sample in a vacuum heating condition to remove impurities on the surface and moisture in pores of the sample. After processing is complete, cool the sample tube to room temperature and remove it from the outgas station. Then weigh the weight of sample tube using balance with accuracy of 0.1 mg, subtract the gross weight and the weight of sample out-gassed is obtained. (3) Sample analysis. Pour fresh liquid nitrogen into the Dewar and ensure that the liquid nitrogen can meet the analysis needs for 60 h. Turn on the computer and start Autosorb-iQ analysis software. Afterwards, click start analysis and set appropriate parameters, and then carry out the experiment. (4) Carry out measurement of adsorption quantity on the basis of the previous settings. The adsorption isotherm of coal samples will be automatically generated.

3 RESULTS OF THE EXPERIMENTAL ADSORPTION ISOTHERM

According to the experimental procedures given by 2.3, adsorption isotherms for five different coal particles were measured by Autosorb-iQ automatic

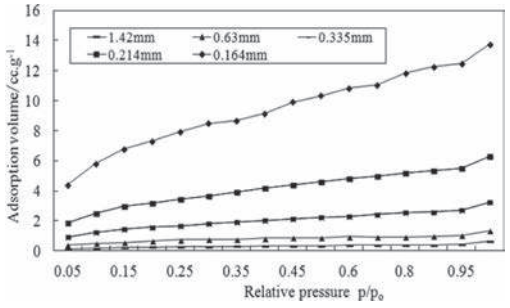


Figure 2. Different coal particles adsorption isotherms.

specific surface area and pore size distribution analyzer. Results are shown in Fig. 2.

It can be seen from Fig. 2 that: the N_2 adsorption isotherm of coal samples in different size show similar trends. The adsorption quantity of N_2 increases with the increase of relative pressure p/p_o, and the adsorption quantity of N_2 also increases with the increase of coal size.

4 CALCULATION AND ANALYSIS OF STRUCTURAL PARAMETERS OF COAL PARTICLES

Parameters that can characterize the structure of coal particles include: specific surface area, pore volume and average pore size. And they have different degrees of influence on the adsorption capacity of the adsorbent. According to the characteristics of the samples' adsorption isotherms, the specific surface area of the adsorbent is calculated by BET method, while the total pore volume and pore size distribution of sample should be calculated by the Kelvin equation (Brunauer. S et al. 1938).

The microstructure characteristic parameters of coal particles in different particle size were calculated according to the above principle and the calculation results were shown in Table 3.

It can be seen from Table 3 that, within a certain range of coal size, the specific surface area and total pore volume of coal particles increase gradually with the reduction of coal particle size, at the same time, the corresponding average pore size decreases. The results are consistent with the research results of literatures (Ren Gengpo et al. 2007).

5 THE FRACTAL CHARACTERISTICS OF PORE STRUCTURE OF COAL PARTICLES

5.1 *Fractal dimension*

Fractal refers to shapes that are similar in global and local in some way. Fractal dimension is one of the main parameters of fractal, which depicts the essential characteristics of fractal set quantitatively. The solution of fractal dimension is the key to solve practical problems with fractal concept (Sun Xia 2006). Methods to determine fractal dimension include physical methods and chemical methods (He Long 2010) Physical methods used frequently include electron microscopy and low-frequency Raman scattering, while chemical methods consist mainly of adsorption method and thermodynamic method. Adsorption method is a method to solve fractal dimension using adsorption isotherms, adsorption volume, capillary condensation and the relationship between physical and chemical parameters of adsorbate. Studies have shown that: it is the best way to solve fractal dimension with adsorption method.

Therefore, fractal is applied to describe the surface and structural inhomogeneities of coal particles and adsorption method is selected to solve fractal dimension. The value of fractal dimension D of coal particles ranges from 2 to 3. It can be demonstrated that the surface of coal particles is smoother when the value of fractal dimension D is closer to 2. However, the surface of coal particles is rougher and the heterogeneity of pore distribution is stronger when the value of fractal dimension D is closer to 3.

Studies have shown that: the definition formula of surface fractal dimension is as follows:

$$n \propto r^{-D} \tag{1}$$

Where D is surface fractal dimension, n indicates the number of molecules with radius r required for covering the surface of material.

According to Frenkel-Halsey-Hill (FHH)model, the calculation equation of fractal dimension is (Pfeifer P & Liu K 1997):

$$\ln\left(\frac{v}{v_m}\right) = \ln k + S \bullet \ln\left[\ln\left(\frac{p_0}{p}\right)\right] \tag{2}$$

Where v_m indicates the adsorption volume of complete monolayer adsorption, v is the adsorption volume under equilibrium pressure p, S, k are constants related with adsorption mechanism and fractal dimension, p_0 indicates saturation pressure.

Based on Fig.1, consider that the adsorption interface is controlled by capillary cohesion (i.e. surface tension) in the process of coal adsorption of nitrogen, the following can be obtained:

$$S = D - 3 \tag{3}$$

According to the calculation expression of FHH model, there is a linear relationship between

Table 3. Coal particle structure parameters experimental results.

Size (mm)	Pipe GW (g)	Pipe and coal weight (g)		Surface area ($m^2 \cdot g^{-1}$)	Total pore volume ($cm^3 \cdot g^{-1}$)	Average pore size (nm)
		Before degassing	After degassing			
1.42	20.6335	23.6972	23.6278	0.960	0.000998	4.159
0.63	20.6338	23.6258	23.5495	2.478	0.002130	3.438
0.335	20.6328	23.7196	23.6516	5.927	0.005029	3.394
0.214	20.6334	23.6293	23.5705	11.95	0.009752	3.264
0.164	20.6359	23.8288	23.7671	27.66	0.02126	3.074

Table 4. Fractal dimension results.

Coal	1.42 mm	0.63 mm	0.335 mm	0.214 mm	0.164 mm
Slope S	0.1847	0.171	0.1605	0.1579	0.1535
D	2.8153	2.8290	2.8395	2.8421	2.8465

$\ln(\frac{v}{v_m})$ and $\ln[\ln(\frac{p_0}{p})]$. Therefore, the relationship diagram between them can be made according to the adsorption isotherm of coal samples and the slope of the straight line obtained is S. Then, fractal dimension D can be solved with formula (3).

Based on the analysis theory above, the calculation results of fractal dimension of different coal particles are obtained by Quantachrome Autosorb-iQ software, as shown in Table 4.

5.2 *Coal particles fractal structure*

According to the data in Table 3 and Table 4, the relation between pore structure of coal particles and fractal dimension can be obtained, as shown in Table 5.

It can be known from Fig. 3 that, in a certain coal particle size, the number of holes inside coal particles increase with the decrease of coal particle size. Besides, with the decrease of coal particle size, the pore structure become more and more complex, and the heterogeneity of pore distribution of coal particles is stronger, moreover, the surface structure of coal particles also tends to become complex, indicating that the surface of coal particles become more rough. As a result, the fractal dimension of coal particles increases to be more and more close to 3, which conclusion is similar to literature (Jiang Xiumin et al. 2003). There is a simple linear relationship between the two:

$$y = -0.0237x + 2.8476, R^2 = 0.9628. \quad (4)$$

It can be known from Fig. 4 and Fig. 5 that the fractal dimension of coal particles increase with the increase of coal surface area and total pore volume. The increase of surface area inside coal particles strengthens the roughness of pore surface. Furthermore, the increments of pore surface area and the promotion of pore surface roughness provide more adsorption sites, therefore, the adsorption capacity of coal is reinforced. It can be seen that, the value of fractal dimension inside coal particles can reflect the adsorption capacity

Table 5. The relation between pore structure of coal particles and fractal dimension.

Size (mm)	Surface area ($m^2 \cdot g^{-1}$)	Total pore volume ($cm^3 \cdot g^{-1}$)	Average pore size (nm)	D
1.42	0.960	9.981×10^{-4}	4.159	2.8153
0.63	2.478	2.130×10^{-3}	3.438	2.8290
0.335	5.927	5.029×10^{-3}	3.394	2.8395
0.214	11.95	9.752×10^{-3}	3.264	2.8421
0.164	27.66	2.126×10^{-2}	3.074	2.8465

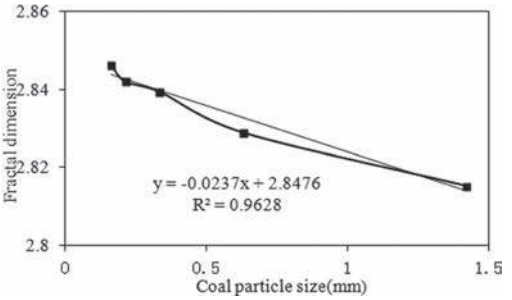


Figure 3. Correlation between fractal dimension and coal particle size.

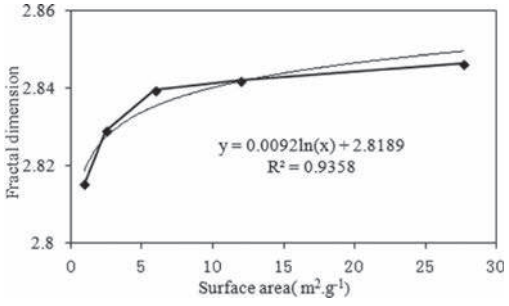


Figure 4. Correlation between fractal dimension and surface area.

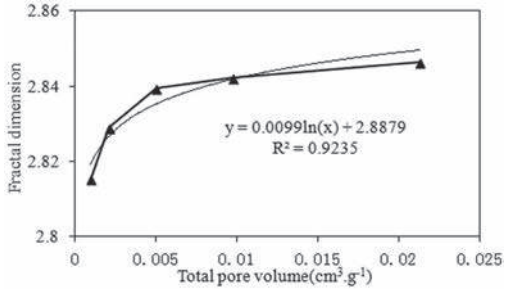


Figure 5. Correlation between fractal dimension and total pore volume.

of coal. Once the fractal dimension increases, the adsorption capacity of coal will also increase.

6 CONCLUSIONS

1. The adsorption isotherm of coal particles with different size were studied using Autosorb-iQ automatic specific surface area and pore size distribution analyzer based on low temperature nitrogen adsorption principle.
2. The fractal dimension of the internal surface of coal particles is calculated with FHH fractal theory. In addition, the relationship between fractal dimension and pore structure parameters together with the adsorption capacity of coal particles is analyzed.
3. The studies on the microscopic pore structure characteristics of coal particles can provide certain theoretical references for mechanism studies such as gas adsorption, desorption and seepage in coal body.

ACKNOWLEDGEMENTS

The authors gratefully acknowledge foundation by the China National Key Basic Research Development Project Program (2011CB201202 and 2012CB724206).

REFERENCES

Brunauer. S, et al. 1938. Adsorption of gases in multimolecular layers. *Journal of the American Chemistry Society*, 60:309–319.

He Long 2010. Experimental Research on Activated Carbon Fibers Used for the Separation of CH_4/N_2. Beijing: China University of Mining & Technology (Beijing) (in Chinese).

Jiang Wenping, et al. 2011. Research on the pore properties of different coal body structure coals and the effects on gas outburst based on the low-temperature nitrogen adsorption method. *Journal of China Coal Society*, 36(4):609–614 (in Chinese).

Jiang Xiumin, et al. 2003. Fractal Characteristic of Surface Structure of Micro-Pulverized Coal. *Proceedings of the Csee*, 23(12):165–169 (in Chinese).

Li Guoxi 2006. Adsorption science. Beijing: Chemical Industry Press, 107–110 (in Chinese).

Liu Fangbing 2008. Experimental study on the mechanical property of coal containing gas. Beijing: China University of Mining and Technology (Beijing) (in Chinese).

Pfeifer P & Liu K 1997. Multilayer adsorption as a tool to investigate the fractal nature of porous adsorbents. *Studies in Surface Science and Catalysis*, 104:625–677.

Qi Lingling, et al. 2012. Study on porosity of coal samples based on low temperature nitrogen adsorption method and mercury porosimetry. *Coal Science and Technology*, 40(8):36–39 (in Chinese).

Ren Gengpo, et al. 2007. Analysis of Surface Area and Pore Structure of Datong Coal. *Journal of Combustion Science and Technology*, 13(3):265–268 (in Chinese).

Song Xiaoxia, et al. 2013. Fractal characteristics of adsorption pores of tectonic coal from Zhongliangshan southern coalmine. *Journal of China Coal Society*, 38(1):134–138 (in Chinese).

Sun Xia 2006. Fractal Theory and Application. Hefei: China Science and Technology University Press (in Chinese).

Tong Hongshu & Hu Baolin 2004. Research on the fractal characteristics of pore of coal reservoirs tested with cryogenic nitrogen adsorption in the ordos basin. *Coal Technology*, 23(7):1–3 (in Chinese).

Xing Deshan & Yan Weiping 2007. Analysis to pore structure of typical semi-cokes by mercury porosimetry. *Journal of North China Electric Power University(Natural Science Edition)*, 34(5):57–63 (in Chinese).

Yu Bufan 2000. Prevention of Coal-mine Gas Hazards and Utilization Manual. Beijing: Coal Industry Press (in Chinese).

Zhang Yutao, et al. 2007. Features of fissure sharp in coal borehole and variation law with temperature. *Coal Science and Technology*, 35(11):73–76 (in Chinese).

This page intentionally left blank

Progress in Mine Safety Science and Engineering II – He et al. (Eds)
© 2014 Taylor & Francis Group, London, ISBN 978-1-138-00122-0

Research on experiment test system of mechanism of fame propagation for gas and coal dust explosion

Licong Zhang, Liping Liu & Jingde Xu
North China Institute of Science and Technology, Beijing, China

ABSTRACT: The experiment test system of gas and coal dust explosion is constructed in this paper, which mainly include body of pipe system, measuring system of explosion pressure and flame data, gas distribution system, delay system of laser trigger, laser schlieren system and vacuum chamber (pumping vacuum before experiment), in order to study the mechanism of propagation for gas and coal dust explosion in pipeline and ensure the change characteristics of main physical qualities characterizing gas and coal dust explosion. Gas circuit, data acquisition cable and power line are integrated in console with gas filling and distribution system through isolated slots respectively. Special optical windows are set in both experimental and transition section, which are used for flow visualization and spectral measurement (component and temperature). Multichannel pressure (piezoelectric and piezoresistive sensors), flame speed measuring and data acquisition systems designed. The experiment test system can simulate complex burning, explosion and mechanism of propagation in coal mine, so it has broad application prospects in studying equipment of anti-explosion and explosion-proof, surveying accident scene and basic research of gas explosion in gas explosion accident of coal mine.

1 INTRODUCTION

With the analysis of the reason of gas and coal dust explosion accident in mine, it can be known that gas and coal dust result in explosion when they meet the explosion concentration limit and encounter source of ignition, then they propagate rapidly and cause damage to mine equipment and the safety of human life. In the process of explosion propagation, the amount of damage of explosion accident is depended on the change characteristics of flame wave, so it's greatly important to study the propagation law of flame and shock wave of gas and dust explosion (Si et al. 2007). Meanwhile, it has widespread and profound significance for the study of occurring mechanism of gas and coal dust disaster, the characteristics of gas and dust explosion and its law of evolution and propagation with the method of advantaged test.

2 OVERALL DESIGN

In coal mine, although gas and dust may explode in any place, most of explosion accidents often occur in coal mining and tunneling faces. Normally, the layout of roadway space of coal mining and tunneling faces can be simplified into pipeline space model of one end being closed and the other one

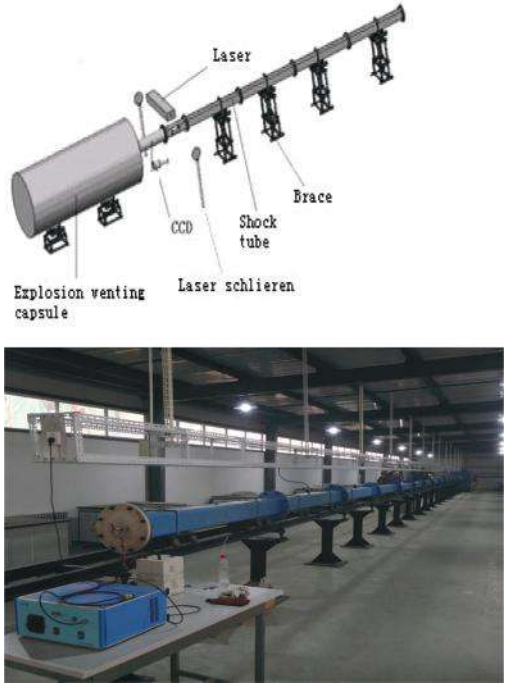


Figure 1. Brief diagram of overall layout of experiment test system.

being open or both ends being open, which is used in this experiment (Donald & Henry 1974).

The overall arrangement of the experiment test system of gas and coal dust explosion is as follows, which includes body of pipe system, flow visualization system, data measuring system and gas distribution system.

3 SUBSYSTEM DESIGN

3.1 *The design of pipe body system*

Pipe body system includes ignition section (ignition flange and ignition section), switching section, experiment section and vacuum tank.

The pipe body uses cold-drawing square pipe with 200 mm × 200 mm in area of section and 40 m in length, inside and outside the wall of which can be electroplated in order to increase its life span and be convenient for spectrum measurement (Zhang et al. 2004).

Ignition section and ignition system: they are needed for combustible gas ignition with low pressure or ignition in other faces and simple shock experiment.

Igniter: capacitive igniter with high ignition energy. The ignition energy can be adjusted by means of adjusting voltage and capacitor. The discharge frequency and pulse width both can be adjusted. A charging voltage indicator is also included (Lin & Qian 2004).

Ignition end cap of low initial pressure is used to keep igniter and shell of pipe from discharging because of the difference of gas dielectric constant and initial pressure, which is as shown in Figure 3.

Mechanism of double membrane: it can be used combined with detonation initiation and to study the evolution of flame which is caused by deflagration wave getting through inert agent, in order to learn about and evaluate the mechanism and effectiveness of fire retardant.

The observation window of experimental section is as shown in Figure 5. Transmission diameter of circular window is 300 mm; K9 glass and quartz glass (S1) are used in flow optical display and spectral measurement respectively. Considering optical measurement (spectral measurement, flow imaging) needing observation window, we weld metal frame outside of tube wall, which is regarded as support of glass installation. In addition, to keep glass from damage, glass is preloaded into glass frame of knock-down so that it only needed to dismantle the metal frame every experiment.

Experimental section of optical measurement is the most important and complicated link in the whole equipment design (Wu et al. 2005). In measurement of optics, it's needed that the upstream of experimental section provides the signal of xenon lamp of trigger laser such as electric signal obtained from flame surface or shock wave. Sensor need to be located on the experimental section when it's required.

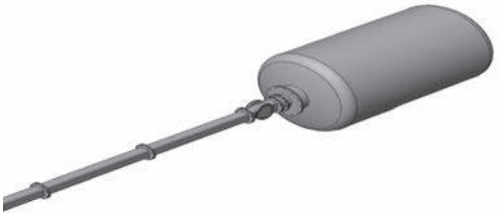


Figure 2. The diagram of pipe body.

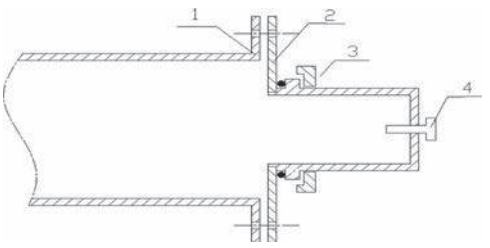


Figure 3. Brief diagram of ignition section.

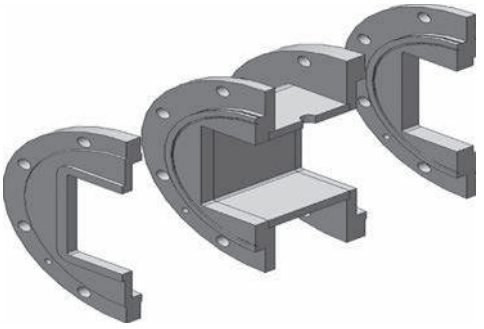


Figure 4. Brief diagram of double membrane section.

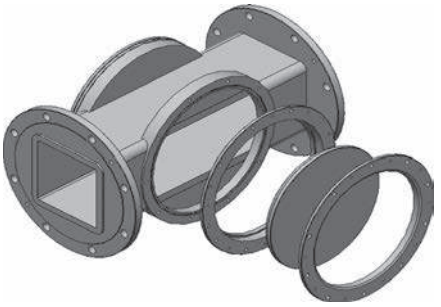


Figure 5. Brief diagram of experimental section.

Design of vacuum tank. It is shown that the volume of vacuum chamber should be 5–10 times the total volume of pipeline, which can ensure the safety of experiment with avoiding end face reflection shock wave damaging observation window because of overpressure (Zhang & Xu 2010). Besides, the vacuum chamber requires a certain length to prevent explosion gas products or the reflection wave of shock wave from rushing into experimental section, which may interferes the flow observation and measurement in relatively slow process of experimental section. This pipeline system is one of the relatively long experimental pipelines in our country currently and the pressure after the reflected shock of deflagration and detonation is very high, so, in the experiment of optical measurement, diaphragm needs to be placed between the experimental pipeline and vacuum chamber to ensure safety. Shock wave reflects on the diaphragm then the pressure inside pipeline will be unloaded quickly.

The situation inside monitoring module: CCD is designed and installed to test the change of explosion gas jet-flow in vacuum module and whether vacuum module is damaged or not in the experimental process.

Safety window: safety window that can cover rubber need to be installed in the tank to guarantee the safety of vacuum module. The safety rubber will automatically break and unload when the pressure inside vacuum module is higher than scheduled critical value.

Empty module operation: vacuum need to be pumped before experiment, which means waste gas of the last experiment need to be pumped, vacuum module and experimental section need to be separated with diaphragm (Xu et al. 2012).

Size estimation:

$$V_{管} = s \cdot L = a^2 \cdot L \tag{1}$$

$$V_{罐} = \mathrm{A} \cdot \mathrm{L}_1 = \frac{\pi d^2}{4} \cdot L_1 \tag{2}$$

$$NV_{管} = \mathrm{V}_{罐} \tag{3}$$

$$\Rightarrow d^2 L_1 = Na^2 L \cdot \frac{\pi}{4} = 4Na^2 L / \pi \tag{4}$$

若$a = 0.4$, $L = 40$, $N = 10$

$$\Rightarrow 2a\sqrt{\frac{NL}{\pi L_1}} = d \tag{5}$$

For overall consideration, we let $N = 5$, and then we have $L = 6.3$ m, $d = 1.6$ m

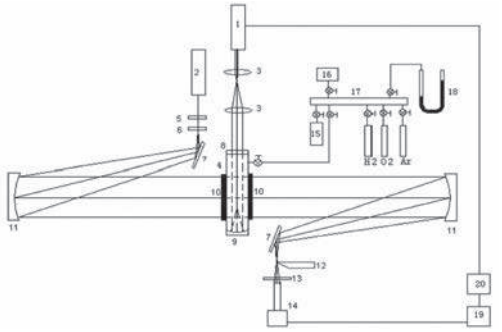
3.2 *Design of flow visualization*

The layout of measuring hole: measuring hole is placed on the three sides of a designated spot (usually every 1 meter) of every section and sensors with special support are installed on these measuring holes. Optical measurement leads flame emitted light to spectrograph through fibre-optical to do component and temperature measuring. Piezoelectric or piezoresistive sensor need to be preposed to avoid signal interference and serious attenuation (Zhang et al. 2011).

The display instrument in flow field is laser schlieren system, the diagram of typical schlieren system is as shown in Figure 6.

The theory of laser schlieren system: schlieren system is that reflecting the first order partial derivative with the change of refractive index in flow field and it can capture the shock wave and contact discontinuity. To combustion flow field with self-luminous light, the light given in flow field and illuminant will both cause film exposion.

The light path of He-Ne laser of ruby laser 2 is adjusted and aligned by the other He-Ne laser 1 through semi-permeable mirror 4. The concave reflector 11 has a focal length of 1.5 m, and the beam expander 6 has a focal length of 5 mm. After getting through dimmer 3 and light beam regulator 5, laser beam is expanded by beam expander 6, and only the relatively even part in the center of light spot gets through the reflector. Collimated light with 150 mm in diameter is focused by another concave reflector after getting through experimental section. The light beam after focused images at the film with photographic objective 14. Using filters to filter the detonation reaction of luminescence, camera B is allowed to be opened for several minutes with no film exposure. The signal of piezoelectric sensor close to the experimental section triggers ruby laser after preset delay.



1 Nd: YAG laser; 2 He-Ne laser; 3 concave mirror; 4 combustor; 5 beam adjustor; 6 expander; 7 turning mirror; 8 quartz glasses; 9 532 nm convex mirror; 10 window; 11 convex mirror; 12 knife edge; 13 filter; 14 high-speed photograph;15 tank; 16 vacuum pump; 17 gas distributor; 18 vacuum gauge; 19 signal generator; 20 delay generator.

Figure 6. Layout of experimental facilities.

The schlieren system includes light source system, reflector system, imaging system and filter.

Light source system: the light source can generally be divided into continuous and pulse light source, which is suitable for taking flow image of continuous and transient change process respectively.

Continuous light source contains lamp bulb, focusing system and slit. The lamp bulb is halogen tungsten lamp with 24 volts of voltage and 150 watts of power. Condenser system: condensing lens is consisting of two doublets. It images the filament on slit so that secondary light source (actual light source) is formed. One doublet is set to move back and forth in order to focus accurately. The slit has two movable simultaneously blades with 0.01 mm of minimum reading. The slit mechanism can make 360 degrees rotation round optical axis to choose different orientation. Male tabs with little holes are installed on the blade surface of slit for shadow photography. In addition, in order to test whether the image of light source seats properly on the slit plane or not, magnified equipment may be prepared.

Pulse light source contains spark discharge and pulse laser. Pulse illuminant need to use external signal (such as pressure or strain signal) to trigger and synchronous control circuit with a time delay unit. Pulse laser, such as ruby laser of monopulse (with $\lambda = 694.3$ nm of wavelength), uses external signal directly to trigger xenon lamp, and then glares time-delay with adjusting Q.

Reflector system: the focal length of spherical reflector generally is 10 times its caliber. The error of machining surface of the spherical mirror is less than or equal to $\lambda/4$ or $\lambda/8$ (interference display). Spherical reflector needs to be plated aluminized reflective film; the strain of glass blank is not more than 2 degree after precise annealing. Schlieren picture frame is designed specially, which takes three point supports. Schlieren mirror is stress-uniform after put in the frame which prevents local deformation. There are appropriate gap between schlieren mirror and its frame, which serves as temperature expansion allowance to prevent the influence of the room temperature change. Schlieren mirror frame has pitching and rotating adjusting mechanism of free degree which can be locked.

Imaging system: it ordinarily contains little reflector, cutter point, filter, special lens and imaging medium. The cutter point includes black-white and color edge and is the key component of schlieren apparatus. It is parallel to the source slit and is located in the focal plane of reflector. When there is no disturbance in the flow field, if the knife cut off part of the image of the source, light intensity on photographic plane will weaken uniformly. Black and white edge has steel sheet with a straight edge. Color edge is spliced with optical module or slide film which is precise finished by optical glasses of three different colors. It is blue in the middle, red and yellow in the two sides. The two cutter points can be replaced conveniently. Its edge can translate along the vertical direction of edge with displacement distance of ±5 mm and the minimum scale of 0.01 mm. The edge mechanism can make 360 degrees rotation round optical axis and can move back and forth along optical axis. It is located accurately at the focal point of reflector.

The parameter choice of filter: in the burning field (such as detonation), self-luminous light has to be filtered out in order to get clear schlieren photos. The measures which should be taken are: (i) the light source adopt ruby laser with pulse width of 40 ns, central wavelength of 694.3 nm, and pulse power of 20 mJ and light beam diameter of 6 mm. (ii) Filter is placed in front of the camera, it allows ruby laser to get through and filter out other lights. The parameter of filter is as follows: its central wavelength is 694.3 nm, its semiband width is 15 nm, and its transmissivity is bigger than 60% when 694.3–7.5 nm $\leq \lambda \leq$ 694.3 + 7.5 nm, its transmissivity is less than 1% when $\lambda \leq$ 694.3–7.5 nm or $\lambda \geq$ 694.3–7.5 nm.

3.3 *Parameter measurement platform*

The measurement of flame speed: the detonation study is usually concerned about the measurement of flame speed. Strictly speaking, flame is the concept of Engineering Combustion. Flame is not unidimensional and its speed measurement is based on average measurement. The main components of measuring channel of every flame speed are as shown in Figure 7. The use of fiber-optical is to increase the adaptability of measuring system.

The measurement of components (photomultiplier and spectrograph): the channel 3 spectrograph is used, chromatograph measures reaction product of detonation and combustion or main number of free radical. This system uses system that emission or absorption spectrum measure the component concentration.

Temperature measurement: using emission spectrum of double wavelength, self-developed.

Stress measurement: 20 channels, multi-channel data acquisition card of high speed, piezoresistive and piezoelectric sensors.

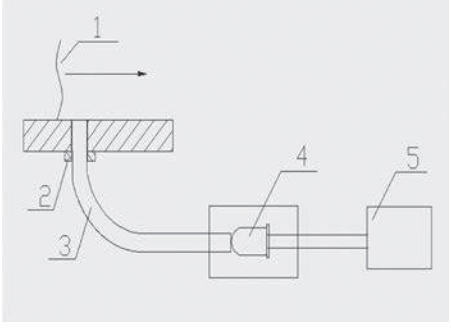
3.4 *Gas distribution, vacuum and control system*

These three subsystems are all integrated on the experiment table. The main role of gas distribution system is pumping vacuum in pipeline, filling with specified pressure and mixture concentration and displaying pressure. The system mainly contains

pressure gauge, mercury column (and vacuum pressure gauge), gas distribution tank, gas bottle, electromagnetic valve, hand valve, connecting windpipe, which is shown in Figure 9.

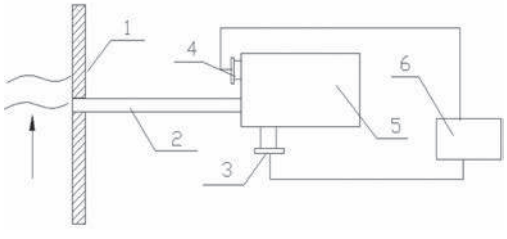
The integration of vacuum system and gas distribution is mainly for pumping vacuum in pipeline, vacuum chamber and gas distribution tank. It consists of vacuum pressure gauge, vacuum pump, electromagnetic valve and jointing pipeline.

The control system serves as valve operating, igniting, date collecting, the monitoring of experiment field and warning. In pipeline, the parts that connect the experiment pipeline all use hand valve and the other adopt electromagnetic valve to drive air operated valve. In order to be convenient for unified operation and control, we design an operation desk that is as shown in the following Figure, which integrates the above three subsystem on the control panel (shown in Figure 10). There are valve controlling system, warning system and data acquisition system of main parameters (pressure, temperature and speed).



1. Flame surface; 2. Platen; 3. Fiber-optical; 4. Photoelectric sensor; 5. Oscilloscope or A/D card.

Figure 7. The measurement of flame speed and data acquisition system.



1. Wall surface; 2. Fiber-optical; 3. ICCD camera; 4. Photomultiplier; 5. personal computer.

Figure 8. The diagram of spectrograph measuring component concentration.

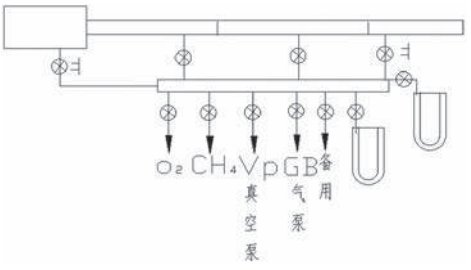


Figure 9. Theory diagram of gas distribution and vacuum system.

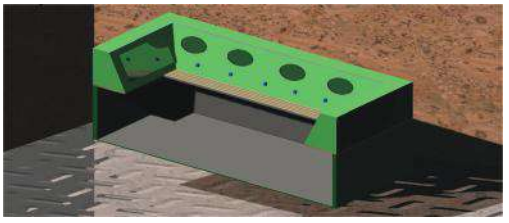


Figure 10. Control desk of operation.

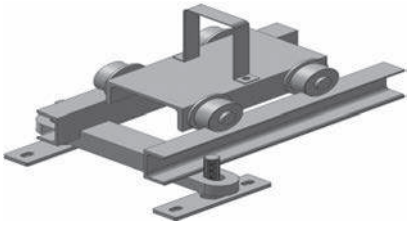


Figure 11. The diagram of lead rail of little car

3.5 *Support design*

The equipment support contains support, lead rail and little car system. The wheeltrack of the little car moves flexibly and has small lateral displacement. The whole lead rail is placed on the shore which can adjust height and horizontal shift. It is shown in experiment that it matches with the pipe body integrated with dowel of every pipeline section and it's a high-precision support system of flexible operation. This support is self-designed and manufactured.

3.6 *Layout of pipeline*

The gas circuit and signal measuring circuit, power and monitor cable should be installed separately to keep clean and beautiful, be convenient for checking. The intake pipe uses high-pressure hose; valve fast joints should be adopted as many as possible for convenient operation.

4 CONCLUSION

The subsystem is modularized designed and convenient for operation and maintaining. The test technology (mainly for optical measurement) is advanced and can display accurately the detonation and deflagration flow field of high speed and transient state in the transmission process of gas and dust explosion, it also can capture the shock wave and connect discontinuity in the flow field. For self-luminous combustion flow field, the light given out from flow field and light source will both cause film exposure.

On the height-adjustable support, the pipeline support is on the special rail to guarantee moving flexibly back and forth.

To ensure the safety of experiment, CCD monitoring system and prompt system of alarm lamp and bell are designed. The alarm lamp is starting to ring when the pipeline is filled with gas and the alarm bell will prompt when starting the ignition system, which is convenient for the irrelevant personnel of experiment to leave the scene.

The test system can measure the process of seepage, spread, ignition and DDT of high pressure gas. Deflagration propagating in a tube with complex geometry; dust explosion induced by shock or deflagration wave; ignition induced by shock wave.

REFERENCES

Donald. N.H.C, Henry E.P (1974). Mathematial Study of Propagating Flame and Its Aerodynamics in a Coal Mine Passway. *Report of Investigation, Pisttsburgh Mining and Safety Research Center, Pisttsburgh, Califomia(USA),* 12, 23–26.

Lin Baiquan and Qian liping. (2004) Research and application on the risk evaluation technology of gas explosion based on the WINDOM 2000. *Mining Science and Technology(China),* 6, 227–232.

Si Rongjun, Wang Chunqiu, Zhang Tingsong, Li Runzhi. (2007) Summarization and prospect of transmission research on gas and dust explosion. *Mining Safety & Environmental Protection(China),* 1, 55–59.

Wu Bing, Zhang Licong, Xu Jingde. (2005) Numerical simulation of shock wave induced by moving flame for gas explosion. *Journal of China University of Mining & Technology(China),* 34, 423–428.

Xu Jingde, Zhang Licong, Li Tifa, Yang Gengyu. (2012) A numerical simulation of stimulating effect of tramcars during the methane explosion propagation. *Explosion and Shock Waves(China),* 32, 47–51.

Zhang Licong, Xu jingde, Wu Bing, Yang Genyu. (2004) Study on numerical value of reaction between barrier and explosion wave of Methane-coal Dust. *China Safety science Journal(China),* 4, 34–37.

Zhang Licong, Xu Jingde. (2010) The study of optical meterage for the flame propagation of gas and coal dust in explosion. *Journal of North China Institute of Science and Technology(China),* 7, 20–23.

Zhang-licong, Xu-jingde, Zhang Yulong. (2011) Numerical Simulation Of Shock Wave Structure In Gas Explosion. *First International Symposium on Mine Safety Science and Engineering, 265–268.*

Progress in Mine Safety Science and Engineering II – He et al. (Eds)
© 2014 Taylor & Francis Group, London, ISBN 978-1-138-00122-0

Numerical simulation of W-type ventilation in goaf of spontaneous combustion and gas migration

Jia-Jia Liu & Dan Wang
College of Safety Engineering, Heilongjiang University of Science and Technology, Harbin, Heilongjiang, China

Jian-Liang Gao
School of Safety Science and Engineering, Henan Polytechnic University, Jiaozuo, Henan, China
Gas Geological State Key Laboratory of Gas Control, Jiaozuo, Henan, China

ABSTRACT They have made a study of numerial simulation in a 2303 mechanized caving face gob of a coking coal group, which is based on Fluent, a Computational Fluid Dynamics (CFD) software, and researched the rules of spontaneous combustion zone and gas migration in the gob, after using W ventilation type. Results indicates that after using W ventilation system on 2303, the face on both ends pressure is smaller, which not only can effectively prevent the coal of gob from self-igniting, but also can play fire protection and outfire because of its pressure balance, can effectively solve the problem of the overrun of the up gas and reduce the explosion limits in gob, we can conclude that when the ventilation quantity of the two air intake ducts is the same, gob's air leakage and the face pressure on both ends can be minimum via the test of the two air intake ducts of W type change from1 1, 12 and 23. The concentration of oxygen we measured is the same as numerical simulation, which had proved the reliability of numerical simulation.

1 INTRODUCTION

With the increasing depth of coal mining, coal-bed gas pressure, gas content increased significantly, and gas emission rapidly increase in mining working face and goaf, seriously restricting the efficiency of safety production in coal mine. According to statistics, mined-out area is one of the main sources of working face and the whole mine gas emission and hazard source, accounting for about working face gas emission of 30%~80% (State Administration of Coal Mine Safety 2007), many serious accidents are related with the mined-out area.

Natural disasters of coal mine goaf are mainly gas accident caused by coal spontaneous combustion and gas overrun two categories. From the theoretical study and field practice, the change of ventilation modes of working face are effective ways to solve the mined-out area two big disaster, according to the working face of combustion and gas migration law of mining W type ventilation system conditions, domestic and foreign experts and scholars to do some research, Zhao Wenhua studies the problem of governance close work group of coal seam top corner gas overrun the partial W ventilation mode, which has important reference value to the similar mine (Zhao Wenhua 2007); Li Zongxiang does research on W type ventilation falling flow field in goaf by Matlab calculation program, and obtains the distribution of flow field (Li Zongxiang 2007); Zhou Aitao and others, through the establishment of Mathematical Physics equations, studied the goaf coal spontaneous combustion and flow field distribution in different working face of air supply and drainage condition, and get the correspondence between the parameters of different goaf gas management and spontaneous combustion (Zhou Aitao et al. 2010); Wu Yuguo studies the goaf gas distribution in the working face of double U type ventilation system by Mining Mobile beam tube sampling, chromatographic analysis system and CFD numerical simulation, and provides a theoretical basis for guiding the drainage measures in goaf gas (Wu Yuguo & Wu Jianming 2011); Qin Yueping compares the characteristics of fully mechanized caving under 3D goaf gas migration between U type and W type ventilation, due to the restrictions on similar simulation experiment from flow disturbances, model size, personal safety and accuracy of measurement, he unable to obtain accurate results (Qin Yueping et al. 2003); Wang Yong studied the advantages and disadvantages of mining face with W type ventilation system, obtained W type ventilation system has good effect for solving methane accumulation, ventilation dust etc (Wang Yong 2009).

At present, little research on goaf spontaneous combustion zone and gas migration law in the working surface with W type ventilation system is done at home and abroad, With the Coal Group mine 2303 working face as an example, the writer uses Computational Fluid Dynamics (CFD) software Fluent to carry out simulation in the W type ventilation system on goaf spontaneous combustion zone, goaf oxygen concentration distribution and the gas migration law.

2 WORKING FACE GENERAL SITUATION AND NUMERICAL SIMULATION

2.1 *The general situation of the 2303 fully mechanized caving face*

2303 fully mechanized caving face which located in the west of three lane of the No. 3 mining area, the north of the No. 4 mining area boundary, is the first mining face of the No. 3 mining area. The trend length of the working face is 1535 m, and it's length of the slope is 100 m. Mining No. 3 coal seam, which is 3.6 deep, belongs to easy self-ignition coal seam. Working face adopt comprehensive mechanization caving, a mining overall height of roof caving mining method. Gas gushing quantity is a little much, absolute gas emission quantity is 24.7 m^3\min. In order to avoid mined-out area of coal spontaneous combustion, The corner of working top gas frequently overrun and other problem. The ventilation system of 2303 working face can adjust to W type ventilation system into one of two.

2.2 *Production of coal samples*

Physical model is built according to the actual situation of 2303 fully mechanized caving face in the scene. Mined-out area to length 200 m, working surface inclination of length 100 m, 10 m long, 3 m wide into the airway, return air lane length 10 m, width 3 m, working width is 5 m. The residual coal in the goaf are located in the caving zone, therefore this model only considers the caving zone, and the caving zone for gas source. Because the gob caving height relative to the mined-out area of length and width is small, so it can be simplified to a two-dimensional model of goaf. The mined-out area towards the direction of X axis, goaf tilt direction as Y axis, the physical model of two-dimensional as shown in Figure 1.

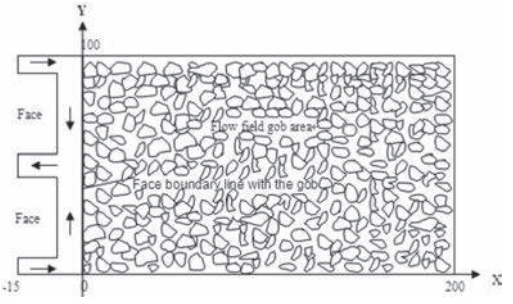


Figure 1. The physical model of 2303 full-mechanized caving mining face goaf.

2.3 *The mathematical models of goaf*

2.3.1 *Typography for references*

The most fresh air entry from into the stope face after in return airway, small part of the drain into the goaf area, the formation of air leakage in gob area, due to the gob porous medium is very complex. the working surface is considered as turbulent flow region while the laminar flow is the goaf gas flow (Li Chengyu et al 2007). For highlight the research, need to make the following assumption

1. Because of the randomness of cave gangue and residual coal distribution, the goaf area is considered as isotropic porous media. Permeability does not change with time;
2. The goaf considered not compressible gas without considering the heat loss caused by the working fluid viscous force assuming the gas flow for steady flow, isothermal process;
3. Assumption the diffusion coefficient of gas unchanged component transport setting for mixed gas of methane, nitrogen and oxygen gas, ignore the water vapor, nitrogen dioxide and so on. In the numerical simulation of gas components need to maximum content of gas in the last.

2.3.2 *The mathematical models of goaf*

According to the law of conservation of mass and the percolation law theory, establish the mathematical model of goaf:

The goaf gas flow continuity equation:

$$\frac{\partial \mathrm{u}}{\partial x}+\frac{\partial v}{\partial y}=0 \tag{1}$$

In the formula:u, v—Components of velocity vector in X, Y direction.

Momentum equation:

$$\frac{\partial(n\rho uu)}{\partial x}+\frac{\partial(n\rho uv)}{\partial y}=\frac{\partial}{\partial x}\left(n\mu_{eff}\frac{\partial u}{\partial x}\right)+\frac{\partial}{\partial y}\left(n\mu_{eff}\frac{\partial u}{\partial y}\right)-\boldsymbol{n}\frac{\partial p}{\partial x}-\frac{\mu}{e}u \tag{2}$$

$$\frac{\partial(n\rho vu)}{\partial x}+\frac{\partial(n\rho vv)}{\partial y}=\frac{\partial}{\partial x}\left(n\mu_{eff}\frac{\partial v}{\partial x}\right)+\frac{\partial}{\partial y}\left(n\mu_{eff}\frac{\partial v}{\partial y}\right)-n\frac{\partial p}{\partial y}-\frac{\mu}{e}v \quad (3)$$

In the formula: μeff = μ + μt; μt- Turbulent viscosity coefficient; μ- Coefficient of kinematic viscosity; n- Porosity of porous medium.

Component transfer equation:

$$\frac{\partial(\rho c_s u)}{\partial x}+\frac{\partial(\rho c_s v)}{\partial y}=\frac{\partial}{\partial x}\left(D_s\frac{\partial \rho c_s}{\partial x}\right)+\frac{\partial}{\partial y}\left(D_s\frac{\partial \upsilon c_s}{\partial y}\right)+S_s \quad (4)$$

In the formula: C_S- The volume concentration of component s; S_S-Component of productivity; D_S-Diffusion coefficient of components;

Standardk-ε equation:

$$\frac{\partial(\rho ku)}{\partial x}+\frac{\partial(\rho kv)}{\partial y}=\frac{\partial}{\partial x}\left(\mu+\frac{\mu_t}{\sigma_k}\right)\frac{\partial k}{\partial x}+\frac{\partial}{\partial y}\left(\mu+\frac{\mu_t}{\sigma_k}\right)\frac{\partial k}{\partial y}+G_k-\rho\varepsilon \quad (5)$$

$$\frac{\partial(\rho\varepsilon u)}{\partial x}+\frac{\partial(\rho\varepsilon v)}{\partial y}=\frac{\partial}{\partial x}\left(\mu+\frac{\mu_t}{\sigma_\varepsilon}\right)\frac{\partial \varepsilon}{\partial x}+\frac{\partial}{\partial y}\left(\mu+\frac{\mu_t}{\sigma_\varepsilon}\right)\frac{\partial \varepsilon}{\partial y}+\frac{\varepsilon}{k}(C_{1\varepsilon}G_k-C_{2\varepsilon}\rho\varepsilon) \quad (6)$$

In the formula: $\mu t = \rho C_\mu k_2/\varepsilon$, there into $C_{1\varepsilon} = 1.44$ $C_{2\varepsilon} = 1.92$ $C_\mu = 0.09$ $\sigma_k = 1.0$ $\sigma_\varepsilon = 1.3$

K-turbulent kinetic energy, m^2/s^2; *ε*-Turbulent Dissipation Rate, m^2/s^3; The turbulent kinetic energy k mean velocity gradient caused by the Gk.

3 THE BOUNDARY CONDITIONS AND THE NUMERICAL SIMULATION PROCESS

3.1 *Boundary conditions*

Face intake working speed entrance, the average wind speed is 3 m/s, the oxygen volume fraction of 20.96%, the gas volume fraction is 0; Return air lane for free export; The working face and goaf solid wall for the no-slip boundary condition, in other Words is u = v = 0; The working face and goaf interface for internal boundary (Interior). Gob permeability in accordance with free accumulation is assumed to satisfy function, $e = 1/D(c + ax + b * (y - L)^2)$, Among them e stands for the permeability of mining area, a or b stands for unbalanced distribution coefficient, c stands for Permeability base, D represents translational coefficient, L stands for Mined-out area width (Wang-Kai 2007, Li Shu-gang et al. 2008). On the adjacent gas emission and the exploitation of coal seam gas emission is a major source of goaf gas. But the goaf, the specific location and strength, it is difficult to determine. Therefore the gob caving zone with a source term for the gas source, the farther distance of working face, the gas emission intensity is small The supporting role of surrounding rock, Mining permeability goaf for O ring of continuous distribution, Using the C language the goaf gas emission intensity, gob permeability is defined as the custom function of continuous distribution.

3.2 *The numerical simulation process*

In the Descartes coordinate system to build the physical model and the mesh model by using modeling tool Gambit, and the physical model for structured grids to form a quadrilateral grid. Use the Fluent software to carry on the numerical simulation calculation, finally, the simulation results will be put into Tecplot to post processing. Laminar flow is the main flow of goaf, but area and working face is regional turbulence model. The governing equations of the control volume method is used to discrete, and the convection and diffusion in Quick format. and it will use calculation of the relaxation factor and the three diagonal matrix algorithm with iterative method, the pressure-Velocity coupled Simple algorithm using (Wang Fujun 2004).

4 THE RESULTS OF NUMERICAL SIMULATION OF GOAF

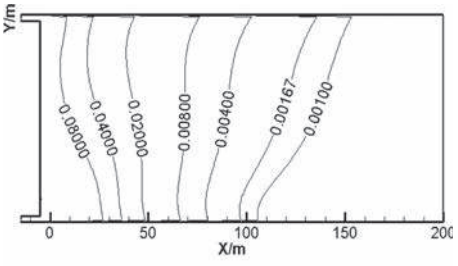
4.1 *Divided into three zones of goaf spontaneous combustion working surface of W type and U type ventilation system*

Goaf spontaneous combustion with air velocity in the three division standard, the wind > 0.004 m/s is radiation belt, the wind speed in the 0.004–0.00167 m/s is the spontaneous combustion zone, Wind speed <0.00167 m/s is suffocative zone, According to this standard can be obtained under different ventilation goaf spontaneous three zones are as shown in Table 1.

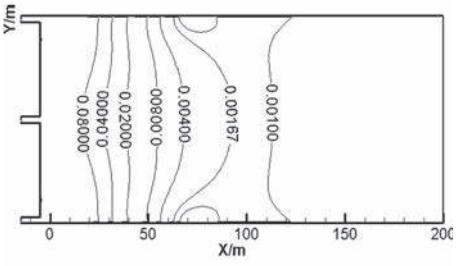
Through the Figure 2 can see, There is great difference between the goaf spontaneous recovery conditions with a range of different ventilation modes, When the u-shaped ventilation system is used, Working on both ends of the pressure

Table 1. Different ventilation modes range of goaf spontaneous combustion zones mingle (m).

Ventilation	Goaf	Scattered tropical	Spontaneous	Suffocation
U-shaped	Into the wind lane	0–80	80–97	97–
U-shaped	Return air lane side	0–102	102–135	135–
W-shaped	Into the wind lane	0–55	55–63	63–
W-shaped	Return air lane side	0–68	68–92	92



(a) U-shaped ventilation



(b) W-shaped ventilation

Figure 2. Distribution of velocity in goaf.

difference is bigger, Working face goaf air leakage range is wide, So brought closer to the deep goaf spontaneous combustion; After adjustment for W type ventilation, Due to the pressure on both ends of the working face of the role, The working surface at both ends of the pressure difference is small, The scope of work for the air leakage of gob area is narrow, Spontaneous combustion zone is closer to coal face, So face using W type ventilation pressure can play a role in preventing and extinguishing the fire.

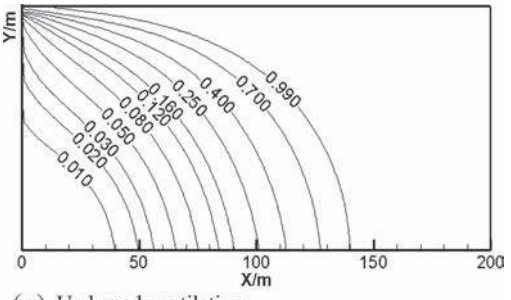
4.2 *Analysis of goaf gas explosion limits of different ventilation modes*

According to the necessary conditions for gas explosion, The gas concentration in 5%~16%; Gas firing temperature is 650°C~750°C; Oxygen concentration >12%, The 2303 fully mechanized caving face ventilation before and after adjusting the gas explosion limit range of width.

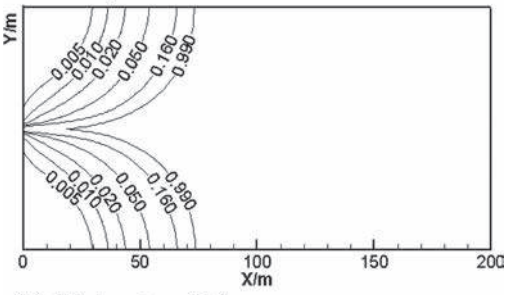
It Can be seen from Figure 3, the 2303 fully mechanized face ventilation mode after adjusting scope of gob gas explosion limits have very big difference. Under the condition of u-shape ventilation mode, Working face goaf air leakage range are more wide, Goaf gas explosion limits of 65 m~90 m (Into the wind lane side), the width is 35 m, Gas explosion limit width gradually narrowed (Return air lane side); Under the condition of W type ventilation mode. Due to the differential pressure at the ends of the working face is smaller, Working face goaf air leakage of the range is narrow, Goaf gas explosion limits for 54 m~72 m (Into the wind lane side), the width is 18 m, Goaf gas explosion limit is much smaller than the conditions of U type ventilation modes, So the 2303 fully-mechanized face way W type ventilation goaf reduces the width of the explosion limit range, And can effectively prevent the gas explosion accidents.

4.3 *"Two into one" W type ventilation into the ventilation airflow is different on the result of simulation*

For the 2303 fully mechanized caving face with W two ventilation system into a back, Two different air volume of goaf air leakage into the wind lane, stress field distribution, the oxygen concentration



(a) U-shaped ventilation



(b) W-shaped ventilation

Figure 3. Distribution of gas in goaf.

field distribution has great influence. The author of 2303 fully mechanized face two into the ventilation air volume ratio is 11, 12 and 23, respectively goaf air leakage, pressure distribution, the oxygen concentration field distribution are analyzed, As shown in Figures 4 and 5.

From the simulation results of Figure 4 we can know that the 2303 fully mechanized face when u-shaped ventilation mode is adopted, Working pressure difference on both ends of 56.7 Pa, Based on the working face and goaf on the border of curvilinear integral calculation, Working face goaf of leakage air volume is 0.625 m^3/s, The 2303 fully mechanized face is adjusted for the "two into one" W type ventilation mode, When two into the ventilation air volume ratio of 11, 23 and 12 condition, the working pressure difference on both ends are respectively 28.5 Pa, 34.2 Pa, 36.9 Pa, Working face goaf of leakage air volume is 0.348 m^3/s, 0.422 m^3/s,

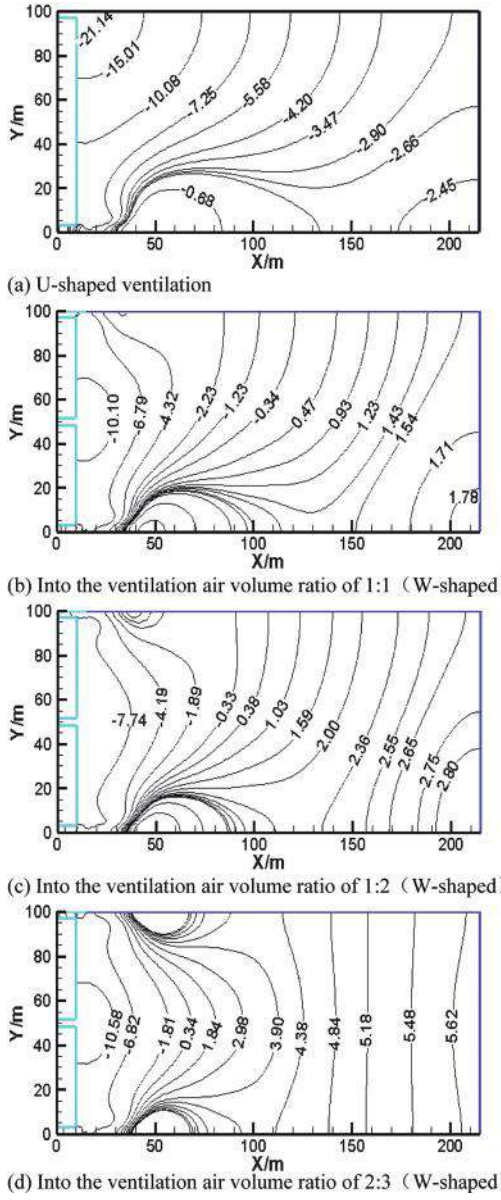


Figure 4. Pressure field distribution in goaf.

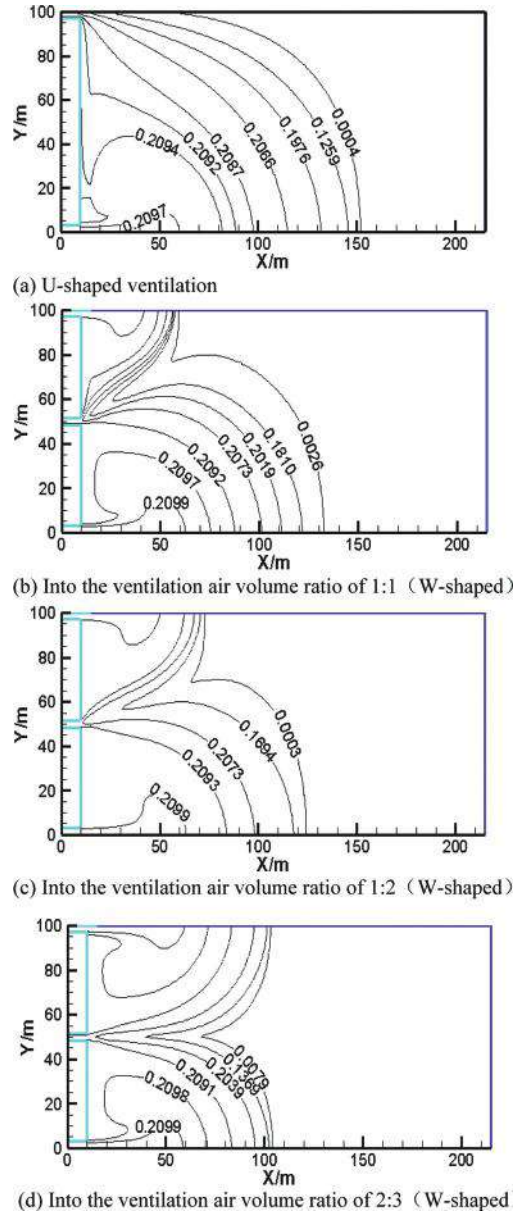


Figure 5. Oxygen concentration distribution in goaf.

0.435 m^3/s, Based on the analysis comparison, 2303 fully mechanized face with two into the wind lane volume ratio of 11 W type ventilation mode, Working face goaf of leakage air volume at least, Working on both ends of the pressure difference is minimal, but The working face goaf air leakage is one of the main factors of goaf coal spontaneous combustion, So 2303 fully mechanized face with W type ventilation mode can effectively reduce the risk of goaf coal spontaneous combustion, In 2303 fully mechanized face stoping combining mined-out area in the process of nitrogen injection and three-phase foam can fundamentally solve the problem of goaf coal spontaneous combustion.

From the Simulation result by Figure 5 we can know that 2303 fully mechanized face is adjusted for W type ventilation mode, the goaf oxygen concentration field distribution has great influence, When U ventilation mode is used, Goaf air leakage is larger, due to the inhibition of coal self-heating in goaf of the oxygen concentration in the lower limit (Inhibition of coal self-heating oxygen concentration in the lower limit of 8%) of about 150 m at the working face; The 2303 fully mechanized face is adjusted for the two into one W type ventilation mode, And when the two ventilation air volume ratio of 11, 23 and 12 conditions respectively, Mined-out area in inhibition of oxygen (Inhibition of coal self-heating of oxygen concentration in the lower limit is 8%~10%) concentration of coal self-heating floor respectively at the working face 130 m, 120 m, 105 m, Through the analysis can be seen, when the 2303 fully mechanized face with two into the wind lane volume ratio of 11 W type ventilation mode, it Can significantly reduce the coal spontaneous combustion caused by the scope of the oxygen concentration field play an important role in inhibition of goaf coal spontaneous combustion.

5 ANALYSIS OF FIELD TEST RESULTS

Analyzing the gas sample collection on the surface by embedding pipe in 2303 caving working face and gob, masterring drawing speed of working face and gas concentration changes in gob and observing relative parameters of working face to gob, such as air leakage at the same time, according to 2303 caving working face's gas concentration and working face recovery in Analyzing field test data (100 m away from working face) as shown in the Table 2.

Comparing the Analyzing field test data of oxygen concentration with the numerically obtained alternant structure of oxygen concentration, as shown in the Figure 6.

We can conclude from Figure 6 that Analyzing field test data is nearly the same as numerical simulation, which proved that numerical simulation can provide accurate tri-zone of coal spontaneous combustion in goaf and the gas distribution rule and also, confirming the reliability of spontaneous combustion zone gas distribution rule after adopting to Fluent, a CFD software.

Table 2. Analyzing field test data.

(x,y)	O_2/%	(x,y)	O_2/%	(x,y)	O_2/%
(5,0)	21.0	(5,10)	20.2	(5,20)	19.8
(5,30)	18.6	(5,40)	17.8	(5,50)	18.2
(5,60)	17.4	(5,70)	15.6	(5,80)	15.1
(5,90)	14.4	(5,100)	13.59		

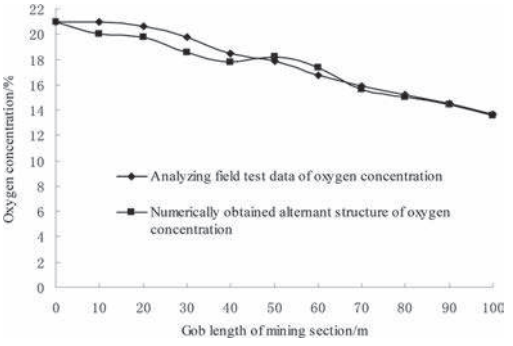


Figure 6. Analyzing field test data of oxygen concentration with the numerically obtained alternant structure of oxygen concentration.

6 CONCLUSIONS

1. After using w-type ventilation method in 2303 caving working face, Pressure effects on both ends of the working face, The working surface at both ends of the pressure difference is small, The scope of work for the air leakage of gob area is narrow, spontaneous combustion zone is closer to working face, Spontaneous combustion belt width is getting more narrow, Can effectively prevent the spontaneous combustion of coal in Goaf, can also pressure balance for air control. besides, under the condition of w-type, we can not only effectively solve Gas in upper corner overrun but also could Reduce the goaf gas explosion limit width, as a result, it Can effectively prevent the goaf gas explosion accident.
2. 2303 caving working face adopts to Article two in airway volume 11, which is called w-type, Can effectively reduce the risk of spontaneous

combustion of coal in Goaf and significantly reduce the oxygen concentration range, play an important role of Inhibition of the spontaneous combustion of coal in goaf. Meanwhile during 2303 caving working face's backstopping, Combined with nitrogen injection goaf and three-phase foam technology to fundamentally solve the problem of spontaneous combustion of coal in Goaf.

3. The comparison results of the Analyzing field test data of oxygen concentration in 2303 and the numerically obtained alternant structure of oxygen concentration, prove The accuracy of goaf spontaneous combustion zone and gas distribution law and confirm reliability of using CFD software to calculate The goaf spontaneous combustion zone and gas distribution law.

ACKNOWLEDGEMENTS

The research project is sponsored by the national natural science foundation of China (Grant No. 51174079) and Research Fund for the Doctoral Program of Higher Education of China (Grant No. 20104116110001).

REFERENCES

Li C.Y. et al. 2007. The mathematical model of goaf gas migration. *Mining letters* (8)17–19.

Li S.G. et al. 2008. Sublevel caving goaf seepage numerical simulation research. *Mining safety and environmental protection* 35(2)1–7.

Li Z.X. 2007. W type ventilation caving goaf flow field numerical simulation. *Journal of liao ning engineering technology university* 26(6)816–818.

Qin Y.P. et al. 2003. Simulation experiments of full-mechanized caving mining goaf gas migration rule research. *Journal of coal science and technology* 31(11)13–16.

The State Administration of production safety supervision and management. 2007. State Administration of Coal Mine Safety safety, *regulations in coal mine*. Beijing China Coal Industry Publishing House.

Wang F.J. 2004. Computational fluid dynamics analysis. Beijing Tsinghua university press.

Wang K. 2007. Numerical simulation of goaf flow field and gas migration to J type ventilation in fully mechanized mining. *Journal of China university of mining* 36(3)277–282.

Wang Y. 2009. Coal mining working face W type ventilation system analysis and application. *Journal of shandong coal technology*, 156–157.

Wu Y.G & Wu J.M. 2011. Pairs of fully mechanized top-coal caving goaf gas distribution of u-shaped ventilation system. *Journal of coal* 36(10)1705–1708.

Zhao W.H. 2007. Working face of close distance coal seam group of partial W type ventilation mode and its application. *Journal of mining safety and environmental protection* 34(2)44–45.

Zhou A.T et al. 2010. Easy to goaf spontaneous combustion and fire work numerical simulation. *Chinese journal of safety science* 20(8)49–53.

This page intentionally left blank

Progress in Mine Safety Science and Engineering II – He et al. (Eds)
© 2014 Taylor & Francis Group, London, ISBN 978-1-138-00122-0

Numerical simulation study on permeability and humectant properties of coal seam water injection under high water pressure in long drilling hole

Y.B. Yu, W.M. Cheng, G. Zhou, L.J. Chen, L. Zhang & G.M. Liu
Key Laboratory of Mining Disaster Prevention and Control, Shandong University of Science and Technology, Qingdao, Shandong Province, China

ABSTRACT: Based on ANSYS numerical simulation method, the 50 m and 80 m drilling length of the coal seam water injection physical model are established, the numerical simulation study of coal seam water seepage pressure, velocity field variation and water wetting distribution is conducted under injection pressure of 20 MPa. The results show that permeability and humectant properties concentrate within the drilling hole and decrease on both sides to a certain gradient. Meanwhile, the 80 m long drilling coal seam water injection pressure and moist coal distribution range increase, the minimum of moisture increment value reaches 1.2%, higher than the 50 m drilling layout. The sealing section of longer drilling hole does not appear the pressure distribution, which helps to prevent the leakage of water injection. The results show that longer drilling of the coal seam under high pressure water can achieve better effect, which provide a basis for optimizing the design of water injection parameters.

1 INTRODUCTION

According to the borehole layout position, length and direction, the coal seam water injection can be divided into many patterns such as short drilling, deep drilling, long drilling, one-way drilling and bidirectional drilling. In the practical process, it is necessary to optimize the way of water injection according to the actual conditions, and the changed relationship of coal seam water injection process and infiltration moisture scope in time and space is what we must grasp at the same time in order to make the water injection more efficiently. So injection parameters is optimized and the water injection process is reasonably controlled. However, due to the unpredictability of coal seam occurrence, empirical design is largely based on the existing water injection equipment and process conditions, so the parameters design of systematic accurate process is lacked in practical application. With the rapid development of modern computational mechanics and simulation software, the changed relationship of coal seam water injection process and infiltration moisture scope is described effectively by using numerical simulation method, which makes up for the deficiency of the traditional process design, so as to better guide the technology application of optimization coal seam water injection.

At present, the related theories of coal seam water injection and the practical technology are systematically researched by many scholars. When it comes to the theory research of coal seam water injection, the mechanism of inhibiting gas emission and preventing impact pressure by coal seam water injection was discussed by some scholars such as Guo Hongyu, Su Xianbo, Wu Yaokun (Wu et al. 1989, Guo & Su 2010); Pore volume and surface integral shape features were analyzed and relation equation between those and performance of coal water absorption was established by Qin Yueping, Fu Gui (Qin & Fu 2000). Coal seam water injection was regarded as the displacement process of water driving gas and the motion law of water in coal seam was studied through seepage mechanics by Zhang Mengtao, Song Weiyuan, Pan Yishan etc (Liang & Pan 2006, Zhang & Song 2006, Zhang et al. 2003). The process of wetting coal by water injection was microcosmically analyzed from the pore perspective and the mathematical model for the related solution was established by some scholars such as Zhang Yansong, Qin Wengui, Nie Baisheng (Nie et al. 2004, Qin & Zhang 2000, Zhang 1995b, Zhang 1995a).

In the aspect of confirming injection parameters reasonably and the numerical simulation, the mathe-matical prediction model between injection parameters and effect was established through quantification theory, and the injection parameters combination was designed for optimizing by Qin Shuyu, Hai guozhi etc (Hai et al. 1994, Qin & Qin 2003). The dynamic process of coal seam water

injection under water pressure was described in de-tail through numerical simulation method and the dynamic changed relationship between injection pres-sure, time and moisture scope was simulated for calculating by Li Zongxiang, Pan Yishan etc (Li et al. 2005, Li et al. 2001). The researches show that there is a obvious threshold when drilling begins to water after water pressure reach-ing a certain value (Ye 1991, Zhang 2001). But with the increase of mining depth, the native fracture pores are not developed and its injection pressure threshold is not increasing under high geostress conditions. Therefore, high pressure is necessary for deep coal seam water injection in order to achieve better water injection effect.

So far, the water change law of seepage pressure and speed about the process of high pressure water injection in coal is barely studied at home and abroad. The research both on the changed law of the seepage pressure field and velocity field and the distribution law of moisture increment in the process is significant for the reasonable design of process parameters and the confirmation of seepage rule, and then better serving the practical work. Therefore, the physical models of numerical calculation is established with the actual conditions in this paper. By using ANSYS numerical simulation method, the seepage pressure field and velocity field change law in the process of long borehole water injection under high pressures including the distribution of wet coal are numerically simulated, in order to reasonably determine the coal seam water injection process parameters, which especially providing the basis for the parameter design of high-pressure water injection in deep coal seam.

2 THE MATHEMATICAL MODEL OF SEEPAGE IN THE HIGH-PRESSURE WATER INJECTION COAL SEAM GENERAL INSTRUCTIONS

In general, the temperature change caused by the flow of fluid is very small, which is regarded as an isothermal process and the energy equation is not considered under this condition. Therefore, the seepage process of high-pressure water injection coal is expressed and calculated in mathematical model by using the Darcy law, continuity equation and state equation in this paper.

2.1 *The seepage law of orientated loss about water in the coal*

The general momentum equation of water as the fluid flowing in the coal seam can be written as (Kong 2010):

$$\frac{\partial(\rho U_i)}{\partial t}+\frac{\partial(\rho U_j U_i)}{\partial x_j}=\frac{\partial(p)}{\partial x_i}+\rho g_j+\frac{\partial \tau_{ji}}{\partial x_j}+S_i^M \quad (1)$$

In this equation, S_i^M is the the momentum source term, which can be obtained by the following equation. That is:

$$S_i^M=-C^{R_1}U_i-C^{R_2}|U|U_i+S_i^{spec} \quad (2)$$

In this equation, C^{R_1} is the coefficient of linear impedance and C^{R_2} is the coefficient of secondary impedance; S_i^{spec} contains other momentum source term; U_i, U are all apparent velocity.

The process of coal seam water injection can be regarded as water flow at low speed in porous medium. Therefore, based on darcy's law, the seepage mathematical model of high-pressure water injection coal is solved (J. et al. 1983, R.E. 1984, Kong 2010).

The general form of darcy's law is:

$$-\frac{\partial p}{\partial x_i}=\frac{\mu}{K}U_i-K_{loss}\rho|U|U_i \quad (3)$$

In this equation, μ is dynamic viscosity; K is permeability; K_{loss} is coefficient of experience loss.

The equations including (2), (3) are overall contrasted, then the following formula is:

$$C^{R_1}=\frac{\mu}{K}C^{R_2}=K_{loss}\rho \quad (4)$$

2.2 *The continuity equation of fluid*

The continuity equation of slightly compressible fluid is:

$$\frac{\partial(\rho\Phi)}{\partial t}+\nabla\cdot(\rho V)=0 \quad (5)$$

The continuity equation of radial flow at plane is:

$$\frac{\partial(\rho\Phi)}{\partial t}+\frac{1}{r}\frac{\partial}{\partial r}(r\rho V)=0 \quad (6)$$

The continuity equation of parallel flow at plane is:

$$\frac{\partial(\rho\Phi)}{\partial t}+\frac{\partial}{\partial x}(\rho V_x)=0 \quad (7)$$

2.3 *The equation of flow and solid state*

The compressibility of fluid is a measure of its volume change when the normal pressure or normal tension

on the liquid change. Under the isothermal condition, the compressibility of fluid is defined as (J. et al. 1983, R.E. 1984, Kong 2010, Erwin et al. 1984):

$$c_f = -\frac{1}{V}\frac{dV}{dp} = \frac{1}{\rho}\frac{d\rho}{dp} \tag{8}$$

In this equation, V is the volume of a certain quality of fluid, the integral gives the following equation as:

$$\rho = \rho_0 \exp[c_f \Delta p] \tag{9}$$

When the pressure difference $\Delta p = p(r,t) - p_0$ is small, the formula above can be approximately expressed as:

$$\rho = \rho_0 (1 + c_f \Delta p) \tag{10}$$

In this equation, ρ is fluid, ρ_0 is the density under the condition of reference pressure ρ_0.

This relation between density and pressure is called the state equation of the fluid. Oil and water are usually called slightly compressible fluid. The state equation (10) is applicable to most of the liquid.

The effective compressibility of coal and rock, that is to say unit pressure change causing the relative change of pore volume V_p, is equal to pore compressibility c_Φ:

$$c_p = -\frac{1}{V_p}\frac{dV_p}{dp} = \frac{1}{\Phi}\frac{d\Phi}{dp} = c_\Phi \tag{11}$$

Through integrals, the following equation is obtained.

$$\Phi = \Phi_0 \exp[c_\Phi \Delta p] \tag{12}$$

In this equation, Φ_0 is medium porosity when reference pressure is p_0. Solid is only considered here in the range of elastic deformation, the pressure difference is not very big, so the (12) can be approximated as:

$$\Phi = \Phi_0 (1 + c_\Phi \Delta p) \tag{13}$$

The formula is called state equation of solid skeleton elastic deformation or state equation of porosity changes.

3 CALCULATING THE PHYSICAL MODEL NUMERICALLY AND SETTING BOUNDARY CONDITION

3.1 *Calculating the physical model numerically*

For long borehole water injection pattern of two arrangement forms including the 50 m and 80 m drill-ing length are established, the numerical simulation study of pressure field, velocity distribution and coal water wetting distribution of water in coal seam in the process is conducted under injection 20 MPa pres-sure. The model is established as shown in the Figure 1.

As shown in the Figure 1 that when drilling's length is 50 m, those number of the work face length of wa-ter mode, coal thickness, the diameter of injection hole, the length of sealed hole, the distance between opening position and floor, hole spacing respectively are respectively 120 m, 6 m, 0.065 m, 10 m, 1.5 m, 20 m. While when drilling's length is 80 m, those number of the work face length of water mode, coal thickness, the diameter of injection hole, the length of sealed hole, the distance between opening position and floor, hole spacing are respectively 120 m, 6 m, 0.065 m, 10 m, 1.5 m, 15 m.

3.2 *Setting the boundary conditions and initial parameters*

Boundary condition is used for solving the shape position of area geometric boundary and playing a

Table 1. Numerical simulation of initial parameters of coal seam water infusion.

Name of parameter	Numerical value	The unit of parameters
water density	1000	kg/m^3
water viscosity	1.04e^{-3}	Pa·s
the absolute permeability of coal seam	2.174×10^{-8}	Darcy
density of seam	1430	kg/m^3
elastic modulus of coal seam	2150	MPa
poisson ratio	0.219	/
porosity of coal seam	4.9	%
cohesion	4.285	MPa
frictional angle	31.8	°

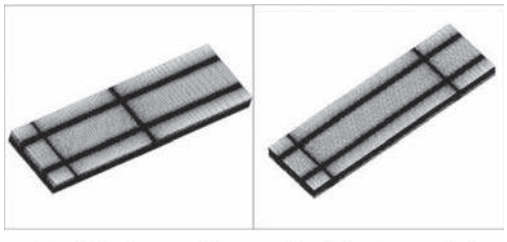


Figure 1. Numerical simulation of water injection model.

dominant role on the border, the boundary conditions of this simulation are as follows:

The upper and lower, left and right boundary of water injection hole are setted as constant pressure permeable boundary.

The Mohr-Coulomb criterion is regarded as coal yield condition.

4 ANALYSIS ON NUMERICAL SIM ULATION RESULTS OF COAL SEAM WATER INJECTION

Physical model of high pressure water injection in coal seam is established by using FLUENT software, relevant boundary conditions and initial parameters are setted. Then seepage pressure field, velocity field distribution and coal wet conditions of water in coal seam under different water pressure are numerically simulated.

4.1 *Analysis on simulation results of coal seam water injection seepage pressure field*

Water injection borehole whose length are 50 m and 80 m is simulated. Results are shown in the figure below, at the same time the cross sections are respectively setted from drilling radial center, central loca-tion of two hole and different axial spacing orifice location. The simulation results are shown in the Figure 2.

As is seen from the Figure 2, the water pressure distributes intensively in the hole, and decays gradually towards both sides of the hole in a certain gradient. Pressure decay by 87.78% in the scope of the drill hole radial 4 m under the condition of 50 m length hole and 20 MPa pressure. Pressure distribution of sealing section, middleend, terminal and the center of two holes under the action of high pressure is shown in the seepage pressure field profile map, and water pressure distribution appears in the coal of sealing section under the action of high pressure. Water injection pressure range of 80 m length borehole is not only amplify, but also the degree of water pressure attenuation have dropped. Pressure decay by 76.97% in the scope of the drill hole radial 7.5 m under 20 MPa pressure, Compared with 50 m length borehole in both the water pressure range and pressure effects, water seepage pressure distribution of 80 m length borehole and the effects significantly improve. Especially sealing section of 80 m length borehole appears pressure distribution of 50 m length borehole when injecting under the high pressure. That is to say that high pressure water injection of long drilling in coal seam increases the pressure range of deep water, and reduces actuating range of

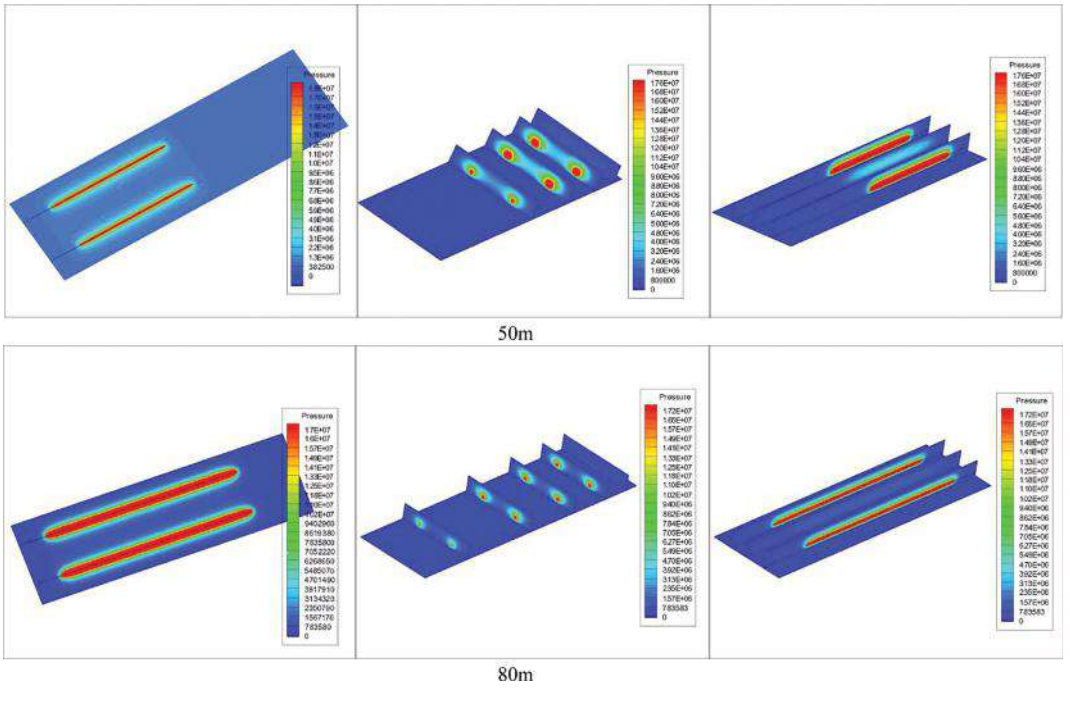


Figure 2. Coal seam water-seepage pressure field simulation results.

pressure water in sealing setion, which is helpful to prevent pressure water from running.

4.2 *Analysis on simulation results of coal seam water injection seepage velocity field*

Water injection process of borehole is simulated, the simulation results of velocity field distribution is shown in the figure below.

As is seen from the Figure 3, correspond to the water injection pressure, water seepage velocity decays gradually towards both sides of the hole in a certain gradient. Maximum seepage speed of 50 m length hole reachs more than 18.75 m/s under 20 MPa pressure. Pressure decays by 87.78% and reachs 3.75 m/s in the scope of the drill hole radial 7 m. But the seepage velocity is relatively high.

Similar to water seepage velocity field of 50 m length borehole, water seepage velocity of 80 m length drilling decays gradually towards both sides of the hole in a certain gradient. Maximum seepage speed reach more than 14.52 m/s under 20 MPa pressure, and the minimum velocity is 2.9 m/s. Compared with water seepage velocity field of 50 m length borehole, water seepage velocity of 80 m length borehole is relatively small. But for that coal has a wide range of seepage, it can achieve a good water injection effect that coal is wetted in a bigger range under the condition of equal pressure.

4.3 *Analysis on simulation results of coal seam water injection wet coal*

In order to better reflect the wetting effect of high pressure water injection, the moisture increment of coal of 50 m, 80 m length borehole after injecting water under 20 MPa pressure is numerically simulated by using numerical computational physics model, the addition of water is shown in the Figure 4.

As is known from the simulative Figure 4, the addition of water in coal reduces gradually from the center of hole to both sides under the action

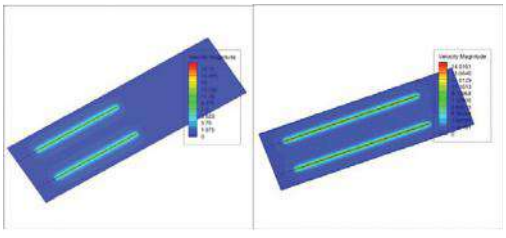


Figure 3. Coal seam water injection seepage flow velocity field simulation results.

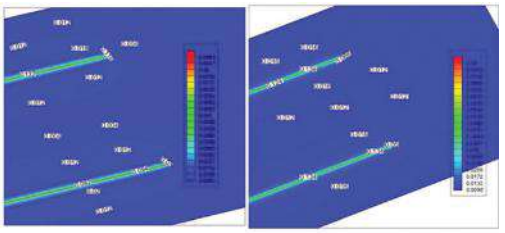


Figure 4. Simulation results of water incremental about coal seam water infusion increment.

of different injection parameters, and the effective wetting radius can reach about 7 m under the conditions of 50 m length borehole and 20 MPa pressure. But the radial ef-fective wet scope covers the whole coal between drilling, the water addition distribute between 13%~1%, and its minimum addition is 1.2%, which is higher than the 0.4% of the 50 m drilling conditions.

5 CONCLUSIONS

1. The numerical simulation results show that water injection pressure, seepage velocity and wetting effect distribute intensively in the borehole under the water injection arrangement of 50 m length hole under the condition of 20 MPa pressure. Pressure decay by 87.78% in the scope of the drill hole radial 4 m, and water pressure distribution appears in the coal of sealing section under the action of high pressure. Pressure decays by 87.78% and reachs 3.75 m/s in the scope of the drill hole radial 7 m. the effective wetting radius can reach about 7 m, the minimum water addition is 0.4%.
2. The water injection pressure, seepage velocity and wetting effect distribute intensively in the borehole under the water injection arrangement of 80 m length hole under the condition of 20 MPa pressure have the same variation characteristics with 50 m length hole. Pressure decay by 76.97% in the scope of the drill hole radial 7.5 m under 20 MPa pressure, maximum seepage speed reach more than 14.52 m/s, and the minimum velocity is 2.9 m/s, the water addition distribute between 13% ~ 1%, and its minimum addition is 1.2%.
3. Compared with seepage pressure field, velocity field and coal wet conditions of pressure water under the conditions of 20 MPa pressure and 50 m and 80 m two kinds borehole, the seepage velocity of 80 m length borehole is lower than that of 50 m borehole when injecting coal

seam. But the pressure and scope of wet coal increases, and the pressure scope of sealing section reduces, which is useful to prevent water from flowing.

ACKNOWLEDGEMENTS

The authors would like to thank The Key Project of Coal Joint Fund National Natural Science Funds of China (U1261205), Natural Science Foundation of China (51074100) and the Science Research Innovative Group of Shandong University of Science and Technology (YC130301) for providing the financial support for conducting this research.

REFERENCES

Erwin Schrodinger, Wang Hongxun & Zhang Chaochen 1984. *Porous medium seepage physics.* BeiJing: Petroleum Industry Press.

Guo Hongyu & Su Xianbo 2010. Research on the Mechanism of Gas Emission Inhibition in Water-flooding Coal Seam. *Journal of China Coal Society* 35(6): 928–931.

Hai Guozhi, Qin Shuyu, Li Zongxiang & Song Hualing 1994. Numerical Analysis and Forecast of the In-Seam Water Infusion Effectiveness. *Journal of China Coal Society* 19(5): 486–492.

J. Bear, Li Jingsheng & Chen Chongxi 1983. *Porous media fluid dynamics.* BeiJing: Chinese Architectural Press.

Kong Xiangyan 2010. *Higher seepage mechanics (second edition).* HeFei: Press of University of Science and Technology of China.

Li Zongxiang, Pan Yishan, Ti Zhengyi & Zhang Zhihui 2005. Numerical Simulation Study on the High-Pressure Water Injection into Coal Seam in Muchengjian Coal Mine. *Chinese Journal of Rock Mechanics and Engineering* 24(11): 1895–1899.

Li Zongxiang, Sun Guangyi & Wang Jibo 2001. Numerical simulation of water injection into coal seam through long drill hole and determination of its reasonable parameters. *Journal of China Coal Society* 26(4): 389–393.

Liang Baoxia & Pan Yishan 2006. Analysis of Plane-Parallel Flow Model for Water Injection in Thin Coal Seams with High gas Content. *Journal of Mining and Safty Engineering* 23(2): 206–209, 214.

Nie Baisheng, He Xueqiu, Wang Enyuan & Zhang Li 2004. Micro-Mechanism of Coal Adsorbing Water. *Journal of China University of Mining & Technology* 33(4): 379–383.

Qin Shuyu & Qin Weihan 2003. Engineering Experiment Research of the Quantity Theoretical Orthogonal Design Optimal Method for the Coal-seam Injection Parameters. *Engineering Science* 5(10): 52–55, 77.

Qin Wengui & Zhang Yansong 2000. Relation of pore distribution of coal with water infusion increment in seams. *Journal of China Coal Society* 25(5): 514–517.

Qin Yueping & Fu Gui 2000. Study on fractal characteristic of pore in coal and moisture-absorbing property of coal. *Journal of China Coal Society* 25(1): 55–59.

R.E. Colins 1984. *The flow of fluid through a porous material.* BeiJing: Petroleum Industry Press.

Wu Yaokun, Wang Shukun & Zhang Wanbin 1989. Discussion on Mechanism of Rock Burst Prebention by Water Infusion. *Journal of China Coal Society* (2): 69–80.

Ye Zhongyuan 1991. *Mine dust prevention and control.* XuZhou: Press of China University of Mining & Techology.

Zhang Mengtao, Song Weiyuan & Pan Yishan 2003. Study on Water Pouring into Coal Seam to Prevent Rock-burst. *China Safety Science Journal* 13(10): 69–72.

Zhang Xiaomei & Song Weiyuan 2006. The theoretical study on water's driving gas displacement as for double medium of coal petrography. *Journal of China Coal Society* 31(2): 187–190.

Zhang Yansong 1995a. The Analytic Resolutions and Applications of the Nonlinear Seepage Flow Equations of Coal Infusion. *Applied Mathematics and Mechanics* 16(11): 991–996.

Zhang Yansong 1995b. Study of Wetting Coal by Seam Infusion. *Journal of China Coal Society* (S1): 1–7.

Zhang Yongji 2001. *Coal seam water injection technology.* BeiJing: Coal Industry Press.

Progress in Mine Safety Science and Engineering II – He et al. (Eds)
© 2014 Taylor & Francis Group, London, ISBN 978-1-138-00122-0

Dimensionless analysis in mathematical model of gas emission in coal particles

Yue-Ping Qin, Yong-Jiang Hao, Peng Liu & Jian Wang
School of Resources and Safety Engineering, China University of Mining and Technology (Beijing), Beijing, China

ABSTRACT: According to Darcy law, the mathematical model of gas emission in the coal particle was established, the gas flow equations were simplified by dimensionless, and Finite Difference Method was used in the program for calculation. The number of condition substitutions in calculating was reduced and some dimensionless quantities were got. The change rule of the gas pressure and the cumulative desorption amount in the coal particle was obtained from the analysis on the dimensionless graphs. Therefore, the introduction of the dimensionless quantity can simplify the solving process of the equations and the writing of the program, and the gas emission laws of the coal particle which are got from it are more universal.

1 INTRODUCTION

Studying gas emission of the coal particle by establishing the mathematical model is the general method to study the gas desorption process, the gas flow rule and the gas flow mechanism of coal seam. In 1960s, some scholars thought that the flow of the coal seam gas basically conforms to Darcy law, and the unidirectional, radial and spherical flow models of the gas in coal seam are established according to the percolation theory (Zhou & Sun 1965), most of which have no analytical solution and the solution can be found only with the aid of computer. In 1980s, some scholars thought that the theoretical basis of gas diffusion from coal cuttings is Fick law, and the theoretical solution of the gas diffusion equation is obtained by means of the solution of the heat conduction equation (Yang & Wang 1986, Yang 1987). In addition, there are some other mathematical models (Wu & Guo 1999).

Once the mathematical model of gas emission in coal particle is set up, how to choose the specific conditions is vital for the solution. The conditions of coal samples with different particle size are varied greatly, even the physical parameters of the same coal sample under different pressures change a lot, and bringing all conditions into the model is almost impossible, so an effective method is needed to simplify the solution (Zhou & Lin 1999). Actually the gas flow in coal particle has much in common, and the dimensionless method can combine several meaningful physical parameters to reflect the common (Zhang et al. 2001, Qin et al. 2009, Qin et al. 1998), which can not only simplify the mathematical model, but also improve the efficiency of the calculation. For this reason, the dimensionless based on the mathematical model of gas emission in coal particle is introduced in order to find out the universal laws of gas emission in coal particle, which can guide the mine production practice.

2 THE ESTABLISHMENT OF GAS FLOW MATHEMATICAL MODEL AND DIMENSIONLESS

Coal is a porous medium, and there are many factors influencing gas emission in coal particle. In order to simplify the problem, several main factors affecting the emission law are found, and the hypotheses are as follows:

1. Coal particles are homogeneous and isotropic sphere.
2. Adsorption gas satisfies Langmuir Equation and free gas in the micropore is ignored. Gas content can be expressed as:

$$X = \frac{abp}{1+bp} \tag{1}$$

where a is the first adsorption constant, m^3/t; b is the second adsorption constant, 1/MPa; p is the gas pressure in the coal, MPa; X is the gas content of the coal per unit mass, m^3/t.

3. When the gas flows in the coal particle, the temperature remains constant.

4. The changes of gas pressure and density satisfy the state equation of ideal gas.
5. The flow of the gas in the coal particle is regarded as laminar flow movement, according with Darcy law:

$$u = -\frac{K}{\mu}\nabla p \tag{2}$$

Where u is the gas flow rate, m/s; K is the permeability of the coal seam, m^2; μ is the gas viscosity coefficient, MPa's; ∇p is the gas pressure gradient, MPa/m.

The gas flow is converted into the volume flow under a standard atmospheric pressure, and Formula (2) can be transformed into

$$q = -\lambda\frac{\partial P}{\partial n} \tag{3}$$

Where q is gas ratio flow, $m^3/(m^2 \cdot s)$; λ is permeability coefficient, $m^2/(MPa^2 \cdot s)$, $\lambda = K/2\mu p_n$, p_n is standard atmospheric pressure, 0.101325 MPa; P is square gas pressure, $P = p^2$, MPa^2; n is the penetration distance on the normal direction, m. According to the law of mass conservation Formula (3) and the symmetry of the sphere, the gas flow equation under the spherical coordinates can be got:

$$\frac{\partial\left(\frac{a}{1+1/b\sqrt{P}}\right)}{\partial t} = \frac{\lambda}{\rho}\frac{1}{r^2}\frac{\partial}{\partial r}\left(r^2\frac{\partial P}{\partial r}\right) \tag{4}$$

Where t is time, s; ρ is the apparent density of the coal, t/m^3; r is the radius, m. The initial conditions and boundary conditions are:

$$\begin{cases} P = P_0 = p_0^2, & 0 \le r \le R, \quad t = 0 \\ \dfrac{\partial P}{\partial r} = 0, & r = 0, \quad t > 0 \\ P = P_W = p_w^2, & r = R, \quad t > 0 \end{cases} \tag{5}$$

Where p_0 is the initial gas pressure of the coal particle, MPa; p_w is the surface gas pressure of the coal particle, MPa; R is the radius of the coal particle, m.

Formula (4) can be transformed into

$$\frac{\partial\left(\frac{1}{1+1/\sqrt{b^2P}}\right)}{\partial\frac{\lambda t}{\rho a R^2 b^2}} = \frac{1}{\left(\frac{r}{R}\right)^2}\frac{\partial}{\partial\frac{r}{R}}\left[\frac{r^2}{R^2}\frac{\partial\left(b^2P\right)}{\partial\frac{r}{R}}\right] \tag{6}$$

To introduce the following dimensionless variables:

Dimensionless pressure:

$$Y = b^2P \tag{7}$$

Dimensionless radius:

$$Z = \frac{r}{R} \tag{8}$$

Dimensionless time:

$$T = \frac{\lambda t}{\rho a R^2 b^2} \tag{9}$$

The Formula (6) can be turned into

$$\frac{\partial\left(\frac{1}{1+1/\sqrt{Y}}\right)}{\partial T} = \frac{1}{Z^2}\frac{\partial}{\partial Z}\left(Z^2\frac{\partial Y}{\partial Z}\right) \tag{10}$$

The initial conditions and boundary conditions are:

$$\begin{cases} Y = Y_0, & 0 \le Z \le 1, \quad T = 0 \\ \dfrac{\partial Y}{\partial Z} = 0, & Z = 0, \quad T > 0 \\ Y = Y_W, & Z = 1, \quad T > 0 \end{cases} \tag{11}$$

3 THE FINITE DIFFERENCE CALCULATION MODEL AND THE DIMENSIONLESS

3.1 *The finite difference calculation model*

First, the spherical coal particle is divided into N sections along the radius from the spherical center to the spherical surface, as is shown like the solid line in Figure 1, and the node numbers are 0, 1, 2, 3……N. Considering the change of the parameters such as pressure, gas content, seepage velocity at the spherical center is less than that near the spherical surface, the node spaces use the equal ratio changes, and the node spaces decrease from spherical center to spherical surface. Taking the 0 node as the spherical center make the concentric spherical surfaces across the center of the two adjacent nodes, as shown like the dashed line in Figure 1, and the spherical coal particle is divided into 1 solid sphere and N spherical shells.

Taking the differential quotient into difference quotient can establish difference equations, also they can be established according to the mass conservation of the spherical shells in Figure 1.

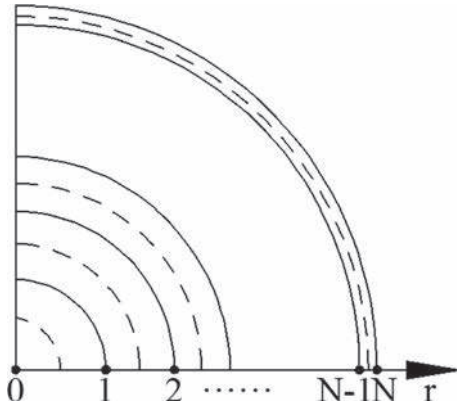


Figure 1. The node division schematic diagram under the spherical coordinate system.

Except the center sphere and the spherical shell where the outer surface node N stands, the interior and exterior surfaces of the rest spherical shells are the spherical surface of the center between two nodes. The non-steady flow difference equation of the gas from 1 to $N-1$ node in Figure 1 is

$$\frac{\left(P_i^j + P_i^{j-1}\right) - \left(P_{i+1}^j + P_{i+1}^{j-1}\right)}{r_{i+1} - r_i}\left(r_{i+1} + r_i\right)^2 - \frac{\left(P_{i-1}^j + P_{i-1}^{j-1}\right) - \left(P_i^j + P_i^{j-1}\right)}{r_i - r_{i-1}}\left(r_{i-1} + r_i\right)^2 = \frac{ab\rho\left(P_i^{j-1} - P_i^j\right)}{6\lambda\Delta t_j\left(1 + b\sqrt{\frac{P_i^j + P_i^{j-1}}{2}}\right)^2\sqrt{\frac{P_i^j + P_i^{j-1}}{2}}} \times \left[\left(r_{i+1} + r_i\right)^3 - \left(r_{i-1} + r_i\right)^3\right] \quad (i = 1,2,\ldots\ldots,N-1 \quad j = 1,2,\ldots\ldots) \tag{12}$$

Where subscript $i-1$, i, $i+1$ are node numbers; superscript $j-1$ and j are time node numbers; Δt_j is the j time step.

For the point at the centre of the sphere, i.e. the sphere where the 0 point stands, its difference equation is

$$\left(P_0^j + P_0^{j-1}\right) - \left(P_1^j + P_1^{j-1}\right) = \frac{ab\rho r_1^2\left(P_0^{j-1} - P_0^j\right)}{6\lambda\Delta t_j\left(1 + b\sqrt{\frac{P_0^j + P_0^{j-1}}{2}}\right)^2\sqrt{\frac{P_0^j + P_0^{j-1}}{2}}} \tag{13}$$

For the outer surface of the spherical coal particle, i.e. when $r = R$, according to the boundary conditions it can be got

$$P_N^j = P_W \tag{14}$$

Formula (12)~(14) constitute the complete system of equations where the unknown quantities are the pressure square of the N nodes at the j moment. If give a time step and the pressure at the last moment, the pressure at the next moment can be calculated. Accordingly, the gas pressure of the coal sphere at any time can be calculated, and the computing time step uses the equal ratio step.

In Formula (12) and (13), the right of the equation is the nonlinear expression of the node pressure square, and thus the iterative approach should be used in the solution. The iterative method is that assume $P_i^j = cP_i^{j-1}$ and calculate the number of the square root. The quasi linear equation system and a set of solutions can be obtained, according to which the number of the square root can be calculated, then the quasi linear equation system is solved again and a set of new solutions can be got. Do this recursion until the relative error of the two calculative solutions is less than a small value.

After the gas pressure square at each time is obtained, the gas desorption amount of the spherical coal particle in the j time step is

$$\Delta Q_j = 2\pi R^2\lambda\Delta t_j\frac{\left(P_{N-1}^j + P_{N-1}^{j-1}\right) - \left(P_N^j + P_N^{j-1}\right)}{r_N - r_{N-1}} \tag{15}$$

The gas accumulative desorption amount of the coal sphere is the sum of the desorption amount at each period.

3.2 *The dimensionless of the finite difference calculation model*

Taking the dimensionless variables in Formula (7)~(9) into the finite difference equation, Formula (12) can be turned into

$$\frac{\left(Y_i^j + Y_i^{j-1}\right) - \left(Y_{i+1}^j + Y_{i+1}^{j-1}\right)}{Z_{i+1} - Z_i}\left(Z_{i+1} + Z_i\right)^2 - \frac{\left(Y_{i-1}^j + Y_{i-1}^{j-1}\right) - \left(Y_i^j + Y_i^{j-1}\right)}{Z_i - Z_{i-1}}\left(Z_{i-1} + Z_i\right)^2 = \frac{\left(Y_i^{j-1} - Y_i^j\right)}{6\Delta T_j\left(1 + \sqrt{\frac{Y_i^j + Y_i^{j-1}}{2}}\right)^2\sqrt{\frac{Y_i^j + Y_i^{j-1}}{2}}} \times \left[\left(Z_{i+1} + Z_i\right)^3 - \left(Z_{i-1} + Z_i\right)^3\right] \quad \left(i = 1,2,\ldots\ldots,N-1 \quad j = 1,2,\ldots\ldots\right) \tag{16}$$

Formula (13) can be turned into

$$\left(Y_0^j + Y_0^{j-1}\right) - \left(Y_1^j + Y_1^{j-1}\right) = \frac{Z_1^2\left(Y_0^{j-1} - Y_0^j\right)}{6\Delta T_j\left(1+\sqrt{\frac{Y_0^j + Y_0^{j-1}}{2}}\right)^2\sqrt{\frac{Y_0^j + Y_0^{j-1}}{2}}} \quad (17)$$

For the outer surface of the spherical coal particle, i.e. when $Z = 1$, according to the boundary conditions it can be got

$$Y_N^j = Y_W \quad (18)$$

By Formula (15) it can be got

$$\frac{\Delta Q_j}{\rho a R^3 \Delta T} = 2\pi \frac{\left(Y_{N-1}^j + Y_{N-1}^{j-1}\right) - \left(Y_N^j + Y_N^{j-1}\right)}{Z_N - Z_{N-1}} \quad (19)$$

To introduce the dimensionless variable:

$$M = \frac{Q}{\rho a R^3 \Delta T} \quad (20)$$

The Formula (20) can be expressed as

$$\Delta M_j = 2\pi \frac{\left(Y_{N-1}^j + Y_{N-1}^{j-1}\right) - \left(Y_N^j + Y_N^{j-1}\right)}{Z_N - Z_{N-1}} \quad (21)$$

3.3 *Compilation and operation of the program*

According to established dimensionless calculation model of the finite difference and the corresponding boundary conditions above, the Visual Basic language is used to design and compile the computer programs, and the flowchart of the program structure is shown in Figure 2.

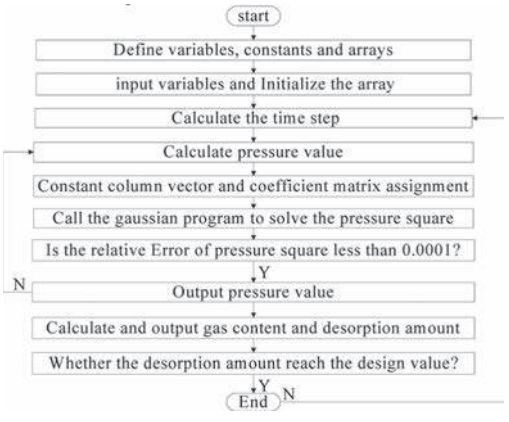


Figure 2. Flowchart of the program structure.

4 ANALYSIS OF THE RESULTS

According to the experiment performed (Qin et al. 2012), the external original gas pressures of the coal particle are respectively taken as 0.5 MPa, 1 MPa, 2 MPa, 4 MPa. After the calculation, the gas pressure distributions at the different time and the gas desorption amount in the coal particle are obtained under the different initial gas pressure and when the external pressure is a standard atmospheric pressure.

4.1 *The change laws of the gas pressure in the coal particle*

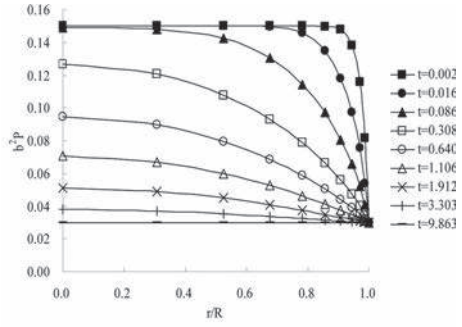
Using VB program to calculate, the curves of gas pressure in the coal particle at the different time and the different node are obtained. Figure 3 shows the curves of gas pressure in the coal particle when the initial pressure is respectively 0.5 MPa, 1 MPa, 2 MPa, 4 MPa.

As can be seen in the figure above: (1) At the beginning of the desorption, the gas pressure at the outer boundary of the coal particle begins to decrease first, which drives the gas pressure in the coal particle reducing. With the passage of time, the change rate of the gas pressure in the coal particle slows, and the gas pressure is gradually close to that in the outer space. (2) In the initial stage of the gas desorption, the greater the initial pressure outside the coal particle is, the gentler the distribution curve of the pressure within the coal particle is. Namely the decreased amplitude of the pressure at each point in the coal particle is more uniform and the gas flow speed is faster, which also accords with Darcy law.

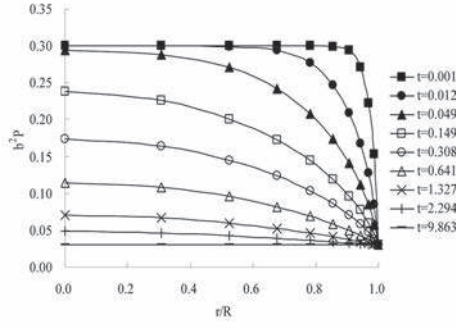
4.2 *The accumulated gas desorption amount in the coal particle under the different pressures*

Using VB program to calculate, the gas desorption amount in the coal particle with the same size and under different pressures is obtained. Figure 4 shows the change curves of the accumulated gas desorption amount in the coal particle under the different pressures.

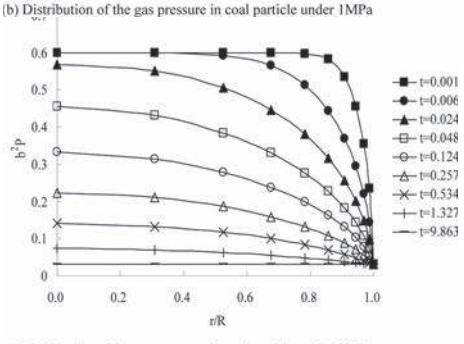
As can be seen in Figure 4: (1) The greater the gas pressure in the coal particle is, the larger the coal gas adsorption amount is. Therefore, the gas desorption amount is more, and the rate of the gas desorption is faster. (2) With the extension of time, the gas in the coal particle gradually desorbs, the differential pressure between inside and outside gradually decreases, and the desorption rate is gradually slow.



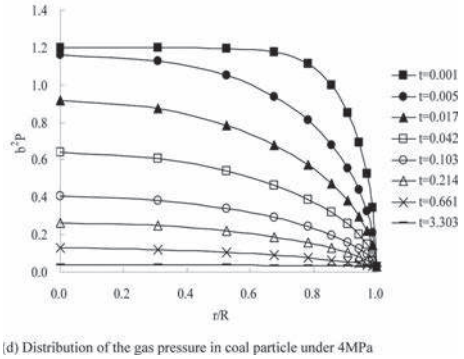
(a) Distribution of the gas pressure in coal particle under 0.5MPa



(b) Distribution of the gas pressure in coal particle under 1MPa



(c) Distribution of the gas pressure in coal particle under 2MPa



(d) Distribution of the gas pressure in coal particle under 4MPa

Figure 3. Distributions of the gas pressure in the coal particle under different gas initial pressure.

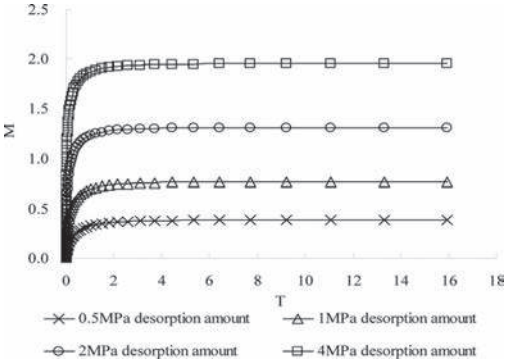


Figure 4. The accumulated gas desorption amount in the coal particle under different pressure.

5 CONCLUSION

1. According to Darcy law, the mathematical model of gas emission in the coal particle and its boundary conditions is established, by means of which the dimensionless pressure, the dimensionless time and the dimensionless radius are put forward to simplify the model.
2. Divide the spherical coal particle into units and using the finite difference method establish the mathematical equations and make them dimensionless, the purpose of which is to simplify the equations and decrease the number of conditions substitution for the model solution. By means of VB programming and calculation, finally the gas pressure distributions at the different time and the gas desorption amount in the coal particle are obtained.
3. Dimensionless quantity is the combination of the multiple physical parameters, that a result considers the combined action of multiple factors. Through the analysis, as can be known the law of the gas emission in the coal particle got from this method is more universal, which also provides a prerequisite for the application of the engineering practice.

REFERENCES

Qin, Y.P. et al. 1998. Dimensionless analysis on heat dissipation of rock surrounding in coal face. *Journal of China Coal Society* 23(1): 62–66.

Qin, Y.P. et al. 2009. Numerical simulation of gas migration in goaf in extracting stage. *Mineral Engineering Research* 24(4): 26–29.

Qin, Y.P. et al. 2012. Mathematical model of gas emission in coal particles and the numerical solution. *Journal of China Coal Society* 37(9): 1466–1471.

Wu, S.Y. & Guo, Y.Y. 1999. Study on the characteristics of coalbed methane migration. *Journal of China Coal Society* 24(1): 65–69.

Yang, Q.L. & Wang, Y.A. 1986. Diffusion theory and application of coal gas. *Journal of China Coal Society* 9(3): 87–93.

Yang, Q.L. 1987. Experimental research on coal gas Diffusion. *Satety in coal mine*.

Zhang, C.L. et al. 2001. The normalization processing and application of dimensionless fluid production index in low permeability Oilfield. *Science Technology and Engineering* 11(11): 2582–2587.

Zhou, S.N. & Lin, B.Q. 1999. *The theory of gas flow and storage in coal seams*. Beijing: China Coal Industry Publishing House.

Zhou, S.N. & Sun, J.Z. 1965. Flow theory and application of coal seam gas. *Journal of China Coal Society* 2(1): 24–36.

Progress in Mine Safety Science and Engineering II – He et al. (Eds)
© 2014 Taylor & Francis Group, London, ISBN 978-1-138-00122-0

Analytical study of the time varying diffusion law of the gas in the pea coal

B. Cheng & H.Q. Zhou
National Key Laboratory of Gas Disaster Detecting, Preventing and Emergency Controlling, Chongqing, China
Chongqing Research Institute, China Coal Technology and Engineering Group, Chongqing, China

ABSTRACT: Analyzed the mechanism of the occurrence of time-varying diffusion coefficient in the process of diffusion in the pea coal on account of Fick diffusion, measured the relationship between time and the diffusion coefficient of Nantong coal samples, by the formula of seeking for the variant diffusion coefficient. Got the mathematical model of variant diffusion coefficient by analysis of the experimental data, derived the analytic solution of time varying diffusion equation.

1 INTRODUCTION

Gas flow in coal seams was an integrated process which included diffusion in pore and seepage in fracture. Free gas flow to the lower gas pressure location along the fracture network occurring in coal seams, and Permeability Coefficient of the seams was closely related to the network. At the same time, adsorbed gas on block coal is desorbed and flowed to the fracture, thus the flow status of gas was determined by the permeability and diffusion coefficient of the gas. As the gas molecules do not move freely in the pore which diameter was smaller than the mean molecular free length of gas, the mass flow of gas was proportional to its concentration gradient, which was in accordance with Fick's law (Nie Baisheng et al.2000, Nie Baisheng et al.1998). While diffusion coefficient of the coal as porous media continues to change with the gas concentration through diffusion process, depends strongly on the concentration and presents time variation. Based on the experiments on desorption-diffusion in the pea coal on account of Fick diffusion at present, it had been found that diffusion quantity Qt over t time in the initial stage of process of desorption-diffusion still had a relationship $Q_t/Q_\infty = K\sqrt{t}$ between with the limiting diffusion quantity Q∞ at t→∞, even though diffusion coefficient D was about the gas concentration (Yang Qiluan et al.1986, Liu Zhongmin et al.1995), it was proved that the Changing Patterns of diffusion process with varying diffusion coefficient was similar to that of diffusion process with invariable diffusion coefficient.

This paper analyzed the time-varying diffusion coefficient in the process of diffusion in the pea coal on account of Fick diffusion, got the formula of seeking for the variant diffusion coefficient by time-quantity curve of gas diffusion, measured the relationship between time and the diffusion coefficient of coal samples, got the mathematical model of variant diffusion coefficient and the analytical solution. The variant diffusion coefficient was especially significant for the prediction of coal and gas outburst hazard, prediction of gas content and calculation of fallen coal gas emission.

2 ANALYSIS OF THE RELATIONSHIP BETWEEN TIME AND THE DIFFUSION COEFFICIENT DURING DIFFUSION

Based on the theory of modern chemistry, effective diffusion coefficient of molecule was related to the bending coefficient calculated from porosity and average pore diameter of porous media, that is:

$$D_{eff} = \frac{D\phi}{\varsigma} \tag{1}$$

Where D_{eff} indicates effective diffusion coefficient, D is diffusion coefficient, Φ is porosity, ζ indicates bending coefficient, correcting for the resistance caused by bending of the channel.

Eq.1 indicates that effective diffusion coefficient of gas in the pea coal was influenced by the porosity and bending coefficient. Swelling of coal matrix owing to gas adsorption reduced the porosity; meanwhile gas adsorption changed the bending coefficient of the diffusion channel and led to the increase of the diffusion resistance. Conversely, gas emission had an impact on the diffusion resistance of gas on the condition of isothermal and isobaric after gas adsorption saturation (Chen Ruijun

et al.1995, Yang Zhenjun 2004). As a result, diffusion coefficient altered continuously affected by changes of gas concentration in the process of diffusion. So the actual diffusion process was different from the ideal model $Q = k\sqrt{t}$ because of the changing diffusion coefficient. Therefore, it's more in line with the actual process that formulating the diffusion coefficient as a function of time and describing the diffusion by Fick's law.

3 SEEKING TIME-VARYING DIFFUSION COEFFICIENT D_T

Combined with the above analysis, following hypothesis was set aiming at the diffusion model with varying diffusion coefficient.

1. The pea coal was spherical particles which was homogeneous and isotropic;
2. Gas flow in the pea coal followed mass conservation law and continuity principle;
3. The solution of the diffusion model with varying diffusion coefficient was the product of the solution of model with invariable diffusion coefficient and the time function X_t.

Put forward the diffusion equation and boundary conditions according to the diffusion model with invariable diffusion coefficient as follows:

$$\begin{cases} \dfrac{\partial c}{\partial t} = \left(\dfrac{1}{r^2}\right)\dfrac{\partial}{\partial r}\left(r^2 D \dfrac{\partial c}{\partial r}\right) \\ c(r,0) = c_0; c(R,t) = c_1 \\ \left.\dfrac{\partial c}{\partial r}\right|_{r=0} = 0 \end{cases} \tag{2}$$

Where R is radius of the pea coal, $c(r,t)$ is the radial concentration of the pea coal.

It had done certain processing to the Eq.3:

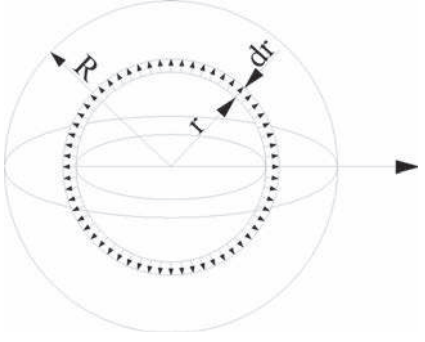


Figure 1. Diffusion of gas in the pea coal.

$$\frac{c_{at} - c_1}{c_0 - c_1} = X_t \left\{ 1 - \left(\frac{6}{R}\right)\left(\frac{D_t t}{\pi}\right)^{1/2} \times \left[1 + 2\pi \sum_{n=1}^{\infty} ierfc \frac{nR}{\sqrt{D_t t}} \right] + \frac{3 D_t t}{R^2} \right\} \tag{3}$$

Where c_{at} is average concentration of the pea coal which radius was R at time t, c_0 is homogeneous concentration at the initial time, c_1 is homogeneous concentration of pea coal surface, X_t is a time function about concentration, time, adsorption properties of coal, etc., D_t is diffusion coefficient that possibly corresponds to the concentration c_{at}.

When diffusion time t tended to time τ it had the relationship as follows based on the continuity of the time-quantity curve of gas diffusion:

$$X_t \to X_\tau, D_t \to D_\tau \tag{4}$$

Describe the curve of diffusion as follows combined with the above functions:

At diffusion time t

$$\frac{c_{at} - c_{a\tau}}{c_1 - c_0} = X_\tau \left(\frac{6}{R}\right)\left(\frac{D_\tau}{\pi}\right)^{1/2} \left(t^{1/2} - \tau^{1/2}\right) \tag{5}$$

In Eq.5:

$$X_\tau = \left(1 - Q_\tau / Q_\infty\right) + X_\tau \left(\frac{6}{R}\right)\left(\frac{D_\tau}{\pi}\right)^{1/2} \tau^{1/2} \tag{6}$$

$$Q_\tau / Q_\infty = \left(c_{a\tau} - c_0\right) / \left(c_1 - c_0\right) \tag{7}$$

The later section on the right-hand side of this equality was the intercept of the line consisted by $c_{at} - c_{a\tau}/c_1 - c_0$ and $t^{1/2}$ in formula (5); Q_τ/Q_∞ was the relative diffusion amount at time τ.

If the diffusion time was long:

$$\ln \frac{c_1 - c_{at}}{c_1 - c_{a\tau}} = -\frac{\pi^2}{R^2} D_\tau (t - \tau) \tag{8}$$

The value of diffusion coefficient D_τ and function X_τ could be determined used by the linear relation presented by above formulas. The diffusion coefficient and function corresponded to any bit on the curve of diffusion (Liu Zhongmin et al.1995).

4 EXPERIMENTAL VERIFICATION

Chongqing Research Institute of China Coal Technology & Engineering Group Successfully

manufactured a set of test device which was used to research the law of desorption and diffusing process of pea coal, according to *Determine method of methane adsorption capacity in coal* (MT/T752-1997), Ministry of Coal Industry. The complete set of the experimental device include vacuum degassing system, gas adsorption-desorption system and high-pressure gas cylinder.

According to the analysis of the part 1, the curve of gas diffusion of 6# coal samples of Yutianbao coal mines, Nantong mining bureau was measured by the diffusion test device. Determined the pore characteristics of coal samples by the mercuric density method, the results showed that the numbers of Knudsen of the coal samples Kn ≥ 10 and the condition of Fick diffusion was met. The particle size of coal samples was 0.2~0.25 mm and weight 30.0003 g. First put coal samples into vacuum drying oven and kept drying them for 24 hours, then charged gas with concentration 99.99% and some pressure into Coal sample tank, kept the samples adsorbing gas after 48 hours and record the equilibrium pressure, worked out the adsorption quantity of samples with the industrial analysis and adsorption constant. After that, determined the diffusion quantity and its corresponding times, the gas diffusion coefficient D_t at different times were worked out by using the formula in part 2.

From Fig.5 can be obtained: the order of magnitude of gas diffusion coefficient was 10–9, the gas diffusion coefficient moderated at the beginning and ending period basically, showed a sharp increase over the medium term at a certain time period. So there was an error for describing the diffusion process of gas in coal particle by using the Fick law. By regression analysis of experimental data in Fig. 4, it was found that the D_t meet the Eq.9 with time.

$$\begin{cases} D_t = D_0 e^{At}, [0 < t < t_1) \\ D_t = D_0 \left(B - Et^{-m} \right), [t_1 < t < \infty) \end{cases} \quad (9)$$

The factor of *A, B, E, m* is fit coefficient, and $e^{At_1} = B - Et_1^{-m}$.

Coal particles aperture and gas molecular free length had about the same size, after adsorption equilibrium coal particles aperture waned, therefore gas molecular were in great diffusion resistance in the early stages of the diffusing process. Along with the gas concentration of lower of

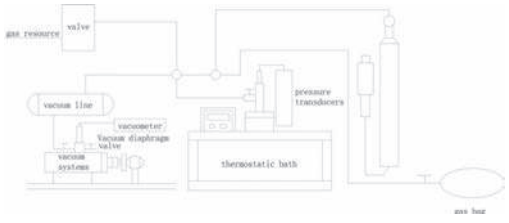


Figure 2. Sketch of diffusion experimental device.



Figure 3. Physical map of diffusion experimental device.

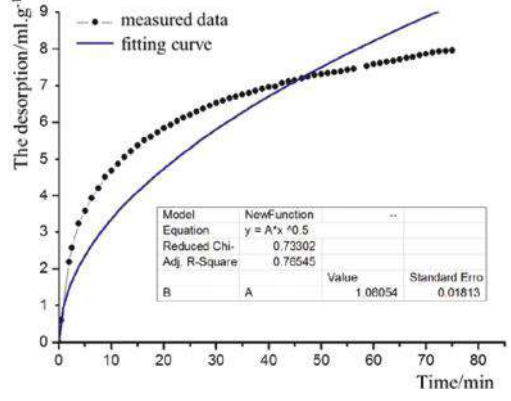


Figure 4. Relationship curve between the diffusing capacity and time.

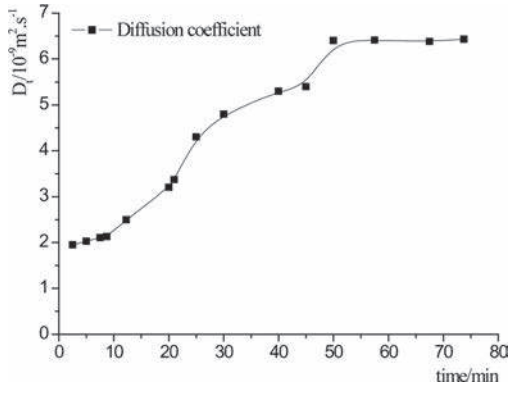


Figure 5. Relationship curve between the diffusion coefficient and time.

coal particles, coal particles became increasingly large, but in the early stages of the diffusing process, the change extent of aperture compared with molecular free length smaller, therefore in the early stages, gas diffusion coefficient had little change. The change of coal particles had obvious influence for the diffusion of gas molecular along with gas evolution. In the end of the diffusing process, Coal particles size change gradually diminished and the change extent of aperture compared with molecular free length smaller still, therefore the gas diffusion coefficient Changed smaller in this period of time, it could be deemed to one constant.

5 THE DIFFUSIVITY MODEL FOR SPHERICAL FLOW IS BASED ON TIME-DEPENDENT DIFFUSION COEFFICIENT

Made u = cr and introduced into the diffusivity equation for spherical flow, could be obtained

$$\begin{cases} \dfrac{\partial u}{\partial t} = D\dfrac{\partial^2 u}{\partial r^2} \\ u = 0\left(r = 0, t > 0\right) \\ u = Rc_1\left(r = R, t > 0\right) \\ u = rc_0\left(0 < r < R, t = 0\right) \end{cases} \tag{10}$$

But the second Fick's law established one of the premise was the diffusion coefficient was assumed to be constant, when considering D was a time-dependent function of the Eq.2, could use variable substitution, make D_t to be variable quantity $\partial f = D_t \partial t$ and be introduced into the diffusivity equation, can be obtained,

$$\frac{\partial u}{\partial t} = D_t \frac{\partial^2 u}{\partial r^2} \Rightarrow \frac{\partial u}{\partial f} = \frac{\partial^2 u}{\partial r^2} \tag{11}$$

Mad u(f,r) = T(f)N(r) and introduced into the Eq.11, could be obtained,

$$\frac{1}{T(f)}\frac{\partial T}{\partial f} = \frac{1}{N(r)}\frac{\partial^2 N}{\partial r^2} \tag{12}$$

The left, right both ends of the Eq.12 were function of f and r, f and r were two independent variables, if the equality holds, they must be constant. Mad this constant to be $-\varepsilon^2$, two partial differential equations could be obtained

$$\frac{\partial T}{\partial f} + \varepsilon^2 T = 0 \tag{13}$$

$$\frac{\partial^2 N}{\partial r^2} + \varepsilon^2 N = 0 \tag{14}$$

The General Solution of the Eqs.13 and14 were separate

$$T = Ce^{\left(-\varepsilon^2 f\right)} \tag{15}$$

$$N = G\cos\left(\varepsilon r\right) + H\sin\left(\varepsilon r\right) \tag{16}$$

C, G, H were undetermined coefficients of the Eqs.15 and 16 and Complicate these two equations, then be introduced into u(f,r) = T(f)N(r), can be obtained the General Solution of the Eq.12,

$$u = Ce^{\left(-\varepsilon^2 f\right)}\left[G\cos\left(\varepsilon r\right) + H\sin\left(\varepsilon r\right)\right] \tag{17}$$

Finished u = cr and the Eq.17 could be obtained,

$$c = \frac{Ce^{\left(-\varepsilon^2 f\right)}}{r}\left[G\cos\left(\varepsilon r\right) + H\sin\left(\varepsilon r\right)\right] \tag{18}$$

The Boundary Conditions introduced into the Eq.18 could be obtained,

$$CHe^{-\varepsilon^2 f}\sin\varepsilon R = Rc_1 \tag{19}$$

$$CHe^{-\varepsilon^2 f_0}\sin\varepsilon r = rc_0 \tag{20}$$

Solutions of the transcendental Eqs.19 and 20 could be obtained the parameters ε and CH, but this solution was the infinite number, so Eq.10 was carried out by employing the Laplace transformation and could be obtained,

$$c = c_0 + \frac{R\left(c_1 - c_0\right)}{r} \times \sum_{n=0}^{\infty}\left\{erfc\frac{(2n+1)R - r}{2\sqrt{f}} - erfc\frac{(2n+1)R + r}{2\sqrt{f}}\right\} \tag{21}$$

The parameters erf of the Eq.21 was error function, $f = \int_0^t D_t dt$.

At diffusion coefficient in front of methane diffusion changes over time in line with: $D_t = D_0 e^{At}$,$[0 < t < t_1]$. And the analytical solution of Eq.21 was:

$$c = c_0 + \frac{R\left(c_1 - c_0\right)}{r} \times \sum_{n=0}^{\infty}\left\{erfc\frac{(2n+1)R - r}{2\sqrt{\frac{D_0}{A}\left(e^{At} - 1\right)}} - erfc\frac{(2n+1)R + r}{2\sqrt{\frac{D_0}{A}\left(e^{At} - 1\right)}}\right\} \tag{22}$$

After methane diffusion at diffusion coefficient changes over time in line with:

$$D_t = D_0\left(B - Et^{-m}\right),[t_1 < t < \infty)$$

then $$f = \int_0^t D_t dt = \int_0^{t_1} D_0 e^{At} dt + \int_{t_1}^t D_0 (B - Et^{-m}) dt$$

And the analytical solution of Eq.22 was:

$$c = c_0 + \frac{R(c_1 - c_0)}{r} \times \sum_{n=0}^{\infty} \left\{ erfc \frac{(2n+1)R - r}{2\sqrt{\frac{D_0}{A}\left(e^{At_1} - 1\right) + D_0 B\left(t - t_1\right) - \frac{D_0 E\left(t^{1-m} - t_1^{1-m}\right)}{(1-m)}}} - erfc \frac{(2n+1)R + r}{2\sqrt{\frac{D_0}{A}\left(e^{At_1} - 1\right) + D_0 B\left(t - t_1\right) - \frac{D_0 E\left(t^{1-m} - t_1^{1-m}\right)}{(1-m)}}} \right\} \quad (23)$$

6 CONCLUSIONS

1. Because of the adsorption of coal and gas-phase, the porosity and bend factors of coal grain would be changed in desorption and diffusing process, proceed to the next step make the diffusion coefficient will be changed in the whole diffusing process.
2. Making use of the equation Dt calculate the diffusion coefficient of Nantong coal (pantoprazole Kn ≥ 10) in different dispersion time, the results show that, the gas-diffusion coefficient basic tend to be gentle in the initial stage and last phase of dispersion process, but it appear peaking in the middle of a time period. Through the analysis of experimental data, the relationship of diffusion coefficient and time was found to conform following equations,

$$\begin{cases} D_t = D_0 e^{At}, [0 < t < t_1) \\ D_t = D_0 (B - Et^{-m}), [t_1 < t < \infty) \end{cases}$$

Therefore, the diffusion coefficient was regard as the time function for processing and then used the Fick's law to describe the process of the Coal Particle in methane diffusion; this method is more suitable to the actual.

3. Through the mathematical model of the time-dependent diffusion coefficient of the experiment, the analytical solutions of the time-dependent equation was derived.

ACKNOWLEDGEMENTS

This work was financially supported by the National Science and Technology Major Project (ID: 2011ZX05040-003-003).

REFERENCES

Chen Ruijun, Wang Dongan. Na Tong mining area coal microspores and gas storage, migration relationship. *Coal Geology & Exploration (Xi'an)*. 23: 29–31 (in Chinese).

Liu Zhongmin, Zheng Lvbin, et al 1995. Diffusion coefficient to calculate the Dt with concentration related. *Science in China Series B (Beijing)*.1995(25):704–709 (in Chinese).

Nie Baisheng 1998. Coal particle gas desorption diffusion dynamic process of the experimental research, *Taiyuan university of science and technology mining system (Taiyuan)*, 4: 417–421 (in Chinese).

Nie Baisheng, He Xueqiu, et al 2000. Mechanism and Modes of Gas Diffusion in Coal Seams. *Journal China Safety Society (Beijing)*. 10: 24–28 (in Chinese).

Yang Qiluan, Wang Youan 1986. Theory of methane diffusion from coal cuttings and its application. *Journal China Coal Society (Beijing)*. 3: 87–93 (in Chinese).

Yan Zhenjun 2004. Mathematical physics equations. University of Science and Technology of China Press (Hefei), 37–176.

This page intentionally left blank

Progress in Mine Safety Science and Engineering II – He et al. (Eds)
© 2014 Taylor & Francis Group, London, ISBN 978-1-138-00122-0

Safe and high-efficient mining model in old mining area and resource integration mines

H.T. Li, L. Zhang & Y.F. Weng
North China Institute of Science and Technology, Sanhe, Hebei, China

H.T. Li
Hebei Province Key Laboratory of Mine Disaster Prevention, Sanhe, Hebei, China

J.G. Yang
China Pingmei-Shenma Group, Pingdingshan, Henan, China

ABSTRACT: In the context of resource integration in old coal mining area in China, taking China Pingmei-Shenma group as research object, by investigating and summarizing its' practical experience in the course of constructing safe and high-efficient mining in old mining area and resource integration mines, connotation and features are preliminarily expounded on safe and high-efficient mining model in old mining area and resource integration mines. Elements are analyzed on safe and high-efficient mining model, and theoretical framework which is based on three dimension (i.e. aim dimension, path dimension and type dimension) and elements is founded to analyze safe and high-efficient mining. Based on theoretical framework, general model and three special models (i.e. production-distribution optimized model, resources optimization deployed model and safety production improved model) are induced on safety and high efficiency mining by analyzing main points in constructing safe and high-efficient mining in old mine area and resource integration mines.

1 INTRODUCTION

At present, since earlier development, there are the backward mining technology and low level technique equipment in Chinese old mine area with longer mining history. Again, according to the government's proposal, a number of large coal enterprises with rich mining experience participate recently in integrating coal resources and merger and reorganization of enterprises one after another. They integrate plenty of local mines with characteristic of small production scale of mine, low yield and poor safety guarantee capability.

In order to adapt old mine area and resource integration mine to present new situation of mine maximization, mining technology modernization and production mechanization. Only if they have to improve largely, even just revolutionary change in all aspects of production, safety and management, the construction can be promoted on safe and high-efficient mine (Pu 2007, Wang 2010, Zou 2007), safety production can be guaranteed in whole mining area, and economic and social benefits can be improved.

Taking mining coal as main body extra large type enterprise, China Pingmei-Shenma group have actively explored in the aspect of safe and high-efficient mining construction in old mine area and resource integration mine.

By investigating and summarizing the experience and ways in practice, the model is abstracted on safe and high-efficient mining in old mine area and resource integration mines. The model will provide important reference and guidance role for old mine area and resource integration mines in the aspect of safe and high-efficient mine construction.

2 CONNOTATION OF SAFE AND HIGH-EFFICIENT MINING MODEL IN OLD MINE AREA AND RESOURCE INTEGRATION MINE

"Safe and high-efficient mining model in old mine area and resource integration mines" basic connotation is insisting on the principle of safety first and prevention first, comprehensive treatment, and production and safety equal attention in the context of integrating and rebuilding local mine in old mine area. To take safety, high efficiency and environment friendly as aim.

According to coal resources hosting and mining basic condition, to take rebuilding and upgrading of

mine production system as basis, mining equipment upgrading to a higher level as breakthrough (Wu 1995), management innovation as guarantee, and technology innovation as relying on, Optimizing and integrating systematically Human-Machine-Environment, information, and mining, excavation, machinery, conveying and ventilation to promote construction of safe and high-efficient, and essential safety mine (Wang 2007, Du et al. 2007, Liu et al. 2007), then improve mine capacity and form long-term mechanism of safe production.

For safe and high-efficient mining model in old mine area and resource integration mine, its main features are as follow:

Firstly, based on characters of new mine existing in old mining areas, achieving sustainable and common development of coal industry by old mine driving new mine, new mine promoting old mine, in old mine area and resource integration mine.

Secondly, establishment of safe and high-efficient mining model with four main aims, that is, safety, high production, high efficiency and environment-friendly (Qian et al. 2008).

Thirdly, paying equal attention to production and safety should be insisted in the course of safe production. One ventilation and three preventions should be taken as emphasis, eliminating firmly gas, coal dust, water disaster, and fire and roof major accidents, and at the same time, eliminating electromechanical, conveying, second-class and upwards non-casualty accidents, and putting an end severe injury and upwards. Achieving the object of mortality rate fell to 0 per million tons and establishing and perfecting long-term mechanism.

Fourthly, the rebuilding and upgrading of mine system is construction basis of high-efficient mining model, it is mainly to resource integration mines which capacity and safety level have to be improved.

Fifthly, there are three realization ways for safe and high-efficient mining model, that is, equipment, management and technology; they support each other with the software and hardware method. They are different fields of safe and high-efficient mining as well as inter-coupling system modules. Their coordination will promote formation of safe and high-efficient mining model.

Sixthly, establishment of safe and high-efficient mining model need mobilize, allocate and integrate systematically, scientifically and organically inner human-machine- environment and information. These aren't unilateral, partial, tactical, microscopic, miniature, mended and short-term measure, but comprehensive, systematic, strategy, macroscopic, large, innovative and long-term measure.

Seventhly, from the view of upgrading equipment to a higher level, mining mechanization degree is more than 95%, loader mechanization degree is more than 95%, and synthetic mechanization degree is more than 40%.

3 ELEMENTS ANALYSIS ON SAFE AND HIGH-EFFICIENT MINING MODEL IN OLD MINE AREA AND RESOURCE INTEGRATION MINES

According to above connotation and characters, safe and high-efficient mining model can be scanned and analyzed from three dimensions degree; it can be disassembled as follow:

The first dimension degree: the aim dimension (Aim, A for short), that is, the aim of safe and high-efficient mine construction; the aim can be concluded to safety (A_1), high yield (A_2), high efficiency (A_3) and environment-friendly (A_4).

The second dimension degree: the path dimension (Path, P for short), that is, the path of safe and high-efficient mine construction; the path can be concluded to equipment (P_1), management (P_2) and technology (P_3).

The third dimension degree: the type dimension (Type, T for short), that is, the type of mine in resource integration old mine area; the type can be concluded to principal production mine (T_1), resources decline mine (T_2) and resource integration mine (T_3).

By mathematical form, three dimensions can be expressed as:

$$A = (A_1, A_2, A_3, A_4)$$

$$P = (P_1, P_2, P_3)$$

$$T = (T_1, T_2, T_3)$$

By three-dimensional coordinate, three dimensions can be is described as Figure 1.

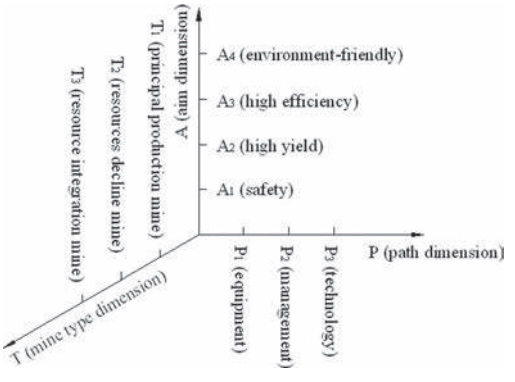


Figure 1. System decomposition maps of on model of safe and high-efficient mining.

The combination of three dimensions can be considered, if a value is chose from each dimension, and then there are 36 combination methods. For example:

Firstly, the combination $A_1P_1T_1$ is to characterize main mines achieve the aim of high production by the path of equipment upgrading to higher level.

Secondly, the combination $A_2P_3T_1$ is to characterize main mines achieve the aim of high production by the path of technology innovation.

Thirdly, the combination $A_4P_2T_2$ is to characterize resources decline mines achieve the aim of environment-friendly by the path of management innovation.

Fourthly, the combination $A_3P_1T_3$ is to characterize resource integration mine achieve the aim of high production by the path of equipment upgrading to higher level.

Of course, since it isn't single for path, it isn't also exclusiveness between aims; there are sharing and input-output in management, technology and human resources between mines, and so on. So the same dimension element can also be combined together. For example, the combination $A_1A_3P_1P_2P_3T_3$ is to characterize resource integration mines should innovate and improve in equipment, management and technology in order to achieve the aim of safety and high production because they have larger improving space in all aspects.

4 THE GENERAL AND SPECIAL MODEL OF SAFE AND HIGH-EFFICIENT MINING IN OLD MINE AREA AND RESOURCE INTEGRATION MINE

Mines pursue and practice safe and high-efficient mining with similarities, at the same time, since geological and production technology conditions are complexity and diversity, safe and high-efficient mining is particularity and diversity. In other words, in the framework of general model, according to different mine condition, different condition correspond to different type special model.

4.1 *The general safe and high-efficient mining model in old mine area and resource integration mines*

In the course of investigating constructing practice on safe and high-efficient mine constructing in Pingmei-Shenma group, major theoretical issue and practical effect are anatomized and summarized deeply and thoroughly. A set of general model is explored which take mining equipment upgrading to a higher level as exerting point to improve safe and high-efficient mining-level in old mine area and resource integration mine.

The general model refer to the basic line that all mines should follow in the course of constructing safe and high-efficient mine in old mine area and resource integration mine. Its basic content is to take connotation of safe and high-efficient mining model as theory evidence, an omni-bearing analysis are given about basic situation and existing problems in equipment, technology and management, and so on. The overall conceptual scheme is made scientifically to promote production and safety. All efforts should be mobilized to promote scheme implementing, improve scheme, and achieve to continuously promote safe and high-efficient mining.

About the general model of safe and high-efficient mining in old mine area and resource integration mine, its basic character is shown as follow:

Firstly, take scientific development view as the lead.
Secondly, take necessary input as basis.
Thirdly, take scientific planning as premise.
Fourthly, take science and technology innovation as motive powers.
Fifthly, take management upgrade as guarantee.
Sixthly, take quality improving as support.
Seventhly, take technical reformation and system upgrading as key link (Yang 2010).

The concrete operation flow of general model is shown as Figure 2 on safe and high-efficient mine constructing in old mine area and resource integration mine.

4.2 *The special model of safe and high-efficient mining in old mine area and resource integration mine*

The special model is based on the framework of general model on safe and high-efficient mining in old mine area and resource integration mine, and

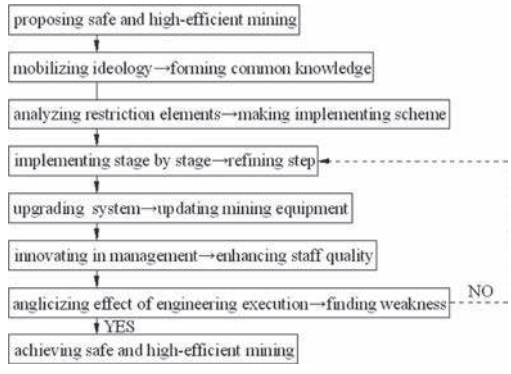


Figure 2. The general model of safe and high-efficient mining.

different models are made by combining different condition of concrete mine. The characteristic pattern is proposed in order to study different emphases which achieve safe and high-efficient mining for different mine, thus make mine more prominence self features when implementing mining equipment upgrading to higher level so as to achieve larger effect.

According to different condition of 34 mines affiliating them with Pingmei-Shenma group, based on general model, three special models are further summarized, that is, production-distribution optimized model, and resources optimization deployed model and safety production improved model.

4.2.1 *Production-distribution optimized model*
Production-distribution optimized model mainly correspond to principal production mine. Taking Pingmei-Shenma group as example, for the first mine, fourth mine, sixth mine and eighth mine example. Such as mines with rich resource, strong technical force, they are main body to improve mine capability, and are main undertakers which achieve great-leap-forward development for coal enterprises.

For above mines, based on adopting new technology and new equipment, production- distribution optimized model is the model which makes mine achieve safety and efficiency by optimizing production—distribution under certain natural resources condition and requirement of mine capacity.

Significance of the model means achieving mine develop to concentrated producing, large, continuous conveying, diversified mining method, single layer and full coal tunnel collocation modern mine, by optimizing production systems (i.e. conveying, hoisting, ventilation and power supply system and so on.), mining method, excavating method, and auxiliary conveying.

According to the mine features, emphasis should be laid on optimizing further production–distribution and production systems, and improving efficiency of mining equipment and mine capability by constructing safe and efficient mine based on mining equipment upgrading to a higher level.

In the course of implementing safety and high efficiency mining model for the principal production mine. The key nodes include forming common knowledge by mobilizing ideology, optimizing production–distribution by setting clear engineering implementing objectives, making implementing scheme by analyzing restriction elements, optimizing production–distribution by implementing stage by stage, updating mining equipment by upgrading and rebuilding of system, enhancing staff quality by innovating in management, finding weakness by anglicizing effect of engineering execution.

According to above key nodes, production—distribution model is formed which the principal production mine achieve safe and high-efficient mining, as shown in Figure 3.

4.2.2 *Resources optimization deployed model*
Resources optimization deployed model mainly correspond to reserves decline mine. Taking Pingmei-Shenma group as example, for the second mine, third mine and ninth mine example. Such mines are faced with dilemma of resources decline or exhaustion because of longer mine life.

For above mines, from sustainable development of mine area view point, resources optimization deployed model is the model which makes every mine balanced development by redistricting and allocating coal resource, human resources, equipment resource, at the same time, implementing technology reformation.

Significance of the model means making resources exhaustion mines gain rebirth to achieve sustainable development by allocating staff (administrator and technologist), updating equipment and technology, and allocating resource to supply more reserve resources for resources exhaustion mines, and so on.

According to the mine features, emphasis should be laid on allocating optimally mine area resource, supplying more reserve resources for resources exhaustion mine, then laying a foundation of resources guarantee. At the same time, speeding up updating of mining equipment and further optimizing mine staff. Thus, achieving mine sustainable and rapid development.

In the course of implementing safe and high-efficient mining model for the mine capacity decline mine.

The key nodes include forming common knowledge by mobilizing ideology, optimizing resources deployment by analyzing restriction elements,

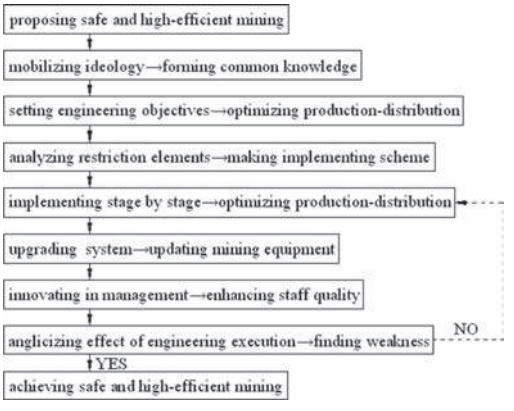


Figure 3. Production-distribution optimized model.



Figure 4. Resources optimization deployed model.

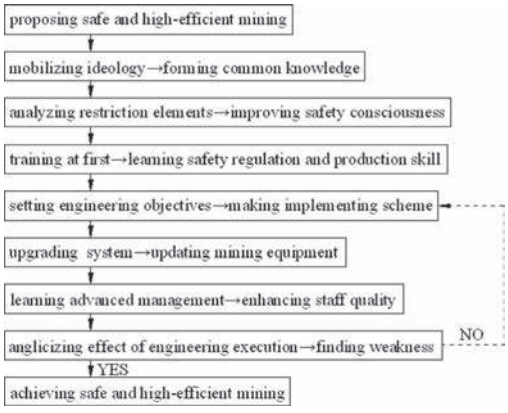


Figure 5. Safety production improved model.

learning production skill by training at first, making scheme by setting clear objectives, updating mining equipment by upgrading of system, improving staff quality by learning advanced management skill and finding weakness by anglicizing engineering implementing effect.

According to above key nodes, resources optimization deployed model is formed which resources exhaustion mines achieve safe and high-efficient mining, as shown in Figure 4.

It should be pointed out that legitimacy issue must be paid attention to optimization deployment of coal resources because reconfiguration of coal resources is involved in optimization deployed model. That is, the currently relevant laws and regulations must be strictly carried out about mineral resources exploitation in the course of implementing resources optimization deployed model in China.

4.2.3 *Safety production improved model*

Safety production improved model mainly correspond to resource integration mine. Taking Pingmei-Shenma group as example, such as Chaochuan mine, Xiang-shan mine and Rui-ping mine. Such mines are weak link to build safety production mine area because of low starting point and poor safety technology basis.

For above mines, safety production improved model is the model which makes safety and management significantly improve by updating or rebuilding full system, and training staff safety consciousness and skill.

Significance of safety production improved model means making operation level and capability of former workers improve to adapt to new condition of mine production by making standards, regulations and laws, and training staff, and updating or rebuilding technology and equipment, and so on.

According to the mine features, emphasis should be laid on building further safety sound foundation, introducing actively technician, speeding up the upgrading of equipment, then achieving maintaining and increasing coal production in the condition of ensuring safety.

In the course of implementing safe and high-efficient mining model in the resource integration mine. The key nodes include forming common knowledge by mobilizing ideology, improving safety consciousness by analyzing restriction elements, learning safety regulation and production skill by training at first, making scheme by setting clear objectives, updating mining equipment by upgrading and rebuilding of system, enhancing total quality by learning advanced management and finding weakness by anglicizing effect of engineering execution.

According to above key nodes, safety production improved model is formed which the resources conformity mine achieve safe and high-efficient mining, as shown in Figure 5.

5 CONCLUSIONS

Firstly, in the context of resource integration in old coal mining area, taking China Pingmei-Shenma group as analyzing object, connotation and major features are preliminarily expounded on safe and high-efficient mining model in old mine area and resource integration mines.

Secondly, according to connotation and features of safe and high-efficient mining model, the theoretical framework is founded by anglicizing elements and three dimensions which refer to aim dimension, path dimension and type dimension.

Thirdly, Under the guidance of theoretical framework of three dimensions and elements, the

general and three special models are concluded by anglicizing and summarizing major nodes in course of constructing safety and high efficiency mine, in which three special models refer to production-distribution optimized model, resources optimization deployed model and safety production improved model.

ACKNOWLEDGEMENTS

This work was financially supported by "the Fundamental Research Funds for the Central Universities" (2011 A01) and "the Fundamental Research Funds for the Central Universities" (3142013035).

REFERENCES

Du, C.Y. et al. 2007. Study on Connotation of Coal Mine intrinsic safety management. *China Coal* 33(4):62–64.

Liu, H.B. et al. 2007. Study on Characteristics of Coal Mine Intrinsic Safety and Strategies of Management. *China Safety Science Journal* 17(4):68–72.

Pu, H.J. 2007. *Annual report on constructing safe and high-efficient mine to coal industry in China* (2005). Xuzhou: China University of Mining and Technology Press.

Qian, M.G. et al. 2008. On Scientific Mining. *Journal of Mining & Safety Engineering* 25(1):1–10.

Wang, C.X. 2007. Connotation and extension on intrinsic safety. *Safety in Coal Mines* (10):85–87.

Wang, X.Z. 2010. *Annual report on constructing safe and high-efficient mine to coal industry in China* (2009). Xuzhou: China University of Mining and Technology Press.

Wu, R.K. 1995. Accelerate constructing high-Productive and high-efficient mine by developing deeply mining mechanization. *China Coal* 33(1):26–29.

Yang, J.G. 2010. Practice and Enlightenment in mining and excavation mechanization level in China Ping-Mei ShenMa Group. *Coal Economic Research* 30(4):96–98.

Zou, X.Z. 2007. *Safe and high-efficient mine technology*. Xuzhou: China University of Mining and Technology Press.

Progress in Mine Safety Science and Engineering II – He et al. (Eds)
© 2014 Taylor & Francis Group, London, ISBN 978-1-138-00122-0

A numerical simulated study on the permeability and the rule of stress distribution on working face

Xiaoyan Song
Key Laboratory of Mine Disaster Prevention of Hebei Province, North China Institute of Science and Technology, Beijing, China

Zhongpeng Xie
Safety and Environmental Engineering Institute, Capital University of Economics and Business, Beijing, China

ABSTRACT: The stress distribution rule along the normal of working surface can be acquired through stress stimulation on the working surface by ANSYS, and further analyze goes on the impact that can be done on the coal seam permeability by the changes of stress. By which technical support on the gas control as well as the forecast of coal and outbursts of gas can be achieved.

1 INTRODUCTION

The rock and coal in the stratum are under the power of ground stress. In the research progress of the gas dynamics in the mine, the ground stress plays a decisive role in the Permeability of rocks and coal mines. However, the permeability has an important guidance for the research of gas storage, pressure distribution, desorption of drainage as well as the movement law of gas.

2 MATHEMATICAL MODEL OF ROCK'S STRESS DISTRIBUTION

The rocks stay in balance under the natural stress before the mines are explored. This natural stress is called the original stress of rocks, and it is also known as the ground stress. The components of ground stress are complex. It mainly consists of gravity and tectonic stress. Heim, the geologist from Switzerland, first announced that the ground stress is in the state of hydrostatic pressure through his observation on the working state of surrounding rock in big tunnels. In other words, he means that the horizontal and vertical components of the ground stress are equal, and both of them can be decided by the product of the volume and depth of rocks. In 1925, according to the analysis of the elastic theory, the Russian scholar Kinnik brought forward that the vertical stress: $\sigma_v = \gamma H$, and the horizontal stress: $\sigma_H = \frac{v}{1-v}\gamma H$ (v stands for the Poisson's ratio of rock mass). According to the large amount of figures that has been measured, calculation of the vertical and the horizontal stress of the original stress can rely on both Kinnik and Heim's formula.

2.1 *Method to solve the stress of rocks*

At present, the finite-element method is the main method, which is carried out in the analysis of stress on rocks. It is an effective numerical way that grows more available with the development of computers. The essence of the finite element is to idealize the continuum with infinite degree of freedom into the unit with limited degree of freedom and simplify the problem to a structure, which is suitable for numerical solutions.

ANSYS is large-scale general software with powerful solver and processing function before and after which is developed for the calculation of finite-element method by ANSYS Software, U. S. In its working process, the operator will simply set the initial and boundary conditions and the rest will leave to the computer. This provides us a good working environment, and leaves us free from the conventional tedious and monotonous finite-element-programming (Liu & Yang 2008). In this paper, we use ANSYS for the simulated analysis on the stress of coal rocks.

2.2 *Set condition for stress of rock*

Let's set the floor of coal seam is fixed, in other words it is constrained by the vertical and horizontal stress. And the vertical stress on the roof of the coal seam is the rock's gravity (measured by the rock stress measure instrument). And the exposed face of coal is not constrained.

The selection of load is determined by the following calculation: assuming that the average density

above the roof is 2.4 t/m^3, the depth to the old roof is –600 m, then the average pressure on upper surface of the rock $q = 600 \times 2.4 \times 10^3 \times 9.8 = 14.112$ MPa, on the condition of ignoring the surface load and dynamic load which is allowed in actual situation. Table 1 provides the selected parameters of the rock for calculation, and the calculation adopts the 8-nodes-hexahedron element. This model consists of 5469 elements and 11972 nodes (Xie 2003, Xie 2004).

3 DISTRIBUTION OF SIMULATED STRESS RESULTS IN FRONT OF THE WORKING SURFACE

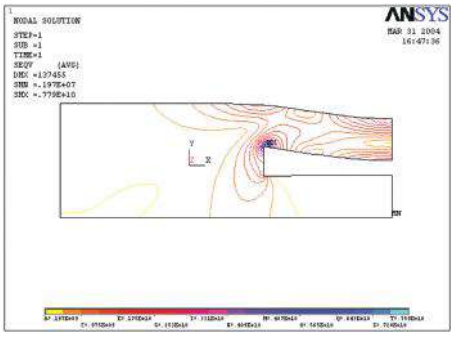


Figure 1. The equivalent stress distribution on the working surface.

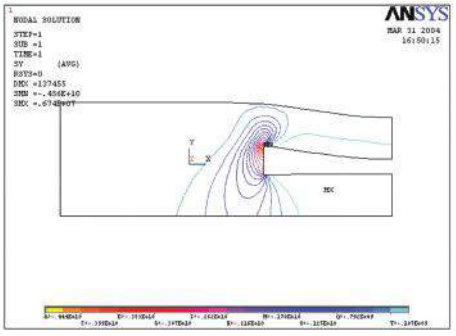


Figure 2. The stress distribution in Y's direction on the working surface.

Table 1. Parameters of rock and coal.

Rock stratum	Thickness	Bulk modulus of elasticity	Elastic shear modulus	Gravity density	Angle of internal friction	Cohesion	Uniaxial compressive strength	Uniaxial tensile strength
	m	Mpa	Mpa	kN·m^{-3}	°	MPa	MPa	MPa
Sandstone	15	40000	8000	2500	45	10	34.4	3.44
Coal	3	10000	2000	1300	40	1.0	16	1.6
Siltstone	15	40000	8000	2500	45	10	42.4	4.24
Shale	17	13000	3000	2500	40	8	23.9	2.39

4 IMPACT OF GROUND STRESS ON PERMEABILITY

According to studies abroad and at home, with mechanical stress the permeability decreases rapidly. But when stress is stronger, the decrease can be very limited and remains basically stable (Sheng 2007). The relationship between the permeability and stress is available to be presented by the following formula in the stress range from 0~4 MPa to 15~40 MPa:

$$k = k_0 e^{-b\sigma} \tag{1}$$

where k = permeability of the stressed coal samples, md; k_0 = permeability of the unstressed coal samples, md; b = empirical coefficient, 1/MPa; and σ = Stress on coal samples, MPa.

Therefore, in the decompress zone ahead of the working surface, the mighty decrease of ground stress leads to the significant increase of air permeability than original permeability in coal body (Feng 2008). And the air permeability will decrease because of the higher ground stress in the stress-concentrated zone (Wu 2009):

According to the results of B. B. Hodot, the distance from the surface to where the vertical stress increases as the original rock stress γH is called the length of pressure-relief area. And it can be calculated in the following formula

$$l = \frac{S}{\pi f_r K_p} \ln \frac{\gamma H}{\sigma_c} \tag{2}$$

where l = the length of pressure-relief area in front of the working surface, m; S = the seam exposed section area, m^2; γ = the overburden Rock stratum Bulk density, t/m^3; and H = the coal seam mining depth, m;

The remaining symbols Ibid.

The vertical stress in pressure-relief area:

$$\sigma = \sigma_c e^{\frac{\pi f_r K_p}{S} x} \tag{3}$$

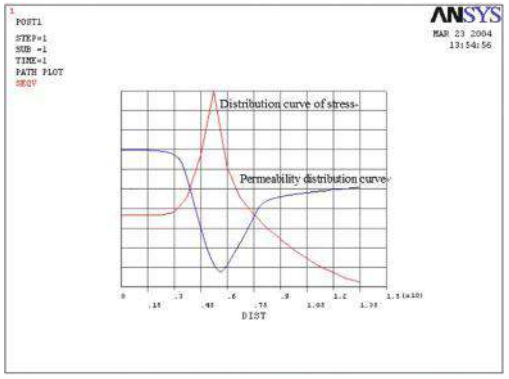


Figure 3. The simulated distribution diagram of coal bearing stress and permeability in front of a mining face.

Therefore, the coefficient of permeability of coal in pressure-relief area can be determined (He et al. 2010).

$$\lambda = \lambda_* e^{-\beta_b \sigma} \tag{4}$$

where λ = the coefficient of permeability where the coal's vertical stress of is σ in the pressure-relief area, $m^2/(MPa^2 \cdot d)$; λ_* = the coefficient of permeability of the coal wall in working surface, $m^2/(MPa^2 \cdot d)$; and β_b = the growth coefficient of permeability in pressure-relief area in front of the working surface, 1/MPa.

The distribution of coal seam stress and permeability in front of the mining face is showed in Figure 3.

5 ANALYSIS OF SIMULATED RESULTS

First point coal mining has destroyed the original formation of the equilibrium state of stress and rearranged the distribution of stress. Under normal circumstances, in a relatively short period of time when the mining space is formed, high concentrated stress (also called bearing pressure) is formed in the vicinity of mining spatial interface firstly. When the concentrated stress reached the peak that the coal could stands, the coal body will yield deformation to transfer the stress deeper down. After a certain period of time, three areas will be formed. These areas are called the pressure-relief area (also named the loose-stress area), the concentrated stress area and the original stress area, as shown in Figure 1, Figure 2, shown in Figure 3. In the three districts, the stress and deformation properties of coal body are different.

Second point according to the stimulated result, the stress is concentrated near the corner of working face. Because the intensity of coal cannot bear the concentrated stress, the decompress zone, the stress concentration zone and the original stress zone are formed along the normal direction of coal wall. The permeability coefficient is biggest in decompress zone, and smallest in stress concentration zone. While after the original stress zone the permeability coefficient tends to be stable, as shown in Figure 3.

6 CONCLUSION

The peak stress in the plastic zone and the decompress zone exceeds their maximum carrying capacity; however, the coal mine in this areas normally could only stand a part of the concentrated stress. And in most occasions, not only the coal mine in the decompress zone which is close to the mining space but also the ordinary country rock cannot bear the concentrated stress. Normally they can only bear a part of it. Therefore, the stress upon the coal in limited zone and the volume of gas in gas-contained coal body, especially the length and carrying capacity of decompress zone can deeply affect the outburst of gas and mine. According to practice, if there always has a certain length decompress zone ahead of the mining face, there would be no outburst of mine and gas. Otherwise, the outburst would happen frequently.

REFERENCES

Feng, Z.-Z. (2008) Theory and Application of Gas Drainage in Low Permeability Coal Seam Rreinforcement (M). *Beijing, Science Press,* 115–117.

He, W.-G., Tang, S.-H., Xie, X.-D. (2010) the Stress of Coal Seam Permeability Effects, *Journal of Liaoning Technical University (Natural Science Edition) (China)*, 19, 353–355.

Liu, G.-Q., Yang, Q.-D. (2008) ANSYS Application Tutorial. *China Railway Press*, 45–46.

Shen, B.-H. (2007) Liu see medium, Technical Measures, Coal Mine Gas Control in China. *Journal of China Coal Society,* 32, 673–679.

Wu, H.-J. (2009) High Gas and Low Permeability Coal Seam Pressure Relief and Permeability Increasing Research on Theory and Technology (D). Xuzhou, *China University of Mining and Technology*, 201–203.

Xie, Z.-P. (2003) A Study on Coal Seam Gas Flow Parameters Inversion. *Research and Development of Mine Disaster Prevention and Control Strategy (China).* China University of Mining and Technology Press, 12, 236–239.

Xie, Z.-P. (2004) Research on Coal Mine Gas Flow Theory and Inverse Problems. *Master Thesis of China University of Mining and Technology (China)*, 6, 112–114.

This page intentionally left blank

Progress in Mine Safety Science and Engineering II – He et al. (Eds)
© 2014 Taylor & Francis Group, London, ISBN 978-1-138-00122-0

Study on the optimization of ventilation system in Zhongxing coal mine

Xiaoyan Song
Safety Engineering College, North China Institute of Science and Technology, Beijing, China

Zhongpeng Xie
Safety and Environmental Engineering Institute, Capital University of Economics and Business, Beijing, China

ABSTRACT: The mining is quite concentrated in east and west wing of Zhongxing Coal mine and the Coalmine has two mining areas, number 1 and number 3. According to the high resistance in the ventilation system, the unreasonable setting of ventilate facilities and the shortage of air support in air-using area, this paper makes a simulated study on the current situation of the mine as well as the schemes using the mine ventilation software of decision support system on the basis of measurement of resistance in ventilation system. The result shows the resistance in ventilation system is greatly reduced and which is of great significance to the safety production as well as the energy saving in the mine.

1 INTRODUCTION

The ventilation system plays an important role in mining. It relies on the force of ventilation to input a quantity of fresh air underground along the established vent line to meet the needs of ventilation in working face, heading face, chamber and so on. Meanwhile it dilutes and discharges the toxicity, blackdamp and explosive gas and dust in the underground. It also reduces the heat and creates a good working environment for the workers (Huang 2010, Lu & Li 2006). In all, the ventilation system prevents the damage and explosive accidents underground and guaranteed the safety of workers. It protects the property of country. So, in order to ensure an efficient, economic and safe work, timely optimization should be adopted to the change of ventilation system.

2 GENERAL SITUATION OF THE MINE

Zhongxing Coal Mine belongs to Fenxi Mining Group of Shanxi Coking Coal Group Company. It is a gassy mine. This mine used the "three two" method for ventilation. Air is blowing in by materials inclined shaft, pedestrian inclined shaft and belt inclined shaft and returned by Mazhuang vertical shaft and Maoshang inclined shaft. There are two BDK618-8-No 28 explosion-proof contra-rotating axial flow ventilators in Maoshang inclined shaft which are in charge of ventilation in wind-using sections in mining area number 1. There are two FBCDE No 34/2 × 630 explosion-proof contra-rotating axial flow ventilators in Mazhuang vertical shaft which are in charge of ventilation in wind-using sections in mining area number 2. As the main power of ventilation, two Typhoon aircraft in two ventilating shaft worked organized. One of them operated while the other backup.

At present, Zhongxing Coal mine has two mining areas: mining area number 1 and mining area number 3. In mining area number 1, there are 2 mining faces (the 1203 and 1204 working faces), and number 3 has 1 mining face (the 3215 working face). What's more, there is a driving face in both mining areas: haul road number 1208 and number 3217. The total air volume that blew in is 15792.2 m^3/min, and the total air volume that returned is 16198.1 m^3/min (the volume of air returned is 7553.0 m^3/min in Maoshang ventilating shaft and 8645.1 m^3/min in Mazhuang ventilating shaft). Systemic resistance in Maoshang ventilating shaft is 2218.6 Pa, and in Mazhuang ventilating shaft it is 2486.5 Pa. The total wind resistance of mine tunnel is 0.032403 $N.s^2/m^8$; the area of equivalent orifice A is 6.611 m^2.

3 DETERMINATION OF RESISTANCE IN MINE VENTILATION

3.1 *Determination of resistance of ventilation*

First point the analysis and optimization of ventilation system depends on the possession of the distribution of mine ventilation resistance and the parameters of resistance on roadway of braches of the ventilation net.

Second point in order to guarantee the precision, measurement was taken point by point with better control barometer. The specific method was

to use 2 precise digital barometers. One stayed on the base point and measured the changes of barometric pressure. The other one was carried along the determined route and measured at every setting point. Only in this way the impact by the changes of barometer pressure and downhole pressure can be avoided and the result would be more reliable (Hong & Wang 2009).

And so on the longest ventilation line is chosen as the main determination route because it can reflect the characteristics of the mine ventilation system (Tao 2009). It contains a larger air volume of working surface, while the other ventilation lines can work as assistance routes (As shown in Figure 1).

A The order of measure points in 1204 working face in Maoshang ventilating shaft:
1→2→3→4→4'→5→6→7→8→9

B The order of measure points in 3215 working face in Mazhuang ventilating shaft:
25→26→27→18→19→20→21→22→23→24

3.2 *Analysis of results*

Based on arrangement of the measured data of the ventilation system results can be achieved. Table 1 shows the resistance in high resistance roadway. The distribution of resistance of the inlet section, the wind-using section and the return section were showed in Figure 2 and Figure 3.

Results can be achieved through determination of the whole mine ventilation resistance and resistance distribution figures:

First point the distribution of resistance is unreasonable both in the east and west wing of the

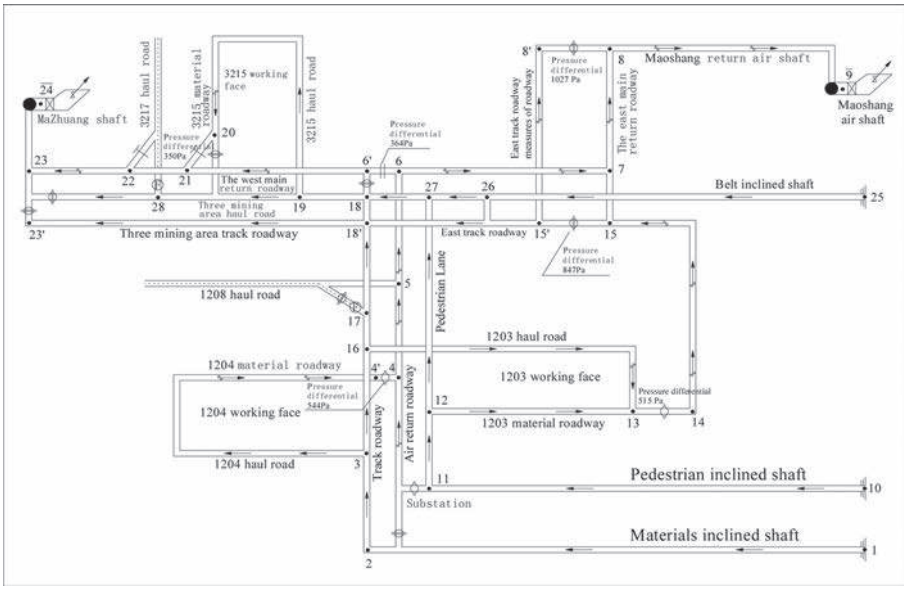


Figure 1. Schematic diagram of Zhongxing Coal Mine Ventilation System.

Table 1. parameters of high-resistance roadway.

		Air quantity	Length	Section	Resistance	Wind resistance	A hundred wind resistance	Percentage
Code	Name	m^3/min	m	m^2	Pa	$N.s^2/m^8$	$N.s^2/m^8$	%
8–9	Maoshang wind-return inclined section	7656.5	944.0	10.6	602.9	0.037024	0.003922	27.2%
26–27	parallel tunnel of east rail and Maoshang inclined shaft	1952.8	373.1	15.5	269.7	0.254626	0.068245	10.8%
21–22	The main west air return roadway	5045.3	224.5	14.9	211.5	0.029912	0.013324	8.5%
22–23	The main west air return roadway	6229.3	1111.6	16.1	1056.1	0.097977	0.008814	42.4%

mine. The wind-using section has a large percentage of resistance. And the reasons are the much more ventilation facilities underground as well as the unreasonable arrangement of them. For example: in 1204 working face, pressure differential in air regulator (4'-4 section) of air return tank is 544Pa, pressure differential in air regulator (13-14 section) of air return lane is 515 Pa in 1203 working face. pressure differential in air regulator (20-21 section) of air return lane is 350 Pa in 3215 working face.

Second point the airway resistance in the main return tunnel is too high. For example: the resistance in 21-23, west main return airway in Mazhuang ventilating shaft system is 1267.6 Pa, about 51% of the total. the resistance in 8-9, Maoshang inclined shaft in Maoshang ventilating shaft system is 602.9 Pa, about 27.2% of the total. The main reason is that the air is too concentrated, the roadway's maintenance is neglected for a long time and the section of the roadway is too small.

And so on some roadways are not fully used. For example, the three mining area track roadway and the east rail measures lane have air doors and the air passes through them is limited which leads to their due functions are not fulfilled.

Table 2. Working condition of major ventilators

Names	Model number	Wind pressure Pa	Wind quantity m^3/min	Power KW
Ventilator in Maoshang ventilating shaft	BDK618-8-No 28	2214.8	7553.0	278.8
Ventilator in Mazhuang ventilating shaft	FBCDE No 34/ 2 × 630	2327.2	8645.1	335.3

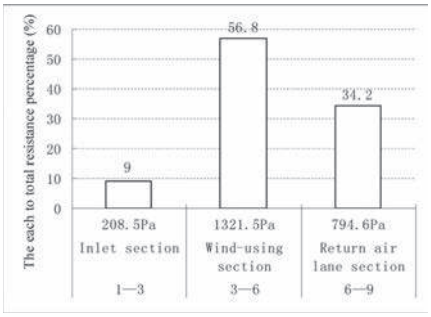


Figure 2. The distribution of resistance in 1204 working face of 1 Mining area, Maoshang ventilating shaft.

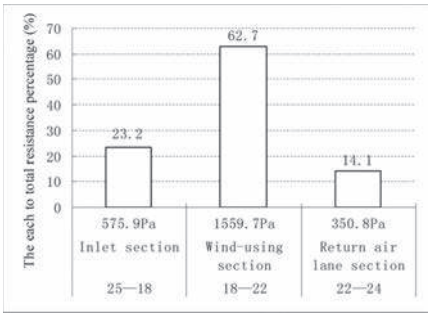


Figure 3. The distribution of resistance in 3215 working face of 3 Mining area, Mazhuang ventilating shaft.

4 ANALYSIS AND OPTIMIZATION OF MINE VENTILATION SYSTEM SCHEME AND THE SOLUTION OF NETWORK

4.1 *Scheme 1: Determine the route of the maximum ventilation and simplify the analysis of ventilation network*

Make the route of 3215 working face as the maximum ventilating resistance line through the demolition of air regulator (20-21) in 3215 working face. Meanwhile, increase the wind area of air regulator (4'-4) in air return tank of 1204 working face and air regulator (13-14) in air return period of working face number 1203. Through the solution of network, the wind pressure is 1961.6 Pa in Maoshang, reduced by 253.2 Pa. The wind pressure in Mazhuang is 2230.7 Pa, reduced by 96.5 Pa. At the same time, the volume of air increased from 1773.1m^3/min to 2230.8m^3/min in 3215 working face, from 1856.1 m^3/min to 2369.8 m^3/min in 1203 working face, and from 2164.7 m^3/min to 2370.3 m^3/min in 1204 working face. This scheme has the advantage of reducing the wind resistance, improving the air quantity, a short construction period as well as a little investment. And there is no disadvantage by far.

4.2 *Scheme 2: analysis of network after decreased the resistance in high resistance roadways*

The resistance can be decreased through the enlargement of roadways which are the parallel tunnel of east rail and Maoshang main inclined shaft 26-27 section, the 21-22-23 section in the west main return roadway and 8-9 section in Maoshang air return inclined shaft. Through the solution of network, the wind pressure is 1855.2 Pa in Maoshang, reduced by 359.6 Pa. The wind pressure in Mazhuang is 2601.7 Pa, reduced by 265.5 Pa. At the same time, the volume of air is slightly increased in wind-using places. And the parameters of the roadway are shown in Table 3. This scheme has the

Table 3. Comparison of the wind resistance between before and after the expansion of lane.

Code of the well lane	Name of wind lane	Length	Before the expansion		After the expansion	
			Section	Wind resistance	Section	Wind resistance
		m	m^2	$N.s^2/m^8$	m^2	$N.s^2/m^8$
8–9	Maoshang inclined shaft	944	10.6	0.037024	16.2	0.012822
26–27	Parallel tunnel of east rail and Maoshang inclined shaft	373.1	15.5	0.254626	16.2	0.023916
21–22	The main west air return roadway	224.5	14.9	0.029912	16.2	0.024267
22–23	The main west air return roadway	1111.6	14.1	0.097977	16.2	0.069841

advantage of reducing the wind resistance, improving effective air quantity. And the disadvantages include long constructive period, large investment that has a certain impact on production.

4.3 *Scheme 3: analysis of network in multiple air return*

Make the 15'-8' section in east rail measurement roadway as the parallel roadway of the main east air return roadway, and demolish the ventilating door in 8'-8 section and remove the ventilating door in 15-15' section to the left of measure point number 15' at the same time. Make the three mining area track roadway as the parallel roadway of the main west air return roadway, and demolish the ventilating door in 23'-23 section and fix a ventilating door in the left of measure point number 18' at the same time. Connected roadway can be built between the main west air return roadway and three mining area track roadway. Through the solution of network, the wind pressure is 1433.6 Pa in Maoshang, reduced by 771.2 Pa. The wind pressure in Mazhuang is 1780.5 Pa, reduced by 546.7 Pa. At the same time, the volume of air is slightly increased in wind-using places. The advantages of this scheme: in spite of the short construction period and low investment wind resistance in west wind-return can be greatly reduced tunnel especially when the three mining area track roadway is changed to wind-return tunnel. The disadvantage: the construction would have certain effect on the production.

5 CONCLUSIONS

First point by analysis and comparison, great effects are achieved in improving the quantity of wind in wind-using section and decreasing the resistance through some adjustments in ventilation facilities in scheme 1. In scheme 2, through the maintenance and enlarge the roadways that are high resistance, concentrated air quantity and severe disfiguration, the decrease of resistance is quite clear. However, the increase of investment has an impact on the production. In scheme 3, great effects are achieved through transverse some smaller air tunnel into parallel tunnels of high resistance tunnels, and the constructive period is short as well as the small investment.

Second point Conclusion can be reached that scheme 1 and scheme 3 are better in economy, constructive period and effect than pan 2 by comparison. Therefore, according to their own situation, the mine shall carry out scheme1, scheme 3 and scheme 2 in a planned step.

And so on According to some problems through the measurement of resistance in Zhongxing Coal mine, a series of schemes are struck out and scientific calculation, analysis and determination are made. This kind of real-time simulation of working mine ventilation and prediction of ventilation stimulation as well as the comparison between scheme of the adjustment of ventilation system and the optimization plays an important role in realizing the current problems and guiding the optimization of ventilation system. The optimization of ventilation system includes the optimization of ventilator, adjustment of air quantity in mine and adjustment of structure of network that has an important practical significance to improve the control capacity of ventilation system as well as the disaster prevention ability.

REFERENCES

Hong, S., Wang, H.-T. (2009) The Donglin Coal Mine Ventilation System Optimization. *Mine Ssafety (China)*, 2, 76–79.

Huang, Y.-P. (2010) Mine Ventilation [M]. Beijing, *China University of Mining and Technology Press*, 128–132.

Lu, Y.-Y., Li, X.-G. (2006) Mine Ventilation and Safety [M]. Chongqing, *Chongqing University press,* 203–206.

Tao, M.-H. (2009) Optimization Designs of Ventilation System Reform in Cuijiazhai Mine. *Hydraulic Coal Mining and Pipeline Transportation (China)*, 4, 115–119.

Progress in Mine Safety Science and Engineering II – He et al. (Eds)
© 2014 Taylor & Francis Group, London, ISBN 978-1-138-00122-0

Multifractal characteristics of coalfield faults and gas-geological significance

P. Chen, E.Y. Wang, Z.T. Liu & Z.Y. Sun
School of Safety Engineering, China University of Mining and Technology, Xuzhou, Jiangsu, China
Key Laboratory of Gas and Fire Control for Coal Mines, Ministry of Education, Xuzhou, Jiangsu, China

ABSTRACT: The multifractal characteristics of faults in Jiaozuo Coalfield were studied and its gas-geological significance was expounded. Based on the gas-geological analysis and multifractal theory, the multifractal spectra f(α) of different regions were calculated and then characteristic parameters were compared. The results show that 1) the fault distribution has multifractal characteristics in Jiaozuo Coalfield which were formed gradually after experiencing a multi-phase evolution controlling gas outburst distribution; 2) different tectonic evolution regions have different multifractal spectra which are related to complexity of tectonic evolution; 3) the characteristic parameters of multifractal spectra such as the symmetry Δf, the width Δα etc. reflect the differences in tectonic background, fault combinations and movement ways. In addition, their magnitudes are well corresponded to the degree of gas outburst. Taking together, coalfield fault multifractal analysis can be used as a new means for gas-geological analysis and to forecast regional coal and gas outburst.

1 INTRODUCTION

Coal and gas outburst causes major natural disasters in coal mines and seriously threaten coal miner safety and production operations. In China, its annual occurrence accounted for more than one-third of the world total. Especially in recent years, with increasing mining depth, it will become more frequent and serious. Mining experiences showed that outburst occurrence displays regional distribution, and that disastrous regions only account for 8% to 20% of entire mining areas (Yu 2005). Researchers carried out extensively studies on many methods to forecast its possibility of occurrence in mining regions (Zhang 2009, Zhang & Lowndes 2010). A large number of studies indicated that faults were often associated with outburst zones. Therefore, clearly locating faults in a coal mine area is very important for forecasting coal and gas outburst. Among regional outburst-forecasting methods, Gas-geology was well developed and widely used to evaluate plate tectonic setting and regional tectonic evolution in order to identify outburst prone areas (Zhang 2009).

Since the 1980s, the fractal theory (Mandelbrot 1983) has been fairly applied in a variety of research areas including geology and geophysics. Some Chinese scholars explored the relationship between the fractal characteristics of coal mine area faults and gas outburst (He et al. 2002). They quantified the fault complexity using the fractal dimension as the index and further compared the fractal dimension values with regional outburst risks.

Multifractal analysis provides a complete description of fault-network fractal properties. It could more veritably describe the complexity and essentiality of fault structure compared to single fractal analysis. The multifractal theory has been widely applied in various fields of earth science. More details about the properties of multifractal spectra in earth sciences applications can be found in References (Agterberg et al. 1996, Zhao et al. 2011, Kiyashchenko et al. 2004). Fault tectonic has multifractal structure characteristics (Panahi and Cheng 2004). But it was not found on the coalfield fault tectonics.

It was widely accepted that the characteristics of outburst's partitions and zones are controlled by the fault structure largely, further, the fault's mechanical property and distribution are determined by the evolution process of its tectonic (Zhang 2009). So it is necessary to apply the multifractal theory to study the fault of coal mining areas for the purpose of revealing the relationships of the fault's multifractal characteristics and tectonic evolution process to coal and gas outburst. In this study, the multifractal theory was applied to study the multifractal characteristics of different regional faults in Jiaozuo Coalfield, Henan Province, China, then based on the domination of tectonic evolution process over coal and gas outburst, the relationship of fault's multifractal characteristics and outburst

distribution was analyzed, finally the gas geological significance of fault's multifractal characteristics was studied. This research aimed at providing scientific means to forecast regional coal and gas outburst.

2 MULTIFRACTAL THEORY

Multifractal can be considered as an alternate superposition of a large number of monofractals with different dimensions and mainly characterized by the multifractal spectrum f(α) or the generalized dimension Dq. The multifractal spectrum f(α) is visually described through the multifractal curve f(α)-α, which contains a set of parameters to precisely and intuitively describe multifractal (Evertsz & Mandelbrot 1992).

At first, the box counting method is used to calculate fault's probability distribution (Walsh & Watterson 1993), the related statistical physics theory is applied to solve the multifractal spectrum of irregular fractal. A two-dimensional orthogonal grid (box) with the side length ε is used to cover the two-dimensional plane on which the faults in different regions are located. By continuously changing ε, the fault number in each box $n_i(\varepsilon)$ (i = 1,2,3…, $N(\varepsilon)$) is calculated, respectively. The probability measure $p_i(\varepsilon)$ represents the probability of the fault falling into the i-th box of the side length ε, it has,

$$p_i(\varepsilon) = n_i(\varepsilon) \Big/ \sum_{i=1}^{N} n_i(\varepsilon) \tag{1}$$

A partition function χq(ε) is defined as the q-th probability measure pi(ε)

$$\chi_q(\varepsilon) = \sum p_i(\varepsilon)^q = \varepsilon^{\tau(q)} \tag{2}$$

where q is any real number. If the second equation in Eq. (2) is true, that is, the partition function χ is the power function of ε, then τ(q) has the following relationship with q:

$$\tau(q) = \lim_{\varepsilon \to 0} \frac{\ln \sum \left[p_i(\varepsilon) \right]^q}{\ln \varepsilon} \tag{3}$$

τ(q) is called as the mass exponent.

In the actual calculation, the least square method is used to fit performed unary linear regression fitting, i.e.,

$$\ln \sum \left[p_i(\varepsilon) \right]^q = a + b \ln \varepsilon \tag{4}$$

Where the slope b yields τ(q). Then the mass exponent can be found from the linear slope, that is τ(q) = b. If τ(q) is nonlinearly related to q, the research object has multifractal character.

The singularity α(q) can be obtained from the following equation:

$$\alpha(q) = \frac{d\tau(q)}{dq} \tag{5}$$

By bringing Eq. (3) into Eq. (5) and differentiating the resulting with respect to q, the singularity function is found as follows:

$$\alpha = \lim_{\varepsilon \to 0} \frac{\sum p_i(\varepsilon)^q \cdot \ln p_i(\varepsilon)}{\sum p_i(\varepsilon)^q} \Big/ \ln \varepsilon \tag{6}$$

which is the same result as that from Chhabra and Jensen algorithm theory (Chhabra & Jensen 1989). Thus, the value of α can be calculated from Eqs. (3) and (4).

By performing the Legendre transformation with respect to τ(q) and q, the following relation is obtained

$$f(\alpha) = q\alpha(q) - \tau(q) \tag{7}$$

By bringing α value to Eq. (5), the relationship f(α)-α is graphed, that is the so-called multifractal spectrum. In Eq. (7), for single fractal, f(α) is reduced to a constant; for multifractal, f(α) becomes a smooth, single peak function. Typical multifractal spectrum is a bell—or hook—shaped curve (Sun 2003).

3 CASE STUDY

3.1 *Gas-geology profile of Jiaozuo Coalfield*

Jiaozuo Coalfield is located at the are turning part from near NS to WE direction in the southern uplift region of the Taihang Mountains on the North China plate, and also in the transitional zone from Taihang Mountains' orogenic belt southward the North China tectonic zone. The coal measure strata of this area has experienced at least 4 tectonic movement periods as below (Coal Industry Department of Henan Province & Henan Polytechnic University 2010): Indo-China period (T_1-J_1), Yanshanian period (J-K_2), Paleogene period (E_1-Q_1) and Neotectonic period (Q_2 to now).

The multi-period tectonic movements formed the present fault system (Fig. 1). The tectonics of faults are spatially characterized by sequence control. The secondary structure distribution along

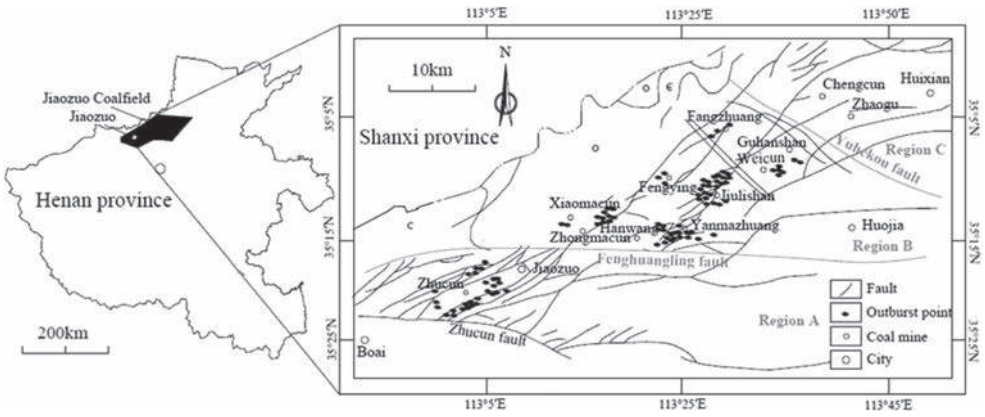


Figure 1. Distribution map of fault structures in Jiaozuo Coalfield.

the main fault plane in the fault zone constitutes a fractal distribution pattern. The fault system produced in this process generally has the fractal structure (Li 2000). Because the tectonic movement generally has a multi-period nature, the fault system formed by a set of faults with different periods of tectonic movement is characteristic of multifractal distribution (Liu et al. 2006), such a multifractal system formation provides the prerequisite for applying the multifractal theory to study faults and its control over gas outbursts.

The distribution of gas outburst points is nonuniform in Jiaozuo Coalfield. They have obvious characteristics of regional distribution. Affected by the regional structure and tectonic evolution, the gas enrichment distribution in Jiaozuo Coalfield has two large dominant faults and can be divided into three regions, Region A, Region B, and Region C, by two large dominant faults namely Fenghuangling fault and Yuhekou fault (Fig. 1) (Coal Industry Department of Henan Province & Henan Polytechnic University 2010). Region A includes the Fenghuangling fault with its southern area with near WE and NE trending. Zhucun mine is located at the southern Region A, where in history gas outburst occurred occasionally. Region B is located between the western Yuhekou fault and the northern Fenghuanling fault, where distributed 9 mines of Zhongmacun, Xiaomacun, Fengying, Hanwang, Jiulishan, Yanmazhuang, Weicun, Fangzhuang, and Guhanshan, respectively. All of them outbursted up frequently in history, especially Jiulishan and Yanmazhuang mines, the outbursts of greater than 1000 tons coal erupted. Region C is located at the eastern Yuhekou fault, on which lying mainly low-gas coal mines such as Chengcun and Zhaogu mines (Fig. 1).

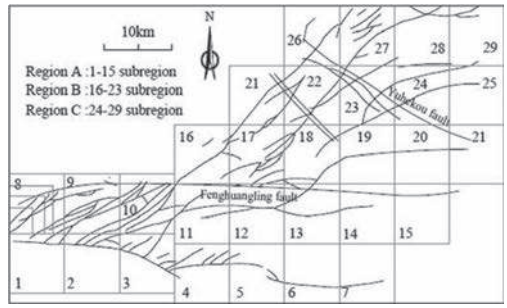


Figure 2. Grid partition map of Jiaozuo Coalfield.

3.2 *Multifractal computing process*

On condition that Jiaozuo Coalfield is divided into more subregions (Fig. 2). Regions A, B and C contain a number of subregions, respectively. The grid scales ε are taken as 15 km, 12 km, 9.6 km and 6.4 km, respectively. By changing ε continuously, for example, for Subregion 8, the fault number in each box, $n_i(\varepsilon)$ (i = 1,2,3…, $N(\varepsilon)$), can be calculated. The probability measure, $p_i(\varepsilon)$ represents the probability of the fault falling into the i-th box of the side length ε and can be found through Eq. (1).

Based on Matlab platform and multifractal theory, the mass index τ(q), singularity index α, and multifractal spectrum f(α) are calculated, q is assigned in the range of −5 ~ 5 and the step of 0.2 is fixed. Using the fault of Region B as an example for multifractal calculation, for a given value of q, In order to find the slope of the fitting line as τ(q) and α, firstly simple linear fitting

$$\ln\sum\left[p_i(\varepsilon)\right]^q \sim \ln\varepsilon \quad \text{and} \quad \frac{\sum p_i(\varepsilon)^q \cdot \ln p_i(\varepsilon)}{\sum p_i(\varepsilon)^q} \sim \ln\varepsilon$$

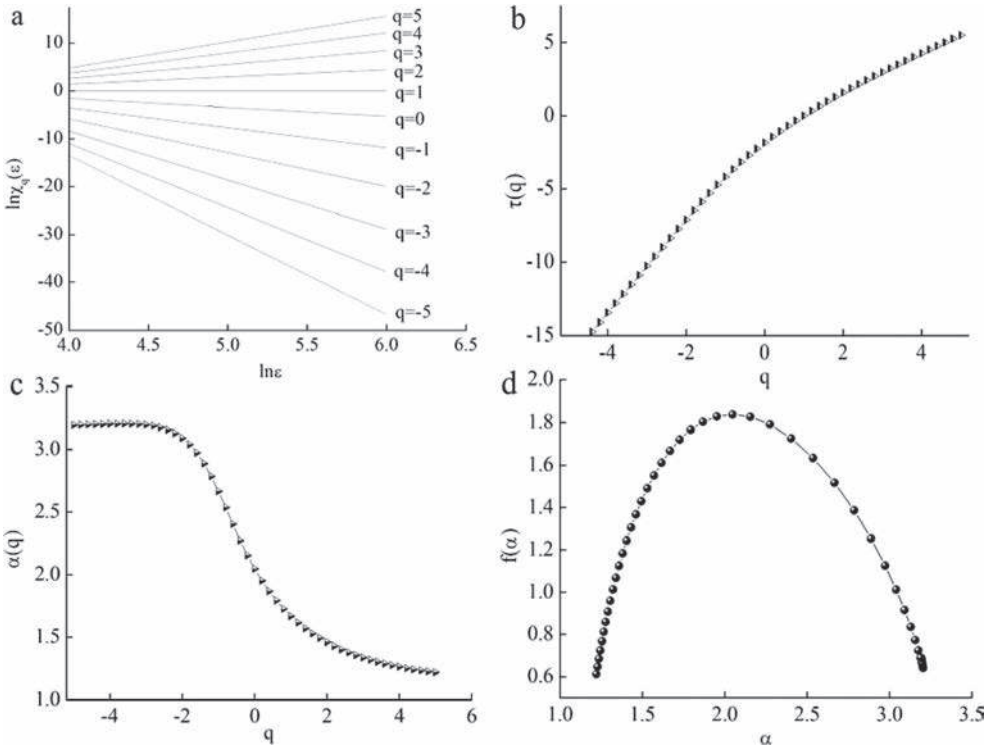


Figure 3. Calculation map of Region B fault multifractal spectrum.
a) ln χq(ε) ~ lnε fitting lines at different q values; b) τ(q) ~ q curve; c) α ~ q curve; d) multifractal spectrum f(α) ~ α curve.

are performed through least squares method, then according to the relationship f(α)-α, the multifractal spectrum is graphed.

3.3 *Results and discussion*

3.3.1 *Multifractal computing results of different regions*

Using the fault system of Region B as an example, the multifractal computing results were shown in Fig. 3. It can be seen from the data fittings in the whole-scale range (Fig. 3a) that 1) $\ln\chi_q(\varepsilon)$ has a good linear relationship to ln(ε), meeting the power law, which indicates that within the scale range, the fault distribution is scale free, i.e., the fault is characteristic of fractal; and 2) $\tau(q)$ is an upward convex function, i.e. it is nonlinearly related to *q,* which indicates that the fault distribution in the stated Region B is indeed characteristic of multifractal.

Similarly, the multifractal spectra of Regions A and C were computed and shown in Fig. 4.

3.3.2 *Multifractal spectrum characteristics of faults in different regions*

The multifractal spectrum reflects the distribution of probability measure of its corresponding fractal body (Sun, 2003). Therefore, it could better reflect the complexity and structural characteristics of the spatial distribution of the fault system. It is clear from Figure 5 that there are great differences in their shapes of the multifractal spectra of different regions.

1. In general, a multifractal spectrum is a hooked curve. If there exists a hooked curve on the left of the multifractal spectrum, the number of subsets with high probability is bigger than that with low probability, indicating that smaller faults are more developed in the region; When there exists a hooked curve on the right of the multifractal spectrum, the number of subsets with high probability is smaller than that with low probability, indicating that bigger faults are more developed and their number is fewer in the region. The symmetry can be expressed as

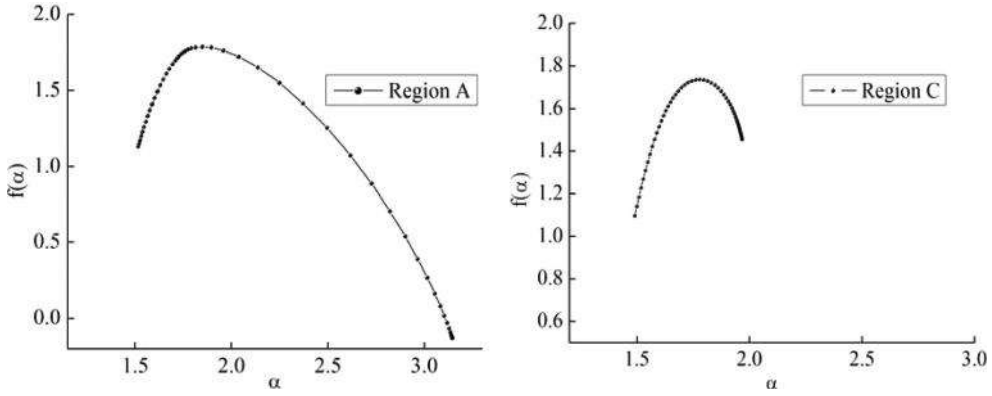


Figure 4. Fault multifractal spectra of Regions A and C.

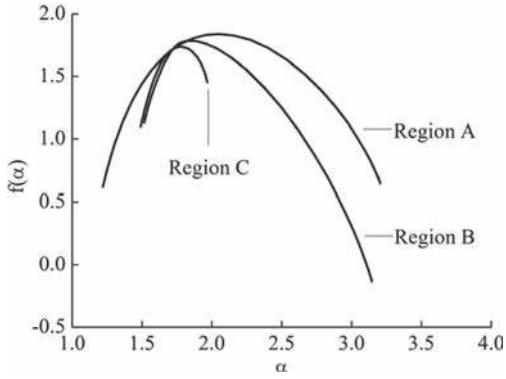


Figure 5. Comparison of fault multifractal spectra of three regions A, B, and C.

Table 1. Characteristic parameters of multifractal spectra.

Regions	α_{max}	$f(\alpha_{max})$	α_{min}	$f(\alpha_{min})$	$\Delta\alpha$	Δf	f_{max}
A	3.14	–0.13	1.52	1.13	1.63	1.26	1.79
B	3.20	0.64	1.22	0.61	1.98	–0.03	1.84
C	1.97	1.45	1.49	1.10	0.48	–0.36	1.74

$\Delta f = f(\alpha_{min}) - f(\alpha_{max})$. It can be seen from Fig. 5 that the curve of the multifractal spectrum of Region B has good symmetry, indicating that a number of smaller faults are produced at the same time as the large fault is well developed.

2. The magnitude of the multifractal spectral width $\Delta\alpha = \alpha_{max} - \alpha_{min}$ reflects the non-uniformity of probability distribution in the whole fractal structure and indicates the differential extent and variation range of the density and length of fault distribution, as well as the non-uniformity of their spatial distribution, etc. Within the study regions, the greater $\Delta\alpha$ is, the more non-uniform the fault probability distribution, the more severe the data fluctuation. It is obvious from Figure 5 that the order of $\Delta\alpha$ in magnitude is Region B> Region A> Region C.

In general, the maximum of multifractal spectrum f_{max} is equal to the capacity dimension (Sun 2003). However, Table 1 shows that the difference in the capacity dimensions of the three regions is very small, thus f_{max} is not considered as a characteristic parameter. It is clear that multifractal analysis could more veritably describe the complexity and essentiality of fault structure compared to single fractal analysis.

3.3.3 *Multifractal gas-geological significance*

The mechanical properties and the scale of fault at the different stages of tectonic evolution not only control the flow and preservation of gas in the coal seams, but also determine the present gas content in the coal seam (Coal Industry Department of Henan Province & Henan Polytechnic University 2010). The multifractal spectrum parameters Δf and $\Delta\alpha$ are related to the tectonic evolution process, there exists great differences among multifractal spectra at different regions (Fig. 5), behind all of these are ubiquitous gas-geology reason. The significances of gas-geology at different regions are discussed as following:

1. Region A has smaller $\Delta\alpha$ than Region B, the uniformity of its fault probability distribution is slightly better, and its multifractal spectrum curve is shaped as a left hook, indicating that small and medium-sized faults are denser. However, its dominant NNE faults are not well

developed compared with Region B, its gas content is higher, generally more than 30 m^3/t. Gas outburst also occurred in Region A. But because its tectonic coal is less developed, the thickness of tectonic coal seam and the number of gas outburst is small.

2. $\Delta\alpha$ of Region B is the greatest, indicating that its fault probability distribution is the most non-uniform and its multifractal spectrum symmetry is better. In addition, due to its bigger α_{max}, its gas geological significance is that the secondary faults associated with the large faults are well developed (Liu et al. 2006). This is because the tectonics in the NE and NNE directions in the north of the Fenghuangling fault underwent many complex tectonic evolutions all of which causing very uneven fault probability distribution. This tectonic evolution could lead to higher gas pressure and gas content in this area. For example, the gas content in Jiulishan Mine reaches 33 m^3/t, the gas pressure in Guhanshan Mine is up to 2.42 MPa, and these mining areas are characterized by higher occurrences and larger scales of gas outburst.
3. The secondary faults associated with the large fault in Region C are fewer, and the tectonic in the direction of this region is well developed and has simple tectonic lines and low complexity. $\Delta\alpha$ in this region is the least, indicating that the fault has better uniformity. Yuhekou Fault on the lower boundary of Region C is a normal fault formed in the Cenozoic Era, while Region C is located on its uprising wall. According to the regional tectonic stress field analysis (He et al. 2002), the NW trending fault during the geological evolution mainly underwent tensile stress. Its fault structural plane belongs to tensional, and its tectonic evolution is simpler. Because the upper part of the fault is subject to uplifting (Coal Industry Department of Henan Province & Henan Polytechnic University 2010), gas escape is obvious and gas content is low, generally lower than 8 m^3/t, much lower than that in the south of Yuhekou Fault. Outburst never happened in Zhaogu Mine and Chengcun Mine in Region C.

4 CONCLUSIONS

In order to truly reflect complexity and natural characteristics of fault structure, the multifractal theory was applied to study fault structure of Jiaozuo Coalfield and to calculate the multifractal spectra of three different regions. The results showed that the fault distribution of all the studied regions has multifractal characteristics.

Through comparative analysis it's found that there are obvious differences in the characteristics of multifractal spectrum curves of all three regions. The symmetric parameter Δf and the spectrum width $\Delta\alpha$ were extracted and analyzed. Both are closely related to the tectonic evolution process and show the differences in tectonic setting, fault combinations, and movement, and determine the distribution characteristics of regional gas outburst. Among the three regions, Region B is the most complex in their tectonic evolution, the next is Region A, and the last Region C. Correspondently, the faults of Region B has the biggest spectrum width $\Delta\alpha$ and the best symmetry. The characteristic parameters of Region A and Region C also well reflect their regional characteristics of tectonic evolution. The characteristic parameters of each of the regions show very good correspondence to the gas outburst degree of risk, indicating that the multifractal characteristics of the fault system are of gas geological significance. This research may have important guidance to forecast regional coal and gas outburst.

ACKNOWLEDGMENTS

The financial supports provided by the "Twelfth Five-Year" Plan for Science & Technology Support of China (2012BAK04B07, 2012BAK09B01) and Project (2012 LWBZ03) supported by "the Fundamental Research Funds for the Central Universities. The authors acknowledge Professor Zimin Zhang of Hennan Polytechnic University for his guidance of Gas-geology analysis, his fruitful research work provides valuable reference material for this paper. We would also thank Doctor RenGuang Zuo of China University of Geosciences for his help in the multifractal calculation.

REFERENCES

Agterberg, F. P., Cheng, Q. M., Brown, A., Good, D. 1996, Multifractal modeling of fractures in the Lac Du Bonnet Batholith, Manitoba. *Computers & Geosciences* 22(5): 497–507.

Chhabra, A. & Jensen R. V. 1989, Direct determination of the *f(α)* singularity spectrum. *Physical Review Letters* 62(12):1327–1330

Coal Industry Department of Henan Province & Henan Polytechnic University. 2010, *Research of gas geology rule of coal mine in henan and drawing of gas geology map*. Beijing: Geology Press.

Evertsz, C. J. G. & Mandelbrot, B. B. Multifractal measures. New York: In: Pitmen, H O, Jurgens, D, Saupe, D (Eds.), *Chaos and Fractals*. Springer Verlag, 1992.

He, J., Liu, M. J., Yan, A. H. 2002. Fractal research of relation between geological tectonic coalfields

and gas outburst. *Journal of China Coal Society* 27(6):623–626.

Kiyashchenko, D., Smirnova, N., Troyan, V., Saenger, E., Vallianatos, F. 2004, Seismic hazard precursory evolution: fractal and multifractal aspects. *Physics and Chemistry of the Earth* 29(4–9):367–378.

Li, G. H. 2000, *Study of regional crustal stability of active tectonic region*. Chinese Academy of Sciences. Beijing, China.

Liu, X. D., Xu, J. Z., Wang, X. F. 1999, Multifractals spectrum behavior of fault system and its application. *Oil Geophysical Prospecting* 34(3): 285–289, 301.

Mandelbrot, B. B. 1983. The Fractal Geometry of Nature (updated and augmented edition). Freeman, New York.

Panahi, A. & Cheng, Q. M. 2004, Multifractality as a measure of spatial distribution of geochemical patterns. *Mathematical Geology* 36:827–846.

Sun, X., Wu, Z. Q., Huang, Y. 2003, *Fractal theory and application*. Hefei: University of Science and Technology of China Press.

Walsh, J. J. & Watterson, J. 1993, Fractal analysis of fracture patterns using the standard box-counting technique: valid and invalid methodologies. *Journal of Structural Geology* 15(12): 1509–1512

Yu, B. F. 2005. *Manual for mine gas disaster prevention, control and utilization*. China Coal Industry Publishing House, Beijing.

Zhang, R. L. & Lowndes, I. S. 2010. The application of a coupled artificial neural network and fault tree analysis model to predict coal and gas outbursts. *International Journal of Coal Geology* 84(2): 141–152.

Zhang, Z. M. 2009. *Gas geology*. China University of Mining and Technology. Xuzhou.

Zhao, J. N., Chen, S. Y., Zuo, R. G., Emmanuel, J. M. C. 2011, Mapping complexity of spatial distribution of faults using fractal and multifractal models: vectoring towards exploration targets. *Computers & Geosciences* 37(12): 1958–1966.

This page intentionally left blank

Progress in Mine Safety Science and Engineering II – He et al. (Eds)
© 2014 Taylor & Francis Group, London, ISBN 978-1-138-00122-0

The reasonable narrow coal pillar width along gob research of the deep dynamic pressure conditions

Zhu-Wu Zhu
College of Natural Resources and Environmental Engineering, Shandong University of Science and Technology, Qingdao, Shandong, China

Zhi-Jie Wen
College of Natural Resources and Environmental Engineering, Shandong University of Science and Technology, Qingdao, Shandong, China
Key Laboratory of Mine Disaster Prevention and Control, Shandong University of Science and Technology, Qingdao, Shandong, China

ABSTRACT: The reasonable width of narrow coal pillar along gob not only improves the recovery rate of coal resources, but also can reduces the roadway maintenance difficulty and improves the roadway maintenance state. This paper studies the reasonable narrow coal pillar width using the theoretical analysis and numerical simulation of the dynamic pressure, by analyzing the plastic zone of surrounding rock in the different width of coal pillar and the distribution of the vertical stress to determine the reasonable coal pillar width. The application effect demonstrates that the narrow coal pillar width is reasonable, which provides the basis for the narrow coal pillar width setting of the gob side entry driving.

Keywords: gob side entry driving; coal pillar width; the vertical stress; the horizontal displacement

1 INTRODUCTION

In recent years, with the improvement of underground mining strength, in order to ensure mine normal production and avoid the emergence of the island coal face, the contradiction that how to advance in the opposite direction between the gob of leaving narrow coal pillar and its adjacent working face is frequently encountered. Remaining narrow coal pillar along roadway driving is one of the effective ways to improve the coal recovery rate. The coal pillar along gob-side entry driving puts the roadway layout in the reduced stress region of goaf edge (Xie et al. 2006). The width of roadway pillars not only changes its internal mechanical state but also change the adjacent surrounding rock mechanical characteristics, which is bound to influence mechanical characteristics and stability of surrounding rock (Jia & Kang 2002, Li & Guan 2006, Bai et al. 2004). So it is necessary to study systematically.

2 THE BACKGROUND CONDITIONS

The face of 107 is lower Permian. The coal seam has a good storage stability and a simple structure. The seam thickness is 4.6 to 7.2 m, the average is 5.9 m. The seam dips is 5° to 12°, the average is 8°. The seam general hardness coefficient f = 1.8. The strike length is 1200 m, the inclination is 130 m. The fully mechanize sublevel caving and home mining is adopted. In order to maintain the continuity of the face, excavating the mining roadway adjacent the face of 105 in advance is suggested. Thereinto, the track lane of 105 face is separated by narrow coal pillar with the face of 107, which is the typical dynamic pressure roadway along the empty during excavation. The 105 face track lane cross-section is a rectangular with 4.4 m of the designed net width and 3.2 m of the designed net height.

3 THE THEORETICAL CALCULATIONS OF THE NARROW COAL PILLAR WIDTH

The reasonable narrow coal pillar width should be arranged in the internal stress field within the lateral top rock beam fracture line along the roadway, so as to avoid the abutment pressure concentrated area generated during the mining process of the adjacent face. The distance between the basic roof fracture location away from the the adjacent goaf

side of the coal wall can be calculated as following formula:

$$x_0 = \frac{mA}{2\tan\varphi_0} \ln\left(\frac{K\gamma H + \frac{C_0}{\tan\varphi_0}}{\frac{C_0}{\tan\varphi_0} + \frac{P_z}{A}} \right) \quad (1)$$

In the formula:

m—The longwall active high, m = 3 m;
A—Coefficient of lateral pressure, 1.8;
φ_0—The coal internal friction angle, 30°;
γ—The average volume of the overburden force, 25.5 kN/m3;
C_0—Coal cohesion, 5 MPa;
K—Stress concentration factor, 3;
H—Roadway depth, 860 m;
P_z—The support resistance from the adjacent face roadway coal, 1 MPa.

The calculation of X_0 is 9.8 m. Considering roadway width 4.2 m, narrow coal pillar width is less than 5.6 m to meet the requirements. Referring under similar conditions, narrow coal pillar width is generally 4 to 6 m.

4 NUMERICAL SIMULATION OF THE NARROW COAL PILLAR WIDTH

4.1 *Numerical simulation model*

According to the engineering geological conditions, the application of FLAC3D software to build the model size of 180 m × 160 m × 90 m as shown in Figure 1. Simulation of tunnel excavation size is 4 m x 3 m, excavation length 160 m, face excavation size is 109 m × 6 m, face advance length is 160 m. In order to establish facilitate grid, lithology and thickness of roof and floor coal seams must be simplified. Model of the left and right and the lower boundary for the displacement are the boundaries, the left and right boundaries limit the displacement in the x direction, the lower boundary limits the displacement in the y direction; the top fabric weight stress is 22.5 MPa.

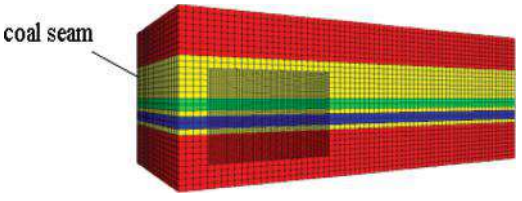


Figure 1. Initial model diagram.

4.2 *Rock Mechanical Parameters*

The model of coal rock composition and parameters from top to down as shown in Table 1.

4.3 *Numerical simulation analysis*

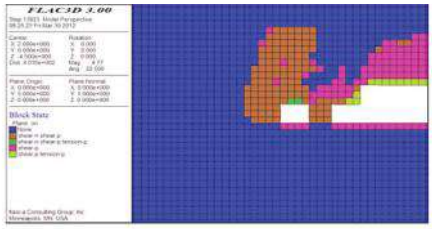
The coal pillar of 3 m, 5 m, 10 m, 15 m, 20 m and 25 m width is respectively selected to adopt a numerical simulation. Fig. 2 and Fig. 3 are respectively the distribution map of surrounding rock mass plastic zone and vertical stress of roadway under different coal pillar width.

Through the Figure 2 and 3, under the mining influence of the adjacent working face, there is a plastic failure to the coal on its both sides. The coal stress is decreased while the vertical stress is transferred to the deep part of the coal pillar. There emerges the vertical stress concentration area in the inner coal pillar, and the vertical stress decreases outward from the concentration area. Under the mining influence of the adjacent working face, the narrow coal pillars often all enter into the stat of the plastic zone, and at this time the bearing capacity of the coal pillar is limited; the concentration degree of the vertical stress in the coal pillar is not too large. But if the width of the coal pillar is large enough, the elastic nuclear zone will appear in the coal pillar. Thus the coal pillar can bear more pressure from overlying strata, and the vertical stress concentration degree in the coal pillar will reach a very high level.

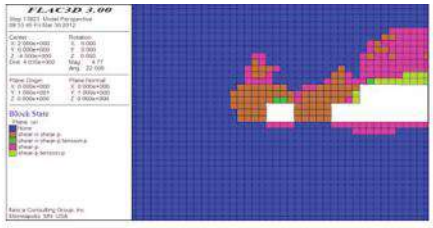
By the analysis of Table 2 and Fig. 4, the deformation of surrounding rock of roadway under coal pillar width of 5 m is less than the coal pillar width of 3 m, then the deformation of surrounding rock increases with the amount of the increasing coal pillar width. When coal pillar width is 10 m to 15 m, there is a large deformation, and when coal pillar width is greater than 15 m, the surrounding rock deformation reduces, but when coal pillar

Table 1. The table of coal rock mechanical parameters.

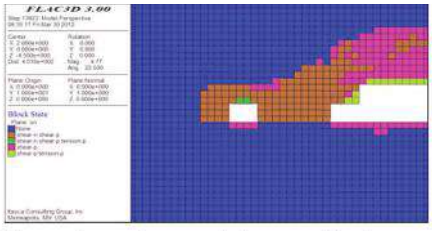
material	elasticity modulus GPa	poisson ratio GPa	mass density kg/m3	cohesion MPa	internal frictional angle °	thickness m
packsand	45.61	0.29	2763	23.8	29.8	24
siltstone	35.76	0.23	2696	16.6	28.9	21
packsand	34.73	0.14	2600	20.3	30.4	6
sandy mudstone	28.56	0.16	2650	12.2	29	3
3rd Seam	4.87	0.34	1500	5.3	30	6
mudstone	19.56	0.15	2580	10.8	28	3
packsand	27.27	0.18	2643	20.7	23.7	27



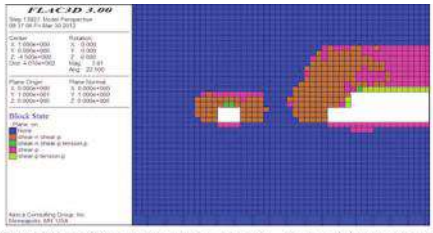
(a) Surrounding rock mass plastic zone of roadway under 3m coal pillars



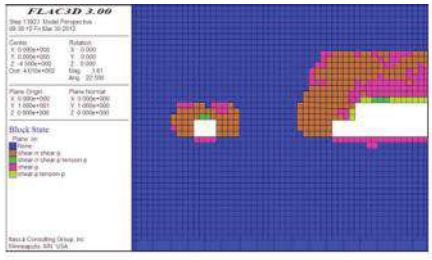
(b) Surrounding rock mass plastic zone of roadway under 5m coal pillars



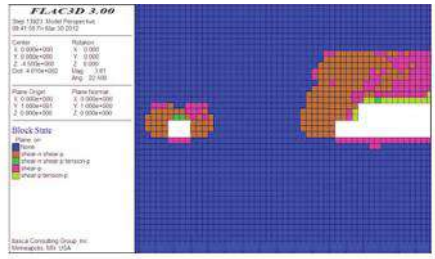
(c) Surrounding rock mass plastic zone of roadway under 10m coal pillars



(d) Surrounding rock mass plastic zone of roadway under 15m coal pillars

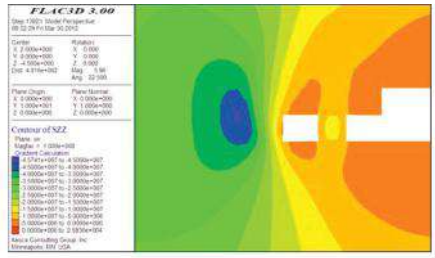


(e) Surrounding rock mass plastic zone of roadway under 20m coal pillars

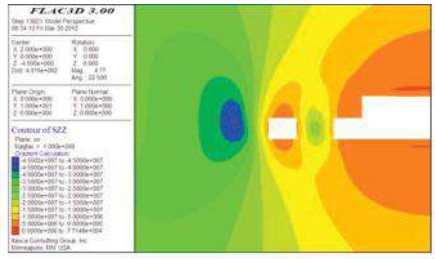


(f) Surrounding rock mass plastic zone of roadway under 25m coal pillars

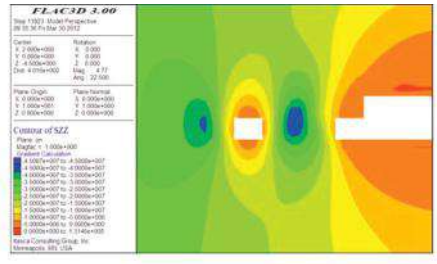
Figure 2. The distribution map of surrounding rock mass plastic zone of roadway under different coal pillar width.



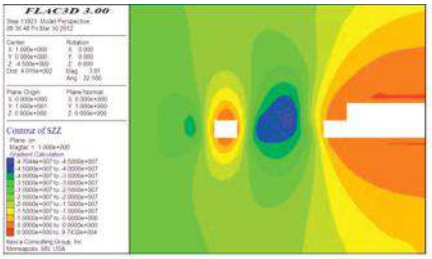
(a) Surrounding rock vertical stress of roadway under 3m coal pillars



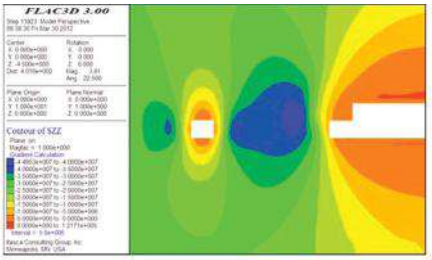
(b) Surrounding rock vertical stress of roadway under 5m coal pillars



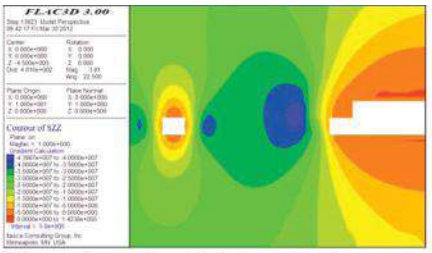
(c) Surrounding rock vertical stress of roadway under 10m coal pillars



(d) Surrounding rock vertical stress of roadway under 15m coal pillars



(e) Surrounding rock vertical stress of roadway under 20m coal pillars



(f) Surrounding rock vertical stress of roadway under 25m coal pillars

Figure 3. The distribution map of surrounding rock vertical stress of roadway under different coal pillar width.

Table 2. The statistics of surrounding rock mass displacement amount of roadway under different coal pillar width.

coal pillar width m	3	5	10	15	20	25
roof to floor convergence m	360	350	400	420	340	340
convergence of roadway two sides m	530	500	610	650	490	490

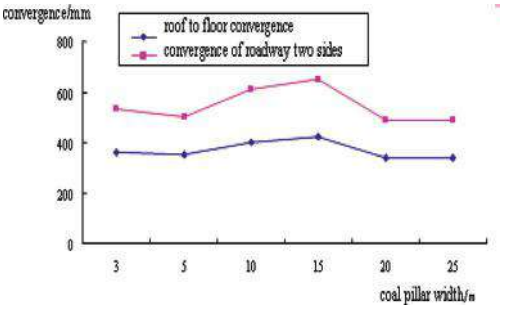


Figure 4. The curve diagram of surrounding rock mass displacement amount of roadway under different coal pillar width.

width is greater than 20 m, there is no significant correlation between surrounding rock deformation and coal pillar width.

Through analyzing the simulation on the surrounding rock stress field and displacement field of different width of coal pillar along goaf dynamic pressure roadway, some conclusions can be made as follows:

1. When the coal pillar width between 3 m and 5 m, the lateral abutment pressure peak area can be avoided and with the increase of coal pillar width, the coal bearing capacity is strengthened while the deformation of surrounding rock of roadway is decreased. In this range, an appropriate increase of coal pillar width is beneficial to control roadway surrounding rock deformation.
2. When the coal pillar width between 10 m to 15 m, the carrying capacity of coal pillar is further enhanced with increasing coal pillar width. The elastic nuclear area begins to appear, and pillar stress concentration increases meanwhile the deformation of surrounding rock of roadway is further increased, which shows that coal pillar width within this scope is unbeneficial to control roadway surrounding rock deformation.
3. When the coal pillar width is more than 20 m, the elastic nuclear area is further expanded and two stress concentration areas are gradually appeared within the coal pillar. The roadway side coal pillar stress peak value and the range is reduced, and the surrounding rock stress level is reduced meanwhile the surrounding rock deformation is small. The large coal pillar width, however, will cause serious waste of coal resources, therefore, it is not recommended to keep a wide coal pillar.

To sum up, although the roadway deformation of 5 m narrow coal pillar is bigger than that of the more than 20 m narrow coal pillar, it can

avoid lateral support pressure peak area, and the narrow coal pillar has a certain capacity. Adopting the reasonable supporting can not only realize the effective control of surrounding rock of roadway, but effectively improve the recovery rate of coal resources. Consequently, 5 m narrow coal pillar is reasonable and feasible, which is in accord with theoretical analysis.

5 EFFECTS IN ENGINEERING PRACTICE

The site engineering practice shows that under the influence of the recovery pressure ahead, the convergence of two-sides roadway is about 485 mm meanwhile roof to floor convergence is relatively closer to the amount of 271 mm, which meets the need of safety production and achieves the desired design requirements. The successful practice of the narrow coal pillar width setting provides a strong guidance and reference for the gob side entry driving in the later period of the coal mine.

ACKNOWLEDGMENTS

This work is supported by National Basic Research Program of China under Grant No. 2012CB72310402, National Natural Science Foundation of China under Grant No. 51244010, Science Research Innovative Group of College of Resources and Environmental Engineering of SDUST No. 2012ZHTD06. New Teachers' Fund for Doctor Stations of Ministry of Education under Grant No.20123718120009.

REFERENCES

Bai J.B. et al. 2004. Hou Chaojiong, Huang Hanfu. Numerical Simula-tion Study on Stability of Narrow Coal Pillar of Roadway Driving along Goaf. *Chinese Journal of Rock Mechanics and Engineering* 23(20):3475–3479 (in Chinese).

Jia G.S. & Kang L.J. 2002. Study on the Chain Pillar Stability of the Developing Entry in Long Wall Top-coal Min-ing. *Journal of China Coal Society* 27(1):6–10(in Chinese).

Li Z.H. & Guan F.H. 2006. Calculation of Stress Field of Elasto-plastic Coal Pillar. *Journal of Mining & Safety Engineering* 23(1):79–82 (in Chinese).

Xie G.X. et al. 2006. Effect of Coal Pil-lar Width on the Stress Distribution Law of Surrounding Rocks in Fully Mechanized Top-coal Caving Mining Face, *Journal of University of Science and Technology Beijing* 28(11): 1005–1008 (in Chinese).

This page intentionally left blank

Progress in Mine Safety Science and Engineering II – He et al. (Eds)
© 2014 Taylor & Francis Group, London, ISBN 978-1-138-00122-0

The mechanism of coal fatigue failure and its numerical analysis under pulsating water pressure

Hongqing Zhu, Minbo Zhang, Jian Shen, Bolong Lei & Guowei Jia
School of Resource and Safety Engineering, China University of Mining and Technology (Beijing), Beijing, China

ABSTRACT: In order to reveal the microscopic mechanism of coal fatigue damage by pulsating hydraulic fracturing, based on damage mechanics, the expression of quantitative relationship between the coal accumulated plastic strain and the number of pulsating water pressure was established. Due to the big difficulty of making experiment of pulsating hydraulic fracturing on the big coal samples, based on the parameters of the actual site, the numerical simulation method was used to study the evolution process of the plastic deformation of the large coal sample under pulsating water pressure. By using the built mathematical model to fit the data of the numerical simulation, it can be obtained that the fitting results of the model were basically consistent with the numerical results, indicating that the correctness of the built model. Finally, the study results can provide some reference for the implementation of the pulsating hydraulic fracturing on-site.

1 INTRODUCTION

China is a country using coal as its main energy and the coal will still account for more than 50% of the total energy consumption in the next 30 to 50 years (Yuan, L et al. 2013). However, there are up to 49% of coal seams in the coal mines of China with the characteristics of high gas content and low permeability, which will lead to the drainage effect of pre-drainage boreholes is poor, so the purpose of safety production can't be achieved (Zhai, C et al. 2011, Lin, B.Q. 2010). Therefore, the methods used to effectively increase the seam permeability, and expand the range of drainage influence of the pre-pumping boreholes are technical problems which should be solved at present (Fu, X. 2011).

In response to these problems, many scholars have studied the hydro-based permeability increasing measures which include hydraulic slotting, hydraulic fracturing, hydraulic punching and so on, despite a certain effect, but there are so many problems. For example, it is difficult to achieve the desired effect by using the ordinary hydraulic fracturing in the soft coal seams even with very high injection pressure, and the phenomenon of stress concentration in the local zone is easy to form (Lin, B.Q et al. 2011). Therefore, many scholars began to study the pulsating hydraulic fracturing technology.

At present, the equipment and field applications of pulsating hydraulic fracturing technology have been studied by many scholars, but there are still many shortages of the research on the mechanism of coal fatigue failure. Therefore, based on the damage mechanics, this paper deduced the relational expression between the accumulated plastic strain and the number of the cycles under pulsating water pressure and analyzed the accumulated plastic strain of large-size coal sample which was applied triaxial pressure under pulsating water pressure by using the method of numerical simulation experiment.

2 THE FAILURE MECHANISM OF COAL UNDER THE ACTION OF THE PULSATING WATER PRESSURE

Studies have shown that (Li, X.Q et al. 2011) coal will produce fatigue damage under pulsating water pressure. When the fatigue damage accumulates to a certain extent, coal will generate a lot of new cracks which will be gradually connected with the effect of continuous pulsating water pressure. At last, the coal will produce fatigue damage at the time of a large number of new cracks developed into the macroscopic fracture. Through further analysis, it is not difficult to find that the damage is caused by accumulated plastic deformation. Therefore, the fatigue failure of coal under the action of the pulsating water pressure is to study the process of cumulative plastic strain of coal. The characteristic parameters of pulsating water pressure are shown in Figure 1.

In Figure 1, σmax is the upper limit of pulsating water pressure; σmin is the lower limit of pulsating water pressure; σm is the average value of pulsating water pressure; $\Delta\sigma$ is the range of pulsating

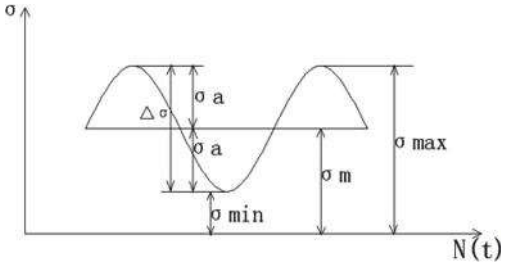


Figure 1. The characteristic parameters of pulsating water pressure.

water pressure; σa is the amplitude of pulsating water pressure (Zhang, A.G et al. 2006).

3 THE CUMULATIVE PLASTIC STRAIN MODEL UNDER THE ACTION OF PULSATING WATER PRESSURE

Based on the theory of damage mechanics, when the material is in one-dimensional state, the relationship between the damage development rate and the cumulative plastic strain rate satisfies the following equation (Li, S.C et al. 2009).

$$D' = (\frac{Y}{Q})^q \cdot p' \tag{1}$$

Where: D' = damage development rate; Y = damage energy consumption rate; P' = cumulative plastic strain rate; Q and q = parameters.

In one-dimensional state, the free energy density function is shown as follows.

$$\phi = \frac{\sigma^2}{2\rho E(1-D)} + K \tag{2}$$

Where: Φ = free energy density function; σ = calculation stress; E = elastic modulus of coal; D = damage variable; ρ = density; and K = a term which is independent of D.

The damage energy consumption rate is shown as the following formula.

$$Y = -\rho \frac{\partial \phi}{\partial D} = \frac{1}{2E}(\frac{\sigma}{1-D})^2 \tag{3}$$

The formula (4) can be obtained by putting the formula (2) and the formula (3) into the formula (1).

$$D' = [\frac{1}{2EQ}(\frac{\sigma}{1-D})^2]^q \cdot p' \tag{4}$$

The relational expression between the damage variable and the cumulative plastic strain can be obtained by integrating the equation (4).

$$\int_0^D (1-D)^{2q} dD = \int_{p0}^{p} \frac{\sigma^{2q}}{2EQ} dp + c_1 \tag{5}$$

The final equation is shown as follows by considering the boundary conditions that are $P = P_0$, $D = 0$; $P = P_d$, $D = 1$.

$$(1-D)^{2q+1} = 1 - \frac{p - p_0}{p_d - p_0} \tag{6}$$

Where: P = cumulative plastic strain at a certain time during the cycles; P_0 = cumulative plastic strain at the beginning of the cycles; and P_d = cumulative plastic strain at the point of fatigue failure.

Because of $0 \le D \le 1$, the expression of the damage variable can be shown as the following equation by taking the q as zero in practice.

$$D = \frac{p - p_0}{p_d - p_0} \tag{7}$$

XIE He-ping and LI Shu-chun who have derived the theoretical equation of coal and rock between the damage variable and the number of cycles, and the equation is shown as follows (Xie, H.P. 1990, Yang, H. W. 2011).

$$D = 1 - [1 - (\frac{N}{N_F})^{1-c}]^{\frac{1}{b+1}} \tag{8}$$

Where: N = number of the cycles at a certain time; N_F = number of the cycles when the material is fatigue failure. b and c = the parameters.

Therefore, the relational expression between the cumulative plastic strain and the number of cycles can be obtained by making the formula (7) equal the formula (8).

$$p = p_d - (p_d - p_0)[1 - (\frac{N}{N_F})^{1-c}]^{\frac{1}{b+1}} \tag{9}$$

4 THE NUMERICAL ANALYSIS OF COAL PLASTIC STRAIN UNDER THE ACTION OF PULSATING WATER PRESSURE

4.1 *modeling*

Because it is very difficult to make triaxial compression experiments on large-size coal sample

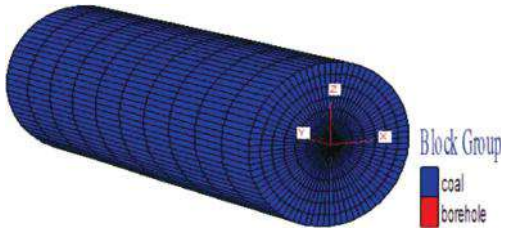


Figure 2. The physical calculation model of pulsating hydraulic fracturing.

in the laboratory, this paper used FLAC3D software to simulate the process of coal plastic strain under the action of pulsating water pressure. The FLAC3D software is an explicit finite difference program developed on the basis of the Lagrange algorithm. It can be used to simulate the mechanical behavior of failure and plastic strain when the coal and rock reach to the strength limit or yield limit. It can also be used for the coupled analysis of fluid calculation and mechanical calculation (Zhu, H.Q et al. 2012, Chen, Y.M & Xu, D. P. 2011).

The 1202 working face of Pinggang coal mine was used as a research example. The characteristics of the 1202 working face are that the buried depth is from 450 to 500 meters, the coal seam is single and low permeability, the permeability coefficient is from 0.023 to 0.026 $m^2/MPa^2.d$, the thickness of the coal seam is from 1.8 to 2.15 meters and the dip angle of the coal seam is from 10 to 15°.

On the basis of the Mohr—Coulomb model, the numerical calculation of the process of coal cumulative plastic strain around the borehole will be realized by the embedded FISH program language of FLAC3D writing pulsating injection function. The model is mainly used to study the strain and damage of the coal around the borehole under the action of pulsating water pressure. The shape of the model is a cylinder with the size of 7×20 m, which contains 86400 units and 88601 nodes. The excavated portion at the center of the model is a water injection borehole with a diameter of 113 mm. The model is shown as Figure 2.

4.2 *Determining the parameters of the model*

In order to reflect the field situation of pulsating hydraulic fracturing, all parameters of numerical simulation are in accordance with the actual situation of the 1202 working face of Pinggang coal mine. The error caused by the size of the model can be ignored, so the confining pressure of the model was set as vertical ground stress and the axial compression is set as horizontal ground stress. The calculation formulas are as follows (Wang, W.M et al. 2009).

Table 1. Physical and mechanical parameters of simulative coal seam.

Bulk moludus	Shear moludus	Internal friction angle	Cohesion strength	Tensile	Density
GPa	GPa	MPa	MPa	kg.	m^{-3}
0.119	0.036	20	1	1.6	1400

$$\sigma_Z = 27H/1000 \tag{10}$$

$$\sigma_X = \sigma_Y = \sigma_Z/\lambda \tag{11}$$

Where: σ_z = vertical ground stress, MPa; H = burial depth, m; σ_X and σ_Y = horizontal ground stress, MPa; and λ = lateral stress coefficient, taking 1.2.

Through calculation, the vertical ground stress is 12.8 MPa and the horizontal ground stress is 10.7 MPa. Other physical and mechanical parameters are in Table 1.

A pulsating water pressure changing with sinusoidal waveform was applied to the borehole at the center of the model during the process of numerical simulation. The upper limit of the water pressure was selected on the basis of the "threshold value" of the fatigue failure. If the upper limit of the water pressure was lower than the "threshold value", the coal would not appear fatigue failure even the number of the cycles were so many. YANG Yong-jie has obtained that the "threshold value" of the fatigue failure does not exceed 81% of the uniaxial compressive strength of coal by making experiments (Yang, Y.J. et al. 2007). Thus, the variation range of the pulsating water pressure is set as from 0 to 25 Mpa and the cycle is set as50 seconds.

4.3 *The analysis of numerical simulation*

When the time of simulation reached to 95 minutes and the number of pulsating water pressure achieved 114, the plastic fatigue damage of outer surface of the middle part of the model began to appear, which showed that the model had been damaged. Figure 3, Figure 4 and Figure 5 showed that the relationship between the damage area of the model and the numbers of pulsating water pressure. It was concluded from Figure 3, Figure 4 and Figure 5 that the cumulative plastic strain at the radial direction of the borehole increased with the number of the cycles increasing until the whole model was damaged. The results of $1 - c = 0.3983$ and $1/(b + 1) = 0.5559$ were obtained

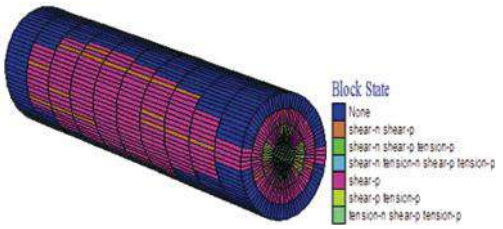


Figure 3. The damage area of the model when the number of the cycles was 30.

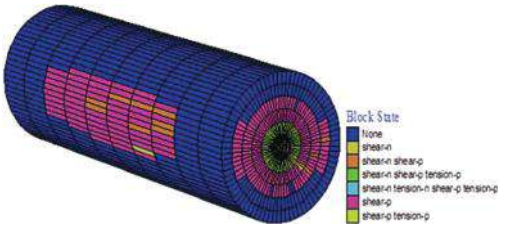


Figure 4. The damage area of the model when the number of the cycles was 100.

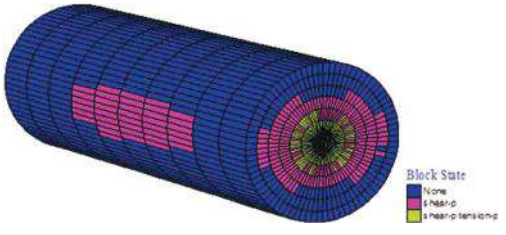


Figure 5. The damage area of the model when the number of the cycles was 114.

by using the equation (9) to making fitting analysis for the results of the numerical simulation. The initial cumulative plastic strain was mainly due to the formation of the fracturing borehole and the value was 0.2 meter. Based on these parameters, the cumulative plastic strain evolution equation under the action of pulsating water pressure was concluded. From Figure 6, it concluded that the theory equation was consistent with the results of numerical simulation. Therefore, the expression of the cumulative plastic strain can be used to describe the evolution process of coal cumulative plastic strain under the action of pulsating water pressure in this paper.

For further analysis, it can be obtained from the Figure 6 that the cumulative plastic strain of coal has the obvious feature of three stages under pulsating hydraulic fracturing.

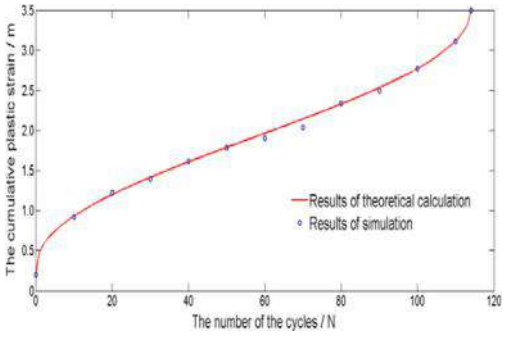


Figure 6. The result of the theoretical model vs the numerical simulation.

The first stage is the rapid increase stage. At the beginning of pulsating hydraulic fracturing, the cumulative plastic strain increases rapidly with the number of pulsating water pressure increased, which is mainly due to the large number of original crack in coal was gradually pushed together and a small amount of new crack began to initiate and propagate. The second stage is steadily increasing phase. The cumulative plastic strain will be steady growth after a certain amount of pulsating water pressure. The third stage is the stage of coal fatigue failure. The new crack will be gradually connected together at this stage when the plastic strain accumulates to a certain extent. Then, the coal will be damaged.

5 CONCLUSIONS

1. The fatigue damage of coal under the pulsating water pressure is caused by plastic strain which will continue to accumulate with the action of the continuous water pressure. When the plastic strain accumulates to a certain degree, the coal will be damaged. As a result, the purpose of increasing permeability will be achieved.
2. Based on the damage mechanics, the relational expression between the accumulated plastic strain and the number of pulsating water pressure was established. Then, the model of large-size coal sample was used to make a numerical simulation experiment. After a comparative analysis, the simulation results were consistent with the fitting results of the theoretical equation, indicating that the correctness of the theoretical equation.
3. The purpose of increasing permeability can be achieved at a lower pressure by using pulsating hydraulic fracturing. Meanwhile, the numerical simulation results can predict the fracturing

radius which can be used as the reference for designing the space between the drainage boreholes on the site.

ACKNOWLEDGEMENTS

The authors gratefully acknowledge the financial support of PHD Top-notch innovative personnel training foundation and the financial support of National Nature Science Foundation of China (51074168).

REFERENCES

Chen, Y.M. & Xu, D.P. 2011. FLAC/FLAC3D foundation and project examples[M]. Beijing: China Water Power Press: 21–31.

Fu, X. 2011. Study of underground point hydraulic fracturing increased permeability technology [J]. *Journal of China Coal Society* 36(8):1371–1321.

Lin, B.Q. 2010. Mine gas prevention theory and technology (The second edition)[M]. Xuzhou: China University of Mining and Technology press:264–269.

Lin, B.Q. etal. 2011. Pressure Relief and Permeability-Increasing Technology Based on High Pressure Pulsating Hydraulic Fracturing and Its Application [J]. *Journal of Mining & Safety Engineering* 28 (3): 452–455.

Li, S.C. et al. 2009. Low cycle fatigue damage model and damage variable expression of rock[J] *Rock and Soil Mechanics* 30(6):1611–1615.

Li, X.Q. et al. 2011. Experimental study on deformation and seepage properties of outburst coal samples under cyclic loading[J]. *Chinese Journal of Rock Mechanics and Engineering* 29 (extra issue 2): 3498–3504.

Wang, W.M. et al. 2009. Rock Mechanics[M]. Xuzhou: China University of Mining and Technology press:150–167.

Xie, H.P. 1990. Damage Mechanics of Rock and Concrete[M]. Xuzhou: China University of Mining and Technology press.

Yang, H. W. 2011. Study on Coupling Mechanism of Rock and Pore Water under Cyclic Loading [D]. Chongqing: Chongqing University:185–188.

Yang, Y.J. et al. 2007. Experimental study on characteristics of strength and deformation of coal under cyclic loading[J]. *Chinese Journal of Rock Mechanics and Engineering* 26(1):201–205.

Yuan, L. et al. 2013. Scenario predication for medium-long term scale of coal mine methane drainage in China [J]. *Journal of China Coal Society*38 (4): 529–534.

Zhai, C. et al. 2011. Research and application of coal seam pulse hydraulic fracturing technology [J]. *Journal of China Coal Society* 36 (12): 1996–2001.

Zhang, A.G. et al. 2006. Fatigue, Fracture and Damage[M]. Chengdu: Southwest Jiaotong university press:1–30.

Zhu, H.Q. et al. 2012. Numerical Simulation of Crack Extension Laws of Hydraulic Fracturing[J]. *Safety in Coal Mines* 43(11), 30–33.

This page intentionally left blank

Progress in Mine Safety Science and Engineering II – He et al. (Eds)
© 2014 Taylor & Francis Group, London, ISBN 978-1-138-00122-0

The law of gas releasing in heating and oxidation process of coal

Haiyan Wang, Bo Yu, Xiaolong Cui, Meizhen Chen & Lan Geng
Faculty of Resources and Safety Engineering, China University of Mining and Technology, Beijing, China

ABSTRACT: In order to study the law of coal spontaneous combustion and oxidation process in different particle sizes, according to the theory of all-stage coal spontaneous combustion experiment by using a new designed oven, a set of temperature programming experiments using Wuhu coal samples selected in Inner Mongolia Autonomous Region were conducted. CO, C2H4, C2H6 and C3H8 generated in the experiment were analyzed, the corresponding relationship between gas generation and coal sample temperature was found, and indicator gases for the Wuhu coal were obtained. CO can be used as the indicator gas, C2H4, C2H6 can be auxiliary indicator. When the particle size of coal samples is smaller, the crossing-point temperature will be lower, the spontaneous combustion tendency can be stronger. The wider the coal granule size range is, the easier it can be self-ignited. The results can be helpful in terms of safety and prediction of the spontaneous combustion tendency.

1 INTRODUCTION

The spontaneous combustion tendency of coal is an important factor of coal mine spontaneous fire. It will result in waste of coal resources and the destruction of the local ecological environment and bring serious casualties and great economic losses. As one result of the larger coal production, the frequenty of coal spontaneous combustion is getting higher. So the research of coal spontaneous combustion tendency is more and more important. Now coal spontaneous combustion tendency and indicator gases of coal spontaneous was studied by many scholars at home and abroad; Deng's relational analysis and the slope of the relational analysis are used in the quantitative analysis of experimental data by Chen Ruhao, Wang Deming, etc (Chen et al. 2012). The result shows the influence law of gas by Initial temperature, the quality of coal sample and the heating rate. Zhu Linqi, Zhou Xinquan eliminate the influence of environmental factors by using of the experiment and the field experience obtain CO concentration difference and using of the proportion between CO concentration and oxygen consumption eliminate the influence of air volume change. Indicator gases has been corrected based on the above two points (Zhu et al. 2008). Zhang Yanni determine the crossing-point temperature of coal spontaneous combustion by using the oil bath temperature programming experiments, obtaining the influence of the different particle sizes on combustion crossing-point temperature (Zhang et al. 2010). Deng Jun used multivariate regression to forecast the spontaneous combustion of coal which intuitively reflected the ash content of coal, volatile sulfur content and oxygen content on the impact of coal spontaneous combustion and qualitative predictions for coal spontaneous combustion period (Deng et al. 2011). In this paper, the author used the temperature programming experiment to test with different particle sizes of coal samples, obtaining the corresponding relationship between gas generation and temperature change.

2 EXPERIMENTAL

2.1 *Experimental facility*

This experimental system consists of coal spontaneous combustion experiment platform, computer monitoring, control system, gas collection and analysis system as shown in Figure 1. Coal spontaneous combustion experiment platform mainly includes air pump, coal sample reaction tank, oven, oil-gas separator, water tank, volumetric flowmeter etc. Computer monitoring and control system includes responsible for data acquisition, signal processing hardware system and the software of the experimental oven process control system.

2.2 *Coal sample*

Sample of new coal put into a sealed bag in order to oxidative deterioration. Bring back to the laboratory in time. Grind the coal sample at first and select different particle size of coal samples, such as 0–1 mm, 1–3 mm, 3–7 mm, 7–10 mm. Then seal save using reagent bottle with ground stopper.

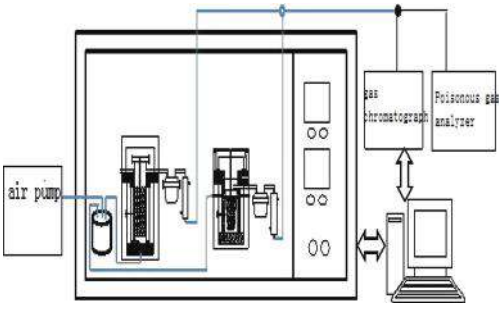


Figure 1. The programmed temperature experiment.

2.3 *Experimental process*

This experiment adopts Xinjiang Wuhu coal sample. Select 1–3 mm, 3–7 mm, 7–10 mm, and the first to four size mixing coal blend for experiments after affirming device normal. Select 200 g coal samples. The heating rate is 1°C/min. The inlet flow rate is 90 ml/min. Take a set of gas sample every 20°C in 30–300°C. After 300°C every 30°C take a set of gas sample. These gas samples are detected by gas chromatograph.

3 EXPERIMENTAL RESULTS AND ANALYSIS

3.1 *The selection of index gases*

The Generation of CO, C2H4, C2H6, C3H8 is shown with temperature in the Figure 2–5.

Different size of the Wuhu coal sample were regularly produce CO, C2H4, C2H6, C3H8 gases shown in above figures. The generation of CO is shown as the Figure 2. The generation increased when temperature is getting higher. And it increases obviously at 100°C. It means coal samples has been strong oxidation reaction with the action of oxygen. CO, C2H4, C2H6, C3H8 began to produce after 30°C. It means these gases exist in the coal sample at 100°C. And it shows coal samples have been strong oxidation reaction with oxygen. CO, C2H4, C2H6, C3H8 began to produce after 30°C. It shows these gases exist in the coal sample first. And these gases begin to release when temperature rises.

These gases increased obviously after 100°C. It means that coal sample started cracking and reacting with oxygen after the heat. The reaction between oxygen and coal has two processes. One is adsorption process, another is oxidation. The first process is physical adsorption. The next is chemical adsorption and chemical reaction. Only conducting the chemical adsorption and chemical reaction can CO and hydrocarbon gas released. Nowadays

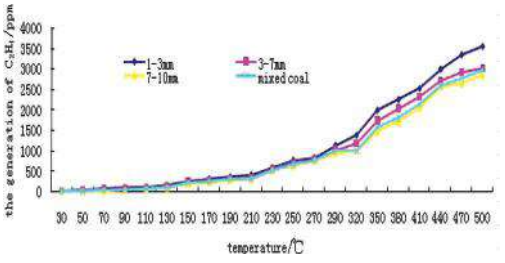


Figure 2. The generation of C2H4 with temperature.

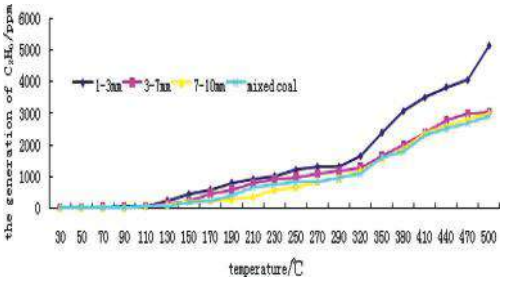


Figure 3. The generation of C2H6 with temperature.

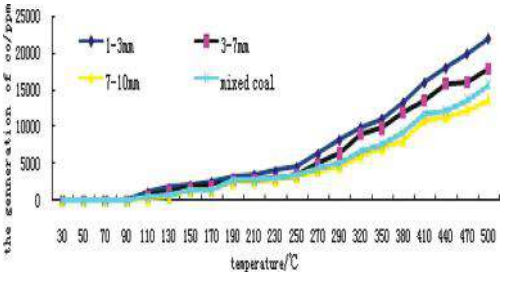


Figure 4. The generation of CO with temperature.

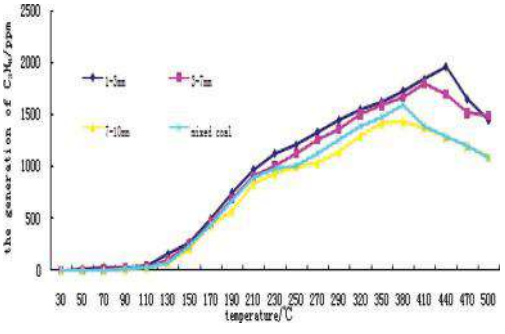


Figure 5. The generation of CO with temperature.

it is widely believed that the relationship between generation of C2H4 and temperature is very simple and clarity. The impact of environment on C2H4 is small.

The characteristics of the indicators of coal gas are Sensitivity, measurability, uniqueness, regularity, monotonous change (Zhu et al. 2008). The forecast of coal spontaneous combustion using indicator gas has two forms. The one is using the change of gas concentration and types of gas to forecast coal spontaneous combustion. Another is using the absolute generation to forecast coal spontaneous combustion. According to these features, Wuhu coal sample can select CO as indicators gas, Choose C2H4, C2H6 gas as auxiliary indicators, rather than C3H8. Because C3H8 gas started falling when the temperature reach 400°C.

3.2 *Influence of particle size*

The crossing-point temperature is the first temperature point when Coal and oxygen compound acceleration during coal sample in heating process. Its macro performance is the sharp increase of CO content. It can get a general idea of crossing-point temperature trend by studying the generation of CO at 50–110 °C.

As the difference of particle sizes, porosity and surface area of the coal is different. The probability of oxygen combining with hydrogen in the various groups in the body of coal is different. Intensity of CO decreases when the particle size increases shown as Table 1. It means coal sample particle sizes reduction increased coal sample surface area in contact with the air so that the active factor of the coal body more exposure in the air. The probability of oxygen combining with hydrogen in the various groups in the body of coal increases. Chemical reaction enhances and releases more heat. So the crossing point temperature drops. In addition, the crossing-point temperature of mixed coal is much lower than 7–10 mm particle size. It shows that the wider the coal granule size range is, the easier it can be self-ignited. Because of the wider range of coal granule has abundant active structure, it can meet with more oxygen and make the chemical reaction process more intensely.

Table 1. The generation of CO in low temperature.

temperature/°C	1–3 mm	3–7 mm	7–10 mm	Mixed coal
50	50.25	32.19	12.12	10.2
70	65.42	50.2	41.1	35.98
90	158.01	98.73	70. 04	50.74
110	1089.63	672.78	312.12	440.32

4 CONCLUSION

It is found that the generation of CO, C2H4, C2H6 increase as the coal temperature getting higher, the quantity of the C3H8 will reduce after 400°C, and CO can be used as the indicator gas, C2H4, C2H6 can be auxiliary indicator.

The generation of CO, C2H4, C2H6 increased rapidly after 130–150°C. It means coal sample began combustion oxidation. And this period is the best opportunity for coal spontaneous combustion prevention. When detecting CO, C2H4, C2H6 gas, the goaf has reached the high temperature area of more than 130°C. And it is time to take measures to deal with spontaneous combustion area.

The generation of CO indicates strength of crossing-point temperature and spontaneous combustion tendency when temperature variation condition remains the same. Experimental study has found that the smaller the particle size of coal samples, the lower the crossing-point temperature, the stronger the spontaneous combustion tendency.

ACKNOWLEDGEMENTS

This work was financially supported by Chinese Academy of Sciences (No. XDA05030000).

REFERENCES

Jun Deng, Zhen Xing, Li Ma. Application of multiple regression analysis for the coal spontaneous combustion prediction. *Journal of Xi 'an University of Science and Technology* 2011; 31(6): 645–648.

Linqi Zhu, Xinquan Zhou. Jianguo Xie, Yingcun Zhu. Spontaneous combustion indicator gases experiment analysis and optimal selection. *Journal of Mining and Safety Engineering* 2008; 25(4): 440–444.

Liqi Zhu, Xinquan Zhou, Yingcun Zhu. Spontaneous combustion index gases optimal selection of donghuantuo coal. *Journal of Xi 'an University of Science and Technology* 2008; 8(2): 288–290.

Ruhao Chen, Deming Wang, Kai Cao. Influence factor correlation analysis of coal during Low oxygen combustion process. *Mineral Engineeering Reseach*, 2012; 27(1): 34–37.

Yanni Zhang, Jun Deng, Yongfei Jin. The oil bath temperature programmed experimental research of Coal spontaneous combustion characteristics. *Safety in Coal Mines* 2010; 31(4): 7–10.

This page intentionally left blank

Progress in Mine Safety Science and Engineering II – He et al. (Eds)
© 2014 Taylor & Francis Group, London, ISBN 978-1-138-00122-0

A new mathematical model of the relationship between gas desorption index of drill cuttings and gas content

K. Shen & H.Q. Zhou
National Key Laboratory of Gas Disaster Detecting, Preventing and Emergency Controlling, Chongqing, China
Chongqing Research Institute, China Coal Technology and Engineering Group, Chongqing, China

ABSTRACT: The relationship between gas desorption index of drill cuttings K_1 and gas pressure was measured for four coal samples from Daning mine based on the measuring principle of index K_1. Then the variation characteristics of k_1 with gas content W were researched combined the proximate analysis of these samples. The results showed that: There is a significant correlation between K_1 and W; This correlation can be expressed by an exponential function, and the two also are in accordance with the linear relation when the gas constant is low. The results provide critical value study of coal and gas outburst prediction index and effective inspection index for regional outburst prevention theoretical with guidance.

1 INTRODUCTION

Gas desorption index of drill cuttings K_1 is a characterization factor of the gas desorption velocity, reflects the gas content of a coal seam and the magnitude of the gas desorption velocity at the initial time of pressure relief (State Administration of Work safety 2008), and comprehensively reflects the gas parameters and pore structure of the coal which are related closely with the coal and gas outburst. The study on the relationship between gas desorption index of drill cuttings and the coal seam gas content is especially significant for determining the critical value of outburst effect inspection index, also provides the research on rapid method of determining gas content (Qiu Haisheng 2007) and scientific-theoretical basis for determining the critical value of outburst effect inspection index in case of regional gas pre-drainage with the experimental base.

With the above mentioned, the relationship between gas desorption index of drill cuttings K_1 and gas pressure was measured at four coal samples from Daning mine in Jincheng City Shanxi Province by experiments. The K_1 corresponding to the various gas content were worked out by combining with the proximate analysis of these samples. Then got the functional relationship between K_1 and W by numerical analysis and studied this relationship by physical chemical method.

2 THE SAMPLES AND EXPERIMENTAL METHOD

Selected four samples of soft coal at tectonic anomaly locations or the locations where happened dynamic phenomenon of No.3 coal seam Daning mine in Jincheng City Shanxi Province. The experimental method and procedures were executed according to the AQ/T 1065-2008 "The Determination Method of Gas Desorption Index of Drill Cuttings". Proximate analysis and gas parameters of coal samples can be seen in the Table 1.

Table1. The proximate analysis and gas parameters of coal samples.

	Industrial analysis				Adsorption constant	
Number	Aad (%)	Mad (%)	Vdaf (%)	Porosity (%)	A (m^3/t)	B (MPa^{-1})
1#	16.78	1.34	6.40	5.03	41.6549	1.3918
2#	13.43	2.17	7.48	6.17	42.6603	1.7142
3#	34.56	1.76	10.79	5.11	43.1303	2.0250
4#	24.83	1.68	8.71	7.78	44.9784	1.7068

3 EXPERIMENTAL RESULTS AND ANALYSIS

The curves between K_1 and gas pressure P were drawn in Fig. 1 according to the experimental results.

The K_1 and P got from experiments were nonlinear fitted and the K_1–P curves fit into the power function $K_1 = AP^B$ and the fitting functions are shown in Table 2. A and B are regression coefficients in the function, the number range of A is 0.9314~1.6386, the number range of B is 0.4595~0.5123.

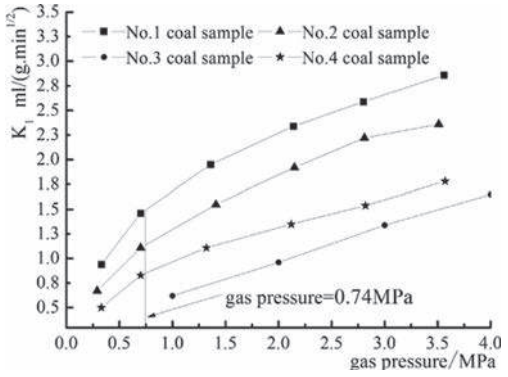


Figure 1. The experiment results of samples K_1–P relationship.

Table 2. Fitting functions of the relationship between K_1 and P.

Number	Fitting functions	Correlation coefficients
1#	$K_1 = 1.6386P^{0.4595}$	0.99388
2#	$K_1 = 1.2910P^{0.5092}$	0.99518
3#	$K_1 = 1.1044P^{0.4828}$	0.988
4#	$K_1 = 0.9314P^{0.5123}$	0.99332

The gas content corresponding to the gas pressure were calculated out by Langmuir equation for getting the relationship between K_1 and W.

$$W = \frac{VpT_0}{Tp_0\xi} + \frac{abp}{1+bp} \cdot e^{n(t_0-t)} \cdot \frac{1}{1+0.31M_{ad}} \cdot \frac{100 - A_{ad} - M_{ad}}{100} \quad (1)$$

In function (1), V is the pore volume of unit mass coal, m³/t; P are the gas pressure of the coal seam, MPa; T_0 and P_0 is the absolute temperature (°C) and pressure (MPa) under the standard state. ξ is the compressibility of gas; a is ultimate gas adsorption capacity of coal, m³/t; b is adsorption constant, MPa^{-1}; t_0 is the experimental temperature, °C; t is the coal seam temperature, °C; A_{ad} and M_{ad} are the ash content and moisture content of coal,‰.

The Fig. 2 intuitively shows that there is a significant correlation between K_1 and W. This correlation can be expressed by an exponential function as function (2). The functions and correlation coefficients are shown in Table 3.

$$K_1 = Ae^{W/B} + C \quad (2)$$

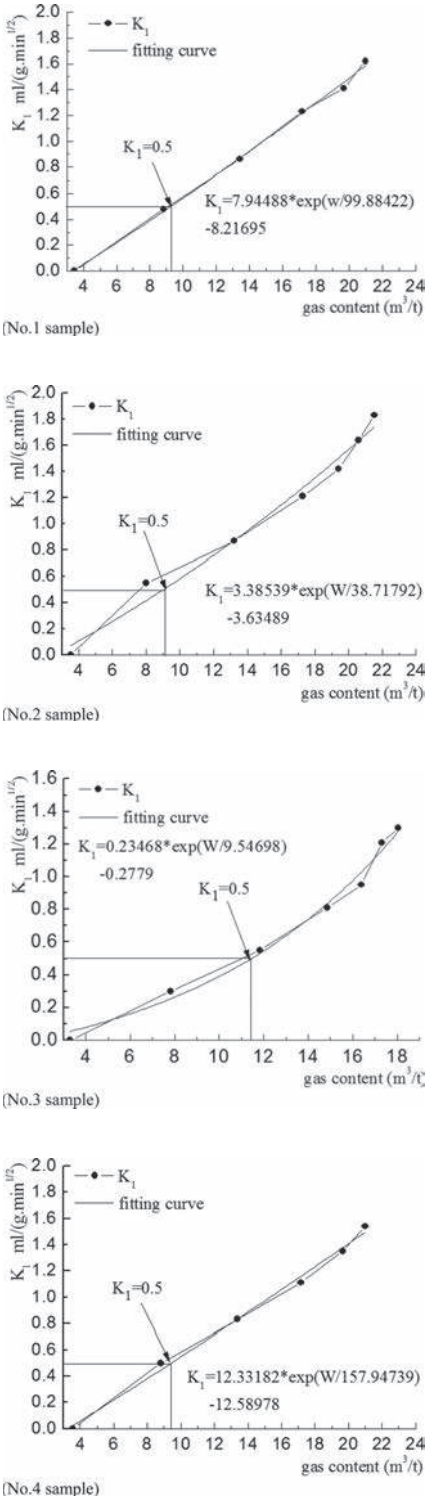


Figure 2. The K_1–W curves of Daning coal samples.

Table 3. Fitting functions of the relationship between K_1 and W.

Number	K_1—W fitting functions	Correlation coefficients
1#	$K_1 = 7.94488 * \exp(W/99.88422) - 8.21695$	0.99637
2#	$K_1 = 3.38539 * \exp(W/38.71792) - 3.63489$	0.97719
3#	$K_1 = 0.23468 * \exp(W/9.54698) - 0.2779$	0.97529
4#	$K_1 = 12.33182 * \exp(W/157.94739) - 12.5898$	0.99166

In function (2), A, B, C are regression coefficients.

K_1 and W are also in accordance with the linear relation when the gas constant is low. The curve presents an obvious uptrend with the W rises.

4 IMPACT OF THE GAS CONTENT ON K_1

The theoretical foundation of the gas desorption index of drill K_1 is that gas diffusion in coal obeys Fick law, the permeation flux of gas is proportional to its concentration gradient. The follows can be got from Fick law (Yang Qiluan 1986).

$$Q_t = K_1\sqrt{t} \tag{3}$$

In function (3)

$$K_1 = Q_\infty \frac{12}{d}\sqrt{\frac{D_{eff}}{\pi}} \tag{4}$$

Q_t is the desorption quantity at the gas desorption time t; Q_∞ is the ultimate desorption quantity of the coal particles under atmospheric pressure; d is diameter of the coal particles; D is the gas effective diffusion coefficient.

Related studying achievements show that the gas effective diffusion coefficient of the coal is not a constant, its value presents time variant characteristics with the decrease of the gas content (Zhang Zhigang 2012). Based on the theory of modern chemistry, effective diffusion coefficient of molecule is related to the bending coefficient calculated from porosity and average pore diameter of porous media, that is:

$$D_{eff} = \frac{D\phi}{\varsigma} \tag{5}$$

In function (5), D_{eff} is the effective diffusion coefficient; D is the diffusion coefficient; φ is the porosity of the coal; ζ is the bending coefficient, correcting for the resistance caused by bending of the channel.

The function (5) indicates that the effective diffusion coefficient of gas in the pea coal is influenced by the porosity and bending coefficient. The Swelling of coal matrix owing to gas adsorption reduced the porosity. Meanwhile, gas adsorption changes the bending coefficient of the diffusion channel and led to the increase of the diffusion resistance. Conversely, gas emission has an impact on the diffusion resistance of gas on the condition of isothermal and isobaric after gas adsorption saturation. As a result, diffusion coefficient alters continuously affected by changes of gas concentration in the process of diffusion. So the actual diffusion process is different from the ideal model $Q = k\sqrt{t}$ because of the changing diffusion coefficient. Therefore, it's more in line with the actual process that formulating the diffusion coefficient as a function of time and describing the diffusion by Fick's law.

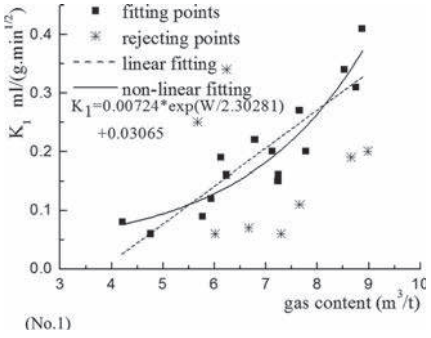
5 SITE VALIDATIONS

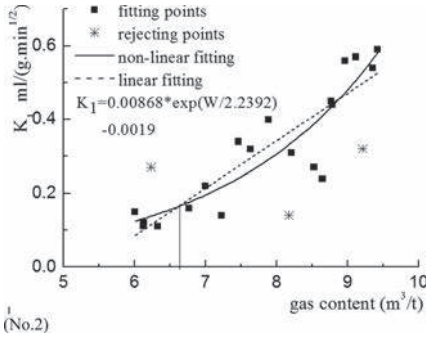
The spot investigation about the relationship between K_1 and W of No.3 coal seam had been down at Daning coal mine for verifying the reliability and correctness of the above research results,. Because the gas occurrence is inhomogeneous and there are inevitable errors when measuring gas parameters underground, make the max gas parameters as the true value for objectively reflecting the coal and gas outburst hazard furthest. The results were drawn into K_1-W curves in Fig. 3.

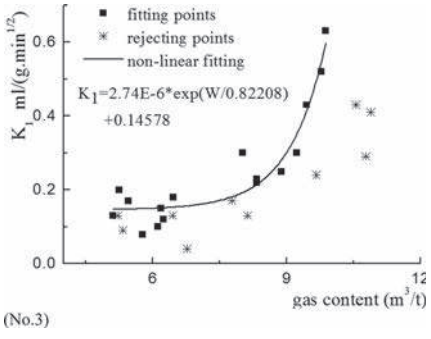
From the Fig. 3, there is a high correlation degree mathematical relation between K_1 and the gas remainder content of the No.3 coal seam. Based on the rational data screening principle, the spot investigation results are consistent with the above mathematical relation model built from the experimental results.

6 CONCLUSIONS

Measured the relationship between the gas desorption index of drill cuttings K_1 and gas pressure of the coal samples in the laboratory, and draw the relation-curves of K_1 and gas content W combined with the proximate analysis of the samples. The relation between K_1 and W is in accords with exponential function by performing analysis of the measured data. According to the physical chemistry theory, the non-linear characteristic between the two is caused by the diffusion coefficient changing constantly with the gas content in







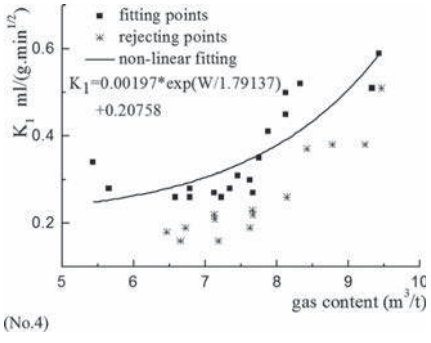


Figure 3. Measured K_1–W curve at each sub-areas in 3202 roadway.

the diffusion process. The K_1–W curves measured at No.3 coal seam of Daning coal mine were also in accords with exponential function as the above experimental results. The achievement of the paper provides a scientific basis and theoretical guidance for the critical value study of coal and gas outburst prediction index and effective inspection index for regional outburst prevention.

ACKNOWLEDGEMENTS

This work was financially supported by the National Science and Technology Major Project (ID: 2011ZX05040-003-003).

REFERENCES

Liu Yanboa, et al 2010. Experimental Study of Swelling Deformation Effect of Coal Induced by Gas Adsorption. *Chinese Journal of Rock Mechanics and Engineering*. 29(12): 2484~2491 (in Chinese).

Qiu Haisheng & Zhang Baoquan 2007. Gas Content of Coal Seam Measurement by Gas Desorption Index of Drill Cuttings. *Safety In Coal Mines*, 07: 18~20 (in Chinese).

State Administration of Work safety 2009. GB/T 23250-2009 The Direct Method of Determining Coal Bed Gas Content in the Mine. *China Standard Publishing House* (in Chinese).

State Administration of Work safety 2009. AQ/T 1065-2008 The Determination Method of Gas Desorption Index of Drill Cuttings. *China coal industry publishing house*. (in Chinese).

Yang Qiluan & Wang Youan 1986. Theory of Methane Diffusion from Coal Cuttings and its Application. *Journl of China Coal Societ*y, 3: 87~93 (in Chinese).

Wang You'an, et al 1993. Adsorption deformation and deformation force of coal. *Safety In Coal Mines*, 6: 19~26 (in Chinese).

Zhang Zhigang 2012. Resolving of Methane Time-varying Diffusion Rule in Coal Grain. *Coal mining Technology*, 17(2): 8~11 (in Chinese).

Zhou Shining & Lin Baiquan 1999. The Theory of Gas Flow and Storage in Coal Seams. Beijing: *China Coal Industry Publishing House* (in Chinese).

Progress in Mine Safety Science and Engineering II – He et al. (Eds)
© 2014 Taylor & Francis Group, London, ISBN 978-1-138-00122-0

Based on simulate test to research the law of CO newly generated when external oxygen involved during the coal breaking process

Xian Wu, Qing Jie Qi, Xin Hua Zhou, Ziwen Dong & Shenghe Huang
College of Safety Science and Engineering, Liaoning Technical University, Fuxin, Liaoning, China

Zhao Liu
Shenyang Coal Science Research Institute, Shenyang, Liaoning, China

ABSTRACT: This paper carried out two different simulate tests under two different scenarios, simulated the process of cutting and crushing coal, the one is in air scenarios and the other is in nitrogen atmosphere scenarios, measuring the difference of gas composition during the process, the purpose is further demonstrate whether to produce new CO and clarify the proportion of CO new generated when external oxygen involved in the all process of cutting and breaking coal. The Coal sample used in experiments is brown coal from 6–3B fully mechanized caving face of feng shui mine Ping hang. The result show that there is new generate of CO from oxidation reaction during all the process of cutting and breaking coal in normal condition of production, the amount of CO newly generated when external oxygen involved is 23.27% of all the CO emission quantity from the total process of cutting and breaking coal. Pointed out the ratio of CO newly generated when external oxygen involved is different, because of the conditions of cutting and breaking coal in normal condition and the Coal types are different, proposed the direction of further research on mechanism of CO emission and newly generated during all the coal breaking process.

Keywords: simulate test, coal breaking, external oxygen, CO, generate, law

1 SIMULATION EXPERIMENT ON BREAKING COAL TYPE AREA

The Coal sample used in experiments is brown coal from 6–3B fully mechanized caving face of feng shui mine Ping hang[1]. After sampling in the field, use sealed plastic bag sealed it up in timely. Back to the lab, daglocked it, then chunks of coal samples from the heart part of coal. Be placed in a special pulverize grinding, the grinding process is divided into two types, one is under nitrogen atmosphere, and the second is in the Naturally air environment. For both of the experimental conditions, the first was measured the gas composition under respective conditions before breaking coal, after the completion of broken coal, after completion of cutting coal determined the gas composition again, all of that use the 3000 Micro GC Gas Chromatograph detect gas component concentration.

1.1 *Determination of gas component before and after coal broken in air environment*

Take about 100 grams of coal sample into a special full-closed pulverize, Leads to nitrogen continuous about three minutes, then detect the gas within the device. Measured oxygen, carbon monoxide, listed in Table 1.

According to table 1, the coal samples poured out mass gas one of O_2 occupy on percentage of 4.6717 which under nitrogen environment when coal was no broken, while concentration O_2 was 0 at this time. At this point the extra oxygen is poured out of the coal samples. We can know these O_2 was come from coal samples. There was no carbon monoxide before Coal samples broken, but we

Table 1. Gas component before and after coal broken in nitrogen environment.

Processing	Keeping time/min	Species	Area/μV*s	Content/Area	Content/%	Gas
before coal broken	0.558	VP	1.34e5	3.47e-7	4.67	O_2
	1.966	–	–	–	–	CO
after coal broken	0.556	VP	1.99e5	3.47e-7	6.92	O_2
	1.956	PB	816.66	3.37e-7	0.023	CO

weren't sure that the raw coal samples not contain carbon monoxide. Because according to the basic theory of gas adsorption-extraction, adsorption of carbon monoxide analytic conditions are relatively strict.

Under nitrogen gas environment, opening the power of the grinder to grinding, the coal samples crushed about spend two minutes. Then close the nitrogen source and analysis on gas that came from grinder. Test results are shown in table 1.

According to table 1, the coal samples poured out mass gas one of O_2 occupy on percentage of 6.91581 which under nitrogen environment when coal broken, while concentration O_2 was 0 at this time. We can know these O_2 was come from coal samples. There was a little of carbon monoxide was test after coal samples broken. We can't know that carbon monoxide was original adsorption or new production, this reason to do further discussion.

The content of process of CO during breaking coal is 0.02256%, under nitrogen environment, comparison in table 1 to break the coal gas composition and concentration changes at before and after. Shows that although in nitrogen environment without external oxygen in Wells have CO, but we weren't sure that carbon monoxide was original adsorption or new production, two situations are more likely to be the combination of the results; Coal sample in crushing process due to chemical reactions produced CO, suppose in the outside world did not exist O_2 nitrogen gas environment, adsorption of oxygen in coal sample that in the process of broken coal are involved in the oxidation reaction. Oxidized coal samples of some of the more active the activation site and fat hydrocarbon, generation some of CO. In order to verify whether the oxygen participate in the reaction during the process of breaking coal, a similar experiment in air environment should be taken. If the coal samples generated CO in the air environment is more than in nitrogen gas environment. So much out of the part CO must be due to the coal sample oxidation in the outside world.

1.2 *Determination of gas component before and after coal broken in air environment*

In air environment, the experiment method is same with 1.1, statistical results are shown in Table 2, it display that in the air atmosphere the is detected before broken is basically same with the normal levels of standard air.

Table 2 shows that after the coal be broken the O_2 content is 20.41335%, CO content is 0.02948%. Contrast with standard air the content of each component has changed, especially the content of CO a lot, this growth part of CO is out from the process of breaking coal. To determine whether emission from original coal occurrence or occurred during from the oxidation reaction during the process of breaking coal, it should compared with the change of before and after broken coal.

Table 2. Gas component before and after coal broken in air environment.

Processing	Keeping time/min	Species	Area/μV*s	Content/Area	Content/%	Gas
before coal broken	0.547	BPA	6.27e5	3.47e7	21.779	O_2
	1.942	BB	24.41	3.374e7	0.0008	CO
after coal broken	0.549	BPA	5.88e5	3.47e7	20.413	O_2
	1.951	PB	873.63	3.37e7	0.0294	CO

Compare with the change of before and after broken coal in air scenarios, O_2 decreased 1.36601 percentage points after the broken coal, CO increased 0.02866 percentage points. A significant reduction of O_2 in air scenarios may be due to the oxygen reaction consume more oxygen in the breaking coal process, CO increased may be due to CO emission from original coal occurrence or occurred from the oxidation reaction during the process of breaking coal, or there may be result of the joint action of the two reasons.

The detected O_2 is increased after broken coal in nitrogen atmosphere, while in oxygen-rich air environment is indeed reduced; but CO is increased in the two different experimental conditions, Putting aside the cause of increase, CO is increasing either in cutting or caving coal process are likely to be appeared during the actual production coal mining work, that bring greater threat to mining personnel and work, and also bring problems to the underground fire forecasting, leading to false positives and so on.

2 ANALYSIS OF CO PRODUCED DURING THE PROCESS OF BROKING COAL

2.1 *Comparative analysis of the amount of CO increased after coal broken*

Compare with the change of O_2 before and after broken coal under two different environmental conditions, can be seen that oxygen Was sufficiently consumed a lot in broking coal process under the air conditions, as long as breaking coal in the coal mining process there will be vigorous oxidation reaction; Compare with the increased amount of CO before and after broken coal under two different environmental conditions, the amount of CO increased 0.02256 percentage

points under nitrogen condition, but it increased 0.02866 percentage points under air condition, the increased amount of CO under air is much greater than the amount of under nitrogen condition, the extra part in the process of breaking coal under the air conditions show that because of oxygen supply is sufficiently that the oxidation reaction is more severe, so that produced larger amount of CO, instructed that a large number of CO is generated newly in breaking coal work of the coal mining process.

2.2 *Assumptions about the reason of produced CO during the process of broking coal*

The possible reasons for a large number of CO increased during the process of broking coal under nitrogen atmosphere are: (1) a large amount of adsorbed CO poured out from original coal during broking coal process in this case absence of external oxygen and the adsorbed O_2 could not taken part in the oxidation reaction, all CO resolved and poured from original coal; (2) absence of external oxygen and there is no adsorbed CO in original coal, the adsorbed O_2 taken part in the oxidation reaction, adsorbed O_2 and some active sites and aliphatic hydrocarbons in original coal occurred oxidation reaction have produced CO, in this case all of CO poured out from oxidation reaction that only adsorbed O_2 taken part in and absence of external oxygen; (3) there be result of the joint action of (1) and (2), some part of CO resolved and poured from original coal and the other part of CO poured out from oxidation reaction that adsorbed O_2 taken part in and absence of external oxygen.

To research on the law of CO produced during breaking process in actual working environment, makes assumption 1, assuming the reasons (1) is established, the amount of CO from broking coal process under the normal production environment is much larger than the amount of adsorbed CO poured out from original coal during broking coal process in this case absence of external oxygen and the adsorbed O_2 could not taken part in the oxidation reaction. the extra part is entirely due to the external oxygen taken part in oxidation reaction, in this case produced larger amount of CO and released it.

Table 3. Results of nitrogen and air atmosphere.

Processing	Increased percentage points	Gas
before and after coal broken under nitrogen atmosphere	2.23964	O_2
	0.02256	CO
before and after coal broken under air atmosphere	–1.36601	O_2
	0.02866	CO

Makes assumption 2, assuming the reasons (2) is established, the amount of CO from broking coal process under the normal production environment is much larger than the amount of CO that poured out from oxidation reaction that only adsorbed O_2 taken part in and absence of external oxygen. The presence of external oxygen could not affect adsorbed O_2 taken part in the oxidation reaction, so that the extra part is entirely due to the external oxygen taken part in oxidation reaction, that produced larger amount of CO and released it.

Makes assumption 3, assuming the reasons (3) is established, the amount of CO from broking coal process under the normal production environment is much larger than the amount of CO that joint action of (1) and (2), some part of CO resolved and poured from original coal and the other part of CO poured out from oxidation reaction that adsorbed O_2 taken part in and absence of external oxygen. So that the extra part is entirely due to the external oxygen taken part in oxidation reaction also.

In summary, regardless of any assumptions is established, compared with anaerobic conditions and normal operating conditions, in the moment of cutting coal, the oxygen could completely contact with coal fully, and the oxidation reaction occurred, the extra part of the latter is due to more external oxygen involved in oxidation reaction, so that there must be new CO generated in the process of breaking coal. The amount of CO is 0.02256% during broking coal process under nitrogen condition and absence of external oxygen, the amount of CO is 0.02948% during the broking coal process under the normal production environment, the mount of CO new generated because of the external oxygen participated in oxidation reaction is account to 23.47% of all the emission amount from the process of breaking coal under normal manufacturing conditions.

However, the intensity of role of coal-oxygen action are varies, free radical can provides a good explanation for the role of law and intensity, the oxygen, the free radical theory is a microscopic interpretation methods to the process of coal-oxygen action, in this paper the Coal sample is lignite coal, the level of lignite deterioration is very low, so that the free radicals concentration of lignite is lowest among the all the coal types; Sometimes as the increasing of the degree of crushing, the higher temperature produced during broking coal, the longer oxidation of coal, the concentration of free radicals is increasing[2–3]. However, the difficulty of coal-oxygen action does not depend on the degree of the original concentration of free

radicals in coal, it depend on the relative growth rate of free radicals during the process of coal-oxygen action, The higher relative growth rate the more prone to coal-oxygen action, the relative growth rate of free radicals concentration of lignite is largest among the all the coal types. So that, on other conditions being the same, the mount of CO produced from the lignite used in this simulation experiment is relatively higher when the external oxygen participated in it.

3 CONCLUSION

This paper carried out two different simulate tests under two different scenarios, combined with data analysis, put forward 3 assumptions about CO produced during the process of breaking coal, after analyzed the 3 assumptions, prove that there must be new CO generated in the process of breaking coal; to the lignite and the degree of crushing used in this simulation experiment, the mount of CO new generated because of the external oxygen participated in oxidation reaction is account to 23.47% of all the emission amount from the process of breaking coal under normal manufacturing conditions. Because the different of coal types, molecular structure of coal complex and diverse of coal origin, history, and age, different states of coal storage and breaking intensity and degree of coal and other reasons, the amount of carbon monoxide produced from the crushing process in different coal is not the same, and the ratio of CO produced when external oxygen participated in oxidation reaction is different. To this paper the further research will be undertake, for example, Preservative law of CO in original Coal, morphological, analytical characteristics, emission law and so on; It should be also in-depth study on the impaction of coal Oxidation that from adsorbed oxygen and other aspects, all the in-depth researches will be undertake is order to clarify the CO emission mechanism during the process of breaking coal.

REFERENCES

[1] Liu Zhao. Study on Fire Prevention and Research on The Goaf of Special Thick Coal Seam on Feng-shuigou Coal Mine. FuXin: degree, 2013.

[2] Wang De-ming. Mine Fires. XuZhou: Macmillan; 2008.

[3] Song Wan-xin, Yang Sheng-qiang, Jiang Chun-lin. Experimental research on the formation of CO during coal spontaneous combustion under the condition of methane-contained airflow. J China Coal Society 2012, 37:1322–1324.

Progress in Mine Safety Science and Engineering II – He et al. (Eds)
© 2014 Taylor & Francis Group, London, ISBN 978-1-138-00122-0

Feasibility of mining under water based on detecting height of water flowing fractured zone

Baobin Gao, Yunpeng Liu & Tian Yuan
School of Safety Science and Engineering, Henan Polytechnic University, Jiaozuo, Henan, China

ABSTRACT: To accurately detect the height of water flowing fractured zone in overlying roof strata after the mining face has been mined and ensure that mining underwater is safe and reliable, use borehole sealing technology to observe the development of water flowing fractured zone through drilling upward holes and calculate the height of water flowing fractured zone by empirical formula calculation, then make them verify each other to ensure the accuracy of detection results and obtain the result which indicates that using borehole sealing technology to detect the height of water flowing fractured zone is reasonable and reliable, and it doesn't travel to the influence sphere of surface water, which not only provides a theoretical support for Sitai Coal mining underwater, but also provides reference for other coals to detect overburden bed's three zones.

1 INTRODUCTION

With coal mining, the roof will move, break up, and even generate the mining-induced fracture. According to the phenomena, the overlying rock can be divided in three zones, which are caving zone, fractured zone and bending zone (Qian 2010). It is not only important for prevention and control of the mine water and mining under water to study the distribution range of the three zones, but also important for prevention and control of mine gas disaster and the utilization of coal-bed methane (State Bureau of Coal Industry 2000).

The development height of overburden bed's three zones and the distribution of new fractures after mining are very complicated, which is not only effected by the lithology characteristics of the overlying rocks and the engineering geological conditions, but also effected by the coal seam thickness and coal mining method. At present, there are many methods to determine the height of the overburden bed's three zones, such as Formula method, Geophysical prospecting method and Drilling piecewise injection method, and so on (Gao et al. 2012). (Qian & Liu, 1991, Coal science research institute Beijing mining 1981, Liu, 1998 & 1996) made a lot of theoretical research and practice tests to determine the height of the overburden bed's three zones after mining, and obtained the empirical formula to calculate the height of the overburden bed's three zones through statistical analysis on that base. (Liang & Wen 2000) accurately divided the roof strata's three zones by using the theory of composed rock beam and key strata theory and the result of finite element analysis; (Liu et al. 2000) use drilling plugging technology and obtain the development of fracture under through observing the injected water, then determine overburden bed's two zones; (Xu et al. 2009, Xu et al. 2012) use theoretical analysis and engineering exploration to study the effect of the location of the key stratum on height of water flowing fractured zone, which turns out that normal distance of key layer and mining coal directly affect the development of water flowing fractured zone; (Hu et al. 2012) use multiple regression analysis in 39cases of measured data of height of water flowing fractured zone in fully-mechanized face, drawing the nonlinear statistical relation of the height of water flowing fractured zone in fully-mechanized face with mining height, robustness coefficient of hard rock, working face length, mining depth, mining velocity and other factors.

For the different mining area geological conditions are complex and different, such as thickness of miming coal seam, mining depth, and strata lithology coal winning technology, it is difficult to determine the height of three zones with empirical formula, or it can be used in some mining area through the location of the key layer, whose scope is relatively limited. For the given reasons above, various reasons must be taken into account to accurately obtain the height of water flowing fractured zone when mining underwater for ensuring the security and effectively of mining underwater. Aiming at geological and mining conditions of Sitai Coal, this paper use a simple and effective method of field test-plugging drilling technology

to detect the scope of rock damage, observe the development of the fracture of the overlying rock intuitively and quantitatively, and get the height of water flowing fractured zone accurately, which provides the technical support for mining safely underwater of Sitai Coal.

2 ENGINEERING SITUATION

Sitai Coal mine of Tongmei Group is 27 kilometers from Datong, design production capacity of 500 000 t/a, the service life of 82 years. Currently 11# and 12# coal seam are main coal seams. Among 11# coal seam thickness is 4.73~4.85 m, the average thickness is 4.79 m, coal seam is more stable; 12# coal seam thickness is 1.22~1.98 m, the average thickness is 1.59 m, the coal seam inclination is 0°~12°, average inclination is 6°, the two coal seams are away from 17 m.

The middle reaches of Shili River flows through the Sitai coal mine, sideways through the mine, causes of coal resources of the mine pressure hysteresis, seriously affected optimization of the layout of the Sitai mine production system.

The mining working face of Sitai Mine is 8205 working face; the mining coal seam is 11# seam.

3 PRINCIPLE OF UNDERGROUND UPHOLE DETECTING THE HEIGHT OF OVERLYING FRACTURED ZONE

3.1 *Research method*

This study uses the patterned product by Henan Polytechnic University-drilling double circuit (put) the water injection system to detective, as Figure 1 shows.

The principle of double side water plugging device is showing in Figure 2. It consists of two connected capsule and corresponding channel. The bulge of the capsule and injecting water into the drilling hole are controlled by two sets of systems.

Basing on the basis of quantitative analysis, use GD3Q-GM downhole drilling television detecting system made in Wuhan DE Technology Company to reflect the development of the drilling's internal rock as pictures through underground borehole imaging. Combining the quantitative analysis with qualitative analysis is not only crystal clear, but also verifies the accuracy of detection results.

The downhole drilling television detecting system is showed as Figure 3.

3.2 *Principle of observation*

Using underground up hole section water leak to detect the height of water flowing fractured zone,

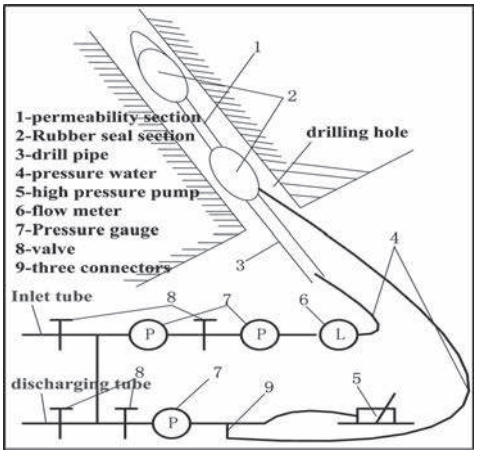


Figure 1. Schematic diagram of underground up-hole observation system.

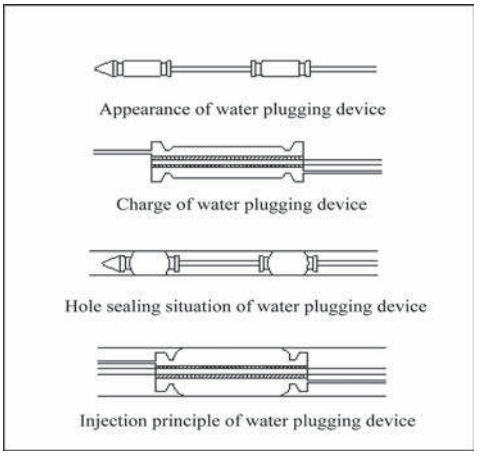


Figure 2. Structure principle of double-side water plugging device.

construct different position and dip angle of the inclined drilling upward through selecting the appropriate location underground. The observation sketch of the borehole in the mine is in Figure 4.

This method of drilling construction requirements is not high, it is simple, safe and reliable, and the observation method is intuitive and easy to understand, its advantages mainly has the following several aspects:

First point: The drilling depth is small, around 70 m per hole, simple operation, saving investment, and compared with the surface borehole flushing fluid consumption observation, it can save the engineering cost about 70% ~ 80%;

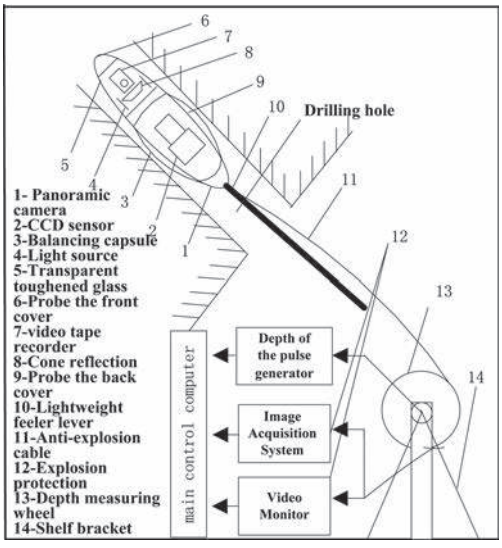


Figure 3. Schematic diagram of boreholes television.

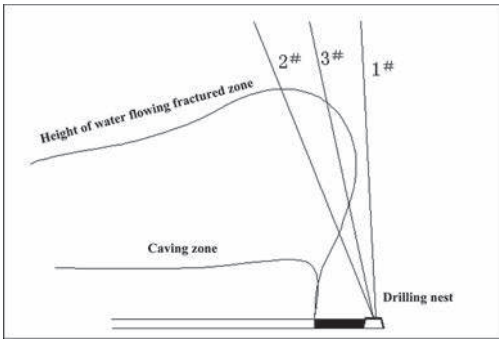


Figure 4. Observation sketch of the borehole in the mine.

Second point: The observation position is accurate, and the observations are reliable. Leak sensitivity is 0.01 L/min, the accuracy is ±5%; detecting depth can reach more than a hundred meter and the depth error is not more than ±1%;
Third point: It is not limited by ground conditions, and it does not take up farmland, so it is suitable for detecting height of water flowing fractured zone in the large water area;
Forth point: It can be well-adapted, and can be observed in any angle upward and down hole;
Fifth point: The water-filled section is small in the hole, and the water injection (discharge) time is short, improving the efficiency of observation;
Sixth point: It can directly measure the water injection (discharge) rate, improving the efficiency of the observation;
Seventh point: It can realize continuous observation, ensuring the continuity of the observations, so the result is not changes about points, but rather changes about the whole rock mass within the observation scope.

Specific observations steps:

First point: Put all the parts of the equipment together, and make sure the sealing effect of each interface is reliable.
Second point: When it is working, connect the push rod and push by root, and connect the hose to the water plugging device with two sides, with the help of the push rod to send the water plugging device with two sides to the specified measurement depth.
Third point: When observing, open the valve first, seal up both ends of the test hole segment through capsule bulged, and then open the water injection system, offer certain water injection pressure (but less than capsule pressure), for the hole of water injection flow rate and water injection leak volume to achieve dynamic balance, finally measure per unit time of water injection by flow meter, namely water injection water leakage.
Forth point: After the test, open the capsules drain valve to release the pressure, capsule contract, the water of the enclosed section flows out, then close the injection valve, and read out the locations of water injection pipeline hydrostatic pressure.
Fifth point: Repeat step 1~4 work, until you finish all the reading.
Sixth point: Basing on the measured water leakage quantity size, determine the crack situation of overburden and determine the development of height of water flowing fractured zone.

4 FIELD CONSTRUCTION

4.1 *Layout of observation borehole*

Before determine the position and orientation of observation drilling (drilling nest), we need to punch observation before mining and leave a rich time to punch observation after mining, then we need to consider the integrity of the surrounding rock around drilling nest, convenient water, ventilation, pedestrians should also be considered.

Considering the above factors and the actual situation in the field, put the observation drilling (drilling nest) at haulage gate of 8205 working face. There are three drillings: one before mining and two after mining. Layout of the drillings is showed in Figure 5.

In order to achieve the desired purpose of this experimental study and get the accurate and reliable

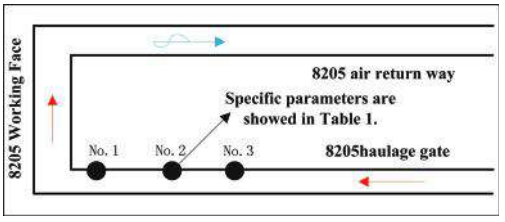


Figure 5. Layout of the drilling hole.

observational data, construct one drilling before mining and two drillings after mining to compare the development of the fracture with each other: the one before mining shows the original crack existing in overburden and the ones after mining show new fractures existing in overburden. Then we approximately get the height of water flowing fractured zone through comparison.

The specific parameters of the three drillings are showed in Table 1.

4.2 *Observation after injecting water*

First point: Observation time: After drilling into the hole.

Second point: Observation number: once before mining, twice after mining.

Third point: Observation way: according to the upward way, observe from where the depth of the drilling is 10 m, and read once when sending two drill pipes (1.36 m) until the vertical depth of the drilling is 50 m.

The observed data of the drillings is showed in Table 2–4, and then we describe the change charts of the water loss (showed in Figure 6–8) both before mining and after mining and the comparison charts (showed in Figure 9 and Figure 10).

4.3 *Observation trough drilling television detecting system*

According to the results of observation of injecting water, the water loss of before mining and after mining has a significant change when the vertical depth is 20~30 m, from which we can get this scope just is the water flowing fractured zone. So, fetch in this scope and the results are showed in Figure 11.

5 ANALYSIS OF THE RESULTS

We can get the flowing conclusion from the data of Table 2–4 and the change chart of Figure 6–8.

First point: The fracture of the overlying rock is not developed before mining for it is not affected. The water loss change of No. 1 borehole is not obvious, which is because that the injecting water flows into the original fracture.

Second point: It produces a large number of new fractures after mining for the overlying rock is affected by the mining work, so the water loss of No. 2 borehole and No. 3 borehole is much more than No. 1 borehole at the same location.

Third point: The water loss is significantly decreasing with the increasing of the vertical depth of No. 2 borehole and No. 3 borehole, and finally trends steady.

Table 1. Parameter table of drilling construction.

Number	Name	Diameter (mm)	Azimuthal angle (°)	Dip angle (°)	Hole depth (m)
1#	Drilling before mining	75	0	40	80
2#	Drilling after mining	75	0	40	80
3#	Drilling after mining	75	0	40	80

Table 2. The observed data of No. 1 borehole.

Slope distance (m)	Vertical depth (m)	Hydrostatic pressure (MPa)	Water injection pressure (MPa)	Average flow rate (L/min)
16	10.28	0.1	0.2	32.20
18.34	11.79	0.111	0.22	32.36
20.68	13.29	0.123	0.243	32.80
23.02	14.8	0.148	0.251	32.46
25.36	16.3	0.162	0.26	32.88
27.7	17.81	0.175	0.273	32.66
30.04	19.31	0.192	0.286	32.46
32.38	20.81	0.205	0.309	32.50
34.72	22.32	0.22	0.317	32.66
37.06	23.82	0.232	0.328	32.84
39.4	25.33	0.242	0.341	32.86
41.74	26.83	0.255	0.353	33.14
44.08	28.33	0.268	0.366	33.10
46.42	29.84	0.283	0.378	32.88
48.76	31.34	0.297	0.386	32.70
51.1	32.85	0.311	0.401	32.66
53.44	34.35	0.325	0.418	32.50
55.78	35.85	0.339	0.424	32.40
58.12	37.36	0.351	0.437	32.40
60.46	38.86	0.364	0.45	32.20
62.8	40.37	0.378	0.466	32.22
65.14	41.87	0.396	0.488	31.60
67.48	43.38	0.412	0.512	31.40
69.82	44.88	0.431	0.534	31.40

Table 3. The observed data of No. 2 borehole.

Slope distance (m)	Vertical depth (m)	Hydrostatic pressure (MPa)	Water injection pressure (MPa)	Average flow rate (L/min)
16	10.28	0.1	0.2	36.24
18.34	11.79	0.111	0.22	36.44
20.68	13.29	0.123	0.243	35.80
23.02	14.8	0.148	0.251	35.62
25.36	16.3	0.162	0.26	35.60
27.7	17.81	0.175	0.273	35.40
30.04	19.31	0.192	0.286	35.22
32.38	20.81	0.205	0.309	34.90
34.72	22.32	0.22	0.317	34.34
37.06	23.82	0.232	0.328	34.12
39.4	25.33	0.242	0.341	33.68
41.74	26.83	0.255	0.353	33.14
44.08	28.33	0.268	0.366	32.96
46.42	29.84	0.283	0.378	32.76
48.76	31.34	0.297	0.386	32.44
51.1	32.85	0.311	0.401	32.22
53.44	34.35	0.325	0.418	32.12
55.78	35.85	0.339	0.424	32.06
58.12	37.36	0.351	0.437	31.88
60.46	38.86	0.364	0.45	31.80
62.8	40.37	0.378	0.466	31.80
65.14	41.87	0.396	0.488	31.60
67.48	43.38	0.412	0.512	31.40
69.82	44.88	0.431	0.534	31.40

Table 4. The observed data of No. 3 borehole.

Slope distance (m)	Vertical depth (m)	Hydrostatic pressure (MPa)	Water injection pressure (MPa)	Average flow rate (L/min)
16	10.28	0.1	0.2	36.60
18.34	11.79	0.111	0.22	36.50
20.68	13.29	0.123	0.243	35.50
23.02	14.8	0.148	0.251	35.48
25.36	16.3	0.162	0.26	35.44
27.7	17.81	0.175	0.273	35.10
30.04	19.31	0.192	0.286	34.62
32.38	20.81	0.205	0.309	34.46
34.72	22.32	0.22	0.317	34.30
37.06	23.82	0.232	0.328	34.10
39.4	25.33	0.242	0.341	33.70
41.74	26.83	0.255	0.353	33.34
44.08	28.33	0.268	0.366	33.10
46.42	29.84	0.283	0.378	32.66
48.76	31.34	0.297	0.386	32.60
51.1	32.85	0.311	0.401	32.60
53.44	34.35	0.325	0.418	32.44
55.78	35.85	0.339	0.424	32.32
58.12	37.36	0.351	0.437	32.30
60.46	38.86	0.364	0.45	32.24
62.8	40.37	0.378	0.466	32.20
65.14	41.87	0.396	0.488	32.20
67.48	43.38	0.412	0.512	32.22
69.82	44.88	0.431	0.534	32.20

We can get the conclusion from the comparison of the injecting water loss of No. 1 borehole and No. 2 borehole in Figure 9 and No. 1borehole and No. 3 borehole in Figure 10.

First point: Because the mining caused the development of the water flowing fractured zone, the water loss of No. 2 borehole and No. 3 borehole is significantly higher than No. 1 borehole at the beginning of the injection.

Second point: As drillings go up, the injecting water loss of the three boreholes final tends steady and roughly equal.

Third point: In the vertical depth of 25 m to 30 m, the water loss of No. 1 borehole is flat with No. 2 borehole and No. 3 borehole fluctuating up and down in the vicinity of one number.

Forth point: The loss of injecting water loss of the three boreholes varies a lot before and after the intersection in the two figures. It can be concluded that the height is the water flowing fractured zone in the position before. No. 1 borehole and No. 2 borehole intersect at a vertical depth of 26.83 m in Fig. 8, and No. 1 borehole and No. 3 borehole intersects at a vertical depth of 28.33 m in Fig. 9, and the higher is the height of water fractured zone, so the height of water flowing fractured zone is 28.33 m in Sitai Coal.

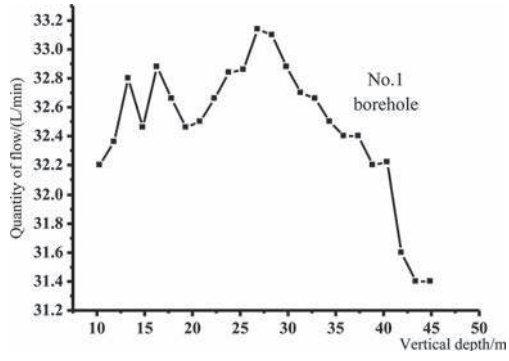


Figure 6. The change chart of injection water leakage of No. 1 borehole.

6 CONCLUSION

First point: The mining height of Sitai Coal is 2.2 m, and the measured height of water flowing

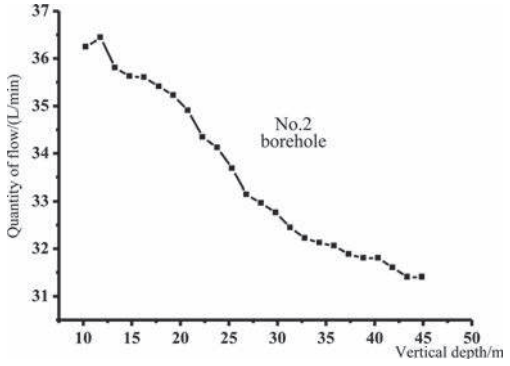


Figure 7. The change chart of injection water leakage of No. 2 borehole.

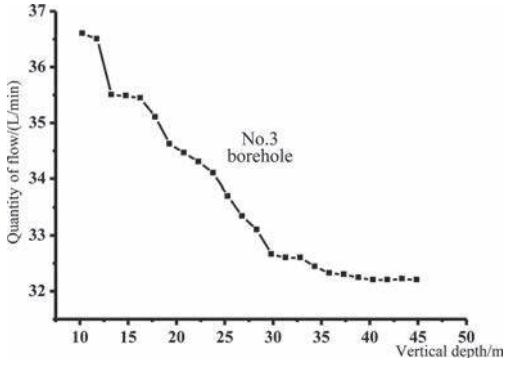


Figure 8. The change chart of injection water leakage of No. 3 borehole.

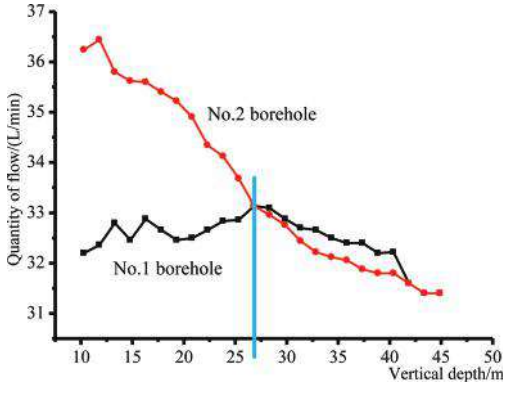


Figure 9. The comparison chart of injection water leakage of No. 1 borehole and No. 2 borehole.

fractured zone is 28.33 m. The ratio of the latter with the former is 12.88:1.

Second point: According to the characteristics of the overburden in Sitai Coal, it is calculated

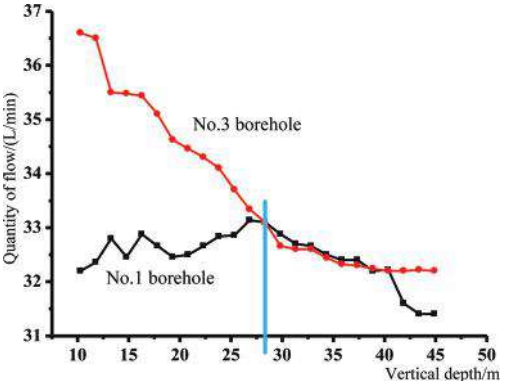


Figure 10. The comparison chart of injection water leakage of No. 1 borehole and No. 3 borehole.

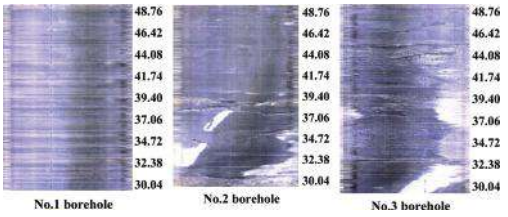


Figure 11. Contrast figure of the drillings' pictures.

that height of water flowing fractured zone is 24.56~34.84 m with the reasonable empirical formula. The measured height of water flowing fractured zone is 24.56~34.84 m. By comparison, it is reasonable and accurate to use underground uphole section water leak to detect the height of water flowing fractured zone.

Third point: Protective coal pillar is 50 meters in the mining process of Sitai Coal, which accords with the relevant provisions of coal mine safety regulation and meets security reliability requirements for mining underwater through the determination of water flowing fractured zone showing that new-born fractures in the mining process of Sitai Coal have no effect on it.

REFERENCES

Coal science research institute Beijing mining 1981. Surface movement of coal mine and law of overburden rock fracture and its application [M]. Beijing: Coal industry publishing house.

Gao B B, Wang X L, Zhu M L & Zhou J W 2012. Dynamic Development Characteristics of Overburden Strata "Two-Zones" under Conditions of Compound Roof, Highly Gassy and Thick Coal Seam in Full-mechanized Top Coal Caving Faces[J]. *Chinese Journal of Rock Mechanics and Engineering,* 31(1): 3444–3451.

Hu X J, Li W P, Cao D T & Liu M C 2012. Index of Multiple Factors and Expected Height of Fully Mechanized Water Flowing Fractured Zone [J]. *Journal of China Coal Society,* 37(4): 613–620.

Liang Y P & Wen G C 2000. Comprehensive Analysis Method of "Three Zone Classification" on Mine Roof Strata. [J]. *Coal Science and Technology,* 28(5): 39–42.

Liu T Q 1986. Safe extraction of near soft layer underlying a thick loose aquifer [J]. *Coal Science and Technology,* 13(2): 14–18.

Liu T Q 1998. Theory and techniques for optimal design of outcrop coal pillar [M]. Beijing: China coal industry publishing house.

Liu W T, Song C W & Ma Y C 2000. Bends downhole probe testing technology for rock area of damage [J]. *Coal Science and Technology,* 28(6): 14–18.

Qian M G & Liu T C 1991. Mining pressure and strata control [M]. China coal industry publishing house.

Qian M G, Shi P W & Xu J L 2010. Mining pressure and strata control [M]. China university of mining press.

State Bureau of Coal Industry 2000. Buildings, water, railway and main shaft and this coal pillar and press coal Mining regulations [M]. Beijing: China coal industry publishing house: 225–233.

Xu J L, Wang X Z, Liu W T & Wang Z G 2009. Effects of Primary Key Stratum Location on Height of Water Flowing Fracture Zone [J]. *Chinese Journal of Rock Mechanics and Engineering,* 28(2): 380–385.

Xu J L, Zhu W B & Wang X Z 2012. New Method to Predict the Height of Fractured Water-conducing Zone by Location of Key Strata [J]. *Journal of China Coal Society,* 37(5): 762–769.

This page intentionally left blank

Progress in Mine Safety Science and Engineering II – He et al. (Eds)
© 2014 Taylor & Francis Group, London, ISBN 978-1-138-00122-0

Study on the deformation mechanism of deep soft rock tunnel and its control

Hebing Luan, Dezhong Kong, Zhaohui Wang & Weishun Sun
School of Resources and Safety Engineering, China University of Mining and Technology (Beijing), Beijing, China

ABSTRACT: The key of deep soft rock tunnel maintaining is to accurately grasp the deformation characteristics. Based on the typical deep soft rock tunnel in some coal mine, the variation of the stress state in the tunnel is analyzed. In addition, the formation process of the plastic zone in the deep soft rock tunnel is presented and the effects of deep mining on the tunnel deformation are studied. In the end of the paper, according to the characteristic of large deformation, the optimal supporting methodology is proposed and applied in the coal mine, which efficiently controls the deformation in the deep soft rock tunnel.

Keywords: deep soft rock tunnel, plastic zone, deep mining, optimal supporting methodology

1 INTRODUCTION

The stability of the surrounding rock of underground tunnel has always been the primal concern during the process of mining, especially in the deep soft rock tunnels (Li et al. 2008). In recent years, plenty of qualitative researches have been conducted on the stability of the surrounding rock. At present, there are a large number of research achievements about the supporting of deep tunnel and the deformation mechanism in the dynamic pressure area (Lin 2006). However, the study on deformation mechanism of deep soft rock tunnel and the related control techniques are still insufficient until now. In particular, few studies, which combine the form two factors, are on the problems of tunnel stability under the condition of high stress and ultrahigh abutment pressure (Bai et al. 2008). Based on the deformation characteristic of deep soft rock tunnel, combined with the theoretical research and the engineering project, the rudimentary deformation mechanism of deep soft rock tunnel is proposed and the control measures are proved to be efficient.er use more than one space after each other.

2 THE ENGINEERING SITUATION

The northern haulage tunnel, railway transportation gateway and air returning gateway are the passages of transportation and ventilation in the north part of the coal mine. The buried depth of these tunnels is approximately 900 m. The lithologies of the surrounding rock are dominated by mudstone and fine sandstone. Rock columnar section is shown in Figure 1. The geological structure and the hydrogeological condition are relatively simple. There are no fault structures whose drop is more than 4 meters according to the geological survey. Because the three tunnels are basically located in the same layer and their the similar conditions,

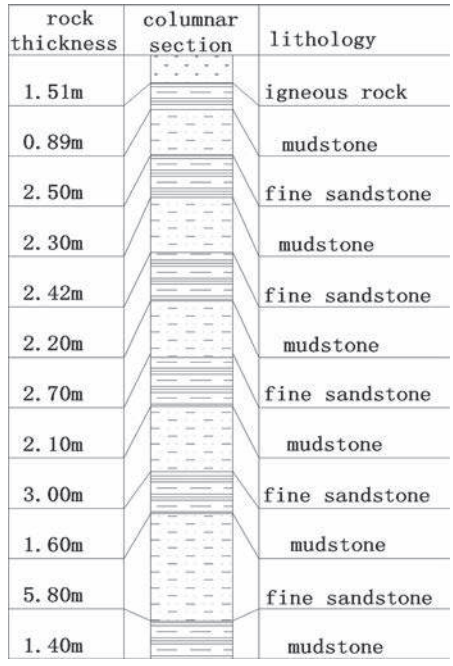


Figure 1. Rock columnar section.

the northern haulage tunnel is selected to be the research subject.

3 ANALYSIS ON THE DEFORMATION MECHANISM OF THE DEEP SOFT ROCK TUNNEL

3.1 *The formation of deep soft rock tunnel plastic zone*

The essence of the deformation failure of the deep soft rock tunnel is the generation of remarkable nolinear and non-smooth plastic deformation, which indicates that it belongs to large deformation. Before the tunnel excavating, the underground rock mass remains triaxial stress equilibrium. After that, the natural stress field is redistributed due to the excavation. As is shown in Figure 2, maximum principal stress is along the tangential direction of the wall. The closer that it move to the gob, the bigger that the tangential stress becomes. The tangential stress research the maximum at the surface of rib. On the other hand, the minor principal stress is along the radial direction It is zero around the tunnel and increases when it moves forward to the deep of the surrounding rock.

If the tunnel buried depth exceeds the soft critical depth, failure will occur in partial rock mass whose stress exceeds the rock mass strength. Failure will tack place firstly in the rock mass which is closed to the wall surface, and then the maximum principal stress will move inward to the interior of the surrounding rock. Accordingly, four regions emerge due to the redistribution of the stress. From the wall surface to the deep-seated rock mass are, in order, plastic flow region, plastic softening region, plastic hardening region and elastic region. The mechanical behaviour in these regions is corresponding to the relevant sections of the rock mass complete stress-strain curve. To be specific: plastic flow region corresponds to the loosening destruction stage; plastic softening region corresponds to the post-peak softening stage; plastic hardening region corresponds to the plastic hardening stage; elastic region corresponds to the elastic deformation stage.

The in situ rock stress increases with the increasing of the mining depth. On the other hand, the strength of the surrounding rock and the stress in the surrounding rock affect the tunnel stability. Surrounding rock displacement rate is relatively small when the stress is less than the strength. And with the increasing of the stress, deformation and failure begin to emerge in the the surrounding rock. Afterwards, with the increasing of the mining depth, radical deformations will take place when the stress exceeds the strength of the surrounding rock, which can trigger the plastic zone extending to the deep. With the expansion of plastic zone, the strength of rock mass in plastic zone decreases, which induces the instability of tunnel. In addition, the temperature will rise with the increasing of mining depth. The generated high temperature will alter the mechanical properties of the rock mass. As a result, the rock mass will turn into plastic body from brittle body and plastic deformation would take place more easily.

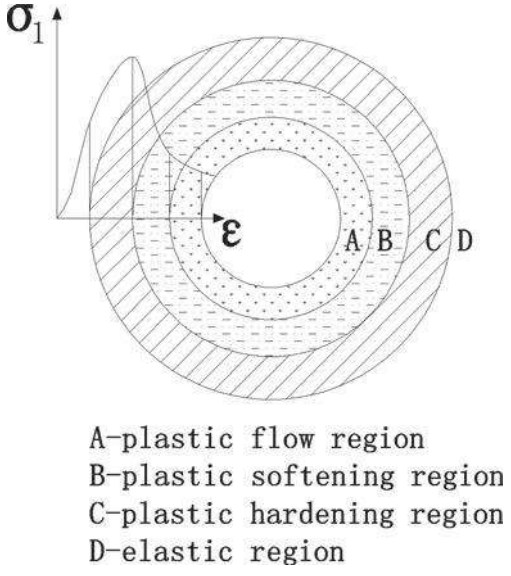


Figure 2. Subregions of the surrounding rock.

3.2 *The characteristics of deformation and failure in deep soft rock tunnel*

The rock formation that northern haulage tunnel is buried in is mainly mudstone. The surrounding rock is loose and the overall strength is low. Through monitoring data, we can conclude that a certain amount of deformation emerges at the beginning of excavation and then the deformation increases rapidly soon. This could trigger severe roof fracture and great tunnel convergence (Wang et al. 2005). What is more, collapse and roof falling may be easily induced in the jointed areas. In summary, the deformation characteristics of deep soft rock tunnel are as follows:

1. High degree of deformation. The convergence displacements are often more than 500 centimetres with the maximum reaching more than one meter (Wang et al. 2008). From the deformation failure prospective, the extrusion large deformation is the dominant form. To be specific, tensile extrusion failure takes place in the lateral

wall; extrusion sink takes place in the roof; floor heaving takes place in the floor.

2. Obvious time effect: At the beginning of excavation, the deforming rate is high. After that, under the influence of high stress, the stability is tending towards stability (Niu et al. 2011). However, the flowing deformation which lasts long still exists.
3. Evident space effect: For the high stress tunnel engineering, the buried depth of tunnel has massive influence on the deformation and stability of the surrounding rock (Meng et al. 2010). Even though the rock strength is relatively high, the damage is still severe due to the great depth and it is very difficult to maintain the tunnels.
4. Upper extrusion failure, later wall cracking and heaving floor are the major failure model (Du & Sun 2007). When there is water erosion the heaving floor is even more severe.
5. Sensitivity to the disturbed stress and environment change: When the deep soft rock tunnels are closed to the excavation, water erosion, blast vibration and mining effect, the surrounding rock can see a rapid rise in its deformation and failure.

4 SUPPORTING SCHEME

According to the former analysis, a supporting scheme is selected for the deep soft rock tunnel in the coal mine. Specifically, the combination of anchor cable, anchor bolt, steel belt, steel mesh and sprayed concrete is applied for the comprehensive supporting in the tunnels. For the sections with severe floor heaving, concrete buffers should be used and forepoling bolts should be applied to support the fractured roof.

Concrete scheme is shown in Figure 3.

The tunnel section, which is 3920 mm high and 4840 wide, is designed to be straight-wall-top-arch.

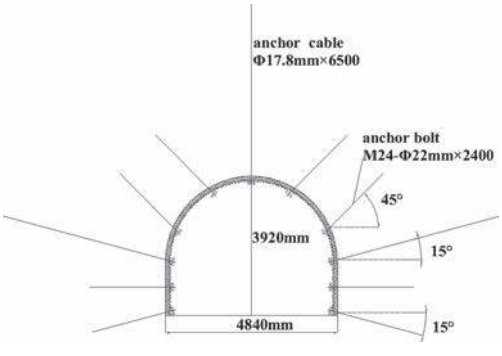


Figure 3. Sectional drawing of roadway support parameters.

Specific supporting parameters are illustrated in Figure 3: M24-Φ22 mm × 2400-type anchor bolt which is composed of high strength twist steel and Φ17.8 mm × 6500-type anchor cable. The space between anchor bolts should be controlled at 800 mm × 800 mm. The pre-tension torque of the anchor bolts is designed to be more than 300 N·m. Also, 12#rhombic metal mesh and W steel belt are used in the supporting system and the spray layer should be 30~50 mm thick.

The proposed comprehensive supporting scheme was applied in the three deep soft rock tunnels. And the deformation rate was monitored for two months. Through the analysis on the monitoring data, it is concluded that the scheme were well correspond with the deformation mechanism of deep soft rock tunnel. The deformation was effectively controlled and its value was with the permitted range. Until now, the tunnels were still not renovated and the deformation tended towards stability, which can meet the requirement of mine full-rate production.

5 CONCLUSION

According to engineering project in some coal mine, combined with its monitoring data of the deep soft rock tunnel, the deformation mechanism of deep soft rock tunnel is analyzed, especially the formation of the plastic zone and its subregions. In addition, the specific control measures are proposed. Through the application of the support scheme, the deformation of the deep soft rock tunnel is controlled in a permitted range.

REFERENCES

Gang Li & Bing Liang et al. 2009. Deformation Features of Roadway in Highly Stressed Soft Rock and Design of Supporting Parameters. *Journal of Mining & Safety Engineering*. 26(2):183–186.

Jian Lin. 2006. Application of High Strength, High Stiffness and Powered Anchor Supporting System in Deep, High Stress and Soft Rock Roadway. *Coal Mining Technology*. 11(6):59–62.

Jianbiao Bai & Xiangyu Wang et al. 2008. Theory and Application of Supporting in Deep Soft Roadways. *Chinese Journal of Geotechnical Engineering*. 30(05):632–635.

Lianguo Wang & Mingyuan Li et al. 2005. Study on Mechanisms and Technology for Bolting and Grouting in Special Soft Rock Roadways under High Stress. *Chinese Journal of Rock Mechanics and Engineering*. 24(16):2889–2893.

Qisheng Wang & Xibing Li et al. 2008. Surrounding Rock Deformation Properties and Determination of Support Parameters of Soft Rock Roadway in Deep Mine. *Journal of China Coal Society*. 33(4):364–367.

Shuangjian Niu & Hongwen Jing et al. 2011. Study on Control Technology of Surrounding Rocks in Deep Soft Roadway and its Application. *Journal of China Coal Society*. 36(6):914–919.

Xianrui Meng & Ruiming Feng et al. 2010. Study on New Support System of Mine Soft Rock Roadway in Kailuan Mining Area. *Coal Science and Technology*. 38(7):6–9.

Zhijun Du & Guowen Sun. 2007. Roadway Supporting of Mine in View of High Geo-stress Soft Rock. *Journal of Xi'an University of Science and Technology*. 27(3): 356–358.

Progress in Mine Safety Science and Engineering II – He et al. (Eds)
© 2014 Taylor & Francis Group, London, ISBN 978-1-138-00122-0

Theoretic seepage model of "water-rock-structural plane" considering the hydro-mechanical coupling mechanism

Ke Man, Ju Wang & Rui Su
Division of Environment Engineering, Beijing Research Institute of Uranium Geology, Beijing, China
Key Laboratory of China National Nuclear Corporation on High Level Radioactive Waste Geological Disposal, Beijing, China

Xiaoli Liu
State Key Laboratory of Hydroscience and Engineering, Tsinghua University, Beijing, China

Yang Zhao & Biao Zhao
Institute of Rock Mechanics and Fractals, China University of Mining and Technology, Beijing, China

ABSTRACT: This paper analyzed the coupling mechanism between stress and seepage in the fractured rock, especially considering the hydrostatic pressure and hydrodynamic pressure on the rock surface. Moreover, the *JRC-JMC* parameters have been incorporated in the model through the topographical method. Then a seepage model has been proposed, i.e. "water-rock-structural plane" model. This model can describe the seepage mechanism clearly and distinctly, even under 3D stresses. From the point of the deformation of the structural plane and the variation of the surface characteristic, the relation between permeability and the 3D stresses and the geometry of the rock surface has been derived. Then, the effective of the seepage model has been clarified deeply and it shows that the seepage model can be applied to the mine excavation and other engineering projects.

1 INTRODUCTION

The physical defects have existed widely in the natural rock, such as fracture, joint and fault and other discontinuous structural plane. The physical and mechanical characteristics of the rock have been influenced seriously by the structural plane, and also the seepage and thermodynamic features and other characteristics have been determined mostly according to the structural plane. It involves mine excavation, environment protection, water conservancy construction, radioactive waste disposal and reservoir induced geologic hazard etc.

For the rock engineering, the projects are subject to the geological environment, which is coupled with the flow field, stress field, thermo field and chemical field and other physical or chemical fields. All these fields have influenced each other and formed a multi-field system in the rock, and it has leaded the rock mass system in a dynamic balance (Lu 2010). To explore the fluid law of the rock with a single fracture under 3D stresses is a fundamental and critical direction. The coupling of solid and fluid of the rock is a significant issue and it arouses extensive interests. And there are numerous researchers focus on it through theoretical and experimental methods.

These papers proposed the cubic law of the water fluid using the single fracture parallel plane test (Louis 1969), and proved that the fluid flow and gap width is proportional to three times. The small variation of the gap width would bring out significant change of the fluid flow. And the gap width was mostly subject to the stress on the structural plane. Meanwhile, the stress also be directly influenced by the seepage pressure, therefore, the seepage field and stress field has been interaction. This feature is called water-rock coupling characteristic. Chang et al (2004) have been built the relation between permeability and stress of the rock and obtained the seepage and stress law through single fracture flow. Zhou (2008) proposed the coupling model of seepage and stress fields, and got the relation between permeability and stress. C. Louis considered the permeability in the fractured rock is much higher than it in the porous rock. And he pointed out that the fractured network is the main channel for the water flow. Therefore, it is necessary to research the single fracture properties of the rock, and then to study the hydro mechanical of the rock mass. Generally, the parameters to measure the joint roughness is *JRC* (Joint Roughness Coefficient) and *D* (fractal dimension).

N. Barton (1973) considered that the shear strength of the joint surface is subject to the residual friction angle φ_n and the incremental friction angle $\Delta\varphi$ due to the roughness of the joint. The *JRC* was defined by the following formula,

$$\Delta\varphi = JRC \lg \frac{JCS}{\sigma_n} \quad (1)$$

In which, *JCS* is the joint wall compressive strength, it could be considered equaling to the joint compressive strength, and σ_n is the normal stress of rock. From the above formula (1), the *JRC* is defined by the shear strength of the joint surface roughness. B.B.Mandelbrot (1983) proposed the fractal dimension theory to measure the joint roughness. N. Fardin (1984) thought the size effect has also existed in the fractal dimension, and there is a size threshold of the joint surface, as long as the *D* more than the threshold value, the *D* of the joint surface could be stable. Although the fractal dimension *D* is accessed by a lot of researchers, it has much more defects. Such as there will be different *D* values for one surface, as using different dimension definition or different size. W.A. Unstrulid and G.A. Johnson (1990) has also taken that accepting the *D* is not suitable and appropriate for the joint surface measurement. Meanwhile, as the *JRC* has a closer connection with the joint mechanical properties (Xiong, 2009), adopting the *JRC* to measure the joint surface roughness is suggested by the ISRM (International Society for the Rock Mechanics). Through studied seepage property of the replica natural fracture, Liu (1999) proposed the remedied cubic law, and pointed out that revised parameter is only connect with the embossing height of the fracture surface. According to the aperture width varies with the stream which is perpendicular to the fracture surface (Neuzil, 1981), it derived the revised method of width density distribution, and the size effect has also been included in another paper (Tsang et al 1983). As the width can be remedied directly by the width function when it is known, paper (Tsang 1984) has setup the remedy formula of the width. However, the accurate width is hardly measured, and another approach method has been proposed by Goodman (1986). The geometry of the aperture is approached by the standard sine curve or saw tooth curve, which are regular curves, to obtain the width function by the compression or dislocation of the aperture. The revised *JRC* method on the joint roughness was raised through a lot of tests in 1985 by Barton (1985). And Iwai discovered the influence of joint roughness on the rock seepage was mainly reflected by the connection area of the aperture surface. From this point, Zhou (1996) has derived the revised formula containing the connection area ratio using pure mathematic derivation.

Above all, for the single fractured rock model, it suffers normal and shear stress on the rock surface. The natural rock has born 3D action, so exploring the rock under 3D stresses is more meaningful. It appears a meaning way to get the seepage regular using the revised cubic law incorporated the joint surface, through analysis the coupling mechanism of seepage and stress interaction, and attempts to find the theoretical formula between permeability and 3D stresses of the rock.

2 SEEPAGE MODEL OF "WATER-ROCK-STRUCTURAL PLANE"

The flow fluid has been influenced by the stress field through the gap width of the structural plane. And the influence of fluid to the stress mechanism through two aspects, one is hydrostatic pressure, another is hydrodynamic pressure. Among the interaction, the structural plane shows the expanding effect along the normal direction and the hauling effect along the shear direction. It distinctly shows that the interaction between flow field and the stress field occurs on the structural plane, and then the coupling effect occurs and influences the rock seepage. So the structural plane between the water and the rock mass is not only a physical medium in the process of water-rock coupling, but also a mechanical medium.

Then the seepage model of "water-rock-structural plane" has been showed in Fig. 1.

This model consists of a structural plane and two rock masses. It consumes that the rock mass does not permeability, and the elastic modulus of the rock is E, and the Poisson ratio is *v*.

Through the seepage model of "water-rock-structural plane", the stress field and the flow field has been decoupled, and it integrates the interactional object to the structural plane.

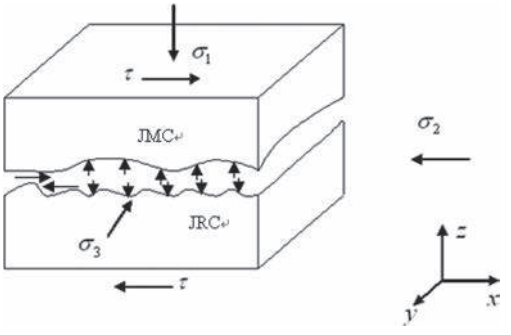


Figure 1. Seepage model of "water-rock-structural plane".

3 THE COUPLING MECHANISM OF THE WATER-ROCK WITH THE STRUCTURAL PLANE

3.1 *Fluid flow on the stress analysis*

As the effect of the fluid field on the stress field, most discussions have just taken into account the hydrostatic pressure, which adopted the effective pressure to solve the coupling problem. However, it has not considered the hydrodynamic pressure on the stress field, which would induce hauling effect.

Assumed that there is a single fracture exists in the rock, and the gap width is constant, the fracture surface is smooth and extension infinite. The length of the structural plane is far great than the width. Then the flow in the structural plane can be considered as narrow flow in parallel plane. The effective pressure is showed in this formula,

$$p = \gamma(H - z) \tag{2}$$

In which, p is hydrostatic pressure, γ is water volume weight, H and z is water head on the structural plane and position individually.

Meanwhile, the hydrodynamic pressure on the stress field has reflected through hauling force on the structural plane. It has driven the hauling force formula,

$$t_w = \frac{b\gamma}{2} J_f \tag{3}$$

In which, t_w is hauling force, b is gap width, J_f is the hydraulic gradient.

In brief, the fluid flow effect on the stress includes two aspects, hydrostatic pressure and hydrodynamic pressure. The former can induce expansion perpendicular to the structural plane, and the later would bring shear displacement along the flow direction.

3.2 *Stress on the fluid flow analysis*

To investigate the stress on the fluid flow effect through the gap width variation, and this effect is responded by the permeability change. Numerous study has on the influence of normal stress to the fluid field, and has obtained many experienced formulas, such as,

$$k = k_0 e^{-a\sigma} \tag{4}$$

In which, k is the permeability when the stress is σ, k_0 is the permeability when the stress is zero. a is parameter.

But the shear stress to the fluid field has not been so widely studied. For the rock subjected to 3D stresses, as show in Fig. 1, according to Mohr—Coulomb standard, the normal stress and shear stress on the structural plane are,

$$\begin{cases} \sigma = \frac{1}{2}(\sigma_1 + \sigma_3) + \frac{1}{2}(\sigma_1 - \sigma_3)\cos 2\beta \\ \tau = \frac{1}{2}(\sigma_1 - \sigma_3)\sin 2\beta \end{cases} \tag{5}$$

For this model, the structural plane is perpendicular to σ_1, so $\beta = 0$, and there are,

$$\sigma = \sigma_1 \tag{6}$$

$$\tau = 0 \tag{7}$$

The hydrostatic pressure is p, and the direction is opposite to σ_1 The hauling force is t_w, and the direction is same to the seepage direction. As the two rocks connect with each other in part, it draws a parameter β here, to indicate the connected area compared to the total area. So the actual hydrostatic pressure on the structural plane is βp.

Because the rock mass is not water-conductivity, the normal stress and shear stress on the structural plane are,

$$\sigma_s = \sigma_1 - \beta p \tag{8}$$

$$\tau = \tau_w \tag{9}$$

Then, the normal deformation of the structural plane is,

$$\varepsilon_s^n = \frac{\sigma_s}{K_n} \tag{10}$$

Here, K_n is normal stiffness of the structural plane.

Simultaneously, the normal deformation of the rock mass is,

$$\varepsilon_r = \frac{\sigma_1 - \upsilon(\sigma_2 + \sigma_3)}{E} \tag{11}$$

And the shear stress also induces the Poisson effect, so the influence of shear deformation to the normal deformation is,

$$\varepsilon_s^s = -\upsilon \frac{\tau_w}{K_s} \tag{12}$$

Here, K_s is shear stiffness of the structural plane.

Above all, the gap width strain of the structural plane can be gotten,

$$\varepsilon = \varepsilon_s^n + \varepsilon_r + \varepsilon_s^s \tag{13}$$

3.3 *The fluid flow law of the stress-seepage coupling*

Considering the rock is elastic material, and it can obtain the normal deformation of the structural plane,

$$\Delta = b_0 \varepsilon \tag{14}$$

In which, b_0 is the initial width of the structural plane.

Now, the width of the structural plane is,

$$b = b_0 - \Delta = b_0(1-\varepsilon) \tag{15}$$

According to the cubic law, the seepage flow and gap width is proportional to three times, and the permeability is directly proportional to the width to square, these can be showed as,

$$q = \frac{\gamma b^3}{12\mu} J_f \tag{16}$$

$$k = \frac{\gamma b^2}{12\mu} \tag{17}$$

In which, k is permeability, μ is motion viscosity coefficient.

The cubic law is driven from the smooth parallel plane, however, the natural rock has rough surface. Through studied the natural surface of the rock and got the revised cubic law, it is,

$$k = \frac{\gamma b_e^2}{12\mu} \tag{18}$$

In which, b_e is equivalent hydraulic width, here the equivalent hydraulic width equals the gap width.

Put the formula (15) into (18), it is,

$$k = \frac{\gamma b_0^2}{12\mu}(1-\varepsilon)^2 \tag{19}$$

Order $k_0 = \frac{\gamma b_0^2}{12\mu}$, then it has,

$$k = k_0(1-\varepsilon)^2 \tag{20}$$

In which, k_0 is the initial permeability of the fractured rock mass.

Through formula (20), it can be concluded that, the permeability is the initial permeability when the stress does not existed. The effective width decreases with the stress increases, and therefore the permeability decreases. This is also accord with the actual situation.

4 THE COUPLING MECHANISM CONSIDERING THE ROUGHNESS OF THE SURFACE

4.1 *JRC and JMC*

Roughness is well described by the *JRC,* which is the index to measure the inherent surface unevenness and waviness of the discontinuity relative to its mean plane (Barton, 1972). Matching is a term used to describe the "pattern agreeness" or "fitness" of the two joint surfaces. When the two surfaces completely fit together, the joint is totally matched. On the other hand, if the two surfaces cannot be fitted together, the joint is then mismatched. The degree of matching is therefore represented by the degree of "pattern agreeness" or "fitness" of the joint surfaces (Zhao 1997a, 1997b). Through various geological processes, joints may suffer from weathering, shearing, loading and thermal cycles, all of which may alter the joint surfaces.

In general, joints that have been weathered, sheared or under loading and thermal cycles are smoother in roughness, but poorer in matching compared to fresh tensile fractures. Clearly, it is not possible to represent the degree of matching by the degree of roughness. The joints of the rock maybe have the same roughness, but differ from the fitness. It is possible huge in the matching aspect. Both these two have significant influences on the mechanical, hydraulic and thermal properties of the joints.

In another words, for example, large joint aperture and joint hydraulic conductivity may be associated with poorer matching of the joint surfaces when the roughness is similar, and the mechanical behavior may also differ due to different degrees of matching. Tsang (1982) used the numerical investigation to correlate the relation between fracture roughness characteristics, and fracture mechanical and hydraulic properties. They used the term aperture density, to describe different matching for the same fracture surface roughness. The results showed that both mechanical fracture closure and water conductivity were affected by different matching of the fracture.

The investigation showed that as the mismatching deeper, the aperture width increased correspondingly, and the variation of normal stress with aperture closure becomes less steep. Or in other words, the hydro mechanical properties of the mismatched and the matched joints showed huge differences. Other researchers also showed the similar observations (Bandis 1983). During an experimental investigation, Zhao also found that the joint hydro mechanical properties were different for natural and freshly induced granite joints

having similar roughness but different matching degrees.

All these observations suggest that joint matching is an important factor in governing the joint hydro mechanical behavior. In order to account for this influence, an index is sought to represent the condition of joint matching. Zhao (1992, 1997) proposed the degree of joint matching coefficient (*JMC*). The *JMC* is the parameter which describes the geometry of the two joints surfaces matching, and is an individual parameter from the *JRC*. The value of *JMC* can be obtained from connection area of the joint compared to the total joint surface area. And the defined *JMC,* scaled from zero to one, obviously. A *JMC* value of one represents a perfectly matched joint with totally surface contact. On the other hand, a *JMC* value close to zero indicates a totally mismatched joint with minimum surface contact. For the natural joint, the *JMC* value varies with the degree of the matching.

Generally, *JMC* values can be estimated from the percentage of the joint connection area. Also, the *JMC* value of the fresh joint is greater than the natural one. Meanwhile, the fresh joint also has higher roughness, i.e. *JRC* value. Incorporating the *JRC* and *JMC* coefficients could better represent the geometry characteristics of the joint surface, thus to determine the hydro mechanical property.

Both *JRC* and *JMC* have an important influence on the normal closure, stiffness, shear strength and conductivity of the joint and so on. The joint physical and mechanical properties are defined by the two parameters. The degree of joint matching and roughness are directly related to the mechanical and hydraulic properties of a joint.

For example, rich roughness of the joint will induce the conductivity more huge. And shear displacement can reduce joint matching and poor joint matching can produce large joint apertures and flow channels. This section focus on the initial aperture variation with the *JRC* and *JMC,* simultaneously, the cubic law has considered, and the joint geometry is incorporated. Thus, the revised cubic law has obtained.

The apertures of a joint are dependent upon the joint surface geometrical properties, i.e. the *JRC* and *JMC*. For a matched joint, despite its roughness, the joint is completely closed, and hence the aperture is at a minimum. For a mismatched joint, the aperture of a rough joint will increase when the joint becomes mismatched and reach a maximum when the joint is totally mismatched. The aperture tends to increase rapidly for a rough joint at a small change of the *JMC,* from completely matched to less matched.

For a smooth joint, the initial aperture is minimum. For a rough joint, whatever the *JMC* is, the aperture increases with the roughness. Compared to the roughness joint, the aperture of the smooth joint is smaller when the *JMC* is similar. And the aperture reaches the maximum value under the roughness is at a higher waviness and unevenness.

Meanwhile, joint with roughness always has higher rock wall, thus the mismatching will induce a much huge aperture. For a mismatched joint, the aperture will increase rapidly when the joint roughness from totally smooth to less smooth at a relative small change.

4.2 *The seepage property of the joint*

The cubic law is a famous and suitable law describing the water movement under parallel and smooth plate. It assumed the fracture was constituted of two straight less and infinite long plates. And the water in it is un-compressive, viscous and laminar stream.

From the cubic law, we know that the quantity of flow has a cubic relation with the aperture, and the permeability has a twice times proportional to the aperture.

As the cubic law widely accepted to judge the water movement, here we use it and the aperture should be revised, because of the roughness of the joint surface. However, just considering the equal aperture is not enough, as it is the quantity obtained through reverse calculation, and has no relation with the practical engineering.

Then, it is urgent to revise the cubic law from the joint itself, and illustrate it totally and seriously.

As the limitation of the cubic law is inevitable, the geometry of the joint surface should be considered, therefore, through the above discussion and analysis of the influence of *JRC* and *JMC* on the aperture, the *JRC-JMC* seepage model has been setup.

Furthermore, according to the model, the cubic law has revised as,

$$k = \frac{\gamma b_e^2}{12\mu} \frac{JRC}{JMC} \tag{21}$$

From the above formula, it can be concluded that permeability of the joint is proportional to *JRC,* and inversely proportional to *JMC*. As the *JRC* increases, the permeability also increases. As the *JMC* matched, the aperture is less small, and the permeability decrease correspondingly. All of these are consistent with the actual seepage conditions.

It should be noted that the permeability has a twice proportional to the aperture, so the conductivity of the joint has a much serious relation varies with the aperture.

5 THE SEEPAGE LAW OF THE FRACTURED ROCK CONSIDERING THE H-M COUPLING

The single joint of the fracture surface is the fundamental element of the fractured network. Meanwhile, the permeability of the fractured rock is not only subject to the growth and incision of the networks, but also to the geometry characteristics, such as the aperture width, direction, roughness and so on. The rock permeability is influenced by the stress on the rock, the aperture width, roughness, filling and other factors. All these factors must be considered carefully and should not be ignored. And the influence of stress on the permeability has been studied widely, but the geometry of the joint on the permeability is few.

For the natural fracture surface, the cubic law is not suitable any more. In that the roughness of the surface in the natural rock is different from the parallel and smooth surface in the cubic model.

And then we should pay more attention to the suitable measurement to get the precise geometry of the joint roughness. Furthermore, through the revised cubic law to research the seepage law of the fractured rock.

So, incorporating the two influence factors (3D stress and joint surface) together, the formula describing the 3D stress, including the hydrostatic pressure and hydrodynamic pressure, the morphology of the rock surface has drawn as follows,

$$k = \frac{\gamma b_0^2}{12\mu}\frac{JRC}{JMC}(1-\varepsilon)^2 \tag{22}$$

In which, the above formula includes three items. The first item ($\gamma b_0^2/12\mu$) illuminates the classic cubic law for the ideal flow channel situation. While, the second item (JRC/JMC) illuminates the influence of the rock surface, which is the fundamental influence factor for the seepage. And the third item $(1 - \varepsilon)^2$ shows the normal and shear stress on the rock mass, especially for the structural plane, which should be considered seriously.

6 CONCLUSIONS

It can be obtained the following conclusions from this paper,

1. The structural plane between the water and the rock mass is not only a physical medium in the process of water-rock coupling, but also a mechanical medium. It would be more exact and effective considering the normal stress, shear stress, hydrostatic pressure and hydrodynamic pressure.
2. From the point of the structural plane deformation, and through the *JRC* and *JMC* parameters, the relation between permeability and the 3D stresses and the rock surface has been derived, which could be more exactly and physically. This model is consistent with the actual seepage conditions.
3. It investigates that the aperture width increase with the *JRC* and decrease with the *JMC,* and the flow conductivity varies correspond with the aperture, and also the effective of the seepage model has been clarified. Meanwhile, the seepage model should be researched in detail from the seepage tests. And it should be considered and expected that the seepage model could be applied to the mine excavation and other engineering projects.

ACKNOWLEDGEMENTS

The author's work has been sponsored by the National Natural Science Foundation of China (No. 41202207).

REFERENCES

Bandis S, A C Lumsden & N R. Barton, 1983, Fundamentals of rock joint deformation [J]. *Int. J. Rock Mech. Min. Sci. Geomech. Abstr.,* 20:249–268.

Barton N R., 1972, A model study of rock joint deformation[J]. *Int. J. Rock Mech.*, 9:579–602.

Barton N.R., 1973, Review of a new shear strength criterion for rock joints[J]. *Engineering Geology,* 7(4):287–332.

Barton N, Bandis S & Bakhtar K, 1985, Strength, deformation and conductivity coupling of rock joints[J]. *Int. J. Rock Mech. Min. Sci. and Geomech. Abstr.,* 22(3):121–140.

Chang Z X, Zhao Y S, Hu Y Q, etc. 2004, Theoretic and experimental studies on seepage law of single fracture under 3D stresses[J]. *Chinese Journal of Rock Mechanics and Engineering,* 23[4]:620–624. (in Chinese).

Elsworth D & Goodman R E., 1986, Characterization of rock fissure hydraulic conductivity using idealized wall roughness profiles [J]. *Int. J. Rock Mech. Min. Sci. and Geomech. Abstr.,* 23(3):233–243.

Fardin, 1984, The effect of tortusosity on fluidflow through a single fracture [J]. *Water Resour. Resear.,* 20(9):1209–1215.

Liu Y R & Tang H M, 1999. Rock Mass Mechanics [M]. Wuhan: China University of Geosciences Press.

Louis C. 1969. A study of groundwater flow in jointed rock and its influence on the stability of rock masses[R]. London: Imp. Coll.

Lu Zude. 2010. Experimental and theoretical analysis on mechanical properties of fractured rock under water-rock interaction[D]. Wuhan: Chinese Academy of Science, (in Chinese).

Mandelbrot B., 1983. The fractal of nature[M]. New York:[s.n.].

Neuzil C E & Tracy J V., 1981, Flow through fractures[J]. *Water Resour. Resear*., 17(1):191–194.

Tsang Y W. & Witherspoon P A. 1983, The dependence of fracture mechanical and fluid flow properties on fracture roughness and sample size[J]. *J. of Geophys. Research,* 88(B3):2359–2366.

Tsang Y W. 1984, The effect of tortusosity on fluidflow through a single fracture [J]. *Water Resour. Resear.,* 20(9):1209–1215.

Tsang Y W & Witherspoon P A., 1982. Correlation between fracture roughness characteristics and fracture mechanical and fluid flow properties[C]. Proc. 23rd US Symp. on Rock Mech.,:560–567.

Unstrulid W.A.& Johnson G.A., 1990. Rock mechanics contributions and challenges[C]. Proceeding of the 31st US symposium on rock mechanics. Rotterdam: A.A. Balkema:471–478.

Xiong X B, Zhang C H, Wang E Z. 2009, A review of steady state seepage in a single fracture of rock [J]. *Chinese Journal of Rock Mechanics and Engineering,* 28(9):1839–1847.

Zhao J. & Brown E T, 1992, Hydro thermo mechanical properties of joints in the Carnmenellis granite [J]. *Engng. Geol*., 25:376–388.

Zhao J., 1997a, Joint surface matching and shear strength. Part A: joint matching coefficient(JMC) [J]. *Int. J. Rock Mech. Min. Sci. Geomech. Abstr*., 34(2):173–178.

Zhao J., 1997b, Joint surface matching and shear strength. Part B: JMC-JRC shear strength criterion [J]. *Int. J. Rock Mech. Min. Sci. Geomech. Abstr.,* 34(2):179–185.

Zhou C B & Xiong W L., 1996, A generalized cubic law for percolation in rock joints [J]. *Rock and soil mechanics,* 17(4):1–7.

Zhou C B, Chen Y F, Jiang Q H, etc. 2008, An interfacial layer model for coupled hydro mechanical analysis in geological discontinuities[J]. *Chinese Journal of Rock Mechanics and Engineering,* 27[6]:1081–1093. (in Chinese).

This page intentionally left blank

Progress in Mine Safety Science and Engineering II – He et al. (Eds)
© 2014 Taylor & Francis Group, London, ISBN 978-1-138-00122-0

Laboratory study and prediction on coal permeability of Qinshui Basin

Guiqiang Zheng, Biaocan Ling, Xuezheng Zhu & Jianxu Pan
School of safety Engineering, North China Institute of Science and Technology, Langfang, P.R. China

Zhejun Pan & Luke D. Connell
CSIRO Earth Science and Resource Engineering, Ian Laboratory, Clayton, Victoria, Australia

Shuheng Tang
School of Energy and Resources, China University of Geosciences, Beijing, P.R. China

ABSTRACT: As one key parameter for coalbed recovery, cleat compressibility has not been well studied in China. In this study, a Chinese coal sample from Qinshui Basin, Shanxi province, was measured using different gases, including He, N_2, CH_4 and CO_2 with different effective stresses and temperatures. Based on the experimental data, the Langmuir constants were calculated and curves of adsorption and permeability were drawn, respectively. The experimental results show that effective stress has important effect on permeability. Permeability decreases with increasing effective stress under the same pore pressure for all four kinds of gases at constant temperature of 35°C. On the basis of experimental results, cleat compressibility was calculated by fitting data to equations. The calculated results also show that cleat compressibility decreases with increasing pore pressure at 35°C for all four gases. Moreover, with increasing temperature, cleat compressibility increases only a little. Based on the analysis the experimental data and summary of literature, effective stress is considered by the authors as the key.

1 INTRODUCTION

The CBM exploration and production potential in China is huge. However, because of the "three-low" character of Chinese coal seams, which is low reservoir pressure, low permeability and low gas saturation, the production recovery is quite low in the past few decades. Since permeability is one of the critical parameters for the success of CBM recovery process while cleat compressibility can significantly affect the permeability, it is necessary to study the characters and change laws of cleat compressibility with different effective stresses and temperatures. These laboratory-tested data can be converted to in-situ data, so it will provide important guidance to the field production (Gu 2009, Pattison et al. 1996, Reiss 1980).

Some studies about cleat compressibility have been made during the past couples of decades. At an early stage of studying, cleat compressibility was treated as a constant parameter by some researchers and some other studies indicated that the value of C_f has no effect on production. Later, some studies showed that C_f is not a constant parameter and has important effect to the production. The exact C_f value, which is 9.24 E-4 psi^{-1} (1 psi^{-1} = 0.145kpa^{-1}) tested in San Juan Basin of America, was early reported by Mckee et al. (1988). However, those results were tested by using conventional method which has historically been difficult, for example equipment constrains, and it is expensive to measure and the results of such measurements are often ambiguous (Charles 2001, Close 1993, Scorer & Miller 1974).

In brief, all the above studies are either using the conventional tests which are expensive and time-consuming, or just giving a general trend of cleat compressibility, or the experimental condition is relative simple. Furthermore, a conclusion drawn from an overseas coal may be not suitable for China, so the laboratory study of cleat compressibility on Chinese coal is quite necessary.

The purpose of this study is to analysis the tested permeability result and corresponding laws of cleat compressibility that change with effective stresses and temperatures. This will provide important guidance to the field production and evidence to the following project step of ECBM process.

2 EXPERIMENT METHODS

2.1 *Experiment apparatus*

Experimental apparatus used in this study is designed and produced by Ian Wark Laboratory of CSIRO themselves. A triaxial permeability

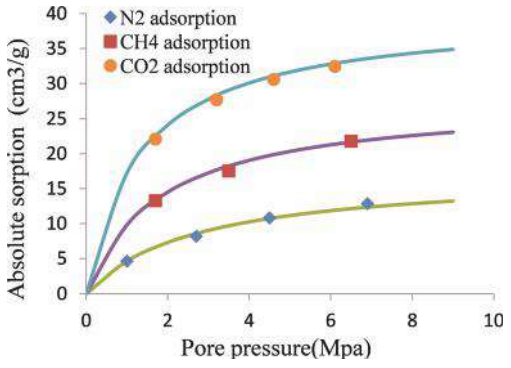


Figure 1. Adsorption result of N2, CH4, CO2 and Langmuir curve at 35°C.

cell was used for the experimental measurement of gas adsorption and permeability under hydrostatic conditions. The sample cell and other parts of the apparatus are in a temperature controlled cabinet to maintain constant temperature during the experiment. The sketch map of experimental apparatus is shown in Figure 1.

2.2 *Sampling site and preparation*

Coal sample used in this work is from Changzhi city of Qinshui Basin, which is one of the eight largest basins in China. Qinshui Basin is one of the hottest CBM exploration and production regions in China at present. Many data-testing and pilot projects, for example the first CO_2 injection to ECBM, were started in Qinshui Basin (Wong et al., 2006). Therefore, the experimental testing result will have representative and guidance to Chinese CBM production.

Following China National standards of GB 474–83 and to maximize sample size, the coal sample is prepared as a cylindrical shape with 50 mm in diameter and 100 mm in height, and is numbered as CZ–1. In order to avoid destroying for partly stress overburden and to smooth the sample, the procedure of filling the fractures and flattening the surface with plaster must be done first. After that, the sample needs to be put into a vacuum oven for several days to remove the moisture, measuring weight twice a day to make sure it is totally dry. Moreover, the sample needs to be wrapped with a thin lead foil then a rubber sleeve before it is installed in the cell.

2.3 *Calculation methods*

2.3.1 *Adsorption capacity*

Calculation method of adsorption capacity is through the measurement of volumetric change to calculate the adsorption capacity. The formula of the adsorption capacity calculation is illustrated as below (Pan et al., 2010):

$$n_{ads}^{Gibbs} = n_{inj} - n_{unads}^{Gibbs} \tag{1}$$

In this study, all gas compressibility factors and densities of He, N_2, CH_4 and CO_2 are calculated from the NIST webbook: http:// webbook.nist.gov/chemistry/fluid/(Brace et al 1968).

2.3.2 *Permeability*

Permeability calculation method in this study adopts the transient method of Brace. This method need to observe the decay of a differential pressure between upstream and downstream vessels. The pressure decay curve can be modeled as:

$$\frac{(p_u - p_d)}{(p_{u,0} - p_{d,0})} = e^{-\alpha t} \tag{2}$$

Using decaying curve to observe the α value, i.e. the gradient of the curve, and then use the following Eq. (3) to calculate the permeability k.

$$K = \alpha\mu\beta L^2 \left(\frac{v_u v_d}{v_u + v_d}\right) \tag{3}$$

2.3.3 *Cleat compressibility*

In this experiment, four kinds of gases, which are He, N_2, CH_4 and CO_2, are used in sequence to test the permeability with different effective stresses and temperatures, and then to calculate the cleat compressibility by fitting permeability curves.

The defining of Cleat compressibility (C_f) is:

$$C_f = \frac{1}{\phi_f}\frac{\partial \phi_f}{\partial p_p} \tag{4}$$

The calculation formula of cleat compressibility used in this study is shown in follows:

$$K = K_0 e^{-3C_f(\sigma - \sigma_0)} \tag{5}$$

Before calculating, the fitting curve of k/k_0 and $\sigma - \sigma_0$ should be drawn firstly, And then fitting above equation to experimental data will yield cleat compressibility (Dabbous et al. 1974, Mckee et al. 1988, Puri & Seidel, 1991, Pomeroy et al 1974).

3 EXPERIMENTAL RESULTS

3.1 *Adsorption capacity*

Based on the experimental data, Langmuir volume V_L and Langmuir pressure P_L are calculated and

Table 1. Langmuir constants of N_2, CH_4 and CO_2.

Gas type	V_L(m3/t)	P_L(Mpa)
N_2	17.24	2.72
CH_4	27.78	1.83
CO_2	40.00	1.32

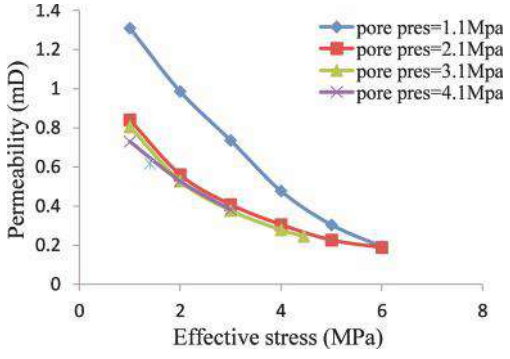


Figure 2. Permeability using He with different stresses.

summarized in Table 1. The adsorption isotherms of N_2, CH_4 and CO_2 then can be plotted in Fig. 1. We can see that all the isotherms can be modeled by the Langmuir model with reasonable accuracy.

From Table 1 we can see that Langmuir volume increases and Langmuir pressure decreases when tested using N_2, CH_4 and CO_2 in sequence. The Langmuir volume is 17.24, 27.78 and 40.00 m^3/t, and the Langmuir pressure is 2.72, 1.83 and 1.32 Mpa in sequence separately. We can also see from Fig. 4 that Adsorption amount of CO_2 is about 1.5 times than that of CH_4 and is about 3 times than that of N_2 over the measured pressure range.

3.2 *Effective stresses influence on permeability*

Permeability curves measured using He, N_2, CH_4 and CO_2 are shown in the following Figs. 3–6. All the above four permeability was tested under the same temperature of 35°C but different effective stresses. Effective stress here equals confining press minus pore pressure.

Permeability measured using He at a constant pore pressure but different effective stresses is shown in Fig. 5. From the figure we can see that Permeability decreases with increasing effective stress. Permeability decreases from 1.3 md to 0.2 md when effective stress varies from 1 Mpa to 6 Mpa at pore pressure of 1.1 Mpa. We can also see that permeability decreases with increasing pore pressures roughly. It decreases from 1.3 md to about 0.8 md when pore pressure varies from 1.1 Mpa to 5.1 Mpa at effective stress of 1 Mpa, which decreases almost 40%.

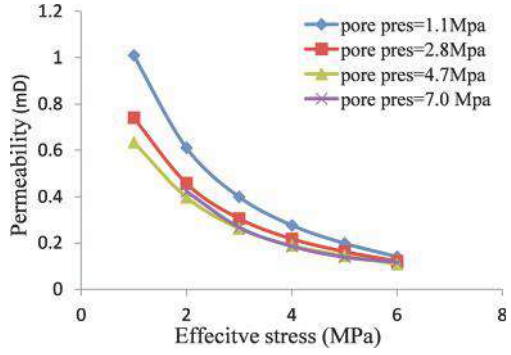


Figure 3. Permeability using N_2 with different stresses.

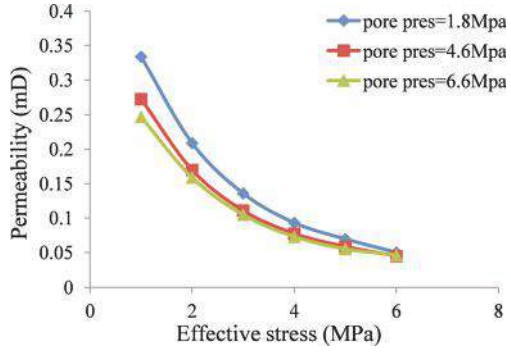


Figure 4. Permeability using CH_4 with different stresses.

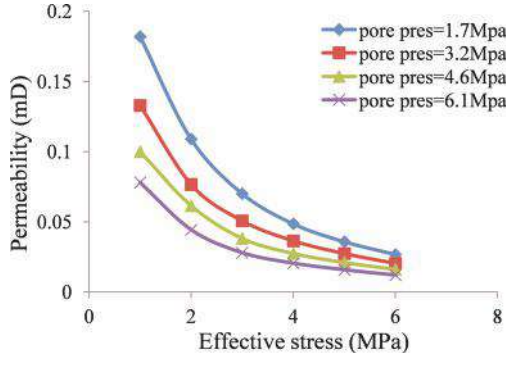


Figure 5. Permeability using CO_2 with different stresses.

Permeability measured using N_2 is shown in Fig. 3. The figure shows that Permeability decreases with increasing effective stress. Permeability decreases from 1 md to 0.1 md when effective

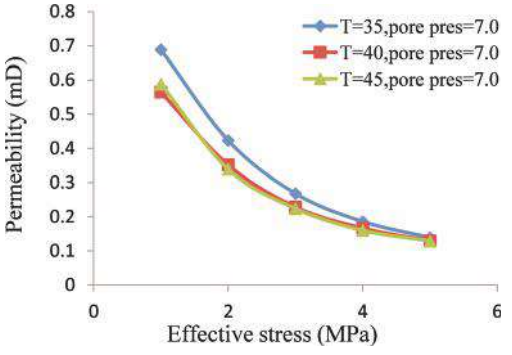


Figure 6. Permeability using N_2 with different temperatures.

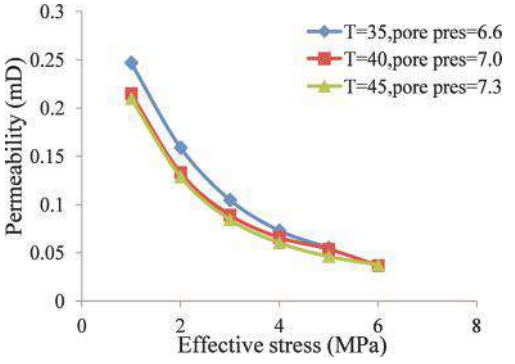


Figure 7. Permeability using CH_4 with different temperatures.

stress varies from 1 Mpa to 6 Mpa at pore pressure of 1.1 Mpa. Permeability decreases with increasing pore pressures, it decreases from 1 md to about 0.7 md when pore pressure varies from 1.1 Mpa to 7 Mpa at effective stress of 1 Mpa, which decreases almost 30%. Moreover, permeability values are quite close to each other at high pore pressures, which are 2.8 Mpa, 4.7 Mpa and 7.0 Mpa. When effective stress reaches nearly to 6 Mpa, permeability for all pore pressures becomes the one same value, which is 0.1 Mpa. Permeability measured using CH_4 is shown in Fig. 4.

It can be seen that permeability decreases with increasing effective stress. Permeability decreases from 0.34 md to 0.05 md when effective stress varies from 1 Mpa to 6 Mpa at pore pressure of 1.8 Mpa. Permeability decreases with increasing pore pressures, it decreases from 0.35 md to about 0.25 md when pore pressure varies from 1.8 Mpa to 6.6 Mpa at effective stress of 1 Mpa, which decreases nearly 30%. Permeability measured using CO_2 is shown in Fig. 6. We can see from the figure that permeability decreases with increasing effective stress. Permeability decreases from 0.18 md to 0.02 md when effective stress varies from 1 Mpa to 6 Mpa at pore pressure of 1.7 Mpa.

It can be seen from the above four Figures 2–5 that: (1) Effective stress has important effect to permeability. With increasing effective stress, permeability decreases at the same pore pressure. (2) With increasing pore pressure, permeability decreases for all four kinds of gases at the same effective stress. For this four kinds of gases, permeability decrease about 30–55% when pore pressure rises from nearly 1.1 Mpa to 7 Mpa at effective stress of 1 Mpa. (3) Permeability decreases when measured using He, N_2, CH_4 and CO_2 in sequence at the same conditions. For example, the permeability is 0.12 for CH_4 and 0.04 for CO_2 at effective stress of

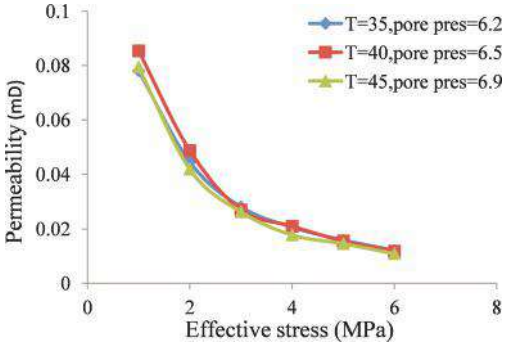


Figure 8. Permeability using CO_2 with different temperatures.

3 Mpa and pore pressure of 4.6 Mpa. (4) For He, N_2 and CH_4, the permeability at low pore pressure, for example 1.1 Mpa for He, is bigger than that at higher pore pressures; at which permeability is very close. However, for CO_2, the permeability values are quite different at different pore pressures. That is maybe because the Klinkenberg effect has major effect for He, N_2 and CH_4 at low-pressure stage, while adsorption capacity has bigger effect than Klinkenberg effect for CO_2. (5) When effective stress reaches nearly 6 Mpa, permeability measured using the four kinds of gases closes up to one value at different pore pressures individually. It is about 0.2 for He, 0.1 for N_2, 0.05 for CH_4 and 0.02 for CO_2.

3.3 *Temperatures influence on permeability*

The permeability curves measured using N_2, CH_4 and CO_2 with different temperatures are drawn in the following Fig. 6–8, respectively. The above three permeability are all tested under the pore pressure

of nearly 7.0 Mpa but different temperatures, which are 35°C, 40°C and 45°C, respectively.

Permeability measured using N_2 with different effective stresses at different temperatures is shown in Fig. 6. Similar to the law of permeability changes with the pore pressure, permeability decreases with increasing temperature at the same effective stress. Permeability is a little higher at 35°C than at 40°C and 45°C, at which permeability is very close to each other. This maybe also contributes to the Klinkenberg effect, which has bigger effect at low temperature while it is not so obvious at a high one. This law is similar with that tested using CH_4 but a little different with CO_2, which will be show in the following Figures.

Permeability measured using CH_4 is shown in Fig. 7. It can be seen that with increasing temperature, permeability decreases at the same effective stress. Permeability is a little higher at 35°C than at 40°C and 45°C, at which permeability is very close to each other. It is about 0.25 md, when effective stress is 1 Mpa and temperature is at 35°C; while it is around 0.20 md at 40°C and 45°C. Permeability measured using CO_2 is shown in Fig. 8. Different from N2 and CH_4, permeability measured using CO2 is quite close to each other at all 35°C, 40°C and 45°C. For example, permeability is about 0.08 md, when effective stress is 1 Mpa for all three temperatures. It has the same law with N_2 and CH_4, when effective stress reaches nearly 6 Mpa permeability gets close to one same value, which is 0.01 Mpa.

It can be seen from the above three Figures 6–8 that: (1) Temperature has some effect to permeability for N_2 and CH_4, it decreases with increasing temperature at the same effective stress. While temperature has no obvious effect for CO_2, it is very close to each other at 35°C, 40°C and 45°C. (2) Permeability is a little higher at 35°C than 40°C and 45°C for N_2 and CH_4, at which the value is close to each other under the same effective stress; while permeability is very close to each other for CO_2 at all 35°C, 40°C and 45°C, which means temperature has no obvious effect to permeability for CO_2. (3) When effective stress reaches nearly 6 Mpa, permeability value gets close to one value for all temperatures. It is 0.15 for N_2, 0.04 for CH_4 and 0.01 for CO_2.

4 CLEAT COMPRESSIBILITY CALCULAITON

Based on the experimental data of permeability, Cleat compressibility can be calculated with fitting permeability curves using Eq. (5). The calculation result has been illustrated in Table 2. Furthermore, the cleat compressibility (C_f) curves measured using different gases with different temperatures are drawn in Fig. 9 and Fig. 10, respectively. All these tests were conducted with almost the same pore pressure of 7 Mpa.

Table 2. Calculated result of cleat compressibility.

Type	Cf	35°C			
Helium	P	1.1	2.1	3.1	4.1
	C_f	0.1289	0.0997	0.113	0.1075
N_2	P	1.1	2.8	4.6	7
	C_f	0.1293	0.119	0.1158	0.1197
CH_4	P	1.8	4.6	6.6	–
	C_f	0.1252	0.1195	0.1132	–
CO_2	P	1.7	3.2	4.6	6.2
	C_f	0.1264	0.1215	0.1209	0.1212

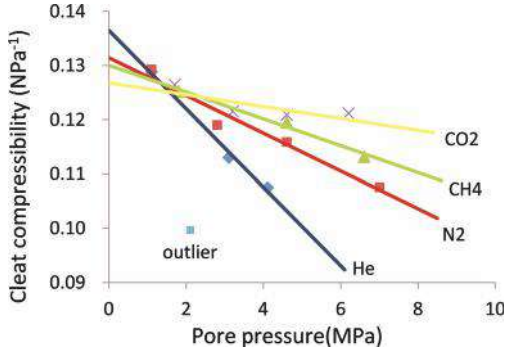


Figure 9. Cleat compressibility by He, CH_4 and CO_2 at 35°C.

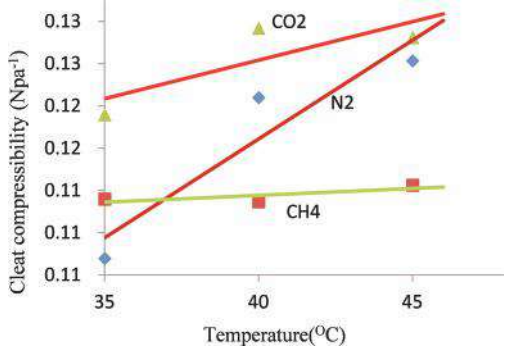


Figure 10. Cleat compressibility by He, CH_4 and CO_2 at 35°C.

It can be seen from Table 2 that the cleat compressibility by He is about 0.10 Mpa^{-1}, it is about 0.11 by N_2 and CH2, and it is about 0.12 by CO_2 at 35°C. This result on a Chinese coal sample is about twice than that that of Australian coal, which reported that the cleat permeability was

about 0.05 by He, CH_4 and CO_2. However, this result is smaller than what had reported of McKee et al. (1988), where the cleat compressibility was 9.24 E-4 psi^{-1} and 1.87 E-3 $psi^{-1,}$ which equals to 0.134 Mpa^{-1} and 0.27 $Mpa^{-1,}$ in San Juan Basin and Warrior Basin, separately. Table 2 also shows that when temperature rises to 40°C and 45°C, cleat compressibility becomes very similar for the same kind of gas. It is about 0.12 by $N_{2,}$ is 0.11 by CH_4 and 0.13 by CO_2. This means that when temperature rises from 35°Cto 40°C and 45°C, cleat compressibility increases by 0.01 by N_2 and CO_2 but it keeps the same value by CH_4.

From Fig. 9 we can see that at constant temperature of 35°C, cleat compressibility decreases with increasing pore pressure for all He, $N_{2,}$ CH_4 and CO_2 gases. This changing law corresponds what have been found by Mckee ea al. (1988). It is reported in his study that compressibility declines with increasing stress, but on some samples it may increase. For this Chinese sample, it fits the general rule. However, decrease trend by different gases is different. Roughly, the decreasing trend is He> N_2> CH_4> $CO_{2,}$ which means cleat compressibility of CO_2 has the smallest decrease trend, while He has the sharpest decline with increasing pore pressure. From Fig. 13 we can see that when temperature rise from 35°C to 45°C, cleat compressibility increase gradually for all three kinds of gases, which are $N_{2,}$ CH_4 and CO_2. However, the increase trend is quite different. Roughly, it changes sharply for N2 while it mainly keeps flat for CH4 with increasing temperature. This means that temperatures have little effect to cleat compressibility for $CH_{4,}$ but it has large effect to N_2. When temperature raises from 35°C to 45°C, cleat compressibility increases from 0.109 to 0.128 for N_2; it increases from 0.123 to 0.130 for $CO_{2,}$ while it keeps the value at about 0.114 for CH_4. It also can be seen that Cleat compressibility of CO_2 is bigger than N_2 and CH_4 at the same temperature. It is around 0.113 for $CH_{4,}$ is 0.117 for N_2 and 0.125 for CO_2 at 37°C; while it is 0.114 for $CH_{4,}$ and is 0.124 for N_2 and 0.128 for CO_2 at 43°C.

5 APPLICATION TO MODEL

In order to predict the permeability change during CBM production, cleat compressibility and adsorption-induced volumetric swelling strain should be studied firstly. According to Fu et al. (2003), the Young modulus and Poisson's ratio of middle rank coal under at the depth of 500–800 m in central and southern part of the Qinshui Basin is 3.05 Mpa and 0.19, respectively. The sample used in this study belongs to middle rank coal and is from about 700 m depth in Changzhi area, south

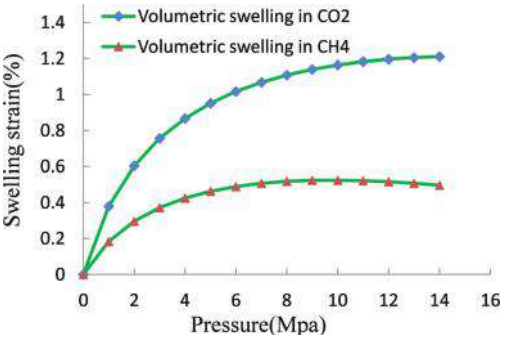


Figure 11. Modeling curve of CH4 and CO2 adsorption-induced swelling.

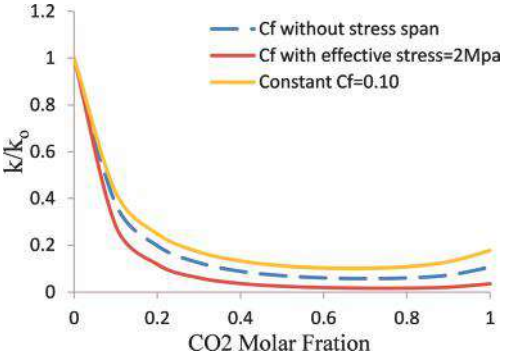


Figure 12. Permeability prediction with CO_2 fraction.

Qinshui Basin, so we can use the two parameters directly to calculate the swelling strain. According to Pan and Connell (2007), mixed-gas adsorption-induced swelling stain can be predicted, on assuming that linear swelling strain is approximately one third of volumetric swelling strain (Palmer & Mansoori 1996, Palmer & Mansoori 1998, Pekot & Reeves 2003):

Through calculation, the swelling strain changes with different pressure can be drawn in the following Fig.11.

Moreover, we need to compare the permeability change with a constant C_f and with the gas composition changing from pure CH_4 to $CO_{2.}$ The changing C_f is defined by following Eq. (6):

$$C_f = y_{co2} C_{f,co_2} + y_{CH_4} C_{f,CH_4} \quad (6)$$

Fig. 12 presents an example using the S&D permeability model with two constant C_f of 0.05 and 0.10 and a variable C_f for a constant pore pressure of 7 Mpa. From this figure, we can see that

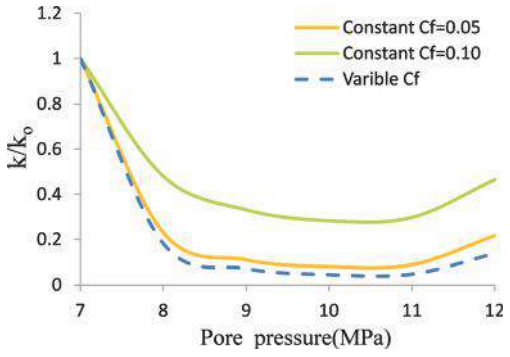


Figure 13. Permeability prediction with changing pressure.

permeability declines more significantly with variable cleat compressibility. Moreover, k/k_0 has the minimum at the CO_2 fraction of 0.7, before which the curve of k/k_0 is decline and after which it raises.

Fig. 13 presents another example of pore pressure varies from 7 Mpa to 12 Mpa and CO_2 composition decreases linearly from 1 to 0 at the same time. From this figure we can see that permeability decline using variable cleat compressibility is much larger than using constant compressibility. Moreover, using different Cf has important effect to permeability. We can see from both Fig. 12 and Fig. 13 that permeability decline using 0.10 is much larger than using 0.05. These permeability decline curves with gas composition and pore pressure changing drawn in Fig. 12 and Fig. 13 have important guidance to field production during the ECBM process. The roughly permeability value and variable trend can be conducted through these figures when we know the gas composition and the pore pressures during CBM production.

6 CONCLUSION

Cleat permeability study has been reported by Mckee early in 1988, but this result is based on the conventional test, which are expensive, time-consuming and often yield ambiguous results. Other studies either based on giving the general trends of cleat compressibility or the testing condition is comparatively simple. Furthermore, all those studies mainly focused on Basins in America, the result of which may not be suitable to Chinese coal. Therefore, this laboratory study about permeability and cleat compressibility is quite necessary and has important guidance to the exploration of Chinese CBM.

After experimental testing, calculation and analysis, some conclusions can be drawn:

The Langmuir volume is 17.24, 27.78 and 40.00 m^3/t, and the Langmuir pressure is 2.72, 1.83 and 1.32 Mpa when tested using N_2, CH_4 and CO_2 in sequence. Adsorption amount of CO_2 is about 1.5 times than that of CH_4 and is about 3 times than that of N_2 over the measured pressure range. Effective stress has important effect to permeability. With increasing effective stress, permeability decreases at the same pore pressure. With increasing pore pressure, permeability decreases at the same effective stress when using four kinds of gases, which are He, N_2, CH_4 and CO_2. When effective stress reaches nearly 6 Mpa, permeability gets close to the same value individually for four kinds of gases. Cleat compressibility by He is about 0.10 $Mpa^{-1,}$ is about 0.11 by N_2 and CH_4 and is about 0.12 by CO_2 at 35°C. While it is about 0.12 by N_2 is about 0.11 by CH_4 and 0.13 by CO_2 at both 40°C and 45°C. This result is about twice than that of Australian coal, which is about 0.05 Mpa^{-1}. Furthermore, cleat compressibility decreases with increasing pore pressure for all gases; while cleat compressibility increases at the same pore pressure with increasing temperature.

The reasons that permeability and cleat compressibility has corresponding laws may contribute to the following factors: effective stress, Kelinkenberg effect, cleat spacing, geological structure, asperities in the cleats, adsorption capacity and so on. After analyzing the experimental data and summarizing literature, effective stress is considered as the principle control factor to both permeability and cleat compressibility. The experimental data was used in the S&D model. The modeling result show that permeability declines more significantly with variable cleat compressibility than a constant one. Moreover, k/k_0 has the minimum at the CO_2 fraction of 0.7, before which the curve of k/k_0 is decline and after which it raises. This modeling curve changing with CO_2 Molar fraction can be used to predict the permeability value during the ECBM process in China.

ACKNOWLEDGEMENTS

This research is funded by National Major Research Program for Science and Technology of China (Grant No. 2011ZX05042-001); National Natural Science Foundation (Grant No. 41272176); National Natural Science Foundation (Grant No. 41072188); 973 plan (Grant No. 2013CB227903).

REFERENCES

Brace, W. F et al. 1968. Permeability of granite under high pressure. *Journal of Geophysical Research.* 73(6), 2226–2236.

Charles, R. N 2001. Geologic controls on effective cleat porosity variation in San Juan Basin Fruitland formation coalbed reservoirs. The International Coalbed Methane Symposium. *The University of Alabama, college of Engineering* 0108 11–16.

Close, J.C 1993. Natural fractures in coal. In hydrocarbons from coal, AAPG studies in geology #38, *American Association of Petroleum Geologists, Tulsa, Oklahoma,* pp.651–655.

Dabbous, M.K et al. 1974. The permeability of coal to gas and water. *SPEJ,* Dec 563–72.

Gu Fagang 2009. Reservoir and Geomechanical Coupled Simulation of CO2 Sequestration and Enhanced Coalbed Methane Recovery. *University of Alberta.*

McKee, C. R et al. 1988. Use of barometric pressure to obtain In-situ compressibility of a coalbed methane reservoir. *SPE* 17725(13–15).

Palmer, I & Mansoori, J 1996. How permeability depends on stress and pore pressure in coalbeds, a new model. *Annual Technical Conference and Exhibition Denver, Colorado,* SPE 36737.

Palmer, I & Mansoori, J 1998. How permeability depends on stress and pore pressure in coalbed: a new model. *SPEREE* 1(6), 539–544.

Pattison, C.I et al. 1996. Nature and origin of fractures in Permian coals from the Bowen Basin, Queensland, Australia. Coalbed Methane and Coal Geology, *London.* Pp 131–150.

Pekot, L. J & Reeves, S.R 2003. Modeling the effects of matrix shrinkage and differential swelling on coalbed methane recovery and carbon sequestration. Proceedings of the 2003 International Coalbed Methane Symposium. *University of Alabama,* 0328.

Pomeroy, C. D & Robinson, D.J 1967. The effect of applied stresses on the permeability of a middle rank coal to water. *Int. J.Rock Mech. Min.* Sci 4, 329.

Puri, R & Seidle, J.R 1991. Measurement of Stress Dependent Permeability in Coal and Its Influence on Coalbed Methane Production. Coalbed Methane Symposium, *Tuscaloosa* May, 13–16.

Reiss, L.H 1980. The reservoir engineering aspects of fractured formations. *Gulf Publishing Company*.

Scorer, J. D & Miller, F.G 1974. A review of reservoir rock compressibility and its relationship to oil and gas recovery. *Institute of Petroleum Study* IP, 74–003.

Progress in Mine Safety Science and Engineering II – He et al. (Eds)
© 2014 Taylor & Francis Group, London, ISBN 978-1-138-00122-0

Impact of air-return lane and gas drainage lane spacing on surrounding rock stress

You-Chang Lyu, Man Wang & Ying-Wei Wang
Institute of Energy and Chemical Industry, China Pingmei Shenma Group, Pingdingshan, China

ABSTRACT: The spacing between gas drainage lane and air-return lane has a direct influence on stress concentration caused by tunneling. Typically, the stress concentration increases with reducing distance. However, the design of very large pillar width has consequences such as: ①reducing the gas emission effect from gob through gas drainage lane; ②increasing costs of tunneling; ③lowering recovery rate of coal and resulting in waste of resources; and ④adverse impact in mining next level coal. In order to research an appropriate spacing between air-return lane and gas drainage lane, the stress state of various widths of the pillar is simulated based on Mohr-Coulomb plastic failure criteria using FLAC3D. According to the numerical simulation results of wall rock stress and goaf stress in different coal pillar width, determine an appropriate spacing between air-return lane and gas drainage lane. This research results provide theory guidance for improving the safety in roadway excavation and reducing coal and gas dynamic disasters.

1 INSTRUCTION

The spacing between gas drainage lane and air-return lane has a direct influence on stress concentration caused by tunneling. In general, the degree of the stress concentration will be low and the interaction between two tunnels will be small if the spacing is large. But the very large pillar width results in a low gas emission rate. All these result in waste of resources, and the coal pillar as a stress concentration area also has an effect on mining the coal seam lying bellow it (Khalib & Antonin 1979, Ji et al. 2010). For large depth of the first mining face, the stress and gas pressure are large, so there is a problem what is an appropriate spacing between gas drainage lane and air-return lane will control the wall rock stress values in a reasonable range, in order to reduce the risk of dynamic disasters (He & Duan 2003). So we need to simulate stress of pillars of different widths, in order to analyze the stress distribution and determine a reasonable distance (Siebrits & Elbel 2000).

The model was built based on actual geological mining conditions of Ji_{15}–32020 Face in Mine No. 5 of Pingdingshan Coal Group (PCG). It is a protective layer mining face at close range, the seam dip angle is 12°–13°, recoverable coal seam thickness is 1.2 m–1.5 m, and it is 3 m–17 m away from Ji_{16} and Ji_{17} long wall face. Since the upper layer of coal used protection layer mining measures, while mining the protective layer, a large number of gas emissions which is a serious impact on coal mining safety. Especially as the first mining face in this level, too broad coal pillar will impact for follow mining. Ji_{15}–32020 as a protective layer for Ji_{16} and Ji_{17} coal mining, the relief arising from recovering will lead to a large number of gas emission. Gob also led to a stress concentration around gas emission lane, the deformation of the lane will also have some effect on gas drainage in goaf. Also, the gob has a large impact on the support of gas emission lane and return air lane before recovering layer.

2 NUMERICAL SIMULATION MODEL

According to the actual geological mining situation of the work face (Figure 1), a numerical simulation model is established (Economides & Nolte 2000). The model size is 220 m (length) × 140 m (width) × 100 m (height).

The displacement of vertical is fixed by bottom boundary, around the direction of the boundary fixed their horizontal displacement. A 27 MPa uniform load is given to the top of the boundary in the model. The original size and direction of principal stress are decomposed by testing results, and were given to the border around of the model (Wang 1994). This model uses the Mohr-Coulomb plastic failure criteria (Cyhbiob 1965). This model is used to analyze the impact of air-return lane and gas drainage lane spacing on wall rock stress.

Because of the boundary effect, a 20 m-wide boundary region is set on the up-side of gas drainage lane (Figure 1). In order to study the influence on wall rock stress after coal mining, a 200 meters'

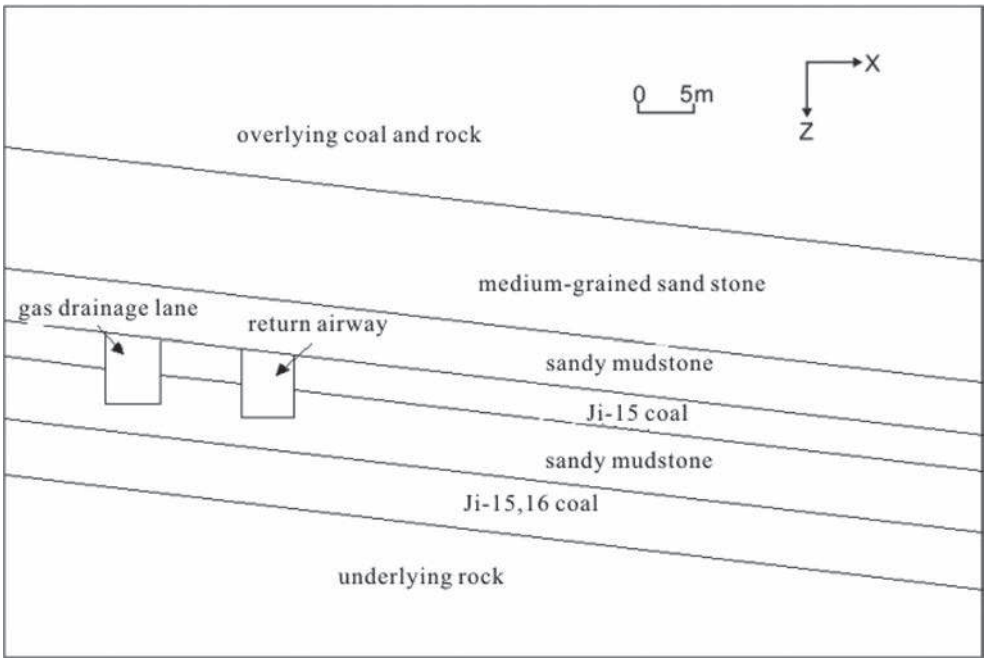


Figure 1. Longitudinal cross-sectional schematic view of lithology and structure.

Table 1. Mechanical Parameters of Model Material.

Litho logy	Bulk modulus (GPa)	Shear modulus (GPa)	Friction angle (o)	Cohesion (MPa)	Dilation angle (o)	Tensile strength (MPa)
Medium-grained sandstone	13.4	7	39	30	15	10
Underlying rock	8.8	5.4	37	15	0	5
Ji-15 coal	4.2	2	20	1	0	1
Sandy mudstone	10.8	5.8	35	27	9	8
Ji-16, 17 coal	4.2	2	20	1	0	1
Overlying cal and rock	13.4	7	39	30	15	10
Mudstone	8.8	5.4	37	15	0	5

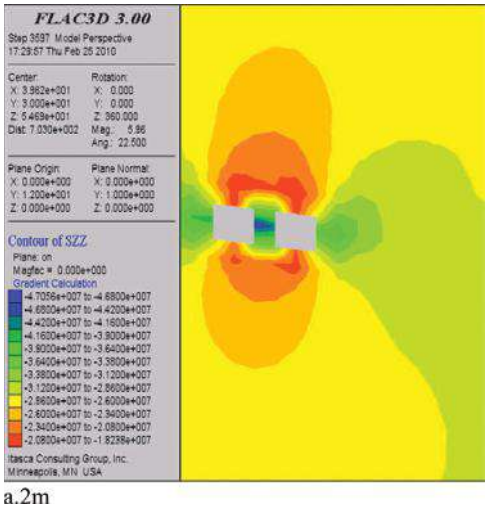
model unit was built at the low-side of the air-return lane, which is used to simulate the 190 m in the face length, seam dip is 7°. The parameters of different coal seams are given in Table 1 (Marchuk 1973), the data come from laboratory determination of field samples and calculated according the Wang Youan Formula (Wang et al. 2013).

3 ANALYSIS OF SIMULATION RESULTS

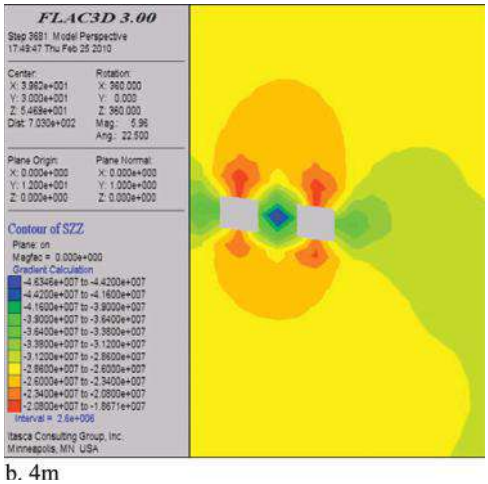
3.1 *Air-return lane and gas drainage Lane pitch on the stress distribution of wall rock*

Four cases were simulated, including two lane pitch 2 m, 4 m, 6 m, 8 m, then vertical stress near the two lanes were compared. Roadway vertical stress cloud about different pitch were given in Figure 2, in this Figure we can see that stress superposition region in the overlying rock tunnel began to separate and the stress concentration zone decreased significantly while the pitch was increased from 4 meters to 6 meters, so 6-m interval is a more appropriate spacing than 2-m and 4-m. Next discuss the two of 6-m and8-m interval which is more appropriate.

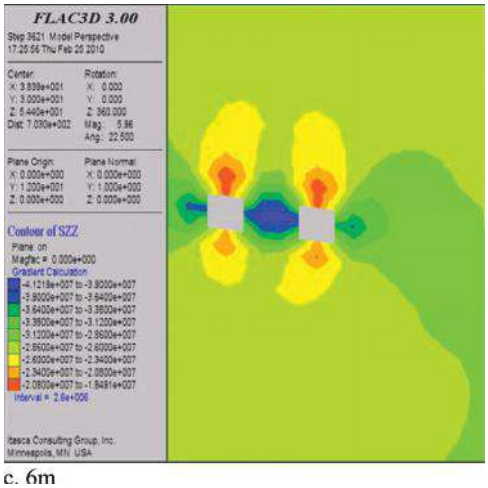
In Figure 3 and Figure 4 the vertical stresses of two sides of air-return lane and gas drainage lane were analyzed separately. The vertical stress rapidly reduces because the relief role of roadway excavation at the central axis between the two lanes, in order to facilitate observation and analysis, these points are canceled in the figure.



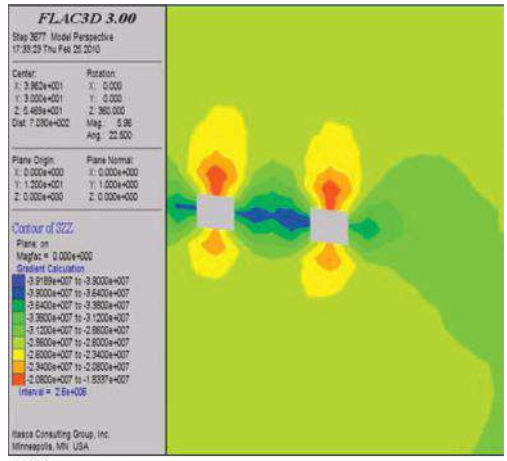
a.2m



b. 4m



c. 6m



d. 8m

Figure 2. Vertical stress contour of different roadway pitch.

Based on the analysis of simulation results, it can be seen that the peak value of stress concentration induced while these two lanes were tunneled appeared in the coal column between them. The stress concentration eased and the maximum peak stress decreased while the distance between two lanes increase. Compare the vertical stress distribution of low-side of air-return lane in different roadway spacing, we can see that the range of stress concentration area reduced. while the pillar width increased. While the pillar width increased from 6 m to 8 m, the value of vertical stress and stress gradient increase in the low-side wall of gas drainage lane and air-return lane, the possibility of dynamic disasters increase. This situation also appears at the up-side of air-return lane. Therefore, a 6 m interval is a more appropriate spacing than 8 m.

So a 6-m interval is a more appropriate spacing than 8-m, 4-m and 2-m interval.

3.2 *Impact of goaf on wall rock stress of air-return lane and gas drainage lane*

The coal mining gradually after gas drainage lane and air-return lane excavation completed. Considering the recovery of mined areas and the overlying rock caving situation, the bulk modulus and shear modulus were taken to 1/10. Then we compare and find the changes of vertical stress in gas drainage lane and air-return lane before and after sloping.

The vertical stress distribution of work face before and after recovering was shown in Figure 5 and Figure 6. Based on the simulation results, we

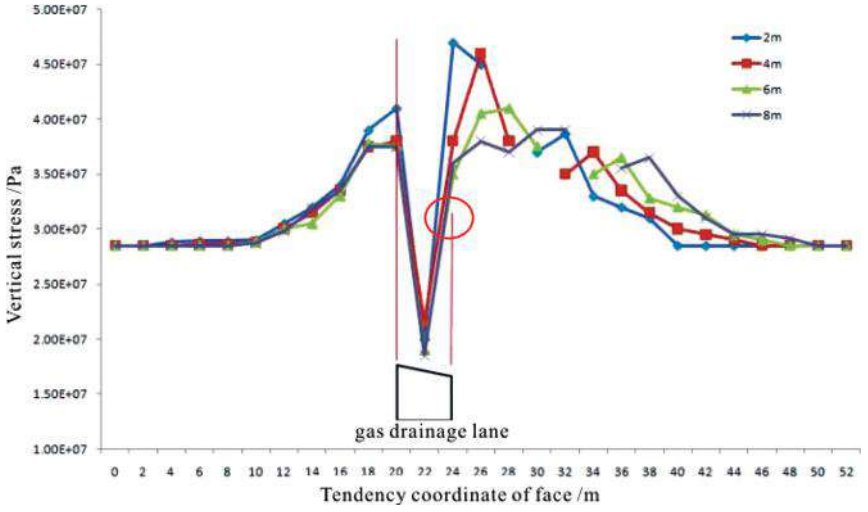


Figure 3. Vertical stress of two sides of gas drainage lane in different distances.

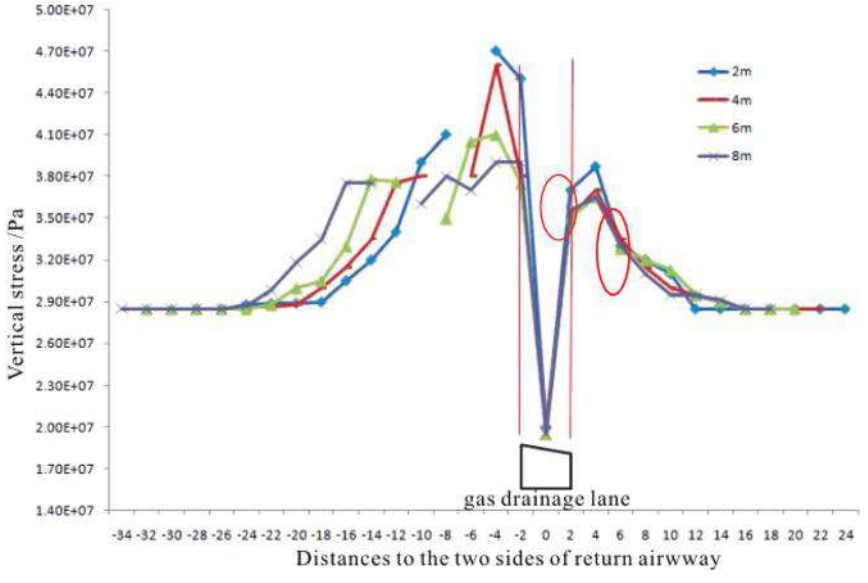


Figure 4. Vertical stress of two sides of return air lane in different distances.

can see that resulting in the recovering of mined areas, vertical stress in mined areas has re-distribution and the concentration of stress at low-side of the gas emission lane increasing dramatically, to nearly 80 MPa, which is more than 2 times before recovering. At the same time, the vertical stress gradient at gas drainage lane also increases and the relief zone width decreases. In this case, if the coal pillar deformation is not sufficient, a high degree of stress concentration will be the main reason that rockburst and coal outburst.

Therefore, the recovery of work face should note the falling of gob and fracture situation of overburden.

Figure 7 and figure 8 show a vertical stress distribution of before and after recovering while 20 m

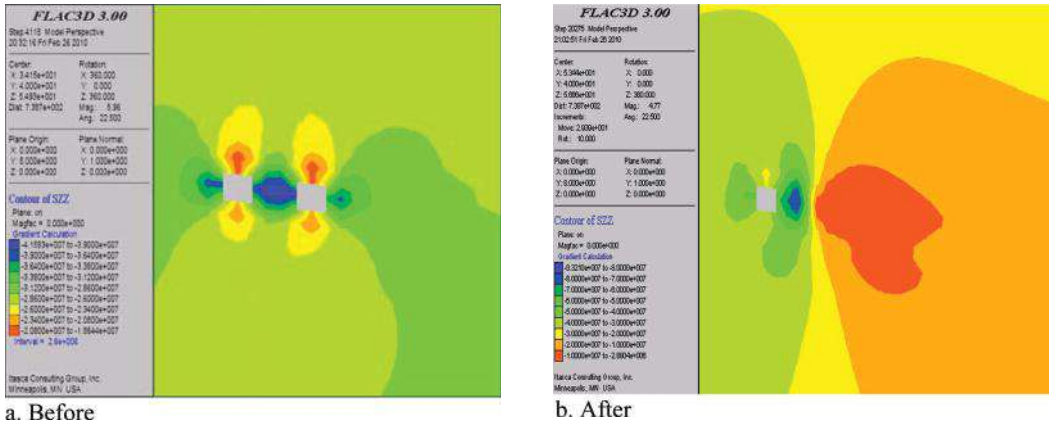


Figure 5. Vertical stress cloud mined area 40 m from mining line before and after mining.

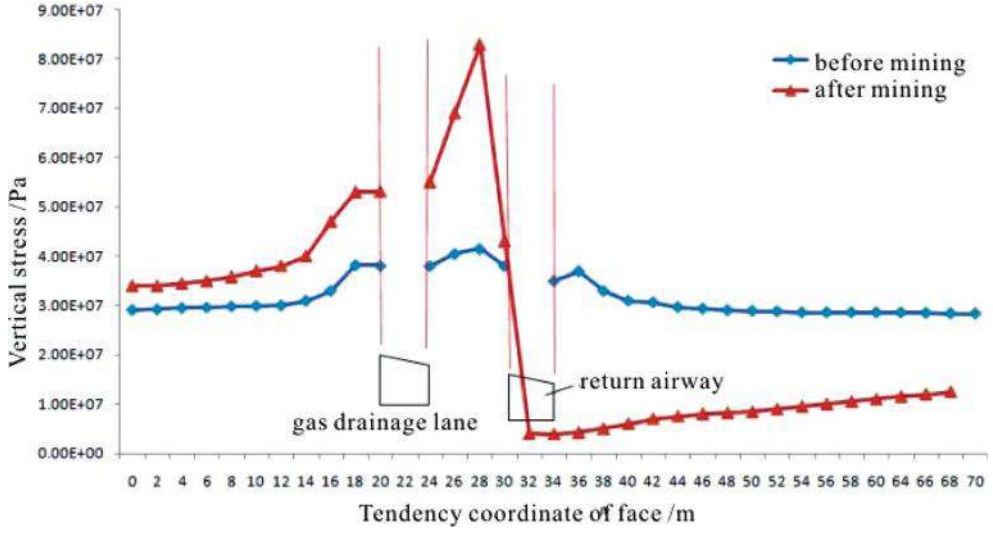


Figure 6. Vertical stress comparison in mined area 40 m from mining line before and after mining.

ahead of coal face. With the advance of mining face, the vertical stress gradually transfer to front coal of recovering coal face. At the same time, stress concentration of gas drainage lane and return air lane at both sides of work face was also increased significantly, pillar peak stress increases, stress gradient increases. Stress gradient reflects the size of accumulation energy of coal and rock (Wang G, 2013), the higher the stress gradient, the greater the energy savings of coal and rock, the greater risk of occurrence of dynamic disasters like rockburst, coal and gas outburst which can cause death. So for the deep mining work face, we should strengthen the roadway in the range of 20 m in the mining face.

4 CONCLUSION

1. The results show that the range of stress concentration region narrows gradually while the pillar width increases. The simulation results show that 6 m is a suitable interval for reducing dynamic disaster risk and improving gas emission efficiency.
2. After goaf forms, wall rock stress redistribute. The vertical stress concentration at low-side of gas drainage lane increases rapidly.
3. Spatial relationship between the roadway caused by the different stress distribution is different.

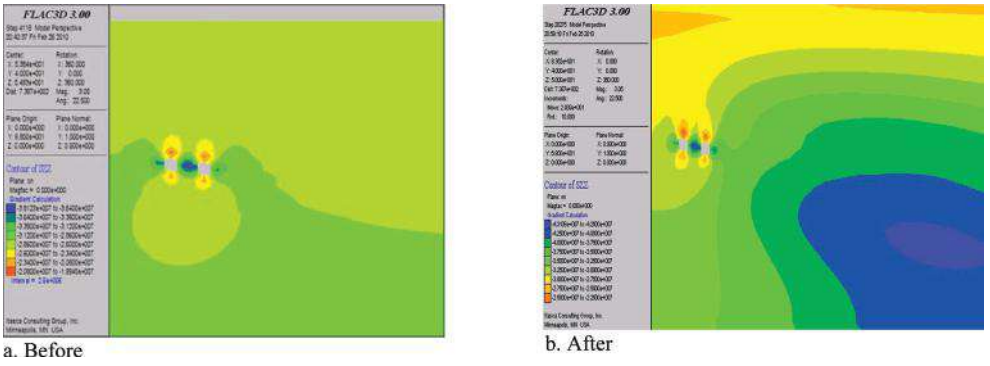


Figure 7. Vertical stress cloud mined area 20 m mining line before and after mining.

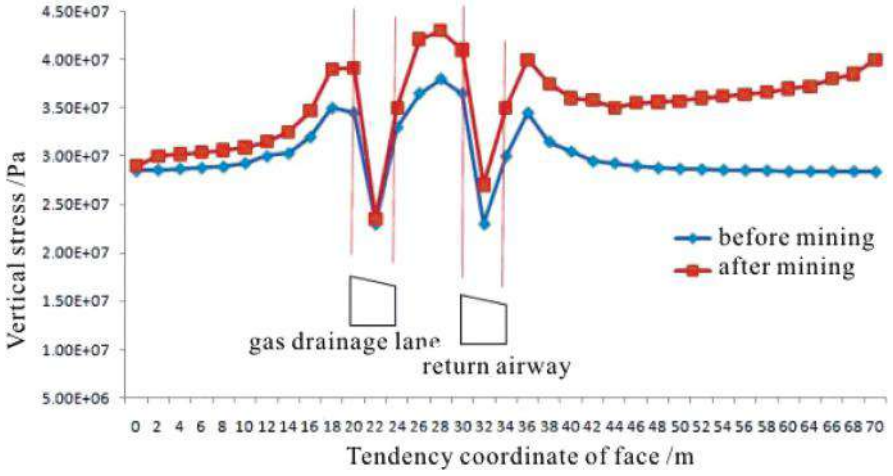


Figure 8. Vertical stress comparison in mined area 20 m mining line before and after mining.

So mining roadway should be designed below the mined-out area where the wall rock stress reduces and the wall rock stress change rate is the minimum.

ACKNOWLEDGEMENTS

This work was financially supported by National Basic Research Program of China (973 Program) (2011CB201201).

REFERENCES

Cyhbiob, H.H., 1965. Underwater and air explosions base. National Defence Industry Press, Beijing.

Economides, M.J., Nolte, K.G., 2000. Reservoir Stimulation. John Wiley & Sons Ltd, New York.

He, G.G., Duan, C.Y., 2003. Energy saving engineering research and application of water pressure blasting. *China Engineering Science,* 5(3):43–46.

Ji, W.P., Liu, C.Y., Guo, W.B., 2010. Numerical Simulation of Coal Pillar Width for Protecting Main Roadway in Extremely Thick Coal Seam. *Coal mining Technology,* 15(5):32–34.

Khalib, A., Antonin, S., 1979. Petroleum Reservoir Simulation. Applied Science Publishers Ltd, London.

Marchuk, G.I., 1973. Methods of Numerical Mathematics. Springer-Verlag Berlin-Heidelberg, Berlin.

Siebrits, E., Elbel, J.L., 2000. Refracture Reorientation Enhances Gas Production in Barnett Shale Tight Gas Wells. SPE Annual Technical Conference and Exhibition, Dallas.

Wang, G., Cheng, W.M., Sun, L.L., 2013. Analysis of Influencing Factors for Coal Seam Gas Pressure and Gas Pressure Gradient. *Safety In Coal Mines,* 44(2):152–156.

Wang, Y.A., 1994. Mine gas control. Coal Industry Press, Beijing.

Progress in Mine Safety Science and Engineering II – He et al. (Eds)
© 2014 Taylor & Francis Group, London, ISBN 978-1-138-00122-0

Research on distribution and evolution patterns of abutment pressure in front of the fully-mechanized working face of "three-soft" coal seam isolated island

W.Q. Xu
Shaanxi Coal and Chemical Technology Institute Co., Ltd., Shaanxi, Xi'an, China
Xi'an University of Science and Technology, Shaanxi, Xi'an, China

E.Y. Wang & Z.T. Liu
Faculty of Safety Engineering, China University of Mining and Technology, Xuzhou, Jiangsu, China

E.K. Hou
Xi'an University of Science and Technology, Shaanxi, Xi'an, China

S.J. Wang & Z.S. Deng
Shaanxi Coal and Chemical Technology Institute Co., Ltd., Shaanxi, Xi'an, China

ABSTRACT: Combining a self-developed mining-induced stress monitoring system and numerical simulation, the front abutment pressure of the fully-mechanized island workface in three-soft coal seam is studied. The effect of abutment pressure distribution on strata behavior is also discussed. Research results show that mining-induced advanced influence distance of the fully-mechanized island workface in three-soft coal seam is larger than that of the general working face. Besides, the fracture zone in front of the working face is widened to some extent, and the influence range caused by loosening on both roadways becomes larger with working face advancing ahead. Moreover, it is revealed that mining work has significant effect on strata behavior at fully-mechanized island workface in three-soft coal seam. And strata behaviors mostly emerge in stress concentration area. The research results have an important reference value for revealing the distribution pattern of front abutment pressure of the fully-mechanized island working face in three-soft coal seam and for controlling coal and rock dynamic disasters occurring under similar mining conditions.

1 INTRODUCTION

The mining-induced stress is resulted from the redistribution of original rock stress caused by underground mining engineering. When the redistributed stress exceeds the limit of coal-rock bodies, self-stabilization of surrounding rocks will fail and sudden instability may occur in severe cases, causing coal-rock dynamic disasters such as coal and gas outburst and rock burst, etc. (Cao and Miao et al., 2001; Cao et al., 2011; Kang 2008; Lv et al., 2011; Qian and Shi, 2003; Wang, et al., 2008). As "three soft" coal seam has low compressive strength and weak bearing capacity, coal and gas outburst easily occurs under the combined action of gas and stress. Influenced by stress superposition of adjoining goaf, the degree of stress concentration for working face of isolated island will be intensified. Meanwhile, the possibility and severity of some coal-rock dynamic disasters such as burst and wall caving, etc will be higher and more serious (Yan et al., 1996), so that the problem of "three soft" coal seam is the key for preventing some coal-rock dynamic disasters such as coal and gas outburst. Nowadays, emphasis for domestic mining-induced stress studies at the working face is on the vertical stress in front of the working face, that is, the abutment pressure. e.g. Qin et al. (2004) has analyzed and studied the distribution of abutment pressure and its transmission pattern in floor at the fully mechanized caving face of isolated island in 4303 deep shaft of Dongtan Coal Mine; Cheng et al. (2008) has simulated and studied the distribution pattern of stress formed during the formation process of folding structures and the variation pattern of local stress filed caused by mining at the working face using FLAC2D software; Liu et al. (2007) has correlated and analyzed the distribution characteristics of abutment pressure of the working face of super long isolated island using FLAC3D

software; Huang et al. (2007) has simulated and analyzed the distribution pattern of abutment pressure of the fully mechanized caving face of isolated islands with different lengths and the deformation and failure patterns of coal pillars with different widths using FLAC3D software. However, there are few measurements and researches on the abutment pressure, especially the abutment pressure of fully-mechanized working face of "three-soft" coal seam isolated island.

The paper bases the coal seam occurring conditions of fully mechanized working face of 11061 "three soft" coal seam isolated island of Liangbei Coal Mine of Henan Shenhuo Group Co. Ltd and adopts the self-developed mining-induced stress testing system to measure stress distribution and evolution patterns of the working face, and also comprehensively studies the distribution pattern of coal abutment pressure in front of the working face of "three soft" coal seam isolated island by combining FLAC3D simulation technique, thereby analyzing the effect of distribution of abutment pressure in front of the working face of "three soft" coal seam isolated island on the mine strata behavior, which can provide accurate space evolution data of abutment pressure for preventing the coal-rock dynamic disasters of fully-mechanized working face of "three-soft" coal seam isolated island such as coal and gas outburst, etc.

2 FIELD TEST OF MINING-INDUCED STRESS

2.1 *Field overview*

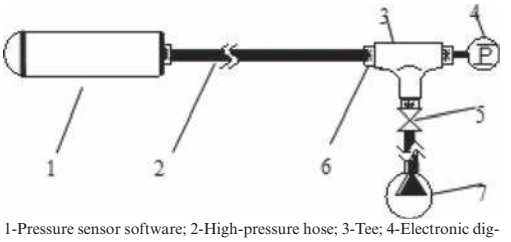
The coal seams for 11061 working face of Liangbei Coal Mine of Henan Shenhuo Group Co. Ltd have a buried depth of 455–486 m, an average thickness of 3.4 m and a dip angle ranging from 10 degrees to 12 degrees 30 minutes and averaging 12 degrees, the coefficient of firmness of coal seam f is 0.2. The direct roof of coal seam consists of sandy mudstones and has a thickness of 5.41 m, with well-developed horizontal bedding, while the old roof consists of medium-to-coarse-grained sandstones and has a thickness of 3.2 m, with horizontal and small bedding. The direct floor consists of the interbed of banded mudstones and siltstones, with a thickness of 7.68 m, and mudstones are in stripped form, while the old floor consists of interbed of sandy mudstones or fine-grained sandstones, with the transparent thin bedding. The 11061 working face is 120 m long and adopts retreating long-wall fully mechanized coal mining methods for mining. Above and below are 11041 working face goaf and 11081 working face goaf respectively and they are typical fully mechanized working faces "three soft" coal seam isolated island. Influenced by some faults such as FS1 and DF29, etc nearby the mining zone, some secondary geological structures occur within the working face, and folds, faults and fracture zones are well-developed in the area, and the integrity of roof of conveyor roadway is worse than that of wind road.

2.2 *Mining-induced stress testing system*

The self-developed mining-induced stress testing system includes one new inductive probe, and its highest initial abutment pressure can reach 40 MPa and maximum radial expansion amount is 20 mm, which can ensure the automatic adaptation and coupling between sensor and coal and rock bodies (including broken coals and rocks), thereby accurately monitoring stress intensity and variation of the coal seam. Using the system, the continuous and real-time testing on original coal and rock bodies and the mining-induced stress of coal and rock bodies under complex geological conditions can be achieved. The Mining-induced stress measuring equipment system is as shown in Figure 1.

2.3 *Measuring point layout*

The measuring points for the mining-induced stress in front of the fully mechanized working face of 11061 "three soft" coal seam isolated island of Liangbei Coal Mine are laid out as follows: six measuring points are laid out horizontally in the coal at the lower side of wind road and four measuring points are laid out horizontally in the coal at the upper side of conveyor roadway. Space between each measuring point of wind road and conveyor roadway is 3 m. Among them, the measuring point 1# at the lower side of wind road is 142 m from the working face, while the borehole depth of measuring points 1# to 6# is 10 m, 9 m, 8 m, 6 m, 5 m and 4 m respectively; the measuring point 1# at the upper side of conveyor roadway is 145 m from the working face, while the borehole depth of measuring points 1# to 4# is 10 m, 9 m, 8 m and 5 m respectively. Site layout schematic diagram is as shown in Figure 2.



1-Pressure sensor software; 2-High-pressure hose; 3-Tee; 4-Electronic digital hydraulic converter; 5-Valve; 6-Quick coupler; 7- High pressure pump

Figure 1. Schematic diagram of device for continuous stress measurement.

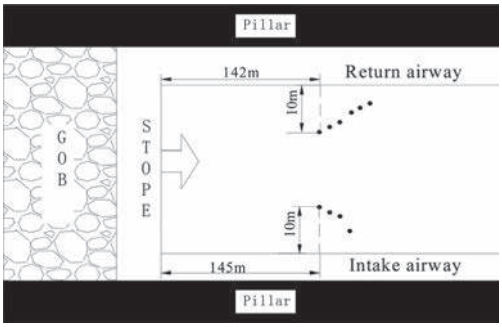
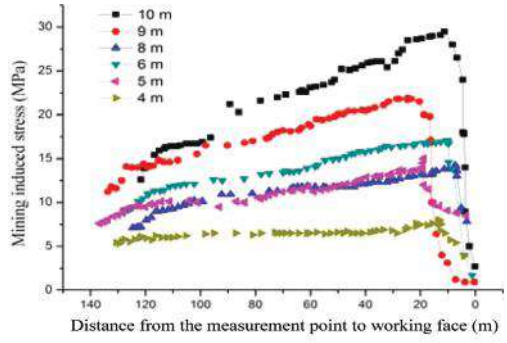


Figure 2. Schematic diagram of stress measuring monitor of entity coal in front of working face.

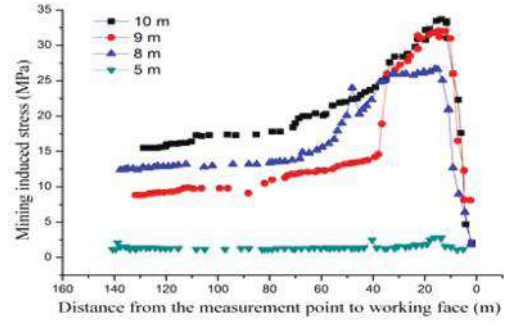
By this layout way of measuring point, the abutment pressures and their variations that occur in different locations and have different distances to the side wall of roadways along the strike of coal bodies in front of the working face can be monitored simultaneously. In the strike, with the advance of working face, the distance from the measuring point to the working face gradually decreases until the working face arrives at the measuring point. While in the dip, the variations of abutment pressures of coal body at both sides that have different distances to side wall can be tested simultaneously. At each measuring point, the abutment pressure can be continuously measured during the process when the working face reaches the place where the measuring point is located, and thus the real-time monitoring on the stress value of each measuring point can be achieved under the premise that the production doesn't be influenced, moreover, according to different distances from working face to measuring point and different buried depths of measuring points along the dip, the distribution and variation patterns of the abutment pressure in front of the working face of "three soft" coal seam isolated island in different locations to the working face and at different distances to the side wall of roadways, as well as the effects on strata behavior, are analyzed and revealed.

2.4 *Testing results analysis*

The Figure 3 is the curve of abutment pressure variation caused by the advance of working face at each measuring point in the wind road and conveyor roadway at 11061 working face. It can be seen from the Figure that the pressure value at the measuring point along the strike gradually increases to a peak value and sharply decreases with the advance of working face, while the range of increase of stress in the dip tends to increase with the increase of distance from the measuring point to the side wall of roadways.



(a) Return airway



(b) Intake airway

Figure 3. Curve of abutment pressure changing with the distance to working face.

(1) Distribution and evolution patterns in the strike

It can be seen from the Figure 3 (a): curve of stress variation at each measuring point in the wind road that when the working face is 125 m from the measuring point 1#, the sensor of partial measuring points has had the tendency to rise, which indicates that the influencing distance of mining in the wind road is about 125 m. When the working face is about 95 m from the measuring point 1#, the pressure values at the measuring points 1# and 2# increase by leaps and bounds one after another, while the pressure values in other measuring points begin to increase slowly; when the working face is 30 m from the measuring point 1#, the pressure value at the measuring point 1# rapidly increases within a certain range and then increases slowly as that in other measuring points; when the working face is 9 to 13 m from the measuring point 1#, the pressure value at each measuring point successively reaches a peak value and sharply decreases later, the peak pressure of 1# is 29.5 MPa and its relative

initial is 12.5 MPa, and the stress concentration coefficient is 2.4.

It can be seen from the Figure 3 (b) that in the conveyor roadway, when the working face is 120 m from the measuring point 1#, the sensor of each measuring point contacts with the wall of borehole in a coupled way, and the pressure value tends to remain stable. When the working face is 110 m from the measuring point 1#, the pressure value increases slightly at the measuring point 1#, in the case above, the measuring point 1# has been influenced by mining, and the advanced influencing distance of mining in the conveyor roadway is about 110 m, after that the pressure value at the measuring point 2# changes to some extent, while the pressure value in other measuring values increase gently. When the working face is 70 m from the measuring point, the pressure value at the measuring point in deep borehole begins to increase rapidly and shows a periodic and step increase process. When the working face is 40 m from the measuring point, the pressure value at the measuring point increases sharply, the pressure value at the measuring point 2# shows a substantial and jumpy increase process, but due to that coal bodies at the measuring point 3# are crushed and the stress is transferred, so that the increasing range of pressure value is greatly influenced. When the working face is 10 to 15 m from the measuring point, the pressure value at each measuring point reaches a peak value, and stress concentration coefficient of the measuring point 1# is 2.1. After that, the pressure value in each measuring point decreases sharply and all measuring points successively arrive at the fracture zone.

It can be seen from the correlation between the curves of abutment pressure variation along the strike at the measuring point on both roadways that the pressure value at the measuring point in wind road increases slowly, while the pressure value in conveyor roadway increases sharply after a gentle increasing process, which is directly caused by the roof of working face, namely that the roof of the wind road has good integrity but the roof of the conveyor roadway is relatively crushed, the crushed roof absorbs parts of energies under periodical coming pressure, and thus the velocity of increase of abutment pressure is low and the range of increase is weak, moreover, under the condition that the roof is crushed, the stress transfer is weakened and the advanced distance caused by mining in conveyor roadway is smaller than that in wind road. It is calculated that the advanced influencing range of distance in wind road caused by the mining at the fully mechanized working face of "three soft" coal seam isolated island is 125 m, the peak value is 9 to 13 m in front of the working face and the range of abutment pressure decreasing zone is about 6 m. While, the advanced influencing range of distance in conveyor roadway is about 110 m, the peak value is 12 to 15 m in front of the working face and the range of abutment pressure decreasing zone is about 9 m.

(2) Distribution and evolution in the dip

It also can be seen from Fig. 3 that in the dip, the pressure values at the measuring points within 10 meters of the lower side wall of wind road and the upper side wall of conveyor roadway tend to increase with the increase of the distance from the measuring point to the side wall of roadways, moreover, during the stoping process, the range of increase of pressure value at the measuring point in deep borehole is larger than that in shallow borehole.

In the wind road, with the increase of distance from side wall of roadways, the abutment pressure values at the measuring points from 6# to 1# generally tend to increase and the increment of mining-induced pressure at the measuring points from 6# to 1# is 2.1, 4.6, 5, 4.7, 7.2 and 13.9 MPa respectively. It can be seen that the increment of pressure value at the measuring point 1# is far larger than that at other measuring points and reasons are that the stresses at other measuring points are influenced by wall rock loosening to different extents, the coal bodies suffer from plastic deformation and the stresses are transferred. The pressure value at the measuring point 4# is larger than that at the measuring points 3# and 5#, moreover, during the stoping process, the range of increase of pressure value at the measuring point 4# is also larger than that at the measuring points 3# and 5#, which is caused by the superposed stresses of goaf in 11041 working face. A small peak value of pressure has already appeared in the place about 6 m from coal bodies in the lower side wall of wind road prior to mining; in addition, this peak value of pressure always exists with the stoping of the working face.

In the conveyor roadway, with the increase of borehole depth, the pressure values at the measuring points from 4# to 1# also generally tend to increase, and the increment of mining-induced pressure at the measuring points from 4# to 1# is 1.4, 9.5, 22.5 and 16.4 MPa respectively and the range of increase generally tends to increase with the increase of borehole depth, from which it can be seen that the pressure value at the measuring point 3# is larger than that at the measuring point 2# and reasons are that the peak value zone of superposed pressure of goaf in 11081 working face is closer to the measuring point 3# and this peak value of pressure always exists with the stoping of the working face. When the stope is 35 m from the measuring point 3#, influenced by the periodic coming pressure and stress superstition in lower goaf, coal bodies at the measuring point 3# are crushed and can't bear more pressure no longer. The pressure value

at the measuring point 3# decreases sharply after keeping a higher peak value in a range for a period of time. Although the pressure value at the measuring point 2# substantially increases, its peak value is still smaller than that at the measuring point 1#.

It can be seen from the correlation between the abutment pressures of coal bodies at both sides that the plastic deformation of coal body has great effect on the range of increase of abutment pressure, in the area with more serious plastic deformation, the compressive strength is lower, coal bodies are more likely to be deformed and the stresses are transferred, and thus the change of abutment pressure is more unobvious. The superposed stresses formed in adjoining goaf also have great effect on the abutment pressures in front of the working face. A small peak value of pressure appears in the range where the coal body is 6 to 8 m from the side wall of roadways, while the large peak value of pressure is more than 10 m from the side wall of roadways. As roofs of wind road and conveyor roadway have different integrity, so the peak value of superposed stresses formed in adjoining goaf has different distance to the side wall of roadways.

3 SIMULATION RESEARCH ON DISTRIBUTION PATTERN OF ABUTMENT PRESSURE AT FULLY MECHANIZED WORKING FACE OF "THREE SOFT" COAL SEAM ISOLATED ISLAND

3.1 *Establishment of model*

The numerical model is established based on FLAC3D simulation software (Su et al., 2001) by taking geological conditions of fully mechanized working face of 11061 "three soft" coal seam isolated island of Liangbei Coal Mine as the prototype. With the adoption of Mohr-Coulomb failure criterion, contact coulomb gliding mode is used by the joint surface, and for the mining part, zero unit simulation is used through the full-seam mining. Load of the model is obtained from the measuring result of original stress of the site, and physical and mechanics parameters of coal seam and immediate roof are given in accordance with the test result of coal-rock samples provided by the laboratory.

3.2 *Simulation results and analysis*

The Figure 4 is the cloud picture of coal-rock body abutment pressure in front of the working face by simulating 11061 working face entering the whole isolated island.

It can be seen from the Figure 4 that the advanced influencing distance caused by mining

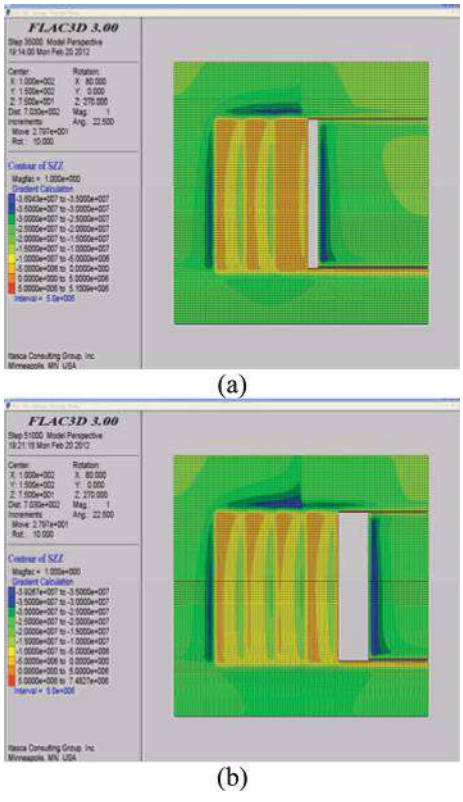


Figure 4. Nephogram of abutment pressure distribution of 11061 working face.

is about 80 m in the vertical direction with the stoping of the working face. The stress rapidly increasing zone is within 6 to 50 m in front of the working face and stress peak is 6 to 10 m in front of the working face, and stress concentration factor is about 2.9. The effect of adjoining goafs on stress distribution in front of the coal wall is different. The scope of coal bodies at the upper side of conveyor roadway affected by superimposed stress in adjoining goaf is obviously greater than that at the lower side of wind road; however, the superimposed stress peak zones are approximately symmetrically from the center of working face, and they are separately located in coal bodies within 6 to 10 m from the upper side of conveyor roadway and the lower side of wind road.

3.3 *Comparison between numerical simulation results and site monitoring results*

The Figure 5 is the curve of comparison between numerical simulation results and site monitoring results. It can be seen that the simulation is

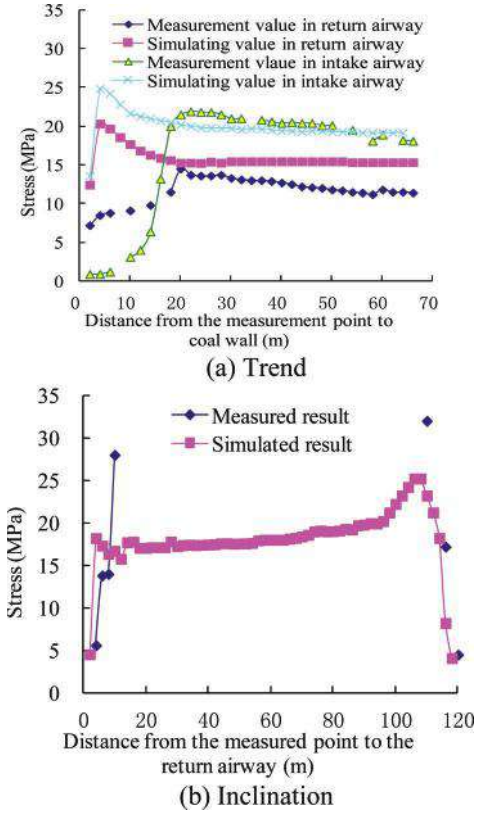


Figure 5. Comparison curve of abutment pressure between numerical simulation and field measurement.

basically anastomotic with the actually measuring results and vertical stress relief zone, stress concentration zone and original stress zone in front of the working face have an obvious distribution. It can be seen from the Figure (a) that, stress peak zone shown in the simulation results is closer to the coal wall, stress distribution curve is smooth and stress rapidly increasing zone is obvious; affected by the periodic weighting, the curve of site monitoring results rises with fluctuations, stress peak zone is about 20 m in front of the working face and stress relief zone is wider, which is more aligned with features of "three soft" coal seam and also can reflect periodic weighting time. It can be seen from the Figure (b) that, both numerical simulation and site monitoring results can reflect stress rising pattern of coal bodies at the side wall of roadways. Site monitoring can't monitor stress distribution pattern at the coal depth affected by the site environment, so numerical simulation can better remedy such defects. Site monitoring results can better reflect real situations of the monitoring scope and are more reliable by combining site environment and comparing between numerical simulation and site monitoring results. The combination of these two methods is complementary each other, through which mining-induced stress distribution and evolution patterns can be more accurately grasped.

4 INFLUENCES OF ABUTMENT PRESSURE DISTRIBUTION OF WORKING FACE OF "THREE SOFT" COAL SEAM ISOLATED ISLAND ON STRATA BEHAVIOR

Influenced by the occurring conditions of coal seam, the structures of wall rocks at the working face and other factors, the advanced influencing distance caused by mining during the mining process of fully mechanized working face of "three soft" coal seam isolated island increases, the fracture zone in front of the working face is widened, and the strata behavior becomes more obvious. As a typical fully mechanized working face of "three soft" coal seam isolated island, coal bodies at the 11061 working face have low compressive strength, and strata behaviors such as wall caving, etc are very likely to occur on the side wall of roadways, so that they can't bear a larger stress. In the wind road, the roof has a better integrity, the abutment pressure begins to increase influenced by mining and two walls obviously approach together within 40 to 70 meters in front of the working face, while within 40 meters in front of the working face, the roadway is severely deformed and the severe strata behavior like wall caving, etc occurs. The roof of conveyor roadway has relatively poor integrity and strata behavior occurs more obviously. Within 40 to 70 meters in front of the working face, some strata behaviors such as floor heave, roof caving or wall caving of roadways or deformation of I-beams occur, while within 40 meters in front of the working face, strata behaviors such as roadway floor heave, roof caving and wall caving, etc are extremely serious. Moreover, parts of single hydraulic props have bursting phenomenon, so that the degree of strata behavior is obviously lager than that in wind road.

5 CONCLUSIONS

5.1 *Equations*

Following conclusions can be obtained by the field testing and numerical simulation research on the distribution pattern of abutment pressure in front of the fully mechanized working face of 11061 "three soft" coal seam isolated island of Liangbei Coal Mine and the effect on strata behavior:

1. The self-developed mining-induced stress testing system can accurately test the variation of mining-induced stress in front of the working face with the advance of working face under "three soft" coal seam geological conditions.
2. The mining-induced advanced influencing distance at the fully mechanized working face of "three soft" coal seam isolated island is 110 to 125 m, while the relative concentration coefficient of abutment pressure is 2.1 to 2.4. There is a small peak value of superposed pressure in a distance of 6 to 8 m along the dip of coal body at the working face in adjoining goaf, while the large peak value zone of pressure is more than 10 m wide. The mining-induced advanced distance at the fully mechanized working face of "three soft" coal seam isolated island is relatively large, so distance from pressure peak value zone to the coal wall also has a certain increase.
3. The abutment pressure at the fully mechanized working face of "three soft" coal seam isolated island has significant effect on strata behavior and strata behaviors such as floor heave, deformation or wall caving of roadways or explosion of props, etc mostly occur in the stress concentration zone. Moreover, roof integrity also has great affect on strata behavior.

REFERENCES

Cao, S.G. and Miao, X.X. 2001. Ground pressure controlling on super-length fully-mechanized mining face with top-coal caving. *Journal of China Coal Society* 26(6): 621–625.

Cao, A.Y., Dou, L.M., Jiang, H., 2011. Characteristics of Energy Radiation and Stress Drop in Different Failure Modes of Mining-induced Coal-Rock Mass. *Journal of Mining & Safety Engineering* 28(3): 350–355.

Chen, G.X., Dou, L.M., Qian, Z.D., 2008. The Stress Field Distribution in Folding Structure Areas and Its Impaction on Rock Burst. *Journal of China University of Mining & Technology* 37(6): 751–755.

Huang, B.X., Liu, C.Y., Zhen, B.S., Cheng, Q., 2007. Distribution abutment pressures on laneway pillars for super wide isolated fully mechanized top coal caving face. *Chinese Journal of Geotechnical Engineering,* 29(6): 932–937.

Kang, H.P., 2008. Analysis on types and interaction of stress fields in underground coal mines. *Journal of China Coal Society,* 33(12): 1329–1335.

Liu, C.Y., Huang, B.X., Meng, X.J., 2007. Research On Abutment Pressure Distribution Law of Over length Isolated Fully-mechanized Top Coal Caving Face. *Chinese Journal of Rock Mechanics and Engineering* 26(1): 2761–2766.

Lv, M.J., Li, X.Z., Li, Y.S., 2011. Study on Mining Stress Distribution Law of Fully Mechanized Coal Mining Face in Thick Seam with Soft Roof. Soft Coal and Soft Floor. *Coal Science and Technology* 39(7): 21–24.

Qian, M.G. and Shi, P.W., 2003. *Mining Pressure and Strata Control*. Xuzhou: China University of Mining & Technology Press.

Qin, Z.C. And Wang, T.X., 2004. Abutment Pressure Distribution And Its Transfer Law In Floor Of Deep Isolated Fully-mechanized Mining Face using Sublevel Caving. *Chinese Journal of Rock Mechanics and Engineering* 23(7): 1127–1131.

Su, S.W., Lin, H., Ren, L.W., 2011. *FLAC3D in geotechnical engineering.* Beijing: China Water Power Press.

Wang, L.G., Song, Y., He, X.Q., 2008. Side Abutment Pressure Distribution by Field Measurement. *Journal of China University of Mining & Technology* 18(4): 527–530.

Yan, J.T., Liang, G.F., An, M.L., 1996. Fore east of Underground Pressure for a Fully-Mechanized Sublevel Caving Face with Four Mined Boundaries. *Journal of China University of Mining & Technology* 25(4): 98–103.

This page intentionally left blank

Progress in Mine Safety Science and Engineering II – He et al. (Eds)
© 2014 Taylor & Francis Group, London, ISBN 978-1-138-00122-0

Study on safety theory of rheology-mutation based on system life cycle

Xue-Qiu He
North China Institute of Science and Technology, Beijing, China

Dai-Ying Zhao
Explosion Science and Technology, State Key Laboratory of Beijing Institute of Technology, Beijing, China
School of Environment Science and Safety Engineering, Tianjin University of Technology, Tianjin, China

ABSTRACT: In order to study the relationship between the theories of rheology-mutation and system life cycles, the two theories and the relationships between the variables they measure are analyzed graphically and via case studies. The results indicate that the two theories exist in a coupling relationship.

1 INTRODUCTION

Safety science addresses the issue of how to assess the degree of risk in systems, and how this risk develops. Accidents and natural disasters are the prime research subjects of safety science.

The general safety law—the theory of safety rheology and mutation and its mathematical model—was put forward by He Xue-qiu in 1998 (He Xue-qiu 1998) and was elaborated by him in 2000 (He Xue-qiu 2001, 2004, 2006). Seventeen safety concepts such as safety damage, safety rheology and mutation were defined in the theory. The mechanisms of change in the emergence, development and dying out of damage in systems were analyzed in detail through use of examples.

Safety and danger are important yet distinct concepts that run throughout system life cycle theory. While safety is relative, danger is absolute. This is because safety is defined as the condition where danger is below a certain acceptable level, and that acceptable level is chosen subjectively. Danger is absolute in the sense that some degree of danger will exist in the system at all times, and cannot be reduced to zero. The curve of safety rheology and mutation represents the status of the damage and its development through every phrase within the system's operation, as per Figure 1(a). On the other hand, the development of every process can also be represented by phases in which it is commencing, growing, stable, declining and withering, and such representation is termed the system life cycle (Cheng Fu-sheng 2009, Hong-Bae Jun 2007, Yu Hai-ying 2011), as per Figure 2(a).

The safety rheology-mutation curve and system life cycle curve both show the path of development from emergence to extinction. Is there any contradiction between them? Is there any relative relationship? Clarifying the relationship between them has important significance in judging the current phase of a system and thus preventing damage.

2 SAFETY RHEOLOGY-MUTATION THOERY

Danger comes into existence with the emergence of a particular thing and runs throughout its life cycle. The status of the danger changes along with that item's development in space and time. The degree of danger faced by the item at a particular time can be represented as damage. The item's safety rheology and mutation process can be expressed as follows, as per Figure 1(a): in the initial phase (OA phase), the growth rate of damage decreases and new order comes into being, increasing gradually; when the new order develops to the mature phase, the perfect new order makes the damage grow slowly (AB phase); after this phase, the order develops chaotically again and the growth of damage accelerates (BC phase). Any particular thing has an inherent damage endurance capability or limit (D point). If damage exceeds its catastrophe limit point, safety mutation will happen and the damage at the mutation point will be the item's critical damage outcome. After the old order is destroyed, the item will develop a new safety status. The physical world exists and develops between safety and danger cycles (He Xue-qiu 1998).

Some typical catastrophic processes, such as mine disasters, people's injury and death, societal reform and mechanical accidents, all have characteristics that can be expressed in terms of safety rheology and mutation theory. Some scholars (He Sha, et al 2011, Ma Shang-quan, et al 2000, Wang Shu-ming, et al. 2009) have also analyzed

construction fires, the spontaneous combustion of oil, traffic accidents and blowout accidents by safety rheology and mutation theory and the results show that those systems conform to the expected characteristics.

3 SYSTEM LIFE CYCLE CURVE

Every system has its own life cycle. For example, the product life cycle is the period of time from a product entering the market to its withdrawal from the market. The equipment life cycle is the length of time from equipment coming into service to its loss of function. A safety measure's life cycle is the period encompassed by the processes of conceiving, designing, applying, using and discarding it.

The S-shaped curve is a kind of system behavior which includes two phases, of exponential and asymptotic growth. Many systems in society exhibit behavior that fits the S-shaped curve, such as the growth of animals or plants, the process of study, and the spread of infectious diseases (Forrester, et al. 1976).

The life cycle processes of growing and withdrawing both conform to the S-shaped curve, so the life cycle curve consists of two S-shaped curves placed symmetrically, as per Figure 2(a). In order to describe the changes in a system's level of order, a variable, sate level, to describe the state is imported. In the initial phase of system, the state variable increases rapidly (OS phase), and then later slows (SA' phase). The system enters a steady-state phase (A'B' phase) after point A' and then enters a withdrawing phase (B'C' phase) after point B'. Point C' is another significant point, because the state variable decreases rapidly before the C' point, but decreases at a much slower rate after that point.

4 ANALYSIS OF SAFETY RHEOLOGY AND MUTATION BASED ON LIFE CYCLE THEORY

Safety rheology and mutation theory and life cycle theory are both general models of item development processes. There are not only similarities but also large differences between them, and hence clarifying the relationships between them will help facilitate effective comparative analysis and elucidate the rules governing the interrelations between their behaviors.

4.1 *Comparative analysis of safety damage, safety degree and state level*

The primary variable used in safety rheology and mutation models is "safety damage", which is denoted by "D". Safety damage reflects the quantity of potential destruction in a system at a particular time. The variable representing a system's safety level is "safety degree", which is denoted by "S". There is a mutually complementary relationship between safety degree and safety damage. The primary variable used in system life cycle theory is "state level", which is denoted by "LEV" (Donella Meadows, et al. 2004, Wang Qifan, et al. 1987.). State level reflects the degree of development of state in that process.

Safety damage and state level are both accumulation variables, however they have different meanings in relation to the systems they describe. The relationship of safety damage to the system is negative, whereas the relationship of state level to the system is positive. For example, environmental pollution, fire temperature, blast pressure and the gas in a coal mine are considered safety damage variables. In contrast, the vision acuity of the eyes, the immunity of the body, the sales volume of products, the quantity of people in society and the reliability of a machine are considered state level variables.

The state variable exists in any particular system at all points in time, and can offer information upon which decisions and actions may be based.

4.2 *Comparative analysis of curve illustrations*

In order to understand the processes that are modeled in safety rheology and mutation theory and system life cycle theory, the development phases and the rate changes will here be analyzed comparatively.

4.2.1 *Comparative analysis of safety damage, safety degree and state level, via illustrations*

Safety damage changes along with lifecycle phase. It goes through a slow growth phase and a rapid growth phase, then comes to the limit point of the system, before finally withering away, as in Figure 1(a). The safety degree variable of the system also varies across the phases, first going through a phase of slow decrease and then one of rapid decrease, until it reaches a zero point as the system withers away, as in Figure (3). Compared to the safety damage variable, the system state variable exhibits a different pattern of change across phases of the process's life. It skips over the growth phase and reducing phases to arrive straight at the dying out phase, as per Figure 2(a).

A comparison of Figure 1(a) with Figure 2(a) shows a strong correspondence between point A and point A', point B and point B', point C and point C', and even between point D and point D'.

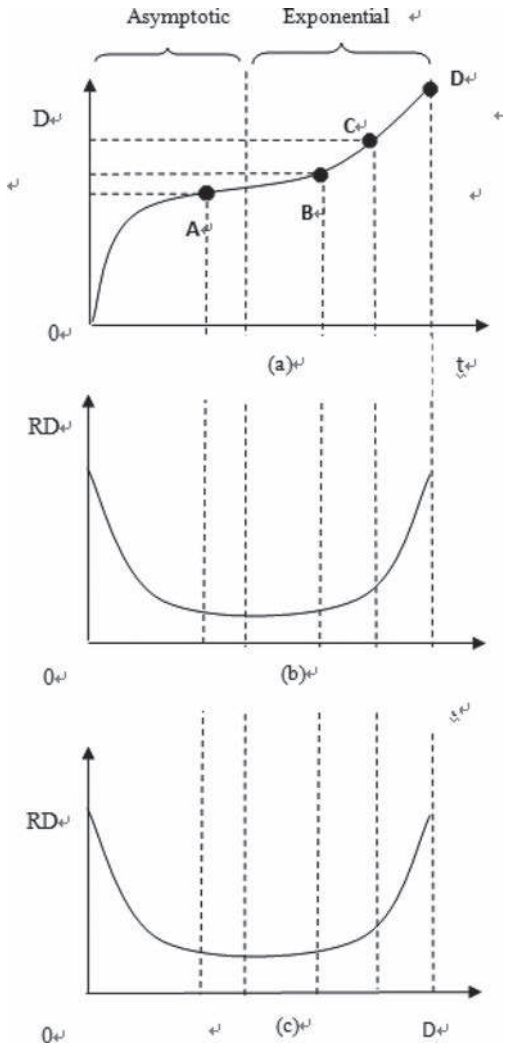


Figure 1. (a) Safety rheology-mutation curve; (b) Change of safety damage over time; (c) Change of safety damage over damage.

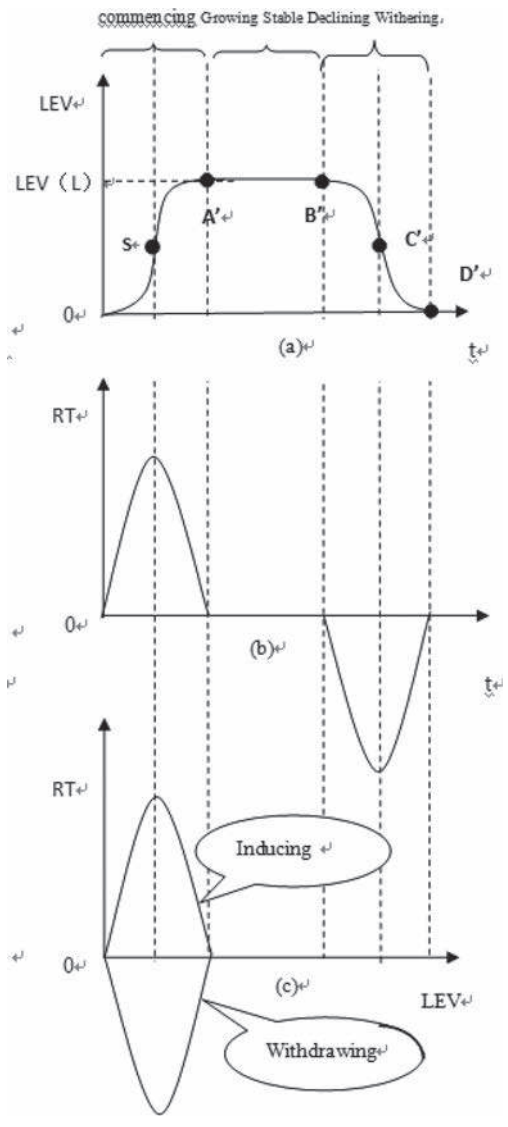


Figure 2. (a) System life cycle curve; (b) Change of state over time; (c) Change of state over state.

The correspondences assist in judging the mutation points.

4.2.2 *Analysis rate of safety damage diagrams*

The rate safety damage variable, denoted by RD, illustrates the changes in safety damage across time, in Figures 1(b) and 1(c). According to Figure 1(b), the curve has three parts: one decreasing, one steady, and one increasing, which match the three periods described by the bathtub curve of reliability: the earlier failure period, the random failure period and the loss failure period.

The bathtub curve represents the curve of the failure rate of a product, which is denoted by $\lambda(t)$ (L. Scheidt, et al. 1994. Niu Peng-zhi, et al. 2007. Wang Rong-hua, et al. 2002) In terms of the maintainability of a product, the failure rate points to the malfunction rate. The rate of failure is also called the rate of damage failure. The rate of safety damage shows the damage probability of system, which is the same as the rate of failure. RD (t) is thus equal to $\lambda(t)$.

Safety damage is the result of accumulation of the rate of safety damage, which is demonstrated

by integral formula (1), so we can define safety rheology and mutation curve as "accumulative damage curve".

$$D = \int_0^t RD(t)d_t = \int_0^t \lambda(t)d_t \tag{1}$$

According to the theory of reliability engineering, the rate of accumulative failure (malfunction) is $H(t) = \int_0^t \lambda(t)d_t$, so D = H(t). Furthermore, the system safety damage function can be calculated according to the distribution of accumulative failure, as follows.

Normal distribution:

$$D = H(t) = -\ln\left\{1 - \phi\left(\frac{t-u}{\sigma}\right)\right\} \tag{2}$$

Logarithmic normal distribution:

$$D = H(t) = -\ln\left\{1 - \phi\left(\frac{\ln t - u}{\sigma}\right)\right\} \tag{3}$$

Exponential distribution:

$$D = H(t) = -t/\theta \tag{4}$$

Weilbull distribution:

$$D = H(t) = t^m/t_0 \tag{5}$$

Extreme value distribution:

$$D = H(t) = e^{(t-u)/\sigma} \tag{6}$$

4.2.3 *Analysis of rate of state diagrams*

The rate of state variable, denoted by RT in Figures 2(b) and 2(c), shows the changes in the value of state over time. Where the rate of state is a positive value, it has periods of in-crease and decrease when in the initial and growing phases; when the rate is a negative value, it has the same periods in the declining and withdrawing phases as in the initial and growing phases respectively. The two curves are placed symmetrically.

5 ANALYSIS OF TYPICAL EXAMPLES

In order to clarify the relationship between safety rheology and mutation theory and system life cycle theory further, some relevant examples are studied as follows:

(1) Machine accidents

According to the cumulative fatigue damage model, there are three phases in the life of a process: damage formation, propagation and damage-instability. These are the same as the trends in rate of change on the accumulative damage curve. On the other hand, the failure rate of a system conforms to a bathtub curve, so it changes along with the accumulative damage. When the accumulative damage reaches the mutation point (C point), an accident will happen.

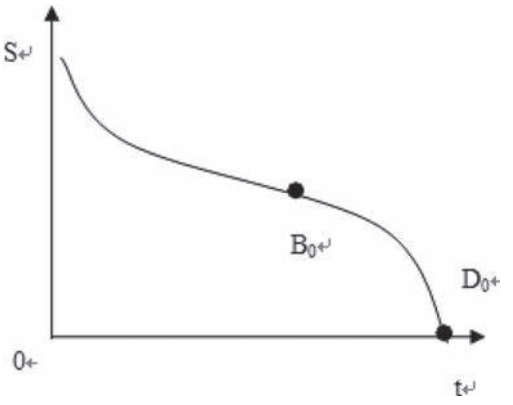


Figure 3. Safety degree curve.

(2) Human life process

The human body will pass through growing, stable and declining stages in life. On the other hand, the probability of sickness changes with changes in immunity. This probability of sickness curve has declining, stable and growing phases, the same as the bathtub curve. When the damage to the body reaches the mutation point (C point), the life will be over.

(3) Mine accidents

The functionality of a coal mine is determined by coal output. It will pass growing, stable and declining stages in the life cycle of the mine. The failure rate, on the other hand, changes with the changes in the amount of order. New order is established step by step in the initial phase of the system life cycle, and is destroyed in the withering phase. The failure rate curve has three phrases: declining, stable and growing, the same as the bathtub curve. When the damage accumulated by the coal mine is enough that the mutation point (C point) is reached, its operation will cease.

(4) Societal reform

A society also will also pass through growing, stable and declining stages in throughout its lifetime. On the other hand, the amount of social conflicts changes with changes in the amount of order. New order is established step by step in the initial phase

of the system's life cycle, and is destroyed in the withering phase. The curve representing social conflict has declining, stable and growing phases, the same as a bathtub curve. When the damage of accumulated by society reaches the mutation point (C point), it will end.

The coupling relationship between safety rheology and mutation theory and life cycle theory has thus been demonstrated by the examples above. Understanding of the phases described can allow for better comparative analysis between the two.

6 CONCLUSIONS

1. The distinction between safety damage and state level was analyzed.
2. The variables involved in safety rheology and mutation theory and life cycle theory models were illustrated graphically.
3. The safety rheology and mutation curve was shown to be equivalent to an accumulative damage curve depending on the degree of accumulative failure, which thus enriches safety rheology and mutation theory.
4. The relationship between damage and its rate of change and the relationship between state level and its rate of change were illustrated graphically.
5. The variables of damage and state were illustrated by figures and the result showed a tight coupling relationship between safety rheology and mutation theory and system life cycle theory.
6. Some typical examples were analyzed and the above relationship between safety rheology and mutation theory and life cycle theory was proved further.

REFERENCES

Cheng Fu-sheng 2009. Life-cycle curve analysis of three-whee led vehicle, *Mechanical Research & Application,* 04: 30–31+35 (in Chinese).

Donella Meadows, et al. 2004. Limits to Growth: The 30-Year Update. UK: Earthscan.

Forrester, et al. 1976. The system Dynamics National Model: Understanding Socio-Economic Behavior and Policy Alternatatives, *Technological Forecasting and Social Change,* 9: 51–68.

He Xue-qiu. 1998. Basic Characteristics of Occupational Safety in China. *China safety Science Journal,* 8: 5–9 (in Chinese).

He Xue-qiu, et al. 2001. Research on Model of "R-M" Theory in Safety Science. *Journal of China University of Mining & Technology,* 30: 425–428(in Chinese).

He Xue-qiu. 2004. Safety Engineering Science. XuZhou: China University of Mining & Technology (in Chinese).

He Xue-qiu, et al. 2006. The New Progress in Study on Safety Rehology-mutation Law of System, *Journal of basic science and engineering,* 14:159–165 (in Chinese).

He Sha, et al. Application of Safety Rheology-Mutation Models in well blowout accidents, *Natural Gas Industry,* 31:109–112.

Hong-Bae Jun, et al. 2007. Product Life-Cycle Metadata Modeling and Its Application with RDF, *Transactions on Knowledge and Data Engineering.*19:1680–1693.

Ma Shangquan, et al. 2000. Application Research on Rheoloy and Mutation Mechanism in Coal and Gas Outbursts, *Jiangsu Coal,* 3:13–15.

Niu Peng-zhi, et al. 2007. Fatigue Accumulative Damage Model of RC Beam Strengthened with Carbon Fiber Laminate, *Journal of South China University of Technology (Natural Science Edition),* 35:23–26(in Chinese).

Scheidt L., et al. 1994. An Approach to Achieve Reusability of Electronic Modules, *Int'l Symp. Electronics and the Environment (ISEE '94)*:331–336.

Wang Shu-ming, et al. 2009. Safety Input Decision2 making Based on Theory of "Rheology-mutation", *China Safety Science Journal,* 19: 46–51.

Wang Rong-hua, et al. 2002. The Failure Rate Function of W eibull Distribution in Progressive Stress Life Testing for the TFR, TRV and CE Models, *Operations Research and Management Science*. 11:47–55 (in Chinese).

Wang Qifan, et al. 1987. Theory and Application of System Dynamics. Beijing: New Times Press.

Yu Hai-ying, et al. 2011. Application of Life Circle Curve Model in High-tech Product Sales Forecasting, *Logistics Technology,* 233:98–100 (in Chinese).

This page intentionally left blank

Progress in Mine Safety Science and Engineering II – He et al. (Eds)
© 2014 Taylor & Francis Group, London, ISBN 978-1-138-00122-0

The law of gas accumulation in top-carving area of roadway and its treatment method

Chen Chen, Bing Wu, Haiyan Wang, Yaoyao Ding, Xiaolong Cui & Yingchun Zhu
School of Resources, Safety Engineering, China University of Science and Technology (Beijing), Beijing, China
Beijing Huayu Engineering Co., Ltd., Beijing, China

ABSTRACT: The gas storage of top-carving area in roadway may be dangerous factor; meanwhile, there exists spontaneous combustion. By analyzing gas distribution of top-carving area, sampled Tashan coal mine, the physical model and mathematical model related to gas accumaltion process are set up. The mathematic equation established consisted of time-averaged motion equations of flow and diffusion equations of gas composition. The law of gas distribution under finished top-carving area and unfinished caving top-carving area are analyzed. The increasing of flow speed could efficiently lower the gas concentration gathering in complete caving top-carving area, which results are better in complete caving than non-complete. By analyzing the effect of applications, the author concluded that top-carving area should be filled, that thermal storage and gas concentration should be detected, and that air deflector should be laced. The research conducted a profound meaning to prevent explosion disaster causing by overlying of gas storage and spontaneous combustion.

1 INTRODUCTION

Roof carving is the cavity which located in roof of roadway. According to the Te Jeer theory (Tur et al., 1981), the cavity is a stable structure with a inverted parabola shape. Depth and area of carving are related to multiple factors, such as construction quality of tunnel, geological structures, and so on. Top-carving area, which meets the factor of the Jeer theory, is named as complete caving area. For gas density is lower than air (Yu et al., 1992), when top-caving appears, gas will accumulate in and near the cavity. Top-carving occur frequently in heading face or working face under unstable coal petrologic situation, which volume and area of these differ a great extent. Therefore, the existence of these different kinds of top-carving bring dangers to safety production, for the concentration of gas accumulated in and near carving area usually exceeds explosion limits, which brought a hidden danger to safety production. The prevention work of top-carving accident, to some extent, is difficult. On one aspect, quantity is larger, which takes time and labor force to discover and monitor. On the other aspect, gas accumulation exists in and near carving as well as spontaneous combustion, where exist possibility of gas explosion hazard. Thus, the research on treatment of how to prevent gas explosion hazard conducted an all-important meaning.

In the field of theoretical research, some researchers put forward gas diffusion-ventilation model (Jiang et al., 2008), which based on the law of Fick and the Brinkman equation, to study the law of gas migration in top-carving area at working face. Researchers (Li et al., 2006; Xu et al., 2009) took simple numerical simulations to simulate gas concentration distribution near fan and shearer by using PHOENICS program (Wu et al., 2001). But the simulations of gas accumulation and gas distribution while exhausting were carried out under single flow velocity condition. Thus, further research is needed to improve scientific nature of the practical experiment measures.

During the process of production and roadway expansion in Tashan, a number of top-carving areas were formed on the roof in roadway in which gas accumulated. Therefore, top-carving area becomes a significant risk in production. This paper conducted a simulation to the law of gas accumulation and migration in top-carving area, and evaluated the effect of treatment methods which is used to eliminate the gas accumulation in area.

2 THE NUMERICAL SIMULATION OF GAS MIGRATION-ACCUMULATION IN TOP CARVING AREA IN TASHAN

Tashan coal mine was designed as 20 Mt/a. The coal seam is compound coalbed with a thickness of 17 m, which covers Jurassic and permo-carboniferous period. The coal is easily combustible.

Table 1. Data collected from 380 m and 720 m caving.

Location	CH_4 (%)	CO (ppm)	CO_2 (%)	4×5 (m^2)	Air velocity (m/s)
720 m top-carving	0.29	9	0.1	20.1	2.03
380 m top-carving	0.3	11	0.1	19.9	1.92

The data used in simulation model were collected from 380 m (distance from starting point) and 720 m of return airway locating in 5208 working face, considering auxiliary haulage roadway of the second district as starting point. The 380 m top-caving is a complete top-carving area with a height of 3.5 m and a proportion of 2 m^2, which depth of carving is deeper than that of the Te Jeer theoretical depth. The 720 m top-caving is a incomplete-collapsed carving with a height of 3 m and a proportion of 2 m^2. The paper conducted some numerical simulations by using FLUENT6.3. The data used in the paper is shown in table 1.

2.1 *The physical model*

The model take parameters of 380 m top-caving and 720 m top-caving as simulation objects. The cross-sectional area in 380 m and 720 m locations of the return air way both with a trapezoid shape are 19.95 m^2 and 20.1 m^2, respectively. In order to analyzing the law of the gas accumulation in fall roof caving area and region near carvings, the simulation selected a length of 500 m airway as object.

2.2 *The mathematic model*

The gas emitted from coal wall inrush into top-carving area continuously. So the process can be seen as a process of diffusion of gas and air. For the low air-speed, gas can not be driven out from top-carving area, which methane cluster formed. Finally, the distribution and concentration of gas and air is interaction of field of air and gas concentration. For top-carving area is place gas accumulated with high concentration, which the existence of gas changed the physical mechanical property of air flow, the concentration of mixed air, kinematic viscosity and flow-speed should be the weighted mean of two kind.

In order to study gas migration and accumulation process in the top-carving area, the hypothesis is put forward as follows:

1. Assuming that the flow in the top-carving area is incompressible;
2. For the variance of flow-temperature is not large, the process of gas diffusion in top-carving area is assuming as an isothermal;

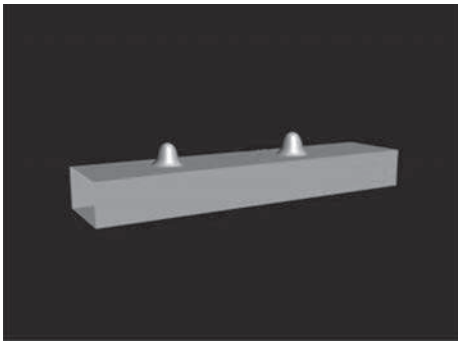


Figure 1. Calculation mesh in top-caving area of the roadway.

3. According to the Boussinesq effect on density approximation, the effect of accumulation was take into account when calculating the volume force.

Basing on assumptions listed above, the mathematical model of gas migration-accumulation is consisted of the time-averaged motion equations of flow and diffusion equations of gas composition, which gas concentration diffusion equation conform to the Fick diffusion law. So the basic equation is as follows:

$$\partial U_i / \partial X_i = 0 \tag{1}$$

$$\frac{\partial U_i}{\partial t} + U_j \cdot \frac{\partial U_i}{\partial X_j} = G_i - \frac{1}{\rho_d} \cdot \frac{\partial P}{\partial X_i} + \frac{\mu_d}{\rho_d} \cdot \frac{\partial^2 U_i}{\partial X_i X_j} \tag{2}$$

$$\frac{\partial c}{\partial t} + (U_i + U_{pi}) \cdot \frac{\partial c}{\partial x_i} = (D_i \cdot \frac{\partial c}{\partial x_i}) + D_t \cdot \frac{\partial c}{\partial x_j} \cdot \frac{\partial c}{\partial x_i} + S \tag{3}$$

U_i: velocity components
i: x, y, z;
G_i: body force (buoyancy);
C: time-averaged concentration of gas;
ρ_d: density of the gas and flow;
P: absolute pressure of mixed gas;
μ_d: kinematic viscosity of the gas and flow;
U_{pi}: Displacement flow velocity in the direction of the component;
D_i: The molecular diffusion coefficient of the mixed gas;
D_t: Turbulent diffusion coefficient of the mixed gas;
I: Gas source term;

$$\rho_d = \rho_{air} + (1 - M_r) + S \tag{4}$$

$$Gi = -\frac{g}{\rho_{air}} \cdot [\rho_{air} + (1 - M_r)] \cdot C = -[\frac{g}{\rho_{air}} \cdot (1 - M_r)] \tag{5}$$

ρ_{air}: air density;
M_r: density ratio of air and gas;

When the gas accumulated in the top-carving area reaches a state of dynamic equilibrium, the gas concentration no longer varies with time, at time of $\partial c/\partial t = 0$. About the stability of stratified fluid, Planck pointed out that the stability of stratified fluid depends on gradient R_i and Richardson Number in 1929,

$$R_i = [(g/\rho) \cdot (\partial p/\partial y)]/(\partial u/\partial y)^2 \cdot W] \quad (6)$$

y: vertical Length, m, vertically upwards is positive;
W: subscript of the side wall
g: acceleration of gravity, 9.8 m/s^2;
ρ: gas density, kg/m^3;
U: gas flow rate, m/2.

R_i as a measure of the probability of the standard turbulence effect disappeared, Numerator represents the revolt buoyancy acting on the lighter gases $[(\cdot \rho VL^2) \cdot (d\rho/dy)^2]/2$, Denominator represents the turbulent kinetic energy of flowing gas, the kinetic of the turbulent mass that volume is V is $[(\cdot \rho VL^2) \cdot (d\rho/dy)^2]/2$ (L is the distance of the flow regiment moved in the vertical direction). The Richardson Number is an important parameter to describe the gas stratified.

Planck hold that when $R_i < 0$, stratified fluid is unstable stratification; when $R_i = 0$, sstratified fluid is homogeneous fluid; when $R_i > 0$, sstratified fluid is stable stratification; when $R_i > 2$, turbulence is inhibited. In 1931, Taylor, after further analysis that the upper limit of stability of stratified fluid: $R_i \geq 1$.

Equation(3), it can be decomposed into three coordinate axes equation, so equation (1), (2) and (3), are five partial differential equations. After the wind speed U and boundary conditions are given, turbulence model using the standard κ-ε model, using SIMPLE algorithm to solve, top-carving area are obtained to roadway large gas flow field velocity and concentration distribution. The article to study two types of measures the increase of wind speed and wind guide, both belong to change the dynamic nature of the air, to change the time-averaged velocity and velocity fluctuations of flow. The nature of dilution effect is the convection-diffusion process that the gas in the flow. Therefore, the mathematical model of the above still applies.

2.3 *The initial conditions*

The simulation assumes that the gas emission position locates at the top of the roof-fall carving in the return airway. The relative methane emission rate is 1.78 m^3/t and the absolute rate is 0.0033 m^3/s. According to the Coal Mine Safety Regulations, the gas concentration of airflow in return airway can not over 0.05%. The air inlet is set as velocity inlet with a air velocity of 2.03 m/s, which is same as actual velocity in 5208 working face. The airway outlet is set as pressure outlet. The initial temperature is set as 300 K and the pressure is set as standard atmospheric pressure.

2.4 *The analysis to the simulation*

Fig. 2 and Fig. 3 show the gas concentration distribution in roof-fall area as speed of 2.03 m/s:

According to Figure 2 and Figure 3, the gas concentration accumulating at the top of the roof-fall area is about 0.3%, which is consistent with the on-site data.

Fig. 4, Fig.5 and Fig. 6 show the gas concentration distribution along the roadway direction that the distance away from the floor is 3.8 m, 3.5 m and 2 m as air velocity of 2 m/s.

It can be concluded that gas concentration around fall roof carving appears different layer distribution along the direction of air flow. The movement mode of gas in carving is relative static,

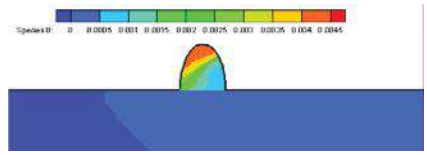


Figure 2. Gas concentration distribution at 720 m top-caving.

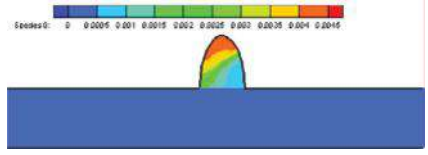


Figure 3. Gas concentration distribution at 380 m top-caving.

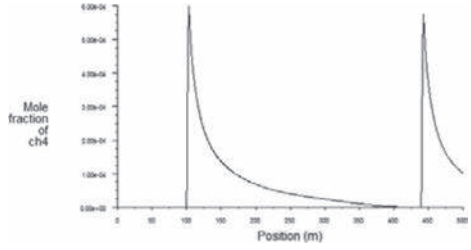


Figure 4. Gas concentration distribution at 3.8 m.

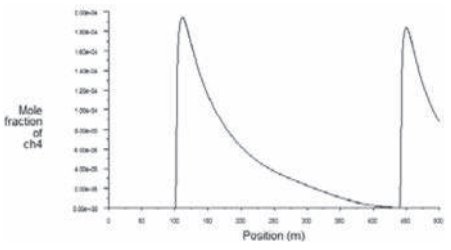


Figure 5. Gas concentration distribution at 3.5 m.

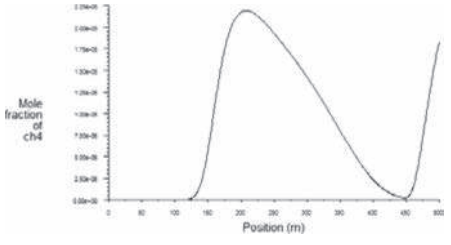


Figure 6. Gas concentration distribution at 2 m.

for molecular diffusion and expansion movement. At the same time, it should be noticed that the gas concentration of 380 m top-caving is lower than that of 720 m top-caving. There is an oxidation reaction of coal spontaneous occurring in carving (Liu et al., 2008; Zhang et al., 2000; Song et al., 2002; Guan et al., 2001; Zhang et al., 2006; Ma et al., 2007), and then the thermal force generated by oxidation reaction pushs gas into airway. Safety supervision personnel should attach importance to monitor the roof-fall carving whether there is a continuous thermal storage effect in it.

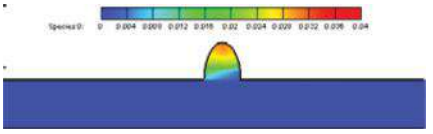


Figure 7. Gas concentration distribution at 720 m top-caving.

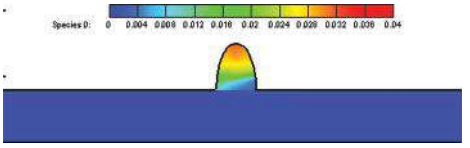


Figure 8. Gas concentration distribution at 380 m top-caving.

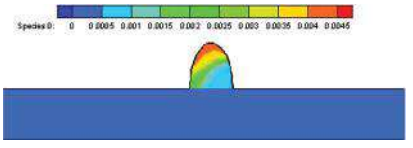


Figure 9. Gas concentration distribution at 720 m top-caving.

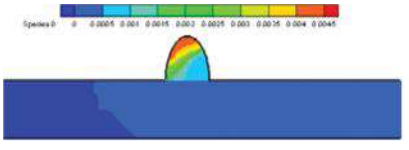


Figure 10. Gas concentration distribution at 380 m top-caving.

3 THE SIMULATION OF GAS CONCENTRATION FIELD DISTRIBUTION OF DIFFERENT TREATMENT METHODS

According to the analysis to the gas accumulation treatment methods in top-caving area, the paper conducted a number of numerical simulations to evaluate the effect of measures by changing flow velocity. Air velocity in airway selected are 4 m/s, 2.03 m/s and 1 m/s.

3.1 *The effect of changing flow-speed*

Figure 7 and Figure 8 show that the gas concentration distribution in roof-fall area under air velocity of 1 m/s. It shows that the gas concentration rises up to 3% from 0.3%, when air velocity goes down from 2.03 m/s to 1 m/s at 720 m and 380 m. For the thickness of gas bed in 380 m caving is over that of The Te Jeer theory, which the gas accumulated at the top will not be able to influent by airflow force and the thickness of 3% gas layer becomes larger, gas concentration will be get in the range of explosion triangle, which increases the possibility of explosion hazard.

Fig. 9 and Fig. 10 show the gas concentration distribution in roof-fall area under the wind velocity of 4 m/s. It can be concluded that the gas concentration in roof-fall area has basically no different under speed of 4 m/s from that of 2.03 m/s (showen in Fig. 2 and Fig. 3). The gas layer in roof-fall area at 380 m top-caving is thicker than that of 720 m top-caving.

By analyzing, it can be concluded that gas concentration would go down if flow-speed is continuously increased. But when flow-speed is over a certain limit, the variance of gas concentration

will tent to keep constant which gas concentration will no longer decrease as flow-speed goes up. Thus, high flow-speed which is over the limit, on one aspect, will cause fugitive dust; on the other aspect, it cause energy waste.

At the same time, the study also shows that increasing flow-velocity has a better effect to eliminate gas accumulation which the depth of carving is less than that of Te Jeer theory.

3.2 *The evaluation of other treatment approaches*

First, sealing method is suitable for larger gas emission coal mine and relative lower air volume. If the gas emission in the roof-fall area is large and lacking of the quantity of air flow in the roadway, the method not only can take away gas accumulated, but also increasing the gas concentration in airway [12]. Namely, if the quantity of gas emitted is beyond the limits of standard, sealing approach can be applied. But the method has heavy workload.

Second, filling method is to lay board or wattle in the shed of area, and then to fill the cavity with loess or high-powered foam, which can eliminate the space and there will be no gas storage in. This is usually applied to the depth is lower than that of Te Jeer theory.

In a word, increasing flow-speed has an effect on eliminating accumulation. But it is hard to have a further noticeable effect when the flow-velocity exceeds a certain value. The method of directly blowing gas into current adds up gas concentration of current. If the gas emission is higher and the air quantity is insufficient, the gas concentration in downwind near-wall-side will easily beyond the limits and there exists hidden danger. According to the analysis, backfill operation at 720 m top-caving in the airway of 5208 working face in Tashan coalmine had been carried, and heat storage monitoring to the area should be done after backfill, for the seam is easily spontaneous combustion.

4 CONCLUSIONS

1. CFD physical model was proved to be effectively verified the simulation of the gas accumlation in the roof-fall area of the airway;
2. Increasing airflow velocity can effectively reduce gas accumulation in top-carving area, especially in those carving which depth is lesser than that of the Te Jeer theory;
3. Gas concentration in top-caving area would go down if airflow velocity is continuously increased. But when air velocity is over a certain limit, the gas will tent to keep constant concentration as airflow velocity goes up. On the contrary, with the decrease of the airflow velocity, the gas accumulated in top-caving area and the gas concentration reached the dangerous level of the gas explosion triangle and spontaneous combustion appeared in the roof-fall area, which gas explosion disasters will happen.

REFERENCES

Guan Jinha. 2001. Reasons and treatment methods of gas accumulating underground. *Coal Sci-tech.*3 (3):54–55.

Jiang Wenzhong. 2008. The establishment of gas diffusion-convection model and calculation method of ventilation in gob caving zone. *Safety in Coal Mine*. (8):81–83.

Li Li. 2006. Analysis on indication gases of different coal's oxidized spontaneous combustion. *Mining Safety & Environmental Protection.* (5):69–71.

Liu Guozhong. 2008. Analysis and practices on micro circulation theory of coal spontaneous combustion in high falling zone of mine roadway. *Coal Science and Technology.*36 (7):60~63.

Ma Yan. 2007. The treatment of high gas coal seam roof caving zone by using polymer material. *Energy Technology and Management*. (1):39–40.

Song Chengwen. 2002. The characteristics and preventions about methane accumulation. *Shanxi Agchitecture*. 28(2):47–48.

Tur M Channing Andrianof. 1981. Foundation of mining rock mechanics. *China Coal Industry Publishing House*.

Wu Qiang. 2001. Application of CFD technology in the ventilation in Engineering. *China University of Mining and Technology press*. (11).

Xu Bobo. 2009. Analysis on indication gases of coal's oxidized spontaneous combustion. *Safety in Coal Mines*. (2):33–34.

Yu Qixiang. 1992. Gas accident prevention and control in coal mine. *China University of Mining and Technology press*.

Zhang Yandong. 2006. Treatment of gas accumulation in the mine. *Mining & Processing Equipment.*34 (2):35–36.

Zhang Ying. 2000. Processing method of gas accumulation in Xinji Mine. *Mining Safety & Environmental Protection*. 27(3):23–24.

This page intentionally left blank

Progress in Mine Safety Science and Engineering II – He et al. (Eds)
© 2014 Taylor & Francis Group, London, ISBN 978-1-138-00122-0

Unsafe act analysis on major and particular major flood accident in coal mine

Yang Chun, Jiye Dong, Baojun Lu, Shanghong Shi, Shasha Yuan, Ping Gao, Zhongqian Chang, Ze Chen & Gui Fu
Faculty of Resources and Safety Engineering, China University of Mining and Technology (Beijing), Beijing, China

ABSTRACT: Flood accident is the second biggest accident in Chinese coal mine currently, bringing huge casualty and economic loss to safety production. However, a prevalent way to prevent flood accident is to focus on the improve equipment and strengthen techniques, but the factor of "people" and their unsafe acts in the accident have been ignored. Taking behavior-based accident causation 2-4 model as theoretical base, this paper analyzed the unsafe acts from samples of major and particular major flood accidents in coal mine from 2005 to 2006. Through analysis, a conclusion can be drawn that township coal mine takes up over 80% of major and particular major flood accidents in case of both the number of times and the death toll it caused. Therefore, the main target to prevent major and particular major flood in coal mine should be township coal mine. 11 kinds and 44 pieces of unsafe acts were gotten by analyzing 17 major and particular major flood accidents from 2005 to 2006, and the first 3 kinds of unsafe acts (failure to take effective measures to detect and remove water according to rules, illegal production, illegal cross-border exploitation) were the most common causes of major and particular major flood accidents. The way how unsafe act leads to accident is shown in this paper by analyzing unsafe acts in accident. It proves unsafe act will lead to accident at the same time, and the real-situation accident proves that safe acts can reduce casualty and save lives.

1 INTRODUCTION

China is one of countries suffering from the most serious coal mine flood in the world (HU WY 2005), and flood is the second biggest disaster of Chinese coal mine considering its death toll and occurrence frequencies (SAWS 2013). Flood leads to a lot of casualties and property loss every year. Statistics indicates that major accident and particular major accident in coal mine happened for over 500 times, and caused about 3000 people's death from 2000 to 2009 (XU LC et al. 2010). The particular major accident at Daxing Coal Mine in Guangdong province on August 7th 2005 resulted in 121 deaths, having an undesirable influence on society (SAWS 2007). In the meantime, it brings about huge economic loss when flood in coal mine damages its equipment, and later drainage work delays manufacturing. Therefore, the prevention of major flood accident and particular major flood accident becomes the main duty for safety production of coal mine nowadays.

Currently, a prevalent way to prevent flood in coal mine is to enhance techniques, including strengthening forecasting and equipping special equipment to detect and remove water, which indeed plays an important role, but it is far from enough from the perspective of accident prevention (RMWPC 2009). A conclusion can be drawn that "88 per cent of accidents were caused by people's unsafe act, and only 10 per cent of accidents were caused by object's unsafe condition" according to Heinrich's research on large numbers of accident (HEINRICH WH et al. 1980). Almost the same conclusion can be gotten that "over 80 per cent of accidents were caused by people's unsafe act" from the research of DuPont, National Safety Council and the related statistics from China (CHE HQ 2003, XU L 2005). Besides, 30 particular major accidents were all caused by "management problem", including 2 particular major flood accidents, announced by State Administration of Work Safety in China, and investigated and handled from December 23rd 2007 to August 28th 2012. The announcement indicates the major causation was "people", not "object" (SAWS 2012). Therefore, the factor of "people" must become the starting point for fundamentally preventing major and particular major flood accident in coal mine.

2 BEHAVIOR-BASED ACCIDENT CAUSATION "2-4 MODEL" AND UNSAFE ACT

Out of all kinds of methods of preventing accident, BBS (Behavior Based Safety) plays a significant role in the control and improvement of personal behavior, but the time it works lasts too long. BBS cannot satisfy the need of Chinese safety production, as far as the characteristic of instantaneity of accident occurrence and Chinese accident-prone situation are concerned. In fact, BBS is seldom used in Chinese coal mine in order to prevent accident and improve safety.

Behavior-based accident causation 2-4 model (FU G et al 2013) is a modern accident causation chain established on the ground of existed accident causation chains and organizational behavioral science. Behavior-based accident causation 2-4 model identifies accident reasons through 2 levels and 4 behavioral stages. "2 levels" refers to the level of organizational behavior and the level of personal behavior of organization members. "4 behavioral stages" means organizational directed behavior, organizational operating behavior, behavior and act, which respectively corresponds to root cause, radical cause, indirect cause and direct cause, and these causes are respectively equivalent to safety culture, safety management, safety knowledge and safety consciousness and safety habits, unsafe acts and unsafe conditions, as is shown in Table 1. Behavior-based accident causation 2-4 model will locate the reason for the accident in one or more parts of 2 levels and 4 behavior stages accurately, which has a very good effect on analyzing the cause of accident, taking countermeasures, and preventing similar accident from happening again.

Behavior-based accident causation 2-4 model is an accident causation chain based on the analysis of the unsafe act of accident trigger. Among direct causes of accidents, the identification of unsafe act is grounded on the common direct cause of classical Heinrich's accident causation chain, modern accident causation chain (like the accident causation chain proposed by Bird and Loftus), existed contemporary accident causation chain (STEWART JM 2002). Additionally, the accident can be impeded by preventing the "domino" of unsafe act from falling down on the basis of Domino Theory in Heinrich's accident causation chain. Furthermore, over 80% of accidents were caused by people's unsafe act, so if the problem of people's unsafe act can be solved, the over 80% of accidents will be impeded. Behavior-based accident causation 2-4 model is theorized on a large number of research findings (FU G et al. 2005) and accident cases (FU G et al. 2005) on the ground of organizational behavior science (Ricky. W. Griffin et al. 2010), which makes accident prevention more efficient.

3 ANALYSIS ON MAJOR AND PARTICULAR MAJOR FLOOD ACCIDENT CASES

Taking behavior-based accident causation 2-4 model as a theoretical base, the major and particular major flood accidents from 2005 to 2006 were systematically analyzed. (The choice of a certain period is because there is no major difference among accident patterns in some particular period of time, so the accidents happening from 2005 to 2006 are very representative.) Starting from the accident triggered by direct unsafe act, this paper attempts to find out the direct cause of accident in order to provide a reference for avoiding similar accident and give a reference to the indirect cause of accident.

3.1 *Analysis on flood accident in coal mine of different forms of ownership*

From 2005 to 2006, 13 major flood accidents and 4 particular major flood accidents happened. The name of the accidents, year, form of ownership and death toll are listed in Table 2.

Based on the number of times of flood accident and the percentage of death toll in different forms of ownership in Table 2, pie charts are generated in Figure 1 and Figure 2. The two figures show that township coal mine owns over 80% of the flood accidents

Table 1. Behaviour-based accident causation "2-4 model".

Name of chain	Behaviour developing process				Consequence	
	Organizational behaviour		Personal behaviour			
	Phase 1	Phase 2	Phase 3	Phase 4		
Developing stages	Directing behaviour	Operating behaviour	Behaviour	Act	Accidents	Loss
Types of causes	Root cause	Radical cause	Indirect cause	Direct cause	Accidents	Loss
Causation chain of accident	Safety culture	Safety management	Safety knowledge Safety consciousness Safety habits	Unsafe acts Unsafe conditions	Accidents	Loss

Table 2. Major and particular major flood accidents (2005–2006) and related data.

Name of accident	Year	Form of ownership	Death toll
"3•18"major flood accident at Fanjiashan coal mine in Shanxi province	2006	State-owned local	28
"4•9" major flood accident at Qinyoumian coal mine in Heilongjiang province	2006	Town	12
"7•15" major flood accident at Pianpoyuan coal mine in Guizhou province	2006	Town	18
"5•18" particular major flood accident at Xinjing coal mine in Shanxi province	2006	Town	56
"4•1" major flood accident at Guida coal mine and Shihuiyao coal mine in Hunan province	2005	Town	20
"5.28" major flood accident at Chikeng coal mine in Fujian province	2005	Town	10
"7•7" major flood accident at Yongsheng coal mine in Jiangxi province	2005	Town	15
"7•14" major flood accident at Fusheng coal mine in Guangdong province	2005	Town	16
"8•19" major flood accident at the 5th coal mine Sulan Mining Bureau in Jilin province	2005	State-owned key	16
"9•10" major flood accident at Dahao coal mine in Guizhou province	2005	Town	10
"10•4" major flood accident at Longtan coal mine in Sichuan province	2005	State-owned key	28
"11•19" major flood accident at Yuanda coal mine in Hebei province	2005	Town	14
"11•24" major flood accident at Gaocun coal mine in Hebei province	2005	Town	18
"12•28" major flood accident at Baoyuan Mining Co., Ltd. in Shanxi province	2005	Town	17
"4•24" particular major flood accident at Ji'an coal mine and Tengda coal mine in Jilin province	2005	Town	30
"8•7" particular major flood accident at Daxing coal mine in Guangdong province	2005	Town	121
"12•2" particular major flood accident at Shigou coal mine in Henan province	2005	Town	42

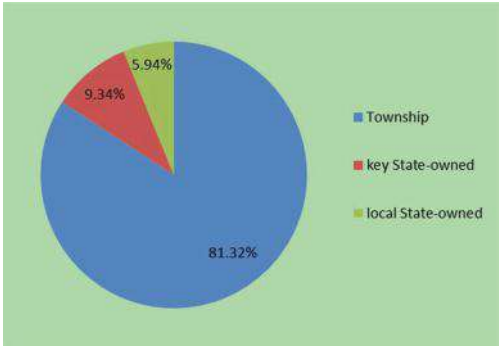


Figure 1. The percentage of number of times of flood in different forms of ownership.

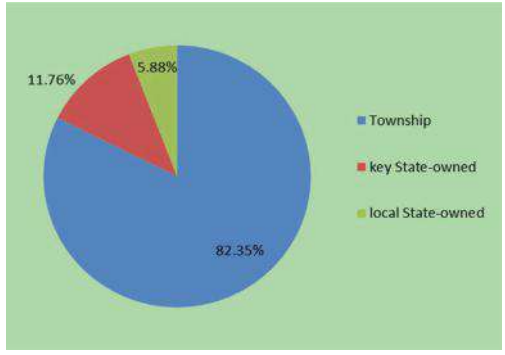


Figure 2. The percentage of death toll in different forms of ownership.

judging from both the number of times and the death toll. This figure makes it clear that the township coal mine should be the main target to prevent major and particular major flood in coal mine.

3.2 *Analysis on unsafe act*

According to the book "Major Accident and Particular Major Accident Casebook in Chinese Coal Mine From 2003 to 2006" published by State Administration of Work Safety in China, direct unsafe acts were counted in 17 major and particular major flood accidents from 2005 to 2006. 11 kinds and 44 pieces of unsafe acts were classified, and the average probability of each unsafe act appearing in every accident and the proportion of each unsafe act in the total number of unsafe acts were calculated in Table 3.

It can be seen from Table 3 the unsafe acts leading to major and particular major flood accidents in coal mine from 2005 to 2006 include: Failure to take effective measures to detect and remove water according to rules; illegal production; illegal cross-border exploitation; Under the condition that signs of obvious flooding and injured miners, leader workers continue blasting and mining in violation of regulations; Blasting in violation of regulations under the condition of signs of obvious flooding; During blasting the borehole did not ring. Inspection in violation of regulations without any safety operation procedure, causing injury; no monitoring and no instant measures, when underground hydrological observation point changed; did not do backfilling in time when day-to-day heavy rain caused a rise in water level and backfill elevation was submerged; constructing safety facilities in violation of regulations with no authorization; did not report the sign of flooding to the next team when handing over work; getting out of coal mine and off work in advance.

Table 3 also shows that the unsafe act—failure to take effective measures to detect and remove water according to rules—appears for 18 times in 17 major and particular major flood accidents, which means the probability of this unsafe act appearing in every accident reaches 105.88% and this unsafe act will happen for at least one time among the direct causes of a piece of major and particular major flood accident on average. In accordance with the third article in general provisions of "Regulations on Mine Water Prevention and Control", water prevention and control should insist on the principle of detecting water in case of any doubt about safety, and the principle

Table 3. Unsafe acts and related data.

Unsafe act	The number of times unsafe act appearing	Average probability of each unsafe act appearing in every accident	Proportion of each unsafe act in the total number of unsafe acts
Failure to take effective measures to detect and remove water according to rules	18	105.88%	40.91%
Illegal production	9	52.94%	20.45%
Illegal cross-border exploitation	6	35.29%	13.64%
Under the condition that signs of obvious flooding and injured miners, leader workers continue blasting and mining in violation of regulations	3	17.65%	6.82%
Blasting in violation of regulations under the condition of obvious signs of flooding	2	11.76%	4.55%
During blasting the borehole did not ring. Inspection in violation of regulations without any safety operation procedure, causing injury	1	5.88%	2.27%
No monitoring and no instant measures, when underground hydrological observation point changed	1	5.88%	2.27%
Did not do backfilling in time when day-to-day heavy rain caused a rise in water level and backfill elevation was submerged	1	5.88%	2.27%
Constructing safety facilities in violation of regulations with no authorization	1	5.88%	2.27%
Did not report the sign of flooding to the next team when handing over work	1	5.88%	2.27%
Getting out of coal mine and off work in advance	1	5.88%	2.27%

of detecting must come before tunneling. However, the 17 accidents were all caused by not holding to this principle. Figures in Table 3 reveal that the unsafe act—failure to take effective measures to detect and remove water according to rules—is the main cause of most major and particular major flood accidents. Therefore, the principle work for preventing flood in coal mine is to enforce the execution of detecting and removing water, and needs special attention from all coal mining enterprises.

The unsafe act—failure to take effective measures to detect and remove water according to rules—specifically includes 7 pieces: ①Front line staff, managers(team leaders), and leaders of coal mine take a blind eye on the sign of flooding and keep on tunneling and blasting without any measures to detect and remove water; ②When the sign of flooding is reported and then a discussion is held, it is believed to be safe and operation continues without any measure to detect and remove water; ③When front line staff report the sign of flooding, manager or leader of coal mine carries on directing operation in violation of regulations under the circumstance of not taking detecting and removing measure; ④In only some areas, taking measures to detect and remove water in the process of mining and tunneling; ⑤When the sign of flooding is already discovered, people do not retreat back to the ground and ineffective measures are taken without permission; ⑥Not detect and remove water by following the regulation of "detecting water if there was any doubt about safety"; ⑦Not detect and remove water by following the regulation of "detecting must come before tunneling".

At the same time, the unsafe act—illegal production—appears for 9 times in 17 accidents, illustrating that there is one accident directly caused by the unsafe act of illegal production in every 2 major and particular major flood accidents. In the process of production, many enterprises pay little or even no attention to safety warning given by safety supervision department after checking. For example, they ignore the safety warning of "production suspension and rectification" and the warning of "rectification ahead of deadline", but hold on producing illegally. This seriously weakens the function of safety supervision. This paper suggests that coal mine enterprises should attach high attention to the safety warnings by safety supervision department and strengthen their own investigation into unsafe act and hidden danger in enterprises. Illegal production in reality specifically include: ①Resume production without authorization after the Spring Festival; ②Refuse to follow the "Close Order", re-produce or construct without authorization when facility was blown up for several times; ③Re-produce illegally during time of "production suspension and rectification"; ④Incomplete licenses; ⑤Mining beyond coal mine ability (beyond layer or beyond a fixed number of staff); ⑥Mining protecting coal pillar in violation of regulations.

Illegal cross-border exploitation includes cross-border exploitation, beyond-layer mining, mining waterproof isolation pillar illegally, and mutual cross-border exploitation between mines competing for resources, etc. According to Table 3, accidents caused by the unsafe act of illegal cross-border exploitation take up over 1/3 of all accidents, so the related departments and enterprises should strengthen their management and prevention.

Some explanation is needed for the unsafe acts listed above. The 3 kinds of unsafe acts are mainly conducted by managers. They appear to be the management behavior of managers, but the managers' unsafe act in fact. For instance, a leader makes a speech or signs a document ordering workers to blast and tunnel without detecting and removing water. Although the speech and document function as management behavior, the leader's behavior cannot represent the whole organization. It is personal unsafe act.

Besides, by making the percentage of the first 3 kinds of unsafe acts of the total number of unsafe acts in Table 3 into pie chart, we got Figure 3. From Figure 3, two points are obvious. The first is that the unsafe act—failure to take effective measures to detect and remove water according to rules—accounts for over 40% of the total number of all unsafe acts. The second is the first 3 unsafe acts (failure to take effective measures to detect and remove water according to rules, illegal production, and illegal cross-border exploitation) take up 75% of total number of unsafe acts. The two points indicate that the first 3 unsafe acts are the main preventative objects of major and particular major flood accidents, especially the first unsafe act needs high attention.

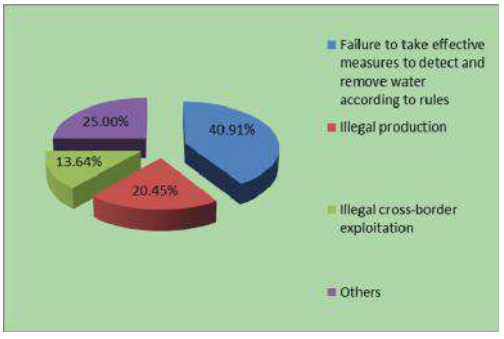


Figure 3. The proportion of the first 3 kinds of unsafe acts to the total number of unsafe acts.

4 CASE STUDY OF FLOOD ACCIDENTS

Statistical analyses of unsafe act from 2005 to 2006 are mainly introduced above. Next the flood accident in coal mine will be taken as case study to illustrate how unsafe acts lead to accident and how safe act can save lives and avoid casualty.

Case description: At 21:15 on October 4th 2005, a major flood accident happened in Longtan, an under construction coal mine of Sichuan Huayingshan Longtan Coal Co., Ltd. The accident caused 28 deaths and its direct economic loss was 7 million Yuan. Accident investigation reported that the direct cause of the accident was blasting induced karst flooding under the condition that the operational worker did not conduct detecting-water drilling and tunneling in violation of regulations.

Then the analysis of unsafe act in this accident will be conducted according to behavior-based accident causation 2-4 model.

Background: The operation mode of three shifts (morning, middle and night) and 24 hours nonbreaking work are adopted by this coal mine.

Brief accident process: In the morning shift, driver A did not conduct detecting-water drilling; there was black mud and water emitting on the left face in the process of constructing blast hole. When drilling is stopped, dripping arose on the right tunneling face. When morning shift was over, the vice-captain attendant B did not report the situation as required and did not hand it over to the next shift. In the middle shift, the tunneling monitor and tunneling worker C did not conduct detecting-water drilling; when the sign of flooding arose in the process of tunneling, C kept on tunneling without taking any safety measures; on-duty vice-monitor D, who is responsible for overall production safety and quality of the project, failed to participate in the job and got off duty and got out from mine ahead; blaster E's blasting in violation of regulations with the sign of obvious flooding triggered the accident.

Analysis: Judging from the process, there are 6 unsafe acts in this accident, including driver A did not conduct detecting-water drilling; B did not report and did not hand over the signs of flooding to the next shift as required; C did not conduct detecting-water drilling; C kept on tunneling in violation of regulations, when the sign of flooding arose in the process of tunneling; D failed to participate in the job and got off duty and got out from the mine ahead of time; E blasted in violation of regulations under the condition that the sign of flooding was obvious. A brief flow chart of accident and unsafe acts is shown in Figure 4.

It can be seen from the above analysis that the combined effect of those unsafe acts resulted in the 28-death-accident. So, the purpose of accident prevention can be reached by strengthening the research and prevention of unsafe acts. By researching on and classifying the unsafe acts which triggered accidents, unsafe act library about flood accident can be built; by using accident cases and other ways to train related workers with

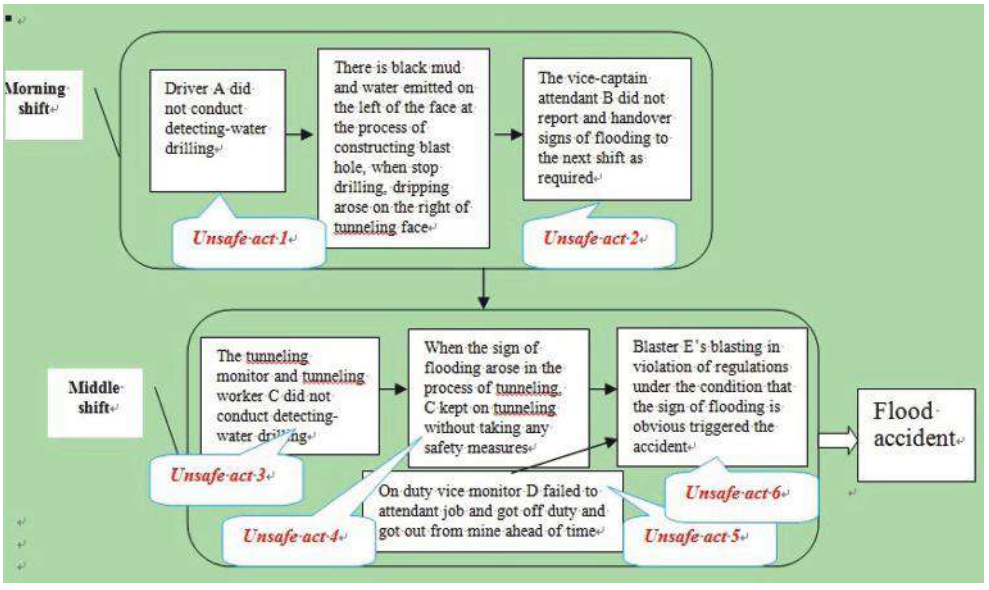


Figure 4. The brief flow chart of accident happening and unsafe acts.

the knowledge about unsafe act in the unsafe act library, they can realize what accident the unsafe act will bring about and which accident was triggered by the unsafe act. It can make related workers remember what correct acts and safe act are in order to avoid similar accidents and unsafe acts.

Besides, in the "9•10" major flood accident at Dahao coal mine in Guizhou province, WU took correct and safe acts by reporting the sign of flooding and taking efficient measures to hide himself and his colleagues in a safe place under the condition that the sign of flooding was obvious and the condition that the manager gave orders to continue working though in violation of regulations. WU's safe act saved his colleagues and himself. This example illustrates safe and correct act can save lives in emergency.

5 CONCLUSIONS

From the above analyses, conclusions can be drawn.

1. Township coal mine takes up over 80% of major and particular major flood accidents in coal mine from 2005 to 2006 in case of both the number of times and the death toll it caused. Therefore, the main target to prevent major and particular major flood in coal mine should be township coal mine.
2. 11 kinds and 44 pieces of unsafe acts were gotten by analyzing 17 major and particular major flood accidents from 2005 to 2006. The 11 kinds of unsafe acts are: Failure to take effective measures to detect and remove water according to rules; illegal production; illegal cross-border exploitation; Under the condition that signs of obvious flooding and injured miners, leader workers continue blasting and mining in violation of regulations; Blasting in violation of regulations under the condition of signs of obvious flooding; During blasting the borehole did not ring. Inspection in violation of regulations without any safety operation procedure, causing injury; no monitoring and no instant measures, when underground hydrological observation point changed; did not do backfilling in time when day-to-day heavy rain caused a rise in water level and backfill elevation was submerged; constructing safety facilities in violation of regulations with no authorization; did not report the sign of flooding to the next team when handing over work; getting out of coal mine and off work in advance.
3. Judging from the data analysis, the first 3 kinds of unsafe acts (failure to take effective measures to detect and remove water according to rules, illegal production, illegal cross-border exploitation) are the most common causes of major and particular major flood accidents, especially the unsafe act of failure to take measures to detect and remove water according to rules. This should attract special attention.
4. The way how unsafe acts lead to accident is shown in this paper, and it proves unsafe act will lead to accident; real-situation accident proves that safe act can reduce casualty and save lives.

ACKNOWLEDGEMENTS

Great thanks for National Natural Science Foundation of China (NO.51074167), The Special Research Foundation on Doctoral Program in University in the Year 2010 (NO.20100023110005) and Special Funds for Fundamental Research in Central Universities (NO.2010YZ04).

Sincere thanks for the guidance from my tutor, because he has always given me detailed guidance in every step of my study career.

REFERENCES

Che Hongqin. 2003. 96% of Accident Can Be Avoided. *China National Conditions and Strength,* (2):57.

Fu Gui et al. 2005. Common Factors Leading to Accidents and Behavior Type Research Based on Prevention. *China Safety Science Journal,* 5 (1): 80–83.

Fu Gui et al. 2005. Behavior Based Model for Organizational Safety Management. *China Safety Science Journal,* 15 (9): 21–27.

Fu Gui et al. 2013. Behavior-based Accident Causation: The "2-4" Model and Its Safety Implications in Coal Mines. *Journal of China Coal Society,* 38 (7): 1123 –1129.

Heinrich W H et al. 1980. Industrial Accident Prevention. McGraw-Hill Book Company, New York.

Hu Weiyue. 2005. Theory and Method on Flood Accident Control in Mine. China Coal Industry Publishing House, Beijing.

Regulations on Mine Water Prevention and Control. 2009. The 28th Regulation from State Administration on Work Safety.

Ricky. W. Griffin et al. 2010. Organizational Behavior. China Market, Beijing.

State Administration on Work Safety. 2007. Major Accident and Particular Major Accident Casebook in Chinese Coal Mine From the Year 2003 to the Year 2006. State Administration on Work Safety, Beijing.

State Administration on Work Safety. 2012. The Particular Major Accident Handling. http://www.chinasafety.gov.cn/newpage/zwgk/tdsgdccl/zwgk_tdsgdccl_lm.htm.

State Administration on Work Safety. 2013. National Science and Technology Major Project "Key Technology and Equipment Research and Development To Control Flood Fire And Other Major Accidents in Coal Mine, "Launched in Beijing. http://www.chinasafety.gov.cn/newpage/Contents/Chan-el_21140/2013/0514/204740/content_204740.htm, 3013-05-13/2013-05-29.

Stewart JM. 2002. Managing for World Class Safety. John Wiley & Sons, 1–31.
Xu Liang. 2005. Analysis on Causes of Safety Accident and Problem about Supervision System. *Science paper Online* http://www.paper.edu.cn/releasepaper/content/200512-703.html.
Xu Liangcai et al. 2010. Brief Discuss on Chinese Main Types of Flood Accident in Coal Mine and Its Technical Prevention. *Safety in Coal Mines,* 42 (1): 53–56.

Progress in Mine Safety Science and Engineering II – He et al. (Eds)
© 2014 Taylor & Francis Group, London, ISBN 978-1-138-00122-0

Numerical study of fluid flow and convention heat transfer in sandstone as a porous media

W.L. Gong, D. Liu, P.Y. Guo, H. Zhang, Y.B. Wang, Y. Zhang, B.J. Liu & Y.Q. Sun
State Key Laboratory for Geomechanics and Deep Underground Engineering, Beijing, China
School of Mechanics and Civil Engineering, China University of Mining and Technology, Beijing, China

ABSTRACT: It has a great significant to research on the convection heat transfer caused by permeability in rock as a kind of porous media for deep underground heat hazard control. In this paper, a porous media model was constructed by non-equal diameter spherical particles for the studying of sandstone or sandy mudstone which are categorized into granular geology material and commonly exist in tunnels. The permeability, convection heat transfer coefficient, particles' heat transfer characteristics, effective thermal conductivity coefficient in various seeping velocities were numerically simulated or studied. The influence of porosity and particle size for the heat transfer coefficient were also analyzed. At last, the obtained parameters of sandstone were used to simulate the cooling channel of Zhangshuanglou Mine, the calculated results were coincided with the practical data well.

1 INTRODUCTION

The scope of underground engineering extents to the deeper layer in a fairly high speed which cause the temperature of tunnels and underground space getting higher and higher due to the intensify of heat emited from the surrounding rock which leading to severer heat hazard for the underground workers, equipment and instrument (Cluver 1932, He et al. 2010) In order to improve the conditions, a lot of scholars developed falling temperature technique and acquired a great achievement. However, research for the thermal conduction in the surrounding rock still leaves much to be desire, for example, the insufficient theory leads to cold load calculate inaccuracy. Therefore, studying on the phenomenon and mechanism of convection heat transfer in the deep underground material has great significance. The common roadway surrounding rock is granular porous material, such as sandstone, sand mudstone and mudstone, the permeability has great influence on their heat transfer process, so study on the heat transfer in porous media is a key to solve the proposed problems. In this paper, the representative roadway surrounding rock, sandstone, is chosen as the investigate subject as porous media. In order to promote better understanding of convection heat transfer phenomenon and mechanism in different seeping velocities, we're going to numerical simulate the whole process.

Much effective work have been done to research on the permeability and thermal conduction in porous media. After Darcy-Law was found, Forchhermer (Forchheimer 1901) and Brinkman (Brinkman 1949) brought out modified Darcy-Forchheimer equation and modified Darcy-Brinkman equation which could react the fluid flow more precisely in porous media separately. Whitaker (Whitaker 1969) pioneered the use of continuum mechanics for establishing the basic conservation equations in porous media. C.T. Hus and P. Cheng (Hsu & Cheng 1990) investigated the thermal dispersion conductivity in porous media via the volume averaging method. They analyzed the thermal dispersion tensor in porous media with various porosities, various particle diameters, various velocities and various temperatures. They found that, for high Reynolds number and low Reynolds number porous media flows, the velocity and porosity dependencies in the thermal dispersion conductivity tensor are different. Whitaker and Slattery (Whitaker 1973) investigated heat transfer in porous media combined with the classic transport theory and volume averaging method, they assumed that there's no temperature difference between the different phases in porous media that satisfies the local thermal equilibrium model. The mathematical description of this method is more rigorous, especially for the multiphase coupling heat and mass transfer problem in porous media. Carbonell and Whitaker ect (Carbonell & Whitaker 1984) proposed local thermal non-equilibrium model and obtained the two-equation of energy transport for solid phase and fluid phase. Vafai and Tien (Vafai & Tien 1981) studied the boundary and inertial effects on the flow and heat transfer in porous meida. They pointed out that the boundary effects only exist in

a very thin momentum boundary layer and often have no significant effect on the overall flow field, however, it's very important for the heat transfer. In recent years, Lattice Boltzmann method was introduced in investigating the permeability in porous media which gives out more reliable results to the actual situation (Abe 1997, Qian et al. 1992, Shan & Chen 1993, Chen & Doolen 1998, Adler & Thovert 1993). Meanwhile, some scholars utilized the fractal theory studied the heat and mass transfer in porous media which is fruitful (Pierre et al. 1992, Adler & Thovert 1993, Chen & Shi 1999, Yu 2003). Models such as particle model, capillary tube bundles model, stochastic model, processing model, fractal model and image reconstruction model were used to reconstruct the porous media, and these models have played significant role in the study of porous media (Jacob & Yehuda 1990).

These researches laid the foundation for the heat transfer of deep underground, and have positive effect on the deep roadway heat transfer mechanism recognization and heat load calculation. These works gained various degrees of success. However, most of the researches considered the heat transfer surface as rigid boundary, ignored the influence from the permeability of the porous media, led to inaccurate understand of surrounding rock heat transfer and calculation of heat load.

2 SANDSTONE MODEL AND BOUNDARY CONDITIONS

As shown in Fig. 1, the reconstructed porous media is placed into adiabatic boundary channel, there's a heat conduct plan at the top of the model with a constant heat flux q_0. We will survey and evaluate the permeability and heat conductivity coefficient of this model with different inlet velocities.

General form of three-dimensional non-steady-state heat conduction differential equation in Cartesian coordinate system can be written as:

$$\rho c\frac{\partial t}{\partial \tau}=\frac{\partial}{\partial x}\left(\lambda\frac{\partial t}{\partial x}\right)+\frac{\partial}{\partial y}\left(\lambda\frac{\partial t}{\partial y}\right)+\frac{\partial}{\partial z}\left(\lambda\frac{\partial t}{\partial z}\right)+\Phi \quad (1)$$

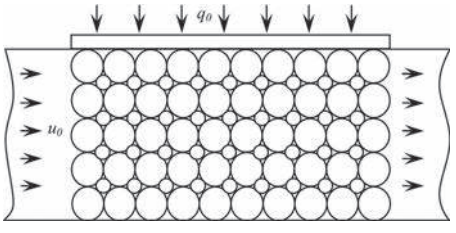


Figure 1. Physical model and boundary condition.

Assume that the solid in the model is constant, no inertial heat source, steady, so the heat conduction equation was given as:

$$\nabla\cdot(\lambda\nabla T)=0 \quad (2)$$

The continuity equation for the fluid in Cartesian coordinate represent as:

$$\frac{\partial\rho}{\partial t}+\frac{\partial}{\partial x}(\rho u)+\frac{\partial}{\partial y}(\rho v)+\frac{\partial}{\partial z}(\rho w)=0 \quad (3)$$

Quality increment per unit volume is zero,

$$\frac{\partial\rho}{\partial t}=0 \quad (4)$$

Therefore, the continuity equation can be abbreviated as:

$$\nabla\cdot(\rho U)=0 \quad (5)$$

The momentum equation for the fluid is:

$$\rho\frac{DU}{Dt}=\rho F_b-\nabla p+\nabla\cdot(2\mu\mathbf{S})-\frac{2}{3}\nabla(\mu\nabla\cdot U) \quad (6)$$

3 NUMERICAL RESULTS AND DISCUSSION

3.1 *Permeability and inertial coefficient*

The momentum equation for fully developed one-dimensional flow in porous media is represented in Eq.7 and can be written in the form of Eq.8

$$-\frac{dp}{dx}=\frac{\mu}{K}u+\frac{F}{\sqrt{K}}\rho u^2 \quad (7)$$

$$-\frac{dp}{dx}\frac{1}{\mu u}=\frac{1}{K}+\frac{F}{\sqrt{K}}\frac{\rho u}{\mu} \quad (8)$$

The results for the pressure drop of four kinds of porosities at various velocities were extracted and squares analyzed as Fig. 2.

We cans see from Fig. 2, with the increase of inlet velocity the pressure drop between the inlet and outlet increases, and they show a linear relationship. In the condition of same inlet velocity, with the decrease of porosity, the pressure drop between the inlet and outlet becomes larger, the slope of the line increase.

3.2 *Effective thermal conductivity*

In the present paper, we simply consider that the skeleton of sandstone all to be quartz granules,

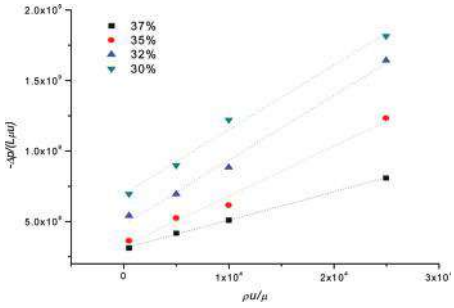


Figure 2. Calculated flow resistances in the porous media for different velocities.

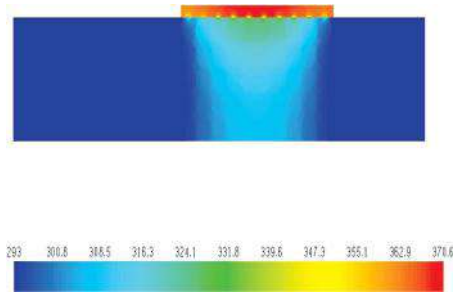


Figure 3. The temperature contour of the model when the inlet velocity is 0 m/s.

the particle's thermal conductivity is 7 W/m•K, the special heat capacity is 966 J/Kg•K, the constant heat flux from the top wall is q_0 = 14650 W/m^2, the boundary conditions of the inlet and outlet were set as adiabatic boundary, velocity of the fluid from the inlet is 0 m/s, then we could obtain the thermal distribution condition in the model by computational simulation, and the thermal conductivity could be obtained. Fig. 3 shows the temperature contour when the porosity is 37%.

The heat flux of the top plan is constant, $q_{w0,}$ the temperature difference between the top plan and the bottom plan is, the thickness of the porous media is Δt, so the effective thermal conductivity of the porous media could be calculated by Fourier's Law $q = -\lambda(\partial T/\partial x)$. The value of λ is 1.94 W/m•K when the porosity is 37%. By the same method, thermal conductivities for the other 3 models could be calculated, the values of λ are shown in Table 1 and Fig. 4.

Sugawara and Yoshizawa (Shen 1988) proposed the following empirical formula based on quantities of experiments for calculating the thermal conductivity coefficient:

$$\lambda = (1 - A)\lambda_s + A\lambda_f \tag{9}$$

Where,

$$A = \left[\frac{2^n}{(2^n - 1)}\right] \cdot \left[1 - \frac{1}{(1+\phi)^n}\right] \tag{10}$$

$n = 2$, when saturated with liquid water.

We could obtain the empirical value of thermal conductivity when porosity is 37%, 35%, 32%, 30% individually.

Table 2 shows the calculate and empirical values of λ and the deviation, which is about 20%, which indicates that the calculate value have a better identical with the empirical value. The main reason for the deviation is that the contact state

Table 1. Calculated values of effective thermal conductivities for different porosities.

ϕ	37%	35%	32%	30%
λ(W/m·K)	3.57	3.60	3.63	3.67

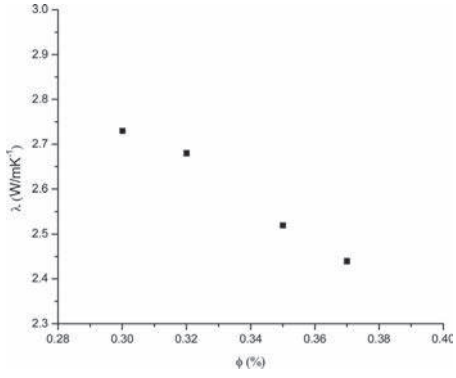


Figure 4. Relationship between porosity and thermal conductivity coefficient.

of the granules in the natural rock is much more complicate than the model we used, the total contact surface for thermal conduct is larger, and the cementing material can also conduct thermal. So this is the reason why the value we got is a bit small compared with empirical value.

3.3 *Convection heat transfer coefficient between the solid and the fluid*

The heat transfer between the solid particles and the fluid follows the local thermal non-equilibrium model. The volumetric heat transfer coefficient hv represents the heat exchanger capacity of the porous media. In the current paper, we will investigate the volumetric convection heat transfer coefficient by numerical simulation results of the

Table 2. Comparison between empirical calculated and numerical results for λ

φ	37%	35%	32%	30%
λ(W/m·K)	2.44	2.52	2.68	2.73
λ_{emp}(W/m·K)	2.94	3.08	3.30	3.46
Deviation (%)	17.0%	18.1%	18.7%	21.1%

non-equal spherical model find out the influence factors of the coefficient.

Dixon and Cresswell (Dixon & Cresswell 1979) proposed the equation for calculating the convection heat transfer as follow:

$$\frac{1}{h_{sf}} = \frac{d_p}{Nu_{sf}\lambda_f} + \frac{d_p}{\beta\lambda_s} \tag{11}$$

$$Nu_{sf} = \frac{0.255}{\varepsilon} Pr^{1/3} Re^{2/3}, \beta = 10 \tag{12}$$

$$Re = \varepsilon\rho u_p d_p / \mu \tag{13}$$

The volumetric heat transfer coefficient between the solid particles and the fluid is:

$$h_v = h_{sf} \cdot 6(1-\varepsilon)/d_p \tag{14}$$

First of all, when the porosity is constant, in case of porosity equals to 37%, we focus on the convection heat transfer coefficients between the large spheres and the fluid and coefficient between the small spheres and the fluid when the inlet velocity is 0.001 m/s, 0.01 m/s, 0.05 m/s separately. The average coefficient value of every vertical line are shown in Fig. 5

Fig. 4 shows that when the inlet velocity is constant, the surface convection heat transfer coefficient between the same size of the solid particles and the fluid is basically unchanged, however, in the same condition the large spheres' surface convection heat transfer coefficient is less than the small spheres'. The surfaces convection heat transfer coefficient increase while the fluid inlet velocity grows up. The gap between the surface convection heat transfer coefficient between the different diameter spheres get larger.

Fig. 5 shows that on the condition of the inlet velocity is 0.001 m/s, the average value of large & small particle's convection heat transfer coefficients while the porosity is various.

According to Fig. 6 in this model, the convection heat transfer coefficient between the particles and the fluid tend to decrease with the porosity increasing. We could conclude from Fig. 6 that velocity plays an important role in the convection heat transfer coefficient which grows up while the

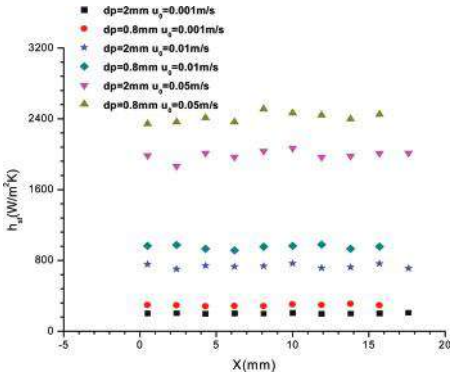


Figure 5. Average surface convection heat transfer coefficients of vertical particles, porosity 37%, inlet velocity 0.001 m/s, 0.01 m/s, 0.05 m/s.

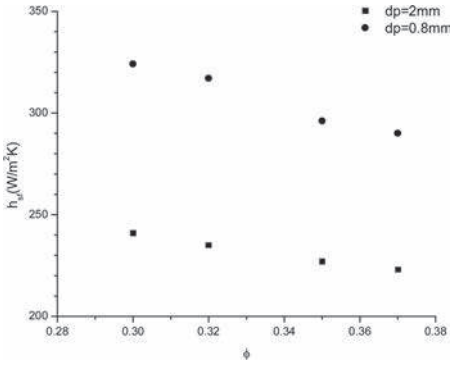


Figure 6. Average surface convection heat transfer coefficients of large & small particle, the inlet velocity is 0.001 m/s, porosity 37%, 35%, 32%, 32%.

velocity increases. The porosity increase so the channels for the fluid flow occupy a larger dimension, the average velocity of the fluid drops, therefore, the fluid velocity around the particles declines, the heat brought away becomes smaller in unit time that lead to the decreasing of the convective heat transfer coefficient.

The volumetric heat transfer coefficient between the solid skeleton and the fluid in the porous media was obtained by Eq.14. Fig. 7 shows the volumetric heat transfer coefficient of different porosities and different inlet velocities.

As can be seen from Fig. 7, in current model, volumetric heat transfer coefficients increase with the increasing of the fluid inlet velocity, while the increasing ratio decrease gradually. On the condition that the inlet velocity is constant, the smaller the porosity the larger the volumetric heat transfer coefficient. With the porosity gets smaller, the increase

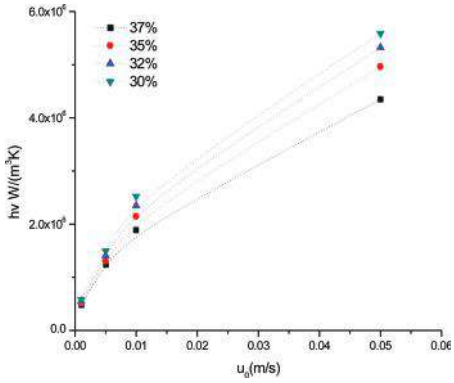


Figure 7. Volumetric heat transfer coefficient of different porosities and different inlet velocities.

ratio of volumetric heat transfer coefficient gets smaller. Because the volumetric heat transfer coefficient is related to specific area, fluid flow velocity around the particles, temperature of the porous media, and so on. In condition that the inlet velocity is constant, reduction of the porosity in current model, on one hand, could increase the fluid flow velocity in the porous media on the other hand, the specific area would decrease meanwhile. In these two factors' combined effect, the current model shows the characteristics as what is depicted above.

4 ENGINEERING EXAMPLE

State key laboratory for GeoMechanics and deep underground engineering carried out a cooling project for Zhangshuanglou Mine, which reached 1000 m deep and the temperatrue of the roadway reached up to 40 centigrade. The project was completed in 2011 successfully, the work condition was greatly improved. In present paper, we will use the parameters obtained from work above to simulate the cooling effect, and compare with the actual cooling condition.

4.1 *Cooling overview of roadway 7119*

The main strata of Zhangshuanglou minefield are sandstone and conglomerate, rich aquifer water. The average original rock temperature is 40°C, the humidity is high. The cooling project adopted HEMS cooling system which utilize full-face cooling mode.

4.2 *Cooling overview of roadway 7119*

For the surrounding rock is sandstone, we set that the model of the surrounding rock to be porous

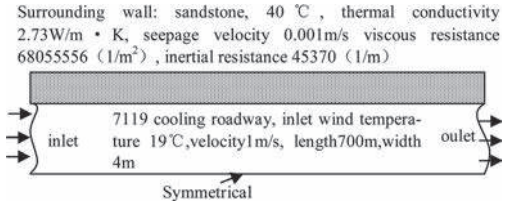


Figure 8. Model of 7119 cooling roadway and boundary conditions.

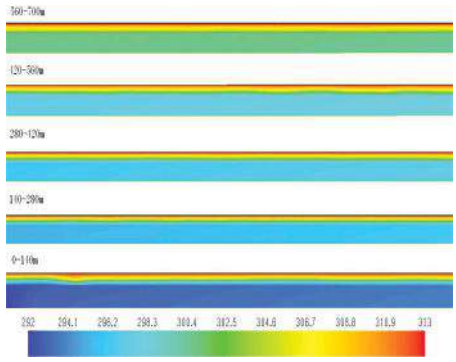


Figure 9. Simulated temperature contours of 7119 cooling roadway.

media whose parameters are obtained from previous work, porosity is 30%, viscous resistance is 68055556(1/m²), internal resistance is 45370(1/m), thermal conductivity is 2.73 W/m•K. The thickness of the rock is 1 meter, temperature of the wall is 40°C, seepage velocity is 0.001 m/s, the roadway is 700 meters long with width of 4 meters, inlet velocity is 1 m/s, temperature of the wind is 19°C. The model is shown in Fig. 8.

Fig. 9 shows the simulated temperature of 7119 roadway after cooling.

We could conclude from Fig. 10 that the simulated temperatures fit well with the actual temperatures, so the parameters we obtained from the non-equal diameter particles model are reliable and could be used in designing and predicting projects.

5 CONCLUSION

The present study reconstructed the sandstone's physical model with non-equal diameter sphere, obtained and analyzed the sandstone's permeability coefficient, thermal conductivity and volumetric heat transfer coefficient, by numerical simulation.

We analyzed the surface heat transfer coefficient of the particle and the volumetric heat transfer

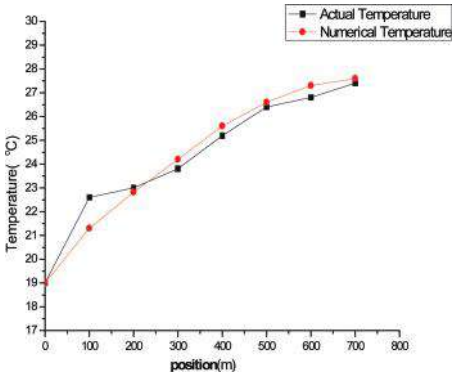


Figure 10. Comparison of actual and simulated temperature in 7119 roadway.

coefficient under the condition of different seepage velocities and porosities of the porous media. The higher the flow velocity, the larger the surface convection heat transfer coefficient will be. When the porosity and inlet velocity are fixed, the small particles' surface convection heat transfer coefficient is higher than the larger particles' which indicates particle size is one of the influence factors for the surface heat transfer coefficient.

In this model, the smaller the porosity is, the higher the volumetric heat transfer coefficient will be. The cause of this phenomenon was explained: Volumetric heat transfer coefficient was influenced by the specific surface, the porosity, and the fluid flow velocity in porous medium. But the trend is not invariably, the next job will focus on studying turning point of the porosity-volumetric heat transfer coefficient curve.

The non-equal diameter spherical particle model can be used to simulate the flow and heat transfer phenomenon in porous media which matches well with the actual situation, especially it make up the lack of equal diameter model in simulating the flow issue. This method proposed a new idea for predicting the flow and heat transfer properties for granule composed porous media, and has positive effect upon the heat load calculation.

ACKNOWLEDGEMENT

Financial support from the Special Funds for the National Natural Science Foundation (Key Project) under Grant No. 51134005 is gratefully acknowledged.

REFERENCES

Abe Takashi. 1997. Derivation of the lattice Boltzmann method by means of the discrete ordinate method for the Boltzmann equation. *Journal of Computational Physics,* 131 (1).

Adler Pierre M., Jacquin Christian G., Thovert Jean François. 1992. The formation factor of reconstructed porous media. *Water Resources Research,* 28 (6): 1571~1576.

Adler P.M., Thovert J-F. 1993. Fractal porous media. *Transport in Porous Media,* 13 (1): 41~78.

Bear Jacob, Bachmat Yehuda. 1990. Introduction to modeling of transport phenomena in porous media.: *Kluwer Academic Pub*.

Boming Yu. 2003. Advances of fractal analysis of transport properties for porous media. *Advances in mechanics,* 3.

Brinkman H.C. 1949. *A* calculation of the viscous force exerted by a flowing fluid on a dense swarm of particles. *Applied Scientific Research,* 1 (1): 27~34.

Carbonell Ruben G., Whitaker Stephen. 1984. *Heat and mass transfer in porous media*. Springer,: 121~198.

Chen Shiyi, Doolen Gary D. 1998. Lattice Boltzmann method for fluid flows. *Annual review of fluid mechanics,* 30 (1): 329~364.

Chen Yongping, Shi Mingheng. 1999. Determination of effective thermal conductivity for real porous media using fractal theory. *Journal of Thermal Science,* 8 (2): 102~107.

Cluver E.H. 1932. An analysis of ninety-two fatal heat stress cases on Witwatersrand gold mines. *South African Medical Journal,* 615~23.

Dixon Anthony G., Cresswell David L. 1979. Theoretical prediction of effective heat transfer parameters in packed beds. *AichE Journal,* 25 (4): 663~676.

Forchheimer Philipp. 1901. Wasserbewegung durch boden. *Z. Ver. Deutsch. Ing,* 45 (1782): 1788.

He Manchao, Cao Xiuling, Xie Qiao, et al. 2010. Principles and technology for stepwise utilization of resources for mitigating deep mine heat hazards. *Mining Science and Technology (China),* 20 (1): 20~27.

Hsu C.T., Cheng P. 1990. Thermal dispersion in a porous medium. I*nternational Journal of Heat and Mass Transfer,* 33 (8): 1587~1597.

Qian Y.H., D'Humieres D., Lallemand P. 1992. Lattice BGK models for Navier-Stokes equation. *EPL (Europhysics Letters),* 17 (6): 479.

Shen Xianjie. 1988. Thermal physical proerties of rock and test.: *science press*.

Shan Xiaowen, Chen Hudong. 1993. Lattice Boltzmann model for simulating flows with multiple phases and components. *Physical Review E,* 47 (3): 1815.

Vafai K., Tien C.L. 1981. Boundary and inertia effects on flow and heat transfer in porous media. *International Journal of Heat and Mass Transfer,* 24 (2): 195~203.

Whitaker Stephen. 1969. Advances in theory of fluid motion in porous media. *Industrial & engineering chemistry,* 61 (12): 14~28.

Whitaker Stephen. 1973. The transport equations for multi-phase systems. *Chemical Engineering Science,* 28 (1): 139~147.

Progress in Mine Safety Science and Engineering II – He et al. (Eds)
© 2014 Taylor & Francis Group, London, ISBN 978-1-138-00122-0

Research on the adaptability large mining height fully-mechanized mining equipment to panel mining of unstable coal seam

He-Xing Wen
School of Mining Engineering, Inner Mongolia University of Science and Technology, Baotou, Inner Mongolia, China

Yu-de Liu
School of Safety Engineering, North China Institute of Science and Technology, Langfang, Hebei, China

Xiang-Tian Meng
School of Mining Engineering, Inner Mongolia University of Science and Technology, Baotou, Inner Mongolia, China

ABSTRACT: Huoluowan coal mine was mining the 2^{-2} coal seam, does the selection in panel 1 5.0 m large mining height fully-mechanized equipment can be apply to the unstable coal seam in panel 2 become a problem need to be solved urgently. In this paper, According to the application analysis and theoretical calculation to parameters of the main equipment, such as the working resistance of powered support, support height, support strength and coal cutter mining height, installed power and so on, then combination with mining experience and equipment operation effect in panel 1, analyze the feasibility to the equipment mining adaptability in panel 2, It demonstrated the applicability of large mining height fully-mechanized mining equipment to unstable coal seam, this research conclusions has the universal significance and promotion value to similar conditions seam exploitation.

1 INSTRUCTIONS

Underground coal seam conditions in most parts of the country are changes, because of fully mechanized coal mining equipment were expensive, generally under the same conditions of coal seam used with same set fully mechanized coal mining equipment, research on the equipment adaptability to unstable coal seam mining can increase the economic benefit of coal mine and coal resource recovery, conducive to the sustainable exploitation of mine and therefore unstable coal seam equipment adaptability of general relevance and promotion value. Reasonable selection of equipment only while fully mechanized, support appropriate, safe and practical, to really bring the automation advantage of mechanization, better guarantee safety and high efficiency mining in coal mines.

This paper intends to 22110 face (end face) conditions on the basis of theoretical calculation method and effect analysis of actual mining, mining machines, hydraulic, scrapers and other analytical studies are widely promoting the use of research results.

2 GENERAL SITUATION

HuoLuowan'2–2 coal mine burying depth 149.6 m~187.2 m, near shallow, seam dip angle 0°~6°, f = 2~3 seam Proctor coefficient 4.71 m~6.76 m was the unstable coal seam, layout Panel-type. Roof integrates column, Panel layout and thickness of coal seam as shown in Figure 1, 2, 3, 4. Panel 1 mining has near end, continued of Panel 2 was different in seam thickness and roof conditions with Panel 1 (floor changes very little), seam almost thick 0.7 m~1.1 m, according to Panel 1 of excavation, and mining situation, seam thickness in 4.8 m~5.46 m; Panel 1 by 1 and 2 face of road way excavation situation, seam thickness in 5.16 m~6.55 m, average in 5.66 m. Direct variable-thickness 0.3 m, thinning old 0.92 m, rock did not change, was hard ~ super hard.

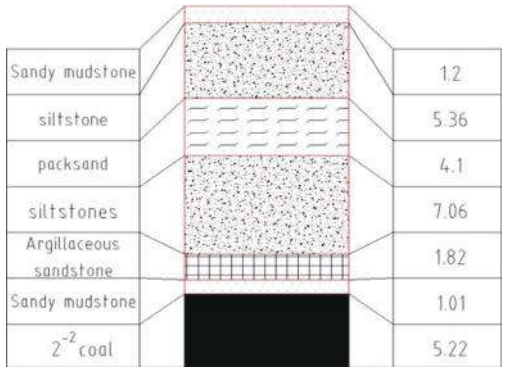


Figure 1. Synthesis Histogram of panel 1 roof.

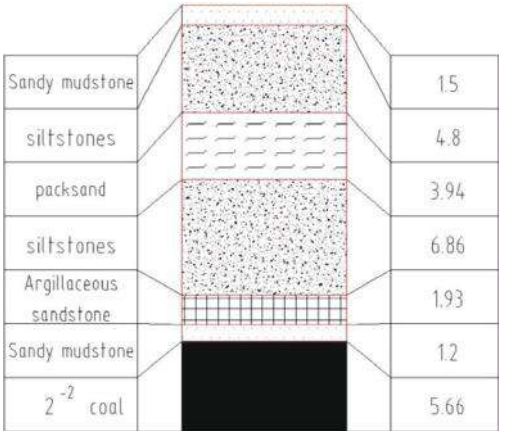


Figure 2. Synthesis Histogram of panel 2 roof.

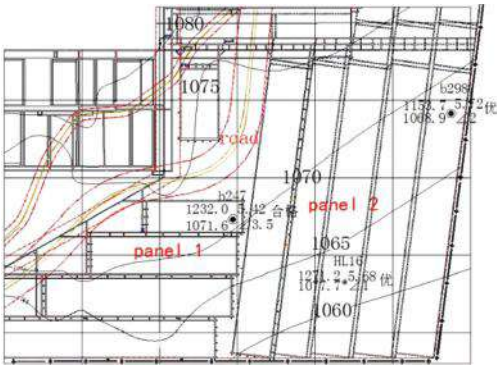


Figure 3. Layout panel in Huo coal mine.

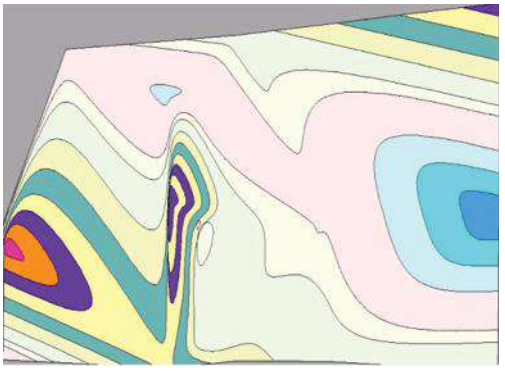


Figure 4. Contour of coal in panel 1 & 2.

Table 1. Main equipment.

No	Equipment name	Type No	Argument
1	Support	ZY86400/25.5/55	8640 kN
2	Coal cutter	MG800/2040-WD	2040 kW
3	conveyor	SGZ1000/1400	2500 t/h
4	Transfer conveyor	SZZ1200/400	3500 t/h
5	crusher	PLM4000	4000 t/h

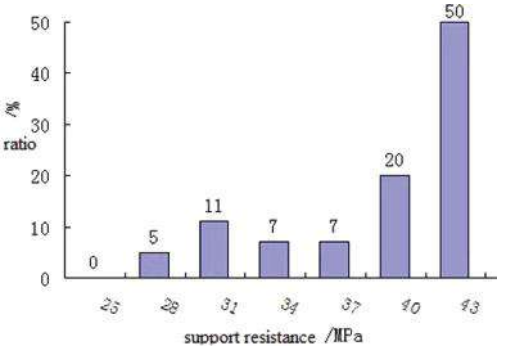


Figure 5. Support pressure distribution.

3 THE EQUIPMENT MATCHING OF FACE

3.1 *Equipment matching*

22, 107 face for HuoLuowan mine was first using 5.0 m large mining high fully mining equipment, Beijing Coal Mine Machinery Co., Ltd according to Unstable Coal Seam production the support mining machine select Jixi Coal Mine Machinery Co., Ltd. Made special mining high mining machine, conveyor machine was matching hydraulic bracket support, used Ningxia Tiandi Benniu industrial group Co., Ltd products. All is shown in Table 1.

3.2 *Panel 1 mining equipment production effect*

In Panel 1, four mining processes, designing mining height 5.0 m, get good Mining Recovery Index, reached 96%, the highest production per day was 19, 700 tons. during pressure change: roof control well, less roof falling slicing, apart from the Central head 35 frames left and right support to achieve maximum resistance, overset, the others has 10%~30% surplus, periodic Weight support pressure distribution shown in Figure 5. Conveyor machine, Crusher, belt conveyor is working well, coal blockage, overloading does not occur.

4 ADAPTABILITY ANALYSIS OF LARGE MINING HEIGHT FULLY-MECHANIZED MINING EQUIPMENT

4.1 *Main parameters and selection of Hydraulic support*

4.1.1 *Support height*

To adapt to the change of coal seam thickness and ensure support, usually selecting holder maximum structure height larger than the maximum cutting height max 0.2 m~0.3 m, $H_{max} = M_{max}+0.2$; support minimum height should be met minimum height roof setting, coal cutter and conveyor equipment, taking 0.3 m less than the minimum height, Hmin = Mmin–0.3. Face design for maximum cutting height 5.3 m, requires support maximum height 5.5 m, face minimum cutting height 4.0 m, support minimum required height of 3.7 m, now the support was range in 2.55 m~5.5 m meet the requirements.

4.1.2 *Support strength*

According to the formula determine the support strength which provided by MT554–1996.

$$Ps = 72.3Hm + 4.5\ Lp + 78.9Bc\text{-}10.24\ N\text{-}62.1 \quad (1)$$

In the equation: P_s as a support strength, kN/m^2; Hm was high, take 5.2 m; Lp as a basic first step, take 50 m; Bc was the Face-to-gob distance, take 5.97 m; N filling factor, N = Hi/Hm; Hi for immediate roof thickness, take 3.13 m. so:

Ps = 1003.733 kN/m^2 = 1.004 MPa.

4.1.3 *Working resistance*

Loads of pressure on each support Q_1 (kN) according to the following formula:

$$Q_1 = K\frac{M}{k-1}b(L+C)\gamma \bullet 9.8 \quad (2)$$

In the equation:

K—the coefficient of dynamic load in periodic weighting, take 1.8;

M—the maximum cutting height, take 5.4 m;

k—the hulking coefficient of rock, take 1.3;

L—the canopy of the support, take 4.685 m;

C—beam distance, 0.485 m;

b—supports spacing, 1.75 m;

γ—density of roof rock, 2.617 t/m^3.

$$Q_1 = 2 \times 5.4 \times 1.75 \times (4.685 + 0.485) \times 2.617 \times 9.8/(1.3–1) = 7518.1 \text{ kN}.$$

According to the calculation result, the Support working resistance surplus.

4.2 *Coal cutter*

4.2.1 *production capacity*

Base on the past production practices, coal cutting average 3.5 m/min, Coal cutter production capacity use the following formula:

$$Q_c = 60V_cLM\gamma_1 \quad (3)$$

In the equation: Q_c was actual production capacity, V_c for average speed, 3.5 m/min; L for cutting deep, 0.8 m; γ_1 mean density of coal, 1.29 t/m^3.

$$Q_c = 60 \times 3.5 \times 0.8 \times 1.29 \times 5.3 = 1148.6 \text{ t/h}$$

Normal daily output of 18, 000 t, fully meet 3 Mt per year production tasks.

4.2.2 *Installed power*

Based on experience, tons of coal mining required 0.6 kW/h~0.8 kW/h energy, taking into account the theoretical maximum total power for the cutter to fast cutting coal in Central and productivity 1804.98 t/h, the required power11443.97 kW. In actual production, mining machine of installed power more than normal cutting needed, also needed to consider mining machine broken rock capacity, so mining machine capacity should consider rich coefficient, take 1.15, thus, mining machine of total power for 1660.57 kW, take round numbers for 1700 kW, so 2040 kW of coal machine full has surplus.

5 FEASIBILITY ANALYSIS OF MINING IN PANEL 2

5.1 *Mining conditions analysis*

Thickness change, according to Panel 2 01 & 02 excavation roadway, judging coal seam thickness 5.16 m~6.55 m, 5.66 m average. Calculate with recovery more than 93% requires, mining height design 5.3 m~5.4 m.

Angle change, Angle is getting large, according to the excavation roadways; angle of coal seam was 3°~8°, had no effect on three machines met and Panel mining.

Roof pressure, floor thickness change very small but in the roof was big, rock property was the same, it will affect the roof weighting step and pressure, influence the support Working resistance. In Panel 1 the coefficient of dynamic load in periodic Weighting was 1.51, take 1.8 into calculate, support has surplus.

Other conditions, the advancing length is to two or three times more, so mining time will be longer, it can reduce the impact of mining dynamic pressure to mining in nearby coal face.

5.2 *Feasibility analysis*

According to the coal mining machine drum diameter of 2.7 m, the installed power 2040 kW, and the application effect in panel 1 under the condition of 5.0 m mining height show that, the thickness of the unstable panel 2, 5.5 m mining height can be adapted to. But as a result of mining height increase, the frequencies of large coal increase, to reduce coal cutting speed, can effectively reduce the generation of large coal, so need to formulate corresponding measures, at the same time actually reduce large coal, reducing load of crusher.

For the local coal seam dip angle is bigger (8°) and mining height increase (5.5 m), if use traditional tolerate clearance, the stability of the support couldn't be ensure, Maybe will appears deflection, torsion, even falling. when design, using the four-bar linkage, its primary to improves the support stress condition and ensure tilt stable of the support, because roof beam trajectories was smallest, can withstand greater horizontal and lateral forces. use the most stable structure: the front and behind double form of connecting rod, under center distance of 1750 mm, the two connecting rods distance increased to 960 mm, Enhances the deflection and torsion resistance ability of the stent itself, The stability of the support was good.

Mining height increase obvious influence on rock pressure control, the manifestation of support use in panel 1 mining and itself parameters show that: the support height enough, support strength meet, but there may be a large number of safety valve open in the first weighting, need to take forced roof caving when the period of primary mining, It can reduce the main roof Fracture length at the first time, and really reduce first weighting cause huge impact load on support, so the three machines meet unstable coal seam mining.

6 CONCLUSION

The selected device in Panel 1 with large mining height coal mining area of 5.0 m, works well, good adaptability.

The seam mining conditions in panel 2 was complicated than panel 1, mainly in: change of coal seam thickness, mining height increase also; coal seam dip angle is getting bigger, influence the stability of support; and the original selection of 5.0 m fully mechanized coal mining equipment mining 5.5 m thick coal seam.

By forced roof caving of primary mining period, slowing the cutting machine travel speed, support closely and manual fragmentation of large coal timely, make large mining height Fully-mechanized mining coal equipment better adapted to the complex conditions.

REFERENCES

Cheng, Y.T. 2008. 6.2 m large mining height in sihe mine fully-mechanized coal mining equipment lectotype. *Coal* 17(2): 24–27.

Hao, C.J. & Chen, P. & Li W.S. 2005. Discussion on fully mechanized coal mining equipment selection and matching principles. *Coal engineering* (10): 37–39.

Lei, Y.J. & Luo, W. 2007. 12 million t/a selection of fully-mechanized face equipment. *Coal engineering* (7): 5–7.

Liu, X.L. 2008. Technology of automatic fully-mechanized equipment with large mining height. *Coal* 17(6): 12–14.

Li, D.Z. 2009. Papaya Nissan tons of coal mine fully mechanized equipment selection. *Coal technology* 28(1): 57–59.

Ma, W.X. & Liu, X.M. 2011. 6.2 m mining height face complete study on stability and application of domestic equipment. *Coal engineering* (5): 43–45.

People's Republic of China coal industry MT554–1996 code for design of hydraulic support. 1996. Beijing: *China coal industry publishing house.*

Wang, C.C. & Zhang, Y. 2008. 7, 211 in renlou coal mine working face with large mining height equipment selection. *Coal technology* 27(8): 143–144.

Yao, Y. & Zhou, M.L. 2001. Full-height fully mechanized mining of thick seam mining equipment type selection calculation. *Coal technology* 20(2): 25–27.

Yin, D.W. 2005. Unstable coal seam mining technology study. Qingdao, *Shandong University of science and technology.*

Progress in Mine Safety Science and Engineering II – He et al. (Eds)
© 2014 Taylor & Francis Group, London, ISBN 978-1-138-00122-0

The study on dynamic early-warning of coal face gas emission based on extension theory

Baiwei Lei, Bing Wu, Yan Peng & Chao Wang
Faculty of Resources and Safety Engineering, China University of Mining and Technology (Beijing), Beijing, China

ABSTRACT: In order to prevent the occurrence of coal face gas disasters, the early-warning model of coal face gas emission is established. Based on the identification and analysis of coal mine gas hazards, the evaluation model of danger level of coal face gas hazards has been built by using extension theory to make coal mine gas emission factor index matter-element, through the computation of membership degree to determine the danger level of coal face gas hazards, and combine with gas monitoring data to realize the dynamic early-warning of abnormal gas emission finally. The early-warning model is applied to the Tongxin coal mine, the result shows that the model can accurately identify danger level of gas emission caused by hazards change, and through a combination of gas monitoring data it can do dynamic early-warning of coal face gas emission, which provide the scientific basis for the prevention and control measures.

1 INTRODUCTION

Mine gas is one of the important hidden trouble to influence coal mine safety production (Shi et al., 2006), the abnormal gas emission will usually lead to coal mine gas accident. Gas emission is affected by many factors (Zhu et al., 2007; Guo et al., 2009; He et al., 2008), the judgment of abnormal gas emission is not only important to the real-time monitor of the gas concentration (Zhang et al., 2012), but also important to the discrimination of the reason of abnormal gas emission. Therefore, the dynamic evaluation of gas emission hazard danger level combined with gas monitoring data plays an important role on gas prevention and gas disaster control when it does dynamic early-warning of coal face gas emission (Lv et al., 2006; Gong et al., 2012).

The related theory about extenics is founded by the Chinese scholars Cai wen to solve the problem of subjective and objective contradictions in 1983 (Cai, 1983), it bases on the matter-element theory and extension set theory and does research on the influence degree of the described problems about "quantity" and "quality", so as to completely know the system features (Guo et al., 2009). Due to the complexity production conditions of underground working face, there are a variety of factors that affect gas emission, how to quickly and accurately judge the reasons that why the gas emission is abnormal is an important task of gas early-warning, the extension theory can calculate the abnormal gas emission level by using the normalized correlation function. Under the condition of correct identification of gas hazard in coal mine, using the extension theory to establish the gas hazard danger level evaluation model, evaluating the change of hazard grade every day, and combining with gas monitoring system to determine an acceptable level of gas emission under different conditions, which can do real-time early-warning of abnormal gas emission.

2 GAS HAZARD EXTENSIBLE SYNTHETIC EVALUATION MODEL

Extenics puts forward the concept of matter-element, records as: R = (matter, characteristic, value) = (N, C, X), which can formally describe objects, things and relationships, exactly describe the change process of objective things. Gas emission is a result of complex factors, single index can not accurately evaluate the reasons of abnormal gas emission. The comprehensive evaluation model of various hazards of gas emission can be built based on matter-element analysis method, by setting different weights to quantitatively calculate the results of the evaluation (Cai et al., 2008; Yang and Cai, 2007).

The basic idea using the extension model to evaluate hazard danger level of gas emission is as follows (Yang et al., 2008):

- Divided the alert degree of early-warning objects into several levels;
- Determined the range of the data of each level by synthesizing expert advice;
- Then put the index of early-warning object into the set of various levels to do multi-index evaluation;

- Compared the evaluation results according to the comprehensive correlation degree of the set of various levels, the greater the comprehensive correlation degree is, the better the degree of compliance with evaluation objects and level set, the alert degree of early-warning object is the level.

2.1 *Determine the classical domain and the evaluated matter-element*

The matter-element of classical domain, records as:

$$R_i = (N_i, C, X_i) = \begin{bmatrix} N_i & c_1 & X_{1i} \\ & c_2 & X_{2i} \\ & \cdots & \cdots \\ & c_n & X_{ni} \end{bmatrix} = \begin{bmatrix} N_i & c_1 & \langle a_{1i}, b_{1i} \rangle \\ & c_2 & \langle a_{2i}, b_{2i} \rangle \\ & \cdots & \cdots \\ & c_n & \langle a_{ni}, b_{ni} \rangle \end{bmatrix} \quad (1)$$

Where N_i represents hazard level of coal face gas, ($i = 1, 2, \ldots, m$);C represents hazard evaluation index of coal face gas; X_i represents the range of corresponding evaluation index.

The evaluated matter-element, records as:

$$R = (P, C, X_p) = \begin{bmatrix} P & c_1 & v_1 \\ & c_2 & v_2 \\ & \cdots & \cdots \\ & c_n & v_n \end{bmatrix} \quad (2)$$

Where P represents specific coal face; v_i represents specific value of hazard evaluation index of evaluated coal face gas.

2.2 *Determine the correlation function value*

Calculation for correlation function value of hazard evaluation index of evaluated coal face gas about the state of different hazards level.

$$K_i(x_j) = \begin{cases} -\dfrac{\rho(x_j, X_{ji})}{|X_{ji}|} & (x_j = X_{ji}) \\ \dfrac{\rho(x_j, X_{ji})}{\left[\rho(x_j, X_{pi}) - \rho(x_j, X_{ji})\right]} & (x_j \neq X_{ji}) \end{cases} \quad (3)$$

and $\begin{cases} \rho(x_j, X_{ji}) = |x_j - (a_{ji} + b_{ji})/2| - (b_{ji} - a_{ji})/2 \\ \rho(x_j, X_{Pi}) = |x_j - (a_{Pi} + b_{Pi})/2| - (b_{Pi} - a_{Pi})/2 \end{cases}$,

$|X_{ji}| = |a_{ji} - b_{jii}| \quad (j = 1, 2, \ldots, n; i = 1, 2, \ldots, m)$

2.3 *The calculation of weighting coefficient*

Through the analytic hierarchy process to determine the relative importance of the evaluation index, ultimately determine the corresponding index weights λ_j ($j = 1, 2, \ldots, n$).

2.4 *Determination of membership and evaluated sample level*

Membership reflects the degree of proximity of sample under test for different levels, it also be called as comprehensive correlation degree, calculated by the following formula:

$$K_i(p) = \sum_{j=1}^{n} \lambda_j K_i(x_j) \quad (4)$$

Where $K_i(p)$ represents comprehensive correlation degree of face gas hazard level; If $K_i(p) = \max K_i(p) (i = 1, 2, \ldots, m)$, the hazard level of face gas will be i.

3 DYNAMIC EARLY-WARNING OF GAS EMISSION

3.1 *Hazard evaluation index classification*

Coal mine gas hazard evaluation index can be divided into three parts: static class index, dynamic class index, key monitoring index(Guo, 2012). Among them, static class index includes the indexes that do not change or rarely change and the degree of change was not significant during the entire coal production; dynamic class index includes the indexes that change constantly, need daily statistics or real-time monitoring; key monitoring index mainly includes some of the danger indexes, if it happens, it will directly lead to changes of danger level. In practical applications, static and dynamic index value is the value of the corresponding monitoring index; the value of key monitoring index is "yes" or "no", that is, whether there is a case mentioned in the index.

3.2 *Hazard evaluation index grading*

The hazards of face gas divided into five levels as safe (I), general (II), dangerous (III), very dangerous (IV), extremely dangerous (V), respectively express with colorless, blue, orange, yellow, red that shown in table 1.

3.3 *Dynamic early-warning*

After using extension theory model to determine the gas hazard level, marking different danger level

Table 1. Gas hazard danger level.

Security status	Safe	General	Dangerous	Very dangerous	Extremely dangerous
Early-warning criterion	[0, a]	(a, b]	(b, c]	(c, d]	(d, +∞]

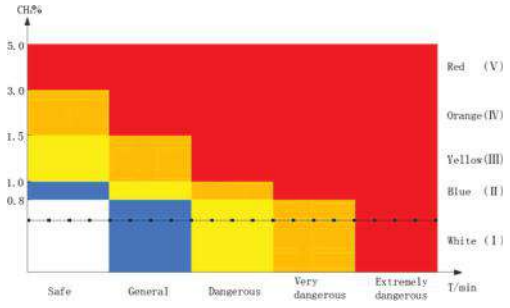


Figure 1. Example of early-warning trend.

with corresponding color, and then combining the monitoring value of gas concentration and eventually determining the risk level of gas emission, to achieve the dynamic early-warning of gas emission combined with extension theory and dynamic critical factor. As shown in figure 1, the early-warning level of gas under the same condition of gas concentration will be different if hazard level of gas is different.

4 ANALYSIS OF APPLICATION EXAMPLE

4.1 *Overview of application mine*

Tongxin mine's design production capacity is 10.0 Mt/a, the mine service life is 67.5 years. The relative gas emission of mine is less than 6 m^3/t, so the mine is the low gas mine, but the local coal seam gas content is high. In order to do early prediction and prevention of gas disasters accidents, using dynamic early-warning model to do dynamic monitoring and timely early-warning of gas emission in 8100 coal face.

4.2 *Evaluation index classification*

According to the principle of classification of three types of indexes, determining the coal face gas emission evaluation index of Tongxin coal mine(shown in table 2).

According to the relevant provisions of "coal mine safety regulation" and "coal and gas outburst prevention regulations", combining with Tongxin mine history data and expert opinion to determine the boundary of the early-warning indexes, shown in table 3.

Table 2. Indexes of gas emission exception in coal face.

Static index	Dynamic index	Key monitoring index
U_1:Coal seam depth(m)	U_{10}:Actual wind speed(m/s)	U_{12}:First caving (enhancing I risk level when it appearing)
U_2:Coal seam thickness(/Mpa)	U_{11}:Actual face advancing speed(m/d)	U_{13}:Roof pressure (enhancing I risk level when it appearing)
U_3:Coal seam gas content		U_{14}:Geological tectonic belt (enhancing I risk level when it 5 m from the tectonic)
U_4:Coal seam gas mission(ml/s)		U_{15}:Gas overrun (enhancing I risk level when it long-term or repeated overrun)
U_5:Sturdiness coefficient(m^3/t)		
U_6:Coal seam gas pressure(m^3/min)		
U_7:Initial velocity of diffusion(m)		
U_8:Mining methods(Expert decision)		
U_9:Goaf treatment(Expert decision)		

4.3 *Evaluation index classification*

The hazard evaluation parameters of 8100 face shown in table 4.

According to the importance of evaluation indexes (Ye et al., 2006)and the research of the literature (Zhang, 2011), determining the weight set:

$$\lambda_j = (\lambda_1, \lambda_2, \ldots, \lambda_{11})$$
$$= (0.021, 0.069, 0.026, 0.042, 0.088, 0.113, 0.033, 0.144, 0.053, 0.229, 0.182)$$

Table 3. Limit table of hazard danger level of gas emission.

Static index	Safe	General	Dangerous	Very dangerous	Extremely dangerous
Coal seam depth(U_1)	[0, 100]	(100, 160]	(160, 600]	(600, 800]	(800, 1000)
Coal seam thickness(U_2)	[0, 0.5]	(0.5, 0.74]	(0.74, 1.0]	(1.0, 1.5]	(1.5, 3)
Coal seam gas content(U_3)	[1, 2]	(0.5, 1]	(0.4, 0.5]	(0.26, 0.4]	(0, 0.26)
Coal seam gas mission(U_4)	[0, 5]	(5, 10]	(10, 15]	(15, 20]	(20, 30)
Sturdiness coefficient(U_5)	[0, 2]	(2, 6]	(6, 8]	(8, 10]	(10, 15)
Coal seam gas pressure(U_6)	[0, 0.85]	(0.85, 1.05]	(1.05, 1.5]	(1.5, 3]	(3, 5)
Initial velocity of diffusion(U_7)	[0, 1.3]	(1.3, 3.5]	(3.5, 10.0]	(10.0, 15.0]	(15.0, 20)
Mining methods(U_8)	[90, 100]	(80, 90]	(70, 80]	(60, 70]	(0, 60)
Goaf treatment(U_9)	[90, 100]	(80, 90]	(70, 80]	(60, 70]	(0, 60)
Actual wind speed(U_{10})	[2, 4]	(1, 2]	(0.5, 1)	(0.25, 0.5]	[0, 0.25)
Actual forward speed(U_{11})	[0, 6]	(6, 6.6]	(6.6, 7.8]	(7.8, 9]	(9, 10.8)

Table 4. Geological structures of 8100 face in Tongxin coal mine.

Index	U1	U2	U3	U4	U5	U6	U7	U8	U9	U10	U11
Value	420	0.7	0.5	8	2.31	2.23	13.67	90	80	1.9	6.1

Table 5. The degrees of the predicting results at Tongxin Coal Mine 8100 face.

Level	Safe membership	General membership	Dangerous membership	Very dangerous membership	Extremely dangerous membership	Early-warning level
Value	–0.156545	0.014852	–0. 260785	-0.213641	–0.328049	General safety

and putting the data under test and the early-warning index weights into the extension synthetic evaluation model to determine the gas hazard danger level, shown in table 5.

As seen from the table 5, "general" is the maximum membership, combined with key monitoring index into account, since the first caving, roof pressure, gas overrun, geological tectonic belt were not appearing, the gas hazard risk level of 8100 face is "normal". Combining with the October 30 gas concentration data of 8100 face listed in table 5.6 and the danger classification of dynamic critical gas concentration under "general" rank, get the figure 2, the figure shows that the gas concentration is in the blue area, and belong to grade II, it is acceptable risk, so the system can maintain normal operation, it doesn't require danger alarm.

5 ANALYSIS OF APPLICATION EXAMPLE

By studying the coal face gas emission characteristics, dividing the gas emission evaluation index into three types: static index, dynamic index and key monitoring index. For different types of index, using different methods to evaluate the risk level, which can dynamically monitor the changes of hazard which can impact gas emission.

As coal face gas emission affected by many factors, it has to synthetically consider qualitative factors and quantitative factors to get more reasonable early-warning results of coal face gas emission, the extension theory can effectively considering factors of quantitative and qualitative index and quantitatively calculate the evaluation results to ensure that evaluation results are reasonable.

After using extension theory model to determine the evaluation results of gas emission, through a combination of gas concentration monitoring data to achieve a dynamic early-warning of gas emission combined with extension theory and critical dynamic factor, avoiding the single and static risk early-warning level of gas emission, and it's guiding role on actual production is more accurate and practical.

REFERENCES

Cai Wen. 1983. So ution of incompatible problems via structural transformation. *Gdit journal,* 1:76–88.

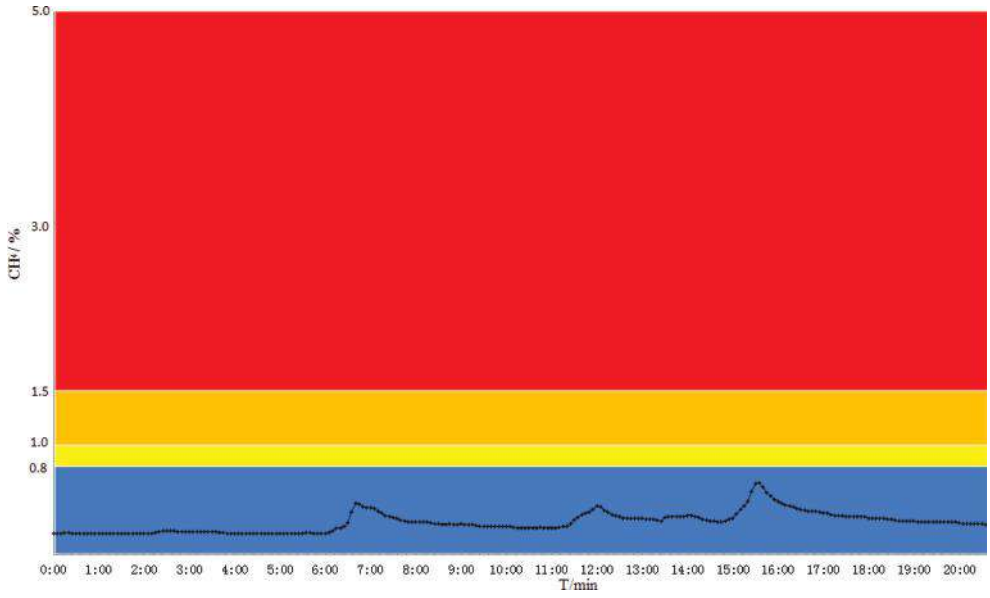


Figure 2. The real-time early warning of gas concentration curve (2012.10.30).

Cai Wen, Yang Cunyan, Chen Wenwei, Li Xingmiao. 2008. *The extension set and extension data mining*. Bei Jing: Science Press.

Gong Xiaoyan, Yan Donghui, Xue He. 2012. Predictive model of excavation ventilation gas concentration in high gas coal mine. *Journal of Xi'an University of Science and Technology,* 32(3): 275–279.

Guo Deyong, Zheng Maojie, Guo Chao. 2006. Hu Dianming, Zhang Xiaoke. Extension clustering method for coal and gas outburst prediction and its application. *Journal of China Coal Society,* 2009, 34(6): 783–787.

Guo Deyong, Zheng Maojie, Ju Chuanlei, Hao Xianglong. 2009. Stepwise regression method for predicting gas emission from coal faces. *Journal of University of Science and Technology Beijing,* 31(9): 1095–1099.

Guo Hai. 2012. Research on Identifying and Early Warning Technology of Coal Mine Gas and Fire Hazards. Doctoral dissertation, China University of Mining and Technology(Bei Jing), Bei Jing.

He Liwen, Shi Shiliang, Song Yi, Liu Ying. 2008. Complexity and measurement of complex degree of gas gush in heading faces of coal mine. *Journal of China Coal Society,* 38(5): 547–550.

Lv Ping, Ma Yunge, Zou Xinquan. 2006. Research and application on dynamic forecasting model of gas consistence in top corner. *Journal of China Coal Society,* 31(4): 461–465.

Shi Shiliang, Song Yi, He Leliwen. 2006. Research on determination of chaotic characteristics of gas gush based on time series in excavation working face of coal mine. *Journal of China Coal Society,* 31(6): 58–62.

Yang Cunyan, Cai We. 2007. *Extension engineering*. Bei Jing:Science Press.

Yang Yuzhong, Feng Changgen, Wu Liyun. 2008. Research on Early-warning Model for Coal Mine Safety Based on Extension Theory. *China Safety Science Journal,* 18(1):40–45.

Ye Yicheng, Ke Lihua, Huang Deyu. 2006. *Technology and application of comprehensive evaluation system.* Bei Jing:. Metallurgical Industry Press.

Zhang Hongling. 2011. *Study on Coal Mine Underground Gas Explosion Early Warning Association Model. Master dissertation*, China University of Mining and Technology(Bei Jing), Bei Jing.

Zhu Hongqing, Chang Wenjie, Zhang Bing. 2007. Differen-tsource gas em ission prediction model of working face based on BP artificial neural netw ork and its application. *Journal of China Coal Society,* 32(5): 504–508.

Zhang Shihe, Cai Qinxiang, Chen Kaiyan. 2012. Characteristics of the Gas Emission Rate Based on the Monitoring Data in the Fully-Mechanized Working Face. *Journal of Ming & Safety Engineering,* 29(4):586–590.

This page intentionally left blank

Progress in Mine Safety Science and Engineering II – He et al. (Eds)
© 2014 Taylor & Francis Group, London, ISBN 978-1-138-00122-0

Study on mining pressure appearance feature in shallow-buried fully-mechanized longwall face

Yan-Fang Ren
Tiandi Science and Technology Co., Ltd., Beijing, China

ABSTRACT: Using field observation combined with data simulation research methods to study mine pressure characteristics and influence factors aimed to the typical shallow-buried long wall face, we master hydraulic support adaptability and mine pressure appearance rule in shallow-buried long wall face. The research results show that, overlying rock structure's stability of shallow-buried long wall face is also affected by mining parameters, such as mining height and length of mining face, etc., besides objective geological conditions. Fissure zones conducting surface (namely, the bedrock layers are all broken periodically) and main roof breaking periodically are key causes that make the roof of shallow-buried long wall face exist two different cycles. And the results provide better references for roof supporting and support selection in mining shallow-buried fully-mechanized working face.

1 INTRODUCTION

1.1 *Shallow-buried long wall face mining*

Generally believed, due to the particularity of the occurrence condition in shallow-buried coal seam, in the process of coal mining, the bedrock layers will be all broken, which directly leads to instability failure of overlying rock structure and then causes a strong pressure appearance in working face (Huang 2000). There are great differences between shallow-buried and conventional-buried depth of coal seams after mining (Qian & Zhao 1987). According to the existing theory and research results, overlying rock structure's stability of shallow-buried long wall face is also affected by controllable factors, such as mining height, length of mining face and mining speed, etc., besides objective geological conditions (Huang & Qian 1999). If mining height and length of a shallow-buried long wall face were not too big, the face will only cause a limited damage to roof strata after mining, and bedrock layers may not be all broken, in addition, mine pressure of working face would appear similar rule as conventional-buried coal seams (Ren 2011). Therefore, through comparison and analysis of mine pressure characteristics in the typical shallow-buried long wall face, we can master factors of mine pressure appearance, and provide better references for roof supporting and support selection in mining coal seams of similar conditions (Ren 2008).

1.2 *General situation of working face*

316-04 working face of Nayi mine mines 6_{-2}^{upper} coal seam of China Dongsheng coal field, and the dip angle of coal seam is 1°~3°, the thickness is 1.85~2.31 m, 2.2 m on average, the ground elevation is +1282~+1209 m, the floor elevation +1152~+1164 m. Average buried depth of working face is 109 m. The average thickness of unconsolidated layers is 42 m, the average thickness of bedrock is 67 m. The working face length in the strike direction is 1635 m, the inclination length is 180 m, which belongs to the typical shallow-buried long wall face.

2 DATA ANALYSIS OF MEASURED MINING PRESSURE

2.1 *Layout scheme of observation instruments*

The study of mine pressure regularity is mainly achieved through the analysis of hydraulic support column pressure. Hydraulic support column pressure measurement instrument adopts CDW-60 type hydraulic support pressure recorder. Support pressure measurement uses the station layout namely, 3 stations were set up along the incline direction of working face, which locate in the upper, middle and bottom of working face respectively. Measurement instruments of the upper station are installed on No.34, No.35 and No.36 supports, and measurement instruments of the middle station are installed on No.67, No.68 and No.69 supports, while measurement instruments of the bottom station are installed on No.92, No.93 and No.94 supports.

2.2 *Results analysis of observation data*

Analysis of roof weighting data in 316-04 working face is shown in table 1. From table 1, we know

that periodic weighting interval of the main roof in 316-04 working face is 14.2 m on average, and the maximum interval is 19 m, the minimum 6 m.

All statistics of dynamic load factors during main roof weighting are shown in table 2 and figure 1.

Though analyzing table 2 and figure 1, we know that the main roof pressure strength of 316-04 working face exist the obvious long and short cycle phenomenon. The main reason is that after extracting shallow-buried mining face, crack zone generally conducts to surface, and the two phenomena of the main roof breaking and crack zone conducting to surface happen periodically, which lead to form the big and small sizes of cycle phenomenon.

3 NUMERICAL SIMULATION ANALYSIS

In order to analyze the mechanical process of surrounding rock force and deformation in the shallow-buried coal seam comprehensively and systematically, the paper uses FLAC^{3D} numerical simulation software to study the changing rule of the overlying rock strata structure of 316-04 fully-mechanized face.

Figure 2 and 3 are distribution characteristics of surrounding rock principal stress along the strike and incline directions, when the 316-04 working face advances to 400 m.

Though analyzing figure 2 and 3, it is known that, at the beginning of 316-04 working face mining, the bearing arch structure was formed in overlying rock strata. When working face advanced to 40 m, the height of bearing arch structure is about 8 m, which is about four times that of mining height. The maximum principal stress along bearing arch axis is 1.8 MPa.

Figure 4 to 7 are the distribution characteristics of surrounding rock principal stress field as well as the maximum principal stress isocline along the strike and incline directions, when the working face advanced to 200 m, which means achieves fully mining.

Figure 8 shows the distribution characteristics of the maximum principal stress in sandy mudstone strata under the unconsolidated layers 52 m over the coal seam (the working face advanced to 200 m and achieves fully mining).

From figure 4 and 5, it is known that when working face advanced to 200 m (when achieves fully mining), the bearing arch structure has already had an instability failure. The bedrock layers of the middle working face have already been broken along the inclination direction of working face

Table 1. Periodic weighting interval of every support.

	Location of face	Upper		Middle		Under			
Pressure order	Support number	35	36	67	68	69	92	93	94
1		11	10	14	13	14	15	13	13
2		11	10	19	19	14	18	18	12
3		15	16	6	8.4	13	18	18	13
4		9.6	9	14	12	13	15	15	13
5		14	11	13	14	14	10	12	14
6		17	12	15	13	16	17	16	13
7		18	16	16	16	17	16	18	17
8		15	15	16	15	17	15	16	19
9		15	15	12	13	12	12	13	13
10		14	13	14	14	14	15	15	14
Avg./m		13.33		14.01			14.86		

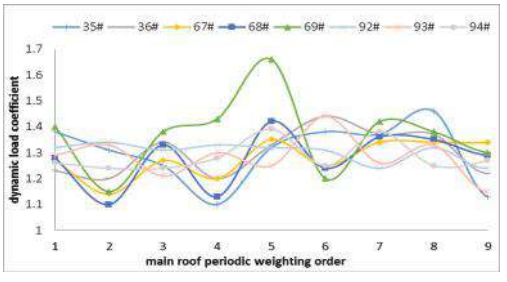


Figure 1. Changing rule of periodic weighting strength.

Table 2. Statistics of dynamic load factors of the main roof periodic weighting.

S/N		35	36	67	68	69	92	93	94	Avg.
Periodic weighting order	1	1.38	1.23	1.27	1.28	1.40	1.32	1.29	1.26	1.3
	2	1.31	1.20	1.14	1.10	1.15	1.34	1.33	1.24	1.23
	3	1.25	1.34	1.27	1.33	1.38	1.31	1.21	1.24	1.3
	4	1.10	1.20	1.20	1.13	1.43	1.33	1.30	1.28	1.25
	5	1.32	1.33	1.35	1.42	1.66	1.32	1.25	1.39	1.38
	6	1.38	1.44	1.25	1.24	1.20	1.31	1.44	1.25	1.32
	7	1.37	1.37	1.34	1.36	1.42	1.24	1.26	1.38	1.34
	8	1.46	1.37	1.34	1.35	1.38	1.32	1.33	1.25	1.35
	9	1.13	1.22	1.34	1.29	1.30	1.24	1.15	1.27	1.24
	10	1.30	1.38	1.37	1.32	1.32	1.36	1.33	1.35	1.34

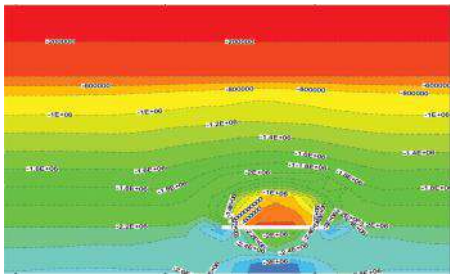


Figure 2. The distribution characteristics of maximum strike principal stress isoline.

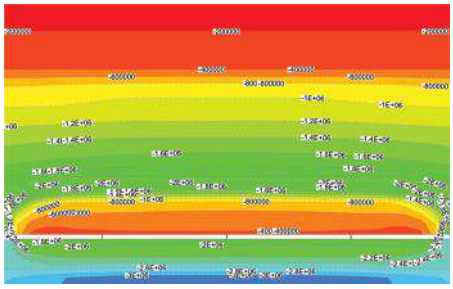


Figure 3. The distribution characteristics of maximum incline principal stress isoline.

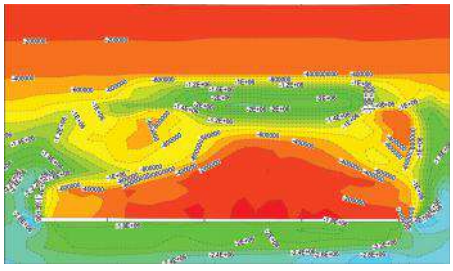


Figure 4. The distribution characteristics of maximum strike principal stress isoline.

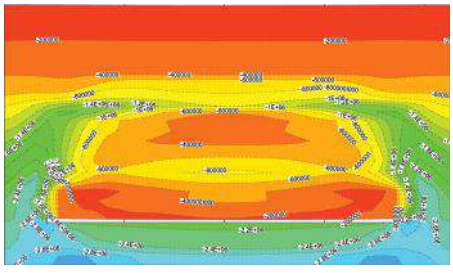


Figure 5. The distribution characteristics of maximum incline principal stress isoline (10 m ahead starting open-off cut).

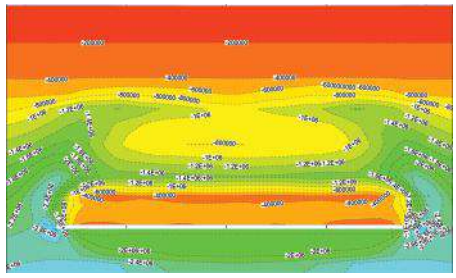


Figure 6. The distribution characteristics of maximum incline principal stress isoline (30 m behind coal wall).

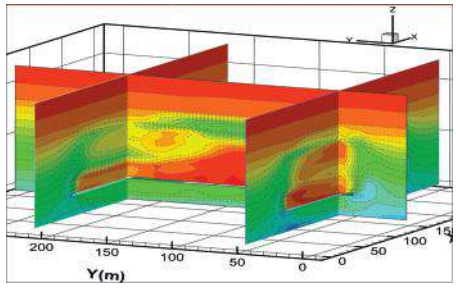


Figure 7. The distribution characteristics of maximum principal stress isoline of surrounding rock.

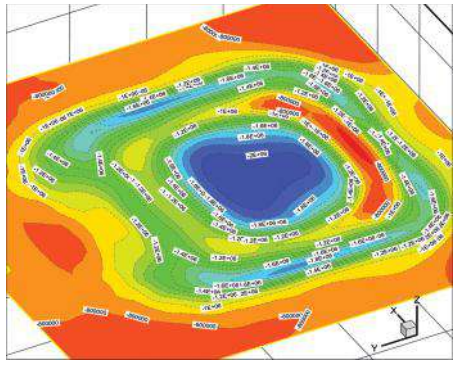


Figure 8. The distribution characteristics of the maximum principal stress in sandy mudstone strata.

from 10 m ahead starting open-off cut to 30 m behind coal wall, which shows that the bearing arch has already been broken. From figure 6 and figure 7, we can learn that the upper rock strata that near starting open-off cut has been influenced by mining for a long time relatively. So this part of the roof strata has been all broken. After rock masses above the coal mining face break, a new bearing arch structure has been formed again, between the

Table 3. Analyze the influence of mining face parameters to the law of mine pressure appearance.

S/N	Entry	Experimental face	316-04 face	326-01 face
1	Coal seam	6	$6_{-2upper}$	6_{-2}
2	Buried depth	89 m	109 m	88 m
3	Mining height	2.2 m	2.2 m	5.8 m
4	Face length	70 m	180 m	180 m
5	Dip angle	1~3°	1~3°	1~3°
6	Support model	ZH1600/16/24	ZY6800/14/32	ZY13000/28/63
7	Intervals of roof weighting	4.8~12 m	9~18.6 m	4~16 m
8	Strength of roof weighting	1.01~1.21	1.01~1.48	1.10~1.66
9	Actual supporting force	950 kN	6460 kN	9256 kN
10	Bearing arch status	Stable	Unstable	Unstable

front coal body and gangue caving and compacted in the goaf. Along with advancing of working face, the new forming bearing arch structure will continue to evolve and change, that is formation—development—instability failure—re-formation. As the length of 316-04 working face is rather large, the bedrock layers over the middle working face have been all broken, and bearing arch structure has an instability failure. Then, synchronous falling of surface unconsolidated layers and the bedrock layers will severely affect the 316-04 working face.

4 PROJECT COMPARATIVE ANALYSIS

In order to analyze the influence of mining face parameters to the law of mine pressure appearance in the shallow-buried mining face, the changing characteristics of overlying strata structure in Rongda experimental mining face, 316–04 and 326-01 coal mining face of Nayi mine have been analyzed by field observation, which are several typical shallow-buried longwall mining faces, and the comparison results are shown in table 3.

From table 3, it is known that because the experimental mining face's length and mining height are both small, face mining caused little effect on roof strata's damage. After achieving fully mining, bedrock layers were not all broken, and the bearing arch structure still exist. The law of mine pressure appearance between the experimental mining face and the regular appears were alike. As the length and mining height of 316-04 and 326-01 working face increase, the bedrock layers have been all broken in the process of mining, and the bearing arch structure also appears instability, but cannot exist stably.

5 CONCLUSION

Through the analyzes of pressure appearance and stress distribution of surrounding rocks of the typical shallow-buried long wall mining face and draws, the following conclusions were obtained:

1. The periodic weighting interval of the main roof in 316-04 typical shallow-buried long wall mining face is 14.2 m on average, and the maximum interval is 19 m, the minimum is 6 m. The average periodic weighting dynamic load coefficient is 1.3, while the maximum is 1.66, the minimum is 1.10.
2. Overlying rock structure's stability of shallow-buried long wall face is also been affected by mining parameters, such as mining height and length of mining face, etc., besides objective geological conditions.
3. Fissure zones conducting surface (namely, the bedrock layers are all broken periodically) and main roof breaking periodically are key causes that make the roof of shallow-buried long wall face exist two different cycles.

REFERENCES

Huang, Q.X. 2000. *Study on roof structure and ground control in shallow seam long wall mining*. Xuzhou: China University of mining and technology press.

Huang, Q.X. & Qian, M.G. 1999. Structural analysis of main roof stability during periodic weighting in long waII face. *Journal of China Coal Society*24 (6):581~585.

Qian, M.G. & Zhao, G.J. 1987. The behavior of the main roof fracture in long wall mining and its effect on roof pressure. *Rock Mechanics (Proceedings of the 28th U.S. Symposium)* 1123–1128.

Ren, Y.F. 2008. Study on structure characteristics of overlying strata in shallow coal seam under long wall mining. Beijing: China Coal Research Institute.

Ren, Y.F. 2011. Study on Monitoring Technology of the Overlying Strata Spatial Structures' Failure in Shallow Seam Long Wall Face. *Procedia Engineering*Vol.26:928–933.

Progress in Mine Safety Science and Engineering II – He et al. (Eds)
© 2014 Taylor & Francis Group, London, ISBN 978-1-138-00122-0

Numerical simulation of blasting effects on soft coal under different confining pressure

H.Q. Zhu, S.H. Zhu, G.W. Jia & Z.Y. Song
China University of Mining and Technology (Beijing), Beijing, China

ABSTRACT: Blasting effects on soft coal under five different types of confining pressure are analyzed numerically using the commercial code Ls-dyna. *X*-stress of a selected element, global kinematic energy, global internal energy and Von Mises stress are investigated, respectively. The results show that confining pressure imposes an influence on the action mode of blasting, and it reduces the peak value of *x*-stress in compressive phase and increases its counterpart in tensile phase. A slight change of the transverse, longitudinal or vertical loading imposes a stronger impact on tensile stress than that on compressive stress. The results also show that a slight change of transverse loading imposes a stronger impact on tensile stress than that of the longitudinal and vertical loading. Confining pressure increases kinematic energy after the peak value and enhances storage of internal energy in soft coal. Von Mises stress field after 20μs of blasting under condition I and II shows that high stress zones under the former locate in the vicinity of the borehole at the beginning of detonation, while those under the latter concentrate both around the borehole and along the edges of the model.

1 INSTRUCTIONS

Pre-blasting has been an effective way for gas drainage to prevent gas outburst, and thus has been widely applied in coal mine. It is well known that detonation in sealed borehole produces intense shock wave and a large amount of exploding gas with high temperature and high pressure (Cai 2009). As the shock wave propagates through the coal, a dynamic stress field is generated and cracks begin to form. And then the detonation gas penetrates into the initial cracks and furthers their extension. These cracks or fractures provide an access for gas flowing in the coal and thus facilitate gas drainage. However, blasting design in underground mine is in most cases empirical, and research in the past has attempted to illustrate the fracture and fragmentation processes in infinite or semi-infinite coal subjected to either static or dynamic loading only (Song & Kim 1996, Yang et al. 1996, Donze et al. 1997, Li & Yang 2002, Sun 2004, Gong et al. 2008, Li et al. 2009, Xing et al. 2010, Onederra et al. 2013). The coal, however, in engineering practice experiences the coupling loading of static stress field induced by confining pressure and dynamic stress field induced by blasting.

Li (2005) proposes a mathematic model to demonstrate rock behavior undergoing static-dynamic coupling loading. In this model rock is characterized with both statistical damage and visco-liquid, and is regarded as a combination of damage mass and visco-piston. The model is also used in this study to investigate *x*-stress variation after detonation under different confining pressure.

It is vital and necessary to study blasting effects under different confining pressure, since the static stress field varies throughout the mining operations. However, it is difficult to map and change in situ stress field for research. Numerical simulation offers an efficient way to untangle this problem and to tailor blasting design in underground coal mine. The work presented in this paper focuses on numerical simulation of blasting effects on soft coal under different confining pressure using the commercial code Ls-dyna. The *x*-stress evolution, global kinematic energy, global internal energy and Von Mises stress after detonation under different conditions are calculated to explore the influence of confining pressure on blasting process.

2 MATHEMATICAL AND PHYSICAL MODEL

2.1 *The coupling of static and dynamic loading*

The coal is assumed to be viscoelastic mass before damage, and is characterized with both statistical damage and visco-liquid (Li et al. 2005, Shan 2003). The constitutive model of visco-piston is expressed as:

$$\sigma_b = \eta \frac{d\varepsilon_b}{dt} \tag{1}$$

Where σ_b = stress of visco-piston, ε_b = strain of visco-piston and η = viscoelastic coefficient.

The relationship between stress and strain of a 3D rock mass is given by:

$$S_{ij} = 2Ge_{ij} \tag{2}$$

$$\sigma_m = 3K\varepsilon_m \tag{3}$$

Here into,

$$\sigma_{ij} = S_{ij} + \delta_{ij}\sigma_m \tag{4}$$

$$\varepsilon_{ij} = e_{ij} + \delta_{ij}\varepsilon_m \tag{5}$$

Where S_{ij} = the partial tensor of stress, e_{ij} = the partial tensor of strain, σ_m = spherical tensor of stress, ε_m = spherical tensor of strain, G = shear modulus, K = volume modulus, σ_{ij} = stress tensor, δ_{ij} = Dirac delta function and ε_{ij} = strain tensor.

The 3D constitutive equation of viscoelastic mass undergoing static-dynamic coupling loading is derived as follows (Li et al. 2006):

$$\begin{aligned}\sigma_x(t) = {} & \frac{9KE_{ld}}{(3K+E_{ld})\eta} \\ & \left\{\eta\left[\varepsilon_{x0}+\varepsilon_r(t)\right]+\frac{E_c-\beta\eta}{\beta}\left[\varepsilon_{x0}+\varepsilon_r(t)-C\right]\right. \\ & \left.-\frac{E_c-\beta\eta}{\beta}\left(\varepsilon_{x0}-C\right)e^{-\frac{\beta\varepsilon_r(t)}{C}}\right\} \\ & +\frac{S_{y0}+S_{z0}}{2(3K+E_{ld})\eta}\left[\gamma+\delta e^{-\frac{\beta\varepsilon_r(t)}{C}}\right]\end{aligned} \tag{6}$$

Here into,

$$\beta = \frac{3K(E_c+E_{ld})+E_cE_{ld}}{(3K+E_{ld})\eta} \tag{7}$$

$$\gamma = \frac{3K(E_c+E_{ld})-2E_cE_{ld}}{\beta} \tag{8}$$

$$\delta = (3K-2E_{ld})\,\eta-\gamma \tag{9}$$

Where E_c = Young's modulus of coal, E_{ld} = linear elastic modulus of coal experiencing coupling loading, S_{y0} = initial loading in y direction, S_{z0} = initial loading in z direction, ε_{x0} = initial strain induced by initial loading in x direction and C = strain rate of dynamic loading.

As seen in the equation (7), if initial static loadings of other two directions (S_{y0} and S_{z0}) exist, the last term of the equation (7) is positive, i.e. static loadings increase x-stress in coal.

2.2 *Physical model*

The commercial code Ls-dyna is used to simulate x-stress, global kinematic energy, global internal energy and Von Mises stress in soft coal after blasting under different confining pressure. Figure 1 shows scheme of simulation model with 500 mm × 500 mm × 500 mm. Borehole is set to be a rectangular solid with 42 mm × 42 mm × 100 mm for the convenience of model building. One fourth of the model is selected to facilitate meshing and calculation. In order to reduce mesh-dependency on dynamic field analysis, the mesh size should be as small and uniform as possible. Fine meshes with the density of 10 × 10 × 20 are used for the explosive in order to embrace the increase of computational efficiency towards achieving the final results. Figure 2 shows the mesh layout of the selected model part with 80, 000 elements.

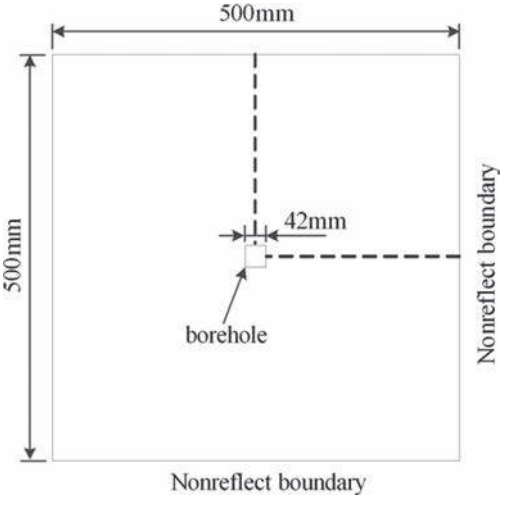


Figure 1. Model layout.

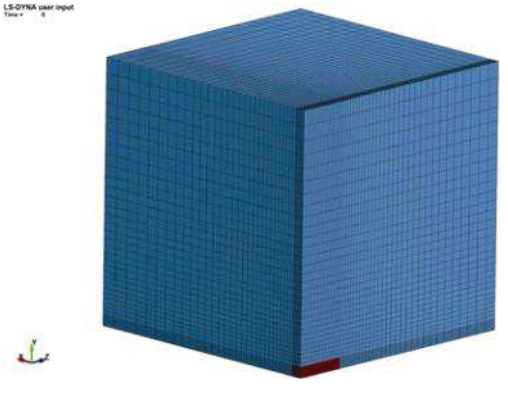


Figure 2. Mesh of simulation model.

One of the working faces in longitudinal direction is excavated for operation space, so the confining pressure is only imposed on the rest five faces of the model, i.e., the coal in working faces bears different crustal stress from five directions instead of six. The scheme of different loading on different faces of the model is presented in Figure 3. Five types of confining pressure conditions are taken into account:

- all the three loadings are set 0 MPa (condition I)
- all the three loadings are set 6 MPa (condition II)
- transverse loading is set 5 MPa, while other two loadings are set 6 MPa (condition III)
- longitudinal loading is set 5 MPa, while other two loadings are set 6 MPa (condition IV)
- vertical loading is set 5 MPa, while other two loadings are set 6 MPa (condition V)

*MAT_HIGH_EXPLOSIVE_BURN as the key word is adopted in the code to describe explosive with Jones-Wilkins-Lee (JWL) equation of state to model the pressure generated by the expansion of the detonation product:

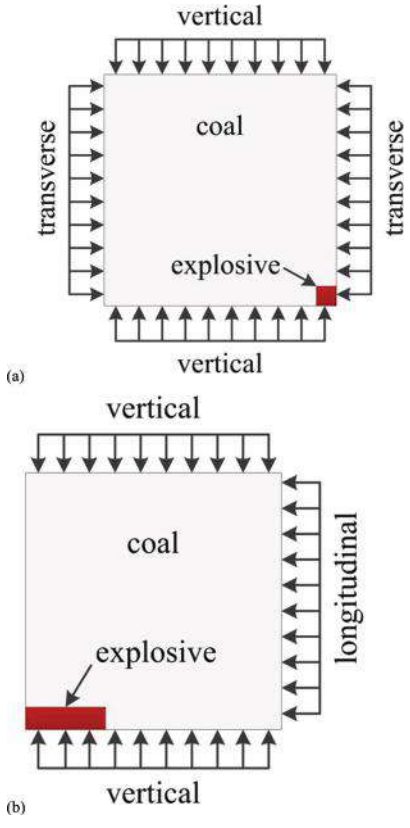


Figure 3. (a) front view and (b) side view of the scheme of different loading on different faces.

Table 1. Material parameters of RDX.

ρ_c kg/m^3	E_c GPa	υ	σ MPa
1330	5	0.26	2.91

Table 2. Material parameters of soft coal.

ρ_c kg/m^3	D m/s	A GPa	B GPa	R_1	R_2	ω	E_0 Gpa
1630	6930	371	7.43	4.15	0.95	0.3	7

$$P = A\left(1-\frac{\omega}{R_1V}\right)e^{-R_1V} + B\left(1-\frac{\omega}{R_2V}\right)e^{-R_2V} + \frac{\omega E}{V} \tag{10}$$

Where A, B, R_1, R_2 and ω are material constants in JWL equation of state, P = the pressure of detonation products, V = the specific volume and E = initial value of the specific energy.

The high explosive properties are presented in Table 1. And the coal is modeled as plastic kinematic material with parameters listed in Table 2.

3 RESULTS AND DISCUSSION

3.1 *X-stress*

An element located at (29.9018, 24.4375, 0) is selected to present x directional stress time-history (shown in Figure 4) after blasting under different conditions.

The peak value of X-stress both in the tensile and compressive phase is also present in the figure to give a contrast of blasting effects under different confining pressure.

As is shown in Figure 4, x-stress curves of the selected component under five different conditions share the same pattern, and peak at the same time in both compressive phase and tensile phase. However, x-stress presents a short tensile phase for about 80.5 μs, and then a compressive phase (of the order of 60 μs) followed by another tensile phase for almost 40 μs under condition II, III, IV, and V, while x-stress under condition I only occupies a compressive phase for about 80 μs, and then a tensile phase for about 40 μs. It also shows that the same loading of confining pressure brings down the peak value of x-stress in compressive phase by 4 MPa and increases its counterpart in tensile phase by 2.7 MPa. This means confining

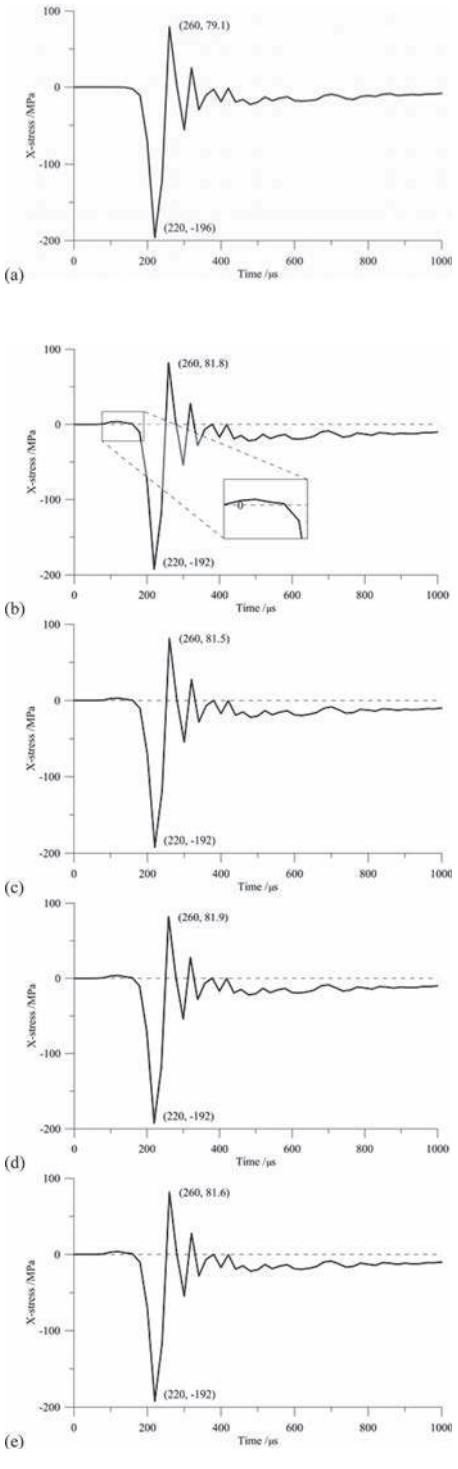


Figure 4. *X*-stress time-history under (a) condition I; (b) condition II; (c) condition III; (d) condition IV; (e) condition V.

pressure imposes an influence on the action mode of blasting.

The maximum value difference of x-stress in tensile phase under condition III, IV, and V with that under condition I is 3 MPa, 1 MPa and 2 MPa, respectively, while the peak value in compressive phase equals to 192 MPa under all these four conditions. It means that a slight change of the transverse, longitudinal or vertical loading imposes a stronger impact on tensile stress than that on compressive stress. It also shows that a slight change of transverse loading imposes a stronger impact on tensile stress than that of the longitudinal and vertical loading.

Although the increment of the peak value of x-stress in tensile phase agrees well with the theoretical analysis in equation (7), the mathematical model still suffers from the lack of an illustration of the x-stress decrease in compressive phase and the diversity of the peak value under different conditions. The reason is that this equation is formulated under intermediate strain rate, while detonation is characterized with high strain rate.

3.2 *Kinematic energy and internal energy*

Global kinematic energy and global internal energy under five conditions are depicted against time in Figure 5.

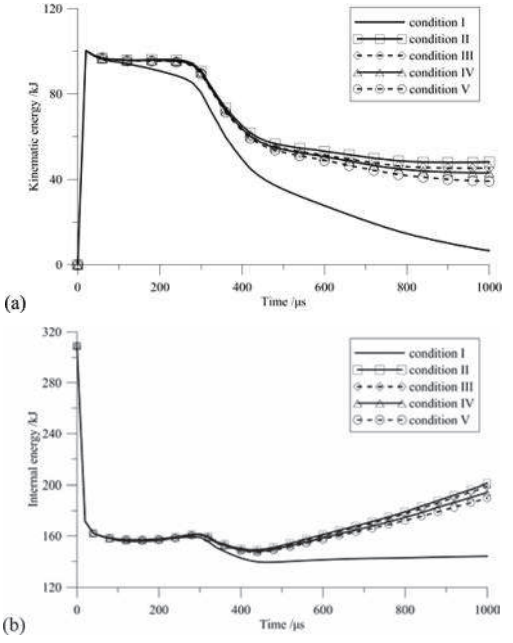


Figure 5. Time-history of kinematic energy (a) and internal energy (b) under five conditions.

The analysis of global kinematic energy presents its dissipation during blasting in coal under different confining pressure, while the analysis of internal energy gives the energy storage in the blasting process and also shows the compressibility of coal under different conditions.

Global kinematic energy under five different conditions shown in Fig. 5(a) all peaks to 100 kJ at the same time. Afterwards, this energy takes the form of two stages of steady decrease until to 7 kJ within solution time under condition I, while it is kept at a constant of kJ for about 220 μs, and decreases slowly to 48 kJ, 45 kJ, 43 kJ and 39 kJ under other four conditions, respectively. Global internal energy under five different conditions shown in Fig. 5(b) all decreases sharply at the beginning, and maintains at about 160 kJ for 220 μs before 300 μs. After that time this energy decreases to 144 kJ under condition I, while it embraces a steady increase under other four conditions within solution time. The above results show that confining pressure increases kinematic energy after the peak value and enhances storage of internal energy in soft coal.

3.3 *Von mises stress*

Von Mises stress is originally formulated to describe plastic response of ductile materials. It is also applicable for the analysis of plastic failure for coal undergoing high strain rate. The von Mises yield criterion suggests that the yielding of materials begins when the second deviatoric stress invariant J2 reaches a critical value. In materials science and engineering the von Mises yield criterion can be also formulated in terms of the von Mises stress or equivalent tensile stress, $\sigma_{v,}$ a scalar stress value that can be computed from the stress tensor:

$$\sigma_v = \sqrt{\frac{(\sigma_1 - \sigma_2)^2 + (\sigma_2 - \sigma_3)^2 + (\sigma_1 - \sigma_3)^2}{2}} \qquad (11)$$

Where $\sigma_{1,}$ σ_2 and σ_3 are principal stresses.

In this case, a material is said to start yielding when its von Mises stress reaches a critical value known as the yield strength, σ_y.

Von Mises stress fields after 20 μs of blasting under condition I and II are presented in Figure 6.

As is illustrated in Figure 6, high stress zones of the left model under condition I (i.e. all confining pressure is set 0 MPa) locate in the vicinity of the borehole at the beginning of detonation, while high stress zones in the right one under condition II concentrate both around the borehole and along the edges of the model.

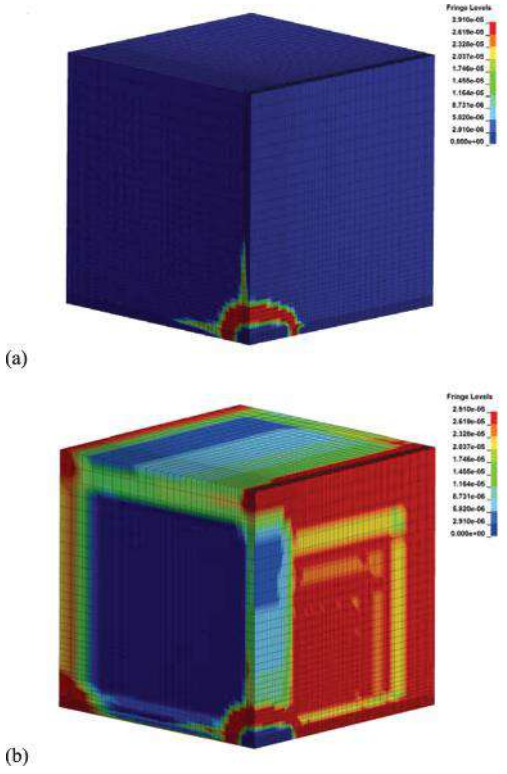


Figure 6. Von Mises stress fields after 20μs of blasting under (a) condition I and (b) condition II.

4 CONCLUSIONS

1. Confining pressure imposes an influence on the action mode of blasting, and it reduces the peak value of x-stress in compressive phase and increases its counterpart in tensile phase.
2. A slight change of the transverse, longitudinal or vertical loading imposes a stronger impact on tensile stress than that on compressive stress.
3. A slight change of transverse loading imposes a stronger impact on tensile stress than that of the longitudinal and vertical loading.
4. High stress zones under condition I locate in the vicinity of the borehole at the beginning of detonation, while those under condition II concentrate both around the borehole and along the edges of the model.

REFERENCES

Cai, F. 2009. Study on Effect of Intensified Increasing Permeability by Deep-hole Presplitting Blasting in High Gas and Low Permeability Coal Seam: 29–37. Anhui University of Science and Technology, Anhui.

Donze, F.V. Bouchez, J. Magnier, S.A. 1997. Modeling fractures in rock blasting. *Int. J. Rock Mech. Min. Sci* 34(8): 1153–1163.

Gong, M. Huang, Y.H. Wang, D.S. et al. 2008. Numerical Simulation on Mechanical Characteristics of Deep-hole Presplitting Blasting in Soft Coal Bed. *Chinese Journal of Rock Mechanics and Engineering* 27(8): 1674–1680.

Li, Q. & Yang, R.S. 2002. Stress Intensity Factor and Fracture Behavior for Crack Propagation under Blasting Load. *Journal of China Coal Society* 27(3): 290–293.

Li, S.B. Dong, Z.X. Qi Y.J. et al. 2009. Numerical Simulation for Spread Decay of Blasting Shock Wave in Different Media. *Journal of Vibration and Shock* 28(7): 115–117.

Li, X.B. Zuo, Y.J. Ma, C.D. 2005. Failure Criterion of Strain Energy Density and Catastrophe Theory Analysis of Rock Subjected to Static-dynamic Coupling Loading. *Chinese Journal of Rock Mechanics and Engineering* 24(16): 2814–2824.

Li, X.B. Zuo, Y.J. Ma, C.D. 2006. Constitutive Model of Rock under Coupled Static-dynamic Loading with Intermediate Strain Rate. *Chinese Journal of Rock Mechanics and Engineering* 25(5): 865–874.

Onederra, I.A. Furtney, J.K. Sellers, E. et al. 2013. Modeling blast induced damage from a fully coupled explosive charge. *Int. J. Rock Mech. Min. Sci* 58: 73–84.

Shan, R.L. Xue, Y.S. Zhang, Q. 2003. Time Dependent Damage Model of Rock under Dynamic Loading. *Chinese Journal of Rock Mechanics and Engineering* 22(11): 1771–1776.

Song, J. & Kim, K. 1996. Micromechanical Modeling of the Dynamic Fracture Process During Rock Blasting. *Int. J. Rock Mech. Min. Sci. & Geomech* 33(4): 387–394.

Sun, Z.Q. 2004. How to Judge Fracture Mode Under Arbitrary Loading: Mode I or Mode II Fracture. *Journal of China Three Gorges University (Natural Sciences)* 26(1): 27–30.

Xing, S.R. Xiao, L. Zhang, J.P. 2010. An Analysis of Fracture Theory on the Expansion of Complex Macroscopic Cracks Caused By Pre-fracturing of Coal Seams. *China Coal* 36(10): 107–111.

Yang, R. Bawden, W.F. Katsabanis, P.D. 1996. A New Constitutive Model For Blast Damage. *Int. J. Rock Mech. Min. Sci. & Geomech* 33(3): 245–254.

Progress in Mine Safety Science and Engineering II – He et al. (Eds)
© 2014 Taylor & Francis Group, London, ISBN 978-1-138-00122-0

The research of high-altitude mine ventilation optimization decision theory based on Analytical Hierarchy Process (AHP)

Hongliang Wang & Kechun Zhang
Department of Safety Engineering and Technology, Heilongjiang University of Science and Technology, Harbin, Heilongjiang, China

ABSTRACT: According to the special production environment of high-altitude mine, the new requirements were proposed for mine ventilation system design and selection. Therefore, this paper gives a high-altitude Mine Ventilation Optimization decision theory based on analytical hierarchy process. From a number indexes which reflect the characteristics of high-altitude mine ventilation system, according to four levels about echnical, economic, safety, environmental impact, it formed a optimizing evaluation index system of high-altitude mine ventilation system. Analytic hierarchy process was used to determine the weight of each index value. The design schemes of high-altitude mine ventilation system were carried out optimization decision by the method of multi-objective decision, the research in Nang Mute mine has achieved good application effect, The results show that: The research of high-altitude mine ventilation optimization decision theory based on analytical hierarchy process has important application value and practical significance.

1 INTRODUCTION

Plateau in western China (Qinghai-Tibet Plateau) is rich in mineral resources, the development of these resources can be effective in promoting western development, but also will help relieve the shortage of mineral resources in China. However, owing to the rarefied air, bitter cold and other severe conditions in plateau area. People who reach the plateau first, will get a series of altitude sickness (such as headache, dizziness, enlargement of the heart, indigestion, respiratory tract mucosa damage, etc.), a significant impact on the body. Underground production environment of high-altitude mine, as a major problem of constrained mine production have proposed a major challenge for traditional coal mine safe production. Thus, the choice and establish of mine ventilation system, improving mine production environment, raising labor productivity, are the key to safe production for high-altitude mine, Which has important scientific value and practical significance.

2 THE DETERMINATION OF OPTIMIZATION INDEXES AND WEIGHTS OF HIGH-ALTITUDE MINE VENTILATION SYSTEM

2.1 *The determination of optimization indexes of high-altitude mine ventilation system*

In high-altitude mines, each mine ventilation system has its own advantages and disadvantages. So if we determine the optimal design of the ventilation system, we must determine the optimal evaluation indexes first. We determined the optimization indexes relying on experience and comprehensive analysis capabilities according to the requirements of high-altitude mine ventilation system shown in Figure 1

2.2 *The determination of optimization indexes weights of high-altitude mine ventilation system*

All sorts of indexes for judging the importance of the system requirements are different. Therefore, In order to reflect the exact degree of importance of each evaluation index, we used analytic hierarchy process (AHP method) for high-altitude mine ventilation system to determine optimization of index weight.

1) The determination of judgment matrix elements Judgment matrix elements value adopted 1~9 scale and reciprocal scale method, as table 1 (JING Quanzhong 2006). we quantized the relative importance which is between indexes according to certain scale by method of 1 ~ 9 scale and then it compose the Judgment matrix.

According to Method of 1~9 scale, and we obtained single ordering of all levels and importance weights by using power method. as table 2.

1. The judgment matrix was calculated according to the next type:

$$\overline{w_i} = \sum_{j=1}^{n} \frac{y_{ij}}{\sum_{k=1}^{n} y_{kj}} \quad \text{i, j = 1, 2, …, n} \tag{1}$$

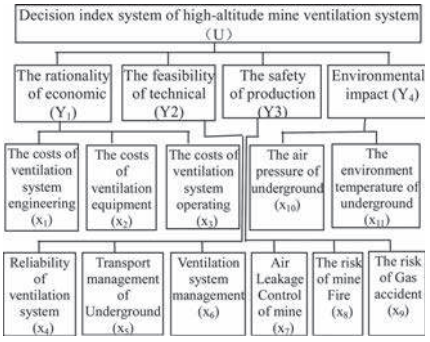


Figure 1. Decision index system of high-altitude mine ventilation system.

Table 1. Method of 1~9 scale.

Scale	Meaning
1	meaning x_i and x_j have equal importance
3	meaning x_i is more important than x_j
5	meaning x_i is significantly important compared with x_j
7	meaning x_i is very important compared with x_j
9	meaning x_i is very top compared with x_j
2, 4, 6, 8	mean value of the two adjacent
Reciprocal	Comparison of x_j and x_i

2. Making vector $\overline{w_1} = \left[\overline{w_1}, \overline{w_2}, \cdots \overline{w_n}\right]^T$ regular:

$$w = \frac{\overline{w_i}}{\sum_{j=1}^{n} \overline{w_i}} \tag{2}$$

The w = $w = \left[\overline{w_1}, \overline{w_2}, \cdots \overline{w_n}\right]^T$ is the eigenvector accordance with requests, namely the weights of factors.

3. The maximum characteristic root of matrix is $\lambda_{max} = \Sigma_{i=1}^{n} \frac{(Aw)_i}{nw_i}$ (A_{wi}) is the component vector "i".
4. Consistency index.
5. The discriminant of Consistency Check is, when CR < 0.10, It is considered that judgment matrix has satisfied consistency, The matrix was passed by the test, Otherwise, we need to adjust judgment matrix. The RI as mean values of random consistency indexes, such as shown in table 3.

Through the inspection, the judgment matrix had satisfactory consistency test. Each evaluation indexe value was ealculated. Such as shown in table 4: According to this method we can give the indexes weights

Table 2. Various levels single sorting and important weight.

U	Y_1	Y_2	Y_3	Y_4	ω_k
Y_1	1	1	1	1/2	0.20
Y_2	1	1	1	1/2	0.20
Y_3	1	1	1	1/2	0.20
Y_4	2	2	2	1	0.40
Y_1	X_1	X_2	X_3		ω_{1j}
X_1	1	1/2	1/3		0.161
X_2	2	1	1/2		0.309
X_3	3	2	1		0.529
Y_2	X_4	X_5	X_6	X_7	ω_k
X_4	1	1	1	2	0.286
X_5	1	1	1	2	0.286
X_6	1	1	1	2	0.286
X_7	1/2	1/2	1/2	1	0.143
Y_3	X_8	X_9			ω_{1j}
X_8	1	5			0.833
X_9	1/5	1			0.167
Y_4	X_{10}	X_{11}			ω_{1j}
X_{10}	1	9			0.9
X_{11}	1/9	1			0.1

Table 3. Random consistency index mean value RI of n-order matrix.

n	1	2	3	4	5	6	7	8	9	10
RI	0.00	0.00	0.58	0.90	1.12	1.24	1.32	1.41	1.45	1.49

3 THE MULTI-OBJECTIVE DECISION OF HIGH-ALTITUDE MINE VENTILATION SYSTEM

Multi-objective decision is the method of comprehensive application of experts collective wisdom, nowledge, experience and comprehensive analysis ability. The wisdom of the collective focus on "value" form. the high-altitude mine ventilation system contains multiple selection index, index between comparable, because of different weight for the different indexes, we can only analyze indexs according to the comprehensive function. Therefore, we adopted multi-objective decision to treat.

3.1 *The matrix of optimization schemes evaluation*

Let *n* be the number of schemes, and let *m* be the number of indexs which was set to high-altitude

Table 4. The weight of each basic evaluation index.

Index			Weight
The rationality of economic	The costs of ventilation system engineering	λ_1	0.032
	The costs of ventilation equipment	λ_2	0.062
	The costs of ventilation system operating	λ_3	0.106
	the Reliability of ventilation system	λ_4	0.057
The feasibility of technical	Transport management of Underground	λ_5	0.057
	Ventilation system management	λ_6	0.057
	Air Leakage Control of mine	λ_7	0.029
The safety of production	The risk of Gas accident	λ_8	0.167
	The risk Of mine Fire	λ_9	0.033
Environmental impact	The air Pressure of underground	λ_{10}	0.360
	The environment temperature of underground	λ_{11}	0.040

mine ventilation system plays an important role. The optimization of each scheme for each index composed $f_i = \{f_1, f_2, \ldots, f_m\}$ (qualitative indexes adopts expert estimation method). The $m \times n$ matrix "A"of optimization scheme evaluation was constituted by specific index value of the schemes, it can be expressed as:

$$A = \{f_{ij}\} = \begin{bmatrix} f_{11} & f_{12} & \cdots & f_{1j} & \cdots & f_{1n} \\ f_{21} & f_{22} & \cdots & f_{2j} & \cdots & \\ \vdots & \vdots & \vdots & \vdots & \vdots & \vdots \\ f_{i1} & f_{i2} & \cdots & f_{ij} & \cdots & f_{in} \\ \vdots\cdots & \vdots & \vdots & \vdots & \vdots & \vdots \\ f_{m1} & f_{m2} & \cdots & f_{mj} & \cdots & f_{mn} \end{bmatrix} \quad (3)$$

3.2 *The determination of evaluation value*

When the indexes are qualitative indexe, it adopts expert estimation method to confirm the index. When the indexes are quantitative index, because of the physical meaning of the different indexes, including some indexes are the bigger the better, such as air pressure, some indexes are the smaller the better, such as electricity charge. Therefore, in order to facilitate unified calculation, according to the characteristics of each index, we calculate the index value by two kinds of case (Wang Jianming 2004).

1. The bigger Index value the better
   If the indexes for the bigger the better, it makes the same index in the maximum value f_{ibj} for the best, namely:

$$\max(f_{ij}) = f_{ibj} \ (i = 1,2,3,\cdots, m, \ 1 \le j \le n \quad (4)$$

   The scheme for the evaluation index value:

$$E_{ij} = \frac{f_{ij}}{f_{ibj}} \times 10 \quad (5)$$

2. The smaller Index value the better
   If the index value is the smaller the better, make the minimum as the best index value f_{ibj} in the same index in Programs.

$$\min(f_{ij}) = f_{ibj} \ \ (i = 1,2,3,\cdots, m, \ 1 \le j \le n) \quad (6)$$

Then the evaluation of index value in programs, namely:

$$E_{ij} = \frac{f_{ij}}{f_{ibj}} \times 10 \quad (7)$$

$$M_j = \max \sum_{i=1}^{m} W_j E_{ij} \quad (8)$$

3.3 *Selection of the optimal system solution*

The "weight" of preferred index is $W_1, W_2, \ldots, W_i \ \ldots, W_m$. The comprehensive index M_j were composed of product sums of evaluation values of index for each program and the "weight", the largest M_j were the optimal solution. Mathematical model representation, namely:

$$M_j = \max \sum_{i=1}^{m} W_j E_{ij} \quad (9)$$

4 THE APPLICATION OF OPTIMIZATION DECISION THEORY ABOUT HIGH-ALTITUDE MINE VENTILATION SYSTEM

4.1 *General situation of the mine*

Nang Mute Mine, is located in South of Datong river in northeastern Qinghai Province, the Altitude is Between+3800 mand +4100 m in the region, the Altitude of Nang Mute Mine is about +3850 m, it is a plateau, alpine and hypoxia zone, atmospheric pressure is about 0.6317 times the standard atmospheric pressure. Average temperature is between –4.2 and 5.1°C. design production capacity of

mine is 1.2 million t/a. it uses inclined shaft multi-level development and central parallel ventilation. Simultaneously it is a low-gas coal mine and the coal seam does not have a spontaneous tendency.

4.2 *Drafted program of mine ventilation system*

Based on the objective circumstances in which Niang Mute mine Located, we put forward three kinds of designs (Wang hongliang 2009).

Program Setting of Program 1 as follows:

Using exhaust ventilation methods and increasing the air volume in order to increase the oxygen volume supply into the mine as Major measures. at same time, Depend on the personnel training and selection as auxiliary measures to improve mine production environment.

The program 1 has three advantages. ①exhaust ventilation methods Due to less external leakage, therefore the mine ventilation is easy to manage. ②it is no need to set the ventilation structures in the main air routes, so ventilation resistance is small and easy to transport. ③ if the main fan stops for any reason, the airflow pressure will increase in underground, which can inhibit the gas emission and is of help gas management, so the mine is relatively safe.

At the same the program 1 has three disadvantages. ① The atmospheric pressure which is in exhaust ventilation mine is lower than that in the underground, it make the mine environmental deterioration.② The air density of exhaust ventilation is lower, so the air expansion will lead the degree to a certain decreasing. ③ easy Affected by mining active process, it forms interlinked fissures with the ground and lead to air leakage condition serious, It is harmful to gas emissions.

Program setting of program 2 as follows: Using the same ventilation methods with program 1. using pressure chamber which was established in the face to improve local pressure. Depend on the personnel training and selection, as auxiliary measures to improve mine production environment.

The program 2 has three advantages. ① Because of using exhaust Ventilation methods, it have the same advantages with the program 1. ② air pressure can be increased in working face to improve the production environment. ③ The program can improve the production conditions in the mine by local supplement oxygen and personnel training.

The program 2 has three disadvantages. ①Because of using exhaust Ventilation methods, it have the same disadvantages with the program 1. ② The establishment of pressure chamber in face crossheading lead to the transportation inconvenience and economy unreasonable. ③The air pressure has no change in other locations.

Program setting of program 3 as follows: It uses the forced ventilation method and artificial pressurization techniques to improve air pressure production environment as Major measures. Depend on the local supplement oxygen, personne l training and selection as auxiliary measures to improve mine production environment.

The program 3 has three advantages. ①the atmospheric pressure was improved comprehensively inside the mine. ②It uses artificial pressurization techniques to improve air pressure in the work space. ③The Program can improve the production conditions in the mine by local supplement oxygen and personnel training.

The program 3 has three disadvantages. ①It is generally believed that forced ventilation is not suitable for high-gas coal mine. ②ventilation management is a little difficulty. ③there are ventilation structures in the ventilation routes, lead to inconvenient transportation for personnel, vehicles and hoisting container.

4.3 *Drafted program of mine ventilation system*

The optimal indexs value of the mine ventilation system determined by specific parameters of each program. Qualitative indexes determined by expert Estimation. such as Table 5.

According to $M_j = \Sigma W_i E_{ij}$, total points of programs are calculated, as follows $M_{\mathrm{I}} = 9.24$; $M_{\mathrm{II}} = 8.94$; $M_{\mathrm{III}} = 9.56$, According to the optimal system selection model $M_j = \max \Sigma W_i E_{ij}$ program III was determined for the first. after Nang Mute mine have used the forced ventilation method and artificial pressurization techniques, the mine not only has Realized the normal ventilation, but also the production conditions of mine has been greatly improved, After using the program III, the air pressure in face has been markedly improved, the the air pressure of face was measured about 68100pa, equivalent to atmospheric pressure of altitude 3200 m, labor productivity of workers has increased by 50%.

5 MAIN CONCLUSIONS

Through the research bout three sets design program of high-altitude of mine ventilation systems, in this paper, High-altitude mine ventilation optimization evaluation index system and weight were determined by analytical hierarchy process (AHP) and multi-objective decision technical, form economic, security and environmental impact four levels, thus we obtained High-altitude mine ventilation optimization design program. the optimization design program applied in the practical engineering, the mine production environment and mine labor efficiencyhave had great improvement in Nang Mute mine improve. it achieved good effect. It is show that, the research of High-altitude mine ventilation optimization decision theory, which Based on the analytical hierarchy process, has important application value and practical significance.

Table 5. Optimization index value of Nang Muter coal mine ventilation system scheme.

No	Index	Index value		
		1	2	3
1	The costs of ventilation system engineering	37500	50000	45000
2	The costs of ventilation equipment (million)	2.78	2.90	2.78
3	The costs of ventilation system operating (million)	1.53	1.84	1.90
4	The Reliability of ventilation system	90	70	80
5	Transport management of Underground	90	60	80
6	Ventilation system management	90	80	80
7	Air Leakage Control of mine	80	60	80
8	The risk of Gas accident	20	20	20
9	The risk of mine Fire	10	10	10
10	The air pressure of underground	Equal to 4000 m altitude	Equal to 3500 m altitude	Equal to 3200 m altitude
11	The environment temperature of underground	80	85	90

Table 6. Integral table of each scheme.

No	Index	Weight	Integral of each scheme wright (Ei × Wi)		
			1	2	3
1	The costs of ventilation system engineering	0.032	0.32	0.24	0.27
2	The costs of ventilation equipment	0.062	0.62	0.59	0.62
3	The costs of ventilation system operating	0.106	1.06	0.88	0.85
4	The Reliability of ventilation system	0.057	0.57	0.44	0.51
5	Transport management of Underground	0.057	0.57	0.38	0.51
6	Ventilation system management	0.057	0.57	0.51	0.51
7	Air Leakage Control of mine	0.029	0.29	0.22	0.29
8	The risk of Gas accident	0.167	1.67	1.67	1.67
9	The risk of mine Fire	0.033	0.33	0.33	0.33
10	The air pressure of underground	0.360	2.88	3.3	3.6
11	The environment temperature of underground	0.040	0.36	0.38	0.4

ACKNOWLEDGEMENTS

This work was financially supported by Scientic Research Fund of Heilongjiang provincial Education Department (12533064).

REFERENCES

Jing Quanzhong. Study on Index System of Capability of Production Safety in Coal Mine Based on AHP [J]. *China Safety Science Journal, 2006(9)*. (in Chinese);

Wang Hongliang. The Research of Ventilation System based on artificial increasing pressure echnology in the high-altitude mines [J]. *Jourenal of Hei Longjiang Institute of Science and Technology. 2009. 6.*(in Chinese).

Wang Jianming. Study on Theories and Application of Multiobject Fuzzy Pattern Recognition Decision Making [D]. *Dalian: Dalian University of Technology. 2004.*

This page intentionally left blank

Progress in Mine Safety Science and Engineering II – He et al. (Eds)
© 2014 Taylor & Francis Group, London, ISBN 978-1-138-00122-0

Study on the stability of roof based on Mathews method in deep mining

Binchuan Zhang, Chunlai Wang & Lei Wang
Faculty of Resources and Safety Engineering, China University of Mining and Technology, Beijing, China

ABSTRACT: The roof stability is a prerequisite of ensuring safety in deep mining. Because of the different engineering geology factor and the complexity engineering geology structure, a base problem is how solved for roof stability in coal mine. In light of the characteristic of store condition at Xiezhuang coal mine, the rock mass engineering geology was surveyed on the site for the safety and successful controling the coal layer. The rock mass mechanical parameter was measured in laboratory, the rock mass quality was obtained. The Mathews method was used to evaluate the roof stability. The important material and foundation were provided for safety exploitation at Xiezhuang coal mine.

1 INTRODUCTION

The reserve achieves 200 million tons in Xiezhuang coal mine of Xin Mine Group in Shandong province, and the recoverable reserve reachs more than 60 million tons. The exploit method is multi-level inclined shaft, which includes 1 main shaft, 2 auxiliary shafts and 3 air shafts. At present, mining depth has reach 1212 m, the horizontal stress is 39 MPa with testing in situ stress in early stage, there are significant creep characteristics in rock surrounding roadways, including floor heaves have been produced and rock surrounding roadways have been large deformation. Now, the high pre-stress bolting-steel mesh-shotcreting support (diameter 22 mm, length2.4 m) was used to control the deformation of rock surrounding. However, it cannot achieve satisfying result. Therefore, it is urgent problem in safe and efficient mining aspects how to solve the key problems about support of soft rock roadways in the process of deep mining in Xiezhuang coal mine.

The stability of surrounding rockmass in driving face and roof in working face is difficult problems in the process of mining with deep high stress (Guo et al. 1999, Li 2006, Sun 1998, Tang 1997). To solve technological problems about roof falling in working face, the field work and indoor testing were conducted for analysis roof stability, including engineering geological survey, physical and mechanical parameters testing, coal and rock mass quality evaluation, working face size parameter measurement. It is important to ensure the safe and efficient mining.

2 PHYSICAL MECHANICAL PARAMETERS TEST OF COAL AND ROCK

Mechanical parameters of the main coal seam have obtained to evaluate for engineering geological condition, select for support methods and provide the basis parameters for optimization of working face. The test parameters include coal and rock density, uniaxial compressive strength, uniaxial tensile strength, elastic modulus and Poisson's ratio, these results are shown in Table 1.

3 EVALUATION OF ROCKMASS ENGINEERING GEOLOGY CONDITION

Classification of surrounding rock stability is important reference to choice supporting methods in deep mining. Classifications of rock mass structure reflect geological characteristics, which can evaluate rock mass stability and be used in a wide range of practice. *RMR* classification and

Table 1. Test Results.

	ρ t/m^3	σ_c MPa	σ_t MPa	E MPa	μ	C MPa	φ (°)
A	2.33	68	10.43	74.09	0.19	13.31	47.22
B	2.25	37	3.46	44.11	0.24	8.86	55.93
C	1.46	17	1.59	73.48	0.21	18.53	60.00

(Note: Rock properties A: Fine Sandstone; B: Sandy Shale; C: Coal Seam).

Table 2. Classification of coal and rock mass quality evaluation.

Classification/ petrofabric	Fine Sandstone	Clay shale	Coal seam
RQD	General	General	General
RMR	Medium	Medium	Medium
Q	Medium	Medium	Medium
Results	General	General	General

Table 3. The largest span of different strata without supporting.

	Rock properties	Fine Sandstone	Clay shale	Coal seam
	Q Value	1.5	2.2	3.56
D(m)	ESR = 1.6~2	3.6~4.5	4.3~5.4	5.3~6.6
	ESR = 3	6.8	8.1	9.9
	ESR = 5	11.3	13.5	16.5

Q system methods are used to evaluate rock mass quality.

According to the results of rock mass physical and mechanical parameters test and engineering geological survey, rock mass quality evaluation results were obtained. As shown in Table 2 and 3.

The classification results of fine Sandstone, clay shale and coal seam are general.

4 ROOF STABILITY ANALYSIS

4.1 *Introduce of mathews method*

Mathews diagrammatize method is used to analyze roof stability of working face, it need to calculate two major variables, one is the shape factor, which is represented with structure size and shape of working face, and another is stability coefficient, which is the self-stability of rock mass under stress condition (Milne et al. 1998). Shape factor is hydraulic radius of structure size of working face. Mathews diagrammatic stability coefficient is been expressed as:

$$N = Q' * A * B * C \quad (1)$$

Where N—Mathews stability coefficient, Q'—Revised Q value, *A*—stress coefficient, *B*—joint position coefficient, *C*—gravity adjustment coefficient.

a. Q′ Value

NGI tunnel quality index (Q) was used to be classification in Mathews diagrammatize method, there are main differences between revised NGI tunnel quality index (Q′) and Q value, which is 1.0 in stress reduction factor (SRF) and joint water seepage reduction factor (J_w), Q′ value computational formula:

$$Q' = \frac{RQD}{J_n} \cdot \frac{J_r}{J_a} \quad (2)$$

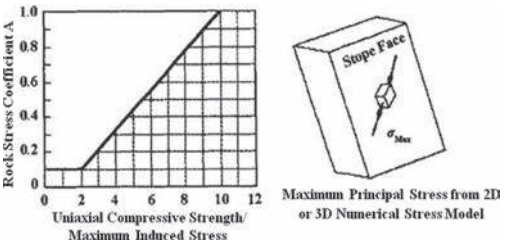


Figure 1. The diagram of stress coefficient *A*.

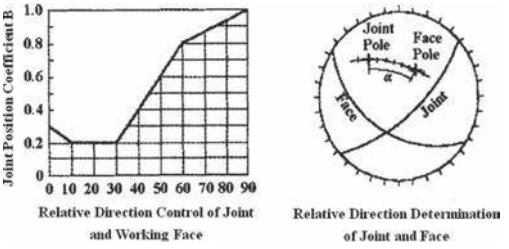


Figure 2. The diagram of joint position coefficient *B*.

b. Stress coefficient *A*

A value is considered effect factor of rock mass stability under high stress condition in Mathews diagrammatize method. *A* value is a ratio of uniaxial compressive strength and maximum principal stress of parallel working face with complete block of coal and rock. The relationship of *A* value and σ_c/σ_1 shows a linear, and its variation range is from 0.1 to 1.0.

c. Joint position coefficient *B*

B value is considered effect factor to cut direction of rock mass discontinuity surface, which decided by control joint and relative direction of working face roof. When the angle of joint surface and working face roof is 90°, *B* coefficient is 1. When the angle of discontinuity joint surface and working face roof is 20°, *B* coefficient is 0.3.

d. Gravity adjustment coefficient *C*

The roof of working face is influenced by dead weight in deep mining, roof stability of working face is smaller than slide. The gravity adjustment coefficient (*C*) is considered effect factor of self-gravity of coal and rock mass to slide roof collapse

and rock mass sliding. The relationship of gravity adjustment coefficient (*C*) and dip angle of working face roof is shown as follows:

$$C = 8 - 6\text{Cos}\ (A\text{angle of } D\text{ip}) \quad (3)$$

f. Hydraulic radius (HR)
Hydraulic radius is used to analyze a ratio between surface area of working face and its exposed roof perimeter.

4.2 *Stability analysis of working face roof*

A. Q′ value.
According to formula (2), the revised results of Q value in different surrounding rock mass were shown in Table 4,

b. Rock stress coefficient *A*
As shown in Table 5.

C. Joint position coefficient *B*
B value is determined by the relative azimuth angle of control joint surface and working face roof. Based on classification method, joint fissure survey results in field and coal and rock physical and mechanical parameters test results. The dip angle of controlled joint surface is steep dip in working face roof. Working face roof is normally horizontal. The joint position coefficient *B* of surrounding rock is 0.85 when it is classified by the unfavorable principle. This value is used to improve safety factor.

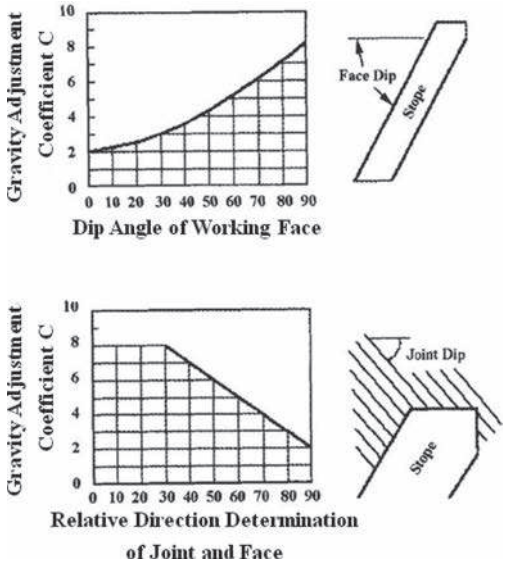


Figure 3. The diagram of gravity adjustment coefficient *C*.

d. Gravity adjustment coefficient *C*
Roof stability becomes worse because of self-gravity. When immediate roof of working face is horizontal, the gravity adjustment coefficient *C* is shown as:

$$C = 8 - 6\text{Cos}\ (A\text{angle of } D\text{ip}) = 8 - 6\text{Cos}0 = 2.0 \quad (4)$$

Hydraulic radius of immediate roof surrounding rockmass is calculated by the working face roof of Xiezhuang mine in deep mining, as shown in Table 6, 7.

The results of the largest span without supporting in different strata and allowable hydraulic radius are obtained based on the revised NGI tunnel quality index classification.

Fine sandstone roof might fall in the process of mining. Strata variation tendency of immediate roof should be monitor in the process of mining

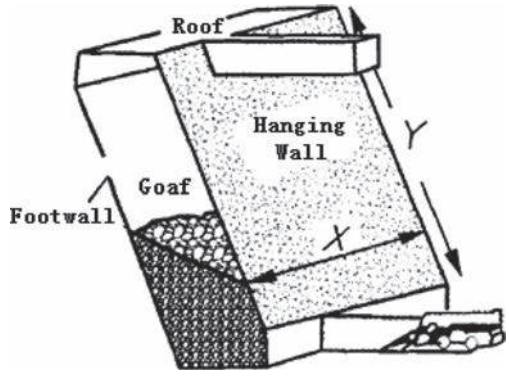


Figure 4. The diagram of Hydraulic radius.

Table 4. Q′ value results.

Rock properties		Fine Sandstone	Clay shale	Coal seam
Revised Q′ value	RQD	65	76	65
	J_n	6	6	6
	J_r	1.0	1.0	2.0
	J_a	4.0	4.0	4.0
	Q′ value	2.71	3.17	5.42

Table 5. Rock stress coefficient *A*.

Rock properties	Fine Sandstone	Clay shale	Coal seam
Rock stress coefficient *A*	σ_c/σ_1		
	1.74	0.95	0.44
	0.13	0.07	0.03

Table 6. Results of hydraulic radius of immediate roof mine rock.

No.	Stope No.	Width (m)	Length (m)	Hydraulic radius calculated value	Remarks
1	1	5	100	4.55	mined

Table 7. Stability coefficient N results.

Area	Rock properties	Q′	*A*	*B*	*C*	N	HR
Immediate roof of working face	Fine Sandstone	2.71	0.13	0.85	2.0	0.6	4.55

because of the F8 fault, which can avoid to roof fall with larger-scale.

5 CONCLUSION

Based on store condition of coal seam and survey results and tests of joints surface in Xiezhuang mine, rock mass structure types are analyzed, and rock mass quality is quantificationally evaluated. The conclusion shows that engineering geological conditions of the working face roof belong to medium. Allowable hydraulic radius are calculated based on stability analysis of working face roof with Mathews diagrammatize method, which provides a foundation for safe and efficient in deep mining.

ACKNOWLEDGEMENTS

We thank the financial support from the Specialized Research Fund for the Doctoral Program of Higher Education (No. 20120023120008), the Fundamental Research Funds for the Central Universities (No. 2011QZ01), and by National Students' Innovation and Entrepreneurship Training Program (No. 201211413013).

REFERENCES

Guo R., Yu R.C. & Zhang W.R. 1999. Mathews method application in mining methods and design. *Metal mine* (9):22–25.

Li Z. 2006. Study on mining stability of 2# ore body in Anqing copper min. *Hu Nan nonferrous metallurgy* 22(5):1–3.

Milne D, Hadjigeorgiou J &Pakalnis R. 1998. Rock mass characterization for underground hard rock mines. *Tunnelling and Underground Space Technology* (13): 383–391.

Sun G.Z. 1998. Structural mechanics of rock mass, *Beijing: science press*.

Tang S.H. 1997. Study on engineering geology of rock mass stability in Anqing copper mine. *Mine research and development* 17(1):30–33.

Progress in Mine Safety Science and Engineering II – He et al. (Eds)
© 2014 Taylor & Francis Group, London, ISBN 978-1-138-00122-0

Burning characteristics of No. 6 coal seam at mine field's two wings in Cuijiazhai mine

Y.H. Wang, H.T. Li, Q.F. Zhao & J.J. Ren
Hebei Province Key Laboratory of Mine Disaster Prevention, Sanhe, Hebei, China
North China Institute of Science and Technology, Sanhe, Hebei, China

S.S. Yang & Z.J. Shu
Chinese People's Armed Police Force Academy, Langfang, Hebei, China

ABSTRACT: Under the condition of radiation energy given 50 KW/$m^{2,}$ by using cone calorimeter, experiments are made to research burning characteristics of 4 coal samples which are taken from two wings of No. 6 coal seam in Cuijiazhai mine. Results show that CO peak concentration and average produce amount which are produced in the course of coal samples taken from east wing burning are more than that of coal samples taken from west working face. Coal sample taken from west wing are more than that of coal samples taken from east wing in heat release rate, total heat release and specific extinction area. In respect of smoke produce rate and total smoke release, there is certain difference that the first coal sample taken from 11605 working face in west wing is the highest, and the first coal sample taken from 11606 working face in east wing takes second place.

1 INTRODUCTION

Mine fire is one of the largest hazards in coal mine, which not only makes coal mine suffer tremendous losses in physical material, but also is the main cause of miners' casualty (Xian et al. 2001). The spontaneous combustion of coal is one of main reasons to mine fire. According to statistics, the mines with spontaneous combustion tendency account for 51.3% of state owned key coal mines in China. There are poisonous material such as CO, CO_2 and dust in the course of coal spontaneous combustion, and so on. The statistical results show that over 95% victims died from above poisonous smoke and gas in mine fire (Jukka et al. 1999).

The coal types are mainly brown coal and long flame coal in Cuijiazhai coal mine, there are spontaneous combustion tendency for coal seams, and the coal seams appeared several spontaneous combustion accidents and hazards. To study the release law of poisonous smoke and gas in the course of coal spontaneous combustion in order to prevent mine fire in the mine, experiments are to be done to study burning characteristics of No. 6 coal seam by using the cone calorimeter.

2 WORKING PRINCIPLE OF EXPERIMENT INSTRUMENT

Coal sample is tested by using the cone calorimeter (CONE) made by the British Fire Testing Technology Corporation; the instrument is composed of six parts including firebox, load-table, oxygen-analyzing instrument, smoke-measuring system, ventilation device and correlative assistant facilities. The standard ISO5660 (Babrauskas & Grayson 1995) for fire characteristic testing with cone calorimeter was published by ISO in 1993. At present, the cone calorimeter has been ideal experiment instrument to research fire and evaluate burning characteristics of materials.

Cone calorimeter is an instrument to test burning heat according to oxygen consumption principle. The principle of oxygen consumption is that the equivalent amount of heat is produced when the per-unit combustible material is burned completely, that is, oxygen consumption burning heat (E) is basically equal (Wang & Zhang 2003). By using oxygen consumption principle, Huggett found that the average value of burning heat of oxygen consumption is 13.1 kJ/g and the deviation

value E is 5% among different materials. Therefore, burning of material can be computed by measuring change of oxygen in the system of burning in the course of actual testing.

3 EXPERIMENT RESULTS AND ITS' ANALYSIS

3.1 *Experiment results*

The tested coal samples are taken from No. 6 coal seam in Cuijiazhai coal mine, in order to analyze and compare, the two coal samples are taken from 11606 working face in east wing of mine field, and the other two coal samples are taken from 11605 working face in west wing of mine field.

Experiments are abide by standard ISO5660 by adopting horizontal test, in the course of testing, the irradiance is given 50 KW/$m^{2,}$ and the calibration constant C is given 0.039694 (Wang et al. 2006).

In the course of experiment, the four coal samples' burning characteristics are measured, the parameters include CO, heat release rate (HRR), total heat release (THR), smoke produce rate (SPR) and total smoke release (TSR), and so on. Each parameter is shown in Figure 1–6.

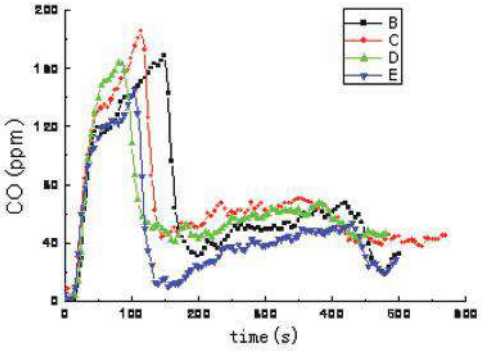
3.2 *Analyses on experiment results*

The following conclusions can be achieved by analyzing the above data.

3.2.1 *Ignition time of coal samples (Tign)*

Ignition time of coal samples reflect easy degree of coal samples ignited, the shorter ignition time is, the easier burning for coal samples. The ignition and extinguishment time of four kinds of coal samples are shown in Table 1.

Ignition time which the two coal samples are taken from west wing of mine field is less than that of east wing. Three coal samples aren't significant



Where B=the second point at 11606 working face in east wing; C=the first point at 11606 working face in east wing; D=the first point at 11605 working face in west wing; E=the second point at 11605 working face in west wing.

Figure 1. The release of CO in the course of coal sample burning.

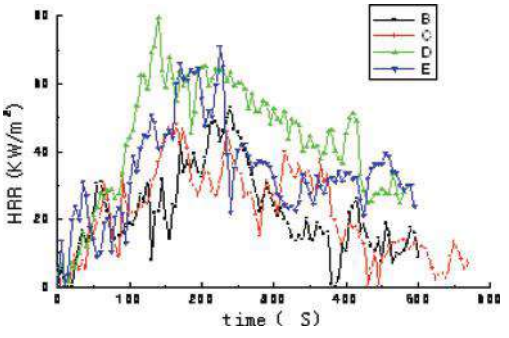


Figure 2. Four coal samples HRR in the course of burning.

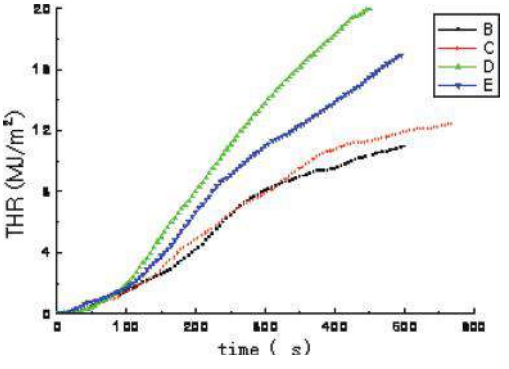


Figure 3. Four coal samples THR in the course of burning.

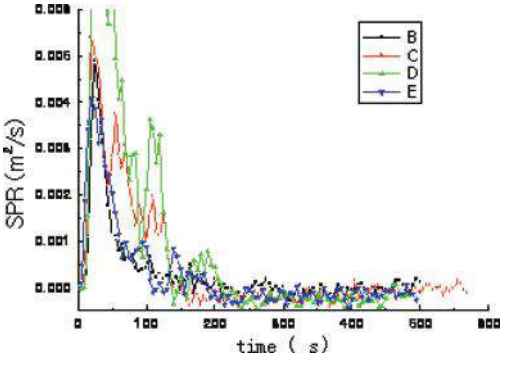


Figure 4. Four coal samples SPRR in the course of burning.

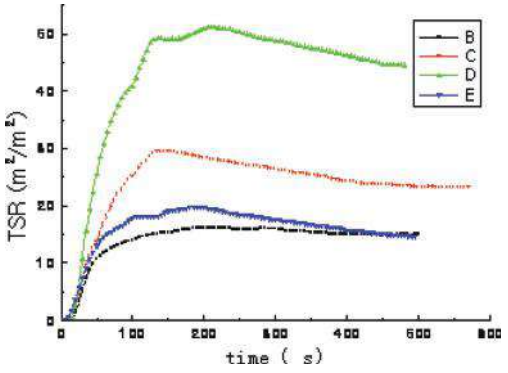


Figure 5. Four coal samples TSR in the course of burning.

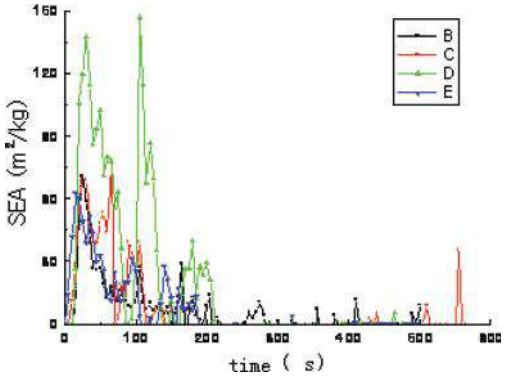


Figure 6. Four coal samples SEA in the course of burning.

difference among four coal samples. Therefore, under the same condition, there is more fire possibility at the 11606 working face in west wing of mine field than 11605 working face in east wing for No. 6 coal seam in Cuijiazhai Coal mine.

3.2.2 *CO concentration and produce amount*

CO is one of mainly released poisonous gases in the course of spontaneous combustion, it is an important significance for preventing and dealing with coal spontaneous combustion to study release law of CO in the course of coal sample burning. The released CO is shown in Figure 1, the results show that the average amount of CO which coal sample produces at 11606 working face in east wing is more than that of 11605 working face in west wing, and nearly as 2 times as 11605 working face. Therefore, CO is the largest danger in mine fire nearby 11606 working face in east wing.

Table 1. Coal samples ignited and extinguished time.

	Sample B	Sample C	Sample D	Sample E
Tign* (s)	149	114	90	95
Text* (s)	236	219	249	232

* Tign = Time of ignition, Text = Time of extinguishment.

Table 2. CO produced in the course of burning.

	Sample B	Sample C	Sample D	Sample E
Apro* kg/kg	0.0731	0.0606	0.0387	0.0397
Ppro* kg/kg	0.137	0.1492	0.2322	0.1197
Peak time (s)	200	145	220	110

* Apro = Average production, Ppro = Peak production.

Table 3. Four coal samples HRR in the course of burning.

	Sample B	Sample C	Sample D	Sample E
Average (KW/m^2)	35.23	37.51	59.94	50.67
Peak (KW/m^2)	47.8	48.88	79.47	71.17
Peak time (s)	165	220	140	225

Table 4. Four coal samples SEA in the course of burning.

	Sample B	Sample C	Sample D	Sample E
Average (m^2/kg)	2.63	3.22	17.89	3.83
Peak (m^2/kg)	19.77	28.91	147	31.27
Peak time(s)	110	165	105	95

3.2.3 *Heat release rate (HRR) and total heat release (THR)*

HRR is an important characteristic parameter to indicate fire intensity; the peak of HRR shows the greatest heat release degree when material is burning.

THR is the total heat release from which material is ignited to be extinguished. Experiment results show that the HRR and THR of two coal samples in west wing are higher obviously than that of other two coal samples in east wing, as shown in Figure 2 and Figure 3.

Therefore, if mine fire break out nearby 11605 working face in west wing of mine field, a large amount of heat will be produced.

3.2.4 *Smoke produce rate (SPR) and total smoke release (TSR)*

SPR and TSR are two important characteristic parameters to indicate smoke produce capacity degree when material is burning. Experiment data show TSR of coal samples which are taken from the first point at 11605 working face in west wing of mine field is higher than others coal samples. Taking SPR and TSR into comprehensive consideration, there is the largest danger at 11605 working face in west wing after mine fire. TSR of coal sample is higher at first point of 11606 working face in east wing.

The other two coal samples are little difference in SPR and TSR.

3.2.5 *Specific extinction area (SEA)*

The larger the SEA is, the more difficult for disaster relief and evacuation. The experiment data show that SEA average of the first coal sample which is taken from west wing of mine field is much larger than other coal sample, and that of the second coal sample is also more than the two coal samples which are taken from east wing of mine field. Therefore, if mine fire break out in west wing of mine field, the difficulty of disaster relief will be more than east wing.

4 CONCLUSIONS

Firstly, ignition time which the two coal samples are taken from west wing of mine field is less than that of east wing.

Secondly, the average amount of CO which coal sample produces at 11606 working face in east wing is more than that of 11605 working face in west wing.

Thirdly, after coal samples taken from west wing burning, their THR is more than that of coal samples taken from east wing.

Fourthly, in respect of smoke produce rate and total smoke release, there is certain difference that the first coal sample taken from 11605 working face in west wing is the highest, and the first coal sample taken from 11606 working face in east wing takes second place, and there is little difference in the others coal samples.

Fifthly, after coal samples taken from west wing burning, SEA is more than that of coal samples taken from east wing. The average SEA of one coal sample from west wing is 5.5~6.8 times as large as coal sample taken from east wing.

ACKNOWLEDGEMENTS

This work was financially supported by “the Fundamental Research Funds for the Central Universities” (2011 A01), “the Fundamental Research Funds for the Central Universities” (3142013035), “the Fundamental Research Funds for the Central Universities” (3142013100), “the Fundamental Research Funds for the Central Universities” (AQ1202B).

REFERENCES

Babrauskas, V. & Grayson, S.J. 1995. *Heat release in fires*. London: Chapman & Hall.

Jukka, H. et al. 1999. Burning characteristics of selected substances: production of heat, smoke and chemical species. *Fire and Materials* 23(4): 171–185.

Wang, Q.G. & Zhang, J. 2003. Principle and application on cone calorimeter. *Modern scientific instruments* (6): 36–39.

Wang, Y.H. et al. 2006. Experiment Research on Burning Characteristic of Combustible Materials in Coal Mine. *Journal of North China Institute of Science Technology* 3(1): 1–4.

Xian, X.F. et al. 2001. The summarization of the investigation on coal mine fire prevention & fire extinguishing techniques in China. *Engineering Science* 3(12): 28–32.

Progress in Mine Safety Science and Engineering II – He et al. (Eds)
© 2014 Taylor & Francis Group, London, ISBN 978-1-138-00122-0

Study on influence of propane for the generating kinetics of multi-component gas hydrate

Qiang Wu & Qiong Wu
Department of Safety Engineering, Heilongjiang University of Science and Technology, Harbin, Heilongjiang, China

Baoyong Zhang
National Engineering Research Center for Coal Gas Control, China University of Mining and Technology, Xuzhou, Jiangsu, China

Xia Gao
College of Civil Engineering, Heilongjiang University of Science and Technology, Harbin, Heilongjiang, China

ABSTRACT: Aimed at curing, storing, and transporting the multi-component gas at a faster speed, this paper is focused on using visualization hydrate equipment facility to investigate the hydration curing processes of four kinds of multi-component gas, as occurs in complex solution consisting of 0.2 mol/L sodium dodecyl sulfate (SDS). The paper obtains the induction time and growth rate in the formation process, analyses and calculates the experimental data combined with the model of growth rate. The results show that it is shortened that the induction time of mixture containing propane gas hydrate formation significantly due to the activation energy of the transition reduce, for propane and methane coordination number in accordance with the structure II hydrate coordination number. Meanwhile propane gas has promoting effect on hydrate growth rate since it is easier to form hydrate compared with methane which the ability of stabilizing the large cage of structure II is lower than propane.

1 INTRODUCTION

Coal mine gas (called Coal bed Gas) is a kind of associated gas from the coal seam in coal mine exploitation process in different forms, which is one of the main reasons of the coal mine accident. As the first fatal factor in coal mine, the gas accident not only causes a large number of casualties and huge economic losses, and imperils the safety of coal mine production seriously once it occurs. Gas concerns the major issues of environmental pollution, the greenhouse effect and the future of new energy. It can be used after recovered rapidly if the coal mine gas develops, storages and transports high-efficiently in moderate environment. Meanwhile it will be reduced that the cost, the hidden safety trouble and the gas emission pollution to the environment. Thus it is badly in need of a new type of gas utilization technology to make up for the current technical defects. Hydrate method is an optional way.

Gas hydrate is a similar ice and non-stoichiometric crystalline solid composed of water and coal mine gas (CH_4, C_2H_6, N_2, O_2, CO_2 etc.) under a certain temperature and pressure conditions. Gas hydrate has three characteristics: formation easer, storage stability, and high gas storage rate. It is the key difficulty to realize industrialized application of gas curing storage and transportation for the stable formation rapidly of the multi-component gas hydrate. Many scholars promote the hydrate formation from the accelerant, the porous medium, and the physical method. Moreover it can accelerate hydrate reaction rate with adding a certain amount of hydrocarbons in hydrate reaction system, such as cyclopentane which can accelerate hydrate reaction rate and shorten the induction time of hydrate reaction to the original quarter. However, heavy hydrocarbon such as cyclopentane is liquefied easily and the high cost. As a new promotes method, the research on propane is less in the promotion of gas hydrate formation kinetics. Therefore, it is quite necessary to study the promoting effect of propane on the kinetics of mixture gas hydration process. In view of this, this paper studies the formation process of mixture gas hydrate in SDS solution environment and the promoting effect of propane on gas hydration process. The indexes are described quantitatively through induction time and growth rate.

2 EXPERIMENT PART

This paper studies four kinds of mixture gas hydrate formation experiment in SDS solution, the sample gas mixture (I: 85%CH_4, 7%N_2, 3%O_2, 5%CO_2; II: 70%CH_4, 22%N_2, 3%O_2, 5%CO_2; III: 85%CH_4, 5%C_3H_8, 22%N_2, 3%O_2, 5%CO_2; IV: 70%CH_4, 10%C_3H_8, 12%N_2, 3%O_2, 5%CO_2), 0.25 mol·L^{-1} SDS solution, and homemade distilled water, etc.

The concrete experimental parameter is shown in Table 1. In this paper, the main part of experimental is a visual hydrate experiment equipment, with precision temperature controller and the control rage of –10~60°C. It can realize the precision control of the system temperature with the control accuracy of 0.1°C in the kinetics experimental process. The equipment forms gas hydrate kinetics experiment system with the visual and high pressure reaction kettle, increases and relief pressure system, temperature pressure measuring system, data acquisition system together. The hydration reaction kettle is 150 ml transparent reaction kettle which carried the solution (temperature range of –10°C to 50°C, the pressure limiting 20 MPa). It can be observed directly those hydrate formation, growth and decomposition process. This experiment equipment can record temperature and pressure data of each stage in the process of decomposition of hydrate formation synchronously, and real-time plotting the P-T curve to analyze the experimental process. It is proceeded the determination experiment of hydrate phase equilibrium conditions for the four kinds of mixture gas at first. Based on the condition of the obtaining phase equilibrium essential data, this paper proceeds hydrate formation kinetics experiment with the initial pressure of 4.0 and 5.0 MPa under the same drive temperature $\Delta T = 5$°C.

3 EXPERIMENTAL RESULTS AND ANALYSIS

3.1 *Influence of propane on induction time*

3.1.1 *Experimental result*

System 3–2nd starts refrigeration experiment in 0.25 mol/L SDS, with the initial pressure of 5.00 MPa and initial pressure of 13.5°C. At 73 min, A needle shape ice crystals are generated in right section of transparent reaction kettle, and produced to air above, as shown in figure 1 (a). At this point, the reaction system temperature is 13.48°C with the pressure of 4.82 MPa. At the 125 min, needle shape hydrate is growing upward along the kettle wall, and growing rapidly to the direction of liquid at the same time, translucent crystals hydrate overgrows the kettle wall gradually. Solid hydrate is full of almost all solution as shown in figure 1 (b). Gas phase pressure of the kettle doesn't change any more, and the wall of kettle almost covered by translucent hydrate at 215 min. It is mean the hydrate formation ended largely, at this point, the reaction system temperature is11.89°C with the pressure of 4.25 MPa.

It is shown in Table 2 that macroscopic induction time and the thermodynamic parameters of mixture gas hydrate formation in each experimental system. In system 3–2nd experiment, transformation situation of P-t-T is shown at Figure 2(a).

From the contrast experiment result Table 2, it can be seen that the longest induced time of hydrate formation is 180 min, and the shortest is 106 min in no propane contain system in experiment 1 and 2; in experiment 3 and 4, the longest induced time of hydrate formation is 81 min, and the shortest is 68 min in propane contain system. The result indicates that the inducted time is shortened due to propane adding. The curve of gas hydrate induction time of four systems is shown

Table 1. The experimental conditions parameters of hydrate formation.

Experiment system	Gas sample	SDS/ mol·L^{-1}	Experiment number	Initial pressure/ MPa	Phase equilibrium temperature/ °C	Initial temperature/ °C	Condition	
							Temperature/ °C	Pressure/ MPa
1	I	0.25	1st	4	5.4	0.5	2.45~17.51	3.27~4.08
		2nd		5	6.8	2.0	2.34~16.75	3.51~5.18
2	II		1st	4	4.9	0.1*	1.85~19.2	3.41~4.12
		2nd		5	5.0	6.5	1.46~18.87	3.81~5.12
3	III		1st	4	16.5	11.5	16.5~27.2	4.33~4.95
		2nd		5	18.6	13.5	18.0~27.9	5.25~6.08
4	IV		1st	4	18.5	13.5	18.2~26.9	4.14~5.02
		2nd		5	20.2	15.0	19.8~27.5	4.88~5.91

* The initial temperature try to avoid falling below 0°C to produce ice to block observe hydrate formation, thus fine-tuning to 0.1°C in 2–2nd experiment system.

in Figure 2(b). Compared with the inducted time between system 3 and 4, inducted time of hydrate formation is shortened with the propane content increased instead of lengthened with the methane content reduced. For instance the induction time of experiment 4–1st is 72 min; it is shorter 9 min than system 3–1st which is 81 min.

3.1.2 *Mechanism analysis*

Sloan and Christiansen [14] research shows that the less unstable cluster which the water molecules number in clusters needs to change in hydrate formation, the faster transformation process, and leading to shorten the inducted time of hydrate formation. Water molecules form unstable clusters around the dissolved guest molecules. The number of water molecules in each cluster is CH_4 20, C_2H_6 24, C_3H_8 28, N_2 20, and H_2S–20. Coordination number depends on the size of the gas molecules. Because each hydrate structure has two types of different coordination number cavities, it is demanded that instability clusters need to correspond with coordination number, too.

As shown in Figure 3, coordination number which the molecular cluster is 20 and 24 combined with the cavity of 5^{12} and $5^{12}6^2$, forming structure I; coordination number which the molecular cluster is 20 and 28 combined with the cavity of 5^{12} and $5^{12}6^4$, forming structure II. When pure methane dissolved in water, aqueous phase will form instability cluster of coordination number 20, but methane forms the structure I hydrate with coordination number 20 and 24 two cavity size (the size cavity ratio of large and small is 3:1). In order to form methane hydrate, only 1/4 coordination number of cluster needn't change in the unstable cluster, the remaining 3/4 cluster have to experience a process that the coordination number translates from 20 to 24. In the case of pure propane dissolved in water, coordination number of propane is 28. It needs 2/3 the cluster to translate coordination number into 20, so as to form structure II (the size cavity ratio of large and small is 1:2). For the coordination number translating need a certain activation energy, the less unstable cluster of coordination number which need to translate, the faster transition process, so that the inducted time of hydrate formation is shorter. Thus it can be deduced the inducted time of pure propane is slightly shorter than methane. However, the coordination number of methane and propane just match the structure II hydrate with 20 and 28 molecular clusters; almost no the coordination number needs to translate early in the formation of structure II hydrate. Therefore, due to the propane added, whole process decreases the change of coordination number, reduces the activation energy consumption and speeds up the transition process turns, and then the mixture hydrate formation induction period is shortened. Moreover the higher propane content, the higher the ratio of structure II hydrate formation, the less coordination number needs to translate, and the shorter the inducted time is.

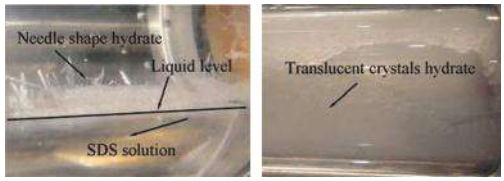


Figure 1. Typical pictures of gas hydration curing process of system 3–2nd, (a) 73 min (b) 125 min.

3.2 *Propane gas effect on the growth rate*

3.2.1 *Experimental result*

It can be obtained that the gas phase pressure changing with time curve of various experimental systems from the experimental data which gained from the data acquisition system, as shown in Fig. 4 (a). Growth rate can be indicated by the range of the pressure changed with the time (curve slope

Table 2. Experimental data of hydrate formation for gas hydration curing in SDS water.

Experiment system	Gas sample	SDS/ mol·L^{-1}	Experiment number	Initial pressure/MPa	Induction time/min	Condition	
						Temperature/°C	Pressure/ MPa
1	I	0.25	1st	4	5.4	2.75	3.788
			2nd	5	6.8	2.70	4.582
2	II		1st	4	4.9	2.10	3.794
			2nd	5	5.0	1.98	4.644
3	III		1st	4	16.5	12.62	3.863
			2nd	5	18.6	13.48	4.819
4	IV		1st	4	18.5	13.13	3.488
			2nd	5	20.2	12.71	4.694

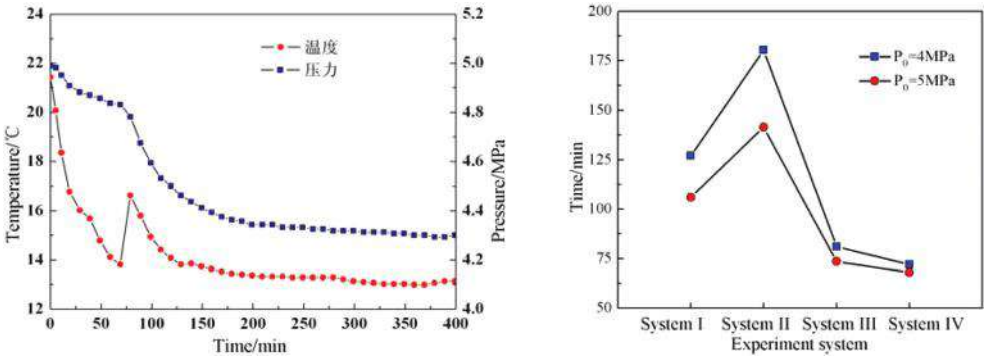


Figure 2. (a) The variation curves of pressure and temperature with time of gas hydration curing process in of system 3–2nd; (b) The curves of gas hydrate induction time with C_3H_8 in four systems.

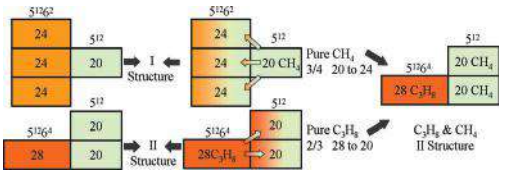


Figure 3. Schematic diagram of the coordination number transformation of hydrate.

of the initial stage). After reaching the induction time, the greater the slope showed that the faster hydrate growth rate. Aim at 4–2nd experiment in the system, according to the changes of the system gas phase pressure hydrate formation process can be divided into gas dissolution, nucleation induction process, macroscopic growth process, slow and generate over five stages. The curve slope can be used to tan α of initial stage in said. Under the condition of P_0 = 5 MPa, the decrease amplitude of gas phase pressure in hydrate formation process is small and the experiment 2–2nd growth rate is minimal in system 1 and system 2. Due to the initial pressure change curve slope is bigger and the amplitude decrease of gas phase pressure is bigger, so that the experiment 4–2nd growth rate is the largest in system 3 and system 4. From this the resulting the law of growth rate is the 4–2nd system > 3–2nd system > 1–2nd system > 2–2nd system.

Combined the characteristics of gas hydrate, this paper introduces the hydrate formation rate calculation model, in order to analyze the influences of the kinetics of gas hydrate formation process quantitative, such as formula (1).

$$\frac{dV_{hyd}}{dt} = \left(V_W + \left(\frac{1}{\rho_H} - \frac{1}{\rho_W} \right) \times m_W \right) \times 10^{-6} / \frac{\tau}{60} \qquad (1)$$

V_W is the volume of water transforming into a cavity in hydration reaction process and unit is cm^3. m_W is the quality of the hydration reaction process of removing water and unit is gcm^{-3}. ρ_H is the density of hydrate cavity and take the 0.796 $g \cdot cm^{-3}$ of structure I hydrate and take the 0.786 $g \cdot cm^{-3}$ of structure II hydrate. According to hydrate formation during the process of hydrate formation time leg between and end moment equations (min), the gas state equation can calculate the hydrate growth rate ($m^3 \cdot h^{-1}$) combined with the hydrate volume equation. It is shown that the hydrate growth rate of experimental systems which calculated by the hydrate growth rate calculation model in Table 3. The curve of hydrate growth rates changed with propane concentration is shown in figure 4 (b).

From Fig. 4(b), it is observed that the hydrate growth rate decreases with the loss of the methane content for system 1 and system 2. The growth rates in system 3 and 4 rise sharply when gas containing propane and with the increase of the content of propane and growth. Such as the gas hydrate without propane growth rate are 1.219 × 10–^{6} $m^3 \cdot h^{-1}$ and 1.1176 × 10–^{6} $m^3 \cdot h^{-1}$, respectively, and the gas hydrate with propane growth rate are 13.453 × 10^{-6} $m^3 \cdot h^{-1}$ and 18.873 × 10^{-6} $m^3 \cdot h^{-1}$ in four experiments P_0 = 5 MPa. At the same time, P_0 = 5 MPa growth rates are slightly higher than the four groups of P_0 = 4 MPa in four experiments. It can be obtained that the high pressure has promotion on hydrate growth rate in 5%~10% propane content scopes.

3.2.2 *Mechanism analysis*

The analyses shows that thermodynamic driving impetus influence on rate of hydrate formation, the ability of stabilizing large cavity of hydrate structure also has important effect on hydrate growth rate. Understanding from the angle of hydrate stability, the ratio(S) of object diameter and the cavity diameter can estimate the stability of cavity. In Table 4,

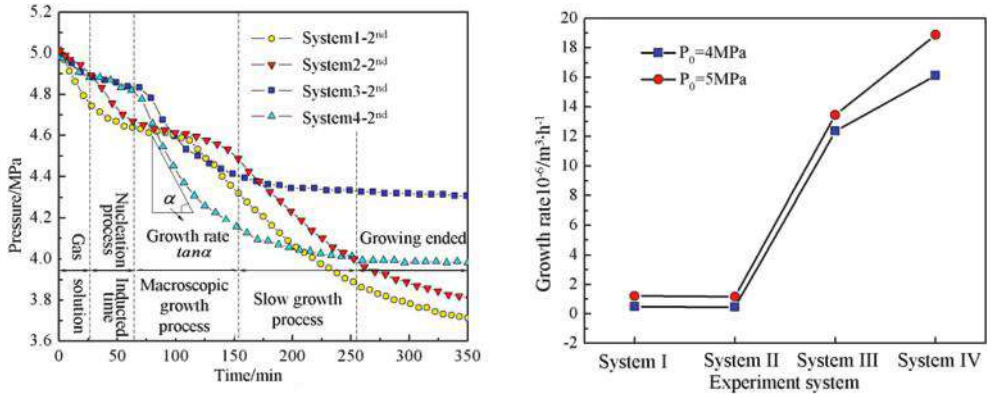


Figure 4. (a) Pressure curves with time in gas hydrate formation process for $P_0 = 5$ MPa (b) The curves of gas hydrate formation rates in four systems.

Table 3. Formation rates of gas hydrates in experimental systems of dynamic study.

System	1–1st	1–2nd	2–1st	2–2nd	3–1st	3–2nd	4–1st	4–2nd
Growth rate $10^{-6}/m^3 \cdot h^{-1}$	0.477	1.219	0.446	1.176	16.126	13.453	12.356	18.873

Table 4. The diameter ratio between Hydrate gas molecules and the hydrate cavity.

Molecule	Object diameter/nm	Crystal structure	S_I-5^{12}	S_I-$5^{12}6^2$	S_{II}-5^{12}	S_{II}-$5^{12}6^4$
N_2	4.1	II	0.804	0.700	0.817	0.616
CH_4	4.36	I	0.855	0.744	0.868	0.655
CO_2	5.12	I	1.00	0.834	1.02	0.769
C_3H_4	6.28	II	1.23	1.07	1.25	0.943

the value S of $5^{12}6^4$ cavity which is 0.943contained propane molecule is higher than the value S (S = 0.855) of methane occupied 5^{12} cavity. It shows that the ability of propane to stable large cavity of structure II is better than that of methane, which is more stable relatively. It can be concluded that large cavity containing propane forms more easily than the small cavity containing methane. Propane forms structure II rapidly to effective supporting the large cavity of structure II hydrate, in order to accelerate the speed that small cavity contents small molecules such as methane. At the same time, propane is consumed to form structure II hydrate at the time of gas hydrate generating at first, and methane and propane etc. gas is consumed together in the process of hydrate formation. Propane is consumed at a higher rate with hydrate formatting constantly. The higher propane content, the higher the ratio of structure II hydrate formatting, the growth rate is faster. Thus propane added accelerates the hydrate growth rate, and the rising of propane content increases hydrate growth rate.

4 CONCLUSION

1. It is studied that hydrate formation induction time of four different gas mixtures in the SDS solution. Induction time of hydrates formation is shorten due to the propane adding, and with the increase of propane content, induction time shortens significantly. The generated induction time of 10% propane gas hydrate is the shortest.
2. Propane has effect on improving mixture gas hydrate growth rate. When the mixture gas containing propane, the growth rate of gas hydrates increase rapidly, and the amplification is larger with the increase of the propane content.
3. As a method of promotion, propane improves conditions of gas hydrate formation kinetics observably from air aspect. The method reduces the cost of curing gas storage and transportation, and promotes the industrialization development of gas hydration solidification separation and storage and transportation.

ACKNOWLEDGEMENTS

This work was financially supported by the National Natural Science Foundation of China (51274267, 51174264, 51104062), and Key Laboratory of Marine Hydrocarbon Resources and Environmental Geology, Ministry of Land and Resources (GZH201100310-wx03).

REFERENCES

Baoyong Zhang, Qiang Wu & Denglin Sun 2008. Effect of surfactant tween on the induction time of gas hydrate formation. *Journal of China University of Mining and Technology,* 18:18.

Baoyong Zhang, Qiang Wu & Yumei Zhu 2009. Effect of THF on the thermodynamics of low-concentration gas hydrate formatiion. *Journal of China University of Mining & Technology,* 38(2):203–208.

Baoyong Zhang, Yuanping Cheng & Wu Qiang 2011. Sponge effect on coal mine methane separation based on clathrate hydrate method. *Chinese Journal of Chemical Engineering,* 19(4)610–614.

Cuiwei Hu 2002. *Preparation Technology of stable methane-hydrate*. Chengdu:Southwest Peroleum University.

Jianzhong Zhao, Suping Han, Dingxian Shi & Xiangping Guo 2005. Application Prospects of coalbed methane hydrate technology. *Mining Technology Institute,* 25(5): 40–43.

Maekawa T 2008. Equilibrium conditions for clathrate hydrate formed from methane and aqueous propanol solutions. *Fluid Phase Equilibria,* 267(1):1–5.

Mingjun Yang, Yongchen Chen & Yu Liu 2010. Effects of porous media and salinity on phase equilibrium of methane hydrate. *Journal of Dalian University of Technology,* 24(5):972–978.

Peng Baozi, Luo, Hu Sun, Chang-Yu Ma, Qinglan Zhou, Wei Chen & Guang-Jin*. Study on growth kinetics of methane hydrate film. *State key laboratory of heavy oil processing, China University of Petroleum,* 102–249.

Qiang Wu & Baoyong Zhang 2010. The Effect of THF-SDS on separation of methane-hydrate from mine gas. J*ournal of China University of Mining & Technology,* 39(4):484–489.

Qiang Wu, Qiang Zhang & Baoyong Zhang 2012. Influence of super-absorbent polymer on the growth rate of gas hydrate. *Safety Science,* 50, 865–868.

Qiang Wu, Yumei Zhu & Baoyong Zhang 2009. Effects of sodium dodecyl sulfate and kaolin on low-concentration mine gas hydration separation. *CIESC Journal,* 60(5):1193–1198.

Sloan E D 2008. *Clathrate hydrate of natural gases*. New York: Taylor & Francis Group LLC.

Vorotyntsev V M, Malyshev V M & Mochalov G M, et al. 2001. Separation of gas mixtures by the gas hydrate crystallization method. *Theoretical Foundations of Chemical Engineering,* 35(2):119.

Zhenquan Lu, Sultan N & Chunshuang Jin 2008. Semi-quantitative analysis of factors affecting gas hydrate formation conditions and its fractions. *Chinese Journal of Geophysics,* 51(1):125–132.

Progress in Mine Safety Science and Engineering II – He et al. (Eds)
© 2014 Taylor & Francis Group, London, ISBN 978-1-138-00122-0

Microcirculation of air leakage of gob-side coal pillar in fully-mechanized face

H.Q. Zhu, S.H. Zhu, S.L. Feng & G.W. Jia
China University of Mining and Technology (Beijing), Beijing, China

ABSTRACT: Microcirculation of air leakage among the gob behind the working face, the gob-side coal pillar and the adjacent gob is investigated theoretically by nonlinear seepage equation. The 2D model is built containing two gobs with heterogeneous porosity distribution and one gob-side coal pillar. Velocity field and streamline distribution of the microcirculation are simulated by the commercial code Fluent. Causes of the microcirculation are also discussed. The results show that fresh air flows into the gob behind the working face, and penetrates into the adjacent gob through the gob-side coal pillar. Microcirculation of air leakage increases air volume that flows into the gob and promotes the spontaneous combustion of residual coal. Gob breathe is also initiated by the oxidation process in which the consumption and supplement of oxygen alternates and thus results in the fluctuation of concentration of CO and O_2.

1 INSTRUCTIONS

Air leakage in the gob of coal mine is the main factor that influences gas emission and spontaneous combustion (Shao et al. 2011). The leakage, persistent or intermittent, provides an access for the penetration of fresh air into the gob, and thus results in the variation of gas component (Li 2008, Wang & Wu 2011, Zhu & Liu 2012), temperature (Li 2008) and pressure in the gob. As the working face advances, the gob is filled with rock mass and residual coal generated in the process of roof caving, which limits the field measurement of air leakage in the gob (Shao et al. 2011). Therefore, some technologies are proposed to study this phenomenon, such as tracer gas (Li 2013), air volume analysis and numerical simulation (Li 2008, Zhu & Liu 2012). Considerable efforts have been directed towards the analysis of spontaneous combustion caused by the air leakage in the gob behind the working face. The present study, however, focuses on a local microcirculation of air leakage.

Coal pillar between fully-mechanized working face and adjacent gob is subjected to mining-induced fragmentation failure. Under pressure gradient of air leakage, air flows into the gob behind the working face, and then penetrates into the gob adjacent the working face through the fragmented coal pillar. The air leakage presents a local circulation among the working face, the gob (behind and adjacent the working face) and gob-side coal pillar, and is named microcirculation of air leakage. The long-term impact of this phenomenon promotes the spontaneous heating and combustion of residual coal in gob, and accordingly shortens the spontaneous combustion period. As such, research on microcirculation of air leakage should be attached importance to. However, a literature review shows that few results have been reported on this phenomenon.

The microcirculation of air leakage is theoretically investigated and numerically simulated using the commercial code Fluent in this paper.

2 MATHEMATICAL MODEL

Air flow in fragmented coal pillar is assumed to be steady seepage in porous media, and is investigated based on the fluid mechanics in porous media. Since air flows slowly in the coal pillar, it can be expressed by the Darcy's law. Oxidation of residual coal in gob results in the temperature increase and thus the air pressure rise (the volume of the gob is assumed to be constant). Under this pressure and air leakage pressure, flow field of the air leakage among the working face, the gob and gob-side coal pillar is expressed by nonlinear seepage equation proposed by Bachmat (Jacob 1972, Ding & Wang 1990, Li 2005, Xu 2011):

$$\boldsymbol{E}\frac{\partial p}{\partial \boldsymbol{n}} = \frac{v}{g}\left(1+\frac{V\beta d}{nv}\right)\boldsymbol{V} \tag{1}$$

where p = the air pressure; $\boldsymbol{E}$ = permeability tensor of porous media, $\boldsymbol{n}$ = the directional vector, g = gravity acceleration, $\boldsymbol{V}$ = penetration velocity

of air, n = porosity, d = harmonic mean particle diameter, v = coefficient of kinematic viscosity and β = particle shape factor.

It can be written as:

$$-\frac{\partial p}{\partial \boldsymbol{n}} = (a + bV)\boldsymbol{V} \tag{2}$$

where $a = v/(eg)$, $b = \beta d/(egn)$ and e = scalar of permeability of porous media.

For the two dimensional plane flow, equation (2) is written as:

$$-\left(\frac{\partial p}{\partial x}\boldsymbol{i} + \frac{\partial p}{\partial y}\boldsymbol{j}\right) = (a + bV)(V_x\boldsymbol{i} + V_y\boldsymbol{j}) \tag{3}$$

Flow conversation is also taken into consideration by:

$$\frac{\partial V_x}{\partial x} + \frac{\partial V_y}{\partial y} = 0 \tag{4}$$

Therefore, the differential equation of 2D nonlinear plane flow is give by:

$$-\nabla(c(\psi)\cdot\nabla\psi) = 0 \tag{5}$$

Where $c(\psi) = -\left(a + b\sqrt{\left(\frac{\partial \psi}{\partial x}\right)^2 + \left(\frac{\partial \psi}{\partial y}\right)^2}\right)$, and ψ denotes the flow function:

$$V_x = \frac{\partial \psi}{\partial y}, \quad V_y = -\frac{\partial \psi}{\partial x} \tag{6}$$

The equation (5) can be solved given the first, the second or the third boundary conditions or any combination of them.

The first boundary condition is given by:

$$\psi\big|_\Gamma = \psi(x, y) \tag{7}$$

The second boundary condition is written as:

$$\frac{\partial \psi}{\partial \boldsymbol{n}}\Big|_\Gamma = \psi(x, y) \tag{8}$$

The third boundary condition is given by:

$$\left(\frac{\partial \psi}{\partial \boldsymbol{n}} + k\psi\right)\Big|_\Gamma = \psi(x, y) \tag{9}$$

where Γ denotes the boundary and k is an arbitrary coefficient.

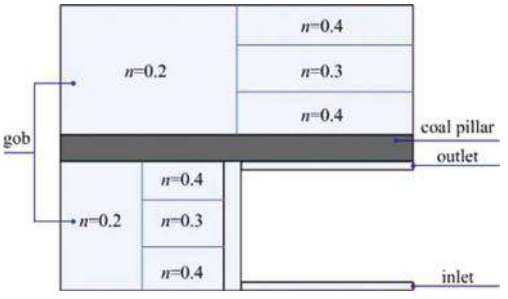


Figure 1. Layout of model with different porosity in gob.

3 PHYSICAL MODEL

Figure 1 shows layout of the 2D model containing the gob behind the working face (120 m × 150 m), the gob-side coal pillar (350 m × 6 m) and the adjacent gob (350 m × 150 m). The velocity inlet is imposed in fresh air inlet surface with the velocity of 2 m/s (the second boundary condition), and the outflow boundary condition is imposed in contaminated air outlet surface.

The gob behind the working face, the gob-side coal pillar and the adjacent gob are described as porous media. Since the pile density of residual coal and rock varies in different area in the gob as the working face advances forward. Both the two gobs are divided into four parts with different porosity (Liu 2008, Liang et al. 2009, Che 2010, Lu et al. 2011), while the porosity of the coal pillar is set 0.1. The mesh density of 1 × 1 is used in this study in order to embrace the increase of computational efficiency towards achieving the final results.

In the model, fresh air flows into the working face through the inlet, and flows out through the outlet. Since the two gobs and the gob-side coal pillar are assumed porous medium, the fresh air flows into the gob behind the working face and penetrates into the gob-side coal pillar and the adjacent gob. Energy equation is not considered in this model since the velocity field of the air leakage microcirculation is the main focus in the present study.

4 RESULTS AND DISCUSSION

4.1 *Flow field of air leakage*

Velocity field of the local microcirculation is presented in Figure 2(a), while streamlines are shown in Figure 2(b).

As seen in Figure 2, air flows into the gob behind the working face and penetrates into the adjacent gob through the fragmented coal pillar. Since the porosity in two gobs is low, the air volume that pen-

etrates into the gob is unmeasured. Therefore, the air flow velocity is relatively low. Figure 2(a) illustrates the velocity profile in the microcirculation of air leakage ranging from 10^{-6} m/s to 10^{-4} m/s. Although the air flow velocity is relatively low, the long term effect of this phenomenon still provides sufficient conditions for the oxidation and spontaneous combustion of residual coal both in the two gobs.

4.2 *Causes of microcirculation of air leakage*

Coal pillar with mining-induced fragments provides an access for air leakage into the adjacent gob, while the gradient of pressure inside and outside of the gob initiates this effect.

One of the reasons inducing the pressure gradient is the fluctuation of air pressure in working face. Air in shaft fails to flow smoothly along lifting equipments, since these equipments in underground coal mine occupies part of shaft space, fluid viscosity and fractions imposed by air on the shaft wall and equipments' surfaces show a stronger impact than they do in open area. The frequent up-down movement of lifting equipments results in piston effect and dynamic variation of air pressure in ventilation system, i.e. the fluctuation of air flow.

Seasonal variation of air pressure also presents an influence on absolute air pressure in ventilation system. It is well known that air pressure in winter is higher than that in summer (the difference of them in certain area reaches to 9500 Pa). As the air pressure drops outside the gob, the relatively higher pressure inside pushes the air to penetrate out of the gob through fragments in gob-side coal pillar. Otherwise, the air in the roadway flows into the gob.

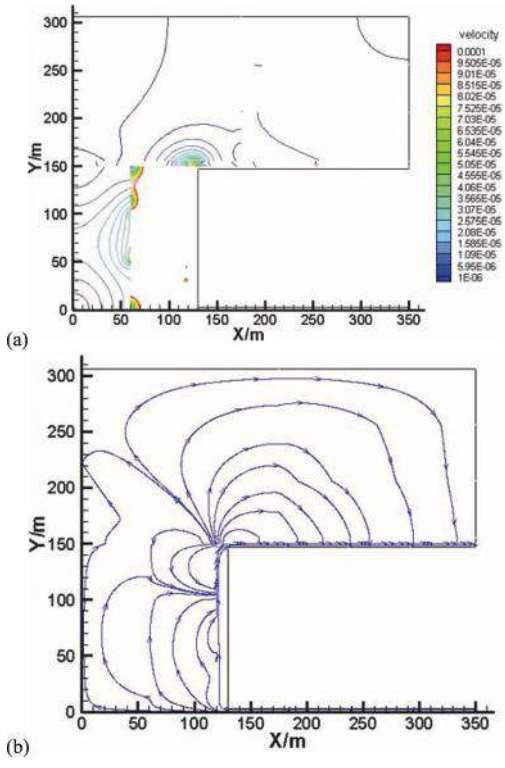


Figure 2. Velocity field (a) and streamlines (b) of the local microcirculation.

4.3 *Influence of microcirculation on the spontaneous combustion*

As the gob-side coal pillar is fragmented, a complex air leakage network forms among the gob behind the working face, the gob-side coal pillar and the adjacent gob. Fresh air in crossheading provides oxygen for the oxidation of residual coal in the gob. The air leakage in mining operation is serious through the gob behind the working face and the fragmented gob-side coal pillar into the adjacent gob. Air leakage control in gob confronts great difficulties as the local air leakage area connects with the three zones in the gob behind the working face and promotes the oxidation and spontaneous combustion of residual coal.

The other consequence of the microcirculation is gob breathe. Gob breathe is described as periodical variation of air leakage volume, air pressure and gas composition in the gob. Evolution of relative air pressure attained from 1301# gob in Geting coal mine from February to March is presented in Table 1 where—stands air-in and + denotes air-out.

Table 1. Evolution of relative pressure from February to March in 1301# gob.

Date	Pressure	Date	Pressure	Date	Pressure
2	–	15	–	28	+
3	–	16	–	1	+
4	–	17	–	2	+
5	+	18	–	3	+
6	+	19	–	4	+
7	+	20	–	5	–
8	+	21	–	6	–
9	+	22	+	7	–
10	+	23	+	8	–
11	+	24	+	9	–
12	+	25	+	10	–
13	–	26	+	11	–
14	–	27	+		

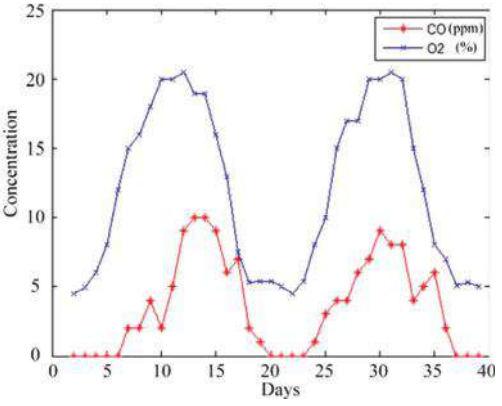


Figure 3. Concentration evolution of CO and O_2 in the adjacent gob.

Figure 3 illustrates the concentration evolution of CO and O_2 in the adjacent gob in 40 days since February 2nd. As seen in the figure, both the two evolution curves show periodic fluctuation. However, it is noted that the change of the two curves is not completely identical.

Gob breathe is mainly induced by the consumption and supplement of oxygen in oxidation process of the residual coal. Temperature increase initiated by the oxidation of residual coal in the gob results in the air volume expanding and according pressure rise (Zhang 2004). As the pressure in the gob outstrips that in the roadway, the air in the gob penetrates out presenting expiration mode. Simultaneously, the oxidation process reduces the volume of oxygen. This process ceases as it suffers from the lack of sufficient oxygen volume and leads to the decrease of temperature and air pressure in the gob. The relative lower pressure than that in the roadway pushes the air to flow into the gob through the fragmented coal pillar presenting inspiration mode. The supplement of fresh air provides sufficient oxygen again for a new circle of oxidation. And then a new alternation of expiration and inspiration mode begins.

The gob breathe is also caused by cyclic change of atmospheric pressure and unsteady working state of main fan, since those factors exert influence on the fluctuation of air pressure.

4.4 *Prevention and control of microcirculation of air leakage*

An important factor that influences air leakage in the gob is the quality of airproof wall. Thus, improving the tightness of airproof wall is an effective way to prevent the air leakage.

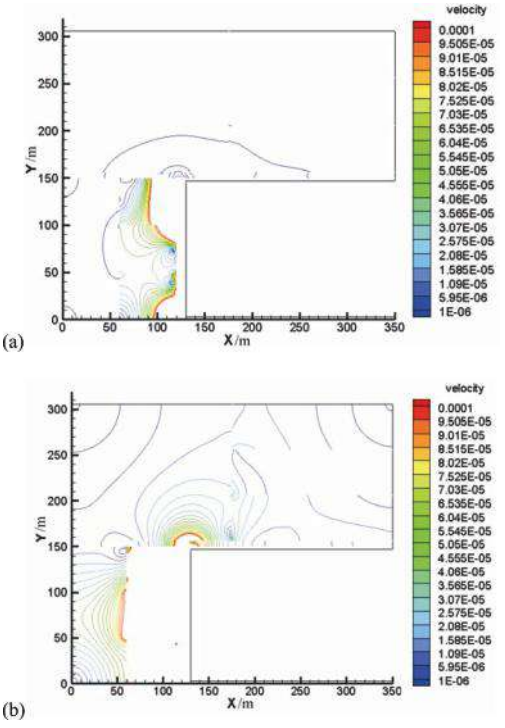


Figure 4. Velocity field of the local microcirculation with the velocity of 3 m/s (a) and 1 m/s (b) imposed on the inlet face.

A high velocity of fresh air also aggravates the microcirculation of air leakage. Figure 4 shows the velocity profile of air leakage microcirculation with the velocity of 3 m/s (a) and 1 m/s (b) imposed on the inlet surface.

The comparison between figure 2(a) and figure 4 shows that a higher velocity of fresh air increases air volume that penetrates into the gob, while a lower velocity results in a narrow microcirculation of air leakage.

Equal-pressure regulation in gob is also an effective method to control microcirculation of air leakage, since it dilutes the oxygen concentration to a certain degree, and correspondently controls the spontaneous combustion of residual coal (Li 2008).

5 CONCLUSIONS

A local microcirculation of air leakage exists among the gob behind the working face, the gob-side coal pillar and the adjacent gob. Coal pillar with mining-induced fragments provides an access for the

air leakage, while the pressure gradient inside and outside of the gob initiates this phenomenon. The microcirculation of air leakage supplies the oxidation process with sufficient oxygen, results in the gob breathe, and promotes the spontaneous combustion of residual coal in the gob accordingly.

REFERENCES

Che, Q. 2010. Study on coupling law of mixed gas three-dimensional multi-field in goaf: 7–13. *China University of Mining & Technology (Beijing)*: Beijing.

Ding, G.X. & Wang, D. 1990. The nonlinear infiltration flow on two-dimensional goaf and its solution. *Journal of Hunan University of Science & Technology (Natural Science Edition)* 5(2):19–25.

Jacob, B. 1972. Dynamics of fluids in porous media. American Elsevier Publishing Company, *Inc.*

Li, Y.C. Zhang, S.Q. Zhang, S. 2013. The qualitative identification of air leakage channels in goaf based on the tracer gases. Safety in Coal Mines 44(1): 185–188.

Li, Z.X. 2005. Numerical simulation of spontaneous combustion process of residual coal in goaf. *China Safety Science Journal* 15:15–19.

Li, Z.X. 2008. CFD simulation of spontaneous coal combustion in irregular patterns of goaf with multiple points of leaking air. *Journal of China University of Mining & Technology* 18(2008):0504–0508.

Liang, Y.T. Zhang, T.F. Wang, S.G. et al. 2009. Heterogeneous model of porosity in gobs and its air flow field distribution. *Journal of China Coal Society* 34(9):1203–1207.

Liu, Z.C. 2008. Research on numerical simulation of airflow field in gob areas of long-wall coal mining: 38–46. *Xi'an University of Science and Technology*: Xi'an.

Lu, C.R. Yang, S.Q. Guo, X.Y. 2011. Analysis on seepage features in goaf and numerical simulation prediction of flow field. *Coal Science and Technology* 39(9):55–59.

Shao, H. Jiang, S.G. Wang, L.Y. et al. 2011. Bulking factor of the strata overlying the gob and a three-dimensional numerical simulation of the air leakage flow field. *Mining Science and Technology (China)* 21(2011):261–266.

Wang, H.G. & Wu, F.L. 2011. Method of calculation of a methane concentration field in gob areas with a known velocity field based on the model of stream tubes. *Mining Science and Technology (China)* 21(2011):277–280.

Xu, J. 2011. The research of seepage in porous medium of the Rujigou coalfield: 39–50. *Xi'an University of Science and Technology*: Xi'an.

Zhang, G.S. 2004. Ventilation Safety. (3rd ed). Jiangsu: Xuzhou.

Zhao, H.B. Pan, W.D. Wang, X. 2011. Numerical simulation on distribution of gas concentration in goaf under condition of mining thin coal seam. *Journal of China Coal Society* 36(2):440–443.

Zhu, H.Q. & Liu, X.K. 2012. Theoretical investigation on the relationship between tail roadway methane drainage and distribution of easily spontaneous combustible region in gob. *Safety Science* 50(2012):618–623.

This page intentionally left blank

Progress in Mine Safety Science and Engineering II – He et al. (Eds)
© 2014 Taylor & Francis Group, London, ISBN 978-1-138-00122-0

Effect of hydrate crystal type on mechanical properties of gas hydrate-bearing coal

Qiang Wu & Fuliang Zhu
Department of Safety Engineering, Heilongjiang University of Science and Technology, Harbin, Heilongjiang, China

Xia Gao
College of Civil Engineering, Heilongjiang University of Science and Technology, Harbin, Heilongjiang, China

Baoyong Zhang
National Engineering Research Center for Coal Gas Control, China University of Mining and Technology, Xuzhou, Jiangsu, China

ABSTRACT: Triaxial compression tests for gas hydrate-bearing coal with different crystal types were performed, using self-developed gas hydrate formation and triaxial compression integrated equipment. Effects of crystal type on mechanical properties of hydrate-bearing coal are studied, based on Mohr-column theory. The crystal types are measured with Raman spectrometer. The relationships between stress-strain and strength parameters are obtained under different confining pressures. The results show that: (1) the larger the confining pressure, the higher the elastic modulus and the inner cohesion angle; (2) the larger the confining pressure, the lower the cohesion; (3) the compression strength of SII gas hydrate bearing coal slightly higher than that of SI gas hydrate bearing coal under the same confining pressure; (4) cohesion of SII gas hydrate bearing coal is larger than SI gas hydrate bearing coal, indicating the lower cohesion between the particles of the SI hydrate-bearing coal. This study has some scientific meanings and practical values for illustrating the mechanical properties of gas hydrate type—bearing coal and for preventing coal and gas outburst.

1 INTRODUCTION

Coal and gas outburst is an extremely complex phenomenon of Mine gas power in the production of coal underground, which is one of the great challenges during mining sector worldwide. Nowadays, the outburst accident of Coal and gas has become increasingly frequent, with the increasing of mining depth. The coal and gas outburst is the process of release of energy and mechanical damage; at the same time, is the result of the interaction of stress, gas pressure, and mechanical properties of coal itself. Qiang Wu et al. proposed technology of preventing coal and gas outburst using methane hydration (Qiang Wu & Xueqiu He 2003; Qiang Wu et al. 2005; Baoyong Zhang & Qiang Wu 2010). The key issue of application of preventing coal and gas outburst using methane hydration is coal in gas hydrate pre and post curing stress distribution and the change of physical properties of coal change under different conditions. Gas hydrates has three types of crystals, which is determined by gas compositions, therefore it affects the physical properties of the hydrate bearing coal. However, studies on physical properties of gas hydrate bearing coal with different crystal type were few, due to its difficulty and complexity. It has been reported the research of hydrate mechanical properties of porous media at home and abroad. Winters and his teammates have analyzed the test results of hydrate-bearing sand of Ottawa, Affirmed the role of hydrates in sediments with reinforcement (Winters WJ et al. 2004; Winters WJ et al. 2007; Waite WF et al. 2004). Masui and his teammates have analysis comparatively the mechanical properties of Natural gas hydrate deposits and Synthetic hydrate sediments (Masui et al. 2007). Xiaobing Lu et al. & Xuhui Zhang et al. performed a series of triaxial test are conducted on the THF hydrate, CO_2 hydrate and CH_4 hydrate with fine sand and Mongolia sand as the skeleton, analyzing and comparing stress-strain and strength properties of the four kinds hydrate sediments (Xiaobing Lu et al. 2007; Xuhui Zhang et al. 2010; Xuhui Zhang et al. 2011). Yanghui Li et al. synthesized gas hydrate in lab mixed with Kaoline to form core samples, so as to simulate the hydrate-bearing sedimentary layers in the seabed, under conditions of different

confining pressure, triaxial compressive tests were conducted on hydrate-bearing sediments with different volume content of Kaoline (Yanghui Li et al. 2011; Yanghui Li et al. 2012).

The effect of hydrate of structure on hydrate-bearing porous medium has not been reported. At first, we synthetic coal samples, in-situ synthesis gas hydrate-bearing coal in pressure chamber, control hydrate saturation by resistance monitoring. Then, control the crystal type of gas hydrates by changing the composition of gas. The result of experiment is different types of gas hydrate crystals coal samples. At last, we begin to do the experiment of triaxial compression test. We began to triaxial compression test by analyzing the influence of crystal type of gas hydrates on physical properties of gas hydrate bearing coal, we provide a reference for the engineering of prevents coal and gas outburst by hydration solidification.

2 EXPERIMENTAL

2.1 *Test equipment of crystal type of gas hydrates*

The test equipment of crystal type of gas hydrates consists of a laser Raman spectrometer, gas supply system, jacketed cooling type high-pressure visual cell, temperature control system, data acquisition and other parts. The experiment using a laser Raman spectrometer for the JY Co. in French produced Lab RAM HR-800 type visible confocal Raman microscope spectrometer. Laboratory independently designed a cooled jacket visible in situ high-pressure reactor, reactor with sapphire window to ensure full transparency of laser, and high pressure performance, visual reactor effective volume 3 ml, compression 20 MPa effective volume, to achieve characteristics of gas hydrate non-destructive and accurate measurement. The schematic representation of equipment is shown in Figure 1.

2.2 *Testing device and specimen preparation*

Laboratory independently designed and developed the integrated experimental apparatus for syntheses of gas hydrate coal and triaxial tests, for the research needs of strength properties of gas hydrate bearing coal. As shown in Figure 2, it consists of high-pressure injection system, hydration-solidification system, on-line triaxial compression test and impedance measurement system. Hardcore of device is functional core gripper. The core gripper can be used for core of $\Phi 50 \times 100$ mm. The high-pressure pump provided the confining pressure up to 40 MPa and the axial compression.

The sample of coal is from 12th type coal specimen of QiXing mine from the Dragon Coal. The coal seam has been the outburst of coal and gas.

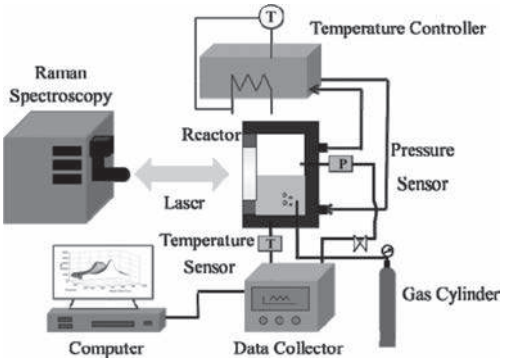


Figure 1. Apparatus for hydrate measurements using in situ Raman spectrometer.

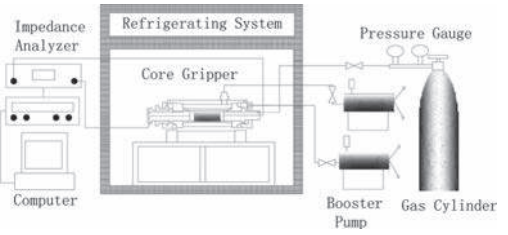


Figure 2. Sketch of the integrated apparatus for gas hydrate coal syntheses and triaxial test.



Figure 3. Moulded coal.

This experiment uses moulded coal, to reduce the discrete caused by individual differences of raw coal, and get general rules, as shown in Figure 3. The specimen size is $\Phi 50 \times 100$ mm, nonparallelism less than 0.05 mm, determined by methods for determining the physical and mechanical properties of coal and rock-part 9.

3 RESULTS AND ANALYSIS OF THE EXPERIMENT

3.1 *Structural characteristics of gas hydrate synthesized in different component of gases*

Test results of Raman spectrum of gas 1(CH_4:100%) hydrate is tested. Shift 2904.8 cm^{-1} is laser Raman spectrum at stretching vibration of big cavity of

CH_4 and shift 2915.6 cm^{-1} is Raman spectrum at stretching vibration of small cavity of CH_4. We see from this figure that the measured Raman intensity (peak area) ratios of large to small cages of CH_4 hydrate are roughly 3:1, so these hydrate are all structure I.

Test results of Raman spectrum of gas 2(CH_4:70%, C_2H_6:10%, N_2:12%, CO_2:5%, O_2:3%) is tested. The crystal structure of gas 2 hydrate is structure II, because molecule-sized of C_2H_6 is bigger than that of CH_4 so it go into big cavity of SII and promote CH_4 going into small cavity of SII. The measured Raman shifts of the C-H bond stretching of large and small cages are, respectively, 992.7 cm^{-1} and 2913.6 cm^{-1}. 992.7 cm^{-1} is Raman shift of C_2H_6 in big cavity of SII, 2913.6 cm^{-1} is Raman shift of C_2H_6 in small cavity of SII, which is consistent with the literature data. So we can conclude that the structure of gas 2 hydrate is SII.

3.2 *Results of mechanical property of hydrate-bearing coal*

Triaxial compression test of SI hydrate bearing coal used gas 1, and the one of SII used gas 2. We adopt heating and cooling of repeated during the course of the experiment, to make distribute hydrate in coal uniformly. We adopt gas consumption calculating and resistance measuring method to controlling gas hydrate saturation at about 70%.

As showed in Figure 4 and Figure 5, the compression strength and elastic modulus of gas hydrate bearing coal increase with confining pressure increasing. The compression strength of SII gas hydrate bearing coal is slightly higher than that of SI gas hydrate bearing coal under the same confining pressure. In the stage of compaction initially, there are large differences between stress-strain curve of gas hydrate bearing coal and the other one, because the character of gas hydrate bearing coal is lower strength and exist external damage poorly. Under confining pressure 1 MPa, mechanical properties of gas hydrate of SII bearing coal, is better than the one of gas hydrate of SII bearing coal, while does not much affect under confining pressures is 3 MPa, this may because structure of hydrate crystal type is different thus affect mechanical property of gas hydrate bearing coal. Even though hydrate can cement coal particles, mechanical property of coal is mainly determined by coal matrix and size of coal particles and other factors.

In this experiment several coal examples have been triaxial shear test under two different confining pressures. We measured c and φ of gas hydrate of different structure bearing coal on the basis of Mohr-column failure criterion, as is showed in Figure 6 and Figure 7. Angle of internal friction of SI gas hydrate bearing coal is 23.5°, while angle of internal friction of SII gas hydrate bearing coal is 18.6°, which means angle of internal friction of SII gas hydrate bearing coal is smaller, bond action

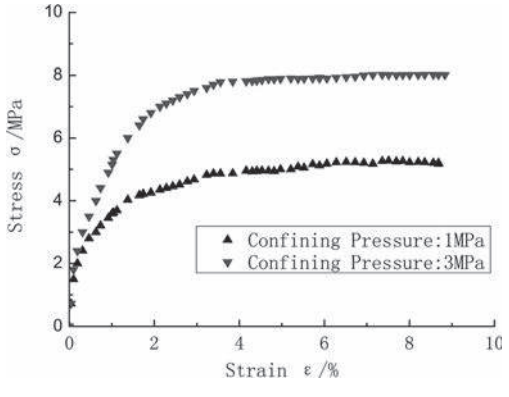


Figure 4. Stress-strain curve of SI hydrate-bearing coal at under confining pressure 1 MPa and 3 MPa.

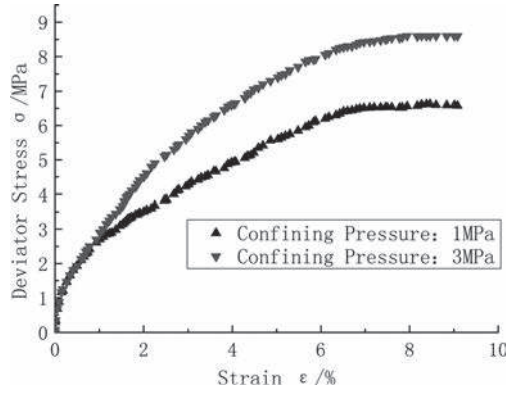


Figure 5. Stress-strain curve of SII hydrate-bearing coal under confining pressure 1 MPa and 3 MPa.

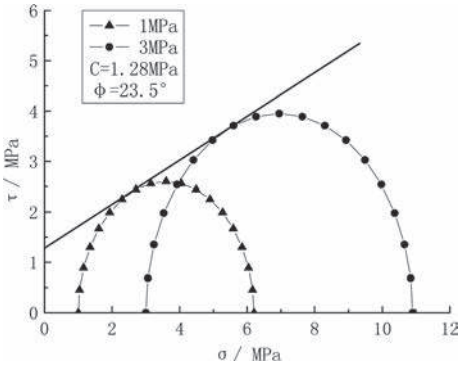


Figure 6. Mohr circle of SI hydrate-bearing coal.

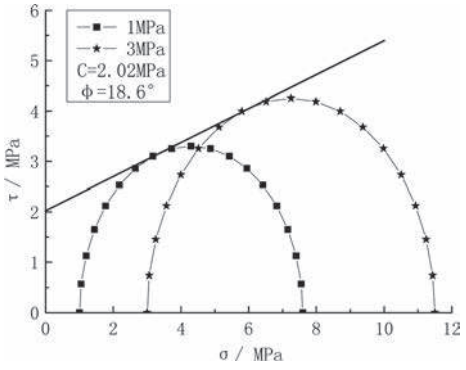


Figure 7. Mohr circle of SII hydrate-bearing coal.

to coal particles is weaker, and the capacity of anti-friction is poorer. The cohesion of SI gas hydrate bearing coal is 1.28 MPa, and the one of SII gas hydrate bearing coal is 2.02 MPa, the one of SII gas hydrate bearing coal is larger.

4 CONCLUSION

On the basis of design and develop the integrated experimental apparatus for syntheses of gas hydrate coal and triaxial tests all by our own, we use two kinds of gas synthesize into gas hydrate coal that contains different types of crystal, we performed a series of triaxial mechanical experiments, measured gas hydrate crystal types by Raman spectroscopic techniques, and control gas hydrate saturation by gas consumption and impedance measurement technology. Accordingly, stress-strain curves and strength parameters of gas hydrate bearing coal are obtained.

1. SI and SII gas hydrate are formed by samples 1 and 2, respectively, used by Raman spectrometer.
2. Plastic failure occurred in the gas hydrate bearing coal; cohesion exists between the gas hydrate and the coal, increasing the stiffness of the coal.
3. The compression strength and cohesion of SII gas hydrate bearing coal slightly higher than that of SI gas hydrate bearing coal, indicating the SII gas hydrate-bearing coal has the higher ability to resist damage, but internal friction angle of SI gas hydrate bearing coal is larger.
4. In the experiment scope, the gas hydrate improves the strength of hydrate-bearing coal, different crystal types have different effects on the mechanical properties of hydrate-bearing coal due to its different micro-scopic structure.

ACKNOWLEDGEMENTS

This work was financially supported by the National Natural Science Foundation of China (51274267, 51174264, 51104062), and Key Laboratory of Marine Hydrocarbon Resources and Environmental Geology, Ministry of Land and Resources (GZH201100310-wx03).

REFERENCES

Baoyong Zhang & Qiang Wu 2010. Thermodynamic promotion of tetrahydrofuran on methane separation from low-concentration coal mine methane based on hydrate. *Energy and Fuels*, 24:2530–2535.

Masui A, Haneda H, Ogata Y, et al. 2007. Mechanical Properties of Sandy Sediment Containing Marine Gas Hydrates in Deep Sea Offshore Japan. *Proceedings of the 17th Imitational Offshore and Polar Engineering Conference*, *ISOPE,* 53–56.

Qiang Wu & Xueqiu He 2003. Preventing coal and gas outburst using methane hydration. *Journal of China University of Mining & Technology*, 13(1):7–10.

Qiang Wu, Chenglin Li & Chuanli Jiang 2005. Discussion on the control factors of forming gas hydrate. *Journal of China Coal Society*, 30(3):283–287.

Winters W J, Pecher I A, Waite W F, et al. 2004. Physical Properties and Rock Physics Models of Sediment Containing Natural and Laboratory-Formed Methane Gas Hydrate. *American Mineralogist*, 89(8–9):1221–1227.

Waite W F, Winters W J, Mason D H 2004. Methane Hydrate Formation in Partially Water Saturated Ottawa Sand. *American Mineralogist*, 89(8–9):1202–1207.

Winters W J, Waite W F, Mason D H, et al. 2007. Methane Gas Hydrate Effect on Sediment Acoustic and Strength Properties. *Journal of Petroleum Science and Engineering*, 56(l-3):127–135.

Xiaobing Lu, Li Wang, Shuyun Wang, et al. 2007. Experimental study of mechanical properties of THF hydrate-bearing sediment. *Proceeding of the Thirteenth China Ocean Engineering*, 681–684.

Xuhui Zhang, Shuyun Wang, Qingping Li, et al. 2010. Experimental study of mechanical properties of gas hydrate deposits. *Rock and Soil Mechanics*, 31(10):3069–3074.

Xuhui Zhang, Xiaobing Lu, Shuyun Wang, et al. 2011. Experimental study of static and dynamic properties of tetrahydrofuran hydrate-bearing sediments. *Rock and Soil Mechanics*, 32(1):303–308.

Yanghui Li, Yongchen Song, Feng Yu, et al. 2011. Effect of confining pressure on mechanical behavior of methan hydrate-bearing sediments. *Petroleum Exploration and Development*, 38(5):637–640.

Yanghui Li, Yongchen Song, Weiguo Liu, et al. 2012. Effect of temperature and strain rate on mechanical behavior of methan hydrate-bearing sediments. *Nature Gas Exploration And Development*, 235(1):50–53.

Progress in Mine Safety Science and Engineering II – He et al. (Eds)
© 2014 Taylor & Francis Group, London, ISBN 978-1-138-00122-0

Numerical study of heat convection caused by two-phase flow confined in underground heat-exchange tunnel

W.L. Gong, D. Liu, Y.Q. Wu, Y.Y. Peng, Y. Zhang & Bingjie Liu
State Key Laboratory for Geomechanics and Deep Underground Engineering, Beijing, China
School of Mechanics and Civil Engineering, China University of Mining and Technology, Beijing, China

ABSTRACT: High temperature geo-thermal disaster has been the major hazards encountered in the exploitation of coal in deep mines. One of the major approach used in extract of the geo-thermal energy in underground mining is the specially designed heat-exchange roadway tunnels. This study presents an numerical investigation on the heat convection between the air-water two-phase flow and the coal rocks in the heat-exchange tunnel. Computational Fluid Dynamics (CFD) and Volume Of Fluid (VOF) were employed for setting up the numerical model and implementing the two-phase flow field. The heat exchange effects between fluid and solid was simulated by using FLUENT 6.3 codes at different boundary conditions including the inlet velocity, wall temperature and air content. The impacts on the fluid-solid heat exchange effects imposed by these three factors were obtained, including the flowing patterns and relations between the output temperature of the tunnel against the three factors respectively. The results of this paper in of general implication in geo-thermal disaster mitigation and heat-reduction system design.

1 INTRODUCTION

With the mining depth goes deeper, very-high rock temperature encounteres more frequently in the underground mining. The high-temperature hazards in the underground mines will bring a lot of safety concerns to the workers and pose damage to the mining equipment. The mitigations and controls of high-temperature hazards in underground mines, become an urgent problem to be solved. (Burrows et al. 1982, Hemp 1985, Wang & Chen 2000, He et al. 2006)

At the current mine cooling technology at home and abroad, generally can be divided into the artificial cooling technology and the artificial refrigeration cooling technology. Artificial underground cooling technology is the core of the formation and heat transfer medium. Researches of fluid-solid heat transfer mainly based on the experiment of experience formula and the fluid heat transfer numerical simulation method, etc. Because the numerical simulation is using a method of approximate solution with the discretization of the discrete analysis method, and it can be solved by computer, and can be repeated, and also can simulate all kinds of ideal state, therefore, it is a major mean of modern engineering design and scientific research.

Fluid-solid heat transfers numerical simulations are mostly betweenrigid boundaries (Lowndes 2006). Considering of the underground heat harm principle, the numerical simulation researches of heat transfer between fluid and rock strata are inadequate. Therefore, it is necessary to carry out the researches of two phase flow of different air-water contents. In this paper, using the VOF method and the numerical software FLUENT to simulate the fluid-solid heat transfer under different air-water contents, different water inlet velocities and different wall temperatures to provide a theoretical support for the deep underground heat transfer engineering optimization designs.

2 FUNDAMENTALS

2.1 *The basic equations for two-phase flow*

k stands for an arbitrary phase, the mass and momentum equations can be written as (Graton & Fraser 1935, Christian & Louis 1963, Hazlett & Bossert 1965, Joshi 1974, Quiblier 1984, Bakke & Ren 1997):

$$\begin{aligned} &\frac{\partial \rho_k u_k}{\partial t} + \nabla(\rho_k u_k) = 0 \\ &\frac{\partial \rho_k u_k}{\partial t} + \nabla(\rho_k u_k u_k) = \nabla T_k + \rho_k f \end{aligned} \tag{1}$$

ρ_k, u_k, T_k stands for the density, velocity and stress tensor; stands for volume force.

At the two-phase interface, the mass and momentum balance equation which is the interface

jump conditions can be expressed as:

$$\sum_{k-1}^{2} \rho_k (u_k - u_i) n_k = 0$$
$$\sum_{k-1}^{2} (\rho_k (u_k - u_i) n_k + T_k n_k = M_m \quad (2)$$

$$X_k(x,t) = \begin{cases} 1 \\ 0 \end{cases} \quad (3)$$

At the instant t, x is in the phase of k, then X_k is equal to 0 at the rest situation. u_i is the interface velocity; M_m stands for the unite surface force. We can combine the mass equation with the momentum equation, and then average through (3) to get a range of local volume averaging conservation equations.

$$\frac{\partial a_k \tilde{\rho}_k}{\partial t} + \nabla a_k \tilde{\rho}_k \tilde{u}_k = \Gamma_k \quad (4)$$

$$\frac{\partial a_k \tilde{\rho}_k \tilde{u}_k}{\partial t} + \nabla a_k \tilde{\rho}_k \tilde{u}_k \tilde{u}_k = -a_k \nabla \tilde{\rho}_k + \nabla a_k (\tilde{\tau}_k + \tilde{\sigma}_k) + \Gamma_k u_{k,i} + (p_{k,i} - \tilde{p}_k) \nabla a_k + M_k^d \quad (5)$$

2.2 *Differential equations for heat transfer process*

We respect the fluid flow to be two-dimensional, incompressible and constant material prosperities flows along the wall. Here are the equations for the convective heat transfer:

Continuity equations:

$$\frac{\partial u_x}{\partial x} + \frac{\partial u_y}{\partial y} = 0 \quad (6)$$

Momentum equations:

$$u_x \frac{\partial u_x}{\partial x} + u_y \frac{\partial u_y}{\partial y} = v \frac{\partial^2 u_x}{\partial y^2} \quad (7)$$

Energy equations:

$$u_x \frac{\partial t}{\partial x} + u_y \frac{\partial t}{\partial y} = a \frac{\partial^2 t}{\partial y^2} \quad (8)$$

Convective heat transfer differential equation:

$$h_x = -\frac{\lambda_f}{(t_w - t_f)} \left(\frac{\partial t}{\partial y} \right)_x |_{y=0} \quad (9)$$

Among the above four equations, there are four unknown parameters: u_x, u_y, t, h_x The equations are closed, so we need these values to solve the above equations:

At $0 < x < L$, $y = 0$ $u_x = u_y = 0$ $t = t_w$
$y \to \infty$ $u_x \to u_f$ $t \to t_f$
At $0 < y < \infty$, $x = 0$ $u_x = u_y$ $t = t_f$

3 PHYSICAL MODEL

3.1 *The field case*

Pangzhuang coal mine is located in Xuzhou, the entire mine is about 5.0 km long from east to west, 3.4 Km south wide from north to south, and the mine area is about 16.944 Km^2. This well is one of the high temperature mine of Xuzhou mining area, the –750 m roadway temperature is 28 °C, up to 32 °C; the –1000 m roadway temperature is 31 °C, up to 37 °C. As the new wells were completed and put into operation, mine mining depth increased, heat harm problem will become more serious.

3.2 *Physical model of the geological strata*

We pick up horizontal roadway of Zhangxiaolou mine to set up the physical model. And then we adopt the VOF method to form the mathematical model for the wall. We define materials as water, turbulent kinetic energy of 0.01, dissipation rate is 0.007 m^2/S. Calculation model select standard k-ε two equations model. The opening size of the parallel wall is 4 m, length of 400 m. As shown in Figure 1.

The determination of the calculation parameters in the model is the most important components. According to the test data and formulas from relevant literatures (David & Vincent 2004, Lin & Barrows 2003, Michael & Rafael 2007, Hiroshi & Blunt 2007, Talabi et al. 2009), the two-phase flow of gas (air) and water thermal physical parameters and wall thermal physical parameters can be determined as shown in Table 1.

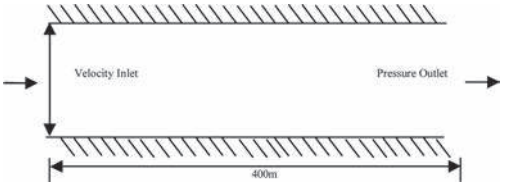


Figure 1. Schematic of the physical Model.

Table 1. Thermal physical parameters.

	Density kg/m^3	Thermal Conductivity $W/m \cdot k$	Specific heat J/kg. K	Kinematic Viscosity (kg °C/m.s)
Air	1.225	0.0242	1006.43	1.79×10^{-5}
Water	998.2	0.6	4182	1.003×10^{-3}
Wall	2440	855	2.56	

4 NUMERICAL SIMULATION

4.1 *Numerical simulation at different air-content*

Here are the simulations of the air-water two-phase flow under the same inlet velocity but different air content. All the parameter values for the fluid in two-phase and wall flow are shown in Table 2. Flow pattern within the model diagram are shown in Figure 2. Figure 3 is the plot of static against position. (Temperature 1 is the temperature value for the upper wall. Temperature 2 is the one for the down wall)

From (a), we can see that the flow pattern at the entrance is typical dine bubbly flow, and the bubble exist corrugated. At the 1/3 inlet, there are bubble which come from the evaporation of the fluid, close to the wall, and then small bubbles gather together to form the plug-shaped air flow pattern map. From (b) we can see that at the entrance, the fine bubbly flow pattern map exists just for a short time, at the 1/4 inlet, forming a gus slug flow pattern map. From (c) we can see that, there is no existence of gas slug flow pattern map at the entire wall. From (d) we can see that the flow pattern map shows a typical gas mist flow pattern, and with the increase of the air-content, the droplets exist as aerosolized between the walls.

The wall outlet section deciles into 40 parts, from Figure 3 we can see the temperature values under different air-content. The maximum value shows at the wall surface and the minimum appears at the middle position of the two-phase fluid inlet. From Figure (a) we can see that the fourth temperature measurement points are equal to the fourth temperature measurement points. When the unit volumes air content varies from 10% to 40%, the plots of static temperature vs. position are almost the same. For Figure (b), it is the seventh. From the cross location coordinates, under the condition of air volume rate changes from 10% to 40%, the maximum fluid heat exchanger radial distances is up to 0.3. When the air volume rate is 80%, the distance is 0.7.

Table 2. Parameters of the variables used in the computation.

No.	Air Content	V. Inlet (m/s)	Inlet T (°C)	T1 (°C)	T2 (°C)
a	10%	50	12	25	45
b	20%	50	12	25	45
c	40%	50	12	25	45
d	80%	50	12	25	45

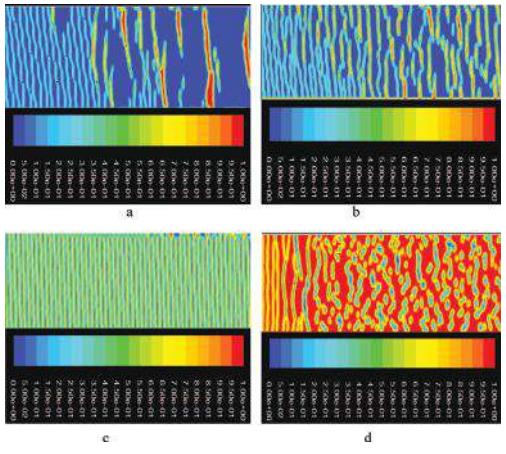


Figure 2. Contour map of flow patterns at different air content; (a) 10% (b) 20% (c) 40% and (d) 80%.

4.2 *Numerical simulation at varied inlet velocities*

Here is the simulation of the air-water two-phase fluid under the same air volume rate, varied inlet velocity. All the parameter values for the fluid in two-phase and wall flow are shown in Table 3. Flow pattern within the model diagram is shown in Figure 4. Figure 5 is the plot of static against position.

When the two-phase flow flows into the wall they are all fine bubbly flow. From Figure (a) we can see that at the 1/4 inlet there comes out a gas slug flow pattern map. From the entrance to the 1/3 inlet, there exists a thin convective heat transfer boundary at the surface of the lower wall. Through 1/3 length, the small bubbles gradually joined together to form a air slug flow pattern map. Figure (b) shows that after the two-phase flow entering 2/5 of the wall, there is bubbles phenomenon at the wall surface of the lower wall. From Figure (c) we can see that, at the 3/5 at the length, there shows

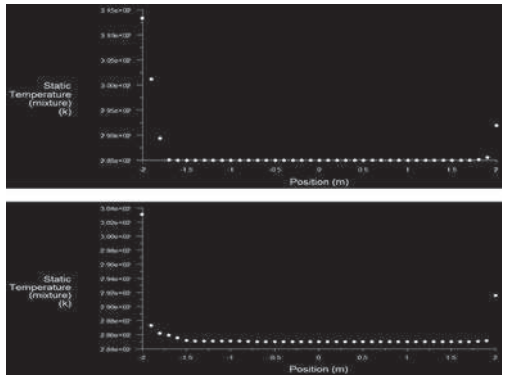


Figure 3. Plot of temperature distribution along the y direction (horizontal coordinate in the plot) at outlet of the tunnel; (a) 10% (b) 80%.

bubbles phenomenon at the surface of the lower wall. At this working condition, the thin convective heat transfer boundary is long, and it do exit from the 1/10 inlet to the outlet. At the two-phase flow through 3/5 of the length, there forms a gas slug flow pattern map. Figure (d) we can see that after the two-phase flow flowing into the 2/3 of the wall, the air flow pattern map began to change into slug flow pattern map. There are little bubbles at the surface of the lower wall. From 1/10 of the inlet to the outlet there is convection boundary layer. This thin layer contains of little bubbles. After the two-phase flow through 2/3 of the length, there forms a gas slug flow pattern map.

The wall outlet section deciles into 40 parts, from Figure 5 we can see that the temperature of the fluid reaches the maximum under the wall wall board surface, and the minimum value occurs in the middle position. When the inlet velocity varies from 5 m/s to 100 m/s, the plots of static temperature vs. position are almost the same. Corresponding to different speeds at different temperature point, the temperature begins to stabilize at 15.2 °C. And the distance of radial heat transfer varies.

Table 3. Parameters of the variables used in the computation.

No.	Air Content	V. Inlet (m/s)	Inlet T(°C)	T1 (°C)	T2 (°C)
a	10%	5	15	25	45
b	10%	10	15	25	45
c	10%	50	15	25	45
d	10%	100	15	25	45

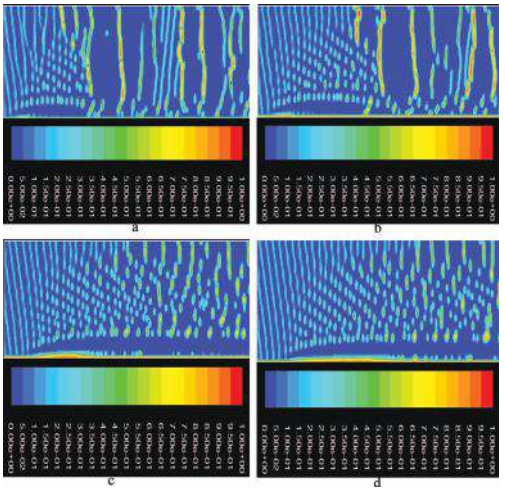


Figure 4. Contour map of flow patterns at varied inlet velocity; (a) 5 m/s (b) 10 m/s (c) 50 m/s and (d) 100 m/s.

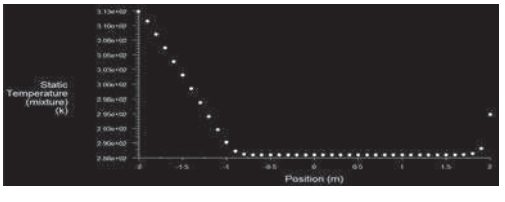


Figure 5. Plot of temperature distribution along the y direction (horizontal coordinate in the plot) at outlet of the tunnel when the inlet velocity is 5 m/s.

4.3 *Numerical simulation at different wall temperatures*

Here is the simulation of the air-water two-phase flow under the same air-content, same inlet velocity, but different wall temperatures. All the parameter values for the fluid in two-phase flow and wall flow are shown in Table 4. Flow pattern within the model diagram as shown in Figure 6. Figure 7 is the temperature scatter plot for the export fluid.

Table 4. Parameters of the variables used in the computation.

No.	Air Content	V. Inlet (m/s)	Inlet T(°C)	T1 (°C)	T2 (°C)
a	10%	50	15	30	45
b	10%	50	15	40	45
c	10%	50	15	50	45
d	10%	50	15	60	45

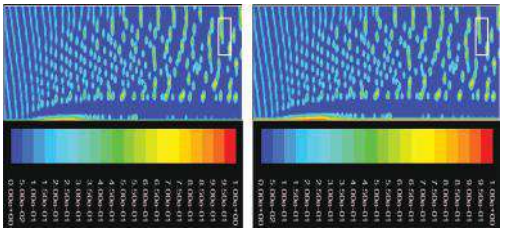


Figure 6. Contour map of flow patterns at different wall temperatures (a) 30 °C (b) 40 °C.

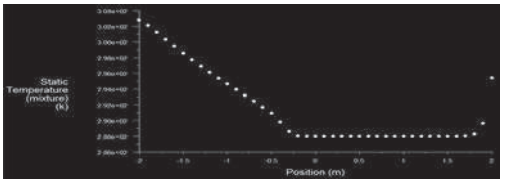


Figure 7. Plot of temperature distribution along the y direction (horizontal coordinate in the plot) at outlet of the tunnel when the wall temperature is 30 °C.

The wall outlet section deciles into 40 parts, from Figure 7 we can see the maximum temperature value occurs at the lower wall wall board surface, and the minimum occurs in the middle position. When the wall temperature varies from 30 to 60, the plot of static temperature vs. position do no change a lot and the temperatures all stabilized at 15.2 °C at the nineteenth measurement points.

5 RESULTS AND DISCUSSION

5.1 *Heat convection against air-content*

Here is the result discussion about the heat transfer effect of air-water two-phase flow under different air-content. Figure 8 is the line chart of static temperature vs. air-content at air-bearing water.

When the air-content rate is the only parametric, the distance of the radial heat transfer in two-phase flow of solid-fluid heat transfer wall model is increases and then decreases and increases again with the changes of air content. The average temperature of the wall export two-phase fluid can be calculated through the scatter plot, and calculate the average export temperature to 12.73 °C when the air content is 80%, higher than the entrance 0.73 °C, which is the minimum temperature rise in the simulation of the same group; We can draw from the temperature rise that under the same working conditions, when the volume containing the air content of 80%, the fluid-solid heat transfer has the worst effect.

5.2 *Heat convection against inlet velocities*

Here is the result discussion about the heat transfer effect of air-water two-phase flow under different inlet velocities, and the volume rate of air is 10%. Figure 9 is the line chart of static temperature vs. inlet velocity of air at air-bearing water.

When the air-content is 10%, and the fluid inlet velocity is the only parametric conditions, the distance of the radial heat transfer in two-phase flow is increase and then decreases, so there is a peak value. The simulation results show: when the inlet velocity is 50 m/s, there is a biggest heat transfer distance value, which is 1.8 m. The smallest one is 1.1 m under the speed of 5 m/s. The average temperature of the wall inlet velocity of two-phase fluid can be calculated through the scatter plot, and the outlet temperature of the outlets in this two-phase flow can be determined by this way, which is 21.21 °C. When the fluid inlet velocity is 5 m / s, the average outlet temperature of the two-phase fluid is 18.24 °C, higher than the inlet 3.24 °C, and it is the minimum temperature rise of the same group. From the temperature rise we can drawn that under the same working conditions, when the fluid inlet velocity is 50 m / s, the effect of heat transfer fluid-solid is the best.

5.3 *Heat convection against wall temperature*

Here is the result discussion about the heat transfer effect of air-water two-phase flow under different wall temperatures. The air-content of air is 10% and the inlet velocity is 50 m/s. Table 7 is the temperature of the export under different wall temperature, and Figure 10 is the line chart of static temperature vs. inlet velocity of air at air-bearing water.

When the wall temperature is the only parametric, the simulation results show that: the distance of radial heat transfer in the two-phase flow heat transfer is increases with the increasing of the wall temperature, showing obvious linear change.

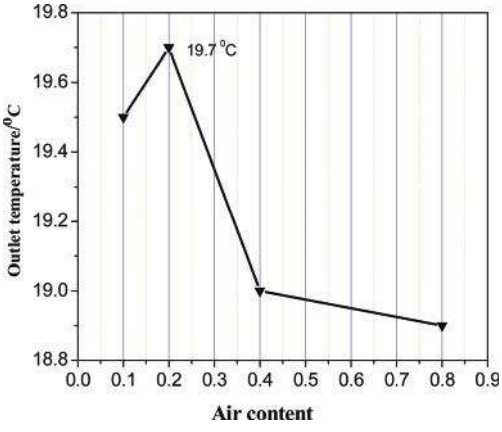


Figure 8. Plot of outlet temperature vs. different air content.

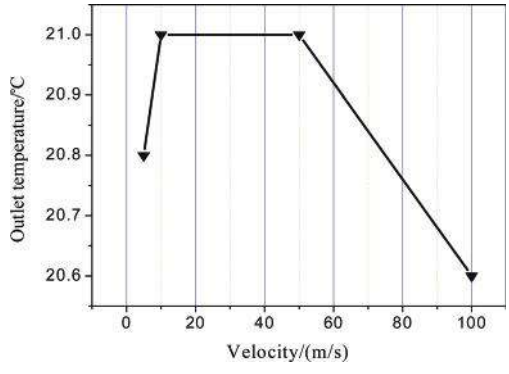


Figure 9. The line chart of static temperature vs. air-content.

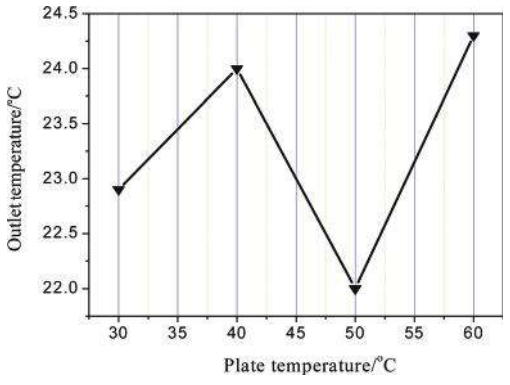


Figure 10. The line chart of static temperature vs. air-content.

6 CONCLUSION

Based on the numerical study of the heat exchange between the coal rock and air-water two-phase flow in the paralleled wall model, with the consideration of varied air contents, inlet velocities and increment of the wall temperatures, following conclusions were made.

In the case of air-content as the unique influencing factor, the air-water two-phase flow exhibits a fine-bubble flowing pattern at air-content less than or equal to 10%; a slug-shaped gas pattern at air-content between 10% and 40%; and a misty pattern with massive fine water droplets at air-content equal to 80%. The output temperature of the tunnel increases with the increase of the air content, and reaches the maximum value. After the peak value, the temperature drops steeply between air content of 20–40% and turns to drop moderately between 40–80% air contents. The simulated results demonstrate that the water based media with the air content ranging from 10% to 40% has better heat-exchange effect than the flow with air content ranging from 40–80%. And the 20% air-contained water flow has the optimal heat exchanging effect.

Under the condition of inlet velocity as the unique factor, the air-content is 10%, the flow pattern of the two phase flow shape from a fine-bubble to a gas-slug pattern. The output temperature of the tunnel increases with the increase of the inlet velocity, and reaches the maximum value. After the peak value, the temperature drops steeply between inlet velocity of 50–100 m/s. The simulated results demonstrate that the inlet velocity ranging from 20 m/s to 50 m/s has better heat exchange effect than the inlet velocity ranging from 50 m/s to 100 m/s and the 100 m/s inlet velocity has the optimal heat exchange effect.

Under the condition of the wall temperature is the unique factor, and the air—content is 10% and the inlet velocity is 50 m/s, the output temperature of the tunnel increase with the increase of the temperature of the wall. When the temperature of the wall is higher than 40 °C, the output temperature drops sharply to the minimum value. After the smallest value, the temperature increases steeply from the wall temperature and reaches the maximum value. The simulated results demonstrate that the wall temperature ranging from 30 °C to 40 °C and from 50 °C to 60 °C has better heat exchange effect than the wall temperature ranging from 40 °C to 50 °C. And the 50 °C wall temperature has the optical heat exchange effect.

7 ACKNOWLEDGEMENT

Financial support from the Special Funds for the National Natural Science Foundation (Key Project) under Grant No. 51134005 is gratefully acknowledged.

REFERENCES

Bakke Stig, Ren P. L-Eric. 1997. 3-D pore-scale modelling of sandstones and flow simulations in the pore networks. *Spe Journal*. 2(2):136–149.

Becker Michael, Kramann Rafael, Franke Andreas, et al. 2007. Impact of left ventricular lead position in cardiac resynchronization therapy on left ventricular remodelling. A circumferential strain analysis based on 2D echocardiography. *European Heart Journal.* 28 10):1211–1220.

Bryant David, Moulton Vincent. 2004. Neighbor-net: an agglomerative method for the construction of phylogenetic networks. Molecular biology and evolution, 21(2):255–265.

Burrows J. 1982. Environmental engineering in South Africa mines [M]. *The mine ventilation society of South Africa*.

Graton Louis Caryl, Fraser H.J. 1935. Systematic packing of spheres: with particular relation to porosity and permeability. Journal of Geology, 785–909.

Hazlett Brian A., Bossert William H. 1965. A statistical analysis of the aggressive communications systems of some hermit crabs. Animal Behaviour, 13(2):357–373.

Hemp R.1985. Air temperature increases in airways [J]. The mine ventilation society of South Africa. 1–20.

He Manchao, Zhang Yi, Guo Dongming, Qian Zengzhen. 2006. Numerical analysis of doublet wells for cold energy storage on heat damage treatment in deep mines. China Journal of Mining & Technology (English Edition), 16(3):278–282.

Joshi Madhusudan Y. 1974. A class of stochastic models for porous media [D]: University of Kansas, Chemical and Petroleum Engineering.

Krumbein William Christian, Sloss Laurence Louis. 1963. Stratigraphy and sedimentation. Freeman San Francisco.

Lin Angela SP, Barrows Thomas H., Cartmell Sarah H., et al. 2003. Microarchitectural and mechanical

characterization of oriented porous polymer scaffolds. Biomaterials, 24 (3):481–489.
Lowndes I S, Yang Z Y, Jobling S, et al. 2006. A parametric analysis of a tunnel climatic prediction and planning model [J]. Tunnelling and Underground Space Technology. 21:520–532.
Okabe Hiroshi, Blunt Martin J. 2007. Pore space reconstruction of vuggy carbonates using microtomography and multiple–point statistics. Water Resources Research, 43(12).
Quiblier Jacques A. 1984. A new three-dimensional modeling technique for studying porous media. Journal of Colloid and Interfact Science, 98(1):84–102.
Talabi Olumide, AlSayari Saif, Iglauer Stefan, et al. 2009. Pore-scale simulation of NMR response. Journal of Petroleum Science and Engineering, 67(3):168–178.
Zhaohui Wang, Guohua Chen. 2000. Heat and mass transfer in batch fluidized-bed drying of porous particles [J]. Chemicao Engineering Science. 55(10):1857–1869.

This page intentionally left blank

Progress in Mine Safety Science and Engineering II – He et al. (Eds)
© 2014 Taylor & Francis Group, London, ISBN 978-1-138-00122-0

The research of realizing the mine safety of ascending vessel undertake force by using 2 force stem mechanical characteristics

A.T. Balkema & G. Westers
A.A. Balkema Publishers, Rotterdam, The Netherlands

Fu-Yin Jia & Meng-Juan Dong
College of Energy Sources and Safety, China University of Mining and Technology, Xuzhou, Jiangsu, China

ABSTRACT: Analysis the mine ascension undertake force, determine the mechanical characteristics of the safety undertake. Developed a concentration workforce, limited force safety protection mechanism for mine lifting undertake by using 2 force stem mechanical characteristics. The mechanism has simple structure, flexible motion, high reliability, adapt to the mine environment, provided guarantee for mine safety, efficient work.

Keywords: Mine ascension undertake force, 2 force stem mechanical, Mechanical Properties

1 OUTLINE

In mine production, vertical ascension is an important part of the production. It is the traffic artery connecting the ground and underground, the safety and reliability of it directly influence production, safety, and even threatening the life of the passenger (Jia F Y & Dong M J 2011, Jia F Y et al. 2008). Therefore, improve the equipment of lifting system, in addition to its reliability, also have to consider the safety. The mechanism in this paper is an equipment for undertaking and stabilizing cage, while the cage is in the middle level of wellhead and the bottom. Its role is, while the cage with a certain speed running in place, to fall in the crawling velocity, the mechanism offer buffer and the cage stop smoothly, and realize the level docking of rail surface in cage and external rail surface. When the cage was too high to speed down in continues on the device, this device in effective after buffer, and can't meet the cage was stopped, buffer tank released in full force, let the cage through without resistance, avoid causing occupant casualties when the reduce speed is more than the allowable value because undertake force is too large (one can withstand 5×9.8 m/s^2) (Jia F Y et al. 2008).The successful development of the device is of great significance to improve conditions for ascending vessel and ensure the safety of ascension significance.

2 THE REQUIREMENTS FOR SECURITY UNDERTAKING FORCE

Undertake device meet the job needs, undertake force must be greater than the load + the dead weight of the cage (Jia F Y et al. 2008).Because every time the cage fall at different rates, said the load change, therefore, set to undertake force must meet (load + heavy of cage) x impact coefficient, impact coefficient select 1.5. Undertake force meet safety requirements, and undertake force in safety limits to ensure that the resulting reducing speed meet safety requirements when the cage high-speed falls (reducing speed a <5 x 9.8 m/s^2)(Li Z J et al. 2009, Dong M J et al. 2008, Deng S J 2004).

2.1 *The analysis of undertake force*

Set the cage own quality for m_1, quality goods for m_2, fall in the tank for the speed on the device for v, to vertical Wells Jane center line for the y axis, down for the positive direction, with China level as the x axis, established for origin coordinate y intersection, as shown in figure is the cage when drawing down forces continues:

As F for elastic cushion resistance, by Newton's second law, have to equation is as follows:

$$m_1 g + m_2 g - F = (m_1 + m_2) y'' \tag{1}$$

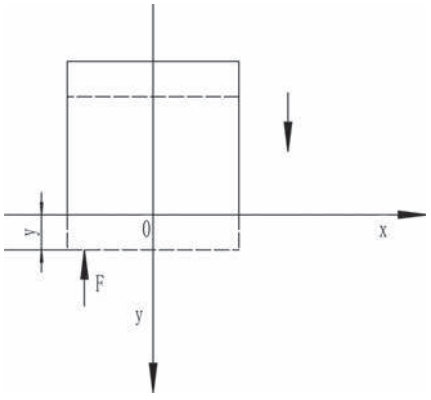


Figure 1. The force of cage undertaking.

As F = ky, (k as equivalent buffer elasticity coefficient)

$$y'' + \frac{k}{m_1 + m_2} * y - g = 0 \tag{2}$$

Given equation for:

$$y = c_1 \cos\sqrt{\frac{k}{m_1 + m_2}} * t + c_2 \sin\sqrt{\frac{k}{m_1 + m_2}} * t + \frac{m_1 + m_2}{k} * g \tag{3}$$

By boundary conditions t = 0, y = 0
Have

$$c_1 = -\frac{m_1 + m_2}{k} * g \tag{4}$$

By t = 0, y′ = v, have

$$y' = c_1\sqrt{\frac{k}{m_1 + m_2}} * \sin\sqrt{\frac{k}{m_1 + m_2}} * t + c_2\sqrt{\frac{k}{m_1 + m_2}} * \cos\sqrt{\frac{k}{m_1 + m_2}} * t \tag{5}$$

As $v = c_2 * \sqrt{\frac{k}{m_1+m_2}}$, $C_2 = v\sqrt{\frac{m_1+m_2}{k}}$, can get:

$$y = -\frac{m_1 + m_2}{k} g * \cos\sqrt{\frac{k}{m_1 + m_2}} * t + \sqrt{\frac{m_1 + m_2}{k}} * v * \sin\sqrt{\frac{k}{m_1 + m_2}} * t + \frac{m_1 + m_2}{k} * g \tag{6}$$

The equation refers the relation of the cage displacement and time when undertake.

2.2 *The requirement of safety limit force*

The reducing speed y "must meet less than one can withstand limits when the cage is forced to slow down due to the undertake force F as a buffer resistance (Chang Y W 2008).

Reducing speed limit is smaller, given the small resistance F, stop the tank good stability. Given the big resistance, stop the cans of reducing speed (Wang H Y 2007, Ma J. 2008, Wiles, T.D. 2006). Choose commonly y″ ≤ 2.5 g.

Obtained by formula (6)
Have

$$y' = \sqrt{\frac{m_1 + m_2}{k}} * \sin\sqrt{\frac{k}{m_1 + m_2}} * t + v * \cos\sqrt{\frac{k}{m_1 + m_2}} * t \tag{7}$$

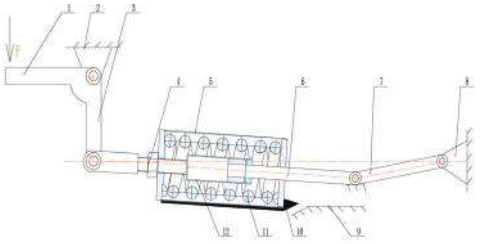
$$y'' = g * \cos\sqrt{\frac{k}{m_1 + m_2}} * t + v * \sin\sqrt{\frac{k}{m_1 + m_2}} * \sin\sqrt{\frac{k}{m_1 + m_2}} * t \tag{8}$$

According to y″ ≤2.5 g, obtain the value of the t;
By t value generation into (6) type work out y, allow buffer quantity.

3 THE STRUCTURE AND WORKING PRINCIPLE OF THE MECHANISM TEXT AND INDENTING

All figures should be numbered with Arabic numerals (1, 2, ..., n). All photographs, schemas, graphs and diagrams are to be referred to as figures. Line drawings should be good quality scans or true electronic output. Low-quality scans are not acceptable. Figures must be embedded into the text and not supplied separately. Lettering and symbols should be clearly defined either in the caption or in a legend provided as part of the figure. Figures should be placed at the top or bottom of a page wherever possible, as close as possible to the first reference to them in the paper.

The figure number and caption should be typed below the illustration in 9 pt and left justified. For more guidelines and information to help you submit high quality artwork please visit: http://www.elsevier.com/wps/find/authorsview.authors/authorartworkinstructions. Artwork has no text along the side of it in the main body of the text. However, if two images fit next to each other, these may



1-Undertaking arm; 2-Support body of bracket arm; 3-Resisting arm; 4- Adjustable force nut; 5- Guide tube outside; 6-Two force stem; 7- After two force stem ;8-Rotary bearing; 9- The instability constraint body ;10-Limit force piece of; 11-Spring ;12-Guide in cone

Figure 2. Floor a action principle diagram.

be placed next to each other to save space, see Fig 1. They must be numbered consecutively, all figures, and all tables respectively.

As shown in figure, the mechanism is made up of 2 force stem (6, 7) in reverse instability state formed under the steady state. 4, 5, 6, 11, 12 buffer organization, 1 and 3 for a whole, 2 for rotary support, 1 be undertaking bracket arm, 3 be a resisting arm for connecting buffer.

The figure for a quarter of F's force, there are four also structure a cage.

When working, the cage with a certain speed (about 0.5 m/s), fell on 1, 1 gives "by a relative work force 3 through the buffering mechanism given, buffering mechanism including two force rods, 6 to 8. Two force rods 7 as counter binding is stable, so cushioning force is stable's work force. When a 4, 5, 6, 11, 12 buffer organization displacement back produce, cushioning force and hold the cage, the initial force size (4) by adjusting the force nut adjustment, when buffer displacement has made the guide tube upper limit of force (10) pushed to the instability constraint body, 6, 7 are 9, 10 push through two force stem the center line, two force bar instability, buffer thrust failure, then lost power system, F to zero, right now for the safety of the buffering mechanism guarantee.

4 MECHANISM SPECIFIC DESIGN

1. The ascertain of instability Angle α
   By 6, 7 of the force of a second with a horizontal bar instability Angle, the selection of big, its good stability, but difficult to lift force, the selection of small, the lift force's stability affected (Dong M J et al. 2008).
2. The buffer mechanism design
   To work out undertake force as the basis, the design of the spring buffering mechanism oriented and the cylinder force agency, satisfy the intensity and the function requirement.
3. The actual application design
   Due to ascend parameters, the cage own quality $m_1 = 11000$ kg, goods quality $m_2 = 12000$ kg, crawling velocity $v = 0.5$ m/s, single force equivalent elastic coefficient $k = 8$ KN/mm, calculated t = 2.5, y = 0.24, the $F = ky = 1.92 \times 10^6$. Set $\alpha = 6°$.
   Set uplifting cage force $F = 1.92 \times 10^6$ as known variables in design, In the cage and relative position known for design measurements, and consider the safety factor of the request, the system design, concrete structure, as shown in figure.

5 CONCLUSION

From what has been discussed above, with 2 force stem mechanical reverse buckling as the release status used in cage safety undertake, it both meet the requirements of the cage smoothly undertake, at the same time ensure that cage high-speed can pass down. It thoroughly solved the problem of the old lap along with the terminal load changes, which the cage to move up and down, in and out of the car is difficult, and is easy to appear the accident. 2 force stem mechanical reverse buckling characteristics can be widely applied to the limited force work and used in the safety function requirements of the device. Its application is of great significance for the safe and efficient production.

REFERENCES

Chang Y W. 2008. Fault diagnosis of a mine hoist using PCA and SVM techniques. *Journal of China University of Mining and Technology* 18(3):327–331. (In Chinese).

Deng S J. 2004. Method of designing the delayed limit velocity for mine hoist. *Journal of China University of Mining and Technology* 33(6):721–725. (In Chinese).

Dong M J, Jia F Y, Zhu C, Jiang X H, Chu L, Qiu S J & Han X D. 2008. ZHT Cage-supported Damping Swing-deck with Self-driven Changing Floor Used in Mine. *Coal Mine Machinery* 29(6):170–171. (In Chinese).

Dong M J, Jia F Y, Jiang X H, Zhu C, Chu L, Qiu S J & Wang Q. 2008. Research on Adjusting Rope Device. *Coal Mine Machinery* 29(7):157–158. (In Chinese).

Jia F Y & Dong M J. 2011. Stabilizing Cage Technology of Deep Shaft Friction Hoist. *Journal of China Coal Society* 36(5):177–180.(In Chinese).

Jia F Y, Li Z J, Wang Y B & Sun J X. 2008. Analysis on safety and reliable braking of sliding rope on frictional hoist. *Coal Mine Enginering* (5):99–100. (In Chinese).

Jia F Y, Bi J M, Bi S H, Chu L & Wang Y B. 2008. SLT Cage Path Rope Online Detect Automatism Modulate Device. *Coal Mine Machinery* 29(4):117–118. (In Chinese).

Jia F Y, Wang Y B, Chu L & Bi J M. 2008. Analysis and Application of Botton of Well Equalize Hold Theory. *Coal Mine Machinery* 29(5):174–175. (In Chinese).

Li Z J, Jia F Y & Dong M J. 2009. Research on ZHT Cage-supported Damping Swing-deck with Automatic Changing Floor Cooperated with Flex Cage Guide. *Coal Technology* 28(1):76–77. (In Chinese).

Ma J. 2008. Distribution of wire deformation within strands of wire ropes. *Journal of China University of Mining and Technology* 18(3):475–478. (In Chinese).

Wang H Y. 2007. Research on Detection Device for Broken Wires of Coal Mine-Hoist Cable. *Journal of China University of Mining and Technology* 17(3):376–381. (In Chinese).

Wiles, T.D. 2006. Reliability of numerical modelling predictions. International. *Journal of Rock Mechanics and Mining Sciences* 43(3):454–472.

Progress in Mine Safety Science and Engineering II – He et al. (Eds)
© 2014 Taylor & Francis Group, London, ISBN 978-1-138-00122-0

Research quantitative model of gas pressure gradient and in-situ stress in complex tectonic outburst coal seam

Dao-Xiong Qin, Ming-Bo Zhang, Bo-Long Lei, Xiao-Yu Kang & An-Yu Zhu
School of Resource and Safety Engineering, China University of Mining and Technology (Beijing), Beijing, China

ABSTRACT: The main factors of affecting coal and gas outburst are gas pressure change rule and in-situ stress distribution regularities in complex tectonic outburst coal seam; Based on the relationship of between Darcy's etc, a quantitative calculation model of gas pressure gradient and in-situ stress is established; Simulating the damage rule in Li Wang-miao coal mine 1152 cross-hole region. The results are stress gradient change obviously and coal first destruction and serious damage in the wing region near stress neutral plane along 15, 20 and 28 m of X direction. Combining the model calculated gas stress gradient distribution regularities in of the region. The results show that gas pressure gradient will change obviously when in-situ stress is 3 MPa, increase sharply when in-situ stress is more than 3 MPa and along X direction 0~5 m and 28~31 m of the calculation model in tectonic coal seam.

1 INTRODUCTION

Coal and gas outburst is an extremely complex dynamic phenomenon and one of the most serious disasters in coal mines. China is the most serious coal and gas outburst in the world and the outburst characteristics consist of the larger number of outburst mines, the more wide distribution range, the larger number of outburst times, the higher outburst frequency, the shallower of beginning outburst depth, the more inclusive outburst types, the greater outburst strength, the more coal and gas of outburst (Zhang Fu-guo 2009, Lin Bo-quan 2010, He Xue-qiu 2009).With increasing mining strength and depth and increasing complexity of geological conditions, especially under the conditions that development of fold and fault is very complicated, the danger of coal and gas outburst is becoming more and more serious. In the coal seams of complex structure, the main influencing factor of coal and gas outburst danger is change rule of gas pressure gradient and distribution rule of in-situ stress(Yu Yan 2012, Jing Guo-xun 2005). It has important engineering practical value and theoretical guide significance that research gas pressure gradient and the quantitative model of in-situ stress in outburst coal seam of complex structure to master its outburst regularity and characteristics and comprehensive prevention and control technology.

2 THE GAS PRESSURE GRADIENT AND THE QUANTITATIVE MODEL OF IN-SITU STRESS

According to Darcy's law, the gas pressure gradient of coal seam is proportional to the gas seepage velocity(Wang Ji-ren 2005, Xu Xue-feng 2003, Sun Jing-lai 2009). Its expression is:

$$q = -\lambda \cdot \frac{dp}{dx} \tag{1}$$

In the formula, q is gas seepage velocity, λ is permeability coefficient of coal seam, dp/dx is gas pressure gradient along the seepage direction.

The expression of permeability coefficient of coal seam is:

$$K = \begin{cases} k_0 e^{-\beta(\sigma_1 - \alpha p)} & D = 0 \\ \varepsilon k_0 e^{-\beta(\sigma_1 - \alpha p)} & D > 0 \end{cases} \tag{2}$$

In the formula, K, k_0, D, ε, β and α respectively are permeability coefficient of coal seam, permeability coefficient of raw coal, damage parameter of coal, increase multiples of permeability coefficient after damage, gas pressure coefficient of pore, coupling coefficient between the stress and the pore gas pressure.

The expression of gas seepage coefficient of coal seam (Sun Jing-lai 2009, Wang Yan-sen 2004, Yang Tian-hong) is:

$$\lambda = \frac{K}{2\mu p_0} \tag{3}$$

In the formula, μ, p_0 respectively are kinetic viscosity of gas and atmospheric pressure.

According to conclusions of related data research, seepage velocity of coal and rock post-peak and rock stress are quadratic relationship (Wang Lei 2010, Ma Dong-xiao 2011, Yin Guang-zhi 2008, Hu Wei-yue 2009, Zhou Dong-ping 2008):

$$q = a\sigma_1^2 + b\sigma_1 + c \tag{4}$$

In the formula, σ_1 is effective stress in the coal. under the conditions that coal quality, damage degree of coal, gas pressure and stress of surrounding rock, formula (1), (2), (3) are substituted in formula (4), then relational expression of gas pressure gradient and in-situ stress can be get:

$$a\sigma_1^2 + b\sigma_1 + c = -\frac{\varepsilon k_0 e^{-\beta(\sigma_1 - \alpha p)}}{2\mu p_0} \cdot \frac{dp}{dx} \tag{5}$$

The expression is:

$$\frac{dp}{dx} = -\left(a\sigma_1^2 + b\sigma_1 + c\right) \cdot \frac{2\mu p_0}{\varepsilon k_0 e^{-\beta(\sigma_1 - \alpha p)}} = -\frac{2\mu p_0}{\varepsilon k_0} \cdot \frac{\left(a\sigma_1^2 + b\sigma_1 + c\right)}{e^{-\beta(\sigma_1 - \alpha p)}} \tag{6}$$

Because α, β are smaller values and the gas pressure P is smaller relative to the surrounding rock stress, formula (6) can be simplified as:

$$\frac{dp}{dx} = -\frac{2\mu p_0}{\varepsilon k_0} \cdot \frac{\left(a\sigma_1^2 + b\sigma_1 + c\right)}{e^{-\beta\sigma_1}} \tag{7}$$

Set:

$$n = -\frac{2\mu p_0}{\varepsilon k_0} \tag{8}$$

$$y = \frac{\left(a\sigma_1^2 + b\sigma_1 + c\right)}{e^{-\beta\sigma_1}} \tag{9}$$

Because of trends consistency of coefficient n and y, the change state of gas pressure gradient in coal mine can be generally reflected by the change trends of y function values. The derivation of in-situ stress in formula (6) is:

$$Y = \frac{\beta a\sigma_1^2 + \left(2a + b\beta\right)\sigma_1 + b + c\beta}{e^{-\beta\sigma_1}} \tag{10}$$

The formula (10) is change intensity of function y values and can reflect change intensity of gas pressure gradient in coal seam.

3 SIMULATION STUDY ON IN-SITU STRESS DISTRIBUTION LAW UNDER COMPLICATED TECTONIC CONDITION

3.1 *The profile of coal seam*

The characteristics of coal seam in LI Wang-miao 1152 working face are: V coal, monoclinal structure, simple structure, Interbedded with gangue, coal seam thickness is 1.8–5.5 m, average thickness is 3.7, etc. The coal primarily is bright coal and presents powder form and metallic luster. The coal seam belongs to the stability coal seam and has lower hardness and bigger coal dust. The Dip Angle of coal seam is 0–50 degrees and average angle is 26 degrees. The gas pressure of coal seam is 0.99 MPa and content of gas is 0.55 m^3/t. The table 1 shows characteristics of coal seam roof and floor and coal bed structure. The figure 1 shows occurrence condition of coal seam.

3.2 *The establishment of calculation model*

In order to eliminate boundary effect, the No. 1 cross-hole of the floor gateway of 1152 working

Table 1. The features of coal seam roof and floor.

Name	Lithology	Thickness (m)
Main roof	Medium sandstone	21.5
Immediate roof	Siltstone	4.6
False roof	Sandy mudstone	0~0.3
Immediate floor	Argillaceous siltstone	0.1
Main floor	Sandy mudstone	26.0

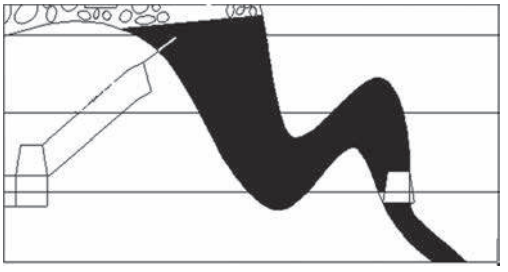


Figure 1. Rock cross-cutting to uncover coal of district raise in 1152 working face floor.

face in Li wang-miao Mine should be considered a variety of factors, so three-dimensional computational model of length, width and height should be set as 31 m, 30 m and 40 m. By adopting CAD to extract the boundary data of the calculation model and using self-compiled program interface to establish the physical calculation model, the result can be shown in Figure 2 which the X-direction is defined as the direction of coal seam and Y-direction is defined as the tendency of coal seam. The physical and mechanical parameters of roof and floor rock are shown in Table 2, While the left and right boundary of the model are exerted pressure load, the front, back and bottom are fixed, and the top is free. In the process, this paper use Moore—Coulomb yield criterion and creep model to present the rock stratum stress distribution and the scope of damage distribution of constructed area.

1. Numerical simulation of stress distribution

In the process of stress simulation, the front, back and bottom of the model are fixed, and each of the left and right boundary of the model are exerted the horizontal compression in 5.2 MPa, then simulate the horizontal stress distribution station along the seam after the fold formation by using the creep model, the result of which is shown in figure 3.

In the procession, there easy exists the phenomenon of horizontal stress concentration in the region of the syncline and anticline on the roof and floor rocks, which the horizontal stress ranges from 12 to 17 MPa and the coefficient of horizontal stress concentration ranges from 2.3 to 3.3 approximately; The horizontal stress shows as vertical layered distribution clearly in the tectonic zone seam, as well as the horizontal stress gradient in the coal seam which is between 0 to 8 MPa, which explains the causes of the phenomenon that coal seam will be damaged like layering and spew outward some in the process of coal and gas outburst layered seams will damage ejected outward.

After the simulation being steady, the horizontal stress distribution will be shown in figure 4. In the picture, the position of the transported lane in the no. 1 cross-hole of the floor gateway of 1152 working face in Li wang-miao mine (physical model in the horizontal direction at 28 m) and the change of horizontal stress is most obvious and the biggest change is stress gradient, which mainly due to, (1) this area is the transition from the anticline to syncline wing, so coal is damaged less severely which can withstand the corresponding stress load; (2) the thickness of coal seam in this area is significantly thinner which will lead the distribution of stress become abnormal; in the same time, looking from the tendency of the change of the horizontal stress, there will be the inflection point of the stress gradient in the vicinity of the wing area of the anticline or syncline, for example, the three position like at 15 m, 20 m and 28 m along the

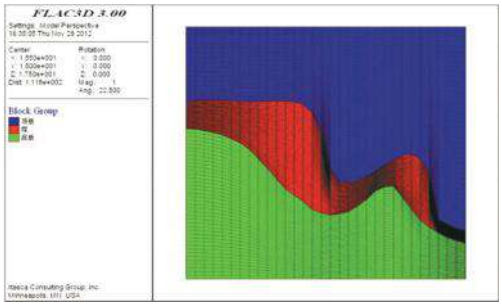


Figure 2. The calculation model of 1 rock cross-cutting to uncover coal area in 1152 working face floor.

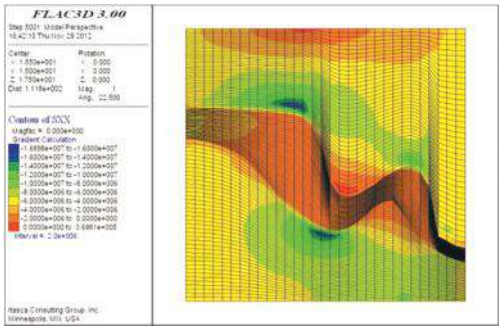


Figure 3. Horizontal stress distribution state of coal and rock.

Table 2. The physical and mechanical parameters of roof and floor rock.

Rock stratum	Bulk modulus (B/GPa)	Shear modulus (S/GPa)	Internal friction angle (F/°)	Cohesion (C/GPa)	Strength of extension (T/GPa)	Density (D/kg · m^{-3})
Main roof	59.14	46.22	38	0.5	0.103	2660
Main floor	20.2	17.09	33	0.41	0.086	2640
Coal	0.119	3.68×10^{-3}	25	2×10^{-3}	3×10^{-5}	1400

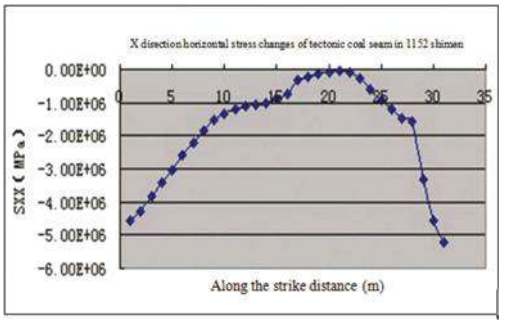


Figure 4. The horizontal stress trends of coal seam.

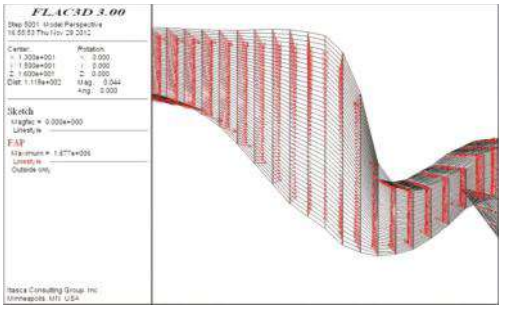


Figure 5. The stress distribution vector of coal seam.

horizontal direction. After the simulation being equilibrium, the stress distribution vector of coal seam will be shown in figure 5. In the picture, there is a neutral surface stress in the rock physics model in the coal fold anticline axis of drape and its vicinity and the horizontal stress approaches to zero in the surface, which mainly because the coal in this area most likely be damaged and the coal scope of the damage be most severe under the action of tectonic stress in the process of geological structure, which lead the coal loss the basic capacity of bearing stress load and then the stress value of the coal in this area become zero essentially.

2. Numerical simulation of the regularities distribution about the scope of damaged coal

In the process of simulation about the scope and state of rock damaged, the front, back and bottom of the model are fixed, and the model is free boundary, and each of the left and right boundary of the model are exerted the horizontal compression in 5.2 MPa, then simulate the horizontal stress distribution station along the seam after the fold formation by using the creep model, at last, every different state of rock damaged of the model will be recorded after a certain number of calculation steps which are shown from figure 6 to 9.

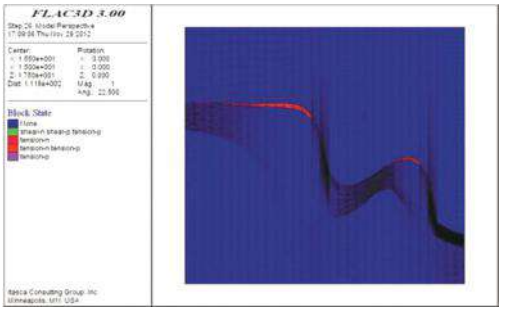


Figure 6. The coal body damage state distribution for creep simulation 20 times.

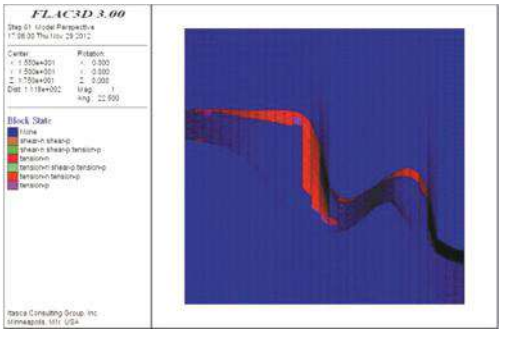


Figure 7. The coal body damage state distribution for creep simulation 60 times.

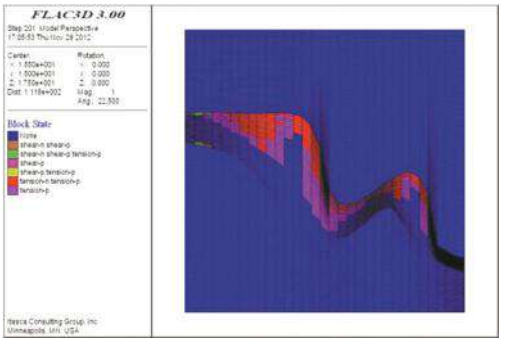


Figure 8. The coal body damage state distribution for creep simulation 200 times.

From the figure 6 to 9, we can see, (1) in this process, neutral surface stress and the coal in area of the alar part of drape and top of anticline produce tensile damage and the extent of damage are most severe; (2) in the process, the coal in the outside of the anticline axis and the inside of the synclinal are also easy damaged region, and the extent of the damage of the coal is too severe.

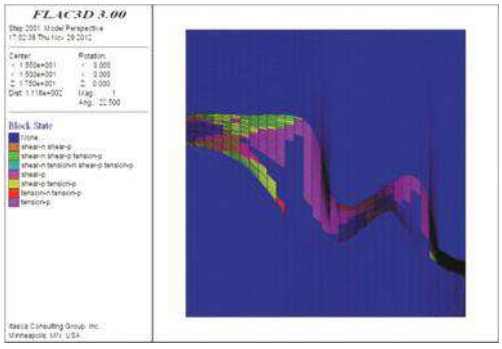


Figure 9. The coal body damage state distribution for creep simulation 60 times.

4 SIMULATION CONCLUSIONS

1. In the coal-rock stratum creep simulation process, the coal seam roof and floor strata in the geologic structure area where the curvature is greater (like synclinal and anticline axis area and coal thickness mutation area, etc) are very prone to appear horizontal stress concentration, in the geologic structure area the coal horizontal stress shows vertical laminar distribution obviously, the coal seam horizontal stress gradient distribution is more obvious, this is also to some extent explains the phenomenon that coal seam appears layered damage and ejection outward in the process of coal and gas outburst.
2. After the coal-rock stratum creep simulation is stable, coal in the geologic structure area in the wing area near synclinal and anticline axis has the inflection point of the stress gradient, stress gradient changes obviously; mainly because in wing area of the fold change, the coal damages not seriously and can stand the stress load, and if the coal thickness changes obviously, it will cause the ground stress changes sharply.
3. After the creep simulation is stable, the stress neutral surface occurs in the anticline axis and the nearby area of the physical computing model, the horizontal stress of the nodes tends to zero on the surface. This is mainly because in the course of geological formations the coal here is prone to be damaged by the tectonic stress, the coal was damaged the most seriously, then the coal almost lost the ability to carry the stress load and the coal stress here tends to zero.
4. In the creep simulation process, coal in the stress neutral surface and the nearby wing area is the first to appear tensile damage and the destruction area is large; In the process, coal of the wing area near the neutral surface gradually experienced the destruction cycle of tensile and shear damage and the extent of the damage is most severe; In the process, anticline axis outside and synclinal axis inside of the tectonic coal are also easily damaged areas, coal extent of the damage is more serious.

5 GAS PRESSURE GRADIENT DISTRIBUTION IN TECTONIC COAL SEAM

According to the related experiments and literature, when gas pressure $P = 0.25$ Mpa, we set $a = 0.81$, $b = -5.476$, $c = 20.375$, $\beta = 0.5028$, calculate the formula (9) and (10) values according to the maximum horizontal stress values in the X direction that gets from the simulation, the distribution shown in figure 10 to figure 11.

According to related research results, when the rock compressive stress is about 5 Mpa and the gas pressure is less than 1 Mpa, gas pressure has little effect on the seepage velocity in the coal seam. Combine the figure 10 and 11 we can obtain:(1) near the 1152 shimen area the gas pressure is between 0 Mpa and 1 Mpa, so when the complex structure coal seam ground stress is about 3 Mpa, gas pressure gradient will appear mutation in the tectonic coal seam; When the ground stress is greater than 3 Mpa, gas pressure gradient will increase sharply; (2) Combine the figure we can obtain that in the 1152 cross-cut calculation model, the 0~5 m and 28~31 m areas in the X direction are in the range of sharp increase in gas pressure gradient. Since the gas pressure and coal seam gas permeation rate are exponential, we can determine the correlation coefficient according to the actual measured gas pressure in the actual

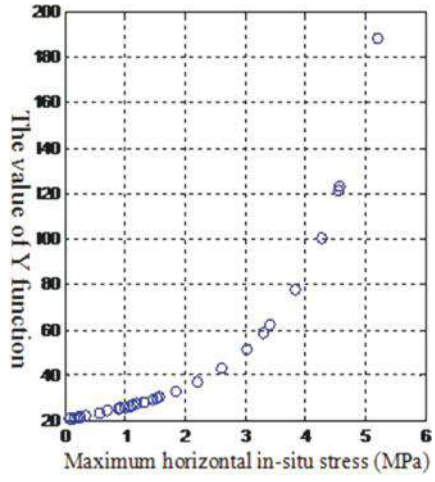


Figure 10. The distribution regularities between y function value and horizontal in-situ stress.

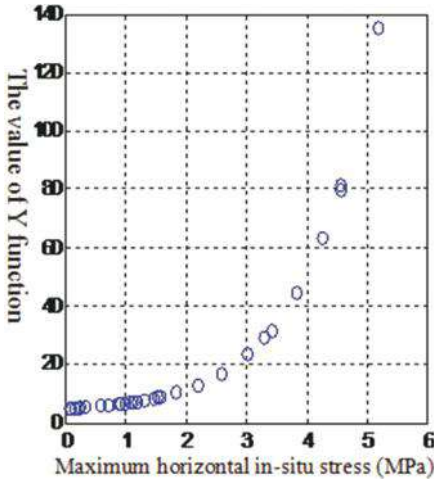


Figure 11. The distribution regularities between Y function value and horizontal in-situ stress.

process, then we can obtain the distribution of gas pressure gradient in the actual geological condition.

6 CONCLUSIONS

1. Based on the relationship between Darcy' low, the gas flow velocity and gas pressure gradient, rock stress, we establish a coal seam gas pressure gradient and ground stress quantitative calculation model.
2. Through the simulation we know the horizontal in the tectonic coal area stress appears obvious vertical laminar distribution, the coal seam horizontal stress gradient is obvious, this explains the phenomenon that coal seam appears layered damage and ejection outward in the process of coal and gas outburst.
3. Through the simulation we can obtain that in the 1152 roadway location(Horizontally at 28 m in the physical model) near 1152-1 shimen structure area in Li Wang-miao mine, horizontal stress changes most obviously At 15 m, 20 m, 28 m in the horizontal direction, stress gradient changes significantly.
4. After the creep simulation is stable, the stress neutral surface occurs in the anticline axis and the nearby area of the physical computing model, coal in the stress neutral surface and the nearby wing area is the first to appear tensile damage and the extent of the damage is most severe.
5. Near the 1152 shimen area when the complex structure coal seam ground stress is about 3 Mpa, gas pressure gradient will appear mutation in the tectonic coal seam, when the ground stress is greater than 3 Mpa, gas pressure gradient will increase sharply;The 0~5 m and 28~31 m areas in the X direction are in the range of sharp increase in gas pressure gradient.

REFERENCES

He Xue-qiu, Shen Bao-hong 2009. Coal mine gas control technology and engineering practice[M]. China University of Mining Press,: 46–257.

Hu Wei-yue, LI Jing, Wang Shou-quan 2009. The flowing and outburst mechanism of gas in coal-based pore and fractured medium[J]. *Coal Geology & Exploration,* 37(4): 6–8, 14.

Jing Guo-xun, Zhang Qiang2005. Study on the role of gas in the coal and gas outburst[J]. *Journal of china coal society,* 30(2): 169–171.

Lin Bo-quan 2010. Mine gas control theory and techniques[M].Xuzhou: China University of Mining Press: 53–299.

Ma Dong-xiao 2011. Research on fold and its effects on gas distribution [D]. Henan Polytechnic University.

Sun Jing-lai 2009. Study on the Penetrability coefficient of the coal[D].China Coal Research Institute.

Wang Ji-ren, Deng Cun-bao, Deng Han-zhong 2005. Study on the microcosmic mechanism for coal-gas outburst[J]. *Journal of china coal society,* 30(2): 131–135.

Wang Lei 2010. Research of Caving Coupling Effects of Stress Field and Gas Field[D]. AnHui University of Science and Technology.

Wang Yan-sen, Ma Li-qiang, Gu Yong-gong 2004. Analysis of Effects of Strata Behaviors on Face Methane Emission Law[J].*Safety in coal mines,,* 35(11):1–4.

Xu Xue-feng 2003. The Research of Influence on Geological structure to Coal and Gas Outburst [D]. LiaoNing Technical University.

Yang Tian-hong. Study on Infiltrate Character and Coupling Analysis of Seepage and Stress in Rock Failure Process [D]. Northeastern University.

Yin Guang-zhi, Li Xiao-quan, Zhao Hong-bao, etc 2008. Experimental research on effect of gestures on outburst coal's gas seepage. Chinese Journal of Rock Mechanics and Engineering, 27(12): 2557–2561.

Yu Yan 2012. Research on Ground Stress Control Action of Gas Permeability of Coal Seam [D]. AnHui University of Science and Technology.

Zhang Fu-guo, Zhang Guo-shu 2009. Mine gas disaster prevention system[M].Xuzhou:China University of Mining Press:1–20.

Zhou Dong-ping, Shen Da-fu, Yu Mo-hua, Guo Chen-ye 2008. Experimental Study on Influence of Strata Stress upon Gas Seepage Characteristics.[J]. *Ming safety and environmental protection,* 39(8) Supplement: 6–12.

Progress in Mine Safety Science and Engineering II – He et al. (Eds)
© 2014 Taylor & Francis Group, London, ISBN 978-1-138-00122-0

Experimental research on movement law of coal-bed methane including temperature and confining pressure effects

Yu Kang, Xia Gao & Changhong Pan
Department of Safety Engineering, Heilongjiang University of Science and Technology, Harbin, Heilongjiang, China
National Central Laboratory of Hydrocarbon Gas Transportation Pipeline Safety, Harbin, Heilongjiang, China

ABSTRACT: Experimental study was conducted on the influence of pressure and temperature upon coal penetration with triaxial test, including sample size, axial force, confining pressure, pore water pressure and temperature effects. The penetration first decreases and then increases as temperature goes up, under the same confining pressure conditions. Additionally, the temperature effect on permeability is no longer significant when the confining pressure is increased to more than 15 MPa. Experimental result provided the basis for factors affecting of coal-bed methane migration in coal.

1 INTRODUCTION

Coal-bed methane (CBM), as an emerging energy, has characteristics of big storage capacity, shallow burial depth (compared with conventional natural gas), low development cost, which can be used as high quality energy and chemical material (Chunhe Yang, et al. 2000). Coal-bed methane will surely become a strategic 'alternative energy', under the increasing tense situation of our energy, after coal, oil and natural gas. CBM formation is mainly ruled by the capacity to form coal gas which is primarily related to degree of coal metamorphism, air condition including conditions of adsorption, gas pressure and temperature and preservation conditions including burial history and surrounding rock sealing ability (Fengyin Xu, et al. 2008, Fuchang Lu, et al. 2010).

In the study of coal-bed methane seepage, the gas flow linear theory has been put forward according to Darcy's law Chinese scholars. Assuming that coal gas adsorption and desorption process is completely reversible, coal-bed gas flow theory, seepage governing equations, statistical thermodynamic and quantum chemistry are established (Chuanliang Li, et al. 2003). According to the results of experimental calculation, get the research results including empirical equation of gas state etc. Most of scholars agree that coal rock gas seepage field is influenced by stress field, electromagnetic field and temperature field (Hui Zhang 2001, Weiyuan Zhou 1990). Among relevant literature reports about researching of seepage field through temperature field, just Liang Bing and Liu Jianjun, et al set up solid and gas coupling mathematical model considering temperature field, stress field and seepage field, and carried on the numerical simulation for distribution law of different temperature stress on coal and gas pressure on the basis of gas adsorption rule and solid-gas (coal and gas) coupling mechanism (Guangqin Fan 1992). With the increase of embedded depth of CBM, temperature change is bound to increase. In this paper, we carry on experiments on coal-bed methane adsorption parsing and permeability law with coal rock triaxial test apparatus including pore pressure at different surrounding rock and different temperature conditions. And finally determine the relationship between temperature, pressure and permeability of coal.

2 EXPERIMENTAL

2.1 *Experimental principle*

The coal-bed methane has three forms of existence, adsorption, and absorption and free. The transformation between absorption and free is the permeability of coal-bed methane. The factors affecting of permeability of coal-bed methane has Specimen size, Confining pressure, temperature and pore pressure, etc. In this experiment, we adopt way of fixed confining pressure and variable temperature and variable confining pressure and fixed temperature, it is qualitative and quantitative measures, for make sure substance of the factors affecting.

In order to qualitatively and quantitatively calculate coal-bed methane penetration, the following formula is used in laboratory.

$$K = \frac{2Q \cdot P_a \cdot \mu \cdot L}{(P_1^2 - P_2^2)} \times 10^2 \quad (1)$$

Where Q = Gas seepage flow; Pa = the atmospheric pressure; L = Length of the specimen; P1 = Specimen inlet gas pressure; P2 = Specimen export gas pressure; A = he cross-sectional area of specimen; μ = the gas viscosity coefficient.

2.2 *Experimental apparatus*

This experiment was carried out through a self-designed triaxial gas adsorption instrument. The device can simulate the storage environment of coal-bed methane and the changes of absorption and desorption of gas at different pressure and temperature. Its structure and function are as follows.

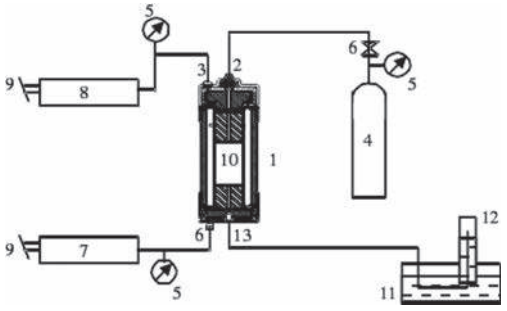


Figure 1. Test equipment schematic of coal-bed methane penetration under three-dimensional pressure. In the figure: 1-parsing permeameter; 2-gas inlet;3-oil pres-sure inlet; 4-gas tank; 5-pressure gauge; 6-control valve;7-manual hydraulic pump; 8-manual oil hydraulic pump; 9-control valve; 10-specimen (coal samples); 11-water trough; 12-measuring cylinder or rotor flow meter; 13-gas outlet; 14-temperature regulator.



Figure 2. Test equipment of coal-bed methane penetration under three-dimensional pressure.

2.3 *Experimental procedure*

The coal samples for laboratory are Ti-rich ash long-flame coal which is collected from Long Jiabao Coal Limited Company, Jilin Province. The coal seam thickness is 18.3 m and gas content is 15.3 m^3/t. According to the experimental requirements, the coal samples are processed into $5 \times 5 \times 10$ cm. In order to get more standard specimens, the specimens are further processed by rock cutting after incising machine so that the specimen error is no more than 0.1 cm. The processed specimen is fastened to a couple of steel ingots with the base area of 5 cm^2 and the center connected with hydraulic equipment that it can load pore pressure. In order to prevent affecting on penetration when water coming during loading pressure, the whole set is put into a 20 cm long laminate tube and heated evenly under the hot air blower for completely sealing. As experiment starts, load the given confining pressure of 4 MPa, 6 MPa, 8 MPa, 10 MPa and 15 MPa firstly. Then load the same axial compression. Slowly Load pore pressure from the 15 MPa CH4 jar through the pressure regulator valve. In order to get the coal-bed methane penetration at different temperature, experiments are carried at 5°C, 30°C, 35°C, 40°C, 45°C, 50°C, 55°C and 60°C respectively.

3 RESULTS AND DISCUSSION

3.1 *Results*

After each loading, just stay for some time, read and record data when the flowmeter coefficient is stable. When the rate of flow is too small to display on the flowmeter, use the cylinder collection method to measure. According to experimental results, use penetration data under the same axial compression, confining pressure and pore pressure but different temperature to draw the curves of penetration with temperatures. As shown in Figure 3 to 6.

3.2 *Discussion*

3.2.1 *Temperature effects on permeability of coal-bed methane*

Under the natural conditions, Coal-bed methane in coal is in the dynamic equilibrium of adsorption and resolution. The change of coal body temperature depends on the adsorption heat and

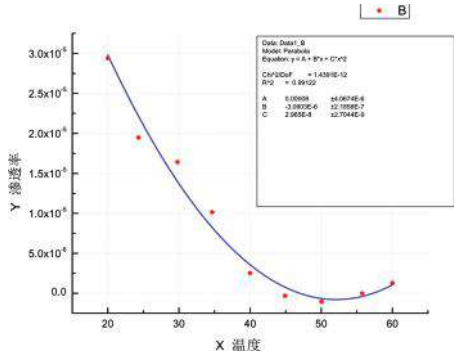


Figure 3. The relationship between penetration and temperature when confining pressure is 4 MPa.

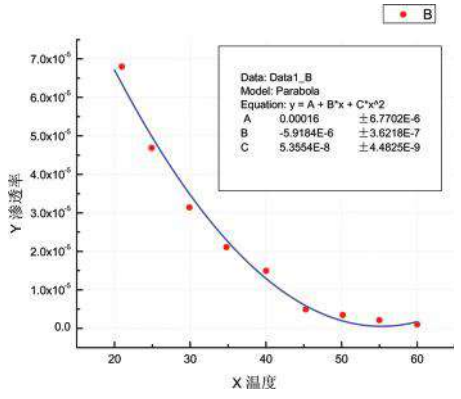


Figure 4. The relationship between penetration and temperature when confining pressure is 8 MPa.

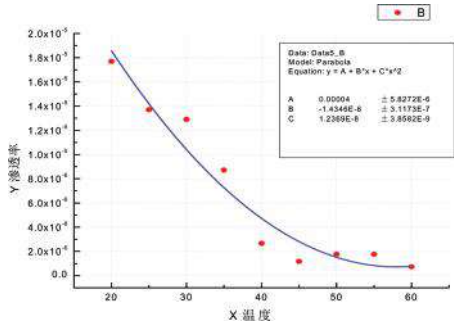


Figure 5. The relationship between penetration and temperature when confining pressure is 10 MPa.

endothermic process, and with the increase of buried depth of coal seam, the temperature of coal has a rising trend generally. In the calculation formula of coal-bed methane penetration, there is no temperature, temperature influences the CBM

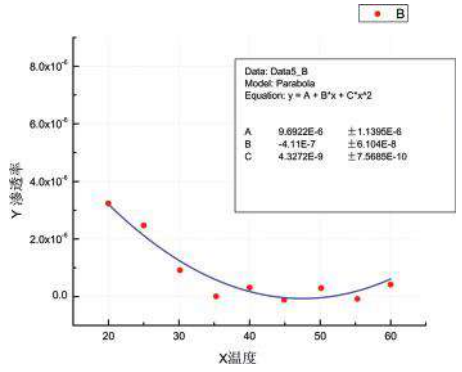


Figure 6. The relationship between penetration and temperature when confining pressure is 15 MPa.

viscosity coefficient and then influences the permeability (Mengcheng Liu, et al. 2002, Xiaoyan Li & Guangxin Xie 2003). Figure 3 to 6 show that, the increase of temperature will lead to the decrease of penetration under the same confining pressure when the temperature is low; the minimum appears between 45 to 55°C. As the temperature continues to rise, penetration appears to be rising, and the qualitative experiment can't be done temporarily due to the limited experimental conditions. Through the experimental data, use the least square method to fit the curve and get the effect of temperature on permeability meeting the quadratic relation function:

$$S(K) = 0.00016 + (-5.9184 \times 10^{-7})T + 5.3554 \times 10^{-8} T^2 \quad (2)$$

3.2.2 *The effect of confining pressure in coal-bed methane temperature—permeability experiments*

The influence of the temperature on permeability decreases gradually with the increase of confining pressure under the four groups confining pressure are 4 MPa, 8 MPa, 10 MPa, 15 MPa, and corresponding pore pressure are 1.5 MPa, 1.5 MPa, 4 MPa, 4 MPa. Especially when the confining pressure is increased to 15 MPa, the influence of temperature is quite limited, which is related to the largely closing of coal pore under the high confining pressure.

4 CONCLUSION

1. Pressure and temperature have significant influence on coal-bed methane penetration at different burring conditions.
2. The increase of temperature will reduce the coal-bed methane penetration under the same

confining pressure and pore pressure. With the increase of confining pressure, the influence of temperature on penetration will decrease. When the confining pressure increases to 15 MPa, the influence of temperature on the coal-bed methane penetration can be ignored. The experimental results can provide reference for the coal-bed methane penetration calculation formula.

ACKNOWLEDGEMENTS

We gratefully acknowledge the financial support provided by National Natural Science Foundation (grant No. 51174264, 51104062, 50904026). Thanks are also extended to all individuals associated with the project.

REFERENCES

Chuanliang Li, Xiangyan Kong & Zhimin Du, et al. 2003. A study on the rheological model of porous media. *Act Mechanic Science,* 35(2):230–234.

Chunhe Yang, Shiwei Bai & Yimin Wu 2000. Stress level and loading path effect on time dependent properties of salt rock. *Chinese Journal of Rock Mechanics And Engineering,* 19(3):270–275.

Fengyin Xu, Shuguang Li & Degui Wang 2008. Development trend of cbm exploration and development theories and technologies. *China Petroleum Exploration,* 5:1–6.

Fuchang Lu, et al. 2010. Diffusion effects on recoverability of coalbed gas. *Fault-Block Oil & Gas Field,* 7(5):17–18.

Guangqin Fan 1992. Rheological mechanics in geotechnical engineering. Beijing: *China Coal Industry Publishing House*.

Hui Zhang 2001. Genetical type of proes in coal reservoir and its research significance. J*ournal of China Coal Society*.

Mengcheng Liu, Yufeng Gao, Hanlong Liu & Kang Fei 2002. Development of study on a large scale triaxial test of coarse-grained materials. *Rock and Soil Mechanics,* 23(2):965–221.

Weiyuan Zhou 1990. High rock mechanics. *Beijing: China Water Power Press*.

Xiaoyan Li & Guangxin Xie 2003. Characteristics and effecting factors of adsorption time of coalbed gas reservoir. *Natural Gas Geoscience,* (6).

Progress in Mine Safety Science and Engineering II – He et al. (Eds)
© 2014 Taylor & Francis Group, London, ISBN 978-1-138-00122-0

Experimental simulation for "sorting" effect after gas and coal outburst in blind draft

Bai-Sheng Nie, Wei-Xi Hu, Long-Long Yang & Jin-Wei Chen
Faculty of Resourses and Safety Engineering, China University of Mining and Technology (Beijing), Beijing, China

ABSTRACT: In order to study "sorting" effect after gas and coal outburst in blind draft the experimental simulation system has been set up. Moreover the sedimentation law for a single coal particle has been analysed based on the theory of pneumodynamics under the action of gas. According to the experimental results the reason why gas-small coal fluid is sorted has been elaborated and the "sorting" flow law for gas-small coal fluid has been analysis. The experimental results show that a larger coal particle falls to the ground faster than a smaller one. In other words the smaller coal particle can be "carried" to a far location by the impact gas flow. It can also be blown up by the impact gas flow once again.

1 INTRODUCTION

Coal and gas outburst is one of the complex dynamic phenomena in coal mine. It is also one of the severe natural disasters in coal mine which threats the safety of production (Cheng 2003, Cheng et al. 2004, Kong et al. 2012, Lang et al. 1998, Yang et al. 2009, Yu 1985, Zhang et al. 2007). The two phase fluid composed by gas and coal which emerges during the coal and gas outburst can flow to the place which is thousands of meters away from the outburst hole. So this two phase fluid can not only destroy the underground production facilities but also flow reversely into the intake airway sometime.

In the process of coal and gas outburst, there is an obvious characteristic that coal is transported to a long distance by the gas outburst from the hole. In the scene of an accident people often can see that the coal and rock can be transported to a far place from the outburst hole. The coal also may be transported to a place passed by a corner. The accumulation angle of coal and rock is less than natural repose Angle. The lager accumulated particles may fall to the bottom near the outburst hole, but the smaller ones can go with the gas to a far place and be covered with the larger particles. This phenomenon is called sorting characteristics of gas-small coal fluid. Many accidents of coal and gas outburst have shown that impact dynamic effect is caused not only by the gas fluid but also by small coal particles jetted from coal and gas outburst hole. So studying sorting and settlement regularity of small coal have an important practical significance.

2 THEORETICAL ANALYSIS FOR SINGLE FINE COAL PARTICLES SEDIMENTATION PROCESS

The Figure 1 is a stress analysis for a single coal particle in vertical direction. This single coal particle belongs to the solid phase in two-phase flow of gas and small coal.

The spherical coal particle can fall freely to the ground under the action of the buoyant-weight (the difference between the gravity and the buoyancy). The falling speed of this particle increases gradually. Finally the small coal particle's velocity increases to a maximum value. At the same time the resistance is equal to the buoyant-weight, This max velocity is called as the sedimentation velocity. This can be described by the following formulas:

$$m\frac{du}{dt} = G - F_b - F_r \tag{1}$$

$$\frac{du}{dt} = \left(\frac{\rho_P - \rho}{\rho_P}\right)g - \frac{3}{4}C_D\frac{\rho}{\rho_P}\cdot\frac{1}{d_P}u^2 \tag{2}$$

Where G = Gravity; F_b = Buoyancy; F_r = Resistance; m = Mass of the small coal; ρ_P = Density of the small coal;ρ = Density of gas; C_D = Drag coefficient; A = Windward area of the small coal; u = Velocity of small coal;

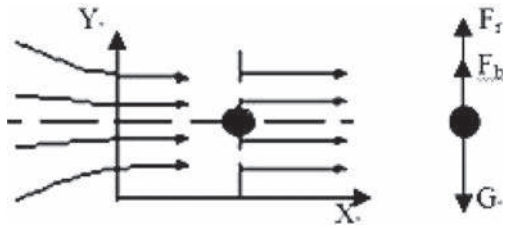


Figure 1. The stress analysis in vertical direction for the single coal particle.

For the spherical small coal:

$$m\frac{du}{dt} = \frac{m}{\rho_P}(\rho_P - \rho)g - C_D A\rho\frac{u^2}{2} \tag{3}$$

When du/dt = 0, the sedimentation velocity of the spherical small coal is:

$$u_m = \sqrt{\frac{4g(\rho_P - \rho)}{3\rho}\cdot\frac{d_P}{C_D}} \tag{4}$$

For Newtonian fluid CD = 0.44, the formula of Newton sedimentation velocity is:

$$u_m = \sqrt{\frac{3g(\rho_P - \rho)}{\rho}\cdot d_P} \tag{5}$$

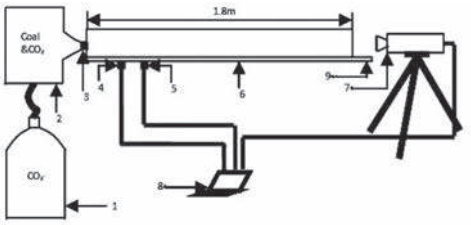
For Stokes fluid CD = 24/Re the formula of Stokes sedimentation velocity is:

$$u_m = \frac{g(\rho_P - \rho)}{18\mu}d_P^2 \tag{6}$$

The conclusion can be draw from the theoretical analysis: The velocity of the small coal is increased and the acceleration decreases until the resistance is equal to the buoyant-weight. The sedimentation velocity of the small spherical coal will be increased with its diameter.

3 EXPERIMENT SYSTEM OF "SORTING" CHARACTER FOR GAS AND SMALL COAL FLUID

The Figure 2 is the principle diagram of the experiment system which will discover the "sorting" characteristic of gas and coal outburst. This experiment system mainly includes: gas cylinder and gas adsorption chamber, outburst hole and rubber membrane, pressure sensor speed sensor and high-speed camera, small coal "sorting" acquisition boards and so on.



1. Gas cylinder 2. Gas adsorption chamber 3. Outburst hole and rubber membrane 4. Pressure sensor 5. Speed sensor 6. Model of roadway 7. High-speed camera, 8. Personal computer 9. Small coal "sorting" acquisition board

Figure 2. Gas-small coal flow separation effect experiment system schematic diagram.

Shown as the Figure 2 the principle of the experimental system is: the CO_2 is filled into the gas adsorption chamber by the gas cylinder. After a period of time the gas is adsorped equilibriumly. The excessive CO_2 is filled into the gas adsorption chamber and then the high pressure CO_2 fracture the outburst rubber membrane. This is a process which simulates the "stress-wall" of coal is fractured by high pressure gas. And then the mixture composed by gas and small coal is jetted into the model of roadway from the outburst hole. The small coal is sorted and accumulated under the action of high speed CO_2. The accumulated small coal is collected by the small coal "sorting" acquisition board. The small coal which is on the acquisition board is sifted and weight segment by segment. The length of every segment is 0.2 m. The length of the model roadway is 1.8 m. The shape is square and the side length is 15 cm. At the same time the high-speed camera is used to shoot the process which records the small coal's motion at the rate of 1000 frames/s.

4 EXPERIMENTAL PROCESS

4.1 *Experimental determination of pulverized coal particle size distribution*

The Table 1 is the coal sample screening data in YuTianPu coal mine near the outburst holes.

The medium particle diameter is deemed as the diameter of those particles and the distribution of the particle diameter is draw as Figure 3. Judged from the curve shown as Figure 3 the diameter of the small coal approximately obey normal distribution. So according to above assumption of normal distribution for small coal diameter, the coal sample is crushed by ball grinder.

And then the mesh number of 6–10, 10–20, 20–40, 40–60, 60–80, 80–100, 100–120 is used to sift the small coal. The different particle diameter of small coal is

Table 1. The coal sample screening data near the outburst holes in YuTianPu coal mine +90 level 4# coal seam.

In the hole		Out of the hole	
Particle size/mm	M%*	Particle size/mm	M%*
0.1	4.6	0.1	3.6
0.1–1.0	39.1	0.1–1.0	38.0
1.0–5.0	23.5	1.0–5.0	31.0
5.0–10.0	16.0	5.0–10.0	17.6
>10.0	16.8	>10.0	9.8

* Mass Percentage.

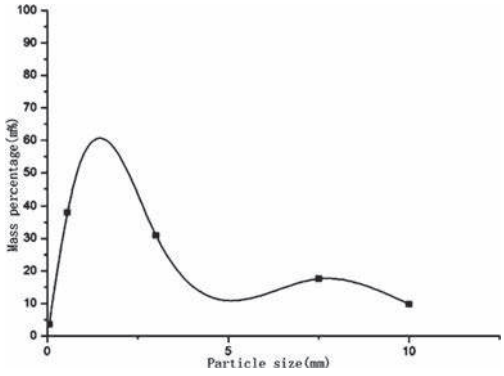


Figure 3. The diameter distribution law of the small coal near the outburst holes in YuTianPu coal mine + 90 level 4 # coal seam.

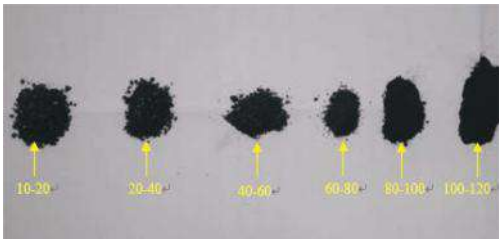


Figure 4. The physical figure of small coal sample.

produced at a certain quality. And then according to the law of normal distribution small coal are prepared. Figure 4 shows the physical Figure of small coal sample which has been sifted in different diameter. The distribution regularity obeys the standard normal distribution, shown as the Figure 5.

4.2 *Pulverized coal flow in the gas analysis "sorting" effect the result of the experiment*

Figure 6 records the distribution of small coal deposited on the model of roadway and the spacing distance between each small picture is 0.1 m.

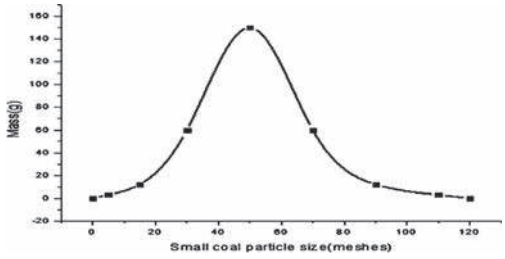


Figure 5. Mixed fine coal particle size—the quality of normal distribution curve.

People can see clearly from the Figure 6: The accumulation of small coal is less at the position of outburst hole where the distance is 0 m or directly below the outburst hole. The main reason is that the small coal stream is accelerated to a high speed by the impact gas. Therefore the inertia effect of the small coal does not make itself sink immediately but migrate forwardly. At the position where the distance is 0.1–0.2 m from outburst hole a lot of small coal accumulates because of the gradually reduced gas desorption quantity and weaken speed of gas. That is to say the gas can not accelerate the small coal to the velocity which make itself move forwardly. So the accumulation of small coal occurs at this position. The place from 0.3 m to 1.0 m can be regarded as uniform distribution area because the phenomenon of accumulation does not appear. The main reason may be due to the high pressure gas which is jetted instantaneously and the gas carries those fine particles to this position. Because of its dead weight those settle to the floor of roadway. In the place from 1.1 m to 1.7 m people also can see that the quality of small coal decreases with the increasing distance from outburst hole. On the other hand the small coal which sinks eventually is usually the smallest ones. To be sure that the green part of the collection board on the model of roadway below model (Shown as distance 1.0–1.3 m) is the color of the piece of paper.

Figure 7a shows the small coal's distribution along the model of roadway of different diameter when the gas velocity is 15 m/s. With the increasing of distance from the outburst hole, all kinds of small coal particles' mass reduce. The bigger of the small coal particle is easier to sink to the ground. Among them the medium diameter fine coal particles can be carried to a long distance such as to the end of the model of roadway. Figure 7b shows the small coal particles with different diameter sink with a different the sinking quality rate along the model roadway: the bigger particle may sink to the ground of model roadway more quickly than the smaller ones. In other words the smaller one can be carried to a long distance. In

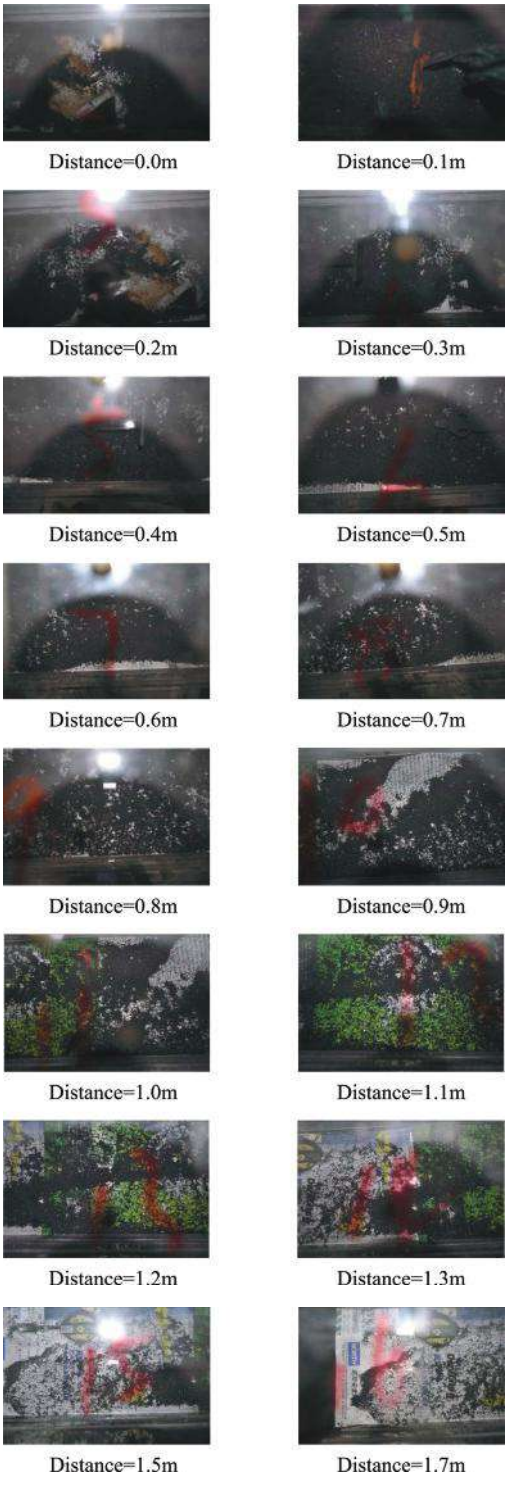


Figure 6. Distribution of small coal along the model of roadway.

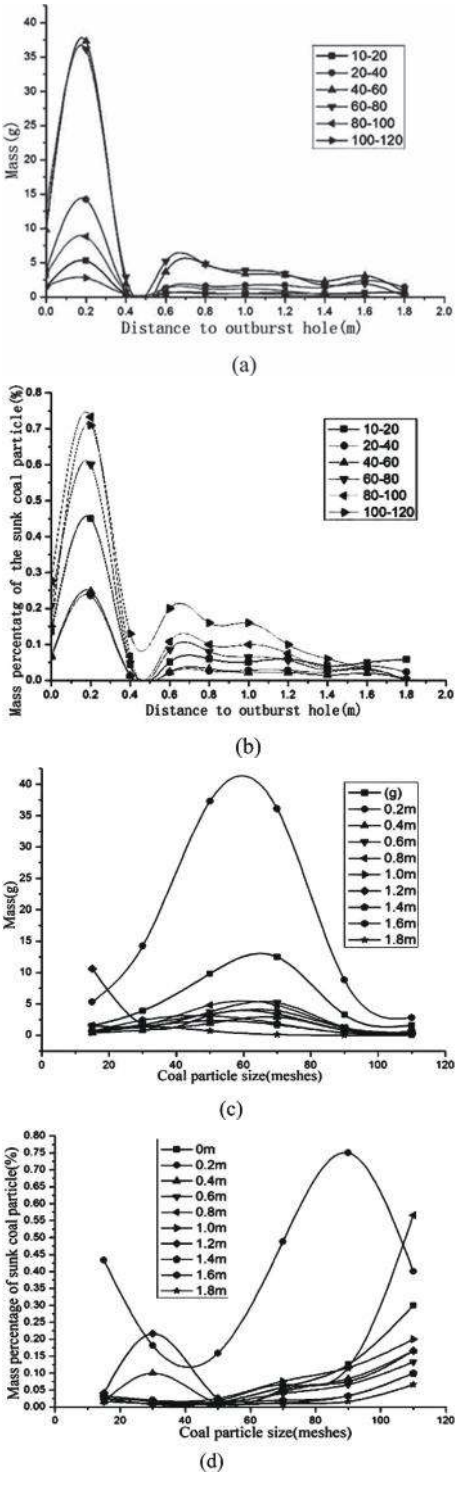


Figure 7. Small coal's "sorting" character after outburst (the velocity of the impact gas is 15 m/s).

practice this phenomenon will increase the risk of dust explosion. This can be proved by the data shown as Figure 7. In the place where the distance to outburst hole is 1.0 m, the small coal particle is arranged with the sinking quality rate: 120–100 mesh >100–80 meshs >80–60 meshs >60–40 meshs >40–20 meshs >20–10 meshs. Figure7c, d shows the proportion of different small coal particle which sink to the ground at the place near the coal and gas outburst hole. It's known from Figure 7c, d that the sunk small coal particles of 40–60 meshs and 60–80 meshs is the most in quality at the place which is 1.2 m far from coal and gas outburst hole. So a conclusion can be draw that the centre diameter fine coal particles which has sunk is more than other ones. But in general the sunk small coal particles' distribution obeys the normal distribution.

5 EXAMPLE ANALYSIS

Those are two pictures which describe characteristics of accumulation for small coal after coal and gas outburst in inclined shaft in ShiBanGou coal mine.

The accumulation of outburst coal in the roadway has an obvious character of "sorting". This character is mainly shown in the following aspects: In the same pile of small coal the diameter is bigger at the bottom than on the surface. The proportion of big particles is more than the smaller ones along the model roadway. But the extrusive coal has not an obvious "sorting" character. On May 4, 2006 the accident of coal and gas outburst happen in ShiBanGou coal mine XianHuanXian Shanxi Province When the coal was uncovered at the place of main inclined shaft. Figure 8 shows the sampled coal in the roadway after this accident. Shown as Figure 8 the coal sample has been gotten in the location where is 14 m far from the outburst hole at the bottom of roadway floor. Figure 8a is the coal sample on the surface of that pile of small coal. Figure 8b is the coal sample at the bottom (1.4 m from the surface). People can see clearly from the picture the "sorting" characteristics of accumulated coal.

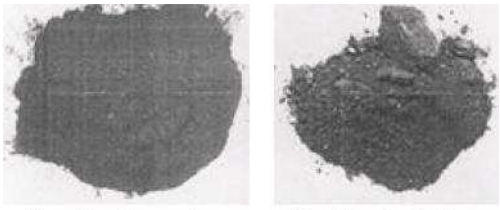


Figure 8. The coal sampling characteristics of roadway accumulation after coal outburst in inclined shaft in ShiBanGou coal mine (Kong et al. 2012).

6 CONCLUSIONS

The small particles of small coal's "sorting" effect is not obvious under the action of impact gas, it can be carried to a far distance.

Seen from the theoretical analysis and the real accident, the mixture composed by gas and small coal has an obvious effect of "sorting" after coal and gas outburst. The closer to the outburst hole, the larger particle of small coal deposited on the floor of roadway priority. Generally speaking, For any pile of small coal in the roadway after coal and gas outburst, there is a lot of tiny coal on the surface. But at the bottom of this pile of small coal there is usually many big blocks of coal. At the place which is closer to the outburst hole the diameter of particle is larger relatively. On the contrary, the diameter of particle is smaller. All those phenomenon show that the bigger coal sink faster than the smaller coal.

It's shown by this experiment that the distribution of small coal is uneven. Most of the small coal accumulates near the outburst hole, while in other place far from outburst hole the distribution of fine coal appears even. So this phenomenon proves the uneven distribution of fine coal.

REFERENCES

Cheng, W.Y. 2000. Coal and gas outstanding impact wave spread formed and the foundation of model. *Safety in Coal Mines* 31(9):23–25.

Cheng, W.Y. et al. 2004. Shock wave front propagating regulation of coal and gas outburst. *Journal of China CoalSociety* 29(1):57–60.

Kong, D.L. et al. 2012. Motion state of coal-gas flow in the process of outburst. *Journal of China Coal Society* 37(3):452–458.

Lang, D. et al. 1998. The mechanism and test research of gas adverse current in roadway air flow. *Journal of China Coal Society* 23(5):476–479.

Yang, S.Z. et al. 2009. Injury study on impact current of gas explosion in coal mine. *Journal of China Coal Society* 34(10):1354–1358.

Yu, B.F. 1985. *Coal and gas outburst mechanism*. Beijing: Coal Industry Press.

Zhang, Q. et al. 2007. The shock wave propagating regulation of coal and gas outburst. *Mining Safety and Environmental Protection,* 34(5):21–23.

This page intentionally left blank

Progress in Mine Safety Science and Engineering II – He et al. (Eds)
© 2014 Taylor & Francis Group, London, ISBN 978-1-138-00122-0

Study on the law of mining-induced fractures field evolution based on similar simulation experiment

Youzeng Wu, Bing Wu, Mingguo Hua & Zhiguo Guo
School of Resources and Safety Engineering, China University of Mining and Technology, Beijing, China

ABSTRACT: Aiming at the problem of insufficient study on the law of roof strata movement destruction space-time evolution under the current conditions of fully mechanized top coal caving, utilizing the method of similarity simulation experiment to aim at doing study on overlying strata movement under the conditions of fully mechanized top coal caving, destruction mechanism, and the distribution law and morphological characteristics in mining-induced fractures, the results show that: with the working surface advancing, the fractures zone gradually upgrade evolving and developing, and this kind of fractures evolution is more rapidly when the key strata cave and fracture, when the working surface mine to 240 m, the bed separation fractures tend to be closed, Mining influence reaches the top of the model, the fractures zone height no longer change with the change of the working face advance distance.

1 INTRODUCTION

As the increasing improvement of the coal mine fully mechanized working surface support and the levels of mining equipment level, ignoring the influences on the development characteristics that roof strata movement, destruction and methane emission and distribution in time and space under the high strength mining conditions of fully mechanized sublevel caving, large mining height and so on (Saghafi A et al 1987, Senseny P E et al 1983). The actual site and research analysis showed that: the high strength mining way such as fully mechanized sublevel caving, large mining height and so on make the mining influence scope and space expand (Somerton W H 1975, Harpalani S & Mopherson M J 1984), caving and destruction mechanism of coal strata, the space-time evolution process of mining-induced overlying strata fractures field play an important part in coal and rock mass relieved methane flow, the law of methane emission, the development evolution that mining-induced overlying strata fractures field in time and space and relieved methane migration relevance and interaction relationship of the two is the theoretical basis for methane control and drainage, and also is the key to control the methane accident. So it has important significance for study on the law of overlying strata fractures field evolution under the conditions of fully mechanized top coal caving.

2 THE ENGINEERING CONDITIONS OF SIMILAR SIMULATION EXPERIMENT PROTOTYPE

Experiments with a coal mine in Shan Xi Lu'an Group on the N3-8 fully mechanized caving working surface as the basic prototype, the 3# coal seam that this working surface mine is stable coal seam in what all mine field mine availably, the buried depth is 342.7~398 m (360 m), the coal seam thickness is 3.53~5.95 m, the average is 5 m. the average of this coal seam is 133.20 m, the length of working surface strike is 758 m, the long of tendency is 150 m, the coal seam dip angle is 5°~16°, the average is 8°. The working surface adopt the mining method that fully mechanized cave overall height of mining at a time, the mining height is 3.0 m, the advance of working cycle is 0.8 m. The structure of coal seam is simple—relatively simple, containing the dirt band of 0–2 layers, N3-8 working surface overburden physical and mechanical properties are shown in Table 2.

3 THE DETERMINATION OF SIMILAR SIMULATION EXPERIMENT PARAMETERS AND THE PRODUCTION OF THE MODEL

According to the every similarity ratio convert to the volume-weight of the Simulation material, com-

Table 1. N3-8 Face model similar parameters.

Model Size/(m)	Time	Geometry	Unit weight	Poisson's ration	Strength	Stress
$1.8 \times 1.3 \times 0.16$	11	100	1.6	1.1	160	160

Table 2. N3–8 working surface overburden physical and mechanical properties.

Stratum name	Unit weight/ (KN·m³)	Modulus of elasticity/(MPa)	Compression strength/(MPa)	Poisson's ration	Cohesion/ (MPa)	Dilatancy angle/(°)	Internal friction angle/(°)
Al mudstone	19.97	19908	19.9	0.201	0.89	7	29
Sandy mudstone	25.89	58686	50.1	0.301	1.26	7	28
Sandrock	25.59	51529	59.8	0.31	2.31	9	29
Charcoal mudstone	14.98	34606	13.9	0.31	0.69	9	23
Fine sandstone	25.19	45151	70	0.32	2.01	9	29
Siltstone	25.88	55686	60.2	0.301	1.2	11	36
Limestone	27.1	45525	89.3	0.19	3.2	11	40
Coal	14.59	14141	13.4	0.276	0.71	8	22
Mudstone	12.99	40499	15	0.26	0.82	7	23

Table 3. Similar model coal and rock physical and mechanical properties.

Lithology	Al mudstone	Sandy mudstone	Sandrock	Charcoal mudstone	Fine sandstone	Siltstone	Limestone	Coal	Mudstone
Unit weight/KN·m³	13.0	16.49	16.62	9.38	16.37	16.32	16.56	9.12	8.12
Elasticity modulus/ MPa	125.11	353.53	315.18	220.21	268.87	342.13	291.49	88.38	253.12
Compressive strength/MPa	0.13	0.30	0.41	0.09	0.44	0.37	0.57	0.08	0.09
Poisson's ration	0.18	0.25	0.25	0.23	0.25	0.23	0.2	0.25	0.24



Figure 1. The similar model along the strike direction panorama.

pressive strength, poisson's ratio and other parameters etc (show Table 1, 3). Selecting material carry out matching, figuring out the quantity of materials each layer, being underway the production of the model, each charge about 1 cm thick, and proper rolling, sprinkling a layer of mica powder in the interlayer as the bedding plane (Harpalain S 1985). Experiments is in progress of the similar simulation lab in China University of Mining & Technology (Beijing). The panorama photos of model that have been maked as shown in Figure 1 the profile of the strike direction) and 2 (the profile of the tendency direction). Similar model totally arrange 210 measuring points, useing to test the changes of the overlying strata displacement and stress in the process of the coal seam mining.

4 THE EXPERIMENTAL RESULTS ANALYSIS

4.1 *The fractures evolution features of roof caving in the progress of mining (along the strike direction)*

When the working surface mine to 33 m, the roof pressure is coming firstly, the medium-grain sandstone (the old roof) fracture and cave, below K2 limestone appear larger bed separation fractures, the height is 9.5 m, the length of rock beam is 19.2 m, as shown in Figure 3. When the working surface mine to 37 m, below K2 limestone appear more obvious bed separation fractures, above K2 limestone appear the bed separation fractures, and there are momentum of developing upward; when continuing to advance to 43 m, the roof firstly appear periodic pressure, the roof pressure step



Figure 2. The similar model along the tendence direction panorama.

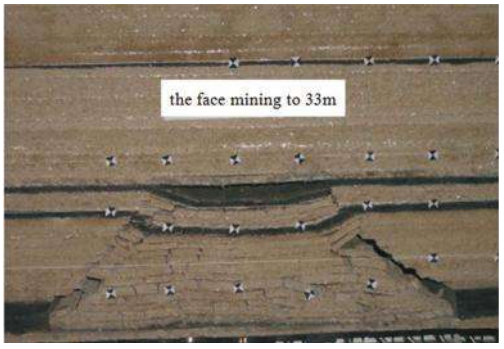


Figure 3. The distribution of fractured roof advance to 33 m.

from 10 m, the caving height is 6.5 m, the development height of the bed separation fractures is 14.7 m, as shown in Figure 4, regarding caving zone and the development boundary of fracture zone as straight line approximatively, we can see simulated experiment images approximatively as trapezoidal shape, the interior of yellow trapezoidal is caving part, blue trapezoidal straight line is the development boundary of the fracture; 2th periodic roof pressure occur when advancing to 55 m (the roof pressure step from 12 m), roof cave in large area, not caving rock beam length up to 29.2 m, the development height of the bed separation fractures is 16.7 m.

Figure 6 is the state that roof strata cave and fractures grow when the roof pressure is coming periodically eleventh times, at the same time, the working surface is 156 m away from cut, the maximum height of fractures is 38 m away from coal seam roof, those the strata cave and the distribution form of fractures are basically same with 10th periodic roof pressure (show Figure 5). The above phenomenon illustrate that with the working surface continuing to advance forward, torsion effects expand continuously, but the development location of the bed separation fractures don't continue to rise, and when some key strata fracture and cave, which is obvious significantly. As

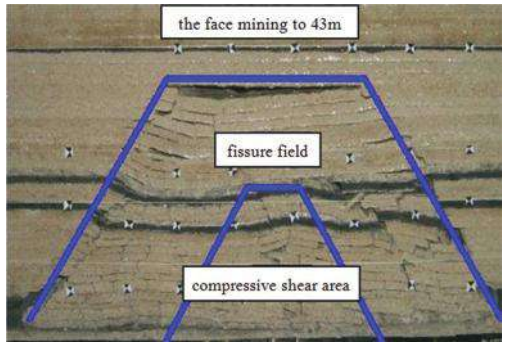


Figure 4. The distribution of fractured roof advance to 43 m.

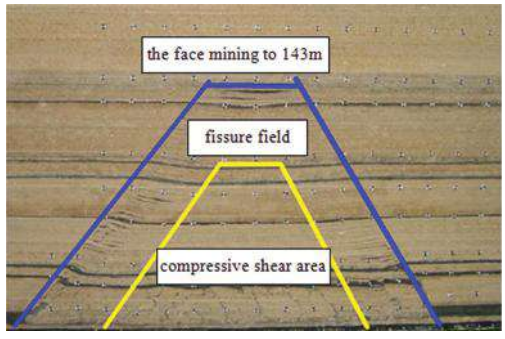


Figure 5. The distribution of fractured roof advance to 143 m.

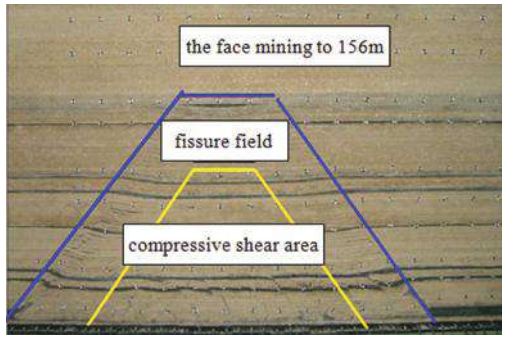


Figure 6. The distribution of fractured roof advance to 156 m.

shown in Figure 7, When the working surface mine to 172 m away from cut, the bed separation fractures develop to 35th floor fine sandstone, height is 43 m, and presents the closed trend. There and when advancing to 240 m, the roof pressure is coming periodically seventh time, Figure 8 show that the bed separation fractures in the middle of

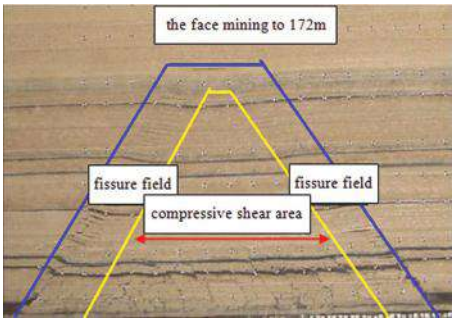


Figure 7. The distribution of fractured roof advance to 172 m.

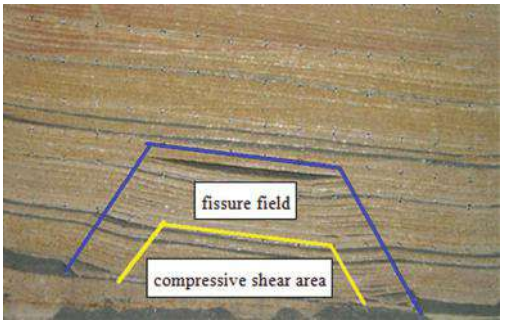


Figure 9. The fissure distribution maps of mining that did not reach the top of the model.

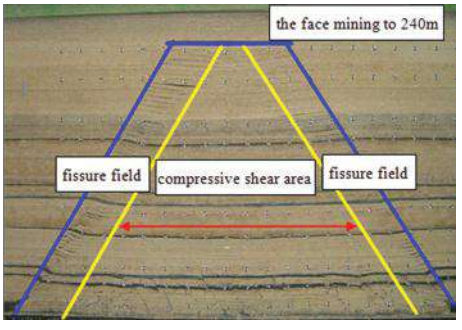


Figure 8. The distribution of fractured roof advance to 240 m.

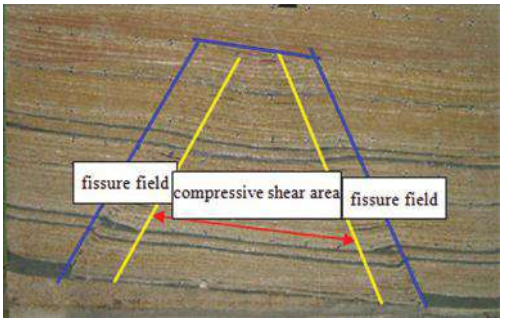


Figure 10. The fissure distribution maps of mining that reached the top of the model.

overlying strata tend to be closed roughly after that continuing to mine and mining-induced fractures don't develop upward, and maintaining a relatively stable value (52 m away from roof of coal seam).

4.2 *The fractures evolution features of roof caving in the progress of mining (along the tendency direction)*

When mining to 33 m, the roof pressure is coming firstly, the old roof cave, with the roof pressure is coming periodically appearing normally, the working surface get into the normal mining stage, as shown in Figure 9, the overlying strata go through the process of moving, bending, damaging, breaking and caving, and in the process the strata that have lower strength and thinner thickness firstly bend or even break due to be affected by mining stress, because of the different of the physical properties, each rock stratum such as strength and hardness etc caused the bed separation phenomenon between layer and layer (Gawuga J 1979, Khodot V 1980), and emerging a lot of crisscross fissures, with the working surface continuing to advance forward, generating the new fissures and carrying out overlying, which makes the original fractures network more complicated and disorderly. The time that the strata that have lower strength and thinner thickness keep stable morphology in the process of the whole overlying strata fractures evolution is shorter„ and which has a little effect on the speed of fractures evolution, in contrast, those the strata that have higher strength and larger thickness, playing a decisive control role in the destruction of the whole overlying strata movement including the formation of the fractures and speed of development. As mining influence reaches the top of the model, the central of goaf are compacted, the bed separation tend to be closed basically, as shown in Figure 10, as can be seen from the figure, in the whole process, not only producing the bed separation fractures of the bedding, but also because of the action of tensile stress produces a large number of vertical fractures or breaks or fractures or breaks of obliquing to the bedding surface.

5 CONCLUSION

This paper aim at doing study on the law of overlying strata fractures field evolution through the

similar model experiment, and summing up the internal movement law of the rock mass. The results show that: (1) The fractures zone height is not have been rising, but only when the breakage of the key strata will have great changes, and before it is relatively stable in a certain period; (2) The time that the strata that have lower strength and thinner thickness keep stable morphology in the process of the whole overlying strata fractures evolution is shorter, and which has a little effect on the speed of fractures evolution, but the strata that have higher strength and larger thickness, playing a decisive control role in the destruction of the whole overlying strata movement including the formation of the fractures and speed of development; (3) When the working surface mine to a certain distance, the bed separation fractures in the middle of overlying strata tend to be closed roughly, after that continuing to mine and mining-induced fractures don't develop upward, and maintaining a relatively stable value.

REFERENCES

Gawuga J. *Flow of Gas Through Stressed Carboniferous Strata* [Ph.D. Thesis]. London: University of Nortingham, 1979 (In UK).

Harpalain S. 1985. *Gas Flow Through Stressed Coal* [Ph.D. Thesis]. California: University of Berkeley (In USA).

Harpalani S, Mopherson M J. 1984. The effect of gas evocation on coal permeability test specimens. *Inernational Journal of Rock Mechanics and Mining Science & Geomechanics Abstracts,* 21(3):361–364 (In Chinese).

Khodot V. 1980. Role of mechane in the stress state of a coal seam. *Soviet Mining Science,* 17(5):460–466 (In Soviet).

Saghafi A, Jeger C, Tauziede C, et al. 1987. A new computer simulation of in seam gas flow and its application to gas emission prediction and gas drainage //Dai G Q, *Proceedings of the 22nd Internation Conference of Safety in Mines Research Institutes.* Beijing: China Coal Industry Publishing House (In Chinese).

Senseny P E, et al. 1983. Influence of deformation history on permeability and specific srorage of masaverde sandstone //Proceeding of 24th U.S. *Symposium on Rock Mechanics.* (In USA).

Somerton W H. 1975. Effect of stress on permeability of coal. *International Journal Rock Mechanics and Mining Sciences & Geomechanics Abstracts,* 12(2):151–158 (In Chinese).

This page intentionally left blank

Progress in Mine Safety Science and Engineering II – He et al. (Eds)
© 2014 Taylor & Francis Group, London, ISBN 978-1-138-00122-0

Study on abrasivity characteristics of surrounding rock in long inclined-shaft of coal mine by TBM techniques

Hua Jiang
China University of Mining and Technology (Beijing), Beijing, China
Beijing Urban Construction Group Co., Ltd., Beijing, China

Yusheng Jiang
China University of Mining and Technology (Beijing), Beijing, China

Jinxun Zhang
Beijing Urban Construction Group Co., Ltd., Beijing, China

ABSTRACT: The abrasivity of surrounding rocks is one of the most important characteristics for the estimation of tool wearing. Itis often described through Cerchar Abrasivity Index (CAI). Based on long inclined-shaft of coalmine excavation by (Tunnel Boring Machine) TBM techniques, CAI and mineral composition are determined by Cerchar abrasivity test and X-Ray diffraction test, abrasivity classification and the relationship between mineral composition and CAI are analyzed. The results turned out that rock samples sampling from construction area mainly consist of quartz, potassium feldspar, anorthose, calcite, pyrite and clay mineral. There is a close linear correlation between CAI and equivalent quartz content. In long inclined-shaft, surrounding rock is slightly and medium abrasive, selection of tools based on CAI and mineral composition is feasible. Therefore it is helpful to combined tests results with practical situation to study the tools selection and reasonable distance of tools changing.

1 INTRODUCTION

With the fast development of social economy and infrastructureconstruction, current coal production techniques are difficult to keep up with the pace of the coal demanding. It is very important and necessary to find and explore more advanced and efficient techniques and methods to improve mining efficiency. Based on characteristics of continue boring, high advancing speed, less environmental pollution and high safety, etc., in order to improve coal mining and transporting capacity significantly, and build a new mining area with annual production capacity of one hundred million tons in Ordos, Inner Mongolia, Shenhua Group Corporation Limited plans to construction long inclined-shaft in coalmine by Tunnel Boring Machine (TBM). TBM has been widely used for rock excavation in tunnelling and underground mining, while it is the first time TBMs are used in long inclined-shaft under the conditions of shaft length over 6 km with dip angle of 6°. The abrasivity of rock is a factor with consideration influence on the wear of tools when TBM tunnelling in rock strata, especially in long inclined shaft which easy to cause uneven wear. Hereby, the wear is a question of material consumption and is an important indicator of rock excavation in tunnelling. On the one hand, the wear depends on the machinery being used for excavation; that are the tools which have contact to the rock or excavation material. On the other hand the rock and the geological conditions can be specified by geotechnical parameters (YARALet al. 2008, KAHRAMANS. 2002, Zhiyong et al. 2012, Michalakopoulos et al. 2005).

The abrasivity of rock can already be described by mineral composition, in particular the contribution of hard minerals like quartz (AL-AMEEN & WALLER 1994, West 1986). Nowadays, more and more technical testing ways are used to determine the abrasivity of rocks. Cerchar abrasivity test is one of the most common used and effectively testing method for studying the rock abrasivity characteristics, and it also can determine the abrasivity classification of tools (Cerchar 1986, Frenzel 1989, Rostami 2005). In the following paper, the Cerchar abrasivity test and the X-Ray diffraction test are used for explaining the abrasivity characteristics of surrounding rock in long inclined-shaft, some technical issues are commented and relationship between CAI and equivalent quartz content is presented.

2 CERCHAR ABRASIVITY TEST

2.1 *Testing principals and technical parameters*

The Cerchar Abrasivity Test has been introduced in 70 s by the Centre d'Etudes et Recherches des Charbonages (CERCHAR) de France for abrasivity testing in coal bearing rocks. The test layout is described in Cerchar and in French standard NF P94-430-1 in general (Cerchar 1986, Frenzel 1989). Test equipment is very important for Cerchar abrasivity test, it's the main influences factors to test results. At first the used testing equipment has to be stiff enough that the steel pin is accurately guided over the rock surface. Secondly and maybe the core point is the steel type and quality. Not only an adequate steel grade has to be used but also required hardness of pin has to be ensured. A worldwide survey at rock laboratory shows that steel pins of Rockwell hardness HRC54-56 and the French standard NF P94-430-1 are used as well as steel pins of a much lower hardness (West 1989). With fast development of underground engineering in China, more and more engineering need to study the abrasivity characteristics of rocks. For that reasons, rock abrasion servo system (Figure 1) of ATA-IGGI is established by Key Laboratory of Engineering Geomechanics, Institute of Geology and Geophysics, Chinese Academy of Sciences, and Cerchar abrasivity test can be carried out base on this system. Detail technical parameters are described in Table 1.

The testing principal is based on a steel pin with defined geometry and hardness that scratches the surface of a rough rock sample over a distance of 10 mm under moving speed of 10 mm/min. The Cerchar Abrasivity Index (CAI) is then calculated from the measured diameter of the resulting wear flat on the pin:

$$\mathrm{CAI} = 10 \cdot \frac{d}{c}$$

Where d is diameter of wear flat (mm); c is unit correction factor (c = 1 mm)

2.2 *Sample preparation*

In addition to the influence of the instrument, sample preparation is also very important to test results. In abrasion servo system, standard sample is the cube with edge length of 30 mm, laboratories carry out the test on plain, saw cut rock surfaces. However, according to the restrictions on the dimensions of samples come from construction site, not all samples can be made into standard sample. In order to get more accuracy results, samples should meet the following requirements after processing in actual tests:

- The surface of sample should be a straight plane and keeping in vertical with blessing face.
- In one direction, the length of test surface should greater than 3 cm. Avoiding the influence



Figure 1. Abrasion servo system of Key Laboratory of Engineering Geomechanics, Institute of Geology and Geophysics, Chinese Academy of Sciences.

Table 1. Maintechnical parameters of rock abrasion servo system (ATA-IGGI).

Technical parameters	Rock abrasion servo system
Effective measurement range of horizontal force	0.4~200 N
Measurement accuracy of horizontal force	±1%
Vertical load of steel pins	70 N
Dimension of steel pins	Diameter:10 mm; Length:100 mm; Taper angle: 90°
Material of steel pins	40CrNiMo; HRC40–45
Displacement accuracy	±1%
Resolution of displacement	1/100000
Magnification of microscope	×60, ×180, ×540
Measurementaccuracy of microscope	0.001 mm

of water in swelling clay mineral, diamond stone sawing machine and abrader machine are used for cutting and smoothing the test face one after another.

Sample preparation consists of two phases: At first filed sampling will be carried out in long inclined-shaft construction area, as shown in Figure 2. And then, samples will be shipped to indoor laboratory for further processing based on the above detailed requirements.

2.3 *Testing process and results*

The detail process of Cerchar abrasivity test is mainly composed of four parts as follows:

- Checking. Prior to the experiment, electron microscope (magnification about 180x) is used to check whether steel pin is in good condition, and whether cone angle is 90°.
- Testing. In order to measure the wear flat diameter of the truncated cone, steel pins are fixed in test apparatus scratching against a freshly broken or saw cut rock surface for a prescribed 10 mm distance in the test velocity of approximately 10 mm/min. This test method is intended for freshly broken rock surfaces; however, saw cut surfaces are covered for when a satisfactory rock surface cannot be obtained.
- Measuring. After testing, steel pins will be put on the stage of electron microscopefor measuring. In particular, the measurement of the wear flat diameter of the truncated cone has to be taken using microscopeas an average of three single readings perpendicular to each other using the cross section of the pin every 90°.
- Dataprocessing. In order to obtain CAI, measured values are converted to abrasion values of steel pins, and according to the empirical parameters, rationality of measurement is ensured. In data processing, taking the arithmetic average of three measurement values in different angle as a single reading, an average of three single readings should be taken and CAI of sample can be got at the average of three single readings. Detailed testing results of Cerchar abrasivity test are described in Table 2 as follows.



Figure 2. Samples come from construction area.

3 X-RAY DIFFRACTION TEST

In order to test the mineral composition of surrounding rock, and make an analysis of the influence of rock abrasivity induced mineral composition, X-Ray diffraction test is carried out in Research Institute of Petroleum Exploration and Development, detailed test results as shown in Table 3.

Table 2. Testing results of Cerchar abrasivity test.

Group	Test number	Measurement values in different angle (um)	(um)	(um)	Average values (um)	CAI 0.1 mm
1	1-A	113.905	125.327	119.582	119.605	1.03
	1-B	89.922	89.204	82.271	87.132	
	1-C	100.352	104.589	102.117	102.353	
2	2-A	83.814	90.810	81.727	85.450	0.88
	2-B	87.002	90.355	88.844	88.734	
	2-C	86.489	89.573	89.002	88.355	
3	3-A	117.078	119.582	107.172	114.611	1.45
	3-B	177.335	149.764	170.803	165.967	
	3-C	143.885	162.106	155.342	153.778	
4	4-A	62.299	67.133	69.865	66.432	0.56
	4-B	48.851	49.965	50.375	49.730	
	4-C	52.990	50.185	55.123	52.766	

Table 3. Minerals composition of rock samples.

Group	Percent and sort of minerals in rock samples						Equivalent quartz content
	Quartz	Potassium feldspar	Anorthose	Calcite	Pyrite	Clay	
1	40.9%	9.8%	27.4%	–	–	21.9%	52.5%
2	33.0%	11.0%	30.2%	7.9%	3.5%	14.4%	47.2%
3	50.3%	10.1%	22.4%	11.8%	–	5.4%	60.8%
4	31.6%	15.6%	11.1%	20.1%	–	21.6%	43.7%

Table 4. Classification of Cerchar abrasivity index.

CAI	Abrasivity classification	Examples
0.0–0.3	Not abrasive	Organic material
0.3–0.5	Not very abrasive	Mudstone, marl
0.5–1.0	Slightly abrasive	Slate, limestone
1.0–2.0	(Medium) abrasive	Schist, sandstone
2.0–4.0	Very abrasive	Basalt, quartzitic, sandstone
4.0–6.0	Extremely abrasive	Amphibolite, quartzite

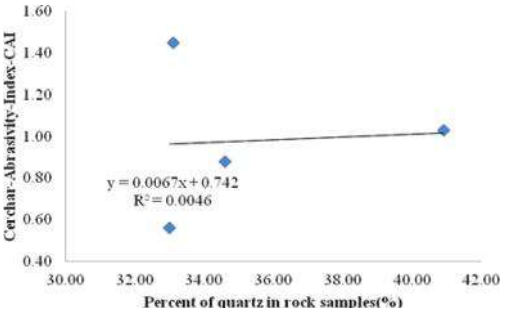


Figure 3. Interrelationship between CAI and percent of quartz in rock samples.

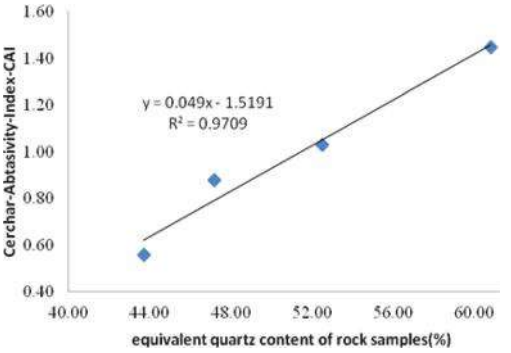


Figure 4. Interrelationship between CAI and equivalent quartz content of rock samples.

4 ABRASIVITY CHARACTERISTICS

For common rock samples, the Cerchar Abrasivity Index varies between 0 and 6, CAI at different scopes has different abrasivity characteristics, as shown in Table 4, abrasivity classification described in detail. Results of the Cerchar abrasivity test indicated that CAI of rock samples in third group is largest, CAI is approximately equal to 1.45, abrasivity classification is medium abrasive. CAI of Rock samples in forth group is smallest, CAI is equal to 0.56, abrasivity classification is slightly abrasive.

According to the X-Ray diffraction test, percent and sort of minerals in surrounding rock are assured. It turned out that rock samples mainly consist of quartz, potassium feldspar, anorthose, calcite, pyrite and clay mineral. At the same time, although quartz is the most important abrasive mineral in rock, the linear correlation between CAI and percent of quartz in rock samples is small, as shown in Figure 3. However, as shown in Figure 4, there is a close linear correlation between the CAI and the equivalent quartz content for the tested rock samples.

5 CONCLUSIONS

The Cerchar abrasivity test is in worldwide use for abrasivity assessment of rocks and wear prediction. The results are directly linked with the prediction model of Colorada School of Mines for TBM cutter wear. Based on rock samples taking from long inclined-shaft, Cerhar abrasivity test and X-Ray diffraction test are carried out, and a series of conclusions is drawn as follows:

– The choice of a suitable testing procedure to determine the abrasivity characteristics of surrounding rock is very important, Cercha abrasivity test and X-Ray diffraction test are considered as two effective tests for studying the abrasivity of rock samples and providing references for cutting tools selection.
– Maximun CAI of tested rock samples is about 1.45, it is shown that rock samples taking from long inclined-shaft area is medium or slightly

abrasive, tool wearing will not very serious during TBM tunnelling.
– There is close linear correlation between the CAI and the equivalent quartz content for the tested rock samples. The linear fitting equation is: CAI = 0.049 Qeq−1.5191 (correlation = 0.9709).

ACKNOWLEDGEMENTS

This work is supported financially by Natural Science Foundation of China. The authors are thankful to Technical Advisory Group of TBM in China University of Mining & Technology, Beijing. Special thanks go to professor LI Xiao and associate proffessor LI Shouding for their cooperation.

REFERENCES

Al-Ameen S.L. & Wallerm. D. 1994. The influence of rock strength and abrasiveness mineral content on the cerchar abrasiveness index. *Engineering Geology,* 36(4):293–301.

Cerchar. 1986. Cerchar Abrasivity Index. 12ed. Verneuil: Centre d'Etudes et Recherches de Charbonnages de France.

Frenzel, Ch. 1989. Kostenprognose für Schneidrollen bei maschinellen Tunnelvortrieben in Festgesteinen. Cost prediction for disc cutters in hard rock TBM tunnelling. Münchner Geowissenschaftliche Abhandlungen, (B) 18, München: Verlag Dr. Friedrich Pfeil. West. Rock abrasiveness testing for tunnelling. *Int. J. Rock Mech. Min Sci. & Geomech*. Abstr. 26:321–327.

Kahramans. 2002. Correlation of TBM and drilling machine performances with rock brittleness. *Engineering Geology,* 65(9):269–280.

Kasling H. & Thuro K. 2010. Determining abrasivity of rock and soil in the laboratory. *Taylor & Francis Group*: 1973–1980.

Michalakopoulos, T.N. et al. 2005. The influence of steel styli hardness on the Cerchar abrasiveness index value. *Int. J. Rcok Mech. Min Sci. & Geomech*. Abstr. 43:321–327.

Rostami, J. 2005. CAI testing and its implications. *Tunnels &Tunnelling International,* 37(10): 43–46.

West G. 1986. A relation between abrasiveness and quartz content for some coal measures sediments. *Inernational Journal of Mining and Geological Engineering,* (4): 73–78.

West G. 1989. Rock abrasiveness testing for tunnelling. *Int. J. Rock Mech. Min Sci. & Geomech*. Abstr. 26:321–327.

Yaral O, et al. 2008. A study of rock abrasivity and tool wear in coal measures rocks. *Inernational Journal of Coal Geology,* 74(3):53–56.

ZhiyongYANG et al. 2012. Abrasivity Characteristics of surrounding rock mass of Shiziyang tunnel. *Journal of PLA University of Science and Technology (National Science Edition),* 13(3):311–315.

This page intentionally left blank

Progress in Mine Safety Science and Engineering II – He et al. (Eds)
© 2014 Taylor & Francis Group, London, ISBN 978-1-138-00122-0

Protected range extension of mining underlying protective seam with long distance

Tao Yu & Jinhua Sun
State Key Laboratory of Fire Science, University of Science and Technology of China, Hefei, Anhui, China

Ping Lu & Houyang Guo
Anhui Jianzhu University, Hefei, Anhui, China

ABSTRACT: Based on mining underlying protective seam with long distance in the panel 1311(1) of ZhangJi mine, and by the contrast of numerical simulation and similar material test, the extended destressed zone was located between the angles of theoretical destressing and normal projection of protective seam border; fully destressed zone was within the limit of theoretical destressing angle. In order to investigate the extended protective range intuitively and correctly, the coal roadway was constructed in overlying protected seam 13–1 to test the coal seam swelling deformation rate, height deformation rate of coal roadway, gas emission and permeability coefficient. The research proved that the destressing angle of 11–2 nearly horizontal coal seam can be expanded to 90° and the equivalent length and width arrangement of protected panel can be realized.

1 INTRODUCTION

It has been proved by the long term practice that mining protective seam is a very effective regional measure to eliminate coal and gas outburst. Reasonably delimiting protective range is very significant for the safety and high-efficient coal mine production (Yuan 2009). At present, outburst prevention rule continues to use the relatively conservative destressing angle of Soviet, and the effective protective range of this rule has some differences from the practical destressed region of protected seam. Thus there is the space in protective range to extend (Liu 2010). Studies about mining protective coal seam mainly focused on the investigation of protection effectiveness index. There were not many differences between identified protective range and the specified zone of rule. The used investigating method needed to construct stone roadway and drill cross-measure boreholes. Moreover, the tests were liable to exist the relatively large error under the environmental influence, and it was not good for determining the really protective range (Shi et al. 2006, Tu et al. 2006, Xiao et al. 2012). Based on mining underlying protective coal seam with long distance of ZhangJi mine, this paper is to investigate the range extension by using the coal roadway of protected seam and monitoring the variation of roadway's height, so as to determine the effective protective range comprehensively.

2 GENERAL SITUATION OF TEST AREA

Test site locates in the panel 1311(1), mining area 11–2 of East No. 2. The panel length is 890 m, panel width is 240 m, and the thickness of coal seam 11–2 is 0.4~4.3 m, 2.82 m in average. The seam dip is 3~8°, 5° in average. The thickness of overlying coal seam 13–1 is 2.1~5.58 m, 3.9 m in average, seam dip is 2~7°, 4° in average. The average distance from coal seam 11–2 to 13–1 is 86.5 m.

13–1 is coal and gas outburst risk coal seam. The original gas pressure is 1.1 MPa, methane content is 5.5 m^3/t, and permeability coefficient is lower, only $0.067(m^2/(MPa^2 \cdot d))$, belonging to difficult drainage coal seam. Therefore, the regional measure of mining protective seam is taken to eliminate coal and gas outburst by first mining 11–2 coal seam of no hazard as the protective seam.

3 NUMERICAL SIMULATION OF THE STRESS AND DISPLACEMENT

Make use of the FLAC^{3D} software to simulate the variation rule of the stress and displacement in coal seam 13–1 during the panel 1311(1) extraction. The height of the model is up to the roof of coal seam 13–1, the mining direction (strike direction) is defined as x-axis, the vertical strike direction of coal seam is y-axis, and the vertical direction of panel is z-axis. The size of the

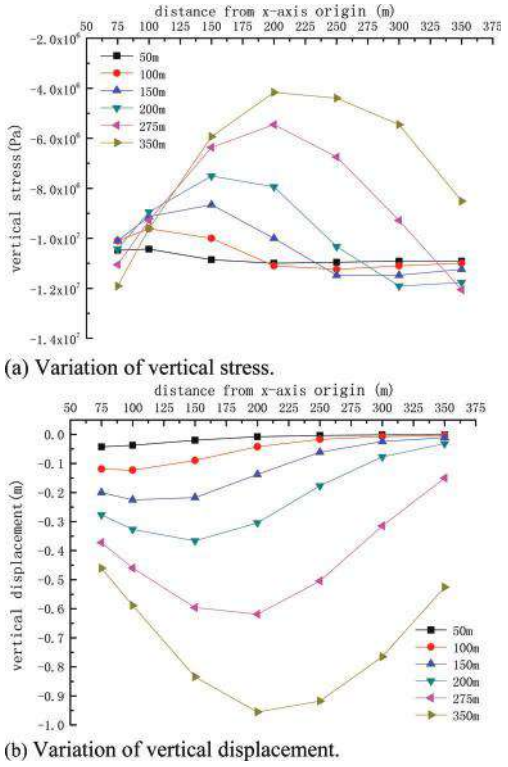


Figure 1. The vertical stress and displacement of coal seam 13–1 roof along the strike direction with the panel advancement.

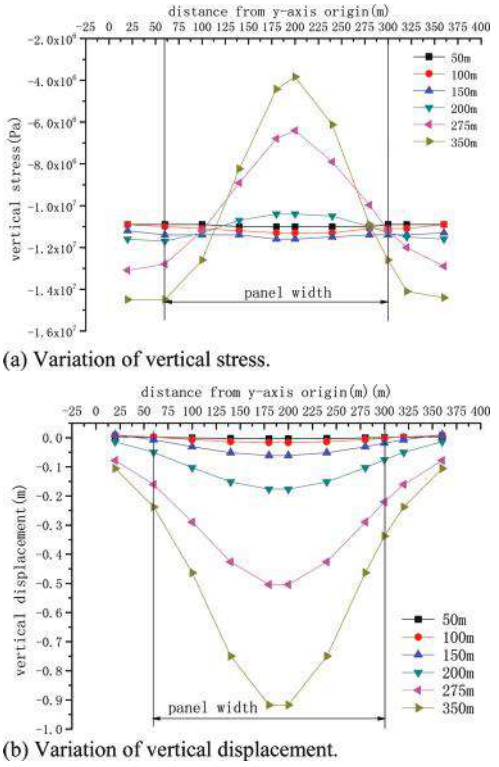


Figure 2. The vertical stress and displacement of coal seam 13–1 roof along the dip direction with the panel advancement.

model is as below: x = 500 m, y = 400 m, z = 200 m, the model boundary in x and y-direction is displacement constraint, at the bottom (z = 0) is fully-constrained and at the top (z = 200) is free with the gravitation load of overlying rock. Because the initial roof weighting step of coal seam 11–2 is about 30 m~40 m, the model extraction begins from the first cut (x = 50 m). The advancement by steps (every 10 m a step) is used to simulate the following six stages: x = 50 m, x = 100 m, x = 150 m, x = 200 m, x = 275 m, x = 350 m. Meanwhile, the vertical stress and displacement of the roof along the strike direction are surveyed as shown in Figure 1, which monitoring points are located in the center of panel.

The vertical stress and displacement of the roof along the dip direction are surveyed as shown in Figure 2, which monitoring points are located at x = 180 m.

Numerical simulation results indicate that the destressed zone in strike and dip direction of coal seam 13–1 extends continuously with the panel advancement, stress is released fully in the mapping center zone of the panel; stress concentration is appeared in the mapping zone of the first cut and working face. The vertical stress along the dip direction is uneven, decreasing continuously from middle to both sides, and the vertical displacement also reduces continuously from center to roadway sides, which result in uneven subsidence, destressed range extension and destressing angle extending to 90°.

4 ANALYSIS OF PROTECTIVE RANGE EXTENSION

Based on the numerical stimulation of destressed range in coal seam 13–1 as mining coal seam 11–2, and combined with the similar simulation test for mining protective coal seam 11–2 of Panxie mine area (Lu et al. 2010) as shown in Figure 3, the results can be summarized as follows: the breaking angle of roof is 45°~50° which scope is caving zone with protected coal seam destressed fully; the wedged destressed swelling zone appears in the scope of angle 50°~90° with destressed gas enrichment; the compressive deformation zone appears in the scope of angle 90°~110° with coal bearing

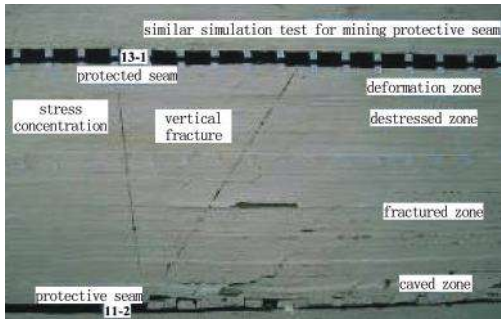


Figure 3. Similar simulation test for mining protective seam 11–2 (Tu 2008).

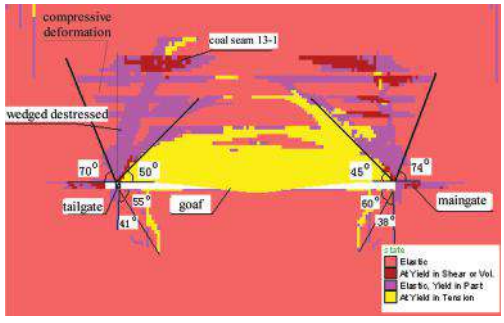


Figure 4. Destressed zone distribution of overlying coal petrography.

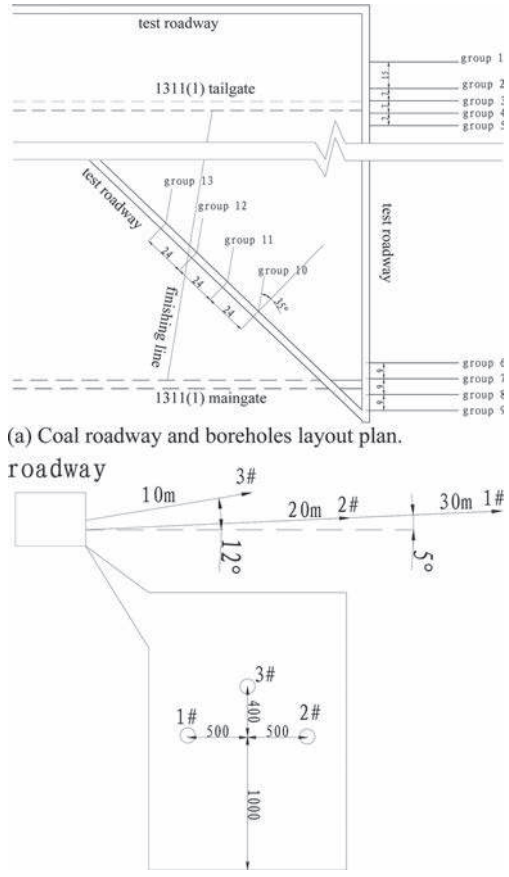


Figure 5. Coal roadway and boreholes layout for testing.

stress increasing and partial stress concentration as shown in Figure 4. Therefore, extended destressed zone exists which was located between the angles of theoretical destressed and normal projection of protective seam border, and fully destressed zone was within the limit of theoretical destressing angle.

5 TEST FOR PROTECTIVE RANGE EXTENSION

5.1 *Test method*

The protection range can be tested by drilling cross-measure boreholes through the roof and floor roadway, but it will waste much more time and energy because quite a few long boreholes are needed to drill and the length is too long, which lead to relatively large error of the swelling deformation data under the environmental influence. Thus the true protective range will be confirmed difficultly. Based on the test site condition, a coal roadway for testing was designed to cave in the protected coal seam 13–1 with the minimum projective distance 50 m from the stop line of panel 1311(1) as shown in Figure 5, and to join existing roadway to form independent ventilation system. The overall length of constructed roadway was about 870 m.

The test roadway in protected coal seam is near the coal seam and convenient to drill boreholes, which lead to the swelling deformation data more correctly. In addition, the destressed range can be confirmed comprehensively by observing the height of coal roadway. The total number of test boreholes is thirteen groups, and every group has three boreholes to measure gas pressure, gas emission and coal seam swelling deformation respectively with the panel 1311(1) advancement. Figure 5 is the drilled boreholes layout, and Table 1 is the corresponding destressing angle of every group.

5.2 *Swelling and deformation rate of coal seam*

According to outburst prevention rule, taking 3‰ swelling and deformation rate of coal seam as

Table 1. Corresponding destressing angle of every group boreholes.

Destressing angle (dip tailgate)					Destressing angle (dip mailgate)				Destressing angle (strike finishing line)			
1	2	3	4	5	6	7	8	9	10	11	12	13
105°	95°	90°	86°	81°	78°	84°	90°	96°	60°	73°	90°	105°

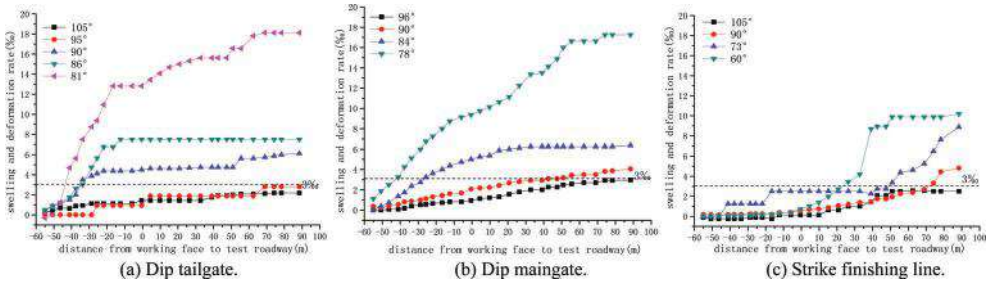


Figure 6. Variation of swelling and deformation rate with panel advancement.

index to confirm the destressed range, the swelling deformation rate of coal seam along dip and strike direction are shown in Figure 6.

When the projective distance from working face to test roadway is 60 m~100 m, the coal seam 13–1 begins to swell and deformation affected by fore-stress. As shown in Figure 6(a) of dip tailgate direction, when the panel advances through the corresponding location of test roadway, the deformation rates of 81°, 86° and 90° angle all exceed 3‰ and reach to 13.4‰, 7.5‰ and 4.6‰ respectively, but the deformation rates of 95° and 105° angle have been less than 3‰ after the working face passing test roadway 88.4 m and beginning to finish. Therefore, the destressing angle along the dip tailgate direction reaches to 90°.

As shown in Figure 6(b) of dip maingate direction, when the panel advances through the corresponding location of test roadway, the deformation rates of 78° and 84° angle all exceed 3‰ and reach to 9.75‰ and 5.25‰ respectively. When the working face advances across the test roadway 40 m, the deformation rate of 90° angle exceeds 3‰ with hysteresis effect, but the deformation rates of 95° angle has been less than 3‰ after the working face passing test roadway 88.4 m and beginning to finish. Therefore, the destressing angle along the dip maingate direction reaches to 90°.

As shown in Figure 6(c) of strike finishing line direction, when the working face passes test roadway 88.4 m and begins to finish, the deformation rates of 60°, 73° and 90° angle exceed 3‰ and reach to 10.19‰, 8.88‰ and 4.81‰ respectively, and 105° angle is 2.5‰. Therefore, the destressing angle in strike finishing line direction reaches to 90°.

5.3 *Deformation rate of roadway*

The test roadway deformed under the influence of fore-stress and post-mining destressed, which caused roof subsidence and floor heave and directly presented the roadway's center height reducing continuously. Protective range can be confirmed visually according to the height variation of coal roadway by observing the roadway's height of each corresponding test groups. The ratio of variable to initial height value is defined as the deformation rate of roadway. The test roadway was supported by bolting and its shape was rectangular. During the panel advancing, the roadway's height changed dramatically. The deformation rate of test roadway of coal seam 13–1 varied with the panel advancement are shown in Figure 7. The timber cribs were added to reinforce support for ensuring ventilation section in fully destressed zone, which leaded to deformation rate less such as 81°, 78° and 60° angle in (a), (b) and (c) of Figure 7.

The roadway deformation results are consistent with the swelling deformation rate of coal seam. When the corresponding coal roadway located in destressed zone, the deformation rate of roadway reached 15%~20%. The destressed effect in lower maingate direction is a little worse than the upper tailgate direction. Because the mine stress is greater in lower level and the destressed effect is relatively hysteretic.

5.4 *Gas emission*

Along with the panel advancement, the variable gas emission of boreholes can be measured to test

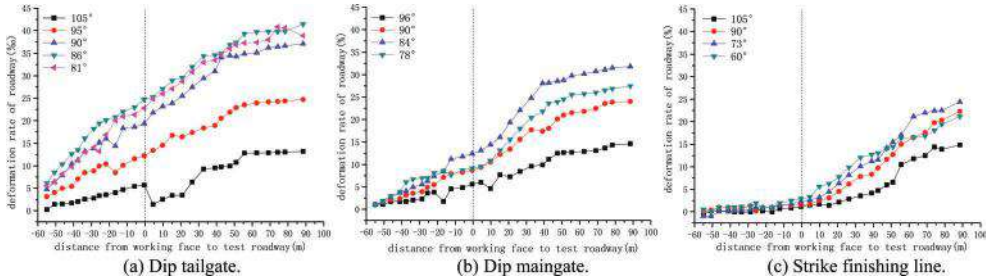


Figure 7. Variation of deformation rate of roadway with panel advancement.

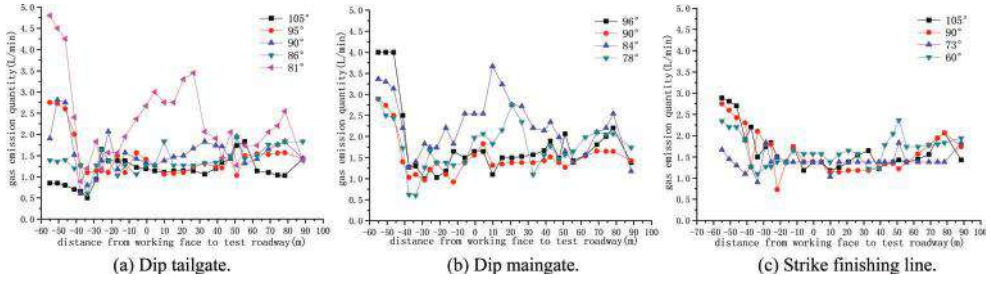


Figure 8. Variation of gas emission of roadway with panel advancement.

destressed effect as shown in Figure 8. Under the influence of fore-stress, the gas emission quantity reaches the minimum value when the distance from working face to test roadway is 30 m~40 m. The gas emission quantity reaches the maximum value when working face passes test roadway 0~30 m, after then it tends to stably. Therefore, the gas emission in range extension zone of 78°~90° angle varies dramatically with the panel advancement and the destressed effect is better.

5.5 *Permeability coefficient*

13–1 is coal and gas outburst coal seam. The measured value of gas pressure is 1.1 MPa, and permeability coefficient is 0.067(m^2/(MPa^2·d)). The coal roadway deformed continuously under the influence of mining fore-stress, which resulted in air leakage in coal wall and measuring pressure of boreholes dropping speedily. When the distance from the working face to test roadway is 80 m, the pressure drops to zero. After mining underlying protective coal seam 11–2, permeability of destressed protected coal seam is increased. According to the gas emission variation of boreholes with the panel advancement, the permeability coefficient of coal seam from theoretical destressing angle in dip direction to 90° angle can be calculated. It is 2.83~6.87(m^2/(MPa^2·d)), 42~101 times the original permeability coefficient and the destressed effect of range extension zone is good.

6 CONCLUSION

The destressed index of protected coal seam was obtained by actual measurement and the consistency of different indexes is good. Research findings show that extended destressed zone is located between the angles of theoretical destressed and normal projection of protective seam border; fully destressed zone is within the limit of theoretical destressing angle by the contrast of numerical simulation and similar material test.

By taking 3‰ swelling and deformation rate of coal seam as index and combining with the height deformation rate of coal roadway, gas emission and permeability coefficient, destressing angle in dip and strike direction can reach 90°after mining the coal seam 11–2 of Zhangji mine. The research proves that the destressing angle of nearly horizontal coal seam 11–2 can be expanded to 90° and the equivalent length and width arrangement of protected panel can be realized.

The roadway of protected coal seam is firstly used to study protective range, which can be investigated intuitively and correctly by observing the deformation rate of roadway. The deformation

rate of destressed zone reaches 15%~20% in bolting support roadway of coal seam 13–1 of Zhangji mine. Making use of roadway deformation to deduce the swelling deformation rate of coal seam should be studied further.

The gas emission in range extension zone of 78°~90° angle varies dramatically with the panel advancement and the destressed effect is better. The permeability coefficient of coal seam in the range extension zone is 2.83~6.87(m^2/(MPa^2·d)), 42~101 times the original permeability coefficient.

ACKNOWLEDGEMENTS

This study is supported by National Natural Science Foundation of China (No: 41172147), Science and Technology Developing Project of Anhui Province (No: 12010402110, Science and Technology Planning Project of Anhui Province (No: 11010401015).

REFERENCES

Liu lin, 2010. *Rational protection range of lower protective layer and application in pressure-relief gas extraction.* Xuzhou: China university of mining and technology.

Lu Ping, Yuan Liang, Cheng Hua, 2010. Theory and experimental studies of enhanced gas drainage in the high-gas face of low permeability coal multi-seams. *Journal of China Coal Society,* 23(4):580–585.

Shi Biming, Yu Qixiang, Wang Kai, 2006. Test Research on coal seam penetrability dynamic changing law by far-distance protecting stratum mining. *Chinese Journal of Rock Mechanics and Engineering,* 09.

Tu Min, 2008. *Analysis of mining rock mechanics in relieved drainage of coal bed methane and its application.* Xuzhou: China university of mining and technology.

Tu Min, Miao Xie-xing, Huang Nai-bin, 2006. Deformation rule of protected coal seam exploited by using the long-distance-lower protective seam method. *Journal of Mining & Safety Engineering,* 23(3):253–257.

Xiao Jia-ping, Zhou Bo, Han Lei, 2012. Pressure relief boundary of protected seam mining with subhorizontal long-distance. *Journal of Xi'an University of Science and Technology,* 32(2):180–185.

Yuan Liang, 2009. Theory of pressure-relieved gas extraction and technique system of integrated coal production and gas extraction. *Journal of china coal society,* 34(1):1–18.

Progress in Mine Safety Science and Engineering II – He et al. (Eds)
© 2014 Taylor & Francis Group, London, ISBN 978-1-138-00122-0

Study on Weijiadi coal mine geological structure characteristics and gas occurrence regularity

Sihua Shao
China University of Mining and Technology, Xuzhou, Jiangsu, China

Jufeng Zhang
WeiJiaDi Mine of Jingyuan Coal Industry Group Co., Ltd., Baiying, Gansu, China

ABSTRACT: Through analyzing the geological structure characteristics of Weijiadi coalfield, and combined with tectonic coal developmental and distributed characteristics and geological structure on gas occurrence control, we concluded what is gas geological law of occurrence in the Weijiadi coalfield, gas content of coal seam NO.1 increases with the increase of coal seam thickness and buried depth; however, gas content of coal seam NO.3 decreases with the increase of coal seam thickness and buried depth. Study on the law of gas geology is to lay the foundation for gas management, which has guiding significance.

1 INTRODUCTION

Gas geology (WANG Dazeng 1992, ZHANG Zixu et al. 2001, XU Kaili & ZHU Zhicheng 1998) is a discipline, which study gas occurrence, migration and distribution in coal seam, and the relationship between gas emission and gas outburst and gas geology factors, and verify these regularities, this discipline is based on absorbing the related theories of geological engineering and safety engineering, through production practice, scientific research and refining theory, and applied in resource, environment and coal mine safety production directly (ZHANG Zhimin & ZHANG Yugui 2005, YUAN Chunfu 1997, Coalfield teaching and research section of Wuhan geological college 1997, Jiaozuo institute of mining gas geology research 1991). Weijiadi coal mine is coal and gas outburst mine, it is very vital significant to research of mine gas geology rules and gas comprehensive control technologies.

2 THE GEOLOGICAL STRUCTURE AND CONTROL CHARACTERISTICS

2.1 *Mine geological and distribution*

Weijiadi coalfield is located in west Gansu extort spiral fold area with middle Songshan ~Huangjiawa Shan folded doming-up area south Baoji Shan~ fold area in the middle of Honghui.

The coal mining field is broad and gentle fold which is composed by anticline NO.1, syncline NO.2, anticline NO.3 and NO.4 from west to east. Tectonic line direction is N60°~70°W, and turn nearly E~W, which shows the angle of 35°~10° with the edge of the coalfield construction line of Dawan fault and F46 fault line, which is presented "S" shape in the plate, and "入" type structure is composed by anticline NO.1, syncline NO.2, anticline NO.3 and NO.4 in the truck of F46 fault.

From the profile view, the entire coal field is a rising wedge form banded geological body, NE side (hanging side) of Dawan fault is up, WS side (heading side) is falling, WS side (hanging side) of F_{46} fault is up, NE side (heading side) is falling. The structure section of Weijiadi coalfield diagram is as shown in figure 1.

2.2 *Tectonic coal development and distribution characteristics*

Through coal mining situation, we could get these conclusions, because the rift tectonic zones of F_{1-2} fault group and the regions which is near the F3

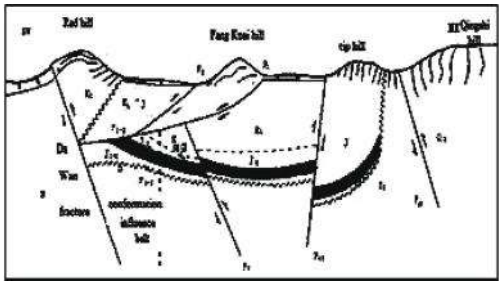


Figure 1. The structure section of Weijiadi coalfield diagram.

fault footwall 100–150 m are affected by F_{1-2} fault group and F_3 fault, cutting layer is fault and fault develops, the original structure appears changes, most of these structures are power structure and the structure of mylonite because of crumpling up between the layers. Coal seam that is in F_{1-2} fault group of mined areas is typical tectonic coal, and four characters are as follows:

1. Because single seams are affected by F_{1-2} fault group, roof and floor is volatile, minor faults and minor wrinkling are very developmental.
2. The thickness of coal seams are easy to change, local thickness is up to 49.08 m, which is the result that coal seams were twisted, pushed and superimposed, meanwhile, which is the result that bedding faults and cutting layer faults superimposed together.
3. Because between layers were crumpled, great changes have taken place in the original structure of coal seams, those shapes are mainly power and scaly.
4. Coal and rock interspersed with each other, which makes the coal seams highly irregular form, and becomes coal and rock broken areas.

According to the situation of coal mining to expose and drilling data, we analyzed and concluded that, tectonic coal of Weijiadi coalfield are mainly distributed in F_{1-2} fault group of fracture tectonic belt and near the F_3 fault footwall, F_{48} fault footwall and F_{46} fault plate of 100~150 m areas.

2.3 *Geological structure on the influence of gas occurrence*

Coalfield geological structure is completed in Weijiadi coal mine, the types of all faults are twisted, and these faults are provided with good sealing ability, especially, more than half of mine field are covered F_{1-2} fault group. From field structure profile and outline drawing view, the entire field become structural assembly that is reverse fault border closed, tectonic cap closed and fault block segment. Secondly, the mining field is an incomplete duplicate syncline, the duplicate syncline is cut by these twisted reverse faults, the geological condition is more advantageous to gas accumulation and storage of coal seam, especially near the fault zones, gas content increased significantly in anticline and syncline axis of the coal seam.

3 GAS OCCURRENCE REGULARITY AND GAS CONTENT PREDICTION

3.1 *Gas occurrence regularity of coal seam*

Gas ingredients of coal seam are mainly N_2–CH_4 in Weijiadi coal mine, heavy hydrocarbon (C_2–C_3) content is relatively much.

Natural gas ingredients mainly include CH_4, CO_2, N_2, C_2—C_3 in the coalfield. N_2—CH_4 is distributed widely in coal seam NO.1, which accounted for about 85% of coal seam mining field. CH_4 is mainly distributed near F_3 fault and the south west of X line, that is those local areas which are anticline NO.1 and NO. 3, syncline axis NO. 2. N_2 and N_2—CO_2—CH_4 are distributed dispersedly. On average, heavy hydrocarbon is accounted for 7.33% of total gas. N_2 —CH_4 is distributed widely in the coal seam NO.3, which is accounted for 90% of coalfield. CH_4 accounted for about 1% of the mining field, which is mainly distributed near F_3 fault local areas.

Areas mined belong to N_2–CH_4 areas (outside of the areas affected by F_{1-2} fault tectonic belt), gas content is relatively less, gas content of coal seam NO.1 is 6~10 m^3/t; gas content is relatively much in the areas which distribute gas, primitive gas content is 10~20 m^3/t; so we predict that primitive gas content of coal seam NO.1 is 6~10 m^3/t in N_2–CH_4 areas; primitive gas content is 10~20 m^3/t in CH_4 areas.

Primitive gas content is less than 6 m^3/t in N_2–CH_4 areas of coal seam NO.3; primitive gas content is 6 m^3/t~10 m^3/t in CH_4 areas.

Through analyzing synthetically the relationship between mine geological structure features and primitive gas content, the conclusions are obtained, gas content is much of coal seam NO.1 and NO.3, and the channels which gas move, diffuse are completely cut off, gas content is rich in Weijiadi coal mine.

We analyzed factors, gas occurrence regularities of coal seam NO.1 are as follows:

1. Gas content is much in which structure of coal seam is extremely complex, predict more than 10 m^3/t.

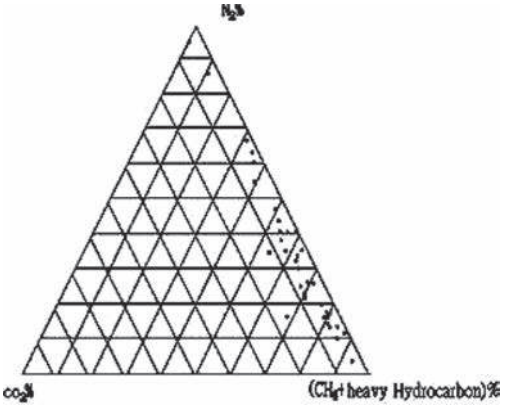


Figure 2. Gas composition distribution of coal seam NO.3.

2. Gas content is relatively much in F_{1-2} fault tectonic belt and $F_{3,}$ F_{48} fault areas; but gas content is less in thin coal seam areas.
3. Gas content of coal seam increases gradually with its buried depth in other areas.

Gas occurrence regularities of coal seam NO.3 are as follows:

1. X IV line west, coal seam is relatively thick, content of gas is much more, predict 6~10 m^3/t;
2. X IV line east, coal seam is relatively thin, content of gas is less, predict 1~2 m^3/t;
3. Gas content increased with the buried depth of coal seam;

3.2 *Prediction of coal seam gas content*

1. Impact on gas content of coal seam thickness

Coal seam is the main reservoir of gas, in general, Coal seam thickness is the important factors that affect gas content and gas emission. Coal seam NO.1 and NO.3 are unstable in Weijiadi Coal Mine, thickness are 1.03–45.47 m, the average is 8.26 m, but local area affected by geological structure, coal seam appears phenomenon that become thick or thin. Through counting digital relationship between coal seam thickness and gas content, we obtain the following relations, as shown in figure 3.

2. Impact on gas content of coal seam buried depth

With the loss of the coal seam bottom elevation and the increase of buried depth, ground stress increases constantly, the permeability of surrounding rock is cutting down, the distance that gas migrate towards the surface, these changes are beneficial to gas occurrence, which makes the gas content and gas emission also increasing. Through counting digital relationship between coal seam buried depth and gas content, we obtain the following relationship, as shown in figure 4.

Through counting digital relationship between coal seam buried depth and gas content, we can find that gas content of coal seam NO.1 increase along with buried depth increasing and bottom elevation lowering; However, coal seam NO.3 lower along with buried depth increasing and bottom elevation increasing, and better linear relationship can be obtained. Although local area is affected by geological tectonic belt, buried depth and bottom elevation of coal seam still be main control factors of gas occurrence.

3.3 *Prediction of coal seam gas content*

Through analyzing qualitatively and quantitatively the affected factors of gas content, although local

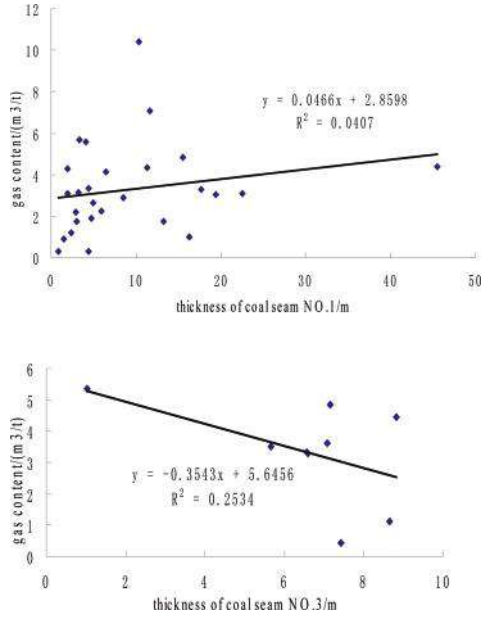


Figure 3. The relationship between thickness of coal seam and gas content.

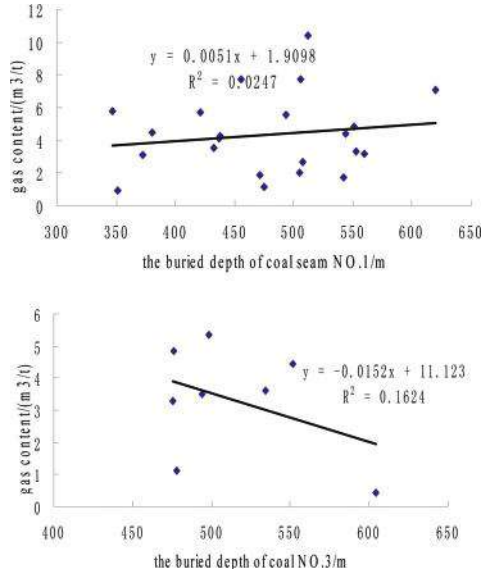


Figure 4. The relationship between buried depth of coal seam and gas content.

coalfield appear abnormal situation in accordance with the influence of geological structure, gas content of coal seam NO.1 increase along with buried depth increasing and bottom elevation lowering; However, coal seam NO.3 lower along with buried

depth increasing and bottom elevation increasing, and buried depth and bottom elevation of coal seam still be main control factors of gas occurrence. Therefore, the model which is relationship between bottom negative level and gas content was set up, which could predict gas content. The relationship model is as follow.

Coal seam NO.1:

$y = 0.0029x + 2.1443$
$R_2 = 0.0117$

Coal seam NO.3:

$y = -0.016x + 11.651$
$R_2 = 0.1809$

Among in them, y represents the gas content (m^3/t), x represents bottom negative level(m), R represents relative coefficient.

4 CONCLUSIONS

1. Weijiadi coalfield is affected by article seven fault, these fault has good sealing coverage ability, which is beneficial for gas accumulation and storage of coal bed, especially, near the fault zones, gas content is significantly increasing in the anticline and syncline axis of coal seam.
2. Through analyzing comprehensively the relationship between mine geological structure features, components of coal and rock, coal seam roof and floor lithology, coal seam thickness and structure, coal seam gas composition distribution and coal seam primitive gas content, we concluded what is gas occurrence law of coalfield coal seam NO.1and NO.3.
3. Through counting and analyzing the relationship between the thickness and buried depth of coal seam and gas content, we concluded that gas content of coal seam NO.1 increases with the increase of coal seam thickness and buried depth; however, gas content of coal seam NO.3 decreases with the increase of coal seam thickness and buried depth.

REFERENCES

Coalfield teaching and research section of Wuhan geological college, 1997. Coal Geology(I).Beijing: *Geological Press*. (in Chinese).

Jiaozuo institute of mining gas geology research, 1991. Overview of geology. Coal Industry Press. (in Chinese).

Wang Dazeng. Gas Geology. *Coal Industry Press,* 1992. (in Chinese).

Xu Kaili & Zhu Zhicheng. 1998. Structural Geology. Beijing: *Geology Press.* (in Chinese).

Yuan Chunfu. 1997. The development and application of gas geology in China. *Journal of China Coal Society* 22(6): 567~570. (in Chinese).

Zhang Zhimin & Zhang Yugui. 2005. Gas Geology Rule and Gas Prediction. *Coal Industry Press*. (in Chinese).

Zhang Zixu et al. 2001. Gas Geology New Progress. Zhengzhou: *Henan Science and Technology Press*. (in Chinese).

Progress in Mine Safety Science and Engineering II – He et al. (Eds)
© 2014 Taylor & Francis Group, London, ISBN 978-1-138-00122-0

Numerical simulation on goaf gas extraction by the ground drilling

Zhipeng Ma, Jufeng Zhang, Yadong Xie, Qingqi Feng & Jun Dang
WeiJiaDi Mine of Jingyuan Coal Industry Group Co., Ltd., Baiying, Gansu, China

ABSTRACT: In order to study the gas distribution in goaf and the gas migration during the ground drilling gas extraction in goaf, based on the theory of gas migration in goaf and the model of Weijiadi East 102 coalface, through establishing the stope model, and FLUENT simulation software was applied on the numerical simulation. The results show that, there is no change in gas concentration before and after ground drilling extraction, but gas concentration is only the overall decline, especially, the area where gas concentration is low expanded significantly near the working face, and gas concentration around the ground drilling is significant low compared to other areas, which shows that the ground drilling has a good effect for gas extraction of goaf.

1 INTRODUCTION

Gas is mainly from goaf the adjacent layer in coal mining space, gas emitted from goaf accounts for 40% of gas emission of the mining space, in some mines, gas emitted from goaf accounts for 60%–70% of total amount of gas emission of the mining space. So, research on goaf gas flow and occurrence regularity has important theoretical significance for prevention and control of mine gas disasters and goaf gas drainage and the implementation of coal and gas mining technology (Yuan Liang 2009, Yuan Liang 2006, ZHAO Hongbao, et al. 2011).

In view of the particularity of goaf gas distribution and migration, experimental study is less, numerical simulation is more, in China, many scholars had studied on the regularity of goaf gas distribution and extraction (HU Qianting, et al. 2007, JIN Longzhe, et al. 2010, LI Zhongxiang. 2002, ZHANG Dongming & LIU Jianzhong 2003), in this paper, CFD software FLUENT 6.32 has been applied, combined with the detail of East 102 full-mechanized caving face of Weijiadi coal mine, goaf gas extraction regularity by the ground drilling was numerically simulated.

2 MODEL ESTABLISHMENT AND PARAMETERS SELECTION

2.1 *The theoretical study on gas migration in goaf*

A small unit is removed from the goaf, that is control volume. Its characteristics are as follows, small control body is fixed on the space of a certain volume, no matter how the fluid affects the control volume, its size, shape and position remains unchanged. Which requires that, unit cell is enough big, make it contains quite a lot coals and rocks and mass pore, in order to get some relevant porosity, stable and meaningful quantities, on the other hand, the unit cell is selected small enough, compared with the goaf, it can be approximate to a point, so that the whole goaf which is composed of porous medium particle is considered to be porous continuous medium. The coordinates of the cell shape heart C is assumed to be (x, y, z), those sides are assumed respectively to be *dx, dy, dz*. The projection of the flow velocity u_i on the axis are u_x, $u_y$and u_z, the density is ρ, which goes through instantaneously point C.

K(r, L) is a porous media cube, whose center and side are defined as r and L, actually, K(r, L) is defined as a measuring unit, the porosity of measuring unit (r, L) is:

$$\varphi(r,L)=\frac{V(Pn(K(r,L)))}{V(r,L)}$$

We assume that the control volume has source item, its intensity is Wg, which is mainly gas resolving from coal, and the control volume has terms, its intensity is Ws, which is mainly gas quantity by gas extraction. Now we calculate the changes of quality fluid, first, quality of fluid on the surface of the hexahedron was calculated.

In t time, the quality difference between gas flow in and out of the control volume is:

$$\begin{aligned} dM &= dM_x + dM_y + dM_z \\ &= \left[\frac{\partial(\rho u_x)}{\partial x}+\frac{\partial(\rho u_y)}{\partial y}+\frac{\partial(\rho u_z)}{\partial z}\right]\varphi dxdydzdt \end{aligned} \quad (1)$$

In addition, considered intensity of W_g, in time, the inflow gas quality is:

$$dM_{wg} = W_g ndxdydzdt \tag{2}$$

Meanwhile, considered intensity of W_s, in time, the outflow gas quality is:

$$dM_{ws} = W_s ndxdydzdt \tag{3}$$

According to the law of conservation of mass, we obtain that:

$$dM + dM_{wg} - dM_{ws} = 0 \tag{4}$$

Equation (1), (2) and (3) are applied to equation (4), the results are:

$$\frac{\partial(\rho u_x)}{\partial x} + \frac{\partial(\rho u_y)}{\partial y} + \frac{\partial(\rho u_z)}{\partial z} + W_g - W_s = 0$$

That is:

$$div(\rho u_i) + \rho_{CH4} w_g - \rho_{CH4} w_s = 0$$

In the equation:

ρ_{CH4}—the density of the gas;
W_g—the gas volume parsing of coal per unit volume and per unit time;
W_s—the gas volume parsing of coal by gas extraction;

2.2 *Stope geometry model and network partitioning*

East 102 working face is the first mining face in the first mining area east of Weijiadi coal mine, located in coal seam NO.1, we establish the model to understand the laws of gas migration in the goaf and the influence of ground drilling for gas migration. The width of base model is 400 m, the highness of the fracture zone in goaf is 120 m. The highness of into the airway and return airway is 3.0 m, the width of roadway is 4.4 m, the length of that is 30 m. Into the wind position was assumed for the origin in the model, that is (0, 0, 0), and the depth direction of goaf was assumed for the x axis, and face direction was assumed for the y axis, height direction was assumed for z axis, the final position of the ground drilling locates in the 100 m distance from transportation roadway, the 30 m distance from return airway, the 36 m distance from the bottom of coal seam, the final coordinate of the ground drilling is (130, 105, 36). The table 1 is the detailed information modeling parameters.

Table 1. The basic parameters of East 102 working face CFD simulation model.

The model parameters	The parameter value
Size of coal mining working face	Length 400 m, width 135 m, height 120 m
Size of roadway	Width 4 m, height 3.0 m (12 m^2)
CFD model size	Height 120 m
The ventilation system, air volume	"U" type ventilation
Gas emission from goaf	
Gas composition	100%
Gas extraction from goaf	No drilling gas extraction in goaf
The position of ground drilling	100 m away from mining working face, 30 m away from air return lane, 36 m away from coal floor

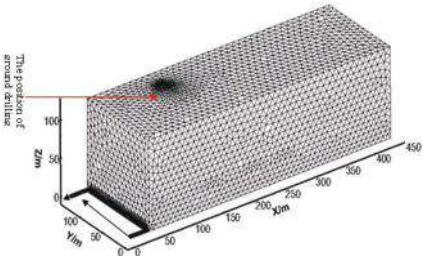


Figure 1. Goaf geometric model and grid.

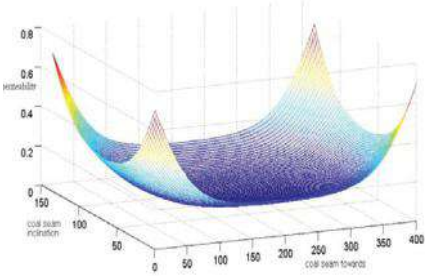


Figure 2. Goaf porosity distribution.

In this program, we can simulate gas flow in goaf of longwall working face by business FLUENT of CFD program. According to the actual mine distribution, the CFD model of East 102 working face was established and dividing the grid by Gambit processor in the FLUENT, about 500,000 cells are as shown figure 1, the simulation was performed by solver. Three-dimensional model of FLUENT software contains tetrahedron cells, hexahedral cells, pyramid cells or wedge cells

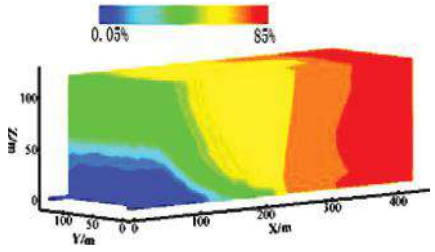


Figure 3. The diagram of three-dimensional gas distribution in goaf.

(or the combination of them).In this time, dividing grid is performed by hexahedral cells. Dividing grip of the CFD model about gas flow in goaf of longwall working face is shown in figure 2. and the porosity distribution diagram of goaf is as shown in figure 3.

3 GAS DISTRIBUTION IN GOAF DURING THE GROUND DRILLING EXTRACTION

Gas volume fraction distribution of goaf when ground drilling extraction is showed in figure 4, 5 and 6, these figures show that ground drilling impacts on gas density of East 102 goaf.

1. Three-dimensional spatial distribution of stope gas

There is no change in gas concentration before and after ground drilling extraction, but gas concentration is only the overall decline, especially, the area where gas concentration is low expanded significantly near the working face.

2. The gas distribution laws along the tendency

The gas distribution laws is similar before and after ground drilling along the tendency, near the working face, gas concentration of goaf increases from into mind lane to return air lane, away from working area, gas concentration first increases, and then decreases, as shown in figure 4e and 4f. Comprared with the ground drilling before extraction, we are easy find that gas concentration field on one side of return air lane decrease significantly and the gas low concentration area becomes big, as shown in figure 6a. On the X = 50 m section, low gas concentration field is expanded in Z direction in the goaf in central location, the main reason is that the ground drilling hole position is located at coal seam floor 36 m, its extraction negative pressure can make the gas migration from low level to high level, on the high level, due to the existence of ground drilling, which makes the surrounding oxygen concentration low, the lowest concentration can reach 30%, as shown in figure 5a.

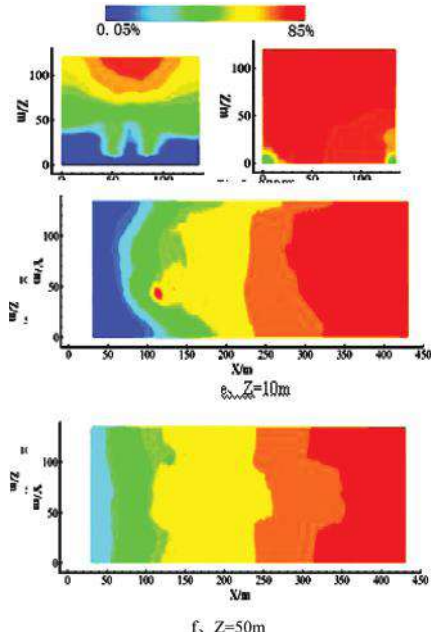


Figure 4. Gas volume fraction distribution from different aspects.

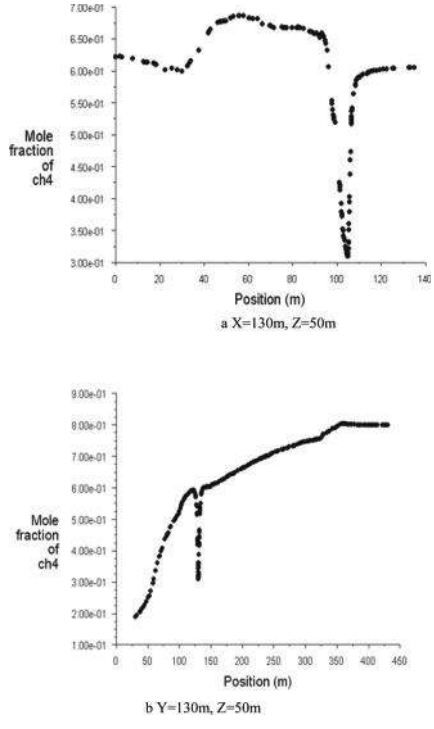


Figure 5. Gas volume fraction distribution from different aspects.

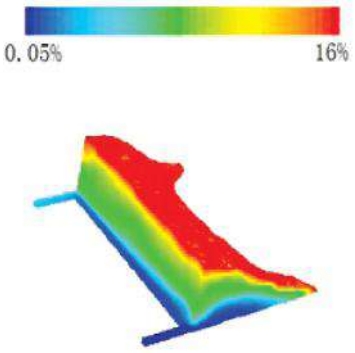


Figure 6. Gas distribution where gas concentration is higher than 16% in goaf.

3. The gas distribution laws along trend

During the ground drilling extraction, gas concentration is high far from working face in the goaf, but near the return air lane side, we can see clearly that, on the low level, low gas concentration field extends along the trend direction, as shown in the figure 4c and 4d. However, on the high level, this variation is not obvious. At the same time, after the ground drilling extraction, bigger changes have taken place in gas concentration gradient near the working face than that in deep area of goaf, which is the results that into the wind lane, return air lane and the ground drilling extraction negative pressure effect jointly, and on the high level, due to the existence of ground drilling, which makes oxygen concentration relatively low around the ground drilling, minimum concentration is only 30%, as shown in the figure 5b.

4. Gas distribution law in different z plane height

Compared with figure 4e and 4f, we can find that, low gas concentration area is expanded compared to the ground drilling without extraction at the Z = 10 plane near the return air lane side. At the Z = 50 plane, due to the effect of the ground drilling extraction, gas which is near the return the return air lane side outflows goaf through the ground drilling, which makes gas concentration low near the return air lane side, and in the figure 5f, we can see clearly that near the ground drilling the gas concentration field is relatively low, which shows that the gas supply near the ground is less than the amount of the ground drilling extraction.

From figure 6, we can see that, due to the effect of the ground drilling extraction negative pressure, the leakage field expands in goaf, which makes the high gas concentration dilute within the goaf, gas concentration decreases, especially in the area of upper corner, gas concentration is reduced to the safe range.

4 CONCLUSIONS

1. The existence of ground drilling can change the original flow of gas in goaf, this change is very obvious near the mining working area, the main reason is that porosity and permeability is bigger near the mining working face, which is easy to affected by the ground drilling extraction negative pressure.
2. After the ground drilling extraction, gas concentration decreases obviously, especially on the return air lane side, gas concentration decreases from 85% to 65%, gas concentration of the upper corner and return air lane also decreases obviously, which is reduced to the safe range.
3. Due to the ground drilling high negative pressure extraction, the oxygen high concentration areas and gas low concentration areas appear around the ground drilling, that is to say, there are big changes in the gradient of the gas composition near the ground drilling.
4. The ground drilling extraction negative pressure also changed the flow of the wind leakage in the goaf, on the above the level of the inlet and return air lane, air leakage flow reduces to the coalface, in a high level with the ground drilling plate, air leakage flow gathers the ground drilling position.

REFERENCES

Hu Qianting, et al. 2007. CFD simulation of goaf gas flow patterns. *Journal of China Coal Society,* 32(7):719–723.

Jin Longzhe, et al. 2010. CFD simulation of gas seepage regularity in goaf. *Journal of China Coal Society,* 35(9):1476–1480.

Li Zhongxiang. 2002. Study on numerical simulation of gas emission regularity and boundary condition of the goaf in coal caving of the fully mechanized. *Journal of China Coal Society,* 27(2):173–178.

Yuan Liang. 2009. Theory of pressure-relieved gas extraction and technique system of integrated coal production and gas extraction. *Journal of China Coal Society,* 34(1):1–8.

Yuan Liang. 2006. Key technique of safe and high efficiency mining inhighly gassy mining area with complex geologic conditions. *Journal of China Coal Society,* 31(2):174–178.

Zhang Dongming & Liu Jianzhong. 2003. Regularity on the distribution of gas moving in gob area of coal mine. *The Chinese Journal of Geological Hazard and Control,* 14(1):81–84.

Zhao Hongbao, et al.2011. Numerical simulation on distribution of gas concentration in goaf under condition of mining thin coal seam. *Journal of China Coal Society,* 36(2):440–443.

Progress in Mine Safety Science and Engineering II – He et al. (Eds)
© 2014 Taylor & Francis Group, London, ISBN 978-1-138-00122-0

Study on the similar experimental model and flow field distribution law of stope

Y. Qin, S.Q. Yang, C.L. Jiang, J.Y. Lun, G.X. Zhang & J. Niu
State Key Laboratory of Coal Resources and Safe Mining, China University of Mining and Technology, Xuzhou, China
Faculty of Safety Engineering, China University of Mining and Technology, Xuzhou, China
Key Laboratory of Gas and Fire Control for Coal Mines, China University of Mining and Technology, Xuzhou, China

ABSTRACT: Using the overburden rock fissure "O"-ring theory, and based on the three-dimensional stope Merry flow continuity equation, differential equations and gas migration momentum dispersion equation, combined with the similarity theory, the similarity criteria relationship of experimental model is established. Such design contains a variety of ways to build a three-dimensional ventilation stope experimental model. Make use of this model as the basis for the test-bed U-shaped ventilation flow field experiment, then input obtained experimental data into MATLAB software for numerical analysis. Finally get the discipline of air leakage field under the U-type ventilation and gas field distribution, then take it as the basis to determine the principles of Spontaneous Combustion Prevention and gas control.

1 INTRODUCTION

In order to more objectively and accurately study characteristics on goaf flow field, analyze goaf caving and overburden breaking features, we apply a mathematical model for three-dimensional flow field stope, simultaneously combine it with the similarity theory then establish stope experimental model. Experimental platform via the control valve can realize transition between ventilation through "U" type, "U + I" type, "U + II" type, "U + L" type, "U + I + high pumping lane" type, "Y" type, "E" type and so son. Implementing the U" type bench for ventilation experiments is discussed in this paper, which obtains the "U" type ventilation patterns goaf distribution of flow field characteristics, while then units flow field distribution law to determine control principles on the gas treatment and prevention of spontaneous combustion.

1 STOPE SIMILAR MODELING THEORY

1.1 *Physical characteristics of goaf*

As we all know, along with the advance of working face, goaf overburden appears to be cyclical caving and breaking, which enables goaf overlying strata in the vertical direction to display "Rounded Rectangle Landings" shape (Lin 2010). There are bottom-up points for the three bands: caving zone, fractured zone and bending sinking zone. Compaction degrees vary in different regions according to horizontal direction, forming a connected each other around the mining-induced fracture zone (Qian & Miao 1995). The compacted middle part is the formation of the so-called the mined crack "O"-ring (Qian & Xu 1998), whose mined crack width and cycle-related pressure are related to the initial pressure, closely near to face side bandwidth (A_1) is about 2–3 times the cycle weighting step ($2L_1 < A_1 < 3L_1$); cut near the eye bandwidth (A_2) is about double period weighting step ($A_2 \approx L_1$); intake and return airway side bandwidth (B_1, B_2) are approximately equal and both are 0.7–0.8 times of the initial pressure step ($0.7\ L_0 < B_1 \approx B_2 < 0.8\ L_0$) (Li et al 2000, Lin et al 2010, Lin et al 2011), goaf overburden mined crack patterns are shown in Figure 1.

1.2 *Basic equation and similar conditions of modeling on stope wind flow and gas migration*

We can conclude, after goaf overburden is caving and breaking, that the action of different caving and breaking forms with mine pressure, make goaf flow field at different position or different space channel, the gas flow state is different. Therefore, based on the theory of average volume (Vafai 2000), nonlinear seepage flow equation and Navier-stokes equation (Huang & Vafai 1994), depending on the working face and goaf for the unity of the different porosity space (Liang et al 2009), keep pure fluid

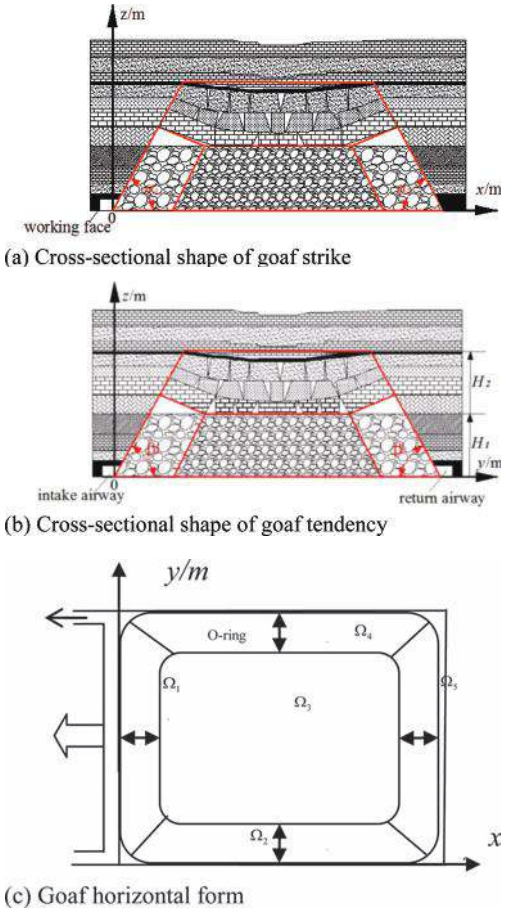


Figure 1. Goaf mined crack morphology diagram. H1-caving zone height; H2-fractured zone height; α_1, α_2—Caving angle, °; β_1, β_1—Fracture angle, °; Ω (i = 1~5)—Goaf different regions.

and porous media interface attributes introduced the approach of continuous single area of the flow field calculation model (Xu 1982), the linear Darcy's law is extended to Brinkman-Forchheime extended nonlinear Darcy's law (Patrick 1995, Sun 1994, Siemek & Nagy 2001), and get the description of three dimensional stope wind flow continuity equation, momentum differential equations and the dispersion equation of gas migration.

$$\frac{\partial u}{\partial x}+\frac{\partial v}{\partial y}+\frac{\partial w}{\partial z}=0 \tag{1}$$

$$\frac{1}{\varepsilon^2}\left(u\frac{\partial u}{\partial x}+\nu\frac{\partial u}{\partial y}+w\frac{\partial u}{\partial z}\right)=-\frac{\lambda}{\psi}u-\frac{F}{\psi}|u|u+\frac{\lambda}{\varepsilon}\left(\frac{\partial^2 u}{\partial x^2}+\frac{\partial^2 u}{\partial y^2}+\frac{\partial^2 u}{\partial z^2}\right)-\frac{1}{\rho}\frac{\partial P}{\partial x} \tag{2}$$

$$\frac{1}{\varepsilon^2}\left(u\frac{\partial v}{\partial x}+\nu\frac{\partial v}{\partial y}+w\frac{\partial v}{\partial z}\right)=-\frac{\lambda}{\psi}v-\frac{F}{\psi}|v|v+\frac{\lambda}{\varepsilon}\times\left(\frac{\partial^2 v}{\partial x^2}+\frac{\partial^2 v}{\partial y^2}+\frac{\partial^2 v}{\partial z^2}\right)-\frac{1}{\rho}\frac{\partial P}{\partial x} \tag{3}$$

$$\frac{1}{\varepsilon^2}\left(u\frac{\partial w}{\partial x}+\nu\frac{\partial w}{\partial y}+w\frac{\partial w}{\partial z}\right)=-\frac{\lambda}{\psi}w-\frac{F}{\psi}|w|w+\frac{\lambda}{\varepsilon}\left(\frac{\partial^2 w}{\partial x^2}+\frac{\partial^2 w}{\partial y^2}+\frac{\partial^2 w}{\partial z^2}\right)-\frac{1}{\rho}\frac{\partial P}{\partial x} \tag{4}$$

$$\varepsilon\frac{\partial c}{\partial t}+u\frac{\partial c}{\partial x}+v\frac{\partial c}{\partial y}+w\frac{\partial c}{\partial z}=\varepsilon D_d\left(\frac{\partial^2 c}{\partial x^2}+\frac{\partial^2 c}{\partial y^2}+\frac{\partial^2 c}{\partial z^2}\right)+\varepsilon F_c \tag{5}$$

Where u = x-direction velocity, m/s; v = y-direction velocity, m/s; w = z-direction velocity, m/s; ε = porosity; λ = fluid viscosity, m^2/s; ψ = permeability, m^2; F = friction coefficient, $F = 1.75/\sqrt{150\cdot\varepsilon^3}$; ρ = fluid density, Kg/m^3; P = fluid pressure, Pa; c = nevas concentration goaf, Kg/m^3; D_d = hydrodynamic dispersion coefficient, m^2/s; and F_c = gas emission source, $(g/m^3)/s$.

Since it is impossible to strictly satisfy similar modeling (Yang et al 2002), we can only use approximate modeling approach, and just focus on playing a decisive role in the flow field conditions that are similar to modeling (Bear 1972). Therefore, this paper adopts the improved test method, introduces into the model's all relevant variables and constants with corresponding values for the ratio of the prototype (where the subscript p represents the prototype, and the model expressed by the subscript m) (Jones & Lourie 1993). Its dimensionless is:

$$x_r=\frac{(\delta x)_m}{(\delta x)_p}\quad y_r=\frac{(\delta y)_m}{(\delta y)_p}\quad z_r=\frac{(\delta z)_m}{(\delta z)_p}\quad u_r=\frac{(\delta u)_m}{(\delta u)_p}$$

$$v_r=\frac{(\delta v)_m}{(\delta v)_p}\quad w_r=\frac{(\delta w)_m}{(\delta w)_p}\quad \varepsilon_r=\frac{\varepsilon_m}{\varepsilon_p}\quad \lambda_r=\frac{\lambda_m}{\lambda_p}$$

$$D_{nr}=\frac{D_{nm}}{D_{np}}\quad \rho_r=\frac{\rho_m}{\rho_p}\quad P_r=\frac{P_m}{P_p}\quad D_{dr}=\frac{D_{dm}}{D_{dp}}$$

$$F_{cr}=\frac{F_{cm}}{F_{cp}}\quad c_r=\frac{c_m}{c_p}\quad t_r=\frac{(\delta t)_m}{(\delta t)_p}$$

Simultaneously

$$\psi_r=\frac{\psi_m}{\psi_p}=\frac{D_{nr}^2\varepsilon_r^2(1-\varepsilon_p)^2}{(1-\varepsilon_m)^2}=\frac{D_{nr}^2\varepsilon_r^2(1/\varepsilon_p-1)^2}{(1/\varepsilon_m-1)^2}$$

$$F_r=\frac{F_m}{F_p}=\frac{1}{\varepsilon_r\sqrt{\varepsilon_r}}$$

Experimental models and prototypes equation should be the same or proportional (Li 2008), but when geometrically similar ratio (i.e. $x_r = y_r = z_r$) is to be determined $u_r = v_r = w_r$, on this basis, the dimensionless variable is put into the formula (2), (3), (4), (5). Reduce and extract the model order simplified equation coefficient corresponding to each of before, the ratio between the following can be obtained:

$$\frac{\varepsilon_r^2 x_r}{u_r^2} = \frac{D_{nr}^2 \varepsilon_r^2 (1/\varepsilon_p - 1)^2}{\lambda_r u_r (1/\varepsilon_p - \varepsilon_r)^2} = \frac{D_{nr} \varepsilon_r^2 \sqrt{\varepsilon_r} (1/\varepsilon_p - 1)}{u_r^2 (1/\varepsilon_p - \varepsilon_r)} = \frac{\varepsilon_r x_r^2}{\lambda_r u_r} = \frac{\rho_r x_r}{P_r} \quad (6)$$

$$\frac{t_r}{c_r \varepsilon_r} = \frac{x_r}{u_r c_r} = \frac{x_r^2}{\varepsilon_r D_{dr} c_r} = \frac{1}{\varepsilon_r F_{cr}} \quad (7)$$

The model ignores flow of airflow diffusion term in the momentum equation, just considers goaf Merry Darcy seepage. Meanwhile, when the Reynolds number exceeds a second stope Merry Renault value ($R_e \geq 2300$) (Jiang & Wang 1995), the stope air current steps into the automatic modeling. Models face section size is 0.04 x 0.03 m, then the critical velocity is:

$$V = \frac{2300 \times 2 \times (0.04 + 0.03) \times 14.4 \times 10^{-6}}{4 \times 0.04 \times 0.03} = 0.966\ m/s$$

Actual speed is 1 ~ 4 m/s, already exceeding the critical speed. The model Reynolds criterion cannot be considered. In addition, the porosity of experimental models and prototypes is small and substantially equal, so the formula (6), (7) can be further simplified to

$$\frac{x_r}{u_r} = \frac{D_{nr}^2}{\lambda_r u_r} = \frac{\rho_r x_r}{P_r} \quad (8)$$

$$\frac{t_r}{c_r} = \frac{x_r}{u_r c_r} = \frac{x_r^2}{D_{dr} c_r} = \frac{1}{F_{cr}} \quad (9)$$

Similarity criterion equation (8), (9) includes an experimental model to be followed by all the criteria relationship, λ_r, ρ_r, D_{dr}, which in the condition of there is no significant difference between prototype and the model flow field thermal properties, can be considered equal to a constant one, and only have two independent relationship, except $P_r = 1$ as a constraint, the remaining six variables x_r, u_r, D_{nr}, c_r, t_r, F_{cr}, can be arbitrarily selected four variables, such as selecting x_r, u_r, c_r, t_r, after then, through a combination dimensionless equation (8), (9), D_{nr}, F_{cr} is obtained.

2 MODEL TEST BENCH

The designed model test station is shown in Figure 2, including five parts, namely, the body of the model, gas releasing system, fan power system, sampling system, test system and attachment means.

2.1 *Main body of the model*

Main body of the model is designed according to the geometry ratio of 1:100, using 2-inch stainless steel angle frame and welding them together. The external part is 10 mm riveting plexi-glass, with the inside and outside both being made of glass and plastic seal. Its goaf strike length is 200 cm, tend length is 160 cm, height of caving zone is 20 cm, and fractured zone height is 64 cm. The mining fractured zone near the face side bandwidth equals to 35 cm, the zone close to the cut side of the bandwidth equals to 25 cm, and intake and return airside of the bandwidth equals to 22 cm. Goaf caving zone and fractured zone are divided into five regions. The internal of each region is filled with foam balls that are reduced by a certain percentage (when $x_r = 100$, $u_r = \lambda_r = \rho_r = P_r$, then $D_{nr} = 10$) and a very small amount of foam particles after crushing load sealed in gauze. The amount usage of pellets and the volume of bubble being broken are determined by the porosity of different area size, and porosity values according to the physical characteristic described in literature, whichever each region use number of average, analog stent uses 1 mm plexi-glass plate bonding processed in accordance with 1:100; simulated roadway uses hydraulic radius equal to rectangular roadway round plexi-glass tube, while arranges control valve disposed thereon, for the purpose of controlling airflow and partial pressure, so that the air volume and pressure will meet specific requirements.

2.2 *Gas release system*

The system consists of high pressure gas bottle with gas of 99% concentration, reducing valve, gas

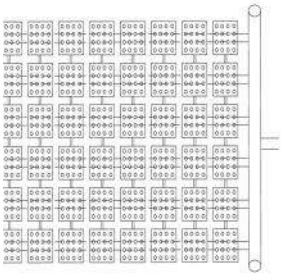


Figure 2. Dimensional flow model goaf bench.

shunt regulator, flowmeter, connecting hoses, gas release plate, shown in Figure 3(a). The gas from High-pressure gas bottle passes through reducing valve to flow into the gas regulator connection hose splitter, and then through the glass rotameter for gas flow distribution, gas distributed at a certain flow through the hose connected to the gas release plate connection injecting gas release hole on the goaf. Gas release plate has multiple releases from the above cloth rectangular plate that is composed of holes along goaf tendency with each direction through the hose connected to a rectangular plate. Hose on the front to the backset of holes are of different sizes. While plugging one end of the hose, connect the other end to the external interface. Along the goaf, the hose is connected to the respective rectangular plates. The rectangular orifice communicates with each other to form a hole, as shown in Figure 3(b). To ensure the release plate propane gas release realistic gas emission characteristics, hose on the pore size and pore size on rectangular plates are obtained experimentally determined through fuming Figure 3(c) below.



(a)Physical Map of Gas Release System



(b) Schematic of Gas Release Plate Geometry



(c) Fuming Experiments

Figure 3. Gas release system diagram.

2.3 *Fan power system*

Models bench uses exhaust ventilation, returns airway connected inverter type axial fans, and tails roadway directly vented to the air. in order to ensure the negative of tail Lane meet the requirements, the tail is also connected to an inverter Lane axial fan speed adjustment and controlled range from 0 m/s to 4 m/s, and high drainage roadway is connected to vacuum pumping to meet high negative pressure requirements.

2.4 *Sampling and testing system*

The model is three-dimensional. In order to comprehensively analyze the distribution of flow field, 260 sampling points for 4 levels in goaf are sampled in a short time, and then the gas concentration of samples was analyzed and tested by GC-4000 A gas chromatograph. The sampling points are also used as pressure measurement points. The static pressure of points are absorbed by the YJB-1500-type compensator micro-manometer, and the wind speed and static pressure of intake and return airway were measured by electronic wind instrument and U-type differential pressure meter.

2.5 *Attachment*

Attachments mainly include control valves and thermometers installed in the tubes of the simulated roadway.

3 U-TYPE VENTILATION EXPERIMENTS, RESULTS AND DISCUSSION

Different inlet and return air pressure are carried out for four U-shaped ventilation experiments. Along goaf tendency the distance for x = 0 cm side is the inlet side, and x = 160 side is the return airside. The mined negative pressure and gas content for each point are tested respectively. Use MATLAB to analyze the pressure and gas concentration values and draw a three-dimensional contour map. The conditions of the gas concentration and pressure distribution get under differential pressure between inlet and return airway.

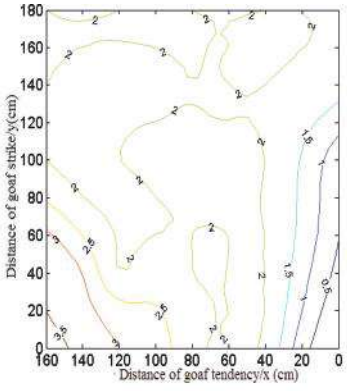
3.1 *Pressure distribution*

In order to avoid unstable impact on the pressure distribution from the changes in atmospheric pressure and wind turbines, the relative pressure is adopted. The measuring point at down-corner

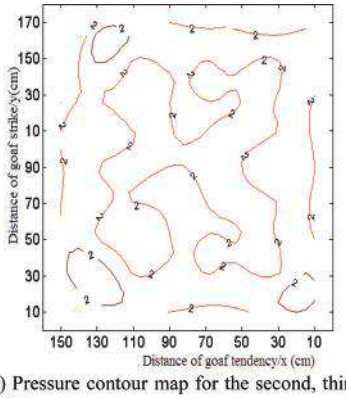
angle is as zero basis points. The rest of the pressure measuring points are relative pressure at that point. Select the results of the second and fourth experiments. The pressure distribution is shown in Figure 4 and Figure 5:

Through the Figure 4 and Figure 5 can be obtained experimental results obtained:

1. U-type ventilation conditions. When determining the physical characteristics of mined-out area, although air pressure on both sides of intake and return airway are different, the pressure distribution of the goaf is basically the same. The negative value is only determined by air pressure difference on both sides for the intake and return. However, goaf leakage Merry is vertical line with the isobars, which

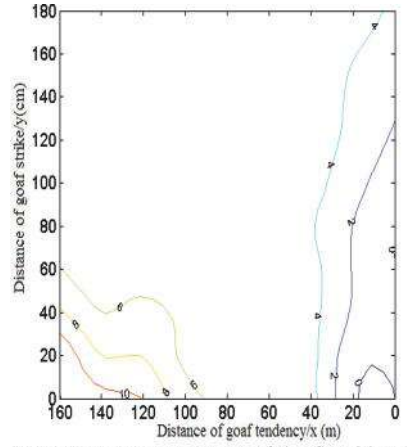


(a) Pressure contour map of the first hierarchy

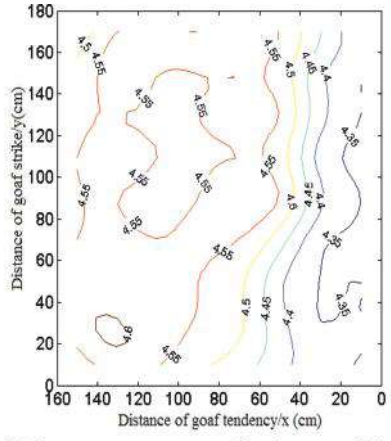


(b) Pressure contour map for the second, third and fourth hierarchy

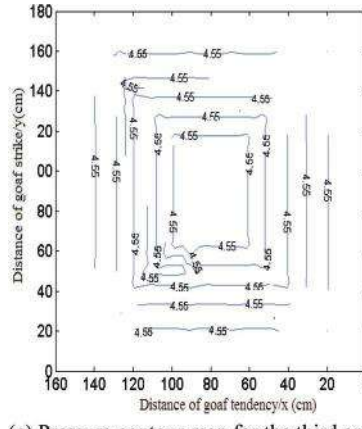
Figure 4. The pressure contour map of second Experiment, (pressure difference of 40 Pa between inlet and return air).



(a) Pressure contour map of the first hierarchy



(b) Pressure contour map for the second hierarchy



(c) Pressure contour map for the third and four hierarchy

Figure 5. The pressure contour map of fourth experiment (pressure difference 100 Pa between inlet and return air).

can fully explain that when the physical characteristics is determined of the flow field in goaf, the flow field in goaf remained unchanged. Different intake and return air pressure make the goaf negative values of different sizes and goaf varying intensity. The greater the pressure, the greater the wind speed; the greater the intensity goaf, the smaller pressure; the smaller wind, the smaller air leakage in goaf. Therefore, for the purposes of spontaneous combustion in goaf, try to keep the equalized state of the inlet. The return airside is the most effective way to prevent Goaf.

2. There is a high-pressure area in the inlet side, while relatively low pressure is for the whole goaf area in the return airside. The pressure gradient in the inlet side is smaller than that in the return airside, which indicating when Merry Lane from the inlet end enters the flow direction perpendicular goaf in the form of jet, dynamic pressure is converted into static pressure and decreases rapidly. In addition, because the porosity of mining coverage fissure "O" circle is greater than that of compaction zone, it makes the inlet air flow along at the end to cut air leakage, resulting in flow field in goaf asymmetry.
3. Pressure gradient of side and the return air inlet side in goaf is significantly greater than that in other regions, while the pressure gradient and the overburden rock "O"-rings are closely linked, in close proximity to face side 35 cm (corresponding to the prototype 35 m), forward, return airway side 22 cm (corresponding to the prototype 22 m) within the pressure gradient is more obvious. It can be concluded that goaf in the overburden rock "O"-ring close to the face side of the bandwidth and feed, return airway side bandwidth is more obvious, and the flow velocity is significantly greater than in other regions. In the vertical direction, when the height exceeds certain value, pressure goaf is substantially a constant value. The air leakage is very small, and the flow velocity is almost zero.
4. Inlet and return air pressure exceeds a certain value, and air leakage happens in vertical between goaf caving zone and fractured zone.

3.2 *Distribution of gas concentration*

When gas emission is under the same conditions, gas concentration distribution and pressure distribution in goaf are mutually sealed. Each experiment for four experimental gas concentration variation in the vertical direction is almost the same, so a second test gas concentration distribution and a second select only the first hierarchical layer, as shown in Figure 6; gas concentration distribution for 4th experiment is to select the first to fourth

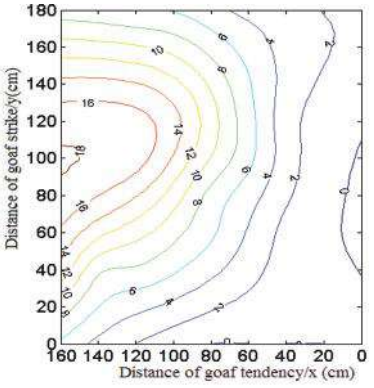
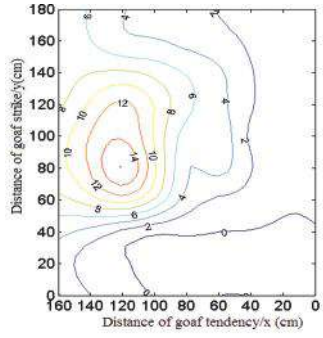


Figure 6. Gas density contour map of each layered of second experiment (pressure difference 40 Pa between inlet and return Air).

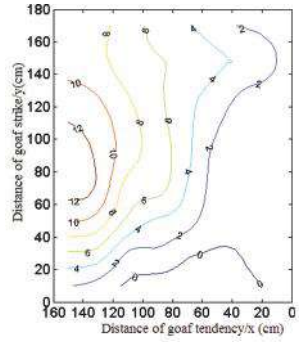
hierarchical layers, as shown in Figure 7. Along the dip, the direction tends to 0 cm is the inlet side, dip at 160 cm distance is the return airside.

Through the Figure 6 and Figure 7, experimental results can be obtained:

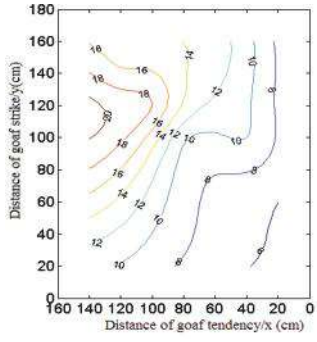
1. Goaf makes inlet end face gas concentration gradient is small, while the return airside gas concentration gradient is large. The inlet side and into the inlet end of the gas close to the face side of the gas concentration along goaf tendency by the return air inlet side to side increases, the methane concentration at the upper corner reaches the maximum. Along goaf leakage toward the inlet side so gas concentration greater increases along strike, combined with pressure distribution goaf compaction pressure gradient region smaller amount of gas leakage romantic take significantly less than in other regions. Because of gas emission from adjacent layers, gas concentration increased first strike



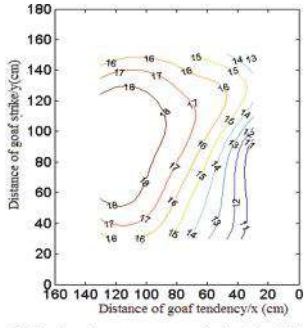
(a) Gas density contour map for the first hierarchy



(b) Gas density contour map for the second hierarchy



(c) Gas density contour map for the third hierarchy



(d) Gas density contour map for the fourth hierarchy

Figure 7. Gas density contour map of each layered of fourth experiment (pressure difference 100 Pa between inlet and return Air).

after a large decrease by the increase of distance in goaf central in the return airside. The gas concentration in return airside is becoming bigger with the increase of toward distance along goaf.

2. When air pressure difference increases, the gas concentration at the upper corner reduced, but for air leakage increasing, the oxygen concentration distribution and gas concentration distribution are counter. For high gassy and spontaneously combustible seam, the goaf is with the coal spontaneous combustion and gas explosion double disaster. Once the left coal combustion caused gas explosion, it will form the dual ignition and explosion hazards that are caused by the chain reaction. Thus, for high gassy and combustible goaf, we must keep rational air pressure conditions for inlet and return to ensure that spontaneous combustion does not occur in the goaf.
3. Gas Emission from adjacent seam creates higher methane concentrations in the fracture zone. However, the pressure gradient is almost zero, for the floating effect gas will gradually accumulate in the upper. When a cycle of pressure takes place, a lot of gas will be pressed into the face, causing gas exceeding the limit.

4 CONCLUSIONS

Combined with the overburden rock fissure "O"-ring theory, three-dimensional heterogeneous flow field in goaf Merry flow continuity equation, momentum differential equations and gas migration dispersion equation, obtained between experimental models similarity criteria style. and designing and constructing three-dimensional stope experimental model, carrying out flow field characteristics under the U-type goaf ventilation, using MATLAB software for numerical analysis of experimental results, obtaining flow field and distribution of gas flow field under the U-type ventilation at goaf. flow field in goaf homogeneous asymmetric distribution, import and return airside of the gas concentration along goaf towards gradually increased, but due to cut air leakage, making goaf central goaf gas concentration along strike first increases and then decreases, basis on these, we summarized the prevention and control principles for spontaneous combustion at goaf.

ACKNOWLEDGEMENTS

I am grateful to professor S.Q.Yang for his useful discussion and comments on the manuscript as well as to all participators who have supported me dur-

ing the writing. Support for this work was obtained from the National Natural Science Foundation of China (No. 51174198) and Independent Subject of State Key Laboratory of Coal Resources and Safe Mining (No. SKLCRSM11X01).

REFERENCES

Bear, J. 1972. Dynamics of fluids in porous media. New York: *American Elsevier Publishing Company.*

Huang, P.C & VafaiK. 1994. Analysis of forced convection enhancement in a channel using porous blocks. *Thermo-physic and Heat Transfer* 8(3): 563–573.

Jiang, S.G & Wang, X.S. 1995. Study on3-D Modeling of airflow and methane transfer in top-coal drawing fields. *China University of Ming & Technology* 25(4):85–89.

Jones, A.D & Lourie, S. 1993. Applications of aero dynamic scale model simulations to predicting the accumulation of methane gas and airborne pollutants in modern of coal mines[R].*Edinburgh: Institute of Occupational Medicine.*

Li, S.G, Qian, M.G & Shi, P.W. 2000. Study on bed-separated fissures of overlying stratum and interstice permeability in fully-mechanized top coal caving. *Rock Mechanics and Engineering* 19(5): 604–607.

Li, Z.X. 2008. CFD simulation of spontaneous coal combustion in irregular patterns of goaf with multiple points of leaking air. *China University of Mining and Technology* 18(4):504–508.

Liang, Y.T, Zhang, T.F, Wang, S.G, et al. 2009. Heterogeneous model of porosity in gobs and its airflow field distribution. *China Coal Society* 34(9):1203–1207.

Lin, H.F, Li, S.G, Cheng, L.H, et al. 2010. Model experiment of evolution pattern of mining-induced fissure in overlying strata. *Xi'an University of Science and Technology* 30(5): 507–512.

Lin, H.F, Li, S.G, Cheng, L.H, et al. 2011. Experimental analysis of dynamic evolution model of mining-induced fissure zone in overlying strata. *Mining and Safety Engineering* 28(2):298–303.

Patrick, L. 1995. Numerical simulator for3-D unsteady-state dual-porosity modeling of gas flow within a coal structure. Lexington; KY; USA: *Soc for Mining, Metallurgy & Exploration Inc*.

Qian, M.G & Miao X.X. 1995. Theoretical analysis on the structural form and stability of overlying stkata in long wall mining. *China University of Ming and Technology* 14 (2):97–106.

Qian, M.G & Xu, J.L. 1998. Study on the "O shape" circle distribution characteristics of mining induced fractures in the overlaying strata. *China Coal Society* 23(5):466–469.

Siemek, J & Nagy, S. 2001. The early time condensation in the near well zone during non-stationary and non-isothermal flow of gas condensate system. *Archive of Mining Sciences* 46 (3):319–336.

Sun, P.D. 1994. Coal gas dynamics and it applications. *Scientia Geologiea Sinica* 3(l):66–72.

Vafai K. 2000. Handbook of porous media. New York: *Marcel Dekker*.

Xu, T. 1982. Similar to the theoretical and experimental models. Beijing: *China Agricultural Machinery Press.*

Yang, S.Q, Yu, Q.X, Wang, K. 2002. The study of theory and experiment on which pulsed ventilation brings the methane accumulating under control in upper corner of working face. Xuzhou: *China University of Mining and Technology Press.*

Progress in Mine Safety Science and Engineering II – He et al. (Eds)
© 2014 Taylor & Francis Group, London, ISBN 978-1-138-00122-0

Uncertainty analysis and evaluation of gas flow measurement

Ping Lu
Chongqing Institute of Coal Science Research Institute, Chongqing, China

ABSTRACT: Wind speed measurement is an important part of safe operation for the mine ventilation system, and it requires the uncertainty analysis and evaluation of flow velocity measurement in engineering applications. A velocity measurement device based on the principle of pitot tube is proposed in this article. First, the influence factors of velocity measurement are analyzed. Then evaluation methods of type A and type B are adopted to combine the relative uncertainty. The method is demonstrated in a standard wind tunnel laboratory environment, where the measurement uncertainty of the velocity is calculated.

1 INTRODUCTION

In the process of coal mining, mine ventilation system is an important part of safe production in coal mines. Reasonable and reliable design of ventilation system can reduce accidents when the mine disasters include gas outburst and fire accidents happen. The wind speed measurement is an important part of safe operation for the ventilation system. Pitot tube has became a widely used velocity sensing device due to its advantages such as its simple structure, easy to use, inexpensive and undergo a rigorous calibration and proper correction, and it can acquire a high accuracy within a certain speed range.

Usually the pitot tube is connected with a soft rubber tube to the micro pressure gauge, and calculates the velocity based on a certain formula[1]. But in the process of actual usage, the velocity measurement precision is affected by a number of environmental factors. It needs to analyze the influencing factors of measurement results and acquire the measurement uncertainty of instruments. A velocity measurement device based on the principle of pitot tube is proposed in this article. The influence factors of velocity measurement are analyzed, and the measurement uncertainty of the device is calculated afterwards.

2 PRINCIPLE ANALYSIS OF FLOW VELOCITY MEASUREMENT DEVICE

Standard pitot tube is composed of two different diameter pipes, two tubes of concentric sockets together. The inner pipe connecting pipe straight tail, as the full pressure connector; another branch pipe and tube side is communicated, static pressure connector. Pitot tube of S-type is welded with two equal tubes. In the face of air flow is a full pressure side, while the back flow is a static pressure side. The number and type information are marked at the joints, which should be sure to true. The side pointing rod is in the same direction with the probe, and the direction can be determined to ensure the probe to align the flow direction. This article selects S-type pitot tube as a differential pressure detection device. Compared to the standard pitot, S-type pitot tube has some advantages such as its holes not easy to be blocked by high concentrations of dust, without bending tube, no need to open too larger measuring hole, with clear readings and easy measurement for differential pressure.

Gas flow measurement device is composed of S-type pitot tube, the pressure tube, differential pressure measurement, pressure measurement, temperature measurement, ARM processor unit, liquid crystal display components. Architecture block diagram looks like this.

This velocity measurement device uses pitot tube to measure differential pressure. It's an indirect way to measure flow rate. In accordance with Bernoulli equation, resulting in:

$$V = \alpha\sqrt{\frac{2\Delta P}{\rho}} \tag{1}$$

Because gas concentration is affected by factors such as the impact of gas temperature, pressure,

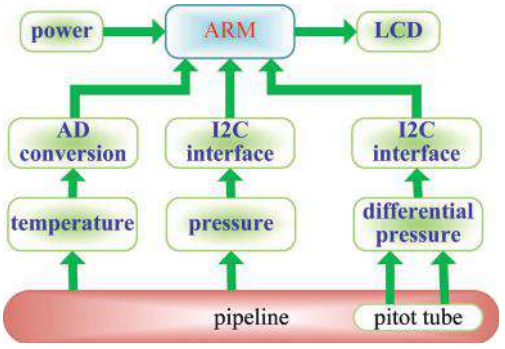


Figure 1. Architecture block diagram for measurement.

humidity and other factors, velocity calculation formula is as follows:

$$V = 2.194\alpha\sqrt{\frac{P\Delta P}{(273.15+t)}} \tag{2}$$

V: gas flow rate.
α: pitot tube coefficient.
ΔP: pitot dynamic pressure. ΔP is total pressure-static pressure.
P: gas pressure.
t: gas temperature.
ρ: gas concentration.

3 EVALUATION OF UNCERTAINTY IN MEASUREMENT

3.1 *Evaluation of uncertainty*

General uncertainty of measurement is said to be dispersed between the measured values and parameter values that are interrelated. In other words, in the course of measurement of physical quantities, such as personnel, equipment and measurement of environmental impact, the degree of uncertainty for measurement result. And evaluation of uncertainty in measurement is by means of a quantitative determine the extent of such uncertainty, the purpose of which is to determine the distribution of measurement range and measurement result reliability level. Observation column evaluation results of the statistical analysis of standard uncertainty is called type A standard uncertainty. Are different from those used for observing statistical analysis to evaluate the uncertainty of standard uncertainty is known as type B standard uncertainty[1].

Type A uncertainty is obtained by a set of observed frequency distribution probability density function that is exported; Type B uncertainty is based on level of trust on the occurrence of an event. They are based on a probability distribution, and characterization by variance or standard deviation. Uncertainty of type A and type B is used in the synthesis of uncertainty standard uncertainty[2, 3].

Using pitot tube as a differential pressure detection device, it need to consider factors that affect measurement accuracy, including the pitot tube coefficient, air density, temperature, pressure, thermal expansion coefficient, kinematic viscosity, and installation locations.

3.2 *Type A evaluation*

Type A standard uncertainty assessing is the adoption of a set of measured data for statistical analysis, with methods of the experimental standard deviation characterizing uncertainty. Single experimental standard deviation of measurements data commonly uses the Bessel formula to calculate:

$$s = \sqrt{\frac{\sum_{i=1}^{n}(x_i - x)^2}{n-1}} \tag{3}$$

The standard uncertainty u(x) for input quantity is used to represent experimental standard deviation of the averages of the measured data:

$$u(x) = s/\sqrt{n} \tag{4}$$

3.3 *Type B evaluation*

Type A evaluation requires uncertainty through a large number of experiments, statistical methods are used, and need to spend a lot of time and energy. Type B evaluation of standard uncertainty can be used with type A assessing reliability. Especially when type A assessing when a small number of independent measurement, access to type A standard uncertainty may not be more reliable than the uncertainty evaluation for the type B. Type B standard uncertainty of information requires a certain amount of experience and have some understanding of this information. Type B uncertainty evaluation of standard content generally includes a previous measurement or assessment of data; understanding of relevant technical characteristics of information and measurement instruments and experience; manufacturing sector to provide technical documents; calibration certificate provides the data, accuracy or level of hierarchy, including temporary use limits of error; manual or information to reference data and uncertainty and so on. This design of gas flow measuring equipment is assessed from the following aspects.

3.3.1 *Uncertainty of pitot tube coefficient u(α)*
Pitot tube as a measuring device, when manufacturing it need to be calibrated. Due to the uncertainty of standard instruments, uncertainty u(α) in the pitot tube coefficient appears.

3.3.2 *Uncertainty of gas pressure u(P)*
Gas pressure inside the wind tunnel is measured by pressure component collection. In conjunction with its error to calculate gas pressure uncertainty u(P).

3.3.3 *Uncertainty of gas temperature u (t)*
Gas temperature with Pt resistance is measured in a wind tunnel, with its error calculating gas temperature uncertainty u (t).

3.3.4 *Uncertainty of differential pressure u (ΔP)*
Between static pressure and total pressure holes producing gas differential pressure, it is measured by differential pressure element, with its error to calculate measuring differential pressure value uncertainty u (ΔP).

3.3.5 *Uncertainty of measurement location u(C_1)*
Pitot tube measurement of differential pressure is point differential pressure value. According to the specification of the wind tunnel and wind field inhomogeneity errors and concluded that measurement uncertainty u(C_1).

3.3.6 *Uncertainty of probe deflection u(C_2)*
By Verification regulation of pitot tube, velocity measurement with a pitot tube as standard, pitot probes should be consistent with the direction of flow, but due to the randomness of the operation and installation, cannot be absolutely consistent with the direction of flow, the resulting measurement error. In conjunction with its error to calculate installation probe deflection into uncertainty u(C_2).

3.4 *Synthesis of relative standard uncertainty U(V)*

When the standard uncertainty of measurement results is made up of several standard uncertainty components of time. By the square and the square root of synthesis be combined standard uncertainty. Formula is as follows:

$$U(V)=\sqrt{\begin{array}{l}u^2(V_A)+u^2(\alpha)+\left(\frac{1}{2}\right)^2 u^2(P)+\left(\frac{1}{2}\right)^2 \\ u^2(t)+\left(\frac{1}{2}\right)^2 u^2(\Delta P)+u^2(C_1)+u^2(C_2)\end{array}} \quad (5)$$

4 CASE

Gas flow measurement device is installed in the wind tunnel laboratory. After a period of time, correlation parameter reaches a steady state. The temperature is 22°C, and pressure is 98 kPa, and air gas density is 1.205 kg/m^3. Using standard identification system to measure flow velocity, it is 4.435 m/s.

4.1 *Type A evaluation*

Insert the pitot tube in the wind tunnel, and measure the air velocity. The insertion depth is 50 mm. 10 sets of measured data representation for Vi. They are 4.47, 4.5, 4.4, 4.43, 4.44, 4.43 and 4.47 m/s. Average velocity V is 4.458 m/s.

Using Bessel formula to calculate the standard deviation. Set data sequence is Vi, (i = 1, 2, ... n). The mean velocity is V. The standard uncertainty is calculated as:

$$U(V)=\sqrt{\frac{\sum_{i=1}^{n}(V_i-V)^2}{n(n-1)}} \quad (6)$$

From the above formula the standard uncertainty of U(V) is 0.0095 m/s. The relative standard uncertainty of u(V_A) is 0.21%.

4.2 *Type B evaluation*

According to the pitot tube verification regulation of requirements, the pitot tube coefficient using the allowable limits of error is ±0.1%. Set to a normal distribution, k = 2, pitot tube relative standard uncertainty u(α) is 0.05%.

Wind tunnel gas pressure within the error range is ±1.5%. Set to a normal distribution, k = 2, pitot tube relative standard uncertainty u(P) = 0.75%.

Wind tunnel gas temperature range is ±0.5°C. Set to a normal distribution, k = 2, pitot tube relative standard uncertainty is

$$u(t)=\frac{0.5}{2*(273.15+22)}=0.085\% \quad (7)$$

In the holes between the static pressure and total pressure differential pressure is created, and differential pressure measurement error is ±0.75%. Set to a normal distribution, k = 2, pitot tube relative standard uncertainty u (ΔP) = 0.375%.

Inhomogeneity of wind error is 0.5%. The uncertainty caused by the measurement location is set to uniform distribution. Get

$$u(C_1)=0.5\%/\sqrt{3}=0.288\% \quad (8)$$

Experiments show that, when the angle between the pitot probes and air reaches 5°, maximum error of measurement of wind speed is 0.25%. Set to uniform distribution, and k = 3, the uncertainty is

$$u(C_2) = 0.25\% / \sqrt{3} = 0.144\% \quad (9)$$

In conjunction with that analysis, using equation (5) maximum error of measurement of wind speed is 0.57%.

5 CONCLUSIONS

This article adopted the measurement uncertainty assessment methods, which contains type A and type B evaluation methods, to evaluate the uncertainty of gas flow measurement via pitot tube. The synthesis of relative standard uncertainty is acquired for the flow velocity measurement.

It can be indicated from the analysis above: for the flow velocity measurement with lower measuring limit, the proportion of the differential pressure measurement uncertainty is larger. While for the compressible gas measurement, the impact of gas pressure measurement uncertainty is larger. Thus the pressure compensation measurement is required in the actual measurement.

In addition, from the perspective of uncertainty evaluation process, the external environmental factors mainly focus on both the distribution of flow and the repetitive terms.

ACKNOWLEDGEMENTS

The author would like to thank the project supported by the National Natural Science Foundation of China (Grant No. 61174006).

REFERENCES

Liu Zhimin 2000. *Uncertainty and its practice*. Beijing: China Standard Press.

SG Etemad et al. 2003. Calculation of the Pitot tube correction factor for Newtonian and non-Newtonian fluids. *ISA Transactions* 42(4): 505–512.

Wang Chi 2002. *Analysis of uncertainty in measurement of flow.* Beijing: China Measurement Publishing House.

Progress in Mine Safety Science and Engineering II – He et al. (Eds)
© 2014 Taylor & Francis Group, London, ISBN 978-1-138-00122-0

Coupling model and its application to dynamic failure for hard coal containing gas

Chunfu Wei
State Key Laboratory Cultivation Base for Gas Geology and Gas Control, Henan Polytechnic University, Jiaozuo, China
School of Mathematics and Information Science, Henan Polytechnic University, Jiaozuo, China

Huamin Li
School of Energy Science and Engineering, Henan Polytechnic University, Jiaozuo, China

Bo Li
State Key Laboratory Cultivation Base for Gas Geology and Gas Control, Henan Polytechnic University, Jiaozuo, China

ABSTRACT: Gas-solid coupling model of hard coal containing gas was studied in this paper, the coupling model was resolved by RFPA and the process of dynamic failure for hard coal containing gas was analysized. According to the simulation results, the process was divided into four phases as follows: stress concentration, coal rock fracture induced by ground and gas stress, protection coal pillar was damaged by gas stress (outburst start), Crushed coal was thrown out by gas pressure (outburst development). And three conclusions were obtained in the paper: the ground stress is very important in the hard coal containing gas outburst because the coal structure needs to be damaged by high stress in the phases of outburst start and development; Gas pressure increases the strength of the outburst destruction and reduces the threshold of the outburst destruction, but it's non-dominant effect in the phases of outburst start and development; Hard coal containing gas out-burst endurance is bad and its termination is rapid.

1 INTRODUCTION

Dynamic failure of coal containing gas is a very complex and challenging research topic and it is also a research focus of coal and rock dynamic disaster. Coal and gas outburst induced by dynamic failure of coal containing gas is a complex dynamic disaster along with the coal mining, which is an urgent problem in order to ensure safe mining. Therefore, scholars both at home and abroad have done a lot of research work in order to know dynamic failure of coal containing gas better. Coal deformation affected by swelling stress of adsorption and porosity gas pressure has been researched (Borisenko A. 1985); Mathematical model of gas solid coupling of coal containing gas was presented and given its numerical solution, and the re-search result laid the foundation of the research field (Zhao Y. S. 1994); The mathematical model of gas solid coupling of coal containing gas based on internal variable theory have been developed (Zhang M.T. & Liang B. 1990); Failure process of coal containing gas and outburst mechanism based on numerical simulation software of RFPA has been researched(Xu T. et al. 2008); The constitutive relation of coal containing gas by a series of physical experiment (Yi G.Z. et al. 2008) and unstable failure of the coal containing gas and its acoustic emission characteristics (Zhao H B. 2010) have been studied.

However, the current research results mostly focus on unstable failure and outburst mechanism of soft coal containing gas; and coal and gas outburst that usually happens in soft coal seam is adopted by most scholars, meanwhile, according to Chinese current the control of the coal and gas outburst regulations, Consistent coefficient ($f \leq 0.5$) and failure types (III, IV, V) of coal are regarded as the indexes whether the coal seam is outburst coal or not on the basis of Chinese current the control of the coal and gas outburst regulations. With the increasing of min-ing depth, phenomenon of unstable failure that hap-pens in hard and half-hard coal seam increases dra-matically. Because gas plays its role in the process of unstable failure of hard coal, dynamical phenomenon seems to have the characteristic of outburst. For this reason, dynamic failure for hard coal containing gas will be researched in the following passage.

2 MATHEMATICAL MODEL OF GAS-SOLID COUPLING OF COAL CONTAINING GAS

In this paper, a series of numerical simulations have been done, which is based on dynamic failure for hard coal containing gas with RFPA2D-Flow numerical simulation software developed (Xu T. 2004). On the one hand, evolution of stress field, fracture field and seepage field can be known clearly in the process of dynamic failure for hard coal containing gas. On the other hand, vacancy of data in the physical experiment can be made up.

Permeability change in the process of damage evolution of coal is taken into consideration in the establishment of permeability coefficient-stress action equation based on rock damage equation and fluid running equation of porous media. And Permeability coefficient-stress action equation adopts the numerical simulation software that is developed by finite element numerical method, which is developed into the numerical model of RFPA2D-Flow. The model has been put into practice and proved in many spots, furthermore, it has been used in theoretical research and technical guidance of failure for hard coal containing gas and gas migration of coal seam. Mathematical model of gas-solid coupling of coal containing gas is as follows:

$$\alpha_p \cdot \nabla^2(\lambda_i \cdot P) = \frac{\partial P}{\partial t} \tag{1}$$

$$(\kappa + G) \cdot u_{j,ji} + G u_{i,jj} + f_i + \left(\alpha \cdot \sqrt{P}\right)_{,i} = 0 \tag{2}$$

$$\lambda = \begin{cases} \lambda_0 e^{-\beta(\sigma_1 - \alpha p)} \\ \xi \lambda_0 e^{-\beta(\sigma_1 - \alpha p)} \end{cases} \text{ (uniaxial compression)} \tag{3}$$

$$\lambda = \begin{cases} \lambda_0 e^{-\beta(\sigma_3 - \alpha p)} \\ \xi \lambda_0 e^{-\beta(\sigma_3 - \alpha p)} \\ \xi' \lambda_0 e^{-\beta(\sigma_3 - p)} \end{cases} \text{ (uniaxial tension)} \tag{4}$$

$$\sigma = \sigma_\infty + (\sigma_0 - \sigma_\infty) \cdot \exp(-B \cdot t) \tag{5}$$

Where ξ: permeability sudden jump coefficient when primitives damage; ξ': permeability sudden jump coefficient when primitives damage completely; λ_0: initial permeability coefficient when there is no stress; α: pore pressure coefficient; β: coefficient of stress on pore pressure; p: pore pressure; P: square pore pressure, $P = p^2$, MPa^2; f_i: Components of coal body force, MPa.

3 NUMERICAL SOLVING AND ANALYSIS

3.1 *Model*

Numerical model was made based on geologic setting and mechanical parameters of coal in order to simulate the whole process of dynamic failure for hard coal containing gas. The model can be divided into three parts, the middle part is coal seam, and the other two parts are roof and floor. Roof and floor are solid sandstone without gas. Geometry size of rock is 10 m × 20 m, which is divided into 200 × 400 = 80000 constant-area units. Plane strain analysis is adopted in the model.

3.2 *Mechanical parameters*

In RFPA2D simulation software the mechanical properties (including elastic modules, strength, etc.) of material element have been assigned by Weibull distribution, which is shown as follows:

$$\varphi(\alpha) = \frac{\mathrm{m}}{\alpha_0}\left(\frac{\alpha}{\alpha_0}\right)^{\mathrm{m}-1} \cdot e^{-(\frac{\alpha}{\alpha_0})^{\mathrm{m}}} \tag{6}$$

Where m is the shape parameter of distribution function (Tang C.A. et al. 2003). In the formula, its physical meaning reflects the homogeneity of the rock medium and it ranges from 1 to 100; the larger m-value, the more uniform rock is. Parameter α is the value of the unit mechanic property; α_0 is the average value of all units; $\varphi(\alpha)$ is the micro mechanic non-uniformity distribution of rock primitives. The coal rock mechanics parameters of model are shown in Table 1.

3.3 *Loading conditions*

This paper mainly studies the dynamic failure for hard coal containing gas. The loading conditions are as follows: upper and lower boundary are airtight seal, that is to say, there is no gas; gas pressure of left boundary is 0.1 MPa in order to simulate atmospheric pressure of working face; gas pressure of right boundary is 5 MPa; ground stress is 20 MPa, equivalently 800 m burial depth; modulus

Table 1. Mechanical and seepage parameters of numerical model.

Mechanic parameter	Coal seam	Roof and floor
Average degree m	2	10
Modulus E_0/GPa	15	50
Strength σ_0/MPa	25	300
Poisson's ratio μ	0.3	0.25
Permeability $\lambda/m^2/(MPa^2 \cdot d)$	0.3	0.0001
Porosity ration	2	0.01
Poro-water pressure α	0.5	0.01
Coupling Coeff β	0.2	0.1

and strength of roof and floor are bigger than the coal's; there is a 5 m coal pillar head on, the initial gas pressure is 0.1 MPa. Loading conditions of model are as shown in Figure1.

4 NUMERICAL SIMULATION AND RESULT ANALYSES

Outburst process and shear stress field are shown Figure 2 respectively. According to the following two figures of numerical simulation, the results can recover the process of dynamic failure for hard coal containing gas. And the process can be divided into four sub-processes as follows: stress concentration, coal rock fracture induced by ground and gas pressure, protection coal pillar was damaged by gas stress (outburst start), and crushed coal was thrown out by gas pressure (outburst development). The four sub processes will be described and analyzed as follows:

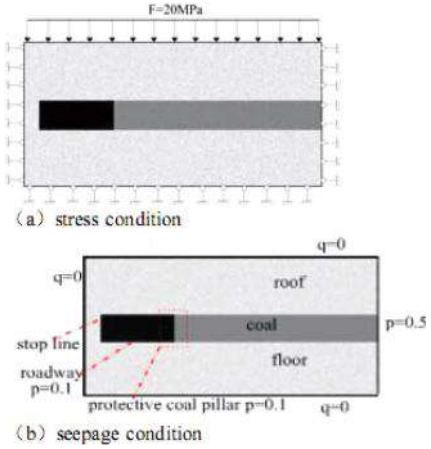


Figure 1. Numerical mechanical and seepage model of coal and gas outbursts.

1. Stress concentration

New coal body was uncovered after mining, and stress concentration area is formed in the front of the new coal body because of abutment pressure. The gas pressure before peak stress was low due to the gas released near the free surface, so distressed zone emerged (see Figure 3). Coal body just revealed has the characteristics as follows: low initial damage, good integrity, high shearing modulus and strong shear capacity. Tangential stress that acted on the coal body on a range of wall was high because of stress concentration. Stress acting on coal body was non-equilibrium because of stress concentration and gas gradient. The coal body was damaged, and the evolution rate of damage was changing from slow to fast. Evolution rate of damage in coal body from the working face approached to zero because of the low ground stress.

2. Coal rock fracture induced by ground and gas pressure

The existence of high abutment pressure in the coal body near the exposed surface (the front of driving end) compressed the coal body in stress peak area, closed fractures, plugged the gas tunnels and hindered the gas seepage. Therefore, high gas pressure gradient appeared in the area, which loaded high pulling stress on two sides of coal body. A large number of cracks that paralleled to the exposed surface appeared in coal body under the force of gas pressure (see Figure 2b). From Figure 2b, some conclusions can be drawn as follows: Coal body was damaged due to tensile stress along with high gas pressure gradient; Strength of coal body reduced; Up stress transferred to two sides; Damage of coal body increased dramatically because of stacked stress in the external coal body.

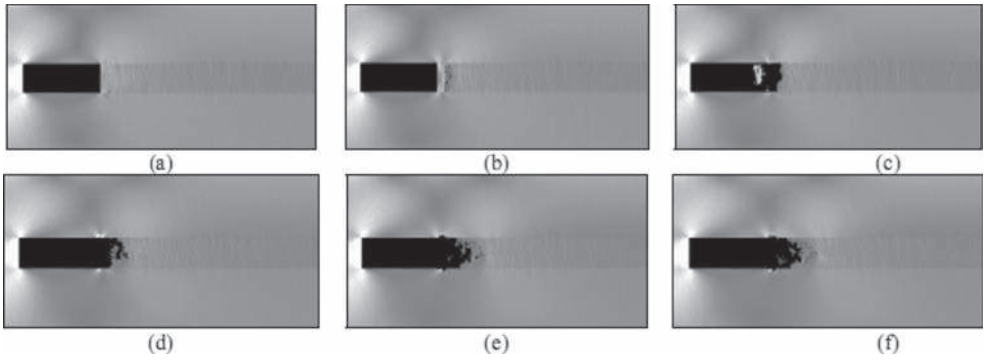


Figure 2. Shear stress field in gas outburst process (3–11).

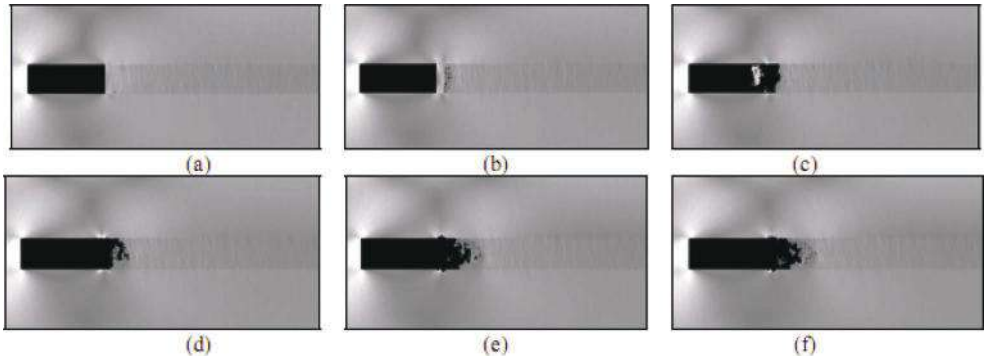


Figure 3. Gas pressure in the initiate stage of outburst (3–13).

3. *Protection coal pillar was damaged by gas pressure (outburst start)*

With the cracks extension and transfixion, during the formation of the tensile ruptured zone, gas did work by expansion and made the cracks further extend paralleling to free face until they are transfixed. However, coal of pressure released zone near exposed surface has lost bearing capacity in the combined force of stress concentration and gas pressure. The coal will be thrown out primarily by gas. Crushed coal of crack propagation region and pressure released zone was thrown out by gas ex-panding power, whose process was shown in Figure 2c. The detailed process of gas pressure field changes and pillar damage can be seen in Figure 3. Gas released after heading face revealed. Gas pressure released zone was formed in the coal that was near the exposed surface. High gas pressure gradient appeared in the Inner-edge of gas pressure released zone. A lot of free gas accumulated because of fissure development, then expansion energy of gas multiplied and load on the protection coal greatly increased. At the same time, the coal damaged and stress transferred to two sides under the tension effect of gas pressure. Coal pillar of pressure released zone damaged and strength lost, then it was thrown out by gas pressure. Obviously, the "out-burst" needs three premises: high coal mass strength, high gas pressure and high primary stress.

4. Crushed coal was thrown out by gas pressure (outburst development)

Exposed surface reached a new instant equilibrium state with the constant thrown-out of crushed coal. The coal near the new exposed surface was fractured and thrown out sequentially. Exposed surface developed continually toward distant coal (see Figure 2d–2f). The simulative outburst stopped after 3~4 m, which is mainly caused by the high strength of coal. In other words, because of the high strength of hard coal, gas can't damage the coal and make outburst develop, moreover, the stress concentration needs long time to damage the coal. In detail, because gas pressure and ground stress have affected the new exposed surface and nearby coal, fractures became more developed, bearing capacity was lower and concentrated stress transferred to inner coal.

5 CONCLUSIONS

In this paper, the authors researched some phe-nomena caused by the outburst are as follows: integrality of coal is damaged, crushed coal is thrown out by gas pressure, peak of abutment pressure transferred to inner coal, pressure released zone became wide and gas pressure reduced fast with the outburst. The outburst will stop fast if the combined force of gas pressure and ground stress can't damage the little-by-little wider pressure released zone. Three conclusions can be obtained in the process of dynamic failure for hard coal containing gas from the numerical simulation as follows: The ground stress plays a very important role in the hard coal containing gas outburst because the coal structure needs to be damaged by high stress in the phases of outburst start and development; The strength of the outburst destruction is increased and the threshold of the out-burst destruction is reduced by gas stress, but the gas stress is a non-dominant effect in the phases of out-burst start and development; Hard coal containing gas outburst endures shortly and terminates rapidly.

ACKNOWLEDGEMENTS

The work is supported by the National Natural Science Foundation of China (51274086), the Ministry of education Doctoral Foundation of China—priority areas (20124116130001), the State

Key Laboratory Cultivation Base for Gas Geology and Gas Control (Henan Polytechnic University) (WS2012 A10) and Operational Research and Cybernetics Key Discipline of Henan Polytechnic University.

REFERENCES

Borisenko A. 1985. Effect of gas pressure in coal strata. *Soviet Mining Science.* 21(5): 88–91.

Tang C.A., Wang S.H., Fu Y.F. 2003. *Numerical Test of Rock Failure.* Beijing: Science Press, 180–185.

Xu T. 2004. Solid gas coupling numerical test of Coal and rock failure process[D]. Shenyang: *Doctoral Dissertation of Northeastern University.*

Xu T., Tang C.A., Yang T.H. 2008. Rupture process and Outburst mechanism of Coal containing gas. Beijing: *China Coal Industry Publishing House,* 150–157.

Yi G.Z., Wang D.K., Zhang D.M. 2008. Research on solid gas coupling dynamic model and simulation of coal contain gas. *Chinese Journal of geotechnical engineering.* 30(10): 1430–1436.

Zhang M.T., Liang B. 1990. Mathematical model and mathematical analysis of gas in coal flow under mining. *The Second Nation wide Symposium Numerical and Model Test of Rock Mechanics.* Tongji University press, 423–428.

Zhao H.B. 2010. Theoretical and Experimental study on unstable failure and AE characteristic of Coal Contained Gas. *Chongqing: Doctoral Dissertation of Chongqing University.* 130–138.

Zhao Y.S. 1994. Coal-gas coupled mathematical model and its numerical solution. *Chinese Journal of Rock Mechanics and Engineering*. 13(3): 229–239.

This page intentionally left blank

Progress in Mine Safety Science and Engineering II – He et al. (Eds)
© 2014 Taylor & Francis Group, London, ISBN 978-1-138-00122-0

Experimental investigations on gas emission rules during fully-mechanized developing entries in deep and high-gas coal seams

Fang-Bin Liu
Planning and Design Research Institute of Coal Industry, Beijing, China

Yuan-Sheng Wang
School of Safety Science and Engineering, Henan Polytechnic University, Jiaozuo, Henan, China

ABSTRACT: As underground mining activities are going deeper and deeper, gas disasters have been a potential risk of explosion especially when high rate and large amounts of developing activities in deep and gas-rich coal mines. In order to understand gas emission from rib-wall changing with time during fully-mechanized developing entries in deep and high-gas underground mines, in-situ experiments were conducted to systematically research and get the characteristics of gas emission strength from rib-wall, and hyperbolic function relationship curves between gas emissions and exposing time were established. After analyzing of experimental results, two empirical equations for rib-wall gas emissions from two experimental coal seams were derived from regression studies performed on experimental data. Research results provide theoretic foundation and safeguard for fresh air supply and gas drainage as well as safety and fast development of fully-mechanized developing entries.

1 INTRODUCTION

At present, many coal mines in China have entered into the stage of deep mining. Because of deep coal resources have the characteristics of high stress, high formation temperature, pore pressure and rock mechanical properties of weak immunity, coal and gas outburst and rock burst disaster have become challenging puzzles in deep coal mining (Yu 2005, He et al. 2006).

From 2003 to 2011, fifteen times of major and extraordinary serious gas outburst accidents have happened (one-time death more than ten people), and eight times occurred in coal roadway heading face. With coal mining level extending deeper, coal and gas outburst danger gradually increases. The original coal seam without outburst danger is likely to become the one with such danger. With the coal seam gas occurrence condition is complex and changeable and unpredictable factors gradually increase, it brings a great threat to coal mine safety excavation (HU & Lin 2006, Leszek (Les) & W. Lunarzewski 1998, Klaus, N. 1998, He et al. 2003).

In coal lane tunneling, with continuous improvement of coal mining mechanization level, digging machines are widely used. This reduces labor intensity and improves driving efficiency. But in high outburst mine, because of high gas effusion intensity and easily overrun, the use of digging machines is limited (Xie & Zhao 2005, Liu & Cheng 2006). In general, gas emission quantity is affected by coal gas content and its permeability, and is related with space and time and other factors at the same time. Continuous properties of mechanical coal, mining, loading, transport of digging machines make emission characteristics of fully mechanized workface be different from that of blasting driving face. The first, relative average exposure time of coal wall on fully mechanized working face is short, and its average gas emission is larger than that of blasting driving face (Yuan et al. 2003). The second, different from the characteristics of gas influx into mining space when coal blasting, with continuous coal drop, the gas in the running chain plate and belt conveyor will continue to pour out. Therefore, gas emission of fully mechanized working face depends not only on the original coal-seam gas content, permeability and digging machine production capacity, but also on the chain plate machine, belt conveyor and the length of coal lane (Zhang & Yuan 1999).

At present, the main production of coal mine in Huainan mining area has entered the stage of deep mining. Gas content of main coal seam is high, ventilation is poor, and its drainage is difficult. The paper takes 13 coal seam and 11 coal seam of No.1 Xinji Mine in Huainan mining area and Liu Zhuang Coal Mine as the research object. Based on the field test, this paper studies gas emission law

on the tunneling process of coal roadway in deep high gas mine.

2 PROFILE OF TEST COAL MINE

No. 1 Xinji Mine in Huainan mining area and Liu Zhuang Coal Mine belong to Huainan mine area. The main coal seams are 13 coal seam and 11 coal seam. And among them.

The elevation of 13 coal seam is from −569 m to −724 m (floor elevation). The average thickness of coal seam is 3.75 m, the average angle is 12.5°, its gas content is about 11 m^3/t, gas pressure is 2.6 MPa. The direct roof is mudstone, and its thickness is 1.2 m.

The elevation of 11 coal seam is from −605 m to −852 m (floor elevation). The average thickness of coal seam is 4.2 m, the average angle is 12°, its gas content is about 12.9 m^3/t, gas pressure is 2.9 MPa. The direct roof is mudstone, and its thickness is 1.1 m.

3 THE GAS EMISSION LAW OF FULLY MECHANIZED WORK FACE

The gas emission of fully mechanized working face depends on many factors such as occurrence characteristics of coal seam, mining technical conditions and so on. Under normal circumstances, gas emission in the coal roadway tunneling process contains gas emission of coal wall and of coal drop. In case of coal roadway is long, gas emission of coal wall accounts for 60% to 90% in the total gas emission of full mechanized roadway excavation face (Izmailov, I. V. et al. 2004, Buslaev, V. I. & Buslaeva, S. F. 2005).

Coal pores and fractures constitute the main channels of gas migration. In coal roadway tunneling process, equilibrium state of gas pressure around the roadway in coal seam continues to be broken, gas pressure and geostress redistribute, the seam permeability increases and pressure relief gas zone forms. Because of the existence of gas pressure gradient between the coal body and coal wall, in the role of gas pressure gradient, gas of coal body gushes to tunnel along the fracture and pore in unloading zones. The strength of coal gas emission decreases with the increase of exposure time. Gas emission quantity depends on the emission intensity of emission sources. Usually, gas emission amount per square meter of coal wall in unit time indicates gas emission strength in coal wall.

Gas emission intensity depends on the gas pressure in coal seam, the structure of pores and fissures, adsorption characteristics of coal methane and the time and space conditions. When other conditions are fixed, gas emission intensity of coal wall is a function of time of exposure.

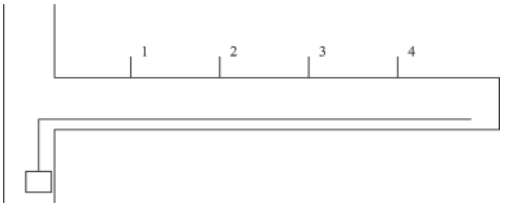


Figure 1. The layout of monitoring points.

3.1 *Method for determination*

In order to study the relationship between gas emission characteristics of coal wall and the exposure time, this paper goes on a lot of actual measurement in roadway and airway heading face of 121102 working face in Liu Zhuang Coal Mine, and of 150605 working face in No.1 Xinji Mine. This paper adopts method of tunnel assay.

Tunnel assay is currently a widely used method, simple and practicable, and determination process does not affect the production. To reduce the error of determination, it needs more data. The specific method is setting a measuring point every certain distance in the normal continuous tunneling roadway (Figure 1). When digging machine carries out normal coal drop and continuous shipment, regularly determines air quantity and gas concentration data of each measuring point, and using the measured data, the paper obtains the gas flow through the measuring point per unit time. Then the paper calculates gas emission intensity according to exposed area of coal wall in each section of roadway, and on the basis of driving speed, calculates corresponding average time of exposure in each section of roadway.

Gas emission intensity of coal wall can be calculated by equation (1):

$$V_t = \frac{Q_2 \cdot C_1 - Q_2 \cdot C_1}{200 L \cdot h} \tag{1}$$

In the formula:

V_t—gas emission intensity of coal wall after a time of t + l, m3/m2.d;

C_1, C_2—gas concentration at measuring points of 1 and 2 in the tunnel, l%;

Q_1, Q_2—air quantity at measuring points of 1 and 2 in the tunnel, m3/min;

H—the average thickness of coal seam at measuring points of 1 and 2, m;

L—the distance between the measuring points of 1 and 2, m.

3.2 *Experimental data analysis*

The relationship between gas emission intensity and exposure time of coal wall at comprehensive driving roadway in Huainan mining area was measured with the roadway assay. Through data processing and regression analysis, the results show that this relationship is in hyperbolic function. The form is:

$$V_t = \frac{V_0}{(1+t)^{\beta}} \tag{2}$$

In the formula:

V_t—coal gas emission intensity of the wall after a time of t + 1, $m^3/m^2.d$;

V_0—coal gas emission intensity of the wall at the zero time, $m^3/m^2.d$;

β—attenuation coefficient;

T—the average exposure time of coal wall, d.

Put formula(2)into a linear equation:

$$\log V_t = \log V_0 - \beta \log(1+t) \tag{3}$$

In the formula, V_t and t is the measured value of each measuring point. β and V_0 is the undetermined coefficient. Through putting n groups of measured values which are getting from the V-t curve after data processing into formula(3), determined equations are obtained as follows:

$$\sum_{i=1}^{m} \log V_i = \sum_{i=1}^{m} \log V_0 - \beta \sum_{i=1}^{m} \log(1+t_i) \tag{4}$$

$$\sum_{i=m+1}^{m} \log V_i = \sum_{i=m+1}^{m} \log V_0 - \beta \sum_{i=m+1}^{m} \log(1+t_i) \tag{5}$$

Calculate out the value of β and V_0 through uniting and solving formula (4) and (5).Therefore, using the least square method, the experimental data are substituted into the linear regression, exponential regression and hyperbola regression respectively. Each standard deviation measuring the corresponding regression coefficient is calculated out. And verify the empirical formula determined.

3.3 *Empirical formula of the gas emission law of coal wall at comprehensive driving roadway*

The V-t curves drawn according to the results measured at 150605 face convey gateway, return air mechanized excavation Lane and 121, 102 face convey gateway, return air mechanized excavation lane are shown in Figure 2, 3, 4 and 5.

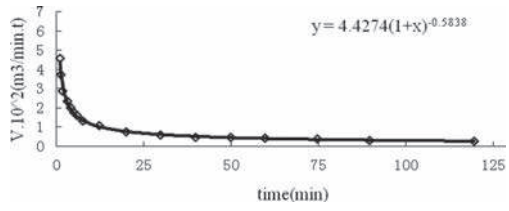


Figure 2. The V-t relationship curve of gas desorption intensity of the coal wall at 150, 605 machine lane in Xinji Mine.

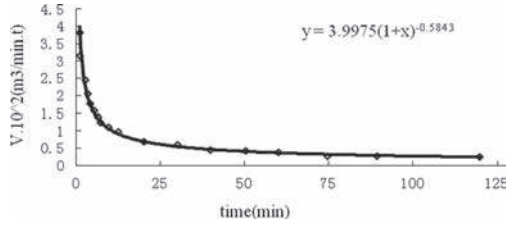


Figure 3. The V-t relationship curve of gas desorption intensity of the coal wall at 150, 605 return air lane in Xinji Mine.

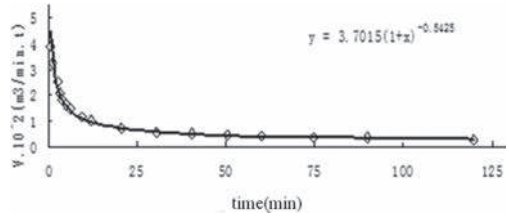


Figure 4. The V-t relationship curve of gas desorption intensity of the coal wall at 121, 102 machine lane in Liuzhuang Mine.

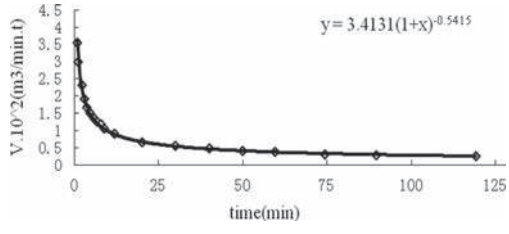


Figure 5. The V-t relationship curve of gas desorption intensity of the coal wall at 121, 102 return air lane in Liuzhuang Mine.

Through the processing and analysis of the measured raw data, this paper obtained the gas emission regularity of coal wall. The V-t relationship fitted out is approximate to power function relationship. The empirical formula of V-t

relationship from analysis are shown in formula (6) and (7).

Coal 13:

$$V = 6.76(1+t)^{-0.6843} \quad (6)$$

Coal 11:

$$V = 5.53(1+t)^{-0.6843} \quad (7)$$

4 CONCLUSIONS

Through systematical analysis of the gas emission regularity at the comprehensive driving roadway in two typical highly gassy mines which are deep mining in Huainan mining area, this paper obtained the relationship of gas emission intensity varing with exposure time of coal wall in highly gassy mines which are deep mining and the gas emission regularity of coal wall at the comprehensive driving roadway.

The study results provide certain theoretical basis for effective allocation of fresh air volume, dilution and extraction of gas and safety rapid excavation at full-machined mining working face. This paper also has reference significance of the research of gas emission law at comprehensive driving roadway under the similar geological condition.

REFERENCES

Buslaev, V.I. & Buslaeva, S.F. 2005. Poincare theorem for difference equations. *Mathematical Notes* 78 (5~6): 877~882.

He, J.H. et al. 2003. Gas emission law in heading and wining faces of Lu Ling mine. *Mining Safety & Environmental Protection* 30(supplement):26–27.

He, M.X. et al. 2006. Gas emission law in coal road heading face of driving of Lu Ning Coal Company. *Mine Safety* 9:56–58.

Hu, D.D. & Lin, B.Q. 2006. Coal Seam Gas Occurrence Law and Control Technology. Beijing. *China University of Mining and Technology Press*.

Izmailov, I.V. et al. 2004. Spatial deterministic chaos in optical systems and methods of its modeling. *Russian Physics Journal* 47 (12): 1289~1296.

Klaus, N.1998. Control of gas emissions in underground coal mines. *International Journal of Coal Geology* (35): 57–82.

Leszek(Les) & W.Lunarzewski. 1998. Gas emission prediction and recovery in undergroundcoal mines. *International Journal of Coal Geolog* 35: 117–145.

Liu, C.C. & Yun, G. 2006. Analysis of gas emission law in mechanical rapid excavation roadway. *Mining Safety & Environmental Protection* 6(1): 19–21.

Xie, S.R. & Zhao, Y.J. 2005. The Law of Gas Emission For Full-Machanized Mining Working Face and The Prediction of Gas Emission Quality. *Journal of Taiyuan University of Technology* 36(5): 553–556.

Yu, B.F. 2005. Coal Mine Gas Disaster Prevention and Utilization Technology Handbook. Beijing: *China Coal Industry Publishing House*.

Yuan, D.S. et al. 2003. Application of gas emission into mine by the methods of 3D grey trend surface analysis. *Journal of Liaoning Technical University* 22(4): 478–479.

Zhang, Z.R. & Yuan, C.F. 1999. Study on mathematical model of coalbed gas geology used to prediction of mine gas emission. *Journal of China Coal Society* 24(4): 8.

Progress in Mine Safety Science and Engineering II – He et al. (Eds)
© 2014 Taylor & Francis Group, London, ISBN 978-1-138-00122-0

Application of optical fiber oxygen sensor in coal mines

Yanjie Zhao, Yubin Wei, Yanfang Li, Tingting Zhang, Weisong Zhao, Lei Lv, Tongyu Liu & Chang Wang
Laser Institute of Shandong Academy of Sciences, The Key Laboratory of Optical Fiber Sensing Technology of Shandong Province, Jinan, Shandong, China

ABSTRACT: This paper proposed a novel all fiber optic multipoint oxygen monitoring system for detecting the concentration of oxygen gas in coal mines. A 760 nm Distributed Feedback (DFB) laser is used as the light source. An optical gas chamber is employed to analyze the absorption lines of oxygen. By taking the triangular signal to modulate the wavelength of the DFB laser, the concentration of oxygen can be monitored. Since the gas chamber is made without any active electrical components, it is intrinsically safe when used in the hazard environment such as coal mines. The system can provide remote monitor information by employing an optical fiber link between monitor and gas chamber, which makes this system particular suitable for the safety monitoring in the coal mines. The oxygen sensor works in the concentration range 0–100% oxygen with good performance in stability and sensitivity. The results show that it will have an important application in coal mines spontaneous combustion.

1 INTRODUCTION

Oxygen is an immensely important species in spontane-ous combustion of coal mines. It is urgent to timely and accurately monitor the oxygen gas concentration in coal mine. Considerable effort has been spent over the years in developing suitable techniques for measurement of oxygen concentrations. The typical oxygen sensors in-clude solid-state potentiometric, equilibrium sensors [Mogensen M., et al., 2000, Sammes N.M., et al., 1999], limiting current amperometric sensors [Usui T., et al., 1989], semi-conducting metal oxide sensors [Tan W. et al., 2004], and optical sensors [Amao Y., 2003, Kolling M., et al., 2001]. Optical methods for detecting oxygen concentra-tion have attracted the attention of researchers. Com-pared with many other methods, tunable diode laser ab-sorption spectroscopy has attracted a growing attention from a laboratory specialty to an accepted, and reliable technology for gas sensing, because of their high preci-sion, remote detection capability, safety in hazardous environments, and so on.

In this paper, a fiber optic remote sensing multiplexed oxygen monitoring system is designed based on tunable diode laser absorption spectroscopy technique. It is an intrinsic sensing method to provide long term stability without the need of frequent calibrations.

2 PRINCIPLE

Many gases of molecules have unique characteristic absorption spectrum. The proposed sensor is based on the absorption spectrum of oxygen gas, which measures the absorption of light at specific wavelengths by the target gases located within a gas chamber. The absorption of light by a gas is governed by the Beer-Lambert law [Bernath P.F., 1995, Edisbury J.R., 1966], given simply by:

$$\frac{I(\lambda)}{I_0(\lambda)} = \exp[-\alpha(\lambda)LC] \tag{1}$$

Where I(λ) is the laser power at the wavelength λ after transmitted though the target gas of optical path length L, I0(λ) is the original laser power, α(λ) represents the coefficient of the gas, C denotes the concentration of the target gas. I(λ), I0(λ) and α(λ) is determined by the wavelength of the light source.

The oxygen gas absorption is very weak in this range. So, it is obtained:

$$\left|\alpha(\lambda)LC\right| << 1 \tag{2}$$

According to (1),

$$I(\lambda) \approx I_0(\lambda)[1-\alpha(\lambda)LC] \tag{3}$$

Hence, the concentration of the oxygen gas can be gotten:

$$c \approx \frac{1}{\alpha(\lambda)L}\left[1-\frac{I(\lambda)}{I_0(\lambda)}\right] \tag{4}$$

3 PRINCIPLE

Figure 1 shows the absorption spectrum of oxygen molecule according to HITRAN database [Rothman L. S., et al. 2005]. The absorption intensity with maximum at wavelength of 760.8 nm is obtained. Figure 2 shows the configuration of the optic fiber oxygen monitoring system. A narrow linewidth Distributed Feedback (DFB) laser of 760 nm is used as the light source. And it could effectively eliminates the cross sensitivity to moisture or other gases.

The wavelength of the DFB laser is modulated by a taking the triangular signal, while the center wavelength is slowly ramped over the oxygen absorption line of interest. The output wavelength

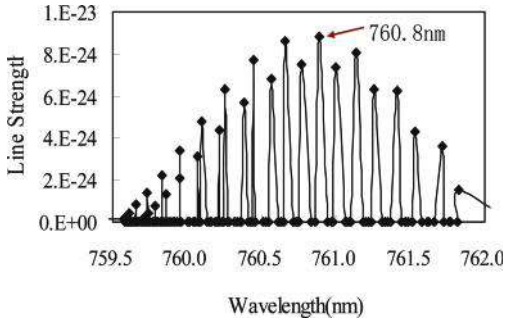


Figure 1. Absorption spectrum of oxygen gas.

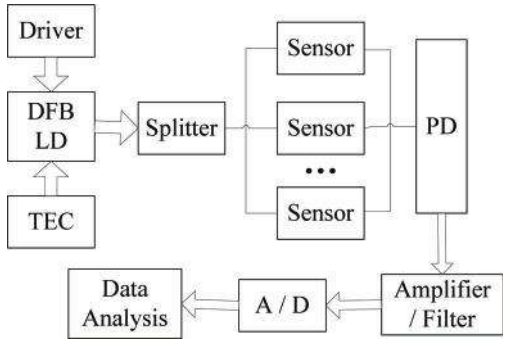


Figure 2. System construction.

can be tuned finely by the current controller and tuned coarsely by the temperature controller. When the system is switched on, a laser beam in the monitor will be transmitted to the sensor chamber via the optic fiber cable, and is detected with a high sensitivity photo detector via another fiber. When oxygen gets into the sensor chamber, a portion of laser intensity will be reduced due to the oxygen molecule absorption, thus the oxygen concentration can be detected.

The system is composed of the gas chamber (probe) and the monitor, by employing optic fiber between them to provide a remote and on-line measurement. The oxygen monitoring unit is often placed in a control room. The probe is installed at the monitored location. The fiber cable is used to transmit signals between the probe and monitoring unit. The passive probe makes it more suitable for being deployed in the hazard environment. The monitor unit can be connected up to multiple optic fiber oxygen probes.

In order to avoid the background noise disturbance and give net absorption for different concentrations of oxygen, pure nitrogen only is first introduced into the chamber and the signal of received by the detector is stored with the data acquisition software. Then a calibrating oxygen gas is introduced into the chamber, and the signal is collected. By subtracting the stored background signal from the sample signal, we can get the normalized absorbed signal from the sample oxygen. Figure 3 shows normalized absorbed signals obtained through background subtraction for different concentrations of oxygen. The oxygen concentrations are increased from 5%, 15%, and 25% by volume. All normalized absorbed signals for various concentrations of oxygen are recorded together for comparison purpose. Obviously, the

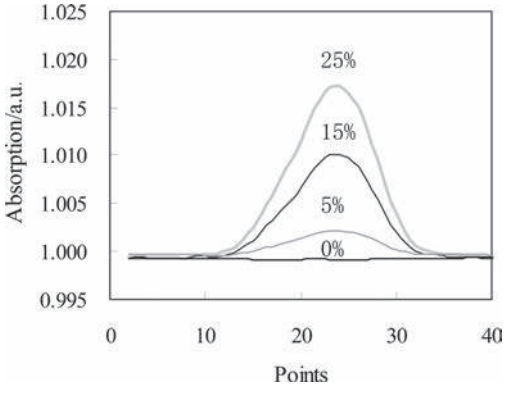


Figure 3. Absorption intensity of different oxygen concentrations.

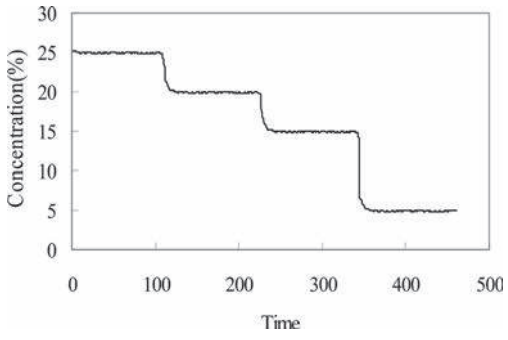


Figure 4. Different oxygen concentrations.

normalized absorbed signals intensity increases with the increase of oxygen concentration. To further improve the stability of the reading, output signals were averaged over 100 samples through software filtering. Based on least square fitting, the target gas concentration can be obtained by comparison the normalized absorbed signals of the known concentration gas and the target gas. We measured calibration oxygen at 4 concentrations: 25%, 20%, 15% and 5%. A time response trace of the instrument output is shown in Figure 4.

4 CONCLUSION

We designed an optic fiber oxygen sensor based on DFB laser wavelength scanning and spectrum absorption technique. With the use of the optical fiber links between monitor and sensor header, the system can provide remote and online monitor information. Since the sensor head is made without any active electrical components, it is intrinsically safe when used in the hazard environment such as coal mines. The oxygen sensor works in the concentration range 0–100% oxygen with good performance in stability and sensitivity. The results show that it will have a great potential application in the harsh environments.

ACKNOWLEDGEMENT

This work was supported by Natural Science Foundation of Shandong Province (ZR2010FM039), National Key Technology R&D Program of the Ministry of Science and Technology (2012BAI25B04), and the key projects of Shandong Province (2011ZHZX1 A0107).

REFERENCES

Amao Y., 2003. Probes and polymers for optical sensing of oxygen, *Microchim, Acta.,* 143, 1–12.

Bernath P.F., 1995. *Spectra of atoms and molecules,* Oxford University Press: New York.

Edisbury J.R., 1966. Practical hints on absorption spectrometry, London: A. Hilger, .

Kolling M., et al., 2001. A simple plastic fiber based optode array for the in-situ measurement of ground air oxygen concentrations, *Proceedings of SPIE,* 4576, 75–86.

Mogensen M., et al., 2000. Physical, chemical and electrochemical properties of pure and doped ceria, *Solid State Ionics*:129 (1–4), 63–94.

Rothman L.S., et al. 2005, The HITRAN 2004 molecular spectroscopic database. *Journal of Quantitative Spectroscopy & Radiative Transfer,* 96(2), 139–204.

Sammes N.M., et al., 1999. Bismuth based oxide electrolytes—structure and ionic conductivity, *J. Eur. Ceram. Soc*. 19 (10), 1801.

Tan W. et al., 2004. Nano-structured oxide semiconductor materials for gas-sensing applications, *Ceram. Int*. 30 (7), 1127–1133.

Usui T., et al., 1989. Gas polarographic oxygen sensor using an oxygen/zirconia electrolyte, *J. Electrochem. Soc*. 136 (2), 534–542.

This page intentionally left blank

Progress in Mine Safety Science and Engineering II – He et al. (Eds)
© 2014 Taylor & Francis Group, London, ISBN 978-1-138-00122-0

Variation characteristics of coal and gas outburst accident and its quantitative analysis based on FAHP

Xiu-Jiang Lv
Faculty of Resources and Safety Engineering, State Key Laboratory of Coal Resources and Safe Mining, China University of Mining and Technology (Beijing), Beijing, China

Mei-Hua Geng
New Institute, Gouda, Netherlands Hebei Province Mine-Building Engineering and Technological Research Center, Hebei University of Engineering, Handan, China

Xiao-Gang Zhang
Faculty of Resources and Safety Engineering, State Key Laboratory of Coal Resources and Safe Mining, China University of Mining and Technology (Beijing), Beijing, China

ABSTRACT: In order to research the variation characteristics of coal and gas outburst accident in China in recent years, the outburst accidents during 2000–2012 were statistically analyzed. The features of outburst accidents in the past 13 years were explained. The evaluation model was established by utilizing fuzzy analytic hierarchy process. The weight matrix of influencing factors of coal and gas outburst was set up by analytic hierarchy process, annual evaluation matrix was obtained through expert evaluating method, and the influencing factors were quantitatively analyzed. The variation characteristics of coal and gas outburst accident over the past 13 years were revealed through method above. The characteristics include that in the past 13 years the accidents increased in the prophase and reduced in the anaphase, the accidents grew rapidly in the prophase and reduced slowly in the anaphase, there were ups and downs in the development process, the influence of subjective factors remained stable throughout and the influence of objective factors were in unstable oscillations, i.e. And some suggestions are proposed for the further outburst-prevention and outburst-control.

1 INTRODUCTION

Compared with other countries in the world, the coal and gas outburst phenomenon in China is one of the most serious (Deng et al. 2010). In recent years, with the concerted efforts of the government, enterprise, science and technology workers, the overall situation of safety production has improved markedly, but the coal and gas outburst accident situation is still serious, especially the proportion of the big and serious coal and gas outburst accident is evident at increased risk. In the 12th Five-Year Plan of coal mine safety production, it has clearly pointed out about 91% of China's coal mines are underground mines, the mining conditions is most complex among the world's major coal-producing countries. Depth of coal mining has an average annual increase of more than 20 meters, with the increasing mining depth and mining intensity, relative gas emission has an average annual increase of 1 cubic meter per ton, an annual increase of 4% in the number of high-gas coal mine, the number of coal and gas outburst mine have increased by 3% per year. So the danger of coal and gas outburst increases and the disaster prevention are become more difficult (SACMS. 2012).

Chinese scholars make a abundant of studies in coal and gas outburst accident, the single mine's coal and gas outburst hazard assessment is mainly concentrated in references (Pang et al. 2012, Zhang 2012, Ou & Wu 2010, Cheng. 2012), the corresponding evaluation model is established in references (Zheng et al. 2012, Xiao et al. 2011, Gong et al. 2008, Qin et al. 2012) via the fault tree analysis method, fuzzy comprehensive evaluation, unascertained measure theory, principal component analysis and other methods, to make a macroscopic evaluation in coal and gas outburst danger; the quantitative changes situation of coal and gas outburst accident hasn't been involved in these literature, and the problem that how does the

evaluation matrix affect the results of the evaluation with the changed factors every year. In this text, the variation characteristics of 13 years, from 2000 to 2012, on coal and gas outburst accident are statisticed, and based on which, FAHP, fuzzy analytic hierarchy process, has been used to analyze the variation characteristics of coal and gas outburst accident, and reveal the change rules of coal and gas outburst accident for 13 years.

2 VARIATION CHARACTERISTICS OF COAL AND GAS OUTBURST ACCIDENT

2.1 *Change features of coal and gas outburst accident*

A statistic analysis about the coal and gas outburst accident in the 13 years, from 2000–2012, is made in this article. There were 253 documented coal and gas outburst accidents, in which some workers died, on the website of the State Production Safety Supervision Administration, based on which, the 13-years change characteristics of the coal and gas outburst accident are analyzed in this paper.

The "coal mine production safety accident reporting and investigation and handling regulations", issued by the State Production Safety Supervision Administration in 2008, divided coal mine accidents into four levels, namely general accident (deaths 1–2), the larger of the accident (deaths 3–9 people), major accident (deaths 10–29), serious and the worst accidents (death of 30 people and above).The situations of coal and gas outburst accident were made from 2000–2012 according to the four levels.

On the view of the number of accidents in the past 13 years, general accidents were 41 cases, accounting for 16% of the total number of the accident; There were 176 larger accidents, accounting for 70% of the total number of the accident; The major accidents were 32, accounting for the accident from the total number of 12%; The serious accidents were 4, accounting for 2% of the total accidents.

From the perspective of deaths toll in the past 13 years, the deaths toll of general accident was 64, accounting for 4% of the total number of deaths; Larger accident's deaths toll was 812, accounting for 52% of the total number of deaths; The deaths toll of the major accident was 459, accounting for 30% of the total number of deaths; The serious and the worst accident's deaths was 216 people, accounting for 14% of the total number of deaths. Each grade accident's distribution is shown in Figure 1.

Figure 1 (a) shows that the number of larger accident in coal and gas outburst accident is much larger than other levels of the accident, up to 69%,

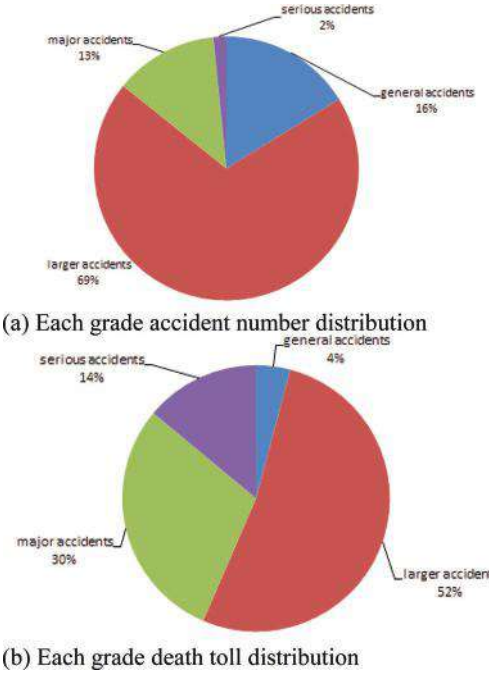


Figure 1. The class distribution of coal and gas outburst accidents.

amounts to twice of the sum of other three levels accident, which fully demonstrates once the coal and gas outburst accident occurred, it is likely to cause serious consequences, and makes harm to coal mine safety production.

Be seen in Figure 1 (b), the largest number of deaths is also the larger accident, accounted for half of the total deaths. Contrast the two figures also finds that, particularly serious and the worst accidents from the number of only 2%, but the number of deaths toll is as high as 14% of the total number; the major accidents occurred from the count of the total number of the 13%, but its deaths is as high as 30% of the total number, which fully demonstrates that the significant, serious and the worst accident have enormous threat to the lives security of the coal mine workers. So to prevent the serious and the worst coal and gas outburst accident has significant meanings, which are the reasons why the State Administration of Work Safety requires coal mines at all levels take as effective as possible measures to prevent the serious and the worst coal mine accidents.

2.2 *Analysis of annual change features about coal and gas outburst accident*

Outburst accident in the past 13 years conducted an annual statistical analysis, is shown in Figure 2.

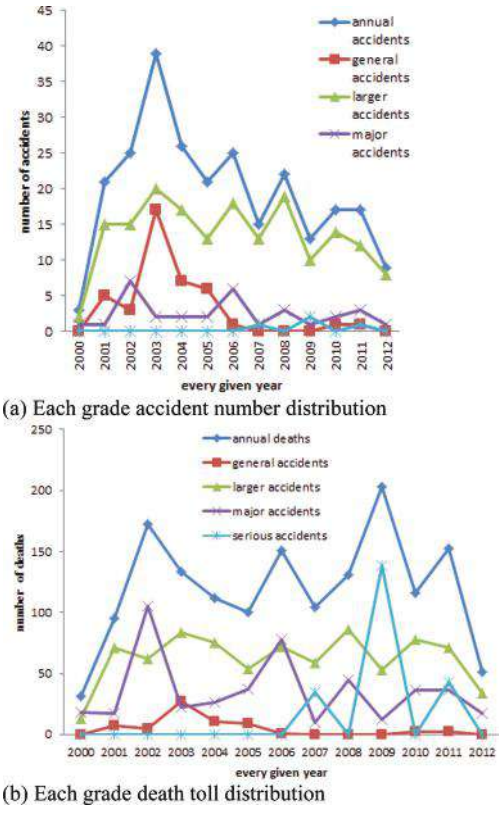


Figure 2. The annual distribution of coal and gas outburst accidents.

Known from the Figure 2 (a), on the view of the number of accidents, the number in 2000 is very little, the total number is 3, including 2 larger accidents and one serious accident. In 2001, 2002 and 2003, the number of accidents has skyrocketed, peaked in 2003, up to 39 accidents. In the next nine years, the number of accidents twists and turns of sexual down to 9, 2012. From the perspective of accident types at all levels, there was only one serious and the worst accident occurred in 2007 and 2011, twice in 2009, and zero in other years; Seven major accidents occurred in 2002, six in 2006, the number in the other years remained no more than 3, had tiny flexural change from 2007–2012; The number of general accident was, except at a high level in 2003 and five from top to bottom, small-amplitude oscillation in 2001, 2002, 2004 and 2005, at the level from 0–1 in other years; most noteworthy is the larger accident, which had a right ascension from 2 accidents in 2000 to 15 in 2001, and fluctuated in the range of 12–20 in subsequent years, down to 8 in 2012 but still was far higher than the number of other types of accidents. Throughout these 13 years, the number of larger accident is more than others, and accounts for more than half every year. There is another aspect deserves attention that the annual number of the accident shows a decline in total number, general accident and larger accident, but the number of serious and the worst accident has ups and downs, so the prevention and control of these accidents should be taken seriously enough.

From the view of Figure 2 (b), the number of deaths in 2000–2002 skyrocketed in the way of straight line, plummeted in the same way in 2011–2012, in the years between the two shown an oscillating trend; the same law was also suitable for the number of the larger accident deaths. From all levels of the types of accident, the deaths toll of serious and the worst accident was zero in 2000–2006, started ups and developed in 2007, up to 4 times, but the number of deaths was large, a total of up to 216 people, so once the serious and the worst accident happened, it would bring about great impact by owning the large proportion and the high total number of deaths; The deaths of the major accident was always at a high level in the past 13 years, which should be paid attention to; The deaths of the larger accident was always in a leading position in the past 13 years, except in 2002, 2006 because of the increasing number of the major accident, and in 2009 due to two serious and the worst accidents took place (The deaths toll of the larger accident was not the largest in 2002, 2006 and 2009, which owing to the increased number of the major accident in 2002 and 2006 and proportion of the serious and the worst accident in 2009.) In addition, the serious and the worst accident hadn't been found between 2000 and 2006, and began to appear in 2007, so it should cause great concern in the industry by considering its great danger.

3 THE FAHP MODEL OF COAL AND GAS OUTBURST ACCIDENT CHANGES

We can see from the above data and charts, the number of accidents which experienced twists and turns declined markedly in 2012, the death toll which went through ups and downs plummeted in 2012, all of which didn't conform the increasingly harsh mining conditions. However, what factors which combined in what way gave rise to this situation, is worth studying. Targeted to solve this problem, the fuzzy analytic hierarchy process can be used to analyze this problem (Guo et al. 2007, Zhong & Gu 2010) (FAHP analysis of the problem of fuzzy Analytic Hierarchy Process), analyzing the developments and changes law of coal and gas outburst accident, meanwhile noting the impact

factors of the coal outburst prevention, both of which can provide technical support for the coal and gas outburst prevention and treatment.

3.1 *Analysis of ideas of fuzzy analytic hierarchy Process*

Firstly, the weights of each factor were determined using FAHP. Secondly, the expert scoring method can be applied to determine the different annual evaluation in order to establish the evaluation matrix. In addition to, the fuzzy comprehensive evaluation method can be used to calculate the annual risk of the coal and gas outburst, and ultimately arrive at the results of the evaluation.

3.2 *The quantitative analysis of outburst accident based on the FAHP*

3.2.1 *The selection of evaluation index*

Summarize the results of previous studies [3–11] to select seven factors of impacting coal and gas outburst accident (A) as the evaluation indicators of outburst risk, the seven indicators are: C1, coal production; C2, outburst prevention equipment and facilities; C3, quality of personnel; C4, ventilation system; C5, outburst prevention and management; C6, outburst prevention regulation and supervision; C7, mining environment.

3.2.2 *The build of the judgment matrix*

Based on the proportional scale in Analytic Hierarchy Process, factors are compared with each other according to the relative importance of each index to show the results Table 1.

Therefore, the judgment matrix of the coal and gas outburst risk is:

$$A=\begin{vmatrix} 1 & 1/8 & 1/2 & 1/3 & 1/7 & 1/4 & 1/5 \\ 8 & 1 & 3 & 5 & 1/2 & 5 & 2 \\ 2 & 1/3 & 1 & 4 & 1/5 & 2 & 1/2 \\ 3 & 1/5 & 1/4 & 1 & 1/6 & 1/2 & 1/4 \\ 7 & 2 & 5 & 6 & 1 & 6 & 4 \\ 4 & 1/5 & 1/2 & 2 & 1/6 & 1 & 1/3 \\ 5 & 1/2 & 2 & 4 & 1/4 & 3 & 1 \end{vmatrix} \quad (1)$$

3.2.3 *The calculation of the weight vector*

Use sum method to calculate the weight vector, the basic solution is:

(a) Integrate the elements of A as columns to contain a matrix:

$$Q=(q_{ij})_{n\times n} \quad (2)$$

Table 1. Compare of parameters of mine and gas outburst.

A	C1	C2	C3	C4	C5	C6	C7
C1	1	1/8	1/2	1/3	1/7	1/4	1/5
C2	8	1	3	5	1/2	5	2
C3	2	1/3	1	4	1/5	3	1/2
C4	3	1/5	1/4	1	1/6	1/2	1/4
C5	7	2	5	6	1	6	4
C6	4	1/5	1/2	2	1/6	1	1/3
C7	5	1/2	2	4	1/4	3	1

among them:

$$q_{ij}=a_{ij}/\sum_{k=1}^{n}a_{kj} \quad (3)$$

(b) The elements of Q is added to each other by the line-by-line to achieve a vector:

$$\alpha=(\alpha_1,\alpha_2,...,\alpha_n)^T \quad (4)$$

among them:

$$\alpha_i=\sum_{j=1}^{n}q_{ij} \quad (5)$$

(c) Make the Vector normalization, get the weight vector:

$$W=(w_1,w_2,...,w_n)^T \quad (6)$$

among them:

$$w_i=\alpha_i/\sum_{k=1}^{n}\alpha_k \quad (7)$$

(d) Find out the maximum eigenvalue:

$$\lambda_{\max}=\frac{1}{n}\sum_{i=1}^{n}\frac{(AW)_i}{w_i} \quad (8)$$

(e) Substituted judgment matrix A into the formula:

$$W=(0.031,0.242,0.094,0.048,0.372,0.068,0.145)^T \quad (9)$$

$$\lambda_{\max}=7.418 \quad (10)$$

3.2.4 *Consistency test*

$$CI=\frac{\lambda_{\max}-n}{n-1}=\frac{7.418-7}{7-1}=0.070 \quad (11)$$

Table 2. Random index RI values.

Dimensionality	3	4	5	6	7	8
RI values	0.58	0.90	1.12	1.24	1.32	1.41

Look-up table we can see that when n = 7, look-up table 2 and the Stochastic RI = 1.32.
so

$$CR = \frac{CI}{RI} = \frac{0.070}{1.32} = 0.053 < 0.1 \tag{12}$$

Therefore, the judgment matrix satisfies the requirements of conformance test, the weights can be accepted.

3.3 *The risk assessment of coal and gas outburst accident*

Aiming at the indicators of seven factors' control to the coal and gas outburst accident in each year, consulting 20 experts in the field of mine safety to score themselves, each score range is (0–10). Added to each other and then take the methods of average number to arrive at a year average score for each indicator, and at last get the following evaluation matrix:

$$R = \begin{vmatrix} 3.125 & 2.164 & 3.225 & 3.875 & 4.325 & 2.385 & 2.126 \\ 4.315 & 4.725 & 4.760 & 6.650 & 7.425 & 3.650 & 5.772 \\ 4.924 & 5.850 & 5.856 & 8.285 & 8.780 & 6.495 & 5.025 \\ 5.580 & 8.936 & 8.825 & 8.950 & 9.500 & 8.125 & 5.625 \\ 5.924 & 6.250 & 5.725 & 8.137 & 8.806 & 6.325 & 5.750 \\ 4.326 & 5.052 & 4.760 & 6.650 & 6.246 & 6.240 & 5.590 \\ 4.890 & 7.364 & 8.825 & 8.125 & 8.552 & 8.036 & 5.950 \\ 4.253 & 5.024 & 4.520 & 6.327 & 6.062 & 6.150 & 6.025 \\ 4.368 & 7.165 & 8.368 & 8.520 & 8.340 & 7.936 & 6.050 \\ 4.658 & 9.087 & 8.954 & 9.250 & 9.850 & 8.874 & 6.462 \\ 4.228 & 5.052 & 4.364 & 6.250 & 6.163 & 6.050 & 6.512 \\ 4.050 & 5.355 & 6.856 & 8.085 & 7.950 & 6.195 & 6.625 \\ 3.525 & 4.784 & 4.225 & 4.036 & 5.325 & 2.125 & 6.625 \end{vmatrix} \tag{13}$$

According to the Fuzzy Comprehensive Evaluation Method, when the weight vector W and evaluation matrix R is known, the fuzzy change can be used to make the comprehensive evaluation, the mathematical model is:

$$B = W \cdot R \tag{14}$$

Substituted the matrix W and R in the formula (9) and (13) accordingly, the result is shown in Table 3.

Table 3. Annual evaluation results.

Year	2000	2001	2002	2003	2004	2005	2006
B	3.189	5.772	6.953	8.497	7.164	5.734	5.744
Year	2007	2008	2009	2010	2011	2012	
B	5.623	7.585	8.834	5.712	6.679	4.945	

4 THE ANALYSIS OF THE CHANGE CHARACTERISTICS OF THE COAL AND GAS OUTBURST ACCIDENT

Thus it can be seen that the risk of the coal and gas outburst is lower in 2000, followed by increased as a straight line, peaked in 2003, the risk of outburst twists and turns and decreased in the next few years, down to a lower level in 2012. Several important changes characteristics can be seen from this process:

4.1 *Accident hazards firstly rise but later decline*

It can be seen from the value changes of various factors in the evaluation matrix R, and combined with the actual situation, that the coal industry achieved profitability in 2000, and came out of the plight of loss over the years of the last century, since then coal production greatly improved year after year, the long-term under-investment in safety lead to outdated outburst prevention equipment and facilities and poor ventilation system, lacking of technical staffs and managements of the outburst prevention, the deficient management of the outburst prevention and the deteriorative mining environment. Therefore, the number of the coal and gas outburst accident presented a linear surge from 2001–2003; after 2003, the investment in outburst prevention equipment and facilities, the strengthened supervision in management, improving the quality of personnel and other favorable conditions made the accident hazards decrease slowly, achieve the best level in 2012 in the new century.

4.2 *Accident hazards early surge and later descend slowly*

Among 2000–2003, that the coal production increases rapidly lead to the work of outburst prevention was difficult to timely follow-up, and all of which made coal and gas outburst accident surge in large growth rate; In 2004–2012, the outburst prevention work was paid more attention to, but the upgrading of coal production and the mining environmental degradation resulted in some new

problems of the outburst prevention work: the management experience of the outburst prevention lacked long-term accumulation, the scientificalness and validity of the equipment and facilities were required to be improved, the professional talents of outburst prevention were trained difficultly, scientific ventilation system was difficult to become universal, all of these negative factors caused the outburst accident situation declined slowly.

4.3 *The flexural development of accident hazards*

The changes and development of coal and gas outburst accident twist and turn in the past 13 years, the situation was good in times and bad in others. Visible from the evaluation matrix R, the reason is that the values of weighted factors fluctuate, these weight factors are listed in follows: outburst prevention management, the equipment and facilities of outburst prevention and the quality of personnel. Therefore, the situation of coal and gas outburst accident can achieve a fundamental improvement on the premise that these factors are controlled effectively.

4.4 *The proportion of objective factors is stable, but the proportion of subjective factors volatile*

Objective factors include coal production and mining environment. Coal production, this factor has a significant effect on the accident early, but later the impact of the accident are become slow and the proportion drop; The incessant deterioration of mining environment makes its weight continue to increase and impact ascend slowly, which should be attached great importance. From now on, it's known to all that Coal production is remain at a high level and will continue to grow; With the increasing mining depth, relative gas emission, the number of high-gas coal mine and coal and gas outburst mine is also increasing year by year, all of which make the mining environmental further deteriorate and will largely boost the threat of coal and gas outburst.

Subjective factors, including outburst prevention management, outburst prevention equipment and facilities, quality of personnel, ventilation systems, safety supervision and other factors, are affected by subjectivity and also by the impact of the difficult outburst prevention work t and arduous task, and make accidents fluctuate. Because of the large proportion of subjective factors and relatively controllable, the effective control of these subjective factors becomes the emphasis and difficulty of the outburst prevention work, it should be paid more attention.

4.5 *Reach the best level in 2012 in the new century*

Throughout the coal and gas outburst accident in the past 13 years from 2001–2012, no matter the number of accidents or deaths in 2012, both reached the best level in the new century, the situation of coal and gas outburst accident has improved prominently. However, it still need to put more effort in turning the significant improvement into a fundamental transformation. According to the study results of this text, strengthen outburst prevention management, improve outburst prevention equipment and facilities, enhance outburst prevention staff skills, reinforce supervision and control and so on, are the directions and focuses of outburst prevention work in the future.

5 CONCLUSIONS

In the past 13 years, the number of coal and gas outburst accident increased rather than decreased. In recently, the serious and the worst accident of coal and gas outburst has occurred from time to time, caused tremendous harm to the lives safety of miners and property of the State. The situation of outburst in 2012 has been significantly improved, but whether this situation can be maintained or not will be an important issue of outburst prevention in the future. Finding the aporia and kernel of the flexural changes of the outburst accident through the development and changes law of coal and gas outburst accident in the past 13 years, is an important reference to sustaining this improved situation. Applying these laws has great significance to carry out outburst prevention work in the future.

ACKNOWLEDGEMENTS

This research are the National Natural Science Foundation of China (Grant No. 51274206) and upported by State Key Laboratory for Coal Resources and Safe Mining, China University of Mining & Technology (Grant No. SKLCRSM11 KFB02).

REFERENCES

Cheng J.S.2012. The Analysis of Outburst Hazard of 1606 Working Face in Pinggou Coal Mine. Mine Safety 7:169–171.

Deng M., Zhang G.S. & Chen Q.H. 2010. Forecast of coal and gas outburst based on time series of gas concentration. Journal of China Coal Society 2:260–264.

Gong F.Q., Li X.B. & Dong L.J. 2008. Underground Goaf Risk Evaluation Based On Uncertainty Measurement Theory. Chinese Journal of Rock Mechanics and Engineering 2:323–330.
Guo D.Y., Fan J.Z. & Ma S.Z. 2007. Prediction method of coal and gas outburst by analytic hierarchy process and fuzzy comprehensive evaluation. Journal of University of Science and Technology Beijing 7:660–664.
Ou Z. & Wu C.F. 2010. Study on prediction of coal and gas outburst danger in No121030 coal mining face of Liangbei Mine. Coal Engineering 10:40–42.
Pang Y.Q., Jia H.Y. & Xiong W. 2012. Research and Application of Coal and Gas Outburst Risk Assessment on Under Coal Seam in Baijigou Coal Mine. Coal Technology 10:94–95.
Qin Y., Yang S.Q. & Ma X.D. 2012. Evaluation of Coal and Gas Outburst Risk Based on Principal Component Analysis. mine safety 9:215–217.
State Administration of Coal Mine Safety.2012. The 12th five-year plan of coal safety production in coal mines.
Xiao J.X., Li X.J. & Meng Z.J.2011. Coal and Gas Outburst Risk Prediction Based on Fuzzy Comprehensive Evaluation. Coal Technology 6:112–114.
Zhang Z.P., Cheng Y.P. & Liu H.B.2012. Analysis on Influence of Geological Factors on Gas Storage and Outburst Risk in Coal Seam of Cuimiao Coal Mine. Mine Safety 3:128–130.
Zheng Y.F., Ju W.J. & Zhu G.Y.2012. Application of FTA method on hazard assessment for coal and gas outburst. China Mining Magazine S:509–511, 516.
Zhong H.R. & Gu X.P.2010. Assessment of Power System Black start Schemes Based on Fuzzy Analytic Hierarchy Process and Its Sensitivity Analysis. Automation of Electric Power Systems 16:34–37, 49.

This page intentionally left blank

Progress in Mine Safety Science and Engineering II – He et al. (Eds)
© 2014 Taylor & Francis Group, London, ISBN 978-1-138-00122-0

The causes of sinking columns in North China coal fields and their permeability identification

Luqin Xu
China National Administration of Coal Geology, China

Jingming Wang
North China Institute of Science and Technology, China

ABSTRACT: The mechanism caused by open or inner circulation of groundwater was put forward based on analyzing the relationship between the distribution and development of the sinking columns with the strength of coal metamorphism in north China coal field. It is considered that the heat due to mantle upwelling cause the water to circulate within Ordovician limestone aquifer and that CO2 brought by the mantle plume from deep inside of the earth into water increase solution of the water—the sinking columns developed. This is the mechanism of sinking column formation due to inner circulation of water. In contract, the sinking columns caused by gravity flow from recharge areas to discharge areas with CO2 from atmosphere attendant—open circulation groundwater system—are much less developed than those in inner circulation system due to low temperature and Pco2 in the water. According to the mechanism proposed in the paper for sinking column formation, the paper gave the 7 indexes to predict the locations and to identify the permeability of sinking columns in order to direct groundwater control engineering.

1 INTRODUCTION

Snikingcolumus (SCs), a populous hydrogeological phenomenon in north China coalfields, have drown broad attentions from hydrogelogists due to the influence on coal mining and harmful to mine safety. A lot of researches have been done to find the distribution regularity and the forming mechanism of the phenomenon. The former researchers assume that the SCs develop along syncline axes and faults (Yin 2004, Zhang 2000). The latter researchers assume that main cause of SCs is gypsum solution (Jia & Hu 1998)or downward caving (Wang 1982, Si & Ma 2001) of limestone. However, these theories con not explain the relationship between SCs with coal rank or geothermal. The author's 20 years research has found the relationship between SCs and geothermal convection or gravity flow of groundwater. The development mechanism of SCs caused by inner Groundwater Circulation (GC) or open groundwater circulation was proposed.

Abnormal geothermal or coal metamorphism has strong relationship with SCs in north China coal fields. For example, SCs are broadly developed in the coal mines where geothermal is abnormal, such as in Renlou mine, Wanbei mining areas, Sanhejian mine, Xuzhou mining areas, Xieqiao mine, Huainan mining areas, Liangbei mine, Yuzhou mining areas, Nanding—lingzi mine, Zibo mining areas. Therefore, it is significant to study the development mechanism about SCs caused by inner and open GC in order to find their distribution regularity and identify their permeability.

2 DISTRIBUTION REGULARITY OF THE SINKING COLUMNS

2.1 *The relationship between Scs and coal ranks*

Author'sinvestigation discovers that the development of SCs is strongly related with coal metamorphism. The higher the coal metamorphism is, the denser is the SCs. For example, in the north end of Fengfeng coal mining areas is Cishan dioriteporphyrite. From the dioriteporphyrite to the south, the coal rank goes down, ranking anthracite, meager coal, lean coal, coke and fat coal and the dense get lower, as shown in fig 1. The SC area is 457, 600 m2 in anthracite regions, sharing 93.5% of total area. In meager regions, it is 2, 1900 m2, sharing 4.47%. In lean region it is 6, 800 m2, sharing 1.41%. In coke regions, it is 3, 100 m2, sharing 0.63%. In fat area, there is no SC.

In other anthracite regions in north China, the SCs are also dense like in the north part of Fengfeng, such as the coal mining areas of Yangquan and Jincheng, the famous places for SC development.

The investigation also shows that most SCs are located in high coal metamorphic regions. Nonof them is located in low metamorphic regions unless the regions are geothermal abnormal, as shown in Table 1.



Figure 1. Fengfeng mining area coal zoning map.

2.2 *The relationship between SCs and groundwater running-offs*

(1) The relationship between SCs and inner GC
According to the investigation, many SCs are located in the mines which are deeply buried by Quaternary system or isolated. In these regions, groundwater exchanges with outside is week and salinity and temperature are low. For example, Ordovician limestone is 900 m covered by overlying formations in Wutongzhuang coal mine located in a horst. The faults in both sides of the horst with throws of 380 m and 440 m respectively are impermeable. The data from boreholes show that the water heads, water temperature, salinity in different walls are quirt different, as seen in Table 2, 4.93 m~10.24 m difference in water head, 18°C~19°C in temperature, 4.03 g/L~5.39 g/L in salinity. 28 SCs weredetected out in the mine. In this kind of isolated areas densely develop SCs in north China coal field. For example, Yangquhe coal mine, Fengfeng region and Xiandewang coal mine, Xingtai region are both located in horsts and the SCs are impacted. It was thought that the groundwater is poor in horsts because the faults in both sides ware water resisting. When exploration data showed that all borehole unit flow over 5l/s.m and water inrushes from coal floor were all located in horsts, the original view was denied. The discharge test data showed that the flow from limestone aquifer in horsts was much bigger than that in grabens. For example, in the horst in Yangquhe coal mine was 2400 m^3/h of bore flow from Daqing limestone with 1.8 m of water table drop. In contract, in a graben in Wangfeng coal mine was only 180 m^3/h of the flow from the same aquifer with 75 m of water table drop. Besides, the

Table 1. Coal ranks and geothermal in the coal mining areas where SCs developed.

Mining areas	Coal ranks	°C in O_2	Remark
Yangquan	anthracite		Igneous stock in outside of the mine
North part of Fengfeng	Coke—anthracite		Basic igneous stock to the north
North part of Fengfeng	oke	43	Abnormal geomagnetism
Jingxing	Lean—anthracite		Basic igneous stock to the east
Luan	Lean—anthracite		Basic igneous stock to the nort
Center part of Xinftai	Coke-lean coal		Abnormal geomagnetism
Yongcheng	Lean coal		Basic igneous stock in the center
Jincheng	Coke—lean coal		Abnormal geomagnetism
Dongshan, Taiyuan	Lean coal		Basic igneous stock to the east
Xishan, Taiyuan	Coke-lean coal		Basic igneous stock in the outside
Xiaoxi, Huaibei	Lean coal		Basic igneous stock to the east
Zhahe, Huaibei	Lean-anthracite		Basic igneous stock in the outside
Linhuan, Huaibei	1/3 coke	43	
Panji, Huainan	Fat coal	43	Basic igneous stock in the outside
Banqiao, Huainan	Fat coal	43	
Sanhejian, Xuzhou	Fat coal	42	
East part of Xingtai	Fat coal	41	

Table 2. Geochemical, temperature, and water table of boreholes in the walls of fault F_{26}.

Locations	Borehole	Water table /m	Geochemical types	Salinity/g·L^{-1}	Temp/°C
Upper wall	668	+133.95	HCO_3–SO_4	0.31	17
	W305	+141.90	SO_4·Cl–Ca·Na	1.17	17
Fault zone	22–35	+132.65	SO_4·Cl–Ca·Na	3.02	24.5
Lower wall	1501	+129.02	Cl·SO_4^-–Ca·Na	5.7	36
	2206	+131.66	Cl·SO_4–Na·Ca	5.2	35

geothermal abnormal areas in Table 1 are all located in isolated and deep buried coal mines. For examples, in Linhuan coal mining area, the bedrock lies 170 m beneath Quaternary system and SCs developed in the two geothermal abnormal coal mines within the area. 3 SCs in Renlou coal mine are transitive and caused the mine flooded and 8 unconfirmed columns are located in Xutuan coal mine which are dangerous because they will betransitive. In contract, there are no any SCs found in other 4 normal geothermal coal mines.

(2) The relationship between SCs and strong running-offs of groundwater

SCs usually develop along faults because they are strong running-offs. This phenomenon is populous in Hedong coal field. The original review that some SCs developed along syncline axels has been changed because the reverse faults paralleled syncline axels ware found. Forexample, 10 discovered SCs developed along Liuqiaosyncline axel were considered to be caused by the syncline. This review was changed when Chenji reverse fault found by some mini faults connection emerged to go along Liuqiao syncline axel. The fault and limestone aquifer conspired a water hazard in a working face in the upper wall and the water level in observation well S13 which went through the fault and down to Taiyuan limestone aquifer became abnormally high. Than the SCs were considered to be caused by Chenji reverse fault rather than Liuqiao syncline. The mining engineering has confirmed that syncline axels are not strong running-offs of groundwater. Therefore, it has no theory basis for SCs caused by folding to develop along syncline axels. The true cause of this kind of SCs in areas may be the uncovered reverse faults going along the syncline axels.

Some SCs in north China coalfields were located neither in isolated or geothermal abnormal regions nor along confirmed faults. These columns seem irregular. But author's investigations discovered that these columns were located in the hidden faults—only cutting Ordovician limestone aquifer under coal floor strata. For example, No.1 SC developed in the zone of the a only fault going north to south in Relou mine, but the No.2 and No.3 developed in its extension line. That is Ordovician limestone strata were cut by the fault, but the coal seam was not.

3 ANALYSES OF SINKING COLUMN FORMATION

3.1 *Formation due to inner circulation of groundwater*

Inner GC is an antigravity circulation caused by geothermal without recharge areas or discharge areas in circulation system withoutprecipitationdirect attendant. The geothermal resource is mantle upwelling. The temperature can be reckoned by coal metamorphism. Accordingto coal petrology, coal metamorphism results from temperature (Yang 1999). The higher the temperature is and the longer the coal was coked, the higher the metamorphism goes. Based on the normal geothermal gradient and the thickness of coal system analyses, the coal seams burn in C-P strata in north China, the highest degree the coal metamorphism can reach is fat coal. This means that coke ~ anthracite should be heated by additional geothermal. Calculation according to vitrinitereflectivity (Yang 1999) shows that coke coal was coked at 254°C at least. Water temperature in Ordovicianlimestone layers should be over 272°C, because the forming temperature of α-quartz is over that degree (Chen, et al 1999). The regions of high coal ranks are mainly located in mountainTaihang coal basins and the north wing of Songshan-Bengbu uplifting which are located in the periphery of mantle upwelling induced by sub mantle plume in north China basin. The mantle plume originated in the interface between core and mantle became lateral flow and the upwelling took the mushroom shape when the upward flow reached the bottom of the lithosphere. About at the depth of 100 km the mantle branches were burn in the periphery of the plume, as shown in Fig. 2, The figure shows that mantle branches are much developed in the regions of Mountain Taihang, Jiaodong

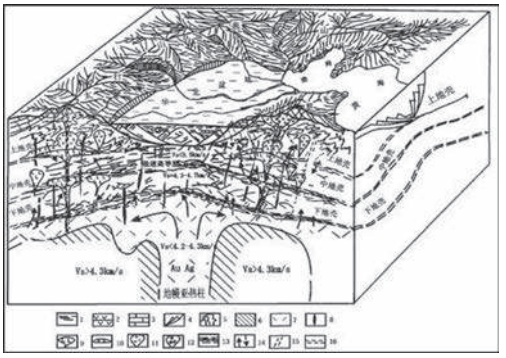


Figure 2. The geothermal model resulted from sub-mantle plume-mantle branches in north China (from Niushuyin).
1. Cenozoic sediment; 2. Mesozoic volcanic rock; 3. sedimentary; 4. detachment zone; 5. Ar metamorphic rock; 6. cold mantle rock; 7. sub mantle plume; 8. mafic dike; 9. mafic intruded rock; 10. basults; 11. nuetral intruded rock; 12. acidic intruded rock

and Songshan-Bengbu where geothermal was high and SCs developed. In Jiaodong region, mantle braches were much unevenly distributed compared with Mountain Taihang region. The earth crust uplifted intensively and the coal bearing strata were eroded out. Coal seams were reserved in the region where mantle branches were sparse and geothermal was not so high as, and the SCs were not so dense as inMountainTaihang region.

CO_2 karst needed stemmed from mantle and skarnrather than from atmosphere. According to the references, there are 3 "gas spheres" with huge reserves ininside ofthe earth. The major content is CO_2 (Sugisaki R.1983). The CO_2 was carried into groundwater in Ordovician limestone by mantle branches. Besides, a large amount of CO_2 would be relieved when magma intruded into limestone, as flowing,

$$CaCO_3 = CaO + CO_2$$
$$CaCO_3 + FeO + 2SiO_2 = CaFeSiO_3 + CO_2$$
$$CaCO_3 + SiO_2 = CaSiO_3 + CO_2$$
$$CaCO_3 + MgCO_3 + 2SiO_2 = CaMgSiO_3 + 2CO_2$$
$$CaCO_3 + Al_2O_3 + 3SiO_2 = Ca_3Al2Si_3O_{12} + 3CO_2$$
$$2CaCO_3 + 5\,MgCO_3 + 8SiO_2 + H_2O = Ca_2$$
$$Mg_3Si_8O_{22}(OH) + 7CO$$

The hot water with high CO_2 content dissolved the limestone rapidly and karst caves formed when the magma intruded. Therefore, the closer to the magma, the higher CO_2 concentration was in the water, and the more intensively the limestone dissolved, and the more the SCs developed.

3.2 *Formation due to open circulation groundwater*

The open groundwater circulation is a kind of gravity flow under normal temperature with direct precipitation attendant in a complete geodrogeological unit consisting of recharge areas, running off areas and discharge areas. According to limestone solution experiments. Dreybrodt (D, W. & B, D. 1991), the temperature influents $CaCO_3$ on solution speed significantly. The higher the temperature is, the fast the $CaCO_3$ solutes. The partial pressure of CO_2 (Pco_2) has positive relationship with limestone solution. The higher the Pco2 is, the faster dissolves the limestone. The Pco2 and temperature are low because CO_2 come from the atmosphere and because the open circulation runs under normal conditions. Therefore, $CaCO_3$ dissolves much slow and SCs much less develop in the open GC regions compared with the inner GC areas. The low coal ranks in open GC regions means that the regions can be identified if they are the inner GC ones or open ones according to coal ranks.

3.3 *Formation due to mixed circulation*

Inner and open GC can coexist in many regions. The heat brought by mantle branches did not change the open system. Therefore, groundwater could both circulated within the system and flow in the open system. For example, Fengfeng belong to Heilongdong spring region, an open system as a whole. The north part is the upstream, closing to Cishan stock. In this area, coal ranks are higher and SCs denser. This kind of areas arecharacterizedby both inner and open GC regions. In the areas of fat coal and lower rank of coal in Fengfeng, even in other coal fields in north China, SCs do not develop at all according to statistical data. This means that it is the inner GC that control SC development, rather than open GC.

4 SC PREDICTION AND ITS WATER TRANSMISSIBILITY IDENTIFICATION

According to the above theory about SC formation, the following deductions can be made.

①In the regions where coal ranks from coke to anthracite develop SCs and the higher the coal rank, the denser the SCs are. The SCs in these area are impermeable.

Coal petrology confirms that under normal geothermal gradient condition coal can only be metamorphosed as high as fat coal. If the coal ranks from coke to anthracite in the region, additional geothermal should be added. The strong heat convection once existed in the regions of high

coal ranks and the condition was favorable for SCs developing. The higher temperature was, the stronger was the groundwater convection and the denser were SCs.

Prof. Yangqi confirmed that these coals got the ranks in Jurassic Period. Groundwater stopped convectional flow because heat consumed out. The materials in the columns become too compacted to be permeable.

②In the current abnormal geothermal regions develop SCs and the SCs are permeable. Groundwater is in the state of thermal convectional flow in the current abnormal geothermal region where SCs are developing. The materials in the columns are so loose as to be permeable.

③In the areas of normal geothermal gradient and low coal ranks, SCs can only sparsely develop in fault zones in a complete hydrogeological unit. Under such conditions, water temperature, flow rate and Pco_2 are low. Karst can only develops in fractured zones where groundwater flow fast and the SCs are sparse.

④The declined SCs are impermeable. The SCs were perpendicular when they were formed. Orogenic movement made the columns declined. This implied that the columns formed before the movement. They are so old as to be compacted and impermeable.

⑤The SCs up to bedrock surface are impermeable, but the ones harden under coal floor or in quaternary strata are permeable. The former developed in Mesozoic Yanshan period. The materials in the SCs are so old as to be compacted and impermeable. The latter ones are developing and the materials in the SCs are too young to be compacted and they are permeable.

⑥The SCs are permeable if the circle fractures surround the SCs and vice versa. According to mechanicalanalyses and practical investigation, SCs are associated with concentricallycircled fractures surround themselves. Their transmissibility is identical to SC's. The transmissibility of the fractures is the effective index to predict permeable SCs.

5 CONCLUSION

Based on the research bout the distribution regularity of SCs and the relationship between SCs and coal ranks or geothermal in north China coal fields, the fowling conclusions can be drawn:

1. The majority of SCs develop in the regions of high coal ranks and current abnormal geothermal. The higher the coal ranks and the current geothermal are, the denser are the SCs.
2. The mechanism theory to form SCs because of inner or open GC is raised. The paper demonstrates: ①Mantle upwelling raised geothermal gradient, sped groundwater convection in Ordovician limestone aquifer; ②The resources of geothermal and CO_2 brought by mantle branched increased Pco_2 and $CaCO_3$ dissolution; ③The SCs densely develop in inner and mixed GC regions. In contract, they sparsely develop along strong running-offs of groundwater in the open GC regions. Inner and maxed GCs are the control factors of SCs.
3. The SCs located in the regions where coal ranks from coke to anthracite, declined, up to the bedrock surface are impermeable. The SCs hidden under coal seams or in Quaternary system and SCs located in abnormal regions are permeable. The SCs are permeable if theassociated and theconcentricallycircled fractures surround the columns are and vice versa.

REFERENCES

Author introduction: WangJingming, PHD, professor, 1958-, graduated from Anhui University of Science & Technology, engaged in research in hydrogeology since graduation, Xinming248@ncist.edu.cn.

Chen Zenfzhi, et al. 1999. Modeling and application geothermal flow history in the ancient basin with multiple geological movements. *Journal of China shiyouuniversity(natural science),* 2(1):91~101.

Dreybrodt, *Prosesses in Karst system. Springer series in Physical Environment,* 1988. Springer, Heideberg, 288.

Dreybrodt, W. & Buhmamn, D.1991. A mass transfer model for dissolution and precipitation of calcite from solution in turbulent motion. *Chem. Geol.*, 90: 107~122.

Jiaguiting & Hu kuanrong. 1998. The causes and distribution of sinking columns in North China coal field, 8 (4), 261~266.

Sano Y, et al., 1992. Secular variations of helium and carbon isotopes at active valcano, *29th Int. Geol, Congr. Abstracts Vol.* 3 of 3, Kyoto, Japan. 609~614.

Si Suping & Ma Jianmin, 2001. Causes and distribution of sinking columns in coal bearing system, *Fault-block oil & gas field,* . 3, 15~18.

Sugisaki R. 1983. Origin of hydrogen and carbon dioxide in fault gases and its relation to fault activity, *Jour. GeolVol.*(91):239~258.

Wang Rui, 1982. Investigation of cause of sinking columns in North China, *Hydrogeology and engineeringjeology,* 9.(1), P37~41.

Yang Qi, 1999. The complex metamorphism of the coal in China, *Earth science frontiers,* 5, Vol.5, Suppl, 1–7.

Yin Shangxian, et al. 2004. nvestigation on the characteristics and the causes of sinking collumnsinNorth China coal mining areas *Chinese Journal of rock mechanics and engineering,* No. 1, Vol. 23 (1), 120~123.

Zhang Yongshuang, et al. 2000. Investigation on the sinking columns in North China coalfield, *Journal of engineering geology.*8(1).35~39.

This page intentionally left blank

Progress in Mine Safety Science and Engineering II – He et al. (Eds)
© 2014 Taylor & Francis Group, London, ISBN 978-1-138-00122-0

Characteristics of in-situ stress field in northern Tianshan Mountain mining areas

S.K. Zhao
Mine Safety Technology Branch of China Coal Research Institute, Beijing, China

ABSTRACT: Based on the measurement of in-situ stress field in coal mine, a combination method of the regional geological structure and field measurement of in-situ stress is used to analyze the distribution rule of in-situ stress of northern Tiashan mining areas, so does the reasons of intense strata behaviors in Sikeshu mining area. Suggest that the best azimuth of the axis of subsequent roadway workface is 16.3° on NNE according to the distribution characteristics of in-situ stress and the situation of mine exploitation, improves the scientific and reliability of ground pressure control in the condition of complex structures.

1 GENERAL INSTRUCTIONS

With the increase of mining depth and intensity underground coal mines, effect of in-situ stress influencing the stability of rock around roadway play outstanding roles (Luo & Li. 2010, Cai 1993). In-situ stress which is the initial stress natural occurrence in rock mass without engineering disturbance, is not merely a important factor determining stability of region al rock-mass structures, and an essential force causing deformation and failure of various underground and ground geotechnical engineering (Hou 2004). Especially under the effect of tectonic stress, the maximum horizontal stress of rock mass in mining stope can reach 1.5–5.0 times more than vertical pressures (Zhao & Chen. 2007). Coal seam and strata in a additive effect of initial in-situ stress (including gravity stress and tectonic stress) and disturbance stress, often causes intense strata behaviors workface and serious deformation of roadway surrounding rock, even induces the coal mine dynamic disaster (Yin & Xian. 1997, Qiao & Li. 2008). Even many scholars has measured and analyzed the relationship between in-situ stress and mine pressure appearance for many years (Zhang & Song. 2010, Kang & Lin. 2010), the causes of in-situ stress are complex, the formation and changes are caused by various earth dynamic behaviors of earth plates, plate extrusion, earth rotation, earth's mantle thermal convection, etc. It exists in an unsteady situation with spatial-time location changing. Magnitude and direction has a strong discreteness. The limit measured points result of in-situ stress could not reflect the whole characteristics of stress in coal mine, especially in mining area of complex tectonic movement. No. 2 inclined shaft in Sikeshu mine in Wusu, Xinjiang province is in northern Tianshan typical mining area affected by multi-period geotectonic movement, the distribution of in-situ stress field is complex. Large roadway deformation and serious floor heave of roadway caused by the process of mining, so this paper based on the measurement of stress in coal mine, analyzes the distribution law of in-situ stress of northern Tianshan mining area by a method of combining the regional geological structure and field measurement of in-situ stress, and gives optimization suggestions for mining scheme, improves the scientific and reliability of ground pressure control in the condition of complex structures.

2 THE RELATIONSHIP BETWEEN IN-SITU STRESS AND TECTONIC MOVEMENT

In-situ stress consists of gravity stress caused by the gravity of rock and tectonic stress caused by geotectonic movement. Gravity stress is only relative to rock gravity and buried depth, easy to determine magnitude and direction. Tectonic stress is not only relative to the rock tectonic movement (including the movement of type, scale, combination of temporal evolution and times), but to geological structure types, topography and geomorphology of rock occurrence. Existence of geological structure (fault, etc) have influence on continuity and uniformity of in-situ stress. The greater scale the fault structure have, the lager influence of extension and intensity in-situ stress will have, especially closing to fault zone of deep,

far fracture extension scale or group development, mutually superimposed fault structure may play domination role in the distribution of in-situ stress in the region. The horizontal tectonic stress have more obvious influences in deep mining, tectonic stress often become the main stress controlling stability of roadway surrounding rock. In addition mechanical property of deep coal and rock mass have a plastic transition influenced by high ground temperature stress, high gas pressure and high seepage water pressure, affecting the distribution of deep in-situ stress. So in-situ stress now could not describe by functional form, especially the distribution of in-situ stress influenced by geological structure only determine by field measurement. There are lots of in-situ stress measurements now, including indirect method indirectly calculating in-situ stress by measuring strain and deformation of rock and geophysics method by measuring propagation law of acoustic and electric. Now hydraulic fracturing method and stress relieving method have more application in geotechnical engineering. As a result of large work quantity and High test cost in deep well measurement drilling from the ground, Hydraulic fracturing method could not realize fast measurement of in-situ stress in local region underground, measure in-situ stress in by using Stress relieving method in No. 2 inclined shaft in Sikeshu mine in XinJiang province.

3 CHARACTERISTICS OF GEOLOGICAL STRUCTURE IN NORTHERN TIANSHAN MINING AREAS

Tianshan Mountains are results of collision by the block of Tarim and Kazakhstan and the orogeny in cenozoic era, having experienced by a complex process. North tianshan orogenic is a nww forward system constituted by a series of fault, fracture, crack. Mainly including yilianhabierga and boged a mountain. As a result of low velocity layers in the lithosphere, a ductile detachment in the crust under horizontal, S-N trending compressive stress and mantle deformation stress, current tectonic stress field shows the south and the north thrust along the fracture surface, appearing as a S-N to a NWW extrusion.

Sikeshu coal mine in Wusu city is located in north tianshan eugeosyncline north-edge in the west piedmont depression of Urumqi mountain. It is a meso-cenozoic depression formed on the Paleozoic basement. Under yanshan movement and himalayan movement, piedmont depression of Urumqi mountain in the mesozoic strata form a series of fasciculation or minor axis fold, form kinds of anticline and syncline structures, mainly including Kerry Ackert—the four tree river anticline and four tree syncline, tectonic line mainly is NWW. In addition faults are developed In this region Influenced by quaternary neotectonic movement, mainly including guidike-aileqigen fracture located in the region of northern and laowugouxiaerhedingbieli fracture located in the region of southwesten. Faults and fractures are developed in Sikeshu mine, tectonic line is in the same direction as region, mainly in E-W direction, Fig 1. The fold in mining area mainly develop in jurassic coal-bearing stratum, keliateke-wusudianchang-walantuoliga syncline is the main part of fold structure in mining area. The faults in mining area mainly include the compressive shear faults striking near E-W and trending towards N or S, associate torsional (shear) fractures in N-W or N-E. The maximum principal stress in mining area is the N-S or NNE direction.

4 IN-SITU STRESS MEASUREMENT IN SIKESHU MINING AREAS

4.1 *Measurement method and arrangement of measuring points*

The field measurement in Sikeshu mining area in Wusu, Xinjiang province is carried out by boring stress-relief method, using improved hollow inclusion strain gauge of higher precision. The main part of the improved hollow inclusion is a hollow cylinder made by epoxy resin, with three resistance strain gage embedded in middle part circumferentially and equally (120°). Each of resistance strain gage consists of four strain gauges with 45°interval, 12 strain gauges in total. The arrangement mode of improved hollow inclusion strain gauges is just as shown in Fig. 2.

In order to ensure that the measurement data could quite accurately reflect the distribution law of in-situ stress in the whole measuring area from the space, synthetically considers arrangement demand of points measured by stress relief method, geological characteristics of rock in coal mine and



Figure 1. Geological structure in Sikeshu mining area.

the roadway layout underground. Choose three measuring points in No. 2 inclined shaft in Sikeshu mining area, respectively for A505 air door in haulage gate (altitude + 1128 m, hole depth10.8 m), No. 1 refuge chamber (altitude + 1145 m, hole depth 10.4 m), shaft station (altitude + 1160 m, hole depth 9.6 m). It could accurately reflect in-situ stress change law in three-dimensional along depth and horizontal direction. The arrangement of measuring points is as shown in Fig. 3.

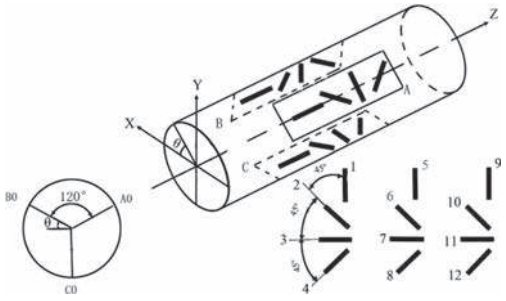


Figure 2. Arrangement mode of improved hollow inclusion strain gauges.

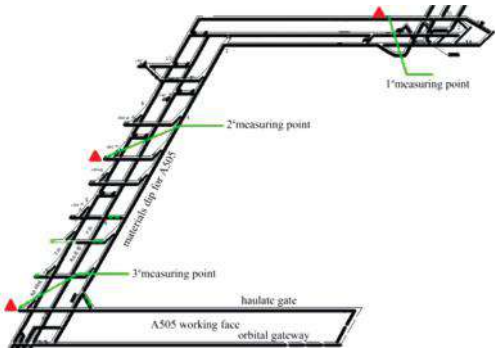


Figure 3. The arrangement of measuring points.

4.2 *Analysis of the results of measurement*

Strain data measured underground measured by improved hollow inclusion strain gauge is collected and preserved by the instrument for measuring stress. Then give the curves of stress relief, the changing curves of strain value of strain gages with the depth of stress relief changing after the data is imported into computer ground, as shown in Fig. 4. Most of the curves of stress relief in Fig. 4 are according to laws, so they are in normal operation and can be involved in calculation of in-situ stress. 12 reliable strain value are obtained in every measuring points through the curves of stress relief, and based on laboratory measurement of modulus elasticity and poisson's ratio in 3 measuring points, calculate the values, direction and angle of the maximum principle stress, the intermediate principal stress and the minimum principle stress by a computation programme for the in-situ stress measurement, as shown in Table 1.

From the results of in-situ stress at 3 measuring points in No. 2 inclined shaft, the regularity of in-situ stress distribution is as follow.

1. There are 2 principal stress nearly horizontal at measuring points, the maximum angle with horizontal plane is 9.28°, the minimum is 0.40°, the average is 4.5°. Another principal stress is near in vertical direction, the maximum angle with horizontal plane is 84.23°, the minimum is 80.70°, the average is 7.93°.
2. The direction of maximum principal stress is nearly horizontal direction. The minimum angle between the maximum principal stress and horizontal plane is 0.4°at 3 measuring points, nearly horizontal. The maximum is 9.28°, nearly horizontal.
3. The style of mine in-situ stress is $\sigma_H > \sigma_h > \sigma_v$, namely: the maximum horizontal stress is larger than the minimum horizontal stress, the vertical principal stress is the minimum. The maximum horizontal stress is averagely 2.16 times more than the gravitational stress, showing that the horizontal stress is in the dominating position

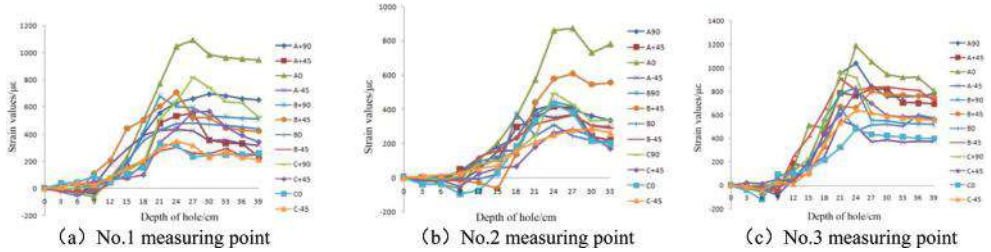


Figure 4. The curves of stress relief at measuring points.

Table 1. Calculation of principal stress in measuring points in No. 2 inclined shaft.

Measuring points	Depth/m	Maximum principle stress			Intermediate principal stress			Minimum principle stress		
		Value/ MPa	Direction/ (°)	Angle/ (°)	Value/ MPa	Direction/ (°)	Angle/ (°)	Value/ MPa	Direction/ (°)	Angle/ (°)
1	234	13.42	181.43	–9.28	8.64	–88.63	0.46	6.47	178.53	80.70
2	249	16.33	208.73	0.40	8.22	–61.32	–8.73	6.74	121.36	–81.26
3	266	14.88	198.76	–1.54	8.31	–71.39	5.56	7.37	124.23	84.23

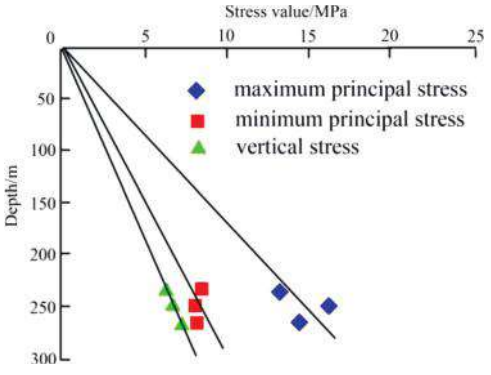


Figure 5. Schematic diagram of the linear regression relationship.

in No. 2 inclined shaft. The maximum horizontal stress is averagely 1.77 times more than the minimum horizontal stress. The difference of 2 kinds of horizontal principal stress is beneficial to formation of faults, joints, etc.

4. The direction of maximum horizontal principal stress should be directed towards SN or NNE. Vertical stress is more or equal to overburden stress. It is 1.00~1.03 times more than the gravitational stress, the average is 1.02 times.
5. The maximum horizontal stress ($\sigma_{h,\max}$), the minimum horizontal stress ($\sigma_{h,\min}$), the vertical principal stress (σ_v) increases linearly with the depth (measurements given are in m), the linear regression equation is as follow.

$$\begin{cases} \sigma_{h,\max} = 0.0052 + 0.0558H \\ \sigma_{h,\min} = 0.088 + 0.0330H \\ \sigma_v = 0.002 + 0.0270H \end{cases} \quad (1)$$

Linear regression relationship of value of $\sigma_{h,\max}, \sigma_{h,\min}$, σ_v changing with the depth is as shown in Fig. 5.

5 ANALYSIS OF INTENSE STRATA BEHAVIORS IN NORTHERN TIANSHAN NO. 2 INCLINED SHAFT

Sikeshu mining area in Xinjiang is located in northern Tianshan eugeosyncline north-edge in the west piedmont depression of Urumqi Mountain. The main characteristics of the contemporary tectonic stress field in northern Tianshan is affected by the compression of Yanshan movement and himalayan movemen, the direction of compressional stress is closed to SN-NNE direction. Meanwhile, the direction of the regional principal stress and the maximum principal stress is nearly horizontal, located in NNE direction. The direction of the tectonic stress fields is consistent with the maximum principal stress. Compared with plan view of excavation, obtain that direction of the layout of main stope face is vertical with tectonic stress or in-situ stress. Near E-W direction fold and fault structure in Sikeshu mine are formed by the compressive stress in northern Tianshan area, local high stress accumulate, which make preparation roadway severe deformation and floor heave, hard to maintain. The incorrect distribution of working face which is nearly vertical to the direction of in-situ stress or tectonic stress is another reason of severe appearance of the mine pressure. The impact of horizontal stresses on roof and floor of the roadway are much greater than that of vertical stresses, so vertical stresses mainly have impact on roadway sides. Therefore, suggest that the best azimuth of the axis of subsequent roadway workface is 16.3° on NNE according to the distribution characteristics of in-situ stress.

6 CONCLUSIONS

In the light of complex geological structure and inhomogeneous distribution of in-situ stress in northern Tianshan region, xinjiang affected by multi-term movement, analyze the distribution law of in-situ stress of northern Tianshan mining area

by a method of combining the regional geological structure and field measurement of in-situ stress, analysis of reasons for intense strata behaviors in Sikeshu mining area.

1. The main characteristics of the contemporary tectonic stress field in northern Tianshan is affected by the compression of Yanshan movement and himalayan movement, the direction of compressional stress is close to SN-NNE direction. Under the tectonic stress field which is maximum horizontal principal stress, the mine suffers the regional principal stress and the maximum principal stress nearly horizontal, mainly in NNE direction.
2. Nearly E-W direction fold and fault structure in Sikeshu mine are formed by the compressive stress in northern Tianshan area, local high stress accumulate, which make preparation roadway severe deformation and floor heave, hard to maintain. The incorrect distribution of working face which is nearly vertical to the direction of in-situ stress or tectonic stress is another reason of severe appearance of the mine pressure.
3. Suggest that the best azimuth of the axis of subsequent roadway workface is 16.3° on NNE according to the distribution characteristics of in-situ stress and the situation of mine development, improve the scientific and reliability of ground pressure control in the condition of complex structures.

ACKNOWLEDGEMENTS

The author wish to acknowledge the financial support and permission to publish this paper by the China Coal Research Institute (CCRI) and the supported by the State Key Development Program for Basic Research of China (Grant No. 2010CB226806), the National Natural Science Foundation of China (Grant No. 51174112 and Grant No. 51174272).

REFERENCES

Cai M F. 1993. Commentary of principle and techniques of rock stress measurement. *Chinese Journal of Rock Mechanics and Engineering.*12 (3): 275–283.

Hou M X. 2004. Studies on new method and principle of three dimensional crustal stress measurement in deep borehole and related issues. *Chinese Journal of Rock Mechanics and Engineering,* 23(24): 4258–4258.

Kang H P. & Lin J. 2010. In-situ stress measurements and distribution laws in Lu'an underground coal mines. *Rock and Soil Mechanics,* 31(3):827–833.

Luo C W. & Li H B. 2010. Study of distribtion characteristics of stress in surrounding rock mass and in-situ stress measurement for deeply buried tunnels. *Chinese Journal of Rock Mechanics and Engineering,* 29(7): 1418–1 423.

Qiao W. & Li W P. 2008. Distribution law of in-situ stress field in engineering subzone of deep coal mine and application in forecast of outburst. *Journal of Engineering Geology,* 16 (Supp):124–127.

Yin G Z. & Xian X F. 1997. The effect of crustal stresses on rock burst and evaluation of zone prone to rock burst. *Journal of China Coal Society,* 22(2):132–137.

Zhao D A. & Chen Z M. 2007. Analysis of distribution rule of geostress in China. *Chinese Journal of Rock Mechanics and Engineering,* 26(6): 1265–1271.

Zhang Y X. & Song C S. 2010. Geostress Measurements by hydraulic fracturing method at great depth of boreholes and numerical modelling predictions of stress field. *Chinese Journal of Rock Mechanics and Engineering,* 29(4): 778–787.

This page intentionally left blank

Progress in Mine Safety Science and Engineering II – He et al. (Eds)
© 2014 Taylor & Francis Group, London, ISBN 978-1-138-00122-0

Distribution and genesis of H_2S abnormity area in gas of Shigejie Coal Mine

Lu Lu
School of Resources and Geoscience, China University of Mining and Technology, Xuzhou, Jiangsu, China

Xue-Hai Fu
School of Resources and Geoscience, China University of Mining and Technology, Xuzhou, Jiangsu, China
College of Geology and Mining Engineering, Xinjiang University, Urumchi, Xinjiang, China

Ye He & Chun-Lin Jiao
School of Resources and Geoscience, China University of Mining and Technology, Xuzhou, Jiangsu, China

ABSTRACT: Coal seam No. 15 of Taiyuan Formation is been mined in Shigejie Coal Mine, usually accompanying large amount of H_2S, which seriously threatens the safety of miners and mine production. In order to find out the distribution and genesis of H_2S abnormity area in gas of this coal mine, this paper firstly discussed the distribution from two aspects of vertical and horizontal through underground observation and previous coal geological data analysis. And then it analysed the genesis from two aspects of internal and external causes.

1 INSTRUCTIONS

There have been lots of study on coal mine gas abnormity and H_2S abnormity in gas (FU et al. 2006, LIU et al. 2012, WU et al. 2011, CHEN et al. 2009, WANG & FU 2007). While there were few researches on distribution of H_2S abnormity in gas of coal mine. Coal seam No. 15 of Taiyuan Formation in Lu'an Mining Area is been mined in Shigejie Coal Mine, with the emission of highly toxic H_2S gas, whose concentration heavily exceeded the national standard of *Coal Mine Safety Regulation,* 6.6 ppm. This paper discussed the distribution and genesis of H_2S abnormity area in gas of this coal mine through underground observation and previous coal geological data analysis, to provide useful information for the prevention and management of H_2S in coal mine gas.

2 DISTRIBUTION OF H_2S ABNORMITY AREA IN GAS

This paper discussed the distribution of H_2S abnormity area in gas of Shigejie Coal Mine from two aspects of vertical and horizontal.

2.1 *Vertical distribution*

Coal seam No. 15 of Taiyuan Formation includes such three coal delamination as No. 15–1, No. 15–2 (not the research emphasis of this paper) and No. 15–3. Each of them exists H_2S abnormity (Table 1).

There locally exist two thin nodule layers of pyrite at roadway No. 15302 of coal delamination No. 15–3. The thickness of the upper part is about 2 cm, lower is about 4 to 5 cm (Fig. 1). If the coal located on upper nodule layers of pyrite is knocked, a rotten egg smell would be smelled.

2.2 *Horizontal distribution*

East and west of Central Roadway (that is, 725 horizontal central roadway, east of it is uphill and west downhill. The strike of the coal-bearing strata is nearly north south, dip 2°.) exist different distribution of H_2S in gas: east of Central Roadway is H_2S normal area in gas and west abnormity area. H_2S abnormity in gas was tested in west of Central Roadway at roadway No. 15302, 15102, 15106, 15108, 15110 and 15112. The highest concentration of H_2S could come to 100 ppm (In Fig. 2, only roadway No. 15302 belongs to coal delamination No. 15–3, the others belong to coal delamination No. 15–1). On the contrary, H_2S abnormity in gas was not tested in east of Central Roadway at roadway No. 15101, 15103, 15105 and 15107.

3 GENESIS OF H_2S ABNORMITY IN GAS

BSR (Bacterial Sulfate Reduction), TSR (Thermochemical Sulfate Reduction) and magmatism are the main causes of H_2S gas formation in coal mine gas (Liu et al. 2011). H_2S is the intermediate

Table 1. Characteristics of each coal delamination of coal seam No. 15.

Coal seam	No. 15–1	No. 15–2	No. 15–3
The average thickness of coal seam (m)	1.12	0.43	1.82
The average percentage content of sulfur/ St, d (%)	2.76	/	1.43
Existing H_2S abnormity or not	Yes	/	Yes

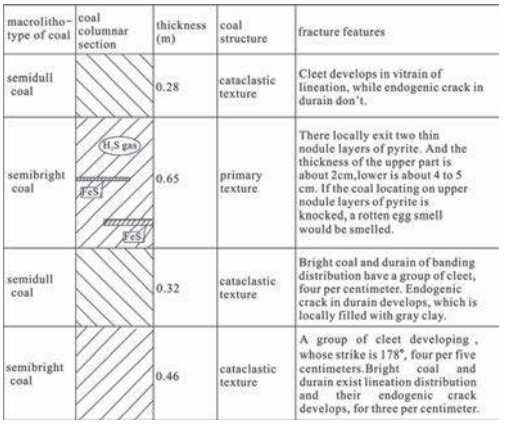


Figure 1. Columnar section of coal structure, coal lithotype and fracture characteristics of coal seam No. 15–3.

of pyrite formation in coal and part of organic sulfur formation. The direct evidence is high content of organic sulfur and pyrite in coal. Pyrite is widespread in Carboniferous-Permian Taiyuan and Shanxi Formation coal of North China (LIU et al. 2011, CHAMBERS & TRUDINGER 1979, BERNER 1984). The following analyses distribution of H_2S abnormity area from such aspects as pyrite, sulfur content and geological processes.

3.1 *Internal factor*

H_2S gas in coal gas is the intermediates of organic sulfur and inorganic sulfur in coal seam. It turns into organic sulfur and metal sulfides mainly consisting of pyrite through a series of complex thermochemical process during TSR (Fu et al. 2006, LIU et al. 2011, ZHOU et al. 2000). During the formation process of coal seam No. 15 in this coal mine, there were large amounts of H_2S gas generating by the redox between organic carbon and sulfate in coal at high temperature (above 120°C, leading to TSR) after the metamorphic grade of coal reached the coking coal stage. Finally pyrite was formed by a series of complex reactions of H_2S gas and available iron in coal (may be iron oxides, such as goethite). The equations can be described as the following:

$$2C + SO_4^{2-}(\text{sulfate}) + 2H_2O \rightarrow H_2S + 2HCO_3^-$$
$$\downarrow$$
$$3H_2S + 2FeO \cdot OH(\text{goethite}) \rightarrow 2FeS(\text{tetragonal pyrite}) + S^0 + H_2O$$
$$\downarrow$$
$$3\,FeS(\text{tetragonal pyrite}) + S^0 \rightarrow Fe_3S_4(\text{melnikovite})$$
$$\downarrow$$
$$Fe_3S_4(\text{melnikovite}) + 2S^0(\text{elemental sulfur}) \rightarrow 3Fe_3S_4(\text{pyrite})$$

There should be a positive correlation relationship between H_2S and total sulfur content as well as H_2S concentration and total sulfur content. That is, the higher total sulfur content, the higher H_2S content and concentration (LIU et al. 2011). Pyrite content generally tended to be high when total sulfur content become high, and pyrite was transformed by H_2S (above equations), leading to more production of H_2S gas in geological evolution stage. There is high sulfur content in both coal seam No. 15–1 and No. 15–3. Coal seam No. 15–1 mainly consists of high sulfur coal and coal seam No. 15–3 mainly consists of middle-high sulfur coal (Table 1). The pyrite nodules were found in the roof and floor layers of each delamination of coal seam No. 15 from the coal geological data of Shegejie Coal Mine. The appearance of nodular pyrite indicates that pyrite formed in the diagenetic stage (TANG & REN 1996, LIU et al. 1999), proving that each layers of coal seam No. 15 formed large amounts of H_2S gas in this stage.

3.2 EXTERNAL FACTORS

3.2.1 *Characteristics of coal structure*

The coal lithotype of coal layer No. 15–1 and No. 15–3 are both semibright and semidull coal (Table 2), and coal structures of each delamination of coal seam No. 15 are all from types of primary texture to cataclastic texture, which are advantageous to preservation of H_2S generated from the buried and evolution stage of coal seam No. 15 and provide prerequisite for H_2S abnormity in certain areas of coal seam No. 15.

3.2.2 *Characteristics of hydrological geology*

In the Shigejie mine field, the aquifer group of Taiyuan formation in Upper Carboniferous (C_{2t}^2) has hydraulic connection with coal seam No. 15. Among this group, the limestone karst fractured aquifer K_2 is widely distributed and has an average separation of 4.33 m away from the roof of coal

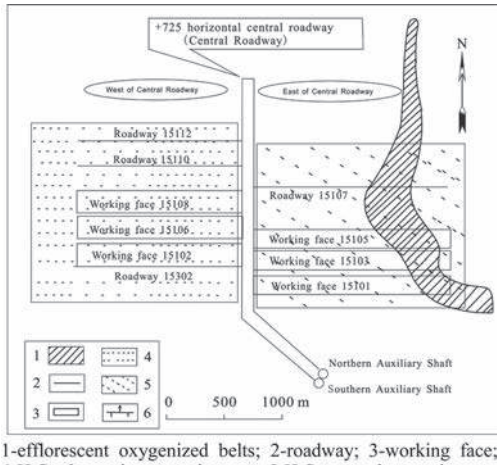
Table 2. Macroscopic characteristics of coal seam No. 15.

Coal seam	Macroscopic component of coal	Texture and structure	Macrolitho-type of coal
No. 15–1	Mainly consisting of bright coal and dull coal, with little vitrain of banding distribution.	Banding distribution on texture; Layered structure; Mainly consisting of primary texture coal and cataclastic texture coal.	semibright and semidull coal
No. 15–3	The same as above	The same as above	The same as above

seam No. 15–1 and 10.28 m away from the roof of coal seam No. 15–3. The limestone aquifer K_2 has 2.20–17.95 m thick with an average thick of 7.80 m. In the aquifer K_2, vertical fractures develop, part of them is full of calcite and dissolved pore can be seen partly. Water inflow at early time generally is about 1300 m^3/d at working place. Some shallow area in the east of Central Roadway can get in touch with atmospheric precipitation, bedrock weathering aquifer and the Quaternary aquifer, where most of H_2S gas in coal seam No. 15 escaped, that is, H_2S abnormity is not obvious.

3.2.3 *The roof and floor of the coal seam and efflorescent oxygenized belts*

The lithology of roof and floor of each delamination of coal seam No. 15 in this coal mine are all mudstone. Mudstone is a kind of dense rock, with low permeability and low porosity, which is disadvantageous to the diffusion of H_2S gas in coal seam No. 15 to surrounding rock. However, there is efflorescent oxygenized belts in east of Central Roadway, which influencing the stability of the roof of each delamination of coal seam No. 15, increasing the difficulty of mine support. Survey in the pit showed that the type of mine support has ranged from active support in west of Central Roadway to passive support in east of Central Roadway. The mudstone roofs of roadway No. 15101, 15103, 15105 and 15107 located in east of Central Roadway become mostly loose and flabby, H_2S gas of each delamination of coal seam No. 15 in east of Central Roadway escaped constantly from these loose and flabby roofs during the long geological history. And these loose and flabby roofs can get in touch with the limestone karst fractured aquifer K_2, making roofs of this place increasingly loose. At the same time, limestone water of K_2 coming from this place absorbed a great quantity



1-efflorescent oxygenized belts; 2-roadway; 3-working face; 4-H_2S abnormity area in gas; 5-H_2S normal area in gas; 6-reversed fault F151-1.

Figure 2. Schematic diagram of distribution of H_2S abnormity area in gas of Shigejie Coal Mine.

of H_2S gas which can quite easily dissolve into water. Water inflow in east of Central Roadway at local area is above 1300 m^3/d according to survey in the pit. Legend 1 in Fig. 2 represents efflorescent oxygenized belts. Legend 5 in Fig. 2 represents influenced area of efflorescent oxygenized belts, where H_2S abnormity in coal seam No. 15 was not tested, that is, concentration of H_2S gas was below 6.6 ppm or not being detected, belonging to H_2S normal area.

3.2.4 *Reversed fault F151–1*

Along the Central Roadway, there existed a reversed fault F151–1 (Legend 6 in Fig. 2), extending nearly for 900 m in the mine, whose strike is nearly north south in accord with Central Roadway. Actually, reversed fault F151–1 prevent H_2S gas of each delamination of coal seam No. 15 in west of Central Roadway from migration and dissipation to east, which are advantageous to preservation of H_2S gas of coal seam No. 15 in west of Central Roadway.

4 CONCLUSIONS

On vertical aspect, each delamination of coal seam No. 15 appeared H_2S gas. On horizontal aspect, the concentration of H_2S gas of each delamination of coal seam No. 15 in west of Central Roadway was more than 6.6 ppm, the highest concentration of which could come to 100 ppm. H_2S abnormity in gas was not tested in east of Central Roadway, that is, concentration of H_2S gas was below 6.6 ppm or

not being detected. In conclusion, west of Central Roadway is H_2S abnormity area in gas, while east is not.

The causes of distribution of H_2S abnormity area in gas have two aspects: Internal factors are prerequisite. The direct evidence of H_2S formation is high content of organic sulfur and pyrite in coal. Each layers of coal seam No. 15 contained large amounts of H_2S gas during the diagenetic stage. On external factors, coal structures of each delamination of coal seam No. 15 are advantageous to preservation of H_2S generated from the buried and evolution stage. However, some shallow area in the east of Central Roadway can get in touch with atmospheric precipitation, bedrock weathering aquifer and the Quaternary aquifer. At the same time, there exist efflorescent oxygenized belts in the east of Central Roadway, both of which almost leading to the dissipation of H_2S in gas fully. Besides, reversed fault F151–1 is advantageous to preservation of H_2S in gas of coal seam No. 15 in west of Central Roadway. In a word, all factors above caused H_2S abnormity in west of Central Roadway, while not in east.

ACKNOWLEDGEMENTS

This work was supported by the National Natural Science Foundation of China (41272177).

REFERENCES

Berner, R.A. 1984. Sedimentary pyrite formation: an update. *Geochimica et Cosmochimica Acta* 48: 605–615.

Chambers, L.A. & Trudinger, P.A. 1979. Microbiological fractionation of stable sulphur isotopes: areview and critique. *Geomicrobiology* 1(3): 249–293.

Chen, K.Y., Zhang, Z.G. and Lin B.Q. et al. 2009. Characteristics of Gas Emission and Distribution of Fully Mechanized Top-Coal Caving Face Under Gas Drainage Conditions. *Journal of Mining & Safety Engineering* 26(4): 418–422.

Fu, X.H., Wang, W.F. and Yue J.H. et al. 2006. Genesis analyses of H_2S gas abnormity in gas of Bayi coalmine in Zaozhuang. *Journal of China Coal Society* 31(2): 206–210.

Liu, D.M., Yang, Q. and Zhou C.G. et al. 1999. Occurrence and geological genesis of pyrites in Late Paleozoic coals in North China. *Geochimica* 28(4): 340–349.

Liu, M.J., Li, G.Q. and Hani M. et al. 2011. Genesis modes discussion of H_2S gas in coal mines. *Journal of China Coal Society* 36(6): 978–983.

Liu, X.F., Fang, Q.C. and Hang Y.Y. et al. 2012. Study on Gas Distribution Law of Driving Process in Blind Seam Gateway. *Coal Science and Technology* 40(3): 62–64, 69.

Tang, Y G., Ren, D.Y. 1996. The Genesis of Pyrite in Coal. *Geological Review* 42(1): 64–70.

Wang, K.X., Fu, X.H. 2007. Analysis on controlmethod of H_2S anomaly in mine gas. *Coal Science and Technology* 35(1): 94–96.

Wu, Y.G., Wu, J.M. and Wang J.F. et al. 2011. The law of gas distribution in goaf of fully mechanized top-coal caving working face with "double-U" ventilation system. *Journal of China Coal Society* 36(10): 1704–1708.

Zhou, C.G., Yang, Q. and Kang X.D. et al. 2000. Sulfur-Isotope Evidence of Pyrite Generation in Coal of Late Palaeozoic in Northern China. *Coal Geology of China* 12(1): 19–22.

Progress in Mine Safety Science and Engineering II – He et al. (Eds)
© 2014 Taylor & Francis Group, London, ISBN 978-1-138-00122-0

Rock slope surface monitoring technologies with focus on ground-based synthetic aperture radar

Hani Mitri & Isaac Vennes
McGill University, Department of Mining and Materials Engineering, Quebec, Canada

ABSTRACT: The stability of rock slopes in open pit mines is crucial to the safe and efficient operation of a surface mine. When not planned for, rock slope failures can cause injuries, equipment damage or loss, delayed production schedule, and even loss of economic ore. Slope monitoring has emerged as a viable engineering tool to help mine operators better understand rock slope behaviour and response to mining activities and environmental conditions during the life of the mine. This paper presents a state-of-the-art review of slope monitoring technologies with focus on the most recent development of Ground-Based interferometric Synthetic Aperture Radar (GB-SAR). Discrete slope surface monitoring systems such as laser prism surveys and surface extensometers provide very accurate and precise point measurements. The data obtained from strategically placed discrete monitoring systems is generally sufficient to accurately describe simple, local failures. For large scale, complex failures however, monitoring systems that produce full-face scans such as radar are necessary. For the purpose of providing near real-time slope displacement data, the most suitable method is ground-based radar interferometry. High resolution, combined with large area coverage, thanks to the possibility of installing the radar at long distances from the slope, and short scan time, make GB-SAR one of the most effective slope monitoring technologies available today. In this paper, it is shown that the GB-SAR systemis able to timely detect and provide alarms on large scale slope movements for both gentle and steep slopes, as well as local scale movements at bench-scale which is equally important to the safety of mine operators at the work face.

Keywords: slope stability radar, Slope surface monitoring

1 INTRODUCTION

The extraction of large scale, low-grade near surface ore deposits in recent decades has been made possible thanks to the development of powerful and more efficient loading and haulage equipment. With high production rates of more than 50,000 tons per day, this trend has resulted in the creation of large and deep open pit mines that are prone to pit wall instability. Thus, interest in rock slope stability has grown substantially over the last decade, particularly that in large scale pits of low-grade deposits, an increase of one degree in the overall pit wall angle could result in significant economic savings. Rock slope stability studies are briefly reviewed in this paper. One of the challenges faced by the mine planner is that often enough, the pit slopes are determined at the planning stage of the project when little geotechnical data is available about the host rock. Information such as rock mass structure and strength and geological features such as shear zones and faults are often not well characterized at an early stage of the project. Therefore, it is important to deploy additional tools to monitor the movement of pit walls during the life of the mine, and to be able to interpret the data obtained from such tools so a decision is made with regard to ensure the safety of the operation. This paper presents a review of the most modern technologies used for rock slope monitoring with focus on Ground-Based Synthetic Aperture Radar (GB-SAR). In this paper, it is shown that the GB-SAR system is able to detect and provide alarms on large scale slope movements as demonstrated by the recent Bingham Canyon failure in Utah, USA where two GB-SAR units tracked the movement of the landslide and provided early warning alarms to support the mine operators in the decision making process. It is also shown that GB-SAR systems are capable of detecting local scale movements at bench-scale which is equally important to the safety of mine operators at the work face.

Nomenclature

ΔR	Range resolution
ΔCR	Cross-range resolution
θ	Radar beam width
D	Radar aperture

λ Radar wavelength
B Radar bandwidth
τ Pulse length
μ Linear frequency modulation coefficient
ϕ Phase shift

1.1 *Rock slope stability methods*

Many empirical slope classifications adapted to assess the stability of slopes are available in the literature. These include for example the Slope Mass Rating (SMR) (Romana, 1985), the Slope Rock Mass Rating (SRMR) (Robertson, 1988), and the Chinese Slope Mass Rating (CSMR) (Chen, 1995). The methods rely on initial characterization of the rock mass based on Bienawski's RMR, with factoring for slope structure, blasting, and weathering. The output is a qualitative rating with which one can assess stability; a low rating indicating complete instability and a high rating indicating complete stability.

To quantitatively assess the stability of a slope, either numerical or analytical methods can be used depending on the complexity of the slope. For small scale, simple failures, controlled by bedding planes and joints, such as planar, wedge, or toppling failure modes, limit equilibrium analysis can be used (Wyllie and Mah, 2004). The output is a factor of safety, which is the ratio between resisting force and driving force. For larger slopes, with no well-defined structural pattern, rock mass failure will occur along a form of circular slide surface. Many analytical methods exist to determine the factor of safety of a slope susceptible to circular failure, ranging from non-rigorous methods such as the Fellenius method of slices to the more rigorous Bishop and Morganstern-Price methods (McCarthy, 2007).

More complicated slope geometries and geology, such as rock masses with major geological features, require numerical analysis as limit equilibrium methods can over-simplify the problem. Contrary to analytical methods, the factor of safety obtained with numerical modelling (Shear Strength Reduction analysis) is often defined as the actual shear strength over the minimum shear strength required to prevent failure. Numerical modelling can also be used to simulate the failure mechanism stages of high walls (Sjöberg, 2000), or, for a slope failure that has already occurred, conduct a back analysis to better understand the failure modes and mechanisms, such as for the slope failure at Jeffrey Mine at J.M Asbestos Inc (Tsomondo and Mitri, 1993).

However, these methods of analysis are primarily used in the planning stage to determine the critical slope angle, and cannot reliably predict the occurrence and time of slope failure, highlighting the importance of slope monitoring. By interpreting slope monitoring data, using for example Fukuzono's inverse velocity method (Fukuzono, 1985), or by determining site-specific threshold movement rates, one can predict the time of failure (Farina et al., 2012, Little, 2005, Harries, 2006). Well established slope surface monitoring techniques exist, such as crack width monitoring, prism surveys, laser imaging, GPS, tiltmeters, airborne radar and finally ground-based radar (Wyllie and Mah, 2004). For the purpose of providing near real time slope displacement data, ground-based radar interferometry is the most suitable monitoring technique available today.

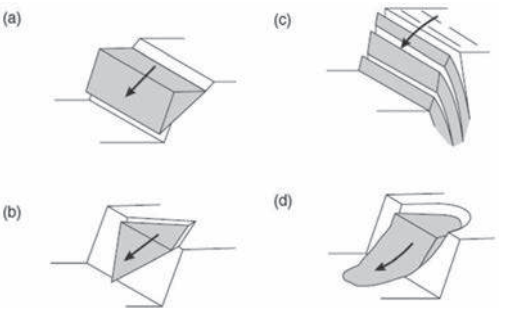


Figure 1. Failure modes for limit equilibrium analysis: a) planar b) wedge c) toppling d) circular (Wyllie and Mah, 2004).

2 RADAR

Radar is an electromagnetic system for the detection and location of reflecting objects (Richards, 2005). It operates by radiating energy into space and detecting the echo signal reflected from the object. The reflected energy indicates presence of the object, and the comparison between the emitted signal and the returning signal can also give other target related information. Conventional radars generally operate in the microwave region. Frequencies range from 100 MHz to 36 GHz (Richards, 2005).

Interferometric radar is currently used in the mining industry to detect slope displacements. Since radar systems are coherent, the phase shift of the echo signal between two pulses can be compared to determine displacement with a precision up to 1/10 mm for the most recent devices. Continuous scanning of the slope coupled with high precision allows the monitoring of slope displacement in "real time".

Two different interferometric radar slope monitoring systems are available. These are Synthetic Aperture Radar (GB-SAR) and Real Aperture Radar (RAR). To be useful, a radar map must have adequate resolution for its intended. A radar system that obtains a low resolution image will not adequately capture displacements leading up

to small failures, as the displacement measured for a resolution cell is an average of all displacements within the cell. Therefore, high resolution translates to high sensitivity. The focus of the last section of the paper is to determine and compare the resolution obtained with RAR or GB-SAR in the mining environment.

2.1 *Radar range determination and range resolution*

Radar uses time of flight to determine the range of a target. The resolution of the range measurement is a function of the emitted signal properties. For a constant frequency pulse train of duration τ and period T, if the pulse is transmitted at $t = 0$ the radar receives at T0 the echo of the leading edge of the pulse from scatterers at range of cT0/2. In the same way at T0 the radar also receives the trailing edge of the echo of the pulse from scatterers at range c(T0 – τ)/2. Therefore, targets over c τ/2 in space will contribute simultaneously to the received signal. This length along the range of the radar is called the range resolution, which expresses the ability of a radar system to distinguish between two or more scatterers at different ranges. The equation indicates that to improve (reduce) the range resolution of a constant frequency pulse train, one must compress the pulse (decrease τ).

$$\Delta R = c\tau/2 \tag{1}$$

The range resolution reduction can also be achievied with alternate techniques such as frequency modulated continuous wave.

The most common frequency modulated continuous wave-form employs a linear frequency pattern (Richards, 2005), where B is the swept bandwidth, f_o is the starting frequency, T is the sweep duration and μ the linear frequency modulation coefficient.

$$s(t) = \cos(2\pi(\text{f_o} \cdot t + 1/2\ \mu[\![\cdot t]\!]^2)) = \cos(2\pi f(t))\ 0 \le t \le T \tag{2}$$

$$\mu = B/T \tag{3}$$

In Figure 2 the linear frequency continuous waveform and frequency evolution in time are shown.

The range resolution with the IBIS radar series is obtained with the Frequency Modulated Continuous Wave technique. In this case, the range resolution is related to the total swept bandwidth B as follows (Taylor, 2000):

$$\Delta R = c/2\text{B} \tag{4}$$

where ΔR is the range resolution (Figure 3) and c is the speed of light. Compared to equation (1), the linear frequency modulation waveform obtains the performance of a synthetic pulse with a duration $\tau = 1/\text{B}$ (IDS, 2011). The total bandwidth of a linear frequency modulated continuous waveform is therefore determined by the desired range resolution. This can be realized by changing the sweep duration as well the modulation coefficient. For example, the IBIS-FS, with the maximum possible bandwidth of 300 MHz, reaches a range resolution of 0.5 m (Rodelsperger et al., 2010).

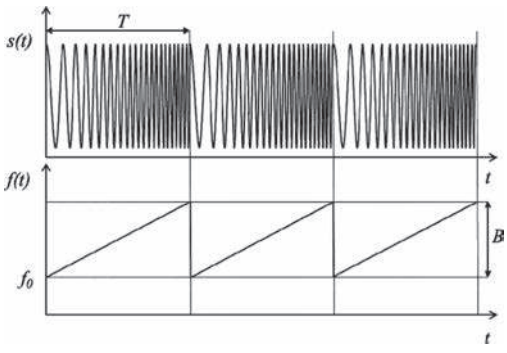


Figure 2. Linear frequency modulated continuous waveform.

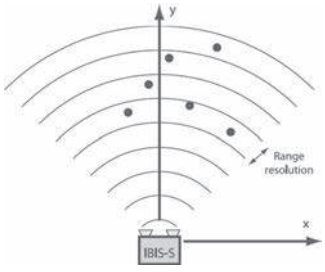


Figure 3. Range resolution of IBIS-FS (Rodelsperger et al., 2010).

2.2 *Radar beamwidth and cross-range resolution*

The azimuthal radiation pattern half power beamwidth of a reflector antenna is described as:

$$\theta\, az = k\ \lambda/\text{D_az (rad)} \tag{5}$$

where Daz is the width of the antenna in the azimuth direction and λ is the emission wavelength. The beamwidth factor k depends on the antenna design, and ranges from 0.89 for an ideal aperture antenna to 1.22 for practical antenna designs (Richards, 2005). For a parabolic antenna the azimuth Daz and elevation dimension Del are the same, as well as the azimuthal θ_az and elevation

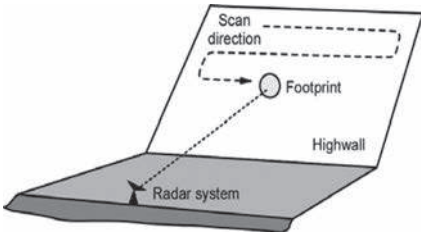


Figure 4. Two dimensional scanning configuration (McHugh et al., 2006). Footprint size is determined by vertical and horizontal antenna beam width.

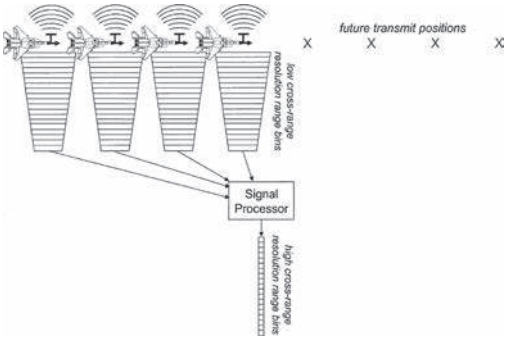


Figure 5. Concept of SAR (Richards, 2005).

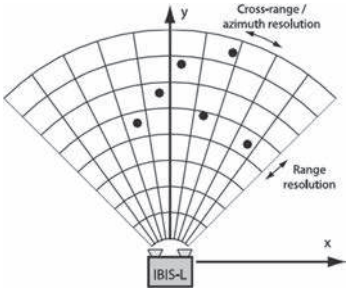


Figure 6. IBIS-FL and IBIS-FM resolution cells (Rodelsperger et al., 2010). By moving along the x-axis, the IBIS-FL is able to distinguish targets at the same range but different azimuths, as opposed to the IBIS-FS.

θ_elradiation pattern beamwidth. Assuming a beamwidth factor of 1, the azimuth resolution also said cross range resolution of real beam radar is given as:

$$\Delta[\![\mathrm{CR}]\!]_(\text{real beam}) = \theta_\mathrm{az} = \lambda/\mathrm{D_az} \quad (6)$$

Equation (6) highlights 2 different methods to obtain better resolution: increase the antenna size or decrease the wavelength of the emitted signal. Alternatively, one can resort to synthetic aperture radar.

2.3 *Synthetic aperture radar*

Synthetic Aperture Radar (SAR) is a technique used for high resolution radar imaging. This technique was developed to overcome resolution restriction of radar images from satellites, and consists of using the forward motion of the satellite (or airplane) to synthesize a larger antenna. Ground based SAR is based on the same principal as airborne SAR, with the antenna moving on a rail. The cross range resolution of GB-SAR is expressed as:

$$\Delta\mathrm{CR} = \theta_\mathrm{SAR} = \lambda/(2\mathrm{D_SAR}) \quad (7)$$

where DSAR is the travel distance of the antenna and λ is the emission wavelength.

2.4 *Interferometry*

Radar systems used for slope displacement monitoring use the phase data the echo signal to detect displacement rather than time of flight calculations as exemplified by laser scanners. The phase shift between the signal and the echo signal at t1 is compared to the phase shift between the signal and echo signal at t2. The difference in phase shifts between the two measurements at different times is a sum of all the following components:

$$\phi = \phi_\mathrm{disp} + \phi_\mathrm{atm} + \phi_\mathrm{diel} + \phi_\mathrm{noise} - 2\pi \cdot n \quad (8)$$

ϕ_disp: Phase difference of the returning wave due to a displacement of the reflecting surface along the line of sight of the radar;

ϕ_atm: Phase difference due to change in atmospheric properties (especially humidity) over space and time;

ϕ_diel: Phase difference to the dielectric properties of the reflecting surface;

ϕ_noise: Measurement noise;

n: integer number of full phase cycles.

The parameter of interest is ϕ_disp, and the remaining effects have to be corrected for. The most predominant phase shift to be corrected is due to changes in humidity over space and time. These atmospheric artifacts are corrected for by determining a stable point, either manually for older radars, or automatically for newer models (IDS, 2011). Once the phase difference due to displacement is found, the displacement along the line of sight is calculated as follows (Rodelsperger et al., 2010):

$$\phi_\mathrm{disp} = \lambda/4\pi \cdot d \quad (9)$$

2.5 *Radar in mining industry*

The advantages of slope monitoring interferometric radar, as opposed to other techniques such as tachymeters, tiltmeters and extensometers are:

- No requirement for survey reflector installation
- No requirement for instrumentation in failure area
- High accuracy and spatial resolution
- Independence of daylight and weather. Can perform its function under conditions impervious to optical and infrared sensors, such as in haze, for, rain or snow (Skolnik, 2001).
- Continuous scanning of the slope, which provides "real time" data.

GB-SAR and RAR radar also share these challenges:

- Necessity to filter the atmospheric component from the phase signal
- Detects displacements in line of sight only

The main limitation of the radar map is that it only measures line of sight movements. However, the radar map obtained with RAR and GB-SAR can be integrated with other slope monitoring equipment like total stations, providing point wise information on the 3D displacement vector for the moving area identified and monitored in its entire extension by the radar. Alternatively pseudo-3d displacement can be measured by combining data from multiple radars (Severin et al., 2011). Also, both RAR and GB-SAR can provide 3D maps. However, the feature is not exploited in favour of more accurate 3D digital models obtained with laser photogrammetry, where the radar map is overlaid on a DTM provided by a laser scanner (Mazzanti and Brunetti, 2010).

3 COMPARISON OF RAR AND GB-SAR SPATIAL RESOLUTION IN MINING ENVIRONMENT

3.1 *Resolution cell area*

GB-SAR produces an image based on range resolution and horizontal cross range resolution. The height of the resolution cell projected on the slope ΔVs is a function of the radar range resolution ΔR and the grazing angle $\gamma - \alpha$ (see figure 7):

$$\Delta V_s = -R\cos(\gamma-\alpha) + \sqrt{R^2\cos(\gamma-\alpha)^2 + \Delta R^2} \tag{10}$$

where γ is the slope incline with respect to the horizontal, and α is the elevation angle of the radar. Note that since resolution cell height is resolved with range, and assuming the berm width is larger than the range resolution, there will always be a new resolution cell at each berm. The maximum resolution cell height is therefore the height between berms.

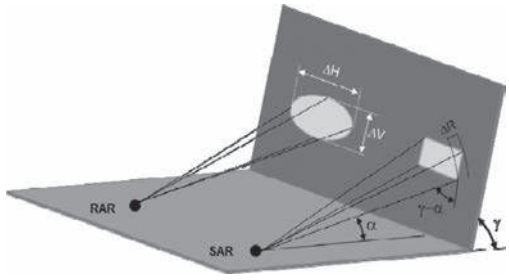


Figure 7. Ground resolution cell. Grazing angle is defined as $\gamma - \alpha$.

The width of the resolution cell projected on the slope wall ΔHs is equal to the cross range resolution at range R:

$$\Delta H_s = \frac{\lambda R}{2D_{SAR}} \tag{11}$$

The resolution cell area is therefore:

$$A_{SAR} = \frac{\lambda R}{2D_{SAR}} \times \left[\sqrt{R^2\cos(\gamma-\alpha)^2 + \Delta R^2 + 2R\Delta R} - R\cos(\gamma-\alpha)\right] \tag{12}$$

On the other hand, the resolution cell area of RAR projected on the slope surface is a function of the azimuthal cross range resolution in the horizontal and vertical directions. The height of the resolution cell projected on the slope is equal to:

$$\Delta V_s = \frac{R\lambda}{D_{el}\sin(\gamma-\alpha)} \tag{13}$$

Similarly, the width of the resolution cell is equal to:

$$\Delta H_s = \frac{R\lambda}{D_{az}} \tag{14}$$

yielding a cell area of:

$$A_{RAR} = \frac{(R\lambda)^2}{D_{az}D_{el}\sin(\gamma-\alpha)} \tag{15}$$

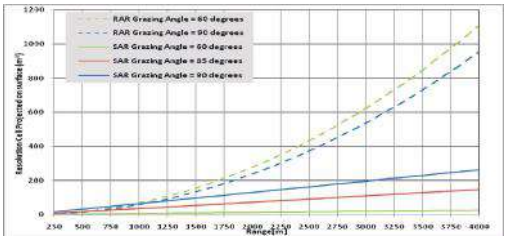


Figure 8. Radar resolution cell area vs. target range.

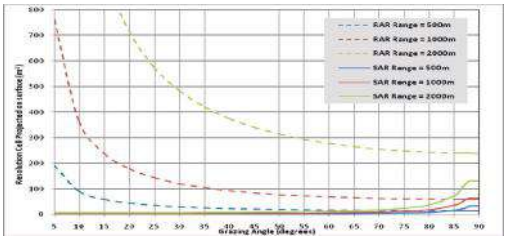


Figure 9. Radar resolution cell area vs. grazing angle.

3.2 *Case study*

RAR curves were plotted using equation (16), assuming a 17.2 GHz emission frequency, a 1.8 meter wide antenna (Ground Probe, 2011), and a beam width factor of 0.89 (ideal reflector antenna), leading to an azimuthal and elevation beam width of 8.72 mrad.

For the purpose of comparison, GB-SAR data was plotted using equation 13 and assuming the performance of IBIS-FL model by IDS, thus 17.2 GHz emission frequency, a synthetic aperture of 2.0 meter and a range resolution of 0.75 meters.

Resolution cell area for RAR and GB-SAR are plot for target ranges between 0 and 4000 m and grazing angles ranging between 60 and 90 degrees. GB-SAR is less sensitive to range than RAR, but more sensitive at high grazing angles. However, given the geometry of an open pit wall, GB-SAR will always have at least 1 resolution cell per bench, meaning it is guaranteed to detect inter-bench failures no matter the range or grazing angle. On the other hand, RAR obtains better resolution at very short ranges (lower than 500 m) with steep grazing angles (greater than 88°).

4 CONCLUSIONS

While both radar systems provide unmatched slope coverage, precision, and range, radar by no means entirely replaces other slope monitoring systems. Both RAR and GB-SAR complete mine wide slope monitoring systems, as seen at Pprust (Little, 2005) where slope monitoring radars are placed close to critical faces, or Bingham Canyon, where 2 real aperture radars and 3 synthetic aperture radar provided real time data to the mine operators, allowing them to anticipate the April 10, 2013 slide (Walker, 2013). Simple equations were presented to estimate to resolution of a radar system based on the radar scanning technique (RAR or GB-SAR), the target range, and the beam grazing angle.

REFERENCES

Chen, Z. Recent developments in slope stability analysis. ISRM 8th Int. Cong. Rock Mech., 1995 Tokyo.

Farina, P., Leoni, L., Coppi, F., Babboni, F., Mayer, L. & Coli, N. 2012. Monitoring open pit slopes through Slope Monitoring Radar based on synthetic Aperture Radar.

Fukuzono, T. 1985. A New Method for Predicting the Failure Time of a Slope. *IVth International Conference and Field Workshop on Landslides.* Tokyo.

Groundprobe. 2011. *SSR-XT* [Online]. GroundProbe. Available: http://www.groundprobe.com/docs/ssr/SSR-XT%20brochure%202011.pdf [Accessed August 24 2012].

Harries, N. 2006. Case studies of slope stability radar used in open cut mines. *The South African Institute of Mining and Metallurgy International Symposium on Stability of Rock Slopes.*

Ids. 2011. *IBIS Image by Interferometric Survey Working Principles* [Online]. IDS. Available: http://www.associazionealig.it/alig/Eventi/PISA_NUOVE%20TECNOLOGIE%20RADAR/IBIS_Working_Principle_Coppi.pdf [Accessed June 6 2012].

Little, M. 2005. Slope Monitoring Strategy at Pprust Open Pit Operation. *The South African Institue of Mining and Metallurfy International Symposium on Stability of Rock Slopes in Open Pit Mining and Civil Engineering*.

Mazzanti, P. & Brunetti, A. Assessing rockfall susceptibility by Terrestrial SAR Interferometry. Mountain Risks International Conference, 24–26 November, 2010 2010 Firenze, Italy. 109–114.

Mccarthy, D.F. 2007. *Essentials of Soil Mechanics and Foundations—Basic Geotechnics, Pearon Prentice Hall.*

Mchugh, E.L., Long, D.G. & Sabine, C. 2006. Applications of Ground-Based Radar to Mine Slope Monitoring. *Report of Investigations 9666.* National Institute for Occupational Safety and Health.

Richards, M.A. 2005. *Fundamentals of Radar Signal Processing,* New York, McGraw-Hill.

Robertson, A.M. Estimating weak rock strength. SME Annual Meeting, 1988 Phoenix, Arizona. Society of Mining Engineers.

Rodelsperger, S., Laufer, G., Gerstenecker, C. & Becker, M. 2010. Monitoring of displacements with ground-based microwave interferometry: IBIS-S and IBIS-L. *Journal of Applied Geodesy,* 4, 41–54.

Romana, M. New adjustment ratings for application of Bieniawski classification to slopes. ISRM Int. Symp. on the Role of Rock Mech., 1985 Zacatecas. 49–53.

Severin, J., Eberhardt, E., Leoni, L. & Fortin, S. Use of ground-Based Synthetic Aperture Radar to Investigate Complex 3-d Pit Slope Kinematics. International Symposium on Rock Slope Stability in Open pit Mining and Civil Engineering, 2011 Vancouver.

Sjöberg, J. 2000. Failure Mechanisms for High Slopes in Hard Rock. *In:* Hustrulid, W.A., Mccarter, M.K. & Zyl, D.J.A.V. (eds.) *Slope Stability in Surface Mining.* SME.

Skolnik, M.I. 2001. *Introduction to Radar Systems,* New York, McGraw-Hill.

Taylor, J.D. 2000. *Ultra-Wideband Radar Technology*, CRC Press.

Tsomondo, C.M. & Mitri, H.S. 1993. Interpretation of non-structural slope failure in open-pit mining - a numerical modelling approach. *In:* MITRI, H.S. (ed.) *First Canadian Symposium on Numerical Modelling Application in Mining and Geomechanics.* Montreal: McGill university.

Walker, S. 2013. Careful Monitoring: The Key to Pit-wall Safety. *Engineering and Mining Journal.* Englewood, Colorado: Mining Media.

Wyllie, D.C. & Mah, C.W. 2004. *Rock Slope Engineering: Civil and Mining*, Taylor & Francis Group.

This page intentionally left blank

Progress in Mine Safety Science and Engineering II – He et al. (Eds)
© 2014 Taylor & Francis Group, London, ISBN 978-1-138-00122-0

Stability analysis on pillar for point-pillar mining of karst water mine

Shi-Gen Fu
Northeastern University, Shenyang, Liaoning, China
China Academy of Safety Science and Technology, Beijing, China

Kai-Li Xu
Northeastern University, Shenyang, Liaoning, China

ABSTRACT: Gujiatai Iron Mine is karst water mine and upward horizontal slicing stoping filling method with points and pillar shall be used to mine when ore body roof curtain grouting is used for waterproof. Aiming at stability of pillar, stress, displacement and distribution of plastic zone between stope point pillar and barrier pillar shall be quantificationally calculated and analyzed with method of FLAC3D finite difference numerical simulation under different mining steps after stope filling during mining of ore body so as to simulate their dynamic change process as mining stress and strain change on each step. The simulation shows that barrier pillar is obviously better than point pillar at supporting upper ore body so that it is suggested that barrier pillar shall be kept between each chamber of the mine under consideration on the basis of comprehensive evaluation of economic benefit in order to fulfill safe and high-efficient mining of mine.

1 INSTRUCTIONS

Arrangement of pillars is very important for mining of chamber, pillars can not only maintain chamber stable but also keep maximum ore recovery ratio, and therefore pillar stability study has always been one of core subjects for mining engineers and rock mass mechanics researchers over the years. Due to pivotal role of pillar, its failure mode, failure mechanism and its stability and reliability are the core contents to be study with various methods. Point safety factor and reliability index of pillar are respectively calculated by Liu Muyu, Liu xuezenget al (Liu & Xu 2000, Liu & Zhai 2000). by application of point safety method and analytical method of reliability; engineering geological survey, on-site stress change detection, acoustic wave test and combination of numerical analytical method three-dimensional finite element are adopted by Zhao Kui (Zhao & Cai 2003), formula for calculating maximum allowable span of roof is derived by Li Junping, et al (Li et al. 2002)by application of theory of mechanics of materials in accordance with rock beam hypothesis to determine pillar space accordingly; and numerical simulation method is adopted by Zhao Xingdong, et al (Zhao et al 2012) to analyze and simulate stope pillar failure process. Based on the catastrophe theory, a cusp catastrophic model of the destabilization of mine pillar was proposed and used in the destabilization mechanism analysis of mine pillar by Wang lianguo, et al (Guo & Dou 2008). Those researches made good progress and provided theoretical guidance and practical reference value for designing stope.

In order to analyze stability of stope pillar of Gujiatai karst water mine, stress, displacement and distribution of plastic zone between stope point pillar and barrier pillar are quantificationally calculated and analyzed with method of FLAC3D finite difference numerical simulation (Wang & Miao 2006, Wang & Sui 2013, Fu et al 2010) under different mining steps after stope filling during mining of ore body so as to simulate their dynamic change process as mining stress and strain changes for each steps and to provide reference for designing stope pillar for mine in the research.

2 PROJECT OVERVIEW

As typical water-contained karst water mine, Gujiatai Iron Mine is characterized with complicated hydrogeological conditions, a river cuts through middle of the ore body on the earth's surface and there are mainly two aquifers, which are quaternary glutenite and Ordovician system limestone developed from karst, and tertiary aquiclude between the two aquifers. The ore body lies in contact zone of marble and diorite and presents stratoid. Direct roof of ore body is mostly marble and its footwall is skarn, sometimes skarnized diorite and alteration diorite.

In order to realize safe mining of karst water mine, first conduct curtain grouting for roof of ore

body in the expected mining area to form water-plugging barrier zone with thickness of 20 m and then adopt point pillar horizontal slicing stoping filling method.

3 MODELING

Chamber shall be arranged on the strike with length of 27.5 m, width of 20 m, stage height of 40 to 50 m and segment height of 10 m, a barrier pillar with width of 5 m shall be constructed every two chambers, and it shall stope every segment in three layers with shallow-hole blasting open-stoping method with layer height of 3 to 4 m. Regular point pillar of 5 m × 5 m shall be arranged in stope with center distance of 12 m and both barrier pillar and point pillar are permanent natural pillars.

Three-dimensional nonlinear numerical model is adopted in the research with width of computation model in X direction of 600 m, length in Y direction of 315 m and height of approximate 152 m. The three-dimensional model is totally divided into 25, 422 units and 29, 836 nodal points. General drawing and cross-section drawing are shown in Figure 1.

Minimum thickness of quaternary on the earth's surface is 12 m with minimum thickness for tertiary aquiclude of 20 m, thickness for ore body layer of 20 m, dip angle of 37° and thickness for grouting roof of 20 m and waterproof pillar of 10 m is reserved. Iron mine is reserved for height of 20 m and is excavated from the position underground –102 m with excavation height of 50 m. Computation model contains two chambers each of which contains two point pillars in each segment and between which there is one barrier pillar. For details, refer to Figure 2.

In accordance with the field sampling and rock mechanics test results, the rocks presented clear plastic deformation characteristics at different confining pressure conditions. In this paper, Mohr—Coulomb yield criterion was used to determine the

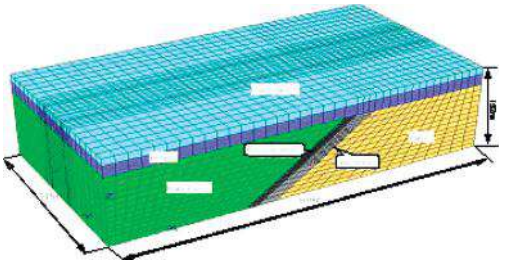


Figure 1. Lithology distribution map of computation model.

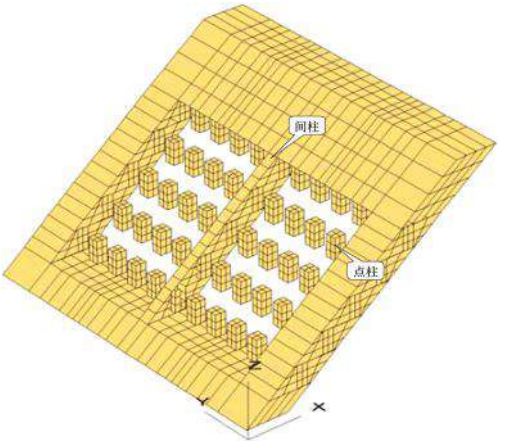


Figure 2. Iron Mine Final State Diagram.

Table 1. Physico-mechanical properties of rocks.

Name	Density (kg/m³)	Modulus Elasticity E (MPa)	Poisson Ratio υ	Cohesion c (MPa)	Internal Friction Angle φ (°)
Quaternary	2000	300	0.3	0.15	22
Tertiary	2300	3780	0.26	.025	27
Limestone	2700	10000	0.22	0.3	30
Magnetite	3700	11300	0.24	0.3	37.8
Skarn	2800	14200	0.18	1.2	25

damage of rock mass, and the computation formula was as follows:

$$f_s = \sigma_1 - \sigma_3 \frac{1+\sin\phi}{1-\sin\phi} - 2c\sqrt{\frac{1+\sin\phi}{1-\sin\phi}} \quad (1)$$

Where, σ_1 = maximum stress; σ_3 = minimum stress; c = cohesive force; φ = friction angle. When $f_s > 0$, the material will suffer shear failure. Under the normal stress conditions, the tensile strength of soil is low, and hence it is able to determine whether the rock has suffered tensile failure in accordance with the tensile strength criteria ($\sigma_3 \geq \sigma_T$). The rock mechanical parameters used in this paper were listed in Table 1.

4 STABILITY ANALYSIS OF PILLAR

The whole mining history and mining process shall be systemically simulated in order to study conditions which possibly occurred to surrounding rock of ore body due to mining. It shall be excavated step by step with one segment excavated once and mining full-seam.

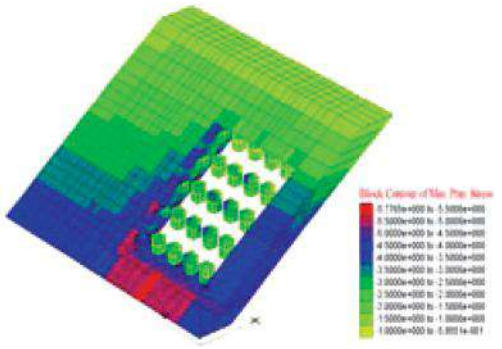


Figure 3. Maximum principal stress envelope of point pillar after mining of chamber.

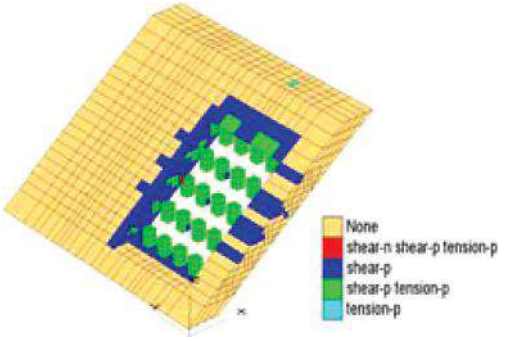


Figure 4. Failure field distribution diagram of point pillar after mining of chamber.

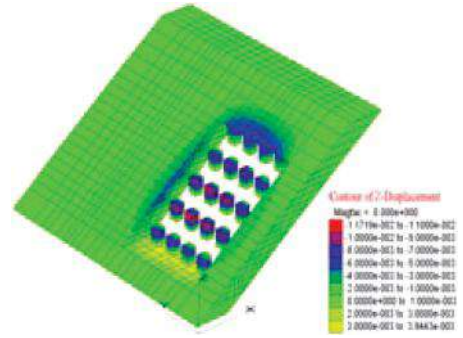


Figure 5. Vertical displacement field distribution diagram of point pillar after mining of chamber.

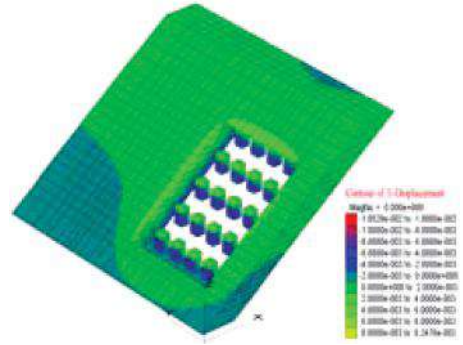


Figure 6. Horizontal displacement field distribution diagram of point pillar in x direction after mining of chamber.

4.1 *Stability analysis of point pillar*

Figure 3 is the maximum principal stress envelope of point pillar after skip-mining of first chamber and second chamber. It is observed from the figure, maximum internal stress of point pillar is 4.25 MPa, maximum stress of primary rock at point pillar is 2.9 MPa and minimum concentration factor for internal stress of point pillar is 1.47, which shows that point pillar supports upper ore body to a certain extent.

Figure 4 is the failure field distribution diagram of point pillar. It is observed from the figure, influenced by disturbance of chamber mining, all the point pillars turn into plastic state and the failure is shear combined failure along strike of ore deposit.

Maximum vertical displacement of point pillar is 1.17 cm and it occurs at upper-middle part of the point pillar (Figure 5) while maximum horizontal displacement of point pillar in X direction is 1.06 cm and it occurs at lower-middle part of the point pillar (Figure 6).

4.2 *Stability Analysis of Barrier Pillar*

Figure 7 is the maximum principal stress envelope of barrier pillar after skip-mining of first chamber and second chamber. It is observed from the figure, stress concentration occurs in lower part of the barrier pillar with maximum stress of 5.78 MPa and concentration factor of 1.99 which is larger than that for internal stress of point pillar and it shows that supporting role of barrier pillars is better than that of point pillar and they play key role to support upper ore body and maintain chamber stable.

Figure 8 is the failure field distribution diagram of barrier pillar. It is observed from the figure, influenced by disturbance of chamber mining, part of barrier pillars turns into plastic state, the failure zone is not cut through and the failure is shear combined failure along strike of ore deposit.

It is observed that from displacement field distribution diagrams of barrier pillar, figure 9 and figure 10, maximum vertical displacement of barrier pillar mainly occurs at hanging side of barrier

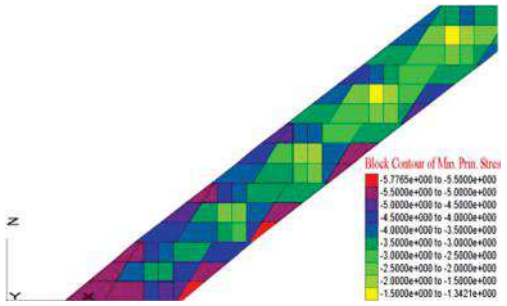


Figure 7. Maximum principal stress envelope of barrier pillar after mining of chamber.

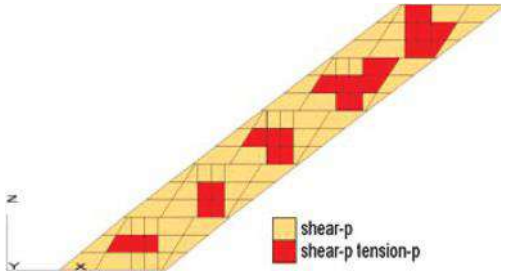


Figure 8. Failure field distribution diagram of barrier pillar after mining of chamber.

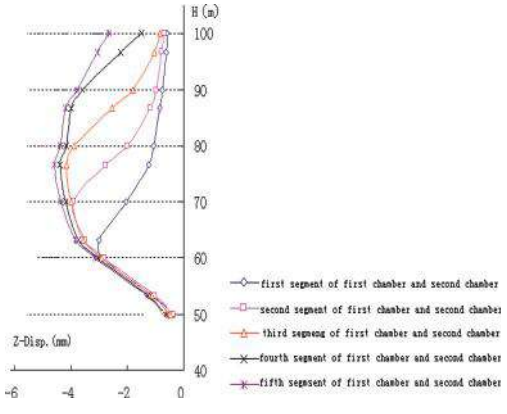


Figure 9. Vertical displacement curve of barrier pillar at segments (negative numbers stands for downward).

pillar and is 4.6 mm; maximum horizontal displacement of barrier pillar in X direction occurs at heading side of barrier pillar and is 3.18 mm; maximum horizontal displacement in Y direction occurs at central position of barrier pillar corresponding to segment height of chamber and is 9.55 mm; and the above shows that barrier pillar mainly bears extrusion from roof and footwall, supports roof well and maintains chamber stable.

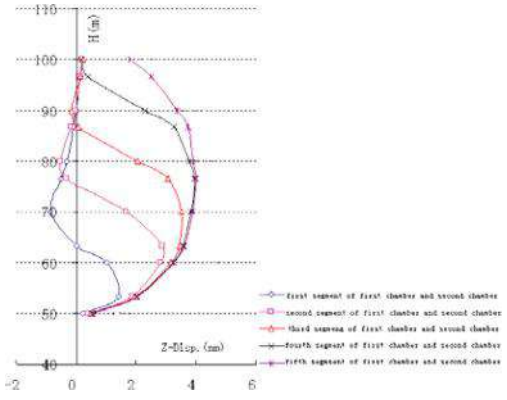


Figure 10. Horizontal displacement curve of barrier pillar roof in x direction at segments.

5 CONCLUSION

Through systematic analysis and study of internal stress field distribution of pillar, development of failure field and changes of displacement field with numerical simulation method, it reaches a conclusion as follows:

1. There is stress concentration in point pillar and the point pillar supports upper ore body to a certain extent. As mining space of chamber increases, concentration factor of internal stress of point pillar gradually decreases and supporting role of point pillar for upper ore body becomes weaken gradually. Influenced by disturbance of chamber mining, all the point pillars turn into plastic state and the failure is shear combined failure along strike of ore deposit.
2. Internal stress concentration of barrier pillar occurs below the barrier pillar. As mining space of chamber increases, internal stress factor of barrier pillar gradually increases and it is larger than the internal stress concentration factor of point pillar, which shows supporting role of barrier pillar is better than that of point pillar and the barrier pillars play key role to support upper ore body and maintain chamber stable.

ACKNOWLEDGEMENTS

This reseach was funded by the National "Twelveth Five-Year" reseach subject of atate science and technology support program (2012BAK09B02–06).

REFERENCES

Fu S.G et al. 2010. Numerical analysis on the stability of impedim ent zone grouting to plug-up water. *Journal of Safety Science and Technology,* 6(3):60–64.

Guo J.J & Dou Y.D 2008. Num erical simulation research on disturbance and failure lawof ore pillar and wall rock bym ining process, *Gold,* 29(6):30–32.

Li J, P et al. 2002. A Study on Pillar Parameter Calculations. *Journal of Beijing Institute of Technology,* 5:662–665.

Liu, M.Y & Xu C.Y 2000. Stability Analysis of Pillars in Mined-out Area. *Mining and Metalurgica Engineering,* 20(1):19–21.

Liu X.Z & Zhai D.Y 2000. The Reliability Desing Pillar. *Chinses Journal of Rock Mechanics and Engineering,* 6:86–88.

Wang L.G & Miao X.X 2006. Study of Mechanism of Destabilization of the Mine PillarBased on a Cusp Catastrophic Model. *Journal of Mining & Safety Engineering,* 23(2):137–139.

Wang H.T & Sui S.F. 2013. Mining Method and Stability Analysis of Barrier Pillar of Dongguashan Copper Mine. *Metal Mine,* 441(3):39–42.

Zhao K & Cai M.F 2003. Stability Analysis of Pillars of a Gold Mine. *Coloured Meta*l, 55(02):83–85.

Zhao X.D, et al. 2012. Numerical Analysis on Pillar Failure Process of Stope in Hongtoushan Copper Mine. *Metal Mine,* 9:5–8.

This page intentionally left blank

Progress in Mine Safety Science and Engineering II – He et al. (Eds)
© 2014 Taylor & Francis Group, London, ISBN 978-1-138-00122-0

Characters and control measures of unsafe operation behaviors in colliery accidents

M. Shang-Quan, M. Zheng, X. Li & F. Jing
North China Institute of Science and Technology, Beijing, China

ABSTRACT: China is a big country with coal production and consumption, but also many accidents take place in collieries. They impacts on our country's national economic and social stability. The direct reason for accidents is the unsafe manipulation. This paper analyzes the cause of mine accidents and discusses the irregular characters of the human malpractice, as well as the relationship between the conductive and psychological states. By analyzing the irregular characters, the author comes up with the system management and psychology control to reduce the occurrence human unsafe manipulation so that the coal safe production can be improved.

1 INTRODUCTION

People operating behavior is an action which under a state of motivated behavior during the process of production. It is also the external behavior about one's inner psychological activities. The mainly unsafe behaviors in coal mines are the coal mine operation and illegal commands, and unsafe operation behaviors, are commonly called the peccancy operation behavior, for illegal operation behavior, mainly refers to a violation of the relevant safety rules (regulations, procedures and system, etc.), which can lead to the accident directly. In the safe production activities, people's psychological activities play an important role. It has affected on safe activities and can lead to different kinds of accidents indirectly.

According to the model of safe behavior, the unsafe behavior of the people and subject are the causes for the accident together. Accident statistics show that in the world, 70% ~ 80% have a direct link to human wrong and unsafe operation. It is one of the important hazards to people's life and seriously endanger the normal operation of production and operation enterprises(WANG 2007). Lutness even said that 95% of accidents are caused by people's unsafe behaviors(LUTNESS 1987). In China, coal mines for unsafe operation behavior is also an important cause of the accident, 97.67% are caused by people's unsafe behavior. So how to take effective measures to control the happening of unsafe behavior is the most important thing.

According to the researchers' statistics in China, people's unsafe actions take up 85% (XU 2005). According to the statistics in the last decade, first three coal mines with high frequent accidents on the list: methane explosion accident (63.16%), Water damage(18.42%), coal and methane outburst accidents (10.53%). In these accidents, for the key reason is due to workers deliberate violation of the rules and regulations, management mistakes. Thus, to avoid the unsafe actions is one of the urgent things to decrease the number of accidents in coal mines.

2 UNSAFE OPERATION BEHAVIOR CHARACTERISTICS AND PERFORMANCE

2.1 *Unsafe operation behavior characteristics*

Unsafe operation is the abnormal behavior that conflicts with the psychological characteristics of people. Behavior which has caused or may cause accident must be an unsafe behavior during production activities. Once unsafe behavior in a person's life does not necessarily occur, it causes harm. Often unsafe actions, however, definitely lead to accidents. Even though the objects are the main reason for the accident, it also can't rule out human wrong behavior transformation hidden behind the unsafe state. Simply speaking, unsafe behavior has the following characteristics.

1. All employees, regardless of age, work years or work, have the possibility of violating the rules at anytime or anywhere. Continuous repetition of the same illegal behaviors may lead to unsafe operations, and even the bad habits of potential consequences often pass down to the workers of the next generation.
2. Consequences have potentials. Operations without regulations have hidden dangers. A certain

illegal action may not lead to any consequences at certain time, but it may lead to accidents in other certain conditions. There are no direct consequences to most of the illegal operations. It leads to the mine workers to follow each other, so relax alert, leading to the accident.

3. Unpredictability. Violations are random events, it is impossible to predict. Mine is a special work environment, different working conditions and working environment, different types, different workplaces may occur unsafe behavior, leading to accidents.
4. Being Stubborn. Mainly workers' abilities in some of the old mine are not good, but they have strong confidence. They have vanity, ignore the masses, leadership, and the rules and regulations; or they are unwilling to learn rules. They work according to their imagination and experience. They emulate others illegal operations blindly.
5. Being Fraudulent. Illegal operations are divided into intentional and unintentional violations, both of which are difficult to distinguish between the two. Even though the operators are clear, due to various reasons, they will admit unintentional violation and will not be punished seriously.

2.2 *Expression and influencing factors of unsafe actions*

1. Physical problems. They may work with insensitive sense, unhealthy body, inadaptable age and inadaptable craft and other problems.
2. Greenhands. The new comers are so curious about whatever they see that they touch equipments unsafe by touching them carelessly. What's more, they are poor in working skills and unfamiliar with the technique.
3. Counting on luck. This always exists on old workers. They want to save time and effort, counting on luck and lack of recognition of safe rules. Their work abilities are not bad, but just counting on luck even they know it is wrong.
4. Unhealthy psychological status. All workers in the coal mines have such characters. Because some are influenced by society, family and other factors, they will be agitated and distracted. It shows that they do not have a correct attitude towards work; they often have bad moods; they suffer a lot of working pressures and have unsafe mind; they have insobriety and acts especially when faced with so many insipid operations. They may have mental fatigue that leads to the colliery accidents.
5. Lack of knowledge. Their careless attitudes are shown in pre-post training. They have lower education, lack of safe knowledge, weak in working skills and poor skills of solving sudden accidents, shown in Table 1, Figure 1, Figure 2.

Table 1. Unsafe operation behavior affecting factors.

Unsafe operation behavior affect factors	Physiological factors	Perception
		Fatigue factor
		Biological Rhythms
		Biomechanics
		Physiological parameters
	Psychological factors	Emotion
		Willing
		Motivation
		Individual
		Personality
	Environmental factors	Ability
		Temperature
		Humidity
		Noise
		Illumination
		Dust
	Management factors	Social factors
		Managers factors
		Leadership factors
		Management model

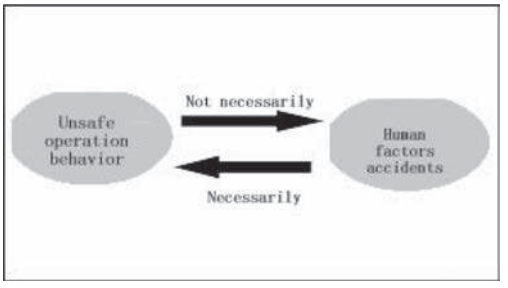


Figure 1. Relationship between accidents and unsafe operation behaviors.

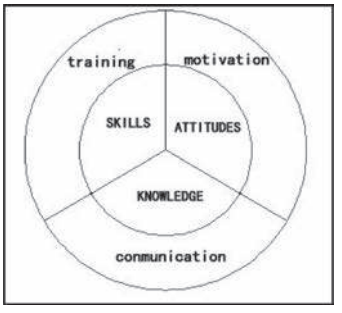


Figure 2. Specific analysis of the causes of accidents.

3 UNSAFE BEHAVIORS AND DAMAGE

3.1 *Unsafe operation behavior rules*

Violation occurs in the following three periods: ①before and after holidays; ②during shifting time;

③3–6 o'clock in the early morning. During the above periods, the operators are often disturbed and are more difficult to focus on ideas, thus they miss an operation or have intentional violations. As for coal mines, the accidents are mainly caused in the following situations:

1. Blasting operation. Accidents are triggered by blasters: in the process of simplifying the blasting procedures, they are not in accordance with the provisions foam padding mud, use of explosives for blasting of rock, such as a charge repeatedly blasting illegal operations; or because of underground mine workers smoking; mine workers operate with electricity, etc. These lead to methane explosion.
2. Mining operations. In the mining process, due to mining staff daze, distracted, etc. inattention performance, it's easy to get the roof accidents, flooding accident, for example, when coal and methane outburst accident occurs and we can't make accurate judgments and cause undue command and operation, which leads to the accident. In addition, the various monitoring and control instruments and equipment chirping in the mining face cannot cause mining work to proceed, so when some staff cover this operation, the occurrence of the accident has played a very important effect.
3. Lifting operations. As the underground lifting equipments overload and the workers are absent from work, mining workers ride lift, cans, pedal cars, pedal hooks and climb cars. Transporting staff drive against regulations.
4. Operating with pollution. When workers work in the underground mining face or near the fan, they are subjected to the interference of the environment. So they will get hallucinations, which cause accidents.
5. Monotonous monitoring tasks. In most cases, machines run well. People work with small load, but they can not leave the work area or do other things that can easily get mental fatigue. This often causes violations.
6. Blind roadway. Since roadway warning signs within the roadway door are not written clear enough, they provide the conditions for the accident. Careless staff mistake into and then die

3.2 *Hazards of unsafe operation behaviors*

Operation against rules lies in not only direct individual harms, but also the potential indirect harm to the enterprises. That unsafe operation behaviors continues to occur leads to enterprises security hazards and they are difficult to troubleshoot. That affects the lives and safety of workers. If a person's death causes the direct economic loss of 800, 000 yuan, losses caused by accidents are very serious, shown in Table 2.

In the coal mine enterprises, there is also another kind of form. Blind impulse but misguiding also lead to accidents. For example, in 2013, when Babao coal mine methane accident occurred for the first time in Jilin Province, in order to quickly resume production after the explosion, they acted against the regulations and sent staff dealt with fire disaster again, which led to the tragic second explosion. Security management objective is the "people-oriented' to protect the lives of workers, thereby controlling the operation of unsafe behaviors and the control of accidents is significant.

3.3 *Unsafe operation behavior causes*

For the purposes of unsafe operation behavior can be roughly divided into the following two categories, unintentional and intentional violation, and the violation of unintentional causes are divided into behavioral and psychological causes.

A. Inadvertent behavior

1. Working environment and work overload cause poor mental and physical exhaustion. The working conditions are poor and the working environment under adverse conditions often overworks. That will lead to the human biological rhythm disorders, physiological function obstacles. Mining work is tough. When the mine staff workload up to a certain limit, their fatigue will accumulate,

Table 2. 2001–2010, the overall accident's situation of China'scoal mine of suffocation accidents.

A Particular year	2001	2002	2003	2004	2005	2006	2007	2008	2009	2010
The Number of accidents	3082	3112	4143	3639	3341	2945	2421	1901	1616	1403
Deaths	5670	6995	6436	6027	5986	4746	3786	3215	2631	2433
Direct loss/one hundred million yuan	45.36	55.96	51.48	48.21	47.88	37.96	30.28	25.72	21.04	19.46

Table 3. Accident cases identified unsafe operation behavior unsafe use of equipments.

The serial number/ type	Unsafe operation behavior	The accident types	Occurrences (times)
1	Downhole smoking	Methane explosion, Fire disaster, Methane combustion	13
2	Downhole repair cap lamp	Methane explosion, Methane combustion	13
3	Charged drag cable	Methane explosion	2
4	Dummy plug pin	Methane explosion	1
5	Go by mining car	Transport accidents	2
6	Charged connecting pin	Methane explosion	1
7	Violation Blasting "three inspection" Provision	Carbon monoxide poisoning	1
8	Blasting withdraw into the safe zone not in time	Coal and methane outburst	1
9	Special operations personnel is not strict	Methane explosion	1
10	Empty the top job	Roof accident, Coal and methane outburst	5
11	Use of facilities not solid enough	Methane explosion	1
12	Part-time workers to operate the equipment without authorization	Methane explosion	4
13	Windless area Job	Methane explosion, Methane combustion	24
14	Not wearing self-rescuer	Coal and methane outburst, Poisoning, fire disaster	32
15	Take off work	Methane explosion	13

Table 4. Downhole environment requirements and workers can save psychological analysis the management decision (WANG 2007).

The serial number/type	Underground environment	Response measures	Adverse effects of using	Result of the unused
1	Low temperatures	Cotton clothes	Clumsy, Increased labor intensity, Muggy	Body cold
2	High Wind speed			Easy to get skin diseases, rheumatism, etc.
3	Water	Raincoat, rubber boots		Affect the work
4	Mine Pressure	Safety hat		Unable to resist impact damage
5	Carbon monoxide, methane	Self-rescuer	Increase the weight	When disaster difficult to escape
6	Dark	Head lap	The power cord of the restrictions	Visual Impact
7	Noise	Protective earmuffs	Unable to hear outside	Auditory effects
8	Dust	Dust mask	Difficulty breathing	Olfactory impact, pneumoconiosis

accumulate to a certain extent, the workers can occur unintentionally against rules of behaviors.

2. Poor social environment and family conflicts cause their lack of power. Production and life of the adverse factors will lead to the person's abnormal mood. When a person's mood is in an abnormal state, he or she often has abnormal behaviors which may cause the violations.
3. Depending too much on others. Such situations occur in cooperation with others, they are not active, not strictly in accordance with their share of the action items and operating procedures. In the case of absent teammates, they are unable to work independently.

Table 5. Intentional unsafe behavior analysis.

Methane explosion	Simplify blasting procedures	Roof	Project quality is poor	Casualties	Live working
	Multi-bus shooting	Blasting	In violation of the three chains blasting system	Water damage	in violation of carry out prospecting drainage principle
	Do not fill the foam mud in accordance with the regulations	Transportation, Upgrade	overburdened		the hidden trouble of accident have no result
	Using rock blasting of explosive		Absent without leave		Illegal operation
	A charge blasting for many times		Illegal to ride		Dereliction of duty
	Smoke		Violation by tank	Fire disasters	Light bulb to keep warm
	Live working		Violation of pedalling		Dereliction of duty
Methane poisoning, suffocation	Illegally entering danger zone		Illegal pedaling hook		Smoke
	Illegal blasting		Illegal driving		Not wear oxygen breathing apparatus
Electrical	Live working		Illegal climbing car		Without security measures
	Violation of pedalling	Other	Illegal construction	Methane outburst	Illegal blasting
	Illegal operation		Absent without leave		

B. Psychological reasons for inadvertent unsafe operation

1. Bad cognitive. Because of the material insecurity, lack of some relevant expertise or lack of experience as a result of violations or illegal operation, people often make wrong judgment. The cognitive adverse is roughly divided into two parts: one is a person's vanity, pretending to understand, irresponsible underground conclusion, whim, chaotic operation, originally did not have the appropriate skills; another part of the psychological quality is poor, conservative thinking. Once they encounter accidents, they will know what to do, not according to a predetermined manner to continue working or to escape, thereby increasing the risk of accident.
2. Fault or negligence. Negligence to the violation of regulations or procedures often leads to real violation. but the offenders do not recognize. If there is no troubleshooting, no good protection and warning, they use unsafe equipments or
3. Character. Every character is not the same, compared with mood swings or lack of concentration, etc., so angry forget the class that indirectly led operations in accordance with operating procedures, which lead to accidents. Or the presence of this serious "rebellious" mentality, the leadership team and other opinions are opposite to work, shown in Table 3.
4. For luck. Performing in strict accordance with rules and regulations is too cumbersome or mechanical, so it is not fully in place to implement or to enforce strict accordance with rules and regulations. In practice, there are several ways: ① task to catch omitted safety measures; ② as much time and eliminates the necessary checks; ③ stingy workers and removed the custodial staff, resulting in accidents caused due to people's violation. These categories of unsafe operations in coal mine production safety accidents account for a large proportion.
5. "Fame and fortune" mentality. In order to improve labor productivity, business managers made the wrong decision which causes accidents or the pursuit of individual workers as well as self-expression desire bonuses and other reasons, the regulation and operation of sequential steps behind. 2013 Babao coal mine disaster occurred in the second error was due to

C. Intentional acts of psychological causes unsafe operations

1. "Paralysis" mentality. Psychological paralysis is one of the main factors causing the accident, because of China generally lack awareness of safety awareness, and thus lead to "paralysis" mentality prevalent in our country many coal mines. Owing to frequent dry work, operators are accustomed to feel there is any danger, shown in Table 4. Violation is blieeved that the pursuit of their own minimum cost to get maximum results. This is a common psychological phenomenon that people, so there is the presence of illegal basis. For example, to go down without a helmet, "a gun seized three" not in accordance with the provisions to do, to cut corners to save energy psychology; miner damage as well as in the case of unauthorized repairs in the underground miner situation.
2. "Conceited" mentality. Workers are not relying on rules and regulations operate, but relying on their habits and nature, self-righteous work; or some technical staff think they have a wealth of experience, and then came out on top during the operation should not have occurred accidents (XIA 2006).
3. "Adventure" mentality. Violation does not necessarily produce an accident. In the production process, there may be recurrent emergence of the production site conditions are extremely bad. If the strict implementation of the system in accordance with relevant regulations does have difficulties, in such conditions, "adventure" psychological mischiefs may result in accidents. For example, in the underground, not a "one shot three inspection" will not necessarily produce a methane explosion; does not necessarily lead for methane pumping methane accumulation, etc.; using various articles covering the detector probe. These are against rules (HE 1988), shown in Table 5.

4 THE WAYS TO SOLVE UNSAFE OPERATION BEHAVIORS

4.1 *Unsafe operation behavior control and management systems*

1. Strengthen education accident cases. Make full use of our experience which has occurred mine safety accidents for workers education. In the educational process using the way that new and old are "equal", and thus avoid the occurrence of habitual unsafe operation. When the conditions permit, we can set up an accident exhibition showroom, with photos, videos and other forms to show. To improve the management level of Managers
2. Ability to achieve acceptable risk value. Depending on the manager's level of management, management of resources and technological capabilities, which is the key level managers. Both managers violations can be very rational analyzed, but also can be very humane treatment, insisting on serious, strict, strict management principles (FANG 2007).
3. Strengthen inspection, supervision, control illegal risks as much as possible to reduce violations. Management is not intended to eliminate illegal violations, but to control the risks of violation, so that minimize violations, but also to reduce losses to a minimum illegal. This is the one of the most important organization of the accident factors.
4. Strengthening security evaluation method using fault tree, safety checklist and other methods, in the presence of various coal mine hazard evaluation were made? By theoretical data to guide the actual work, and through practical work to come back to the theory, constantly the cycle to improve mine safety values.
5. Establishment of a multi-level fault tolerance measures. Through the refuge chamber, mobile rescue capsule, dampers and blind alleys, etc. some food and water supplies are placed. Restricted security alarm signal device is set. This will improve mines' safety.

4.2 *Psychological control illegal operation*

1. Using secure employment mechanism. To change impressionistic, relying on the experience of the management of the old tradition, the establishment of scientific personnel, selection mechanism, based on individual personality to arrange a suitable job. On the human potential for scientific excavation. Strengthen the psychological exploration and development of the staff.
2. In accordance with the rules of the provisions of the technical staff requests start starting, and then to manage. Staff for different mines them varying degrees of heart counseling and potential of the excavation. So that in the event of unexpected circumstances can win time for disaster relief and other activities.
3. Improve management thinking. Improve management thinking and understanding, so that they can lead in unexpected situations the majority of mine workers to make timely and effective measures are very important.
4. Enhance safety incentive system. ① adding "Top Ten security expert", "Security Qishou" honorary title; ② mine workers and their fami-

lies to carry out similar to the "Safe Home", "security assistance and education" campaign, ③ conduct job skills contest improving their motivation and creative, motivating staff techniques, learning management, knowledge, to understand device performance, master methods of operation, familiar with the process, safety in production.

5. Violations from the analysis of the objective reasons to proceed. To be good at summing mine accident objective reasons, there is no shortage of help to create a relaxed yet rigorous, realistic atmosphere, so that avoid mines working illegally dare to speak their minds and illegal behavior. The only way to be able to better analyze subjective reasons.

REFERENCES

He Xin-Qin, Labor Personnel Psychology[J].*Beijing Institute of Economic Publishing House,* 1988.

Lutness, J. Measuring up: Assessing Safety with Climate Surveys[J]. *Occupational Health and Safety,* 1987, 56: 20~26.

Wang Jie-Jun. Analyse the Enterprise Production in Violation of the Cause and the Measures Against Violations[J]. *Inner Mongolia Technology and Economy,* 2007 (8): 95~97.

Wang Lingxiang. Introduction to the Habitual Peccancy [J], *Economic Review,* 2007, (1):136.

Xia Li-Ming. Analysis of Error Causes and Countermeasures[J]. *Engineer,* 2002.

Xu Liang, Research on the Cause of the Accident and Problem of the Regulatory System in Coal Mine, *China Science and Technology Papers Online,* 2005.

This page intentionally left blank

Progress in Mine Safety Science and Engineering II – He et al. (Eds)
© 2014 Taylor & Francis Group, London, ISBN 978-1-138-00122-0

High gas drainage lane design parameter simulation research

Zhengang Wang & Huishuang Li
LuAn environmental energy development Co., Ltd., Chang Cun Coal Mine, Changzhi, Shanxi, China

ABSTRACT: 470 level single coal seam working face roadways of Chang Cun ore using the "two into two back " design, coal loss is big, gas drainage efficiency is low; Using FLAC3D simulate damage rule of overburden in stopping process, determined the distance of 3# coal seam roof 31 m, about 5 ~ 6 m thick sandstone (K8 rock) is a key stratum, it plays an important role on the fracture development and distribution of 3# coal seam of overburden; Using UDEC simulate the fracture development and distribution rule of overburden in stopping process, obtained working face towards the direction of fracture area is about 5 ~ 48 m from cut; Vertical direction vertical fracture area high about 21 ~ 24 m from coal seam roof; From starting cut about 40 to 45 m, old top appeared the pressure of first time; starting cut above goaf fault zone width is about 40 m, working surface above the fault zone width is about 48 m; Lane to help on both sides of the fracture zone width is slightly smaller than 40 m. According the site of the 2103 working face the test results of near surface fissure zone to of, fitting out the relationship curve of the 3# coal seam overburden caving zone, fracture zone and vertical height of fractured zone and working face strike; Based on FLAC3D, UDEC and the field test results, determined the design parameters of 2103 working face of high gas drainage lane.

1 THE WORKING FACE

Chang Cun 2103 working face strike length is 1150 m, long tendency is 310 m, coal thickness is 5.66 m, with a thick layer 0–1, the average thickness is 0.05 m, recoverable length is 1100 m, the recoverable reserves is 2.7 million t, coal seam angle is 0°~8°. The overall shape of the working face is back and composite syncline structure, expected the relative gas emission quantity is 11.43 m^3/t, the geological columnar distribution of working face as shown in Figure 1.1.

Maximum horizontal principal stress is 7.45~13.50 MPa, minimum horizontal principal stress is 6.49 ~ 6.49 MPa, rock density 26.5 KN/m^3, the vertical principal stress SV is 12.93~16.03 MPa, crustal stress state is $S_V > S_H > S_h$.

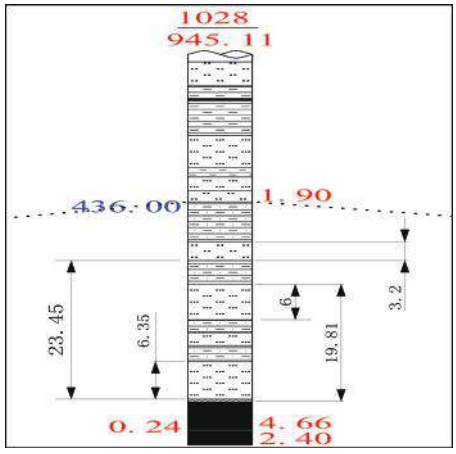


Figure 1.1. Mining geology histogram.

2 THE DETERMINATION OF KEY STRATA OF OVERBURDEN

The fracture of Key layer of overlying strata play an important role on rock fracture condition and distribution, It is determined key parameters of the high gas drainage roadway horizon (Qian Minggao et al. 2003).

2.1 *Introduction FLAC3D*

FLAC3D mainly suitable geological materials and mining simulation process on the mechanical behavior. Especially material can generate plastic flow after reach the yield limit, materials can be represent via unit and regional, according to the shape of calculation object form the corresponding grid. Under the outside load and boundary constraint conditions of each unit, in accordance with the contract of linear or nonlinear stress-strain relationship produce mechanical response (Zeng Lei & Xiang Yifan, 2007. Liu Zenghui &

Table 2.1. The overlying rock physical and mechanical parameters.

Rock types	Modulus of volume elasticity B/Pa	Shear modulus S/Pa	Angle of internal friction F/°	Cohesive force C/Pa	Tensile strength T/Pa	Density D/kg.m^{-3}
Siltstone	2.02e9	1.709e9	33	4.1e6	0.86e6	2400
Sandstone	5.833e9	4.375e9	38	5e6	0.97e6	2610
Coal	1.19e9	0.368e9	25	2e6	0.03e6	1400
Mudstone	1.613e9	1.26e9	34	3.5e6	0.06e6	2100
Fine sand stone	5.914e9	4.622e9	38	5e6	1.03e6	2660

Yang Benshui, 2006. Chen Yumin & Xu Dingping, 2010. Chen Ronghua et al, 2006).

2.2 *Simulation calculation model*

Due to calculation model is mainly study the coal seam and roof deformation, damage, and the division unit number of calculating model is limited, so the division unit of the calculating model should not equal, the study area of working face and laneway with fine cell division, using sparse around central dense division unit, division of region of external surrounding rock units is gradually increased, to build a strike length 400 m, long tendency 250 m, physics calculation model of rock thickness is 114.6 m. Overlying rock physical and mechanical parameters are shown in Table 2.1.

2.3 *Simulation results*

Three-dimensional simulation process: generation model→calculating the original rock stress→coal seam mining→calculation stability→each step calculate balance→output the calculation results. The 2103 working face implement mining step by step, after open cut, mining step by step, circular 10 steps, each step is 20 m, excavation ends at 200 m, as shown in Figure 2.2 to Figure 2.5.

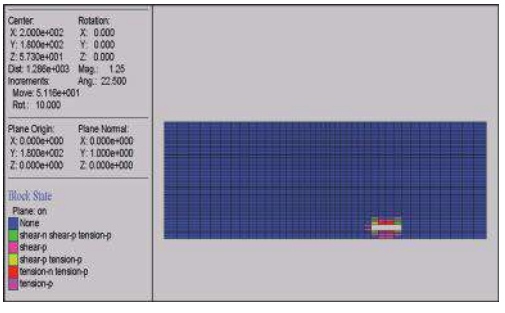


Figure 2.2. Stopping 40 m model unit damage state.

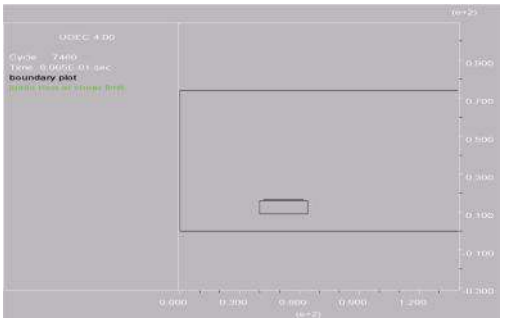


Figure 2.3. Stopping 100 m model unit damage state.

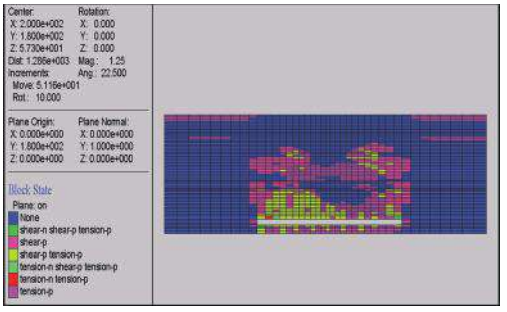


Figure 2.4. Stopping 120 m model unit damage state.

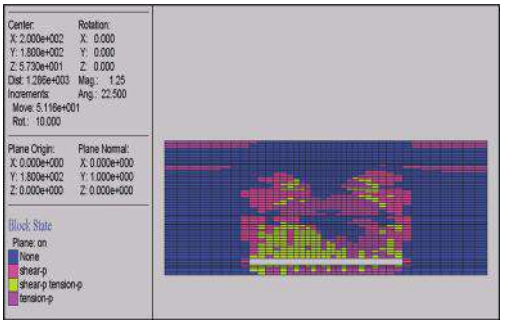


Figure 2.5. Stopping 200 m model unit damage state.

3 THE ROCK FISSURE DISTRIBUTION SIMULATION

Caving face after fully mining of initial pressure, pressure and other process cycles, the overburden rock elliptic band will disappear, mining-induced fracture belt on both sides of the fault zone will be formed; Fracture zone of level distribution is still the approximate ellipse area, called the circle of mining fissure elliptic.

Many times simulation test can be found (Li Shugang 2000): mining-induced fractured zone is not constant, and has a close relationship with the distance of first weighting and periodic weighting interval of fully-mechanized caving mining. That is the width of cut above goaf fault zone is approximately the first weighting step distance, while the fault zone width above the working face is change, the change range is about 1 ~ 2 times the cycle pressure. Fault zone width of along the sides of their tendency is slightly smaller than the first pressure step distance, as shown in Figure 3.1, namely A1 is about the first pressure step; A2 is about 1 ~ 2 times periodic, B1 and B2 is slightly less than the first weighting interval.

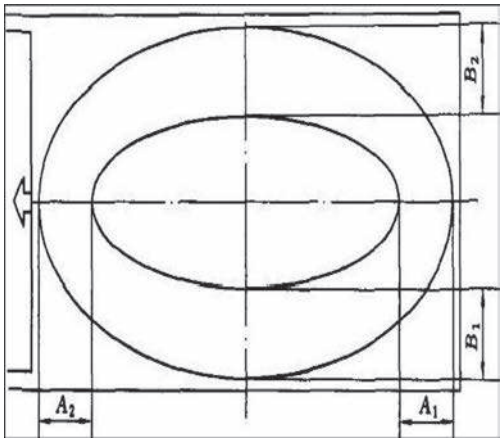


Figure 3.1. Oval ring strata by mining fissure level.

It can be seen from Fig. 2 that: the N_2 adsorption isotherm of coal samples in different size show similar trends. The adsorption quantity of N_2 increases with the increase of relative pressure $p/p_{o,}$ and the adsorption quantity of N_2 also increases with the increase of coal size.

3.1 *Introduction UDEC*

UDEC is used to simulate the discontinuous medium (such as joints and fissures in rock mass, etc.) under static load and dynamic load under the action of the response. Discontinuous medium is represented via discrete block assembly. Discontinuity handling for the block between the boundary surfaces, allow the block along the discontinuity occurs larger displacement and rotation which include fully out, and in the process of computing, automatic identification the new interface(Hao Zhiyong et al. 2007. Song Genxiang, et al. 2009).

3.2 *Simulation models*

Because calculation model mainly study the coal and overburden deformation, damage and fracture distribution, and the dividing unit number of calculation model is limited, so partitioning unit of the calculation model is not equal, build a strike length 300 m long, the physical calculation model of which the strata thickness is 74 m, rock mechanics physical parameters are shown in Table 3.1, the mechanical parameters of rock joints are shown in Table 3.2.

3.3 *Simulation results*

Simulation process: generation model→calculating the original rock stress→coal seam mining→ calculation stability→each step calculate balance →output the calculation results. the 2103 working face implement mining step by step, after open cut, mining step by step, gradually circulation, until the end of extraction and analysis of the results (Xu Fuli 2010, Li Qingbai & Li Wenzhou.2010), as shown in Figure 3.2 to Figure 3.6.

Table 3.1. Physical parameters of rock mechanics.

Parameters Lithology	Bulk density (KN/m^3)	Modulus of volume elasticity (Gpa)	Shear modulus (Gpa)	Cohesion (MPa)	Angle of internal friction (°)
Fine sandstone	27	25.8	17.8	2.6	36
Mid Sandstone	26.6	22.2	16.67	2.4	38
Coal	14	9	5.4	1.2	25
Mudstone	25	12	7.2	1.7	32
Sandy mudstone	25	12	7.2	1.8	32

Table 3.2. Mechanical parameters of rock joints.

Parameters Lithology	Normal stiffness (Gpa)	Tangential stiffness (Gpa)	Cohesion (MPa)	Angle of internal friction (°)
Fine sandstone	15	15	3.5	36
Mid Sandstone	15	15	3	35
Coal	15	15	0.1	30
Mudstone	15	15	2.2	30
Sandy mudstone	15	15	2.4	32

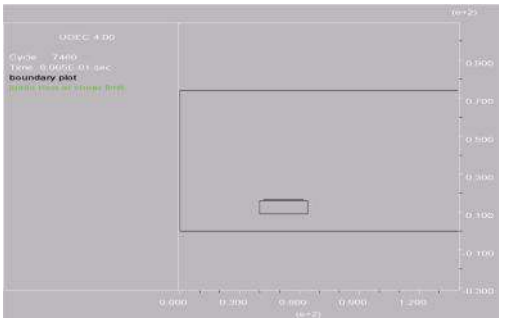


Figure 3.2. The distribution state of mining 20 m overburden fracture.

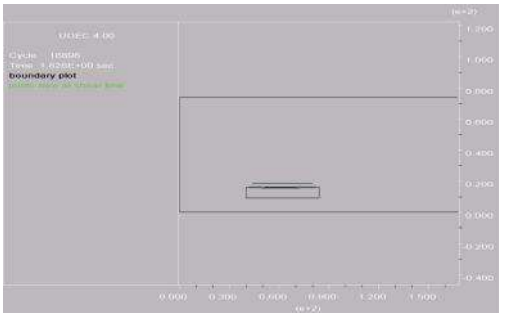


Figure 3.3. The distribution state of mining 40 m overburden fracture.

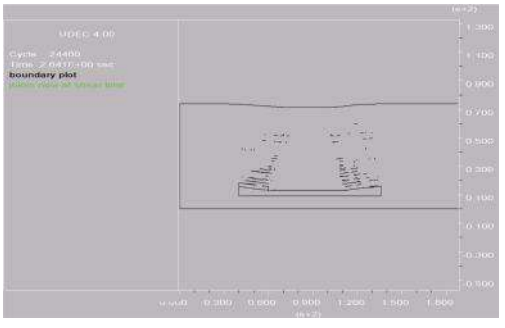


Figure 3.5. The distribution state of mining 90 m overburden fracture.

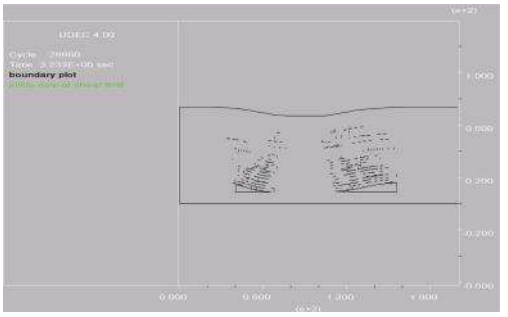


Figure 3.6. The distribution state of mining 120 m overburden fracture.

In the working face trend direction, fracture development zone is about 5~48 m from the cut-hole; vertically fracture development zone vertical distance is about 21~24 m from the coal seam roof; when mining face is about 40 m, the old roof appears initial pressure at about 40~45 m from the open-off cut; in the face mining process, after the key stratum of overburden K8 initial fracture, the central region of the overburden is began to compaction, fracture development parts is reduced significantly; Figure 3.1 shows above the cut-hole goaf fault width is A1 = 40 m, above the working face fault width is A2 = 48 m; in the two sides of the roadway wall the fractured development area width is B1 = B2 < 40 m.

4 THE VERTICAL "THREE ZONES" FIELD TEST

2103 working face of +470 level is in the excavation period, the face has not been formed, therefore, S3–9 working face is selected to study, which is near to 2103 working face of the +470 level and have the same coal seam thickness, in order to study the development regularity of the goaf overburden rock of S3–9 working face, determine the horizon of the trend high drainage roadway, drilling 7 holes in the coal side of rail roadway (return airway), also investigating the original 13# and 14# hole, Through the observation of the relationship between the orifice pressure difference and the working face advance, to determine the development regularity of the overburden, Drilling parameters are shown in Table 4.1, the relationship between working face advancing distance and various orifice pressure difference is shown in Figure 4.1~Figure 4.5.

1) The caving zone height curve fitting

Observed by measuring the change of 1~7# hole orifice differential pressure with working

Table 4.1. Test drilling parameters.

Hole number	The angle with roadway side (°)	Elevation angle (°)	Final hole length (m)	Drilling projection in the roadway direction (m)	Drilling vertical height (m)	The distance of final hole projection with the roadway side (m)
1	23.6	15.8	90.7	80	24.7	35
2	23.6	21	93.7	80	33.6	35
3	23.6	26	97	80	42.4	35
4	23.6	30.5	101.4	80	51.5	35
5	23.6	34.5	106	80	59.9	35
6	23.6	38	111	80	68.6	35
7	23.6	41.5	116.7	80	77.4	35
13	60	18	150	71	42	123.5
14	60	18	150	71	42	123.5

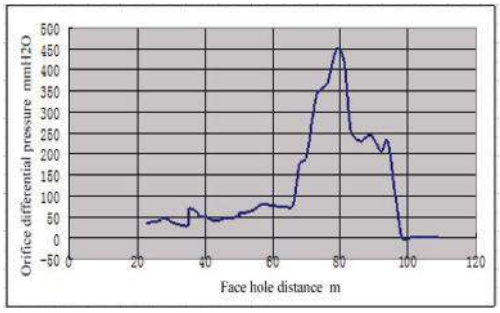


Figure 4.1. The relationship between face advancing distance and orifice pressure difference of 1# hole.

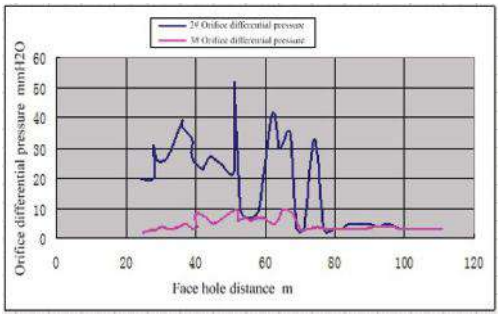


Figure 4.2. The relationship between face advancing distance andorifice pressure difference of 2# and 3#.

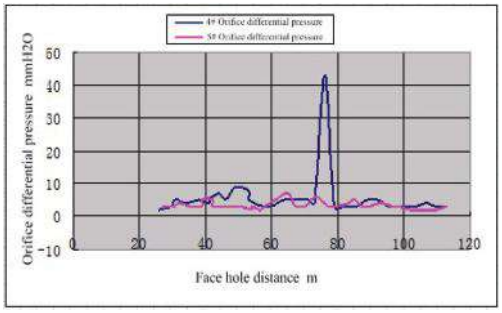


Figure 4.3. The relationship between face advancing distance and orifice pressure difference of 4# and 5# hole.

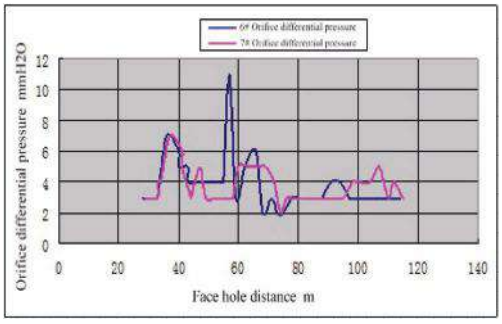


Figure 4.4. the relationship between face advancing distance and orifice pressure difference of 6# and 7# hole.

face advancing distance, it can been see: 1# hole in 70 m and 35 m working face is away from the opening hole, orifice differential pressure and gas drainage concentration fell sharply, because of its working surface roof periodic pressure, 1# hole caving at this location, and the working face roof control distance is about 5 m, by calculation, 1# hole caving in oblique direction is 32.727 m and 17.476 m respectively from the return airway, while the vertical height (from seam roof height) were 18.96 m and 8.15 m respectively; in the measurement period, 2# hole orifice pressure do not dramatically reduce, therefore, with the working face roof periodic pressure, it can been drawn 2# hole caving phenomenon do not occur, and the vertical of the 2# hole height at which the 1# hole cave

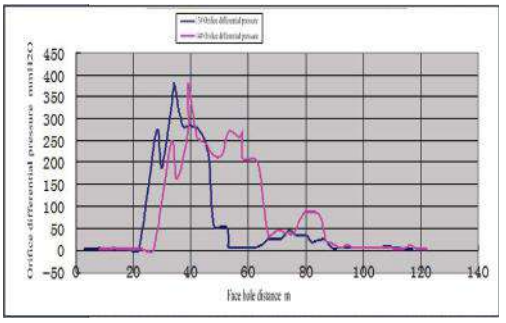


Figure 4.5. The relationship between face advancing distance and orifice pressure difference of 13# and 14# hole.

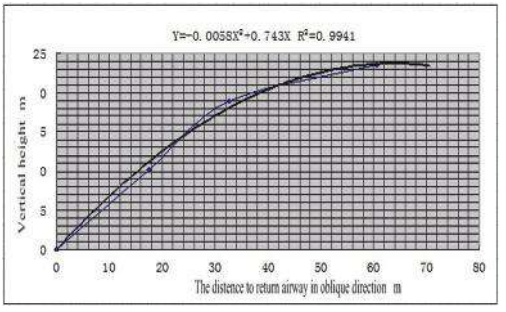


Figure 4.6. Overburden caving zone height curve fitting.

is 27.64 m and 12.59 m respectively. Therefore, in 17.476 m away from the return airway, the overburden caving in between 8.15 m and 12.59 m, take a height of 10.15 m. Because roof pressure, drilling occurs caving, fractured zone 13 # and 14# hole, etc. basically in the face about 30 m away from the hole, orifice differential pressure reduced dramatically, by calculating, in oblique direction, the fracture zone drill hole caving is at 60.6 m away from the return airway, vertical height is 18.34 m; when the last time the old roof press, the fractured zone drilling vertical height is 28.94 m, therefore, in this position, the top height of overburden caving zone is between 18.34 m and 28.94 m and greater than 18.96 m, take its height of 23.5 m. Fitting overburden caving zone height curve shown in Figure 4.6.

2) Fracture development zone height curve fitting

By observing 1~7# hole measured data it can be seen: 1# hole in which the face is on the end hole position (along the inclined is 35 m apart from the return airway), orifice differential pressure and the mixed gas quantity are sharply higher and bigger, and at this time, the 2 # hole orifice differential pressure and the mixed gas quantity is almost no significant change. Therefore, in 35 m the inclined away from the return airway, the fractured development zone top is between 1# and 2# end hole height and deviation of 2# hole; by calculating, the 1# final hole height is 20.5 m, 2# final hole height is 29.4 m, take its height of 27.3 m; 2 # hole in the working face 60 m from the opening hole (along the inclined 26.4 m away from the return airway), namely roof periodic pressure, orifice differential pressure and mixed gas volume is stable but not too high, but at this location, 3 # hole the orifice differential pressure is increased, but not obvious, therefore, in the inclined 26.4 m from the return airway, the overburden fractured development zone top is between 2# and 3# hole height and deviation of 2# hole; by calculating, the 2# final hole height is 20.93 m, 3# hole height is 29.27 m, take its height of 24.5 m; 2 # hole in 40 m the working face away from the opening (along the inclined 15.7 m and 17.5 m away from the return airway), namely after roof periodic pressure, orifice differential pressure is stable but not too high, and at this location, 3 # hole the orifice differential pressure is increased, but not obvious, therefore, along the inclined 15.7 m and 17.5 m away from the return airway, the overburden fractured development zone top is between 2# and 3# hole height and deviation of 2# hole; by calculating, in this position the 2# hole height is 12.56 m and12.97 m respectively, 3# hole height is 18.09 m and 18.62 m respectively, take their height of 14 m and15.8 m respectively. Through comparative analysis 2 # and 3 # hole data changes, arrive at the location of working face overburden fractured development zones, fitting overburden fracture development zone height curve shown in Figure 4.7.

3) Fracture zone height curve fitting

By observing 1~7# hole measured data it can be seen: During the investigation of gas drainage, when the first old roof press, namely the working face get to 74 m from the opening hole, 5# hole orifice differential pressure increase suddenly, while the 6# hole is always low and no obvious change. Therefore, the top height of fractured zone is about the height of 5# hole, along the inclined direction 32.3 m from the return airway, vertical height is 52.3 m; but the second roof pressure, namely the work surface get to 57 m from the opening hole, 6# hole orifice differential pressure increase suddenly, while 7# hole is always low and no obvious change. Therefore, the top height of fractured zone is about the height of 6# hole, namely along the inclined direction the 24.9 m from the return airway, vertical height is 45.39 m; but the third roof pressure, namely the working face get to 40 m from the opening hole, 6# hole drainage gas

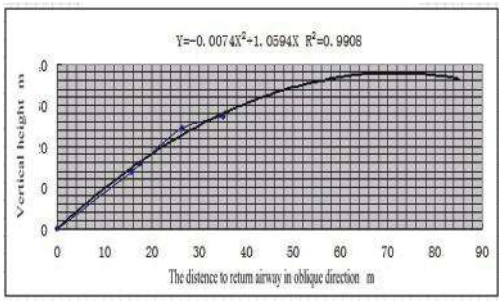


Figure 4.7. Overburden fracture development zone height curve fitting.

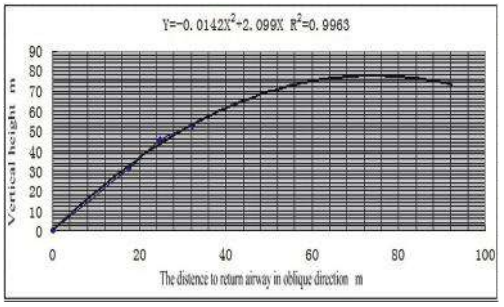


Figure 4.8. Overburden fracture zone height curve fitting.

concentration and pure gas quantity is stable and high, while 7# hole is always low and no obvious change. Therefore, the top height of fractured zone is about the height of 6# hole, along the inclined direction 17.47 m from the return airway, vertical height is 31 m. Through comparative analysis 6# and 7# hole data changes, arrive at the working face overburden fractured zones height, fitting overburden fracture zone height curve shown in Figure 4.8.

5 HIGH GAS DRAINAGE ROADWAY DESIGN PARAMETERS

Because 3 # coal seam is the single coal seam, the role of the high gas drainage roadway is mainly used for the current seam gas drainage in the coal mining process, based on the results of FLAC3D, UDEC and the field test, determine the design parameters of high gas drainage roadway of 2103 working face:

1. Section: 2.5 m × 2.5 m;
2. Level is about 30~45 m away from the return airway, suggest to choose the range of 35~40 m.
3. Vertical horizon is about 23 m away from coal seam roof, begin to excavate along the first layer floor of the 3# coal seam overburden sandstone;
4. At about 120 m away from open-off cut, begin to dig along with the level down to 8° ~10° direction, until the first layer sandstone of the roof, drainage roadway end vertical is about 7 m away from coal seam roof.
5. The gas drainage roadway floor heave is the main mode of failure in the mining process, high drainage roadway need high strength support, in both sides of roadway bottom need to use the 4~6 m cable support.

6 CONCLUSIONS

1. According to FLAC3D simulation results obtained: At 31 m away from 3# coal seam roof, the sandstone of about 5~6 m thickness (K8 stratum) is the key layer, has important effect on the overburden fractured development and distribution of the strata 3# coal;
2. According to UDEC simulation results obtained: Fracture development zone is about 5~48 m away from the cut in the direction of face trend; vertically fracture development zone is about 21~24 m at the vertical distance to coal seam roof; at about 40~45 m from the open-off cut, the old roof appears the initial pressure; goaf fault width is A1 = 40 m above cut, and the fracture width is A2 = 48 m above the working face; fractured development zone width is B1 = B2 < 40 m on the both sides of roadway wall.
3. According to the fissures zone field test results of the working face which near to 2103 working face, the relationship curve between vertical height and working face trend is fitted, which is the vertical height of 3# overburden rock caving zone, fractured development zone and fracture zone;
4. According to the FLAC3D, UDEC and field test results, the design parameters were determined of 2103 working face high gas drainage roadway.

REFERENCES

Chen Ronghua, et al. 2006. Determination of the Height of Water Flowing Fractured Zone in Overburden Strata above Fully-Mechanized Top-Coal Caving Face. *Journal of Mining and Safety Engineering,* 23 (2): 220–223.

Chen Yumin & Xu Dingping.2010. FLAC/FLAC3D foundation and project examples. *Beijing: Mechanical Industry Press*:10–64.

Hao Zhiyong, et al. 2007. Numerical simulation and analysis of the law of overlaying strata movement in the mining of protective layers of coal seams based on UDEC. *China Mining Magazine,* 16(7): 81–84.

Li Shugang 2000. Surrounding rock movement and gas migration of fully mechanized caving face. *Jiangsu: China University of Mining and Technology Press*:127–133.

Li Qingbai & Li Wenzhou. 2010. Optimized Design for Methane drainage Roadway Location in Roof. *Coal Mining Technology,* 15 (5): 28–30.

Liu Zenghui & Yang Benshui. 2006. Determine the height of water flowing fractured development zone numerical simulation method. Mining. *Safety and Environmental Protection,* 33 (5): 16–19.

Qian Minggao, et al. 2003. The key strata theory in rock control. *Xuzhou: China University of Mining and Technology Press*.

Song Genxiang, et al. 2009. Numerical simulation study on main roof weighting step in fully-mechanized working face. *Zhong Zhou coal,* 10:3–5.

Xu Fuli 2010. Application of high roof road to Jixi mining area. *Coal Technology,* 29 (3): 127–128.

Zeng Lei & Xiang Yifan. 2007. Discussions on the 3D mine pressure simulation realization of fully mechanized caving face using FLAC3D. *Coal Engineering,* (6): 86–88.

7 *Occupational health and safety in mines*

This page intentionally left blank

Progress in Mine Safety Science and Engineering II – He et al. (Eds)
© 2014 Taylor & Francis Group, London, ISBN 978-1-138-00122-0

SWOT analysis of aging mines' low carbon development

Hui Ma
Safety Engineering College, North China Institute of Science and Technology, Beijing, China

Huiqing Lian
Safety Engineering College, North China Institute of Science and Technology, Beijing, China
School of Resource and Safety Engineering, China University of Mining and Technology (Beijing), Beijing, China

Hongjie Zhu
China Shenhua International Engineering Co., Ltd., Beijing, China

ABSTRACT: The limits of coal resources storage, which determines that the coal mine production is a process from growth to aging. The aging mines produce a lot of coal and simultaneously face many problems, such as unsatisfactory depositary conditions, insufficient reserves, simplex industrial structure, high energy consumption, low products extra value, and what's more, the "waste" coal gangue, mine water, and waste heat are just ignored of their value and completely wasted. Based on comprehensive analysis of the current situation of the development of coal enterprises in china, the paper will research in the definition of aging mines and their development bottleneck, and connecting with the SWOT comprehensive analysis of the domestic and foreign aging coal mine's low carbon development, the analysis proves that development of "it is the inevitable choice of aging mine to lose control of all kinds of adverse conditions, prolong the mine life cycle through the low carbon transition".

1 INTRODUCTION

Coal is the major source of energy in China, accounting for 94.3% of the proven fossil energy resources, 76% of primary energy production and 70% of the primary energy consumption. In China's energy production and consumption of the composition, coal has always accounted for about 70% of the proportion and power is the main flow of the coal consumption. In 2007, coal accounted for only 27.8% of the world's primary energy consumption, while the number was less than 20% as for most of the developed countries, however, the proportion of coal in China's energy consumption was up to 69.5%. At the same time, National Economic and Social Development Statistics Bulletin published by the National Bureau of Statistics says that from 2008 to 2012, coal consumption in China's total energy consumption, had increased 3.0%, 9.2%, 5.3%, 9.7%, 2.5%, year by year, showing that the important position of coal in China's energy consumption will not change at all in the long period.

Coal industries produce large amount of energy, but also are energy-hungry. Carbon emission sources in China's coal mines are mainly three: First, the coal mine gas emissions, more than 15 billion m^3/a (equivalent of 225 million t/a carbon dioxide), which destruction of the ozone layer is seven times that of carbon dioxide, the greenhouse effect is quite 21 times that of carbon dioxide. The main component of the coal mine gas; second indirectly caused by carbon dioxide emissions of coal production (coal mining, transportation, lighting, shaft antifreeze, coal Mine industry Square surface buildings, etc.) and coal washing and processing; third the auxiliary production energy consumption, energy consumption in mine insulation, underground lighting, the wellhead canteen, laundry, wellhead baths.

2 THE DEFINING OF AGING MINE

The formation of Mine production capacity and the end of the service cycle experience from exploration, infrastructure, commissioning of production, stable to aging (Change), this time span is called the mine life cycle. Therefore, the mine life cycle of an regular coal mine is divided into four stages of the infrastructure, growth, stable and aging period, as shown in Figure 1 (LU Gang et al. 2009, REN Yixin et al., 2008).

Aging mine is an old problem. Aging mines with the problem of the depletion of resources and to be closed in relevant literatures are expressed in a variety of ways and the titles are not yet uniform.

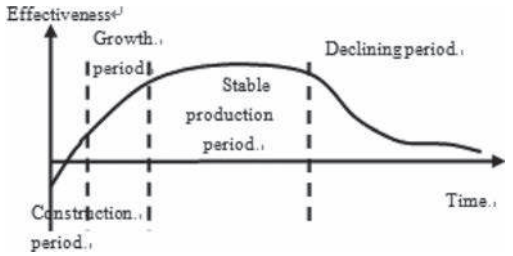


Figure 1. Life cycle of common coal mine.

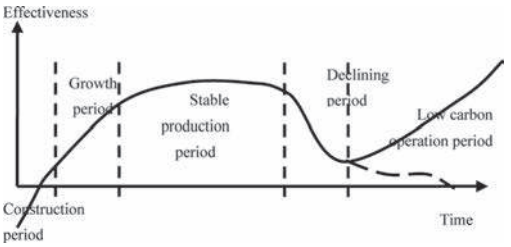


Figure 2. Life cycle of aging mine's in low carbon developent.

Common titles are old mine, aging mine, the resource depletion mine, resource crisis mines, aging mines, late in the mines and crisis mine, and so on, even though the same object as discussed, the meaning of the expressions are broadly similar, but each statement is not the same, not only different title, but also to understand differently.

There are different points of view for the determination of the mine recession and for the definition of Aging Mine.

1. According to the facts of Kailuan Coal Mine, Jia Yanjie puts the aging period into four signs: the exploitation and consumption reserves of more than 2/3 of the mine recoverable reserves or the service life is less than 10 years; tons of coal usage reached 3 people, and more than doubles of the development of a stable of mine; investment reached more than 80 yuan per ton of coal, more than 60% of the development of stable production of the mine; mine production began to decline, daily output has dropped to the level of design capability or stable ability.
2. Su evaluates weather a mine should be closed or not based on the comprehensive evaluation of the asset-liability ratio, reasonable economic losses and economic benefits of mining depth and coal resources etc.
3. The former State Bureau of Coal Industry developed on the basis of the research, resource depletion, high ash and high sulfur and losses hopeless standard coal mine with one of the following two conditions may be regarded as the aging period and resource depletion. According to the provisions of the former Ministry of Coal Document No. 211 May 13, 1991, the mine may preclude the reserves to reduce the deep and surrounding scalable resources, remaining recoverable reserves of the original design is about 20% of the recoverable reserves. The actual mine recoverable reserves, mine design capacity of and consider coal reserves coefficient calculated remaining service period of not more than 5a mine.
4. Huang Shude proposed different shaft types, different production years and under different production conditions in the mine aging scrapped the best point in time study, production and operation of the mine development trend of mine into the aging point index system.

In summary, it can be seen, the Aging Mine defined standard feature selection, mainly reflected in the following indicators: recoverable reserves; length of service; economic benefits; efficiency; production capacity.

Entered the aging of mine to be solved firstly is the depositary conditions are not ideal, lack of reserves, a single industrial structure, high energy consumption, low value-added products, coal gangue, mine water, valuable "waste" such as waste heat not to be utilized and bottlenecks encountered in the development process of the waste and other issues, it must be a new opportunity to explore the aging mine development, the transformation of economic development mode to achieve efficient low energy consumption, low pollution (zero pollution), low-emission (zero emissions) and from the aging of the energy, high efficiency, high efficiency, low-carbon development of running in transition, ushered in the enterprise has a rapid development period, as shown in Fig.2.

3 THE BOTTLENECK OF AGING MINE'S DEVELOPMENT

3.1 *The limit of resource storage*

Due to the characteristic of the coal's limited storage, the regional coal mining production is the process of growth to decline. Because of long time mining, the period of stable and high production mining has passed. The production is affected by the increase of mining depth, the deterioration of mining conditions and so on. The fact that the reserve resources are inadequate could result in a serious shortage of available reserves and lack of ability in coal mine. And then the coal mines enter the last period of their lifecycle with the production ability beginning to decline until they are

finally shutting down, which seriously restricts the sustainable development of coal enterprises.

The core problem of aging mines is that the remaining resources are inadequate, which is a big bottleneck of restricting aging mines' development.

3.2 *Restriction of production system*

Mine is a complicated system of artificial, machinery, mining engineering, geological conditions and natural environmental coexistence. Coal production is a complex systematical engineering and if we want to develop a coal production project, we need to go through the resource exploration, project argumentation, feasibility study and mine construction. Then coal production is formed. Coal production system consists of the production system, development system, mining system, ventilation system, mechanical and electrical transport system, power supply system, drainage system, communication system and other complex systems. Every subsystem should function properly in order to meet the needs of normal production.

All of the above determines the complexity of coal mine production system. The restriction of production system is mainly manifested in the following aspects:

1. *Restriction of production and safety conditions*

1. The aging coal resources are exhausted and the original coal seam is basically exploited. We normally exploit residual mining village coal pillar, stage coal pillar, corner pillar, pillar, fault pillar, industry square pillar and etc.
2. The mine goaf surface is covered by water and from the roof sandstone, fault water, floor water, igneous rock fissure water and the adjacent mine goaf water form a large area goaf seeper with a complicated hydrogeological conditions.
3. On both sides the work of mining roadway has ended. The stress concentration in the roadway is surrounding. The loose of broken coal is easy to form the roadway roof leakage, often causing spontaneous combustion.
4. Roof management is difficult.
5. Aging mine generally has the characteristics of wide and long transportation, which causes the difficulty of mine ventilation, transportation, drainage and other production conditions. It also causes the low level of mechanization, technology and equipment as well as low recovery rate.
6. The aging coal mine mainly exploits residual mining's lower layered face and all kinds of coal pillar.
7. The old equipment also restricts the mine production (WANG Wenjuan 2011, WANG Chun et al. 2006).

2. *Restrictions of production layout*

For a long time because of low mine geological guarantee system reliability, exploration and penetration equipment technology cannot effectively promote. And they cannot provide reliable geological data for the mine exploiting in time, causing a certain blindness of mine development layout and roadway drivage. What's more, it brings bigger impact to the mine, mining, machine, transportation, communication, power supply and etc. That the production layout is not reasonable seriously restricts the efficient production of the mine.

3. *Limit of production efficiency*

Whether the exploitation of mine is reasonable or not, it directly related to the whole mine production stable high yield and benefit. Because of bad geological conditions, mining working face causes more invalid footage increase and increases the quantity of tunneling engineering. At the same time sustained and stable production capacity must also be ensured.

The aging mines have entered the deep and final level mining. The complex of geological condition, the difficulty in mining technology and the low level of mechanization result in the cost increase. At the same time, affected by the geological conditions, commercial coal quality cannot be guaranteed. The reduction of coal production and high production cost result in inferior position for the enterprises in market competition. Profit ability is reduced and the mine maintain simple reproduction investment is insufficiency, which caused the narrow space for enterprise development.

4. *Limit of human resource*

The phenomenon of brain drain is serious in aging coal mine. Mine resource depletion, reduced production capacity, economic benefits glides, reduced income for technical management personnel, abandoned mines and bad employing mechanism seriously affect the production enthusiasm of workers, resulting in some engineering and technical personnel leaving the coal flow to other industry. New technology supplement does not come, which caused the lack of safety technical management personnel. It is not conducive to the safety production in coal mines.

4 SWOT ANALYSIS OF AGING MINES' LOW CARBON DEVELOPMENT

4.1 *Advantages analysis*

1. Policy support: national, provincial, coal group, aging mine own 4 levels policy supported system has been formed together, which provides

policy support and guidance for the old mine developing low carbon economy.
2. Feasible technology: many foreign countries have done a lot of research in sustainable development and low carbon transformation for coal enterprise at present, such as the development and utilization of coalbed methane exploration. A handful of countries such as the United States, Canada and Australia have formed industrial scale production, which is mainly used for civil and industrial fuel, power, etc. Domestic currently rely on the improvement of the level of mechanization, no pillar continuous mining science system, downhole primary system, coal gangue backfilling technology, coal gangue power generation and power plant flue gas desulfurization, waste heat recycling technology, in order to improve the recovery rate and the utilization rate of resources. Extending the industrial chain has been confirmed. From the technical perspective, it is feasible for aging mines development energy conservation, emissions reduction, and efficiency of low carbon operation mode.
3. Reasonable economy: developing low carbon economy can do to energy conservation, environmental protection and mine "three wastes" used together, achieving high efficiency comprehensive exploitation and utilization of coal resources development at last. The social and economic benefit from developing low carbon economy is remarkable, which is not only beneficial to the people and countries, but also can make the coal enterprises turning around, self-perfection, self-development and towards a low carbon road of healthy development.

4.2 *Disadvantages analysis*

1. Resources condition characteristic: for the aging mines having long mining history, the insufficient remaining reserves, relatively backward production system and other adverse conditions, which the difficult of determines the single coal production and operation to achieve the efficient development of the coal mine. It must rely on low energy consumption, low pollution, low emission and high performance, high efficiency, high benefit of operating mode of low carbon to improve enterprise comprehensive competitiveness.
2. Early large input: without coal pillar continuous mining science system, intelligent thin fully mechanized coal mining technology, downhole coal washing and backfilling technique, and the heavy washing technology, coal gangue power generation technology, and multistage efficient spray flue gas desulfurization technology, cement production and waste heat power generation technology, water source heat pump technology and low carbon technologies such as sewage treatment technology, in really applied to production, preliminary research time and inputs are relatively large.
3. Aging mine's low carbon development mode in our country is still exploring stage: it is not much of running the low-carbon ecological mining development mode of research and exploration of mine in our country at present, more representative of Jizhong Energy, Yan Coal Mine, Fengfeng group, Xishan coal and electricity, etc, in view of the characteristics of the low carbon cycle of ecological mining beneficial exploration. But the few studies of aging mines and practice, can be the object of reference and reference, pioneering.

4.3 *Opportunity analysis*

1. Countries and world environment: from the Kyoto protocol, the UK energy white paper in 2003, the Copenhagen conference in cancun, industries in our country and the world will be focused on the development of low carbon economy.
2. The national policy and financial support: in October 2007, revised through the energy conservation law of the People's Republic of China clearly put forward "the state encourages and supports the development and utilization of new energy and renewable energy", the state will introduce tax preferential policies, financial incentives and market oriented.
3. Group leadership attention: to prolong the life-cycle of the old mines, establishing ecological mining development low carbon operation orientation and target of enterprise development, the coal group will continue to encourage others especially similar caol mine, innovate and practice size for low carbon operation system as the core, the circular economy industrial chain for the soul, and technical support system as the key guarantee of low carbon operation mode, improve coal group's overall competitiveness.

4.4 *Threat analysis*

Carbon economy development goals and the development of high carbon economy reality have formed the dilemma in China's development. energy the body of the coal industry of China are also put forward challenge that can be said to be the of life and death, which is the inherent in the concept of traditional industries and is eliminated for the sunset industry into history, or the transformation idea, forming a new development

concept, conforming to the low carbon economy development trend of a member of the new energy to get new life. This is not just a technical upgrading, more important it is the development of the industry a revolutionary change in concept. Facing the current global inflation expectations, it must be a problem had been dealed with to keep the enterprise value and profit growth, at the same time, technical analysis and implement low carbon ecological mining, construction, operation.

4.5 *SWOT matrix*

Using SWOT matrix to determine the old mining area of low carbon economy development strategy, on the whole the SWOT can be divided into two parts: the first part is the SW, is mainly used to analyze internal conditions, focusing on enterprise's own strength and its comparison with competitors; The second part is the OT, is mainly used to analyze the external conditions, emphasising on the external environment change and the likely impact of enterprises. According to own actual situation in our country and the objective environment, and SO strategy combined settlement, ST strategy combination, combination strategy, WT strategy combinations corresponding countermeasures and Suggestions.

1. SO strategic combination—increase capital investment to build low carbon ecological mining operation
2. ST strategy combination—on the basis of economic growth to implement low carbon ecological operation
3. ST strategy combination—introduce capital investment in technology, will be incorporated into the social benefits of accounting
4. WT strategy combination—technical and economic analysis, the reasonable control of investment proportion

The above SWOT method analysis and the SWOT matrix method, get the following conclusion:

1. From the superiority of the enterprise internal and external opportunity comprehensive consideration, to the development of old mining area of low carbon economy is positive, is in line with the enterprise own development and the national basic policy inevitably.
2. From the perspective of the internal disadvantages of aging mine resources conditions are not ideal, lack of resources, because of that only have to choose a kind of high technology content, low energy consumption, low pollution, low emission and high performance, high efficiency, high benefit model of development. Run construction low carbon ecological mining resources can not only overcome the disadvantage of occurrence condition and improve the resources comprehensive utilization, but also energy conservation and emissions reduction, from "black economy" to "white" transformation.
3. Lack of reference, pioneering is not only the internal disadvantages of construction low carbon ecological mining operation, but the result of the practice on the development of other mines has the important exemplary role of guidance.
4. In the early period of the enterprise investment is larger, according to the input-output analysis of economics, want to get output has to

Table 1. SWOT matrix of old mine's low carbon development.

Internal conditions	(Strength)—internal advantage	(Weakness)—internal disadvantage
	• policy support • feasible technology • reasonableeconomic	• resource conditions features • early large inpu lack of reference and pioneering
(Opportunity)—external opportunities	SO countermeasures	WO countermeasures
• country and the world's environment • national policies and financial support • group attaches the great importance	Increasing financial investment to build low carbon ecological mining operation	Introduction of capital investment in technology, will be incorporated into the social benefits of accounting
(Threat)—external threats	ST countermeasures	WT countermeasures
Carbon economy development goals and enterprise development of the relationship between its growth	realizing low carbon ecological operation on the basis of sustaining economic growth	Technical and economic analysis, reasonable control of investment proportion

be input, proved that the construction of low carbon ecological mining operation of economic and social benefit is very significant.

5. From the perspective of the external threats to deal with low carbon economy development goals and the relationship between the growth of enterprise development, the implementation of coal output and profits "greening", is achievable.

Therefore aging mine construction low carbon mine is feasible, advantage is obvious.

5 CONCLUSIONS

Long mining history, lack of resources, production system aging factors determine the quality and quantity of aging mine resources alone, so it is not realistic to have the advantage in the market competition, must to potentialities of mine development, adhere to the "coal resources eat dry bleed" basic train of thought, improve the comprehensive utilization of coal resources, to achieve low energy consumption, low pollution, low emission and high performance, high efficiency, high benefit (clear and three highs) model of development, with as little as possible of ecological disturbance to realize enterprise low carbon, green, ecological and sustainable development.

Developing low carbon economy is the inevitable choice of aging mine, the main reason has the following three aspects:

1. Aging mine developing low carbon economy fits the requirement of the current low carbon economy development situation at home and abroad;
2. Aging mine developing low carbon economy is in line with the coal group company's overall development and the overall layout;
3. Aging mine developing low carbon economy for the national coal industry similar type of aging mine second development provides a good model and example, has a strong demonstration effect.

In conclusion, developing low carbon economy is aging mine out of all kinds of adverse conditions, through the low carbon transition achieve prolong the mine life cycle of the inevitable choice.

REFERENCES

Lu Gang, et al. 2009. Simulation study on the life cycle identification of the aged coal mine and mine. Journal of Henan Polytechnic University (Natural Science Edition). 2009, 28 (5):659~694.

Ren Yixin, et al. 2008. Construction of circular economy mode of old coal mine. Mining and Metallurgical Engineering. 2008, 28(4):108~113.

Wang Chun, et al. 2006. Research and practice of old coal mine mining technology. Coal Technology, 2006, 25(2):48~50.

Wang Wenjuan. 2011. Study on the coal industrial chain optimization based on low carbon economy. Fudan University, 2011.

Progress in Mine Safety Science and Engineering II – He et al. (Eds)
© 2014 Taylor & Francis Group, London, ISBN 978-1-138-00122-0

Study on the information management mode of occupational hazard supervision

Hongbin Bai & Yifei Weng
North China Institute of Science and Technology, Sanhe City, Hebei Province, P.R. China

ABSTRACT: Regarding domestic occupational hazards and the prevention and treatment of serious occupational hazards, government management loopholes, and corporate occupational hazards sense of strong randomness of the Occupational Health and rating agencies, and many other issues, combined with domestic and international occupational hazards informatization status, this paper proposes the establishment of an occupational hazards management model based on information technology, to achieve information exchange and business integration of the three enterprises, testing bodies, regulatory bodies, government regulators to provide scientific and efficient for testing and evaluation of occupational hazards management tools and adequate basis; effective accumulation of first-hand data on the occupational hazards occupational hazard management for the enterprise to provide strong technical support, provide a rigorous and efficient processes for the evaluation of occupational health rating agencies, to study occupational diseases occur, development, control and prevention of authoritative data.

1 OCCUPATIONAL HAZARDS AND THEIR SEVERITY

Since the reform and opening up, China's economy to achieve high-speed development, energy is the power source of economic development as China's most important form of energy, coal, plays a decisive role in the national economy, but also China's most important primary energy in the primary energy The proportion has remained at about 70%. It can be said that China is the world's largest coal producer and consumer countries. However, with the increase of the raw coal production of coal mining enterprises, over the frequent occurrence of coal mine safety accidents gripping. Relative to the concern of mine accidents, occupational hazards is more like a lingering shadow of death in the head of the coal mining enterprises.

Occupational diseases that affect the health of workers, to cause premature workers lose the ability to work the main factors. Mine occupational hazards in dust (coal dust, rock dust, cement dust, etc.), chemicals (nitrogen oxides, carbon oxides, sulfur dioxide, hydrogen sulfide, etc.) and physical factors (noise, vibration, thermal radiation, high temperature, etc.) three categories. Which is the most serious to dust hazards caused by pneumoconiosis. 2009, 14,495 cases of pneumoconiosis new cases, the CWP and sand lung accounted for 91.89%. The incidence of pneumoconiosis shorten the length of service, the mass of pneumoconiosis have occurred. Actual cases is much higher than the number of reported new cases of occupational diseases is now released from the coverage of about 10% of occupational health surveillance found. Coal mine accident deaths decreased year by year due to pneumoconiosis deaths rose steadily (song 2012). Pneumoconiosis can cause fibrosis of the lungs, this process is irreversible, according to expert estimates, pneumoconiosis caused each year by the economic losses of tens of billions of pneumoconiosis as the representative of occupational disease situation is grim, a heavy burden for enterprises and national will become a social problem can not be ignored.

2 GOVERNMENT, ENTERPRISE AND AGENCY OCCUPATIONAL HAZARD PREVENTION AND CONTROL WORK

2.1 *Government regulatory loopholes exist in the prevention and treatment of occupational hazards*

For some time, the lack of prevention and control of occupational hazards in China's coal mine supervision, coordination between government departments adverse regulatory difficulty. Most of the occupational hazards of long incubation period, in addition to acute poisoning, in most cases not the incidence, regulatory or bad can not be concluded, some two years or even three years

to ten years before problems, which gives after the monitoring of buried "curse".

In response to these circumstances, the State Administration of Work Safety issued in 2010 the second coal mine Workplace Occupational Hazard Prevention Regulations (the total safety supervision coal tune [2010] No. 121). The provisions of the introduction of coal occupational hazards prevention and disposal of the basis for enforcement, shows the determination of the state of the importance of occupational hazards and governance. However, in the process of the implementation of the provisions, we found that the occupational hazards of coal mining enterprises the universality and regulatory monitoring team deficiencies in the quantity and quality of this contradiction is very prominent, there is not enough monitoring of coverage, hazards can not be timely discovered, the corporate existence of significant occupational risk factors can not fully grasp and control can not be an effective and timely manner to eliminate hidden dangers that may cause significant occupational hazards. Meanwhile, in the process of dealing with major occupational hazards, due to the lack of day-to-day monitoring data the regulatory inspectors analyze the cause of the accident and response measures can not be targeted.

2.2 *The enterprise occupational hazards not pay enough attention*

The enterprise legal awareness of the law, practitioners of workers self-protection awareness is poor. Most enterprises have not the prevention of occupational diseases included in the legal term target management responsibility system, establish and improve the prevention and treatment of occupational diseases organizations, institutions or organizations, the system becomes a mere formality, the lack of effective implementation. Some companies still use the traditional and backward technology, facilities and technology, not equipped with the necessary occupational protective equipment, not to grant the necessary labor protection products. Some companies do not enter into labor contracts with employees, to organize the employees medical examination does not accept the monitoring and inspection of the relevant departments. Some practitioners workers simply work to earn money, without regard to occupational hazards, poor self-protection awareness and rights awareness, to pay the cost of the health and even life. Their mobility, instability, and the various occupational hazards increased significantly worsening the damage caused by the labor population health, but also to occupational health supervision increases the difficulty (guo et al. 2008).

2.3 *Occupational health service institutions engaged in occupational health activity behavior for discretion*

At present, some of the technical services practice in accordance with the law consciousness, occupational health work in non-standard behavior, driven by the interests, can not be correct and true reflection of coal mining enterprises the status quo. Parts of the organization professionals an accurate understanding of the standards and norms ability to apply standards or technical specifications using the wrong or non-standard, lead to the conclusion incomplete or error; identified occupational hazards evaluation or evaluation is not given too simple conclusion or conclusions; scope of the evaluation description is too general and not specific enough; simple evaluation of occupational protective measures, the evaluation recommendations pertinence; some occupational health service institutions in the case of staying at home and will be able to complete the so-called "real" report on social harmony and anti-work, occupational, physical and mental health of workers are not at all responsible.

In short, the occurrence of coal mine occupational hazards will have serious consequences. Accidents and occupational diseases directly harm the health of workers and even life-threatening; occupational hazards not only affect the workers and their families, but also affect the safety of the community as a whole, stable; occupational hazards will be caused huge losses to the national economy; excessive occupational hazards accident, serious damage to the international image of our country, is not conducive to international exchanges. Therefore, the establishment of a coal mine occupational hazard assessment and management system, the the contact government occupational hazards regulatory authorities, occupational health services and coal mining enterprises, for the evaluation and supervision of occupational diseases, as well as on the occupational disease prevention and research has great practical significance.

3 RESEARCH PROGRESS

3.1 *Foreign occupational hazard information systems research status*

With its state-of-the-art software and hardware development and the development of the advantages of the developed countries in terms of supervision of occupational hazards has been in a leading position, are more representative of countries such as United States, Australia and so on. They have set up their own occupational hazard supervision information system. In addi-

tion, many other countries have established their respective occupational hazard supervision information system. In Brazil, for example, is currently being implemented to enhance Brazil occupational health and safety "(Enhancement of Occupational Health and Safety in Brazilian Industry) (referred to EOHSBI), the project by the Brazilian National Institute of Industrial Social Service, the Canadian Centre for Occupational Health and Safety Association shared.

Developed countries, occupational health information system main contents include:

- Detection and evaluation of industrial establishments, occupational hazards.
- In the industrial field collection, recording and analysis of accidents, injuries, illness, and death data.
- The development of the industrial sector occupational health database to declare occupational health practices and programs.
- The establishment of occupational health information system, and its operations sustained, effective. To meet the industry, epidemiological and health requirements.

3.2 *Occupational hazards information systems research status*

In the country, the widespread implementation of the technology and application-oriented research projects has laid a good technical foundation. First, the of domestic occupational injury hazard classification and grading monitoring technology research, has achieved some success, the results of their research has been started in some provinces and cities learn from the implementation; Second, the current multi-level, multi-permissions transmission technology of network and information security has become increasingly mature, widely used in many government departments; Third, China's existing statistical indicators of occupational diseases has been applied for many years (wang & guo 2011). However, in high-risk industries, such as coal mines, non-coal mines, hazardous chemicals, and other industries, similar occupational hazard testing and evaluation system there is no national, former National Security Administration of the online occupational hazard reporting system just to stay in the information one-way current level, can not play a regulatory role.

4 OCCUPATIONAL HAZARDS INFORMATION MANAGEMENT PLATFORM

By means of information, establish a set of integrated regulators, intermediaries, enterprise management platform to collect the enterprise occupational hazards monitoring data, and occupational hazards analysis of data, achieve regulatory authorities to obtain information for the management of occupational hazards unified management, data analysis, decision support, implementation of the results and evaluation work, to tease out a set of occupational hazards regulatory management model, and to promote the country to other high-risk industries, promotion of safe production major accident prevention is of great practical significance and strategic significance.

By combing the existing occupational hazard supervision work, the platform should have the following features:

- The platform should support automatic, semi-automatic and manual matching of data collection methods. For enterprises with comprehensive data acquisition conditions, support automatic monitoring system installed in workplaces, automatically obtain the relevant occupational hazard data, and real-time, reliable, convenient transmitted to the monitoring center, connect to the network server to receive and enter the occupational hazards regulatory information the database server of the system to achieve real-time monitoring of the occupational hazards source-to-multipoint (occupational hazard source monitoring points) state parameters (central station). With some data collection capabilities but can not work on-site networked enterprise, support for portable mobile device to import data; enterprises do not have the data acquisition conditions, you can use the manual entry of data collected system data.
- The platform should support the collected data and system settings of indicators for automatic comparison and show the way different than the calculated results, the use of graphics, SMS, mail warning. Early warning information can be automatically fed back to the inspection department, regulators, the system will automatically prompt and dealt with accordingly. On the other hand, early warning information can be connected to the enterprise early warning sensor display warning status and readings remind the attention of the staff.
- The platform should support the construction project occupational health "three simultaneous" management functions, supervision of the project design, construction, construction of different periods of pre-evaluation of occupational hazards, occupational hazards monographs for design, occupational hazards assessment and should have support issue occupational hazards pre-assessment, control assessment, now rating, daily inspection report of the occupational

hazards, guidance coal mine occupational health service agencies to provide technical services to the coal mining enterprises, "Occupational Disease Prevention Law" requires the timely publication of the occupational hazards of day-to-day test results.

- The platform should support the inspection activities of the regulatory authorities, test results, treatment advice, rectification, analysis summarizing cycle monitoring and management, to provide strong information security management work.
- The platform should be the regulatory authorities, testing organizations monitoring the basic information. Such as regulatory authorities the hierarchical regulatory functions of the enterprise, to distinguish between different levels of enterprises have different functions. Lower risk enterprises, the main guidance, to provide occupational hazard prevention and control of information, to promote self-discipline; guidance and oversight to the medium-risk businesses, in order to facilitate enterprises to further improve the management system and preventive measures; compared with the risk high enterprises, strengthen supervision, to encourage enterprises to work hard to rectify, to take effective engineering technology, personal protection and organizational management and other measures to reduce the risk of occupational hazards and gradually establish a more comprehensive occupational health management system and preventive measures. To focus the work, and the limited resources to the most needed link.
- The platform should support extensive reporting capabilities. To provide users with a variety of testing the occupational hazards indicators, activities, accidents, time, regional dimensions, graphs, line charts, bar charts, pie picture shows the means of expression, through data analysis, data drill reports and statistical reports to guide the behavior of industrial enterprises, assist with the monitoring and management sector decision-making.
- The platform should provide the rules and norms of the industry. Such as occupational health laws and regulations of the database, the database of occupational health standards and technical specifications, technical measures of prevention and treatment of occupational diseases, occupational hazards case, the auxiliary enterprises to standardize its occupational hazards management systems.

5 CONCLUSION

The platform-oriented factories and mines, testing agencies, regulatory authorities, provide different business functions, from the establishment of the occupational hazards intermediaries management model, data acquisition, authentication management, indicators and early warning, detection report, analysis of statistics and other aspects of full cycle Ocupational hazards management, factories and mines, inspection department, the exchange of information among regulatory authorities and service interworking, to achieve regulatory authorities for the testing and evaluation of occupational hazards scientific and efficient management tools and sufficient basis; system of occupational hazards first effective accumulation of first-hand data provide strong technical support, to study the occurrence of occupational diseases, occupational hazards management, development, control, prevention authoritative data.

ACKNOWLEDGEMENTS

This work was financially supported by Shanxi Coalmine Safety Product Examination Center as a scientific research project (2013). Meanwhile I appreciate Prof. & Director Song Hongzhi's help for this thesis.

REFERENCES

Guo Jinyu, Sun Qinyun & Zhang Zhongbin. 2008. Analysis and research on influencing factors of in occupational hazard supervisions. *Journal of Safety Science and Technology* 5(4): 91~95.

Song Shengcheng. 2012. Investigation on the status of coal dust workers health. *Chinese Journal of Industrial Hygiene and Occupational Diseases* 30(2):158~161.

Wang Xueni & Guo Jinping. 2011. Study on the Occupational Hazards Evaluation System of Underground Mine. *METAL MINE* (4):130~133.

Progress in Mine Safety Science and Engineering II – He et al. (Eds)
© 2014 Taylor & Francis Group, London, ISBN 978-1-138-00122-0

Study on factors of asphyxiation & poisoning and its preventive measures in underground mining

Guodong Mei
China Academy of Safety Science and Technology, Chaoyang, Beijing, China

ABSTRACT: The data on China's accidents of blasting-fume asphyxiation & poisoning in metal and non-metal underground mining from 2001 to 2012 has been analyzed. The death toll from asphyxiation & poisoning totaled to the fifth highest among all 20 categories of accidents. We made a study on local ventilation and the distribution of airflow under different distances from air duct outlet to tunneling end face, and found that forced local ventilation functioned better than withdraw-able blasting-fume dilution. This paper proposes a sequence model of blasting-fume asphyxiation & poisoning, and accordingly suggests a few technical measures to dispel the blasting-fume, e.g., adopting explosives of zero-oxygen balance and fine granularity and adding inhibitors. It also makes suggestions to purify the blasting-fume by neutralizers and gas purification equipment. Five management measures are proposed in this paper to help reduce and control the accidents of blasting-fume asphyxiation & poisoning.

1 PREFACE

During the mining operations in metal and non-metal underground mines, explosives are necessary tunneling roadways or blast mining. Speaking of composition, explosives are usually made of four elements, i.e., carbon (C), hydrogen (H), oxygen (O) and nitrogen (N), wherein carbon and hydrogen are combustible elements and oxygen is a combustion element (WANG Xuguang 2010, PEI Haixing 2008) In essence, explosion is a violent process of oxidation-reduction reaction between combustible elements and combustion elements. In the process, CO_2, CO, H_2O and N_2 are generated along with a large emission of heat. According to the amount of oxygen, explosives can be categorized to zero oxygen balance, positive oxygen balance and negative oxygen balance (SU Lijun 2007). In zero oxygen balance, the oxygen contained in explosives is just enough to completely oxidize the combustible elements with H_2O and CO_2 as products; in negative oxygen balance, the oxygen contained in explosives is insufficient to completely oxidize the combustible elements, and there will be products of CO and H_2; and in positive oxygen balance, the contained oxygen still has remains after completely oxidize the combustible elements, so there will be NO, NO_2 and other gases (LIANG Feng 2005, WANG Yujun 2009).

When the working face of underground mining blasts, many factors are subject to changes, such as blasting conditions, detonation mode, blast-hole depth and layout, loading dose and the amount of stemming, so explosives designed as zero oxygen balance are actually explored in the manner of positive or negative oxygen balance. Therefore, the blasting-fume will contain toxic gases, mainly carbon monoxide and nitrogen oxides. When the ore contains sulfur or sulfur compounds, the blasting-fume will contain toxic gases such as hydrogen sulfide and sulfur dioxide, which impose great danger to people who breathe in a certain amount of such toxic gases. Its symptoms will be as minor as headaches, palpitations, vomiting, weakness and fainting, or as heavy as spasm, respiratory arrest and even death (REN Chunfang et al. 2007).

From 2001 to 2012, China's non-coal mines claimed 1662 lives due to blasting-fume asphyxiation & poisoning, averagely more than 138 deaths each year. It accounts for 7.15 percent of the total mortality, ranking the fifth highest among various types of accidents (State Administration of Work Safety 2013). This paper is to analyze the factors causing blasting-fume asphyxiation & poisoning in metal and non-metal underground mining as well as the impact factors. It also proposes appropriate techniques and administrative & preventive measures to reduce blasting-fume asphyxiation & poisoning accidents and steadily improve the production safety of metal and non-metal mining.

2 STATE ADMINISTRATION OF WORK SAFETY

As can be seen from the Figure 1, in 12 years, there were 18,401 accidents, which claimed 23,237 lives.

Averagely, it presented an annual rate of 1533.4 accidents and 1,936.4 deaths. Among them, there were 721 asphyxiation & poisoning accidents and 1662 deaths. Each year on average, there were about 60 accidents and over 139 deaths.

Asphyxiation & poisoning ranked fifth, only second to Collapse, Hit by an object, Cave-in and Falls Accident. However, since 2006, among heavy accidents with more than 3 deaths at one time, there were 87 asphyxiation & poisoning accidents caused by fire and blasting-fume, with a death toll reaching 348, respectively accounting for 36.9% of heavy underground mining accidents and 47.2% of total mortality. Both percentages ranked highest among underground mining accidents. As can be seen, asphyxiation & poisoning was one of the chief culprits causing group death and injuries in metal and non-metal mining. In the current task of production safety, top priority should be placed on effectively preventing asphyxiation & poisoning accidents in underground mining and reducing the total number of underground mining accidents.

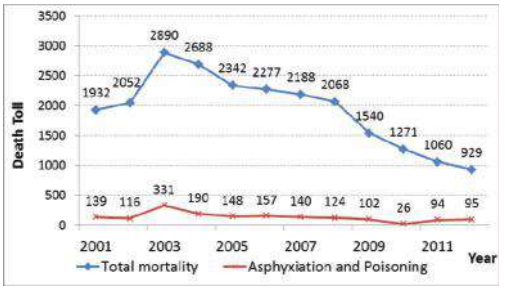


Figure 1. The trend of total mortality and the death toll from asphyxiation & poisoning from 2001 to 2012 in China.

3 ANALYSIS ON THE IMPACT FACTORS IN ASPHYXIATION & POISONING ACCIDENTS

3.1 *The impact of the ventilation system*

Numerical simulation has been adopted to analyze the impact of local ventilation methods. Figure 2 and Figure 3 show the distribution of airflow in tunneling roadways respectively with forced ventilation and withdraw-able ventilation, where the roadway had a length of 100 m and a height of 2.4 m; the diameter of air duct was 0.4; and the distance from air duct outlet to tunneling end face was set to 5 m.

When the distance from air duct outlet to tunneling end face was 5 m, fresh air could reach the tunneling end face and form a vortex in the front area of the roadway (from Figure 2). The flow direction of the vortex was conducive for fresh air to form a convection mix with blasting-fume gases and then get out of the roadway. When adopting withdraw-able ventilation (from Figure 3), the air in the roadway was discharged outwardly, forming a vortex at the tunneling end. But the direction of vortex rotation was not conducive to the diffusion of blasting-fume gases near the tunneling end face, and the negative pressure at the entrance of air duct only impacted a small scope. By comparison we can see that, forced ventilation has better effect of blasting-fume dilution, and it can fast dilute the blasting-fume to safety concentration. Therefore, in the actual production of mine tunneling, we should maximize the use of forced ventilation.

The physical model, the distance from air duct outlet to tunneling end face was respectively set to 5 m, 35 m and 65 m, have been simulated. The results are shown in Figure 4, Figure 5 and Figure 6.

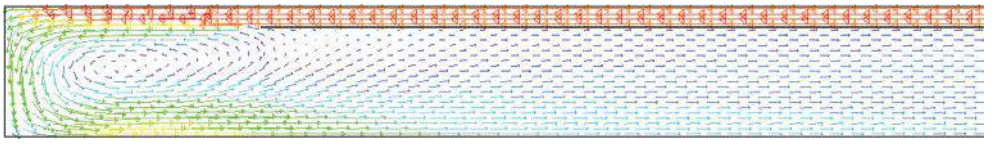


Figure 2. The distribution of airflow in the tunneling roadway with forced ventilation.

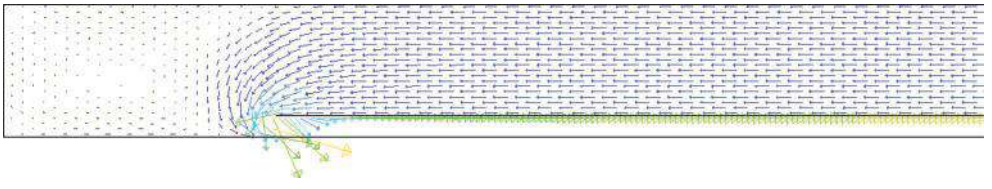


Figure 3. The distribution of airflow in the tunneling roadway with withdraw-able ventilation.

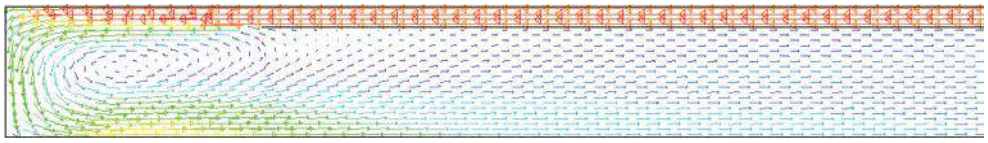


Figure 4. The distribution pattern of airflow when the distance set to 5 m.

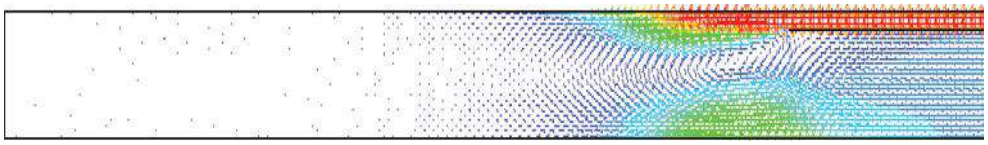


Figure 5. The distribution pattern of airflow when the distance was set to 35 m.

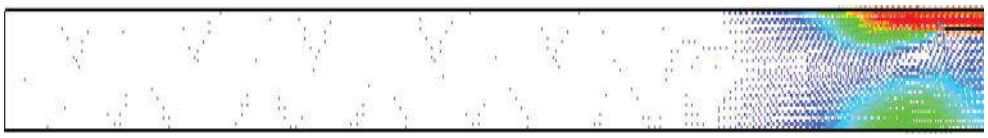


Figure 6. The distribution pattern of airflow when the distance was set to 65 m.

When the distance from air duct outlet to tunneling end face was set to 5 m, the airflow could reach the tunneling end face and it formed a vortex in the vicinity of the tunneling end face. The direction of vortex was conducive to the diffusion of blasting-fume gases. When the above distance was set to 35 m and 65 m, there was a vortex formed in the vicinity of the air duct outlet. It facilitated the diffusion of blasting-fume gases around the area, but the entire front of the roadway widely saw a low rate of air flow, and there was a weak "secondary vortex", whose direction was adverse to the dilution of blasting-fume in this region. The above analysis shows that, as the distance from air duct outlet to tunneling end face increases, the amount of fresh air in the front of roadway will be reduced, and there will be two vortexes rotating in opposite directions. The vortex which is close to the tunneling end face is not conducive to the diffusion and dilution of blasting-fume.

3.2 *The impact of management factors*

The accidents of blasting-fume asphyxiation & poisoning can be largely attributed to objective insecurities in the production process. The direct cause of asphyxiation & poisoning accidents includes people's unsafe behavior (e.g., insufficient ventilation time, venturing into the working face against rules, etc.) and physical insecurity (e.g., malfunction of local fans, the failure to remove blasting-fume). However, the root resulting in "human errors" and "physical failures" can usually be traced to management flaws. Although mismanagement is an indirect cause, it is a background factor that often turns out to be the radical cause of asphyxiation & poisoning accidents.

As shown in Table 1 and Figure 7, a causation sequence model of asphyxiation & poisoning accidents is proposed according to Heinrich's and Adams' accident causation sequence theories (JIAO Xia 2007, SUI Pengcheng et al. 2005). Such model is targeted to blasting-fume asphyxiation & poisoning accidents.

The unsafe behavior of miners (mainly refers to the blasters working on mining face and related workers) and the physical insecurities on mining work face and other field mistakes were due to the mismanagement of mining managers and accident-preventing staff (security officers, blasters, team leaders, leaders taking charge of mining). The mining production safety and the work for accident prevention are decisively impacted by managers' errors or omissions in their management and mining leaders' wrong decisions or lack of decision. Mismanagement reflects the problems in the system of mining enterprise management. It relates to the management system, namely, how to carry out organized management of production safety, how to determine management objectives, how to plan and achieve established goals, and other issues. Management system reflects the purposes, goals and norms of the mining leader, who is the center of decision-making. I determines the work priorities, benchmarks and guidelines for

Table 1. Asphyxiation & poisoning accidents based on Adams' accident-causing theory.

Management system	Mismanagement		Field mistakes	Accidents	Injuries or damages
Target	Managers' wrong decisions or lack of decision	Security professionals' wrong decisions or no decision	Unsafe behavior		Injuries
Organization	Policy target authority responsibility duty	Behavior responsibility authority rules guide	Unsafe state	Accidents	Damages
Functional operation	Attentive scope permission grants	Initiatives Positivity Operational activities			

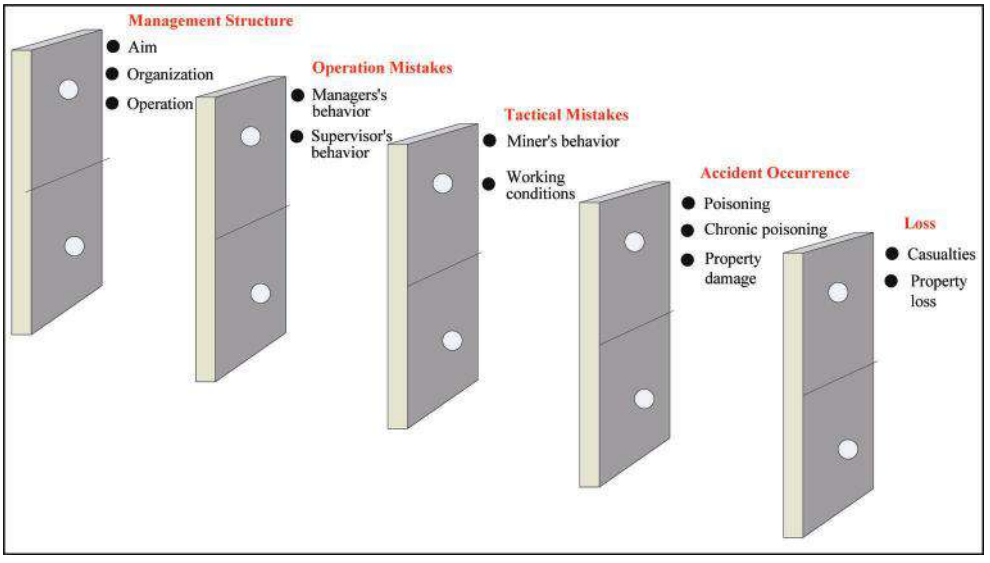


Figure 7. The sequence model of asphyxiation & poisoning accidents based on Adams' accident causation sequence theory.

managers at all levels to ensure safety production and organize work.

4 PREVENTION MEASURES FOR ASPHYXIATION & POISONING ACCIDENTS

4.1 *Technical measures*

A) Measures for eliminating and purifying toxic blasting-fume gases
The fundamental measure to prevent blasting-fume asphyxiation & poisoning is to reduce or eliminate the produce of toxic blasting blasting-fume gases, mainly including:
a) Technical measures for eliminating blasting-fume
First, choose explosives with good quality and strictly control the dose of a detonation, e.g., adopting explosives of zero-oxygen balance and fine granularity and ensuring the quality of explosive processing or adding active catalysts of alkali metal salts. Another measure is to replace clay mud with foam mud to eliminate blasting-fume, e.g., adding manganese dioxide (MnO_2) into 1% lye to turn it into colloidal liquid suspension and stuffing it in a polyethylene bag as stemming.
b) Technical measures for purifying blasting-fume
First, choose a neutralizer to eliminate toxic blasting-fume gases, e.g., in the roadway of working face after blasting, using a compressor to spray a solution of 0.5% MnOH or the 20th-mesh hydrated lime to remove NO_2. Second, using a gas purification apparatus to eliminate toxic gases, e.g., putting hoplite with granularity of 3 mm (main components include MnO_2, CuO) and soda lime with granularity of 3~5 mm onto the working

face and starting the air blower to have the CO and NO_2 in blasting-fume changed into absorbable CO_2 by making it interact with the chemicals in the filter.

c) Management measures for eliminating or purifying blasting-fume
First, strengthen the management of explosives' transport and storage and ensure that the moisture does not exceed 0.5%. Second, ensure the length and quality of blast-hole stemming. Third, adopt water infusion blasting or shooting spray. The last is to apply back detonation.

B) Optimization and control technology for ventilation system
If the concentration of toxic blasting-fume gases remains the same, an essential measure for preventing blasting-fume asphyxiation & poisoning in underground mining is to dilute the concentration of toxic blasting-fume gases by effective ventilation. First, optimize the system of mines' ventilation system, ensure effective ventilation of all mining faces, and ensure the toxic gases can be diluted after blasting within a prescribed time. Second, improve the systems of local ventilation and local air blower is a must for the ventilation in poorly ventilated pits and single-head tunneling roadway. At last, strengthen the management of ventilation structures and timely fix failures to ensure normal operation of equipment.

4.2 *Management measures*

a) Setting centralized blasting time
Blasting operators shall make the blast in strict accordance with the prescribed time, and other operators must be evacuated from the blasting danger zone within a prescribed time.

b) Enhancing blasting vigilance
Vigilance shall be in strict accordance with the provisions of blasting procedures, and all channels leading to working faces of blasting operations shall hang signs and be on sentry duty. The vigilance guards must make sure that no irrelevant person is left in areas affected by the blasting or in adjacent working faces.

c) Making more strict measures to organize blasting
When there are more than two people in charge the blasting, a responsible person should be designated. Understand and grasp the relation between blasting operation-points and surrounding working faces, make a co-ordination and devise sound security measures and organizational measures.

d) Strengthening safety training
Improve blasting techniques and safety training, enhance the quality of blasting operators and increase the underground operators' self-defense capability to prevent blasting-fume asphyxiation & poisoning.

e) Individual protection
Operators of underground mining must carry a self-rescuer with them. A filtering self-rescuer is composed of a headband, shell, exhalation valve, dust filter cartridge, nose clip, tooth bite, oral tools, heat exchangers, chin strap, catalysts, coarse filters and other equipment. The filtering self-rescuer should meet the requirements of GB8159 Filtering Self-rescuer of Carbon Monoxide for Mining.

5 CONCLUSION

a) Blasting-fume asphyxiation & poisoning is a main type of metal and non-metal underground mining accidents, and its total mortality reaches the fifth highest among the 20 categories of accidents. It ranks first among those accidents claiming more three lives at one time. With an average annual death toll of more than 139 people, asphyxiation & poisoning is one of the chief culprits causing group death and injuries, and top priority should be placed on production safety of China's underground mining.

b) Forced ventilation dilution effect of blasting-fume than draw-well, will be able to quickly dilute to safe blasting-fume concentration below the concentration, so the actual production of the mine excavation should maximize the use of forced ventilation.

c) As the distance from air duct outlet to tunneling end face increases, there will be two vortexes rotating in opposite directions. The vortex which is close to the tunneling end face is not conducive to the diffusion and dilution of blasting-fume. From the tunneling end face to the exit of roadway, the distribution of blasting-fume in the entire roadway can be divided into three regions: the retention zone of blasting-fume, the zone for ready diffusion of blasting-fume, and the zone for diffusion of blasting-fume.

d) The direct cause of asphyxiation & poisoning accidents can be attributed to field mistakes including people's unsafe behavior and some physical insecurity, and the field mistakes such as unsafe acts and unsafe status of mining working face were due to the mismanagement of mining managers and accident-preventing staff.

e) In order to reduce asphyxiation & poisoning accidents, we must focus on the root measures to eliminate, suppress and reduce blasting-fume, and develop concrete and feasible measures, e.g., improving the selection and adoption

of explosives and its blasting conditions, adding neutralizer, installing purification devices, enhancing ventilation and establishing critical operations of blasting-fume inspection. Only by doing so can we effectively prevent and control asphyxiation & poisoning accidents.

ACKNOWLEDGEMENTS

This research was funded by the projects of special funds in basic research and operation of China Academy of Safety Science & Technology (2013JBKY01) and the major project of the Ministry of Science and Technology of China (2011ZX05040-001).

REFERENCES

Jiao Xia. 2007. Discussion on the Inspiration of Heinrich Causal Chain Theory on the Safety Management of Enterprise. SCI—*Tech Information Development and Economy* 17(36):181–182.

Liang Feng. 2005. Application of FTA on Poisoning Choke. *Journal of Safety Science and Technology* 1(2):74–76.

Pei Haixing. 2008. Present Situation and Development Trend of Explosives for Metallurgic Mines. *Express Information of Mining Industry* 469(5):7–9.

Ren Chunfang et al. 2007. Compiling the Emergency Rescue Preplan for Blasting Fume Poisoning Accident. *Yunnan Metallurgy* 36(4):3–7.

State Administration of Work Safety. 2013. Notice on Special Management of ant-poisoning in underground metal and nonmetal mines.

Su Lijun & Lu Wenbo. 2000. Study on Diffusion of Blasting Fumes and Ventilation Technique during Construction of Underground Tunnel. *Blasting* 7(1):1–6.

Sui Pengcheng et al. 2005. *Safety Principle*: 33–40. Beijing: Chemical Industry Press.

Wang Xuguang. 2010. *Handbook of Blasting*: 3–25. Beijing: Metallurgical Industry Press.

Wang Yujun et al. 2009. Fault Tree Analysis of Explosion Smoke Poisoning Accidents at Heading Face. *Journal of Kunming Metallurgy College* 25(1):5–8.

8 *Petroleum and natural gas exploitation*

This page intentionally left blank

Progress in Mine Safety Science and Engineering II – He et al. (Eds)
© 2014 Taylor & Francis Group, London, ISBN 978-1-138-00122-0

Preventive maintenance planning strategy of natural gas pipelines based on risk inspection

Hai-Xia Li, Wen-He Wang & Bao-Jiang Sun
Chongqing University of Science and Technology, Chongqing, China

Rui-Zhi Dong
China University of Petroleum, Qingdao, Shandong Province, China

ABSTRACT: Fuel gas pipelines, as the lifelines of cities, are highly vulnerable to sudden and disastrous accidents due to the factors of long-term operation, material aging and corrosion, environmental changes, system capability expansion and urbanization etc. Moreover, gas lines show higher risks as time changes, accordingly to prepare a gas line Preventive maintenance planning is of great significance for guaranteeing the security, functionality and economy of the gas lines. Taking the gas lines in some area, by using risk-based inspection, this paper performs a quantitative analysis on the eight main gas lines in the research area. Based on the risk levels, Reliability-Centered Maintenance is employed for regular inspection and maintenance of the eight gas lines. The results indicate that Risk-level-based preventive maintenance planning features desirable economy and applicability, offering valuable reference to the risk predication and maintenance of city lifelines.

1 INTRODUCTION

Urban gas pipelines, together with water & power supply systems, and traffic roads, constitute the public infrastructures of modern cities, and are an important component of urban lifelines. However, due to the factors of long-term operation, material aging and corrosion, environmental changes, system capability expansion and urbanization etc., gas pipelines are highly vulnerable to sudden and disastrous accidents, making the security issue of gas lines get worse and worse. In the entire life cycle of the gas pipeline network, the accident rate of urban gas lines follows a bathtub curve as time goes by (Li 2006, Dai & Kang 2001). Since the fault probability of urban Filter area takes three perspectives into consideration: gas lines varies with the use age, to prepare a gas line Preventive maintenance planning is of great significance for guaranteeing the security, functionality and economy of the gas lines. Therefore, it is necessary and significant to conduct researches on risk inspection and preventive maintenance of gas line network.

Preventive maintenance refers to inspection, test and varied maintenance activities performed in the specified state of the devices so as to discover fault signs and to avoid fault occurrence. Reliability-Centered Maintenance (RCM) follows a basic thread: performing a function and fault analysis of the devices, understanding the fault consequence clearly, using normalized logical decision to determine the preventive maintenance measures of different failures and faults. Preparation of preventive maintenance plan based on RCM conduces to cost saving since it focuses on key devices or devices with high reliabilities, accordingly achieving significant effect (Sunil 2008, Guo et al. 2009).

In this Paper, based on the traditional RCM, the concept of risk and risk matrix is introduced into the decision-making flow of RCM, and the risk matrix diagram is generated based on comprehensive consideration of device security, mission fulfillment and economy. Furthermore, the traditional RCM decision making logics is improved in order to enhance the effectiveness and precision of analysis process, to work out reasonable and scientific preventive maintenance period for gas lines and to achieve unification of economic profit and security (Das et al. 2011).

2 RISK-BASED RCM PREVENTIVE MAINTENANCE PLANNING

2.1 *Basic concept of risk-based RCM*

Risk-based RCM is to divide the traditional RCM decision-making process into two parts: filtration area and decision-making area. Firstly, if some fault mode brings minor risk and limited economic

loss, then it is not worthy of specially-organized maintenance. Next, if the fault mode shows no degeneration sign (random fault), then it is unnecessary to consider preventive maintenance measures. Regarding the cost and degradation in the transition area, any trained professional engineers with experience in using the device are able to give a consistent answer. If some risk is significantly high or low, then the analytic flow can be continued with answers of "yes/no", and if there is any doubt about any risk, risk matrix diagram can be used for detailed analysis (Figure 1). If the risk level is high or midhigh, then analysis in decision area should be performed, yet for low risk level, the answer to risk should be "no" (Chen & Gong 2006, Zhang 2008).

The goal of providing a decision area in decision making process is for the convenience of choosing the best maintenance method corresponding to the fault mode. As the majority of less important issues (such as simple function degradation) have been eliminated in the filter area, analysis in the decision area will be more specific and purposeful by contrast with the traditional RCM. Based on the RBI-based analysis of pipelines, different maintenance plans are worked out for pipelines with different fault probability and consequent influences in accordance with the varied degree of security, mission fulfillment and economy and based on RCM strategy.

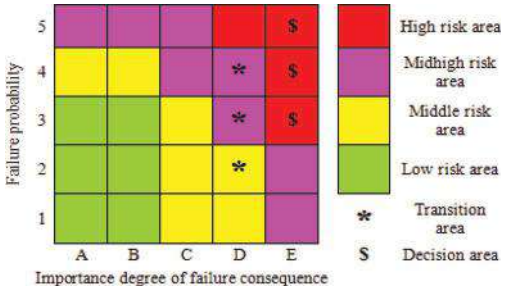


Figure 1. Risk matrix diagram.

2.2 *Risk level defining of each functional component*

Regarding the consequent influences of RCM component (here pipe wall, connectors and valves are selected) on the whole devices, there are influences on security, mission fulfillment and economy. The content of maintenance work type varied with the consequent influences. The introduction of risk concept actually indicates that the severity of three different consequent influences can be divided into different risk levels. For the convenience of statistics, the fault probability and consequence are classified into five degrees (as shown in Table 1 and 2) (Zhang 2008).

Based on the above level classification of risk probability and consequence, the risk level of each component is defined in accordance with the failure modes and consequent influence (Table 3). After determination of risk level, a preliminary judgment can be conducted. For low-risk area, generally it is unnecessary to adopt any measures and the devices can be used continuously with proper extension of inspection time intervals; With respect to the middle risk area, the devices can be used within the specified inspection period, yet more importance should be attached to inspection or monitoring with moderate arrangement of maintenance plans, wherein the determination of inspection period subject to the fact that the risk level remains middle level in the next inspection; As for the midhigh risk area, the reasons for the risks should be analyzed, and the inspection time intervals should be shortened, while the main positions causing midhigh risk should be restricted, or

Table 1. Failure probability level classification.

Probability	Fault probability	Management measures	Inspection and remedy measures
5	Occur frequently in normal circumstances	Never inspect, lack of operation procedures	No measures or measures never been used
4	Occur frequently or as anticipated	Inspect occasionally, with operation procedures which is occasionally implemented (or consummated in content)	With measures which is only a part or unconsummated
3	Occur frequently in the past or in abnormal circumstances	Inspect monthly, with operation procedures which are just partially implemented	With measures which are often not used effectively
2	Occur occasionally in the past	Inspect weekly, with operation procedures which are not implemented occasionally	With remedies which fails to function well or makes mistakes occasionally.
1	Highly unlikely to occur	Inspect daily, with operation procedures which are strictly implemented	With effective preventive control measures

Table 2. Failure consequence level classification.

Consequence levels	Casualties (security)	Property damage (economy)	Downtime (mission fulfillment)	RCM influences
E	Cause death, permanent disability, permanent incapacitated	(10 million Yuan	Downtime of over 3 devices for more than 3 days	Severe influences on security
D	Partial loss of ability to work and material injuries	10–1 million Yuan	Downtime of 2 devices for 2 days	Influences on Security
C	Minor injuries, (amputations, fractures, loss of hearing, and chronic diseases, etc.)	1 million–100 thousand Yuan	Downtime of 1 device for 1 day	Influences on mission fulfillment
B	Slight traumas, and short-time physical discomfortableness	Less than 100 thousand Yuan	Downtime of partial device for half-day	Influences on economy
A	No injury	No	No downtime	No influence

Table 3. Risk levels of the component of gas pipelines.

Items	Failure mode	Influence consequences	Risk probability	Risk consequences
Pipe wall	Inner wall corrosion	Corrosion reduction	3	E
	External wall corrosion	Corrosion reduction	3	E
	Pitting corrosion of wall	Gas leaks	2	D
Connectors	Corrosion	Corrosion reduction	2	A
	Wearing	Gas transmission efficiency decrease	1	A
	Scaling	Gas transmission blocked	1	C
Valve	Corrosion	Corrosion reduction	2	B
	Inflexible, jammed	Security performance reduces	1	B

Table 4. Risk-based RCM establishment.

Risk and influences	Maintenance type	Specific maintenance measures
1/A	Regular abandonment	Replacement of worn-out connector
1/B	Preventive Maintenance	Preventive Maintenance, and lubricate in time
1/C	Preventive Maintenance	Maintenance and cleaning of impurities and oil contaminations
2/A	Regular monitoring and maintenance	Regular monitoring and anti-corrosive coating thickening
2/B	Regular monitoring and maintenance	Regular monitoring and anti-corrosive coating thickening
2/D	Regular abandonment	Replacement of perforated pipelines
3/E	Regular abandonment	Replacement of the pipelines with severe corrosions, and anti-corrosive coating thickening

particular inspection and control should be performed if using such risky positions in case of any accidents, and the inspection method used should be highly effective. For high risk area, it should be halted immediately to implement maintenance or replacement so as to eliminate the factors causing high risks and to control the risk within a middle or lower level (Chen & Gong 2006, Zhang 2008).

2.3 *Establishment of RCM maintenance types*

The varied risk levels of different functional components in the pipeline network are specified, then after preliminary decision making of the countermeasures, RCM final decision analysis is performed in combination with the risk matrix diagram (Table 4). The same maintenance type or replacement strategy can be applied to components at the same high risk level, different maintenance types should be used based on the specific failures and judgment on logic decision diagram. Maintenance types are generally divided into preventive maintenance, on-condition maintenance and potential risk maintenance and inspection. Preventive maintenance therein include regular abandonment, and regular maintenance.

2.4 *Determination of the maintenance time interval*

After establishing the maintenance types, the maintenance time interval should be determined. Maintenance time interval refers to the interval between the maintenance work and inspection. Maintenance time interval directly influences the security and economy of devices. Over long maintenance time interval may fail to guarantee the security and usability of devices for those faults bringing consequences in security and usability. As for the fault with consequences in economy, over short or long maintenance time interval will influence the economy. When new devices come into service, due to the lack of information, it is hard to determine the maintenance time interval. Accordingly a conservative initial maintenance interval will be established based on the former experience. Therefore, the initially established time interval are conservative and will be revised accordingly with the accumulation of information during the use process of devices (Chen & Gong 2006, Zhang 2008, Tan et al. 2010).

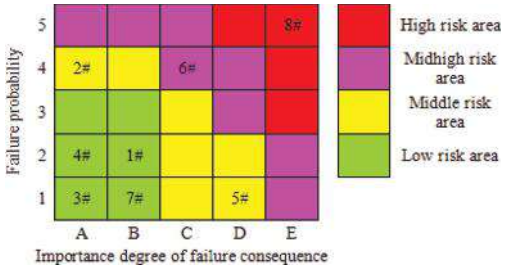


Figure 2. Risk matrix diagram of 8 pipes.

3 CASE ANALYSIS

Taking the gas pipeline network in some area as the research object. In this paper, the risk matrix diagram (Figure 2) is cited in order to plan the preventive maintenance of the 8 pipelines.

Table 5 shows the risk level standards. The results indicate that: 8# pipeline should be replaced partially or wholly because of its high risk level and severe pipeline corrosion; 6# pipeline should be provided with regular inspection with an interval of about one and a half years, and its anti-corrosion wall should be thickened; The rest 6 pipelines are at a low risk level, thus their test interval can be extended with regular inspection and maintenance (Table 6).

4 CONCLUSIONS

1. During the life cycle of urban gas pipes, the accident rate follows the principle of bathtub curve. To deal with the pipelines with high risk

Table 5. Risk levels.

Risk levels	Device inspection strategies
High risk	Reinforce management, implement rectification, strength monitoring, eliminating potential risks, perform annual inspection, and increase the inspection frequency if necessary
Midhigh risks	On-line monitoring and non-destructive testing; once a year
Middle risks	Regular inspection and maintenance, regular comprehensive examination, inspection frequency can be once every two years
Low risks	Reduce inspection, extend the inspection interval, sampling inspection is also applicable, inspection frequency can be once every three years

Table 6. Maintenance plan of gas pipe network.

Items	Specific Maintenance rules	Maintenance interval.
8# pipe	Replacement of the perforating pipe	Require replacement
	Replacement of badly corroded connectors	Require replacement
	Replacement of fault valves	Require replacement
6# pipe	Replacement of pipe with badly corroded wall	Require replacement
	Replacement of badly corroded connectors	Once every 1–1.5 years
	Regular monitoring of valve and thickening of anti-corrosion layer	Once every 1.5 years
Pipe 2, 5#	Thickening of anti-corrosion layer for the badly corroded pipes	Once every 2 years
	Thickening of anti-corrosion layer of connectors, regular decaling	Once every 2.5 years
	Regular monitoring of valves	Once every 3 years
Pipe 1, 3, 4, 7#	Regularly monitoring and data recording	Once every 3 years

levels, preventive maintenance plan is proposed by giving consideration to the maintenance experience of relevant components and the truth that over long preventive maintenance period may increase the accident rate and risk of gas pipe network, while over short preventive maintenance period may result in more costs for maintenance and inspection.

2. The results of case indicate that: 8# pipeline should be replaced partially or wholly because of its high risk level and severe pipeline corrosion; 6# pipeline should be provided with regular inspection with an interval of about one and a half years, and its anti-corrosion wall should be thickened; The rest six pipelines are at a low risk level, thus their test interval can be extended with regular inspection and maintenance.

ACKNOWLEDGEMENTS

This work is supported by National Natural Science Foundation of China (51254001), the Project (2012M511418) supported by China Postdoctoral Science Foundation and Central South University Postdoctoral Science Foundation; Project (CK2010B17, CK2013Z03) supported by the Fund of Chongqing University of Science & Technology; Project (2013A02) supported by the opening Fund of Guangdong Provincial Key Laboratory of Fire Science and Technology.

REFERENCES

Chen, Y.J. & Gong, S.Y. 2006. Reliability-centered Maintenance Ideas. *Industrial Safety and Environmental Protection* 32(6):60–62.

Dai, R.& Kang, Y. 2001. RCM Decision Processes and Risk Assessment. *Aviation maintenance* 12(6):10–11.

Das Adhikari Manik. et al. 2011. Landslide Hazard and Risk Analysis in India at a Regional Scale. *Disaster Advances* 4(2):26–39.

Guo, Z.L. et al. 2009. On the Inspection Periodicity of Urban Gas Pipelines. *Storage and Transportation of Gas and Oil* 28(3):25–28.

Li, Y.H. 2006. Application of RBI-based Ethylene Unit. Tianjin: Tianjin University Publishing House.

Sunil, C.H. 2008. Configuring Disaster Risk Reduction into Development Processes. *Disaster Advances* 1(2):20–28.

Tan, H.X. et al. 2010. Empirical study on the safety factors in mining production. *Disaster Advances* 3(4):473–478.

Zhang, C.Y. 2008. RBI Quantitative Risk Assessment of Gas Transmission System. Lanzhou: Lanzhou Institute of Petrochemical Technology Publishing House.

This page intentionally left blank

Progress in Mine Safety Science and Engineering II – He et al. (Eds)
© 2014 Taylor & Francis Group, London, ISBN 978-1-138-00122-0

Collision behavior mechanism between drill pipe and coal hole wall during gas extraction drilling

Xiaoming Han, Zhanxu Tie, Dongsheng Li & Longlie Zhang
School of Mechanical and Power Engineering, Henan Polytechnic University, Jiaozuo, Henan, China

Chaoyang Shi
Wangzhuang Coal Mine, Lu'an Environmental Protection and Energy Development Co., Ltd., Changzhi, Shanxi, China

ABSTRACT: In order to reveal the collision behavior regularity between the drill pipe and the coal hole wall in the process of gas extraction drilling, the nonlinear dynamic equations of the drill pipe and the finite element model of the collision between the drill pipe and the hole wall are established. The collision stress variation between the drill pipe and the hole wall with different diameters are analyzed. The results show that with the decrease of the coal hole diameter, the collision stress value between the drill pipe and the hole wall increases and the hole wall is more instability to collapse. When the hole diameter increases to a certain extent, the collision stress variation become gentle and the hole wall become stable. The research provides the theoretical law to select the proper drilling parameters, which can improve the coal hole wall stability in the process of the gas extraction drilling.

1 INTRODUCTION

In the process of the gas extraction drilling in coal mine, the collision between the drill pipe and the coal hole wall can cause the instability phenomenon such as the coal hole wall collapse and the jam of the drilling tool which reduce the gas extraction effect and prolong the gas extraction drilling time. At the same time, the collision can also cause the damage of the drilling equipment (Xu et al 2009, Liu et al 2011, Fu et al 2011).

This paper establishes the finite element model of the collision between the drill pipe and the coal hole wall to reveal the collision behavior in the process of the gas extraction drilling. The results provide the theoretical law to select the proper process parameters of the drilling, which improve the hole wall stability during the gas extraction drilling.

2 DRILL PIPE NONLINEAR DYNAMIC EQUATIONS

The drill pipe is dispersed into some beam elements. Then, the dynamic equations of each unit in the local coordinate system are established. After simplified, the dynamics equations of the drill pipe in the overall coordinate system can be obtained (Ritto et al 2013).

In the local coordinate system, the unit generalized vectors of displacement, velocity and acceleration of the arbitrary beam element at t time are as follows:

$$f(t) = N d_e(t) \tag{1}$$

$$\dot{f}(t) = N \dot{d}_e(t) \tag{2}$$

$$\ddot{f}(t) = N \ddot{d}_e(t) \tag{3}$$

Where, N is the shape function matrix. According to the multi-degree freedoms of the Lagrange equations, the unit motion equation is derived:

$$\frac{d}{dt}\left[\frac{\partial(T-U)}{\partial \dot{d}_e}\right] - \left[\frac{\partial(T-U)}{\partial d_e}\right] + \left[\frac{\partial R}{\partial \dot{d}_e}\right] = \{0\} \tag{4}$$

Where, T is the unit kinetic energy. U is the unit potential energy and R is the unit dissipation energy function.

After derivation and simplification, the nonlinear dynamic equations of the drill pipe are:

$$M^e \ddot{d}_e(t) + C^e(t)\dot{d}_e(t) + \left(K_0^e + K_N^e(t) + K_\sigma^e(t) + K_G^e\right) d_e(t) = F_e(t) + R_G^e(t) \tag{5}$$

Where, K_0^e is the unit linear stiffness matrix. K_N^e is the unit large displacement stiffness matrix. K_σ^e is the unit geometrical stiffness matrix. K_G^e is the dynamic gap element stiffness matrix. F_e is the equivalent nodal force vector and R_G^e is the dynamic gap element additional force vector.

3 COLLISION FINITE ELEMENT MODEL BETWEEN DRILL PIPE AND HOLE WALL

The collision between the drill pipe and the coal hole wall is a complex nonlinear problem. The conventional calculation method is more complicated and the calculation precision is low. However, the problem can be solved effectively with the large-scale finite element analysis (Wang & Shao 1997).

So, this paper uses the LS-DYNA module of the ANSYS software to establish the 3D collision model between the drill pipe and the hole wall which is shown in Figure 1.

Where, the drill pipe diameter is 73 mm, the elasticity modulus of the drill pipe is 2.1×10^{11} Pa, the Poisson ratio is 0.3 and the density is 7800 kg/m^3. In the model, the drill pipe is looked as a rigid pipe, and the boundary conditions and the external loads which include the drilling pressure, the drilling torque, the centrifugal force and the friction force are applied.

4 COLLISION BEHAVIOR SIMULATION BETWEEN DRILL PIPE AND HOLE WALL

In the process of gas extraction drilling, if the drill bit encounters with the rocks in the coal seam, the drill pipe will deviate from the expected trajectory direction. And the drill pipe will be in a similar "pendulum" movement to collide with the hole wall (Luiz & Franca 2011, Royal ea al 2010).

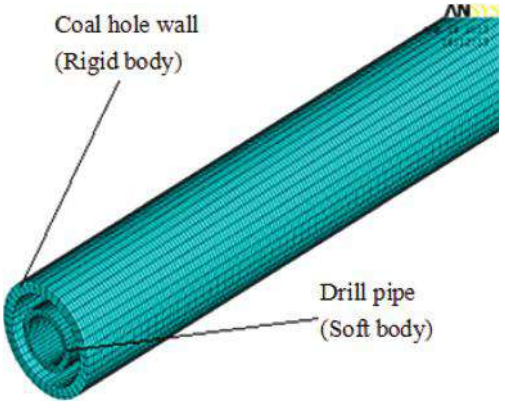


Figure 1. Collision finite element model.

The collision direction and position in different time are random distributed which are shown in Figure 2.

The collision between the drill pipe and the coal hole wall is finished in a short time. In the process of drilling, the drill pipe generates the elastic deformation to collide with the coal hole wall under the influence of the drilling pressure, the torque and the gravity. The impact between the drill pipe and the hole wall is the main reason of the instability and the failure of the coal hole wall. The gas extraction drilling under high ground stress makes the stress be redistributed. The collision between the drill pipe and the hole wall will lead to the local collapse in the coal hole which can cause the accidents of drill pipe breaking and drill tool jamming (Thomas ea al 2009, Mo et al 2011).

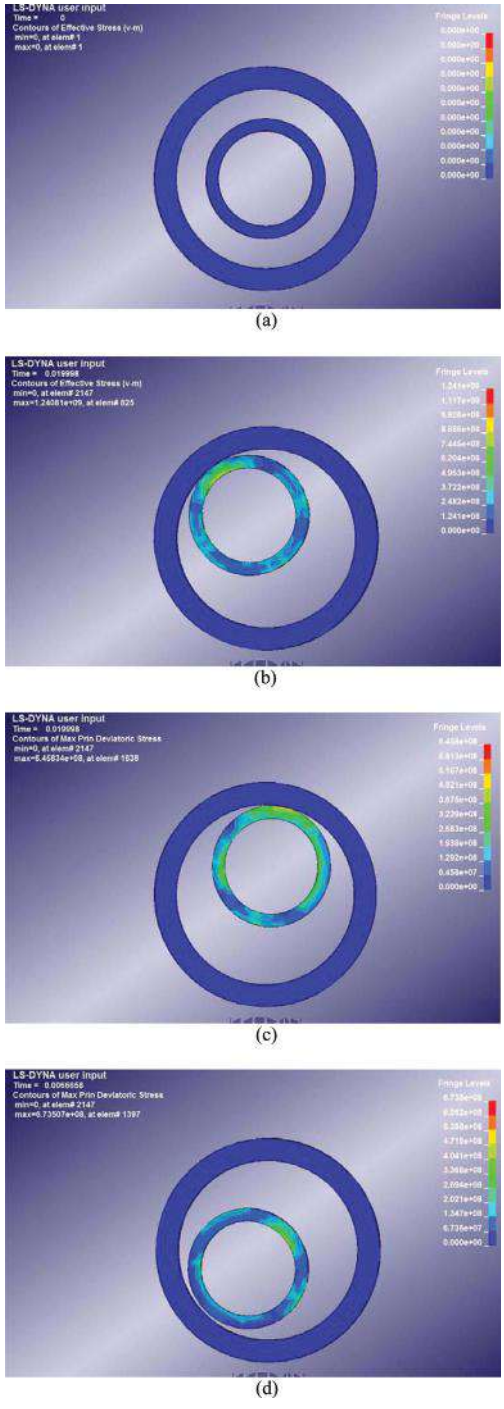
5 COLLISION STRESS ANALYSIS BETWEEN DRILL PIPE AND HOLE WALL

The collision stress in different time between the drill pipe and the hole wall in the diameters of 98 mm, 108 mm, 118 mm and 128 mm are shown in Figure 3.

In the process of drilling, the drill bit plays a role of breaking and guiding. Under the joint action of the elastic deformation energy of the drill pipe and the drilling pressure, the coal rock are squeezed and broken further when the drill pipe collides with the coal hole wall. Because the coal rock is a kind of brittle hard material, the coal produces a lot of shattered zone during the drilling in the coal seam. With the vibration and collision of the drill pipe, the coal slack in the hole begins to fall and discharge with the pressure gas supplied by the pump station.

In Figure 3a, the drill pipe collides with the hole wall along the radial direction. At time t = 0.0089s, the collision stress between the drill pipe and the coal hole wall increases rapidly to 169 MPa. In the subsequent time, the collision stress increases constantly and reaches the maximum of 243 MPa at time t = 0.0235s. Subsequently, the collision stress value begins to decline. And at time t = 0.0613s, the stress value reaches 242 MPa once more.

In Figure 3b, due to the stress waves caused by the collision conduct in the drill pipe, the stress waves superimpose mutually. The elastic performance energy of the drill pipe accumulates and releases constantly. At time t = 0.0312s, the collision stress value reaches 117 MPa. Then, the stress



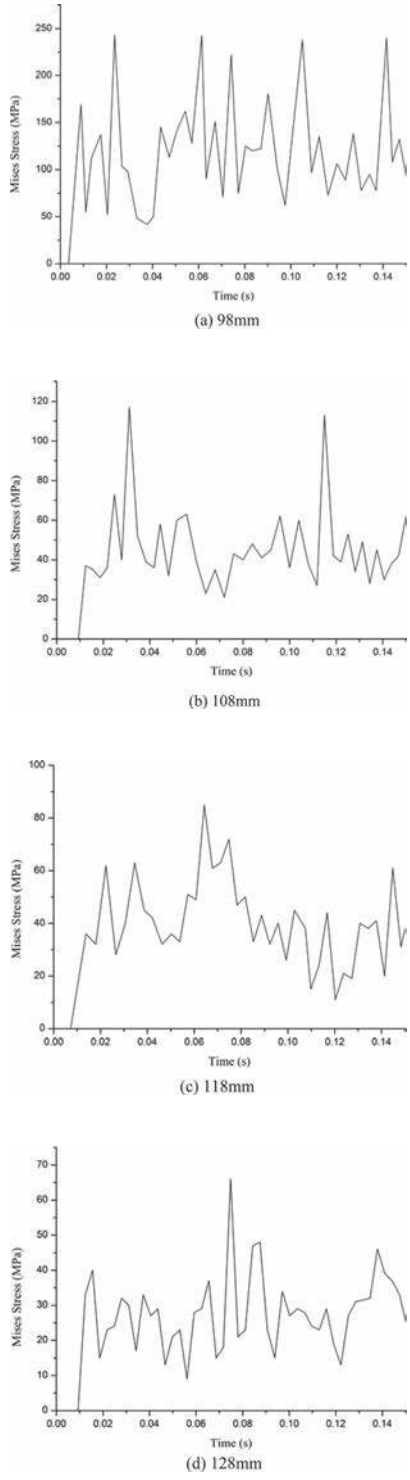
(a)

(b)

(c)

(d)

Figure 2. Collision state between drill pipe and hole wall.



(a) 98mm

(b) 108mm

(c) 118mm

(d) 128mm

Figure 3. Collision stress between drill pipe and hole wall in different aperture.

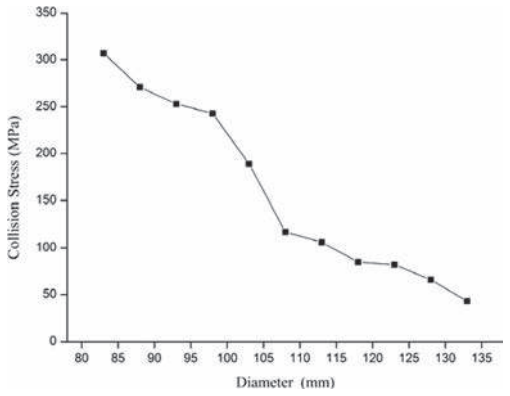


Figure 4. Collision stress variation tendency in different coal hole diameter.

value drops rapidly. And at time t = 0.115 s, the collision stress value increase to 113 MPa rapidly.

In Figure 3c, with the collision between the drill pipe and the hole wall, the coal slack flakes from the coal hole wall and the coal hole diameter expands constantly. At time t = 0.0643s the collision stress reaches the maximum of 84.9 MPa. With the annulus clearance becomes bigger, the bending elastic deformation energy of the drill pipe reduces obviously. As shown in Figure 3d, when the hole diameter is 128 mm, the stress value is lower significantly comparing with these of the former three diameters. The maximal collision stress value is 66 MPa.

From the collision stress variation analysis in each coal hole diameter, we can see that the appearance of the maximum of the collision stress is periodic, which is caused by the periodic vibration of the drill pipe. With the increases of the hole diameter, the period of the appearance of the maximum of the collision stress increases. When the hole diameter is small, the collision probability between the drill pipe and the hole wall is higher than that of the hole with the bigger diameter, and the collision stress is larger than that of the hole with the bigger diameter. Therefore, with the increase of the diameter of the coal hole, the collision stress reduces, the failure and fatigue fracture phenomenon of the drill pipe decrease, and the stability of the hole wall during drilling becomes better, which improve the drilling operation efficiency and increase the gas extraction effectiveness significantly.

The collision stress variation tendency of the drill pipe in different coal hole diameter is shown in Figure 4.

It can be seen from the curve in Figure 4 that the stress state of the drill pipe is from unstable to stable during the drilling. When the coal hole diameter in coal seam increases from 83 mm to 133 mm, the collision stress between the drill pipe and the coal hole wall reduces from 307 MPa to 43 MPa. As the coal hole diameter widening, the collision stress of the drill pipe decreases gradually. When the coal hole diameter increases to a certain degree, the collision stress variation tendency of the drill pipe becomes gentle and the hole wall becomes stable relatively. The reduction of the collision stress will decrease the fatigue failure of the drill pipe effectively and be beneficial to maintain the stability of the hole wall.

6 CONCLUSION

Through the derivation and the establishment of the nonlinear dynamic equations of the drill pipe, the collision behavior between the drill pipe and the coal hole wall is analyzed using the LS-DYNA module of the ANSYS software. The results shows that the coal hole diameter is smaller, the collision stress value between the drill pipe and the hole wall is bigger and the instability of the coal hole wall is more serious. When the coal hole diameter increases to a certain extent, the collision stress variation tendency becomes gentle and the hole wall is in a relatively stable state.

The research results provide the theoretical guidance to avoid the coal hole wall collapse and the jam of the drilling tool caused by the collision between the drill pipe and the hole wall. In the process of gas extraction, the drilling process parameters will be reasonable chosen to improve the efficiency of the gas extraction drilling.

ACKNOWLEDGEMENTS

This project is supported by 2012 Technology Development Plan of Safe Production in Henan Province (H12–094) and Henan Provincial Key Technology Project (102102210211).

REFERENCES

Fu, J.W., Fu, X.H. & Hu, X. 2011. Research into comprehensive gas extraction technology of single coal seams with low permeability in the Jiaozuo coal mining area. *Mining Science and Technology* 21:483–489.

Liu, Y.W., Liu, M.J. & Wei, J.P. 2011. Regional Outburst-prevention Technique by Gas Predrainage Based on Large Diameter Boreholes along Coal Seams under Deep Mining. *Procedia Engineering* 26:623–629.

Luiz, F.P. & Franca. 2011. A bit–rock interaction model for rotary–percussive drilling. *International Journal of Rock Mechanics & Mining Sciences* 48:827–835.

Mo, H.T., Shi, Z.J. & Hao, S.J. 2011. Analysis and Application of Treatment Techniques in Horizontal Directional Drilling Borehole Accident. *Procedia Earth and Planetary Science* 3:273–279.

Ritto, T.G., Escalante, M.R. & Sampaio, R. 2013. Drill-string horizontal dynamics with uncertainty on the frictional force. *Journal of Sound and Vibratio* 332:145–153.

Royal, A.C.D, Riggall, T.J. & Chapman, D.N. 2010. Analysis of steering in horizontal directional drilling installations using down-hole motors. *Tunnelling and Underground Space Technology* 25:754–765.

Thomas, G., Nathan, D. & Richard, J.C. 2009. A method to predict geomechanical properties and model well stability in horizontal boreholes. *International Journal of Coal Geology* 78:149–160.

Wang, M.C. & Shao, M. 1997. *Basic principle of finite element method and numerical method*. Bei Jing:Tsinghua university press.

Xu, T., Tang, C.A. & Yang, T.H. 2009. *Containing gas soot failure process and mechanism*. Bei Jing:Coal industry press.

This page intentionally left blank

Progress in Mine Safety Science and Engineering II – He et al. (Eds)
© 2014 Taylor & Francis Group, London, ISBN 978-1-138-00122-0

Research on leak accident risk of typical heavy-caliber long-distance natural gas transportation pipeline

Shengzhu Zhang
China Academy of Safety Science and Technology, Beijing, China

ABSTRACT: Use of heavy-caliber, high pressure pipeline is the development direction in long-distance natural gas transportation. This technique not only improves transportation efficiency but also increases the risk of the long-distance transportation pipeline system itself and its surrounding area. Identifying the leak risk of heavy-caliber long-distance natural gas transportation pipeline is significant for guaranteeing the safety of the personnel surrounding the pipeline and safe operation of pipeline itself. According to the consequence analysis of long-distance natural gas transportation pipeline leak accident, its major hazards include the thermal radiation generated by jet fire and vapor cloud explosion overpressure caused by delay burning. Calculating the two kinds of accident consequences by simplified Croce model and TNT equivalent method respectively, the results show that their influence area is proportional to leak size and pipeline operating pressure. The influence distance of thermal radiation of large rupture leak and complete rupture are about 86 m and 1570 m. The influence distance of overpressure of large rupture leak and complete rupture are about 156 m and 520 m, respectively. In large rupture leak, the overpressure influence area is greater than that of jet fire thermal radiation, in complete rupture, the jet fire thermal radiation influence area is much larger than that of overpressure. In extreme cases, both kinds of accident consequences impose serious impact on a large area around the pipeline.

1 INTRODUCTION

With the rapid development of economy, the demand of natural gas in urban and industrial production is becoming more and more extensive, and usage of natural gas increases significantly especially due to the requirements of environmental protection. Natural gas is mainly transported by pipeline system. West-east gas transportation pipeline, Sichuan-east gas transportation pipeline and extension pipeline network in natural gas consumption areas were widely constructed in recent years. Long-distance natural gas transportation pipeline is affected by many factors, including corrosion, external force, third-party damage, etc, which lead to pipeline ruptures. Due to the characteristics such as inflammable and explosive, once leaking, natural gas easily leads to fire and explosion accidents. The accidents will cause severe casualties and economic loss and bring serious damage on the surrounding environment, especially in densely populated areas. Natural gas pipeline accidents occurred frequently in China since 2010, such as Wuhan natural gas pipeline leak accident on March 15th and Jinzhou gas leak accident on June 18th and so on. Heavy-caliber and high-pressure transportation technology is widely used in long-distance natural gas transportation pipeline in China. This technology improves transportation efficiency and at the same time increases the risk of the transportation system itself, once leaking, the accident influences the surrounding area greatly. This paper studies the leak risk in typical heavy-caliber long-distance natural gas transportation pipeline based on the analysis of the characteristics of natural gas leak accident.

2 ACCIDENT CONSEQUENCE ANALYSIS

Because of the high compressibility of natural gas, the resulting leak hole attachments maintain high energy in a long time, and it may lead to leak hole changes from small to big, and even lead to pipeline rupture completely under specific conditions. For long-distance transportation pipeline, types of the consequence and related forms of damage depend on the failure mode of the pipeline, manner of leak and burning time of the natural gas (UNECE 2005, Kent 1992, Kent 1996).

Natural gas is flammable and explosive gas, once leaking from long-distance transportation pipeline, in case of encountering ignition source and igniting immediately, it will cause jet fire or explosion. It also may spread at the direction of the wind and

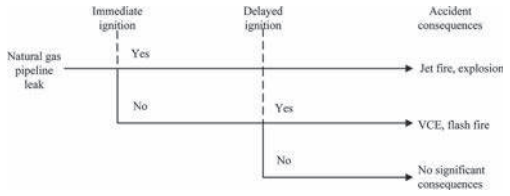


Figure 1. Long-distance natural gas transportation pipeline leak accident consequences.

mix with the surrounding air to form inflammable and explosive mixture. If encounters ignition source at this time, it can cause Vapor Cloud Explosion (VCE) or a flash fire, and have a huge impact. The density of the natural gas is relatively smaller than air, with the floating properties, if the natural gas is not impeded after leak, a large number of air is entrained in the gas, thus reduces gas concentration, and the flashover probability of distance retarded combustion is low, and the main forms of harm are thermal radiation generated by jet fire and shockwave overpressure generated by vapor cloud explosion (Kiefner & Vieth 1989, ASME 1991, Jo & Ahn 2002, Dziubinski & Fratczak 2006, Huang et al. 2012, Hopkins 2011). The accident consequences of long-distance natural gas transportation pipeline leak are shown in Figure 1.

3 ACCIDENT CONSEQUENCE CALCULATION MODEL

3.1 *Thermal radiation of jet fire*

Calculate the thermal radiation of jet fire by simplified model proposed by Croce and Mudan (Croce & Mudan 1986, Mudan 1987).

1. Calculation of flame height

Calculate flame length according to the following formula:

$$\frac{L}{d_j}=\frac{5.3}{C_T}\sqrt{\frac{T_f/T_j}{\alpha_T}\left[C_T+(1-C_T)\frac{M_a}{M_f}\right]} \tag{1}$$

Where L is flame length; d_j is diameter of jet pipe; C_T is the mole fraction of fuel in fuel—air measurement chemical reaction; T_f is adiabatic temperature of combustion flame; T_j is adiabatic temperature of injection fluid; α_T is the moles of reactants generate per mole combustion products in fuel—air measurement chemical reaction; M_a is air molar mass; and M_f is fuel molar mass. For the most of fuel, C_T is far less than 1, α_T approximate equal to 1, the ratio of T_f and T_j is between 7 to 9.

2 Calculation of thermal radiation flux

Calculate thermal radiation flux of the target received according to the following formula:

$$q(r)=\tau_a\eta\dot{m}\Delta H_c F_p \tag{2}$$

Where q(r) is thermal radiation flux received at a distance from target r; τ_α is atmospheric transmission rate; η is thermal radiation coefficient; $\dot{m}$is mass flow rate of the fuel; ΔH_c is combustion heat; and F_p is view factor.

3.2 *Shockwave overpressure of vapor cloud explosion*

Use TNT equivalent method (Zheng et al. 2004, Joann 1995) to calculate the shockwave overpressure of vapor cloud explosion, and estimate TNT equivalent according to the following formula:

$$W_{TNT}=\frac{AW_fQ_f}{Q_{TNT}} \tag{3}$$

Where W_{TNT} is TNT equivalent of vapor cloud; A is TNT equivalent coefficient of the Vapor cloud; value range is 0.02~14.9%; the mid-value of the range is 3~4%; W_f is total mass of the fuel in vapor cloud; Q_f is combustion heat of the fuel; and Q_{TNT} is explosion heat of the TNT.

Calculate death radius of vapor cloud explosion according to the following formula:

$$R_{0.5}=13.6\left(\frac{W_{TNT}}{1000}\right)^{0.37} \tag{4}$$

Where $R_{0.5}$ is individuals death radius.

Calculation of injury radius and minor injury radius is according to shockwave overpressure ΔP_S by the following formula:

$$\begin{cases}\Delta P_S=1+0.1567Z^{-3} & \Delta P_S>5\\ \Delta P_S=0.137Z^{-3}+0.119Z^{-2}+0.269Z^{-1}-0.019 & 1<\Delta P_S<10\end{cases} \tag{5}$$

$$Z=R\cdot\left(\frac{P_0}{E}\right)^{1/3} \tag{6}$$

Where R is horizontal distance from target to explosion source; P_0 is environmental pressures; and E is total energy of the explosion source.

4 DETERMINE CALCULATION CONDITIONS

According to the design parameters of the West-east natural gas transportation pipeline under

construction, and combining with actual operating parameters collected in the research process and design parameters currently under planning and construction, simulation range and the representative values for calculation are determined.

4.1 *Gas composition*

Natural gas is a multi-component mixture, composed of a variety of combustible and non-combustible gases. Its main ingredients are alkanes of which methane (CH_4) accounts for vast majority, a small amounts of ethane (C_2H_6), propane (C_3H_8) and butane (C_4H_{10}), in addition, it also contains hydrogen sulfide (H_2S), carbon dioxide (CO_2), nitrogen (N_2) and water vapor (H_2O), as well as trace amounts of inert gases, such as helium (He) and argon (Ar). Because methane accounts for vast majority, and is easily calculated at the same time, all leak gas is set in methane.

4.2 *Leak rate*

Natural gas leak rate gap in long-distance transportation pipeline is closely related to its flow state. Determine the state of the gas flow and then calculate the leak. Its flow state is divided into sonic and subsonic flow. According to formula (7) and (8), when formula (7) is established, it belongs to sonic flow; when formula (8) is founded, it belongs to subsonic flow.

$$\frac{P_0}{P} \le \left(\frac{2}{k+1}\right)^{\frac{k}{k-1}} \tag{7}$$

$$\frac{P_0}{P} > \left(\frac{2}{k+1}\right)^{\frac{k}{k-1}} \tag{8}$$

Where P_0 is standard atmospheric pressure; P is actual pressure of the gas; and k is adiabatic coefficient of the gas.

Adiabatic coefficient of methane k is 1.32, substituting into formula (7) and (8) in the calculation, the critical value of P is $1.8P_0$. Due to the current long-distance natural gas transportation pipeline design pressure is above 6 MPa, and its work pressure is greater than $1.8P_0$, so its flow is sonic flow, and the leak rate is calculated according to the following formula (SINOPEC Safety Engineering Institute 2007).

$$Q = YC_dA\rho\sqrt{Rk\left(\frac{2}{k+1}\right)T\left(\frac{2}{k+1}\right)^{\frac{1}{k-1}}} \tag{9}$$

$$Y = \sqrt{\left(\frac{1}{k-1}\right)\left(\frac{k+1}{2}\right)^{\frac{k+1}{k-1}}\left(\frac{P}{P_0}\right)^{\frac{2}{k}}\left[1-\left(\frac{P_0}{P}\right)^{\frac{k-1}{k}}\right]} \tag{10}$$

Where Q_0 is gas leak rate; C_d is gas leak coefficient, circular cracks take 1.0, triangle rip take 0.95, rectangular rip take 0.9; A is leak hole area; ρ is gas density; R is gas constant; and T is gas temperature.

4.3 *Pipeline diameter*

In the currently built west-east Phase II gas pipeline, the trunk diameter is 1219 mm, and the branch trunk diameter includes 1016 mm and 660 mm. 1016 mm diameter pipes are more used. In this simulation, main consideration is given to the diameter of the 1219 mm pipe.

4.4 *Pressure*

The west-east Phase II gas pipeline adopts design pressure 12 MPa and 10 MPa, respectively, and the branch lines' design pressure all uses 10 MPa. Due to the different transport task and site location, the actual change in pressure during operation is great. In this simulation, main consideration is given to 11 MPa situation.

4.5 *Leak mode*

Typical leak size is usually divided into small, medium, large and extra-large level. In this simulation, in order to determine the consequences of the accident in the ordinary and extreme cases, main consideration is taken into pipeline medium aperture leak and large aperture leak. According to the criteria recommended by DNV (TNO 1997, TNO 1992, TNO 1988, TNO 1999), this paper determines the representation of aperture 100 mm (large aperture) and 1200 mm (complete rupture).

4.6 *Meteorological conditions and topography*

Choose a typical weather condition, and select the average wind speed at 2.0 m/s, and the atmospheric stability is E. Assume surrounding terrain conditions are the plains, and there are no obstructions around the leak point.

5 CALCULATIONS OF TYPICAL ACCIDENT CONSEQUENCES

Adopt ALOHA to calculate typical accident consequences of long-distance natural gas transportation pipeline, and analyze separately thermal radiation and shock wave overpressure's influence distance in a typical accident condition. For the leak of long-distance natural gas transportation pipeline, when the gas is released from the crevasse, if encounters an ignition source immediately, it

will form a jet flame; if not encounter an ignition source immediately, natural gas will be diffused in the form of turbulent jet, and the natural gas that is leaked and diffused will mix with air to form an explosive region, which will explode after encountering an ignition source.

5.1 *Analysis of the influence of jet fire thermal radiation*

At 1219 mm diameter, 11 MPa pressure and large aperture leak (100 mm), thermal radiation influence range of jet fire is shown in Figure 2. Under complete rupture (1200 mm) condition, thermal radiation influence range of jet fire is shown in Figure 3.

Figure 2 shows that in large aperture leak, the radius is about 38 m in $q_c \geq 8$ kW/m^2 region, the width is about 10 m in 8 kW/m^2 > q_c ≥ 5 kW/m^2 region, the width is about 38 m in 5 kW/m^2 > q_c $1.5 kW/m^2 region. Under such condition, thermal radiation's farthest influence distance of jet fire is about 86 m. As shown in Figure 3, in complete rupture, the radius is about 700 m in $q_c \geq 8$ kW/m^2 region, the width is about 170 m in 8 kW/m^2 > q_c ≥ 5 kW/m^2 region, and the width is about 700 m in 5 kW/m^2 > q_c ≥ 1.5 kW/m^2 region. Under such condition, thermal radiation's farthest influence distance of jet fire is about 1570 m.

5.2 *Analysis of VCE overpressure influence*

At 1219 mm diameter, 11 MPa pressure and large aperture leak (100 mm), shockwave overpressure's influence range of VCE is shown in Figure 4. Under complete rupture (1200 mm) condition, shockwave overpressure's influence range of VCE is shown in Figure 5.

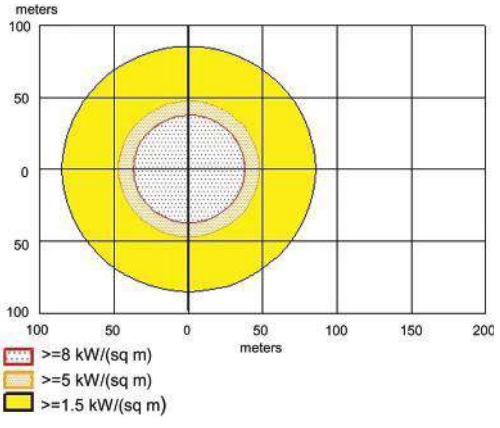


Figure 2. Thermal radiation influence range of jet fire under Φ100 aperture leak (d = 1219, P = 11 MPa).

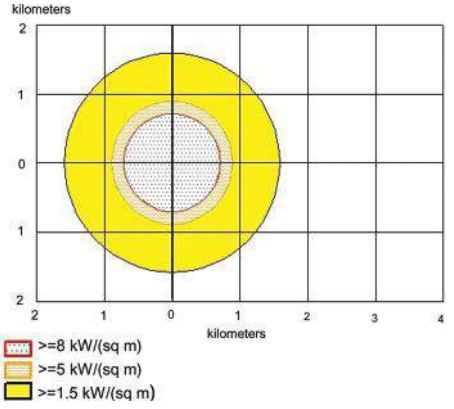


Figure 3. Thermal radiation influence range of jet fire under Φ1200 aperture leak (d = 1219, P = 11 MPa).

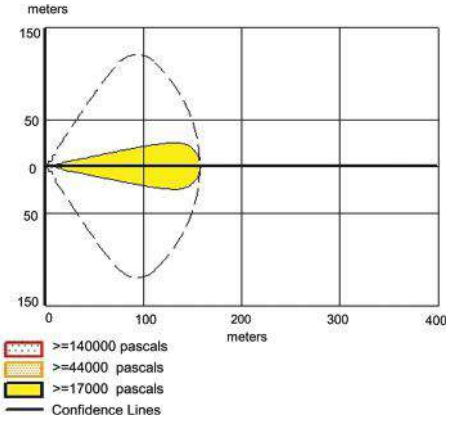


Figure 4. Shockwave overpressre's influence range of VCE under Φ100 aperture leak (d = 1219, P = 11 MPa).

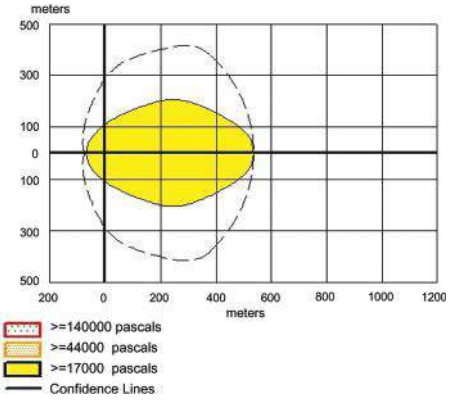


Figure 5. Shockwave overpressure's influence range of VCE under Φ1200 aperture leak (d = 1219, P = 11 MPa).

As shown in Figure 4, if large aperture leaks, minor injuries zone's maximum distance is about 156 m on one side of the pipe when $\Delta P \geq 0.017$ MPa. As shown in Figure 5, in complete rupture, minor injuries zone's maximum distance is about 520 m on one side of the pipe and 200 m along the pipeline route when $\Delta P \geq 0.017$ MPa.

6 CONCLUSIONS

Once the long-distance natural gas transportation pipeline leaks, in case of immediate ignition, it will lead to jet fire or explosion, while in case of delayed ignition, it will cause vapor cloud explosion or flash fire. The main damage form of the leak is thermal radiation produced by jet fire and overpressure caused by vapor cloud explosion.

Thermal radiation's influence range of jet fire is proportional to leak aperture size and pipeline operating pressure. The farthest influence distance of thermal radiation is about 86 m in large aperture leak, while in complete rupture, thermal radiation's influence distance will be up to 1570 m, and the death radius is also increased significantly.

Overpressure influence range of VCE is also proportional to leak aperture size and pipeline operating pressure. The farthest influence distance of overpressure is about 156 m in large aperture leak, while in complete rupture the influence distance will be 520 m. Compared with the influence distance in large aperture leak, overpressure is greater than jet fire thermal radiation; while in complete rupture, the influence distance of jet fire thermal radiation is greater than that of overpressure. The two accident consequences both impact the surrounding area seriously under extreme conditions.

ACKNOWLEDGEMENTS

The study was supported by National Science and Technology Support Program (2013 BAK04B03-02).

REFERENCES

ASME. 1991. *Manual for determining the remaining strength of corroded pipelines*. ASME B31G–1991.

Andrew, H. 2011. Risk-management and rule-compliance: Decision-making in hazardous industries. *Safety Science* 49(2): 110–120.

Croce, P.A. & Krishna, S.M. 1986. Calculating impacts for large open hydrocarbon fires. *Fire Safety Journal* 11(1–2): 99–112.

Dziubinski, M. & Fratczak, M. 2006. Aspects of risk analysis associated with major failures of fuel pipelines. *Journal of Loss Prevention in the Process Industries* 19(5): 399–408.

Huang, Z. et al. 2012. Numerical simulation and study on the transmission law of flame and pressure wave of pipeline gas explosion. *Safety Science* 50(4): 806–810.

Jo, Y.D. & Ahn, B.J. 2002. Analysis of hazard areas associated with high-pressure natural-gas pipeline. *Journal of Loss Prevention in the Process Industries* 15: 179–188.

Joann, M.G., et al. 1995. Risk assessment/management program evolves with experience. *Pipe Line & Gas Industry* 7: 45–47.

Kiefner, J.F. & Vieth, P.H. 1989. *A modified criterion for evaluating the remaining strength of corroded pipe*. Final Report on Project PR 3–805. Columbus: Battelle Memorial Institute.

Krishna, S.M. 1987. Geometric view factors for thermal radiation hazard assessment. *Fire Safety Journal* 12(2): 89–96.

Muhlbauer, W.K. 1992. *Pipeline risk management manual*. New York: Gulf Publishing Company.

Muhlbauer, W.K. 1996. *Pipeline risk management manual, 2nd ed*. New York: Gulf Publishing Company.

SINOPEC Safety Engineering Institute. 2007. *A guide for quantitative risk assessment of petrochemical plant*. Beijing: China Petrochemical Press.

TNO. 1988. *Methods for determining and processing probabilities*. Directorate General of Labour, CPR 12E. Voorburg.

TNO. 1992. *Methods for the determination of possible damage to people and objects resulting from releases of hazardous materials*. Directorate General of Labour, CPR 16E. Voorburg.

TNO. 1997. *Methods for the calculation of physical effects; Resulting from releases of hazardous materials (liquids and gases)*. Directorate General of Labour, CPR 14E, 3rd edition. Voorburg.

TNO. 1999. *Guidelines for Quantitative Risk Assessment*. Directorate General of Labour, CPR 18E. Voorburg.

Zheng J.Y. et al. 2004. *Long-distance transportation pipeline safety*. Beijing: Chemical Industry Press.

This page intentionally left blank

Progress in Mine Safety Science and Engineering II – He et al. (Eds)
© 2014 Taylor & Francis Group, London, ISBN 978-1-138-00122-0

Safety evaluation model of oil depot based on BP neural network

Yi Yang, Geng Luo, Yuhua Gu & Chengping Zhu
Aviation Fuel and POL Equipment Test Center, Beijing, China

ABSTRACT: The safety of oil depot is threatened by many factors and the results of safety evaluation are limited by the evaluation method, the accuracy of evaluation results also has been largely affected by personnel subjective factors. To overcome these defects, based on the analysis of influence factors of oil depot safety hierarchical structure safety evaluation model of oil depot is built by BP neural network method in this paper, and the evaluation model of neural network is trained by sample data. Evaluation results proved that BP neural network method is very suitable to evaluate the safety status of oil depot.

1 INTRODUCTION

From the safety point of the view fuel is the dangerous liquid, it is inflammable, explosive, volatile, toxic and so on, safety is always occupied in the first place of oil depot. For objectively evaluating the safety status of the oil depot, scientific evaluation method and calculation method should be adopted to obtain the correct analysis results. People commonly used comprehensive scoring method and linear weighting method to evaluate safety status of complex system, but these methods are easily affected by the randomness of evaluation process and subjective uncertainty of evaluation personnel, their applications in safety evaluation are limited. By simulating human brain activity artificial neural network method has many superior performances, such as nonlinear conversion capabilities, large-scale parallel processing, self-training and self-organization [1, 2], this method can absorb experts' experience and has higher calculation efficiency, and gradually applied to industrial field [3–15]. In this paper artificial neural network method is used to evaluate the safety status of oil depot, and evaluating model which is more close to the thinking mode of human beings is built.

2 SAFETY EVALUATION MODEL BASED ON BP NEURAL NETWORK

2.1 *Influence factors and index system*

According to the structure and function of oil depot, safety status can be evaluated by four units: personnel, facilities, safety management and environmental. Each unit includes several influence factors respectively, its evaluation index system is shown as Fig 1.

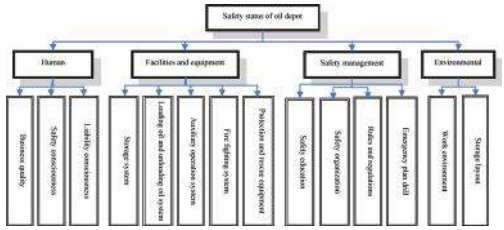


Figure 1. Structure diagram of safety evaluation index system of oil depot.

2.2 *Safety evaluation process of bp neural network*

BP network used in this paper is a multilevel feedback network, this network consists of input layer, intermediate layer and output layer. Learning process of the BP network includes forward propagation and error back propagation of information. When given a set of input mode, the input mode will be trained by BP network as follow manners: firstly, input mode is transferred from input layer to hidden layer, after processed layer by layer in hidden layer, a new input mode comes into being and is transferred to output layer, this process is called forward propagation; Secondly, in comparison with output and the expected value, if the expected expectations is not achieved, error Back Propagation is adopted and the error returned along the original path, by modified the connection weights of each layer neurons, error signals become smaller. Forward propagation and back propagation alternate with each other, and a memory training process is formed. The two processes are continuously circulated in system until the output value and the expected value of the error are reduced to an acceptable range. When the

new samples are inputted to the trained network, the corresponding output value can be calculated. Safety evaluation process of BP neural network is shown as Fig 2.

The establishment steps of BP neural network safety assessment model of oil depot are as follows:

1. Ascertaining the neuron number of input layer. According to the safety comprehensive evaluation index system of oil depot (shown as Fig 1, 14 basic factors can be obtained and become input neurons of the model. So, the neuron number of input layer is 14.
2. Ascertaining the neuron number of output layer. Evaluation results is the output of network, the output layer number is 1.
3. Ascertaining the neuron number of hidden layer. Hidden layer can be one layer or multilayer. Kolmogrov theory has proved that the three layer Sigmoid neurons in the BP neural network can approximate any continuous function as long as it has enough hidden nodes. So the hidden layer number is 1 in safety assessment model of oil depot.
4. Ascertaining the node number of hidden layer. The universal approximation theore requires enough number of hidden layer nodes, but too many layers and excessive neuronal data of hidden layer cause excessive number of connections and make a worse result of network generalization ability. To overcome this defect the value range of hidden node number should be ascertained and the maximum value in this range is the number of hidden layer nodes. The value range of hidden node number m is $\sqrt{nl} \le m \le \left[n(l+3)+1\right]$. In this paper, $6 \le m \le 9$, its maximum value is 9.

Evaluation model structure diagram of three layer neural network is shown in Figure 3.

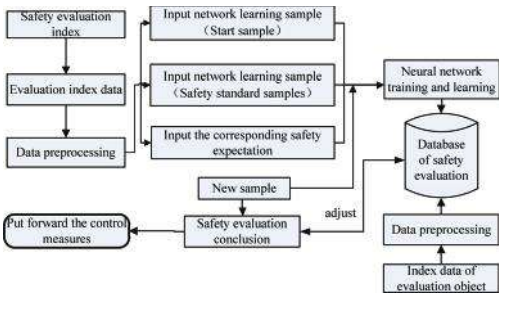


Figure 2. Safety evaluation process diagram of BP neural network.

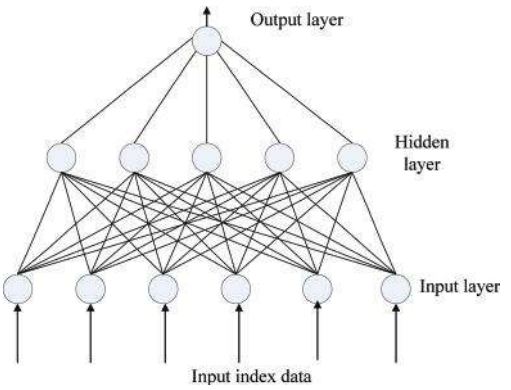


Figure 3. Structure diagram of three layer neural network.

2.3 *Bp neural network model*

There are 3 layer neural network. The k layer Input sum of i unit is U_i^k, its output is V_i^k, combination weight of the j neuron in k-1 layer and the i neuron in k layer is W_{ij}, input and output function of Each neuron and is f, the relationship between each variable is shown as follows.

$$V_i^k = f\left(U_i^k\right) \tag{1}$$

$$U_i^k = \sum W_{ij} V_j^{k-1} \tag{2}$$

Error function r is the mean square deviation of desired output and actual output:

$$r = E\left[\left(V_j^m - Y_j\right)^2\right] \tag{3}$$

Weight is changed along negative gradient direction of error function by LMS method, updated weight is:

$$\Delta W_{ij}^{(k+1)} = \in d_j^k V_j^{k-1} + \Delta W_{ij}^{(k)} \tag{4}$$

Where

$$d_j^l = V_j^l\left(1 - V_j^l\right)\left(V_j^l - Y_j\right) \tag{5}$$

$$d_j^k = V_j^k\left(1 - V_j^k\right)\sum W_{ij} d_i^{k+1} \tag{6}$$

The calculating process of error function is a back propagation process. Through repeated training of large number samples and modifying the weight, finally a well trained network is obtained.

3 SAFETY EVALUATION MODEL BASED ON BP NEURAL NETWORK

According to the relationship structure of basic safety evaluation factors of oil depot, hierarchy structure neural network of safety evaluation is built and is composed of 2 layers and 4 neural network units, the parameters of neural network structure is shown in table 1.

3.1 *Fuzzy processing of sample input value*

Because neural network requires that input must meet [0, 1] interval, data normalization processing of input unit is necessary by applying fuzzy theory. Processing rules is: The unit set is $U = \{U_1, U_2, U_3, U_4\}$, the factor sets are $U_1 = \{u_{11}, u_{12}, u_{13}\}$, $U_2 = \{u_{21}, u_{22}, u_{23}, u_{24}, u_{25}\}$, $U_3 = \{u_{31}, u_{32}, u_{33}, u_{34}\}$, $U_4 = \{u_{41}, u_{42}\}$; Evaluation result of oil depot can be divided into 5 levels: $V = \{v_1, v_2, v_3, v_4, v_5\}$. $x_i = u_{ij}$ o V, where x_i is the input value of i factor; "o" is the vector product; j express the j level, $i = 1, \ldots, 4$, $j = 1, \ldots, 5$.

3.2 *Network training*

When network is built, the samples need to be selected to train the network. There is big difference in the value of samples and the values cannot directly be compared with each other, so sample data need to be initialized during network training, i.e. sample input value of the last step should be fuzzy normalization processed. In principle number of samples is as much as possible for training network. In this paper 15 groups of samples is selected to train the network, when the network is converged, that trained neural network of safety evaluation of oil depot is obtained. The trained network can be used to evaluate the safety status of oil depot, meanwhile, the weight of factors affecting the safety of oil depot also can be analyzed and calculated. The following factors described the relationship between input factors and output factors.

1. Correlation coefficient

$$r_{ij} = \sum_{k=1}^{p} W_{ki} \left(1 - e^{-x}\right) / \left(1 + e^{-x}\right), \quad x = w_{jk} \tag{7}$$

2. Index of correlation

$$R_{ij} = \left|\left(1 - e^{-y}\right) / \left(1 + e^{-y}\right)\right|, \quad y = r_{ij} \tag{8}$$

3 Absolute influence coefficient

$$S_{ij} = R_{ij} \Big/ \sum_{i=1}^{m} R_{ij} \tag{9}$$

In formulae (7)–(9): i is the input unit of neural network, $i = 1, \ldots, m$; j is the output unit of neural network, $j = 1, \ldots$; k is the hidden unit of neural network, $k = 1, \ldots, p$; W_{ki} is the weight coefficient of input neuron i and hidden neuron k; W_{ki} is the weight coefficient of output neuron j and hidden neuron k. Using formulae (7)–(9) to sum up the trained network weights, the factors' weight of safety evaluation of oil depot can be calculated, the results are listed in table 2.

3.3 *Safety level*

By training and studying the network, evaluation result of the oil depot safety status can be obtained from the output of network. It has 5 levels of the output value Z of safety evaluation. When, $0.85 \le Z < 1.0$, the safety status of oil depot is excellent, belonging to intrinsic safety level; $0.70 \le Z < 0.85$, the safety status of oil depot is good, belonging to safety level; $0.60 \le Z < 0.70$, the safety status of oil depot is average, belonging to basic safety level; $0.30 \le Z < 0.60$, the safety status of oil depot is poor, belonging to criticality safety level; $0 < Z < 0.30$, the safety status of oil depot is bad, belonging to dangerous level.

4 EXAMPLE ANALYSIS

The factor value of evaluation system of the oil depot is known as table 1, the input value of network can be calculated by fuzzy normalization processing, shown as table 3.

Table 1. The parameters of neural network structure of oil depot.

Parameters	Safety status	Human	Facilities and equipment	Safety management	Environmental
Unit number of input layer	4	3	5	4	2
Hidden layer number	1	1	1	1	1
Unit number of hidden layer	7	6	8	8	3
Unit number of output layer	1	1	1	1	1

Table 2. The factors' weight of safety evaluation of oil depot.

Evaluation unit	Unit weight	Factor	Factor weight	Relative error
Human	0.32	Business quality	0.463	0.65
		Safety consciousness	0.307	2.28
		Liability consciousness	0.230	4.35
Facilities and equipment	0.33	Storage system	0.304	1.97
		Loading oil and unloading oil system	0.309	2.91
		Auxiliary operation system	0.115	4.35
		Fire fighting system	0.228	0.88
		Protection and rescue equipment	0.044	9.09
Safety management	0.21	Safety education	0.287	1.05
		Safety organization	0.213	1.41
		Rules and regulations	0.488	0.20
		Emergency plan drill	0.012	9.09
Environmental	0.14	Work environment	0.697	0.43
		Storage layout	0.303	0.99

Table 3. Input value of network processed by fuzzy normalization.

Evaluation unit	Factor	Excellent $v1 = 0.9$	Good $v2 = 0.8$	Average $v3 = 0.7$	Poor $v4 = 0.6$	Bad $v5 = 0.3$	Input value x_i
Human U_1	Business quality u_{11}	0.081	0.358	0.347	0.106	0.108	0.698
	Safety consciousness u_{12}	0.657	0.311	0.021	0.009	0.002	0.861
	Liability consciousness u_{13}	0.137	0.401	0.315	0.129	0.018	0.747
Facilities and equipment U_2	Storage system u_{21}	0.146	0.310	0.343	0.182	0.019	0.734
	Loading oil and unloading oil system u_{22}	0.132	0.417	0.306	0.111	0.034	0.743
	Auxiliary operation system u_{23}	0.279	0.308	0.211	0.198	0.004	0.765
	Fire fighting system u_{24}	0.115	0.325	0.297	0.183	0.080	0.705
	Protection and rescue equipment u_{25}	0.087	0.335	0.327	0.131	0.120	0.698
Safety management U_3	Safety education u_{31}	0.071	0.271	0.489	0.153	0.016	0.720
	Safety organization u_{32}	0.083	0.357	0.376	0.163	0.040	0.733
	Rules and regulations u_{33}	0.379	0.333	0.214	0.073	0.001	0.801
	Emergency plan drill u_{34}	0.101	0.275	0.384	0.201	0.039	0.712
Environmental U_4	Work environment u_{41}	0.211	0.337	0.343	0.102	0.007	0.763
	Storage layout u_{42}	0.088	0.321	0.331	0.215	0.005	0.698

Input the network input value to trained multilayer network, output value of safety level of oil depot is 0.75, it means the safety status of oil depot is good and the oil depot is belong to safety type, but there also exist some potential risks.

5 CONCLUSIONS

1. Because artificial neural network has the excellent characteristics of self learning, nonlinear dynamic processing, it provides a new method to solve the uncertainty, fuzzy and dynamic complexity problem of safety evaluation. Meanwhile, the difficulties of building complicated mathematical models to describe the nonlinear relationship can be solved.
2. To overcome the one-sidedness of safety evaluation, based on the characteristics of parallel structure and parallel processing, safety status of oil depot can be evaluated comprehensively by choosing suitable evaluation index; Using the fault tolerant characteristics of neural network, non numerical index can be calculated by choosing suitable function and data structure to realize fuzzy safety evaluation of oil depot.
3. Safety evaluation of oil depot belongs to pattern recognition category, and artificial neural network in pattern recognition has been widely used. Artificial neural network used in safety evaluation is feasible.

REFERENCES

[1] Y. Jiangang. 2003. *Artificial neural networks*. Zhejiang University Press.

[2] Z. Zhihua, C. Cungen. 2004. *Artificial neural networks and its application*. Qinghua University Press.

[3] Omran M G H, Mahdavi M. 2008. Global-best harmony search. *Applied Mathematics and Computation* 198: 643–656.

[4] Wasileski R F, Henselwood F. 2011. A retro-synthesis approach for hazard evaluation and risk screening. *Journal of Loss Prevention in the Process Industries* 24: 377–382.

[5] Dengyou Xia. 2007. Fire Risk Evaluation Model of High-Rise Buildings Based on Multilevel BP Neural Network. *Fuzzy Systems and Knowledge Discovery*: 24–27.

[6] Shen Xiaoyan, Liu Haoxue, Yan Yuanchun. 2009. A renovated safety evaluation model based on the principal component analysis and BP neural network. *Journal of Safety and Environment*: 180–184.

[7] Y. Lihua, L. Xinxing. 2010. Application of Neural Network Algorithm in Security of Oil Storage Depot. *Journal of Hubei Automotive Industries Institute* 24: 54–58.

[8] L. Huaijun. 2010. Safety Evaluation Model of Hazardous Chemical Transportation Enterprises Based on BP Neural Network and Its Application. *Logistics technology* 3: 88–89.

[9] L. Lixia, H. Guiming. 2001. Fuzzy comprehensive evaluation and its application based on BP neural netword. *Compution and application* 22: 5–7.

[10] Wang Yingbo, Wang Lin, Li Zhongxue. 2012. Safety evaluation of mine tailings facilities based on HS-BP algorithm. *Systems Engineering—Theory & Practice* 32: 2585–2590.

[11] Liu sheng, Liu Na, Yang Yu. 2013. Safety evaluation of hazards based on discrete Hopfield neural network. *Journal of Chongqing University (Natural Science Edition)* 36: 26–32.

[12] Liu Xinxi, Yan Echuang, Wang Penghui, et.al. 2003. Nonlinear Method for Evaluating the Landslide Stability. *China Safety Science Journal*: 58–61.

[13] Liu qiiuhong, Xu Guangfei. 2013. Role Exploring of Neural Network in Computer Network Security Assessment. *Coal Technology* 32: 270–272.

[14] Fan Yongjian, Mai Jianying, Shen Yanguang. 2009. Study of the Safety Assessment Model of Coal Mine Based on BP Neural Network. *Intelligent Computation Technology and Automation International Conference*: 103–106.

[15] Chen Jun, Li Congying, Ding Guangming. 2008. Traffic Safety Assessment of Freeway Based on BP Neural Network. *Journal of Tongji University* 36: 56–60.

This page intentionally left blank

9 *Other related topics*

This page intentionally left blank

Progress in Mine Safety Science and Engineering II – He et al. (Eds)
© 2014 Taylor & Francis Group, London, ISBN 978-1-138-00122-0

Protection for the occupational safety right of workers and China's legislative practice

Fanghua Lu
School of Humanities and Social Sciences, China University of Mining and Technology (Beijing), Beijing, China

ABSTRACT: The eighteenth National People's Congress report suggested that we should strengthen public safety system and safe production infrastructure, curb the rate of serious safety accidents, which fully reflects the attention central government pays to production safety. Protection for occupational safety rights of workers is helpful to maintain a good social order and social justice as well as to promote economic development. In this regard, we should learn from foreign experience in the relevant legislation and continue to improve the existing law to establish an independent legal system of occupational safety and enhance the systematization of the existing law as soon as possible.

1 INTRODUCTION

In recent years, China's national economy has maintained rapid growth but more and more serious occupational safety problems are hidden behind rapid economic growth. According to statistics, China's coal mine mortality rate of per million tons of production is as 200 times as that in the United States. The number of 2011 annual identified injuries is 120.1 million, There is an increase of 6.1 million over the last year. Annual assessment of disability was 51.0 million, containing an increase of 9.2 million over last year. There are many reasons for frequent accidents in production. One of which is the lagging in protecting workers' occupational safety. National basic occupational safety principles, guidelines, supervision, management system and measures are not legalized, standardized and do not form a comprehensive system and a systematic architecture. In order to improve legal system of production safety, protect and promote the development of market economy effectively and build a harmonious society, we must combine theoretical and practical demonstration of independence and mechanization of the protection for occupational safety of workers.

2 AWARENESS OF OCCUPATIONAL SAFETY AND HUMAN RIGHTS

Broadly speaking, the so-called human right refers to the right that people must possess based on the human nature for self development and sustenance, under certain economic structure and cultural development within specific social and historical context. Human rights are involved with morality, politics, law, people's subjective mental activity and other aspects. labor rights, as a basic human right, taking the right of employment as its core, is the sum of internal related and interactional rights. Narrow definition of labor rights is only the right of being employed and means that citizens are legally enfranchised to combine their labor with production to realize the value of the labor (Ren Guoyou 2013). Since the emergence of 'labor rights', it does not only include the right of employment, work selection and getting paid, but also includes rights arising out of labor, such as the right to be protected, the right to rest, the right to work safely, the right to get vocational training, the right to join work union and so on. Occupational safety, given to workers by the labor law, is in order to avoid harms caused by risk factors at workplace. According to provisions in the International Labor Conventions and Recommendations, occupational safety should be related to the issue arise from the 'main working domain' of 'relations between material requirement and the worker, and mental and physical adaptation to machine, assets, work time, work organization and working process. The term of 'work-related health' not only means the elimination of disease or health weakness, but also includes the physical and mental health, which is directly related to the occupational safety, hygiene." Obviously, occupational safety is based on the rights of life and health. Occupational safety is a basic expression of human rights.

From the perspective of content and structure of human rights, occupational safety right includes individual right such as right of refusal, as well as group right such as right of suggestion. On the

other hand, there are both procedural right like right of claim and substantive right like right of necessity. It also includes the right within working process like right of information and out of working process like right of getting trained and work insurance. Human right, labor rights and occupational safety right are the same process in different levels, the execution of occupational right will influence the realization of labor rights and human right both directly and indirectly. Thus, it has great practical significance.

3 INTERNATIONAL PROTECTION OF LABORER'S OCCUPATIONAL SAFETY RIGHTS

Occupational safety right is brought up by the early 19th century at the birth of the labor law. The initial scope of labor rights in legislation is extremely narrow, restricted to child labor, protection of women as well as maximum working hours and other basic working conditions. The protection is not only insufficient but also minimum, as in the case of fault liability in the claim of work injury. The result of which is frequent injury and occupational disease, and the increase of the mortality rate. The dire situation of the working class, which will inevitably lead to the increasingly tense labor relations and the rising of workers' movement, makes social order unstable. At the end of 19th century, with the uprising of working class struggle, accompanied by the enlightenment and French revolution, some political force sympathize and support the demand of workers, and they force bourgeois state to make constraint on the exploitation on the workers. Different country has a huge turn in the attitude of occupational safety and protection, where they tend to treat workers as vulnerable social group. In the "German code of labor protection" 1884 and "English code of worker's claim", the principles of employer's no-fault liability and employer's responsibility are set up, which makes responsibility of redemption by employer absolute.

Since the 20th century, labor safety and protection has entered a new realm. Occupational safety is no longer just government pushing employers to protect workers' rights, while it is the positive legal protection of workers in the safety production. Since the 1970s, Western countries forged the Occupational Safety by mixing the injury prevention and relief with the occupational safety, comfort, dignity and health, which promotes labor safety and protection to the level of human rights protection, and achieves integrated legislation of protection. The effect is prominent in the case like Sweden in 1978, the "Working Environment Act," 1970 U.S. "Occupational Safety and Health Act", Japan's "Labor Safety Law" in 1972. The ILO also passed "Convention on occupational safety and working environment", which sets the international labor safety standards. It also advocates in developing a more comprehensive and widely-accepted occupational safety standard, and an occupational safety administrating system encompasses government, employer and worker. In 2002, the Protocol approved in the International Labor Conference made further adjustment on Convention No. 155 on the issue of occupational accidents, occupational diseases and other content in registration and reporting. And it constructed a relatively thorough system of the International Labor Occupational Safety.

4 THE PROTECTION BY "SAFETY PRODUCTION LAW" TO OCCUPATIONAL SAFETY

China pays much attention to the legislation in occupational safety. From the middle of last century, a lot of code and regulation has been enacted. In 1990th, the "Mine Safety Law," "Trade Union Law", "Labor Law", "Occupational Disease Prevention Law," "Production Safety Law" and a series of important laws have been approved, while the State Council and its labor administration sector and the local government have also issued a number of administrative rules and regulations, which has basically formed a multilevel legal system led by Constitution. In addition, the state also has developed more than 100 national standards for labor safety. Generally speaking, China's legislation in protecting workers' right of occupational safety is basically the same with international labor conventions in contents and requirements.

On November 1, 2002 "Production Safety Law" has come into effect. "Production Safety Law" is China's first comprehensive special law in regulating safety protection. Compared with the previous occupational safety laws and regulations, "Production Safety Law" has the following characteristics:

To begin with, it defined the rights and the dominant position of workers in legislation for the first time, while also human spirit and harmonious society's values is profoundly embodied. Law explicitly endows employees in the production process with the right of information, right of suggestion, criticisms, reports and accusing, the right of emergency refuge, the right to refuse dangerous work, right of work injury insurance, right of civil claims and some other rights. Breaking the previous limit of only stipulating the obligation of employer, the new law turns the worker from passive beneficiary to active right owner.

Second, law is more integrated. Legislative activities cover the protection of production safety and the prevention of occupational diseases, requirement of investment of safety construction, obligation of education and training of employees, safety management systems, safety supervision and inspection system, and the rights and obligations of the "tripartite management" in government, trade unions and enterprises, as well as the punishing system of violations.

Third, it strengthens the legal responsibility. "Production Safety Law" made a more detailed provision in violation of labor safety and sanitation liability. In light of administrative, civil and criminal liability, it has formed a comprehensive accountability system, which is a tort liability system that is more complete. Congress Standing Committee approved No. 155 proposal of "Convention on occupational safety and the working environment." in 1981.

5 DEFECT OF CHINA'S PROTECTION FOR THE OCCUPATIONAL SAFETY RIGHT OF WORKERS

With the further development of socialist market economy and the continuous improvement of the legal system construction in China, consciousness of occupational safety protection has been strengthened. The basic frame of legal system has been enhanced. But, presently, the status of safety at work in the mine is not good, and serious accidents occur frequently that destroy people's lives. The reason is that the covering rate of production safety law and Law of Occupational Disease Prevention and Treatment of P. R. is low, driving by financial interests, capital consuming labor rights. It also has the key reason for it that is unsound legal system, administrative nonfeasance, poor supervision, evade laws.

5.1 *Priority of economic security over the right of occupational safety*

"Production Safety Law" Article begins with the provision: "In order to strengthen production safety supervision and management to prevent and reduce accidents in production, the law protects people's lives and property safety, and promotes economic development", which clearly shows its focus—economic sense of security. The aim lies behind is the protection of the production safety. Production safety is the process of accrue and sustain capital in the production process. As long as there are no major accidents in production, the aim of the law is achieved. However, in the production process, security of capital doesn't necessarily follows by security of occupational safety, for the difference exist in the notion of capital security and work safety.

This requires the design of the "Production Safety Law" should balance the interests, change the landscape of unequal distribution of interest. Specifically, it should divert the focus to the obligations of employers and rights of workers, especially the safety right. Meanwhile, when drafting the liability, we should increase the punishment of illegal act. A clear personal responsibility should be delineated and a strictly enforcement of law should be practiced.

5.2 *Narrow coverage of occupational safety and protection of the right*

China's "Production Safety Law" coverage is very low (Zhou Min 2005). According to ILO, implementation of a national occupational safety laws and regulations can be determined by the data of the industrial injury insurance coverage rate. Injury insurance coverage rate refers to ratio between workers who own injury insurance with all active workers nationwide. According to 2011 Annual Labor and Social Security Development Statistical Report by China's Ministry of Labor and Social Security, there are 17,6960 thousand people with work insurance and total employed are 76,4200 thousand people nationwide. The coverage rate is thus 23.1%, while 98% in Japan, Germany and other countries. With a large gap, striving to improve the implementation of occupational safety protection coverage is an important task for us at the moment.

5.3 *Weak idea of human rights in legislative style and legislation concept*

Current legislation adopted a legislative system in which the protection of occupational safety and prevention of occupational diseases were divided, and this is presented in the two most important existing laws, namely "Production Safety Law" and "Occupational Disease Prevention Law." "Production Safety Law" is the legislation of protection of labor safety and accidents prevention, "Occupational Disease Prevention Law" is a legal system which is relevant to industrial hygiene and occupational diseases prevention. These two laws have their own legislative systems, and are parallel. Occupational safety and health are closely related, which cannot be artificially separated, and both of them are serving the workers' safety and health. In regard to the concept of legislation purpose, the spirit of the legislation focuses on "economy", which lacks "sociality" and tends to take the production safety and promotion of

economic development as the theme. The concept of people-oriented ultimate concern is not revealed, and it's not conducive to establish a comprehensive national management system of the prevention of occupational danger (Shi, Meixia 2011). Compared with international labor legislation and labor safety laws in some Nordic countries, the occupational safety legislation shows a gradual comprehensive development, which covers all aspects of economic and social life of labor. And they regard the "decent work" as the highest goal of occupational safety and rights. In order to promote the harmonious physical and mental development of labor, we should also take previous mentioned goal as the direction of development of occupational safety right.

5.4 *Deficiency of legal system of occupational safety rights protection*

At present, China has promulgated a series of laws and regulations dealing with occupational safety, including important laws such as "Production Safety Law," "Mine Safety Law," "Occupational Health Prevention Law". Most of these laws and regulations are divided and fragmented in accordance with departments. They are comparatively more concerned about the economy of security, ignoring the social effect of occupational security protection, and are lacking of organic links between laws. The legislative technology is insufficient too, the case of occupational safety rights and role of workers in the dominant position remain to be improved. Provisions concerning protection of the rights of workers lack maneuverability. Liability and punishment are too light. These have seriously weakened the role of law.

6 CONCLUSION

Safety is related to the life and health as well as property safety of the majority of workers, and it is also related to the overall coordinated and sustainable development of the national economy (He Xueqiu 2000). In recent years, China's average rate of economic growth is above 8%. This kind of overspeeding development brought great pressure to national production security and occupational safety protection of workers. At present, the Chinese government pays more attention to economic development and ignores the protection of workers' rights. Its reasons include both insufficient legislation in occupational health and safety, and the enforcement of the law. To change this situation, the government should adopt a variety of ways to create a better environment for employment, build the law system of occupational safety and health, strengthen labor protection, improve working conditions, and, on the basis of expanded production, increases remuneration and benefits of workers, show the strength of Chinese harmonious development, coordinated development of social and ecological values.

ACKNOWLEDGEMENTS

The authors gratefully acknowledge foundation by the Basic Scientific Research Fund Project of Central Universities (3142013104).

REFERENCES

He Xueqiu 2000. *Security Engineering*. Xuzhou: China Mining University Press, 23–50 (in Chinese).

Ren Guoyou 2013. Local work safety supervision and management system: problems, reasons and improvement paths. *Journal of Safety Science and Technology*, 9(2):182–187 (in Chinese).

Shi Meixia 2011. China's Labor and Social Security Protection under the Globle Financial Crisis, *Human Rights*, 10(1): 4–17 (in Chinese).

Zhou Min 2005. Optimization of safety production supervision mode of coal mining enterprises. *Journal of China University of Mining and Technology*, 15(4):348–353 (in Chinese).

Progress in Mine Safety Science and Engineering II – He et al. (Eds)
© 2014 Taylor & Francis Group, London, ISBN 978-1-138-00122-0

Analysis on the styles of young miners subculture

Yuanwu Fang & Xiaozhuan Tian
North China Institute of Science and Technology, Beijing, China

ABSTRACT: The young miners subculture means values and act ways shared by some young miners groups, which has the enormous influence to person's thought and behavior and coalmine safety production. In order to promote the construction of coalmine culture, the paper analyse the style of young miners subculture basically from its characterization, construction and integration.

1 INTRODUCTION

The youth is the main force of miners, and style is the core of subculture, which is very important to coalmine safety production. To promote the construction of coalmine culture, we should analyse the styles of young miners subculture carefully.

2 CHARACTERIZATION OF STYLE

Stuart Hall of "Birminghan school" said: "youth culture mostly able to reflect essence of changes in society " (Dick Hebdige 2009) , therefore it is necessary to analyze and study mine youth subculture. In order to reflect the identity and avoid the loss of identity, coal mine youth create all kinds of styles, forming a meaningful whole, establishing a collective identity. This subculture styles are mainly composed of three elements: image, character, jargon, mainly occurs in the leisure time (Tao Dongfeng. & Hu Jiangfeng 2011).

The young miner subculture means that the young miners want to solve the problems of love, marriage, empty, life situation, social status, income, injustice, oppression, or reflects their efforts to solve these problems. Because some problem lack of existing solutions, resulting in symptoms of anxiety, tension and uneasiness, which can be expressed through subculture forms.

2.1 *Daily performance*

Mostly the young miners are dependable, simple, kind, with the spirit of hard-working and persistence. Some young people can't get the material and spiritual satisfaction in the mines. For self-esteem needs, they formed a small group in the leisure time. In their opinion, the core value of culture, such as sober, ambition, are replaced with hedonism, contempt for authority and the pursuit of stimulation and adventure, sometimes their values are showed in a strong way. They like to wear colorful clothes, to listen powerful and emotional music, jollification and comparisons. some are rather rude, arrogant, with a strong sense of community, and try to from a faction behind the curtain, sometimes fight with others. Because of tired work, they participate in sports activities occasionally, often not many people in attendance, but once form a small team, they can persist generally. Compared with their parents, they tend to be more fashionable and trend, and accept new things faster, they send messages by using the mobile phone almost every day, often surf on the net, with the influence of network information, they like shopping on internet, like to express their opinions and ideas over the internet. They are tired of the leader's long talk, don't like the leaders to read the manuscript at the meeting, They are reluctant to accept nagging or criticizing.

2.2 *Occupation targets*

The reasons for the young miners to work in the mine, partly because they can't find another better job, but entered the mine helplessly; Some young think coal mine work relatively stable, near parents, close to home, comparative comfort, but most are not willing to work in the frontline units, hoping to work in the office or some second units. When the young miners just go to work, they are full of freshness, but when really contact with the job, monotonous work environment may spend part of young people's willpower, and they will have the feeling of disappointment, which may lead to the emergence of the negative and neglect emotions, low work quality, lack of mental stability. Safety consciousness and operation skills of young miners are uneven, which cause them to violate regulations or codes of conduct. Also some young people

witnessed the hardships of miners life, because their ancestors are miners, so they have a deep understanding of coal mines and miners, they took the miner's lamps from the hands of clan elders, the youth may become outstanding young miners recognized by the main culture. Their continuous learning as an intellectual pursuit, they combine the theory learning with practice, to improve comprehensive quality, continuous innovation as a goal, to show their talents in the most difficult places, to forge ahead, to explore bravely, tracking the forefront of world science and technology, continuously improving the capability of independent innovation, to be diligent and thrifty as a habit, practicing safe production as a conscious act, the pursuit of excellence in ordinary posts, slowly they will become the backbone of the mine.

3 STYLE CONSTRUCTION

3.1 *Collage*

Collage is a word initially used by Lévi-Strauss to describe primitive people daily creation activities, which refers to "in a general guidance system, sort the object and recombine the context to convey new meaning" (Chen Dianlin 2010). In the process of the young miners subculture style formation, collage refers to the use safety culture system of young miners to transform the safety culture, the specific means mainly include exaggeration, move, transfer. The young miner often spoof, imitate voice and behavior especially speaking tone or manner of walking of the safety supervisors or managers, to satirize them seriously, stubborn or muddle with their duty, corruption and omission. When work in the underground, some young people imitate sound and action of managers, shortening the distance with other miners; some young miners move the safety equipments to unsuitable position, such as "pay attention to ventilation," "attention slippery" sign to the place where needn't be labeled, offside and absence of some emergency relief devices in space layout, graffiti on the wall, these are the means for young miners to express their subculture values. Some enterprises flaunted how much input increased in facilities of safety, how advanced the equipment be, but when you come to the coal mine, you will find the aging equipment, absence of safety facilities, which reflects the managers ' subculture values.

Collage content appear mainly for young miners to express discontent of the main culture, when young miners use this method, they tend to borrow latest achievement from fashion, science and technology, and result of the collage often is to form backlash against safety culture in the heart.

3.2 *Isomorphism*

The term "isomorphism" comes from the structural anthropology, Paul Willis as a representative scholar of "Bermingham school" firstly applied the concept of "isomorphic" to subculture phenomenon, referring to the symbolic agreement between group values and the life styles. The young miners pay more attention to safety, to cherish life and the right to life in dealing with the relationship between individual and collective, when the individual's rights to life are in conflict with collective interests, they will put the right to life on a more important position, the values of young people have "isomorphism" with their styles, forming disregard of the collective interests, such styles and values are often recognized in a small range firstly, through personal or media transmission, then be recognized in a wide range, even will awaken inner consciousness of some miners.

The values and styles of young miners also have consistency with people-oriented idea in some aspects, so that now once accident happened, no matter big or small, as long as caused casualties, everyone is intolerable, things different what it used to be before 2004, reflecting the people-oriented idea winning support among the people.

4 THE INTEGRATION OF SUBCULTURE STYLES

Part of young miners subculture in same direction with the main culture, part will produce repulsive interaction, to dispel adverse effects of young miners subculture, we should try to integrate from the following aspects.

4.1 *Combining with the characteristics of youth, respecting real life, solving the key problems*

Focus on young miners' growth, to solve the employment problem of the miner kids. Miner kids live in the mining area, nearly, therefore if they work in the mine, which have certain positive effects on the long-term stable development of mine, but some miner kids' specialty are not suitable, which can be considered that the miner kids go to institutions for second professional education, after completion of second professional, they can be arranged to work. Shanxi Lu'an and Datong Coal Mine Group adhere to the long-term training cooperation with China University of Mining and Technology and North China Institute of Science and Technology, which can play the resource advantages of the colleges, but also reserve talents for enterprise, and solve the serious problems for miners' family, achieving win-win results.

To realize intrinsic safety, we must have the good equipment. In order to reduce the risk of accidents, we must vigorously carry out technological transformation. The young miners witnessed the changes brought by technology each passing day, and they worship the power of technology, so in technology we should fully trust the young people's creativity, passion and ability. We can't blindly devote to speed in technological transformation, a mature technology must be tested for thousands of times, for various certification, promotion to large scale from small scale of trial operation.

In addition, we should implement education and guidance according to the characteristics of young miners, because they like to use the network and mobile phone, to express their demands, and hate empty political slogans, so we should adopt new management and countermeasures. For a new generation of young miners, we can't criticize at random, and we should rationally analyze the new features, trust them, respect them, and try to establish a good relationship, which is the premise for us to guide and obtain actual effect. According to the characteristics of young miners, we must focus on solving practical problems, not on empty talk. Don't be anxious for success mentality, we must have strategic vision, and don't hope that the young miners completely change in short time, should pursue long-term effect. Keeping pace with the times in the guide way, use new technology and new words.

4.2 *Strengthening the training awareness, improving training methods, selecting the training content*

To improve the quality of the training, we must strengthen the training awareness, select the appropriate training methods, and improve learning consciousness. Nowadays the training effect for the young miners is not very ideal, the reasons include: the training consciousness is not strong; using tension funds as an excuse; easy to be diluted by the professional work; The pertinence of training is too strong and the training ways are rigid; Self-consciousness of young miners in learning is not high.

In order to enhance the effect of training, we need to adopt a variety of measures and forms of education and training to strengthen education and training efforts, institutionalized way to keep training and education in an important position, and the education and training as an important aspect to appraise performance of grassroots cadres, which won't be shaken at any time, many coal mines often strengthened education and training when an accident happened, but underestimated education and training when there was no an accident. In the content of training, according to the objective to choose, as long as in line with the real, good and beauty requirements, the range can be wide, not too strong pertinence, combination of content and the acceptance, some content seem to has nothing with the safety, but reflect the social hot spots, close to the life of young miners, through which can improve their quality of and rich their knowledge, such training can be arranged more, from another angle to raise awareness of safety in production, to achieve good results, too strong pertinence training is easy to cause antipathy. In ways, the use of different training methods according to different types, and forms should be more vivid, which can be a movie, a lecture, a debate, a play; Organized by spontaneous organizations, also can invite the family members, and play positive role of multimedia means, not to abandon the traditional education training means; In places, from indoor to outdoor, from the meeting to the scene.

4.3 *Focusing on grass-roots workers, paying attention to practical activities, improving the quality of propaganda*

Seize the image soul of the young miners, much publicity to advanced models from the front-line. In the enterprise propaganda work, set more sights on the grass-roots workers, and try to tap advanced people and things from ordinary miners, let young miners see that from the ordinary things and posts can also make great career, close to experience character strength of mortals and almsdeed; Seize the essence through the phenomenon, much publicity to swallow humiliation and bear a heavy load, firm and indomitable, not the image of insanitation and swearing.

Pay attention to the publicity in the practical activities, highlight of the timeliness and effectiveness. To guide more people to pay attention to safety, the mine can carry out safety pledge, watching the safety publicity and warning films, attending the fire fighting training, emergency rescue drills, inviting family visit work on-site activities. Sum up after the activities, and expand the influence through the report and achievements exhibition, further to improve staff awareness of production safety, and create atmosphere that "all talk safety, all understand safety, all protect safety ".

SUMMARY

Report at 18th Party Congress puts forward "developing a Strong Socialist Culture in China", highlights the significance of cultural construction in the strategic level. In such specific background,

as an important component of coal mine culture, construction of coal mine subculture will be further strengthened.

ACKNOWLEDGEMENTS

Fund Project: Fundamental Research Funds for the Central Universities (No. 3142013104).

REFERENCES

Chen Dianlin. 2010. *Research on the influence mechanisms on youth subculture on university students*.

Dick Hebdige. 2009. *Subcultures: the meaning of style*.

Shi Zongbao. 2009. *Investigation and case analysis of coalmine accidents*.

Tao Dongfeng. & Hu Jiangfeng. 2011. *Subcultures: A reader*.

Progress in Mine Safety Science and Engineering II – He et al. (Eds)
© 2014 Taylor & Francis Group, London, ISBN 978-1-138-00122-0

The industry transformation in resource-exhausted city based on safety science

H. Yao
Editorial Department of Journal of North China Institute of Science and Technology, Yanjiao, Beijing-East, China

ABSTRACT: The appearance of resource exhausted cities and a series of social safety problems arisen from it, has become a global problem. There are 118 resource exhausted cities in our country, which face difficult choice of transformation because of extensive development and the lack of overall planning. The geological disasters arisen from illegal exploitation and the social damage emerged during the period of social transformation such as violence, poverty and disease can not be neglected in the industrial transformation of resource exhausted cities. To achieve the succeed of industrial transformation and social stability, the experience and lessons of success and failure at home and abroad should be drawn on and diversified comprehensive strategy should be carried out with the combination of government guidance and market regulation.

1 THE HISTORICAL PROCESS OF THE EMERGING OF RESOURCE EXHAUSTED CITIES

1.1 *The dutch disease being global problem*

During the period of industrial engineering, there are many resource cities established all over the world. Along with the depletion of non-renewable resources, resource cities have gradually become resource exhausted cities. Many researchers have proposed that many countries or resource cities have developed "the Dutch disease" since 1980s (Fan 2013, Yin 2012, Zhou 2003).

The Dutch disease is a phenomenal that a certain primary products division being abnormal prosperous results in the decline of other divisions in a country, especially a medium-sized and small country. In 1950s, there has been a large amount of oil and natural gas discovered in Dutch, which has already been main country of manufactured products export. Then the Dutch government has vigorously developed oil and natural gas industry, the export has risen sharply, the international balance of payment was surplus and the economy was prosperous. However, the vigorous natural gas industry has hit hard the agriculture and other industrial sectors of Dutch, and has weakened the international competition of export industries. Till the early 1980s, Dutch has suffered rising inflation, the fall of manufactured goods exports and the increase of unemployment, which was called the Dutch disease internationally.

We enlarge the extension of the Dutch disease, the exploitation of coal mine, mental mine and oil mine has brought about prosperous economy once. However, once the resources has exhausted, the original mining industry, relative manufacturing industry and service industry would withered consequently, the existing of resource cities would be the burden of their country and society, the remaining equipments were left unused and devalued, a large number of people were unemployed, which would arisen a series of economic and social problems and bought many restraining factors to the development of their countries. There are many cities existing the Dutch disease in China from this perspective.

1.2 *Mining cities of our country have got into the resource exhausted period instantly*

Our country has already defined 69 resource exhausted cities in three equal lots and 9 counties (city, territory and district) that enjoy the policies in the Xiaoxing'anling and Daxing'anling forest areas. There are batches of cities that have already become and are becoming resource exhausted cities other than the 69 cities that our country has announced, which reaches 118 cities by adding both.

The main industries of resource cities are coal, oil, iron mine and copper mine. In the 118 resource cities, there are 63 coal cities which accounts for 53%, 21 forest industrial cities for 18%, 12 colored metal cities for 10%, 9 oil cities for 8%, 8 ferrous metallurgy cities for 7%, and 5 other cities for 4%. From the structure of administrative level of cities, there are 47 prefecture-level cities and 71 county-level cities.

As the national energy and raw material security bases, these cities have made great contributions to national economic construction. Because of over-exploitation and resource exhaustion, these cities are generally in trouble of resource exhaustion and city decline: single industrial structure, serious damaged ecologic environment, prominent security risk and high pressure of employment stability.

2 THE SAFETY AND SOCIAL PROBLEM CAUSED IN MINING CITIES BY RESOURCE EXHAUSTION

Although resource cities are more and more prosperous from small to big cities, they depend too much on the advantage of resources which causes single economic composition. When the resources get little and little even exhausted, crisis will begin to come into being.

2.1 *Mining condition deteriorates and coalmine accidents happen frequently*

The operators of mine often make a reckless move and take a risk to manufacture to meet the rigid requirements of local economic development needing energy, people's life needing heating supply and workers needing wages and bonus, because resources exhaust, mining conditions gradually deteriorate, many manufacture equipments age, the update of equipments is lack of capital, plus inadequate supervision, unsound systems and unscientific management. The manager of Chenjiashan coal mine in Tongchuan of Shanxi province, caused accident because of insisting mining for overfulfilling the production target under the condition of the two ex-managers being dismissed because of safety accidents, safety workers under mine reporting gas leak and open fire again and again.

Haizhou vertical shaft in Sunjiawan coal mine of Fuxin was put into production before the rebuilding and extension engineering of it is completed and checked before acceptance. Its management of productive technology was in chaos, its annual output in 2005 was 1.86 million tons, which was more than two times of the approved annual productive capacity (0.9 million tons). Under the background of energy shortage and the price of coal being soaring, state-owned coal mines go full steam ahead and mine with super-capacity to gain high returns and huge economic benefits instantly.

2.2 *Resource exhaustion brings about a series of economic and social problem*

As a famous coal and electric city in the last century, the productive scene at nights of china's well-known Haizhou open-air coal mine in Fuxin city was marked with a paper money of 5 yuan printed in 1960. However, in 2005, Haizhou coalmine which has produced at night and day for 24 billion tons of coal came to a stop because the coal in it had been mined out. What's worse, around 2000, there were tens of coalmines closed one after another in Fuxin with coal resource gradually exhausting. Several major coal mines basically have gone bankrupt, a large number of industrial workers have been facing unemployment, coal resources have gradually exhausted, which made the city of coal and electricity-- Fuxin produce big confusion. According to statistics, above 1/3 of the industrial enterprises in Fuxin were off production or in semi-shutdown state, 156,000 industrial workers have been laid off, accounted for 36.7% of the total number of employees. From the city's point of view, there were 198,000 people being in the lowest living security line. In addition, Fuxin was also facing the embarrassing situation of crowded shanty towns and continuous subsidence in goaf.

Gejiu, being famous with the title of "china's capital of tin" and its reserves account for 10% of world's reserves and a third of china's reserves, rapidly expanded after its building in 1951. In 1958, Gejiu even become the capital of Honghe prefecture by replacing Mengzi. Several generations of industrial workers have built a once prosperous mining city out of this small border town since 1950, which is the same as every resource city full of mines. During the period of large industrial leap, those resources cities have depleted their reserves, got into trouble and been left behind without people. Mine robbers hollowed out the bottom of cities, which caused the collapse of the housing, subsidence and road crack. In 2001, the raw ores, which were stolen in mining area of Yunxi Group, have reached more than 200,000 tons, which has caused hundreds of millions Yuan worth of damage. 12,000 industrial workers were laid off. The recoverable deposits of tin in mining area of Gejiu were less than 10% of known reserves and can only last for 3 to 5 years in 2008.

Since 1990s, original workers have become the law income group and led a hard and monotonous life, and then Gejiu has consequently become one of the most serious drug abuse cities in Yunnan. In March, 2008, Gejiu was placed in the first list of 12 resource exhausted cities. Till 2009, there were more than 30 state-owned enterprises in Gejiu going broke one after another and more than 30,000 people have become unemployed, which accounts for one sixth of Gejiu's urban population.

With rapid development in China, Yumen, the once oil city, was one of the few dying towns. On the main streets of old urban district in Yumen, there were rows of high buildings, huge billboards

everywhere, offices, businesses and enterprises with full functions, from which we can imagine the once prosperous and rich Yumen. However, for today, rows of closed shop-front houses have showed the decline of the city. Daqin, the oil city, has faced with production reduce for a time and the workers have had no things to do.

In 2002, it was discovered by the investigation of Research group for "the economic structure transformation of resources cities" of the national development and reform commission that one third of the state-owned mines building in the middle of the 20 century have got into gerontic period and there were 50 ones out of 390 cities falling into resource exhaustion.

In mining cities of resource exhaustion, there are generally serious problems of group poverty and social environment deterioration. And the crime rate and numbers are also large.

3 THE INDUSTRIAL TRANSFORMATION OF MINING CITIES WITH RESOURCE EXHAUSTION

The existing mining cities of resource exhaustion are facing difficulties and there will emerge new resource exhausted cities in the future. Either the existing mining cities of resource exhaustion or the future ones face a same choice: where should they go?

After resource exhaustion, there are only three outcomes. Firstly, they disappear in-place just like many ghost towns in USA. Secondly, they migrate entirely as Tongchuan City of Shanxi. And last, they can make transformation, which is the best outcome and the thinking under the guidance of the scientific outlook on development.

3.1 *The experience and lessons from the mining cities transformation of resource exhaustion overseas*

The industrial revolution of 18–19 centuries has brought a batch of mining towns into being in Europe and North America. With the universal development of industrial process, resource towns, large and medium-sized industrial and mining cities which have developed based on it and depended on resources, which were both called resource cities, have gradually around all over the world. Until 1950 and 1960, resource cities have started to face two big problems: one is that resource exhaustion arises, the reserves of mining resources get little and little through long-term exploitation and their quality also declines; the other is the competition of cheap substitutes, there is not only the competition of cheap mining products of the same kind in third world countries, but also the competition of coal from cheap oil. Both cases will lead to the recession of the original industry.

The main approach to solve this problem is industrial transformation. USA and South Africa both are worldwide great powers of mining industry with many resource cities. The industrial transformation problem of resource cities has appeared early in Germany and was basically already solved. But those ones in Ukraine and Nauru were basically failed.

Several countries' practice on industrial transformation in resource cities are summarized as follows:

1. Pittsburgh: Since 1980s, the steel and machinery industries in Pittsburgh have lost their competitive power so that the unemployment rate has once exceeded 15%. Later on, conventional industries were emigrated, universities' scientific research was taken advantage of to develop emerging and service industries (such as software) and the environment was rectified. It not only has solved the environment brought by the steel and manufacture industry and made Pittsburgh become one of the livable cities in USA, but also made it become a city taking the service industry and computing software as orientation.
2. Butte: Butte is a mining city over hundred years, it has taken University of Montana Institute of Technology, which was established in 1900, as its pillar, its economy has started to diversification after its economic has recessed and its population has decreased. Except the tourism, medical and health services and energy industries, high-tech enterprises have been developed actively and fight for being settled. In 1997, the processing plant of ASIMI has settled down in Butte. The natives also have established several new technology application company.
3. Rhodell: Rhodell is located in the middle of coal belt of West Virginia, coalmines have been discovered in 1930s and then were developed comprehensively, it was in its booming period in late 1940s, both shops and entertainment service equipments were complete. Since 1950s, because the coal resource has gradually exhausted and the difficulty of exploitation was getting bigger and bigger, coal companies have began to evacuate one after another, so the workers and businesses also have evacuated consequently. The town was given up, then it finally became a ghost city without people.
4. Ruhr: Since the early 1960s, the exploitation price of coal has risen, the exploitation output has reduced annually. Coalmines have gradually shut down, the steel plants have emigrated one after another and he population

of unemployment has increased enormously. Meanwhile, the quality of environment has declined and the ecological environment has deteriorated. The government has taken a series of measures to support the transformation of resource cities and the rebuilding of old industries area. The mine law of Germany stipulates that the reclamation of mining area must be proposed concrete and reliable measures, the emerging industries, like information and biotechnology, settle down in the locality. Its transformation belongs to the type of the combination of government and market. The reclaimed cultivated land, grassland, forest and artificial water are well-proportioned so that the city takes on a brand new look. The output value of coal and steel only accounts for 16% of the output value of whole district, the emerging industries has developed vigorously.

5. Kyushu: Since the early 1960s, Japan has gradually decided to give up the high-cost protect of coal industry and adjusted the coal policy 9 times. Region economy development corporation was established to be in charge of the industrial revitalization of coal production. Industrial development zone has been set up to promote the structural optimization with preferential policies of investment. 80% tax exemption has been resupplied regions by the state and tilt fiscal policy and infrastructure construction policy have been implemented to Kyushu. The large-scale unemployment arising in the transformation period was paid high attention. The transformation was led by governments and has taken high prices.
6. Yubari: In order to decrease the influence of coal industry's recession, on the one hand, taking the advantage of the features of local weather and geography, Yubari has cultivated Yubari Muskmelon and competitively featured agriculture that takes Yubari Muskmelon as the flagship product; and on the other hand, it has taken efforts to develop the tourism industry through being in debts and build the robot hall of science, museum, zool and adventure playground one after another, it also has done a lot of work around ski, hot spring and film festival, but all haven't achieved desired effect. Until 2000, the city's population has declined from 120,000 in peak to 14,000, the financial index was only 20%, and the per capital debt has reached 4,800,000 yen. The government of Yubari announced bankrupt in July, 2006, and it became a city that was under the direct management of central government. Its transformation was failed.
7. Dundee: Dundee has prospered because of coal and was called coal capital. Since 1980s, the coal industry has begun to recess and the quantity of employment from 1981 to 2000 was down by 84%, because resources have gradually exhausted, mining infrastructures has aged and the local requirement for coal has declined. Then the government has actively carried out attracting investment and implemented regional economic development strategy. However, the locals were lack of enterprising spirit and entrepreneur practicing, the residents who were proficiency in a particular line have migrated out so that the scale of the city was so small, then the outside world has had no confidence in the local economic development.

3.2 *The exploration of mining cities transformation of resource exhaustion in china*

Since 1990s, China's mining cities of resource exhaustion have started to grope for the industrial transformation. Currently, there are a part of cities achieving remarkable results and creating successful experience (Dai 2010, Wang 2009, Research Center of Socialism Theory with Chinese Characteristics in Gansu Province 2012). Other cities can draw lessons from their experience. The explorations of mining cities transformation of resource exhaustion in China are summarized as follows:

1. Shizuishan: On the one hand, the traditional industries like coal, electric power and metallurgy were reformed and promoted; on the other hand, the new featured industries such as new materials, nonferrous metal, equipment manufacturing and fine chemistry were cultivated and expanded. Funds were invested, many kinds of jobs were set up, the reemployment and social security of the whole city were propelled actively, vocational education was developed vigorously and let the vocational education promote employment. The reformed and cultivated industries of new features have achieved 2.88 billion yuan worth of added value for the whole city by the end of 2007. It has created a stable social environment for economic transformation. During 5 years, it has achieved jobs for 870,000 people in town and has taken the lead in the implementation of the new rural cooperative medical care and basic medical insurance system for urban residents in Ningxia.
2. Baiyin: It has focused on the establishment of economic support, fostering multi-pillar industry, accelerated the fostering of non-ferrous metals and rare earth new materials, fine chemical industry integration, energy and new energy sources which were "the eight pillar industries",

adhered to the extension of industrial chain as a breakthrough, focused on the cultivation of strong industries, chosen a good direction of industrial development and sped up the construction of the "five bases". A number of multi-pillar industries have boomed. "Eight pillar industries" has completed 4.683 billion yuan worth of investment, accounting for 50.35% of the city's investment in fixed assets, which has achieved 8.727 billion yuan worth of the added value, accounting for 43.64% of the city's GDP.

3. Fushun: It has constructed a national fine chemical industry base, to accelerate the transformation from a resource-based city to a resource city of deep processing. In Fushun High-tech Industrial Development Zone, a land of 9.9 square kilometers of was planned as the core of Fine Chemical Industry Park base. A public test platform for services to small and medium enterprises of fine chemicals and test base for the transformation service to science and technology achievements. It was identified as national fine chemical industry base by the National Ministry of Science and Technology and was China's first national industrialization base which was named as "fine chemicals". It can realize the extension of the industry chain after its completion and drive Fushun to become fine chemical industrial agglomeration area with obvious advantages in China.
4. Zaozhuang: It has closed 82 small coal mines in 3 years, decreased a production capacity of about 3 000 000 tons, shutdown 43 cement production lines and decreased a production capacity of 2,710,000 tons. Secondly, relying on resource advantage, it has developed the coal industry of deep processing, and built a number of chemical enterprises depending on the coal chemical industrial chain such as water coal slurry gasification, market competitiveness has been enhanced. At the same time, Zaozhuang has taken paper, machinery manufacturing, beer brewing as an alternative industry to develop. The transformation was successful and has changed the original single structure relying on coal industrial structure.
5. Fuxin: It has developed modern agriculture and planned to use 9 years to achieve economic transformation. During the 5 years from 2006 to 2010, it has basically set up a modern agricultural system and initially built a national model city of ecological agriculture construction. Fuxin has hired 8000 hectares of land of 12 neighboring township farmers, and constructed 50 agricultural parks and 200 professional communities emphasizing on aquaculture, arranged 42000 job-transfer workers in employment and promoted 10000 workers to develop towards the tertiary industry. Fuxin currently has 156,000 unemployed workers, there are 114,000 people left with 42000 people employed. In addition to the modern agriculture, Fuxin is also considering the tertiary industry, to solve the way out of laid-off workers.
6. Pingding Mountain: In addition to coal chemical industry and tourism, it will develop the salt chemical industry. The revenue of Pingtai Mountain tourism ranks fifth in our country, more than the Imperial Palace income.
7. Kelamayi: It will construct oil and gas, and processing industrial cluster and develop the tourism industry and modern agriculture. During the 12th five-year plan, Petro China will invest 300 billion yuan in Xinjiang to develop oil and gas and processing industry. This initiative will contribute to Xinjiang's oil and gas and processing industry cluster rise. In recent years, it has carried out preparatory work for key regional planning and major construction projects, and has made important progress.
8. Daqing: The main measures of future development is the development of petrochemical industry, striving for new large petrochemical projects in Daqing construction and production, to form a large chemical industry production base, and gradually make Daqing take transformation from the exploitation of oil and natural gas to a chemical industry as the first industry and from the "oil economy" into "oil and chemical economy". In the next few years, Daqing oil field production will decline by about 1500000 tons every year, local economic growth is difficult to compensate for the decrease in oil production. The economy of Daqing has only 10 billion Yuan worth of scale, even if the continuous maintenance of over 30% growth rate, it only can increase 3 billion Yuan worth of output value. Daqing concerned admits, there may be local sustained economic growth in the future, the city's economy is still in situation of zero growth or even negative growth.
9. Datong: In accordance with the concept of "one axis with two cities, separate development, considering both ancient and modern, two benefits of new and old, cultural heritage, create characteristics", it has opened a grand project for overall protection of historical and cultural city of china. And it has vigorously developed cultural undertakings and cultural tourism industry. A "great harmony mode" of culture protection, harmonious development of city construction has been proposed. City construction is in progress.

4 PROSPECT FOR INDUSTRIAL TRANSFORMATION IN MINING CITIES OF EXHAUSTED RESOURCE IN CHINA

4.1 *Thinking on historical experience*

The hard transformations of mining cities from home and abroad after entering into the stage of resource exhaustion bring about a lot of thinking:

1. It is a historical necessity that mining cities enter into the stage of resource exhaustion. Any city that has developed depend on resource exploitation has its prosperous and decline periods, because resources are limited and aren't last forever. Both governors of cities and residents from home and abroad should save against rainy days, other than being forced to look for a way out when resources exhaust and environment deteriorates seriously. The government should not catch the fish by draining the pool in early days and begin to dig a well when feeling thirsty in later period. For those resource cities that are still in their blooming days, planning for the future should be made in early days to avoid single development and taking old paths that predecessors have taken.
2. There are successful and failed cases in the industrial transformation of mining cities from home and abroad. For those relatively good transformations, firstly, their natural conditions are great; secondly, those cities have long histories and high population quality; thirdly, the combination of government leading and market adjusting plays an important role.
3. The industrial transformation is not only economic problem but also social problem. If it isn't solved well, it will influence the stability of society, and also bring biological environment problems which will influence environment for hundreds of years even thousands of years. Therefore, the implement of transformation strategies should take overall consideration, make a long-term planning and avoid taking old path only for the pursuit of GDP.
4. The safety problem, which includes production safety in the remaining resource exploitation and the living safety of workers and residents, is extraordinary remarkable during resource exhaustion and must be given enough attention.

4.2 *The prospect for future development*

1. Insisting on diversified development strategy. Either for Fuxin or Zaozhuang model, china's resource cities should insist on diversified development strategies, prolong the deep processing train of mining products, and maximize the added value of resources, for instance, oil cities can vigorously develop petrochemical industry and deep processing industry of petrochemical products; coal cities can use coal to make electricity and use electricity to make aluminum in order to achieve all-in-one service of coal, electricity and aluminum. Meanwhile, other industries' development should be encouraged, especially the development of tertiary industry, so as to cultivate new economic growth point.
2. The combination of government leading and market regulation. From the successful experience from home and abroad, it shows that the practices of depending purely on government leading or market regulation both have drawbacks. Government leading and market regulation should be combined to exert dual function of "visible hand and invisible hand". The government should provide financially transfer payment in order to guarantee the safeguard ability of basic public service and maintain the social stability during the period of transformation; and set industry policies to encourage the development of emerging industries and service industry. At the same time, enterprises should develop new technologies, introduce capital, expand the ways of employment and gradually expand reproduction according to the market law, in order to create new economic growth point.
3. Insisting on safety and green development. During the period of looking for transformation paths because of resource exhaustion in cities like Fuxin and Gejiu, the contention and super-mining of surplus resources have caused new coalmine accidents, damaged the original fragile ecological environment and brought about social crisis, which makes a greatly profound lesson. In the starting and running of the government leading transformation, we should insist on safety and green development and can't owe new debts while old ones are not still paid off. During the period of transformation, there are prominent contradictions which are apt to trigger safety problems and group events. We mustn't take a casual attitude.
4. Acting according to circumstances to avoid to copy by rote. Currently, some cities breed a low vision, they only stare at the old economic model and surplus resources so they couldn't explore a new path. Other cities introduce new projects blindly, those with poor transportation conditions and being lack of travel resources also carry out travel projects, only they get little return with huge input. So we should get a clear understanding of the advantages and disadvantages of cities, act according to their own circumstances and make best use of the

advantages and bypass the disadvantages. And we also should avoid seeking quick success and instant benefits. It is practical that most of cities achieve transformation successfully in 20–30 years except few cities with good conditions.

REFERENCES

Dai, X.F. 2010. How to make transformation for resources exhausted cities from international experiences. *Chinese Reform Forum* (2): 96–99.

Fan, C.G., Shao, S.W. & Jiang, C.Z. 2013. Workers county of Gejiu under the charm of resources exhaustion. *Southern Weekend*.

Research Center of Socialism Theory with Chinese Characteristics in Gansu Province. 2012. Exploration on the transformation of resource exhausted cities. *Economic Daily*.

Wang, Z.J. 2009. Discussion on how to make good transformation for resources exhausted cities. *Modern Business* (32): 90.

Yin, Y. 2012. After resources exhaustion. *Jiangxi Daily* (*Nanchang*).

Zhou, C.M. 2003. China is confronted with the crisis of resource exhaustion. *Worker Daily*.

This page intentionally left blank

Progress in Mine Safety Science and Engineering II – He et al. (Eds)
© 2014 Taylor & Francis Group, London, ISBN 978-1-138-00122-0

Application of the analytic hierarchy process on the tender invitation and evaluation of mine safety equipments

Y. Song
Department of Assets Management, North China Institute of Science and Technology, Yanjiao, Beijing-East, China

L.P. Liu
Editorial Department of Journal of North China Institute of Science and Technology, Yanjiao, Beijing-East, China

ABSTRACT: With Analytic Hierarchy Process (AHP), this paper sorts hierarchically various index on the impact of tender invitation and evaluation for mine safety equipments and forms an orderly hierarchical structure. By means of calculation, its weight is determined. Then a objective and scientific evaluation system of bid scheme is established with the combination of quantitative evaluation and qualitative evaluation, which reduces the influence of subjective elements and reflects an open, fair and just principle of competition.

1 INTRODUCTION

In recent years, with the development of safety engineering specialty and the constant expansion of its enrollment scale at colleges and universities, the number of students in this study field has increased steeply. China government and the universities increase the investment of funds of teaching equipments in mine safety yearly in order to guarantee the teaching quality, the procurement of the equipments also gets onerous gradually. The work of procurement is a specific systematic engineering with powerful policy, it also is widespread, complicate with various elements and has high requirements for technology (Duan et al. 2005, Zhang & Hu 1997, Zheng & Chen 2005). Under the principles of following market economy and based on our country's policies and regulations, for example, the Bidding Law Interpretation, and universities' stipulations, the bid winner is determined through a series of procedures such as invitation, submission, opening, evaluation and confirmation of tender by means of competition, then the contract is signed. Thus the influence of subjective elements on the process of decision-making is reduced, which reflects the principle of competition to be open, fair, just and honesty. However, sometimes it obtains different bid winner with various methods of bid evaluation.

Analytic Hierarchy Process (AHP) is a concise and effective method that can make decisions for complicate problems (Zhao & Xu 1986). It meets this need to some extent that applying AHP on the invitation and evaluation of tender for mine safety equipments. According to the overall goal of problem, with the combination of qualitative and quantitative analysis, AHP separates the problem into several factors in a systematic view point and constructs a hierarchical structure model based on its dominance relationship, then confirms the relative materiality of decisions by means of comparison of every two decisions, which reduces the influence of subjective factors, finally obtains a satisfying decision with picking over and objective evaluation.

2 AHP COMPUTING MODEL

2.1 *Determining bid evaluation conditions and establish the hierarchical structure*

There are three companies participating in the bidding competition for mine safety equipments of a certain university. According to the factors considered in the purchase of equipments and the requirements of the bid invitation documents, a hierarchical structure model is built as shown in Figure 1 with evaluation from 4 aspects and 16 factors. The factors are denoted by 16 letters as in Table 1.

2.2 *Constructing judgment matrix*

The weight of evaluation index is the evaluation's quantitative expression of the relative importance of evaluation index. Firstly, the judgment matrix is constructed, the elements of which is comparing every two dominant elements in this hierarchy in

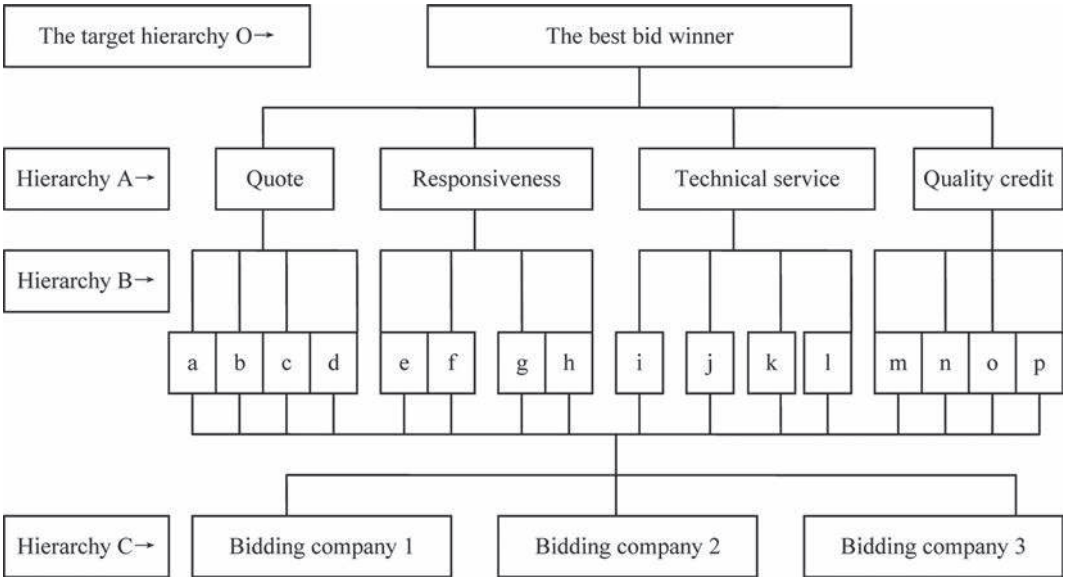


Figure 1. Hierarchical structure model of evaluation condition.

Table 1. Letters denoting the factors.

Letters	Factors
a	Rhe level of total price
b	Complete quotation
c	Favorable terms
d	The rationality of the itemized price
e	Qualification certificates in accordance with the requirements
f	Technical standard response
g	Business standard response
h	Bidding statement accurately clear
i	Program integrity and feasibility
j	Roject personnel structure and quality
k	Technical training plan
l	Service guarantee system and efficiency
m	Business standing
n	Manufacturing capacity
o	The implementation of the Convention in recent three years
p	Similar achievement

terms of some element in the last hierarchy. The comparison adopts 1-9 rating scale method which gives its relative importance a certain numerical value (Zhao & Xu 1986). The specific scale is defined as shown in Table 2.

Experts in the field of safety engineering are invited to quantize the importance of each influence factor, then the judgment matrix of every two factors' comparison is as follows.

Table 2. The definition and scale of judgment matrix.

Scale	Definition and instruction
1	Two elements are of equal importance towards a certain property
3	One element is a little bit more important than the other element while the two elements are compared
5	One element is obviously more important than the other element while the two elements are compared
7	One element is quite more important than the other element while the two elements are compared
9	One element is extremely more important than the other element while the two elements are compared
2, 4, 6, 8	Representing medium scale between the above two standards
$1/a_{ij}$	Reversal comparison of two elements

Taking the hierarchy O of the overall goal as the criteria, the judgment matrix OA of every two factors' comparison of hierarchy A is

$$OA=\begin{bmatrix} 1 & 2 & 2 & 4 \\ 1/2 & 1 & 1 & 3 \\ 1/2 & 1 & 1 & 3 \\ 1/4 & 1/3 & 1/3 & 1 \end{bmatrix}.$$

Similarly, taking the indexes of hierarchy A as the criteria, the judgment matrices A_1B, A_2B, A_3B,

A_4B of every two factors' comparison of hierarchy B are

$$A_1B=\begin{bmatrix}1 & 3 & 3 & 5\\ 1/3 & 1 & 1 & 2\\ 1/3 & 1 & 1 & 2\\ 1/5 & 1/2 & 1/2 & 1\end{bmatrix},\ A_2B=\begin{bmatrix}1 & 2 & 2 & 4\\ 1/2 & 1 & 1 & 3\\ 1/2 & 1 & 1 & 3\\ 1/4 & 1/3 & 1/3 & 1\end{bmatrix},$$

$$A_3B=\begin{bmatrix}1 & 2 & 3 & 4\\ 1/2 & 1 & 1 & 2\\ 1/3 & 1 & 1 & 3\\ 1/4 & 1/2 & 1/3 & 1\end{bmatrix},\ A_4B=\begin{bmatrix}1 & 2 & 3 & 5\\ 1/2 & 1 & 3 & 5\\ 1/3 & 1/3 & 1 & 3\\ 1/5 & 1/5 & 1/3 & 1\end{bmatrix}.$$

Taking the indexes of hierarchy B as the criteria, the judgment matrices B_1C, B_2C, B_3C, B_4C, B_5C, B_6C, B_7C, B_8C, B_9C, $B_{10}C$, $B_{11}C$, $B_{12}C$, $B_{13}C$, $B_{14}C$, $B_{15}C$, and $B_{16}C$ of every two factors' comparison of hierarchy C are

$$B_1C=\begin{bmatrix}1 & 2 & 5\\ 1/2 & 1 & 2\\ 1/5 & 1/2 & 1\end{bmatrix},\ B_2C=\begin{bmatrix}1 & 1/2 & 3\\ 2 & 1 & 5\\ 1/3 & 1/5 & 1\end{bmatrix}.$$

$$B_3C=\begin{bmatrix}1 & 1/2 & 2\\ 2 & 1 & 3\\ 1/2 & 1/3 & 1\end{bmatrix},\ B_4C=\begin{bmatrix}1 & 1/3 & 2\\ 3 & 1 & 5\\ 1/2 & 1/5 & 1\end{bmatrix}.$$

$$B_5C=\begin{bmatrix}1 & 2 & 3\\ 1/2 & 1 & 2\\ 1/3 & 1/2 & 1\end{bmatrix},\ B_6C=\begin{bmatrix}1 & 1/3 & 2\\ 3 & 1 & 5\\ 1/2 & 1/5 & 1\end{bmatrix}.$$

$$B_7C=\begin{bmatrix}1 & 1/2 & 1/3\\ 2 & 1 & 1\\ 3 & 1 & 1\end{bmatrix},\ B_8C=\begin{bmatrix}1 & 1/3 & 3\\ 3 & 1 & 8\\ 1/3 & 1/8 & 1\end{bmatrix}.$$

$$B_9C=\begin{bmatrix}1 & 1/3 & 1\\ 3 & 1 & 2\\ 1 & 1/2 & 1\end{bmatrix},\ B_{10}C=\begin{bmatrix}1 & 1 & 1/2\\ 1 & 1 & 1/3\\ 2 & 3 & 1\end{bmatrix}.$$

$$B_{11}C=\begin{bmatrix}1 & 1/2 & 1/3\\ 2 & 1 & 1\\ 3 & 1 & 1\end{bmatrix},\ B_{12}C=\begin{bmatrix}1 & 1 & 1/3\\ 1 & 1 & 1/3\\ 3 & 3 & 1\end{bmatrix}.$$

$$B_{13}C=\begin{bmatrix}1 & 1/2 & 2\\ 2 & 1 & 3\\ 1/2 & 1/3 & 1\end{bmatrix},\ B_{14}C=\begin{bmatrix}1 & 1 & 1/2\\ 1 & 1 & 1/3\\ 2 & 3 & 1\end{bmatrix}.$$

$$B_{15}C=\begin{bmatrix}1 & 1/3 & 1/2\\ 3 & 1 & 2\\ 2 & 1/2 & 1\end{bmatrix},\ B_{16}C=\begin{bmatrix}1 & 1/3 & 1/4\\ 3 & 1 & 1\\ 4 & 1 & 1\end{bmatrix}.$$

3 THE CONSISTENCY CHECK OF EACH JUDGMENT MATRIX

The consistency of each judgment matrix is determined by its random consistency ratio CR. The judgment matrix is determined to be consistent if $CR<0.1$, otherwise the values of matrix elements need to be adjusted. The random consistency ratio CR is obtained by the following formula.

$$CR=\frac{CI}{RI} \tag{1}$$

where RI = mean random consistency index, which is relevant to the order p of the judgment matrix. For 3 and 4 of the order p, RI is 0.58 and 0.9 respectively (Zhao & Xu 1986); CI = the consistency index of the judgment matrix, which is relevant to the maximal eigenvalue λ_{max} and is of the following form.

$$CI=\frac{\lambda_{max}-p}{p-1} \tag{2}$$

The calculation results are listed in Table 3. It is shown that the CR values of the all 21 judgment matrices in a single order are less than 0.1 so that they all meet the requirements of consistency.

Table 3. The maximal eigenvalue λ_{max} of every matrix, CI, RI and CR.

Matrix	λ_{max}	CI	RI	CR
OA	4.0206	0.0069	0.90	0.0076
A_1B	4.0042	0.0014	0.90	0.0015
A_2B	4.0206	0.0069	0.90	0.0076
A_3B	4.0623	0.0208	0.90	0.0231
A_4B	4.1042	0.0347	0.90	0.0386
B_1C	3.0055	0.0028	0.58	0.0048
B_2C	3.0037	0.0018	0.58	0.0032
B_3C	3.0092	0.0046	0.58	0.0079
B_4C	3.0037	0.0018	0.58	0.0032
B_5C	3.0092	0.0046	0.58	0.0079
B_6C	3.0037	0.0018	0.58	0.0032
B_7C	3.0183	0.0091	0.58	0.0158
B_8C	3.0015	0.0008	0.58	0.0013
B_9C	3.0183	0.0091	0.58	0.0158
$B_{10}C$	3.0183	0.0091	0.58	0.0158
$B_{11}C$	3.0183	0.0091	0.58	0.0158
$B_{12}C$	3.0000	0.0000	0.58	0.0000
$B_{13}C$	3.0092	0.0046	0.58	0.0079
$B_{14}C$	3.0183	0.0091	0.58	0.0158
$B_{15}C$	3.0092	0.0046	0.58	0.0079
$B_{16}C$	3.0092	0.0046	0.58	0.0079

4 THE CONSISTENCY CHECK OF THE TOTAL ORDERING OF HIERARCHIES

When the total number of hierarchies $n \geq 3$, the consistency of the total ordering of hierarchies is needed to be checked other than the single ordering of hierarchies, and the consistency ratio of the overall goal of each hierarchy should be less than 0.1. The consistency ratio CR^k of the hierarchy k towards the overall goal is

$$CR^k = CR^{k-1} + CI^k / RI^k \quad (3 \leq k \leq n) \tag{3}$$

where CI^k = the consistency index of the hierarchy k to the overall goal; RI^k = the random consistency index of the hierarchy k towards the overall goal. CI^k and RI^k is obtained by the following formulae respectively.

$$CI^k = \left[CI_1^{(k-1)}, CI_2^{(k-1)}, \ldots, CI_{n_k}^{(k-1)} \right] \mathbf{w}^{(k-1)} \tag{4}$$

$$RI^k = \left[RI_1^{(k-1)}, RI_2^{(k-1)}, \ldots, RI_{n_k}^{(k-1)} \right] \mathbf{w}^{(k-1)} \tag{5}$$

where $CI_i^{(k-1)}$ = the consistency index of each element's comparison matrix of the hierarchy k, taking the index i of the hierarchy k–1 as the criterion; $CR_i^{(k-1)}$ = the random consistency index of each element's comparison matrix of the hierarchy k, taking the index i of the hierarchy k–1 as the criterion. $\boldsymbol{w}^{(k-1)}$ = the total ordering vector of the hierarchy k–1 to the overall goal and is obtained from the following formula.

$$\mathbf{w}^{(k-1)} = \mathbf{W}^{(k-1)} \mathbf{W}^{(k-2)} \cdots \mathbf{w}^{(2)} \tag{6}$$

where $\boldsymbol{w}^{(2)}$ = the ordering of each index of the hierarchy 2 (hierarchy A) towards the overall goal, namely the corresponding eigenvector of the largest eigenvalue of matrix OA, that is $\boldsymbol{w}^{(2)} = [0.4337, 0.2389, 0.2389, 0.0886]^T$; $\boldsymbol{W}^{(k-1)}$ = the matrix constructed by the weight vector of each element of the hierarchy k–1 towards each index of the hierarchy k–2.

$$\mathbf{W}^{(k-1)} = \left(\mathbf{w}_1^{(k-1)}, \mathbf{w}_2^{(k-1)}, \ldots, \mathbf{w}_{n_{k-1}}^{(k-1)} \right) \tag{7}$$

where $w_i^{(k-1)}$ = the weight vector of each element of the hierarchy k–1 towards the index i of the hierarchy k–2.

For the maximal eigenvalue λ_{max} of every matrix listed in Table 3, its corresponding eigenvector is calculated. The ordering matrix $\boldsymbol{W}^{(3)}$ of the hierarchy 3 (Hierarchy B) towards each index of the hierarchy 2 (hierarchy A) and the ordering matrix $\boldsymbol{W}^{(4)}$ of the hierarchy 4 (hierarchy C) towards each index of the hierarchy 3 (hierarchy B) are gained.

$$\mathbf{W}^{(3)} = \begin{bmatrix} 0.5320 & 0 & 0 & 0 \\ 0.1854 & 0 & 0 & 0 \\ 0.1854 & 0 & 0 & 0 \\ 0.0971 & 0 & 0 & 0 \\ 0 & 0.4337 & 0 & 0 \\ 0 & 0.2389 & 0 & 0 \\ 0 & 0.2389 & 0 & 0 \\ 0 & 0.0886 & 0 & 0 \\ 0 & 0 & 0.4760 & 0 \\ 0 & 0 & 0.2114 & 0 \\ 0 & 0 & 0.2157 & 0 \\ 0 & 0 & 0.0969 & 0 \\ 0 & 0 & 0 & 0.4600 \\ 0 & 0 & 0 & 0.3248 \\ 0 & 0 & 0 & 0.1486 \\ 0 & 0 & 0 & 0.0665 \end{bmatrix},$$

$$\mathbf{W}^{(4)} = \begin{bmatrix} 0.5954 & 0.2764 & 0.1283 \\ 0.3090 & 0.5816 & 0.1095 \\ 0.2970 & 0.5396 & 0.1634 \\ 0.2297 & 0.6483 & 0.1220 \\ 0.5396 & 0.2970 & 0.1634 \\ 0.2297 & 0.6483 & 0.1220 \\ 0.1692 & 0.3874 & 0.4434 \\ 0.2363 & 0.6817 & 0.0819 \\ 0.2098 & 0.5499 & 0.2402 \\ 0.2402 & 0.2098 & 0.5499 \\ 0.1692 & 0.3874 & 0.4434 \\ 0.2000 & 0.2000 & 0.6000 \\ 0.2970 & 0.5396 & 0.1634 \\ 0.2402 & 0.2098 & 0.5499 \\ 0.1634 & 0.5396 & 0.2970 \\ 0.1260 & 0.4161 & 0.4579 \end{bmatrix}^T.$$

From the formula (6), the ordering of each index of hierarchy B towards the overall goal is [0.2307, 0.0804, 0.0804, 0.0421, 0.1036, 0.0571, 0.0571, 0.0212, 0.1137, 0.0505, 0.0515, 0.0231, 0.0408, 0.0288, 0.0132, 0.0059]^T.

The ordering of hierarchy C towards the overall goal is [0.35067, 0.42081, 0.22852]^T, which shows that the order of quality of the three bidding com-

panies towards the overall goal is the Company 2,1,3, so that the Company 2 is the best.

The consistency index CI of hierarchy 3 towards the total goal is 0.0103, the corresponding random consistency index RI = 0.9000, the consistency ratio $CR = 0.0191 < 0.1$, which meets the requirement of consistency.

The consistency index CI of hierarchy 4 towards the total goal is 0.0049, the corresponding random consistency index $RI = 0.5800$, the consistency ratio $CR = 0.0274 < 0.1$, which also meets the requirement of consistency.

5 CONCLUSION

With the application of analytic hierarchy process, the index of bid evaluation is quantized by means of constructing judgment matrix, which is convenient for the operation on computers. It provides scientific reference for better determining the final bid winner for the mine safety equipments with the reduction of the interference of the subjective factors. It also makes the decision-making process of the submission of tenders more procedural and scientific with the increase of the transparency of appropriation expenditure and reflects the bid evaluation to be fair and reasonable. It is quite a effective and practical method of bid evaluation and worth to be promoted everywhere.

REFERENCES

Duan, A.L., Wang G.P. & Li, Y.G. 2005. The application of analytic hierarchy process on the bid evaluation of equipments purchase. *Computer and Information Technology* 12: 39–41.

Zhang, G.X. & Hu S.L. 1997. Inviting and evaluating tenders with the application of analytic hierarchy process. *Optimization of Capital Construction* 18(1): 23–27.

Zhao, H.C. & Xu, S.B. 1986. *Analytic hierarchy process-a easily new decision-making method*. Beijing: Science Press.

Zheng, Y.Q. & Chen, B.W. 2005. The application of fuzzy analytic hierarchy process on project bidding. *Journal of Hunan City University* (*Natural Science Edition*) 14(1): 11–14.

This page intentionally left blank

Progress in Mine Safety Science and Engineering II – He et al. (Eds)
© 2014 Taylor & Francis Group, London, ISBN 978-1-138-00122-0

Fault characteristics and the tectonic evolution in Changdi area of the Bohai Bay Basin

Xuemei Li, Wei Wang, Benqun Zhang & Lifang Zhou
College of Geoscience and Surveying Engineering, China University of Mining and Technology, Beijing, China

ABSTRACT: Based on the analysis of 3D seismic data and drilling wells, this paper studies the main fault and its associated structures in Changdi area of the Bohai Bay Basin. Fault activity has the characteristics of episodic by the influences of the Jiyang movement and the Dongying Movement. The larger two unconformity interfaces are closely related to the fracture episodic activities in Changdi area. The multi-phase unconformity interface reflects the tectonic evolution of the experience of polycyclic depression in the Cenozoic. According to the analysis of the major balanced cross section and identification of the important interface, combined with regional subsidence history, the tectonic evolution of the Changdi area can be divided into three stages: fold formation stage, extensional rift stage and stable depression stage. Extensional rift stage further divided into I episode in Eocene ($E_2 s_3$–$E_2 s_2$) and II episode in Oligocene ($E_3 s_1$–$E_3 d$).

1 INTRODUCTION

Changdi area is located at northeast of shallow water area in Dong Ying, Shandong Province (Fig. 1), it has more than 30 years of exploration history since the beginning of being developed in 1970s. After years of exploration and development, there were great discoveries in the fault terrace zone of the west side and the slope belt of the east side of Changdi faults, which has already been put into exploration. The research (Chen et al. 2001, Chen 2000, Ma 2004, Tian et al. 2005) to the regularity of petroleum entrapment in this zone done by predecessors has further revealed that this area is an petroliferous zone which is multi-type, multi-layer, extremely rich of petroleum and gas resources, it has great potential for exploration and development. In consideration of that the structure is a key factor on controlling petroleum entrapment, and for the purpose of providing geological supports to continuous exploration, this article studies the fracture development period, combined styles and tectonic evolution characteristics in Changdi area.

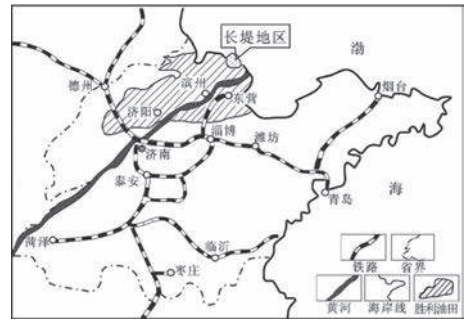


Figure 1. The geographical location map in Changdi area.

2 GEOLOGICAL BACKGROUND

Bohai Bay Basin is a superimposed basin in Mesozoic and Cenozoic that developed on the basis of North China Craton (ancient crystalline basement), which was composed of a series of NNE and NE directive depressions and uplifts among. They are, from north-west to south-east, Jizhong depression, Cangxian uplift, Neihuang uplift, Huanghua depression, Linqing depression, Dongpu depression, Chengning uplift, lower Liaohe depression, Liaodong Bay depression, Bozhong depression and Jiyang depression, etc. (Guo et al. 2007).

Changdi area is located at south central of Bohai Bay Basin, the position of its structure is located at north-east of Zhanhua sag in Jiyang depression, which is composed of Changdi fault and the drape structural belt in Changdi buried hill. The drape structural belt in Changdi buried hill is low uplift belt surrounded by sub-sag, it extends into Zhuangdong sag by the direction of north and east, divided by Gudong fault and the drape structural belt in Gudong buried hill by the direction of south-east, connected with Gunan sag at the south, divided by Changdi fault and Wuhaozhuang sag at west, laid against Chengbei sag at north-west

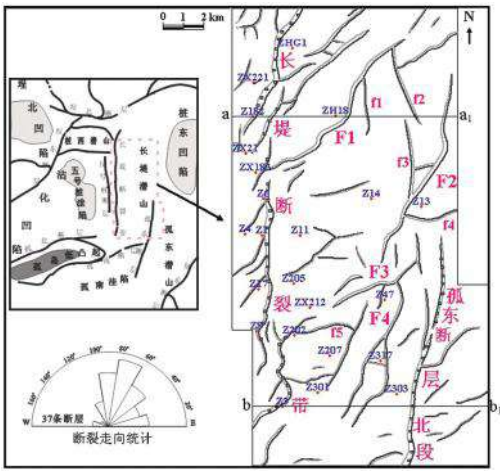


Figure 2. Fault distribution in Changdi area.

(Fig. 2). The drape structural belt is a positive structure of NNE direction grown based on the background of Mesozoic buried hill, it is an asymmetrical anticline which is located at the up-thrown side of Changdi fault and is also divided by other secondary faults. The strata of buried hill is mainly the Pre-Paleogene, the overlying strata is Shahejie formation and Dongying formation in Paleogene, Guantao formation and Minghuazhen formation in Neogene (Wang & Qian 1992).

2 FAULT CHARACTERISTIC

2.1 *Fault of order*

There are 50–70 faults with differences of scale, shape and attributes in Changdi area, those faults are extensive normal faults which controls the tectonic framework and formative evolution in this area. Fault are also the main reason of controlling of petroleum and gas generation, migration, accumulation, storage and allocation, such fault can be divided into 5 scales according to the different controlling effect of petroleum and gas reservoir allocation and scale (Luo 1999). Deep fracture (Fracture L1) controls the extension and allocation of petroleum and gas zone, basement fractures (Fracture L2 & 3) control the formation of multiple petroleum and gas accumulation belt, superficial fracture (Fracture L4 & 5) control the allocation of water in the petroleum and gas and complicate it. This article, combines with above category, gives 4 levels to the fractures according to the fault controlling effect to the different structural unit of basins and depressions, they are—main basement fractures (Fracture L1), secondary basement fractures (Fracture L2 & 3) and superficial fractures (Fracture L4).

Level-one fracture, "controlling basin fault", controls the deposition and allocation of petroliferous basins, and cut through basement. The faults have a long evolutionary history, hundreds of kilometers of extended length with up to ten thousand meters gap, such as Tan-Lu fault in Bohai Bay Basin. There is no Level-one fracture in this area.

Level-two fracture, "controlling depression fault", controls the deposition and allocation of the depression (sag) and uplift. The faults extend length of about ten kilometers with up to 200–1000 meters gap. There are Changdi fault and Gudong fault in this area. They control the formation of Changdi buried hill and the migration and accumulation of petroleum and gas.

Level-three fracture, "controlling zoning fault", divides fault block zones and controls the history of geological development of fault block zones. The faults extend length of several kilometers with up to 100–200 meters gap, such as the fault terrace on the northern of ZH18 well fault (F1) and Changdi low uplift on the southern of F1 fault.

Level-four fracture controls the local structures and complicates relations of oil-gas-water in petroliferous fault block zones. They are the secondary faults, and are huge in quantity, formed lately and with short-lived activity characteristic. The faults extend length of about 1–2 kilometers with up to 10 meters gap, such as f1 fault and f2 fault in Figure 2.

The faults developed in Changdi area are all L3 and L4 fractures except Changdi fault and Gudong fault.

2.2 *The main characteristic of fracture*

Affected by the strike-slip of Tan-Lu fault, Changdi fault and Gudong fault has a consistent strike with NS trending. The main feature is an en-echelon structure in plane. There developed two groups of the secondary faults, strike of NS trending and nearly EW trending between the two main faults. These faults are with skew-type or bifurcation-type in plane, and this type of tectonic activity forms a number of fault nose (Chen et al. 2005). These faults are the hinge and the channel of connection Paleogene and Neogene.

Changdi fault is located in the west of Changdi buried hill, with significant characteristic of strike-slip structure (Liu et al. 2005). It is the boundary fault and controlled the formation and development of the drape structural belt. This fault was constitutive of the three main faults in en echelon arrangement and the secondary fault is intersected with the main fault. The middle part of the fault is the main body, strike of near NS trending. The

south part turns to SW and the north part turns to NE. The overall fault is "S" type with a total length of the 26 km, W tendency and 40°~65° dip angle. From south to north the fault becomes gradually steepen and the biggest gap developed in the north part has a drop that is up to 300 meters. From capwise seismic profiles, the fault showed obviously the normal fault feature that the fault plane is the listric shaped of steep upper and flat lower (Fig. 3a). Both sides of Changdi fault are developed Mesozoic. The downthrown side deposited thick Paleogene while the up-thrown side subjected to uplift and erosion, resulting in hiatus of Kongdian formation and the No. 4 section of Shahejie formation. It shows that the fault activity began in Early Paleogene, and controlled the deposition of Paleogene above its strata in Changdi buried hill.

Gudong fault was also constitutive of a series of fault in en echelon arrangement as well as Changdi fault. The north part of Gudong fault controlled the deposition of Changdi buried hill. It is the normal fault with a length of the 7 km, strike of near NS trending, dip of NW trending and 60°~70° dip angle, the biggest gap is up to 400 meters. Figure 3b shows that the combined type of Gudong fault and Changdi fault is fault terrace, the combined type of Gudong fault and the antithetic fault is "Y" type.

Changdi fault and Wuhaozhuang fault formed the fault terrace zone. The north part of Changdi fault and F1 fault of NE trending formed the fault terrace zone of west-dipping (Fig. 3a). Figure 4 shows that the southern F1 fault formed Changdi low uplift (anticline) and near Z11 well developed culmination due to the uplift of footwall controlled by Changdi fault and F1 fault. The middle part of Changdi fault and the north part of Gudong fault formed horst block. The south part of Changdi fault and Gudong fault formed the fault terrace zone of west-dipping. The north part of Gudong fault controlled the structural framework of southeastern buried hill which developed culmination near the western of Gudong fault Z303 and Z47 wells. The eastern of Gudong fault formed Gudong uplift. Since there is no impact by Changdi fault and Gudong fault, only a series of NE trending step faults in fault terrace (F1, F2, F3), the northeast of Changdi area formed slope. Changdi area showed tectonic framework of "High in the south, low in the north; High in the east, low in the west" and "E-W zoning and N-E blocking".

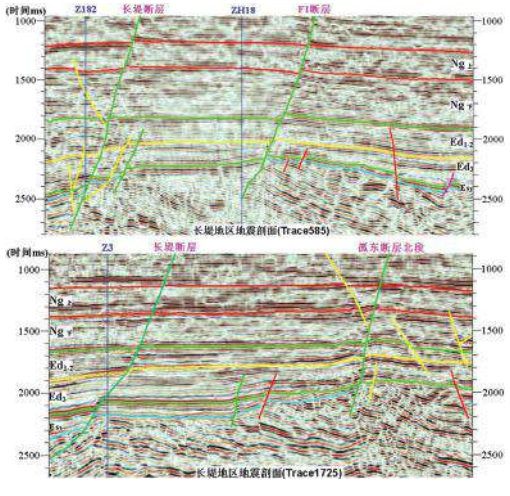


Figure 3. Main fault profile feature (a) aa1 seismic survey line in fig. 2; (b) bb1 seismic survey line in fig. 2.

2.3 *Fault control over petroleum and gas*

Fault is the channel of petroleum and gas migration, but is also the advantage of petroleum and gas gathering area. Z1 and ZX221 wells in Changdi fracture zone shows the existence of petroleum and gas while away from the fault or oil source wells there is almost no petroleum and gas existed. Changdi fault is connected with Wuhaozhuang Sag and Changdi buried hill (Lu et al. 2004). Petroleum and gas of Wuhaozhuang Sag migrated to Changdi fault through the sandstone layers. Under the condition of lateral sealing of north section of Changdi fault and the seal of regional caprocks, petroleum and gas gathered in fault nose or fault block traps of the downthrown side of fault to form rich reservoirs in Changdi fault terrace zone. Sand body of both

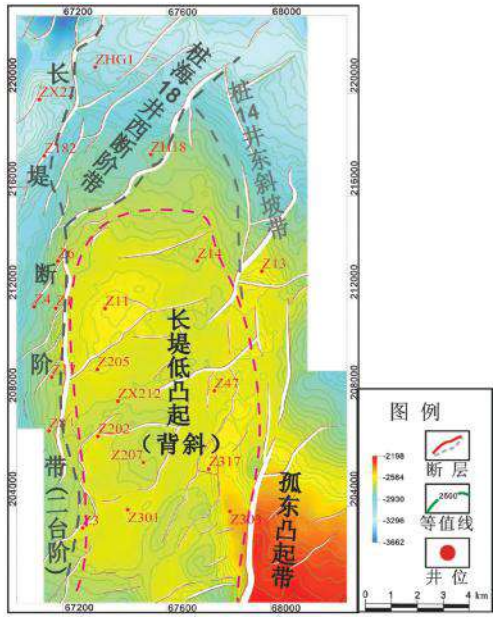


Figure 4. Tectonic map of Es_3 reflector in Changdi area.

sides of fault can be connected in South section of Changdi fault. Across the fault petroleum and gas moved along up-dip strata, and finally gathered in the favorable traps of Shahejie formation, Dongying formation and Guantao formation. The NE trending faults in the northeast slope of the study area are orthogonal to structural lineament and cutting a few series of strata. It is not conductive to petroleum and gas migration and accumulation. Petroleum and gas migrated to the culmination along the unconformity, under the condition of lateral sealing of F3 fault and north section of Gudong fault, and can gather in stratigraphic traps.

3 TECTONIC EVOLUTION

In the current study, tectonic evolution of Bohai Bay Basin has the characteristics of multi-episodic rift and multi-cycle evolution (Gong et al. 2007, Allen et al. 1997, Qi et al. 1995, Hou et al. 2001). That there are multiple tectonic movements since Cenozoic era: tectonic uplift events during the final deposition of Kongdian formation, the No. 4 and No. 3 section of Shahejie formation and Dongying formation in Paleogene, Minghuazhen formation in Neogene. Good evidence of tectonic evolution is the evidence of unconformity surface between sedimentary strata.

In the case of Changdi area, two period unconformity surfaces, which were formed during the final deposition of the No. 4 section of Shahejie formation and Dongying formation, showed the most intense and the strongest regional character. The former represented tectonic movement is commonly known as the "Jiyang Movement", the latter is commonly referred to as "Dongying movement". Tectonic evolution of Changdi area is closely related to these movements. It has significant episodic characteristics, divided into three stages: fold formation stage, extensional rift stage and stable depression stage. Extensional rift stage further divided into I episode in Eocene (E_2s_3–E_2s_2) and II episode in Oligocene (E_3s_1–E_3d).

3.1 *Fold formation stage in Cretaceous*

It began with effect of strong intracontinental rift and lithospheric thinning in early Cretaceous Eastern China. Strong extension had led to the NW basement fault activity in this region, huge amount of lava gushed along the fault (Zhang et al. 2004). Along Tan-Lu fault zone generated the dextral strike-slip motion, it controlled of the formation and development of rift basin of the west of fault zone (Zhang & Dong 2008).

Late Cretaceous Eastern China entered into the NW–SE trending tectonic compression and shrinkage strain stage due to the late episode of Yanshan movement (Yang & Chen 2005). During this stage fault activities strengthened, such as Gudong-Wuhaozhuang-Zhuangxi NW trending fault, began to activity. Changdi area was subjected to squeeze, resulted in fold uplift and erosion Mesozoic strata. Changdi buried hill has an initial shape with a clear fold shape of EW axial trend and East pitch.

3.2 *Extensional rift stage in Paleogene*

3.2.1 *I episode in Eocene (E_2s_3–E_2s_2)*

After the experiences of short-lived uplift in late Cretaceous, Bohai Bay Basin entered into rift stage in early Paleogene. Under the influence of fault depression, the earth's crust fractured and a series of small rift lacustrine basin formed. The lacustrine basin is commonly filled with Kongdian formation and the No. 4 section of Shahejie formation in Bohai Bay Basin. But the study area is still in the stage of uplift and erosion, resulting in hiatus of Kongdian formation and the No. 4 section of Shahejie formation in Changdi buried hill.

Jiyang Movement, occurred in the final deposition of the No. 4 section of Shahejie formation was recognized as the result of the conversion of tectonic regime in the tectonic evolution of Jiyang Depression (Chen 1993, Jia et al. 2007, Ren 2004). The motion direction of the Pacific plate transformed NNW trending into NWW trending at latest middle Eocene, and the Indian plate and Eurasian plate during this period occurred in the hard collision, making the regional stress field of Changdi area changed (Wu et al. 2004). The regional stress field turned into the NW–SE tensile stress field from S–N trending. In the course of transformed stress field the succession activity of Wuhaozhuang fault caused to form the secondary fault-Changdi fault. Trending near NS of Changdi fault is in parallel with Wuhaozhuang fault, and between the two faults formed the fault terrace zone. Changdi buried hill extends at NNW trending. Now regional tectonic framework began to take shape.

After the formation of Changdi buried hill, its deposition was controlled by Changdi fault and Gudong fault. Bohai Sea is similar to a pull-apart basin and the uplift area began rift after Jiyang Movement. The No. 3 section of Shahejie formation began to deposit and within this period the subsidence rate of basin basement is the largest in the rift stage (Guo et al. 2007). From south to north section of Changdi fault the intensity of fault activity in turn strengthened. The north section of Gudong fault began to activate in southeast part of the study area. The fault block uplift is simultaneously with the rift subsidence. The No. 3 section of Shahejie formation formed deposition only in the downthrown side of Changdi fault

and the downthrown side of Gudong fault, having angle unconformity with the underlying Mesozoic strata (Tr). The unconformity interface has the meaning of tectonic change in Changdi area, because of the transformation of tectonic stress field and change arid paleoclimate into moist. The depositional and subsidence center of Bohai Bay Basin has begun to migrate towards sea area in this period. The No. 3 section of Shahejie formation mainly developed near-shore subaqueous fan and was a sufficient thickness of gray mudstone.

Lake Basin became gradually small during the deposition of the No. 2 section of Shahejie formation. Changdi buried hill exposed above water and subjected to erosion because of short-lived lifting during the final deposition. The No. 2 section of Shahejie formation has stratigraphic gap.

3.2.2 *II episode in Oligocene (E_3s_1–E_3d)*

Oligocene regional stress field has been completely transformed into dextral shear stress, in this period fault with weak activity or inactivity. The deposition of No. 2 section of Shahejie formation has the feature of filling and leveling up, led to flat terrain in Changdi area. Lake water abundantly invaded during the deposition of the No. 1 section of Shahejie formation. This stratigraphy is mainly composed of dark oil shale of shallow lake-semi-deep lake facies. The bottom of the No. 1 section of Shahejie formation developed bio-accumulated limestone in Changdi buried hill high parts. The distribution of sediments was dominated by paleotopography and terrigenous supply. During the deposition of Dongying formation lake water was further deep and the depositional and subsidence center continually migrated towards north (Han & Zheng 2007). The lower part of Dongying formation developed the inter-bed of a sufficient thickness of dark mudstone and thin carbonate formation.

Late Paleogene Himalayan orogeny caused uplift of the Qinghai-Tibet Plateau. Affected by this, the transition from rift stage to overall settlement stage in eastern China, the landform turned from west-dipping into east-dipping (Wang 2005). This movement is referred to as "Dongying movement" in Bohai Bay Basin (Shi et al. 1999). Under the influence of Dongying movement, Bohai Bay Basin was subjected to strong uplift and erosion to form the regional angular unconformity between Paleogene system and Neogene system (T_1). Analysis on the rates of vertical fault motions (Fig. 5) showed that Changdi fault and Gudong fault once again began the activity and produced the secondary faults nearby (Ji et al. 2008) and controlled the formation of fault nose and fault block trap.

The late deposition of Dongying formation is the final rift stage of basin. At this stage lake basin

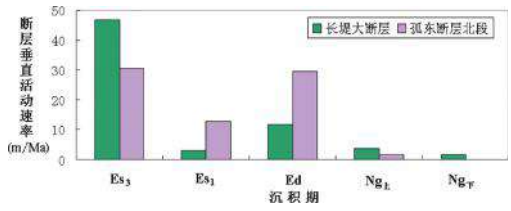


Figure 5. Vertical activity rate of Changdi fault and Gudong fault.

shrunk and lake water became shallow. The upper part of Dongying formation developed the inter-bed of sandstone and mudstone. Sedimentary environment turned from fan delta in the lower part to braided river in the upper part.

3.3 *Stable depression stage from Neogene to Now*

Dongying movement makes a period transferring of Bohai Bay Basin from the rifting period to the stable depression period. Neogene sedimentary environment became stable and tectonic activity became weak in Changdi area. Neogene system layers developed a few of small fault with NEE trending. During Miocene Changdi fault may have little activity, but it cannot control the development of the strata. Late Pliocene Changdi fault and the secondary fault were basically inactivated. The subsidence center of Jiyang Depression has moved into Zhanhua Sag in the late deposition of Dongying formation, and further moved into Bozhong Sag in the deposition of Guangtao formation. During this period Changdi area belongs to the intrabasinal depression. The stratigraphy sedimentation of Changdi buried hill significantly thickened in northeast by the impact of the sag in north and east. The Guantao formation developed the inter-bed of conglomerate, conglomerate-bearing sandstone and mudstone, from braided river sediments to meandering river sediments. Covered by the Guandao formation, Minghuazheng formation and Quaternary system, the strata became gradually thicker towards Bohai sea area, which formed the drape structural belt of Neogene and Quaternary.

4 CONCLUSION

1. Experienced a complex evolutionary process, Changdi fault is the fracture structure of long-term inheritance activities. In the Cenozoic, Changdi fault strongly subsided. The downthrown side of Changdi fault deposited thick Paleogene strata through oil and gas migration to Changdi fault direction. Continuing the

up-thrown side uplift, it formed the drape structural belt in Changdi buried hill.

2. Affected by "Jiyang Movement" and "Dongying movement", fault activity has episodic characteristics in Changdi area. Jiyang Movement caused a series of syn-sedimentary fault to development, such as Changdi fault and Gudong fault. The upper part of Changdi buried hill exposed above water and subjected to erosion to form the No. 3 section of Shahejie formation and Mesozoic strata with angular unconformity (Tr). Dongying Movement made Changdi fault and Gudong fault once again activate and produced the secondary faults nearby. It was subjected to strong overall uplift and erosion to form Dongying formation and Guantao formation with angular unconformity (T_1) in Changdi area.
3. Tectonic evolution of Changdi area is closely related to "Jiyang Movement" and "Dongying movement". It has significant episodic characteristics, and was divided into three stages: fold formation stage, extensional rift stage and stable depression stage. Extensional rift stage further divided into I episode in Eocene (E_2s_3-E_2s_2) and II episode in Oligocene (E_3s_1-E_3d).

REFERENCES

Allen M.B., McDonald D.I.M., Zhao X, et al. Early Cenozoic two-phase extension and late Cenozoic thermal subsidence and inversion of the Bohai basin, northern China. *Mar Petrol Geol*, 1997; 14:951–972.

Chen Guangjun. Discussion on hydrocarbon-bearing in Changdi buried hill of Zhanhua Sag. *Multiple Oil-Gas Field*, 2000; (4):6–10.

Chen Guangjun, Shang Yanan, Zhuang Wenshan, et al. Discussion on hydrocarbon-bearing possibility in east flank of drape structural zones of Changdi buried hill. *Petroleum Geology and Recovery Efficiency*, 2001; 8(1):27–30.

Chen Haiyun, Yu Jianguo, Shu Liangshu, et al. The structural styles and their relation with petroleum-gas resources of the Jiyang Depression. *Geological Journal of China Universities*, 2005; 11(4):622–632.

Chen Jiashu. Features of the Jiyang movement and its effects on the evolution of the Jiyang Depression. *Experimental Petroleum Geology*, 1993; 15(1):86–99.

Gong Zaisheng, Cai Dongsheng, Zhang Gongcheng. Dominating action of Tanlu fault on hydrocarbon accumulation in eastern Bohai Sea area. *Acta Petrolei Sinica*, 2007; 28(4):1–10.

Guo Xingwei, Shi Xiaobin, Qiu Xuelin, et al. Cenozoic subsidence in Bohai Bay Basin: characteristics and dynamic mechanism. *Geotectonica et Metallogenia*, 2007; 31(3):273–280.

Hou Guiting, Qian Xianglin, Cai Dongsheng. The tectonic evolution of Bohai Basin in Mesozoic and Cenozoic time. *Acta Scientiarum Naturalium Universitatis Pekinensis*, 2001; 37(6):845–851.

Han Huijun, Zheng Deshun. Characteristic contrast of Mesozoic and Cenozoic faults of eastern and western structure units in Jiyang Depression and its controlling factors. *Petroleum Geology and Recovery Efficiency*, 2007; 14(3):12–15.

Ji Shuangwen, Yan Zijie, Jiang Nengdong. Discuss on tectonic and sedimentary evolutions of Bohai Bay Basin—taking Jiyang Sag as an example. *Petroleum Geology and Engineering*, 2008; 22(3):21–25.

Jia Hongyi, Yang Changchun, Yu jianguo, et al. Structual transition and hydrocarbon accumulation during early eocene in Dongying Sag of the Jiyang Depression. *Progess in Geophysics*, 2007; 22(4):1312–1319.

Liu Gang, Wu Shiguo, Zou Dongbo. The discussion about the property of Changdi fault. *Petroleum Geophysics*, 2005; 3(1):53–56.

Lu Youliang, Song Haitao, He Youbin, et al. Analysis of hydrocarbon reservoir formation characteristics and its key control factors. *Journal of Jianghan Petroleum Institute*, 2004; 26(2):50–52.

Luo Qun. An outline of theory of fracture-controlling hydrocarbon. *Petroleum Explorationist*, 1999; 4(3): 8–14.

Ma Hongfei. Analysis on oil-gas reservoir-forming rule in Changdi buried hill drape structural belt. *Petroleum Geology and Recovery Efficiency*, 2004; 11(5):33–35.

Qi Jiafu, Zhang Yiwei, Lu Kezheng, et al. Cenozoic tectonic evolution in Bohai Bay Basin province. *Journal of the University of Petroleum, China (Edition of Natural Science)*, 1995; 19(suppl.):1–6.

Ren Jianye. Identification of Cenozoic fold-thrust structure and its dynamic setting in Jiyang Sag. *Geological Science and Technology Information*, 2004; 23(3): 1–5.

Shi Buqing, Wu Zhiping, Wang Jixiang, et al. A study of the geological characteristics and geodynamic origin of Dongying movenment, Bohai Bay Basin. *Experimental Petroleum Geology*, 1999; 21(3):196–200.

Tian Bo, FengBin, Ji Youliang. Oil-gas reservoir forming system and pattern in Changdi area. *Petroleum Geology and Recovery Efficiency*, 2005; 12(5):28–30.

Wang Binghai, Qiankai. Geology research and exploration practice in the Shengli petroleum province. *Dongying: The Petroleum University Press*; 1992.

Wang Pinxian. Cenozoic deformation and history of sea-land interactions in Asia. *Earth Science-Journal of China University of Geosciences*, 2005; 30(1):1–17.

Wu Zhiping, Li Wei, Zheng Deshun, et al. Analysis on features and origins of the Mesozoic and Cenozoic faults in Zhanhua Sag. *Geological Journal of China Universities*, 2004; 10(3):405–417.

Yang Chao, Chen Qinghua. Tectonic evolution and tectono-stratigraphic classification of Jiyang Depression. *Petroleum Geology and Recovery Efficiency*, 2005; 12(2):9–12.

Zhang Yueqiao, Dong Shuwen. Mesozoic tectonic evolution history of the Tan-Lu fault zone, China: Advances and new under-standing. *Geological Bulletin of China*, 2008; 27(9):1371–1390.

Zhang Yueqiao, Zhao Yue, Dong Shuwen, et al. Tectonic evolution stages of the early Cretaceous rift basins in eastern China and adjacent areas and their geodynamic background. *Earth Science Frontiers*, 2004; 11(3):123–133.

Progress in Mine Safety Science and Engineering II – He et al. (Eds)
© 2014 Taylor & Francis Group, London, ISBN 978-1-138-00122-0

Regression model analysis on relativity between coal mine output and safety

Li Song, Li Yang & Cheng-Jun Zhang
Anhui University of Science and Technology, Huainan, Anhui, P.R. China

ABSTRACT: This paper quantitatively analyzed effect of production performance on organizational accidents using Pearson correlation and regression model analysis. Results showed that coal mine output have significant effects on safety. Specifically, this paper posits that there is a U-shaped curve relativity between production yields and accident rate, along with yields increase, death toll occurred in accidents initially decrease, then increase.

1 INTRODUCTION

Although the death rate for one million tons of coal output steadily decreased, the coal industry also sees the most severe and frequent accidents, resulting in more than 2000 deaths every year. Two third of the industry's fatalities occurred in township and village coalmines with small size. It seems that smaller firms tend to have higher accident rates than larger firms. However, several coal mines' disasters astonishingly occurred in modern coal mines which have been regarded as higher safety, even some key state-owned coal mines with advanced gas supervisory system. For example, a methane gas explosion in 2009 killed 78 miners at the Tunlan mine in Sanxi province; in 2005, at the Sunjiawan mine in Liaoning province, 214 more perished. Whether coalmines' size may be related to organizational safety or not aroused our research interest (Xueqiu He & Li Song 2012). On the one hand, larger firms generally have more slack resources and are thus better able to withstand setbacks and adapt to changing circumstances and to have more slack resources to devote to support functions, including safety specialists and safety management (Karen Page 2009, Abay Asfaw et al. 2013, Benjamin Brooks 2008). On the other hand, larger firms have more complex social-technical system in which system components can interact in unexpected ways (Charles Perrow 1998, Trond Kongsvik & Petter Almklov 2010). And more employees increase the likelihood that multiple human errors will interact in unanticipated ways to create an accident. As the repercussions of organizational accidents reverberate through organizations and are felt from human resources to accounting, firms are beginning to incorporate messages of safety in their missions and strategies. Safety is often not the reason for the existence of an organization, but it is one of the desirable attributes of its performances. Since safety is not the sole organizational output and concern, coal mine managerial decisions and organizational practices seek to strive a balance between different organizational outcomes, they are faced with decisions on how to structure their activities among safety and other performance (Rasmussen J & Svedung I 2002; Zohar D 2010). Therefore, an organizational safety causal model should consider the interaction of safety performance with other organizational performances. In order to explore relativity between output and safety, this paper made a statistically analysis based on data in China mining.

2 METHODS

2.1 *Data and variable*

Coal mine output data were obtained from databases collected in the book "Coal Mine Safety Accidents and Typical Cases" which was compiled by HENAN ADMINISTRATION OF COAL MINE SAFETY (Henan Administration of Coal Mine Safety 2001). Coal mine output was used to describe coal mine size. Deaths toll was used to describe coal mine safety.

2.2 *Model*

Data during 1980–2000 were used to build regression models (Guosheng Ding & Tao Li 2010). To built regression model, we must test correlation between coal mine output and coal mine safety. We used SPSS 13.0 software to operate data.

3 RESULTS OF MODELS

3.1 *Pearson correlation analysis*

Shown in Table 1, all of correlation coefficient was significant, which means that coal output have relativity with safety. Comparing five coal mines, obvious difference would be found. As to JZ, correlation between coal output and death indexes were positive significant (.606*, .541**), which means that safety risk would be increase along with rise of output. But in other coal mines (PDS, HB, XZ), correlation between coal output and death indexes were negative significant, which means that death occurred in accidents would decrease with increase in output.

3.2 *Regression analysis*

Table 2 and Figure 1 to Figure 4 present the results of both linear and quadratic regression analysis where the exposure variable is death toll in each mine, independent variable is mine output. It is obviously

Table 1. Descriptive statistics and correlations for key variables.

Coal mine	Variable	1	2	3
JZ	1 coal output	1		
	2 death toll	.606**	1	
	3 fatality rate per Mt	.541*	.975**	1
PDS	1 coal output	1		
	2 death toll	–.671**	1	
	3 fatality rate per Mt	–.690**	.994**	1
HB	1 coal output	1		
	2 death toll	–.436*	1	
	3 fatality rate per Mt	–.527*	.987**	1
XZ	1 coal output	1		
	2 death toll	–.730**	1	
	3 fatality rate per Mt	–.787**	.986**	1

*Correlation is significant at the 0.05 level (2-tailed).
**Correlation is significant at the 0.01 level (2-tailed).

Table 2. Results of linear and quadratic regression of 4 coal mines.

Coal mine	Equation	R2	F	Constant	b1	b2
JZ	M1-Linear	.37	9.29	–19.30	.068	
	M2-Quadratic	.49	7.22	107.84	–.64	.001
PDS	Ml3-Linear	.45	15.55	298.60	–.16	
	M4-Quadratic	.49	8.60	970.89	–.99	.000
HB	M5-Linear	.19	4.46	44.43	–.07	
	M6-Quadratic	.23	2.61	226.67	–.78	.001
XM	M7-Linear	.53	21.71	42.82	–.06	
	M8-Quadratic	.77	29.83	173.32	–.56	.000

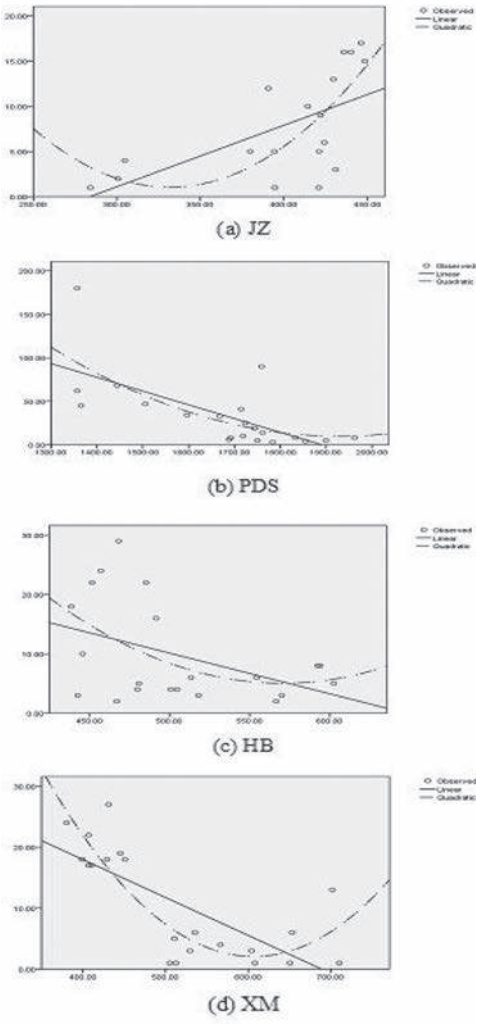


Figure 1. Linear and quadratic regression of 4 coalmines.

that quadratic regression results were better than those of linear regression. Models showed that the quadratic model testing a possible curvilinear effect of output on the accident death toll, which posits a U-shaped curve relationship between the output of the coal company and the accident death toll. In other words, as output are increased in a mine company, the death toll occurred in accidents initially decrease, then increase.

4 DISCUSSION AND CONCLUSIONS

The essence of the argument was that at the corporate level, firms are removed from the immediate

dangers of the work environment and can bring time, resources, and rationality to bear on the issues surrounding workplace safety. As they accumulate a variety of accident experiences across organizational units, firms can analyze and integrate their findings. There are many factors that promote coal output to increase, such as expanding scale, increasing labor number and improve mining technology. As to a colliery, coal reserves is fixed, they are two mutually alternative mode of coal output growth, one is mining technique progress, the other is labor investment, the first is lean production, the later is labor-intensive. Added labors obviously increase safety risks at work place. Besides, each mine has a life cycle. With the increase of mining depth, environment safety risks generated by ground pressure, terrestrial heat and gas would rise. JZ, PDS, HB and XM are all state-owned key mines, compared with PDS, HB and XM, JZ is a coal company with a long history. It was proposed that size would increase the relative danger for each employee because of the notions of physical factors and unexpected interactions risks at workplace.

While management contemplates important issues such as safety investment and safety culture on organizational accidents, the results of this paper suggest that they should also consider the size and life cycle of the companies. Where the size do not favor workplace safety, managers should consider substitutes for these factors through networks or other forms of organization.

ACKNOWLEDGEMENTS

This work is supported by the National Natural Science Foundation of China (71071003), Humanities and Social Science plan foundation of the MOE (12YJAZH119), and the key project of Humanities and Social Science of Anhui education department (2011sk139zd).

REFERENCES

Abay Asfaw, Christopher Mark & Regina Pana-Cryan. 2013. Profitability and occupational injuries in U.S. underground coal mines. Accident Analysis and Prevention 50(1):778–786.

Benjamin Brooks. 2008. The natural selection of organizational and safety culture within a small to medium sized enterprise (SME). Journal of Safety Research 39(1):73–85.

Charles Perrow. 1998. High-risk Technology with the "Normal" Cccident:34–36. Science and Technology Literature Publishing House, Beijing.

Guosheng D & Tao L. 2010. SPSS statistics: form research design to data analysis:259–261. Machine Industry Publishing House, Beijing.

Henan administration of coal mine safety. 2001. Henan coal mine production safety accident statistics and typical case:15–44. China Coal Industry Publishing House, Beijing.

Karen Page. 2009. Blood on the coal: The effect of organizational size and differentiation on coal mine accidents. Journal of Safety Research 40(2): 85–95.

Rasmussen J & Svedung I. 2002. Graphic representation of accident scenarios: mapping system structure and the causation of accidents. Safety Science 40(5):397–417.

Trond Kongsvik & Petter Almklov. 2010. Organisational safety indicators: Some conceptual considerations and a supplementary qualitative approach. Safety Science 48(10):1402–1411.

Xueqiu He & Li Song. 2012. Status and future tasks of coal mining safety in China. Safety Science 50(4):894–898.

Zohar D. 2010. Thirty years of safety climate research: reflections and future directions. Accident Analysis and Prevention 42(5):1517–1522.

This page intentionally left blank

Progress in Mine Safety Science and Engineering II – He et al. (Eds)
© 2014 Taylor & Francis Group, London, ISBN 978-1-138-00122-0

Construction of mine safety explicit knowledge map

Wensheng Wang, Wei Dai & Qianying Sun
School of Management, China University of Mining and Technology (Beijing), Beijing, China

ABSTRACT: According to WBS in project management, the article forwards decomposition and classification methods in the explicit knowledge of mine safety, discusses theme indexing method in the application of mine safety knowledge mapping, gives some suggestions about reducing or eliminating the inconsistent in mine safety explicit knowledge, and realizes the construction through related knowledge.

1 INTRODUCTION

Knowledge map is an important skill in constructing knowledge management system, it associates knowledge resources into knowledge network. Its main function is to find the needed knowledge fast and correctly through knowledge map index. Mine safety knowledge map is a comprehensive set where mine safety knowledge's location and relationship store. (Chen & Liao 2006, Su & Jiang 2005). Therefore, after we search and arrange the related explicit knowledge, we should break the complex knowledge into easy and understandable unit, and also need to associate the related knowledge according to their relationship.

2 THE DECOMPOSITION AND CLASSIFICATION OF MINE SAFETY EXPLICIT KNOWLEDGE

2.1 *Preparing the new file with the correct template*

In order to manage the process of projects implementation conveniently, in the management of projects, we often decompose the project, and control it by procedure step by step, this method in projects management is called Work Breakdown Structure (WBS). Referring to this thought, we can also decompose the mine security explicit knowledge, through the decomposition of mine security knowledge we can realize goals as follow (Zhu & Li 2011):

1. Decompose big mine security explicit knowledge into small ones, thus can let the mine workers understand the whole content of knowledge quickly.
2. Decompose mine security explicit knowledge can visualize and embody the abstract knowledge, let workers more easily master the lower level mine security knowledge. Therefore, the fear of accepting new knowledge can reduce dramatically, and, studying step by step can improve workers' enthusiasm of study and bring them sense of achievement.
3. The smaller mine security explicit knowledge units are more easy for search and link. (Yuan & Zhang 2006)

Figure 1 is an example of decomposition of mine security influence factor knowledge system. This knowledge decompose diagram is showing that mines security is influenced by four factors such as workers' unsafe action, machines' unsafe status, environment's unsafe factor and management drawback. If you want to learn mines security knowledge, you can from these four factors. These four factors have knowledge system separately and can continue to decompose, meanwhile, they have tight connections and disasters' reason theory is just about their connections.

The decomposition of mines security knowledge must enforce by the basic rule of the knowledge forming, and the knowledge decomposition is limited. We must make sure that lower level of knowledge is including enough knowledge, do not have much more quantity and layers, to prevent the final knowledge overflow, let workers are hard to study and search for.

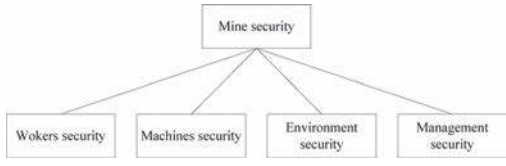


Figure 1. An example of decomposition of mine safety knowledge.

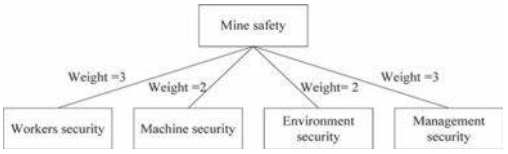


Figure 2. An example of weight of decomposition of mine security knowledge.

Each knowledge point's importance is different. After decomposition of mine security knowledge, we should weight each knowledge unit, determine the key knowledge. As shown in Figure 2, management security and workers security can guide security management directly, so they are more important, therefore we can give them higher weight (Ren & Zhang 2011). The other two points are ordinary so their weights can be lower.

After the decomposition of knowledge, we then label each point, including date, author, source and store mode, etc.

3 MINE SAFETY EXPLICIT KNOWLEDGE MAP INDEX

3.1 *Text and indenting*

After decomposing the collected and organized mine safety explicit knowledge, then the important task is to indexing the knowledge, making more convenient. Indexing is to make the natural language (title) to controllable humanities language (intelligence language). Through analysising related mine safety paper, web document, we can determine the identification, construct the indexing project, and then provide more index point. Indexing process need to be correctly, reasonably and objectively, especially to reveal knowledge content, practical, targeted and consistent character is needed, so that the user can find the specific point from a lot of resources.

Now, indexing technology is mainly divided it two classes: theme indexing and classification indexing. Theme, usually refers to the object in the resource set that we talk about, including phenomenon, things and problems. Subject indexing is to reveal kinds of knowledge and data from subject angle. Theme indexing is give the corresponding words identification according to the valuable content and character in the knowledge set. China Classification Theme words List is needed before we analysis and check theme. Theme index can be divided into yuan morphology, key morphology, title method and Syria lexical, according to is different, word selecting methods.

To reduce or eliminate the inconsistency in subject indexing process finish indexing work effectively, we should pay attention to the following problems. (Liang & Zhang 2008)

1. Improving indexing personnel's professional knowledge level. As to indexing mine safety knowledge, mastering indexing techniques and methods is not enough, the professional field of mine safety is preferred. Theme analysis is a key point in indexing, to refine the theme accurately, indexing staff must master the related knowledge in mine safety. In addition, indexing personnel should have seriously pragmatic style of work, can not only based on the classification number is given in the corresponding bar to find a few key words, one-sided pursuit of quantity is easy to cause the error indexing.
2. Improving indexing personnel's quality. Staff's educational background, thinking style and knowledge level influence indexing work directly. Indexing personnel should pay attention to keep learning, improve the quality, enlarge scope of knowledge, to solve new theory, new knowledge in the application of Chinese Classification Subject Words List flexibly, avoiding all sorts of wrong.
3. Keeping the same indexing personnel in professional field stable. Indexing personnel can't please everyone, and grasps each professional domain knowledge. In other words, each index personnel's indexing knowledge is limited to a relatively stable professional range, not only can improve the accuracy of the subject analysis and the speed of document indexing, but also help improve the consistency of the literature indexing.
4. Paying attention to subheading's indexing. Paying attention to subheading's index is not at random, indexing accurately can improve retrieval efficiency rapidly.
5. Refining theme accurately. Analysis is the key link of the indexing, the correct or not of the indexing is related to the stand or fall of the theme analysis. The process is to enrich and refine the contents of the literature and the central idea. They should browse the original content paragraph by paragraph. If only by using title or provided key words, it will end up in leakage scale, wrong standard, too thick index.

4 PHOTOGRAPHS AND FIGURES MINE SAFETY EXPLICIT KNOWLEDGE MAP ASSOCIATED

Mine safety explicit knowledge map is an icon that shows the location and the relationship. So after we mark, classification, and store each knowledge

Table 1. Typical relations between mine safety explicit knowledge.

Classification	Description	Explanation
Equivalence Relation	Kind of equivalence between the two knowledge units, including a sense of equivalence and numerical equivalent.	A = B
Generic Relation	The specific part of knowledge is universal knowledge.	A can be divided into B, C, D
Structural Relation	A knowledge system can be divided into a number of subsystems.	C is formed of A, B.
Sequential Relationship	Obvious chronological relationship between knowledge unit.	A happened before B; A happened after B.
Topological Relation	Spatial structure relations between knowledge unit.	A is above of B; C is in the right of D
Casual Relation	There is a causal relationship between the knowledge unit.	A is the reason of B; B is the result of A.
Conditional Relation	A knowledge unit is another knowledge unit's conditions.	B occurs only if A occurred.
Similar Relation	The meaning of the expression of the two knowledge unit is similar.	A and B have similar meanings.
Dependent Relation	The existence of a knowledge unit depends on another knowledge unit.	A is responsible for B.



Figure 3. Typical relations between mine safety explicit knowledge.

unit, the main work of build knowledge is to establish the relationship of each unit, which is the core step as the relationship is the main part of knowledge map. The typical relationship is listed in followed form.

Complex internal relations. After we establish various relationships between knowledge, we link each knowledge unit as network hyperlinks link each different knowledge dot, then the knowledge map builds, as picture 3 shows. To show mine safety knowledge map through visualization techniques, both traditional directory hierarchy in tree structure or reticular structure can be used.

Varieties of complex internal relationships. Established various associations between knowledge, knowledge unit are various meanings cable, the like Network hyperlinks, knowledge connects the dots, so that the formation of enterprise knowledge map, Figure 3 shows. Can choose to make use of visualization techniques to mine safety knowledge map unfolded, both traditional directory hierarchy in tree structure or other the reticular structure (Lu & Du 2010, Peng & Yang 2009) can be used.

5 CONCLUSION

Knowledge map is a compass of knowledge resources. When some kind of knowledge is needed, we can acquire "line" through knowledge map. Knowledge map can help people establish the link between knowledge, make messy, unstructured knowledge into structured, and can also help users find the desired look for knowledge and information quickly and correctly. Explicit knowledge in the field of mine safety is widely applied, varieties of explicit knowledge is distributed in different nodes and body, the complex relationship between the knowledge is existed, therefore, the clearly classification and define is the basis of establishing Mine Safety knowledge management system.

ACKNOWLEDGMENTS

We wish to thank the financial supports from the Program for New Century Excellent Talents in University (Grant No. NCET-12-0963), and the Doctoral Foundation of Ministry of Education of China (Grant No. 20100023120008), and the Ministry of land and resources public industry welfare fund (Grant No. 201211003).

REFERENCES

Chen Qiang & Liao Kaiji. 2006. Knowledge Map Research and Prospect. Journal of Information 24(05):43–46.

Liang Yong & Zhang Chenzhi. 2008. Based on CSSCI journals knowledge map. *Modern Library and Information Technology* 22(02):18–22.

Lu Qiaochu & Du Hui. 2010. System design knowledge map-based Learning Content Management System. *Silicon Valley* 35(08):57.

Peng Runhua & Yang Zhenqing. 2009. New product development ontology-based knowledge management research. *China Management Informationization* 6(10):76–79.

Ren Hao & Zhang Hong. 2011. Knowledge map-based enterprise knowledge management system. *Magement* 54(09):195.

Su Hai & Jiang Zuhua. 2005. Construction of product development-oriented knowledge map. *Journal Of Shanghai Jiaotong University* 11(12):34–39.

Yuan Zonglei & Zhang Chenhong. 2006. Xu Zhengchuan, Process-oriented enterprise knowledge map. *Computer Integrated Manufacturing Systems* 51(09):30–3.

Zhu Jing & Li Daquan. 2011. On China's mine safety standardization problems and countermeasures. *Management & Technology (HEAD)* 5(01):61–66.

Progress in Mine Safety Science and Engineering II – He et al. (Eds)
© 2014 Taylor & Francis Group, London, ISBN 978-1-138-00122-0

The distribution and influencing factors analysis of coal consumption of China based on quantile regression

Pingping Cheng
Jiangsu Jianzhu Institute, Xuzhou, Jiangsu, China

Yuan Kong
The Thirty-Eighth Research Institute of China Electronic Technology Group Corporation, China

ABSTRACT: This paper uses quantile regression and OLS regression to analysis the factors of coal consumption of china. In contrast, we find a lot of differences between quantile and OLS, quantile regression gives more conditions. This gave us more theoretical support for China economic sustainable development.

1 INTRODUCTION

China's coal resource has not only large-quantity production, but also tremendous consumption as well as the single consumption structure problem exist relatively at the same time. The main consumption of coal are focus on electricity and manufacturing industry, though the coal chemical industry is booming, there is till far way to go forward. The consumption is distributed unevenly both in industry and region. By comparing the four provinces which has largest consumption of coal in east region with the four provinces which consume mostly in middle-west region, we can find that the consumption percentage of four provinces in east region has been keeping upon 40% since 2005, but the consumption percentage of four provinces in middle-west region has been keeping around 16% generally since 2000. So to speak, the comparison of coal consumption between provinces is as important as between industry. In consideration of the huge different data comes from provinces, we are going to set up Regression quintile model to analyze the influence factors and distribution feature of coal consumption.

2 QUINTILE REGRESSION MODEL

Quintile regression model proposed by Koenker and Basset in 1978's, is readily extended to the linear model (Koenker R & Bassert G 1978, Wu Jiannan & Ma Wei 2006, Zhang Weiying, et al. 2005). Quintile regression equation can be described as:

$$y_t = x_t\beta_\theta + \mu_t \tag{1}$$

$$Quant_\theta(y_t / x_t) = x_t'\beta_\theta \tag{2}$$

$$Quant_\theta(\mu_t / x_t) = 0 \tag{3}$$

Where θ means Conditional Quantile determined by the regression matrix.

Then the θ th sample quantile, $0 < \theta < 1$, may be defined as solution to the minimization problem:

$$\min \sum_{t=1}^{n} \rho_\theta(y_t - x_t'\beta_\theta) \tag{4}$$

(4) Where checking function is defined as follows:

$$\rho_\theta \begin{cases} \theta\lambda, \lambda > 0 \\ (\theta - 1)\lambda, \lambda < 0 \end{cases} \tag{5}$$

(5) solving the weighted value of the least error, that is the sum of the weighted value of the least error, where the positive error endowed θ, the negative error endowed (1 – θ).

Note that for the θth sample quantile ($0 < \theta < 1$), the estimated value –is $\hat{Quant}_\theta(y_t | x_t) = x_t'\hat{\beta}_\theta$, that is the conditional distribution of y_t is under the condition x_t. On the basis of empirical study, 0.1, 0.25, 0.5, 0.75 and 0.9 are a few commonly used in the estimation of sample quantile. Note that, the 5th sample quantiles estimated functions relative to each other, so the estimated standard deviation can be attained by the bootstrapping method. OLS regression coefficients can be described as marginal change of non explanatory variables caused by unit change of explanatory variables.

Regression quintile meaning that estimated coefficients are the θth sample quantily conditional distribution caused by marginal change of the t-th variable x_t.

3 DATA DESCRIPTION AND INDEX SELECTION

3.1 *Data Description*

To ensure the representability and comprehensive of the sample, increasing the robustness of regression estimation and the reliability of testing, this paper selected total 30 provinces (excluding Tibet) as a sample, using a total of seven years (2000–2006) array about 210 observations, making empirical analysis using both the cross-section data and time-series data. In the models, the missing data use the mean of Observation data. At the same time, we set the time dummy variables (Zhang Hong & Li Zhong-xue 2007).

All data are from the China Infobank and china statistical yearbook (2005–2007).

3.2 *Index selection*

3.2.1 *Explanatory variables*

There are complex factors of coal consumption, also many uncertainties. This paper examines the factors commonly accepted by the dominant theory. This paper selects five main variables: Gross fixed asset formation (GDZC), price (P), population (R) and industrial structure (CYJG) and GDP.

3.2.2 *Controlled variables*

In order to study dynamic change of factors that influencing the coal consumption, introducing the time dummy variables, this paper constructed five dummy variables to represent the years 2000–2006, for example in the year of 2000, we make D2000 valued 1, others take 0, when other variables have taken the value of 0, denote the time data of year of 2006.

By analyzing, we can get the influencing factors of coal consumption quintile regression model:

$$Quant_{\theta}(y_n|x_n) = \beta_0 + \hat{\beta}_{\theta} x_n + \gamma' z_1 \quad (6)$$

Where y_n the θ-th ($0 < \theta < 1$) random quantile, x_n denote explanatory variables, ψ_0 is constant terms, z_1 is other influencing factors. In this paper, let coal consumption be explanatory variables, and explanatory variables with Gross fixed asset formation (GDZC), price (P), population (R) and industrial structure (CYJG) and GDP.

4 REGRESSION QUANTILE

Uses (6) formulas, we can estimate the explanatory variables θ-th quintile on coal consumption. Regression results are shown in Table 1. Unlike the least squares estimator, high efficiency over a wide rang of error distributions.

5 CONCLUSIONS AND SUGGESTIONS

5.1 *The Influence of Industrial structure to coal consumption*

In this paper, using the proportion of the second industry to measure industrial structure, through the comparative analysis of OLS estimation and quantile regression estimation we find that except in the 75% and 90% percentiles are statistically insignificant, other regressions are highly significant. With the rise of quantile, the coefficient of regression estimation rose from 53.935 to 143.32, as shown in Figure 1. This show that the influence factors of industrial structure is constantly expanding, it also reflect from the side under the conditions of the larger proportion of the second industry, the pressure of the coal consumption is greater. This rise is not a simple linear. Easing the pressure of the coal consumption and reducing the proportion of the second industry have a crucial relationship. The investment of fixed assets is a good alternative of total industrial investment, and it strengthens this conclusion from the industrial side.

5.2 *The population impact on coal consumption*

If the proportion of the second industry and investment in fixed assets is a good representative of industry, then the population is a good representative of the people's living consumption. The regression coefficient of population to coal consumption also reflects an increasing relationship. It also shows that in the present consumption system, coal consumption is still the main source of energy. Rising quantile brings the expansion of coefficients and the similar conclusion of industrial structure, it also reflects a positive reinforcing relationship. Conversing the energy consumption mode is good way to ease the non-renewable energy.

5.3 *Economic growth and coal consumption*

The regression results don't get the expecting positive relationship. It cannot exclude in the factors of industry and people's life, due to the multicol linearity exists the possible regression parameter distortion. But a negative correlation between the

Table 1. Results of coal consumption quintile regression (2000–2006).

	OLS	Q5	Q10	Q15	Q25	Q50	Q75	Q90
d2000	–245.375	709.639	1192.314	1198.236	646.407	271.315	126.285	1609.164
	(–0.190)	(0.640)	(1.200)	(1.280)	(0.790)	(0.280)	(0.070)	(0.300)
d2001	–100.900	619.896	977.266	1387.012	931.286	179.673	574.990	1516.511
	(–0.080)	(0.530)	(0.970)	(1.440)	(1.130)	(0.160)	(0.310)	(0.270)
d2002	21.458	744.348	1239.880	1095.028	573.524	140.617	–203.410	255.377
	(0.020)	(0.750)	(1.450)	(1.330)	(0.770)	(0.150)	(–0.110)	(0.050)
d2003	–78.436	628.227	552.910	404.898	253.009	–134.083	–158.669	570.473
	(–0.070)	(0.8300)	(0.800)	(0.580)	(0.370)	(–0.150)	(–0.080)	(0.110)
d2004	–391.612	501.251	342.670	249.116	362.282	–342.747	–10.980	–708.696
	(–0.390)	(0.660)	(0.530)	(0.340)	(0.540)	(–0.380)	(–0.010)	(–0.160)
d2005	477.999	475.298	316.996	446.806	297.763	284.287	343.901	645.129
	(0.500)	(0.590)	(0.390)	(0.560)	(0.440)	(0.310)	(0.230)	(0.150)
CYJG	260.52***	53..935	89.401***	111.94***	114.63***	143.32***	156.787	234.669
	(6.330)	(1.380)	(2.720)	(4.440)	(4.990)	(4.140)	(1.130)	(1.410)
GDZC	3.457***	1.849**	2.469***	2.816***	2.482***	3.470***	4.288***	4.020**
	(5.170)	(2.490)	(3.460)	(4.100)	(3.050)	(3.370)	(4.550)	(2.090)
p	–0.752	4.794	14.917	43.712	43.028	1.901	117.424	255.034
	(–0.010)	(0.110)	(0.330)	(1.040)	(1.100)	(0.040)	(0.550)	(0.570)
R	0.821***	0.431***	0.428***	0.448***	0.455***	0.905***	1.202***	0.821
	(5.910)	(7.470)	(6.100)	(5.780)	(4.960)	(6.540)	(5.180)	(1.640)
GDP	–0.874***	–0.236	–0.401**	–0.510**	–0.438	–0.812**	–1.068**	–1.003
	(–4.000)	(–1.220)	(–2.100)	(–2.630)	(–1.810)	(–2.390)	(–2.830)	(–1.540)

* (1) ***, **, * denote the 1%, 5% and 10% significance level.
** (2) Numbers in parentheses are t-test values.
*** (3) Numbers of the regression observed value is 210, using six time dummy variables.

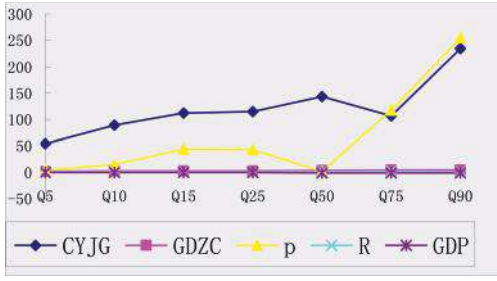


Figure 1. Results of the explanatory variables quintile regression.

weak also reflects a strengthening of relations, and the relationship is positive, can't change the mode of energy consumption, simple rely on investment to satisfy the economic growth of coal consumption will give greater pressure, this model is not sustainable.

REFERENCES

Koenker R & Bassert G 1978. Regession quantile. Economica.(46).

Wu Jiannan & Ma Wei 2006, Estimating Behavioral Models of Extreme Behavior: Quantile Regression Method and Its Real ization and Appl ication. Application of Statistics and Management.(9).

Zhang Weiying, et al. 2005. The Gr owth of High—New—Tech Firms and its Determinants: An Application of the Quantile Regr ession Model. Management World.(10).

Zhang Hong & Li Zhong-xue 2007, Affecting factors and projected scenarios for coal demand in China, Journal of china coal society.

This page intentionally left blank

Progress in Mine Safety Science and Engineering II – He et al. (Eds)
© 2014 Taylor & Francis Group, London, ISBN 978-1-138-00122-0

Coal fines production in different drainage stages and its influence on productivity

Shihui Hou, Xiaoming Wang, Min Wu, Xinjing Wang & Zhenhua Jing
China University of Geosciences, Wuhan, Hubei, China

Aiwei Zheng
China University of Geosciences, Wuhan, Hubei, China and Key Laboratory of Coalbed Methane Resources and Reservoir Formation Process, Ministry of Education, China University of Mining and Technology, Xuzhou, Jiangsu, China

ABSTRACT: Investigation about coal fines flow in different drainage stages and its influence on well productivity was based on parameters, such as the peak gas rate, the peak water rate, the peak change of producing fluid level (PFL) and duration of coal fine flow, and also combined with analysis of coal primary texture. It can be concluded that the key factor that influences well productivity is coal fines migration, deposition, and block in pore and fracture; coal fines production in different drainage stages is influenced both by coal structure and drainage system, and the latter determines quantity of coal fines in late production process; while continuous and steady drainage system will control coal fines flow and thus improve well productivity, by effectively avoiding pressure and velocity sensitivity induced by dramatic pressure change, and also Jamin Effect caused by coal fines accumulation.

1 INTRODUCTION

Controlling coal fines production is an important part in dewatering process of CBM wells, which has an important influence on gas production (Xian et al. 2005). Coal fines production can lead to a significant decline in production, besides, to clean out the coal fines on a continuous basis is a costly work over issue (Magill et al. 2010). Therefore, controlling coal fines production is the key to decreasing issues of stuck pump, bury pump and workover, and also the key to keeping high and stable gas production.

In terms of production mechanism of coal fines, Liu et al (2011) concluded that coal fines production is mainly induced by drilling, wellbore collapsing and coal matrix cracking in coalbed methane horizontal well. Chen et al (2009) proved that coal fines production is associated with coal property, drill rig abrasion, proppant grinding and coal matrix collapsing affected by ground stress change. In order to investigate coal fines production mechanism and its influencing factors during the production process in CBM wells, Cao et al (2012, 2013) conducted relevant physical experiments with single-phase water flow displacement, and came to that coal property is the basis of coal fines generation, while disturbance affected by engineering process is one of its inducements.

In terms of relationship between coal fines and well productivity, Zou et al (2012) suggested coal fines accumulation will bridge pores, damage reservoir, and finally cause decline on gas production. Based on coal reservoir-pressure-drop model, Zhang et al (2013) indicated that deposition of coal fines in gas production channel will decrease reservoir permeability and thus damage reservoir and influence gas production. Li et al (2009) suggested rapid drainage rate could lead to the closure of fractures, the damage of permeability and the decline of gas production. Quan et al (2012) suggested the unreasonable drainage system could easily cause the phenomenon of reservoir damage, damage of coal petrography and jam of coal fines, and impact on the coalbed methane production. Luo et al (2012) analyzed production factors and pointed that coal fines could enter and block gas production channel with fluid, causing influence on gas production.

Liu et al (2012) suggested coal fines production in different phases is responding to different stages of drainage. Li et al (2012) indicated coal fines production is different within different drainage stages.

In brief, previous researches are mainly on mechanism of coal fines production and relationship between coal fines and well productivity, but few talks about coal fines flow in different drainage process and its influence on well productivity.

Therefore, this paper takes 4 drainage wells for example, and investigates coal fines flow in different drainage process and its influence on well productivity, based on researches about coal structure and drainage system.

2 GEOLOGICAL SETTINGS

The study area is located in SE of Ordos Basin, the joint between Jinxi ply belt and Shanbei slope (Fig. 1). It spans within a monoclinal structure, with strata flattish and trend NS. The two parallel faults, which are reverse faults, runs 20 km long, trends NNE and dips ES, with the angle of dip 60° and distance of displacement 25–60 km; and depth of the target 2# coal, within Shanxi Formation, runs ranging from 600 m to 1500 m, which indicates a favourable exploration area for coalbed methane (CBM).

3 DATA SOURCE

4 CBM wells: A1, A2, A3 and A4, are selected for this research. And parameters, such as the peak gas rate, the peak water rate, the peak change of producing fluid level (PFL) and duration of coal fine flow, are listed in Table 1. As indicated by the table, drainage system of the 4 wells above is not the same and there is great difference in their rate and duration of coal fine flow. For A1 well, there is no fine flow and its peak gas rate can be up to 3534.34 m^3/d during the whole drainage process, however, plenty of coal fine flows out in A4 well and time of fine flow is as high as 255 days, while its peak gas rate is only 460 m^3/d.

Figures 2(a)-2(d) are coal cores drilled out of the four wells. Cores, which are from A1 and A3 wells and in blocks, indicate that coal is mainly clarain in lithotype and bright coal in macroscopic type. Coal cores from both A1 and A3 wells bear entire primary texture, while those from A2 and A4 wells present broken texture, in detail, coal from A2 well is cracked and that from A4 well is polished into powder, with fine being easy consolidated into block.

Table 1. Parameters of CBM wells.

Wells	Max change of PFL* (m/d)	Peak water rate (m^3/d)	Coal fines production	Duration of coal fine flow (d)	Peak gas rate (m^3/d)
A1	65.0	5.52	None	0	3534.34
A2	48.0	7.04	Slight	81	2632.0
A3	83.87	10.13	Some	15	1115.0
A4	134.9	14.37	Mass	255	460.0

* PFL: producing fluid level.

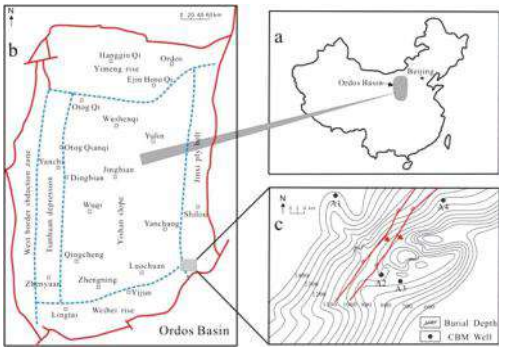


Figure 1. (a) Location of Ordos Basin in China, (b) Ordos Basin, (c)The study area.

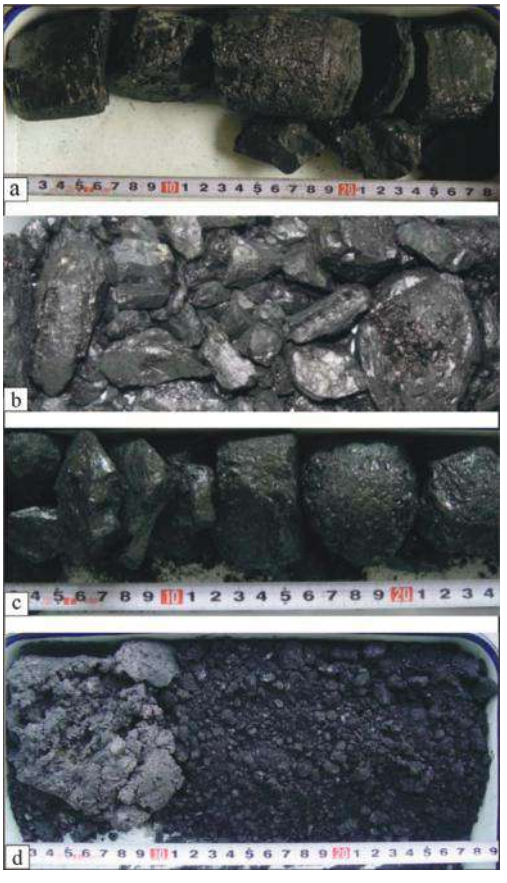


Figure 2. (a) Coal cores of well A1, (b)Coal cores of well A2, (c) Coal cores of well A3, (d) Coal cores of well A4.

4 RESULTS AND DISCUSSIONS

Gruesbeek & Collin (1982) concluded that fine concentration in porous media is related with flow speed. The density remains constant in steady flow, while it will boost in scales influenced by transient flow. Accordingly, the transient drainage system will lead to fine production and migration in coal seam, and destruction in coal texture within area of primary coal developed is the main cause of coal fines.

The change in producing fluid level (PFL) indicates that in drainage system. Figures from 3 to 6 show PFL fluctuation, gas rate and coal fine production from wells of A1, A2, A3 and A4 respectively.

Production curves of A1 well (Fig. 3) indicate there is no fine and gas flow during the early steady depressurization process. After drop of 65 m in PFL, A1 well commences to produce gas on the 125th drainage day. And gas rate increases with no fine flow under the steady PFL. The main reasons for no fine flow of A1 well are: a) coal primary texture is intact because of the simple structure nearby, and accordingly there is few coal fine (Fig. 2(a)); b) the pressure drop induced by steady PFL is too small to broke coal texture, accordingly there is no fine produced and no influence on productivity of this well.

Production curves of A2 well (Fig. 4) indicate there is great change in PFL both during the steady-depressurization and come-to gas production processes, which leads to fluctuant speed of flow migration in formation. The unsteady flow will cause: a) increasing grain in fluid, including coal fine and proppant, which has been confirmed by Gruesbeek & Collin; b) decreasing conductivity of both hydraulic and nature fracture system, induced by coal fine block; c) decreasing desorption speed of coalbed methane, controlled by increasing pressure in porous media, which influences effect of depressurization, area of desorption and finally the productivity of CBM well.

The fluctuation in gas rate is also associated with fine flow induced by great change in PFL. Coal from this well presents in block, with some in powder (Fig. 2(b)), which is controlled by faults within the study area. The extreme change in PFL leads to quick pressure drop, gas desorption within reservoir near wellbore, and thus the high gas rate in a short time. However, quick and fluctuate drainage system can contribute to coal fine concentration increase in fluid, fine accumulation in pore and finally a dramatic gas rate decrease; after present fine production, gas rate will increase in a short time as a result of the better permeability and conductivity.

After the original fines in the coals discharged entirely, there was no coal fine produced when changed the PFL, and the main reasons were considered as a), the coal fines had been flown out in the early production, and because of the relative integrity of coal structures in well A2, the fluctuant pressure, attributing to the PFL in the later period, did not produce new fines; b), In the later production, PFL became stable gradually as well as the daily gas production rate was about 1000 m^3/d.

As indicated in Figure 5, in well A3 (similar as well A1), the PFL, in the stable pressure decline period, kept relatively high resulting in the pressure fluctuation. And because of this, the fluid began to flow unstably and brought residual coal fines out of the coalbeds. On the 162nd drainage day, the PFL reached 83.87 m/d, but the steep fluctuation of the PFL did not cause the coal fines production. Except for the original structure integrity of the coals in well A3 (Fig. 2(c)), the phenomenon also

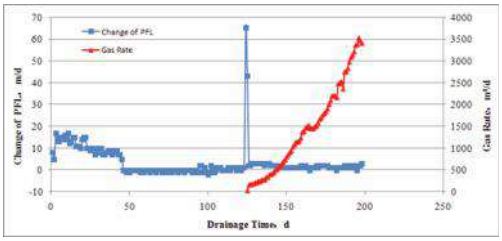


Figure 3. Production curves of well A1.

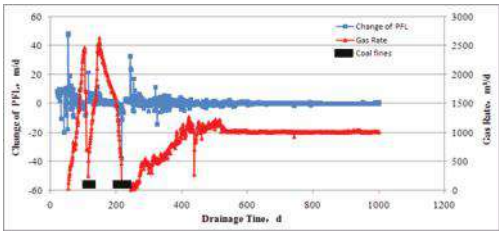


Figure 4. Production curves of well A2.

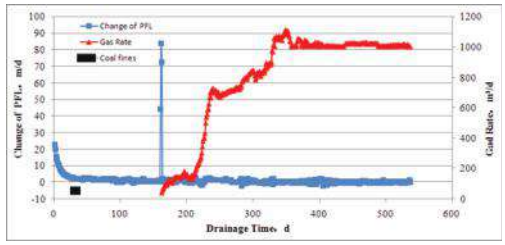


Figure 5. Production curves of well A3.

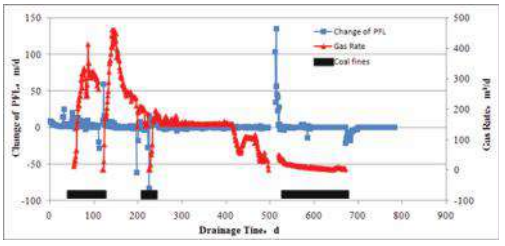


Figure 6. Production curves of well A4.

indicates that the coalbed could be tolerant of this PFL, and the pressure fluctuation resulting from the PFL variation did not destroy the coal structure, and thus did not produce coal fines. With the PFL remaining stable in the later production, the daily gas production rate increased gradually to approximate 1000 m^3/d.

Production curves of A4 well (Fig. 6) indicate there is extreme fluctuation in PFL both in the steady-depressurization and come-to gas production processes, which induces to fluctuant speed of flow migration in formation. While coal from this well is badly damaged and in powder (Fig. 2(d)), so coal fine is easy to be flowed and can block fracture system, which is so-called velocity sensitivity and to damage the reservoir.

The daily gas production rate in well A4 experienced a dramatic variation with relative low peak value, and after the peak, the daily gas production rate declined drastically. On the 240th day, the daily gas production rate, only around 150 m^3/d, tends to be at a stable level. On the 514th day, the drainage system was changed with the PFL 134.9 m/d, and then the coal fines were produced again resulting in the decline of daily gas production rate. Based on the data listed in Figure 6, it could be seen clearly that the frequent variation of drainage system made the pressure fluctuate and thus the coal structure was destroyed accordingly, because of which a vast numbers of coal fines were produced. Consequently the stress sensitivity, velocity sensitivity and Jamin effect, which is due to the discontinuous drainage, happened and contributed to the decrease of coalbed permeability as well as the permanent reservoir damage. In spite of the stable tendency of PFL in the later production, the daily gas production rate could not be able to restore, and steadily descended to zero.

Accordingly, unreasonable drainage system can easily contribute to fluctuant pressure, reservoir damage, such as velocity and pressure sensitivity, and finally decreasing gas rate of CBM wells; as a result, it's necessary to ensure continuous and steady drainage in order to control fine flow and better well productivity.

5 CONCLUSIONS

1. Coal fines production is one of the key factors that affect the production of the CBM wells. No coal fines are produced in Well A1 and the peak gas rate of this well is 3534.34 m^3/d. Plenty of coal fines are produced in Well A4 with low peak gas rate of 460 m^3/d. By analyzing the production process of Well A4, coal fine production is the archcriminal of low gas production. When the fluid level is significant changed, coal fines are tended to produced, migrated and deposited in the coal cleats or fractured, finally reduced coal permeability thus this process will lead to low production.
2. The production of coal fines is not only affected by the primary texture of coal but also the drainage system. The primary texture of coal in Well A1 and Well A3 is intact, and the drainage systems of these two wells are reasonable therefore there is no or some coal fines produced in these two wells. The primary texture of coal in Well A2 is crushed thus in-situ coal fines would be produced with fluid flowing during stable pressure decline period and the beginning of production when the fluid level is fluctuant. However, in the late stage of production, Well A2 achieved a stable gas rate for the reason of a reasonable of drainage system and no production of coal fines. The primary texture of coal in Well A4 is crushed and the drainage system is unstable in the whole production history. So a lot of coal fines would be produced by the above internal and external factors. Velocity sensitivity and solidification during coal fines production would block cleats and decline production.
3. Based on the production comparison of the four wells, this study concludes that the stress sensitivity, velocity sensitivity and Jamin effect which are caused by fluctuant pressure could be avoided under continuous and steady drainage system. Coal fines could be controlled thus it would improve production. In the late period of production, it should maintain continuous and steady drainage system and reduce coal fines production to enhance production.

ACKNOWLEDGEMENTS

The research is sponsored by National Natural Science Foundation for Distinguished Young Scholars of China (NO.41102098), National Science Foundation of China (NO.41072112), the Scientific Research Foundation of Key Laboratory of Coalbed Methane Resources and Reservoir Formation Process, Ministry of Education (China University of Mining and Technology)

(NO.2013–001) and Open Foundation of Teaching Lab of China University of Geosciences(Wuhan) (NO.SKJ2012180).

REFERENCES

Cao, Daiyong et al. 2012. Comprehensive classification study of coal fines genetic mechanism and origin site. *Coal Geology of China* 24(1): 10–12.

Cao, Daiyong et al. 2013. Rules of coal powder output under physical simulation experiments of single-phase water flow displacement. *Journal of China Coal Society* 38(4): 624–628.

Chen, Zhenhong et al. 2009. Destructive influences and effectively treatments of coal powder to high rank coalbed methane production. *Journal of China Coal Society* 34(2): 229–232.

Gruesbeek & Collin 1982. Entrainment and deposition of fine particles in porous media. *SPE 8430:* 847–856.

Li, Jinhai et al. 2009. Relationship between discharge rate and productivity of coalbed methane wells. *Journal of China Coal Society* 34(3): 376–380.

Li, Mengxi et al. 2012. Characteristics of production of CBM vertical well in fanzhuang block, Qinshui Basin. *China Coalbed Methane* 9(3): 3–7.

Liu, Shenggui et al. 2011. Production mechanism and control measures of coal powder in coalbed methane horizontal well. *Journal of Liaoning Technical University (Natural Science)* 30(4): 508–512.

Liu, Shenggui et al. 2012. Regularity of coal powder production and concentration control method during CBM well drainage. *Journal of China Coal Society* 37(Supp.2): 412–415.

Luo, Zhenxing et al. 2012. The division of coalbed methane wells production curves and analysis of production factors. *Journal of Chongqing University Of Science & Technology (Natural Science)* 14(4): 56–59.

Magill, D. et al. 2010. Controlling coal-fines production in massively cavitated openhole coalbed-methane wells. *SPE134031:* 1–11.

Quan, Fangkai et al. 2012. Reservoir damage mechanism and system optimization of in-situ coalbed methane drainage and production. *China Coalbed Methane* 9(4): 42–44.

Xian, Baoan et al. 2005. Analysis on applied mechanism ofmultiple laterals horizontal well in developing coalbed methane. *Coal Geology & Exploration* 33(6): 34–37.

Zhang, Fenna et al. 2013. Analysis of the impact of gas production channel for coalbed methane well by pulverized coal. J*ournal of China University of Mining &Technology* 42(3): 428–435.

Zou, Yushi et al. 2012. Damage mechanism of coal powder on fracture conductivity. *Journal of China Coal Society* 37(11): 1890–1894.

This page intentionally left blank

Progress in Mine Safety Science and Engineering II – He et al. (Eds)
© 2014 Taylor & Francis Group, London, ISBN 978-1-138-00122-0

Research on the relationship among safety labor division, safety specialization and safety marketization

Yifei Weng
North China Institute of Science and Technology, Beijing, P.R. China

ABSTRACT: In this thesis, the ternary relationship among safety labor division, safety specialization and safety marketization is researched. Based on three pairs among these three objectives are described respectively, conclusions can be drawn that safety activities separating from production activities is the inevitable result of economic and social development, which will inevitably improve safety, economy and efficiency of production; Safety labor division is the professionalization and specialization of safety activities, for the best operational efficiency of safety specialization, the answer can only be safety marketization.

1 INTRODUCTION

Safety and health is an important goal for economic and social development of countries over the world and one of the starting points for policy-making, and it is also the ideal state of human production and life that haves been pursued. Safety is one of the most basic needs of human's survival and development. Safety and operation is a contradiction, there must be safety problems in the production process, and the safety always exists in the whole process. Safety plays both restrain and promoting role on production. If safety work is not settled, there might be accidents frequently, which not only cause huge economic losses and increase production costs, but also lead to bad social impact, thus hindering the development of production. Since safety and production is a pair of twin sisters, with the economic development in the production process, "safe" gradually emerges the trend of independence, specialization and marketization, which in turn promote the progress of the production.

2 RELATIONSHIP BETWEEN SAFETY LABOR DIVISION AND SAFETY SPECIALIZATION

Social division of labor is one of the hallmarks of human civilization, but also the basis for the development of the commodity economy. Without social division of labor, there is no exchange; the market economy will be out of the question. The advantage of the social division of labor is to let people do what they are good at, so that the average social labor time is greatly reduced. Production efficiency is improved significantly. People who provide products of good quality and high efficiency can gain high profits and value in the market competition. The most profound meaning that derived from the social division of labor is to make the best of human resources and materials. Therefore, safety labor division is the social division in all kinds of labor and its independence, specialization.

Division and specialization is a pair of opposites and the two aspects of a thing, both closely linked and difficult to separate: the division of labor leads to specialization; specialization depends on division and develops it. In the long history of human process, after an initial natural division of labor based on gender, age, or physical strength, the first great social division of labor—division of animal husbandry and agriculture, the second social division of labor—division of handicraft industry and agriculture, the third social division of labor—the emergence of the merchant class, and the separation of the Fourth—the social division of mental and manual labor. The specialization of production continues to develop in depth, which promotes the transformation of the mode of production and process of productivity. In modern society, along with the development of large industrial machines and new technological revolution, comply with the requirements of large-scale socialized production, new production departments and enterprises separate from departments and enterprises of the past, varieties of products from single enterprise reduce increasingly, or even only does part of the production of a product or in a single process, so the social division of labor become more and

more specialized. Further, the meaning of division and specialization can be understood statically or dynamically. From a static point of view, it refers to the degree or status of division and specialization; from a dynamic point of view, it refers to the process or trends of division and specialization. In book Wealth of Nations, when Smith discusses the division of labor and handicraft workshop, he considers that the production activities is constitute of a series of different "Action". Smith pointed out that the manufacturing of pins is divided into 18 kinds of operations, from the 18 specialized workers. Stigler wrote in his analysis of the manufacturers: "It's better to see that manufacturers are engaged in a range of different 'operation' (including the purchase and storage of raw materials, raw materials into semi-finished products and semi-finished products into the final product, storage and sale of products and extend the purchase of credit, etc.)" So, the economic activities of enterprises can be explained as a range of different operating forms and then to explain the division and its specialization, which seems to be a "consensus". This indicates that the "operation" for explanations of the division and specialization is more certain and accurate than using "production activities "or" labor "to explain and illustrate the division and specialization. "Operation", as the elements or the basic unit constituting the "productive activities" or "labor", can not be separated in a fixed technical level. On the other hand, "production activities" or" labor "is a complete set of economic activity posed by many most basic operations, we can see them as production activities that a micro item for the production of one or several products, they can also be seen as production activities of an individual or a tribe or an economic organizations to meet their own needs. Safety can be seen as a unique "Operation" that different from production operation.

Therefore, in general, Safety labor division and specialization, in essence, refer to the deepening process of such a mode of production of an economic actor (a person, a sector) who tends to bear only one or several safety economic activity or one or several safe operation of a safe economic activity.

3 RELATIONSHIP BETWEEN SAFETY LABOR DIVISION AND SAFETY MARKETIZATION

3.1 *Safety division enlarges the safety market*

The development of the division of labor expands the size of the market, because the social division of labor makes the labor of commodity producers unilateral and his needs multifaceted. The development of the social division of labor and improvement of the professional level can help to improve labor productivity, thereby increasing the total market supply of goods. At the same time, the specialization of production increase the total market supply also increased the total market demand. Firstly, the division of labor increases labor productivity and per capita income, so that the purchasing power is improved, the scale of market demand is enlarged. Secondly, the social division of labor enlarges the gap between people's production activities and its own needs, that is to say people have to get more diverse and larger number of goods from the transaction to meet their own needs, so that the size of the market expands. Thirdly, the market expansion can be explained by lengthened "Roundabout Production Act" and "division of labor chain". "Roundabout Production" is an indirect production method access to the goods, before getting the goods, first for the ability to manufacture goods. Human activities are universal roundabout, and the social division of labor, as a part of the production, must be roundabout production method, which is split off from the different nodes in the production chain. The deepening of specialization indicates that the increase in the division of labor chain node will multiply the scale of economy. Assuming that the market as a function of the division of labor chain and the initial size of the market can ensure the lowest economic specialization, the marginal division (deepening division of labor) will bring geometric progression expansion of marginal market. Safety separates from the production and forms safety products market, including safety services and safety products.

3.2 *Safety division requires the safety market*

The division of labor depends on the market; the safety division of labor depends on the safety market. Therefore, reasonable safety market is required in the internal science division. This is because the division and trade are two sides of the question of the mode of production, division of labor do not exist without trading, therefore, safety division requires trade. Smith pointed out that "the division of labor is a source which promotes national wealth"; at the same time "the level of division is determined by the size of the market". So we can consider that the size of safety division of is determined by the level of safety (quantity and quality of safety products), the wider the range of market transactions, the more trading partners, which can support the people in special service industry better, the degree of division of labor will be higher, this is the theoretical roots of improving the internal

market. Division of labor does not exist without trading, the safety division of labor needs trading, which is the root causes of the internal safety market management. Market demand, capacity constraints the degree of social division. Only when the market demand for certain products is large enough, the middle part of the production of such products (operation) can be separated.

3.3 *Safe transaction cost is the evolution of safety division and the core of safety market expansion*

The division and trade are two sides of the mode of production; division does not exist without trade. Deepening division gains labor economy, at the same time, it increases the costs of division coordination—transaction costs. The division of labor depends on the size of the market range; the size of the market range is determined by the transaction costs, and more accurately determined by the level of transaction efficiency. This shows that the scientific pricing of in-house safety services is conducive to expanding the scope of the internal safety market. The so-called "transaction costs" is expense of transaction among people's bargaining, contract negotiations, disputes solving. Transaction costs are divided into endogenous transaction costs and exogenous transaction costs. Endogenous transaction cost is that people compete for the interests of division in the transaction, at the expense of reducing the interests of others from the division, such cost unable to measure prior caused by moral hazard, adverse selection and other opportunistic behavior (corruption, deception and unreliable commitments). The exogenous transaction fee is, directly or indirectly, the costs incurred in the transaction process that people can see the size (such as taxes, transportation costs, etc.) before making decisions. Whether endogenous transaction costs or exogenous transaction costs has a decisive impact on the level of division. Endogenous transaction costs have a larger impact on the division of labor. Endogenous transaction costs can be reduced through the creation of the system, the formation of habits to curb opportunistic behavior. In order to reduce the transaction costs of the safety division of labor, the price of the safety service and form need intermediaries for pricing and determination.

3.4 *Safety transaction costs and safety institutional arrangements*

In general, the safety market exchange achieves the benefits of safety specialization production, and induces the evolution of the safety division structure by the safety price mechanism. However, due to the presence of transaction costs, producers may not make timely and accurate response to price signals, this is what we call price failure. The new institutionalism economic school thinks that it is the price failure related to the transaction costs that leads to the emergence of the organizational and institutional arrangements aimed at reducing transaction costs. The level of transaction costs depends on the institutional arrangements of a society. Commons divided trading activities into three categories: market transactions; management transactions and quota transactions. In correspondence, there are three basic institutional arrangements in the modern society, markets, corporate (industrial organization) and the government. The most basic function of the system is to reduce the transaction costs. Economists believe that, the main reason leading to national disparity between the rich and the poor is whether there is a good system effective in reducing endogenous transaction costs. With the deepening of division, transaction cost continues to increase. In order to gain benefits from division, while deepening specialization, people make institutional innovation to reduce transaction costs. System innovation can effectively reduce the uncertainty in the market, inhibit the tendency of people's opportunistic behavior, and thus has the function of saving endogenous transaction cost. In all the systems that reduce transaction costs, the market system is undoubtedly the most important. Enterprises (industrial organization) make transactions which originally belong to the market "internal" to save transaction costs. For the safety market management of the enterprise, developing scientific and rational pricing system and the implementation system, can help to reduce the transaction costs in the safety market operation, effectively improve the safety level of the enterprise, to achieve safety.

4 THE RELATIONSHIP BETWEEN SAFETY SPECIALIZATION AND SAFETY MARKETIZATION

Generally, division of labor has gone through several major stages of development so far: (1) product specialization stage, that is, a single enterprise produces all parts and intermediate goods they need and completes the final product independently; (2) intermediate products specialization stage, that is, a single enterprise only does part of the production of a final product (for example, in automobile production, some companies only produce engines, and some companies only produce control instruments); (3) specialization stage of the components and the process, a single enterprise only does one or several parts of the final product,

or only responsible for the completion of production process of a product or components (e.g., specifically for casting, electroplating, heat treatment, etc.); (4) In addition, there is a specialization stage which parallels to the production process, out of the direct production process but serves the production process, such as a number of specialized enterprises responsible for equipment maintenance, and others dedicated to the transportation of products. The safety marketization belongs to this category. Because economic agents' "safe" products can be entrusted to another individual, department or organization to produce or supply, and checked by the other organizations. Therefore, from the perspective of economic efficiency, safety specialization must finally result in safety marketization.

5 CONCLUSIONS

In short, safety activities separating from production activities is the inevitable result of economic and social development, which will inevitably improve safety, economy and efficiency of production; Safety labor division is the professionalization and specialization of safety activities, for the best operational efficiency of safety specialization, the answer can only be safety marketization.

ACKNOWLEDGEMENTS

This work was financially supported by the Basic Scientific Research Fund Project of Central Universities (No.: 3142013104). Meanwhile I appreciate Prof. Yan Ye, Prof. Liuwei and Prof. Wang Dan's help for this paper.

REFERENCES

Weng, Yifei. Safety Administration [M]. *China Waterpower Press*. 2000.

Weng, Yifei. Research on the Complexity of System Safety Management [J]. *Safety and Environmental Protection of Mining Industry*. Vol 35. 2 (2008): p. 78–80.

Progress in Mine Safety Science and Engineering II – He et al. (Eds)
© 2014 Taylor & Francis Group, London, ISBN 978-1-138-00122-0

Study on effectiveness of coal mine reorganization systems based on game model

Yajing Bi
China Safety Science and Research Institute, Beijing, China
China Mining University, Beijing, China

Xingkai Zhang
China Safety Science and Research Institute, Beijing, China

ABSTRACT: Under the unreasonable situation of uncoordinated structures and imbalance regions in coalmine industry with the increasing rate of death accidents, this paper used game theory to study effectively on the system of rectification and closure of coal mines, and proposed the best strategy of establishing a new pattern of coal industry to achieve a fundamental improvement in the safety production of the coal industry.

1 INTRODUCTION

In 2012, SACSS focused on closing small coal mines in conjunction with related departments to promote and propel the backward mines. There are 628 mines are closed, 662 mines are enhanced by technology innovation, 388 mines are restructured, which forced out the backward coal production capacity of 978 million tons, and the death is decreased within 1500 persons, the death rate per million tons (DRPMT) of downtown coal mines reduced by 31.7% from 1.104 to 0.754. And the situation of uncoordinated structures and imbalance regions of coalmine coal industry is quite unreasonable; the proportion of small coal mines with low productivity makes up 80% of whole national coal industry, which concentrated in both the southern areas of Guizhou, Yunnan, Hunan, Sichuan, Chongqing and the north-eastern provinces of Heilongjiang etc, and the output value of national downtown coal mines makes up 34.6% of the whole industry. But the rate of accidents and death are nearly 65.0% and 69.7%. According to the statistic in last year, the death of these five provinces and one city mentioned above is 54.4%. At the aim of building a prosperous society, it is the inevitable requirement or objective criteria to fulfill by the complete improvement of the safety production in mining industry. The main direction to speed up the economic development is promoting the strategic adjustment in the economic structures.

2 COMPETITION ANALYSES BETWEEN THE COALMINE ENTERPRISES

Here assume that in one area that has a n coalmine enterprises, their production decision are independent, and they can choose to produce any production under their capacity, production enterprises neither negotiate between each other, nor have any restriction, and also decided to their respective production, This constitutes a game between n production enterprises on coalmine production (Li Haofeng, et al. 2004).

In the strategy that each coal mines enterprise can choose the production value q_i (i = 1,2,…n) to produce and put in the market. Because production is restricted by the production capacity, so in theory the output of each production enterprise is to have a cap (Li Ying 2007). The total output of the n production enterprises is $Q = q_1 + q_2 + \cdots + q_n = \Sigma_{i=1}^{n} q_i$ the relationship of the mines market price p and the total production is

$$p = p(Q) = p\left(\sum_{i=1}^{n} q_i\right) \tag{1}$$

Assumption, at stage A,

$$\frac{dp(Q)}{dQ} > 0 \tag{2}$$

Namely, the stage of supply less than demand, the market price will be increased as the increasing of output.

At stage B,

$$\frac{dp(Q)}{dQ} < 0 \tag{3}$$

That is in the later stage of supply has exceeded demand, the market price will be decreased as the increase of output.

Supposed the fixed costs of production enterprise i for f_i, variable costs for c_i and set its profit for u_i

$$u_i = q_i\left(p(Q)\right) - q_i c_i - f_i = q_i\left(p(Q) - c_i\right) - f_i \tag{4}$$

From the formula(4) can see that, the profit of production enterprise i depends not only on the fixed cost f_i, variable cost c_i and production value q_i, but also on the production value of the other production enterprises. Therefore, the production enterprise i in decision-making must consider the decisions of the other production enterprises and the possible react of the decision it made.

Solution to a first-order:

$$p\left(\sum_{i=1}^{n} q_i^*\right) - c_i + q_i^* \frac{\partial\left(p\left(\sum_{i=1}^{n} q_i^*\right)\right)}{\partial q_i^*} = 0 \quad i = 1,2,\ldots n \tag{5}$$

Second order conditions meet:

$$2\frac{\partial p\left(\sum_{i=1}^{n} q_i^*\right)}{\partial\left(\sum_{i=1}^{n} q_i^*\right)} + q_i^* \frac{\partial^2 p\left(\sum_{i=1}^{n} q_i^*\right)}{\partial\left(\left(\sum_{i-1}^{n} q_i^*\right)^2\right)} < 0 \quad i = 1,2,\ldots n \tag{6}$$

For n production enterprises, naturally there are n equations, namely

$$\begin{cases} p\left(\sum_{i=1}^{n} q_i^*\right) - c_1 + q_i^* \dfrac{\partial\left(p\left(\sum_{i=1}^{n} q_i^*\right)\right)}{\partial q_1^*} = 0 \\ p\left(\sum_{i=1}^{n} q_i^*\right) - c_2 + q_2^* \dfrac{\partial\left(p\left(\sum_{i=1}^{n} q_i^*\right)\right)}{\partial q_2^*} = 0 \\ p\left(\sum_{i=1}^{n} q_i^*\right) - c_n + q_n^* \dfrac{\partial\left(p\left(\sum_{i=1}^{n} q_i^*\right)\right)}{\partial q_n^*} = 0 \end{cases} \tag{7}$$

Get the optimal output $(q_1^*, q_2^*, \ldots, q_n^*)$ through solving the pair of simultaneous equations, again put it into the formula (4) then we can get

$$u_i^* = q_i^*\left(p\left(\sum_{i=1}^{n} q_i^*\right) - c_i\right) - f_i \tag{8}$$

This is the stable results that they act according to the principle of realizing their max interests when they made their production decision independently.

At stage A, supposing that the relationship between product price p and output Q is $p = a + bQ$, and $a > 0$, $b > 0$, $0 \le Q \le Q_0$, so $\frac{dp(Q)}{dQ} = b > 0$ meet the condition (2) $\frac{dp(Q)}{dQ} > 0$, but can't meet the condition (6), its profit is

$$u_i' = q_i^*\left(a + bQ - c_i\right) - f_i \tag{9}$$

This kind of situation does not disappear until the demand of the market reach its saturation point Q_0 (Yu Mingjie 2008). The profit of this enterprise depends on the size of its production capacity fully. This is the reason why each production enterprise enlarges its production scale and the early incentive of the competition.

At stage B, supposing the relationship between product price p and the market input Q is $p = a - bQ$ and $a > 0$, $b > 0$, $Q > Q_0$. Obviously the formula $\frac{dp(Q)}{dQ} = -b < 0$ meet (3) and (6), use (7), get,

$$q_i^{*\prime} = \frac{1}{b}\left[\frac{1}{n+1}\left(a + \sum_{i=1}^{n} c_i\right) - c_i\right] i = 1,2,\cdots,n \tag{10}$$

The formula above is the best production of every mining enterprise. At this time any enterprise cannot get profit by changing the output. So the profit of the enterprise is

$$u_i^{*\prime} = \frac{1}{b}\left[\frac{1}{n+1}\left(a + \sum_{i=1}^{n} c_i\right) - c_i\right]^2 - f_i, \quad i = 1,2,\ldots,n \tag{11}$$

3 COOPERATION ANALYSES OF MINING ENTERPRISES

Assume that the n enterprises in order to achieve the enterprise's maximum profits, reached a cooperation agreement. Each coalmine enterprise's production is not the same for the different production capacity. But once come to an agreement, the share of the production they get can be undertook by their production capacity. That is to say the share of the production is decided by enterprise's internal production capacity, and has nothing to do with external environment. So they can be thought of as a constant. Established that the share of production that coalmine enterprises get are as follows $\lambda_1, \lambda_2, \ldots, \lambda_n$; and $\lambda_1 + \lambda_2 + \cdots + \lambda_n = 1$, that is to say $\Sigma_{i=1}^{n} \lambda_i = 1$, $\lambda_i > 0$,; So the distributions of production of each coalmine enterprise are $\lambda_1 Q$, $\lambda_2 Q$, …, $\lambda_n Q$.

Obviously, the coalmine enterprises may also have cooperation risk between each other. A

certain proportion of the enterprise production's cost is called risk coefficient k_i (Zhang Weiying 2004). Then profit function of each coalmine enterprise is $u_i = p(Q)\, q_i - c_i q_i - f_i - k_i c_i q_i = p(Q)\, \lambda_i Q - (1 + k_i) c_i \lambda_i Q - f_i$ So the profit function of all coalmine enterprises $U = u_1 + u_2 + \ldots + u_n$,

$$U = Q\left(p(Q) - \sum_{i=1}^{n} \lambda_i (1 + k_i) c_i \right) - \sum_{i=1}^{n} f_i \tag{12}$$

The solution of the first-order conditions

$$p(Q^*) - \sum_{i=1}^{n} \lambda_i (1 + k_i) c_i + Q^* \frac{\partial p(Q^*)}{\partial Q^*} = 0 \tag{13}$$

Second-order condition meets

$$2\frac{\partial p(Q^*)}{\partial Q} + Q^* \frac{\partial^2 P(Q^*)}{\partial Q^{*2}} < 0 \tag{14}$$

Give Q^*, and substitute it into equation (4),:

$$U^* = Q^*\left(p(Q^*) - \sum_{i-1}^{n} \lambda_i (1 + k_i) c_i \right) - \sum_{i=1}^{n} f_i \tag{15}$$

At stage A, assuming that the relationship between price p of coal and the market data Q is still $p = a + bQ$, obviously, $\frac{\partial p(Q)}{\partial Q} = b > 0$, meet the condition (2), but does not satisfy the condition (6). At this time, the profit of coalmine enterprise is

$$u_i'' = \lambda_i Q^* \left(a + bQ - (1 + k_i) c_i \right) - f_i \tag{16}$$

At stage A, the cooperation between enterprises is clearly non-existent cooperation risk,

so $k_i = 0$. So there is

$$u_i'' = \lambda_i Q^* \left(a + bQ - c_i \right) - f_i \tag{17}$$

Compare (17) with (9),

$$u_i'' - u_i' = \left(\lambda_i Q - q_i \right)\left(a + bQ - c_i \right) \tag{18}$$

When $\lambda_i Q > q_i$, the coalmine enterprises should take the cooperative strategy, when $\lambda_i Q < q_i$, the coalmine enterprises should take the competitive production strategy.

At stage B, assuming that the relationship between price of coal p and market data Q

Is still $p = a - bQ$, obviously $\frac{\partial p(Q)}{\partial Q} = -b > 0$, meet the condition (2) and condition (6), using (13) gets

$$q_i^{*''} = \frac{\lambda_i}{b}\left[a - \sum_{i=1}^{n} \lambda_i (1 + k_i) c_i \right], \; i = 1, 2, \ldots, n \tag{19}$$

The benefit of the enterprise as follows

$$u_i^{*''} = \frac{\lambda_i}{b}\left[a - \sum_{i=1}^{n} \lambda_i (1 + k_i) c_i \right] \times \left[\frac{1}{2}\left[a + \sum_{i=1}^{n} \lambda_i (1 + k_i) c_i \right] - (1 + k_i) c_i \right] - f_i \tag{20}$$

Compare (20) with (11)

$$u_i^{*''} - u_i^{*'} = \frac{1}{b}\left\{ \left[\frac{\lambda_i}{2}\left(a - \sum_{i=1}^{n} \lambda_i (1 + k_i) c_i \right) \right] \times \left[\frac{1}{2}\left[a + \sum_{i=1}^{n} \lambda_i (1 + k_i) c_i \right] - (1 + k_i) c_i \right] - \left[\frac{1}{n+1}\left(a + \sum_{i=1}^{n} c_i \right) - c_i \right]^2 \right\} \tag{21}$$

To discuss the different situations of type (21) get

1. If you don't consider the risk of cooperation, that is $k_i = 0$, and each coalmine enterprise distribute production quotas on average, that is to say, $\lambda_i = \frac{1}{n}$, meantime, $c_1 = c_2 = \cdots = c_n = c$, so $u_i^{*''} > u_i^{*'}$;
2. If you don't consider the risk of cooperation, that is $k_i = 0$, and each coalmine enterprise distribute production quotas on average, that is to say, $\lambda_i = \frac{1}{n}$, but the cost of each are not the same, if $c_i \geq \frac{(n-1)}{2n(n+1)}(a - w) + w$, $a > w$, which average cost is w, that is, $w = \frac{1}{n}\Sigma_{i=1}^{n} c_i$, so $u_i^{*''} > u_i^{*'}$;
3. If you consider the risk of cooperation, $k_i \neq 0$, and share the risk on average, that is $k_1 = k_2 = \ldots k_n = k$. And each coalmine enterprise distribute production quotas on average, that is $\lambda_i = \frac{1}{n}$, meantime, $c_1 = c_2 = \ldots c_n = c$, at this point, if $k = \frac{a-c}{2c}$, it is $u_i^{*''} > u_i^{*'}$
4. If you consider the risk of cooperation, $k_i \neq 0$, and share the risk on average, that is $k_1 = k_2 = \ldots k_n = k$. And each coalmine enterprise distribute production quotas on average, that is $\lambda_i = \frac{1}{n}$, but the cost of each are not the same, if $c_i < \frac{w}{2}$, it is $u_i^{*''} > u_i^{*'}$
5. Other situations require according to type (21) for evaluating, and determine to take the competitive or cooperative production strategy.

4 CONCLUSION AND SUGGESTION

From the above analysis, we can see that if the production cost and ability of one enterprise correspond to another, the cooperative production strategy can maximize profits between enterprises.

Otherwise, the strength are very different, it should adopt competitive manufacturing strategy. The strong enterprises in the production scale can achieve maximum profits; the weak enterprises achieve limited profits for small production scale and are forced out eventually. Also need to point out that the production of each enterprise is less in cooperation model, but benefit function is larger than maximum profit interest function separate decision of each enterprise and the profits of cooperation model increase with the enterprises increasing in the market. Therefore, it is wise for the same strength manufacturing enterprises to adopt cooperative game when they are under the conditions of market economy.

The State Administration of Work Safety clarified that the death caused by accidents happened in coalmine enterprises must be decreased more than 50% in 2020 than that happened in 2010. At present, in some areas, China's coal mines department have achieved the initial success by carrying out integration strategy. But the total safety production accidents in coal mines is very huge still, and the DRPMT of coal mines is higher than that of developed countries, such as USA, Australia etc. Especially we cannot control the accidents well for the reason of lacking advanced security devices and facilities.

From analysis, it will be best way of rectification and closure of small size coal mines, and here proposed the best strategy of establishing a new pattern of coal industry from smaller size to bigger size, from companies to group, to achieve a fundamental improvement of structure in whole coal industry.

ACKNOWLEDGEMENTS

The authors gratefully acknowledge foundation by the China National Science and Technology Support Program (2013BAK04B03–02).

REFERENCES

Li Haofeng, et al. 2004. Game Analysis of Our Coal Mine Production Safety Supervision. Coal Economic Research, (7), 72–75 (in Chinese).

Li Ying 2007. Game Analysis of Local Mine Safety Supervision Based on the Game Theory of Incomplete Information. Industrial Safety and Environmental Protection, 33(12), 55–56 (in Chinese).

Yu Mingjie 2008. Research on Safety Input Incentive Mechanism Based on the Principal-agent Theory of Coal Mine. Xi'an: Xi'an University of Science and Technology Press (in Chinese).

Zhang Weiying 2004. Game theory and information economics. Shanghai: Shanghai People's Publishing House, 403–407 (in Chinese).

Progress in Mine Safety Science and Engineering II – He et al. (Eds)
© 2014 Taylor & Francis Group, London, ISBN 978-1-138-00122-0

A study on accounting and measurement of resources and environment value in Beijing region

Pengfei Bai
University of Chinese Academy of Sciences, National Earthquake Response Support Service, Beijing, China

Qianqian Duan
School of Management and Economics, Beijing Institute of Technology, Beijing, China

ABSTRACT: Scientific index and effective model are essential for Beijing resources and environment evaluation. In this paper, we divided the Evaluation system into six parts respectively, and according the six parts, we build an index system and a model to make evaluations of Beijing resource and environment. Finally, an instance is given to explain how to apply the model. By comprehensive analysis and data statistics of Beijing resource and environment, some useful information can be gained for Beijing public policy making.

Keywords: urban resource & environment, index system, evaluation model, beijing region

1 INTRODUCTION

Resources and environment is the natural foundation and guarantee of the human society as non-regenerative elements of human development. Since the reform and opening up in China, the process of urbanization and industrialization develops rapidly. Problems such as resource shortage, environment pollution emerges, and these problems are becoming more and more seriously.

Scientific index and effective model are essential for the urban resources and environment evaluating. An ideal evaluation system should not only reflect the status of resources and the environment, but also reflect the potential impact on urban resources and environment, such as the activities of human beings, regional features.

By comprehensive analysis and evaluation of urban resource and environment, we can get a lot of useful information for public policy making. In this paper, we divided the Evaluation system into six parts respectively, there are atmospheric environment, acoustic environment, water environment, radiation environment, the meteorological environment, water resources, land resources. According the six parts, we build a index system and a model to make evaluations of urban resource and environment.

Firstly, we set level 2 indicators according the nine parts, analysis every indicator by using Delphi-AHP method, estimate the value and the weight of the indicators.

Then, we calculate the integrated index value by K-means algorithm, the function is

$$E = \sum_{t=1}^{k} \sum_{p \in C_t} \left\| p - c_t \right\|^2 \tag{1}$$

Where p denotes the data object, c_t denotes the cluster-head of mass c, and E denotes the sum of the Squares of the Errors of all objects.

Secondly, we give the weight of level 1 index according their composition proportions, the weight was denoted by p_i, the integrated index was calculated by the following function:

$$C_i = \frac{\sum c_i \cdot P_i}{\sum P_i} \tag{2}$$

Where c_i denotes the value of the ith evaluation unit.

Finally, we evaluate the object by comparing the calculated value and the real value.

2 INDEX SYSTEM

Resource environmental monitoring and evaluation index system is composed by many index, Different types of index have different meanings and some of the index are similar. Different index are also have different weight.

Based on the principles of practical applicability, comprehensiveness, scientificity and representativeness, we taking Beijing as the example, build an index system of evaluation of urban resource and environment by using the Delphi-AHP methods. The index system has three levels, level 2 includes atmospheric environment, sound environment, water environment, meteorological environment, water resources and land resources. Index of level 3 is derived from level 2, level 3 is more complicated specific than level 2.

2.1 *Atmospheric environment*

Atmospheric environment is evaluated mainly through the level of air quality and average concentration of inhalable particulate matters.

The air quality can be calculated by API (Air Pollution Index). API is a conceptual concentration index which combines the several common air pollutants. API can represent the level of air pollution and quality of air condition.

The diameter of inhalable particulate matters is less than 10 microns in general, the units of measurement is mg/cubic meters. The monitoring time includes daily mean and hour mean.

2.2 *Sound environment*

Sound environment is evaluated mainly through the level of traffic noise and the level of ambient noise, which can be download from the website of environmental protection bureau. The traffic noise is statistic from the motor vehicles in the urban. The ambient noise is divided into 5 levels, the following is the table of ambient noise classification.

Table 1. API and the air quality.

API	Quality of air condition	Level of air quality
0–50	Excellent	Level I
51–100	Good	Level II
101–150	Normal	Level III
151–200	Light Pollution	
201–250	Intermediate Pollution	Level IV
251–300	Medium-Heavy Pollution	
>300	Heavy Pollution	Level V

2.3 *Water environment*

Water environment is evaluated mainly through the surface water quality and the groundwater quality of the city.

Surface water includes rivers, glacier, lakes and swamp. The condition of Beijing's surface water can be calculated by monitoring the water of the 18 large and medium-sized reservoirs, 17 lakes and 5 rivers. Groundwater is water located beneath the ground surface in soil pore spaces and in the fractures of rock formations.

2.4 *Meteorological environment*

The Meteorological environment is evaluated by four indicators including daily maximum temperatures, daily minimum temperatures, relative humidity and Pollution meteorological condition. Specially, the index of pollution meteorological condition reflects

Table 2. The classification of urban ambient noise.

Level	Zone division	Night	Daytime
0	Special Quiet Zone	50	40
1	Living Area, Authorities District	55	45
2	Mixed Zone of Living, Commercial and Industrial Area	60	50
3	Industrial Area	65	55
4	Neighboring area of Traffic track	70	55

Unit: dB.

Table 3. The classification of groundwater.

Level	Description
I	Applicable for all purposes. Classified by chemical composition.
II	Applicable for all purposes. Classified by chemical composition.
III	Applicable for drinking, agricultural using and industrial using. Classified by baseline health parameter.
IV	Applicable for agricultural using and industrial using, applicable for drinking after purifying treatment. Classified by the requirement of agricultural and industrial using.
V	Not Suitable for drinking, used for special purposes.

Table 4. Index of meteorological pollution condition.

Index	Description
1	The meteorological condition aggravates the diffusion of air pollutants severely.
2	The meteorological condition aggravates the diffusion of air pollutants slightly.
3	The meteorological condition at intermediate level.
4	The meteorological condition is not conducive to the spread of air pollutants.
5	The meteorological condition is very detrimental to the spread of air pollutants.

the relations between meteorological condition and pollutant diffusion. The index can be used to analysis that what pollution meteorological condition exacerbates the atmospheric pollution.

2.5 *Water resource*

Water resources in is evaluated mainly through the average flow of the river, poundage of the reservoir, the numbers of the reservoirs, accumulated precipitation and accumulated available water. About 5 main rivers and 17 large and medium-sized reservoirs are monitored in Beijing.

Accumulated precipitation is a key index reflecting the city rainfall condition, and this index should be compared to the same period in previous years during the calculation. Other index such as poundage of the reservoir, accumulated available water also should be compared to the same period in previous years in evaluation.

2.6 *Land resource*

According the situation of land using, Land resource can be classified as cultivated area, garden area, forest area, grassland area, water area, construction land and unutilized land. In this paper, we choose forest area, industrial land, residential land and water area as the low level index of the land resources.

The forest area includes all sorts of forest such as economic forest, shelter forest, fire wood forest and timberland. Water area includes continental water area and water resources conservancy lands.

3 EVALUATION MODEL

3.1 *Delphi-AHP method*

Delphi method and AHP method are comprehensively applied to gain the weight of index which are used to evaluate the urban resource and environment. And this integrated approach is mainly from the view of qualitative analysis.

Delphi method is based on structural surveys and makes use of the intuitive available information of the participants, who are mainly experts. Therefore, it de-livers qualitative as well as quantitative results and has beneath its explorative, predictive even normative elements. There is not the one Delphi methodology but the applications are diverse. There is agreement that Delphi is an expert survey in two or more rounds in which in the second and later rounds of the survey the results of the previous round are given as feedback. Therefore, the experts answer from the second round on under the influence of their colleagues' opinions. Thus, the Delphi method is a relatively strongly structured group communication process, in which matters, on which naturally unsure and incomplete knowledge is available, are judged upon by experts.

The Analytic Hierarchy Process (AHP) is a structured technique for organizing and analyzing complex decisions. Based on mathematics and psychology, it was developed by Thomas L. Saaty in the 1970s and has been extensively studied and refined since then. The procedure for using the AHP can be summarized as:

1. Model the problem as a hierarchy containing the decision goal, the alternatives for reaching it, and the criteria for evaluating the alternatives.
2. Establish priorities among the elements of the hierarchy by making a series of judgments based on pair-wise comparisons of the elements. For example, when comparing potential real-estate purchases, the investors might say they prefer location over price and price over timing.
3. Synthesize these judgments to yield a set of overall priorities for the hierarchy. This would combine the investors' judgments about location, price and timing for properties A, B, C, and D into overall priorities for each property.
4. Check the consistency of the judgments.
5. Come to a final decision based on the results of this process.

Delphi method is Suitable for qualitative analysis while AHP is Suitable for quantitative analysis. By compounding these two kinds methods' advantages, we use Delphi-AHP methods to identify the key indices of urban resource and environment system and give the weight of every index. Then, we calculate the collected date set and get the evaluate result by using K-means algorithm.

3.2 *K-means algorithm*

The K-Means is a simple clustering algorithm used to divide a set of objects, based on their attributes/

features, into k clusters, where k is a predefined or user-defined constant. The main idea is to define k centroids, one for each cluster. The centroid of a cluster is formed in such a way that it is closely related (in terms of similarity function) to all objects of that cluster.

Given a set of observations $(x_1, x_2, \ldots, x_n)$, where each observation is a d-dimensional real vector, k-means clustering aims to partition the n observations into k sets ($k \leq n$) $S = \{S_1, S_2, \ldots, S_k\}$ so as to minimize the within-cluster sum of squares:

$$\arg\min_{S} \sum_{i=1}^{k} \sum_{x_j \in S_i} \left\| x_j - \mu_i \right\|^2 \tag{3}$$

where μ_i is the mean of points in S_i. The following is how the algorithm works:

1. The algorithm arbitrarily selects k points as the initial cluster centers.
2. Each point in the dataset is assigned to the closed cluster, based upon the Euclidean distance between each point and each cluster center.
3. Each cluster center is recomputed as the average of the points in that cluster.
4. Steps 2 and 3 repeat until the clusters converge. Convergence may be defined differently depending upon the implementation, but it normally means that either no observations change clusters when steps 2 and 3 are repeated or that the changes do not make a material difference in the definition of the clusters.

The two key features of k-means which make it efficient are often regarded as its biggest drawbacks: (1)Euclidean distance is used as a metric and variance is used as a measure of cluster scatter. (2) The number of clusters k is an input parameter: an inappropriate choice of k may yield poor results. That is why, when performing k-means, it is important to run diagnostic checks for determining the number of clusters in the data set.

3.3 *Evaluation modeling*

According to the classification above, Individual Index are set and statisticed, the weight of every index was given. Then, the weighted average method is used to calculate the comprehensive index value by the function:

$$c_i = \frac{\sum t_i \cdot p_i}{\sum p_i} \tag{4}$$

Where c_i denotes the evaluating value of the ith evaluation unit, t_i denotes the value of the ith individual index, p_i denotes the weight of the ith individual index, and the weight is given according to the index's composition proportion.

Then, the evaluation object is assessed by comparing the calculated value and the real value.

Table 5. Index system with the weight.

	Level 2 index	Weight	Level 3 index	Weight
Urban Resource and Environment	Atmospheric environment	0.1646	Air Quality	0.1243
			Average Concentration Of Inhalable Particulate Matters	0.0403
	Sound environment	0.1102	Traffic Noise	0.0563
			Ambient Noise	0.0539
	Water environment	0.1702	Surface Water Quality	0.0906
			Groundwater Quality	0.0796
	Meteorological environment	0.1521	Maximum Temperatures	0.0406
			Minimum Temperatures	0.0392
			Relative Humidity	0.0376
			Pollution Meteorological Condition	0.0347
	Water resource	0.2714	Average Flow of The River	0.0492
			Poundage Of The Reservoir	0.0537
			The Numbers of The Reservoirs	0.0264
			Accumulated Precipitation	0.0769
			Accumulated Available Water	0.0652
	Land resource	0.1315	Forest Area	0.0417
			Water Area	0.0329
			Industrial Land	0.0325
			Residential Land	0.0244

Table 6. Monitoring data of atmospheric environment and sound environment.

Index		Levels and scores I	II	III	IV	V	Units
Atmospheric	Air Quality	0–50	50–100	101–200	201–300	>300	API
Environment	Average concentration of Inhalable Particulate Matters	<123	123.6–245.2	245–1451	1451–2181	>2181	$mg/m^3 \cdot day$
Sound	Traffic Noise	50	55	60	65	70	db
Environment	Ambient Noise	50	55	60	65	70	db

Resource: Beijing Environmental Protection Bureau, December, 2008.

The following are the specific steps of the model building: firstly, evaluation threshold is set which is divided into incomplete segment, relatively complete segment and complete segment. Then, evaluation is made by comparing the real value which is calculated and the standard evaluation valve. It's conveniently to make a quantitative evaluation by centesimal system scoring which combined the index classification method and the centesimal system. The following is the index classification table, and the weight of the index has been given by the approach above mentioned.

4 CASE ANALYSIS AND CONCLUSION

The following demonstrates how to apply the model to make evaluations by taking the atmospheric environment and sound environment as examples. For the convenience of index monitoring, the collecting data was classified into 5 levels which are represented by I, II, III, IV, V, and we can give the scores according the different level.

Atmospheric environment is evaluated mainly through the level of air quality and average concentration of inhalable particulate matters, and the data can be collected from the website (http://www.bjee.org.cn/cn/index.php). Table 6 is the monitoring data at December 2008. The level I, II, III, IV, V represents the scores of 100, 80, 60, 40, 20.

Besides, we statistic that the average concentration of inhalable particulate matters is 132.712. The corresponding score is 80 and the level is II. Based on the evaluation model above, the score of atmospheric environment evaluation in Beijing is 78.05 which is close to level II. That is to say the condition of atmospheric environment is good.

Sound environment is evaluated mainly through the level of traffic noise and the level of ambient noise. The data can be collected from the website (http://www.bjepb.gov.cn/publish). By the same way, we can make evaluation of the sound environment. The score of sound environment is 53.7 which is also close to the level II. That is to say the condition of sound environment is good and acceptable to the urban residents.

REFERENCES

Amorim, R. C & Mirkin, B. Minkowski metric, feature weighting and anomalous cluster initializeing in K-Means clustering. *Pattern Recognition*, 2012, 45 (3): 1061–1075.

Chris Ding & Xiaofeng He. K-means Clustering via Principal Component Analysis. *Proc. of Int'l Conf. Machine Learning (ICML 2004)*.

Honarkhah, M & Caers, J, Stochastic Simulation of Patterns Using Distance-Based Pattern Modeling, *Mathematical Geosciences,* 2010, 42: 487–517.

Little, M.A & Jones, N.S. Generalized Methods and Solvers for Piecewise Constant Signals: Part I. *Proc. Roy. Soc. A.* 2011.

Press, W.H. Gaussian Mixture Models and k-Means Clustering. *Numerical Recipes: The Art of Scientific Computing (3rd.)*. New York: Cambridge University Press. 2007.

Vattani., A. k-means requires exponentially many iterations even in the plane. *Discrete and Computational Geometry*, 2011, 45 (4): 596–616.

This page intentionally left blank

Progress in Mine Safety Science and Engineering II – He et al. (Eds)
© 2014 Taylor & Francis Group, London, ISBN 978-1-138-00122-0

Early-warning models of regional work safety risk in Chongqing city and Ningbo city, China-based on partial least squares regression

Tian-Han Jiang
China Academy of Safety Science and Technology, Beijing, China

Dai-Ying Zhao
Explosion Science and Technology, State Key Laboratory of Beijing Institute of Technology, Beijing, China
School of Environment Science and Safety Engineering, Tianjin University of Technology, Tianjin, China

ABSTRACT: In the process of industrialization of China, regional work safety situation is still grim. It is of great significance to coordinate the relationship between work safety and economic growth by constructing macro early-warning models for local work safety risk management. With the data of economic and social development obtained from local governments, early-warning models were established to assess regional work safety risks in Chongqing City and Ningbo City, China, based on partial least squares regression method. The results showed that the work safety risk in Chongqing City and Ningbo City declined year by year in the coming years, but the former is much higher than the latter. The alarm level in Chongqing City is "dangerous" and Ningbo is "attention". The models are effective and feasible.

1 INTRODUCTION

1.1 *Type area*

Previous studies have found that there is an inherent certain relationship between work safety risk and economic development (Vilanilam, 1980, van Beeck, et al., 2000, Gerdtham & Ruhm, 2006, Klinische, 2007, Barth, et al., 2007). All of these studies concluded that some factors such as economic growth, industrial structure, employment structure, etc, might be important influecing factors of occupational or traffic accidents, injuries and occupational diseases according to long-term observation (Song, 2010). Work safety indicators of China fluctuate with the rapid economic development in recent years (Liu, et al., 2005, Wang, 2006, He, et al., 2008, Song, et al., 2011). Yearly fatality rate per 105 workers of China in 2003 was about 10.8, which was much higher than those of other developed countries (Wang, 2006). He et al.(2008) found that there existed regional difference in work safety risk for regional economic wealth in China (He, et al., 2008). Song, et al. (2011) presented that variation of economic speed had important influence on occupational accidents in short term in China. At present, compared with other developed countries, China work safety situation is rather grim.

This study aimed to establish macro early-warning models for work safety risk in Chongqing City and Ningbo City based on partial least squares regression. It is of great significance to coordinate the relationship between work safety and economic growth for local governments.

2 MATERIALS AND METHODS

2.1 *Study scope*

In this study only industrial and traffic accident risks are discussed in Chongqing City and Ningbo City, China, which is typical developing and developed area, respectively. Industrial accident risk is described by yearly industrial accident death toll (IAD) and yearly fatality rate per 105 workers (FRW) and traffic accident risk is composed of yearly traffic accident death toll (TAD) and yearly mortality rate per 104 vehicles (MRV).

2.2 *Economic and accident data*

Song (2010) proved that economic growth scale, economic structure as well as economic cycles all have effects on accident risks (Song L, 2010). However, economic growth scale is not the only element which influences accident risks spatial distribution. Economic growth structure is the dominant element, globalization and marketing are important complex elements. In this study, some key factors are selected as the early-warning indices of work safety risk in Chongqing City and Ningbo City, China as shown in Table 1. The data are listed in Table 2 and Table 3.

Table 1. The early-warning indices of work safety risk in Chongqing City and Ningbo City, China.

Types of risk	Work safety indicators	Early-warning indices of risk
Industrial accident risk	Yearly industrial accident death toll (IAD)(person)	Yearly growth rate of gross domestic product (RGDP)(%)
	Yearly fatality rate per 10^5 workers (FRW)(10^{-5})	Yearly growth rate of fixed assets investment (RFAI)(%)
		The proportion of secondary industry in gross domestic product (PSI)(%)
		The proportion of tertiary industry in gross domestic product (PTI)(%)
Traffic accident risck	Yearly traffic accident death toll (TAD) (person)	Yearly growth rate of motor vehicle population (RMVP) (%)
	Yearly mortality rate per 10^4 vehicles (MRV)(10^{-4})	Yearly growth rate of gross domestic product (RGDP)(%) yearly urbanization rate (UR)(%)

Table 2. The risk, economy and accident data in Chongqing City, China.

Year	IAD	FRW	TAD	MRV	RGDP	PSI	PTI	RFAI	RMVP	UR
2003	1070	13.44	1566	13.78	11.5	40.5	44.6	31.8	15.43	43.6
2004	825	10.24	1502	18.62	12.2	41.3	42.8	32.34	18.98	44.8
2005	867	10.61	1484	13.32	11.5	41	43.9	26.14	28.24	45.18
2006	704	8.49	1299	9.74	12.2	43.5	45.3	24.06	20.2	46.69
2007	701	8.08	1218	8.46	15.6	45.9	42.4	30	7.96	48.33
2008	646	7.18	1043	6.44	14.3	47.7	41	27.24	13.25	49.98
2009	605	4.95	1031	4.6	13.8	52.81	37.89	31	13.12	51.59

Data source: IAD and FRW data came from Chongqing Administration of Work Safety; TAD, MRV, and RMVP data came from Chongqing Traffic Management Bureau; RGDP, PSI, PTI, RFAI, and UR data derived from Chongqing Statistics Yearbook, 2003–2009.

Table 3. The risk, economy and accident data in Ningbo City, China.

Year	IAD	FRW	TAD	MRV	RGDP	PSI	PTI	RFAI	RMVP	UR
2003	109	3.66	947	13.4	20.36	54.54	39.19	39.02	20.38	30.74
2004	109	3.45	1038	11.14	20.59	55.34	38.94	32.05	32.31	31.88
2005	106	3.13	938	9.35	16.02	48.39	39.77	21.06	7.89	32.8
2006	107	2.98	923	8.46	17.45	49.15	40.16	12.46	8.9	33.72
2007	95	2.57	860	7.23	18.93	49.82	40.18	6.31	9.25	34.4
2008	81	2.16	839	6.72	15.44	49.6	40.26	8.18	5.18	34.94
2009	74	2.4	773	5.62	9.7	48.76	41.2	15.97	10.32	35.38

Data source: IAD and FRW data came from Ningbo Administration of Work Safety; TAD, MRV, and RMVP data came from Ningbo Traffic Management Bureau; RGDP, PSI, PTI, RFAI, and UR data derived from Ningbo Statistics Yearbook, 2003–2009.

2.3 *Modeling approach*

2.3.1 *Basic model*

Partial Least Squares Regression (PLSR) can analyze data with strongly collinear, noisy, and numerous X-variables, and also simultaneously model several response variables (Wold, et al., 2001). However, standard regression will fail in these cases. The basic model based on PLSR is built as follows:

$$Y = XB + E \quad (1)$$

where Y is 7 by 2 risk matrix, and Y = [IAD, FRW] for industrial accident risks while Y = [TAD, MRV] for traffic accident risks;X is 7 by 4 matrix of early-warning indices, and X = [RGDP, PSI PTI, RFAI] for industrial accident risks, while X is 7 by 3 early-warning indices, and X = [RGDP, RMVP, UR] for traffic accident risks;B is a 2 by 4 regression coefficient matrix for industrial accident risks while B is a 2 by 3 regression coefficient matrix for traffic accident risks;E is a noise term for the model which has the same dimensions as Y.

2.3.2 *Eearly-warning index*

With the output of the above early-warning model Eq. (1), the comprehensive risk of regional work

safety can be obtained from the following Eq. (2):

$$CRI = \alpha \cdot IRI + \beta \cdot TRI \quad (2)$$

where *CRI* is the comprehensive risk index, *IRI* is industrial accident risk index, and *TRI* is traffic accident risk index. α and β are their weights with the default value 0.5.

$$IRI = \gamma \cdot IDI + \delta \cdot FRWI \quad (3)$$

where *IDI* is the industrial accident death index, and *FRWI* is the fatality rate per 10^5 workers index. γ and δ are their weights with the default value 0.5. *IDI* and *FRWI* are normalized to the range [0, 1] with the same scale, respectively.

$$IDI = \frac{ID_i}{\overline{ID}} \times 100 \quad (4)$$

where ID_i (i = 1, 2, ……) is the industrial accident death toll in the i th year, and $\overline{ID}$ is the average industrial accident death toll in all years.

$$FRWI = \frac{FRW_i}{\overline{FRW}} \times 100 \quad (5)$$

where $FRWI_i$ (i = 1, 2, ……) is the fatality rate per 10^5 workers in the i th year, and $\overline{FRW}$ is the average fatality rate per 10^5 workers in all years.

$$TRI = \mu \cdot TDI + \lambda \cdot MRVI \quad (6)$$

Where *TDI* is the traffic accident death index, and *MRVI* is the mortality rate per 10^4 vehicles index. μ and λ are their weights with the default value 0.5. *TDI* and *MRVI* are normalized to the range [0, 1] with the same scale, respectively.

Table 4. The alarm levels of local work safety risk.

Alarm levels	CRI	Description
I	CRI > thr1	Dangerous
II	thr2 ≤ CRI ≤ thr1	Warning
II	thr3 ≤ CRI ≤ thr2	Attention
No alarm	CRI < thr3	Safe

$$TDI = \frac{TD_i}{\overline{TD}} \times 100 \quad (7)$$

where TD_i (i = 1, 2, ……) is the traffic accident death toll in the i th year, and $\overline{TD}$ is the average traffic accident death toll in all years.

$$MRVI = \frac{MRV_i}{\overline{MRV}} \times 100 \quad (8)$$

where $MRVI_i$ (i = 1, 2, ……) is the mortality rate per 10^4 vehicles in the i th year, and $\overline{MRV}$ is the average mortality rate per 10^4 vehicles in all years

2.3.3 *Alarm levels*

In this study alarm levels are set according to the Annual Control Target (ACT) of local work safety. The ACT of Chongqing City is different from that of Ningbo City. The default targets are obtained by annual trend extrapolation based on annual decline rate which is about 3%. The fist threshold value is just equal to ACT (marked as thr1, red color), the second threshold value is 85 percent of ACT (marked as thr2, yellow color), and the third threshold value is 70 percent of ACT (marked as thr3, blue color). All the alarm levels are also normalized to the range[0, 1] with the above scale. The alarm levels are shown in Table 4.

3 RESULTS

With their natural logarithm, the data in Table 2 and Table 3 were input to the Eq. (1) to build early-warning models in R environment (Wold, et al., 2001, Mevik & Wehrens, 2007), respectively. The model parameters in Chongqing City and Ningbo City were shown in Table 5. One was called Chongqing Model, the other was named Ningbo model. All the models were assessed by Leave-One-Out Cross Validation method (LOOCV), and the maximum model error was less than 15%.

Base on the Twelfth Five-Year Plan for National Economic and Social Development of Chongqing City and Ningbo City, firstly the annual values of RGDP, PSI, PTI, RFAI, RMV, and UR during 2010–2015 were predicted. Then the values of IAD, FRW, TAD, and MRV were obtained with Eq. (1).

Table 5. The parameters of early-warning models in Chongqing City and Ningbo City, China.

Models	B		E
Chongqing model	IRI	[–0.464, –0.927, 0.898, 0.741; –0.819, –1.469, 1.676, 0.728]	[5.481, 1.098]
	TRI	[0.060, –2.784, 0.021;2.963, –9.8382, 0.583]	[17.675, 20.984]
Ningbo model	IRI	[0.348, –0.251, –3.282, 0.012;0.137, 0.977, –2.775, 0.081]	[16.646, 6.8402]
	TRI	[0.136, –0.921, 0.023; 0.482, –3.657, 0.012]	[9.596, 13.507]

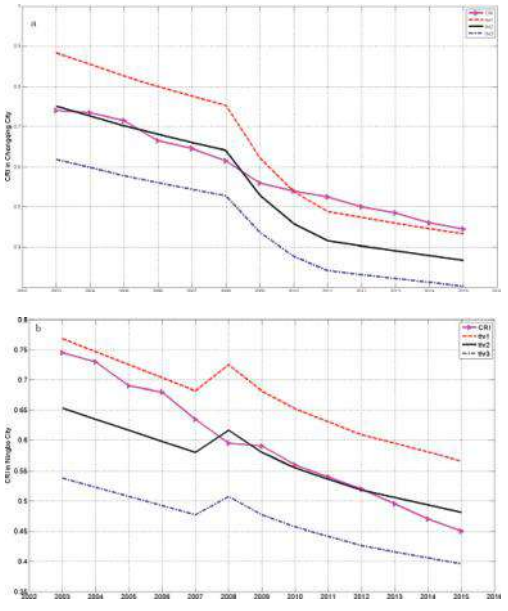


Figure 1. (a) CRI in Chongqing City, China; (b) CRI in Ningbo City, Zhejiang province, China.

Finally, CRI of Chongqing Model and Ningbo Model were calculated with Eq. (2)–Eq. (8). The results were shown in Figure 1.

Figure 1(a) and Figure 1(b) described the evolutions of regional work safety risk in Chongqing City and Ningbo City during 2003–2015, respectively. The data during 2003–2009 were real, while the data during 2010–2015 came from the early-warning models. Figure 1 showed that the CRI in the two cities all declined year by year, but their evolutions were very different. Figure 1(a) showed that the work safety risk in Chongqing City was in "attention" situation before 2009. Since then, it became worse and was in "dangerous" situation. Figure 1(b) showed that the work safety risk in Ningbo City was in "attention" situation before 2012. Since 2013, it became better and better, and would be in "safe" situation. In fact, the FRW in Chongqing City was 4.95, which was much higher than 2.4 in Ningbo City.

4 DISCUSSION OF RESULTS

The general trend of work safety in China have entered the turning point since 2003, and the accident death toll declined continuously over our country, for rapid economic development and implementation of some important policies (Liu, 2009). In the context of safe development in China, the CRI in those two cities have all declined year by year since 2003.

The work safety situation in Chongqing City was severer than that in Ningbo City. The gross domestic product per capita (per-capita GDP) rose from 9098 yuan in 2003 to 22920 yuan in 2009 in Chongqing City. At the meantime the IAD declined from 1070 person in 2003 to 605 person in 2009 as well as the FRW decreased from $13.44(10^{-5})$ to $4.95(10^{-5})$ in its industrial accident risk. The TAD declined from 1566 person in 2003 to 1031 person in 2009 as well as the MRV decreased from $13.78(10^{-4})$ to $4.6(10^{-4})$ in its traffic accident risk. The per-capita GDP rose from 31943 yuan in 2003 to 76012 yuan in 2009 in Ningbo City. At the meantime the IAD declined from 109 person in 2003 to 74 person in 2009 as well as the FRW decreased from $3.66(10^{-5})$ to $2.4(10^{-5})$ in its industrial accident risk. Meanwhile the TAD declined from 947 person in 2003 to 773 person in 2009 as well as the MRV decreased from $13.4(10^{-4})$ to $5.62(10^{-4})$ in its traffic accident risk. In our recent workshop report, we found that if RGDP or PSI increase by 1%, IAD would increased 0.86% or 0.90%; if PTI or RFAI increase by 1%, IAD would decreased 0.71% or 0.17%. Analogously if RGDP or RMVP increase by 1%, TAD would increased 0.53% or 0.16%; if UR increase by 1%, TAD would decreased 1.38%. With the implementations of the Twelfth Five-Year Plan for National Economic and Social Development of Chongqing City and Ningbo City, the regional difference of local work safety risk would still exist for the coming years. The deep factors of this phenomenon were economic growth, industrial structure, employment structure, and urbanization, etc..

5 CONCLUSIONS

In summary, the purpose of this study was to establish early-warning models to assessment regional work safety risks in Chongqing City and Ningbo City, China. The major results were as follows: Firstly, the work safety risk in Chongqing City and Ningbo City declined year by year in the next few years. Secondly, the work safety risk in Chongqing City is much higher than that in Ningbo City, China. Finally, the models are effective and feasible. However, short of valuable data of employment and labors which couldn't be attained for no complete registration system in China, the early-warning models might have some model errors, and would be further improved.

ACKNOWLEDGEMENTS

The authors would like to thank National Natural Science Foundation of China for supporting

this research under Contract Nos. 91024031 and 90924303. The support and ideas provided by Deng Yunfeng is gratefully acknowledged.

REFERENCES

Barth, A. et al. 2007. Economic growth and the incidence of occupational injuries in Austria. *Wiener Klinische Wochenschrift,* 119(5–6).

Gerdtham, U.G. & Ruhm, C.J. 2006. Deaths rise in good economic times: evidence from the OECD. *Economics and Human Biology,* 4:298–316.

He, X, Song, L, Baisheng, N. Basic features of occupational safety in china. *China Safety Science Journal,* 2008, 1(1):5–9 (in Chinese).

Klinische, W. 2007. Wochenschrift Economic growth and the incidence of occupational injuries in Austria. *Springer Wien,* 119(5):23–49.

Liu T.M. et al. 2005. Industrial accidents: Challenges for China's economic and social development [J]. *Safety Science,* 43:503–522.

Liu T.M. 2009. The general trend of work safety in China have entered the turning point——macro-early warning and analysis of trend of work safety [J]. *Journal of Safety Science and Technology,* 5(3):5–12 (in Chinese).

Mevik B.H. & Wehrens R. 2007. The pls Package: Principal Component and Partial Least Squares Regression in R [J]. *Journal of Statistical Software,* 18(2):1–24.

Song L. 2010. Dynamic Econometric Analysis on Relativity between Accident Disasters and Economic Growth & Its Application [D]. *China University of Mining & Technology (Beijing),* Beijing, China (in Chinese).

Song L. et al. 2011. Longitudinal relationship between economic development and occupational accidents in China. *Accident Analysis and Prevention,* 43:82–86.

Van Beeck, E.F. et al. 2000. Economic development and traffic accident mortality in the industrialized world, 1962–1990. *International Journal of Epidemiology,* 29:503–509.

Vilanilam, J.V. 1980. A historical and socioeconomic analysis of occupational safety and health in India. *International Journal of Health Services: Planning, Administration, Evaluation,* 10(2):233–249.

Wang, X. 2006. Report on Occupational Safety vs Economic and Social Development. *China Coal Industry Publishing House,* Beijing, 39–40 (in Chinese).

Wold, S. et al. 2001. PLS-regression: a basic tool of chemometrics [J]. *Chemometrics and Intelligent Laboratory Systems,* 2001, 58(2):109–130.

This page intentionally left blank

Progress in Mine Safety Science and Engineering II – He et al. (Eds)
© 2014 Taylor & Francis Group, London, ISBN 978-1-138-00122-0

Study on the hydrogeochemistry and isotope characteristics of Ordovician groundwater in Yanzhou coalfield, North China

Yong Han, Guiqiang Zheng & Jianxu Pan
Hebei Province Key Laboratory of Mine Disaster Prevention and Control, Sanhe, Hebei, China
North China Institute of Science and Technology, Sanhe, Hebei, China

Guangcai Wang
China University of Geosciences (Beijing), Beijing, China

Zhikun Li
Liaocheng Jingkai Real Estate Co., Ltd., Liaocheng, Shandong, China

ABSTRACT: In order to get a clear understanding of water circulation and lay the foundation for discriminating the water source of mine water inrush, it's necessary to study the hydrogeochemistry and isotope characteristics of the Ordovician limestone groundwater in study area. The main water type of Ordovician limestone groundwater is $Ca^{-}Mg^{-}SO_4$. The main ions are SO_4^{2-} and Ca^{2+}. There was very good linear correlation between the concentration of $Ca^{2+,}$ SO_4^{2-} and TDS ($R_{Ca}^2 = 0.978$, $R_{SO4}^2 = 0.996$), and the increase velocity of the Ca^{2+} and SO_4^{2-} concentration was the largest. Calcite and dolomite were oversaturated, but gypsum and anhydrite were unsaturated. The distribution of Cl^- and TDS was analogous to groundwater flow field. The representative meteoric water line of the study area is $\delta D = 7.80\delta^{18}O + 6.28$, and Ordovician limestone groundwater was not recharged from local precipitation.

1 INTRODUCTION

The North China Coal field is one important coal areas in our country, its coal output accounts for more than 60% of China's total coal output (Gao et al. 2009). At present, the shallow coal in North China coal mines has nearly been mined out, so the mining of the deep coal resource is extremely urgent. The mining depth of the eastern part of North China coal mines increased rapidly, and the mining depth of the main coal mines had reached about 600 m and it is still increasing at the speed of about 12 m/a (Hu 2010). The significant difference between deep and shallow mining of Coal mines is the special environment (three high and one disturbance); namely, high stress, high temperature, high Karst water pressure and mining disturbance (Chen et al. 2003, He 2007).

The main coal seams of North China Coalfield (Permo-Carboniferous coal) deposited on the Ordovician limestone, in which the karst was well developed and groundwater was rich. The water head of the underlain Ordovician limestone groundwater gradually increaseand the water pressure to the floor also keep increasing with the raising of mining depth. Besides, mining disturbance may make the faults or fractures active, which may become the new underground watercourse (Wu & Wang 2006). Therefore, the threat to the mining of the main coal seams of North China Coalfield (Permo-Carboniferous coal) gradually increases. In order to ensure the safety of coal mining, the hydrogeochemistry and isotopes characteristics of the Ordovician limestone water need to be studied.

The theory and method of hydrogeochemistry and isotope could effectively reveal the characteristics of groundwater circulation, and it plays an important role in identifying the water source of the mine water inrush, determining the groundwater runoff channels, discriminating the hydraulic connection of different aquifers, and confirming the effect of the water prevention (Wang et al. 2000, Ma 2006). There are more study on the groundwater circulation characteristics and water prevention of coal mine by the hydrogeochemical and isotopic theories and methods (Li et al. 2006, Liu et al. 2008).

However, there is very little study on the hydrogeochemical and isotopic characteristics of Ordovician limestone water in our study area. Therefore, the purpose of this paper is to study the hydrology-geochemistry, isotope and water circulation characteristics of Ordovician limestone groundwater, and lay the foundation for discriminating the water source of mine water inrush.

2 STUDY AREA

Our study area (Dongtan, Baodian, Xinglong Coalmine) which is part of coalfield of North China is located in the central part of Yan Zhou Coalfield, Shandong Province, China and Si river and Baima river flow through Dongtan, Baodian and Xonglong coalmine respectively (Fig. 1). Yanzhou coalfield is an incomplete eastward syncline with the axial direction NE–SW and formation dip angle less than 10 degree (Fig. 2). The NE folds, SN faults and EW faults are the main geological structures (Fig. 1). On the whole, large-medium faults were not well developed (Liu & Yu 2002). The top-down strata are Quaternary, Jurassic, Permian, Carboniferous, Ordovician, Cambrian and Archean formations (Fig. 2). The C-P formations are the coal-bearing strata. The thickness of Ordovician stratum are from 450 to 750 meters.

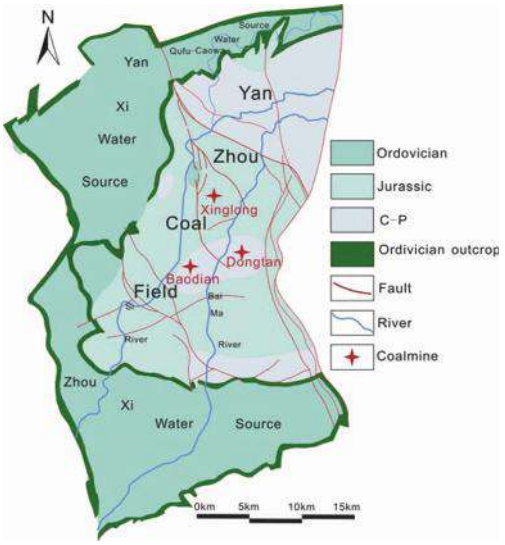


Figure 1. Sketch geological map of study area.

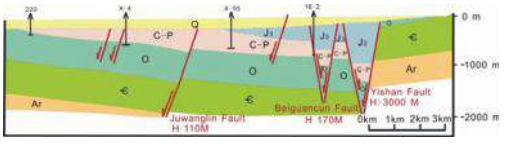


Figure 2. Geological cross section from west to east.

The main top-down aquifers affecting mining are the gravel aquifer of the lower Quaternary group, the Jurassic sandstone aquifer, the Permian sandstone aquifer, the Carboniferous thin limestone aquifer and the Ordovician limestone aquifer. In the south, north and west part of Yanzhou coalfield, Ordovician groundwater is confined fracture and solution cavern groundwater. And Zhouxi, Yanxi, Qufu-Caowa Ordovician water source are located out of coalfield periphery (Fig. 1). There is directly hydraulic connection between Ordovician groundwater in coalfield and out of coalfield. Generally, the Ordovician groundwater flows from north to south.

3 SAMPLES AND METHODS

In order to study the hydrogeochemical evolution, 96 groundwater Samples for chemical analysis were collected from 48 ground boreholes or tunnel boreholes in the Ordovician limestone aquifer when pumping test or drainage test were done during January 2005 and July 2009, filtered through a 0.45-lm filter, and preserved with appropriate additives (HNO_3). The samples were kept in sealed polyethylene bottles on ice until analyzed in the laboratory. The depths of these 48 boreholes range from 472 meters to 1180 meters.

pH and temperature were measured in situ, and the concentrations of K^+, Na^+, Ca^{2+}, Mg^{2+}, HCO_3^-, SO_4^{2-}, Cl^- were measured in Hydrochemistry Laboratory, the Institute of Hydrogeology and Environmental Geology, CAGS. Ca^{2+} and Mg^{2+} were analyzed by atomic absorption spectrophotometry, K^+ and Na^+ were analyzed by atomic emission spectrophotometry, Cl^- and SO_4^{2-} by ion chromatography. The chemical results were only accepted when the charge balance error was within ±5%. Total dissolved solid (TDS) was calculated as summation of all major ions. The tritium in water was analyzed by 1220 Quantulus Liquid Scintillation Spectrometer. The ^{18}O was analyzed by CO_2–H_2O equilibrium method and the ^2H was analyzed by metallic zinc reduction method.

4 HYDROGEOCHEMISTRY CHARACTERISTICS

4.1 *Water type*

All the groundwater samples concentratively scattered on the upper part of the Piper diagram (Fig. 3). Water types of Ordovician limestone groundwater were very single. Water type of 93 water samples

was $Ca^{-}Mg^{-}SO_4$, and water type of other 3 water samples was $Ca^{-}Mg^{-}SO_4^{-}HCO_3$. Therefore, the main water type of Ordovician limestone water is $Ca^{-}Mg^{-}SO_4$. The groundwater with this water type is relatively usual in marine limestone formation with gypsum intervals, and is in the middle stage transferring from $Ca^{-}HCO_3$ to $Na^{-}Cl$.

4.2 *Total dissolved solution*

The value of TDS of Ordovician groundwater was relatively bigger, varying from 1,330.3 mg/l to 3,555.4 mg/l with the average value of 2,464.4 mg/l. The Ordovician groundwater belonged to middle mineralization (1,000~3,000 mg/l) and high mineralization water (Table 1).

The TDS decreased from the North to South, which indicated the groundwater in the mass flowed from North to South and the water circulation condition in North was better than that in South. So, the variation of TDS in space must be considered to raise the accurate of water inrush distinguishing when TDS was used to identify the source of groundwater as a factor.

4.3 *The main ions*

The main anion was SO_4^{2-}, and the main cations were Ca^{2+} and Mg^{2+}. The concentration of SO_4^{2-} varied between 238.6 mg/l and 695.0 mg/l, and the concentration of Ca^{2+} varied between 803.3 and 2,296.5 mg/l (Table 1). They accounted for a high proportion in Ordovician groundwater. The concentration of $K^+ + Na^+$ and Mg^{2+} was not high, and the average of them individually was 126.3 and 111.8 mg/L. The concentration of Cl^- and HCO_3^- largely varied, with the value 17.0~538.3 mg/L and 32.1~331.4 mg/L. The concentration of ions was consistent with the main water type of most groundwater samples. The concentration of Ca^{2+} and SO_4^{2-} could be used as characteristic ions to distinguish the Ordovician limestone groundwater with the groundwater from other aquifers.

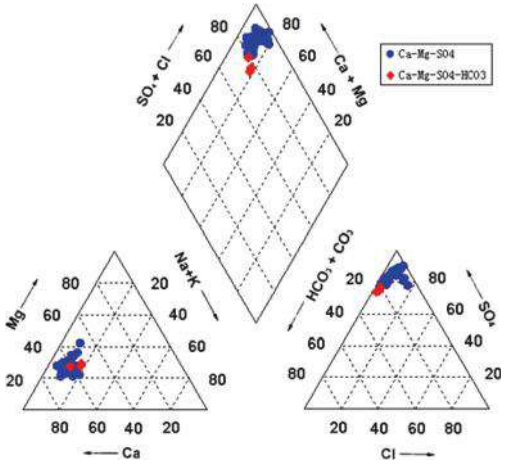


Figure 3. Piper diagram.

Table 1. The statistic of the main ions and TDS (Units: mg/L).

	$K^+ + Na^+$	Ca^{2+}	Mg^{2+}	Cl^-	SO_4^{2-}	HCO_3^-
Average	126.3	439	112	87.9	1467	218.9
Maximum	867.7	695	173	538	2402	331.4
Minimum	24.3	8.7	27.4	17	537.1	32.1

4.4 *Ions' contribution to TDS*

The relationship between TDS and major ions can intuitively reflect the variation of ion concentration in the process of hydrogeochemical evolution, which could be used to deduce the sources of ions in groundwater. For cations, there was very good linear correlation between the concentration of Ca^{2+} and TDS ($R^2 = 0.978$), and the increase velocity of the Ca^{2+} concentration was the largest one. Also, there was relatively good linear correlation between TDS and the concentration of Mg^{2+} and $Na^+ + K^+$, the increase velocities of them were much smaller than the increase velocity of Ca^{2+} (Fig. 4).

For anions, there was the best linear correlation between TDS and the concentration of SO_4^{2-} ($R^2 = 0.996$) and the concentration of SO_4^{2-} had the fastest increase. The concentration of Cl^- also increased, but it was a little slower; and in general the concentration of HCO_3^- decreased (Fig. 5). The main minerals of Ordovician aquifer are calcite, dolomite, gypsum and pyrite. These indicate that more minerals containing Ca^{2+} and SO_4^{2-} dissolved. Considering the analysis of SI of gypsum and anhydrite, gypsum or anhydrite is the main sources of Ca^{2+} and SO_4^{2-}. Mg^{2+} may derive from the dissolution of dolomite, and from the reduc-

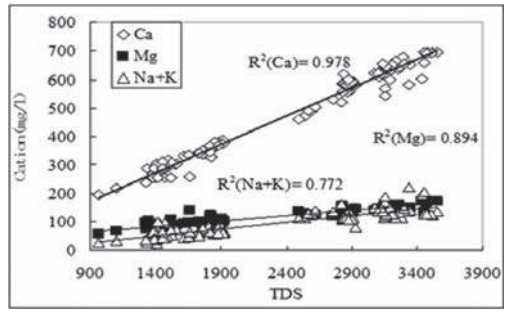


Figure 4. Plot of TDS vs Cation concentration.

tion of HCO_3^- the conclusion may be that calcite precipitated when dolomite dissolved.

All these variation indicated that Ca^{2+} and SO_4^{2-} were the main factor for the growth of TDS. And Cl^- had the relatively good relationship with TDS, which could be used to analyze the direction of groundwater flow, because the TDS usually increases along the flow path.

4.5 *Saturation index*

Saturation Index (SI) can be employed to determine the chemical equilibrium between water and minerals. Phreeqc is used to calculate the SI of main minerals. SI of calcite and dolomite was all greater than 0, which indicated they were oversaturated. SI of gypsum and anhydrite of most groundwater samples was less than 0, suggesting gypsum and anhydrite were unsaturated and gypsum or anhydrite kept dissolving along flow path until SI of gypsum or anhydrite was a little greater than 0.

SI of calcite and dolomite varied above 0, and there is no linear relationship between SI of them and TDS with TDS increasing (Fig. 6). This indicated that calcite and dolomite did not keep dissolving or precipitating. SI of gypsum was less than 0 and keep increasing, and there was very good linear relationship between it and TDS. This indicated groundwater always had the capacity to dissolve gypsum. Fig. 7 confirmed the dissolution of gypsum, and Ca^{2+} and SO_4^{2-} exponentially increased. And there was a very good correlation between Ca^{2+} and SI of gypsum, SO_4^{2-} and SI of gypsum, respectively R^2 were 0.994 and 0.987. All these indicated groundwater kept getting Ca^{2+} and SO_4^{2-} along the total flow path.

4.6 *Variation of Cl^- and TDS in groundwater flow field*

From the analysis above, Cl^- and TDS had a relative coefficient. Generally, Cl^- and TDS keeps increasing along the groundwater flow directions in the closed groundwater system, therefore Cl^- and TDS can be used to deduce groundwater flow direction.

Groundwater head was a little higher in North than that in South, which indicate the groundwater mainly flowed from north to south. But there were locally some low values in X-FO2-2C, D-O2-DX3 and D-O2-D1 (Fig. 8), because the discharge of groundwater during coal mining induced the decrease of water head in these areas. By contrasting Fig. 8 with Fig. 9, the trend was obvious. The distribution of Cl^- and TDS was coincident in groundwater flow field. TDS and the concentration of Cl^- was higher in North than that in South, and TDS and the concentration of Cl^- were higher in the places where the water head was low, which indicated the coincidence of the groundwater flow direction with the variation of TDS and the concentration of Cl^-. This commendably demonstrated the coincidence of variation between the groundwater head and the distribution of TDS and the Cl^-. So, the distribution of TDS and Cl^- can represent the groundwater flow field to a certain extent.

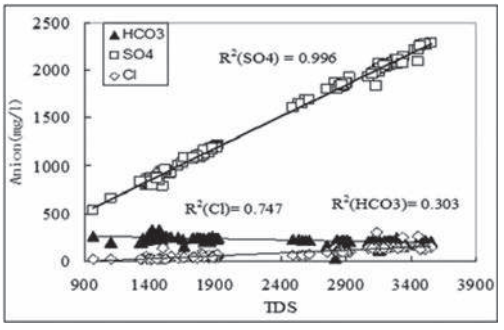


Figure 5. Plot of TDS vs Anion concentration.

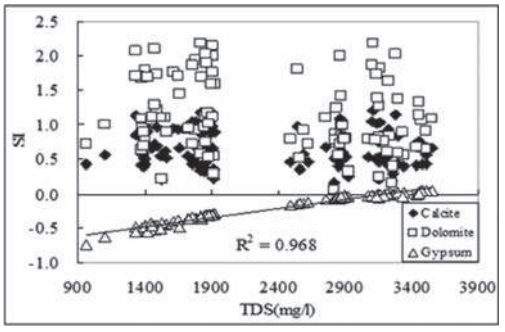


Figure 6. Scatter plot of TDS vs SI.

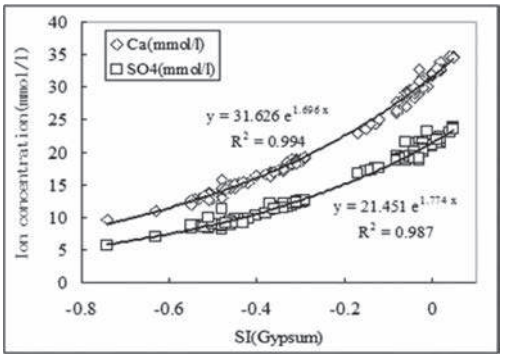


Figure 7. Plot of SI (calcite) vs Ion concentration.

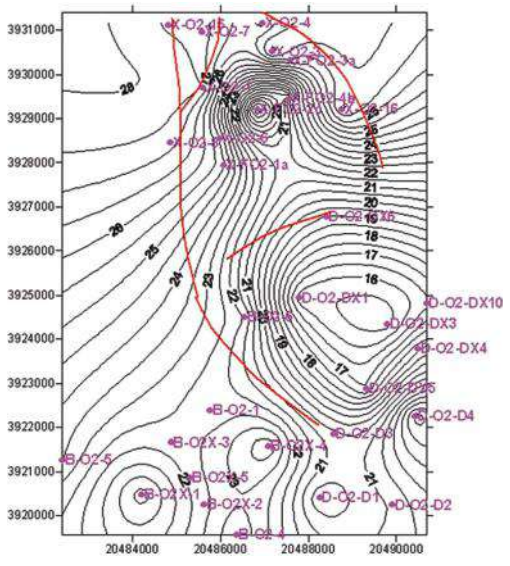


Figure 8. Contour map of groundwater head.

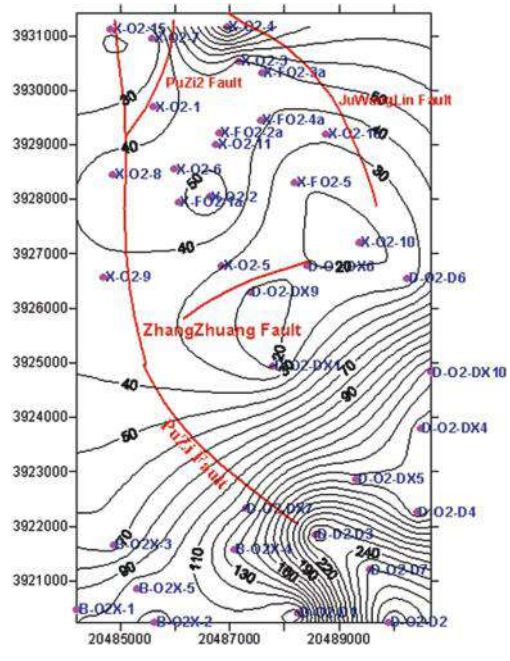


Figure 9. Contour map of Cl^-.

5 ISOTOPE CHARACTERISTICS OF ORDOVICIAN GROUNDWATER

5.1 *$\delta^{18}O$ and δD*

LWML is the foundation of analyzing the characteristic of $\delta^{18}O$ and δD, but there is no ready-made and representative LWML in our study area and we did not obtain the precipitation samples. So, the LWML must be deduced. The data of $\delta^{18}O$ and δD from GNIP about Tianjin, Shijiazhuang, Zhengzhou, Taiyuan and Yantai were used to establish the LWML for our study area by weighted average: $\delta D = 7.80\delta^{18}O + 6.28$ (VSMOW).

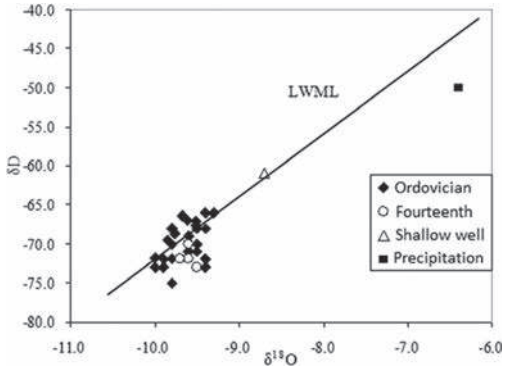


Figure 10. Plot of δD and $\delta^{18}O$.

Ordovician limestone groundwater distributes in the deep aquifer, the $\delta^{18}O$ and δ^2H can indicate this. $\delta^{18}O$ varied between –9.3‰ and –10.0‰ with average value –9.7‰, and δD varied between –66‰ and –75‰ with average value –69.9‰. The $\delta^{18}O$ and δD of Ordovician groundwater were located on the bottom left corner, and near the LWML (Fig. 10), which indicated there was close relationship between precipitation and Ordovician limestone groundwater and the precipitation was the ultima source of Ordovician limestone groundwater.

The value of $\delta^{18}O$ and δD of Ordovician groundwater was much less than that of shallow well and Precipitation. This indicated the groundwater was not recharged from local precipitation which was coincident with former study on the Ordovician outcrop, and was recharged in relatively colder environment.

5.2 *Tritium*

There are no continuous data about Tritium in China and only some concentration of Tritium was recorded, such as 400 TU in 1963. So, some key spot was used to analyze it as showed in Fig. 11.

1. There is tritium in five samples (13, 16, 20, 22 and 23) no more than 1 TU, which indicated the groundwater in these places was recharged before 1960.
2. There is tritium in five samples (1, 2, 3, 4, 5, 6, 7, 8 and 29) varying between 15.2 and 23.7 TU. They were located between 1962~1964, 1978 and 1986~1993, 1996~2002, which indicated

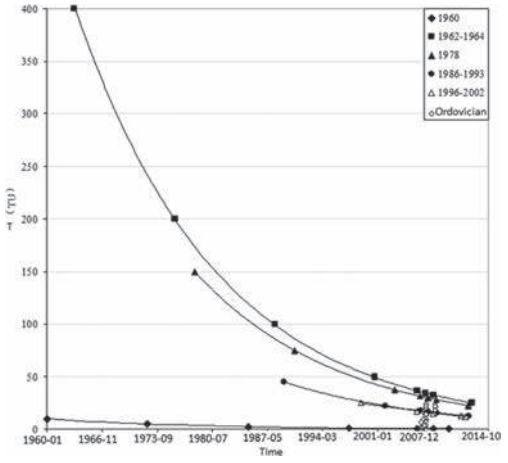


Figure 11. The variation of tritium with time in China (Yang 2004).

the groundwater in these places was recharged by mixing of groundwater recharged during 1962~1964 and 1986~1993 or 1996~2002. To estimate the idiographic recharge time is impossible.

3. There is tritium in fourteen samples (9, 10, 11, 12, 14, 15, 17, 18, 19, 21, 24, 25, 26 and 28) varying between 2.2 and 14.5 TU. They were located between 1960 and 1986~1993, 1996~2002, to estimate the idiographic recharge time is also difficult. But groundwater of these samples should be recharge by mixing of the water before1960 and after 1986.

6 CONCLUSIONS

The main water type of Ordovician limestone water is $Ca^{-}Mg^{-}SO_4$. SO_4^{2-} was the main anion, and the main cations were Ca^{2+} and Mg^{2+}. The concentration of SO_4^{2-} and Ca^{2+} varied during 238.6–695.0 mg/L and 803.3–2,296.5 mg/L, individually. TDS varied during 1,330.3–3,555.4 mg/l with the average value of 2, 464.4 mg/l. There was very good linear correlation between the concentration of Ca^{2+} and TDS ($R^2 = 0.978$), and the increase velocity of the Ca^{2+} concentration was the largest one. Also, there was the best linear correlation between TDS and the concentration of SO_4^{2-} ($R^2 = 0.996$) and the concentration of SO_4^{2-} had the fastest increase velocity. All these indicated groundwater kept getting Ca^{2+} and SO_4^{2-} along the total flow path.

SI of calcite and dolomite was all greater than 0, which indicated they were oversaturated. SI of gypsum and anhydrite of most groundwater samples was less than 0, suggesting gypsum and anhydrite were unsaturated. This was coincident with the fastest increase of Ca^{2+} and SO_4^{2-}. The distribution of Cl^- and TDS was analogous to groundwater flow field. They was higher in North than that in South, and they were also higher in the places where the water head was low, which indicated the coincidence of the groundwater flow direction with the variation of TDS and the concentration of Cl^-. This commendably demonstrated the coincidence of variation between the groundwater head and the distribution of TDS and Cl^-. So, the distribution of TDS and Cl^- can represent the groundwater flow field to a certain extent.

The representative meteoric water line of the study area is $\delta D = 7.80\delta^{18}O + 6.28$. There was close relationship between precipitation and Ordovician limestone groundwater and the precipitation was the final source of Ordovician limestone groundwater. The value of $\delta^{18}O$ and δD of Ordovician groundwater was much less than that of shallow well and Precipitation, which indicated Ordovician limestone groundwater was not recharged from local precipitation. The tritium age of Ordovician limestone groundwater can be only qualitatively analyzed because of the absence of the observation data. The Ordovician limestone groundwater containing less than 1 TU, 18.4–23.7 TU, 2.2–14.5 TU tritium was individually recharged before 1960, partly recharged after 1960, before 1960 and after 1986.

ACKNOWLEDGEMENTS

Thanks are given to the Natural Science Foundation of China (No. 51204069), the Fundamental Research Funds for the Central Universities of China (No. AQ2013B01) and the project "Study on the groundwater chemistry law of three soft coal seams in Zhengzhou Coalmine" for financial supports and our staffs for sample collections. The authors would like to thank the reviewers of this paper for their useful comments.

REFERENCES

Chen LW, et al. 2003. Study of hydrochemical characteristics in Karst water of coal seam floor in the Mining District of North Anhui (in Chinese). *Coal Geology and Exploration* 31(2):27–31.

Gao B, et al. 2009. Advances in the study of hydrogeochemistry of karst groundwater in coal mines in North China (in Chinese). *Hydrogeology and Engineering Geology* (3):59–63.

Hu WY. 2010. The characteristics of karst and deep coal mine karst water hazards in eastern North China (in Chinese). *Coal Geology and Exploration* 38(2):23–27.

He MC. 2007. Study on the control of deep mining rock mechanics and engineering disaster (in Chinese). *Support in Coal Mine* (3):1–14.

Li XQ, et al. 2006. Study on the geochemistry-isotope characteristics of the groundwater systems in Taiyuan Basin (in Chinese). *Journal of Arid Land Resources and Environment* 20(5):109–113.

Liu FT, et al. 2008. Application of isotope techniques in determining the depth of groundwater circulation (in Chinese). *Yellow River* 30(4):52–54.

Liu XX & Yu KJ. 2002. Hydrogeologic characteristic of Ordovician system in West Yanzhou, Shandong Province (in Chinese). Coal geology and exploration 30(1):38–40.

Ma ZY. 2006. Application of the environmental isotope technique to the study of Karst groundwater in Pingliang City (in Chinese). *Geological Review* 25(6):757–761.

Wu Q & Wang MY. 2006. Characterization of water bursting and discharge into underground mines with multilayered groundwater flow systems in the North China coal basin. *Hydrogeology Journal* 14:882–893.

Wang GC, et al. 2000. Hydro-geochemical exploratory method in mine groundwater hazard control (in Chinese). *The Chinese Journal of Geological Hazard and Control* 11(1):33–37.

Yang YC, et al. 2004. The age and origin of groundwater in the Ordos basin. *Northwestern Geology* 36(1):97–100.

This page intentionally left blank

Progress in Mine Safety Science and Engineering II – He et al. (Eds)
© 2014 Taylor & Francis Group, London, ISBN 978-1-138-00122-0

Discussion on application of strength reduction FEM based on bishop method of soil slope

Wei Yu
Taiyuan University of Technology, Taiyuan, Shanxi, P.R. China
CPI Shanxi Aluminum Co., Ltd., Yuanping, Shanxi, P.R. China

Jingluo Cai
Taiyuan University of Technology, Taiyuan, Shanxi, P.R. China
North China Institute of Science and Technology, Beijing, P.R. China

ABSTRACT: The stability coefficient of soil slope is achieved on the basis of the safety factor calculated by the strength reduction FEM. Through the reduction of values, the FEM computation will not converge when the model reaches plastic zone linking, and the safety factor is just the reduction coefficient at this state. In addition, the stability coefficient obtained by Bishop is fairly closed to the result used by strength reduction FEM. That is, it may indicate the strength reduction FEM has certain applicability in stability coefficient the determination of soil slope.

1 INTRODUCTION

The problems of applicability of strength reduction FEM to the stability of soil slope have attracted Geotechnical sector widespread attention in recent years, but the supportive faction and questioning faction have never stopped arguing. Some people, including Zhao Shangyi and Zhen Ying, carried on the thorough research in the field and obtained certain achievements. At the same time some scholars like Liu Jinlong believe that there exist many problems in the method. Based on Bishop arc surface of sliding stability calculation method the author explores the applicability of this method in soil slopes.

2 CALCULATING THE SLOPE STABILITY COEFFICIENT WITH FINITE ELEMENT STRENGTH REDUCTION FACTOR METHOD

2.1 *Calculating principle e*

In theory, finite element strength reduction factor method can be expressed as: in the finite element static steady-state calculation, if the system is unstable, finite element calculations will not converge. Based on this principle, in the nonlinear finite element slope stability analysis, we obtain formula (1), using equation (1) to adjust the surface of the structure strength (cohesion c and friction angle φ) for reduction, dynamically adjust reduction factor ω, so that the system reaches a critical failure state when finite element static calculation does not converge, then the reduction factor ω is the safety factor of slope stability (ZHAO 2005).

$$\left.\begin{aligned} c' &= \frac{c}{\omega} \\ \tan\phi' &= \frac{\tan\phi}{\omega} \\ F &= \frac{\alpha}{\omega} I_1 + \sqrt{J_2} = \frac{k}{\omega} \end{aligned}\right\} \tag{1}$$

The expression of the formula, α, k is

$$\left.\begin{aligned} \alpha &= \frac{\sin\phi}{\sqrt{3}(\sqrt{3}\cos\theta_S - \sin\theta_S \sin\phi)} \\ k &= \frac{\sqrt{3}\cos\phi}{\sqrt{3}\cos\theta_S - \sin\theta_S \sin\phi} \end{aligned}\right\} \tag{2}$$

In formula (1), I_1, J_2 respectively represent the first invariant of the stress tensor partial second invariant in the stress tensor. Different α, k are constants related to c and ϕ, different α, k represents different circles on plane π, Zhao Shangyi, Zheng Yingren, Deng Weidong gave elaboration and derivation in the relevant articles.

2.2 *Establishment of the model and the solving of its safety coefficient*

We adopted ANSYS finite element program to analyze and calculate and set up the model accord-

ing to the plane strain problem. Soil material is simulated by PLANE82 unit. D-P model is used to describe the constitutive model. Model is built in x-y plane, and the top of the model is free boundary, the left and right sides are level constraint, the bottom is fixed constraint; Unit grid will be refined according to the estimates in the high stress gradient near the sliding zone, in order to save computational resources coarse grid should be applied to low stress gradient and the places far away from the sliding body. The corresponding grid and displacement boundary conditions are shown in figure 1, the soil physical and mechanical indexes are shown in table 1 (LIU 2005).

2.3 *Results and analysis of the finite element calculation*

First, for a certain strength reduction factor ω the entire loading process will be applied to. The conventional elastoplastic numerical calculation will be carried out in accordance with the strength indexes after reduction. In elastoplastic numerical calculations we use incremental iterative nonlinear iteration based on corrected Newton-Raphson method and judge its convergence by the displacement convergence judgment. The soil slope increases with reduction coefficient, the plastic zone development trends are shown in Figures 2–7.

According to the results of numerical simulation, with the increase of reduction factorω, the plastic strain of the slope extends from the bottom of the slope, and when the reduction factor reaches a certain value, the plastic strain zones in the slope goes from top to toe. Then, it can be regarded as the slope safety factor. Through the finite element strength subtraction calculation, when the reduction factor is 1.55, the slope is in critical damage condition, when the reduction factor is 1.60, the finite element calculation no longer converges, so the safety coefficient of the slope is 1.60. The chart of the plastic zone in the slope model destruction when it is perforated (not converged) is showed in Figure 6. The perforation of plastic zone doesn't mean the model is completely destroyed, when the plastic zone developed to a certain extent, and with other factors unfavorable to the slope stability, soil will be overall damaged, and it will generate other perforated plastic zone (HUANG 2006).

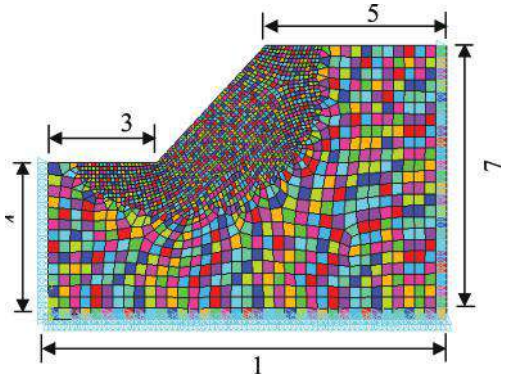


Figure 1. Finite element mesh and displacement boundary conditions (the slope angle $\beta = 45^{o}$).

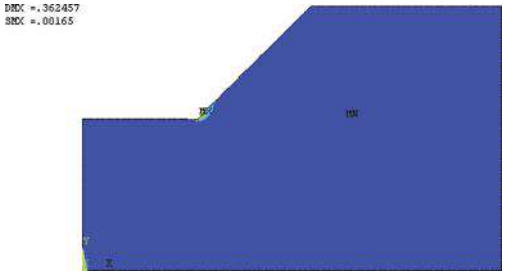


Figure 2. $\omega = 1.00$ plastic strain slope model.

Table 1. Physical and mechanical properties of soil.

	Calculated parameters				
Reduction factor	Cohesive force C(kPa)	Angle of internal friction φ(°)	The natural density γ(kN/m^3)	Modulus of elasticity E (MP)	Poisson's ratio v
1.00	38.00	28.00	19.5	100	0.3
1.20	31.66	23.33	19.5	100	0.3
1.40	27.14	20.00	19.5	100	0.3
1.50	25.33	18.66	19.5	100	0.3
1.55	24.52	18.06	19.5	100	0.3
1.60	23.75	17.50	19.5	100	0.3

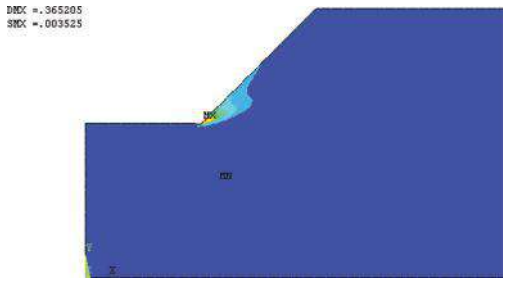


Figure 3. $\omega = 1.20$ plastic strain slope model.

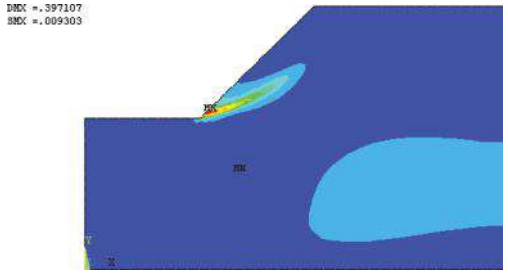


Figure 4. $\omega = 1.40$ plastic strain slope model.

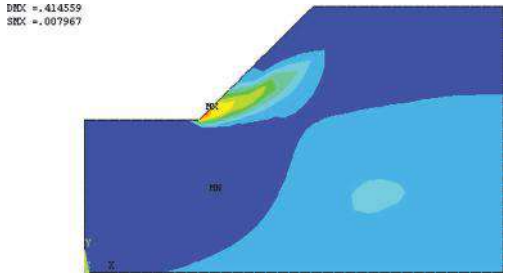


Figure 5. $\omega = 1.50$ plastic strain slope.

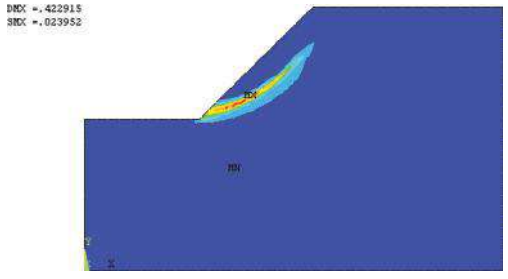


Figure 6. $\omega = 1.55$ plastic strain slope model.

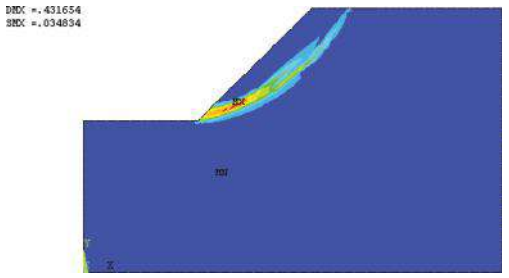


Figure 7. $\omega = 1.60$ plastic strain slope model.

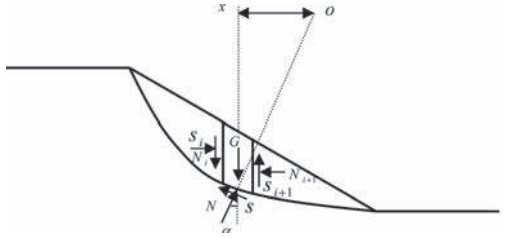


Figure 8. Bishop Method of sliding stability of the circular surface.

3 THE SOIL SLOPE STABILITY COEFFICIENT CALCULATED BY BISHOP METHOD

When the slope of rock is soft and structural plane is in the opposite direction against the slope plane, slope will slide along a curved surface of a slide, rather than flat sliding. Most circular surface soil slope is sliding, therefore, this paper calculates the soil slope stability factor with Bishop method (LI 2006).

Circular surface sliding slope stability coefficient is defined as the ratio of the anti-sliding torque and the sliding torque. As Figure (8) shows, we provided the surface center of the arc is O, and a small block i is chosen, the bottom surface diagonal length is l, width is b. According to slice thought, considering lateral force between soil strips, coefficient of stability can be obtained for the simplified formula.

$$\eta = \frac{\sum (CL\cos\alpha + G\tan\varphi)}{\sum G\sin\alpha \left(\cos\alpha + \frac{\tan\varphi}{\eta}\sin\alpha \right)} \tag{3}$$

In view of the slope in the example, according to formula (3) it is easier to calculate the soil

slope stability coefficient which is 1.52 (calculation process omitted). The value is slightly less than the results of finite element calculation. Thus, the calculating results of finite element strength subtraction and the Bishop calculating results are basically identical. Indeed, that the Bishop method to verify finite element strength reduction that applies to all types of slope safety factor obtained uniqueness requires further in-depth study.

4 CONCLUSIONS

1. The soil side slope, this paper uses the finite element method of strength subtraction for itself which is in the traditional sense of the safety coefficient of stability coefficient, until plastic zone linking. At this time the reduction factor is the required stability coefficient. The coefficient is very close to the result calculated by the Bishop method, which shows the feasibility in engineering application.
2. To some degree, the finite element strength subtraction provides another way for slope stability evaluation, and this method can be used in determining complex slope stability, which can yield twice the result with half the effort. And, of course, the approach in dealing with groundwater elevation, atmospheric precipitation and other issues still needs to solve.
3. Response to some questions about finite element strength subtraction: some scholars believe that "non-convergence of finite element solution as a standard slope failure does not have applicability because there are many affecting factors of the non-convergence." The author thinks that, with the finite element program for slope stability coefficient in the process of determining, in view of the different safety factor, the only change is C and ϕ, and there is no change in using the unit types, constitutive model, geometric shape, meshing, loading way and load step, step, time control and the solving method of select. So the other reasons of non-convergence program can be eliminated, the most possible reason program does not converge is the linking of plastic zone of slope to broken edges.

REFERENCES

Huang Xian-Gui. Application of strength reduction finite element method to slope stability assessment at BEIMENGOU site. *Journal of Engineering Geology,* 2006, 15(5): 665~669.

Li Rong-Jian, Yu Yu-Zhen, Li Guang-Xin. Application of strength reduction FEM to analysis on stability of unsaturated soil slope. *Water Resources and Hydropower Engineering,* 2006, 37(3): 42~45.

Liu Jin-Long, Luan Mao-Tian, Zhao Shao-Fei. Discussion on criteria for evaluating stability of slope in elastoplastic FEM based on shear strength reduction technique. *Rock and Soil Mechanics,* 2005, 26(8): 1345~1348.

Zhao Shang-Yi, Zheng Ying-Ren, Zhang Yu-Fang. Study on slope failure criterion in strength reduction finite element method. *Rock and Soil Mechanics,* 2005, 26(2): 332~336.

Progress in Mine Safety Science and Engineering II – He et al. (Eds)
© 2014 Taylor & Francis Group, London, ISBN 978-1-138-00122-0

Experimental study on macro-micro mechanism of the marble during unloading damage process

Yu Cong, Zaiquan Wang & Liming Zhang
School of Science, Qingdao Technological University, Qingdao, Shandong, China

ABSTRACT: With aim to explore unloading failure mechanism, the unloading confining pressure of marble specimens are carried out. The unloading damage process has been discussed by combining with a variety of analysis methods. The present results show: (1) During the process of unloading confining pressure, the increasing rate of strain energy is gradually increasing until specimens damage; there are inflexion point both axial strain energy curve and total strain energy curve. (2) Acoustic emission events are related to fractures variation of rock sample, the maximum value of ring-down count rate appears at the failure of rock samples, accumulated acoustic emission events appear an inflection point obviously. (3) The failure zones caused by compression have a gradually connecting trend during process of unloading tests, cracks caused by compression are in the majority of cracks. (4) The trend of concentration of shear failure is the direction that failure surfaces develop in.

1 INTRODUCTION

Rocky material has the unique physical mechanical nature that obviously shows characteristics of particle agglomeration under microscopic perspective of microscope, usually deemed to the kind of porous medium material between continuum medium and discontinuous medium. Failure mechanism of the material is urgently needed to be recognized along with extension of human engineering activities. In this situations, the methods, such as energy, discrete element simulation, acoustic emission, are applied to further study of failure mechanism.

Shear failure was inferred(Wang et al. 2003, Wang 2007) through uniaxial compression and criterion of strain instability based on energy through shear test; Tri-shear energy criterion was deduced theoretically (Gao et al. 2007), further coming to the conclusion that M-C criterion is more conservative compared with tri-shear strength criterion considering single shear plane. Acoustic characteristics of three types of unloading way under triaxial stress state were analyzed (Wu & Zhao 1998). Characteristics of acoustic emission of rock failure process was analyzed (Li et al. 2004, Mansurov 1994), under uniaxial compression, such as granite, diabase, limestone, ore, schist. Damage of jointed rock caused by microseism was quantitatively analyzed (Liu et al. 2008, M 2007, M et al. 2001) under the process of underground excavation, discussed failure mechanism of intermittent jointed rock mass under direct shear loading conditions; researched peak and residual strength of joint rock with PFC^{2D}.

The above achievements promote the research of evolution mechanism on material damage, but it is difficulty for understanding of destroying process due to the constraints of current technology, the research with combinations of several analysis methods is rare at the same time. So in this article unloading confining pressure tests of marble had been performed, the unloading evolutionary process is analyzed with combinations of macro-micro methods, such as energy, acoustic emission, discrete element simulations, results that provide references for research of rock material failure mechanism.

2 PRINCIPLE

In the process of deformation and failure, rock releases strain energy in the way of elastic wave called acoustic emission (Wang 2007).

Deformation and failure process of rock is associated with accumulation and release of energy that equals to force times the distance through which the forces acts in physics. Energy analysis of laboratory experiments mainly represents strain energy.

The axial energy absorbed by rock samples, that is, test machine doing axial work to rock samples:

$$E_{axial} = \int \sigma_1 d\varepsilon_1 \tag{1}$$

In the above formula, σ_1 means axial stress, ε_1 means axial strain.

Total energy actually absorbed by rock samples under triaxial stress state:

$$E_{total} = \int \sigma_1 d\varepsilon_1 + 2\int \sigma_3 d\varepsilon_3 \quad (2)$$

In the above formula, σ_3 means confining pressure, ε_3 means circumferential strain, while positive, it means compressed.

Numerical experiments discuss absorption and dissipation of energy during damage process from microscopics. Bond energy is work overcoming the bond force between particles; Friction energy is equal to the product of the friction force and displacement; Boundary energy is equal to the product of the boundary forces and displacement, the sum of the energy of loading system acting on the samples; Kinetic energy is energy of particle motion; Strain energy means stress times strain.

3 TESTING PROGRAM

3.1 *Laboratory test*

According to international rock mechanics testing requirements, Marble was taken with the same batch, fine grained texture, uniform fine texture. After processing into cylinder in the laboratory, diameter 50 mm, height 100 mm, samples were carefully grinded on both ends. The density of samples is about 2500 kg/m^3. In order to reduce the discreteness of testing, rock samples with joint obviously were rejected, then wave speed of rock samples were selected before testing, about 4500 m/s.

The unloading test of marble completed on MTS815.02 electro-hydraulic servo rock mechanics testing machine. According to interval being set, acoustic emission events synchronization was monitored during the whole damage process, by AE21C acoustic emission testing equipment.

Steps: increasing confining pressure to setting value (10, 20, 30, 40 MPa) under hydrostatic pressure condition; the confining pressure remaining unchanged, increasing axial pressure to 60% of peak of samples; simultaneously applying axial stress by displacement rate 0.003 mm/s until rock samples damage.

3.2 *Numerical experimentation*

Unloading simulation test of Marble complete on the discrete element software PFC^{2D}, contact constitutive between particles of model is parallel-bond.

Model specimen parameters: diameter 50 mm; height 100 mm; grain density 2527 kg/m^3; the minimum radius of particle 0.3 mm. The appropriate micro-parameters were debugged based on macro-parameter of laboratory tests: intergranular contact modulus 32 GPa; parallel-bond elastic modulus 25 GPa, mean value of parallel-bond normal strength 60 MPa, mean value of parallel-bond shear strength 70 MPa; intergranular friction coefficient 0.4.

Steps: same as steps of laboratory experiments.

4 ANALYSIS OF THE RESULTS

4.1 *Evolution process of stress*

Stress-strain relation directly reflects parameter evolution rule of laboratory experiments of marble.

Confining pressure is 10 MPa in Fig. 1. The unloading point is elastic stage, in the increasing process of axial pressure, stress-strain curve is almost linear, the slope of axial strain is less than circumferential strain, that is, the rate of increase of axial strain of specimens is more that circumferential strain.

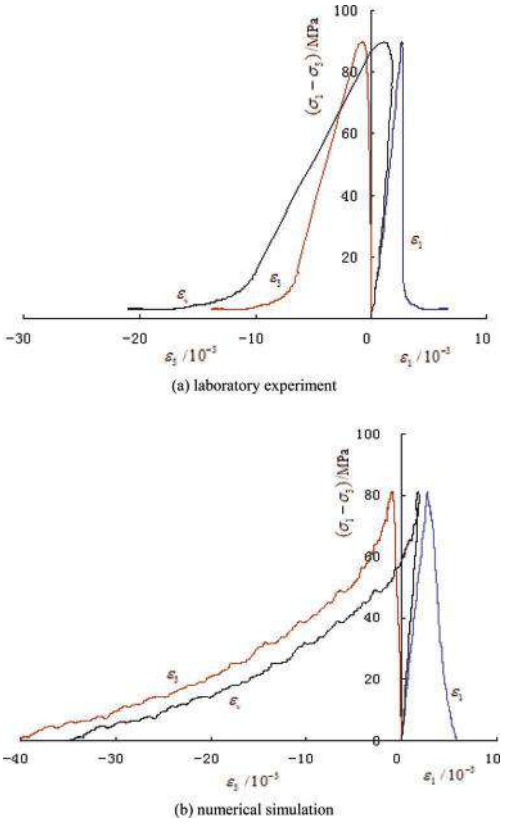


Figure 1. Curves of axial stress-strain.

The slope of axial stress-strain curve increases until unloading confining pressure, while which of circumferential stress-strain slows down, that is, the samples appear volume expansion in the process of unloading confining pressure. Sample is yield stage, which created by tiny cracks or joint surface pressure of rock sample. Past-peak of test specimen, carrying capacity is decreasing with the increment of strain, stepping into the stage of strain softening, until sample damages.

There are some differences in elastic segment between laboratory experiments and numerical experiments (shown in Fig. 1), major reason: micro-fractures of marble internal primitive existed cause load increasing, deformation parameters of test specimen changing, on the contrary, internal of numerical samples are relatively uniform.

The peak of carrying capacity increases with increasing of confining pressure. Specific results, as shown in Table 1. In the view of evolution of stress and specific data, the results of laboratory experiments and numerical simulations are basically consistent, the last one could be used as a complement of the first one.

4.2 *Failure mode*

Failure mode of unloading test specimens is shear forms. As shown in Fig. 2(a), color yellow and black represents same meaning in the below figure of damage of numerical simulation, zones of color yellow represents failure of compression and color black represents failure of tension or shear.

In the figure unloading failure form of samples is under the condition of 10 MPa confining pressure, sample of laboratory experiments appears shear failure, as shown in Fig. 2(a), angle of main failure surface damage is about 51°, there is no obvious dislocation displacement, and there are multiple fractures near the main damage surface. A connectivity main failure surface also exists in the numerical experiments, as shown in Fig. 2(b), the angel is about 53°, failure surface appears along the diagonal to the center of sample, fracture surface is mainly formed by compression, failure of tension or shear also exists on the compression failure surface, and there are several secondary failure surfaces that connected with main damage surface.

Table 1. Experimental data.

Confining pressure /MPa	Peak of axial stress/MPa	
	Laboratory experiments	Numerical simulations
10	94	90
20	110	106
30	131	120
40	149	146

4.3 *Energy response*

Strain energy of laboratory experiment changes in Fig. 3. Stress-strain curve of marble damage, curve of axial energy-strain, curve of total energy-strain.

The laws of evolution of stress-strain curve are shown in Fig. 1. At the beginning of experiments energy absorbed by rock samples is basically used for initial crack such as crack closure, friction sliding et al. Just as stage AB of axial energy-strain of axial energy curve increased by nonlinear parabolic, with a smaller rate of increasing, while value of energy is 0.012 MJ/m^3, increasing rate of curve of axial energy and total energy are essentially coincident. The stage is interpreted as compaction.

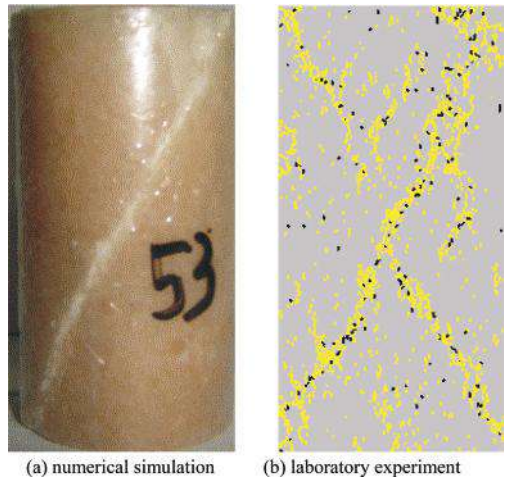


Figure 2. Failure mode of loading test.

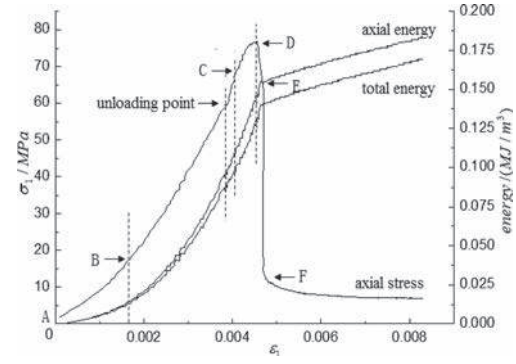


Figure 3. Curves of destructive tests by loading axial stress and unloading confining pressure.

In further experiments, due to stress concentration, generation and propagation of micro-crack, the initial fracture of rock sample had been compacted, the rate of curve is not totally elastic genuinely, but gradually increasing, just as linear elastic stage *BC* of axial energy-strain. The growth rate of axial energy is gradually greater than total energy, axial energy growing to 0.095 MJ/m^3, total energy 0.085 MJ/m^3.

The phenomenon of generation and propagation macro-cracks further improved the proportion of dissipation energy in the energy distribution, just as stage *CE* of axial energy. The curve approximately linearly increased with axial stress increasing slowly and circumferential deformation increasing faster. The growing rate reduced, until breakdown point *E*. The change is evident, even forms a inflection point, energy of point *E* of axial energy is 0.155 MJ/m^3, and total energy almost 0.14 MJ/m^3.

After the inflection point *E*, circumference deformation of rock sample increases rapidly along with axial deformation, shear failure surface appears, rock samples break down. Rate of total energy is apparently higher than axial energy, until point *F*, energy absorbed by rock sample is mainly used for dissipation of frictional energy caused by plastic slipping of rock sample. Growing rate of energy maintained stability.

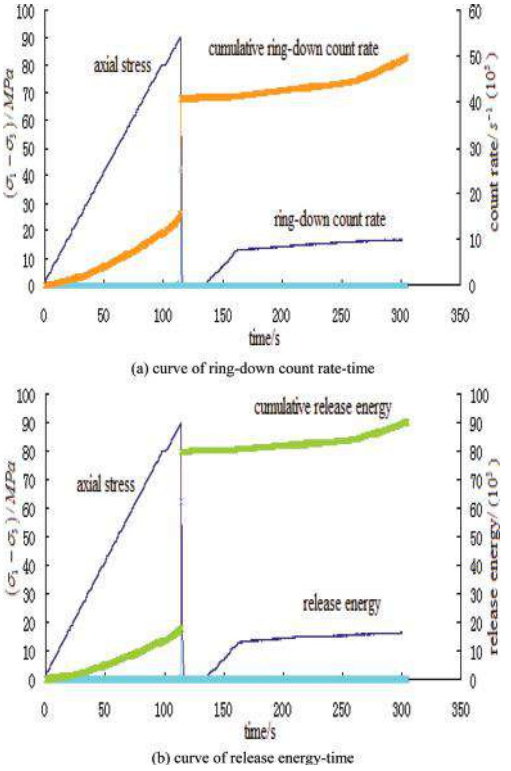


Figure 4. Curves of specimen under unloading confining pressure test.

4.4 *Acoustic emission response*

In the whole process of unloading confining pressure, acoustic emission events appear along with the failure of sample. Before rock sample destroyed, acoustic emission events are gradually increasing, just as cumulative ring-down count rate-time curve in Fig. 4(a), and the increasing rate is also increasing slowly. As shown in Fig. 4(a), the corresponding inflexion point in the stress-strain curve, the largest value of ring-down count rate appears, approximately 110s, at the same time the inflexion point of the cumulative ring-down count rate appears.

After maximum counting rate of acoustic emission events appears, acoustic emission events don't disappeared along with failure of test specimen, active occasionally under the condition of certain level of counting rate. The rate is still linearly growing.

The evolution law of energy of ring-down count rate (shown in Fig. 4(b)) is the same as ring-down count rate.

4.5 *Crack propagation*

The crack extension of failure of Marble has been shown in Fig. 5.

At the beginning of unloading process, rock sample just steps into plastic state, internal specimen appears damage of tension, shear, or compression, but the plastic zones distribute discretely, as shown in Fig. 5(a). There is not directly relationship between the failure zones, but density of distribution all around is higher than the center region.

In further experiments, plastic zones of sample changes along with the different stress state. The failure zones of shear, tension, or compression of central region are increasing in different zones. Tension or shear failure zones of upper increase significantly, but in the bottom compression failure zones increase significantly, and failure surface of compression failure appears firstly. Failure surface of bottom of specimen connects from central region near the outer wall to outer wall, failure zones of bottom keep increasing. Failure zones increase obviously, and there is a trend that points becomes surface in the upper of specimen. Until peak of axial stress, shown in Fig. 5(b), in a short time multiple failure surfaces form, but without connecting between them. Failure surface of upper connect with outer wall, the part in front of individual damage surface appears accumulation of tension or shear, and distribution of surface is higher than others.

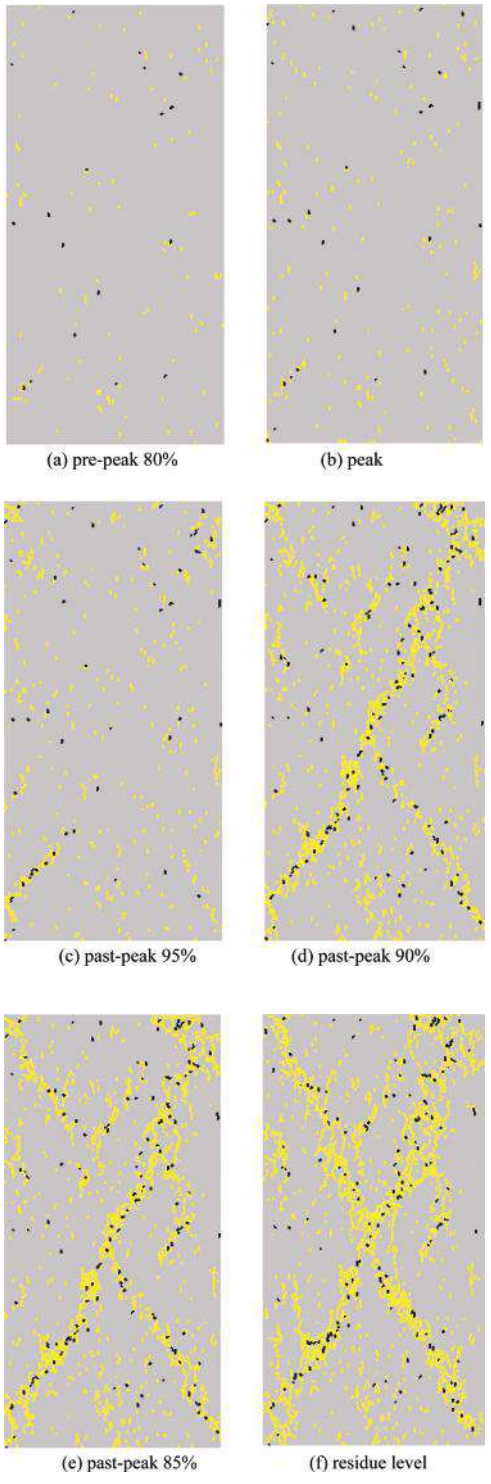


Figure 5. Failure mode of different point of axial stress in unloading process under 10 MPa confining pressure.

The failure surface has been basically formed in past peak stage of axial stress, plastic zones of internal sample mainly focus on secondary failure surface. In past-peak 95%, shown in Fig. 5(c), the main failure surface of upper of specimen connects with secondary failure surface, failure surfaces of upper and bottom that connected with outer wall almost connect. In past-peak 90%, shown in Fig. 5(d, e), due to failure surfaces connecting from upper of specimen to bottom, strength of specimen reduce. Compression is the main cause of failure surface, and failure zones of tension or shear mainly focus on the connected surface, the rest is rarely. In residue level, shown in Fig. 5(f), the change of tensile or shear is not very obvious.

In the unloading process, failure caused by compression is more than tension or shear, there is a trend that failure surface of compression is gradually connecting. At the beginning of experiments, compression failure zones distribute discretely, distribute density of compression failure zones in both sides of sample is gradually higher than others. The trend of concentration of shear failure is the direction that failure surfaces develop in, the connecting shear surface caused by compression is the main factor that caused failure of rock sample. Decreasing of strength of sample is caused by shear failure and connected surface of compression mainly.

5 CONCLUSIONS

This article, based on analysis of unloading of marble, with combinations of several methods, such as energy, acoustic emission and discrete element, comes to the following conclusions:

1. Under different conditions of unloading confining pressure, the evolution law of stress and failure mode of numerical experiments are very similar to laboratory experiments of Marble, this phenomenon shows discrete element numerical experiments could displace the laboratory experiments to some extent.
2. In the process of unloading tests of marble, both axial strain energy and total strain energy are gradually increasing until rock specimens damage. The inflexion point appears in the point of strain energy curves corresponding peak of stress-strain curve.
3. During unloading confining pressure, acoustic emission events are related to fractures variation of rock sample, the maximum value of ring-down count rate appears at the failure of rock, accumulated acoustic emission events appear an inflection point obviously. The evolution laws of Energy of ring-down count rate are similar to what gained from ring-down count rate.

4. The failure zones caused by compression have a gradually connecting trend during process of unloading tests, cracks caused by compression are in the majority of cracks. The trend of concentration of shear failure is the direction that failure surfaces develop in.

ACKNOWLEDGEMENTS

This work is supported by the National Natural Science Foundation of China (41002109, 51074095), The Research Fund for the Doctoral Program of Higher Education (20103721110002) and Shandong Provincial Natural Science Foundation of China (ZR2010DQ021).

REFERENCES

Cai. M. et al. 2007. Peak and Residual Strengths of Jointed Rock Mass and Their Determination for Engineering Design. *Rock Mechanics,* 259–267.

Cai, M. et al. 2001. Quantification of rock mass damage in underground excavation from microseismic event monitoring. *International Journal of Rock Mechanics and Mining Science,* 1135–1145.

Gao Hong, et al. 2007. Study on energy yield criterion of geomaterials. *Chinese Journal of Rock Mechanics and Engineering,* 26: 2437–2443. (in Chinese).

Li Shulin, et al. 2004. Studies of acoustic emission characteristics of uniaxial compressive rock failure. *Chinese Journal of Rock Mechanics and Engineering,* 23:2499–2503. (in Chinese).

Liu Shungui, et al. 2008. Direct shear tests and PFC^{2D} numerical simulation of intermittent joints. *Chinese Journal of Rock Mechanics and Engineering,* 27:1828–1836. (in Chinese).

Mansurov V A. 1994. Acoustic emission from failing rock behavior. *Rock Engng.,* 173–182.

Wang Xuebin. 2007. Unstable criterion of rock specimen subjected to shear failure in uniaxial compression based on energy principle. *Engineering Mechanics,* 24:153–156. (in Chinese).

Wang Xuebin, et al. 2003. Analysis of strain (or the ratio of strain) in the shear band and a criterion on instability based on the energy criterion. *Engineering Mechanics,* 20:111–115. (in Chinese).

Wu Gang & Zhao Zhenyang. 1998. Acoustic emission character of rock materials failure during various stress states. *Chinese Journal of Geotechnical Engineering,* 20: 82–85. (in Chinese).

Progress in Mine Safety Science and Engineering II – He et al. (Eds)
© 2014 Taylor & Francis Group, London, ISBN 978-1-138-00122-0

Graded classification of mine environment geological problems

Qi Chen
China University of Mining and Technology (Beijing), Beijing, China
China University of Geosciences (Beijing), Beijing, China

Wenjie Sun & Qiang Wu
China University of Mining and Technology (Beijing), Beijing, China

Sha Xi
Beijing Keli Huaan Geological Disaster Monitoring Technology Co., Ltd., Beijing, China

ABSTRACT: This paper presented a graded classification of mine environment geological problems, which is based on geology background, sorts of mineral resources, mining methods and mine environment geological problems, and the basis and characteristics of this classification were explained. According to this classification, the causes and dynamic characteristics of mine environment geological problems were well analyzed. This classification can well pinpoint mine environment geological problems, and better guide mine environment recovering treatment projects.

1 THE SUMMARIZATION OF MINE ENVIRONMENT GEOLOGICAL PROBLEMS

1.1 *The current state of study*

The classification of mine environment geological problems is an important part of environment geology, and theoretical basis of scientific management, monitoring of mine environment, as well as precaution and treatment of mine environment geological problems. Correct understanding and scientific classification of mine environment geological problems can guide mine geological environment investigation, evaluation, precaution and treatment effectively. Up to now, many scholars in China and abroad had done much research on mine environment geological problems and put forward various classifications from different perspectives.

We had put forward some classifications according to the nature of problems, sorts of mineral resources and stages of mine development (Wu 2003). Xu Youning et al. had discussed a comprehensive classification according to various basis, and had classified concretely according to the situation in north-west areas (Xu 2006). Zhang Jinde et al. had set mine environment geological problems into four kinds of types according to their forms and influence effects.

1.2 *The genetic classification of mine environment geological problems*

Recently, the author continues research on mine environment geological problems from perspective of treatment demand, holds that the mine environment geological problems are caused by mining actives and changes in mine geological environment, and greatly affected by human being activities, and finally puts forward the genetic classification of mine environment geological problems (Chen 2009).

According to the law of geological environment changes and research on various forming conditions and inducing factors, the causes of mine environment geological problems can be divided into four types: dynamic unbalance in rock and soil mass, change of hydrodynamic condition, dispersion of contamination and multiple restricted factors (Table 1).

1.3 *Classification based on mine environmental effects*

The classification of mine environmental effects, based on the effects of mine environment geological problems, is put forward according to the requirements of mine environment management (Hu 2004, Jiang 2004). In the process of mineral

Table 1. The genetic classification of mine environment geological problems.

Genetic type	Mine environment geological problems	Relevant mining behavior
Dynamic unbalance in rock and soil mass	Mined out area breakdown, ground fissures, collapse, mountain cracking, landslide, slope failure in accumulation	Evacuation, blast working, unloading slope, solid waste accumulation
Change of hydrodynamic condition	Karst collapse, land subsidence, ground fissures, soil erosion, land desertification, seawater invasion, etc.	Pumping and drainage, liquid waste discharge
Dispersion of contamination	Rock and soil pollution, surface and ground water pollution, spontaneous combustion in coal gangue	Solid waste accumulation, waste liquid discharge
Multiple restricted factors	Mine debris flow, tailings dam failure	Slope cutting, solid waste accumulation, tailings dam construction

resources exploitation, mine environment geological problems appear with characteristics of time and space, and there is causal relationship between parts of these problems. When sorts of these problems occurred and overlapped simultaneously, their seriousness will be increased and cause comprehensive environmental effects, which can be divided into four types: land resources effects, water environment effects, secondary disaster effects as well as landscape and ecology effects (Table 2).

No matter what perspectives (such as sorts of mineral resources, mining methods and mine exploitation history) the classifications consider about, each classification has its own perspective, emphasis and sound basis. Therefore, each classification is reasonable and practicable. However, these classifications have their own limitations because of their insufficient analysis on relationship between various inducing factors. Considering conflict between current mine environment situations and mining development as well as requirement of mine environment management, graded classification, which is based on geology background, sorts of mineral resources, mining methods and mine environment geological problems, was put forward on the basis of further discussion.

Table 2. Classification based on mine environmental effects.

Environmental effects	Relevant mine environment geological problems	Analysis on effect form
Land resources effects	Solid waste accumulation and contamination, ground surface deformation, water loss and soil erosion, desertification, etc.	Cut down the total of land resources by occupation, mechanical damage, chemical contamination, etc.
Water environment effects	Liquid (solid) waste permeation and leaching pollution, great fall of water level caused by mine drainage and gushing	Damage water resources by cutting down water quantity because of cone of depression's presentence and contaminating surface and underground water resources by liquid (solid) permeation and leaching pollution
Secondary disaster effects	Ground surface deformation, water loss and soil erosion, desertification, solid waste occupation, tailings dam failure, spontaneous combustion in coal gangue, radioactive contamination, etc.	Mine secondary geology disasters are induced or aggravated by mismanagement of many problems
Landscape and ecology effects	Water loss and soil erosion, desertification, ground surface deformation, solid waste occupation, naked mountain rock, collapse and landslide, etc.	Transformation in landform and landscape overwhelms its capacity at the cost of landscape damage and decline in resources and species

This classification puts more emphasis on mine environment geological problems' characteristics, which are progressive increase, overlap, complication and dynamic change property. So it can better guide mine geology environment treatment engineering projects and achieve better effect.

2 GRADED CLASSIFICATION

As for the productive mines, various mine environment geological problems have occurred or are occurring, but seriousness of these problems differ from it in closed mines. If these problems were solved only by prevention, they would definitely restrict exploitation and aggravate the conflict between mine environment protection and mine development. If these problems were not treated properly, it means chronic suicide and runs counter to the aim of sustainable development.

How to treat these mine environment geological problems, on the promise of protecting mine environment and accelerating mine development, is an urgent task. Therefore, the graded classification, which is a useful attempt to meet the requirement of mine geology environment treatment, is put forward.

This classification try to analyze mine environment geological problems from the angles of geology background, sorts of mineral resources and mining methods (Figure 1), and accurately explain the causes, characteristics, seriousness and law of dynamic changes.

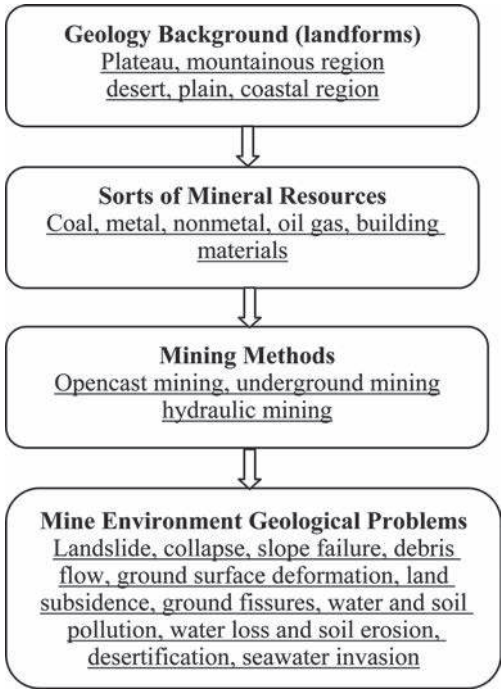


Figure 1. The diagram of graded classification of mine environment geological problems.

3 THE BASIS OF GRADED CLASSIFICATION

The graded classification includes four gradations: mine geology background, sorts of mineral resources, mining methods and mine environment geological problems. These four gradations are the analyzing contents, basic conditions and dynamic inducing factors of mine environment geological problems. The basis of classification is as follows (Table 3).

3.1 *Geology background*

The gradation of mine geology background concludes regional structure, geologic history, formation lithology, rock mass structure, topography characteristic, climate, hydrological conditions, etc (Figure 2). These are basic conditions of mine environment geological problems. The mine environment geological problems always vary in different geology backgrounds. Collapse, landslide, debris flow, water loss and soil erosion and other secondary mine disasters possibly take place in mountainous area; while in plain, it is likely to occur ground surface deformation as well as water and soil pollution. In contrast, it is possible to occur seawater invasion in coastal region. The consideration aspects are as follows:

Table 3. The contents of graded classification.

Gradation	Contents	Representation content
Geology background	Regional structure, formation lithology, topography characteristic, climate and hydrological conditions	The basic gradation
Sorts of mineral resources	Coal, metal, nonmetal, oil gas, building materials	Reflect storage conditions of ore body
Mining methods	Opencast mining, underground mining, hydraulic mining	Reflect the strength of man-mad interference
Mine environment geological problems	Landslide, collapse, slope failure, debris flow, ground surface deformation, land subsidence, ground fissures, water and soil pollution, water loss and soil erosion, desertification, seawater invasion	Reflect characteristics of concrete problems

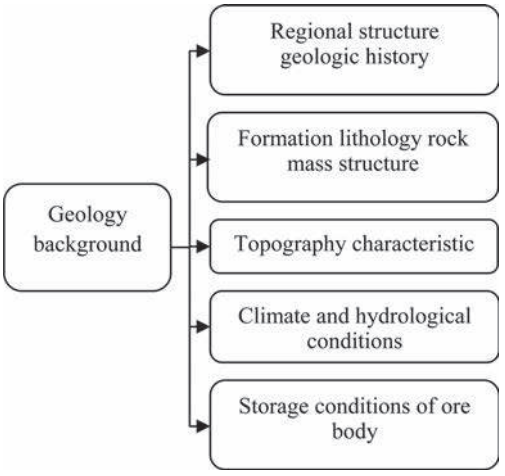


Figure 2. Factors of the geology background.

(1) Being the main factor of environment geological problems

Geology background can better reflect basic conditions of occurrence and distribution law of mine environment geological problems. Meanwhile, geology background concludes the storage conditions of ore body.

Geology background is the primary factor of mine environment geological problems, which restricts the occurrence and seriousness of these problems. If geology background is good enough, not every mining action can cause mine environment geological problems, or these problems are in slight condition. Otherwise, the environment capacity is low and mining action can surely cause environment geological problems which are probably serious.

(2) Restricting other relevant factors

Geology background is the basic gradation of graded classification, and restricts other factors. As to sorts of mineral resources, the formation of mineral resources have something to do with tectonic movement in history, rock metamorphism, changes of paleoclimate and paleogeography, etc. The storage conditions of ore body are decided by geology background. As for mining method, the exploring way is related to sorts of mineral resources and geology background. For instance, the exploring way of gold bearing rocks, whether using opencast mining or underground mining, is decided by the location where the ore body is, while the exploring way of alluvial gold is always hydraulic mining.

(3) Deciding the characteristics of mine environment geological problems

The characteristics of mine environment geological problems are restricted by geology background to a great extent. When it comes to the problems of stability of slope, there are great differences in rock slope and soil slope. Compared to soil slope, because the rock slope has structure property, it is always in high completeness and strength. While the temporal slope formed by solid waste accumulation is always with poor stability because of its fast accumulation, uneven grains and different ingredients. As for the ground fissures caused by mining subsistence, the one in different geomorphic units, like mountain district and plain district, has different effects. In mountain district, if the fissure approaches the free face, unstable rock, formed by distension fissure, is likely to collapse and should be taken into account. While if the ground fissure is located in the outer fringe of depressive basin, its effect is obvious and is easy to be solved.

(4) Affecting the application of treatment measures

The application of treatment measures is closely relevant to mine geology background. As for rock slope, anti-slide piles and pre-stressed anchor cable can be used; retaining wall and lattice frame are applied to treat soil slope; pruning the shape and controlling the angle of the slope are often used in treatment of loose accumulations. With ground fissures mentioned above, anchoring is used to reinforce the unstable rock, and fulfilling and grouting are applied to treat the outer fringe ground fissures.

Mine environment geological problems are greatly decided by geomorphic unit, complexity of geological structure and storage conditions of ore body. Landforms are obvious in different geology background, so we use topographic feature as basis of classification. According to different geomorphic unit, the areas, including mountainous region, plateau, desert, inland plain and ocean-front are divided (Table 4).

3.2 *Sorts of mineral resources*

The characteristics of major mine environment geological problems in different mines vary. In mental mines, because of huge volume of excavation, the solid waste is numerous, and it is more likely to occur heavy metal pollution and to cause serious pollution. Some resources like coal are buried beneath the ground. The direct problems in these mines are mining subsidence and gangue spontaneous combustion, no matter opencast mining or underground mining is used. It is more likely to occur land desertification in the process

Table 4. Mine environment geological problems in different geology background.

Geology background	Mine environment geological problems
Plateau	Land subsidence, ground fissures, water loss and soil erosion, water and soil pollution
Mountainous region	Landslide, collapse, mountain cracking, debris flow, failings dam failure, water loss and soil erosion, water and soil pollution
Desert	Land desertification, salinization, water loss and soil erosion, water and soil pollution
Inland plain	Land subsidence, ground fissures, water and soil pollution
Oceanfront	Land subsidence, ground fissures, water and soil pollution, seawater invasion

of exploitation of oil and gas, and expose rock and destroy landscape in building materials mines.

The sorts of mineral resources restrict the kinds of mine environment geological problems. They are as follows.

(1) Reflect the differences of ore body storage conditions. The metallogenic conditions and storage conditions of different mineral resources are varied.

Basically, the storage conditions depend on geology background, especially in large-scale structural movement and multistage magmatic activities in the long geologic period. Different formation causes and generating environment cause diverse mine environment geological problems.

(2) Decide mining methods. Different sorts of mineral resources use various mining methods.
Diverse mining methods decide different mine environment geological problems. For example, underground mining of coal resources often causes mining subsidence; opencast mining often causes slope failure and air pollution.

Using sorts of mineral resources as basis to classify, there can be four types: coal, mental, soil and gas, as well as building material. Besides ground deformation, solid waste occupation, water and soil pollution and secondary disasters, some special and representative mine environment geological problems of all sorts of mineral resources are all concluded below.

Table 5. Different sorts of mineral resources of mine environment geological problems.

Sorts of mineral resources	Universal mine environment geological problems	Special mine environment geological problems
Coal	Ground surface deformation, solid waste occupation, water and soil pollution, secondary geology disasters	Gangue spontaneous combustion
Mental		Heavy metal pollution
Oil and gas		Organic pollution, land desertification
Building maters		Naked rock, landscape damage

3.3 *Mining methods*

The relationship between mine environment geological problems and mining activities should not be neglected. In general, mine environment geological problems are always caused by mining activities.

Almost all environment geological problems have something to do with mining activities. Different mining methods decide diverse environment geological problems. Effect of mining method towards environment geological problems concludes disturbance, rebuilding, and damage of rock and soil around mining objects.

Opencast mining always causes readjustment of internal stress in steep slope formed by excavation, change of slope stress condition by shock wave, and decrease of strength in open-pit rock and soil slope, and finally induces some environment geological problems like landslide and collapse.

While, underground mining always causes environment geological problems like mining subsistence or collapse of mind-out area. The formed mined-out area, the ratio of mining depth to mining thickness, tunneling ways and roof managements are all related to mining method. If full face driving and caving roof management were used, it would probably cause mining subsidence with serious consequences. However, if reserved coal or rock pillar roof management were used, the occurrence of mining subsistence would be less and the consequences would be slight. Moreover, miss-management of all kinds of solid waste and disordered accumulation, not only destroy landscapes and create pollution, but increase the possibility of mine debris flow.

Mining method and mining intensity decide whether the mine environment geological problems occur and control their seriousness. Therefore, if mining activities were controlled properly, and advanced technology and scientific management were used, mine environment geological problems would be protected to a certain degree.

Table 6. Different mining methods of mine environment geological problems.

Mining method	Mine environment geological problems
Opencast mining	High and steep slope failure, water loss and soil erosion, solid waste occupation, tailings dam failure
Underground mining	Land subsidence, ground fissures, solid waste occupation, tailings dam failure
Hydraulic mining	Landscape damage, river pollution

Using mining methods as basis to classify, there are three types: opencast mining, underground mining and hydraulic mining. They are as follows.

3.4 *Mine environment geological problems*

In specific geology background, as to a kind of mineral resources with a specific mining method, several mine environment geological problems may be generated. If one of these factors above changes, the mine environment geological problems probably change accordingly.

As the mining production continues, mine geological environment changes and mine environment geological problems become serious. Mine environment geological problems have time effect, and these problems will become more serious with long history and large-scale mining. The seriousness of mine environment geological problems is reflected by mining methods, mining intensity and the extent of damage to mine environment.

The characteristic, seriousness and complexity of mine environment geological problems together determine the difficulty of treatment towards mine environment.

(1) The characteristic of mine environment geological problems

The characteristic of mine environment geological problems is the main basis of treatment mode. Technical measures of different environmental problems vary and they are the key of successful treatment.

In the process of mining, physical property changes, strength decrease, local deformation and displacement as well as global failure of rock and soil, which are caused by mining activities, always induce problems like slope failure, ground deformation, etc. Therefore, the treatment measures should be emphasized on deformation and failure mode, scale and other properties. Moreover, the problems like water loss and soil erosion and desertification are all caused by obvious hydro-geological condition changes. The conflict between surface water permeation and surface runoff should be put more attention. When solving problems like disorder emission of solid and liquid waste, which will cause water and soil pollution, we should put emphasis on chemical constituent changes in water and soil so to prevent them from permeation. Considering characteristics, technical property and applicability of treatment measures, the graded classification can be generally formed.

(2) The seriousness of mine environment geological problems

The seriousness of mine environment geological problems is judged by influence sphere, damage consequences and seriousness of environment pollution. Single or multiple problems, environmental effects, and slight or seriousness influence of these problems should all be taken into account.

Generally, there is a single mine environment geological problem with slight, unobvious influence and pollution in the early stage of mining. Therefore, the single mode can be chosen. With the increase of mining, there are multiple and serious environmental problems, and environmental effect gradually appear. As a result, the treatment measures should consider the complexity and overlapping of these problems, and a comprehensive treatment mode should be applied.

(3) Difficulty of management

There are positive correlations between difficulty of management and complexity and seriousness of these problems. In addition, the difficulty of management technology, management quantity, personnel and equipment investment and expenses for project are all concluded.

The difficulty of management technology is decided by project scale and technology complexity. In general, the scale effect of management object restricts the project management level and difficulty of management technology. The management technology difficulty of large-scale and small-scale projects varies. The large-scale project probably needs pre-stressed anchor with anti-slide piles or other measures, specific investigation and accurate design calculation before construction, while the small-scale one may just need simple slope protection measures. The more serious the mine environment geological problems are, the more difficult the management is, companied by more project quantity and expenses. Under this circumstance, comprehensive management mode is generally available.

4 THE CHARACTERISTICS OF GRADED CLASSIFICATION

As to most productive mines, mine environment geological problems have occurred disproportionally.

Most mines had single problem initially but overlapping problems later on. And these problems become more and more serious. The task of mine geology environment protection and mine environment geological problems management become arduous.

Therefore, the presentation of graded classification is a good idea to enhance management effectiveness of mine environment geological problems, which is depended on correct measures and reasonable design. Absolutely, correct measures are based on clear understanding of complex and comprehensive mine environment geological problems. As a result, the graded classification is the basis of research on management technology and mode, and is also the theory of management practice.

This comprehensive classification considers the restriction of geology background, sorts of mineral resources and mining methods.

The characteristics of this classification are as follows.

(1) Well targeted
This classification is based on the analysis of geology background, focuses on basic conditions of mine environment geological problems, specifies the inducing mechanism and major inducing factors, and analyzes these problems progressively and exactly.

(2) Reflecting dynamic characteristics
This classification emphasizes the influence and restriction of mining methods. Therefore, it can effectively reflect the influence on environment and dynamic characteristics of mine environment geological problems.

(3) With practical significance
This classification is put forward with the purpose of guiding management practice. So, it emphasizes the effect of management mode. Because of the characteristics of this classification, the management mode based on this classification is well targeted so as to guarantee management effectively.

Anyway, the classification of mine environment geological problems is the theory basis of mine geological environment management. This classification focuses on productive mines, and through easy and in-depth analysis, this classification can better guide mine geological environment management.

ACKNOWLEDGEMENTS

This study was financially supported by the Fundamental Research Funds for the Central Universities (2013QD03), which we gratefully acknowledge.

REFERENCES

Chen Q., 2009. Research of Treatment Technology of Mine Environment and Treatment Model. *China University of Mining and Technology(Beijing)*: 90–102.

Hu D., 2004. Brief Introduction on International Mine Environmental Protection Management and the Suggestions for China. *Environmental protection,* 13(2): 39–40.

Jiang J., 2004. Guide on Geological Environment Management of Mine. *Beijing: the Earthquake Publishing House*.

Wu Q., 2003. Study of Classification of Geologic Environmental Problems in Mines in China. *Hydrogeology and Engineering Geology,* (5): 107–111.

Xu Y., 2006. Survey and Assessment on Environment geological problems of Mine in Northwest China. *Bejing: the Geological Publishing House*.

This page intentionally left blank

Progress in Mine Safety Science and Engineering II – He et al. (Eds)
© 2014 Taylor & Francis Group, London, ISBN 978-1-138-00122-0

Preliminary study on safety audit

Shu-Ming Wang & Juan Xu
Jinling Institute of Technology, Nanjing, China

Xiao-Fei Liu
Faculty of Safety Engineering, China University of Mining and Technology, Xuzhou, China
Post-doctoral Scientific Research Workstation of Jizhong Energy Group Co., Ltd., Xingtai, China

ABSTRACT: Safety development is the important guarantee of sustainable development of human society. Safety audit could help enterprises; especially mining companies to implement the safety responsibility effectively and establish a long-term mine safety production mechanism. This research is based on the theoretical framework of the establishment of safety audit and the discussion of operation of practical safety audit cases.

Keywords: Safety; Audit; Safety investment; Safety Theory

1 INTRODUCTION

Mine is one of the main energy resources and mining provides the most important production resource for China's economic and social development. As a result, Mine safety relates closely to state property and people's lives and safety as well as the harmony and stability of the whole society. Overall, in the recent years, with the efforts of every aspects, the development of technology and standardized enterprise management continued to improve, China mine safety and production on the whole showed relatively stable. But on the other hand, serious safety accidents occurred along with the huge amount of total accidents. In a word, mine production safety situation is still grim. As is proved by practice, in order to realize the permanent stability of the mine safety production, we must establish an effective long-term mechanism of safe production in mines. We should carry out active audit work effectively, mine safety audit should play the role of supervision and inspections, promoting mining earnestly implement the safe production responsibility. It would conscientiously implement the various laws and regulations of production safety ensure safety in production of the necessary inputs, the implementations of safety measures continue to improve the safe production conditions. In order to promote the mine safety production status of fundamental improvement, the whole system should be standardized, including the mine production of operation management and supervision system on the right track.

2 THE CONNOTATION OF THE SAFETY AUDIT AND ITS ROLE

Safety audit sprang up in the 1970s and it is a new branch of audit system. At present, the research of safety audit is still in the exploratory stage, and it has not formed a theoretical model of the system. In the 1970s, British Road Traffic Ordinance (1974) first put forward the necessity of safety audit for new roads. In 1990, the ministry of transport issued a "standard of road safety audit". Later, this method is introduced rapidly to Australia, New Zealand, Canada, the United States and other many countries, and became a kind of important method of road traffic safety management. In recent 10 years, many countries are in the process of safety protection and governance, they began to attach importance to the participation of the independent audit supervision and evaluation functions. Safety audit has been preliminary application in e-government, aviation safety, road traffic safety, and other fields. But in the grim situation of safety production industry has not been widely used in mines, the lack of related basic theory support is one of the key factors.

As a new branch of audit, what is a safety audit has not been determined yet. Considering all aspects of the comprehensive point of view, the authors think that, the safety audit is that audit institutions and their staff used, according to the laws, regulations and policy provisions of the state of production safety responsibility fulfillment situation evaluation or verification to promote coal enterprises earnestly implement production safety

responsibility. It is also an independent surveillance activities which improves production safety conditions and makes it conform to the requirements of the safe development. As an independent category, the supervision of safety audit has unique features which other economic supervision do not contain.

Compared with the developed countries, there is still a big gap of production safety guarantee mechanism between China and other developed countries. One of the reasons is that Safety agency did not play a necessary role. The application of intermediary institutions for evaluation, certification and identification of occupational safety and health, is an important means of national production safety supervision work and this method has been a practice in many developed countries. As the number of safety agency and their management level continue to increase, safety agencies promote safety production standard. Safety auditing theories contribute to the development of intermediary organizations of safety audit activities and help them expand their business scope.

As safety audit is an independent audit activity for safe production supervision and evaluation, it helps enterprises to comply with safety laws and regulations. Besides, it helps enterprises to enforce safety facility realize the "three simultaneous". What's more, safety audit helps related departments to It helps to supervise production accidents compensation in place in time. It contributes urge enterprises to secure investment in a timely manner and in full, etc. Thus safety audit ensures production safety situation improved fundamentally.

3 THEORETICAL STRUCTURE OF SAFETY AUDIT

3.1 *Auditing theory structure*

Theoretical structure of audit is the internal system audit linkages between various elements, the manner and order in the interaction, for example, the internal arrangement of the elements and combinations. The key of theoretical structure of the audit is to determine what the logical starting point for research is. After this key step, the following permutations and combinations of the elements of the problem is very simple manners. Whether the auditing theory and its structure is correct depend heavily on the proper selection and scientific logical of starting point. In order to play a constructive role in the coal mine safety management, safety audit, we must understand the theoretical structure of coal mine safety audit at first.

Domestic and foreign scholars hold different perspectives on the theoretical structure of the specific content of the audit, and the logical starting point for the theoretical structure can be divided into the following five typical views:

1.To audit philosophical basis as the logical starting point.

In 1961, two professors: Mertz and Sharaf published "Auditing theoretical structure", and the book created a structure of audit theory of precedent. They think that theoretical structure of the audit: Audit philosophical foundation—Audit assumption—auditing concepts—application of standards—the practical application. Two professors considered that "to audit the philosophical basis for the logical starting point" and they were in favor of a more philosophical level of auditing theory, in the absence of systematic audits of theoretical research it was very important. However, it seems that this is too abstract to audit the philosophical basis for the logical starting point now. If on a broader scope, the content is not easy to determine. Thus, they should choose a more specific and more relevant auditing theory logical starting point.

2. To audit hypothesis as the logical starting point

This view is to audit hypothesis as the basic starting point. The auditing concepts to be applied, forming a series of auditing standards, thereby affecting audit practice and guidance. It can generally be described as the concept of an audit, assuming an audit auditing standards an audit practice. Audit assumption can not explain many phenomena, and as is proved in the history, auditing hypothesis as the logical starting point is not the right choice.

3. To audit the environment as the logic starting point

This view showed the emergence and development has always been audited by the environmental impact and disposal. Audit environment and external environment affect the sum of the audits; internal audit environment determines the nature and functions of the external environment determines the objectives of the audit. By auditing, the environmental audit can reveal the logical starting point in the development of all the factors and the objective law. However, I believe it will affect the audit environment audit theory, though it just auditing theory building is a prerequisite or external condition. In the theoretical structure, audit is inseparable from any one part of the investigation on the environment, but it is not a theoretical structure of the internal audit of the logical starting point.

4. To audit the essence as the logical starting point

This view is revealed that only accurate audit nature could establish audit theoretical structure in order

to grasp the development direction of auditing theory. Audit essentially theoretical starting point in our study of auditing theory has been dominant. We thought that audit nature cannot be put a direct reflection of the changing economic environment in the theoretical structure of the audit, which often results in the disconnection between theory and practice. Meanwhile, the same as the truth, one can only infinitely close to nature in essence and cannot be grasped. Moreover, people have different interpretations of the nature auditing to audit the essence of the theory as a starting point will lead to the audit system and the economic environment is not from the audit practice guidance.

5. The logical starting point to the audit objectives Audit target is under certain historical condition, the main body of audit achieves the desired outcome through the auditing practice. The audit goal starting point theory believes that, as a system, the audit should understand objectives at first, if there is no target the systems will be unthinkable. Meanwhile, only based on the consistent goal, auditing standards can be useful and effective. The audit-goal-based starting point of audit theory research is the most popularin the current. prevalent, it is subject to the impact of the Accounting Research and the emergence of goal-oriented, "the Montgomery Auditing" is an example. Some people think that in order to audit the audit objectives theoretical structure as the logical starting point is inappropriate. Audit objective is to guide the audit practice can only say that the starting point for the audit theory as a guide if the logical starting point, it may cause incomplete audit theory structure and biased.

3.2 *Safety audit theoretical structure*

Governments receive the public's tax, so they have a responsibility to protect the public interest. Due to safety and public properties of the "external effect", it is difficult for the market mechanism to achieve optimal allocation of resources in mine safety production; the public began to demand the government from the perspective of the public interest for the mine production safety management. Safety responsibility will be the government's fiduciary duty. It is entrusted with the responsibility to expand the field of mine safety. Safety audit will become an important element of the audit.

To play a safety audit in safety production of construction, you must first clear theoretical structure of safety audit. Since the entire audit objectives play a guiding role in the theoretical structure, this paper starts from the safety objectives of the audit and establishes the theoretical construct structural framework of safety audit, shown in Figure 1.

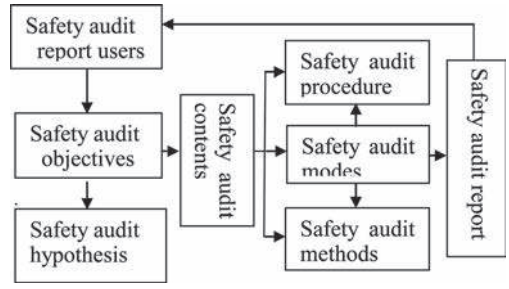


Figure 1. Theoretical framework of safety audit.

According to the realistic environment faced by the safety audit and safety audit report users determine the purpose of the safety audit objectives, only by determining the safety audit objectives at first, can we define the direction of activities. The theoretical structure of safety audit in the target is a priority position which reflects and embodies the essence of the safety audit requirements. To achieve the audit objectives, we need to clear the contents of the safety audit, scientific design of safety audit model and select the appropriate audit procedures and methods. Meanwhile, we should ultimately the formation of appropriate safety audit reports through information disclosure and accountability mechanisms in order to achieve the established safety audit functions of development services for safety audit external environment.

4 SAFETY AUDITING PRACTICE

Safety audit in our country has not carried out large-scale, and it's still in exploring in many aspects. In the light of the realistic situation of mine safety audit in china, the author advocates the establishment of practical structure as shown in Figure 2.

4.1 *Safety audition preparation*

Saying goes, "forewarned is forearmed." Do anything, we will succeed by considering the preparation beforehand, otherwise you will fail. Safety audition preparation was essential to the audit goal. It's mainly focused on the following aspects.

1. The establishment of safety audit service type
Pre audit preparation should be due to different types of audit. Enterprise safety audit is generally divided into three types: (1)commissioned by the government department in charge of production safety. The central or local government department in charge of production safety according to the safety production situation in the region, com-

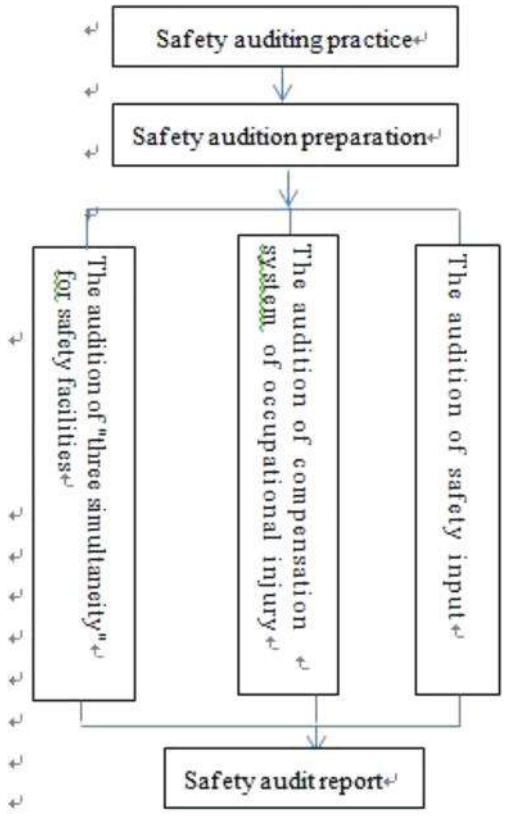


Figure 2. Safety auditing practice framework.

bined with the actual needs of the supervision and administration of production safety, entrusted with the safety audit qualification implemented safety audit of enterprises. (2) the form of consultation with the enterprise. Based on recognizing the importance and role of safety audit, audit unit with the audited entity signed a safety audit agreement (or contract), to determine the objectives and content of the work, the time to carry out audit work; (3) invited and commissioned by the enterprise. According to their own safety production management, enterprises take the initiative to invite audit unit to audit themselves.

2. Clear objectives and scope of safety audit

Safety audit can be large or small, can be complicated or simple. Different audit objectives determine the different scope of the audit; will determine the type of audit resources. For different types of safety audits and their specific audit objectives is not the same. Safety audit specific goals should be based on the audit conclusion using objective and preparing work process. Emphasis on the development of enterprises, the safety and sustainable development has an important influence, there are important matters to the enlightenment to the management of the enterprise, should focus on risk control and audit activities governance process.

3. Determine the safety audit staff and work arrangements

Safety audit unit should be based on the project's objectives and its safety audit risk level selected auditors, determination of audit project leader. In determining the audit staff should strictly implement the avoidance system, and maintain the independence of the audit team members. In considering the staff, attention should be paid to the professional knowledge structure and competence, hire safety professionals when necessary. Audit project manager carry on the division of the members according to the specific target of auditing projects.

4. Make safety audit program

Before the development of the audit program, Before making the audit plan, auditors need to be audited entity related aspects of understanding. In the specific implementation of audit project, safety audit project leader should be aware of the following information concerning the audited entity to initially grasp the audited units of production safety situation: (1) the characteristics of safety production and general situation of audit unit; (2) for safety audit content laws, rules and regulations; (3)the design and operation situation of the audited units safety control system; (4)the important meeting record; (5)important contracts and agreements; (6)the relevant safety assessment documents.

In the specific implementation of a safety audit project, safety audit project leader should be fully aware of the following circumstances, an initial assessment of the importance of this safety audit and audit risk: (1) ask the audited entity related personnel and related management; (2) access to the audited entity's operations manual, the internal control manual and other information; (3) access to the audited entity annual production and safety plans, financial budget and other documents; (4) check the safety activities or safety issues certificates and records; (5) examine the audited unit production, business activities and the implementation of internal control; (6) select the number of safety events to be tested.

The audit plan should be made by the leader of safety audit project based on this safety audit objectives, preliminary information and preliminary assessment of internal control and risk level. The audit program shall include the following contents: (1) the basis for preparing the audit program; (2) the name of the audited entity and

the basic situation; (3) the audit objectives; (4) the audit scope, content, key, methods and audit procedures; (5) the scheduled audit date; (6) the importance of identifying and audit risk assessment; (7) the leader of audit project, members and their division of labor; (8) the staff and date; (9) other related content.

4.2 *The audition of "three simultaneity" for safety facilities*

The audition of "three simultaneity" for safety facilities, refers to the production and business units new construction, renovation, expansion project (hereinafter referred to as construction projects) safety facilities, with the main project must be designed, constructed and put into production and use at the same time. In the safety facilities "three simultaneous" audit, the following content should focus on the review and appraisal of the audited units and safety facilities "three simultaneous" related: (1) the audited entity in the process of production and operation of the relevant safety production laws and regulations, policies, planning, budget, contract compliance program, etc.; (2) safety project risk identification, assessment and response measures; (3) the appropriateness and effectiveness of relevant safety control activities; (4) safety liabilities assets, safety, safety-related expenditure items such as financial and non-financial information acquisition, processing, and delivery.

Safety auditors should collect the following safety facilities and non-financial information related to the project: (1) the written request for the project construction units; (2) safety preassessment report; (3) safety specific report and relevant documentation about project preliminary design; (4) written approval of preliminary design safety facilities of construction projects; (5) the project completion report and related construction drawings; (6) the safety assessment report; (7) safety facilities construction project completion and acceptance approval letter; (8) technical indicator information applies to the audited entity 's safety facilities "three simultaneous". Safety facilities "three simultaneous" can be audited by audit, supervision, observation, inquiry, confirmation, calculation, analysis and review and other conventional methods of audit. Due to the comprehensive and technology of safety audit project, safety auditors should also use cost-benefit analysis and economic evaluation of safety and other methods.

4.3 *The audition of compensation system of occupational injury*

Occupational accidents, refers to workers in enterprises in order to produce and work in production time and production activities in the region, due to the effect of risk factors in the production process, or not on the production and jobs, but because of the business environment, equipment, or other adverse working conditions, causing bodily harm, either temporarily or long-term incapacity of the accident.

No uniform standard of compensation of work-related accidents, the majority of enterprises to industrial injury accident compensation has many man-made factors and random factors, generally at a failed to follow State, the amount of compensation is generally low, and the compensation is often not in place in time. Conflicts between employers and employees in turn, affects the social harmony and stability, and become an urgent social problems. Lower compensation amount, the objective is also to make some employers do not pay attention to safety work, or even ignore the occurrence of accidents, further exacerbated by the frequent occurrence of accidents, injuries caught in the vicious cycle, is not conducive to safety. Meanwhile, the workers' life, health, safety and other legal rights are not adequately protected.
Injuries compensation audit focused on two points:

1. the compensation standard is compliance with the law ? In different industries, different regions and different times compensation standards are not always consistent, such as low compensation standards for mining industry. From January 1, 2011 onwards, according to " Work Injury Insurance Regulations " requirement, death caused due to a production safety accident of the workers, their lump-sum death benefits on your national standards adjusted to the annual per capita disposable income of urban residents at 20 times, paid to the dead workers near relatives. At the same time, according to the law to ensure that workers killed one-off funeral allowance, dependent relatives pensions have been issued.
2. whether the amount of compensation in full and on time? This is often the focal point of dispute between employers and employees. Third party provide relevant audit opinion, help to the safety supervision department of law enforcement, effective protection of injured employees to the legitimate rights and interests.

4.4 *The audition of safety input*

Safety input, is an enterprise operating in the production process in order to ensure production safety and improve the working environment and the prevention of occupational hazards and consumption of manpower, material and financial

resources. During safety input audits, review and evaluation should focus on the audited entity with the following safety—related inputs to perform conformance testing: (1) the audited entity operating in the production process of the relevant safety laws and regulations, rules, policies, plans, budgets, procedures and other compliance; (2) the extraction cost standard of safety production, extraction time, extraction using scope and regulatory measures. (3) concerning safety assets, safety liabilities, safety expenditure items such as the financial information and non-financial information acquisition, processing, transmission.

Safety auditors should collect the following financial information relating to safety input: (1) If there is safety assets? (2) Safety spending does take place? (3) Safety assets are owned by the audited entity? (4) Structural condition of safe assets; (5) Safety assets records are complete? (6) The safety asset valuation is appropriate? (7) Ending balance of safe assets is correct? (8) Disclosure of safety assets in the accounting statements is appropriate?

Safety auditors should collect the following non-financial information relating to safety input: (1) Enterprise safety culture and safety management activities; (2) The safety awareness of employees.

4.5 *Safety audit reports*

Safety audit reports are written document which the auditors compile in accordance with relevant laws and regulations in order to realize the implementation of a safety audit of the audited entity on the basis of production safety audit opinion. Safety audit report is the direct results of audit work. Safety auditors should work in accordance with the content, scope and requirements of safety audit. And the auditors should also process work papers by sorting and analysis, comprehensive, classification, analysis of audit evidence to identify problems and correct the audit opinion as well as conclusions What's more, those responsible should be asked to sign in safety audit reports.

Safety audit report written records, together with the audited entity feedbacks are responsible for safety audit for review, modification to form an audit report. Then the reports should be submitted to the audited entity and signed by management layer.

Safety audit report body should include the following contents:

1. audit summary: To clarify safety audit project basis, objectives and scope of the audit, the audit focus and the content such as auditing standards.
2. audit basis: safety audit should declared that it is in accordance with the provisions of technical standards for safety audit of Jiangsu province, if it is not follow the standard case, auditors should add explanation and illustration.
3. the audit conclusion: According to the facts that have been identified, the unit being audited safety operations and internal controls to evaluate performance in the affirmative, while the audit results was found that the main problem was described in detail. Auditors should give the corresponding treatment advice. If necessary, a separate audit decisions issued independently.
4. the audit proposals: Auditors should focus on the main safety issues where safety audit findings affect the safety of production, business activities and internal control in order to strengthen and improve safety audit quality.

5 CONCLUSIONS

1. Safety audit as a special supervision and evaluation of the enterprise safety in production of the independent auditing activities, actively and effectively carry out mine safety audit work, to play the role of audit supervision and inspection, contribute to the promotion of mines to implement the main responsibility for production safety, serious implementation of the laws and regulations of production safety, ensure the safety of the necessary inputs production, the implementation of various safety measures, improve the conditions for safety production.
2. The development of safety audit theory contributes to the intermediary institutions to carry out the safety audit activities, expand their business scope.
3. Since the audit objectives in the structure theory of the entire audit has a guiding role in the security audit security, audit objectives are a priority in the theoretical structure reflect and embody the essence of the security audit requirements, but they also fully reflects the real needs of safe production practices. Therefore, the authors advocate the establishment of objectives for the logical starting point security audit security audit theoretical framework.
4. Security audit units should do a good job the following audit preparation work: establish security audit service types; clear security audit objectives and scope; determine the safety audit staff and the organization of work; develop safety audit program.
5. We believe that the current security audit work should focus on the following three aspects: security facility "three simultaneous" audit; injuries compensation audits; investment in safety audits.

ACKNOWLEDGEMENTS

This paper was supported by Jinling Institute of Technology doctoral scientific research foundation(jit-b-201230) and Safety Technology Project of Jiangsu Provine(2010–49). Here we express our appreciation.

REFERENCES

Cai, C. & Chen, X.Y. 2006. *On the Environmental Auditing*. Beijing: China Economic Times Press.

Chen, B. & Guo, Y.H. 2007. *Analysis of Road Factors in Traffic safety and Safety audit*. Chengdu: Southwest Jiaotong University press.

Chen, D.K. et al. 2004. Study on Compensation System of Occupational Injury in China. *China Safety Science Journal*. 2004(9):12–15.

Huang, R.B. 2011. Guarding State Environmental Safety With Audit Supervision. *Environmental Protection,* 2011 (9):23–29.

Liu, M.H. 2003. The Use of Auditing Environment Point to Build up the Auditing as Logical Starting Theory Structure, *Audit & Economy Research,* 2003(7):3–7.

Liu, R.Q. 2009. Discussion on Audit preparation. *Finance Aspect*.2009 (12):37–39.

Liu, W. 2006. How to Build Audit Theory Structure. *Economic Forum,* 2006 (14):139–140.

Li, X. et al. 2002. Study on Environmental Auditing Theory Structure. *Finance and Trade Research,* 2002(5):107–111.

Shen, Z. 2000. Analysis on the Auditing Theory Structure. *Modern Finance & Economics.* 2000 (1):26–29.

Wang, S.M. & He, X.Q. 2008. Study on Safety Accounting. *Friends of Accounting,* 2008(6):32–34.

Wu, J.J. & Bi, X.L. 2003. On the Structure of Audit Theory. *Journal of Shandong University of Finance,* 2003 (1):78–82.

Yang, L.J. 2011. Industrial Accidents Compensation Model: Choice, Confusion and Prospects. *Journal of Shanxi Academv of Governance,* 2011(4):94–97.

This page intentionally left blank

As societies continue to grow and develop, the demand for energy has increased worldwide. In China, coal is still one of the principal energy resources and it is expected that more coal mining projects are needed in the future. As mining operations continue to increase their production rates and discover more ore reserves, mine safety issues have become more urgent. Even more than in the past there is a greater need to understand these issues better. **Progress in Mine Safety Science and Engineering II** discusses mine safety techniques and technologies, methods and approaches, as well as problems and issues. The contributions cover a wide range of topics:

- Coal mine safety
- Metal and non-metal mine safety
- Mine product testing technology and safety symbol management
- Mine rescue tools and techniques
- Mine safety management and standardization
- Mine safety science and theory
- Occupational health and safety in mines
- Petroleum and natural gas exploitation

Progress in Mine Safety Science and Engineering II will be invaluable to academics and engineers interested or involved in mine safety issues.

CRC Press
Taylor & Francis Group
an **informa** business
www.crcpress.com

6000 Broken Sound Parkway, NW
Suite 300, Boca Raton, FL 33487
Schipholweg 107C
2316 XC Leiden, NL
2 Park Square, Milton Park
Abingdon, Oxon OX14 4RN, UK

ISBN 978-1-138-00122-0

an **informa** business